

SCIENCE ABSTRACTS, SERIES A

Physics Abstracts

U. of ILL. LIBRARY

OCT - 7 1968

CHICAGO CIRCLE

1968 Subject Index Number
Part I (January-June)

An INSPEC Publication
The Institution of Electrical Engineers



Digitized by the Internet Archive
in 2025

SUBJECT INDEX-PART I

INTRODUCTION

The entries in this index refer to the abstracts by their serial number, not by the page number. The entries are grouped under headings (printed in bold type, e.g. "**Abrasion**") which represent, in the main, general categories or concepts rather than specific names. If a heading for a particular subject does not appear, a more general heading should be consulted; for example, "Zone plates" would be listed under "**Diffraction/light**"; "Barkhausen discontinuities" under "**Magnetization process**". There are numerous cross-references directing attention to related headings in other parts of the index.

Many of the headings are subdivided by the use of subheadings, which are indented (i.e. printed slightly to the right) and commence with a small letter (for example, see the subheadings under "**Absorption**").

ARRANGEMENT OF HEADINGS AND SUBHEADINGS

The headings are arranged throughout the index in alphabetical order according to British Standard 1749:1951 (the "word by word" system, not "reading right through"). The subheadings, with a few exceptions, are themselves arranged in alphabetical order under their respective headings. The exceptions (for example, see the subheadings under "**Spectra**", "**Crystal structure, atomic**") are cases where a more logical order is preferable to a purely alphabetical one.

ARRANGEMENTS OF ENTRIES UNDER HEADINGS

Entries are arranged in two alphabetical groups as follows. First group: generalities and named substances (in words); second group: named substances (chemical formulae). If a search is being made for a particular substance, both the first and second alphabetical groups should be inspected since, for example, alumina may also be listed as Al_2O_3 .

COLLECTED LIST OF SUBJECT HEADINGS

The alphabetical arrangement of the headings is the most convenient for locating a known heading quickly, but there may be other related headings elsewhere in the index of which the reader is unaware, and which he would only come across by accident. To assist the reader to discover all the headings appropriate to his subject, a collected list of the headings is given on pages S2 to S16, which follow this page; they should be consulted as a matter of routine each time a search is made. In this list, the headings are not arranged in alphabetical order, but are grouped into sections by subject on the same basis as the arrangement of the abstracts in the monthly issues of Physics Abstracts. By using this list, the reader can quickly determine which are the headings appropriate to his subject, and they are then easily found in the main index in their alphabetical position.

HEADINGS WITH NO ENTRIES

Because physics is a developing subject, it is not possible to maintain the list of headings unchanged from year to year; it is subject to a continuous process of revision, with the introduction of new headings and subheadings, and the alteration and elimination of old ones. This process is a gradual one, however, and the great majority of the headings are the same as those of the previous year. To assist in maintaining the continuity of the index, all the headings in current use in a given year are printed, even those for which there are no abstracts to be recorded. The latter are followed by the announcement "No entries"; this supplies confirmation that these headings have not been dropped from the index, and entries may reappear under them in the next issue of the index.

ELEMENTS, COMPOUNDS AND OTHER SUBSTANCES

The names of elements, their compounds, a few compounds of special interest (e.g. "**Ruby**", "**Water**") and a few common materials (e.g. "**Wood**", "**Paper**") are included as headings or subheadings (e.g. "**barium titanate**" under "**Barium compounds**"). Under these, as well as under the appropriate "subject" headings, are listed any abstracts which contain significant physical information about the element, compound or substance named; except however, that abstracts listed under headings referring to nuclear properties, including radioactivity, are not necessarily also listed under the substance name. The entries under these headings are themselves arranged in alphabetical order of substance or nuclide names, so that a given substance can be readily located.

Inorganic compounds of the elements are listed under the first element in the chemical formula, and all the compounds of a given element are grouped under a single heading (e.g. "**Sodium compounds**"). Alloys are listed under compounds of the base or first-named constituent, e.g. Au-Ag alloys under "**Gold compounds**". There are also four special headings for the common alloys: "**Aluminium alloys**", "**Copper alloys**", "**Iron alloys**", "**Nickel alloys**". Organic compounds are grouped under "**Organic compounds**", "**Polymers**", "**Plastics**" and under special substance headings such as "**Paper**", "**Proteins**", etc.; all the latter are listed in the collected list of headings at the end of the index.

BEFORE USING INDEX, CONSULT LIST OF SUBJECT HEADINGS ON PAGES S2-S16,
WHICH FOLLOW THIS PAGE

LIST OF SUBJECT INDEX HEADINGS

The headings used in the Alphabetical Index are listed below. The headings are grouped into sections on the same basis as the arrangement of the abstracts in the monthly issues of Physics Abstracts. Each section lists the headings which concern its subject and it follows that many of the headings are listed in several places.

An introduction to the Subject Index will be found on page S1

GENERAL

Bibliographies
Biographies
Books

Collections of physical data
Conferences
History

Laboratories
Laboratory apparatus and technique
Nomenclature and symbols

Physics
Physics fundamentals
Reviews

EDUCATION

Biographies
Books
History

Laboratories
Laboratory apparatus and technique

Physics
Physics fundamentals

Reviews
Teaching demonstrations

UNITS · MEASUREMENT · METROLOGY

Acceleration measurement
Alignment
Anemometers
Angle measurement
Angular velocity measurement
Area measurement
Balances
Constants
Density measurement

Dimensions
Dynamometers
Force measurement
Instruments
Interferometry
Length measurement
Manometers
Measurement errors

Mechanical measurement
Micrometry
Nomenclature and symbols
Particle size
Pressure measurement
Recording
Standards
Strain gauges
Stroboscopes

Surface measurement
Thickness measurement
Time interval measurement
Time measurement
Units
Vapour pressure measurement
Velocity measurement
Volume measurement

MATHEMATICAL PHYSICS

Algebra
Differential equations
Equations
Field theory, classical
Fluctuations
Fourier analysis
Functions

Geometry
Group theory
Hysteresis
Information theory
Integral equations
Integrals

Mathematics
Matrices
Probability
Radiation
Relaxation
Series

Statistical analysis applications
Tensors
Transformations, mathematical
Vectors
Waves

MATHEMATICAL METHODS COMPUTATION

Calculating apparatus
analogue apparatus
digital computers
digital computer programmes
Calculation
Graphs

Nomograms
Sliderules
Statistical analysis applications
Tables, mathematical

MECHANICS

Ballistics
Centrifuges
Dynamics
Friction
Gravitation
Gyroscopes
Impact
Kinematics

Mechanics
Pendulums
Pressure
Rockets
Rotating bodies
Torsion
Velocity

Elasticity · Plasticity

Bending
Compressibility
Damping
Deformation
Elastic deformation
Elasticity
Photoelasticity
Plastic deformation

Plasticity
Relaxation
Rheology
Stress analysis
Stresses, internal
Thermoelasticity
Viscoelasticity

GRAVITATION · RELATIVITY

Gravitation
Relativity
general
special
unified field theories

STATISTICAL PHYSICS

Bosons
Brownian movement
Electron gas
Fermions
Fluctuations
Hysteresis
Information theory
Kinetic theory
Probability

Quantum theory
many-particle systems
Random processes
Relaxation
Statistical analysis applications
Statistical mechanics
Thermodynamics

Thermodynamics

Entropy
properties of substances
Equations of state
gases
liquids
solids

Joule—Thomson effect
Thermodynamic properties
Thermodynamics applications

TRANSPORT PROCESSES

Diffusion
Radiation

Radiative transfer
Transport processes

VIBRATIONS · WAVES · ACOUSTICS

Oscillations
Vibrations
Waves

VIBRATIONS · ELASTIC WAVES

Damping
Elastic waves
Membranes
Oscillations
Piezoelectric oscillations
Relaxation
Resonators
Seismic waves

Shock waves
 effects
Vibrating bodies
Vibrations
 excitation
 measurement
Waves

Diffraction/
 acoustic waves
 acoustic waves, ultrasonic
Diffusion/
 acoustic waves
Dispersion, acoustic
 ultrasonic
Doppler effect
Echo
Helium/
 liquid, sound propagation
Holography
Intensity measurement/
 acoustics
Interference/
 acoustic waves
Interferometers/
 acoustic waves
Interferometry/
 acoustic waves
Magnetoacoustic effects
Microphones
Musical instruments
Noise/
 acoustic
Noise abatement
Physical effects of radiations
Radiation pressure

Reflection/
 acoustic waves
 acoustic waves, ultrasonic
Refraction/
 acoustic waves
 acoustic waves, ultrasonic
Reverberation
Scattering/
 acoustic waves
 acoustic waves, ultrasonic
Schlieren systems
Sound ranging
Sound recording
Sound reproduction
Speech
Stroboscopes
Transmission/
 acoustic waves
 acoustic waves, ultrasonic
Ultrasonics
Velocity/
 acoustic waves
 acoustic waves, ultrasonic
Velocity measurement/
 acoustic waves
 acoustic waves, ultrasonic

SHOCK WAVES

Detonation
Explosions
 nuclear
Schlieren systems

Shock tubes
Shock waves
 effects
Supersonic flow

ACOUSTICS

Absorption/
 acoustic waves
 acoustic waves, ultrasonic
Acoustic analysis
Acoustic generators
Acoustic impedance
Acoustic radiators
Acoustic receivers
Acoustic resonators
Acoustic streaming
Acoustic transducers
Acoustic wave propagation
 ultrasonic

Acoustic waves
 effects
Acoustical laboratories
Acoustical measurement
Acoustics
 musical
Acoustoelectric effects
Architectural acoustics
Atmospheric acoustics
Biological effects of radiations
Chemical effects of radiations/
 acoustic waves

Hearing · Speech

Ear
Hearing

Noise/
 acoustic
Speech

HEAT

Bolometers
Calorimeters
Calorimetry
Combustion
Conductivity, thermal
Convection
Cooling
Cryostats

Emissivity
Flames
Heat
Heat conduction
Heat transfer
Heat treatment
Heating
High-temperature production
 [and effects]

Latent heat
Pyrometers
Radiation
 heat
Radiation detectors
Radiation pressure
Radiative transfer
Specific heat
Temperature

Temperature distribution
Temperature measurement
 spectral methods
Thermal expansion
Thermal measurement
Thermocouples
Thermometers
 resistance
Thermostats

LOW-TEMPERATURE PHYSICS

Cryostats
Joule-Thomson effect
Liquefaction, gases
Low-temperature phenomena
Low-temperature production

Low-temperature technique
Magnetic cooling
Quantum theory/
 many-particle systems
Superconductivity

Liquid and Solid Helium

Helium/
 liquid
 liquid, sound propagation
 solid
Superfluidity

ELECTRICITY AND MAGNETISM

Electricity
Electromagnetism
Magnetism

**ELECTRICAL MEASUREMENTS
AND CIRCUITS**

Amplifiers
Circuits
Counting circuits
Dielectric measurement
Electrical measurement
Fluctuations/
electrical
High-voltage production
Image convertors and amplifiers
Plasma/
measurement technique

Direct Conversion

Electricity/
direct conversion
Magnetohydrodynamics

ELECTROSTATICS · DIELECTRICS

Breakdown, electric
Contact potential
Dielectric devices
Dielectric phenomena
Electrets
Electric charge
Electric fields
effects
Electric strength
Electroluminescence
Electrostatics
Electrostriction
Ferroelectric phenomena
High-voltage production
Hysteresis
Piezoelectric oscillations
Piezoelectricity
Pyroelectricity
Relaxation
Space charge
Triboelectricity

CURRENT ELECTRICITY

Acoustoelectric effects
Conduction, electrical
Conductivity, electrical
measurement
Contact potential
Contact resistance
Current, electrical
Eddy-currents
Electric charge
Electrical properties of subst.
Electrokinetic effects
Electromotive force
Electron gas
Electrons
Electro-optical effects
Electrophoresis
Fluctuations/
electrical
Hall effect
Inductance
Magnetoelectric effects
Magnetoresistance
Photoconductivity
Photoelectricity
Photoelectromagnetic effects
Photovoltaic effects
Piezoresistance
Rectifiers
Resistance, electrical
Semiconductors
Skin effect
Space charge
Superconductivity
Thermocouples
Thermoelectricity

MAGNETISM

Antiferromagnetism
Compasses
de Haas—van Alphen effect
Diamagnetism
Ferrimagnetism
Ferromagnetism
spin-wave theory
Gyromagnetic effect
Gyromagnetic ratio
Hall effect
Magnetic devices
Magnetic field measurement
Magnetic fields
effects
Magnetic films
Magnetic measurement
Magnetic resonance and relaxa
Magnetism
Magnetization process
Magnetization state
Magnetoacoustic effects
Magnetoelectric effects
Magnetomechanical effects
Magneto-optical effects
Magnetoresistance
Magnetostriction
Magnetothermal effects
Magnets
Paramagnetism

ELECTROMAGNETISM

Eddy-currents
Electromagnetism
Electromagnetic fields
Electromotive force
Inductance

ELECTRODYNAMICS · PARTICLE OPTICS

Electrodynamics
Particle optics
Particle range
Particle velocity analysis

**ELECTRON BEAMS
ELECTRON OPTICS AND TUBES**

Electron beams
effects
Electron diffraction
Electron gas
Electron lenses
electrostatic
magnetic
Electron microscopes
Electron microscopy
Electron optics
Electron tubes
Electrons
absorption
ionization
radiation
scattering
Fluctuations/
electrical
Gas-discharge tubes
Image convertors and amplifiers
Photomultipliers
Space charge

**ION BEAMS
ION OPTICS AND SOURCES**

Bremsstrahlung
Ion beams
effects
Ion microscopes
Ion optics
Ion sources
Ion velocity
Ions
recombination
scattering
Sputtering

**MAGNETOHYDRODYNAMICS
MAGNETOGASDYNAMICS**

Electricity/
direct conversion
Magnetohydrodynamics
Plasma/
magnetohydrodynamics
Shock waves
effects

ELECTROMAGNETIC WAVES AND OSCILLATIONS

Electromagnetic oscillations
 Electromagnetic waves
 Light/
 electromagnetic theory
 Radiation

GENERATION AND PROPAGATION

Absorption/
 electromagnetic waves
 Amplifiers
 Diffraction/
 electromagnetic waves
 Diffusion/
 electromagnetic waves
 Doppler effect
 Electromagnetic oscillations
 Electromagnetic wave
 atmosphere [propagation
 ionosphere
 guided waves
 Electromagnetic waves
 radiators

Interference/
 electromagnetic waves
 Interferometers/
 electromagnetic waves
 Interferometry/
 electromagnetic waves
 Plasma/
 electromagnetic wave propagation
 Reflection/
 electromagnetic waves
 Refraction/
 electromagnetic waves
 Scattering/
 electromagnetic waves

**RADIOFREQUENCY SPECTROSCOPY
MAGNETIC RESONANCES**

Antiferromagnetic resonance
 Cyclotron resonance
 Ferrimagnetic resonance
 Ferromagnetic relaxation
 Ferromagnetic resonance
 Magnetic resonance and
 [relaxation
 Nuclear magnetic resonance and
 measurement [relaxation
 Nuclear quadrupole resonance
 Paramagnetic resonance and
 measurement [relaxation
 Spectra
 Spectrometers, radiofrequency
 Spectroscopy, radiofrequency

MASERS

Amplifiers
 Masers

Optical pumping

Lasers

Amplifiers
 Holography
 Lasers
 gaseous
 solid

Light
 coherence
 Optical pumping

OPTICS

Doppler effect
 Electro-optical effects
 Light
 coherence
 e.m. theory

Light sources
 Optics

Photons
 Photophoresis
 Radiation
 Radiation pressure

Velocity/
 light
 Velocity measurement/
 light

PHOTOMETRY · COLORIMETRY

Bolometers
 Brightness
 Colorimetry
 Colour
 Densitometry
 Emissivity

Illumination
 Photometers
 Photometry
 light sources
 Pyrometers
 Radiation detectors

Spectroscopy

Astronomical spectra
 Atmospheric spectra
 Monochromators
 Spectral line breadth
 Spectrochemical analysis
 Spectrometers
 accessories
 Spectrophotometers

Spectrophotometry
 Spectroscopy
 light sources
 Stark effect
 Temperature measurement/
 spectral methods
 Zeeman effect

GEOMETRICAL OPTICS

Aberrations, optical
 Dispersion, optical
 Lenses
 aspherical
 photographic
 Mirrors
 Optical images
 Optical systems
 Optics/
 geometrical

Prisms, optical
 Reflection/
 light
 Refraction/
 light
 Refractive index/
 light
 Resolving power, optics
 Schlieren systems
 Stereoscopy

PHYSICAL OPTICS

Absorption/
 light
 Diffraction/
 light
 Diffraction gratings
 Diffusion/
 light
 Dispersion, optical
 Doppler effect
 Double refraction
 flow
 mechanical
 Electro-optical effects
 Filters, optical
 Holography
 Interference/
 light
 Interferometers/
 light
 Interferometry/
 light
 Magneto-optical effects

Optical constants
 Optical films
 Optical pumping
 Optical rotation
 Photoelasticity
 Pleochroism
 Polarimeters
 Polarized light
 Reflection/
 light
 Reflectivity
 Refraction/
 light
 Refractive index/
 light
 Scattering/
 light
 Transmission/
 light
 Transparency

INSTRUMENTAL OPTICS

Aberrations, optical
 Dispersion, optical
 Filters, optical
 Glass
 Image convertors and
 Lasers [amplifiers
 gaseous
 solid
 Lenses
 aspherical
 photographic
 Light sources
 Luminescent devices
 Microscopes
 Microscopy
 Mirrors
 Optical constants
 Optical films
 Optical images
 Optical instrument testing

Optical instruments
 Optical materials
 Optical systems
 Prisms, optical
 Projectors, optical
 Quartz
 Reflection/
 light
 Refraction/
 light
 Refractive index/
 light
 Refractive index measurement
 Refractometers
 Resolving power, optics
 Schlieren systems
 Stereoscopy
 Stroboscopes
 Telescopes

PHOTOGRAPHY

Cameras
Cinematography
Densitometry
Lenses/
 photographic
Light sources
Nuclear track emulsions
Photographic materials
 sensitivity

Photographic process
 development
Photography
 applications
 colour
 high-speed
Radiography

VISION

Eye
Colour vision

Stereoscopy
Vision

X-RAYS · TUBES AND TECHNIQUES

Dosimetry
High-voltage production
Radiation monitoring
Radiation protection
Radiography

X-ray absorption
X-ray diffraction
X-ray examination of materials
X-ray measurement

X-ray monochromators
X-ray reflection
X-ray scattering
X-ray spectra
 absorption
 emission

X-ray spectrometers
X-ray spectroscopy
X-ray tubes
X-rays
 effects

QUANTUM THEORY

Collision processes
Dispersion relations
Indeterminacy

Parity
Quantum electrodynamics

Quantum theory
 application methods
 many-particle systems
 quantization
 wave equations

Scattering

QUANTUM FIELD THEORY

Current algebra
Dispersion relations

Field theory, quantum
 interactions
 interactions, strong
 interactions, weak
 meson field
 quantization

Nuclear forces
Parity
Quantum electrodynamics
Quantum theory
 application methods
 many-particle systems
 quantization
 wave equations

S-matrix theory
Scattering

ELEMENTARY PARTICLE AND NUCLEAR MEASUREMENTS**APPARATUS · PARTICLE DETECTORS**

Alpha-ray spectrometers
Beta-ray spectrometers
Counters
 accessories
 Cherenkov
 crystal
 Geiger
 operation technique
 proportional
 scintillation
 semiconductor
 spark
 statistical analysis

Dosimetry
Gamma-ray spectrometers
Ionization chambers
Neutron spectrometers
Nuclear bombardment targets
Particle accelerators
Particle detectors
Particle optics
Particle spectrometers
Particle velocity analysis
Photomultipliers
Radioactivity measurement/
 apparatus

Counting Circuits

Amplifiers
Counting circuits

Track Visualization

Bubble chambers
Cloud chambers
Luminescence chambers
Nuclear track emulsions

Particle range
Particle tracks
Particle track visualization
Spark chambers

PARTICLE ACCELERATORS

High-voltage production
Ion sources

Particle accelerators
 linear
 orbital
 orbital, cyclotrons

ELEMENTARY PARTICLES

Bosons
Elementary particles
Fermions
Parity
Particle range
Particle velocity analysis
Quarks
Scattering, particles
Strange particles

Elementary Particle Theory

Bosons
Collision processes
Current algebra
Dispersion relations
Elementary particles
Fermions
Field theory, quantum
interactions
interactions, strong
interactions, weak
meson field
quantization
Nuclear forces
Parity
S-matrix theory
Scattering, particles
Strange particles

Photons · Gamma-rays · X-rays

Bremsstrahlung
Cherenkov radiation
Compton effect
Gamma-ray spectrometers
Gamma-rays
absorption
angular distribution
detection, measurement
effects
scattering
Mössbauer effect
Photons
interactions
polarization
scattering
X-ray absorption
X-ray diffraction
X-ray measurement
X-ray reflection
X-ray scattering
X-rays
effects

Leptons

Leptons

Neutrinos

Neutrinos and antineutrinos

Electrons

Beta-ray spectra
conversion electrons
Beta-ray spectrometers
Beta-rays
absorption
angular distribution
detection, measurement
effects
polarization
scattering
Electron pairs
annihilation
production
Electron theory
Electrons
absorption
ionization
radiation
scattering
scattering, electron-proton
Positronium
Positrons

Muons

Muons
capture
decay
detection, measurement
interactions
production
scattering
Muonium

Hadrons

Hadrons

Quarks

Mesons

Mesons
absorption
capture
decay
decay observations
detection, measurement
effects
interactions
magnetic moment
mass
production
scattering
spin and parity
Pions
decay
interactions
interactions, pion-nucleon
interactions, pion-pion
interactions, pion-proton
production
scattering
scattering, pion-nucleon
scattering, pion-pion
scattering, pion-proton
Strange particles

Meson Resonances

Mesons
resonances

Baryons

Baryons

Nucleons

Nuclear forces
Nucleons and antinucleons
antinucleons
interactions
interactions, nucleon-nucleon
scattering
scattering, nucleon-nucleon

Protons

Proton spectra
Protons and antiprotons
absorption
angular distribution
antiprotons
detection, measurement
effects
interactions
interactions, proton-proton
magnetic moment
polarization
production
scattering
scattering, proton-deuteron
scattering, proton-proton

Neutrons

Neutron diffraction
Neutron spectra
Neutron spectrometers
Neutrons and antineutrons
absorption
angular distribution
detection, measurement
diffusion
effects
interactions
moderation
polarization
production
reflection
scattering
scattering, proton-neutron

Hyperons

Hypernuclei
Hyperons
absorption
capture
decay
decay observations
detection, measurement
effects
interactions
magnetic moment
mass
production
resonances
scattering
spin and parity
Strange particles

Baryon Resonances

Baryons
resonances
Hyperons
resonances
Nucleons

Deuterons

Deuterons
effects
interactions
photodisintegration
polarization
scattering

Tritons

Tritons

Alpha-particles, He Nuclei

Alpha-particles and He nuclei
Alpha-ray spectrometers
Alpha-rays
absorption
angular distribution
detection, measurement
effects
scattering

COSMIC RAYS

Cosmic rays
 absorption
 apparatus
 composition
 alpha-particles
 deuterons
 electrons
 mesons
 muons
 neutrons
 photons
 protons
 effects and interactions
 origin
 primary
 showers and bursts
 variation

NUCLEAR PHYSICS

Nuclear physics

NUCLEUS. ENERGY LEVELS

Beta-ray spectra
 conversion electrons
 Gamma-ray spectra
 Gamma-rays
 angular distribution
 internal conversion
 Gyromagnetic ratio
 Hypernuclei
 Mössbauer effect
 Nuclear excitation
 Nuclear forces

Nuclear isomerism
 Nuclear magnetic resonance and
 measurement [relaxation]
 Nuclear orientation
 Nucleus
 electric moment
 energy levels
 magnetic moment
 models
 size
 spin and parity
 theory

NUCLEAR REACTIONS

Alpha-rays/
 scattering
 Chemical analysis/
 by nuclear reactions
 Collision processes
 Deuterons/
 scattering
 Electrons/
 scattering
 Gamma-rays/
 scattering
 Hyperons/
 scattering
 Mesons/
 scattering
 Muons/
 scattering
 Neutrinos and antineutrinos
 Neutrons and antineutrons/
 scattering
 Nuclear bombardment targets
 Nuclear excitation
 Nuclear forces
 Nuclear reactions
 chemical effects

Nuclear reactions due to/
 alpha-rays
 cosmic rays
 deuterons
 electrons
 helium-3
 mesons
 muons
 neutrinos
 neutrons
 nuclei of $Z > 2$
 photons
 protons
 tritons
 Nuclear spallation
 Nucleons and antinucleons/
 scattering
 Photons/
 scattering
 Pions/
 scattering
 Protons and antiprotons/
 scattering
 Radiation monitoring
 Radiation protection
 Scattering, particles

NUCLEAR DECAY. RADIOACTIVITY

Alpha-particles and He nuclei
 Alpha-ray spectra
 Alpha-ray spectrometers
 Alpha-rays
 absorption
 angular distribution
 detection, measurement
 effects
 scattering
 Beta-decay theory
 Beta-ray spectra
 conversion electrons
 Beta-ray spectrometers
 Beta-rays
 absorption
 angular distribution
 detection, measurement
 effects
 polarization
 scattering
 Biological effects of radiations
 Chemical effects of radiations/
 ionizing radiations
 Dosimetry

Fallout
 Gamma-ray spectra
 Gamma-ray spectrometers
 Gamma-rays
 absorption
 angular distribution
 detection, measurement
 effects
 internal conversion
 scattering
 Nuclear decay theory
 Nuclear bombardment targets
 Physical effects of radiations
 Radiation monitoring
 Radiation protection
 Radioactive dating
 Radioactive tracers
 Radioactivity
 decay periods
 decay schemes
 electron capture
 Radioactivity measurement
 apparatus
 Radiochemistry

Nuclear Fission

Explosions/
 nuclear
 Nucleons

Nuclear fission
 products
 uranium

**Thermonuclear Reactions
Nuclear Fusion**

Explosions/
 nuclear
 Nuclear fusion

Plasma
 Thermonuclear reactions

NUCLEAR POWER STUDIES

Biological effects of radiations
 Chemical analysis/
 by nuclear reactions
 Chemical effects of radiations/
 ionizing radiations
 Dosimetry
 Neutrons
 absorption
 angular distribution
 detection, measurement
 diffusion
 effects
 interactions
 moderation
 polarization
 production
 reflection
 scattering

Nuclear fission
 products
 uranium
 Nuclear fusion
 chemical effects
 Nuclear reactors, fission
 materials
 operation
 theory
 Nuclear reactors, fusion
 Physical effects of radiations
 Plasma
 devices
 Radiation monitoring
 Radiation protection
 Radiochemistry
 Thermonuclear reactions

ATOMIC AND MOLECULAR PHYSICS

Collision processes
Orbital calculation methods
Quantum theory

MASS SPECTROMETERS

Mass spectra
Mass spectrometers
accessories
applications

ATOMS

Atomic beams
Atomic mass and weight
Atoms
electron scattering
excitation
magnetic moment
structure
Collision processes
Electron emission/
photoelectric
Elements
origin
relative abundances

Gyromagnetic ratio
Ionization potential
Luminescence
gases
Optical pumping
Orbital calculation methods
Periodic system
Spectra
atoms
Spectral line breadth
Stark effect
X-ray spectra
absorption
emission
Zeeman effect

Isotopes

Isotope effects
Isotope exchanges
Isotope separation
Isotopes
detection
relative abundances
Mass spectra

Mass spectrometers/
applications
Radioactive dating
Radioactive tracers
Radiochemistry
Tracers

Mesic and Muonic Atoms

Atoms, mesic and muonic

MOLECULES

Molecules

Structure · Internal Mechanics**Spectra**

Bonds
Chemical structure
Isomerism
Luminescence
gases
Molecular weight
Molecules
configuration and dimensions
inorganic
organic
excitation
internal mechanics
electronic structure
electronic structure, inorganic
electronic structure, organic
nuclear coupling
rotation
vibration
moments
Optical pumping

Orbital calculation methods
Raman spectra
inorganic
organic
Spectra
inorganic molecules
diatomic
diatomic, radiofrequency
polyatomic
polyatomic, radiofrequency
inorganic liquids and solutions
inorganic solids
radiofrequency
organic molecules and substances
infrared
radiofrequency
Spectral line breadth
Stark effect
Valency
Zeeman effect

Magnetic Resonances

Magnetic resonance and
[relaxation
Molecules/
nuclear coupling
relaxation

Nuclear magnetic resonance
[and relaxation
Nuclear quadrupole resonance
Paramagnetic resonance and
[relaxation

Dissociation · Free Radicals

Association
gases
Free radicals
Heat of dissociation

Molecules/
dissociation
dissociation energies

Intermolecular Mechanics

Collision processes
Molecular beams

Molecules/
intermolecular mechanics

Macromolecules · Polymers

Association
Heat of formation
Isomerism
Macromolecules

Molecules/
configuration and dimensions,
Polymers [macromolecules
Proteins

Mesic and Muonic Molecules

Molecules, mesic and muonic

ELECTRIC DISCHARGES

Arcs, electric
Breakdown, electric
gases
Corona, electric discharge

Discharges, electric
glows
high-frequency
Gas-discharge tubes
Lightning
Sparks, electric
Sputtering

IONIZATION

Dissociation
Ion velocity
Ionization
gases
Ionization potential
Ionization, surface

Ions
recombination
scattering
Shock waves/
effects
Space charge

PLASMA

Discharges, electric
glows
high-frequency
Electron gas
Ionization
gases
Nuclear fusion
Nuclear reactors, fusion

Plasma
electromagnetic wave propagation
magnetohydrodynamics
measurement techniques
Shock waves/
effects
Space charge
Thermonuclear reactions

Plasma Confinement

Plasma/
confinement

Plasma Oscillations and Stability

Plasma/
magnetohydrodynamics
oscillations
stability

Plasma Devices

Nuclear reactors, fusion
Plasma/
devices

FLUIDS

Flow
Fluids
Hydrodynamics
Hydrostatics

Oscillations
Turbulence
Viscosity
Vortices
Waves

MECHANICS OF GASES

Acoustic streaming
Aerodynamics
Anemometers
Compressibility/
 gases
Condensation
Density/
 gases
Diffusion in gases
 thermal
Flow/
 gases
Flowmeters
Gases
Humidity

Hygrometers
Jets
Manometers
Moisture
Pressure
Pumps
Radiation pressure
Supersonic flow
Turbulence
Viscometers
Viscosity/
 gases
Vortices
Waves

GASEOUS STATE

Absorption/
 acoustic waves
 acoustic waves, ultrasonic
 electromagnetic waves
 light
Association/
 gases
Breakdown, electric/
 gases
Conductivity, electrical/
 gases
 measurement
Conductivity, thermal/
 gases
 measurement
Dielectric properties of substances/
 gases
Diffraction/
 acoustic waves
 acoustic waves, ultrasonic
 electromagnetic waves
 light
Diffusion/
 acoustic waves
 electromagnetic waves
 light
Electrical properties of substances
Electroluminescence
Equations of state/
 gases
Gases
Helium/
 gas
Interference/
 acoustic waves
Joule-Thomson effect
Kinetic theory/
 gases
Lasers/
 gaseous
Luminescence/
 gases

Magnetic resonance and relaxation
Molecules/
 intermolecular mechanics
Nuclear magnetic resonance and relaxation
Nuclear quadrupole resonance
Optical properties of substances
Paramagnetic resonance and relaxation
Reflection/
 acoustic waves
 acoustic waves, ultrasonic
 electromagnetic waves
 light
Refraction/
 acoustic waves
 acoustic waves, ultrasonic
 electromagnetic waves
 light
Scattering/
 acoustic waves
 acoustic waves, ultrasonic
 electromagnetic waves
 light
Sorption
Specific heat/
 gases
Spectra
Statistical mechanics
Thermoluminescence
Transmission/
 acoustic waves
 acoustic waves, ultrasonic
 light
Velocity/
 acoustic waves
 acoustic waves, ultrasonic

Viscosity • Diffusion

Diffusion in gases
 thermal
Transport processes
Viscosity/
 gases

VACUUM PHYSICS

Glass-metal seals
Leak detection
Manometers
Sputtering

Vacuum apparatus
Vacuum gauges
Vacuum pumps
Vacuum technique

MECHANICS OF LIQUIDS

Acoustic streaming	Drops	Hydrostatics	Sprays
Bubbles	Elasticity/ liquids	Jets	Surface energy
Capillarity	Emulsions	Liquid oscillations	Surface tension
Cavitation	Films/ liquid	Liquid waves	Surface tension measurement
Compressibility/ liquids	Filters	Lubrication	Thixotropy
Density/ liquids	Flow/ liquids	Moisture	Turbulence
Diffusion in liquids	Flowmeters	Pressure	Viscometers
Double refraction/ flow	Foams	Pumps	Viscosity/ liquids
	Hydrodynamics	Radiation pressure	Vortices
		Rheology	Wetting
		Schlieren systems	

LIQUID STATE

Liquids

**Theory and Structure of Liquids
Solutions**

Association/ liquids	Liquids structure
Electron diffraction examination	theory
Equations of state/ [of materials	Neutron diffraction examination of
liquids	Neutrons/ [materials
Films/ liquid	scattering
Heat of solution	Polymers
Liquid crystals	Solubility
	Solutions
	X-ray examination of materials/ liquids

Viscosity • Surface Tension • Diffusion

Diffusion in liquids	Sorption
thermal	Surface tension
Filters	Surface tension measurement
Membranes	Transport processes
Osmosis	Viscosity/ liquids

Optical Properties of Liquids

Absorption/ electromagnetic waves	Raman spectra
light	inorganic
Diffraction/ electromagnetic waves	organic
light	Reflection/ electromagnetic waves
Diffusion/ electromagnetic waves	light
light	Refraction/ electromagnetic waves
Double refraction	light
flow	Scattering/ electromagnetic waves
Electroluminescence	light
Luminescence/ liquids and solutions	Spectra/ inorganic liquids and solutions
Optical pumping	Thermoluminescence
Optical properties of substs.	Transmission/ light

Thermal Properties of Liquids

Conductivity, thermal/ liquids	Specific heat/ liquids
measurement	Thermal expansion
Heat of solution	Thermodynamic properties

Acoustical Properties of Liquids

Absorption/ acoustic waves	Refraction/ acoustic waves
acoustic waves, ultrasonic	acoustic waves, ultrasonic
Acoustic wave propagation	Scattering/ acoustic waves
ultrasonic	acoustic waves, ultrasonic
Diffraction/ acoustic waves	Transmission/ acoustic waves
acoustic waves, ultrasonic	acoustic waves, ultrasonic
Diffusion/ acoustic waves	Velocity/ acoustic waves
Interference/ acoustic waves	acoustic waves, ultrasonic
Reflection/ acoustic waves	
acoustic waves, ultrasonic	

**Electrical and Magnetic Properties
of Liquids**

Absorption/ electromagnetic waves	Ionization, liquids
Breakdown, electric/ liquids	Magnetic properties of substs.
Conductivity, electrical/ liquids	Magnetic resonance and relaxation
liquids, electrolytic	Metals
measurement	Nuclear magnetic resonance and [relaxation
Dielectric properties of substs./ liquids and solutions	Nuclear quadrupole resonance
Electrical properties of substs.	Paramagnetic resonance and [relaxation
	Semiconducting materials
	Semiconductors

DISPERSIONS • COLLOIDS

Aerosols	Filters	Osmosis	Solubility
Centrifuges	Foams	Particle size	Solutions
Colloids	Gels	Precipitation	Surface phenomena
Disperse systems	Heat of solution	Sedimentation	Suspensions
Electrophoresis	Membranes	Sols	Thixotropy
Emulsions			

CHANGE OF STATE

Boiling	Equations of state	Heat of sublimation	Phase equilibrium
Boiling point	gases	Heat of transformation	Phase transformations
Condensation	liquids	Heat of vaporization	Sublimation
Critical constants, thermal	solids	Humidity	Supercooling
Distillation	Evaporation	Liquefaction, gases	Vapour pressure
Drying	Freezing	Melting	Vapour pressure measurement
	Heat of fusion	Melting point	Vaporization

SOLID-STATE PHYSICS

Bonds
Crystals
 internal fields
Crystal properties

Equations of state/
 solids
Metals
 theory

Mössbauer effect
Nuclear orientation
Orbital calculation methods

Solids
 structure
 theory

STRUCTURE OF SOLIDS · ALLOYS

Alloys
Crystal structure
Density/
 solids
Fibres
Filters
Granular structure
Heat treatment
 alloys
Membranes

Particle size
Permeability, mechanical
Polymorphism
Porous materials
Powders
Sintering
Solids
 structure
Solid solutions
Solubility

Solid-State Phase Transformations

Heat treatment
 alloys
Phase equilibrium

Phase transformations/
 solid-state
Polymorphism
Precipitation

Surfaces

Surface energy
Surface measurement

Surface phenomena
Surface texture

Films

Evaporation
Films/
 solid
Magnetic films

Optical films
Sputtering
Sublimation

Adsorption

Adsorbed layers
Adsorption

Heat of adsorption
Sorption

NON-CRYSTALLINE STATE

Amorphous state
Glass
Plastics
Polymers

Rubber
Vitreous state
Waxes

CRYSTALLOGRAPHY

Crystal chemistry
Crystal properties
Crystal structure
Crystallization
Crystallography
Crystals
 etching
 faces
 growth
 orientation
 twinning
 whiskers

Minerals
Polymorphism
Precipitation
Solids/
 structure
Surface texture
Zone melting and refining

MICROSTRUCTURE OF SOLIDS

Amorphous state
Crystal structure/
 microstructure
Electron diffraction examination
 [of materials]
Electron microscope examination
 [of materials]
Electron microscopy
Fibres
Granular structure
Ion microscopes

Metallurgy
Microscopy
Neutron diffr. exam. of mater
Particle size
Porous materials
Powders
Radiography
Surface texture
X-ray examination of materia
 microstructure
 molecular structure

CRYSTAL LATTICE STRUCTURES

Crystal structure, atomic
 elements
 alloys
 inorganic compounds
 organic compounds
Electron diffraction crystallography
Electron diffraction examination
 [of materials]
Electron microscope examination
 [of materials]
Neutron diffraction crystallography
Neutron-diffraction examination
 [of materials]
Polymers

X-ray absorption
X-ray crystallography
 apparatus
 calculation apparatus
 calculation methods
 technique
X-ray diffraction
X-ray examination of materia
 molecular structure
X-ray measurement
X-ray monochromators
X-ray reflection
X-ray scattering
X-ray tubes

LATTICE MECHANICS

Crystals/
 lattice mechanics

Mössbauer effect

ACOUSTICAL PROPERTIES OF SOLIDS

Absorption/
 acoustic waves
 acoustic waves, ultrasonic
Acoustic wave propagation
 ultrasonic
Acoustoelectric effects
Diffraction/
 acoustic waves
 acoustic waves, ultrasonic
Dispersion, acoustic
 ultrasonic
Magnetoacoustic effects

Reflection/
 acoustic waves
 acoustic waves, ultrasonic
Refraction/
 acoustic waves
 acoustic waves, ultrasonic
Scattering/
 acoustic waves
 acoustic waves, ultrasonic
Transmission/
 acoustic waves
 acoustic waves, ultrasonic
Velocity/
 acoustic waves
 acoustic waves, ultrasonic

THERMAL PROPERTIES OF SOLIDS

Conductivity, thermal/
 measurement
 solids
Equations of state/
 solids

Heat conduction
Specific heat/
 solids
Thermal expansion
Thermodynamic properties

DIFFUSION IN SOLIDS

Diffusion in solids

Permeability, mechanical

DEFECT PROPERTIES OF SOLIDS

Cold working

Creep

Crystal imperfections

dislocations

interstitials

vacancies

Crystal structure

Crystals

etching

twinning

Deformation

Elastic deformation

Electron diffraction examination

[of materials

Electron microscope examination

Heat treatment [of materials

alloys

Internal friction

Neutron diffraction examination

Plastic deformation [of materials

Plastic flow

Slip

Stresses, internal

Work hardening

X-ray examination of materials/
microstructure**Colour Centres**

Absorption/

light

Colour centres

X-rays/

effects

RADIATION EFFECTS IN SOLIDS

Acoustic waves/

effects

Alpha-rays/

effects

Beta-rays/

effects

Deuterons/

effects

Electron beams/

effects

Gamma-rays/

effects

Hyperons/

effects

Ion beams/

effects

Mesons/

effects

Neutrons and antineutrons/

effects

Physical effects of radiations

Protons and antiprotons/

effects

Sputtering

X-rays/

effects

MECHANICAL PROPERTIES OF SOLIDS

Abrasion

Adhesion

Bending

Brittleness

Cold working

Compressibility

Corrosion

Cracks

Creep

Deformation

Density/

solids

Elastic constants

measurement

Elastic deformation

Elastic fatigue

Elastic limit

Elastic relaxation

Elasticity

Fracture

Friction

Hardness

Heat treatment

alloys

High-pressure phenomena

Hysteresis [and effects

Impact

Internal friction

Lubrication

Magnetomechanical effects

Mechanical properties of substs.

Mechanical strength

compressive

shear

tensile

Photoelasticity

Physical effects of radiations

Plastic deformation

Plastic flow

Plasticity

Rheology

Slip

Strain gauges

Stress analysis

Stress effects

Stress/strain relations

Stresses, internal

Thermoelasticity

Thixotropy

Torsion

Viscoelasticity

Wear

Work hardening

ELECTRON STATES IN SOLIDS

Crystal electron states

band structure

excitons

Fermi level

Fermi surface

plasma

polarons

surface

Crystal properties

Cyclotron resonance

Electron beams/

effects

Electron gas

Electron pairs/

annihilation

Electrons

absorption

radiation

scattering

Hall effect

Magnetoacoustic effects

Metals

theory

Piezoresistance

Solids

theory

Surface phenomena

ELECTRICAL PROPERTIES OF SOLIDS

Acoustoelectric effects

Conduction, electrical

Conductivity, electrical/
measurement
solids

Contact potential

Metals • Conductors

Electron gas

Hall effect

Magnetoelectric effects

Magnetoresistance

Superconductivity

Superconductivity

Superconducting Materials and Devices

Superconducting materials and devices

Semiconductors

Acoustoelectric effects

Contact potential

Contact resistance

Electron gas

Electro-optical effects

Fluctuations/

electrical

Semiconducting**Materials**

Semiconducting materials

gallium arsenide

germanium

indium antimonide

silicon

Contact resistance

Crystal electron states

Eddy-currents

Electrical properties of substs.

Electron gas

Metals

theory

Piezoresistance

Skin effect

Electro-optical effects

Fluctuations/

electrical

Hall effect

Magnetoelectric effects

Magnetoresistance

DielectricsBreakdown, electric/
solids

Contact potential

Dielectric devices

Dielectric materials

Dielectric measurement

Dielectric phenomena

Dielectric properties of substs./
solids

Electrets

Electric charge

Electric fields

Electric strength

THERMOELECTRIC PROPERTIES OF SOLIDS

Thermocouples

Thermoelectricity

PHOTOCONDUCTIVITY • PHOTOVOLTAIC EFFECTS

Photoconductivity

Photoelectricity

Photoelectromagnetic effects

Photovoltaic effects

ELECTRON AND ION EMISSION BY SOLIDS

Cathodes

oxide

Electron emission

field emission

photoelectric

secondary

thermionic

Ion emission

secondary

thermionic

Ionization/

solids

Ionization, surface

Work function

MAGNETIC PROPERTIES OF SOLIDS

Antiferromagnetism	Ferromagnetism	Magnetic properties of substs.	Magnetoacoustic effects
de Haas—van Alphen effect	spin-wave theory	antiferromagnetic	Magnetoelectric effects
Diamagnetism	Gyromagnetic ratio	diamagnetic	Magneto-optical effects
Electron diffraction examination	Hall effect	ferrimagnetic	Magneto-resistance
[of materials]	Hysteresis	ferromagnetic	Magnetostriction
Electron microscope examination	Magnetic devices	paramagnetic	Magneto-thermal effects
[of materials]	Magnetic fields/	transitions	Neutron diffraction examination
Ferrimagnetism	effects	Magnetism	[of materials]
Ferrites	Magnetic films	Magnetization process	Paramagnetism
	Magnetic materials	Magnetization state	Zeeman effect
		domains	

Paramagnetic Properties

Magnetic properties of substances/ Paramagnetism
paramagnetic

Ferromagnetic Properties

Ferromagnetism	Magnetic properties of substances/
spin-wave theory	ferromagnetic
Hysteresis	Magnetization process
Magnetic devices	Magnetization state
Magnetic films	domains

Ferrimagnetic Properties • Ferrites

Ferrimagnetism	Magnetic films
Ferrites	Magnetic properties of substs./
Hysteresis	ferrimagnetic
Magnetic devices	

Antiferromagnetic Properties

Antiferromagnetism	Magnetic properties of substs./
	antiferromagnetic

MAGNETIC RESONANCES IN SOLIDS

Antiferromagnetic resonance	Ferromagnetic relaxation	Magnetic resonance and relaxation	Nuclear quadrupole resonance
Cyclotron resonance	Ferromagnetic resonance	Magnetomechanical effects	Optical pumping
Ferrimagnetic resonance	Gyromagnetic ratio	Nuclear magnetic resonance and measurement [relaxation]	Paramagnetic resonance and measurement [relaxation]

OPTICAL PROPERTIES OF SOLIDS

Absorption/	Lasers/	Refraction/	Spectral line breadth
electromagnetic waves	solid	electromagnetic waves	Stark effect
light	Magneto-optical effects	light	Transmission/
Diffraction/	Optical constants	Refractive index/	light
electromagnetic waves	Optical films	light	Transparency
light	Optical materials	Scattering/	Velocity/
Diffusion/	Optical properties of substances	electromagnetic waves	light
electromagnetic waves	Optical pumping	light	X-ray spectra
light	Optical rotation	Spectra/	absorption
Dispersion, optical	Photoelasticity	inorganic solids	emission
Double refraction	Pleochroism	radiofrequency	Zeeman effect
mechanical	Polarized light	organic molecules and	
Electromag. wave propagation	Raman spectra	infrared [substances	
Electro-optical effects	inorganic	radiofrequency	
Emissivity	organic		
Interference/	Reflection/		
light	electromagnetic waves		
	light		
	Reflectivity		

Luminescence of Solids

Colour centres	Luminescence/
Counters, scintillation	solids, inorganic
Electroluminescence	solids, organic
	Luminescent devices
	Thermoluminescence

PHYSICAL CHEMISTRY

Atomic mass and weight	Distillation
Balances	Elements
Bonds	origin
Centrifuges	relative abundances
Chemical structure	Filters
Chemical technology	Isomerism

THERMOCHEMISTRY • REACTIONS

Association	Heat of adsorption
gases	Heat of combustion
liquids	Heat of dissociation
Catalysis	Heat of formation
Chemical reactions	Heat of reaction
Combustion	Isotope exchanges
Corrosion	Oxidation
Crystal chemistry	Phase equilibrium
Detonation	Phase transformations
Dissociation	Polymerization
Exchanges, chemical	Polymers
Explosions	Reaction kinetics
Flames	Sorption

ELECTROCHEMISTRY

Conductivity, electrical/	Electrolysis
liquids, electrolytic	Electrolytic deposition
Dissociation/	Electrophoresis
electrolytic	Ion velocity/
Electrochemistry	electrolytic
electrodes	Ions, electrolytic
Electrokinetic effects	

Laboratory app. and technique	Physical chemistry
Macromolecules	Precipitation
Molecular weight	Pumps
Molecular weight determin.	Quantum chemistry
Periodic system	Sedimentation
	Valency

PHOTOCHEMISTRY**RADIATION CHEMISTRY****RADIOCHEMISTRY**

Chemical effects of radiations	Nuclear reactions/
acoustic waves	chemical effects
ionizing radiations	Photochemistry
	Radiochemistry

PHYSICAL METHODS**OF CHEMICAL ANALYSIS**

Chemical analysis	Chromatography
adsorption	Radioactive tracers
by mass spectrometry	Spectrochemical analysis
by nuclear reactions	Tracers
electrochemical	
radioactive	
X-ray	

GEOPHYSICS

earth age composition electricity heat rotation	Geodesy Geophysical prospecting Geophysics Glaciers	Gravity Minerals Oceanography Radioactive dating	Radioactivity Seawater Seismic waves Seismology Soil
--	--	---	--

ATMOSPHERE

anemometers atmosphere composition humidity movements precipitation radioactivity structure temperature thermodynamics	Atmospheric acoustics Atmospheric electricity Atmospheric optics Atmospheric pressure and [density] Atmospheric spectra Atmospherics Clouds Condensation	Electromagnetic wave atmosphere [propagation] Evaporation Fallout Fog Humidity Hygrometers Ice Lightning Meteorological instruments	Meteorology Rain Rockets Satellites, artificial Sky brightness Snow Sunlight Thunderstorms Twilight Wind
---	---	--	---

UPPER ATMOSPHERE

auror glow atmosphere composition movements radiation belts radioactivity structure temperature thermodynamics upper atmospheric electricity atmospheric optics atmospheric pressure and [density]	Atmospheric spectra Atmospherics Aurora Fallout Ionization, atmosphere Meteors Rockets Satellites, artificial Sky brightness Sunlight Twilight Zodiacal light	Ionosphere Atmospherics Aurora Electromag. wave propagation ionosphere Ionization, atmosphere	Ionosphere D-region E-region F-region Ionosphere meas. apparatus
--	--	---	--

SPACE RESEARCH TECHNIQUES

Rockets Satellites, artificial Space research	Space vehicles instrumentation
---	-----------------------------------

GEOMAGNETISM

compasses earth/ magnetic field magnetic field, variations

Magnetic storms Rock magnetism

ASTROPHYSICS

astronomical instruments astronomical observations astronomical spectra astronomy and astrophysics celestial mechanics cosmic rays cosmology	Elements/ origin relative abundances Gravitation Interstellar matter Telescopes/ astronomical
--	---

STARS · GALAXIES

cosmic radiations, r.f. galaxies the Galaxy interstellar matter magnetohydrodynamics nebulae novae	Quasars Stars composition evolution magnetism radiation spectra structure Thermonuclear reactions
--	---

SOLAR SYSTEM · SUN

Comets Cosmic rays Earth rotation Gravitation Interplanetary magnetic field Interplanetary matter Meteorites Meteoroids Moon Planets Solar system	Sun corona eclipses flares magnetism prominences radiation radiation, corpuscular radiation, r.f. spectra Sunspots Zodiacal light
--	--

RADIOASTRONOMY TECHNIQUES

Cosmic radiations, r.f.	Radioastronomy
-------------------------	----------------

BIOPHYSICS

biological effects of radiations biological technique and [instruments] biology biophysics blood cosimetry	Medical science Physiology Proteins Radiation protection Radiography Zoology
---	---

TECHNIQUE · MATERIALS

Biological technique and instruments Chemical technology Heat treatment alloys Laboratory apparatus and technique Leak detection Low-temperature technique Materials	Metallurgy Vacuum technique Zone melting and refining
---	---

**HIGH-PRESSURE
TECHNIQUES**

High-pressure phenomena [and effects]
--

SUBSTANCES

Chemical elements and inorganic compounds

All the chemical elements are listed by name, followed by their compounds, e.g. "Cadmium", "Cadmium compounds".

"Hydrogen" is subdivided by the subheadings "neutral atoms", "neutral molecules", and "ions". "Deuterium" and "Tritium" are independent headings. "Hydrogen compounds" is supplemented by "Ice", "Steam", and "Water".

"Oxygen" is supplemented by "Ozone", and "Carbon" is supplemented by "Diamonds" and "Graphite".

The following inorganic compounds are further subdivided by subheadings as shown:-

Barium compounds	Nitrogen compounds
barium titanate*	ammonia
Cadmium compounds	ammonium compounds
cadmium sulphide	Potassium compounds
Calcium compounds	potassium bromide
calcium fluoride	potassium chloride
Gallium compounds	Sodium compounds
gallium arsenide**	sodium chloride
Indium compounds	Zinc compounds
indium antimonide**	zinc sulphide
Lithium compounds	
lithium fluoride	

* Ferroelectric properties are listed under "Ferroelectric materials/barium titanate"

** Semiconducting properties are listed under the corresponding subheadings of "Semiconducting materials"

Organic compounds

Organic compounds are grouped under headings "Organic compounds", "Polymers", "Plastics", "Proteins". "Rochelle salt" is an independent heading.

Substance groups

In addition there are the following headings for groups of elements, compounds or substances:-

Actinides	Metals
Actinide compounds	Minerals
Alkali metals	Rare-earth metals
Alkali-metal compounds	Rare-earth compounds
halides	Semiconductors
Alkaline-earth metals	Semiconducting materials
Alkaline-earth compounds	gallium arsenide**
Ferrites	germanium**
Ferroelectric materials	indium antimonide**
barium titanate*	silicon**
Garnets	Transition metals
Halogens	Transition-metal compounds
Inert gases	

* Used for ferroelectric properties only

** Used for semiconducting properties only

Alloys

General papers on alloys are indexed under "Alloys". Alloys of specified composition are listed under, either

- (i) special alloy headings (there are five of them: "Aluminium alloys", "Copper alloys", "Iron alloys", "Nickel alloys", "Steel"), e.g. Al-Ni alloys under "Aluminium alloys", or
- (ii) compounds of the base or first-named element, e.g. Mn-Zn alloys under "Manganese compounds", and silicon-iron under "Iron alloys".

Special substances and materials

There are also the following special headings for certain common substances:-

Air	Paper
Blood	Porous materials
Ceramics	Powders
Clay	Quartz
Coal	Rubber
Concrete	Ruby
Fibres	Sand
Gelatin	Seawater
Glass	Soil
Mica	Waxes
Optical materials	Wood

ADP (ammonium dihydrogen phosphate). See Nitrogen compounds/ammonium compounds.

Abacs. See Nomograms.

Aberrations, optical

See also Electron lenses; Ion optics; Optical instrument testing; Optics/geometrical; Particle optics.
 aplanatic Fresnel system correction 8=20048
 astigmatism of noncentred multipass-cell system 8=6490
 cemented doublets and triplets, localized var. of two paraxial ray paths 8=20047
 chromatic, rel. to optimum image plane position 8=477
 coma, elimination in Mangin mirror system 8=20041
 "condenser-objective" for microscope up to 700 kV, spherical, and resolving power 8=19790
 correction by aspherical surfaces 8=3347
 corrective aspherical surface calc. 8=20042
 diffraction gratings, geometrical theory 8=6500
 electron microscope, emission, spherical aberration and limit of resolution 8=10902
 electrostatic sector fields, ion image aberrations 8=19802
 rel. to frequency-contrast characts. calc. by Hopkins method 8=20045
 hologram, evaluation by ray tracing 8=11216
 human eye, meas. methods 8=15571
 lens, longit. spherical aberration, determ. by simple tech. 8=470
 monochromator, non-symmetrical with plane diffraction grating 8=3345
 off-axis, of photographic lens 8=15503
 of optical systems, Hauser's formula for modulation transfer function 8=15504
 Seidel, differentials for thick lenses and air spaces and use in pancratic lens systems 8=471
 spherical, of laser beams in low-loss liquids 8=15442
 superconducting e lens, aperture and chromatic, calc. 8=19791
 telescope objective, cemented, 5th order spherical aberration 8=3351
 triplets, method for evaluation of spherical aberration 8=15501
 two-lens system of Ramsden type, primary 8=6493

Abrasion

See also Hardness; Wear.
 diamond, surface damage and strains 8=8826
 CdS single crystal polishing by phosphoric acid 8=9705

Absorption

See also subheadings of Alpha-rays; Beta-rays; Cosmic rays; Electrons; Gamma-rays; Hyperons; Mesons; Neutrons and antineutrons; Protons and antiprotons; and also Sorption; X-ray absorption.
 in catalysts 8=14402
 gases in a turbulent liquid 8=12745
 grain boundary gas bubbles, equilib. conditions 8=1986-9
 liquids, far infrared, survey 8=12886
 magnetoplasma dielectric in resonant cavity, spectrum 8=21352
 multiphoton, damage to materials in laser 8=403
 semiconductors, Beers law and charge carrier absorpt. 8=5102
 Ba getters, of Ar, liberation obs. 8=17161
 He-CF₄, nonresonant, and dispersion in compressed mixtures 8=1486
 LiNbO₃, shear-wave attenuation 8=2059
 NaBr-KBr solid solutions, fundamental spectra 8=18549
 PbO, single crystal, yellow form, optical coeffs. 8=5628
 SbSI, ferroelectric semiconductor, fund. edge profile 8=9120
 TiCl₄, two photon absorption, angular dependence 8=9561

acoustic waves

See also Noise abatement; Transmission/acoustic waves.
 absorber systems, impedance ratio rel. to coeff., charts 8=10739
 air, rel. to humidity, pressure var. obs. 8=23268
 antiferromagnets, hypersound 8=8620
 dibromomethane, gaseous, multiple relaxation 8=1475
 duct with nonlinear wall impedance, attenuation 8=15066
 elastic pulses in media with coeff. proportional to freq. or freq. squared 8=10743
 ferro-, and antiferromagnets, attenuation 8=13344
 fibrous layers, scale-modeling of large silencing devices 8=19563
 free induction in quadrupolar spin system 8=5543
 gases, critical, using Mori's continued fraction representation 8=16706
 gas, critical, sound attenuation 8=12688
 gas, rel. to free energy associated with critical density fluctuations 8=16703
 gases, organic mixtures in air, optical-acoustic effect using cm e.m. waves 8=21520
 glycerol and water mixture, complex form. 8=8057
 hydrodynamic by forced alternating viscous fluid flow 8=3058
 insulation in presence of flanking paths, meas. 8=19582
 kaolinite and kaolinite-sand, water saturated, 4-600 kHz obs. 8=1857
 l.f. attenuation coeffs. in ocean, analytic description 8=5786
 liquids, calc. from optical scatt. meas. 8=8059
 light modulators and scanners, u.s. driven, photoelastic criteria of materials 8=9496

Absorption—contd

acoustic waves—contd

metals, electronic attenuation, magnitude meas. 8=4919
 metal, giant oscillations, electron scatt. effect 8=5136
 metals, transport eqns. 8=17492
 methane-water vapour mixture, vib. Napier relax. time 8=4481
 NMR meas. on systems of nuclear spins 8=389
 panels, double, transmission loss, calc. allowing for absorption by cavity walls 8=10740
 pipe organ, due to resonant vib. of pipe walls 8=3068
 provided by ear plugs, fingers, palms and tragi 8=213
 radiative damping for arbitrary wavelength to photon mean-free-path ratio 8=190
 in receiving room, by steady-state and decay rate methods 8=191
 resonance line, width and shift dependence on temp. 8=13342
 reverberation room, edge effect in absorption coeff. meas. 8=6181
 semiconductors, spin-cyclotron-phonon resonance 8=2352
 silencers with quasisonant living, attenuation freq. characteristics 8=10738
 solids, re-entrant excitation of hypersonic waves rel. to air-gap effect 8=8621
 spherical volume absorber, coefficient calc. 8=10742
 transmission loss meas. using vibr. transducers 8=10754
 volume, individual, by small chamber method 8=10755
 walls, double and single 8=10741
 Bi-Ca-V garnet 8=18397
 CO₂-D₂O mixture, rel. to vibr. relaxation of CO₂ 8=21071
 Ge, attenuation coeff. by donor spins 8=22096
 He II, below 0.6°K 8=6235
 KMgF₃:Ni²⁺, near acoustic paramag. reson. 8=22912
 Nb, superconducting, mixed state, u.s. attenuation rel. to transverse mag. field 8=17502
 O₂, H₂O vapour mixtures, obs. 8=1476
 Si, attenuation coeff. by donor spins 8=22096
 YFe garnet, ferroacoustical reson. absorpt. 8=18397

acoustic waves, ultrasonic

in A₂B₆ type crystals, effect of illumination 8=4915
 acetate-alcohol binary mixtures 8=4571
 antiferromagnetic insulators, rel. to lattice and Heisenberg spin systems 8=9388
 benzene and furan vapours obs. 8=12687
 crystals, usefulness of thermal cond. obs., for determ. attenuation at high and low temp. 8=22092
 dielectric crystals with high impurity concs. 8=17491
 ferroelectric, near phase transition rel. to long range dipole-dipole effects 8=18181
 by free electrons in quantizing mag. field 8=6165
 gases at high temp., rot. collision and vibr. relax. determ. 8=4478
 graphite, stress wave packet, attenuation effect on freq. content 8=8626
 Heisenberg paramagnets, attenuation asymptotic behaviours near critical points 8=22757
 ice crystals in supercooled water rel. to crystal growth 8=22102
 metal in quantizing mag. field by free electrons, calc. 8=22093
 paramagnetic crystals, quantum theory of resonance and relax. absorpt. 8=17487
 propionic acid 8=12860
 pyridine and thiophene vapours obs. 8=12687
 resonance reverberation method, 10 to 300 kc/s 8=12858
 Rochelle salt, u.s. relaxation near ferroelec. transition 8=1858
 rock samples in lab., meas. by bending vib. method 8=22095
 shallow water propag. loss at sonar freqs. 8=1554
 silicones, # 200 series, 30-350 MHz and -30° to +30°C rel. to viscosity 8=8063
 solids, attenuation consts., resonance meas. 8=17489
 superconductor, anisotropic, attenuation in gl < limit 8=22090
 in superconductors, in intermed. state 8=4914
 superconductors, type II, anisotropy of attenuation 8=22091
 triglycine sulphate, u.s. relaxation near ferroelec. transition 8=1858
 two-zone superconducting alloys, theory 8=22535
 Ag, attenuation rel. to Fermi surface deformation 8=1851
 Au, attenuation rel. to Fermi surface deformation 8=1851
 Ar, liquid 8=1553
 CO₂, 300°-1300°K 8=4478
 CO₂-water-vapour mixtures, at 1.25, 3.3, 4.8, 9.9 and 14.0 MHz 8=7931
 CS₂, var. with impurity 8=12861
 CoO, antiferromagnetic, attenuation-frequency relationship near Neel point 8=22106
 Cu, attenuation rel. to Fermi surface deformation 8=1851
 Cu, shear waves, attenuation at low temps. 8=22099
 D₂, H₂, and sound velocity at high temp. obs. 8=1251
 Eu, polycrystalline, attenuation and elastic moduli from 4.2 to 300°K 8=17781
 Ga, geometric oscillations 8=4922
 GaAs, infrared radiation effect 8=13352
 Gd, critical attenuation near Curie temp. 8=22101
 Ge, attenuation, low temp. 8=8629
 Ge-Si alloys, decrease on alloying 8=1853

Absorption—contd**acoustic waves, ultrasonic—contd**

- In, normal and superconducting, electronic contribution to attenuation 8=13354
- In, waves, quasi-longitudinal, superconducting electronic attenuation 8=22103
- K, by conduction electrons 8=22104
- KCl deformed crystals, by dislocations, rel. to freq. 8=8630
- MnO, antiferromagnetic, attenuation-frequency relationship near Neel point 8=22106
- N₂, 300°-1300°K 8=4478
- Nb, superconducting, attenuation, temp. and mag. field depend. 8=17503
- N₂, O₂, and sound velocity at high temp. obs. 8=1251
- O₂, 300°-1300°K 8=4478
- RbMnF₃, F¹⁹ nuclear acoustic resonance 8=22922
- RbMnF₃, near magnetic critical point, attenuation 8=17504
- Sn, doped, rel. to superconductivity 8=22572
- Sn, longitudinal, by electrons, near supercond. transition 8=4924
- Sn, supercond., at various u.s. amplitudes 8=5213
- Te, meas. and dislocation loop length calcs. 8=8619
- ZnSO₄ soln. in H₂O-glycol, viscosity effect 8=8062

electromagnetic waves

- See also Spectra (radiofrequency subheadings).
- cosmic, rel. to solar microwave bursts 8=23710
- elementary particle behaviour 8=20279
- ground abs. of cm and dm radio waves 8=23230
- infinite strip, with arbitrary face impedances, back scatt. 8=6388
- interstellar grains, effects of impurities 8=10238
- metal, giant oscillations, electron scatt. effect 8=5136
- plasma, effect on inter-antenna transmission coeff. 8=7783
- radioastronomy meas., relating data to atmospheric opacity 8=2595
- ruby, microwave resonance spectra 8=14089
- superconducting films, thick, far-infrared spectra 8=22939
- superconductor, surface relax. 8=9022
- superconductors, thin-film, far-infrared, mag. field depend. 8=22938
- thermal radiation in anisotropic medium 8=10763
- transhorizon tropospheric propagation, book 8=14630
- transparency effect of multiquantum resonance 8=499
- tropospheric attenuation over range 0.4-10 GHz 8=9887
- water vapour, gaseous 8=12689
- X-rays, powder grain size determ. 8=17018
- Bi, u.h.f. penetration at cyclotron resonance 8=5588
- C₂ClF₂-He compressed mixtures, meas. 8=7936
- Hg, 1849Å in saturated vapour 8=1166
- Ho, spectrum, 3mm microwave radn., mag. structures effects 8=14226
- Pb films, thin superconducting, in far i.r. 8=13759
- Pb films, threshold effect on Josephson tunnel junction characts. 8=9063
- Pb, superconducting, microwave, in surface-sheath regime, depairing effect of mag. field 8=13760
- O₂, atmospheric, radiowave absorpt. coeff. 8=9888
- Sn films, threshold effect on Josephson tunnel junction characts. 8=9063
- SO₂ asymmetric mol., microwave absorpt. 8=16302

light

- See also Atmospheric optics; Densitometry; Filters, optical; Optical constants; Optical films; Pleochroism; Transmission/light; Spectra.
- air, humidity and pressure influence, experimental apparatus 8=7935
- alkali borate glasses, binary, u.v. absorpt. of Cr(VI) 8=18519
- alkali or halide, i.r., impurity-induced 8=9481
- alkali halides, i.r. spectra of U-centres, sidebands 8=4991-2
- alkylbenzenes crysts. spectra rel. to mol. config. 8=5645
- all-trans β carotene, i.r. and electronic absorpt. spectra 8=2465
- analysis, conditions for maximum reliability 8=3367
- anthracene crystals, and fluorescence spectra symmetry 8=18631
- anthracene effect of radiation damage 8=9565
- artificial fogs, visible and i.r. 8=1606
- atmosphere, coeffs. from ocean spectrophotometry 8=9872
- atoms, excited by modulated light, modulation of absorption of resonance emission 8=20972
- beam stabilization effect 8=18487
- benzene crysts. spectrum rel. to mol. config. 8=5645
- Bouger's law, in rel. to beam dia. 8=6537
- cell, spectra meas., volatile solns., under press., up to 300°C 8=8084
- collimated beams in turbid media, attenuation 8=11194
- concentric spheres, efficiency factors 8=512
- condensed media, rel. to spectroscopic parameters of component mols. 8=22932
- by crystal hot atoms vibrs. due to lattice displacement near charged impurity 8=2393
- crystal, rel. to quantum transitions 8=10763
- diamond, i.r. rel. to Lave spike refls., obs. 8=22014
- 2,3-dimethyl-naphthalene in n-hexane rigid matrix at 77°K, and emission spectra 8=14286
- electronic edge in strongly anisotropic substs. 8=9482
- emulsion, and thickness, rel. to hologram reconstruction 8=15556

Absorption—contd**light—contd**

- extinction coeff., collimated and diffuse fluxes, reln. between 8=3375
- f. c. c. lattice, monatomic, impurity-induced i.r. absorpt. 8=9480
- films, thin metal, vectorial selective surface effects 8=22950
- filters, in Barnes ES-100 Educational, spectrometer absorpt. 8=491
- Franz-Keldysh effect, spectral broadening representation 8=17853
- gases, absorption function of overlapping spectral lines 8=498
- gas ionization, influence on Townsend coefficients 8=7699
- graphite, n-irradiated 8=14202
- graphite, study of pi-electrons in light-binding model 8=18511
- high pressure cell for studies at 77°K 8=6502
- infrared, crystal lattice dynamics 8=14176
- infrared, impurity-induced in interstellar dust 8=23571
- i.r., by semiconductors 8=9479
- laser radiation, by atmosphere 8=18878
- linear diatomic chain, band-mode 8=9477
- liquid, i.r., cell for low temp. use 8=8069
- liquids and solns. in elect. field, Kerr effect relationship 8=4573
- metal halides and oxides, i.r. freq. and charact. Debye temp. 8=14190
- mixed cryst., deep-trap impurities rel. to host spectrum 8=17865
- by molecular excitons, form of bands 8=5127
- monochromators, resonance, for absorpt. meas. in visible and u.v. 8=11155
- multiphoton processes, anal. rel. to coherence of the light source 8=11165
- naphthalene, four-photon absorpt. from laser beam 8=18517
- naphthols, triplet state, rel. to electronic struct. 8=21152
- negative, poss. mech. from quantum theory of collision broadening of spectral lines 8=2395
- nitrates, molten mixtures, u.v. spectra 8=8085
- optical cell, null press., for liquids at elevated temp. and press. 8=21676
- organic dye solns, two-photon absorpt., geometrical model and meas. 8=16834
- organic molecules, quantum studies 8=4128
- paramagnetic crystals, and emission, by impurity centres, theory 8=5574
- perfluoro-aza-propene, CF₃N = CH₂, u.v. band of NCF₂ radical 8=7626
- phenolphthalein and congeneric mol. crystals, colour deepening on plastic deform 8=23033
- pigments in white emulsion paint, rel. to colour strength and shade 8=9574
- polythene films, of laser-light rel. to formation mechanism of plasma 8=23034
- polyvinylthalimide rel. to triplet-triplet energy transfer, 15000-40000 cm⁻¹ 8=12389
- pulse shape functions rel. to absorption and loss coefficients 8=2394
- quasars, spectra 8=23621
- ruby, linear Stark effect in U band 8=9501
- ruby, R, R' and B linewidth and phonon-induced relaxations 8=14194
- saturable, reversible depend. on incident flux of high intensity laser 8=12873
- semiconducting II-IV compounds with wurtzite structure, intrinsic, rel. to exciton creation 8=5224
- semiconductors, of exciton condensate 8=5128
- semiconductors, intrinsic, polaron effects in interband magneto-optic absorpt. 8=18493
- semiconductors, magneto-optical, interband, optical phonons 8=18492
- semiconductor multiphoton absorpt. rel. to saturable transmission 8=9478
- semiconductors, two-photon absorpt. coeff. formulation 8=18516
- silver halides, spectra of T_{2g} → E_g transitions of Ti³⁺ and Fe²⁺, Jahn-Teller effect 8=14193
- smoke, laser beam attenuation rel. to Buger's law validity, obs. 8=21739
- solids, 2-photon processes intermediate states lifetime meas. 8=14173
- sphalerite:Fe²⁺, i.r. spectra of Fe²⁺ 8=18570
- by substrate rel. to reflectivity of single-layer coating 8=6539
- transparency effect of multiquantum resonance 8=499
- thermal effect causes self-focusing of light beam 8=14170
- triphenylmethylanionium-tetracyanoquinodimethan single crystals by reflectance technique 8=14287
- two-photon absorpt. processes, model calcs. 8=16286
- two-photon process, theory using density matrix formalism 8=3339
- 2-photon transitions to exciton states in semiconductor, oscillator strengths 8=8953
- uniaxial crystal, complex indices 8=5579
- Urbach's optical absorpt. edge shape, interpretation 8=1417

Absorption—contd

light—contd

water, relative spectral attenuation coeffs. 8=12888
 water vapour, atmospheric, i.r., over slant path 8=18879
 weakly absorbing layers, rel. to optical consts. of solids 8=18486
 xanthane rel. to mols. $\pi\pi^*$ and $n\pi^*$ levels location 8=1302
 Ag foils, thin, rel. to struct. and surface characts. 8=18502
 Ag in irradi. metaphosphate glass 8=4990
 AgCl absorpt. edge, polaron states 8=22955
 AgIn, u. v. spectral bands, system A, vibrational analysis 8=16262
 As-S glasses, origin of 800 cm^{-1} bands 8=5584
 Au film, absorption band edge 8=5585
 Au foils, thin, rel. to struct. and surface characts. 8=18502
 Ba silicate glasses, γ -ray effects 8=13479
 BaF_2 , X-ray coloured, by colour centres, temp. dependence 8=17683
 n- BaTiO_3 , single-domain ferroelectric, 26-130°C 8=9506
 C particles, computation: results discussed 8=513
 CO fundamental band, spectral absorpt. coeff. at high temp. 8=21067
 CO_2 , atmospheric, i.r., over slant path 8=18879
 Ca films, between 0.5 and 5.5 eV 8=14204
 CaCO_3 , complex indices 8=5579
 CaF_2 , proton irradiated, band strength, and change in microhardness, kinetics 8=22320
 CaF_2 - Sm^{2+} crystals, optical spectrum 8=9513
 CaF_2 , X-ray coloured, by colour centres, temp. dependence 8=17683
 CaS films, and SrS conc. effects 200-450 μm 8=9511
 Cd crystals, interband absorpt., 32° and 295°K 8=18545
 CdS, doping, heat treatment and deform. effects, 4.2°K 8=9606
 CdS, exciton effects 8=22965
 CdS, 2-photon processes intermediate states lifetime meas. 8=14173
 CdS with Te as isoelectronic trap, and fluorescence 8=23048
 CdSe, doping, heat treatment and deform. effects, 4.2°K 8=9606
 CdSe, and reflection spectra in i.r. at low temps. 8=23026
 CdSnAs_2 , polarized 8=22966
 n-CdTe:In, free carrier 8=22967
 CeO_2 , spectra obs. 8=1740
 CoBr_2 , spectra high temp. and pressure 8=1580
 CoCl_3 , spectra high temp. and pressure 8=1580
 CoF_2 , polarized spectrum rel. to magnon sidebands 8=22974
 CoO, semiconducting, i. r., 0.5-700 μm , by small polarons 8=23008
 Cs in Cs-Ar low-pressure discharges 8=7401
 CsBr, Raman and i. r. spectra at second order, interpretation 8=5595
 Cs_2Sb , time depend. of absorpt. and photoemission 8=13937
 Cu film on Si, in spectral region from 1.5-7 μ 8=14212
 Cu film, spectra 8=5596
 Cu films, thin, and transmission in spectral region between 0.6 and 4 μ 8=22972
 Cu ions in NaCl crystals 8=18521
 Cu and Cu-Ni alloys, rel. to Ni conc. effects 8=2411
 CuCl exciton spectrum, 4.2°K 8=9523
 CuCl exciton states rel. to spectrum oscils. 8=8932
 CuCl rel. to photocond. spectrum, 4°K 8=9251
 CuCl weak lines and luminesc. rel. to exciton complexes 8=9525
 CuO_2 crysts. excitons photoionization, assoc. absorpt. coeff. calc. 8=9529
 Cu_2O rel. to exciton-phonon interactions, n=1 line profile, 4.2-112°K 8=9527
 Cu_2O exciton spectrum, uniaxial press. and n irradi. effects obs. 8=9521
 Cu_2O spectrum rel. to band struct., obs. 8=9524
 $\text{Cu}_{1-x}\text{Zn}_x\text{Ni}_x$, $x < 0.25$ and $0.08 < y < 0.10$, at room temp. 8=22976
 Dy, M_{IV} and M_V lines and edges 8=5602
 Er ferrite-garnet, dichroism and mag. anisotropy 8=18523
 GaAs, edge shift, influence of magnetic field 8=9531
 n-GaAs in mag. field, circularly polarized waves, doping effect 8=22981
 n-GaAs:S, Se, Te, i. r. spectra 8=18528
 GaP, intrinsic 8=2417
 GaP: Ni, spectrum 8=22983
 GaP, uniaxially stressed, interband absorpt. rel. to band-to-band threshold 8=18529
 GdAlO_3 , antiferromag. order, from optical absorption studies 8=22880
 Gd, M_{IV} and M_V lines and edges 8=5602
 Ge, amorphous, rel. to elec. conductivity 8=18066
 Ge, amorphous, i. r. bands rel. to electronic struct. 8=22987
 Ge, electron irradi., absorption edge 8=9534
 Ge, interband, rel. to photon-assisted magnetotunnelling in elec. and mag. fields 8=5260
 Ge:Li(P), i. r. bands rel. to impurity vibrational modes 8=9532
 Ge thin films, piezoabsorption, above fundamental energy gap 8=22986

Absorption—contd

light—contd

H in solution in liq. Ar, translational spectrum in far i. r. 8=12889
 $\text{H}_2\text{NH}_4\text{PO}_3$ films, i. r. spectra in polarized light, 400-4000 cm^{-1} rel. to internal vibrations 8=14224
 He liquid, by excess electrons 8=19687
 $(\text{HgTe})_3\text{-In}_2\text{Te}_3$ alloys, single-crystals, optical energy gap 8=5608
 InAs, free carrier absorpt. coeffs. 300°K and 80°K obs. 8=18536
 n-InSb, in 0.2-4 mm. range at 4.2°K 8=18537
 InSe crystal, 0.4 \rightarrow 25 μ range 8=5609
 K, thin films 8=5612
 K_2 vapour, nonlinear absorpt. of ruby laser light, and resonance fluoresc. 8=7527
 $\text{K}_2\text{B}_2\text{O}_7$ glass, γ -irrad., induced absorption bands assoc. with Ti^{4+} , Pb^{2+} or Bi^{3+} 8=5639
 KBr, Ca doped, growth of bands by X-irrad. 8=2429
 KBr, F-band absorpt., u. s. strain modulation 8=22232
 KBr:OH, i. r. spectra rel. to temp. dependence of intensity of OH vibrations 8=18538
 KCl, constant, and reflectivity spectra rel. to exciton states 8=14230
 KCl, in i. r., induced by monovalent impurities 8=9544
 KCl, transform. of OH centres into U centres by electrolytic decoloration 8=13456
 KCl:Ag (from AgI), of impurity rel. to E-band models 8=14228
 KCl(Br) foils, P-polarized light band at plasma frequency 8=2123
 KCl, F-band absorpt., u. s. strain modulation 8=22232
 KCl-KBr solid solns. 8=2431
 KCl and KF, dichroism, mag. circular, of R, band 8=14235
 KClO_3 , new bands in i. r. after X-ray irradi. 8=22993
 KCl:OH, i. r. spectra rel. to temp. dependence of intensity of OH vibrations 8=18538
 KDF_2 , i. r. study of lattice vibrations 8=5617
 KHF_2 , i. r. study of lattice vibrations 8=5617
 KH_2PO_4 films, i. r. spectrum, internal vibrations 8=9545
 KI-NaI (-RbI), (-KCl) solid solns., temp. dependence, 80-100°K 8=22994
 KI:Ti⁴⁺, B band symmetry assignment 8=5616
 KNbO_3 crystals, ferroelectric, absorpt. edge temp. dependence 8=2430
 KNiF_3 , antiferromagnetic, anomalous temp. depend. 8=22996
 KX, (X = Cl, Br, I), rel. to U centre electronic structure 8=2001-2
 LaCoO_3 , p- and n-type, by small polarons 8=2434
 LiBr, fine structure near K-edge 8=18544
 LiCl, fine structure near K-edge 8=18544
 LiF, fine structure near K-edge 8=18544
 LiF, and LiH, rel. to F-centres exchange interactions 8=17684
 $\text{LiH}_3(\text{SeO}_3)_2$, fundamental edge near ferroelectric phase transition pt. 8=9548
 LiI, fine structure near K-edge 8=18544
 Mg crystals, interband absorpt., 32° and 295°K 8=18545
 MgF_2 , i. r., selection rules 8=5621
 MgO, "mirror", fluorescence 8=9620
 $\text{MnCsCl}_2 \cdot 2\text{H}_2\text{O}$, spectrum rel. to Mn^{2+} crystalline field parameters 8=8197
 α -MnS, rel. to elec. conductivity 8=18057
 MoS_2 , thin anisotropic, crystals, delocalized excitons from magneto absorpt. study 8=13674
 N_2 , in shock tube, vac. u. v. absorpt. 8=7532
 NO, solid, rel. to mol. excited states, 2300-1100 Å 8=14243
 NO in solid Ne, Ar and Kr rel. to excited states, 2300-1100 Å 8=14243
 N_2O , coeff. 600-1000 Å 8=16447
 N_2O , i. r. spectral bands rel. to isotopic mols. and crystal lattice vibrations 8=14251
 Na, liquid rel. to electronic structure 8=8111
 NaCl:Eu rel. to luminesc. centres structure, obs. 8=9623
 NaCl, F-band absorpt., u. s. strain modulation 8=22232
 NaCl:OH, i. r. spectra rel. to temp. dependence of intensity of OH vibrations 8=18538
 NaClO_4 , X-ray irradiated crystals 8=18548
 NaHF_2 , i. r. study of lattice vibrations 8=5617
 NaI, in i. r., induced by monovalent impurities 8=9544
 NaI, i. r. vibrational by U-centres 8=9557
 NaNO_3 , absorpt. spectra from 450-5700 cm^{-1} 8=9556
 in Nd^{3+} laser glass, saturable absorpt. of colour centres rel. to self Q-switching 8=11107
 in Nd^{3+} - Yb^{3+} laser glass, saturable absorpt. of colour centres rel. to self Q-switching 8=11107
 Ni^{2+} in MgO, spectra, line shift rel. to temp. 8=2442
 NiBr_2 , spectra high temp. and pressure 8=1580
 NiO, semiconducting, i. r., 0.5-700 μm , by small polarons 8=23008
 Pb, supercond., far i. r. rel. to critical energy gaps 8=18555
 PbBr_2 :Mn and luminesc. excit. and emission spectra 8=9622
 PbCl_2 :Mn and luminesc. excit. and emission spectra 8=9622
 $\text{Pb}_{0.85}\text{Sn}_{0.15}\text{Te}$, energy gap 8=2446

Absorption—contd**light—contd**

- Pb_{0.93}Sn_{0.07}Te, energy gap 8=2446
 PbI₂, in region 0.5–15 μ and photoconduction at 0.525 μ 8=2444
 PrF₃, i.r., dichroism 8=9560
 RbCl, F-band absorpt., u.s. strain modulation 8=22232
 SO₂, with ketones, nitriles, esters or alcohols, u.v. absorpt. spectra 8=18688
 Se, amorphous, rel. to elec. conductivity 8=18066
 Si, amorphous, i.r. bands rel. to electronic struct. 8=22987
 Si, amorphous, rel. to elec. conductivity 8=18066
 Si, B-doped, broadening 8=2452
 Si, rel. to bound excitons 8=5132
 Si, three-photon process 8=5635
 SiC polytypes, infrared 8=23013
 SiO₂ film, i.r., rel. to temp. of deposition 8=21889
 SiO₂ vitreous films, i.r. 8=5637
 SnO₂, thin films, u.v. edge spectrum 8=2458
 SnTe, visible and i.r. obs. 8=18562
 Sr films, thin, between 0.5 and 5.5 eV 8=23014
 SrF₂, X-ray coloured, by colour centres, temp. dependence 8=17683
 Su film, edge due to quantum transition from d-band 8=5585
 Te, amorphous, rel. to elec. conductivity 8=18066
 ThO₂, spectra obs. 8=1740
 TlBr:Mn and luminesc. excit. and emission spectra 8=9622
 TlCl:Mn and luminesc. excit. and emission spectra 8=9622
 TiO₂ layers, rel. to electronic carrier props. 8=23017
 V₂O₅, absorption coefficients 8=23020
 Yb, M_{IV} and M_{II} lines and edges 8=5602
 Zn crystals, interband absorpt., 32° and 295°K 8=18545
 ZnO:Ni(Co), lattice-vibration effects 8=9563
 ZnS luminesc. reabsorption rel. to equilib. emission kinetics 8=9641
 ZnSe, and reflection spectra in i.r. at low temps. 8=23026
 ZnTe, and reflection spectra in i.r. at low temps. 8=23026

Abundance ratio. See Elements/relative abundances; Isotopes/relative abundances.

Acceleration. See Dynamics; Kinematics.

Acceleration measurement

See also Velocity measurement.

- absolute, of "g", review 8=38
 g absolute 8=37
 gravity, using laser-interferometer system 8=10487
 due to gravity, Poland, determ. 8=14515
Accelerators. See Particle accelerators.
Accommodation coefficient. See Gases; Kinetic theory/gases; Surface phenomena.

Acids, inorganic. See Individual compounds, and Hydrogen compounds.

Acids, organic. See Organic compounds.

Acoustic amplification in solids. See Acoustoelectric effects.

Acoustic analysis

- bell, amplitude-time distribution of partial tones 8=19572
 elastic surface waves on acoustical optical branches 8=15041
 engine, multicylinder, air-induction system 8=6174
 field new infinite photo driven by point source 8=10725
 field of point source in fluid wedge with compliant boundaries, amplitude and phase structure 8=10723
 focusing system, double mirror 8=19576
 gases, optical-acoustic, selectivity and sensitivity on gas pressure 8=23192
 matrix formulation in analysis of mechanically driven fluid systems 8=175
 media, non-linear props. 8=194
 point emitter in absorbing waveguide, total field of damped normal modes 8=10724
 pressure correlation for cylinder in diffuse field 8=173
 radiation from solid object moving in helical path, press. field, directivity and total energy 8=10726
 ray tracing in layered atmosphere, analogue computer solution 8=14637
 sound field freq. spectrum laser appl. 8=19552
 sound field by striaoscope-photometer method 8=3046
 WKB approx. applied to wave propag. in split-beam sound field 8=19567

Acoustic field. See Acoustic radiators; Acoustics; Intensity measurement/acoustics.

Acoustic generators

See also Musical instruments.

- coated infinite plate backed with baffle, driven to point and line source 8=3043
 driven infinite plate backed with baffle, far field acoustic pres. 8=3047
 laser, mag. pumped paramag. salts appls. 8=15473
 matrix formulation in analysis of mechanically driven fluid systems 8=175
 plasma, ion removal 8=12569
 r.f. electromagnetic radiation rel. to acoustic wave generation and effect on metal surface impedance 8=180
 Ryke tube, sound generation zones 8=10728
 sonar dome, vibrating, generalised field formulation and noise loading 8=15062

Acoustic generators—contd

- of travelling, transverse modes, by rotating radial gas jet at centred short cyl. cavity 8=15063
 underwater, impulsive high power, using elect. discharge 8=6157
 MgO:Cr, hyper- and terasound generation by ruby lasers 8=10727

Acoustic impedance

- absorbent systems, absorption coeff. rel. to impedance ratio, charts 8=10739
 air layer, thin, correction for parabolic diaphragm deformation 8=19554
 cylinder, uniformly vibrating, Robey's first reactance integral evaluation 8=181
 input admittance of plates with radiation load 8=19559
 mutual between flexible different-size disks in infinite rigid plane, calc. 8=6160
 orifice, meas. of nonlinearity 8=3053
 plane wave confronting circular device, analog equivalent cct. 8=6158

Acoustic paramagnetic resonance. See Paramagnetic resonance and relaxation.

Acoustic radiators

See also Doppler effect.

- arrays, directivity pattern in Fresnel zone, error compensation 8=19550
 by dislocation motion in ionic crystal 8=17637
 impedance, mutual between flexible different-size disks in infinite rigid plane, calc. 8=6160
 jet, free with periodic structure, radiation 8=10722
 loudspeaker casings, dimensioning for bass reflection using equivalent electric circuits 8=10730
 monopole in reverberation chamber, calc. of power radiated 8=178
 moving, Doppler correction of spectra 8=19577-8
 moving in helical path, press. field, directivity and total energy 8=10726
 plane base, properties 8=19593
 plate, thin elastic, under random loading 8=10729
 plates, circular vibrating, nearfield press. distribution calc. 8=6152
 point emitter in absorbing waveguide, total field of damped normal modes 8=10724
 spark underwater 8=12863
 spherical, calc. of radial vel. at surface for prescribed pressure distrib. 8=19553
 wave generation by r.f.e.m. radiation and effect on metal surface impurities 8=180

Acoustic receivers

See also Microphones.

- arrays, directivity pattern in Fresnel zone, error compensation 8=19550
 design using signal detectability theory 8=184
 detection of incoherent finite signal using sensors in isotropic noise field 8=6159
 earphones, free-field frequency response determination 8=3050
 line arrays, inter-element coupling effect on signal to noise ratio and beam steering 8=10734
 Luneberg fluid lens, acoustic field 8=19562
 nonlinear mixing, detect. by optical Bragg diff. 8=10732
 plane wave confronting circular device, analog equivalent cct. 8=6158
 point array directional response major and minor lobe structure of response by 2-parameter calc. 8=15065

Acoustic resonators

- air in tube, forced vibrations of finite amplitude 8=16705
 jet, choked, radiation from 8=10722
 LiNbO₃:Cr³⁺ hypersonic, propag. of 10⁴ Mc/s, room and He temps. 8=8631
 YFe garnet single crystal, magnetoacoustic resonance obs. 8=22891

Acoustic streaming

- bubble in liquid, u.s. 8=21590
 bubble mass transfer, effect of u.s. streaming 8=21584
 fluid, elastico-viscous, near cylindrical obstacle 8=6169
 fluid, flow field method for heat transfer from transverse oscill. cylinder 8=3098
 induced by finite amplitude sound 8=3067

Acoustic transducers

See also Acoustic generators; Acoustic receivers; Microphones; Sound reproduction.

- displacement type, effects of air compression between parallel plates 8=7892
 infrasonic, role in obs. geoaoust. phenomena due to artificial sources 8=9804
 piezoelectric, acoustic dispersion in thin cylindrical rods 8=4913
 piezoelectric ceramics, sensitivity to high stress perpendicular to polar axis obs. 8=19556
 piezoelectric ceramics, stress sensitivity of permittivity reduced by heat treatment 8=19555
 piezoelectric, mechanical responses 8=5379
 piezoelectric plate, with prescribed input, electrical response 8=15064
 piezotransducers, equivalent circuits, for u.s. analysis 8=196
 reactor structural damage due to vibr. of high pressure gas, meas. 8=20885

Acoustic transducers—contd

- rotational displacement, construction and design 8=6000
- spark chamber readout system, matching and backing problems 8=3485
- systems, flush mounted, as spatial and spectral filters for turbulent boundary press. field 8=10731
- ultrasonic and liquids viscosity meas. 8=8028
- wedge, for Rayleigh wave excitation 8=182
- LiNbO_3 , resonant and antiresonant freq. constants rel. to rot. angle 8=9226
- LiTaO_3 , resonant and antiresonant freq. constants rel. to rot. angle 8=9226

Acoustic wave propagation

- See also Absorption/acoustic waves; Dispersion/acoustic; Doppler effect; Helium/liquid, sound propagation; Shock waves; Velocity/acoustic waves.
- acoustic nonlinearity of an orifice, meas. 8=3053
- anomalous, in atmosphere around nuclear explosions 8=9898
- atmosphere after nuclear explosion 8=2583
- cavitation and streaming due to sound waves of finite amplitude 8=12753
- cross-section of a circular cylinder with an impedance-loaded strip along a generatrix 8=176
- dielectric crystal, excitation by interaction of charged particles 8=8625
- far field pressure from driven coated plate with baffle 8=3048
- far-field pressure from driven infinite plate with baffle 8=3047
- fluid nearly incompressible, inviscid. due to time depend. motion of arbitrary submerged body 8=21662
- gases, monatomic 8=1474
- in gas-particle mixture, and acoustic combustion instability 8=16704
- in highly rarefied gases, effect of gas-surface interaction 8=21519
- infrasonic, from aurora, shock-wave model 8=19533
- interaction with electrons in strong elec. field, Boltzmann eqn. 8=13343
- lens, liquid, aberration theory, focusing props. 8=19573
- liquids, finite-amplitude waves 8=12856
- liquid force on bubble in standing wave 8=16826
- in liquid metals, attenuation 8=12859
- liquid, viscous, non-Newtonian 8=16830
- methane-water vapour mixture, vib. Napier relax. time 8=4481
- mode-conversion in the long-wavelength limit 8=186
- ocean, sound fluctuations and random inhomogeneities 8=3054
- in ocean, spherical waves, induced nonlinear losses and cavitation 8=9820
- panels, double, transmission loss, calc. allowing for absorption by cavity walls 8=10740
- physical acoustic, principle and methods: the effect of imperfections, book III A 8=17485
- piezoelectric semiconductors, I-V characteristic under sound amplification conditions 8=18021
- in pipe, hydraulic analogy 8=187
- plane longit. waves in bar, vel. gains for free free mode-resonator case 8=3057
- pulsed, in layered inhomogeneous medium, time struct. depend. on vertical coordinate 8=3056
- quartz, hypersound generation by stimulated Brillouin scatt. 8=2451
- radiation-driven acoustic waves in confined gas 8=4483
- radiation, flexurally vibr. plates, abatement, by dampers 8=3019
- radiation from underwater spark 8=12863
- ray theory expressions for a wide class of vel. functions 8=19560
- ray tracing, 3D, Frenet formulation 8=6161
- sand, propagation parameters for various grades 8=22107
- scattering by front rows of audience, experimental model 8=15068
- semiconductors, piezoelec., amplification critical electron drift velocity 8=19571
- semiconductors, piezoelectric interaction of growing sound noise 8=22094
- shock-front-vortex interaction, sound generation, maths. 8=188
- solids, non-isotropic second sound dispersion and damping 8=4910
- solids, phonon amplification, spatially inhomogeneous 8=4917
- sound amplification in gas, radiation induced, possibility 8=21516
- sound propagation in highly rarefied gases, effect of gas-surface interaction 8=21519
- split-beam sound field, ray representation of diffraction effects 8=19567
- standing wave in rigid-walled tube containing air, theory and obs. 8=21518
- turbulent media, statistical properties, book 8=10735
- 240 nsec r. f. pulse, compression by Bragg diffraction of light with microwave sound 8=8618
- underwater acoustics 8=4569
- underwater, effect of internal water wave propag. 8=3051
- underwater, nonlinear, transmission 8=6164
- underwater signals, cross correlation 8=3059

Acoustic wave propagation—contd

- underwater sound-pulse distortion by converging lens 8=4570
 - underwater, theory, book 8=10751
 - underwater, waveguide layer model 8=3055
 - walls, double and single 8=10741
 - water, parametric amplification, with uniformly distributed bubbles 8=12864
 - water, standing wave, forces on bubble 8=12855
 - in waveguides with arbitrary cross-section, calc. of eigenvalues 8=3052
 - waveguide, with inhomogeneities in medium and at boundaries 8=10737
 - in wind-tunnel, press. grad. effect on turbulent-boundary layer press. fluctuations 8=4480
 - BaTiO_3 , ferroelectric modes, and soft optic modes, mixing 8=22665
 - Bi, plasma, theory 8=17498
 - CdS, Rayleigh wave amplification at 30 MHz 8=13350
 - He^4 liquid, 3-phonon mechanism incompatibility with obs. 8=258
 - in Hg discharge, ion-acoustic 8=4313
 - K, shear wave magnetoacoustic effect 8=22105
 - KBr, phonons, first and zero sound, elastic const. variation 8=13357
 - $\text{LiNbO}_3 \cdot \text{Cr}^{3+}$, 10^4 Mc/s hypersound perp. to optical axis, room and He temps. 8=8631
 - α -Mn, longitudinal and transverse velocities and ultrasonic attenuation betw. 4.2–300°K 8=17501
 - SiO_2 , vitreous, shear wave losses and phase vel. vars. obs. 8=13358
- ultrasonic**
- amplification, Love type in dielectrics with thin CdS layer 8=4921
 - amplifiers, parametric, misalignments 8=3066
 - butyl alcohol, stimulated and thermal Mandel'shtam Brillouin dispersion 8=21665
 - gases, molecular, kinetic theory 8=4479
 - graphite, stress wave packet, attenuation effect on freq. content 8=8626
 - holography, recording technique 8=6176
 - laminated materials, forbidden frequency bands 8=6166
 - liquid, cavitating, parametric effects 8=21664
 - liquids rel. to volume viscosity, theory 8=16804
 - metals, compressional and shear waves generated electromagnetically, meas. 8=4920
 - metals, e. m. waves and interaction with u. s. waves, theory 8=22951
 - metals, shear wave circular polarization 8=17488
 - mixed salt solns., interferometric obs. 8=16827
 - phase velocity, pulse-echo-overlap method incorporating diffraction phase corrections 8=6177
 - piezoelectric semiconductors, rel. to non-linearity of elec. props. in a. c. field 8=18022
 - piezoelectrics, ultrasound generation under Gunn effect 8=22100
 - polyelectrolyte solns., vibr. potentials 8=8061
 - in polymers, cryst. 8=1859
 - polystyrene in chlorinated biphenyl solns., dynamic mech. props. 8=12818
 - position sensing device in air 8=19579
 - pulse attenuation meas. for dynamic modulus 8=17715
 - pulse compression, using Bragg scatt. of light by u. s. waves 8=8617
 - quantizing mag. field, free electron absorpt. 8=6165
 - semiconductors, multilayer, amplification by carrier drift 8=17855
 - in solids, u. s. and hypersonic waves 8=1842
 - surface waves, generalized, in cubic crystals. 8=1855
 - CdS, longit., amplification 8=8627
 - He liquid 8=10806
 - RbMnF_3 , near magnetic critical point, attenuation and velocity 8=17504
 - SrTiO_3 , reduced, at low temps. 8=17505

Acoustic waves

- See also Diffraction; Interference, etc.; Elastic waves; Shock waves; Ultrasonics.
- combustion chamber with self-oscillatory system 8=243
- Epstein normal-mode model of surface duct 8=174
- finite amplitude, dynamics of propagation in free space 8=10736
- in gas, generation by entropy discontinuities flowing past an area change 8=177
- hypersound generation using magnetic surface film 8=1841
- ion in collisional plasma, damping study using Focker-Planck eqns. 8=12550
- ionic, electron temp. variation effects 8=16574
- ionic, interaction with transverse waves and oscillations in plasma 8=16569
- ionic, propagation in bounded plasma 8=16575
- in non-simple elastic materials 8=19389
- plasma magnetized by dipole field, model for magnetosphere 8=1393
- in plasma, nonlinear ion wave evolution 8=16463
- radiation, by vibr. nonuniform wall 8=3049
- rattles, swings and subharmonics 8=179
- Rijke thermoacoustic oscills., literature review 8=21515

Acoustic waves—contd

- from solid object moving in helical path, press. field, directivity and total energy 8=10726
- Sondhauss thermoacoustic oscills., literature review 8=21514
- sound field, pulsating ring on cylinder 8=3045
- in stratified atmos., generation by turbulent motion motions 8=23270
- ultrasonic in crystals., as light diffraction grating 8=22944
- waveguides with arbitrary cross-section, calc. of eigenvalues 8=3052
- I_2 -Ar mixtures, vibr. relax. time meas. 8=7932
- I_2 -He mixtures, vibr. relax. time meas. 8=7932

effects

- See also Chemical effects of radiations/acoustic waves.
- aerosols, particle interaction at high press. 8=21732
- drying of capillary-porous materials 8=19575
- flames modulation rel. to sound reproduction 8=10750
- heat transfer in gases 8=12680
- interaction with light and applications 8=11120
- ionic, l.f., coupling to longitudinal plasma oscills. 8=16579
- ionsphere, irregularities ascribed to earthquake 8=23395
- light diffraction in anisotropic media 8=9476
- nonlinear interactions 8=6153-4-5
- particle aggregation, in sound field 8=6156
- on, plasma dipole impedance 8=4386
- plasma, trapped, fast randomization of electron gas 8=16580
- quartz, light scatt. by u.s. surface waves 8=5636
- sonic bangs and explosions subjective estimation 8=15075
- sphere, small rigid, radiation press. in fluid 8=6151
- structural element, modal density expressions 8=19591
- Ag film growth, ultrasonic vibrations of substrate 8=4827
- Au film growth, ultrasonic vibrations of substrate 8=4827
- KBr, u.s. strain modulation of F-band absorpt. 8=22232
- KCl, u.s. strain modulation of F-band absorpt. 8=22232
- NaCl, u.s. strain modulation of F-band absorpt. 8=22232
- RbCl, u.s. strain modulation of F-band absorpt. 8=22232

Acoustical laboratories

- anechoic chamber, small, for acoustical meas. 8=3074
- Danish Technical University 8=19583
- free-field listening for psycho-acoustic expt. 8=19584

Acoustical measurement

- See also Interferometry/acoustic waves; and under separate subjects e.g. Intensity measurement/acoustics.
- anechoic enclosures, freq. inhomogeneities 8=19585
- architectural, method 8=10752
- external-ear replica for testing of props. 8=3082
- geoacoust. phenomena resulting from artificial sources, instrumental role 8=9804
- harmonic analysis of guitar string tone for different excitation methods 8=6172
- imaging of microwave acoustic beam, cross section in rutile by Bragg laser 8=6175
- infrasonic signals from field expt., analog system for rapid approx. analysis 8=6179
- insulation in presence of flanking paths 8=19582
- meas. in reverberating conditions using a correlation method 8=15077
- noise, total exposure evaluation 8=19589
- phase velocity, u.s., pulse-echo-overlap method incorporating diffraction phase corrections 8=6177
- scattering by front rows of audience, experimental model 8=15068
- by spectrometry, time-delay, in reverberant environment 8=6180
- spectrum analysis of transients and sonic band loudness 8=10753
- stiff strings, normal freq. 8=6171
- striograms, graphical resolution by strioscope-photometer method 8=3046
- transducer face, vibrational displacement and mode shape, by laser interferometer 8=6178
- transmission loss using vibr. transducers 8=10754
- ultrasonic surface wave amplitude from diffraction pattern of interacting light beam 8=6553
- volume absorbers, individual, small chamber method 8=10755
- P and S waves in rock, velocity meas. by pulse transmission method 8=14542

Acoustics

- See also Acoustic resonators; Architectural acoustics; Atmospheric acoustics; Hearing; Noise/acoustic; Sound reproduction; Speech; Ultrasonics; Vibrations.
- diffraction, extension of ray representation into shadow zone 8=10747
- hammer mill sounds, comparative study 8=6186
- hearing aid output baffle and shadow effects of head 8=10733
- hologram, laser reconstruction of image 8=524
- marine geology, application 8=23248
- periodic room reflections, repetition pitch threshold 8=3096
- physical acoustic, principle and methods: the effect of imperfections, book III A 8=17485
- principles and methods: application to quantum and solid state physics, book IV A 8=17486
- rotating jet, energy density spectrum 8=19551

Acoustics—contd

- sand in desert, "singing" phenomenon 8=23232
- shocks, generated by diaphragm rupture in tube 8=15051
- solid acoustic thermometer 8=19664
- sound fields, subjective investigation 8=19549
- teaching films 8=19548
- thermometer for reactor fuel 8=4018
- underwater, theory and applications, book 8=10751
- underwater, utilization of nonlinear effects 8=19574

musical

See also Musical instruments.

- concert halls, levels of reflection masking 8=19594
- violin woods, unseasoned and aged 8=3070

Acoustoelectric effects

- amplification, Love waves in dielectrics with thin CdS layer 8=4921
 - amplification in piezoelectric semicond., critical electron drift vel. 8=19571
 - amplification of sound in crystals, effect of elec. field 8=1846
 - attenuation theory and appl. to semiconductors ultrasonics 8=1845
 - domains, approx. analysis 8=13347
 - ferrites, dielectric props., influence of ultrasound 8=9370
 - ferroelectrics, acoustic and polarization waves interaction, elastic consts. 8=18182
 - low-temperature thermometry appl. 8=19663
 - measurement, comparison method 8=1847
 - metal surface impedance changes on acoustic wave generation by r.f. e.m. radiation 8=180
 - piezoelectrics, self-excited vibration prod. by current in separate semicond. layer 8=9223
 - in plasma, microwave nonlinear coupling to electro-acoustic resonances 8=12506
 - p-n junctions, forward and reverse sensitivity to small deformations 8=13842
 - semiconducting piezo-elec. crystals, transient phenomena 8=13346
 - semiconductors, amplification and negative differential cond. rel. to traps 8=1843
 - semiconductors, magnetic field effect on gain 8=13345
 - semiconductor plate 8=17496
 - semiconductor with traps, and sound amplification, theory 8=9078
 - semiconductors, piezoelectric, acoustoelec. domain formation during thermal noise amplification 8=18001
 - semiconductors, piezoelectric, stimulated Brillouin scattering. 8=17495
 - in semiconductor, wavelength of sound \ll mean free path of electrons, theory. 8=17494
 - solids, sonic wave effect on current carrier mobility 8=22415
 - superconductors type I, microwave absorption by surface states 8=2142
 - CdS crystal, transverse u.s. wave amplification at 87 MHz. 8=22098
 - CdS light scanner 8=5309
 - CdS, photoconducting, rel. to field distrib. and current saturation 8=9250
 - CdS, 3- and 4-phonon processes obs. 8=1850
 - CdS, u.s. amplification, temp. dependence 8=2081
 - CdS, u.s. dispersion meas. 8=1849
 - CdS wideband transducer using diffusion layer 8=19557
 - CdSe, in regime of continuous intense supersonic electron stream 8=8628
 - InSb, domain form. and amplifiers d.c. loss mag. fields effect 8=13355
 - n-InSb, oscillation rel. to microwave emission at 77°K 8=13823
 - InSb, oscillations in presence of magnetic field field-dependent period 8=4923
 - n-InSb at 77°K in crossed electric and magnetic fields 8=13356
 - ZnO, oscillations, 1-5 GHz range 8=22613
- Acoustomagnetic effects.** See Magnetoacoustic effects.
- Actinides**
No entries
- Actinide compounds**
group IVA-VIA, with NaCl structures, lattice constants and melting pts. 8=4867
- Actinium**
Ac²²⁸ in Ra²²⁸ solns, separation and purification by solvent extraction method 8=16047
- Actinium compounds**
No entries
- Actinometry.** See Photometry.
- Activation analysis.** See Chemical analysis/by nuclear reactions.
- Active nitrogen.** See Nitrogen.
- Active oxygen.** See Oxygen.
- Adhesion**
coefficients at very low temperatures 8=7954
electronic theory 8=2046
moist powder, to solid in temp. field 8=22303
of pneumatic tyre to wet road, simulation, and theory of viscous hydroplaning 8=17752
polycapromamide fibres to polyvinylalcohol, CF₃ radiation grafting effects, obs. 8=22410
polyethylene, cross-bindings prod. by reactor irradi., showed by n scatt. 8=16969

Adhesion—contd

- polyethylene, filled, effect of chem. nature of substrate 8=13617
 polyethylene, relation with wettability 8=8879
 polyethylene, and wettability 8=8874
 polymers to porous substrates, formation of joints, and strength 8=17751
 polymers, wettability data 8=17841
 polypropylene fibres to polyvinylalcohol, CF_3 radiation grafting effects, obs. 8=22410
 polyethyleneterephthalate fibres to polyvinylalcohol, CF_3 radiation grafting effects, obs. 8=22410
 rubber, cross-bindings prod. by reactor irradi., showed by n scatt. 8=16969
 75 Cu-25Ni laminate on Cu core in coinage composite, bond degradation mechanism 8=22329
 spherical particles, effect of capillary liq. 8=8150
 styrene, cross-bindings prod. by reactor irradi., showed by n scatt. 8=16969
 surface energy of, role in metalworking 8=5034
 ZnS:CdS:Cu phosphor-silicic acid sol. to glass, obs. 8=8157

Adiabatic demagnetization. See Magnetic cooling.

Adion. See Adsorption.

Adsorbed layers

- dyes on solids, ionization energy 8=5424
 intermolecular nucl. mag. relax., theory 8=8330
 metals, desorption of multiple additives, rel. to thermionic diodes 8=17154
 monolayers, capillary ripple 8=1514
 organic, on metal films, polymerization 8=2251
 polycyclic cpds. monolayers, isotherms rel. to mol. struct. obs. 8=17178
 poly(methylmethacrylate), interface tension, tacticity determ. 8=4551
 polystyrene, conformation meas. by attenuated total reflect 8=8350
 stripping, double-layer charging 8=2535
 vapour deposition, obs. by mass spectra 8=17155
 on n-Ge, conductivity hydrostatic pressure dependence 8=18045
 U on W, study by field emission work function 8=22715
 H_2O mols. in oxide films on Si, dielectric relax. 8=1706
 W, Ce and Ba, e emission, Thomas-Fermi-Dirac theory 8=5414
 Zn, on W emitter, adconc. rel. to following crystallite nucleation 8=1746

Adsorption

- See also Chemical analysis/adsorption; Chromatography; Films; Heat of adsorption; Sorption.
 amylose, asymm. adsorpt. of DL-mandelic acid and DL-ethyl mandelate. 8=18696
 anions on metal surface 8=4760
 asbestos, adsorpt. of gases 8=21898
 by atmospheric particles, of radioactive I 8=9892
 biotite, adsorpt. isotherms of alkyl ammonium ions in aqueous solns. 8=13106
 carbon, adsorpt. of polyethers at soln.-solid interface 8=1708
 carbon blacks, graphitized, of Xe rel. to surface heterogeneity, obs. 8=17162
 carbon black of poly(dimethyl siloxane) from CCl_4 and xylene solns. 8=8336
 cations on metal surface 8=4760
 cell for study by i. r. spectrography 8=17157
 charcoal, activated, of ethylene, n-scattering studies rel. to adsorbant mol. motions 8=21901
 charcoal, surface heterogeneity meas. 8=8293
 clay minerals—Al oxide, hydrous, mutual adsorption 8=8341
 direct electrical meas. on electrodes 8=9767
 effect on orbiting pressure gauge errors 8=5838
 gas-covered surfaces, kinetic electron ejection model 8=16435
 gas-solid interface study, i. r. cell 8=6530
 glass, of acetone vapour, increase in surface conductivity 8=4766
 glass, of methanol vapour, increase in surface conductivity 8=4766
 glass of water vapour, increase in surface conductivity 8=4766
 graphite, of CO_2 , anisotropy of polarizability 8=21900
 graphite grains, interstellar 8=23572
 graphite, localized 8=8339
 graphite, of various gases and vapours, by fresh surface 8=8338
 Graphon, adsorpt. of isopropyl alcohol 8=1700
 Graphon and Spheron 6, monocarboxylic acids and methyl esters 8=8340
 heats of, calorimeter obs. 8=6221
 heterogeneous surfaces, defined adsorpt. sites and free energies 8=13103
 hydroxyapatite catalysts, H content 8=14395
 immersion and adsorpt. heats, thermodynamic relations and lateral interactions effects 8=17152
 isotherms, analysis 8=13102
 large atoms, configurational entropy 8=13104-5
 liquid phase adsorpt. fractionation in fixed beds, anal. 8=17151
- Adsorption—contd**
 low pressure adsorpt and pot. theory 8=21895
 metallic lattice, calculation by method of stochastic processes 8=8334
 montmorillonite, Na and Li, of trimethylcarbonil, by i. r. spectra 8=1705
 nylon, adsorpt. of polyethers at soln.-solid interface 8=1709
 oil molecules, mean adsorpt. time obs. 8=17156
 organic crystals as adsorbents for gas-solid chromatography 8=18763
 oxide-film on metals, passivity theory 8=9702
 packed powders with fluids, at liquid/solid interface, rel. to permittivity 8=22648
 phthalocyanine blue of poly(dimethyl siloxane) from CCl_4 and xylene solns. 8=8336
 portland cement component hydration products, of Ca lignosulphonate and salicylic acid 8=21902
 powders, adsorpt. of He at room temp. 8=21899
 preferential, prep. of o- H_2 and p- D_2 8=17158
 rutile, adsorpt. at solid-liq. interface from binary soln. 8=1710
 second layer adsorpt. model allowing for energy losses in primary layer 8=17150
 silica, adsorpt. of aliphatic aldehydes and ketones, i. r. study 8=8346
 silica gel, surface meas. 8=21742
 soda-lime glass with adsorped water spreading of org. liqs. 8=1520
 on solids from non-ideal solutions 8=8331
 soluble surface active material at oil/water interface 8=16811
 solute at gas-liquid interface 8=5760
 steel, of H_2 in Cd plating 8=17163
 on substrate, of vapour, rel. to kinetics of film nucleation 8=8305
 surface localized vibration mode 8=17153
 Teflon 6, N_2 and Ar isotherms 8=13047
 thermodynamic treatment for substrate in equilb. with ionized vapour, and emission 8=18263
 time-dependent impurity adsorpt., influence on metal electrocrystallization 8=17225
 trons-dichloroethylene on silica gel, laser Raman spectra 8=23031
 vacuum microbalance techniques, conference Newport Beach USA (1966) 8=14919
 vapour-solid interactions in effusion oven 8=7899
 zeolite/water, methanol, methylamine or propane systs. 8=18454
 zeolites LiX and NaX, of Xe and Kr, press. and temp. depend. 8=1713
 AgI, adsorpt. of methanol vapour 8=8337
 AgI: KNO_3 nuclei, of water vapour obs. 8=8335
 Al, of H_2O , effect on electron emission 8=9270
 Ar, adsorbed in equilibrium with gas in ultrahigh vacuum, obs. 8=21530
 Ar f. c. c. crystal, of inert gases, potential energy profiles 8=17159
 BeO, hot-pressed, effect of adsorbed sulphate and fluoride on density 8=21821
 Br on silica gel, laser Raman spectra 8=23031
 Ca_2 aluminate hydration product, of Ca lignosulphonate and salicylic acid 8=21902
 Ca_2 aluminoferrite hydration product, of Ca lignosulphonate and salicylic acid 8=21902
 Ca_2 silicate hydration product, of Ca lignosulphonate and salicylic acid 8=21902
 Ca_2 silicate hydration product, of Ca lignosulphonate and salicylic acid 8=21902
 CCl_4 on silica gel, laser Raman spectra 8=23031
 CO_2 , radiolysis in adsorbed state 8=18741
 CS, on silica gel, laser Raman spectra 8=23031
 CdS films, of O_2 , effect on elec. props. 8=13791
 Cr, adsorpt. of polar organic mols. 8=13107
 Fe, (011) surface, O adsorption, low energy electron diffraction study 8=1701
 Fe_2O_3 of poly(dimethyl siloxane) from CCl_4 and xylene solns. 8=8336
 Fe_2O_3 powder, of the anions VO_3^- , WO_4^{2-} , MoO_4^{2-} and $\text{Cr}_2\text{O}_7^{2-}$, pH depend. 8=8342
 He, by condensed gas layers 8=8329
 Hg/methanol interphase 8=18721
 Hg-Mo system, desorption 8=21903
 Hg-W system, desorption 8=21903
 Ir, of Cs rel. to film formation and electron emission 8=9268
 K, on W, desorption from emitter of field emission microscope 8=3211
 KBr, adsorpt. of water vapour on cleavage surface 8=17166
 KCl, adsorpt. of water vapour on cleavage surface 8=17166
 LiF, adsorpt. of water vapour on cleavage surface 8=17166
 Mg-Fe mixed hydroxides, of benzene, rel. to surface area 8=17023
 Mg-Fe mixed hydroxides, of cyclohexane, rel. to surface area 8=17023
 Mg-Fe mixed hydroxides, of N, rel. to surface area 8=17023
 MgO , adsorption of nitro-cpds. rel. to electron donor props. on surface 8=8343

Adsorption—contd

- MgO, of OH, retention props. 8=1703
 MnO₂, radiochem. separations 8=9763
 Mo crystals, of O₂, from surface exam. by LEED and work function studies 8=17165
 Mo films on W crystal, and electron emission 8=9269
 Mo, fluorinated, adsorpt. of Cs, structure of adsorbed layer, and effect on thermionic conversion 8=17154
 Mo tip, of O₂, H₂, and N₂, field emission study 8=21905
 NH₃ on supported Fe catalyst, Mössbauer spectra 8=13108
 NaBr, adsorpt. of water vapour on cleavage surface 8=17166
 NaCl, adsorpt. of water vapour on cleavage surface 8=17166
 Ni of Ar, temp. dependence. 78-120°K 8=17168
 Ni, clean {100}, of CO 8=21906
 Ni films, of O₂, effect on Hall effect and elec. conductivity 8=17936
 Ni(110), of CO, behaviour model 8=17169
 Ni surfaces, of H₂, electron probe surface mass. spectrometer obs. 8=21908
 Ni and W ribbons exposed to water, low-energy electron bombardment 8=21907
 Pb-Sn alloy, of Na, at grain boundaries 8=8344
 PbCrO₄, of poly(dimethyl siloxane) from CCl₄ and xylene solns. 8=8336
 Pd, i.r. spectra of adsorbed CO 8=4764
 Pt electrodes, adsorpt. of hydrocarbons 8=9714
 Pt electrodes, adsorpt. of n-hexane 8=5737
 Pt, oxidative adsorpt. of propane 8=2534
 PuO₂ of O, sintering effects and adsorpt. sites, obs. 8=8345
 Re-Nb alloy, adsorpt. of H₂O vapour, study by work function behaviour 8=13927
 Rh electrodes, adsorpt. of CO 8=18726
 Rh electrodes, adsorpt. of CO + H 8=18727
 Si(111) surface, of PH₃, LEED study 8=4765
 SiO₂, adsorpt. of polyethers at soln.-solid interface 8=1707
 Ta ribbon, work function changes on Cs, O₂ and H₂ adsorpt. 8=9276
 TiO₂, adsorption of CO, i.r. spectroscopy 8=8347
 TiO₂ of poly(dimethyl siloxane) from CCl₄ and xylene solns. 8=8336
 U, surface potential of H₂ 8=21909
 W, adsorption of N₂, rel. to work function 8=1711
 W, carbon, field emission pattern 8=2276
 W, of CO, effect of surface O 8=4762
 W field emitter tips, of Hg, nucleation obs. 8=1702
 W, of I₂ vapour 8=18699
 W film, of N₂, sticking probability obs. 8=4761
 W, of Mo rel. to film formation and electron emission 8=9269
 W, of N₂, phase changes of N₂ on e-impact 8=21913
 W, (112) and (100) oriented crystal surfaces, surface potentials of CO 8=21910
 W polycrystals, of CO, behaviour model 8=17169
 W surface, adsorpt. of CsF, influence on work function 8=18270
 Xe f. c. c. crystal, of inert gases, potential energy profiles 8=17159
 Y₂O₃, of ethanol, methanol, ethylene, acetaldehyde and H₂O i.r. obs. 8=4768
 ZnO, of gases, rel. to electoreflectance 8=9564
 ZnO, impure, of O₂, i.r. absorpt. studies 8=4769
 ZnO powder, cond. effect of O₂ 8=22612

Aerials. See Electromagnetic waves/radiators.

Aerodynamics

- See also Flow/gases; Jets; Shock waves; Supersonic flow; Turbulence.
 aerofoil in non-uniform stream 8=21488
 aerofoil problems in magnetoaerodynamics 8=19804
 aerospace vehicles, gliding, aerodynamic manoeuvre 8=14708
 air flow over boundary between smooth surface and small waves 8=1460
 air, jet, cold, axisymmetric, turbulent mixing with room temp. stagnant, obs. 8=16669
 airborne dust sampling through orifice, cross-wind effect 8=16907
 atmosphere, high-altitude, acoustics 8=9905
 axisymmetric jet, exhausting into quiescent atmos., length of supersonic core 8=16680
 blunt body heat transfer, shock wave effect 8=19538
 boundary layer, compressible, mixing length and kinematic eddy viscosity 8=21489
 boundary layer flows with large injection 8=21485
 boundary layer transition, anemometry 8=21486
 circular cylinders, flow field in far wake 8=16674
 compressible fluid flow in wake of symmetrically positioned body 8=7862
 compression corner, boundary layer separation 8=21484
 conical body, 8° half angle, boundary layer transition at Mach 5.5, shock tunnel investigation 8=12670
 critical points, determination using wire heater and differential thermocouple 8=12668
 discontinuities in charged aerosol jets as cause of ionization 8=4301
 drag coeffs. for cones, supersonic 8=23460
 electric arc in transverse aerodynamic and mag. fields, heat transfer and flow 8=16424
 expansion flows behind incident shock waves, probe studies 8=15049

Aerodynamics—contd

- exponentially sheared in vert. dirn., effect on induced drag of elliptically loaded lifting line 8=16677
 flag waving motions, wind tunnel experiments 8=21477
 flexure-torsion flutter of aerofoils 8=16679
 flow between parallel plates, meas. parabolic profile 8=7902
 flow visualization using holographic moire fringes 8=6572
 hypersonic flow blunted bodies, soln. valid for whole field 8=16654
 inviscid, past delta, wing, field near centre of rolled-up vortex sheet 8=1459
 laminar compressible boundary layer, heat transfer 8=21491
 laminar-turbulent transition, small parameter method 8=12655
 lift and drag in free-molecule flows, applic. fo Nocilla wall reflection model 8=21495
 magnetoaerodynamic flow, supersonic, blunt body, theory 8=355
 momentum defect superposition, wind-tunnel obs. 8=21481
 motion of gas behind diverging detonation wave 8=4461
 Navier-Stokes eqns., non-uniform Mach number expansion 8=21479
 near wake flow field, theoretical soln. 8=16670
 non-adiabatic temp. distrib. behind detached shocks 8=15053
 particle deposition on vertical surfaces 8=16909
 rarefied flow past thin wedge 8=21487
 Reynolds number effect on Apollo near-wake temp. 8=23459
 sharp cones in rarified hypersonic flow, surface pressure distribns. 8=16681
 shock wave diffr. in fluid by supersonic wedge 8=21492
 shock wave structure, from fluorescence meas. 8=3033
 shock wave velocity distribution function, gas of rigid spheres, using model and computer 8=6139
 shock waves in air, ion density profiles 8=4460
 shock waves in fluid with steady uniform flow, 8=21447
 of solar stills, coeffs. rel. to leakage of steam-air mixture 8=19678
 solid particle in gas flow behind sloped diaphragm 8=7906
 space vehicles, pitch-damping coeffs. calc. 8=23458
 sphere, steady motion in dusty gas 8=12669
 supersonic real gas flow over solid of revolution, perturbations damping 8=21480
 supersonic entropy layers, linearized perturb. 8=16652
 thin-ring air foil, loading calc. anal. in viscid source flow field 8=21473

Aeronomy. See Atmosphere: Meteorology.

Aerosols

- See also Foams.
 artificial fogs, attenuation in visible and i.r. 8=1606
 atmosphere, concentration and size distribution 8=18870
 atmosphere, evidence for layer at 71 km 8=9875
 atmospheric, condensation nuclei vertical distrib. in boundary layer 8=9835
 atmospheric, particles removal by raindrops and snow crystals. 8=23275
 atmospheric, rel. to haze, microstruct. from polarization ellipticity of scatt. light 8=9877
 atmospheric, and condensation process from optical obs. 8=9834
 atomizer, ultrasonic, particle size-capillary wave amplitude relation 8=21734
 charged jets, ionization caused by aerodynamic discontinuities 8=4301
 cloud droplet growth by hydrodynamic capture, stochastic model 8=18869
 and cloud microphys. props. at Hawaii, comp. of inland and sea forming clouds 8=9859
 dioctylphthalate, particle conc., by turbidity meas. 8=8153
 dispersing device, dry-powder, with long-time output stability 8=21738
 droplet size distribution determ. 8=4635
 dust particle sampling through orifice, cross-wind effect 8=16907
 flow, non-symmetrical, near obstacles 8=21737
 fluorescent photography using Q-switched laser light source rel. to particle size determ. 8=4636
 fog, laser beam attenuation rel. to Buger's law validity, obs. 8=21739
 ionically irradiated, particle interaction at high press. 8=21732
 latex, high-speed beam 8=12952
 light scattering by extremely small particles, photons detection 8=21740
 liquid flows around obstacles for small Stokes numbers 8=4634
 metals, prep. by evap., electron microscopy 8=4839
 metal smoke particles prep. by evap. 8=4839
 microstructure, optical estimation parameters 8=18871
 particle aggregation, in sound field 8=6156
 particle deposition on vertical surfaces 8=16909
 particle size analysis by flame ionization 8=16908
 particle size comparator 8=5
 photophoresis, kinetic theory 8=4629
 polystyrene latex particles, aqueous suspensions, atomization 8=8154

Aerosols—contd

- radioactive dust in neighbourhood of accelerator 8=6690
 radioactive, mass-transfer between airstreams and surfaces, rel. to pollen travel 8=23298
 separation, viscous momentum transfer effect 8=21736
 shock waves effects in gas-dust medium 8=10239
 smoke diffusion from high stacks, time-average ground concentration 8=14614
 smoke distribution in turbulent jets using pulsed laser obs. 8=8152
 smoke, laser beam attenuation rel. to Buger's law validity, obs. 8=21739
 smoke, laser light absorpt. and scatt. 8=18878
 solution drops in binary gas mixt., diffusive phoresis 8=21741
 in sound field under Oseen flow, hydrodynamic particle interaction calc. 8=21731
 spectrophotometric emission particle analyzer 8=21733
 stearic acid, particle conc., by turbidity meas. 8=8153
 thermal conduction props. 8=21735
 triphenylphosphate, particle conc., by turbidity meas. 8=8153
 AgI for cloud seeding, hygroscopicity and chemical composition 8=1605
 H₂SO₄, light scatt. studies 8=12951
 Na, produced by burning, characts. 8=12950
 Pu, produced by burning, characts. 8=12950

Afterglow. See Discharges, electric.**Ageing.** See Alloys; Metallurgy; Phase transformations/ solid-state.**Air**

See also Atmosphere.

- acoustic impedance of thin layer, correction for parabolic diaphragm deformation 8=19554
 adhesion coefficients at 4.2° and 20°K 8=7954
 adsorption on Molecular Sieves 5A, 10X, and 13X, at 77.3°K and press. range 10² to 10⁻³ torr, effect of preadsorbed H₂O 8=21897
 air-pentane mixtures, effect of vessel size and turbulence on explosion press. 8=6147
 air-water vapour mixtures, third virial coeff. 8=4468
 between parallel plates of displacement transducer, effects of compression 8=7892
 breakdown, elec. 7.5-20 cm gap 8=16414
 convecting layer, temp. gradient reversal, interferometric obs. 8=4475
 discharge voltage, comparison with SF₆ 8=16421
 drying by molecular sieves 8=18644
 electric breakdown, humidity effect 8=12691
 flow, laminar, between parallel plates, parabolic profile meas. 8=7902
 flow, low speed, study of skewed turbulent boundary layers 8=21475
 flow, in tubes, acoustic reflection coeff. of discontinuous changes of cross-section 8=19565
 free convection from vertical flat plate with step discontinuities in surface temp. 8=21458
 glow discharge in toroidal tube, expt. investigation 8=4286
 glow discharge, secondary electron energy distrib. 8=16409
 high-temperature, meas. of continuum and atomic line rad. spectra 8=16198
 high-temperature, microwave breakdown 8=21244
 high-temp. plasma, l.p. growth rate calc. 8=21390
 humidity control system for small chamber 8=16645
 hydrodynamic boundary layer at a disc 8=4449
 ion density profiles in expanded shock tube flows 8=15050
 ionization energy per ion pair formed by H⁺₂ particle 8=4315
 ionized, Joule heating by low-voltage d.c., 6700-7800°K and 10-20 atm. 8=12421
 jet, cold axisymmetric, turbulent mixing with room temp. stagnant, obs. 8=16669
 jet, nozzle-fluid concentration field 8=4453
 laminar forced convection in entrance region between parallel flat plates 8=21459
 light absorption, humidity and pressure influence 8=7935
 in organic gaseous mixtures, optical-acoustic effect 8=21520
 plasma containing electrophilic gases, microwave meas. behind shock waves 8=7754
 plasma excitation in e.m. shock tube 8=1337
 plasma flames, induction-coupled, spectroscopic obs. 8=21411
 plasma, permittivity and conductivity variations with freq. and electron density 8=4346
 pre-breakdown currents rel. to temp. at high pressure 8=16417
 pressure and acoustic wave propagation after nuclear explosions 8=2583
 shock heated, elect. conductivity obs. 8=4486
 shock tube, electrodeless, using θ -pinch effect 8=6136
 shock wave front, luminance temp. obs. 8=21483
 shock waves, ion density profiles 8=4460
 spark, by focused laser beam, development 8=4292
 sparkover in mixtures with water vapour 8=12412
 steam-air mixture leakage from solar still, rel. to aerodynamic coeffs. 8=19678
 stream, arc heated, temp. fluctuations and autocorrelation function 8=12653

Air—contd

- thermal conductivity, hot-wire cell meas., 30°-100°C, 120-150 torr 8=16700
 thermals, observations 8=2578
 turbulent flow through concentric annuli, experimental study 8=12650
 turbulent thermal convection between horizontal plates, velocity and temp. obs. 8=12686
 vibrations, forced, of finite amplitude in a tube 8=16705
 Ar-air mixture, shock wave front luminance temp. 8=21483
 CO₂-air interface, plane shock refraction and expansion wave generation 8=4482
 H₂-air system, free convection, heat transfer and binary diffusion 8=4491
 He-air system, free convection, heat transfer and binary diffusion 8=4491
 TiO₂ surface discharge, channel development 8=1330

Airglow

- See also Atmospheric spectra; Aurora; Sky brightness; Twilight; Zodiacal light.
 afterglow from recombination of e and ions temp. depend. obs. 8=7719
 arcs, intertropical, movement and shape rel. to ionospheric equatorial anomaly peaks 8=23390
 conjugate photoelectron flux onset timing, solar cycle variation, from 6300 Å and Te obs. 8=23331
 dayglow, O₂ emissions 8=9925
 day, during solar eclipse, λ 3914 Å and λ 6300 Å, 30 May 1965 8=2628
 grenade glow clouds, spectral energy distrib. 8=9924
 Lyman α dayglow, degree of polarization, meas. 8=14646
 night, [O I] 5577 Å and 6300 Å, Na D-lines and continuum at 5300 Å, rocket obs. 8=18935
 night, 3100-10 000 Å spectrum 8=23333
 nightglow, long-term correls. 8=2632
 nightglow, OH rotational temps. and intensities 8=14647
 nocturnal, and mag. storms, low and middle latits., obs. analysed 8=2752
 optical research, 20 year review 8=19066
 twilight, far u.v., rocket photometry obs. 8=9927
 O 45%, O₂ 10% and N₂ 45% mixture, daytime, photoelectron excitation calc. 8=2627
 OH emission bands in nightglow, photometric obs. 8=9928
 OH(8, 3) band, OI 5577 Å line and continuum at 5775 Å, nocturnal, mid-latit., rocket obs. 8=2631
 OSO-B2 satellite obs. 8=23332

Albedo. See Cosmic rays; Earth; Nuclear reactors, fission.**Alfvén waves.** See Magnetohydrodynamics; Plasma/oscillations.**Algebra**

- Adler-Weisberger sum rule, rigorous derivation 8=773
 antilinear operators, canonical form 8=6016
 associative, for mass formula problem 8=15688
 B*, integral representations of invariant states 8=2879
 C*-algebra A, covariance, generalization 8=6009
 C*, extremal invariant states 8=6010
 of currents, derivation of Regge poles 8=3558
 Fock-space language for drone theory of ferro-magnetism 8=13975
 Galilean, translational invariant in describing nuclei 8=3765
 γ, σ , rel. to spinor theories, graphical methods 8=11268
 Lie, deformation and contraction 8=6026
 Lie, dynamical variables in classical mechanics 8=10490
 Lie, infinite-dimensional, one-particle representations, tensor product 8=6724
 Lie, inhomogenization condition for isomorphism 8=2878
 Lie, nonintegrable representations, mass-splitting theorem 8=11375
 Lie, rotation R₃ group, new representations 8=11360
 Lie, rel. to transformation of Bhabha's equation 8=648
 Lie, in unitary representations of non-compact groups 8=14932
 projector-operator, applic. to decay of unstable system 8=11262
 spherical harmonic expansion of $f(\mathbf{r}_{AB})Y_{lm}(\theta_{AB}, \phi_{AB})$, radial depend., integral form. 8=19354
 spinors and 3-D rotations, relation extended to n dimensions 8=660
 U(6, 6) group, matrix elements of generators 8=14934
 von Neumann, types rel. to extremal invariant states 8=6013

Algol. See Calculating apparatus/digital computer programmes.**Algorithms.** See Calculation.**Alignment**

- orientation system for balloon-borne γ -telescope 8=19328
 quadrupole magnet systems, tolerances 8=15277
 supporting system, tilt, accurate meas. method 8=6001

Aliphatic compounds. See Organic compounds.**Alkali metals**

See also the individual metals.

- alkali-Noble gas mixture, partially ionized, e vel. distrib. calc. 8=12423
 atomic vapour, optical pumping, polarization effect 8=4088
 atoms charge transfer, Gryzinski procedure tested 8=12424
 atoms, collision with inert gas, fine-structure transition cross sections 8=4106
 atoms, electron scatt. 8=1190

Alkali metals—contd

- atoms, g. determ. by atomic beam resonance technique 8=12089
 atoms ^{23}P , fine structure transitions in adiabatic collisions, calc. 8=1162
 atoms, long-range interactions 8=12108
 atoms, optical orientation rel. to meas. of weak mag. fields 8=20934
 atoms, reson. states lifetimes, inert gases and vapour press. effects 8=20976
 atoms, thermal excitation and deactivation in atmosphere of inert gas 8=12088
 condensation, boundary thermal resistivities 8=8049
 continuum theory, nonlinear, based on quantum mechanics 8=17711
 doping of semiconductors, in small quantities, by electrolysis of fused salt 8=18017
 electron-ion pseudopotentials 8=22427
 gas, Cotton-Mouton effect in optically oriented 8=4485
 gas, ionization by p impact classical binary approx. calc. 8=12417
 interionic potential modified in conduction electron presence 8=4671
 ion distrib. in surface layer of glass, diffusion theory 8=21146
 ionic crystals, cohesion with noble gas atoms 8=8193
 ions scatt. at He atoms 8=7464
 liquid phase m. h. d. 8=15384
 liquid, resistivity and thermopower pressure depend. 8=9010
 pseudo-atom phase shifts 8=8910
 purification by preferential contact in magnetoplasma device 8=4302
 solid, resistivity and thermopower pressure depend. 8=9010
 vapour, with buffer gas, optical pumping rate eqns. 8=20978
 vapour detect. by mass spectrometer 8=21532
 vapours, optical pumping and relaxation 8=12086
 NH_3 solutions, phase separation model 8=12808

Alkali metal compounds

- See also the compounds of the individual metals.
 alkali borate glasses, co-ord. equilib. of Ni(II) 8=21836
 aluminogermanates, high press. transforms rel. to geochem. 8=8261
 aluminosilicates, high press. transforms rel. to geochem. 8=8261
 antimonides, photoelectric emission, double-photon 8=18278
 beryls, structure dependence on tempering at 600-1200°C 8=17345
 borate glasses, binary, u.v. absorpt. of Cr(VI) 8=18519
 dilute binary alloys, liq., resistivity theory 8=12919
 multialkali-antimonide, anomalous vector effect of photoemission 8=2282
 nitrates- AgNO_3 , molten ternary mixtures, thermodynamics 8=21648
 nitrates and thiocyanates, refractometry 8=1556
 nitrates, binary mixtures with $\text{Ca(NO}_3)_2$, relax. processes in supercooled melts 8=1586
 nitrates, molten, thermal cond. 8=16820
 silicate glass, validity of Nernst-Einstein eqn. 8=8354
 silicate glasses, X-irrad., e.p.r. study of trapped hole centres 8=1998
 silicates, molten, elec. cond. 8=4601-2
 solutions, rel. to passivation studies on Sn electrodes 8=18733

halides

- See also the compounds of the individual metals.
 aqueous solns., influence on struct. of water 8=4527
 aqueous solns., spin-relax. of Li^+ and Na^{23} rel. to conc. 8=1593
 aqueous solns., X-ray diffraction 8=12800
 B-centre in Ag^+ doped crystals 8=17681
 bromides, aq. solns., Soret effect 8=4557
 bromides, aq. solns., partition coeffs. by thermal diffusion 8=4559
 cathodoluminescence, electron-probe meas. 8=1754
 colour centres, dichroic absorption, appln. to information storage 8=13461
 colour centres and sputtering, induced by slow electron bombardment, formation theory 8=13472
 colour centre studies by pulsed irradiation 8=13460
 colourability and luminescence, activating impurities 8=17682
 conductivity, electrical, kinetics of radiational change 8=22501
 crystals, box model 8=1627
 crystals, i.r. absorpt. spectra, local vibrs. of mol. impurity ions 8=14197
 crystal ion overlap meas. by strain polarizability 8=23003
 crystal with nitrate ion impurities, lattice vibrations and i.r. absorption spectra 8=17471
 crystal thermal expansion, m.p. calc. 8=16970
 e' bound states 8=13694
 energy band params. and plasmon energy, e energy loss obs. 8=8938
 entropy of vacancy pair formation, calc. 8=1943
 etch figures of fission fragments, flat-bottomed 8=8707
 in far i.r. transmission filters, prep. and use 8=20063

Alkali metal compounds—contd**halides—contd**

- F-centers, book 8=17680
 impurities, divalent cation and dipolons, conc. correlations 8=8701
 i.r. absorption, impurity induced 8=9481
 infrared absorption of injected molecular ions 8=5583
 i.r. spectra of cyanate ion complex in solid soln. 8=14233
 inner-electron excitation spectra 8=7529
 interstitial cations, dielec. props. calc. 8=1948
 iodides, e.s.r. of Se_2^- and SSe^- 8=14123
 ionization temperature meas. in flames 8=7946
 luminescence, r.f., and carrier motion rel. to phosphors F centres, obs. 8=18594
 luminescence, r.f., and phosphors, storage props. obs. 8=9591
 luminescence, r.f., and scintillation props. of inactivated crystals, obs. 8=9592
 luminescence, thermal quenching of O_2^- and S_2^- 8=2485
 magnetic susceptibility additivity 8=13959
 melting, Born treatment calc. 8=12966
 melting parameters 8=12969
 melting under high pressure 8=1612
 mixed crystals, Sr^{++} doped, Zr^- and Zn^- centres 8=22225
 optical birefringence 8=18501
 optical spectra, comparison with absorpt. formula 8=8947
 paramagnetic resonance of Cu atoms 8=22897
 Peierls stress estimation 8=1968
 phosphors, temp. depend. of X-ray luminesc. and optical flash 8=5653
 photoelectrons created by soft X-rays, energy spectra 8=18274
 radiation defect formation 8=13487
 Reststrahlen freq. in rel. to elastic props. 8=13580
 shell-model treatment of harmonic vibrs., localized modes of V-centres 8=13321
 spectrum, two-photon, theory using two-band model 8=22935
 thermal expansion at low temps. 8=22133
 triplet state of self-trapped exciton, and intrinsic recomb. rad. 8=2476
 two-photon absorpt. with pulsed N_2 laser 8=5578
 X-ray diffuse scattering from deformable ions 8=13330
 Ca-doped, Zr^- bands, absorpt. energies and osc. strengths 8=13455
 ClO_4^- and ClO_3^- solid soln. i.r. spectra 8=22968-9-70
 CsCl structure, low temp. thermal expansion coeffs. and related thermodynamic props. 8=8648
 CsCl-structure, Schottky defects, energy of formation 8=8694
 F-band, pressure shift: ion-size effects 8=22226
 F-centre luminescence under hydrostatic pressure 8=9599
 F-centre multipole polarizability 8=13453
 K-absorption of Cl and q.s.s. 8=2410
 KCl-KBr solid solutions, elec. props. 8=22504
 KCl, K-L_{II,III}, M_{II,III} and quasi-stationary states 8=2432
 OH⁻ and divalent cations, removal in zone refining 8=21931
 U-centre-induced i.r. absorpt. spectra, sidebands 8=4991-2
 Z centres 8=13454

Alkaline earth metals

See also the individual metals.

- bromides, aq. solns., partition coeffs. by thermal diffusion 8=4559
 bromides, aq. solns., Soret effect 8=4557
 compressibility subjected to high press., effect of electron structure 8=17724
 strain critical systems 8=13524

Alkaline earth compounds

See also the compounds of the individual metals.

- in alkali halides, with cyanate ions, i.r. spectra 8=14233
 dicarbide formation when diffusing in graphite 8=4950
 fluorides, F-centre electronic structure from wave functions 8=1997
 orthophosphates, double, Sn-activated luminescence 8=14309
 oxides, e.s.r. of F centres 8=13456
 pyrophosphates, Eu^{2+} activated, luminesc. 8=9628

Allotropes. See Phase transformations; Polymorphism.

Alloys

See also Crystal structure, atomic/alloys; Heat treatment/alloys; Solid solutions; Steel; and under alloys or compounds of the base of the first-named element.

- AB binary, triplet probabilities rel. to pair correlations 8=9313
 above solidus temp., mech. for deformation, strength and fracture 8=22304
 alloys oxidation, high temp., scales form. mechanism 8=5711
 analysis by X-ray fluorescence 8=9750
 binary, freq. spectrum of lattice vibrs., calc. with quantum Green functions 8=8605
 binary, interatomic energies from short-range-order meas. by diffuse scattering 8=17331
 binary, liq. of equi-valent metals, Knight shift charges rel. to conc. 8=12927
 binary, slab, unidimensional solidification rel. to time-dependent surface temp. 8=21757
 bonds, atomic interactions 8=4666
 composite growth from melts 8=4647
 conductivity, thermal, 4.2-273°K 8=22129

Alloys—contd

contacts for GaAs semiconducting devices suitability, fabrication and ohmic props. 8=5291
 crystallization, dendritic, general soln. of eqn. for binary alloys 8=8174
 deformed f. c. c., intrinsic stacking-fault tetrahedra formation 8=22215
 dendrites and interdendrite spaces, distribution 8=4823
 dilute binary, liq., theory of resistivity 8=12919
 Dilute, new magnetic, characteristic, temp. var. 8=1659
 dislocation motion mechanism for coherent, ordered, stresses precipitates 8=1978
 dislocation structure and grain size effect on validity of Cottrell-Stokes law 8=8721
 e state density around an impurity 8=5112
 electron cell model 8=21815
 equilibrium petition between ferrite and cementite, temperature dependence 8=17279
 eutectics, multicomponent, brittle rupture of Cd and Sn during contact melting 8=8832
 f. c. c., stacking fault energies, extrinsic to intrinsic relative magnetudes 8=17666
 ferromagnetic, additivites of electronic states 8=5446
 ferromagnetic, neutron elastic diffuse scatt. 8=22766
 ion emission, secondary, rel. to chemical analysis 8=18286
 Ising model, Onsager's results using Green's function 8=2964
 Ising models, ordering conditions 8=4686
 liquid and amorphous, structure and correl. by X-ray and n diffraction 8=12795
 liquid, atomic distrib. and electronic transport props. from X-ray diff. 8=12799
 liquid, binary expt. and theory of mixing 8=12844
 liquid binary, model for anal. of enthalpies and entropies of mixing 8=12846
 liquid, Hall coeff. and elec. resistivity 8=16880
 liquid, interatomic distances from X-ray diff. pattern peaks 8=12784
 liquid, reln. between pair pots. and radial distrib. functions of ions 8=16787
 liquid, thermodynamic props. effect of electronic and structural characts. 8=12845
 liquid, Wagner interaction parameters determ. 8=8016
 liquid, Ziman pseudo-atom phase shifts calc. for monovalent ions 8=16882
 macrosegregation on solidification, and mold design effect 8=16930-1
 magnetic, dilute, low temp. props. 8=18289
 magnetic, effect of electrons of opposite spins on elec. resistivity 8=22432
 magnetic impurity degenerate orbitals, Kondo and Anderson Hamiltonians 8=13008
 magnetic meas., prep. of ball-shaped samples 8=10859
 magnetic, sp. ht. calcs. 8=13367
 magnetic, sp. ht. rel. to Kondo model 8=17510
 magnetoacoustic effect, theory and experiment 8=8624
 mechanical relax. due to changes in short-range order produced by stress 8=5009
 metallic, crystalline structure changes at early stages of ageing and order-disordering 8=17036
 metal, structural characts. from solubility method 8=17001
 of metals from groups IB and IV B, liquid, elec. resistivities 8=12912
 metals oxidation, high temp., scales form. mechanism 8=5711
 microanalysis, electron probe data analytic correction 8=14472
 Nimonic type, stability of dislocation structures 8=17643
 of noble metals, liq., Hall coeff., resistivity and electron states 8=12923
 noble metals, surface preparation for optical meas. 8=14163
 non-ferrous, thermomechanical deformation 8=23777
 ordered, containing antiphase domains, X-ray diffr. 8=4863
 ordered, effect of crystal symmetry on field ion images 8=4881
 ordered, grain boundary theory 8=17258
 ordering, dislocations and antiphase boundaries rel. to plastic deformation 8=17634
 ordering of ternary b. c. c., having three types of sites, theory 8=17033
 oxidation, high temp., scales form. mechanism 8=5711
 oxidation mechanism, isotopic study 8=23092
 f. c. c. polycrystals, plastic deformation computer simulation and derived rolling texture 8=13512
 shear stress increase due to coherent precipitates 8=5017
 solid solution, field ion emission patterns, computer simulation 8=8453
 sormite type, influence of Nb on hardness and structure 8=5066
 strength, time and temp. depend., non-equilib. state 8=8811
 structural, tensile work hardening, exponential relation 8=22282
 superconducting, worked, critical current density rel. to dislocation distrib. 8=9029
 thermodynamic props. and heat processes meas. in twin calorimeter 8=250
 two-phase, finely dispersed, recrystn. behaviour 8=8395

Alloys—contd

two-zone superconducting, u.s. adsorpt. theory 8=22535
 X-ray microanalysis data corrections for complex alloys 8=14471
 Zener relax. 8=5009
 Al-base, unidirectionally solidified eutectic, structure 8=4685
 Al-Al₃Ca, unidirectionally solidified eutectic, structure 8=4685
 Al-Al₃Ce, unidirectionally solidified eutectic, structure 8=4685
 Al-Al₃Y, unidirectionally solidified eutectic, structure 8=4685
 Co-Ni-Al-Cu-Ti-Fe, solid soln. struct. 8=17010
 CsCl-type ternary, hyperfine fields and electronic structure 8=14156
 Cu₃Au, ordering conditions, cubic-to-tetragonal structural transition 8=4687
 Fe-rich, with various transition elements, magnetization values 8=22811
 In-Sb-Ni, the quasibinary section InSb-NiSb in 8=4691
 K-Na, density 0 to 300 °C 8=21624
 Mg, binary, isothermal growth of Mn precipitates in 8=4688
 Mg-Zn, dendrite arm spacing and grain size, influence of coarsening 8=4849
 Mn with Dy, Ho and Er, X-ray fluorescence analysis 8=2552
 Na-K liquid metal reactor coolants, role of possible impurity admixtures, O, H, C and N 8=7328
 Na-K, K:49, 51 and 74% viscosity at 300 °C 8=21627
 Ni-bearing steels, ageing rel. to martensitic structure 8=1762
 NiPb formation by simultaneous evaporation of NiPb 8=21852
 V₂VL_{3+x}, Te and Se phase and grain boundary detection by chem. etching 8=17102
Alnico alloys. See Nickel alloys.
Alpha decay. See Nuclear decay theory; Radioactivity/decay periods; Radioactivity/decay schemes.
Alpha-particle model. See Nucleus/models.
Alpha-particles and helium nuclei
 See also Alpha-rays.
 cluster and 4-body scatt. correl. rel. to 4 particle-4 hole states in O¹⁶, Ca⁴⁰ 8=15958
 d- α , 42 MeV α projectile, d break-up, spectrum 8=15868
 d + He³ \rightarrow He³ + pp, pick-up and charge-exchange 8=6990
 e + He⁴, elastic scatt. cross section, 30-59 MeV 8=15732
 e-He⁴ high energy scatt. and N-N correlation 8=891
 form factor, charge, Irving wave function calc. 8=11657
 γ + He³ \rightarrow π^+ + H³, using PCAC and current algebra 8=15765
 γ + He⁴ \rightarrow H³ + n + π^+ , impulse approximation 8=888
 γ + He⁴ \rightarrow ρ^- + He⁴, determ. of particle scattering amplitudes 8=11858
 ground state props. with Hamada potential 8=885
 ion source for Van de Graaff accelerator improved by K vapour exchange 8=6693
 K⁻ + He⁴ \rightarrow Λ^0 + π^- + p + d obs., impulse model fit, via intermediate Σ + nucleus + π^- state 8=20417
 model for nuclear matter 8=11650
 μ capture rate in channel n + n + p + ν 8=6817
 μ^- + He³ \rightarrow H³ + ν_μ , asymm. in recoil of H³ 8=15740
 μ^- + He³ \rightarrow H³ + ν , rate, phenomenological treatment of exchange effects 8=20589
 n + He³ \rightarrow p + H³ rel. to "elementary particle" model of nuclei 8=15873
 N-He⁴ high energy scatt. and N-N correlation 8=891
 photodisintegration cross-section calc., normalization anomaly 8=11655
 photoreactions, cloud chamber for investigation 8=7000
 π^- -He³ reaction π^0 yield obs. 8=7220
 π^- + He³ \rightarrow γ + t by PCAC generalization of Kroll-Ruderman theorem 8=7217
 π^- + He⁴, inelastic at 140 MeV, excited and multineutron final states 8=6848
 plastic track detectors 8=20220
 p photo-absorpt. sum rule 8=3577
 states of odd-parity, trans. prob. 8=887
 in AgCl crystals, track recording technique 8=15644
 Al²⁷-He³ scatt., 37.7 MeV rel. to structure of Si²⁸ 8=15963
 B¹⁰(d, $\alpha\alpha$) α 3α sequential decay process obs. 8=11718
 C¹²(He³, He^{3'}, γ_{4-43})C¹², angular correlation symmetry angle 8=20831
 D(t, n)He⁴, as polarized n generator 8=15844
 D(p, γ)He³, cross-section from p+d wave function 8=11593
 H²(He³, γ)Li³, 2-5.5 MeV, resonances obs., applic. of S-matrix theory 8=20581
 He⁺ ion source using Cs vapour exchange 8=15872
 He⁻ source using charge exchange between He and K vapour 8=15871
 He⁺⁺ + N \rightarrow He⁺ + N⁺, classical cross-section calc. 8=7461
 He²⁺ + H(1s) \rightarrow He⁺(1s) + H⁺, back-coupling and distortion 8=7466
 He³ binding energy of 3-body system, with 2 charged particles 8=20587
 He³, charge density function calc. from e-He³ scatt. 8=20393
 He³, Coulomb energy and e.m. radius, perturbation calc. 8=3740

Alpha-particles and helium nuclei—contd

- He³, Coulomb energy in non-local potential and binding energy diff. 8=11654
 He³(d, p)He⁴, d tensor polarization degree (P_{33}) obs. 8=6994
 He³(d, p)He⁴, p polarization and asymmetry 8=7002
 He³ Fadeev calc. of binding energy, T matrix perturbation theory 8=20584
 He³ + $\gamma \rightarrow$ d + p, with Cabibbo-Radicati sum rule 8=6999
 He³-H⁴ current algebra sum rule possible test 8=3756
 He³(He³, n) for Be⁹ ground state search, 18.0–26.0 MeV 8=3790
 He³(He³, 2p)He⁴, dependence of B⁸ solar neutrino flux on rate of reaction 8=5969
 He³-He⁴ interaction, resonating group theory in single channel approx. 8=20588
 He³ inelastic scatt. on Li^{6,7}, B¹⁰, F¹⁹ and Al²⁷ at 10 MeV 8=7233
 He³, μ capture rate calc. using charge form factor and vacuum polarization corrections 8=20393
 He³, p-d final states, 5.5–12.0 MeV rot. obs. in p reactions on Li⁶, 9–10 MeV 8=7187
 He³ photodisintegration, Cabibbo-Radicati sum rule appls. 8=695
 He³, photodisintegration cross section 8=11652
 He³ photodisintegration, two- and three-body cross section calc. 8=15870
 He³ prod. at interaction of 660 MeV protons with light nuclei 8=16071
 He³-p scatt., 30 MeV no evidence for excited state of He³ 8=20586
³He, search for excited states in reaction ³He(p, p')He* 8=11653
 He⁴ charge form factors and charge distrib. calc. 8=886
 He⁴, excited levels rel. to particle hole interaction 8=7003
 He⁴(γ , p)H³, 50 MeV, cross-section 8=889
 He⁴(p, B)He⁴, magnitude and phase of baryon scatt. amp. 8=890
 He⁴, photodisintegration, calc. using Levinger-Bethe sum rules and vel. depend. pot. 8=11658
 He⁴(π , M)He⁴, magnitude and phase of meson scatt. amp. 8=890
 He⁴, product of nuclear reaction, excited states, obs. 8=15953
 He⁴, radius meas., use of impulse model 8=20590
 He⁴ second order corrections to negative parity excited states 8=15932
 He⁴-beam prod. by charge exchange of He⁴⁺ with K vapour 8=15347
 HF, search for analog states in Li⁷(p, t)Li⁵, Li⁷(p, He³)He⁵ 8=11659
 He⁶, search for T = $\frac{1}{2}$ states 8=11659
 He⁸ production rate from pp, π^- , K⁻ interactions with emulsion nuclei 8=892
 Li⁹-He³ scatt., 8–20 MeV, optical model parameters deduced 8=20833
 Nb⁹³, emission, energy obs. 8=1041
 T(d, n)He⁴, as polarized n generator 8=15844
 T(p, n), He³, obs. 8=882

Alpha-ray spectra

- See also Nuclear decay theory.
 fission accompanying, probability in spontaneous and induced 8=3977
 rare-earth metals, fine structure obs. 8=16038
 Ac^{209, 215} decay, energy determ. 8=20759
 Ac²²⁵ decay, energy obs. 8=16048
 Au^{177, 178, 179, 181, 183, 185, 187} decay 8=16045
 Au^{179, 181, 183, 185} decay 8=7148
 Bi²¹¹ decay 8=7150
 C¹¹ hindered α -decay 8=11950
 Fm²⁵³ \rightarrow Cf²⁴⁹ 8=11836
 Hg^{179, 180, 182} decay 8=7148
 Ho^{152, 153, 154}, radioactive decay 8=3883
 Ne²⁰, delayed emission for meas. β -decay 8=3865
 Np²³⁷ accompanying fission, probability rel. to fragment mass asymm. 8=3977
 Po²¹¹ decay 8=7150
 Pt^{176, 177, 178, 180} decay 8=7148
 Pu²³⁹ \rightarrow U²³⁵ decay 8=11789
 Th²³² accompanying fission probability rel. to fragment mass asymm. 8=3977
 U²³³ 8=11830
 U^{235, 238} accompanying fission, probability rel. to fragment mass asymm. 8=3977
 103^{256, 257} decay 8=7151

Alpha-ray spectrometers

- cellulose nitrate target, particle energy meas. for hole diameter 8=11293
 n detector using (n, p) reaction on He³ 8=6959
 n detector to 20 MeV 8=6967
 semiconductor detector, resolution and stability, temp. effects 8=884
 with Si detector, design and operation 8=6998
 Si:Li surface barrier detector, prod. and resolution, 8.78 MeV 8=20201

Alpha-rays

- See also Alpha-particles; Cosmic rays/alpha-particles; Radioactivity.
 He⁴⁺ ions, multiple freq. acceleration 8=6714

Alpha-rays—contd**absorption**

- range, simple stand for determination 8=883
 in water, slowing-down, fast neutron irradiation 8=644
angular distribution
 from projectile nuclei, in nucleus-nucleus collisions prod. by cosmic ray primaries 8=16126
 B¹⁰(d, d₀)Be⁸ 8=16112
 Be⁹(He³, α)Be⁸ \rightarrow α + α , for spin-parity assignment to Be⁸ 8=20834
 C¹²(He³, $\alpha\gamma$)C¹¹, $\alpha\gamma$ correls., C¹¹ energy levels 8=953
 C¹²(O¹⁶, α)Mg²⁴, cross-section fluctuations 24.3–27.7 MeV 8=1105
 C¹²(O¹⁶, α)Mg²⁴, fluctuations, statistical analysis compound nucleus model 8=1104
 Ca⁴⁰(d, α)K³⁸, 9.2 MeV 8=7230
 Np²³⁷, fission-accompanying, to distinguish from prior-emitted α 8=3977
 O¹⁶(n, α)C¹³, 14.1 MeV stripping and knock on process fits 8=3936
 S³²(He³, α)S³¹, 7.6 MeV meas. 8=3966
 Th²³², fission-accompanying, to distinguish from prior-emitted α 8=3977
 U^{235, 238}, fission-accompanying, to distinguish from prior-emitted α 8=3977
detection, measurement
 See also Alpha-ray spectrometers; Dosimetry; Particle detectors; Radioactivity measurement.
 cellulose nitrate target, particle energy meas. from hole diameter 8=11293
 counting efficiency for case of widespread solid α sources 8=20591
 cyclohexane as dosimeter 8=20592
 high counting rate circuit 8=6997
 Injun 4, Si surface barrier with four electronic discrimination levels 8=18961
 liquid scintill. for α -p discrimination 8=1075
 pair and single low level counting system 8=6996
 range, simple stand for determination 8=883
 scintillator, noble gas 8=6643
 spark-chamber, He-alcohol, lowest pressure for sparks 8=11328
 spark counter for α -activity meas. 8=7120
 spectrometer parameter calibration and evaluation 8=20585
 B¹⁰(n, α)Li⁷, use of semiconductor detector 8=852
 He-Xe gas scintillation counter, linearity 8=20193
 Nb⁹³, emission, energy obs. 8=1041
 Si detector, channeling effect 8=3467
 Z-102 isotopes half-lives and energies in 8=1206

effects

- See also Nuclear reactions due to/alpha-rays.
 alkali-metal and alkaline-earth radioactive source prod. 8=7121
 light output from some organic scintillators 8=2495
 metal embrittlement, produced by thermal neutron reactions 8=22237
 noise pulses from photomultiplier tubes 8=3216
 scintillation prod. in He, He-Ar and He-Ne, due to decay of 3α mol. 8=12202
 Au, cold-worked, recrystallization during α -irrad. 8=21943
 UI, self irradiation investigated 8=17105
 ZnS-Ag single crystal, luminescence 8=5674

scattering

- α - α and the ground state energy and lifetime of Be⁸ 8=7072
 A=12–124 rel. to nuclear dimensions 8=15949
 Austern-Blair theory modified to include non-adiabatic effects 8=3963
 d- α , double scatt., rel. to polarized d beams 8=876
 d- α , 3–14 MeV, negative parity states of Li⁶ 8=11651
 d + α , phase shifts, and odd parity P level in Li⁶ 8=15869
 e-He rel. to α charge form factor 8=11657
 even-even nuclei, energies between 12 and 16 MeV 8=7235
 group theory, resonating, in single channel approx. 8=20588
 nuclei about A = 60, abs. compared to optical model 8=7237
 optical model parameters, influence of expt. errors 8=11941
 p- α , 1 GeV obs. rel. to π cross-sect. 8=1052
 p- α , 6–11 MeV, p polarization obs. 8=837
 p- α 22–25 MeV, Li⁶ resonance obs. 8=20532
 phase shift analysis with hard-core potential 8=3738
 p-He³, low energy, spin-dependent interaction theory 8=832
 p + He⁴ \rightarrow B + He⁴, B-N scatt. factor 8=3736
 π^- - α , 24 MeV, π e. m. form factor 8=3616
 π + He⁴ \rightarrow M + He⁴, M-N scatt. factor 8=3736
 rare earth nuclei Y₄₀ and Y₆₀ shape component determ. 8=11713
 Al²⁷ optical model parameters rel. to Al²⁷(He³, α)Al²⁶, 10 MeV 8=11945
 As⁷⁵, 3.5–8.1 MeV, multipolarities, spins and parities of levels 8=3816
 Be⁸ inelastic at 28.5 MeV 8=7234
 Bi, 20 MeV, yield depend. on orientation of crystal and beam 8=20801
 C¹², 3.6–3.8 MeV, optical-model parameters 8=3965
 C¹², 22.5 MeV, ang. correl. function symm. angle rel. to mass-transfer reactions 8=11843

Alpha-rays—contd**scattering—contd**

- Ca^{40,42,44,48}, 31 MeV, new multipole states, spin-parity assignments 8=3807
 Ca⁴⁰, 31 MeV, states obs. 8=11746
 Cd¹¹¹, new transitions, B(E2) values, energy level lifetimes 8=20712
 Co⁵⁹-He³, 37.7 MeV optical model fit, level structure of Ni⁶⁰ 8=15981
 Cr^{50,52,54}(He³, α), 18 MeV, DWBA analysis tested 8=3969
 Fe⁵⁴, expt. data and optical model parameters 8=16120
 Fe⁵⁶, 21 MeV cross-section to first 2⁺ level, optical model fit ambiguity 8=11940
 H³-He³, using 2-body pot. calc. compared to expt. 8=11656
 He³-He³, using 2-body pot. calc. compared to expt. 8=11656
 He³-He³, levels of Li⁷ and Be⁷ 8=7001
 (He³, t) quasi-elastic, differential cross section analysed 8=7231
 In¹¹⁵, 8 MeV, deduced levels 8=3822
 K⁻ α , differential cross section, low-energy elastic 8=11549
 Li⁷(α , α')Li^{7*}, rel. to Li⁷(α , γ)B¹¹ investigation of B¹¹ levels 8=11721
 Mg²⁴, 29 MeV, optical-model parameters 8=1097
 Mg²⁴, 42 MeV, optical and Fraunhofer models 8=11939
 Ni^{58,62}, 21 MeV cross-section to first 2⁺ level, optical model fit ambiguity 8=11940
 Ni⁶⁰, expt. data and optical model parameters 8=16120
 Pb^{204,206} rel. to transition strengths in the Pb region 8=995
 Re^{185,187}, γ -vibrational state obs. 8=16000
 Re^{185,187}, 16.6 MeV, vibrational band obs. 8=3954
 S³², elastic, 10-17.5 MeV, optical model analysis 8=20831
 Si²⁸, 22.5 MeV, ang. correl. function symm. angle rel. to mass-transfer reactions 8=11843
 Sm^{148,150}, inelastic, 15.1 MeV cross-section obs., E2, E3 transitions 8=20824
 Sm^{152,154}, inelastic, 15.1 MeV cross-section obs., E2, E3 transitions 8=20824
 Te isotopes, excitation of one- and two-phonon states 8=1098
 Zn⁶⁴, 21 MeV cross-section to first 2⁺ level, optical model fit ambiguity 8=11940
 Zn⁶⁶, expt. data and optical model parameters 8=16120

Altimeters. See Length measurement.

Aluminium

- absorption in L_{II,III} region, structure 8=22956
 analysis, Cu determ. by at. absorpt. spectrometry 8=2545
 annealed, commercially pure, strain ageing 8=5042
 annealed, helices and large loops, in prismatic dislocations X-ray topography 8=17647
 anodic oxidation in presence of hydrated oxide 8=18729
 APW band structure calcs, systematic numerical error 8=17883
 Bauschinger effect in quenched samples 8=5020
 bed to polyurethane coats, effect on network density in surface layer 8=17145
 binary rare earth systems arrangement 8=13286
 block, indented by opposed steel punches, deformation, theoretical and actual, comparison 8=10562
 brazing sheet with improved corrosion behaviour 8=10462
 cladding with stainless steel rel. to composite sheet prod. 8=10461
 coating on Ir, u.v. reflectivity calc. 8=14227
 cold-worked, nucleation of recrystallization 8=8397
 collective motions of atoms in liq. state, compared with polycryst. solid 8=12796
 composite bar of hard and soft section response of plastic deform. wave on junction 8=19395
 content and distrib. in schistic biotites, phengites and chlorites 8=13055
 corrosion of anodized, electrolytic quality test evaluation 8=23097
 crystal, 15 eV plasma loss, damping 8=2121
 cylinders, thin wall, expt. plastic buckling at 500°F 8=17757
 deformation bands and (111)-(001) fibre texture formation 8=5045
 deoxidation of liq. Fe, form. of cloud group of oxide inclusions 8=22183
 diffusion of Ag. 8=22147
 diffusion coeff. meas. by n. m. r. 8=4949
 diffusion in Ge 8=13406
 diffusion in Mo 8=1911
 diffusion of Pd, Ag, Cd, In and Sb 8=8671
 dislocations, formation during slow heating and cooling 8=8723
 distribution of sputtered atoms by electron microprobe 8=21876
 effect on grain coarsening temp. of austenite 8=8462
 elastic modes, e. m. excitation 8=17760
 elasto-plastic behaviour study of pure monocrystalline sheets 8=8848
 electrical resistivity recovery after low temp. electron and neutron irradiation 8=2134
 electrode, electrochemical behaviour at d. c. and a. c. polarization 8=18725

Aluminium—contd

- electron diffraction, energy dependence from 100 keV to 1 MeV 8=4868
 electron emission, effect of abrasion in air, O₂, N₂ and H₂O vap. 8=9270
 electron-irradiated, deformation at 20°K rel. to dislocation model with defect barriers 8=13523
 electron irradi., resistivity recovery, kinetics study 8=5171
 electron-irradiated, stage III annealing study 8=13475
 e-irradiated, state II and III recovery temp. and impurity conc. dependence 8=1935-6
 electron slowing-down spectrum 8=13474
 electroplating, alkaline Zn pretreatment soln. 8=14431
 electroplating using stannate activation and bronze strike deposit and plated Al corrosion 8=14430
 electropolished, form. of surface tops and pits during heat treatment 8=17117
 energy loss of fission fragments, range-energy relation 8=2021
 excitation of L-shell electrons by 20-keV electrons 8=22495
 exoelectronic emission due to sliding friction obs. 8=18254
 extrusion, recovery and recrystallization during 8=4841
 fatigue-crack propagation, 2024-T3 cantilever 8=5043
 fatigue mechanism, 0.5-0.85 Tm°K 8=8806
 50 kV electron mean free path for plasmon excitation, diffr. condition effect 8=13696
 film on glass, vacuum deposition 8=17123
 films with organic molecular inclusions, enhancement of critical temp. 8=12965
 film, oxidation effect on photocurrent 8=18221
 films, oxidation in low-pressure O₂ atmosphere 8=18669
 films, plasma oscillatory modes at surface, energy rel. to intensity 8=8946
 films on Ta (110) surface, growth studied by LEED 8=8311
 fine particles, surface plasma oscillations 8=8967
 flow stress, effect of specimen diameter 8=8820
 foil, dislocations, dynamic behaviour on deformation, continuous obs. 8=13433
 foil membrane, circular, deform, under hydrostatic pressure 8=5044
 foils, microstructure, by transmission electron microscopy 8=4840
 foils, range-energy for α -active products of Pb²⁰³(O₁₆, X)Y, Bi²⁰⁹(O₁₆, X)Y 8=11952
 freezing pt., as fixed pt. 8=244
 γ -beam scatt., differential albedo obs. 8=16844
 grain boundary sliding, constant-stress shear test 8=22220
 grain boundary sliding, isothermal shear test 8=22221
 Hall coeff., high field, from helicon resonances 8=5169
 Hall effect and mag. resist. var., 2.5° to 300°K 8=5170
 hardening, influence of quenching temp. 8=13530
 heat capacity between 2.7 and 20°K 8=22114
 heavy ion penetration along low index channels, effect of atomic thermal motion 8=2024
 hemispherical reflectance, rel. to λ and surface roughness 8=2399
 high speed impact extrusion 8=19340
 hydrostatic tension on solidification 8=21758-9
 internal friction, room temp. peak 8=13532
 lattice defects recovery after tensile deformation 8=22184
 lattice distortion in plastic deform., e microprobe-Kossel obs. 8=21978
 lattice vibrations, 6% accuracy in freqs. 8=22080
 liquid, effective ion-ion potential 8=8237
 liquid, rare earth impurities, mag. susceptibility and Knight shift changes 8=21724
 magnetoresistance and resist. of plastically deformed 99.999% pure, \leq 175 kOe and 4.2-77°K 8=17926
 microdeformation measuring technique 8=22273
 with microrough or dispersed surface, increase of thermal rad. compared with polished surface 8=22139
 molten, electronic band struct., density of states, and resistivity calc. 8=16789
 n-irradiation damage and recovery rel. to defect doping effect 8=1953
 neutron monochromator 8=854
 nucleation of vacancy clusters 8=1944
 n. m. r., strongly saturated, modulation and cross-relaxation effects on line shape 8=18455
 1 μ thick, filtered electron diffraction obs. 8=8455
 oxidation, controlled, in radio-frequency-excited glow discharge 8=8310
 oxidation and diffusion removal of Mg impurity 8=18670
 phonon damping at low temp. due to electron-phonon interact. 8=17477
 phonon-frequency distrib. and ht. capacity 8=1868
 plasma produced by laser beam, energy spectra 8=2122
 plastic stress relaxation rel. to stacking fault energy 8=13529
 plates of constant cross section, high order Lamb wave excitation and reception 8=19491
 plates, fatigue crack propag. under extension and bending, effect of mean stress 8=17758
 polycrystalline, deformation at high strain rates 8=13533
 polycrystalline films, influence of annealing on block structure charact. 8=4741
 polycrystals, temp. depend. of thermal diffuse X-ray scattering 8=5581

Aluminium—contd

positron annihilation meas. cf Se 8=5150
 pure single cryst. growth by strain-annealing from zone-refined Al 8=8398
 purification by fractional crystallization 8=4801
 quenched and degassed, form. of dislocation loops 8=1966
 quenched, interaction of point defects with dislocations 8=8690
 quenched, nucleation rate for dislocation loops 8=17645
 range of Kr and Xe ions, 500 KeV to 2 MeV 8=13481
 rapid self-diffusion along dislocations rel. to void annealing 8=13432
 reoxidation in Al electrolysis 8=23151
 resistance at He boiling temp. for purity determ. 8=9741
 rods, polycrystalline, texture changes rel. to mech. forming processes 8=22308
 rolled, texture representation by biaxial pole figures 8=17778
 rolling and recrystallization texture orientation relationships 8=1755
 rolling and recryst. textures, relationships 8=21938
 SAP and normal, elect. cond. 8=13707
 sections and wires, reinforced by continuous steel wires 8=10459
 sheet free of streaks by cladding 8=10460
 shock wave attenuation 8=8814
 single crystals, dynamic deformation 8=22310
 single crystals grown from melt, direct observation of sub-boundaries 8=17678
 solid, liquid and vapour states, X-ray emission spectra 8=9502
 solidifying, continuous radiographs of solid-liq. interface 8=4646
 solubility in cryolite melts, comp. and temp. dependence 8=21618
 stacking fault energy calcs. using pseudopotentials 8=17673
 stacking fault removal via n irradi., Frank loops change to perfect loops 8=17670
 stage I recovery recoil energy dependence from e-irrad. data 8=4961
 strain accumulation, second-order, at u. s. freq. 8=13527
 strengthening rate in slow loading process 8=22311
 stressed, thermally cycled, temp. after-effect rel. to strength and creep 8=13534
 stress-strain curves for shear deformation, zone refined 8=17761
 superconducting cylinders, mag. field periodicity in flux quantization expts. temp. depend. 8=22539
 superconducting transition temp. calcs. 8=5201
 superconducting transition temp. change due to 3d transitional impurities 8=9041
 surfaces, dispersion of surface plasma oscillns. 8=12547
 surfaces, (111), (100) and (110), atomically clean, prep. and props. 8=4728
 surface rearrangement involving chemisorbed O₂ 8=5726
 surface stacking faults after mechanical working, e-microscopy obs. 8=17675
 target for ion emission, bombard by Ar⁺ 8=6626
 thermal conductivity at low temp. 8=17542
 thermal conductivity 2.5-33.5°K 8=22132
 thermal radiation increase from microrough surface compared with polished one 8=22139
 thermoelectric power, and elec. resist. high press. effects 8=13902
 thermopower meas. rel. to electronic diffusion and phonon drag contributions 8=5382
 thin film strips, direct obs. of electro-transport 8=17927
 thin film, thickness monitor 8=17118
 u.s. shearwave, attenuation and rot. in mag. field 8=17497
 vacancy diffusion rate calc., Debye model 8=22172
 Wiedemann-Franz ratio and anomalous lattice cond. 8=8990
 wires, deformed, double fibre texture rel. to orientation 8=4832
 work function changes during and following low press. oxidation 8=5407
 X-ray atomic scatt. factors, Slater approx. 8=8506
 X-ray emission, K α doublet 8=5582
 X-ray K-satellites and K-absorption spectra 8=2398
 X-ray prod. and e backscatt. rel. to microanalysis, obs. and calc. 8=18794
 X-ray production on p-bombardment 8=4995
 zone-refined, strain-anneal grown, dislocation densities and configs. during heating and cooling 8=22198
 Al⁺, atomic interaction potential calc. 8=7456
 Al²⁺, pseudopotentials 8=7409
 Al²⁶ in oceanic sediment, atm. origin 8=23236
 Al II, spectra, transition probabilities 8=7411
 Al II, theoretical multiplet strengths 8=7410
 Al II, III, beam-foil excitation 8=12079
 Al(III) coord. no. in aq. mixtures 8=16888
 Al III, vacuum u. v. spectra 8=16202
 Al-Al₂O₃-Ag sandwich, electroluminescence rel. to electron emission 8=9277
 Al-Al₂O₃-Al sandwich photoemission studies 8=13858
 Al-Al₂O₃-Al, superconducting tunnel junctions, temp. dependence of energy gap 8=17958
 Al-Al₂O₃-Al thin film diodes, noise meas. 8=13851
 Al-Al₂O₃-Al thin film structures, electrode props. rel. to photocurrent direction 8=22689

Aluminium—contd

Al-Al₂O₃-Au film system, contact barrier height determ. by photoelectric meas. 8=18277
 Al-Al₂O₃-Au thin film structures, internal photoemission yields, Monte Carlo calcs. 8=22722
 Al-Al₂O₃-metal diodes, negative resistance obs. 8=5377
 Al-Al₂O₃-M film diodes electroluminescence 8=9598
 Al-Al₂O₃-metal structures, int. photoelectric effect, attenuation length 8=13910
 Al + Cl reaction, from 500 to 650°K, kinetics and rates 8=14358
 Al-MgF₂-Al bandpass, filter, far vac. u. v. 8=20065
 At beam range-energy studies 8=13473
 Fe content, by absorption spectrometry at 2483Å 8=9756
 in Fe liquid, heat of solution 8=16799
 O₂ content determ. by radioactivation anal. 8=5764
 Po beam range-energy studies 8=13473
 in Si, impurity redistrib. in oxidation and depletion depth, obs. 8=22606
 in YFe garnet rel. to spin wave susceptibility saturation above instability threshold, obs. 8=22864

Aluminium alloys
 See also Aluminium compounds.
 age-hardenable, vacancy conc. 8=1941
 ageing, natural, effect on subsequent artificial ageing 8=17764
 AlNi₃ A, magnetization coercive field strength, time- and temp.-depend. 8=5460
 Alnico V cylindrical bar magnets, meas. of axial field near magnet 8=19749
 analysis, Cu determ. by at. absorpt., spectrometry 8=2545
 analysis, Mn determ. by at. absorpt. spectrometry 8=2547
 cavitation damage resistance 8=5035
 cracking, during welding 8=5047
 cryogenic, high strength with good weldability 8=17762
 dislocations multiplication, transmission electron microscope obs. 8=13435
 duralumin, mass ejection by laser pulse 8=8759
 dynamic indentation, conical projectile, up to 550°K 8=17780
 electroplating, surface pretreatments 8=14429
 fatigue behaviour, thin anodic oxide films effects 8=2049
 irradiated, tensile and shear props. at cryotemps. 8=17763
 lattice defects recovery after tensile deformation 8=22184
 mechanical props., short-transverse, thick plate 8=13531
 microstructural changes, during and after hot working 8=21979
 secondary ion emission 8=18287
 shear deformation up to fracture under reversed loads 8=17759
 sheets, stress corrosion cracking at cutting planes 8=8818
 surface bubble formation during fatigue, rel. to humidity 8=4729
 surface preconditioning for electroplating, electron microscopy 8=8291
 2014-T6, crack propag. under low cyclic load rates 8=17746
 2219-T87 and 2219-T6, mechanical props. at elevated temp. 8=5048
 wrought, strength and ductility rel. to ingot structure 8=5046
 Al-Ag(20%) films, dynamical multiple reflections in electron diffraction patterns 8=13256
 Al-Ag, plasticity and tensile tests 8=8821
 Al-Al₃Ca, unidirectionally solidified eutectic, structure 8=4685
 Al-Al₃Ce, unidirectionally solidified eutectic, structure 8=4685
 Al-Al₃Ni, stability of eutectic stressed at elevated temps. 8=4842
 Al-Al₂O₃, dispersion strengthened, compression and cold rolling 8=8812
 Al-Al₃Y, unidirectionally solidified eutectic, structure 8=4685
 Al-Au, solid-liq. interface, radiographs 8=4646
 Al-4%Cu, deformational instability 8=8816
 Al-Cu alloys, dendrite arm spacing rel. to coarsening effect 8=4820
 Al-Cu alloy, dendrite structure at chill surfaces 8=4821
 Al-Cu, dendritic solidification 8=8177
 Al-4.5%Cu, macrosegregation on solidification, and mold design effect 8=16930-1
 Al-4 wt.%Cu, precip. phase microanalysis by e-microscopy and energy analysis 8=17276
 Al-Cu, X-ray Al-K β , emission bands 8=9502
 Al-Cu-Ag, precip. nucleation 8=17040
 Al-Cu-Cd alloys, deformation before and during ageing, effects on precip. 8=17039
 Al-Cu-Cd, resistivity, in artificial ageing 8=13708
 Al-Cu-Mg, atomic diffusion within lattice on ageing 8=17041
 Al-Cu-Mg with 1%Fe and 1%Ni, intermetallic phases comp. rel. to age hardening obs. 8=14495
 Al-Cu-Mg, stress-corrosion props. 8=8819
 Al-Dy-U system, phase equilib. 8=13060
 Al-Fe, Al activity at 1315°K 8=21651
 in Al-Fe alloys, activity at 1315°K 8=21651
 Al-Fe, disordered and ordered, soft X-ray emission spectra 8=5624

Aluminium alloys—contd

- Al-0.25 wt.% Fe, internal friction 8=5049
 Al-Fe, 12.42-12.8%, u.s. sound speed, effect of mag. polarization and temp. 8=13348
 Al-Fe-Si, Al-rich, phases 8=13058
 Al-Fe-Si-Mg-Zn, magnetoacoustic effect obs. 8=8624
 Al-Li, neutron irradi., grain boundary migration and gas bubble growth 8=8456
 AlM, (M = Mg, Ga, Ag), e-irradiated, stage II and III recovery temp. and impurity conc. dependence 8=1935-6
 Al-2%Mg, dislocation network knitting on stress-induced climb 8=17644
 Al-Mg, Mg atom clustering, electronic origin 8=13636
 Al-Mg, oxidation and diffusion removal of Mg 8=18670
 Al-Mg, Portevin-le Chatelier effect, rel. to comp. and testing temp. 8=22309
 Al-5%Mg with small Ag additions, X-ray investigation of ageing 8=13528
 Al-Mg, structure dependence on plastic deformation and ageing 8=17004
 Al-Mg, various ageing conditions and recovery 8=17765
 Al-Mg, X-ray Al-K β , emission bands 8=9502
 Al-Mg-Zn, brittle, precipitates, grain boundaries and dislocation movements 8=17646
 Al-Mn 1.04% dilute, solute atom-vacancy binding energy 8=8693
 Al-Si eutectic, modified, struct. 8=13155
 Al-Si, interaction between dislocations and precipitates 8=13431
 Al-Si, solidification process, study 8=1619
 Al-Sn system, above solidus temp., deformation, strength and fracture 8=22304
 Al-Ti, tensile creep at 250°C 8=8813
 Al-U-Sm system, phase equilib. rel. to use as nuclear fuel 8=13059
 Al-Y, phase analysis and crystal structure studies 8=22045
 Al-1 at.%Zn, electron irradiation hardening 8=8822
 Al-Zn eutectoid alloy, superplasticity rel. to grain boundary shear 8=17766
 Al-Zn eutectic, undercooling 8=17003
 Al-Zn, lattice defects and aging phenomena 8=13536
 Al-Zn, neutron-irradiation effect on Guinier-Preston zone formation 8=17274
 Al-10%Zn, neutron-irrad., pre-precipitation rate at 78°K 8=21980
 Al-Zn-Mg alloys, quenching rate rel. to age hardening 8=8817
 AlZn-Mg cast, surface structure rel. to stress corrosion cracking 8=22312
 Al-Zn-Mg, lattice defects and aging phenomena 8=13536
 Al-Zn-Mg, precipitation and ageing 8=13062
 Fe content, by absorption spectrometry at 2483Å 8=9756
 O₂ content determ. by radioactivation anal. 8=5764
 Zn determ. by atomic absorpt. spectrometry 8=23184

Aluminium compounds

- See also Aluminium alloys; Ruby.
 alumina, adsorpt. of He at room temp. 8=21899
 alumina, anodic layer analysis by X-ray fluorescence 8=18595
 alumina ceramics-Mb seals, bonding mechanism obs. 8=16743
 alumina, pure, γ -irrad., and magnesia-doped, thermoluminescence 8=5652
 aluminate i. r. glasses, optical, mech. and thermal props. 8=22954
 aluminosilicate catalyser in sludge, concentration by recording permittivity 8=15167
 corundum, complexes of bound impurity ions, group-theoretical classification 8=8887
 corundum crystals, large, hydrothermally produced 8=8400
 corundum, far u. v. polarizing power 8=15551
 corundum, H etched, orientation meas. by optical back reflection 8=17206
 corundum macroparticles accel. by laser radiation 8=10885
 corundum, mean strain curves, 0-900°C rel. to uniform dilatometric meas. 8=6
 corundum plates, elec. domains, and elec. effects rel. to plate-like whisker formation 8=21972
 corundum, thermal expansion, mean curves 8=17534
 cryolite-alumina melts in contact with Al, Al reoxidation process 8=23151
 erionite and offretite, differentiation 8=13153
 garnets, mag. structure by n-diffr. 8=22865
 garnet, phase change with symmetry enhancement as function of magnetic field 8=21839
 leuco-sapphire crystal, destruction by powerful laser radiation, mechanism 8=22247
 methyl ammonium aluminium sulphate dodecahydrate, thermal expansion 8=8647
 mica, tracks caused by e showers 8=22246
 oxide, X-ray emission, K α doublet 8=5582
 sapphire, critical surface tension 8=13080
 sapphire, Fe²⁺-doped, u.s.-induced changes in e. s. r. spectra 8=18407
 sapphire, filament growth from melt 8=21973
 sapphire, pulse compression by Bragg diff. of light with microwave sound 8=8618

Aluminium compounds—contd

- sapphire, Raman effect and vib. anal. 8=2401
 sapphire rod thermosensor 8=19668
 sapphire, spin-lattice relax. time meas. 8=9416
 sapphire, Si chemical-vapour deposition obs. 8=4826
 sapphire, with Si film, space-charge limited currents 8=2213
 sapphire, single crystals, alloyed with Ti, increased hardness and fracture strength 8=17767
 sapphire window mountings for low temp. spectroscopy 8=3362
 silicates, irradiated, thermoluminescence and e. s. r. 8=23044
 zeolites in liquid, proton relax. meas. 8=18454
 zeolites, synthetic, ion exchange theory 8=18651
 Al in Cr solid solution, antiferromagnetism obs. 8=14063
 Al-AlO interface, ionic diffusion 8=1912
 AlB₂, ht. of formation 8=2512
 AlB₁₀, crystal structure 8=8507
 AlB_{1n}, crystal structure by convolution mol. method 8=17337
 β -AlB₁₂ containing <2%Si, prep., stoichiometry and structure 8=17199
 α -AlB₁₂, ht. of formation 8=2512
 AlBeB₄, prep., stoichiometry and structure 8=17199
 Al₂Be₃Si₂O₁₈, crystal chemical analysis and structure refinement 8=17338
 AlBr phthalocyanine luminesc. singlet-singlet transitions 8=18591
 AlCl₃, in binary solvent mixtures, n.m.r. 8=8138
 AlCl₃, monomeric, mol. structure from gas e-diffr. exam. 8=16264
 AlCl₃, p. m. r. determ. of coord. no. in aq. mixtures 8=16888
 AlCl₄⁻ ion, h.f. i. r. active ν_2 vibr., correction 8=4142
 AlCl₆, force field and thermodynamics 8=4143
 AlF₃, anhydrous cryst., enthalpy 273°-1173°K 8=4929
 AlF₃, assoc. with NaF in saturated vapour 8=9692
 AlF₃, ht. of sublimation and i. r. spectrum 8=12997
 α (AlFeSi), crystal structure 8=8508
 α -AlFeSi, 4 possible phases 8=13057
 AlH₃, thermodynamic props. 8=4928
 AlK alum, cryst. growth rate, rel. to super-saturation 8=21940
 Al₂Me₆, force field and thermodynamics 8=4143
 Al₂Me₆Cl₂, force field and thermodynamics 8=4143
 Al-Mg alloys, liq., atomic distrib. and electronic transport 8=12799
 AlN:Cr photo-, cathodo- and electroluminesc. and S and Zn impurity effects, obs. 8=9595
 AlN, electrical and optical properties 8=2185
 AlN:Eu photo-, cathodo- and electroluminesc. and S and Zn impurity effects, obs. 8=9595
 AlN, i. r. lattice vibrations 8=8609
 AlN:Mn photo-, cathodo- and electroluminesc. and S and Zn impurity effects, obs. 8=9595
 Al oxide, hydrous, adsorption, mutual, with clay minerals 8=8341
 Al-O tetrahedral distances in aluminosilicate framework structures 8=21795
 AlO, absorption spectrum, dissociation energy 8=12169
 AlO clouds, night sky radiation obs. 8=18872
 AlO, new $2\Sigma^+-X^2\Sigma^+$ band, Franck-Condon factors 8=16263
 AlO trail spectra rel. to upper atmosphere densities and temps. 8=2613
 Al₂O₃, amorphous and polycrystalline, charact. energy-loss spectra and -Im ϵ^{-1} 8=13695
 Al₂O₃, amorphous, range distrib. of Na, K, Kr and Xe ions 8=13476
 Al₂O₃, rel. to anodic oxidation of Al in presence of hydrated oxide 8=18729
 Al₂O₃, anodized and crystalline, absorption in L_{III} region, structure 8=22956
 Al₂O₃ ceramic, for testing surface roughness rel. to directional emittance if thermal rad. 8=22138
 α -Al₂O₃, containing oxygen ion, electronic quadrupole polarizability 8=8232
 α -Al₂O₃, (corundum), vacuum deposition of Si 8=5281
 Al₂O₃ (corundum), V³⁺ ions, longit. relax. at simple electron levels 8=5541
 Al₂O₃:Cr³⁺, e. p. r. and acoustical mag. reson. in elec. field, profiles 8=18406
 α -Al₂O₃, crystal whisker sizing and testing 8=17248
 Al₂O₃, Cs activated, semicond. low work function films, props. 8=17999
 Al₂O₃, excitation of L-shell electrons by 20-keV electrons 8=22495
 Al₂O₃, dispersion of surface plasma oscilns. 8=12547
 Al₂O₃ films on Al in boric acid-formamide electrolyte 8=13089
 Al₂O₃ films, breakdown electric strength rel. to thickness 8=5351
 Al₂O₃ films, chem. deposition and props. 8=4740
 Al₂O₃ films e beam evaporation and dielec. props. 8=22652
 Al₂O₃ films, photoluminescence, spectral distrib. curves 8=9596
 Al₂O₃ films, plasma oxidized, breakdown field strength, thickness variation 8=22651
 Al₂O₃ films, pyrolytically grown, voltage-current charac. 8=13873

Aluminium compounds—contd

- Al₂O₃, film-thickness by tunnel emission and capacitance obs. 8=8312
- Al₂O₃ grain, effect of environments on fracture strength 8=13526
- Al₂O₃, irradiation damage on exposure to 5×10^{21} fast neutrons cm⁻² 8=22244
- Al₂O₃, large-area planar and non-planar films 8=13088
- Al₂O₃, lattice expansion and density decrease rel. to n irradi. 8=13249
- Al₂O₃, m. p., environment effects 8=1613
- α -Al₂O₃, n irradi. induced macroscopic growths 8=13132
- Al₂O₃ powders, reflection and polarization properties 8=14266
- Al₂O₃:Rh, fluoresc. 8=14300
- Al₂O₃ (sapphire), crack-branching, vel. meas. and stress effects 8=8815
- Al₂O₃, single crystal and sintered, γ photo-conductivity 8=18222
- Al₂O₃, sintered, fast n-irrad., effects on lattice, thermal cond., microstruct., density etc. 8=22245
- α -Al₂O₃, sintered, non-basal, dislocations, Burgers vectors 8=1967
- Al₂O₃, sintering, activation enthalpy 8=13052
- Al₂O₃, sintering, kinetics, data correlation 8=8258
- Al₂O₃, sintering kinetics, resonant freq. meas. 8=17027
- Al₂O₃, solubilities of MgO, TiO₂ and MgTiO₃, in H₂ atmos., temp. dependence 8=21818
- Al₂O₃, sputtering by Cs ions, 2.5-10 keV 8=8760
- Al₂O₃ systems, surface photochemistry 8=14441
- Al₂O₃, thermal cond., with Cr/Mn impurity, γ -irrad. effect 8=1886
- Al₂O₃, thermal expansion 8=13381
- Al₂O₃, tunnel structures, interface trapping 8=5381
- Al₂O₃, vapour-deposited, transitions from 300°C to 1200°C 8=13061
- Al₂O₃.V³⁺, Zeeman effect of absorption lines, up to 79 kOe at 4.2°K 8=9500
- Al₂O₃, X-ray analysis, qualitative and quantitative 8=9762
- Al₂O₃ whiskers, structure and mech. props. rel. to size and geometry 8=5050
- α -Al₂O₃-Cr₂O₃ solid solns., crystalline parameters 8=8241
- Al₂O₃-Y₂O₃ system, formation of compounds 8=4720
- Al₂O₃-Y₂O₃ system, liquidus curve meas. 8=16921
- Al₂O₃/SiC powders, reflection and polarization properties 8=14266
- 3Al₂O₃.2SiO₂, free energy of reaction of formation from CoO-Al₂O₃-SiO₂ 8=9669
- Al(OH)₃, nordstrandite, structure determ. by X-ray powder analysis 8=17339
- AlP, Raman and i. r. active modes 8=18500
- AlSb superconductivity 8=9043
- AlSb, Te and Se donors, photoexcitation spectra 8=22953
- Al₂SiO₅F₂, e. p. r. of Fe³⁺, hyperfine structure 8=2368
- Al₂SiO₅F₂, e. s. r. spectrum of Fe³⁺, fine structure 8=9412
- AlTiBO₆ (B=Nb, Ta, Sb), crystal structure and fluorescence 8=4879
- Al₂WO₆ bronzes, struct. evolution with temp., phase stability 8=17048
- AlZn, ageing rel. to metastable α' phase appearance and stability 8=8262
- MgO-Al₂O₃-Cr₂O₃ system, coherent precip. 8=21848
- PbO-Al₂O₃-B₂O₃-SiO₂ system glasses, elec. props. temp. and comp. dependence 8=18170

Americium

isotope shift constants 8=16234

Americium compounds

AmO₂²⁺, M-O bond force consts. in various media 8=21094

Ammonia. See Nitrogen compounds/ammonia.**Ammonium compounds.** See Nitrogen compounds/ammonium compounds.**Amorphous state**

See also Vitreous state.

- electron diffraction examination, background intensity 8=8443
- electronic processes in low mobility solids, conference, Sheffield, England, April 1966 8=5101
- films, dielectric, tunneling model 8=18155
- free radicals, local conc. meas. 8=4682
- optical method for analysing micrographs of spinodal decomposition structures 8=17268
- Bi, double structure of spherical close packing and layer lattice 8=12786
- Bi, strong-coupling superconductivity and phonon structure 8=5202
- C, electronic model 8=8998
- Ge, i. r. absorpt. bands and electronic struct. 8=22987
- Ge, structure and elec. transport phenom. 8=22597
- Sb₂S₃ films, photo-e. m. f. meas. 8=9255
- Se, atomic radial distrib. function rel. to quenching from different melt temps. 8=1714
- Si, i. r. absorpt. bands and electronic struct. 8=22987
- Si films, structure 8=13092
- Si, structure and elec. transport phenom. 8=22597
- Si₃N₄ films, structure dependence on deposition parameters 8=17179
- SiO₂ films, MOS capacitors, noncrystalline structure electronic conduction 8=9234

Amplifiers

- analogue, with two Hall-effect multipliers 8=19374
- crossed-field distributed-emission, computer simulation, space-charge and secondary emission effects 8=19712
- current pulse for 4π proportional counter used to standardize β -emitters 8=16012
- differential voltage, wide-band, high-gain 8=19709
- double delay-line, modification for coincidence time resoln. 8=20219
- electrometer with response curve α to argument of \sin^4 8=10832
- exponential, of lasers, to give energy densities of 10^{17} - 10^{25} ergs cm⁻³ 8=6421
- FET operational amplifiers, use as fast electrometers 8=3131
- ferrite magnetostatic degenerated-type with resonator coupling 8=358
- ferrite magnetostatic degenerated-type with waveguide coupling 8=359
- gas laser, solution of wave equation in frequency domain 8=11040
- generator of pulses of precise amplitude 8=11320
- high input impedance, for electrophysiological meas. 8=5983
- klystron, multi-cavity, e stream bunching theory 8=19827
- laser, amplification of amplitude-modulated light signal 8=19977
- laser, regenerative, theory, expt. and apps. 8=11027
- linearity in Ge(Li) γ -ray spectrometer 8=11440
- liquid, stimulated Brillouin scattering phonon lifetimes meas. 8=21666
- logarithmic, for β -ray spectroscopy 8=11469
- logarithmic, based on follower type circuits 8=6668
- logarithmic, MOS and Si planar transistors for space instrumentation 8=5342
- low Q, h. f. rectangular modulated pulse response, parametric envelope and overshoot probability 8=360
- magnetic, appl. in millivoltage to current converter 8=10831
- magnetic, single-core, output-circuit transmittance 8=6282
- maser, low-noise, basic characteristic meas. methods 8=396
- masers, travelling-wave and reflex type cavity, estimation of signal distortions 8=394
- modulated light signal, amplification 8=19945
- "molecular-ringing", in molecular oscillator, invest 8=10940
- multistage, resonant, low-Q-factor, pulse response 8=3143
- noise calc. time domain method 8=619
- nonlinear, for pulse-time reduction of Q-switched lasers 8=11002
- nuclear, pulse shaping circuits 8=15641
- optical appl. to fast spectrometer 8=20076
- optical parametric oscillation, theory and appl. to threshold cond. deriv. 8=11029
- parametric excitation, mech. of limiting oscs. 8=6368
- parametric, for ultrashort laser pulse 8=11015
- piezoelectric semiconductors, I-V characteristic under sound amplification conditions 8=18021
- preamplifier allowing use of 10-stage photomultiplier with particle spectrometer 8=3474
- preamplifier based on Ge FET 8=3473
- preamplifier, charge-sensitive, time constant reduction 8=618
- preamplifier, cooled FET, for semiconductor detectors 8=6651
- preamplifier, low noise, charge sensitive, for Ge gamma detector 8=6780
- preamplifiers, semi-conductor detector ensemble, waveforms 8=611
- preamplifiers used with semi-conductor detectors 8=610
- pulse height logic unit amplification 8=3476
- pulse shaping, nanosecond pulse integrator 8=15643
- pulse systems, time-domain calc. of noise of integrators 8=20213
- pulse, wide-band 8=6247
- pulse window, employing area meas. 8=6669
- r. f., driving cavities of accelerators, exciting circuit 8=11334
- second-emission tubes in linear-gain cond., operation 8=15173
- for semiconductor counters, universal pre-amplifier 8=20212
- semiconductor surface wave amplification in strong mag. fields, theory 8=9090
- semiconductor sound amplification and acoustoelectric effects, theory 8=9078
- sound amplification in gases, radiation induced, possibility 8=21516
- spectrum analysis by section, circuit 8=3475
- superconducting parametric, for d. c. voltage meas. 8=15166
- transistor, double-tuned transformer design 8=15162
- u. s. parametric, misalignments 8=3066
- ultrasonic, Love waves in dielectrics with thin CdS layer 8=4921
- van de Graaff accelerator voltage control, for improved energy resoln. 8=20234

Amplifiers—contd

- CdS crystal 8=5337
- CdS, u. s. amplification, temp. dependence 8=2081
- CO₂ laser, dispersion meas. by interferometric method 8=11052
- CO₂ laser, 10.6 μ , gas flow effect on gain 8=11053
- GaAs, microwave, Gunn oscillators 8=5302
- GaAs, two-port amplification 8=5251
- KH₂PO₄ optical parametric, quantum noise, 0.5-0.6 μ 8=15526
- Nd: glass laser, gain saturation 8=447
- NH₃ maser, characteristics: theory, exp. 8=397
- R-C, compensating circuit for low and high-frequency 8=271
- TWT and BWT, parametric, with premodulation 8=6369
- 100 kHz, signal and power, for e. s. r. instrumentation 8=6406

Analogue computers. See Calculating apparatus/analogue apparatus.

Analysis. See Chemical analysis; Statistical analysis.

Anechoic rooms. See Acoustical laboratories.

Anelasticity. See Internal friction.

Anemometers

- constant temp. hot-wire, further studies 8=16666

Angle measurement

- See also Alignment.
- carriage, rotational movement, accurate method 8=6001
- deflection, recording, automated 8=4637
- optical incidence, accuracy, reflectometer design 8=15517
- spin-rate sensor, two-mirror c. w. laser 8=6004
- transducer for rotational displacement using light sensitive resistors 8=6000

Angular distribution. See Gamma-rays/angular distribution;

Neutrons and antineutrons/angular distribution; Protons and antiprotons/angular distribution.

Angular velocity measurement

See also Stroboscopes.

No entries

Annealing. See Heat treatment.

Annihilation of electrons. See Electron pairs.

Anodic films. See Electrochemistry; Films/solid.

Antennae. See Electromagnetic waves/radiators.

Antiferroelectric materials. See Ferroelectric materials.

Antiferromagnetic resonance

- in orthorhombic weak ferromagnetics, frequencies at 0°K and temp. dependence 8=18306
- α -Fe₂O₃, anomalies in magnetization curve, lattice dynamics 8=2360
- α -Fe₂O₃, mm. wave expts. 8=22892
- CoCO₃, hexagonal anisotropy of line position 8=5514
- CoCO₃, rel. to mag. structure 8=18372
- Cr₂BeO₄, orthorhombic 8=14084
- CuBr₂Cl₂(H₂O)₂, 2H₂O mixed crysts. 8=2359
- CuCl₂·2H₂O, relax. effects 8=2358
- MTiO₃, (M=Mn, Fe, Co and Ni), meas. 8=9398
- MnCO₃, rel. to mag. structure 8=18372

Antiferromagnetism

- See also Magnetic properties/antiferromagnetic.
- easy-axis critical fields and resonance involving Dzyaloshinsky interaction 8=22871
- e. m. waves, fluctuations and scatt., theory 8=5497
- exchange interaction, antisymmetrical, and change of multiplicity 8=22767
- gyromagnetic effect at low temps. 8=14058
- Heisenberg antiferromagnet dynamical props. near critical point, generalized scaling laws appl. 8=2346
- Heisenberg antiferromagnet, spin-wave theory of impurity states, negative impurity-host exchange coupling 8=22868
- Heisenberg antiferromagnet, spin-wave theory of impurity states, positive impurity-host exchange coupling 8=22867
- Heisenberg linear chains, alternating, theory 8=14060
- Kondo problem, perturbation instabilities 8=22869
- Kondo scattering problem, ground state 8=5098
- neutrons slow and light fluctuations and scattering in strong magnetic field 8=5498
- phase transitions, in a mag. field, mol. field treatment 8=14062
- semiconductor, magnetic polaron suggested 8=9068
- sound attenuation near critical points 8=13344
- spin pair correlation, longit., by thermal Green function method 8=9387
- spins $\frac{1}{2}$, chain, X-Y model 8=2306
- spin wave theory, kinematical interaction 8=2345
- spin waves instability with "easy axis" anisotropy (linear approximation) 8=18370
- spiral spin systems, probability distrib. 8=13994
- surface spin-flop state 8=14057
- thermodynamic props. and correlation functions in strong magnetic fields, theory 8=18369
- Al in Cr solid solution, X-ray and neutron diffraction obs. 8=14063
- Al garnet, phase change with symmetry enhancement as function of magnetic field 8=21839
- Dy garnet, phase change with symmetry enhancement as function of magnetic field 8=21839
- KNiF₄, magnetic exchange dichroism 8=14257

Antimony

- acoustic cyclotron resonance in inclined magnetic field 8=22488
- in brass, embrittlement mech., and effects of U additions 8=22326

Antimony—contd

- crystal growth mode rel. to cleavage planes 8=17243
- diffusion in Al 8=8671
- diffusion in polycrystalline Ag, volume and grain-boundary diffusion 8=17563
- dislocations in single crystals, multiplication 8=8732
- effect of small amounts on self-diffusion of Fe in γ -phase 8=1930
- electromigration of small amount in liq. Bi 8=12815
- Fermi surface and Seebeck coeff. 8=22467
- films, thin, conductivity quantum oscill. obs. 8=17940
- galvanomagnetic coeffs. temp. and pressure dependence 8=17938
- impurity addition to steel, effect on temper brittleness 8=17797
- impurity in Fe or Ni, internal nucl. mag. field 8=8198
- magnetic resistance anisotropy, temp. depend. 8=5432
- n. q. r. in SbCl₃CH₃CN, SbCl₃POCl₃, and SbCl₅ 8=2391
- phase transition, shock-induced 8=4715
- resistance in magnetic field 8=9016
- tunnel junction, conductance maxima rel. to band structure 8=13859
- Fe-Sb systems, α - γ equilb. 8=4709
- Sb¹²⁴ implanted in Fe, hyperfine mag. field 8=8199
- Sb¹²⁵ in crude Pb 8=14499
- in Si, implanted atoms location and lattice disorder, obs. 8=17414

Antimony compounds

- isoelectronic cpds., Sb¹²¹ Mössbauer effect, isomer chem. shifts 8=16987
- multialkali-antimonide, anomalous vector effect of photoemission 8=2282
- In-Sb-Ni, ternary alloy, the quasibinary section InSb-NiSb in 8=4691
- PbTe-Sb₂Te₃ alloy system, thermoelectric props. and phase relations 8=4716
- Sb Menshutkin complexes, electric field gradient, asymmetry parameter temp. depend. 8=21802
- SbCl₃, NQR of Sb^{121,123} and Cl³⁵, temp. dependence, 20-150°K rel. to mol. motions and intermol. forces 8=22929
- SbCl₄F, crystal structure 8=17418
- SbCl₅, n. q. r. and phase transition 8=2391
- SbCl₅, polymerized with methyl methacrylate, methacrylonitrile and acrylonitrile 8=2527
- SbCl₅POCl₃, n. q. r. 8=2391
- SbH and SbD radicals, absorpt. spectra 8=12354
- SbI₃, refl. spectrum doublet structure rel. to spin-orbit interaction, 1-5 eV 8=9509
- Sb₂O₄:Mn luminescence, impurity effects obs. 8=18613
- Sb₂S₃ trap levels and recomb. centres, photocond. and obs. 8=22698
- SbSI, anomalous dispersion of permittivity and reson. absorpt. of microwaves 8=9218
- SbSI, light polarization near ferroelec. phase transition 8=18559
- SbSI, photo-induced microwave response obs. 8=5630
- SbSI, photosensitive phase transition 8=2159
- SbSI, refractive indices rel. to temp. and wave-length 8=2448
- SbSeI crystals, pyrocurrent props. 8=9228
- Sb(SiH₃)₃, i. r. and Raman spectra, and struct. 8=4144
- Sb-Sn alloys, magnetoconductivity tensor evidence for second set of holes 8=2086
- Sb-Sn alloys, oxidation products, e-diff. study 8=13287
- Sb₂S₃ amorphous films, photo-e. m. f. meas. 8=9255
- Sb₂S₃, anomalous dispersion of permittivity and reson. absorpt. of microwaves 8=9218
- Sb₂S₃ crystals, pyroelectric effect 8=9229
- Sb₂S₃, dielectric props., anomalies 8=9217
- Sb₂S₃ evaporated film microstructure 8=17126
- Sb₂Se₃ films, optical anisotropy 8=14259
- Sb₂Se₃-In₂Se₃, thermal and microscopic analysis 8=21828
- p-Sb₂Te₃, de Haas-van Alphen susceptibility meas. 8=9293
- Sb₂Te₃-In₂Te₃, thermal and microscopic analysis 8=21828

Antineutrinos. See Neutrinos and antineutrinos.

Antineutrons. See Neutrons and antineutrons.

Antinucleons. See Nucleons and antinucleons.

Antiparticles. See Under corresponding particle.

Antiphase domains. See Alloys; Crystal structure/microstructure; Solids/structure.

Antiprotons. See Protons and antiprotons.

Antireflection coatings. See Optical films.

Apodization. See Optical images.

Apparatus. See Cosmic rays/apparatus; Instruments; Ionosphere measuring apparatus; Laboratory apparatus and technique; Radioactivity measurement/apparatus; Vacuum apparatus; X-ray crystallography/apparatus. Further entries describing apparatus for specific purposes are included under the headings of the appropriate subjects.

Appearance potential. See Ionization potential.

Architectural acoustics

- See also Echo; Noise abatement; Reverberation; Transmission/acoustic waves.
- anechoic enclosures, freq. inhomogeneities meas. 8=19585
- angular distribution of lower room modes 8=198
- insulation in presence of flanking paths, meas. 8=19582
- booth, lightweight, design and construction 8=6184
- double walls, optimum parameters 8=3079

Architectural acoustics—contd

- meas. method 8=10752
- modal densities of shallow structural elements 8=19591
- noise and vibration control, conference 8=3076
- panels, multimode response to sonic booms, normal and travelling 8=6123
- reflection masking levels in concert halls 8=19594
- reverberation obs. 8=19590
- reverberation room, absorption coeff., edge effect 8=6181
- reverberation room, effect of boundary conditions 8=6182
- rooms, sound propagation and design for improvements 8=10759
- sonic booms, building excitation 8=10758
- speech distortion in reverberating hall 8=19592
- Stadthalle Gottingen, model, reverberation obs. 8=10756
- Toka-gaku-do concert Hall, Japan 8=199
- wall material, choosing type and distribution 8=6185

Arcs, electric

- a. c., influence of substance transferred on spatial distrib. of sample atoms 8=4295
- aerodynamic behaviour and heat transfer when stationary in aerodynamic and mag. fields 8=16424
- cascade arc chamber for high power 8=12413
- coaxial, nonsteady in fully developed plasma flow 8=7689
- combustion stability in gas flow 8=4293
- cross-section determ. from discharge meas. 8=4294
- direct-current, stability and critical parameters 8=21255
- distribution of emission lines 8=7684
- free-burning, oscill. strengths, systematic errors 8=7683
- gas heating, enthalpy meas. 8=19672
- ionization, non-equilibrium 8=21254
- Knudsen, hot-cathode low-voltage, electron energy distribution 8=12414
- low-pressure columns with positive V-I characteristics, low-pressure 8=12403
- low-temp., for emission anal. of solns. 8=23185
- oxides in graphite electrodes thermochemical reactions, rel. to spectral line intensity 8=14385
- plasma, electron beam disintegration 8=16425
- transient, in dielectric liquid, electrode erosion 8=21252
- transverse magnetic fields, expt. data, correl 8=21251
- thermionic converters, V-A charact. 8=6271
- ultraviolet sources, book 8=20012
- unipolar-d. c. conversion with coal electrodes 8=1345
- vacuum arc voltage rel. to plasma frequency of electrons in cathode 8=16426
- vacuum, initiation by field emission 8=7688
- vacuum, initiation by microprojections 8=7687
- vacuum, thin-film cathode drop meas. 8=7686
- Ar, anode melting and fall determ. 8=16427
- Ar cascade arc with O_2 , absorpt. oscill. strengths of O I lines in vac. u.v. 8=7417
- Ar discharge, model of interstellar medium, light scatt. by non-spherical particles 8=4296
- Ar, electron density in current perturbation by laser interferometry 8=7694
- Ar, short moving, effective drag width 8=4298
- Ar, temp. meas. 8=4297
- Ar II capillary, effect of mag. field on lower level inversion population 8=7692
- Ar II, stationary population inversion in 4s and 4p states 8=7693
- As(SiH_3)₃, i.r. and Raman spectra, and struct. 8=4144
- C, d. c., for steel oxygen content determ. 8=9751
- C, electrode erosion, particle trajectory photography 8=16428
- CoO crystals, growth by arc-transfer 8=4806
- Cu contacts rel. to wear 8=12415
- Fe₂O₃ crystals, growth by arc-transfer 8=4806
- He, pulsed, spectrographic meas. 8=21253
- Hg, effect of TII on temp. 8=485
- Hg, tube producing large volume 8=16606
- Mn₂O₃ crystals, growth by arc-transfer 8=4806
- N cascade, conductance decay after switch-off 8=7685
- NiO crystals, growth by arc-transfer 8=4806
- Xe, high-pressure, device for stabilizing radiant output 8=12416

Area measurement

- in histological sections, integration method 8=20058

Area measurement, porous substances. See Surface measurement.**Argon**

- absorption in Ba getters, obs. 8=17161
- accommodation coeff. in impact on Al, Ag, Au and Pt, 500-12 000 eV 8=12685
- additive in Cs arc diode, effect on performance 8=15225
- adhesion coefficients at 4.2° and 20°K 8=7954
- adsorption on Ni, temp. dependence, 78-120°K 8=17168
- afterglow, msec microwave pulses nonlinear interactions 8=21340
- alloys, above solidus temp., fracture-stress values 8=22304
- arc, anode melting and fall determ. 8=16427
- arc, current-perturbed, electron density meas. by laser interferometry 8=7694
- arc, cylindrical cascade, temp. meas. 8=4297
- arc plasma, Stark broadening of Ar I lines 8=12057
- arcs, short moving, effective drag width 8=4298
- atom, collision broadening and shift of Kr spectrum 8=20956

Argon—contd

- atom, $Ar^+ + Ar \rightarrow Ar^{m+} + Ar^{n+} + (m+n-1)e$, final change states and discrete loss mechanism 8=4107
- atom, $Ar-p$ e capture excitation of 3s, 4s states of H 8=7462
- atom collision with H_2^+ , H_3^+ , prod. of H atom in 3s state 8=21191
- atom, $(3p^4 4s)^2P$, state, lifetime obs. 8=1164
- atomic beams, secondary electron emission from gas-covered surface 8=22731
- atoms, ionization cross-sections to ground and excited states of Ar^+ 8=21267
- atoms and ions, multielectron ionization in close collisions 8=21012
- atoms and ions, multielectron ionization in close collisions with Ar^+ and K^+ ions 8=21012
- atoms, electron scatt., 40 keV 8=7447
- atoms, Van der Waals interact. with Si, rel. to shift of Si I lines 8=7423
- benzene luminesc. excit. in solid solns., obs. 8=13036
- binary mixtures, fast channel ions in glow discharge 8=7665
- bulk mod. and Debye temp. at T=0°K, anharmonic contribs. 8=13594
- collision cross sections, elastic differential, meas. 8=4108
- condensation coeff. at 4.2°K 8=12981
- conductivity, thermal, for partly ionized gas, equilibrium calc. 8=7900
- conductivity, thermal, line-source transient-heat-transfer technique 8=16701
- conductivity thermal near critical point 8=12683
- critical self-diffusion obs. 8=16716
- crystalline, dielec. and optical props. rel. to growth parameters 8=2238
- dimers and clusters in nozzle beams 8=12379
- discharge, elec., h.f., electrodeless, props., meas. 8=21234
- discharge, h. f. electrodeless, e density cinematography 8=16398
- discharges, high-freq. unipolar, spectral diagnostics, 1 to 12 atm. press. 8=4290
- discharge ionization rates, spectrographic measurement 8=7709
- discharge, medium press., neutral gas temp. 8=16408
- discharge positive column contraction 8=21231
- discharge, radio-frequency, temp. determ. using reversal technique 8=21223
- discharge tubes for 10 GHz noise source 8=7664
- dissociation react. with F₂O 8=12335
- electric discharge positive column, electrons energy distrib. 8=7655
- electrical conductivity, tensor, Cs seeded 8=12432
- f. c. c. crystal, adsorpt. of inert gases, potential energy profiles 8=17159
- Faraday effect theory of excitons for weak mag. field 8=5130
- free-carrier drift-velocity studied in liquid and solid state 8=8119
- gas discharge study, rel. to operation of Ar^+ laser 8=12402
- gas in equilibrium with adsorbed phase in ultrahigh vacuum system 8=21530
- gas, He-Ar mixture excited by α , scintillation mechanism 8=12202
- gas, for sputtering of films in crossed e.m. field 8=7651
- gas, ionized, shock wave interferometry 8=4311
- gas, laser induced ionization, mechanism 8=16434
- gas, photoelectron spectrometer, single grid 8=16441
- gas, spectral self-broadening and oscillator strengths 8=7416
- glow discharge in toroidal tube, expt. investigation 8=4286
- heat of fusion at high pressures and random close packing 8=8181
- h.f. discharge plasma torch, at atmos. press., power developed 8=21236
- hydromag. gas-ionizing shock fronts, nonequilibrium structure 8=16504
- ion bombardment on Ag, LEED study 8=22240
- ion density profiles in expanded shock tube flows 8=15050
- ion, energy loss in passing through ZnS:Ag film 8=8758
- ion laser, mode interactions 8=15458
- ion laser, single-freq. operation at 5145 Å 8=19957
- ionization chamber as extreme u.v. absolute detectors, comparison with thermopile 8=11162
- ionization cross-sections for 100-2000 eV electrons 8=12446
- ionization energy per ion pair formed by $H^3\beta$ particle 8=4315
- ionization near threshold by electron impact 8=7711
- ionization recombinations and wall effects 8=1363
- ionizational relax. behind shock front 8=1356
- ionized by shock wave, electron density and collision freq., microwave obs. 8=12431
- ions, incident on polycrystalline targets rel. to sputtering coeff. 8=8766
- isotope mixtures, thermal diffusion props. 8=1492
- jets, subsonic, electron densities, Langmuir probe 8=1409
- laser action in thermionic hollow cathode discharge 8=15457

Argon—contd

laser for colour television display 8=11068
 laser-heated plasma radiation spectra 8=16200
 laser lines, high gain, identification 8=7395
 laser lines, i.r., isotopic displacements 8=7397
 laser, long life construction 8=6439
 laser, mode-locked quieting 8=15466
 laser mode sustained by excitations, single frequency operation 8=6440
 laser, pulsed, upper level population obs. 8=19956
 laser, spectrum stable, magnetic field-tunable and line-width determ. 8=11043
 liquid, activation particle detector 8=20203
 liquid, charge transport temp. dependence 8=18161
 liquid, H in solution, translational H absorpt. spectrum in far i.r. 8=12889
 liquid, at 85-9°K, calc. of atomic self-motion 8=21603
 liquid, cold-n scatt. at 94.4°K, analysis using computer molecular-dynamics expts. 8=21611
 liquid, collective motion, evidence from n scatt. 8=16793
 liquid, quasielastic scattering of cold neutrons 8=1524
 liquid, scattering, inelastic, of cold neutrons, at high temps. 8=16792
 liquid, sound velocity and law of corresponding states 8=1552
 liquid, thermal conductivity calc. using Green correlation function 8=8053
 liquid, thermodynamic functions calc. using geometric theory 8=8042
 liquid, thermodynamic props. calc. 8=8041
 liquid, u.s. absorption 8=1553
 liquid, velocity autocorrelation function calc. 8=12777
 liquid viscosity, shear, meas., elec. method 0-200 Kg/cm² and 86-146°K 8=12820
 mass spectra, obtained with static operation, mass 80 peak 8=12056
 melting curve to 30 kb, obs. 8=1610
 melting, significant struct. theory 8=12967
 mol. beam reflection at Al surface, energy meas. from 100-7500 eV 8=16382
 mol. beams at high intensity, condensation forming single crystals 8=16383
 molecular flow through capillary, interaction with tube wall 8=7893
 monatomic, partially ionized, transport props. 8=4304
 neutral, transition probabilities in intermediate coupling 8=12055
 normal ionizing shock wave, structure 8=21490
 I and II, interferometric wavelength meas. in region 5000-7000 Å 8=4070
 paraboloid eroded by ion bombardment 8=13466
 partially ionized, supersonic source flow expansion into vacuum 8=16658
 Penning discharge modes characts., <10⁻⁴ torr 8=1332
 physisorption on silica at low temps., process and mean adsorpt. time 8=17172
 plasma containing alkali metal additions, elect. conductivity 8=12482
 plasma, flames, induction-coupled, spectroscopic obs. 8=21411
 plasma, flowing, specific energy and electric field for intense stable discharge 8=16402
 plasma, l.p. growth rate calc. 8=21390
 plasma jet, heating of condensed powder particles, calc. 8=12574
 plasma, laminar flow heat transfer in entrance region of circular tube 8=16477
 plasma, meas. of refractive index 8=4378
 plasma, microwave induced for spectrochem. anal. of metals 8=18785
 plasma, with N₂ admixture, applicability of two temp. model 8=12460
 plasma, permittivity and conductivity variations with freq. and electron density 8=4346
 plasma viscosity and thermal conductivity, partially ionized 8=7734
 polycrystalline, elastic constants calcs. 8=17768
 positive column, direct display of electron temp. var. 8=16407
 pumping speed-press. data, getter-ion pump 8=1495
 reactor, Ar-filled, thermionic, with thermionic convertor 8=298
 refractive index, real part, calc. from Kramers-Kronig dispersion relation 8=1670
 resonance-line lamp for u.v. photochemistry 8=18738
 scattering ionization, short range forces 8=1364
 scintillation counter, characts. and light spectrum, impurities effects, obs. 8=20194
 self-consistent phonon theory, phonon spectrum and bulk thermodynamic props. 8=13336
 shock compression, Thomas-Fermi-Dirac theory 8=16994
 shock layer e density meas. 8=21265
 shock wave front, luminance temp. obs. 8=21483
 shock waves, explosively generated, radiation 8=1480
 solid, charge transport temp. dependence 8=18161
 solid, compressibility 8=5075
 solid, excitons and band gap from e energy loss obs. 8=9194
 solid, free carrier mobility 8=17863

Argon—contd

solid at 0°K, parameters from interact. potential of gas 8=1468
 solid, with trapped Ru atoms, optical and X-band e.s.r. spectra 8=18558
 solid, zero-point energy, effect of long-range 3-body forces 8=22083
 solubility in H₂O-methanol system 8=12809
 solidified, vapour pressure, binding energy and mean vibration freq. 8=16960
 superradiant transitions 8=7398
 supersonic flow, by h.f. induction, electronic and ionic properties. 8=21266
 on Teflon 6, isotherms 8=13047
 test gas in ballistic compressor, thermodynamic conditions 8=1470
 thermal conductivity, between 24 and 73°K 8=4940
 thermal conductivity, hot-wire cell meas., 30°-100°C, 120-150 torr 8=16700
 thermal conductivity meas. with hot-wire cell 8=6210
 thermal plasma, continuous emission spectrum 8=16207
 in thermionic diodes, effect on performance 8=15216
 thin solid films, microstructure, electron diffraction study 8=8313
 translation accommodation coeff., on W surface 8=17113
 transport properties, single-component model 8=1438
 Ar ions reflected from Cu crystal incident obliquely 8=8767
 Ar self diffusion coeff. and atoms interaction-energy 77.5-121°K and 294°K 8=1489
 Ar-like ions, phys. props. rel. to electronic config. for excited states 8=1148
 Ar II capillary arc discharge, effect of mag. field on inversion population of levels 8=7692
 Ar II laser, polarization in perturbed spontaneous emission spectrum 8=11042
 ArII lines, Stark broadening parameters, obs. 8=20949
 Ar II, stationary arc discharge, population inversion in 4s and 4p states 8=7693
 Ar II, transition probabilities 8=1163
 Ar', highly excited, autoionization prod. by electron impact 8=12430
 Ar' laser operation, study of relevant characts. of Ar gas discharge 8=12402
 Ar' laser, spectroscopic study 8=3307
 Ar₂, ground state, wavefunctions and potential curves 8=7526
 Ar₂, 2nd virial coeff. obs. 8=7913
 Ar₂, thermal conductivity at 100-300°C, 1 atmosphere, obs. 8=4477
 Ar²⁺ + Ar, reaction cross-sections 8=4310
 Ar³⁹ 'excess' in stone meteorites, origin 8=19277
 Ar³⁹, nuclear spin and magnetic moment, spectroscopic measurement 8=11739
 Ar-C₂H₂ mixture, ionization defect meas. 8=7710
 Ar+Cs positive column contraction 8=21231
 Ar Cs system, electron density in plasma prod. by fission fragments 8=15215
 Ar-F₂ cryst. state, phase diagram 8=1670
 Ar-H₂ plasma jet radial temperature distribution, determination 8=12571
 Ar-5%He gas mixture scintillation props. 8=11301
 Ar-Hg low-pressure discharge luminescence efficiency 8=4287
 ArI, mean lives of some 4p levels 8=4069
 Ar-Kr binary mixture, spectra in vapour, liq. and solid states 8=7425
 Ar-N₂ mixture, meas. of thermal-diffusion factors 8=1488
 Ar-N₂ mixtures, virial coeffs. from Burnett meas. 8=16691
 Ar-O₂ gas lasers, mechanism of laser action 8=11975
 Ca IX, spectra, transition probabilities 8=7411
 He-Ne laser wavelength increase due to Ar addition 8=11063
 In-doped solid film, absorption spectra 8=9541
 K-Ar, interatomic potential, χ^2 minimum method 8=12205
 L₁ shell, Coster-Kronig and Auger spectrum 8=7396
 N₂-Ar gas mixtures, thermal conductivity 8=4474
 O₂-Ar gas mixtures, thermal conductivity 8=4474
 TiO₂ surface discharge, channel development 8=1330
 Xe-Ar couples in binary mixtures, translation spectra 8=7425
 in ZnO:Zn, ions energy losses obs. 8=18624

Argon compounds
 AsH and AsD, A, ³I, -X, ³S⁻ band systems 8=21062

Aromatic compounds. See Organic compounds.

Arsenic
 impurity addition to steel, effect on temper brittleness 8=17797
 inhibitor, in Cu-Zn alloys, selective corrosion 8=23100
 ions, registration in olivine and hypersthene crystals. 8=11325
 polarizability 8=9505
 X-ray K absorption spectra, chemical effects 8=22957
 p-GaAs, photoluminescence, affect of heat treatment with excess As pressure 8=23054
 in Ge, solid solution, supersaturated, decomposition mechanism 8=17005
 n-InP crystal doping, elec. effects 8=9113

Arsenic—contd

in Si, implanted atoms location and lattice disorder,
obs. 8=17414

Arsenic compounds

X-ray K absorption spectra, chemical effects 8=22957
AsF₃, general force field 8=4157
AsF₃, mean amplitudes of vibration 8=16298
AsO, potential curves of electronic states 8=1236
As-S glasses, origin of 800 cm⁻¹ absorpt. 8=5584
As-S-Se partially vitreous system, sintering obs. 8=13053
As-Se glasses, thermal expansion 8=13382
As-Se system, thermal conductivity in glassy
state 8=1887
As-Se vitreous alloys, introduction of Cu atoms 8=13111
AsSe_x glass, refractive index 8=14198
As₂S₃, amorphous, carrier mobilities from conductivity
studies on e-irradiation 8=18162
As₂Se₃, crystal structure refinement by NQR
method 8=17340
As₂Se₃-4As₂Te₃, thermal cond. in glassy and cryst.
states 8=1887
Ga-As-M (M = Au, Ag or Cu), equil. ternary liquidus-
solidus phase diagrams 8=4639

Assistors. See Semiconducting devices: Resistance. electrical.

Association

hemoglobin with O₂, theory 8=13111
ion pair, constants and solvent composition 8=8009
tetracene dimer, association const., absorpt. and emission
spectra 8=1301
thiobutylolactam, dimerization, values of ΔH° , ΔG°
and ΔS° 8=4241
thiocaprolactam, dimerization, values of ΔH° , ΔG°
and ΔS° 8=4241
thiovalerolactam, dimerization, values of ΔH° , ΔG°
and ΔS° 8=4241

gases

azo compounds in vapour phase 8=16958
I, at h. p. 8=23080
NaF + AlF₃ in saturated vapour mixture 8=9692

liquids

See also Colloids.
alcohols, tertiary, from dielec. consts. 8=12908
dispersion interact. energy as molar vol. /int. press.
prod., rel. to H bonding energies 8=12779
methyl viologen cation, aq. and alcoholic solns., water
induced dimerization, e.s.r. spectra obs. 8=8123
molten salts containing water, quasi-lattice model 8=8015
phenols, from dielec. consts. 8=12908
tetracyanoquinodimethane anion, aq. and alcoholic solns.,
water induced dimerization, e.s.r. spectra obs. 8=8123
tungstate solns., aggregation study, by W¹⁸⁵ 8=21607
LiClO₄ in acetonitrile-dioxane, ion pairs 8=8108
LiClO₄ in H₂O-dioxane, ion pairs 8=8107
LiClO₄ in methanol-dioxane, ion pairs 8=8108
Zn(NO₃)₂·xH₂O, molten, ion assoc. 8=16868
ZnSO₄ soln. in H₂O-glycol, ion assoc. 8=8062

Astatine

beam, range energy in Al, Al₂O₃ 8=13473
At^{209, 211} beam, recoil prod., for bombard. of Al
foil 8=11952

Astatine compounds

No entries

Asteroids. See Planets; Solar system.

Astigmatism. See Aberrations, optical.

Astronautics. See Space research.

Astronomical instruments

See also Radioastronomy; Telescopes/astronomical.
achromatization, partial, device for u. v. stellar
research 8=10319
camera, electronic, US Navy, linearity and information
gain over photography 8=14742
camera, wide-angle, all-reflecting Schmidt 8=10107
Danjon astrolabe, reflecting modification 8=10105
echelle spectrometer-spectrograph for astronomical
use 8=14740
electronic camera and spectroscope for use at high
dispersion 8=14743
glass-filters in photometry, effect of temp. changes 8=10103
gratings to increase intensity of u. v. spectrum 8=10102
image intensifier, two-chamber, for telescope
obs. 8=11147
interferometer, optical intensity, for stellar temps.
meas. 8=19134
lens, 535 mm, objective of coronagraph, investigation
of 8=536
meteor visual observations recorder 8=19264
micrometer, photoelectric for meridian passage
times 8=10104
optical device for spacial filtering of photo-
graphs 8=14744
photometer, small-diaphragm, for faint objects photoelec.
obs. 8=23498
photomultiplier as photon counter of very faint light
sources 8=10904
polarimeter, two-cell photoelectric using rotatable
achromatic half-wave plate 8=10106
solar radio spectrograph, 30-300 MHz 8=14869
solar spectrometer, large Echelle grating 8=10385
spectracon, for obs. of stellar rotations 8=19105

Astronomical instruments—contd

spectrograph, multi-slit, for simultaneous slit
spectra 8=23498
stellar amplitude interferometer 8=19135
stellar spectrum analysis, reading of diagram
coordinates 8=14763
telescope fixing on star, clock-controlled drive 8=2772
two-cell photoelectric polarimeter, Uppsala,
Sweden 8=19168
two-channel spectroelectrophotometer with pulse-
counting registration 8=19104

Astronomical observations

See also Radioastronomy.
atmospheric scintillation, spiking probability
calc. 8=18876
Ephemeris time corrections rel. to revised lunar
theory 8=10485
inertial frames of reference, planetary and
galactic 8=14739
new variable stars, around globular cluster NGC6304,
6638 and 7099 (M30) obs. 8=19182
photoelectric polarization meas. on faint stellar objects,
detection principle 8=19143
practical amateur observatory, construction 8=23499
radar astronomy, fundamental principles and recent
research 8=19326
stellar magnetic field, var. observer effect 8=19115
stellar magnitudes directly from in-focus images,
method 8=5852
stellar photometry, direct elimination of sky
background 8=23542
sun, observatory, Hawaii 8=10374
telescope dome, microthermal slit obs. rel. to image
quality 8=14741
Tokyo, time and latitude bulletins 8=10068
FK₄ catalogue, periodic errors 8=14745

Astronomical spectra

See also Atmospheric spectra; Cosmic radiations,
radio-frequency; Stars/spectra; Sun/spectra; and
other individual astronomical bodies.
Compton effect, energy-differential cross
section 8=3571
extra galactic radio sources 8=23607
 γ Pegasi, from electronic photography and spectros. at
high dispersions 8=14743
nebulae gaseous, A₂ recombination lines relative
intensities 8=14793
quasistellar objects, absorption spectra 8=23628
radio galaxies rel. to fine struct. const. time var., O III
emission obs. 8=14727
radio source spectra and cosmological red shift, hyperbolic
model 8=14812
r.f., two planetary nebulae, optical depths and electron
temp. obs. 8=23561
stellar spectrum automatic reduction, automation 8=14763
u. v., intensity increase by means of gratings 8=10102
Venus, atm. light scatt. props. rel. to CO₂ bands
intensities 8=14846
CO₂, relative intensities, 160°-280°K calc. 8=7506
OD transition B² Σ^+ -A² Σ^+ , high resolution obs. of excited
water vapour jet 8=21095
OH 18 cm lines, cosmic, polarization theory 8=7543
OH-18 cm rad., anomalous elec. polarization 8=23582
OH transition B² Σ^+ -A² Σ^+ , high resolution obs. of excited
water vapour jet 8=21095
N₂O-CO mixture, study of overlapping absorpt.
bands 8=7507
Si II superposition of configuration applied to a
series of states 8=19158
Si II λ 4128 and λ 4130Å in model atmospheres and B
stars 8=19163

Astronomical telescopes. See Radioastronomy; Telescopes/
astronomical.

Astronomy and astrophysics

See also Cosmology; Radioastronomy.
astronomical observatory, influence of night cloud on
choosing site 8=14579
astronomical society of Australia, conference, Sydney
Australia (1966) 8=14722
black-body radiation in cold universe 8=23473
calibration of correl. between abs. magnitude and K line
width, use of small parallaxes 8=19110
Cambridge Institute of Theoretical Astronomy 8=23464
catalogue, astrographic, new plate const. for N. Hyderabad
Zone 8=19075
convention of Italian Astronomical Society, Catania
Italy (1966) 8=19111
extra terrestrial observational astronomy,
advantages 8=14721
fields of force generating motion on family of
spirals 8=10100
rel. to interstellar matter fragmentation, wave propag.
in plasma with Coriolis force 8=16515
model atmospheres in theory of stellar classifi-
cations 8=2777
non-equilibrium and enhanced mixing at a plasma-fitted
interface 8=5841
optical positions of bright galaxies south of 20°
declination 8=10259

Astronomy and astrophysics—contd

photometry, temp. effects on U, B, V glass filters 8=10103
plasmas, gravitating, with mag. field and rot., 2-stream
instability 8=19085
proton whistlers, dispersion, Injun 3 and Alouette 1
data 8=18958
seeing, verification by isophote of vertical
satellite 8=14746
spatial filtering of photographs, and Fourier integral
representation, theory 8=10108
stars, ionized, thermomagnetic instability and thermo-
dynamic waves 8=10109
stratified atmos., acoustic and gravity wave emission by
turbulence 8=23270
unit determination by dynamical method 8=2765
H atom—fast H⁺ and He⁺ collision processes 8=16230

Atmosphere

See also Air; Electromagnetic wave propagation/
atmosphere; Ionosphere.
absorption of 5.65 mm waves 8=5789
aerosol and condensation process from optical
obs. 8=9834
aerosol, condensation nuclei vertical distrib. in boundary
layer 8=9835
albedo, Tiros VII obs. 8=23285
albedo from 2 colour photoelectric earthshine obs.,
S. Africa 8=2594
atom-atom collision processes 8=16230
barotropic, nonlinear geostrophic adjustment 8=2573
boundary layer, appl. Ekman spiral instability 8=14601
boundary layer, Eulerian rel. to Langrangian correlation
coeffs. 8=14593
boundary layer, flux of momentum, heat etc., scale
handover 8=14578
boundary layer over oceans, importance in synoptic
meteorology 8=14582
boundary layer turbulence over land and sea 8=14596
boundary layer, turbulent variables, joint probability density
functions 8=14592
clouds, noctilucent, and jet streams detect. by satellite
i.r. obs. 8=9855
convection below cloud base 8=2578
cosmic -ray at re-entrant albedo intensity calc. from
balloon obs. 8=903
density from satellite orbital decay and instruments 8=5796
'earth-atmos.' outgoing rad. correl. with total cloudiness
etc. 8=9861
energy, annual var. and spectrum, (1963-64) 8=23252
explosion, geomagnetic disturbance due to shock
waves 8=2746
frontogenesis, narrow zone, from field having only large-
scale var., numerical expt. 8=18860
general circulation, computer model for global
study 8=9822
global, research programme, study conference 8=23250
gravity wave instability 8=2584
ground layer, turbulent transfer for quasi-homogeneous
flows 8=15610
high altitude fronts, theory of types and anal. of velocity
fields 8=9830
laser backscatter, Raman component, obs. 8=23263
laser and nonlaser light propag., comparison 8=9867
lower layers, model for two-dimens. heat and mass
transfer 8=23267
lower, meteorological analysis and predictions 8=18848
magnetosphere, hydromag. emission rel. to
perturbations 8=2739
meson monitoring, meteorological corrections 8=3753
mesosphere, thermal behaviour 8=2575
meteors fragmentation, deform. and ablation and
luminous intensity 8=10364
microboroms origin and rel. to microseisms 8=9773
millimetre transfer radiation from O₂¹⁶ molecules, influence
of Earth's mag. field 8=23284
momentum, relative angular, and day length vars. 8=14510
morning magnetospheric perturbations, relation with
v.l.f. emissions 8=23318
and ocean surface, dynamical and thermal inter-
actions 8=9829
particle spectrum calc., by small-angle scatt.
pattern 8=23251
planetary boundary layer, appl. Ekman spiral
instability 8=14601
planetary, energy loss functions for electrons and
protons 8=23658
pollutant effect on electrical contacts 8=8988
potential energy, available zonal and eddy, earth i.r.
radiation generation obs. 8=23262
radiation, outgoing terrestrial 7-26 μ , statistical characts.
from Cosmos obs. 8=23283
radiation transfer, with reflection from boundaries 8=9862
radiation, measurement of 8=10066
radio refractivity, world atlas 8=18905
radiowave refraction and attenuation, book 8=14629
Rayleigh-scattering, of large optical thickness, global
radiation 8=14831
ring current growth and polar magnetic
substorms 8=19056

Atmosphere—contd

shear flows, thermally stratified, rel. to laboratory
models 8=14599
smoke diffusion from high stacks, time-average ground
concentration 8=14614
solar type stars, non-gray model 8=2775
stratified, acoustic and gravity-wave emission by turbulent
motions 8=23270
strato-mesospheric, temp. and density from hypersonic
sphere obs. 8=9831
stratospheric circulation, southern hemisphere 8=2574
temp. stratified, wind speed components, spectral
structure 8=14607
top, solar e.m. flux incident, numerical calc. 8=2840
troposphere, scintillation of discrete sources 8=23287
troposphere, structure factor from radio data 8=2603
turbulence effect on optical surveillance systems 8=14598
Van Allen radiation changes rel. to polar substorms,
Alouette 1 obs. 8=18966
whistlers and v.l.f. emissions, obs. and theories 8=14672

composition

above 30 km, i.r. absorption meas. by balloon-borne
diffusing system 8=9840
alkali metals, optical meas. 8=9925
chemi-ionization in upper atm., model 8=23307
electron flux at synchronous altitude, variations,
ATS-1 obs. 8=18924
ion-temp. and relative composition, low altitude polar
satellite obs. 8=18919
magnetosphere, He ions effect on micropulsation 8=9921
mass spectrometer obs. above 100 km 8=9901
particles in Antarctic atmosphere, near surface 8=23264
precipitation of low-energy particles at high latitudes
results of satellite meas. 8=9954
radioactivity and O₂ at Antarctica (90°S) 8=9897
radio astronomy meas., relating data to opacity and
source brightness 8=2595
60-100 km altitude range 8=14590
sodium, upper 8=18916
sodium, upper 8=18917
tropical oceanic air, sea-salt particles, var. of ion ratios
with size 8=9837
upper, meteoric dust, detection from sounding
rocket 8=18918
water, isotopic fractionation at liquid-vapour and solid-
vapour transformations below 0°C 8=2503
CO₂ gas constituent, number density determ. using laser
beams 8=14585
CO, low concentrations in air, spectrophotometry
analysis 8=14589
Cl, natural gaseous, origin rel. to volcanic action 8=9841
H².³, cosmic ray produced, balloon obs., June
1965 8=3752
H₂O gas constituent, number density determ. using laser
beams 8=14585
Na, daytime distrib. and origin, 92.4 km 8=2616
Na distribution 8=9903
Na, rel. to meteoric origin 8=9902
O, atomic, at 120 km, mass spectrometric meas. 8=18920
O₃ concentration, mesospheric rocketsonde obs. 8=18852
O₃ concentration above S. Africa up to 45 km,
obs. 8=14588
O₃, heating and radiative equilibrium in
stratosphere 8=2579
O₃, oscillation, quasi-biennial, from monthly O₃
data 8=2581
O₃, from satellite meas. 8=2576
O₃ and submicron dust soundings, N and central America
troposphere and stratosphere 8=18851
O₃ vertical distribution, troposphere and stratosphere
obs. 8=18853
O₂ gas constituent, number density determ. using laser
beams 8=14585

humidity

See also Humidity.
ceramic sensing device, obs. 8=18855
condensation of moisture from tropical maritime air
masses as freshwater source 8=18854
moisture determ. from absorption of solar
radiation 8=14586
moisture flux, diurnal fluctuations in Caribbean 8=2580
at north pole of cold, 1.38 and 1.87 μ bands obs. 8=9874
vertical structure parametrization 8=9836
water vapor, stratosphere, absorption spectra obs. 8=14587
water vapour transfer, turbulent, at different stability
condns. 8=14611
BaF₂ film hygrometer element, storage stability 8=18856

ionization. See Atmospheric electricity; Ionization, atmosphere; Ionosphere.

movements

See also Wind.
aerodynamic-acoustic theory, high-altitude
fluctuations 8=9905
baroclinic flow, stability in zonal magnetic field 8=2582
boundary layer, alternating and horizontally rolling
vortices with axes in mean flow direction 8=14600
in boundry layer, mass transfer from radioactive tracer
obs. 8=14594

Atmosphere—contd

- movements—contd**
 boundary layer, turbulence 8=14595
 circulation in equatorial region, model eqns. for stationary case with zonal press. fields 8=9846
 circulation rel. to solar activity 8=23253
 diffusion in wind direction, and surface layer 8=9847
 diurnal variation of winds over eastern Hawaii 8=9849
 exchange studies by Na²² meas. 8=18857
 fluctuation data, in surface layer over sea, analysis 8=23266
 governing equations and spectra, transports in freq., wave-number space 8=23269
 hydromagnetic oscs., structure polarization and propag. 8=2609
 ionosphere drifts, comparison of anal. methods 8=19000
 ionospheric drift meas., statistical method 8=19001
 ionospheric drifts, winter, during quiet-sun period 8=19004
 jet streams, origin 8=18862
 large-scale, eddy diffusion and viscosity coeffs. 8=23237
 long waves with cross-wind 8=9843
 lower layers, model for two-dimens. heat and mass transfer 8=23267
 mesosphere, tidal oscs. and summer flow near subpolar mesopause, obs. over Alaska 8=18863
 nongeostrophic effect on baroclinic wave disturbances 8=9845
 nuclear debris, interhemispheric transfer 8=23297
 oscillations, free, rel. to mean wind 8=9844
 pressure and acoustic wave propagation after nuclear explosions 8=2583
 stratosphere, lower, circulation from radiometric temp. obs., Tiros VII 8=18858
 stratosphere, turbulence obs. 8=14580
 stratospheric winds over Panama, obs. 8=14606
 structure, a model, between 85 and 110 km 8=2617
 suspended particles, diffusion theory 8=18861
 thermal turbulence in forced convection, model and analysis 8=12638
 thermosphere, diurnal vel. oscill., new anal. 8=14602
 tidal eqns., β plane form, asymptotic solution of Cauchy problem 8=9771
 tropospheric wind field above low-level jet, diurnal oscillations 8=23271
 turbulence in boundary layer over sea, spectra and stress meas. 8=18859
 turbulence due to mountain disturbance of airflow 8=14597
 turbulence, locally isotropic, veloc. and temp. derivatives cross-correl. moment 8=14604
 turbulence parameters, discussion 8=14591
 turbulence, rel. to fluctuations in light waves from edge of solar disc 8=14623
 turbulence, spatial coherence of 3.2 mm e.m. wave 8=18900
 turbulence, spherical e.m. waves propag. 8=18897
 turbulent boundary layer, contaminant transport with unstable stratification 8=14608
 varying turbulence rel. to intensity fluctuations of propag. light beam 8=14618
 velocity spectra, one- and three-dimens., comparison 8=9848
 vortices, free, generation, governing parameters 8=7904
 waves due to Pyrenees, wind and temp. meas. 8=5790
 waves, instability rel. to billow clouds and clear-air turbulence, obs. 8=23265
 wind profiles, boundary layer eqns. approx. soln. 8=23273

precipitation

- See also Ice; Rain; Snow.
 aerosols, concentration and size distribution 8=18870
 aerosol particles removal by raindrops and snow crystals. 8=23275
 cloud droplet growth by hydrodynamic capture, stochastic model 8=18869
 cloud nuclei production and droplet concentration, effect of sugar cane fires 8=18868
 contaminant washout and rainout, theory 8=9852
 droplets and nuclei in cloud, number concentration comparison, obs. 8=18867
 drops in elect. field, free falling, mass loss and distortion 8=21586
 freezing level altitude by radar obs. 8=9856
 hailstones, liquid water content 8=23276
 ice nuclei sizes 8=2587
 ice from supercooled H₂O, particles growth and struct., obs. 8=23274
 near earth's surface and 500-1000 m, microstruct. obs. 8=9854
 particle size and charge, meas. 8=23279
 precipitation—evaporation ocean surface, balanced by heat exchange 8=9814
 raindrop distribution and growth, deduction from vertical wind tunnel obs. 8=1519
 statistical studies, on local, national and continental scales 8=18865
 suspensoid stratification and cloud-top accumulation of droplets 8=14609
 AgI-KNO₃ nuclei, water vapour adsorption obs. 8=8335

Atmosphere—contd**precipitation—contd**

- NO_x ions, role in thunderstorm electrification 8=23290
radiation belts
 alpha particles, trapped in mag. field, OGO 1 obs. 8=2643
 betatron acceleration by geomag. storm, adiabatic 8=2645
 cosmic ray cut-off rigidity, effect 8=20630
 and cosmic ray cutoffs, magnetosphere model 8=18960
 cyclotron instability limit allowing for wave absorption in ionosphere 8=18956
 cyclotron instability, nonlinear theory 8=18957
 diffusion, radial, of particles with arbitrary pitch angle due to extensive mag. disturbances 8=18962
 dose rate meas. graphs 8=23347
 electron lifetimes, 1 MeV, at mirror altitudes of 350, 500 and 750 km, calc. 8=18959
 electrons trapped in low L shell, 1962-1965 obs. 8=2644
 high-energy proton data, from Telstar 1, stat. anal. and modeling 8=9955
 inner, Brazilian magnetic anomaly, proton components, Proton 1 and 2 data 8=18954
 inner, electron flux and spectra following Starfish test, satellite obs. 8=9953
 inner, energy fluxes of low energy protons and positive ions 8=23348
 inner zone electrons, temporal behaviour, 1965/66 Pegasus 1 obs. 8=23344
 ionospheric effects of e precip. 8=23360
 mag field study by means of belts 8=19028
 magnetosphere (B, L) coord. system allowing for distortion by ring current 8=23434
 magnetosphere v.l.f. emissions, discrete, gyroresonance model 8=2647
 outer boundary with zone of unstable radiation, location and props. 8=23345
 outer, disturbances rel. auroral irregular phenomena 8=993
 outer, electron energy spectra, Elektron 1 and 2 data 8=18953
 outer, high-latitude boundary, local time asymmetries, Alouette II data 8=18955
 outer at mag. equator, electron omnidirectional intensity contours 8=23350
 outer, proton diffusion 8=18964
 outer, proton events rel. to mag. bays in auroral zone, 1961 Explorer 12 obs. 8=2648
 outer, relativistic electrons, pitch angle diffusion obs. by Hitch-hiker I 8=2650
 α particles, geomag. trapped, Injun 4 obs. 8=18961
 particle motion in dipole field, mag. moment adiabatic invariant 8=2649
 precipitation of low-energy particles at high latitudes results of satellite meas. 8=9954
 proton motion in geomagnetic trap 8=9958
 proton whistlers, dispersion, Injun 3 and Alouette 1 data 8=18958
 protons and electrons, differential energy spectra rel. to mag. field, OGO 3 obs. 8=2646
 storm, polar, trapped particle accel. Explorer 26 obs. 8=23349
 storm-time, rel. to magnetic and auroral substorms 8=19046
 trapped electrons, low-altitude, boundary collapse in mag. storms 8=14656
 trapped flux, processes and future levels 8=23346
 Van Allen boundaries and electron increases beyond boundary from IMP-B satellite 8=9956
 Van Allen electrons scattering by e.m. transverse waves travelling along mag. field 8=18965
 Van Allen, energetic electrons by satellite obs. 8=2651
 Van Allen, proton meas., electron contamination 8=9957
 Van Allen, r.f. synchrotron radiation 8=14654
 Van Allen zone, outer, intensity maxima, position depend. on electron energy 8=14655
 H and charged particles, interaction and consequent Lyman α emission 8=18963
radioactivity
 See also Fallout.
 I adsorption by atmos. particles 8=9892
 aerosol transport across trade wind inversion at Hawaii 8=9896
 aerosols and vapours, mass transfer, appl. to travel of spores and pollen 8=23298
 α -activity meas. for environmental surveys 8=16013
 fallout, north east Pacific ocean 1961-62, particles sinking rate 8=14633
 in layer above ground, emanation vertical propag. theory 8=9894
 thermonuclear explosion γ -glow 9 July 1962, riometer obs. validity 8=14636
 Be⁷ over Australia, 1965 obs. 8=23299
 Br⁸⁷, γ and β rays 8=2611
 C¹⁴, excess deposit after nuclear explosion, decay calc. 8=2610
 C¹⁴ prod. by cosmic ray processes, obs. 8=20620
 CO₂ from troposphere, C¹⁴ content obs. 8=2566
 Cd¹⁰⁹ in USSR from Jan. 1964 to June 1966 8=23302
 Rn decay products, conc., seasonal variation 8=5794

Atmosphere—contd

radioactivity—contd

- Rn exhalation changes, rel. to changes in conc. and of decay products 8=9891
 Rn²²⁰ and prods. 8=9893
 Rn²²² distrib. over Atlantic, Antarctic and Paris 8=14635
 Sr90, global budget, implications of changes 8=14634
 Th exhalation changes, rel. to changes in conc. and of decay products 8=9891
 W¹⁸⁵ distribution and stratospheric transport processes 8=23300

structure

- Hartree-Fock eqns. solns., stability conditions 8=16174
 troposphere, from radio data 8=2603
 O₃ vertical distribution, troposphere and stratosphere obs. 8=18853

temperature

- and cosmic ray intensity var. 60 m.w.e. underground, London 8=11678
 equilibrium gradient 8=9824
 equilibrium gradient, rel. to discussion 8=9826
 freezing level altitude by radar obs. 8=9856
 and geomag. disturbances 8=10051
 mesosphere from O₃ microwave spectra 8=23258
 radiative heating, meas., in surface layer 8=23261
 solar-terrestrial physics, The Inter-Union Symposium Belgrade, 1966 8=10325
 at South Pole, rel. to O isotope ratio in snow and firn 8=23227
 spectra, one- and three-dimens., comparison 8=9848
 stratosphere, rocket altitudes, height-lag correlations of density with press. and temp. 8=23255
 stratospheric profile from O₃ microwave spectra 8=23256
 stratosphere, radiometric meas. from Tiros VII rel. to circulation 8=18858
 temperature grads with heat flux equal to zero 8=9825
 troposphere and solar wind 8=18850
 upper, neutral, response of F2 region to changes 8=10018
 upper, optical meas. 8=9925
 H⁺ ionosphere, determ. from proton whistlers 8=23356
 O₃ absorption lines, equivalent width obs. 8=2577

thermodynamics

- boundary layer, momentum rel. heat vertical transfer 8=14584
 earth i.r. radiation rel. to zonal and eddy available pot. energy generation, obs. 8=23262
 heat conduction waves propag. 8=2614
 heat, water vapour and momentum transfer in lower 8=14583
 latent heat exchange with ocean in low latitude synoptic scale systems 8=9828
 lower layers, model for two-dimens. heat and mass transfer 8=23267
 thermally stratified surface layer flux-gradient relations 8=23259
 thermobaric seishes, origin 8=9827
 H₂O vapour and heat turbulent transport in unstable atm., obs. 8=23260

upper

- acoustic-gravity waves, due to nuclear explosion and to earthquake 8=14641
 alpha particles trapped in geomag. field, OGO
 auroral-zone precipitation event, simultaneous balloon and satellite obs. Sept. 20, 1963 8=9944
 boundary layer, l.f. limit of inertial subrange 8=9906
 bow shock compression, IMP 2 and OGO 1 simultaneous obs. 8=23329
 chemi-ionization, model 8=23307
 composition above 100 Km mag. deflection mass spectrometer obs. 8=9901
 concepts, definition and explanations, review 8=18911
 conjugate photoelectron flux onset timing, solar cycle variation, from 6300 Å and Te obs. 8=23331
 corpuscular heating effect near sunspot max., Explorer 6 obs. 8=18915
 cosmic ray secondary electrons, flux and energy spectrum calc. 8=11669
 cosmic ray shower production of combined optic and e.m. pulse 8=3750
 counter-electrojet in equatorial latitudes 8=2642
 current system and polar mag. disturbances, IGY winter obs. 8=23442
 current systems, quiet day, of solar-diurnal mag. vars., construction by graphic integration 8=19039
 densities at high altitudes from satellite accelerations 8=5832
 density changes, 140-160 km, from solar X-ray absorption obs. 8=9900
 density, by low altitude satellite drag 8=14640
 density at 100 km altitude, variations meas. by Thompson scattering 8=18912
 density, satellite magnetron ionization gauges 8=16733
 density, semi-annual var. near 200 Km, 1966-67 8=23306
 density variations at 280 km from satellite air drag 8=5797
 density, var. rel. to heating, and geomag. var., satellite drag obs. 8=14695
 density var., semiannual, analogy with mag. activity var. 8=10035

Atmosphere—contd

upper—contd

- density var. near 150 km, satellite obs. 8=18913
 dust layer at 85 km, optical radar evidence 8=23309
 e and ion accel. by mag. solitary waves 8=2620
 electrojet current layers, equatorial, explanation of formation 8=9952
 electrojet, equatorial, latitude movements possible cause of ionospheric drifts 8=19016
 electrojet equatorial Sq currents, S. America IGY obs. 8=2640
 electrojet equatorial Sq currents on individual quiet days, obs. 8=2641
 electrojet, equatorial, in India, prelim. results 8=18948
 electrojet, Indian equatorial, 1958 and 1964 8=9949
 electrojet, seasonal movement over India 8=9950
 electrojet, seasonal movement over India 8=9950
 electron beam attenuation at different levels 8=18972
 electron conc. diurnal vars. and temp. changes, 160-200 km 8=23355
 electrons in earth's magnetotail, obs. by Vela satellites 8=23431
 electron flux at synchronous altitude, variations, ATS-1 obs. 8=18924
 exosphere plasma conc., hydromag. sounding 8=23314
 exospheric density var. near 1100 km from satellite orbits calc. 8=18914
 fluorescence, molecular, accompanying the twilight injection of triethylborane 8=9926
 geomagnetic bays as superposition of effects due to Hall current system and westward electrojet 8=19047
 geomag. field-solar wind boundary, appl. of ideal-case analysis 8=7750
 geomagnetic neutral sheet acting as particle source by accelerating solar wind 8=2618
 geomag. tail detection by Luna 10 8=23313
 geomagnetic tail at 10³ earth radii, Pioneer 7 obs. 8=2748
 heat conduction waves propag. 8=2614
 hydromag. emissions (Pc1), narrow band, nature and origin 8=10048
 hydromagnetic toroidal resonance, math. viability 8=2723
 infrasound spectra of rocket flight and take-off 8=197
 ionospheric irregularities, large scale, radio interferometer obs. 8=9986
 ionospheric winds, nocturnal variation from gun projectile luminous trail obs., Barbados 8=2683
 ion-temp. and relative composition, low altitude polar satellite obs. 8=18919
 magnetic tail, IMP 3 rel. to Lunik 10 obs. 8=23315
 magnetosheath, mag. noise of freq. 3-300 Hz, OGO 1 obs. 8=2621
 magnetosheath, shock aligned mag. oscills. 8=9920
 magnetosheath, structure and pulsations at 18 earth radii, Vela 3 obs. 8=2744
 magnetosphere, anomalous charged-particle diffusion 8=2625
 magnetosphere, attached 2nd standing shock wave 8=2624
 magnetosphere, balloon obs. 8=23319
 magnetosphere, bulk motion and associated elect. field 8=9919
 magnetosphere, closed, neutral points on boundary 8=9911
 magnetosphere, convection limitation by ionospheric dissipation 8=9918
 magnetosphere, deformed, charged particle motion by Stormer theory and Euler pots. 8=14644
 magnetosphere, elect. field generation and auroral particle acceleration 8=18930
 magnetosphere, elec. field meas. with probes, necessary conditions 8=9907
 magnetosphere, excitation by solar wind 8=9923
 magnetosphere, guided propag. of Alfvén waves 8=23327
 magnetosphere, importance and theory of elec. fields 8=9914
 magnetosphere, interaction of moon with 8=2815
 magnetosphere ionization density profiles and whistler propag. 8=9909
 magnetosphere at L = 5, electron response rel. to solar wind during April 17-18, 1965 storm 8=23321
 magnetosphere, lower, electron concentration diurnal var. from lunar radar echo obs. 8=23326
 magnetosphere, mag. field merging across neutral sheet 8=23323
 magnetosphere, meas. of elec. fields 8=9913
 magnetosphere meas., high-latitude, rel. to closure of auroral electrojet circuit 8=9951
 magnetosphere, m.h.d. resonances, guided poloidal mode 8=350
 magnetosphere m.h.d. waves rel. sudden mag. storm commencement 8=10043
 magnetosphere, model experiments 8=12465
 magnetosphere, neutral sheet, position and shape 8=18926
 magnetosphere, night-time, origin of v.l.f. auroral hiss 8=5801
 magnetosphere, nondipole part of geomag. field influence on boundary 8=18932
 magnetosphere, one-dimens. model of transition layer, motion of charged particle 8=14645
 magnetosphere, outer, coupling with ionosphere, depend. on geomag. field topology 8=9910

Atmosphere—contd**upper—contd**

magnetosphere, outward plasma flow in tail after negative geomag. bays, Vela 2 obs. 8=18928
 magnetosphere, particle energy storage and higher-order ring currents 8=18927
 magnetosphere, planetary, magnetized plasma partial corotation 8=14834
 magnetospheric plasma, collisionless, viscosity in weakly turbulent mag. field 8=18929
 magnetosphere plasma resonances, axially symmetric modes obs. 8=9922
 magnetosphere props. from OGO 1 whistler obs. 8=23322
 magnetosphere, proton escape 8=9958
 magnetosphere, proton events rel. to auroral mag. bays, 1961 Explorer 12 obs. 8=2648
 magnetosphere, separable case of poloidal m. h. d. resonances of plasma 8=18925
 magnetosphere, solar-atmos. reaction times, accentuation rule and variations 8=18931
 magnetosphere, solar cosmic ray injection 8=23721
 magnetosphere, solar ejected plasma interaction, lab. analog 8=2622
 magnetosphere-solar wind interact, scaling for model plasma gun-terrella expts. 8=14643
 magnetosphere and tail, proton flux Explorer 33 obs. 8=23324
 magnetosphere, trapped radiation shells, and cosmic ray cutoffs, model 8=18960
 magnetosphere v.l.f. emissions, discrete gyroresonance model 8=2647
 magnetosphere, whistler mode propag., effect of longitudinal elect. field 8=19008
 magnetospheric ionization, 1.9 to 2.6 Re, from whistler radio records, 1957-1966 8=23317
 magnetospheric particle motion, appl. of model 8=23343
 magnetospheric plasma, flow past satellites nonmagnetized lab. simulation 8=12475
 magnetospheric tail, associated mag. storm effects 8=9912
 magnetospheric tail, electrons within neutral sheet 8=23320
 magnetospheric v.l.f. noise triggering by 60 watt transmission 8=23325
 magnetospheric v.l.f. propag., France to S. Africa 8=9915
 magnetospheric waveguide propagation along field aligned irregularities 8=18986
 mapping of earth's bow shock and mag. tail by Explorer 33 8=23430
 meteoritic dust, detection from sounding rocket 8=18918
 micrometeor flux at 60 to 145 km, rocket obs. 8=2829
 neutral motions, review 8=18921
 oscillations, interactions between 8=23310
 particle asymmetries, local-time, ATS 1 synchronous orbit obs. 8=9916
 physics, book 8=23305
 plasmopause down minimum equatorial distance rel. to mag. activity, obs. 8=2747
 plasmopause, shape, location and rel. to 3 hr K_p index, IMP 2 obs. 8=9917
 polar cap absorption, anomalous separation into 2 types 8=10407
 pressure meas., airstream adsorption errors 8=5838
 processes and solar optical radiation, review 8=18910
 properties from satellite orbits 8=5795
 protons, secondary, and re-entrant albedo from balloon and satellite obs. 8=3751
 radio scattering, incoherent, at perpendicular intersection with geomag. field 8=9983
 re-entry plasma stability near photoemission surface 8=7842
 rel. to ionosphere D-layer form., >40 keV e flux at ≤ 100 km 8=14680
 rotational speed rel. to orbital inclination of satellite calc. 8=18922
 rotational speed above 200 km 8=14642
 satellite lifetime rel. to density vars., nomogram 8=14711
 secondary electrons spectrum and intensity rel. to IMP-A data 8=7020
 sodium distribution 8=9903
 sodium, and stratospheric warning at high latitudes 8=18917
 sodium and stratospheric warnings at high latitudes, comments 8=18916
 solar proton precip. over poles, obs. of nonuniformity Feb. 1965 lat. 68° to 82°S 8=905
 space, neutron flux after PCN event of November 15, 1960, Atlas ballistic flight obs. 8=2623
 spectroscopic and photometric studies, Canadian survey 8=14639
 stratosphere, electron streams, riometer obs. 8=18951
 temp. and density from AIO trail obs., 105-165 km 8=2613
 temperature, optical meas. 8=9925
 thermal anisotropies, solar wind, Vela 3 and IMP3 obs. 8=10406
 thermosphere, acoustic-gravity waves, equation solved 8=2686
 thermosphere, middle and upper, wind system, deviation 8=9996
 thermosphere, spectral energy distrib. from grenade glow clouds 8=9924

Atmosphere—contd**upper—contd**

tides at 90 to 120 km from wind distribution obs. 8=18998
 topside, sunrise effect in summer, onset time and plasma temp. rise 8=23402
 triethylborane rocket injection, obs. of yellow-green luminosity 8=9904
 turbulence, energy balance 8=23311
 turbulence, energy balance 8=23312
 twilight layer noctilucent cloud, satellite detection 8=2626
 BO_2 emission from injection of triethylborane 8=23330
 H distribution, in thermosphere up to 800 km, solar cycle and diurnal variations 8=2615
 N and NO, distribution and lifetimes in 100 to 280 km 8=23308
 N_2^+ intensity distrib. among bands, obs. 8=18933
 Na, daytime distrib. and origin, 92.4 km 8=2616
 Na, meteoric origin 8=9902
 O, atomic, at 120 km, mass spectrometric meas. 8=18920
 O₂, 8mm absorption and emission 8=18934
 IMP-2, magnetosphere and near space, meas. of magnet. field, results 8=2832
 PCA, cosmic noise, midday recoveries 8=9969

Atmospheric acoustics
 acoustic-gravity waves, wind effects rel. to grandpress. 8=23303
 aerodynamic-acoustic theory, fluctuations, high-altitude 8=9905
 anomalous propagation of powerful signals 8=9898
 infrasound generated by nuclear explosion, period < 1 minute effect of wind structure on propag. 8=23304
 oscillations excited by surface waves 8=9899
 ray tracing in layered atmosphere, analogue computer solution 8=14637
 sound absorpt. rel. to humidity, pressure depend. obs. 8=23268
 standing wave in rigid-walled tube containing air, theory and obs. 8=21518
 stratified atmos., acoustic and gravity-wave emission by turbulent motions 8=23270
 thunder, dominant 200 Hz peak 8=18909

Atmospheric disturbances. See Atmosphere/movements; Thunderstorms.

Atmospheric duct. See Electromagnetic wave propagation.

Atmospheric electricity
 See also Atmosphere/radioactivity; Atmospheric; Aurora; Electromagnetic wave propagation/atmosphere; Ionization, atmosphere; Ionosphere; Lightning; Thunderstorms.
 auroral electrons velocity distribution 8=9945
 characteristics, indirect methods 8=9881
 contribution from sea water evaporation 8=4307
 charge transfer associated with temperature gradients in ice 8=14625
 counter-electrojet' in equatorial latitudes 8=2642
 distribution in thunderstorms, effect of particle interactions 8=18891
 electrode effect 8=9882
 electrojet, polar 8=18950
 electrojet current layers, equatorial, explanation of formation 8=9952
 electrojet, equatorial, in India, investigation Sep. (1958) 8=18948
 electrojet, equatorial, model involving meridional currents 8=18949
 electrojet, Indian equatorial, 1958 and 1964 8=9949
 electron fluxes at 1000 km, auroral substorms 8=18952
 electron-plasma interaction, v.l.f. noise bands 8=23291
 ionosphere electron content increases rel. to solar flares 8=18967
 lightning, interval between strokes and initiation of dart leaders 8=18888
 noise fluctuations affecting cm. wave radio-astronomy 8=18894
 point discharge during rapid field changes, rel. to pot. gradient and winds 8=9883
 radio pulses from extensive air showers, effect 8=7015
 S-current ascent and descent in intense and weak sunspot cycles 8=18968
 space charge meas., guarded double field meter 8=15163
 stratosphere, electron streams, riometer obs. 8=18951
 thunderstorm charge generation and separation model 8=2586
 thunderstorms, non-disruptive currents 8=2585
 transient effects caused by wire launched by mortar shell 8=14626
 v.l.f. spheric counting rates, Uppsala and Ankara 8=18893
 water drop discharge e.m. pulses, microwave superheterodyne receiver, epoch sensitivity 8=14624

Atmospheric optics
 See also Airglow; Sky brightness; Sunlight; Twilight.
 absorption of CO_2 laser radiation 8=6441
 absorption by H_2O vapour and CO_2 , i.r., over slant path 8=18879
 absorption at 1.15 μ of gas laser radiation 8=7935
 rel. to aerosol and condensation process, obs. 8=9834
 albedo from 2 colour photoelectric earthshine obs., S. Africa 8=2594

Atmospheric optics—contd

binary communications link, atm. scintillation rel. to bit error probability 8=9869
 brightness of multiply forward-scattered light 8=18885
 depolarization by turbulent inhomogeneities 8=14619
 extinction and absorpt. coeffs. from ocean spectro-photometry 8=9872
 glow clouds from explosion of aluminized grenades, spectral energy distrib. 8=9924
 haze, small-grained, characteristics 8=18882
 image propagated through turbulence, processing 8=9873
 images propag. through turbulence, max. likelihood processing 8=23288
 i.r. detectors of thermistor flake arrays immersed in Ge and Si lenses 8=9143
 laser beam, mode degeneration calc. 8=8067
 laser beam modulation by turbulence 8=404
 laser light absorpt., gaseous, as function of atm. pressure and methane pressure 8=9880
 laser light propag. and scatt. 8=18878
 laser scatter, mesosphere and above, obs. 8=9875
 light scatt. by air, ellipticity of polarization, rel. to aerosol microstruct. 8=9877
 light scatt. impulse in semi-infinite layer 8=9878
 light scatt. by surface layer, polarization phase functions 8=9876
 longwave rad., outgoing, influence of refraction 8=9889
 opacity from radio astronomy 8=2595
 particle density distrib., from spectral and angular data 8=18881
 photographic detectors, air to ground viewing, meas. of contrast and range 8=20126
 polar zodiacal light, terrestrial origin 8=5961
 polydisperse particles optical scatt., non-spherical randomly aligned 8=12942
 Rayleigh scattering, as function of altitude 8=18873
 refraction, corrections in surveying 8=23286
 refractive index differences, amplitude distrib., Deam refractometer obs. 8=2596
 refractive index gradient, optical meas. 8=9870
 refractive index of tropospheric layers 8=2603
 Rylov approximation, limitations of applicability 8=18883
 Rylov solution, multiple-scattering interpretation 8=18884
 scattered radiation at small angles, intensity aerosol spectrum 8=18880
 scattering, optical radar performance 8=9879
 scattering, small-angle, particle spectrum determ. 8=23251
 seeing, by resistance analogue obs. 8=14622
 scintillation, spiking probability calc. 8=18876
 solar disk flattening, obs. 8=2597
 thick layers, light transmission 8=6538
 transmittance at north pole of cold, i.r. and sub-mm obs. 8=9874
 transparency, anomalous and twilight vars., u.v. obs. 8=9871
 transparency, rapid determ. from obs. of sky brightness 8=18886
 turbulence, limitations on planetary photography 8=14835
 turbulence, validity of ray optical calc. 8=18877
 N₂ intensity distrib. among bands, obs. 8=18933

Atmospheric pressure and density

baroclinic wave disturbances, non-geostrophic effect 8=9845
 barometer with digital output 8=9832-3
 cosmic ray barometric coefficient calc. allowing for variations in primary spectrum and cut-off rigidity 8=909
 cosmic-ray intensity data, barometric correction 8=893
 density, exosphere, variations near 1100 km from satellite orbits 8=18914
 density at 100 km altitude, variations meas. by Thompson scattering 8=18912
 density var. near 150 km, satellite obs. 8=18913
 double wave rel. to moisture flux diurnal var. 8=2580
 at high altitudes, density from orbital drag coeff., computer estimation 8=2612
 isobaric surfaces in N. hemisphere, altitude changes after solar flares 8=18923
 magnetron ionization gauges for neutral particle density, press. conversion consts. 8=7958
 orbiting gauges, airstream adsorption errors 8=5838
 pressure changes at ground level due to nuclear explosions 8=2721
 sound absorpt. with varying humidity, effect 8=23268
 strato-mesospheric, from hypersonic sphere obs. 8=9831
 stratosphere, rocket altitudes, height-lag correlations of density with press. and temp. 8=23255
 tropospheric responses to chromospheric flares, search 8=23257
 upper, density, semi-annual var. near 200 Km, 1966-67 8=23306

Atmospheric spectra

See also Atmospheric optics.
 airglow, night 3100-10 000 Å 8=23333
 i.r. absorpt. of minor constituents above 30 km, meas. with diffusing system 8=9840

Atmospheric spectra—contd

5577 and 6300 Å regions using a prism grating spectrometer 8=5966
 5577/3914 Å intensity ratio, in auroras, mechanism explaining obs. 8=5800
 m.m. and sub m.m. spectral range, rel. to absorpt. by water vapour 8=9865
 molecules in mesosphere, temp. determ. 8=23258
 particle, calc., by small-angle scatt. pattern 8=23251
 Raman scatt., pulsed N₂ u.v. laser obs. 8=23289
 reflected solar, and emitted thermal rad. of natural surfaces and clouds, 1.6 to 5.4 μ 8=9866
 sky temp., apparent, at mm wavelengths 8=2593
 1 mm to 130 μ obs. aboard aircraft at 40 000 ft. 8=9863
 BO₂ emission from injection of triethylborane 8=23330
 Na in dayglow rel. to atmospheric distrib., 92.4 km 8=2616
 O₂, 8mm absorption and emission 8=18934
 O₂ equivalent width, atmospheric temp. determination 8=2577
 O₂ microwave emission, stratosphere, and temp. profile deduction 8=23256
 O₂ microwave, mesosphere, means of temp. determ. 8=23258
 O₂, microwave, satellite obs. to obtain vertical sense 8=2762
Atmospherics
 auroral zone, 0-30 kHz hiss, morphological obs. 8=18947
 e.l.f. attenuation rates, nonreciprocal, from slow tail obs. 8=9890
 e.l.f. slow tail waveforms, direction dependence, nocturnal obs. 8=9982
 e.l.f. and v.l.f. radio noise and lightning currents, amplitude statistics 8=2602
 fluctuations affecting c.m. and m.m. wave radio-astronomy 8=18894
 ionospheric reflection type, amplitude spectra 8=9977
 lightning corona currents and e.l.f. emissions 8=2598
 nocturnal, amplitude spectra, 70 Hz to 30 kHz 8=18994
 phase spectra, 1-20 kHz, and freq. rel. to source distance 8=2600
 precursor whistler generation obs. 8=18895
 proton temp., ionosphere, determ. from whistlers 8=23356
 sun, lower chromosphere, CaII and MgII lines 8=2859
 thunderstorm sources, book 8=19005
 u.l.f. radiations, depend. on mag. bays and state of ionosphere 8=9971
 v.l.f., long period fading 8=14628
 v.l.f. spheric counting rates, Uppsala and Ankara 8=18893
 whistlers in low latitudes, dispersion and occurrence freq. in IGY 8=2601
 whistler propag. and magnetosphere ionization density profiles 8=9909
 whistlers, subprotonospheric 8=23373

Atomic beams

See also Particle velocity analysis.
 alkali metals, g factor determ. 8=12089
 for coherent light prod. of stable freq., theory 8=6438
 reflection from crystal surface, rel. to surface micro-structure 8=13201
 time-of-flight velocity analysis 8=16379
 Ag, electron-impact ionization cross-sections 8=12429
 Ar, secondary electron emission from gas-covered surface 8=22731
 Ba, electron excited, lifetimes and light emission polarization 8=21019
 Cs, scatt. by benzene and cyclohexane, comparison 8=1205
 Cs, surface ionization on W and Pt, temp. depend. 8=12110
 F, interaction potentials with inert gases 8=12104
 H, control of excited state distrib. 8=21276
 H, prod. by thermal dissociation, dissociation temp. var. 8=7474
 H, photoionization 8=21020
 H, polarized source, atomic conc. from H₂ dissociation in h.f. discharge 8=21018
 H, ZnO crystal change in surface conductivity 8=7475
 K lamp, line shape dependence on current 8=15523
 K, scatt. by benzene and cyclohexane, comparison 8=1205
 K, surface ionization on W and Pt, temp. depend. 8=12110
 N, photoionization 8=21022
 Na, scatt. from polyat. gases, quenching of glory undulations 8=7633
 Na, scattering by Cs beam, total elastic cross section, vel. depend. 8=21091
 O, interaction potentials with inert gases 8=12104
 O, photoionization 8=21021
 Rb, scatt. by benzene and cyclohexane, comparison 8=1205
 Rb, surface ionization on W and Pt, temp. depend. 8=12110
 Tl, surface ionization on Pt and oxide-coated W 8=12110

Atomic clocks. See Time measurement.

Atomic frequency standards. See Time measurement.

Atomic mass and weight

See also Isotopes; Mass spectra.
 coriolis coupling in ethylene type mols., effect 8=4195
 Fe⁵⁶-Fe⁵⁷ mass difference, from mass-spectroscopic and reaction Q-value analysis 8=21017

Atomic orbitals. See Atoms/structure; Orbital calculation methods.

Atomic scattering factors. See Crystal structure, atomic; X-ray crystallography; X-ray scattering.

Atomic spectra. See Spectra/atoms.

Atoms

See also Atoms, mesic; Elements; Nucleus; Positronium.
advances in atomic and molecular physics,
book I and II 8=16171-2
alkali ion scatt. at He atoms 8=7464
alkali-metal, optical orientation rel. to meas. of weak
mag. fields 8=20934
alkali metals, long-range interactions 8=12108
in anharmonic crystals, mean-square velocity 8=13035
atom-diatomic mol. collision, compound state
resonances 8=4255
atomic ensemble, quantum statistics of multi-mode
radiation 8=19452
collision problems, slowly converging radial integrals,
evaluation 8=21003
collision processes rel. to astrophysics 8=16230
collision processes rel. to planetary atmospheres
phenomena 8=14832
collisions, 3 body, rearrangement for high energies, linear
model 8=16228
concentration for line with complex structure using
reabsorption method 8=4051
coupled bimodal system, photon cross correlations 8=12102
dark-filled images form by electron microscope, nearly
incoherently illuminated 8=1145
diamagnetic susceptibility calc. and temp.
dependence 8=18294
discharge-flow system, and free radicals, reactions 8=9700
dynamic polarizability, coupled and uncoupled approx.
for many open shells 8=7368
earth-ionosphere cavity resonances 8=2608
e capture p impact on He, Ar, Ne, N₂, H₂, C₂, with transition
to 3s, 4s states of H, obs. 8=7462
e capture in He⁺-He collision, with excitation,
probability calc. 8=7463
electron affinity, rel. to reaction rates 8=14357
electron-impact ionization, empirical formula 8=1351
electron spectroscopic method for study 8=16180
electronic energy calcs. by modified local-energy
method, reliability 8=1146
electrons interact. in infinite square well, quantum
mechanics 8=3403
e quadrupole moment induced by nuclear quadrupole
moment, hyperfine structure effect 8=7402
energy calc. by method of local moments 8=12025
exchange energy in SCF method, using non-orthogonal
basis functions 8=4046
exchange interactions in different perturbation
formalisms 8=12361
exchange interactions, three- and four-atom, in Gaussian
effective-electron model, perturbation anal. 8=21793
exchange interacts, Schrödinger perturb. formalism 8=4256
excited states, press. shift in gaseous medium 8=4052
interact. of 2 not in ⁴S state, elastic and resonant
exchange cross-sections 8=4104
interactions, second-order three-body, with Gaussian
wavefronts 8=7457
interaction potentials for different electron
distributions 8=7456
inert gases, interaction potentials with O and F
atoms 8=12104
ion transport in solids, under conditions including large
elec. fields 8=21813
isoelectronic systems, phys. props. rel. to electronic
config. for excited states 8=1148
linear chain, fast vib. excited mol. collision, exchange
energy and momentum loss 8=16381
Long-range interatomic forces 8=12232
low Z, asymptotic reln. between press. for Thomas-Fermi
and Thomas-Fermi-Dirac models 8=1151
magnetic, ground state spin in non-mag. metal
host 8=16991
many-electron problem, perturb. theory from Hirschfelder
eqn. 8=7369
in masers, photons interaction with atoms with angular
momenta 8=19921
metal ion promoted atom-transfer oxidation-reduction
reactions 8=14401
metals in flames, detect. by atomic fluoresc. 8=14460
metals, radii calcs. from shock-wave eqn. of state
meas. 8=8225
multiphoton absorpt., laser and thermal light relative
prob. 8=20975
one-electron wavefunctions, simple approx. 8=1156
1¹S state of two-electron isoelectronic series, lower
bounds for energy-eigenvalues comment 8=1150
orientation by superposition of interactions separately
not orienting 8=7374
periodic table and atomic props. 8=20918
polarizability calc. for e systems with several open
shells 8=1142
polarizability increase by induced deformation, new
nonlinear effects 8=20910
positronium atom conversion on O₂ and NO 8=7476
primary, distrib. function for total paths 8=7365

Atoms--contd

quantum orbital calc. using convolution theorem 8=1228
in radiation field, coupled, correlations 8=19458
radiation propagation in a resonance medium 8=21000
rare-earth ions, electric multipole interactions 8=16977
recoil accompany α -emission, charge 8=16014
retarded interaction energies between like atoms in
different energy states 8=21006
r. f., l. f. and v. l. f. radio propagation, conference,
London, England (1967) 8=14671
rigidity of gyromagnetic prop., eqn. of motion 8=4047
scattering, from continuous media 8=2017
scattering, iteration-variation convergence methods 8=7454
scattering, light, three-photon, in fluids 8=4044
screening effect on internal conversion decay 8=15946
6-12 gas-atom-solid atom pairwise model rel. to gas-solid
interaction 8=8332
in solids, energy loss and range of energetic,
neutral 8=13469
solids interatomic forces, moderately long-range
and meas. 8=16993
space quantization of ang. momentum, simple Stern-
Gerlach apparatus 8=1144
spontaneous emission, line shape for imperfect mixing
of degenerate levels 8=4049
Stark effect consts, quadratic, computation for 8
elements 8=20935
S-state, dipole polarizabilities, bounds, from oscillator-
strength sum rule 8=7373
stimulated rad. during interact. of cascade
transitions 8=417
terminal position determ. by X-rays, rel. to charge
distribution effect 8=1261
with three energy levels, 1-dimens. medium, polychromatic
scatt. of radiation 8=16186
two-photon processes in 2-level system, photon field
statistics 8=20948
Van der Waals coeffs. bounds from Padé approxi-
mants 8=16229
Van der Waals constant for atom-atom force, self-
consistent calc. 8=21002
van der Waals forces, macroscopic, macroscopic
derivation 8=4105
van der Waals interactions, dipole-dipole term
calc. 8=7550
vibrations, thermal, rel. to X-ray anomalous
transmission 8=13222
weak interactions, new perturbation procedure 8=12103
X-ray scatt., He atomic form factor 8=12053
Al, distribution of sputtered atoms by electron micro-
probe 8=21876
Ar-like ions, phys. props. rel. to electronic config. for
excited states 8=1148
Ar and Kr, multielectron ionization in close collisions
with Ar⁺ and Kr⁺ ions 8=21012
CO, interaction energy for 6³ Σ state 8=4109
Cu, p-irradiated, platelets of interstitial atoms rel.
to dislocation loops 8=22202
Fe, ground state, universal potential field calc. 8=20952
H, α -particle capture of electrons, collision
process 8=12101
H, coherent elastic scatt. of photons 8=7379
H, energy of interact. in ground-state, by Gaussian-
type functions 8=1198
H, ground state, differential polarizability 8=12048
H, long-range interact., appl. of electrostatic Hellman-
Feynman theorem 8=1197
H⁺ or H⁺ + H⁺ fluxes, 1-10 keV, an energy independent
detector 8=7381
H-fast H⁺ and He⁺ collision processes rel. to
astrophysics 8=16230
H⁺ on Kr scattering, charge transfer 8=1203
H, quantum-mechanical treatment without complicated
mathematics 8=12046
H, relax. of F = 1 level of ground state, appl. to H
maser 8=12049
He³, gas, nucl. spin relax. by surface interactions
suppression 8=1160
He⁴, Ramsauer-Townsend effect 8=1200
He isoelectronic sequence multipole polarizabilities 8=16199
He sequence, 1s²S-1snp¹P transitions, calc. 8=7388
H-H interaction pot. using isotope effect in dissociative
attachment 8=21075
He-He interaction, quantum calc. 8=4110
He-He interaction, SCF-MO approx. 8=21013
He-Li⁺ interaction energy at small internuclear
distances 8=21014
Hg, 6s6d levels, collision cross-sections with inert
gases 8=1201
MnHg, atomic thermal vibration amplitudes at 298°K 8=8236
N-(p-bromophenyl) benzene sulphonamide, intramolecular
van der Waals interactions 8=1278
Ne, metastable, conc. in glow discharge at low
temp. 8=1368
Ne-like ions, phys. props. rel. to electronic config. for
excited states 8=1148
O, charge distribution effect on terminal position determ.
by X-rays 8=1261
Pd fission fragments, highly ionized, electron binding
energies 8=1112

toms—contd

- RaA, charged capture metal disk 8=1370
 Rb, optically pumped, relax. in collisions with Kr atoms, correl. times 8=7472
 $^{15}\text{S}_0$ systems, magnetoelectric susceptibilities 8=4053
 Sm fission fragments, highly ionized, electron binding energies 8=1112
 Sn, on silica gels and zeolite, states and dynamics 8=16912
 Sr fission fragments, highly ionized, electron binding energies 8=1112
 Tl, oscillator strengths for np, \rightarrow ms $_{1/2}$ and np \rightarrow md transitions 8=4086
 Xe fission fragments, highly ionized, electron binding energies 8=1112

electron scattering

- alkali metals, neutral atoms 8=1190
 atomic props. investigation, periodic table investigation 8=20918
 collision processes 8=12091
 elastic, ang. and energy depend. of Mott polarisation at 100–2000 eV 8=7439
 elastic scatt. amplitudes calc. for Z = 1 to 54 8=4100
 in electron-avalanche, impacts of second kind on excited atoms 8=21243
 excitation and ionization study using Coulomb wave approx. 8=7427
 40–100 keV electrons, amplitudes for atoms in solids 8=13240
 Gell-Mann-Goldberger theory 8=12420
 integral expressions for scattering amplitudes 8=20989
 long-range interaction, dominant nonadiabatic contrib. 8=12092
 low energy, relativistic effects by Fredholm method 8=1189
 optical pot., partial wave expansion 8=20992
 plasma, ion line width shifts 8=12511
 quasi-free, of low and middle-energy electrons 8=12093
 Rydberg states excitation 8=20970
 subshells, incomplete of any number, h.f. approx. calc. 8=12094
 variational methods of Hulthén, Kohn and Malik comparison 8=7448
 Ar, $(3p^4s)^3P_1$, lifetime obs. 8=1164
 Ar, 40 keV gas electron-diffr. 8=7447
 Ba, Rydberg states obs. 8=20941
 Ca, Rydberg states obs. 8=20941
 Cd I, $5^3P_{0,1,2}$, effective cross sections 8=20993
 H, correlation method for extension of S-wave to higher partial waves 8=7441
 H, elastic resonance 8=16222
 H, exchange scattering amplitudes 8=12090
 H, excitation analysis using many-channel resonance theory 8=7443
 H, excitation to n = 2 level, theory and expt. 8=7442
 H, low energy, expansion approach 8=20994
 H, in 1s state, e-impact ionization cross-section obs. 8=21273
 H, in magnetic bottle for prod. of polarized e beam 8=15304
 H, positronium formation in e⁻-H, field theory cross-section calc. 8=16223
 H, simplified second Born approx. 8=20996
 H, six-state close-coupling at low energy 8=7440
 H, variational methods of Hulthén, Kohn and Malik, comparison 8=7448
 H, zero-energy positrons, elastic scatt 8=20995
 H, e-H compound states, 5 parameter wave function for lowest two 8=20997
 He, atomic form factor and incoherent-scatt. function 8=12053
 He, differential and total cross-sections, 100–400 KeV, Born approx. anomaly 8=16218
 He, excitation of 2^1P and 2^3P states 8=7446
 He, positron annihilation in gas 8=20998
 He, zero-energy positrons, elastic scatt 8=20995
 Hg, angular distribution and spin polarization, influence of plural scatt. 8=16225
 Kr, 40 keV gas electron-diffr. 8=7447
 Mg, Rydberg states obs. 8=20941
 Ne, 40 keV gas electron-diffr. 8=7447
 Ne, transition between levels, excitation 8=20947
 O, polarization effects, and photodetachment from O⁻ 8=4101
 Si II, inelastic, collision contributions to ion linewidths 8=20991
 Sr, Rydberg states obs. 8=20941
 Xe, 40 keV gas electron-diffr. 8=7447

excitation

- alkali-metal, cross sections for fine-structure transitions in adiabatic collisions 8=4106
 alkali metals, by electrons, first threshold 8=1190
 alkali metals, by low energy electrons, absolute cross sections 8=12087
 alkali metals 2P , fine structure transitions in adiabatic collisions, calc. 8=1162
 alkali-metal, thermal, and deactivation, in inert gas atmosphere 8=12088
 alkalis reson. states lifetimes, inert gases and vapour press. effects 8=20976

Atoms—contd

excitation—contd

- anticrossing signals from $6s^1P$, level 8=16211
 atomic collisions, molecular-orbital theory 8=7451
 broadening of spontaneously emitted line in presence of laser beam 8=12040
 coherent and incoherent, magnetization equations 8=121
 decay of excited states, lineshape of double resonance signals 8=7428
 depolarization cross-section in medium 8=4089
 echoes, radiative 8=3274
 electron-atom collisions, threshold cross-sections 8=12077
 electron impact, Coulomb wave perturbation theory 8=7427
 electron impact, determ. of excited state lifetimes 8=7429
 electron and proton collisions, classical adiabatic perturbation theory 8=7460
 e scatt., Gell-Mann-Goldberger theory 8=12420
 energy, average, of states of given multiplicities 8=12034
 energy levels, perturbation by e.m. wave 8=7375
 fluorescent X-rays from γ -irradiated target, absolute yield meas. 8=23039
 forbidden lines, $2p^3$, $2p^4$, $3p^2$ and $3p^4$ isoelectronic sequences 8=12076
 free-free transitions, survey of theoretical results 8=11454
 by h.f. discharge, orientation of excited states 8=16215
 p impact induced, ID model 8=20152
 interaction, perturbation theory for exchange forces 8=4043
 laser, ionization photoelectron counting statistics, quantum theory 8=20987
 laser, spontaneous emission, polarization 8=7430
 lifetimes determ. by single-photon counting 8=7429
 lifetime of excited-states, meas. by Hanle effect 8=1181
 long-lived highly excited, collisional ionization 8=4303
 metallic target, electron emission by Auger de-excitation of atoms by sputtering 8=5422
 by modulated light, modulation of absorption of resonance emission 8=20972
 noble gases, lifetime of at. excited levels by time analyser 8=20926
 optical lifetime obs., using positive ion Van de Graaff accelerator 8=16183
 optical pot. in terms of self-energy of single particle Green's function 8=20992
 optical, by simultaneous beams, step-wise fluoresc., coherency matrix calc. 8=20974
 oxygen, $^5S^0$ metastable state 8=1304
 photoelectric effect, multiquantum, and laser coherence meas. 8=20986
 plasma, distrib. eqns. and solns. 8=7730
 population and r.f. coherence transfer by spontaneous emission 8=16220
 radiative transitions, retarded pot. calc. of probability 8=16212
 resonance fluorescence, applic. of projection-operator decay theory 8=11262
 secondary radiation, theory of intensity beats 8=12078
 silver halides, optical absorpt. spectra of transitions of Ti^{3+} and Fe^{2+} , Jahn-Teller effect 8=14193
 spectrum of linear chain of paramag. atoms with spin-phonon interaction 8=20977
 spontaneous emission from a system of 2 level atoms interacting with relaxation mechanism 8=20971
 three-level system, obtaining inverse repopulation of levels 8=20924
 Ag, Rydberg state by e collision 8=20970
 Al II, III, beam-foil excitation spectra 8=12079
 Ar, to ground and excited states of Ar⁺, cross-sections 8=21267
 Ar, Rydberg state by e collision 8=20970
 Ar I, mean lives of some 4p levels 8=4069
 Ar I, transition probabilities in intermediate coupling 8=12055
 Ba, electron excited, Rydberg states 8=20941
 Ca, electron excited, Rydberg states 8=20941
 Cd, decay of excited states, lineshape of double resonance signals 8=7428
 Cd $5^3P_{0,1,2}$ levels lifetimes and transitions, obs. 8=1183
 Cd I, $5^3P_{0,1,2}$ electron excitation, effective cross sections 8=20993
 Cu, $1s^2s^2p^3s^2p^3d^4f$, universal potential field calc. 8=20952
 Fe XVII, electron impact, Coulomb-Born calc. 8=12081
 Ga V, $3d^9$ – $3d^84p$ transition spectra 8=12082
 Ge, As and Sb impurities, spectra, under uniaxial compression 8=13424
 Ge, Auger electrons, energy spectra, surface contamination detection 8=1688
 Ge VI, $3d^9$ – $3d^84p$ transition spectra 8=12082
 H, by e scattering, excitation to n = 2 level 8=7442
 H, by e scattering, resonances analysis 8=7443
 H, elastic resonance in electron scattering 8=16222
 H, Lyman- α prod. by electron collisions on H₂ 8=12050
 H, $1s \rightarrow 2s$ and $1s \rightarrow 2p$, by e and p impact 8=20996
 H(1s, 2s, 2p) in electron capture reaction $\text{H}^+ - \text{He}(1s^2)$ 8=7465
 H, Balmer- α line, by electron impact, cross section and polarization meas. 8=20979

Atoms—contd

excitation—contd

- H*, highly excited, production by H_2^+ and H_3^+ passing through Ne, H, Na and Mg 8=21082
 H, by scattering, correlation method analysis 8=7441
 H-C collisions, levels 8=1193
 H-O collisions, levels 8=1193
 H, 2^1 -pole oscillator strength sum rules 8=7380
 He, adiabatic exchange approx. calc. 8=7434
 He aligned depolarization of resonance fluorescence when in Zeeman rf field. 8=20982
 He, by electron impact, determ. of excited state lifetimes 8=7429
 He, by 100-400 eV electrons, cross sections rel. to Born approx. 8=16218
 He, 4^1P to $4F$, evidence by population studies of $4F$ state 8=12054
 He-like, Hartree-Fock equations for $1s2p$, 3p and 1P states, perturbation treatment 8=20921
 He, in hollow cathode, balance eqns for 2^3S , and 2^3P levels 8=20981
 He, impact of H^+ , D^+ , H_2^+ and H_3^+ 8=16217
 He ionization by e impact, cross-section calc. 8=12084
 He, metastable, Penning ionization of gases 8=21258
 He, metastable states, dipole props. 8=20980
 He, from metastable 2^3S He, cross-section 8=4055
 He, by fast protons and H atoms 8=7433
 He, n^1S , n^1P , n^1D states by 0.15-1 MeV p bombard. 8=7384
 He, para- and ortho-, ratios of cross sections 8=7431
 He⁺, $2s$ state, close-coupling calc. of electron-impact 8=4091
 He⁺, $2s$ state, electron-impact expt. 8=4092
 He, 2^1P and 2^3P states by e scatt. 8=7446
 He, 3^1P - 2^1P transition, polarization 8=7432
 He, 3^1P , 4^3S and 4^1D levels, lifetime obs., using positive ion Van de Graaff accelerator 8=16183
 He, by p, d, 0.15-1.0 MeV impact, obs. compared with theory 8=7385
 He, 1S , 1D , 1P states by d bombard. 8=7384
 He², electronic orientation, from previously oriented nuclei 8=16226
 He, Rydberg state by e collision 8=20970
 He², transverse optical pumping and detection of modulation resons. 8=16195
 He-like atoms, 1^1S state conservation prob. in β -decay 8=7426
 He⁺-He collisions, with e capture probability calc. 8=7463
 He(n^1p) \rightarrow He(n^1D), validity of Wigner spin rule 8=21015
 He-Kr mixture in d. c. discharge 8=4093
 He-Ne mixture optical pumping by He-Ne laser, Hanle and saturation effects obs. 8=20983
 Hg, 6^3P_2 level, relaxation anisotropy 8=7609
 Hg, 6^3P_1 state depopulation, effect of N_2 and CO 8=7405
 Hg, 7^3S_1 - 6^3P_1 - 6^1S_0 cascade correlation, and 6^3P_1 coherence time 8=4078
 Hg(6^3P_1), energy transfer with gaseous paraffins 8=9688
 Hg, 3^1P_2 metastable state, coherent, by e impact, rel. to res. absorpt. 8=4094
 Hg*(6^3P_1), quenching by H_2 , phase-space theory 8=14436
 Hg, $6s6d$ levels, lifetime, magnetic meas. 8=4095
 Hg, lifetime of 3^1P_1 state, meas. by Hanle effect 8=1181
 Hg¹⁹⁹ and Hg²⁰¹ isotopes, 6^1P_1 level structures 8=7404
 I($5^2P_{1/2}$), time resolved emission obs. 8=4079
 In¹¹³, L and K Auger spectra from Sn¹¹³ capture decay 8=4099
 K, $4^2P_{1/2}$, collisional mixing with inert gases 8=12064
 Kr, by electron-atom collisions, for 3^3 spectral lines 8=4096
 Kr, excitation cross sections for some of the states of $4p^4$ - $5p$ configuration 8=20973
 Li, adiabatic exchange approx. calc. 8=7434
 Li ground-state levels by slow electrons, cross sections obs. 8=7435
 Li to Kr, by β decay, probabilities calc. 8=4090
 Mg, electron excited, Rydberg states 8=20941
 Mg, oscillator strengths, semiempirical calc. 8=20959
 Na, depolarization cross-section by collision with inert gases 8=7436
 Na, by electrons, cascade transitions 8=20962
 Na-like, autoionization, structure of curves 8=21256
 Na-Na collisions, energy transfer in sensitized fluorescence 8=16213
 Na, resonance fluorescence quenching in inert gases 8=1185
 Ne, excitation cross sections for some of the states of $2p^4$ - $3p$ configuration 8=20973
 Ne, multiply ionized, mean lines of some excited levels 8=4097
 Ne, population transfer and alignment by spontaneous emission 8=20985
 Ne, probability of $3s_2$ - $2p_4$ transition in Ne 8=3317
 Ne, Rydberg state by e collision 8=20970
 Ne, $2S_{1/2}$, $2P_{1/2}$ and $3P_{1/2}$, Landé factors 8=1186
 Ne, X-ray $\kappa\alpha$ satellites (non-diag. lines) intensity 8=1170
 O, multiply ionized, mean lines of some excited levels 8=4097
 O, on e-collisions and excitation of extreme u.v. radiation 8=7722

Atoms—contd

excitation—contd

- O(1D) deactivation 8=4098
 O, 1D_2 - 3P_1 forbidden transition origin 8=1182
 Rb⁺, following β decay of Kr⁸⁵ in solid 8=8226
 Si, Auger electrons, energy spectra, surface contamination detection 8=1688
 Sr, absorption spectrum, u. v. extension of arc spectra 8=20967
 Sr, electron excited, Rydberg states 8=20941
 Sr, lifetime of $5s5p^3P_1$ state 8=7437
 Srl, $5s^2$ 1S_0 - $4dnp$, nf spectrum, analysis of autoionization resonance structure 8=20968
 Tm, Auger e intensities meas 8=20988
 W, transition probabilities, 9 lines, 4700-5300 Å 8=20969
 Xe, Rydberg state by e collision 8=20970
 Yb⁷⁰, transitions, from L spectrum 8=23023
- magnetic moment**
 See also Gyromagnetic ratio.
 dipole formation in atomic collisions rel. to dielectric constant of gas mixtures 8=12692
 resonant freq. shifts in mag. fields rel. to electrostatic potentials 8=312
 Co²⁺ in KCoF₃, polarizabilities and dipole moments from i.r. studies 8=2426
 Mg²⁺ in KMgF₃, polarizabilities and dipole moments from i.r. studies 8=2426
 Mn²⁺ in KMnF₃, polarizabilities and dipole moments from i.r. studies 8=2426
 Ni²⁺ in KNiF₃, polarizabilities and dipole moments from i.r. studies 8=2426
 Pa, Fe impurity atom, range of spin perturbation 8=1655
 Rb²⁺ in RbMnF₃, polarizabilities and dipole moments from i.r. studies 8=2426
- structure**
 See also Nucleus; Spectra/atoms.
 configurational entropy of large atoms 8=13104-5
 configuration interaction using open-shell functions 8=12028
 core, closed-shell, polarization by outer electron 8=7413
 correlation effects in calc. of ordinary and rotatory intensities 8=12023
 correl. energy calc., role of e density gradient 8=10659
 correlation factors, effective range 8=20938
 diffraction studies, importance of small angle domain 8=12045
 doublet-term inversion, non-central electrostatic corrections 8=4054
 effective pot., calc. from spectroscopic data 8=12038
 e bound state energies and low-energy e scatt. 8=1189
 e pots., binding energy and the periodic table 8=20918
 electron shell filling order, pressure effects 8=7364
 electrostatic interaction integrals using screened hydrogenic orbitals calc. 8=7394
 energy levels, bound-state, in continuum 8=4061
 energy level calc. by variational perturbation method based on the principle of moments 8=20919
 energy levels, perturbation by e.m. wave 8=7375
 energy levels of systems, lower bound, ΔE method 8=561
 Hartree-Fock expectation values for phys. props. 8=4038
 Hartree-Fock problem, multiple solns. 8=20933
 Hartree-Fock-Rootham eqns., numerical solns. 8=7349
 Hartree-Fock wave functions, Compton line shapes 8=20940
 integrals for correlated wavefunctions 8=7371
 lanthanides (IV), free ion $4f^n$ levels 8=21814
 laser, gaseous, transitions and population inversion 8=11041
 magnetic hyperfine anomaly, nonrelativistic derivation 8=12042
 many-electron, fine-structure splitting, use of Hartree-Fock functions 8=20923
 many-electron levels, relativistic corrections 8=16190
 many-electron wavefunctions, GF method 8=20911
 matrix elements involving interelectronic coordinates, ang. coeffs. 8=20925
 in molecule, definitions of charge 8=21053
 multielectron, inner electron binding energy using generalized WKB approx. 8=4050
 one- and two-electron-pair systems, spherical Gaussian orbital model calc. 8=12154
 optical pot., single particle states for resonances and inelastic scatt 8=20992
 orbit-orbit interaction in many-electron atoms 8=4058
 perimetric coordinates 8=4045
 periodic features with exchange and correlation 8=16184
 radial wave function calc., new method 8=20931
 reduced density matrices 8=4037
 repulsion theory, chemical bonds 8=1229
 Schrödinger eqn. test in shell rearrangements 8=3407
 shell-struct. effects in inelastic collisions 8=7452
 shell theory, recast by abandoning total spin quantum number S 8=4048
 shielding factors for nuclear moments 8=1155
 Thomas-Fermi eqn., soln. improved by flexible choice of boundary conditions 8=20936
 three-electron ions, ground-state energy, perturbation theory 8=16206
 three-electron systems, mag.-dipole and elec.-quadrupole hyperfine elements 8=12036

Atoms—cont'd

structure—cont'd

- transition metals, binding energies 8=8976
 transition metal, limited-basis-set SCF wave functions in ground state 8=12075
 two-centre moment integral, general formulation 8=16185
 two-electron atom in spherical potential box, correl. energy 8=16182
 two-electron atoms, Eckart-type wavefunctions for excited states 8=20928
 two-electron closed-shell systems 8=20933
 two-electron, correction of Breit approximation 8=12035
 two-electron, Hartree-Fock energy, saddle-point character 8=7370
 two- and four-electron systems, Hartree-Fock calc. 8=12037
 two-particle integrals, recursive evaluation 8=4056
 two valence electrons, specific mass effect 8=16181
 wave function, many electron, natural expansion 8=20920
 wavefunctions, integral coalescence conditions 8=12026
 X-ray scattering factors calc. from Hartree-Fock wave functions 8=16189
 Al²⁺, pseudopotentials 8=7409
 Ar, shock compression, Thomas-Fermi-Dirac theory 8=16994
 Ar, (3p⁴s)³P₁ state, lifetime obs., e excitation method 8=1164
 Ar II, transition probabilities 8=1163
 Au III, transition strengths between 5d⁶6s and 5d⁶6p configurations 8=4071
 B, ²P ground state, electronic structure 8=20950
 Ba, g_J-values of lowest ³P₁ states 8=7424
 Be isoelectronic sequence, diagram, calc. 8=12058
 Be⁺, pseudopotentials 8=7409
 C I electrostatic interaction integrals using screened hydrogenic orbits calc. 8=7394
 C I and II, wave functions and oscillator strengths, from superposition of configs. 8=4073
 C, term splitting for p² ground-state configuration 8=20951
 Ca⁺, ²F and ²G levels, polarization by outer electron 8=7413
 Ca⁺, pseudopotentials 8=7409
 Ca²⁺, dipole polarizability from spectra 8=7414
 Ca II, Hartree-Fock multiplet strengths 8=4081
 Cm³⁺, low-lying levels 8=4074
 Co²⁺, energy levels in MgO 8=23050
 Cs, one-electron energy levels for extended pot. 8=1167
 Cs-inert gas, collisional J reorientation and e spin polarization from D₂ pumping 8=1194
 Cs 6p and Rb 5p doublets, depolarization 8=7471
 Cs¹³⁴, h.f.s. of 8²P_{3/2} state 8=7400
 CSCP and e partition energy in hydrogenic atom 8=1157
 Cu⁸⁺, configuration interactions, polarization corrections from quadrupole moment determ. 8=12061
 Cu I, lifetime of 3d⁹4s4p⁴P_{3/2} state 8=12062
 Cu, pseudopotentials 8=7409
 Dy³⁺, energy levels in Dy₂O₃ cryst. 8=18522
 Er(III), in YPO₄ and YVO₄, angular overlap treatment 8=4075
 Eu³⁺ in garnet struct., hypersensitivity of ⁵D₀-⁷F₂ transition 8=18602
 Gd I, g values of levels from Zeeman effect 8=4077
 Gd²⁺, energy levels in LaCl₃ 8=16975
 Gd³⁺ ion, according to reflection spectrum of Gd₂O₃ and GdF₃ powders 8=2421
 e-H compound states, 5 parameter wave function for lowest two 8=20997
 H, and Coulomb potential energy of two charges 8=7378
 H, Green function 8=4035
 H⁺, hyperpolarizability, computer calc. 8=20942
 H, improved Gaussian wave functions 8=21080
 H, interaction with radiation field, Coulomb-Green's function calc. 8=12047
 H-like, hypervirial operators 8=3408
 H, ²-pole oscillator strength sum rules 8=7380
 He, atomic form factor and incoherent-scatt. function 8=12053
 He, correlation factors, effective range 8=20938
 He e excitation of triplet states, relativistic effects 8=7445
 He, ground state dynamic polarizability, variational calc. 8=20945
 He, ground state, variational calc. of expected values 8=7386
 He, hyperpolarizability, computer calc. 8=20942
 He isoelectronic sequence shielding factors 8=16199
 He isoelectronic sequence, ¹S states eigenvalues calc. 8=7391
 He isoelectronic sequence, ³S states eigenvalues and wave functions calc. 8=7392
 He isoelectronic sequence, 1snp¹P and ³P states, wave functions calc. 8=7390
 He isoelectronic series, ground-state wavefunctions and energies 8=4067
 He-like, Hartree-Fock equations for 1s2p, ³P and ¹P states, perturbation treatment 8=20921
 He-like, ¹S state, Hartree-Fock equations 8=7389
 He, lower bounds to eigenvalues 8=11253
 He params. from wave functions with pole-eliminating correl. factors 8=16197

Atoms—cont'd

structure—cont'd

- He, 0.15-1.0 MeV p and d impact, quadrupole and dipole transition theory compared to obs. 8=7385
 He, S limit, energy surface in parameter space 8=16196
 HF eqns, modification involving Slater p^{1/2} term 8=1149
 K⁺, dipole polarizability from spectra 8=7414
 K, ²F levels, polarization by outer electron 8=7413
 K-shell electrons, correl. energy, and relativistic and Lamb-shift correction 8=4068
 K, one-electron energy levels for extended pot. 8=1167
 K, pseudopotentials 8=7409
 K I, Hartree-Fock multiplet strengths 8=4081
 L²⁺, (L=Ce, Pr, Nd, Sm, Gd, Dy, Er and Yb), 4f electron radial wave functions 8=1168
 Li-donor in Si, ground state chemical splitting 8=1950
 Li, ground-state energy, perturbation theory 8=16206
 Li⁺, hyperpolarizability, computer calc. 8=20942
 Li and ions of isoelectronic sequence, wavefunctions calc., using effective potential 8=20958
 Li, Kerr dispersion, theory 8=12068
 Li⁺, lower bounds to eigenvalues 8=11253
 Li, pseudopotentials 8=7409
 Li sequence, transition energy, state eigenvalues 8=20957
 Li, 2p²P levels, hyperfine coupling constants 8=7408
 Lu, K Auger spectrum, from Hf¹⁷⁵ decay 8=1187
 Mg²⁺, dipole polarizability from spectra 8=7414
 Mg⁺, ²F and ²G levels, polarization by outer electron 8=7413
 Mg⁺, pseudopotentials 8=7409
 Mg, wavefunctions and oscillator strengths, semi-empirical calc. 8=20959
 Mo, O₂₄ ion in a crystal of ammonium heptamolybdate tetrahydrate 8=8234
 N I, N II electrostatic interaction integrals using screened hydrogenic orbitals calc. 8=7394
 N spectrum obs. in p-N₂ 0.15-1.0 MeV collisions 8=12213
 Na⁺, dipole polarizability from spectra 8=7414
 Na and ions of isoelectronic sequence, wavefunctions calc., using effective potential 8=20958
 Na isoelectronic sequence, dipole polarizabilities and shielding factors 8=7415
 Na, Kerr dispersion, theory 8=12068
 Na, pseudopotentials 8=7409
 Na, ²F levels, polarization by outer electron 8=7413
 Nd³⁺ ions in rare-earth trichlorides, new satellite structure 8=12070
 Nd³⁺ in LaF₃, energy levels 8=14328
 Ne, 2p levels, average lifetime 8=20963
 Ni²⁺, energy levels in MgO 8=23050
 O I, energy levels 8=12072
 O II electrostatic interaction integrals using screened hydrogenic orbitals calc. 8=7394
 P, 3d-radial functions in sp²d config. 8=1172
 Pu²³⁹, e binding energy determ. from conversion electron spectra 8=4085
 Rb 5p and Cs 6p doublets, depolarization 8=7471
 Rb⁸⁵, h.f.s. of ⁷2P_{1/2} state 8=7421
 Rb, pseudopotentials 8=7409
 Rb^{85,87} g₁/g₂ optical pumping determ. 8=1173
 Rb⁸⁵ in ²S_{1/2} electronic ground state, hyperfine structure 8=20708
 SCF theory, open-shell, coalescence conditions as constraints 8=16173
 SCF theory for N-electron system 8=20917
 Sc III, Hartree-Fock multiplet strengths 8=4081
 Se(p⁴ ↔ p³s), excited-state wavefunctions and oscillator strengths 8=16209
 Si and Si cpds. valence bonds, X-ray emission spectrum 8=2454
 Sn in cpds. rel. to Mössbauer spectra 8=12233
 Sr, g_J-values of lowest ²P₁ states 8=7424
 Sr, lifetime of 5s5p³P₁ state 8=7437
 Ti(III) hexahydrated ions, electronic struct. 8=16995
 V(III) hexahydrated ions, electronic struct. 8=16995
 WKB approx. for radial problems, 2nd and 3rd order correction terms 8=12039
 Xe, I and II, Hartree-Fock wavefunctions and parameters 8=1177
 Xe III, ground state Slater integrals 8=4087
 XeIII(5p⁴, ³P) HF calc. of ground state wave functions 8=1178
 Yb³⁺ in LaF₃, energy levels 8=14328
 Zn⁺, pseudopotentials 8=7409
- Atoms, mesic and muonic**
 helium, liquid, pionic and muonic X rays 8=1211
 muonic 2p-1s transition energies in light nuclei, charge radii deduction 8=3785
 muonic, X-ray spectrum rel. to nuclear rotations vibrations and multipole oscillations 8=20655
 μd, rate of μ transfer reaction with Y₂ (He, N, Ne, Ar, K, Xe) 8=12115
 μp mesoatom capture rate 8=721
 π, fine structure formula, reduced mass corrections 8=4114
 π mass meas. from 4f-3d transition in pionic Ca and Ti 8=6839
 pionic 2p-1s transitions Ge counter obs. 8=1179
 strong interactions and finite nuclear charge radius effects 8=7482

Atoms, mesic and muonic—contd

- X-radiation as a parameter of nuclear size and form. 8=7069
 Bi²⁰⁹, X-rays for study of nuclear structure 8=20672
 Ca, K series X-rays 8=1209
 K-mesic X-rays 8=11914
 K, nonmesonic decay processes 8=1210
 Li⁶, muon total capture rate assuming nuclear clustering 8=3915
 Mg, K series X-rays 8=1209
 S, K series X-rays 8=1209
 Si, K series X-rays 8=1209

Attenuation. See Absorption.**Auger effect.** See Atoms/excitation; Atoms, mesic; Radioactivity.**Auger showers.** See Cosmic rays/showers and bursts.**Aurora**

See also Airglow; Atmospheric spectra.

- absorption of cosmic noise in conjugate high latit. regions 8=23335
 absorption structure over 300 km and conjugate region correlation, obs. 8=18987
 in atmosphere, upper, excit. theory and H arc emission 8=9925
 blackouts rel. to solar wind activity, 1957-65 8=23363
 bombardment rel. to transverse drift l.f. plasma instability 8=4356
 channel multiplier instrumentation for low-energy e and p 8=5799
 cosmic noise absorption pulsations obs. 8=2639
 cosmic noise absorption, short period pulsations 8=23334
 day side, elementary disturbance obs. 8=18940
 diurnal activity pattern, Tixie Bay obs. 8=9940
 dynamical model of morphology, particularly substorms 8=9932
 electric field from electron conc. rocket obs. 8=23339
 elect. fields parallel to mag. field in auroral ionosphere, expt. investigation 8=23354
 electrojet circuit closure, soln. from high-latitude magnetosphere meas. 8=9951
 electrojets, rel. to micropulsation of non-impulsive Pi subtype 8=2736
 electrojet and polar mag. substorm 8=18950
 electron, low energy, multiplier for det. 8=10903
 electron precip. bremsstrahlung obs. 8=2635
 electron temp. and flux obs. indicating geomag. caused layer structure 8=9938
 electrons, energizing mech., from laboratory plasma meas., theory 8=16594
 electrons, nearly monoenergetic, flux and energy variations, rocket obs. 8=18936
 electrons velocity distribution 8=9945
 energetic electron, precipitation, daytime Nike Apache obs. 8=18942
 E region sporadic, 'flat-type' rel. to mag. disturbance 8=10005
 exceptional periods, historical review 8=23336
 extended forms, diurnal patterns 8=9935
 5577/3914 Å intensity ratio, mechanism explaining obs. 8=5800
 rel. to fluctuations in earth's e.m. field 8=2727
 frequency during min. solar activity 8=9941
 frequency in years of max. and min. solar activity, obs. 8=9933
 geomagnetic neutral sheet acting as particle source by accelerating solar wind 8=2618
 hiss, measured on OGO 2 and at Byrd station, interpretation in terms of incoherent Cerenkov radiation 8=23342
 Hiss, v.l.f., origin from night-time magnetosphere 8=5801
 hydrogen arc, Balmer α emission rel. to incident H flux obs. 8=2636
 infrasonic radiation, shock-wave model 8=19533
 infrasonic waves, northern zone 8=2633
 ionosphere, electron density, r.f. capacity probe obs. 8=2666
 ionosphere, winter, total electron content and variations 8=9960
 ionospheric irregularities, sub-auroral, satellite scintillation transition obs. 8=18945
 irregular phenomena rel. outer radiation belt disturbances 8=9939
 low-freq. radio hiss, 0-30 kHz, morphological obs. 8=18947
 luminescence intensity pulsations rel. to geomag. Pi2 8=19048
 luminescence var. rel. pearl pulsations, 1964-1965 8=9936
 luminosity, λ 3914(N₂⁺), λ 5577[OI] and λ 6300[OI], spatial var. obs. 8=14649
 luminosity rel. to absorption, narrow beam obs. 8=23338
 lunar variations in auroral zone 8=10331
 magnetic and optical features of low latitude class II event, 25-6 May, 1967 8=10054
 and magnetic storms, night, at low and middle latits., obs. analysed 8=2752
 N, atomic, enhancement at 100 km with natural incidence of auroral electrons 8=9929
 N. zone, electron bremsstrahlung rel. geomag. micro-pulsations, obs. 8=10047
 1957, 13 Sept., solar flare effects 8=9934
 optical, review 8=18937

Aurora—contd

- oval, boundaries, position rel. mag. disturbance intensity 8=9937
 oxygen forbidden transitions, obs. 8=1182
 particle acceleration due to elect. field generation in magnetosphere 8=18930
 particle precipitation satellite obs. rel. to radar echoes 8=9942
 photographic, visual and radio studies, Canadian report 8=14639
 polar, correl. with cosmic X-radiation 8=18939
 polar glows 8=14648
 poles, theory 8=18941
 precipitation event, simultaneous balloon and satellite obs. Sept. 20, 1963 8=9944
 proton precipitation and H emissions 8=18946
 proton, precip., spectra and ang. distrib., rocket meas., also electrons 8=5798
 proton, secondary ionization processes 8=14683
 radar echoes, wavelength dependence and aspect sensitivity 8=2637
 radio absorpt., apparent poleward expansion 8=18988
 radio absorpt. events, differences between conjugate regions 8=14653
 radio absorpt. at 3 pairs of mag. conjugate sites, occurrence in statistical props. 8=14652
 radio, and ionospheric electric current, two-stream plasma instability model 8=2638
 radio pulsating echoes 8=9948
 radio, review 8=18938
 radio, v.h.f., at sunspot maximum, echo movement obs. 8=9947
 red, 1946-1951, correl. with solar activity 8=9930
 space vehicle instrumentation 8=5837
 storms, theoretical review 8=19043
 sub-storm rel. to magnetic sub-storm and radiation belt 8=19046
 substorms, electron fluxes at 1000 km 8=18952
 v.h.f. radio, simultaneous obs. of ionization by 2 separated radars 8=14651
 v.h.f., sunspot maximum, diffuse and discrete 8=9931
 v.l.f. hiss at very low L values, obs. 8=23353
 visual, conjugacy obs. 8=23337
 X-ray event, intense, in 4-5 sec period range 8=9946
 X-ray events, pulsating, E-W movement balloon obs. 8=18943
 X-ray pulsations, energy dependent modulation 8=9943
 H α line, variation in width over 1 hour 8=14650
 N₂⁺, 3914 and 4709 Å, ratio of spectral intensity to H β 8=23340
 N₂ second positive system, vibrational development 8=1894
 N₂-p, N₂-H collision processes, optical emission 8=12212
 O I, 5577 and 6300 Å, ratio of spectral intensity to H β 8=2334
 O, O₂ and N₂, electron impact cross sections used to calc. auroral intensities 8=2634

Austenite. See Iron alloys; Steel.**Avogadro's number.** See Constants.**Axicons.** See Lenses.**BCS theory.** See Nucleus/theory; Superconductivity.**Backscattering.** See Scattering, particles; and under "scattering" subheadings of the appropriate particles.**Backward wave oscillations.** See Electromagnetic oscillations; Electron tubes.**Balances**

- electric strain-gauge scales 8=10478
 microbalance for molecular beam forces 8=16380
 micro, vacuum for 77.3°K operation 8=7965
 quartz fibre ultramicrobalance for microgram loads 8=2876
 remote controlled for high radiation environment 8=6005
 thermal gravimetric apparatus, sample 8=9658
 thermo, continuously recording using strain gauges 8=9659
 torsion, precision standard masses 8=19349
 vacuum microbalance techniques, conference Newport Beach USA (1966) 8=14919
 vibrating quartz microbalance, transistorized temp. regulator 8=19671

Ballistics

- See also Impact.
 arc jet, thrust calc., mass flow rate 8=4421
 bullet velocity meas., paper screen method 8=10488
 internal, of orthodox guns, composite change 8=39
 metal cylinder, penetration into massive target 8=10534
 projectile deform. on impact, direct. anal. of dynamic behaviour 8=17728

Band theory of solids. See Crystal electron states/band structure; Solids/theory.**Bardeen-Cooper-Schrieffer theory.** See Nucleus/theory; Superconductivity.**Barium**

- atomic beam, excited levels, alignment by electron impacts 8=21019
 diffusion in MgO rel. to dislocation densities 8=4954
 films, methane sorption 8=17160
 film, sorption capacity for O₂ in colour picture c. r. t. 8=15324

- Barium** — contd
- getters, absorpt. of Ar, obs. 8=17161
- g_J -values of lowest 3P_1 states 8=7424
- optical properties and band structure 8=5598
- plasma, resonance radiation scattering obs. rel. ion density 8=4331
- plasma source, fully ionized 8=4419
- Rydberg states obs. from electron collision 8=20941
- vapour absorpt. spectra, using modified King furnace 8=7393
- Ba^{133} isotope, use in Mossbauer effect investigation of bone surfaces 8=14902
- Ba I-II transition, pressure determ. with single-piston apparatus 8=4702
- Ba II spectrum, isotope shifts and mag. h.f. s., 4.934 Å 8=16204
- W, adsorbed, e emission, Thomas-Fermi-Dirac theory 8=5414
- W surface ionization coeff. meas. 1800-2600°K 8=18288
- Barium compounds**
- barium-ferrite magnets as "self-crystallizing" molecular models 8=16375
- crystallization with Ra as radioactive tracer 8=21962
- leucophanite, crystal structure 8=13252
- silicate glasses, γ -ray induced defects 8=13479
- Ba silicate glasses, internal friction due to condensation 8=13537
- $BaAl_2Si_3O_{10} \cdot 4H_2O$, proton resonance and H atom position 8=18456
- $Ba + Ba_2O_3$ ferrites, dielectric props., influence of ultrasound 8=9370
- $BaCO_3$, aragonite/disordered rhombohedral polymorphic transition 8=21840
- $BaCa_2Al_3(Si, Al)_{12}O_{30} \cdot 2H_2O$, crystal chemical analysis and structure refinement 8=17338
- $BaCl_2$ - $CaCl_2$ system, analysis by β -ray backscatt. 8=18796
- $BaCl_2 \cdot 2H_2O : Mn^{2+}$ e.s.r. 8=14115
- $BaClF : Sm^{2+}$, fluoresc. 8=14332
- $BaClF : Sm^{2+}$, phonon annihilation in 5D_1 and 5D_0 states 8=9600
- $Ba(ClO_3)_2 \cdot H_2O$ and $Ba(ClO_3)_2 \cdot D_2O$, irradiated with X-rays, e.p.r. 8=18409
- $Ba(ClO_3)_2 \cdot H_2O$, X-irradiated, e.p.r. spectral changes in u.v. irradiation 8=18410
- $BaCo^{2+}Fe^{2+}Fe^{3+}_2O_{27}$, hexagonal, spin structure and anisotropy 8=22849
- $Ba_2Cu(H, COO)_6 \cdot 4H_2O : Cu^{2+}$ e.s.r. obs. 8=14103
- BaF , gaseous, rotation of $A^2\Pi$ and $B^2\Sigma^+$ states 8=7502
- BaF_2 , additively coloured, phonon-assisted colour centre fluorescence 8=14306
- BaF_2 , colorability enhancement by plastic deformation 8=22228
- $BaF_2 : Eu^{2+}$, e.p.r. spectrum at 77-964°K 8=9424
- BaF_2 , F-centres 8=22227
- $BaF_2 : Gd^{3+}$, Stark splitting and centre of gravity of $^6P_{7/2}$ and $^6P_{5/2}$ 8=23015
- $BaF_2 : H, D$, polarization 8=8206
- BaF_2 , lattice theory, elastic consts., dielectric const. 8=13178
- $BaF_2 : Mn^{2+}$, hyperfine coupling constants temp. dependence 8=18429
- BaF_2 , X-ray coloured, absorpt. by colour centres, temp. dependence 8=17683
- $BaF_2 : Yb^{3+}$, spin-lattice relax. 8=18444
- $BaFe_{12}O_{19}$, complex permeability and mag. loss in cm. and mm.-wave range 8=5489
- $BaFe_{12}O_{19}$, ferromag. resonance 8=9403
- $BaFe_{12}O_{19}$, polycrystalline samples, mag. dispersions 8=5490
- $BaFe_{12-x}Sc_xO_{19}$ hexagonal ferrite, magnetization temp. dependence 8=18358
- $BaFeSi_4O_{10}$, Fe^{2+} Mossbauer spectrum 8=13026
- BaGe, crystal structure 8=8557
- Ba-M alloys (M=Pt, Pd, Rh, Au), work function 8=18245
- $Ba_{1-x}Me_x^{2+}Fe_2O_7$, hexagonal ferrites, crystal structure and stacking sequences 8=17342
- $Ba_2Me_2Fe_{24}O_{41} (Me_2Z)$, magnetic structure 8=9373
- $Ba(NO_3)_2 \cdot H_2O$, single crystal, elastic, piezoelectric and pyroelectric props. 8=5051
- $Ba_2NaNb_3O_{15}$, electro-optic and nonlinear optic characts. 8=22959
- $Ba_2NaNb_3O_{15}$, nonlinear optical coeffs. 8=9508
- BaO cathode emission affected by residual gases 8=18663
- $BaO \cdot Al_2O_3 : Mn$ Th and Ce sensitized luminescence 8=14303
- $Ba(OH)_2$ impurity in ice, dielec. dispersion obs. 8=18188
- $Ba(BrO_3)_2 - BaBr_2$, solid solution formation during thermal decomposition of $Ba(BrO_3)_2$ 8=21816
- BaS:Bi luminesc. rel. to activator and $BaSO_4$ phase concs., obs. 8=9601
- BaS-Cu and BaS-Mn, freq. depend. of shape of light pulse 8=5676
- BaS:Cu luminesc. rel. to activator and $BaSO_4$ phase concs., obs. 8=9601
- BaS:Mn luminesc. rel. to activator and $BaSO_4$ phase concs., obs. 8=9601
- BaS:Mn phosphors, luminescence 8=23045
- BaSi, crystal structure 8=8557
- $Ba_2Si_{2n}O_{3n+1}$, multiple chain structure 8=17343
- BaSn, crystal structure 8=8557
- $Ba, Sr_{1-y}F_2$, far i.r. reflectivity spectra 8=9507
- Barium compounds—contd**
- (Ba, Sr, K)Na(Ti, Fe)TiSi₂(O, OH, F)₉, lamprophyllite, structure 8=17344
- $Ba_{2-x}Sr_xZn_2Fe_{12}O_{22}$, quasi-spiral ordering, n diffraction obs. at 4.2°-400°K 8=9372
- $BaTa_2O_6$, polymorphism 8=4780
- $Ba_2TiSi_2O_8$, fresnoite, i.r. absorpt. spectra and X-ray powder data 8=18506
- $Ba(UO_2AsO_4)_2 \cdot nH_2O$, metaheinrichite, e-diffr. meas. 8=17360
- $Ba_2Zn_2Fe_{11}O_{22}$, Bloch wall structure determs. 8=5496
- $BaZnFe_3O_{11} (ZnY)$ crystals, mag. props. 8=22744
- $Ba_xZr_{1-x}Si_3O_8$ (x = 1, 2; y = 1, 2; z = 9, 12), phys. and luminesc. props. 8=9624
- Bi-Ba titanate (IV), ceramic, Fe^{3+} doped, model and props. 8=5236
- barium titanate**
- See also Ferroelectric materials/barium titanate.
- cold conductor ceramic, working mechanism, electron microscopic investigation 8=21982
- doped with Sb_2O_3 , surface states 8=13790
- electrical conductivity between 600 and 900°C 8=5363
- films, spark discharge along surface 8=7682
- hysteresis and dielec. props. 8=13881
- micro electron diff. investigation of at. structure 8=8510
- optic lattice l.f. vibration, temp. dependence 8=17479
- optical phonon, i.r.-active, directional dispersions at room temp. 8=17478
- in polycarbonate, films dielec. props. 8=22661
- in polysulfone, films dielec. props. 8=22661
- porous, firing temp. and pore volume 8=8256
- reduced, interpret. of e.s.r., as resonance of Ti^{3+} ion 8=2375
- shock-wave compression 8=13538
- single domain ferroelectric, optical absorpt. 26-130°C 8=9506
- sintering behaviour of high purity samples 8=17024
- small polaron problem rel. to reflectivity and conductivity 8=5587
- $BaTiO_3 - Cr_2O_3$ systems, phase transformations 8=17045
- $BaTiO_3 : Eu^{3+}$, vibronic structure in luminescence spectra 8=14333
- Eu^{2+} e.s.r. in cubic and tetragonal phases 8=14094
- Barkhausen effect.** See Magnetization process.
- Barnett effect.** See Gyromagnetic effect.
- Baryons**
- See also Hyperons; Nucleons and antinucleons.
- axial vector currents in terms of baryons and bosons, divergences 8=6743
- baryon number inhomogeneity rel. to early history of universe 8=23474
- $B + \bar{B} \rightarrow \mu + \nu$, with π as Regge particle 8=11502
- B-B scatt., quark model, cross-section calc. 8=11577
- $B\bar{B}$ scatt., superconvergence sum rules assuming Regge-pole theory 8=6917
- BBM rel. to MMM coupling constant from πN scatt. superconvergence relations 8=3640
- B-N scatt. factor from $p + d \rightarrow B + d$ 8=3736
- B-N scatt. factor from $p - He^4$ B prod. interaction 8=3736
- bibaryon suppression except for d as members of TO SU(3) multiplet 8=20512
- coupling constant for Y_1^* BP from $K + N \rightarrow \Sigma + \pi$ 8=20580
- current, baryon, vacuum expectation value sum rules, saturation 8=20513
- decay, accounted for by SU(3) mixing 8=3690
- data on properties, updating 8=15671
- decay mode, B + pseudoscalar meson, classification of particles 8=6766
- Δ_0 and N_α Regge exchanges rel. to π^+p backward elastic scatt. 8=15778
- $\Delta^{*+}(1238)$ in $K^+ + p \rightarrow K^0 + \Delta^{*+}(1238)$ 8=3662
- Δ^{*+} in $\pi^+ + p \rightarrow \eta + \Delta^{*+}(1238)$, cross-section and Δ^{*+} spin density 8=6855
- Δ prod. in $\pi B \rightarrow V\Delta$, Regge-pole couplings 8=6903
- electric and mag. polarizabilities, in quark model 8=6823
- e.m. mass differences using Reggeized tadpole model 8=11575
- exchange, evidence from K^+p backward elastic scatt. 8=803
- excited, search in nucleon-nucleon interactions 8=20517
- high spin, model for Regge recurrences of inelastic resonances 8=6918
- isobar, T = J = 3/2, photo- and electroproduction, soln. of dispersion relations 8=3732
- K-B coupling constants from K-N scatt. sum rules 8=20483
- K-p scatt., resonance state formation calc. 8=6897
- leptonic decay, two-angle Cabibbo theory rel. to data anal. 8=6819
- leptonic decays, e.m. finite state interaction and T-odd correlations 8=11576
- leptonic three-body decays 8=15822
- magnetic moment relations from ρB scatt. 8=6900
- magnetic moments, form factors and mass spectrum 8=15823
- mass differences, e.m., of $1/2^+$ baryons, Dashen-Frautschi method 8=3689
- mass formula, empirical 8=6915

Baryons—contd

- mass formula, unified, in quark model 8=738
 masses spectrum from saturation of baryon current 8=20513
 mass-splitting, e. m. from source theory of gauge fields 8=20158
 meson-baryon interactions in quark model, prod. cross-sections 8=20405
 meson-baryon scatt. cross-sections, in SU(3), asymptotic limits 8=742
 meson-baryon scatt., mass difference effect, Wali-Warnock model 8=3692
 meson-baryon scattering, quark model 8=20418
 meson-baryon scatt., with Regge poles and SU(3) symmetry 8=740
 meson-baryon scatt., response of masses to perturbations in N/D model 8=3691
 meson-baryon scatt. saturation of superconvergence relations 8=15818
 meson-baryon scatt. test of a superconvergent relation 8=11494
 meson-baryon, SU(n) crossing matrices 8=741
 meson-baryon S-wave scatt. length calc., pseudo-scalar 8=20420
 meson-B scatt. p-wave, low energy sum rules 8=6833
 MN Reggeized scatt. model, B exchange 8=825
 model, of 4 quarks and one antiquark 8=817
 N isobars, regularity of mass spectrum 8=3639
 N_{1-} (1575) production in K^+p at 5 GeV/c 8=869
 N^+ production in pp, pn reactions, 2.8 GeV/c 8=844
 nuclear shell model with quarks, finite of mass 8=15819
 octet and decuplet, e. m. mass differences 8=11574
 paraquark dynamics 8=816
 π -B scatt, dispersion relations, sum rules 8=3635
 $\pi B \rightarrow V\Delta$, Regge-pole couplings 8=6903
 quark-diquark model, approx. in variant under SU(6)) 8=20511
 quark model, field-theoretic restriction on 8=15817
 quark model, parity and wave functions 8=3687
 quark model rel. to S-wave hyperon decay 8=6975
 quark model with three-body interaction forces 8=11573
 radiative decays, calc. in pole approx. 8=6914
 radii, Dirac and axial vector mean square rel. to SV_0 predictions 8=20344
 representation mixing in $U_{6,6}$, applic. to weak and e. m. interactions 8=15820
 scattering BM couplings in quark model, soln. to super-convergence relations 8=20404
 spinor field and axial vector currents commutation relationship 8=819
 stable, and $3/2^+$ resonances, mixing of weak and e. m. parameters 8=818
 sum rule connecting $1/2^+$ and $1/2^-$ spectra 8=819
 SU(3) mixing among $3/2_2$ to account for decay widths 8=3690
 three-quark model of baryonic states with nonlocal separable potl. 8=3688
 vector meson-B scatt. lengths, symm. breaking and Ademollo-Gatto theorem 8=6916
 $He^4(p, B)He^4$, magnitude and phase of baryon scatt. amp. 8=890

resonances

- conference, Varenna, Italy July 1964 8=6745
 couplings with normal B and pseudoscalar mesons 8=6983
 isobars, representation for the group of strong-coupling theory 8=20577
 $\Delta(1238) + \pi$ in $\pi^-p \rightarrow \pi^+\pi^-n$, 870 MeV 8=20445
 Δ Regge-pole model for π -N isospin- $3/2$ partial wave amplitudes 8=15784
 Δ , rel. to static model of π -N scatt. 8=11533
 Δ trajectory and superconvergence relation for π^+p scatt. 8=20328
 $\gamma^* \rightarrow \Delta\pi$ quark model, exchange currents 8=15821
 higher spin, strong decay in O(4, 2) theory 8=867
 $J^P = 1/2^-$, possible decuplet 8=15863
 $J^P = 3/2^-$, SU_3 27-plet structure 8=3731
 N^* electroprod. cross-section calc. 8=20514
 N^* , form factors for electroprod. 8=20579
 N^* in $\gamma N \rightarrow \pi N^*$, threshold cross-section calc. from current algebra 8=11504
 N^* isovector form factor rel. to photoprod. 8=15864
 N^* , 9 new resonances in range 1680-2190 MeV form πp phase shifts 8=15865
 $N^*N_\gamma(1238)$ coupling constant current algebra calc. 8=3733
 N^*, N^*N^*, N^*N^* , decay distrib. using statistical tensors 8=20505
 $N^*, N\pi, N\eta$ decay modes, s, d wave contrib. 8=11637
 $N^*(1236)$, photoproduction by polarized γ -quanta 8=868
 $N^*(1236)$ rel. to π prod., 500-700 MeV 8=20438
 $N^*(1238)$ from $\gamma + p$, test of e. m. C noninvariance 8=694
 $N^*(1238)$ prod. rel. to $I = 1$ P-wave phase-shift calc. for K^+p interactions 8=15805
 $N^*(1400)$ domination of N form factors, test in calc. of $g_{\pi N N}/g_{\pi N N}$ 8=20515
 $N^*(1400)$ $I = 1/2$ prod. from π^+p at 6 GeV/c 8=15775
 $N^*(1400)$, Roper, in $\pi^+p \rightarrow \pi^+\pi^-\pi^+p$, 8 GeV/c 8=20447
 $N^*(3245)$ evidence in π^+p scatt. at 180° 8=11540
 $N^*(3/2_1, 3/2_2)$ in $\pi p \rightarrow \pi\pi N$, 720 MeV 8=15772

Baryons—contd**resonances—contd**

- N^* polarization in $\nu_1 + N \rightarrow N^* + l$ 8=3586
 N^* prod. and decay to (hyperon + K) in $p + p \rightarrow$ hyperon + K + N, 6 BeV/c obs. 8=20480
 N^* prod. $\gamma + N \rightarrow N^* + \pi$ as test for Regge cuts 8=20331
 N^* prod. in $\gamma + p \rightarrow N^*(1238) + \pi^-$ OPE model anomaly 8=6986
 N^* prod. in $K^+p \rightarrow K\pi N$, 735, 785 MeV/c 8=3686
 N^* production in $\nu_1 + N \rightarrow N^* + l$ and $\bar{\nu}_1 + N \rightarrow N^* + l$ 8=3585
 N^* prod. in $\pi^+ + p \rightarrow N_{1238}^* + \pi^0$ 0.5-1.46 GeV, ang. distrib. of π^0 8=15780
 N^* prod. in $p + p \rightarrow p + N^*$, 6-30 BeV obs. 8=15828
 N^* πN coupling constant related to that for πNN^* 8=11554
 N^* rel. to π -N scatt. amplitude second order energy terms 8=11532
 $N^*, \pi N$ scatt. exchange contrib. 8=761
 $N^* \pi N^*$ scatt. Regge-pole theory, constraint eqns. 8=20321
 N^* in $\pi p \rightarrow \rho N^*, \rho N^*$, ang. correls. in decay 8=11636
 N^* pNN, pNN*, pNN $_{33}$ coupling from current algebra 8=11564
 N^* in $pp \rightarrow N^*p$, 2 π exchange contrib. 8=3650
 N^* Regge trajectory clans with parity degeneracy 8=15866
 N_{15}^* (1688) excitation function, by missing mass method 8=11638
 N_{33}^* $\rightarrow N\pi$, quark model, exchange currents 8=15821
 N_{33}^* (1236) from $\gamma + p$ reaction, and current algebra 8=6985
 N_{33}^* in π^+p 900 MeV interactions, single π prod. 8=11523
 $N^{*++} + N^{*0} - 2N^{*+}$ mass difference, e. m., superconvergence dispersion relation approach 8=11485
 $N^{*++}(1236)$, in $\pi^-p \rightarrow \pi^-\pi^+\pi^-p$, 8 GeV/c 8=20447
 $N^{*++}(1238)$ in $\pi^-p \rightarrow \pi^+\pi^-\pi^-p$, 3 GeV/c 8=20446
 $N^{*++}(1238)$ prod. in $\pi^-p \rightarrow N^{*++}(1238) \pi^-\pi^-$, 3.2, 4.2 GeV/c obs. 8=20448
 N^{*++} , in $\pi^+p \rightarrow \rho^0 N^{*++} \rightarrow \pi^+\pi^-\pi^+p$, peripheral models 8=11515
 N^{*++} in $pp \rightarrow N^{*++}n$, 10 GeV/c, OPE model 8=11591
 N^{*+} in π -N scatt., mass, spin and isospin determ. 8=20452
O(4, 2), evidence, assignment of hadron levels 8=15747
 $\pi N \rightarrow \pi N^*$ 8=6849
in πN scatt. 8=6866
 πN^* , superconvergent sum rules 8=3634
 $p + \bar{p} \rightarrow B^+ + B^*$, absorpt. model 8=20526
 P_{11} mass shift in $pp \rightarrow pN^*$ in compound structure model 8=11592
 P_{11} in πN channel, model 8=11513
paraquark dynamics 8=816
quark model prediction 8=20404
quark symm. model, derivation of mass formula 8=6980
Regge recurrences of SU(3) multiplets 8=6981
as rotational states 8=866
 $(7/2^-)$ octet, possibility 8=20578
 $3/2^-$ decay in SU(3) symm. 8=11635
 $3/2^-$, SU(3) struct. rel. to decuplet-octet-singlet combination 8=6984
vector meson-B couplings from superconvergence relations 8=6900
 Ξ^* prod. in K^+p , 10 GeV/c 8=15803
 Y^* rel. to K^+ photoprod. at 4.0-6.1 BeV 8=15859
 Y_0^* BP coupling from $\bar{K} + N \rightarrow \Sigma + \pi$ 8=20580
 $Y_0^*(1820)$ in K^+p scatt. 0.8-1.2 GeV/c 8=6894
 Y_0^* prod. in πp , 1.5-4.2 BeV/c 8=6860
 $Y_0^* - Y_0^*$ mixing rel. to baryon resonance strong decay 8=11635
 $Y_1^*(1385)$ from K p interaction 8=800
 $Y_1^*(1760)$ in K-p scatt. 0.8-1.2 GeV/c 8=6894
 $Y_1^*(1942)Y^*(2097, 2299)\Sigma^*(1933)$ and AY^* with $I = 2$ 8=11571
 Y_1^* spin and parity 8=870
 Y_1^* , spin and parity determination from $K^+p \rightarrow Y_1^*(1660) + \pi^- \rightarrow \Sigma^+\pi^+\pi^-\pi^-$ 2.1-2.7 GeV/c 8=6987
 $Y_1^* + Y_1^* - 2Y_1^{*0}$ mass difference, e. m., superconvergence dispersion relation approach 8=11485

Barysphere. See Earth.**Bauschinger effect.** See Deformation.**Bayard-Alpert gauges.** See Vacuum gauges.**Bays.** See Earth/magnetic field; Magnetic storms.**Bells.** See Musical instruments.**Bending**

- See also Stress analysis; Torsion.
 anticlastic deform. problems solns. 8=19392
 bar under its own weight, strain tensor components 8=19397
 beams, elastic-plastic, large deflections calc., equiv. multipoint cross-sections method 8=10556
 beam, loaded and supported at two points 8=10545
 beams, plastic, asymmetrical 8=10558
 circular block, anisotropic compressible, finite 8=6052
 circular plates, uniformly loaded, various supporting conditions, deflections 8=14951
 cylinder, in second order elasticity 8=10536
 elastic frame system with var. cross-section under its own weight 8=6042
 elastic stability of curved beams, extensible and inextensible theories 8=10547
 glass, microporous, accompanied by shrinkage 8=17021

ending—contd

- half-space, loaded, strain tensor components 8=19397
- hollow notched round bar, stress-intensity factor 8=5024
- oscillations of three-layer beam with various end constraints 8=10698
- parallelogram plates, elastic support 8=19384
- plates, effect of mean stress on fatigue crack propag. 8=17758
- plates, elastic 8=10535
- rod, inhomogeneous, internal stresses and loading capacity 8=10553
- shell, shallow spherical 8=2925
- of thin circular plates, on equally spaced point supports 8=10555
- thin plates, material with nonlinear stress-strain relation 8=10548
- thin plates with non-linear stress/strain reln., comments and reply 8=22264-5

ending of light. See Gravitation; Light.

erkeium

No entries

eryllium

- abundancies estimated in expanding hot universe 8=5840
- atoms, isoelectronic sequence, diamag. calc. 8=12058
- atoms, isoelectronic series, Rydberg spectra, Slater-Condon parameters 8=12059
- corrosion, retarding by fluoride coating 8=23098
- crystal, gliding prismatic 8=1981
- de Haas-van Alphen data for Fermi surface, non-local pseudopotential model 8=8923
- ductility rel. to prestraining, and cracks, 50, 100, and 200°C 8=8825
- electrical resistivity recovery after low temp. electron and neutron irradiation 8=2134
- electron back-scattering from Be-Au 2-layer target 8=3203
- electron emission, secondary, for large incident angles of primary beam 8=5421
- e secondary emission, calibration with Faraday cup 8=6808
- films, self-supporting, 5-10 $\mu\text{g}/\text{cm}^2$ 8=4744
- ionization cross-section, electron impact 8=7700
- irradiated by electrons and neutrons, recovery meas. 27-77°K 8=22249
- laser induced emission of electrons, ions and X-rays 8=13947
- mass spectrum of isotopes prod. in p-O¹⁶ reaction 8=20792
- moderators, neutron thermalization analysis 8=7303
- polishing and etching by metallographic technique 8=4790
- range of Ar, Kr and Xe ions, 500 KeV to 2 MeV 8=13481
- sheet rolled from ingots, grain boundary precipitation 8=17046
- target for ion emission, bombard by Ar⁺ 8=6626
- target nucleus, thermonuclear reaction rates 8=11976
- X-ray Raman scatt. of Cu K α rad. 8=2396
- Be₂, potential curves, MO calc. 8=16267
- Be⁺ over Australia, 1965 obs. 8=23299
- Be⁻ e affinity calc. by superposition of configurations 8=21281
- Be⁺ in Na(K)Cl, substituent behaviour from ionic thermo-current spectra 8=8702
- Be⁺, pseudopotentials 8=7409
- Be-Au two-layer target, electron energy losses 8=22496
- Be-BeO-Au sandwich, electroluminescence rel. to electron emission 8=9277

eryllium compounds

- alloys, superconducting, magnetization meas. 8=17959
- beryls, alkaline, structure dependence on tempering at 600-1200°C 8=17345
- beryl and beryl melts, thermal decomposition at high temps., press. depend. 8=18645
- beryl, i.r. spectra of foreign mols. 8=2400
- beryllia-based fuels with dispersions of (U, Th)O₂, irradiation effects 8=22248
- hambergite, integrated intensities, expt. test of general formula 8=13480
- Be₂BO₃OH, integrated intensities, expt. test of general formula 8=13480
- BeF, emission spectra in vacuum u.v. 8=21064
- BeF, $^2\Sigma^+$ state and $^2\Pi$ levels, calcs. from Hartree-Fock equations 8=7503
- BeH₂, configuration-interaction calc. 8=16252
- BeH₂, Hartree-Fock limit 8=1238
- Be₃N₂ vaporization, enthalpy and enthalpy of activation, vapour pressure and evap. coeff. 8=1624
- BeO, crystal growth and its dislocation dependence 8=1736
- BeO, e.p.r. of Cu 8=2366
- BeO excited by 6328Å line of a He-Ne laser, Raman spectrum 8=18507
- BeO, grain growth and rupture props, effects of SiC and MgO additions 8=22315
- BeO, Hertzian stress cracks 8=13540
- BeO, hot-pressed, effect of adsorbed sulphate and fluoride on density 8=21821
- BeO, n-irrad. at high temps., dislocation loops 8=8761
- BeO neutron irrad., determ. of Li⁶ conc. and diffusion 8=8672

Beryllium compounds—contd

- BeO, n-irrad. induced defect clusters, obs. by n-scatt. 8=22177
 - BeO, polycrystalline, high temp. defects and deform. 8=13539
 - BeO, radiation damage, electron microscope investigation 8=22250
 - BeO single crystals, dislocations, slip, fracture 8=1969
 - BeO, twin boundary and dislocation decoration by n-irrad. at high temps. 8=22199
- Bessel functions.** See Functions.
- Beta-decay theory**
- See also Nuclear decay theory.
 - book 8=3858
 - electron mass values maximization of ratio Γ/Q 8=3601
 - elementary particles, coupling constant sum rule derived 8=11482
 - Fermi function evaluation including charge distrib. and e screening effect 8=7126
 - first forbidden transitions, anomalies in lifetimes 8=11822
 - ft values for 0⁺-0⁺ transitions calc., suggested change of definition 8=7125
 - Gamow-Teller, speed rel. to M1 γ transition 8=11731
 - inner bremsstrahlung, correction effects 8=11804
 - ionization probability, energy depend. 8=12419
 - isospin hindered transitions, second-order contrib. 8=1005
 - lepton-charged ρ vector coupling, radiative convection 8=20374
 - Nilsson model for Re^{186,9}, Tm¹⁷⁰ 8=1021
 - N in presence of strong interactions, e.m. corrections 8=11581
 - n, quark shell model of baryons, finite mass correction 8=15819
 - review, and anal. d expts for determ. of decay Hamiltonian 8=1003
 - simple interaction model, A=6, 18, 42, lifetime calc. 8=11689
 - spectrum shape factor in calc. of longitudinal polarization and isobaric spin impurity 8=1019
 - time reversal invariance 8=7127
 - 2s-1d shell nuclei, calc. using projected HF wave functions of ft values 8=11802
 - T violation, e.m. interactions 8=3863
 - O⁻ \rightarrow O⁺ transitions and μ capture in conflict 8=3862
 - O⁺, ground level rate difference due to spin-quadrupole force 8=11801
 - Tm¹⁷⁰, conserved vector current in first forbidden decay 8=16040

Beta-ray spectra

- See also Nuclear decay theory.
- β - γ directional correlation in retarded allowed β -transitions, higher order effects 8=11803
- double, and neutrino properties 8=6798
- e⁺ in K₁⁺ decay obs. 8=20477
- hadron decay Fermi part, radiative corrections 8=20409
- hyperon decay, relative rates estimated 8=3727
- instellar medium due to cosmic ray collisions 8=19094
- from μ decay spectrometer and visual method obs. 8=11472
- Nilsson, and β -decay of Re^{186,9}, Tm¹⁷⁰ 8=1021
- nuclear polarization meas. from asymm. 8=3955
- repetitive correction for finite resolving power of collimator in scintiscanning 8=20366
- scintillation detector, unfolding by numerical methods 8=6810
- shape factor for forbidden decays 8=1004
- Au¹⁹⁸, beta-gamma correlations 8=3887
- Au¹⁹⁹ decay 8=20753
- B¹² recoil nucleus stopped in foil asymm. as meas. of nuclear polarization 8=3955
- Be⁹(He⁶, α)Be¹¹ 8=3964
- Br⁸⁷ decay, in atmosphere 8=2611
- C¹⁰, rel. to anomaly in obs. lifetime of 1.74 MeV state of B¹⁰ 8=16015
- Ce^{133, 133m} \rightarrow La¹³³ 8=20722
- Ce¹⁴¹, decay 8=20753
- Cs¹³⁴ \rightarrow Ba¹³⁴, shape, endpoint energy, log ft values 8=16030
- Er¹⁷³, new radioactive isotopes 8=20756
- Eu¹⁵⁶, 0⁺-0⁺ transition, spectrum shape factor 8=1019
- Fm²⁵³ \rightarrow Cf²⁴⁹ 8=11836
- In¹¹³ K, L-Auger lines 8=20387
- Mg²², positron branchings 8=3866
- Mn⁵⁴ \rightarrow Cr⁵⁴, upper limit to positron decay 8=7132
- Na²⁰ \rightarrow Ne²⁰, by meas. delayed α emission 8=3865
- Na²², positron obs. 8=20746
- Nb⁹⁰ decay, e⁺ endpoint energy 8=11813
- Pr¹³⁹ \rightarrow Ce¹³⁹, positron decay 8=7141
- Pr¹⁴⁰, e⁺ decay, rel. to photoneutron cross-section of Pr¹⁴¹ 8=16060
- Pr¹⁴⁴, Nd¹⁴⁴, O⁻-O⁺ transition, pseudoscalar interaction 8=3880
- RaE rel. to time-reversal invariance violation 8=11829
- Re^{186,9}, Nilsson model for decay 8=1021
- Sr⁷ \rightarrow Cs¹³⁷ 8=16018
- Se⁸³-Br⁸³ 8=3871
- Si²⁶ \rightarrow Al²⁶ used to calc. speed of M1 transition in Al²⁶ 8=11731

Beta-ray spectra—contd

- Sn^{113} , K, L-Auger lines 8=20387
 Ta^{182} , decay, sum coincidence studies 8=3884
 in Tl^{204} decay, continuous, and K Auger-line spectrum 8=1026
 Tm , Auger spectrum obs. 8=20988
 Tm^{170} Nilsson model for decay 8=1021
 V^{48} , β - γ circular polarization correl. meas. 8=7131

conversion electrons

- atomic screening effect 8=15946
 Mossbauer effect, efficient geometry 8=691
 spectrometer obs. 56 cm radius, double focusing 8=11470
 Ag^{102} , unsuccessful search in isomeric transition 8=7094
 $\text{Ba}^{133} \rightarrow \text{Cs}^{133}$ decay 8=16031
 Ba^{133} decay, K, L, M coeffs. determ. 8=11820
 $\text{Cd}^{117,117m} \rightarrow \text{In}^{117}$, K-conversion coeff. obs. 8=15984
 $\text{Ce}^{133,133m} \rightarrow \text{La}^{133}$ 8=20722
 Ce^{135} decay 8=20721
 Co^{57} , K shell coeffs. obs., 122 and 136.4 keV 8=3812
 Dy^{165} , and transition multipolarities 8=989
 $\text{Er}^{169} \rightarrow \text{Tm}^{169}$ disint. obs. 8=16039
 $\text{Eu}^{149} \rightarrow \text{Sm}^{149}$, K coeff. 8=7143
 Ga^{72} decay, K coeff. 8=16021
 $\text{Gd}^{149} \rightarrow \text{Eu}^{149}$, K coeff. 8=7143
 Gd^{154} , E2 transition, anomalies 8=1020
 In^{115} , from β^- decay of Cd^{115m} , 8=3822
 $\text{Lu}^{172} \rightarrow \text{Yb}^{172}$, multipolarities of K=3 rot. band deduced 8=15996
 Nb^{90} , K, L coeffs. 8=11813
 Np^{239} , in elec. field, e binding energy var. in Pu^{239} 8=4085
 Os^{182m} , neutron emission 8=16001
 Pt^{184m} , neutron emission 8=16001
 Pt^{195m} decay 8=3837
 Pt^{197m} and Pt^{197} decays 8=7110
 $\text{Pu}^{245} \rightarrow \text{Am}^{245}$ 8=11833
 Re^{188} , following thermal n capture by Re^{187} 8=11780
 Ru^{103} decay spectrum 8=11815
 Sm^{152} , E2 transition, anomalies 8=1020
 $\text{Sn}^{117m,119m}$, of M4, M1 transitions to ground state 8=20717
 Te^{131m} , decay, multipolarities of transitions 8=3878
 $\text{Tb}^{155} \rightarrow \text{Gd}^{155}$, decay, Nilsson model 8=988
 Xe^{123} decay, and energy level scheme 8=7138

Beta-ray spectrometers

- background signals, decay depend. 8=11467
 double-focusing based on $\text{H}=\text{H}_0 a/r \sin \nu$ 8=11468
 electronic integrator to control magnetic field 8=3597
 for $4\pi\beta$ - γ coincidence meas. on activated Au, improved correction 8=6966
 Heidelberg $\frac{1}{2}\pi\sqrt{13}$ instrument, high-resolution 8=15736
 high-resolution production by cooling 8=6811
 iron-free mag. double-lens, construction and performance 8=6809
 lens, magnetic, condenser, computer study of behaviour 8=20389
 long-lens, with triangular mag. field 8=11471
 (n, γ) conversion e spectra meas. 8=11470
 $\pi/2$, post-focusing acceleration allowing det. below 150 eV 8=20387
 refractive electron systems 8=16175
 scintillation, plastic, 2-20 MeV 8=20388
 scintillation type with logarithmic amplifier 8=11469
 spectrograph for meas. of e irradi. effects on semiconds. 8=11466
 $\text{Eu}^{155} \rightarrow \text{Gd}^{155}$ decay, investigation by double focusing iron free instrument 8=11769
 H bubble chamber, calibration for low momentum e 8=11465
 Si(Li) cooled detector 8=3598
 Si:Li surface barrier detector, prod. and resolution, 35-40 keV 8=20201

Beta-rays

- See also Electrons.
 from infinitely-thick sources, energy from transmission through Al 8=20744
 in stars evolution, ν radiation from β decay 8=10138

absorption

- See also Electrons/absorption.
 in water, slowing-down, n-irrad. 8=644
 Ni^{63} , self-absorpt. as metallic Ni 8=16020

angular distribution

- β - γ - γ correlation, CP violation in strong interactions 8=669
 n decay, $e\nu$ correlation 8=3712
 $\pi^+ \rightarrow \mu^+ \rightarrow e^+$, in 140 000 Oe field, e^+ asymmetry 8=3618
 Eu^{154} , 1855-123 keV β - γ directional correl. energy depend. obs. 8=7142
 Sm^{153} , β - γ ang. correl. obs. 8=16035

detection, measurement

- See also Beta-ray spectrometers; Dosimetry; Particle detectors; Radioactivity measurement.
 backscattering deformation, experimental corrections 8=3850
 β emitter standardization, proportional counter 8=16012
 channel multiplier for space research 8=5799
 Cherenkov counter, Pb glass for det. 8=6877
 coincidence expts., magnetic steering device 8=3596
 'curtain-discharge' spark chamber, for β -rays from radioactive source 8=624

Beta-rays—contd**detection, measurement—contd**

- Faraday cup, calibration of secondary emission 8=6808
 $4\pi\beta$, γ -counting efficiency 8=605
 helicity, from μ^- decay 8=3593
 infinitely-thick sources, energy meas. by transmission through Al 8=20744
 liquid scintillator, compensation for extinction using auxiliary source 8=20740
 low-energy emitters, quenching correction in liquid scintillation counting 8=11805
 moisture-detection efficiency and geometry 8=9842
 p-e discrimination by Owen-Batchelor method, theory of high-energy limit 8=6672
 by plastic scintillators, effects of absorpt. of and contamination by gases and liqs. 8=20386
 proportional counter, gas for low level β emitters 8=3852
 satellite instrumentation for auroral studies 8=5837
 in solution, by Cherenkov counting, channels ratio colour quenching correction 8=20382
 tritium evacuation of scintillation probe 8=3853
 C^{14} , evacuation of scintillation probe 8=3853
 $\text{ZnS}(\text{Ag})$ and glass probes, two types, efficiency for β particles from tritium gas 8=15735

effects

- See also Electron beams/effects; Nuclear reactions due to electrons.
 lepton pair production, trident expts. 8=3584
 noise pulses from photomultiplier tubes 8=3216
 polycarbonate, elec. conductivity 8=9204
 polyethylene, elec. conductivity 8=9204
 thin film, space charge effect on transmission 8=13470
 Li to Kr, atoms excit. and ionization by β decay, probabilities calc. 8=4090

polarization

- Au^{199} decay 8=20753
 Ce^{141} decay 8=20753
 from Eu^{152} decay, relative obs. of longitudinal polarization 8=20754
 Pr^{144} - Nd^{144} , O^- - O^+ transition, pseudoscalar interaction 8=3880
 RaE rel. to time-reversal invariance violation 8=11829

scattering

- See also Electrons/scattering.
 backscattering, total coeff. determination using GM and scintillation counters 8=712

Betatrons. See Particle accelerators/orbital.**Bethe-Salpeter equation. See Field theory, quantum.****Bethe-Uhlenbeck equations. See Statistical mechanics.****Bevatron. See Particle accelerators/orbital.****Bibliographies**

- electromagnetic devices, simulation of dynamic characts. 8=6285
 electron collision cross section data, low energy 1925-1966 8=20990
 electrosorption of neutral substs. 8=9716
 FET transistors 8=9169
 flame spectroscopy, analytical applications, 1800-1966 8=23182
 health and safety in U.K.A.E.A., 1966, research and development work 8=19329
 Hertizian resonances, optical methods 8=20929
 laser devices 8=11011
 optical space research, 1946-66 8=19066
 organic mols., proton chemical shifts 8=7498
 photonuclear data index 8=19343
 in polyacene solid solns., energy transfer, (1965-66) 8=14162
 Rijke thermoacoustic oscillations 8=21515
 semiconductors, organic, r. f. spectroscopy 8=14088
 solar radio bursts 8=2845
 Sondhauss thermoacoustic oscillations 8=21514
 CO, lasers, development 8=11050

Binary stars. See Stars.**Binding energy, solid state. See Bonds; Solids.****Bingham plastics and solids. See Rheology.****Biographies**

- Mme. Curie, centenary article 8=3
 resonant elastic response of matter to intense light pulse 8=19925

Biological effects of radiations

- cat, single unit activity of primary auditory vortex 8=19618-9
 hair, use for personal dosimetry 8=11315
 laser hazards to eye, He-Ne continuous wave 8=14900
 linear accelerators, safety in radiotherapy 8=5985
 local tissue heating, appl. of laser microscope 8=6503
 neutron depth dose meas. in tissue-equiv. phantom 8=1584
 neutron dose in air depend. on distance from neutron source 8=10444
 neutron dosimetry in radiological protection 8=14894
 proton recoil dose from DD and DT neutrons, LET distrib. 8=15837
 rat, startle depend. on sensation level 8=19595
 soft X-ray analysis, conference, Boston, June 1967 8=8445
 sunlight deficiency u.v. installations correction 8=14899
 u.s., effect of static pressure 8=23767
 ultrasound in medical diagnosis, harmful effects 8=5986
 vertex pot. obs. rel. to acoustic input 8=19605

Biological effects of radiations—contd

- Al, electron slowing-down, total electron flux, energy spectrum 8=13474
- Cu, electron slowing-down, total electron flux, energy spectrum 8=13474
- Biological technique and instruments**
- amplifier, high input impedance, for electrophysiological meas. 8=5983
- analytic ultracentrifuge, automata acceln. and speed control 8=9742
- aquatic organism detection, capacitive method 8=19332
- autofluoroscope, digital, addressing of crystal mosaic 8=5984
- autofluoroscope, scintillation camera, data processing 8=5982
- bacterial colony automatic counter 8=19333
- biochemistry, soft X-ray microanalysis appls. 8=18795
- chamber for elec. recording, mammalian nervous tissue 8=14896
- colour photomicrography, app. using image intensifier 8=11226
- drug assay, automatic, controlled sequence 8=6245
- electroretinography, use of c.w. laser 8=11233
- extinction and area meas., integration method 8=20058
- films, solid, X-ray microanalysis 8=14482
- 4 π plastic scintillator detector with clinical applications 8=11304
- γ -ray camera with image intensifier 8=15719
- γ -scanning, heart, separation of blood flow and muscle 8=5981
- gravitational compensator for space simulation 8=10446
- hydroxide of hyamine 10-X, chemiluminescence 8=11305
- liquid crystals, applications 8=1527
- macromolecules, diffusion consts. from scatt. spectra 8=12381
- membranes, device to meas. V-I characts. due to ion flux 8=5988
- microkymography, new method and apparatus 8=15566
- microscope ruby laser 8=6503
- Mössbauer spectroscopy, use 8=692
- myocardial stimulation, photon-coupled isolator 8=19331
- optical differentiation of amoebic ectoplasm and endoplasmic flow 8=2869
- phase difference meas. of objects using four part quartz plate 8=15512
- radiometer, biothermal 8=6204
- radiotherapy, particle accelerators 8=6689
- retinal rods and cones, differentiation by staining 8=19330
- u.s. detection, cardiac valves and muscle, motion 8=2868
- ultramicrotome for hard tissue 8=10445
- ultrathin sections, Pb contrasting 8=19336
- urinary U determ. for radiation protection 8=23181
- Au colloids, use in radiotherapy 8=14893
- LiF thermoluminesc. dosimeter 8=14890
- Pu²³⁸O₂, depleted in O¹⁸ for radiation minimization 8=10443

biology

- See also Medical science; Physiology; Zoology.
- animal tissues, e. s. r. spectroscopy, and possible medical appls. 8=14891
- bacteria flagella, surface structure by X-ray exam. 8=23769
- charge-transfer molecular compounds 8=14895
- faunal extinction at last geomag. field reversal, causal reln. 8=23435
- genetic investigations in space 8=14901
- microscope, dry-mass determ. of biological substs., ext. of Pehland-Hager theory to optically anisotropic systems 8=20098
- nervous tissue, mammalian, electrical recording chamber 8=14896
- one-electron or radical group transfer, e. s. r. study rel. to biological intermediates 8=12341
- orgueil carbonaceous meteorite, electron microscopy 8=2830
- redox reactions of living cell, separation of positive and negative charges 8=23762
- signals 20 Hz from under Central Pacific 8=23256
- Venus, surface, life possibilities 8=23675

Physics

- acoustic stimulation aftereffects 8=6197
- auditory nerve fibres in cats, threshold rel. to stapes displacement 8=10761
- auditory and visual sensory modalities, interaction 8=10449
- biological membranes, device to meas. V-I characts 8=5988
- biological systems studied by complementary X-ray diff. and electron microscopy 8=14897
- biomolecules with radiosensitizers, molec. complexes, spin transfer, e. p. r. meas. 8=10450
- bone crystal surfaces, Mossbauer effect appl. to ion uptake mechanism study 8=14902
- cat's ear, olive S-segment cells, encoding of stimulus frequency and intensity 8=218
- DNA with complexed carcinogen, elec. and optical props. 8=18093
- eye's interior structure, u. s. visualization 8=19581
- genetic investigations in space 8=14901
- hearing thresholds underwater at 12 and 35 ft 8=6193

Biophysics—contd

- helical structure with the parameters of the Pauling-Corey α -helix 8=10447
- human body, influence on neutron dose meas. 8=855
- human tissue, ionization chamber response 8=606
- laryngoscopic technique using fiber optics 8=14892
- lichen depsides and depsidones, i. r. and u. v. spectra 8=4191
- memory role in hearing 8=19604
- nuclear reactions in living tissue 8=3891
- one-electron or radical group transfer, e. s. r. study rel. to biological intermediates 8=12341
- pig-skin surface contamination by U 8=5987
- plant tissues and isolated chloroplasts, e. s. r. study of photoinduced changes in Mn²⁺ 8=23763
- protein, myosin monolayers structure 8=2870
- psychophysics, testing for sequential dependencies 8=15086
- tubes, thin-walled, non-absorbing, in living cells, visibility conditions in electron microscope 8=6501
- u. s. detection, cardiac valves and muscle, motion 8=2868
- ultrasonic diagnostic scan within body, localisation employing Doppler shift 8=15074
- Ca⁴⁵ deposition in bone, obs. 8=23766
- Ru¹⁰⁶ in Black Sea seaweeds, identification and separation 8=9734
- Y⁹¹ deposition in bone, obs. 8=23766
- Zn⁶⁵ deposition in bone, obs. 8=23766
- Biot-Savart law.** See Electromagnetism.
- Birefringence.** See Double refraction.
- Bismuth**
- Alfvén wave damping, theory 8=8963
- Alfen waves, high mag. fields 8=5146
- amorphous, strong-coupling superconductivity and phonon structure 8=5202
- atomic-absorpt. characts. using turbulent-flow total-consumption burner 8=18780
- atom, e-binding energy effect on incoherent γ scatt. 8=17703
- band structure, relativistic calcs. using augmented plane wave method 8=8925
- collective motions of atoms in liq. state, compared with polycryst. solid 8=12796
- conduction, electrical, size-depend. 8=22515
- conductivity, thermal, temp. dependence, 1. 3-2°K 8=8656
- crystal growth in furnace using zone cooling 8=4802
- crystal growth mode rel. to cleavage planes 8=17243
- crystallographic modification, condensed on surface, 2-4°K, superconducting props. 8=2155
- dislocations in single crystals, multiplication 8=8732
- distribution coefficient and donor valency of Te 8=22517
- effect of small amounts on self-diffusion of Fe in γ -phase 8=1930
- elec. electromigration of small amounts of Ag, Cd, In and Sb 8=12815
- electrical properties, effect of pressure 8=5173
- electrical properties, 300-540°K 8=13710
- elec. resist. and Hall coeff. of films, temp. var. 8=8995
- electron energy spectrum parameters, variation 8=17880
- electron spectrum, effect of deformation 8=17870
- electron structure from quantum oscillatory phenomena, 1. 2-4. 2°K 8=13659
- Fermi level, quantum variation at high mag. field 8=17882
- films, condensed, crystal structure defects 8=8705
- films, field effect at 4. 2°K 8=17928
- films, thermoelectric power and elec. resist. 8=5383
- films, thin, quantum and classical dimension effects 8=22516
- galvanomagnetic effects 8=8994
- growth of large crystals from supercooled melt 8=17227
- liquid, electromigration of small amounts of Ag, Cd, In and Sb 8=12815
- liquid, optical consts and dielec. const ϵ , + it, 8=12877
- liquid, X-ray diffraction investigation 8=21610
- luminescence in rare-earth oxides 8=14304
- magnetoacoustic waves, microwave phase velocity 8=22097
- magneto resistance in high magnetic field 8=5172
- magneto-Seebeck effect 80°K, effect of surface recombination 8=18211
- mechanical props., deformation and twinning, and elec. props. 8=5052
- plasma two-stream instability, dispersion relations 8=8968
- plasma waves, acoustical, theory. 8=17498
- screening of fixed charge in metal 8=8924
- Shubnikov-de Haas effect meas. at 15 kbar 8=5237
- solid amorphous and molten, spherical close packing and lattice layer structure 8=12786
- solid and liquid, angular correlation of positron annihilation 8=8974
- tunnel junction, conductance maxima rel. to band structure 8=13859
- u. h. f. penetration at cyclotron resonance 8=5588
- u. s. attenuation, amplitude of giant quantum oscs. 8=1848
- valence-band maximum location from recombination and phonon dispersion expts. 8=13660
- Ag¹¹⁰ diffusion, dependence on crystallographic direction 8=13407

Bismuth—contd

- Bi, phonon dragging obs. using thermal e. m. f. and
Nernst effect 8=22435
Bi I, $^2D_{3/2}$ and $^2P_{1/2}$ levels hyperfine structure, $6p^3$
ground configuration 8=4072
Bi $^{3+}$ -activated phosphors 8=23046
Bi $^{3+}$ in $K_2B_2O_4$ glass, γ -irrad., induced absorption
bands 8=5639
Bi $_2$ and Bi $_4$, electron-impact fragmentation and dissoc.
energies 8=4239
BiMn $_2O_6$, mag. structure and ordering 8=22844
Bi:Sb, diamagnetic susceptibility max. and depend. on
Sb content 8=22745
Bi-Sb, transformation of semiconductor into metal, obs.
using magnetoresistance 8=22581
in Si, photoexcitation lines, anomalous broadening rel. to
optical phonons, obs. 8=5601
Sn and Te doped, solid and liq. phase boundary, Peltier
coeff. 8=9238
Sn-doped, galvanomag. effects at low fields at 77°K
rel. to doping 8=2186

Bismuth compounds

- electron structure from quantum oscillatory phenomena,
1.2-4.2°K 8=13659
Ba-Bi titanate (IV), ceramic, Fe $^{3+}$ doped, model and
props. 8=5236
Bi halide complex salts, cryst. struct. 8=8574
Bi $_{1-0.5}Ca_{0.5}Fe_{0.75}V_{1.25}O_{12}$, magnetoelastic inter-
action 8=22850
BiCl, dissociation energy 8=1309
BiCl, A'-X system rotational analysis 8=7504
Bi $_{1-x}Cu_xMnO_3$ solid solns., mag. props. in pulsed mag.
field of 160 kOe 8=18330
BiFeO $_3$, atomic and mag. structure from time-of-flight
n-diff. 8=17346
BiFeO $_3$ with Pb(Ti, Zr)O $_3$, solid solns., dielectric props. at
high temp. and freq. 8=13885
Bi $_2GeO_{20}$, ferroelec., cryst. struct. 8=13254
Bi $_2GeO_{20}$, photo-induced changes in optical
polarization 8=2404
Bi-Hg alloy, angular correlation of positron
annihilation 8=8974
BiI $_3$ refl. spectrum doublet structure rel. to spin-orbit
interaction, 1-5 eV 8=9509
BiO, absorption bands rotational structure 8=12171
BiO molecular absorption bands rotational
structure 8=12171
BiO molecules, magnetic interactions in Hund's
case 8=12172
Bi-O system, new tetragonal phase, crystal
structure 8=17347
Bi $_2O_3$, electrical properties and defect structure in
range 175-250°C 8=8996
Bi $_2O_3$ -WO $_3$ and Bi $_2O_3$ -MoO $_3$ system, crystal structure and
comp. of phases 8=17047
BiOCl, variation of electron diff. intensities 8=1784
Bi-Sb alloys, electron energy spectrum meas. 8=5104
Bi $_2S_3$, evaporated film microstructure 8=17126
Bi-Sb alloy, Shubnikov-de Haas effect vanishing under
pressure 8=22514
Bi-Sb films, 2-layer, struct. defects by Moiré
method 8=22186
Bi $_{1-x}Sb_x$, ($0 < x \leq 0.15$), galvanomag. props. at
77°K 8=22518
Bi-Se layers, vitreous, as near-infrared photo-
detectors 8=22704
Bi-Se vitreous system as semiconductor 8=22579
Bi $_2Se_3$ -Bi $_2Te_3$, thermoelect. props. of cryst. and pressed
powder 8=18212
Bi-Sn eutectic alloys, of type 304 stainless steel,
dissolution kinetics, convective-diffusion study 8=4558
Bi-Sn, superconductivity transition temp. under
pressure 8=2156
BiTe, electrotransport of Ag, Au and Cu, 150 and 250 A/cm 2 ,
 $\leq 400^\circ\text{C}$ 8=17564
Bi $_2Te_3$ alloys sintered, orientation 8=21922
Bi $_2Te_3$, electronic band structure calc. 8=17881
n-Bi $_2Te_3$, thermal diffusivity variations between -200
and +50°C 8=4941
Bi $_2Te_3$, diffusion of Cu, etching technique
investigation 8=1914
Bi $_2Te_3$ -Bi $_2Se_3$ alloys, n-type, thermoelectric props. 8=9237
BiTe:I, I electrotransport, obs. 8=17564
Bi $_2Te_3$ -PbTe alloys, thermoelect. props. 8=22680
Bi $_2Te_3$ -In $_2Te_3$, thermal and microscopic analysis 8=21828
Bi $_2(Te, Se)_3$ system, reflectivity, rel. to effective mass
of conduction electrons 8=2096
Bi-Tl-Te systems, phase equilibrium in Te-rich
regions 8=4703
SnTe-Bi $_2Te_3$ alloy system, thermoelectric props. and
phase relations 8=4716

Bitter patterns. See Magnetization state/domains.**Bitumen.** See Materials.**Block walls.** See Ferromagnetism; Magnetization state/domains.**Blood**

- aortic flow meas., isolation of myocardial
stimulus 8=19931
catalase, crystal structure 8=8575

Blood—contd

- γ -scanning, heart, separation of blood flow and
muscle 8=5981

Boiling

- See also Distillation.
di-ethyl ether, heat transfer in nucleate boiling 8=16948
forced liquid flows, critical heat flux 8=4656
Freon 113 horiz. strip, transition and film boiling, heat flux
and surface temp. fluctuations 8=12986
heat transfer data at low heat flux 8=21773
methane, h. p. heat transfer apparatus 8=16944
nucleate, delay time of bubbles from artificial sites rel. to
surface orientation 8=12987
nucleate pool boiling, bubble freqs. and departure vols., at
subatmos. press. 8=12984
nucleation, third factor 8=12991
pool boiling, effect of subcooling on wall
superheat 8=21772
propyl alcohol, subcooled in tube, heat-transfer
rate 8=21657
simulated, heat transfer coeff. on submerged heating surface
rel. to bubbles 8=16945
in two-phase flow system, transient behaviour of vapour
volumetric conc. 8=12988
vapour pressure, improved boilers for ebulliometric
determ. 8=16952
water, forced convection, flow patterns and burnout 8=4657
water, saturated pool boiling heat transfer, effect of
interfacial vibration 8=12985
water, subcooled in tube, heat-transfer rate 8=21657
water, surface, in vertical tube, local fluid friction 8=12989
N $_2$, h. p. heat transfer apparatus 8=16944

Boiling point

- He, thermodynamic temp. scale 8=19689

Bolometers

- aerial measurements of sea surface temperature in the
infra-red 8=308
development trends, review 8=15098
metal, impedance and noise 8=224
semiconductor, for infrared 8=226
semiconducting thermosonde, use for investigation of
Umov-Poynting's flux distribution in waveguides 8=19880
thin strip, theory 8=19627
p-Ge, using Hall effect 8=6205
p-InSb, using Hall effect 8=6205

Boltzmann equation. See Transport processes.**Bonding of materials.** See Adhesion.**Bonds**

- See also Molecules.
alkali metals, ionic crystals, cohesion with noble gas
atoms 8=8193
n-alkanes, anisotropies of polarizability 8=12248
alloys, atomic interactions 8=4666
ammonium acetate, H bond studies 8=8503
angle, and correl. energy 8=16252
aromatics conjugated π -bonds rel. to absorpt. spectra
obs. 8=4178
atoms X-ray emission spectra distortion 8=16191
aziridines, mag. anisotropy, variation with H bonding,
n. m. r. obs. 8=16895
bent XY $_2$ molecules, bond energy-force constant
relationship 8=7493
biphenyl, phosphoresc. state 8=12288
butatriene, parallel and perpendicular components of
polarizability calc. 8=12264
carbides, stoichiometry and bonding rel. to carbon κ and
metal emission bands 8=2406
charge-transfer complexes, Cl 35 n.q.r. 8=14158
chemical, electronic repulsion theory 8=1229
decane, C-C and C-H bond electrons momentum distrib.
rel. to β^+ annihilation 8=16324
diamond, bending and stretching model for photoelastic
constants 8=8830
diamond, covalent, X-ray diff. meas. 8=4869
diamond-type crystals, bending and stretching model for
photoelastic constants 8=8830
diamond, valence force potentials for calculating cryst.
vibrs., especially rel. to covalent bonding 8=16968
diatomic crystals, force consts. and cohesive
energies 8=8192
diatomic hydrides, binding and molec. charge
distrib. 8=7496
dimethyl amides 8=21150
diphenyls, 4-monosubstituted, conjugated π -bonds rel.
to absorpt. spectra, obs. 8=4212
1,4-distyrylbenzenes, 4-monosubstituted, conjugated
 π -bonds rel. to absorpt. spectra, obs. 8=4212
ethanol, strong intermolec. H bonding at room temp. 8=1523
glasses, nature, det. by spectral char. of Mn 8=8194
halogens, rel. to electron density and space groups 8=17328
hexane, C-C and C-H bond electrons momentum distrib.
rel. to β^+ annihilation 8=16324
s-hybrid charact. of bonding orbitals 8=16251
hydrocarbon molecules, C 13 -H coupling 8=7510
hydrogen bond stretching vibr. in phenol and substituted
phenols 8=4211
intermetallic cpds., length dependence on hybrid character
of bond orbitals 8=13004
ion removal from square lattices 8=21791

Bonds—contd

lattice energies of heavy ionic crystals 8=21794
length corrections using 'riding' model 8=16966
lysozyme, bent H bonding 8=10447
malonic acids, intramolec. H-bonding 8=16894
metal-metal, in coordination complexes 8=8594
metals and alloys, electronic, rel. to diffusivity in metals 8=17559
metals and alloys, using pseudo-atom phase shift model 8=8910
metals and solid solns., cohesive and volume props., ab initio calc. 8=4665
methanol, strong intermolec. H bonding at room temp. 8=1523
methylacetylene, methyl-triple bond interact. MO calc. anal. 8=1291
mixed cryst., impurity-host coupling rel. to intermol. pot. energy 8=17865
molecular complexes exhibiting polarization bonding 8=8585
molecular complexes, quantum theory 8=16249
molecules, π electron, MO's calc. 8=21049
myoglobin, bent H bonding 8=10447
oxides of metals, X-ray spectroscopic investigation 8=9499
paraffins, e irradi., dissoc. probability for specific bond, calc. 8=4206
pentamethylenetetrazole-ICl complex, ligand struct. 8=17453
 π electron systems and mol. packing in crystals 8=13031
piperidinium picrates, stability of cation-oxygen ligand complexes (ligands=triphenylphosphine, tetrahydrofuran) in chlorobenzene, by elec. cond. meas. 8=16338
polarizabilities, effect of internal field on additivity 8=4132
polymethylacrylate and copolymers solns. networks rel. to rheological props., obs. 8=21552
polyphenoxyacetylene, substituents in conjugated bonds, effects 8=4266
polyphenylacetylene, substituents in conjugated bonds, effects 8=4266
quinaldic acid, H-bonding from dimer formation studies at low temp. 8=1825
 σ and π , effects in coordination of CN group 8=12181
7, 7, 8, 8-tetracyanoquinodimethane-anthracene complex structure rel. to polarization bonding 8=17460
in silicate melts, rearrangement in Newtonian flow 8=21628
sydnone ring 8=12299
terphenyls, 4-monosubstituted, conjugated π -bonds rel. to absorpt. spectra, obs. 8=4212
transition metal complexes, ligand exchange and e.s.r. linewidths 8=4616
transition metal cpds. rel. to thermodynamic stability, effective bonds calc. 8=4669
transition metals, electronic 8=8976
transition metals, 5th and 6th periods, valency structure 8=16967
transition-metal fluorides, MO calc. of 10 Dq 8=4667
trans-stilbenes, 4-monosubstituted, conjugated π -bonds rel. to absorpt. spectra, obs. 8=4212
triphenyl boron and phenyl boron halides, boron-phenyl bond strength from thermodynamic props. 8=1863
2, 2, 2-trifluoroethanol H bonding acid, spectroscopic study 8=16863
in X-ray microanalysis, bonds prod. wavelength shifts compensation 8=14481
Al-Mn 1.04% dilute alloy, solute atom-vacancy binding energy 8=8693
Al-O tetrahedral distances in aluminosilicate framework structures 8=21795
Ar, solidified, vapour pressure, binding energy and mean vibration freq. 8=16960
B₂O, planar cpds., B-O bond lengths, mol.-orbital treatment 8=16268
BO₂, vibr. spectrum in alkali halides obs. 8=22946
C-F, positive hyperfine interaction 8=16358
C-H bond strengths, student expt. 8=21109
(CH₃)₃CCl, rupture in γ irradi. at 77°K 8=12349
(CH₃)₂CCl₂, rupture in γ irradi. at 77°K 8=12349
(CH₃)₃SiCl, rupture in γ irradi. at 77°K 8=12349
Co(III) ethylenediamine, secondary coordination shell 8=12319
C-O, bond strength in NCO 8=16369
Eu complex, ligand exchange kinetics 8=23085
Ge, bending and stretching model for photoelastic constants 8=8830
Ge-O-Ge in germanium fluoro- and hydroxyfluoro-compounds and thermal polymerization products, i.r. vibr. freqs. 8=4170
H, between phenol and N, N-dimethylacetamide, solvent effects 8=1571
H-bonded complexes, proton transfer meas. by F n.m.r. 8=12157
H bonding energies in liqs. and dispersion interact. energy, estimation 8=12779
H, in carboxylic acids, i.r. spectra 8=7571
H, in crystals, rel. to elec. cond. 8=13704
H, effect of bond strength on stretching vibr. freq. 8=21141
H, ht. of formation in chloroform-triethylamine system 8=18649

Bonds—contd

H, intramolec. in ethylenediamines 8=1283
H, intramolec. in o-phenylenediamine 8=1295
H, isotope effect on vapour press. 8=4662
H, nature of, and water structure 8=4529
H, in salicylaldehyde soln., n.m.r. obs. 8=16883
H, stretching force const. 8=18532
H, in succinimide-dimethyl sulphoxide 8=12334
H, two approaches to heats of formation 8=12156
H₂⁺, binding energies 8=12194
H₂, intramol. bridging, pot. 8=7497
HCl.2H₂O, H bonding and crystal structure 8=8504
HCl.3H₂O, H bonding and crystal structure 8=8505
HCo(CO)₄, metal-H distance, anal. from n.m.r. with quadrupole coupling 8=5559
HMn(CO)₅, metal-H distance, anal. from n.m.r. with quadrupole coupling 8=5559
H₂O, H bonds and liquid structure from thermodynamic functions, n. scatt. meas. 8=1525
InAsTe, chemical structure analysis 8=1760
K-Ar, interatomic potential, χ^2 minimum method 8=12205
K-F, lattice energy at 0°K and Debye temp. calc. from elastic constants meas. 8=2056
Kr, solidified, vapour pressure, binding energy and mean vibration freq. 8=16960
MnSe, K absorption spectra rel. to chemical bonding 8=14242
Na₂Tl, Tl tetrahedra, model 8=8536
Nb-Mo alloys, atomic bond strength, Debye temp., Young's modulus 8=1626
Nb-Ta alloys, atomic bond strength, Debye temp., Young's modulus 8=1626
Nb-Ti alloys, atomic bond strength, Debye temp., Young's modulus 8=1626
Nb-V alloys, atomic bond strength, Debye temp., Young's modulus 8=1626
Nb-W alloys, atomic bond strength, Debye temp., Young's modulus 8=1626
Ni complex, bis-salicylaloximate-nickel, bond lengths 8=8549
NO, hybridization of O atom effect on terminal atom position determ. by X-rays 8=1261
O-methyl O-(2, 4, 5-trichlorophenyl)N-alkylphosphoramidates, H bonds in soln., i.r. spectra obs. 8=7591
OH-stretching, vibration in solid alcohols, band-width 8=8228
P, covalent, mag. rot. and partial ionic charact. 8=21098
S...H-N in thiourea 8=13339
Si, bending and stretching model for photoelastic constants 8=8830
Si, covalent, X-ray diffr. meas. 8=4869
Si-Fe alloys, rel. to elec. resist. at 800-1700°C 8=9017
Si-O in silicates, rel. to haradaite, SrVSi₂O₇, crystal structure 8=17416
Si-O tetrahedral distances in aluminosilicate framework structures 8=21795
S-N cpds., bond stretching freqs. 8=1299
Sn with Co, Mn, Mo and Re in organo-Sn cpds., Mössbauer obs. 8=4668
Sn-O-Sn in tin fluoro- and hydroxyfluoro-compounds and thermal polymerization products, i.r. vibr. freqs. 8=4170
Sn(O, S, Se or Te) cpds. rel. to chem. shifts of K_α X-ray line 8=9558
Ti-I, in tetraiodothallates 8=18477
Ti-Tl, rel. to Na₂Tl crystal structure 8=17399
[V(CN)₆]³⁻→⁴⁻CN⁻, central ion-ligand charact. 8=23088
VN, electronic state from X-ray diffr. intensity meas. 8=22414
Xe, solidified, vapour pressure, binding energy and mean vibration freq. 8=16960
Bone. See Materials.
Books
advanced optical techniques 8=15489
advances in applied mechanics 8=16683
advances in applied mechanics, IX 8=16747
advances in atomic and molecular physics, I and II 8=16171-2
advances in low temp. physics, V 8=19680
advances in nuclear science and technology, III 8=17691
anelastic and dielectric effects, in polymeric solids 8=22658
annual review of nuclear science, XV 8=15628
applied underwater acoustics 8=10751
atmosphere, upper, main concepts and classification 8=18911
atmosphere, upper, neutral motions review 8=18921
atmospheric radiowave refraction and attenuation 8=14629
aurora, optical 8=18937
aurora, radio 8=18938
auroral and geomag. storms, theory 8=19043
 β -decay 8=3858
elastic systems, stability and oscillations 8=15030
electromag. fields, plane wave spectrum representation 8=15392
e.m. wave propag. homogeneous medium 8=18982
e.m. wave propag. inhomogeneous medium 8=18983
F-centers in alkali halides 8=17680
ferroelectricity 8=5361
foundations of mechanics 8=10518

Books—contd

- fundamentals of quantum mechanics 8=6589
geomag. and ionospheric storms 8=19002
geomag. micropulsations and ionospheric noise 8=18995
Guide to the Solar Corona 8=14886
hadrons, interaction 8=6830
introduction to strong interactions 8=20278
ionosphere F-region irregularities, effects on radio communication 8=18978
ionosphere, lower regions 8=19011
ionosphere, outer region to 2000 km 8=19018
ionospheric and atmospheric radio behaviour 8=19005
ionospheric drift and diffusion 8=18999
ionospheric F-region 8=19017
ionospheric st absorption of solar cosmic rays 8=18997
luminescence of inorganic solids, 1966 8=18593
mathematics for scientists 8=6007
microwave breakdown in gases 8=16411
nuclear interactions 8=11386
particles and accelerators 8=11353
physical acoustics, principles and methods: application to quantum and solid state physics, IV A 8=17486
physical acoustic, principle and methods: the effect of imperfections, IIIA 8=17485
plasma, statistics of non-equilibrium processes 8=16472
plasma theory, MHD, waves, Vlasov-plasmas 8=16455
progress in elementary particle and cosmic ray physics, IX 8=15875
progress in heat transfer 8=15104
progress in nuclear physics, IX 8=15627
progress in nuclear techniques and instrumentation, II 8=15648
progress in optics, VI 8=15541
progress in optics, V 8=15542
quantum mechanics 8=20133
quantum mechanics of applications in chemistry 8=11247
radioastronomy antennas and receivers 8=19005
radio wave transhorizon tropospheric propagation 8=14630
review of plasma physics, I 8=16460
reviews of plasma physics, II 8=16461
reviews of plasma physics, IV 8=16462
semiconductor devices, physics and technology 8=5287
SIDs and geomag. effects rel. to solar activity 8=18996
solar optical radiation, and upper atmospheric processes 8=18910
solar radiation and rel. to geomag. activity 8=19303
space vehicles, interaction with ionized atmosphere 8=14706
spin relaxation theory 8=18446
studies of nuclear reactions 8=16050
thermal stress analysis of composite cylinder 8=19408
transmission electron microscopy, fundamentals 8=15316
ultraviolet radiation, sources and material props. 8=20012
unified theory of nuclear models and forces 8=3760
unitary symmetries, SU(3) and SU(6) 8=20256
upper atmospheric physics 8=23305
wave propagation and turbulent media 8=10735
- Bootstrap theory.** See Elementary particles; Field theory; quantum.
- Bordoni effect.** See Acoustic wave propagation/ultrasonic; Damping; Internal friction.
- Boron**
abundancies estimated in expanding hot universe 8=5840
acceptor states in Si, effects of ext. and int. elec. fields 8=2208
amorphous, tensile strength obs. 8=2050
atom, ^{10}P ground state, electronic structure 8=20950
in austenitic steel, distrib. inferred from He gas bubble obs. after α -irrad. 8=13040
in borosilicate glasses, determ. by neutron transmission 8=23196
diffusion in Ge 8=13406
diffusion in Si, dislocation motion rel. to coefficient 8=1925
diffusion in Si, appl. of dynamical theory of X-ray scattering 8=13412
diffusion in Si, lattice contractions, contrast reversal in filament material, Young's and shear moduli meas. 8=5003
fraction of four-co-ord. B atoms present in borate glasses 8=21915
interaction with O_2 in Ge melt 8=23104
ion bombardment of Si, distrib. profiles in doped material 8=18071
ionization cross-section, electron impact 8=7700
layers, ultra-pure, technique for preparation 8=8315
in low-alloy steel, vacuum spectrometric determ. 8=23188
mass spectrum of isotopes prod. in p-O^{16} reaction 8=20792
solubility in graphite, 1800–2500 °C 8=17006
thermopower and resist. of polycryst., temp. and press. effects 8=18210
trace element determ. by mass spectrometry 8=18769
X-ray Raman scatt. of Cu $K\alpha$ rad. 8=2396
X-ray spectra 8=18503
B rich lattices, ferromag., antiferromag. and superconductivity 8=22870
 B^{10} isotope content, determ. 8=14456
 $\text{B}^{10,11}$, fractionation between BF_3 and additional cpds. 8=5698
OBE pot. in N–N scatt. 8=11583

Boron—contd

- $\text{PbO-Al}_2\text{O}_3\text{-B}_2\text{O}_3\text{-SiO}_2$ system glasses, elec. props. temp. and comp. dependence 8=18170
in Si, nuclear methods of determ. 8=5765
Ta content, spectrochemical determ. 8=9749
- Boron compounds**
borates, crystal chemistry classification 8=13119
borate glasses, e. p. r. of Mn^{2+} , 293–4 °K 8=18408
borate photolysis, aq. Na tetraaryl borates 8=5746
borazine, i.r. spectra and vibr. modes 8=4145
boron oxide, "washing out" effect in mol. e.-diff. pattern 8=16266
diphenylboron halides, thermodynamic properties 8=1863
ferromagnetic compounds, electronic configuration 8=13658
hydrides, crystal chemistry rel. to electron deficient valencies 8=13118
phenylboron dihalides, thermodynamic properties 8=1863
tricyclohexylboron, thermodynamic properties 8=1863
triphenylboron, thermodynamic properties 8=1863
X-ray spectra 8=18503
B complex, $(\text{CH}_3)_2\text{OBF}_3$, isotope separation by exchange distillation 8=18656
 BaTe , photoelectric emission 8=2280
 B_4C , effect of low porosity on elastic props. 8=22313
 B_4C , sputtering with Cd^+ ions, 100–500 eV energies, coeffs. 8=8762
 BF_3 , diamagnetic molecular susceptibility calc. 8=12176
 BF_3 , force consts. calc. 8=21047
 BF_3 , fractionation of $\text{B}^{10,11}$ with additional cpds 8=5698
 BF_3 , isotopic exchange with liq. BF_3 :dimethyl sulphide complex 8=1569
 BF_3 , radiative lifetimes of u.v. emission systems 8=7501
 BH_3 , in lowest bent state, effects of quasi-linearity 8=1243
 BH_3 , thermodynamic functions 8=7624
 B_2H_6 , liq., significant struct. theory 8=4526
 $\text{B}_{12}\text{H}_{12}^{2-}$, electrochem. oxidation in acetonitrile 8=5732
 BL_3 , solid vapour press., surface tension, rel. to nucleation studies 8=12998
 BO_2 , emission spectrum, upper atm. 8=23330
 BO_2^- ion in alkali halides, vibr. spectrum and bonds, obs. 8=22946
 B_2O_3 films on Al in boric acid-formamide electrolyte 8=13089
 B_2O_3 glass, permanent densification by hydrostatic press. 8=22314
 B_2O_3 , molten high-temp., high-pressure viscometer obs. 8=8022
 B_2O_3 planar cpds., B–O bond lengths, mol.-orbital treatment 8=16268
 $\text{B}_2\text{O}_3\text{-SiO}_2$ system, metastable immiscibility 8=21748
BN, cubic, band struct. calc. 8=8922
B–N chains and rings, MO calc. 8=1237
 HBF_4 , microwave spectrum, molec. struct. 8=21063
 $\text{H}_2\text{B}_2\text{O}_4$, cyclic, microwave spectrum and molec. structure 8=12170
- Borrmann effect.** See X-ray diffraction.
- Bose gas.** See Bosons.
- Bosons**
See also Elementary particles; Quantum theory/many-particle systems.
approximation of N pair 8=15917
axial vector currents in terms of baryons and bosons, divergences 8=6743
BCS theory of superconductivity, Freidrichs-Berezin transformation reformulation 8=5190
Bose–Einstein condensation criterion and canonical commut. relns. represent. 8=6108
commutators, equal-time involving divergences of currents 8=6729
condensation of ideal gas, conds. of box size 8=127
creation and annihilation operators rel. to quantum optics 8=11425
 δ^+ resonance, 960 MeV, no evidence in $\text{p} + \text{p} \rightarrow \text{d} + \delta^+$ 8=6982
exchange theory of nuclear forces 8=15916
Fermi-Bose mixtures, phase-separation 8=6109
fluid, λ transition, in lattice model of planar 'spins' 8=126
gas, fermion quasiparticle soln., model for He^3 in He^4 8=6232
gas thermodynamic props. at transition 8=19459
gas, 3-body correl. function with hard-sphere interaction 8=2993
Goldstone, in symmetry breaking 8=3438
graviton-spin-0 particle scatt., low-energy theorem 8=20283
intermediate vector, contrib. to μ mag. moment 8=3602
many-boson problem, operators of zero-momentum states considered as q-number quantities 8=10652
model, one-dimensional, of interacting electrons, flux quantization 8=19460
in nuclei, approximation and antisymmetry, description of anharmonic corrections 8=7030
OBE model for nuclear pot. 8=15919
OBE model for $\text{pp} \rightarrow \text{YKN}$ 8=20522
off-mass-shell matrix elements, conditions for use of partial integration 8=20291
one-boson-exchange model for Y–N scatt. 8=20573
 π leptonic decays with intermediate boson, e.m. corrections 8=6836

- Bosons—contd**
 propagators, covariant and vertex functions for any spin 8=20336
 quasi-free states 8=15676
 Regge trajectories, coalescence, at $t \leq 0$ 8=688
 resonance, δ^- (960 MeV) search in $\pi^- + p \rightarrow p + X^-$ at 1.8 GeV/c 8=756
 resonance empirical mass formula 8=6915
 resonances, $I=1$, $Y=0$, Regge daughter trajectory 8=3557
 resonances R, S, T and U rel. to bootstrap hypothesis and Regge trajectories 8=11411
 resonance 3π in $\pi^-\pi^+\pi^0$, 8 GeV/c, decay to $\pi^-\pi^0$ 8=20447
 statistics, at gravitational transitions 8=14969
 superfluid system, Green's functions 8=10653-4
 system, attractive interact. at zero temp., by quantum field theory 8=2992
 system, Bose fluid, Brownian motion, theory 8=125
 system, energy spectrum of elementary excitations with liq.-structure function 8=3115
 system, interact. with Fermi system, in partially finite geometries 8=127
 system, phase transformations, second kind, quantum theory 8=10651
 system, phonon interaction with individual particles 8=2991
 system, wave function and order-parameter function used for superfluid 8=19696
 vector, leptonic decay model, validity 8=20497
 vector, neutral weak, that couple to $\mu^+\mu^-$ only 8=720
 vector theory of weak interactions 8=6726
 He³ in superfluid He⁴, dilute mixtures 8=15152
 N-N scatt., exchange in N potential 8=3700
 W-intermediate in weak interaction theory 8=3418
- Boundary layer flow.** See Flow.
Bragg reflection. See X-ray crystallography.
Brass. See Copper alloys.
Bravais lattice. See Crystal structure, atomic.
Breakdown, electric
 See also Discharges, electric; Electric strength.
 cathode surface, submicroscopic projections 8=1343
 concentric hemispheres, impulse discharge current expt. 8=16413
 dielectric surface, pulsed discharge in uniform field 8=9188
 dielectric surface, pulsed discharge in non-uniform field 8=9189
 in dielectrics, solid, rel. to collision ionization 8=18153
 electrical insulation and dielectric phenomena, conference Pocono Manor USA (1966) 8=18154
 insulator surface discharge in vacuum 8=7673
 multipacking discharges between coaxial electrodes 8=21225
 partial discharge hazards in elec. equipment 8=16412
 p-n junctions, effect of imperfections on 8=9150
 positive-point/negative-plane, surge shape dependence 8=12408
 SiO₂ layers on Si 8=18080
- gases**
 air, comparison with SF₆ discharge voltage 8=16421
 air, high temperature, microwave 8=21244
 air, laser spark region 8=7670
 air, by focused laser beam, development 8=4292
 air, prebreakdown phenomena and humidity effect 8=12691
 air, 7.5-20 cm gap at atm. pressure 8=16414
 air, temp. effect on pre-breakdown currents at high pressure 8=16417
 atoms and free radicals produced, reactions in fast flow 8=9700
 delay meas., short gaps with intense field 8=7669
 electromechanical conversion, optimum pressure 8=7672
 electron avalanches statistics, influence of energy distrib. 8=4289
 laser-induced, dynamics 8=1344
 microwave, book 8=16411
 noble gases, by laser action radiative equilb. theory 8=7937
 optical-primary using laser, electron-avalanche explanation 8=21243
 preliminary ionization, spark channel parameters 8=7671
 space charge effect in coaxial resonator 8=7647
 space charge effect in coaxial waveguide 8=7646
 Ar; Cs, K and Na seeded, elevated temp., atmos press 8=21247
 CO₂, temp. effect on pre-breakdown currents at high pressure 8=16417
 H, multiphoton ionization 8=12440
 He; Cs, K and Na seeded, elevated temp., atmos press 8=21247
 He-Ne mixture tubes, electron temp. and conc. factors 8=7676
 N₂, prebreakdown Townsend discharge development 8=7677
 N₂, temp. effect on pre-breakdown currents at high pressure 8=16417
 N₂, wave shape effect 8=21246
 Ne afterglow, e density determ. 8=12451
 Ne; Cs, K and Na seeded, elevated temp., atmos press 8=21247
 Ne, secondary ionization mechanisms, theory 8=16419
 SF₆, comparison with air discharge voltage 8=16421
- Breakdown, electric—contd**
liquids
 electrode erosion due to transient arc discharge in dielectric liquid 8=21252
 oil, mineral, in point-to-plane gap, prebreakdown luminosity waves 8=4598
 water, pulsed discharge, dimensional and similarity analysis 8=8114
- solids**
 glasses, and fracture, laser-induced 8=8851
 glasses, laser induced, rel. to photocond. 8=18239
 insulating materials, time dependence 8=22646
 insulation, thermal breakdown under radioactive radiation 8=9190
 insulator, spectrum of discharges occurring in gaseous occlusions 8=18157
 plastic films, effect of corona discharge 8=22645
 semiconductor, mechanisms, review 8=18009
 transparent, laser-induced 8=13865
 Al₂O₃ films, plasma oxidized, thickness variation of field strength 8=22651
 Al₂O₃ films, rel. to thickness 8=5351
 BaTiO₃ rel. to movement of colour centres 8=13884
 Ge, p-i-n and p-n-i-n diodes, avalanche voltage evaluation 8=13855
 Ge:As, at 4.2°K 8=13809
 InAs, avalanche theory 8=22599
 InSb, avalanche theory 8=22599
 KCl, single crystals, directional 8=18167
 Mo-Si epitaxial Schottky, diodes, avalanche voltages obs. 8=13857
 Si n+p junctions, large area, high voltage, destructive reverse breakdown 8=18109
 Si, p-i-n and p-n-i-n diodes, avalanche voltage evaluation 8=13855
 Si, p-n junctions, diffused, breakdown voltage 8=5317
 Si p-n junction, Zener and avalanche breakdown, distinguishing criteria and temp. effects 8=9155
 Si p-n junction, Zener and avalanche breakdown, reverse characteristics, analysis 8=9154
 Si rectifiers, avalanche 8=18123
 SiO, thin film capacitors, a. c. 8=2253
- Breaking strength.** See Mechanical strength.
Breeders. See Nuclear reactors, fission.
Bremsstrahlung
 See also Electrons/radiation; Gamma-ray spectra; Gamma-rays; X-ray spectra/emission; X-rays.
 absorption by potassium halide crystals 8=6795
 angular distribution, definite energy loss of outgoing electron 8=701
 cross section in large-angle Compton scattering 8=15715
 crystal target, photon beam prod., polarization close to 100% 8=13465
 e⁺e⁻ backward scatt., dble.-log asymptotics 8=702
 e-e, in quantum plasma 8=3581
 electron in crystal, spectrum distortion by e scatt. 8=15723
 electron energy spectra production in graphite and Al absorpt. at 10, 20, 40 MeV 8=20769
 electron-ion, spectrum and energy loss rate for extreme relativistic plasma 8=21344
 electron-muon collision theory 8=722
 electron scattering, interference with nuclear γ radiation 8=6796
 electron scatt., stimulation in strong field 8=7172
 experimental programme at Desy 8=11349
 e gas, extreme-relativistic, spectrum 8=12503
 $\eta \rightarrow \pi^+\pi^-\gamma$, emission rate not negligible 8=20488
 graviton, quantum theory of gravitation 8=3452
 inner, correction effects 8=11804
 inverse processes in laser induced ionization in gases 8=16434
 leakage of energy from calorimeter absorber, ionization chamber for meas. 8=11447
 linac beam, reproducibility with pneumatic transfer system 8=6695
 magnetic, ang. distrib. and pressure anisotropy 8=16593
 magnetic, quantum effects by operator method 8=700
 plasma density meas. in θ -pinch 8=12525
 plasma, relativistic correction 8=21343
 p-p interactions, cross-section 8=830
 p-p scatt. calc. 8=833
 p-p, theory 8=6928
 production, e. m. form factor of the medium, multiparticle approach 8=6797
 reflection from single crystal, spectrometry 8=6794
 specimen activation for radioactivity meas. 8=7117
 synchrotron-radiation model for meson prod. in p-p collisions 8=11492
 thin-target, linear polarization 8=11446
 titanium isotopes, proton yields from nuclei excitation 8=7168
 total spectrum of ultrarelativistic electrons 8=20367
 from X-rays on thick anodes, absolute spatial and spectral meas. 8=699
 K* radiative decay process 8=6911
 K₂⁰ $\rightarrow \pi^+ + \pi^-$, calc. 8=3659
 Li gas, absorption cross section as function of wavelength 8=7717
 NaI scintillation spectrometer meas. 8=3582

Bremsstrahlung—contd

- P^{32} , inner, ang. correl. and energy spectrum obs. 8=11811
 Pr^{139} activation, γ -ray spectra 8=986
 Sm^{143} activation, γ -ray spectra 8=986
 U^{238} photofission, Cd^{115} yield, 5.3-6.5 MeV 8=16135
 Y^{90} inner, ang. correl. and energy spectrum obs. 8=11811

Brightness

See also Illumination.

- colour vision, spatially induced changes in rel. to wave-lengths 8=15579
 photographic detector, accuracy and stability 8=11225
 spectral irradiances, spectroradiometric determ. 8=462
 spectrometers with concave-diffr. gratings, image illuminance distrib. calc. 8=487

Brillouin scattering. See Scattering/light.

Brillouin zones. See Crystal electron states.

Brittleness

See also Breaking strength.

- brass, Sb embrittlement, effects of U additions and low-temp. annealing 8=22326
 failure of materials subjected to thermal shock by cooling, statistical analysis 8=22295
 steel, due to NbC precip. 8=22358
 steel, nodular graphite ductility rel. to heat treatment, 800-850°C 8=8843
 steel, on tempering, rel. to structural imperfections 8=17626
 steel, temper, effects of alloying with Ni and Cr and adding Sb, P, Sn or As impurities 8=17797
 steels, ausforming effect on ductility 8=13561
 steels, notch-brittleness occurring during time-to-rupture tests, theory 8=17753
 stress-intensity factor for edge-notched specimen 8=5023
 stress-intensity factor for hollow notched round bar 8=5024
 Ag, H embrittlement obs. 8=22307
 Al- Al_2O_3 , dispersion strengthened, causes 8=8812
 Al-Mg-Zn alloys, rel. to precipitates, grain boundaries and dislocations 8=17646
 Cd, brittle rupture, on contact melting with multi-component eutectics 8=8832
 16/13 CrNi steels, high temp. embrittlement after n irradiat. 8=22362
 Fe, intergranular weakness rel. to fatigue damage 8=5060
 Fe-Cr(0-53%) alloys, aged at 475°C 8=8841
 MgO whiskers, ductility obs. 8=13586
 Rh and Ir, in hot and cold working 8=22390
 σ -FeCr alloy, rel. to atomic ordering and co-ordination 8=17030
 σ -2NbAl alloy, rel. to atomic ordering and co-ordination 8=17030
 Si, plastic deform. in fracture region 8=5084
 Sn, brittle rupture, on contact melting with multi-component eutectics 8=8832
 W, ductile-to-brittle transition, effect of non-metallic trace additions 8=17835

Bromine

- adsorbed on silica gel, laser Raman spectra 8=23031
 analysis, γ -activation method 8=14502
 atomic, new Rydberg absorpt. series and ionization pot. 8=1165
 chemical shift in NaBrO₃ cryst. 8=18457
 liquid, dielectric constant, 20°C, 8.2-18 GHz 8=4596
 meteorites, stony, analysis by thermal neutron activation 8=19271
 molecule, Br₂, continuum and line absorption, 6328 Å, half-width meas. 8=12173
 solid film at 80 K, u.v. absorpt. rel. to intermol. interactions 8=18510
 Br-Br system, 2nd virial coefficient for different electron states at 2000-6000°K 8=1469
 Br₂(Σ^+), improving molec. consts. 8=21065
 Br₂ beam, reaction kinetics with K, Rb and Cs atoms 8=1202
 Br₂, complete pot. energy curve for $^3\Pi_{0+u}$ state 8=7511
 Br₂, orientation of transition moment in photo-dissociation 8=1307
 Br⁻, passivity breakdown of stainless steel 8=23147
 Br^{79,81} quadrupole spectra in paramag. NdBr₃ 8=9469
 Br⁸², flow meas. of Fe(OH)₃ suspension 8=21727

Bromine compounds

- tribromide ions, n.q.r. in different crystals. 8=5567
 Br⁻ and BrO₃⁻ crystals, K⁸³ Mössbauer studies 8=8221
 Br₃CNO₂ mols. dielec. relax. in solid and liquid, 9GHz, 10 and 200kHz 8=18179
 BrF₃, quadrupole coupling consts. 8=16276
 BrHBr⁻ and BrDBr⁻ ions, vibr. spectra 8=12174
 BrO, dipole moment, from gas-phase electron reson. 8=12345
 BrO gaseous free radical, e.s.r. study 8=12340
 BrO, gas-phase electron reson., double quantum transitions 8=12308
 BrO₂⁻ and Br⁻ crystals, K⁸³ Mössbauer studies 8=8221
 BrO₃Na monocrystals, reflection spectrum, effect of cooling 8=18509
 HOBr, matrix i.r. spectra 8=12175

Brownian movement

- classical fluids, h.f. linear response to Brownian oscillators 8=4446

Brownian movement—contd

- coagulation, particle size distrib. 8=8148
 colloidal micelles distrib. density rel. to Boltzmann's theory for perfect gases 8=16905
 Bose fluid, theory 8=125
 critical point, near, interaction with velocity field 8=14989
 fluctuation-dissipation theory, conference Oiso Japan (1965) 8=10641
 Langevin eqn. of Moni and Kubo derived from theory of stochastic processes 8=10616
 lattices, harmonic, motion of heavy impurity 8=19440
 from model of oscillations of autocorrel. function of individual particle vel. in liquid 8=12727
 organic liquids, combination scattering model 8=1559
 particle deposition on vertical surfaces 8=16909
 particle within wave, quantum mechanics 8=91
 polystyrene soln., laser scatt., using photon counting statistics 8=1557
 positive definite kernels on homogeneous spaces and certain stochastic processes 8=10615
 quantal, mean square displacement, Gibbs method calc. 8=6095
 quantum fluid, theory 8=92
 quantum mechanics 8=6094
 relaxation equations and renormalisation, derivation 8=14988
 Smoluchowski eqns., functional integral 8=10614
Brush discharges. See Corona, electric discharge.
- Bubble chambers**
 analysis, error formulae, contribution of small angle nuclear scattering 8=6681
 bubble density and coordinates on photographs, simultaneous meas. 8=20223
 experimental programme at Desy 8=11349
 exposures, co-ordinate measurements, electronic 8=482
 holograms of tracks 8=6567
 large H type, sealing of glass illuminators using pneumatic packing 8=15645
 light scattering by bubbles 8=16835
 3D-picture, rel. to camera characteristics 8=11324
 H, with H target 8=6682
 H as low momentum β spectrometer 8=11465
 H, track momentum and direction multiple scatt. effect 8=6683
 Ne-H cryogenic 8=20224
 Ne-H with H target 8=6682

Bubbles

See also Foams.

- acoustic microstreaming effect on mass transfer 8=21584
 in acoustic wave, standing, force 8=16826
 air bubbles bursting at water surface, elec. charges carried on ejected drops 8=1117
 air in ice, spiral formation 8=4989
 alkali silicate melts, formation, wet atmosphere effect 8=7996
 aut propulsion by rocket effect, applications 8=7894
 cavitation due to sound waves of finite amplitude 8=12753
 in cavitation, pulsations in u.s. wave 8=12862
 coalescence in aq. electrolyte solns. 8=12769
 coalescence, effect on acoustic cavitation threshold 8=12755
 dissolving gas bubbles in liquid 8=12763
 explosive liquids, cavitation by shock wave 8=171
 in flexible liq. filled cylinder, induced by longit. vib. 8=16781
 frequencies and departure vols. in nucleate pool boiling at subatmos. press. 8=12984
 gas, collisional coalescence in solids 8=4695
 gas-filled in fluid, nonlinear oscs. 8=4520
 gas, imploding rel. to trailing microjet 8=12658
 gas in liquid, resonant frequencies and damping 8=21585
 gas, in solids, rel. to surface tension and surface energy 8=21452
 in glass, crystal growth, contamination-nucleated, at surfaces 8=21937
 light scattering, in bubble chamber 8=16835
 in liquid cavity, implosion energy and multiplication 8=12754
 in liquid, microstreaming 8=21590
 in liquid, rising along tube axis, velocity 8=4518
 micro, motion due to cavitating liquid under ultrasonic field 8=21664
 in nucleate boiling, delay time from artificial sites rel. to surface orientation 8=12987
 production of uniform, small bubbles, vibrating capillary 8=4516
 production, use as cavitation nuclei 8=12766
 rising velocities of large bubbles 8=12770
 sphere pulsating in fluid, theory 8=21585
 spherical cap, rising in liquids, velocities and shapes 8=12768
 in streamers associated with acoustic cavitation annihilation obs. 8=1512
 on submerged heating surface, in simulated boiling, heat transfer coeff. 8=16945
 vapour bubble-growth calc., importance of non-equilib. region at bubble wall 8=21767
 wakes behind two-dimens. air bubbles 8=12767
 water, in standing sound wave, forces 8=12855
 water, uniformly distributed, and parametric sound amplification 8=12864

Bubbles—contd

- water vapour, in solid Ag, formation and growth 8=22307
 Al alloy, surface formation during fatigue, rel. to humidity 8=4729
 CO_2 , fixed position in flowing water, interphase mass transfer at high Reynolds numbers 8=12764
 CO_2 in water, volume strain and laminar flow 8=21591
 H_2 in electrolytic dissoc., size rel. to added solutes 8=23149
 He , in Al-Li alloys, neutron irradiation 8=8456
 N in water, decay constants and pulsation frequencies determ. 8=21588
 N_2O in water, volume strain and laminar flow 8=21591
 Zn liquid, vibration rel. cavitation intensity 8=4521

Burgers vector. See Crystal imperfections/dislocations.

CPT (charge, parity, time) conservation. See Field theory, quantum/interactions; Parity.

Cadmium

- addition to Zn, effect on dislocation density and substructure 8=17295
 atom, Stark effect obs. 8=20966
 atoms $5^2\text{P}_{0,1,2}$ levels lifetimes and transitions, obs. 8=1183
 brittle rupture during contact melting with multi-component eutectics 8=8832
 crystal interband absorpt., 82° and 295°K 8=18545
 crystal, vapour-grown, patterns from screw dislocations 8=4803
 diffusion in Al 8=8671
 dislocations and slip planes in single crystals 8=8725
 electric cond., isotopic composition effect 8=13712
 electromigration of small amount in liq. Bi 8=12815
 etch figures 8=1726
 Fermi surface and band structure, calc. 8=2111
 freezing pt., as fixed pt. 8=244
 galvanomagnetic props., evidence for anisotropic electron-phonon scattering probabilities 8=8901
 gravimetric determ., appl. of tetrazoline-5-thiones 8=14188
 ions, effect on photographic process 8=533
 Knight shift anisotropy, reversal at low temps. 8=5552
 laser c.w. oscillation at 4416 Å obs. 8=6460
 liquid, optical consts and dielec. const $\epsilon_1 + i\epsilon_2$ 8=12877
 molten, ultrasonic velocity 8=12867
 moving boundaries, solute profile 8=8468
 ratio in $\text{U-H}_2\text{O}$ subcritical assembly, meas. by scintillation detector 8=7314
 resistance below 3.7°K, temp. variation meas. with supercond. bolometer 8=22573
 resonance fluorescence, modulation effects and lifetime meas. 8=9609
 sheathing of H_2 radiation counter 8=852
 steel plating, H_2 adsorption 8=17163
 texture study by magnetores. and Hall effect 8=8454
 vapour impinging on W, film nucleation in two phases 8=8305
 whisker growth from vapour on Cd substrate, and orientation 8=1747
 Cd I , $5^2\text{P}_{0,1,2}$ electron excitation, effective cross section 8=20993
 Cd^+ ions, 100-500 eV energies, sputtering coeffs. of metal carbides 8=8762
 Cd^+ sputtering of metal nitrides and borides by Cd^+ ions, coeff. determ. 8=17705
 Cd_2^+ , trapped in inert gas matrices, spectra 8=8227
 Cd^{2+} , diffusion in NaCl single cryst. 8=4956
 Cd^{3+} -containing phases, e.p.r. rel. to molecular and structural props. 8=9436
 Cd-Bi solder joints, thermal transport near 0.1°K 8=5203
 Cd^{109} , atmospheric fallout in USSR from Jan. 1964 to June 1966 8=23302
 Cd^{109} and Cd^{111} n.m.r. frequency ratio between 8=16232
 Cd^{109} and Cd^{111} oriented by optical pumping, relaxation on silica walls 8=16233
 K -absorption spectrum, variations rel. to beam direction 8=2408

Cadmium compounds

- alloys, magnetic properties 8=22755
 EDTA chelates of Cd^{2+} , comp. study by ultrasonic vel. meas. 8=23170
 oxide, controlled resistors 8=18034
 Cd(II) , sulphosalicylic acid chelates, of, u.s. velocity and adiabatic compressibility lowering 8=8633
 Cd_3As_2 , Righi-Leduc effect meas. 8=9289
 Cd-Bi eutectic solder, superconductivity 8=2161
 $\text{CdCl}_2 \cdot \text{Mn}^{2+}$, e.s.r. study 8=22902
 CdCO_3 , crystal growth, e.p.r. study rel. to antiferromagnetism 8=18372
 $\text{CdCl}_2 \cdot \text{Ag}$, γ -irradiated, e.p.r. and optical spectra 8=9419
 $\text{CdCl}_2 \cdot \text{Cu}^{2+}$ layer, e.s.r., exchange coupled pairs spectrum 8=18416
 $\text{CdCl}_2(\text{ZnCl}_2) \cdot \text{H}_2\text{O}$, crystn. interphase equil. 8=21933
 $\text{Cd}(\text{ClO}_4)_2 \cdot \text{HClO}_4 \cdot \text{H}_2\text{O}$ saturated solution, thermodynamics 8=12847
 Cd-CdCl_2 soln., radiometric study 8=21615
 $(1-X)\text{CdCr}_2\text{S}_4 \cdot \text{XCdCr}_2\text{Se}_4$ system, mag. and crystallographic props. 8=14006
 CdCr_2Se_4 , magnetostriction constants, resonance linewidth, anisotropy constant and Curie temp. 8=2316

Cadmium compounds—contd

- CdCr_2Se_4 , ferromagnetic, semiconducting props. 8=2189
 CdCr_2Se_4 , ferromagnetism rel. to electrical transport props. 8=18031
 $\text{CdCr}_2\text{Se}_4 \cdot \text{Ag}$, mag. semiconductor, helicon-spin wave interaction 8=18329
 CdF_2 , carrier mobility 8=18029
 CdF_2 crystal activated by rare earth ions, semiconduction and electroluminescence 8=5658
 CdF_2 single crystals, growth and phys. props. 8=8409
 CdGeAs_2 , semiconducting, high-temp. modifications 8=21842
 $\text{Cd}_{0.23}\text{Hg}_{0.77}\text{Te}$ alloy, n-type, determ. of lifetime and recombination mechanism 8=5238
 $\text{CdH}_2\text{IO}_6 \cdot 3\text{H}_2\text{O}$, crystal structure 8=8558
 CdI band spectrum, 3586 to 3495 Å C-system representation by vibr. quantum eqn. 8=21070
 CdI films, vac.-deposited, structure 8=8317
 CdI_2 , absorpt. spectra and luminesc. 8=5660
 CdI_2 , thermoluminescence curves, use of computer anal. 8=5659
 CdI_2 , two new polytypes crystal structure 8=1786
 $\text{CdI}_2(\text{Eu})$, absorpt. spectra and luminesc. 8=5660
 Cd-In alloys, liq., abs. thermoelec. power 8=12913
 $\text{CdI}_2(\text{Pb})$ phosphoresc. and fluoresc. excit., e transitions 8=9605
 Cd-Mn alloys, low temp. electrical resistivity, influence of magnetic ordering 8=2136
 CdO , u.v. reflection, influence of lattice vibrations 8=9514
 $\text{Cd}_2\text{P}_2 \cdot \text{Cd}_3\text{As}_4$ solid soln. system, semicond. 8=22582
 CdSe , absorption and reflection spectra in i.r., low temps. 8=23026
 $\text{Cd}[\text{SC}(\text{NH}_2)_2]_2 \cdot \text{SO}_4 \cdot 2\text{H}_2\text{O}$, crystal structure 8=8513
 $\text{Cd}[\text{SC}(\text{NH}_2)_2]_2 \cdot \text{SO}_4 \cdot 2\text{H}_2\text{O}$, crystal structure 8=8514
 Cd-Sb molten alloys, free energy of mixing and elec. resistivity 8=12842
 CdSb , alloyed with Au, acceptor level depth 8=22456
 CdSb , growth, poly and monocrystalline, electrical and thermal properties, investigation 8=13698
 CdSb , thermoelec. eddy currents 8=5386
 CdSb , thermoelec. efficiency 8=2254
 CdSb_2O_7 ($x=1, 3; y=4, 6$), prep. and props. 8=14363
 CdSb , Te donor level energy position 8=9097
 CdSe , acoustoelectric effect in regime of continuous intense supersonic electron stream 8=8628
 CdSe , conductivity spectra dependence on light intensity over 0.55-0.75 μ 8=18226
 CdSe , control of photocond. props. 8=18231
 CdSe crystals, photoconductivity at high injection levels 8=18224
 CdSe , p-type, Hall effect measurement 8=5239
 CdSe luminescence, absorpt. and refl. spectra rel. to doping, heat treatment and deform., 4.2°K 8=9606
 CdSe , luminescent yield from radiative electron capture by sensitizing recombination centres 8=18598
 CdSe photoconductive layers, current saturation and negative resistance 8=18229
 CdSe , photoconductivity, microwave and d.c., spectral distribution 8=5400
 CdSe powder, surface investigation by e.p.r. method 8=8294
 CdSe , as target in vidicon 8=3215
 CdSe , splitting of exciton lines by uniaxial stress 8=14273
 CdSe , stoichiometric, preparation in thin film 8=17127
 Cd-Se system, phase equilibria 8=16955
 CdSe whiskers, photoinjected space-charge-limited currents 8=18230
 CdSe-CdS mixed crystals at 4.2°K, photoluminescence 8=5656
 CdSe:Mn , photoconductivity rel. to Mn deep donor level 8=2259
 CdSe(S) , band structure rel. to optical props. 8=8928
 CdSnAs_2 , absorption of polarized light 8=22966
 CdSnAs_2 , conduction band structure 8=8929
 n-CdSnAs_2 , magnetoresistance, influence of spin 8=2290
 CdSnAs_2 , n-type, magnetoresistance at 77° and 300°K, obs. 8=5241
 CdSnAs_2 , semiconducting, high-temp. modifications 8=21842
 Cd(S;Se) powder, cathodic luminescence 8=9604
 Cd(SSe) , sintered, photoconductivity decay, rel. to temp. 8=2262
 CdS-SiO_2 film system, heat-stimulated currents, and 'quenched' cond. 8=9096
 CdTe , absorption edge, imperfections effect 8=5603
 CdTe , far i.r. spectrum, 30 cm^{-1} to 4000 cm^{-1} 8=14207
 CdTe films, polymorphism from multiple refl. studies 8=1694
 CdTe , n-type, Gunn effect 8=5242
 CdTe , Gunn effect, rel. to current instabilities 8=5243
 CdTe , Gunn effect and impact ionization, influence of ionized impurity scatt. 8=22583
 CdTe , i.r. absorpt. spectrum 8=14208
 CdTe , metal vacancies formation energies rel. to Te-Te covalent bonding 8=17608
 n-CdTe , photoelectromag. effect 8=18225
 CdTe , pressed, far i.r. optical properties 8=18518
 CdTe solar cell, photovoltaic barrier form. by Pt sputtering 8=10856
 CdTe solar cells, spectral response and integrated array fabrication 8=10856

Cadmium compounds—contd

- CdTe solar cells, 28 V module and roll-up array 8=10857
 p-CdTe, thermostimulated currents and trap levels 8=2260
 CdTe thin film solar cell 8=19735
 CdTe, thin films, structure, obtained by coevaporation 8=4747
 CdTe, wedge-shaped films, photo-voltages rel. to incident angle of illum. 8=5398
 CdTe-Cu₂-Te heterojunction photoconverter 8=6276
 CdTe-HgTe, mass transfer by evaporation-diffusion 8=8673
 CdTe:Mn²⁺ e.p.r. and forbidden transitions 8=14119
 n-CdTe:In, free carrier absorpt. 8=22967
 CdTeS₂, semicond., crystal structure and elec. characts. 8=17354
 Cd₂V₂O₇, cryst. struct. 8=8512
 Cd-Zn solder alloys, high-strength, props. 8=5056
 Cd_{1-x}Zn_xAs₂, thermal and elec. cond. and thermoelec. power 8=5385
 Cd_{1-x}Zn_xS, mixed single crystals, optical, photoconductive and thermoelectric props. 8=18227

cadmium sulphide

- absorption, 2-photon, intermediate states lifetime meas. 8=14173
 acoustic waves, longit., amplification 8=8627
 acoustoelectric effect 3- and 4-phonon processes obs. 8=1850
 acoustoelectric light scanner 8=5309
 application, soleil i.r. compensator 8=15550
 capacitive changes in thin crystals under d.c. bias 8=9195
 cathodoluminescence, electron-probe meas. 8=1754
 cathodoluminescence temp. dependence 8=18597
 chemical sensibilization 8=22584
 crystal amplifier 8=5337
 crystals, bulk, closed system vapour growth from Cd and S 8=17228
 crystal growth from liq. Cd soln. 8=17229
 crystal, single, polishing by phosphoric acid 8=9705
 dislocations origin in vapour growth, obs. 8=8726
 double injection, current kinetics 8=22692
 edge emission, peak shift with excitation intensity 8=2478
 elastic constants between 4.2-300°K, Debye temp. calc. at 0°K 8=13542
 electrical conductivity in strong electric field 8=18030
 electroabsorption, exciton effects 8=22965
 electroacoustic transducer, wideband, using diffusion layer 8=19557
 electroluminescence, d.c. excit. mechanism obs. 8=9608
 electron emission, secondary, and cathodoluminesc., e microprobe obs. 8=14317
 electrooptical effect, meas. at 10.6 μ 8=18515
 etched in KOH(NaOH) soln., light sensitization investigation 8=14294
 exciton stimulated emission for excitation by 50 keV electrons 8=14311
 excitons lines, emission intensity variation rel. to excitation intensity, 4.2°K 8=22964
 exciton lines splitting by uniaxial stress 8=14273
 film on dielectric, ultrasonic Love wave amplification 8=4921
 films, structure and phase composition by electron diffr. investigations 8=4746
 first and second current saturation, build-up time 8=2188
 fluorescence, green-edge, 4.2°K 8=2479
 growth, improved furnace, rel. to fluorescence 8=1739
 hexagonal, band structure calc. by orthogonalized-plane-wave analysis 8=2097
 laser induced refractive index inhomogeneities and absorption saturation effects 8=9515
 laser transition at 90°K using two-photon excitation 8=11091
 lattice Raman scattering theory 8=2397
 layers on Ge, elastic surface wave behaviour 8=8850
 longitudinal optical phonon-plasmon coupling 8=14206
 luminescence, absorpt. and refl. spectra rel. to doping, heat treatment and deform., 4.2°K 8=9606
 luminescence centres nature, heat treatment and impurity effects obs. 8=8741
 luminescence excit. by high photon densities, 4.2 and 77°K 8=9607
 luminescence induced by double photon absorpt. 8=14313
 luminescence, i.r., and thermally stimulated currents 8=5661
 luminescence of photochemically sensitized and unsensitized 8=9603
 luminescence in two-photon excitation case 8=18599
 optical longitudinal phonon-plasmon coupling rel. to reflectivity and wavelength 8=14206
 paramagnetic centres on surface 8=18415
 phase structure recovery to room press. at 77°K 8=1671
 photoconducting, field distrib. and current saturation 8=9250
 photoconducting, optical quenching spectrum temp. dependence 8=9249
 photoconduction induced by double photon absorpt. 8=14313
 photoconductive, h.f. current oscillations on multiple band illumination 8=5397

Cadmium compounds—contd**cadmium sulphide—contd**

- photoconductivity at low temps. 8=9248
 photoconductivity, impurity, stationary lux-ampere characts. 8=22693
 photoconductivity, microwave and d.c., spectral distribution 8=5400
 photoconductivity, ruby laser excited 8=22690
 photoelements, sintered, with p-n-heterotransitions 8=22710
 photoconductivity, thermally stimulated, influence of electric field 8=9239
 photo Hall mobility at high electric field 8=2187
 photoluminescence efficiency, and photocond. response 8=14312
 photoluminescence spectrum, emission bands rel. to N₂ impurities 8=5657
 photosensitive layers, field effect freq. and temp. dependence 8=18228
 photothermoelec. effects 8=22681
 piezoelectric polarons, cyclotron resonance theory 8=9220
 piezoelectric semicond., elec. field distrib. determ. by optical probe 8=18033
 polycrystalline bulk crystals and thin films, orientation inversion 8=8374
 Rayleigh wave amplification at 30 MHz 8=13350
 recombination centres, sensitizing, radiative capture yield of electrons 8=9602
 refractive index, from interference max. on transmission curve 8=2409
 single crystal, photo-Hall mobility and elec. field 8=17860
 solar cell deployable rigid-frame array, performance obs. 8=10845
 solar cells environmental thermal cycling test obs. 8=10848
 solar cell, thin film 8=19735
 solar cells, thin film on Cu and plastic, characts. and stability 8=10855
 solar film cell mechanism obs. 8=10847
 structure, rel. to shift of exciton lines 8=13673
 surface and volume conductance, kinetics comparison 8=18032
 transducers for coherent optical systems 8=15072
 trapping spectrum, effects of optical radiations and water vapour 8=5396
 2-photon transitions to exciton states, oscillator strengths 8=8953
 u.s. amplification, mobility temp. depend. rel. to electron trapping 8=2081
 u.s. dispersion, by acoustoelec. effect 8=1849
 u.s. vibrations, diffr. of light 8=18514
 u.s. wave amplification, 87 MHz transverse, and signal to noise ratio 8=22098
 CdS-Au alloy recombination centre parameters in single crystals 8=14293
 CdS-Au, photosensitive carrier e.s.r. 8=2362
 CdS-CdSe films, thermal quenching of photoconductivity 8=5399
 CdS_{1-x}-CdSe_{1-x}, laser generation freq., temp. depend. 8=11092
 CdS_x-CdSe_{1-x}, stimulated rad. during two-photon excitation 8=23049
 CdS-Co₂S solar cell, mobile impurity ions model 8=10846
 Cd(S;Se) photocond. spectral distrib. and band gap, 100 and 300°K 8=2261
 CdS_{1-x}Se_x, birefringence rel. to concs. of components 8=5763
 CdS_{1-x}Se_x films, prep., structure and props. 8=4748
 CdS-SiO₂ film devices, thermostimulated currents and "frozen" cond. 8=5388
 CdS:Ti²⁺, e.p.r. 8=22900
 S₂ annealing pressure effect on resist. homogeneity 8=8980
 with Te as isoelectronic trap, optical fluorescence and absorpt. 8=23048

Caesium

- additive in thermionic converter emitters, correl. of emission processes 8=15214
 absolute values of ionization cross-section close to threshold 8=12436
 adsorption on Ta ribbon, work function changes 8=9276
 arc diode, effect of Kr, Xe, I and Ar as additives 8=15225
 atom, Cs-inert gas collisional J reorientation, e spin polarization determ. from D, pumping 8=1194
 atom, collisional depolarization of doublets 8=7471
 atom, h.f.s. of 8²P_{3/2} state 8=7400
 atom, Stark effect obs. 8=20966
 atomic beam, scatt. by benzene and cyclohexane beams, comp. 8=1205
 atomic beam, surface ionization on Pt and W 8=12110
 atoms in Cs-Ar low-pressure discharges rel. to light absorpt. 8=7401
 atoms, excitation by low energy electrons, absolute cross sections 8=12087
 atoms, reaction with Br₂ and I₂ molec. beams, kinetics 8=1202
 atomic, two-quantum photoionizations rate 8=12437
 concurrent neutralized by electrons, behaviour of potential after neutralization 8=15350

Caesium—contd

- elastic moduli and pressure derivs. at absolute zero 8=17818
 electrode vapour pressure effect on work function 8=18246
 electron recombination at 6P and 5D levels, cross section obs. 8=12080
 films on Ir, adsorption and electron emission 8=9268
 frequency standard, comp. with H for average freq. and freq. stability 8=10483
 frequency standard, errors 8=15160
 heat capacity, 2°-4°K 8=13374
 impurity states in thermionic converter 8=10842
 ion beam, synthesized, electrostatic oscillation obs. 8=16584
 ions, antishielding factors, by nucl. acoustic quadrupole reson. in CsI 8=9470
 ions Cs⁺ on Hg electrode, partial charge transfer react. 8=18722
 ions, linear acceleration in crossed e.m. fields 8=318
 liquid, density in range 100-750°C 8=12813
 liquid, elec. resistivity, appl. of structure factor and pseudo pot. relation 8=12920
 liquid and solid on Re substrate, mode of growth 8=1696
 liquid, thermal conductivity obs. 75-700°K 8=12851
 l.v. arc, plasma measurements with Mo probe 8=7782
 molecular-ion formation by collision of two excited atoms 8=12438
 nuclear spin relax. below 77°K 8=9463
 one-electron energy levels, for extended Thomas-Fermi-Dirac pot. 8=1167
 plasma converter, migration of ions and electrons, diffusion theory 8=15212
 plasma diagnosis by interpret. of spectra, molec. effects 8=12527
 plasma, diffusion coeff. of ions, and reflection coeff. from plasma boundary, meas. 8=12473
 plasma diode, ion current and Schottky effect 8=339
 plasma diode, meas. of pot. and particle energies by obs. of ion and electron energy spectra 8=15210
 plasma, effective electron-Cs heavy particle momentum transfer collision freq. 8=12476
 plasma, ion-acoustic wave, non-linear Landau damping 8=4375
 plasma, particle losses due to charge exchange 8=21288
 plasma, prod. by resonance rad. from Cs discharge, and parameters 8=4362
 plasma, surface ionization in mag. confinement 8=1415
 plasma in vapour, physical props. 8=12474
 plasmas, electron current flow under influence of d.c. fields and plasma grads. 8=12477
 plasmas, thermally ionized, and field-modified emitting electrodes, plane collisionless sheaths 8=21365
 scattering of Na, atomic differential spin-exchange scattering 8=12109
 spectral absorpt. of vap., temp. depend., Fabry-Perot interferometer 8=501
 standard, servo-system, freq. 8=9
 thermionic converter, anal. of dominant ionic species 8=15211
 thermionic converter, departure from Saha-Langmuir surface ionization rehn. 8=15238
 thermionic converters, electrode inhomogeneity influence 8=297
 thermionic converter, spacing and press. effect on electron temps. and ion densities 8=15242
 thermionic converter, use of O as steady-state electro-neg. additive 8=15224
 thermionic diode, collector work function meas, effect of electron scatt. 8=15243
 vapour, charge exchange H⁺ to H⁻ 8=12441
 vapour, effect on electron emission of Pt-group metals 8=18265
 vapour, effect on thermionic emission of Hf, Th and Ti 8=18264
 vapor interaction with ZrC powder under thermoelectron transformation conditions 8=10843
 vapour, rel. to instability of Ag-O-Cs photocathodes 8=18275
 vapour, ionization decay, microwave cavity studies 8=21271
 vapour, viscosity meas. by transpiration tech-from 800 to 2000°K 8=12702
 vapour, viscosity meas. in temp. range 1000° to 2400°K by transpiration method 8=16714
 work function on W crystal faces 8=13926
 Cs⁺, abundance sensitivity improvement on low mass side 8=12029
 in Cs methoxide-methanol ions coordination number and solvates comp. obs. 8=2497
 Cs plasma diodes, identification of dominant ion species 8=15322
 Cs¹³³, self-diffusion in CsI single crystals and polycrystalline samples 8=8674
 Cs¹³⁷, activity, rain water, Sydney 8=14633
 Cs¹³⁷-Ba^{137m} isotope generator 8=1207
 Cs-F vapour, effect on electron emission from transition metals, model 8=18261
 in He, thermal diffusion calc. 8=21525
- Caesium compounds**
 additives effect on work function of W 8=18251

Caesium compounds—contd

- halides, i.r. windows, polishing 8=495
 Cs graphites, Knight shift of Cs¹³³ rel. to comp. and temp. 8=2382
 Cs halides, defect form. energies and migration energy barriers 8=13422
 Cs halides, low temp. thermal expansion coeffs. and related thermodynamic props. 8=8648
 CsAl(SO₄)₂·12H₂O single crystals, e. s. r. of Ti³⁺ 8=18418
 CsBr, colloid band, effect of particle size 8=1604
 CsBr crystals with F- and M-centres, photoconductivity wavelength and temp. dependence 8=22694
 CsBr, elastic and fourth order elastic constants, and nonlinear pressure dependence 8=13544
 CsBr:P radioluminesc. rel. to hole storage at centres, obs. 8=9625
 CsBr, Raman and i. r. absorption spectra at second order, interpretation 8=5595
 CsCl, e. p. r. spectrum of Mn²⁺, spin-Hamiltonian parameters 8=5534
 CsCl, elastic and fourth order elastic constants, and nonlinear pressure dependence 8=13544
 CsCl, Schottky defect energies for Pm3m and Fm3m structures 8=22178
 CsCl, sp. ht. and dispersion curves, using shell model 8=8610
 CsCl-structure alkali halides, Schottky defects, energy of formation 8=8694
 CsCl transition energy at 470°C 8=1672
 CsCl(g) effusion, ang. number distrib. 8=12706
 Cs₂DyF₇, fluoresc. and absorpt. spectra 8=21814
 CsF additive effect on performance of W-emitter thermionic converter 8=15244
 CsF adsorpt. on W surface, influence on work function 8=18270
 Cs¹³³F¹⁹, h. f. s. molec. beam meas. 8=16278-9
 CsF:Na⁺, impurity displacement calcs. 8=8243
 CsHCO₃, CsDCO₃, i. r. cryst. spectra 8=18556
 CsI, charged dislocations 8=17649
 CsI dislocation etching 8=1727
 CsI, elastic and fourth order elastic constants, and nonlinear pressure dependence 8=13544
 CsI, excitation density of slow secondary electrons, distrib. determin. 8=18283
 CsI, isothermal annealing effect on dislocation density 8=17650
 CsI, nucl. acoustic quadrupole reson., antishielding factors of Cs ions 8=9470
 CsI photoelec. emission, two-photon, 6-8.5 eV 8=18279
 CsI, self-diffusion of Cs¹³³ and I¹³¹ 8=8674
 CsI(Na) fluorescent response function 8=5665
 CsI(Tl) fluorescent response function 8=5665
 CsMnCl₃, prep. and crystallographic props. 8=13138
 CsMnO₄, Raman spectra 8=21085
 Cs₂NiCl₆, effect of melting on spectra 8=9519
 CsNiCl₃, effect of melting on spectra 8=9519
 Cs₂Sb, time depend. of absorpt. and photoemission 8=13937
 CsUF₆, crystal structure 8=1787
 Cs[UO_2Br_4], crystal structure 8=17359
 (Li, Cs)₂SO₄, differential thermal anal. 8=8270
 RbNO₃ molten, refr. index meas. by interferometry 8=4583
- Calcium**
 atom, pionic, 4f-3d transition rel. to π mass 8=6839
 calutron, ionized spectrum, Doppler shift due to charge exchange 8=6334
 determination in picomole range by emission photometry 8=9757
 films, absorpt. of light between 0.5 and 5.5 eV 8=14204
 f. c. c., elec. resistivity from 4.2 to 300°K 8=5175
 ionized solar lines, mean and core profiles of H and K lines 8=23706
 ionized vapour laser, pulse efficiency from cyclic excitation and relax. 8=11056
 ions, CaII reson. lines rel. to photosphere-chromosphere transition zone temp. distrib. 8=19319
 muonic K series X-rays 8=1209
 vapour absorpt. spectra using modified King furnace 8=7393
 Rydberg states obs. from electron collision 8=20941
 Sun, CaII resonance line, emission peaks 8=23744
 Ca⁴⁵ deposition in bone, obs. 8=23766
 Ca²⁺, dipole polarizability from spectra 8=7414
 Ca⁺, pseudopotentials 8=7409
 Ca⁺, ²F and ²G levels, polarization by outer electron 8=7413
 CaII, H and K lines in solar spectrum, rel. to chromosphere model 8=23707
 Ca II, Hartree-Fock multiplet strengths 8=4081
 CaII solar line in lower chromosphere 8=2859
 CaII, spatial extent in twilight, airborne obs. 8=9868
 CaII stellar lines near H I clouds, search for 8=5880
- Calcium compounds**
 apatite crystallites, carbonate effects on morphology during growth 8=1720
 apatites, luminesc. and stoichiometry 8=2477
 calcite, Brewster angle generalization 8=22947
 calcite, elastic compliances temp. dependence 273-90°K 8=5055
 calcite, motional effects in e. s. r. of CO₂ 8=22899
 calcite, optical consts. in region of fund. freq. 8=9512

Calcium compounds—contd

- calcite, refractive indices, variation with pressure to 7 kbar 8=22961
 calcite, stimulated Raman effects 8=5591
 calcite, window in double spectrometer, X-ray diffr. profile exam. with monochromatic radiation 8=22004
 calcium fluoxytantalate: Eu^{3+} , Sm^{3+} , crystalline field parameters of ions 8=16973
 chlorospodiosite ($\text{Ca}_2\text{PO}_4\text{Cl}$), e. s. r. and optical spectra of CrO_4^{2-} 8=14099
 dicarboxylates, i. r. spectra and thermal decomp. 8=23095
 F-centres, X-ray prod. 8=1999
 hydroxyapatite catalysts, H content 8=14395
 manganates, CaMnO_3 , $\text{Ca}_2\text{Mn}_2\text{O}_{10}$, $\text{Ca}_2\text{Mn}_2\text{O}_7$, and Ca_2MnO_4 , mag. props. 8=9390
 manganates, localized v. collective d electrons and Néel temps. 8=9391
 phosphate, nucleation from soln. 8=13135
 portland cement component hydration products, adsorpt. of Ca lignosulphonate and salicylic acid 8=21902
 whitlockite and cerite, isotypy 8=4778
 Ca aluminate hydrates, lamellar, crystal structures 8=8511
 Ca aluminate hydration product, adsorpt. of Ca lignosulphonate and salicylic acid 8=21902
 Ca₄ aluminoferrite hydration product, adsorpt. of Ca lignosulphonate and salicylic acid 8=21902
 Ca hydrosilicate, crystallization in presence of gypsum and Al_2O_3 rel. to cement setting 8=1738
 Ca lignosulphonate adsorpt. on portland cement component hydration product 8=21902
 Ca₂ silicate hydration product, adsorpt. of Ca lignosulphonate and salicylic acid 8=21902
 Ca₃ silicate hydration product, adsorpt. of Ca lignosulphonate and salicylic acid 8=21902
 Ca sulphoaluminate hydrates, expansion characts. 8=21831
 CaAl_2O_4 - CaAl_2O_3 - $\text{Ca}_2\text{Al}_2\text{SiO}_7$ - MgAl_2O_4 , liquidus relations in quaternary subsystem 8=21763
 $\text{Ca}[\text{B}(\text{OH})_4]_2$ modifications, crystal structure 8=17353
 Ca-Bi eutectic melt, displacement of inactive marks during diffusion 8=17565
 CaCl_2 aq. soln., phenomenological coeffs. for elect. cond. and diffusion 8=12924
 CaCl_2 - BaCl_2 system analysis by β -ray backscatt. 8=18796
 CaCl_2 , in Mg fused electrolyte, elec. cond. and density obs. 8=23143
 CaCO_3 , absorbing crystal, complex indices 8=5579
 CaCO_3 aragonitic oolites, solubility in sea water pressure coeff. obs. 8=8012
 CaCO_3 (calcite), lattice parameters, precision, and thermal expansion 8=22015
 CaCO_3 in H_2O , surface charge form. and zero point, obs. 8=16903
 CaCO_3 phase-matched 4-freq. mixing obs. 8=14203
 CaCO_3 , X-irrad., electron-hole trapping 8=5105
 CaCO_3 , X-ray luminesc., empirical decay law 8=14307
 $\text{CaCr}_2\text{Fe}_2\text{O}_4$, antiferromag. structure rel. to CaFe_2O_4 8=18371
 $\text{Ca}_2\text{Cr}_2\text{Fe}_2\text{O}_4$, antiferromag. structure rel. to CaFe_2O_4 8=18371
 CaDPO_4 and dihydrate, i. r. spectra obs. 8=5594
 CaF molecule, A-X and B-X band spectra 8=21069
 CaFe_2O_4 , Mossbauer study of spin relax. 8=21804
 $\text{Ca}_2\text{Fe}_2\text{O}_5$, Néel temp. 8=5499
 $\text{Ca}_2\text{Fe}_2\text{Si}_2\text{O}_9$, F^{3+} 3d⁵ configs. splitting by cryst. field 8=1654
 $\text{CaH}_2\text{IO}_6 \cdot 3\text{H}_2\text{O}$, crystal structure 8=8558
 CaHPO_4 and dihydrate, i. r. spectra obs. 8=5594
 CaI_2 , optical, luminesc. and scintillation props. 8=5654
 $\text{Ca}(\text{IO}_3)_2 \cdot 6\text{H}_2\text{O}$, crystal structure 8=8558
 $\text{CaMg}[\text{B}_5\text{O}_{13}(\text{OH})_{12}] \cdot 6\text{H}_2\text{O}$, inderborite, crystal structure 8=17349
 $2(\text{Ca}_2\text{Mg}_2\text{Si}_2\text{O}_{22}(\text{OH})_2) \cdot \text{Mn}^{2+}$, e. s. r. 8=18414
 CaMoO_4 : Er^{3+} , e. p. r. spectra at 4.2 and 10°K 8=18412
 $\text{Ca}(\text{NO}_3)_2$, binary mixtures with MNO_3 (M = Na, Cs, Rb, K), relax. processes in supercooled melts 8=1586
 $\text{Ca}(\text{NO}_3)_2 \cdot 4\text{H}_2\text{O}$ melts, p. m. r. 8=12938
 $\text{CaNa}_2(\text{CO}_3)_2 \cdot 2\text{H}_2\text{O}$, pirssonite, crystal structure 8=1785
 $\text{Ca}_2\text{Nb}_2\text{O}_7$, eight linear electro-optical coeffs. 8=18513
 CaO, colorability enhancement after plastic deformation 8=22229
 CaO, elastic constants at 80-270°K 8=8831
 CaO, effect on elec. cond. of ferrites 8=13715
 CaO e. s. r. of F centres 8=13456
 CaO, neutron or γ irradiated, O_2 chemisorption rel. to surface states 8=5724
 CaO, sound velocity obs. rel. to Birch's law 8=13349
 CaO, thermoluminesc., unirrad. 8=14308
 CaO, water vapour effect on sintering kinetics, 920-1123°c 8=21833
 $3\text{CaO} \cdot \text{Al}_2\text{O}_3 \cdot 3\text{CaSO}_4 \cdot 32\text{H}_2\text{O}$, crystal structure and chemistry 8=13253
 $\text{CaO} \cdot \text{Al}_2\text{O}_3$: Mn Th and Ce sensitized luminescence 8=14303
 CaO: Mn^{2+} , impurity ion hyperfine coupling constant temp. dependence 8=8196
 $3\text{CaO} \cdot \text{SiO}_2$ hydration in Portland cement, obs. 8=14362
 $\text{Ca}(\text{OH})_2$, thermoluminesc., unirrad. 8=14308
 $\text{Ca}_{10}(\text{PO}_4)_6(\text{Cl})_2$, single crystals, conversion to $\text{Ca}_{10}(\text{PO}_4)_6(\text{OH})_2$ by hydrothermal bomb. method 8=4776
 $\text{Ca}_2\text{P}_2\text{O}_7$: Eu^{3+} activated, luminesc. 8=9628

Calcium compounds—contd

- $\text{Ca}_2\text{Sb}_2\text{O}_7$ ($x = 1, 2, 3$; $y = 4, 5, 6$), prep. and props. 8=14363
 $\text{CaS} \cdot \text{SrS}$ phosphors absorpt., excit. and i. r. flash stimulation spectra 8=9511
 Ca_2SiO_5 and Ca_2SiO_4 in Portland cement clinker, high-temp. microscopic investigation 8=21841
 Ca_2SiO_5 and solid solns., polymorphism 8=13064
 $\text{Ca}(\text{SO}_3\text{F})_2$, i. r. spectra and mag. props. 8=9562
 CaSO_4 : Mn, X-ray luminescence, accumulation capacity 8=5655
 CaSO_4 : Mn^{2+} , e. s. r. allowed and forbidden transitions 8=14116
 CaSO_4 : Sm^{2+} , luminescence 8=23047
 CaTiO_3 films, spark discharge along surface 8=7682
 $\text{Ca}_2\text{V}_{10}\text{O}_{28} \cdot 17\text{H}_2\text{O}$, pascoite, structure determ. and refinement 8=17350
 CaWO_4 : Ce, charge-compensated sites, e. s. r. 8=9418
 Ca_2WO_6 bronzes, struct. evolution with temp., phase stability 8=17048
 CaWO_4 , diffusion of Ca 8=13408
 CaWO_4 laser crystals, light loss, possible scattering contribution 8=19994
 CaWO_4 : Nd, role of Nd in reduction coloration 8=22962
 CaWO_4 : Nd^{3+} , e. s. r., uniaxial pressure effect meas. 8=14121
 CaWO_4 : Nd^{3+} , quasicontinuous laser 8=440
 CaWO_4 , quantum efficiency of Nd^{3+} absorpt. and excitation spectra 8=5667
 CaWO_4 , tunnel structures, interface trapping 8=5381
 CaWO_4 : Nd^{3+} , spin-lattice relaxation time obs. 8=22914
 CaWO_4 : Yb^{3+} , absorpt. spectrum and Zeeman effect 8=14205
 CaWO_4 : Yb^{3+} , symmetry of Yb^{3+} on charge compensation by Na^+ , e. p. r. study 8=18413
 CaY_2O_6 , crystal structure, rel. to Ca ferrite isomorphism 8=4870
 $\text{CaZr}(\text{Hf})_2\text{O}_9$ system of type RTiO_5 structure, and stability relations 8=1719
 CaZrO_3 : Mn^{2+} , paramag. resonance spectrum 8=14118
 CuO - FeO - SiO_2 solid solutions, activity-composition relns. 8=17004
calcium fluoride
 colorability enhancement by plastic deformation 8=22228
 colour centre fluorescence, phonon-assisted, in additively coloured sample 8=14306
 dielectric loss in crystals doped with O^{2-} ions 8=5350
 doped with Ce^{3+} and Yb^{3+} at tetragonal sites, charge compensation 8=22918
 e. p. r., dielectric loss 8=2371
 e. p. r. of Ho^{3+} , stress effects 8=14128
 enthalpies of solution, Born model calculation 8=21650
 F centre, ENDOR meas. 8=9417
 F-centres, fourth shell isotropic h. f. s. constants 8=13457
 fluoride, far u. v. polarizing power 8=15551
 lattice theory, elastic const., dielectric const. 8=13178
 n. m. r. in rotating crystal, decay of transverse magnetization 8=14136
 nuclear spin-lattice relax. via paramag. centres 8=18459
 paramagnetic rare-earth activated, magnetooptic rotation 8=5590
 photochromic crystals, thick hologram storage 8=20118
 proton irradiated, change in microhardness, kinetics 8=22320
 thermoluminescence and thermostimulated exo-emission, obs. 8=14305
 X-ray coloured, absorpt. by colour centres, temp. dependence 8=17683
 CaF_2 (111) face, epitaxial growth of Pt 8=4752
 CaF_2 , and MgF_2 and Na_3AlF_6 , i. r. antireflectant suitability 8=2435
 CaF_2 : Dy^{3+} , giant pulse laser, with high repetition rate 8=11090
 CaF_2 : Dy^{3+} , behaviour of F⁻ interstitials during reduction of Dy^{3+} 8=1949
 CaF_2 (Eu) fluorescent response function 8=5665
 CaF_2 : Eu^{2+} , stress induced nuclear quadrupole splitting 8=22928
 CaF_2 : Eu^{3+} , radiochemical reduction giving Eu^{2+} centres 8=18740
 CaF_2 : Er^{3+} , stimulated emission at $\lambda_1 = 8456 \text{ \AA}$ and $\lambda_2 = 8548 \text{ \AA}$ 8=22963
 CaF_2 , F⁻-treated, photocathodes, spectral characts. 8=18281
 CaF_2 : Gd^{3+} , thermoluminescence, Stark splittings of $^6\text{F}_{7/2}$ and $^6\text{P}_{5/2}$ levels 8=14310
 CaF_2 : GdF_3 , surface-layer dielec. relax. 8=18163
 CaF_2 : H_2D , F^{19} nuclear polarization 8=1640
 CaF_2 : Ho^{2+} , magneto-optical rot. 8=18512
 CaF_2 : Mn^{2+} , hyperfine coupling constants temp. dependence 8=18429
 CaF_2 : Nd^{3+} , new laser line, oscillations from ions at noncubic sites 8=3335
 CaF_2 : Sc^{2+} , paramagnetic reson. in ^2E state, effect of linear Jahn-Teller coupling 8=18402
 CaF_2 : Nd^{3+} , stimulated emission, high-temp. effects 8=22960
 CaF_2 : Sm^{2+} crystals, optical spectrum 8=9513
 CaF_2 : Sm^{2+} , fluoresc. 8=14332
 CaF_2 : Sm^{2+} laser action from giant pulse ruby laser excitation 8=11089
 CaF_2 : Sm^{3+} , tetragonal field, energy levels 8=13009
 CaF_2 : Ti^{3+} optical and e. s. r. spectra 8=14126
 CaF_2 : Yb^{3+} , anisotropy of spin-lattice relax. for Kramers doublets 8=9414
 CaF_2 : YF_3 , Nd^{3+} activated, 'ageing' and photoreduction to Nd^{2+} by stimulated rad. conds. 8=8765

Calcium compounds—contd**calcium fluoride—contd**

- CaF₂:Yb³⁺, new laser line, oscillations from ions at noncubic sites 8=3335
- CaF₂:Yb³⁺, polarization effects in cubic cryst. field from e.p.r. and optical spectra 8=21800
- CaF₂:Yb³⁺, spin-lattice relax. 8=18444
- with Cu²⁺ impurities, e.p.r. spectrum 8=9422
- with Eu²⁺ impurity, e.p.r. spectrum at 77-964°K 8=9424
- F dynamic polarization of 45% 8=18458
- with Fe³⁺ impurity, e.p.r. spectrum 8=9437
- H-doped crystals, spin-lattice relaxation time meas. 8=8206

- Nd³⁺ activated, 'ageing' and photoreduction to Nd²⁺ by stimulated rad. conds. 8=3765
- Nd³⁺ doped, cubic e.p.r. spectrum 8=5539
- Nd³⁺ doped, mag. rotatory dispersion curves 8=5592
- Nd³⁺ optical centre, effect of rare earth impurities 8=5593
- with Ni²⁺ impurity, e.p.r. spectrum 8=9437
- with Ti²⁺ impurities, e.p.r. spectrum 8=9422

Calculating apparatus

- See also Fourier analysis; X-ray crystallography/calculation apparatus.
- analytical cont. of 2-dimens. pot. fields into lower half space, computational scheme 8=23428
- autofluoroscope, scintillation camera, data processing 8=5982
- character recognizer, using domain wall motion in Permalloy wire 8=10876
- computer-generated subjects, 3-d images, recording and reconstruction by Lippmann integral photography 8=20127
- data handling system for sonic spark chamber 8=3484
- data recording, paper-tape punches, solid-state drive circuit 8=6035
- magnetic film memories, written by focused light, thermal cycle-time and read bandwidth 8=10874
- memory, increase of effective storage 8=19371
- memory system, delay line for pulse height analyzer 8=20216
- optics, role in information processing 8=20020
- ratio recording, on-line, simple method 8=6037
- space vehicle radiation meas., data handling system 8=10067
- system for instantaneous plotting of scintillation spectrometer output 8=15636
- wideband magneto-optic readout from rotating disc thin film 8=10871

analogue apparatus

- See also Nomograms; Sliderules.
- acoustic ray tracing in layered atmosphere 8=14637
- beam waveguide stability simulation, effect of lens transverse shifts 8=377
- computer, particle tracks and beam envelopes 8=6680
- computer programme for Josephson radiation effects 8=9064
- computer for strain-gauge deformation measurements 8=10476
- crystal growth rate, simulation 8=8387
- device with two Hall-effect multipliers 8=19374
- for dynamical behaviour of systems, network models, theory 8=6038
- e.m. method for computing gravity and mag. effects of 2-dimens. bodies 8=18807
- fields with rel. motion, elec. network simulation 8=19372
- for infrasonic signal analysis, rapid approx. 8=6179
- integration system using temp. variation for mag. field stabilization study 8=19740
- mass spectrometry, photographic intensity assessment 8=18769
- readout using dynamic magneto-optic detector 8=19750
- simulation of flux reversal in mag. films by uniform rotation 8=14001
- for stress-strain diagrams 8=2919
- viscoelastic materials, dynamic shear, thermistor analog study 8=62
- transmission-line, quadrupole network analogue, precision criterion 8=19373

digital computers

- activity of radioisotope after n bombard. in reactor 8=4025
- analogue-digital conversion, improvement by random noise 8=14942
- appl. of Permalloy wire devices using domain wall propag. 8=14034
- for boundary value problems in cylindrical reactors, in p-θ geometry 8=3989
- CAT, computer of average transients, for rapidly changing spectra 8=6405
- for data anal. in correl. Cherenkov spectrometer system 8=11308
- data collection and computation simultaneously 8=19377
- data collection, nuclear physics, event selector hardware 8=6036
- dislocation loops in superlattices, analysis 8=8719
- display units using storage-CROs for small lab. computers 8=6320
- electronic dig. voltmeter as voltage integrator 8=15168
- ellipsometer, following, operation for film growth monitoring 8=6562

Calculating apparatus—contd**digital computers—contd**

- e produced e.m. showers in solids, study 8=8753
- flocs, random, computer-simulated 8=16906
- formulation of eqn. of state from thermodynamic data 8=10666
- gamma-ray spectrum, complex, decomposition 8=15943
- generation of dislocation pictures in electron microscopes 8=8709
- heart K⁴² clearance, separation of blood flow and muscle 8=5981
- holograms, binary Fraunhofer, generation and reconstruction 8=6576
- ionospheric sounding data processing 8=2703
- and laboratory model of rigid sphere gas, shock wave velocity distribution determination 8=6139
- laser rate equations for pulse reflection and transmission modes 8=409
- on-line in closed loop high-energy physics experiments 8=11350
- mass spectra, digital recording and automatic data reduction 8=1137
- memory circuits, optico-elec., static params. theory and obs. 8=6039
- nuclear spectroscopy, small computer for time-saving analysis 8=6636
- particle accelerators, data collection and analysis 8=6704
- stellar spectra, automatic data reduction 8=23540
- system for stabilizing gain of semicond. γ-spectrometer 8=11439
- time-averaging, baseline slope elimination, in n.q.r. spectra 8=6409
- time-of-flight meas., front end 8=6960
- digital computer programmes**
- activation anal. counting errors 8=14500
- algorithm for atmospheric ray height, with continuous nonlinear refractive index profile 8=23379
- amplifier, crossed-field distributed emission, space charge and secondary emission effects in simulation 8=19712
- atmosphere general circulation model for global study 8=9822
- atomic e. scatt., h.f. approx. calc. 8=12094
- collision probability code for reactor, Minos 8=7295
- cosmic ray μ defl. from primary direction by geomag. field 8=20619
- crystal cell dimensions refinement using I.C.T. Fortran programme 8=8483
- crystal constant calc. 8=4860
- crystal growth eqn., numerical soln. 8=4793
- crystal growth process applic. 8=4793
- crystal structure, field-ion image simulation 8=8494
- crystallization of binary cpds. rel. to kinetic phase transitions 8=4794
- crystallography, electron diffraction pattern, diffuse intensity calcs. 8=13232
- crystallography, for solving complex centrosymmetric structure problems 8=13114
- curve smoothing, stars spectra 8=2785
- data entry, manual, for multichannel analyzer system 8=2909
- density of atmosphere at high altitudes, from drag coeffs. on satellites 8=2612
- dynamic programming, inverse problem in transport theory, applications 8=11613
- electrode field uniformity calc. 8=16395
- e gun, soln. of field and space charge eqns. 8=15284
- electron optical devices simulation 8=6307
- electron probe absorpt. corrections 8=14478
- e.m. wave scatt., 3-d 8=19858
- for energy band calc. in tight-binding approx., and population anal. 8=17878
- equations of motion, formulation using tensor notation 8=19380
- f. c. c. alloy polycrystals, plastic deformation simulation and derived rolling texture 8=13512
- f. c. c. metal polycrystals, plastic deformation simulation and derived rolling texture 8=13512
- Ferraro-Rosenbluth problem 8=1384
- film scanner for particle track measurements 8=3481
- fluid, classical, with Lennard-Jones pot., computer expt. 8=12576
- FORTAN dimensional analysis, for IBM 1620 8=28
- FORTAN IV for analysis of e. scatt. from multipole excited nuclei 8=20773
- Fortran IV for multi-region multi-group reactors one-dimens. reactor computing programme 8=16142
- frequency response calc. for linear systems involving time-delayed terms, FRP Mk 2 8=19376
- function of one variable, uniform polynomial approximation 8=19375
- gravity gradiometer model for simulated gradient contour mapping 8=5771
- Hartmann test reduction, Fortran programme 8=20050
- high-energy physics experiments 8=11350
- for ionograms, polynomial coefficient calc. 8=2698
- ionosphere N(h) profile computation, determ. matrix of coeffs. 8=23399
- ionospheric propagation oblique, digital recording and short-term prediction 8=5806

Calculating apparatus—contd**digital computer programmes—contd**

- Keplerian elliptic motion, expansions 8=10095
- lens, magnetic, condenser, computer study of behaviour 8=20389
- light vel. determ. using rotational spectra of mols. 8=11122
- liquid, laminar viscous film flow on a rotating disc, effect of R number and flow rate 8=4522
- lunar theory, literal developments on Titan 8=23648
- magnetic spectrograph, split-pole, ion optics 8=3228
- MAGOG, 3-d, 2 group diffusion code with burnup 8=20868
- mass spectrometry, high resolution 8=20916
- mean-rate analysis for multiparameter data, PDP8 analyser 8=20182
- melting transition and entropy of solid phase 8=16923
- metallic couples, interdiffusion kinetics description 8=1906
- MHD generators, efficiency calc. 8=3156
- molecular dynamics expt. rel. to cold-n scatt. in liquid Ar 8=21611
- molecular e-energy, linear eqn. method 8=1248
- molecular force consts. 8=21042
- molecular rotational consts. 8=21044
- molecular wavefunctions 8=4137
- Monte Carlo calc. of efficiency of Gd loaded scintillator 8=20558
- Monte Carlo calc. of the transmission of ion-optical system 8=19801
- Monte Carlo methods for finite geometry and multiple scatt. effects in n polarization expts. 8=11610
- multidimensional integrals, evaluation 8=16247
- n spectrometer, fast, semiconductor using Li⁶ and He³ reactions 8=6968
- noise in Markoffian continuous-parameter system, Lax calc. modified for computer evaluation 8=3152
- noise in waveforms, smoothing 8=3153
- non-linear programming, conditions of Kuhn and Tucker 8=2910
- nuclear data mean rate analysis 8=6633
- nuclear instrumentation appl. 8=6624
- nuclei g-factor by differential perturbed angular correlation in Algol 8=7066
- nuclear reactor, time optimal control 8=4015
- optical model fit to n scatt. from Ca and K 8=3933
- photopeak analysis, Ge(Li) and NaI(Tl) spectrometers 8=6792
- for potential field, 2-dimens., analytical continuation 8=17
- particle trajectory in magnetic field, simulation 8=3192
- proton, inelastic scattering by light nuclei, excitation function meas. 8=16068
- pulse height analysis programmes 8=6670
- radar cross section calc., geometrical optics approach 8=20040
- radioactive spheroidal γ -ray source, spheroidal, dose rate on axis 8=3855
- radioisotope sediment tracing studies 8=18835
- reaction rate of H₂ + O₂ 8=18678
- satellite minimum distance from observer 8=19069
- SCAT and SLAB, thermal neutron cross sections 8=20540
- scattering phase shifts, multichannel processes 8=672
- scintillation spectrometry, Fortran IV 8=11295
- single-crystal diffractometer, on-line computer-controlled, counting time optimization 8=13214
- source to target geometry, soln. of activation eqn. 8=3854
- spark chambers, filmless for use with synchro-phasotron 8=3486
- spectrograms, for absolute intensities 8=493
- spectroscopic data, automatic reduction 8=15534
- stellar spectrum analysis, IBM 1620 8=14763
- for structure of monoclinic centrosymmetrical crystals. 8=1769
- symmetry projections for electronic states in magnetic solids 8=17877
- time-of-flight S neutrons, analysis of resonances 8=856
- VEGAS, calc. of N reaction with nucleus ~ 380 MeV 8=20776
- weather forecasting 8=18849
- X-ray diffr. photograph interpretation 8=1770
- X-ray propagation in perfect and nearly perfect crystals, calc. using Takagi's theory 8=13212
- C particle light absorption and scattering 8=513
- CdI₂, thermoluminescence curves, computer anal. 8=5659

Calculation

See also Graphs; Nomograms.

- ab initio molec. potential curves, adjustment 8=12150
- beams, elastic-plastic, large deflections equiv. multipoint cross-sections method 8=10556
- β -ray spectrum, unfolding by numerical methods 8=6810
- Cartesian coords. calc. from internal molec. coords. 8=7500
- Chebyshev polynomials, fitting to equidistant points 8=14941
- computer formulation of ionogram real-height problem 8=2701
- data extraction from ionograms using computers 8=2702
- discharges, elec., gaseous, between parallel plates field distortion 8=21248
- electron density profiles from multifreq. ionograms 8=2695

Calculation—contd

- experimental data, with equal and nonequal spacing 8=27
- initial-value problems, numerical stability, exptl. testing 8=19368
- interface location, coord. stretching method 8=19367
- JWKB phase shifts, efficient computation 8=10514
- Monte Carlo and S_i calc. for Li⁶ loaded glass scintill. detectors 8=6645
- preliminary processing of results from multidimensional analyzer 8=11318
- reduction of $h'(f)$ curves to $N(h)$ profiles using phase refractive index 8=2697
- single polynomial, manual, of ionospheric parameters 8=2694
- thermodynamics of gases, corresponding states law correl. method 8=16697

Calculus. See Differential equations; Integrals; Mathematics. Californium

No entries

Californium compounds

No entries

Calorimeters

- adiabatic, for 20-300°C, construction and use 8=10790
- with adiabatic shell, CH₃OH-H₂O solns., sp. ht. obs. 8=21647
- bomb, two-compartment for combustion 8=15129
- capillary flow, for specific heat of gases 8=7921
- conduction, differential for enthalpy meas. at low temp. 8=15126
- diathermic, for meas. of temp. depend. of specific heat of metals at high temp. 8=1864
- dimensional changes and thermal properties simultaneous obs. 8=6221
- for heat capacity meas. from 1.2°K to room temp. 8=22116
- micro, Tian-Calvet, calibration 8=6222
- pyroelectric, for laser pulse meas. 8=15128
- twin, high-temp., for heat processes and thermodynamic props. of metals and alloys 8=250
- Au plating technique 8=14428
- C cone, for pulsed lasers 8=6223
- Cu, 700 kg for 15 kW e beams 8=11462

Calorimetry

See also Heat of adsorption, etc; Specific heat.

- anatase-rutile transformation enthalpy 8=13074
- appl. to energy ang. distrib. of plasma coaxial accelerator 8=16610
- asymptotic calc. measurements, mathematical interpretation 8=252
- coaxial system, reduced emissivity meas. method 8=223
- gas flow, arc-heated, enthalpy meas. 8=19672
- heat of soln. calorimeter with Peltier cooling for operation at const. temp. 8=9677
- laser microcalorimeter, c.w. He-Ne 8=19673
- low-temp. Cu standard, atomic heat meas. 8=17517
- low-temp., use of pure Cu standard 8=15127
- plasma jet temp. meas. technique 8=12572
- polypropyleneoxide, isothermal crystallization, calorimetric study of kinetics 8=4811
- pulse for specific heat determ. 8=4927
- rare earths, hyperfine interactions obs. 8=17514
- solids, integral emissivity meas. 100-1100°C 8=13400
- solid-solid transformations study 8=17069
- CsCl transition energy at 470°C, differential method 8=1672
- Cu-Be-Al alloys, ageing characts. obs. 8=22335
- KD₂PO₄, order-disorder, ferroelectric, phase transition studies, calorimetric investigations 8=22668

Cameras

- characteristics, rel. to accuracy of stereoscopic pictures of particle tracks 8=11324
- electronic US Navy, linearity and information gain over photography 8=14742
- γ -ray, image intensifier system 8=15719
- image converter, high speed, operation and applications 8=20125
- Polaroid-Land for Wilson cloud chamber photography 8=20222
- Schmidt, wide-angle, all-reflecting, astronomical instrument 8=10107
- strobocameras, use of polaroid projection film 8=534
- TV system for e microscope, image intensification 8=15527
- Weissenberg, crystal orientation correction 8=17208

Candoluminescence. See Luminescence.**Capillarity**

See also Bubbles; Drops; Films/liquid; Foams; Surface tension.

- cylinder withdrawal, gravity corrected theory for speed range extension 8=12762
- moist powder, adhesion to solid in temp. field 8=22303
- ripples on monolayers 8=1514

Capture cross-sections. See Nuclear reactions and subheadings.**Carathéodory's principle. See Thermodynamics.****Carbon**

See also Diamonds; Graphite.

- activity in alloyed austenite at 1000°C 8=17008
- activity in liq. Fe-C-Cr solns. 8=21653
- adsorption of polyethers at soln.-solid interface 8=1708

Carbon—contd

- alternant hydrocarbons, in valence state rel. to atomic orbital changes 8=4135
- amorphous, electronic model 8=8998
- analysis, in bulk materials, nuclear meas. 8=18801
- arc electrode, particle trajectory photography 8=16428
- atom, energy level calc. from ground state configuration 8=20951
- atom, spectral absorption coeffs. compilation 8=12060
- black, sample prep. for elec. meas. 8=2135
- blacks, graphitized, surface heterogeneity, Xe adsorpt. obs. 8=17162
- burning stars, evolution, and pre-supernova models 8=5874
- in carbides of heavy elements, X-ray micro-analysis 8=14475
- carbon black, adsorpt. of He at room temp. 8=21899
- carbon blacks, interact. with gaseous Cl 8=9685
- carbon blacks prod. from coals, X-ray study of structure 8=8351
- charcoal, activated/adsorbed ethylene system, n-scattering rel. to adsorbant mol. motions 8=21901
- charcoal, activated, adsorpt. of He at room temp. 8=21899
- charcoal, surface heterogeneity meas. 8=8293
- chemisorption of O₂ 8=5725
- chondrites, ordinary, total content of 86 specimens 8=19272
- cone calorimeter, for pulsed lasers 8=6223
- contacts in microphones, resistance increase due to surface deterioration 8=19558
- diamond, drilling by electron beams 8=14906
- diffusion, in Fe-Ni alloys, mag. and mech. anisotropies 8=22814
- e. s. r. effect of halogens 8=18411
- effect on creep strength on niobium at 800-1200°C over stress range 1500-5000 lb/in² 8=13593
- fibres, high modulus, structure 8=8457-8
- fibres, preferred orientation 8=1664
- films, evap. reaction with heated metal substrates 8=4745
- furnace, i. r. source 8=15093
- galactic source 3C 191, Si:C ratios 8=14810
- gaseous, oxidation 8=5699
- glassy, X-ray scattering, small-angle, rel. to pore structure and conc. 8=21983
- grains, production in discharge, light scatt. and interstellar matter 8=4296
- graphite, band structure critical points from temp.-modulated reflectance meas. 8=14100
- graphite, stress wave packet, attenuation effect on freq. content 8=8626
- Graphon and Spheron 6, adsorption, monocarboxylic acids and methyl esters 8=8340
- ionization cross-section, electron impact 8=7700
- laser action in electrical discharge containing C 8=12398
- laser-induced 'blow-off' plasma, density and temp. 8=12467
- laser induced emission of electrons, ions and X-rays 8=13947
- low-temperature meas., resist., calibration 8=19682
- in microanalysis probes for light elements, contamination reduction 8=14468
- particles, light absorption and scattering, computation 8=513
- plasma, laser-produced, two-wavelength interferometry 8=21357
- poly(dimethyl siloxane) adsorpt. on black from CCl₄ and xylene solns. 8=8336
- pyrolytic, Hall effect 8=5174
- pyrolytic, thermal diffusivity variations between -200 and +50°C 8=4941
- pyrolytic, tracer-level diffusion of Th, rel. to structure 8=1915
- range of Ar, Kr and Xe ions, 500 KeV to 2 MeV 8=13481
- in refractory metals, diffusion, investigation over wide temp. range 8=17586
- resistors, low-temp. resistance and magneto-resistance 8=17929
- resonance lamp for spectroscopy 8=15538
- soft, structural defects, heat treatment 8=1955
- in steel, quenched, behaviour 8=22354
- steel wire, stress relax. obs. 8=17789
- stopping cross-section for ions with $21 \leq Z_1 \leq 39$ betw. 200-1500 KeV 8=13482
- surface reaction between CO₂ and CO 8=2502
- target for ion emission, bombard by Ar⁺ 8=6626
- X-ray microanalysis using network method analyser, obs. 8=14489
- X-ray Raman scatt. of Cu K α rad. 8=2396
- C black, domain structure study 8=8352
- C I electrostatic interaction integrals using screened hydrogenic orbitals calc. 8=7394
- CI lines in solar EUV limb spectrum, relative intensities 8=19324
- CI lines in solar spectrum, rel. to CH(A² Δ -X²II) transition 8=10389
- C I and II, wave functions and oscillator strengths, from superposition of configs. 8=4073
- C₂ in comet Ikeya-Seki (1965f), (1,0) emission band polarization obs. 8=10360
- C₂, dissoc. energy determ. 8=12336
- C₂, electronically excited in hydrocarbon flames 8=7509

Carbon—contd

- C₂, solar lines, centre-limb anal. in five photospheric models 8=23697
- C₃ radical absorpt. spectrum, diazopropyne photolysis obs. 8=16368
- C⁴⁺ ionization by e impact, cross-sections calc. 8=12435
- C⁵⁺ ionization by e impact, cross-sections calc. 8=12435
- C¹²/C¹³ ratio in interstellar gas, a lower limit 8=5919
- C¹²/C¹³ ratio in solar photosphere 8=23726
- C¹²/C¹³ solar abundance ratio from spectral meas. 8=10429
- C¹³ in tetramethyldiphosphine used in X spectra of X_AAA¹X_A¹ spin systems 8=4235
- C¹⁴, excess atmospheric deposit after nuclear explosion, decay calc. 8=2610
- C¹⁴ in tree rings, rel. to sunspot cycle and Tunguska meteor 8=23225
- in α -Fe, diffusion 8=17572
- in α -Fe, precipitation, n-irrad. effects 8=17059
- in Na-K liquid metal reactor coolants, effect on efficiency of coolant, corrosion activity and residual radioactivity 8=7328
- in Mo, solubility limit and diffusivity 8=17007
- Carbon compounds**
- See also Organic compounds.
- carbides, carbon κ and metal emission bands rel. to bonding 8=2406
- carbides, formation in reaction of oxides in graphite electrodes burnt in d. c. arc 8=14385
- carbides, of heavy elements, C X-ray micro-analysis 8=14475
- carbides, spherical fuel particles prepared from solutions of metal salts 8=16166
- composite sintered materials, elec. resistivity, temp. depend. 8=22502
- ionization energy per ion pair formed by H³ β particle 8=4315
- metal carbonyls, i. r. spectra 8=4189
- mol. beams at high intensity, condensation forming single crystals 8=16383
- sintered materials, effect of heat treatment on electrical resistivity 8=2129
- C_xCs, Knight shift of Cs¹³³ rel. to comp. and temp. 8=2382
- CN⁻ in alkali halides, environmental perturbation of motion 8=2405
- CN bands, red system, electronic transition strength 8=12180
- CN in comet Ikeya-Seki (1965f), (0,0) emission band polarization obs. 8=10360
- CN, electronically excited in active N₂ flames, vibr. population 8=12179
- CN free radical, N¹⁴ quadrupole coupling const. in ground and excited states 8=1316
- CN group, effects of σ and π bonding on coordination 8=12181
- CN halides, photoionization 8=12433
- CN laser, far i. r. 8=11054
- CN mol. Franck-Condon factors rel. to mol. constant var. 8=4173
- CN, solar lines, centre-limb anal. in five photospheric models 8=23697
- CN, spectral band, assuming gaussian line profile, calc. 8=7488
- C₂N₂, photoionization 8=12433
- CNI, i. r. spectrum of vapour 8=12184
- CO, adsorbed on Pd, i. r. spectra 8=4764
- CO, adsorption on clean {100} Ni 8=21906
- CO adsorbed on transition metals, entropy changes on desorption 8=17174
- CO, adsorpt. with H on Rh electrodes 8=18727
- CO, adsorpt. on Ni(110) and W polycrystals 8=17169
- CO, adsorpt. on Rh electrodes 8=18726
- CO adsorption by TiO₂, i. r. spectroscopy 8=8347
- CO, adsorption on W surface partly covered with O 8=4762
- CO-air flames, burning velocities 8=15109
- CO, atomic interaction energy for 6³ Σ^+ state 8=4109
- CO catalytic oxidation rel. to Ag surface struct., chemisorpt. obs. 8=18706
- CO, chemisorbed on Pt-Aerosil surfaces, i. r. spectra 8=9704
- CO, diamagnetic molecular susceptibility calc. 8=12176
- CO, electron removal during d. c. discharge afterglow 8=21233
- CO, equilibrium vapour pressure data 8=21779
- CO, evolution from Ni by vacuum heating 8=16745
- CO, fundamental band at high temp., spectral absorpt. coeff. 8=21067
- CO, incubation time in dissociation 8=21184
- CO ions, appearance potential and kinetic energy 8=7721
- CO, laser oscillation characteristics on electronic transitions 8=11069
- CO lines in solar spectrum, near 2.3 μ , interpret. rel. to no. of mols. 8=19294
- CO molecular vibration and kinetic temperature in solar photosphere 8=10412
- CO mols. dissoc. in solar photosphere-chromosphere transition zone 8=12337
- CO mols. energy transfer to solar photosphere particles 8=12377

Carbon compounds—contd

- CO, O low temp. flame, kinetic calc. 8=9699
 CO oxidation on Pd film, induction period 8=5700
 CO plasma in comets, prod. and flow under influence of solar wind 8=14854
 CO, reaction with O atoms in shock tube 8=1342
 CO, residual, in colour picture c. r. t., mass spectrometry 8=15324
 CO, residual, effect on BaO cathode emission 8=18663
 CO spectrophotometric determ. of low concentrations in air 8=14589
 CO, solar lines, centre-limb anal. in five photospheric models 8=23697
 CO solubility in Ta-O-C solid solns. and equil. press., 1700-2000°C 8=21787
 CO, sorption on Mo, physical and chemical processes from low energy electron interactions 8=18702
 CO sorption on Pt. 8=18701
 CO stretching vibs. in Ni(CO)₄, corrections 8=1570
 CO thermal cond., mag. field effects, 290°K 8=4469
 CO, 3ν band, streng. h.s, widths and shapes 8=16269
 CO, vibr. relax. in shock-wave and nozzle expansion-flow 8=16270
 CO + p collisions 8=1357
 CO from W desorption, electron impact 8=21911
 CO, from W, desorption by electron impact 8=21912
 CO⁺ + CO₂, reaction cross-sections 8=4310
 CO₂, radiolysis in adsorbed state 8=18741
 CO₂, relative intensities, 160°-280°K calc. 8=7506
 CO₂, residual, effect on BaO cathode emission 8=18663
 CO₂ sealed laser tube, life expectancy rel. to form. and adsorpt. of CO and O₂ 8=15461
 CO₂, second virial coefficient, -10 to 200°C 8=12675
 CO₂, solubility in molten salts influence on current efficiency in Al electrolysis 8=12805
 in CO₂ solns., Zn corrosion rel. to predominance diagrams 8=2523
 CO₂, thermal cond. 8=16699
 CO₂ from troposphere, C¹⁴ content obs. 8=2566
 CO₂, u. s. velocity and absorpt., 300°-1300°K 8=4478
 CO₂, vibr. relax. times 8=4146
 CO₂ vibrational relaxation in D₂O from sound absorpt. and vel. meas. 8=21071
 CO₂-water-vapour mixtures, ultrasonic absorption obs. 8=7931
 CO₂ 1.049 μ band rel. to Mercury atmosphere search 8=10352
 CO₂, 10.4 μ band, strength and half-width 8=12178
 CO₂-CO atom., stainless steel corrosion, behaviour of C 8=2515
 CO₂ in calcite, motional effects in e. s. r. 8=22899
 CO₂²⁺Π_g → ²Π_g vibrational transition probabilities 8=21066
 CO₂²⁺, CO₂⁻ ions, injected in alkali halides, i. r. absorption 8=5583
 CO⁺ + CO, reaction cross-sections 8=4310
 CO₂, D content by neutron spectrometry 8=9765
 CO₂-SF₆, critical binary fluids, spectral width temp. and angular dependence 8=21778
 CO₂-N₂ plasma, i. r. emission spectra 8=12510
 CO₂-N₂-He laser, radiation prod., effect of water vapour addition 8=11045
 CO₂-N₂-He laser, multikilowatt in modular form construction 8=11046
 CO₂-N₂-He laser, Q-switching, appls. and progress 8=11047
 CO-N₂O mixture, study of overlapping absorpt. bands 8=7507
 CO₂, N₂O, mixtures, separation in thermal diffusion column 8=7945
 CO₂-N₂ gas laser, use of multipath cell 8=419
 CO₂-N₂-He, Pt catalysed laser system 8=3308
 CO₂ + N₂ mixture, vib. relax. time of ν₃ mode of CO₂, meas. with spectrophone 8=7508
 CO₂⁺, study of the ²Π_g → ²Π_g transition 8=16277
 CO₂^{12,13} laser, selective isotope emission 8=19959
 CO₂, adsorpt. on graphite, anisotropy of polarizability 8=21900
 CO₂-air, CH₄-air interfaces, plane shock refraction and expansion wave generation 8=4482
 CO₂, atmosphere, gas constituent number density determ. using laser beams 8=14585
 CO₂, atmospheric, i. r. absorption over slant path 8=18879
 CO₂ atm., stainless steel corrosion, behaviour of C 8=2515
 CO₂, band emissivities, evaluation 8=16272
 CO₂ bands intensities, rel. to Venus atm. light scatt. props. 8=14846
 CO₂, Brillouin scatt. in critical temp. region and isothermal compressibility, obs. 8=16708
 CO₂ bubble, fixed in flowing water, interphase mass transfer 8=12764
 CO₂ bubble in water, laminar flow obs. 8=21591
 CO₂, cryst. Raman spectra 8=9510
 CO₂, diffusivity and solubility in solid solns. of phosphors in polyvinyltoluene 8=20386
 CO₂, electron-impact dissoc. 8=4133
 CO₂, e impact, ionization and excitation, absolute cross sections 8=21268
 CO₂, eqn. of state for region 0-1000°C and 0-1000 bars 8=10666
 CO₂, equilibrium vapour pressure data 8=21779

Carbon compounds—contd

- CO₂, exchange of O with CO on carbon surface 8=2502
 CO₂, fluoresc. excited by transfer from heated N₂, rel. to chem. laser 8=16271
 CO₂, gasification of graphite, transient phenom. rel. to impurities 8=9678
 H₂-CO₂ gas mixtures, thermal conductivity 8=4473
 CO₂, H⁺, H₂⁺, He⁺ charge exchange, 40-1500 eV 8=21275
 CO₂, heat cond., extension of Saxena-Saksena-Gambhir theory 8=16702
 CO₂, ions and fragments, sequential mass spectrometry 8=21270
 CO₂, ionization curves due to electron impact 8=12434
 CO₂ ionization by Fe atoms, ionization ratio meas. 8=1359
 CO₂, i. r. emission from low vib.-rot. levels in discharges, rel. to laser action 8=12177
 CO₂, i. r. maser, i. r. freqs. by O¹⁸ substitution for O¹⁶ 8=10993
 CO₂ laser amplifier, 10.6 μ, gas flow effect on gain 8=11053
 CO₂ laser amplifier gain characteristics at 10.6 μ 8=6445
 CO₂ laser amplifier, nonresonant multipass 8=6446
 CO₂ laser, atmospheric absorpt. of radiation 8=6441
 CO₂ lasers, development review 8=11050
 CO₂ laser discharge, gain 8=19963
 CO₂ laser, effect of tube structure on power and efficiency 8=11044
 CO₂ laser, excited, population inversion time 8=3309
 CO₂ laser, flux limits for continuous and Q-pulse gain for 10.6 μ line 8=19960
 CO₂ laser freq. of oscill., press. and current depend. shifts 8=15460
 CO₂ laser levels, lifetimes, effects of CO₂, He and N₂ 8=420
 CO₂ lasers, inversion mechanism 8=11049
 CO₂ laser, oscillations and amplifiers dispersion meas. by interferometric method 8=11052
 CO₂ laser output visual obs. 8=15463
 CO₂ lasers, plasma temp. obs. 8=15459
 CO₂ laser, pulse recovery time 8=6443
 CO₂ lasers, power output increase, inexpensive 8=6444
 CO₂ laser radiation, obs. using i. r. image converter 8=19962
 CO₂ laser, sealed-off, high output and long lifetime 8=11048
 CO₂ laser; selective oscillation of P and R branches 8=11051
 CO₂ laser transitions, Lamb dip, obs. 8=15462
 CO₂ laser, vibr. levels population calc. 8=15464
 CO₂, liq. and solid, near i. r. spectra 8=21685
 CO₂, melting curve to 30 kb, obs. 8=1610
 CO₂, molec. collisions rel. to vib. deactivation 8=1321
 CO₂ near critical point, admixture density distrib. 8=21744
 CO₂, near critical point, forced convection heat transfer 8=16915
 CO₂-N₂ laser, modulation of optical cavity 8=19961
 CO₂ oxidation of U-Ti alloys at 450°C 8=5718
 CO₂, pre-breakdown currents rel. to temp. at high pressure 8=16417
 C₃O₂-olefin mixture, photolysis, product isomerization 8=5747
 C₃O₂ reaction with O atoms and active N 8=14360
 CS₂, gaseous, thermal cond. 8=16699
 CS₂, ν₃ bands, gas and liq. 8=12265
 CS₂, impure, ultrasonic absorpt. 8=12861
 CS₂, induced combination scatt. of light, and self-focusing 8=4581
 CS₂, ions and fragments, sequential mass spectrometry 8=21270
 CS₂, laser action, P-branch vibrational transition 8=3310
 CS₂, laser beam filament formation, linearized calc. 8=8067
 CS₂, liquid and crystalline state, sub-millimeter wave spectra 8=7568
 CS₂-N₂ laser, interpretation and mechanism 8=19958
 CS₂, soln. of acetone, thermal diffusion coeff. by heterodyning light 8=4553
 CS₂, stimulated Brillouin scatt., quasi-steady state 8=21687
 CS₂, stimulated, scattering spectrum, amplification of ruby-laser radiation line R₂ 8=9520
Carbon tetrachloride (CCl₄). See Organic compounds.
Carcinotrons. See Electromagnetic oscillations; Electron tubes.
Carrier mobility. See Crystal electron states; Semiconducting materials; Semiconductors.
Carrier scattering. See Crystal electron states; Semiconducting materials; Semiconductors.
Catalysis
 See also Reaction kinetics.
 aspirin, substituted, hydrolysis rel. to intramolec. catalysis 8=5727
 benzene hydrogenation to cyclohexane, effect of support on Ni catalyst 8=9707
 butadiene polymerization by π-crotyl NiII and -NiCl rel. to structs., obs. 8=8576
 catalyst, exo-emission, chem. stimulation 8=22711
 diethyl ether decomposition on W film 8=14404
 diffusion in catalysts 8=14402
 di-n-propyl ethers, decomp. on W film 8=14404
 ethylene oxidation rel. to Ag surface struct., chemisorpt. obs. 8=18706
 formic acid dehydration over Al₂O₃ and SiO₂ gel 8=9701

Catalysis—contd

- heterogeneous reactions, forward and reverse rate const., dynamic method of calc. 8=14403
- hydroxyapatite catalysts, H content 8=14395
- lysozyme enzymatic props., crystallographic study 8=23128
- metal ion promoted atom-transfer oxidation-reduction reactions 8=14401
- D-neopentane exchange, effects of desorption, diffusion and surface exchange 8=23083
- oxidative, catalyst valence transitions energy rel. to oxidised subst. ionization pot. 8=2526
- propylene polymerization, with α -TiCl₃-Al(C₂H₅)₃-H₂O 8=5730
- recombination system of H₂-O₂-gases in BER reactor 8=4014
- selective action of developers on photographic layers, mechanism 8=20124
- wustite reduction in CO, promoters 8=5702
- xanthine oxidase, mech. of action, e. s. r. study 8=14406
- Ag catalysts, form. of oxide layer 8=9706
- Ag, oxidation of acetate ion by K₂S₂O₈ 8=23094
- CO oxidation rel. to Ag surface struct., chemisorpt. obs. 8=18706
- Cu films, epitaxial, activity and topographical changes on exposure to H₂-O₂ combination at 325°C 8=8318
- CuI, defect struct. and catalytic props. 8=22169
- Fe support for NH₃ adsorption, Mössbauer spectra 8=13108
- H oxidation rel. to Ag surface struct., chemisorpt. obs. 8=18706
- Mo, N₂ isotope equilibration 8=18655
- N₂ afterglow, surface catalytic efficiency 8=21239
- W film catalyst, effect of H₂O vapour interact. and absorpt. 8=14405

Cathoporesis. See Electrophoresis.**Cathode-ray oscillographs.** See Electrical measurement.**Cathode-ray tubes.** See Electron tubes.**Cathode rays.** See Electron beams.**Cathodes**

See also Electron emission.

- cleavage by plasma shock wave near axis 8=1336
- cold, for He-Ne gas lasers 8=11067
- electrodes, 90° Rogawski, 120° Rogawski, Bruce, computer calc. of field uniformity 8=16395
- erosion by pulsed discharge 8=7649
- gas discharge, electron back-scattering 8=1331
- gas discharge lamp, noise expt. 8=15521
- glow-discharge tubes, sputtering variation with current 8=2019
- magnetrons, surface-wave, enhanced heating 8=15334
- metal, electron plasma frequency rel. to vacuum arc voltage 8=16426
- microprojections initiating vacuum arc 8=7687
- photocathodes, current-limiting protective circuit 8=13923
- photocathode deposition, vapour detect. by mass spectro-meter and ionization gauge 8=21532
- photocathodes, enhancement of i. r. response 8=18276
- photocathodes, enhancement of quantum efficiency in near i. r. 8=13933
- point-cathode electron source, simplified analysis 8=9273
- point, electron emission energy distrib. 8=9274
- scintillation counter, non-uniformity 8=6642
- semiconductor, high-density, field-emitting, produced by voltage-breakdown process 8=18257
- submicroscopic projections, role in elec. breakdown 8=1343
- thin-film, vacuum arc voltage drop meas. 8=7686
- virtual, in arcing thermionic convertors 8=6271
- Ag-O-Cs photocathodes in convertor tubes, instability caused by residual Cs vapour 8=18275
- Al-Al₂O₃-Al thin film structures, electrode props. rel. to photocurrent direction 8=22689
- CaF₂, F-treated, photocathodes, spectral characts. 8=18281
- Ce containing afterpulses in photomultiplier 8=5418
- MgF₂, F-treated, photocathodes, spectral characts. 8=18281
- O⁺ ion poisoning from feralma anode 8=15330
- ThO₂-Mo cermet, thermoemission constants at high temp. 8=13932
- W, carbon adsorbed high temp. field emission, effect of oxygen and air 8=2276

oxide

- emissivity in low-pressure pulse discharge 8=18258
- growth mechanism, effect of creep rate 8=8801
- space charge effect 8=18259
- surface temp. meas. during pulsed emission 8=9275
- Ba, emission affected by residual gases 8=18663

Photoluminescence. See Luminescence.**Causality.** See Physics fundamentals.**Cavitation****Cavitation**—contd

- and induced nonlinear losses in spherical acoustic waves in ocean 8=9820
 - liquid, acoustic, effect of gaseous nuclei coalescence on threshold 8=12755
 - liquid, bubbles, implosion energy and multiplication 8=12754
 - liquid surface films destruction in sound field at elevated static press., photographic obs. 8=12775
 - liquid transients in pipes, problem of column separation 8=16757
 - liquid, translating cavity, equilibrium and stability 8=7982
 - liquid under ultrasonic field, parametric effects 8=21664
 - metals destruction in magnetostriction oscillator 8=22306
 - n detection in water 8=3721
 - noise modelling parameters 8=19587
 - nuclei, use of single bubbles, production 8=12766
 - by sound waves of finite amplitude 8=12753
 - in standard flow nozzles, effect on discharge coeff. 8=21579
 - ultrasonic shock waves, emitted in Venturi tube 8=19530
 - unsteady cavity flows, extension of Woods theory for hydrofoil design 8=16768
 - vapour cavity in rot. cylindrical tank, oscillations of curved interface with liquid 8=16772
 - Cu, damage by magnetostrictive vibratory method 8=22339
 - H₂O, in vibratory and venturi apparatus, damage prediction 8=16767
 - Hg, liq., in vibratory and venturi apparatus, damage prediction 8=16767
 - Li, liq., in vibratory and venturi apparatus, damage prediction 8=16767
 - Pb-Bi alloy, liq. in vibratory and venturi apparatus, damage prediction 8=16767
 - Zn, liquid, intensity rel. vibration of bubbles 8=4521
- Cavity resonators.** See Acoustic resonators; Electromagnetic oscillations.
- Celestial mechanics**
- in barred spirals, high-energy orbits 8=10099
 - blackbody radiation, Eddington-Lemaitre model 8=23494
 - Brownian motion in a stellar system 8=19109
 - Burrau three-body problem, historical review and soln. 8=19100
 - change of independ. variables in dynamical systems, appls. to regularization 8=23497
 - collective processes in gravitating systems, considering finiteness of parabolic velocity 8=19103
 - control problems, optimal, gradient method 8=2883
 - correction manoeuvres in interplanet. flight, theory 8=2758
 - dynamical friction enhancement of travelling massive particle by stellar co-operative effects 8=19108
 - earth-moon system, solar perturb. of motion near collinear libration points 8=19070
 - epochs of minimum. determ. 8=23559
 - escape vel. effect on dist. of residual velocities 8=14800
 - fields of force generating motion on family of spirals 8=10100
 - field stars system, dynamics of test star 8=10211
 - foundations of and stability problems, book 8=10518
 - Galaxy, mass model velocity dispersions 8=2797
 - gaseous masses, uniform rot., dynamic stability 8=23495
 - Gröbner's method, applications 8=19099
 - inertial frames of reference, planetary and galactic 8=14739
 - interplanetary trajectories correction, by radial heliocentric velocity impulses 8=2760
 - interplanetary trajectories correction, systems requirements 8=2759
 - Keplerian elliptic motion, computerized expansions 8=10095
 - Kepler motion, relativistic spinor regularization 8=19418
 - Kepler problem, formulation invariant with respect to SO₄, SO_{3,1} groups 8=14943
 - liquid-gas media dynamics under zero-gravity, surface effects 8=4506
 - non-linear coupling of two harmonic oscillations 8=14738
 - particle tracks near massive star, relativistic eqns. of motion 8=10110
 - persecution trajectories in central gravitation field, method of construction 8=19098
 - planet, unspherical, motion in gravitational field 8=10096
 - planetary general theory, application of von Ziepel method 8=10338
 - planetary precession derived without use of Einstein's field eqns. 8=19421
 - planets, unspherical, particle motion in gravitational field, appl. of method of averaging 8=23660
 - polytropes, slow rot., non-radial oscills. 8=23496
 - relaxation time in an infinite uniform stellar medium 8=19112
 - restricted three-body problem, props. of soln. of first-order variational eqns. 8=10094
 - retrograde satellites and possible past planets, loss due to tidal forces 8=23653
 - satellite, equatorial, resonance phenomena 8=19074
 - satellite resonance with longitude-dependent gravity 8=19073
 - in solar gravit. field, motion of variable mass particle 8=10093
 - stellar dynamics in a discrete phase space 8=19107

Cavitation

See also Vortices.

- acoustic, associated streamers, bubble annihilation obs. 8=1512
- bubbles, pulsations in u. s. wave 8=12862
- damage resistance to metals using rotation disc in water 8=5035
- explosive liquids, detonation by shock wave 8=171
- finite-amplitude waves, variation of α/γ^2 , explanation 8=12856
- in flow past a cylinder, equiv. vel. and boundary effects 8=16769
- hydrodynamic and u. s., gas diffusion, into void 8=4497

Celestial mechanics—contd

- stellar system, self-gravitating, with uniform rotation, kinetic theory 8=23502
- Sun-Earth-Moon-artificial satellite system, equations of motion 8=2808
- three bodies problem, new periodic soln. 8=19097
- three body problem, Pythagorean, complete numerical soln. 8=10098
- three body problem in space, regularization of singularities 8=10533
- 3-body problem, 3 dimensional, dispersion of fragments 8=19102
- triple systems, trajectories in plane problem, computer calc. 8=19101
- OH mols. and charged particles, in interstellar space, maser action mechanism 8=5927

Cell model. See Liquids, theory.

Centrifuges

- analytic ultracentrifuge, automata acceln. and speed control 8=9742
- centrifugal force explanation, by two problems 8=35
- temperature distrib. in liquid 8=21654
- ultracentrifuge sedimentation during period of const. accn. 8=19379
- ultracentrifugation, simultaneous, automatic sequence and photo control system 8=4631

Ceramics

- alundum, Al-90 and Al-100, X-ray analysis, qualitative and quantitative 8=9762
- anatase formation at high temps. 8=1684
- β spodumene-silica in $\text{Li}_2\text{O}-\text{Al}_2\text{O}_3-\text{TiO}_2-\text{SiO}_2$ glass ceramic 8=1661
- electron bombardment luminescence, viewing by optical microscopy 8=14296
- ferroelectric condenser, use in thermodielectric generator 8=9231
- glass-ceramic from $\text{SiO}_2-\text{Li}_2\text{O}-\text{ZnO}$ system, plastic deformation 8=17829
- glass-ceramics, strengthening by application of compressive glazes 8=22322
- as heating element core in creep test furnace, influence on properties of metals 8=13543
- laminated, residual stress development at interfaces, rel. to mech. props. 8=17723
- magnetic meas., prep. of ball-shaped samples 8=10859
- magnetic, spinels and related structures 8=18291
- mechanical props., deformation and fracture, review 8=17726
- nuclear and engineering, conference Harwell 1965 8=16168
- nuclear science and technology for ceramists, conference, Washington USA (1966) 8=16167
- permanent magnets for quadrupole lens 8=3226
- piezoelectric ceramics, sensitivity to high stress perpendicular to polar axis obs. 8=19556
- piezoelectric readout device for spark chamber 8=3485
- piezoelectric stress sensitivity of permittivity reduced by heat treatment 8=19555
- porcelain, electrotechnical, Ag diffusion rate temp. dependence 8=17584
- porcelain, thermal cond. and specific heat 8=1893
- portland cement component hydration products, adsorpt. of Ca lignosulphonate and salicylic acid 8=21902
- quartz-kaolin-microdine reactions during firing, i.r. studies 8=18690
- sensing device for meas. atmospheric humidity 8=18855
- tensile strength meas. 8=22321
- whitewaves, quartz-free, flexural strength rel. to elasticity mod. 8=17733
- window for microwave plasma diagnostic systems at 8, 4 and 2mm 8=7789
- Ba-Bi titanate (IV), Fe^{3+} doped, model and props. 8=5236
- BaTiO_3 doped with Sb_2O_3 , surface states 8=13790
- Be_3N_2 vaporization, enthalpy and enthalpy of activation, vapour pressure and evap. coeff. 8=1624
- $\text{CaAl}_2\text{O}_4-\text{CaAl}_4\text{O}_7-\text{Ca}_2\text{Al}_2\text{SiO}_5-\text{MgAl}_2\text{O}_4$, liquidus relations in quaternary subsystem 8=21763
- Fe caked powder, porosity and thermal conductivity 8=13388
- Mo-alumina ceramic seals bonding mechanism, obs. 8=16743
- Ni: Al_2O_3 , sintered, compressive strength grain size dependence 8=2048
- PbCrO_3 , high pressure synthesis 8=23110
- $\text{Pb}(\text{Zr}, \text{Sn}, \text{Ti})\text{O}_3$ ferroelectric, Nb-doped, elec. props. 8=2246
- $\text{Pb}(\text{Zr}-\text{Ti})\text{O}_3$, addition of Cr_2O_3 8=13043

Cerenkov radiation. See Cherenkov radiation.

Cerium

- effect on cast iron, austenitic, struct. 8=21988
- isotopes, four natural, shift 8=21025
- sensitizer for $\text{CaO} \cdot \text{Al}_2\text{O}_3 \cdot \text{Mn}$ emission 8=14303
- Ce(III) exchanged faujasite, crystal structure 8=8515
- Ce^{44} , activity, in rain water, Sydney 8=14632
- Ce^{3+} -activated phosphors 8=18600
- Ce^{3+} , in silicate glass, Faraday rotation, freq. depend. 8=18531
- W, adsorbed, e emission, Thomas-Fermi-Dirac theory 8=5414
- in YFe garnet, magnetostriction 8=2344

Cerium compounds

- cerite and whitlockite, isotopy 8=4778
- Ce ethyl sulphate, Schottky anomaly and spin-phonon coupling 8=8636
- Ce ethylsulphate, spin-bath relaxation, Kapitza resistance 8=19700
- Ce magnesium nitrate and He^3 , boundary resistance due to spin fluctuation 8=10800
- CeAlO_3 , chemically homogeneous, crystal structure 8=17355
- CeO_2 , sublimation and high-temp. X-ray diffrn. 8=21785
- CeCl_3 , e. s. r. and susceptibility meas. 1.07°-4.2°K 8=14097
- $\text{CeCl}_3 \cdot 7\text{H}_2\text{O}$, paramag. spin-lattice and cross relaxation, 1.1°K to 4.2°K 8=14096
- Ce-Ni-Si system, ternary cpd. formation, comp. and structures 8=17200
- CeO_2 crystal, conduction mechanism from electrolyte reduction study 8=18164
- CeO_2 , molec. geometry 8=7550
- CeO_2 , non-stoichiometric, defect structure model 8=22166
- CeO_2 single crystals, Er^{3+} centers spin relaxation times 8=5530
- CeO_2 single crystal growth for laser and optical components 8=1740
- CeO_2 , transients and non-ohmic behaviour 8=9196
- CeS, gaseous, dissociation energies 8=7616
- Ce_2S_3 , γ -phase stabilization with additives 8=8264
- $\text{CeO}_2-\text{ZrO}_2$ mixtures, high-temp. semicond. 8=22614

Cermets. See Ceramics; Metals.

Change of state. See Boiling; Condensation; Freezing; Melting; Phase transformations; Sublimation; Vaporization.

Characteristic temperature. See Specific heat.

Charcoal. See Carbon.

Charge. See Electric charge.

Charge carriers. See Crystal electron states; Semiconducting materials; Semiconductors.

Charge exchange. See Collision processes; Ionization/gases.

Chelates. See Molecules; Organic compounds.

For inorganic chelates see under various element headings

Chemical analysis

- See also Spectrochemical analysis.
- alloys by secondary ion emission 8=18286
- analytic ultracentrifuge, automata acceln. and speed control 8=9742
- atomic absorpt. flame photometry, instrument developments 8=18777
- by cathodoluminescence, scanning e microprobe meas. 8=14493
- crystals, improved method 8=14254
- EDTA chelates of Cd^{2+} and Hg^{2+} , comp. study by ultrasonic vel. meas. 8=23170
- electron absorpt. microanalysis, microscope band-pass filter and obs. 8=15303
- electron probe secondary emission effects meas. 8=13941
- by electron probe specimen current meas., binary targets backscatt. coeffs. 8=14467
- inert gases isotopes anal. in Te ore 8=14455
- lunar surface by scatt. α particles aboard Surveyor V 8=23463
- microanalysis, point-anode proportional counters, for X-ray detection 8=14497
- n.m.r., acetone-chloroform system 8=2498
- ores and slags, analysis with unipolar arc 8=1345
- particle optics appls. to microanalysers 8=14464
- pre-concentration in trace analysis 8=18753
- pre-concentration in trace analysis 8=18754
- standard silicate rocks, scheme for anal. 8=9802
- trace analysis, pre-conc. techniques 8=18753
- trace analysis, pre-conc. techniques, sampling and reagents 8=18754
- trace, by electron and optical microscopy 8=17269
- trace characterization based on elec. meas. 8=18757
- trace characterization based on elec. props. of mats. 8=18756
- trace characterization rel. to physical props. of materials 8=18755
- Al purity by resistance meas. at He boiling temp. 8=9741
- Cd, gravimetric, use of tetrazoline-5-thiones, complexing agents 8=14188
- Co(II)-Ni(II)-Mn(II)-V(V)-Mo(VI) chloride systems, extraction separation studies 8=23077
- Cu-Ni alloys, electron-probe microanalysis, atomic no. effect 8=9764
- H_2O isotopic anal. of micro quantities 8=22151
- $\text{H}_2\text{O}-\text{D}_2\text{O}$ mixtures, comp. determ. by F^{19} n.m.r. 8=14454
- Mg alloys, electrographic 8=18762
- N determ. in Cr alloys 8=9740
- Pb in air, estimation by chromatography 8=9754
- Pd, gravimetric, use of tetrazoline-5-thiones, complexing agents 8=14188
- Se phase detection in V_2V_{1-x} alloys, by etching 8=17102
- Si, electronic grade, by frozen drop method 8=14509
- Sm_2O_3 , verification of existence 8=9738
- Te phase detection in V_2V_{1-x} alloys, by etching 8=17102
- Zr alloys, electrographic 8=18762
- ZrO_2 , phase transitions and polymorphism investigations 8=4722

adsorption

- See also Chromatography.
- direct electrical meas. on electrodes 8=9767

Chemical analysis—contd

electrochemical

- polarography, impedance meas. 8=5735
 polarography, controlled-potential differential 8=14507-8
 selenocystine-selenocysteine, polarography 8=18760
 trace, techniques review 8=18758-9
 BaCl₂-CaCl₂ system, 8-ray backscatt. 8=18796
 WO₄²⁻ ion in HCl, polarography 8=18736
 Zn in ethylenediamine medium, polarography 8=18761
 Zr(IV), polarographic behaviour 8=18735

by mass spectrometry

- See also Mass Spectrometers/applications.
 analog computer technique for assessing photographic intensity 8=18769
 colour picture c. r. t., residual gas analysis 8=15324
 gas chromatograph application 8=5761
 gas flow meas. in e tube manufacture 8=18770
 gases from overheated power transformer 8=23173
 inert gases, 90°-sector instrum. 8=12033
 isotope abundance ratio meas. 8=7355
 LKB 9000 with gas chromatograph, testing and application results 8=7363
 oil diffusion pumps back-streaming fluid analysis 8=9746
 oxide matrices, trace element determ. 8=18769
 polyacrylonitrile, pyrolytic products 8=23174
 polyvinyl alcohol, pyrolytic products 8=23175
 polyvinylidene chloride, pyrolytic products 8=23174
 PVC, pyrolytic products 8=23175
 reactor radiation chemistry, continuous sampling method 8=23165
 refractory materials, trace element determ. 8=18769
 research mass spectrometer 8=23172
 spark source, ion beam chopper 8=18767
 spark source, trace analysis of solids 8=18768
 tetraethyl compounds, group IV elements 8=18766
 tetramethyl compounds, group IV elements 8=18766
 trace characterization 8=18769
 trace characterization in solids by spark source mass spectrometry 8=18768
 Be, trace element determ. 8=18769
 U, trace element determ. 8=18769

by nuclear reactions

- activation anal. counting errors, binomial distrib. statistics 8=14500
 light elements, by γ 's and charged particles 8=14503
 nuclear activation analysis in trace characterization 8=18798
 trace characterization-chemical and physical, symposium NBS, USA, Oct. 1966 8=8437
 trace characterization by nuclear activation analysis 8=18798
 trace elements in chromatographic paper, by neutron activation 8=14501
 2.8 MeV neutron, from (D, d), activation analysis 8=18800
 Ag, by (γ , γ') reaction 8=14502
 B in Si, determ. by irradiating with thermal neutrons 8=5765
 Ba, 2.8 MeV neutrons inducing (n, n' γ) reactions 8=18800
 Br, by (γ , γ') reaction 8=14502
 Br, 2.8 MeV neutrons inducing (n, n' γ) reactions 8=18800
 C, in bulk materials, 4.43 MeV γ -rays from n scatt. 8=18801
 D in gases, neutron time-of-flight spectrometry 8=9765
 Eu, in Eu₂WO₃ by γ -activation 8=9766
 Gd, in Gd₂WO₃ by γ activation 8=9766
 H determ., neutron activation analysis 8=2553
 He³ activation anal., rapid calc. methods 8=18799
 In, by (γ , γ') reaction 8=14502
 N¹⁵ tracer detection in solids 8=14504
 O₂ stable isotopes, microanal. 8=14453
 Si film evaporated, radioisotope analysis following n-activation 8=4756
 U²³³-U²³⁵ mixtures, isotope abundance anal. 8=4113
 Y, 2.8 MeV neutrons inducing (n, n' γ) reactions 8=18800

radioactive

- See also Radiochemistry.
 metal oxides, dehydration processes, investigation by emanation methods 8=14369
 from photoactivation prods. with 20 MeV bremsstrahlung 8=7163
 radiochemical separations by adsorpt. on MnO₂ 8=9763
 rare earth elements, by photoactivation with 20 MeV bremsstrahlung 8=7161
 scintillation counting, gelation technique 8=15638
 semiconductor research, appl. of autoradiography to tracer studies 8=18019
 trace characterization, symposium 8=18797
 tritiated water, water vapour counter 8=9748
 Co⁵⁸, carrier-free extraction using 1-phenyl-3-methyl-4-capryl-pyrazolone-5 8=18750
 Fe⁵⁹, carrier-free extraction using 1-phenyl-3-methyl-4-capryl-pyrazolone-5 8=18750
 Mn⁵⁴, carrier-free extraction using 1-phenyl-3-methyl-4-capryl-pyrazolone-5 8=18750
 O₂ in Al determ. by 14 MeV-neutron bombardment 8=5764
 Pu containing sample, preparation for microanalysis 8=4831
 Sb¹²⁵ in crude Pb 8=14499

Chemical analysis—contd

radioactive—contd

- U, ore, content of Ra, Th, and K, comparison with NaI scintillation method 8=14528

X-ray

See also X-ray examination of materials.

- alite comp. and hydration, obs. 8=14362
 alloys, complex, microanalysis data correction 8=14471
 alloys, electron microprobe data analytic correction 8=14472
 automatic high-speed continuous analysis of wet and dry processes 8=2550
 biochemistry, soft X-ray microprobes appls. 8=18795
 bonds prod. wavelength shifts compensation 8=14481
 ceramics, alundum, Al-90 and Al-100, qualitative and quantitative, method 8=9762
 curved surfaces microanalysis 8=14483
 diamond by concave diffr. grating system, CK spectrum obs. 8=14491
 electron beam analyser and light elements obs. 8=15588
 electron energy analysis and charact. loss energy electrons use 8=14465
 electron microprobes performance standard obs. 8=14486
 electron microprobe resolving power meas. 8=15314
 electron microprobe spatial resolution, nomogram and e scatt. and fluoresc. effects 8=15313
 electron penetration and X-ray prod. in solid targets, Monte Carlo calc. 8=18793
 electron probe absorpt. corrections, computer calc. 8=14478
 for electron probe microanalysis, absorpt. correction tables 8=14470
 electron probe microanalysis in Japan 8=14466
 electron probe system specifications and testing 8=14484
 elements Z < 12 by ultrasoft X-rays, obs. 8=14474
 energy dispersion spectrometer using Si lithium drifted detector 8=23195
 films, solid, and thickness meas. 8=14482
 fluorescence anal., glass disks casting technique 8=2551
 garnet, fluoresc. method 8=9761
 geological samples, fluoresc. method 8=14498
 light elements by fluoresc., spectroscopy 15-150 Å 8=22945
 light elements by non-dispersive spectroscopy 8=14488
 light elements, concave diffr. grating system 8=14491
 microanalyser with network method pulse analysis 8=14489
 microanalysis, X-ray absorpt. and Z effects, computer calc. 8=14473
 microbeam analyser for industrial lab. use 8=14492
 minerals quantitative microanalysis, errors 8=14485
 minerals, standards and correction methods 8=14480
 non-dispersive, matrix effects elimination 8=23194
 phase-contents by e microprobe 8=17260
 phase diagram determ. by e probe microanalysis 8=17034
 proportional counter system, evaluation 8=14490
 quantitative elementary, by fluorescence, absolute and general method 8=23193
 silicates, microprobe standards prep. from gels 8=14496
 solids X-ray prod. depth distrib. calc. from e absorpt. obs. 8=17693
 steel, stainless, inclusion identification and counting by e probe 8=17616
 steel, stainless, Cr content, e beam analyser obs. 8=15588
 steel, stainless, CrC precipitation at grain boundaries, e probe obs. 8=17677
 steel surface comp. vars., e probe obs. 8=14494
 trace characterization, fluorescence and microprobe analysis 8=18789
 trace characterization, techniques survey 8=18790
 trace characterization by X-ray diffr. topography 8=17602
 trace impurity effects in diffr. topography 8=18791
 X-ray fluoresc. microprobe meas. 8=14487
 Al, rel. to microanalysis, X-ray prod. and e backscatt. obs. and calc. 8=18794
 in Al target, charact. radiation depth distrib., Mg tracer obs. 8=15587
 Al-Cu-Mg alloy with 1% Fe and 1% Ni, intermetallic phases comp. rel. to age hardening 8=14495
 Al₂O₃, qualitative and quantitative, method 8=9762
 Au microanalysis, e backscatt. correction obs. 8=14469
 Au, rel. to microanalysis, X-ray prod. and e backscatt. obs. and calc. 8=18794
 Au-Ag-Cu natural alloys, e probe obs. 8=14477
 B, using paraffin reflector in ultrasoft X-ray wavelength identification technique 8=3392
 C contamination reduction in light element probes and e backscatt. meas. 8=14468
 C microanalysis in heavy element oxides carbides 8=14475
 C by network method pulse analysis micro-analyser 8=14489
 C, using paraffin reflector in ultrasoft X-ray wavelength identification technique 8=3392
 in Cu microanalyser target, K α depth distrib. obs. 8=15586
 Cu microanalysis, e backscatt. correction obs. 8=14469
 Cu, rel. to microanalysis, X-ray prod. and e backscatt. obs. and calc. 8=18794
 F, using LiF mirror in ultrasoft X-ray wavelength identification technique 8=3392
 Fe, MnWO₄ atomic number effect correction, obs. 8=14479
 Fe-Cr alloys for fluoresc. and absorpt. corrections evaluation 8=14476

Chemical analysis—contd**X-ray—contd**

- Fe-Ni phase diagram, e probe microanalysis obs. 8=17034
 FeS₂, atomic number effect correction, obs. 8=14479
 Mn alloys with Dy, Ho and Er, fluorescence analysis 8=2552
 N by network method pulse analysis micro-analyser 8=14489
 N, using LiF mirror in ultrasoft X-ray wavelength identification technique 8=3392
 O microanalysis in heavy element oxides 8=14475
 O by network method pulse analysis micro-analyser 8=14489
 O, using LiF mirror in ultrasoft X-ray wavelength identification technique 8=3392
 PbS, atomic number effect correction, obs. 8=14479
 Pt-Fe natural alloys, e probe obs. 8=1477
 U-Nb-Zr alloy, absorpt. edge technique 8=18792
 ZnS, atomic number effect correction, obs. 8=14479

Chemical effects of radiations

See also Nuclear reactions/chemical effects; Photo-chemistry.

- annual review of nuclear science, book XV 8=15628
 cyclohexane-benzene mixtures, emissivity and charge transfer 8=9731
 ethylene in solution, reactions in presence of O by pulse radiolysis and γ -irrad. 8=14446
 gas meas. system, Toepler pump, automatic 8=14442
 polymerization, in glassy phase 8=18711
 rare-earth ions, trivalent, in fluorite-type crystals, reduction giving divalent centres 8=18740
 reactor analysis, continuous sampling method 8=23165
 Al, electron slowing-down, total electron flux, energy spectrum 8=13474
 CaF₂:Eu³⁺, reduction giving Eu²⁺ centres 8=18740
 Co complex ions, Szilard-Chalmers reaction, interpret. of specific activity values obtained 8=18749
 Cu, electron slowing-down, total electron flux, energy spectrum 8=13474
 KI aqueous solution, possible applications as dosimeter 8=6664
 Pb(NO₃)₂, photo-annealing 8=9732
 TiCl₄-heptane solns., γ -radiolysis obs. 8=18747

acoustic waves

- oxidation in solid systems 8=9735

ionizing radiations

- alkaline ices, e.p.r. of trapped electrons 8=2370
 aromatic hydrocarbons, induced tritium substitution 8=23166
 cyclohexane-2,2,4-trimethyl pentane mixture H₂ yield 8=18748
 dipolar systems, thermal electron escape 8=2541
 ethylene, H, production as dosimeter 8=614
 glycine, kinetics of γ -radiolysis 8=5757
 heavy-ion expts. 8=5755
 heavy and light water Fricke dosimeter solutions, ferric ion yield from 14.6 MeV n and Co⁶⁰ γ 8=9733
 hydrocarbon-alcohol mixtures, carbonium ion yield and ion-mol. reactions 8=5756
 hydrocarbons, saturated, perturbed orbital energies in radiolysis 8=18742
 hydrogenated terphenyls, e-irrad. effects on comp. and props., rel. to reactor coolant 8=14445
 ice, pH depend. of reducing species 8=2540
 ionic recomb. rate, electrostatic model 8=4611
 isobutane, gas-phase radiolysis 8=23158
 liquids, γ radiolysis at high press. 8=14444
 nonpolar liqs, X- and γ -irrad., ionization and theory of separated ion pairs 8=2539
 methanol, X-irrad., u.v. photolysis at 77°K 8=5750
 2-methylbutane, condensed-phase radiolysis 8=18739
 organic glasses, γ -irrad., e.s.r. of trapped electrons 8=9729
 pyridine, pulse radiolysis 8=18746
 radiolysis systems, ion lifetimes meas. 8=23163
 triglycine sulphate, kinetics of γ -radiolysis 8=5757
 vinyl cpds., pulse radiolysis and free radicals 8=18745
 water-methanol vapour, competitive solvation of H⁺ 8=14443
 water+10% ethanol, γ -radiolysis, yield of solvated electrons 8=23167
 CaF₂, behaviour of F⁻ during reduction of Dy³⁺ 8=1949
 CO₂, radiolysis in adsorbed state 8=18741
 HCl, gaseous, γ -irrad., ion lifetimes 8=23164
 NF₃, new compound by fission-fragment radiolysis 8=9730
 NH₃ gas, decomp., effect of H and e scavengers 8=23162
 NH₃ gas, radiolysis by electrons 8=18743-4

Chemical equilibrium. See Chemical reactions.**Chemical exchanges. See Exchanges, chemical.****Chemical kinetics. See Reaction kinetics.****Chemical reactions**

See also Exchanges, chemical; Heat of formation; Heat of reaction; Oxidation; Photochemistry; Polymerization; Reaction kinetics.

- acetates, rare earth, Pb and Cu, i. r. spectra and thermal decomp. 8=23095
 amylose, asymm. interaction with DL-mandelic acid and DL-ethyl mandelate 8=18696

Chemical reactions—contd

- aromatic hydrocarbons, pyrolysis, e.s.r. 8=2513
 aromatic-oxygen complex, stabilization constants from aromatics solubility in O₂ 8=2499
 aryl oxalates, electronegatively substituted, reactions with H₂O₂ and fluorescent compounds, chemiluminescence 8=18672
 atom-transfer oxidation reduction, metal ion promoted 8=14401
 atoms and free radicals in fast flow systems 8=9700
 azo-compounds decomp. tracing by n.m.r. spectroscopy 8=8127
 benzene hydrogenation to cyclohexane, effect of support on Ni catalyst 8=9707
 benzene ion reactions with benzene 8=16452
 benzotropones, reactivity indices 8=18673
 contaminants on glass with Na-NH₃ solns. at -78°C 8=21868
 carbon blacks, surface interact. with gaseous Cl 8=9685
 carbon, chemisorption of O₂ 8=5725
 carbonyl cpds., reversible hydration study, limitations of u.v. spectroscopy 8=9682
 cation hydration, charge-dipole model 8=9670
 cellulose hydroxyl groups, reactivity to N oxides in presence of P₂O₅ 8=5721
 chemiluminescence in solution 8=1574
 chemi-ionization in upper atm., model 8=23307
 chemisorption, meas. apparatus 8=5723
 chemisorption, surface mobility parameter 8=14400
 in chloroethylene, ion-molecule, study by ion cyclotron reson. spectroscopy 8=16453
 chloroform-triethylamine system, equilib. and H-bond formation 8=18649
 in chloroethylene, reactions with ions, study by ion cyclotron reson. spectroscopy 8=16453
 chromic (III) cpds., stability, by spectrophotometry 8=23079
 collision-induced, with Dempster mass spectrometer 8=4309-10
 dibenzoylperoxide decomp., tracing by n.m.r. spectroscopy 8=8127
 diffusion and absorpt. in catalysts 8=14402
 di-p-chlorobenzoylperoxide decomp. tracing by n.m.r. spectroscopy 8=8127
 dissociation field effect relax. apparatus, square wave, for rapid reaction rate obs. 8=9665
 effect on soln. of stagnation point laminar boundary layers and viscous shock layers eqns. 8=16671
 energy-surface treatment, state-area principle for phase transitions 8=12963
 extraction of NO₂, U and fission prods. with tri-n-octylamine, temp. effects 8=5708
 electrical contact degradation effect 8=8987
 electrical contacts, tarnishing effect of atmospheric pollutants 8=8988
 electron tubes, residual gases 8=18663
 ethylene, shock pyrolysis, chem. overshoot 8=9690
 exothermic, behind reflected shock waves 8=23120
 exothermic front in condensed medium (k-phase), theory of stationary propag. vel. 8=18660
 flash excitation, obs. with modulated optical null spectrophotometer 8=3359
 formic acid dehydration over Al₂O₃ and SiO₂, i.r. study of chemisorbed species 8=9701
 form. of Ni(II) complexes of glycine peptides in aqueous soln. 8=9664
 free radicals, direct i. r. spectrometry 8=16367
 gas mixtures in chem. equilib., separation in temp. gradient 8=21526
 gas production kinetics, pen recorder 8=14353
 gas reactions, bimolecular and termolecular, tables 8=10466
 gas reactions, transition state and Arrhenius parameters 8=4465
 gases, use of e.s.r. to study of kinetics 8=14351
 in graphite gasification by pure CO₂, transient phenom. 8=9678
 graphite, interact. of gases and vapours with fresh surface 8=8338
 graphite, nuclear reactor, gasification with CO₂ and H₂O 8=2514
 heterogeneous, transient multicomponent diffusion 8=14354
 hexafluoroethane, secondary ion-mol. reactions ion cyclotron reson. 8=21284
 high temp. use of thermal plasmas as environment 8=21410
 hydrides, gaseous, decomp. in r.f. glow discharge rel. to films deposition 8=21872
 hydrogen ion solvation by H₂O mols. in gas phase, kinetics and thermodynamics 8=18661
 hydrolysis of substituted aspirin rel. to intramolec. catalysis 8=5727
 ion-molecule, studied in corona discharges 8=12409
 iron metallurgy, homogeneity and interface reactions 8=5704
 jacketed blender-reactor 8=23091
 layer structures, enhancement at dislocations 8=8710
 metal oxides, dehydration processes, investigation by emanation methods 8=14369
 methane, shock pyrolysis, chem. overshoot 8=9690

Chemical reactions—contd

- monitoring, by synchronous operation of mass spectrometer 8=20914
muonium reactions 8=5713
nickelous nitrate-water-magnesium oxide system low-temp. cementation effects 8=14374
non-equilibrium boundary-layer problems, finite-difference soln. 8=18662
nuclear magnetic resonance spectra, explanation 8=8128
nuclear magnetic resonance spectra for tracing rapid reactions 8=8127
organic cpds., interaction with superconductors 8=9668
organic, liq. phase, under press., differential thermal analysis 8=9684
oxalic anhydrides, reactions with H_2O_2 and fluorescent compounds, chemiluminescence 8=18685
oxides in graphite electrodes burnt in d. c. arc, rel. to spectral line intensity 8=14385
phosphine oxides, $R_1R_2R_3PO(R_{1-3})$ are different hydrocarbon radicals, preparation 8=16345
polymethacrolein reduction with $LiAlH_4$ and polymethyl alcohol prep., obs. 8=23107
polyvinylchloride plasticization by aromatic and condensed ring cpds., obs. 8=23141
propane ions with benzene, butadiene, H_2S and NO 8=14381
propane, pyrolysis in shock tube for temp. range 830 to 1180°C 8=14380
pyridines, electrophilic substitutions 8=18687
quartz-kaolin-microdine, during firing, i. r. studies 8=18690
quartz rocks, hydrolytic weakening at high temp. and press 8=14561
quartz in water soln., 400-500°C, 1 kb, molecularity obs. 8=2520
radical ions formed by electron addition to unsaturated mols., e. s. r. rate study 8=14350
slags, dephosphorizing capacity effect of BaO and CaF_2 8=9676
solid state, theory of nucleation 8=23090
in solutions under pressure 8=14356
in stationary droplets of solns. of salts, study by radio-active tracers 8=14355
steel, analysis of decomposition process and inter-element effect 8=14392
steelmaking, homogeneity and interface reactions 8=5704
superconductors, interaction with organic cpds. 8=9668
surface, exam. by simultaneous X-ray emission and electron diffr. 8=8290
systems far from equilb, oscillations round steady state 8=2500
teflon, and I and AgCl, melting and pyrolysis, high pressure 8=4644
thiophenes, reactivity theory 8=5720
trimethylplatinum(IV) iodide and methylsodium, structural identification of product 8=14382
xanthine oxidase, mech. of action, e. s. r. study 8=14406
Ag, sulphiding by H_2S , effect of surface Fe 8=23096
Al + Cl, from 500 to 650°F, mechanism and rates 8=14358
 Al_2O_3 films prep. from pyrolysis of Al alkoxide 8=4740
 Al_2O_3 -glass composite, effects of hot-pressing 8=18671
 $Be_3N_2 \rightarrow 3Be(g) + N_2(g)$, enthalpy and enthalpy of activation, vapour pressure and evap. coeff. 8=1624
C atoms with Cl, to form free radical CCl , 8=1315
C, evap. films, with heated metal substrates 8=4745
 C_2H_2 with H- and O- atoms, e. s. r. investigation 8=2511
 C_3O_2 with O atoms and active N 8=14360
 $C_{10}OH_{12}N_2O_8$, condensation product of diaminosuccinic acid and pyruvic acid 8=17437
Ca dicarboxylates (malonate to sebacate), i. r. spectra and thermal decomp. 8=23095
 $CaF_2:Dy^{3+}$, behaviour of F⁻ interstitials during reduction of Dy^{3+} 8=1949
 $CaCl_2$ -NaCl- H_2O systems, chem. pot. 8=12848
 $Ca(OH)_2$, thermal decomp. activation energy 8=14308
 $3CaO \cdot SiO_2$ hydration in Portland cement, obs. 8=14362
 $Ca_3Sb_2O_7$, ($x = 1, 2, 3$; $y = 4, 5, 6$), prep. from CaO and Sb_2O_3 and stability 8=14363
Ca-Sr ion exchange props. of synthetic zeolites 8=23081
CdS single crystal polishing by phosphoric acid 8=9705
CdS from Cd and S, bulk crystals, closed system vap. growth 8=17228
CdS, sensibilation 8=22584
 $Cd_3Sb_2O_7$ ($x = 1, 3$; $y = 4, 6$), prep. from CdO and Sb_2O_3 and stability 8=14363
 CrO_3 , reduction into C_4O_2 and Cr_2O_3 , under high press. and temp. 8=9674
Co complex-ions, Szilard-Chalmers reaction, interpret. of specific activity values obtained 8=18749
Fe, liq., deoxidation by Al, rel. to form. of cloud group of inclusions 8=22183
FeO, high-press. synthesis of stoichiometric cpds. 8=13259
 $2GaS_2 = 2Ga_{(g)} + S_{2(g)}$, equilb. const. and thermal stability 8=21786
Ge hydrides, pyrolysis rel. to Ge epitaxial film production 8=17130
Ge with MoO_3 in powder form., reaction mechanism 8=14365

Chemical reactions—contd

- H atoms with F⁻ ions, formation of hydrated electrons 8=18679
H catalytic reduction 8=18735
H, free atoms with simple hydrocarbons, e. s. r. study 8=14376
 $H^2(P)$ with O_2 , luminesc. of OH 8=14366
 H_2 flames, chemiluminesc., effects of SO_2 8=18693
 $He^+ + H_2$ and $He^+ + HD$ reactions 8=21277
InOF, by $In_2O_3 + InF_3$ at 1000°C 8=8414
 $K + NaCl = KCl + Na$, electronic pot. energy surfaces 8=23106
 K_2O-SiO_2 solns., activity 8=21620
 Li_2-SiO_2 solns., activity 8=21620
 $Mn_3Sb_2O_8$, prep. from $MnCO_3$ and Sb_2O_3 and stability 8=14363
Mn-Zn ferrite, oxidation rate from cation diffusion coefficient 8=9691
 M_2WO_3 , ($M = La, Y$), solid state preparative reactions 8=5709
 Mg_2SiO_4 with related minerals in mantle, required temp. and press. calc. 8=2556
of Na_2CO_3 , during prep. of KCl pressed discs 8=14373
 Na_2O-SiO_2 solns., activity 8=21620
 Nb , vacuum deposited on MgO , rel. to substrate-condensate interaction 8=8326
 NH_4Cl formation from $NH_3 + HCl$ 8=12217
 NH_4ClO_4 , thermal decomp., mass spectra 8=9693
 NO_2 chemiluminescence, rad. from far wake of hypersonic spheres 8=21478
Ni-base alloys, refractory-melt reactions in vacuum induction melting 8=9694
O + CO, shock-heated system, radiation 8=1342
O, free atoms with simple hydrocarbons, e. s. r. study 8=14376
 O_2 chemisorbed on Al films, stability and work functions changes 8=5726
 $O_2 + H \rightarrow OH + O$, in oxyhydrogen detonation waves obs. 8=170
O + P(PH_3), stoichiometry and chemiluminescence 8=23109
OH with oximes, free radical intermediates, e. p. r. 8=14394
P(N and S), rel. to use as nuclear fuel 8=12017
 $PbCrO_3$, high-pressure synthesis 8=23110
PbTe compatibility with metals 8=18686
PuZr₂ synthesis from Pu and Zr, obs. 8=8279
Si and Ti carbides, formation by chemical vapour deposition 8=23112
Si hydrides, pyrolysis rel. to Si epitaxial film production 8=17130
 $SiCl_4$ with water vapour, SiO_2 film deposition 8=21889
 SiH_4 decomp. in r. f. glow discharge rel. to films deposition 8=21872
SnTe compatibility with metals 8=18686
 SO_2 , with ketones, nitriles, esters or alcohols, u. v. absorpt. spectra 8=18688
 $SrCl_2$ cryst., e. s. r. of reaction intermediate with F_2 8=14124
 $Sr_xSb_2O_y$ ($x = 1, 2$; $y = 4, 5$), prep. from SrO and Sb_2O_3 and stability 8=14363
Th phosphides, prep. 8=23116
Ti, 4-valent, with OH and O_2 radicals, e. s. r. and chemiluminescence 8=2522
 $TiCl_3 + H_2O_2$, e. s. r. 8=2521
U(N, P and S), rel. to use as nuclear fuel 8=12017
 U^{VI} extraction by methyl propyl ketone 8=20898
U phosphides, prep. 8=23116
 $UCl_4 + Al + H_2S$, for prep. of U_3 , 8=23114
 UO_{2+x} lattice defects rel. to thermochem. and non-stoichiometry 8=23113
Zn ferrite form. at 400°C, obs. 8=23117
W, surface interactions of I_2 vapour 8=18699
- Chemical structure**
See also Bonds.
acetone-chloroform system, n. m. r. study 8=2498
azidopurine from 6-hydrazinopurine + HNO_2 , and crystal structure 8=21117
(3:1) bullvalene- $AgBF_4$ complex 8=4890
complexes formed by H-bonding 8=12242
ethylene oxide- H_2O clathrates, nonstoichiometric 8=17447
hydroxyapatite catalysts, H content 8=14395
manganese vanadate, and O_2 parameters, determ. 8=8534
3-methoxy-5 β , 19-cyclo-5, 10-secoandrosta-1(10), 2, 4-trien-17 β -ol p-bromobenzoate 8=22063
polycarbonate films, rel. to deformation and tensile strength 8=22403
sulphur cpds., determ. by ESCA (electron spectroscopy for chem. anal.) 8=21100
triphenyl boron and phenyl boron halides, rel. to phenyl-boron bond strength 8=1863
 C_7H_8 isomers, chem. ionization mass spectra 8=9745
Cs methoxide-methanol solvates comp. and Cs ions coordination number obs. 8=2497
InAsTe, analysis 8=1760
K methoxide-methanol solvates comp. and K ions coordination number obs. 8=2497
Li methoxide-methanol solvates comp. and Li ions coordination number obs. 8=2497
 $Mn_{a-x}V_x[Mn_{b-x}V_{b-y}]O_2$, and O_2 parameters, determ. 8=8534
Na methoxide-methanol solvates comp. and Na ions coordination number obs. 8=2497

Chemical structure—contd

- Pu²³⁹, var. in ϵ binding energy in strong elec. field 8=4085
 Rb methoxide-methanol solvates comp. and Rb ions
 coordination number obs. 8=2497
 Si sesquioxide, formula 8=9662
 Sn(O, S, Se or Te) cpds, chem. shifts of K_{α} X-ray
 line 8=9558
 TaC_x, stoichiometric effect 8=1881

Chemical technology

- cement setting, rel. to crystallization of Ca hydrosilicate
 in presence of gypsum and Al₂O₃ 8=1738
 metal fume concentration, measurement by atomic
 absorption method 8=5992
 rehydration monitoring, appl. of n.m.r. 8=23770
 Ac²²⁸ in Ra²²⁸ solns, separation and purification by
 solvent extraction method 8=16047
 Al purification using fractional crystallization 8=4801
 BN as a diffusion source for Si 8=8684
 Mg, silico-thermal prod., mechanism from radioactive
 tracer study 8=23776

Chemiluminescence. See Chemical reactions; Luminescence.

Chemisorption. See Chemical reactions; Sorption.

Cherenkov radiation

- See also Counters/Cherenkov; Electrons/radiation.
 Cherenkov emission of Alfvén waves by moving force
 source 8=6343
 coherence effects 8=20027
 density fluctuations in air showers at seas level 8=7013
 density fluctuation in EAS at sea level 8=7013
 EAS det. using r. f. port 8=20597
 incoherent, interpretation of auroral hiss, measured on
 OGO 2 and at Byrd station 8=23342
 lucite, time resolution function 8=5690
 non-linear dielectric, losses of modulated
 current 8=277
 photomultiplier residual light emission 8=6327
 plasma heating in radially non-uniform cylinder 8=16485
 plasma, helically moving test particle 8=12501
 point charge moving parallel to interface between two semi-
 infinite dielectrics 8=6363
 relativistic charged particle passing through classical
 changed oscils. 8=3583
 teaching misconceptions 8=7027
 two-correlated spectrometers system with computer
 data anal. 8=11308
 Vavilov-Cherenkov, by motion of charged ring in
 transparent crystal 8=22949
 in waveguide with elliptic cross section, frequency
 modes 8=6394
 H₂O, time resolution function 8=5690

Chirality. See Elementary particles; Field theory, quantum.

Chlorine

- in alkali-chlorides, K-absorption and q.s.s. 8=2410
 atom, K_{α} line calc. from M/L ϵ capture ratio of
 Ar³⁷ 8=20748
 atomic, new Rydberg absorpt. series and ionization
 pot. 8=1165
 electrodes, high current density, impurity effects 8=18730
 gaseous, interact. with carbon blacks 8=9685
 isotope mixtures, thermal diffusion props. 8=1492
 natural gaseous atmospheric, origin rel. to volcanic
 action 8=9841
 n. q. r. in SbCl₃CH₃CN, SbCl₃POCl₃, and SbCl₅ 8=2391
 reaction with O atoms 8=9696
 vibrational relax. calc. 8=4259
 Cl⁻, passivity breakdown of stainless steel 8=23147
 Cl + Al reaction, from 500 to 650°F, kinetics and
 rates 8=14358
 Cl-Cl system, 2nd virial coefficient for different electron
 states at 2000-6000°K 8=1469
 Cl⁻, effect on transparency of Hf and Th oxide
 films 8=5605
 Cl₂, anomaly of ground-state reduced potential
 curve 8=16275
 Cl₂, complete pot. energy curve for ³ Π_{0^+} state 8=7511
 Cl₂ radical, i.r. spectrum 8=7620

Chlorine compounds

- halides trapped in inert-gas crystals, theory of
 spectra 8=8230
 perchlorates, explosive props. and electronic
 struct. 8=1259
 Cl₃CNO₂ mols. dielec. relax. in solid and liquid, 9GHz,
 10 and 200kHz 8=18179
 ClF₃, quadrupole coupling consts. 8=16276
 ClH, ground-state props. calc. 8=7514
 ClO, dipole moment, from gas-phase electron
 reson. 8=12345
 ClO gaseous free radical, e.s.r. study 8=12340
 ClO, gas-phase electron reson., double quantum
 transitions 8=12308
 ClO₃ in alkali-halide lattices, i.r. spectra 8=22968-9-70
 ClO₄ in alkali-halide lattices, i.r. spectra 8=22968-9-70
 ClOO radical, matrix i.r. spectra 8=12344
 ClO radicals, kinetic obs. 8=23125
 CO₂-NiO/Ni system, isotopic exchange reaction between
 O¹⁶ and O¹⁸ 8=9663
 HCl aq. soln., phenomenological coeffs. for elect. cond. and
 diffusion 8=12924
 HCl as electrolyte for WO₄²⁻ ion, polarography 8=18736

Chlorine compounds—contd

- HCl, hexadecapole moment 8=8230
 HCl₂ symmetrical ion, Cl n. q. r. 8=5568
 HClO₄ aq. soln., phenomenological coeffs. for elect. cond. and
 diffusion 8=12924
 HOCl, matrix i.r. spectra 8=12175
Chondrites. See Meteorites.
Chromatic aberration. See Aberrations, optical.
Chromatography
 See also Adsorption; Chemical analysis/adsorption.
 amino acid analyser, sensitive linear flowing-stream
 photometer 8=5762
 effluent retention time meas. 8=14451
 gas chromatograph, application of fast scan mass
 spectrometry 8=5761
 gas, electrodeless discharge as detector 8=23169
 gases, purification by cataphoresis 8=2536
 gas, for partition coeffs. of organic vapours between gas
 and non-polar solvent phases, rel. to molec. dimens.
 determ. 8=1485
 gas-liquid, use of electronic digital integrator 8=10817
 gas, with mass spectrometer, interface separators 8=14506
 gas, Ni⁶³ electron absorpt. detector 8=14505
 gas, spectral-emission type detector 8=18764
 gas, gas-liq. interface and solid support effects 8=5760
 gas-liquid analysis of irradiated organic compounds,
 sample injection port 8=14450
 gas-liquid, stationary phases selectivity 8=5759
 gas-solid, organic crystals as adsorbents 8=18763
 interdiffusion of gases, study using electrodeless discharge
 as ionization detector 8=14452
 lanthanide fission products 8=9739
 paper, trace elements determ. by neutron activation 8=1450
 polar isotopic mol. separation 8=9744
 rare earths, use of phosphoric-acid treated paper 8=18765
 silica gel, surface meas., absorption method 8=21742
 Co, thin-layer, followed by complex formation and
 reflectance spectros. detect. 8=23176
 Cu, thin-layer, followed by complex formation and
 reflectance spectros. detect. 8=23176
 Ni, thin-layer, followed by complex formation and
 reflectance spectros. detect. 8=23176
 Pb in air, colorimetric method 8=9754
 WO₃ film, Pt-activated, sensitivity as gas detector 8=13098
Chromium
 adsorption of polar organic mols. 8=13107
 alloying with steel, effect on temper brittleness 8=17797
 antiferromagnetic, band structure by Green's
 function 8=2348
 antiferromagnetic, spin density wave studies by n-diffr.,
 high pressure effects 8=22876
 antiferromagnetic, X-ray line splitting above and below
 Néel point 8=17358
 antiferromagnetism, itinerant, rel. to resist. and Néel temp.
 press. depend., obs. 8=5500
 deposition from low-energy ion source 8=19796
 deposits, pseudomorphic, on Ni 8=21886
 diffusion in Fe and low C steels, experimental obs.
 in 950-1265°C range 8=4951
 electrodeposits, internal stress development,
 obs. 8=22325
 electronic structure, photoemission investigation 8=22457
 elinvar alloys, influence on mag. props. 8=9348
 film, reflection and transmission coeffs. in
 0.4-1- μ range 8=5580
 films, thin, glow discharge rel. to resist. 8=17128
 Hall effect at 4.2, 77 and 273°K, rel. to applied mag.
 field 8=8855
 Hall effect at 4.2°K, 77°K and room temp., magnetic fields
 up to 147 kOe 8=9002
 L-emission spectra, fine structure 8=14270
 resistance, elec., near Néel point 8=5177
 self-diffusion 8=17566
 solid solns. in Cu, mag. moments 8=22760
 surface oxidation rel. to Cr₂O₃ epitaxial growth 8=4828
 X-ray emission bands fine struct. rel. to e band struct.,
 obs. 8=18527
 Cr³⁺ in alum lattice, relaxation behaviour 8=22903
 Cr³⁺ in ruby, resonance, microwave second harmonic
 generation 8=22896
 Cr³⁺ trivalent ion hyperfine structure obs. using ENDOR
 technique 8=5553
 Cr⁺ in ZnS, photo-induced e.s.r., decay obs.
 77°-325°K 8=18441
 Cr⁺ in ZnTe, photo-excited paramag. reson. 8=5525
 Cr³⁺ ions in ruby maser, L-band appl. 8=15439
 Cr³⁺ in LaAlO₃, e.p.r. spectrum at room temp. 8=18426
 Cr³⁺ in LiNbO₃, e.p.r. 8=18428
 Cr³⁺ in tungstates (ZnWO₄-type), third crystal-field
 constant meas. 8=16974
 Cr³⁺ in Y(Al, Cr)₃(BO₃)₂, e.p.r. at room temp. 8=18439
 Cr³⁺ in ZnWO₄, e.p.r. electric broadening of
 lines 8=18442
 Cr³⁺ spin-lattice relax. in ZnWO₄ 8=10994
 Cr(VI) in binary alkali metal glasses, u.v.
 absorpt. 8=18519
 Cr/Co layered films of high coercive force, for digital
 mag. recording 8=14009
 Cr₂O₃-BaTiO₃ systems, phase transformations 8=17045

Chromium—contd

- Cr-SiO cermet films, elec. props. 8=8981
 Nd:Cr:YAG, sidelight fluorescence changes, due to lasing at 1.06 μ 8=6473
 ZnWO₄:Cr³⁺, theory 8=14085
- Chromium compounds**
 alloys, antiferromagnetic, transport props. 8=18374
 alloys with Co and Ni, antiferromag. props. rel. to Co/Ni conc. 8=22875
 alloys with d-transition group elements, n-mag.-scattering studies 8=18349
 alloys, high-temp. tensile creep, influence on properties by ceramic environment 8=13543
 alloys, N determ. from nitride behaviour 8=9740
 chromel-alumel thermocouples for small difference meas. 8=15121
 chromic potassium (methylamine) alums, temp. scales from nuclear orientation 8=8205
 chromic (III) cpds., stability, by spectrophotometry 8=23079
 halides (CrBr₃ and CrF₃), paramag. phase, exchange integrals by neutron scattering 8=13971
 methylammonium chromium alum, crystal structure 8=22017
 selenides, elec. and thermal cond., thermoelectric power, lattice parameters 8=13703
 α -Al₂O₃-Cr₂O₃ solid solns., crystalline parameters 8=8241
 Cr alloys, antiferromagnetism from time-of-flight n-diff. studies 8=18375
 Cr³⁺ alum, e. s. r. weak fine struct. components 8=14098
 Cr³⁺ diopside, absorpt. 10 000–20 000 cm⁻¹, 1.7–290°K 8=18520
 Cr(II) bistoluene complex, e. s. r. spectra 8=12311
 Cr(V) complexes, liquid solutions, Overhauser effect 8=21725
 Cr-Ag film, reflection and transmission coeffs. in 0.4–1 μ range 8=5580
 (Cr:Al)K(SO₄)₂·12H₂O, Cr³⁺ relaxation behaviour 8=22903
 Cr₂BeO₄, orthorhombic, antiferromagnetic resonance 8=14084
 Cr₂BeO₄, spin-flopping 8=5506
 [Cr(CNS)₆]³⁻-¹⁴CNS⁻, isotopic exchange rel. to structure study 8=23087
 Cr(CO)₆ halogen and pseudohalogen derivs., i. r. spectra 8=14209
 Cr(CO)₆, crystal structure 8=8516
 Cr(CO)₆, space group R factor, significance tests 8=8517
 [Cr(C₂O₄)₃]³⁻-¹⁴C₂O₄²⁻, radioisotopic exchange 8=21796
 Cr-Fe alloys, Cr rich, antiferromag. ordering rel. to energy changes 8=8931
 Cr-Fe alloys, dilute, antiferromag. props. rel. to Fe content 8=2347
 Cr-Fe-C-N alloys, 18%Cr, constitutional diagrams 8=21822
 Cr-Ge alloys, elec. resist. at 20–300°K, Curie points and ferromag. props. 8=9338
 Cr-Mn alloys paramag. susceptibility rel. to band struct., obs. 8=22759
 Cr-Mo alloys, Hall effect and sp. ht. meas., between 125–625°K rel. to comp. 8=4931
 Cr(NH₃)₆NO⁺ ion in soln., e. s. r. and N hyperfine splitting 8=1592
 16/13 CrNi steels, high temp. embrittlement after n irradi. 8=22362
 CrO₂, reduction from CrO₃, under high press. and temp. 8=9674
 CrO₃, reduction into C₄O₂ and Cr₂O₃, under high press. and temp. 8=9674
 CrO₄²⁻, e. s. r. and optical spectra in chlorospodiosite 8=14099
 Cr₂O₃, acoustic spin waves, studied by neutron scattering 8=14065
 Cr₂O₃, addition to Pb(Zr-Ti)O₃ solid solution 8=13043
 Cr₂O₃, epitaxial growth due to Cr surface oxidation 8=4828
 Cr₂O₃ films, optical props. 8=9517
 Cr₂O₃, magneto-electric susceptibility versus temp. 8=5427
 Cr₂O₃ particles in pre-mixed flames 8=23118
 Cr₂O₃ protective scales on Fe-Cr alloy, mechanism of lifting and cracking 8=23099
 Cr₂O₃-Al₂O₃ solid solns., mag. susceptibility 8=13972
 Cr₂O₇²⁻ anion, pH depend. of adsorpt. of Fe₂O₃ powder 8=8342
 Cr₂O₃Cl₂, cryst., electronic absorpt. spectrum 8=22971
 Cr₂K₂, γ and n irradiated, e. s. r. 8=18417
 CrO₂(NH₄)₂, γ and n irradiated, e. s. r. 8=18417
 Cr(ONO)₃(H₂O)₃ 1.5 KNO₂, formation and struct. in crystalline state and in soln. 8=9518
 Cr-Os alloys paramag. susceptibility rel. to band struct., obs. 8=22759
 Cr-Re alloys, dilute, antiferromag. props. 8=18373
 Cr-Ru alloys paramag. susceptibility rel. to band struct., obs. 8=22759
 Cr₂Si, superconductivity, band structure 8=5216
 Cr-Si alloys, electrical resistivity 8=9001
 Cr-SiO cermet films, resistivity and struct. 8=1695
 CrTiBO₆ (B=Nb, Ta, Sb), crystal structure and fluorescence 8=4879
 Cr_{1-x}Te_{1+x} alloys, transport phenomena in paramagnetic state 8=9300

Chromium compounds—contd

- Cr₂WO₆, mag. structure 8=22873
 Li_{0.5}Cr_{1.5}Fe_{1.5}O₄, spontaneous magnetization rel. to compensation temp. 8=14049
 MgO-Al₂O₃-Cr₂O₃ system, coherent precip. 8=21848
 V and Ti alloyed, elec. resist. anomalous decrease 8=9000
- Chromosphere.** See Sun.
- Chronographs.** See Time measurement.
- Cinematography**
 See also Cameras.
 high-speed photomicrography 8=11220
- Circuits**
 See also Amplifiers; Counting circuits.
 a. c. voltage stabilizer, with high efficiency, and small output distortions 8=15182
 automatic plotter of electron beam current density profile 8=3197
 blanking, for mag. electron multiplier in time-of-flight mass spectrometer 8=20913
 bridge oscillator freq. stabilization 8=3145
 character recognizer, using domain wall motion in Permalloy wire 8=10876
 coincidence, for simultaneous (p, p') ang. correlations 8=20794
 coincident current store performance rel. to ferrite core characts. 8=14043
 communication systems in schools for semi-deaf 8=10748
 comparing frequency reference standard and quartz clock 8=15160
 constant-current power supply for H or D lamp 8=19714
 contactless system for measuring deformation and temperature 8=10780
 controller, programmed, for sequential laboratory operations 8=6245
 converter d. c.-d. c., regulated, providing low standby current for portable radiation instruments 8=3455
 current comparison, automatic 8=10826
 current-voltage converter with output voltage proportional to argument of sinh (input current) 8=10832
 digital pulse-shape analyser 8=6168
 discharge circuits with flash lamps, current and voltage 8=4291
 double-pulse variable-delay, for electron-hole plasma decay meas. 8=15177
 electrical feedthrough, compact 60 kV UHV, construction 8=3140
 electrical lead for high-pressure gas systems at low temp. 8=3147
 e. m. f. to current converter, solid-state, mag. amplifier improvement 8=10831
 electronic components conference, Jackson USA, 1967 8=6244
 equivalent, for plasmas 8=7746
 equivalent, piezotransducers, for u. s. analysis 8=196
 exciting circuit of r. f. amplifier driving cavities of accelerators 8=11334
 exploding-wire, current meas. 8=15171
 filter, linear, giving max. intelligibility over noisy channel for peak power limited transmitter 8=15080
 four coils of square-cross-section, for prod. of uniform mag. fields 8=3162
 frequency follower for sustaining resonance in a plasma 8=16406
 frequency multiplier, phase-locked 8=2877
 frequency reducer, aperiodic 8=272
 function generator, digital, reciprocal 8=3468
 gamma ray spectrum stabilizer 8=20357
 generator, double-phase, infrasonic 8=10833
 helium waves, h. f. phase sensitive detection 8=5138
 h. f. electronics and stimulated radiation of classical oscillators 8=3298
 high voltage supply, d. c., for electron beam machine 8=15290
 hysteresisless nonlinear reactive elements, energy exchange between harmonic sources 8=10829
 ignition switching for inductive energy storage 8=15187
 induced polarization apparatus for metalliferous mineral prospecting 8=2561
 integration system, using temp. variation, to study mag. field stabilization 8=19740
 integrator, electronic to control magnetic field in β spectrometers 8=3597
 integrator, gated, for pulsed n. m. r. 8=14134
 ionization gauge, for detect. of shock and reflected detonation waves 8=3041
 klystron-oscillator power supply for mm spectroscopes 8=15425
 linear gate, with stretcher 8=275
 linear gate, specifications 8=10828
 linear gate, 30 nanosec., high precision parallel-switch type 8=3137
 low-freq., thermistors as circuit elements 8=22619
 magnetic, loudspeaker 8=15258
 magnetometer, transistorized with 10⁻⁴ accuracy 8=19914
 memory elements, optico-elec., static params. theory and obs. 8=6039
 microwave beam pulsing system of nuclear energy level lifetimes 8=7058
 microwave mixing with weakly coupled superconductors 8=15386

Circuits—contd

- nanosecond pulse integrator 8=15643
 microwave receivers, superheterodyne, epoch sensitivity to e.m. pulses from water drop discharges 8=14624
 Nernst glower control 8=3364
 network analogues for heat conduction calc. 8=19646
 nonlinear capacitor in series with inductor, forced oscills. 8=19710
 qoscillation, 100 Mc/s gated clock 8=6246
 oscillator, vibrator-controlled, for measuring elastic constants and internal friction 8=8785
 oscillatory, stabilized, effect of variable attenuator 8=15174
 parallel-to-serial converter, using domain wall motion in Permalloy films 8=10875
 phase-control, automatic, phase following behaviour in noise 8=274
 phase-lock, for 100 MHz spectrometer 8=15430
 phase-locked pulsed oscillator 8=15180
 photocathode current-limiting protection 8=13923
 photomultiplier, automatic gain control 8=6324
 polarization in high resistivity electrolytes, modified Wheatstone bridge 8=18715
 power transmission network, d.c. three-wire, relaxation method, solution 8=281
 pulse-echo apparatus for v. h. f. 8=15073
 pulse, for investigation of weak pulse currents in high-resistance semiconductors 8=22576
 pulse generator for nuclear spectroscopy 8=15632
 pulse generator high current and fast 8=6249
 pulse generator, spark gap system, subnanosec., description 8=6248
 pulse generator using three-electrode spark gap 8=7680
 pulse limiter, for protection of high speed logic circuits 8=19711
 pulsed system operations, use of supercond. coils as energy storage elements 8=13766
 RLC filter, efficiency with Ge(Li) counter 8=20198
 radio thermoluminescent research, electronic instrument for 8=9585
 receiver, l.f. time signals 8=8
 rectangular current pulse generator, using Si controlled rectifier 8=15178
 redundant, electrical continuity checking method 8=3136
 relaxation generators of pulses using secondary emission tubes 8=15179
 relaxation oscill., tunnel diode 8=5330
 sequential recognition system for spoken digits in real time 8=3084
 simulation of fields with rel. motion 8=19372
 single channel recorder, device for conversion to multi-channel sequential recorder 8=6239
 solid state drive for paper-tape punches 8=6035
 spark commutator, pulse correction with heterogeneous shaping line 8=10830
 spark-gap-switch deionization det. 8=7679
 stabilizer, small d. c. currents, semiconductor 8=15183
 static decade register with visual presentation 8=15175
 superconducting oscillator-detector 8=15172
 superconductor, in current magnetometer 8=15253
 superhigh freq. power simulator, for operation in 3 cm band 8=15389
 switching using parallel bank of spark gaps, performance 8=273
 for synchronous operation of mass spectrometer 8=20914
 systems analysis using thermodynamic and nonlinear circuit eqns. 8=26
 thermoelectric generator, use of ferroelectric ceramic capacitor 8=9231
 time mark generator for X-Y recorder 8=15176
 time-to-amplitude converter for photoelectric optical field meas. 8=15496
 timing and control system for radioactive activation by accelerator bombardment 8=11799
 twin-T bridges for impedance and inductance meas. at 10 MHz 8=303
 u. h. f. fast pulse generator using charge storage diode 8=18122
 valves, packing for cryogenic service 8=3139
 voltage-controlled attenuator with photoresistors 8=15181
 voltage integrator, using electronic digital voltmeter 8=15168
 voltage integrator, using electronic digital voltmeter 8=15168
 voltage stabilizers, stabilization coefficient of 8=15184
 wide-band linear amplifiers using secondary emission tubes 8=15173
 wide-band n. m. r. dispersion detector 8=15435
 wideband pulse compression via Brillouin scatt. in Bragg limit 8=10948
 wire loop, e.m. excitation and loading 8=19895
 X130 standard attenuator, with rotating plate, in super-high freq. 8=15415
 zero-crossing detector of bipolar pulses with long cross-over times 8=3141
 zero crossing timing, accurate, using tunnel diodes 8=3142
 GaAs, oscillators, microwave characteristics 8=5301
 Pt resistance thermostat for $\pm 25^\circ\text{C}$ 8=15123
 Si-controlled rectifier switching circuit, for prod. pulsed mag. fields 8=3164

Clathrates. See Molecules; Organic compounds.**Clay**

- adsorption, mutual, with Al oxide, hydrons 8=8341
 electrophoretic filtration, forced-flow, elec. field effects 8=16898
 kaolinite, water saturated, acoustic props. at 4-600 kHz, obs. 8=1857
 mineral mixtures, high-temp. reactions and ceramic props., dimensional and weight changes on refining 8=22323
 surface contour meas. using gas laser probe 8=19339
 ultrasonic dispersal for particle size meas. 8=13046

Cleavage. See Crystals/faces; Fracture.**Clebsch-Gordan coefficients.** See Field theory, quantum; Nucleus/theory; Quantum theory.**Climatology.** See Meteorology.**Clock paradox.** See Relativity.**Clocks.** See Time measurement.**Cloud chambers**

- cosmic rays, large air shower obs. 8=7016
 photoreactions on He³, investigation 8=7000
 Wilson expansion, Polaroid-Land photography 8=20222

Clouds

- aerosol and microphys. props. at Hawaii, comp. of inland and sea forming clouds 8=9859
 rel. to atmosphere waves instability, billow clouds characts., obs. 8=23265
 and back radiation formulae, long wave 8=2590-1
 below base, convection 8=2578
 characteristics correl. with outgoing rad. of "earth-atmos." system 8=9861
 collision efficiencies for small droplets in Stokes flow, theory 8=14616
 condensational growth of NaCl soln. drops 8=9853
 condensation nuclei in air free from aerosols, formation in light and dark 8=18864
 cumulonimbus, large sheared, updraught outflow mixing, obs. 8=23281
 cumulus and cumulonimbus, radio emission during solar eclipse 31st June 1962 8=23282
 droplet coalescence, analytic studies 8=23277
 droplet growth by hydrodynamic capture, stochastic model 8=18869
 droplets and nuclei, number concentration comparison, obs. 8=18867
 evaporation in air, continuum model 8=8184
 gas, expansion in a vacuum 8=4447
 grenade glow clouds, spectral energy distrib. 8=9924
 infrared radiation transfer by spherical harmonics method 8=18866
 microstructure, optical estimation parameters 8=18871
 night, influence on choosing site for astronomical observatory 8=14579
 noctilucous, recent advances 8=2588
 nuclei production and droplet concentration, effect of sugar cane fires 8=18868
 physical processes during formation of layers 8=14617
 radioactive, γ -ray dose calc. 8=10448
 rain water, elec. conductivity, over Hawaii 8=9857
 satellite i. r. obs. for noctilucous cloud detect. 8=9855
 seeding, by AgI aerosols, hygroscopicity and chemical composition 8=1605
 seeding, results and benefits in Australia 8=23280
 short-wave radiation fluctuations relationship 8=9860
 sky conditions, Cerro Tololo Observatory, predictions for 1968 8=14621
 spectral meas. from 1.6 to 5.4 μ 8=9866
 warm over Hawaii, elec. charge on raindrops 8=9858
 Al grenade glow, night radiation obs. 8=18872

Clusius-Dickel columns. See Isotope separation.**Coal**

- agglomerating, specific electrical conductivity, temp. depend. 8=22507

Cobalt

- chromatographic separation, complex formation and reflectance spectros. detect. 8=23176
 critical magnetic scattering of neutrons 8=2317
 deposits, pseudomorphic, on Cu 8=21881
 diffusion studies 8=17575
 domain structures on perpendicular surfaces, obs. with electron microscope 8=13991
 doped MnF₂, magnon sidebands and local order 8=23001
 electrical resistance compared with Fe and Ni 8=17930
 electronic structure, photoemission studies 8=22723
 f. c. c. - h. c. p. martensitic transformation, thermodynamic props. 8=17049
 ferromagnetic lattice, hyperfine magnetic field on Sm¹⁵⁰ 8=2335
 film on Cu, magnetization under circular alternating and longitudinal static fields 8=9335
 films, electrolytically deposited, growth rate rel. to structure and ferromag. props. 8=13999
 films, electron diffraction images of periodic domain struct. 8=22772
 films, galvanomagnetic effect, in rotating mag. field 8=17931
 films, phase changes, thickness depend. 8=17050
 foils, ferromagnetic domain width depend. on thickness 8=22791

Cobalt—contd

- galvomagetic effect obs. in thin film specimens 8=5475
 hexagonal Co films, dynamical multiple reflections in
 electron diffraction patterns 8=13256
 hexagonal single crystal surface plastic deformation due
 to friction against sapphire ball 8=17771
 hexagonal single crystal, Young's modulus dependence
 on thermal expansion 8=22324
 lattice, (0001) surface states calc. using tight binding
 approx. 8=5121
 magnetic recording films, deposition and props.,
 obs. 8=22790
 magnetized, polarized n transmission 8=2031
 magneto-caloric effect near Curie temp. and determ.
 sp. ht. 8=9337
 magnetocrystalline anisotropy and temp. dependence 8=9336
 magneto-optical props., u.v., visible and i.r. 8=18550
 magnetoresistance and electrical resistance 8=8999
 magnetothermal effect during the $\epsilon\epsilon_2\gamma$ phase
 transition 8=13961
 micromosaic block size and misorientation in zone-
 melted crystals, impurity depend. 8=8470
 nuclear polarization in Fe from Fe^{57} Mössbauer expts. at
 1-0.08°K 8=4676
 reflectance meas. 8=22975
 specific heat from magneto-caloric effects near Curie
 temp., specific magnetization 8=9337
 X-ray emission bands fine struct. rel. to e band struct.,
 obs. 8=18527
 in Ag, liquid, diffusion 8=12836
 Co^{56} , extraction from aqueous soln. using 1-phenyl-3-
 methyl-4-capryl-pyrazolone-5 8=18750
 Co^{60} underwater source, γ -ray flux density 8=1008
 $\alpha\text{-Co}$, hexagonal cryst. magnon obs. 8=14008
 Co/Cr layered films of high coercive force, for digital
 mag. recording 8=14009
 Co(II) ions, sublation studies, by radioactive
 tracers 8=23075
 Co^{2+} ion hydration, n.m.r. 8=12937
 Co^{2+} , near i.r. fluoresc. and absorpt in MgO 8=23050
 Co^{2+} in MgO, anisotropy of spin-lattice relax. for
 Kramers doublets 8=9414
 Co^{2+} in MnF_2 , antiferromagnetic, radiationless processes
 and afterglow kinetics 8=23058
 Co^{2+} in $\text{Zn}(\text{NH}_4)_2(\text{SO}_4)_2 \cdot 6\text{H}_2\text{O}$, forbidden hyperfine
 e. p. r. spectra 8=9420
 in Si p-i-n, current oscillations 8=2227
 with Sn, bonds in organo-Sn cpds., Mössbauer obs. 8=4668
 $\text{TiMnF}_3\text{:Co}$, antiferromag. zero anisotropy Co conc.
 dependence 8=9401

Cobalt compounds

- alloy films, meas. of mag. transitions with vib. head
 magnetometer 8=19745
 alloys, f. c. c., ageing effects after cold working
 deformation 8=17622
 alloys, structural defects and precip. 8=17621
 complex, trans-dichloro(1, 4, 8, 11-tetraazaundecane) cobalt
 (111), isomerism 8=7512
 complexes, Co^{99} quadrupole interaction 8=22919
 Co(III) complex, chloropentamminecobalt(III)dichloride,
 crystal structure 8=22016
 Co complex, decammine- μ -amido-dicobalt pentanitrate,
 crystal structure 8=17357
 Co complex, decammine- μ -peroxo-dicobalt pentanitrate,
 crystal structure 8=17356
 Co complex, dichlorobis(2-picoline) Co(II), ligand exchange
 kinetics by n.m.r. 8=2501
 Co complex, tris-dipyridyl Co(111) perchlorate, trihydrate,
 $^{57}\text{Co}^{2+}$ -doped 8=2082
 Co complexes, inversion-vibr. levels and splitting 8=4121
 Co complexes, stereospecificity rel. to conformational
 analysis 8=5691
 Co(III) ethylenediamine complexes, p.m.r. and secondary
 coordination shell 8=12319
 Co(II) halides, absorption spectra at high temp. and
 pressure 8=1580
 Co^{2+} octahedral systems, theory of nuclear resonance
 shifts 8=1597
 Co(II) perchlorates, water solns., u.s. velocity 8=12865
 Co-Al alloy, effect of Ni addition on magnetic
 properties 8=13960
 Co-Al alloy, 'Malcolloy', effect of V addition on mag.
 props. 8=22793
 CoAl, elec. resist., temp. and comp. depend. 8=13721
 Co-Al magnetic alloy, effect of Mo addition 8=22792
 CoAl-Co eutectic, mechanical props. 8=17770
 CoB, transfers of electronic states 8=5461
 Co-Be alloy, ferromag. props. rel. to transfer of
 electron states 8=14018
 $\text{CoBr}_2 \cdot 2\text{H}_2\text{O}$, cryst. structure 8=1798
 Co-Cr alloys, growth of spheroidal graphite crystals 8=13156
 $\text{Co}(\text{CN})_3^{3-}$, molec. and electronic struct. 8=4147
 CoCO_3 , antiferromag. resonance line position, hexagonal
 anisotropy 8=5514
 CoCO_3 , crystal growth, e. p. r. study antiferromagnetism
 and resonance 8=18372
 $\text{Co}(\text{CO})_{12}$, C^{14}O isotope exchange 8=2506
 $\text{Co}(\text{CO})_2\text{NO}$, dipole moment 8=12185
 $[\text{Co}(\text{C}_2\text{O}_4)_2]^{3-}$ - $^{14}\text{C}_2\text{O}_4^{2-}$, radioisotopic exchange 8=21796

Cobalt compounds—contd

- CoCl_2 , in binary solvent mixtures, n.m.r. 8=8138
 $\text{CoCl}_2\text{:MCl}$ (M=Rb, K, Na, Li), symmetry changes rel. to
 CoCl_2 conc. 8=9516
 $\text{CoCl}_2 \cdot 6\text{H}_2\text{O}$, antiferro-paramagnetic transitions at low
 temps. 8=9392
 $\text{CoCl}_2 \cdot 6\text{H}_2\text{O}$, antiferro-paramag. transition rel. to
 Fisher's relation 8=9393
 Co-Cr alloy with W, Ta or Nb, cpd. formation and structure
 on precip. 8=17621
 Co-Cr 10% alloys, contrast effect at cubic-hexagonal
 interface 8=8459
 CoCr_2O_4 , mag. study by neutron diffr. 8=9374
 CoCr_2O_4 , sp. ht. in 80-273°K range 8=17516
 CoCr_2S_4 , mag. structure determ. by n-diffr. 8=18332
 Co-8Cr-Ta, precip. on hardening at 700°K 8=17621
 CoF_2 , optical spectrum 8=22974
 CoFe_2O_4 , coprecipitated particle size distribution 8=4843
 CoGa, elec. resist., temp. and comp. dependence 8=13721
 CoMo alloys, hard magnetic props., structure 8=5462
 $\text{Co}[(\text{NH}_4)_2\text{CS}_4]\text{Cl}$, thermal cond., anomalous enhancement
 rel. to magnon cond. 8=13391
 Co-Ni alloys, effective field distribution at Co^{59}
 nuclei 8=8195
 Co-Ni mag. recording films, deposition and props.,
 obs. 8=22790
 Co-Pd alloys, ferromag., Co^{59} and Pd^{105} n.m.r.
 studies 8=2381
 Co-Pd alloys, (8, 3 to 0.03 at. % Co), effective mag. field at
 Co^{60} nuclei 8=5463
 Co-Ni-Al-Cu-Ti-Fe, solid soln. struct. 8=17010
 CoO, antiferromagnetic, u.s. attenuation 8=22106
 CoO, crystal dynamics and magnetic
 excitations 8=22086
 CoO crystals, growth by arc-transfer 8=4806
 CoO, Néel temp., effect of hydrostatic pressure 8=9394
 CoO, paramagnetic, anomalous Hall effect 8=17914
 CoO, semiconducting, near and far i.r. absorpt. by small
 polarons 8=23008
 $\text{CoO-Al}_2\text{O}_3\text{-SiO}_2$, formation of mullite, free energy of
 reaction 8=9669
 CoO:Li , Seebeck-effect, thermogravimetric effect,
 high temps. 8=1956
 CoO:Li , ($\text{Li}^+ - \text{Co}^{3+}$) dipole relax. losses rel. to free hole
 movement 8=18165
 CoO:Na , ($\text{Na}^+ - \text{Co}^{3+}$) dipole relax. losses rel. to free hole
 movement 8=18165
 Co-P mag. recording films, deposition and props.,
 obs. 8=22790
 Co-Pd and Co-Pt, giant moments theory 8=9302
 Co-Pt binary solns, interdiffusion coeff. conc. dependence,
 by X-ray analysis 8=17570
 CoSi , scattering mechanism and band structure 8=2098
 Co_2Sn , Mössbauer effect 8=1645
 CoTiO_3 , mag. props., theoretical interpretation 8=9399
 CoTiO_3 , mag. resonance and susceptibility 8=9398
 CoW alloys, hard magnetic props., structure 8=5462
- Cochlea.** See Ear.
- Coherence.** See Electromagnetic waves; Lasers; Light/coherence;
 Masers.
- Cohesive energy.** See Bonds; Solids.
- Coincidence circuits.** See Counting circuits.
- Cold working**
 See also Plastic deformation; Slip; Work hardening.
 h. c. p. metals and alloys, X-ray study 8=22283
 polyethylene, effect of cold drawing on sorption of
 organic vapours 8=8349
 rolling materials between 4.2 and 300°K, roller
 design 8=19335
 rolling theories, validity 8=5033
 steel, low-carbon, sheets, rolling and annealing
 textures 8=17799
 steel, mild, rolling, yield stress rel. to strain 8=22368
 Zircalloys-2 and -4, effect on terminal solubility and
 thermodyn. activity of H_2 in these and $\alpha\text{-Zr}$ 8=8249
 Al, rolled, textures 8=21938
 $\text{Al-Al}_2\text{O}_3$, dispersion strengthened, workability
 examination 8=8812
 $\beta\text{-AuMn}$, transform. to f. c. c. structure 8=17042
 Co alloys, f. c. c., ageing effects after cold-working 8=17622
 Cu-Fe alloys, effects on mag. props. and elec.
 resistivity 8=17934
 Fe, effect on oxidation in water vapour at 550°C 8=23101
 Pu-Ga (3 at. %) alloy, α -phase precipitation in
 δ -phase 8=21855
 Rh and Ir, poor ductility 8=22390
 $\alpha\text{-Zr}$, effect on terminal solubility and thermodyn. activity
 of H_2 in this, Zircaloy-2 and Zircaloy-4 8=8249
- Collections of physical data**
 Only comprehensive works of reference are listed here.
 ancient geomag. field intensities, geological and historic
 and archeological data 8=23426
 ancient geomag. field intensities, past 10 000 yrs 8=5811
 atmospheric radio refractivity, world atlas 8=18905
 bimolecular rate constants, table for e, H and OH in
 aqueous solns. 8=2510
 crystallographic Fourier map atomic peak heights and
 corresponding Patterson functions 8=1771
 crystallographic symmetry groups up to 3-dimensions,
 geom. symbols 8=8365

Collections of physical data—contd

- electric dipole moments, molecules in gas phase 8=21050
etchants for crystal defect studies, table 8=17597
gas isotope mixtures, thermal diffusion props. 8=1492
gas reactions, bimolecular and termolecular, tables 8=10466
illumination from moon intensity received on earth for any phase and altitude 8=5951
molecular vibrational frequencies, 54 molecules 8=21036
nuclei, $Z = 11 - 21$, energy level props. 8=7054
particles and resonant states, updating 8=15671
photonuclear data index 8=19343
radioactivity, environmental, National Nuclear Research Centre, Pelindaba, S. A., 1966 8=18908
radio emission of 47 bright galaxies 8=5931
210 radio sources, accurate positions 8=23617
spectral-line intensities, revised tables below 2450 Å 8=1152
source between declinations +27° and -30°, identification 8=23615
USSR State Service of Standard Reference Data, organization 8=2
X-ray crystallography, cylinder absorpt. corrections 8=1774
X-ray diffraction powder patterns, 80 substances 8=17327
Cu alloys, low-temp. mechanical properties 8=17779
Cu, low-temp. mechanical properties 8=17779
Si, stopping power for p, d, t, α 8=8778

Collision processes

- See also Atoms/electron scattering; Elementary particles; Field theory, quantum/interactions; Ionization; Nuclear forces; Nuclear reactions; Scattering, particles; and under the individual particles.
accelerators with colliding particle beams 8=639
advances in atomic and molecular physics, book I and II 8=16171-2
alkali-metal atoms with inert gas, fine-structure transition cross sections 8=4106
alkali-metal atoms, thermal excitation and deactivation in atmosphere of inert gas 8=12088
alkali vapours buffer gas mixing, evidence from optical pumping 8=20978
anthracene, singlet-exciton collisions 8=17891
rel. to astrophysics, atom-atom processes 8=16230
asymmetric molecule-atom scatt., classical theory 8=12368
atom-atom, inelastic, investigated by perturbed stationary state method 8=12101
atom-diatom mol., compound state resonances 8=4255
atoms by diatomic mols, resonances in elastic scatt. 8=21193
atom-molecule energy exchange, variation procedure 8=20150
atoms and charged particles, matrix elements for large energy or momentum transfer 8=4103
atoms or mols., exchange interacts, Schrödinger perturb. formalism 8=4256
atoms, not in 1S states, elastic and resonant exchange cross-sections 8=4104
atoms, scatt. of changed particles, total cross-section, Bethe cross-section sum rule 8=12107
atoms, 3 body, rearrangement collisions for high energies, linear model 8=16228
atomic, autoionization 8=7714
atomic interaction potentials for different electron distributions 8=7456
atomic, with fast e ejection, molecular-orbital model 8=7451
atomic and molecular interactions, weak, new perturbation procedure 8=12103
atomic rel. to planetary atmospheres phenomena 8=14832
atomic scatt., validity of semiclassical method 8=1191
atomic-shell struct. effects in inelastic collisions 8=7452
atomic, slowly converging radial integrals, evaluation 8=21003
atomic, spectral line breadth, effect 8=7372
bimolecular reactions, velocity spectra 8=7635
broadening of spectral lines 8=21197
broadening of spectral lines, semi-classical calculations 8=7459
charge-transfer, high-energy, involving rare gases, adiabatic hypothesis 8=21005
Coulomb interaction, matrix elements, method of quasispin 8=21011
cross-section determ. from meas. on arc discharges 8=4294
deoxidation product growth and separation, model 8=18658
diatomic gas, accommodation coeffs. 8=7629
diatomic mols., rotational relax., theory 8=12365
diatomic mols., vibr. energy transfer 8=21190
differential cross-sections at thermal energies, transformations and averaging 8=21199
elastic, influence on broadening of ion lines 8=12099
electron-atom, classical perturbation theory of atomic excitation 8=7460
electron-atom, excitation cross-sections 8=12077
electron-atoms 8=12091
Collision processes—contd
e capture, classical theory $H^+ - O$, (N) and $He^+ - N$ 8=7461
e-e, e-ion in partially ionized gas mixtures, subject to elect. and mag. fields 8=12423
e-ion, in taking away energy from ion recombination 8=1355
focused sequence generation, inverse-square potential calcs. 8=17696
Fokker-Planck equation and conservation equations 8=4488
gas-solid, study by scatt. modulated molec. beams 8=1323
gases, effects of excited particles 8=16373
heavy particle and electronic states of molecules 8=4249
heavy particles, exchange matrix elements, evaluation 8=12100
highly excited atoms, ionization 8=4303
Holtmark, between Hg isotopes 8=7468
inelastic atomic, effect of pseudo-interaction on adiabatic transitions 8=21010
inelastic, effects on electron transport 8=7939
inert gas ions, doubly charged, cross-section for momentum transfer 8=7458
inert gases, scattering ionization 8=1364
interatomic scatt., interference effects using modified Lennard-Jones potential 8=7453
interelectron, effect on plasma distrib. function 8=1328
ion molecule reactions at pressure $8 \cdot 10^{-6} - 10^{-3}$ mm Hg 8=4258
ion-polar mols., capture 8=7696
ions, multiple acceleration in electric field 8=630
iron, liq. -silica, deoxidation product growth and separation, model 8=18658
low-energy "orbiting" collisions, semiclassical phase shifts 8=12366
metallic lattice, collision of atom, accommodation coeff. 8=22238
molecular beam, shock-tube produced, for O atoms at 3 eV 8=7640
molecular rot. absorpt. lines, broadening 8=12121
molecular scatt. in presence of angle depend. pot. 8=4254
molecule, fast vib. excited, collision with linear chain of atoms, exchange energy and momentum loss 8=16381
molecule-noble gas atom, ang. mom. reorientation cross-section 8=21524
mols., polyatomic, unimolecular reactions activation mechanism 8=4260
molecules and recoil atoms in condensed media, effective interaction range by nuclear γ resonance obs. 8=21198
non-equilibrium ionization, gas in electric field 8=288
nuclear and atomic, Doppler broadening of energies of emitted particles 8=20763
paraffins-electrons, energy transfer to vibr. degrees of freedom 8=4206
phase shifts for inverse-power force field 8=20142
physisorption, angular distrib. of desorbed mols. 8=17146
 $\pi^- - N_2$, π^+ yield obs. 8=7220
plasma, Coulomb system Green's functions 8=7739
plasma, electron-atom interactions and triple collisions 8=7730
plasma, electron-ion reflection thermodynamics 8=7736
plasma, non-linear mixing of waves, velocity dependence 8=16578
plasma, rate calc. for ions 8=12470
in precipitation deoxidation kinetics, model 8=18658
primary atoms, distrib. function for total paths 8=7365
proton-atom, classical perturbation theory of atomic excitation 8=7460
quasi-particles rel. to transformation properties of the kinetic equations 8=14996
resonance multichannel, T matrix expansion 8=20274
semiclassical approx. for elastic scatt. and eigenvalues 8=20151
slow electron scattering by molecules 8=21061
 3α formation in He, He-Ar, He-Ne gases bombard. by α rel. to scintillation mechanism 8=12202
3-body, approx. from Lovelace-Faddeev eqns. 8=20305
translational-vibr. energy transfer, steric factor 8=4250
transport processes, quantum theory 8=19475
vibrational transition probabilities, reaction matrix calc. method 8=21196
vibrational-translational energy transfer, molec. orientation effect 8=7632
vibrators and librators perturbed by collisions 8=100
wave-packet formulation, semiclassical approx. time-depend. 8=20153
wave packets, relativistic 8=15609
of water drops, in steam atmos., energy dissipation 8=21593
 $Ar^+ + Ar \rightarrow Ar^{m+} + Ar^{n+} + (m+n-1)e$, final change states and discrete loss mechanism 8=4107
 Ar^{2+} , in parent gas, mobility calc. 8=7458
Ar, accommodation coeff. in impact on Al, Ag, Au and Pt, 500-12 000 eV 8=12685
Ar, elastic differential collision cross sections meas. 8=4108
Ar and Kr ions and atoms, multielectron ionization in close collisions 8=21012
Ar-p, e capture excitation to 3s, 4s states of H, cross-section obs. 8=7462
Ar, spectral self-broadening and oscillator strengths 8=7416
Br₂ with K, Rb and Cs atoms, reaction kinetics 8=1202

Collision processes—contd

- CO mols. energy transfer to solar photosphere particles 8=12377
 CO₂, vib. deactivation by collision of mols. in presence of Fermi resonance 8=1321
 CO₂, e impact, ionization and excitation, absolute cross sections 8=21268
 Cs-inert gas collisional J reorientation, e spin polarization determ. from D₂ pumping 8=1194
 Cs plasma, effective electron-Cs heavy particle momentum transfer collision freq. 8=12476
 Cs, 6p and Rb 5p doublets, depolarization 8=7471
 Cs, two excited atoms, rel. to formation of molecular ion 8=12438
 D⁺-rare gas, radiation polarization in charge transfer collisions 8=21004
 D₂ with inert gases, total scatt. cross-sections 8=7634
 D₂ with alkanes and alkenes, rel. to deactivation 8=1358
 H and other ions, cross-sections determ. by ion cyclotron reson. 8=12442
 H atom pairs, hyperfine splitting of energy 8=12105
 H atoms—fast H⁺ and He⁺ rel. to astrophysics 8=16230
 H-C, level excitation 8=1193
 e + H, polarization of Lyman-alpha radiation produced 8=12096
 H-e for prod. of polarized e beam 8=15304
 H-H, 1.25–117 KeV, e transfer and ionization obs. anomaly 8=21276
 H-H, spin exchange cross-section from H maser oscils. 8=21008
 H-H, 2–60 keV, ionization fraction obs. 8=21007
 H-H₂, 2–60 keV, ionization fraction obs. 8=21007
 H(1s) + He²⁺ → He⁺(1s) + H⁺, back-coupling and distortion 8=7466
 H-O, level excitation 8=1193
 p+H, electron capture probability 8=1199
 p-H, 1D model for high-energy charge transfer 8=20152
 H⁺-H, 2–60 keV, ionization fraction obs. 8=21007
 H* formation, by H₂⁺ and H₃⁺ prsing through Ne, H₂, Na and Mg 8=21082
 H⁺-H(1s), elastic and resonant exchange collisions, nuclear symmetry 8=12106
 H⁺, H₂⁺ in N₂, O₂, CO₂, H₂O, charge exchange 40–1500 eV 8=21275
 H⁺ + He(1s²) → H(1s, 2s, 2p) + He⁺(1s), e capture cross section calc. 8=7465
 H⁺ + N(O) → H + N⁺(O⁺), classical calc. of cross-section 8=7461
 H⁺-rare gas, radiation polarization in charge transfer collisions 8=21004
 H₂, accommodation coeff. in impact on Al, Ag, Au and Pt, 500–12000 eV 8=12685
 (H₂, D₂) exchange reaction, vib. versus translational energy importance 8=4257
 (H₂, H₂) exchange reaction, vib. versus translational energy importance 8=4257
 H₂ with inert gases, total scatt. cross-sections 8=7634
 H₂—p, e capture excitation to 3s, 4s states of H, cross-section obs. 8=7462[~]
 H₂—p cross-section obs., Balmer emission 8=12190
 H₂⁺ formation, by H₂⁺ and H₃⁺ passing through Ne, H₂, Na and Mg 8=21082
 H₂⁺ + H₂ → H₃⁺ + H, cross-section obs. 0.1 ≤ W ≤ 10 eV 8=21192
 H₂⁺—H₂, He, Ar, Ne, 20–120 keV, cross-section for H atom in 3s state prod. 8=21191
 H₂⁺—N₂, 100 keV, cross-section for H atom in 3s state prod. 8=21191
 H₂⁺—H₂, He, Ar, Ne, 20–120 KeV, cross-section for H atom in 3s state prod. 8=21191
 He, accommodation coeff. in impact on Al, Ag, Au and Pt, 500–12000 eV 8=12685
 He⁴ atoms, Ramsauer-Townsend effect 8=1200
 He beam on H₂ scatterer, total cross section meas. using high intensity nozzle beam source 8=7639
 He-He, validity of Wigner spin rule 8=21015
 He with inert gases, total scatt. cross-sections 8=7634
 He-Ne laser, field modulation method 8=11061
 He—p, e capture excitation to 3s, 4s states of H, cross-section obs. 8=7462
 p + He → H(2p) + Ne⁺, cross-section 8=21009
 p + He → H(2p) + He⁺, cross-section 8=21009
 He, positron annihilation in gas 8=20998
 He⁺—He, excitation and e capture probability calc. 8=7463
 He⁺ in N₂, O₂, CO₂, H₂O, charge exchange 40–1500 eV 8=21275
 He⁺⁺ → He⁺ + H⁺, e capture probability calc. 8=1192
 He⁺⁺ + N → He⁺ + N⁺, classical calc. of cross-section 8=7461
 He²⁺, in parent gas, mobility calc. 8=7458
 He³⁺—He, 7.2–181 KeV, single and double e-capture cross-sections obs. 8=21278
 He³⁺—N₂, 7.7–166 KeV, cross-sections for single and double e capture 8=21279
 Hg, cross-sections of rare gases 8=7469
 Hg, 6s6d levels, with inert gases 8=1201
 Hg²⁰¹, hyperfine levels, population transfers 8=7467

Collision processes—contd

- I₂ with K and Cs atoms, reaction kinetics 8=1202
 e + K, differential spin-exchange cross section and differential cross section, 0.5 eV 8=12097
 K-inert gas, collisional mixing rel. to selection rules for atomic spectrum 8=12064
 K + O₂, atomic differential spin-exchange scattering 8=12109
 Kr-Ne, Ar, He, spectrum broadening and shift effect 8=20956
 Kr, spectral self-broadening and oscillator strengths 8=7416
 Kr²⁺, in parent gas, mobility calc. 8=7458
 N ions in N drift vels. and reactions at 300°K, 0.5–1 Torr in elec. field 8=7718
 N + O → NO⁺ + e, ionization cross section calc. 8=4111
 N₂, accommodation coeff. in impact on Al, Ag, Au and Pt, 500–12000 eV 8=12685
 N₂ ionization by e collisions 8=16448
 N₂ mols., scattering ionization 8=1364
 N₂ second positive system excited by impact with a metastable Ar atom 8=12209
 N₂—H, spectrum rel. to aurora, cross-section calc. 8=12212,
 N₂—p, e capture excitation to 3s, 4s states of H, cross-section obs. 8=7462
 N₂—p, 0.15–1.0 MeV, spectra of N and N₂⁺ 8=12213
 N₂—p, spectrum rel. to aurora, cross-section calc. 8=12212
 N₂⁺—e, dissociation cross-section 8=1312
 N₂⁺ + O₂ → O₂⁺ + N₂, low-energy cross sections 8=16372
 Na, resonance fluorescence quenching in inert gases 8=1185
 Na + Cs, atomic differential spin-exchange scattering 8=12109
 Na-Kr interference effects using modified Lennard-Jones potential 8=7453
 Na-Xe, interference effects using Modified Lennard-Jones potential 8=7453
 Ne, elastic differential collision cross sections meas. 8=4108
 Ne, spectral self-broadening and oscillator strengths 8=7416
 Ne-He plasma, cross section for second kind collisions, meas. 8=21016
 Ne—p, e capture excitation to 3s, 4s states of H, cross-section obs. 8=7462
 Ne²⁺, in parent gas, mobility calc. 8=7458
 O⁺ + N₂ → NO⁺ + N rate constants energy var., drift tube meas. 8=14667-8
 O⁺ + O₂ → O₂⁺ + O rate constants energy var., drift tube meas. 8=14667-8
 O₂ ionization by e collisions 8=16451
 O₂—p, e capture excitation to 3s, 4s states of H, cross-section obs. 8=7462
 O₂⁺—e, dissociation cross-section 8=1312
 OH mols. and charged particles in interstellar space, maser action 8=5927
 p with He, Ar, Ne, N₂, H₂, O₂, excitation to 3s, 4s states of H obs. by e capture 8=7462
 Rb, optically pumped, with Kr atoms, relax. correl. times 8=7472
 Rb, 5p and Cs 6p doublets, depolarization 8=7471
 Tl 2p_{1/2} state depolarization 8=7473
 Xe+D₂, compound state resonances 8=4255
 Xe+H₂, compound state resonances 8=4255
 Xe²⁺, in parent gas, mobility calc. 8=7458
 ZnS:Ag film, ion beam energy loss anomalies 8=8758
- Colloids**
 See also Electrophoresis; Emulsions; Gels; Sols; Thixotropy.
 aggregates, shape analysis, from electron micrographs 8=16906
 amine oxide micellar solns., potentiometric studies 8=8158
 diffusion const., rot., by transient elec. light scatt. 8=8073
 distribution density rel. to Boltzmann's theory for perfect gases 8=16905
 drilling muds in tubes, laminar and transitional flow 8=8151
 ferric oxides, hydrous, mineralogical comp. 8=12954
 light scatter study of turbulence 8=4440
 metal salts solution, preparation of spherical fuel particles 8=16166
 moisture absorpt., chemical potential 8=21730
 stability of precipitating systems 8=12949
 stability, role of water structure 8=12948
 3-layer body, kinetics of temperature field 8=4633
 ultracentrifugation, simultaneous automatic sequence and photo control system 8=4631
 Ag, colour centres form. in KCl:Ag phosphors, obs. 8=8746
 Ag solutions in water, extinction light curves 8=4579
 Al oxide, hydrous, adsorption, mutual, with clay minerals 8=8341
 Au, radioactive, Ag coated for radiotherapy 8=14893
 Au solutions in water, extinction light curves 8=4579
 CsBr, effect of particle size on colloid band 8=1604
 Li, in pile irradiated LiF crystals 8=12947
- Colorimeters.** See Colorimetry.

Colorimetry

- See also Spectrochemical analysis; Spectrophotometry.
 colour matching and specifications 8=465
 colour temp. meas., luminance ratio method 8=20039
 compact colour perception test device 8=20131
 equivalent luminance of a colour meas. for a number of chromaticities and luminance levels 8=15499
 metameric object colours, spectral reflectance intersections 8=15498
 monochromators, resonance, for absorpt. meas. in visible and u.v. 8=11155
 specifications, inter-source transformation 8=11123
 white surface reference standards, U.S.S.R. specimens 8=466
 Pb in air, chromatography appl. 8=9754

Colour

- See also Photography/colour.
 equivalent luminance meas. for a number of chromaticities and luminance levels 8=15499
 indices of some cosmic and earth surfaces 8=2816
 moon, by photometric analysis 8=14825
 phenolphthalein and congeneric mol. crystals, deepening on plastic deform 8=23033
 pigments in white emulsion paint, strength and shade from light absorpt. meas. 8=9574
 television display using lasers 8=11068

Colour centres

- alkali earth oxides, e.s.r. of F centres 8=13456
 alkali halide, Ag⁺ doped, B-centre 8=17681
 alkali halides, Ca doped, Z₁-bands, theoretical studies 8=13455
 alkali halide crystals with activating impurities, colour-ability and luminesc. 8=17682
 alkali halides, dichroic absorption, appln. to information storage 8=13461
 alkali halides, F-band peak, Mollwo relation 8=17688
 alkali halides, F-band, pressure shift: ion-size effects 8=22226
 alkali halides, F-centre, luminescence, under hydrostatic pressure 8=9599
 alkali halides, F-centre multipole polarizability 8=13453
 alkali halides, formation and decay meas. by pulsed e beam 8=13460
 alkali halides, formed by two-photon absorpt. of pulsed N₂ laser 8=5578
 alkali halide phosphors F-centres rel. to radioluminesc. and carrier motion obs. 8=18594
 alkali-halide phosphors, temp. depend. of optical flash from F band 8=5653
 alkali-halides, props. rel. to divalent cation impurities and dipolons, conc. 8=8701
 alkali halides: Sr⁺⁺, mixed crystals, Z₁- and Z₂-centres 8=22225
 alkali halides, and sputtering induced by slow electron bombardment, formation theory 8=13472
 alkali halides, U-centre-induced i.r. absorpt. spectra, side bands 8=4991-2
 alkali halides, U-centre localized mode, shell model harmonic treatment 8=13321
 alkali halides, Z-centres 8=13454
 alkali silicate glasses, X-irrad., trapped hole centres 8=1998
 alkaline earth fluorides, F-centre electronic structure from wave functions 8=1997
 aluminophosphate glasses, radiocolouration and luminescence kinetics 8=1996
 anthracene, γ -irrad. 8=17689
 crystal lattice, theory of quantum absorption and appearance of electrons developed 8=8739
 crystals, as models of positronium atoms and mols. of chem. cpds. 8=13451
 excitation and recomb. near fundamental absorpt. limit 8=9580
 F, in alkali halides, book 8=17680
 F-centre wave functions calc. 8=13646
 F-centres luminesc. as phosphor hole processes meas. 8=8888
 F, diffusion, lecture demonstration 8=13452
 F', theory of photo-ionization 8=8740
 magnetoacoustic reson., double electron-nuclear 8=8623
 metaphosphate glass, Ag radicals 8=4990
 recombination, effect of high mag. field 8=22223
 R-centre, linear Stark effect 8=1992
 ruby, luminescence meas. 8=1995
 rutile, partially reduced, F-centres from e.p.r. study 8=18436
 sodalites, photochromic, e.s.r. 8=14120
 zircon, natural, obs. of two types of centres 8=9649
 AgBr:Se, e.s.r. studies of Se₂⁻ centres 8=13464
 AgCl:Se, e.s.r. studies of Se₂⁻ centres 8=13464
 Ba silicate glasses, γ -ray effects 8=13479
 BaF₂, additively coloured, fluorescence, phonon-assisted 8=14306
 BaF₂, enhancement of colorability by plastic deformation 8=22228
 BaF₂, F-centres 8=22227
 BaF₂, X-ray coloured, absorpt. by colour centres, temp. dependence 8=17683
 BaTiO₃, movement rel. to electrical breakdown 8=13884
- Colour centres—contd**
 CaF₂, additively coloured, fluorescence, phonon-assisted 8=14306
 CaF₂, ENDOR study of F centre 8=9417
 CaF₂, enhancement of colorability by plastic deformation 8=22228
 CaF₂, F-centres, fourth shell isotropic h.f.s. constants 8=13457
 CaF₂, F-centres, X-ray prod. 8=1999
 CaF₂:Nd³⁺, effect of rare earth on Nd³⁺ optical centre 8=5593
 CaF₂, X-ray coloured, absorpt. by colour centres, temp. dependence 8=17683
 CaO, colorability enhancement after plastic deformation 8=22229
 CaO, e.s.r. of F centres 8=13456
 CaWO₄:Nd, reduction coloration, role of Nd 8=22962
 CdS, luminescence of photochemically sensitized and unsensitized, spectra 8=9603
 CdS luminesc. centres nature, obs. 8=8741
 CdS, sensitizing recomb., radiative capture yield of electrons 8=9602
 CsBr crystals with F- and M-centres, photoconductivity wavelength and temp. dependence 8=22694
 Cu₂O, neutron-irrad., rel. to absorption and photocond. 8=5597
 KBr, aggregated H centres 8=2005
 KBr, Ca doped, F-centres rel. to growth of absorpt. bands by X-irrad. 8=2429
 KBr, F-band absorpt., u.s. strain modulation 8=22232
 KBr, F-centre props. rel. to photocurrent wavelength dependence 8=2264
 KBr, F, thermal stability 8=8750
 KBr, formation and decay meas. by pulsed e beam 8=13460
 KBr, irrad.-induced low temp. vol. expansion from relaxs. at Frenkel defects 8=13486
 KBr, KBr:Ti, F-centres photostimulated e emission mechanisms, obs. 8=9278
 KBr:NO₃, CO₃²⁻, SO₄²⁻ and Cu, luminesc. centres nature, obs. 8=8745
 KBr:Ti F-centres luminesc. rel. to hole processes, obs. 8=8888
 KBr, Ti⁺ and In⁺ activated, F-centre form. spectrum rel. to mechanisms, 5-21.2 eV 8=2008
 KBr, V-bands, effect of stress, obs. 8=2000
 KBr, vacancy conc. changes during electrolytic coloration at 460-670°C 8=17609
 KCl:Ag, Ag centres form. rel. to point defects, obs. 8=8746
 KCl:Ag (from AgI), optical absorpt. of impurity rel. to E-band models 8=14228
 KCl:Ag, assoc. e.p.r. absorpt. rel. to relax. process 8=8743
 KCl:Ag, B-centre, luminescence and photocond. 8=2006
 KCl:Ag:OH, Ag centres form. rel. to point defects obs. 8=8746
 KCl:Ag, Pb and Ti, Cl₂⁻ centres conc. temp. depend., e.p.r. obs. 8=8742
 KCl:Ag:Sr, Ag centres form. rel. to point defects obs. 8=8746
 KCl with blocking electrode, photoelectric charge 8=22230
 KCl with blocking electrode, photoelectric polarization 8=22231
 KCl Cl₂⁻ centres conc. temp. depend., e.p.r. obs. 8=8742
 KCl crystals, transform. of OH centres into U centres by electrolytic decoloration 8=13458
 KCl, excited F centre lifetime below 100°K 8=2004
 KCl, F-band absorpt., u.s. strain modulation 8=22232
 KCl, F-centre half-width and effective lattice freq. calcs. 8=4993
 KCl, F, thermal stability 8=8750
 KCl, γ -irradiated near room temp., F-centre saturation concentration 8=8696
 KCl, irrad.-induced low temp. vol. expansion from relaxs. at Frenkel defects 8=13486
 KCl, KCl:Ti, F-centres photostimulated e emission mechanisms, obs. 8=9278
 KCl:Na, dichroic absorption, appln. to information storage 8=13461
 KCl:Na, F₂ luminescence 8=9615
 KCl:RbCl crystals, Q₁ centre e.s.r. study 8=22905
 KCl:Sr, F-Z₂ thermal equilibrium kinetics 8=2007
 KCl, Ti⁺ and In⁺ activated, F-centre form. spectrum rel. to mechanisms, 5-21.2 eV 8=2008
 KCl, U₂-centre, electronic structure rel. to correlation effects 8=13459
 KCl, X-irradiated, α -centre production and thermal annealing 8=17685
 KCl, Z-centre, Faraday rotation 8=14229
 KClO₄, X-ray irrad., absorpt. spectrum 8=22233
 KI, F-centre formation quenching 8=8744
 KI, Ti⁺ and In⁺ activated, F-centre form. spectrum rel. to mechanisms, 5-21.2 eV 8=2008
 KX, (X = Cl, Br, I), U centre electronic structure 8=2001-2
 LiF, F centres ENDOR 8=18465
 LiF, isotopic, shift of U-center local mode 8=13462
 LiF M-centre luminesc. excit. spectra and transitions, obs. 8=8747

Colour centres—contd

- LiF, M-centre, upper excited states 8=2010
 LiF, n-irradiated, F-centre exchange interactions from optical and e.p.r. spectra 8=17684
 LiF, R-centre, linear Stark effect 8=1933
 LiF, 6955Å zero-phonon line, pseudo Stark and uniaxial stress splitting 8=18542
 LiF, V_K centre, lattice distortion 8=2009
 LiH, form. rel. to u.v. irradi. and crystal growth conditions 8=8748
 LiH, n-irradiated, F-centre exchange interactions from optical and e.p.r. spectra 8=17684
 LiH, for red luminesc. 8=18608
 MgO production, atomic displacement effects 8=2011
 Mn-activated alkaline earth aluminate phosphors, sensitized luminescence 8=14303
 NaCl:Ag, assoc. e.p.r. absorpt. rel. to relax. process 8=8743
 NaCl:Ag F-centres thermal stability rel. to dislocations, microspectrophotometry obs. 8=749
 NaCl:Ag and Pb_2 , Cl_2^- centres conc. temp. depend., e.p.r. obs. 8=8742
 NaCl:Ag phosphors, photo-excited F-colour centres, microdefect interactions 8=2013
 NaCl:Ag, Sr phosphors, F centre thermal ionization mechanism 8=17687
 NaCl Cl_2^- centres conc. temp. depend., e.p.r. obs. 8=8742
 NaCl, electron centres form. by Co^{60} - γ -irrad. 8=22235
 NaCl, F-band absorpt., u. s. strain modulation 8=22232
 NaCl, F-centre first-stage formation, X-ray induced 8=2012
 NaCl, F-centre half-width and effective lattice freq. calcs. 8=4993
 NaCl F-centres photostimulated emission mechanisms, obs. 8=9278
 NaCl, F-centres, photostimulated exo-emission 8=5409
 NaCl, F-centre prod., electric field effects 8=13463
 NaCl, F, thermal stability 8=8750
 NaCl with Sr, Cd, Ag, Ca and Tl impurities, F-centres stability rel. to cryst. defects 8=8751
 NaCl-type, endor. of F-centres, in external electric fields 8=14137
 NaF, F-aggregate centres 8=17686
 NaI, U-centres, i. r. vibrational absorption 8=9557
 $NaPO_3$, γ irradi. effect 8=22234
 in Nd^{3+} laser glass, saturable absorpt. rel. to self Q-switching 8=11107
 in Nd^{3+} - Yb^{3+} laser glass, saturable absorpt. rel. to self Q-switching 8=11107
 Ni centres in molten LiCl-KCl 8=8087
 Ni centres in molten $MgCl_2$ -KCl 8=8086
 RbCl, F-band absorpt., u. s. strain modulation 8=22232
 RbCl, Z_1 centre circular dichroism 8=22224
 RbI:Ti, luminesc. and formation of excitons 8=5131
 $SrCl_2$, electron centres form. by Co^{60} - γ -irrad. 8=22235
 SrF_2 , additively coloured, fluorescence, phonon-assisted 8=14306
 SrF_2 , enhancement of colorability by plastic deformation 8=22228
 SrF_2 , F-centres, e. s. r. and optical data 8=2014
 SrF_2 , X-ray coloured, absorpt. by colour centres, temp. dependence 8=17683
 $(Sr_{0.99}Mg_{0.11})_2(PO_4)_2$:Eu yellow luminesc. centres 8=9629
 SrO, colorability enhancement after plastic deformation 8=22229
 ZnS:Cl excit. peaks of green and blue centres from emission obs. 8=9642
 ZnS:Cu excit. peaks of green and blue centres from emission obs. 8=9642
 ZnS:Ho $^{3+}$ blue luminesc. centres rel. to lattice-activator energy transfer, obs. 8=9643
 ZnS:Sm $^{3+}$ blue luminesc. centres rel. to lattice-activator energy transfer, obs. 8=9643
 ZnS:Tm, Tm luminesc. centres form rel. to Zn vacancies obs. 8=8434

Colour photography. See Photography/colour.

Colour vision

- compact colour perception test device 8=20131
 chromatic threshold, dominant wavelength and purity 8=11239
 difference judgments, monochromatic stimuli 8=11238
 difference perception, method of analysis 8=15580
 eye spectral sensitivity, visual task effect 8=3390
 fovea, central blue-brightness 8=11237
 heterochromatic threshold reduction factor, flicker modification 8=15581
 human, transfer of spatial chromaticity-contrast at threshold 8=3389
 spatially induced brightness changes in rel. to wavelengths 8=15579

Colubium. See Niobium.

Coma. See Aberrations, optical.

Combustion

- See also Explosions; Flames; Heat of combustion; Reaction kinetics.
 chamber with thermo-acoustic self-oscillatory system 8=243
 compact metallic materials 8=2524

Combustion—contd

- drops, single, of liquid fuel, influence of initial diameter 8=19657
 dust flammability, critical O_2 conc. determ. 8=18694
 electric arc in gas flow, stability 8=4293
 flame configuration in guided flow 8=19655
 gas explosions, transient heat convection 8=15108
 gaseous fuels in fluidized beds 8=23119
 gas-particle mixtures, acoustic combustion instability 8=16704
 laminar diffusion flame behind parabolic cylinder, const. press. Oseen-flow model 8=19656
 pure bipropellant droplet, wake-type diffusion flame shape, rel. to free and forced convection 8=15113
 rocket motors, instability rel. to detonation waves interaction with flow field 8=10721
 two-compartment bomb calorimeter 8=15129
 wood, wet and dry, ignition by radiation 8=15110
 $2C_2H_2+SO_2$ mixture, continuous in annular channel, rot. rate of luminesc. heads 8=23121
 H_2 ignition, slot-injected in supersonic air stream 8=15112
 Na, characts. of aerosol produced 8=12950
 Pu, characts. of aerosol produced 8=12950

Comets

- dissociation and ionization 8=2827
 Halley, irregularities in motion in 1910, and physical behaviour 8=23677
 Halley, nongravitational forces 8=19260
 Iyeka-Seki (1965f), airborne photography 8=19258
 Ikeya-Seki (1965f), emission band intensities of C, (1, 0) and CN(0, 0) 8=10359
 Ikeya-Seki 1965f, Na D lines near perihelion passage 8=14852
 Ikeya-Seki (1965f), polarization of head and tail emission and continuum, 3890-5875Å 8=10360
 Ikeya-Seki, tail polarization plane and degree obs. 8=10358
 rel. to meteor shavers origin, Canada and N. Zealand radar obs. comparison 8=19265
 m. h. d. effects in solar wind 8=19262
 Morehouse 1908 III, rays distrib. and movement 8=14850
 Morehouse, vels. of streamers and condensations in tail 8=14851
 observations with 15 in. wide-field astrographic camera 8=23661
 1965f, "sun-grazing" effect on solar radiation, Oct 21 obs. 8=2846
 solar wind interaction, laboratory simulation 8=23678
 in solar wind, motion 8=19261
 "spontaneously" split, fracture mechanism 8=14853
 sungrazing group, orbit determ. 8=19259
 tail, spectral obs., inelastic collisions between CO molecules and pistons 8=1357
 CO plasma, prod. and flow under influence of solar wind 8=14854

Compasses

No entries

Complimentarity. See Physics fundamentals; Quantum theory.

Compressibility

- See also High-pressure phenomena and effects.
 aggregate of particles of 4 sizes, fluid-saturated, and compressional wave vel. 8=22270
 alkali halides, in rel. to Reststrahlen freq. and elastic constants 8=13580
 axial extension by cyclic straining, at ultrasonic freq., second-order strain accumulation 8=13527
 granodiorite shocked mechanically and by nuclear explosion 8=23212
 graphite, foamed, shock compression 8=22316
 inert gases, solid, bulk modulus temp. dependence 8=5075
 iodine, solid 8=13578
 metals, effect of superimposed u.s. vibration 8=8795
 metals, electron orbital, under shock-wave compression 8=8225
 metals, subjected to high press., effect of electron structure 8=11724
 organic crystals, rel. to derivation of oscillation spectrum and charact. temp. 8=17470
 polyurethane, compression modes, obs. 8=22271
 quartz, X, Y and Z cut, elastic shock obs. 8=13608
 shock-velocity-particle-velocity relationship in study of solids under pressure 8=8787
 solid-filled pistons, u. s. meas. of expansion rel. to internal press. 8=10580
 stishovite, anomalous compression curve 8=22039
 Ag_2Al , calc. from elastic constant meas., 77-700°K 8=5040
 Al- Al_2O_3 , dispersion strengthened, workability 8=8812
 Ar solid, bulk modulus temp. dependence 8=5075
 BaTiO $_3$, shock-wave 8=13538
 CO $_2$, isothermal, critical divergence, Rayleigh and Brillouin scatt. obs. 8=16708
 Cd(II), sulphosalicyclic acid chelates of, adiabatic, lowering of 8=8633
 D, polycrystalline, calc. from sound velocity meas. at 2 and 16°K. 8=17499
 Fe, 4.2-300°K 8=5061
 Ge, metallic modification formation under shock compression 8=17083

Compressibility—contd

- KBr, shock wave, compression and phase transitions 8=22376
 KCl powders, energy absorption during compression 8=13592
 KCl, shock wave, compression and phase transitions 8=22376
 KNO₃, dynamic compression by explosive impact loading 8=22377
 Kr solid, bulk modulus temp. dependence 8=5075
 Li⁷H and Li⁷D, to 40 kbar 8=13581
 Mg, plane-strain compression, anisotropy 8=17814
 Mg-Li alloy, plane-strain compression, anisotropy 8=17814
 Mg-Th alloy, plane-strain compression, anisotropy 8=17814
 NaCl powders, energy absorption during compression 8=13592
 NaCl-KCl powder mixture, powders, energy absorption during compression 8=13592
 NaF, ionic crystal, and elastic constants, calc. 8=2062
 Ne crystals, isothermal, and volume coeff. of thermal expansion 8=1803
 Ni, 4.2-300°K 8=5061
 Pb(Zr_{0.96}Ti_{0.04})O₃, shock-wave 8=13538
 Se, calcs. rel. to structure 8=17827
 Si, metallic modification formation under shock compression 8=17083
 Th(II), sulphosalicylic acid chelates of, adiabatic, lowering of 8=8633
 TlBr, temp. and pr. dependence, obs. 8=2068
 Tl and polymorphism and thermal expansion 8=1683

gases

- air, between plates of displacement transducer, effects of compression 8=7892
 linear relation of temp. and density at unit compressibility factor 8=16690
 n-paraffins, adiabatic, and sound vel. 8=21517
 CO₂ bubble in laminar flow of water 8=21591
 N₂O bubble in laminar flow of water 8=21591

liquids

- benzene, hypersonic velocity, from Brillouin shifts, temp. dependence 8=1502
 toluene, hypersonic velocity, from Brillouin shifts, temp. dependence 8=1502
 CCl₄, hypersonic velocity, from Brillouin shifts, temp. dependence 8=1502
 Co(II) perchlorates, water solns., adiabatic 8=12865
 Cu(II) perchlorates, water solns., adiabatic 8=12865
 H₂O, hypersonic velocity, from Brillouin shifts, temp. dependence 8=1502
 Mn(II) perchlorates, water solns., adiabatic 8=12865
 Ne, isothermal, at press. to 1000 atmos. 8=21555
 Ni(II) perchlorates, water solns., adiabatic 8=12865
 S and Se, and sound velocity 8=12866
 Zn(II) perchlorates, water solns., adiabatic 8=12865

Compressive strength. See Mechanical strength/compressive.

Compton effect

- in astrophysics for intense radiation 8=21296
 cosmic black-body radiation interacting with radio galaxies 8=19213
 "edge", teaching misconceptions 8=7027
 energy-differential cross section 8=3571
 forward high energy and Drell-Hearn-Gerasimov sum rule 8=690
 γ -ray scatt., excitation of nuclear resonance fluoresc. 8=20666
 γ spectrometer for n radiative capture, anti-Compton 8=6785
 γ spectrometer, weak, using summing principle with 2 detectors 8=6789
 hadrons, J^P = 1⁻, 3/2⁺, sum rules 8=6901
 harmonic oscill., 3-D, e. m. field coupling, Fabini sum rules satisfied 8=3427
 in intense fields, freq. shift 8=20349
 inverse, motion of e in radiation field, energy spectrum of scatt. photons 8=20346
 inverse, resultant energy losses and thermal instability 8=5944
 large-angle scattering, double logarithmic approximation 8=15715
 light waves standing, obs. of deflection of 1.6 keV electrons 8=20378
 low energy theorem 8=20341
 low-energy theorems for nucleon Compton scatt. 8=20521
 nucleon amplitudes, sum rules 8=6942
 N, with π photoprod., analysis 8=20345
 photon scatt. from electrons, in field of intense laser ray 8=20354
 polarized photons off spin 1/2 particle with charge and anomalous magnetic moment 8=20348
 p scatt., subtraction constants in sum rules 8=20347
 quasars, inverse process and circular polarization 8=23631
 spectral profile of second harmonic in scatt. 8=11426
 spin-0, -1/2 targets, low-energy theorems from dispersion theory 8=20350
 on uncharged fermions, with anom. mag. moment 8=675
 virtual photon, high energy behaviour in O(3,1) symm. compared to Regge pole model predictions 8=20353
 white dwarfs, energy loss 8=10150

Compton effect—contd

- Ge crystal, comparison with Klein-Nishina prediction 8=11435
 Ge(Li) γ -spectrometer, reduction of background by use of single crystal 8=697
 InSb, and thermal agitation in X-ray diffusion 8=13332
 V, and thermal agitation 8=13300

Computation. See Calculation.

Computer memories. See Calculating apparatus/digital computers; Magnetic devices; Magnetic films; Superconducting materials and devices.

Computers. See Calculating apparatus.

Concrete

- creep, high temp. effect 8=2042
 diffusion of water between 50 and 95°C, further comments 8=22148
 heat resistance, elect. insulating props. dependence on temp. and atmosphere 8=13900
 C steel wire stress relax. obs. 8=17789

Condensation

- See also Drops; Fog.
 alkali metal vapours, thermal resistivities of liquids 8=8049
 atmospheric, process from optical obs. 8=9834
 cloud droplets collision efficiencies, theory 8=14617
 controlled by heat transfer on large droplets in pure vapour, perturb. anal. 8=16942
 forced convection type, effect of noncondensable gases and interfacial resistance 8=16941
 growth of liq. drop in subcooled vapour mixture 8=12983
 homogeneous nucleation theory, thermodynamic aspects 8=23278
 jet streams detect. by satellite i.r. obs. 8=9855
 metals in metal vapour-CO-CO₂-neutral gas system 8=8182
 nuclei in air free from aerosols, formation in light and dark 8=18864
 oblique shock waves 8=19541
 physical-cluster theory 8=4654
 of saturated steam, rel. to interfacial heat-transfer resistance 8=16940
 of saturated steam, laminar film cond. on vertical plate, effect of variable phys. props. 8=21771
 solar loop prominences, theory 8=5973
 on substrate, quasi-equilib. models and surface defect structure theories 8=21782
 surface resistance in transport from vapour to liq. 8=12975
 within thermal boundary layer, rel. to enhancement of vaporization rates 8=4658
 Ar, coeff. obs. at 4.2°K 8=12981
 in Ar, mol. beams forming single crystals 8=16383
 Bi on 2-4°K, superconducting modification 8=2155
 in CO₂ mol. beams forming single crystals 8=16383
 Cu, in vacuum, structural transitions 8=16943
 H₂-Ne liquid-vapour phase equilib., 26°-42.5°K, 10-25 atm. 8=16937
 K vapor, associated shock 8=12982
 K, saturated vapour, film condensation 8=21770
 Kr, coeff. obs. at 4.2°K 8=12981
 LaF₃, coeff. from thin film meas. 8=4655
 LiF, coeff. from thin film meas. 8=4655
 NaCl soln. drops, growth on nuclei with radius 0.01-100 μ 8=9853
 Xe, coeff. obs. at 4.2°K 8=12981
 Y, in vacuum, temp. effect on purity 8=4652

Condensation of gases. See Liquefaction, gases.

Conduction, electrical

- See also Conductivity, electrical; Contact resistance; Current, electrical; Photoconductivity; Resistance, electrical; Semiconductors; Skin effect; Superconductivity.
 anthracene, hole injection from electrolyte and space-charge-limited current 8=18177
 coupled electron-phonon system, transport theory, variational approach 8=2080
 crystals containing H bonds 8=13704
 dielectric liquids, prebreakdown current meas. 8=8115
 electron energy spectrum in ferro- or antiferromagnets, near Curie temp. 8=5099
 electron in external field, one-band approx. 8=17871
 electrons, quasiorbital mag. moments and electro-dipole 8=323
 electron scattering by impurity with unity spin 8=22426
 hydrocarbon chains, effective masses estimation 8=17873
 insulating films with ionic space charge, conduction process 8=2232
 metal crystal with oxide film, ionic diffusion and thermionic emission model 8=5710
 m. i. s. tunnel junctions, conductance extrema 8=22620
 nonlinear theory of h.f. field penetration 8=13706
 non-metallic crystals, space-charge-limited transient currents 8=5161
 oxide layers, thin unsaturated, phenomenological model 8=8979
 plastic films, in high fields 8=13877
 power transmission network, d.c. 3-wire, relaxation method solution 8=281
 solutions, effect of non-Brownian motion 8=21718
 space charge, review 8=18002

Conduction, electrical—contd

- temperature-dependent, elec. field and temp. distrib. 8=3151
- 10^{-9} Ω joints to superconducting Al by ultrasonic soldering 8=17995
- transport coeffs., calc. using Schwinger's variational principle 8=17916
- α -Ag₂S mixed conductor, electronic and ionic processes 8=22500
- Ar, charge transport temp. dependence in liq. and solid state 8=18161
- Ar, solid and liq. free-carrier drift-velocity meas. by oscilloscope 8=8119
- As₂S₃, amorphous, carrier mobilities from conductivity studies on e-irradiation 8=18162
- Bi, size-dependent 8=22515
- CeO crystals, mechanism from electrolyte reduction study 8=18164
- CuSO₄ · 5H₂O crystals, proton conductance 8=8982
- Fe-Cu ferrites, mixed mechanisms from resistivity and Seebeck meas. 8=18035
- FeO, mechanism from elec. meas. at high temp. rel. to defect structure 8=18166
- Ge: Au double injection diodes, N- and S-type negative resist. and relax. oscs. 8=22628
- n-Ge, small-field d.c. conduction in presence of large microwave field 8=13811
- Kr, solid and liq. free-carrier drift-velocity meas. by oscilloscope 8=8119
- Ne, solid and liq. free-carrier drift-velocity meas. by oscilloscope 8=8119
- Pb-Ag system, galvanic cell studies using PbO-SiO₂ melts 8=23150
- Pb-Sn alloy polycrystalline vs. impurity concentration obs. of two maxima 8=8803
- Pt/rare-earth alloys, conduction electron polarization 8=17857
- S, orthorhombic, electron hopping transport and orbital overlap 8=18064
- Se, polycrystalline, hexagonal, local (conduction) levels, X-ray-induced 8=18236
- Si-Fe alloys, rel. to bonds, at 800-1700°C 8=9017
- SrCl₂, pure and Y³⁺(Na⁺) doped, ionic, and diffusion mechanisms 8=8983
- TiO₂ films with large ionic space charge, conduction process 8=2233
- Xe, solid and liq. free-carrier drift-velocity meas. by oscilloscope 8=8119

Conduction, heat. See Heat conduction.

Conduction bands. See Crystal electron states.

Conduction electron scattering. See Crystal electron states.

Conductivity, electrical

- See also Resistance, electrical; Semiconducting materials; Semiconductors; Skin effect; Superconducting materials and devices; Superconductivity.
- electron-impurity interacting system, h.f. cond., calc. 8=2999
- ferromagnetic metals, anomaly in resist. near T_c 8=13985
- generator, segmented-electrode m. h. d., electron temp. effect 8=15200
- glasses in PbO-Al₂O₃-B₂O₃-SiO₂ system, temp. and comp. dependence 8=18170
- increase following impact ionization in Gunn-effect domain 8=5142
- β -methyl-naphthalene in polycrystalline, dissolved and melted state 8=16866
- naphthalene in polycrystalline, dissolved and melted state 8=16866
- phenanthrene in polycrystalline, dissolved and melted state 8=16866
- plasma, particle impenetrability 8=7745
- of plasma, in strong mag. field 8=21321
- two-phase flow, high-void-fraction, in MHD generator, effective cond. 8=15202-3
- C, amorphous, rel. to electronic model 8=8998
- SF₆ plasma, 2400-9000°K, meas. 8=7737
- gases**
- m. g. d. flow, temp. dependence 8=16491
- air, air-teflon mixture, shock heated, obs. 8=4486
- air plasma variation with freq. and electron density 8=4346
- electron drift velocity meas. 8=12694
- of electron-ion plasma, with drifted electrons, h. f. resistivity 8=4324
- ionized multicomponent mixtures, rel. to thermodynamic parameters 8=1354
- ionized, weakly, approx. calc. 8=4487
- plasma, multi-ion rel. temp. calc. 8=4345
- Ar plasma containing alkali metal additions 8=12482
- argon plasma variation with freq. and electron density 8=4346
- N₂ with LaB₆ powder suspension, m. h. d. generator working fluid 8=15199
- Pb-cpds, contribution to gas purification 8=4488
- Zn-cpds, contribution to gas purification 8=4488

liquids

- alkali metals, pressure depend. 8=9010

Conductivity, electrical—contd**liquids**—contd

- alkali metals, resistivities, appl. of structure factor and pseudopot. relation 8=12920
- alkali silicates, molten 8=4601-2
- alloys, anomalous resistivity meas. 8=16880
- alloys, electronic transport props. from X-ray diff. 8=12799
- alloys of metals from groups IB and IV B, rel. to comp. and temp. 8=12912
- benzene, electrode effect 8=8116
- binary mixtures rel. to dielec. const. and isotherm calc. 8=4609
- dilute binary alloys, resistivity theory 8=12919
- electroconducting fluid flow between rough plates 8=8110
- hexane, behaviour of negative charge carriers 8=21717
- n-hexane after irradi. by γ -rays, theory, applic. to ionization chamber 8=6628
- n-hexane, u. v. and γ -radiation effects 8=21714
- metals, conduction-electron states, variational soln. 8=12903
- metals, ion interact. via model pseudo pot. rel. to resistivity and band struct. 8=16789
- metals, resistivity Born approx, reply to criticism on X-ray testing 8=12916
- metals, resistivity, Born approx., X-ray testing, comments 8=12915
- metals, resistivity, failure of Born approx. calc. 8=12914
- metals, Ziman pseudo-atom phase shifts calc. for monovalent ions 8=16882
- mixed salt solns., h. f. obs. 8=16827
- nitrate melts, binary mixtures of Ca(NO₃)₂ and MnO₃ (M = Na, Cs, Rb, K), supercooled, rel. to relax. processes 8=1586
- noble metal alloys, resistivity depend. on temp. and cond. 8=12923
- piperidinium picrates in chlorobenzene containing ligands tetrahydrofuran and triphenylphosphine rel. to cation-oxide ligand complexes stability 8=16338
- pure metals, nearly-free-electron diff. theory compared with expt. 8=12911
- rain water in cloud over Hawaii 8=9857
- tetrabutyl ammonium perchlorate soln. in H₂O-dioxane 8=8105
- tetraethylammonium perchlorate soln. in H₂O-dioxane 8=8105
- Ag-In alloys, resistivity depend. on temp. and conc. 8=12923
- Ag₂S_{1-x}, dependence on S vapour pressure above melt 8=16876
- Cd-Sb molten alloys, resistivity rel. to free energy 8=12842
- Hg, press. depend. of resistivity, thermopower and phonon dispersion 8=16879
- Hg, resistivity rel. to temp. and press. 8=12900
- In-Bi molten alloys, resistivity rel. to free energy 8=12842
- In-Sb molten alloys, resistivity rel. to free energy 8=12842
- (Li, K)₂, (SO₄, WO₄) system, molten, up to 1100°C 8=8112
- Li-Mg dilute alloys, resistivity theory 8=12919
- LiNO₃ solns., ion assoc. 8=21715
- NH₄ salts, quaternary, in water-glycine, mixtures 8=8104
- Na, resistivity pressure dependence rel. to lattice dynamics model calcs. 8=1838
- NaClO₄ solns., ion assoc. 8=21716
- Pb-Bi molten alloys, resistivity rel. to free energy 8=12842
- Sn-Bi molten alloys, resistivity rel. to free energy 8=12842
- Sn-BiCl₃ solutions 8=17000
- Te, high pressure meas. 8=1588
- Te_{1-x}Se_x alloys, 0 ≤ x ≤ 0.5, rel. to electron states 8=12918
- liquids, electrolytic**
- See also Chemical analysis/electrochemical; Ion velocity/electrolytic.
- acetic acid in propanol-H₂O mixtures 8=21720
- cell for aqueous solns., 1-3000b and 25-225°C 8=14424
- contact ion pairs, equilib. const., effect of ion polarizability 8=8118
- ethanol-H₂O mixtures, with electrolytes in soln. 8=4604-5
- fixed-charge ionic systems, convective contrib. 8=8037
- polarization in high resistivity electrolytes, modified Wheatstone bridge circuit 8=18715
- propanol-H₂O mixtures, with HCl in soln. 8=4607
- propanol-H₂O mixtures, with NaCl in soln. 8=4606
- seawater activated AgCl-Mg battery electrolytes 8=16875
- strong solns., polarization contribs. to thermodynamic props. 8=4599
- thermal equilb. of intrinsic ionic cond. 8=4603
- tracer detection, in flow systems 8=8109
- CaCl₂ aq. soln., phenomenological coeffs. 8=12924
- HCl aq. soln., phenomenological coeffs. 8=12924
- HClO₄ aq. soln., phenomenological coeffs. 8=12924
- HNO₃ aq. soln., phenomenological coeffs. 8=12924
- I₂ molten salt solns. 8=21719
- KCl solns., under high press. 8=12922
- LaCl₃ aq. soln., phenomenological coeffs. 8=12924
- LiCl aqueous solns., for formation of pulse discharges 8=4608

Conductivity, electrical—contd

liquids, electrolytic—contd

- LiClO₃ in acetonitrile-dioxane mixtures 8=8108
 LiClO₃ in H₂O-dioxane mixtures 8=8107
 LiClO₃ in methanol-dioxane mixtures 8=8108
 Mg fused, NaCl, KCl, CaCl₂ additives, obs. 8=23143
 MnSO₄ in water-glycol, viscosity effect 8=12921
 NaCl aq. soln., phenomenological coeffs. 8=12924

solids

- albite, high press. and high temp. 8=8978
 alkali halide crystals, kinetics of radiational change 8=22501
 alkali metals, pressure depend. 8=9010
 anisotropic mats, meas. from small specimens 8=5156
 anthracene, resistivity obs. on single crystals 8=22523
 basalt, high press. and high temp. 8=8978
 binary cpds., inorganic, rel. to point defects 8=8689
 β -brass, resistivity, effect of heat treatment 8=13714
 β carotene, all-trans, and elec. activation, obs. 8=2465
 coal, agglomerating, temp. depend. 8=22507
 conducting slab, e. m. waves transmission, cyclotron reson. peak 8=19838
 conductor shape changes during "wire explosions" 8=6150
 crystals with high permittivity, theory 8=8897
 crystalline mixtures, rel. to thermal diffusion 8=22144
 DNA with complexed carcinogen 8=18093
 earth, crystalline basement struct., e. m. meas. 8=18821
 earth's surface, rel. to mag. field vertical component variation 8=23441
 earth's surface, review 8=9791
 epoxy compound, rel. to elec. field strength 8=22498
 epoxy resin, polymerization from resistivity studies 8=18707
 excitonic insulator, transport props. 8=13652
 ferrites, effect of CaO and SiO₂ proportions 8=13715
 films, metallic, thickness determ. by Leonard and Ramey method 8=17119
 film, metallic, thin, quantum theory of perp. cond. 8=22510
 flat, circular samples, anisotropy study by four probes method 8=5163
 glass, porous, surface increase by adsorption of water vapour 8=4766
 glasses, transition metal oxide and chalcogenides based 8=22522
 Kondo anomaly, frequency depend. calc. with e-spin interactions 8=13642
 low temp. resistivity meas., eddy current method, contactless, 1-10 000 n Ω cm range 8=5162
 magnetic alloys, effect of electrons of opposite spins on elec. resistivity 8=22432
 mechanisms for current flow and band theory 8=17917
 metals 8=22508
 metals, digital meas. of current decay 8=17922
 metal films, Fuchs geometry, size effects 8=13631
 metals, with impurities, freq. depend. 8=17920
 metal, influence of electron fluctuation pairing, theory 8=17919
 metal to insulator transitions 8=22451
 metals, isotopically disordered 8=13630
 metallized plastic films for source mounts 8=5153
 polyethylene film, I-doped, current oscillations at high field strengths 8=8985
 polyethylene films, I-doped, meas. 8=8984
 polymers, effect of electron irradiation 8=9204
 polysulphimide 8=9138
 polysulphimide 8=22615
 porous, model for cell level 8=18149
 quartz, in a.c. field, 10⁸-10⁹ Hz, 20-700°C 8=18197
 rare-earth sesquisulphide crystals 8=9119
 rock, moist, meas. in lab. 8=13899
 semiconductors, elemental, hot-carrier microwave conductivity 8=13779
 n-type semiconductors as function of impurity 8=5226
 semiconductor with negative bulk differential cond., stationary state 8=13782
 semiconductors, negative differential cond. and sound amplification 8=1843
 semiconductors, organic, temp. dependence meas. in metal chamber 8=9092
 size effects, theory, assuming diffuse surface scatt. 8=13699
 solid solns., resistivity dependence on short range order 8=17915
 space charge, with introduced carriers 8=5158
 superconductors, ordinary and gapless, effect of phonon-bogolon processes 8=13730
 superconducting wire in composite conductor, min. propag. current rel. to int. thermal resistance 8=17993
 TMPD-chloranil crystals, meas. 8=8595
 toluene glow discharge prod. polymer films, obs. 8=21894
 transitional metals, dependence on atomic wt. 8=17924
 vanadites, metallic, rel. to growth 8=4819
 wüstite, hole mobility obs. 1 000-1 300°C 8=13697
 Ag film, vapour-deposited, resistivity annealing temp. and thickness dependence 8=17925
 AgCl, effect of ultrasonic field 8=2237
 AgCl, negative resist., and current-voltage characts. 8=17918
 Al at He boiling temp. for purity determ. 8=9741
 Ag-Mg solid solns., Ag-rich, long-range order dependence 8=21820

Conductivity, electrical—contd

solids—contd

- Ag-Mg solid soln., Ag rich, short-range order dependence 8=21819
 Al, electron irradi., resistivity recovery, kinetics study 8=5171
 Al, plastically deformed 99.999% pure, resist. and strain effects, 4.2-77°K 8=17926
 Al, resistance, and thermoelectric power, high press. effects 8=13902
 Al, resistivity recovery after low temp. electron and neutron irradi. 8=2134
 Al, sintered (SAP) and normal 8=13707
 Al, Wiedemann-Franz ratio and anomalous lattice cond. 8=8990
 Al-Al₂O₃-Au tunnel structures, interface trapping 8=5381
 Al-CaWO₄-Au tunnel structures, interface trapping 8=5381
 Al-Cu-Cd alloy, resistivity, in artificial ageing 8=13708
 Al₂O₃ films, pyrolytically grown, voltage-current charc. 8=13873
 α -Ag₂S, mixed conductor: electronic and ionic 8=22500
 As₂Se₃, vitreous, effects of heat treatment 8=8991
 Au film on quartz glass and BaTiO₃ substrates 8=13709
 Au films, thin, and thermoelectric props., -100 to +100°C in ultrahigh vacuum 8=22513
 Au, resistance, and thermoelectric power, high press. effects 8=13902
 AuMn, spin-disorder resist., anisotropic 8=14064
 Au/Ni-Cr, contacts and conductive paths 8=8993
 Au-V alloys, resistivity, near Kondo temp. 8=8992
 Au-V alloys, resistivity and mag. susceptibility temp. dependence rel. to s-d interaction 8=13657
 B, polycryst., thermopower and resist., temp. and press. 8=18210
 BaTiO₃, anomalies 8=9208
 BaTiO₃ application of small polaron problem 8=5587
 BaTiO₃, between 600 and 900°C 8=5363
 Be, resistivity recovery after low temp. electron and neutron irradi. 8=2134
 Bi, effect of pressure 8=5173
 Bi film, resistivity voltage dependence at 4.2°K 8=17928
 Bi films, temp. dependence 8=8995
 Bi, Shubnikov-de Haas effect meas. at 15 kbar 8=5237
 Bi, thin films, resistivity and thermoelectric power 8=5383
 Bi, 300-540°K 8=13710
 Bi₂O₃, and defect structure in range 175-250°C 8=8996
 Bi_{1-x}Sb_x, (0 < x \leq 0.15), at 77°K rel. to band structure 8=22518
 Bi₂Te₃-PbTe alloys, low temp. obs. 8=22680
 C composite sintered materials, resistivity heat treatment on 8=2129
 C composite sintered materials, resistivity, temp. depend. 8=22502
 C resistors at low temp. 8=17929
 Ca, f.c.c., resistivity from 4.2 to 300°K 8=5175
 CaF₂-GdF₃, surface layer 8=18163
 Cd, isotopic composition effect 8=13712
 Cd oxide, semiconductors, possibility of obtaining controlled resistors 8=18034
 CdCr₂Se₄, ferromagnetic 8=2189
 Cd-Mn alloys, low temp. resistivity, influence of magnetic ordering 8=2136
 CdS film 8=13852
 CdS, resist. homogeneity, S₂ annealing pressure dependence 8=8980
 CdS in strong electric field 8=18030
 CdS, surface and volume conductance, kinetics comparison 8=18032
 CdS, thermally stimulated, influence of electric field 8=9239
 CdS-SiO₂ film devices, "frozen" cond. and thermo-stimulated currents 8=5388
 CdSb 8=13698
 Cd_{3-x}Zn_xAs₂, 80°-400°K meas. 8=5385
 Co, resistivity comparison with Fe and Ni, -190° to 1450°C 8=17930
 Co, resistivity up to 1000 Oe 8=8999
 CoAl and CoGa, temp. and composition depend. 8=13721
 Cr, alloyed with V and Ti, anomalous decrease 8=9000
 Cr films, rel. to glow discharge 8=17128
 Cr resist., mag. contribution temp. depend. rel. to itinerant antiferromag., obs. 8=5500
 Cr selenides, cond. and thermal cond., thermoelectric power, lattice parameters 8=13703
 Cr-Fe alloys, Cr rich, resistance meas. and antiferromag. ordering rel. to energy changes 8=8931
 Cr-Ge alloys, 20-300°K, Curie points and ferromag. props. 8=9338
 Cr-Si alloys, resistivity 8=9001
 Cr-SiO cermet films, resistivity 8=1695
 Cr-SiO cermet films, and temp. coeff. of resistance and Hall coeff. 8=8981
 Cr_{1-x}Te_x alloys, in paramagnetic state 8=9300
 Cu alloys, high-temp. resistivity 8=9003
 Cu complexes, tetraphenylporphine and tetraphenylchlorine 8=9117
 Cu, defect concentrations study from cyclic stressing at room temp. 8=17604

Conductivity, electrical—contd**solids—contd**

- Cu, 99.999% pure, rel. to theory, 78-400°K 8=22134
 Cu oxide semiconductors, possibility of obtaining controlled resistors 8=18034
 Cu, polycrystalline, resist. of dislocations, exptl. determ. 8=9004
 Cu, resistivity, effect of transition elements 8=22133
 Cu, resistivity and susceptibility studies of localized Fe moments 8=22796
 α -Cu-Ag alloy, resistivity and Hall coeff. interpretation 8=13641
 Cu-Be alloys, Guinier-Preston zone formation, from resistance meas. 8=17606
 CuCr₂Se₄, ionic config. from neutron diff. and elec. trans. props. 8=1788
 Cu-Fe alloys, resistivity rel. to cold working 8=17934
 CuFeMn₂O₄, temperature dependence 8=17932
 p-Cu₂S, and thermo-electric power and Hall effect 8=22585
 Eu, contribution to hyperfine field 8=1633
 Fe, electron irradi., resistivity studies 8=5180
 Fe, as function of temp. and magnetization 8=13716
 Fe, reproducible residual resistance measurement 8=5179
 Fe-Al alloys, resistivity 8=9005
 FeCr₂Se₄, rel. to d-orbital interaction clarification 8=5391
 Fe-Ni (35 wt. %)-Cr (0-20 wt. %) alloys (in as-cold worked state), resistivity temperature dependence 8=9006
 GaAs, ultrasonic absorpt. max. for infrared irradiation 8=13352
 GaAs:Zn polycrystalline films, obs. and theory 8=5255
 p-GaSb, effect of pressure and temp. 8=13804
 GaSb-InSb alloys, resistivity at high temps. rel. to comp. and impurity doping 8=4944
 Gd, contribution to hyperfine field 8=1633
 Gd-Yt alloy, spin-disorder resistivity meas. 8=9007
 n-Ge, effect of dislocations on galvanomag. props. 8=22593
 Ge, microwave freq., rel. to impurity conc. and temp. 8=13829
 Ge-Si alloyed heterojunctions, and Hall coeff. at interface region 8=2217
 HfO₂ crystals, defect struct. 8=13419
 HfO₂ films, and resistors characts. 8=22654
 HfO₂, high temp. 8=9198
 Hg, low temperature variation meas. 8=5181
 HgTe-ZnTe system, determination 8=5263
 HgTe-ZnTe, at low temperatures 8=13816
 In₂O₃ films, pyrolytically grown, voltage-current charac. 8=13873
 InSb alloy films, vacuum-evaporated 8=9008
 n-InSb, Corbino, Hall effect 8=9114
 InSb, High pressure dependence 8=13819
 n-InSb, and magnetoresist. below 1°K 8=13820
 p-InSb, 90% compensated, and mobility coeff., 4.2-300°K 8=13822
 InSb, n-type, anomaly at very low temps. 8=5265
 IrO₂, temperature dependence 8=17939
 KAg₄I₅, ionic cond. rel. to cryst. struct. 8=17379
 KBr:Ca, and capacitance, distortion at low freq. 50 and 330°C obs. 8=5154
 KBr:In, thermally stimulated, rel. to impurity C excits. delocalization mechanism 8=8903
 KBr rel. to self-diffusion entropy and enthalpy 8=8679
 KCN single cryst. 8=5352
 KH₂(D₂)PO₄, rel. to isotope effects 8=2130
 KHF₂ and KDF₂ 8=13704
 KI:In, thermally stimulated, rel. to impurity C excits. delocalization mechanism 8=8903
 KNO₃, resistivity rel. transforms, thermodynamic props. 8=18191
 K(Rb, NH₄)Ag₄I₅, electrolytes 8=18719
 KTA_xNb_{1-x}O₃, resistivity comp. dependence and effect of Sn doping 8=22503
 La_xWO₃, resistivity temp. dependence 8=5709
 Li₂O.nB₂O₃ (n = 1, 2), charge with n-irrad. 8=6953
 MgO, at low temps. 8=22506
 Mn ferrites, and Seebeck voltage influence of Mn²⁺ clustering 8=13720
 Mn steel, rel. to martensitic transform. 8=17061
 MnO₂ films 8=4750
 Mo containing Co, resistivity meas., Kondo temp. obs. 8=9009
 Mo, zone refined, residual resistivity, effect of W content 8=17935
 Mo-Al intermetallic resistor films, sheet resistivity and temp. coefficients of resistance 8=22520
 Na aluminosilicate glass, relation with Na self-diffusion 8=22158
 Na-Ca-aluminosilicate glass, relation with Na self-diffusion 8=22158
 NaCl:CaCl₂ + NaOH crystal, and dielectric loss maxima 8=5164
 NaCl, var. with particle size and temp., obs. 8=17913
 NaCl-Sr(Ba)Cl₂, ionic, 200-670°C rel. to assoc. enthalpies of Sr and Ba 8=5165
 NaNO₃ resistivity rel. transforms, thermodynamic props. etc. 8=18191
 Na_{0.35}V₂O₆, single cryst. 8=22601
 Nb, resistivity, linear increase rel. to amt. of dissolved O₂-N₂ mixture 8=9011

Conductivity, electrical—contd**solids—contd**

- NbN, effect of N content variation 8=13702
 Nb₃Sn, Fermi level motion rel. to temp. depend., model 8=5118
 NH₄Ag₄I₅, ionic cond. rel. to cryst. struct. 8=17379
 NH₄ClO₄ 8=2128
 Ni alloys, K-effect 8=13723
 Ni alloys, plastically deformed, resistance recovery 8=13722
 Ni films, electrolessly deposited surface resistivity 8=17136
 Ni films, and Hall effect dependence on O₂ adsorption 8=17936
 Ni, low-temp. obs. 8=17937
 Ni, temp. coeff. of resistivity, divergence at Curie temp. 8=9012
 NiAl and NiGa, temp. and composition depend. 8=13721
 NiCr₂Se₄, rel. to d-orbital interaction clarification 8=5391
 Ni-Cu alloys, rel. to Hall effect 8=9014
 Ni-Cu solid solns., and thermoelectric power rel. to temp. and Cu % 8=5389
 Ni-Fe films, vacuum deposited, resistivity method of thickness meas. 8=17135
 NiFe films and mag. props. rel. to vacuum deposition press., 10⁻⁶-10⁻³ torr. 8=22822
 NiFe₂O₄, thin films 8=2343
 Ni₂Ge alloy in the range 77°K < T < 1300°K 8=18215
 NiO, neutron irradi. effect 8=18058
 NiO, stoichiometry 8=13826
 NiS, semiconductive-metallic transition pressure dependence 8=22885
 Pb, interband transitions 8=14253
 Pb, resistivity and two-band conduction model 8=2107
 PbSe, rel. to forbidden band width 8=5272
 PbTe films, thin, and resistivity and Hall mobility 8=22603
 PbZrO₃ near antiferroelec.-ferroelec. transition, rel. to ageing and relax. polarization 8=2249
 Pd, Lorentz number from 2.5-19°K 8=5184
 Pd-Ni alloys, at 2-30°K rel. to s-electron-paramagnon scattering 8=9015
 PdNi alloys, dilute, resist. and mag. susceptibility, local exchange enhancement effects 8=13634
 Pt film on quartz glass and BaTiO₃ substrates 8=13709
 Pt, resistivity and two-band conduction model 8=2107
 RbAg₄I₅, ionic cond. rel. to cryst. struct. 8=17379
 Re, and thermal resistivity from 2°K to 20°K 8=17546
 RuO₂, temperature dependence 8=17939
 Sb crystals in mag. field up to 420 kOe at liquid He temp. 8=9016
 Sb films, quantum oscill. obs. 8=17940
 Se, conductance during n and γ -irrad., rel. to temp. 8=18067
 Se, high-purity, rel. to Na and O₂ impurity admixture 8=5276
 Si deposited on corundum, resistivity 8=5281
 Si ion implanted with Sb, Ga and As, sheet resist. obs. 8=18072
 Si, microwave props., rel. to impurity conc. and temp. 8=13829
 Si single crystals, repeated alternating bending effects 8=17828
 SiO film, Poole-Frenkel eqn. 8=13705
 SiO₂ films, pyrolytically grown, voltage-current charac. 8=13873
 Sn oxide films, electron emission from high resist. regions 8=22713
 SnO₂, natural 8=5167
 SnTe films, thin, prep., Hall effect and cryst. props. 8=13096
 SrCl₂, pure and Y³⁺(Na⁺) doped, rel. to ionic conduction and diffusion mechanisms 8=8983
 TaN, effect of N content variation 8=13702
 Te, rel. to dislocations, theory 8=4984
 ThC_x, nonstoichiometric, resistivity 8=2140
 Th_xN_y, (x = 1, 3; y = 1, 4), rel. to electronic props. 8=2139
 Ti, resistivity in thickness range 75-350 Å 8=9019
 U-M alloys, (M=Fe, Al and Si), irradiated, resistivity changes rel. to phase comp. 8=8283
 UO₂, nearly stoichiometric 8=18089
 UO_{2+x} and U₄O_{9-y}, and Hall coeff. rel. to carrier mobility investigation 8=18090
 V, pure and H-alloyed, resistivity temp. dependence rel. to H₂ content 8=5186
 VCr₂Se₄, rel. to d-orbital interaction clarification 8=5392
 W, effects of neutron irradi. and subsequent annealing 8=2141
 W, resistivity and two-band conduction model 8=2107
 YH₂, resistivity meas. at 1000-1200°K 8=17942
 Y₂WO₆, resistivity temp. dependence 8=5709
 Zn complexes, tetraphenylporphine and tetraphenylchlorine 8=9117
 ZnCd_{1-x}Sb, rel. to temp. and conc. of acceptors 8=2131
 Zn-Mn alloys, low temp. resistivity, influence of magnetic ordering 8=2136
 ZnO crystals, effect oxygen chemisorption 8=5160
 n-ZnO, neutron irradi., resistivity vs time and temp. 8=2109
 ZnO: (Ni, Co) crystals, liquid N₂ to room temp. 8=9132
 ZnO powder, adsorbed O₂ effect 8=22612
 ZnO rel. to radicaloluminesc. excit. mechanism, obs. 8=9635

Conductivity, electrical—contd**solids—contd**

- ZnO single crystal, γ -irradiated, defect structure 8=22168
 ZnO, surface as detector of atomic H beams 8=7475
 ZnS:Cu rel. to electroluminesc. obs. 8=9133
 ZnS; S^{3+} radioactive, dark, photoluminescence spectrum 8=5000
 ZnSb and ZnSb-CdSb mixed crystals 8=13698
 ZrC₂H₂ cpd. formed in Zr-H-C system 8=17433
 ZrC₂H₂ cpd. formed in Zr-H-N system 8=17433
 ZrH_{1.99-1.96}, resistivity meas. at 1000-1200°K 8=17942
 ZrO₂, cubic, influence of neutron irradiation on ionic mobility 8=5152
 ZrO₂-CeO₂ mixtures, high temp. 8=22614

measurement

- crystals, anisotropic, mech. method 8=18160
 films, thin, meas. and ion bombardment apparatus 8=17121
 plasma induction method, theory reviewed 8=4380
 recorder, multi-range, with linear scale 8=6243
 rocks and minerals, high temp. and press. 8=8978
 semiconductors, resistivity, volume, surface and contact 8=18020
 GaAs, Sn doped 8=2191

Conductivity, thermal

See also Heat conduction.

- argon, partly ionized, equilibrium calc. 8=7900
 cell, modified hot wire type 8=6210
 contact, empirical formula 8=17540
 contact resistance in vacuum 8=19628
 co-ordination crystals, dependence on anion vacancies (produced by chem. reduction) 8=17543
 cylinders, hollow, sectors, radiation at boundaries 8=238
 disperse systems, theory and expt. compared 8=16901
 furnace wall, temp. dependence, effect on temp. distrib. 8=19659
 gas, rarified, appl. of conventional eqn. for conductivity and boundary temp. jumps 8=12682
 granular sphere to contact plates, calc. 8=19629
 heat-impulse method for rapid determ. of constants 8=233
 at liquid-gas critical point 8=21745
 manometer applic., error in formula 8=21544
 negative eddy, production in presence of buoyancy and shear 8=21441
 nonsteady state, inverse problem soln. for monotonic heating of bodies 8=10773
 one-dimensional heat flow, problems, use of boundary sources 8=234
 planetary interiors, minerals calc. 8=23654
 superconducting solder joints near 0.1°K, thermal transport 8=5203
 Ce magnesium nitrate and He³, boundary resistance due to spin fluctuation 8=10800
 KCl crystals, Ca-doped, 20-90°C, influenced by segregation processes 8=13394
 Li_{0.5}Fe_{2.5}O₄, vacancy depend. 8=8660
 MgFe₂O₄, polycrystalline, dependence on anion vacancies (produced by chem. reduction) 8=17543
 MgFe₂O₄, vacancy depend. 8=8660
 Pt, and elect. resistivity, 373 to 1373°K, obs. 8=22521
 SF₆ plasma, 2400-9000°K, meas. 8=7737
 ZnFe₂O₄, polycrystalline, dependence on anion vacancies (produced by chem. reduction) 8=17543
 ZnFe₂O₄, vacancy depend. 8=8660

gases

- acetylene 8=16699
 diatomic, influence of ang. momentum anisotropy 8=12681
 diatomic, low-temp. in stationary mag. field 8=7919
 diethyl ether, rel. to temp. 8=7925
 dust laden, electronic component of coefficient of cond., calc. 8=1472
 gray, unsteady energy transfer by thermal radiation 8=7923
 heat transfer from wall, hot-film sensor 8=16822
 heat transport medium, Conference, London, March 1967 8=7326
 inert-gas mixtures, binary, ternary, and quaternary 8=21509
 ionosphere, model for e.m. wave propag. effects 8=19903
 with micron-size particles, props. 8=21735
 molecular, in perpendicular stationary and varying fields 8=21493
 multi-component mixtures, computation 8=21509
 quadrupolar gases 8=16699
 rarefied gases between parallel plates, heat transfer and density-distribution obs. 8=21505
 steam, 149-180°C at atmospheric press., obs. 8=4477
 thin films, contactless method 8=270
 Ar, line-source transient-heat-transfer technique 8=16701
 Ar, near critical point 8=12683
 Ar plasmas, partially ionized 8=7734
 Ar₂, 100-300°C at atmospheric press., obs. 8=4477
 CH₄, mag. field effects at 290°K 8=4469
 CH₄-CF₄ dense mixtures 8=21511
 CO, mag. field effects at 290°K 8=4469
 CO₂ 8=16699
 CO₂, extension of Saxena-Saksena-Gambhir theory 8=16702
 CS₂ 8=16699
 D₂-He, normal composition variation 8=7924
 H₂, dense, calc. by lattice theory 8=4476
 H₂-He, normal composition variation 8=7924

Conductivity, thermal—contd**gases—contd**

- H₂-N₂ and H₂-CO₂ gas mixtures 8=4473
 He, line-source transient-heat-transfer technique 8=16701
 N₂, mag. field effects at 290°K 8=4469
 N₂, 100-300°C at atmospheric press., obs. 8=4477
 N₂-Ar and O₂-Ar gas mixtures 8=4474
 N₂O 8=16699
 N₂O, extension of Saxena-Saksena-Gambhir theory 8=16702
 N₂O₄ \rightleftharpoons 2NO₂ system by hot-wire method, relaxation effects 8=7929
 NH₃-Ar, 39° to 199.6°C 8=4470
 NH₄-He, 39° to 199.6°C 8=4470
 NH₃-Ne, 39° to 199.6°C 8=4470
 NO, mag. field effects at 290°K 8=4469
 Ne, line-source transient-heat-transfer technique 8=16701
 2. NOBr \rightleftharpoons 2NO + Br₂ system, 290-900°K 8=12684
 O₂, mag. field effects at 290°K 8=4469
 O₂-Ar mixture, and N₂-Ar 8=4474
 O- and n-D₂, at 18.5, 19.8 and 21.1°K 8=7930
 SO₂, rel. to temp. 8=7925

liquids

- alkali metals, condensation boundary resistivities 8=8049
 alkali nitrates, molten 8=16820
 application of theory to insulating crystals 8=8649
 Bridgman equation, and reln. between sonic vel. and latent heat of vaporization given 8=12852
 calculation from theory of corresponding states 8=4564
 chalcogen group, semiconducting 8=12850
 cryogenic liqs, correl. with viscosity and self-diffusivity 8=15132
 freezing, in rel. to Stefans problem 8=8176
 heat exchanger, response to flow rate disturbances 8=8048
 heat-generating liq. in vertical cylinder, heat-transfer due to convection 8=7916
 heat transfer from wall, hot-film sensor 8=16822
 heat transfer in square ducts 8=12854
 laminar flow in circular tube 8=21656
 metal rot. in magnetic field 8=8054
 mixtures, two-continuum model 8=21655
 monatomic, using Green correlation function 8=8053
 organic, temp. depend. rel. to radiative transfer, obs. 8=12853
 plug, viscous, laminar flow 8=4566
 solutions, two-continuum model 8=21655
 temperature distribution, in circular pipe 8=8055
 CCl₄, temp. depend. rel. to radiative transfer, obs. 8=12853
 Cs, liquid, 75-700°C 8=12851
 H₂, calc. by lattice theory 8=4476
 He³-He⁴ mixture, \leq 0.6°K, due to phonons 8=10801
 He³, pressure dependence, spin-fluctuation theory 8=19693
 He³ spin rel. to Rice theory of nearly ferromagnetic Fermi liquids 8=10800
 Pb-Bi alloys 8=16823

solids

- alloys, radiation correction, 4.2-273°K 8=22129
 calculation of radiant-heating case 8=13386
 chalcogen group, semiconducting 8=12850
 contact conductance, transient sensitivity coeffs. 8=17538
 crystals, non-conducting, linear response function theory 8=13399
 crystals, usefulness obs. for determining u.s. attenuation at high and low temp. 8=22092
 dispersed system having irregular pore sizes comparative study 8=8142
 electron gas, degenerate, due to interaction between electrons 8=8960
 excitonic insulator, transport props. 8=13653
 fibrous insulation, radiant ht. transfer 8=1883
 flat plate, effect on heat transfer 8=22126
 glycine, single crystals, obs. at 60° and 82°C. 8=22135
 graphite, quasi monocrystalline, quantitative description 8=13390
 graphite, quasi monocrystalline, measurement between 6 and 300°K 8=13389
 hafnium iodide, and blackness 8=1890
 heat resistant, high m.p., coefficient meas. at high temps. 8=1885
 insulating crystals, application of liquid transport theory 8=8649
 metals, radiation correction, 4.2-273°K 8=22129
 metal surfaces, low-temp. resistances 8=22130
 minerals, diffusivity from 300° to 1100°K at 1 atm 8=22131
 normal process relaxation times, from thermal cond. data 8=22424
 packing in packed bed of spheres, with fluid stream, determ. of heat transfer and dispersion coeff. 8=13363
 paramagnetic salts, effect of spin-phonon coupling 8=18405
 polymeric and refractory heat shield materials, ablation obs. 8=1860
 porcelain, rel. to structure 8=1893
 powders, insulating, meas. 8=8651
 PTFE 8=17544
 Pyrex glass, 0.4°-4°K in 0-90 kG fields 8=17525
 rocks, ring heat source probe for rapid determ. 8=8654
 sandwich plates 8=2040
 n-type semiconductors as function of impurity 8=5226
 semiconductors, photothermal effect due to illumination of 8=8650

Conductivity, thermal—contd**solids—contd**

- superconductor, type II flux flow state, apparent negative figure 8=2148
 superconductors, intermediate state 8=8652
 superconductors with strong electron-phonon interaction 8=17508
 surface layer of oxide cathode 8=9275
 temperature wave propagation, second sound excitation 8=1882
 textiles of Egyptian cottons, disc-type meas. apparatus 8=13392
 variable, transient temp. field 8=22127
 Al, pure, 2.5-33.5°K 8=22132
 Al, at low temp. 8=17542
 Al, Wiedemann-Franz ratio and anomalous lattice cond. 8=8990
 Al₂O₃, decrease due to fast n-irrad. 8=22245
 Al₂O₃, with Cr/Mn impurity, γ-irrad. effect 8=1886
 Ar, between 24 and 73°K 8=4940
 As-Se system in glassy state 8=1887
 As₂Se₃-4As₂Te₃, in glassy and cryst. state 8=1887
 Bi, temp. dependence, 1.3-2°K 8=8656
 Bi₂Te₃-PbTe alloys, low temp. obs. 8=22680
 CdF₂ 8=8409
 Cd_{1-x}Zn_xAs₂, 80°-400°K meas. 8=5385
 CdSb, poly and monocrystalline, doped and undoped 8=13698
 CdSnAs₂ and CdGeAs₂, semiconducting, rel. to high-temp. modifications 8=21842
 Ce ethyl sulphate, mag. field effect, spin-phonon scatt. 8=13393
 Co(NH₄)₂CS₂Cl₂, anomalous enhancement rel. to magnon cond. 8=13391
 Cr selenides, cond. and elec. cond., thermoelectric power, lattice parameters 8=13703
 Cu, effect of transition elements 8=22133
 Cu, high temp. 8=8657
 Cu-4.6 at. %Ga, decrease due to dislocation density increase 8=8658
 Cu, 99.999% pure, rel. to theory, 78-400°K 8=22134
 Cu-Al-Zn alloys, rel. to dislocation phonon scattering 8=22203
 Fe powder, influence of porosity 8=13388
 FeCr₂Se₄, rel. to d-orbital interaction clarification 8=5391
 Ga single crystals, size effects 8=17545
 GaAs, rel. to Gunn device design 8=5297
 GaSb-InSb alloys, at high temps. rel. to comp. and impurity doping 8=4944
 Ge, lattice cond., effect of impurities 8=1888
 Ge-Si alloys, decrease on alloying 8=1853
 Ge_{1-x}Si_x, effect of defects on lattice thermal conductivity 8=1892
 He isotope mixtures, rel. to lattice distortion scattering due to isotope impurity 8=1889
 He⁴ and isotopic mixtures at high densities 8=15154
 He⁴ oriented single crystals, h.c.p. 8=8659
 InSb-GaSb solid solns., 80-500°K 8=1891
 LiF, 0.05 → 2°K cryostat obs. 8=22112
 MgO, decrease due to fast n-irrad. 8=22245
 MgO, doped, mag. field depend. 8=13395
 Mo, meas. and analysis, 100-400°K 8=4943
 NaCl, resonant phonon scattering 8=8661
 Nb alloys for nuclear reactors 8=5082
 Nb, superconducting, thermal conductivity rel. to energy gap and mag. hysteresis 8=2166
 Nb temperature dependence of temp. coefficient 8=13387
 NbN, effect of N content variation 8=13702
 Ni-60 at. %Co, decrease due to dislocation density increase 8=8658
 NiCr₂Se₄, rel. to d-orbital interaction clarification 8=5391
 PbSe, rel. to forbidden band width 8=5272
 p-PbTe, doped, rel. to Lorenz number and interband interactions of holes 8=9116
 p-PbTe heavily doped betw. 80-400°K 8=8662
 PbTe_{1-x}Se_x, effect of defects on lattice thermal conductivity 8=1892
 Pd, Lorentz number from 2.5-19°K 8=5184
 RbCl:CN, and specific heat, rel. to rot. degrees of freedom of mols. 8=22120
 Re, and elec. resistivity from 2°K to 20°K 8=17546
 Si, containing O₂, neutron irrad. effects at 80°K 8=8663
 Si, 100 to 1300°K 8=22136
 Sn, pure and Cd-doped, effect of superconductivity energy-gap 8=4942
 Sn, superconducting films, in mag. field 8=22137
 Ta temperature dependence of temp. coefficient 8=13387
 TaN, effect of N content variation 8=13702
 ThO₂-UO₂, in-reactor, from thermal simulation expts. 8=1130
 TiSe 8=17547
 UO₂, depend. on temp. and temp. gradient 8=8665
 UO₂, effect of porosity 8=13397
 UO₂ powder compacted fuel, effective cond. in simulation expt. 8=13398
 UO₂, in-reactor, from thermal simulation expts. 8=1130
 UO₂-SiO₂ vitroceraamics, 100 to 400°K rel. to SiO₂ conc. 8=8664
 UO₂-ZrO₂-CaO, nuclear fuel, out-of-pile tests 8=17527

Conductivity, thermal—contd**solids—contd**

- VCr₂Se₄, rel. to d-orbital interaction clarification 8=5391
 W, meas. and analysis, 100-400°K 8=4943
 ZnSb and ZnSb-CdSb mixed crystals, poly and mono-crystalline, doped and undoped 8=13698
measurement
 air, hot-wire conductivity cell, 30°-100°C, 120-150 torr 8=16700
 cryostat for 0.05 → 2°K 8=22112
 dielectrics, temp. dependence 8=17539
 gases, cond. cell 8=4469
 heat resistant high m.p. materials, coefficient at high temp. 8=1885
 hot-wire cell for liquids and gases 8=7852
 insulating materials, new device 8=8655
 at liq. He temp., device using zeolites 8=3106
 method, based on transient change of temp. gradient 8=13396
 potentiometric method, radiation correction for Fourier formula 8=22129
 refractory materials, heat resistance determination, review 8=1894
 rocks, ring heat source probe for rapid determ. 8=8654
 semiconductors, cylindrical specimens, in He bath 8=3107
 semiconductors, temp. dependence 8=17539
 textiles of Egyptian cottons, disc-type meas. apparatus 8=13392
 Ar, hot-wire conductivity cell, 30°-100°C, 120-150 torr 8=16700
 Bi₂Te₃, n-type, diffusivity variations between -200 and +50°C 8=4941
 C, pyrolytic, diffusivity variations between -200 and +50°C 8=4941
 D₂, hot-wire conductivity cell, 30°-100°C, 120-150 torr 8=16700
 He, hot-wire conductivity cell, 30°-100°C, 120-150 torr 8=16700
 KNO₃ molten, optical method, plane source technique 8=21658
 Kr, hot-wire conductivity cell, 30°-100°C, 120-150 torr 8=16700
 NaNO₃ molten, optical method, plane source technique 8=21658
 Ne, hot-wire conductivity cell, 30°-100°C, 120-150 torr 8=16700
 Xe, hot-wire conductivity cell, 30°-100°C, 120-150 torr 8=16700

Conferences

- antennas and propagation, Ann Arbor 1967 8=15401
 applied mechanics convention, Cambridge, England (1966) 8=13490
 astronautics and aviation Conference, Israel 1966 8=5822
 astronomical society of Australia, Sydney Australia (1966) 8=14722
 atmospheric research, global 8=23250
 calculation of the properties of vacancies and interstitials, Skyland, USA, (1966) 8=22165
 chemisorption and physisorption, Rome, March 1967 8=8333
 coherence and quantum optics, Rochester University, New York, June 1966 8=6484
 convention of Italian Astronomical Society, Catania Italy (1966) 8=19111
 cyclotrons, Krakow (1966) 8=6701
 definition, realization and use of time and frequency London 1967 8=10
 discussion, metallurgical problems of heat deform. 8=22277
 earth upper mantle, Newcastle-upon-Tyne, England Feb. 1966 8=9787
 electrical conduction properties of polymers, Pasadena USA (1966) 8=13701
 electrical insulation and dielectric phenomena, Poc. no Manor USA (1966) 8=18154
 electronic components conference, Jackson USA, 1967 8=6244
 electron, ion and laser beams technology, Berkeley, USA (1967) 8=15283
 electron microprobe analysis, Boston, June 1967 8=8445
 electronic processes in low mobility solids, Sheffield, England, April 1966 8=5101
 electronic properties of thin films, Orsay, France (1967) 8=22499
 elementary particle, Liperi Summer School in Theoretical Physics Helsinki, 1966 8=6715
 fast critical experiments and their analysis, Conference, Argonne National Laboratory, Oct. 1966 8=7240
 fracture of metals, polymers and glasses, Boston, USA (1966) 8=13518
 galaxies evolution and structure, Brussels Belgium (1964) 8=19210
 gas as heat transport medium, London, March 1967 8=7326
 geophysical theory and computers, Cambridge 1966 8=18809
 high-energy physics and nuclear structure, Israel 1967 8=15672
 high-energy physics, Oiso Japan (1965) 8=11348
 ice symposium, Pittsburg U.S.A. (1966) 8=21867
 Institute of Metal Finishing, Brighton, England (1967) 8=14419

Conferences--contd

- isotopic ratio measurements, Japan 1966 8=16235
 u.s. and hypersonic wave propag., in solids 8=1842
 Liperi Summer School in theoretical Physics 1966 8=7028
 lubrication and wear, Plymouth, England (1967) 8=13521
 magnetic-fluid and plasma dynamics, New York
 USA (1965) 8=16459
 magnetic materials and their applications, London,
 1967 8=9286
 magnetohydrodynamic electrical power generation,
 Salzburg, Austria (1966) 8=15355
 magnet technology, Oxford England (1967) 8=15259
 magnetic resonance and relaxation, Ljubljana
 (Yugoslavia), 1966 8=22889
 many-body theory, Oiso Japan (1965) 8=10641
 meteorite research in U.K., Leicester, (1966) 8=19274
 molecular spectroscopy, Copenhagen Denmark
 (1965) 8=16239
 molecular structure and spectroscopy, Ohio
 USA (1966) 8=16238
 neutron monitoring for radiological protection, Vienna,
 Austria (1966) 8=15852
 new materials and processes in instrument manufacture,
 Eastbourne, 1965 8=2872
 new methods of instrumental spectroscopy, Orsay,
 France (1966) 8=20071
 noise and vibration control 8=3076
 non-compact groups in particle physics, Milwaukee,
 USA (1966) 8=11352
 nuclear and engineering ceramics, Harwell 1965 8=16168
 nuclear and space radiation effects, Columbus
 U.S.A. (1967) 8=22578
 nuclear science and technology for ceramists, Washington
 USA (1966) 8=16167
 nuclear structure, Dacca Pakistan (1967) 8=15925
 nuclei heavy and medium, Bordeaux (France)
 1967 8=20640
 nucleon-nucleon interaction, Florida (USA) 1967 8=20516
 nuclides far off the stability line, Lysekil Sweden
 (1966) 8=15911
 particle symmetries, International School of Physics
 "Ettore Majorana", ERICE 1965 8=6721
 perturbation theory for exchange forces, seminars
 at University of Wisconsin 8=4043
 phase changes in inorganic solids, Rennes
 April 1965 8=8259
 photovoltaics, Florida USA 1967 8=9242-4
 plasma, e.m. wave phenomena, I.E.E.E., New York,
 1967 8=1398
 plasma, m.h.d., lasers, geophys. solid-state devices and
 electrical material, Dallas 1967 8=12480
 polarized targets and ion sources, Saclay
 France (1966) 8=15629
 power source cells, fuel cells and thermoelectric
 generators Brighton, England 1966 8=286
 radiation research, space radiation biology, Berkley USA
 (1966) 8=23456
 r.f., l.f. and v.l.f. radio propagation, London, England
 (1967) 8=14671
 residual gas in electron tubes and vacuum systems, inter-
 national symposium, Rome, March 1967 8=6317
 semiconductor devices meas. and test methods Budapest,
 1967 8=9144
 solar-terrestrial physics, The Inter-Union Symposium
 Belgrade, 1966 8=10325
 solid state, 2nd Nordic, Tyllösand, Sweden 1966 8=8191
 stars and galaxies, gravitational instability, formation and
 structure, Belgium 1966 8=14734
 static electrification, London May 1967 8=6255
 statistical mechanics and thermodynamics, Copenhagen
 Denmark (1966) 8=15007
 strong and weak interactions, present problems, Erice
 Italy (1966) 8=15695
 strong interactions, Varenna, Italy July 1964 8=6745
 structure and crystal growth, Moscow, July 1966 8=8362
 structure and properties of liquids, Exeter England
 (1967) 8=16784
 surfaces structure, 8-9th Nov, 1966, Durham,
 North Carolina 8=17115
 theoretical and applied mechanics, Haifa Israel
 (1967) 8=16750
 theoretical physics, Providence USA (1966) 8=20246
 theoretical spectroscopy, Yerevan (1966) 8=11148
 thermionic conversion specialist conference, California
 USA, (1967) 8=19731
 thermionic conversion Specialists Conference San Diego
 USA October 1967 8=6273
 trace characterization-chemical and physical,
 symposium NBS, USA, Oct. 1966 8=8437
 the triplet state, Beirut Lebanon (1967) 8=16347
 turbulence and boundary layers with geophysical appl.,
 Kyoto, Japan 1966 8=7850
 vacuum metallurgy, New York USA (1966) 8=16746
 vacuum microbalance techniques, Newport Beach
 USA (1966) 8=14919
 vacuum techniques, Warsaw Poland, 1966 8=21531
 weak interaction and high-energy neutrino physics
 Varenna, Italy, July 1964 8=6747
 X-ray optics and microanalysis, Orsay, France,
 Sept. 1965 8=8441

Confinement of plasma. See Plasma/confinement.**Constants**

- Avogadro's number, determination by scintillation
 counter 8=7483
 dielectric, of liquids, calculation 8=8102
 gravitation, sign implications of conformal theory 8=10594
Contact angle. See Capillarity; Surface tension; Wetting.
Contact potential
 difference measurement, direct comparison of Kelvin and
 electron-beam methods 8=13700
 glass-metal in vacuum, charge transfer 8=18159
 metal-semiconductor, small area, voltage-current characts.,
 within diffusion theory 8=9089
 nylon 66, static electrification, rel. to metals 8=5356
 polythene-metal in vacuum, charge transfer 8=18159
 superconductors, double point contact without applied
 d.c. 8=13732
 in GaAs-metal, ohmic multilayer contacts 8=9145
 Si-metals, characts. 8=18082
 Ta ribbon, adsorpt. of Cs, O₂ and H₂, determ. of work
 function changes 8=9276

Contact resistance

- microscopic obs. of chemical reactions 8=8987
 tarnishing studies atmospheric pollutant effect 8=8988
 thermal, empirical formula 8=17540
 Ag and Ag alloy contacts, effect of H₂S
 contamination 8=22512
 Cu-M (M = Cu, Mo, steel, constantan), rel. to normal
 loading 8=8986

Continuous creation hypothesis. See Cosmology.**Convection**

- air layer, temp. gradient reversal, interferometric
 obs. 8=4475
 air, turbulent thermal between horizontal plates, velocity
 and temp. obs. 8=12686
 below cloud base 8=2578
 Benard, cellular motion, Rayleigh number
 intervals 8=6213
 cellular, boundary-layer theory 8=10777
 cellular, finite amplitude stability rel. to extremum
 principle 8=6212
 cellular, in fluid layer, effects of surface curvature and
 property variation 8=21417
 cellular in liquid, induced by surface tension in semi-
 infinite layer 8=1503
 earth, mantle, graphical representation 8=23220
 evaporation, nonadiabatic, from porous system 8=8183
 explosions, gaseous, transient heat transfer 8=15108
 flow, non-Newtonian fluids, boundary layer equation
 solution 8=7857
 fluid, cylinder subject to transverse oscills. 8=3098
 fluid in box heated from below 8=6214
 fluid cell heated from below, finite amplitude 8=6215
 fluid heated from below, Rayleigh cells of arbitrary wave
 numbers, 2D, evolution 8=10775
 fluids laminar and turbulent flow, variational and
 physical analysis 8=7870
 fluid layer, forced, thermal turbulence 8=12638
 fluid of high thermal diffusivity, instability in heated
 layers 8=16639
 fluid unevenly heated from below, nonlinear model 8=16637
 fluid, rotating, large amplitude Benard 8=12616
 free and forced, in field droplet, rel. to wake-type
 diffusion flame shape 8=15113
 free, effect on heat transfer in forced pipe flow 8=16623
 heat pipes, operating characts. when capillarity-
 limited 8=6216
 heat transfer due to natural convection in vertical
 cylinder with heat-generating liq. 8=7916
 horizontal fine wire, effect of vibration 8=19649
 laminar boundary layer, ht. and mass transfer 8=240
 laminar boundary layers, incipient instability 8=4430
 liquid dielectrics, electric field effects 8=21659
 liquid, with internal heat generation, theory 8=4511
 liquid, rotation-induced heat transfer in zero-gravity
 field 8=4562
 liquid, stabilized turbulent flow in tube, heat transfer
 at supercritical press. 8=1550
 in low-loss liqs, rel. to self-defocusing of passing laser
 beams 8=15442
 magnetosphere, limitation by ionospheric
 dissipation 8=9918
 Malkus' transition in thermal turbulence 8=19653
 mixed, high temp., mass transfer between spherical
 particle and medium 8=1473
 natural, in horizontal liq. layers 8=19650-1
 natural laminar, from plane vertical surface in non-
 isothermal surroundings 8=19654
 nichrome ribbon, rel. to heat flux 8=17548
 origin in horizontal fluid layer 8=3108
 plane isothermal sheet in turbulent flow 8=241
 plasma, nonequilibrium, effect on current
 patterns 8=16486
 porous layer, critical temp. gradient 8=10776
 Rosseland approximation appl. 8=19633
 sea surface layer, organized, due to slicks and wave
 radiation stress 8=14571
 self-gravitating fluid sphere 8=10122
 silicone oil heated under constant temp. air
 surface 8=1504

Convection—contd

- stellar zone, density gradient inversion 8=2778
- surface in laminar boundary layer effect of thermal conduction of wall 8=6211
- transient natural, from vertical plate, leading edge effect 8=19652
- vertical impermeable flat surface, turbulent natural convection, theory 8=10778
- viscous liquid, appl. of numerical method 8=21626
- water, acoustical effects on free convective transfer from horizontal wire 8=21663
- water, lower boundary at 0°C and upper at above 4°C, interpenetration 8=16825
- CO₂, near critical point, forced convection heat transfer 8=16915
- ZnSO₄ soln., due to electrolytic heating, obs. 8=1509

Conversion electrons. See Beta-ray spectra/conversion electrons; Gamma-rays/internal conversion.

Cooling

- See also Joule-Thomson effect; Low-temperature production; Magnetic cooling; Supercooling.
- β , γ -spectrometers, improved resolution 8=6811
- electromagnets, appl. of liq. Ne 8=15261
- gas and liquid compared in nuclear reactor 8=20887
- generator, m. h. d., by water, temp. distrib. in channel wall 8=19726
- reaction, radiation cooling, thermionic for space flight, review 8=1114
- tempered metal in non-vaporizable liquid 8=8044
- ultraviolet spectra of molecules, recording device 8=22930
- Al-Zn eutectic, undercooling 8=17003
- He Dewar, fast precooling to N₂ temp. 8=3114
- Na-cooled fast reactor kinetics 8=12002

Copper

- annihilation radiation, momentum distrib., Brillouin zone boundary effect 8=13691
- anodic oxidation in LiCl-KCl 8=5738
- APW band structure calcs, systematic numerical error 8=17883
- atom, polarization corrections for shielding and anti-shielding configurations 8=12061
- atom, λ 3247.5 Å -resonance line profile from hollow-cathode source, by interferometry 8=3365
- atomic state, by absolute meas. of X-ray scattering factors 8=13030
- atomic vapour laser, pulse efficiency from cyclic excitation and relax. 8=11056
- atoms, pseudopotentials 8=7409
- atoms, stabilized in alkali-halide crystals, paramag. reson. 8=22897
- band structure rel. to lattice spacing 8=22458
- Bauschinger effect in quenched samples 8=5020
- Bauschinger effect recovery mechanisms 8=17775
- calorimetry, low-temp. standard 8=15127
- cavitation damage, by magnetostrictive vibratory method 8=22339
- chromatographic separation, complex formation and reflectance spectros. detect. 8=23176
- cold-rolled electrolytic crystallization and Fourier anal. of elastic anisotropy 8=8404
- cold-rolled and recrystallization textures, n-diffraction study 8=17278
- cold worked, impurities rel. to modulus effect 8=22332
- condensate, in vacuum, structural transitions 8=16943
- conductivity, thermal, and resistivity, elec., effect of transition elements 8=22133
- constant thermocouples 8=22686
- contacts rel. to wear and arc current 8=12415
- crack form. and propag. in cyclic deform rel. to coarse slip, obs. 8=22330
- creep at const. and variable loads using tubular specimens 8=17776
- creep at 650-700°C rel. to deformation at 77 and 4.2°K 8=17824
- creep, 78°K and room temp. 8=22256
- crystals with dispersed Co/SiO₂ phases and dislocation distrib. 8=4974
- crystals, generalized surface wave propag. 8=1855
- crystals, nearly perfect, intensities of X-rays diffracted in anomalous transmission 8=4873
- crystal, n-irradiated slip band development 8=22212
- crystal, neutron-irradiated, annealing effect on lattice parameter 8=1937
- crystal, u.v. emission using proton beam 8=2025
- crystals, well-annealed, stress at which dislocations multiply 8=13545
- cubic crystals, thermal expansion coeff., temp. depend. 8=8646
- cubic texture formation during recrystallisation 8=4809
- defect concentrations from cyclic stressing at room temp. 8=17604
- deformed, elastic mod. and creep recovery, role of dislocation rearrangement 8=22337
- deposits, pseudomorphic, of Co 8=21881
- diffusion of Au, detect. by deuteron elastic scatt. 8=8675
- diffusion in Bi₂Te₃, etching technique investigation 8=1914
- diffusion in GaAs, defect centres, Hall effect 8=1954
- dislocation mobility rel. to shear stress 8=1970
- dislocation motion, nature of obstacles 8=22200

Copper—contd

- dynamic indentation, conical projectile, up to 600°C 8=17780
- electric field gradient due to charge density redistribution around dislocations 8=5176
- electrode, anodic behaviour in NaCl aqueous solution 8=2532
- electrodes in H shock tube plasma, V-I characts. 8=21359
- electrode pot. in Brussels mains water, influence of light and cords of circulation 8=18728
- electron irradiated, yield stress increase 8=17773
- electron slowing-down spectrum 8=13474
- electroplating to graphite, rel. to graphite soldering to metals 8=5998
- erosion by liquid droplets 8=22333
- evaporation from Fe-Cu alloys at 1600°C under vacuum 8=12993
- excited state, 1s²2s²2p⁶3s²3p³3d¹⁰4f, universal potential field calc. 8=20952
- exploding wire plasma, temp. meas. 8=7784
- explosive formation, residual strains and hardening 8=13564
- explosively deformed, dislocation structure 8=17651
- f. c. c. angular forces in lattice dynamics model 8=8612
- fatigue cracks, initiation 8=5058
- fatigue life improvement by cyclic strain dispersal, obs. 8=5031
- fatigues, at low strain amplitude, surface and interior structure relationships 8=17774
- Fermi surface, galvanomag. invest. 8=13713
- film, absorpt. spectra 8=5596
- films, creep, elastic lattice strains 8=13548
- films, epitaxial growth, and activity and topographical changes on exposure to H₂-O₂ combination at 325°C 8=8318
- film deposited by sputtering in crossed e.m. field 8=7651
- films, grain boundary cavity form. during high temp. creep 8=13547
- films, obliquely deposited, struct., effect of atom mobility 8=8296
- films, plasma oscillations, interband transitions 8=5117
- film on Si, transmission and absorpt. in spectral region from 1.5-7 μ 8=14212
- film, reflectance and transmittance, anomalous skin and size effects 8=9498
- film, thickness depend. on heat generated by 9 to 100 keV electron beam 8=17699
- films, thin, optical props. in spectral region between 0.6 and 4 μ 8=22972
- foils, ion irradi., agglomerates formation and density 8=13417
- foils, ion irradi., analysis of type and configuration of defect clusters 8=13416
- fracture when fatigued in Hg 8=5057
- γ -ray absorpt. and scatt., stress effects 8=13483
- grain boundary diffusion of Ag and Au 8=17568
- grain struct. prod. in hot working, obs. 8=21984
- heat capacity, temp. dependence, effect of crystal lattice defects 8=13368
- helicon wave excitation by a.c. 8=5147
- high speed impact extrusion 8=19340
- hot, pseudomorphic growth of Fe 8=21880
- hydrostatic tension on solidification 8=21758-9
- impurity in NaI, effect on X-ray luminesc., 8=23062
- interstitial migration kinetics at low temps. 8=8699
- ions, effect on photographic process 8=533
- ions, in NaCl crystal, optical absorption 8=18521
- n-irradiated, small dislocation loops, type 8=13437
- isochromat at 8 kV compared QSS energies and X-ray absorption 8=2414
- isochromats at Cu K α , wavelength 8=2416
- length change, after e irradiation 8=22338
- low-temp. calorimetric standard, atomic heat meas. 8=17517
- oxidation of vacuum deposited films, rel. to temp. 8=18674
- magnetoresistance coeff. at 4.2°K 8=8997
- magnetoresistance, longitudinal from 4.2 to 35°K, electron scattering effects 8=22511
- mass ejection by laser pulse 8=8759
- mechanical properties, low-temp., collection of data 8=17779
- metals analysis, determ. by at. absorpt. spectrometry 8=2545
- microdeformation measuring technique 8=22273
- n-irradiated, with vacancy dislocation loops, thermally activated motion 8=22189
- neutron irradi., dislocation pinning 8=1974
- neutron monochromator 8=854
- O.F.H.C., furnace and foundry equipment for production 8=5997
- oxidised single crystals, exam. by diff. of slow electrons 8=13258
- p-irradiated, platelets of interstitial atoms rel. to dislocation loops 8=22202
- phonon freq. determs. at 49 and 298°K 8=8611
- plastic stress relaxation rel. to stacking fault energy 8=13529
- plastically deformed, annealing behaviour, effect of dispersed phases 8=17772

Copper—contd

- polycrystalline, elec. resist. of dislocations, exptl. determ. 8=9004
 polycrystalline target, sputtering coeff. rel to incident angle of Ne, Ar and Kr ions 8=8766
 polycrystals, grain boundary cavity stability 8=13448
 polycrystals, temp. depend. of thermal diffuse X-ray scattering 8=5581
 positron annihilation ang. depend. rel. to Fermi surface 8=22493
 powder, X-ray study 8=4844
 quench hardening, study 8=22334
 quenched, vacancy annihilation kinetics 8=1946
 recrystallization, deformed with tension, at low temp. 8=17230
 recrystallization and mech. props., rel. to plastic deform. at low temps. 8=8403
 rolled, dislocation structure effect on mechanical props. 8=13550
 rolled high purity crystals, orientation distribution 8=1756
 rolled, texture representation by biaxial pole figures 8=17778
 rolling texture development at room temp. and -196°C 8=22328
 secondary electron emission, H^+ bombardment 8=5423
 shear strength in grossly deformed sample at high temps. 8=8833
 shock waves, prod. by electron beam pulses 8=13484
 single crystals in stressed condition, dislocation arrangement, electron microscope obs. 8=22201
 single crystal film, effect of ion bombardment on texture and structure 8=17124
 solid solns. with Ti, V, Cr and Mn, mag. moments 8=22760
 solubility and diffusion in InAs 8=17011
 stacking fault energy calcs. using pseudopotentials 8=17673
 strong proximity effects: superconductivity in fine Nb-Cu composite 8=22553
 surface self-diffusion coeff. temp. dependence, $600-1030^{\circ}\text{C}$ 8=17567
 susceptibility and resist. studies of localized Fe moments 8=22796
 target for ion emission, bombard by Ar^+ 8=6626
 texture development deformation dependence, pole figure 8=17777
 thermal cond., elec. resist. and Seebeck coeff. of 99.999% pure, $78-400^{\circ}\text{K}$ 8=22134
 thermal diffusivity meas. 8=1898
 thermal smoothing of single crystals. 8=4788
 thin films, Hall effect 8=2133
 thin films, thermopower size-effect for determination of electronic structure 8=13903
 transport properties at high temperatures 8=8657
 ultrasonic attenuation rel. to Fermi surface deformation 8=1851
 ultrasonic shear waves, attenuation at low temps. 8=22099
 u.s. work hardened, flow and recovery 8=22336
 vacancy diffusion rate calc., Debye model 8=22172
 vapour laser, 5106\AA , pulsed, theoretical model 8=15465
 wire, drawing process with lubricant under externally generated pressure 8=2052
 wires, electric explosion, temp. variation during first stage 8=1622
 wires, explosion discharges initiated at the surface and inside the wire 8=4272
 X-ray microanalyser target, K_{α} , depth distrib. obs. 8=15586
 X-ray K-absorption spectra of (100), (110), and (111) structures 8=2413
 X-rays, K_{α} , films and solid targets direct and fluoresc. components 8=14179
 X-ray microanalysis e backscatt. correction, obs. 8=14469
 X-ray prod. and e backscatt. rel. to microanalysis, obs. and calc. 8=18794
 X-ray production on p-bombardment 8=4995
 X-ray transmission temp. dependence (Borrmann effect) from $77-377^{\circ}\text{K}$ 8=14210
 Young modulus and modulus of rigidity, variation-latitude dependence 8=2051
 Ag cementation, in perchloric acid and alkaline cyanide solns., kinetics 8=14427
 As-Se vitreous alloys, introduction 8=13111
 in BeO , e.p.r. 8=2366
 in BiTe , electrotransport, 150 and 250 A/cm^2 , $\leq 400^{\circ}\text{C}$ 8=17564
 $\text{CaF}_2:\text{Cu}^{2+}$, impurity ion e.p.r. spectrum 8=9422
 $\text{CdCl}_2:\text{Cu}^{2+}$ layer, e.s.r., exchange coupled pairs spectrum 8=18416
 Cu^+ , atomic interaction potential calc. 8=7456
 Cu ions reflected from Cu crystal incident obliquely 8=8767
 Cu: Cu-12.5 wt.%Al multiphase couple, interface comps., motion and lattice transformations 8=17552
 Cu and Cu-Ni alloys, optical absorpt. rel. to Ni conc. effects 8=2411
 Cu^{2+} rhombic e.s.r. spectra angular dependence of applied mag. field 8=5526
 Cu^{2+} in Rochelle salt, e.p.r., external elect. field effect 8=14111
 Cu^{2+} , in ZnO crystal, absorption spectra 8=14211

Copper—contd

- Cu^{2+} in ZnWO_4 , e.p.r. spectrum 8=5527
 Cu^{63} , n.m.r. in Cu-Mn alloys, and spin-lattice relax. 8=9464
 in Fe liquid, heat of solution 8=16799
- Copper alloys**
 See also Copper compounds.
 β -brass, band structure calc. using LCAO approximation 8=8906
 brass, Bauschinger effect recovery mechanisms 8=17775
 β -brass, creep, influence of crystallographic order 8=13549
 β -brass, elastic consts, temp. and composition depend. 8=13546
 brass, hardness rel. to grain size 8=8835
 β -brass, hexagonal dislocation networks 8=22204
 α -brasses, internal friction and elastic props. 8=13552
 β -brass, martensitic transform., deformation effects 8=21843
 β -brass, order-disorder transition, study by n diffraction 8=17051
 β -brass, resistivity, effect of heat treatment 8=13714
 brass, rolled, texture representation by biaxial pole figures 8=17778
 brass, rolling texture development at room temp. 8=22328
 brass, Sb embrittlement, effects of U additions and low-temp. annealing 8=22326
 brass, 70-30, texture development deformation dependence, pole figure 8=17777
 α -brass, stress corrosion cracking 8=8844
 α -brasses, Young modulus and modulus of rigidity, variation-latitude dependence 8=2051
 constantan wires, electric explosion, temp. variation during first stage 8=1622
 constantan wires, explosion discharges initiated at the surface and inside 8=4272
 dilute, high-temp. resistivity 8=9003
 electrodiffusion with small additions of Sn, Sb, Ni 8=1916
 mechanical properties, low-temp., collection of data 8=17779
 phonon-drag thermoelectric power 8=18214
 solid solution, latent heat of deformation 8=13551
 thermopowers interpret. rel. to resistivity and band structure 8=18213
 with transition impurities, non-mag., elec. field gradient 8=9458
 Ag-4.09%Cu binding energy and vibration amplitude 8=13029
 Au-Cu single crystal film, effect of ion bombardment on texture and structure 8=17124
 AuCu_3 , vibration amplitude, temp. depend. 8=13029
 Cu-base mats., oxidized, appl. of u.s. vibs. to pickling process in dilute H_2SO_4 8=23780
 α -Cu-Ag alloys, Hall effect. and resistivity interpretation 8=13641
 Cu-Ag(0.083 at.%), internal friction and elastic modulus measurement at low frequencies 8=8784
 Cu-Al, annihilation radiation, momentum distrib., Brillouin zone boundary effect 8=13691
 Cu-Al solid solution, latent heat of deformation 8=13551
 Cu-Al, structure of martensites 8=4871-2
 Cu_3Al , stacking faults in β' -martensite phase 8=17674
 Cu-Al-Mn, surface relief rel. to supercond. transition 8=19686
 Cu-Al-Zn, dislocation-phonon scattering rel. to thermal conductivity meas. 8=22203
 Cu-Au, electron scatt. from disorder, rel. to anomalous absorpt. of rad. 8=17362
 CuAu II films, dynamical multiple reflections in electron diffraction patterns 8=13256
 Cu_3Au , low order, vacancy clustering 8=8695
 Cu-2 wt.%Be, ageing investigated by electron microscopy 8=17056
 Cu-Be, Guinier-Preston zone formation, conc. and ageing dependence 8=17606
 Cu-2%Be, precip. and twins appearing on ageing 8=17625
 Cu-Be, as secondary electron emitters 8=13943
 Cu-Be, quenched and aged, vacancy role in solute clustering 8=17607
 Cu-Be-Ag, precip. nucleation 8=17040
 Cu-Be-Al, ageing characts. obs. 8=22335
 Cu-Co, liquid, solubility and activity coeff. of O 8=8011
 Cu-Cr, dilute, low-temp. theory and magnetoresistance obs. 8=17933
 Cu: Cu-12.5 wt.%Al multiphase couple, interface comps., motion and lattice transformations 8=17552
 CuFe alloy, Kondo resistivity, magnetic field dependence 8=5178
 Cu-Fe, magnetoresistance and magnetization meas. 8=22519
 Cu-Fe, mag. props. and elec. resistivity, rel. to cold working 8=17934
 Cu-Fe mixed whiskers, strength, hardness and growth mechanism 8=17249
 Cu-4.6 at.%Ga, deformed, thermal conductivity decrease rel. to dislocation density increase 8=8658
 Cu-Mn, Cu^{63} n.m.r. and spin-lattice relax. 8=9464
 Cu-Mn, interdiffusion kinetics, by X-ray microprobe 8=22149

Copper alloys—contd

- CuMn alloy, Kondo resistivity, magnetic field dependence 8=5178
 Cu-Mn-Al system, effect of quenching and ageing on mag. phases 8=14010
 Cu₂MnAl and associated structures (Heusler alloys), studies 8=22794
 Cu₂Mn₂Al (Heusler alloy), structure studies 8=22795
 Cu-Ni diffusion pairs, pore migration during counter-current diffusion 8=17569
 Cu-Ni, electron-probe microanalysis, atomic no. effect 8=9764
 75 Cu-25Ni laminate on Cu core coinage composite, bond degradation mechanism 8=22329
 Cu-Ni, optical absorpt. rel. to Ni conc. effects 8=2411
 Cu-Ni, specific heat, anomalous, at low temps. 8=22118
 Cu-Ni, stacking fault density, conc. depend., by X-ray analysis 8=17671
 Cu-Ni, thermal expansion, rel. to ferromag. Curie point of Ni 8=17532
 Cu-Ni-Co alloys, critical shearing stress temp. dependence 8=1971
 Cu-Pt foils, n. m. r., quadrupole effects 8=2383
 pCu₂S-nZnS:MnCu, Cl films, d.c. electroluminescence mechanism 8=23051
 Cu-Sb, stacking fault X-ray meas. 8=17672
 Cu₂Se-In₂Se₃, constitution diagrams, structure 8=8266
 CuSn, liq., Hall coeff. rel. to bound state form. round Sn atoms 8=12917
 Cu-Sn, structural changes on natural ageing 8=17052
 Cu-Sn structures of metastable states during eutectoid transform. 8=17055
 Cu₂Sn₅ liquid, partial structure factors 8=12788
 Cu₂Te-In₂Te₃, constitution diagrams, structure 8=8266
 Cu-Ti, precipitation, direct obs. 8=13065
 Cu-Zn alloys with (Cr, Mn, Fe, Co) impurities, magnetic props. 8=9339
 Cu-Zn alloys, decomposition of β' 8=4706
 β'-CuZn, binary and ternary, cross slip 8=8834
 Cu-Zn brasses in NaOH, anodic dissoln. 8=18732
 Cu-Zn, dendritive crystallization under optimal cooling 8=4822
 β₁ Cu-Zn, martensite, transform. after repeated thermal cycling 8=17053
 β₁ Cu-Zn, martensitic transformation temps. from elec. resistivity meas. 8=4704
 CuZn(β brass) mechanical props., hydrostatic extrusion effects obs. 8=5059
 CuZn(β brass), ordering conditions 8=4686
 β'-CuZn, reflectance and other optical props. 8=2402
 Cu-Zn, rolling textures, X-ray methods 8=21985
 Cu-Zn, selective corrosion 8=23100
 Cu-Zn solid solution, latent heat of deformation 8=13551
 Cu-Zn system, phase equilib. 8=13546
 Cu_x-Zn_{1-x}Ni_y, x < 0.25 and 0.08 < y < 0.10, optical absorpt. at room temp. 8=22976
 Cu-Zn-Si β-phase, inhomogeneity effect on martensite transform. 8=4707
 Cu-Zr, supersaturated solid soln., n. m. r. study of decomposition 8=8265
 MgO, Kikuchi patterns rel. to anomalous absorpt. of rad. 8=17362
 Zn determ. by atomic absorpt. spectrometry 8=23184

Copper compounds

- See also Copper alloys.
 acetate, i. r. spectra and thermal decomp. 8=23095
 copper sulphide (digenite), cubic high temp., defect equilibria obs. 8=1942
 cupric complexes, e. p. r., F¹⁹ hyperfine splittings 8=21168
 oxide, controlled resistors 8=18034
 phthalocyanine, luminesc. singlet-singlet transitions 8=18591
 salts, ammonium sulphate, n. m. r. obs. 8=2385
 Cu chelate of polyethylenimine, spectrophotometric analysis 8=16393
 Cu complex, N-salicylidene-glycinato-cuprocopper(II) hemihydrate, structure 8=8518
 Cu complexes, tetraphenylporphine and tetraphenylchlorine, as photosemiconductors 8=9117
 Cu phthalocyanine films, thin, trap distrib. 8=22586
 Cu(I) complex, dipotassium bis(glycylglycinato)cuprate(II) hexahydrate, structure 8=17363
 CuI, defect struct. and catalytic props. 8=22169
 Cu(II)azide, crystal structure 8=22018
 Cu II complex, NH₄CuTiF₇·4H₂O, crystal structure 8=13280
 Cu(II) perchlorates, water solns., u. s. velocity 8=12865
 Cu-Al solid solution dislocation structure and grain size effect on validity of Cottrell-Stokes law 8=8721
 Cu-Au, α-phase, charging and mag. susceptibility, electron states variation, electronic sp. ht. 8=13970
 Cu₂Au, ordering conditions, cubic-to-tetragonal structural transition 8=4687
 Cu₂Au, shear modulus change during ordering 8=17769
 Cu₂Au solid solutions, determ. from short-range order parameters 8=16996
 Cu-Be, lattice particle X-ray and electron scattering on new phase form. 8=1773
 CuBr, exciton luminescence 8=23052
 CuBr₂Cl₂·xH₂O, antiferromag. res. 8=2359
Copper compounds—contd
 Cu³Br³, rotational structure of the C band system 8=1239
 Cu(C₂H₃N)₃(CH₃COO)₂, crystal structure 8=17456
 CuCl band struct. and excitons rel. to absorpt. spectrum, calc. 8=8932
 CuCl crystals, two-photon absorption spectrum m 8=2412
 CuCl, Czochralski growth and crystal imperfections 8=4804
 CuCl emission line lifetimes, positions and intensities, 4.2-300°K 8=9526
 CuCl exciton absorpt. spectrum, 4.2°K 8=9523
 CuCl, exciton luminescence 8=23052
 CuCl, factors influencing growth in silica gel 8=21944
 CuCl, growth of clear crystals in gels 8=8405
 CuCl, growth for optical modulators 8=8407
 CuCl, growing single crystals with flux 8=17231
 CuCl luminesc. and weak absorpt. rel. to exciton complexes 8=9525
 CuCl photocond. and absorpt. spectra rel. to excitons, 4°K 8=9251
 CuCl X-ray spectra rel. to distrib. of states, obs. 8=9522
 Cu₂Cl₂, crystals, gel growth 8=8406
 Cu₂Cl₂, second harmonic generation under laser radiation 8=14213
 CuCl₂·2D₂O, spin density distrib. 8=22877
 CuCl₂·2H₂O, antiferromag. resonance, relax. effects 8=2358
 CuCl₂·2H₂O, dipolar mag. field at proton site 8=18378
 CuCl₂·2H₂O e. p. r., thermal detect. obs. 8=14100
 CuCl₂·2H₂O, mag. ordering 8=18377
 CuCl₂·2H₂O, wave function of unpaired electrons 8=18376
 CuCr₂Se₄, ionic config. from neutron diff. and elec. trans. props. 8=1788
 CuCr₂Te₄, ferromag. spinel, Te¹²⁵ Mössbauer effect study of hyperfine field 8=8223
 CuF₂, layer growth conditions 8=17232
 CuF₆⁻ ions, absorpt. spectrum and struct. 8=16280
 Cu-Fe system, susceptibility and resist. studies 8=22796
 CuFeMn₂O₄, temperature-dependent electrical resistance 8=17932
 CuFeMn₂O₄, tetragonal distortion 8=17205
 CuFeS₂, (chalcopyrite), Fe⁵⁷ Mössbauer effect rel. to configuration 8=1649
 Cu₂FeS₃ (cubanite), mag. coupling and Mössbauer spectra 8=14066
 Cu-Ga solid solution dislocation structure and grain size effect on validity of Cottrell-Stokes law 8=8721
 Cu(HCOO)₂·4H₂O, magnetic susceptibilities and crystal fields 8=5501
 CuI, equilib. internuclear distance, determ. from rot consts. 8=1240
 CuI, exciton luminescence 8=23052
 CuI layers, low-temp. spectra rel. to nature of substrate 8=9528
 CuK₂(SO₄)₂·6H₂O, heat capacity below 1°K, meas. 8=13372
 Cu₂Mg, mode of precipitation from solid solutions of Mg in Cu 8=4705
 Cu₂-Mg, Fe₂O₄, O content and thermomag. props. 8=2516
 CuMn ferrites mag. props., Sc₂O₃ effects, obs. 8=18359
 CuMn₂O₄, cation distrib. determ. 8=17364
 Cu(NH₃)₄SO₄·H₂O, exchange and "10/3 effect" 8=2365
 Cu(NH₃)₄SO₄·H₂O, proton magnetic resonance, 0.25-4.2°K 8=14138
 Cu(NH₃)₄·SO₄·H₂O, proton n. m. r. at low temp. 8=2384
 Cu(NH₃)₄Br₂·2H₂O, e. s. r. 8=9423
 Cu₂NbS₄(Se₄), crystal growth 8=8408
 Cu-Ni, Kirkendall and Frenkel effect 8=8676
 CuO, isochromat structure 8=2415
 CuO X-ray spectra rel. to distrib. of states, obs. 8=9522
 CuO₂ cryst. excitons photoionization, assoc. absorpt. coeff. calc. 8=9529
 CuO₂, isochromat structure 8=2415
 Cu₂O absorpt. and refl. spectra rel. to band struct., obs. 8=9524
 Cu₂O band struct. and excitons nature 8=8933
 Cu₂O, Debye temp. calc. from elastic constants 8=1869
 Cu₂O exciton spectrum, uniaxial press. and n irr. effects obs. 8=9521
 Cu₂O, 4 exciton line series, effect of plane stress 8=22973
 Cu₂O rel. to exciton-phonon interactions, n=1 line profile, 4.2-112°K 8=9527
 Cu₂O, luminescence non-linear dependence on photexcitation intensity 8=18601
 Cu₂O magneto-absorpt. and Zeeman effect in pulsed fields, 4.2°K 8=11157
 Cu₂O, multielectron theory of excitons in semiconductors 8=22478
 Cu₂O, plastic deformation by motion of a {100} dislocations on {100} glide planes 8=22327
 Cu₂O, 2-photon transitions to exciton states, oscillator strengths 8=8953
 Cu₂O X-ray spectra rel. to distrib. of states, obs. 8=9522
 Cu₂P monocrystals, prep. and props. 8=21948
 α-Cu₂P₂O₇, crystal structure 8=17367
 CuRh₂Se₄ and CuRh₂S₄ with spinel structure, superconductivity obs. 8=13749
 Cu₂S, nonstoichiometric, mag. props. meas. 8=9290
 p-Cu₂S, thermoelectric power, elec. cond. and Hall effect 8=22585

Copper compounds—contd

- Cu₂S-CdS p-n heterojunction, photovoltaic response 8=13843
 Cu(SO₃F)₂, i. r. spectra and mag. props. 8=9562
 CuSO₄, crystal growth from aqueous soln. under X-irrad. 8=21947
 CuSO₄, e. s. r. of anhydrous cryst. 8=2364
 CuSO₄-H₂O system, phase boundaries to 40 kilobars 8=4640
 CuSO₄·5H₂O crystals, proton conductance 8=8982
 CuSO₄·5H₂O e. p. r., thermal detect obs. 8=14100
 Cu₂Se, nonstoichiometric, mag. props. meas. 8=9290
 Cu₂Se₃, umangite, crystal structure 8=17366
 Cu-Si solid solutions, dislocation motion, nature of obstacles 8=22200
 Cu₃TaS₄(Se₄), crystal growth and optical props. 8=8408
 CuTe, liq. Hall coeff. rel. to possible semicond. nature 8=12917
 Cu-Te system, phases investigated by e-diffr. 8=17057
 Cu-Te system in thin films, phase transformations and structure 8=17054
 Cu₂-Te-CdTe heterojunction photoconverter 8=6276
 CuTiF₆·4H₂O, crystal structure 8=17365
 Cu(UO₂AsO₄)₂·2H₂O, meta-zeunerite, e-diffr. meas. 8=17360
 CuX, (X=Cl, Br and I), band structures 8=2190
 ε Cu-Zn phase, dissolved Fe, low-temp. resistance minimum 8=9340
 Ni-Cu solid solns., variation of thermoelectric power and resist. 8=5389

Corbino effect. See Current, electrical.

Coriolis forces. See Dynamics.

Cornea. See Eye.

Corona, electrical discharge

- See also Breakdown, electric.
 direct current, effects of wind 8=12411
 from EHV transmission lines, effect on radio interference, model 8=16422
 ion-molecule reactions, method 8=12409
 in lightning, and e.l.f. emissions 8=2598
 onset field in air, lowering due to breakup of supercooled water drops 8=21595
 plastic films breakdown mechanism 8=22645
 pulsed and quasi-stationary, in dielectric-bounded cavity 8=7681
 surface discharge with ring-type electrodes 8=12397
 Trichel pulses, long-tailed, effect of solid dielectrics 8=7678
 water, impulsive, hydrodynamic characteristics 8=21250

Corona, solar. See Sun/corona.

Coronagraphs. See Sun/corona.

Corpuscular streams. See Cosmic rays; Sun/radiation, corpuscular.

Correspondence principle. See Quantum theory.

Corrosion

- cast iron, austenitic, effect of Ce 8=21988
 cell for stress corrosion studies 8=8793
 electrical contact degradation effect 8=8987
 erosion rate meas. and flaw detection by microwave interferometry 8=5032
 gases, pressure meas. 8=4448
 gas-tight thermobalance-load seal for studies 8=5991
 Institute of Metal Finishing, conference, Brighton, England (1967) 8=14419
 ionic, of polycrystalline metal surfaces 8=13522
 in liquids, heat transfer influence, review 8=18667
 metals in acids, kinetics rel. to organic inhibitors specificity 8=2509
 metals, with heat transfer, test apparatus 8=18665
 in steam, influence of temp. 8=18666
 steel, anodic dissolution and corrosion potential 8=9723
 steel, by HCl vapour 8=23103
 steel, by H₂O, solid-state diffusion of O₂ 8=22151
 steel, mild, by NaCl solns., NaNO₂ inhibition, 20°C 8=2517
 steel, mild, stress-corrosion cracking in NaOH solns. with various additions 8=22366
 steel, rate as function of minor element content, and distrib. of FeC 8=18664
 steel, stainless, in CO₂ and CO₂-CO, C behaviour 8=2515
 Zircalloy-2 in LiOH solns., hydrating rate, 300°C 8=5719
 Ag, elec. erosion, obs 8=22342
 Ag, sulphiding by H₂S, effect of surface Fe 8=23096
 Ag-Cd alloy, elec. erosion, obs. 8=22342
 AgCdO, sintered and internal oxidized, elec. erosion, obs. 8=22342
 Al alloys, stress corrosion cracks, at cutting planes 8=8818
 Al, anodized, electrolytic quality test evaluation 8=23097
 Al brazing sheet, improved behaviour 8=10462
 Al, electroplated strike 8=14430
 Al-Cu-Mg alloy, effect of quenching rate 8=8819
 Be, coating with BeF₂ as retardant 8=23098
 Cr-Ni stainless steel, intercrystalline, theory 8=8460
 Cu, in Brussels water, rel. to electrode pot., effect of light and circulation conds. 8=18728
 Cu-Zn alloys, selective 8=23100
 Fe, rel. to impurities 8=18664
 Fe-Cr-Al alloys, by S at high temp. 8=23102
 Fe in H₂SO₄, thiourea inhibition and K₂Cr₂O₇, NH₄CNS and KI effects 8=2518

Corrosion—contd

- LiOH-LiF-H₂O, molten, of metals 8=14368
 Nb alloys, stability in nuclear reactors 8=5082
 Ni alloys, heat transfer effects 8=15102
 SF₆, degradation in electrical equipment 8=14383
 Si-steel in silicate glass film removal rel. to magnetostriction, obs. 8=22843
 Ti alloy in non-electrolyte, stress cracking susceptibility 8=8863
 Ti-6Al-4V alloy, stress-corrosion cracking in methanol 8=22394
 U₂Si, reactor fuel possibility 8=4019
 Zn alloys in atmosphere, acrylic and polyurethane protective layers 8=14389
 Zn in CO, solns., predominance diagrams appls. 8=2523
 Zn, surface pitting at dislocation sites 8=13440
- Cosmic dust.** See Interplanetary matter; Interstellar matter; Meteorites.
- Cosmic noise.** See Cosmic radiations, radiofrequency.
- Cosmic radiations, radiofrequency**
 See also Quasars; Radioastronomy; Sun/radiation, r. f.
 Andromeda nebula (M31), 11-cm obs. 8=10268
 ang. struct. meas. at 0.73 m with tracking 12 sources, interferometer 8=10285
 atmospheric absorpt. of 5.65 mm waves 8=5789
 auroral noise absorption, short period pulsations 8=23334
 background, 4080 MHz, isotropy 8=10295
 background, microwave at 3.2 cm and 1.58 cm meas., blackbody spectrum evidence 8=5846
 background radiation at 3.2 cm, measurement 8=2866
 background, microwave 8.56 mm, meas. 8=5845
 background temperature, 9.24 mm 8=14728
 black-body and galaxy formation 8=14809
 blackbody, rel. to isotropic γ obs. 8=23485
 bright galaxies, data for 47 8=5931
 Cassiopeia A, 113 Mc/s for scintillation studies 8=2801
 Cassiopeia A spectrum, 5.8-25 Mc/s 8=10304
 Cassiopeia scintillations freq. depend., 30-400 MHz 8=2800
 Centaurus XR-2, variability obs. 8=23598
 clusters of galaxies, radio emission obs. 8=19211
 coherent, generation mechanism rel. to quasar and local source in Crab Nebula 8=10311
 Crab Nebula circularly polarized radiation upper limit 8=10309
 Crab nebula, sky survey of cosmic X-rays and source spectra 8=10230
 Cyg A spectrum, 5.8-25 Mc/s 8=10304
 Cygnus loop supernova remnant obs. at 41, 195 and 430 MHz 8=5904
 Cygnus scintillations freq. depend., 30-400 MHz 8=2800
 e ~ p charge difference, cosmological consequence 8=23480
 emission in 7m waveband, meas. 8=7006
 extra galactic radio sources 8=23606
 extra galactic radio sources 8=23607
 extra galactic radio sources, mechanisms 8=23608
 flux density obs. at 153 MHz 8=19228
 4C sources, angular scales in declination 20°-40° and weak sources spectral props. 8=10306
 4C sources in declination 40°-44°, spectra, 38, 178, 610-5 and 1417 Mc/s 8=10297
 4C sources declinations and optical identifications 8=10305
 4C sources identified with blue objects 8=5940
 frequency spectrum, 10-207 MHz, high galactic latitudes 8=23612
 Galactic noise, ionospheric attenuation, 25 and 21.3 MHz, Ahmedabad, 1957-64 8=14673
 galactic, region l^{II} = 140°, b^{II} = 6° 8=23595
 Galaxy radio sources at 4170 MHz, high resolution obs. 8=5928
 interferometer using 2 steerable paraboloids, of 425 metres baseline, operation at λ 21 cm 8=10441
 isotropy of faint sources, evidence for 8=10293
 Jupiter, decametric bursts, wide bandwidth obs. 8=23666
 Jupiter, 11 cm radiation, radio rotation period 8=23667
 Jupiter radio emission stimulation by Io 8=10345
 Jupiter, S-bursts, long-baseline interferometry 8=23668
 linear polarization of distributed rad., meas. 8=14888
 maser action of interstellar H₂ at 21cm 8=5923
 M31, extent of radio emission 8=23596
 metagalactic radiophone intensity in evolutionary models of Universe 8=10076
 microwave, anisotropy rel. to velocity of Sun 8=23609
 microwave background rel. to density inhomogeneities in universe 8=10082
 microwave spectral line in sources NGC 2024 and IC 1795 8=10307-8
 microwave 3°K background, fluctuation limits 8=23486
 microwave 3°K spectrum 8=23610
 NRAO radio positions reduction to system of optical positions 8=10281
 night-time noise var. with solar activity 8=10283
 noise absorption by ionosphere F region, electron temp. calc. from 8=10015
 noise absorption, ionosphere, 25 MHz, effect of solar eclipse of May 20, 1966 8=9979
 noise, cosmic, sudden, absorption and X-ray flares 8=2653

Cosmic radiations, radiofrequency—contd

- noise, PCA, midday recoveries 8=9969
 nonthermal sources, energy and lifetime of relativistic electrons 8=19224
 planetary nebulae, 14, at 408 MHz 8=5909
 from planetary nebulae, obs. at 3 microwave freqs. 8=10218
 polarization, linear, obs. at 3.6 cm wavelength 8=19230
 polarization, linear, of 950 MHz emission 8=14806
 quasars and radio galaxies contrasted 8=5945
 quasars and remnants of supernova stars, coherent plasma radioemission 8=14813
 radio galaxies, cosmic black-body radiation interactions 8=19213
 radio galaxies, 1418 MHz, upper limits to degree of circular polarization 8=23600
 radio-sources, extra-galactic, conference, Brussels Belgium (1964) 8=19210
 radio source spectra and cosmological red shift, hyperbolic model 8=14812
 radio source 3C 273B, 9.10⁶ wavelength baseline interferometer obs. 8=10286
 radio sources, 38 MHz, interferometric obs. 8=10287
 radio survey of sky at 81.5 Mc/s north of declination 70°, using tech. of 2-dimens. aerial synthesis 8=10294
 radiostar existence? 8=2799
 relict emissions at 8.2 mm, abs. meas. rel. to black body temp. 8=19227
 Sgr A, discrete source, obs. of flux density at 2.11 mm 8=19226
 sky temp. calc. from radio and other galaxies 8=5936
 source between declinations +27° and -30°, identification 8=23615
 source counts, fitting cosmological models 8=23467
 source, diffuse X-rays background between 4 and 40 keV 8=10282
 source, magnetic field, i.r. spectra obs. 8=23613
 source 3C31(NGC383), beamwidth obs. 8=10267
 sources 3C 225 and 3C 267, obs. 8=10298
 source 3C338(NGC6166), beamwidth obs. 8=10267
 source W49, anomalous OH emission 8=10290
 sources, consequences of inverse Compton effect 8=23619
 sources, diameters new limits rel. to interplanetary scintillations obs. 8=10296
 sources, extended, inertial confinement 8=23618
 sources, in 4 C catalogue, identifications with bright galaxies 8=10288
 sources, Fornax A 8=23601
 sources, 458 with declination in range +18° to +20° at 750 and 1410 MHz, pencil beam survey 8=23605
 sources, model in terms of gravitationally bound current loop 8=14811
 sources, 9.55mm, flux density obs. 8=23599
 sources, non-thermal, thermal X-ray emission 8=5941
 sources polarization, of arbitrary optical thickness 8=5942
 sources, position and models from lunar occultation observations 8=10301
 sources previously identified with clusters of galaxies 8=19212
 sources spectral indices distrib. rel. to freq., obs. 8=23614
 sources, survey, in declination ranges -07° to 20° and 40° to 80° 8=2803
 sources, theory of multiple constitution 8=23611
 sources, 210, accurate positions 8=23617
 sources, 31, between 40 and 130 MHz, obs. 8=23616
 sources, wavelength depend. of linear polarization, stochastic theory 8=10300
 spectra, rel. to Fermi accn by shocks in source 8=10292
 stellar and interstellar, interaction red-shift 8=5922
 supernova remnants CTA₁ and HB₃ struct. and spectral indices, 81.5 and 178 MHz 8=10191
 survey of emission at 178 MHz using pencil-beam radio telescope 8=19225
 synchrotron emissivity, correction 8=23604
 T = 3°K background radiation 8=10083
 Taurus A (Crab Nebula) at 1420 MHz, occultation obs. 8=5917
 Taurus A, discrete source, obs. of flux density at 2.11 mm 8=19226
 3C sources flux intensity and spectral indices, 86 and 38 Mc/s 8=10303
 3C79 and 3C192, structure obs. 8=23603
 3C84, 3C273, 3C274, 3C279, flux and linear polarization at cm. wavelength 8=10302
 3C 273, optical polarization 8=19229
 3C273, photographic obs. 8=10175
 3°K blackbody, evidence for singularity 8=23466
 Venus, microwave obs. from Mariner 2, anal. 8=5957
 Vir A, discrete source, obs. of flux density at 2.11 mm 8=19226
 W49 galactic source 8=10249
 X-ray emission and stellar accretion 8=10310
 X-ray sources, galactic, 1964-65 survey 8=10252
 zenith temp. at wavelength 3.2 cm 8=23754
 H, nebulae vels. from $n_{106} \rightarrow n_{104}$ line obs. 8=10233
 H II regions, higher-order high-quantum H recombination lines 8=23569
 OH emission from H¹¹ regions, mechanisms 8=10258

Cosmic radiations, radiofrequency—contd

- OH galactic, brightness and temporal variation of emission 8=10253
 OH in H I regions, excitation temp. of 18-cm line 8=10299
 OH radical interstellar absorpt. 8=23581

Cosmic rays

- anisotropic stage and determ. interplanetary inhomogeneity parameters 8=23688
 distribution over sphere and acceptance vectors of detectors 8=894
 11-year cycle, and solar wind props. 8=14874
 energization of charged particles by arbitrarily moving spherical magnet 8=19769
 energy spectrum, Kosmos 53 obs. 8=19089
 galactic, low energy, intensity obs. from balloon flights 1961-65 8=2770
 galactic, modulation by solar activity 8=10419
 in galactic mag. field, transverse e.m. waves effect 8=5850
 hard X-ray fluxes from Mars, Venus and Jupiter, upper limits 8=23670
 as high-energy particle source 8=7004
 and interplanetary features, large-distance 8=10088
 interstellar matter heating and ionization by 25 MeV subcosmic rays and star form. 8=10245
 interstellar path length calc. from p/He⁴, d/He⁴ and He³/He⁴ + He³ ratios 8=11676
 at last geomagnetic field reversal, rel. to faunal extinction 8=23435
 and magnetic fields 8=23585
 measurement by "automatic interplanetary stations" 8=19090
 measurements by space vehicles 8=5849
 in meteorites, radioactive particles distrib. in meteorites calc. 8=10367
 in meteorites, tracks, identification 8=20596
 Monte Carlo simulation of EAS, possibility of distinguishing primary 8=11667
 nuclei, rigidity spectra obs. 8=20603
 neutrinos, solar, use in search for (νe)(νe) scatt. 8=14871
 ν, μ production, 7500 m.w.e. 8=3590
 ν rate at 8800 m.w.e., meas. and obs. 8=3591
 plasma, synchrotron and gyromag. relativistic, amplification dependence on polarization 8=21345
 progress in elementary particle and cosmic ray physics, book IX 8=15875
 quark production in galaxy, search 8=3604
 quarks, unit and fractional charges in region $m_s > m_p$, search at 3200 m above sea 8=15888
 radial density gradient and rigidity dependence obs. at solar minimum 8=5970
 space flux obs. rel. to predictions on basis of balloon ionization chamber obs. 8=11666
 solar, enhancement obs. 8=23319
 solar high energy particles in new cycle, ground-based neutron monitoring 8=23723
 solar, and polar cap absorption 8=14736
 solar, low energy cut-off dependence on latitude in geomag. field 8=897
 in solar system, energy changes rel. to energy balance in solar wind 8=14872
 space weathering of lunar and asteroidal surfaces 8=19246
 storm, Feb. 1962, rel. to interplanetary structure 8=2833
 stream of fast particles, spectra of plasma and e.m. waves induced by stream instability 8=19305
 T = 3°K background radiation 8=10083
 X-ray bursts, correl. with polar aurora 8=18939
 X-rays, celestial, polarization 8=2802
 B^a solar neutrino flux dependence on heavy element composition 8=5968
 B^b solar neutrino flux dependence on rate of the reaction He³(He³, 2p)He⁴ 8=5969
 OH radiation, polarization, and of amplifying medium 8=19916

absorption

- atmospheric, spectrography 8=20623
 auroral, noise pulsations obs. 8=2639
 intensity data, barometric pressure correction 8=893
 interstellar matter, effect on composition and energy spectrum, calc. 8=11668
 mass coefficient, solar-cycle variation, Climax and Chicago neutron monitors 1953-65 8=7024
 muons, energy spectrum incident on medium rel. to spectrum within medium 8=15889
 muon spectra and change ratio at sea-level at zenith angle of 45° 8=900
 nucleons, energies > 10¹¹ eV, elim. of contradictions by hypothesising a passive baryon state 8=15907
 π attenuation length 8=899
 range fluctuations for muons of energy up to 10⁶ GeV 8=15906

apparatus

- See also Particle detectors.
 anisotropy beyond geomagnetic field, response of function 8=895
 charge determ. of heavy particles 8=20598
 Cherenkov r.f. pulses associated with EAS, antenna det. 8=20597
 counters, secondary production in shielding material 8=902

Cosmic rays--contd**apparatus--contd**

- detectors, acceptance vector concept introduced 8=894
dielectric plastic particle detector using rate of chemical etching 8=11331
emulsion chamber, 10^{13} eV interactions at height 2640m 8=627
extensive air showers, detect. and meas. 8=7006
galactic and solar, OGO data analysis system 8=5847
gas discharge counter, satellite-borne 8=19089
gas proportional counter array to distinguish p and π , about 100 GeV 8=7009
ground-based neutron monitors, in earth-centred system, directions of viewing 8=20593
Haverah Park E.A.S. array description 8=7019
installation at Tyan'-Shan', for study of pion and proton strong interacts. 8=15881
ionization calorimeter at depth of 130 m.w.e., for high-energy muon study 8=15876
liquid scintill. for e density and time-of-arrival meas. of E.A.S. 8=7008
multiplate spark chamber, simplified system 8=624
n monitors, lifetime of n inside 8=15877
primary, high energy gamma quanta, obs. 8=15879
proportional counters and electronic systems for obs. in space 8=5848
scintillation counters for e density digitalization in E.A.S. 8=7007
scintillator, plastic, non-linear response 8=7005
with solar-energy power units, optimization 8=15880
spark chamber assembly for muon flux meas. in EAS 8=15883
spark emulsion chamber for photon, e cascades 8=20594
spectrometer, high-transmission, nuclear charge of primary rays 8=15878
"telescope", giant, 250 sq. km., Australia 8=10091

composition--

- chemical, solar flare origin 8=20603
heavy nuclei energy spectrum during solar min. 1965 8=3742
interstellar absorption affects, calc. 8=11668
heavy long-lived particles, search for in air showers 8=15887
low energy spectra, June 65, rocket determ. 8=3743
massive elementary particle search 8=11661
oblique component, coupling coeffs. determ. 8=20609
primary, charge, and energy spectra, 200 MeV to 5 GeV/nucleon, Cerenkov-scintillation counter 8=11665
primary, flux of nuclei, time var. obs. 8=20611
primary, high energy gamma quanta, obs. 8=15879
primary, nuclear component, investig. by satellite 'proton-2' 8=15893
quarks, negative evidence 8=11474
quark search at sea level 8=20402
search for quarks of charge $\geq \frac{1}{2}e$ 8=15742
stars in photographic emulsion at high altitude 8=15882
teaching misconceptions 8=7027
in terrestrial radiation belt, Kosmos 53 obs. 8=19089
H, low energy det. summer 1966 8=11676
He, low energy det. summer 1966 8=11676
O and elements of lower atomic number, low energy det. summer 1966 8=11676

alpha-particles

- rigidity spectra obs. 8=20603
He isotopes, production 8=20607

deuterons

- flux, lower limit from $p + p \rightarrow d + \pi^+$ reaction 8=19092

electrons

- atmosphere, upper, energy absorption at different levels 8=18972
at energies > 12 GeV, rel. to models and related astrophysical quantities 8=11660
energy losses in interstellar transit 8=23492
extraterrestrial, spectrum and origin, 70-2000 MeV 8=3745
fluctuation of numbers in EAS, expt. analysis 8=15897
fluctuation of numbers in EAS, theoretical analysis 8=15896
flux meas. and recording, balloon apparatus 8=20601
flux meas. and sign ratio, review 8=7010
galactic and prod. of background X-radiation. 8=19095
galactic secondary spectrum rel. to prod. and confinement in galaxy and halo 8=19198
high energy, proton 1 and 2 obs. 8=20604
intensity diurnal var. near poles, low-energy, obs. 8=913
positron-electron ratio, energy dependence in primary cosmic radiation in 1965 8=5843
positrons, evidence for secondary origin 8=19093
primary, energy spectrum 10-40 MeV obs. 8=15890
primary, 25-600 MeV 1964-66 obs. 8=11664
secondary electrons, upper atmosphere, flux and energy spectrum calc. 8=11669
secondary, low-energy, at balloon altitudes 8=7020
spectra prod. by cosmic ray collisions with interstellar matter 8=19094
synchrotron, Compton scattering of virtual photons 8=3571

mesons

- atmospheric correlations with counting rate 8=3753
change during magnetic storm 8=11673

Cosmic rays--contd**mesons--contd**

- diurnal intensity wave at high latitudes 8=20626
 K/π ratio from muonic intensity 8=896
pions, strong interact. in 100 to 1000 BeV range, installation for study 8=15881
 π -N interactions, recoil p transverse momentum and four-momentum transfer obs. 8=11589
 π -p distinction with gas proportional counter arrays 8=7009

muons

- electron pair production in medium and low Z elements 8=7178
energy spectrum, study by electron-photon showers, for large zenith angles 8=15892
fluctuation of numbers in FAS, expt. analysis 8=15897
fluctuation of numbers in EAS, theoretical analysis 8=15896
flux at 8800 m.w.e., meas. and obs. 8=3591
flux meas. in EAS using spark chamber, at 20m water equiv. 8=15883
geomagnetic field defl. from primary direction, telescope obs. correction programme 8=20619
incident on dense material, absorpt. curve and energy spectrum 8=15889
 μ pair prod. 8=15909
muon spectra and charge ratio at sea-level at zenith angle of 45° 8=900
muons and atmospheric coefficients near geomag. equator, intensity 8=11671
 ν induced and atmospheric, 7500 m.w.e. 8=3590
nonelectromagnetic interacts. shown by cascade shower initiation 8=15891
positive-to-negative charge ratio at sea-level, 3-360 GeV 8=20606
production process of $> 10^{12}$ eV μ , angular distrib. obs. 8=15886
range fluctuations, energy up to 10^6 GeV 8=15906
solar daily, variation at a depth of 60 m water equivalent 8=7023
spectrum 3-1000 GeV/c obs., agreement with π prod. theory 8=20605
study with complex installation inc. ionization calorimeter, at depth of 130 m.w.e. 8=15876
underground, energy spectra 8=15885
underground penetration, invest. using scintillator stack 8=15884

neutrons

- air-land interface, density obs. 8=20620
annual variations, atmospheric temperature effect 8=914
coupling coeffs. determ. 8=20608
energy spectrum at sea level, 20-4000 GeV 8=15894
flux in atmosphere, energy range thermal -100 eV, Yakutsk balloon obs. 8=907
ground-based monitors, in earth-centred coordinate system, directions of viewing 8=20593
intensity sudden var., correl. with solar minima 8=20638
lifetime monitors 8=15877
and magnetic storms 8=7011
monitor yield functions, Gross transform and nucleonic component m.p.p.'s during solar min. 8=20595
multiplicity during solar increase of January 28, 1967, obs. 8=915
multiplicity, low latitudes, 1 GY monitor obs. 8=906
multiplicity monitor, 1965 obs. 8=901
secondary flux after solar event November 15, 1960, Atlas ballistic flight obs. 8=2623
solar-diurnal var., Antarctic (1963-64) 8=20635
spectrum, 0.05-2.0 MeV near sea-level 8=20602
27 day cycle, quasi-spiral variation with solar activity 8=912

photons

- aerial γ -spectrometer, calibration 8=20364
 γ background due to inverse Compton scattering of $3^\circ K$ photons by galactic electron rays 8=23487
 γ -ray beyond atmosphere, obs. 8=19096
gamma-ray intensity in an expanding universe, calculation 8=10085
high energy, due to inverse Compton scattering of universal microwave photons in Crab nebula 8=14795
intensity, vertical, rel. to depth of atmosphere, hard γ obs. 8=20639
OSO 1 high energy expt. 8=908
primary, large air shower prod. 8=11662
primary γ spectrum, effects of decaying nucleon isobars and hyperons 8=23489
synchrotron, Compton scattering of virtual photons 8=3571
X-radiation, due to galactic e interaction with cosmic black body radiation 8=19095
X-ray background between 4 and 40 keV, diffuse 8=10282
X-rays, proportional counters and electronic systems for obs. 8=5848

protons

- anti-protons abundance upper limit in low energy galactic radiation 8=14730
atmospheric, secondary, and re-entrant albedo from balloon and satellite obs. 8=3751
large angle elastic scatt., contrib. of statistical scatt. 8=15836

Cosmic rays—contd**protons—contd**

- low-energy, elektron satellites recording 8=20610
 momentum 24 BeV/c, nuclear reactions, energy and ang. characts. 8=16074
 π -p distinction with gas proportional counter arrays 8=7009
 primary, cross-section for inelastic interact. with air nuclei 8=16075
 radial intensity gradient obs. from the orbit of Earth 8=5970
 recoil, in N-N interact., transverse momenta and four-momentum transfer 8=898
 solar, low energy cut-off dependence on latitude in geomag. field 8=897
 solar low energy cutoff diurnal vars. and pitch angle distributions 8=20631
 solar, precipitation over polar caps, nonuniformity obs., Feb. 1965 8=905
 strong interact. in 100 to 1000 BeV range, installation for study 8=15881
 spallation reactions for Li, Be, B formation 8=3922
 C interaction cross section at $E_{\pi}=10^{10}$ - 10^{12} eV, Proton 1 satellite obs. 8=16080

effects and interactions

- albedo, re-entrant, intensity calc. from balloon obs. 8=903
 atmosphere, high energy shower, combined optic and e.m. pulse production 8=3750
 barometric coefficient calc. allowing for variations in primary spectrum and cut-off rigidity 8=909
 cascades in Pb-Fe absorber, 'multiplicative effect' of EAS 8=904
 emulsion chamber, 10^{13} eV interactions at height 2640m 8=627
 extensive air, radio pulses due to slow electron movement in atmospheric elect. field 8=15900
 Fermi gas model for nuclear reactions not confirmed by 10^3 BeV cosmic ray obs. 8=20777
 fireball hypothesis for meson resonances, obs. 8=20622
 interstellar medium, e spectrum prod. calc. 8=19094
 K^0/π^+ ratio in collisions, calc. including η prod. 8=20617
 lunar surface, neutron emission 8=19240
 meteorites, nuclear particle tracks obs. of intensity 8=20599
 μ pair prod. on nucleus 8=15909
 N-N interact., transverse momenta of recoil p's 8=898
 nucleons, energies $> 10^{11}$ eV, elim. of contradictions by hypothesising a passive baryon state 8=15907
 nucleons, prod. photons, distrib. of fraction of primary energy transferred 8=16103
 neutron multiplicity monitor, 1965 obs. 8=901
 nucleus-nucleus collisions, prod. by primaries 8=16126
 π -N interactions, recoil p transverse momentum and four-momentum transfer obs. 8=11589
 π prod. of μ , rel. to μ spectrum at sea level 8=20605
 pion, prod. photons, distrib. of fraction of primary energy transferred 8=16103
 π^+ prod. in very high energy nuclear interactions obs. 8=20618
 particle groups, in EAS, shower prod. ability 8=15899
 protons, secondary, and re-entrant albedo from balloon and satellite obs. 8=3751
 with relic radiation 8=10089
 secondary particles, transverse momenta data compared with predictions of hydrodynamic theory 8=15908
 secondary production in shielded counters 8=902
 solar modulation effect 8=11676
 solar, rel. to electron density and radio absorpt., in ionosphere, 1961 ionosphere, report 8=2655
 stars in photographic emulsion at high altitude 8=15882
 300 BeV, cascade process in Fe obs. with ionization calorimeter 8=20621
 C^{14} prod. near sea level obs., meson, photon, n induced 8=20620
 Fe ion tracks in olivine 8=8768
 H^2 - 3 production in atmosphere, balloon obs., June 1965 8=3752
 Na^{22} prod. meas. for atm. exchange studies 8=18857

jets. See Cosmic rays/showers and bursts.

origin

- e ~ p charge difference, cosmological consequence 8=23480
 electrons, extraterrestrial, and spectrum 70-2000 MeV 8=3745
 extragalactic, interpretation of spectrum 8=10092
 meteorite data, early history of solar system 8=23493
 X-ray sources, spectral and location meas. 8=2835

primary

- asymptotic directions, calc. 8=20613
 charge composition and energy spectra, 200 MeV to 5 GeV/nucleon, Cerenkov-scintillation counter 8=11665
 composition and propagation in interstellar space 8=10090
 electron energy spectrum, 10-40 MeV obs. 8=15890
 electrons at energies > 12 GeV, rel. to models and related astrophysical quantities 8=11660
 electron flux using balloon obs. 8=20601
 electrons, spectrum and origin, 70-2000 MeV 8=3745
 electrons, 25-600 MeV 1964-66 obs. 8=11664
 energy estimation 8=3747
 energy spectrum obs., 10^{10} - 10^{14} eV 8=20600

Cosmic rays—contd**primary—contd**

- energy spectrum var. 8=20612
 flux of nuclei, time var. obs. 8=20611
 galactic, anisotropy in intensity distribution 8=23488
 galactic electrons and protons, 70 MeV to 2 GeV, solar modulation obs. 8=11679
 galactic escape rate 8=23491
 galactic, evolution of element abundances 8=23490
 galactic, solar modulation and p and He source spectra 8=2771
 galactic and solar, solar modulation theory and e component obs. 8=23717
 γ background due to inverse Compton scattering of $3^{\circ}K$ photons by galactic electron rays 8=23487
 γ spectrum, effects of decaying nucleon isobars and hyperons 8=23489
 heavy nuclei and solar cycle modulation, Texas, March 1962 8=3744
 high energy gamma quanta, measuring instrument 8=15879
 intensity analysis, role of worldwide vertical cut-off rigidity grid 8=11672
 intensity evaluation from nuclear particle tracks in meteorites 8=20599
 interstellar and plasma interactions, theories review 8=23578
 measurements by "automatic interplanetary stations" 8=19090
 modulation, solar, from neutron monitor data 8=7021
 Monte Carlo analysis of EAS distinguishes p from Fe 8=11667
 μ telescope direction obs., geomag. field defl. correction 8=20619
 neutrino max. energy calc. 8=14796
 neutron, monitor, yield functions, Gross transform and nucleonic component m.p.p.'s during solar min. 8=20595
 nuclear charge, high-transmission spectrometer 8=15878
 nuclear component, investig. by satellite 'proton-2' 8=15893
 nuclei, intensity vars. with A, 1964-65, rel. to solar generation 8=11680
 nuclei, tracks in plastic solids 8=3741
 photon, large air shower prod. 8=11662
 radiation in 1965, positron-electron ratio, energy dependence 8=5843
 satellite elektron, obs., 30 Jan 1964 and 9 Feb 1965 8=19088
 solar electrons > 40 keV and protons > 500 keV 8=2850
 solar heavy nuclei accel. rel. to ionizing capacity increases obs. 8=11663
 solar injection into magnetosphere 8=23721
 solar modulation, neutron monitor and direct space obs., 1958-65 8=11677
 solar protons and electrons, interplanetary diffusion 8=23686
 stellar-diurnal var. correction for solar-diurnal amplitude-phase modulation 8=7026
 superhigh energy ($E_0 > 10^{15}$ eV), rel. to EAS spectrum 8=15898
 in terrestrial radiation belt, Kosmos 53 obs. 8=19089
 X-ray background between 4 and 40 keV, diffuse 8=10282

showers and bursts

- air showers above 10^{12} eV, sidereal time variation 8=20616
 cascade showers non. e.m., initiated by muons nuclear, reactions 8=15891
 e density digitalization and core location, scintill. counters 8=7007
 e.m. showers, muon initiated, lateral and ang. distrib. of particles 8=15903
 energy spectrum of neutrons at sea level, 20-4000 GeV 8=15894
 EAS axis-detector dist. rel. to shower size and age param. 8=20615
 EAS, calc. of longit. and transverse development, inc. fluctuations 8=15901
 EAS, Cherenkov radiation density fluctuation at sea level calc. 8=7013
 EAS, detect. and meas. 8=7006
 EAS, development in upper atmos., expt. compared with theory rel. to π^0 prod. 8=15904
 EAS with fixed numbers of e and μ , characts. and energy flux densities 8=15895
 EAS, fluctuations of muon and electron numbers, expt. 8=15897
 EAS, fluctuations of muon and electron numbers, theory 8=15896
 EAS in lower atmos., contrib. of leading particle undergoing interacts. with fluctuations 8=15902
 EAS, meas. of coherent r.f. emission in meter wavelength range 8=15905
 EAS, Monte Carlo simulation, p and Fe primaries compared 8=11667
 EAS, nuclear-active parts. rel. to generation of cascade in absorber 8=904
 EAS, radio pulses det. at large zenith angles 8=3748
 EAS, radio pulses due to slow electron movement in atmospheric elect. field 8=15900
 EAS, shower prod. ability of particles in non-Poisson groups 8=15899
 EAS spectrum for $N_s > 10^7$, rel. to superhigh energy primary rad. 8=15898

Cosmic rays—contd**showers and bursts—contd**

- EAS theory and cloud-chamber obs. 8=7016-18
 due to extra-galactic primary photons 8=11662
 fluctuations rel. to principle components, simulation 8=3749
 Haverah Park E.A.S. array description 8=7019
 heavy long-lived particles, unsuccessful search 8=15887
 high energy, detection by combined optic and e.m. pulse 8=3750
 jets, primary energy estimate by $\langle \log \cot \theta \rangle$, effect of secondary momentum and ang. distrib. 8=20614
 jets, transverse momenta of recoil p in N-N interact. 8=898
 jets, centre of mass system velocity, estimation 8=3747
 jets, 2-centre fireball model, wider applic. 8=3746
 liquid scintill. for e density and time-of-arrival meas. of E.A.S. 8=7008
 muons penetrating underground, invest. using scintillator stack 8=15884
 progress in elementary particle and cosmic ray physics, book IX 8=15875
 radio emission from extensive air showers, mechanism 8=7012
 radio pulses from air showers, theory 8=7014
 radio pulses, atmospheric electric field as possible cause 8=7015
 shower electrons in Cu, Fe, Al and graphite, calc. of integral spectra 8=16059

variations

- air showers above 10^{12} eV, sidereal time variation 8=20616
 anisotropy associated with magnetic storms 8=11673
 anisotropy in galactic space, 10^{10} – 10^{12} eV 8=19087
 annual, attributed to solar corona asymmetry 8=3755
 atmospheric correlations with counting rate 8=3753
 barometric coefficient calc. allowing for variations in primary spectrum and cut-off rigidity 8=909
 classification of variations and origin, criticism 8=20624
 cut-off rigidity correl. with McIlwain parameter 8=20629
 cut-off rigidity, radiation belt effects 8=20630
 cyclic, with solar activity 8=20632
 data on properties of interplanetary space, 11-year cycle 8=19283
 diurnal anisotropy magnitude variation 8=11675
 diurnal, intensity, diffusion 8=11674
 diurnal, study of periodic fluctuations during quiet sun period 1962-64 8=910
 electrons, low energy, diurnal intensity variation new poles, obs. 8=913
 equator of intensity, location 8=20628
 Fermi accel., ionization loss and energy spectra 8=11670
 Forbush decrease Sept., Oct. 1962 8=20633
 Forbush decrease effect, rocket obs. 8=3743
 galactic electrons and protons, 70 MeV to 2 GeV, solar modulation obs. 8=11679
 γ -rays, hard, vertical intensity rel. to atmospheric depth 8=20639
 intensity modulation, interplanetary 8=19091
 intensity monthly average, data rel. to solar activity 8=20636
 latitude effect, stratosphere meas. (1964-5) 8=20627
 local atm. pressure correction 8=3754
 magnetic charges in dipole field, allowed cone 8=19031
 in magnetic storms, nuclear component Forbush decreases obs. 8=15910
 magnitude of diurnal anisotropy 8=11675
 mesons, diurnal intensity wave at high latitudes 8=20626
 muon solar daily, at depth of 60 m water equivalent 8=7023
 muons, atmospheric coeff. at Hong Kong 8=11671
 n component solar diurnal var., Antarctic (1963-64) 8=20635
 neutron component, atmospheric temperature effect 8=914
 nuclei with A, 1964-65, rel. to solar generation 8=11680
 periodic, simultaneous amplitude-phase modulation 8=7025
 primary component, energy spectrum 8=20612
 primary flux of nuclei, time var. obs. 8=20611
 radionuclides, cosmogenic, in Pearce River and Harleton chondrites, deductions 8=14858
 review, book on cosmic ray physics 8=15875
 rigidities, vertical cut-off, worldwide trajectory derived and appl. to expt. meas. 8=11672
 solar cycle effect from IGY data 8=3754
 solar-cycle, mass absorption coeff. Climax and Chicago neutron montiros, 1953-65 8=7024
 solar-diurnal, correl. with type IV radio bursts 8=19298
 solar diurnal and semidiurnal, seasonal changes 8=916
 solar flare effects, var. with solar activity 8=20634
 solar modulation from neutron monitor data 8=7021
 solar modulation, neutron monitor and direct space obs., 1958-65 8=11677
 solar proton low energy cutoffs, diurnal and pitch angle distributions 8=20631
 spatial-rigidity distrib., analysis (1965) 8=20625
 spectrography by atm. absorpt. 8=20623
 stellar-diurnal correction for solar-diurnal amplitude-phase modulation 8=7026
 study of, zonal harmonic, spherical analysis and diurnal var. methods 8=7022
 sudden intensity change, correl. with solar activity minima 8=20638

Cosmic rays—contd**variations—contd**

- 27-day cycle, correl. with solar and geomagnetic activities 8=20637
 27 day cycle, quasi-spiral variation with solar activity 8=912
 27-day, effect of solar plasma stream 8=911
 underground, 60 m.w.e. London, rel. to atmospheric temp. 8=11678
 variations from 1954 to 1958 to 1965 8=14737

Cosmogony. See Cosmology.**Cosmology**

See also Elements, origin.

- Alfven-Klein metagalaxy, rel. to background black body rad. in Universe 8=19078
 background radiation, X-ray, due interaction of galactic e with black body radiation. 8=19095
 binaries, models approximating possible remnants after mass loss 8=19126
 black-body background radiation origin of universe and det. of gravitational waves 8=14959
 blackbody radiation, Eddington-Lemaître model 8=23494
 black-body radiation in cold universe 8=23473
 blackbody radiation, spectral corrs. using quantum electrodynamics 8=23479
 Brans-Dicke gravitation theory, and solar neutrino flux 8=14731
 Brans-Dicke theory implications 8=23478
 charge fundamental unit constancy, geological evidence 8=15728
 Compton effect in astrophysics for intense radiation 8=21296
 consequence of $e \sim p$ charge difference 8=23480
 constant, and perihelion precession 8=10343
 cosmic background radiations, 4080 MHz, isotropy 8=10295
 density inhomogeneities, large scale, in universe 8=10082
 distribution of neighbours around a star 8=14747
 dust-filled space-time, general relativity 8=2941
 "electrovac" universe with axial symmetry 8=19077
 and elementary particles 8=20247
 equilibrium properties of matter at very high temp. and densities 8=19167
 expanding universe, gravitation of charged particles 8=10600
 expanding universe, thermal instability 8=14733
 expanding universe thermodynamic instabilities 8=10080
 extra galactic radio sources 8=23606
 extra galactic radio sources, mechanisms 8=23608
 fine structure const. time var., radio galaxies OIII emission obs. 8=14727
 fluctuations in the primordial fireball 8=10075
 Friedlich-Forbes empirical const., physical meaning 8=2839
 Friedman models, curvature of space-like surface 8=23475
 Friedmann models, e scatt. of photons 8=23465
 galactic cosmic radiation, abundance of anti-protons 8=14730
 galaxies, elliptical, statistical mechanics of collisionless relax. 8=10273
 galaxies, models of concentration of matter in expanding universe 8=14724
 gamma-ray intensity in an expanding universe, calculation 8=10085
 general relativity and Mach's principle rel. to origins of space-time and inertia 8=10598
 geodesic motion in internal Schwarzschild field 8=72
 ghost images in inhomogeneous Friedman universes 8=19080
 gravitating systems absolute and convective instability 8=10261
 rel. to gravitation and general relativity 8=80
 gravitation Treder theory, non-singularity of models 8=10596
 gravitational instability, formation and structure of stars and galaxies, conference Belgium 1966 8=14734
 gravitational var. with time 8=6085
 graviton density in universe 8=19422
 hot model of universe 8=14723
 hypersurfaces, null, treatment by Ricci rotation 8=2951
 light propag. rel. to local inhomogeneities statistical effects 8=10078
 matter in e.m. field, Gödel-type soln. 8=19082
 matter survival in matter-antimatter stage due to inhomogeneity of baryon number 8=23474
 metagalactic radiophone intensity in evolutionary models of Universe 8=10076
 metagalactic turbulence and fragmentation of matter, rel. to microwave relict. rad. 8=19079
 metagalaxy anisotropic expansion, rel. to weakly interact. particles 8=5844
 models containing radiation and matter 8=23476
 model at the galactic cluster scale 8=5839
 model with both radiation and matter, analytical solution 8=10074
 model universe with magnetic field, imbedding in a pseudo-Euclidian space 8=10069
 models, fitting to radio source counts 8=23467
 models, homogeneous, with bounded gravitational potential 8=23477

Cosmology—contd

- nuclear astrophysics, conference Israel 1967 8=15672
- nuclear cosmochemistry 8=23472
- open magnetic model of universe, imbedding in a pseudo-Euclidean space 8=23482
- p charge time var. from Re^{187} , Os^{187} terrestrial occurrence 8=15826
- primordial fireball transport processes 8=14729
- pulsating model of closed universe 8=10079
- quantum considerations 8=10084
- quasars, lagging-core model rel. to Universe model 8=10314
- quasars, origin, evidence of emission-line variability 8=23627
- quasars, spatial distribution 8=14814
- red-shift effect caused by distance, log N-log S curve for 70 objects 8=14815
- red shift effects on inverse Compton reactions black-body radiation in radio galaxies 8=19213
- red shift, gravitational, disagreement with Fock's hypothesis 8=2955
- red shift, rel. to quasar spectral energy distrib. 8=19233
- relativistic gas, non-relativistic bulk motion, e. m. effects and suprathermal waves 8=5925
- relativistic models, numerical calculations 8=10077
- relativistic models, rel. to radio galaxies 8=23597
- relic radiation, interaction with cosmic rays 8=10089
- Schwarzschild's instability criterion, influence of mag. field 8=10072
- Schwarzschild universe, gravitational energy det. 8=2946
- self-gravitating fluid layer, in comp., of finite thickness, stability 8=10237
- singularity, evidence from 3°K black-body radiation 8=23466
- solar system, cosmogony 8=19236
- space homogeneity criteria rel. to models 8=10081
- spontaneous creation in de-Sitter space 8=10070
- star clusters and universe ages rel. to models 8=19076
- stellar system, one-dimensional, a variational principle 8=19209
- $T = 3^\circ\text{K}$ background radiation 8=10083
- theoretical physics, conference Providence USA (1966) 8=20246
- 3°K microwave radiation spectrum 8=23610
- uniform, homogeneous and isotropic models, classification 8=10071
- universe, electrogravitational, construction from Klein-Gordon-Maxwell-Einstein field eqns. 8=19423
- universe, expanding hot, formation of Li, Be, B 8=5840
- universe, Friedman and steady-state models from Q.S.S. data 8=2768
- universe, Gödel-type, investigation using general relativity 8=2767
- Universe, helium abundance 8=10073
- universe, isotropic 8=19081
- universe model with magnetic field, imbedding in a pseudo-Euclidean space 8=23481
- universe models vibr. normal modes and stability 8=14732
- Universe models rel. to quasars redshift 8=10317
- universe, open Friedman type model 8=2766
- universe, semi-closed mag. model 8=23469
- universe, topology, non-orientable 3D space 8=23470

Cosmotron. See Particle accelerators/orbital.

Costa Ribeiro effect. See Dielectric phenomena; Phase transformations.

Cotton-Mouton effect. See Magneto-optical effects.

Cottrell atmosphere. See Crystal imperfections/dislocations.

Couette flow. See Flow; Hydrodynamics.

Counters

See also Ionization chambers.

- bacterial colony, automatic instrument 8=19333
- chamber, free-air, elect. field distortion 8=15633
- chamber for simultaneous (p, p') ang. correlations 8=20793
- cylindrical capacitor as analyser for non-relativistic particles 8=3208
- dead time meas. by coincidence method, validity of approx. formula 8=20185
- $4\pi\beta$, gas, γ counting efficiency 8=605
- γ -ray, geometric imaging props. 8=11437
- ion detector for fast scanning mass spectrometer 8=1141
- neutron, 0-14 MeV 8=850
- portable radiation survey instruments, regulated d. c. - d. c. converter for low standby current 8=3455
- recoil p for n flux meas. 8=3720
- spinner using the sensitivity of centrifugally stressed liquid to radiation 8=20202
- telescope for μ reactions, rejection of stops 8=1048
- water vapour, for tritiated water analysis 8=9748

Cherenkov

- channels ratio colour quenching correction 8=20382
- correlated system of two, with computer data anal. 8=11308
- cosmic rays, large air shower detection 8=7017
- image intensifier application 8=608
- optical system for focusing Cherenkov light 8=6511
- in shower spectrometer, resolving time 8=11307
- K^{42} in aqueous media, det. 8=3867
- Pb glass total absorpt. for π , e 8=6877

Counters—contd**crystal**

- diamond, particle-counting props. 8=6647
- γ spectrometer, Ge(Li)-Na(Tl), high efficiency 8=20365
- n spectrometer for use with reactor 8=3725
- shape factor and directional diagram, and coaxial telescope 8=3462
- CsI(Tl) for γ , X radiation monitor 8=11444
- Ge(Li) γ -spectrometer, reduction of background by use of single crystal 8=697
- LiF monochromator, n det. correction factors 8=3724
- NaI(Tl) in Fe room underground as low-level γ spectrometers 8=6790
- NaI(Tl) for meas. e^+ annihilation radiation, efficiency 8=17905
- NaI(Tl) used with paraffin pile for n det. in KeV range 8=11624
- NaI(Tl), Pb impurity effect 8=6646

Geiger

- efficiency for γ -beam, rel. to incidence angle 8=6639
- exo electron emission 8=15634
- liquid quenches of light pulse, properties 8=11297
- multicounter probe, channel remote control and pulse transmission 8=20189
- self-quenching, aging, anode role 8=6638
- teaching misconceptions 8=7027

proportional

- β emitter standardization, current pulse amplifier, and dead time circuit 8=16012
- gas array for π -p distinction in cosmic rays 8=7009
- gas for H^3 , C^{14} low-level β activity 8=3852
- high pressure, use of Au coated quartz fibre 8=11298
- n-d scatt., interaction, part of counter telescope system 8=11646
- point-anode, for soft X-ray detection 8=14497
- for solar X-ray spectrum 8=23709
- solid state, possibility 8=6648
- synchrocyclotron system for μ^- capture rate in $p + \mu^- \rightarrow n + \nu_e$ 8=3457
- X-ray microanalysis system evaluation 8=14490
- Ar-5%He, scintillation props. 8=11301
- Ar-N₂ scintillation wavelength shifter effect 8=11303
- He-42.5%Xe scintillation props. 8=11301

scintillation

- α pair counting system, low level 8=6996
- anthracene, efficiency with 2 to 40 keV electrons 8=716
- anthracene, light output under influence of α -particles 8=2495
- antineutron det. following annihilation and π prod. 8=6970
- benzoxazoles, for liquid scintillation counting 8=15637
- benzoxazolyl-thiophenes, for liquid scintillation counting 8=15637
- β -ray spectrometer 2-20 MeV, plastic 8=20388
- β -ray spectrum, unfolding by numerical methods 8=6810
- borazine and borazorene derivatives for n detection 8=6963
- collimator, finite resolving power, repetitive correction 8=20366
- cosmic rays, large air shower detection 8=7017
- determination of Avogadro's number 8=7483
- fast coincident circuit with NaI(Tl) scintillator 8=6677
- γ -ray back-scatter meas. of soil density 8=23231
- γ -source activity meas., corrections 8=3851
- gas with position independent pulse height 8=11302
- hydroxide of hyamine 10-X, chemiluminescence 8=11305
- image intensifier application 8=608
- large area for e density digitalization in E.A.S. 8=7007
- large-area isochronous for time-of-flight obs. 8=15631
- liquid, automatic external standardization, Fortran IV programme 8=11295
- liquid, B loaded, n- γ pulse-shape-discrimination 8=20563
- liquid, compensation for extinction using auxiliary source 8=20740
- liquid, counting doubly labelled quenched samples 8=23171
- liquid, counting efficiency determ., new method 8=11306
- liquid, criterion for selection of solutes 8=15637
- liquid, dating by radio carbon count 8=9798
- liquid, for α -p discrimination 8=1075
- liquid for EAS e density and time-of-arrival meas. 8=7008
- liquid, gelation technique 8=15638
- liquid for meas. ratio of n capture and fission events 8=11958
- liquid, method of quench correction 8=11805
- liquid, photon collection by photomultiplier as fraction of total yield 8=11300
- liquid, quenching corrections using relative quenching factor 8=20195
- liquid scintillation cell, for use with photomultipliers 8=11299
- low-efficiency, coincidence method for standardizing β - γ emitters 8=11797
- minimum time resolution, rel. to photoelectron generation 8=20192
- n detectors with spherical moderators, energy response 8=11623
- neutron monitoring for radiological protection, conference Vienna, Austria (1966) 8=15852
- noble gas, characteristics 8=6643
- n- γ pulse-shape-discrimination in B loaded liq. scintillation detectors 8=20563

Counters—contd**scintillation—contd**

- n spectrometer employing p recoil in 10s of keV range 8=11628
- organic doped crystals, α -particle bombardment 8=2472
- organic, efficiency determination with linear accelerator 8=6961
- organic fast neutron detector with controlled γ -back-ground 8=15853
- organic, fast neutron response 8=15855
- organic to improve sensitivity of Compton polarimeters 8=6788
- oxadiazoles, for liquid scintillation counting 8=15637
- photomultipliers for severe environment 8=6328
- photoneutron liq. detector, cross section meas. 8=20560
- plastic for n det. 10-70 MeV 8=11621
- plastic, glass and liquid, for neutron detect. 8=6956
- plastic, light output under influence of α -particles 8=2495
- plastic, muonium behaviour 8=723
- plastic, non-linear response in terms of knock-on e 8=7005
- plastic phosphors, γ -ray detection 8=11304
- plastic scintillator, efficiency with 2 to 40 keV electrons 8=716
- plastic, use of 2 light-guide-photomultiplier assemblies for uniformity 8=3458
- pulse height trigger, for optimum time resolution 8=20191
- pulse shape discriminator 8=11321
- use of pulse-shape discrimination system, wide-range 8=20218
- radiation 'colour' of short flashes, due to different particles 8=14297
- β radioactivity meas., evacuation technique 8=3853
- resolution and cathode uniformity 8=6642
- resolution time reduction 8=6678
- scintillation camera, autofluoroscope, data processing for 8=5982
- semiconductor oxygen conc., activation spectrometry 8=18083
- for shower absorpt. from e-photon cascade in Pb 8=6804
- spectrometer, liquid 8=6644
- spectrothermal emission aerosol particle analyzer 8=21733
- stilbene use as n spectrometer 8=6965
- system for instantaneous plotting of output 8=15636
- time resolution anomalies and photomultiplier triggering level 8=3218
- timing props. of scintillation photomultiplier system' 8=3459
- transmitter, resolution meas. by amp. pulse analyzer, statistical error 8=3460
- tritium counter, water/toluene/triton system, reproducibility 8=3856
- used with crystal diffraction γ spectrometer 8=11442
- water, tritiated, monitoring probe 8=3737
- Ar gas, characts. and scintillations spectrum, impurities effects, obs. 8=20194
- Ar-5%He, scintillation props. 8=11301
- Ar-N, characteristics 8=3461
- Ar-N, proportional, wave-length shifter effect 8=11303
- CdS, integration of α, β, γ dose rates 8=5404
- CsI crystals, Na-activated, characteristics 8=6641
- CsI(Tl), efficiency with 2 to 40 keV electrons 8=716
- CsI(Tl) for γ, X radiation monitor 8=11444
- Gd loaded for meas. of (n, 2n) cross-sections 8=20558
- Ge:Li, coaxial detector, electron-hole collection time 8=20391
- He-42.5%Xe, scintillation props. 8=11301
- He gas-Xe mixture, linearity and resolution 8=20193
- KI(Tl), efficiency with 2 to 40 keV electrons 8=716
- Li⁶ loaded glass detectors, Monte Carlo and S_n calc. 8=6645
- NaI crystal scintillation gamma-spectrometer for Ra, Th, K content in U ore 8=14528
- NaI(Tl) crystals, Pb²¹⁰ impurity effect 8=6646
- NaI(Tl), efficiency with 2 to 40 keV electrons 8=716
- NaI(Tl) layers for low energy X-ray det. 8=3580
- NaI(Tl), single cryst., with oxygen-containing impurities, photoluminesc. and gamma ray response 8=18610
- NaI(Tl) 64-channel γ -spectrometer probe, 0.05-9.6 MeV 8=20363
- PPO + o-xilen, and butyl-borate, radioluminescent properties 8=1578
- Xe-He mixture as simultaneous monitor and target for n-induced reactions 8=3942
- ZnS(Ag) and glass probes, two types, efficiency for β particles from tritium gas 8=15735

semiconductor

- α -spectrometer, stability, temp. effects 8=884
- in charged-particle detector expts. for students 8=609
- coincidence resolution improvement by energy-time correl. 8=6649
- collected charge fluctuations 8=612
- current-pulse method, use of preamplifiers 8=610
- digital system for gain stabilization 8=11439
- high-resolution production by cooling 8=6811
- high temp. detectors, survey 8=6652
- ion-implantation, efficiency due to low damage effects 8=6653

Counters—contd**semiconductor—contd**

- junction detector, wave form anal. of signal pulse 8=3463
- junction type, survey of detection mechanism 8=6648
- n spectrometer, sandwich, using Li⁶ and He³ reactions 8=6968
- n spectrometry to 20 MeV, part of He³ sandwich 8=6967
- neutron monitoring for radiological protection, conference Vienna, Austria (1966) 8=15852
- particle detectors, 28 compounds listed 8=15639
- p-d discrimination 8=6937
- preamplifier design, cooled FET 8=6651
- preamplifier, universal 8=20212
- review 8=20197
- suppression of interference pulses by anti-coincidence tech. 8=6650
- surface barrier detectors, pulse, shapes obs. and compared with theory 8=9141
- surface barrier detector for p spectroscopy 8=6939
- waveforms, current and voltage from equivalent circuits 8=611
- GaP miniature photodiode nsec light source 8=15525
- CdTe, γ detector 8=3578
- Ge, activation meas. of oxygen conc., by He³ bombard. 8=18083
- Ge, full registration efficiency for γ -rays 8=11429
- Ge, γ -ray detectors for reactor meas. 8=1127
- Ge p-type, Li ion drifting, rate determ. 8=22594
- Ge spectrometer, multiple element 8=6656
- Ge 2 detector telescope for separation of p and heavier particles 8=6654
- Ge(Li) array for meas. thermal n capture γ -rays 8=3576
- Ge(Li) annular, for γ -ray spectroscopy 8=6787
- Ge(Li), calibration with Ba¹³³ 8=6655
- Ge(Li), Compton recoil distribution, comparison with Klein-Nishina prediction 8=11435
- Ge(Li) Compton, reduction of background by use of single crystal 8=697
- Ge(Li), cryostat with liquid N₂ and automatic refilling 8=11310
- Ge(Li), cryostat for low temp. work 8=3113
- Ge(Li) detectors, high resolution, fabrication and use 8=6782
- Ge(Li) detectors in parallel, as γ -ray spectrometer 8=6781
- Ge(Li) detectors, review of properties and applications in gamma spectrometry 8=11443
- Ge, Li drifted, production by a.c. drifting 8=6659
- Ge, Li-drifted, technique in nuclear radiation study 8=6657
- Ge(Li) drift, U-junction permitting large vol. fabrication 8=6658
- Ge(Li), efficiency of RLC filter 8=20198
- Ge(Li), γ -ray spectrometer, 30 c.c., coaxial 8=6786
- Ge(Li), for low energy γ using summing principle 8=6789
- Ge(Li) ionization, current pulse generation 8=11430
- Ge(Li) photopeak analysis by computer programme 8=6792
- Ge(Li) as pulse dosimeter 8=7347
- Ge(Li), pulse height defects due to dead layer, correction 8=6777
- Ge p-i-n detector, width of sensitive region, meas. with electrophotography 8=9152
- L and U-type, with fast current pulses 8=11309
- NaI(Tl) photopeak analysis by computer programme 8=6792
- Si, activation meas. of oxygen conc., by He³ bombard. 8=18083
- Si, α -particle detection, channeling effect 8=3467
- Si for chemical analysis of lunar surface using scatt. α particles 8=23463
- Si detector in α -spectrometer, design and characts. 8=6998
- Si, fast n dosimeter using crystal damage 8=4030
- Si, ion implanted, position detector 8=20196
- Si, stopping power for p, d, t, α 8=8778
- Si surface barrier detectors, transient response to fission fragments 8=20199
- Si surface barrier, effective window 8=6661
- Si surface barrier, pulse height defect due to recomb. 8=3465
- Si, theory and simple laboratory applications 8=11311
- Si, B and P implantations, X-Y sensitive 8=3466
- Si(Li) β spectrometer 8=3598
- Si(Li), cooled, linearity of charge conversion 8=6778
- Si-Li drifted detectors, monoenergetic electron back-scattering obs. 8=11464
- Si, Li drifted n-i-p⁺ diodes, prep. and characts., obs. 8=20200
- Si, Li drifted, simplified manufacture procedure 8=6662
- Si(Li) for n-d scatt., interaction, part of counter telescope system 8=11646
- Si:Li surface barrier, prod. and e and α resolution obs. 8=20201
- Si, p-n operating 77°K-150°C 8=6660
- ZnO crystal, change in surface conductivity as detector for atomic H beam 8=7475

spark

- for fission fragment detect. in presence of intense α -rad. 8=16134

Counters --contd**spark--contd**

- multiwire, time resolving power 8=607
- progress in nuclear physics, book IX 8=15627
- progress in nuclear techniques and instrumentation, book II 8=15648

accessories

- See also Counting circuits.
- semiconductor detector for neutron distribution 8=852

operation technique

- See also Counting circuits.

No entries

statistical analysis

- activation anal. counting errors 8=14500
- dead time correction by coincidence method 8=11296
- level curves, automatic tracing 8=11289
- nuclear data mean rate analysis 8=6633
- nuclear physics, peak separation, applic. of prediction analysis 8=6632
- quantum stimulated emission counters probability distrib. 8=20183
- random trend removal in parity violation expts. 8=6630
- semiconductor junction type, energy resolution 8=6648

Counting circuits

- analyzer, linearity in Ge(Li) γ -ray spectrometer 8=11440
- analyzer, multichannel with automatic folding through forward backward operation for Mössbauer expts. 8=3787
- analyzer, time for high energy particle beams 8=617
- baseline shift reduction with capacitive pulse transmission 8=20207
- chronotron to meas. time diff. between discrete pulse levels 8=6666
- coincidence delayed, appl. problems rel. to circuit parameters 8=3480
- coincidence, with pulse shaping by saturated transistors 8=6676
- coincidence, zero crossover time resoln. and pulse shaping 8=20219
- converters for energy level life-time meas. 8=3859
- converter, weighted, pulse stretcher effect on linearity 8=3471
- converter, weighted, improvement in linearity 8=3471
- count rates, average, relative, by digital reciprocal function generator 8=3468
- dead time correction, rel. to linear accelerators 8=3489
- decision electronics for multiscanner expts. 8=20209
- discriminating for n spectrometer 8=6965
- discriminator high stability for use in multiple channel pulse height analyzer 8=20217
- discriminator, for photomultiplier time resolution improvement 8=6330
- discriminator, pulse, for space appl. 8=6674
- discriminator, tunnel diode, switching theory 8=5332
- discriminators, voltage, tunnel diode, charge sensitivity 8=5331
- ENCODER time-of-flight, multi-stop 8=3472
- fast coincident circuit with NaI(Tl) scintillator 8=6677
- fast logic for counter expts. in high energy physics, system approach 8=20208
- 500 MHz ring counters using tunnel diodes 8=3469
- $4\pi\beta$ - γ coincidence meas. for n-activated Au, corrections 8=6966
- high counting rate circuit 8=6997
- high-speed, single-cycle, ferrite-transistor ring counter circuits 8=11316
- linear gate, high precision 8=3477
- linear gate, 30 nanosec., high precision parallel-switch type 8=3137
- multichannel data acquisition system, parametric stabilization, review 8=11319
- multidimensional analyzer, preliminary mathematical processing of results 8=11318
- multi-input, with automatic information output 8=11317
- neutron supermonitor radio channel, dead time instability rel. accuracy 8=6955
- n. sec bifilar wound transformers 8=3470
- photomultiplier gating method 8=6331
- for photons, reversible precounter to spectro-fluorimeter 8=3573
- pulse amplitude, effect of "baseline restoration" on signal-to-noise ratio 8=3478
- pulse discrimination, generator with temp. stabilization 8=6250
- pulse discrimination, Owen-Batchelor method, theory of high energy limit 8=6672
- pulse discriminator, analogue output 8=11322
- pulse discriminator for low level α pair counting system 8=6996
- pulse discriminator, zero crossing for time of arrival of accelerator beam 8=6675
- pulse generator for precise amplitude pulses 8=11320
- pulse-height analyzer for charged-particle spectroscopy on lunar surface 8=20214
- pulse height analyzer, delay line memory system 8=20216
- pulse height analyzer, 400-channel 8=621
- pulse-height analyzer, high stability discriminator for use with 8=20217
- pulse height analyser, linear gate 8=3477

Counting circuits--contd

- pulse height analyser, 16 channel 8=620
- pulse-height analysers, statistics of digital stabilizers 8=20215
- pulse height analysis programmes 8=6670
- pulse height discrimination with compensation for time dispersion and broadening 8=3479
- pulse height discriminator with small time slewing 8=6673
- pulse height logic unit, input amplifier 8=3476
- pulse height trigger for scintillator-photomultiplier system 8=20191
- pulse meas., active D-C restoration 8=6671
- pulse-shape discrimination system, wide-range 8=20218
- pulse shape discriminator, used with liquid scintillator 8=11321
- pulse shaping for nuclear amplifiers 8=15641
- random signal quantization effect 8=6260
- resolution time reduction, using slow scintillators 8=6678
- resolving time improvement by energy-time correl. 8=6649
- ring counter for fast decimal scalars 8=6667
- shift register and scaler for derandomization, comparison 8=15640
- space vehicle radiation meas. data handling system 8=10067
- static decade register with visual presentation 8=15175
- time-amplitude converters, pulse height compensator 8=20211
- time analyses of nuclear particle beams 8=622
- time-of-flight, computer front end 8=6960
- time to pulse height conversion, pulse transformer with two ferrox cube cores 8=616
- time-to-pulse-height converter for pulsed accelerator 8=20210
- time resolution, photomultiplier pulse processing 8=6665
- ultrasonic pulse-echo detector, variable width gate 8=3073
- unstable resolution-correction problems, stabilization 8=15642
- X-ray for electron-probe microanalyzers, non-linearity corrections 8=4837
- zero-crossing detector of bipolar pulses with long cross-over times 8=3141

Cracks

- in cyclic-loaded structures, numerical anal. of crack growth 8=17745
- diffusion, forced, in 3D region with uniformly moving boundary 8=13403
- extension, ultrasonic detection of 8=8807
- fatigue fracture, anal. of initiation and propag. 8=5030
- flaw detection and erosion rate meas. by microwave interferometry 8=5032
- fracture of metals, photographic apparatus for study 8=22293
- fracture toughness, plane strain, determ. 8=5027
- glass, branching, vel. meas. and stress effects 8=8815
- glass, rel. to Hertzian stresses 8=13540
- glass, ring cracking by spherical indenters 8=17747
- glassy materials, propagation and bifurcation velocity 8=22296
- glazes of dolomite earthenware 8=2044
- graphite, deformation mechanism, tensile stress 8=5053
- in graphite, polycryst. form. and growth 8=22318
- in infinite elastic solid, stress intensity factor for penny-shaped cracks 8=22298
- under longitudinal shear, behaviour considering plastic and cohesive forces 8=13519
- Makrolon films stress cracking obs. 8=8473
- metals, fatigue crack growth, dislocation model 8=17740
- metals, fatigue crack propag., anal. 8=5038-9
- microcracks, clarification of terminology 8=8808
- mild steel, alternating stress requirement, tensile mean stress dependence 8=8838
- nucleation from dislocation pile up, criterion 8=17744
- in orthotropic plates, appl. of fracture mechanics to extension 8=22294
- parallel elastic, interaction 8=17743
- plastic zone length in moving brittle crack path direction, theory 8=57
- in plates, fatigue propag. under extension and bending, effect of mean stress 8=17758
- polyester resins, water damage 8=13622
- propagation law for infinite and finite width specimens, by dimensional anal. 8=17746
- propagation in viscoelastic media 8=2045
- in rectangular beams, stress anal. and soln. of mixed boundary-value problems 8=22297
- resistance to propag. in modern high strength composites 8=5025
- semi-circular edge, stress intensity factor, for axial bending and thermal loads 8=22299
- silicon iron, notched, nucleation and growth rel. to fracture topology 8=17793
- steel, C, fatigue crack propagation, effect of atmosphere 8=17794
- steels, low-alloy, heat treated, propagation obs. 8=5072
- steel, medium-strength, fracture toughness 8=17808
- steel, mild, stress-corrosion cracking in NaOH solns. with various additions 8=22366
- steels, notched, nucleation and growth rel. to fracture topology 8=17793

Cracks—contd

- steel, slow growth, effect of moisture 8=5071
 steel, structural, toughness, effect of temp. and strain rate 8=5070
 Zircaloy-2 tubing, hydride layer, under stress 8=13615
 Al alloys, stress corrosion, at cutting planes 8=8818
 Al alloys, during welding 8=5047
 Al cantilever, propagation under random excitation 8=5043
 Al₂O₃ (sapphire), branching, vel. meas. and stress effects 8=8815
 AlZn-Mg cast alloys, stress corrosion, influence of surface structure 8=22312
 Ag, formation on H embrittlement 8=22307
 Be, grain boundary blocking, 200°C 8=8825
 BeO, rel. to Hertzian stresses 8=13540
 in Cu cyclic deform., form. and propag. rel. to coarse slip, obs. 8=22330
 Cu, fatigue, initiation 8=5058
 Fe, fatigue damage from intergranular weakness 8=5060
 Fe-30% Cr, propagation after stress 8=13558
 n-GaAs, formation at high pressures 8=22369
 MgO bicrystals, transgranular cleavage fracture studies 8=8854
 Ti alloy in non-electrolyte, stress corrosion cracking susceptibility 8=8863
 Ti-6Al-4V alloy, stress-corrosion cracking in methanol 8=22394
- Cracking model.** See Nucleus/theory.
- Creation of electron pairs.** See Electron pairs.
- Creep**
 See also Slip.
 apparatus, for low temp. meas. 8=22256
 austenitic steel, structural changes 8=17284
 beams, deformation, iterative procedure 8=8797
 β -brass, influence of crystallographic order 8=13549
 circular plates, effect of random temperature distributions 8=10572
 comprehensive model, applicable to deforms. at increasing temp. and varying load 8=17730
 concrete, high temp. effect 8=2042
 cylinder, thick walled, under internal press. 8=17731
 diffusional mechanisms 8=22279
 graphite, irradi. induced under const. stress 8=8828
 helical spring specimens, stress redistrib. analysis 8=5021
 Magnox ZR-55, heat-treated, behaviour in 350-450°C range 8=5078
 in mantle of Earth, due to thermal grad. 8=14539
 metals, and high-strain fatigue, correlation of data 8=2060
 Nimonic 80A, damage and recovery by annealing, 600-750°C 8=5083
 nonlinear viscoelasticity, form of generalized function 8=60
 nuclear fuel, effect on coated particle 8=20900
 plane creep of free surface in viscous fluid, kinematic reversibility conds. 8=22281
 plastics, solids, under hydrostatic press. and vol. decrease with time 8=22280
 poly- α -methylstyrene, monodisperse, tensile 8=5094
 polyethylene, high-density, follows a Ramberg-Osgood type law 8=22408
 polymers, unoriented crystalline, mechanisms 8=13619
 polyvinyl chloride films, rheo-optical properties during experiments 8=2076
 polyvinyl chloride, mechanism of Andrade creep 8=13624
 pressurized shell, near sealed opening effect of stress-strain rate relationship 8=10560
 rate, effect on cavity growth mechanism 8=8801
 of rocks, temp. and stress effects, rel. to isostasy and tide damping 8=14559
 shallow trusses and arches, nonlinear creep buckling 8=22278
 shells, inelastic, membrane, with rotation symmetry, creeping at finite deformations 8=10571
 stainless steel, type 310, creep-rupture props. to 2000°F 8=17755
 steel, austenitic, liquid Na environment on secondary and tertiary 8=22359
 steel, austenitic type 304, creep-rupture props, influence of N and other elements 8=17754
 steel, carbide transformations during creep 8=17081
 steel, stainless with high N content, at cryotemps. rel. to dislocation behaviour 8=17784
 strain of a polycrystal, contribution of grain boundary sliding 8=8802
 viscoelasticity, generalized function 8=61
 voids formation and competition from sintering processes 8=8800
 Al, stressed, thermally cycled, temp. after-effect 8=13534
 Al-Al₃Ni eutectic, microstructural stability, during creep 8=4842
 Al-Ti alloy, tensile, at 250°C 8=8813
 BeO polycrystals, high temp. obs. 8=13539
 Cr alloys, influence of ceramic environment 8=13543
 Cu, at 650-700°C rel. to deformation at 77 and 4.2°K 8=17824
 Cu, films, elastic lattice strains 8=13548

Creep—contd

- Cu films, high temp, mechanism of grain boundary cavity formation 8=13547
 Cu, tubular specimens, at const. and variable loads 8=17776
 Fe, crystalline, strengthening by step-wise low temp. creep 8=2054
 Fe-Mn-N alloys, resistance rel. to effects of stress changes 8=5064
 Fe-Ni alloy, phase-hardened, condition for thermal stability 8=17066
 Fe-Ni alloy, rapid heating effect during reverse martensitic transform. on high temp. stability 8=17065
 HK-40 alloy, creep-rupture props. to 2000°F 8=17755
 In, high-temp., pressure dependence 8=8852
 MgO grain shape change 8=13584
 MgZn, plastic deformation, test 8=5081
 Mo, 950°C to 1385°C, 3500 to 12 000 lb/in² stress 8=13588
 Nb, effect of O and C on strength at 800-1200° C over stress range 1500-50 lb/in² 8=13593
 Nb-Ta-W alloys, influence of carbide and boride additions 8=22384
 Nb-W alloys, influence of carbide and boride additions 8=22384
 Ni, at 700°C rel. to deformation at 77 and 4.2°K 8=17824
 Ni, crystalline, strengthening by step-wise low temp. creep 8=2054
 Ni-base alloy, temperature cycling effects 8=2066
 Ni-1% Cr alloy, prestrain effect 8=13600
 Ni, recrystn. models criticism 8=8857
 Ni, strength increase after thermomechanical treatment 8=13601
 Ni-Al₂O₃ alloys, dispersion-strengthened 8=22388
 Ni-20Cr-2ThO₂ alloys, fracture 8=8858
 Pb, stress sensitivity at low stresses, article discussion 8=17825
 Pb-Tl alloys, superplasticity 8=13603
 Si-Fe alloy, effect on dislocation structure and ductility, low temp. 8=13571
 Si-Fe, dislocation structure changes 8=8734
 SiC, polycrystalline 8=22393
 SiC, 'self-bonded', delayed creep 8=22391
 Th, during fission 8=8866
 U, α and β mono- and poly-crysts., mechanisms 8=8867
 U containing small alloying additions, strength 8=8868
 U-C alloys, around UC comp., high-temp. creep and hot extrusion 8=22396
 Zn-Al, alloy, superplastic, deformation behaviour 8=5090
 Zn-Al, alloy, superplastic effect of stress, temp. and heat-treatment 8=5090
 α -Zr, polycrystalline, at steady-state rel. to strain-rate dislocation-velocity dependence 8=4986
 Zr and alloys, behaviour rel. to vacancy diffusion 8=4964
- Critical constants, thermal**
 ferromagnets, behaviour theory 8=13978
 ferromagnetic metals, anomaly in elec. resist. near T_c 8=13985
 gas, critical, sound attenuation 8=12688
 gas, sound attenuation near critical point 8=16706
 for heat capacity meas. from 1.2 to 300°K 8=22116
 Ising model, transport eqns 8=10669
 liquid-gas critical point, transport coeffs. 8=21745
 mixtures, shear viscosity nonlinear effect 8=8163
 particle distrib. function near crit. pt. 8=12964
 physical-cluster theory 8=4654
 supercritical fluid, thermodynamic props. calc. 8=12575
 surface tension near crit. pt., quasichem. approx. 8=21635
 thermal cond. and sp. ht. meas., 0.05 to 2°K 8=22112
 thermodynamics of critical pt., liq.-vapour systems 8=16916
 transport coeffs. in gas critical region 8=4490
 Al films, organic molecular inclusions, enhancement of critical temp. 8=12965
 Ar, thermal conductivity near critical point 8=12683
 CO₂, near critical point, forced convection heat transfer 8=16915
 Ga, superconducting boundary scattering rel. to critical temp. shifting 8=13747
 He-n-butane system, gas-gas equil. with crit. temp. above crit. temps. of components 8=12979
 He*, density measurement near critical point to test $\beta(\delta + 1) + \alpha^2 \geq 2$ 8=259
- Critical mixtures.** See Solutions.
- Critical opalescence.** See Phase transformations; Solutions.
- Crowdions.** See Crystal imperfections/interstitials.
- Cryopumping.** See Vacuum pumps; Vacuum technique.
- Cryoscopy.** See Freezing; Low-temperature production; Low-temperature technique.
- Cryostats**
 continuous flow for mag. reson., room temp. to 4.2°K 8=10793
 cryogenic liquids, differential density meas. 8=19347
 cryopump, design and performance 8=15134
 cryopump for ultrahigh vacuum 8=7951
 demagnetization, for Mössbauer effect expts. 8=1642
 electron irradiation damage meas. apparatus 8=17692
 for e. s. r. spectra at liq. He temps, effects of illumination 8=15135

- Statistics**—contd
 for ferromagnetic resonance meas. at liq. He temp. 8=6226
 Joule-Thomson refrigerator, for n diffraction at liq. N temp. 8=8501
 for ~100kbar studies at liq. He temps. 8=3112
 for -190 to +200°C temp. range, and suitable for ferromag. resonance meas. 8=253
 for Raman spectra of crystals. 8=22941
 sample holder, two degrees of freedom 8=18292
 semiconductor detectors in low temp. work 8=3113
 using charcoal adsorption pumps for liq. He⁴ and He³, without mech. vacuum pump 8=15133
 variable temp., for magneto-optical studies 8=5592
 Ge(Li) detectors, liquid N₂ automatic cooling 8=11310
 He, liquid, for use with torque magnetometer down to 4.2°K 8=15140
 He⁴ liquid, for 0.9°K 8=15146
- Superconductors.** See Superconducting materials and devices.
- Crystal chemistry**
 borates, classification 8=13119
 cerite and whitlockite, isotypy 8=4778
 diamond, valence force potentials for calculating cryst. vibrs. 8=16968
 geometrical basis, props. of net planes 8=13116
 intermetallic cpds. of CsCl structure, defect formation energies rel. to comp. and ordering 8=17623-4
 ions with incomplete shells, spectra calcs. rel. to chemical structure analysis 8=13033
 iron oxide scale, hematite phase physico-chemical state 8=17201
 isomorphous replacements 8=13120
 metallides, isomorphous substitution of atoms in crystals 8=17195
 minerals of murmanite-lomonosovite group 8=17198
 multisublattice, cation distrib. rel. to stoichiometric restrictions and solid soln. parameters 8=4775
 neptunite, oxidation state of Fe, by Mössbauer effect 8=8369
 organic, studies in USSR, review 8=8368
 pyrochlores 8=13117
 rare-earth germanides and silicides, 5:4 and 5:3 compositions 8=8554
 rare-earth-manganese cpds., prep. by amalgam process and structures 8=17203
 semiconductors and stoichiometric vacancies 8=17197
 silicates, and structural anal., review 8=8466
 of sulphosalts 8=17204
 transition metal thionibates, MNb₂S₄ 8=8560
 transition metals, 5th and 6th periods, valency structure 8=16967
 trimethylplatinum(IV) iodide and methylsodium, reaction product identification 8=14382
 Ag-Cu-Sn system, electronic phases rel. to chemical displacements 8=17002
 β-AlB₁₂ containing <2%Si, prep., stoichiometry and structure 8=17199
 AlBe₂₃, prep., stoichiometry and structure 8=17199
 Al₂Be₃Si₂O₁₈, crystalchemical analysis and structure refinement 8=17338
 B hydrides, rel. to electron deficient valencies 8=13118
 BaCa₂Al₂(Si, Al)₁₂O₃₀·2H₂O, crystalchemical analysis and structure refinement 8=17338
 3CaO·Al₂O₃·3CaSO₄·32H₂O, and structure 8=13253
 Ca₁₀(PO₄)₆(Cl)₂, single crystals, conversion to Ca₁₀(PO₄)₆(OH)₂ by hydrothermal bomb, method 8=4776
 CaZr(Hf)₄O₉ system of type RTiO₃ structure, structure and stability relations 8=1719
 Ce(III) exchange fawcites, and crystal structure 8=8515
 CeAlO₃, chemically homogeneous prep. and structure determ. 8=17355
 Ce-Ni-Si system, ternary cpd. formation, comp. and structures 8=17200
 CeO₂, non-stoichiometric, defect structure model 8=22166
 Ce₂Si₃, γ-phase stabilization with additives 8=8264
 Co complex, trans-dichloro(1,4,8,11-tetraazaundecane) cobalt (III), isomerism 8=7512
 CoCl₂:MCl (M=Rb, K, Na, Li), symmetry changes rel. to CoCl₂ conc. 8=9516
 CuFeS₂, from Fe⁵⁷ Mössbauer spectrum 8=1649
 Cr(ONO)₃(H₂O)₃·1.5 KNO₃, formation and struct. in crystalline state and in soln. 8=9518
 CsMnCl₃, and structure 8=13138
 EuAl borate, nonstoichiometry 8=8410
 GdB_x, (x=4, 6), X-ray investigation 8=17384
 H₂O* in HClO₄·2H₂O, HCl·2H₂O and HCl·3H₂O 8=17196
 HgX₂-TiX₂ (X=I, Br, Cl) systems, cpds. formed 8=17085
 KCa₂(Be, Al)₂Si₂O₁₀·0.8H₂O, crystalchemical analysis and structure refinement 8=17338
 KMnCl₃, and structure 8=13138
 La telluride phases 8=17202
 LaB₆, X-ray investigation 8=17384
 LiMSiO₄ and related sulphates, (M=Al with Ga and Ge substitution) 8=17013
 Mn₃GaC_{1-x}, non-stoichiometric effects on mag. props. 8=22819
 Mn₂SiC_x, non-stoichiometric effects on mag. props. 8=22819
 MgAl₂O₄ fibres and platelets in growth process 8=21956
 NaI(Tl) growth from melt, effect of Cl⁻ ions 8=14327
- Crystal chemistry**—contd
 NaMnCl₃, and structure 8=13138
 Nd telluride phases 8=17202
 Ni_{0.5}Fe_{0.5}O₄, oxygen stoichiometry rel. to magneto-crystalline anisotropy 8=9385
 PaCl₃, stoichiometry and structure 8=13283
 Pr telluride phases 8=17202
 Pu(N and S) cpds., rel. to use as nuclear fuel 8=12017
 RGe-Si system, (R=Gd, Tb, Dy, Ho and Er), 5:4 stoichiometry and mag. props. 8=4779
 R-Ni-Si, (R=rare-earth), system, ternary cpd. formation, comp. and structures 8=17200
 RbMnCl₃, and structure 8=13138
 Sb₂S₃, dielectric props., lattice structure anal. rel. to anomalies 8=9217
 Sb₂S₃ and SbSI, anomalous dispersion of permittivity and stoichiometry, microwave freq. 8=9217
 U(N, P and S) cpds., rel. to use as nuclear fuel 8=12017
 YB_x, (x=4, 6, 12), X-ray investigation 8=17384
- Crystal classes.** See Crystallography; Crystal structure, atomic.
- Crystal counters.** See Counters, crystal.
- Crystal electron states**
 See also Colour centres.
 adiabatic potential of complex system, calc. using perturbation theory 8=13626
 absorption edge in strongly anisotropic substs. 8=9482
 alkali halides band params., e energy loss obs. 8=8938
 alkali halides, e⁺ bound state 8=13694
 alkali metals, electron-ion pseudopotentials 8=22427
 alkali metals, interionic potential modified in conduction electron presence 8=4671
 alkali metals, resistivity and thermopower under pressure using pseudo-atom model 8=9010
 alloys, additivites 8=5446
 alloys, ordered, grain boundary theory 8=17258
 alloys, structure using pseudo-atom model 8=8910
 Anderson and s-d exchange models, comparison 8=8886
 anthracene, carrier decay from pulsed photoconductivity meas. 8=2267
 anthracene rel. to carrier prod. 8=22434
 anthracene, exciton annihilation and autoionization 8=17890
 anthracene, space-charge-limited currents, temp. dependence 8=17859
 anthracene, u. v. irradiated, fluorescence and photoconductivity rel. to carrier generation 8=2266
 antiferromagnets in strong mag. fields, correlation functions 8=18369
 aqueous solution, frozen, electron hole pairs 8=8950
 atoms embedded in electron gas, statistical model calcs. 8=22486
 binary crystals, one-dimensional, electronic states by MO-LCAO method 8=2091
 bound states of cond. electrons and mag. impurity atoms, "soluble" case 8=17848
 carriers, hot, thermoelectric effect analyzed as Bernoulli effect 8=13629
 colour centres excit. and recomb. near fundamental absorpt. limit 8=9580
 conduction electrons energy spectrum in ferro- or antiferromagnets, near Curie temp. 8=5099
 conduction electron scattering by impurity with unity spin 8=22426
 conduction electrons, theory of interaction with a strong hypersonic flux 8=17854
 conduction in dilute alloys, density around an impurity 8=5112
 conductivity electrons, dynamics during interband mag. breakdown 8=5100
 conference Työlsand, Sweden 1966 8=8191
 corundum, complexes of bound impurity ions, group-theoretical classification 8=8887
 coupled electron-phonon system, transport theory, variational approach 8=2080
 crystallization and mag. ordering of electron gas 8=22484
 cubic crystal field on covalence 8=17875
 current carrier mobility, effect of sonic wave 8=22415
 current carrier scatt. by impurities, kinetic eqn. 8=22423
 deep-trap impurities rel. to host absorpt. spectrum 8=17865
 density of energy levels rel. to scattering centre distrib. 8=5108
 diamond, charge density calcs. by OPW method 8=8927
 diamond monovacancy distortion by Jahn-Teller effect, mol. model 8=17605
 diamond, theory of hole motion in mag. field 8=22436
 1,4-dibromonaphthalene, triplet states 8=2467
 disordered system, exact expression for average propagator 8=17850
 disordered systems, comments on Gubanov's theory 8=17849
 drift mobility experiments rel. to trapping effects 8=8896
 durenene, doped, energy transfer 8=18637
 d-transition, formulae of Slater-Koster interpolation procedure 8=8885
 e and hole mobility and density in phosphors, Hall effect meas. 8=8898
 effective mass theory using one-electron Green's function 8=8921

Crystal electron states—contd

- electron diamagnetism, case of inhomogeneous mag. moment, thermodynamics 8=17896
 electron density, complex distrib. 8=8883
 electron-electron correlation and instabilities 8=22788
 electron-impurity interactions, h.f. elec. cond., calc. 8=2999
 electron-impurity interactions, master eqns. 8=2998
 electron-impurity interactions, one-particle evolution eqns. 8=2997
 electron momentum distrib., rel. to Compton scatt. of X-ray 8=17907
 electron-phonon density fluctuations, non-linear excitation mechanism 8=9070
 electro-optical effects and e transitions rel. to cryst. anisotropy 8=9495
 electronic band structure, approx. calculations 8=13650
 electronic conductors, magnetic field effects 8=13635
 electronic processes in low mobility solids, Conference Sheffield, England April 1966 8=5101
 electronic theory of adhesion 8=2046
 electron transmission through periodic pile by Schrödinger equation 8=3406
 electroreflectance use for band struct. meas. 8=9494
 epitaxial films, propag. of growth striae 8=17129
 epoxy resin, polymerization, interpretation of elect. resistivity meas. 8=18707
 exchange coupling, effect of multiplicity of mag. ions 8=22412
 excitation by absorption and scatt. expts. 8=5095
 F-centre wave functions calc. 8=13646
 ferromagnetic s-f interaction, ground state energies 8=17898
 finite translations in solid-state physics 8=13648
 Franz-Keldysh effect, spectral broadening representation 8=17853
 grain growth, excessive, during recrystallization after deformation, mechanism 8=17259
 graphite, pi-electrons, study by optical absorpt. 8=18511
 ground-state energy of Anderson Hamiltonian 8=13627
 Hamiltonians, symmetric, order of levels 8=13625
 heated-electron distribution, energy relaxation, role of two-phonon processes 8=8893
 Heine-Abarenkov model potential, screening reformulation 8=5107
 helicon propag., low-field, band structure effects, perturbation calc. 8=5140
 helicon relaxation of electron spins 8=17901
 high-permittivity crystal, conduction theory 8=8897
 high pressure modification of electronic spectra 8=8914
 hot-electron diffusion theory for space-charge-limited current flow 8=9129
 ice, low frequency optical spectra, interpretation using crystal lattice model 8=13326
 indene polyassociates, conjugated, photoelectric emission 8=13938
 insulating thin films, effective mass, meas. 8=8944
 insulators, electron, hole and exciton binding to dislocations 8=5349
 inverse overlap matrix, cluster expansion 8=5096
 Kondo problem, perturbation instabilities 8=22869
 Kondo scattering problem, ground state 8=5098
 Landau electrons, exact dynamics 8=8891
 Landau levels near singular or saddle point, quantization and magnetoacoustic effects 8=22439
 luminescence, delayed, apparatus for decay time study, used on organic substs. 8=9579
 magnetic alloys, effect of electrons of opposite spins on elec. resistivity 8=22432
 magnetic structure representation analysis 8=13951
 magnetic subs., symmetry-adapted basis states for energy level calc., comp. program 8=17877
 magnetic symmetry groups, representation 8=5111
 magnetoresistance, negative transverse, in low-temp. inelastic scattering by optical phonons 8=8892
 many-electron model, rudimentary 8=22413
 metal crystal oxide film growth rel. to ionic and electronic currents 8=5710
 metal, electron density near chemisorbed atom or molecule 8=8908
 metal, free-electron, impurity screening, preasymptotic form 8=8907
 metals, band struct. and interatomic exchange effects on spin fluctuations 8=2092
 metals, containing impurities, energy spectrum 8=2077
 metals, coupled cyclotron and spin waves 8=13682
 metals, configuration and orbital compressibility rel. to shock waves 8=8225
 metals, disordered, electron-phonon interaction 8=13630
 metals, electronic optical transitions, self-consistent theory 8=5394
 metals, form. of bound states with localized spins 8=5168
 metals, helicoid instability of sound oscs. 8=5139
 metals and impurities possessing spin, scatt. and exchange interact. of electrons 8=8899
 metals, Kondo spin-compensated impurities, low temp. props. 8=8882
 metals, localized spin and singlet bound state 8=8884

Crystal electron states—contd

- metals, oscillatory size effects with arbitrary quasi-particle dispersion law 8=22441
 metals, positron momentum distrib. relax. 8=8973
 metals, structure using pseudo-atom model 8=8910
 metal surface impedance changes on acoustic wave generation by r.f. e.m. radiation 8=180
 minority carrier lifetime of MOS capacitor from transient response 8=9177
 minority carriers, space charge effects on mobility, diffusion and recombination 8=22429
 Mott and Wigner transitions and excitonic phases 8=2083
 naphthalene-d₈-naphthalene-h₈ mixed crystals in triplet state, e.s.r. =18433
 nearly free electrons, linear response rel. to skin effect in layer lattices 8=5115
 negative absorption rel. to collision broadening of spectral lines 8=2395
 nonadiabatic transitions 8=13039
 non-adiabatic transitions between bound states 8=21054
 normal process relaxation times, from thermal cond. data 8=22424
 one-dimensional mixed crystals, by matrix method 8=2090
 paramagnetic impurities in metals, ground-state and low-temp. props. 8=22440
 Permalloy, magnetoresistance and effect of 3d orbital degeneracies 8=13724
 phonons and excitons, excitation by strong elect. field 8=17889
 phonon drag effect, contribution to thermomagnetic phenomena 8=5103
 phonon-electron interaction, piezoelectric rel. to nonlinear phonon damping 8=2079
 phosphors hole processes, F-centres luminesc. meas. 8=8888
 piezoelectric, charge carrier motion, kinetic power theorem 8=22672
 p-n junction characteristics, band gap variation rel. to hydrostatic pressure 8=5304
 polar semiconds., mobility and temp. of electrons or holes 8=17856
 in polyacene solid solns., energy transfer, 1965-66 bibliography 8=14162
 positron annihilation in pure Fermi gas, ladder-graph approx. 8=22492
 positrons, complex bound systems 8=6812
 pyridazine, singlet-triplet transitions 8=9573
 quasi-particle excitation attenuation, ferrite temp. theory 8=2120
 radioactive atoms spacial effect on electron and positron emission, wave mechanical treatment 8=17910
 rare gas solids, free carrier mobility 8=17863
 review 8=8881
 rhombohedral, laws of dispersion, at symm. points of Brillouin zone 8=8918
 rutile, electronic mobility at high pressures 8=2087
 scattering theory for muffin-tin ionic potentials 8=8895
 screening around ion cores in electron gas 8=22485
 semiconducting films, thin, electron-phonon interactions at low temps. 8=22428
 semiconductor, degenerate, meas. of band-tail spreading energy 8=13781
 semiconductor diodes, minority carrier lifetime, mag. field effect 8=13853
 semiconductor, electron exchange eqns., between surface and vol. zones 8=22431
 semiconductor, graded-band-gap, electronic transport 8=9083
 semiconductor non-linear props. governed by electron-phonon interactions 8=18004
 semiconductor, screened electron-phonon interact. rel. to carrier mobility 8=9075
 semiconductor trap level conc. deter. using thermo-stimulated conductance 8=18012
 superconductor, type II, two-band model props. 8=13736
 semiconductor with negative bulk differential cond., stationary state 8=13782
 semiconductors, Beers law and absorpt. of charge carriers 8=5102
 semiconductors, carrier temp., electric field depend. 8=8900
 semiconductors, compensated, electron mobility rel. to ionized impurity scattering 8=9080-1
 semiconductors, coupled cyclotron and spin waves 8=13682
 semiconductors, displacement of energy levels by interactions 8=5109
 semiconductors, double injection, effects of diffusion and thermal generation 8=22419
 semiconductors, effects of electron-lattice interaction on free-carrier magneto-optics 8=8890
 semiconductors, elec. characts. of diffusion layers 8=22418
 semiconductors, electron-hole gas, correlation energy 8=8889
 semiconductors, electronic band parameters determination from optical and magneto-optical properties 8=9493
 semiconductors, elemental, hot-carrier microwave conductivity 8=13779
 semiconductors, extrinsic, carrier thermalization, recombination mechanism 8=18010

Crystal electron states—contd

semiconductors, free carriers, magnetic resonances in higher harmonics 8=5223
semiconductors, g-factor and valence band spin-orbit splitting, laser induced, determ. 8=9094
semiconductors, helicoid instability of sound oscs. 8=5139
semiconductors, hot-electron Faraday effect 8=22420
semiconductors hot e diffusion rel. to current instability 8=13773
semiconductors, hot e relax. times, effect on bulk-microwave oscillators 8=22422
semiconductors, multilayer, ultrasound amplification by carrier drift 8=17855
semiconductors, polar, charge carrier scatt. by optical phonons 8=13628
semiconductors, polar, electron temp. approx. 8=13775
semiconductors, polar, hot electron mobility 8=22430
semiconductors, randomly doped, hole-electron pairs regeneration-recombination 8=13632
semiconductors, rel. to electro-acoustical attenuation theory 8=1845
semiconductors with non-uniform charged ion conc., Hall effect, mobility and magnetoresist. 8=22421
spatial correlation of valence electrons distorted by core electron correlation 8=17851
spins, nuclear or ionic, ferromagnetic s-f interaction, ground state energies 8=17898
spins, nuclear or ionic, indirect interaction derivation from ground state energies 8=17897
steady current in strong electric fields 8=22425
superconductivity, electronic mechanism, pairing criterion 8=17943
superconductors, quantum generation and phonon detection 8=17954
superconductors with overlapping bands, nonmagnetic impurity effect 8=2147
superconductors with strong electron-phonon interaction, thermal props. 8=17508
tetragonal, lattice Γ_q^* , laws of dispersion, in symm. points of Brillouin zone 8=8917
transition-metal monophosphides 8=22847
transition metals, itinerant electron correlation and ideal Lorenz number 8=8905
transport phenomena involving low temp. optical phonon scattering, theory 8=8894
transport theory for strong electric fields 8=2078
tunneling anomalies, zero-bias, temp., voltage and mag. field depend. 8=13860
two valence systems, model potential rel. to excited impurity states 8=23035
Urbach's rule, interpretation 8=14172
vibration spectra, molecular, by inelastic electron tunnelling 8=13633
vibrational excitation, relaxation 8=17866
walk-counting method for c. p. lattices rel. to energy bands and impurity states 8=8604
water, positron lifetime, temp. depend. 8=16871
Wurster's blue perchlorate 8=14288
wüstite, hole mobility obs. 1000-1300°C 8=13697
zero bias anomalies due to paramagnetic impurities, theory 8=13784
Ag, free and bound, γ -scatt., Thomas-Fermi model 8=17703
Ag, magnetoresistance, electron scattering effects 8=22511
Ag-Cu-Sn system, electronic phases rel. to chemical displacements 8=17002
Ag-Zn alloys, ϵ -phase, Zn thermodynamic activity dependence on density of states 8=22109
Al, helicon resonance determ. of high field Hall coeff. rel. to holes 8=5169
Al, phonon damping at low temp. due to electron-phonon interact. 8=17477
Al, pure, thermopower meas. rel. to electronic diffusion and phonon drag contributions 8=5382
Al, thermal conductivity 2.5-33.5°K 8=22132
Al-Mg alloys, Mg atom clustering, electronic origin 8=13636
AlSb, Te and Se donors, photoexcitation spectra 8=22953
Ar, free-carrier drift-velocity studies 8=8119
Au films on MoS₂, epitaxially grown under u. h. vacuum, defect structure 8=17125
 β' -AuZn, inter- and intraband transitions rel. to optical props. 8=2402
B compounds, ferromagnetic, electronic configuration 8=13658
Ba, band structure rel. to optical properties 8=5598
BaCl₂:Sm²⁺, phonon annihilation in ⁵D₁ and ⁵D₀ states 8=9600
BaF₂, additively coloured, phonon-assisted colour centre fluorescence 8=14306
Bi alloys electronic band structure from quantum oscillatory phenomena, 1.2-4.2°K 8=13659
Bi, band structure from quantum oscillatory phenomena, 1.2-4.2°K 8=13659
Bi, fixed charge, screening-charge density 8=8924
Bi, free and bound, γ -scatt., Thomas-Fermi model 8=17703
Bi, phonon dragging obs. using thermal e. m. f. and Nernst effect 8=22435
Bi, superconducting modification, e energy gap 8=2155
Bi thin films, quantum and classical dimension effects 8=22516

Crystal electron states—contd

Bi-Sb alloys, energy spectrum meas. 8=5104
Bi₂(Te, Se)₃ system, effective mass from reflectivity meas. 8=2096
CaCO₃, X-irrad., electron-hole trapping 8=5105
CaF₂, additively coloured, phonon-assisted colour centre fluorescence 8=14306
CaS, SrS, Ce:Sm, trapping rel. to i. r. flash stimulation obs. 8=9511
CaWO₄:Nd³⁺, spin-phonon interaction 8=14121
Cd, anisotropic electron-phonon scattering probabilities, evidence from galvanomagnetic props. 8=8901
Cd band structure, non-local pseudopot. calc. 8=2111
CdF₂, carrier mobility 8=18029
CdI₂(Pb) phosphoresc. and fluoresc. excit., e transitions 8=9605
CdS film, carrier conc. and electron mobility 8=13852
CdS hexagonal, band calc. by orthogonalized-plane-wave analysis 8=2097
CdS, photo-Hall mobility and scatt. 8=17860
CdS, temp. dependence of mobility for u. s. amplification rel. to electron trapping 8=2081
CdS trapping spectrum, effect of optical radiations and water vapour 8=5396
CdSb, alloyed with Au, acceptor level depth 8=22456
CdSe:Mn, photoconductivity rel. to Mn deep donor level 8=2259
CdSe(S), band structure rel. to optical props. 8=8928
Cd(S:Se) band gap and defect centres ionization energy, 100-300°K 8=2261
p-CdTe, trap levels from thermostimulated currents 8=2260
Cl in alkali-chlorides, K-absorption and q. s. s. 8=2410
Co complex, tris-dipyridyl Co(III) perchlorate, trihydrate, ⁵⁷Co²⁺-doped, 8=2082
CoB, transfers of electronic states 8=5461
CoSi, semimetal band structure 8=2098
Cr, antiferromag., band structure by Green's function 8=2348
Cr₂Si, band structure, superconductivity 8=5216
Cu alloys, electron-phonon interactions and high temp. resistivity 8=9003
Cu alloys with non-mag. impurities, elec. field gradient 8=9458
Cu, helicon wave excitation by a. c. 8=5147
Cu, magnetoresistance, electron scattering effects 8=22511
 α -Cu-Ag alloys, Hall coeff. and resistivity, interpretation 8=13641
CuCl from X-ray spectra obs. 8=9522
CuCl₂·2H₂O, unpaired, wave function calc. 8=18376
Cu-Cr alloys, low-temp. theory and magnetoresistance obs. 8=17933
CuO from X-ray spectra obs. 8=9522
Cu₂O band struct. rel. to absorpt. and refl. spectra obs. 8=9524
Cu₂O from X-ray spectra obs. 8=9522
Cu, QSS energies, isochromat and X-ray spectra compared 8=2414
CuX, (X=Cl, Br and I), band structures 8=2190
 β -CuZn, inter- and intraband transitions rel. to optical props. 8=2402
Eu, band structure rel. to optical properties 8=5598
Fe borides, phosphides and carbides, transfers of electronic states 8=5461
Fe, electronic sp. ht. by band model 8=4932
Fe-based alloys, charge screening 8=13661
Fe-group ions, e. p. r. spectrum calcs. allowing for electron-phonon interaction 8=9410
Fe(III) porphyrins, energy levels of Fe³⁺ from zero-field splitting 8=2469
Ga, effective mass in ab plane by ultrasonic cyclotron resonance 8=2099
Ga, r. f. size effect, temp. and freq. dependence 8=9099
Ga, velocity of open-orbit electrons 8=13640
GaAs, carrier concentration rel. to elastic constants 8=13575
GaAs density-of-state effective mass 8=5256
GaAs, i. r. spectral reflectivity rel. to free carriers 8=2418
GaAs, laser-heated, band pinch effect 8=13662
GaAs-GaP 50% alloy, charge transport 8=18038
GaAs, O₂ doped, high electric field domain behaviour 8=9103
Ga_{1-x}In_xAs alloys, electroreflectance rel. to band structure 8=2419
Ga_{1-x}In_xAs alloys, optical energy gap variation 8=18040
Ge, carrier lifetime, determination through self-associated cyclotron resonance 8=13831
Ge, conduction electron g-tensor from k-p theory 8=9110
Ge diodes, minority carrier lifetimes and reverse current, anisotropic press. 8=9163
n-Ge, effect of dislocations on galvanomag. props. 8=22592
Ge films, thin, piezoabsorption, above fundamental energy gap 8=22986
n-Ge, i. r. spectral reflectivity rel. to free carriers 8=2418
n-Ge, lattice mobility at low temps. 8=8902
n-Ge, phonons stimulated emission by supersonic electrons, 4.2°K 8=5257

Crystal electron states—contd

- n-Ge, small-field d.c. conduction in presence of large microwave field 8=13811
- Ge, photoexcited carriers, observed trapping parameters, rel. to Hall number anomalies 8=13637
- Ge, photon emission from indirect band-to-band Auger recombination 8=14221
- Ge, velocity field charact. of electrons 8=22590
- H, Mott transition and excitonic phases 8=2083
- HgTe, carrier model rel. to Hall coeff. and magneto-resistance 8=2200
- I₂, insulator-metal transition from diatomic bond destruction under high pressure 8=2084
- In, density, nearly-free-e model and photoemission obs. 8=13718
- InAs, optical second-harmonic generation by laser interact. with drifting carriers 8=5610
- InSb, electron drift velocity and mobility calc. 8=9112
- n-InSb, electron shielding rel. to impurities 8=2202
- InSb, electron-TO- and electron-LO-phonon interactions 8=13817
- InSb, helicon wave propag. 8=5141
- InSb, Landau levels, electron-hole pair effects 8=5113
- p-InSb, lifetime of nonequilibrium carriers, influence of illumination on 8=5271
- p-InSb, 90% compensated, hole density and deep level activation energy, 55–130°K 8=13822
- InSb, thin films, electron mobility rel. to temp. 8=8323
- InSb-oxide-metal structure, osc. tunnel conductance induced by L.O. phonons 8=13862
- K, helicons, surface impedance near cyclotron edge 8=13686
- KBr, electron transport props. in high fields at low temps. 8=2264
- KBr:In, impurity C excitations delocalization mechanism, obs. 8=8903
- KCl self-trapped holes temp. depend., e.p.r. obs. 8=8742
- KCl, tunneling states of OH⁻ 8=2101
- KBr:Tl hole processes, F-centres luminesc. meas. 8=8888
- KCl:Ag, Pb and Tl, self-trapped holes temp. depend., e.p.r. obs. 8=8742
- KCl:Tl, induced local 3p states on Cl⁻ ions nearest Tl⁺, calc. 8=8930
- KCl:Tl, optical and thermal electrons roles in recomb., photostimulated luminesc. 77–300°K 8=9617
- KCl:Ag relax. process temp. depend., colour centres e.p.r. absorpt. obs. 8=8743
- KCl, M₁-centres 8=2003
- KCl, U₂-centre, electronic structure rel. to correlation effects 8=13459
- KFeF₃, exchange and spin-orbit coupling 8=22881
- KI:In, impurity C excitations delocalization mechanism, obs. 8=8903
- Kr, free-carrier drift-velocity studies 8=8119
- LaBr₃, multiphonon orbit-lattice relaxation 8=13334
- La-Ce film, gapless supercond., resonant scattering 8=5205
- LaCl₃, multiphonon orbit-lattice relaxation 8=13334
- LaF₃, multiphonon orbit-lattice relaxation 8=13334
- LaF₃:Nd³⁺, Yb³⁺, energy transfer 8=14328
- Li alloys, conduction spin-lattice relaxation time 8=9430
- LiF, importance in theoretical detm. of elastic constants 8=17812
- LiF, thermal activation energies 8=18609
- Mg, electronic structure from optical properties 8=14239
- Mg₂Ge, and selection rules for transitions and intervalley scattering 8=22437
- Mg₂Si, and selection rules for transitions and intervalley scattering 8=22437
- Mg₂Sn, and selection rules for transitions and intervalley scattering 8=22437
- MnB, transfers of electronic states 8=5461
- Mn₂Fe₃O₄, hopping of electrons, meas. via dielec. loss peaks 8=14050
- Mo, anisotropy of effective masses, cyclotron resonance 8=2126
- Mo, features from electron field emission 8=5411
- Mo, optical props. rel. to conduction band transitions 8=9553
- Mo, superconducting, energy gap anisotropy, u.s. investigation 8=9048
- Na, electron-self-energy, phonon contrib., numerical calc. rel. to temp. 8=17862
- NaCl self-trapped holes temp. depend., e.p.r. obs. 8=8742
- NaCl, theory of hole motion in mag. field 8=22436
- NaCl, thermal activation energies 8=18609
- NaCl, valence band, three-centre corrections 8=2104
- NaCl:Ag and Pb, self-trapped holes temp. depend., e.p.r. obs. 8=8742
- NaCl:Ag relax. process temp. depend., colour centres e.p.r. absorpt. obs. 8=8743
- NaF, thermal activation energies 8=18609
- NaNO₃, X-irrad., electron-hole trapping 8=5105
- Nb, helicon resonances near H₂ 8=9049
- Ne energy levels, radiative lifetimes, population mechanism 8=1171
- Ne, free-carrier drift-velocity studies 8=8119
- Ni, band theory and low energy electron diffraction 8=2105
- Ni, density of states from soft-X-ray spectrum studies 8=8940

Crystal electron states—contd

- Ni, electronic band structure and de Haas-van Alphen effect 8=9360
- Ni, electronic sp. ht. by band model 8=4932
- Ni₃Ga, density of states curve in Fermi region, mag. susceptibility 8=9359
- O, and D_{3h} double groups, basis functions calc. 8=5097
- Pb, dislocation-electron interactions, temp. independence 8=17864
- Pb, phonon spectrum, energy shifts, observed by electron-tunneling 8=2085
- Pb, supercond., crit. energy gaps and thresholds from far i.r. absorpt. 8=18555
- Pb, two band conduction 8=2107
- β⁻PbIn, inter- and intra-band transitions rel. to optical props. 8=2402
- PbSe, forbidden band width and temp. depend. 8=5272
- p-PbSe, hole mass and valence band, from free carrier Faraday rot. 8=2445
- Pb_{0.85}Sn_{0.15}Te, thermal and optical energy gaps 8=2446
- Pb_{0.93}Sn_{0.07}Te, thermal and optical energy gaps 8=2446
- PbTe, anomalously high-mobility from Hall meas. rel. to sample prep. 8=2138
- PbTe, helicon-phonon coupling at 4.2°K 8=18063
- PbTe, stimulated emission of phonons, obs. 8=9115
- Pb-Tl alloys, electron-phonon coupling and phonon spectra, electron tunnelling studies 8=22555
- PdNi alloys, dilute, elec. resist. rel. to s electron scattering in d band, mag. susceptibility 8=13634
- Pd-Ni alloys, s-electron-paramagnon scattering 8=9015
- Pt, free and bound, γ-scatt., Thomas-Fermi model 8=17708
- Pt/rare-earth alloys, conduction electron polarization 8=17857
- Pt, two band conduction 8=2107
- S, orthorhombic, electron hopping transport and orbital overlap 8=18064
- S, orthorhombic, hole and electron traps 8=8904
- S, orthorhombic, transient space-charge perturbed currents 8=18171
- Sb, effective mass and drift vel. rel. to Doppler effect obs. 8=22488
- Sb₂S₃ trap levels and recomb. centres, photocond. obs. 8=22698
- Sb-Sn alloys, second set of holes, magnetoconductivity tensor evidence 8=2086
- Se, polycrystalline, hexagonal, local (conduction) levels, X-ray-induced 8=18236
- Si, B-doped, deformed in elec. fields, hole relax. times at low temps. 8=18074
- Si, carrier lifetime, determination through self-associated cyclotron resonance 8=13831
- Si deposited on corundum, carrier mobility 8=5281
- Si e distrib. from autophotoemission energy 8=22726
- Si, drift mobility, e-phonon scatt. 8=22438
- Si, effects of elec. field on B acceptor states 8=2208
- Si, effective mass, intrinsic concentration 8=5119
- Si, hot carrier drift velocity, Stratton theory 8=9130
- Si, minority carrier lifetime from transient response of MOS capacitor 8=9179
- Si, p-type, hole velocity depend. on elec. field and hole density 8=13832
- Se, vitreous, electron and hole drift mobilities, temp. depend. 8=13639
- Si, photoexcited carriers, observed trapping parameters, rel. to Hall number anomalies 8=13637
- SiO₂, electron Hall effect 8=9124
- Sm²⁺ in host lattices 8=14332
- SnO₂, electron scattering polar optical modes 8=22611
- SnTe, i.r. reflectivity rel. to free carrier dispersion theory 8=2457
- SrF₂, additively coloured, phonon-assisted colour centre fluorescence 8=14306
- Te, effective masses from cyclotron resonance 8=22490
- Te in Bi, distribution coeff. and donor valency 8=22517
- Te, p-band absorption at 4°K 8=8945
- Te, magnetoabsorption meas. 8=23016
- Th, N₂, (x = 1, 3; y = 1, 4), from elec. props. 8=2139
- Ti³⁺ in SrTiO₃, ground state 8=9445
- Ti₂O₃, effective mass, calc. from magnetic susceptibility data 8=5120
- TlCl, holes, transient magnetoresistance 8=9020
- Tl₂O₃ layers, effective mass in conduction band from optical meas. 8=23017
- U cpds., systematics 8=17852
- UO_{2-x} and U₂O_{7-y}, carrier mobility investigation 8=18090
- VN, from X-ray diff. intensity meas. 8=22414
- V₃Si, band structure, superconductivity 8=5216
- V₃Si type compounds, in cubic phase, rel. to elastic consts. temp. depend. 8=13611
- W, features from electron field emission 8=5411
- W, phonon drag effects below 2.6°K 8=5106
- W, two band conduction 8=2107
- Xe, band structure, deform. potential and exciton states 8=2108
- Xe, free-carrier drift-velocity studies 8=8119
- YFe garnet, hopping of electrons, meas. via dielec. loss peaks 8=14050
- Y-Tb alloys, conduction electron and Y ion, exchange interaction 8=2299

tal electron states—contd

- Zn band structure, non-local pseudopot. calc. 8=2111
- Zn—base alloys, study from Hall coefficient 8=17941
- Zn, g factor determ. by de Haas—van Alphen meas. 8=2110
- Zn, Cd_{1-x}Sb, hole mobility rel. to elec. and thermoelec. props. 8=2131
- Zn, K $\beta_{2,s}$ band fine structure 8=23027
- ZnS, band structure rel. to optical props. 8=8928
- ZnS e and hole mobility, Hall effect obs. 8=8898
- ZnS phosphors, carrier redistrib. among traps under i.r. irradi., obs. 8=9135
- ZnS trapping levels and recomb. mechanisms 8=9258
- ZnS—Cu electroluminescent phosphor, filling of traps during electric field excitation 8=14314
- ZnS:Mn, Cl, rel. to electroluminescence i.r. enhancement 8=5678
- ZnSe, electron mobility rel. to prep. by direct fusion 8=2210
- ZnTe films, electroabsorpt. rel. to determ. of reduced effective mass 8=18566

and structure

- alkali halides, two-photon spectroscopy theory using two-band model 8=22935
- b. c. c. transition metals, isochromat spectroscopic invest. 8=17876
- Bloch functions, transform. props., in k.p perturbation theory 8=13649
- compressibility of metals under high. press., effects 8=17724
- conduction, and electron effective mass from double resonance data 8=17874
- conduction electron in external field, one-band approx. 8=17871
- conductivity mechanism 8=17917
- disordered linear chain, new calc. by density of states vs energy function expression 8=22450
- effective masses for nineteen elements 8=13651
- electron density in perfect lattice, one with single vacancy and one with impurity 8=22443
- energy gap, and critical current of superconducting film with current flowing 8=22528
- excitonic insulator, transport props., elec. cond. 8=13652
- excitonic insulator, transport props., thermal cond. 8=13653
- ferromagnetic metal, band model 8=22764
- forbidden bands and electron reflection, dependence on crystal thickness 8=2095
- graphite, critical points from temp.-modulated reflectance meas. 8=14200
- group theory and crystal symm., calcs. 8=8906
- Hall coefficient, weak-field, new computation method 8=13645
- h. c. p. alloys of later 4d and 5d transition metal series, from mag. susceptibilities 8=18296
- hydrocarbon chains, effective masses estimation 8=17873
- interband interaction and spontaneous polarization of crystal lattices 8=9210
- interband transitions in optical range, pseudopotential Fourier components determ. 8=17869
- itinerant-electron magnetism 8=9287
- for LEED intensities, treatment 8=5110
- magnetoresistance, mag. breakdown by Kubo formula 8=13954
- metal to insulator transitions 8=22451
- metals, interband transitions due to Bragg reflection 8=22442
- mixed crystals, persistence and amalgamation types 8=22452
- non-conductors, calc. from spectra 8=8915
- non-transition metals, rel. to superconductivity 8=17868
- perovskite oxides in paraelectric and ferroelectric phases, optical props. 8=18504
- point change model and covalence theory 8=17875
- polymers, relevance of theory to conduction and optical studies 8=17872
- population anal., computer program 8=17878
- p-quaterphenyl polycrystals, thermally stimulated currents 8=13906
- principles and pseudopot. 8=8912
- P, red, energy levels from X-ray spectroscopy data 8=9559
- p-type semiconductors (Ge, GaAs, GaSb, InAs, ZnTe), Faraday rotation, band transitions 8=14216
- rare-earth sesquisulphides 8=9119
- reflectance, modulated, at oblique incidence for analysing band structure 8=14168
- rare-earth metals, heavy, mag. ordering and electronic props. 8=22466
- semiconductor films, effective density of electron states per unit volume 8=22448
- semiconductor with InSb-type valence band, statistics 8=22449
- semiconductor, two-band model in intense photon field 8=17867
- semiconductors, Green's function method 8=8913
- semiconductors, piezoelectric, stimulated Brillouin scattering. 8=17495
- semiconductors rel. to quantum efficiency 8=13907
- semiconductors, transitions and saturation effects, rel. to laser theory 8=15475

band structure

- semiconductors, two-photon absorpt. coeff. formulation 8=18516
- spin density wave in mag. field, one-band model 8=13980
- spin-polarized, exchange effects 8=13655
- superconducting films, energy gap dependence on mag. field 8=22529
- superconductivity, gapless, induced by metallic contact, I-V curves interpret. 8=13739
- superconductivity theory, cryst. lattice study 8=22534
- superconductors, energy gap eqn., linearized, boundary conditions 8=13726
- superconductors, gapless, expts. 8=13744
- superconductors, incomplete inner bands 8=17951
- temperature dependence of self-energy of electron interacting with acoustic phonon 8=13647
- transition metal alloys 8=22444
- transition metal compounds, broad band versus d-level semiconductors 8=17886
- Π -VI compounds, obs. and calcs., review 8=8911
- tunnel transitions between bands, theory 8=17879
- wurtzite, symmetrized combinations of plane waves 8=13666
- A'B₃ VII type crysts., prohibited zone width, temp. depend. 8=22453
- AB-type mixed crysts., dependence on comp. 8=13667
- Ag alloys, thermopowers interpret. rel. to resistivity and band structure 8=18213
- Ag, anomalous skin effect theory, in i.r., verification 8=14192
- Ag 2-band model for calc. of dielectric constant and polarizability 8=18498
- AgPd alloy, localized states from permittivity obs. 8=13656
- Al, APW calcs, systematic numerical error 8=17883
- Ar, solid, band gap, hole effective mass and exciton params. obs. 8=9194
- AuMn, spin-disorder resist., anisotropic 8=14064
- AuPd alloy, localized states from permittivity obs. 8=13656
- Au-V alloys, s-d interaction from elec. resistivity and mag. susceptibility meas. 8=13657
- Bi, calculation of experimental data 8=22454
- Bi, relativistic calcs. using augmented plane wave method 8=8925
- Bi, rel. to oscillatory nature of resistivity voltage dependence 8=17928
- Bi, subjected to press., variation of e energy spectrum parameters 8=17880
- Bi tunnel junction, conductance maxima rel. to band structure 8=13859
- Bi tunnel junction, semimetal-insulator, phonon-assisted tunnelling, band-edge energies 8=22455
- Bi, valence-band maximum location from recombination and phonon dispersion expts. 8=13660
- Bi—Sb alloy, Shubnikov-de Haas effect vanishing under pressure 8=22514
- Bi_{1-x}Sb_x, (0 < x \leq 0.15), from galvanomag. props. at 77°K 8=22518
- Bi₂Te₃, calc. using pseudopotential method 8=17881
- BN, cubic, band struct. calc. 8=8922
- CdSb, Te donor level energy position 8=9097
- CdSAs₂, conduction band structure 8=8929
- Co-Be alloy, ferromag. props. rel. to transfer of electron states 8=14018
- CoF₂, magnon sidebands rel. to polarized absorpt. spectra 8=22974
- Cr, antiferromag. energy gap rel. to i.r. reflectivity temp. depend. dip. 8=22874
- Cr, electronic structure, photoemission investigation 8=22457
- Cr—Fe alloys, Cr rich, energy gap rel. to antiferromag. ordering 8=8931
- Cu, momentum distrib. of annihilation radiation, Brillouin zone boundary effect 8=13691
- Cu, rel. to lattice spacing 8=22458
- Cu—Al alloy, momentum distrib. of annihilation radiation, Brillouin zone boundary effect 8=13691
- Cu, APW calcs, systematic numerical error 8=17883
- CuCl band struct. and spin-orbit splitting, calc. 8=8932
- Cu₂O band struct., APW calc. 8=8933
- Fe, b. c. c., density of states 8=22460
- Fe, rel. to X-ray K and L emission bands fine struct., obs. 8=18527
- Fe—Be alloy, ferromag. props. rel. to transfer of electron states 8=14018
- FeF₂, near i.r. spectrum, rel. to magnon sidebands 8=18525
- GaAs, interband magneto-optical absorpt. meas. at 2°K, 77°K and room temp. 8=22985
- GaP, from interband piezoabsorpt. 8=18529
- GaSb, from Faraday rotation, spectral emittance and Hall effect 8=22587
- p-GaSb at 4.2°K, by magnetoresistance and Hall effect meas. 8=13803
- Ge acceptor impurity states and valence-band in mag. field 8=22991
- Ge, amorphous, valence-band wave function, and i.r. absorpt. bands 8=22987
- Ge, complex, and real energy-lines 8=9125

Crystal electron states—contd**band structure—contd**

- Ge, double group k, p expansions, approx. symmetry relations 8=22461
- Ge, and electroreflectance spectra, at int. pts. in interband transitions 8=13663
- Ge, interband electro-optical props., electro-absorption 8=22595
- Ge, interband electro-optical props., electroreflectance 8=22596
- p-Ge:Ga, impurity photoconductivity spectra, nature of oscs. 8=13912
- In, and Fermi surface and Knight shift 8=22463
- InSb, acceptor impurity states and valence-band in mag. field 8=22991
- InSb, hot electron polar scattering 8=13638
- InSb interband magnetoabsorption polaron induced anomalies, Coulomb effect 8=22818
- InSb, shallow donor levels, in mag. field 8=22462
- La, density of states, periodic table position 8=8936
- Lu, density of states, periodic table position 8=8936
- Nb, by modified OPW method 8=8939
- Nb-Re alloys rel. to paramag. susceptibility, obs. 8=22759
- Nb, superconducting, anisotropic energy-gap meas. by tunnelling 8=22552
- Ni-Be alloy, ferromag. props. rel. to transfer of electron states 8=14018
- Pb, superconducting, energy gap pressure dependence 8=22557
- Pb, superconducting, tunnelling meas. of energy gap, 1.3 to 4.2°K, at high pressures 8=22554
- PbS, and electronic props., investigation 8=22465
- PbSe, and electronic props., investigation 8=22465
- p-PbTe, doped, interband interactions of light and heavy holes rel. to Lorenz number 8=9116
- Pd, density of electronic states from X-ray spectroscopy of alloys 8=17884
- Pt, cyclotron effective mass, anisotropy and mass enhancement 8=22487
- ReO₃ metal, optical props. including effective mass and band models, 0.1-22 eV 8=14258
- Sb tunnel junctions, conductance maxima rel. to band structure 8=13859
- Sc, and density of states by cellular method 8=8942
- Sc₂In phase, magnetization meas. and press. depend. of Curie point 8=17885
- Se Green's function method 8=8913
- Se, relativistic KKR-calculations 8=22468
- Si, amorphous, valence-band wave function, and i.r. absorpt. bands 8=22987
- Si Brillouin zones symm. elements obs. by e⁻ annihilation 8=13690
- Si, complex, and real energy-lines 8=9125
- Si, effects on photoelectromag. effect 8=13916
- Si, impact ionization, transition probability 8=13665
- Si p-n junctions, anisotropic stress effects 8=13847
- Si, localized state energies rel. to neutral divacancy 8=9123
- n-Si:As, electric props. 8=13830
- SnTe 8=8943
- Te Green's function method 8=8913
- Te, relativistic KKR-calculations 8=22468
- Tl, and density of states by cellular method 8=8942
- Tl₂ rel. to X-ray K and L emission bands fine struct. obs. 8=18527
- TiFe_{1-x}Co_x alloys, ⁵⁵Co Knight shift constant rel. to electronic structure 8=14156
- TiO₂ (rutile), vac. reduced, sp. ht. below 4.5°K, rel. to impurity band model 8=13380
- USn₃, interband mixing effects on Sn¹¹⁹ n.m.r. 8=18474
- Yt, and density of states by cellular method 8=8942
- ZnS Green's function method 8=8913
- Zr, and density of states by cellular method 8=8942

excitons

- alkali halides, self-trapped, triplet state, rel. to intrinsic recomb. rad. 8=2476
- amorphous solids, theory 8=13669
- anthracene, band theory and photoconductivity meas. 8=13671
- anthracene, distinction by recombination luminesc. meas. 8=18632
- anthracene, recombination luminescence in mag. field 8=18630
- anthracene, rel. to carrier formation and charge transport 8=17858
- anthracene, rel. to low temp. reflection spectra anomalies 8=23030
- anthracene, rel. to polarization of triplet factor group states 8=2494
- anthracene, singlet-exciton collisions 8=17891
- anthracene, triplet diffusion and triplet-triplet interaction delayed fluoresc. obs. 8=23066
- anthracene, triplet dynamics, spectroscopic approach 8=13672
- aromatic molecular crystals, theory 8=13671
- aromatics, triplet excitons props. theory 8=22479
- benzene molecular crystal, lowest states, Faraday effect and spin-orbit interaction calc. 8=9568
- benzene, vibr. exciton spectrum 8=9567

Crystal electron states—contd**excitons—contd**

- dielectrics, transitions in 2-photon stimulated luminesc. 8=9583
- disordered molec. crystals, theory of exciton bands 8=8949
- energy spectrum in crystals with complex band structure 8=13668
- excitation by strong elect. field 8=17889
- exciton-photon coupling and retarded interactions in molecular crystals 8=22473
- Faraday effect in exciton absorpt. region in strong mag. field 8=18491
- Frenkel, collective properties, Bose operator represent 8=5122
- insulating (excitonic) phase in semiconductors and semimetals, anisotropy effects 8=9192
- insulating phase in presence of normal impurities, excitonic props. 8=8951
- insulators, binding to dislocations 8=5349
- insulators, optical absorpt. from exciton resonances 8=8947
- insulators, rel. to lattice Raman scattering theory 8=2397
- interchange symmetry concept 8=4118
- lattice scattering in molec. crystals. 8=8948
- luminescence rel. to annihilation and bound complexes 8=9582
- metals, rel. to infinite hole mass 8=5129
- molecular crystals, excitation spectrum and ground-state energy 8=18479
- molecular crystals, weak-coupling theory of vibr. struct. 8=5126
- molecular, form of bands of light absorpt. and reflection 8=5127
- rel. to Mott and Wigner transitions, phases 8=2083
- Mott exciton in strong mag. field, energy depend. on transverse momentum 8=5125
- multielectron theory in semiconductors 8=22478
- naphthalene, rel. to polarization of triplet factor group states 8=2494
- naphthalene in solid solution of PMMA, triplet-triplet annihilation 8=2114
- nonpolarizing, multielectronic theory 8=5124
- organic mol. crystals, meas. and obs. 8=8952
- phenazine, rel. to polarization of triplet factor group states 8=2494
- polyphenyls, spin-spin interactions 8=2374
- radiation damping of exciton states 8=22477
- rare-gases, Faraday effect theory, for weak mag. field 8=5130
- reflection and transmission coeffs. at lowest exciton level calc. from polariton model 8=22480
- semiconducting II-IV compounds with wurtzite structure, creation rel. to intrinsic absorpt. edge 8=5224
- semiconductors, condensate form, and absorpt. of light 8=5128
- semiconductors, intrinsic, transitions in 2-photon stimulated luminesc. 8=9583
- semiconductors, superfluidity 8=22476
- spectra, rel. to crystal thickness 8=22475
- triplet, coherent and incoherent migration 8=22474
- the triplet state, conference Beirut Lebanon (1967) 8=16347
- 2-photon transitions to exciton states in semiconductor, oscillator strengths 8=8953
- vibronic coupling, rigid-lattice model of molec. crystals. 8=13670
- Wannier-Mott capture by shallow traps, in nonpolar crystals 8=5123
- Würster's blue perchlorate, triplets rel. to susceptibility and transition heat 8=22763
- rel. to X-ray absorpt. spectra 8=9492
- Ar, solid, binding energy and reduced mass obs. 8=9194
- CdS, absorpt. spectrum, structure rel. to line shift 8=13673
- CdS, electroabsorption, exciton effects 8=22965
- CdS, emission intensity of lines, variation rel. to excitation intensity, 4.2°K 8=22964
- CdS, pure crystals, submission to excitation of 50 keV electrons 8=14311
- CdS, splitting of exciton lines by uniaxial stress 8=14273
- CdSe, splitting of exciton lines by uniaxial stress 8=14273
- CdS(Se) semiconductor lasers, free exciton annihilation 8=11088
- CoF₂, optical spectrum 8=22974
- CuBr, rel. to luminescence 8=23052
- CuCl, absorpt. spectrum and e and hole masses, 4.2°K 8=9523
- CuCl, dissociation energy and rel. to absorpt. spectrum oscils. 8=8932
- CuCl, from two-photon absorption spectrum 8=2412
- CuCl luminesc. and weak absorpt. rel. to exciton complexes 8=9525
- CuCl rel. to emission line lifetimes, 4.2-300°K 8=9526
- CuCl, rel. to luminescence 8=23052
- CuCl rel. to photocond. and absorpt. spectra, 4°K 8=9251
- CuI, rel. to luminescence 8=23052
- Cu₂O, nature 8=8933
- Cu₂O absorpt. spectrum, uniaxial press. and n. irradi. effects obs. 8=9521
- Cu₂O rel. to exciton-phonon interactions, n=1 line profile, 4.2-112°K 8=9527

Crystal electron states—contd**excitons—contd**

- CuO₂, photoionization, assoc. absorpt. coeff. calc. 8=9529
 n-Ge, impact ionization rel. to elec. breakdown on carrier photoinjection 8=18050
 Ge, obs. with optical wavelength wobbles 8=5573
 I₂, intermediate triplet excitons props., theory 8=22479
 InSb, Landau levels, electron-exciton interaction modifications 8=5113
 KCl, rel. to reflectivity spectra and absorpt. constant 8=14230
 KI-NaI, (-RbI), (-KCl) solid solns., exciton absorpt. tail and peaks 8=22994
 MoS₂, thin anisotropic, delocalized excitons from magneto-absorpt. study 8=13674
 PbI₂ on different substrates, absorpt. and refl. spectra 8=13675
 PbI₂, effective mass from optical absorpt. and photo-conduction meas. 8=2444
 RbI:Ti, formation, and luminesc. 8=5131
 Si, bound, rel. to absorption 8=5132
 Si, obs. with optical wavelength wobbles 8=5573
 Xe, and band structure and deform. potential 8=2108
 ZnO, semiconductor lasers, free exciton annihilation 8=11088
 ZnO single crystal, transmission spectrum, rel. to exciton absorpt. and exciton-phonon complexes 8=14272
 ZnO, splitting of exciton lines by uniaxial stress 8=1427
- Fermi level**
 Hartree-Fock approximation, thermal, consequences at zero temperature 8=8919
 metals, spin susceptibility, dynamic, Fermi liquid theory 8=22447
 recombination through centres, effect of high mag. field 8=2223
 Ag-Au alloys, mag. susceptibility, and electronic sp. ht. 8=13970
 Al-Al₂O₃-Au tunnel structures, interface trapping 8=5381
 Al-CaWO₄-Au tunnel structures, interface trapping 8=5381
 Bi, quantum variation at high mag. field 8=17882
 Cu-Au alloys, α -phase, mag. susceptibility, and electronic sp. ht. 8=13970
 GaAs, influence of volume dope 8=8934
 GaAs:Zn, rel. to Zn diffusion coeff. 8=1918
 n-GaSb, Shubnikov-de Haas oscs., beating effects 8=9102
 HgSe, inversion-asymmetry splitting rel. to magneto-resistance 8=2100
 Nb₃Sn, motion rel. to normal-state susceptibility, resist. and elastic const. temp. depend. 8=5118
 PbO layers, vapour-deposited 8=8941
 Ti₂O₃ layers, effect on free carrier absorpt. from optical meas. 8=23017
 V₃Ga, motion rel. to normal-state susceptibility, temp. depend. 8=5118
 V₃Si, motion rel. to normal-state susceptibility, temp. depend. 8=5118
 n-ZnO, neutron irradi., transmuted-centre spectroscopy 8=2109

Fermi surface

- graphite, pressure effects 8=8926
 magneto-oscillatory components of electron transport kinetic coeffs. 8=8916
 magnetoacoustic resonance effects in metals in inclined mag. fields 8=1844
 metallic surface, oscillations of impedance, quantum spectroscopy 8=2094
 metals, ground state of magnetic impurity 8=8909
 one-dimensional case, impulse-distribution ("sharpness") 8=129
 oscillatory free energy for nearly free electrons and their mag. props. 8=2088
 positron annihilation rotating specimen method meas. 8=13689
 transition metals, electron-magnon interaction 8=2300
 Al, range of g-factors, conduction e.s.r. 8=5522
 Au films, optical absorption edge due to quantum transition from d-band 8=5585
 AuAl₃, topological props. 8=5116
 BCS theory of superconductivity, Freidrichs-Berezin transformation reformulation 8=5190
 Be, de Haas-van Alphen data, non-local pseudopotential model 8=8923
 Bi, effect of deformation on electron spectrum 8=17870
 Bi-Sb alloys, energy spectrum meas. 8=5104
 Cd, non-local pseudopot. calc. 8=2111
 Cr-Mn alloys, density of states rel. to paramag. susceptibility, obs. 8=22759
 Cr-Os alloys, density of states rel. to paramag. susceptibility, obs. 8=22759
 Cr-Ru alloys, density of states rel. to paramag. susceptibility, obs. 8=22759
 Cu, from magneto res. and transverse effect data 8=13713
 Cu, rel. to positron annihilation ang. depend. 8=22493
 Cu, thin films, electronic structure from thermopower size-effect 8=13903
 α -Cu-Ag alloys, rel. to Hall coeff. and resistivity interpretation 8=13641
 Eu metal, and antiferromagnetism 8=22459
 Fe, shape in para- and ferro-magnetic states 8=2089

Crystal electron states—contd**Fermi surface—contd**

- Ga, study, by u.s. geometric reson. 8=8935
 In, and band structure and Knight shift 8=22463
 Li, by positron annihilation 8=8937
 Mg, from de Haas-van Alphen studies 8=2102-3
 Mo, investigation by cyclotron resonance meas. to 1.6°K and 9.7 GHz 8=13664
 Mo, r.f. size effect 8=22464
 Mo, rel. to that of W 8=17887
 Mo-Re alloys, density of states rel. to paramag. susceptibility, obs. 8=22759
 Na, distortion rel. to lattice dynamics model calcs. 8=1838
 Na, from positron annihilation and enhancement factor 8=8975
 Ni, X₂ hole pockets, study by de Haas-van Alphen effect 8=2106
 Pb, calc. from Kohn anomalies 8=5114
 Pt, s- and d-like carriers, from de Haas-van Alphen effect 8=22752
 Re-Os alloys, theory of superconducting transition temp. h.p. anomaly 8=17972
 Rh, and de Haas-van Alphen effect 8=13643
 Sb, anisotropy, rel. to mag. resistance anisotropy 8=5432
 Sb, and Seebeck coefficient 8=22467
 Sc, calc. by cellular method 8=8942
 p-Sb₂Te₃, de Haas-van Alphen susceptibility meas. 8=9293
 Th, from de Haas-van Alphen studies 8=2294
 Ti, calc. by cellular method 8=8942
 W, "jacket" orbits and cyclotron resonance 8=13688
 W, rel. to that of Mo 8=17887
 Yt, calc. by cellular method 8=8942
 Zn, from cyclotron resonance meas. 8=13725
 Zn, non-local pseudopot. calc. 8=2111
 Zr, calc. by cellular method 8=8942
- plasma**
 alkali halides plasmon energy, e energy loss obs. 8=8938
 cathode metal electrons, plasma frequency rel. to vacuum arc voltage 8=16426
 coupled plasmon-particle excitation in electron gas 8=17900
 density waves in electron-hole plasma, classical study 8=2118
 electron gas collective description in generalized r.p.a. rel. to plasmon freq. 8=5143
 electron gas, electron-plasmon coupling approx., single-particle spectrum 8=5144-5
 electron-hole decay meas. by double-pulse variable-delay circuit 8=15177
 graphite, pyrolytic, two-stream instability, dispersion relations 8=8968
 Gunn effect domain, conductivity, temporary increase 8=5142
 Gunn effect, domain field distrib. for inhomogeneous doping 8=13783
 helicon waves, h.f. phase sensitive detection 8=5138
 helicon waves in solids 8=8965
 helicon waves, interaction with adjacent drift current, theory 8=2119
 high density, lifetime in semiconductor, obs. 8=13685
 insulator/semiconductor interfacial magnetoplasma wave instability 8=2116
 metal foil scattered radiation at plasma frequency 8=8958
 metal, giant oscillations, electron scatt. effect 8=5136
 metals in quantized mag. field, sound-like waves in electron plasma 8=17895
 metals, plasmon satellite in soft X-ray spectra, theoretical interpretation 8=13680
 micro plasma generation rel. to material damage in lasers 8=403
 plasmon excitation, mean free path of fast electrons 8=2117
 plasmons, two-phonon decay 8=17899
 polythene film, laser-produced formation mechanism 8=23034
 resonance emission process, quantum theory 8=8961
 semiconducting rod, lifetime and density distrib. 8=9069
 semiconductor bulk oscillator by self-excitation of plasma waves 8=18098
 semiconductor, collision induced instability 8=8964
 semiconductor crystal, conditions for oscillations generation 8=8957
 semiconductors, current oscs., growth rate calc. 8=13774
 semiconductor, electron-hole, excitation of l.f. waves 8=13683
 semiconductors, intrinsic, pinch effect and its mag. field dependence 8=9072
 semiconductors, ionization waves theory 8=18056
 semiconductors, Landau damping and phonon, plasmon and photon wave dispersions 8=9093
 semimetals, m.h.d. waves, plasma-phonon 8=5135
 surface plasmon, indirect coupling of photons 8=13684
 white tin films, plasmon energy-loss function from optical data analysis over 0.1 to 27.5 eV energy region 8=2456
 Ag, by photoexcited electrons, discrete energy loss 8=2279
 Al 15 eV loss, dependence of damping on scattering angle and crystal size 8=2121

Crystal electron states—contd**plasma—contd**

- Al, 50 kV electron mean free path for plasmon excitation, diffraction condition effect 8=13696
- Al, fine particles, surface oscillation 8=8967
- Al foils, oscillatory modes at surface, energy rel. to intensity 8=8946
- Al foils, plasmon excitation cross-sections by electrons 8=8966
- Al, produced by laser beam, energy spectra of ions 8=2122
- Bi, Alfen waves, high mag. fields 8=5146
- Bi, Alfvén wave damping, theory 8=8963
- Bi, two-stream instability, dispersion relations 8=8968
- CdS, longitudinal optical phonon-plasmon coupling 8=14206
- Cu, films, oscillations, interband transitions 8=5117
- GaAs, coupled optical-phonon-plasmon modes rel. to Raman scattering 8=22984
- n-GaAs, Raman scatt. by mixed plasmon-phonon modes, polarization and intensity obs. 8=5599
- n-Ge, electron hole plasma, helical density waves and oscillator effect, theory 8=17903
- Ge, pinch effect and breakdown in pure material 8=8956
- p-HgTe, i.r. reflection in region of plasma minimum 8=5262
- n-HgTe, magnetoplasma reflection at 296 and 85°K 8=13815
- InAs, light scattering by plasmons and Landau levels of electron gas 8=22990
- InSb, appl. of ionization wave theory, predictions of instabilities 8=18056
- InSb, n- and p-type, current instability under crossed electric and magnetic fields 8=2201
- n-InSb, magnetic-field-free electron-hole, and gigahertz radiation 8=8969
- n-InSb microwave emission during plasma formation 8=22600
- InSb θ pinch effect, 250°K 8=13821
- InSb, waves, X-ray scattering 8=5148
- KCl(Br) foils, resonance absorption of P-polarized light 8=2123
- MgO, optical props. rel. to plasma and electron energy losses 8=9550
- Na, electron sea polarization enhancement factor from positron annihilation 8=8975
- Na, random electric field stabilization 8=16599
- Na and K, helicon waves, nonlocal damping 8=17904
- Pd, by photoexcited electrons, discrete energy loss 8=2279

polarons

- antiferromagnetic crystal, magnetic polaron suggested 8=9068
- bound, ground-state energy 8=5133
- ferroelectric of 'light plane' type, interaction with spin waves 8=22481
- Hall mobility from perturbation treatment of Kubo's formula 8=13678
- Hall mobility temp. variation in Holstein model 8=8954
- hopping conduction, Hall effect theory 8=17998
- ionic crystal, single phonon electron lattice interaction 8=5134
- ionic, cyclotron resonance 8=2125
- low-mobility theory, range of validity extension 8=17892
- piezoelectric, motion at zero temp. 8=13677
- piezoelectric, strong coupling limit 8=8955
- α -quartz, polaron spectrum 8=2115
- rutile, rel. to carrier props. 8=17894
- semiconductors, intrinsic, rel. to interband magneto-optic absorpt. 8=18493
- theory 8=17893
- variational ansatz, theory based on Fröhlich's Hamiltonian 8=13676
- AgBr, internal states detection using piezo-optical transmission 8=13679
- in AgCl absorpt. edge structure 8=22955
- BaTiO₃, optical props. of small polarons 8=18505
- BaTiO₃, small, rel. to reflectivity and conductivity 8=5587
- CoO, hopping and narrow-band conduction 8=18059
- CoO, hopping model for elec. conduction 8=18060
- CoO, semiconducting, in near and far i.r. absorpt. 8=23008
- α -Fe₂O₃, hopping model for elec. conduction 8=18060
- InSb, abnormalities of donor spectrum in magnetic field 8=13817
- InSb, rel. to anomalies in interband magnetoabsorpt., Coulomb effect 8=22818
- KBr, cyclotron resonance 8=2124
- LaCoO₃, optical props. of small polarons 8=18505
- LaCoO₃, p- and n-type, rel. to optical absorpt. 8=2434
- NiO, hopping model for elec. conduction 8=18060
- NiO, hopping and narrow-band conduction 8=18059
- NiO, semiconducting in near and far i.r. absorpt. 8=23008
- SrTiO₃, optical props. of small polarons 8=18505

surface

- b.c.c. (100), calc. using tight binding approx. 8=5121
- conduction electrons, scattering by localized charges, meas. 8=22640
- f.c.c. (111), calc. using tight binding approx. 8=5121
- linear-atomic-chain models, Hartree-Fock calc. 8=17888
- in linear chain with next-nearest-neighbour interactions, existence of localized states 8=22470
- metals, electron states near boundaries 7=2113

Crystal electron states—contd**surface—contd**

- metallic interfaces, electron-gas model, exchange-correlation and lattice potentials effects 8=2112
- semiconductors, 1/f noise theory 8=13787
- semiconductor, rel. to voltage rectification across potential barrier 8=13786
- superconductor, e.m. wave absorpt. 8=9022
- AB-type mixed crystals, MO-TBA method 8=13667
- Al foils, plasma oscillatory modes at surface, energy rel. to intensity 8=8946
- BaTiO₃ doped with Sb₂O₃ 8=13790
- Co-hexagonal lattice, (001) surface, calc. using tight binding approx. 8=5121
- p-Ge, complicated hole energy spectrum, effect on low field transport props. 8=18055
- Ge, on clean surface, study of origin 8=13814
- PbO layers, vapour-deposited, elec. behaviour 8=8941
- Se, vitreous, electronic processes in photocrystallization 8=22471
- Si, from charges in oxide coating 8=22469
- Si, from field effect kinetics study 8=22472
- Si shallow donors ground and optically excit. states calc. 8=9126
- Si-SiO₂ interface, thermal oxidation, effect of Na impurity 8=14384
- Crystal energy.** See Bonds; Crystals; Solids/structure.
- Crystal fields.** See Crystals/internal fields.
- Crystal imperfections**
- See also Colour centres.
- alloys, deformed f. c. c., intrinsic stacking-fault tetrahedra formation 8=22215
- alkali-halide crystals, containing CO₂, NO₂, NO₂, SO₂ impurities, local vibr., i.r. absorpt. spectra 8=14197
- alkali-halides, divalent cation impurities and dipolons, conc. correlations 8=8701
- alkali halides, etch figures of fission fragments, flat bottomed 8=8707
- alkali halide, induced i.r. absorption by substituted alkali or halide ions 8=9481
- alkali halides, radiation defect formation 8=13487
- alkali iodides, e.s.r. of Se⁻ and SSe⁻ impurities 8=14123
- anthracene rel. to delayed fluoresc. decay time, vars., 2-300°K 8=23065
- anthracene, vapour- and melt-grown 8=21942
- atom impurity, velocity, anharmonic contrib. 8=13035
- binary cpds., inorganic, point defects rel. to stoichiometry 8=8689
- brass, 70-30, deformation texture development rel. to stacking fault frequency, pole figure 8=17777
- conductors, macroscopic defects, detect. by elec. tests 8=8706
- carbons, soft, structural defects, heat treatment 8=1955
- cold worked, impurities rel. to modulus effect 8=22332
- corundum, complexes of bound ions, group-theoretical classification 8=8887
- defects annealing in crystals, observation 8=1933
- diamond, etch pits and trigons 8=1725
- diamond, particle-counting effect 8=6647
- diamond, trigon origin in defects and relation to growth failure 8=4787
- diffusion kinetics, pressure influence 8=8669
- disordered molec. crystals, theory of exciton bands 8=8949
- disordered, one-dimensionally, close-packed structures with stacking faults, diffraction theory 8=8476
- distortions, non-spherical, diffraction contrast 8=8688
- disturbed lattices, dispersion dynamics 8=1834
- doping, non-uniform, effect on Gunn domain propag. 8=13783
- excited impurity states from model potential of two-valence electron systems 8=23035
- f. c. c. lattice, monatomic, impurity-induced i.r. absorpt. 8=9480
- f. c. c. materials, interpretation of defects in field ion images 8=22196
- ferromagnet, Heisenberg, with magnetic impurity, diffuse inelastic neutron cross section 8=9319
- ferromagnets, non-mag. impurities, local magnetization calc. 8=13987
- field-ion images, from asymmetric specimens, streak contrast 8=8452
- foils with stacking fault, fine structure of weak electron diffraction beams 8=1781
- gas bubble collisional coalescence in solids 8=4695
- grain boundary gas bubbles, equilib. conditions 8=1986-9
- grain boundaries, growth of pores rel. to tensile stresses 8=17676
- grain-boundaries, high-angle, development of island model 8=22218
- grain-boundary precipitates, growth kinetics 8=13445
- hardening, atomic block theory, existence of extremums of property impurity curves 8=8803
- h.c.p. metal (Y and rare earths) hydride habit and deformation planes 8=8728
- ice cavities filled with air, vapor and brine, migration under temp. gradient 8=1991
- ice, spiral air bubbles, formation 8=4989
- impurities and current carrier scatt., kinetic eqn. 8=22423

Crystal imperfections—contd

impurities, effect on force constants 8=1952
 impurities, effect on phonon spectrum 8=1960
 impurities in crystals with stoichiometric vacancies, thermodynamic model 8=17614
 impurities, trace, effects in X-ray diff. topography 8=18791
 impurity atoms, vibrational and optical props. from impurity, density of conduction e states in dilute alloy 8=5112
 impurity ion, lowering of Slater parameters 8=8700
 inclusion, cuboidal, diff. contrast 8=8688
 inclusions, influence on ductile fracture with rotation 8=17729
 insulators, meas. by complex dielectric constant method of trace characterization 8=18757
 intermetallic cpds. of CsCl structure, formation energies rel. to comp. and ordering 8=17623-4
 ionic compounds, stacking fault energies 8=13441
 irradiated material, coalescence, dislocation loops and pores 8=17632
 lattice with one substitutional impurity, electron density calc. 8=22443
 laser-beam thermal effects in transparent crystals 8=4926
 lattice defects conc., effect on diffusion, using radionuclides 8=22141
 lattice dynamics, influence of defects: appl. of new formalism 8=13312
 metal, impurity microsegregation on liq. stream interaction with solidification front 8=17224
 metal, impurity screening, preasymptotic form 8=8907
 metal oxide, hypostoichiometric, partially ordered defects, statistical model 8=17600
 metals, b.c.c., radn. effects rel. to production, and diffusion 8=17702
 metals, cause of increase in positron lives 8=2127
 metals, electrostatic energy calc. of growth and deformation stacking faults 8=8201
 metals, h.c.p., deformation planes after dehydrogenation and hydride habit planes 8=8728
 metals, mechanical properties, rel. to stacking faults 8=22305
 metals, quenched, rel. to Bauschinger effect 8=5020
 microscopic exam., optical and electron 8=17269
 Nimonic 80A grain boundary cavities rel. to creep props., 600-750°C 8=5083
 nonstoichiometric compounds, point defects, thermodynamic considerations 8=1934
 optical absorption in diatomic chain, impurity effect 8=9477
 optical, e-microscope and diffraction studies, technique and limitations 8=17597
 p-n junctions electrical breakdown due to 8=9150
 paramagnetic crystals, impurity centres, absorpt. and emission of light 8=5574
 in Permalloy films, caused by plastic deform., effect on mag. anisotropy 8=14031
 phosphors, Tb³⁺ activated, radiative transition probabilities in Tb³⁺ 8=4683
 physical acoustic, principle and methods: the effect of imperfections, book III A 8=17485
 point defects, rel. to bulk and local elastic constants 8=22260
 point defect location by X-ray diff. topography 8=17602
 point defect, rel. to thermodynamic characts. calcs. 8=13362
 point defects and disorder, effects on vibrs. of crystals 8=13327
 point defects, influence of force-const. changes on lattice dynamics 8=13319
 point defects, interaction with dislocation ribbons, elastic-modulus effect 8=17603
 point defects, long range effects on dislocation-free crystal growth 8=4797
 point defects, rel. to mag. after effects in ferromag. mats. with domains 8=18321
 polyethylene, fold-surface struct. 8=17214
 polyethylene, point defects, molecular mechanics 8=1938
 potash feldspar, Rb impurities effect on Al-Si order 8=17618
 quartz impurities on annealed semiconductor surfaces 8=9087
 scattering of long wavelength neutrons, mathematical formulation 8=22167
 Schottky defects, energy of formation 8=8692
 semiconducting devices, internal structural defects, testing by electrical methods 8=18100
 semiconductors, differentiation of lattice defect types 8=9067
 semiconductors, displacement of energy levels by interactions 8=5109
 n-type semiconductors, effect on transport props. 8=5226
 semiconductors, impurity redistrib. during thermal oxidation 8=18015
 semiconductors, impurity redistribution for out-diffusion 8=5229
 semiconductors, micro-inhomogeneities 8=18013
 space charge conduction for studying 8=5158
 stacking fault energies, extrinsic to intrinsic relative magnitudes, in f.c.c. solids 8=17666
 stacking-faulted, electron-diff. image calcs. 8=13234

Crystal imperfections—contd

stacking faults, X-ray diff. image 8=13442
 stacking faults in close-packed AB₃ superlattices 8=17667
 static distortions, Borman effect from diffuse scatt. 8=13415
 steel, austenitic, B impurity distribution 8=13040
 steel, stainless, grain boundary CrC precipitation, e probe obs. 8=17677
 steel, stainless, inclusion counting by e probe micro-analyser 8=17616
 steel, stainless, n-irradiated, voids obs. 8=22251
 steel, structural, rel. to temper brittleness reversibility 8=17626
 steel surface, mechanically worked, stacking faults obs. by e-microscopy 8=17675
 steel, surface segregation of Cr obs. by Auger electron emission 8=22730
 steel, surface segregation of S obs. by Auger electron emission 8=22730
 steel, surface segregation of Sb obs. by Auger electron emission 8=22730
 steels, intergranular fracture 8=22222
 striations, due to temp. fluctuations, in flux growth 8=13449
 structural defects in epitaxial thin films, role in nucleation 8=1735
 superconductors, type II, lattice defects of flux lines 8=13734
 transitions of electrons, theory 8=13039
 vibrational modes associated with defects 8=4900
 walk-counting method for c.p. lattices rel. to energy bands and impurity states 8=8604
 wustite, Mg doping and grain size dependence of Seebeck coeff. rel. to p to n transition 8=5387
 X-ray detect. by pseudo-Kossel lines, obs. 8=17598
 X-ray scattering by Coulomb displacement fields of defects, kinematic theory 8=13223
 Zircaloy-2, grain boundary effects in deformation 8=13447
 Ag alloys, dilute, stacking-fault energy from extended node meas. 8=17669
 Ag, effect on temp. dependence of heat capacity 8=13368
 Ag, on hydrogen embrittlement 8=22307
 AgBr microcrysts., rel. to impurities and surface reactions 8=8698
 AgCl, state of Fe impurity ions 8=1657
 AgCl + CdCl₂, state of Fe impurity ions 8=1657
 AgI, state of Fe impurity ions 8=1657
 Ag-Ni alloys, f.c.c. stacking and twin faults 8=4988
 Ag-Zn alloys, deformed, stacking faults and twin-fault probability 8=17668
 Al, e-irradiated, deformation at 20°K rel. to dislocation model with defect barriers 8=13523
 Al, grain boundary sliding, isothermal shear test 8=22221
 Al, lattice defects recovery after tensile deformation 8=22184
 Al, n-irradiation damage and recovery rel. to impurity doping effect 8=1953
 Al, quenched, interaction of point defects with dislocation 8=8690
 Al, stacking fault energy calcs. using pseudo-potentials 8=17673
 Al, stacking fault removal induced by n irradi. 8=17670
 Al, stage I recovery atomic recoil energy dependence from e-irrad. data 8=4961
 Al, sub-boundaries in single crystals grown from melt, direct observation 8=17678
 Al surface, mechanically worked, stacking faults obs. by e-microscopy 8=17675
 Al alloys, lattice defects recovery after tensile deformation 8=22184
 Al-Ag alloys, stacking faults, in GP zones and matrix rel. to plasticity 8=8821
 Al and AlM, (M = Mg, Ga, Ag), e-irradiated, stage II and III recovery temp. and impurity conc. dependence 8=1935-6
 Au-Cd binary system, point defect segregation at melting rel. to comp. 8=17624
 Al-4% Cu, deformational instability rel. to defects 8=8816
 Al-Mg alloys, Mg atom clustering, electronic origin 8=13636
 Al-Zn, lattice defects and aging phenomena 8=13536
 Al-Zn-Mg, lattice defects and aging phenomena 8=13536
 Al₂O₃, irradiation damage on exposure to 5 × 10²¹ fast neutrons cm⁻² 8=22244
 Au, collapsed tetrahedra and stacking fault energy 8=22216
 Au, effect on temp. dependence of heat capacity 8=13368
 Au, quenched, defect behaviour and slip channel formation on plastic deformation 8=17663
 Au, quenched, stacking fault tetrahedra as vacancy sinks 8=13443
 Au-Pt alloys, annealed, rel. to X-ray diff. "tails" 8=17341
 Be, n-irrad. induced, obs. of clusters by long-wavelength n-scatt. meas. 8=22177
 BeO, twinned, twin boundary decoration by n-irrad. at high temps. 8=22199
 Bi films, condensed, structure defects 8=8705
 Bi, Ag¹¹⁰ diffusion, dependence on crystallographic direction 8=13407

Crystal imperfections—contd

- Bi-Sb films, 2-layer, struct. defects by Moiré method 8=22186
 CdS rel. to luminesc. centres 8=8741
 CdS: Au, photosensitive carrier e.s.r. 8=2362
 CdSe: Mn, photoconductivity rel. to Mn deep donor level 7=2259
 CeO₂, non-stoichiometric, defect structure model 8=22166
 CdTe, rel. to absorption edge 8=5603
 Co alloys, f. c. c., rel. to ageing effects after cold-working 8=17622
 Co complex, tris-dipyridyl Co(III) perchlorate, trihydrate, ⁵⁷Co²⁺-doped, electron exchange 8=2082
 Co-M alloys (M = Cr, Fe, Ni, Cr-Ni), structural defects and precip. 8=17621
 Co-Cr 10% alloys intrinsic stacking faults, cubic-hexagonal interface, contrast effect 8=8459
 CoO: Li, Co interstitials, contribution to defect structure rel. to conductivity 8=1956
 CsCl-structure alkali halides, Schottky defects, energy of formation 8=8694
 CsF: Na⁺, impurity displacement calcs. 8=8243
 Cu, cold worked, impurities rel. to modulus effect 8=22332
 Cu crystal, slip band development on n-irradiation 8=22212
 Cu, defect concentrations from cyclic stressing at room temp., resist. studies 8=17604
 Cu, deformation texture development rel. to stacking fault frequency, pole figure 8=17777
 Cu, effect on temp. dependence of heat capacity 8=13368
 Cu, fatigued at low strain amplitude, surface slip lines and interior planes 8=17774
 Cu films, grain boundary cavity form. during high temp. creep 8=13547
 Cu foils, ion irradi., agglomerates formation and density 8=13417
 Cu foils, ion irradi., analysis of type and configuration of clusters 8=13416
 Cu, neutron-irradiated, annealing effect on lattice parameter 8=1937
 Cu polycrystals, grain boundary cavities 8=13448
 Cu, rel. to quench hardening 8=22334
 Cu, stacking fault energy calcs. using pseudo-potentials 8=17672
 Cu-Al alloy, stacking faults in β'-martensite phase 8=17674
 CuCl, and Czochralski growth 8=4804
 CuI, defect struct. and catalytic props. 8=22169
 Cu-Ni alloys, stacking fault density, conc. depend., by X-ray analysis 8=17671
 75 Cu-25 Ni laminate on Cu core in coinage composite, voids in bond degradation mechanism 8=22329
 Cu₂O rel. to n=1 exciton line profile, 4.2-112°K 8=9527
 Cu-Sb alloys, stacking fault X-ray meas. 8=17672
 Fe, coarse grained polycrystalline, under tensile deformation 8=1985
 Fe, form. of cloud group of inclusions by Al deoxidation 8=22183
 Fe, intergranular weakness rel. to fatigue damage 8=5060
 Fe, point defects recovery after low-temp. deform. 8=13418
 Fe, (Al, Ga, Si, Ge, Sn, Sb) impurities, magnetization distribution 8=9349
 FeCl₂: Fe³⁺, Mn²⁺, impurity spin resonance at low temps. 8=14108
 FeCo alloy, grain boundary theory 8=17258
 FeO, defect structure rel. to conduction mechanism at high temps. 8=18166
 Fe-Rh alloys, structural defects, phase transformations 8=9395
 GaAs, impurity effect on ultrasonic absorpt. subject to infrared radiation 8=13352
 GaAs, impurity photoionization, quantum defect study 8=2207
 GaAs, Zn-diffused, precipitates 8=17617
 p-Ge, bombardment-produced defects at low temps. 8=22170
 Ge, rel. to absorption edge 8=5603
 Ge, effect on dust elec. charge 8=13812
 Ge, impurity photoionization, quantum defect study 8=2207
 in Ge, As and Sb impurities, excitation spectra, under uniaxial compression 8=13424
 Ge: Li(P), impurity vibrational modes rel. to i.r. absorpt. 8=9532
 HfO₂, structural 8=9198
 InSb, Corbino magnetoresistivity effect 8=5266
 K halides, monatomic impurities rel. to phonon scattering 8=4904
 KBr, impurity anion form. conditions 8=8745
 KCl, electric breakdown, directional, single crystals 8=18167
 KCl, γ-irradiated near room temp., defect production and annihilation 8=8696
 KCl: Ag point defects rel. to Ag colour centres form. obs. 8=8746
 KCl: Ag: OH point defects rel. to Ag colour centres form. obs. 8=8746
 KCl: Ag: Sr point defects rel. to Ag colour centres form. obs. 8=8746
 KCl: Be⁺, substituent behaviour from ionic thermocurrent spectra 8=8702

Crystal imperfections—contd

- KCl(Br): Li⁺, impurity displacement calcs. 8=8243
 KCl: OH⁻, cooling to 0.36°K by adiabatic depolarization of OH⁻ 8=1874
 KH₂PO₄, after reactor and fission fragment irradi. 8=8773
 KI, analysis of TI impurities 8=17237
 KI: Ti⁺, Ti⁺ clustering from absorpt. and emission spectra at 77°K 8=23056
 KX: Cu⁺, (X = Br, Cl, I), lifetime of excited Cu⁺ 8=23057
 Li, point defects, thermo- and electrotransport 8=22157
 Li ferrite, X-ray topography of defects 8=8708
 LiF, lattice distortion around V_K centre, ENDOR study 8=2009
 LiF, radiation defect formation 8=13487
 Mg aluminate spinels, defect structure and mech. props. 8=22187
 Mg, stacking fault energy calcs. using pseudo-potentials 8=17673
 Mg₂Cd, antiphase boundaries, size, shape and orientation 8=17679
 MgO, grain boundary sliding strain prod. 8=13584
 MgO, impurity distribution 8=13450
 MgO lattice, Mn impurity, h.f.s. of spectrum 8=14238
 Mn ferrites, Mn³⁺ clustering, influence on elec. props. 8=13720
 Mn steel, effect of multiple γ = (ε, ε') transformations on structural defects 8=17785
 Mn-Fe spinels, Mn-rich, Mn³⁺ clustering effect on ferromagnetic resonance linewidth 8=18396
 NaCl-type crystals, lattice distortion by impurities and n.m.r. line splitting 8=9455
 NaCl: Ag phosphors, photo-excited F-colour centres, microdefect interactions 8=2013
 NaCl: Be⁺, substituent behaviour from ionic thermocurrent spectra 8=8702
 NaCl: Cd, aggregation of divalent impurities 8=13425
 NaCl: CaCl₂ + NaOH crystal, dielectric loss maxima and conductivity 8=5164
 NaCl: Mn²⁺, lattice defect effect on hyperfine interactions 8=18431
 NaCl, pure and doped, pot. differences due to plastic deform. temp. dependence 8=16978
 NaCl with Sr, Cd, Ag, Ca and TI impurities, rel. to F-centres stability 8=8751
 NaI(Tl) crystals, Pb⁺ impurity effect on particle detector props. 8=6646
 Nb, superconducting, defects produced on n-irradiation 8=2169
 NH₄Br, Cu²⁺ doped, e.p.r. 8=14102
 NH₄ClO₄, lattice defects, enthalpy of formation 8=2128
 Ni, surface segregation of S obs. by Auger electron emission 8=22730
 NiO, nonstoichiometric, defect model 8=13826
 Ni₂Sn, antiphase boundaries, size, shape and orientation 8=17679
 Pa, Fe impurity atom, range of spin perturbation 8=1655
 Pb-Sn alloys, degenerate structure and fault formation on solidification 8=4785
 Pb-Sn alloy polycrystalline, atomic block theory of hardening investigation 8=8803
 Pb-Sn, Na conc. at grain boundaries 8=8344
 Se, oxygen impurity and crystallinity on photosensitivity spectrum 8=18237
 Si, deep-level impurities, interact. with lattice defects, other impurities, and i.r. absorpt. 8=22607
 Si, electron-beam heated, triangular macrodefect, X-ray topography 8=1862
 Si, epitaxial layers, "hillock" formation 8=17619
 Si epitaxial layers, stacking faults, cause and cure 7=8736
 Si, extrinsic faults, climb 8=22217
 Si, impurity diffusion anomaly 8=13427
 Si, impurities testing by non destructive neutron activation method 8=18086
 Si, impurity photoionization, quantum defect study 8=2207
 Si, paramag. centres produced along proton range 8=8704
 n-Si, e-irradiated, elec. props. rel. to impurity and irradiation-temp. dependence 8=5282
 n-Si, n-irradiated, elec. props. rel. to defect structure and annealing 8=5283
 p-Si thermally quenching effects on 8=18084
 Si web dendrite, stacking faults, contrast in X-ray topographs 8=1983
 Si, Au-diffused, precipitates formation 8=17620
 Si, B-doped, impurity redistrib. during thermal oxidation 8=18015
 Si, B-doped by ion bombardment, B distrib. profiles 8=18071
 Si: B, "internal" impurity spectrum, conc. depend. 8=13428
 Si: Li, e irradi. prod., and annealing at 20°C, 1 MeV 8=22604
 Si: Li, radiation defects, effect on annealing rate 8=2067
 Si: P, defect production on e-irradiation rel. to spin-lattice relax. 8=18434
 Si, P-doped, irradi., annealing of the Si-E centre 8=2209
 Si: Sb, melt-grown, tetrahedral defects 8=1958
 Sn alloys, dilute, microsegregation nodes and cellular solidification substructures 8=16919
 SrCl₂, pure and Y³⁺ (Na⁺) doped, rel. to ionic conduction and diffusion mechanisms 8=8983

Crystal imperfections—contd

- SrCl₂, reaction intermediate with F₂ 8=14124
 SrF₂, Gd³⁺ impurity centres, temp. effects 8=8703
 SrO, defect structure studies 8=22171
 Te, low-angle subgrain boundaries and dislocation motion 8=8737
 TiC, B-doped, TiB₂ precip. as defects 8=4967
 Ti₂O₃ single crystal, impurity segregation during growth from melt 8=4817
 TiCl₃, Schottky defects, form. and motion from conductance meas. 8=9200
 UO_{2+x} lattice defects rel. to thermochem. props. 8=23113
 W, neutron irradi., rel. to elec. resist. and hardness 8=2141
 W, point defects due to n-irrad., migration in annealing 8=17601
 W, stacking faults, electron micr. obs. 8=1984
 YFe garnet rel. to domain configs., obs. 8=22863
 Y₂O₃ grain-boundary segregation and final-stage sintering 8=13444
 Zn, damage caused by electric spark discharge machining 8=1959
 Zn, stacking fault energy calcs. using pseudo-potentials 8=17673
 Zn-0.03 at.%Cd, Al, Cu or Ag, substructure rel. to impurity distrib. coeff. 8=17296
 ZnO single crystal, γ -irradiated 8=22168
 ZnS, polytype families, from recurrent slip 8=8564
 ZnSe crystals, recombination centre parameters 8=18627
 α -Zr, deformed, form. of polygonized sub-structure 8=22219
 (Zr,Hf)_{0.955}N, defect structure by chem. and lattice studies 8=17434

dislocations

- alkali halides, and optical birefringence 8=18501
 alkali halides, Peierls stress estimation 8=1968
 alloys with coherent, ordered, stressed precipitates, motion, derived mechanism 8=1978
 alloys, deformed f. c. c., rel. to intrinsic stacking-fault tetrahedra formation 8=22215
 alloys, Nimonic type, stability of structures 8=17643
 alloys, ordering, and antiphase boundaries rel. to plastic deformation 8=17634
 alloys, worked, superconducting, distrib. rel. to critical current density 8=9029
 anisotropic crystals, stresses of piecewise straight type, forces at bend, and motion 8=17628
 anthracene 8=17648
 austenitic stainless steel foil, formation of loops 8=17654
 β -brass, hexagonal networks 8=22204
 calcite, topographical study 8=13436
 climb forces 8=4972-3
 continuum theory, boundary problems 8=17636
 Cottrell atmos. formation around dislocations, kinetics rel. to strain ageing 8=4969
 crack nucleation from pile up, criterion 8=17744
 deformation twin growth, effect on 8=13124
 dipole accumulations in planes, rel. to dilatation 8=8714
 dissociation width dependence on dislocation velocity in f. c. c. crystals 8=17638
 distribution effects on crystal volume changes 8=17631
 in Earth's mantle, velocities rel. to deformation 8=14544
 edge, direct viewing 8=1962
 edge, X-ray diffr. contrast exam. 8=13207
 electron microscope pictures, computer generation 8=8709
 f. c. c. crystals, configuration of ions near edge dislocation 8=22191
 f. c. c. crystals, new configurations 8=22190
 f. c. c., equilib. configuration of dissociated jogs 8=8718
 f. c. c. metals, elastically anisotropic, shear stresses of tilt boundaries of {111}, 1/2 {110} dislocations 8=22195
 f. c. c. structure, sequence of partials 8=13429
 faulted dipoles, contrast calcs., and stacking-fault energy meas. 8=8717
 ferromagnet, elastic and magnetic fields around dislocation 8=18316
 ferromagnets, relaxation by two-magnon scattering 8=14078
 field-ion micrograph interpretation of contrast from dislocation loops 8=17633
 flexible, equilib. shape under internal and external stress influence 8=1961
 force on dislocations emerging at free surfaces 8=22188
 geometrical eqn. of Hollander, criticism 8=8712
 graphite:ICl, impurity-dope effects on anelasticity 8=13541
 graphite, rel. to electronic props. 8=5384
 ice, and plastic deformation 8=4977
 insulators, binding with electrons, holes and excitons 8=5349
 internal friction rel. to optical properties of dielectrics 8=14165
 ionic crystals, NaCl-type, dissociation on {110} planes 8=22192
 in ionic mats, rel. to necessary conds. for plastic deformation 8=13511
 irradiated material, coalescence, dislocation loops and pores 8=17632
 lattice disturbed by dislocation, model 8=17307
 layer structures, enhanced chemical reactivity at

Crystal imperfections—contd**dislocations—contd**

- linear defects, imaging in 'spectral' position, with X-rays 8=4968
 loops from contrast in field-ion micrographs 8=17633
 loops, elastic interact. rel. to plastic flow velocity 8=8720
 loops in superlattices, computer analysis 8=8719
 martensite carbon strength rel. to thermally activated deformation 8=22351
 metals, dynamics rel. to repeated discontinuous yielding 8=22274
 metals, elastically anisotropic f. c. c., shear stresses and energies of $\frac{1}{2}$ {110}, {111} edge, new data 8=17640
 metals, f. c. c., formation and configurations of faulted dipoles 8=8716
 metals, rel. to fatigue crack growth model 8=17740
 metals, hexagonal, stress fields due to dislocation pile-ups on anisotropic treatment 8=1963
 motion, thermally activated, in periodic internal stress field 8=8711
 motion, uniform, at transonic and supersonic velocities 8=8713
 movement in ionic crystal, radiation of electromagnetic and acoustic waves 8=17637
 nodes, equilib. of pinned triple node, and stable configs. of single node 8=17635
 nucleation on external and internal surfaces 8=1964
 nylon, dislocation motion interpretation of plastic flow rates 8=2074
 partial, central, of triple ribbons, anomalous contrast 8=13428
 Peierls barrier calcs. from Frenkel-Kontosova model 8=17642
 piezoelectric, fields, and of linear charges 8=5375
 pile-ups, associated to amplitude-dependent internal friction 8=13496
 polyethylene, mechanism for deformation 8=2072
 problems in theory, present status and prospects for advance 8=22193
 quartz, screw, optical striations 8=4982
 ruby, examination by X-ray topography 8=13434
 screw, image evaluation using kinematical theory of e-diffr. 8=22194
 screw type, effect on cryst. growth 8=13131
 semiconductors, effect of non-uniformity on kinetic phenomena 8=13780
 solid containing multiple spectrum of dislocation obstacles, thermally activated motion 8=22189
 solid, internally stressed, mobility 8=8715
 steel Armco, rel. to work hardening 8=5067
 steel, austenitic stainless, in different fatigue stages, structure 8=22205
 steel EI702, effect on deformation 8=13570
 stress-assisted diffusion theory and strain ageing 8=4969
 symmetry considerations 8=13430
 sucrose 8=4983
 thermodynamic force 8=17641
 thick plate surface loops rel. to sinusoidal surface temp. cycling 8=17630
 two-phase materials, equilib. eqns. for pile-ups 8=17639
 widths in anisotropic b. c. c. crystals 8=4970-1
 work of core tractions, importance rel. to total energy, and meaning 8=17629
 Zorski theory, extension to superfluid vortex 8=10807
 Ag, Bordoni relaxation 8=22197
 Ag crystals, well-annealed, stress at which dislocations multiply 8=13545
 Ag, effect of impurity 8=8722
 AgCl, etching 8=1965
 Al, annealed, helices and large loops, X-ray topography 8=17647
 Al, e-irradiated, deformation at 20°K rel. to dislocation model with defect barriers 8=13523
 Al foil, dynamic behaviour on deformation continuously observed 8=13433
 Al, formation during slow heating and cooling 8=8723
 Al, Frank sessile loops transform. to perfect loops on n irradi. 8=17670
 Al, quenched and degassed, form. of loops 8=1966
 Al, quenched, nucleation rates for loops 8=17645
 Al, void annealing by self-diffusion along dislocations 8=13432
 Al, zone-refined, densities and configs. during slow heating and cooling 8=22198
 Al alloys, multiplication, transmission electron microscope obs. 8=13435
 Al-2%Mg alloy, network knitting on stress-induced climb 8=17644
 Al-Mg-Zn alloys, rel. to ductility, inc. precipitate zones and boundaries 8=17646
 α -Al₂O₃, sintered, non-basal, Burgers vectors 8=1967
 Au crystals, well-annealed, stress at which dislocations multiply 8=13545
 Au, quenched and aged, structure 8=22185
 Au-Cd alloys, quenched and aged, structure 8=22185
 Au-Zn alloys, quenched and aged, structure 8=22185
 BaTiO₃, -90° domain boundary interactions 8=8724
 Be single crystals, formal during growth and deformation 8=1969

Crystal imperfections—contd

dislocations—contd

- BeO, emergence on crystallization and effect on crystal growth 8=1736
 BeO, n-irrad. at high temps., loops 8=8761
 BeO polycrystals, high temp. obs. 8=13539
 BeO, twinned, n-irrad. decoration at high temps. 8=22199
 Bi crystals, multiplication 8=8732
 Bi₂Te₃, diffusion of Cu, etch pits of Cu along dislocations 8=1914
 Cd, slip planes in plastic deformation 8=8725
 Cd, vapour-grown, rel. to growth patterns 8=4803
 CdS, growth of bulk crystals, containing 10³ dislocation/cm² 8=17228
 CdS, rel. to shift of exciton spectrum lines 8=13673
 CdS, vapour grown, origin obs. 8=8726
 Co, on Cu, pseudomorphic deposits 8=21881
 Cr on Ni, pseudomorphic deposits 8=21886
 CsI, charge density and behaviour 8=17649
 CsI, density, isothermal annealing effect 8=17650
 CsI etching 8=1727
 Cu crystals, plastically deformed, distrib. rel. to dispersed phase effect 8=4974
 Cu crystals, well-annealed, stress at which dislocations multiply 8=13545
 Cu, density, effect on mechanical props. 8=13550
 Cu, explosively deformed, structure 8=17651
 Cu, mobility rel. to shear stress 8=1970
 Cu, neutron irrad., pinning 8=1974
 Cu, n-irradiated, small loops, type 8=13437
 Cu, n-irrad., with vacancy dislocation loops, thermally activated motion 8=22189
 Cu, p-irradiated, platelets of interstitial atoms rel. to loops 8=22202
 Cu, rearrangement role in elastic mod. recovery after deform. 8=22337
 Cu single crystal in stressed condition, dislocation arrangement, electron microscope obs. 8=22201
 Cu, resist. and density, expl. determ. 8=9004
 Cu, screw, charge density redistribution, electric field gradient 8=5176
 Cu and Cu-Si solid solutions, motion, nature of obstacles 8=22200
 Cu-Al solid solution validity of Cottrell-Stokes law 8=8721
 Cu₃Au alloy, low order, loops, and stacking faults 8=8695
 Cu-Al-Zn alloys, rel. to phonon scattering 8=22203
 Cu-4.6 at.% Ga, density increase causing thermal conductivity decrease 8=8658
 Cu-Ga solid solution validity of Cottrell-Stokes law 8=8721
 Cu-Ni-Co alloys, movement from critical shearing stress temp. dependence 8=1971
 Cu₂O, plastic deformation by motion of a {100} dislocations on {100} glide planes 8=22327
 Fe, b.c.c., screw dislocation core structure 8=4976
 Fe, crystalline, rel. to strengthening by step-wise low temp. creep 8=2054
 Fe, H-charged internal friction rel. to H interstitial-dislocation binding 8=4965
 Fe on hot Cu, rel. to pseudomorphic growth 8=21880
 Fe, moving, frictional forces 8=22206
 α-Fe, rel. to plastic deform. and strength 8=4975
 Fe, purified, motion studied by amplitude-dependent internal friction and induced modulus defect 8=13557
 Fe-Al 40 oil quenched alloy, influence of ordering 8=13438
 FeCl₃-graphite cpd. 8=1972
 Fe-Ni-Cr aged alloy validity of Cottrell-Stokes law 8=8721
 Fe-3%Si, movement in elastic deform. 8=17661
 α-Fe₂O₃, whiskers on Fe 8=17250
 Fe₃O₄, fine grained, coercivity 8=9343
 Fe-3.5 at.% V alloy moving, frictional forces 8=22206
 GaAs, rosette structure temp. dependence, 20-800°C rel. to doping effects 8=17809
 GaAs, vapour grown, twins and stacking faults obs. 8=1982
 GaSe, on basal planes, visualization with established optimal etchant 8=1973
 n-Ge, edge, rel. to surface recombination changes 8=22591
 Ge, edge-type, cyclotron resonance study 8=9106
 n-Ge, effect on galvanomagnetic props. 8=22592
 Ge films, charge-carrier mobility, scattering in bulk material 8=9107
 Ge, Hall effect, optical effects 8=1979
 Ge, investigation by Borrmann's method: appl. of asymmetric exposures 8=17655
 Ge lattice, rel. to structure of kinks and steps 8=8727
 Ge point contact diode, etch pits due to plastic deform. 8=5326
 Ge, screw and edge damping in internal friction 8=22370
 n-Ge single crystal, effect on electrical properties 8=18053
 Ge, n-type, space-charge cylinders, overlapping phenomena 8=17656
 Ge, thin foils, arrangements after crystallization 8=1975
 KBr, dynamic characts. by internal friction method 8=8730

Crystal imperfections—contd

dislocations—contd

- KBr, mobilities, temp. depend. 8=8729
 KBr, n. m. r. rel. to type and orientation of dislocation 8=14146
 KCl, absorpt. of ultrasound, rel. to freq. 8=8630
 KCl crystal, density dependence on compressive force obs. 8=8731
 LiF, mobility, effect of hydrostatic pressure 8=1976
 LiF single crystals, sub-grain boundaries by limited projection topography 8=13446
 LiF, surface layer structure, props. after annealing 8=8378
 MgO:Ba, effect on Ba diffusion 8=4954
 Mo crystals, velocity-stress relations from strain-rate sensitivity of flow stress 8=17657
 Mo, etch pitting 8=4978
 Mo, impurity effects on strain hardening 8=22380
 Mo, mobility rel. to amplitude depend. of internal friction 8=22209
 N₂ solid, electron microscope investigation 8=8465
 NaBr, n. m. r. rel. to type and orientation of dislocation 8=14146
 NaCl, crystal etching by formic acid 8=17658
 NaCl crystal density dependence on compressive force obs. 8=8731
 NaCl, mobility, photoexcitation 8=4979
 NaCl, quenched, structure on {100} faces 8=22207
 NaCl, structure on light impulse exposure 8=17659
 NaCl:Ag rel. to F-centres thermal stability, microspectrophotometry obs. 8=8749
 NaI, density, isothermal annealing effect 8=17650
 NaNO₃ and cryst. growth, obs. 8=21957
 Nb crystals, structures, chemical and electro-etched, optical microscope obs. 8=22208
 Nb foil, density and flow stress, effects of grain size 8=4980
 Nb, mag. flux lines interaction, 4.2°K 8=22210
 Nb, mobility rel. to amplitude depend. of internal friction 8=22209
 Nb, superconducting, rel. to n-irradiation 8=2169
 Ni, crystalline, rel. to strengthening by step-wise low temp. creep 8=2054
 Ni, density deformation-dependence and upper temp limit 8=2064
 Ni, effect on mag. susceptibility. 8=22830
 Ni, polygonization rel. to recrystallization 8=4808
 Ni alloys, effect on γ' particles form. 8=21993
 Ni-base alloy, fatigued at several temps. 8=4981
 Ni:Al₂O₃, sintered, movement resistance rel. to flow stresses 8=2048
 Ni-60 at.% Co, density increase causing thermal conductivity decrease 8=8658
 Ni₃(MnCo) ordered alloy validity of Cottrell-Stokes law 8=8721
 Ni-Mn-Fe order alloy validity of Cottrell-Stokes law 8=8721
 Ni₃Mn order alloy validity of Cottrell-Stokes law 8=8721
 Ni₃Si alloy with coherent ordered stressed precipitates, motion mechanism 8=1978
 NiO, etch pits, shape and size rel. to etching time 8=1977
 O₂ solid, electron microscope investigation 8=8465
 Pb, dislocation-electron interactions, temp. independence 8=17864
 Pb, superconductive, rel. to structure of intermediate stage 8=22556
 PbSe_(1-x)Te_x, from etching 8=1689
 Pt, annealed, rel. to relax. effect of internal friction at low temps. 8=22211
 Sb crystals, multiplication 8=8732
 Si containing oxygen, effect on precip., X-ray diff. obs. 8=13073
 Si, diffusion of B, motion rel. to coefficient 8=1925
 Si, diffusion of P, motion rel. to coefficient 8=1925
 Si, Hall effect, optical effects 8=1979
 Si, motion under e-bombardment during e-microscope investigations 8=17660
 Si, prod. in region of indentation in brittle fracture area 8=5084
 Si, rosette structure temp. dependence, 20-800°C rel. to doping effects 8=17809
 Si:B rel. to Li drift mobility, obs. 8=20200
 Si-Fe alloy, structure and ductility, low-temp. creep effects 8=13571
 Si-Fe, structure changes during creep 8=8734
 Si:Ga rel. to Li drift mobility, obs. 8=20200
 SiO₂-openings, diffusion induced dislocations, arrangement rel. to transistor simulation 8=8733
 Ta, impurity effects on strain hardening 8=22380
 Te, loop-lengths from u.s. wave absorpt. meas. 8=8619
 Te, theory and plastic behaviour 8=4984
 β-Ti, rel. to diffusion behaviour from thermo- and electro-transport meas. 8=17589
 U, α and β mono- and poly-crysts., rel. to creep mechanisms 8=8867
 US single crystals, slip behaviour 8=17834
 W, impurity effects on strain hardening 8=22380
 W, pinning, rel. to strain amplitude 8=1980
 Zn, basal dislocation mobility meas. 8=8735

Crystal imperfections—contd**dislocations—contd**

- Zn, behaviour on basal slip rel. to Al impurity effects 8=17836
 Zn, in compression along [0001] axis, strain, mobility and density 8=22214
 Zn, density, effect of Cd additions 8=17295
 Zn, etch pits at dislocations 8=4985
 Zn, etch-pit revealing technique 8=13439
 Zn, slip planes in plastic deformation 8=8725
 Zn, surface corrosion pitting at dislocation sites 8=13440
 Zn, and vacancies rel. to isotope effect in self-diffusion 8=4959
 ZnS, hexagonal, rel. to electroluminescent intensity distrib. 8=18621
 ZnS, single crystals, grown from melt 8=21969
 α -Zr, polycrystalline, rel. to steady-state creep 8=4986
 β -Zr, rel. to diffusion behaviour from thermo- and electro-transport meas. 8=17589

interstitials

- alkali halides, cations, dielec. props. calc. 8=1948
 calculation of the properties of vacancies and interstitials, conference 8=22165
 diffusion, isotope effect, model 8=1901
 diffusion, isotope effect, model 8=1902
 f. c. c. metal, recovery kinetics, model 8=2015
 impurities rel. to Ising mag. problem 8=1951
 metal-interstitial systems, phase boundary motion and polyphase diffusion 8=17035
 metal wires, recording accurate Snoek spectra at low freq. 8=8786
 metals, b. c. c., diffusion of impurities 8=17558
 Ba silicate glasses, γ -ray effects 8=13479
 CaF_2 , behaviour of F^- during reduction of Dy^{3+} 8=1949
 $\text{CoO}:\text{Li}$, Co interstitials, contribution to defect structure rel. to conductivity 8=1956
 Cu, migration kinetics at low temps. 8=8699
 α -Fe, and vacancies, calcs. 8=22179
 Fe, H-charged internal friction rel. to H interstitial-dislocation binding 8=4965
 Fe, metallic, C impurity effects on Mössbauer spectrum 8=20704
 Fe-V-C Snoek peak, anomalous obs. 8=13559
 Ge, impurity of Cu, irradi. induced, obs. 8=2027
 H, in Fe, anomalous behaviour at low temps. 8=22182
 KBr, vol. expansion, X-irrad. induced, by relax. at Frenkel defects 8=13486
 KCl, vol. expansion, X-irrad. induced, by relax. at Frenkel defects 8=13486
 KX, (X = Cl, Br, I), H_2O mols. 8=4953
 Li_2^+ mol-ion in LiF , stability study 8=22181
 Mo, impurity effects on strain hardening 8=22380
 Mo, n-irradiated and annealed, and vacancy loops identification 8=17610
 Nb-Hf, (-W), (-Mo) alloys, interstitial solid solubilities of O, N, C 8=17015
 Pt, annealed, effect on further damage on e-irradiation at 90°K 8=1947
 Si, Li-donor ground state, chemical splitting 8=1950
 Ta, impurity effects on strain hardening 8=22380
 W, impurity effects on strain hardening 8=22380
 W, and vacancies, calcs. 8=22179
 V, calcs. 8=22179

vacancies

- alkali halides, entropy of vacancy pair formation, calc. 8=1943
 alkali halide, impure, generation during electrolysis 8=9718
 aluminium alloy, age-hardenable, vacancy conc. calc. 8=1941
 calculation of the properties of vacancies and interstitials, conference 8=22165
 copper sulphide (digenite), cubic high temp., defect equilibria obs. 8=1942
 cubic, migration energy, calcs. 8=22173
 diamond-like solids, Jahn-Teller effect for single vacancy 8=8691
 diamond monovacancy distortion by Jahn-Teller effect, mol. model 8=17605
 f. c. c. lattices, diffusion calcs. using Debye model 8=22172
 fluorite-related systems, gross anion sub-stoichiometry, statistical aspects 8=22175
 formation and migration energy rel. to Debye temp. 8=1865
 inorganic substances, formation enthalpy calcs. 8=22176
 ionic cpds., prep. with ordered vacancies by exchange reactions 8=23082
 lattice with one vacancy, electron density calc. 8=22443
 mechanism for thermal mass transport 8=4947
 metals, Debye temp. rel. to energies of form. and migration 8=17509
 metals, f. c. c., self-diffusion coeffs. allowing for divacancies 8=8681
 phosphates, γ -irrad., O vacancies 8=22913
 relaxation of elect. and mechanical modes in NaCl structure allowing for 1st and 2nd neighbours 8=22174
 relaxation energy in cubic crystals 8=1939
 rutile, partially reduced, defect nature from e.p.r. study 8=18436

Crystal imperfections—contd**vacancies—contd**

- semiconductors with stoichiometric vacancies, crystalline, chemical and thermal props. 8=17197
 Ag, diffusion rate calc. using Debye model 8=22172
 Ag-Au alloys, flow, effect on tracer diffusion coeff. 8=4948
 AgCl single, Fe ions enter into complexes with vacancies 8=8215
 Al diffusion rate calc. using Debye model 8=22172
 Al, vacancy cluster nucleation 8=1944
 Al-Mn 1.04% dilute alloy, solute atom-vacancy binding energy 8=8693
 Au-Ni alloys, in modulated structure formation 8=17044
 Al-Zn alloys, n-irradiation effect on Guinier-Preston zone formation 8=17274
 Au, and divacancy behaviour from elec. resistance meas. on quenching and annealing 8=1945
 Au, annealing, three different experiments 8=13421
 Ba silicate glasses, γ -ray effects 8=13479
 CaWO_4 , rel. to self-diffusion of Ca 8=13408
 CdTe, metal vacancies formation energies rel. to Te-Te covalent bonding 8=17608
 Cs halides, defect form. energies and migration energy barriers 8=13422
 CsCl, Schottky defect energies for $\text{Pm}3\text{m}$ and $\text{Fm}3\text{m}$ structures 8=22178
 Cu, diffusion rate calc. using Debye model 8=22172
 Cu, quenched, annihilation kinetics 8=1946
 Cu_3Au alloy, low order, clustering 8=8695
 Cu-Be alloys, Guinier-Preston zone formation, conc. and ageing dependence 8=17606
 Cu-Be alloys, quenched and aged, role in solute clustering 8=17607
 α -Fe, and interstitials, calcs. 8=22179
 Fe-Ni alloys, annealed, rel. to X-ray diffr. "tails" 8=17341
 Fe-Si alloys, ferromagnetic after-effect from annealing of vacancies 8=5466
 Ge, n-type, rel. to quenching expts. 8=4962
 HfO_2 , elec. cond. meas. 8=13419
 HgTe, metal vacancies formation energies rel. to Te-Te covalent bonding 8=17608
 KBr, conc. changes during electrolytic coloration at 460-670°C 8=17609
 $\text{K}_2\text{SO}_4:\text{Mn}^{2+}$ 8=22910
 $\text{Li}_2\text{O}_3\text{Fe}_2\text{O}_4$, scattering of phonons on lattice distortions, non-stoichiometric vacancies 8=8660
 LiH, gap modes 8=22180
 LiI, gap modes 8=22180
 MgFe_2O_4 , scattering of phonons on lattice distortions, non-stoichiometric vacancies 8=8660
 MgFe_2O_4 , anionic, (produced by chem. reduction), rel. to thermal conductivity 8=17543
 Mo, n-irradiated and annealed, and interstitial loops identification 8=17610
 MoS_2 , detect. by etch-decoration method 8=4963
 MoS_3 surfaces, detection, and monatomic steps 8=4730
 NaCl:Mn, ratio of concentrations of nnn to nn complexes at low temp. 8=13420
 NiAl, ordered b. c. c., supersaturation on quenching 8=17611
 P_2O_5 , γ -irrad., O vacancies 8=22913
 Pt, annealed, effect on further damage on e-irradiation at 90°K 8=1947
 Pt, deuteron-irradiated, damage and recovery rel. to vacancy behaviour 8=8697
 Pt, and divacancies and self-diffusion from quenching and recovery expts. 8=17612
 Pt, n-irradiation damage and recovery rel. to defect doping effect 8=1953
 Pt-Rh alloy, formation and recovery, quenched 8=13423
 Si, diffusion of P, enhancement by vacancy generation 8=1926
 Si, localized state energies rel. to neutral divacancy 8=9123
 ThC_x , nonstoichiometric contribution to resistivity rel. to conc. 8=2140
 Zn, and dislocations rel. to isotope effect in self-diffusion 8=4959
 ZnFe_2O_4 , anionic, (produced by chem. reduction), rel. to thermal conductivity 8=17543
 ZnFe_2O_4 , scattering of phonons on lattice distortions, non-stoichiometric vacancies 8=8660
 $\text{ZnS}:\text{Tm}$ rel. to Tm luminesc., Zn vacancies, obs. 8=8434
 ZnTe, metal vacancies formation energies rel. to Te-Te covalent bonding 8=17608
 Zr and alloys, diffusion rel. to creep behaviour 8=4964
 W, and interstitials, calcs. 8=22179
 W, doped, annealed, evidence for voids 8=17613

Crystal properties

- Cauchy relations, deviation rules from expt. 8=5004
 conductivities, appl. in low-temp. elec. termination 8=15137
 ionic, polarization theories 8=9186
 laser-beam thermal effects in transparent crystals 8=4926
 metallic lattice, collision of atom, accommodation coeff. 8=22238
 molecular rigid-body motion rel. to triclinic coordinates 8=8231

Crystal properties—contd

- packing calc., phase problem, new approach 8=13311
- physical, correlation with space group 8=13164
- rare earth cobalt compounds with CaZn_2 structure, and mag. props. 8=22753
- symmetry dependence 8=4858
- transition-metal molybdates, and structure 8=13296
- volume changes rel. to non-uniform dislocation distrib. 8=17631
- Ar, optics and dielectrics 8=2238
- Bi-MnBi eutectic single crystal, growth dependence 8=8402
- GaS, thermal stability 8=21786
- KCl:KBr solid soln, ion shift in lattice due to different sizes 8=17378
- KCl:OH⁻, cooling to 0.36°K by adiabatic depolarization of OH⁻ 8=1874
- ZnS, effective ionic charge calc. 8=17304

Crystal structure

- See also Polymorphism.
- Alnico, structure on formation at different ageing temps. (300-800°C) 8=17077
- analogy in study of antagonism in pharmaceuticals: vit. and antivit. K 8=23765
- anthracene, morphology 8=8381
- apatite crystallites, carbonate effects on morphology during growth 8=1720
- austenite, grain coarsening temp. effects of Al and Nb 8=8462
- benzene sulphonyl chlorides, parasubstituted, determination 8=13133
- bond sphere grinder, modifications 8=4830
- cubic, equilibrium shapes rel. to surface energy 8=13001
- diamond crystals, cube form, structure studies 8=8370
- diamond hexagonal polymorph, "lonsdaleite", and natural occurrence 8=13121
- erionite and offretite, differentiation 8=13153
- faulted dipoles, contrast calcs., and stacking-fault energy meas. 8=8717
- geometrical basis of crystal chemistry, props. of net planes 8=13116
- higher order crystals, relation to other super-phases 8=8363
- ions with incomplete shells, spectra calcs. rel. to structure 8=13033
- lonsdaleite, diamond hexagonal polymorph and natural occurrence 8=13121
- metallic alloys, changes at early stages of ageing and order-disordering 8=17036
- metals, f.c.c. formation and configurations of faulted dipoles 8=8716
- models for teaching 8=10470
- molecular-crystals, structural class and subclass determ. 8=21917
- Mössbauer effect rel. to structure determinations 8=17326
- ordering of ternary b. c. c. alloys having three types of sites, theory 8=17033
- organic, rel. to thermodynamic props. 8=13360
- piezoelectric ceramics, alteration of pseudocrystal symm. obs. due to compressive stress perpendicular to polar axis 8=19556
- polyethyleneterephthalate, cryst., fraction content, determ. from i. r. spectra 8=17190
- polyvinylchloride, crystallinity degree determ. by X-ray analysis 8=1717
- rare-earth-manganese cpds., types and prep. by amalgam process 8=17203
- rare gas probe, diffusion eqns. 8=13404
- semiconductors and stoichiometric vacancies 8=17197
- silicates, anal. and crystal chemistry, review 8=8466
- sormite type alloys, influence of Nb conc. 8=5066
- symmetry, theory and applications in crystallography review 8=8364
- Ticonal, structure on formation at different ageing temps. (300-800°C) 8=17077
- titanomagnetite, from thermal variation of magnetization 8=14054
- twinning, procedure for solving struct. 8=4857
- vinylchloride with vinylidenechloride copolymers, crystallinity degree 8=1717
- vitamin K and antivitamin K, rel. to antagonism studies in pharmaceuticals 8=23765
- Al distrib. in schistic biotites, phengites and chlorites 8=13055
- $\beta\text{-AlB}_{12}$ containing < 2% Si, and crystal chemistry 8=17199
- AlBeB₂, and crystal chemistry 8=17199
- Al-Cu alloy, dendrite structure at chill surfaces 8=4821
- $\alpha\text{-Al}_2\text{O}_3\text{-Cr}_2\text{O}_3$ solid solns., parameters 8=8241
- Be, gliding prismatic 8=1981
- Bi, growth mode rel. to cleavage planes 8=17243
- C, in quenched steel, behaviour 8=22354
- (nC_3H_7)₄NBr, non centrosymmetric, morphology 8=22054
- CdS, rocksalt, recovery, room pressure 8=1671
- Ce-Ni-Si system, ternary cpd. formation, comp. and structures 8=17200
- Co films, electrolytically deposited, lamellar, rel. to growth rate 8=13999
- Cr(ONO)₃(H₂O)₃ 1.5 KNO₃, formation and struct. in crystalline state and in soln. 8=9518

Crystal structure—contd

- Cr-SiO cermet films 8=1695
 - CrZr(Hf)₂O₆ system of type RTiO₆ structure, structure and stability relations 8=1719
 - CsMnCl₃, and prep. 8=13138
 - Cu, (111), from X-ray K-absorption spectra 8=2413
 - Cu₂P monocrystals, and prep. 8=21948
 - Fe films, electrolytically deposited, lamellar, rel. to growth rate 8=13999
 - $\delta\text{-Fe}_2\text{O}_3$, mag. props., effect of struct. and chem. alterations 8=17627
 - K(Ta-Nb), by electrooptic obs. 8=9199
 - KF-SnF₂-H₂O system 8=4781
 - KMnCl₃, and prep. 8=13138
 - Li-B system, class identification after cpd. formation 8=8244
 - Li-C system, class identification after cpd. formation 8=8244
 - Mg₃Cd, degree of order effect on critical resolved shear stress for slip 8=5079
 - Mn steel, phase changes on heat treatment 8=17090
 - Mn₃GaC_{1-x}, non-stoichiometric effects on mag. props. 8=22819
 - Mn₅Si₃C_x, non-stoichiometric effects on mag. props. 8=22819
 - Mn-Ni system, and mag. structures rel. to phase transformation 8=17088
 - Mo, and low-temp. ductility, deform.-induced changes 8=13589
 - NaH₂(SeO₃)₂ and NaD₂(SeO₃)₂, phase transitions, isotope effects in symm. and nature 8=21849
 - NaMnCl₃, and prep. 8=13138
 - Ni base superalloy, carbide phases, composition and morphology 8=8246
 - Ni_{1-x}Fe_{2x}, coprecipitate, comp. and structure 8=23078
 - Ni films, electrolytically deposited, lamellar, rel. to growth rate 8=13999
 - PbO, single crystal, yellow form, some props., and optical absorption coeffs. 8=5628
 - PbO₂ electrodeposits rel. to electrolyte impurities 8=21919
 - PbO₂ from PbSO₄, Pb₃O₄, 2PbCO₃, Pb(OH)₂ and PbO anodization, obs. 8=23148
 - R-Ni-Si, (R=rare-earth), system, ternary cpd. formation, comp. and structures 8=17200
 - RbMnCl₃, and prep. 8=13138
 - Sb, growth mode rel. to cleavage planes 8=17243
 - Se, rel. to compressibility 8=17827
 - Se, photosensitivity spectrum dependence on crystallinity and oxygen impurities 8=18237
 - SiC polarity by etching method 8=21999
 - Ti, non-basal slip planes, vector identification 8=17665
 - Ti-Al alloys, non-basal slip planes, vector identification 8=17665
 - W oxide bronzes, evolution with temp., and phase stability 8=17048
 - W-Re alloys, from H reduction of WF₆ and ReF₆, rel. to phases 8=17100
 - ZnS polypotypes of family 24L-72R, unit cell and Zhdanov symbols 8=17194
- microstructure**
- See also X-ray examination of materials/microstructure alloys, ordered, grain boundary theory 8=17258
 - Armco iron, grain size rel. to lower stress yield 8=17798
 - austenite, retained in precip. hardening of stainless steel, X-ray meas. 8=4848
 - austenitic steel, changes during creep 8=17284
 - brass, rolled, texture representation by biaxial pole figures 8=17778
 - brass, rolling texture development at room temp. and -196°C 8=22328
 - brass, 70-30, rel. to deformation texture development, pole figure 8=17777
 - cast iron, austenitic, effect of Ce 8=21988
 - diamonds, synthetic, growth hillocks on (100) faces 8=17213
 - diamond twins, (111) faces, micromorphology 8=1723
 - electron-probe microanalysis, heat flow problems 8=1753
 - ethylene-trifluoropropylene copolymer, study by i. r. spectra 8=17298
 - excessive grain growth mechanism during recrystallization after deformation 8=17259
 - f. c. c. polycrystals, plastic deformation computer simulation and derived rolling texture 8=13512
 - ferrites, elec. cond., effects of CaO and SiO₂ in grain boundaries 8=13715
 - fibrous, in modern high strength composites 8=5025
 - field-ion images from asymmetric specimens, streak contrast 8=8452
 - glass, thin, transmission electron microscopy 8=21995
 - glass, thin, transmission electron microscopy 8=21996
 - grain boundaries, cavity growth mechanism, effect of creep rate 8=8801
 - grain-boundaries, high-angle, development of island model 8=22218
 - grain structure in metal castings, enforced fluid motion during solidification 8=8435
 - graphite pyrolytic, bisulphate interaction obs. 8=18731

Crystal structure—contd

microstructure—contd

graphite, pyrolytic, X-ray study 8=13134
 graphite, spheroidal, in Fe-C, Ni-C, Co-C, Au-C and Fe-C-Si alloys 8=13156
 hastelloy X-280, thermomechanical effects 8=17288
 ice, grain orientation, in growth from melt 8=21924
 Inconel 600, twin and grain boundaries free energy ratios, from e-micros. exam. 8=17287
 lamellar mixtures of 2 c.p. phases, by e-microscopy 8=21974
 lucite, disintegration under tension and strength, obs. 8=17843
 Makrolon films, spherulites and non-amorphous struct. form., 180°C 8=8473
 metal surfaces, ionic corrosion 8=13522
 metals, texture study by magnetores. and Hall effect 8=8454
 muscovite, superstructure when heated in vacuum 8=17285
 oligomers, reticulate crystalline nature from X-ray and thermomechanical tests 8=17192
 18Ni(250) maraging steel, banding effect on mechanical props. 8=8463
 orientation depend. of grain size, X-ray meas. 8=8832
 phase-contents and grain size distrib. by e micro-probe 8=17260
 polyethylene, crystallinity degree, X-ray and density obs. 8=8472
 polyethylene, fold-surface packing from moiré patterns 8=17299
 polyethylene, point defects, molecular mechanics 8=1938
 polymers, rel. to orientation birefringence temp. dependence 8=9577
 polymers, polylamellar habits 8=1766
 polymers, from ultrathin sections 8=17297
 poly(4-methylpentene-1), fold-surface packing from moiré patterns 8=17299
 polyoxymethylene, fold-surface packing from moiré patterns 8=17299
 precipitates in thin foils, electron-microscope images 8=13152
 reflection patterns, Kikuchi-like, by scanning electron microscope 8=8446
 reflection patterns, Kikuchi-like, by scanning electron microscopy, comments on interpretation 8=8447
 steel, annealed low-carbon and cold-rolled, orientation distrib. function of crystallites 8=21923
 steel, austenite grain size, high temp. microscope obs. 8=13157
 steel, continuous casting, alternating e. m. fields 8=4847
 steel, Cr-Ni stainless, intercrystalline corrosion 8=8460
 steel grain size rel. to mech. strength, hot working effects 8=22356
 steel, low-carbon, sheets, rolling and annealing textures 8=17799
 steels, carbon, volume fraction analysis, X-ray diffraction 8=8464
 surface, from reflection of atom and ion beams 8=13201
 surface growth spirals on crystals from molten salts 8=4838
 Teflon, disintegration under tension and strength, obs. 8=17843
 texture, cold-rolled and recrystallization, appl. of n diffraction 8=17278
 thoria gel, crystallite size obs. 8=12960
 trace characterization-chemical and physical, symposium NBS, USA, Oct. 1966 8=8437
 Udimet 700, Ni-base, sigma phase 8=13158
 vinyl plastic, disintegration under tension and strength, obs. 8=17843
 Zircalloys-2 and -4, effect of grain size on terminal solubility and thermodyn. activity of H₂ in these and α -Zr 8=8249
 Ag surfaces, ethylene, CO and H catalytic oxidation effects, obs. 8=18706
 Al alloys, during and after hot working 8=21979
 Al alloys, wrought-, strength and ductility rel. to ingot structure 8=5046
 Al, during extrusion, recovery and recrystallization 8=4841
 Al foils, by transmission electron microscopy 8=4840
 Al rods, polycrystalline, texture changes rel. to mech. forming processes 8=22308
 Al, rolled, texture representation by biaxial pole figures 8=17778
 Al, rolling and recrystn. textures 8=21938
 Al, rolling and recrystallization texture orientation relationships 8=1755
 Al vacuum condensates, annealing effects 8=4741
 Al, wires, deformed, double fibre texture rel. to orientation 8=4832
 Al-Al₃Ni alloy, stability of eutectic stressed at elevated temps. 8=4842
 Al-4wt.%Cu alloy, microanalysis of precip. phases by e-microscopy and energy analysis 8=17276
 Al-Li alloys, neutron irradi., grain boundary migration 8=8456
 Al-Mg alloy, dependence on plastic deformation and ageing 8=17004

Crystal structure—contd

microstructure—contd

Al-Si eutectic alloy, modified 8=13155
 Al-10%Zn alloy, n-irrad., pre-precipitation rate at 78°K 8=21980
 Al-Zn eutectoid alloy, superplasticity rel. to grain boundary shear 8=17766
 Ag on Mo, moiré fringes, dynamical effects 8=21977
 Ar, thin solid films, electron diffraction study 8=8313
 Au electrodeposits, pores and cryst. struct. 8=21981
 B distrib. in austenitic steel, from obs. of He gas bubbles after n-irrad. 8=13040
 BaTiO₃, cold-conductor-ceramic, working mechanism, electron microscopic investigation 8=21982
 BaTiO₃, grain growth inhibition 8=2244
 BeO, effects of SiC and MgO additions on grain growth 8=22315
 BeO, n-irrad. at high temp., dislocation loops 8=8761
 Bi₂S₃ evaporated films 8=17126
 C, glassy, X-ray scattering, small-angle, rel. to pore structure and conc. 8=21983
 Cd, texture study by magnetores. and Hall effect 8=8454
 Co, micromosaic block size and misorientation in zone-melted crystals, impurity depend. 8=8470
 CoAl-Co eutectic, mechanical props. 8=17770
 Co-Cr 10% alloys, cubic-hexagonal interface, contrast effect 8=8459
 Cr electrodeposits, epitaxy rel. to internal stress development, obs. 8=22325
 Cu, cold-rolled and recrystallization texture, study by n-diffraction 8=17278
 Cu, rel. to deformation texture development, pole figure 8=17777
 Cu, hot worked, grain struct. prod., obs. 8=21984
 Cu, powders, X-ray study 8=4844
 Cu, rolled high purity crystals, orientation distribution 8=1756
 Cu, rolled, texture representation by biaxial pole figures 8=17778
 Cu, rolling texture development at room temp. and -196°C 8=22328
 CuFe₂Mn₂O₄, tetragonal distortion 8=17205
 Cu-Zn alloys, rolling textures, -196° to 275°C 8=21985
 Er₂O₃ foils, grain boundary energetics by transmission e-microscopy 8=21986
 Fe, coarse grained polycrystalline, changes under tensile deformation 8=1985
 Fe, cubic lattice, microcontours, wide temp. range, in vacuo 8=2053
 Fe and Mg multilayered films, X-ray diffraction 8=1758
 Fe, technical, during fatigue tests 8=13566
 Fe-whiskers, ferromag. nucleation, theor. investigation 8=18335
 Fe whiskers surfaces, scanning e microscope obs. 8=17281
 Fe-(9.75-11.66%)Al alloys, nature of K-state 8=9005
 Fe-Au-Cu, ordered G.P. zones 8=8461
 FeCo alloy, grain boundary theory 8=17258
 Fe-Cr-N ternary system, and nitrides 8=4845
 Fe-Cr-N ternary system, diagrams and phase reactions 8=4846
 FeCl₃-graphite cpd. 8=1972
 FeCo superstructures in (Fe, Cr)Co, (Fe, Mn)Co and Fe(Co, Ni) alloys 8=1757
 Fe-12 at.%Ni alloy, finely dispersed system, rel. to particle size and oxidation 8=17280
 Fe-Ni base alloy: 9 at.%Cu, changes on ageing 8=1759
 Fe-Ni-Al-Ti alloy, after thermomech. treatment 8=21987
 Fe-Ni-Ti alloy, changes during martensite ageing 8=17064
 α -Fe₂O₃ whiskers on Fe 8=17250
 Ga-Fe system phases, obs. 8=21749
 InSb, layer distrib. effect on Corbino magneto-resistivity 8=5266
 Ir films, ultra-thin, vacuum-deposited, by e-diffr. and microscopy 8=17292
 Li colloidal aggregates in LiF, e. p. r. study 8=9431
 MgAl₂O₄, hot-pressed, rel. to mech. props., quadratic multivariable analysis 8=21991
 Mg₂Cd, direct obs. of antiphase boundaries, size and shape 8=17679
 Mg-Fe mixed hydroxides, dehydration effects, obs. 8=17023
 Mg-Mn ferrite composition microinhomogeneities 8=21990
 Mo, micromosaic block size and misorientation in zone-melted crystals, impurity depend. 8=8470
 Nb with precip. nitride 8=8274
 Nb-Zr alloy with precip. nitride 8=8274
 Ni, a. c. electrodeposited from NiCl₂ soln., obs. 8=22035
 Ni alloys, growth, distrib. and shape 8=21993
 Ni-base alloys, melt-refractory contact regions 8=9694
 Ni-base alloy, fatigued at several temps., structural charges 8=4981
 Ni-base superalloys, metallurgical props. 8=4850
 Ni-bearing steels, martensitic during ageing 8=1762
 Ni, changes under supersonic air streams at 900°C 8=17290
 Ni films, condensed polycrystalline 8=17286
 Ni layers, electrolytically deposited, orientation rel. to deposition inhibitor effect 8=1805
 Ni, twin and grain boundaries free energy ratios, from e-micros. exam. 8=17287

Crystal structure—contd**microstructure—contd**

- Ni:Al₂O₃, sintered, compressive strength grain size dependence 8=2048
 Ni₃Cr alloy, short-range order parameters from n-diffr. data 8=17291
 Ni₃(Fe, Mn), Ni₃(Fe, Cr), Ni₃(Mn, Cr), (Ni, Co)₃Mn, (Ni, Co)₃Fe_{0.5}Mn_{0.5} analysis of superstructure 8=1763
 NiFe₂O₄, thin films 8=2343
 NiMn, tetragonal, order twins and antiphase boundaries 8=17289
 Ni₃Sn, direct obs. of antiphase boundaries, size and shape 8=17679
 Pb stearate, optimization for X-ray diffraction 8=14254
 Pb-0.4wt%Mg alloy, G. P. zone formation in early stage of ageing 8=22389
 Pb-Sn alloys, lamellar stability on solidification 8=4785
 Pb-Sn, Na conc. at grain boundaries 8=8344
 PbSe_{1-x}Te_x, from etching 8=1689
 Pt₃-Co alloy, ordered, field-ion microscope study 8=1764
 Pu containing sample preparation for electron probe microanalysis 8=4831
 Pu, electrorefined, recrystallization and concurrent plastic deformation, 24-115°C 8=21961
 Sb₂S₃ evaporated films 8=17126
 Si, channeling of 2 MeV protons 8=2034
 Si web dendrite, X-ray topographs, stacking fault contrast 8=1983
 SiC, from thermal decomp. of methyl trichlorosilane, texture 8=21994
 Si-WSi₂-Si, epitaxial struct. 8=17257
 Sn vacuum condensates, annealing effects 8=4741
 Sn-Bi alloys, dendrite morphology 8=4825
 Ta films, ultra-thin, vacuum-deposited, by e-diffr. and microscopy 8=17292
 Te, low-angle subgrain boundaries 8=8737
 ThO₂-UO₂, in-reactor, from thermal simulation expts. 8=1130
 Ti alloy, VT15, solution-treated and aged, by e-microscopy 8=17293
 Ti-Al-Co alloys, rel. to Ti-rich corner 8=4851
 Ti-3 wt.% Fe alloy, quenched from β -phase, martensite study 8=21859
 U-M alloys, (M=Fe, Al and Si), irradiated, phase comp. changes rel. to resistivity meas. 8=8283
 U-1.5wt% Mo, transforms rel. to cooling rate from γ phase, obs. 8=8285
 UO₂, columnar grains, in thermal cond. meas. at high temps. and large temp. gradients 8=8665
 UO₂, columnar grains, obs. 8=21997
 UO₂, irradiated 8=8469
 UO₂, in-reactor, from thermal simulation expts. 8=1130
 US crystals, precipitation phenomena 8=21862
 US single crystals, transmission electron microscopy obs. 8=17834
 V₂V_{1+x} alloys, chalcogenide grain boundaries from etching technique 8=17102
 W, grain boundary porosity, effect of non-metallic trace additions 8=17835
 W, fast n irradi., changes rel. to changes in mech. props. 8=21998
 W, micromosaic block size and misorientation in zone-melted crystals, impurity depend. 8=8470
 W sheet, thermochemically deposited sheet, effect of deformation on grain structure 8=8471
 W, thermochem. deposited, effect of F impurities on high temp. grain stability 8=17294
 W wires, on secondary recrystallization, from electron optical meas. based on emission 8=1765
 Zn, effect of Cd additions 8=17295
 Zn, texture study by magnetores. and Hall effect 8=8454
 Zn-0.03 at.% Cd, Al, Cu or Ag, substructure rel. to impurity distrib. coeff. 8=17296
 α -Zr, deformed, form of polygonized sub-structure 8=22219
 α -Zr, effect of grain size on terminal solubility and thermodyn. activity of H₂ in this, Zircaloy-2 and Zircaloy-4 8=8249
 Zr rich alloys, effect of rolling temp. on texture developed 8=22399
 Zr-Nb alloy/oxide system 8=14390
 ZrO₂, Y₂O₃ and MgO-stabilized, rel. to stress relief mechanism 8=17839

Crystal structure, atomic

- See also Crystal electron states; Crystals/lattice mechanics; Electron diffraction crystallography; Neutron diffraction crystallography; X-ray crystallography.
 analysis based on inadequate data 8=8480
 anomalous scatterers, X-ray diffraction 8=13150
 anomalous scattering in structural analysis 8=13202
 b. c. c. lattices, Green's functions 8=4859
 b. c. c. to σ -phase, phase transformations, atomic mechanism 8=17030
 bond length corrections using 'riding' model 8=16966
 Bravais lattice in {4} derivation and point structure symmetry 8=13179
 cation off-centre displacements in octahedral environments 8=13172

Crystal structure, atomic—contd

- changes of lattice parameters around interface in transformation 8=8489
 circles packed in the plane, conditions evaluated using lattice complexes concept 8=13173
 classification of 8795 substances by space group, etc. 8=8474
 close-packed, stability and axial ratios 8=4866
 coloured point groups Shubnikov, stereographic projections 8=13170
 complexes, crystal, analysis using N.Q.R. 8=22927
 coordination complexes, metal-metal bonding 8=8594
 conference, Moscow, July 1966 8=8362
 convolution in direct and reciprocal space, new relationships 8=13192
 D_{2h} symmetry lattice sites, Jahn-Teller effect 8=17308
 defective, X-ray scattering, kinematic theory 8=13223
 diamond lattice, second order dipole moments 8=1629
 dielectric, elastic, homogeneously deformed and uniformly polarized, lattice theory 8=13177
 dielectric, elastic, lattice theory rel. to fluorites 8=13178
 dislocation disturbed lattice, model 8=17307
 disordered, one-dimensionally, close-packed structures, diffraction theory 8=8476
 displacements in electron cascade 8=8754
 distribution rule of factors for non-uniform atomic distrib. 8=13180
 dynamic scattering theory, fundamental eqns. for imperfect crystal 8=13196
 electron diffraction study of atomic surface structure 8=22012
 end of series effect influencing the apparent shape of atoms 8=17303
 extended internal defects, effect on Debye-Waller factor 8=1779
 f. c. c. lattices, second order dipole moments 8=1629
 field ion images, interpretation 8=8493
 film shrinkage effect on lattice parameter determination by X-ray diffraction 8=13219
 geometry, teaching in introductory course 8=1767
 (hkl) plane type (mesh shape) in Bravais lattice, algorithm for determ. 8=13165
 habit planes in martensite-austenite transformations with the aid of Kossel diagrams 8=4853
 hexagonal reciprocal lattice, four-axis, rel. to transmission e-diffr. pattern indexing 8=17309
 hexagonal structure, field-ion image computer simulation 8=8494
 homometric structures 8=13161
 imperfect, fundamental eqns. of dynamic scattering theory 8=13196
 ionic, Schottky defects, energy of formation 8=8692
 Kikuchi band, line in middle, many-beam dynamical theory 8=13272
 lamellar mixture of two phases, anomalous spots in electron diffraction patterns 8=13235
 Landau theory of 2nd-order phase transitions, $|\Gamma|^2$ and $\{\Gamma\}^2$ for crystallographic point groups 8=17031
 lattice cell vol. depend. in calc. of two-point function in quantum mech. 8=4856
 lattice complexes applied to sets of equivalent points in planar groups 8=13176
 lattice complexes concept in evaluation of conditions for circles packed in the plane 8=13173
 lattice distortions, elastic, interaction energy of interstitial atoms 8=8477
 lattice generalization and classification 8=17306
 lattice, magnetic symmetry groups representation 8=5111
 lattice parameters, precise det., likelihood ratio method 8=8479
 lattice parameters and orientation from Kossel lines 8=21920
 lattice strengths and structure sensitive 8=17735
 magnetic or Shubnikov groups, and black and white Bravais lattices, theory 8=13171
 magnetic structure, 3-dimensional, described by Shubnikov groups 8=13956
 maximal sub-groups of all space groups, derivation 8=13168
 molecular crystals, computer calc. 8=22002
 molecular, lattice energy calcs. rel. to unit-cell parameters 8=13012
 molecular packing from potential function symmetry 8=13169
 molecular rigid-body motion rel. to structure refinements 8=17311
 monoclinic centrosymmetrical crystals, comp. programme for refinement 8=1769
 morphology in rhombohedral space groups 8=13163
 Mössbauer effect rel. to determinations 8=17326
 multisublattice, cation distrib. rel. to stoichiometric restrictions and solid soln. parameters 8=4775
 noncentrosymmetric, partial structure information combined with tangent formula 8=17319
 non-crystallographic symmetry problem, linear analysis 8=8475
 pair, related, probability distributions of normalized intensities 8=22006

Crystal structure, atomic—contd

- parameters from electron-diffr. intensities 8=13230
 perfect lattice, thermodynamic quantities in harmonic approx. 8=4854
 phase correction method for solving partially known structures 8=13215
 phase determination based on larger structure phases 8=13184
 phase determination involving mols. in different environments 8=13160
 phase-determining techniques in solving complex structures 8=13114
 point structure symmetry and Bravais lattice in {4} derivation 8=13179
 polychromatic symmetry groups, planar, exhaustive generation algorithms 8=13166
 potential function symmetry approach to mol. packing 8=13169
 reciprocity in electron diffraction and microscopy 8=13241
 reciprocal lattice dimensions from meas. angular co-ordinates 8=17320
 scattering amplitudes in solids for 40-100 keV electrons 8=13240
 semiconductors, changes due to high static press. 8=4699
 Shubnikov groups, derivation 8=17310
 Shubnikov groups, three dimensional periodic mag. structure 8=8367
 space group correlation with physical props. 8=13164
 space group representation, irreducible, operational projection 8=17305
 spin-orbit coupling, crystalline field with magnetic point group symmetry 8=1632
 space symmetry and induced polarization 8=9206
 superconductivity theory, cryst. lattice study 8=22534
 superlattice lines, axiomatic definition and assembly theory 8=13162
 superlattices, close-packed, AB_3 , stacking faults 8=17667
 superlattices, field-ion image computer simulation 8=8494
 surface lattice distortion rel. to Debye-Waller factors 8=1780
 symmetry of crystals with dislocations 8=13430
 symmetry groups classified by character of independent translations 8=13167
 symmetry groups up to 3-dims., geom. symbols 8=8365
 symmetry rel. to physical props. 8=4858
 symmetry, theory and appls. review 8=8364
 tetragonal spinel lattices, Néel ionic migration law 8=8502
 tetrahedral lattice, self-avoiding walks 8=1768
 trial structure generation rel. to mol. symmetry and space groups 8=17302
 X-ray diffuse scattering in reciprocal space 8=13205
 X-ray scattering intensity distrib. of (hk) interferences in lattices with preferred orientation 8=13216
 H atom localization by electronographic method 8=13233
 NaCl-type crystals, lattice distortion by impurities and n. m. r. line splitting 8=9455

elements

- diamond, Lave spike refls. rel. to i. r. absorpt. and impurity N location, obs. 8=22014
 electron momentum distrib. by Compton X-ray scattering 8=17907
 lattice perfection, degree determ. by p scatt. 8=4997
 metallic lattice, coefficients of accommodation and capture 8=8334
 metals, atomic distrib. connection with liq. state 8=12787
 metals, changes due to high static press. 8=4699
 non-centrosymmetric, Bijvoet differences rel. to temp. effects in X-ray diffr. 8=13273
 Z=10-98, anomalous scattering corrections 8=4886
 Al, atomic scatt. factors, Slater approx. 8=8506
 Al distortion in plastic deform., e microprobe-Kossel obs. 8=21978
 Al, electron energy dependence from 100 keV to 1 MeV 8=4868
 Ar, at 0°K, calc. from interact. pot. of gas 8=1468
 Au, quenched and aged 8=22185
 C (pyrolytic graphite, electron momentum distrib. by Compton X-ray scattering 8=17907
 Ce(111) exchanged faujasite 8=8515
 Cr, antiferromag., X-ray line splitting above and below Néel point 8=17358
 Cu, anomalous X-ray transmission 8=13257
 Cu, atomic state, by absolute meas. of X-ray scattering factors 8=13030
 Cu films, obliquely deposited, effect of atom mobility 8=8296
 Cu, neutron-irradiated, annealing effect on lattice parameter 8=1937
 Cu, oxidised single crystals, exam. by diffr. of slow electrons 8=13258
 Fe, absolute atomic scatt. factor 8=8519
 Fe, lattice parameters of powders, ferromagnetic props. 8=14033
 Ga 8=22024
 Ge films, grown from liq. films 8=1741
 Ge, lattice location of implanted group V elements 8=22160
 Ge, lattice theory of third order elastic consts. 8=13261
 Ge, Pendellösung meas. 8=13262
 Ge, scattering factor, Pendellösung meas. 8=22025

Crystal structure, atomic—contd

- elements—contd**
 Ge, structure of kinks and steps on dislocations 8=8727
 H and D, changes during transitions in ortho- and para-states, X-ray exam. 8=13263
 H, ortho-, solid, orientational order; h. c. p. molecular lattice 8=22026
 o-H₂, orientational ordering of mols. in c. c. p. lattice 8=1793
 o-H₂, solid, self-consistent model, Pca2, ordering 8=17375
 He isotope mixtures, lattice distortion and thermal conductivities 8=1889
 I₂, press. effect 8=13578
 In, diffuse X-ray reflections in order-disorder transition near melting pt. 8=8525
 Kr, at 0°K, calc. from interact. pot. of gas 8=1468
 Li, electron momentum distrib. by Compton X-ray scattering 8=17907
 α -Mn, atomic parameters, refinement 8=8532
 α -Mn, non-centrosymmetric, Bijvoet differences rel. to temp. effects in X-ray diffr. 8=13273
 Ne crystals, lattice constants, thermal expansion and isothermal compressibility 8=1803
 Ne, at 0°K, calc. from interact. pot. of gas 8=1468
 Ni, lattice distortion under supersonic air streams at 900°C 8=17290
 Ni, lattice parameters of powders, ferromagnetic props. 8=14033
 Ni layers, electrolytically deposited, lattice deformations rel. to deposition inhibitor effect 8=1805
 α -O₂, rel. to mag. props. 8=17406
 α -O₂, n-diffr. study 8=4882
 Pd films, obliquely deposited, effect of atom mobility 8=8296
 Pt films, obliquely deposited, effect of atom mobility 8=8296
 Se, α -monoclinic and hexagonal modifications, refinement 8=13288
 Se, hexagonal, atomic displacement rel. to conductivity 8=1808
 Se, non-centrosymmetric, Bijvoet differences rel. to temp. effects in X-ray diffr. 8=13273
 Si, elastically distorted, X-ray topography 8=13198
 Si epitaxial films on Ge(111) surfaces, LEED struct. obs., 870°K 8=17140
 Si epitaxial films on Si(311) surfaces, LEED struct. obs., 870°K 8=17140
 Si, implanted Sb, Ga, As, In and Xe location and lattice disorder, obs. 8=17414
 Si, lattice location of implanted group III elements 8=22160
 Si(111), LEED study of Ni induced surface structure 8=4732
 Si, lattice theory of third order elastic consts. 8=13261
 Si wafers, orientation, by proton channelling 8=8376
 Si, with diffused B (and P), appl. of dynamical theory of X-ray scattering 8=13412
 Sn films, obliquely deposited, effect of atom mobility 8=8296
 Te, bond distances, Mössbauer effect 8=4887
 Te films, vac. -evaporated, forbidden reflexes in e-diffr. 8=17141
 Te, isomorphous, non-centrosymmetric, Bijvoet differences rel. to temp. effects in X-ray diffr. 8=13273
 Xe, at 0 K, calc. from interact. pot. of gas 8=1468
- alloys**
 Armco iron, parameters by X-ray flat film back reflection technique 8=8521
 binary, interatomic energies from short-range-order meas. by diffuse scattering 8=17331
 ordered alloy containing antiphase domains, X-ray diffr. 8=4863
 ordered, effect of symmetry on field ion images 8=4881
 rare-earth germanides and silicides, 5:4 and 5:3 compositions 8=8554
 solid solution, field ion emission patterns, computer simulation 8=8453
 steel, high-C, α' and κ' -martensite 8=17373
 steel, low-C, rapidly annealed to 700°C, quench-ageing at 240°C 8=17806
 Al-Cu-Mg, atomic diffusion within lattice on ageing 8=17041
 ζ -Ag-Ga, lattice spacings on addition of Cd 8=17335
 AuAg order rel. to optical consts., 276-1200 nm 8=22958
 Au-Cd alloys, quenched and aged 8=22185
 AuCu order rel. to optical consts., 276-1200 nm 8=22958
 AuCu₃ order rel. to optical consts., 276-1200 nm 8=22958
 Au-Mg system 8=17043
 Au-Ni spinodal, re-calc. 8=13245
 Au-Pt alloys, annealed, defects rel. to X-ray diffr. "tails" 8=17341
 Au-Zn alloys, quenched and aged 8=22185
 Cu-Al, martensites 8=4871-2
 Cu-Sn, of metastable states during eutectoid transform. 8=17055
 Fe-Al, paracrystals from X-ray powder patterns rel. to comp. and annealing treatments 8=17368
 Fe-20 at. %Al, structure factor variations for electrons with accelerating voltage 8=13260
 Fe-C steel, atomic displacements from X-ray diffr. meas. 8=17371
 Fe-Co, lattice parameters of powders, ferromagnetic props. 8=14033
 FeCr, σ -phase, atomic ordering and co-ordination rel. to mech. props. 8=17030

Crystal structure, atomic—contd**alloys—contd**

- Fe-N alloys, martensite lattice meas. 8=8522
 Fe-N, quenched, X-ray diffraction and interferometry study 8=8522
 Fe-Ni alloys, annealed, vacancies rel. to X-ray diffr. "tails" 8=17341
 Fe-Rh, parameters, structural defects, phase transformations 8=9395
 Mo steel, orientation relationship and coherency between Mo_2C and ferrite matrix 8=17369
 2NbAl, σ -phase, atomic ordering and co-ordination rel. to mech. props. 8=17030
 Nb-Ni-Al, M phase 8=17403
 Ni-Fe films, lattice contractions by electron diffraction 8=1806
 Ni₃Mo ordered, symmetry effects on field ion image 8=4881
 Ni-Ti, changes on martensite transformations 8=21851
 Pb₂Sn₃-Te, lattice parameters, redeterm. 8=22037
 PtCo ordered, symmetry effects on field ion image 8=4881
 PuZr peritectoid reaction, 615°C 8=8279
 ReAl₃ 8=8555
 Sb-Sn oxidation products, by e-diffr. 8=13287
 Tb-Y solid solns., 77-300°K 8=22040
 TcAl₃ 8=8555
 Ti-Al alloys, dilute, hydride formation in thin foils 8=17016
 UN-ThN pseudobinary system 8=22044
 V-Fe-Si, D phase 8=17403
 Y-Al, X-ray powder photographs 8=22045
 ZrM₂-H₂ system cpds., (M = Cr, V, Mo), by X-ray diffr. 8=4723

inorganic compounds

- Al₂S₃-type phases, binary, containing transition elements, atomic ordering 8=17419
 actinide cpds., group IVA-VIA, with NaCl structures, lattice constants 8=4867
 alkali-halide crystals, i.r. absorpt. spectra, local vibrs. of mol. impurity ions 8=14197
 alkaline beryls, dependence on tempering at 600-1200°C 8=17345
 alkaline earth silicides with BaGe, BaSi, BaSn, CrB, SrGe, SrSn 8=8557
 aluminosilicate frameworks, Si-O and Al-O tetrahedral distances 8=21795
 analyt. method of representing structure 8=13246
 b.c.c. metals, lattice rotations, axisymmetry flow, computer solution 8=8373
 botryogen 8=4876
 chlorapatite 8=17352
 chrysotile asbestos, microfibres and lattice parameters from electron microscopy 8=1796
 ferric oxyhydroxide, by Mössbauer absorpt. spectroscopy 8=17370
 ferrites, hexagonal, type Ba₂Me_x²⁺Fe₂O₇, and stacking sequences 8=17342
 fluorapatite 8=17352
 fresnoite, Ba₂TiSi₂O₈, cell dimensions from X-ray powder data 8=18506
 garnet-type cpds., Sn⁴⁺ coordination from Sn¹¹⁹ Mössbauer effect 8=17415
 goethite dehydration and haematite/magnetite formation rel. to c.c.p. orientations 8=4875
 goethites, by Mössbauer absorpt. spectroscopy 8=17370
 halogens, space groups dependence on electron density 8=17328
 hambergite, integrated intensities, expt. tests of general formula 8=13480
 haradaite, SrVSi₂O₇, and Si-O bond lengths 8=17416
 hauyne, polysynthetic structure 8=17348
 hydroxyapatite 8=17352
 ice V 8=17377
 intermetallic cpds., bond length dependence on hybrid character of bond orbitals 8=13004
 kernite, by X-ray diffraction 8=8542
 labradorite, supersatellite reflections 8=13255
 lamprophyllite, (Ba, Sr, K)Na(Ti, Fe)TiSi₂(O, OH, F)₃ 8=17344
 Laves structure formation rel. to MgM₂, (M = Cu, Zn, Ni) 8=13071
 lepidocrocite, by Mössbauer absorpt. spectroscopy 8=17370
 leucophanite 8=13252
 magnetic structure representation analysis 8=13951
 manganese vanadate, determ. of O₂ parameters and degree of conversion 8=8534
 meliphanite 8=17351
 metallic lattices stability rel. to highest density principle 8=17329
 metallic lattices stability rel. to space-filling and coordination number 8=17330
 methylammonium chromium alum, rel. to Lipson classification 8=22017
 mica, lattice spacing, particle size effects 8=17301
 oxiodates of Sr, Ca and Cd 8=8558
 pascoite, Ca₃V₁₀O₂₈, 17H₂O, and refinement 8=17350
 perovskite-type crystals, lattice dynamic modes rel. to atomic displacements 8=17332
 potash feldspar, Al-Si order and Rb impurity effect 8=17618
Crystal structure, atomic—contd
inorganic compounds—contd
 pyrosmalite 8=17393
 α -quartz, integrated intensities, expt. test of general formula 8=13480
 α -quartz, structure factor ratios by Pendellösung method 8=13291
 rare-earth aluminides, RAl, rel. to DyAl and CeAl structures 8=1789
 rare-earth aluminides, RAl₃, closest-packing super-structures 8=17410
 rare earth-aluminium systems, binary 8=13286
 rare-earth metal-aluminium system, closest-packing superstructures 8=17410
 rare-earth cobaltides, RCo₃, and mag. props. 8=13967
 rare-earth cobaltides RCo₅, rel. to Curie temp. dependence 8=18350
 rare-earth-gallium compounds 8=1812
 rare-earth nickelides, R₂Ni 8=13247
 rare-earth oxide, R₂O₃-M₂O₃, (R=rare earth, M=Nb, Ta or Pa) 8=1802
 rare earth sulphate hydrates, X-ray and thermo-gravimetric analysis 8=17385
 rare-earths, stability and axial ratios 8=4866
 rinkite, and rel. to analogous silicates 8=8543
 spinels, equilibrium order-disorder 8=13282
 stishovite, effect of press. on parameters, and compression curve 8=22039
 thortveitite, (Y, Sc)₂Si₂O₇ 8=9447
 transition metal chalcogenides, MM₂X₄, M(M') = trans. metal, X = S, Se, Te 8=13294
 transition-metal molybdates, and props. 8=13296
 transition metal thionitobates, Mn₂S₄ 8=8560
 triclinic mica polytypes giving monoclinic diffr. patterns, symmetry enhancement phenomena 8=13290
 X-ray diffraction powder patterns, 80 substances 8=17327
 Ag(1) complex, monothiosemicarbazidesilver(1)chloride and mol. structure 8=22013
 Ag₃AsS₃, xanthoconite 8=13248
 Ag₂C₄H₄N₂ClO₄, X-ray diffraction 8=17333
 AgCl, rel. to electron distrib. 8=17334
 Al-serpentine, hexagonal 8=17336
 AlB₁₀, analysis by convolution mol. method 8=8507
 AlB₁₀, by convolution mol. method 8=17337
 Al₂Be₂Si₂O₈, structure refinement 8=17338
 α (AlFeSi) 8=8508
 Al₂O₃, distortion due to n-irrad. 8=22245
 Al₂O₃, lattice expansion rel. to n irrad. 8=13249
 Al(OH)₃, nordstrandite, by X-ray powder analysis 8=17339
 Al-Si, interaction with precipitates 8=13431
 AlTiMO₆, (M=Nb, Ta, Sb), and fluorescence 8=4879
 As₂Se₃, refinement by NQR method 8=17340
 Au₇Mg₂₃ phase 8=13251
 β -AuMn, change to f.c.c. structure on cold working 8=1704
 BaCa₂Al₂(Si, Al)₁₂O₃₀·2H₂O, structure refinement 8=17338
 Ba₂Me_x²⁺Fe₂O₇, hexagonal ferrites, and stacking sequences 8=17342
 Ba₂Si₂O₈, multiple chain structure 8=17343
 (Ba, Sr, K)Na(Ti, Fe)TiSi₂(O, OH, F)₃, lamprophyllite 8=17344
 BaTiO₃, micro electron diffr. investigation 8=8510
 Ba₂TiSi₂O₈, fresnoite, cell dimensions from X-ray powder data 8=18506
 Ba(UO₂AsO₄)₂·nH₂O, metaheinrichite, e-diffr. meas. 8=17360
 Bi single, backward elastic scattering of 5 MeV protons and 20 MeV α particles 8=20801
 BiFeO₃, and mag. structure from time-of-flight n-diffr. 8=17346
 Bi₂GeO₂₀, ferroelec. 8=13254
 Bi-O system, new tetragonal phase 8=17347
 Bi₂O₃-WO₃ and Bi₂O₃-MoO₃ system, and comp. of phases 8=17047
 BiOCl, lamellar crystals, and 'thinning' effect on electron diffr. 8=1784
 Ca aluminate hydrates, lamellar 8=8511
 Ca₂B(OH)₄ modifications 8=17353
 CaCO₃ (calcite), lattice parameters, precision, and thermal expansion 8=22015
 CaH₂IO₆·3H₂O 8=8558
 Ca(IO₃)₂·6H₂O 8=8558
 CaMg₂B₃(OH)₅·2H₂O, inderborite 8=17349
 CaNa₂(CO₃)₂·2H₂O, pirssonite, by X-ray diffr. 8=1785
 3CaO·Al₂O₃·3CaSO₄·32H₂O 8=13253
 Ca₂Sb₂O₇ (x = 1, 2, 3; y = 4, 5, 6), X-ray powder diffr. patterns 8=14363
 Ca₂V₁₀O₂₈·17H₂O, pascoite, and refinement 8=17350
 CaWO₃·Yb³⁺, symmetry of Yb³⁺ on charge compensation by Na⁺, e.p.r. study 8=18413
 CaYb₂O₇, rel. to Ca ferrite isomorphism 8=4870
 CbBe₃, data 8=17426
 (1-X)CdCr₂S₄·XCdCr₂Se₄ system, and mag. props. 8=1400
 CdH₂IO₆·3H₂O 8=8558
 CdI₂, two new polytypes with uncommon space-group symmetry 8=1786
 Cd₂Sb₂O₇ (x = 1, 3; y = 4, 6), X-ray powder diffr. patterns 8=14363
 CdS, Se_x films from vacuum deposition, structure 8=4748
 Cd[SC(NH₂)₂]SO₄·2H₂O rel. to S bridging 8=8514
 Cd[SC(NH₂)₂]SO₄·2H₂O 8=8513

Crystal structure, atomic—contd

inorganic compounds—contd

- CdTiS₂, new semicond. cpd, unit cell and space group 8=17354
 Cd₂V₂O₇ 8=8512
 CeAlO₃, chemically homogeneous 8=17355
 CeC₂, high-temp. lattice parameter 8=21785
 Co(III) complex, chloropentamminecobalt(III)dichloride, re-determination 8=22016
 Co complex, decammine-μ-peroxo-dicobalt pentanitrile 8=17356-7
 CoBr₂·2H₂O 8=1798
 CoCl₂·MCl (M=Rb, K, Na, Li), symmetry changes rel. to CoCl₂ conc. 8=9516
 Cr(CO)₆ 8=8516
 Cr(CO)₆, space group R factor, significance tests 8=8517
 CrO₂K₂, γ and n irradiated, e.s.r. 8=18417
 CrO₂(NH₄)₂, γ and n irradiated, e.s.r. 8=18417
 CrTiMO₆, (M=Nb, Ta, Sb), and fluorescence 8=4879
 CsUF₆, and isomerism with KOF₆ 8=1787
 Cs₂[UO₂Br₄] 8=17359
 Cu(II)azide, single-crystal X-ray exam. and refinement 8=22018
 Cu complex, dipotassium bis(glycylglycinate)cuprate(II) hexahydrate 8=17363
 Cu complex, N-salicylidene-glycinato-aquocopper(II) hemihydrate 8=8518
 CuCr₂Se₄, ionic config. from neutron diff. and elec. trans. props. 8=1788
 Cu_{1-x}Mg_xFe₂O₄, lattice constants on quenching in high oxygen pressure furnace 8=2516
 Cu₂Mn₃O₄, cation distrib. determ. 8=17364
 α-Cu₂P₂O₇ 8=17367
 Cu₂Se₂, umangite 8=17366
 CuTiF₆·4H₂O 8=17365
 Cu(UO₂AsO₄)₂·2H₂O, meta-zeunerite, e-diff. meas. 8=17360
 DyAlO₃, X-ray diff. 8=8544
 Fe carbonyl tolane complex, by X-ray analysis 8=4874
 Fe complex, tetracarboxyl (fumaric acid) iron racemate 8=1790
 Fe martensite, atomic displacements 8=4877
 Fe oxyhydrates, computation of bond distances and angles 8=22022
 Fe oxides, computation of bond distances and angles 8=22022
 Fe-C martensite, static atomic displacements by X-ray diffractions 8=4878
 Fe₂C₂, Hägg iron carbide 8=17372
 FeCl₃·6H₂O 8=1791
 FeCr₂Se₄, lattice parameters, rel. to d-orbital interaction clarification 8=5391
 FeLiO₂, Q₁₁ (or β) phase, X-ray diff. results rel. to periodic antiphase model 8=17386
 Fe-Mn carbides, cell volume obs. 8=22019
 Fe₂Mn₃O₄, cation distrib. determ. 8=17364
 Fe₂Mn_{1-x}TO₃, (T = rare earth), and mag. props. dependence on x value (0 to 1) 8=22851
 Fe₂(MoO₄)₃ 8=8526
 Fe₂(MoO₄)₃, refinement and structure formation 8=17374
 FeO, stoichiometric cpd. 8=13259
 δ-Fe₂O₃ (hydrate) 8=22023
 Fe₃O₄, diffraction of slow electrons at octahedral surface 8=8520
 GaAs, Sn doped, lattice parameter meas. 8=2191
 GaTiMO₆, (M=Nb, Ta, Sb), and fluorescence 8=4879
 Gd phosphate-vanadates 8=14330
 GdCl₃ 8=8523
 HCl·2H₂O, and H bonding 8=8504
 HCl·2H₂O and HCl·3H₂O, rel. to proton hydration 8=17196
 HCl·3H₂O, and H bonding 8=8505
 HClO₄·2H₂O, rel. to proton hydration 8=17196
 H₂O, dynamics in Na₂S₂O₆·2H₂O and Li₂S₂O₆·2H₂O crystals. 8=8537-8
 H₂O dynamics in Na₂S₂O₆·2D₂O, deuteron m.r. 8=8539
 HfSiO₄, synthesis and X-ray study 8=8524
 Hg(CN)₂·0.80 tetrahydrofuran, morphology 8=1794
 Hg(OH)F 8=17376
 Hg₂S₂Cl₂, confirmation and refinement 8=13264
 HgX₂-TLX, (X = I, Br, Cl) systems, cpds. formed 8=17085
 IBr, and refinement 8=22027
 In₂(MoO₄)₃ 8=8526
 InTiMO₆, (M=Nb, Ta, Sb), and fluorescence 8=4879
 Ir₂Se₃, Rh₂S₃ and Rh₂Se₃, octahedron pairs 8=1807
 KAg₂I₆, rel. to ionic mobility 8=17379
 2K₂CO₃·3H₂O 8=8528
 KCa₂(Be, Al)₂Si₂O₈·0.8H₂O, structure refinement 8=17338
 K₂Ca(SO₄)₂·H₂O, syngenite 8=13268
 KCl monocrystals, slow electron patterns 8=8527
 KCl:KBr(36:64), ion shift in lattice due to different sizes, from diffuse scatt. 8=17378
 K₂Cu(CN)₄, and refinement 8=17361
 K₂CuFe(CN)₆, tetragonal, X-ray analysis, i.r. and e.s.r. spectra 8=13265
 KF monocrystals, slow electron patterns 8=8527
 KH₂PO₄, anomalous incoherent scattering of thermal neutrons in Laue-case 8=13267
 KMnCl₃·2H₂O 8=17411
 K₂MoO₄·F_x·H₂O (x=1, 2, 3; y=5, 4) 8=17381
 K₂NiFe(CN)₆, cubic, X-ray analysis, i.r. and e.s.r. spectra 8=13265

Crystal structure, atomic—contd

inorganic compounds—contd

- K₂PtCl₆, lattice images with electron microscope 8=8500
 KSO₃NH₂, by neutron diff. meas. 8=4897
 KTh₂(PO₄)₃ 8=17382
 K(UO₂AsO₄)₂·3H₂O, abernathyite, e-diff. meas. 8=17360
 La phosphate-vanadates 8=14330
 La telluride system, six phases, and their crystal chemistry 8=17202
 La₂WO₆, lattice constants determ. 8=5709
 Li ferrite, FeLiO₂, Q₁₁ (or β) phase, X-ray diff. results rel. to periodic antiphase model 8=17386
 Li fluorophlogopite, 4-layer, new mica polytype 8=8531
 α-Li₂AlF₆, at room temp. 8=17390
 LiBaH₃, and deuterated cpd., n-diff. study 8=17391
 LiBO₂, β and γ high-press. forms 8=8269
 Li₂EX, E=Cu, Ag, Au; X=Al, Ga, In, Tl, Si, Ge, Sn, Pb, Sb, Bi 8=22028
 LiF, lattice distortion around V_K centre, ENDOR study 8=2009
 LiF:Fe³⁺ system, mag. resonance studies of crystal field distortions 8=13005
 LiN₃, rel. to NaN₃ and Sr(N₃)₂ 8=17387
 LiNaSO₄ 8=8530
 Li₂O-ZB₂O₃, refinement by least squares of 3-dimensional data 8=17389
 Li₂S₂O₆·2H₂O, rel. to H₂O dynamics 8=8538
 Ln₂O₃S₂, rare earth oxydisulfides 8=4883
 Lu phosphate-vanadates 8=14330
 LuTiMO₆, (M=Nb, Ta, Sb), and fluorescence 8=4879
 Mg[B₄O₅(OH)₆]·6H₂O 8=13270
 MgCr_{2-x}Mn_xO₄, tetragonal distortion of Jahn-Teller type study by X-ray and neutron diff. 8=13269
 MgGa_{2-x}Mn_xO₄, tetragonal distortion of Jahn-Teller type study by X-ray and neutron diff. 8=13269
 MgMn₂O₄, cation migration at high temps. rel. to lattice energy calcs. 8=4955
 MgM₂, (M = Cu, Zn, Ni), Laves structure formation 8=13071
 MgO, absolute structure factor meas. 8=17392
 MgO, distortion due to n-irrad. 8=22245
 MgO, lattice expansion rel. to n irradi. 8=13249
 MgO, line in middle of Kikuchi band, many-beam dynamical theory 8=13272
 α-Mg₂P₂O₇ 8=17367
 Mg₂Si, Renninger effect rel. to X-ray reflections 8=13271
 Mg(UO₂AsO₄)₂·nH₂O, novacekite, e-diff. meas. 8=17360
 Mn complex, μ-hydrido-μ-diphenylphosphido-bis (tetracarboxyl-manganese) 8=1799
 Mn complex, tetramethylammonium Mn(II) chloride, by X-ray diff. 7=1795
 Mn ferrite, Mn rich, lattice parameter temp. dependence (293-4, 5°K) rel. to comp. 8=17394
 MnBr₂·2H₂O 8=1798
 Mn₂Fe(CO)₁₄ 8=8533
 MnFe₂O₄, cation distrib. in sample from aq. soln., by n-diff. 8=13274
 MnMoO₄, preliminary data 8=17395
 Mn₃Sb₂O₆, X-ray powder diff. patterns 8=14363
 Mn_(1-x)V_x(Mn_{1-x}V_{x-1})₂O₄, determ. of O₂ parameters and degree of conversion 8=8534
 MnYb₂S₄, a spinel, mag. and structural study 8=5436
 Mo₂C, rhombic modifications and polymorphic transitions 8=8561
 MoCl₃-graphite, by single-crystal electron and X-ray diff. 8=1797
 Mo₂NiB₃, rel. to analogues 8=17396
 MoS₂ polytypes by e-diff. 8=17397
 (MoV_{1-x})₂O₅, (0≤x≤0.30) 8=17425
 NOSO₃Cl 8=13275
 Na tetraborate, Na₂O·4B₂O₃ 8=8541
 Na₂Ca₂Si₂O₉, by X-ray powder diff. 8=22030
 Na₂CdSi₂O₆, lattice struct., obs. 8=22031
 NaCl monocrystals, slow electron patterns 8=8527
 NaCl, structure factors and Debye-Waller factors at 300, 202 and 70°K 8=8535
 NaCl, thermal diffuse scattering contribs. to X-ray reflection intensities rel. to electron density distrib. 8=13277
 NaCl, X-ray structure amplitudes, statistical exam. 8=4885
 Na₂Fe₂O₆ 8=8540
 Na₂Ge₂Sn₂O₁₅(OH)₂, and refinement 8=17402
 NaN₃, and phase transformations 8=17387
 Na₄P₂O₇·10H₂O, improved dimensions 8=17400
 Na₂S₂O₆·2H₂O, rel. to H₂O dynamics 8=8538
 α-Na₂Si₂O₅, new refinement 8=13278
 Na₂SiO₃, improved dimensions 8=17400
 Na₂Si₂O₇, rel. to silicate sheet type 8=1801
 Na₂SnSiO₄ 8=17401
 NaTi₂Al₂O₁₂, from X-ray analysis 8=1800
 Na₂Ti₂O₁₅ 8=22029
 Na₂Tl, structure and bonding model 8=8536
 Na₂Tl, rel. to Tl-Tl bonding 8=17399
 Na₂Zr₂F₃₁, and refinement 8=13276
 Nb complex, (C₂NH₂)₂[NbCl₄O], deviation from superposition structure 8=13279
 Nb₂S₃ 8=22032
 Nd telluride system, six phases, and their crystal chemistry 8=17202
 NdAlO₃, X-ray diff. 8=8544

Crystal structure, atomic—contd**inorganic compounds—contd**

- NH₄AgI₃, rel. to ionic mobility 8=17379
 NH₄BrCl, at 140°K 8=8545
 NH₄CuTiF₇·4H₂O 8=13280
 NH₄I, modifications II and III, lattice parameters 8=17398
 NH₄OHCl, hydroxylammonium chloride 8=8546
 Ni complex, bis(diethyldithiophosphato) nickel (II) 8=8548
 Ni(II) complex, bis-(N,N-di-n-propyldithiocarbamate), pseudo-homometric 8=22034
 Ni complex, bis-(N-isopropyl-3-ethylsalicylaldiminato) nickel 8=8551
 Ni complex, bis-(N-methylsalicylaldiminato) nickel, orthorhombic form 8=8550
 Ni complex, bis-salicylaldoximate-nickel, bond lengths 8=8549
 Ni complex, tetraethylammonium tetrachloronickelate, [(C₂H₅)₄N]₂NiCl₄ 8=8547
 Ni complex, bistrisphenylphosphine-ethylene nickel(o) 8=13281
 NiCr₂S₃, rel. to mag. props. and analogy with Cr₂S₃ 8=22833
 NiCr₂Se₄, lattice parameters, rel. to d-orbital interaction clarification 8=5391
 Ni-H system, lattice parameter H conc. dependence at -40°C 8=17404
 NiMn₂O₄, single crystals, lattice const. 8=21959
 Ni(NO₃)₂·4H₂O 8=17405
 NiO, hydrated, rel. to electrochem. activity, obs. 8=23146
 α-Ni₂P₂O₇ 8=17367
 Ni₃TeO₈ 8=4880
 O¹⁸ in enriched-UO₂ coherent neutron scattering length 8=8553
 OsS₂ 8=8556
 OsTe₂ 8=8556
 PaCl₃, and stoichiometry 8=13283
 PaOCl₂, by X-ray diff. and least-squares refinement 8=22036
 Pb phosphates, M^{II}M^{III}(PO₃)₄, (M^{II}=Pb, M^{III}=NH₄, K, Rb or Tl) 8=13293
 Pb₂CuCrO₄ (As, P)O₄OH, formacite 8=13284
 Pb₂V₂O₇ (chervette) 8=13285
 Pd complex, bis-(N-isopropyl-3-ethylsalicylaldiminato) palladium 8=8552
 Pd complex, trans-dichlorobis(dimethyl sulphoxide) Pd(II), and mol. structure 8=1804
 Pd-Au-D system, α phase, neutron diffraction 8=17407
 Pd-Au-H system, α phase, neutron diffraction 8=17407
 Pr telluride system, six phases, and their crystal chemistry 8=17202
 Pr₂Fe₁₇, refinement 8=17408
 PrH₃ 8=22761
 Pt₃Fe, atomic order effects on mag. structure 8=18348
 Pu₂Zn₂₉ 8=17409
 RbAg₄I₆, rel. to ionic mobility 8=17379
 β-RbMnCl₃·2H₂O 8=17411
 Rh₄(CO)₁₂ twinned 8=17412
 Rh₂S₃ 8=17413
 Rh₂S₃, Rh₂Se₃ and Ir₂Se₃, octahedron pairs 8=1807
 RuS₂ 8=8556
 RuTe₂ 8=8556
 S₈N₄H₄, by neutron diff. meas. 8=4884
 S₈O₃, improved dimensions 8=17400
 SbCl₄F 8=17418
 ScTiMO₆, (M=Nb, Ta, Sb), and fluorescence 8=4879
 Sr phosphates, M^{II}M^{III}(PO₃)₄, (M^{II}=Sr, M^{III}=NH₄, K, Rb or Tl) 8=13293
 Sr(IO₃)₂·XH₂O (X=1, 6) 8=8558
 Sr(IO₃)₂·7H₂O 8=8558
 SrK(PO₃)₄ 8=13293
 Sr(N₃)₂, and refinement 8=17387
 α-Sr₂P₂O₇ 8=13292
 Sr₂Sb₂O₇ (x = 1, 2; y = 4, 5), X-ray powder diff. patterns 8=14363
 SrVSi₂O₇, haradaite, SrVSi₂O₇, and Si-O bond lengths 8=17416
 TaCl₄F 8=17418
 Ta-O system, new phases, e-diff. study 8=17101
 TaO_{2-x} in thin films, e-diff. exam. 8=17417
 Te(NO₃)₄, bond distances, Mössbauer effect 8=4887
 TeO₂, bond distances, Mössbauer effect 8=4887
 Ti complex, diethoxytitanium dichloride, rel. to Ti 5-coordination 8=17421
 Ti complex, di-tetraethylammonium tetrachloroxo-titanate (IV) 8=17422
 TiCl₃·α, X-ray diffraction meas. 8=22041
 TiFe₂, atomic arrangement in homogeneity range of Laves phase 8=1813
 Ti-Fe-Si system, R(M, X)₂ and RMX₂ cpds. 8=17435
 TiGaLiO₄, of ordered phase on annealing at 600°C 8=17423
 Ti(HPO₄)₂·H₂O, synthetic ion exchanger 8=13295
 TiO₂ II modification at 40-120 kbar and 400-1500°C 8=17104
 Ti₂O₃, ordered, by e-microscopy 8=17420
 TL₂Te, rhombohedral, by e-diff. 8=17424
 UC₂, 300-5°K 8=1810
 UF₃, from n diffraction 8=13297
 U₂F₉, body-centred 8=13298
 UO₂, Debye-Waller factors, anharmonic temp. contribs. 8=13299
 UO₂Cl₂, and hydrates 8=22042
 UO₂[S₂CN(C₂H₅)₂]₂·[H₂N(C₂H₅)₂], monoclinic 8=4899
 U₂Ru₃, from X-ray powder data 8=22043

Crystal structure, atomic—contd**inorganic compounds—contd**

- V complex, di(tetraethylammonium) tetrachloroxo-vanadate (IV) 8=17422
 VCr₂Se₄, lattice parameters, rel. to d-orbital interaction clarification 8=5391
 V₂MoO₈ 8=17425
 VN, atomic state, by absolute meas. of X-ray scattering factors 8=13030
 VO₂, domain structure and twinning in low temp. monoclinic phase 8=4889
 VO₂, tetragonal phase, thermal expansion from lattice meas. at 78-415°C 8=13385
 VO₂, phase transformation 8=4719
 V₃Si type, tetragonal modifications 8=4888
 β-W, V₃Si type tetragonal modifications 8=4888
 W, C, rhombic modifications rel. to annealing temp. 8=856
 XeF₆, electron diff. obs. 8=17383
 Y phosphate-vanadates 8=14330
 Y sulphate hydrates, X-ray and thermogravimetric analysis 8=17385
 YAl₃, two polymorphic forms 8=1811
 YAlO₃, X-ray diff. 8=8544
 Y-B system with 1-1½%Y, refinement 8=17429
 YCl(OH)₂, monoclinic, X-ray diff. exam. 8=17428
 Y₂Cl₂O(OH)₂, orthorhombic, X-ray diff. exam. 8=17428
 YNi₂ and YNi₃ 8=17426
 YTaO₄, M^I-phase (fergusonite polymorph) 8=8562
 YVO₄, refinement from single crystal and powder X-ray data 8=17427
 Y₂WO₆, lattice constants determ. 8=5709
 Yb₂Sb₂ 8=17430
 Zn[Co(CO)₄]₂ 8=17431
 Zn₃In₂S₈ 8=8567
 Zn₃In₂S₈, single crystals 8=13301
 Zn₂Mn₂O₄, cation distrib. determ. 8=17364
 Zn(NO₃)₂·XH₂O (X=4, 2) 8=8565
 β-Zn₃(PO₄)₂ 8=8566
 ZnS, effective ionic charge calc. 8=17304
 ZnS polytypes 8=8563
 ZnS, polytype families 8=8564
 ZnS polytypes of family 24L-72R, unit cell and Zhdanov symbols 8=17194
 ZnS-phosphor, vibrational structure in stimulation spectrum 8=2459
 ZrSiF₆·6H₂O and analogous cpds., X-ray exam. 8=17432
 ZrC₂H₂ cpd. formed in Zr-H-C system 8=17433
 ZrF₆, atomic arrangement in homogeneity range of Laves phase 8=1813
 Zr(HXO₄)₂·H₂O, (X = P, As), synthetic ion exchanger 8=13295
 (Zr, Hf)_{0.955}N, defect structure by chem. and lattice studies 8=17434
 ZrN₂H₂ cpd. formed in Zr-H-N system 8=17433
 Zr-Ni-Al system, R(M, X)₂ and RMX₂ cpds. 8=17435
 Zr(OH)₂(MoO₃OH)₂, synthetic ion exchanger 8=13295
 Zr₅Si₄, by X-ray diff. 8=17436
- organic compounds**
 acetoinediol cyclophosphate 8=17438
 4-acetyl-2'-fluorobiphenyl 8=17444
 acetylene-diphenyl Ge addition cpd, (CH₂)Ge(C₆H₅)₂, and mol. structure 8=22046
 acetylene-GeI₄ addition cpd, and mol. structure 8=22046
 aleuritic acids (erythro and threo), powder diffraction data 8=22047
 amino acids derivatives and metal complexes 8=1814
 p-aminobenzamide, and mol. structure 8=22075
 p-aminobenzoic acid 8=8570
 α-p-aminobenzoic acid, and refinement 8=17443
 ammonium acetate, rel. to H bonding 8=8503
 amyl stearate, and other long-chain esters 8=22057
 amylose triacetate I 8=17461
 5α-androstan-3, 17-dione (ANDR), crystal packing calculation 8=13311
 L-ascorbic acid, X-ray analysis 8=13303
 anthraquinone, 1, 5-dihalo derivs., and mol. structure 8=22048
 auramine perchlorate, correl. with refl. spectroscopic obs. 8=13302
 azidopurine from 6-hydrazinopurine + HNO₃, and mol. structure 8=21117
 benzo-thiopyrone 8=22051
 o-benzoyl benzoic acid, space group 8=17441
 4-benzoyloxyphenol, packing relationship 8=17440
 2-(benzylthio) imidazole hydrochloride 8=8582
 2-(benzylthio) tetrahydropyrimidine hydrochloride 8=858
 5, 5'-bisoxazole, and mol. structure 8=22067
 2, 2'-biphenyldisulphide 8=22071
 p-bis(dimethylhydroxysilyl) benzene 8=22065
 p-bromooacetanilide, Br⁷⁹ Zeeman effect obs. 8=4228
 2-bromo-1, 1-diphenyl-prop-1-ene 8=4187
 bromomexicanin E, and mol. structure 8=21151
 (3:1) bullvalene-AgBF₄ complex 8=4890
 canthaxanthin 8=22053
 catalase, electron microscope and X-ray investigations 8=8575
 α-chloro-δ-valerolactam 8=8597
 chlorpromazine 8=8592
 π-crobyl NiX, (X=Cl, I), rel. to butadiene polymerization catalysis, obs. 8=8576

Crystal structure, atomic—contd**organic compounds—contd**

- cryptopine, $C_{21}H_{29}O_3N$ 8=22055
 cyclic paraffins, interatomic distances, molecular structure, chain folding 8=1827
 deca-trans-3, trans-7-dienedioic acid, X-ray analysis 8=8578
 15,15'-dehydrocanthaxanthin 8=22053
 diaminodiphenylsulphone, and mol. structure 8=22075
 1,4-dibenzoyloxybenzene, packing relationship 8=17440
 4,4'-dibromo-dibenzoylperoxide, and mol. structure 8=17442
 2,3-dibromo-1,4-naphthoquinone 8=8588
 dicalcium strontium propionate, $Ca_2Sr(C_2H_5CO_2)_6$, in ferroelectric phase 8=4892
 dicalcium strontium propionate, $Ca_2Sr(C_2H_5CO_2)_6$, in paraelectric phase 8=4891
 dicarboxylic acids, appl. of close-packing principle 8=22056
 4,4'-dichloro-dibenzoyl peroxide, and mol. structure 8=17442
 9-dicyanomethylene-2,4,7-trinitrofluorene 8=8580
 di-iodo-L-tyrosine dihydrate, from X-ray diff. 8=1826
 1,1-dimethoxy-2,4,6-trinitro-benzene ion 8=8572
 2,6-dimethylbenzoic acid 8=8571
 2,6-dimethyl benzoic acid, rel. to distortion of planarity 8=22049
 2,5-dimethyl-p-benzoquinone, and electron density 8=8573
 meso- α , α' -dimethylglutaric acid, refinement and mol. structure 8=1819
 2,3-dimethylnaphthalene, mol. and cryst. structure from i.r. spectra and diagm. anisotropy 8=18574
 2,3-dimethyl-1,4-naphthoquinone 8=8587
 dimethylsilylamine, penta co-ordinated Si 8=4894
 α , α' -dimethylsuccinic acids, and molecular structure obs. 8=22000
 1,1,-diphenyl-2-bromo-prop(1)ene, rel. to chem. activity 8=22058
 dithiono-4-oxo-1,3-thiazane, unit cell and space group 8=4898
 1,1,-di-para-tolyl-2-bromoethylene, rel. to chem. activity 8=22058
 DPPH stable free radical 8=1317
 esters, long-chain and other long-chain esters 8=22057
 estrone-related cpds., lattice constants 8=8579
 ethyl-1-thio- α -D-glucofuranoside 8=8581
 ethylene-butene-1 copolymers 8=8598
 ethylene oxide- H_2O clathrates, thermal and composition expansion 8=17447
 ethylidene-NN-diacetamide, unit cell and space group obs. 8=1817
 ferrocene-tetracyanoethylene complex 8=1792
 furane- α , α' -dicarboxylic acid, and mol. structure 8=17448
 galactital, by sign correlation procedure 8=22059
 α -glycylglycine 8=13307
 gramicidin C, iodohydrate, structural anal. 8=4893
 guanidinium $Al_2(SO_4)_3 \cdot 6H_2O$ 8=17449
 guanidinium aluminium sulphate, $6H_2O$, refinement 8=17450
 guanidinium $Cr_2(SO_4)_3 \cdot 6H_2O$ 8=17449
 haloxine, new alkaloid, and mol. structure 8=17451
 2-imino-4-thiazolidinone 5-acetic acid unit cell and space group 8=4898
 α -iodododecanoic acid methyl ester and other long-chain esters 8=22057
 lanthanide (III) oxalate decahydrates 8=8529
 L-leucine hydrobromide 8=8583
 D-leucyl glycine hydrobromide, min. function Fourier integral approach 8=22061
 lysozyme, rel. to enzymatic props. 8=23128
 magnesium hexa-antipyrine perchlorate, and mol. structure 8=8593
 D-mannitol, α - and β -forms 8=22062
 Meisenheimer salts, rel. to chem. activity 8=22058
 3-methoxy-5 β , 19-cyclo-5, 10-secoandrosta-1(10), 2, 4-trien-17 β -ol p-bromobenzoate 8=22063
 trans N-methyl-N-benzilthioformamide, and mol. structure 8=22050
 1-methyl-1,4-dihydronicotinamide, dimeric acid product 8=1822
 methyl β -maltopyranoside 8=8584
 methyl oxocarboxion ion, Friedel-Crafts acylation intermediate 8=22064
 methylene halides, i.r. data 8=14284
 molecular complexes exhibiting polarization bonding 8=8585
 molecular packing rel. to π electron systems 8=13031
 naphthalene-1,4-diol, and mol. structure 8=8586
 nitrilotriacetic acid, by X-ray crystallography 8=1815
 norbornene-2,3-dicarboxylic acid mono-potassium salt dihydrate, and mol. structure 8=22052
 octylstearate, and other long-chain esters 8=22057
 oxalate, $NH_4Y(C_2O_4)_2 \cdot H_2O$ 8=8590
 L-ornithine hydrochloride 8=8591
 pentamethylenetetrazole-ICI complex 8=17453
 1,10-phenanthroline-mercury (I) nitrate 8=17454
 phenolphthalein and congeneric mol. crystals, lattice disordering on plastic deform 8=23033
 phenoquinone, refinement 8=22070
 phenylhydrazine, X-ray diff. obs. 8=22069
 picolinium tetraiodobismuthate (III) 8=8574
 picolinium tetrabromobismuthate (III) 8=8574

Crystal structure, atomic—contd**organic compounds—contd**

- polyethylene, interatomic distances, molecular structure, chain folding 8=1827
 poly-3-methyl-butene-1, isostatic, single crysts. and growth, obs. 8=8599
 polyphenylacetylene lattice and crystallization structs. obs. 8=8600
 poly-p-xylene, molecular orientation, cell dimensions 8=1828
 promazine 8=8592
 proteins, rapid meas. of large nos. of reflection intensities by precession photography 8=17455
 protopine, $C_{20}H_{15}O_3N$ 8=22072
 pyrene-tetracyanoethylene complex, and refinement 8=22073
 quinaldic acid, at low temps. 8=1825
 quinaldic acid, Reminger effect 8=17457
 quinhydrone, monoclinic, refinement 8=22070
 reserpine, and mol. configuration 8=13310
 retusamine, α' -bromo-D-camphor-trans- π -sulphonate monohydrate 8=1816
 rifamycins B and Y, by X-ray analysis 8=22074
 ring cpds, non-aromatic, conformation 8=8597
 selenocyclopentane dibromide, and mol. structure 8=22068
 sulphanilamide monohydrate, three dimensional refinement 8=17458
 sulphanilamide polymorphs and hydrate, and mol. structure 8=22075
 tetracyanoethylene-naphthalene complex 8=8585
 7,7,8-tetracyanoquinodimethane-anthracene complex, and mol. structure 8=17460
 tetraethylammonium triiodide, two modifications 8=1818
 tetramethylammonium fluoride tetrahydrate 8=1821
 2,2,6,6,-tetramethylpiperidin-4-ol-1-oxide, radical rel. to mol. configurations 8=16370
 1,3,7,9-tetramethyluric acid: 3,4-benzpyrene, 2:1 mol. complex 8=1823
 tetraphenylporphyrin, triclinic 8=4896
 tolane-dimethyl silicon addition cpd, $(C_6H_5C)_2Si(CH_3)_2$, and mol. structure 8=22046
 p-toluidine, and mol. structure by X-ray and n-diff. 8=22077
 2,4,6-tribromoaniline 8=8569
 2,4,6-trichloroaniline 8=8569
 3,4,5-trichlorotetracyclo[4.4.0.0^{3,6}.0^{3,8}] decan-2-one 8=17446
 trimethylaluminium 8=4895
 trimethylplatinum (IV) iodide and its misrepresentation as hexamethyldiplatinum 8=13308
 2,4,6-trinitrophenetole 8=13309
 trioxane, determ. at -170°C 8=22066
 triphenyltin pentacarbonyl manganese 8=8594
 triscyclooctatetraen-dititanium 8=13304
 uracil 8=8596
 $Ag[C_9H_6N]_2ClO_4$, structure 8=17333
 $[Al(CH_3)_3]_2 \cdot C_4H_8O_2$ 8=8568
 $(CH_3)_4NNiCl_2$ 8=22076
 $[(C_2H_5)_xNH_{4-x}]_2Pt(CN)_4$ (X=1 to 3) 8=13306
 $(n_2C_2H_4)_4NBr$, non centrosymmetric, morphology 8=22054
 $C_6H_5N_2O_2 \cdot HCl$, using $CuK\alpha$ radiation 8=17452
 $C_{10}H_{12}N_2O_8$, condensation product of diaminosuccinic acid and pyruvic acid, X-ray studies 8=17437
 $(C_2NH_6)[NbCl_4O]$, deviation from superposition structure 8=13279
 Cs ethylate-ethyl picrate complex, rel. to chem. activity 8=22058
 $Cu(C_6H_5N)_3(CH_3COO)_2$, 3-d Patterson and Fourier methods 8=17456
 $(Et_4N)_2Cu(C_2B_9H_{11})_2$ 8=13305
 K ethylate-ethyl picrate complex, rel. to chem. activity 8=22058
 KH di-p-hydroxybenzoate hydrate, reinvestigation 8=22060
 LiBr(Cl). $2NH_3 \cdot CH_2 \cdot CH_2 \cdot NH_2$, ethylene diamine addition cpds. 8=1820
 $Ni_4(CO)_6[P(C_2H_5CN)_3]_4$, with tetrahedral Ni cluster 8=8589
 Pb diethyl-dithiocarbamates, and refinement 8=17445
 Pb stearate, optimization 8=14254
 Sr tartrate tetrahydrate, gel-grown, X-ray study 8=17459
 $UO_2[S_2CN(C_2H_5)_2]_2 \cdot [H_2N(C_2H_5)_2]$, monoclinic 8=4899
 Zn diethyl-dithiocarbamates, and refinement 8=17445
- Crystal symmetry.** See Crystallography; Crystal structure, atomic.
Crystallites. See Crystal structure/microstructure.
Crystallization
 See also Crystals/growth.
 alloys, binary, general soln. of dendritic crystn. eqn. 8=8174
 alloys, finely dispersed two-phase, recrystn. behaviour 8=8395
 Alnico-alloy permanent magnets, Ti-containing, columnar investigations 8=8399
 from aqueous solution under enforced fluid motion 8=8436
 binary cpds., computer model, rel. to kinetic phase transitions 8=4794
 chains in multicomponent systems 8=1733-4
 column for crystal purification with cyclic solids movement 8=17223
 dendrites and interdendrite spaces, alloy addition distribution 8=4823

Crystallization—contd

- diamond, in catalyst-metal system, graphite impurity crystal growth problem 8-1737
- diamonds, nucleation in growth, evidence 8-21945
- 1,2-diphenyl benzene, solidification kinetics into under-cooled melt 8-8401
- electrocrystallization, surface diffusion interactions 8-9719-21
- flux technique with localized cooling 8-13143
- Makrolon films, spherulites and non-amorphous structs. form., 180°C 8-8473
- metal crystals., electrochem., influenced time-depend. impurity adsorption 8-17225
- metals, growth vel. rel. to supercooling theory of expt. method 8-8419
- metals, on levitation in e. m. field 8-17222
- metals, nucleation, low freq. vibration effect 8-4796
- metals, supercooled, dynamic nucleation 8-21760
- mixtures, thermodynamics 8-4643
- nucleation kinetics, solids, examination of plane sections 8-4798
- n-paraffins, binary mixtures, kinetics 8-1733
- polyalkylacrylates, rel. to lengths of side branches, and struct. formation 8-21941
- polyethylene ethyl and methyl branched copolymers 8-17233
- polyethylene, from melt, regulation of degree of crystallinity, and fixing at given temp. 8-21932
- polymer melts, flow-induced fibre nuclei formation mechanism 8-1532
- polymer melts heterogeneous nucleation rel. to wettability, substrate effects 8-8298
- polymers, chain-folded 8-1734
- polymers, ciliation and fractionation 8-8390
- polymers, kinetics, a modified equation 8-8424
- polymers, rel. to orientation birefringence temp. dependence 8-9577
- polymers, polylamellar habits 8-1766
- polypropyleneoxide, isothermal, calorimetric study of kinetics 8-4811
- poly(tetramethylene oxide), dielec. meas. 8-17240
- polyvinyl alcohol films, i. r. study 8-13101
- polyvinylchloride, influence of high pressure on crystallinity 8-4774
- polyvinyl ethers, rel. to lengths of side branches, and struct. formation 8-21941
- quartz from dil. solns. at low temps. 8-4816
- rubber, stark, partially melted, recryst. 8-4771
- silicate glasses containing fluorides 8-8357
- steel, recrystallization, electron microscope observation 8-337
- u.s. vibration effects, review 8-3071
- white dwarf star 8-10152
- Ag, nucleation on NaCl 8-8188
- Al, cold-worked, nucleation 8-8397
- Al purification using fractional crystallization 8-4801
- Al, recrystn., textures 8-21938
- Al, rolling and recrystallization texture orientation relationships 8-1755
- Al-Cu-Ag alloys, nucleation of precipitates 8-17040
- Ar mol. beams at high intensity, condensation forming single crystals 8-16383
- Au, cold-worked, recryst. during α -irrad. 8-21943
- Au nucleation density on NaCl cleavage surface 8-4742
- Au, thin films, obs. in electron microscope 8-8314
- CO₂ mol. beams at high intensity, condensation forming single crystals 8-16383
- Ca hydrosilicate, in presence of gypsum and Al₂O₃ rel. to cement setting 8-1738
- Ca phosphate, nucleation from soln. 8-13135
- CdCl₂(ZnCl₂)-H₂O, interphase equil., by labelled Zn atoms 8-21933
- Cu, cold-rolled electrolytic, and Fournier anal. of elastic anisotropy 8-8404
- Cu, cubic texture formation during recrystallisation 8-4809
- Cu, deformed with tension, recrystallization at low temp. 8-17230
- Cu, and mech. props., rel. to plastic deform. at low temps. 8-8403
- Cu-Be-Ag alloys, nucleation of precipitates 8-17040
- CuFe₂Mn₂O₄, tetragonal distortion 8-17205
- Cu₂P monocrystals in Sn, and structure 8-21948
- Cu-Zn, dendritic under optimal cooling 8-4822
- Fe-whiskers, nucleation 8-18335
- Fe-whiskers, nucleation mag. field strength investigations 8-5467
- Fe-Cr-Ni-Nb steel, recrystallization obs. 8-21950
- Ge semiconducting films, by zone-melting 8-8320
- Ge, thin foils, dislocation arrangement obs. 8-1975
- InSb, thin films, electron beam re-crystallization, electrical props. 8-8323
- KCl(ZnCl₂)-H₂O, interphase equil., by labelled Zn atoms 8-21933
- (K, Na)(Br, Cl) solid soln., constitutional supercooling, convection cells 8-8417
- Li disilicate, from Li₂O-SiO₂ glasses 8-21953
- N₂ from molten Li, supercooling 8-12814
- NH₄Cl(ZnCl₂)-H₂O, interphase equil., by labelled Zn atoms 8-21933

Crystallization—contd

- NaCl(ZnCl₂)-H₂O, interphase equil., by labelled Zn atoms 8-21933
- Ni, cold-worked, nucleation 8-8397
- Ni, during creep, models criticism 8-8857
- Ni, rel. to polygonization 8-4808
- Ni, weakly deformed, recryst. nucleation 8-8421
- NiCrWTi steel solidifying at high temp., diagrams and results 8-8423
- PbB₂O₃, interface temp. of crystallizing melt 8-21960
- Pu, electrorefined, recrystallization and concurrent plastic deformation, 24-115°C 8-21961
- Ra-Ba mixed crystals., Ra as radioactive tracer 8-21962
- Re, cube texture formation, electron microscopic observations 8-13129
- Se, vitreous, photo-cryst., electronic processes 8-22471
- α -SiC on diamond, directed 8-8428
- Sn, recrystallization, autoradiography 8-13142
- SnO-SiO₂ glasses, and decomposition 8-21965
- Zn crystallite nucleation rates rel. to prior adsorpt. on W emitter 8-1746
- Zn crystals in rod form. prep. 8-8431

Crystallography

- See also Electron diffraction crystallography; Neutron diffraction crystallography; X-ray crystallography.
- achievements in USSR, 1917-1967 8-2874
- anomalous transmission, thermal vibr. contrib. 8-8492
- antisymmetry 8-13113
- classification of 8795 substances by space group, etc. 8-8474
- films, Debye-Waller factor from freq. spectrum 8-13024
- groups of quasi-symmetry (P-symmetry) 8-8366
- groups of symmetry and kinds of antisymmetry, classification scheme 8-1718
- homometric structures 8-13161
- impurity capture coefficient for elementary step 8-8386
- indices of planes in twinned crystals., transform. formulae 8-1722
- isogyres, special forms and props. 8-17193
- lattice generalization and classification 8-17306
- non-crystallographic symmetry problem, linear analysis 8-8475
- oriented cutting of single crystals without external facing 8-13149
- single crystal studies, rotating head apparatus 8-8361
- symmetry groups up to 3-dimensions, geom. symbols 8-8365
- symmetry, theory and applications review 8-8364
- trial structure generation rel. to mol. symmetry and space groups 8-17302

Crystals

- See also Liquid crystals.
- alkali halide, box model 8-1627
- amplification of sound in crystals, effect of elec. field 8-1846
- charges acquired by rubbing with metals 8-18158
- diatomic, force consts. and cohesive energies 8-8192
- inert-gas matrices with trapped mols., rotation-translation coupling 8-8230
- interchange symmetry concept 8-4118
- ion removal from square lattices 8-21791
- Ising model, transport eqns. near critical point 8-10669
- lattice energies of heavy ionic crystals 8-21794
- methyltrichlorosilane, thermal-decomp. and texture of SiC formed 8-21994
- non-linear, tuning for second harmonic in laser beam 8-3322
- particles, fast, charged, reversibility 8-2016
- quantum mechanics, possible use for crystal construction 8-21790
- single, bremsstrahlung reflection spectrometry 8-6794
- Al, as neutron monochromator 8-854
- Cu, as neutron monochromator 8-854
- Cu, recrystall. and cold-rolled textures, study by n diffraction 8-17278
- D⁺ ion channeling, transparency model 8-22243
- HiCuSi single crystals. 8-4777
- KBr, structure factors, and electron distrib. in K and Br ions 8-17861
- KF-SnF₂-H₂O system 8-4781
- KH₂PO₄, anisotropic, analysis of stimulated Raman effects 8-9543
- K(Ta-Nb), characterization by electrooptic obs. 8-9199
- PbGe, as neutron monochromator 8-854
- ThCu₂Si₂ single crystals. 8-4777
- electron states. See Crystal electron states.
- etching
- anthracene 8-8381
- apophyllite, a-face structures 8-17220
- corundum, in H, orientation meas. by optical back reflection 8-17206
- diamond, synthetic, rates on different forms, comparative study 8-21929
- etchants for crystal defect studies, table 8-17597
- feldspar, plagioclase, electron microscopy study 8-21930
- ferrite hexagonal, in 1:1 HCl at 90°C, etch steps height used as standard for electron microscope calibration 8-8450
- particle detector using chemical etching 8-11331

Crystals—contd
etching—contd

- photoetching techs. rel. to precise and fine treatment of integrated circuit fabrication 8=18096
polyethylene, with fuming HNO_3 , after irradi. 8=17216
polyethylene, HNO_3 oxidation technique 8=17214
sucrose, dislocations 8=4983
technique for control of slip and bowing 8=8385
II-VI compounds, new optical-quality etch 8=21928
AgCl dislocations 8=1965
Al, electropolished, thermal etch pits formed during cooling 8=17117
Be, and polishing by metallographic technique 8=4790
BeO polycrystals, etch pitting obs. 8=13539
Cd, prep. and figure-types 8=1726
CdS, in KOH(NaOH) soln., sensitization to light 8=14294
CsI, dislocation, inhibitor ions role in prod. of pits 8=1727
Fe, thermal, in vacuum, around transformation point of α to γ 8=17652
GaSe, optimal etchant for visualization of dislocations on basal planes 8=1973
Ge, by I vapour, reflection coeff. from surface 8=8382
n-Ge, in HNO_3 -HF- CH_3COOH 8=4791
Ge, metallic, rel. to facet forming planes 8=1728
Ge point contact diode, etch pits due to plastic deform. 8=5326
Ge, vac. thermal etching 8=17217
InSb crystal, selective, in HCl solns. of FeCl_3 8=8383
InSb, metallic, rel. to facet forming planes 8=1728
 $\text{KCa}_2\text{H}_2\text{Si}_2\text{O}_8$ (apophyllite), on basal cleavages, rot. 8=8384
Li ferrite, self-decoration effect 8=1729
LiF, with Fe^{3+} soln., rel. to surface morphology 8=1724
Mo, dislocations, etch pitting 8=4978
 MoS_2 , rel. to detect of vacancies 8=4963
NaCl, etch-pit morphology changes on cleavage faces due to water 8=1731
NaCl, use of formic acid 8=17658
NaF, universal etch 8=1730
Nb, dislocation structures, chemical and electro-etched, optical microscope obs. 8=22208
NiO, dislocation etch pits, shape and size rel. to etching time 8=1977
 $\text{PbSe}_{1-x}\text{Te}_x$, dislocation revealing 8=1689
Se, hexagonal, etch pits 8=1990
Se phase identification in V_2V_{1-x} alloys 8=17102
Si films, etch rates in H_3PO_4 , influence of H_2O content 8=17218
Si, in HNO_3 -HF- CH_3COOH 8=4791
Si, in H_2O -amine-complexing agent 8=4792
Si, n-type, etching in aq. h.f. solns. 8=17219
Si, substrate, SiO_2 and Si_3N_4 elimination, epitaxial growth 8=13128
Si and SiO_2 surfaces, use of F^{18} in HF etches for fluoride chemisorption obs. 8=18697
Si, through windows in SiO_2 8=17245
Si, vac. thermal etching 8=17217
 SiC , use for polarity study 8=21999
 Si_3N_4 films, etch rates in H_3PO_4 , influence of H_2O content, and use of SiO_2 mask 8=17218
 SiO_2 film, rel. to temp. of deposition 8=21889
 SiO_2 films, etch rates in H_3PO_4 , influence of H_2O content, and use as mask for etching Si_3N_4 8=17218
 SiO_2 films, on Si, after exposure to electron beam 8=22609
Te phase identification in V_2V_{1-x} alloys 8=17102
 YMnO_3 , ferroelec., for visibility of domain structure 8=2247
Zn, etch pits at dislocations 8=4984
Zn, etch-pit technique, revealing dislocations 8=13439
- excitons.** See Crystal electron states/excitons.
- faces**
alkali halides, cleavage surface, adsorpt. of water vapour 8=17166
angles of prisms, measurement of 8=11124
anthracene, morphology 8=8381
cleaving device, in ultra-high vac. 8=21926
diamond (111), epitaxial growth of SiC 8=8428
diamonds, synthetic, growth hillocks on (100) faces 8=17213
diamond, trigons rel. to growth failure 8=4787
diamond twins, (111) faces, micromorphology 8=1723
dislocation-free growth rel. to long range action of local active centres 8=4797
oriented crystals prep., lapping machine attachment 8=21918
polyethylene, fold-surface struct. 8=17214
polyethylene, surface struct. 8=17215
surface reflection of atom and ion beams rel. to micro-structure 8=13201
thermodynamic classification of surface and ang. depend. of free surface energy 8=8377
X-ray topography, apparatus 8=17262
Ag(III), exam. by LEED rel. to secondary emission 8=17212
AgBr, microcrystals, effect of solvolysis on growth 8=4786
Be, polishing and etching by metallographic technique 8=4790
(nC_2H_7)₄NBr, non centrosymmetric, morphology 8=22054
Cr, oxidation rel. to Cr_2O_3 , epitaxial growth 8=4828
Cu, fatigued at low strain amplitude, surface slip line behaviour 8=17774

Crystals—contd
faces—contd

- Cu films, epitaxial, topographical changes on exposure to H_2 - O_2 combination at 325°C 8=8318
Cu single crystals, thermal smoothing 8=4788
GaAs, prep. for epitaxial deposition 8=9104
Ge, metallic etching rel. to facet forming planes 8=1728
InSb, metallic etching rel. to facet forming planes 8=1728
LiF, surface layer structure, props. after annealing 8=8378
LiF, surface morphology, after etching in Fe^{3+} soln. 8=1724
MgO, primary step growth obs. by direct transmission microscopy 8=4789
NaCl, cleavage, etch-pit morphology changes due to water 8=1731
NaCl, nucleation density of Au on cleavage surface 8=4742
NaCl, (100) surface, study with LEED 8=17116
Ni(III), oriented growth of Ni_3S_2 , e-diffr. study 8=17254
NiO, LEED study 8=8379
Pt, epitaxial growth on NaCl(100) face and CaF_2 (111) face 8=4752
Si, electrical decoration of solid surfaces, new method 8=8380
W, work function of Cs 8=13926
Zn single crystals, stress-wave cleavage 8=21927
- growth**
See also Crystallization; Zone melting and refining.
acetoxine, (CH_3)₂C:NOH from benzine soln., up to 2.5 cm., props. 8=8396
anthracene, vapour- and melt-grown, purity and perfection 8=21942
apatite crystallites, carbonate effects on morphology during growth 8=1720
apophyllite, a-face structures 8=17220
arsenolite epitaxial growth on fluorine rel. to temp. of As_2O_3 vapour and CaF_2 8=17252
benzene sulphanyl chlorides, parasubstituted, single crystals 8=13133
composite growth from melts 8=4647
conference, Moscow, July 1966 8=8362
corundum, weighing up to 1 kg, hydrothermally produced 8=8400
Czochralski, radial solute segregation 8=4815
dendrite tip instability 8=8432
diamond, in catalyst-metal system, graphite impurity crystal growth problem 8=1737
diamond, trigons rel. to growth failure 8=4787
diamond twins, from micromorphology of (111) faces 8=1723
diamonds, nucleation evidence 8=21945
1,2-diphenyl benzene, solidification kinetics into under-cooled melt 8=8401
diphenyl, layer-spiral, influence of constant electric field 8=21949
dislocation-free, rel. to long range action of local active centres 8=4797
f. c. c. dendrites, twin configs. 8=17247
ferrites, nucleation of magnetic domain walls 8=2339
films, nucleation mechanism, role of structural defects 8=1735
flame-fusion method, automatic control system 8=4795
flux method, striations due to temp. fluctuations 8=13449
flux technique with localized cooling 8=13143
in gels, large crystals. 8=21934
glass, contamination-nucleated growth at bubble surfaces 8=21937
graphite, pyrolytic, formation mechanism and structure 8=13134
graphite, spheroidal, in Fe-C, Ni-C, Co-C, Au-C and Fe-C-Si alloys 8=13156
ice from melt, preferred orientation 8=21924
ice, hollow tubes and needles of controlled size 8=8413
ice, in H_2O or NaCl solns., by butane evap. sub-cooling, rates 8=13137
ice in supercooled water and aq. sucrose solns., velocities 8=17236
ice, in supercooled water, ultrasound effects 8=22102
lanthanides, recrystallization and work-hardening characts. 8=5089
large and single with focused light 8=8389
metal films, epitaxial on NaCl and KCl in vacuum, electron diffraction and electron microscope obs. 8=13147
metal, impurity microsegregation on liq. stream interaction with solidification front 8=17224
metallic, depend. on supercooling, theory of expt. method 8=8419
metals, extraction from molten state, thermal regime 8=8175
microscopic rates of growth, determ. in single crystals. 8=17226
models, analysis, for slightly supersaturated solns. 8=21935
multicomponent chains, kinetics 8=8390
naphthalene, zone melting, ultrasound effect 8=13139
niobates, single crystals, Czochralski technique 8=21958
numerical technique for calc. 8=4793
with plane faces, from soln., rates for rough and perfect interfaces 8=8388

Crystals—contd
growth—contd

- PVC single crystals of low mol. wt. 8=17300
polyethylene, supercooled liquid, nucleation rel. to temp. 8=1533
poly-3-methyl-butene-1, isotactic, single crystals and structure, obs. 8=8599
polyoxymethylene, epitaxy and molec. struct. 8=17255
polypropyleneoxide, isothermal, calorimetric study of kinetics 8=4811
polythiomethylene due to radiation effect on trithiane 8=17184
rare-earth sesquioxides, by Verneuil method; radiation effects and optimum conditions 8=4813
rare-earth sesquisulphide single crystals. 8=9119
rate, by analogue computer simulation 8=8387
ruby, by floating zone tech. with resistance heating 8=21939
sapphire, filaments from melt 8=21973
silicate glasses containing fluorides 8=8357
single and large, with focused light 8=8389
from solution at low supersat., error anal. of rate meas. 8=8393
solutions, stirred, diffusive and kinetic processes 8=8391
sphalerites faces in polar direction rel. to surface polarization calc. 8=8392
spirals on crystals, grown from molten salts 8=4838
steel, preferential, secondary grains, during annealing 8=17283
step, capture coeff. of impurities 8=8386
surface processes in electrocrystallization 8=13131
theoretical rate versus rel. supersat. curve, using least squares method 8=13130
thermodynamic surface anal., and ang. depend. of free surface energy 8=8377
triglycerides, long-chain, rates and kinetics 8=8412
vanadites, rel. to elec. transport props. 8=4819
vanadium (III) tris(salicylaldehydes) and tris(salicylaldehydes) complexes 8=16343
vapour deposition, nucleation obs. by mass spectra 8=17155
verneuil method, plasma heat transfer 8=21936
Verneuil tech., high temp., by arc melting 8=4799
wurtzites faces in polar direction rel. to surface polarization calc. 8=8392
Ag films on mica, W substrate nucleation 8=13087
AgBr, microcrystals, effect of solvolysis on faces 8=4786
AgBr microcrystals, rates and defect formation 8=8698
Al, pure thin single crystals by strain-annealing from zone-refined Al 8=8398
Al-Cu alloy, dendrite structure at chill surfaces 8=4821
Al-Cu alloys, dendrite arm spacing rel. to coarsening effect 8=4820
AlK alum., rel. to supersaturation, at low supersaturation 8=21940
 α - Al_2O_3 , n-irrad. induced growth along a and c axes 8=13132
Ar, effect on dielec. and optical props. 8=2238
Au film on MoS_2 , epitaxial, under u. h. vacuum and defect structure 8=17125
Au films, on NaCl, high vacuum 8=21878
Au films on NaCl, high vacuum, model 8=21879
Au, uniform microcrystals, from hydrosols 8=1745
Be single crystals, formation of dislocations 8=1969
BeO, rel. to screw-dislocation appearance 8=1736
Bi, in furnace using zone cooling 8=4802
Bi, large crystals, from supercooled melt 8=17227
Bi, mode rel. to cleavage planes 8=17243
Bi-MnBi eutectic single crystal, rel. to semimetal and ferromag. props. 8=8402
Bi, Te doped, rel. to distribution coeff. and donor valency 8=22517
 $\text{Ca}_{10}(\text{PO}_4)_6(\text{Cl})_2$, single crystals, conversion to $\text{Ca}_{10}(\text{PO}_4)_6(\text{OH})_2$ by hydrothermal bomb. method 8=4776
Cd, vapour-grown, patterns from screw dislocations 8=4803
 CdCO_3 , and e. p. r. study rel. to antiferromagnetism 8=18372
 CdF_2 , and phys. props. 8=8409
 CdS , closed system vapour growth from Cd and S 8=17228
 CdS , improved furnace, rel. to fluorescence 8=1739
 CdS , from liq. Cd soln. 8=17229
 CdS , S₂ annealing pressure effect on resist. homogeneity 8=8980
 CdSb , mono and polycrystalline 8=13698
 CeO_2 , single crystal, for lasers and optical components 8=1740
Co films, electrolytically deposited, rel. to structure and props. 8=13999
 CoCO_3 , and e. p. r. study, antiferromagnetism and resonance 8=18372
CoO by arc-transfer, ambient atmos. and Li doping effects obs. 8=4806
Cr electrodeposits epitaxy rel. to internal stress development. obs. 8=22325
Cu films, epitaxial, and activity and topographical changes on exposure to H_2 - O_2 combination at 325°C 8=8318
Cu-phthalocyanines from vap. phase 8=21946
CuCl, clear crystals, in gels 8=8405
CuCl, Czochralski technique, and imperfections 8=4804
CuCl, for optical modulators 8=8407
CuCl, in silica gel, technique 8=21944

Crystals—contd
growth—contd

- CuCl , single crystals, flux method 8=17231
 Cu_2Cl_2 , by diffusing Cl^- ions into gel 8=8406
 CuF_2 , layer growth conditions 8=17232
 Cu_2P monocrystals in Sn, and structure 8=21948
 $\text{Cu}_2\text{NbS}_4(\text{Se}_4)$ 8=8408
 CuSO_4 , from aqueous soln. under X-irrad. 8=21947
 $\text{Cu}_2\text{TaS}_4(\text{Se}_4)$, and optical props. 8=8408
EuAl borate, nonstoichiometry 8=8410
Fe, form. of cloud group of inclusions during deoxidation of liq. Fe with Al 8=22183
Fe films, electrolytically deposited, rel. to structure and props. 8=13999
Fe-Ni-Co-Al-Ti alloys, added Si, Se and Te effects rel. to coercivity and energy 8=22805
 $\text{Fe}(\text{NH}_4)_2(\text{SO}_4)_2 \cdot 6\text{H}_2\text{O}$, isothermal, high mag. field effect 8=8411
 α - Fe_2O_3 whiskers on Fe 8=17250
 Fe_3O_4 , by arc-transfer, ambient atmos. and Li doping effects obs. 8=4806
GaAs, epitaxial, from Ga soln. 8=4829
GaAs, epitaxial, use of SiCl_4 8=13146
GaAs, epitaxial deposition in Ar 8=17253
GaAs epitaxial films, propag. of growth striae 8=17129
GaAs, high-mobility, grown by liquid-phase epitaxy 8=22589
GaAs-Ge heterojunctions, by iodine process 8=5312
GaP, large crystals, from soln. 8=17234
GaP, vac. deposited, polymorphism 8=21883
GaP, vapour growth, effect of substrate orientation 8=13136
GdFe garnet, epitaxial on YAl garnet by chem. vapour deposition 8=13099
Ge, epitaxial films, prep. by pyrolysis of hydrides 8=17130
Ge, epitaxial growth in open iodine process 8=17131
Ge, thin, from liq. films, structure obs. 8=1741
Ge tubes, by pulling from melt 8=9111
 $\text{GeSe}_{0.75}\text{Te}_{0.25}$, prep. and props. 8=2197
He, solid, electron microscope investigation 8=8465
 He^4 , hexagonal, for birefringence meas. 8=15155
HfC, by arc melting Verneuil tech. 8=4799
 $\text{Hg}(\text{CN})_2 \cdot 0.80$ tetrahydrofuran, morphology and atomic structure 8=1794
HgS, by vapour phase method 8=21955
 $\text{Hg}_2\text{S}_2\text{Cl}_2$, by vapour phase method 8=21955
InAs diode laser prod. 8=11106
InAs epitaxial film on GaAs, orientated growth 8=17132
InAs, epitaxial, preparation and properties 8=1749
InAs-GaAs heterojunctions, by iodine process 8=5312
InOF, by reaction of In_2O_3 and InF_3 at 1000°C 8=8414
n-InP, effect of As doping on electrical properties 8=9113
InSb, epitaxy on single crystal substrate 8=17133
InSb films 8=13091
InSb films, epitaxial, electron diffraction study 8=21884
InSb, mechanism for single crystals using temp.-gradient zone melting 8=21951
 $\text{K}_{0.4}\text{Li}_{1.6}\text{NbO}_3$, single crystals, ferroelec. 8=21952
 $\text{KAl}(\text{SO}_4)_2 \cdot 12\text{H}_2\text{O}$, isothermal, high mag. field effect 8=8411
 $\text{KBr} \cdot \text{NO}_3$, CO_3^{2-} , SO_4^{2-} and SeO_3^{2-} , impurity anion form. conditions 8=8745
KCl, from aq. soln., effect of PbCl_2 8=8415-16
KCl, from soln., distrib. of Pb^{2+} impurities 8=17238
KI with TI impurities using vacuum furnace 8=17237
 KNO_3 , hydrothermal synthesis, 2-3 mm in size 8=8418
 $\text{KTaNb}_2\text{O}_{10}$ and effect of comp. on elec. resistivity 8=22503
 KTaO_3 , hydrothermal synthesis up to 1 mm in size 8=8418
 LiCe_2WO_4 , hydrothermal synthesis 8=21954
 LiF , with various Li isotope ratios, control using Stockbarger-Bridgman method 8=1742
LiH rel. to colour centre form. obs. 8=8748
 $\text{LiNd}(\text{WO}_4)_2$, hydrothermal synthesis 8=21954
 $\text{LiPr}(\text{WO}_4)_2$, hydrothermal synthesis 8=21954
 MgAl_2O_4 fibres and platelets, and crystal chemistry 8=2195
 MgO , primary step growth obs. by direct transmission microscopy 8=4789
 MgO whiskers, ductility obs. 8=13586
 MgO whisker, by vapour-liquid-solid, evidence 8=13144
 $3\text{MgO} \cdot \text{B}_2\text{O}_3$:Ge:Mn phosphors and luminesc. obs. 8=9621
 $\text{MgSO}_4 \cdot 7\text{H}_2\text{O}$, epsomite, left form predominance origin 8=17241
 Mg_2SiO_4 , forsterite, by flame fusion method 8=17242
Mn ferrites, (and mixed with Zn), intermed. phases in formation 8=17087
 MnCO_3 , and antiferromagnetism and resonance 8=18372
 Mn_3O_4 by arc-transfer, ambient atmos. and Li doping effects obs. 8=4806
Mo film on insulating substrates, heteroepitaxial 8=17134
 N_2 solid, electron microscope investigation 8=8465
 NaClO_3 , rel. to supersaturation, at low supersaturation 8=21940
 $\text{NaD}_2(\text{SeO}_3)_2$, ferroelectric 8=8420
 $\text{Na}_2\text{Fe}_2\text{O}_9$ 8=8540
 $\text{NaH}_2(\text{SeO}_3)_2$, ferroelectric 8=8420
 $\text{NaI}(\text{Ti})$, effect of Cl^- ions on activator distrib. 8=14327
 NaNO_3 , and dislocations, obs. 8=21957
 NaNO_3 , epitaxial, rel. to dielec. props. 8=2239
Ni films, electrolytically deposited, rel. to structure and props. 8=13999
Ni, weakly deformed, recrystallization nucleation 8=8421

Crystals—contd

growth—contd

- NiBr₂, surface-spikes, and impurities conc. 8=4807
 Ni-Fe ferrite, using arc image furnace 8=8422
 NiMn₂O₄, single crystals. 8=21959
 NiO by arc-transfer, ambient atmos. and Li doping effects obs. 8=4806
 Ni₃S₂ on Ni(III), oriented, e-diffr. study 8=17254
 O₂ solid, electron microscope investigation 8=8465
 PO₄, in static system, pH effects 8=17239
 PbB₂O₆, interface temp. of crystallizing melt 8=21960
 PbS, in silica gel near ambient temperatures 8=1743
 Pb-Sn alloys, composite growth from melt 8=4648
 PbZrO₃, coprecipitation meas. 8=1744
 Pt, refinement by annealing in air 8=4812
 Pt, uniform microcrystals, from hydrosols 8=1745
 Rb, vapour-deposition on Ag wire 8=13140
 Sb, mode rel. to cleavage planes 8=17243
 Se, hexagonal from orthorhombic, by polymorphic transition 8=8426
 Se, hexagonal single crystals, from supercritical NH₃ 8=8425
 Se, monoclinic by precipitation from solution in CS₂ 8=4814
 Si, epitaxial, effect of surface perturbations 8=17256
 Si epitaxial films on α -alumina, rel. to elect. props. 8=9121
 Si epitaxial films on Ge(111) surfaces, LEED struct. obs., 870°K 8=17140
 Si, epitaxial films, prep. by pyrolysis of hydrides 8=17130
 Si epitaxial films on Si(311) surfaces, LEED struct. obs., 870°K 8=17140
 Si epitaxial layers, "hillock" formation 8=17619
 Si films on W substrate by vacuum evaporation 8=4758
 Si, homoepitaxial, vacuum deposition, low temp. 8=1697
 Si, ingot prod. by Czochralski method 8=13141
 Si on insulators, epitaxy 8=8328
 Si, large area p-n junctions, by epitaxial growth technique 8=5316
 Si, radial solute segregation in Czochralski growth 8=4815
 Si on sapphire by chemical-vapour deposition, electron microscopy obs. 8=4826
 Si, single crystals, on cleaved planes, faults investigation 8=17244
 Si, substrate, SiO₂ and Si₃N₄ elimination, epitaxial growth 8=13128
 Si, through windows in SiO₂ 8=17245
 Si, variable capacitance diodes, low temp. epitaxial growth 8=13856
 α -SiC on diamond, directed 8=8428
 SiC, single crystal films on Si 8=1748
 β -SiC, from soln., C transport kinetics 8=17246
 SiC, vapour-liq.-solid and melt growth 8=21963
 SiO₂, epitaxial systems, vapour deposition 8=13148
 SiO₂ films deposited on n-type Si 8=4757
 SiO₂, film, in microwave discharge 8=4755
 SiO₂ isolation structures, fabrication rel. to integrated circuits 8=21964
 Si-WSi₃-Si, epitaxial struct. 8=17257
 Sn single crystals, by Webb-dendrite method 8=4824
 Sn, whiskers and filamentary growths on film due to d.c. 8=13145
 Sn-Bi alloys, dendrite morphology 8=4825
 Sr_{1-x}Ba_xNb₂O₆, Czochralski technique 8=21966
 TaC, by arc melting Verneuil tech. 8=4799
 ThO₂, single crystal, for lasers and optical components 8=1740
 TiO₂, by chem. transport with TeCl₄ 8=8429
 TiO₂, from the melt, single crystals 8=4817
 TlI, CsI stabilized 8=5640
 U-Cr alloys, martensite nucleation and growth in β - α transform., temp. dependence 8=4717
 US, mechanism, groove etching 8=21862
 β -US₂, single crystal prep. 8=4818
 Y, recrystallization and work-hardening characts. 8=5089
 YFe garnet, epitaxial on YAl garnet by chem. vapour deposition 8=13099
 Zn, effect of mech. vibr. 8=8430
 Zn ferrites, (and mixed with Mn), intermed. phases in formation 8=17087
 Zn, in rod form, prep. by recrystn. 8=8431
 ZnO, vapour phase 8=21970
 ZnS, cubic, epitaxial growth by evaporation in ultra-high vac. 8=21893
 ZnS, from melt, 1850°C, 50 atm Ar press. 8=21969
 ZnS, S³⁵ incorporation, radioactive 8=5000
 ZnS, Tm, and luminesc. rel. to Zn vacancies, obs. 8=8434
 ZnSb and ZnSb-CdSb mixed crystals, mono and polycrystalline 8=13698
 ZnSe, by direct fusion and electron mobility 8=2210

imperfections. See Crystal imperfections.

internal fields

- alkali metals, interionic potential modified in conduction electron presence 8=4671
 alkaline metals, strain critical systems 8=13524
 calcium fluoxytantalate: Eu³⁺, Sm³⁺, crystalline field parameters of ions 8=16973
 chemical shifts from n.m.r. resolution 8=4670
 cubic, lattice energy distrib. and its variation with compression or expansion 8=13000

Crystals—contd

internal fields—contd

- diamond lattice, second order dipole moments 8=1629
 electron momentum distrib. by Compton X-ray scattering 8=17907
 e. p. r. linewidth calc. by methods of moments 8=14086
 f. c. c. lattices, second order dipole moments 8=1629
 hyperfine fields in crystals, with mag. ordering 8=1630
 impurity ion, lowering of Slater parameters on electron exchanges 8=8700
 inhomogeneity effects on n. m. r. quadrupolar satellites 8=22917
 ion 3d⁵ configs. splitting by octahedral field 8=1654
 ionic complexes, overlap contrib. to elec. field gradient 8=21801
 ions with incomplete shells, spectra calcs. from field-theory 8=13033
 d⁷ ions in tetragonal fields, anal. of e.p.r. and optical spectra 8=21798
 lanthanides in fields of cubic symmetry, composite fⁿd configurations theory 8=21799
 lattice strain and Raman-active vibrations rel. to elasticity and piezoelectricity 8=5013
 magnetic hyperfine, sign determ. by Mössbauer-Faraday effect 8=13007
 magnetic impurity, Anderson and Kondo Hamiltonians for impurity orbitals 8=13008
 metals, electrostatic energy calc. by plane wise summation 8=8201
 metals, hexagonal, stress fields due to dislocation pile-ups on anisotropic treatment 8=1963
 metals, mag. moments nonlinear quantum pseudo-resonance 8=1631
 mixed cryst., impurity-host intermol. pot. energy rel. to coupling 8=17865
 molecular, lattice energy calcs. 8=13012
 molecular, strain tensors temp. dependence 8=13508
 parameters determ. using spin-lattice relaxation 8=18445
 periodic, stress thermally activated dislocation motion 8=8711
 polar, thermal eqn. of state, linear model 8=13013
 rare-earth ions, electric multipole interactions 8=16977
 rare-earths, theory of antisymmetric exchange 8=16972
 rectangular prismatic uniformly magnetized, demagnetizing fields 8=5454
 rutile-type with (nd)² ions, field theory explanation of e. s. r. spectra 8=9411
 Scheelites, pot. rel. to tetragonal rare earth centres optical and e. p. r. spectra 8=1637
 self-energy expressed as a continued fraction 8=10613
 62 \leq Z \leq 74, recoil implanted in polarized Fe-, Co- and Ni-environment, hyperfine fields 8=13034
 spin-orbit coupling, crystalline field with magnetic point group symmetry 8=1632
 tetrathiomolybdates 8=2438
 tetrathiotungstates 8=2438
 transition metal ions, octahedral complexes, electric quadrupole transitions 8=16976
 transition metal ion theory, recent Japanese work 8=16992
 transition metal cpds., thermodynamic and optical calcs. discrepancy correction 8=4669
 transition-metal fluorides, MO calc. of 10 Dq 8=4667
 weak octahedral field, matrix elements for config. d⁴ 8=13006
 III-V cpds., antishielding effects 8=14157
 AgCl, van-der-Waals dipole-dipole coeffs. 8=1625
 Ag-4.09% Cu, Ag and Cu binding energies 8=13029
 Ag-Cu-Sn system, electronic phases rel. to chemical displacements 8=17002
 Au-Fe solid soln., magnetic ordering rel. to electric hyperfine interactions 8=2289
 BaTiO₃, fine-grained, high permittivity, theory 8=22664
 CaFe₂O₄, hyperfine splitting rel. to spin relax. from Mossbauer studies 8=21804
 Ca₂Fe₂Si₂O₁₂, Fe³⁺ 3d⁵ configs. splitting 8=1654
 CaF₂:Sm³⁺, tetragonal field, energy levels 8=13009
 CaF₂:Yb³⁺, polarization effects in cubic cryst. field 8=21800
 CaO: Mn²⁺, impurity ion hyperfine coupling constant temp. dependence 8=8196
 CaWO₄:Ce, charge-compensated sites, local elec. fields 8=9418
 CaWO₄:Yb³⁺ 8=14205
 CdS, elec. field and photo-Hall mobility 8=17860
 CdS, piezoelec., field distrib. determ. by optical probe 8=18033
 Ce³⁺-activated phosphors 8=18600
 Co(H₂O)₆³⁺ and Co(NH₃)₆³⁺ thermodynamic and optical calcs., discrepancy correction 8=4669
 Co-Ni alloys, effective field distribution at Co⁵⁹ nuclei 8=8195
 Co-Pd alloys, (8.3 to 0.03 at. % Co), effective mag. field at Co⁵⁹ nuclei 8=5463
 Cr³⁺ in tungstates (ZnWO₄-type), third crystal-field constant meas. 8=16974
 Cu alloys with non-mag. impurities, elec. field gradient 8=9458
 CuCl₂.2H₂O, dipolar mag. field at proton site 8=18378

Crystals—contd

internal fields—contd

- Cu(HCOO)₂·4H₂O, magnetic props. and transitions 8=5501
 CuSO₄·5H₂O, proton conductance 8=8982
 Dy-Al-garnet hyperfine splitting of lowest 2' state of Dy 8=9301
 ErCl₃·6H₂O hyperfine splitting of lowest 2' state of Er 8=9301
 Eu, hyperfine field from conduction-electrons 8=1633
 Eu-M₂ (M = Pt, Pd, Zn, Rh), mag. hyperfine field Mossbauer studies 8=18334
 EuAl borate 8=8410
 EuF₃ 8=14214
 EuPd₃, mag. hyperfine field Mossbauer studies 8=18334
 Fe²⁺, cubic, magnetically induced electric field gradients, theory 8=21803
 FeBr₂, hyperfine structure at 78°K and 4°K Mössbauer effect obs. 8=13025
 FeCl₂, hyperfine structure at 78°K and 4°K, Mössbauer effect obs. 8=13025
 FeCl₃, hyperfine structure at 4°K, Mössbauer effect obs. 8=13025
 FeCl₂·2H₂O, antiferromag., exchange interaction rel. to magnetization process 8=2349
 FeCr₂S₈, effective fields in Fe⁵⁷ Mössbauer spectra 8=1647
 Fe(H₂O)₆²⁺, thermodynamic and optical calcs., discrepancy correction 8=4669
 FeI₂, hyperfine structure at 78°K and 4°K, Mössbauer effect obs. 8=13025
 Fe-In binary sy tem, γ-Fe field contraction, and δ, α expansion 8=8160
 Fe(NCS)₂·4Py, electric field from Mössbauer effect 8=8213
 FeSiF₆·6H₂O, hyperfine interactions from Mössbauer spectra 8=8220
 FeSiF₆·6H₂O, pure and diluted crystals, ligand field behaviour and mag. susceptibility 8=18297
 Gd, hyperfine field from conduction-electrons 8=1633
 H₂, ortho, in solid para-H₂, field splitting by n. m. r. obs. 8=13010
 H₂ solid, 1.6-4.2°K, magnitude of splittings for J=1 rot. manifold deduced from n.m.r. data 8=14141
 Ir¹⁹³ in Ar-rare-earth cpds. 8=1634
 KBr, van-der-Waals dipole-dipole coeffs. 8=1625
 KCl, van-der-Waals dipole-dipole coeffs. 8=1625
 KI, van-der-Waals dipole-dipole coeffs. 8=1625
 LaCl₃·Gd³⁺ 8=16975
 LiBH₄ and LiBD₄ 8=18466
 LiF:Fe³⁺, system, crystal field distortions, resonance obs. 8=13005
 MgAl₂O₄ rel. to optical transition variation with temp. 8=23000
 MnCsCl₃·2H₂O, parameters for Mn²⁺ ion from absorpt. spectrum 8=8197
 NaCl, pure and doped, pot. differences due to plastic deform. temp. dependence 8=16978
 NaI, elastic tensor of gradient elec. field induced by uniaxial stress, n. m. r. obs. 8=13014
 Na_{0.33}V₂O₅, model of electron transport 8=22601
 Nd ethylsulphate, parameters determ. using spin-lattice relaxation 8=18445
 NiF₂, thermodynamic and optical calcs., discrepancy correction 8=4669
 Ni(H₂O)₆²⁺ and Ni(NH₃)₆²⁺ thermodynamic and optical calcs., discrepancy correction 8=4669
 Ni₂Mn alloy, magnetic field at Mn⁵⁵ 8=1635
 Pa, large magnetic moment associated with Fe impurity atom, spin perturbation 8=1655
 Pd-Fe alloy containing H, hyperfine fields and isomer shifts temp. dependence by Mössbauer effect 8=13020
 Pr³⁺, field splitting and exchange interaction with electrons rel. to metal magnetism 8=2292
 PrCl₃, exchange charge effects 8=13011
 Pr₂(SO₄)₃·8H₂O, Pr¹⁴¹ n.m.r. meas. 8=14155
 RbFeF₃, effective fields in Fe⁵⁷ Mössbauer spectra 8=1647
 Sb impurity in Fe or Ni, internal nucl. 8=8198
 Sb Menshutkin complexes, electric field gradient, asymmetry parameter temp. depend. 8=21802
 Sb¹²⁴ implanted in Fe, hyperfine 8=8199
 Sn, oscillatory rel. to Knight shift 8=5566
 SrO:Mn²⁺, impurity ion hyperfine coupling constant temp. dependence 8=8196
 Ti³⁺ in SrTiO₃, electronic structure 8=9445
 Tm, crystalline elec. field determ. by Mössbauer-effect 8=8203
 TmN, exchange effects, e. p. r. study 8=2376
 TmT₃ (T = transition element), Mössbauer effect determ. of elec. field splittings 8=16979
 VO₂, V⁴⁺ electronic structure, field theory explanation of V⁵¹ n. m. r. spectra 8=9411
 Y_{3-x}Ca_xFe_{5-x}Sn_{0.12}, Mössbauer effect of Fe⁵⁷ 8=4677
 YFe garnet, transitions rel. to reflectivity 8=5642
 YFe garnet:Yb³⁺, behaviour on anomalous sites 8=22860
 Y₃Fe_{5-x}Cr_xO₁₂, symmetry by ferromagnetic resonance 8=1636
 Y₃Fe₅O₁₂:Ho³⁺, Faraday effect obs. 8=14271
 YGa garnet, transitions rel. to reflectivity 8=5642
 YbCl₃·6H₂O hyperfine splitting of lowest 2' state of Yb 8=9301

Crystals—contd

lattice mechanics

- See also Mössbauer effect,
 acoustic domains, generation of electroluminescent light 8=18587
 absorption by hot atoms vibrs. due to lattice displacement near charged impurity 8=2393
 alkali halides, expansion and m. p. calc. 8=16970
 alkali halide type crystals, theorem for spectral gaps 8=13314
 alkali halides, shell model treatment of harmonic vibrs., substitutional defects 8=13321
 alkali halide single crystal with nitrate-ion impurities, lattice vibrations 8=17471
 alkali halides, X-ray scattering from deformable ions 8=13330
 alloys, binary substitutional, calc. of freq. spectrum of vibrs. 8=8605
 anharmonic, mean-square velocity of atom 8=13035
 atomic vibrations in solids, survey of basic theory 8=22082
 b. c. c. metals, approx. dispersion relations 8=17480
 b. c. c. and f. c. c. metals, vibrations, freqs. and wave numbers, approx. dispersion relns. 8=17467
 benzene spectra in solid solns., matrix effects rel. to lattice vibrs. coupling, 77°K 8=13037
 channeling phenomena, location of shoulders, incorporating lattice vibrs. model 8=17690
 Coulomb-lattice vibrs., anharmonic effects investigated by s. c. f. method 8=13320
 cubic, energy distrib. and its variation with compression or expansion 8=13000
 defect effects: appl. of new formalism 8=13312
 diamond-like, chain distrib. of freq. in phonon spectrum 8=17515
 diamond, valence force potentials for calculating vibrs. 8=16968
 diamond, zero-phonon 415 mμ line temp. dependence 8=5589
 d' impurity systems, octahedrally coordinated, dynamic Jahn-Teller effect 8=16990
 diatomic disordered chain, freq. distrib. function 8=13316
 dispersion dynamics, new formalism 8=1834
 dynamics at 0°K, new theory 8=13324
 eigenoscillations of double spirals of discrete point masses 8=17473
 electron-phonon interaction, degree of coherence temp. 8=17466
 electron transport theory in strong elec. fields 8=2078
 end of series effect influencing the apparent shape of atoms in crystals 8=17303
 equations in harmonic approx. 8=13322
 excitons, triplet, coherent and incoherent migration 8=22474
 f. c. c. metals, angular forces in lattice dynamics model 8=8612
 f. c. c. metals, approx. dispersion relations 8=22080
 ferromagnet, phonon spectral density near Curie pt. 8=17468
 films, thermal freq. spectrum and Mössbauer effect 8=13024
 force-constant changes due to point defects 8=13319
 fractional phonon hysteresis 8=22081
 graphite, thermal vib. amps of C atoms parallel to e-axis 8=22085
 Green function and freq. spectrum, evaluation of Fourier coeffs. in expansion 8=13315
 halogens, intensities of i. r. -active vibr. 8=22084
 of harmonic and anharmonic shell models 8=8602
 harmonic, stationary nonequib. Gibbs ensemble 8=4901
 Helmholtz free energy, anharmonic contrib., high-temp. limit and zero-point energy 8=8601
 h. c. p., Coulomb sum calc. by Ewald's method 8=4855
 h. c. p. metals, phonon dispersion relations, calc. 8=13329
 ice, low frequency optical spectra, interpretation using crystal lattice model 8=13326
 impurity atoms, vibrational and optical props. from morphic effects 8=4966
 impurities, effect on phonon spectrum 8=1960
 impurity, isotopic composition effect on electronic-vibration lines 8=22937
 infrared absorpt. and Raman scat. calc. 8=14176
 insulators, lattice Raman scattering theory 8=2397
 ionic, finite-size, limiting phonon frequencies, retardation effects 8=1832
 lattice distortion effect on Debye-Waller factor rel. to lattice dynamics 8=1779
 lattice distortion effect on Debye-Waller factor rel. to lattice mechanics 8=1780
 local vibration mode, resonance phenomena 8=13323
 magnetodielectrics, interact. between optical phonons and magnons 8=2231
 metals, b. c. c., vibrational freq. spectrum 8=17465
 metals, Mössbauer effect, shift and intensity calc. 8=1643
 metals, simple, reln. with liq. state props. 8=16789
 metals, thermal expansion: thermodynamic approach to anharmonicity of lattice vibrs. 8=17529
 methane, molec. dynamics, translational and rot. 8=16374
 methylbenzenes, hindered rot., from neutron scatt. 8=17484
 mixed crystals, 3D disordered lattice model 8=10609
 molecular crystals, vibr. struct. of exciton states 8=5126

Crystals—contd

lattice mechanics—contd

Mössbauer effect intensity calc. in case of alocal vibrations for crystals with vacancies 8=8209
 multicomponent systems Mössbauer thermal shift, and Debye-Waller factor 8=13023
 multispin systems, relax. theory in presence of lattice and spin modulating mechanisms 8=9453
 normal vibrations, symmetry props. 8=17474-5
 one-dimensional lattice, stability 8=22079
 organic, oscillation spectrum and derivation of charact. temp., theory and expt. 8=17470
 paraffins, long-chain, intermolec. vibrations 8=13341
 paramagnetic ion nuclear relax. due to spin-phonon interaction 8=18450
 paramagnetic relaxation, phonon superheating, model 8=5518
 paramagnetic, u.s. absorpt. rel. to spin-lattice relax., quantum theory appl. 8=17487
 perovskite-type crystals, distorted, dynamic modes rel. to atomic displacements 8=17332
 perovskite-type, ferroelectric phonon lifetime, at low temps. 8=4908
 phonons with anharmonicity, perturbation theory for retarded Green's function 8=17469
 phonons, heating, influence on magnetophonon resonance 8=8622
 phonons, h.f. longitudinal, decay, perturbation theory calcs. 8=1829
 phonon interactions, use of Green function decoupling and diagrams 8=8603
 phonon processes in magnetic crystals, selection rules 8=13318
 phonon spectrum and mechanical perturbation propag. 8=13317
 phonons, subharmonic, threshold, including "up conversion" 8=13325
 in polyacene solid solns., energy transfer, 1965-66 bibliography 8=14162
 polydioxolane, vib. modes and molec. struct. 8=18584
 polyethylene, intermolec. vibrations 8=13341
 polymethylene chains, longitudinal acoustic vibrs. 8=8608
 polymer, linear chain-polycrystalline, anisotropic dynamics rel. to Mössbauer effect doublet spectra 8=13022
 quartz, stimulated Raman scattering from i.r.-active phonons 8=11112
 quartz α - β transition assoc. modes from Raman scatt. -196-615°C 8=1682
 Raman-active vibrations and internal-strain rel. to elasticity and piezoelectricity 8=5013
 relaxation of elect. and mechanical modes in NaCl structure allowing for 1st and 2nd neighbours 8=22174
 resonance, kinetic, moving source in periodic structure 8=13328
 rotation-translation coupling of trapped mols. 8=8230
 ruby, phonon breakdown theory 8=22952
 ruby, R^1 and B absorpt. linewidth and phonon-induced relaxations 8=14194
 sapphire, vib. assignments from Raman spectra 8=2401
 scattering of excitons in molec. crystals. 8=8948
 scattering of local initial perturbations in ideal lattice 8=17472
 semiconductors, electron-lattice interaction effect on free-carrier magneto-optics 8=8890
 semiconductors, elemental and compound, mean internal lattice potential 8=13833
 semiconductors with magnetic impurities, spin-lattice relaxation of conduction electrons, theory 8=5519
 semiconductor, optical phonons in magneto-optical absorption, interband 8=18492
 semiconductors, polar, optical phonon scatt. of charge carriers 8=13628
 semimetals, m.h.d. waves, plasma-phonon 8=5135
 solid solns., binary metallic, with random and ordered atom distrib. 8=1867
 solid solutions, thermal equation of state and quasi-local vibrations 8=8634
 specific heat calc. from phonon freq. meas. 8=22113
 spin-lattice relax. for Kramers doublets, dynamical spin Hamiltonian and anisotropy 8=9413-14
 spin-lattice relax. rel. to lattice anharmonicity 8=4902
 spin-orbit coupling, crystalline field with magnetic point group symmetry 8=1632
 spin-phonon coupling in conc. paramag. salts, effect on thermal cond. 8=18405
 spin-phonon system, decoupling of Green's functions 8=18404
 thermal phonons and third-order elastic consts. rel. to u.s. attenuation 8=4916
 thermal vibrations of coherently scattering crystals experimental method 8=8607
 thermal vibrations rel. to diamagnetic susceptibility 8=18294
 thermodynamic characts. in harmonic approx. without dispersion low calc. 8=13362
 thiourea, lattice vibr. freq. and intensities calc. 8=13339
 thiourea, l.f. modes, from neutron scatt. 8=13340
 two-component crystals, model problems 8=1833
 U-center local mode absorption, vibrational analysis of sideband 8=1831

Crystals—contd

lattice mechanics—contd

urea, l.f. modes, from neutron scatt. 8=13340
 vibration, conference Tylösand, Sweden 1966 8=8191
 vibrational excitation, relaxation 8=17866
 vibrations, effects of point defects and disorder 8=13327
 vibrations, modes, localized on defect in atom chain 8=4900
 vibrations, quantization 8=8606
 vibronic coupling, rigid-lattice model of molec. crystals. 8=13670
 vibronic spectra, nonlocal polarization effects 8=22078
 walk-counting method for c.p. lattices rel. to energy bands and impurity states 8=8604
 X-rays anomalous transmission, thermal vibr. contrib. 8=8492
 X-ray scattering dynamical theory, role of lattice vibrations 8=13313
 Ag, thermal oscillations frequency, temp. variation 8=17476
 Ag-4.09% Cu, vibration amplitudes, temp. depend. 8=13029
 Al, compared with collective atomic motion in liq. state 8=12796
 Al, phonon damping at low temp. due to electron-phonon interact. 8=17477
 Al, phonon-frequency distrib. and ht. capacity 8=1868
 Al, Wiedemann-Franz ratio and anomalous lattice cond. 8=8990
 AlN, i.r. lattice vibrations 8=8609
 Ar, self-consistent phonon theory, phonon spectrum and bulk thermodynamic props. 8=13336
 Ar, solid, zero-point energy, effect of long-range 3-body forces 8=22083
 Ar, solidified, vapour pressure, binding energy and mean vibration freq. 8=16960
 BaClF:Sm²⁺, phonon annihilation in ⁵D₀ and ⁵D₁ states 8=9600
 BaF₂, additively coloured, phonon-assisted colour centre fluorescence 8=14306
 BaTiO₃, i.r.-active optical phonon directional dispersions at room temp. 8=17478
 BaTiO₃ overdamped vibr. made from 30 ft E mode, Raman line-shape obs. 8=5586
 BaTiO₃, temp. dependence of l.f. transverse optic lattice vibration 8=17479
 Bi, amorphous, strong-coupling superconductivity and phonon structure 8=5202
 Bi, compared with collective atomic motion in liq. state 8=12796
 Bi, condensed on a surface, 2-4°K, phonon spectrum 8=2155
 CCl₄, dissolved coronene and triphenylene mols. deform., phosphoresc. obs., 77°K 8=1577
 CaF₂, additively coloured, phonon-assisted colour centre fluorescence 8=14306
 CaF₂:Yb³⁺, anisotropy of spin-lattice relax. for Kramers doublets 8=9414
 CaO:Mn²⁺, orbit-lattice interaction from lattice vibration amplitude 8=8196
 CaWO₄:Nd³⁺, spin-photon interaction 8=14121
 CdO, lattice vibrations, influence on u.v. reflection 8=9514
 Ce ethyl sulphate, Schottky anomaly and spin-phonon coupling 8=8636
 Ce ethyl sulphate, spin-phonon scatt. in mag. field rel. to thermal cond. 8=13393
 ClO₂⁻, ClO₂⁻ vibr. in alkali halides 8=22968-9-70
 CoO, dynamics and mag. excitations 8=22086
 Cr₂O₃, acoustic spin waves, studied by neutron scattering 8=14065
 CsCl, theoretical study, using shell model, sp. ht. and dispersion curves 8=8610
 Cu, f.c.c., angular forces in lattice dynamics model 8=8612
 Cu, phonon freq. determs. at 49 and 298°K 8=8611
 Cu-Al-Zn alloys, dislocation-phonon scattering rel. to thermal conductivity meas. 8=22203
 Cu-Mn alloys, Cu⁶³ n.m.r. and spin-lattice relax. 8=9464
 α -Fe, phonon dispersion relation at room temp. 8=1835
 Fe, phonon motion of mag. atoms, studied by polarized neutron scatt. 8=14012
 α -Fe, phonons and magnons, dispersion relations 8=13331
 Fe-N quenched alloys, martensite distortion 8=8522
 α -Fe-O₂, new type of antiferromagnetic resonance 8=2360
 FeV₂O₄, vibration, effect of deformation 8=8614
 GaAs, coupled optical-phonon-plasmon modes rel. to Raman scattering 8=22984
 GaP, dielectric dispersion and phonon line shape 8=14215
 H, solid, ortho, low lying excitation and ground state configuration 8=8267
 He, b.c.c., phonon freq. calcs. and thermodynamic props. 8=1836
 He, solid, by n-scattering at 2.9°K and 125 atm. 8=1837
 He³, solid, nuclear relaxation, 0.3-0.04°K, spin-lattice interaction 8=3130
 He⁴, phonon dispersion measurements on single crystals 8=10815
 In film, transverse phonon generation by microwave excitation 8=4903
 InSb, electron-TO- and electron-LO-phonon interactions 8=13817
 InSb, freq. of transverse oscillations along symmetry axes, by X-scattering meas. 8=8613

Crystals—contd

lattice mechanics—contd

- InSb, In¹¹⁵, Sb¹²¹, ¹²³ nuclear spin-lattice relax. rates 8=9471
 InSb, nuclear spin-lattice relax. temp. dependence 8=9472
 K halides, phonon scattering by monatomic impurities 8=4904
 KBr, U-center local mode absorption 8=1831
 KBr:O₂⁻, effect anharmonic vibrations on isotopic displacement of luminescence 8=22937
 KBr:Sm²⁺, one-phonon sideband of 6890 Å transition at 7°K 8=9614
 KCl, effective lattice freq. and F-centre half-width calcs. 8=4993
 KX, (X = Cl, Br, I), rel. to U centre electronic structure 8=2001-2
 K₃Cr(CN)₆, spin-phonon transition probabilities, meas. 8=5544
 KDF₂, vibrations, i.r. absorpt. study 8=5617
 K₄Fe(CN)₆, 3H₂O, ferroelectric phase transition, Mössbauer test for dynamical model 8=22667
 KHF₂, vibrations, i.r. absorpt. study 8=5617
 KI(Cl), phonon dispersion curves by X-ray analysis 8=1333
 KMF₃, (M = Mg, Mn, Co, Ni) rel. to i.r. reflectance spectra 8=2426
 KI-NaI, (-RbI), (-KCl) solid solns., rel. to absorpt. edge 8=22994
 KMF₃ (M = Mg, Mn, Co, Ni, Zn, Mg/Ni), i.r. transmission spectra rel. to multiphonon processes 8=2427
 KMgF₃, vib. anal. and assignments 8=2428
 KNiF₃, vib. anal. and assignments 8=2428
 KZnF₃, vib. anal. and assignments 8=2428
 Kr, solid, phonons anharmonic effects 8=17481
 Kr, solid, zero-point energy, effect of long-range 3-body forces 8=22083
 Kr, solidified, vapour pressure, binding energy and mean vibration freq. 8=16960
 LaBr₃, multiphonon orbit-lattice relaxation 8=13334
 LaCl₃, multiphonon orbit-lattice relaxation 8=13334
 LaF₃, multiphonon orbit-lattice relaxation 8=13334
 Li_{0.5}Fe_{2.5}O₄, phonon scattering by lattice distortions rel. to vacancies 8=8660
 MgF₂, phonons, dispersion relns. 8=13335
 MgF₂:V²⁺, phonon-terminated stimulated emission in vibronic sideband 8=2489
 MgFe₂O₄, phonon scattering by lattice distortions rel. to vacancies 8=8660
 MgO, surface modes of vibrations 8=17482
 MgO:Co²⁺, anisotropy of spin-lattice relax. for Kramers doublets 8=9414
 MgO:Fe²⁺(Ni²⁺), microwave phonon-impurity ion interactions 8=9450
 Mn²⁺ in Mn(Mg)SO₄·4H₂O, e. p. r. temp. dependence and spin-lattice relax. 8=9432
 MnF₂, rel. to i.r. spectra 8=14241
 MnF₂, phonon processes, selection rules 8=13318
 MnHg, thermal vibration amplitudes at 298°K 8=8236
 N₂O, i.r. absorpt. bands rel. to isotopic mols. and crystal lattice vibrations 8=14251
 Na, quasiharmonic calc. 8=1838
 NaCl, effective lattice freq. and F-centre half-width calcs. 8=4993
 NaHF₂, vibrations, i.r. absorpt. study 8=5617
 NaMg[Cr(C₂O₄)₃]·9H₂O, vibronic spectra 8=14247
 NaNiF₃, vib. anal. and assignments 8=2428
 Ne, self-consistent phonon theory, phonon spectrum and bulk thermodynamic props. 8=13336
 Ne, solid, zero-point energy, effect of long-range 3-body forces 8=22083
 Ni ferromag. reson. linewidth anisotropy, rel. to direct relax. to lattice, 25.92 and 9.42 GHz 8=2355
 NiCr₂O₄, vibration, effect of deformation 8=8614
 OCS, i.r. intensity of librational mode 8=14201
 Pb, compared with collective atomic motion in liq. state 8=12796
 Pb, phonon dispersion relations at 80 and 300°K 8=1839
 Pb, phonon-frequency distrib. and ht. capacity 8=1868
 Pb, phonons, freq. and wave vector connection, rel. to dispersion relns. 8=17483
 Pb, supercond., phonon spectrum change by lattice distortion 8=22559
 Pb, thermal vibration spectra, experimental 8=8607
 PbS(Te), by n-spectroscopy 8=13337
 Rb, compared with collective atomic motion in liq. state 8=12796
 RbMnF₃, rel. to i.r. reflectance spectra 8=2426
 RbMnF₃, vibr. modes 8=2449
 SO₂ hydrate, solid, l.f. vib. spectra of H₂O mols. 8=1840
 Se, vibrational props., i. r. spectra rel. to reflectivity and transmission 8=8615
 Si, vibr. freq. spectrum 8=8616
 Sn, compared with collective atomic motion in liq. state 8=12796
 β-Sn, freq./wave-vector phonon dispersion relations at 110°K 8=4907
 Sn, grey, phonon spectrum from inelastic scattering of cold neutrons 8=4905
 β-Sn, group-theoretical vibrational analysis 8=4906
 SnTe, by n-spectroscopy 8=13337
 SrF₂, additively coloured, phonon-assisted colour centre fluorescence 8=14306

Crystals—contd

lattice mechanics—contd

- SrO:Mn²⁺, orbit-lattice interaction from lattice vibration amplitude 8=8196
 SrTiO₃, ferroelectric phonon lifetime, at low temps. 8=4908
 SrTiO₃, optical-phonon freq., electric field depend. 8=5370
 Te, thermal vibration spectra, experimental 8=8607
 (Ti-Be) oxide, energy absorbers of superhigh-freq. vibs. 8=10458
 (Ti-Mg) oxide, energy absorbers of superhigh-freq. vibs. 8=10458
 UO₂, spin lattice interaction, first-order phase transition theory 8=22886
 UO₂, spin-lattice interaction, ground-state and spin-wave excitations 8=18437
 V:Fe⁵⁷, Mössbauer effect, recoil-free fraction and Doppler shift meas., localized modes 8=13338
 W, phonon drag effects below 2.6°K 8=5106
 Xe, solid, zero-point energy, effect of long-range 3-body forces 8=22083
 Xe, solidified, vapour pressure, binding energy and mean vibration freq. 8=16960
 YFe garnet interaction of microwave phonons with domain walls 8=22087
 ZnFe₂O₄, phonon scattering by lattice distortions rel. to vacancies 8=8660
 ZnO:Ni(Co), lattice-vibration effects 8=9563
 ZnS-phosphor, vibrational structure in stimulation spectrum 8=2459
 ZnS:Ho³⁺, lattice-activator energy transfer rel. to blue luminesc. centres, obs. 8=9643
 ZnS, Se_{1-x}S_x, LO and TO optical phonons 8=4909
 ZnS:Sm²⁺, lattice-activator energy transfer rel. to blue luminesc. centres, obs. 8=9643
- orientation**
 b.c.c. metals, lattice rotations for axisymmetric compressions, flow, computer solution 8=8373
 brass, rolled, texture representation by biaxial pole figures 8=17778
 corundum, H etched, meas. by optical back reflection 8=17206
 determ. from Kikuchi patterns, rapid method 8=13122
 determination, visual X-ray method 8=8371
 rel. to electro-optical effects in strongly anisotropic crystals 8=9495
 ferromagnetic films, controlled, rel. to coercive force 8=9333
 graphite, polycryst., effect on Young's modulus, comment 8=22319
 growth orientation in vapour deposited layers, "evolutionary selection" 8=13086
 ice, preferred, in growth from melt 8=21924
 from Kossel patterns, rapid method 8=21921
 lapping machine attachment for prep. oriented crystals 8=21918
 and lattice parameters from Kossel lines 8=21920
 from Laue photographs using vector analysis 8=22003
 Laue X-ray refl. method, puncture collimator 8=17322
 magnesia, hot-pressed, preferred 8=8375
 polymers, biaxially oriented, function plot rel. to spherical harmonic expansion coeffs. 8=17462
 polymers, crystallite randomization, nondestructive methods 8=8440
 polymers, preferred, polarized-fluorescence experiment, mathematics 8=1721
 steel, low-carbon, sheets, rolling and annealing textures 8=17799
 Weissenberg camera correction technique 8=17208
 X-ray diffraction orienting device 8=17207
 X-ray production dependence in e-microscopy 8=17266
 Ag, stability under plane compression 8=17662
 Al, effect on X-ray production on p-bombardment 8=4995
 Al, rolled, texture representation by biaxial pole figures 8=17778
 Bi₂Te₃ alloys, sintered 8=21922
 C fibres, preferred 8=1664
 CdS, polycrystalline, inversions in bulk crystals and thin films 8=8374
 Cu, effect on X-ray production on p-bombardment 8=4995
 Cu, rolled, texture representation by biaxial pole figures 8=17778
 InSb films, growth, structure 8=21884
 KI, reorientation of O₂, 1.5-4.2°K 8=13123
 Li film on W and Re faces, effect of film thickness and substrate orientation on work function 8=18256
 Nb-Mo alloy single crystals, rel. to plastic deformation, -196°C -250°C 8=17819
 n-Si rel. to anodic passivity in NaOH 8=2533
 Si, directional effects in proton scatt. 8=2034
 Si wafers, by proton channelling 8=8376
 Sn, condensed at low pressure, e diffraction pattern anomaly 8=13154
 Ti hydrides, disligning by plastic straining 8=4782
 Ti-Al alloys, dilute, hydride formation in thin foils 8=17016
 W, effect on X-ray production on p-bombardment 8=4995
 W, vapour deposited from WCl₆, rel. to work function 8=18248
 W, rel. to work function and phase changes of adsorbed N₂ on e-impact 8=21913

- Crystals—contd**
orientation—contd
 Zr rich alloys, basal plane normals, rel. to texture developed by rolling 8=22399
polarons. See Crystal electron states/polarons.
twinning
 anthracene, morphology 8=8381
 diamond twins, (111) faces, micromorphology 8=1723
 f. c. c. dendrites, twin configs. 8=17247
 fracture, twin-induced stress needs 8=5028
 growth, processes control of deformation twins 8=13124
 metals, h. c. p., process on {10 $\bar{1}2$ }, structural mechanism 8=13126
 p-aminobenzoic acid 8=8570
 polythiomethylene, radiation effect on trithiane 8=17184
 procedure for solving structure 8=4857
 quartz, synthetic, artificial twinning during plate sawing 8=17210
 steel, high-carbon, rel. to carbide formation mechanism during tempering 8=17073
 transformation formulae for indices of planes and directions 8=1722
 Au and Pd films, formation of twins during diffusion 8=13127
 BeO, twin boundary and dislocation decoration by n-irrad. at high temps. 8=22199
 Bi, due to deformation, rel. to elec. resistance change in deformation 8=5052
 Cu-2%Be alloy, and precip. on ageing 8=17625
 Fe-1.82%C, {110} twins in bct martensite 8=21925
 Fe-4.4%Si, direct observation of formation 8=13125
 Fe-4.5%Si, growth obs. on Neumann bands by high-speed photography 8=4783
 GaAs, vapour grown, twins and stacking faults obs. 8=1982
 InS, on growth and e-irradiation, rel. to phase transformations 8=17209
 Mg, second-order (10 $\bar{1}1$)-(10 $\bar{1}2$) twins, irrational habits 8=4784
 Mg-9 wt.% Al alloy, in age hardening mechanism 8=13583
 NiMn alloy, tetragonal, ordered 8=17289
 Rh₄(CO)₁₂ obs. 8=17412
 VO₂, and domain structure in low temp. monoclinic phase 8=4889
 Zn crystal, kinetics in deformation at 8-10°K 8=17211
- whiskers**
 corundum plates, elec. domains, and elec. effects rel. to formation 8=21972
 grown from solder terminations, in electrotransport process 8=8433
 polycrystalline metals, appl. in high strength materials 8=21971
 straining devices, two, for low temp. 8=22258
 α -Al₂O₃, sizing and orientation method 8=17248
 Al₂O₃, structure and mech. props. rel. to size and geometry 8=5050
 Cd, growth from vapour on Cd substrate, and orientation 8=1747
 Cu-Fe, mixed, (from CuCl/FeCl₂ reduction) growth mechanism and strength 8=17249
 Fe, ferromag. nucleation, theor. investigation 8=18335
 Fe, surface struct., scanning e microscope obs. 8=17281
 α -Fe₂O₃ on Fe, morphology and growth 8=17250
 GaP, vac. deposited, polymorphism 8=21883
 In₂Sn, grown from Sn-In solder terminations 8=8433
 KCl, origin of Bragg spots 8=17380
 MgO, evidence for growth by vapour-liquid-solid mechanism 8=13144
 MgO growth, ductility obs., growth 8=13586
 β -SiC, elastic modulus 8=22392
 SiC, and field emission 8=9272
 Sn, electrodeposited, growth during storage 8=17251
 Sn, growth on film due to d. c. 8=13145
 Sn, grown from Pb-Sn solder terminations 8=8433
 Sn, superconducting, intrinsic thermodynamic fluctuations from depressions of supercurrent and T. 8=22560
 SrTiO₃, superconducting semiconductor films and whiskers, transition temps. 8=9056
 Zn, growth from vapour on Zn substrate, and orientation 8=1747
- Curie temperature.** See Ferroelectric materials; Ferroelectric phenomena; Magnetic properties of substances.
Curie-Weiss law. See Magnetic properties of substances/paramagnetic; Paramagnetism.
- Curium**
 Cm³⁺, low-lying levels 8=4074
- Curium compounds**
 No entries
- Current, electrical**
 See also Conduction, electrical.
 a. c., comparison using thermistors 8=267
 a. c., distribution in cylindrical conductor with elliptical section 8=15194
 a. c. in supercond. Nb-25%Zr wires in mag. field 8=5208
 alloys, worked superconducting, density rel. to dislocation distrib. 8=9029
 conductors, impulse density distrib. 8=8989
 direct current on floating pot., meas. 8=10827
 flux pump with only frictional losses 8=15196
- Current, electrical—contd**
 generator, homopolar without ferromagnetic core for MHD investigations 8=15356
 generator, temp. stabilization 8=6250
 glow-discharge tubes, cathode sputtering variation 8=2019
 leads, He vapour cooled, construction 8=15195
 liquid dielectrics, 'polarization' currents 8=21706
 minimum propag. current in composite conductor with supercond. wire 8=17993
 superconductors, critical current curves, recording 8=13738
 PbS chemical films. effect on photo-e. m. f. 8=18234
- Current algebra**
 A₁ \rightarrow $\rho + \pi$, calc. 8=11565
 axial-vector currents, inverse-mass approx. to saturation 8=20254
 axial-vector current in terms of pseudo-vector field 8=20494
 charge commutation relations for cross section rules of ν and $\bar{\nu}$ nuclear scattering 8=16061
 chiral, rel. to vector and axial vector fields 8=15809
 commutation of currents, equal time, conserved and nonconserved 8=6622
 commutators, equal-time involving divergences of currents 8=6729
 CP-invariant current X current non-leptonic Hamiltonian 8=11630
 current-current theory, role of fld ratios in octet dominance 8=11391
 current, standard identity proved in perturbative model 8=6725
 currents with massive vector particles, positivity and restrictions 8=6730
 current-spectral-function sum rules 8=6727
 density in one-particle spaces 8=6737
 dibaryon state suppression in **TO** SU(3) multiplet 8=20512
 and dispersive sum rules 8=598
 electro and photoprod. identities 8=20376
 $\eta \rightarrow 3\pi$, review 8=15808
 $\eta \rightarrow \pi^+\pi^-\pi^0\gamma$ in terms of $\eta \rightarrow \pi^0\gamma\gamma$ rate 8=20488
 form factors and density algebra 8=6736
 hadron dynamics in terms of currents 8=20397
 hadron dynamics, self-interacting charged meson model 8=20398
 hyperon P-wave decay, similarity to vector meson-dominance model 8=11632
 infinite, of covariant spin densities, giving SU(6) \otimes SU(6) symm. group 8=11272
 as infinite momentum, existence of non-trivial solns. 8=581
 KN interaction, calc. of Λ/Σ ratio 8=15858
 K₈, vector form factor 8=6906
 Lagrangian, phenomenological approach, computational rules, pion mass 8=20251
 meson-baryon scatt. lengths, s-wave 8=6916
 meson pole dominance, results equiv. to Yang-Mills theory 8=11357
 non-compact groups in particle physics, conference Milwaukee, USA (1966) 8=11352
 and Ω^- hadronic decay 8=20576
 on-mass-shell and subtracted dispersion relations 8=20420
 π -emission, calc. avoiding kinematic zeros 8=20468
 pion-hadron, elastic amplitude calc. 8=20451
 $\pi\mu$ and $\pi\beta$ decays, rel. to intermed. boson 8=6836
 π - π scatt., dispersion relation approach 8=20463
 π - π scatt. length 8=15782
 π - π s-wave scatt. lengths, unitarity corrections to calcs. 8=11525
 and poles, fixed, locations and residues 8=3535
 pNN*, pNN₃, pNN₃ coupling calc. 8=11564
 quasi-free states of fermions and bosons 8=15676
 $\rho \rightarrow \pi + \pi$, calc. 8=11565
 SU(3) \times SU(3) space time local current commutators, derivation 8=6611
 strange particle electro- and photo-prod. 8=20344
 strong and weak interactions, present problems, conference Erice Italy (1966) 8=15695
 and sum rules 8=15743
 sum rules, covariant, convergent props. procedure for obtaining 8=20255
 and sum rules group theoretical derivations 8=3522
 theoretical physics, conference Providence USA (1966) 8=20246
 Thirring model, 2D based on currents for hadron dynamics 8=20399
 U(3) \otimes U(3) in special mixing model 8=20253
 vector and axial-vector currents, divergence conditions and low energy meson theorems 8=20495
 vector-meson field theory, coupling parameters, determ. 8=6899
 Weinberg's relation $m_A = \sqrt{2}m_\rho$ derived 8=20506
 Weinberg sum rule validity and Schwinger terms 8=15675
- Curvature measurement.** See Mechanical measurement.
 Cyanogen (C₂N₂). See Carbon compounds.
- Cyclotron resonance**
 Bloch electrons, one-band effective-mass approx. 8=13654
 charge in travelling e. m. wave, Doppler effects 8=15272
 chloroethylene, ion-molecule reactions obs. 8=16453

Cyclotron resonance—contd

- conducting slab, e. m. waves transmission, peak 8=19838
- cyclotron maser, resonator excitation near electron resonance 8=395
- free electrons in mag. field, and proton n. m. r., freq. ratio meas. 8=10989
- hexafluoroethane, secondary ion-mol. reactions. 8=21284
- ion, collision cross-sections determ. 8=12442
- ion, line broadening at high E/P 8=390
- line width theory 8=8970
- in light-electric field, from e. m. waves in conductors 8=5155
- plasma, second-harmonic, electron temp. and density var. 8=1419
- polaron in ionic crystals 8=2125
- semiconductors, spin-cyclotron-phonon resonance 7=2352
- solids, echo signal, theoretical treatment 8=5149
- Bi, u. h. f. penetration meas. 8=5588
- CdS, piezoelectric polarons, theory 8=9220
- Ga cyclotron effective mass obs. 8=13717
- Ga, mass determinations 8=13687
- Ga, ultrasonic, effective mass in ab plane 8=2099
- Ge, carrier lifetime determination 8=13831
- Ge, deformed, due to edge-type dislocations 8=9106
- H ion plasma in mirror machine and nonadiabatic trapping 8=21370
- KBr, of polarons 8=2124
- Mo, anisotropy of effective masses 8=2126
- Mo, meas. at 1.6°K and 9.7 GHz rel. to Fermi surface investigation 8=13664
- Pt, effective mass, anisotropy and mass enhancement 8=22487
- Sb, acoustic, in inclined magnetic field 8=22488
- Si, carrier lifetime determination 8=13831
- Sn, at 9.5 Gc/s obs. in (010), (110) and (001) planes, in inclined mag. field 8=22489
- Te, meas. of diamag. and other resonance phenomena 8=22490
- Tl 8=8972
- TlCl, obs. 8=8971
- W, electron "jackalot" of Fermi surface 8=13688
- Zn, rel. to Fermi surface 8=13725

Cyclotrons. See Particle accelerators/orbital, cyclotrons.
Czocharlski method. See Crystals, growth.

D-layer. See Ionosphere/D-region.

DNA. See Proteins.

DPPH (diphenylpicrylhydrazyl). See Free radicals; Organic compounds.

Damping

See also Internal friction.

- beams, thin cantilever, by air and internal forces 8=19486
- double-beam system, elastically connected, response to cyclic moving load 8=151
- jet, plane, of conducting liquid propagated in mag. field 8=19807
- Landau, ionospheric photoelectrons near 600 km, radar scatt. obs. 8=23362
- longitudinal waves, in viscous fluid 8=1534
- oscillations, non-linear, elliptic functions applied 8=6122
- p and \bar{p} oscills. in storage rings 8=640
- plates, fluxurally vibr., radiation statement 8=3019
- plate, transverse normal modes 8=19491
- simple single-span beam with tuned viscoelastic dampers 8=3018
- of sound waves, radiative, for arbitrary wavelength to photon mean-free-path ratio 8=190
- space vehicles, pitch-damping coeffs. calc. 8=23458
- vibrations, viscoelastic material armoured with rigid sheath 8=19494
- LiF, strain amplitude independent dislocations, recovery 8=13582
- Ni-ThO₂, rel. to magnetoelasticity, 20-500°C 8=17821

Dark space. See Discharges, electric.

Data tables. See Collections of physical data; Tables, mathematical.

Dating. See Earth/age; Radioactive dating.

Daughter. See Nucleus; Radioactivity.

Dawn chorus. See Atmospherics; Ionosphere.

Dayglow. See Airglow.

Debye-Hückel theory. See Conductivity, electrical/liquids, electrolytic; Electrochemistry; Solutions.

Debye-Scherrer cameras. See Cameras; X-ray crystallography/apparatus.

Debye temperature. See Specific heat.

Debye-Waller factors. See Electron diffraction crystallography; X-ray crystallography.

Decay periods. See Hyperons/decay observations; Mesons/decay observations; Pions/decay; Radioactivity/decay periods.

Decay schemes. See Hyperons/decay observations; Mesons/decay observations; Pions/decay; Radioactivity/decay schemes.

Decomposition. See Dissociation.

Decomposition, thermal. See Chemical reactions.

Decoration techniques. See Crystal imperfections/dislocations; Crystals/etching.

Defects. See Crystal imperfections.

Deformation

See also Bending; Elastic deformation; Plastic deformation.

- alkali halides, ions, X-ray diffuse scattering 8=13330
- alloys, above solidus temp., mechanism 8=22304
- anticlastic, hypergeometric series solns. 8=19392
- armco Fe, explosive formation, residual strains and hardening 8=13564
- beams, elastic, plastic and creep, iterative procedure 8=875
- beams, rigid-plastic, permanent, effects of strain hardening and strain-rate sensitivity 8=19402
- bending thin plates with nonlinear stress-strain relation 8=10548
- bodies, elastic/visco-plastic, compressible, plane strain condition 8=10573
- brass, Bauschinger effect recovery mechanisms 8=17775
- brass, 70-30, rel. to texture development, pole figure 8=17777
- buckling of microfibrils in matrix due to cooling, phenom. and effect on strength 8=22289
- ceramics, basic mechanism, survey 7=17726
- circular plate yield-point load sealing an incompressible fluid 8=45
- creep of cylinder, thick walled, under internal press. 8=17731
- cylinder, hollow, changes in geometry during compression 8=10563
- cylindrical wafers, radial and axial press. grads. when between compression plates 7=19394
- EI-702 steel, effect on mechanism of precipitation 8=17078
- EI702 steel, metallographical investigation of mechanism 8=13570
- eigenmodal, under all-round dead loading, in elastic-plastic continua 8=19399
- of elastic bodies, meas. with double-pass interferometer 8=20092
- elastometers, multiaxial, stress/strain relns. 8=5010
- granular materials, impact cratering 8=8253
- graphite, cracking with increasing stress, stress-strain relations 8=5053
- graphite by n irradi. and bromination, 200°C 8=8764
- graphite, nuclear grade A, and anomalous strength 20-2200°C 8=8829
- h.c.p. metal (yttrium and rare earths), deform. planes and hydride habit planes 8=8728
- heat, metallurgical problems 8=22277
- initial finite deform. of simple elastic structures, effect on natural vibs. 8=15031
- liquid drops, shear, second-order theory 8=7993
- martensite carbon strength rel. to thermally activated deformation 8=22351
- measurement in rotating systems 8=10780
- membranes, tensile instability for large deformations. 8=13503
- metal, probability of fracture 8=17736
- metals, effect of u.s. vibration superimposed on static compressive load 8=8795
- metals, quenched, Bauschinger effect 8=5020
- microinhomogeneous bodies rel. to couple stress theory 8=42
- polycarbonate films, rel. to chem. structure 8=22403
- polyethylene, dislocation mechanism 8=2072
- projectile, impact on rigid target, direct anal. of dynamic behaviour 8=17728
- rolling contact fatigue, identification of potential failure nuclei 8=17749
- shallow trusses and arches, nonlinear creep buckling 8=22278
- shell, axisymmetric cylindrical, effects of anisotropy 8=19388
- shells, cylindrical under piecewise pressure, ring forces and moments, and energy losses 8=41
- shell, truncated conical, thin, buckling under uniform static press. 8=19382
- single crystals, explosive 8=17029
- spherulites, ringed, rel. to light scatt. patterns 8=9491
- steel, change in coercive force 8=14015
- steel, maraging, 15 and 18%Ni, influence of small cold deformation preceding ageing, discussion 8=17801
- toroidal shell, perturbation theory 8=10543
- twins, growth processes control 8=13124
- viscoelastic, nonlinear, relation to stress 8=2929
- Zircaloy-2, grain boundary effects 8=13447
- Ag-Ni alloys, f.c.c., stacking and twin faults 8=4988
- Al alloys, tensile, rel. to lattice defect recovery 8=22184
- Al, at high strain rates 8=13533
- Al circular foils, pressure effects 8=5044
- Al, e-irradiated, at 20°K rel. to dislocation model with defect barriers 8=13523
- Al foil, dynamic behaviour of dislocations, continuously observed 8=13433
- Al, quenched, Bauschinger effect 8=5020
- Al, rel. to (111)-(001) fibre texture formation 8=5045
- Al, shear along slip direction, stress-strain curves 8=17761
- Al single crystals, high strain rates 8=22310
- Al, tensile, rel. to lattice defect recovery 8=22184
- Al-Al₂O₃, dispersion strengthened, mechanism from rolling texture analysis 8=8812
- Al-4%Cu, deformational instability 8=8816

Deformation—contd

- Al-Cu-Cd alloys, before and during ageing, effects on precip. 8=17039
 Al_2O_3 , n-irrad. effects on lattices, thermal cond. etc. 8=22245
 AuAg alloy recovery and ordering rel. to optical consts., 276-1200 nm 8=22958
 AuCu alloy recovery and ordering rel. to optical consts., 276-1200 nm 8=22958
 AuCu₃ alloy recovery and ordering rel. to optical consts., 276-1200 nm 8=22958
 Be single crystals, dislocations formation, slip directions, fracture 8=1969
 Bi, and twinning, and meas. of elec. resistance 8=5052
 Bi, effect on electron spectrum 8=17870
 CdS rel. to luminesc., absorpt. and refl. spectra, obs. 8=9606
 CdSe rel. to luminesc., absorpt. and refl. spectra, obs. 8=9606
 Co alloys, f. c. c., ageing effects after deformation 8=17622
 Cr-Ni steel, behaviour 8=5085
 Cu, at 77 and 4.2°K rel. to creep at 650-700°K 8=17824
 Cu, Bauschinger effect recovery mechanisms 8=17775
 Cu, cyclic, coarse slip and crack form. and propag., obs 8=22330
 Cu, explosive formation, residual strains and hardening 8=13564
 Cu, quenched, Bauschinger effect 8=5020
 Cu, rel. to texture development, pole figure 8=17777
 Cu, tension deformed, recrystallization 8=17230
 Cu wire, drawing process with lubricant under externally generated pressure 8=2052
 Cu-Al alloy solid solution, latent heat of 8=13551
 Cu-Ni alloy solid solution, latent heat of 8=13551
 Cu-Zn alloy solid solution, latent heat of 8=13551
 Fe, armco, preliminary, effect on strain ageing 8=17786
 Fe, low-temp., point defects recovery 8=13418
 Fe, microcontours, during fatigue testing 8=2053
 FeCo, causing micro-strain and -hardness 8=13596
 Fe-Ni-C martensites, ferrous, rel. to hardness change 8=22352
 Fe-Ni-Si-C steel, effect of martensite ageing 8=22357
 FeV₂O₄, effect on lattice vibration 8=8614
 para-H₂, solid, stress-strain curves at 4.2°K, mech. constants 8=5074
 and He^{3,4}, relative abundances, implications of Brans-Dicke theory 8=23478
 K, thermally activated at low temps. 8=1957
 Li, under diffusive mass transport 8=22157
 Mg alloy, hydro-explosive loads 8=17815
 Mg, by plane-strain compression rel. to anisotropy 8=17814
 Mg-Li alloy, by plane-strain compression rel. to anisotropy 8=17814
 MgO, n-irrad. effects on lattices, thermal cond. etc. 8=22245
 Mg-Th alloy, by plane-strain compression rel. to anisotropy 8=17814
 Mo, structure and low-temp. ductility, deform. -induced changes 8=13589
 Ni, at 77 and 4.2°K rel. to creep at 700°K 8=17824
 Ni, intermittent, upper temp. limit from Cottrell formula 8=2064
 Ni, weakly deformed, recrystallization nucleation 8=8421
 Ni₃Co, causing micro-strain and -hardness 8=13596
 NiCr₂O₄, effect on lattice vibration 8=8614
 Ni₃Mn, causing micro-strain and -hardness 8=13596
 Ni-2ThO₂, dispersion-strengthened, cyclic behaviour 8=13597
 Si, B-doped, by uniaxial compression in elec. fields, rel. to hole relax. time 8=18074
 Si, elastically distorted, X-ray topography 8=13198
 n-SiC, α -phase, rel. to piezoresistance constants 8=18073
 Sn, supercond., effect on u. s. absorpt. 8=5213
 Ta, effect of Nb and Mo additions 8=8862
 Ta-Mo alloys, mechanism rel. to pure Ta 8=8862
 Ta-Nb alloys, mechanism rel. to pure Ta 8=8862
 Ti, mechanisms, low-temp. 8=8864-5
 Xe, solid, potentials, band structure and exciton states 8=2108
 Zn, at high strain rates in hardening process 8=17837
 Zr-H alloys, thermally-activated mechanisms 8=13613
 Zr-O alloy crystals, rate-controlling mechanism at 77-473°K 8=13614
- de Haas-van Alphen effect**
 See also Diamagnetism; Magnetic properties/diamagnetic.
 oscillations from free energy studies of nearly free electrons 8=2068
 Shubnikov-de Haas effect, additional oscillation due to $4\pi M = B - H_0$ 8=22446
 Shubnikov oscillations, resistance jumps, galvanomagnetic charact. 8=22445
 Be, Fermi surface, non-local pseudopotential model 8=8923
 Bi and Bi alloys, 1.2-4.2°K 8=13659
 Bi-Sb alloys, electron energy spectrum meas. 8=5104
 Mg, rel. to Fermi surface 8=2102-3
 Ni, and electronic band structure 8=9360
 Ni, rel. to band structure and Fermi surface 8=2106

de Haas-van Alphen effect—contd

- Pt, Fermi surface determ. for s- and d-like carriers 8=22752
 Rh, and Fermi surface 8=13643
 p-Sb₂Te₃, susceptibility meas. 8=9293
 Sn, dHvA susceptibility oscillation meas. rel. to Knight shift 8=5566
 Th, rel. to Fermi surface location 8=2294
 Y obs. 8=5434
 Zn, g factor determs. 8=2110
 Zn, in (0001) plane, freq. meas. 8=5435
- Delay lines, ultrasonic.** See Acoustics; Ultrasonics.
Delbrück scattering. See Photons/scattering.
Demagnetization. See Magnetization process.
Dember effect. See Photoelectromagnetic effects.
Demonstrations. See Teaching/demonstrations.
Dendrites. See Crystallization; Crystals/growth.
Densitometry
 He-I mixture, thermal diffusion meas. 8=7942
- Density**
 alkali nitrates and thiocyanates, fused 8=1556
 earth, interior distrib. 8=18826
 stellar gradient inversion, in convection zone 8=2778
 GaSb-GaAs alloy, pressure-sintered, densification and thermoelectric props. 8=4697
 Na borate glasses, and ht. of soln. and refractive index changes under high pressure 8=1715
- gases**
 mass of large volumes, determ. by direct weighing 8=7890
 methane-tetrafluoromethane system, and principle of corresponding states 8=7912
 with shock wave, corrections to Crook's soln. for density, temp. and vel. of gas 8=16667
 CO₂ near critical point, admixture density distrib. 8=21744
 NO, 200°-2000°K and at 1000 bar 8=7918
- liquids**
 densimeter, temp. sensitive, magnetic float 8=4544
 hydrostatic weighing, high precision procedure 8=14920
 methane-propane mixtures, at low temp. and high press. 8=12819
 plasma, spectroscopic 8=16538
 propanol-H₂O mixtures, with NaCl in soln. 8=4606
 Ag-Bi molten alloys with segregation tendencies 8=12812
 Ag-Pb molten alloys with segregation tendencies 8=12812
 Cs, 100-750°C 8=12813
 HeII near critical point, obs. 8=19702
 He³-He⁴ mixtures, dilute, molar density, 1.25-0.025°K 8=6230
 K-Na alloys, 0 to 300°K 8=21624
 K, 0 to 300°C 8=21624
 Li, 400-1125°C 8=12813
 Mg fused electrolyte, NaCl, KCl, CaCl₂ additives, obs. 8=23143
 Na, 0 to 300°K 8=21624
 NaCl solutions at 25°C using temp. sensitive magnetic float densimeter 8=4544
 Ne, at press. to 1000 atmos. 8=21555
 Rb, 50-800°C 8=12813
- solids**
 graphite slabs, meas. of isodensity curves by X-ray absorpt. 8=22317
 packed particles, bulk density, rel. to size and mass ratio, and degree of mixedness 8=17017
 parahydrogen, at up to 400 atmos. 8=16928
 polycapromide, correl. with melting temp. and nature and cond. of filters 8=21914
 Al₂O₃, decrease rel. to n irrad. and annealing 8=13249
 B₂O₃ glass, permanent densification by hydrostatic press. 8=22314
 BeO, hot-pressed, effect of adsorbed sulphate and fluoride 8=21821
 MgO, decrease rel. to n irrad. and annealing 8=13249
 SiO₂ film, rel. to temp. of deposition 8=21889
- Density measurement**
 cryogenic liquid mixtures, differential method 8=19347
 gas solns., up to 1 part in 10⁶ meas. 8=16803
 liquids, simultaneously with dielec. const. 8=1582
 magnetic float densimeter, temp. sensitive 8=4544
 plasma, ion-cyclotron instability threshold 8=7834
 polyacrylonitrile, atomic-pile-irradiated, changes 8=17709
 single small particles, determination by floating in liquid 8=6006
 soil, by γ -ray back-scatter 8=23231
 solids, hydrostatic weighing principle and technique 8=19348
 water at high press. from propag. meas. 8=21623
 He⁴, near critical point 8=259
- Desorption.** See Sorption.
Detonation
 See also Explosions; Shock waves.
 Chapman-Jouguet pressures, simplified calc. 8=23124
 chemistry, buffered equilb. 8=23123
 converging waves propag. 8=19540
 diverging wave, motion of gas 8=4461
 explosive hydrodynamic theory appl. 8=6146
 explosive liquids, by cavitation 8=171
 gas, collapsed cylindrical waves 8=7907
 in gas, self-similar motions 8=4462

Detonation—contd

- imploding, non-uniform self-propag nature 8=15059
- liquid, explosive, low velocity initiation, effect of shape and material of container 8=10720
- in liquids, during gap testing, wall interacts. rel. to shock initiation 8=15057
- nitroglycerine, low velocity, mechanism 8=21582
- nitroglycerine, shock initiation 8=6148
- nitromethane-acetone solns., wave front turbulence 8=6145
- oxyhydrogen mixtures, waves, induction zone obs. at low initial pressures 8=170
- pressure meas. in kbar range 8=6149
- propane-O₂-N₂ mixtures, velocity meas. 8=172
- reflected waves, detect. with ionization gauge circuit 8=3041
- unsteady flow behind, friction and heat transfer effects on transition to steady flow 8=15058
- waves interaction with flow field rel. to rocket motors combustion instability 8=10721
- waves in medium with variable initial densities 8=3039
- waves, rebounding, trajectory: analytical determination 8=169
- wave, spherical, distrib. of flow properties behind 8=15061
- C-H-N-O explosives, calc. of detonation props. 8=23122
- 2C₂H₂+SO₂ mixture, continuous combustion in annular channel rotation of spinning luminesc. heads 8=23121
- T-D gas mixture, propagation of thermonuclear detonation wave 8=21482

Deuterium

- \bar{p} annihilation in H₂ and D₂, rates rel. to initial state 8=20537
- autoionization, kinetic energy 8=12443
- autoionization process, calc. using H atom model 8=21034
- combination with H₂, gas torque effect on heated cylinder 8=1320
- crystal-structure changes during transitions in ortho- and para-states X-ray exam. 8=13263
- diffusion in Pd and Pd alloys, at 0° to 100°C 8=17582-3
- discharge lamp, constant-current power supply 8=19714
- dissociative attachment of e, survival prob. 8=1310
- dissolved in α -Zr, thermodynamic props. 8=8252
- electron transport coeff. 8=21521
- flash lamp pressure and voltage gradient effects 8=15522
- in gases, neutron spectrometry 8=9765
- gas, rotational relaxation, high temp. u.s. obs. 8=1251
- ionization, temporal growth and secondary ions, 0.2-40 keV, deceleration in Ag foil 8=2020
- laser action in electrical discharge containing D 8=12398
- magnetic drift vel. and deflection coeff. for slow electrons 8=7712
- neutron capture, cross-section 8=6988
- ocean content as water mass parameter 8=23238
- π^0 photoproduction, as test of symmetry in e.m. current 8=670
- polycrystalline, sound velocity meas. and elastic constant calcs. 8=17499
- p polarized beam scatt., 300-700 MeV, polarization parameter 8=6927
- p scatt and T = 1/2 state of He³ 8=3739
- in solar system, origin 8=19236
- solid and liquid, Raman spectra, intensity anomaly 8=9536
- solid, pressure changes on phase transitions 8=4711
- solid, Raman spectra anomalies rel. to mol. vibrations 8=9535
- solution in liquefied inert gases, absorption spectra 8=12887
- thermal conductivity, hot-wire cell meas., 30°-100° C, 120-150 torr 8=16700
- thermal cond. of O- and n-D₂, at 18.5, 19.8 and 21.1°K 8=7930
- water, atmospheric, tracer 8=2503
- Zeeman effect, Lamb shift and quantum electro-dynamics 8=1158
- D-neopentane exchange, effects of desorption, diffusion and surface exchange 8=23083
- D-T gas mixture, propagation of thermonuclear detonation wave 8=21482
- D₂ line, wing broadening, expt. 8=16194
- D⁺ ion source, polarization increase 8=10915
- D polarized beam prod. by charge exchange 8=15352
- D', critical angles for channeling in thin Au films 8=17704
- D'-rare gas collision, polarization of Lyman- α radiation 8=21004
- p-D₂ prep. by preferential adsorption 8=17158
- D₂ collisions with inert gases, total scatt. cross-sections 8=7634
- D₂ in liq. Ar, induced rot.-translation spectra 8=1564
- D₂ in liq. Ar, induced rot.-translation spectra 8=1564
- (o-D₂, He) system, translation-rotation energy transfer calc. 8=12374
- D₂-He, thermal conductivity, normal composition variation 8=7924
- D₂-HT mixture, thermal diffusion 8=4495
- D₂O, neutron spectra, time depnd. 8=6948
- D₂⁺ chemical reactions with He, cross section 8=14348
- ²D⁺ in Ge, channelling props., diff. calc. 8=13485
- D₃⁺ ions, reactions with alkanes and alkenes, energy transfer and deactivation 8=1358

Deuterium—contd

- HD, liquid, n.m.r. proton transitions 8=8133
 - HD-D₂ system, thermal diffusion factor 8=1494
 - in NH₃ system, isotopic disproportionation equilibria 8=2505
 - O + D₂ → OD + D reaction, e.s.r. detect. 8=14375
 - α -Ti-D₂ system, thermodynamic props. 8=21858
- Deuterium compounds. See Hydrogen compounds.**
- Deuterons**
- See also Cosmic rays/deuterons; Nuclear reactions due to/deuterons.
 - angular distrib. in Bi^{10,11}(α , d)C^{12,13} 8=1100
 - ang. dist. in Cu^{63,65}(He³, d)Zn^{64,66}, 18 MeV 8=3970
 - binding energy calc. using nonrelativistic sum rules from pot. scatt. 8=11641
 - blocking effects in Au films 8=22241
 - 3-body treatment, with n-p, p-e interactions 8=11639
 - channeling in crystals, transparency model 8=22243
 - disintegration on Au, Rh, Cu, C, Coulomb and nuclear forces 8=11934
 - electrodisintegration differential cross sections, resonance prod. 8=11640
 - ion source for tandem accelerator 8=6694
 - μ d + Y₂ → μ Y₂ + d, rate compared with μ p + Y₂ + μ Y₂ + p 8=12115
 - n-d scatt., Fadeev eqns. and n-n low energy parameters 8=15841
 - in nuclear emulsion nuclei interaction with 9 GeV protons, emission, obs. 8=15867
 - optical potential, from (d, p) stripping 8=1087
 - p + p → π^+ + d, 5 GeV/c cross-section meas. 8=20525
 - production, in He³ + γ → d + p, with Cabibbo-Radicati sum rule 8=6999
 - production, high-momentum 8=3735
 - (\bar{d}) singlet, detect. from reaction Be⁹(p, \bar{d})Be⁸ 8=871
 - singlet state rel. to Be⁹(p, d)Be⁸ 8=20787
 - D⁺ transmission through thin films 8=22242
 - H²(p, 2p), 9 and 10.5 MeV, decay mechanism 8=875
 - Sb^{117,119,121}(He³, d) spectra 8=3971

effects

Pt, damage and recovery rel. to vacancy behaviour 8=8697

interactions

- d- α 42 MeV α projectile, d break-up, spectrum 8=15868
 - D(d, p)T, 8 energies 2.1-14.1 MeV, p polarization obs. 8=11642
 - d-d, use of neutrons for deuterium plasma diagnosis 8=1404
 - d + He³ → He³ + pp, pick-up and charge-exchange 8=6990
 - d-He⁴, 1 MeV, rel. to 2.19 MeV level of Li⁶ 8=20675
 - D(p, γ)He³, cross-section from p μ d wave function 8=11593
 - D(p, p)d, polarization and phase shift at 3.00 MeV 8=6993
 - d-T reaction, n yield 8=874
 - D(t, n)He⁴, as polarized n generator 8=15844
 - K⁺d total cross section at 1.2 GeV/c, I = 0 peak rel. to K → K⁺(890) channel coupling 8=15804
 - K⁺d → $\Sigma^+\pi^0$, 815-, 915-, 1015- and 1115 MeV/c incident K⁺ momenta 8=20574
 - n-d, 14.1 MeV, coincidence meas. 8=11643
 - n + D → p + 2n, counter telescope for energy and ang. distrib. 8=11646
 - pd, at about 2 GeV/c, final state p $\bar{d}\pi^+\pi^-$ 8=15827
 - p + d → B + d and B-N scatt. factor 8=3736
 - p-d, low-energy, resonance charge exchange meas. 8=828
 - p photo-absorpt. sum rule 8=3577
 - π^+ + d → M + d, and M-N scatt. factor 8=3736
 - π^+ + d → p π^0 + p + neutrals, 2.7 GeV/c search for ϵ^0 8=11488
 - T(d, n)He⁴ rel. to polarized d beam prod. 8=11602
 - T(d, n)He⁴, as polarized n generator 8=15844
 - t-d prod. of n with t in Zr or Ta, yield decrease diffusion mechanism theory 8=6921
 - tritium targets, life under bombardment in accelerator 8=11290
 - H²(d, n)H³, below 400 keV, polarization of n emission obs. 8=20582
 - H²(He³, γ)Li⁵, 2-5.5 MeV, resonances obs., applic. of S-matrix theory 8=20581
 - H²(N¹⁴O¹⁵(N¹⁵)), 30 MeV lifetimes of mirror states of O¹⁵ and N¹⁵ 8=3793
 - H²(p, 2p)n, 9 and 10.5 MeV 8=875
 - He³(d, p)He⁴, p polarization and asymmetry 8=7002
 - K⁺d, total cross-sections, new structures 8=796
- photodisintegration**
- Franz-Stech theory 8=16056
 - γ + d → p + n differential cross section, 100-420 MeV 8=873
 - p polarization obs., 170-450 MeV 8=20533
 - π -exchange contribution 8=872
- polarization**
- beam prod. from T(d, n)He⁴ 8=11602
 - e-d scatt. rel. to e helicity and as a test for T invariance 8=20375
 - Lamb shift, 3-body e, p, n treatment 8=11639
 - tensor polarization degree (P₃₃) obs. 8=6994
 - in d- α double scatt., and phase shifts 8=876
 - p-d scatt. obs. 21.7 MeV 8=878
 - p-d scatt., 1.5-11.5 MeV, phase-shift analysis 8=877
 - C¹², 6-10 MeV, scatt. analysis 8=1089
 - Ni¹⁰⁰ scattering, and asymmetry of ang. distrib. of products 8=16110

neutrons—contd
scattering

- See also Protons and antiprotons/scattering, proton-deuteron.
- elastic, spin-orbit effects in optical-model anal. 8=879
- linked-cluster expansion for optical pot. 8=6991
- on nuclei, elastic, tensorial effects in optical model 8=7222
- nuclei, elastic, with tensor spin-orbit interaction 8=3951
- stripping theory 8=3953
- d- α , double scatt., polarization and phase shifts 8=876
- d- α , 3-14 MeV, negative parity states of Li^6 8=11651
- d + α , phase shifts, and odd parity P level in Li^6 8=15869
- (p,n)p, $E_0 = 9$ MeV 8=6989
- e-d quasielastic scatt., forward angle obs. 8=6806
- e-d, for study of e helicity and as test for T-invariance 8=20375
- γ d, sum rule for magnetic and quadrupole moments 8=6992
- γ d, sum rules for forward scatt. 8=6992
- n-d counter telescope for energy and ang. distrib. 8=11646
- n-d Fadeev eqns., sensitivity to n-n parameters 8=15841
- n-d, Hamada potential, variational calc. 8=885
- n-d, length calc. using N-N non-local separable pot. 8=11647
- n-d, length calc. using pair pot. 8=881
- n-d length, obs. anomaly rel. to 3N binding energy 8=11648
- n-d, second quantization formalism appl. 8=11853
- n-d, soln. of Fadeev eqns. 8=11403
- nuclear, differences parameter, energy depend. 8=11918
- π -d, coupling const. derived 8=759
- π p scatt., fully covariant theory 8=6865
- p-d, phase-shift analysis, 1.5-11.5 MeV 8=877
- p-d rel. to T = $\frac{1}{2}$ state of He^3 8=3739
- p-d, 1-2 BeV, cross-section obs. 8=11645
- p-d, p polarization obs. 11.6 MeV 8=11644
- p-d, 17.1 MeV, elastic, cross-section obs. 15°-165° 8=20529
- p-d, 21.7 MeV, vector and tensor polarization obs. 8=878
- Be^9 -d, 9.97 MeV and levels of Be^9 8=20676
- $\text{C}^{12,13}$, 4-6 MeV, rel. to C^{13} (d,p) C^{14} optical model and DWBA analysis 8=16113
- C^{12} , 6-10 MeV, polarization analysis 8=1089
- Ca^{40} , elastic, at 11 MeV, tensor spin-orbit interaction, calc. 8=3951
- Ca^{40} , 5-6.5 MeV, optical model parameters determ. for (d,p), (d,n) reactions 8=16118
- Ca^{40} , 26 MeV, ang. distrib. and excited states 8=7229
- Ca^{41} , stripping channel coupling theory 8=3953
- Ce^{40} , 26 MeV, ang. distrib. and excited states 8=7229
- Co^{59} , levels, multipolarity, spin, lifetimes 8=3813
- in Cu, rel. to study of Au diffusion 8=8675
- Cu, elastic scatt., Akhiezer-Pomeranchuk-Blair model analysis 8=20822
- $\text{Er}^{162,164,166,168,170}$, 12.1 MeV, 2 $^+$, 4 $^+$ states in γ vibr. bands 8=11774
- Fe, elastic scatt., Akhiezer-Pomeranchuk-Blair model analysis 8=20822
- Fe^{56} , 26 MeV, ang. distrib. and excited states 8=7229
- He atom, excitation of ^1S , ^1P , ^1D states 8=7384
- $\text{Li}^{6,7}$, 11.8 MeV, optical model parameters deduced 8=20833
- Mg, elastic scatt., Akhiezer-Pomeranchuk-Blair model analysis 8=20822
- $\text{Mg}^{24,26}$, 26 MeV, ang. distrib. and excited states 8=7229
- Ni^{58} , 26 MeV, ang. distrib. and excited states 8=7229
- Ni^{60} , with polarized d, asymmetry of ang. distrib. of products 8=16110
- Ni^{61} transitions below 1.5 MeV strongly enhanced 8=3815
- $\text{Re}^{185,187}$, γ -vibrational state obs. 8=16000
- $\text{Re}^{185,187}$, 12.1 MeV vibrational band obs. 8=3954
- $\text{Sm}^{147,149}$, levels and ground-state transition 8=987
- $\text{Sm}^{150,150,152,154}$, 12.1 MeV, levels and E2, E3 transitions 8=20824
- $\text{Ti}^{47,48,49,50}$ elastic and inelastic, 2.5-10 MeV, optical model analysis 8=20823
- Tm^{170} , 5.5 and 12 MeV, collective states 8=7106
- U^{238} , energy level obs. 8=16007
- Zn, elastic scatt., Akhiezer-Pomeranchuk-Blair model analysis 8=20822
- Zn, 26 MeV, ang. distrib. and excited states 8=7229
- development, photographic.** See Photographic process/development.
- diamagnetic resonance.** See Cyclotron resonance.
- diamagnetism**
- See also Cyclotron resonance; de Haas-van Alphen effect; Magnetic properties/diamagnetic.
- plasma, meas. using external coil near conducting wall 8=16543
- Mg-Cd, 4.2°K 8=22755
- Pd based double cyanide complexes obeying square planar symmetry, mean susceptibility 8=22751
- TlBr, anisotropy of diamag. susceptibility 8=9295
- TlF, anisotropy of diamag. susceptibility 8=9295
- Zn, at 112°K 8=22755
- Zn-Cd, at 4.2°K 8=22755
- diamonds**
- bonding, covalent, X-ray diffr. meas. 8=4869
- charge density calcs. by OPW method 8=8927

Diamonds—contd

- crystallization in catalyst-metal system, graphite impurity crystal growth problem 8=1737
- cube form, structure studies of natural crystals 8=8370
- epitaxial growth of SiC on (111) face 8=8428
- etch pits and trigons 8=1725
- growth, nucleation evidence 8=21945
- hexagonal in meteorites, implications 8=10369
- hexagonal polymorph, "lonsdaleite", natural occurrence and crystal analysis 8=13121
- hole motion in a mag. field, theory 8=22436
- Jahn-Teller effect distortion of monovacancy, mol. model 8=17605
- Jahn-Teller effect for single vacancy 8=8691
- microanalysis by X-ray diffr. grating system, CK spectrum obs. 8=14491
- natural, luminescence, effect of heat treatment and irradiation 8=18596
- particle-counting props. 8=6647
- permittivity calculation 8=5354
- photoconductivity of particle-counting, model 8=5395
- photoelastic constants, bond stretching and bending model 8=8830
- radiation dosimetry by current glow 8=20205
- strains and damage in abraded surfaces 8=8826
- synthetic, etching rates on different forms, comparative study 8=21929
- synthetic, growth hillocks on (100) faces 8=17213
- trigons, origin and relation to growth failure 8=4787
- twins, (111) faces, micromorphology 8=1723
- valence force potentials for calculating cryst. vibrs. 8=16968
- X-ray Lave spike refls. rel. to i. r. absorpt. and impurity N location, obs. 8=22014
- zero-phonon 415 m μ line temp. dependence 8=5589
- Dichroism.** See Pleochroism.
- Dielectric devices**
- amplifier, surface waves, ultra and hypersonic 8=13897
- capacitors, power, effect of self-reson. on discharge magnitude meas. 8=21228
- capacitors, reference, temperature characteristics 8=10820
- capacitors, voltage shock, dielectric ageing mechanism 8=13898
- ceramic titanate rectifying barriers 8=18125
- coaxial loaded waveguide, inverse hybrid waves 8=3263
- condenser, spherical electrostatic field 8=276
- diode, normal metal, geometrical reson. in E//H tunnelling 8=22674
- electronics, review 8=18203
- electrostatic generator, vertical injector 8=3150
- frequency-controlled quartz oscillators, temp. compensation 8=2252
- insulators, solid, creep discharge in SF $_6$ atm. 8=16420
- i. r. detection by pyroelectric effect, performance 8=5378
- imperfection meas. by complex dielectric constant method of trace characterization 8=18757
- insulators, high-tension, ultrasonic pulse method for non-destructive testing 8=22286
- metal films with polymerized adsorbed layers, equilib. ptl. 8=2251
- metal-oxide-Si, Au-doped, C-V props. 8=13896
- mica-resin superimposed layers subject to alternating field, elec. stress distrib. 8=9235
- nuclear spin relax. and dynamic polarization rel. to electron spin-spin relax. 8=18443
- particle track detector using rate of chemical etching 8=11331
- photocapacitor, application of n-GaAs-Au surface barrier diode 8=13925
- piezoelectric transducer for wave velocity meas. in shock tubes 8=9230
- polarization under shock load 8=22675
- prism between mirrors for e. m. oscillations 8=6361
- resonators, filled with TiO $_2$ dielec. discs, h.f. props. 8=19829
- space charge noise, suppression and amp. rel. to no. of traps 8=5380
- superimposed insulating layers, distrib. of elec. stresses 8=9235
- transducer, piezoelectric, mechanical responses 8=5379
- thermoelectric generators, use of ferroelectric ceramic condenser 8=9231
- transfer surfaces for latent image 8=6580
- Al-Al $_2\text{O}_3$ -Al film, current instabilities 8=18201
- Al-Al $_2\text{O}_3$ -Al, superconducting energy gap 8=17958
- Al-Al $_2\text{O}_3$ -Al thin film structures, electrode props. rel. to photocurrent direction 8=22689
- Al-Al $_2\text{O}_3$ -Au thin film structures, internal photoemission yields, Monte Carlo calcs. 8=22722
- Al-Al $_2\text{O}_3$ -Au tunnel structures, interface trapping 8=5381
- Al-Al $_2\text{O}_3$ -metal diodes, negative resistance obs. 8=5377
- Al-CaWO $_4$ -Au tunnel structures, interface trapping 8=5381
- HfO $_2$ film capacitors, characts. 8=22654
- SbSI, temp. autostabilization element 8=5369
- Si-collodion-Au contacts, photocapacitive effects 8=22673
- SiN films deposited on metal-coated substrates, resistivity and breakdown strength 8=13870
- SiO capacitors, rel. to impurities in vapour source 8=18202

Dielectric devices—contd

- SiO capacitors, thin film, heating effects 8=9233
 SiO capacitors, thin-film, heat treatment 8=22676
 SiO₂ films, pyrolytically grown, conductivity mechanism 8=13872
 SiO₂ films, MOS capacitors, noncrystalline structure electronic conduction 8=9234
 SiO, thin film capacitors, a.c. electrical breakdown 8=2253
 Ta₂O₅ film capacitors, prep. methods 8=13097
 Ta₂O₅-SiO thin film capacitor, prep. and props. 8=9232
 ZnO, polycryst. containing 3% Bi₂O₃, doped, semiconducting and semi-insulating props. 8=18205

Dielectric loss. See Dielectric phenomena; Dielectric properties of substances.

Dielectric materials

- ADP, antiferroelectric, nuclear and e.p.r. studies 8=22671
 alkali halides, nonlocalized dipoles, weak field, low freq. third harmonic generation 8=22653
 anthracene, Hall and drift mobilities of carriers 8=18178
 anthracene, hole injection from electrolyte and space-charge-limited current 8=18177
 crystals with high permittivity, electrical conductivity theory 8=8897
 discharges occurring in gaseous occlusions, amplitude spectrums 8=18157
 dyestuffs, organic, elec. energy storage 8=18176
 elastic, thermodynamic pots. at finite deforms. 8=10541
 electrical insulation and dielectric phenomena, conference, Pocono Manor USA (1966) 8=18154
 electron and ion emission on laser light interaction 8=18272
 exciton resonances, optical absorption 8=8947
 Franz-Keldysh effect, spectral broadening representation 8=17853
 glasses, meas. of losses at 40 Gc/s 8=22649
 glasses in PbO-Al₂O₃-B₂O₃-SiO₂ system, elec. props. temp. and comp. dependence 8=18170
 heterogeneous absorbing medium, realization by oxide absorbent of s.h.f. oscillation energy 8=13867
 inhomogeneous, reflection of e.m. waves 8=10951
 liquids and solids with gas inclusions, permittivity formulae 8=13868
 liquids, thermal convection, elec. field effects 8=21659
 magnetically ordered, two-magnon Raman scattering 8=9487
 mica, LEED obs. of electric dipoles on cleaved surface 8=22650
 nonlinear propag. of laser beam 8=22931
 nonlinear, self-modelling wave beams 8=10835
 paper, insulation, elec. discharge, d.c. detection and meas. 8=21242
 plastics, for specialised applications 8=13876
 polarization as a function of electron displacement 8=15193
 polyethylene, degradation by partial discharge 8=21214
 polymers, anelastic and dielectric effects, book 8=22658
 polymethylmethacrylate, effect of impulse γ -neutrons on permittivity 8=18180
 polymethylmethacrylate, temp. depend. of conformation transitions and dipole moment 8=17111
 space charge conduction, review 8=18002
 stearic acid multi-monolayers thin film, electrical properties 8=13878
 thermal conductivity, temp. dependence meas. 8=17539
 transparent, damage due to laser light 8=8755
 u.s. absorption in crystals with high impurity concs. 8=17491
 Al-Al₂O₃-Au film system, contact barrier height determ. by photoelectric meas. 8=18277
 Al₂O₃, breakdown field strength, thickness variation 8=22651
 Al₂O₃ films, pyrolytically grown, conductivity mechanism 8=13872
 BaTiO₃-Cr₂O₃ systems, phase transformations 8=17045
 CeO₂ crystals, conduction mechanism from electrolyte reduction study 8=18164
 In₂O₃ films, pyrolytically grown, conductivity mechanism 8=13873
 KBr, ionic, structure factors and electron distrib. 8=17861
 KCl, dark currents, space-charge-limited electron 8=18168
 NaCl:Co, props., 90-200°C, 30 c/s-100 kc/s 8=13869
 NaNO₂, infrared dielectric dispersion and apparent ionic charges 8=22670
 NiO films prep. and thin film triodes 8=22602
 TiO₂, current rise due to injection during elec. ageing, hypothesis 8=18194
 TiO₂, effect of H₂O and NH₄Cl traces on ϵ' and ϵ'' 8=18174
- Dielectric measurement**
 agar agar, and soft materials, complex permitt., microwave 8=22659
 capacitance, absolute meas. by cross capacitor 8=15169
 capacitors, reference, temperature characteristics 8=10820
 cavity resonator for 32 GHz, 4.2°-300°K 8=18150
 complex ϵ meas. at microwaves 8=6399
 complex permittivity variations 8=265
 concentration of a solution, continuous, using reactance meter 8=5733
 crystals, anisotropic, mech. method 8=18160

Dielectric measurement—contd

- extremal values recording for excluding fluctuations and errors 8=15167
 liquids, as function of temp. and press. 8=1582
 losses in solids, at v.l.f., meas. using oscs. of solid on torsion suspension 8=2235
 low-loss media, properties, using dipole surface waves 8=13864
 permittivity and loss tangent, automatic, by transformer bridge method, 50 Hz-200 kHz 8=6241
 on polystyrene, mobility and dipole moments of polar mol. solutes 8=9205
 rock, moist, in laboratory 8=13899
 semiconductor diodes, capacitance obs. at h.f. and v.h.f. 8=13850
 semiconductors permittivity of microwave freq. 8=5277
 thin films on metal surface, detection apparatus 8=8299
 Br, liquid, 20°C, improved method 8=4596
 a(Fe₂O₃)+b(Cr₂O₃)+X₁(NiO)+K₂(ZnO) type ferrites, complex const. microwave system 8=9371
 Ge-Si alloyed heterojunctions, capacitance over 77°-273°K 8=2217
 Sn films, in u.v. reflecting power, and optical constants deduced 8=5638
- Dielectric phenomena**
 See also Electric strength.
 alkali halides, interstitial cations, theory 8=1948
 antiferromagnetic ionic dielects., interact. between optical phonons and magnons 8=2231
 breakdown, electric, in solids 8=18153
 constants, classical theories 8=6257
 capacitor charging time, voltage effect 8=280
 capacitors, voltage shock, dielectric ageing mechanism 8=13898
 Cherenkov losses of modulated current, non-linear 8=277
 conductor, nonlinear theory of h.f. field penetration 8=13706
 copper formate tetrahydrate, antiferroelectric phase transition, cell doubling 8=9222
 crystal, interaction of charged particles, theory 8=8625
 cube, capacitance, effect of perturbations from symm. 8=6256
 dipolar actions at short distances 8=3148
 dipole system, permittivity dispersion 8=9187
 effect of dielectric layers on radiation-patterns of e.m. sources 8=10975
 effective dielec. const. tensor of strongly inhomogeneous anisotropic media 8=16492
 elastic dielectric, rel. to thermodynamic theory of higher-order effects 8=2234
 electrical insulation and dielectric phenomena, conference, Pocono Manor USA (1966) 8=18154
 electrification by rubbing, essential conds. 8=6254
 electromagnetic pulse propag. in lossless, inhomogeneous, dispersive media 8=3250
 electromag. waves in periodic pile 8=19837
 electron gas with fixed point charge, dielectric constant 8=8962
 electron transmission through thin films 8=13470
 e.m. waves, reflection and transmission, moving perpendicular to incident plane 8=10947
 e.m.f. due to shock wave, theory 8=5344
 Faraday effect, rel. to Raman scatt. 8=5575
 ferrimagnetic ionic dielects., interact. between optical phonons and magnons 8=2231
 ferroelectrics, spin-wave intensification by charged-particle beam 8=5443
 films, non-crystalline, tunneling model 8=18155
 fluids, motion of conducting particles, enhanced charge transfer 8=16709
 gas, of resonance atoms, permeability theory 8=1481
 guided waves, transformation theory 8=378
 insulating phase in presence of normal impurities, excitonic props. 8=8951
 ionic crystals, polarization theories 8=9186
 liquids, polar microwave to far infrared spectra, relaxation theories 8=8081
 luminescence, 2-photon stimulated, in dielectrics, exciton transitions calc. 8=9583
 magnetoplasma in resonant cavity, absorpt. spectrum 8=21352
 Maxwell-Wagner dispersion, eqns. 8=22647
 metals, dielectric constant, exchange term 8=2137
 metal-dielectric-supercond. structure, electron tunneling in sound field 8=5219
 nonlinear dielectrics, propag. of higher-order coherence functions 8=5570
 plasma-dielec. interface boundary conds. 8=4325
 plasma imbedded in moving dielec. medium, governing eqns. for e.m. fields and waves 8=12507
 polar liquids, longitudinal electrostatic waves, theory 8=4600
 polarizability increase by induced deformation of molecules, atoms and particles 8=20910
 polarization as function of e displacement 8=15193
 polymers, relaxation, book 8=22658
 pulsed breakdown along surface, uniform field 8=9188

electric phenomena—contd

- pulsed breakdown along surface, non-uniform field 8=9189
 reflection and transmission of e.m. waves incident on moving plate 8=369
 relaxation due to chem. rate processes 8=9673
 relaxation in elec. double layer 8=2530-1
 reststrahl anomalous structure rel. to dielectric constant, model 8=5572
 slab excitation by parallel plate waveguide with one plate truncated 8=21335
 solids, relax. effects, meas. by ionic thermocurrents method 8=5346
 spheres, free, e. m. resonance 8=10979
 trace characterization method for imperfection meas. in insulating crystals 8=18757
 transparent, laser-induced breakdown 8=13865
 triglycine selenate, crystalline, transition from ferroelectric to paraelectric at high press. 8=8288
 Van der Waals forces, macroscopic theory 8=19718
 Zwanzig theory of dielec. friction 8=8099
 CaF₂ containing Mn²⁺, OH⁻ and oxygen, loss 8=2371
 CaF₂:O²⁻ ions, dielectric loss 8=5350
 with CdS layer, ultrasonic Love wave amplification 8=4921
 GaP, dispersion, and phonon line shape 8=14215
 Mn₂Fe₃-O₄, loss peaks rel. to electron diffusion 8=14050
 NaNO₂, infrared dispersion and apparent ionic charges 8=22670
 Ti₂O₃, dielec.-metal phase transition rel. to mag. ordering 8=18389
 V₂O₅, dielec.-metal phase transition rel. to mag. ordering 8=18389
 VO, VO₂, dielec.-metal phase transition rel. to mag. ordering 8=18389
 YFe garnet, loss peaks rel. to electron diffusion 8=14050
- ferroelectric.** See Ferroelectric phenomena.
- electric properties of substances**
 See also Electric strength.
 agar agar, and soft materials, complex permitt., microwave meas. 8=22659
 air plasma, permittivity and conductivity variations with freq. and electron density 8=4346
 argon plasma, permittivity and conductivity variations with freq. and electron density 8=4346
 benzene, adsorbed on silica gel, change in dielec. behaviour on gel purification 8=1663
 fluids, constant derived from radiation stress theory rel. to refractive index and thermodynamic props. 8=16615
 light wave interaction in nonlinear medium 8=18487
 lossless, inhomogeneous, dispersive media, e. m. pulse propag. 8=3250
 low frequency, anomalous charging and discharging currents 8=13866
 packed powders with fluids, permittivity 8=22648
 plasma, dielectric response function rel. to turbulent stationary state theory 8=12559
 plasmas, scatt. of e. m. waves by dielect. const. fluctuation 8=21338
 plasma, two temp., permittivity analysis 8=7742
 'polarization' current 8=21706
 polarization as function of e displacement 8=15193
 poly(tetramethylene oxide), during crystallization 8=17240
 random continuum, h. f. spherical wave elect. field component correl. functions 8=15390
 slabs with large permittivity modulation parametric props of 8=18206

gases

- nonpolar, Clausius-Mossotti function, effect of molec. interaction 8=12693
 rare-gas binary mixtures, frequency-depend. dielec. constant 8=12692
 Co(CO)₃NO, microwave determ. of dipole moment 8=12185
 He-CF₄ compressed mixtures, rel. to nonresonant absorpt. and dispersion 8=1486
 NH₃, Lorentz-Lorentz rel. 8=1477

liquids and solutions

- absorption at 2 and 4 mm wavelengths, meas. 8=21709
 alanine, α and β , increments and relax. wavelengths, comparison 8=8098
 alcohols, tertiary, association consts. determ. 8=12908
 aliphatic alcohols, domain theory 8=4550
 benzene, electron-injection from tunnel junction, effective barrier 8=257
 binary mixtures rel. to elec. cond. 8=4609
 chloroform-triethylamine system 8=18649
 Conference, London May 1967 8=6255
 cyclohexane, electron-injection from tunnel junction, effective barrier 8=257
 n-decanol in non-polar solns., microwave relax. 8=21711
 dimethyl sulfoxide, base-catalysed titration and ionization 8=4610
 electrolyte solns. in alcohols 8=8100
 electrolyte solns., dielec. friction 8=8099
 electrostatic purification 8=1543
 ethylenimine, dipole moments meas. by benzene solvent method 8=1583
 gas inclusions, ellipsoidal, permittivity of mixture, formulae 8=13868
 n-hexane, elec. cond., u.v. and γ radiation 8=21714
 n-hexane, as function of temp., press. and density 8=1582

Dielectric properties of substances—contd**liquids and solutions—contd**

- Kerr cell system, high voltage transient waveform meas. 8=6240
 metals, liquid, reln. between pair pots. and radial distrib. functions of ions 8=16787
 methylmethacrylate copolymers with styrene and p-chlorostyrene, relax. 8=12906
 microwave constant, precision meas., corrections to earlier method 8=16874
 nitrate melts, binary mixtures of Ca(NO₃)₂ and MnO₃ (M = Na, Cs, Rb, K), supercooled, relax. processes 8=1586
 nitrobenzene, h. p. effect 8=21713
 nitrobenzene, laser prod. permittivity vars., obs. 8=21712
 oils, blended, power factor calc. from ion content 8=21708
 oil, mineral, prebreakdown luminosity waves 8=4598
 orienting field and dipole polarization 8=8102
 phenols, association consts. determ. 8=12908
 piezo-optic coefficients by pulsed u.s. light diffraction, 24 liquids obs. 8=8064
 piperine, supercooled, dipole polarization relax. time obs. 8=21710
 polar liquids, longitudinal electrostatic waves, theory 8=4600
 polar, proton shielding, role of reaction field 8=12782
 polarizable liquid, correction to Stoke's law for charged sphere 8=12723
 poly-L- γ -benzyl glutamate helices in soln. 8=21705
 poly(ethylene oxide) in benzene soln. 8=12390
 poly(hexene-1 sulphone), dielec. meas. and relax in soln., poly(2-methylpentene-1 sulphone), dielec. meas. and relax in soln., dipole moment obs. 8=1584-5
 polymethylpolysiloxanes, microwave 8=4597
 poly-DL-phenylalanine helices in soln. 8=21705
 poly(tetramethylene oxide) in benzene soln. 8=12390
 prebreakdown impulse current meas. apparatus 8=8115
 propanol-H₂O mixtures, with NaCl in soln. 8=4606
 semiconductors, complex permittivity 8=265
 space charge distrib., after passage through a filter 8=12910
 static electricity in liquids 8=12907
 urea aq. soln., dielec. dispersion 350-3600 MHz 8=8103
 water, electrification accompanying bursting of air bubbles 8=8117
 water, permittivity meas. at 8.6 mm from 1°-60°C 8=16873
 Al acetylacetonate in benzene, microwave absorpt. 8=16872
 Al acetylacetonate in benzene solution, electrical polarization and microwave absorption 8=12905
 Ar, charge transport temp. dependence 8=18161
 Bi, const $\epsilon_1 + it_2$, and optical consts 8=12877
 Br, 20°C, 8.2-18 GHz, dielectric constant 8=4596
 BrC(CH₃)₃, Br₂CNO₂ const. and loss rel. to mols. relax., 9GHz, 10 and 200 kHz 8=18179
 Cd, const $\epsilon_1 + it_2$, and optical consts 8=12877
 ClC(CH₃)₃, Cl₂CNO₂ and ClSi(CH₃)₃ const. and loss rel. to mols. relax., 9GHz, 10 and 200kHz 8=18179
 Cr acetylacetonate in benzene, microwave absorpt. 8=16872
 H₂O, permittivity at 0.85 mm 8=1581
 H₂O, permittivity, 1.2 to 1.6 mm 8=21707
 He, electron-injection from tunnel junction, effective barrier 8=257
 Hg, const $\epsilon_1 + it_2$, and optical consts 8=12877
 NaNO₃, fused, complex permittivity 8=8101
 Pb, const $\epsilon_1 + it_2$, and optical consts 8=12877
 Zr acetylacetonate in benzene, microwave absorpt. 8=16872
- solids**
 alkali halides, nonlocalized dipoles, weak field, low freq. third harmonic generation 8=22653
 alloy, very dilute constants at Fermi level at low temp. 8=1659
 anatase, permittivity rel. to that of rutile 8=18173
 anilines, disubstituted, constant and loss in r.f. region 8=5357
 anthracene, Hall and drift mobilities of carriers 8=18178
 antiferroelectric, permittivity and losses investigated at 37Gc/s 8=18196
 butyl phthalate, relax. compared with spin-lattice relax. 8=9459
 carrier concentration and mobility determ. by surface charge density meas. 8=18152
 ceramic insulators in thermal neutron flux 8=12010
 concrete, heat resistance, elect. insulating props. dependence on temp. and atmosphere 8=13900
 constants cavity resonator meas. at 32 GHz, 4.2°-300°K 8=18150
 Conference, London May 1967 8=6255
 crystals, ionic, permittivity, static and high frequency, calc. from polarization theories 8=9186
 cyanethylacetylcellulose relax. rel. to acetate and cyanethyl groups motion, -160-200°C 8=22662
 cylinders, between reflecting planes, e.m. vibrations 8=10699
 diamond crystal, permittivity calc. 8=5354
 dicalcium strontium propionate, Ca₂Sr(C₂H₃CO₂)₆, structure in paraelectric phase 8=4891

Dielectric properties of substances—contd

solids—contd

- dielectrics, internal friction of dislocations rel. to optical props. 8=14165
 dielectric-coated semicond., equilib. config. and charge distrib. 8=13788
 dipole waves as means of props. determ. 8=13864
 elastic, homogeneously deformed and uniformly polarized, lattice theory 8=13177
 elastic, lattice theory rel. to fluorites 8=13178
 electrical insulation, thermal breakdown under radioactive radiation 8=9190
 electronic processes in low mobility solids, conferences, Sheffield, England, April 1966 8=5101
 excitonic insulator, anisotropy effects 8=9192
 ferrites, influence of ultrasound 8=9370
 ferrites, polycrystalline, relaxation rel. to temp. 8=22644
 gas inclusions, ellipsoidal, permittivity of mixture, formulae 8=13868
 ice, impure, dispersion obs., above -190°C 8=18188
 insulating films, effective mass meas. 8=8944
 insulating films with ionic space charge, conduction process 8=2232
 insulating materials, time dependence of electric breakdown 8=22646
 insulators, dislocation binding with electrons holes and excitons 8=5349
 insulators, e-irradiated, space-charge effects 8=9185
 insulators, hot-electron diffusion theory for space-charge-limited current flow 8=9129
 insulators, lattice Raman scattering theory 8=2397
 ionic, constants and change with hydrostatic pressure 8=5348
 ionic matrix, dipole moment of trapped polar impurity 8=2236
 methylmethacrylate-methylacrylate copolymers, relaxation 8=5358
 molecular crystals, permeability in rel. to polarization operator 8=18480
 molecular crystals, permeability, quantum field theory 8=5347
 multilayer coatings for white light interferometry 8=6540
 permittivity of randomly inhomogeneous anisotropic media 8=19715
 p-n junctions, capacitance rel. to doping 8=18106
 p-n junction with deep donor impurities, capacitance, theory 8=18102
 polyalkyl methacrylates, absorption 8=9203
 polybromoprene polarization rel. to mol. motion, obs. 8=22660
 polycarbonate films, BaTiO_3 and organic cpds., loaded 8=22661
 polychloroprene polarization rel. to mol. motion, obs. 8=22660
 polyethylene, irradiated, at melting point 8=9201
 polyethylene terephthalate, e-irradiated, space-charge effects 8=9185
 poly- γ -benzyl-DL-glutamate, rel. to mol. motion 8=2241
 polymethylmethacrylate, stereoblock, low-temp. 8=18175
 polystyrene, behaviour rel. to molec. weight 8=5360
 polystyrene, rel. to polar molecule solutes 8=9205
 polystyrenes, v. low temp. 8=5359
 polysulfone films, BaTiO_3 and organic cpds., loaded 8=22661
 polyvinylacetate, behaviour rel. to molec. weight 8=5360
 polyvinylchloride, plasticized, dipole-group losses rel. to conformation 8=8360
 porous, permittivity model for cell level 8=18149
 quartz, permittivity as a function of X-ray irradiation 8=13871
 Rochelle salt, permittivity and permeability 8=5371
 rutile, permittivity rel. to that of anatase 8=18173
 sapphire, mech. meas. method 8=18160
 shellac wax, surface charge obs. 8=13892
 silica glass, dielect. loss at low temp., OH^- conc. and irradiation effects 8=18172
 slab, moving, rel. to reflection and transmission of e. m. waves, parallel polarization 8=19836
 space symmetry and induced polarization 8=9206
 TFE-HFP copolymers, γ -irrad. effects 8=9202
 thin films, tunnel and Schottky currents rel. to thickness fluctuations 8=5345
 toluene glow discharge prod. polymer films, obs. 8=21894
 tracking resistance at l. v., dry test using trigger discharge 8=2240
 transport props, low-mobility, exptl. determ. 8=18151
 triglycine fluoroberyllate, under hydrostatic press. 8=9221
 Ag, constant, and bilinear optical polarizability calc. 8=18498
 AgCl, ultrasonic field effect on conductivity 8=2237
 AgPd alloy, localized states from permittivity obs. 8=13656
 Al_2O_3 , amorphous and polycryst., $-\text{Im}\epsilon^{-1}$ and charact. energy-loss spectra 8=13695
 Al_2O_3 and e beam evaporation 8=22652

Dielectric properties of substances—contd

solids—contd

- Al_2O_3 films, chem. deposited 8=4740
 Al_2O_3 , produced by anodic oxidation of Al in presence of hydrated oxide 8=18729
 Ar, charge transport temp. dependence 8=18161
 Ar, crystalline, constant dependence on growth parameters 8=2238
 As-S glasses, dielectric constraints and dissipation factors, obs. 8=9193
 As_2S_3 , amorphous, carrier mobilities from conductivity studies on e-irradiation 8=18162
 AuPd alloy, localized states from permittivity obs. 8=13656
 $\text{Ba}(\text{NO}_3)_2 \cdot \text{H}_2\text{O}$, single crystal, meas. of coeff. in range $80-3000^{\circ}\text{K}$ 8=5051
 BaTiO_3 , ceramic, grain size dependence 8=13881
 BaTiO_3 , field depend. of dielect. consts. at 58.2 GHz 8=13879
 BaTiO_3 , single crystal and polycrystalline, dynamic polarization 8=18183
 BiFeO_3 with $\text{Pb}(\text{Ti}, \text{Zr})\text{O}_3$, solid solutions, at high temp. and freq. 8=13885
 $\text{BrC}(\text{CH}_3)_2\text{Br}_2\text{CNO}_2$, consts. and loss rel. to mols. relax., 9GHz, 10 and 200kHz 8=18179
 $\text{CaF}_2\text{:GdF}_3$, surface-layer relax. 8=18163
 CaF_2 , MgF_2 , Na_3AlF_6 , thin films, rel. to i. r. antireflectant suitability 8=2435
 CdF_2 8=8409
 CdS , thin crystals, capacitance changes under d.c. bias 8=9195
 CdSe , and optical constants 8=23026
 CeO_2 , transients and non-ohmic behaviour 8=9196
 $\text{ClC}(\text{CH}_3)_2\text{Cl}_2\text{CNO}_2$, and $\text{ClSi}(\text{CH}_3)_2$ const. and loss rel. to mols. relax., 9GHz, 10 and 200kHz 8=18179
 CoO:Li , ($\text{Li}^+-\text{Co}^{3+}$) dipole relax. losses rel. to free hole movement 8=18165
 CoO:Na , ($\text{Na}^+-\text{Co}^{3+}$) dipole relax. losses rel. to free hole movement 8=18165
 Cu formate tetrahydrate, sp. ht. and entropy at anti-ferroelectric transition pt. 8=8638
 EuS, magnetically ordered, magnetointernal field emission obs. and model 8=5428
 EuSe, magnetically ordered, magnetointernal field emission obs. and model 8=5428
 FeO , elec. props. at high temp. rel. to defect structure 8=18166
 GaAs, microwave, resonance behaviour 8=13799-802
 Ge-Hg, relax. phenomena 8=2230
 HfO_2 and e beam evaporation 8=22652
 HfO_2 films, and appls. 8=22654
 HgI_2 crystal, polarisation vs field strength under light excitation 8=5373
 InAs, calc. from light absorpt. by free carriers, 300°K and 80°K obs. 8=18536
 KD_2PO_4 , dynamic props. due to deuteron intrabond jumping 8=9212
 KH_2PO_4 , dielectric const. just above transition temp., freq. and temp. depend. 8=22666
 KH_2PO_4 , paraelectric, proton dynamics 8=9214
 KMF_3 , ($\text{M} = \text{Mg}, \text{Mn}, \text{Co}, \text{Ni}$), constants from i. r. reflectance spectra 8=2426
 $\text{K}(\text{Ta-Nb})$ crystals, permittivity with temperature variation 8=9199
 $\text{LiH}(\text{SeO}_3)_2$, const. and spontaneous polarization 8=18190
 LiNbO_3 , single crystal, up to 9 GHz 8=9216
 LiTaO_3 , single cryst. 8=8853
 MgO , electron donor props. at surface, study via adsorbed nitro-cpds. 8=8343
 Mn ferrite, Maxwell-Wagner dielec. dispersion meas. 8=22647
 NaCl , polarization under shock load, obs. 8=5353
 NaCl:Ca , interpretation of obs. relaxations 8=22656
 $\text{NaCl:CaCl}_2 + \text{NaOH}$ crystal, loss maxima, and conductivity 8=5164
 NaCl:Co , 90- 200°C , 30 c/s-100 kc/s 8=13869
 NaNbO_3 , dipole interaction and electronic polarizabilities 8=22655
 NaNbO_3 , loss, d. c. cond. and permittivity, temp. depend. 8=2239
 Pb , interband transitions 8=14253
 $\text{PbTiO}_3\text{-PbZrO}_3\text{-PbMg}_{1-x}\text{W}_{1-x}\text{O}_3$ system, domain orientation processes 8=5367
 PbZrO_3 , l.f. study, rel. to temp. 8=5368
 RbMnF_3 , constants from i. r. reflectance spectra 8=2426
 ReO_2 metal, optical props. including dielectric const., range 0.1-22 eV 8=14258
 S, orthorhombic, transient space-charge perturbed currents 8=18171
 SbSI , anomalous dispersion of permittivity and reson. absorpt. of microwaves 8=9218
 Sb_2S_3 , anomalous dispersion of permittivity and reson. absorpt. of microwaves, temp. depend. 8=9217-8
 Se films, vitreous, space-charge-limited currents and high elec. field effect 8=13828
 Si crystal, permittivity calc. 8=5354
 SiN films deposited on metal-coated substrates 8=13870
 SiO_2 film deposited from SiCl_4 -water vapour reaction 8=21889

electric properties of substances—contd**solids—contd**

- SiO₂, vacuum deposited insulating layer, instability 8=9175
 Sn film, white, constant contrib. from optical data analysis over 0.1 to 27.5 eV energy region 8=2456
 SnO₂, constants rel. to electron scattering polar optical modes 8=22611
 Ta₂O₅ and e beam evaporation 8=22652
 TiO₂, effect of H₂O and NH₄Cl traces on ϵ' and ϵ'' 8=18174
 TiO₂ films with large ionic space charge, conduction process 8=2233
 TiO₂:V⁴⁺, modes rel. to paramag. impurities, multiple electron-spin echoes 8=22657
 TiO₂-x (reduced rutile), relaxation processes at 1.2 to 50°K 8=5355
 Tl halides, consts., temp. and press. depend. 8=13874
 TiCl₃, space-charge polarization capacity, and conductance 8=9200
 ZnO, polycryst. containing 3% Bi₂O₃, doped, semiconducting and semi-insulating props. 8=18205
 ZnS/Cu, Cl, complex constants and luminance, comparison during thermoluminescence 8=13875
 ZnS:Mn films polarization effects in electroluminesc., obs. 8=9638
 ZnSe, and optical constants 8=23026
 ZnTe, and optical constants 8=23026
 ZrO₂ and e beam evaporation 8=22652

solids, ferroelectric. See Ferroelectric materials.**electric relaxation.** See Dielectric phenomena; Dielectric properties of substances.**electric strength.** See Electric strength.**differential analysers.** See Calculating apparatus.**differential equations**

- boundary layer, Laplace transform. solutions 8=6021
 conformal transformation use and relaxation net construction 8=19352
 of diffusion, nonlinear, stability of solns. of simple stationary wave type 8=3008
 first-order, coupled, for waves in inhomogeneous warm magnetoplasma 8=16532
 ith order, numerical solutions, accurate and stable 8=6594
 Laplace, soln. of boundary Dirichlet problem 8=19369
 linear, matrix algorithm for soln. 8=14931
 Maxwell's, soln. for moving source and progressive wave formalism for homogeneous medium 8=3252
 nonlinear, general computational form 8=19357
 nonlinear Lie-series soln. technique 8=10996
 parabolic for 2-dimens. boundary layer, soln. by finite difference procedure 8=19634
 parametric resonance, transition from linear to non-linear state 8=6018
 partial, for probability density of quantum statistical mechanics 8=19447
 polymer chains, hierarchy of eqns. 8=12383
 residual gases in ultrahigh vac. systems, press. eqns. 8=16723
 restricted three-body problem, props. of soln. of first-order variational eqns. 8=10094
 2nd order, existence of forced periodic solutions 8=6019
 second order at a turning point, classification and reduction 8=6020
 Sturm-Liouville, one dimensional upper bounds to eigenvalues 8=2882
 third-order system for oscillations, critical Lyapunov case 8=6120
 Thomas-Fermi, soln. improved by flexible choice of boundary conditions 8=20936
 transformation of non-linear into equivalent linear 8=19359
 WKB, generalized approx. for binding energies of inner atomic electrons 8=4050

diffraction

- crack, penny-shaped, plane longitudinal wave 8=2924
 edge, in arbitrary anisotropic medium 8=6549-50
 elastic waves, by parabolic cylinder, wave function expansions and perturb. method 8=19525
 elastic waves by spherical cavity, anal. in shadow zones 8=19518
 elastic waves in cylindrical wedge 8=10706
 elastic waves, Fraunhofer phenomena 8=15043
 liquid Kelvin waves at corner 8=12758
 liquid surface waves, by a wedge 8=9815
 sampling theorem, axial form 8=24
 shock wave, in fluid by supersonic wedge 8=21492
 shock waves by wedge, corner conditions 8=10716
 theory as singular perturbation problem, matched asymptotic expansions 8=25

acoustic waves

- acoustic holography, with inclined planar reference 8=10744
 convex boundary with propagation velocity change 8=10704
 convex surfaces, smooth, variable curvature, asymptotic theory 8=6382
 elastic tube, semi-infinite, in moving medium 8=3062
 holography account 8=195
 plane, by grating of cylindrical cavities in elastic medium 8=19570

diffraction—contd**acoustic waves—contd**

- ray representation, extension into shadow zone, feasibility 8=10747
 split-beam sound field, propag., ray representations 8=19567
 wall material, choosing type and distribution 8=6185
 by wedge, Sommerfeld's problem soln. for multipole fields 8=10746

acoustic waves, ultrasonic

- crystals, off e. m. waves 8=22942
 line source, vel. pot. on surface of elliptic cylinder, as test of Kellers creeping waves 8=19569

electromagnetic waves

- anisotropic medium subject to u. s. waves 8=22942
 by anisotropically conducting plane ("radial grid") 8=19852
 at arbitrary obs. point behind screen, Kottler theory 8=373
 Babinet's princ. in anisotropic medium 8=374
 by circular aperture in non-planar screen 8=15400
 on conducting half-plane 8=10953
 by conducting half-plate, Wiener-Hopf soln. 8=19849
 by conducting strip in layered medium, rel. to e. m. prospecting for ore deposits 8=23214
 by conical horn, geometrical calc. and obs. 8=19847
 convex surfaces, smooth, variable curvature, asymptotic theory 8=6382
 creeping wave excit. by mode conversion of critically incident ray 8=19826
 at curved interface, rel. between creeping and lateral waves 8=19846
 cylindrical grating, excitation by rotating charge 8=6380
 dipole field by conducting half plane 8=3258
 dipole field, by two spheres 8=15404
 dipole radiation, by ideally-conducting wedge 8=19851
 elementary particle behaviour 8=20279
 Fraunhofer, validity of Babinet's principle 8=22008
 Fresnel and Fraunhofer eqns., derivation by resolving field into angular distribution of plane waves 8=19853
 by half-plane in arbitrary medium, Wiener-Kopf eqns., uncoupling 8=372
 half-plane, conducting, in a layered medium 8=6385
 inhomogeneous medium, appl. of Huygens' principle 8=19854
 integral eqns. for open screens 8=19855
 matrix operators in diffr. problems 8=19843-4
 microwaves, by cylindrical objects 8=19845
 plane, by a rectangular cylinder, numerical solution 8=15399
 radiating functions, pseudo-radiation conditions for derivatives 8=381
 rectangular aperture, side-lobe contribution 8=10954
 scattering from finite edges, geometrical diffr. theory 8=19859
 scattering, specular, geometrical diffr. theory modification 8=19860
 skew grating, Riemann-Hilbert soln. 8=3257
 strip current approx. by Fresnel integrals 8=19862
 surface waves, at junction of half-planes with anisotropic and isotropic conductivity 8=6384
 transhorizon tropospheric propagation, book 8=14630
 by u. s. waves, in anisotropic medium 8=10952
 waveguide, surface wave on semi-infinite anisotropically conducting plane 8=15402
 Wiener-Hopf functional eqns. 8=6381
 X-rays, dynamical theory, appl. to holography 8=530

electrons. See Electron diffraction.**light**

See also Holography.

- in anisotropic media due to acoustic waves 8=9476
 annular and disc-like objects, images under partially coherent illumination 8=11188
 Bragg detect. in acoustic freq. mixing 8=10732
 Bragg type, by chirped acoustic wave, pulse compression of 240 nsec r.f. pulse 8=8618
 Chinese characters, patterns rel. to recognition 8=6556
 coherent beam, energy flow near focus 8=6499
 coherence function depend. 8=20100
 Cornu's spiral, support of Young's theory 8=6557
 creeping waves in shadow of elliptic cylinder, test with acoustic line source 8=19569
 Debye-Sears, with ultrasonic field, line intensity calc. 8=11190
 by elec. and mag. anisotropic media 8=515
 Fresnel of apertures under partially coherent illumination 8=6559
 Fresnel pattern correl. in signal det. 8=14935
 Fresnel zone patterns, variable 8=507
 Fresnel zone plate generation 8=6551
 holograms, inexpensive method 8=6569
 holograms, point, as optical elements 8=6568
 holograms, quantity reproduction process 8=11209
 holographic interferometry appl. to plasma meas. 8=7779
 holographic interferometry in electrochem. 8=2528
 holographic moire fringes, use in flow visualization in aerodynamics 8=6572
 holography, birefringent beam splitting device 8=3379
 holography and spatial filtering, new applications 8=11119
 image of diffuse object using coherent illumination, noise-like structure 8=11217

Diffraction—contd**Light**—contd

- imaging of microwave acoustic beam, cross section in rutile by Bragg laser 8=6175
- intensity distribution due to interaction of monochromatic beam with progressive u.v. surface wave 8=6553
- lasers, holographic application, review 8=6479
- in liquids, by u.s. waves, rel. to vel. of sound determ. 8=8060
- multiple diffraction formula 8=3369
- non-planar, influence of screen geometry 8=11183
- open laser resonator losses 8=15447
- optical imaging systems, significance of nonlinearity 8=11134
- optical relay, effect on useful flux incident on a receiver 8=15505
- parabolic cylinder, illuminated, short wave asymptotics 8=508
- pattern calc. from Schlömlich series 8=6552
- patterns with phase and amplitude vars., apodization and iterated diffr. rel. to waveguides 8=6558
- progress in optics, book VI 8=15541
- ray deviations in optically inhomogeneous field, holographic process 8=526
- Rayleigh-Huygens formulae, boundary conditions 8=11182
- by rectangular aperture, partially coherent illum., diffr. field coherence calc. 8=20101
- sampling theorem, axial form, optical application 8=24
- theory in inhomogeneous media, transition functions 8=20102
- theory, integral-transform formulation 8=11187
- by u. s. waves in cryst., depend of field on u. s. amplitude for cubic crystals. 8=22944
- ultrasonic fields in liquids 8=20035
- wave theory, corpuscular interpretation 8=15547
- zone plates and phase zone plates, efficiencies 8=11185
- zone plate theory, axial intensities, comments 8=6554
- zone plate theory, image intensities, axial, reply to comments 8=6555
- GaAs monocrystal subject to u. s. waves 8=22942
- YFe garnet, for magnetoelastic wave propag. study 8=22861
- YIG, spin and acoustic Bragg, in longitudinal magnetoelastic 8=18482
- ZnO, ZnS crystal ultrasonic waves, obs. 8=18514

neutrons. See Neutron diffraction.

X-rays. See X-ray diffraction.

Diffraction by acoustic waves. See Acoustic waves/effects; Diffraction/light.**Diffraction gratings**

- aberrations, optical, geometrical theory 8=6500
- bevelled, r.f., props. 8=19856
- blazed, prod. from single crystals 8=11186
- calculator, from graphical soln. of grating eqn. 8=3370
- circular 8=6558
- cylindrical, e. m. excitation by rotating charge 8=6380
- grating eqn, graphical soln. rel. to calculator of parameters 8=3370
- light dist. analysis, Fourier 8=11164
- metallic, i. r., properties 8=3371
- moving, translation of light frequency 8=11189
- Rowland's ghosts using lasers, obs. 8=3372
- ruling engine to control motion of diffraction grating during cutting 8=11184
- ruling, interferometric control 8=11180
- second generation, prod. by dividing engine using photographic media 8=11181
- skew, e. m. waves, Riemann-Hilbert soln. 8=3257
- spectrometers with concave gratings, image illuminance and resolving power calc. 8=487
- spectroscopy, predispersion order sorter for high order blazed gratings 8=6534

Diffraction spectroscopy. See Diffraction/light; Optical images.

Diffusion

- See also Neutrons and antineutrons/diffusion; for diffusion of matter, see Diffusion in gases; Diffusion in liquids; Diffusion in solids.
- Burger's nonlinear eqn., viscous and nonsteady solns. 8=4439
- coefficient, in lattice with cavities, variational estimate 8=15026
- collisional, transverse to stable mag. plasma 8=21312
- concentration-dependent, variational formulation 8=16812
- crystal defects, pressure influence 8=8669
- eddy, oceanic and atm. motions, large-scale 8=23237
- effects on double injection in semiconductors 8=22419
- electrolyte kinetics, radiometric methods 8=23144
- electron beams, counter streaming 8=10912
- electron, Einstein generalized ratio for coeff. 8=15025
- finite speed of propagation in all matter 8=239
- forced, Leibnitz series for moving boundary 8=6114
- fluid, turbulent, local concentration fluctuations, variance 8=12631
- fluids, corrections to kinetic theory 8=21416
- gases, in porous media, approx. equations 8=21467
- growth of liq. drop in subcooled vapour mixture 8=12983
- heat, nonlinear equations 8=10771
- Langrangian eqn., appl. turbulent dispersion in incompressible fluid 8=12634
- laser stationary oscills., effect 8=405

Diffusion—contd

- liquid permeation through polyethylene membrane, temp. effects 8=1508
- Lorentz gas, density behaviour of coeff. 8=136
- multicomponent, theory for coeffs. 8=10672-3
- neopentane-D exchange, effects 8=23083
- nonlinear eqn., stability of solns. of simple stationary wave type 8=3008
- nonstationary, of radiation in nonuniform stationary, medium 8=19481
- optimal discounted stochastic control 8=10671
- particles in radiation belt, with arbitrary pitch angle, due to extensive mag. disturbances 8=18962
- particles in stochastic e. m. field 8=10880
- photons in plane layer, number of scatterings 8=3567
- plasma, and instability in uniform longitudinal magnetic induction 8=12564
- plasma, coeff. for turbulent plasma 8=12559
- plasma column across uniform mag. field, kinetic theory 8=4341
- plasma inhomogeneities, eqns. of motion 8=12478
- plasma, in multipoles 8=21318
- radiation from a cavity, moments method description 8=19622
- radiation, source excitation power from spectral line profile 8=5895
- radioactive contamination, model 8=7341
- resonance quenching as diffusion process 8=2471
- rubber + benzene mixtures, tracer diffusion 8=21641
- solid-fluid mixture, thermodynamic analysis 8=19480
- sorption-diffusion in heterogeneous systems 8=17147-9
- spin, in Ising model from master eqn. 8=10669
- transient multicomponent, with heterogeneous reaction 8=14354
- turbulent, expts. in thermal plasma 8=21313
- in two media with moving boundary 8=15027
- ZnO₂ in cellulose membranes 8=21645

acoustic waves

See also Scattering/acoustic waves.

No entries

electromagnetic waves

See also Scattering/electromagnetic waves.

dispersive medium, response time calc. 8=19875

elementary particle behaviour 8=20279

molecular crystals, excitation spectrum and ground-state energy 8=18479

light

See also Reflectivity; Scattering/light.

No entries

Diffusion in gases

See also Flow/gases.

the atmosphere, diffusion in wind direction, and in surface layer 8=9847

atmospheric, turbulent boundary layer, contaminant

transport with unstable stratification 8=14608

charged particles with var. elec. and mag. fields,

by violation of 3rd adiabatic invariant 8=7706

coefficient, organic vapour in air, simple

experiment 8=12709

concentration-dependent, variational formulation 8=16812

convective, into cavitation void 8=4497

dispersion, one-particle, rel. to velocity distribution 8=16

drop, liquid, velocity calc. 8=1482

equations modeling spatially variable stochastic

processes 8=4496

Graham's law, range of validity 8=12708

Graham's laws reviewed 8=12707

ideal gas mixtures, tensor matrix calc. 8=16718

influence on Townsend discharge 8=12395

inter-diffusion, study using electrodeless discharge in gas

chromatography 8=14452

Lorentz gas, non-analytic density behaviour of

coeff. 8=16720

methane-Ar-H₂ system, unsteady diffusion, mean conc.-

time history 8=12712

mixtures, coeff. meas. by cataphoresis 8=12704

mixtures with internal freedom, thermodynamic

treatment 8=21528

multicomponent coeffs. in reacting gases 8=1490

multicomponent mixtures 8=1491

noble gases, binary mixtures, coeffs. as function of temp.

and conc. 8=16719

plasma, weakly ionized, across mag. field, effect of

boundary conditions 8=16502

plasmoid, laser-produced, across mag. field and super-

imposed on oscilln. 8=16505

resistance to relative motion 8=16686

smoke from high stacks, time-average ground

concentration 8=14614

spheres inside diffusers, resultant forces acting and

parameters affecting them 8=16717

ternary mixtures, validity of Stefan-Maxwell

eqns. 8=12710

transport coeffs. from inelastic collisions 8=7939

turbulent, convectionless, above small evaporating water

surface 8=14638

van der Waals gas, Yang-Lee distrib. of zeros 8=12671

Ar self diffusion coeff. and atoms interaction-energy,

77.5-121°K and 294°K 8=1489

Diffusion in gases—contd

- Ar, self-diffusion in critical region 8=16716
- Ar-C₂H₂ mixture, temp. dependence 8=7941
- Ar-Kr mixture, temp. dependence 8=7941
- Au, vapour press. from Knudsen effusion 8=12999
- CsCl(g) effusion, ang. number distrib. 8=12706
- D, electron transport coeff. 8=21521
- H, electron transport coeff. 8=21521
- He atoms, diffusion of metastable He atoms 8=4494
- He, of CF₄, nonresonant absorpt. and dispersion in compressed mixtures 8=1486
- Hg plasma ambipolar coeff., 10⁻⁸ torr 8=21377
- Hg vapour through rare gas, demonstration 8=12711
- Kr⁸⁵ in multicomponent mixtures 8=1491
- Kr-CO system, binary, unlike interactions 8=7943
- Kr-NO system, binary, unlike interactions 8=7943
- Kr-O₂ mixture, temp. dependence 8=7941
- N₂-He mixtures, diffusive separation obs. 8=19537
- Ne-Ar mixtures, coeff. meas. by cataphoresis, 300-650°K 8=12704
- Ne, e-ion determ. 8=12451
- O₂ and org. vapours interdiffusion, and diffusion into N₂ 8=14452
- O₂-SF₆ mixtures, temp. dependence 8=7941
- Xe¹³³ in multicomponent mixtures 8=1491

thermal

- column, expt. test of theory 8=16715
- flames, turbulent, thermal equil. meas. 8=7946
- gas mixtures in chem. equil. 8=9661
- isotope mixtures, theory and meas. 8=1492
- isotope separation apparatus 8=16237
- loaded-sphere gases, kinetic theory 8=4495
- multicomponent mixtures 8=12713
- separation of mixtures in chem. equil. 8=21526
- ternary systems, approach to steady state 8=21527
- transport coeffs. from inelastic collisions 8=7939
- Ar-N₂, factors, meas. by new design swing separator 8=1488
- CO₂-N₂O, separation in column 8=7945
- Cs-He mixture, Enskog-Chapman kinetic theory 8=21525
- D₂-HT mixture 8=4495
- H₂-air mixture, for free convection flows 8=4491
- H₂-CO₂, factors, meas. by new design swing separator 8=1488
- H₂-He mixture, composition depend. of factor 8=1493
- HD-D₂, factor obtained by Murphey (1947) 8=1494
- He-air mixture, for free convection flows 8=4491
- He-I mixture, optical meas. 8=7942
- He³-HD, loaded sphere-smooth sphere model 8=12705
- He⁴-HT, loaded sphere-smooth sphere model 8=12705
- He-Ne, factors, meas. by new design swing separator 8=1488
- UF₆, thermal diffusion factor meas. 8=7944

Diffusion in liquids

- See also Flow/liquids.
- acetonitrile-d₃, rotational diffusion, n.m.r. meas. 8=8140
- chain mol., rotary diffusion const. 8=16816
- concentration-dependent, coeffs. meas. 8=12835
- concentration-dependent, variational formulation 8=16812
- convective, in stagnation flow with imperfect semi-permeable membrane, rel. to reverse osmosis 8=12841
- cryogenic liqs, correl. with thermal cond. and viscosity 8=15132
- deoxidation product growth and separation, collision model 8=18658
- diffusion-controlled processes, kinetics 8=4555
- dispersion of matter in non-Newtonian flow 8=1506
- dye injected into turbulent pipe flow, numerical soln. for mixing 8=21576
- film falling down vertical wall 8=1541
- glass melt, diffusion of Ne bubbles 8=4554
- glycerol, molecular, from n scatt., theory of p motion 8=21609
- n-hexane-nitrobenzene, diffusion in crit. separation region 8=21644
- iron-silica deoxidation product growth and separation, collision model 8=18658
- low-temperature, interferometric meas. 8=8035
- measurement, by filter paper diaphragm 8=12839
- metals, mutual diffusion, absolute rate and corresponding states theories 8=21642
- metals, self-diffusion coeff. using Enskog dense-gas formulation 8=12837
- metals, self diffusion, model using ion pair pot. and number density 8=12833
- metals, self-diffusion, temp. depend. 8=12831
- molecular, from n scatt., theory of p motion 8=21609
- non-electrolytes, mechanism, study by dielectric constant method 8=12834
- polymeric, of low molecular weight 8=1540
- polymethacrylic acid solns. 8=12817
- polystyrene+solvent system, diffusion anomalies 8=12829
- precipitation deoxidation kinetics, collision model 8=18658
- n-propanol molecular, from n scatt., theory of p motion 8=21609
- rotational const., by transient elec. light scatt. 8=8073
- self-diffusion in simple liqs. 8=8032
- solutions, surface diffusion interactions affecting electrocrystallization 8=9719-21

Diffusion in liquids—contd

- in sphere, diffusivity and solubility with error anal., calcs. 8=16813
- surface active monolayers on H₂O substrate, reduction in gas desorption 8=12830
- translational, meas. cell model 8=8034
- volume and surface, models, for cryst. growth 8=21935
- water, molecular diffusion coeffs. of dissolved H and He 8=12828
- water-triethylamine, diffusion in crit. separation region 8=21644
- Ag, diffusion of metal solutes, theory 8=12832
- Ag liquid, of Ru, Fe and Co 8=12836
- Al melt, of Au, coeff. from radiographic obs. 8=4646
- AlK alum, cryst. growth from soln., model 8=21940
- Bi-Sn eutectic alloys, of type 304 stainless steel, dissolution kinetics, convective-diffusion study 8=4558
- in CCl₄, of cyclo-pentane-hexane and heptane, translational diffusion, expt. and theory 8=16814
- CaCl₂ aq. soln., phenomenological coeffs. 8=12924
- Cu, electro, small additions of Sn, Sb, Ni 8=1916
- Fe-C alloys, of N. at 1600°C 8=16815
- HCl aq. soln., phenomenological coeffs. 8=12924
- HClO₄ aq. soln., phenomenological coeffs. 8=12924
- HNO₃ aq. soln., phenomenological coeffs. 8=12924
- H₂O, molec. dia. from diffusion meas. 8=21606
- H₂O vapour, in cation exchange membranes 8=8040
- He³, spin rel. to Rice theory of nearly ferromagnetic Fermi liquids 8=10800
- LaCl₃ aq. soln., phenomenological coeffs. 8=12924
- Na silicates, of Na, self 8=8036
- NaCl aq. soln., phenomenological coeffs. 8=12924
- NaClO₃, cryst. growth from soln., model 8=21940
- Sn, diffusion of metal solutes, theory 8=12832
- TlCl molten, self diffusion of Tl⁺ 8=21643

thermal

- aqueous bromide solns., partition coeffs. 8=4559
- aqueous bromide solns., Soret effect 8=4557
- equation, method of solution 8=4556
- freezing, in rel. to Stefans problem 8=8176
- horizontal diffusion column, description and results 8=12838
- integral characteristics for particular regions 8=8033
- n-propanol, soln. of bromoform, coeff. by heterodyning light 8=4553
- water-ethyl alcohol mixture, separation meas. 8=12838
- CCl₄ + cyclohexane system, flow-cell meas. of Soret coeff. 8=1542
- CS₂, solution of acetone, coeff. liq. heterodyning light 8=4553
- KCl solns., self 8=21640
- Na²² in KCl solns., self 8=21640
- NaCl and Na²²Cl solns., self 8=21640

Diffusion in solids

- See also Permeability, mechanical
- acceleration by irradiation, mechanism 8=1903
- alkali silicate glass, validity of Nernst-Einstein eqn. 8=8354
- Arrhenius plot, study of inherent curvature 8=13401
- Auger electron emission technique for obs. 8=22730
- b. c. c. structures, theory application 8=17551
- binary interstitial solutions, equations 8=17556
- binary systems, coeff. conc. and temp. dependence 8=17554
- in catalysts 8=14402
- concentration distribution near idealized contact spot 8=22143
- concrete, of water, between 50 and 95°C, further comments 8=22148
- creep, diffusional mechanisms 8=22279
- cristobalite, diffusion of He and Ne 8=8247
- crystalline mixtures, thermal, rel. to elec. conductivity 8=22144
- data analysis 8=17550
- data correlation as periodic function of atomic number 8=17549
- doping, concentration distributions 8=1899
- effect of lattice defects conc., using radionuclides 8=22141
- electric fields, effect on diffusion, expt. 8=22145
- F-centre, lecture demonstration 8=13452
- flat boundary interfaces, "absolute" methods 8=8666
- forced in 3D region with uniformly moving boundary 8=13403
- gas bubble collisional coalescence 8=4695
- gas diffusion apparatus 8=8668
- glass, surface layer, rel. to distrib. of alkali ions 8=22146
- grain boundary gas bubbles, equil. conditions 8=1986-9
- grain boundary models, exptl. comparison 8=22142
- graphite, diffusion and escape of captured fission Xe 8=11975
- graphite, of fission products Xe and I 8=12015
- graphite, permeability for gaseous fission products 8=4950
- group-III elements in Si, hot implantation behaviour, comp. with group V in Ge 8=22160
- group V elements in Ge, hot implantation behaviour, comp. with group III in Si 8=22160
- interstitial, isotope effect, model 8=1901-2
- iron meteorites, tritium loss by solar wind hydrogen 8=10370

Diffusion in solids—contd

- isotope thermotransport effects theory 8=1904
 magnetite, self-diffusion of O_2 8=22151
 mass transfer by evaporation-diffusion between solids 8=8673
 measurement, MOS-C-V method 8=13896
 metals and alloys, ferromagnetic 8=17560
 metals, b.c.c., coeffs. by internal friction meas. 8=17557
 metals, b.c.c., of interstitial impurities 8=17558
 metals, b.c.c., rel. to radn. effects and imperfections produced 8=17702
 metallic couples, interdiffusion kinetics description from computer programme 8=1906
 metals, Debye temp. rel. to activation energy of diffusion 8=17509
 metals, f.c.c., Arrhenius plot analysis allowing for divacancies 8=8681
 metals, rel. to electron-concentration concept 8=17559
 metal-interstitial system, polyphase diffusion and phase boundary motion 8=17035
 metals, sintering, surface, vol. and grain boundary 8=21832
 migration of interphase boundaries, effect of coefficient 8=1900
 minerals, thermal diffusivity from 300° to 1100°K at 1 atm 8=22131
 multiphase couples, interface comps., motion and lattice transformations 8=17552
 naphthalene, polycrystalline, self-diffusion 8=4960
 penetration curve variations due to evaporation 8=1905
 polyethylene, drawn and undrawn, of organic vapours 8=8349
 polymethylmethacrylate, O_2 diffusion, meas. by quenching of phosphorescence 8=8687
 polyvinyltoluene + phosphors, solid solns, diffusivity of CO_2 8=20386
 porcelain, electrotechnical, of Ag, rate temp. dependence 8=17584
 rare gases, plane or spherical solids, eqns. 8=13404
 refractory metals, of C, investigation over wide temp. range 8=17586
 rubber vulcanizates, of liqs. 8=1932
 semiconductors, impurity redistribution 8=5229
 solid solns., crystalline, theory, and time evolution of X-ray and thermal neutron scattering 8=8667
 of solute atoms, to dislocations rel. to strain ageing 8=4969
 steels, of carbides rel. to surface friction and wear stability 8=17788
 steel, of Cr, experimental obs. in 950–1265°C range 8=4951
 substitutional alloys, thermal, mass transport by vacancy mechanism 8=4947
 ternary curves using a second integration of the Fick law, anal. 8=17555
 thermal diffusivity, heat resistant materials, theory 8=13405
 thermal, method of meas. 8=1898
 transition metals, b.c.c., theoretical critique 8=17590
 transition metal systems, b.c.c., binary inter-diffusion 8=17577
 tridymite, diffusion of He and Ne 8=8247
 vacancies in f.c.c. lattices, Debye model 8=22172
 wires, sintering by surface diffusion, theory 8=13051
 X-ray microanalysis, fluoresc. effects obs. 8=17553
 zeolites containing H_2O , ethane diffusion 8=8685
 Zircaloy-2, of H_2 , thermal, rel. to terminal solubility 8=8250
 Zircalloys-2 and -4, of H_2 , rel. to terminal solubility and partitioning in these and α -Zr 8=8249
 zirconium carbide powders, of Xe^{133} , activation energy rel. to struct. 8=8686
 Ag, diffusion of Xe from recoil fission of U 8=3981
 Ag, polycrystalline, of In, as impurity 8=8670
 Ag, polycrystalline, of Sb, volume and grain-boundary 8=17563
 Ag, self in crystal containing alumina 8=1909
 Ag, vacancies, Debye model calc. of rate 8=22172
 Ag-Au alloys, of tracers, coeff. rel. to activity-coeff. and vacancy flow effect 8=4948
 AgBr, migration of photoexcited holes, obs. 8=1908
 AgCl, Ag diffusion under pressure 8=1910
 AgI, under high pressure gradient 8=1907
 AgMg, silver-rich, of Ag, re-examination 8=17561
 β -AgMg, stoichiometric, simultaneous diffusion of Ag and Mg 8=17562
 α -Ag₂S mixed conductor, of Ag ions rel. to conduction processes 8=22500
 Al, of Ag. 8=22147
 Al, diffusion removal of Mg, and oxidation 8=18670
 Al of Mo 8=1911
 Al, of Pd, Ag, Cd, In and Sb 8=8671
 Al, pure, n.m.r. meas. of coefficient 8=4949
 Al, rapid self-diffusion along dislocations rel. to void annealing 8=13432
 Al, vacancies, Debye model calc. of rate 8=22172
 Al-AlO interface, ionic diffusion 8=1912
 Al-Mg alloys, diffusion removal of Mg, and oxidation 8=18670
 Au, of Ag, grain-boundary, electrical field effect 8=17568
 Au and Pd films, formation of twins 8=13127
 Au, vacancies, Debye model calc. of rate 8=22172

Diffusion in solids—contd

- Au/Ni-Cr, contacts and conductive paths forced diffusion 8=8993
 Au-Pt system, chem. diffusion coeff., X-ray meas. 8=1913
 BeO neutron irradi., diffusion of Li^9 8=8672
 Bi, of Ag¹¹⁰, dependence on crystallographic direction 8=13407
 BiTe, electrotransport of Ag, Au and Cu, 150 and 250 A/cm² \leq 400°C 8=17564
 BiTe:I, I electrotransport, obs. 8=17564
 Bi₂Te₃ of Cu, etching technique investigation 8=1914
 C of Th, tracer-level, rel. to structure 8=1915
 Ca-Bi eutectic melt, displacement of inactive marks during diffusion 8=17565
 CaO, of water vapour, rel. to sintering kinetics, 920–1123°C 8=21833
 CaWO₄, of Ca 8=13408
 CdTe-HgTe, mass transfer by evaporation-diffusion 8=8673
 Co⁶⁰, diffusion studies 8=17575
 Co-Pt binary solns, interdiffusion coeff. conc. dependence, by X-ray analysis 8=17570
 Cr, self-diffusion 8=17566
 CsI, self-diffusion of Cs¹³⁴ in single crystals and polycrystalline samples 8=8674
 CsI, self-diffusion of I^{131} in single crystals and polycrystalline samples 8=8674
 Cu, of Ag, grain-boundary, electrical field effect 8=17568
 Cu: Cu-12.5 wt.% Al multiphase couple, interface comps., motion and lattice transformations 8=17552
 Cu, diffusion of Au, detect. by deuteron elastic scatt. 8=8675
 Cu in InAs 8=17011
 Cu, surface self-diffusion coeff. temp. dependence, 600–1030°C 8=17567
 Cu, vacancies, Debye model calc. of rate 8=22172
 Cu-Mn alloys interdiffusion kinetics, by X-ray microprobe 8=22149
 Cu-Ni diffusion pairs, pore migration during counter-current diffusion 8=17569
 Cu-Ni, Kirkendall and Frenkel effect 8=8676
 75 Cu-25Ni laminate on Cu core in coinage composite, inter-diffusion in bond degradation mechanism 8=22329
 Fe, b.c.c., O atoms, solubility and migration energy 8=22150
 α -Fe, of C 8=17572
 Fe, of Cr, experimental obs. in 950–1265°C range 8=4951
 Fe, distribution of additions during oxidation 8=1917
 Fe, electromigration of dissolved H_2 8=8677
 Fe in γ -phase, self, effect of traces of Sn, Sb, Pb and Bi 8=1930
 Fe, of H, anomalous behaviour at low temps. rel. to interstitial mobility 8=22182
 Fe, of Ni, volume and grain-boundary 8=17571
 Fe-Cr alloy components, electrotransfer at 1150–1400°C 8=4952
 Fe-Cr alloys of 25–95% Cr comps., oxidation at 1000–1300°C, interdiffusion, rel. to scaling kinetics 8=18677
 Fe-Ni alloys, C, mag. and mech. anisotropies 8=22814
 Fe-Ni binary solns, interdiffusion coeff. conc. dependence, by X-ray analysis 8=17570
 Fe-Si alloys, mechanism for magnetic Zener relaxation 8=9451
 Ga, self-diffusion 8=22152
 GaAs, of Cu, production of defect centres 8=1954
 GaAs(P) p-n junction, of Zn, conc. gradient near junction 8=8678
 GaAs:Si, site transfer 8=17574
 GaAs, of Zn, coeff. Fermi level dependence 8=1918
 GaAs, of Zn, precipitates formation 8=17617
 GaAs, of Zn, under excess As pressure 8=22153
 GaSb, of Li, and solubility 8=13409
 Ge, Al and B diffusion 8=13406
 Ge, SiO₂ and Si₃N₄ films to mask Al and B diffusion 8=13406
 Ge-O system, sticking coeff., orientation dependence 8=22154
 He³-He⁴ mixtures, phase separation, theory 8=15157
 Hg-Mo system, surface 8=21903
 Hg-W system, surface 8=21903
 InAs(Sb)(P), p-n junction, of Zn, conc. gradient near junction 8=8678
 InSb, heat treatment effect rel. to disloc. density 8=1919
 K, of Na²² impurity 8=8680
 KBr, of inert-gas at energies to 85keV and release behaviour 8=22156
 KBr, self-diffusion, activation entropy and enthalpy from elec. cond. 8=8679
 KCl, of Ar^{39,41} and trapping, n irradiated 8=1920
 KCl, doped and pretreated, of Tl⁺ 8=13410
 KCl, of inert-gas at energies up to 85 keV and release behaviour 8=22156
 KCl-KBr diffusion pairs, pore migration during counter-current diffusion 8=17569
 KCl-KBr, Kirkendall and Frenkel effect 8=8676
 K₂Fe(CN)₆·3H₂O, translational diffusion 8=14145
 KI, of inert-gas at energies up to 85 keV and release behaviour 8=22156

Diffusion in solids—contd

$K_2O-SrO-SiO_2$ system, effective binary coeffs., 8=22155
 KX, (X = Cl, Br, I), of H_2O mols, mechanism 8=4953
 Li, in temp. and elec. potential grads, mass transport and deformation 8=22157
 M hydrides, M = Pd, V, Nb and Ta, of H_2 , solubility isotherm in hydride phase 8=1924
 $MgMn_2O_4$, of cations, migration energy at high temps. 8=4955
 MgO , of Ba rel. to dislocation densities 8=4954
 Mo, of C, and solubility limit 8=17007
 Mo, tracer-diffusion studies 8=17575
 N^{15} , detect. by nuclear activation 8=14504
 NH_4BF_4 , ion rotational diffusion 8=5560
 Na, of alkali metal impurities (K^{42} and Rb^{86}) 8=8680
 Na aluminosilicate glass, Na self-diffusion, rel. to elec. cond. 8=22158
 Na mordenite, synthetic, diffusion of methane, ethane, propane and butane 8=13109
 Na salt, of $Ar^{39,41}$ and trapping n irradiated 8=1920
 Na self-diffusion, isotope effect 8=17576
 Na-Ca aluminosilicate glass, Na self-diffusion, rel. to elec. cond. 8=22158
 NaCl single cryst., diffusion of Cd^{2+} 8=4956
 NaCl crystals, thermal diffusion strontium ions, Soret effect obs. 8=1921
 NaCl-NaBr system, Na isotope diffusion, self-diffusion coefficient 8=13402
 Nb^{95} , diffusion studies 8=17575
 Nb, summary of ORNL work 8=17593
 $\alpha-Nb_2O_5$, near-stoichiometric, diffusion of O_2 8=1922
 Ni, kinetics of H_2 permeation 8=8682
 Ni, mobility of $Sn^{113,123}$ obs. 8=17579
 Ni, sintered, effective, volume self-diffusion 8=1923
 Ni-Co binary solns, interdiffusion coeff. conc. dependence, by X-ray analysis 8=17570
 Ni-Cr solutions, interdiffusion, conc. and temp. dependence 8=17578
 Ni-Pt binary solns, interdiffusion coeff. conc. dependence, by X-ray analysis 8=17570
 PbTe, of Na, coeff. meas. by radio tracer technique 8=17580
 Pd, diffusion of H and D at 0° to $100^\circ C$ 8=17582-3
 Pd, mobility of Fe^{59} obs. 8=17579
 Pd-Ag, diffusion of H and D at 0° to $100^\circ C$ 8=17582-3
 Pd-H, α -phase, of H, by small energy transfer neutron scattering 8=13411
 α -Pd-H, diffusion of H, study by n scatt. 8=17581
 Pt, self-diffusion, vacancies and divacancies from quenching and recovery expts. 8=17612
 Si, of Au, precipitates formation 8=17620
 Si of B, dislocation motion rel. to coefficient 8=1925
 Si, B-doped by ion bombardment, B distrib. profiles 8=18071
 Si of B, lattice contraction, contrast reversal in reflection topography 8=1927-8
 Si:B, Li drift mobility, dislocations effects, obs. 8=20200
 Si, BN source 8=8684
 Si, of B (or P), appl. of dynamical theory of X-ray scattering 8=13412
 Si:Ga, Li drift mobility, dislocations effects, obs. 8=20200
 Si impurities, anomalous obs. 8=13427
 Si, isolation diffusion of P, integrated circuits 8=1929
 Si, Li in surface, electron mirror microscope obs. 8=22159
 Si, of Li, Na and K experimental results cf. Weiser theory 8=8683
 Si of P, dislocation motion rel. to coefficient 8=1925
 Si of P, enhancement by vacancy generation 8=1926
 SiO_2 , of Au 8=13896
 SiO_2 film, of borax 8=4957
 SiO_2 films, tracer diffusion of Na, rel. to Na contamination 8=18069
 SiO_2 :Tb, Eu, fused, H diffusion 8=17585
 Sn, Ag^{110} coeff. meas. 8=22162
 Sn self-diffusion, radioactive tracer absorpt. obs. 8=22161
 $SrCl_2$, pure and Y^{3+} (Na^{+}) doped, of Sr^{90} and Cl^{36} , and ionic conduction mechanism 8=8983
 Ta, summary of ORNL work 8=17593
 β -Ti, behaviour from thermo- and electrotransport meas. rel. to dislocation mechanism 8=17589
 β -Ti, impurity, summary 8=17588
 β -Ti, mechanism 8=17594
 Ti, of metallic impurities 8=17596
 Ti, of Ti-44 and V-48 8=17587
 Ti of Au and of Ag, obs. by radiotracer technique 8=22163
 γ -U, mechanism 8=17594
 γ -U, tracer-diffusion 8=17591
 UC, self-diffusion, appl. to activated processes 8=22164
 UN, of N 8=14504
 UO_2 , surface self-diffusion, from decay of scratches 8=13413
 UO_2 of U ions, lattice and grain boundary, 1900-2150°C 8=13414
 UO_{2+x} , O self-diffusion and lattice defects rel. to chem. props. 8=23113
 V^{48} , self-diffusion 8=17592
 V, summary of ORNL work 8=17593
 α -Zr, of H_2 , rel. to terminal solubility and partitioning in α -Zr, Zircaloy-2 and Zircaloy-4 8=8249

Diffusion in solids—contd

Zn, self-diffusion, isotope effect meas. rel. to vacancies and dislocations 8=4959
 ZnS of S, self 8=1931
 β -Zr, behaviour from thermo- and electrotransport meas. rel. to dislocation mechanism 8=17589
 β -Zr, mechanism 8=17594
 Zr, of metallic impurities 8=17596
 β -Zr, summary of ORNL work 8=17593
 Zr in $ZrH_{1.7}$, $ZrH_{1.65}$, 800-1000°C 8=17595
 Zr-2.5wt%Nb, of H_2 , thermal, rel. to terminal solubility 8=8250
Diffusion columns. See Diffusion in gases/thermal; Isotope separation.
Diffusion pumps. See Vacuum pumps.
Digital computers. See Calculating apparatus/digital computers.
Dilatometers. See Length measurement; Volume measurement.
Dimensions
 See also Units.
 magnetic susceptibility calc. 8=15250
 physical quantities, and orientation, rel. to units system 8=19344
Dimers. See Molecules; Polymers.
Dineutrons. See Neutrons.
Diodes. See Electron tubes; Plasma devices; Rectifiers; Semiconducting devices/diodes and /tunnel diodes.
Dipole moments. See Molecules/moments; Nucleus/electric moment; Nucleus/magnetic moment.
Diquarks. See Quarks
Dirac electron theory. See Electron theory.
Dirac equation. See Quantum theory/wave equations.
Discharge tubes. See Electron tubes; Gas-discharge tubes; Ion sources; Particle accelerators; X-ray tubes.
 electrode field, container wall effect, computer calc. of uniformity 8=16395
Discharges, electric
 See also Arcs, electric; Breakdown, electric; Corona, electric discharge; Plasma; Sparks, electric.
 arc columns with positive V-I characteristics, low-pressure 8=12403
 arc, transient, electrode erosion in dielectric liquid 8=21252
 atmosphere, point, during rapid field changes, rel. to pot. gradient and winds 8=9883
 ball lightning, laboratory, formation mechanism 8=18892
 busbar cavities, location by X-rays 8=21245
 capacitors, power type, effect of self-reson. freq. on magnitude meas. 8=21228
 capacitor, simple switch 8=15188
 cavity with variable density plasma, sustaining of resonance 8=16406
 creep, over solid dielectrics in SF_6 atm. 8=16420
 cross-section determ. from meas. on arc discharges 8=4294
 cyanide laser, HCN mm absorption obs. 8=11055
 cylindrical, time dependent, analysis 8=7650
 dense plasma focus discharge 8=21221
 development, laser photographic study 8=12526
 discharge column, constriction, randomization of plasma-sac 8=1338
 electric discharge machining, dynamic evolution of low-voltage discharges 8=12396
 electrical insulation and dielectric phenomena, conference, Pocono Manor USA (1966) 8=18154
 electrodeless, as detector in gas chromatography 8=23169
 electrode, skin effect analysis using semi-bounded plasma model 8=21219
 exploding-wire discharges, current pause rel. to field strength 8=7695
 exploding wire, precursor ionization rel. to gas, wire distance, press. and capacitor energy 8=16433
 exploding wires, time-resolved spectra 8=15537
 explosion of foils by 6 kV discharge between coaxial electrodes 8=7690
 gas, electromechanical energy conversion 8=7672
 gaseous, between parallel-plate electrodes, field distortion, calc 8=21248
 gaseous occlusions in an insulator, amplitude spectrums 8=18157
 gas-flow system, mass spectra of ions 8=16429
 gas, low-freq. noise 8=21226
 gases, mixture, d. c. axial gas transport 8=1333
 high current, vacuum for triode-sputtering 8=7653
 hollow-cathode, for determ. of trace Li in refractory oxides 8=23189
 hollow cathode effect, medium-pressure theory 8=21230
 inert gases, diffuse continua-emitting 8=4273
 inert gases, stationary ion waves 8=1424
 insulator surface phenomena in vacuum 8=7673
 ion beam extraction from gas discharges 8=342
 ion source, Ti anode, desorbed H_2 8=21227
 Langmuir probe curve second derivative plotting devices, comparison 8=1335
 laser action in selected compounds containing C, N, and H or D 8=12398
 laser induced, optical interferometry of 8=16403
 low-pressure column in axial magnetic field, steady-state theory 8=4283

Discharges, electric—contd

- magnetoplasma dynamics accelerator, phenomena in cathode region 8=7652
 microwave, properties of plasma skin slab 8=12394
 multipacking between coaxial electrodes 8=21225
 oscillographic registration of events in discharge 8=12400
 ozonizer, leakage time constant, external radns. effect, and Joshi effect 8=21222
 partial hazards in elec. equipment 8=16412
 Penning as high brightness ion source 8=15345
 Penning, modes theory and obs. < 10^{-4} torr 8=1332
 Penning, toroidal pulsed 8=21371
 Penning, in vacuum, cathode particle currents 8=7648
 plasma acceleration by self-induced mag. field 8=1327
 plasma, in alternating electric field, changes due to perp. magnetic field 8=16490
 plasma, beam instability, heating 8=4285
 plasma current instability 8=7837
 plasma generation in e. m. shock tubes, optical props. 8=1337
 plasma generator, heat transfer meas. in mag. field 8=7847
 point, current rel. to p. d. and wind speed, lab. expt. 8=9884
 polyethylene, dielectric degradation 8=21214
 positive column, kinetic model of Tonks-Dattner resonances 8=4282
 positive column, l.p., in transverse mag. field 8=7661
 positive column plasmas, l.f. impedance, theory 8=7659
 positive low pressure column in limiting case of low electron density, review 8=7654
 preionized gas gap, spark channel parameters 8=7671
 pulsed, cathode erosion mechanism 8=7649
 pulse, low-pressure, emission from oxide cathode 8=18258
 reflex, rot. vane freq. rel. to anode diameter 8=7662
 resonant-electron, space charge effects 8=16399
 self-crowbar air gap, tests 8=12458
 solid insulation, d.c. detection and meas. 8=21242
 space-charge field, electron temp. gradient effect 8=4278
 spark gaps, overvoltage, without trigger electrode 8=16400
 spiralling impulsive, shape obs. 8=12401
 streamer chambers, pulse mechanisms obs. 8=11326
 surface with ring-type electrodes 8=12397
 theta pinch, He plasma electron densities and temp., spectroscopic meas. 8=21349
 thetatron, rarified-plasma microwave, instability excitation and propag. 8=16523
 through small tree in artificial electric field 8=2599
 Townsend, influence of diffusion 8=12395
 underwater as impulsive high power sound generator 8=6157
 Venus microwave emission, model 8=5959
 wires, explosions initiated at surface and inside the wire 8=4272
 z-pinch, press. -depend. transition behaviour 8=4275
 Al, vacuum pulse, coaxial, charged particle concentration from line broadening 8=16203
 Ar duoplasmatron, relative abundance of ions 8=7780
 Ar laser action in thermionic hollow cathode discharge 8=15457
 Ar, medium press., neutral gas temp. 8=16408
 Ar, Penning modes characts., < 10^{-4} torr 8=1332
 Ar plasma, flowing, minimum specific energy and electric field 8=16402
 Ar, positive column contraction 8=21231
 Ar, positive column, electrons energy distrib. 8=7655
 Ar, spectroscopic study of characts. rel. to Ar⁺ laser 8=12402
 Ar-Cs and Ar-K plasma in pulsed discharge with ionization confined to impurity atoms, props. 8=1346
 Ar⁺ Cs, positive column contraction 8=21231
 for CO₂ lasers, plasma temp. meas. 8=15459
 CO₂, laser, pulse recovery time 8=6443
 CO₂ with N₂ and He, laser gain 8=19963
 Cd 5sP_{0,1,2} levels lifetimes rel. to discharge conditions, obs. 8=1183
 Cs-Ar low-pressure, conditions rel. to absorpt. of Cs atoms 8=7401
 H₂, positive column plasma, cross wave of moving striations 8=4281
 He, electrodeless, cyclotron harmonic resonances 8=4274
 He, in hollow-cathode balance eqns for 2S² and 2P levels 8=20981
 He with hot cathode, behaviour in alternating electric field 8=16489
 He, mag. field stabilised, press. built up 8=7691
 He, positive column, electrons energy distrib. 8=7655
 He-Cs and He-K plasma in pulsed discharge with ionization confined to impurity atoms, props. 8=1346
 He-Kr mixture, excitation 8=4093
 He-Ne, cataphoresis and collision processes 8=1334
 He-Ne laser, stimulation rel. to radiation noise obs. 8=19966
 in He-Ne mixture relation between electron temp. and conc., and discharge parameters 8=7666
 He-Ne mixture tubes, electron temp. and conc. factors 8=7676
 He₂, positive column, correlator for 10-200 kHz signals 8=1405

Discharges, electric—contd

- Hg, e channel multiplier as u.v. detector 8=6506
 Hg, ion acoustic waves phase vel. and ambipolar diffusion coeff., 10^{-3} torr 8=21377
 Hg, ion-acoustic waves, propagation and damping 8=4313
 Hg vapour, electron beam-plasma interaction with transverse modulation 8=4368
 K r.f., spectroscopy reson. lamp for kgauss fields use 8=6536
 LiCl aqueous solns., formation of pulse discharges 8=4608
 Mg vapour, colour change 8=12393
 N plasmas, electron velocity distrib., non-Maxwellian form. 8=16418
 N₂, release of secondary electrons by metastable N₂ and its quenching 8=7663
 N₂, Townsend, prebreakdown, development 8=7677
 Ne-N₂ mixtures, microwave, afterglow decay, e and ion recombination, temp. depend. obs. 8=7719
 Na gas plasma, line excitation rel. to cascade transitions 8=20962
 Ne, positive column, electrons energy distrib. 8=7655
 Ne-Ar, cataphoresis and collision processes 8=1334
 O, Au film sputtering due to negative O ions 8=21877
 Se electrophotographic layers, kinetics 8=2265
 TiO₂ surface, channel development 8=1330
 Y, ohmic heating discharges, in C-stellarator, computer description 8=21407
- glows**
 anomalous, mass-spectrometry of positive ions 8=7658
 cathode sputtering, variation with current 8=2019
 glow probes, effect of work function 8=4284
 hollow cathode effect in neg. glow plasma 8=7660
 hot-cathode, passage of fast neutral H atoms, ionization 8=21274
 light source, cathode noise expt. 8=15521
 microwave detect. effect, theory and obs. 8=10938
 moving striations at medium pressures 8=7657
 photomultiplier residual light emission 8=6327
 positive column, constricted, wall control 8=12406
 positive column diffusion theory, low electron density 8=16404
 positive column, longitudinal non-uniformity 8=7656
 positive column, several gases, modes of screw instability 8=12407
 secondary electrons in neg. glow and Faraday dark space 8=16409
 striations, effect of transverse magnetic field 8=4279
 toluene, polymer films form., comp. and elec. props. 8=21894
 toroidal low-pressure r.f., plasma losses 8=21235
 toroidal tube, expt. investigation in air, He, Ar and Ne 8=4286
 in toroidal tube, positive column at low press. 8=1339
 vacuum, short gap pulsed breakdown, e optical obs. 8=16396
 Al oxidation, controlled, in radio-freq.-excited discharge 8=8310
 Ar mixtures, fast channel ion mass analysis 8=7665
 Ar positive column, direct display of electron temp. var. 8=16407
 Ar-Hg, low-pressure luminous efficiency in positive column 8=4287
 CO, electron removal during d.c. afterglow 8=21233
 Cr films, rel. to resist. 8=17128
 H, movement of ions calc. 8=7705
 H₂ and D₂ flash lamps, comparison 8=15522
 He afterglow, light emission rel. to e density, differential level decay 8=21237
 He, after glow, microwave heating by standing wave 8=1340
 He, fast electron energy decrease in negative glow region 8=4288
 He positive column at above critical field 8=16410
 He-Xe plasma positive column, Xe-level population inversion 8=12405
 Hg vapour, pulsed, afterglow, and population of 6₃P levels 8=21238
 Hg vapour, zeroth order distrib. changes 8=7667
 N₂ afterglow, surface catalytic efficiency and decay of atomic N 8=21239
 N₂, positive column, mass spectrometric analysis 8=1341
 N₂, recomb. rates 8=1313
 NH₃, decomp. in flow system 8=18682
 Ne afterglow, e density determ. 8=12451
 Ne column plasma, radial distribution of parameters in subnormal region 8=7668
 Ne, conc. of metastable atoms at low temp. 8=1368
 Ne, hot cathode, electron energy distribution in moving striations 8=12404
 Ne₂⁺ afterglow decay rel. to recombination rate 8=21282
 O + CO, shock-heated system, radiation 8=1342
 O₂ and O₂-N₂ mixtures, e density decay rates, microwave meas. of temp. depend 8=21240-1
 SiC films deposition in r.f. glow 8=21872
 SiN films deposition in r.f. glow 8=21872
 Ta oxidation, controlled, in radio-freq.-excited discharge 8=8310
- high-frequency**
 coaxial resonator, space-charge effects 8=7647
 coaxial waveguide, space-charge effect rel. to spark voltage 8=7646

charges, electric—contd

high-frequency—contd

current measurements in high-voltage 8=4277

excitation of atoms by orientation of excited states 8=16215

fast electron population, conditions 8=21229

low-pressure, r. f., time-averaged potentials, meas. using ion-beam probe 8=21224

multipacting, similarity principle 8=7675

plasma, energy transfer from e. m. field 8=16397

plasma striations, moving, in strong field, obs. 8=4280

plasma transport in 8=16401

torch, power characteristic, and dependence on electrode geometry 8=4299

tritium, atomic, quartz contained 8=4276

turbulent, at 1 atm, numerical calc. 8=4271

Ar, at atmos press., power developed in jet of plasma torch 8=21236

Ar, electrodeless, props., meas. 8=21234

Ar, electrodeless, temp. dependence of specific power 8=16398

Ar, radio-frequency, temp. determ. using reversal technique 8=21223

Ar, unipolar, spectral diagnostics, 1 to 12 atm. press. 8=4290

Ar-Hg, low-pressure luminous efficiency in positive column 8=4287

H₂, dissociation, rel. to polarized atom source 8=21018

He, electrodeless, temp. dependence of specific power 8=16398

He gas, l. p., luminosity of 5875Å yellow line 8=16416

He gas, low-pressure, p. d. meas. 8=16415

N, microwave, spin-relax. effects 8=12098

N₂, microwave excitation, vibrational deactivation 8=12211

N₂, unipolar, spectral diagnostics, 1 to 12 atm. press. 8=4290

O₂, electrodeless, temp. dependence of specific power 8=16398

O, r. f., dark-sheath form. mechanism 8=12399

integration. See Beta-decay theory; Nuclear decay theory; radioactivity.

integration energies. See Radioactivity.

locations. See Crystal imperfections/dislocations.

erse systems

See also Aerosols; Colloids; Emulsions; Foams; Powders; Sols; Suspensions.

adhesion, spherical particles, effect of capillary liq. 8=8150

Bingham plastic, settling of spherical particles 8=21553

coagulation, by Brownian motion, particle size distrib. 8=8148

condensation nuclei in air free from aerosols, formation in light and dark 8=18864

fluidized bed, dense, gas distribution 8=8141

fluidized bed, dense heat transfer with vibrating cylinder 8=8144

fluidized bed, interphase heat transfer, meas. method 8=8145

fluidized beds, mixing model, dense phase dispersion coeff. and cross flow 8=12945

gas-particle mixture in nonequilibrium, continuum approach to flow props. 8=16655

gas-particle reacting system, source flow model 8=21461

gas-solid, supersonic flow in convergent-divergent nozzle, heat transfer obs. 8=16902

heat and mass transfer, interrelationships and mechanisms, anal. 8=16904

heat transfer 8=8142

latex spheres in H₂O, coherent and incoherent light scatt. rel. to Mie theory 8=20104

mass transfer in solid-liquid system 8=4630

particle, moving, in gas, evaporation 8=12943

permittivity of packed powders in fluids 8=22648

polydisperse particles optical scatt., non-spherical randomly aligned 8=12942

polymers in aqueous solutions, reduction in turbulent skin friction 8=12946

polymer latexes, size distrib. from light scatt. 8=16900

spherical particles in oscillating liquid, terminal velocity 8=7988

surfactants, interaction with hydrocarbon liqs. 8=8147

thermal conductivity, theory and expt. compared 8=16901

CaCO₃ in H₂O, surface charge form. and zero point, obs. 8=16903

Cu crystals with dispersed Co/SiO₂ phases deformation and dislocation distrib. 8=4974

Fe powder in perspex, magnetization process and Mössbauer effect 8=5470

He-CF₄, nonresonant, and absorpt. in compressed mixtures 8=1486

ersion, acoustic

ion-acoustic waves, rel. to increase in frequency 8=185

in rods, thin and cylindrical, piezoelectric transducer 8=4913

solids, non-isotropic, second sound 8=4910

KMgF₃:Ni²⁺, near acoustic paramag. reson. 8=22912

trasonic

rotatory, in spin-phonon interaction in paramagnetic crystals 8=5516

CdS, by acoustoelec. effect 8=1849

Dispersion, optical

See also Optical constants; Refractive index/light.

hexafluoroacetone sesquihydrate, fuchsin red prod.

anomalous, for phase-matched third harmonic

generation 8=8072

Kerr effect 8=4578

methyl iodide, i. r. 8=8079

of modulated or time-varying light, anal. 8=6486

organic solvents, i. r. 8=8074

polymers, amorphous, oriented, birefringence

dispersion 8=9578

polystyrene, oriented, birefringence dispersion 8=9578

quartz, anomalous dispersion spectrum due to Si-K

absorption 8=18560

CaF₂ crystal, doped with Nd³⁺, mag. rotatory curves 8=5592

K₂S₂O₆, rotatory, interpretation 8=18539

NaNO₂, infrared dielectric, and apparent ionic

charges 8=22670

SnTe, visible and i. r. obs. 8=18562

Tl₂O₃ layers, in IR, rel. to electronic carrier props. 8=23017

Dispersion relations

See also Field theory, quantum; S-matrix theory.

coaxial loaded waveguide, inverse hybrid waves 8=3263

Compton scatt. off spin-0, $\pi/2$ particles, sum

rules 8=20350

electrodynamics, calc. of traces 8=3439

even-even nuclei, pairing correls. ground-state energy

calc. 8=922

form factor behaviour 8=20269

harmonic oscill., 3-D, e. m. field coupling, all strong

interaction amplitudes superconvergent 8=3427

K-K scatt., extension of analyticity domain 8=6895

K(K)-N elastic scattering, calc. and expt. 8=15830

KN forward scatt., determ. 8=11550

KN scatt., NAK and N π K coupling constants,

SU(3) violation 8=6891

KN superconvergence sum rules and Regge pole

parameters 8=3666

$\bar{K} + N \rightarrow \Sigma + \pi$, use of dispersion relations and Regge

trajectories to calc. Y_0^* BP coupling 8=20580

Kp superconvergent sum rule 8=3667

Kramers-Kronig, real part refractive index calc.

for Ar and Ne 8=16707

Langmuir waves, freq. correction for turbulent

plasma 8=7823

magneto-plasma, nonlinear rel. to instability produced by

pumping wave 8=12485

magnetoplasma, radiative modes of e. m. oscillns. in cold

slab 8=16527

mass difference calc. in hadrons 8=11485

meson-baryon scatt. test of a superconvergent

relation 8=11494

meson-baryon S-wave scatt. length calc., pseudo-

scalar 8=20420

meson-N scatt. amplitude sum rules 8=20469

N leptonic weak decay, PCAC hypothesis 8=3696

nuclear pots., applic. to 8=15919

partial wave, number of subtractions 8=15700

π virtual photoprod. on N dispersion sum rules, static

model 8=20457

π -B scatt, spin-flip amplitudes 8=3635

π -d, coupling const. derived 8=759

π K scatt., extension of analyticity domain 8=6895

$\pi \rightarrow \mu + \nu$, with π as Regge particle, unsubtracted does

not hold 8=11502

π N change exchange scatt., relating high and low energy

data 8=11530

π -N elastic scatt. dispersion sum rules, static

model 8=20457

π N scatt., at fixed u 8=3640

π N scatt., Δ and N trajectories parametrization 8=20328

π N scatt., derivation of AW and spin-flip sum

rules 8=11531

π N scatt., generalized to include S-matrix effects,

partial-wave analysis 8=20430

π N scatt., Roper resonance, magnetic moment relations

using dispersion relations 8=3605

π N scatt. superconvergent sum rules and existence of

resonances 8=6866

π^+ -p elastic scattering, calc. and expt. 8=15830

π^+ p, rel. to Adler Weisberger rule 8=773

π^+ photoprod., $1 < E_\gamma < 3$ GeV, ang. distrib.

predicted 8=20437

π - π phase shifts, low energy behaviour 8=15781

π - π scatt. length 8=15782

π - π scatt. length, numerical bounds 8=20434

π - π scatt., partial wave on first and second Reimann

sheets 8=20463

π - π scatt., soluble model 8=767

plasma, transverse waves due to spatially uniform elec.

field varying sinusoidally with time 8=12557

plasma, two-pole approx. 8=16475

n-pole problem, N/D soln. applic. to S-matrix calc. 8=3552

p-p elastic scattering, calc. and expt. 8=15830

propagators, covariant and vertex functions for any

spin 8=20336

pseudoscalar-vector meson interaction, super-

convergence relations 8=11493

PV \rightarrow VV, superconvergent sum rules 8=15759

Dispersion relations—contd

- q \bar{q} scatt. 8=11478
 Regge cuts, in the presence of 8=11417
 Reggeization of invariant amplitudes 8=11418
 in Regge trajectory eqn. method 8=20412
 scatt. amplitude determ. 8=20300
 scatt. amplitude, oscills. allowed in asymptotic region 8=20299
 Stieltjes transform., asymptotic behaviour 8=6015
 sum rules from current algebra, method Amati, Jengo and Remiddi 8=3551
 superconvergence assumptions rel. to one-meson dominance of a current or its divergence 8=20496
 superconvergence as dynamical assumption unrelated to current algebra 8=3517
 superconvergence conditions in elastic two-particle scatt., relations 8=20298
 superconvergence conditions for scatt. of spinless off arbitrary spin particle 8=6758
 superconvergence in meson-baryon scatt. consequences of saturation in SU(3) symm. 8=15818
 superconvergence props. in helicity formalism 8=11406
 superconvergence relations, construction of solutions 8=20311
 superconvergence, soln. in quark model for M-M, B-M scatt. 8=20404
 superconvergence from strong interaction cases of electro- and photoprod. 8=20376
 superconvergence for all values of momentum transfer, $N\pi$ 8=20455
 superconvergence sum rules for BB scatt. from Regge-pole theory 8=6917
 superconvergence sum rules for meson-meson scatt. 8=20421
 superconvergent sum rules from generalization of chiral symm. 8=20310
 superconvergent sum rules using helicity amplitudes 8=3553
 superconvergent sum rule, model for saturation using Regge pole theory 8=6756
 superconvergent sum-rule technique applied to e.m. form factor of N 8=20514
 3-particle scatt. amplitudes, spinless 8=3548
 vector meson-baryon and symm. for couplings 8=6900
 CsCl, curves and sp. ht., using shell model 8=8610
 α -Fe, phonons and magnons 8=13331

Dispersions. See Disperse systems.

Displacement measurement. See Length measurement; Strain gauges.

Dissociation

- See also Heat of dissociation; Ionization; Molecules/dissociation.
 comets 8=2827
 diethyl ethers, catalytic decomp. on W film 8=14404
 di-n-propyl ethers, catalytic decomp. on W film 8=14404
 formic acid over Al_2O_3 and SiO_2 gel, i.r. study of chemisorbed species 8=9701
 ionic crystals, NaCl-type, of dislocations on (110) planes 8=22192
 metal oxides, dehydration processes, investigation by emanation methods 8=14369
 oxy-halogen radical system kinetics 8=23125
 water, forced convection boiling 8=4657
 As in Ge, solid solution, supersaturated, decomposition mechanism 8=17005
 GaS, thermal stability, and equilb. const. for $2GaS_s \rightleftharpoons 2Ga_{(s)} + S_{2(g)}$ 8=21786
 H_2SnO_3 to SnO_2 , kinetics, Mössbauer obs. 8=14386
 I gas at h. p. 8=23080
 N_2 , stagnation-point dissociation, soln. of nonequilb. boundary layers 8=18662
 O_2 , by e-collisions and excitation of extreme u.v. radiation 8=7722
 $SnO-SiO_2$ glasses, crystallization and decomposition 8=21965

electrolytic

- See also Ions, electrolytic.
 acetic acid 8=4605
 aqueous solutions, computation from ultrasonic relaxation study 8=18712
 hydrazyls form. by hydrazines electrochem. oxidation, e.p.r. obs. 8=5722
 interhalogens in molten I_2 solns. 8=21719
 thermal equilb. in liq. phase 8=4603
 xanthilium salt reagents, dissoc. consts. 8=18713
 H_2 bubbles from aq. soln., rel. to added solutes 8=23149

Dissolution. See Solubility; Solutions.

Distillation

- See also Isotope separation.
 liquid phase adsorpt. fractionation in fixed beds, anal. 8=17151
 macromolecular solns., method of determ. props. 8=8018
 Y, vacuum, for low gas content 8=4652

Domains. See Ferroelectric phenomena; Magnetization state; Superconductivity.

Domains, antiphase. See Alloys; Crystal structure/micro-structure; Solids/structure.

Doping. See Semiconducting materials; Semiconductors.

Doppler effect

- acoustic spectrum of moving source, correction 8=19577-
 acoustic wave reflection from rough surface 8=19566
 attenuation calcs. for low recoil vels., nuclear-lifetime meas. 8=7156
 collision processes, nuclear and atomic, energies of emitted particles 8=20763
 defocusing spectrometer, for MeV range 8=15856
 electrodynamics in travelling e.m. wave 8=15272
 e.m. wave propag. off great-circle path 8=2672
 ideal electron plasma, theory 8=12499
 in ionospherically propagated sea scatter 8=18976
 light wave undergoing multiple reflections between two mirrors in rel. motion 8=15543
 magnetic spectrograph, split-pole, ion-optics 8=3228
 Maxwell's eqns. for moving source, soln. and progressive wave formalism for homogeneous medium 8=3252
 μ capture reactions, rel. to meas ν - γ ang. correl. 8=16065
 in neutron reflection, by rotating crystal, condition for time focusing 8=15845
 in nuclear reactors, broadened functions calc. 8=11616
 in nuclear reactors, maximum 8=11615
 quasars, brightness correlation, explanation of absence 8=23625
 radar sea return dependence on waves 8=23240
 rocket propulsion particle velocity meas. 8=23457
 rotation of e.m. wave radiator-reflector system 8=3270
 satellite signals, data accuracy rel. to ionospheric refraction 8=23371
 Schwarzschild space, and Einstein freq. shift 8=10590
 spectral line broadening, effect of collisions 8=1153
 ultrasonic diagnostic scan within body, localisation 8=1507
 Ca ionized spectrum in calutron, due to charge exchange 8=6334
 B^{10} , lifetime of states obs. 8=11719
 Na^{22} energy level lifetime meas. in C_2F_6 8=11729
 on $U^{238}(n, \gamma)$ reaction at different n energies and high temp. 8=20815

Dosimetry

- See also Radiation monitoring; Radioactivity measurement; X-ray measurement.
 α , cyclohexane appls. 8=20592
 activation meas. for high energy p 8=11603
 alkali halide crystal applications 8=13487
 diamond, by current glow 8=20205
 electron irradiation, sample size restrictions 8=10892
 e-photon cascades induced in water by bombard with e and photons 8=21722
 fast neutron radiometers, power sensitivity 8=20562
 ferrous sulphate in heavy water 8=9733
 Fricke, secondary e effects 8=20206
 γ calibration sources Co^{60} , Cs^{137} and Ra by lead absorber method 8=11436
 γ dose rate in p bombarded spherical shell shield 8=3568
 γ -radiation from gas cloud, calc. 8=10448
 γ radiation, scattered dose rate 8=15718
 γ -rays, energy depend. correction for scintillation detector 8=15720
 γ -ray flux density from reflector-mounted sources 8=1007
 γ -ray, in phantom exposed to fallout and simulated fallout 8=23301
 health and safety in U.K.A.E.A., 1966, research and development work 8=19329
 human body influence on n 8=855
 ionization chamber, human tissue equivalent response 8=606
 ionization chamber, n-hexane, recombination after irradiation with γ -rays 8=6628
 ionizing radiations, dose equivalent 8=20741
 n counter, semi-conductor using crystal damage 8=4030
 neutron depth dose meas. in tissue-equiv. phantom 8=15847
 neutron dose in air depend. on distance from neutron source 8=10444
 neutron dose equivalent rate meas. techniques 8=14894
 neutron equivalent monitor, portable 8=20557
 neutron exposure meas., use of hair 8=11315
 n, fast, thermoluminescent detector 8=20564
 n- γ mixed, dose equiv. and quality factor, organic scintillator meas. 8=20561
 neutrons and gamma rays in paraffin block (human body imitation) 8=615
 neutron monitoring for radiological protection, conference Vienna, Austria (1966) 8=15852
 neutron sensitive foils for thermal neutrons, pocket size ionization chambers 8=851
 n, by ultrasonic cavitation in water 8=3721
 nuclear and space radiation effects, conference 8=22578
 personnel radiation dosimeter with preset alarm 8=7346
 with polyvinyl fluoride plastic film, for γ -rays 8=6779
 proton and neutron secondary doses, equivalent model 8=841
 proton recoil dose from DD and DT neutrons, LET distrib. 8=15837
 radiation research, space radiation biology, conference, Berkley USA (1965) 8=23456
 radiation, ionizing, units 8=613
 reactor γ , n field, using PMMA 8=11313

Imetry—contd

- scintillation camera, autofluoroscope, data processing for 8=5982
- of small β rad. doses, use of nuclear emulsions 8=1001
- spheroidal source, calc. of γ -dose on axis 8=3855
- surface and finger-tip, plastic sachet dosimeter containing LiF 8=20204
- X-rays, high-energy, using ionization chambers 8=15595
- Al 8=13474
- CaF₂:Mn, temperature stability and thermoluminescence during γ -irrad. 8=11314
- CaSO₄(Mn) thin film phosphors as thermoluminesc. dosimeters 8=11800
- CdS cell, integrating appl. 8=5404
- Co⁶⁰, photon emission, exposure meas. 8=11427
- Co⁶⁰ underwater source, γ -ray meas. 8=1008
- Cu 8=13474
- H₂ production, ethylene radiolysis 8=614
- K⁴² in urine, det. meas. 8=3867
- KI aqueous solution, possible applications as dosimeter 8=6664
- LiF, response to thermal neutrons 8=20899
- LiF thermoluminesc. dosimeter, for radiobiological work 8=14890
- LiF thermoluminescence fading characteristics and proper utilization 8=14295
- LiF (TLD 100), temperature stability and thermoluminescence during γ -irrad. 8=11314
- Si(Li) detection for π beams in H₂O 8=7347

Refractive index

- See also Electromagnetic wave propagation; Optical constants; Optical rotation; Polarized light.
- alkali halide crystals. 8=18501
- birefringent beam splitter for holography 8=3379
- chain birefringent filters, anal. of Solc and Lyot type 8=3352
- in crystals, analyt. solns. 8=14183
- crystals, internal and external refl. and refr. 8=14184
- filters, optimum-response synthesis 8=15520
- gases, Cotton-Mouton magneto-optical effects 8=7934
- PDMS solns., birefringence 8=12895
- photoelastic stress analysis, automatic meas. 8=11205
- plagioclase feldspars, birefringence varying rel. to age 8=14182
- polymers, amorphous, oriented, birefringence dispersion 8=9578
- polymers, orientation birefringence temp. dependence rel. to structure 8=9577
- polymethylmethacrylate, rotational isomerism in ester group, prediction 8=4220
- polystyrene, oriented, birefringence dispersion 8=9578
- Portland cement clinker, birefringence meas. of tricalcium silicate and dicalcium silicate phases 8=21841
- Rayleigh scatt. meas. in anisotropic medium, birefringence meas. 8=11197
- solns, birefringence, electric and magnetic field effects 8=12878
- CdS_{1-x}Se_x, birefringence rel. to concs. of components 8=5763
- He⁴, hexagonal crystals meas. 8=15155
- KH₂PO₄, birefringence change by elec. field, rel. to 90° phase-matching 8=14234
- LiTaO₃, ferroelectric, birefringence variation and Curie temp. rel. to melt stoichiometry 8=22669
- Sb₂Se₃ films, birefringence 8=14259
- ZnS polytypes 8=8563

Optical effects. See Electro-optical effects.

Low

- polymer solns., relax. times 8=16849
- polymer solns., streaming birefringence, influence of inter-molecular hydrodynamic interaction 8=4505
- polystyrene solns., mol. wt. depend. 8=8030

Magnetic. See Magneto-optical effects.

Mechanical

- See also Photoelasticity
- polyethylene, dynamic, time-temp. 8=18582
- polyethylene, time-dependent 8=18583
- Relaxance. See Nuclear magnetic resonance and relaxation;**
- Paramagnetic resonance and relaxation.**

Sp

- aerosol, diffusive phoresis in binary gas mixt. of soln. drops 8=21741
- aniline or toluene, charged evaporating, supported by elect. field, instability obs. 8=7992
- cloud droplet coalescence, analytic studies 8=23277
- combustion of single drops of liq. fuel, influence of initial diameter 8=19657
- ejected from air bubbles bursting at water surface, elec. charges carried 8=8117
- liquid, coalescence at interface 8=12765
- liquid, disintegration and electrification subject to electrical forces 8=16782
- liquid, growth in subcooled vapour mixture 8=12983
- liquid interface, drop shape 8=12771
- liquid interface, film rupture 8=12773
- liquid interface, film thickness 8=12772
- in liquid-liquid, immiscible systems, agitated, size distrib. 8=12955

Drops—contd

- liquid, shear deform., second-order theory 8=7993
- liquid, wall migration, in Couette and Poiseuille flows 8=7995
- metal falling in viscous dielectric medium with magnetic field 8=7994
- methyl isobutyl ketone, rising in H₂O and H₂O-sugar soln., vols. of continuous phase translated in water 8=21592
- in methyl isobutylketone-salt water emulsion, size distrib. rel. to mixing and coalesc. 8=12956
- sea spray as function of wind speed and height (<1.2 m) 8=23243
- single drop, mass transfer with continuous phase, convective-diffusion eqns. 8=21594
- size, in liquid spraying, determ. 8=4635
- splashing, distortion obs., computer analysis 8=21587
- spray droplets produced by impact of water drop on water 8=4517
- sprayed electrohydrodynamically, charge-to-mass rel. 8=4519
- toluene-CCl₄ mixtures, rising in H₂O and H₂O-sugar soln., vols. of continuous phase translated in water 8=21592
- toluene, rising in H₂O and H₂O-sugar soln., vols. of continuous phase translated in water 8=21592
- transport in a 2-component gas 8=1482
- water, bouncing off rot. ice ball, effect of NO₃' conc. on charge 8=23290
- water, charged evaporating, supported by elect. field, instability obs. 8=7992
- water, discharge between, microwave superheterodyne receiver epoch sensitivity to pulses 8=14624
- water, distortion and disintegration in elect. fields 8=21595
- water, erosion of Cu surface 8=22333
- water, freely falling in elect. field, mass loss and distortion 8=21586
- water, steam-borne, collision behaviour 8=21593
- water, in vertical wind tunnel, collision, coalescence and breakup obs. 8=1519
- Fe alloy, liquid, voids formation 8=8257
- NaCl soln. drops, growth by condensation on nuclei 8=9853

Drying

- air, use of molecular sieves 8=18644
- porous sphere in air stream, mass conductivity calc. 8=12992

Ductility. See Plastic flow; Plasticity.

Dusts. See Aerosols; Powders.

Dynamics

- See also Ballistics; Kinematics; Rotating bodies; Vibrations.
- acceleration of gravity meas. using laser-interferometer system 8=10487
- amplitude jumps, study 8=10523
- beam oscills. anal., duality relations 8=15037
- bifilar pendulum 8=6043
- body over tangentially vibr. surface allowing for friction 8=19493
- classical, SU_n and O_{n+1} symms. 8=10521
- classical systems, symm. degeneracy problem 8=2912
- classical, Utiyama's Hamiltonian rel. to quantum electrodynamics 8=3435
- collisions on air track, matrix description 8=14946
- constant acceleration flows, appl. to high-speed guns and launchers 8=16668
- continuous media, using field theory 8=2916
- continuous media, foundations 8=2915
- coupled oscillators and normal coordinates 8=10532
- deceleration of long rods after impact, hydrodynamic theory inc. for strength effects 8=19378
- demonstration apparatus 8=10525
- discs, rough rotating, torque due to friction 8=6044
- disk, rigid, on isotropic elastic plate, vibration calc. 8=3015
- dynamometers torsion 8=31
- ellipsoid containing non-central rotating mass, resonance oscills. 8=10522
- force and potential energy, relation, experimental determination 8=14923
- Kepler problem, formulation invariant with respect to SO₄, SO_{3,1} groups 8=14943
- Lie algebra of dynamical variables 8=10490
- linear discrete medium 8=30
- linear vibrations, complementary variations principles 8=10692
- man in boat, paradox 8=36
- mechanisms with more than one degree of freedom, dynamic acceleration analysis 8=34
- motion of a triple rod in a Newtonian field 8=14947
- Newtonian pot. equivalent for relativistic particle in 2-superimposed fields 8=6080
- Newton's second law, formulation 8=10526
- pendulums, inverted, stabilized, small oscillations 8=10527
- pendulums, truncated ring, equivalence 8=10528
- periodic motions of systems with impulsive interaction 8=10530
- polarized system relativistic equations 8=10631
- relativistic, Ehrenfest's paradox of rotating disc 8=14961
- simple harmonic oscillation, SU_n and O_{n+1} symms. 8=10521
- symmetries in quantum mechanics, integrals of motion 8=11246

Dynamics—contd

- swings, and subharmonic generation 8=179
- system of point particles in E_2 space, symmetry theory 8=117
- three body problem in space, regularization of singularities 8=10533
- two-mass vibrator-hammer, contribution to theory 8=10524
- vibration of circular plate, weights or bar on outer boundary 8=15039

Dynamometers

See also Force measurement.

No entries

Dysprosium

- deformation planes after dehydrogenation and hydride habit planes 8=8728
- dimensions of ferromag. correlation range by neutron depolarisation obs. 8=22797
- garnets, mag. structure by n-diffr. 8=22865
- M_{IV} and M_V absorpt. lines and edges 8=5602
- mag. properties, 4-300°K 8=14067
- magnetoelastic effects and mag. props. 8=22799
- microwave absorption phenomena at 4.44 and 35.3 Gc/s, 10-290°K 8=14269
- probability distrib., spiral spin system 8=13994
- uniaxial mag. anisotropy 8=18333
- Dy^{3+} in $LiNbO_3$, e.p.r. 8=18428
- Dy^{3+} , in silicate glass, Faraday rotation, freq. depend. 8=18531
- Dy^{3+} in tungstates and molybdates, u.v. excitation of fluoresc. 8=2473
- in ThO_2 , spectrometric determ. 8=18787
- in YVO_4 , rel. to const. quantum yield 8=5670

Dysprosium compounds

- garnet, phase change with symmetry enhancement as function of magnetic field 8=21839
- Dy^{3+} salts, hyperfine structure of Dy^{161} at 4.2°K 8=1646
- Dy-Al-garnet, hyperfine splitting of lowest $2'$ state of Dy 8=9301
- $DyAl_3$, nuclear magnetic resonance 8=22920
- $DyAlO_3$, crystal structure, X-ray diffr. 8=8544
- $DyFeO_3$, orthoferrite, transition to antiferromagnetism at liq. He temps. 8=9375
- Dy_2O_3 single cryst., electronic spectrum 8=18522
- Dy_2O_3 , sintering, kinetics, data correlation 8=8258
- Dy_2O_3 , sintering kinetics, resonant freq. meas. 8=17027

E-layer. See Ionosphere/E-region.**ENDOR (electron nuclear double resonance).** See Nuclear magnetic resonance and relaxation; Paramagnetic resonance and relaxation.**Ear**

See also Hearing.

- basilar membrane fine displacements, rel. to tonal residue 8=209
- bone conduction improvement when ear is covered rel. to unilateral hearing loss 8=19600
- bone vibrator calibration using artificial mastoid 8=6189
- cat, olive S-segment cells, encoding of stimulus frequency and intensity 8=218
- damage-risk criterion for impulsive noise of 'toys' 8=3083
- external-ear replica for acoustical testing 8=3082
- harmonic distortion produced by ear 8=19606
- human, relative motion between tectorial membrane and reticular lamina 8=3081
- nerve fibres in cats, threshold rel. to stapes displacement 8=10761

Earphones. See Acoustic transducers.**Earth**

- albedo, Tiros VII obs., July 1963-June 1964 8=23285
- rel. to atmosphere available pot. energy generation, i.r. radiation, obs. 8=23262
- bow shock, Explorer 12 magnetometer obs. 8=2619
- Brazilian glauconites, K-Ar age meas. 8=18830
- Chandler wobble, theoretical model 8=14566
- constant of model for mantle, compatibility with surface wave data 8=5777
- core convection and continental drift 8=23217
- core and mantle motions, main geomag. var. 8=14554
- core radius 8=14560
- cosmic ice residuum and astrobleme 8=2562
- creep and damping props. of mantle, by unified viscosity and viscoelasticity theory 8=14538
- creep of rocks, effect of temp. and stress, rel. to isostasy 8=14559
- crust, seismic studies, Far Eastern transition zone, 1963-4 8=9780
- crust, velocity parameters from reflected-wave travel times 8=9786
- crustal fracture at edge zone of Antarctic, rel. to isostatic motions due to variable ice load 8=18823
- dipslip faults in upper mantle, energy released 8=18820
- earth-moon system, solar perturb. of motion near collinear libration points 8=19070
- earth-moon system, Trojan manifold 8=19242
- free modes, dissipating mechanism, linear model with Q almost freq. independ. 8=23204

Earth—contd

- ground abs. of cm and dm radio waves 8=23230
 - isostatic equilb. of crust, and viscosity of asthenosphere 8=14556
 - isostatic equilb. disturbances, rel. to tectonics and internal processes 8=14555
 - mantle, elastic props. from deformation due to tidal loads 8=14545
 - mantle, flow inferred from continental drift and low harmonics of geopot. 8=14551
 - mantle, $NaAlGeO_4$, high pressure form. and crystal structure 8=1678
 - mantle, upper, conference, Newcastle-upon-Tyne, England Feb. 1966 8=9787
 - mantle, upper and lower, viscosities from slow deforms. and solid state theory 8=14550
 - mantle, upper, rigidity and mech. props. from tidal studies 8=14546
 - mantle, upper, viscosity rel. to postglacial uplift of Scandinavia 8=14547
 - mantle, viscosity and finite strength, from transient water and ice loads 8=14548
 - mantle, viscosity variation with depth 8=14549
 - moon system astron. params. optical radar meas. 8=14827
 - motion rel. to sources of ext. mag. field, removal of elec. field components in mag. 8=10344
 - Ordovician rock structures, Victoria (Australia) 8=18824
 - phase change boundary motion rel. to pressure, calc. 8=23201
 - pole movements, free and forced amplitude long period var. 8=9770
 - potential field determ. from satellite obs. 8=9769
 - radiation, outgoing terrestrial 7-26 μ , statistical characts. from Cosmos obs. 8=23283
 - resistivity, prospecting, appl. of reciprocity theorem 8=14541
 - rheological props., influence on seismic regime 8=14537
 - rock density in crust and upper mantle, correl. with longit. wave propag. vel. 8=18816
 - rotatable field e. m. prospecting system, anal. and model studies 8=14540
 - Sahara basins, evolution of water isotopic comp. during evaporation 8=18832
 - snow and firm of South Pole region, O isotope ratio rel. to air temp. 8=23227
 - soil pressure cell, effect of diaphragm flexibility on calibration 8=9803
 - solar light pressure rel. to circumterrestrial motion of dust 8=10342
 - spectra of reflected solar and emitted thermal rad., in 1.6 to 5.4 μ range 8=9866
 - standard silicate rocks, chem. anal. techniques 8=9802
 - state of stress in cryst., and energy of tectonic processes ass. with upper mantle 8=14516
 - surfaces, optical characteristics 8=2816
 - tectonic processes, model expts. of effect of gravity 8=14512
 - torsional vibrations, tables for derivs. of first to fourth harmonics 8=18803
 - tri-partite system earth-Mars-moon 8=23657
 - variable density of horiz. layer, errors in determ. by gravitational anomalies 8=18822
 - Re and Os abundances in 14 igneous and metamorphic rocks 8=18825
- age**
- See also Radioactive dating.
- No entries
- composition**
- alkali aluminogermanates, high press. transforms rel. to geochem. 8=8261
 - alkali aluminosilicates, high press. transforms rel. to geochem. 8=8261
 - aluminous pyroxene peridotite and garnet peridotite, stability fields in upper mantle 8=9789
 - ancient charts, O isotope comp. rel. to Precambrian ocean 8=5779
 - rel. to charge fundamental unit time var. 8=15728
 - crystalline basement internal struct., e. m. meas. 8=18821
 - diffusion creep in mats. due to thermal grad. 8=14539
 - diopside in upper mantle, plastic deform. 8=14557
 - η , departure from chem. homogeneity, allowing for superadiabatic temp.-grad. 8=5782
 - eustatite in upper mantle, plastic deform. 8=14557
 - geological samples, X-ray fluoresc. anal. 8=14498
 - interior density, pressure and rigidity distrib. 8=18826
 - interior, national report, Canada, 1963-66 8=14526
 - lanthanide distrib. between pyroxene and garnet 8=5780
 - low viscosity layer in mantle, effect on convection 8=14591
 - mantle, anelastic props. from seismic wave attenuation 8=14543
 - mantle-core transition zone, theory 8=9788
 - mantle deformation rel. to dislocation velocities 8=14544
 - mantle, upper, preferred mineral orientation by recrystal. under stress 8=14552
 - model, elastic and viscoelastic behaviour 8=14948
 - Old Red Sandstone, effect of heat treatment on mag. props. 8=5821
 - olune in upper mantle, plastic deform. 8=14557

th—contd

composition—contd

phlogopite, possible presence in upper mantle 8=23221
 plagioclase feldspar, age from birefringence
 variation 8=14182
 quartz and silicate rocks, hydrolytic weakening at high
 temp. and press. 8=14561
 rock fracture, effects of triaxial stress systems,
 appl. to earthquakes 8=13516
 sandstones, fracture strength and mechanism 8=13517
 upper mantle, anal. of ultrabasic rocks and nodules 8=5778
 Wairakite, conversion of stilbite and Heulandite
 under very low water s.v.p. 8=2563
 Zuni Lineament in New Mexico, geophys. evidence from
 Pb isotopic meas. 8=5781
 MgSiO_3 - CaSiO_3 - Al_2O_3 system garnet-pyroxene equil.
 press. depend. rel. to mantle 8=1676
 O and H isotope vars., firm core in W. Antarctica 8=14563
 Re^{187} , Os^{187} occurrence rel. to p charge time var. 8=15826

electricity

core resistivity, allowing for impurities, rel. to geomag.
 dynamo 8=18828
 current var. rel. to ionospheric u.l.f. emissions 8=9974
 digital, portable observatory for meas. of two horiz.
 comps. of elec. field 8=14693
 Greenland ice cap, dielectric constant rel. to ice
 density 8=14565
 mantle conductivity distrib. from mag. field var. 8=23223
 moist rock, dielect. constant and conductivity lab.
 meas. 8=13899
 surface conductivity distrib., review 8=9791
 telluric currents, scattering and signal extraction 8=14564

eat

convection hypothesis in upper mantle, criteria for evaluation
 of pertinence 8=14517
 convection in mantle, effect of low viscosity,
 layer 8=14519
 energy release by creep rel. to geothermal flux, rel. to
 convection hypothesis 8=14524
 expansion at high press., eqns. of state 8=18808
 mantle convection cells, graphical representation 8=23220
 mantle convection and continental drift hypotheses,
 criticism 8=14518
 mantle convection, thermal requirements for crustal
 phenom. and magma prod. 8=14521
 mantle, upper, low velocity zone temp. and density
 distributions, thermodynamic approach 8=14553
 terrestrial heat flow distrib., consistent with mantle
 convection 8=14522
 thermal convection theory for mantle, problem of non-
 linearity of eqns. 8=14520
 thermal history 8=9772
 thermal radiation for satellite's vertical determ. 8=2763
 thermal rel. to gravitational anomalies 8=2555
 upper mantle, energy input to crust under Japan since
 Palaeozoic times 8=14523
 Mg_2SiO_4 reactions, required temp. and press. from thermal
 compressibility data 8=2556

magnetic field

acoustic mode for wave in dipole magnetized
 plasma 8=1393
 ancient field intensities, geological and historic and
 archeological data 8=23426
 ancient field intensities, to past 10 000 yrs,
 tabulation 8=5811
 Antarctica, E, Soviet expedition 1960-62 obs. 8=23437
 in auroral ionosphere, expt. investigation of parallel
 elect. fields 8=23354
 bays, effect on u.l.f. e.m. radiations 8=9971
 bow shock, plasma and mag. field correlation obs. 8=23328
 Canadian Arctic, aeromagnetic survey, Taylor
 expansion 8=19024
 Canadian report on geomagnetism 8=14692
 Chukchi sea, N. E., marine magnetometer obs. 8=19034
 Dessler-Parker-Sckopke relation, simple
 derivation 8=23429
 closed magnetosphere, neutral points on boundary 8=9911
 core surface fluid velocity from mag. obs. of 1885, 1912,
 1933 and 1960 8=5813
 cosmic ray μ defl. from primary direction, telescope
 obs. correction programme 8=20619
 Cosmos-49 obs. rel. to computed values 8=10030
 deformation by interior conducting-fluid motion 8=6346
 digital portable observatory for three components of mag.
 fields 8=14693
 dipolar, motion of mag. monopole, model 8=19031
 dipole axis, vib. round geographic N pole in historic
 time 8=5812
 dipole, nonlinear inflation by plasma 8=10028
 dynamos, nearly symm., Braginskii result true to
 second approx. 8=10097
 electrons in earth's magnetotail, obs. by Vela
 satellites 8=23431
 energization of charged particles by
 arbitrarily moving spherical magnet 8=19769
 energy of monopole in dipole field 8=10026
 equivalent current functions, negative and positive
 extrema on maps 8=19026

Earth—contd

magnetic field—contd

errors arising from separation into main and
 anomalous 8=19030
 Euler potentials, calc. by perturbation scheme 8=2722
 flux tubes, approx. flow eqn. and appl. to polar
 substorms 8=10029
 in geological part, intensity 8=10023
 geomagnetic activity, July-Sep. (1965) 8=19053
 geomagnetic activity, Oct-Dec (1965) 8=19054
 geomagnetic activity, Jan-March (1966) 8=19055
 geomagnetic pot., appl. of oblate spheroidal harmonic
 functions for calc. 8=19025
 geomagnetic tail, configuration and
 reconnection 8=23432
 geopotential field at any atmos. level, from satellite
 vel. 8=10027
 gradiometer, for vertical grad. meas. and total field
 intensity 8=14694
 "growth effect" in n. m. r. in earth's field 8=15432
 influence on millimetre transfer radiation from
 atmospheric O_2^{16} molecules 8=23284
 interaction with solar field 8=10375
 ion-beam field-confinement, geomag. appl. 8=1417
 ionosphere-earth cavity model, cylindrical with dipolar
 field, resonances 8=9981
 Km, Kn and Ks indices, from mag. activity obs., northern
 and southern hemispheres, prelim. calc. 8=23316
 last field reversal, cosmic ray effects and faunal
 extinctions 8=23435
 late paleozoic 8=14700
 latitude dependence of solar cosmic ray low energy
 cut-off 8=897
 magnetic time, calc. and definition 8=2726
 m.h.d. dynamo 8=23427
 magnetometers, nuclear, for meas. from rockets 8=14720
 in magnetosheath and beyond, correlation with ≥ 30 -keV
 electron pulses 7=23433
 magnetosheath penetration by interplanetary field, IMP 1
 and 2 obs. 8=14861
 magnetosheath, shock aligned oscils. 8=9920
 magnetosphere, bulk motion 8=9919
 magnetosphere (B, L) coord. system allowing for distention
 by ring current 8=23434
 magnetosphere, higher-order ring current and particle
 energy storage 8=18927
 mapping of earth's bow shock and mag. tail by
 Explorer 33 8=23430
 motion of charged particles in geomagnetic field,
 perturbing forces effects 8=19052
 multidimensional statistical analysis 8=5814
 muon spectra and change ratio at sea-level,
 effect 8=900
 nondipole part, influence on magnetosphere
 boundary 8=18932
 Ntonya ring structure, Malawi, syenitic and granitic
 rocks 8=19061
 OGO-A obs., 4 to 24.5 R_E 8=10024
 'pearl' type oscs. of e.m. field, polarization and time
 variations 8=19032
 penetration of ocean bed, R-C network analogy 8=10025
 polarity transition in Miocene, unstable components
 and paleomag. evidence 8=19057
 radiation belt as means of studying drift shells of
 electrons 8=19028
 in radiation belts, rel. to Lyman α directional intensity
 var. 8=18963
 radiocarbon dating, influence of changes in 8=9796
 representation, analytical, from Cosmos 49 obs. 8=19029
 representation, analytical, using given number of
 dipole sources 8=19027
 representation by 3 eccentric dipoles 8=23436
 satellites, influence on, and means of stabilization 8=5824
 secular variations rel. to core's surface fluid
 motion 8=2724
 sensor, noise cancelling, for proton magnetometer meas.
 near a.c. lines 8=302
 sheath, mag. noise of freq. 3-300 Hz, OGO 1 obs. 8=2621
 solar wind distortion rel. to magnetosphere models,
 $3\frac{1}{2}$ -13 earth radii 8=2751
 and solar wind, interaction rel. to interstellar plasma
 theories 8=23578
 solar wind-magnetopause transition and tail neutral
 sheet, obs. 8=23717
 Stomer problem solution to a restricted case 8=19051
 tail detection by Luna 10 8=23313
 tail at 10^3 earth radii, Pioneer 7 obs. 8=2748
 tail, IMP 3 rel. to Lunik 10 obs. 8=23315
 tertiary, intensity determ. using baked contacts and
 dykes 8=2725
 topology at 3-7R, Elektron 2 obs. 8=19033
 topology, rel. to coupling between magnetosphere and
 ionosphere 8=9910
 2-dimensional pot. fields, analytic continuation into lower
 half space, computational scheme 8=23428
 uncoupling of parallel and perpendicular particle
 motion in neutral sheet 8=19766
 waveguide effect on long radiowaves 8=3273

Earth—contd

magnetic field, variations

- See also Magnetic storms.
 activity, high N latitudes, IGY 8=19037
 activity index, response to interplanetary mag. field,
 obs. 8=10052
 activity, middle and low latitudes, IGY 8=19038
 activity, rel. to nocturnal spread-F at Kodaikanal 8=10010
 activity rel. to outer radiation belt boundary electron
 intensity > 100 keV 8=23345
 anomalous, stationarity of approximating random
 process 8=19042
 Atlantic north-earth, rates of secular variations 8=10031
 aurora electron precip. accompanying impulse,
 bremsstrahlung obs., interpretation 8=2635
 autocorrelation function of anomalous field 8=23446
 bays as superposition of effects due to Hall current
 system and westward electrojet 8=19047
 bays, auroral zone, rel. to proton events in outer
 belts, 1961 Explorer 12 obs. 8=2648
 Brazilian anomaly, chart 8=19035
 British Isles, daily 8=10037
 Canadian Arctic, aeromagnetic survey, Taylor
 expansion 8=19024
 and core and mantle motions 8=14554
 and density variations, rel. to upper atm. heating, satellite
 drag obs. 8=14695
 dipolar, wobbling over last 2000 years, archeomag.
 obs. 8=10034
 dipole moment, evidence from Permo-Carboniferous,
 intensity 8=23453
 disturbances and atmospheric temps. 8=10051
 disturbance indices, power spectra, 27 day subsidiary
 peaks 8=2732
 disturbance rel. to sporadic E, auroral 'flat-type' 8=10005
 diurnal, cartographic representation 8=10033
 dynamo model, self-excitation condition 8=5818
 dynamo region current systems rel. to F2 drift,
 obs. 8=23420
 e. m. field, 'auroral-type' fluctuations 8=2727
 equatorial electrojet, regions below and nearby,
 correlation 8=2745
 extensive disturbances rel. to radial diffusion of trapped
 particles with arbitrary pitch angle 8=18962
 fine structure and polarization of PP 8=19050
 from Explorer 9 drag data 8=5816
 rel. to formation of sporadic-E 8=2707
 geomagnetic micropulsations, spectra analysis 8=10049
 high-latits., quiet days in IGY summer 8=10036
 hydromag. emissions (Pc1), narrow band, nature and
 origin 8=10048
 hydromagnetic emissions, relation to, perturbations in
 magnetosphere 8=2739
 hydromagnetic toroidal resonance, math. viability 8=2723
 "Indo-Pacific" mid-ocean ridge, mag. profiles 8=23438
 intense disturbances, arctic, freq. obs. 8=10042
 ionospheric equatorial anomaly, E. Asian zone of
 Pacific 8=19003
 ionosphere, F2, response 8=10018
 K_p rel. to average L shell of plasmopause, IMP 2
 obs. 8=9917
 Kerguelen archipelago, 2 stations 20 km apart 8=2738
 long period, 4 to 0.002 Hz, dynamic spectra character-
 istics 8=2735
 Lunar, diurnal, semi-diurnal, terdiurnal 8=14696
 lunar diurnal variation at Val-Joyeux 8=2728
 Lunar periodic, Heiss Island obs. 8=19040
 luni-solar daily, at Tananarive during IGY 8=10040
 luni-solar daily variations, in Brit. Isles in 1 GY 8=5815
 magnetite deposit, seismomagnetic effects 8=10032
 mantle conductivity meas. and local vars. origin 8=23223
 micropulsation activity, frequency spectrum rel. to
 planetary magnetic activity 8=10050
 micropulsations, and ionospheric noise, review 8=18995
 micropulsations, Pi and Pc Lerwick obs. 8=23445
 micropulsations, afternoon occurrence 8=5817
 micropulsation rel. to auroral X-ray event 8=9946
 micropulsations due to Geminids meteors 8=2733
 micropulsations, e. l. f. 8=2740
 micropulsations, impulsive Pi subtype rel. to ionospheric
 cosmic absorption 8=2736
 micropulsations, long period, m. h. d. explanation 8=2731
 micropulsations, meteors as possible cause, math.
 model 8=2734
 micropulsations, non-impulsive Pi subtype rel. to auroral
 electrojets 8=2736
 micropulsations, Pc 1 characters, rel. to origin 8=2742
 micropulsations, Pc 1 simulation by bounded p plasma
 model 8=2741
 micropulsations pi 2, frequency analysis 8=2737
 micropulsations polarization, theory and obs. 8=2743
 micropulsations, rel. electron bremsstrahlung, N. auroral
 zone, obs. 8=10047
 micropulsations rel. magnetosphere solar wind 8=10046
 mid-Atlantic ridge anomalies near 27°N 8=23439
 nocturnal sub-e. l. f., rel. to negative ions in
 ionosphere 8=14699
 Pc/micropulsations at College, polarization
 characts. 8=14698

Earth—contd

magnetic field, variations—contd

- pc-type pulsations, correlation with variations of
 much longer period 8=23440
 Pc1 micropulsations, rel. to waves generated by
 proton belt 8=18956
 Pc1, Pi2 + Pc1, and Pi1 microstructure accompanying
 disturbance 8=19049
 Pi2 pulsations rel. to solar activity, 1956-1966
 obs. 8=23447
 Pi2 rel. to auroral luminescence intensity
 pulsation 8=19048
 paleo intensities determ. and mechanisms responsible for
 non-ideal behaviour in Thellier's method 8=10061
 pearl micropulsations production 8=23444
 pearl pulsations rel. aurora luminescence var.
 1964-1965 8=9936
 and plasmopause dawn minimum equatorial distance,
 obs. 8=2747
 polar disturbances and current system, IGY winter
 obs. 8=23442
 polar solar, diurnal, on exceptionally quiet days 8=10038
 polar substorms and ring current growth 8=19056
 polar wandering and continental drift deductions from
 paleomag. Sierra Nevada obs. 8=14701
 pp bursts, short term, as geomag. pulsations 8=10044
 pulsations at Halley Bay, spectrum 8=19041
 quartz variometers, Central Magnetic Observatory U.S.S.R.
 obs. 8=23443
 "seashore" effect, vertical component rel. to surface elec.
 cond. 8=23441
 secular, cyclic, 1879-1961, Tbilisi obs. 8=10039
 secular, regular distrib. law found 8=19036
 semiannual, analogy with upper atmosphere density
 var. 8=10035
 sheath at 18 earth radii, and structure, Vela 3 obs. 8=2744
 shock waves effect from atmospheric explosion 8=2746
 small, from place to place, meas. with Hall effect
 magnetometer 8=3163
 rel. to solar-atmos. reactions, variations, time and
 geographic 8=18931
 and solar cosmic ray diurnal anisotropy obs., corre-
 lation 8=2749
 solar-diurnal, quiet day current systems, construction
 by graphic integration 8=19039
 and solar particle emissions, review 8=19303
 solar radiation, and ionospheric gravit. tides, contrib.,
 calc. 8=14678
 rel. to solar wind in spectrum outside magnetosphere,
 Venus 3 obs. 8=14875
 by solitary pulses, e and ion accel. 8=2620
 and sporadic E, correlation obs. 8=10004
 sporadic E and mag. activity 8=23404
 stellar radiowave var. effect 8=2865
 subpolar and mid-latits. 8=10041
 surface, rel. interplanetary mag. field, IMP 1 and
 terrestrial obs. 8=14860
 travelling pulse due to cosmic ray shower protons and
 electrons 8=3750
 variometer, 3-component portable with resolution better
 than 1 γ 8=6278
 westward drift, correlation with solar activity 8=2750
rotation
 angular momentum, transfer between solid and fluid
 parts 8=14511
 correlation of solar activity with geomagnetic
 drift 8=2750
 day length, annual and semi-annual vars. rel. to geo-
 physical obs. 8=14510
 Ephemerical time det. from lunar occultations 8=5952
 geostrophic adjustment, nonlinear 8=2573
 high-precision timing by radio interferometry 8=18833
 irregularities, rel. to stress state in crust 8=14516
 irregularity, 1955.5 to 1965.0 obs. 8=9801
 nutation, free, damping and relaxation time 8=2569
 radio interferometric meas., implications for
 geophysics 8=18804
Earth satellites. See Satellites, artificial.
Earthquakes. See Seismology.
Eberhard effect. See Photographic materials.
Ebullition. See Boiling.
Echelons. See Diffraction gratings.
Echo
 See also Architectural acoustics; Reverberation;
 Sound ranging.
 quadrupole spin, under 2 frequencies amplitude
 calc. 8=370
 ultrasonic pulse-echo detector, variable width
 gate 8=3073
Eclipses. See Moon; Sun/eclipses.
Eddy-currents
 orbital accelerator magnets, field distortion 8=635
 trace characterization method for electron purity
 meas. 8=18757
 Fe, sintered, losses reduction and mag. props.,
 obs. 8=22807
 Fe-Ni, sintered, losses reduction and mag. props.,
 obs. 8=22807
 Fe-Ni-Mo, sintered, losses reduction and mag. props.,
 obs. 8=22807

ddy-currents—contd

Fe-3%Si, grain-oriented, losses rel. to domain wall motion, obs. 8=22842

Fe-Si, sintered, losses reduction and mag. props., obs. 8=22807

luminescence emission. See Luminescence/solids, inorganic; Luminescence/solids, organic.

education. See Teaching.

diffusion. See Flow/gases.

doublet way. See Elementary particles; Field theory, quantum.

Eden-de Haas effect. See Gyromagnetic effect.

elastin

sensitive spark spectral lines 8=12063

elastic constants

See also Compressibility; Stress/strain relations. acenaphthene monocrystals, determ. of elastic const. by two methods 8=5092

alkali halides, in rel. to Reststrahlen freq. and compressibility 8=13580

α -brasses, Young modulus and modulus of rigidity, variation-latitude dependence 8=2051

anisotropic tensor decomposition for given crystal symmetries 8=17714

anthracene 8=5093

b. c. c. metals, determ. of approx. dispersion relations 8=17480

β -brass, temperature and composition depend. 8=13546

bulk and local, rel. to point defects of crystals 8=22260

bulk, rel. to volume per ion pair of compounds 8=13494

C-steel, hardened, Young's modulus rel. to, carbide transforms., $< 400^\circ\text{C}$ 8=22360

calcite, compliances temp. dependence 273-90°K 8=5055

Cauchy relations, deviation rules from expt. 8=5004

centrosymmetric cubic cryst., model, rel. to free-vib. modes 8=5002

class 3m crystals, meas. 8=9226

composite materials, perfectly disordered, moduli 8=13493

crystals of general symmetry, from sound-velocity measurements 8=8782

cubic crystals, mono- and polycryst., third-order constants relationships 8=13492

earth, interior distrib. of incompressibility and rigidity 8=18826

epoxy composites, filled and porous, Young's modulus obs. 8=13620

f. c. c. metals, detm. of approx. dispersion relations 8=22080

ferroelectrics in acoustic and polarization waves interaction 8=18182

garnet, and derivatives w. r. t. temp. and press., obs. 8=2037

graphite, polycryst. Young's mod., porosity and orientation effects, comments 8=22319

h. c. p. crystals, derivation through third order 8=13491

inert gas solids, contributions of a non-central force 8=22259

isotactic polyvinyl tert. butyl ether, elastic moduli, along and across fibre-axis 8=8877

isotropic ceramic, conversion relations table 8=8783

measurement by vibrator-controlled oscillator system 8=8785

obsidian, by u. s. interferometry 8=17713

para-H₂, solid, deformation curves at 4.2°K, static Young's modulus 8=5074

polycapromide, oriented, depend. on molec. weight 8=22405

polycrystalline, first pressure derivatives rel. to single-crystal acoustic data 8=8781

polyethylene, derived modulus 8=8608

polyethylene, elastic moduli, along and across fibre-axis 8=8877

polymers, high, crystalline regions, elastic moduli, along and across fibre-axis 8=8877

porous epoxy composites, strain-rate dependence 8=13621

rare-earth, polycryst., and Debye temps., 4.2 and 300°K 8=2057

rod, vibrating and heated nonuniformly, stress amplitude rel. to modulus 8=10688

solid solns., temp. coeff. incr. due to heavy component 8=8634

steel, low-alloyed, Young's modulus, change on tempering 8=13560

steel, Murnaghan's n constants by ultrasonic waves 8=13568

stress analysis of plates with stiffened perforations, effective modulus calc. 8=10546

stressed materials, and thermoelasticity 8=2036

third-order, rel. to thermal u. s. attenuation along (110) axis 8=4916

whitewaves, static and sonic Young's mod. rel. to flexural strength 8=17733

Young's modulus, errors due to shear and rotatory inertia in flexural vibrations method 8=17712

Li ferrites, Young's modulus, temp. depend. 8=22378

Ag₃Al, from 77°-700°K 8=5040

AgCl, 4.2 to 300°K 8=5041

Ar, bulk mod. at T=0°K, anharmonic contribs. 8=13594

Ar, polycrystalline, calcs. 8=17768

Au₃Cu, shear modulus change during ordering 8=17769

CaO, at 80-270°K 8=8831

Elastic constants—contd

CdS, between 4.2-300°K, Debye temp. calc. at 0°K 8=13542

Co hexagonal single crystals, Young's modulus dependence on thermal expansion 8=22324

Cs, and pressure derivs. at absolute zero 8=17818

Cu, cold worked, impurities rel. to modulus effect 8=22332

Cu, recovery after torsional deform., role of dislocation rearrangement 8=22337

Cu, Young modulus and modulus of rigidity, variation-latitude dependence 8=2051

Cu₂O, and Debye temp. calc. 8=1869

Cu₃Au, shear modulus change during ordering 8=17769

D, polycrystalline, Poisson ratio calc. from sound velocity meas. at 2 and 16°K. 8=17499

Eu, and u. s. attenuation from 4.2 to 300°K 8=17781

Fe-Al alloys, stiffness coefficients, long range order effect 8=5063

Fe-Al alloys, stiffness coefficients, experimental results and thermodynamic analysis 8=5062

Fe-Mo alloys, Fe-rich, precip. reactions and solid solns. by Young's modulus studies 8=4678

Fe-Ni-Ti alloy of Invar type, Young modulus anomalies 8=17790

GaAs, rel. to charge carrier concentration 8=13575

Ge, lattice energy rel. to elastic deform., electron distrib., internal strain 8=13576

Ge, third order, lattice theory 8=13261

K, and pressure derivs. at absolute zero 8=17818

K, liquid, wavenumber-dependence 8=1499

KBr, acoustic phonons, change during first and zero sound 8=13357

KCl, higher order, theoretical calcs. 8=17811

KCl, third-order, obs. 8=13579

KF, from 300-4.2°K, Debye temp. and lattice energy calcs. 8=2056

LiCl, adiabatic, 300° to 4.2°K, obs. 8=2058

LiF, higher order, theoretical calcs. 8=17811

LiF, theoretical determination 8=17812

LiF, third-order, obs. 8=13579

LiTaO₃, single cryst. 8=8853

Mg, liquid, wavenumber-dependence 8=1499

MgAl₂O₄, hot-pressed, rel. to microstructure, quadratic multivariable analysis 8=21991

MgO matrix composites Young's and shear moduli 8=13585

Mg-Th alloy in temp. range 25°C-350°C 8=5080

Na, and pressure derivs. at absolute zero 7=17818

Na, liquid, wavenumber-dependence 8=1499

NaCl, higher order, theoretical calcs. 8=17811

NaCl, third-order, obs. 8=13579

NaF, ionic crystal, calc. 8=2062

NaI, temp. dependence 8=13591

Nb, superconducting, mixed and normal states, variation 8=2063

Nb-Mo alloys, Young's modulus, Debye temp., atomic bond strength 8=1626

Nb-Ti alloys, Young's modulus, Debye temp., atomic bond strength 8=1626

Nb-Ta alloys, Young's modulus, Debye temp., atomic bond strength 8=1626

Nb-V alloys, Young's modulus, Debye temp., atomic bond strength 8=1626

Nb-W alloys, Young's modulus, Debye temp., atomic bond strength 8=1626

Nb₃Sn Fermi level motion rel. to temp. depend., model 8=5118

Ne, bulk mod. at T=0°K, anharmonic contribs. 8=13594

Ni, ΔE effect, freq. dependence 8=2065

Ni₃Fe in solid solutions, variations of Young's modulus with alloying and temp. 8=4690

Pb_{0.95}Sr_{0.05}(Zr_{0.43}Ti_{0.47})O₃, effect of elec. field on Young's modulus 8=1856

Rb, and pressure derivs. at absolute zero 8=17818

RbCl, adiabatic, 300° to 4.2°K, obs. 8=2058

RbI, temp. dependence 8=13591

Si, third order, lattice theory 8=13261

3% Si-Fe, upper yield stress rel. to etch pitting experiments 8=5065

TaC_{0.90}, by u. s. pulse velocity method 8=8861

TlBr, calc. from vel. of acoustic waves 8=17833

TlBr, temp. and pr. dependence, obs. 8=2068

UO₂, shear modulus, temp. depend., calc. 8=13610

V₃Si type compounds in cubic phase, temp. depend. explanation 8=13611

measurement

automatic recording torsion pendulum for moduli meas. 8=5006

dielectric, from lattice theory calcs. 8=13177

dynamic modulus at elevated temp. using a rapid heating technique 8=5005

inorganic filaments, Young's and shear moduli meas., and data for W and B 8=5003

metals, recording equipment low frequencies 8=8784

monolayers, by capillary ripples 8=1514

plastic, glass-reinforced, at cryotemps. 8=17840

resonant frequency method, rel. to sintering kinetics, four oxides 8=17027

Elastic constants—contd**measurement—contd**

- solid solns., from exam. of diffuse background scattering of X-rays 8=13359
- solids, anisotropy parameter by polarised u. s. frequency method 8=2039
- ultrasonic pulse attenuation method 8=17715
- Young's modulus variation at kHz frequencies using simplified bridge system 8=5007
- Ba(NO₃)₂·H₂O, single crystal, coeff. in range 80–3000°K 8=5051
- CsBr, elastic and fourth order elastic constants and nonlinear pressure dependence 8=13544
- CsBr, nonlinear pressure var. and fourth-order obs. 8=13544
- CsCl, nonlinear pressure var. and fourth-order obs. 8=13544
- CsI, elastic and fourth order elastic constants, and nonlinear pressure dependence 8=13544
- CsI, nonlinear pressure var. and fourth-order obs. 8=13544
- Mg-Th alloy, by pulse transmission technique 8=5080
- α-Mn, polycrystalline betw. 4.2–300°K 8=17501
- Si single crystal between 25 and 300°C from u. s. wave velocity 8=17830
- β-SiC whiskers, Youngs modulus 8=22392

Elastic deformation

See also Bending; Stress/strain relations; Torsion.

bars, rotating, relation between components of strain tensor 8=19397

- beam, loaded and supported at two points 8=10545
- beams, iterative procedure 8=8797
- brass, Bauschinger effect recovery mechanisms 8=17775
- circular inclusions undergoing dimensional changes in elastic half plane 8=6058
- circular plates, uniformly loaded, various supporting conditions, deflections 8=14951
- controllable, of incompressible simple materials 8=13509
- cylinders, orthotropically stiffened, instability under torsion loading 8=19393
- cylindrical shell in elastic casing, stress and displacement fields 8=10538
- earth, free nutation damping and relaxation time 8=2569
- elliptic inclusion in orthotropic stress matrix 8=6057
- finite, propagation of plane loading wave in solid 8=3029
- indentation of sheet, solution of integral equation 8=2920
- inverse deform. infinite elasticity 8=14953
- microdeformation of solids, measuring technique 8=22273
- piezoelectric disc with inhomogeneous rigid inclusion 8=10542
- polyurethane foam plastic, characts. 8=22261
- post-buckling, imperfection-sensitivity, gen. stat. theory 8=19396
- prismatical bar, magnetostriction 8=10552
- rod, linear loading, matrix algorithm for differential eqn. 8=14931
- shell, circular, thick walled, radial oscillations, analysis 8=144
- shells, non-shallow, linear theory of undamped solns. 8=6056
- steel, type 1H18N9T, austenitic, mag. qualities, and influence of plastic deform. 8=9291
- strain-gauge measurements, advantages of analogue computer treatment 8=10476
- stress analysis of plates with stiffened perforations 8=10546
- stringed instruments, analysis of bridge behaviour 8=15070
- Al alloy, up to fracture under reversed loads 8=17759
- Au nuclei on MoS₂ substrate, strain nucleus size and misalignment dependence 8=8823
- Cu, Bauschinger effect recovery mechanisms 8=17775
- Fe-Ni(35 wt. %)-Cr(0–20 wt. %) alloys (in as-cold worked state), strain gauge factor in relation to electrical and magnetic properties 8=9006
- Fe-3%Si crystal, dislocation movement 8=17661
- Ge, rel. to lattice energy, elastic consts., electron distrib., internal strain 8=13576
- Mo crystals, at slow rates of strain 8=13587
- NaI, elastic tensor of gradient elec. field induced by uniaxial stress, n. m. r. obs. 8=13014

Elastic fatigue

- ball bearing, flanged, mounted, Weibull plot of contact fatigue data 8=17741
- fracture, anal. of initiation and propag. of cracks 8=5030
- fuel element with variable axial mechanical stress of canning tube, simulator 8=20896
- high-cycle, new failure theory 8=5029
- metals, crack growth, dislocation model 8=17740
- metals, and elevated temp. creep, correlation of data 8=2060
- metals, mechanism at elevated temperatures 8=8806
- polymethyl methacrylate, cycle dependent fracture 8=2073
- rolling bearings, identification of potential failure nuclei 8=17749
- steel, austenitic stainless, in different stages, dislocation structure 8=22205
- steel, C, crack propagation, atmosphere effect 8=17794
- steel, Cd plated, fatigue strength and delayed brittle failure 8=22361

Elastic fatigue—contd

- steel, cyclic hardening 8=22363
- steel, limit, correlation with true stress-true strain behaviour 8=17783
- steel, under triaxial stresses, influence of principal stress, apparatus design 8=5068
- stress-strain curves under variable stresses 8=14955
- thin walled shells, supported, pressurized, anal. of short endurance fatigue 8=17716
- Al alloy, effects of thin anodic oxide films 8=2049
- Al alloy, surface bubble formation during fatigue, rel. to humidity 8=4729
- Al, 0.5–0.85 Tm°K 8=8806
- Cu, cracks, initiation 8=5058
- Cu, fatigued at low strain amplitude, surface and interior structure relationships 8=17774
- Cu, life improvement by cyclic strain dispersal, obs. 8=5031
- Fe commercial, microcontours, wide temp. range, in vacuo 8=2053
- Fe, intergranular weakness rel. to fatigue damage 8=5060
- Ni-base alloy, fatigued at several temps., dislocation structure 8=4981
- Ni-SPAN-C alloy 902, vacuum remelted versus air-melted, for Bourdon tubes 8=17822
- Ni-2ThO₂, dispersion-strengthened, cyclic deformation behaviour 8=13597
- Pb, 0.5–0.85 Tm°K 8=8806

Elastic limit

See also Slip.

- b. c. c. metal, crystallographic study of yield condition 8=17727
- elastoplastic impact on rigid targets, direct anal. 8=17728
- energetics criterion 8=8789
- HK-40 alloy, creep-rupture props. to 2000°F 8=17755
- metals, repeated discontinuous yielding, mechanics 8=22274
- stainless steel, type 310, creep-rupture props. to 2000°F 8=17755
- steel structure rel. to design 8=8846
- Al, quenched, aging temp. effect 8=13530
- CuZn(ε brass) yield strength, hydrostatic extrusion effects obs. 8=5059
- Fe-Al alloys, yield effect from elevated temp. constant strain-rate tests 8=13555
- Fe-30%Cr, yielding and fracture 8=13558
- LiF crystals, optically determ., in temp. range 300–1.4°K 8=5076
- 3% Si-Fe upper yield stress rel. to etch pitting experiments 8=5065
- TiNi yield strength, hydrostatic extrusion effects obs. 8=5059

Elastic losses. See Internal friction.**Elastic relaxation**

See also Creep.

- α-brasses, props. and internal friction 8=13552
- alloys, Zener relax. 8=5009
- metal wires, recording accurate Snoek spectra at low freq. 8=8786
- polymers, rel. to structure and viscoelasticity 8=8869
- strength, direct measurement 8=13500
- Al-0.25 wt. % Fe, rel. to internal friction 8=5049
- αAgZn, Zener relax. 8=5009
- α-Fe, (b. c. c.), torsional, impurity-induced internal friction peak (Snoek's peak), anisotropy 8=13572
- Fe; purified, amplitude-dependent internal friction and induced modulus defect 8=13557
- Fe-V-C Snoek peak, anomalous obs. 8=13559
- In-Tl f. c. t. alloy, atomic relaxation 8=22375
- LiNbO₃, shear-wave attenuation 8=2059
- Si-Fe, (b. c. c.), torsional, impurity-induced internal friction peak (Snoek's peak), anisotropy 8=13572

Elastic waves

See also Acoustic waves; Seismic waves.

- accelerative, in material of finite thermal, and infinite elect. conductivity 8=15042
- acceleration, in viscoelastic mats., calc. 8=10570
- antiferromagnets, coupled magneto-elastic waves 8=18368
- attenuation, pulses in media with coeff. proportional to freq. or freq. squared 8=10743
- axial shear waves, radial propag. in nonhomogeneous elastic media 8=3026
- bars, circular, cylindrically orthotropic, propag. 8=19514
- boundary between viscoelastic media, reflection and transmission 8=6129
- circular cylindrical shell closed at one end by elastic plate, natural freqs. and mode shapes 8=15034
- comment 8=15040
- composite bar of short soft section glued to long hard one, response at junction 8=19395
- in conducting plate, magnetoelastic effects 8=10708
- coupled thermoplasticity, continuity at wave fronts 8=10577
- couple-stress effects, in elastic half space 8=6131
- crystal, ideal, mechanical perturbation propag. and phonon spectrum 8=13317
- cylinder, solid isotropic conducting, magnetoelastic vibrs. 8=13499
- diffraction by parabolic cylinder, wave function expansions and perturb. method 8=19525

Elastic waves—contd

- diffraction by spherical cavity, anal. in shadow zones 8=19518
- elastic-viscoplastic semi-infinite body, loading and unloading biwaves, numerical analysis 8=10565
- elastic-viscoplastic semi-infinite body, propag. of loading and unloading biwaves 8=10564
- elastic-visco-plastic semi-space, plane biwaves 8=10569
- elastoplastic stress waves, cylindrical and spherical, soln. by unified direct anal. 8=14952
- extensional in bars of rectangular cross section 8=15044
- excitation, freq. and size resons. 8=10710
- flexural, plate, oblique incidence on slender obstacle 8=19521
- Fraunhofer diffraction phenomena 8=15043
- gravitational perturbation rel. to S and P pulses and dispersion curves 8=3030
- guide, cylindrical, phase velocity and damping of longitudinal normal modes 8=19520
- laser excit. threshold for longit. and transverse waves 8=17831
- in linear elastic bars, rectangular, dispersion of longit. or extensional waves 8=19515
- loading and unloading biwaves in elastic-visco-plastic body, strain hardening effect 8=17718
- longitudinal and transverse, interaction 8=10705
- Love waves, propag. in anisotropic medium with hexagonal symmetry 8=23206
- magnetoelastic, in pulsed magnetic fields 8=156
- magnetoelastic, scattering from surface of ferromagnetic medium 8=2301
- in nonconductors, influence of propag. discontinuity in heat supply and body force 8=19517
- with one space variable, soln. by method of characteristics 8=19519
- in piezoelectric semiconductors, propagation and amplification 8=9088
- piezoquartz, surface waves 8=17832
- plane compressional step wave, scatt. by circular obstacle, appl. of Kirchhoff's integral eqn. 8=19523
- plane elastic-plastic waves of 1-dimens. strain, propag. anal. 8=19522
- plane strain-elastic wave propag. at flexibly bonded interface 8=19524
- plastic propagation in a bar 8=2928
- propagation, effect of mag. field, body forces and normal mechanical pressure 8=10703
- propagation of plane loading wave in solid for finite deformations 8=3029
- propagation and reflection in elastic/visco-plastic beams 8=14954
- propagation rel. to identification of one-dimensional medium 8=10702
- quartz, laser excit. threshold for longit. and transverse waves 8=17831
- quartz, X-cut, Rayleigh surface wave vel. 8=155
- quasi linear dynamic eqn., soln. 8=10550
- Rayleigh, conservation of energy 8=10707
- Rayleigh, in liq. layer, on anisotropic half-space 8=6132
- Rayleigh, reflection of light and its resultant scattering 8=9490
- Rayleigh waves, scattering, at elastic body random boundary 8=10700
- Rayleigh, wedge transducer 8=182
- reflection and diffraction in cylindrical wedge 8=10706
- resonance of shock wave, longitudinal, in elastic-plastic bar 8=15052
- in rocks, propag. and absorpt. with rupture 8=13515
- rel. to seismology, refl. and refr. coeffs. of thin-layered media 8=158
- scattered, freq. depend. of amplitudes 8=3027
- scattering of long wavelength plane waves by homogeneous obstacle in infinite elastic medium 8=22262
- scattering by rigid bodies, calc. 8=3031
- seismic wave propag. in friable medium, model 8=157
- shear in viscoelastic half-space 8=15035
- small source radiation, Green's function 8=153
- spherical, finite amplitude, calc. 8=19516
- spherical, propag. and reflection in viscoelast. medium, closed form soln. 8=10567
- strain and velocity meas. 8=3025
- stress waves, laser-generated in pressure bar, meas. 8=6130
- stress waves, plane, produced by moving load in elastic plastic medium 8=10566
- surface, excitation by transient surface heating, piezo-electric and nonpiezoelectric 8=11720
- surface, on optical and acoustical optical branches 8=15041
- surface, travelling, in finite systems 8=10701
- thermo-, non-coupled, particular soln. of nonhomogeneous fundamental set of eqns. 8=10576
- transmission in system of corrugated layers 8=13498
- transmission through a stratified medium 8=13497
- transverse, rotation of polarization by gyrotropic layer 8=3376
- visco-plastic-elastic, longitudinal in finite bar, resonance 8=10568
- visualization of quasilongitudinal and quasitransverse elastic waves 8=8788

Elastic waves—contd

- CdS layered system on Ge surface wave behaviour 8=8850
- LiNbO₃, shear-wave attenuation 8=2059
- YFe garnet, dispersion, optical investigation 8=2070

Elasticity

- See also Compressibility; Mechanical strength; Stresses, internal; Thermoelasticity; Viscoelasticity.
- aeolotropic elliptic plate, stress distribution compressed along major axis 8=47
- alkali metals, nonlinear continuum theory based on quantum mechanics 8=17711
- anisotropic half-space, Boussinesq problems 8=10540
- annulus, circular, aeolotropic non-homogeneous, radial vibrations 8=2922
- asymmetric mixed boundary value problems for half space with a cylindrical cavity 8=6053
- beams, curved, instability, extensible and inextensible theories 8=10547
- bending and buckling of frame system under its own weight 8=6042
- bending thin plates with nonlinear stress-strain relation 8=10548
- bodies, axially symmetric, stationary dynamic problems in thin range of very short waves 8=10537
- circular hole, tangential stress analysis 8=19391
- circular inclusions in elastic half plane 8=6058
- complex structure with spatial dispersion 8=52
- composites with buckled microfibrils 8=22289
- composites, reinforced, fibre-matrix interaction forces calc. 8=22268
- contacting solid bodies, measurement 8=56
- couple stress theory and deformation of microinhomogeneous bodies 8=42
- critical loads, estimation 8=10539
- deformable surface, theory, simple force multipoles 8=2918
- dielectrics thermodynamic pots. at finite deform. 8=10541
- disturbance, longit. propag., in thin inhomogeneous rod 8=2921
- Earth's mantle, anelastic props. from seismic wave attenuation 8=14543
- Earth model, elastic and viscoelastic behaviour 8=14948
- elastic body containing small rigid spheres 8=6055
- elastic-modulus effect in interaction of point defects with dislocation ribbons 8=17603
- elastic-plastic analysis, numerical methods 8=19400
- elastic-plastic continua, eigenmodal deformations crit. conds. and charact. 8=13999
- elastic rings, equilibrium states 8=51
- elastic solid permeated with non-Newtonian fluid 8=19381
- elastic systems, stability and oscillations, book 8=15030
- elastoplastic stress waves, cylindrical and spherical, soln. by unified direct anal. 8=14952
- elliptic inclusion undergoing dimensional changes in orthotropic stress matrix 8=6057
- flush nozzles in pressure vessels, stress analysis 8=10557
- glasses, fibre elongation rel. to approx. of viscosity-temp. data 8=17725
- graphite:ICl, impurity-dope effects on anelasticity 8=13541
- half-space with inclusion, contact problems 8=2923
- indentation of sheet, solution of integral equation 8=2920
- isotropic ceramic, conversion relation table 8=8783
- linear dissipation model with Q almost freq. independ. 8=23204
- liquid films, rel. to thickness and composition, obs. 8=12776
- membranes, tensile instability at large deformations 8=13503
- metals, plastically deformed, residual stresses and latent elastic strain energy 8=22269
- modulus meas. by electronic level indicator 8=54
- nonconductor, amplitude of induced shock and acn. waves, rel. to propag. discontinuity 8=19517
- orthotropic plate parameters of stiffened plates and grillages 8=49
- plate under pressure, polygon-circle paradox 8=19390
- plates, thin, rib-stiffened carrying concentrated masses, vibrations 8=19496
- pulse loading, unloading boundary 8=19385
- polymerized material, statistical mechanics 8=8875
- polymers, cross-linked, under tension 8=17845
- polymer melts 8=16748-9
- polyurethane foam form., surface elasticity 8=8156
- post-buckling, imperfection-sensitivity, gen. stat. theory 8=19396
- quartzite, precursor decay for cylindrical and spherical flow 8=13605
- quasi linear dynamic eqn., soln. 8=10550
- Raman-active vibrations and internal-strain rel. to elasticity and piezoelectricity 8=5013
- rectangular retaining wall, with pressure of loose material, piezoelectric analogue of elastic problems 8=6054
- rocks, displacement field in horiz. layer of elastic and granular material 8=2567
- rod, inhomogeneous, internal stresses and loading capacity 8=10553
- rubber sheet with hole, stress conc. under axially symmetric loading 8=22263
- second order, bending of cylinder 8=10536

Elasticity—contd

- semi-infinite plate with circular inclusion 8=10551
- shallow shell equations; displacement, stress function and mixed solutions 8=48
- shell, axisymmetric cylindrical, effects of anisotropy 8=19388
- shells with variable curvatures, bending 8=19387
- shock loading of nonlinear material 8=5008
- shock-velocity-particle-velocity relationship 8=8787
- sound waves in non-simple elastic materials 8=19389
- space anisotropy, soln. by linear sources 8=14936
- stability of equilibrium, elastic body 8=6040
- steel, Murnaghan's n constants by ultrasonic waves 8=13568
- strain measures, finite, correlation 8=53
- stress distribution in thin strip material 8=5011
- stress state of closed cylindrical shell with doubly periodic holes system 8=19398
- support of parallelogram plates, rel. to bending 8=19384
- thermodynamic props. of elastic materials 8=50
- thin circular plates, symmetrical bending 8=10555
- thin elastic disk, numerical determ. of stress field 8=6059
- three-dimensional problem, Ritz method 8=19386
- toroidal shell, perturbation theory 8=10543
- torsional vibrations of non-homogeneous spherical and cylindrical shells 8=19513
- vibrations of plates on elastic foundations 8=10549
- waves, extensional, in bars of rectangular cross section 8=15044
- "whisker" straining devices, two, for low temp. 8=22258
- Al, elastic modes, e. m. excitation 8=17760
- B₂C, effect of low porosity 8=22313
- Fe-Al, elastic stiffness coefficients, experimental results and thermodynamic analysis 8=5062
- Ni-ThO₂, damping capacity rel. to magnetoelectricity, 20-500°C 8=17821
- ZnS, hexagonal, stiffness conductivity dependence, corrections 8=17838

liquids

- See also Compressibility/liquids.
- elastico-viscous fluid, drag on oscill. sphere 8=21557
- Gibbs, Sheludko eqn., correction 8=7997
- liquid crystals, theory 8=1527
- polyethylene melt, steady flow elasticity 8=12735
- H-bonded, shear rigidity 8=1537
- K, wavenumber-dependence of elastic moduli 8=1499
- Mg, wavenumber-dependence of elastic moduli 8=1499
- Na, wavenumber-dependence of elastic moduli 8=1499
- Rb, wavenumber-dependence of elastic moduli 8=1499

Elastomers. See Rubber.**Elastoplasticity.** See Plasticity.**Elastoresistance.** See Piezoresistance.**Electrets**

See also Electrostatics.

- carboxylic acid C₂₀, persistent electric dipole moment obs. at -78°C 8=13890
- ice, persistent electric dipole moment obs. at -78°C 8=13890
- paraffin wax, persistent electric dipole moment obs. at -78°C 8=13890
- photoelectret regime, trap levels rel. to stable inner polarization 8=5372
- photoelectret state correl. with Gudden-Pohl effect 8=5679
- polymer film, trapping of electrostatic changes in surfaces 8=13891
- shellac wax, surface charge obs. 8=13892
- tetradecanol, persistent electric dipole moment obs. at -78°C 8=13890
- HgI₂ crystal, polarization vs field strength under light excitation 8=5373
- ZnS, photoelectret state correl. with Gudden-Pohl effect 8=5679

Electric breakdown. See Breakdown, electric.**Electric charge**

See also Space charge.

- capacitor discharge switch 8=15188
- charge independence graphs, elementary particle reactions 8=645
- with dielectric and conductors, firmly connected, rel. to higher-order effects in dielectrics 8=2234
- on drops ejected by bursting air bubbles at surface of water 8=8117
- droplets, electrohydrodynamically sprayed, rel. to mass 8=4519
- e, time invariance 8=15690
- e², limit on variation with time 8=15691
- fundamental unit constancy, geological evidence 8=15728
- fundamental unit time var. from Re¹⁸⁷, Os¹⁸⁷ terrestrial occurrence 8=15826
- insulators, mechanism of discharging by ionized air 8=15192
- linear, in piezoelectric crystals, and fields of dislocations 8=5375
- multipole interactions, group theoretical derivation 8=15190
- nature, by rubbing crystals with metals 8=18158
- neutrality of matter, macroscopic determ. 8=11455
- particles, in electrostatic precip., charge magnitude 8=19719

Electric charge—contd

- on rain drops in warm clouds over Hawaii 8=9858
 - static, dissipation and generation on dielectrics in vacuum 8=18159
 - static, measuring instruments 8=279
 - surface density on cylindrical conductor, Fredholm integral eqn. 8=15189
 - Ge, dust, effect of crushing period 8=13813
 - Ge, dust, effect of crystal lattice defects 8=13812
- Electric discharges.** See Discharges, electric.
- Electric fields**
- See also Electromagnetic fields.
- of accelerating charge, for $v < c$ 8=319
 - in auroral ionosphere, parallel to mag. field, expt. investigation 8=23354
 - complex 2-dimensional, approx. calc. 8=19716
 - components of complex, near-zone e. m. fields, new meter 8=269
 - in conductor with temp. depend. conductance 8=3151
 - dipole in motion 8=10505
 - disc beam optics 8=19783
 - double field meter, guarded, for atm. space charge meas. 8=15163
 - electrode produced, computer calc. of uniformity 8=16395
 - electrostatic, approximate calc. method 8=19717
 - electrostatic lens, cylindrical three electrode field analysis 8=19778
 - electrostatic sector fields, ion image aberrations 8=19802
 - field mill, sign-discriminating 8=266
 - gravitationally induced near metals 8=5159
 - homogeneous, in cylindrical set of electrodes, elimination of harmonics 8=15191
 - meas. using probe, gives audible signal for lab. demonstration 8=10822
 - plasma microfield calc. 8=12479
 - potential fields, two dimensional, for given sources, simulation by electrostatic induction method 8=6253
 - in semi-infinite medium whose conduct. varies laterally, calc. 8=19756
 - steady current in strong electric fields 8=22425
 - waveguides with uniform, strength 8=15419
 - BaTiO₃, field depend. of dielect. consts. at 58.2 GHz 8=13879
 - Cu, gradient due to charge density redistribution around dislocations 8=5176
 - He gas, var. across l. p. discharge 8=16415
- effects**
- alkali metal, emission spectra 8=1895
 - beam-plasma system, interaction suppression 8=16507
 - Boltzmann equation for electrons interacting with acoustic waves 8=13343
 - colloid solns., light scatt., rot. diffusion consts. determ. 8=8073
 - diphenyl, crystal growth 8=21949
 - discrete charges in crossed elec. and mag. fields, rotating ring stability 8=6291
 - e. p. r. line profile parameters in crystals 8=18399
 - epoxy compound, strength rel. to elec. cond. 8=22498
 - ethyl acrylate polymerization by a. f. field, obs. 8=9709
 - ferrites, 9400 Mc/s pumping rel. to spin wave excitation 8=18355
 - flames, vibrating, Schlieren survey 8=6217
 - on flute oscillations of tenuous plasma 8=21378
 - frequency modulated, homogeneous plasma electron distrib. function 8=16526
 - gas flow subsonic with crossed mag. field 8=16659
 - gas, partially ionized, e. vel. distrib. function 8=12423
 - ion movement in gases 8=7705
 - latent image of particle track, pulsed-field erasure 8=11330
 - liquid dielectrics, on thermal convection 8=21659
 - liquid drops disintegration and electrification 8=16782
 - MHD, discontinuities 8=15360
 - Mössbauer spectra in fluctuating environment, random gradient variations 8=13018
 - n. m. r. and n. q. r. Stark effect, rel. to electrons 8=14133
 - particle behaviour during electrostatic precipitation, photographic study 8=10836
 - periodic, reduction factor for space-charge field of electron beams 8=322
 - piezoelectric semiconductors, a. c. effects on non-linearity of props. 8=18022
 - plasma, inhomogeneous and imperfectly Lorentzian, non-linearities 8=16480
 - polyethylene film, I-doped, current oscillations at high field strengths 8=8985
 - ponderomotive forces on particles in conical field 8=3149
 - Rochelle salt: Cu²⁺ e. s. r. spectrum influence through external elec. field 8=14111
 - rock salt, luminescence, in ultra-strong fields 8=23059
 - ruby, linear Stark effect in U absorpt. band 8=9501
 - semiconductors, polar, electron mobility at intermediate and high fields 8=18005
 - semiconductors, tunneling in crossed and parallel elec. and mag. fields 8=5227
 - solids, e. transport, including lattice interaction 8=2078
 - solids, ion transport 8=21813
 - sol, birefringence 8=12878
 - 2, 6 di-isopropyl phenol, spectral shift of OH vib. absorpt. line 8=1572

Electric fields—contd**effects—contd**

- vinyl monomers, liquid, polymerization by a.f. field, obs. 8=9709
- Al_2O_3 , Cr^{3+} - Cr^{3+} , luminescence effect 8=2475
- Al_2O_3 : Cr^{3+} , e.p.r. and acoustical mag. reson., profiles 8=18406
- BaTiO_3 , absorption edge anomalous shift 8=13882
- BaTiO_3 , absorpt. edge shift, temp. dependence 8=13883
- Fe-Cr, electrotransfer of components at 1150-1400°C 8=4952
- n-GaAs-Al Schottky barriers, photoelectric barrier energy dependence on electric field 8=13924
- Ge, photon-assisted magnetotunnelling in parallel and crossed, elec. and mag. fields 8=5260
- H⁻, hyperpolarizability, computer calc. 8=20942
- He, hyperpolarizability, computer calc. 8=20942
- n-InSb, electron mobility at intermediate and high fields 8=18005
- KBr, electron transport props. in high fields at low temps. 8=2264
- Li⁺, hyperpolarizability, computer calc. 8=20942
- NaCl crystals, F-centre prod. 8=13463
- O_2 desorption from W, inert-gas enhancement 8=17176
- PbZrO_3 polycrystals, temp. changes of polarization at phase transition 8=13888
- Pu^{239} , e binding energy var. 8=4085
- electric strength**
See also Breakdown, electric.
polyethylene, degradation by partial discharge 8=21214
concrete, heat resistant, volume breakdown and surface flashover voltages, effect of atmosphere 8=13900
 Al_2O_3 films, rel. to thickness 8=5351
- electrical conduction.** See Conduction, electrical; Conductivity, electrical.
- electrical current.** See Current, electrical.
- electrical measurement**
Entries describing measurement methods for specific electrical quantities and effects may also be found listed under the various headings for the subjects concerned.
- a.c., comparison using thermistors 8=267
- cathode-ray oscilloscopes, use in schools 8=10818
- capacitance, absolute meas. by cross capacitor 8=15169
- capacitive transducer, effect of air compression between plates 8=7892
- capacitors, reference, temperature characteristics 8=10820
- cavities, bimodal, wide-band balancing for microwave props. meas. 8=15387
- conductivity of anisotropic mats. with small specimens 8=5156
- critical currents of superconds., with self-balancing current regulator 8=9039
- currents, automatic comparison circuit 8=10826
- current in exploding-wire circuits 8=15171
- current in high-voltage r.f. plasma discharges 8=4277
- digital trace reading potentiometer 8=10816
- direct current on floating pot. 8=10827
- d.c. voltage, by superconducting parametric amplifier 8=15166
- discharge magnitude, power capacitors, effect of self-reson. 8=21228
- double field meter, guarded, for atm. space charge meas. 8=15163
- e/m, modification of experiment 8=10471
- electric drive in cyclotron meas. dev., use of working mag. field 8=11347
- electric-field-strength meter, for components of near-zone e.m. fields 8=269
- electrometer, insulated gate field effect transistor 8=5336
- electrometer, theory and practice 8=3132
- electrometers, use of FET operational amplifiers 8=3131
- electron conc. in plasma, homodyne phase meter 8=7785
- electronic digital integrator 8=10817
- exponentially decaying signals, digital method 8=17922
- gases, electron drift velocity 8=12694
- guarded sphere as gauging electrode in length metrology 8=10823
- h.f. electronic voltmeters, testing and calibrating 8=15164
- impedance, polarographic cell 8=5735
- LCR circuit, ferro-reson. at low freq. 50 Hz, potential difference across inductance 8=6242
- low temp. resistivity meas., eddy current method, contactless, 1-10 000 nΩ cm range 8=5162
- magnetic pickups effects on input transformers of measuring devices 8=10864
- magnetic potentiometer, high precision, description and appl. 8=10819
- oscilloscope, intensity modulation effect on multi-parameter display 8=6238
- piezoresistance of semiconductors 8=268
- potentiometer applications based on Poggendorf's 2nd method 8=3134
- potentiometer, 10⁻⁹ to 10 volts, account 8=19705
- potentiometers, non wire-wound, effective resolution 8=19706
- radiometer signal compensation 8=3271
- random signal quantization effect 8=6260

Electrical measurement—contd

- resistance in series circuit, errors 8=17917
- resistance, very high, electrometric apparatus 8=19707
- resistance, standard ohm 8=19708
- resonators, filled with TiO_2 dielec. discs, h.f. props. 8=19829
- sampling oscilloscope, appl. to meas. of time differences in milli- to picosec. range 8=3138
- semiconductor devices, scattering and transmission parameters 8=9139
- semiconductor, four probe resistivity meas. wander error 8=22577
- single channel recorder, device for conversion to multi-channel sequential recorder 8=6239
- small d.c. voltages, with supercond. parametric amplifier 8=3135
- standard resistors, effect of power dissipation on performance 8=10825
- superconducting bolometer current modulator 8=22573
- voltage meas. using quantum interference device, 10⁻¹⁵ volt sensitivity 8=15165
- voltage ratio, semiconductor magnetoresistance method 8=10821
- voltage, standard cells, electrostatic method 8=10824
- voltage, transient waveform, by Kerr cell system 8=6240
- voltmeter, use of Josephson radiation from superconducting point contact 8=2181
- Ar shock layer, e density 8=21265
- N_2 , electron drift velocity obs. 8=12695
- Electrical properties of substances**
See also Individual properties, e.g. Conductivity, electrical; Dielectric properties of substances, etc.
- benzene, liq., electron-injection from tunnel junction, effective barrier 8=257
- carbon blacks, sample prep. 8=2135
- chalcogenide glasses 8=18028
- conducting mats., rel. to detect. of macroscopic defects 8=8706
- conductors, e. m. wave propag. and light-electric fields cyclotron res. 8=5155
- conference, Dalas 1967 8=12480
- corundum plates, domains, and effects rel. to plate-like whisker formation 8=21972
- current-field non-linear relations in Shubnikov-de Haas conditions 8=17923
- cyclohexane, liq., electron-injection from tunnel junction, effective barrier 8=257
- electrical conduction properties, conference, Pasadena USA (1966) 8=13701
- glasses, chalcogenide, Hall effect meas. 8=13789
- glasses in $\text{PbO-Al}_2\text{O}_3\text{-B}_2\text{O}_3\text{-SiO}_2$ system temp. and comp. dependence 8=18170
- isotropic media, anisotropy induced by intense laser beam 8=8106
- liquid alloys, Hall coeff. meas. 8=16880
- liquid conductors, flow in annular gap, circumferential accn. due to Lorentz force 8=16755
- liquid crystals, review of data 8=1527
- liquid membranes, from ion pair form. and transport 8=4560
- liquid metals, polyvalent, absolute thermoelec. power 8=16881
- liquids, chalcogenide, Hall effect meas. 8=13789
- liquids, electronic wave functions, coherent-wave approx. 8=7998
- macroscopic body, determ. of elect. neutrality 8=11455
- metals, liquids, electronic structure 8=12899
- metals, liq., electron theory and liq. state theory, correl. and meeting points 8=16786
- non-metallic crystals, space-charge-limited transient currents 8=5161
- nylon 66, static, electrification rel. to metals 8=5356
- oxy-acetylene flame, e. m. f. between nozzle and metal target 8=12696
- photo-semiconductors, microwave impedance, dynamic behaviour 8=5288
- polar liquids, collective oscillations, theory 8=21721
- polyethylene film, I-doped, current oscillations at high field strengths 8=8985
- rocks, saturated, resistivity changes in fracture and frictional sliding, obs. 8=23222
- simple cell and mass spectrometer apparatus 8=8668
- solids, current carrier mobility, effect of sonic wave 8=22415
- suspensions, relaxation of transient electric birefringence 8=16899
- thin films, colloquium, Orsay, France (1967) 8=22499
- trace characterization basis 8=18756
- trace characterization basis 8=18757
- transition-metal molybdates, and structure 8=13296
- Ag and Ag alloy contacts, effect of H_2S contamination on contact resistance 8=22512
- Ar, solid and liq. free-carrier drift-velocity meas. by oscilloscope 8=8119
- B, polycryst., thermopower and resist., temp. and press. effects 8=18210
- Bi, liq., electromigration of small amounts of Ag, Cd, In and Sb 8=12815
- Bi-MnBi eutectic single crystal growth dependence 8=8402

Electrical properties of substances—contd

- CdSb, transport properties, temp. range, liquid He to 500°C 8=13698
 CdS, Cu-diffused insulating layers, behaviour 8=13792
 n-CdSe, 4.2 to 300°K 8=13796
 CdSe, stoichiometric, in thin film, and structural and optical props. 8=17127
 CdSnAs₂ and CdGeAs₂, semiconducting, rel. to high-temp. modifications 8=21842
 GaAs injection lasers with compensated p-type region and optical props. 8=15482
 GaP, large crystals, grown from soln. 8=17234
 GaP:S 8=13804
 GaP:S 8=13805
 GaP:Zn 8=13806
 He, liq., electron-injection from tunnel junction, effective barrier 8=257
 Hg-In alloys, liq., electronic struct. and optical consts. 8=16846
 Hg-In, electron transport props. 8=8005
 Hg, liq., electronic struct. and optical consts. 8=16846
 InOF, temp. independent conductor 8=8414
 n-InP, effect of As doping 8=9113
 In-Sb liq. alloys, cell for electrotransport meas. 8=12816
 InSb, thin films, rel. to temp. 8=8323
 KCl-KBr solid solutions 8=22504
 KNbO₃-AgNbO₃ system, and X-ray and thermal expansion studies 8=21823
 Kr, solid and liq. free-carrier drift-velocity meas. by oscilloscope 8=8119
 LiCl aqueous solns., formation of pulse discharges 8=4608
 MnSb, existence region and mag. props. 8=22820
 Ne, solid and liq. free-carrier drift-velocity meas. by oscilloscope 8=8119
 NH₄Cl, solutions, occurrence during freezing 8=1587
 NH₄OH, solutions, occurrence during freezing 8=1587
 Ni and GaAs surface barrier diodes 8=22629
 Pb-Sn liq. alloys, cell for electrotransport meas. 8=12816
 Pb(Zr, Sn, Ti)O₃ ferroelectric ceramics, Nb-doped 8=2246
⁵¹Si, atomic systems, magnetoelec. susceptibility 8=4053
 Si epitaxial films on α -alumina 8=9121
 n-Si:Au 8=13830
 SiC, cond. and Hall coeff. 8=9122
 SiC, vapour-deposited films 8=17137
 Ti₂O₃ single crystal, and growth from melt 8=4817
 Xe, solid and liq. free-carrier drift-velocity meas. by oscilloscope 8=8119
 Yb-Sb phases 8=22754
 ZnS:Cu, irradi., rel. to electroluminesc. quenching and stimulation 8=9640
 ZnSb and ZnSb-CdSb mixed crystals, transport properties, temp. range, liquid He to 500°C 8=13698
 ZnSe interface with electrolyte 8=13837

Electrical units. See Units.**Electricity**

- 50 kV ceramic feed-through plug and socket connector 8=15170
 power transmission network, d.c. 3-wire, relaxation method solution 8=281
 Ni-Mo-Fe core power line de-icing transformer core, obs. 8=22828
 project laboratory, advantages and disadvantages 8=15159

direct conversion

- advanced solar converter, performance rel. to design and mats. 8=15248
 chemical energy engines 8=19723
 collectors in Cs and Cs-Ba vapours, study of low work function region of Re, Mo, Ru and Nb 8=15213
 conference on power source, cells, fuel cells and thermoelectric generators Brighton, England 1966 8=286
 electric pulse, large, prod. by explosive mag. field compression 8=6261
 fuel cells, high temp. 8=9711
 fuel cells, isoporous electrodes 8=9717
 fuel cells, solid electrolyte, 700-1100°C 8=15198
 Gabor-type auxiliary discharge converter, cost of space-charge neutralization 8=15239
 heat radiation into electricity, efficiency 8=15249
 hydromagnetic, thermodynamics of 8=345
 ignited thermionic, ion generation mech. and electron energy distrib. functions 8=15221
 liquid vein m. h. d. generators 8=15207
 MGD generators, graphical display of local characts. 8=15382
 MHD, collision and gyration modes 8=288
 MHD converter, isothermic with electrodes in series 8=6270
 MHD devices using liquid metals 8=6263
 MHD electrical power generation, conference, Salzburg, Austria (1966) 8=15355
 MHD flow distortion by strong Hall effect and effect on power generation 8=15381
 MHD generation, status report 8=15201
 MHD generator 8=10839
 MHD generator, anal. of elec. cond. of high-void-fraction two-phase flow 8=15203
 MHD generator, effect of electrode ends on flow 8=3155
 MHD generator, elec. conductivity of high-void-fraction two-phase flow, expt. 8=15202
 direct conversion
 MHD generator, extreme value of voltage 8=6269
 MHD generator, induction type, fundamentals 8=6268
 MHD generator, liquid vein, sliding field 8=6264
 MHD generator, non-equilib. flow of conducting fluid in channel on sudden short-circuiting 8=6267
 MHD generator, rectangular channel, 2-dimensional flow analysis 8=15209
 MHD generator with peg walls, effect of internal short-circuiting 8=3157
 MHD generators and engines, boundary flow calc. 8=19725
 MHD generators, combustion fired 8=291
 MHD generators from superconducting magnets 8=3166
 MHD generators, liquid vein 8=6262
 MHD generators, review 8=19724
 MHD generators, stability of plasma, voltage oscills. 8=15208
 MHD generators, survey 8=290
 MHD induction generator, flat channel, linear, comparison of three analyses 8=15204
 MHD induction machine, general equations of sliding magnetic field 8=15383
 MHD liquid vein generators, power transfer study 8=6265
 MHD liquid vein generators, pump and flowmeter applications 8=6266
 MHD machines with flat channels, liquid metal efficiency 8=19727
 MHD, molten metal mixing, thermodynamics of cycles 8=294
 MHD power plant 8=19728
 MHD stations, open cycle, thermal efficiency and economics 8=293
 MPD generator, analysis in uniform state 8=10840
 MPD power generation, closed cycle, prospects 8=292
 noble gas mixture thermionic converters, with plasma generation fission-fragment ionization 8=15215
 nuclear reactor heat source, magnetogas dynamic and thermionic systems 8=295
 photoelectromagnetic receivers with optically polished thin elements, sensitivity and inertness 8=6275
 plasma diode, stationary regimes 8=296
 plasma, mag. press. generation of shock wave 8=15054
 plasma, r.f. power into thermal energy, diamagnetic press. obs. 8=12484
 plasma, weakly ionized, transport equations 8=3158
 prototype thermionic, with Re emitters, performance rel. to variable-spaced test diodes 8=15219
 reactor, Ar-filled, thermionic converter 8=298
 reactor for space flight, thermionic, parameters 8=1123
 semiconductor solar cells multistage, selection of optimum combination of materials 8=6277
 sliding-field liquid-vein m. h. d. generator 8=15205
 solar cells, calc. of optimum grid 8=3160
 solar cells, Conference, Florida USA 1967 8=9242-4
 solar cells, distributed model 8=9265
 solar cells for UK 3 satellite 8=19734
 solar cell props. integral covers effects, obs. 8=10854
 solar cell, surface radiative props., effect of scatter, rel. to collector design 8=1686
 solar energy, system of acquisition on space flights 8=10858
 superconducting electromagnets, appl. 8=6281
 supersonic nozzles, gas flow conversion to electrical energy 8=1456
 thermionic, appl. Monte Carlo method to transport processes 8=15246
 thermionic, arc mode operation, anal. 8=6274
 thermionic conversion specialist conference 8=19731
 thermionic conversion Specialists Conference San Diego USA October 1967 8=6273
 thermionic converter 8=19730
 thermionic converter, auxiliary discharge, with extra-electrode, design 8=15232
 thermionic converter, collector work function meas. rel. to Cs press. and interelectrode spacing 8=15243
 thermionic converter, classification of operating regimes 8=3159
 thermionic converter, cylindrical, appl. to nuclear reactors, performance and life test 8=15247
 thermionic converters, electron emission cooling, and optimum collector temp. 8=15236
 thermionic converters, performance, development of parametric eqn. for description 8=15237
 thermionic converters, planar, life-test results and failure mechanisms 8=15233
 thermionic converter plasmas, electron transport phenom., theory 8=15235
 thermionic converter, plasma measurements 8=7782
 thermionic converters, plasma physics, and nine regions of operation 8=15240
 thermionic converter with vapour deposited W emitter, and Mo collector 8=15230
 thermionic converter, vapour-filled, effect of multiple electrodes on efficiency 8=15231
 thermionic converters, V-A characts. in arc regime 8=6271
 thermionic converter, with W emitter, comparison of Nb and Ni as collectors 8=15228
 thermionic, determ. of time-depend. emitter temps. output power and efficiencies rel. to initial values 8=15218

Electricity—contd

direct conversion—contd

- thermionic diode effects of Ar on performance, expt. results 8=15216
- thermionic diode, influence of anode emission on efficiency 8=10841
- thermionic diode, optimization of emitter length 8=15323
- thermionic diode, V-I characts. with grooved-collector 8=15217
- thermionic diodes, structure of adsorbed layer of electropos. and neg. additives 8=17154
- thermionic, dynamic characts, analytical model and expt. 8=15229
- thermionic, effective collector work function variations, interpret. 8=15223
- thermionic emission, Cs-Ne, operation 8=300
- thermionic, (Mo emitter, Nb collector), in-pile tests with nuclear heating 8=15227
- thermionic, Mo emitters, UO_2 fueled, irradiation studies rel. to in-core converters 8=15226
- thermionic nuclear power plant for space flight 8=1122
- thermionic, nuclear reactor, heat transfer simulation apparatus 8=1134
- thermionic, reactor parameters 8=299
- thermionic, sheath-plasma-sheath type anal., boundary conditions 8=15222
- thermionic, space-charge distrib. in neutral plasma 8=16467
- thermionic, theoretical output and efficiency characts, using fundamental princs. 8=15220
- thermionic, transfer of electrons by negative ions 8=287
- thermionic, transport eqns. of 3-component plasma, using irreversible thermodynamics 8=15234
- thermoelectric, review 8=19733
- thermoelectric systems, thermodynamics 8=10844
- thermopile, semiconductor, stationary temp. field calc. 8=22685
- Ar-filled generator, I-V characts. rel. to contact PD between emitter and collector 8=6272
- CdS film solar cell, mechanism obs. 8=10847
- CdS solar cell deployable rigid-frame array, performance obs. 8=10845
- CdS solar cells environmental thermal cycling test obs. 8=10848
- CdS solar cells, thin film on Cu and plastic, characts. and stability 8=10855
- CdS thin film solar cell 8=19735
- CdS-Cu₂S solar cell, mobile impurity ions model 8=10846
- CdTe solar cells, spectral response and integrated array fabrication 8=10856
- CdTe solar cells, 28 V module and roll-up array 8=10857
- CdTe thin film solar cell 8=19735
- Cs, additive emitters, correl. to emission processes 8=15214
- Cs arc diode, effect of additive gases Kr, Xe and I, and Ar 8=15225
- Cs diodes, vapour pressure effect on electrode work function 8=18246
- Cs plasma converter, diffusion theory of Cs ions and electron migration 8=15212
- Cs plasma diode, meas. of pot. and particle energies 8=15210
- Cs plasma diodes, identification of dominant ion species 8=15322
- Cs thermionic converter, anal. of dominant ionic species 8=15211
- Cs thermionic converter, departure from Saha-Langmuir ionization reln. 8=15238
- Cs in thermionic converter, impurity states 8=10842
- Cs thermionic converters, electrode inhomogeneity influence 8=297
- Cs thermionic converter, use of O as steady-state electroneg. additive 8=15224
- Cs thermionic diode, electron temp. and ion density rel. to spacing and press. 8=15242
- Cu₂-Te-CdTe heterojunction, efficiency in solar energy conversion 8=6276
- GaAs solar cells, thin film on Mo and Al, fabrication and props. 8=10853
- GaAs thin film solar cell 8=19735
- Mo emitters with UO_2 , filling, radiation tests 8=15241
- Na vein m. h. d. generator, power transfer to armature 8=15206
- Pt-CdTe solar cell prep. by sputtering 8=10856
- Re cesiated thermionic emitter, evaluation 8=22717
- Re electroetched emitter in variable-parameter diode, output characts. 8=19793
- Re, thermionic emitter, cesiated, evaluation of surface 8=18269
- Si-Ge alloy thermoelectric generator modules 8=19732
- Si p or n solar cell characts. rel. to distributed model 8=9265
- Si solar cell characts. thickness and temp. depend. rel. to power-weight param., obs. 8=10850
- Si solar cell deployable rigid-frame array, performance obs. 8=10845
- Si solar cell, integrated high-voltage 8=10852

Electricity—contd

direct conversion—contd

- Si solar cells, dendritic and refr. back, prod. by implantation 8=10849
- Si solar cells for 0.4 and 0.2 AU from sm use 8=10851
- SrCO_3 -W, conversion/activation, and low work function collector 8=18266
- UC-ZrC, W clad emitter, stability rel. to operating temp. 8=18267
- UO_2 , W clad emitter, stability rel. to operating temp. 8=18267
- W, cesiated, saturated emission and max. output rel. to Cs reservoir temp. 8=18268
- W cesiated thermionic emitter, evaluation 8=22717
- W emitter converter, performance with CsF additive 8=15244
- W emitter, Ni collector thermionic device, effect of emitter mat. evaporated on collector 8=15245
- W, thermionic emitter, cesiated, evaluation of surface 8=18269
- W work function, effect of Cs additives 8=18251
- ZrC powder in vacuum and Cs vapors under thermoelectron transformation conditions 8=10843
- Electroacoustic transducers.** See Acoustic transducers.
- Electrocataphoresis.** See Electrophoresis.
- Electrochemistry**
- See also Chemical analysis/electrochemical; Electrolysis; Electrolytic deposition.
- cation hydration, charge-dipole model 8=9670
- double layer, soln. creeping or dielec. relax. 8=2530-1
- electrolyte boundaries, recording by thermocouples 8=5734
- electrolytes, diffusion kinetics, radiometric methods 8=23144
- fuel cells, high temp. electrolytes 8=9711
- fuel cell, high temp. solid electrolytes, 700-1100°C 8=15198
- holographic interferometry techniques 8=2528
- liquid metal-oxygen solns., solid electrolytic cell for measuring equilb. press. 8=16951
- metal electrocrystallization, influence of time-depend. impurity adsorpt. 8=17225
- nitrosobenzene, oxidation in organic media, e.s.r. 8=14426
- polarization in high resistivity electrolytes, modified Wheatstone bridge circuit 8=18715
- polyelectrolytes, thermodynamics of potentiometric titration 8=5736
- salt, molten concentration cells, electromotive force and association equilibria 8=2529
- seawater activated AgCl-Mg battery electrolytes, elec. cond. 8=16875
- solid-state electrochem. cells 8=14425
- Soret effect determ. in aq. bromide solns. 8=4557
- steel, anodic dissolution and corrosion potential 8=9723
- under weightless conditions 8=14416
- water-phenol-organic electrolyte system 8=18714
- $\text{B}_{21}\text{H}_{12}^{2-}$ controlled oxidation in acetonitrile 8=5732
- Cr-Ni-steels, electrochem. behaviour, rel. to vacuum melt purifying 8=9713
- Mn dioxides reduction and form., obs. 8=18718
- MnO_2 -Zn alkaline cell discharge curves and reactions, obs. 8=18717
- Ni hydroxide oxidation, γ -NiOOH form., obs. 8=18716
- Pb-Ag system, galvanic cell studies using PbO-SiO₂ melts 8=23150
- 2PbCO₃ anodization and PbO₂ struct. obs. 8=23148
- PbO anodization and PbO₂ struct. obs. 8=23148
- Pb₂O₃ anodization and PbO₂ struct. obs. 8=23148
- Pb(OH)₂ anodization and PbO₂ struct. obs. 8=23148
- PbSO₄ anodization and PbO₂ struct. obs. 8=23148
- Zn sulphides, standard free energy of formation 8=9712
- ZnO, cathodic reduction of aqueous $\text{Fe}(\text{CN})_6^{3-}$ 8=14423
- Zn Se interface with electrolyte, chem. and elec. props. 8=13837
- ZrO₂ between O₂ electrodes, thermoelect. power 8=9241
- electrodes**
- anodes, etching, pitting and passivity 8=9702
- carrier distillation, apparatus for rapid prep. 8=14903
- double-layer charging during stripping of adsorbed layers 8=2535
- electrode kinetics of strained wires, cell for study 8=8793
- electrosorption of neutral substs. 8=9716
- erosion by pulsed discharge 8=7649
- glow, during electrolysis 8=18720
- graphite, pyrolytic, bisulphate intercalates form. and elec. props. 8=18731
- Institute of Metal Finishing, conference, Brighton, England (1967) 8=14419
- isoporous diffusion electrodes for fuel cells 8=9717
- manganate-VI-permanganate redox electrode, mechanism 8=18724
- metal in electron, theory 8=5740
- oxygen-peroxide, exchange current density 8=9695
- perforated plates, mass transfer coeffs. 8=23145
- potentials, definition, rel. to work function 8=9715
- scaling, in polarity-reversal water purification 8=18734
- Al, anodic oxidation in presence of hydrated oxide 8=18729

Electrochemistry—contd
electrodes—contd

- Al, behaviour at d.c. and a.c. polarization 8=18725
 Cl₂, high current density, impurity effects 8=18730
 Cu, anodic behaviour in NaCl aqueous solution 8=2532
 Cu, anodic oxidation in LiCl-KCl 8=5738
 Cu, potential in Brussels water influence of light and conds. of circulation 8=18728
 Cu-Zn brasses in NaOH, anodic dissoln. 8=18732
 Cs⁺ on Hg electrode, partial charge transfer react. 8=18722
 GaAs single cryst., H evolution 8=14421
 Hg/methanol interphase, adsorption 8=18721
 I⁻ on Hg electrode, partial charge transfer react. 8=18722
 K⁺ on Hg electrode, partial charge transfer react. 8=18722
 Ni, in In-H₂SO₄, influence of alternating current 8=5739
 NiO, hydration state and electrochem. activity rel. to struct., obs. 8=23146
 Pt, adsorpt. and oxidation of hydrocarbons 8=9714
 Pt, anodic oxidation in LiCl-KCl 8=5738
 Pt, oxidative adsorpt. of n-hexane 8=5737
 Pt, oxidative adsorpt. of propane 8=2534
 Rb⁺ on Hg electrode, partial charge transfer react. 8=18722
 Rh, adsorpt. of CO + H, multipulse potentiodynamics 8=18727
 Rh, adsorpt. of CO, multipulse potentiodynamics 8=18726
 Rh, photoinjection into liq. hydrocarbons 8=8113
 Si, anodic oxide growth behaviour 8=14422
 n-Si anodic passivity in NaOH rel. to cryst. orientation 8=2533
 Sn, passivation in alkaline solns. 8=18733
 Ta, anodic oxidation in LiCl-KCl 8=5738
 Ta, gas-phase anodization 8=14420
 W, anodic oxidation in LiCl-KCl 8=5738

Electro-deposition. See Electrolytic deposition.**Electrodes.** See Cathodes; Electrochemistry/electrodes.**Electrodynamics**

- See also Eddy-currents; Quantum electrodynamics.
 accelerating charge, $v < c$, elec. field calc. 8=319
 Aharonov-Bohm effect, gravitational analogue 8=6060
 anisotropic medium, problems 8=6294
 betatron acceleration of trapped radiation by geomag. storm, adiabatic 8=2645
 calculus, theory and application 8=10491
 charge in anisotropic medium, radiation of 8=6360
 charged fine particle, radial focusing with transaxial electrostatic fields 8=15276
 charged particles in mag. field, exponentially time dependent, directionally constant 8=15273
 charged particle in modulated magnetic field, stability 8=3178
 charged-particle paraxial motion in varying, azimuthally symmetric elec. and mag. fields 8=3184
 charge motion in e. m. field, Lorentz transformation 8=15269
 in circularly polarized waves of time-varying amplitude 8=19765
 classical, amplitude and phase of e. m. field 8=10887
 classical motion of electron in electric-dipole field, finite dipole case 8=19771
 classical motion of electron in elect. -dipole field, point dipole case 8=19772
 collisionless capture of electrons into region of finite motion, distrib. of particles 8=7740
 current through plane diode, solns. obtained by invariant transforms for description of passage 8=15270
 Dessler-Parker-Sckopke relation, simple derivation 8=23429
 dielectric crystal, interaction of charged particles 8=8625
 diffusion, scattering and acceleration of particles by stochastic e. m. field 8=10880
 discharge plasma, eqns. of motion 8=1329
 discrete charges in crossed elec. and mag. fields, rotating ring stability 8=6291
 drift of particle, effect of h.f. field not close to cyclotron freq. 8=3182
 e-e. m. wave scatt., classical theory 8=15408
 e. m. field of charged particle in the presence of interfaces 8=317
 in electric-dipole field, bound states quantization 8=320
 electromagnetic field equations for moving quadrupolar medium 8=6293
 electron interaction with intense e. m. wave 8=19761
 electron trapping in laser beam rel. to scatt. light freq. shift meas. 8=19821
 energization of charged particles by arbitrarily moving spherical magnet 8=19769
 equations of motion of classical radiating charge, derivation 8=11453
 e radius and var. in gravity 8=6085
 Fermat's principle, appl. to trajectories in mag. spectrometers 8=6629
 fields of accelerated dipole, Heaviside-Feynman expression 8=19825
 hollow conducting cylinder, reflecting oscillator 8=3179
 hollow conducting cylinder, transmitting oscillator 8=3180

Electrodynamics—contd

- kinematic parameters of particles from photos of tracks in track chambers 8=11323
 light packet, adiabatic compression 8=10884
 Lorentz and Coulomb gauges, causal relations, comparison 8=10882
 microparticles, acceleration by laser-induced vapour emission 8=19768
 monocurrent similarly charged particles, theory 8=19767
 moving media, elec. and mag. polarization 8=10886
 non-local effects, comparison with quantum theory 8=10883
 opposed beams, stability of motion 8=19762
 paraxial motion in const. spatially modulated mag. field 8=19759
 particle acceleration in uniform delay structure 8=3493
 particle and plasma motion with e. m. field confinement 8=19764
 particle in dipole field, mag. moment adiabatic invariant 8=2649
 particle in travelling e. m. wave near cyclotron resonance 8=15272
 point charge moving over conducting $\frac{1}{2}$ planes, radiation 8=3183
 potentials in anisotropic dispersive medium 8=3173
 radiation from moving dipoles 8=19770
 relativistic electrons in mag. and weak electrostatic field, effect of radiation 8=6292
 relativistic particle, conical trajectories 8=19760
 self-resonant acceleration of particle in inhomogeneous medium 8=10879
 space and time dependent fields, guiding centre approximation in lowest order 8=3191
 stochastic acceleration in mag. mirror 8=15271
 surface wave excitation by moving charge at interface between vacuum and medium 8=3181
 transition probability for multi-photon process with resonance 8=20011
 uncoupling of parallel and perpendicular particle motion in neutral sheet 8=19766
 in weakly modulated axially-symmetric mag. field 8=19763
 Cs ions, linear acceleration in crossed e. m. fields 8=318
- Electroendosmosis.** See Electrophoresis.
Electrojet. See Atmosphere, upper; Atmospheric electricity; Ionosphere.
- Electrokinetic effects**
 See also Electrophoresis.
 gas discharge, electromechanical conversion efficiency 8=7672
 gases, inert, Kerr coeffs. compared with optical third-harmonic generation 8=1479
 hidden momentum, Penfield and Haus formula 8=19722
 CaCO₃ in H₂O, solns. zeta pot. rel. to surface charge form. 8=16903
- Electroluminescence**
 acoustic domains, generation of light 8=18587
 gases, light sources 8=484
 Gudden-Pohl effect, optical image recording, storage and reproduction applns. 8=6496
 memory circuits, optico-elec., static params. theory and obs. 8=6039
 metal sample prep. for electron microscopy 8=17271
 p-n junction, impurity, kinetics 8=18588
 panel as modulatable light source 8=6517
 specimens for electron microscopy, electrolytic polishing 8=17270
 spectroradiometer-luminometer for quantum-yield studies 8=18589
 sulphide phosphors, freq. depend. of shape of light pulse 8=5676
 transport equations, description using two-stage model 8=5651
 Al-Al₂O₃-Ag sandwich, rel. to electron emission 8=9277
 Al-Al₂O₃-Au tunnel structures, interface trapping 8=5381
 Al-Al₂O₃-M film diodes 8=9598
 Al-CaWO₄-Au tunnel structures, interface trapping 8=5381
 AlN:Cr and S and Z impurity effects, obs. 8=9595
 AlN:Eu and S and Z impurity effects, obs. 8=9595
 AlN:Mn and S and Z impurity effects, obs. 8=9595
 AlN:Sm and S and Z impurity effects, obs. 8=9595
 BaS:Bi rel. to activator and BaSO₄ phase concs., obs. 8=9601
 BaS-Cu(Mn), freq. depend. of shape of light pulse 8=5676
 BaS:Cu rel. to activator and BaSO₄ phase concs., obs. 8=9601
 BaS:Mn rel. to activator and BaSO₄ phase concs., obs. 8=9601
 Be-BeO-Au sandwich, rel. to electron emission 8=9277
 CdF₂ crystal, activated by rare earth ions 8=5658
 CdS acoustoelec. light scanner 8=5309
 CdS film in Au-CdS-In diode, d.c. excit. mechanism obs. 8=9608
 pCu-S-nZnS: Mn, Cu, Cl films, d.c. mechanism 8=23051
 GaAs diffused p-n junctions, longwave bands in luminescence spectra 8=5663
 GaAs, diodes, fabrication 8=5323
 GaAs, diode, with thermoelec. cooling, efficiency 8=22684
 GaP diodes, green bands obs. at room temp. 8=9161
 GaP, and elec. props, effects of two zone melting prep. techniques 8=9611

Electroluminescence—contd

- GaP:Ge p-n functions 8=23073
 KI, intrinsic, and excit., 77°K and 5×10^4 V/cm 8=14320
 KI:TI roentgenoluminesc. stimulation mechanism, obs. 8=9618
 M—O—M sandwich rel. to electron emission 8=2977
 NaCl:Ag, by u.v. excitation studies 8=2486
 SiC diodes, properties 8=9627
 ZnO—ZnSe systems as function of band gap 8=9644
 ZnS, and conductivity changes, alternating voltage effect 8=9259
 ZnS brightness wave 8=9634
 ZnS electrolumino-phors, radiation-controlled enhancement 8=14344
 ZnS, hexagonal, intensity distrib. rel. to dislocation structure 8=18621
 ZnS lamp, calibrated for use as standard light source 8=20067
 ZnS phosphors, photoimpedance, a.c. field freq. and excitation intensity dependence 8=14335
 ZnS phosphors, spectra, time constants of build-up and decay 8=5677
 ZnS, photoconductivity changes 8=22701
 ZnS:Cu brightness build-up and electrolysis prod. ageing, obs. 8=9637
 ZnS:Cu, brightness wave variation 8=18620
 ZnS:Cu, effects of grinding, obs. 8=9647
 ZnS:Cu electroroentgenoluminescence brightness non-additivity obs. 8=9636
 ZnS:Cu, irradi., quenching and stimulation rel. to elec. props. 8=9640
 ZnS:Cu phosphor condenser, characts. depend. on props. of crystal barrier layer 8=9657
 ZnS:Cu rel. to elec. cond., obs. 8=9133
 ZnS—Cu phosphor, filling of traps during electric field excitation 8=14314
 ZnS—CuAl(Mn), freq. depend. of shape of light pulse 8=5676
 ZnS:Cu, Al phosphors, luminescent centre interactions 8=18622
 ZnS:Mn films, polarization effects obs. 8=9638
 ZnS:Mn films, pulse excitation characts. obs. 8=9639
 ZnS:Mn, Cl, i.r. enhancement 8=5678
 ZnS(Mn, Cu), high-efficiency d.c. 8=18625

Electrolysis

- See also Conductivity, electrical/liquids, electrolytic; Dissociation/electrolytic; Electrochemistry; Electrolytic deposition; Ion velocity/electrolytic.
 aluminum, sol. of CO_2 in molten salts, influence on current efficiency 8=12805
 concentration of a solution, continuous meas. using reactance meter 8=5733
 conductance cell for aqueous solns., 1–3000b and 25–225°C 8=14424
 cryolite-alumina melts in contact with Al, Al reoxidation process 8=23151
 electrocrystallization, surface diffusion interactions 8=9719–21
 electrode glow 8=18720
 electrolytes, intermediate conc., statistical theory 8=14417
 ice/water interface, electrostatic potentials 8=18723
 mixed salt solns., ultrasonic and cond. parameters 8=16827
 solid electrolytes of high conductivity 8=18719
 solutions, two-structure model 8=23142
 steel, austenitic, passivity breakdown by halide ions 8=23147
 water, polarity-reversal purification, optimum reversal time 8=18734
 CeO_2 crystal, rel. to conduction mechanism 8=18164
 Li_2CO_3 — Na_2CO_3 , molten 8=5741
 Li_2CO_3 — Na_2CO_3 , molten, electrochem. studies 8=5741
 Pb—Ag system, galvanic cell studies using PbO — SiO_2 melts 8=23150
 ZnS:Cu electroluminesc. cells rel. to ageing 8=9637

Electrolytes, theory. See Electrochemistry; Solutions.

Electrolytic conductivity. See Conductivity, electrical/liquids, electrolytic.

Electrolytic deposition

- anodic behaviour of Fe and its oxides in H_2SO_4 and alkaline solutions 8=14432
 anodic oxide films on Al in boric acid-formamide solns., struct. obs. 8=13089
 Institute of Metal Finishing, conference, Brighton, England (1967) 8=14419
 surface interferometry 8=9722
 water, electrode scaling in polarity-reversal purification 8=18734
 Ag cementation on Cu in perchloric acid and alkaline cyanide solns., kinetics 8=14427
 Al alloys plating, surface pretreatments 8=14429
 Al alloys, surface preconditioning, electron microscopy 8=8291
 Al, plating, alkaline Zn pretreatment soln. 8=14431
 Al plating using stannate activation and bronze strike deposit 8=14430
 Au, inside metal containers, regulation 8=14428
 Au, porosity rel. to Cu substrate surface, prep. and undercoats, obs. 8=21981

Electrolytic deposition—contd

- Cd on steel, effect on fatigue 8=22361
 Cd on steel, H₂ absorption 8=17163
 Ce deposits internal stress development, obs. 8=22325
 Co films, growth rate rel. to structure and props. 8=13999
 Fe films, growth rate rel. to structure and props. 8=13999
 Fe—Ni films, conditions effect on internal stresses 8=17653
 Ni, dull plating salt, formulation 8=23152
 Ni film, electroless, and e microscope study 8=17136
 Ni films, growth rate rel. to structure and props. 8=13999
 Ni layers, lattice deformations and crystal orientation rel. to deposition inhibitor effect 8=1805
 Ni from NiCl₂ soln. by a.c., microstruct. obs. 8=22035
 Ni, specified process for electroformation rel. to mech. props. 8=17823
 PbO_2 , cryst. struct. rel. to electrolyte impurities 8=21919
 Pt—Ir alloys from aqueous electrolyte, deposits hardness and stress obs. 8=23153
 Sn, aftergrowth of whiskers 8=17251

Electrolytic tanks. See Calculating apparatus/analogue apparatus.

Electromagnetic fields

- accelerated point charge, exterior vector product 8=3169
 alternating, in continuous casting of steel 8=4847
 of arbitrarily moving particle with mag. and electric moment 8=19770
 averaged equations in nonstationary resonance medium 8=3246
 axial, symmetric, solution 8=10877
 coherent state time development 8=2975
 constant, Lorentz transformation and motion of charges 8=15269
 correlation theory, relativistic formulation 8=19823
 electric-field components, near-zone strength meter 8=269
 electromagnetic induction in conductor bounded by inclined surface 8=18802
 electron gun, computer soln. of eqns. 8=15284
 energy distrib., Maxwell tensor 8=3171
 energy transfer to h.f. discharge plasma 8=16397
 far field scatt. at low freqs. 8=19871
 fluids, relativistic, charged in gravitational field, Larmor and Helmholtz theorems 8=16633
 forces in conductors, relax.-averaging formulae 8=6284
 formal model, based on four-space hyperfluid flow 8=6283
 geometry, energy-impulse tensor treatment 8=3172
 guide field for plasma betatron 8=16563
 impulse-energy tensor from Lagrange function 8=3170
 interaction with warm slightly ionized magneto-plasmas 8=16517
 microwave, redistribution of density in plasma 8=7729
 near to far field, l.f. continuation 8=19870
 null field in Einstein—Maxwell theory propag. vectors and metric tensor 8=316
 null, source-free, energy tensor, differential conds. 8=315
 plane wave, relativistic charge radiation in 8=10881
 plane wave spectrum representation, book 8=15392
 Poyntings theorem, uniqueness theorem concerning energy tensor 8=6288
 produced by rot. bodies, superconductor test proposed 8=3174
 quantization, canonical in Landau gauge 8=3434
 quantized, characteristic states 8=19818
 quantized, fluctuations and correlations 8=20016
 quantum operators, coherent states diagonal representation 8=19820
 radiation from Fermi particles 8=6739
 radiation, Gaussian or laser, statistical props. by photon counting distrib. 8=10998
 radio waveguides, modelling apparatus 8=10962
 relativistic electron motion, effect of radiation 8=6292
 rel. to photon counting statistics, coherence props., dynamical calc. 8=20352
 secondary, due to elementary dipoles, approximation 8=15266
 structural analysis, optimal conditions 8=10878
 for switching thin mag. film near finite permeability keeper and semi-infinite conductor 8=3168
 two-dimensional, integral formula 8=3176

Electromagnetic oscillations

See also Magnetohydrodynamics; Masers; Plasma/oscillations.

- accelerators, coherent, stability 8=638
 avalanche oscillators, freq. locked, relative phase shift 8=10944
 cylindrical resonators with losses, criteria rel. to length 8=6367
 dielectric prism between plane mirrors 8=6361
 exposed cylindrical cavity, excitation coefficient 8=3267
 Gunn effect, freq. modulation by mag. tuning, 9, 300 and 10, 900 MHz 8=361
 laser optical coupled modes, Green functions 8=6430
 laser quantum noise, classical models 8=398
 limiting oscs. in generator during parametric excitation 8=6368
 magnetron electron cloud, calc. of natural freq. 8=15328
 molecular oscillator, investigation with "molecular-ringing" amplifier 8=10940
 multimesh self-excited oscillator, subjected to ext. sinusoidal voltages 8=6371

Electromagnetic oscillations—contd

- optical resonator filled with anisotropic medium, Gaussian beam propag. 8=6373
- oscillators, self-sustained, near threshold, noise exam. 8=6259
- piezoelectric resonator, heat transfer coeff. 8=1884
- quasi-harmonic, self-excited oscillators, fluctuations in case of low noise 8=6370
- radiation, experimental introduction 8=10936
- resonances, free dielect. spheres in infinite medium 8=10979
- resonator formed by concave mirrors, conds. for focusing 8=11025
- resonators, cavity, dependence of e.p.r. sensitivity on geometry 8=387
- resonators, h.f. props. when filled with artificial dielectric 8=19829
- ruby laser, single longitudinal mode production 8=6459
- self-resonance in power capacitors, effect on discharge magnitude meas. 8=21228
- superconducting oscillator-detector 8=15172
- superconducting resonators for oscillators 8=13767
- vibrator on wedge edge, spatial directivity characteristics 8=3249
- whistler resonance temp. dependence rel. to plasma diagnostics 8=3272
- in Fe, purified, rel. to amplitude-dependent internal friction and modulus defect 8=13557
- GaAs, n-type, Gunn oscillators, inhomogeneity effects 8=362

Electromagnetic radiation. See Electromagnetic waves; Gamma-rays; Light; Radiation; X-rays.

Electromagnetic wave propagation

- See also Absorption; Diffraction, etc.; Plasma/electromagnetic wave propagation.
- amplitude modulation by alternating mag. fields 8=15391
- antennas and propagation conference, Ann Arbor 1967 8=15401
- avalanche oscillators, freq. locked, relative phase shift 8=10944
- charged-body plasma sheath effects, book 8=14706
- Cherenkov emission of Alfvén waves 8=6343
- complex permeability and permittivity, meas. of at microwaves 8=6399
- conducting slab, peak at cyclotron reson. 8=19838
- dielectric cylinders, between reflecting planes vibrations 8=10699
- dielectrics, periodic pile, nodes of standing waves 8=19837
- dielectric slab with large permittivity modulation 8=18206
- dipole moving over dielectric medium, spherical waves, radiation 8=383
- earth surface with irregular relief, medium radio wave, attenuation rel. to distance 8=384
- EAS, meas. of coherent r.f. emission in meter wavelength range 8=15905
- by elastic waves incident on conducting plate, freq. and size resons. 8=10710
- electromag. fields, plane wave spectrum representation, book 8=15392
- ferrite dev., superhigh freq. for operation in band 8.2-12.4 Gc 8=10939
- Fresnel's eqn. deriv. in general relativity 8=6082
- Gaussian beams in anisotropic media 8=6373
- harmonic generation in optically active medium, coupled wave solution 8=455
- helicoidal nematic films 8=16837
- h.f. spherical, weak dielectric random continuum, elect. field component correl. functions 8=15390
- holography microwave 8=20109
- inhomogeneous isotropic medium, wave struct. 8=15393
- inhomogeneous media, strong amplitude fluctuations 8=6374
- in isotropic inhomogeneous medium, refraction 8=15398
- laser beam through random medium 8=3251
- light beam, narrow, in turbid medium with highly directive scatt. 8=11161
- light, coherent sources, equi-energy and equi-phase contours paradox 8=6546
- light, in inhomogeneous cosmologies, statistical effects 8=10078
- limiting oscs. in generator during parametric excitation 8=6368
- in lossless nonlinear mag. medium, rel. to shock vels. and discontinuities 8=19832
- microwave system, expt. and demonstration 8=6366
- multimesh self-excited oscillator, subjected to ext. sinusoidal voltages 8=6371
- multiplexer for multifrequency microwave sounding of plasma 8=12524
- near to far field, l.f. continuation 8=19870
- over non-parallel stratified conducting medium 8=6372
- partially-polarized waves in slightly anisotropic medium 8=6375
- permutation symmetry of nonlinear susceptibilities and energy relation 8=19835
- in plane stratified medium, theory and meas. 8=365
- Poynting's theorem for moving media with nonrelativistic velocity 8=6376
- Poynting vector orientation of plane monochromatic wave in homogeneous isotropic medium 8=10950

Electromagnetic wave propagation—contd

- Poynting vector in static fields, correct usage 8=10946
 - quantum coherence theory of propag. in vacuum 8=20172
 - pulsed, in lossless, inhomogeneous, dispersive dielectric media 8=3250
 - r.f. sources in ionized medium, behaviour 8=12495
 - ray focusing between concave mirrors of resonator 8=11025
 - ray statistics in plane layer medium with random inhomogeneity 8=10949
 - self-modelling wave beams in nonlinear dielectric 8=10835
 - semiconductors, electron beam excitation quasilinear theory 8=5151
 - semiconductors, electron temp. not unique function of incident field amp. 8=9084
 - semiconductors, surface wave, and amplification in strong mag. fields, theory 8=9090
 - spherical cavity, symmetric perturbation, appl. of group theory methods 8=10943
 - spherical, expansion of vector pot. 8=15403
 - surface waves on semiinfinite metals 8=14164
 - TEM transient in unbounded radial line 8=15394
 - transmission and reflection by moving dielectric slab, parallel polarization 8=19836
 - transmission cross section of infinite slit in gyrotropic medium 8=15395
 - transmission through coaxial cylinders, phase shifts 8=366
 - turbulent media, statistical properties, book 8=10735
 - wave functions in cylindrical stratified columns 8=19834
 - whistler resonance temp. dependence rel. to plasma diagnostics 8=3272
 - wideband pulse compression via Brillouin scatt. in Bragg limit 8=10948
 - Nd³⁺/glass laser, continuously tunable, 0.5 to 0.8 μ spectral range 8=364
 - SF₆ gas, self-induced transparency using 10.6 μ laser radiation 8=1478
- atmosphere**
- acoustic mode, dipole magnetization field 8=1393
 - atmosphere, cm, mm and sub-mm 8=5793
 - atmospherics, 1-20 kHz phase spectra and freq. rel. to source distance 8=2600
 - D-region electron density distrib. obs. 8=5808
 - decimetre waves, radiation temp., for elevation angles 0.5-10° 8=18896
 - directional h.f., 450-km path, correlation obs. 8=18901
 - earth crust movements meas., refr. effects correction 8=2605
 - earth-ionosphere cavity modes, freq. variations 8=2676
 - earth-ionosphere cavity resonances 8=2608
 - e.l.f. attenuation rates, nonreciprocal, from slow tail obs. 8=9890
 - fog, 0.337 mm maser source 8=2592
 - geomagnetic field, ionization density profiles 8=9909
 - interaction of measuring cavity with stream of rarified gas, special case 8=14631
 - light beam, fluctuations in intensity rel. to varying turbulence 8=14618
 - longwave, outgoing rad., influence of refraction 8=9889
 - in m.m. wavelength range, rel. to absorpt. by water vapour 8=9865
 - microwave, seasonal attenuation 8=2677
 - nuclear explosion, low altitude, radio signal development 8=23296
 - phasemeter, long base, feasibility 8=18902
 - radar target parameters, invariant 8=19864
 - radio, medium wave, over irregular relief earth surface, attenuation as function of distance 8=384
 - ray height for continuous nonlinear refractive index profile, algorithm 8=23379
 - ray tracing study with satellites 8=2672
 - refraction coeff., mm. waves 8=18906
 - refraction, theory and meas., book 8=14629
 - Rytov approximation, limitations of applicability 8=18883
 - Rytov solution, multiple-scattering interpretation 8=18884
 - scattering, incoherent, at perpendicular intersection with geomag. field 8=9983
 - short-wave radiation, correl. with cloud field 8=9860
 - sky wave illumination, phase of field on inhomogeneous earth surface 8=2606
 - spatial coherence in turbulence, 3.2 mm 8=18900
 - spherical array of circularly polarized elements 8=19896
 - spherical waves through atmospheric turbulence 8=18897
 - surface waves, book 8=14629
 - transhorizon, tropospheric, book 8=14630
 - tropospheric absorption by radioastron. methods 8=5792
 - tropospheric attenuation over range 0.4-10 GHz 8=9887
 - troposphere, lower refractive index small-scale irregularities 1966 obs. 8=2604
 - troposphere, radio-meteorological correlations over Bass Strait 8=18899
 - tropospheric scatter propagation and equipment rel. to a system in Korea 8=9886
 - troposphere, stratified, pulse distortion in total internal refl. 8=2607

Electromagnetic wave propagation—contd atmosphere—contd

- troposphere, structure factor determ. 8=2603
- troposphere, super-refractive with nontrapping surface 8=18904
- tropospheric microwave, total internal reflection mechanism 8=18898
- upper air refractivity, world atlas 8=18905
- v.l.f. emissions, obs. and theories 8=14672
- v.l.f., quasi-sinusoidal waveforms of distant atmospherics, Fourier anal. 8=18903
- v.l.f., waveguide effect of geomagnetic field 8=3273
- H₂O vapour in ground layer, 183-31 GHz absorpt. line shape, obs. 8=23295
- O₂, radio wave absorpt. coeff. 8=9888
- ionosphere**
- absorption of cosmic r.f. radiation, during 18 April 1965 disturbance 8=14660
- absorption, winter anomaly identification criteria 8=2680
- auroral absorption 8=18987
- auroral absorpt., apparent poleward expansion 8=18988
- cavity model, cylindrical with dipolar mag. field, resonances 8=9981
- current boundary layer prod. by refl. from ionized medium 8=6378
- D, u.h.f. radar returns from 75 km 8=10002
- E region drift meas., comparison of similar fade and max. cross correl. methods 8=14684
- E-region, scattering propagation caused by field aligned irregularities on v.h.f. band, obs. 8=5809
- E, sporadic, cut-off freq. var. 8=10007
- E_s blanketing freq. vars., latit. $\pm 60^\circ$ 8=2706
- E_s, v.h.f. forward scattering obs. 8=10006
- earth-ionosphere cavity modes, freq. variations 8=2676
- earth-ionosphere cavity resonances 8=2608
- Earth-ionosphere waveguide, calc. mode conversion at sunrise boundary 8=23365
- e.l.f., long distance, calc. 8=15424
- e.l.f. reflection coefficient 8=18993
- e.l.f. slow tail waveforms, direction dependence, nocturnal obs. 8=9982
- e.l.f. and v.l.f. below anisotropic region with dipping static mag. field 8=23370
- fading speed, over Ahmedabad 8=9970
- F layer, radio effect on critical freq. and isoconcentration surfaces 8=19019
- F-region irregularities, effects on radiowave propagation book 8=18978
- h, F2 latitudinal variations of (M-3000)F₂ and statistical result 8=23422
- Faraday effect used to meas. e-content, Early Bird satellite 8=2662-3
- Faraday effect, satellite signal for calcs. of total e content 8=2660
- Faraday effect from Syncom-3, meas. of e-content var. 8=2661
- Faraday effect in transversal propagation zones 8=23366
- Faraday fading near transverse propag. 8=2671
- Faraday fading of satellite signals for ionospheric electron content 8=14669
- Faraday rotation in a stratified ionized medium 8=22948
- Faraday rotation of waves from satellites rel. to electron content over Texas 8=14663
- field strength of 164 kHz λ rel. to solar X-rays λ received signal 8=5807
- frequency, max. usable, allowing for earth's mag. field, calc. 8=23381
- frequency trajectories, 20 and 30 MHz, in presence of horizontal inhomogeneity 8=9975
- Galactic radio noise attenuation, 25 and 21.3 MHz, Ahmedabad, 1957-64 8=14673
- group path-phase path relation 8=385
- homogeneous medium, model 8=18982
- hydromagnetic gradient waves 8=14674
- illumination of inhomogeneous surface 8=19902
- inhomogeneous medium, model 8=18983
- investigations, at NIRFI for 1957-1967 8=23369
- Loran transmissions, Explorer 20 reception obs. 8=2684
- magnetosphere, guidance of waves along field aligned irregularities 8=18986
- Mc/sec signals reflected by free radicals obs. 8=23384
- model for viscosity and thermal cond. effects 8=19903
- modes, theory, direction dependent 8=2678
- no-echo occurrences and absorption of cosmic radio noise 8=9980
- oblique propagation, digital recording and short-term prediction 8=5806
- PCA, and solar cosmic radiation 8=14736
- phase perturbations, v.l.f., produced by solar protons February 5, (1965) 8=18990
- plane wave incident on stratified medium, reflection theorem 8=18979
- proton gyrofrequency, effect on satellite antenna resonance 8=6400
- proton gyroresonance observed in incoherent scattering 8=2669
- radio absorption, conversion from vertical to oblique 8=9972
- radio noise flux, 10.7 cm, Schmidt's phenom. 8=18968

Electromagnetic wave propagation—contd ionosphere—contd

- radio, prediction of conditions on basis of IF2 index 8=18991
- radio signals, incoherently scattered, and meas. electron conc. profiles 8=23398
- ray calc. in quasiparabolic model with no mag. field 8=23380
- ray computations, exact, for tilted ionosphere with no mag. field 8=23378
- ray path eqns. for ionized layer with horizontal gradient 8=23377
- ray path solns., exact, with entry from above or below 8=23376
- ray tracing, extension of Booker's method to v.l.f. 8=23372
- ray tracing at 3 to 30 MHz 8=23382
- ray tracing in anisotropic medium, num. integration of Yobroff's eqns. 8=23375
- reflection atmospherics, amplitude spectra 8=9977
- reflection coefficient for layered media 8=18980
- reflection of radiowaves, nature of signal 8=18989
- refraction of satellite signals used for Doppler data 8=23371
- refractive correction and electron total content latitude variation 8=9965
- refractive index, relativistic, for drifting magnetoionic plasma 8=18977
- resonances by l.f. propagation 8=2679
- r.f., l.f. and v.l.f. radio propagation, conference, London, England (1967) 8=14671
- SCNA and X-ray flares 8=2653
- satellite ORBIS expt. 8=2670
- scintillation meas. with interferometer system 8=2865
- scintillation, seasonal var. 8=2673
- scintillations, radio star and satellite 8=386
- sea scattered h.f. radio waves 8=18976
- signal intensity along short wave link, computing method 8=9976
- signal records of Elektons 1 and 3, electron total no. and gradients from 8=18971
- space vehicle effects, book 8=14706
- in stratified magnetoplasma, using energy propagation 8=23368
- stratified plasma waveguide, orthogonal natural or eigen waves, study 8=10960
- thickness var. Sputniks obs. 8=5805
- topside, delay of remote-resonance ionogram traces, explanatory model 8=2712
- topside, m.f. conjugate echoes, Alouette II sounder obs. 8=18981
- "turbidity", influence of geophysical factors 8=2682
- u.l.f., (dawn chorus and hissing noise), assoc. with mag. bays 8=9971
- u.l.f. emissions, 1.5-3 kHz, conjugate point obs. 8=9974
- v.l.f., across geomag. anomaly, during S.I.D. 8=2675
- v.l.f. and e.l.f. modes, theory 8=2674
- v.l.f., below anisotropic region, model with dipping static mag. field 8=18985
- v.l.f. emissions, obs. and theories 8=14672
- v.l.f. influence of meteoric dust 8=18992
- v.l.f. long path, effect of total solar eclipse 8=23374
- v.l.f. mode structure and polarization below anisotropic region 8=18984
- VLF reception anomalies associated with a natural Earth satellite 8=9984
- v.l.f. wave normals, influence of horizontal e density gradients on direction 8=23367
- wake of space vehicles, radar backscatter 8=14676
- waveguide regions below F₂ layer maximum rel. to distant short wave communication 8=14675
- whispering gallery for satellite-to-satellite HF/VHF waves 8=2716
- whistlers, subprotonospheric 8=23373
- guided waves**
- accelerating system for iron-free synchrotrons, theoretical anal. 8=6702
- active transmission line, with nonlinear loss, dispersion rel. to self-osc. 8=10961
- air-dielectric coaxial-line standards, precision, skin-effect corrections 8=10964
- along plasma column waveguide, for different series of modes 8=19885
- aperiodic waveguide array, radiation 8=19890
- beam, between parallel concave reflectors, theory 8=15420
- beam waveguide stability, effect of lens transverse shifts using computer simulation 8=377
- Cherenkov radiation in waveguide with elliptic cross section 8=6394
- circularly symmetric modes in magneto-ionic cavity 8=10966
- coaxial cable delay lines, delay time meas. method 8=6395
- coaxial dielectric filling, inverse hybrid waves 8=3263
- coaxial guide, space-charge effect in discharge rel. to spark voltage 8=7646
- coaxial resonator, space-charge effects 8=7647
- curved irregular waveguide, scatt. near cut-off freq. 8=19878

Electromagnetic wave propagation—contd**guided waves—contd**

- cylindrical slit guide, excitation by rotating charge 8=6380
- dielectric line, radiation from free end 8=19891
- dielectric line, reception at free end 8=19892
- diffraction of surface wave on semi-infinite anisotropically conducting plane 8=15402
- dipolar modes in magneto-ionic cavity 8=10967
- dispersive media, moving, effect on TE and TM structure in cylindrical guide for nonrelativ. vels. 8=15413-14
- eigenvalues of coupled guides 8=19886
- ferrite amplifier, degenerated-type, with waveguide coupling 8=359
- ferrite cylinders, premagnetized axially 8=10970
- ferrite-loaded waveguides, lossless, non-conservation of energy 8=10963
- gases, ionization time and electron density, microwave meas. 8=12518
- helical guide, Doppler excitation of slow waves 8=19883
- helix in plasma, symmetric wave behaviour 8=7766
- h.f. electronics and stimulated radiation of classical oscillators 8=3298
- ionosphere below anisotropic region, e.l.f. and v.l.f., with dipping static mag. field 8=23370
- ionosphere below anisotropic region, v.l.f. mode structure and polarization 8=18984
- ionosphere-earth spherical guide, v.l.f. propag. during S.I.D. 8=2675
- magnetosphere, along field aligned irregularities 8=18986
- microwave polarization inverter, frequency shift 8=15396
- microwave power coupling to helicon mode in InSb 8=13825
- millimetre and sub-mm wave generation with electron beam devices 8=380
- mode conversion by diaphragms etc. in rectang. wave guides 8=3261
- optical beam waveguides, self-aligning 8=10965
- optical waveguide, nonlinear, crystal class C_{6v} , generation of second harmonic 8=5577
- partial hot plasma filling, dispersion eqns. 8=10959
- partial plasma filling, non-linear coupling 8=10958
- pin comb loaded waveguides, effects of wall deform. 8=15418
- pipes with walls formed by intersection of two orthogonal parabolas 8=6392
- plasma or dielectric slab, excitation by parallel plate guide with one plate truncated 8=21335
- planar dielec. waveguide, field excitation at p-n junctions 8=10969
- plasma, waveguide method for meas. electric characteristics behind shock front 8=1389
- plasma waveguide, nonlinear coupling of slow and fast waves 8=4401
- plasma waveguide, stratified, orthogonal natural or eigen waves study 8=10960
- quasi-optical systems, mode selection 8=3262
- radio waveguides, apparatus for modelling e.m. field 8=10962
- rectangular guide with anisotropic filling 8=15416/7
- rectangular guide excitation by distributed charges 8=3264
- slot compensation in standing wave meter at mm. waves 8=3265
- solid-state plasma waveguide, circular, propag. and Faraday effect 8=10968
- surface wave diffraction at junction of half-planes of different conductivity 8=6384
- surface wave in waveguide with impedance changing along length 8=19881
- symmetric waves in rectangular helix, effect of presence of plasma 8=6396
- threshold field in a waveguide loaded with an ellipsoidal ferrite 8=6393
- transformation theory, in moving media 8=378
- transmission line with distrib. noise sources, classical theory 8=19889
- Umov-Poynting's flux distribution in waveguides, use of semiconducting thermosonde 8=19880
- warm plasma loaded waveguides, surface waves 8=16522
- by waveguide bifurcation and aperture, scatt., ray-optical calc. 8=19882
- waveguide, circular, partly dielec. filled, dispersion eqn. 8=19887
- waveguide, discontinuity problem between empty and ferrite filled 8=6397
- waveguide discrimination method for plasma measurement 8=12520
- waveguide elements, testing at high power levels with super h.f. power simulator 8=15389
- waveguide ferrite diode applications 8=22626
- wave guide partially filled with plasma in infinite axial mag. field 8=3266
- waveguide phase arrays, dielectric loaded and covered, rectangular 8=19884
- waveguide, plasma osc. excitation with low density particle beam near axis 8=16568
- waveguide, rectangular, transmission, refl. and absorption coeffs. of thin metal films in transverse plane 8=21874
- waveguide, Stark, in 258 GHz modulator 8=6365
- waveguide with ferrite, prop. const., Galerkin-Ritz method 8=19888

Electromagnetic wave propagation—contd**guided waves—contd**

- waveguide with semiconducting wall 8=19877
 - waveguides semiconductor loaded 8=19833
 - waveguide walls, radiation pressure 8=19879
 - waveguides with uniform elec. field strength 8=15419
 - waveguide, very short pulses, and group vel. of signals 8=379
 - X130 standard attenuator, for superhigh freq. transmission systems 8=15415
 - Ar, shock ionized, microwave obs. 8=12431
 - Li-Co-ferrite-aluminates, thermostable valves in decimetre range 8=9377
 - SbSI, photo-induced microwave response meas. 8=5630
- Electromagnetic waves**
See also Diffraction; Reflection, etc.; Light/electromagnetic theory.
- Aharonov-Bohm and Mercereau effects, classical analogue 8=585
 - avalanche oscillators, freq. locked, relative phase shift 8=10944
 - cavities, bimodal, wide-band balancing for microwave props. meas. 8=15387
 - circularly polarized, charged particle motion rel. to growth and decay 8=19765
 - compressed inert gas, depolarization with scatt. 8=6387
 - depolarization, backscattered from rough metals 8=19839
 - earth's radiation belts, cyclotron instability, nonlinear theory 8=18957
 - electron beam, radially divergent, interaction 8=6297
 - excitation of shock waves in metals 8=6143
 - fluctuations spectrum analyser, statistical props. 8=10981
 - generation conditions in semiconductor crystals 8=8957
 - generation, use of interacting electron beam theory 8=193
 - gravitational waves, generation 8=81
 - helium waves, h.f. phase sensitive detection 8=5138
 - intense, electron pair production by photons in field 8=717
 - laser radiation, linear and circular polarized, in optical third harmonic generation 8=11016
 - laser radiation, time dependent statistical props. 8=3304
 - linear accelerator, microwave effect on current pulse 8=6697
 - Maxwell's equations, group theoretical derivation 8=10935
 - Maxwell's equations, three derivations 8=10934
 - metals, interaction with u.s. waves, theory 8=22951
 - microwave detect. by glow discharge, theory and obs. 8=10938
 - microwave emission from acoustoelectrically oscillating n-InSb 8=13823
 - microwave, generation and detection by Sn supercond. point contact 8=22570
 - microwave harmonic generators and detectors 8=19830
 - microwaves, amplification by electron beam in plasma 8=12570
 - microwaves, detection, using n-type InSb, influence of mag. field and impurities 8=2224
 - microwaves, magnetization change approximations 8=13955
 - microwave mixing with weakly coupled superconductors 8=15386
 - microwaves, polarization, demonstration 8=375
 - microwave signal processing using ultrasonic devices 8=15072
 - mixing in a ferrite of 10 GHz waves 8=19848
 - modal diversity reception expt. 8=19899
 - mode mixing in nonlinear media, quantum statistics 8=19822
 - moving jump of parameter, interaction with 8=3253
 - from moving source, progressive wave formation for homogeneous medium 8=3252
 - multiple-mode, superposed coherent and chaotic radiation, quantum statistics 8=2984
 - open resonators, whispering-gallery modes 8=6364
 - photoelectromagnetic receivers with optically polished thin elements, sensitivity and inertness 8=6275
 - plane, effect on elementary particles 8=20279
 - polarization angle rel. to impedance matching, small-reflection wall application 8=3256
 - polarized, rotation by gyrotropic layer 8=3376
 - power spectrum modulation for unmodulated signal, 2800 MHz 8=19850
 - progressive rel. to separation of high energy particles 8=15649
 - radiation, experimental introduction 8=10936
 - rays and caustics, complex 8=3247
 - resonance field effect on double radiation 8=10942
 - scattered, spatially coherent detection 8=19831
 - semiconductors, anisotropic, non-linear excitation of electron density fluctuations 8=13772
 - spatial distrib. of flux density, meas. method 8=357
 - spherical cavity, symmetric perturbation, appl. of group theory methods 8=10943
 - 3 cm, superconducting cylindrical iris resonator 8=6362
 - InSb, microwave emission 8=9112

radiators

- antennas for astronomy, 36 in array with resolutions of 1, 3, 9 and 27 seconds of arc at 11 cms 8=10442

Electromagnetic waves—contd
radiators—contd

- antenna, cylindrical, in lossy magnetoplasma, admittance calc. 8=19901
- antennas focused in Fresnel zone, field calc. 8=3268
- antennae, logarithmic periodic, investigation 8=10977
- antenna in plasma, quasi-static approximation 8=15423
- antenna polar diagram, Fresnel zone field meas. 8=19900
- antennas subsurface, impedance properties rel. to localized conductivity perturbation 8=10971
- antenna in weak plasma, current propag. constant 8=16528
- aperiodic waveguide array 8=19890
- circular apertures, Laguerre functions appl. 8=19898
- circular array, fast 360° beam rotation 8=19893
- cylinder, shadow region from slot, increasing radiation level 8=10972
- cylindrical antennas, planar and collinear arrays, current and impedance 8=10973
- decimetre waves, low angle radiation, antenna meas. 8=18896
- dielectric line, radiation from free end 8=19891
- dielectric sheath, enhanced radiation, tuning 8=10978
- dipole emitters, identical, resonance interaction between 2 8=21032
- dipole field, diffraction by conducting half plane 8=3258
- dipole in medium with space dispersion 8=15422
- dipole over moving dielectric medium 8=383
- dipole in plasma, warm, induced acoustic source effect on impedance 8=4386
- dipoles, small, tuned, effect of plasma on 8=6398
- by dislocation motion in ionic crystal 8=17637
- ferrites, rel. to nonlinear spin resonance 8=18395
- field calc. for excitation of transient oscillations in isotropic plasma 8=21332
- fields of accelerated dipole, Heaviside-Feynman expression 8=19825
- field radiated by line sources on wedge covered with finite distrib. of dielectric 8=10974
- hollow conducting cylinders, re-radiation 8=19865
- linear antenna over tapered ground screen, rad. pattern 8=10976
- monopole, quarter wave, impedance meas. in isotropic plasma 8=19897
- moving charges in electric and mag. field, overall emission 8=3269
- plasma antenna in nuclear environment 8=4422
- radiating functions, pseudo-radiation conditions for derivatives 8=381
- radiation from charge moving in magneto-active plasma with l.f. oscillations 8=21385
- radiation-patterns of sources in presence of dielectric layers 8=10975
- radiometer signal compensation 8=3271
- reciprocity of fields and currents 8=15421
- reflector system, Doppler effects due to rotation 8=3270
- reflectors, Laguerre functions appl. 8=19898
- ruby laser radar transmitter, single-mode, characts. 8=11077
- satellite antenna, proton gyrofrequency effect on resonance at electron plasma frequency 8=6400
- single quanta detection using p-n junctions 8=382
- Smith-Purcell effect, theory 8=10941
- spherical array of circularly polarized elements 8=19896
- spherical reflectors, feeds 8=19894
- wire loop antennas, radiation and scatt. patterns 8=19895
- n-InSb microwave emission during plasma formation 8=22600

Electromagnetism

- See also Electrodynamics; Quantum electrodynamics.
- Appell's eqns., appl. to electromechanical systems 8=15268
- atoms in mag. field, resonant freq. shifts rel. to electrostatic potentials 8=314
- complex ϵ and μ meas. at microwaves 8=6399
- devices, simulation of dynamic characts. 8=6285
- electric field in semi-infinite medium whose conduct varies laterally calc. 8=19756
- flow transducers, principles and eqns. 8=16635
- impedance and inductance meas. by twin-T bridges at 10 MHz 8=303
- induction drive for spectrograph shutter 8=15535
- linear motor, induced currents in secondary 8=15197
- magnetic monopole analogue in gravitation theory 8=6078
- magnet, uniform transverse field, coil forces, exact solution 8=19747
- massive circuits, transient behaviour 8=10867
- null field in form of spherical radiation 8=3175
- one-body problem, renormalization of moment of inertia 8=6286
- in orbital accelerators, parasitic current compensation 8=635
- partition method for sol. of equations with partial derivatives extending to impurity 8=15267
- point-particle with mag. dipole moment, Einstein-Maxwell eqn. approx. soln. 8=313
- potentials in Landau gauge 8=312
- potentials, physical non-reality 8=6289
- Poynting vector in static fields, correct usage 8=10946
- relativity, four-potential term, non-positive-definite 8=14980

Electromagnetism—contd

- relativity, unification with gravitation, geodesic principle 8=83
- resonances, free dielectric spheres in infinite medium 8=10979
- shock e.m. waves 8=3254
- tensor Green's function, singularities 8=19758
- theorem, general average force-energy 8=6287
- theory, junior college course 8=19757
- Wiener-Hopf equations, application to boundary value problems 8=2884
- Electromagnets.** See Magnets.
- Electromechanical effects.** See Electrostriction; Piezoelectricity.
- Electrometers.** See Electrical measurement.
- Electromotive force**
 - cells with alkali halide solns. in normal and heavy water 8=4527
- ferromagnetic films, magnetization inversion by Barkhausen-Cisman-Brion method, e.m. aspect 8=22781
- magnetrons, calculations from geometry and magnetic field 8=15333
- in metal conductor, time variation 8=19721
- solid-state electrochem. cells 8=14425
- PbS chemical films, photovoltaic effect of const. current 8=18234
- Electron affinity.** See Atoms; Ionization; Molecules; Solids.
- Electron annihilation.** See Electron pairs/annihilation.
- Electron avalanches.** See Breakdown, electric.
- Electron beams**
 - See also Electron optics; Particle accelerators.
 - aberration in magnetic deflection fields 8=10897
 - absorption coefficient, mean, depend. on Bragg deviation parameter 8=8497
 - accelerator, effect of metallic walls in storage rings 8=15670
 - accelerator, linear, radial motion 8=633
 - alkali halides rel. to band params. and plasmon energy, energy loss obs. 8=8938
 - beam-plasma system, em. wave propag. 8=7765
 - break-up in linear accelerator, asymptotic theory 8=20230
 - Brillouin, in tube of rectangular section 8=15300
 - bunched, microtron injection 8=3494
 - calorimeter, total absorpt. up to 15 kW 8=11462
 - collisional energy transfer 8=3200
 - collisions, radiation correction to scatt. 8=711
 - compression of, by a magnetic field 8=326
 - contact potential difference measurement, and Kelvin method, direct comparison 8=13700
 - current density profile, 10-200 V range, automatic plotter 8=3197
 - deflection by laser standing wave, obs. 8=19784
 - devices for mm and sub-mm wave generation 8=380
 - disc, in electrostatic field 8=19783
 - diffraction study of atomic surface structure 8=22012
 - discrete charges in crossed elec. and mag. fields, rotating ring stability 8=6291
 - disintegration in low-voltage arc plasma 8=16425
 - drilling of diamond dies 8=14906
 - e⁻-e⁺ beam collisions, infrared radiative corrections 8=592
 - e⁻-e⁺ colliding beams in alternating magnetic field storage rings at 280 MeV 8=20243
 - electron, ion and laser beams technology, conference, Berkeley, USA (1967) 8=15283
 - energy anal. of pulsed beam 8=328
 - energy spread from duoplasmatron source 8=16608
 - fine focussed, meas. of semiconductor characts. 8=22575
 - focusing and stability, in periodic mag. fields 8=10895
 - focusing by periodic permanent magnet for mm wave tubes 8=6308
 - focusing device, magnetic, suitable for mm wave tubes 8=10896
 - 40 keV, sharp sporadic increases beyond boundary of distant radiation zone 8=9956
 - gun, computer soln. of design eqns. 8=15284
 - guns, crossed-field, space charge effect on shot noise 8=19781
 - gun with curved cathode, simple model 8=19782
 - guns, effect of press. and kind of residual gas 8=15292
 - gun, high current suitable for use down to ins pulse length 8=15286
 - guns, high perveance three-electrode, theory and applications 8=10889
 - gun for linear accelerator 8=15659
 - guns, low energy 8=329
 - guns, for tuning and mapping of complex mag. systems and fields 8=15289
 - gyrating, interaction with cold plasma in mag. field 8=16501
 - helical, magnetically confined by two-anode electron guns 8=327
 - high current telefocus gun of the triode type 8=15282
 - high voltage, d.c. supply 8=15290
 - injection for accelerator with multiple pulse width and intensity capability 8=15658
 - instability associated with a 35 MeV medical betatron 8=6710
 - interaction with inhomogeneous u.h.f. fields 8=15302
 - interference and polarization relationship 8=10894

Electron beams—contd

- irradiation sample size restrictions 8=10892
 - klystron operation from wave coupling on beam modulation by low freq. 8=1397
 - Landau damping in 8=6299
 - magnetic deflection fields, one-dimensional production and analysis 8=19789
 - magnetically focused, conds. for space-charge compensation 8=6300
 - metal and semiconductor films, thin, transmission, reflection and adsorpt. 8=22494
 - microtron, correction to magnetic fringing fields 8=6708
 - minimum spot size, depend. on space charge 8=15306
 - monitoring by secondary emission 8=3198
 - monochromator for atom excitation cross-section data 8=12077
 - monoenergetic, transmission curves at 100 and 150 keV, rel. to measuring geometry 8=15734
 - 150 kV machine, for machining 8=15297
 - Penning discharge in vacuum, energy spectra 8=7648
 - in periodic electric fields, reduction factor for space-charge field 8=322
 - Pierce gun, beam characteristics for large beam currents and voltages 8=15296
 - Pierce gun, dimensioning, inclusion of relativistic electron speeds 8=15295
 - in plasma, current-convective instability 8=21292
 - plasma, two stream instability rel. to anomalous electron heating during adiabatic compression 8=12471
 - polarized, prod. by trapping in magnetic bottle with polarized H atoms 8=15304
 - probe, focusing props., shadow image meas. 8=15305
 - probing of semiconductor materials and devices 8=18026
 - proportioning by triacetate films 8=10890
 - quasi-neutral, current cut-off, and electron-ion oscs. 8=3199
 - radial, interaction perturbations 8=3193
 - radially divergent, interaction with e.m. wave 8=6297
 - radial, space-charge waves 8=15291
 - reflection coeff. for zero-energy electrons from Ag surface 8=6301-2
 - refraction in intense e.m. wave 8=19761
 - relativistic, partially immersed, equilibrium solutions 8=3196
 - ρ production, e^+e^- collisions 8=812
 - ring beam electron gun, theory 8=15280
 - ripple of, focused by an axially symmetric magnetic field 8=325
 - runaway, quasilinear theory 8=1377
 - slow down spectra for graphite and Al absorpt. at 10, 20 and 40 MeV 8=20769
 - in solids, energy loss rate and X-ray prod. depth distrib. obs. 8=17693
 - sources for linear accelerators, safe radiotherapy 8=5985
 - space charge compensation conditions, high-power 8=10891
 - space charge wave propagation 8=7767
 - in stationary field with rotating axial symmetry 8=15288
 - straight-line, in crossed fields, statistical characteristics 8=15301
 - technology and US standards 8=6298
 - telefocus, one-step reducing technique for microfocus X-ray unit 8=15583
 - thin, in crossed fields, diocotron amplification rel. to shape 8=15294
 - transient phenomena when injected in accelerating cavity with circular iris 8=15287
 - travelling wave tubes, beam interaction with space-harmonic fields 8=10910
 - trochoidal beams, of large space-charge, prod. in crossed elec. and mag. fields 8=15293
 - two-beam approx. for thickness fringes with wedge-shaped crystals, comment 8=8498
 - Wien filter, optimum adjustment 8=10899
 - and X-ray prod. in solid targets, Monte Carlo calc. 8=18793
 - Al, electron slowing-down, total electron flux, energy spectrum 8=13474
 - Al_2O_3 , amorphous and polycryst., charact. energy-loss spectra and $-Im\epsilon^{-1}$ 8=13695
 - Ar, solid, excitons and band gap from charact. energy loss obs. 8=9194
 - in Be-Au, two-layer target, energy losses 8=22496
 - Cu calorimeter for 15 kW beams 8=11462
 - Fe-Al alloys, charact. energy losses 8=17912
 - GaP, energy loss probability, retardation effects 8=22497
 - Si, energy loss probability, retardation effects 8=22497
- absorption.** See Electrons/absorption.
- effects**
- See also Beta-rays/effects.
 - alkali halides, colour centre studies by pulsed irradiation 8=13460
 - alkali halides, colour centres and sputtering, formation theory 8=13472
 - alkali halides, e^+ annihilation spectrum 8=13694
 - anthracene and plastic scintillator, radiation damage by $4 \rightarrow 10$ keV electrons 8=23029
 - atom displacement in collision cascade 8=8754

Electron beams—contd**effects—contd**

- beam-plasma discharge, steady state condition 8=21294
- beam-plasma system, h.f. and l.f. oscillations interactions 8=12539
- bremsstrahlung, from crystal, high polarization 8=13465
- cathodoluminescence, electron-probe meas. 8=1754
- crystalline solids, fusion by shock wave 8=8757
- diamonds, natural, on luminescence 8=18596
- electron-microscope specimens, temp. distrib. calc. 8=1861
- e.m. showers in solids, computer-operated system for studying 8=8753
- excitation of plasma oscs. 8=7813
- foils, e^+ annihilation as f (thickness, Z) 8=13693
- gas fluorescence, for shock wave meas. 8=3033
- graphite electrodes for spectroscopy, purification 8=23187
- hydrogenated terphenyls, comp. and props. charge, rel. to use as reactor coolant 8=14445
- instability of two counter streaming beams, quasi-linear 8=10912
- insulators, rel. to space-charge effects 8=9185
- ion accel. apparatus and meas. 8=15337
- ionizer, weak field for ion source 8=19798
- K-ionization by relativistic electron theory 8=4994
- machining, beam divergence and electron diffusion heating in boundary area 8=15285
- magnetically deflected, coma-dominated aberration 8=333
- metal film rel. to orientation and X-ray production efficiency 8=13221
- metal films, equilibrium potential, during polymerization of adsorbed org. layers 8=2251
- metal irradiation, meas. cryostat 8=17692
- microwave amplification, interaction with plasma 8=12570
- organic liquids, scintillation 8=12893
- paraffins mols. energy transfer to vibr. degrees of freedom and dissoc. probability calc. 8=4206
- penetration in solids at moderation energies, meas. 8=176
- Permalloy, possibility of vaporization 8=8189
- photoresistors, polymerizing threshold and sensitivity to flux 8=22236
- plasma, beat and harmonic generation 8=7758
- plasma column, pseudo-sound wave excitation 8=16570
- plasma, extremely hot electrons prod. 8=21306
- plasma interaction with transverse modulation 8=4368
- plasma, longit. high freq. waves generation 8=21387
- plasma oscillations generated by relativistic beam 8=7818
- plasma prod., temp. distrib. and oscillations 8=21287
- plasma, u. h. f. e. m. waves radiated rel. to instability mechanism 8=16520
- polyethylene terephthalate, rel. to space-charge effects 8=9185
- polymer, etch-resisting, cross-linking, rel. to integrated cct. prod. 8=15279
- probe microanalyzers, X-ray counting systems, non-linearity corrections 8=4837
- quasi-stationary plasma oscillations, amplification 8=7816
- semiconductors, design of β -spectrograph for meas. 8=11466
- semiconductors, e.m. wave excitation, quasilinear theory 8=5151
- Smith-Purcell effect, theory 8=10941
- spot distortion by mag. deflection of beam 8=6306
- steel, stainless, -induced desorption of gas from surfaces 8=17164
- Teflon friction on steel, adhesion component modification, obs. 8=17842
- water, e-photon cascade calc. 8=21722
- X-ray production from crystals, emission yield dependence on diff. conditions of electrons 8=13237
- Ag, rad. prod. at grazing angles, interpret. via surface-waves 8=3181
- Al, on deformation at 20°K rel. to dislocation model with defect barriers 8=13523
- Al, 50 kV electron mean free path for plasmon excitation; diff. condition effect 8=13696
- Al foils, plasmon excitation cross-sections 8=8966
- Al, irradiated, stage III annealing study 8=13475
- Al, low temp. irradi., electrical resistivity recovery 8=2134
- Al, resistivity recovery, kinetics study 8=5171
- Al, stage I recovery atomic recoil energy dependence from e-irrad. data 8=4961
- Al, 20 keV, excitation of L-shell electrons 8=22495
- Al_2O_3 , 20 keV, excitation of L-shell electrons 8=22495
- Al-1 at. %Zn, irradiation hardening 8=8822
- Ar ionization near threshold 8=7711
- As_2S_3 , amorphous, carrier mobilities from conductivity studies on e-irradiation 8=18162
- Ba atoms, polarization of light emitted and lifetimes of excited levels 8=21019
- Be, e-irradiated, recovery meas. 27-77°K 8=22249
- Be, low temp. irradi., electrical resistivity recovery 8=2134
- Be target, secondary emission, calibration monitor 8=6808
- CO_2 , ionization curves 8=12434
- CdSe, acoustoelectric effect in continuous intense super-sonic stream 8=8628
- Cu, e.m. shower study with computer-controlled system 8=8753

Electron beams—contd
effects—contd

- Cu, electron irradiated, yield stress increase 8=17773
 Cu, electron slowing-down, total electron flux, energy spectrum 8=13474
 Cu films, thickness depend. on heat generated, 9 to 100 keV 8=17699
 Cu, shock waves 8=13484
 Fe, irradi., anisotropy of defect production 8=8770
 p-Ge, angular dependence of radiation-induced conductivity and secondary emission 8=18041
 Ge atom displacement in collision cascade calcs. 8=8754
 p-Ge, bombardment-produced defects at low temps. 8=22170
 Ge, e-irradiated, annealing of Hall mobility changes 8=2196
 Ge, fast electrons, optical absorption edge 8=9534
 Ge, interstitial Cu impurity, irradi. induced, obs. 8=2027
 p-Ge, on microhardness 8=17810
 n-Ge, subthreshold damage 8=22252
 Ge, zone melting and recryst. 8=17235
 H₂ and D₂, excitation by trapped-electron method 8=16281
 H₂, Lyman- α prod. 8=12050
 InS crystals, on twinning and phase transformations 8=17209
 KBr, colour centre studies by pulsed irradiation 8=13460
 MgF₂ films, thin, surface charging 8=22505
 Mo/absorbed CO system, physico-chemisorption processes from study of low energy electron interactions 8=18702
 NH₃ gas, radiolysis 8=18743-4
 N₂O, ionization curves 8=12434
 Ni-20%Cu, penetration at moderate energies, meas. 8=17694
 Ni and W ribbons exposed to water, low-energy bombardment 8=21907
 O₂ dissociation and extreme u.v. radiation excitation 8=7722
 Pt, damage on irradiation at 90°K rel. to built-in annealing damage 8=1947
 Si Brillouin zone symm. props. obs. by e⁻ annihilation 8=13690
 n-Si, elec. props. rel. to impurity and irradiation-temp. dependence 8=5282
 Si, heated, stress investigation, X-ray and i.r. studies 8=1862
 Si: Li, irradi. prod. defects and annealing at 20°C, 1 MeV 8=22604
 Si photocells, rectifying props., effect of accelerated electron irradiation 8=22699
 SiO₂ films on Si, damage rel. to etching rate 8=22609
 Si:P, defect production rel. to spin-lattice relax 8=18434
 Ti-Mg oxide, getterizing effect in vacuo 8=10458
 V₂O₅ (010) surface structure transitions in LEED expt. 8=4733
 W, desorption of CO, NO and O 8=21912
 W, of CO, desorption by electron impact 8=21911
 W/N₂ system, rel. to phase changes of adsorbed N₂ 8=21913
 ZnS, u.v. luminesc. excitation 8=18619

ionization. See Electrons/ionization.

Electron capture. See Ions/recombination; Radioactivity/electron capture.**Electron diffraction**

- biprism interference, low energy 8=330
 crystals, LEED intensities, dynamical Bethe theory 8=17325
 extinction distance, several-beam dynamic theory 8=6304
 high resolution, use of electron microscope 8=6316
 inert gases, sector-microphotometer scatt. meas. 8=7447
 intensity meas. methods, comparison 8=6305
 low energy apparatus, improved spot size 8=15306
 low energy intensities, band structure treatment, solid surface 8=5110
 theory, transmission electron microscopy, fundamentals, book 8=15316

Electron diffraction crystallography

- See also Crystal structure, atomic.
 absorption coefficient, mean, depend. on Bragg deviation parameter 8=8497
 anomalous absorpt. when incident beam is Bragg diffracted 8=17362
 atomic scattering amplitudes in solids for 40-100 keV electrons 8=13240
 n-beam theory for diffuse scattering 8=13236
 diffractometer attachment for e microscope 8=19792
 diffuse scattering by lattice particles in new phase on phase transformations 8=1773
 diffuse scattering in diffr. patterns, theory and computational methods 8=13232
 dynamical effects at high voltages 8=13239
 extended internal defects, effect on Debye-Waller factor 8=1779
 filters for thick polycrystalline metal foils 8=8455
 hexagonal crystals, transmission pattern indexing using four-axis reciprocal lattice 8=17309
 indexing reflections on 3- or 4-circle diffractometers, graphical aid 8=17320
 Kikuchi line eqn. from model of origin of P patterns 8=1778

Electron diffraction crystallography—contd

- kinematical theory appl. to screw dislocation image evaluation 8=22194
 LEED intensities, dynamical Bethe theory 8=17325
 LEED intensities, multiple diffr. origin 8=13238
 low energy, sensitivity rel. to surface perfection 8=4726
 low and high combined, ultra-high vacuum system 8=4834
 microscopy, column approx. validity 8=8499
 moiré fringes, dynamical effects 8=21977
 molecular structure in high temp. vapour rel. to excited vibrational populations 8=16245
 one-dimensional crystal models, slow electron scattering 8=22011
 pattern geometry of slow electrons rel. to 2D and 3D reciprocal lattices 8=17324
 quasi-free atoms, electron scattering 8=12093
 R factors for constant-count-per-reflection expts. 8=8491
 reciprocity theorem, and appl. to microscopy 8=13241
 relativistic dynamical theory including inelastic scattering 8=13231
 structure parameters from intensity meas. 8=13230
 surface lattice distortion rel. to Debye-Waller factors 8=1780
 surface, with simultaneous X-ray emission meas. 8=8290
 thin films, Debye-Waller factors calc. from Mössbauer effect 8=8207
 trace characterization-chemical and physical, symposium NBS, USA, Oct. 1966 8=8437
 two-beam approx. for thickness fringes with wedge-shaped crystals, comment 8=8498
 X-ray production from crystals, emission yield dependence on diffr. conditions of electrons 8=13237

Electron diffraction examination of materials

- amorphous, background intensity estimation 8=8443
 boron oxide, in vapour, "washing out" effect 8=16266
 crystal imperfections, techniques and limitations 8=17597
 crystal surfaces, structure and props, study with LEED 8=17116
 diatomic gas, molecular structure determ. 8=4115
 of electronic structures of atoms and mols., importance of small angle domains 8=12045
 ferromagnetic films, Fraunhofer images from single domain walls, characts. 8=22772
 films during growth, small angle filtered method 8=8306
 films, structure of organic and inorganic, and study of minerals 8=8309
 films, thin, filtered and unfiltered intensities 8=1777
 foils with stacking fault or antiphase boundary, fine structure of weak beams 8=1781
 gas-covered surfaces, kinetic electron ejection model 8=16435
 gases, regularization method 8=12698
 growing thin films, scanning reflexion method 8=17265
 lamellar mixture of two close-packed phases, anomalous spots in patterns 8=13235
 magnetrons, space-charge density influencing adiabatic theory 8=15331
 metal films, epitaxial growth on NaCl and KCl in vacuum 8=13147
 metal foils, images calc. rel. to strong simultaneous reflections 8=13234
 metal smoke particles prep. by evap. 8=4839
 mica, LEED obs. of electric dipoles on cleaved surface 8=22650
 muscovite, superstructure when heated in vacuum 8=17285
 polycrystalline solids, validity of Debye scattering equation 8=8444
 PVC single crystals 8=17300
 surface superstructures, pseudo-, and low energy multiple scattering 8=1752
 Ag, 0.16 μ thick, with 50 KV electrons, use of filters 8=8455
 Ag(III) face, by LEED rel. to secondary emission 8=17212
 Al, 1 μ thick, with 50 KV electrons, use of filters 8=8455
 Al-Ag(20%) alloy films dynamical multiple reflections 8=13256
 Al₂O₃, vapour-deposited, transitions from 300°C to 1200°C 8=13061
 Au, foils, filtered intensities, temp. dependence 8=8509
 Au single crystal film, structural and texture changes due to ion bombardment 8=17124
 Au-Cu alloy single crystal film, structural and texture changes due to ion bombardment 8=17124
 Ba(UO₂AsO₄)₂ · nH₂O, metaheirichite 8=17360
 C fibres, high modulus 8=8457-8
 CdS, thin films, structure and phase composition 8=4746
 Co films, ferromag., images of periodic domain structure 8=22772
 Cu, oxidised single crysts., exam. by slow electron diffr. 8=13258
 Cu single crystal film, structural and texture changes due to ion bombardment 8=17124
 Cu-Al alloys, structure of martensites 8=4871-2
 CuAu II films containing Zn, dynamical multiple reflections 8=13256
 Cu-Be-Al alloys, ageing characts. obs. 8=22335
 Cu(UO₂ · AsO₄)₂ · 2H₂O, meta-zeunerite 8=17360

Electron diffraction examination of materials--contd

- Fe(011) surface, O adsorption, low energy study 8=1701
 Fe-20 at. % Al alloy, structure factor variations for electrons with accelerating voltage 8=13260
 Fe_2O_3 , diffraction of slow electrons at octahedral surface 8=8520
 GaO , gaseous, using sector-microphotometer 8=16290
 H atom localization by electronographic method 8=13233
 H_2 solid 8=8465
 In-Al liq. alloys, charact. energy losses of 8 keV electrons 8=12791
 In-Bi liq. alloys, charact. energy losses of 8 keV electrons 8=12791
 InO , gaseous, using sector-microphotometer 8=16290
 InSb films, epitaxial growth 8=21884
 KrF_2 and SiF_4 mixt. identification in sample believed to be KrF_4 , and KrF_2 struct. 8=17383
 Li metaborate, in vapour, "washing out" effect 8=16266
 $\text{K}(\text{UO}_2\text{AsO}_4) \cdot 3\text{H}_2\text{O}$, abermathyite 8=17360
 LiF plates to meas. inelastic diffr. 8=1782
 $\text{Mg}(\text{UO}_2\text{AsO}_4)_2 \cdot \text{nH}_2\text{O}$, novacekite 8=17360
 Mo crystals with adsorbed O_2 surface exam. by LEED and work function studies 8=17165
 $\text{Mo}(\text{CO})_6$, intensity values rel. to structure determ. 8=12236
 MoF_6 , intensity values rel. to structure determ. 8=12236
 MoS_2 polytypes 8=17397
 by NH_3 gas, chem. bonding effect 8=6303
 Nb_2O_5 , high temp. and related phases 8=22033
 Ni, forbidden reflexions viewed from band theory 8=2105
 Ni-Fe films, lattice contractions 8=1806
 NiO crystals, structure study rel. to (100) face 8=8379
 NiO solid 8=8465
 O_2 solid 8=8465
 OsO_4 , intensity values rel. to structure determ. 8=12236
 Sb-Sn alloys, oxidation products 8=13287
 Se films, polycrystalline and single crystal, extra reflections 8=4753
 Si, anomalous scattering coeffs., determ. 8=13289
 $\text{Si}(111)$, study of Ni induced surface structure 8=4732
 $\text{Si}(111)$ surface, low energy study of PH_3 adsorption 8=4765
 Sn condensed at low-pressure, abnormal reflections due to preferred orientation 8=13154
 Te films, vac.-evaporated, forbidden reflexes 8=17141
 TeF_6 , intensity values rel. to structure determ. 8=12236
 UF_6 , intensity values rel. to structure determ. 8=12236
 VBr_4 , in gas-phase 8=16303
 VCl_4 , in gas-phase 8=16303
 V_2O_5 , low-energy study of surface 8=21870
 $\text{V}_2\text{O}_5(101)$ surface structure transitions, e-induced in LEED expt. 8=4733
 $\text{W}(\text{CO})_6$, intensity values rel. to structure determ. 8=12236
 WF_6 , intensity values rel. to structure determ. 8=12236
 XeF_6 , pseudo-Jahn-Teller effect evidence 8=7552
 XeF_6 symmetry obs. 8=17383

Electron emission

- See also Fluctuations/electrical; Photoelectricity.
 emission from and adsorpt. on a substrate surface in equilib. with ionized vapour 8=18263
 exo, in Geiger counter 8=15634
 metal gas interface, Thomas-Fermi-Dirac model of quantum mechanical contrib. 8=5414
 metals, field thermionic and T-emission, current tangential to surface 8=5410
 polymers in vibro-mech. treatment, obs. 8=18253
 radioactive atoms in crystal, spacial dependence, wave mechanical treatment 8=17910
 steel, exoemission due to sliding friction, obs. 8=18254
 Ag catalyst, exo-emission, chem. stimulation 8=22711
 $\alpha\text{-Ag}_2\text{S}$ mixed conductor, surface potential meas. rel. to electronic props. 8=22500
 Al, effect of abrasion in air, O_2 , N_2 and H_2O vap. 8=9270
 Al, exoemission due to sliding friction, obs. 8=18254
 Au-Ba alloys, work function 8=18245
 Ba-Pd, Ba-Pt, Ba-Rh alloys, work function 8=18245
 Be, spacial distrib., due to focused laser beam 8=13947
 C, spacial distrib., due to focused laser beam 8=13947
 CaF_2 exo-emission, thermostimulated, rel. to calcination and X-ray dosage, obs. 8=14305
 Cr, electronic structure investigation 8=22457
 Cs film on Ir, and adsorption, microscopy 8=9268
 Fe, exoemission due to sliding friction, obs. 8=18254
 K surface (100), under proton bombardment 8=18249
 MgF_2 films, solid, Molter emission 8=22732
 Mo, Auger electron yield on Ar⁺ and He⁺ bombardment 8=9279
 Mo films on W crystal, and adsorption 8=9269
 Mo, spacial distrib., due to focused laser beam 8=13947
 NaCl containing F-centres, photostimulated exo-emission 8=5409
 Ni exoemission, photostimulated, during ferro-paramag. transition, obs. 8=2273
 NiO exoemission, photostimulated during antiferro-paramag. transition, obs. 8=2273
 Si, n- and p-type, mechanically treated, surface exoemission 8=18255
 $\text{SiO}_2\text{-C}$ structure, anomalous auto-emission 8=22712
 Sn oxide films, from high resist. regions 8=22713
 Ta, laser induced, using pulsed Ar laser 8=18271
 W, laser induced, using pulsed Ar laser 8=18271

**Electron emission--contd
field emission**

- cathode, high-density, produced by voltage-breakdown process 8=18257
 Nottingham energy exchange process, effect of different surface barrier models 8=13929
 potential barrier, influence of space charge 8=9271
 surface potential barrier in theory 8=22714
 Ge, field emitters, Fowler Nordheim plots 8=5412
 Li film on W and Re faces, effect of film thickness and substrate orientation on work function 8=18256
 Mo, anomalous total-energy distribution 8=5411
 Mo tip, absorption of O_2 , H_2 , and N_2 , study 8=21905
 Nb surfaces, microscope study 8=13930
 SiC whisker 8=9272
 U films on W, work function rel. to state of adsorption 8=22715
 W, carbon adsorbed, high temp. effect of oxygen and air 8=2276
 W, electron total energy distrib. and work function, and effects of Zr-O coating 8=5413
 W, (110) surface, rel. to atomic perfection 8=2275
- photoelectric**
 alkali antimonides, double photon 8=18278
 alkali halides, energy spectra for prod. by soft X-rays 8=18274
 device for large currents from small u.v. sources, for swarm expts. 8=5416
 energy distrib., obs., double modulation method 8=13935
 films, thin, effects of optical parameters 8=13936
 films, thin metal, vectorial selective surface effects 8=22950
 gases, single grid spectrometer 8=16441
 indene polyassociates, conjugated 8=13938
 interference-enhanced 8=18276
 on laser light interaction with conductors, semiconductors and dielectrics 8=18272
 rel. to light statistical props. meas., e emission distrib. 8=15493
 metal-SiO₂-CdSe (metal) contacts, photocurrent studies 8=2281
 M-O-M sandwich, rel. to electroluminescence 8=9277
 metals, due to short laser pulses, many-quantum effect 8=399
 metal surface external photoeffect, theory 8=22720
 metals, vacuum u. v. 8=13934
 method for u. v. reflection spectra 8=15532
 multialkali-antimonide, anomalous vector effect 8=2282
 in near i. r., enhancement of quantum efficiency of photocathodes 8=13933
 particle detectors, single-electron detection 8=11463
 photocathodes in SEM, spectral depend. of quantum yields, 75-300Å 8=19795
 photon counting statistics rel. to anal. of light fluctuations 8=6425
 random-walk models 8=22719
 scintillation counters, rel. to minimum time resolution 8=20192
 screened potential model, Z = 13-92, table of cross-sections 8=7438
 theory of radiation field interacting with photo-detector 8=20037
 thin films, spectral shift and degradation 8=18282
 Ag, laser-induced non-linear photoelectric effect 8=22721
 Ag, plasmon excitation, discrete energy loss 8=2279
 Ag-O-Cs photocathodes, instability caused by residual Cs vapour 8=18275
 Al-Al₂O₃-Ag sandwich, rel. to electroluminescence 8=9277
 Al-Al₂O₃-Au film system, rel. to contact barrier height determ. 8=18277
 Al-Al₂O₃-Au thin film structures, internal yields, Monte Carlo calcs. 8=22722
 Al, 40-411 keV, scatt. cross-section 8=1188
 Au, laser-induced non-linear photoelectric effect 8=22721
 BaTe, using magnetic velocity-analyser tube 8=2280
 Be-BeO-Au sandwich, rel. to electroluminescence 8=9277
 CaF_2 , F-treated, photocathodes, spectral characts. 8=18281
 Co, electronic structure 8=22723
 CsI two-photon quantum yield, 6-8.5 eV 8=18279
 Cs₂Sb, time depend. of absorpt. and photoemission 8=13937
 Eu cpds., determ. of chem. shifts of inner levels 8=16971
 Fe, cross-section for K-Mv subshells for X-rays 412-1332 keV 8=7438
 I cpds., determ. of chem. shifts of inner levels 8=16971
 In rel. to density of states, obs. 8=13718
 InAs, rel. to surface props. and interband transitions 8=5417
 InP-Cs-O 8=22724
 KBr and KBr:Ti, F-centres, mechanisms rel. to surface contamination, obs. 8=9278
 KCl monocrystals, between 3 and 5.5 eV 8=18280
 KCl and KCl:Ti, F-centres, mechanisms rel. to surface contamination, obs. 8=9278
 KI monocrystals, between 3 and 5.5 eV 8=18280
 Mg cpds, energy spectra for prod. by soft X-rays 8=18274
 MgF_2 , F-treated, photocathodes, spectral characts. 8=18281
 NaCl F-centres, mechanisms rel. to surface contamination, obs. 8=9278

Electron emission—contd

photoelectric—contd

- Ni, density of states, rel. to X-ray and ion neutralization studies 8=8940
 Ni, ferromagnetic, energy distrib. and rigid-band model 8=13940
 Ni, laser-induced non-linear photoelectric effect 8=22721
 Ni-Al alloys, ferromagnetic, energy distrib. and rigid-band model 8=13940
 Pd, plasmon excitation, discrete energy loss 8=2279
 Rh, photoelectron into liq. hydrocarbons 8=8113
 Se, amorphous layers and single crystals, studies 8=22725
 Si, autophotoemission energy rel. to e distrib. 8=22726
 Sn, cross-section for K-Mv subshells for X-rays 412-1332 keV 8=7438
 SnO, S-11, S-20, modified S-I and high temp. bi-alkali photocathodes, spectral shift and degradation 8=18282
 SrO, and photoluminescence and enhanced thermionic emission 8=23063
 U, cross-section for K-Mv subshells for X-rays 412-1332 keV 8=7438
 U films, photoelectron attenuation lengths 8=22727
 U monolayer film on polycrystalline W, work function 8=5408

secondary

- Auger electrons for surface segregation obs. 8=22730
 coefficient dependence on energy of primary electrons 8=22728
 crossed-field distributed-emission amplifier, effects in computer simulation 8=19712
 e beam monitoring device 8=3198
 electron-excited Auger electrons for material analysis 8=22729
 gas-covered surfaces, by Ar atoms and ions 8=22731
 glass, degassing by 100-1000 eV bombardment 8=13945
 ion extraction effect in plasma sheath 8=4389
 on laser light interaction with conductors, semiconductors and dielectrics 8=18272
 magnetron diode, space-charge interactions 8=15332
 metallic target, by Auger de-excitation of atoms by sputtering 8=5422
 in microanalysis probe, meas. 8=13941
 negative glow and Faraday dark space 8=16409
 oils, diffusion pump, study by pulsed-beam method 8=13942
 photomultiplier afterpulses, 3:1 ion ratio 8=5418
 Steel, bombarded with H⁺ ions 8=5423
 storage devices, resolution and frequency response 8=10906
 200-2000 eV energy curves, rapid method of determ. 8=5419
 yield, use of Polya statistics in anal. 8=5420
 Ag self-supporting films, and primary electron scatt. 8=2284
 Ag(III) face, rel. to exam. by LEED 8=17212
 Au cathode, rel. to temporal growth of ionization in D 8=12439
 Au films, coeff. on exit side, rel. to energy of primary electrons 8=2285
 Be, Faraday cup for calibration 8=6808
 Be, rel. to large incident angles of primary beam 8=5421
 CdS, e microprobe obs. 8=14317
 CsI, excitation density of slow secondary electrons, distrib. determin. 8=18283
 Cu, bombarded with H⁺ ions 8=5423
 Cu-Be alloys 8=13943
 p-Ge, e-irradiated, angular dependence of emission current 8=18041
 KCl transmission dynode, single electron response, Polya statistics 8=5420
 MgF₂ films, solid, rel. to Molter emission 8=22732
 MgF₂ films, thin, surface charging 8=22505
 Mo, bombarded with H⁺ ions 8=5423
 N₂ discharge, release by metastable N₂ 8=7663
 Ni, bombarded with H⁺ ions 8=5423
 Ni, ionization mechanism in Ne discharge 8=16419
 Ni, polycrystalline, temp. depend, 100 to 600°C 8=13944
 Pb, rel. to large incident angles of primary beam 8=5421
 PbO₂ layers, exptl. results discussed 8=18284
 SnO₂ layers, exptl. results discussed 8=18284
 Ta, bombarded with H⁺ ions 8=5423

thermionic

- See also Cathodes,
 converters, plasma physics 8=2277
 converters with surface ionization, diffusion mechanism for inter-electrode particles 8=2278
 metal crystal with oxide film, and ionic diffusion rel. to oxidation kinetics 8=5710
 metals, effect of surface micropatches on const. 8=18260
 oxide layers, thin unsaturated, phenomenological model 8=8979
 point-cathode electron source, simplified analysis 8=9273
 point cathodes, energy distrib. 8=9274
 from refractory compound surfaces, cesiated, rel. to stable, at 1500°, low work function surface 8=18262
 solid fine powder ionized in cold gas 8=2274
 space charge effect in oxide cathodes 8=18259
 thermionic conversion Specialists Conference San Diego USA October 1967 8=6273

Electron emission—contd

thermionic—contd

- transfer by negative ions 8=287
 transition-metals in Cs and F vapours, model 8=18261
 Au-GaAs Schottky barriers, dominant electron transport mechanism 8=13931
 Cs film in Ir, and adsorption, and field-emission microscopy 8=9268
 Hf, in Cs vapour, emission vs reciprocal temp. curves 8=18264
 Ir filament, periodic Schottky deviations at 1500-2000°K 8=5415
 Pt-group metals, in Cs vapour at T_c=414°K 8=18265
 Re, cesiated, evaluation of emitter surface 8=18269
 Re cesiated surface, evaluation 8=22717
 SrO, enhanced, and photoluminesc. and photoelectric emission 8=23063
 SrWO₄ (mixed normal and basic), and repeatable conversion and activation 8=18266
 Th₃ in Cs vapour, emission vs reciprocal temp. curves 8=18264
 Ti, in Cs vapour, emission vs reciprocal temp. curves 8=18264
 UC-ZrC, W clad, vacuum stability, effect of temp. to 2473°K 8=18267
 UO₂, W clad, vacuum stability, effect of temp. to 2473°K 8=18267
 W, cesiated, evaluation of emitter surface 8=18269
 W, cesiated, saturated emission rel. to energy conversion 8=18268
 W cesiated surface, evaluation 8=22717
 W, in Cs-additive system, work function, rel. to adsorbed mols. 8=15214
 W surface, influence of CsF adsorpt. on work function 8=18270
 W-La₂O₃ system alloys obs. 8=22716
- Electron energy states.** See Crvstal electron states.
Electron gas
 See also Metals/theory; Plasma; Solids/theory; Superconductivity.
 bremsstrahlung, photon spectrum 8=12503
 collective description in generalized r.p.a. 8=5143
 correlation energies at metallic densities 8=5137
 correl. energy calc., in slowly varying high density 8=10659
 coupled plasmon-particle excitation, behaviour of spectral weight function 8=17900
 crystallization and mag. ordering 8=22484
 degenerate, thermal resist. due to interaction between electrons 8=8960
 dielectric constant of dense electron gas with fixed point charge 8=8962
 electrodeless discharge, fast e population conditions 8=21229
 electron-impurity interactions, h.f. elec. cond., calc. 8=2999
 electron-impurity interactions, master eqns. 8=2998
 electron-impurity interactions, one-particle evolution eqns. 8=2997
 embedded atoms, statistical model calcs. 8=22486
 free electrons, ultrasonic absorption in quantizing mag. field 8=6165
 hot-, galvanomagnetic and thermomagnetic size effects 8=19466
 hot ionized, statistical mechanics, and collision theory, book 8=16455
 hydrodynamic equations 8=131
 interacting at high and metallic densities, pair distrib. function 8=17902
 interaction with nuclear or ionic spins via ferromagnetic s-f interaction 8=17898
 kinetic equations, for non-uniform relativistic 8=132
 magnetron cloud, natural freq. calc. 8=15328
 metal, e correlations 8=22483
 metallic interfaces, model, exchange-correlation and lattice potentials effects 8=2112
 plasma, resonant, iemp. and density var. 8=1419
 polarization, static, influence of exchange 8=13681
 polarized free, spin density oscillations 8=22482
 randomization, fast, by trapped electroacoustic waves 8=16580
 scattering of e m. waves in stellar atmosphere 8=15028
 screening around ion cores 8=22485
 semiconductors, dense electron-hole gas 8=8959
 semiconductors, Green function method for density 8=8889
 spectrum, single-particle, electron coupled to plasmons approx. 8=5145
 spectrum, single-particle, spectral weight-function structure 8=5144
 spin-density-wave, 3D case, with magnetic field, existence theorem 8=15022
 superfluid Fermi system, dynamics 8=130
 in thermionic converter plasmas, theory of electron transport phenomena 8=15235
 thermodynamic state with broken geometrical symmetry, existence 8=19465
 virial theorem, alternative proof 8=19464
 rel. to work function calc. 8=18243

Electron gas—contd

- Ar shock layer, density meas. 8=21265
- Fe-based alloys, representation of electron bands 8=13661
- Ga crystal thermal cond., size effects 8=17545
- InAs, light scattering by plasmons and Landau levels 8=22990

Electron guns. See Electron beams.**Electron lenses**

- See also Electron microscopes; Electron optics.
- aberration correction, spherical and chromatic, for fast electrons 8=15308
- objective, spherical aberration coeff., dependence on object position and magnification 8=19788
- quadrupole, aberrations, necessary coeffs. 8=3189
- quadrupole, in scanning microscope 8=334
- quadrupole, third-order aberrations calc. in rectangular model 8=6310
- quadrupole triplets, distortion free image formation 8=332
- refractive systems in spectrometers 8=16175

electrostatic

- "condenser-objective" for microscope up to 700 kV, spherical aberration and resolving power 8=19790
- cylindrical telescopic three-electrode systems 8=3205
- deflection defocussing 8=3206
- intermediate decelerators in electron microscopy 8=6309
- mirror analyser, spherical, comparison with spherical deflectors 8=15209
- quadrupole, linear accelerator beam shaping 8=15655

magnetic

- aberrations, spherical and chromatic, of non-circular lens 8=3207
- coma aberration 8=333
- condenser for e spectrometer 8=20389
- electron microscope objective, soln. for magnetic field 8=336
- iron-less quadripolar 8=15307
- magnetic field meas. at grid of spectrometer, ADI method 8=6337
- magnetron, space charge electrons, lifetimes meas. 8=6319
- quadrupole quadruplet, mech. aberrations 8=15312
- quadrupole quadruplet projector, electron-optical props. 8=15311
- spectrometer analysers, spherical aberration calculation 8=10898
- superconducting, optical characteristics 8=6311
- superconducting, optical constants calc. 8=19791
- three-dimensional with restricted propag. 8=15310
- transmission through aperture, application to retending p.d. 8=3204
- Yoke design rel. to electron beam aberration in magnetic deflection fields 8=10897

Electron microscope examination of materials

- biological systems, complemented by X-ray diffr. 8=14897
- cathodes, submicroscopic projections, in elec. breakdown 8=1343
- clay minerals—Al oxide, hydrous, mutual adsorption 8=8341
- colloidal aggregates, shape analysis 8=16906
- crystal imperfections 8=17269
- crystal imperfections, techniques and limitations 8=17597
- cube recrystallization texture formation 8=13129
- ethylene-butene-1 copolymers, crystalline structure 8=8598
- feldspar, plagioclase, etching and replicating technique 8=21930
- of field-ion specimen tips, interpret. of images 8=18285
- gibbsite in bauxites of Mas Rouge region 8=17275
- glass, thin, transmission 8=21995-6
- lamellar mixtures of 2 c. p. phases, stacking features 8=21974
- magnetic domains, direct obs. by scanning e micros. 8=18315
- of magnetic fields and domain structure 8=13991
- magnetic stripe domains, study 8=22778
- materials, conference, Boston, June 1967 8=8445
- mesomorphic phase 8=16796
- metal disc specimens, electrolytic polishing 8=17270
- metal films, epitaxial growth on NaCl and KCl in vacuum 8=13147
- metal foils, images calc. rel. to strong simultaneous reflections 8=13234
- metal smoke particles prep. by evap. 8=4839
- plastics, elevated temperature, thermal mass thickness variation 8=17186
- polyethylene below 20°K 8=13159
- polyethylene, thin specimens, obtained by xylene-stream method 8=4852
- polymers, microstruct. in ultrathin sections 8=17297
- polymers, sample preparation technique for scanning microscope 8=17180
- PVC single crystals 8=17300
- precip. phase microanalysis with combined energy analysis 8=17276
- precipitates in thin foils, images 8=13152
- silicon iron, notched, fracture topology rel. to crack nucleation and growth 8=17793
- steel, austenite grain size, high temp. obs. 8=13157
- steels, notched, fracture topology rel. to crack nucleation and growth 8=17793

Electron microscope examination of materials—contd

- surface topography charact. with scanning microscope 8=17114
- surface steps, resolution and contrast, meas. 8=13079
- trace analysis 8=17269
- Ag—Cu alloys, age hardenable, precip. 8=21837
- Al, 50 kV electron mean free path for plasmon excitation, diffr. condition effect 8=13696
- Al thin films, distribution of sputtered atoms 8=21876
- Al thin film, obs. of electro-transport 8=17927
- Al-4wt%Cu alloy, precip. phase microanalysis with combined energy analysis 8=17276
- Al—Li alloys, neutron irradiation 8=8456
- Al—Si alloy, interaction between dislocations and precipitates 8=13431
- Au, fine lattice fringes, resolution by dark and light field axial illum. 8=1783
- B₂O₃—PbO—Al₂O₃ glass system, spinodal decomposition structures 8=17268
- BaTiO₃, surface potentials, analysis 8=13880
- BeO, radiation damage 8=22250
- Bi—Sb films, 2-layer, struct. defects by Moiré method 8=22186
- C, evap. films on heated metal substrates 8=4745
- Cu cubic texture formation during recrystallisation 8=480
- Cu films, epitaxial, changes on exposure to H₂—O₂ combination at 325°C 8=8318
- Cu films, obliquely deposited 8=8296
- Cu single crystals in stressed condition, dislocation arrangement 8=22201
- Cu-2 wt.%Be, ageing studies 8=17056
- Cu—Be—Al alloys, ageing characts. obs. 8=22335
- Fe, thermal etching in vacuum 8=17652
- FeC₂—graphite cpd. 8=1972
- H₂ solid 8=8465
- Hg layers adsorbed onto W field emitter tips 8=1702
- Mo, surface structure 8=21992
- MoZr, surface structure 8=21992
- N₂ solid 8=8465
- Nb surfaces, microscope study 8=13950
- Nb₂O₅, high temp. and related phases 8=22033
- Nb—Zr alloy, structure, by photomicrographs and diffr. patterns 8=8245
- Ni films, electrolessly deposited 8=17136
- Ni-2 wt.%Be, ageing studies 8=17056
- O₂ solid 8=8465
- PbTiO₃—PbZrO₃, surface potentials, analysis 8=13880
- Pd films, obliquely deposited 8=8296
- Pt films, obliquely deposited 8=8296
- Pu α -phase foils 8=21887
- Si chemical-vapour-deposition on sapphire, obs. 8=4826
- Si, dislocation motion under e-bombardment 8=17660
- Si, surface diffusion of Li 8=22159
- Sn films, obliquely deposited 8=8296
- UO₂, irradiated 8=8469
- W wire, recrystallized, sample prep. 8=17267
- W, stacking faults obs. 8=1984
- W/N₂ system, phase changes of adsorbed N₂ from field microscope exam. 8=21913

Electron microscopes

- alignment, standard specimen 8=15317
- band pass filter, 8=15303
- calibration, high magnification, using single crystals with known etch steps height as standards 8=8450
- combined with X-ray microanalyzer, illuminating system 8=8442
- condenser-objective for 700 kV accel. 8=6313
- condenser-objective, spherical aberration and resolving power 8=19790
- development, review 8=15516
- diffractometer attachment 8=19792
- electron accelerator, 1MeV, for 8=15319
- energy analyzing, for precip. phase microanalysis of alloys 8=17276
- field emission, desorption of K from emitter 8=3211
- field-emission, ultra-high vacuum metallic dismountable apparatus 8=15320
- filter projection system with image intensification through storage 8=15318
- filters for thick polycrystalline metal foils 8=8455
- 5000 kV, improved fundamental characts. and features 8=8500
- image contrast, theory, elementary account 8=10901
- image intensification, television camera system 8=15527
- lens, quadrupole quadruplet projector, electron-optical props. 8=15311
- objective lens, soln. for magnetic field 8=336
- microprobe resolving power meas. 8=15314
- microprobe spatial resolution 8=15313
- mirror type, spatial frequency response 8=15315
- probe microanalyzers, X-ray counting systems, non-linearity corrections 8=4837
- probes, cathodoluminescent detector 8=5689
- resolution limit of emission type 9=10902
- scanning, experiments with quadrupole lenses 8=334
- scanning, specimen cooling stage 8=6227
- scanning, secondary-electron channel multiplier use 8=3209

Electron microscopes—contd

- scanning microscope with three e.m.lenses 8=17281
thermoelectronic emission type, observation of
recrystallization of steel 8=337
use as diffraction camera, high resolution 8=6316

Electron microscopy

- See also Crystal structure, atomic.
band-pass filter and chem. analysis obs. 8=15303
cartridges, combined and specimen stage 8=17272
column approximation, validity 8=8499
conference, Boston, June 1967 8=8445
diffraction pattern obs. methods 8=6314
e accelerator, 1 MeV, for 8=15319
electropolishing of thin foils, specimen
temperatures 8=4836
embedding media, relative merits 8=6315
field-emission, Fowler-Nordheim data recording 8=15321
field ion micrographs, indexing method 8=8448
foils, simultaneous prep. by chemical thinning 8=8449
image resolution and contrast 8=3210
image contrast, theory, elementary account 8=10901
intermediate electron decelerators 8=6309
Kikuchi patterns rel. to cryst. orientation 8=13122
low temp. specimen, method of thinning, and specimen
holder 8=6228
metal sample prep., electrolytic techniques 8=17271
mirror microscopy, using mag. lenses, optics and
magnification 8=10900
mirror, projection method, electrical contrast 8=15315
optical method for analysing micrographs of spinodal
decomposition structures 8=17268
pictures of dislocations, computer generation 8=8709
planarian normal eye, obs. 8=11240
planarian regenerating eye, obs. 8=11241
preparation of pyrolytic graphite for transmission 8=4835
probe, for electron-lattice interactions 8=1754
probe, heat flow problems 8=1753
reciprocity theorem, and appl. to diffraction 8=13241
reflection patterns, Kikuchi-like, by scanning 8=8446
reflection patterns, Kikuchi-like, by scanning, comments on
interpretation 8=8447
scatt. by specimen-supporting films, effect on
Fresnel fringe formation 8=19787
specimens, temp. distrib. calc. 8=1861
specimens, thin foil, preparation by rotating P.T.F.E
holder 8=8451
strain contrast images due to new phase 8=1773
trace characterization—chemical and physical,
symposium NBS, USA, Oct. 1966 8=8437
transmission, fundamentals, book 8=15316
ultrathin sectioning of polymers 8=17297
X-ray production dependence on crystal orienta-
tion 8=17266
xylene-stream method for obtaining thin polyethylene
specimens 8=4852
zone plate correction of nearly incoherently illuminated
atoms 8=1145

Electron multipliers. See Electron tubes; Photomultipliers.**Electron multiplier phototubes. See Photomultipliers.****Electron nuclear double resonance (ENDOR). See Nuclear magnetic resonance and relaxation; Paramagnetic resonance and relaxation.****Electron optics**

- See also Beta-ray spectrometers; Electron lenses;
Ion optics; Particle optics.
Aharonov-Bohm effect 8=324
beam in crossed fields, statistical characteristics 8=15301
beam interaction with inhomogeneous u. h. f. fields 8=15302
beam ripple, focused by ax. symmetric mag. field 8=325
 β -ray spectrometer with triangular mag. field 8=11471
biprism interference, low energy 8=330
"biprism", polarization of beams 8=10894
of cylindrical capacitor as analyzer for non-relativistic
particles 8=3208
devices simulation on computer 8=6307
disc beam in electrostatic field 8=19783
distortion-free images formation using quadrupole
triplets 8=332
filter projection system with image intensification
through storage 8=15318
focusing device, magnetic, suitable for mm wave
tubes 8=10896
focusing and stability, in periodic mag. fields 8=10895
image contrast in electron microscopes, theory 8=10901
interferometer, magnetic fringe shift 8=335
klystron, multi-cavity, e stream bunching theory 8=19827
lens correction for aberration, possibility for fast
electrons 8=15308
linear accelerator beam, radial shaping 8=15655
magnetic analysers, spherical aberration
calculation 8=10898
magnetic bottle for e, in which polarized e are prod. by
spin-exchange collisions with H atoms 8=15304
for microscopy, band-pass filter and chem. analysis
obs. 8=15303
magnetic effects on transmission and the R. P. D.
technique 8=6312
objective lens, spherical aberration coeff., dependence
on object position and magnification 8=19788

Electron optics—contd

- probes, spot size and current density distribution in
Kodak photoresist, films 8=331
refraction of beam by laser standing wave, obs. 8=19784
refractive index of laser beam, meas. 8=19786
selectors, useful current calc. 8=19773
superconducting lens, aberrations calc. 8=19791
systems with fixed image positions, electrostatic 8=15299
Wien filter, optimum adjustment 8=10899

Electron pairs

See also Positronium.

- bremsstrahlung, test for absence of Poisson dist. 8=702
nuclear transitions, prod., spectrometer 8=20668

annihilation

- alkali halides, positron bound states 8=13694
arbitrarily polarized two-particle, radiation, by tensor
integration 8=718
coincidence counting determ. 8=11848
decane rel. to C-H and C-C bond electrons momentum
distrib. 8=16324
 $e^+e^- \rightarrow \mu^+\mu^-$, backward annihilation amplitude 8=3599
 $e^- + e^+ \rightarrow \mu^- + \mu^+ + \gamma$, non-local theory 8=15737
 $e^+ + e^- \rightarrow \pi^+ + \pi^-$ rel. to π e.m. structure and p-wave
phase shift in π - π scatt. 8=15761
 $e^+ + e^- \rightarrow \pi^+ + \pi^-$ at 775 MeV, Orsay storage ring
obs. 8=15738
Fermi surface study using rotating specimen
method 8=13689
foil, source supporting, spectral shape 8=13693
into hadrons, total cross-section, in vector-meson field
theory and PCAC 8=719
hexane rel. to C-H and C-C bond electrons momentum
distrib. 8=16324
meson pair production, spin current 8=739
in metals, solid and liquid 8=12896
metals, positron momentum distrib. relax. 8=8973
positron annihilation in solids 8=17906
positronium, form. and decay 8=6812
pure Fermi gas, ladder-graph approx. 8=22492
 ρ production, e^+e^- colliding beams 8=812
single-quantum, higher-shell contributions and polarization
correlations 8=22491
statistical unitary-symmetry theory 8=3527
Al, angular correlation of positron annihilation radiation
cf Se 8=5150
Bi-Hg alloy, solid and liquid, angular correlation of
positron annihilation 8=8974
Bi, solid and liquid, angular correlation of positron
annihilation 8=8974
Cu, ang. depend. rel. to Fermi surface 8=22493
Cu, momentum distrib. along [111], Brillouin zone
boundary effect 8=13691
Cu-Al alloy, momentum distrib. along [111], Brillouin zone
boundary effect 8=13691
Ge, angular correlation of positron annihilation radiation
cf Se 8=5150
in He gas 8=20998
Hg, solid and liquid, angular correlation of positron
annihilation 8=8974
Li, Fermi surface by positron annihilation 8=8937
Se, angular correlation of positron annihilation radiation,
cf Al, Si and Ge 8=5150
Se-Te alloys, photon angular distrib. 8=13692
Si, angular correlation of positron annihilation radiation
cf Se 8=5150
Si Brillouin zone symm. element meas. by positron
annihilation 8=13690

production

- e.m. form factor of the medium, multiparticle
approach 8=6797
 $\eta \rightarrow \pi^+e^-e^-$, C-conservation, vector-meson model, decay
width calc. 8=3674
 $\eta^0 \rightarrow \pi^+e^-e^-$, unsuccessful search 8=804
by γ quanta a field and intense e.m. wave 8=717
by muons in medium and low Z elements 8=7178
 $\omega \rightarrow e^+e^-$, following $\pi^- + p \rightarrow \omega + n$ 8=808
 $\phi \rightarrow e^+e^-$, following $\pi^- + p \rightarrow \phi + n$ 8=808
photon polarization meas. method 8=3572
quantum electrodynamics, possible test, high energy
corrections 8=20390
 $\rho \rightarrow e^+e^-$, following $\pi^- + p \rightarrow \rho + n$ 8=808
 $\rho^0 \rightarrow e^+e^-$ and $\pi^+\pi^-$, branching ratio, 600-900 MeV/c² 8=6908
statistically independent, events and energy loss
deter. 8=6813
vector meson decay, boson model 8=20497
C, photoproduction, phase and magnitude of virtual
Compton scattering 8=3904
Pb, photoproduction, phase and magnitude of virtual
Compton scattering 8=3904

Electron paramagnetic resonance. See Paramagnetic resonance and relaxation.**Electron-phonon interactions. See Crystal electron states; Crystals/lattice mechanics.****Electron probe analysis. See Chemical analysis/X-ray.****Electron resonance. See Cyclotron resonance; Paramagnetic resonance and relaxation.****Electron spin resonance. See Paramagnetic resonance and relaxation.****Electron states in solids. See Crystal electron states.**

Electron structure of solids (crystallography). See Crystal structure, atomic.

Electron structure of solids (energy structure). See Crystal electron states.

Electron theory

See also Quantum electrodynamics.

Dirac current, non-relativistic approx. for charge and density 8=707

Dirac, third-order approximation 8=11452

Dirac, scattering by central potential 8=6801-2

$e \sim p$ charge difference, cosmological consequence 8=23480

emission, induced, moving in mag. field 8=6805

equations of motion of classical radiating charge, derivation 8=11453

gravitational field interaction and gravitational field 8=708

history of evolutionary concepts 8=20373

intense laser field, nonrelativistic quantum theory, correction 8=15727

Kapitza-Dirac effect in strong radiation field 8=714

and photon beam, intense, interaction 8=20372

real spinor fields in modified Dirac theory 8=705

Electron theory of metals. See Crystal electron states; Metals/ theory.

Electron traps. See Crystal electron states.

Electron tubes

See also X-ray tubes.

amplifier, crossed-field distributed emission, computer simulation 8=19712

anode materials, omegatron obs. 8=15330

auxiliary electrode for t. w. t. pumping 8=15281

colour picture c. r. t., mass spectrometry of residual gas 8=15324

backward-wave, parametric amplification with pre-modulation 8=6369

channel multiplier as u. v. detector 8=6506

continuous channel electron multiplier detection efficiency for positive ions 8=6635

crossed-field guns, shot noise, effect of space charge 8=19781

electron multiplier, poss. reason for appearance of 'false' pulses 8=6329

electron multiplier, windowless, suitable for use on rockets 8=10903

experimental for emission properties of cathodes at high temp. 8=13932

gun, crossed-field, Brillouin flow production 8=3194

guns, high perveance three-electrode, theory and applications 8=10889

image intensification, television camera system 8=15527

international symposium, Rome, March 1967 8=6317

klystron, multi-cavity, e stream bunching theory 8=19827

klystron operation from wave coupling on beam modulation by low freq. 8=1397

klystron-oscillator power supply for mm spectroscopes 8=15425

klystrons for Stanford center 8=3488

magnetron diode, anode current distribution 8=15332

magnetron injection gun, range 8=3195

magnetron lens, space charge electrons, lifetimes meas. 8=6319

magnetron, non-split anode, electron resonator quality factor 8=15326

magnetrons, applicability of adiabatic theory 8=15331

magnetrons, current flux and h. f. field interaction 8=15333

magnetron, e. m. field fluctuations effect on space charge and anode current 8=338

magnetron electron cloud, calc. of natural freq. 8=15328

magnetron electron cloud, steady-state oscillations 8=6321

magnetrons, cut-off characteristic modified by positive ions 8=10909

magnetrons, strongly cut-off, electron transport 8=10908

magnetrons, cylindrical, cut-off field rel. to space charge 8=19828

magnetrons, surface-wave, enhanced cathode heating 8=15334

magnetron, surface-wave, stabilizing instabilities of electron cloud oscs. 8=15327

mm wave, Co-Pt magnetic device for beam focusing 8=10896

mm waves, beam focusing by periodic permanent magnets 8=6308

manufacture, mass spectrometry of residual gases 8=18770

n image intensification, television 8=6954

non-slotted, pot. distrib. under static conds, meas. by probe and e-beam indicator 8=15329

oscilloscope deflection sensitivity enhancement by scan magnification 8=10907

oscilloscopes, short length, high deflection sensitivity 8=6318

Penning cell, potential in presence of space charge, calc. 8=3212

photo, zero crossing timing, accurate, tunnel diode circuit 8=3142

picture c. r. t., residual gas composition obs. 8=15325

rectangular section, tape Brillouin beam 8=15300

reflex klystron, flicker effect on freq. 8=3214

residual gas chemical reactions 8=18663

secondary-electron channel multiplier use in scanning electron microscopy 8=3209

Electron tubes—contd

secondary emission devices, resolution and frequency response 8=10906

secondary emission, for relaxation pulse generators 8=15179

secondary-emission, in wideband linear amplifiers 8=1517

secondary multipliers, explanation of spurious pulses 8=6322

storage-CRO display units for small lab. computers 8=6320

strophoton, e interact. with travelling-wave field 8=10911

strophoton, exisymmetric 8=3213

thermionic diode, energy convertor, influence of anode emission on efficiency 8=10841

thermionic diode, optimization of emitter length 8=15323

travelling-wave, evacuation by Ti getter pump 8=16731

travelling-wave, parametric amplification with pre-modulation 8=6369

travelling wave tubes, space-harmonic fields, interaction with electron beams 8=10910

vacuum diode detector for high γ flux 8=15721

vacuum switching, use of permanent magnets 8=3154

vidicon for automatic recording of spark chamber events 8=3483

Vidicon camera for simultaneous meas. of density and coordinates on bubble chamber photographs 8=20223

vidicon, with CdSe target 8=3215

Cs diodes, electrode inhomogeneity influence 7=297

Cs plasma diode, anal. of ionic species 8=15211

Cs plasma diodes, identification of dominant ion species 8=15322

Cs vapour thermionic diodes, ion current and Schottky effect 8=339

Re electroetched emitter in variable-parameter diode, output charact. 8=19793

Electrons

This heading includes both negative and positive electrons when the differences between them are of no special significance. See also Beta-rays; Cosmic rays/ electrons; Crystal electron states; Fluctuations/ electrical; Nuclear reactions due to/ electrons; Photoelectricity; Plasma; Positronium; Positrons; Space charge.

accelerators, Tomsk Polytechnic design and performance 8=15667

atomic, Cs-inert gas collisions, spin polarization from D_2 pumping 8=1194

bremsstrahlung, total spectrum of ultrarelativistic electrons 8=20367

capture by μ^+ from H and He atoms 8=7481

classical motion in elect. -dipole field, point dipole case 8=19772

cloud in magnetron, stabilizing instabilities in oscillatory conds. 8=15327

coincidence expts., magnetic steering device 8=3596

collision cross section data, low energy, bibliography 1925-1966 8=20990

collisionless capture into region of finite motion, and particle distrib. 8=7740

Compton line shapes for Hartree-Fock wave functions 8=20940

Compton wavelength determ. 8=15739

concentration profiles during sunspot maximum and minimum 8=23357

conduction, quasioptical mag. moments and electrode dipole 8=323

cylindrical capacitor as analyser, dynamic and optical props 8=3280

depolarization in Al, longitudinal with up to 70% energy loss obs. 8=11460

diffusion coeff., Einstein generalized ratio 8=15025

diffusion in gases, time-of-flight meas. 8=7702

in earth's magnetotail, obs. by Vela satellites 8=23431

in elec. -dipole field, classical motion, finite dipole case 8=19771

e^+e^- binding energy, rel. to three body theory 8=667

e/m measurement, modification of experiment 8=10471

$e-\mu$ e. m. difference from $\mu-p$ scatt. obs. 8=20395

$e^+ + p \rightarrow e^+ + \pi^+ + n$ obs. 8=11505

electroproduction of N^* cross-section calc. 8=20514

electroprod. of N^* , model for form factors 8=20579

electroproduction of π on N as function of momentum transfer 8=6840

electroprod. on spin-1/2 target, superconvergence relation and current-algebra identities 8=20376

electroprod. of strange particles, PCAC and current algebra study 8=20344

e-photon cascades in Pb plates, meas. in scintillator 8=6804

energy decrease in neg. glow region of He discharge 8=4288

F-region, approx. 10 ev, geographic distribution 8=23417

in field of intense e. m. wave, photon emission 8=717

freely falling, gravitational force compared with metallic 8=704

Green function and mobility in random potential, calc. 8=11461

heating in beam plasma system rel. to resonant resistive instability 8=1426

- electrons—contd**
 helicity studied in scatt. off polarized d 8=20375
 high-speed reflection, calcs. 8=3595
 hot, in plasma, due to e beam bombard. 8=21306
 hydrated, absorpt. spectrum 8=5705
 hydrated, bimolecular rate constants in aqueous solns. 8=2510
 hydrated, formation in $H + F^-$ reaction 8=18679
 hydrogen-proton collision, electron capture probability 8=1199
 ice, γ -irradiated, solvated e spectrum obs. at 77°K 8=22989
 inner zone, temporal behaviour, 1965/66, Pegasus 1 obs. 8=23344
 ionosphere, local conc., determ. from Doppler dispersion meas. of satellite radio beacons 8=23358
 ionospheric density detm. by coherent frequency method 8=14670
 isobar $T = J = \frac{1}{2}$, electroproduction, soln. of dispersion relations 8=3732
 low-energy, precipitation at high-latitudes, satellite meas. 8=9954
 magnetic moment anomaly in muonium as test for Q. E. 8=11285
 magnetic moment rel. to self-interaction corrections in q. e. d. 8=20174
 magnetospheric tail, electrons within neutral sheet 8=23320
 mass of Dirac particle as function of spin 8=3592
 mass values maximization of ratio decay rate/Q-value 8=3601
 minimum size in nonrelativistic theory, from hyperfine structure 8=826
 p-e charge inequality determ. 8=11455
 p-e interaction quasi pot., using two-time Green functions, p structure effect 8=11590
 photoelectrons, distrib., quantum optics 8=20013
 photoelectron heating efficiency in ionosphere 8=23359
 photoelectrons, single, detection 8=11463
 photon scatt., in field of intense laser ray 8=20354
 π electroproduction, $e + p \rightarrow e + n + \pi^+$, π form factor meas. 8=6834
 plasma, interaction of proton and electron plasma waves 8=4364
 in polar gases, collision freqs. and drift vels. 8=4471
 polarization, radiative, in mag. field, quasiclassical approx. 8=715
 propagator, analytic behaviour for complex $e^2/\hbar c$ 8=15726
 pulses, ≥ 30 -keV, in magnetosheath and beyond, correlation with mag. fields 8=23433
 quantum electrodynamics, third-order vertex part of single electron line 8=20385
 quantum-relativistic concepts 8=6800
 radio sources, energy and lifetime of relativistic electrons 8=19224
 reflection from target, intensity prop. to Z number 8=20381
 resonant radial oscill. in betatron at 5 and 15 MeV 8=20239
 scintillation response and efficiency of crystal 8=716
 self-energy graph, asymptotic behaviour 8=20170
 solvated, yield in γ -radiolysis of water+10% ethanol 8=23167
 temp. and density in theta pinch plasma, laser scatt. expt. 8=16553
 thermal, capture by O_2 8=7723
 trapped in γ -irrad. organic glasses 8=9729
 trapped, low-altitude, boundary collapse in mag. storms 8=14656
 upper atm. >40 keV flux rel. to ionosphere D-layer form., ≤ 100 km 8=14680
 vel. distrib. function in partially ionized gas 8=12423
 Al L-shell. excitation by 20-keV electrons 8=22495
 Al_2O_3 , L-shell, excitation by 20-keV electrons 8=22495
 in D, mag. drift vel. and deflection coeff. 8=7712
 in H, mag. drift vel. and deflection coeff. 8=7712
 K, conduction, u.s. attenuation 8=22104
 NH_3 gas radiolysis, effect of scavengers 8=23162
 Si-Li drifted detector response, 200 keV-1.7 MeV monoenergetic 8=11464
- absorption**
 See also Beta-rays/absorption.
 polycrystalline foils, temp. effects 8=13467
 Si, anomalous, determ. of coeffs. 8=13289
- ionization**
 impact cross sections, semi-empirical 8=1350
 CO, removal during d.c. discharge afterglow 8=21233
 H ionization, asymptotic form of wave function 8=16443
 NO_2 , rate of attachment of gaseous electrons 8=12449
- radiation**
 See also Bremsstrahlung; Cherenkov radiation; Electrodynamics.
 bremsstrahlung angular distribution 8=701
 bremsstrahlung, on collision of fast muon, theory 8=722
 bremsstrahlung in crystal, spectrum distortion by e scatt. 8=15723
 bremsstrahlung, e-e, in quantum plasma 8=3581
 e^-e^+ beam collisions, infra-red radiative corrections 8=591
 free-free transitions, survey of theoretical results 8=11454
 induced, moving in mag. field, and exposed to e. m. waves 8=6805
- Electrons—contd**
radiation—contd
 polarization effect in mag. field, quasiclassical approx. 8=715
 relativistic, in lamellar media, 60-70 keV spectrum meas. 8=709
 synchrotron, Compton scattering of virtual photons 8=3571
 synchrotron radiation report 8=710
 synchrotron, relativistic, max. polarisation of radiation 8=11456
 synchrotron, resultant energy losses and thermal instability rel. to radio sources 8=5944
 synchrotron, review 8=15664
 X-radiation, due to galactic e interaction with cosmic black body radiation 8=19095
 Cu, length change after e irradiation 8=22338
- scattering**
 See also Atoms/electron scattering; Beta-rays/scattering.
 benzene, large-angle electron-impact spectra 8=16224
 bremsstrahlung, interference with nuclear γ radiation 8=6796
 bremsstrahlung stimulation in strong field, relativistic 8=7172
 central potential, Dirac theory 8=6801
 complex amplitudes, Molière and Born approx. compared 8=3594
 Compton effect, inverse, e moving in radiation field 8=20346
 conduction, by localized surface charges, meas. 8=22640
 in crystal, bremsstrahlung spectrum distortion 8=15723
 crystal, mean free path for plasmon excitation 8=2117
 deuteron electrodisintegration differential cross sections, resonance prod. 8=11640
 dispersion effects, eigenchannel theory calc. 8=20771
 double-scatt. effect on cross-section meas. 8=10893
 diffraction pattern microscopy, 4 methods 8=6314
 $e^- + e^+ \rightarrow \mu^- + \mu^+ + \gamma$, non-local theory 8=15737
 $e-\mu^+$, backward scatt. amplitude, calc. 8=3599
 e-d quasielastic, forward angle obs. 8=6806
 e-d, using polarized d, e helicity studied 8=20375
 e-e cross section calc. and polarization correlations 8=11457
 (e, e'), O^8 elec. monopole and quadrupole excitations 8=20685
 e-e, test of quantum electrodynamics, at $2 \times 43, 2 \times 135$ and 2×160 MeV 8=11458
 e^-e^- , backward scatt. amplitude, calc. 8=3599
 e-He rel. to α charge form factor 8=11657
 $eN \rightarrow eN$ interaction amplitude reconstruction from expt. data 8=6803
 e-N, inelastic, review of kinematics and sum rules, inequalities 8=20377
 e-N, meson field model of excitation 8=3697
 elastic diffraction by polycrystalline solids validity of Debye scattering equation 8=8444
 electromag. waves by free electrons, intensity dependent freq. shift 8=19866
 e. m. waves, frequency mixing in classical theory 8=15408
 by e. m. waves, meas. 8=19786
 e. m. wave non-relativistic quantum field theory 8=15409
 e-phonon as main mechanism in hot e drift in Si 8=22438
 e-spin interactions rel. to Kondo anomaly in elec. cond. 8=13642
 electron transmission through aperture and R. P. D. technique 8=6312
 ethylene, large-angle electron-impact spectra 8=16224
 experimental programme at Desy 8=11349
 ferromagnetic crystal surface, low energy, theory rel. to spin waves 8=5447
 γ -e, Klein-Nishina formula, Legendre polynomial expansion 8=3570
 gas discharge, cathode reflections 8=1331
 grant resonances of medium and heavy spherical even nuclei, partial wave analysis 8=20772
 inelastic, filtering in electron optical projection system 8=15318
 inelastic, form factors, effect of nucleon continua 8=16062
 Kapitza-Dirac effect in strong radiation field 8=714
 ladder processes rel. to Kondo anomaly in elec. cond. 8=13642
 light nuclei, solns. of Dirac eqns. 8=11863
 light waves, laser pulses, deflection obs. 8=20378
 in magnetic field 8=3201
 magnetic spectrometer for recording 400 MeV/c spectra 8=11292
 MOS effective mobility theory rel. to surface conduction model 8=22433
 rel. to microanalysis probe spatial resolution 8=15313
 microanalysis probes low energy backscatt. meas. 8=14468
 rel. to microanalysis by specimen current meas., binary targets backscatt. coeffs. 8=14467
 molecules, homonuclear diatomic, theory 8=12371
 molecules, polar, critical 8=7638
 multiple, modified distrib. functions 8=15730
 multiple, verification of Gavallas-Kagan formula 8=20379
 multipole excitations of nuclei, FORTAN IV cross-section calc. 8=20773
 n-e, rel. to neutron form factors 8=6941

Electrons—contd

- scattering—contd
 nuclear, asymm. function for calc. of nuclear magnetic props. 8=3910
 nuclear level excitation extension of Helm model 8=3773
 nuclear size and form probe 8=7069
 nuclei, light, charge radii data comparison with muonic X-ray meas. 8=3785
 nuclei, light using Woods-Saxon pot. with spin-orbit coupling 8=7173
 nuclei, radiative background compared with muons 8=11868
 nucleon emission, cross section, rel. to nucleus props. 8=11864
 one-dimensional crystal models 8=22011
 p beam oscills., damping in storage rings 8=640
 π electroprod. and photoprod. dispersion relation theory 8=11508
 polar molecules, low-energy cross-sections, mol. taken as rigid rotator 8=1233
 positrons, by various targets 8=1044
 positrons, slow, by mols. 8=12168
 probability, Kapitza-Dirac effect, experimental test 8=19785
 pseudo-nuclei isotope for configuration mixing extended to s-d shell and non-degenerate case 8=20774
 pseudo-nuclei model, test of purity of configurations in shell-model analysis 8=20774
 quasi-free and nuclear shell structure 8=1043
 radiation correction including hard photon emission 8=711
 reflection coeff. for zero-energy electrons from Ag surface 8=6301-2
 Saskatchewan laboratory, facility 8=7171
 2s-1d shell nuclei, form factor calc. from HF wave functions 8=11802
 solids, for muffin-tin ionic potentials 8=8895
 solid targets backscatt. spectra and coeffs., obs. 8=15298
 by specimen-supporting films in electron microscopy, effect on Fresnel fringe formation 8=19787
 in superconductor by impurities 8=2146
 by thin films, incoherent component 8=3202
 in thin films, inelastic, at oblique incidence 8=17911
 Thomson, frequency shift 8=15729
 Ag foil target, 0.52 MeV to 2.0 MeV, 0° to 20° angle, plural 8=16064
 Al, backscatt. and X-ray prod., obs. and e transport calc. rel. to microanalysis 8=18794
 Al foil target, 0.52 MeV to 2.0 MeV, 0° to 20° angle, plural 8=16064
 Au, backscatt. and X-ray prod., obs. and e transport calc. rel. to microanalysis 8=18794
 Au, rel. to X-ray microanalysis, backscatt. correction, obs. 8=14469
 Be foil, multiple, of high-energy electrons 8=20384
 Be⁹, elastic and inelastic, rel. to nucleon clusters 8=11865
 Be-Au 2-layer target, back-scatt., rel. to thickness 8=3203
 Bi²⁰⁸, 28-73 MeV radiative transition probability 8=11785
 C, cross section meas. and sum rules 8=3911
 C¹² and C¹³, inelastic, excitation of 15.11 MeV levels 8=3791
 C¹², inelastic, at 180°, levels excited 8=16063
 C¹² (e, ep)B¹¹, Born approx. and DWIA calc. compared 8=7175
 C¹², first excited state 8=952
 C¹², inelastic, with excitation of levels at 19.5 MeV 8=1045
 C¹², 15.1 MeV level excited 8=3773
 C¹², 19.4 MeV, $J^\pi = 2^-$ 8=20682
 C¹³, in methane, 250 MeV, nuclear charge radius 8=3912
 in Cs thermionic diode, effect on collector work function meas. 8=15243
 Cu, backscatt. and X-ray prod., obs. and e transport calc. rel. to microanalysis 8=18794
 Cu, rel. to X-ray microanalysis, backscatt. correction, obs. 8=14469
 Cu-Au alloy, from disorder, rel. to anomalous absorpt. 8=17362
 GaP, hot-electron-phonon interactions 8=5245
 H₂, Born inelastic differential cross-sections 8=12191
 H₂, dissociative attachment of e, vibrational resonances obs. 8=21182
 H₂, low-energy elastic 8=7516
 He atom, rearrangement collision, spin flip effect 8=7445
 He, large-angle electron-impact spectra 8=16224
 He⁴, high energy scatt. and N-N correlation 8=891
 He⁴ nuclei, elastic scatt. cross section, 30-59 MeV 8=15732
 InSb, hot polar scattering 8=13638
 K, elastic differential spin-exchange cross sections 0.5 eV 8=12097
 La¹³⁹, at 225 ± 0.7 MeV 8=11866
 Li⁶, 60-130 MeV, off 3.56 MeV level 8=11716
 Li^{6,7} elastic and inelastic, rel. to nucleon clusters 8=11865
 Li^{6,7}, elastic at 100-600 MeV nuclear charge form factors 8=1047
 Li⁷, form factor, h.f. calc. 8=3789
 MgO, Kikuchi patterns rel. to anomalous absorpt. 8=17362
 N¹⁴, inelastic, 50, 53 and 57 MeV electrons, determ. of ground state e.m. widths 8=20684
 N₂, large-angle electron-impact spectra 8=16224

Electrons—contd

- scattering—contd
 N₂, struct. of 2 eV resonance 8=12214
 Ni^{58,60,62} form factors 8=3913
 O¹⁶, 19.08 MeV level form factor 8=3794
 Pb foil target, 0.52 MeV to 2.0 MeV, 0° to 20° angle, plural 8=16064
 Pb²⁰⁸, 207, 208, 28-73 MeV radiative transition probability 8=11785
 Pb²⁰⁸, inelastic form factor calc. 8=16003
 Si²⁸, inelastic, transition matrix elements at 100-260 MeV 8=7174
 Sn^{116,120,124}, collective levels obs. 8=11757
 Sn^{116,120,124}, elastic at 150 MeV, charge density changes 8=1046
 SnO₂, polar optical-modes 8=22611
 scattering, electron—proton
 backward, ratio $R = \sigma(e^+ + p)/\sigma(e^- + p)$ meas. 8=15733
 cross-section data up to 1.1 GeV 8=11459
 cross-section ratio to positron-proton scatt. 8=20383
 elastic, differential cross section comparison with e⁻p scattering 8=3600
 high-energy, polarization quantities and cross-sections 8=20380
 high-momentum-transfer obs. 8=15731
 in equality derived from ν -p backward scatt. sum rule 8=6923
 μ -p, e-p comparison as test for quantum electrodynamics 8=11285
 N₁₅^{*} (1688), missing mass determ. of excitation function 8=11638
 proton aurora, spectra and ang. distrib., rocket meas. 8=5798
 resonances, isobaric electrical excitation 8=713
 Electro-optical effects
 See also Electroluminescence; Optical constants.
 alkali niobates with 'filled' tetragonal W bronze-like structs. 8=22959
 anisotropic crystals, rel. to orientation, and e transitions 8=9495
 rel. to band structure determ., electroreflectance 8=9494
 crystals, uniaxial 8=18494
 diamonds, particle-counting, photoconductivity model 8=5395
 dielectric constant and absorption stability effects 8=18487
 dielectric slab with large permittivity modulation, parametric props. 8=18206
 electroreflectance near anisotropic interband edges in cubic crystals 8=14186
 Faraday effect in glasses, and intra-cavity perturb. of gas lasers 8=11059
 Faraday shutter for laser 8=435
 Franz-Keldysh effect, spectral broadening representation 8=17853
 Kerr cells, appl. to laser beam modulation 8=6488
 Kerr cell system, high voltage transient waveform meas. 8=6240
 Kerr effect, dispersion 8=4578
 Kerr effect for h.v. d.c. meas. 8=6564
 Kerr effect in liquids, ang. correl. of anisotropic mols. 8=12871
 Kerr effect rel. to optical absorpt. in elect. field 8=4573
 Kerr effect and striction in self-focusing of light 8=3377
 Kerr, in fluids rel. to laser beam filament formation 8=800
 laser, Pockels and travelling-wave modulators 8=20036
 modulation voltage vars. at filter rel. to photodetector signal: noise ratio 8=2270
 molecular optical rotation in elec. field 8=516
 niobates, ferroelec., single crystals, growth 8=21958
 Pockels effect, from large CuCl cryst. 8=17231
 real-time signal processors with coherent detection 8=6532
 reflectance, modulated, at oblique incidence for analyzing band structure 8=14168
 semiconductor surface parameters from electroreflectance studies 8=5230
 suspensions, transient birefringence relax. 8=16899
 triglycine sulphate, deuterated, rel. to deuteration effects 8=5647
 AgBr, migration of photoexcited holes in electric field, obs. 8=1908
 AgBr, piezo-optical transmission, detection of internal polaron states 8=13679
 Ar, crystalline, rel. to growth parameters 8=2238
 Bi₁₂GeO₂₀, elec.-field biased, photo-induced changes in optical polarization 8=2404
 Ca₂Nb₂O₇, eight linear coeffs. 8=18513
 CdS, electroabsorption, exciton effects 8=22965
 CdS, in field distrib. and current saturation meas. 8=9250
 CdS, meas. at 10.6 μ 8=18515
 CdS, photo Hall mobility at high electric field 8=2187
 CuCl, cryst. growth for modulators 8=8407
 Cu₂TaSe₄, and other optical props. 8=8408
 n-GaAs coeff. from Raman scatt. by mixed plasmon-phonon modes, obs. 8=5599
 GaAs crystals, light amplitude modulation, $\lambda=10.6 \mu$ 8=95
 GaAs diode, reverse-biased, light emission position and waveform 8=9160

Electro-optical effects—contd

- GaAs at 80°K, electric field obs. 8=2193
 GaAs, meas. at 10.6 μ 8=18515
 Ga_{1-x}In_xAs alloys, electroreflectance rel. to band structure 8=2419
 Ge, electroreflectance spectra and band structure, 1.5–6.5 eV 8=13663
 Ge films, piezoabsorption, above fundamental energy gap 8=22986
 Ge, interband props., electroabsorption 8=22595
 Ge, interband props., electroreflectance 8=22596
 He-Ne laser modulation by inactive cavity 8=19965
 HgS, linear, at 0.63 and 3.39 microns 8=14225
 K_{0.4}Li_{0.4}NbO₃, ferroelec., single cryst. growth 8=21952
 K_{0.4}Li_{0.4}NbO₃, stable nonlinear optical material 8=5618
 K(Ta-Nb), crystals, obs. 8=9199
 KH₂PO₄, elec. field alteration of phase matching freqs. 8=14234
 KSR₂Nb₂O₁₅, and ferroelec. props. 8=5365
 KTa_{0.66}Nb_{0.34}O₃, crystal obs. 8=14232
 Li, atomic, theory 8=12068
 LiNbO₃, d. c. constant, temp. and optical freq. dependence 8=9547
 LiNbO₃, spontaneous rel. to induced, temp. depend. of birefringence, polarization and linear coeffs. 8=18543
 LiNbO₃, temp. depend. and model 8=5619
 NH₄H₂PO₄ group, 45°X-cut, use in laser emission control devices 8=6424
 Na, atomic, theory 8=12068
 Si p-i-n, Co-doped, optical excitation of current oscillations 8=2227
 Sr_{1-x}Ba_xNb₂O₆, ferroelec. crystals. 8=21966
 ZnO, electroreflectance rel. to gas adsorption 8=9564
 ZnS crystals in X band travelling-wave light-intensity modulator 8=23025
 ZnTe films, rel. to determ. of reduced effective mass 8=18566
 ZnTe, meas. at 10.6 μ 8=18515

Electrophoresis

- clay suspensions forced-flow filtration, elec. field effects 8=16898
 gases, cataphoretic purification 8=2536
 gas mixtures, diffusion coeff. meas. by cataphoresis 8=12704
 He-Hg vapour mixture, cataphoresis 8=7656
 Na, K radioactive ion separation, spacers 8=5742

Electrophotography. See Photography.**Electrophotoluminescence.** See Electroluminescence.**Electropolishing.** See Surface texture.**Electroproduction.** See Beta-rays/effects; Electrons; Nuclear reactions/due to electrons.**Electrostatic generators.** See High voltage production; Particle accelerators/linear.**Electrostatic lenses.** See Electron lenses/electrostatic; Ion optics.**Electrostatics**

- See also Electrets; Electric charge; Electric fields.
 capacitor plates, induced charge convergent solution 8=10834
 charged ellipsoid, potentials 8=3186
 charge measuring instruments 8=279
 charging of solid surfaces 8=18156
 condenser, spherical, field calc. 8=276
 e emission, metal-gas interface, Thomas-Fermi-Dirac theory 8=5414
 electrification by rubbing, essential conds. 8=6254
 field, elec., complex 2-dimens., approx. calc. 8=19716
 field, homogeneous, in cylindrical set of electrodes, elimination of harmonics 8=15191
 guarded sphere as gauging electrode in length metrology 8=10823
 latent image transfer to dielec. surface 8=6580
 liquid drops disintegration and electrification subject to electrical forces 8=16782
 liquids, static electricity 8=12907
 medium including ellipsoidal particles, equiv. cct. 8=6252
 nylon 66, electrification rel. to metals 8=5356
 particle beam focusing, soln. of Cauchy problem 8=15275
 permittivity of randomly inhomogeneous anisotropic media 8=19715
 point charge screening potential by thin films 8=278
 potential fields, two dimensional, for given sources, simulation by induction method 8=6253
 potential problems for half space with cylindrical cavity, solutions 8=6053
 precipitation, particle charge magnitudes 8=19719
 precipitators, particle behaviour, photographic study 8=10836
 space anisotropy, soln. by linear sources 8=14936
 spherical segments, soln. by paired eqns. 8=6251
 static charge, dissipation and generation on dielectrics in vacuum 8=18159
 static electrification Conference, London May 1967 8=6255
 superconductivity, effect on BCS theory for tiny samples 8=5194
 Van der Waals forces, macroscopic theory 8=19718
 voltmeter, feedback, with transparent probe 8=3133

Electrostriction

See also Piezoelectricity.

Electrostriction—contd

- diamond-like crystals, rel. to photoelasticity and first-order Raman effect 8=9486
 ferroelectrics, acoustic and polarization waves interaction, elastic consts. 8=18182
 ferroelectric ceramics, perovskite-type 8=5362
 fluids, rel. to laser beam filament formation 8=8067
 Kerr effect and striction in self-focusing of light 8=3377

Elementary particles

- See also Baryons; Field theory, quantum; Hadrons; Leptons; Nucleons and antinucleons; Nucleus; Particle detectors; Particle range; Quantum theory; Quarks; Scattering particles; Strange particles; and individual particles, e.g. Electrons; Mesons.
 accelerators, classification 8=6689
 Adler-Weisberger relation, π dominance implication 8=11424
 algebra of vector densities, inverse mass approx. to saturation 8=6738
 annihilation processes, statistical unitary-symmetry theory 8=3527
 annual review of nuclear science, book XV 8=15628
 axial coupling constant, renormalized, current algebra predictions 8=3520
 baryon mass formula in terms of decay products 8=6915
 behaviour in plane e.m. wave 8=20279
 β decay coupling constant, sum rule derived 8=11482
 Bethe-Salpeter amplitudes, normalization methods 8=3540
 Bethe-Salpeter eqn. compared to N/D values of required coupling constants smaller 8=20313
 Bethe-Salpeter eqn. for fermion-antifermion system in 0⁺, 1⁻ states, soln. 8=15687
 binary and nonbinary processes, amplitudes, asymptotic relns. bet. asymptotic expansions 8=665
 Bondi-Metzner generalized, reduction 8=14933
 book, general discussion 8=11353
 bootstrap incompatibility with closure and locality 8=15710
 bootstrap model, unified Fermi-Yang and Chew-low 8=3566
 bootstrap theorems and Lagrangian field theory of self-generating interactions 8=20161
 bootstrap theory in Lagrangian field theory, particle wave-function renormalization 8=20334
 bootstrap theory tested by Ω as bound state of ΞK 8=6978
 bound states, equivalent field theories 8=11273
 bound state, intrinsic size as a function of mass 8=20270
 broken symmetries and sum rules 8=11368
 C-conservation in $\eta \rightarrow \pi^+ K^- e^+$, vector meson model 8=3674
 C independ. in $\pi^- p \rightarrow \Sigma^- K^+$, 1170 MeV/c 8=20449
 C violation in e.m. processes 8=584
 Cabibbos' angle and $\Gamma(K \rightarrow \mu + \nu)/\Gamma(\pi \rightarrow \mu + \nu)$ 8=15798
 charge commutation relations in calc. $\pi-\pi$ S-wave scatt. length 8=20466
 charge independence triangular diagrams 8=645
 charge invariance rel. to model for soft-particle production in scatt. 8=3534
 charge renormalization as spontaneous symm. breakdown 8=3425
 charge superselection rule test 8=666
 chiral dynamics, nonlinear theories significance 8=11358
 chiral symm., nonlinear realizations 8=20262
 chiral symm. rel. to superconvergent sum rules for scatt. amplitudes 8=20310
 classification, Clebsch-Gordan coeffs. for SU₆ groups 8=15683
 classification in three categories 8=15706
 Clebsch-Gordan coefficients for SL(n, C) 8=651
 commutators, equal time, appl. of JLD representation 8=3524
 complex angular momentum method, test of basic assumptions 8=6735
 complex double pole and decay law 8=11379
 composite, infinitely as bootstrap criterion 8=11484
 composite model, the optimum Lagrange problem 8=11390
 composite system with mass a linear function of angular momentum 8=11378
 composite system, nonrelativistic, high-energy collision 8=15012
 composite, in weak interaction, absence of poles 8=20249
 compositeness conditions 8=3501
 compositeness criteria in quantum field theory and S-matrix theory 8=6764
 compound, conditions Z = O and bootstrap 8=6772
 conservation laws, review 8=3430
 conserved vector current theory rel. to μ^- stars in emulsion 8=11872
 conspiracy, test in π photoproduction on N 8=6775
 and cosmology 8=20247
 covariant spin operators 8=20338
 CP symmetry, review 8=11282
 CP violating decay, relation between ordinary, strange β and K $\rightarrow 2\pi$ 8=20467
 CP violation in strong interactions, $\beta-\gamma-\gamma$ angular correlation 8=669
 CP violation and weak interactions 8=11393
 current algebra and group theoretical derivations of sum rules compared 8=3522

Elementary particles—contd

- current algebra and locations and residues of fixed poles 8=3535
 current algebra, standard identity proved in perturbative model 8=6725
 current density algebra and form factors 8=6736
 current \times current hypothesis and $\Delta S = \Delta Q$ 8=15684
 Dashen-Frautschi approach to mass perturbation, modified technique 8=20267
 data on properties, updating 8=15671
 decay, nonleptonic, surface terms connected with reduction formulae 8=3511
 decay processes, soluble model 8=3413
 decaying system, theory 8=659
 deformable sphere model, excitons identified as quarks 8=15673
 density matrix elements in resonance production 8=11381
 de Sitter group, inhomogeneous, structure of generators 8=654
 digital computers in high-energy physics experiments 8=11350
 e. m. current operator, hadronic as linear combination of field operators 8=6831
 e. m. current operator, uniqueness proved in strong-coupling theories 8=6746
 e. m. current, possibility of part with $I=2$, $C=-1$ 8=20252
 e. m. effect on bootstrap model of $NN^*\pi$ dynamics 8=11486
 e. m. form factors of particle with spin 1 8=11376
 e. m. formfactor from inverse mass approx. to the saturation of the algebra of vector densities 8=6738
 e. m. interactions involving photons, dressed amplitudes in S-matrix theory 8=20343
 e. m. mass difference, sum rule calc. from current algebras 8=655
 e. m. mass shifts by dispersion theory 8=3509
 e. m. polarisability, correlation symmetry 8=3514
 experimental programme at Desy 8=11349
 F/D ratios for B + pseudoscalar-meson decaying particles 8=6766
 fermion-vector particles interaction 8=15692
 field theory propagators, variational formalism 8=6608
 Feynman diagram, Cayley eqns. equiv. to Landau 8=3448
 field equations, nonlinear, particle like solutions 8=3505
 fixed poles, existence by asymptotic behaviour of weak amplitudes 8=20249
 forces, short range, N/D representation, Regge trajectory calc. 8=3554
 form factors, canonical, and current commutation relations 8=3512
 form factors, consequences of Wu-Yang theorem for asymptotic behaviour 8=20269
 form factors, exponentially falling, crossing bootstrap model 8=20333
 form factor idealities from current density representations in one particle spaces 8=6737
 form factors weak and modification of GT relation with generalization of PCAC 8=11377
 free, field eqns., heuristic determ. 8=6720
 free spin particle, kinematics 8=11382
 Fubini sum rules relating K-decay form factors, meson-meson, and photon-meson couplings 8=20474
 fundamental charge, time-invariance 8=15690
 Galilei group, physical and nonphysical representations 8=6728
 Gell-Mann current commutators, off mass-shell matrix elements, condition for use of partial integration 8=20291
 Goldberger-Treiman relation, correction 8=20496
 Goldberger-Treiman relation, Nambu and Gell-Mann-Levy versions compared 8=6723
 Goldstone's theorem, rigorous treatment 8=6613
 graviton-graviton scatt. and annihilation 8=3452
 groups, noninvariant 8=3502
 high-energy physics, conference Oiso Japan (1965) 8=11348
 high symmetries, useful tools and SU 8=11366
 Hilbert space of 5D pseudosphere, non-diagonalism of mass-squared operator 8=3417
 impulse model for $K^- + He^4 \rightarrow \Lambda^0 + \pi^- + p + d$, obs. 8=20417
 inelastic interactions, energy and angular distribution of secondary particles 8=3518
 infinite component fields model 8=20248
 interacting, finite theory of 8=20136
 interaction constants, equations 8=6741
 interactions, diffraction and structure, conference Israel 1967 8=15672
 interactions, S-matrix theory 8=683
 interactions, strong, self-induced, simplification in infinite-momentum limit 8=20277
 interactions with spin rel. to representation of Poincaré group 8=15614
 interaction 2 spin-zero particles, relativistic 8=15609
 internal symmetries, significance 8=11365
 inverse scatt. problem, finite-range solns. 8=11394
 isospin symmetry, TCP and local field theory 8=11364
 Klein-Gordon equation for spinors 8=15621
 Klein-Gordon wave equation, transformations by conformable group 8=15681
 Lee model, algebraic solns. of V-O sector 8=20250

Elementary particles—contd

- Lee model, equal-time commutator and zero-energy theorem 8=3529
 Lee model, strong coupling soln. 8=11389
 leptonic decay, book 8=3858
 leptonic decays and unitary symmetry breaking 8=671
 Lie algebra of infinite-dimension, tensor product of one-particle representations 8=6724
 Lie algebra R_n group representation 8=11360
 Liperi Summer School in Theoretical Physics Helsinki, 1966 8=6715
 long-range force due to ν -pair exchange, as r^{-5} 8=20273
 Lorentz group complex, in homogeneous rel. to relativistic S-matrix scatt. 8=20289
 Lorentz group, rel. to lepton field 8=11450
 Lorentz group, unitary representations, rel. to dynamics 8=3507
 Lorentz invariance violation in field theory with unreasonable mass spectrum 8=3426
 magnetic moment determ. in $O(3,2)$, $O(4,2)$ 8=20265
 mass differences, e. m. of baryon octet and decuplet 8=11389
 mass, empirical relation, multiples of e mass 8=6734
 mass formula, associative algebra 8=15688
 mass formula describing mass-spin states using unified wave equations 8=11373-4
 mass formula for Nambu eqns., using Lie-group theory 8=20266
 mass formula, quadratic in SU_3 , evidence against use from $X^0 \rightarrow 2\gamma$ 8=20499
 mass formula rel. to superconvergence sum rules algebraic struct. 8=656
 mass ratios from $SU(3) \times SU(3)$ spectral function sum rules 8=20493
 mass spectrum determ. in $O(3,2)$, $O(4,2)$ theories 8=20265
 mass spectrum in $O(3,3)$ group for relativistic deformable model 8=3503
 mass-splitting models 8=3510
 mass-splitting in scatt., symmetries 8=676
 mass-splitting theorem for nonintegrable Lie algebras 8=11375
 massive, search in cosmic rays 8=11661
 massless, condition for existence 8=11363
 massless fields, $U(2,2)$ algebra unitary representations 8=15689
 massless transforming according to infinite-spin representations of 2D Euclidean group 8=20325
 micro-causality principle, math. formulation 8=6716
 monopole, magnetic Schwinger quantization relation derived by group-theoretic methods 8=20271
 μ^2 operator, diagonalization, extended models 8=6733
 multiparticle prod. processes, high energy bounds deduced from scatt. props. through unitarity 8=20275
 multiple-pole resonance, mean life 8=11380
 multiple-production theory via Toller variables 8=686
 N function integral eqn. reduced to Tamarkin form, removal of singularity 8=20314
 N/D eqns. compared to Bethe-Salpeter, values of required coupling constants larger 8=20313
 N/D eqns., Padé pole approx. 8=20315
 N/D formalism rel. to Y-N scatt. 8=20573
 n interacting, Schrödinger eqn. 8=668
 non-compact groups in particle physics, conference Milwaukee, USA (1966) 8=11352
 nonleptonic decay unified treatment rel. to CP-conservation 8=6750
 nonrelativistic quark model, rel. to classification and decay 8=729
 nuclear interactions, book 8=11386
 nuclear model, test with $n + He^3 \rightarrow p + H^3$ 8=15873
 $O(3,1)$ representation and Regge daughter-poles 8=11413
 $O_{3,1}$ unitary representation from IO_3 8=3506
 $O(3,1)$ rel. to high energy behaviour in Compton scatt. 8=20353
 $O(3,2)$, $O(4,2)$ derivation of mass spectrum and magnetic moments 8=20265
 $O(3,3)$ group for relativistic deformable model, mass and spin spectrum 8=3503
 $O(4,2)$ dynamics and N isoscalar form factor 8=6919
 OPE model for K^+ prod. in $p-p$, 2.5-3.0 GeV 8=20479
 off-shell dynamics relativistic, new covariant integral eqns. 8=20293
 pairs, photon-produced and photon-annihilated 8=11445
 parastatistics and unified theory of identical particles 8=6110
 parities, imaginary rel. to Bhabha's equation 8=648
 parity-violating nuclear forces 8=15915
 partial wave analysis of $\pi^+ p \rightarrow \eta n$ 8=6856
 particle state transformations under $\Theta=CPT$, rel. to internal symms. 8=11370
 particles and antiparticles, scatt., high-energy relations for oscillating scatt. amplitudes 8=11400
 PCAC, generalization to strangeness-changing and axial-vector current rel. to weak form factors 8=11377
 PCAC, implications from presence or absence of poles in weak interactions 8=20249
 PCAC, pionic in calc. $\pi-\pi$ S-wave scatt. length 8=20466
 PCAC in strong interaction Lagrangian 8=15749
 PDDAC hypothesis, tested in K^+ scatt. 8=3668
 peripheral inelastic interacts., theory and consequences 8=15693

Elementary particles—cont'd

- phase-shift analysis of $K^0\pi$ scatt. <1500 MeV/c 8=20484
 phase shift analysis for πN scatt. below 1.6 GeV/c 8=20458
 phase shifts, WKB high energy, produced by repulsive singular potential, expansion 8=20272
 photon processes, $2J + 1$ multipoles, associated low-energy theorem 8=20341
 Poincaré group extension to internal symmetry group, non-physical 8=649
 Poincaré and Lorentz invariant expansions of relative amplitudes 8=11396
 poles complex double in propagator and spectral condition 8=11408
 potential scatt., non-relativistic, effect of CDD poles on long range, behaviour 8=6751
 production processes, multi-Regge-pole hypothesis, group theory Toller analysis 8=6769
 progress in nuclear physics, book IX 8=15627
 propagation functions and field theory 8=6753
 quantum theory of scalar field with nonstatic source 8=11362
 quasiparticles, kinetic eqn. for free fermions 8=15674
 quasi-particles as many-sakaton system 8=20401
 quasi-particles rel. to transformation properties of the kinetic equations 8=14996
 reduced density matrices, permutational symmetry 8=13
 Regge cuts, condensation 8=6768
 Regge pole couplings to N in field theoretic model 8=20327
 Regge-pole model for associated prod. reactions 8=15777
 Regge-pole model with L-S coupling for $PN \rightarrow P^*N$, $PN \rightarrow VN$ 8=20318
 Regge-pole model for partial-wave amplitudes in $\pi-N$ scatt. 8=15784
 Regge-pole model for πN scatt. 1-5 BeV/c, modifications 8=20456
 Regge pole model for $\pi^- + p \rightarrow \eta + n$ 8=11519
 Regge-pole model with L-S coupling applied to $\pi^- p \rightarrow \pi^0 n$, $\pi^- p \rightarrow \eta n$, $\pi^+ n \rightarrow \omega p$ 8=20444
 Regge pole prediction for Compton scatt. and $O(3, 1)$ symm. compared 8=20353
 Regge poles, suppression at $t=0$ 8=11410
 Regge-pole theory in relativistic problems, constrain eqns., general scheme for Reggeization 8=20321
 Regge-pole theory used in model for saturating super-convergent sum rule 8=6756
 Regge residue function, $\beta(s)$, decrease with $\alpha(s)$ as $s \rightarrow \infty$ 8=11420
 Regge theory rel. to real-to-imaginary amplitude ratio for $\pi^+ p$ scatt. 8=20459
 Regge trajectory formulation of dynamics, with unitarity, and narrow-resonance approx. 8=20324
 Regge trajectories, integral eqn. for ρ derived and solved 8=20412
 Regge trajectory for ρ 8=20504
 Regge trajectories for Schrödinger eqn. with Yukawa pot. 8=11421
 Reggeons interaction with vector and scalar currents 8=664
 relativistic quantum mechanical position operator 8=20339
 relativity theory, negative self-energy contribs. by fields rel. to mass discrepancy 8=647
 representation in quantum field theory 8=3446
 resonances, decay rate, implications of infinitely rising Regge trajectories 8=11422
 rigid rotor, relativistic motion 8=11383
 S-matrix theory, uniqueness and symmetry breaking 8=11405
 saturation a good approx. to sum rules? 8=3513
 seniority scheme, quasi-spin methods and pairs of one particle CFP 8=918
 separation by a progressive e. m. wave 8=15649
 $Sh_{2,c}$, Feynman diagrams for unitary representations 8=20180
 SL(6), Casimir operators of Lie algebra determined 8=3508
 SL(6, C) invariant interact., non-linear spinor eqn. 8=646
 $SL_{6,c}$, Weinberg formalism for spin-s particles 8=20259
 $SO_0(4, 2)$ conformal group, physical aspects 8=15682
 sources, anisotropic, path-length formalism 8=7284
 space-time and degrees of freedom 8=11351
 space-time fluctuations as propagator 8=15677-8
 special relativity and high energy physics experiments 8=69
 in spherical potential, classical symmetry group 8=6732
 spin current algebra and relativistic formulation of SU(6) 8=11272
 spin-1/2, in gravitational field 8=2959
 spin, general case in Reggeization of 2-body interactions 8=11412
 spin and isospin, spinor field classification rel. to interacts. 8=706
 spin, Lagrangian formulation of $(2J + 1)$ -component theory 8=6616
 spin, mass-spin depend., unified wave eqn. 8=11373-4
 spin, nonphysical representations the limit of Poincaré group with spacelike momentum 8=6728

Elementary particles—cont'd

- spin-one, polarization effects in scattering 8=6752
 spin particle in outer Maxwell field, kinematics 8=11384
 spin quantization, dynamic reference system 8=3515
 spin- $\frac{3}{2}$ Rarita-Schwinger field, spectral representation 8=6719
 spin, $S_{3/2}$ interacting with gravitational field, covariant wave eqns. 8=11359
 spin and statistics rel. to hyperquantization in quantum field theory 8=20163
 spin theory, non-linear, applic. of Feynman technique 8=20288
 spin-W-spin mixing for B + pseudoscalar-meson decaying particles 8=6766
 spinless, symm. of wave functions, necessity of connected space 8=6602
 spinors and 3-D rotations, relation extended to n dimensions 8=660
 spontaneous creation in de-Sitter space 8=10070
 square of fundamental charge, time-invariance 8=15691
 strong coupling consts., symm. breaking corrections, dispersive calc. 8=15685
 strong coupling group representations 8=6731
 strong interactions as mediator for weak interactions 8=6749
 strong interactions, universal vector and axial-vector theory 8=15771
 strong and weak interactions, present problems, conference Erice Italy (1966) 8=15695
 structure and quantum theory of gravitation 8=6081
 SU(2) and internal symmetry group b, embedding in larger group b 8=652
 SU(2) \otimes SU(2) symmetry of Kepler motion 8=653
 SU(2) and SU(3), rel. between "outer" and "inner" multiplicity 8=3504
 SU(3) generators expressed as differential operators 8=15686
 SU_3 harmonics as basis states for meson resonances 8=11555
 SU(3) and O(4), connection rel. to symms. 8=11371
 SU(3) multiplet, suppression of dibaryon states from PCAC and CA 8=20512
 SU_3 , projection operators and Clebsch-Gordan coeffs. calc. 8=15680
 SU(3) and Regge poles: classification and high-energy scatt. 8=15708
 SU(3) symm. rel. to $\pi^- + p \rightarrow n + \eta$, $\gamma + p \rightarrow p + \eta$ 8=20490
 SU_3 , Wigner coeffs. 8=2885
 SU(3, 1) wave eqn. for dynamical description of h and l 8=20258
 SU(6)_v approach to e.m. form factor of N 8=20514
 subtractions in dispersive approach to SU(3) and SU(2) breaking in medium strong interaction 8=15694
 sum rules and currents, restrictions 8=6730
 sum rules and high energy theorems of current algebra in free field model 8=3550
 sum rule identities from equal-time commutator 8=3526
 sum rule for spectral functions, relation to between $A_1(1080)$ and $K_1(1320)$ 8=20261
 sum rules, Weinberg type, necessary and sufficient condition for validity 8=6727
 superconvergence and e.m. mass differences calc. 8=11372
 symmetries, International School of Physics "Ettore Majorana", ERICE 1965 8=6721
 symm. breakdown, classical model, invariance of solns., mass spectrum and occurrence of zero masses 8=20257
 symmetry breaking and const. gauge transforms. 8=650
 symmetry groups, appl. 8=11361
 symmetry, spherical, breaking into Euclidean rel. to impact-parameter representation 8=15698
 three-body final-state interactions, appl. of unitary symmetry 8=3519
 three-body reaction threshold, scatt. cross-section near 8=3547
 three-particle states, Green's function expansion using spherical harmonics 8=20263
 $3\pi^{1+}$ in three octets, decay 8=733
 3-nucleon system, application of perturbation theory 8=11579
 time-of-flight obs., large-area isochronous scintillation counters 8=15631
 time reversal invariance in $\nu_l + N \rightarrow N^* + l$ and $\bar{\nu}_l + N \rightarrow N^* + \bar{l}$ 8=3585
 two-body charge-exchange processes, in quark model 8=6742
 2-body reactions, simultaneous s-t analyticity from axiomatic field theory 8=6740
 2-particle inelastic interactions asymptotic amplitudes, Mandelstam branch points contrib. 8=663
 2-particle \rightarrow 2 particle transformation relativistic, current algebra 8=662
 U(3) \times U(3) chiral symm. in strong interaction Lagrangian 8=15749
 U(6), relativistic, difficulties 8=11369
 U(6, 6) algebra in harmonic function space 8=14934
 unitary symmetry 8=11367
 unitary symm., change in internal symm. group on going from time-like to space like momentum 8=20337
 unitary symmetries, SU(3) and SU(6), book 8=20256

Elementary particles—contd

- unitary symmetry theory 8=6722
- unstable, and resonances, application of general wave function 8=20268
- vector meson sum rules from current commutators 8=3525
- vertex functions obeying $SU(2) \otimes SU(2)$, calc. 8=744
- Vrkljan linearization eqns., verification 8=6717
- weak interactions of non-strange particles 8=11392
- Weinberg sum rules for spectral functions of vector and axial-vector current propagators, 8=20260
- Weinberg sum rules, finite meson corrections 8=3521
- Yang-Mills field, rel. to conformal group on space-time curve 8=15679
- Yang-Mills theory, equivalent results from current algebra with meson pole dominances 8=11357
- Yukawa potential, bound on double spectra function 8=661
- zero mass in σ model of PCAC eliminated 8=11489
- zero rest-mass particles, wave equation 8=11354

interactions. See Field theory, quantum/interactions; Nuclear reactions. Entries on interactions involving named particles are listed under the particles concerned, e.g. Mesons/interactions; Cosmic rays/effects and interactions.

Elements

- equilibrium properties of matter at very high temp. and densities 8=19167
- f.c.c., stacking fault energies, extrinsic to intrinsic relative magnitudes 8=17666
- new, prod. of, accelerator problems 8=15913
- 126^{210} production possibility calc. 8=3972

origin

- See also Cosmology; Thermonuclear reactions.
- chondritic meteorites, origin from moon or Mars 8=14856
- nucleosynthesis in supernovae shock waves 8=5842
- planets, by accretion of planetesimals, statistical problems 8=19248
- primeval thermonuclear fusion 8=23471
- B, in expanding hot universe, abundancies 8=5840
- Be, in expanding hot universe, abundancies 8=5840
- D, in solar system 8=19236
- Li, Be, B spallation formation in solar system 8=3922
- Li, in expanding hot universe, abundancies 8=5840
- p- O^8 reactions, Li, Be, B isotope ratio obs. 8=20792

relative abundances

- anomalies, explanation by cosmic annihilation 8=7116
- in BL Telescopii primary body 8=10204
- evolution in galactic cosmic rays 8=23490
- HD 122563, iron-peak, from u. v. spectra 8=5862
- HD 30353, H-poor, light elements 8=5882
- meteorites, Fe, inert gas compositions 8=10366
- radioactive Th, U and K, in crystalline shield rocks 8=9794
- solar chromosphere, O, Mg, Cr, Mn, Fe and Ni 8=23742
- solar corona, from u. v. spectrum 8=5976-7
- stellar interiors, heavy ion reactions 8=10151
- stellar surfaces, anomalies produced by nuclear reactions 8=5870-1
- Sun, rel. to diffusion of Li to Bi 8=19285
- supergiants, HD 96248 and HD 14443, N-deficiency 8=5889
- C^{12}/C^{13} solar abundance ratio from spectral meas. 8=10429
- from Ca II forbidden line in solar spectrum 8=19293
- D, $He^{3,4}$, implications of Brans-Dicke theory 8=23478
- Fe 8=2769
- Fe, in sun and meteorites 8=23682
- Fe XIII solar emission lines, photoelectric meas. during eclipse 8=5965
- Fe, in volcanic pigeonite, by Mössbauer meas. 8=9790
- He in Star Groombridge 1830 8=23505
- P^{229} and Pu^{244} in early solar system, obs. from achondrites 8=23468
- Li in the Pleiades and Ursa Major clusters 8=5863
- O/Fe in solar corona 8=23748
- Pb in sun, spectrometry 8=23696
- Pu^{244} and P^{229} in early solar system, obs. from achondrites 8=23468

Emission spectra. See Luminescence; Spectra; X-ray spectra emission.

Emissivity

- cathode, oxide, in low-pressure pulse discharge 8=18258
- cavities, cylindrical, nr. black body 8=220
- coaxial system, reduced emissivities meas. method 8=223
- incandescent light source, angular dependence 8=15524
- infrared, impurity-induced in interstellar dust 8=23571
- nichrome ribbon, natural convection rel. to heat flux 8=17548
- solid bodies, study 8=225
- solids, thermal, integral, 100 to 1100°C, modified calorimetric method 8=13400
- spatial distrib. of emission coeff., in limit of small self-absorption 8=3354
- surfaces, role of scatter, rel. to polar-collector design 8=1686
- synchrotron, for cosmic radio waves, correction 8=23604
- tubular radiator, computer soln. 8=10767
- CO_2-N_2 plasma, i.r. meas. 8=12510
- CdS, exciton lines, intensity variation rel. to excitation intensity, 4.2°K 8=22964
- Eu chelates, u. v. irradi., three-ligand β -diketonates, absence of stimulated emission, causes 8=18571

Emissivity—contd

- LiF film on Mo substrate, at 420°K and 605°K, at 20° and 0° 8=14236
- W, spectral, in visible and i.r. range 8=1897

Emulsions

- See also Colloids.
- alkylbenzenesulphonate-octanol-water systems, phase behaviour 8=8159
- benzene-in-water, particle size and distrib. 8=12953
- immiscible liq.-liq. system, agitated, drop size distrib. 8=12955
- methyl isobutylketone-salt water system, drop size distrib. rel. to coalescence 8=12956
- stabilized, barrier to coalescence, model 8=12957
- thickness and absorption, rel. to hologram reconstruction 8=15556
- tritium counter, water/toluene/triton system 8=3856
- ultracentrifugation, simultaneous automatic sequence and photo control system 8=4631

Emulsions, nuclear. See Nuclear track emulsions.

Emulsions, photographic. See Nuclear track emulsions; Photographic materials.

Energy bands. See Crystal electron states; Metals/theory; Semiconducting materials; Semiconductors.

Energy gaps. See Crystal electron states; Semiconducting materials; Semiconductors; Superconducting materials and devices; Superconductivity.

Energy levels. See Atoms/structure; Molecules; Nucleus/energy levels; Spectra.

Enthalpy. See Thermodynamic properties.

Li plasma, calc. 8=12462

Enthalpy measurement. See Calorimetry.

Entropy

- See also Thermodynamics.
- alkali halides, entropy of vacancy pair formation, calc. 8=1943
- Boltzmann's H theorem, standardization of terms 8=1066
- change rel. to vacancy diffusion in f. c. c. lattices 8=2217
- expansion, adiabatic, of mixture of two phases 8=10662
- fluid, charged, relativistic in e. m. and gravit. fields, adiabatic flow, rel. to pot. 8=16634
- functions existence of as result of relations of inaccessibility between states 8=93
- gas, discontinuities flowing past area change as cause of acoustic wave generation 8=177
- generation equation, derivatives of symmetry relations 8=96
- Hamiltonian system, indefinability 8=2971
- increase principle 8=108
- Landau damping 8=12505
- low temp. behaviour near transition line 8=8260
- magnetic alloys, dilute, low temp. props. 8=18289
- minimum prod. rate conditions in heat-cond. body 8=10663
- neutron diffusion in non-absorbing moderator 8=15850
- plasma, Gibbs entropy calc. outside equilb. 8=4334
- radiative transfer, size of production 8=6118
- solid phase, computer calc. 8=16923
- supersonic layers, linearized perturb. and vorticity due to curved shock waves 8=16652
- rel. to systems analysis by thermodynamics, combined pot. function 8=26
- superconductor, type I, mechanical transport 8=22545
- thermodynamic and information theoretical relationship 8=6104
- weak turbulence in plasma 8=7839
- of KBr self-diffusion from elec. cond. 8=8679
- K_2MoCl_6 , mag ordered and disordered states difference obs. 8=1872
- properties of substances**
- adsorbed large atoms, configurational 8=13104-5
- cyclohexane, gases in solution, rel. to solubility 8=4536
- cyclooctaselenium, changes in formation 8=21207
- cyclooctasulphur, changes in formation 8=21207
- elastic material, no. of parameters 8=50
- hydrogen ion solvation by H_2O mols. in gas phase 8=18661
- ice, square, residual entropy at low temp. 8=4945
- steam, dissociating 8=7917
- transition metals with adsorbed CO, changes on desorption 8=17174
- CO adsorbed on transition metals, changes on desorption 8=17174
- Cu formate tetrahydrate, at antiferroelectric transition pt. 8=8638
- $KCoF_3$, 80°-300°K 8=17519
- Na_2HPO_4 hydrates, low temp. 8=17521
- Th cpds., refractory, and charact. temp 8=13379
- YH_2 , from resistivity meas. 1000-1200°K 8=17942
- $ZrH_{1.69-1.96}$, from resistivity meas. 1000-1200°K 8=1794
- Epitaxy.** See Crystals/faces; Crystals/growth; Films/solid.
- Equations**
- See also Differential equations; Integral equations.
- Bethe-Salpeter, normalization of amplitudes 8=3540
- boundary layer flow, numerical solution 8=7871
- evaporation transient, through a finite region, generalized Galerkin-Kantorovich treatment 8=16946
- exploding loop, second integrals of simplified eqn. 8=613
- gases, diffusion and flow in porous media, approx. 8=214

Equations—contd

- Hartree-Fock-Roothaan eqns., numerical solns. 8=7349
 hierarchy, in fluctuation theory of gases 8=21501
 integral for partial distribution functions 8=10619
 K-G, covariant generalization of soln. 8=11256
 Korteweg-de Vries asymptotic soln. 8=2901
 Korteweg-de Vries, solution 8=2900
 Lagrangian eigenvalue problem $[\omega^2 I - \omega i A - H] \xi = 0$,
 soln. 8=20159
 Laplace, Cauchy problem soln. for particle optics 8=15275
 Laplace, soln. with transport through cylindrical
 constrictions 8=10670
 Liouville for simple fluids, soln. for thermal
 excitations 8=21419
 magnetic induction, use of SI units 8=3177
 Monge-Ampère, and one-dimensional m. h. d. flow 8=19812
 Navier-Stokes, non-stationary, new finite-difference
 scheme 8=21558
 nonlinear diffusion 8=10771
 with partial derivatives extending to impurity, solution
 by partition method 8=15267
 Percus-Yevick eqn. for fluids, soln. method 8=21415
 thermoelasticity, linear 8=10579
 Vlasov, integration in a reduced phase space 8=10499
 wave soln. with transport through cylindrical
 constrictions 8=10670
 Wiener-Hopf with kernel, application to e.m. boundary
 problems 8=2884

Equations of state

- See also Thermodynamics.
 Boltzmann, monoenergetic, spectrum in plane geometry
 with linear-anisotropic scatt. funct. 8=135
 Bose gas at critical point, correl. function 8=19459
 correlation function near critical point, thermodynamic
 behaviour 8=16914
 critical point thermodynamics, fundamental
 problems 8=12962
 fluid of linear mols., 2nd virial coeffs. 8=4252
 fluids, perturbation theory, square-well potential 8=4425
 formulation from thermodynamic data using digital
 computers 8=10666
 nuclear matter at zero temp. and high density rel. to
 neutron stars 8=19166
 plasma free energy, second virial coeff. contribution at
 high temp. 8=12468
 relativistic, condition satisfying principles 8=6065-6
 square-well fluid 8=12581
 stars with phase transition, equilibrium 8=5861
 virial coeffs. of low density fluid, square-well
 model 8=16613
 virial theorem for electron gas, alternative proof 8=19464
 Yvon-Born-Green eqn. for rigid spheres and disks,
 asymptotic modification 8=16616
 Ar, shock compression, Thomas-Fermi-Dirac
 theory 8=16994
 CH₂Cl₂, thermodynamic props., to 750°K and
 200 atm. 8=16819
 Fe-Ta system, liquid and solid δ -phases 8=8161

gases

- air-water vapour mixtures, third virial coeff. 8=4468
 Boltzmann rel. to specific heat of thin film 8=10656
 comparison using spinodal as envelope of isocurve
 family vs. p, T 8=1620
 diatomic, thermodynamic functions with molecules in
 Σ^3 state 8=1467
 ethyl ketone, vapour, second virial coeff. 8=1471
 ethyl propyl ketone, vapour, second virial coeff. 8=1471
 Fermi, hard-sphere at zero temp., thermodynamic
 props. 8=10658
 linear relation of temp. and density at unit compressibility
 factor 8=16690
 methane-tetrafluoromethane system, PVT relations 8=7912
 methyl isopropyl ketone, vapour, second virial
 coeff. 8=1471
 methyl phenyl ether, vapour, second virial coeff. 8=1471
 multi-atomic, temp. dependence of thermodynamic
 props., formulae derived 8=12674
 nitrogen-ethane mixture, Joule-Thomson coeffs. 8=12679
 nonpolar, and mixtures, third virial coeffs. 8=12677
 pentane, enthalpy calc. from Redlich-Kwong eqn. 8=16689
 Rice-Allnatt assumption in low-density limit 8=1464
 second virial coeffs. of unpolar mols. 8=12676
 Van der Waals, fallacies 8=21503
 van der Waals, sound attenuation near critical
 point 8=16706
 virial eqn., based on hard-sphere model 8=21504
 Ar, interact. potentials rel. to parameters of solid
 at 0°K 8=1468
 Ar₂, virial coeff., 2nd., obs. 8=7913
 Ar-N₂ mixtures, virial coeffs. from Burnett meas. 8=16691
 CO₂ for region 0-1000°C and 0-1000 bars 8=10666
 CO₂, second virial coefficient, -10 to 200°C 8=12675
 F-F, Cl-Cl, Br-Br and I-I systems, 2nd virial coefficient
 for different electron states at 2000-6000°K 8=1469
 H-H and O-O, 2nd virial coefficient for different electron
 states at 2000-6000 K 8=1469
 H₂, and nonpolar mixtures, third virial coeffs. 8=12677
 H₂, normal, Is diagram, 16°-100°K, up to 500 kg/cm² 8=7915
 H₂O₂, decomposition thermodynamics and kinetics 8=1466

Equations of state—contd

gases—contd

- He, enthalpy calc. from Redlich-Kwong eqn. 8=16689
 He, and nonpolar mixtures, third virial coeffs. 8=12677
 He-n-butane mixtures, second virial coeffs.
 determ. 8=12980
 He⁺, second virial coeff., for exponential repulsion
 potential 8=12678
 Kr, interact. potentials rel. to parameters of solid
 at 0°K 8=1468
 Kr₂, virial coeff., 2nd., obs. 8=7913
 N₂, enthalpy calc. from Redlich-Kwong eqn. 8=16689
 N₂-hydrocarbon mixtures, enthalpy calc. from Redlich-
 Kwong eqn. 8=16689
 NH₃, enthalpy calc. from Redlich-Kwong eqn. 8=16689
 Ne, interact. potentials rel. to parameters of solid
 at 0°K 8=1468
 Ne, and nonpolar mixtures, third virial coeffs. 8=12677
 Xe, interact. potentials rel. to parameters of solid
 at 0°K 8=1468

liquids

- n-alkanes, correl. with chain length 8=16790
 binary mixtures, hard-sphere model 8=4539
 inert gases, law of corresponding states 8=1552
 parahydrogen, to 350 atm 8=4525
 perturbation theory 8=12783
 polyelectrolytes, 2nd virial coeff. 8=4540
 polymer solutions, rel. to critical opalescence 8=21669
 simple liquids, theory 8=21604
 solutions, 2nd virial coeff., cryometric determ. 8=8017
 transition metals, density of states of non-degenerate
 (s) band 8=12901
 volume change on mixing simple liqs., corresponding
 states calc. 8=4537
 Ar, thermodynamic props. calc. 8=8041
 Hg, density rel. to temp. and press. 8=12900
 N, 63.15° to 140°K and reduced densities from
 1.8 to 3.1 8=4543

solids

- polar crystals, thermal eqn., linear model 8=13013
 solid solns., thermal 8=8634
 Be, mechanical, from stress/strain curves 8=8825
 Ni near Curie temp., approx. eqn. 8=2330

Erbium

- deformation planes after dehydrogenation and hydride
 habit planes 8=8728
 energy/wave vector spin-wave dispersion
 relation 8=22800
 magnetic structure using Mössbauer effect 8=2291
 microwave absorption phenomena at 9.44 and 35.3 Gc/s,
 10-290°K 8=14269
 thin films, oxidation, electron microscope study 8=5701
 Er³⁺ in CaMoO₄ and SrMoO₄, e. p. r. spectra at 4.2 and
 10°K 8=18412
 Er³⁺ centers in CeO₂, spin lattice relaxation times 8=5530
 Er³⁺, energy transfer in Na rare-earth tungstates 8=9610
 Er³⁺ in LiNbO₃, e. p. r. 8=18428
 Er³⁺ in YGA garnet, optical obs. intensities and quantum
 counter action 8=22979
 Er(III), in YPO₄ and YVO₄, angular overlap
 treatment 8=4075
 in Mg crystal, e. s. r. 8=5531
 Sc₂O₃:Er³⁺, absorpt. and emission spectra 8=14260

Erbium compounds

- Er ferrite-garnet, dichroism and mag. anisotropy 8=18423
 α -ErAl₃, nuclear magnetic resonance 8=22920
 ErCl₃·6H₂O, hyperfine splitting of lowest 2⁺ state of
 Er 8=9301
 Er-H₂ system, phase analysis by X-ray exam. 8=17058
 Er₂O₃ foils, grain boundary energetics by transmission
 e-microscopy 8=21986
 Er₂O₃, sintering, kinetics, data correlation 8=8258
 Er₂O₃, sintering kinetics, resonant freq. meas. 8=17027

Ergodic theorem. See Statistical mechanics.

Errors. See Measurement/errors; Random processes.

Esaki diodes. See Semiconducting devices/tunnel diodes.

Esaki effect. See Semiconducting devices/p-n junctions.

Etalons. See Interferometers.

Etching. See Crystals/etching.

Ether drift. See Relativity/special; Velocity/light.

Etingshausen effect. See Magnetothermal effects.

Europium

- elastic moduli and u. s. attenuation from 4.2 to
 300°K 8=17781
 Fermi surface and antiferromagnetism 8=22459
 heat capacity, 5°-300°K 8=17518
 hyperfine field from conduction-electrons 8=1633
 Mössbauer effect measurements, 16°K anomaly 8=8212
 optical properties and band structure 8=5598
 Eu²⁺ activation, alkaline-earth pyrophosphates,
 luminesc. 8=9628
 Eu²⁺ in BaTiO₃, e. s. r. in cubic and tetragonal
 phases 8=14094
 Eu²⁺ in CaF₂, stress induced nuclear quadrupole
 splitting 8=22928
 Eu²⁺, e. p. r. in KCl cryst. 8=5529
 Eu³⁺ in CaF₂, radiochemical reduction giving Eu²⁺ 8=18740
 Eu³⁺ in garnet struct., hypersensitivity of ¹⁵²D₀-⁷F₂
 transition 8=18602

Europium — contd

- Eu³⁺ in MnF₂, antiferromagnetic, radiationless processes and afterglow kinetics 8-23058
 Eu³⁺ in SrTiO₃, vibronic structure in luminescence spectra 8-14333
 Eu³⁺ in tungstates and molybdates, u. v. excitation of fluoresc. 8-2473
 Eu¹⁵² decay, longitudinal polarization of β -rays 8-20754
 Eu WO₃, determ. of Eu by γ -activation 8-9766
 in MF₂ (M=Ca, Sr, Ba), e. p. r. spectra at 77-964°K 8-9424
 in Na₂B₂O₇ glass, luminescence 8-23061
 in ThO₂, spectrometric determ. 8-18787

Europium compounds

- chemical shifts of inner levels, determ. by photoemission 8-16971
 β -diketon complexes, spectron, rel. to laser use 8-22978
 ligand exchange kinetics 8-23085
 salts, hydrated, fluoresc. lifetimes and multi-phonon deactivation, 4, 2°, 77° and 300°K 8-14315
 Eu chelates, mag. props. 8-9306
 EuAl borate, nonstoichiometry 8-8410
 EuF₃, absorpt. and fluoresc. spectra 8-14214
 EuO films, prep., Faraday rot. and mag. props. 8-13090
 EuO, magnetic susceptibility and mag. sp. ht., Padé approximant estimates 8-22861
 EuO, u. v. reflect. spectra 8-18524
 Eu₂O₃, u. v. reflect. spectra 8-18524
 Eu₂O₄, metamagnetism 8-22746
 EuPc₂, EuPd₂, EuPt₂ and EuRh₂, mag. props. by Mössbauer e. p. r. and n. m. r. studies 8-18334
 EuS, magnetic susceptibility and mag. sp. ht., Padé approximant estimates 8-22861
 EuS, magnetically ordered, magnetointernal field emission obs. and model 8-5428
 EuS, magnetocrystalline anisotropy 8-9341
 EuSe, magnetically ordered, magnetointernal field emission obs. and model 8-5428
 EuSe, magnetic moment 8-22802
 EuSe, magnetic structure 8-22803
 EuZn₂, mag. props. by Mossbauer e. p. r. and n. m. r. studies 8-18334

Evaporation

- See also Vaporization.
 capillary transpiration, liquid-vapour mass transfer 8-21776
 clouds and sprays in air 8-8184
 diffusion limited, enhancement by condensation within thermal boundary layer 8-4658
 directed, in high vacuum, for obtaining targets 8-23775
 drops, large, formation of, equation 8-4556
 ethanol, into O₂ and CO₂, effect of interface motion on mass transfer 8-16711
 ethylether, into He and CO₂, effect of interface motion on mass transfer 8-16711
 films, thin, piezoelectric crystal-type instrument for thickness obs. 8-21871
 liquids, coeffs. determ. by jet tensimeter 8-12990
 metals, by powerful heat flux, pulse effect 8-8187
 mass transfer by evaporation-diffusion between solids 8-8673
 metals, "flash" evaporation, high vacuum device for rate metering 8-8186
 nonadiabatic, from porous system, convective heat and mass transfer 8-8183
 particle, moving, in gas, free mol. regime 8-12943
 polymer solvent kinetics at film formation 8-12972
 solids, due to laser irr. heating effect 8-15130
 of solid surface, surface defect structure theories and quasi-equilib model 8-21782
 surface, unsaturated, using energy balance and Dalton-type transport eqn. 8-21777
 thin films, vacuum deposition, substrate heater 8-17122
 transient, through a finite region, generalized Galerkin-Kantorovich treatment 8-16946
 vacuum metallurgy conference New York USA (1966) 8-16746
 water baths, const. temp., minimizing evaporation 8-16947
 water surface, small, at ground level, convectionless turbulent diffusion 8-14638
 Ag films on mica, W substrate nucleation 8-13087
 Be₃N₂ vaporization, coeff., vapour pressure, enthalpy and enthalpy of activation 8-1624
 CdTe-HgTe, mass transfer by evaporation-diffusion 8-8673
 Cu from Fe-Cu alloys at 1600°C under vacuum 8-12993
 of Mg from Ni, rel. to CO evolution 8-16745
 Mn from Fe-Mn and Fe-C-Mn alloys at 1600°C under vacuum 8-12993
 of NaCl and NaCl solns., charge release 8-4307
 Ni and Pb simultaneously for formation of NiPb phase 8-21852
 Pb-glass melts, volatilization of volatile constituent from surface 8-21775
 Se films, viscoelastic properties, obs. 8-21888
 Si films on W substrate 8-4758
 Sn from Fe-Sn alloys at 1600°C under vacuum 8-12993
 ZnS, cubic, epitaxial growth by evaporation in ultra-high vac. 8-21893
 ZnSe, ZnSe_{1-x}Te_x and ZnTe, thin films, prep. by flash evaporation 8-13100

Evershed effect. See Sunspots.

Examination of materials. See Electron diffraction examination of materials; Electron microscope examination of materials; Neutron diffraction examination of materials; X-ray examination of materials.

Exchanges, chemical

See also Isotope exchanges.

- albite crystals in K⁺ solns., hydrothermal Na-K "exchange" process 8-18648
 alkali-metal atoms in atmosphere of inert-gas 8-12088
 benzene radical anion, electron exchange with neutral benzene 8-5692
 chelated amino acids, p exchange and mutarotation via carbanion intermeds. 8-5691
 contact pairs, energetics 8-18650
 cyclopropylcarbinyl cations, equilibrating expts. 8-5699
 e. s. r. line shapes of systems undergoing intermolec. exchange 8-12302
 faujasite crystal in contact with Ce(NO₃)₃, crystal structure 8-8515
 ion-exchange equilibria in mixed solvents 8-18647
 ion, use of Rumanian molecular sieves 8-18652
 ion, synthetic zeolites 8-18651
 ionic cpds., prep. with ordered vacancies by exchange reactions 8-23082
 mixed anion and cation resins, for removal of fission prods. from degraded solvent 8-5694
 2-picoline, with dichlorobis (2-picoline) Co(II), n. m. r. study of ligand exchange 8-2501
 thermal diffusion of gas mixtures in chem. equilib. 8-966
 zeolites, synthetic, ion exchange theory 8-18651
 Au¹⁹⁹ ion exchange removal from n irr. Pt 8-23168
 B complex, (CH₃)₂OB. F₃, isotope separation coeff. 8-1865
 D-neopentane, kinetics, effects of desorption, diffusion and surface exchange 8-23083
 D₂⁺ and He ion-molecular reactions, cross sections 8-14348
 Eu cpds., chem. shifts of inner levels, determ. from photoemission 8-16971
 (H₂, D₂) reaction, vib. versus translational energy importance 8-4257
 (H₂, H₂) reaction, vib. versus translational energy importance 8-4257
 H₂⁺ and He ion-molecular reactions, cross sections 8-14348
 I cpds., chem. shifts of inner levels, determ. from photoemission 8-16971
 N-methyl-N-benzylformamide, rel. to int. rot., compared with n. m. r. method 8-4623
 NaCl uptake by cellophane membrane rel. to ion exchange props., obs. 8-23084
 O between CO₂ and CO on carbon 8-2502
 Ti(HPO₄)₂ · H₂O, synthetic ion exchanger, crystal structure and exchange behaviour 8-13295
 Zr(HXO₄)₂ · H₂O, (X = P, As), synthetic ion exchanger, crystal structure and exchange behaviour 8-13295
 Zr(OH)₂(MoO₄OH)₂, synthetic ion exchanger, crystal structure and exchange behaviour 8-13295

Excimers. See Molecules/excitation.

Excitation. See Atoms/excitation; Molecules/excitation; Nuclear excitation; Vibrations/excitation.

Excitons. See Crystal electron states/excitons.

Excitons, molecular. See Molecules/polymers.

Exoelectron emission. See Electron emission.

Exosphere. See Atmosphere/upper.

exp-6 potential. See Kinetic theory; Molecules/intermolecular mechanics.

Expanding universe. See Cosmology.

Expansion, thermal. See Thermal expansion.

Explosions

See also Detonation; Shock waves.

- in air, parameters rel. to energy of seismic surface wave expt. compared with theory 8-23211
 air-pentane mixtures, effect of vessel size and turbulence on explosion press. 8-6147
 in atmosphere, geomagnetic disturbance due to shock waves 8-2746
 azides, explosive props. and electronic struct. 8-1259
 conductors, wire, ovoid, rel. to shape changes 8-6150
 dust, prevention, critical O₂ conc. determ. 8-18694
 e. m. perturbations 8-3040
 exothermic front in condensed medium (k-phase), theory of stationary propag. vel. 8-18660
 explosive liquids, cavitation by shock wave 8-171
 field limitations in cylindrical flux compression experiments 8-10862
 foils, by 6 kV electric discharge between coaxial electrodes 8-7690
 gaseous, transient heat convection 8-15108
 hydrodynamic theory appl. 8-6146
 impact loading of KNO₃, dynamic compression 8-22377
 nitrates and perchlorates, explosive props. and electronic struct. 8-1259
 shock wave propag. in generalized Roche model 8-15060
 subjective estimation of sonic and explosive bangs 8-15
 Tunguska meteor, energy density 8-23681
 underwater in N. Pacific, location and enumeration 8-23
 underwater, phase shift due to total internal reflection 8-19547

Explosions—contd

- underwater, $\pi/2$ phase shift at caustics 8=19546
- white dwarf into Type I supernova 8=23549
- wire for det. of spark-gap-switch deionization 8=7679
- wires, discharges initiated at the surface and within 8=4272
- wire, electrical, specific energy distrib. of shock waves formed 8=6142
- wire, mathematical description 8=3042
- wires, time-resolved spectra 8=15537
- Ag wires, electric, temp. variation during first stage 8=1622
- Cu wires, electric, temp. variation during first stage 8=1622
- Mg alloy deformation 8=17815

nuclear

- acoustic signals in atmosphere, anomalous propagation 8=9898
- alluvium, cavity press. and temp. time history afterwards 8=14527
- atmosphere, pressure and acoustic wave propagation 8=2583
- atmospheric, products, interhemispheric transfer 8=23297
- controlled, employing dense plasma implosion by hypervelocity macroparticle impact 8=16601
- dating from fresh nuclear debris 8=7119
- effects on ionosphere, and atmos. pressure 8=2721
- γ -glow, 9 July 1962, riometer obs. validity 8=14636
- high-altitude, effect on electron loss rate of F2-region 8=14691
- infrasound, period < 1 minute, wind structure effect on propag. 8=23304
- ionospheric travelling disturbance 8=10016-7
- ionosphere waves, period \sim 1 minute, obs. 8=23388
- Longshot source term, azimuthal variation 8=5772
- low altitude, radio signal development 8=23296
- low altitude, spatial model of F-region ionospheric travelling disturbance 8=23418
- low yield weapons, image furnace for simulation of thermal effects 8=3986
- personal neutron dosimetry, use of hair 8=11315
- in salt dome, deep reflection obs. 8=18815
- Starfish, ionospheric v. l. f. amplitude perturbations July 9, 1962 8=23389
- 30 October 1961, upper atm. acoustic-gravity waves 8=14641
- travel times of P waves from Central Pacific 8=23213
- P wave travel times obs. 8=2557

extensive air showers. See Cosmic rays/showers and bursts.

extensometers. See Strain gauges; Thermal expansion.

extra-terrestrial radiation. See Cosmic radiations, radio-frequency; Sun/radiation.

eye

- See also Vision.
- aberration, monochromatic, meas. methods 8=15571
- asymmetric convergence, stereoscopic frame of reference 8=11227
- cornea, instrument for measuring contour 8=20129
- electrical responses, utilization of Stiles-Crawford effect 8=15572
- electroretinogram, dependence on point of pupil entry 8=3386
- electroretinography, use of c.w. laser 8=11233
- entoptic effect following strong illumination 8=538
- fovea, central blue-brightness 8=11237
- human, control mechanism model 8=6586
- humming vibration, strobe vision effect 8=20128
- interior structure, ultrasonic visualization 8=19581
- lens, thin shell deformation analysis 8=15573
- movements, effect of flicker 8=15574
- occipital and retinal potentials from subjectively faded stimuli 8=11234
- ocular and occipital responses, variation with stimulus patterns 8=11229
- optical picture, and looking through binoculars 8=3383-4
- planarian, normal, electron microscopy 8=11240
- planarian, regenerating, electron microscopy 8=11241
- pupil, corneal distortion meas. 8=3382
- retinal image stabilization with plane mirror on tightly fitting contact lens 8=15575
- retinal injury, pulsed laser induced, melanin granules models 8=20130
- retinal rods and cones, differentiation by staining 8=19330
- retina structure model rel. to Stiles-Crawford effect 8=15570
- sensitivity curve, effect on resolving power of telescope 8=481
- sensitivity to incremental stimulus, threshold comparison 8=3387
- spectral sensitivity, visual task effect 8=3390
- spontaneous saccadic movements, resulting visual threshold changes 8=11228
- turtle retinas, isolated, directional sensitivity 8=3391
- visual potential, modification by monochromatic backgrounds 8=11235
- X-radiation visual response 8=6585
- He-Ne laser continuous wave hazards 8=14900

F-centres. See Colour centres.

F-layer. See Ionosphere/F-region.

Faculae. See Sun.

Fallout

- See also Atmosphere/radioactivity; Nuclear reactions; Radioactivity.
- dating of fresh nuclear debris by activity-ratio determ. 8=7119
- from French 1966 Pacific tests 8=18907
- γ -ray dose distributions in phantom 8=23301
- interhemispheric transfer, atm. model 8=23297
- National Nuclear Research Centre, Pelindaba, S.A., 1966 obs. 8=18908
- radioactive, north east Pacific ocean 1961-62, particles sinking rate 8=14633
- seawater, radioactive contamination spreading regularities 8=9806
- Be⁷ over Australia, 1965 obs. 8=23299
- Cd¹⁰⁹ in USSR from Jan. 1964 to June 1966 8=23302
- Sr⁹⁰, on surface of Atlantic 8=9816
- Faraday effect. See Magneto-optical effects.
- Fatigue. See Elastic fatigue.
- Fermi gas. See Fermions.
- Fermi level. See Crystal electron states/Fermi level.
- Fermi surface. See Crystal electron states/Fermi surface.
- Fermion systems. See Fermions.
- Fermions
 - See also Elementary particles; Quantum theory/many-particle systems.
 - currents, positivity contradiction 8=6730
 - composite model, the optimum Lagrange problem 8=11390
 - density matrices, N representability 8=10657
 - dilute mixture in dense Bose fluid, as model for He³ impurities in liq. He⁴ 8=19688
 - Fermi-Bose mixtures, phase-separation 8=6109
 - Fermi gas model for nuclear reactions not confirmed by 10⁸ BeV cosmic ray obs. 8=20777
 - Fermi gas model for nucleus, anomalous corrections for finite size 8=20648
 - Fermi-gas, soln. of Boltzmann master eqn. rel. to equilibrium in excited nuclei 8=11700
 - Fermi hand-sphere gas at zero-temp., eqn. of state distrib. function 8=10658
 - Fermi liqs., nearly ferromag., theory of viscosity 8=2994
 - Fermi liq., nearly ferromag., re-evaluation of spin fluctuation contrib. 8=2995
 - fermion-antifermion system, accurate soln. to Bethe-Salpeter eqns. for masses in U_1 states 8=15687
 - fermion-antifermion system, by Bethe-Salpeter eqn. 8=3603
 - field in σ model of PCAC, bilinears interpreted 8=11489
 - field theory, interacting with vector meson, derivation of Regge trajectory 8=6770
 - 4F interaction, relativistic and causal theories 8=15615
 - free, in presence of impurities, kinetic eqn. 8=15674
 - gas, 1D, two-body orbitals calc., and applic. to repulsive δ -function interactions 8=19462
 - gases, zero-point kinetic energy 8=15018
 - interacting finite system, continuous energy spectrum 8=128
 - interaction, 4 particles, $U(3)$ invariant, meson masses 8=657
 - interaction with massive vector particles 8=15692
 - interactions, 4-, non-leptonic, $\Delta S=1$, with SU_3 symm. among hadrons 8=20400
 - interactions, strong-coupling quark-model $SU(3)$ invariance limit, mass formula 8=20276
 - massless, interacting with vector meson field in 1D 8=3678
 - meson nonet coupling in field theoretical model 8=3421
 - meson theory of nuclear matter 8=1693
 - neutral, scatt. of e. m. waves, spin effects 8=675
 - N isoscalar form factor for fermion representation space 8=6919
 - nuclear shell model as n-fermion system 8=3761
 - one-dimensional system, impulse-distribution ("sharpness") 8=129
 - parastatistics and unified theory of identical particles 8=6110
 - parities, imaginary rel. to Bhabha's equation 8=648
 - propagators rel. to combinatorial feature of Feynman graphs 8=596
 - propagators, covariant and vertex functions for any spin 8=20336
 - quantum electrodynamics, elimination of double corner diagrams 8=3433
 - quantum electrodynamics, two-fermion, infinite renormalizations elimination 8=15620
 - quasi-free states 8=15676
 - radiation in crossed fields 8=6739
 - scattering, polarization quantities and cross sections 8=20380
 - soln. in boson gas, model for He³ in He⁴ 8=6232
 - spin- $1/2$, ground state problem, reduced to generalized Fredholm equation 8=10648
 - superfluid Fermi gas, dynamics 8=130
 - system, analysis of 2- and 4-point functions 8=15014
 - system, condensed state, phase transitions 8=19463
 - system with direct interaction, retarded temp. Green's functions, perturbation theory 8=15021

Fermions—contd

- system, duality of hypervirial and conservation theorems 8=15015
- system, Fermi liquid, flow along narrow channel, spin diffusion and thermal cond. calc. 8=15017
- system, Fermi liquid, specific heat and magnetic susceptibility 8=15020
- systems, interacting, wave-function and energy of basic state 8=3402
- system, Ising model, chain dynamics 8=10611
- system, low-density zero-temp. superfluidity 8=15019
- system, mean kinetic energy, lower bound 8=15016
- system, non-relativistic, 2-particle Green's function spectral functions 8=2996
- systems, response functions 8=10655
- system, supercond. with P-pairing, theory 8=9026
- thin film, specific heat, size effects 8=10656
- trajectory parametrization, N and Δ in a dispersion relation 8=20328
- He³ in superfluid He⁴, dilute mixtures 8=15152

Fermium

No entries

Ferrimagnetic resonance

- See also Ferromagnetic resonance.
- domain structure, boundary shift resonance effect 8=5512
- Bi_{0.4}Ca_{0.6}Fe_{3.2}Ga_{0.8}V_{1.3}O₁₂, and mag. props. 8=18398
- YIG crystal, influence of domain structure 8=5513

Ferrimagnetism

- See also Ferromagnetism.
- sublattices, mol. field soln. uniqueness 8=14042
- RbNiF₃, magnetic exchange dichroism 8=14257

Ferrites

- See also Magnetic properties of substances.
- anisotropic crystals, magnetodynamic natural oscillations rel. to waveguide passband filters 8=5485
- biased to resonance, time variation of r. f.

- magnetization 8=14079
- conductivity, elec., effect of CaO and SiO₂ 8=13715
- core in coincident current store, characts. 8=14043
- crystal growth using arc image furnace 8=8422
- crystal, hexagonal, etch steps height used on standard for electron microscope calibration 8=8450
- cylinder, axially premagnetized, e. m. wave propag. 8=10970
- dielectric props., influence of ultrasound 8=9370
- diode, waveguide applications 8=22626
- domain walls, $k\pi$ and mobile, origin in induced anisotropy 8=5493
- ferrimagnetic res. and relax., effects of paramag. impurities 8=2357
- ferrite dev., superhigh freq. for operation in band 8.2-12.4 Gc 8=10939
- ferrites: Fe²⁺ powders, electron relax. study 8=18419
- ferromagnetic dielectric, magnetization eqns. of motion and eqn. for temp. change 8=5451
- ferromagnetic resonance, bottleneck in energy flow to lattice 8=9408
- ferromagnetic reson. in polycryst. spheres 8=14081
- ferrox cube cores, 2 in pulse transformer for time to pulse height conversion 8=616
- filled and empty waveguide discontinuity problem 8=6397
- frequency doubler, spin-wave instability 8=18393
- garnets, solid solns. rel. to cation distrib. 8=4775
- hexaferrites, Al-Fe substitution by i. r. spectroscopy 8=16999
- hexagonal, type Ba_{1-x}Me_x²⁺Fe₃O₇, crystal structure and stacking sequences 8=17342
- high-speed, single-cycle, ferrite-transistor ring counter circuits 8=1316
- load, ellipsoidal, in a waveguide, calculation of threshold field 8=6393
- lossless magnetized, in waveguides, study of propag. 8=10963
- in loud-speaker circuits, design and performance characts. 8=15258
- magnetic anisotropy constants, mag. saturation intensity dependence, temp. effects 8=2338
- magnetic domain walls, nucleation 8=2339
- magnetostrictive, electro. mech. coupling coeff., mech. reson. freq., meas. accuracy 8=9368
- mag. resonance spectra rel. to sintering temp. effects 8=2342
- nonlinear phenomena, simplified theory 8=5487
- orthotitanate, solid solns., xM₂TiO₄(1-x)MFe₂O₄ (M = metal), spinel structure 8=18365
- permeability tensor, meas. of wire components 8=14044
- polycrystalline, dielectric relaxation rel. to temp. 8=22644
- porous, firing temp. and pore volume 8=8256
- rare earth orthoferrites, temp. induced spin flop, temp. range 8=14048
- solid solutions, dilute, saturation magnetization and Néel temp. 8=9369
- spin resonance, nonlinear, rel. to e. m. wave radiation 8=18395
- spin wave excitation threshold fields 8=18355
- spinel, orientation superstructures and their effects 8=14046
- spinels, polycryst., temp. depend. of hysteresis props. 8=14047

Ferrites—contd

- spinels, solid solns. rel. to cation distrib. 8=4775
- spinel, spin wave linewidth variations on substitution of transition metals 8=5495
- square-loop, magnetization reversal by domain wall movement, model 8=2337
- square-loop polycrystalline, magnetization reversal by Bloch wall movement, model 8=18356
- uniaxial two-sublattice in a noncollinear phase, reson. freq. 8=5486
- BaCo₄F₂²⁺, Fe₁₂O₂₂, hexagonal, spin structure and anisotropy 8=28849
- BaFe₁₂O₁₉, complex permeability and mag. loss in cm. and mm.-wave range 8=5489
- BaFe₁₂O₁₉, polycrystalline samples, mag. dispersions 8=5489
- Ba₂Me₂Fe₃O₄(Me₂Z), magnetic structure 8=9373
- Ba_{2-x}Sr_xZn₂Fe₃O₂₂, quasi-spiral ordering, n diffraction obs. at 4.2°-400°K 8=9372
- Ba₂Zn₂Fe₁₂O₂₂, Bloch wall structure determs. 8=5496
- Bi_{0.24}Ca_{0.76}Fe_{3.26}V_{1.33}O₁₂, Faraday effect mechanism 8=18508
- Bi_{0.5}Ca_{2.5}Fe_{3.75}V_{1.25}O₁₂, magnetoelastic interaction 8=22850
- CaYb₂O₄, crystal structure, rel. to Ca ferrite isomorphism 8=4870
- Cu, nuclear reson. of Fe and Cu, and nuclear relaxation 8=5554
- Cu_{1-x}Mg_xFe₂O₄, O content and thermomag. props. 8=2516
- CuMn, mag. props., Sc₂O₃ effects, obs. 8=18359
- DyFeO₃, transition to antiferromagnetism at liq. He temps. 8=9375
- Er garnet, dichroism and mag. anisotropy 8=18523
- Fe²⁺ presence, determ. 8=18357
- Fe-Cu, mixed conduction mechanisms from resistivity and Seebeck meas. 8=18035
- Fe-Y garnet for microwaves mixing 8=19848
- a(Fe₂O₃) + b(Cr₂O₃) + x₁(NiO) + x₂(ZnO) type, complex susceptibility and dielec. const. meas. 8=9371
- Li, magnetostriction constants at -170 and +340°C, effect of ion ordering 8=9379
- Li, magnetostriction constants from ferromagnetic resonance 8=14045
- Li, self-decoration effect on thermal etching 8=1729
- Li, X-ray topography of defects 8=8708
- Li, Young's modulus, temp. depend. 8=22378
- Li-Co-ferrite-aluminates, thermostable waveguide valves in decimetre range 8=9377
- Li_{0.5}Cr_{1.25}Fe_{1.25}O₄, spontaneous magnetization rel. to compensation temp. 8=14049
- Li, FeLiO₂, Q₇₇ (or β) phase, X-ray diffr. results rel. to periodic antiphase model 8=17386
- Li_{0.5}Fe_{2.5-x}Al_xO₄ (0 < x < 1), mag. moments and mol. field coeffs. 8=9378
- Mg ferrous, magnetically-induced ordering 8=22857
- Mg, nuclear reson. of Fe and nuclear relaxation 8=5554
- Mg-Cr-Cu, mag. permeability tensor, influence of porosity 8=22852
- Mg-Fe, magnetic diffusion after-effect 8=5491
- MgFe₂O₄, thermal conductivity dependence on anion vacancies (produced by chem. reduction) 8=17543
- Mg-Mn, composition microinhomogeneities 8=21990
- Mg-Mn, impulse mag. reversal in strong fields 8=9380
- Mg-Mn, magnetostriction and mag. anisotropy consts. 8=5492
- Mg_{1-0.03}Mn_{0.123}Fe_{0.783}O_{3.983}, cation distribution changes, kinetics 8=22853
- Me_{0.812}Mn_{0.288}Ni_{0.082}Fe_{1.837}O_{3.998}, cation distribution changes, kinetics 8=22853
- Mg-Mn-Zn, mechanism of ageing 8=9381
- Mn, magnetostriction constants from ferromagnetic resonance 8=14045
- Mn, Maxwell-Wagner dielec. dispersion meas. 8=22647
- Mn, nuclear reson. of Fe and nuclear relaxation 8=5554
- Mn-Fe spinels, Mn-rich, Mn³⁺ clustering effect on ferromagnetic resonance linewidth 8=18396
- MnFe₂O₄, cation distrib. in sample from aq. soln., by n-diff. 8=13274
- MnFe₂O₄ from silicate melts, superparamagnetism 8=1402
- MnFe₂O₄, magnetic anisotropy constant change 8=5488
- Mn_{1-x}Fe_{1+x}Sn_{0.1}O₄, mag. fields at Sn nuclei, Mössbauer effect studies 8=9382
- MnMg, square-loop coercive force temp. depend. 8=14051
- Mn, Mn rich, lattice parameter temp. dependence (293-4.5°K) rel. to comp. 8=17394
- Mn-Zn, high permeability, dynamical magnetization curve 8=18361
- Mn-Zn, oxidation rate and phase diagram 8=9691
- MnZn, comp. rel. to stability and losses and prep. 8=22854
- MnZn, mag. props. rel. to final firing cycle cooling condition and atm. equil. maintenance, obs. 8=22855
- MnZn, monodisperse fractions, prepn. 8=9384
- Mn_{0.8}Zn_{0.2}Fe₂O₄, magnetic anisotropy constant change 8=5488
- Ni-ferrite-chromite, Mössbauer effect on Fe⁵⁷ 8=1649
- Ni ferrous, magnetically-induced ordering 8=22857
- Ni-Co-Mn, shifting of u. s. vel. minima due to mag. polarization changes 8=8632

- Ferrites**—contd
 Ni-Fe memory films, dispersion of anisotropy 8=14052
 NiFe₂O₄ films, single cryst., prep. and props. 8=18362
 NiFe₂O₄, magnetic properties in 14-600°C 8=5494
 NiFe₂O₄, thin films, microstructure, ferrimagnetic props., electrical conductivity 8=2343
 NiO-Fe₂O₃, heating during ferromag. resonance 8=14082
 Ni₁Zn_{1-x}Fe_{2-x}O₄, doped with transition elements 8=22856
 Ni-ZnO-Fe₂O₃ ferro(ferri)mag reson., heat prod. obs. 8=14100
 SmY_{3-x}Fe₂O₁₂, magnetostriction anomalies, 4.2-100°K and < 25 kOe 8=18364
 (Sr, Ba)₂Zn₂Fe₁₂O₂₂(Y), spin ordering using neutron diffraction meas. 8=22858
 TbFeO₃, transition to antiferromagnetism at liq. He temps. 8=9375
 TmFeO₃, magnetic structure 1.6°K-94°K, neutron diffr. determ. 8=22859
 Tm₃Fe₂O₁₂, magnetostriction anomalies, 4.2-100°K and < 25 kOe 8=18364
 Y, magnetostriction constants from ferromagnetic resonance 8=14045
 Y orthoferrite, mag. sublattice switching under mag. pulses 8=18366
 YFe_{0.9}Al_{0.1}O₃ crystal, antiferromag. at 602°K and ferromag. at 600°K 8=14074
 YFe garnet interaction of microwave phonons with domain walls 8=22087
 YFe garnet, Al and Ga substituted, heat treatment effect on mag. props. 8=14055
 YFe garnet domain configs. and rel. to cryst. defects, obs. 8=22863
 YFe garnet, elastic wave dispersion, optical investigation 8=2070
 YFe garnet ferromagnetic resonance, bottleneck in energy flow to lattice 8=9408
 YFe garnet, magnetoelastic wave propag. light diffraction study 8=22861
 YFe garnet, spin wave susceptibility saturation above instability threshold, Al and rare earth doping effects, obs. 8=22864
 YFe garnet: Yb³⁺, behaviour on anomalous sites 8=22860
 Y₃Fe_{3-x}M_xO₁₂, (M = In, Sc, Al, Ga) Faraday rot. and i.r. modulator appls., 1.15 and 3.39 μ 8=23021
 Y₃Fe₂O₁₂:Ho³⁺, Faraday effect obs. 8=14271
 YIG slab, magnetostatic surface waves 8=22862
 ZnFe₂O₄, thermal conductivity dependence on anion vacancies (produced by chem. reduction) 8=17543
 ZnO-NiO-Fe₂O₃, heating during ferromag. resonance 8=14082
- Ferroacoustic resonance.** See Crystals/lattice mechanics;
 Ferromagnetic resonance.
- Ferroelectric devices.** See Dielectric devices.
- Ferroelectric materials**
 acoustic and polarization waves interaction, elastic const. 8=18182
 antiferroelectric, permittivity and losses investigated at 37Gc/s 8=18196
 ceramic condenser and its use in thermodielectric generators 8=9231
 ceramics, perovskite-type, electrostriction 8=5362
 copper formate tetrahydrate, antiferroelectric phase transition, cell doubling 8=9222
 crystals, switching transients, contour and symmetry, theoretical interpretation 8=9207
 dicalcium strontium propionate, Ca₂Sr(C₂H₃CO₂)₆, dielectric critical slowing down 8=2248
 dicalcium strontium propionate, Ca₂Sr(C₂H₃CO₂)₆, crystal structure 8=4892
 dicalcium strontium propionate, Ca₂Sr(C₂H₃CO₂)₆, structure in paraelectric phase 8=4891
 electro-optical effects 8=5647
 guanidinium Al₂(SO₄)₃·6H₂O, cryst. struct. 8=17449
 guanidinium Al₂(SO₄)₃·6H₂O, ferroelec. moment 8=18195
 guanidinium Cr₂(SO₄)₃·6H₂O, cryst. struct. 8=17449
 guanidinium Cr₂(SO₄)₃·6H₂O, ferroelec. moment 8=18195
 ice, impure, dielec. dispersion obs., above -190°C 8=18188
 multiple Curie point films prep. 8=18185
 niobates, single crystals., growth 8=21958
 order-disorder, statistical perturbation theory, Zeroth approximation 8=9191
 perovskite crystals, phonon lifetime, at low temps. 8=4908
 perovskite-type crystals, distorted, phase transitions rel. to lattice dynamics of atomic displacements 8=17332
 polarization vectors, spontaneous, irreversible but divertible 8=2242
 Rochelle salt: Cu²⁺ e.p.r. Stark effect obs. 8=14101
 Rochelle salt, u.s. relaxation near ferroelec. transition 8=1858
 Rochelle salt, X-ray extinction rules and radiation damage effects 8=13266
 thiourea, l.f. modes from neutron scatt. 8=13340
 triglycine fluoroberyllate, e.p.r. study of Cu²⁺ ion 8=14105
 triglycine sulphate crystals, pyroelectric effect, by dynamic method 8=18198
 triglycine sulphate, u.s. relaxation near ferroelec. transition 8=1858
 ultrasound damping and velocity near phase transition rel. to long range dipole-dipole effects 8=18181
- Ferroelectric materials**—contd
 BeSeI, dielec. const. and elec. conductivity meas., -200 to +50°C 8=18193
 BiSI, dielec. const. and elec. conductivity meas., -200 to +50°C 8=18193
 Bi_{1-x}GeO₂₀, cryst. struct. 8=13254
 HBr, solid, lowest temp. phase ferroelec., obs. 8=13889
 HCl, solid, lowest temp. phase ferroelec., obs. 8=13889
 K₃Fe(CN)₆·3H₂O, proton relax. and translational diffusion 8=14145
 KD₂PO₄, Curie temp. and Curie-Weiss constant pressure dependence 8=5366
 KD₂PO₄, dynamical effects of deuteron intrabond jumping 8=9212
 KD₂PO₄, near Curie point (-70°C) 8=1873
 KD₂PO₄, order-disorder, phase transition studies, calorimetric investigations 8=22668
 KH₂PO₄, dielectric const. just above transition temp., freq. and temp. depend. 8=22666
 KH₂PO₄, domain switching by irradiation damage 8=18184
 KH₂PO₄, n.m.r. of K³⁹ at 77°K 8=22924
 KH₂PO₄, transition temp. shift by hydrostatic press 8=18189
 KH₃(SeO₃)₂, fundamental absorpt. edge near phase transition pt. 8=9548
 K_{0.4}Li_{0.4}NbO₃, single crystals., growth 8=21952
 KNbO₃ crystals, absorpt. edge temp. dependence 8=2430
 KNO₃, resistivity rel. to temp. and other props 8=18191
 KSr₂Nb₂O₁₅, charact. and electro-optic coeff. 8=5365
 LiH₃(SeO₃)₂, dielectric const. and spontaneous polarization 8=18190
 LiH₃(SeO₃)₂, fundamental absorpt. edge near phase transition pt. 8=9548
 LiNbO₃ crystal for converting near i.r. to visible light by optical mixing 8=11118
 LiNbO₃ domain structure, single crystal 8=13886
 LiNbO₃, refractive index 20°-900°C 8=5620
 LiNbO₃, single crystal, dielectric properties up to 9 GHz 8=9216
 LiN₂H₃SO₄, mol. reorientation of NH₃ 8=8235
 LiTaO₃, Curie temp. and birefringence variation rel. to melt stoichiometry 8=22669
 LiTaO₃, pyroelec. coeff. temp-dependence, 200-800°C and spontaneous polarization 8=18200
 NaH₃(SeO₃)₂ and NaD₂(SeO₃)₂, crystal growth 8=8420
 NaH₃(SeO₃)₂, fundamental absorpt. edge near phase transition pt. 8=9548
 NaH₃(SeO₃)₂ and NaD₃(SeO₃)₂, crystal symm. and nature of phase transitions 8=21849
 NaH₃(SeO₃)₂, phase transition, second, meas. 8=2245
 NaNbO₃, resistivity rel. to temp. and other props 8=18191
 (NH₄)₂SO₄, deuteron spin-lattice relax. time 8=2386
 (NH₄)₂SO₄, H-bonding below ferroelec. transition 8=23005
 Pb zirconate-titanate ceramics, depolarization at high strain rates 8=2243
 Pb zirconate-titanate, surface potentials, electron-mirror microscope anal. 8=13880
 PbTiO₃-PbZrO₃-PbMg_{0.5}W_{0.5}O₃ system, domain orientation processes 8=5367
 PbZrO₃, current hysteresis loops near Curie point, obs. 8=13887
 PbZrO₃ near-antiferroelec.-ferroelec. transition, cond. rel. to ageing and relax. polarization 8=2249
 PbZrO₃ polycrystals, temp. changes of polarization at phase transition 8=13888
 Pb(Zr, SnTi)O₃ ceramics, Nb-doped, elec. props. 8=2246
 Sb₂S₃ and SbSI, anomalous dispersion of permittivity and reson. absorpt. of microwaves 8=9218
 SbSeI, dielec. const. and elec. conductivity meas., -200 to +50°C 8=18193
 SbSI, light polarization near ferroelec. phase transition 8=18559
 SbSI(Br), dielec. const. and elec. conductivity meas., -200 to +50°C 8=18193
 SbSI, photosensitive phase transition 8=2159
 SbSI, polarization discontinuities caused by illumination 8=18192
 SbSI, temp. autostabilizing props. at <20°C 8=5369
 Sr_{1-x}Ba_xNb₂O₆, hysteresis loops 8=21966
 SrTiO₃, optical-phonon freq., electric field dependence 8=5370
 SrTiO₃, phonon lifetime, at low temps. 8=4908
 SrTiO₃, second-order renormalization and phase stability 8=9219
 YMnO₃, domain struct. made visible by etching 8=2247
- barium titanate**
 absorption edge anomalous shift under electric field 8=13882
 absorption edge shift in elec. field, temp. dependence 8=13883
 acoustic and soft optic modes, mixing 8=22665
 breakdown, electric, rel. to movement of colour centres 8=13884
 ceramics, depolarization at high strain rates 8=2243
 cold-conductor ceramic, working mechanism, electron microscopic investigation 8=21982
 conductivity, elec., anomalies 8=9208
 current rise due to injection during elec. ageing, hypothesis 8=18194

Ferroelectric materials—contd**barium titanate—contd**

- dislocation-90° domain boundary interactions 8=8724
- electrical conductivity between 600 and 900°C 8=5363
- field depend. of complex dielect. consts. at 58.2 GHz 8=13879
- fine-grained, high permittivity, internal field theory 8=22664
- grain growth inhibition 8=2244
- hysteresis and dielect. props. 8=13881
- metal contact, elec. conduction temp. dependence 8=22623
- optical properties 8=18504
- photoconductivity, hole transit time temp. dependence 8=18223
- Raman spectrum rel. to overdamped soft optic mode, obs. 8=5586
- semiconductors, piezoresistance effect 8=9095
- silver-ceramic rectifying junction manufacture 8=18125
- single crystal and polycrystalline, dynamic polarization 8=18183
- space charge conduction 8=18002
- surface potentials, electron-mirror-microscope anal. 8=13880
- switching behaviour, low-field, using pyroelectric effect 8=9209
- n-type, single-domain, optical absorpt. 26-130°C 8=9506
- wall energy calc. 8=5364
- BaTiO₃-SnO₂ solid solns, temp. characts. of varikonds 8=18186
- with Fe and Co impurities, elec. props. temp. dependence rel. to optical props. 8=18187

Ferroelectric phenomena

- crystal lattices, interband interaction and spontaneous polarization 8=9210
- ferroelectricity, book 8=5361
- glycine silver nitrate, probable cause of ferroelectricity 8=5646
- 'light plane' type, interact. of spin waves and polarons 8=22481
- space symmetry and induced polarization 8=9206
- triglycine selenate, crystalline and transition to paraelectric at high press. 8=8288
- Fe-I-boracite, orthorhombic phase, optical study 8=22980
- K₄Fe(CN)₆·3H₂O, dielectric dispersion 8=9211
- K₄Fe(CN)₆·3H₂O, phase transition Mössbauer test for lattice-dynamical model 8=22667
- KH₂PO₄-type crystals, dynamics of phase transition 8=9215
- KH₂PO₄, phase transition, high temp., isotope effect 8=9213
- LiNbO₃ domain structure, single crystal 8=13886
- NaNO₂, ferroelectric phase, N¹⁴ n. q. r. 8=9473
- PbZrO₃, i.f. dielectric study, rel. to temp. 8=5368

Ferromagnetic relaxation

No entries

Ferromagnetic resonance

- See also Ferrimagnetic resonance.
- anisotropy effect on frequency of calc. 8=5510
- coupled spin systems, two, mol. field eqns. 8=9406
- cryostat for meas. at liq. He temp. 8=6226
- cryostat for use in temp. range -190° to +200°C 8=253
- damping by s-d exchange interaction 8=9405
- ferrite, freq. doubler, spin-wave instability 8=18393
- ferrite, meas. of spin wave relax. rates under perpend. pumping 8=14079
- ferrite, nonlinear rel. to e. m. wave radiation 8=18395
- ferrite polycryst. spheres 8=14081
- ferrite, use for determ. of Fe²⁺ presence 8=18357
- ferrites, doped, bottleneck in energy flow to lattice 8=9408
- in ferrites, effect of fast relax. paramag. impurities 8=2357
- ferrites, heating obs. 8=14082
- ferrites, magnetostriction constants determ. 8=14045
- ferrites relaxation, correlation with relaxation in magnetic anneal 8=9407
- ferroacoustic resonance, theory 8=4918
- in ferromagnetic films, theory rel. to boundary conditions 8=18394
- film, due to hypersound in substrate 8=1841
- in films, single-crystal 8=2353
- in garnets, effect of fast relax. paramag. impurities 8=2357
- line broadening, due to cond. currents 8=18392
- nonlinear, energy equil. mechanism 8=14077
- Permalloy, composite films, structure 8=9357
- permalloy films, r. f. reflecto-polarimetry 8=9409
- permalloy, "flash-evaporated", standing spin-wave resonance 8=14083
- relaxation by two-magnon scattering on dislocations 8=14078
- Supermalloy, rel. to spin diffusion 8=9404
- susceptibility tensor under spin-wave resonance excitation 8=9330
- susceptibility depend. on h. f. field 8=2354
- theory, non-linear 8=18391
- thin film, nonuniform magnetization models 8=14080
- thin films, use in fast response magnetometer 8=19744
- BaFe₁₂O₁₉, rel. to multidomain theory 8=9403
- Bi-Ca-V garnet, absorption of longit. acoustical waves 8=18397

Ferromagnetic resonance—contd

- Fe-Ni alloys, heating obs. 8=14082
- Li ferrite magnetostriction constants at -170 and +340°C, ion ordering effect obs. 8=9379
- Mn-Fe spinels, Mn-rich, linewidth rel. to Mn²⁺ clustering 8=18396
- Ni intrinsic linewidth anisotropy rel. to relax., 25.92 and 9.42 GHz 8=2355
- Ni, polycrystalline, variation between -100 and +400°C 8=5511
- Ni powder, heating obs. 8=14082
- Ni-Fe thin films, linewidth rel. to temp. 8=2356
- Ni-ZnO-Fe₂O₃ ferrite, heat prod. obs. 8=14100
- YFe garnet, absorption of longit. acoustical waves 8=1839
- YFe garnet, anomalous effects rel. to paramag. impurities 8=2357
- YFe₂-Cr₂O₃, crystal field symmetry 8=1636
- YFe garnet, Yb doped, bottleneck effects in ferromagnetic resonance 8=9408

Ferromagnetics. See Magnetic properties of substances/ferromagnetic.**Ferromagnetism**

- See also Antiferromagnetism; Ferrimagnetism; Ferromagnetic relaxation; Ferromagnetic resonance; Magnetic properties/ferromagnetic; Magnetization process; Magnetization state.
- Anderson-type localized moments coupling rel. to theory 8=2314
- band model for metals, magnetic isotherms 8=22764
- Bloch walls in b.c.c. crystals, variational calc. 8=2308
- Bloch walls in f.c.c. crystals, variational calc. 8=2309
- Brillouin function and spontaneous magnetization table for J=1/2 to 7/2 and J=∞ 8=9328
- condensed Fermi system, phase transitions 8=19463
- critical behaviour of boundary susceptibility and boundary tension 8=22774
- critical behaviour theory 8=13978
- crystal with induced anisotropy, domain walls fixed and mobile, origin and consequences 8=5449
- crystal surface magnetic scattering of low energy electrons, theory 8=5447
- cubic lattices, Bloch wall orientations, relative energies 8=18312
- dilute, critical behaviour of specific heat 8=9307
- exchange-interaction model, high temp. susceptibility 8=2302
- ferroelectrics, spin-wave intensification by charged-particle beam 8=5443
- Heisenberg ferromagnet dynamical props. near critical point, generalized scaling laws appl. 8=2346
- Heisenberg ferromagnet, Fock-space formulation of drone theory 8=13975
- Heisenberg magnet with magnetic impurity, diffuse inelastic neutron cross section 8=9319
- Heisenberg model, approximate free energies 8=13986
- Heisenberg, quantum statistical mechanics 8=9317
- Husimi-Temperley model, zeros of partition function 8=13977
- Ising model, binary correl. functions, mean-field bound 8=18304
- Ising model, chain dynamics 8=10611
- Ising model, initial perpendicular susceptibility, freq. depend. 8=18310
- Ising model, Onsager's results using Green's function 8=2964
- Ising model, second order 8=14986
- Ising model, time-independ., kinetic eqns. developed 8=14985
- Ising problem for lattice with substitutional and interstitial impurities 8=1951
- Ising systems, first-order transition probability 8=18309
- Ising, three dimens., critical isotherm and exponents 8=18310
- Kondo problem, perturbation instabilities 8=22869
- magnetization, appl. of conventional Bloch wall models 8=9320
- magnetization transition temp. rel. to domain structure 8=9324
- magnon spectrum in band model mag. dipolar coupling 8=2307
- micromagnetic treatment of local fluctuations using Green's function 8=5450
- periodic magnetic structures and phase transitions 8=18310
- phase transition, effect of non-mag. impurities 8=5444
- role of theoretical physics in development of materials, review 8=22733
- saturation magnetization derived 8=8260
- sound attenuation near critical points 8=13344
- spherical model rel. to a Bose gas at transition 8=19459
- spins 1/2, chain, X-Y model 8=2306
- spin polarization round local mag. impurity 8=18317
- thermodynamics, ideal, using diagram techniques 8=5447
- thin films, complex susceptibility 8=22786
- u.s. attenuation near transition temp., phonon interact. with spin system 8=18323
- α-Co, hexagonal cryst. magnon obs. 8=14008

spin-wave theory

- AB binary alloys, triplet probabilities rel. to pair correlations 8=9313

Ferromagnetism—contd**spin-wave theory—contd**

- B-site spinel, critical index of susceptibility in Heisenberg model 8=18305
 collective modes of spins in magnon and critical regions, dispersion theory 8=22769
 dielectrics, mag. ordered, two-magnon Raman scattering 8=9487
 exchange interaction, antisymmetrical, and change of multiplicity 8=22767
 exchange interactions effect on Mössbauer spectrum intensity 8=8208
 films, thin, with surface anisotropy 8=5456
 Heisenberg ferromag., critical and high-temp. behaviour 8=13976
 Heisenberg ferromagnetics, magnetisation and susceptibility comp. dependence near Curie pt. 8=18308
 Heisenberg ferromagnet, thermodynamic behaviour 8=13984
 Heisenberg ferromagnet, thermodynamic props. and spin deviation, surface effects 8=2303
 Heisenberg magnet below transition temp., damping and correl. functions 8=5445
 Heisenberg model of B-site spinel, critical index of susceptibility 8=18305
 Heisenberg model classical, partition function and correl. function 8=2304
 Heisenberg model, expansion parameter and $S = \frac{1}{2}$ Ising model similarity 8=9309
 Heisenberg model, interpolation theory 8=9311
 Heisenberg model, planar classical, spin-correlation function calc. 8=2305
 Heisenberg model, Wick theorem and linked-diagram expansion 8=13983
 Heisenberg system, paramag. phase 8=22756
 helicoidal magnetic structures, coupled e.m., plasma, and spin waves 8=18307
 high-temp. expansion coeff. for lattices with exchange and dipole interactions 8=9352
 intermodulation in spin systems obeying Bloch's equations 8=10992
 Ising model, two-dimensional, Toeplitz determinants and spin correlations 8=9310
 Ising spin $1/2$ system, triplet probabilities rel. to pair correlations 8=9313
 Ising system, disordered, odd-order correlation functions 8=5448
 metals, dispersion in strong field 8=9308
 nuclear and electronic, simultaneous parallel pumping 8=14107
 permalloy films*, flash-evaporated*, standing spin-wave resonance 8=14083
 rare-earth metals, electron interaction 8=22838
 s-f interaction, ground state energies 8=17898
 spin density wave in mag. field, one-band model 8=13980
 spin diffusion in paramag. temp. range 8=9318
 spin- $1/2$ Heisenberg model, high temp. power-series expansion coeffs. 8=9312
 spin waves 8=13988
 spins with planar constraint, critical props. 8=18311
 temperature depend. of spin wave energy, in itinerant electron model 8=13979
 thin film, nonuniform magnetization models 8=14080
 unidimensional lattice, theory of bound states 8=9315
 vapour pressure, dependence on spin ordering 8=16961
 CdCr_2Se_4 , Ag, helicon-spin-wave interaction 8=18329
 $\text{Co}[(\text{NH}_4)_2\text{CS}]_2\text{Cl}_2$, magnon cond. rel. to anomalous enhancement in thermal cond. 8=13391
 Er, energy/wave vector spin-wave dispersion relation 8=22800
 GdCl_3 , with dipolar interactions, magnon spectrum analysis 8=9353
 GdCl_3 , high-temp. expansion coeffs. calc. 8=9352
 H_2 , ortho, solid appl. of Holstein-Primakoff theory to molecular rot. 8=8233
 Tb, exchange interactions and spin-wave spectrum 8=22846
 Tb, spin wave dispersion analysis using exchange coupling 8=9367
 Tb, spin-wave spectrum, temp.-dependent crystal field effects 8=22845
 V^{2+} and Ni^{2+} superexchange interaction in MgO 8=9355

Ferromagnets. See Magnetic properties of substances/ferromagnetic.

Feynman diagrams. See Field theory, quantum/interactions.

Fibre optics. See Optical systems.

Fibres

- cellulose, surface structure, ionic etching effect 8=13083
 chrysotile asbestos, microfibrils and lattice parameters from electron microscopy 8=1796
 elastic with elastic-plastic coating, cyclic extension 8=19403
 glass, drawing apparatus and tensile strength 8=5073
 glass, length rel. to strength 8=1666
 inorganic, Young's and shear moduli meas. 8=5003
 insulating, radiant ht. transfer 8=1883
 length distrib. meas. 8=13054
 nylon, molecular orientation by polarized reflexion spectroscopy 8=16394

Fibres—contd

- optics, wavelength multiplexing 8=15519
 paper, comp. determ. by i.r. absorpt. 8=14462-3
 polymer melts, nuclei formation mechanism, flow-induced crystallization 8=1532
 polytetrafluoroethylene, fibril structure 8=1665
 reinforcement, whisker sizing and orientation 8=17248
 sound absorption in layer, scale-modeling of large silencing devices 8=19563
 synthetic, X-ray small angle scatt., review 8=8438
 textile, viscoelasticity 8=17846
 textiles of Egyptian cottons, thermal conductivity, meas. 8=13392
 in vibroscope, electrostatically driven, polarizing voltage effect on frequency 8=6124
 Al, (111)-(001) fibre texture formation on deformation 8=5045
 C, high modulus, structure 8=8457-8
 C, preferred orientation 8=1664
 PVC, pyrolytic products, analysis by mass spectrometry 8=23175
 SiC, fibrous single cryst., i.r. spectrum 8=2455
- Field emission.** See Electron emission/field emission.
- Field emission microscopes.** See Electron microscopes; Ion microscopes.
- Field theory, classical**
 See also Electromagnetism; Gravitation; Relativity.
 charged particle in expanding universe, gravitation 8=10600
 continuous medium interacting with external fields, Noether's theorem 8=10507
 continuous media, theory 8=2916
 crystal fields, radial integrals 8=1628
 dipole-dipole interaction, distribution theory 8=19364
 double layer on circular surface, potential calc. 8=14937
 electric dipole in motion 8=10505
 inertial mass, positive-definiteness, e. m. coupling and Mach principle 8=14980
 fields of force generating motion on family of spirals 8=10100
 intersection of two dielectrics with free space 8=2896
 magnetic, force free with normal pot. 8=6030
 magnetohydrostatic, application of variation principle 8=305
 Maxwell's eqns. for moving source, soln. and progressive wave formalism for homogeneous medium 8=3252
 potential field, 2-dimens., numerical method for analytical continuation 8=17
 potential theory, vector spatial density 8=2897
 relativistic charge radiation in a plane wave e. m. field 8=10881
 singular potentials, regularization and peratization 8=2898
 space anisotropy, soln. by linear sources 8=14936
 spheroidal harmonic pot. rel. to Laplace eqn. for finite cylinder 8=10670
 stretching and spin tensors of surface and linear material elements 8=40
 temperature, uniform, stability props. 8=19661
 theorem, Schroer-Jost, generalization 8=6031
 vector-potentials of source-free vector fields 8=10509
 Yang-Mills eqns., singularity-free non-Abelian solns. 8=10506
 Yang-Mills, nonexistence of classes 8=10508
- Field theory, quantum**
 See also Dispersion relations; Elementary particles; Physics fundamentals; Quantum theory.
 algebra of fields, derivation of sum rules 8=6727
 algebra, von Neumann, types rel. to extremal invariant states 8=6013
 angular momentum dependent potential 8=11395
 application of techniques to wave system in randomly fluctuating medium 8=2986
 axial-vector current, divergence, corrections to ρ dominance 8=20496
 axiomatic, applic. to scatt. amplitude for $\pi-\pi$ 8=6872
 axiomatic, Haag-Ruelle asymptotic states, uniqueness 8=15623
 axiomatic, M-functions, reduced type defined 8=15625
 axiomatic model 8=15624
 axiomatic, time-averaged, operator domain 8=11287
 axioms for formulation of nontrivial example 8=593
 axiomatic, using Mackey's axioms and another 2 which ensure coordinate and momentum obs. 8=20178
 Bethe-Salpeter scatt., amplitudes rel. to crossing symmetry 8=20282
 Bhabha, Lorentz group transformation 8=648
 Bogoliubov-Parasiuk-Hepp renormalization theorem and spacelike regularization 8=3449
 bootstrap incompatibility with closure and locality 8=15710
 bootstrap restrictions on quark model for baryons 8=15817
 causality cond. for on mass shell elements 8=582
 commutation of currents, equal time, conserved and nonconserved 8=6622
 complex angular momentum method, test of basic assumptions 8=6735
 compositeness criteria of particles 8=6764
 compound particles, conditions $Z = 0$ and bootstrap 8=6772
 conservation laws, review 8=3430
 contraction, elementary particles 8=6753

Field theory, quantum—contd

- covariant spin operators 8=20338
- convolution, hyperbolic, for solutions of general equations 8=575
- C conservation in η decay to $\pi^0 e^+ e^-$, $\pi^+ \mu^- \bar{\nu}_\mu$ 8=20487
- C=-1, possible e. m. current component 8=20252
- CP invariance effects in K-decay 8=20472
- CP symmetry, review 8=11282
- CTP invariance of S-matrix, in theory of local observables 8=583
- current algebra and dispersive sum rules 8=598
- current algebra and sum rules 8=15743
- current x current hypothesis and $\Delta S = \Delta Q$ 8=15684
- degenerate vacuum and infinite component wave equation 8=3444
- de Sitter group, inhomogeneous, particle field equations 8=654
- in de-Sitter space 8=15612
- dielectric permeability of molecular crystals 8=5347
- Dirac spinor field, rel. to theory of spin-1/2 particles in a gravitational field 8=2959
- Einstein eqns., difficulty of combining with Wightman theory 8=19414
- e-e. m. wave scatt. 8=15409
- electron interaction with intense photon beam 8=20372
- e. m. field characteristic states 8=19818
- e. m. field quantization in framework of axiomatic field theory 8=3446
- energy-momentum conservation rel. to translation invariance 8=20169
- energy momentum spectrum 8=11278
- e propagator, sum of all rainbow diagrams 8=15726
- equal-time current commutators, calc. method 8=20164
- equilibrium statistics, cluster development 8=10626
- fermion, spin $1/2$, interacting with vector meson, derivation of Regge trajectory 8=6770
- Feynman diagrams, larger class, leading Landau curves 8=3450
- Feynman graphs, new combinatorial feature 8=596
- Feynman graphs, new topological features 8=595
- Feynman technique in non-linear spin theory of elementary particles 8=20288
- finite system, effective field eqn. 8=920
- free particles, heuristic eqns. 8=6720
- free relativistic multipole field, quantum part 8=15616
- Goldstone theorem, Euclidean proof 8=6607
- Goldstone's theorem, rigorous treatment 8=6613
- gravitational state, superradiating in super-nonradiating electromagnetic state 8=2949
- gravity, manifestly covariant theory 8=3451
- harmonic oscill., 3-D, e. m. field coupling 8=3427
- Hamiltonian for unstable particle, hermitian and non-hermitian 8=15626
- Heisenberg ferromagnet 8=9317
- inhomogeneous Lorentz, manifest covariant representations 8=11274
- introduction to strong interaction, book 8=20278
- inversion problem, and renormalized coupling consts. 8=6610
- isospin symmetry, TCP and local field theory 8=11364
- Isospin=2, possible e. m. current component 8=20252
- Klein-Gordon field, charge density, critical analysis 8=597
- Klein-Gordon field, nonlocal macrocausality 8=11356
- K^0 , C, CP, CPT theory consequences 8=777
- $K_L^0 \rightarrow \pi^+ \pi^-$ decay, CP violation 8=777
- Lagrangian approach to current algebra 8=20251
- Lagrangian, bootstrap theory, particle wave-function renormalization 8=20334
- Lagrangians, chiral-equivalent, construction 8=20262
- Lagrangian eigenvalue problem $[\omega^2 I - \omega i A - H] \xi = 0$, soln. 8=20159
- Lagrangians, equivalent, redundant fields, matrix elements 8=11273
- Lagrangians for fields satisfying wave and Klein-Gordon eqns. 8=572
- Lagrangian, perturbation theory leading to Greens functions formulation 8=20160
- Lagrangian, stripped correlation functions, theory of self-generating interactions 8=20161
- $\lambda \phi^3$, ladder diagrams give imaginary part of scatt. amplitude 8=6754
- Lehmann, Symznzik and Zimmermann, analytical structure of integral reduction method 8=573
- lepton field represented by 4 x 4 component spinor 8=11450
- Lie algebra extensions of the Poincaré group 8=14
- Lie fields, scalar, existence 8=15613
- local, with Lorentz group representations, crossing symm. in vertex functions 8=6609
- localization of relativistic microparticles in space and time 8=580
- Lorentz group, Feynman rules for representation generalized from finite to infinite dimensional 8=20180
- Lorentz invariant generalized functions, use 8=20156
- mass formulae rel. to superconvergence sum rules algebraic struct. 8=656
- mass spectrum and superconvergence relations 8=3427
- multi-photon processes, probability 8=104
- nonanalytic perturbations 8=3412
- non-compact symmetry groups, reln., and unitary S-matrix 8=578

Field theory, quantum—contd

- nonlocal 8=568
- non-local, analyticity in momentum transfer 8=20295
- nonrenormalizable theories, weak local commutativity 8=6621
- N non-relativistic particles, scattering theory 8=10649
- N Regge-pole coupling, model 8=20327
- operators, coherent states diagonal representation 8=19820
- optics, detector field-source coupling 8=20022
- nonlinear spinor theory, new determ. of κI 8=20416
- nucleons, e. m. form factors 8=6941
- particles faster than light, effect precedes cause 8=3500
- perturbation theory, renormalized, A^4 coupling, local field eqn. 8=6612
- phase shifts calc. from Bethe-Salpeter eqn. 8=571
- photodetectors in radiation field, corrls. rel. to photon field commutation 8=6623
- photon, coherent states and gauge invariance 8=3437
- π -N Lagrange functions, chiral-invariant uniqueness of theory 8=6614
- plane waves, generalization for K-G eqn. 8=11281
- p-n mass difference, lack of gauge invariance, consequences 8=11586
- Poincaré group, positive mass representations 8=15614
- possible $(7/2^-)$ -octet 8=20578
- propagators, covariant and vertex functions for any spin 8=20336
- pseudo-vector field, axial-vector current which satisfied current algebra 8=20494
- $P \times SL(6, C)$ group, with infinite multiplets, predictions of model 8=579
- quasiquarks rel. to fibre bundle $C(N)$ cross sections 8=20407
- radiation propag. in vacuum, coherence theory 8=20172
- rainbow graph model for n-p mass difference 8=11587
- Rarita-Schwinger fields and interact. Lagrangians for fields of arbitrary spin 8=11355
- reduced density matrices, permutational symmetry 8=13
- Regge "daughter" trajectories model depend. 8=11419
- relativistic charge radiation in a plane wave e. m. field 8=10881
- relativistic free multipole field, theory 8=11279
- relativistic, Koenig theorem generalization 8=3428
- relativistic quantum mechanical position operator 8=20339
- relativistic, reformulation, independent of Hilbert space 8=574
- relativistic satisfying Wightman axioms exactness of internal group symmetry 8=11280
- relativistic, unreasonable mass spectrum effect 8=3426
- renormalized relativistic perturbation theory from finite local field equations 8=3429
- renormalized theories, existence of stationary singularity of scatt. amp., test 8=20168
- representation physical equiv., rel. to automorphism 8=3447
- scalar, complex, condition for one-quantum and two-quantum particle-antiparticle stationary states 8=2016
- scalar, conform-invariant, mathematical basis 8=15682
- scalar field with nonstatic source 8=11362
- scattering amplitude, impact parameter representation 8=20167
- scattering from Coulomb-like pots, generalized Lippman-Schwinger eqns. 8=680
- Schrödinger equation with Woods-Saxon potential, approximate solution 8=7055
- Schwinger term equality rel. to ϕ - ω mixing 8=11561
- Sh(2C) group, irreducible unitary representations 8=576
- σ model for PCAC, improved 8=11489
- spectral density, asymptotic behaviour in non-renormalizable theory 8=20166
- spectral representations for simple quantum-mechanical system 8=569
- spin, Lagrangian formulation of $(2J + 1)$ component theory 8=6616
- spin-one operators, Wick theorem 8=20181
- spinor theories, graphical methods for γ , σ -algebra 8=11
- spin- $3/2$ Rarita-Schwinger field, spectral representation 8=6719
- stress-tensor commutators and Schwinger terms 8=3422
- superconvergence 8=11399
- superconvergence sum rules and current algebra 8=356
- SU(2) and internal symmetry group b, embedding in larger group b 8=652
- SU(2), and SU(N) correction, fibre bundle theory 8=2040
- SU(3) irreducible representations, quasispin and multiple structure 8=594
- SU(3), set of harmonic functions and commutation rules c generators 8=600
- SU(3) x SU(3) space-time local current commutators, derivation 8=6611
- SU(3) x SU(3) spectral function sum roles and mass ratios 8=20493
- symmetry breaking and const. gauge transforms, 8=650
- symmetry breaking distinctions 8=3438

Field theory, quantum—contd

- symm. groups, continuous and zero-mass states 8=3425
- symmetry groups in nuclear and particle physics 8=11361
- system with Hamiltonian a time-depend. quadratic form of \hat{x} and \hat{p} 8=3423
- time-reversal invariance, expt. in weak decay processes 8=11283
- Thirring model, 2D based on currents for hadron dynamics 8=20399
- T-invariance test in e-d scatt. with d in D-state, polarized 8=20375
- T violation in nonleptonic decays 8=6820
- topological properties of theory 8=20154
- 2-particle \rightarrow 2 particle transformation relativistic, current algebra 8=662
- two point function, lattice-cell-volume depend. 8=570
- unified field, macroscopic gravitation 8=10606
- unitarity and multiparticle prod. reactions 8=20275
- U(3) isoscalar factors, recursion relations 8=3420
- variational formulation, determ. of mass operator, Green's function 8=6608
- vector-meson, coupling parameters from current algebra 8=6899
- violation of CP invariance, review 8=6617
- Weinberg sum rule validity and Schwinger terms 8=15675
- Yang-Mills, axial vector mesons introduced as chiral partners of vector gauge mesons 8=15809
- Yang-Mills field of point charge, integration ambiguities using non-Abelian soln. 8=20162
- Yang-Mills theory, equivalent results from current algebra with meson pole dominances 8=11357
- zero-dimensional, convergence 8=11270
- $Z_0=0$ and $\Phi_0=\Phi$ inequivalence 8=3445
- electromagnetic field.** See Quantum electrodynamics.
- interactions**
 - See also Elementary particles; Nuclear reactions.
 - Entries on interactions involving named particles are listed under the particles concerned.
 - annihilation processes, statistical unitary-symmetry theory 8=3527
 - axial-vector coupling constants by saturation of axial change commutations 8=3520
 - axial vector currents in terms of baryons and bosons, divergences 8=6743
 - axiomatic, rel. to simultaneous s-t analyticity in 2-body reactions 8=6740
 - bootstrap model, unified Fermi-Yang and Chew-Low 8=3566
 - boson system, attractive interact. at zero temp. 8=2992
 - charge superselection rule test 8=666
 - chiral dynamics, nonlinear theories significance 8=11358
 - commutators, equal time, appl. of JLD representation 8=3524
 - commutators, equal-time involving divergences of currents 8=6729
 - C violation in e.m. processes 8=584
 - cross process amplitudes, asymptotic expansion, asymptotic relns. 8=665
 - current algebra and group theoretical derivations of sum rules compared 8=3522
 - current density, algebra representations in one-particle spaces 8=6737
 - currents with massive vector particles, positivity and restrictions 8=6730
 - derivatives, exact soln., model 8=11277
 - elastic scattering of a neutron by a nucleus, time dependent wave packet behaviour 8=20803
 - electromagnetic current, symmetry props., experimental test 8=670
 - e.m. of N, Seigent's theorem and nuclear muon capture 8=11871
 - e.m. of particle with spin $\geq \frac{1}{2}$, in gravitational field 8=11359
 - Faddeev's three-particle theory 8=6604
 - fermion and gravitational fields, stress-tensor operator 8=11269
 - four-fermion, relativistic and causal theories 8=15615
 - four-fermion, renormalizable 8=15621
 - four-fermion, singular scatt. eqns. in momentum space 8=11267
 - hadron reson. splitting and multiple poles 8=11483
 - inelastic, $T \geq 1$ GeV, energy and angular distribution of secondary particles 8=3518
 - Lee model, equal-time commutator and zero-energy theorem 8=3529
 - Mandelstam representation, moment conditions for double spectral functions 8=3543
 - multiple-production theory via Toller variables 8=686
 - N/D equations, S-wave, domain of self-damping interactions 8=6767
 - non e.m., classification with Dirac theory, rel. to spin and isospin 8=706
 - nuclear interactions, book 8=11386
 - octet dominance in weak, strong and e.m., test in K_s^0 and hyperon decays 8=3516
 - 189- and 405-plet of SU(6), decomposition into irreducible subgroups 8=20411
 - PCAC relation and π field 8=11498
 - peripheral inelastic processes, theory and consequences 8=15693

Field theory, quantum—contd

- interactions—contd**
 - phase shifts, lower bound to momentum derivatives 8=20179
 - potentials, light nuclei at large distances 8=921
 - quadratic terms, effects on theory and Hilbert spaces 8=3424
 - Regge trajectories for even-power potentials 8=3560
 - Regge trajectories, infinitely rising, kinematic constraints 8=11422
 - Reggeons interaction with vector and scalar currents 8=664
 - resonance multichannel collisions, T matrix expansion 8=20274
 - scalar particle with massive vector field, non-renormalizable propagator 8=20165
 - Schwinger-Thirring-Wess model, consistency problems 8=15692
 - self-generating rel. to Greens function formulation of Lagrangian field theory 8=20160
 - self-generating, renormalization of single-particle propagators 8=20161
 - square diagram, insertion of complex propagation 8=3528
 - sum rules from current algebra, different families obtained 8=3517
 - sum rule identities from equal-time commutator 8=3526
 - SL(6, C) invariant interact., field operator and components 8=646
 - SU(2) \times SU(2), chiral, method of phenomenological Lagrangians 8=6744
 - SU₃ Wigner coeff. calc. 8=3523
 - three body interact. under Coulomb law 8=667
 - two-body charge-exchange processes, in quark model 8=6742
 - 2-particle inelastic, Mandelstam branch points contrib. to asymptotic amplitudes 8=663
 - unitary symmetry in interactions with 3-body final state 8=3519
 - unitary violation by impulse approx. for 3-body scatt. 8=682
 - U(3) invariant, 4-fermion, meson masses 8=657
 - vector-current spectral functions sum rules rel. to vector-meson dominance 8=3679
 - wave packets, relativistic collision 8=15609
- interactions, strong**
 - baryons high spin resonances decay in 0(4, 2) theory 8=867
 - baryon sum rule connecting $\frac{1}{2}^+$ and $\frac{1}{2}^-$ spectra 8=819
 - Bethe-Salpeter eqn., meaning of amplitudes and relative time 8=11388
 - bootstrap conditions in S-matrix theory, rôle of CDD zeros 8=15712
 - bootstrap model, crossing-symmetric rel. to asymptotic form factors 8=20333
 - canonical, reconstruction of models in terms of e.m. weak and gravitational scatt. 8=11275
 - Chew-Frautschi theory, scatt. systems with high-isospin multiplets, stability 8=6762
 - conference, Varenna, Italy July 1964 8=6745
 - CP violation, $\beta\text{-}\gamma\text{-}\gamma$ angular correlation 8=669
 - currents, strong, conserved used in weak interactions 8=11387
 - dynamics, reln. of current algebras 8=599
 - groups, noninvariant 8=3502
 - gauge field, source theory rel. π e. m. mass and B e. m. mass splitting 8=20158
 - hadrons, using composite particle theory 8=11487
 - Lagrangian with chiral U(3) \times U(3) symm. and PCAC 8=15749
 - Lee model, strong coupling soln. 8=11389
 - multiparticle prod. processes, high energy bounds deduced from scatt. props. through unitarity 8=20275
 - N/D effective range theory with J-independent short-range forces 8=3554
 - octet dominance in weak, strong and e. m., test in K_s^0 and hyperon decays 8=3516
 - phase shifts, WKB high energy, produced by repulsive singular potential, expansion 8=20272
 - potential scatt., non-relativistic, effect of CDD poles on long range, behaviour 8=6751
 - Reggeization in 2-body with general spin 8=11412
 - Regge-pole residues, singularities for processes with external spin 8=11415
 - self-induced, simplification in infinite-momentum limit 8=20277
 - SL(6, C) and U(6, 6) in two meson annihilation of \bar{p} on N 8=15839
 - sum rules and equal-time commutation relations for composite fields 8=15750
 - sum rules from current algebra in perturbative model 8=3530
 - time reversal and detailed balance using DWBA theory 8=11847
 - weak interaction nonrenormalizability not removed by strong inclusion 8=6749
- interactions, weak**
 - appl. of quark model 8=724
 - conference, Varenna, Italy, July 1964 8=6747
 - consistent S-operator theory, and renormalization 8=6748
 - CP-conservation rel. to unified treatment of nonleptonic decay 8=6750

Field theory, quantum--contd**interactions, weak--contd**

- current-current theory, role of fld ratios in octet dominance 8=11391
- e. m. of Bargmann-Wigner fields, with spin 3/2 equivalence with Rarita-Schwinger formulation 8=20157
- elementary or composite particles, existence of fixed poles 8=20249
- hadrons, SU(2) chiral transformation applic. 8=15752
- phase shifts, WKB high energy, produced by repulsive singular potential, expansion 8=20272
- leptonic decays and unitary symmetry breaking 8=671
- Lepton octet, of current-current form governed by current-parity selection rule 8=11449
- model with fermion field coupled to meson nonets 8=3421
- non-leptonic model, CP violation and conservation in non-strange particles 8=11392
- ν interactions, high-energy, as tests 8=3588
- octet dominance in weak, strong and e. m., test in K_s^0 and hyperon decays 8=3516
- optically orientated spin system, magnetization equations 8=121
- $\pi \rightarrow l\nu$ structure-depend. axial-vector form factor, low energy theorem 8=6837
- restrictions on currents rel. to positivity 8=6726
- strong interaction as possible mediator 8=6749
- strong symm. not destroyed, strong currents used 8=11387
- ultraweak, CP-odd, $|\Delta S| = 1$, neutral lepton currents 8=3531
- $U_{\frac{1}{2}}$ rep. mixing, baryon low-lying states 8=15820
- W-intermediate bosons, using perturbations expansions and regularized propagators 8=3418

meson field

- See also Mesons; Nuclear forces.
- anharmonic oscillator and Schrodinger equation for Yukawa potential 8=565
- bound state, relativistic, symmetries of Bethe-Salpeter eqn. 8=3608
- electromagnetic processes and integer quark charge 8=727
- hadronic current operators, e. m. as linear combination of operators 8=6831
- Levinson's theorem, validity for superimposed Yukawa and Coulomb repulsion potentials 8=938
- pseudoscalar, consistent with PCAC 8=20420
- renormalized relativistic perturbation theory 8=3429
- scalar, neutral, without pairing, existence of prod. amplitudes 8=20410
- vector, interacting with massless fermions, 1D, infinite no. of solns. 8=3678

quantization

- See also Quantum theory/quantization.
- antisymmetrical field quantization and functional integration 8=3436
- Bialynicki-Birula model, four dimensional relativistic 8=6615
- e. m. field in Landau gauge, canonical formalism 8=3434
- Heisenberg type particle eqn. field, according to Fermi statistics 8=3419
- hyperquantization method, spin-statistics relation 8=20163
- rel. to light interference, modified second quantization 8=20096
- local and causal infinite-dimensional fields for unitary representations of Sh_{∞} 8=20180
- space-time lattice 8=20171
- spherical homogeneous nuclei, generalized coordinates 8=917
- spin- $\frac{3}{2}$ field, new formalism, limit of infinite masses taken after quantization 8=11276
- spin-statistics theorem, limitations of application 8=11271
- wave eqn. unified, rel. to mass-spin depend. 8=11373-4

Films

- on acoustics and wave motion for teaching purposes 8=19548
- electron scattering, incoherent component 8=3202
- fluoride, Li and La, condensation coeff. 8=4655
- growth orientation in vapour deposited layers, "evolutionary selection" 8=13086
- helicoidal nematic films, e. m. wave propag. 8=16837
- lipid, ultra thin, interface free energy 8=8038
- liquid surface, cavitation destruction in sound field, at elevated static press., photographic obs. 8=12775
- Permalloy, composite films, structure and magnetic props. 8=9357
- polymers, formation from soln., kinetics of solvent evaporation 8=12972
- protein, myosin monolayers structure 8=2870

liquid

- See also Adsorbed layers; Contact angle; Helium/liquid; Superfluidity; Surface tension.
- bearing lubrication, turbulent and laminar flow 8=8810
- contaminated, wind generated waves 8=12756
- elasticity rel. to thickness and composition, obs. 8=12776
- entrainment and drainage 8=21597
- falling, mass transfer with vertical surface, diffusion-controlled electrolytic tech. 8=21598
- in flow, annular 2-phase and falling film, stability, literature survey 8=12774
- fluid inertia effects 8=21589
- Gibbs elasticity, Sheludko eqn., correction 8=7997

Films--contd**liquid--contd**

- glassy materials, unsteady movement on melting surface, calc. using Lagrange's variables 8=16922
- hydrodynamic thin, behaviour in transient state 8=16783
- laminar flow along vertical wall, neglecting surface tension 8=21599
- laminar viscous flow on a rotating disc, energy and motion equations 8=4522
- rupture, under drop at interface 8=12773
- specific heat, size effects in fermion model 8=10656
- steam, saturated, condensation on vertical flat plate, effect of variable phys. props. 8=21771
- surface layer adjacent to high speed gas stream, stability 8=4523
- surface velocities of falling films 8=12731
- thermal instability 8=21596
- thickness under drop at interface 8=12772
- viscoelastic, flow down plane 8=12736
- He, rotating, thickness rel. to superfluid component motion, obs. 8=10796

solid

- See also Magnetic films; Optical films; Thickness measurement.
- absorbing, containing pinholes, light transmission meas. 8=9483
- anodic oxide on Al in boric acid-formamide electrolyte, struct. 8=13089
- anodic oxide, ductility 8=2047
- α -brass, stress corrosion cracking 8=8844
- cathode drop meas. on vacuum arcs 8=7686
- cellulose triacetate, transition temp. for amorphous and cryst. 8=4724
- conductance measurement, contactless method 8=270
- deposition, nucleation and initial growth 8=17120
- dielectric, on metal surfaces, detection apparatus 8=8299
- dielectrics, tunnel and Schottky currents rel. to thickness fluctuations 8=5345
- electron transmission, space charge effect 8=13470
- electronic components conference, Jackson USA, 1967 8=6244
- epitaxial garnet films, chem. vapour deposition 8=13099
- ethane, far u. v. spectra 8=14283
- evaporated, work function substrate roughness dependence 8=9267
- ferroelectric, multiple Curie point, prep. 8=18185
- foils with stacking fault, fine structure of weak electron diff. beams 8=1781
- formation conditions of natural and atomic structure, USSR review 8=8309
- glass diodes, I-V characts. 8=18118
- glass, X-ray total reflection 8=5604
- growth monitoring, computer-operated following ellipsometer 8=6562
- Inconel, stress corrosion cracking 8=8844
- insulating, effective mass meas. 8=8944
- insulating, with ionic space charge, conduction process 8=2232
- insulating materials, time dependence of electric breakdown 8=22646
- latexes of copolymers of alkylacrylates with methacrylamide, struct. rel. to coalesc. 8=17189
- low-temp. behaviour, research in USSR 8=19681
- magnetic, demagnetizing fields 8=9331
- magnetic double layer separated by a dielectric, magnetic reversal quasi-statistical analysis 8=5458
- magnetic, non-planar surfaces, equilib. magnetization and internal field distrib. 8=14000
- magnetic with rectangular coupling loop, flux linkage 8=22782
- magnetic structure and ferromagnetic resonance 8=2278
- magnetic, uniform rotation mode of flux reversal, analogue simulation 8=14001
- Makrolon, stress cracking and crystallization obs. 8=8473
- metal, adsorbate binding state characterization 8=14398
- metal, chemisorpt. of gases, evaluation of sticking probability without gas pressure meas. 8=14397
- metal crystal oxide film growth kinetics: thermionic emission and ionic diffusion 8=5710
- metal, equilibrium potential, rel. to polymerization of adsorbed org. layers 8=2251
- metal, growth, deposition parameters rel. to coalescence stage 8=21873
- metal and semiconductor, thin, transmission, reflection and absorpt. of electrons 8=22494
- metal-SiO₂-CdSe (metal) contacts, photocurrent studies 8=2281
- metal, size-effects in elec. cond. 8=13631
- metal surfaces, rough, plasma resonant radiation 8=948
- metal, temp. changes during vapour deposition 8=8304
- metal, thin, optical absorb. and photoelectric emission, vectorial selective surface effects 8=22950
- metal, thin, props. at microwave freqs. 8=21874
- metallic, thickness determ. by Leonard and Ramey (conductivity and Hall voltage meas.) method 8=17119
- metallic, thin, perp. elec. conductivity, quantum theory 8=22510
- metallized plastic films for source mounts 8=5153

- Films—contd**
solid—contd
 metals, conductivity rel. to electron fluctuation pairing, theory 8=17919
 metals, device for evaporation in a predetermined sequence 8=8186
 metals, epitaxial growth on NaCl and KCl in vacuum 8=13147
 metals, vapour phase deposition, applics. in electronics 8=13840
 methane, far u. v. spectra 8=14283
 melting point of thin films 8=1611
 methyl methoxysilanes on base, i. r. spectra 8=4738
 monomolecular, semiconductor or dielectric on metal, effect on metal work function 8=9091
 Mössbauer effect and freq. spectrum 8=13024
 noble metal, reflectance and transmittance, anomalous skin and size effects 8=9498
 non-crystalline, dielectric, tunneling model 8=18155
 nucleation and initial-growth behaviour 8=8308
 optical constants, non-normal incidence meas. methods 8=14167
 oxide, on Si, adsorbed H₂O mols. dielectric relax. 8=1706
 photoemission, effects of optical parameters 8=13936
 photoemissive, spectral shift and degradation 8=18282
 plastic, breakdown due to corona discharge 8=22645
 plastic, electrical conduction in high fields 8=13877
 polyacrylonitrile drawn film, anisotropy of mech. tan δ 8=17847
 polybenzoxazoles with O and S in chains, props. 8=4772
 polycarbonate, BaTiO₃ and organic cpds. loaded, dielec. props. 8=22661
 polycrystalline foils, electron absorpt., temp. effects 8=13467
 polycrystalline, magnetization ripple wavelength 8=18326
 polyenes, prep. of films for dichroism meas. 8=18580
 polyethylene, I-doped, current oscillations at high field strengths 8=8985
 polyethylene, I-doped, elec. conductivity meas. 8=8984
 polyethylene obtained by xylene-stream method for electron microscopy 8=4852
 polyethylene, oriented, low angle X-ray patterns and structure 8=17144
 polyethylene terephthalate, as solar furnace 8=19675
 polyhexamethyldisiloxane on Al, form. and dielec. props. 8=5731
 polymers on base, i. r. spectra 8=4738
 polymer, trapping of electrostatic changes in surfaces 8=13891
 polymethylmethoxysiloxane on Al, form. and dielec. props. 8=5731
 polypropylene, melting and recryst. or evap. due to laser pulse irradi. 8=17710
 polysulfone, BaTiO₃ and organic cpds. loaded, dielec. props. 8=22661
 polythene, laser-produced plasma, formation mechanics 8=23034
 polyurethane coats, effect of Al bed on density of network in surface layer 8=17145
 polyvinyl alcohol crystallization, i. r. study 8=13101
 polyvinyl alcohol films dyed in solutions of iodine in iodides and bromides, absorption spectra 8=5650
 poly-p-xylene, molecular orientation, cell dimensions 8=1828
 precipitates in thin foils, electron microscope images 8=13152
 production and ion bombardment apparatus 8=17121
 propane, far u. v. spectra 8=14283
 reflexion scanning electron-diffraction crystallography 8=17265
 semiconducting, charge-carrier mobility 8=9107
 semiconductor, effective density of electron states per unit volume 8=22448
 semiconductor, electron-phonon interactions at low temp. 8=22428
 semiconducting thin layers, nature of high voltage photo-e. m. f. 8=9247
 semiconductor, quantum longit. galvanomag. oscs. 8=9074
 sensor for heat transfer to turbulent fluid 8=16822
 single-crystal, ferromag. resonance 8=2353
 sputtering in crossed e. m. field 8=7651
 sputtering, r. f. dielectric system with non-grounded electrodes 8=17138
 sputtering resistive, effect of temp., pressure 8=8303
 standard for electron microprobe analysis by automatic stepping shutter system 8=4737
 stearic acid multi-monolayers dielectric thin film, electrical properties 8=13878
 steel, austenitic, stress corrosion cracking 8=8844
 structural defects, nucleation mechanisms 8=1735
 structure during growth, electron diffraction method 8=8306
 submetallic, quantum longit. galvanomag. oscs. 8=9074
 substrate, glass, low power self heated 8=4736
 superconducting, critical currents rel. to thickness 8=13729
 superconducting, energy gap dependence on mag. field 8=22529
 superconducting, far i. r. absorption, mag. field depend. 8=22938
- Films—contd**
solid—contd
 superconducting, far i. r. spectra 8=22939
 superconducting, Green's function calc. in mag. field 8=5188
 superconducting with current flowing, energy gap and critical current 8=22528
 superconductor, on plane surface of massive supercond., third crit. field 8=5192
 superconducting, as transformer secondary, modulated flux flow 8=17992
 superconducting superimposed, proximity effects 8=9044
 superconducting, surface parallel critical field, calc. 8=13727
 surface reactions exam. by simultaneous X-ray emission and electron diffr. 8=8290
 thickness measurement, dielectric 8=1690
 thickness meas. instrument, vacuum evaporated, piezo-electric crystal-type 8=21871
 thickness meas. by interferometry 8=1692
 thickness meas. using X-ray interferometry 8=8301
 thickness and microanalysis, X-ray meas. 8=14482
 thickness and refractive index meas., method 8=8300
 thin, calc. of Debye-Waller factors from Mössbauer effect 8=8207
 thin, electron scattering within, inelastic, at oblique incidence 8=17911
 thin, electronic properties, colloquium, Orsay, France (1967) 8=22499
 thin film solar cells 8=19735
 thin film techniques, development and application 8=13841
 thin, filtered and unfiltered electron diffraction intensities 8=1777
 thin foil electron microscope specimen preparation by rotating P. T. F. E. holder 8=8451
 thin, grain size distribution, conservative systems 8=13084
 thin, grain size distrib., non-conservative systems 8=13085
 from toluene, polymer, comp., spectra and elec. props. obs. 8=21894
 transistors 8=18135
 transistors, thin-film field-effect, fabrication process, props. 8=13861
 transparent thin (10-600 nm), thickness meas., simple non-destructive interferometric method 8=8302
 triacetate, proportioning electron beam 8=10890
 triacetylcellulose, plastified, thermomech. curves of elongation at const. strength 8=22407
 triode sputtering, new discharge arrangement, high current in 10⁻⁴ torr range 8=7653
 vacuum deposition on heated substrate, and structure X-ray study 8=8307
 vacuum deposition, substrate heater 8=17122
 vapour deposition, obs. by mass spectra 8=17155
 wax polished painted surface, reflectance determ. of thickness and roughness 8=2470
 white tin, optical data analysis over 0.1 to 27.5 eV energy region 8=2456
 zinc evaporated, oxidation 8=1691
 Ag, growth effected by ultrasonic vibrations, of substrate 8=4827
 Ag on mica, W substrate nucleation 8=13087
 Ag, optical constants, ellipsometric meas. 8=11201
 Ag, secondary electron emission from self-supporting films 8=2284
 Ag, structure and surface characts. rel. to optical absorpt. 8=18502
 Ag, thin, Hall effect 8=2133
 Ag, vapour deposited, resistivity annealing temp. and thickness dependence 8=17925
 AgBr plates, ion-sensitive, for mass spectrograph 8=16178
 Al alloys, dislocations multiplication, transmission electron microscope study 8=13435
 Al alloy, effects of thin anodic oxide films, on fatigue behaviour 8=2049
 Al, chemisorption of O₂, stability and work function changes 8=5726
 on Al, deposited from Zn electroplating pretreatment soln, props. 8=14431
 Al, dislocations, dynamic behaviour on deformation, continuous obs. 8=13433
 Al, distribution of sputtered atoms by electron microprobe 8=21876
 Al on glass, vacuum deposition technique 8=17123
 Al on Ta (110) surface, growth studied by LEED 8=8311
 Al, oxidation effect on photocurrent 8=18221
 Al, oxidation in low-pressure O₂ atmosphere 8=18669
 Al oxidised in radio-freq. discharge 8=8310
 Al, plasma oscillatory modes at surface, energy rel. to intensity 8=8946
 Al, thickness monitor of osc. quartz cryst. type 8=17118
 Al, thin strips, electron microscope obs. of electro-transport 8=17927
 Al vacuum condensates, influence of annealing on block structure charact. 8=4741
 Al-Ag (20%), dynamical multiple reflections in electron diffraction patterns 8=13256
 Al-Al₂O₃-Al, current instability 8=18201

Films—cont'd

solid—cont'd

- Al-Al₂O₃-Al diodes, noise meas. 8=13851
 Al-Al₂O₃-M diodes, electroluminescence 8=9598
 Al₂O₃, rel. to anodic oxidation of Al in presence of hydrated oxide 8=18729
 Al₂O₃, breakdown electric strength rel. to thickness 8=5351
 Al₂O₃, Cs activated, semicond. low work function, props. 8=17999
 Al₂O₃, chem. deposition and props. 8=4740
 Al₂O₃ dielectric, pyrolytically grown, voltage-current charac. 8=13873
 Al₂O₃, e beam evaporation and dielec. props. 8=22652
 Al₂O₃, large-area planar and non-planar films 8=13088
 Al₂O₃, photoluminescence, spectral distrib. curves 8=9596
 Al₂O₃ thickness obs. by tunnel emission and capacitance 8=8312
 Ar, thin, microstructure, electron diffraction study 8=8313
 Au, D⁺ transmission 8=22242
 Au, electrical conductivity, island structure, on quartz glass and BaTiO₃ substrates 8=13709
 Au, electron diffr. intensities, temp. dependence 8=8509
 Au, growth effected by ultrasonic vibrations, of substrate 8=4827
 Au, growth on NaCl, high vacuum 8=21878
 Au, growth on NaCl, high vacuum, model 8=21879
 Au, light scattering, thickness and wavelength dependence between 2000–7000 Å 8=14199
 Au, meas. of secondary electron emission from exit side 8=2285
 Au, morphological changes following deposition 8=4743
 Au nuclei on MoS₂ substrate, strain nucleus size and misalignment dependence 8=8823
 Au, nucleation density on NaCl cleavage surface 8=4742
 Au, ohmic and thermoelectric props., –100 to –100°C in ultrahigh vacuum 8=22513
 Au on MoS₂, epitaxial growth under u. h. vacuum and defect structure 8=17125
 Au on NaCl, deposition rate and residual gas effects 8=1693
 Au, optical absorpt. band edge 8=5585
 Au, recrystallization obs. in electron microscope 8=8314
 Au, reflectance and transmittance, anomalous skin and size effects 8=9498
 Au single crystal, effect of ion bombardment on texture and structure 8=17124
 Au single crystals, deuteron blocking 8=22241
 Au, sputtered, due to negative O ions in O discharges 8=21877
 Au, structure and surface characts. rel. to optical absorpt. 8=18502
 Au, thin, Hall effect 8=2133
 Au, X-ray total reflection 8=5604
 Au-Cu alloy single crystal, effect of ion bombardment on texture and structure 8=17124
 B, ultra-pure, technique for preparation 8=8315
 Ba, sorption capacity for O₂ in colour picture c. r. t. 8=15324
 Be, self-supporting, 5–10 µg/cm² 8=4744
 BeF₂ on Be, as corrosion retardant 8=23098
 Bi, condensed, crystal structure defects 8=8705
 Bi, elec. resist. and Hall coeff., temp. dependence 8=8995
 Bi, field effect at 4.2°K 8=17928
 Bi quantum and classical dimension effects 8=22516
 Bi, thin, thermoelectric power and elec. resist. 8=5383
 Bi, transmittance and reflectance meas. rel. to band structure 8=13859
 Bi₂O₃, electrical properties and defect structure in range 175–250°C 8=8996
 Bi₂S₃ evaporated, electron diffr. exam. 8=17126
 Bi-Sb, 2-layer, struct. defects by Moiré method 8=22186
 Bi-Se, vitreous, near i. r. photodetection 8=22704
 C, evap., reaction with heated metal substrates 8=4745
 C, for target backings in reaction studies 8=8316
 Ca, absorpt. of light between 0.5 and 5.5 eV 8=14204
 CaF₂, MgF₂, Na₃AlF₆, i. r. antireflectant suitability 8=2435
 Cd vapour impinging on W, film nucleation in two phases 8=8305
 CdCl₂:Cu²⁺, e. s. r., exchange coupling pairs spectrum 8=18416
 CdI, vac.-deposited, structure 8=8317
 CdS, elec. props. changes on O₂ adsorpt. and ion bombardment 8=13791
 CdS, electroluminesc. d. c. excit. mechanism obs. 8=9608
 CdS in diode, d. c. and a. c. behaviour 8=13852
 CdS polycrystalline, orientation inversions, and in bulk crystals 8=8374
 CdS solar cell mechanism obs. 8=10847
 CdS, thin, structure and phase composition by electron diffr. investigations 8=4746
 CdS-CdSe, thermal quenching of photoconductivity 8=5399
 CdSe_{1-x}, prep. by vacuum deposition from molec. beam 8=4748
 CdS-SiO₂ film devices, "frozen" cond. and thermo-stimulated currents 8=5388
 CdS-SiO₂ system, heat-stimulated currents and 'quenched' cond. 8=9096
 CdSe, non-stoichiometric, elec. and photoelec. props. 8=13795

Films—cont'd

solid—cont'd

- CdSe, stoichiometric, preparation, structural, optical, electrical and photoelec. props. 8=17127
 CdTe, ion bombardment effect on resistance 8=5244
 CdTe, polymorphism by multiple refl. studies 8=1694
 CdTe, thin, structure, obtained by coevaporation 8=4747
 CdTe, wedge-shaped, photo-voltages rel. to incident angle of illum. 8=5398
 Co for mag. recording, deposition and props., obs. 8=22790
 Co, galvomagnetic effect obs. 8=5475
 Co, galvanomagnetic effect, in rotating mag. field 8=17931
 Co, hexagonal, dynamical multiple reflections in electron diffraction patterns 8=13256
 Co, on Cu, pseudomorphic deposits 8=21881
 Co, phase changes, thickness depend. 8=17050
 Co-Ni for mag. recording, deposition and props., obs. 8=22790
 Co-P for mag. recording, deposition and props., obs. 8=22790
 Cr, deposition from low-energy ion source 8=19796
 Cr, glow discharge rel. to resist. 8=17128
 Cr on Ni, pseudomorphic deposits 8=21886
 Cr₂O₃, epitaxial growth due to Cr surface oxidation 8=4828
 Cr₂O₃, reactively evaporated, optical props. 8=9517
 Cr-SiO cermet, elec. props. 8=8981
 Cr-SiO cermet, resistivity and struct. 8=1695
 Cs on Ir, adsorption and electron emission 8=9268
 Cs on Re substrate, mode of growth 8=1696
 Cs₃Sb, time depend. of absorpt. and photoemission 8=13937
 Cu, absorpt. spectra 8=5596
 Cu-constantan thermocouples 8=22686
 Cu, creep, elastic lattice strains 8=13548
 Cu, epitaxial growth, and activity and topographical changes on exposure to H₂-O₂ combination at 325°C 8=8318
 Cu, film on Si, transmission and absorpt. in spectral region from 1.5–7 µ 8=14212
 Cu, K_α emission fluoresc. and direct components 8=14179
 Cu, obliquely deposited, struct., effect of atom mobility 8=8296
 Cu, optical transmission and absorpt. in spectral region between 0.6 and 4 µ 8=22972
 Cu phthalocyanine, trap distribution 8=22586
 Cu, plasma oscillations, interband transitions 8=5117
 Cu, reflectance and transmittance, anomalous skin and size effects 8=9498
 Cu single crystal, effect of ion bombardment on texture and structure 8=17124
 Cu thermopower size-effect for determination of electronic structure 8=13903
 Cu, thickness depend. on heat generated by 9 to 100 keV electron beam 8=17699
 Cu, thin, Hall effect 8=2133
 Cu, vacuum deposited, oxidation rel. to temp. 8=18674
 CuAu II containing Zn, dynamical multiple reflections in electron diffraction patterns 8=13256
 CuI layers, low temp. spectra rel. to nature of substrate 8=9528
 Cu-Pt alloy, n. m. r., quadrupole effects 8=2383
 Cu-Te system, phases investigated by e-diffr. 8=17057
 Cu-Te system in thin films, phase transformations and structure 8=17054
 Er, thin, oxidation, electron microscope study 8=5701
 Er₂O₃, grain boundary energetics by transmission e-microscopy 8=21986
 EuO, preparation, Faraday rot., and mag. props. 8=13090
 Fe on hot Cu, pseudomorphic growth 8=21880
 Fe-2°Cr alloy, early growth of oxide, structure and stability 8=21882
 Fe-28°Cr alloy, early growth of oxide, structure and stability 8=21882
 Fe-Cr alloy, Cr₂O₃ protective scales, mechanism of breakthrough 8=23099
 Fe-Gd, hysteresis loops, by static method 8=9345
 Fe and Mg multilayered structure, X-ray diffraction 8=1758
 Fe-Ni alloys, evaporation characteristics 8=12719
 Fe-Ni alloy, thin evaporated with oblique incidence, structure 8=14017
 Fe-Ni electro-deposited, internal stresses rel. to deposition conditions 8=17653
 FeNi, electrodeposited, mag. props. rel. to struct. 8=9347
 FeNi-FeNiMn, with ferro-antiferromagnetic coupling, study 8=9346
 GaAs, epitaxial, propag. of growth striae 8=17129
 GaAs, high-mobility, grown by liquid-phase epitaxy 8=22588
 GaAs, wedge-shaped, photo-voltages rel. to incident angle of illum. 8=5398
 GaAs:Zn polycrystalline, electrical resistance and Hall effect obs. 8=5255
 GaP epitaxial layers with high mobility 8=9101
 GaP, vacuum deposited, polymorphism 8=21883
 GdFe garnet on YAl garnet, chem. vapour deposition 8=13099
 Ge, degenerate epitaxial, production by iodide method rel. to tunnel diodes 8=8321

- Films—contd**
solid—contd
 Ge, epitaxial growth in open iodide process 8=17131
 Ge, epitaxial, prep. by pyrolysis of hydrides 8=17130
 Ge, polycrystalline, acceptor and scattering centre natures 8=18046
 Ge, recryst. by electron beam zone melting 8=17235
 Ge semiconducting, growth by zone melting 8=8320
 Ge, thin, Seebeck coefficient, Hall mobility 8=2255
 Ge, transition to metallic conduction at high exciton concs. 8=18048
 Ge on Al_2O_3 by vacuum deposition, and elec. mobilities 8=4749
 Ge, X-ray stress topography, rel. to film-crystal interface stresses 8=22371
 Ge, X-ray total reflection 8=5604
 HfO_2 , dielec. and resist. props., and resistors and capacitors characts. 8=22654
 HfO_2 , e beam evaporation and dielec. props. 8=22652
 In-doped Ar, Kr and Xe, absorption spectra 8=9541
 In, longitudinal magnetomorph effect 8=5430
 In, superconducting, Nernst effect 8=2174
 In, superconducting transition temp. thickness dependence 8=9045
 In with superconductive and ferromag. overlays, tunnelling 8=22549
 In surface, oxide layer, kinetics of growth 8=8322
 In, transverse phonon generation by microwave excitation 8=4903
 InAs epitaxial film on GaAs, orientated growth 8=17132
 InAs, growth and electrical props. 8=1749
 InAs, optical props. 8=18535
 InAs, thin, obtained by discrete evaporation, structure 8=8324
 InAs thin film transistor, fabrication and charact. 8=22635
 In_2O_3 dielectric, pyrolytically grown, voltage-current charac. 8=13873
 InSb, epitaxial growth, electron diffraction study 8=21884
 InSb, epitaxy on single crystal substrate 8=17133
 InSb, slow photoconduction 8=9254
 InSb, thin by electron beam re-crystallization, electrical props. 8=8323
 InSb, vacuum deposited, crystallization by electron beam zone-melting process 8=13091
 Ir, ultra-thin, vacuum-deposited, structure from e-diffr. and microscopy 8=17292
 K, optical absorption 8=5612
 KCl(Br) foils, P-polarized light absorption at plasma resonance freq. 8=2123
 KH_2PO_4 , i. r. absorption spectrum, internal vibrations 8=9545
 La, superconducting, electron-tunneling meas. 8=9047
 La-Ce alloy, gapless superconductivity 8=5205
 La-Lu alloy, superconducting, electron-tunneling meas. 8=9047
 Li, on W and Re faces, effect of thickness and substrate orientation on work function 8=18256
 Li_2Bi , prep. and props. 8=8325
 LiF, on Mo substrate, emissivity at 420°K and 605°K 8=14236
 MgF_2 , thin, charging with electrons of average energy 8=22505
 MgF_2 , thin, Molter electron emission 8=22732
 MnO_2 , prep. and props. 8=4750
 Mo, heteroepitaxial growth on insulating substrates 8=17134
 Mo, on W crystal, adsorption and electron emission 8=9269
 Mo-Al intermetallic resistors, sheet resistivity and temp. coefficients of resistance 8=22520
 Nb, for cryotron ground planes 8=2171
 Nb, vacuum deposited on MgO , rel. to substrate-condensate chem. interaction 8=8326
 Ni, condensed polycrystalline, structure and substructure elements 8=17286
 Ni, elec. conductivity and Hall effect dependence on O_2 adsorption 8=17936
 Ni, electrolessly deposited, e microscope study 8=17136
 Ni-Cr sputtering role of H_2 rel. to thickness control 8=8777
 Ni-Fe, lattice contractions by electron diffraction 8=1806
 Ni-Fe, thickness and composition determ. by X-ray fluorescence 8=9750
 Ni-Fe, vacuum-deposited, thickness meas. by elec. resistivity method 8=17135
 NiO, semicond. and insulating, prep. 8=22602
 NIS on Ni in S solns., growth kinetics and mechanisms, obs. 8=2525
 Pb, Josephson tunnel junction characts. 8=9063
 Pb, self-supporting, 250-500Å thick, prep. 8=4751
 Pb, superconducting, far i. r. absorption 8=13759
 Pb, superconducting, frequency conversion in 3 cm band 8=22558
 Pb superconducting, thermal forces on vortices 8=13761
 PbS, photo-e. m. f., effect of const. current 8=18234
 PbTe, elec. characts. and vacuum evaporation 8=8327
 PbTe, resistivity, Hall mobility and cond. 8=22603
 Pd, obliquely deposited, struct., effect of atom mobility 8=8296
 Pd, preadsorbed CO oxidation, induction period 8=5700
 Pt, electrical conductivity, island structure, on quartz glass and BaTiO_3 substrates 8=13709
- Films—contd**
solid—contd
 Pt, epitaxial growth on NaCl(100) face and CaF_2 (111) face 8=4752
 Pt, obliquely deposited, struct., effect of atom mobility 8=8296
 Pu α -phase foils, electron microscope study 8=21887
 Sb, conductivity quantum oscill. obs. 8=17940
 Sb, transmittance and reflectance meas. rel. to band structure 8=13859
 Sb_2S_3 , amorphous, photo-e. m. f. meas. 8=9255
 Sb_2S_3 evaporated, electron diffr. exam. 8=17126
 Sb_2Se_3 , optical anisotropy 8=14259
 Se, evaporated, viscoelastic properties, obs. 8=21888
 Se, photoconductivity, anomalous, activated by Hg 8=9256
 Se, polycrystalline and single crystal, extra reflections in electron diffr. pattern 8=4753
 Se, vitreous, space-charge-limited currents and high elec. field effect 8=13828
 Si, amorphous, structure 8=13092
 Si epitaxial on α -alumina, electrical props. 8=9121
 Si, epitaxial, on Ge(111) surfaces, LEED struct. obs., 870°K 8=17140
 Si, epitaxial growth, Si substrate, SiO_2 and SiN_4 elimination 8=13128
 Si epitaxial layers, "hillock" formation 8=17619
 Si, epitaxial, on Si(311) surfaces, LEED struct. obs., 870°K 8=17140
 Si, epitaxial, prep. by pyrolysis of hydrides 8=17130
 Si, epitaxial, stacking faults, cause and cure 8=8736
 Si, etch rates in H_3PO_4 , influence of H_2O content 8=17218
 Si, evaporated, quantitative determ. by radioisotope analysis following n-activation 8=4756
 Si growth on W substrate by vacuum evaporation 8=4758
 Si grown epitaxially on sapphire, diffused diode charact. 8=18130
 Si, heteroepitaxial on sapphire, space-charge limited currents 8=2213
 Si, homoepitaxial, vacuum deposition, low temp. 8=1697
 Si on insulators, epitaxial growth 8=8328
 Si, on Ni substrate, total reflection of X-rays of different wavelengths 8=22038
 Si, isolation diffusion of P, integrated circuits 8=1929
 Si, large area p-n junctions, by epitaxial growth technique 8=5316
 Si, prep. by rheotaxial method 8=4739
 Si and SiO_2 films, r. f. and d. c., sputtered rel. to re-emission coeffs. 8=2032
 Si, X-ray stress topography, rel. to film-crystal interface stresses 8=22371
 SiC deposition in r. f. glow discharge 8=21872
 SiC, vapour deposited, phys. props. 8=17137
 SiN deposition in r. f. glow discharge 8=21872
 SiN deposition on metal coated substrates 8=13870
 Si_3N_4 , amorphous, structure dependence on deposition parameters 8=17179
 Si_3N_4 , deposited on GaAs, i. r. absorpt. 8=14262
 Si_3N_4 , etch rates in H_3PO_4 , influence of H_2O content, and use of SiO_2 mask 8=17218
 Si_3N_4 , fabrication and characts. 8=21891
 Si_3N_4 , prod. by reactive sputtering 8=17139
 Si_3N_4 , pyrolytically deposited, thermal expansion coefficient 8=4939
 Si_3N_4 , reactively sputtered, evidence of excess Si 8=21890
 Si_3N_4 , vapour deposition on GaAs, by $\text{SiCl}_4\text{-NH}_3\text{-N}_2$ system 8=13094
 SiO_2 , etch rates in H_3PO_4 , influence of H_2O content, and use as mask for etching Si_3N_4 8=17218
 SiO_2 , capacitor appl. 8=22676
 SiO_2 capacitors, heating effects 8=9233
 SiO_2 elect. cond., Pool-Frenkel eqn. 8=13705
 SiO_2 evaporated, forming process variables 8=4754
 SiO_2 , thin 8=2253
 SiO_2 deposited on n-type Si by reaction SiH_4 with water vapour 8=4757
 SiO_2 , deposition from silane 8=13095
 SiO_2 deposition from SiCl_4 -water vapour reaction 8=21889
 SiO_2 dielectric, pyrolytically grown, voltage-current charac. 8=13873
 SiO_2 , diffusion of borax 8=4957
 SiO_2 , growth in microwave discharge 8=4755
 SiO_2 , MOS capacitors, noncrystalline structure, electronic conduction 8=9234
 SiO_2 , in m. o. s. structure, Fowler-Nordheim tunnelling and energy band structure 8=2229
 SiO_2 , Na contamination, and diffusion and drift of tracer Na 8=18069
 SiO_2 on Si, pinhole locating by electrograph method 8=1698
 SiO_2 on Si, thickness (< 900 Å) meas. with reflection tech. 8=13093
 SiO_2 , proton and Na transport 8=9172
 SiO_2 , thermally grown, electronic conduction mechanism 8=18076
 SiO_2 , vitreous, i. r. absorpt. 8=5637
 $\text{SiO}_2\text{-Si}_3\text{N}_4$ on Si, optical thickness obs. 8=1699
 Si- WSi_2 -Si, epitaxial struct. 8=17257
 Sn, Ge coating effect on transition temp. 8=5214

Films—cont'd**solid—cont'd**

- Sn, Josephson tunnel junction characts. 8=9063
 Sn, obliquely deposited, struct., effect of atom mobility 8=8296
 Sn oxide, electron emission from high resist. regions 8=22713
 Sn superconducting and bulk Nb, microwave-photon assisted tunneling 8=17975
 Sn, superconducting, Nernst effect 8=2174
 Sn, superconducting, nonlinear effect at about 10 GHz 8=22562
 Sn, in u.v., reflecting power, optical const. and dielectric const. deduced 8=5638
 Sn vacuum condensates, influence of annealing on block structure charact. 8=4741
 SnO₂, thin, u.v. absorption edge spectrum 8=2458
 SnTe, prep., resist. meas., Hall effect and cryst. props. 8=13096
 Sr, thin, optical absorpt. between 0.5 and 5.5 eV 8=23014
 SrTiO₃, superconducting semiconductor films and whiskers, transition temps. 8=9056
 Ta oxidized in radio-freq. discharge 8=8310
 Ta, ultra-thin, vacuum-deposited, structure from e-diff. and microscopy 8=17292
 Ta₂O₅, e beam evaporation and dielec. props. 8=22652
 Ta₂O₅, prep. by anodizing and sputtering 8=13097
 Ta₂O₅, prep. by gas-phase anodization 8=14420
 Ta₂O₅-SiO₂ thin film capacitor, prep. and props. 8=9232
 Tb chelate phosphors, radiative quantum efficiencies, enhancement 8=18617
 Te, vac.-evaporated, forbidden reflexes in e-diff. 8=17141
 Tl, resistivity in thickness range 75-350 Å 8=9019
 Ti-Al alloys, thin foils, hydride formation 8=17016
 TiO₂, with large ionic space charge, conduction process 8=2233
 TiO₂, spark discharge along surface 8=7682
 Tl, Ge coating effect on transition temp. 8=5214
 U monolayer on polycrystalline W, photoelectric work function 8=5408
 U on W, vac.-deposited, props. in u. h. vac. and H₂ 8=17142
 U, photoelectron attenuation lengths 8=22727
 UAl₃ coatings formed by electrophoretic depos. of Al on U, structure and props. 8=21892
 W, absorpt. and interact. of H₂O vapour, rel. to catalytic activity 8=14405
 W, adsorpt. of N₂, sticking probability temp. dependence 8=14396
 W, L_α emission fluoresc. and direct components 8=14179
 W, sputtered and condensed on cleaved NaCl, structure rel. to temp. 8=4759
 WO₃, Pt-activated, sensitivity as gas detector 8=13098
 YFe garnet on YAl garnet, chem. vapour deposition 8=13099
 ZnS, cubic, epitaxial growth by evaporation in ultra-high vac. 8=21893
 β-ZnS, growth and elect. props. 8=17143
 ZnS:Ag, use of radiation deterioration for meas. ion energy losses 8=8758
 ZnSe, preparation by flash evaporation 8=13100
 ZnSe-Te_{1-x}, preparation by flash evaporation 8=13100
 ZnTe, electroabsorpt. rel. to determ. of reduced effective mass 8=18566
 ZnTe, preparation by flash evaporation 8=13100
 Zr-O coated W, field-emitted electron distrib. and work function 8=5413
 ZrO₂, e beam evaporation and dielec. props. 8=22652

Filters

- axially symmetric. eqn., boundary problems, relaxation method 8=16761
 liquids, insulating, Cottrell electrostatic purification 8=1543
 microwave, with two-pole maximally flat response functions 8=11377
 molecular, appl. to air drying 8=18644
 molecular, Rumanian ion exchangers 8=18652

Filters, electrical. See Circuits.**Filters, optical**

- See also Absorption/light; Optical films.
 in astronomical photometry, temp. effects 8=10103
 in Barnes ES-100 Educational spectrometer absorpt. 8=491
 birefringent, optimum-response synthesis 8=15520
 chain birefringent filters, anal. of Solc and Lyot type 8=3352
 device for spacial filtering of astronomical photographs 8=14744
 distorted images, linear least-squares filtering 8=483
 far i. r. LWP, low temp. transmittance 8=20066
 for far i. r., metal mesh interference type 8=6516
 far i. r. transmission filters, containing alkali halides, preparation and use 8=20063
 frustrated total reflection 8=11143-4
 holograms for filtering spatial frequencies in incoherent light 8=20111
 image restoration after random-media degradation 8=15507
 i. r., effects of variation of angle of incidence and temp. 8=6515
 infrared, water-cell for pyrometer 8=15099
 interference, for i. r. region of spectrum 8=20064
 interference, narrow-band, u. v. region 8=6513

Filters, optical—cont'd

- interference-polarization, with transmission-band shift 8=11203
 Irtran 2, 4 and 6, total hemispherical emittance at low temps. 8=18467
 multilayer, consisting of homogeneous layers or inhomogeneous films, Fourier synthesis 8=11142
 Ross difference filter for Mo K α rad., preparation 8=2437
 ruby laser, smoothing of spikes 8=11141
 spatial filter for character recognition, storage capacity 8=6514
 spatial frequencies, for pattern recognition 8=3353
 Al-MgF₂-Al bandpass, far vac. u. v. 8=20065
 Finlay-Freundlich red-shift hypothesis. See Astronomical spectra; Cosmology; Gravitation; Relativity.
 Fireball model. See Cosmic rays; Elementary particles; Field theory, quantum/interactions; Nuclear reactions.
 Fission. See Nuclear fission.
 Flames
 absorption line profiles, Zeeman scanning 8=12044
 air-N₂O-acetylene, for atomic absorpt. spectroscopy 8=14458
 audible noise, ultrasonic abatement 8=10779
 configuration in guided flow 8=19655
 impinging on plate, e. m. f. 8=12696
 ionization, aerosol particle size analyser 8=16908
 diffusion, turbulent, thermal equil. meas. 8=7946
 electric field effect, Schlieren survey 8=6217
 fuel droplet, free and forced convection, diffusion-flame shape in wake 8=15113
 hydrocarbon, electronically excited CH and C₂ 8=7509
 laminar diffusion, in core of vortex, swirling motion and flow field 8=15111
 laminar diffusion flame behind parabolic cylinder, const. press. Oseen-flow model 8=19656
 metals detect. by atomic fluoresc. 8=14460
 modulated by acoustic waves 8=10750
 oxyacetylene, in air or N₂, temp. determ. from rot.-vib. spectrum of OH 8=18692
 oxyacetylene, low press., absorption and emission spectroscopy of C₂, CH and OH 8=21189
 oxygen-acetylene, temp. meas. by molecular spectroscopy 8=3109
 photometry, atomic absorpt. chemical analysis 8=18777
 plasma, induction-coupled, in air and Ar, spectroscopic obs. 8=21411
 premixed, with diffusion, asymptotic treatment of structure 8=242
 spectral source, evaluation for atomic absorpt. 8=23183
 spectrophotometry, absorpt.-emission intensity ratio 8=18778
 spectroscopy analytical appl., bibliography 1800-1966 8=23182
 spectroscopy, atomic absorpt., atomization of solid samples, use of solid fuel 8=11150
 temp. field in cylindrical chamber, recirculation effect 8=15114
 CO-air, effect of H₂O on burning velocities 8=15109
 H₂, chemiluminesc., effects of SO₂ 8=18693
 H₂+O₂+N₂ pre-mixed, Cr₂O₃ particles obs. 8=23118
 N₂O-acetylene, in emission anal. 8=18782
 O, CO, low temp., kinetic calc. 8=9699
 O, H, low temp., kinetic calc. 8=9699
 Flares, solar. See Sun/flares.
 Flash photolysis. See Photochemistry.
 Flicker noise. See Electron tubes; Fluctuations/electrical.
 Floating zone refining. See Zone melting and refining.
 Flocculation. See Sedimentation.
 Flow
 See also Diffusion; Jets; Plastic flow; Turbulence; Viscosity.
 aerosols, near obstacles, non-symmetrical theory 8=21737
 axisymmetrical free flow with rotation, turbulent, decay of vel. 8=21463
 baroclinic, stability in zonal magnetic field 8=2582
 b.c.c. metals, axisymmetric, lattice rotations, computer solution 8=8373
 between disks, rotating and stationary 8=21571
 Boltzmann eqn., linear, soln. for flow over point source 8=7875
 boundary layer effect on shock wave reflection at rigid boundary 8=6138
 boundary layer growth in non-conducting fluid on a magnetized circular cylinder 8=7872
 boundary layer, simultaneous ht. and mass transfer in convection 8=240
 boundary layer turbulence promoters, improved heat transfer rel. to power reactor systems 8=21510
 boundary layer, turbulent, inactive motion and press. fluctuations 8=4436
 boundary values for uniform wall temp. in non-circular conduits 8=4429
 channel, two-dimensional, reverse transition from turbulent to laminar 8=21430
 circular Couette flow, problem of Taylor instability suppression of effect of geometry 8=21425
 compressible fluid, in wake of symmetrically positioned body 8=7862

Flow—contd

- confined rotating vortex, forced and periodic breakdown 8=21469
- distribution properties behind spherical detonation wave 8=15061
- drag of two-dimensional bluff-plates immersed in turbulent boundary layers 8=21446
- elastic tube, satisfying Windkessel condition, asymptotic uniqueness 8=21428
- elastico-viscous fluid, slow steady motion with heat transfer in wavy channel 8=16624
- eqn. for geomag. flux tubes, and appl. to polar substorms 8=10029
- exact Navier-Stokes solutions including swirl and cross-flow 8=4433
- expanding, behind incident shock waves, probe studies 8=15049
- fluid, along plate with transverse cavity, mass transfer coeff. 8=12600
- fluid boundary layer build-up between concentric rot. cylinders, turbulence development 8=12633
- fluid, boundary layer eqns., dual solns. at point of detachment 8=7873
- fluid boundary layer, laminar, nonlinear instability development 8=12613
- fluid boundary near wall, turbulence, press. rel. to velocity components 8=12632
- fluid boundary, 2D, rot. tank with small inflow, instability 8=12592
- fluid, charged in e. m. and gravit. fields, Hamilton-Jacobi eqn. 8=16634
- fluid, charged, relativistic in e.m. and gravit. fields, Helmholtz and Larmor eqns. 8=16633
- fluid, Coutte, inner cylinder stationary, stability with centrifugal forces 8=16627
- fluid, Couette, plane, nonlinear instability 8=12591
- fluid, Couette and Poiseuille, between parallel plates, appl. couple stress and micropolar theories 8=7874
- fluid, curved, rate of change of vorticity components 8=12609
- fluid, elastico-viscous, acoustic streaming near cylindrical obstacle 8=6169
- fluid, electrically conducting, incompressible near accelerated plate under transverse magnetic field 8=3241
- fluid with finite conductivity, in mag. field 8=10921
- fluid, forced oscillations behind vibrating cylinder 8=12609
- fluid, free boundary layer, statistical behaviour of turbulence 8=12617
- fluid, incompressible, shear, between parallel walls, statistical theory 8=12748
- fluid, induced by thermal oscillation of infinite horizontal cylinder 8=7881
- fluid, laminar boundary layer interaction with free stream turbulence 8=12614
- fluid, laminar-turbulent, stationary mixed, digital obs. 8=12640
- fluid motion induced by surface-tension variation 8=21422
- fluid, periodic pressure gradient 8=7861
- fluid, Poiseuille in pipe, stability when subject to azimuthally periodic disturbances 8=16631
- fluid, re-attaching high-speed, transverse variations obs. 8=12604
- fluid, rot. stratified, second circulation generation 8=12637
- fluid, shear isotropic, turbulent energy spectrum eqn. 8=12599
- fluid, shear, space-time correlation obs. interpretation 8=12605
- fluid, supersonic, forced vibr. of plate in plane of flow 8=10686
- fluid, turbulent boundary layer structure, review 8=12607
- fluid, turbulent boundary layer, 3D, with wall heat transfer 8=12611
- fluid, turbulent, longitudinal dispersion by combination of convection and lateral spreading 8=12622
- fluid, turbulent radial wall jet, mass transfer from axial source 8=1451
- fluid, turbulent separated in rectangular cavity, transport processes 8=12610
- fluid, turbulent shear, waveguide model 8=12598
- fluid, turbulent swirling jet, axial velocity and shear stress profiles 8=12626
- fluid of 2nd order, plane Poiseuille, effect of slight viscoelasticity on hydrodynamic stability 8=16632
- fluid, velocity defect law, surface roughness effect 8=12612
- fluidized bed, mean and variance of local particle conc., rel. to non-uniformity 8=21462
- fluidized beds, solid-to-fluid heat transfer 8=21470
- fluids, boundary layer, velocity space-time correlations, structure with and without freq. filtering 8=12606
- fluids, elec. cond., Hall effect for variable mag. field and high Reynolds numbers 8=16614
- fluids, freezing in forced flow, analysis 8=16926
- fluids, micropolar, between concentric cylinders 8=12590
- fluids, non-Newtonian, natural convection, laminar boundary layer equation solution 8=7857
- fluids, Reiner-Rivlin, in entrance region of channel 8=12601
- fluids, rotating and stratified 8=21427
- fluids, thermodynamically nonequilib., restraints on energy and spectrum of turbulence 8=16641

Flow—contd

- fluids, velocity spikes in limiting layer 8=1448
- fluids, viscoelastic through porous media 8=1446
- fluid, wall turbulence, secondary currents 8=12639
- four-space hyperfluid, as model of electro-magnetism 8=6283
- free-surface waves, interaction with viscous wakes 8=21449
- free turbulent, effects of intermittency on turbulent transport processes 8=16766
- free turbulent shear layer, approx. theory for development 8=21474
- fully developed, in tube with exp. varying heat flux, Nusselt numbers 8=19642
- gas-liquid mixtures in pipes, friction press. grad., Lockhard-Martinelli correl. 8=21564
- gas/liquid, through packing of absorpt. column 8=12737
- gas-particle reacting system, source flow model 8=21461
- gas-solid mixt., supersonic, in convergent-divergent nozzle and heat transfer, obs. 8=16902
- granular material in fluidized bed, heat transfer 8=4628
- gravity currents and related phenomena 8=16626
- heat transfer from a sphere at rest in a fluctuating stream 8=6207
- heterogeneous systems, 2nd law of thermodynamics 8=12595
- homogeneous fluid, inviscid layer, stability under action of uniform adverse temp. gradient 8=12602
- hydrodynamic boundary layer, heat transfer 8=12587
- hydrodynamic mixing in porous media 8=12596
- incompressible, density-current surges at density ratios of 1.05 and 3.0, numerical study 8=16630
- induced by body oscillating in unbounded viscous fluid otherwise at rest, review and extension 8=21556
- interpenetrating electron and ion streams, warm, nonlinear interaction 8=7752
- inviscid source flow field, loading calc. anal. of thin-ring airfoil 8=21473
- laminar boundary layers, free convection, incipient instability 8=4430
- laminar boundary layer on a sphere rotating about a diameter 8=7871
- laminar boundary layers, stability at separation 8=12589
- laminar, conduction-convection critical transition time 8=16692
- laminar, development in rectangular ducts 8=4451
- laminar incompressible viscous, nonlinear stability theory 8=12586
- laminar in parallel plate channel, development stability 8=4428
- laminar, through pipe with small suction 8=7868
- laminar Poiseuille, slightly supercritical, disturbance evolution 8=1450
- laminar source flow between 2 parallel co-axial discs rotating at different velocities 8=21426
- laminar and turbulent, heat transfer, analysis 8=7870
- laminar to turbulent, transition, incompressible fluid obs. review 8=12608
- laminar, of wall-jet over curved surface 8=21443
- linear Maxwell type viscoelastic fluids, near osc. or accelerating plate 8=21559
- MHD in cylindrical pipes with non-uniform mag. field 8=19810
- MHD, in expanding pipe, transverse magnetic field effect 8=6354
- MHD at flat duct entrance, heat transfer 8=19809
- MHD nozzles with end effects 8=6348
- MHD, one-dimensional, and Monge-Ampère eqn. 8=19812
- MHD, solution for small magnetic interaction 8=3236
- MHD stabilization, in plane channel, heat exchange 8=3240
- mass oscillating, in modified Moore variometer configuration 8=4445
- miscible in porous column, one dimens. hydrodynamic dispersion eqn. soln. 8=1441
- non-equilibrium, shock wave formation 8=6141
- non-Newtonian fluid, rotational motion through annulus with porous walls 8=21433
- non-Newtonian fluids, in straight pipes 8=7867
- non-Newtonian fluids, turbulent, through round tubes 8=16638
- ordered aggregates of rigid spheres, disks and rods in plane Couette flow 8=12944
- orifice, circular, numerical soln. of integral eqn. 8=16625
- over yawed cylinder, eqns. for boundary layer and out pot. flow, for cross-wire and spanwise vel. comps. 8=16657
- perfect fluid, over obstacles of finite amplitude 8=21431
- pipe, forced, free convection effect on heat transfer 8=16623
- plane reversible, compressible fluid, singularity of hodograph 8=16662
- plane supersonic, plate vibrations, nonstationary parametric and self excited 8=15033
- Poiseuille flow in parallel channel, with variable fluid props. 8=21472
- Poiseuille over porous surface, boundary conditions 8=1447
- Poiseuille, stability and incipient turbulence, study by difference method 8=12722
- polymer melts, molec. mechanisms 8=16749

Flow—contd

- in porous media, saturated, numerical simulation 8=12594
- potential, numerical solution for flux components 8=19365
- power-law fluids, down inclined plane between parallel plates 8=21435
- pressure drop across sharp-end capillary tubes 8=12588
- progress in heat transfer, book 8=15104
- rate of mass flow of a fluid 8=16629
- Reynolds number, large, Navier-Stokes solutions 8=7863
- shear, past cylinder with inverse ellipse cross section 8=21436
- shear, rapidly rotating, instability rel. to non-axisymmetric disturbances 8=21429
- shearing, influencing motion of sphere 8=7866
- slow viscous, extremum principles and application to suspensions 8=1449
- soap stems, complex, meas. 8=12959
- for sphere transversely moving in rot. fluid 8=4435
- spiral, conformal representation 8=10495
- standard flow nozzles, effect of cavitation on discharge coeff. 8=21579
- steady of visco-elastic fluid in annulus of two cylinders 8=21432
- Stokes, cellular, spatially periodic, induced by time invariant elect. field 8=7883
- Stokes conditions, particle aggregation, in sound field 8=6156
- Stokes, past a circular cylinder in MHD 8=15372
- suction, optimal, of boundary layer, rel. to initial turbulence and surface roughness 8=12597
- supersonic with heat sources through deformable cylindrical shell 8=16649
- of suspension, particle migrations in 8=8146
- suspensions and drilling muds, in tubes, laminar and transitional 8=8151
- Taylor-vortex, perturbation instability 8=12643
- transducers, principles and basic eqns. 8=16635
- transient Couette, kinetic theory 8=21423
- turbulent boundary layer, effect of sudden compressions 8=15055
- turbulent, conduction-convection critical transition time 8=16692
- turbulent boundary layer, structure 8=7876
- turbulent, heat transfer in tube with circumferentially varying thermal boundary conditions 8=19638
- turbulent wakes, two dimensional, self preserving 8=7880
- 2 incompressible immiscible viscous fluids, due to pulses of tangential force on upper surface 8=21434
- two-phase in heated pipe, stability calc. 8=4431
- vapour-liquid mixtures in pipes, friction press. grad., Lockhard-Martinelli correl. 8=21564
- variational principle for hydromagnetic flows 8=15374
- viscoelastic, linear instability of a plane-parallel Couette flow 8=7869
- viscoelastic Maxwell fluid, contained between concentric spheres, motion 8=21421
- viscoelastic, restrictions on velocity probes 8=12603
- viscous, around semi-infinite obstacle 8=7864
- viscous incompressible between parallel plates, appl. of variational principle 8=4432
- viscous under transverse magnetic field 8=6353
- viscous, unsteady temp. distrib. 8=7977
- vorticity, free-stream, effects in region of separated zones 8=12644
- water, small bore, effect of vibrations rel. to laminar and turbulent transition regimes 8=1501
- $\text{Fe}(\text{OH})_3$ suspension, Br^{82} meas. 8=21727

gases

- See also Acoustic streaming; Aerodynamics; Anemometers; Supersonic flow.
- absorbing-emitting, free convection at stagnation point 8=4454
- air/air free jet, nozzle-fluid concentration field 8=4453
- air, arc heated, temp. fluctuations and autocorrelation function 8=12653
- air between parallel plates, parabolic profile meas. 8=7902
- air, free convection from vertical flat plate with step discontinuities in surface temp. 8=21458
- air, hydrodynamic boundary layer at a disc 8=4449
- air, laminar forced convection in entrance region between parallel flat plates 8=21459
- air, low-speed, study of skewed turbulent boundary layers 8=21475
- air, turbulent, through concentric annuli, experimental study 8=12650
- air, in tubes, acoustic reflection coeff. of discontinuous changes of cross-section 8=19565
- air, turbulent, in vertical square duct, temp. inner-law and heat transfer 8=4456
- air over boundary between smooth surface and small water waves 8=1460
- air, turbulent, rel. to effect of waves at gas-liq. interface 8=21464
- air-water interface with progressive water waves, aerodynamic press. distribution 8=5791
- "almost-Lagrangian" formulation 8=21476
- annular duct, boundary elements, flutter, gas flow induced 8=15038

Flow—contd**gases**—contd

- atmospheric shear, thermally stratified, rel. to laboratory models 8=14599
- behind detonation, friction and heat-transfer effects on transition to steady flow 8=15058
- boundary layer, with large injection and heat transfer 8=21485
- boundary layer, low-drag, disturbances induced by suction through slots 8=12667
- boundary layers, turbulent with air injection, transformation 8=12665
- boundary layer transition at Mach 5.5, shock tunnel investigation on 8° half-angle cone 8=12670
- channel, of mixtures in chemical and thermodynamic non-equilibrium 8=7903
- compound-compressible theory for streams through nozzle 8=21455
- conducting, at high vel., influence of Hall currents 8=16653
- conical, holographic interferogram, refined analysis 8=6565
- in conical nozzle, with velocity slip and temp. jump 8=16651
- counter-flow suspension, particle residence time tracing 8=21454
- critical points, determination using wire heater and differential thermocouple 8=12668
- critical, valve sizing 8=7898
- crossed E and H fields, longitudinal stability 8=10923
- cylinder near-wake and separation point, velocity fluctuation obs. 8=12654
- adiabatic internal source 8=1458
- droplet suspension, momentum and heat transfer 8=12663
- dusty, steady, past sphere 8=12669
- effusion apparatus, angular deflection recording, automated 8=4637
- effusion current through cylindrical orifice 8=7899
- Ekman boundary layer, transition and instability 8=12657
- ethane, transpiration through membrane 8=12662
- exponentially sheared in vert. dirn., effect on induced drag of elliptically loaded lifting line 8=16677
- flame, laminar diffusion, in vortex core, field 8=15111
- fluidized bed, dense, gas distribution 8=8141
- free convection, heat transfer and binary diffusion 8=4491
- gas-particle system, turbulent flow, two-phase eqns. with fluctuations of particle cloud 8=16660
- Graham's law, range of validity 8=12708
- Graham's laws reviewed 8=12707
- guided, flame configuration 8=19655
- heat transfer with packing in packed bed of spheres 8=13363
- high-enthalpy, stagnation point heat transfer of a solid 8=22140
- high speed over liquid layer, effect on stability 8=4523
- hypersonic low-density, past thin wedges 8=21487
- hypersonic past blunted bodies, soln. valid for whole field 8=16654
- ideal, magnetohydrodynamic 8=3234
- ideal, with a normal shock 8=15375
- integral characts. method for press. and vel. calc. 8=21460
- inviscid, past delta wing, field near centre of rolled-up vortex sheet 8=1459
- ionized laminar boundary layer, two temp. 8=7900
- ionized, quasi-unidimensional flow in mag. field, stability of transverse oscills. 8=349
- laminar, development in rectangular ducts 8=4451
- laminar diffusion flame behind parabolic cylinder, const. press. Oseen-flow model 8=19656
- laminar hypersonic near wake, theoretical soln. 8=16670
- laminar-turbulent transition, small parameter method 8=12655
- linearized inviscid relaxing, approx. analysis 8=4457
- MGD, elect. conductivity dependence on temp. 8=16491
- MHD, distortion by strong Hall effect and effect on power generation 8=15381
- measurement and recording by capillary method 8=7896
- miniature turbine flowmeter, low flowrates, operation and calibration 8=16665
- molecular, in cylindrical tubes, approximation 8=1453
- molecular flow in long cylindrical tubes, soln. of Clausius's integral eqn. 8=21529
- molecular, interaction with tube walls 8=7893
- in narrow channels, rel. to flow-induced vibs. in rigid plate 8=19497
- nozzle into still air, plume geometry calc. 8=21453
- over yawed cylinder, boundary layer and out pot. flow equations 8=16657
- partially dissociated stream, effect of mass injection on heat transfer 8=21457
- partially ionized, supersonic source flow expansion into vacuum 8=16658
- particle-gas mixture in nonequilibrium, continuum approach 8=16655
- plane Poiseuille, of rarefied gas 8=21456
- plane reversible, singularity of hodograph 8=16662
- plasma, collisionless, over mag. obstacle, wind tunnel obs. 8=16513

Flow—contd**gases—contd**

in porous media, approx. equations 8=21467
 propane, transpiration through membrane 8=12662
 pulsating, particle motion and heat transfer 8=16696
 quasi-one-dimensional, de-excitation shocks 8=12661
 quasi-one-dimensional, reservoir problem 8=12660
 rarefied, axially symmetric stagnation-point flow 8=21468
 rarefied multicomponent over subliming wall, boundary conditions 8=4663
 rarefied, stagnation-point flow 8=1454
 rarified, through cylindrical tube 8=4455
 rate obs. by modified continuous-ionizing method 8=12659
 Rayleigh problem in slip flow, linearized, with modified initial conds. 8=21466
 residual, in e tube manufacture, mass spectrometry 8=18770
 self-similar motions in shock and detonation waves 8=4462
 shock waves in presence of unsteady motion of a gas 8=16656
 short waves, Navier-Stokes equations at shock wavefronts 8=7895
 slip flow over flat plate, new approach using perturb. of Navier-Stokes eqns. 8=21465
 steam-water mixture, in vertical pipes, hydrodynamics 8=21560
 Stokes paradox in kinetic theory of gases 8=21496
 stream formation following shock wave 8=16663
 subsonic in crossed elect. and mag. fields 8=16659
 supersonic, Chaplygin's equation near vacuum line 8=7905
 supersonic of real gas over solid of revolution, perturbations damping 8=21480
 surface transport mechanisms 8=4450
 tangential slot injection into external supersonic stream, associated flow field 8=16675
 in tube, one-dimens., unsteady compressible boundary layer 8=16650
 turbulence downstream of grid, hot-wire meas., nonlinearity effects 8=12664
 turbulence sound field freq. spectrum, laser appl. 8=19552
 turbulent boundary layer, streamwise wall curvature effect 8=12656
 two-phase cocurrent flow, press. drop in packed bed, correl. 8=12651
 two-zone transonic flow in throat region of convergent-divergent nozzle 8=16648
 unsteady, meas. of rapidly varying temps. 8=16694
 unsteady, 3D, vorticity and current density behind magnetogasdynamic shock wave 8=6358
 updrift, ambient circulation about and viscous counter-forces 8=7904
 velocity profile, slip coefficient and perturbed distribution function, calc. 8=16647
 into vacuum with exponential boundary temp. 8=4458
 wake of oscill. cylinder, suppression of turbulence and vortex shedding, expt. 8=12666
 weakly ionized turbulence correl. with Langmuir probe current fluctuation 8=1406
 CO, vibr. relax. in nozzle expansion flow 8=16270
 CO₂, shock wave reflection, normal, with vibrational relaxation 8=1455
 CsCl(g) effusion, ang. number distrib. 8=12706
 H₂-air, free convection, heat transfer and binary diffusion 8=4491
 He-air, free convection, heat transfer and binary diffusion 8=4491
 He₂, rarified, molecular velocity distribution function Doppler obs. 8=16664
 K vapour, adiabatic, associated with supersaturation and condensation shocks 8=12982
 N₂, laminar boundary in stream with coolant mixture injected through porous surface 8=4459

liquids

See also Acoustic streaming; Double refraction/flow; Hydrodynamics; Superfluidity.
 advances in applied mechanics, book IX 8=16747
 aerosols, around impenetrable bodies, for small Stokes numbers 8=4634
 aortic meas., isolation of myocardial stimulus 8=19331
 boiling, in heated pipe, stability calc. 8=4431
 boiling two-phase system, transient behaviour of vapour volumetric conc. 8=12988
 cavitating, past a cylinder, boundary effects and equiv. vel. 8=16769
 in channel, viscous, unsteady heat transfer 8=1546
 conducting, induced by nonuniform m.h.d. pinch 8=10932
 conducting, turbulent, effect of mag. field on heat transfer 8=10930
 conducting viscous, in porous channel with transverse mag. field 8=15363
 conductor, in annular gap, accn. by Lorentz force in circumferential dirn. 8=16755
 convection, cellular, induced by surface tension in semi-infinite layer 8=1503
 convective with internal heat generation, theory 8=4511
 cylindrical shell, vibrations 8=152

Flow—contd**liquids—contd**

drag force on sphere rolling in closed-end fluid-filled tube 8=21629
 dragging by plane walls in presence of magnetic field 8=10926
 drainage of a sand column, capillary conductivity law 8=16762
 drops, migration, from bonding walls 8=7995
 elastic, through curved pipes 8=21570
 electroconducting between rough plates numerical calc. 8=8110
 entrainment and drainage of liquid films 8=21597
 ferromagnetic colloidal suspension, mag. field prod. rotation 8=16622
 field of flow in system of parallel cylinders perpendic. to flow direction 8=1500
 film falling down wall, diffusion-controlled electrolytic mass transfer 8=21598
 films, laminar flow along vertical wall, neglecting surface tension 8=21599
 films stability in annular 2-phase and falling film flow, literature survey 8=12774
 films, surface velocities 8=12731
 forced, critical heat flux 8=4656
 heat exchange in turbulent motion in presence of transverse mag. field 8=12742
 heat exchanger, response to disturbances 8=8048
 hydroxyethyl cellulose aqueous soln, non-Newtonian flow past sphere 8=12724
 ideal, free surface, with a hydraulic jump 8=15375
 laminar boundary, over dielec. disc, in mag. field 8=4507
 laminar, eddies in conduit expansion 8=21569
 laminar, elasticoviscous in annulus with porous walls 8=7978
 laminar at high shear stresses, temp. distrib. 8=4508
 laminar, instability due to film of adsorption 8=7974
 laminar, lubrication of journal bearings 8=8810
 laminar, non-Newtonian, theory of double cone viscometer 8=12821
 laminar, Reiner-Rivlin liq. in circular pipe inlet 8=4509
 laminar viscous film on rotating disc, energy and motion equations 8=4522
 laser Doppler velocimeter, flow-velocity fluctuation obs. 8=21574
 longitudinal wall curvature, effect on nonviscous stability of boundary-layer flow 8=16621
 lubricants, laminar and turbulent flow analysis 8=12733
 Maxwell, in porous annulus 8=21572
 meas., precision techniques 8=21575
 mercury, turbulent in tube in longitudinal mag. field 8=10933
 metal, laminar and transitional, heat transfer 8=21568
 metals, along row of spheres, anal. of heat transfer 8=21660
 metals, turbulent in smooth tubes, heat transfer laws 8=16824
 Navier-Stokes equations, exact solutions in spherical polars 8=1507
 Newtonian, through smooth annuli, turbulent boundary-layer development 8=16765
 non-linear problems in fluid mechanics, Newton's approximation application 8=12721
 non-Newtonian, elasticoviscous, friction factors and velocity profiles in turbulent flow 8=12746
 non-Newtonian, dispersion of matter 8=1506
 non-Newtonian, in porous media 8=7979
 non-Newtonian, through porous media and packed beds 8=12739
 non-Newtonian, of Reiner-Rivlin type, rotating flows over rotating discs 8=21561
 over long circular cylinder, laminar boundary-layer flow and heat transfer 8=21565
 polyethylene oxide aqueous soln, non-Newtonian flow past sphere 8=12724
 polymer, additives in water, effect on turbulent shear flow 8=16764
 polymer solutions, turbulent shear flow 8=12743
 polymers, onset of non-Newtonian flow 8=16759
 polystyrene in benzene solns., birefringence 8=12732
 pipeline capsules, velocity and press. gradient 8=7972
 polyethylene membrane permeation, effect of temperature 8=1508
 polymer, dilute solutions, Pitot tube and hot film obs. 8=7981
 polymer solns., effect of aggregates 8=8023
 polymer solns. in pipes, drag reduction 8=1511
 polymer solns., turbulent in pipe 8=4510
 polymer solns., viscous, conc. depend. of activation energy 8=16807
 1, 2, 3% polyvinyl alcohol laminar-turbulent transition, obs. 8=4512
 progress in heat transfer, book 8=15104
 relaxing, instability and drag reduction through tubes and porous beds 8=1513
 rotating with free cylindrical surface, stability to small inviscid disturbances 8=1505
 shear, with Brownian motion, coagulation 8=8148
 shear, drop deform., second-order theory 8=7993
 shear, generation of surface waves by 8=1515

Flow—contd**Liquids—contd**

- silicate melts, Newtonian, viscosity eqn. and bond rearrangement 8=21628
- slow, nonisothermal, viscous and heat conducting, variational formulation 8=7976
- from sluice gate under gravity 8=21567
- in square duct, laminar flow development meas. using laser-Doppler flowmeter 8=21566
- steady open-channel past solid surface of finite-wave-group shape 8=7973
- Stokes flow, at large Péclet numbers, mass transfer to rear of sphere 8=21563
- suspensions, in porous media 8=12738
- theoretical and applied mechanics, conference, Haifa Israel (1967) 8=16750
- thixotropic, hysteresis experiments 8=7860
- tracer detection, by elec. cond. meas. 8=8109
- transient movement in pipes, problem of column separation 8=16757
- tube, horizontal, and surface tension effects 8=16626
- turbulence near solid wall, electrochemical obs. 8=12747
- turbulent boundary layer on smooth wall, structure obs. 8=12741
- turbulent, conducting, Lorentz force effects 8=16763
- turbulent, non-Newtonian, heat transfer coefficients and friction factors 8=4565
- turbulent, past circular cylinder, drag-reducing effect of polymer solns. 8=16754
- turbulent pipe flow, diffusion and mixing of injected dye, numerical soln. 8=21576
- turbulent skin friction, Preston tube meas. 8=12750
- two-dimensional, under gravity in viscous jet 8=21562
- unsteady cavity flow, extension of Woods theory for hydrofoil design 8=16768
- vertically oscillating, thermal velocities of suspended spherical particles 8=7988
- viscoelastic fluids through porous media 8=21573
- viscoelastic, linear, steady, two-dimens. flows 8=12725
- viscoelastic, turbulent heat flow 8=1510
- viscous, in circular pipe with absorbing walls 8=21630
- viscous, Hele-Shaw cell, breakdown with large wall separation 8=16760
- viscous, numerical method of soln. 8=21626
- viscous with orthogonal magnetic and velocity field distrib., reduction 8=6350
- viscous, in rectangular open channel 8=7975
- viscous in a tube at const. temp. 8=12734
- vortex breakdown, 'conjugate-flow' theory 8=4513
- vortex shedding and transition, wake of cylinder 8=12752
- water, laminar, round CO₂ and N₂O bubbles 8=21591
- water-steam mixture, in vertical pipes, hydro-dynamics 8=21560
- water, viscogravitational in horizontal tube 8=12730
- water, wake of rot. cylinder, obs. 8=12751
- H₂O, in clear tubes, evaluation of H bubble tech. for velocity meas. 8=16756
- He II, heat exchange torques on immersed body 8=3127
- He II in a porous medium, superfluid 8=19698
- He II quantized circulation around a fine wire obs. 1.2-1.9°K 8=19703
- He II, superfluid, subcritical 8=19695
- He, superfluid, through orifices, critical vel. and vortices form. obs. 8=6234
- He⁴, turbulent, λ -point shift 8=19694
- Hg, turbulent in square duct, heat transfer and temp. distribution in wall, obs. 8=1545
- Na conducting, with aligned mag. field, drag obs. 8=6349
- ZnSO₄ soln., convectional due to electrolytic heating, obs. 8=1509

Flow birefringence. See Double refraction/flow.

Flowmeters

See also Anemometers.

- flowmeter, magnetic for Na cooled reactors 8=7317
- laser-Doppler type, for precision meas. of vel. rel. to laminar flow distrib. in square duct 8=21566
- laser Doppler velocimeter, flow-velocity fluctuation obs. 8=21574
- microflowmeter, Benseman type, theory 8=16628
- miniature turbine, with gases at low flowrates, operation and calibration 8=16665
- sensing devices for measuring amount of fluid in tank 8=21575
- transducers, principles and basic eqns. 8=16635

Fluctuations

See also Brownian movement; Random processes.

- cosmic rays showers, rel. to princ. components, simulation 8=3749
- fluctuation-dissipation theorem, steady-state 8=10608
- interferometry, two-beam, signal/noise 8=503
- irreversible processes, fluctuation theory 8=10624
- laser intensity, theories rel. to photon counting distrib. 8=19939
- laser noise, Fokker-Planck solution 8=11023
- in laser rad. at threshold, statistics 8=402
- lasers, gaseous, intensity 8=19951
- light, log amplitude and phase in Gaussian beam, propag. through random medium 8=20089
- light, phase and instantaneous freq. 8=20029

Fluctuations—contd

- noise, harmonic oscillator and atomic sources, quantum theory 8=19438
 - optical parametric devices, quantum noise 8=15445
 - particles, heavy charged, in thin absorbers, energy loss distrib. 8=13471
 - pulse effect in a medium, instabilities, convective and absolute 8=19476
 - quantum noise, rate equation and amplitude noise in lasers 8=11022
 - in quasi-harmonic self-excited oscillators, for low noise 8=6370
 - radiation, detector, meas. theory 8=3010
 - radiation and matter interacting system 8=19819
 - random trend removal in parity violation expts. 8=6630
 - reduced-width amplitude, exact distrib. 8=2908
 - spectrum, statistical props. of analyser 8=10981
- electrical**
- accelerator tubes, suppression of e loading 8=15653
 - amplifier, pulse, noise calc. employing gated active integration 8=619
 - atmospheric, affecting cm.-wave radioastronomy 8=18894
 - capacitor charging time, voltage effect 8=280
 - crystal-mixer noise, rel. to temp., 1400 MHz 8=6258
 - diodes, space-charge-limited, thermal noise 8=18132
 - e.m. perturbations in explosions 8=3040
 - frequency, bridge oscillator, stabilization 8=3145
 - in frequency modulation due to damped waves 8=2902
 - gas discharges, low-freq. noise 8=21226
 - gas laser, multimode, excess photon noise in detected photocurrent 8=11039
 - integrators, in pulse amplitude systems 8=20213
 - interference in sonar detection 8=23241
 - JFET, noise calcs. of meas. values 8=5334
 - laser noise in phase locking region, quantum mech. theory 8=3291
 - laser noise, quantum Fokker-Planck soln. 8=19937
 - magnetron, e.m. field fluctuations effect on space charge and anode current 8=338
 - in Markoffian continuous-parameter system, Lax calc. modified for computer evaluation 8=3152
 - MOS transistors, generation-recombination, theory 8=9174
 - MOS transistors, l.f. noise, surface states 8=9176
 - MOS transistors, thermal noise, theory accounting for substrate doping 8=9170
 - noise source, 10 GHz, Ar discharge tubes 8=7664
 - noise in waveforms, programme for reduction 8=3153
 - oscillators, self-sustained, near threshold, noise exam. 8=6259
 - oscilloscope, intensity modulation effect on multi-parameter display 8=6238
 - photoconductive i. r. detectors, generation-recomb. noise 8=22709
 - photoconductive i. r. detectors, noise limited detectivities 8=22708
 - photodetector signal: noise ratio rel. to electro-optic filter modulation voltage vars. 8=2270
 - photomultipliers, noise factor and photocathode quantum efficiency 8=10905
 - photomultipliers noise pulse, effect of high energy radiation 8=3216
 - plasma, turbulent, intensity of emitted e.m. rad. and noise 8=4370
 - polyethylene film, I-doped, current oscillations at high field strengths 8=8985
 - random signal quantization effect 8=6260
 - reactor interference on n counting system 8=4028
 - reduction method 8=15161
 - semiconductor lasers, population and current noise 8=429
 - semiconductors, piezoelectric, acoustoelec. domain formation during thermal noise amplification 8=18001
 - semiconductor surfaces, l/f noise, theory 8=13787
 - shot noise in crossed-field electron guns, space charge effect 8=19781
 - signal-to-noise ratio in pulse amplitude meas. 8=3478
 - in solids, space charge noise suppression 8=5380
 - spectroscopy, nuclear, improvement of peak to background ratio 8=3453
 - superconductors, type II, rel. to flux-transport 8=17949
 - superconducting foils, flicker noise 8=5220
 - thermal noise across tuned circuits used to meas n.m.r., e.p.r. 8=19906
 - transformer laminations, transversal motion as cause of hum 8=285
 - X-ray tube supply, high voltage waveform, radiographic effects 8=11243
 - Al-Al₂O₃-Al thin film diodes, meas. 8=13851
 - Cs vapour thermionic diodes, ion current and Schottky effect 8=339
 - GaAs at 80°K, electro-optic obs. 8=2193
 - Ge diodes, high freq. noise and double injection, obs. 8=13854
 - Ge, generation-recombination, 100°-350°K 8=22593
 - Ge photodiodes, shot-noise meas. at high freqs. 8=22706
 - He-Ne laser, discharge modulation noise 8=6449
 - InSb, quantum oscillations in photoelec. coeffs. in n-type 8=13913
 - n-InSb, relaxation oscillations rel. to bias current and magnetic field intensity 8=13824

Fluctuations—contd**electrical—contd**

- Se rectifiers, prebreakdown region, I-V fluctuations 8=2225
 Si:In, measurement, and photocond. and Hall effect rel. to
 electron and hole-capture coeff. 8=13915

Fluid flow. See Flow.**Fluid mechanics. See Hydrodynamics.****Fluidized powders. See Flow; Fluids; Powders.****Fluids**

- See also Gases; Liquids.
 binary mixtures, excess thermodynamic functions 8=4423
 boundary flow, 2D, rot tank with small inflow,
 instability 8=12592
 boundary layer and outer potential flow over a yawed
 cylinder 8=16657
 cellular convection, effects of surface curvature and proper
 property variation 8=21417
 cellular convection, finite amplitude stability rel. to
 extremum principle 8=6212
 charged in e.m. and gravitational fields, Larmor and
 Helmholtz theorems 8=16633
 charged, relativistic in e. m. and gravit. fields, Hamilton-
 Jacobi eqn. 8=16634
 classical dense with Lennard-Jones pot., correlation
 function 8=12576
 classical, form factor calc. rel. to n scatt. 8=7851
 classical, high-frequency thermal excitations 8=21419
 classical, Percos-Yevick eqn. generalisation 8=1437
 classical, theory, generalizations of hypernetted chain
 integral eqns. 8=101
 classical, triplet potentials in theory 8=21413
 conducting, Hall effect for variable mag. field and high
 Reynolds numbers 8=16614
 conducting, in motion, mag. field deformation by 8=6346
 convection in box heated from below 8=6214
 convection, cell heated from below, finite
 amplitude 8=6215
 convection, cellular, boundary-layer theory 8=10777
 Couette and Poiseuille flows between parallel plates,
 appl. couple stress and micropolar theories 8=7874
 with deforming microstructure, governing eqns. 8=12577
 dense hard-sphere gas, propag. of density
 disturbances 8=10660
 diffusion, corrections to kinetic theory 8=21416
 elastico-viscous, slow steady motion with heat transfer
 in wavy channel 8=16624
 enthalpies at elevated press. and low temps. 8=21600
 equation of state, square-well potential 8=4425
 ferromagnetic-non-magnetizable interface,
 instability 8=6355
 flow along plate with transverse cavity, mass transfer
 coeff. 8=12600
 flow, boundary layer eqns., dual solns. at point of
 detachment 8=7873
 flow, boundary layer nonviscous stability, effect of long.
 wall curvature 8=16621
 flow, Couette, circular, inner cylinder stationary, stability
 with centrifugal forces 8=16627
 flow, Couette, plane, nonlinear instability 8=12591
 flow, discontinuous one dimensional non-dissipative 8=15375
 flow electrically conducting, incompressible near accelerated
 plate under transverse magnetic field 8=3241
 flow, incompressible, density-current surges at density
 ratios of 1.05 and 3.0, numerical study 8=16630
 flow, induced by thermal oscillation of infinite
 horizontal cylinder 8=7881
 flow, laminar boundary layer on a sphere rotating about
 a diameter 8=7871
 flow, laminar, in parallel plate channel, development
 stability 8=4428
 flow, laminar and turbulent, heat transfer, analysis 8=7870
 flow, large Reynolds number, Navier-Stokes
 solutions 8=7863
 flow over obstacles of finite amplitude 8=21431
 flow, re-attaching high-speed, transverse variations
 obs. 8=12604
 flow in rotating and stratified fluids 8=21427
 flow, shear isotropic, turbulent energy spectrum
 eqn. 8=12599
 flow, with suspended solids, unsteady mass transfer 8=4630
 flow through porous media, numerical simulation 8=12594
 flow, 2 incompressible immiscible viscous fluids, due to
 pulses of tangential force on upper surface 8=21434
 flow, turbulent boundary layer, structure 8=7876
 flow, turbulent shear, waveguide model 8=12598
 flow, velocity spikes in limiting layer 8=1448
 fluid-saturated aggregate of particles, compressional
 wave vel. and compressibility 8=22270
 fluidic amplifier, improved sensitivity 8=4427
 fluidized bed, non-uniformity in particle conc. difference
 between bubble and dense phases 8=21462
 fluidized beds, solid-to-fluid heat transfer 8=21470
 free-surface waves, interaction with viscous
 wakes 8=21449
 freezing in forced flow, analysis 8=16926
 granular material in fluidized bed, heat transfer 8=4628
 gravity waves, internal, at critical level, viscosity and
 heat conduction effects 8=7887

Fluids—contd

- gravity waves, internal, propag. with shear flow and
 rotation 8=7885
 hard sphere, phase transition 8=12578
 heat transfer, cooling of moving cylinder 8=227
 heat transfer domains in variable gravity 8=16692
 heat transfer to porous medium 8=6206
 heated from below, Rayleigh convection cells of arbitrary
 wave numbers, 2D, evolution 8=10775
 heated unevenly from below, nonlinear model 8=16637
 h.f. linear response to Brownian oscillators 8=4446
 homogeneous, inviscid layer, stability under action of
 uniform adverse temp. gradient 8=12602
 ideal, gravitation in Einstein space-time 8=10595
 incompressible cylinder, gravitational
 instability 8=19084
 incompressible, elastic tube flows satisfying Windkessel
 condition, asymptotic uniqueness 8=21428
 incompressible, heat transfer between it and a porous
 medium 8=16821
 incompressible, isotropic homogeneous turbulence,
 evolution of single-time moments of velocity
 field 8=16642
 incompressible, laminar flow through pipe with small
 suction 8=7868
 incompressible, laminar to turbulent flow transition,
 obs. review 8=12608
 incompressible, plane reversible flow, singularity of
 hodograph 8=16662
 incompressible, tangential disturbances, viscosity
 effect on instability 8=12618
 incompressible, turbulent dispersion using Lagrangian
 diffusion eqn. 8=12633
 integral eqn. for pair correl. function, hard-sphere
 solns. 8=12579
 inviscid, rigidly rotating, enclosed, forced oscills. 8=7884
 jets, bulk properties of three dimensional, turbulent,
 incompressible 8=12585
 laminar boundary flow, stability at separation 8=12589
 laminar jets, plumes and wakes, entrainment
 models 8=4437
 linear molecules, statistical mechanics 8=4251-2
 m. h. d. shocks, transition soln. 8=19805
 mechanics, non-linear problems, Newton's approximation
 application 8=12721
 mechanics, use of ruby laser interferometers 8=16618
 micropolar, flow between concentric cylinders 8=12590
 mixtures, semiempirical theory 8=1436
 motion induced by surface-tension variation 8=21422
 motion of sphere near wall boundary of viscous
 fluid 8=7866
 motion of sphere through 8=7865
 multi-layered rotating, normal modes of
 oscillations 8=1452
 non-Newtonian, elasticoviscous, friction factors and
 velocity profiles in turbulent flow 8=12746
 non-Newtonian, incipient flow in straight pipes 8=7867
 non-Newtonian, natural convection flow, laminar
 boundary layer equation solution 8=7857
 non-Newtonian with nonlinear heat conduction law,
 flat-plate thermal boundary layer 8=4424
 non-Newtonian, rotational motion through annulus with
 porous walls 8=21433
 non-Newtonian, turbulent flow through round tubes 8=16638
 Nusselt numbers for fully developed flow in tube with exp.
 varying heat flux 8=19642
 oscillating mass flow in modified Moore variometer
 configuration 8=4445
 with packed powders, permittivity 8=22648
 particle distrib. function near crit. pt. 8=12964
 Percus-Yevick eqn. appl. to Lennard-Jones fluid 8=21415
 Percus-Yevick theory, triplet potentials 8=21414
 pipe flow, Poiseuille, stability when subject to
 azimuthally periodic disturbances 8=16631
 polar, coherent infra-red generation 8=9485
 power-law, flow down inclined plane between parallel
 plates 8=21435
 power-law, heat transfer from vertical plate to 8=8052
 progress in heat transfer, book 8=15104
 quantum, Brownian motion in, theory 8=92
 radiative heat transfer, volumetric absorpt. effects in
 optically dense fluids 8=10675
 Reiner-Rivlin, flow in entrance region of channel 8=12601
 relativistic sphere, Schwarzschild internal
 solution 8=2937
 relativistic, wave propagation 8=7888
 rotating, flow structure for sphere in slow transverse
 motion 8=4435
 rotating, large amplitude Benard convection 8=12616
 rotating, shear layer inertial effects 8=12593
 shear flow past cylinder with inverse ellipse cross
 section 8=21436
 shock waves, Burger's equation, Lagrangian-history
 statistical theory 8=19536
 square-well, eqn. of state 8=12581
 statistics, Eulerian rel. to Lagrangian 8=12582
 stratified rot., secondary circulation generation 8=12637
 stratified, spin-up 8=7855

Fluids—contd

- stratified, stably and unstably, turbulent velocity and temp. fields 8=12624
- superposition approx. for triplet correl. function 8=12580
- surface layer distant from boundary surface, statistical mechanics 8=99
- thermodynamically non-equilib., restraints on energy and spectrum of turbulent motion 8=16641
- thermodynamic props. at supercritical temps., calcs. 8=12575
- three-fluid heat exchanger, NTU-effectiveness relns. 8=19643
- Tietjens function, numerical evaluation 8=21420
- transport processes in single-component 8=1438
- turbulence and boundary layers with geophysical appl., conference, Kyoto, Japan 1966 8=7850
- turbulence, Burger's nonlinear diffusion eqn., viscous and nonsteady solns. 8=4439
- turbulent cylinder-wake, large eddy structure 8=12627
- turbulence, effect on heat transfer from spheres 8=17541
- turbulent, hot-film sensor for heat transfer 8=16822
- turbulent wakes, two dimensional, self preserving 8=7880
- with Van der Waals and dipole-dipole interactions of mols. at large distances, weakening of correlation, Bogoliubov condition 8=21418
- variable, heat transfer in laminar boundary layer 8=10769
- virial coeffs., radial distrib. and direct correl. functions at low density, square-well model 8=16613
- visco-elastic, isotropic turbulence decay, non-Newtonian effects 8=12645
- viscoelastic, linear instability of a plane-parallel Couette flow 8=7869
- viscoelastic Maxwell, contained between concentric spheres, motion 8=21421
- viscoelastic, restrictions on velocity probes 8=12603
- visco-elastic, steady flow in annulus of two cylinders 8=21432
- viscoelastic, stress in oscillatory motion 8=7861
- viscous, dislocation motion theory 8=16617
- viscous flow bet. parallel plates, appl. of variational princ. 8=4432
- viscous, incompressible, laminar flow around semi-infinite obstacle 8=7864
- viscous, Rayleigh instability theory 8=4546
- viscous, slow flow, extremum principles and application to suspensions 8=1449
- vortex breakdown, 'conjugate-flow' theory 8=4513
- wave, nonlinear, resonant, stability criteria 8=7886
- waves in viscous fluid at finite depth, Tsunami problem 8=12648
- wedge with compliant boundaries, point acoustic source, amplitude and phase structure of field 8=10723
- Yvon-Born-Green eqn. for rigid spheres and disks, asymptotic modification 8=16616

Fluorescence. See Luminescence.**Fluorescent screens.** See Luminescent devices.**Fluorimetry.** See Chemical analysis.**Fluorine**

- atomic, new Rydberg absorpt. series and ionization pot. 8=1165
- atoms, interaction with inert gases 8=12104
- dynamic polarization in CaF_2 : U^{3+} of 45% 8=18458
- ionization cross-section, electron impact 8=7700
- n.m.r., dynamic enhancement 8=12323
- n.m.r., dynamic polarization in fluorocarbon solns. 8=4627
- n.m.r. in hexafluoroethane 8=8134
- n.m.r., press. dependent chemical shifts in freon gases 8=12324
- Ar- F_2 cryst. state, phase diagram 8=1670
- F in MoF_6 , spin-lattice relax. in intense r.f. field 8=14139
- F^{19} in CaF_2 :H,D, single crystal nuclear polarization 8=1640
- F^{19} mag. reson. absorpt. in CF_4 and SF_4 clathrate hydrates 8=7607
- F^{19} , n.m.r. in oxygen fluorides 8=4231
- F^{19} in RF_3 (R = rare earth), n.m.r. 8=5556
- F^{19} , spin-lattice relax. in gases 8=21176
- F-Cs vapour, effect on electron emission from transition metals, model 8=18261
- F-F system, 2nd virial coefficient for different electron states at 2000-6000°K 8=1469

Fluorine compounds

- fluoride chemisorption on Si and SiO_2 surfaces, use of F^{18} in HF etches 8=18697
- proton bombard., additivity of stopping power 8=20188
- FCN, microwave spectrum of excited vibrational states 8=12182
- FCN, two vibration-rotation bands 8=12183
- F_2CN_2 , mol. struct. 8=12186
- FH, ground-state props. calc. 8=7514
- F_2O dissociation react. with Ar 8=12335
- KF- SnF_2 - H_2O system 8=4781

Foams

- See also Bubbles.
- polyurethane form., surface chemistry 8=8155
- polyurethane form., surface elasticity 8=8156
- polyurethane, use in construction of faceted solar concentrators 8=19677
- soap systems, complex, flow meas. 8=12959

Focused collision sequences. See Sputtering**Focussons.** See Crystals/lattice mechanics; Sputtering.**Fog**

- artificial, attenuation in visible and i.r. 8=1606
- artificial, scatt. of collimated thermal and laser beams, rel. to Buger law 8=510
- e.m. wave transmission, 0.337 mm maser source 8=2592
- haze, small-grained, characteristics 8=18882
- laser light absorpt. and scatt. 8=18878
- laser and monochromatic incoherent light scattering, comparison 8=14615
- microstructure, optical estimation parameters 8=18871
- Fokker-Planck equation. See Transport processes.
- Foldy-Wouthuysen transformation. See Field theory, quantum.
- Forbush decreases. See Cosmic rays/variations.
- Force. See Dynamics.
- Force constants. See Molecules/vibration.
- Force measurement.

- microbalance for molecular beam meas. 8=16380
- relation between force and potential energy, experiment 8=14923
- torque, low-temp. calibration technique 8=14924

Fortran. See Calculating apparatus/digital computer programmes.**Fountain effect.** See Helium/liquid; Superfluidity.**4 π counters.** See Counters.**Fourier analysis**

- See also X-ray crystallography/calculation methods.
- coiled-coil, modified transforms 8=7643
- convolution theorem, rel. to expansion of 3-dimens. function of spherical harmonics 8=1228
- crystal structure, min. function integral approach 8=22061
- diffraction theory, integral-transform.
- formulation 8=11187
- harmonic, correction for non-cyclic variation 8=6034
- light distribution by means of grating 8=11164
- multilayer optical filters 8=11142
- musical sounds, integral analysis 8=192
- Riemannian spaces with negative Riemannian curvature 8=10496
- Cu, cold-rolled electrolytic of elastic anisotropy, and crystallization 8=8404

Fourier series. See Series; Transformations, mathematical.**Fourier-transform spectroscopy.** See Fourier analysis; Spectroscopy.**Fractionation.** See Distillation.**Fracture**

- See also Mechanical strength.
- alloys, strength, time and temp. depend., non-equilib. state 8=8811
- bombs, tubular, behaviour, and plastic deform. 8=22292
- ceramics, basic mechanism, survey 8=17726
- crack extension in orthotropic plates, appl. of fracture mechanics 8=22294
- crack propagation in viscoelastic media 8=2045
- disks (flat faces insulated), thermal shock, statistical analysis 8=22295
- dry modulus of rupture and drying shrinkage 8=17737
- ductile, with rotation, influence of stress-state and inclusion content 8=17729
- fatigue, anal. of initiation and propag. of cracks 8=5030
- glass blocks, produced by impact 8=2055
- glasses, and breakdown, laser-induced 8=8851
- glass, tempered, rel. to elastic strain energy and rate of crack extension 8=22373
- graphite, polycryst. brittle, form. and growth of cracks 8=22318
- granite compression, microfracture events spatially located by S waves 8=23215
- magnetite film on Fe, crit. tensile fracture strains 8=2187
- mechanism at high temp. rel. to material props. and test conditions 8=17738
- metals, b.c.c., c.p.h., and f.c.c. 8=22290
- metals, fibre reinforced, mechanics 8=8805
- metals, photographic apparatus for study 8=22292
- metals, plane strain fracture toughness, determ. using double cantilever beam specimen 8=17721
- metals, polymers and glasses, conference, Boston, USA (1966) 8=13518
- metal, probability under multiaxial stresses 8=17736
- metal shells rupture rel. to strain rate and thickness obs. 8=5037
- metals, strength, time and temp. depend., non-equilib. state 8=8811
- photographic recording method 8=6584
- plate, thin flat, and plastic flow under uniform stress 8=13513
- polyethylene, fragment shapes in hypervel. impact rel. to lunar surface struct. 8=13609
- polymers, reinforced, spiral characteristics 8=2043
- polymethyl methacrylate, cycle dependent 8=2073
- polyurethane elastomer, triaxial behaviour in tensile field 8=2075
- rock in compression, microfracturing obs. 8=23203
- rocks, effects of triaxial stress systems, appl. to faulting and earthquakes 8=13516
- rocks and similar brittle materials, stress conditions during cutting 8=5012

Fracture—contd

- rocks under confining press., and elastic wave propag. and absorpt. 8=13515
 sandstones, strength and mechanism 8=13517
 sapphire, single crystals, alloyed with Ti, increased fracture strength 8=17767
 silicates, porous, fragment shapes in hypervel. impact rel. to lunar surface struct. 8=13609
 silicon iron, notched, topology rel. to crack nucleation and growth 8=17793
 spalls formed in rolling contact, electron fractographs 8=17750
 steel, creep-resistant 8=17803
 steels, intergranular matt facet weakness 8=22222
 steel, medium-strength, fracture toughness 8=17808
 steel, notch-brittle, torsional prestraining, influence on 8=13563
 steels, notched, topology rel. to crack nucleation and growth 8=17793
 steels, structural, susceptibility, effect of strain ageing of martensite 8=13573
 steel, structural, toughness, effect of temp. and strain rate 8=5070
 stress-intensity factor for edge-notched specimen 8=5023
 stress-intensity factor for hollow notched round bar 8=5024
 -surface energies, double cantilever method, critical analysis 8=22291
 toughness, plane strain, determ. 8=5024
 toughness of sheet, plate, and multilayered adhesive-bonded panels 8=17734
 twin-induced, stress needs 8=5028
 voids formation in creep and competition from sintering processes 8=8800
 Al alloy, shear deformation under reversed loads 8=17759
 Al_2O_3 grain, effect of environments on strength 8=13526
 Be single crystals, dislocations, slip 8=1969
 Cu, fatigued in Hg 8=5057
 Fe, technical, microstructure during fatigue tests 8=13566
 α -Fe, 3.28% Ni addition, effect on behaviour 8=22346
 Fe-30% Cr, yield and fracture stress, before and after ageing 8=13558
 Fe-Cu alloys, obs. 8=22347
 Fe-Ni-Si-C steel, rel. to martensite ageing 8=22357
 Fe-TaC alloys, obs. 8=22347
 MgO bicrystals, transgranular cleavage studies 8=8854
 NaCl, strength, particle size effect 8=22382
 Ni-Cr alloys, creep-resistant 8=17803
 Ni-20Cr-2ThO₂ alloys, creep 8=8858
 Si, plastic deform. in brittle region 8=5084
 SiC, 'self-bonded', delayed in temp. range 20 to 1200°C 8=22391
 Si-Fe crystals, [110], and fracture at 293 and 473°K 8=13607
 Si-Fe, intercrystalline 8=13567
 Ti-6Al-4V alloy, stress-corrosion cracking in methanol 8=22394
 Zn single crystals, stress-wave cleavage 8=21927

Francium

- Fr²¹² beam, recoil prod., for bombard. of Al foil 8=11952

Franck-Condon factors. See Spectra.**Franck-Read sources.** See Crystal imperfections/dislocations.**Fraunhofer lines.** See Astronomical spectra; Spectra; Sun/spectra.**Free radicals**

- acid amides, in liq. photolysis, e. s. r. 8=14435
 advances in atomic and molecular physics, book I and II 8=16171-2
 anion reactions, formed by e addition to unsaturated mols., e. s. r. study 8=14350
 p-benzosemiquinone anion dimers in soln., absorpt. spectra 8=21186
 benzyl, fluoresc. spectrum in methylcyclohexane, cyclopentane and methylcyclopentane, 4°K 8=12342
 benzyl, methyl and benzyl substituted, in solid solns., fluoresc. spectra vibr. analysis 8=13032
 4,4-dimethylcyclohexenone anion, e. p. r. 8=12304
 dinitrobenzene anions, dynamic freq. shifts in e. s. r. 8=4244
 diphenyl-amino dimer 8=7625
 dipyrityl mononegative ion and alkali metal ion biradical, e. s. r. and structure 8=4247
 direct i. r. spectroscopy 8=16367
 discharge-flow system, reactions 8=9700
 DPPH, absorpt. spectra, high press. low temp. effects 8=18579
 DPPH, cryst. structure 8=1317
 durene, irradi. cryst., e. p. r. 8=5528
 e. s. r. spectra, study by computer of average transients 8=6405
 emulsion polymerization, free radical mechanism, kinetics 8=14415
 fluorocarbons in soln., dynamic polarization of F nuclei 8=4627
 formation in polynuclear hydrocarbons, e. s. r. spectra 8=12307
 gaseous, e. s. r. study, results and anal. 8=12340
 hydrazyls form. by hydrazines electrochem. oxidation, e. p. r. obs. 8=5722
 Free radicals—contd
 hydrocarbons, e. p. r. spectroscopy meas. of g factor 8=12301
 imide, in liq. photolysis, e. s. r. 8=14435
 methanol, X-irrad., u. v. photolysis at 77°K 8=5750
 methyl, i. r. spectrum in solid Ar 8=7624
 nitrobenzene in alkaline soln., decay kinetics and electrochemical behaviour 8=21187
 nitrosobenzene, electrochem. oxidation in organic media, e. s. r. 8=14426
 organic, hyperconjugation and spin delocalization 8=4172
 organic, spectra in solid solns. and vibr. analysis 8=13032
 oxalate ion, i. r. and Raman spectra and symmetry 8=21154
 phenolphthalein and congeneric mol. crystals formation on plastic deform at high pressure 8=23033
 in polymerization, liquid phase, and polymer oxidation, e. s. r. study 8=14414
 in polymethylmethacrylate, γ -irrad., e. s. r. spectra obs. 8=4682
 polypropylene, e. s. r. spectra and photoinduced conversion 8=12352
 in polypropylene, γ -irrad., e. s. r. obs. 8=7628
 in powders, production and e. s. r. study in simple chamber 8=7619
 pyridine radical anions, e. s. r. 8=21171
 reactivity, effect of H bonding 8=7623
 RCHSR' type in X-irrad. sulphide-urea cpds., e. s. r. study 8=1314
 semiquinones in alcoholic soln., hyperfine interactions 8=7627
 short-lived, prod. by u. v. flash photolysis, e. s. r. spectrometer for study 8=12339
 in solution with P³⁴, nuclear-electron Overhauser effect, rel. to scalar interacts. 8=4626
 in solution, saturation in e. s. r. spectra 8=3278
 tetracyanoethylene, kinetics of formation 8=9686
 in, tetrafluoroethylene-hexafluoropropylene copolymers, γ -irrad., radical conversions 8=1326
 tetrafluoroethylene-hexafluoropropylene copolymers, γ -irrad., e. s. r. of radicals formed 8=1325
 2,2,6,6-tetramethylpiperidin-4-ol-1-oxide, structure 8=16370
 in toluene glow discharge prod. polymer films, obs. 8=21894
 triradical, electron reson. spectrum 8=12350
 tri-tertiary butyl phenoxy radical, proton-electron double reson. 8=12312
 d,l-valine, hindered rotations, e. s. r. study 8=4248
 vinyl cpds., reactions in pulse radiolysis 8=18745
 Würster's cation dimers in soln., absorpt. spectra 8=21186
 xylol from cryst. xylenes photolysis, fluoresc. spectra vibr. analysis obs. 8=12356
 Ag in irradi. metaphosphate glass 8=4990
 BrO, dipole moment from gas-phase electron reson. 8=12345
 C(CH₃)₃ from (CH₃)₃CCl γ irradi. at 77°K, struct. e. p. r. obs. 8=12349
 C(CH₃)₂CCl from (CH₃)₂CCl₂ γ irradi. at 77°K, struct. e. p. r. obs. 8=12349
 CCl₂, prod., and electronic and vib. spectra 8=1315
 CCl₃, photochemical prod. 8=12343
 CD, C² Σ^+ decay rates and predissociation probability 8=21185
 CF₃, photoionization 8=7724
 CF₃, in photolysis of CF₃I in matrices at 4.2°K 8=14440
 CF₃OO, in low-temp. soln. 8=9727
 CH, absorption and emission spectroscopy, in low-press. oxyacetylene flames 8=21189
 CH, C² Σ^+ decay rates and predissociation probability 8=21185
 CH, relative oscillator strengths and ht. of dissoc. 8=7618
 CH₂(CH₃)₂SiCl from (CH₃)₃SiCl γ irradi. at 77°K, struct. e. p. r. obs. 8=12349
 CH₂OH, ionization potential and heat of form. obs. 8=4245
 CH₃, i. r. spectrum in photolysis of methane 8=18737
 CH₃CO₂⁻ in γ -irrad. Na acetate, e. s. r. spectrum 8=4242
 CH₃-CR₂ radical in X-irradiated acetyl-(d,l)-alanine, spin-lattice relax. time 8=22906
 (CH₃)₂N, ionization potential and heat of form. obs. 8=4245
 C₂, absorption and emission spectroscopy, in low-press. oxyacetylene flames 8=21189
 C₃ absorpt. spectrum, diazopropyne photolysis obs. 8=16368
 C₃H₂ absorpt. spectrum, diazopropyne photolysis obs. 8=16369
 C₅H₅, cyclic radicals, e. s. r., total splitting parameters 8=4243
 Cl₃, i. r. spectrum 8=7620
 ClO, dipole moment from gas-phase electron reson. 8=12345
 ClO, kinetic studies 8=23125
 ClOO, matrix i. r. spectra 8=12344
 CN, Franck-Condon factors rel. to mol. constant var. 8=4173
 CaCO₃, X-irrad. cryst. 8=5105

Free radicals—contd

- GeH₄, struct. and Ge⁷³ coupling 8=12346
 H atoms trapped in irradiated frozen aq. solns. 8=18423
 HO₂ destruction on various surfaces 8=18704
 HO₂, e.s.r. in Ar at 4.2°K 8=18424
 NaNO₂, X-irrad. cryst. 8=5105
 NaSbF₆, e.s.r. of X-irrad. cryst. 8=5538
 NCF₂, u.v. absorpt. bands 8=7626
 NCO, matrix-isolated spectra 8=16369
 NO₂, paramagnetic resonance spectrum 8=7621
 O₂, e.s.r. in H₂O₂-urea addition compound, γ -irradiated at 77°K 8=2373
 OH, absorption and emission spectroscopy, in low-pressure oxyacetylene flames 8=21189
 OH, 18-cm transitions, Einstein A coeffs. 8=12351
 OH hydrated, bimolecular rate constants in aqueous solns. 8=2510
 OH, microwave spectrum, low-field Zeeman effect 8=4246
 OH, predissociation in chemiluminescence spectrum 8=12223
 OH reaction with oximes, e.p.r. 8=14394
 PO, rotational structures and perturbations 8=7622
 SH, dipole moment from gas-phase electron reson. 8=12345
 SO(Δ), dipole moment from gas-phase electron reson. 8=12345
 S³³O¹⁶, gas-phase electron reson. 8=12353
 SbH and SbD, absorpt. spectra 8=12354
 Si²⁹Cl₃, struct. and hyperfine coupling const., e.p.r. obs. 8=12349
 SiH₂, spectrum 8=12355

Freezing

- See also Melting; Supercooling.
 alloy, binary, slab, unidimensional solidification rel. to time-dependent surface temp. 8=21757
 alloys, binary, general soln. of dendritic crystn. eqn. 8=8174
 alloys, hydrostatic tension on solidification 8=21759
 aqueous solns. of macromolecules 8=21761
 aqueous solutions of non-polar gases 8=1618
 benzene under press., differential thermal analysis 8=9684
 benzonitrile, under press., differential thermal analysis 8=9684
 binary eutectic system, solidification, heat-transfer analysis 8=21756
 cast steel slabs, solidification, heat transfer model 8=8179
 composite growth from melts 8=4647
 enforced fluid motion, metal castings, grain structure 8=8435
 fixed points, 233°-661°C 8=244
 of flat casting at constant crystallization temp., Biot variational solution 8=1616
 fluids in forced flow, analysis 8=16926
 hydrostatic tension in solidifying alloys 8=21759
 hydrostatic tension in solidifying materials 8=21758
 ice from aqueous, effect of rate on dendritic solidification 8=8178
 ice, conference 8=21867
 ice formation in supercooled water, ultrasound effects 8=22102
 ice growth in supercooled aqueous solns., electrical effects 8=21762
 ice phases, selective nucleation using different org. nucleators 8=4805
 impurity distribution coefficient during directional solidification 8=16935
 ingot structure comp. dependence 8=16927
 interface vel. rel. to undercooling, impurity effects in thermal wave meas. 8=4651
 liquid-level sensor, superconducting, for slush hydrogen use 8=16929
 macrosegregation on solidification, and mold design effect 8=16930-1
 metals, extraction from molten state, thermal regime 8=8175
 organic mixtures, eutectic forming, normal freezing and constitutional subcooling 8=12973
 parahydrogen, ht. of fusion and density at up to 400 atmos. 8=16928
 n-pentane, solidification at high press. 8=21747
 point determination by differential thermal analysis 8=9684
 problems, analytical solution 8=4650
 rate for semi-infinite slab, effect of heat evolution 8=16932
 solutions, 2nd virial coeff. determ. 8=8017
 Stefans problem, generalized, soln. 8=8176
 supercooled liquids, nucleation of by cavitation 8=16934
 Al and Al-Al alloy, solid-liq. interface, radio-graphs 8=4646
 Al-Cu alloys, dendritic solidification 8=8177
 Al-4.5% Cu alloy, macrosegregation on solidification, and mold design effect 8=16930-1
 Al-Si, solidification process, study 8=1619
 Ge undercooling 8=4649
 He³, freezing curve, press. var. 8=3118
 He³-He⁴ mixture freezing curve, press. var. 8=3118

Freezing—contd

- Hg, invariance of photocurrent and work function 8=13939
 NH₄Cl and NH₄OH electrical effects 8=1587
 α P₄, isenthalpic, solid/liq. interface temps. 8=21755
 Pb-Sn alloys, composite growth from melt 8=4648
 Pb-Sn alloys, lamellar stability on solidification 8=4785
 Pb-Sn eutectic, undercooling at interface 8=16933
 Se, amorphous, atomic radial distrib. function rel. to quenching from different melt temps. 8=1714
 ZrTiO₄, freezing point determ. of incongruently melting material 8=1608
Frenkel defects. See Crystal imperfections/interstitials.
Frequency. See Time measurement.
Friction
 See also Internal friction
 coeff. meas., applicability of results 8=22302
 discs, rough rotating, torque 8=6044
 lubrication and wear, conference, Plymouth, England (1967) 8=13521
 metalworking, role of surface energy of adhesion 8=5034
 motion of body over tangentially vibr. surface 8=19493
 pendulum, design for significant reduction 8=10527
 polymers reinforced with C fibres 8=13618
 reactor, surface factor for coolant flow 8=1131
 steel, exoelectronic emission due to sliding friction, obs. 8=18254
 steel, surface, rel. to carbide diffusion 8=17788
 Teflon on steel, adhesion component modification by γ irradiation, obs. 8=17842
 thermal stresses in elastic half-space, elastohydrodyn. lubrication 8=14958
 thrust bearing, hydrostatic, MHD lubricated, effects of inertia 8=8809
 turbulent flow, meas. with heat transfer 8=12750
 unsymmetrical, pressure loss in high pressure cylinders 8=14909
 vibrating solid, high frequency behaviour 8=3023
 vibration incidence, critical velocity 8=10682
 Al, exoelectronic emission due to sliding friction, obs. 8=18254
 Co hexagonal single crystal surface and sapphire ball rel. to superficial plastic deformation 8=17771
 Fe, exoelectronic emission due to sliding friction, obs. 8=18254
Frictional electricity. See Electric charge; Electrostatics.
Fuel cells. See Electricity/direct conversion.
Fugacity. See Diffusion in gases; Kinetic theory/gases.
Functions.
 analytic, determ. from its modulus on the boundary 8=1576
 Chebyshev polynomials, fitting to equidistant points 8=1499
 control problems, optimal, gradient method 8=2883
 distribution, resolution distortion due to experimental apparatus 8=6008
 Green, in atomic and molec. calc. 8=4035
 Green, iterative solution for $\Delta U = f(M) + g(M)V(M)$ 8=7495
 Greens, formulation of Lagrangian field theory 8=20160
 Green's funct. with boundary conds. containing non-normal directional derivs. 8=6017
 Green's in higher order corrections to particle-hole excitations 8=15932
 H, appl. to resonance radiation transfer 8=6116
 Hermite polynomials, roots and weight factors tables 8=19370
 Laguerre polynomials, roots and weight factors, tables 8=19370
 menomorphic of order <2 , in scatt. length rel. to complex ang. momentum 8=15697
 M, reduced, in S-matrix theory 8=15625
 N, in elementary particle theory, integral eqn. reduced to Tamarkin form, removal of singularity 8=20314
 one-variable, uniform polynomial approximation, computer programme 8=19375
 partial distribution, integral equations for 8=10619
 periodic, calculation of autocorrelation 8=14938
 prolate spheroidal, asymptotic representations 8=19357
 spherical harmonic expansion of $f(r_{AB})Y_L^M(\theta_{AB}, \phi_{AB})$, radial depend., integral form. 8=19354
 thermodynamic Green's, zero-freq. behaviour 8=113
 time-correlation, for nonlinear chem. rate consts. 8=6113
 time-correlation, for transport coeffs. 8=6112
 transition in inhomogeneous media 8=20102
 two-point, field quantized according to Fermi statistics 8=3419
 two variational methods, a comparison 8=19356
Fundamental concepts. See Physics fundamentals.
Fundamental constants. See Constants.
Fundamental particles. See Elementary particles.
Furnaces. See Heating.
Furry theorem. See Quantum electrodynamics.
Fusion. See Heat of fusion; Melting; Nuclear fusion.

g-factor. See Elementary particles; Gyromagnetic ratio; Nucleus; Spectra.

Gadolinium

deformation planes after dehydrogenation and hydride habit planes 8=8728

Gadolinium—contd

- ferromagnetic, critical attenuation of sound near Curie temp. 8=22101
 ferromagnetic lattice, hyperfine magnetic field on Sm^{150} 8=2335
 hyperfine field from conduction-electrons 8=1633
 internal friction obs., magnetic damping effect 8=14020
 M_{IV} and M_V absorpt. lines and edges 8=5602
 magnetic study by neutron diffraction 8=14021
 Gd I, Zeeman effect rel. to g-values of levels 8=4077
 Gd II, Zeeman effect rel. to g values of levels 8=4076
 Gd³⁺ in BaF_2 and SrF_2 , optical spectra 8=23015
 Gd³⁺, energy levels and cryst. field in LaCl_3 8=16975
 Gd³⁺ impurity centres in SrF_2 , temp. effects 8=8703
 Gd³⁺ ion, energy structure 8=2421
 Gd³⁺, e. s. r. in $\text{SmCl}_3 \cdot 6\text{H}_2\text{O}$ single crystals 8=9427
 Gd³⁺: $\text{Sm}(\text{NO}_3)_3 \cdot 6\text{H}_2\text{O}$, e. s. r. 8=18435
 Gd³⁺ in YVO_4 e. p. r. 8=9428
 in ThO_2 , spectrometric determ. 8=18787

Gadolinium compounds

- heat capacity singularities below 1°K 8=22115
 Gd phosphate-vanadates, struct. and luminesc. 8=14330
 GdAlO₃, antiferromag. order, from optical absorption studies 8=22880
 GdB₃, (x=4, 6), prep. and props. 8=17384
 GdCl₃, crystal structure 8=8523
 GdCl₃, with dipolar interactions, magnon spectrum analysis 8=9353
 GdCl₃, ferromagnetic high-temp. expansion coeffs. calc. 8=9352
 Gd-Dy alloys, magnetocrystalline anisotropy 8=9350
 GdFe garnet, epitaxial film on YAl garnet, chem. vapour deposition 8=13099
 GdFe garnet wafer for magneto-optic memory element 8=19755
 Gd₂O₃, u.v. reflect. spectra 8=18524
 Gd₂O₃, vapour pressure from 2350° to 2590°K 8=21789
 Gd-Tb alloys, magnetocrystalline anisotropy 8=9350
 GdWO₄, determ. of Gd by γ -activation 8=9766
 Gd-Y alloys, mag. props. 8=5472
 Gd-Yt alloy, spin-disorder resistivity meas. 8=9007

Galaxies

- See also Nebulae.
 analogue of H-R stellar diagram 8=23590
 background linear polarization at $l^{II} = 140^\circ\text{C}$, $b^{II} = 6^\circ$ 8=23595
 blue compact, Leo A and B clusters, suitability for verification of redshift for light from ultradense galaxies 8=19221
 bright, identification with radio sources in 4 C catalogue 8=10288
 bright, south of +20° declination, optical positions 8=10259
 Centaurus, stellar assoc., statistical obs. 8=10264
 close encounters, possibilities and frequencies 8=19215
 clusters, analysis of clustering distribution 8=2798
 clusters and assoc., nearby, β Cephei stars, photoelectric search 8=2786
 clusters and assoc., nearby, new variable stars, data 8=2787
 clusters formed by compact galaxies, discovery of two new ones 8=19220
 clusters, previously identified radio sources 8=19212
 clusters, radio emission obs. 8=19211
 compact, condensation to neutron-star-studded 8=14808
 cosmic mag. field, generation 8=23583
 cosmic rays, intergalactic, solar modulation and p and He source spectra 8=2771
 counter-jet in M87 8=23591
 cylindrical, in gravitational experiments 8=10086
 disks, time-independent, axisymmetric, self-consistent models 8=10271
 disc, types of vel. distrib. and stability 8=10262
 elliptical, collisionless relax. rel. to light distrib. statistical mechanics 8=10273
 escape vel. effect on dist. of residual velocities 8=14800
 evolution and structure, conference, Brussels Belgium (1964) 8=19210
 formation in early stages of universe due to baryon inhomogeneity 8=23474
 formation from an initial spectrum of primordial fluctuations 8=14809
 formation rel. to fluctuations in the primordial fireball 8=10075
 formation, thermal instability in expanding universe 8=14733
 forms and activity, unifying theory 8=14803
 Fornax dwarf, integrated magnitudes and colour indices from photoelectric scans 8=10276
 4 near groups, conc. of irregular dwarf galaxies 8=19218
 galactic cosmic rays, anisotropy in intensity distribution 8=23488
 halo, selected area 54, stellar density by 2-colour photometry 8=19214
 hydrogen neutral, detection, and model profiles investigated 8=5934
 instability, absolute and convective rel. to evolution 8=10261
 intergalactic arms lifetime and star form. 8=10260
 intergalactic mag. field and density, radar obs. 8=10236

Galaxies—contd

- "integral sign" redshift, vel. field and evolutionary stage 8=10270
 irregular galaxies of M82 type 8=19222
 Jacobi's ellipsoidal figures under influence of halo, gravitational stability 8=14725
 Magellanic Cloud Large, X-rays in 8-80 keV, search with sounding rocket 8=5916
 Magellanic Clouds, obs. rel. to massive stars evolution 8=10274
 mag. fields and cosmic rays, role 8=23585
 mass distribution from radial velocities data 8=14801
 mass distribution from radial velocities and photometry 8=5939
 mass-luminosity ratio, variations 8=19216
 metagalactic radiophone intensity in evolutionary models of Universe 8=10076
 metagalactic turbulence and fragmentation of matter, rel. to microwave relict. rad. 8=19079
 metagalaxy anisotropic expansion, rel. to weakly interact. particles 8=5844
 M31, extent of radio emission 8=23596
 M33, H II, kinematical and physical data from interferometric obs. 8=23568
 M87 jet, radiation and props. 8=23592
 NGC383 (radio source 3C31), beamwidth obs. 8=10267
 NGC 1808, velocity field, rotation and mass 8=10277
 NGC 2403 in the M81 group, stellar content and distance 8=23593
 NGC 3516, nucleus spectral variations 8=23589
 NGC4151, O III fluorescence in u.v. spectrum 8=5937
 NGC 4151, optical and near i. r. spectrum of nucleus 8=23588
 NGC 4449, rotation obs. 8=19217
 NGC 4486 ejection, spectrum 3730-6300 Å 8=10279
 NGC 4631/4656 binary system, neutral H observations 8=10275
 NGC 5548, nucleus electron temp. var. obs. 8=14805
 NGC6166 (radio source 3C338), beamwidth obs. 8=10267
 NGC 6611, 6523 and 7000, electron densities from 4 cm obs. 8=23570
 nonexistence of cluster of clusters of galaxies 8=10269
 normal spiral, radio radiation at 430 and 611 MHz 8=5933
 nuclei and activity 8=23587
 nucleus, i. r. obs. for structure determination 8=10250
 origin, models of concentration of matter in expanding universe 8=14724
 with peculiar nuclei, properties 8=10265
 plasma, synchrotron and gyromag. relativistic, amplification dependence on polarization 8=21345
 proton relativistic anisotropic plasma, transverse e. m. wave effect 8=5850
 radio, as cosmological probes 8=23597
 radio emission of 47 bright galaxies 8=5931
 radio, inverse, Compton effect due to interaction with cosmic black body radiation 8=19213
 radio, 9.55mm, flux density obs. 8=23599
 radio, O III emission rel. to fine struct. const. time var., obs. 8=14727
 radio observations, r. f. spectra of normal spiral, flux densities of radio sources 8=5935
 radio radiation of normal galaxies at 8 cm flux densities and angular dimensions obs. 8=10266
 radio, sky temp. calc. 8=5936
 radio sources 3C79 and 3C192, structure obs. 8=23603
 radio sources in declination range + 18° to +20°, freq. 750 and 1410 MHz, pencil beam survey 8=23605
 radio, 1418 MHz radiation, upper limits to degree of circular polarization 8=23600
 radiogalaxies and quasars, space distribution 8=23630
 radioluminescence function 8=10272
 reddening of light, gravitational contribution 8=14804
 Seyfert, envelopes, structure and masses 8=19176
 Seyfert, new, intrinsically bright 8=14802
 Seyfert NGC 1068, as extragalactic nebula 8=10227
 Seyfert NGC 5548 nucleus props., spectral obs. 8=10263
 Seyfert, nuclei struct., spectrophotometry obs. 8=10278
 spiral arm, magnetic field and gas outflow association 8=10280
 spiral, orbits and velocity distribution of population I stars 8=5932
 stars and gas evolution in 8=19132
 Stephan's Quintet, 3 colour photometer obs. 8=5938
 structure and evolution 8=23586
 containing supernovae, class and absolute value distrib. 8=19223
 systematic red shift, explanation 8=19219
 3C191, Si/C ratios 8=14810
 3C revised catalogue, re-examination 8=23602
 Triangulum spiral, M33, spectrophotometric studies of diffuse nebula NGC 604 8=19193
 triple, dynamics, trajectories and decay, computer calc. 8=19101
 HI regions, i. r. emission and m. h. d. shock waves 8=23566
 H II regions, higher-order high-quantum H recombination lines 8=23569
 H_{II} regions, radial velocities and kinematics 8=19208
 H II regions, temperature obs. 8=10251
 H II, stimulated emission of r. f. lines, enhancement by small departures from thermal equil. 8=23567

Galaxies—contd

- OH galactic, radio emission, brightness and temporal variation 8=10253
- the Galaxy**
- anticentre, stellar distrib. obs. 8=19207
- central globular cluster 8=5929
- central region, photographic obs. 8=2796
- Circinus (SA195), photographic UB_V photometry of 634 stars, catalogue 8=19202
- cosmic ray e prod., model from secondary spectrum 8=19198
- cosmic ray trapping 8=23491
- Crux regions, photometric standard sequences 8=19205
- Gould's belt, kinematics from simple model as projection from Orion spiral arm 8=10255
- inertial frame of reference in stars near the earth 8=14739
- interstellar hydrogen, radial motion 8=10243
- magnetic field strengths 8=14798
- mass model, velocity dispersions 8=2797
- Milky Way, southern, distrib. of OB star groups 8=10111
- neutral hydrogen in Gould's belt, influence on modelling 8=10256
- north galactic spur, structure of mag. fields 8=10254
- precessional corrections, in systems GC, FK3, N3O and FK4 8=23584
- proto-, He and metal abundance vars. from globular cluster to cluster 8=14799
- I Puppis and Norma, OB stars radial vels. rel. to struct., obs. 8=23594
- Puppis, three regions, magnitudes and colours for 78 stars 8=19204
- radio noise, ionospheric attenuation, 25 and 21.3 MHz, Ahmedabad, 1957-64 8=14673
- radio sources at 4170 MHz, high resolution obs. 8=5928
- rotation, in systems GC, FK3, N3O and FK4 8=23584
- Scorpius, interstellar K line and λ 4430 absorption band 8=19201
- South Pole, new C star 8=14755
- spiral arm population distrib. 8=10248
- spiral arms, shape, stellar positions, movement of gases etc. 8=19203
- survey of southern sky at 85 MHz 8=10257
- two new variables found 8=23548
- u. v. emission in drapason 1225-1340 Å and in L α line in dira of Milky Way 8=19206
- X-ray sources, 1964-65 survey 8=10252
- HI region, OH, excitation temp. of 18 cm line 8=10299
- HII regions, electron temperature 8=2795
- H γ regions, H recombination line 158 α , obs. 8=5930
- H β regions, OH emission mechanism 8=10258
- HII regions, W49 radio source 8=10249

Gallium

- crystal structure 8=22024
- cyclotron effective mass obs. 8=13717
- cyclotron resonance, mass determinations 8=13687
- Fermi surface study, by u.s. geometric reson. 8=8935
- glasses, e. s. r. study 8=18420
- line-broadening collisions, cross-sections 8=12083
- liquid, structural sensitivity of thermoelectric props. 8=16878
- open-orbit electrons in crystal, velocity 8=13640
- periodic size effect in high magnetic field meas. 8=3161
- self-diffusion 8=22152
- r.f. size effect, temp. and freq. dependence 8=9099
- single crystals, therm. cond., size effects 8=17545
- specific heat near 1.7°K, no anomaly, rel. to absence of mag. transition 8=1871
- superconducting boundary scattering rel. to critical temp. shifting 8=13747
- superconducting energy gap and anisotropy meas. by tunneling effect, 0.36-1.1°K 8=22546
- ultrasonic wave absorption 8=4922
- velocity of sound, quantum oscs. 8=13351
- Ga in GaAs and GaP X-ray K-absorption spectra 8=2420
- GaBr phthalocyanine, luminesc. singlet-singlet transitions 8=18591
- in Si, implanted atoms location and lattice disorder, obs. 8=17414
- in Si, photoexcitation lines, anomalous broadening rel. to optical phonons, obs. 8=5601

Gallium compounds

- gallate i. r. glasses, props. 8=22954
- junction laser, e. m. cavity properties 8=19996
- suboxide, structure in gaseous phase by e-diff. 8=16290
- Ga $_x$ Al $_x$ As diodes, stimulated emission at 77°K 8=19997
- n-GaAs, in mag. field, circularly polarized waves, doping rel. to optical absorpt. 8=22981
- GaCl phthalocyanine, luminesc. singlet-singlet transitions 8=18591
- Ga-Fe system, mag. props. 8=22817
- Ga-Fe system phase transform temps., comp. and struct., obs. 8=21749
- Ga $_{0.85}$ Fe $_{0.15}$ O $_3$ magnetically ordered crystal, electron resonance spectrum 8=14087
- Ga $_2$ -Fe $_2$ O $_3$, Mössbauer investigations 8=13028
- GaH, mol., $a^3P_1 \rightarrow X^1\Sigma^+$ transition 8=7515
- Ga $_x$ In $_{1-x}$ As alloys, electroreflectance rel. to band structure 8=2419

Gallium compounds—contd

- Ga $_x$ In $_{1-x}$ As alloys, optical energy gap variation 8=18040
- 5Ga $_2$ O $_3 \cdot 3M_2$ O $_3$, (M = rare earth), mag. props. 8=2340
- GaP crystals, anomalous photoconductivity response 8=18241
- GaP, dielectric dispersion and phonon line shape 8=14215
- GaP diffused single crystal layers p-n junctions photoelectric properties 8=5406
- GaP, electron energy loss probability, retardation effects 8=22497
- GaP epitaxial layers with high mobility 8=9101
- GaP films, vacuum deposited, polymorphism 8=21883
- GaP, Ga X-ray K-absorption spectra 8=2420
- GaP, Hall coefficient and conductivity, 4.2-300°K 8=9100
- GaP, hot-electron-phonon interactions 8=5245
- GaP, inter-band piezoelectr. 8=18529
- GaP, intrinsic optical absorption 8=2417
- GaP, large crysts. soln. grown, prep. and props. 8=17234
- GaP miniature photodiode 8=15525
- GaP: Ni, absorption spectrum 8=22983
- GaP p-n junctions, microplasma obs. 8=5310
- GaP, photoelastic props. rel. to use as acoustic light modulators and scanners 8=9496
- GaP, thermal expansion coeffs. from -62° to 200°C 8=1880
- GaP, vapour-grown crystals, effect of substrate orientation 8=13136
- GaP-Cl $_2$ -H $_2$ system, vapour transport in open tube, thermodynamics 8=12699
- Ga-P-Te system, phase equilibrium 8=17082
- GaSb, vapour press. as function of temp., and thermal stability 8=21786
- GaSb, diffusion and solubility of Li 8=13409
- n-GaSb, electron mobility carrier conc. dependence at 77°K 8=2195
- GaSb, Faraday rotation, spectral emittance and Hall effect 8=22587
- GaSb injection laser, emission in pulsed conditions 8=6462
- GaSb, laser diode, spectrum fine structure 8=444
- GaSb, photoelectromagnetic receivers with optically polished thin elements, sensitivity and inertness 8=6275
- n-GaSb, Shubnikov-de Haas oscs., beating effects 8=9102
- GaSb, surface stress in polished and clean (111) surfaces 8=8849
- GaSb, thermal expansion from 2-40°K 8=4937
- GaSb-InSb alloys, thermal and elec. props. at high temps. rel. to comp. 8=4944
- GaSb-GaAs alloy, pressure-sintered, densification and thermoelectric props. 8=4697
- GaSe crystal, dislocations and optimal visualization etchant 8=1973
- GaSe, generation of second optical harmonic 8=5600
- GaTiBO $_5$ (B=Nb, Ta, Sb), crystal structure and fluorescence 8=4879
- gallium arsenide**
- See also Semiconducting materials/gallium arsenide.
- coated with Si $_3$ N $_4$ film, i. r. absorpt. 8=14262
- diffusion of Zn under excess As pressure 8=22153
- elastic constants rel. to charge carrier concentration 8=13575
- electrodes, single cryst., H evolution 8=14421
- e. m. diffraction when subject to u. s. waves 8=22942
- electrooptical effect, meas. at 10.6 μ 8=18515
- electroreflection meas. 8=2422
- epitaxial deposition in Ar 8=17253
- epitaxial films, propag. of growth striae 8=17129
- epitaxial growth from Ga soln. 8=4829
- epitaxial p-n junctions, spontaneous and coherent light emission 8=6466
- Fermi level, influence of volume dope 8=8934
- growth of InAs films on 8=17132
- Gunn oscillators, inhomogeneity effects 8=362
- injection laser, catastrophic degradation 8=6461
- junction laser, operation on diamond heat sinks at 200°K 8=6465
- junction laser, threshold current calc. 8=6467-8
- laser diode, c.w.-operated, junction temp., current depend. 8=442
- laser diodes, influence of junction structure on parameters 8=6464
- laser diodes, low threshold 8=19995
- laser diode operating at room temp. 8=441
- laser, dual type, quenching resonance 8=443
- laser, excited by electron beam, pulsed operation 8=6469
- laser threshold current density temp. dependence 8=6463
- luminescence, stepwise excitation 8=23055
- magneto-optical absorpt., interband, meas. at 2°K, 77°K and room temp. 8=22985
- n-type, Raman scatt. by mixed plasmon-phonon modes, polarization and intensity obs. 8=5599
- photoelastic props. rel. to use as acoustic light modulators and scanners 8=9496
- photo-Hall effect, high field 8=9105
- piezoelectric, ultrasound generation under Gunn effect 8=22100
- p-n junctions, diffused, luminescence spectra 8=5663
- p-n junction laser, direct investigation method 8=445

Gallium compounds—contd

gallium arsenide—contd

- p-n junction, max photo-e.m.f. on laser excitation 8=9252
 Raman scattering by coupled optical-phonon-plasmon modes 8=22984
 semi-insulating, light amplitude modulation, $\lambda=10.6\mu$, using electro-optical effect 8=9530
 solar cell, thin film 8=19735
 solar cells, thin film on Mo and Al, fabrication and props. 8=10853
 thermal expansion coeffs. from -62° to 200°C 8=1880
 tunnel-diode p-n junctions, alloying temp. rel. to characts. 8=22631
 twins and stacking faults obs. for vapour grown crystal 8=1982
 vapour pressures and phase equilibria, 900-1200°K 8=4664
 wedge-shaped, photo-voltages rel. to incident angle of illum. 8=5398
 X-ray K-absorption spectra of Ga 8=2420
 Ga-As-M (M = Au, Ag or Cu), equil. ternary liquidus-solidus phase diagrams 8=4639
 GaAs-Cs-O photoemission 8=22718
 GaAs-Ga(AsP) heterojunctions, photocurrent, forward current injection modulation 8=13844
 Ga(As, P), thermal expansion coeffs. from -62° to 200°C 8=1880
 GaAs:Zn, photoluminescence, effect of As pressure 8=23053
 Ga-As-Zn system, gas phase equilibria 8=21764
 (GaIn)As-GaAs heterojunctions, photocurrent, forward current injection modulation 8=13844
 Si diffusion, site transfer 8=17574
 SiCl₄, use in epitaxial growth 8=13146
 Si₃N₄ deposition, by SiCl₄-NH₃-N₂ system 8=13094
 Zn-diffused, precipitates formation 8=17617
 Galvanomagnetic effects. See Magnetoelectric effects.
 Galvanothermomagnetic effects. See Magnetoelectric effects;
 Magnetothermal effects.
 Gamma-ray sources. See Gamma-rays.
 Gamma-ray spectra

- See also Nuclear decay theory.
 computer decomposition 8=15943
 cosmic, effects of decaying nucleon isobars and hyperons 8=23489
 differential energy and angle spectra in water and air, for Cs¹³⁷ point source 8=11819
 of fission gases released from n-irrad. UO₂ graphite pellets 8=4016
 fission-product contamination of earth, aircraft meas. 8=9895
 μ capture reactions, Doppler broadening rel. to meas. ν - γ ang. correl. 8=16065
 from n reactions on 14 elements, prompt γ rays and prod. processes, 14.7 MeV 8=7211
 photopeak analysis by computer programme 8=6792
 of products from U fast-n fission, at selected times after fission 8=3984
 radioactive nuclei 8=16019
 stabilizer correcting gain drifts of detector heads, transition probabilities E_0 , M_1 and E_2 , lifetimes of excited states 8=936
 Ag^{108m} \rightarrow Pd¹⁰⁸ 8=7092
 from Ag^{110m} 8=982
 Al²⁷(p, γ)Si²⁸, Q-value meas. of γ -ray energy 8=3574
 Au¹⁹⁸, beta-gamma correlations 8=3887
 Ba¹³⁴ following Cs¹³⁴ \rightarrow Ba¹³⁴ decay 8=7139
 Be⁹(He⁹, α)Be¹¹ 8=3964
 Bi²⁰⁵ \rightarrow Pb²⁰⁵, to determ. which transitions feed 13/2⁺ isomeric level 8=997
 Bi²⁰⁷, 569.6, 1063.6, 1771 keV obs. 8=11440
 Bi²¹⁴, energies and rel. intensities above 1 MeV 8=11788
 Br⁸⁷ decay, in atmosphere 8=2611
 Ce¹³⁶ decay 8=20721
 Ce¹³⁶ and K-conversion coeffs. and transitions multiplicity, 119-1469 keV 8=11763
 Co^{58m} \rightarrow Co^{58g}, obtained by radiating nickel-foil with deuterons 8=1011
 Co⁶⁰, by Ge p-i-n detector 8=16010
 Co⁶⁰, n.m.r., orientation destruction by resonant absorption 8=18331
 Cs¹³⁶ and decay scheme, obs. 8=11761
 Cs¹³⁷, by Ge p-i-n detector 8=16010
 Eu¹⁵⁵ levels from Sm¹⁵⁵ decay 8=7105
 Er¹⁶⁷ from thermal n capture by Er¹⁶⁶ 8=1083
 Er¹⁷³, new radioactive isotopes 8=20756
 Fe⁵⁷(n, γ)Fe⁵⁸, thermal n-capture 8=1080
 Fm²⁵³ \rightarrow Cf²⁴⁹ 8=11836
 Fr²²¹, γ transitions studied by α - γ coincidences 8=3845
 Gd¹⁴⁹ \rightarrow Eu¹⁴⁹ \rightarrow Sm¹⁴⁹ decay chain 8=7143
 Gd¹⁵³, by Ge p-i-n detector 8=16010
 Ge, from thermal neutron capture 8=3810
 Hg²⁰⁸, by Ge p-i-n detector 8=16010
 Ir, from thermal neutron capture 8=3810
 Ir¹⁹⁵, ^{195m} decay 8=11827
 K⁴¹, resonances in proton bombardment 8=16082
 Lu¹⁷⁶ decay 8=1023
 Mn, from thermal neutron capture 8=3810

Gamma-ray spectra—contd

- Mn⁵⁴ n.m.r., orientation destruction by resonant absorption 8=18331
 Na²², from F¹⁹(α , n γ)Na²², and Ne²⁰(He³, p γ)Na²², reactions, Doppler broadening 8=3801
 Nd¹⁴³, ¹⁴⁵, following neutron capture 8=16032
 Nd¹⁴⁷, decay using Ge(Li) spectrometer 8=1018
 Ne²⁰ 4.97 MeV 2⁻ and 7.02 MeV 4⁻, states weak decay, obs. 8=15959
 of Np²³⁷, obtained with Ge-Li detector 8=20732
 Os^{162m}, neutron emission 8=16001
 Os¹⁹¹ β decay 8=3886
 Os¹⁹³ \rightarrow Ir¹⁹³, levels assigned 8=11826
 Pd¹⁰⁶, linear polarization correl., solid angle correction 8=11433
 Po²¹⁴, 10 new γ -rays 8=3844
 Pr¹³⁹, bremsstrahlung-induced activity 8=986
 Pr¹³⁹ \rightarrow Ce¹³⁹ decay 8=7141
 Pt^{194m}, neutron emission 8=16001
 Pt¹⁸⁸, from Au spallation 8=1024
 Pt^{197m} and Pt¹⁹⁷ decays 8=7110
 Pu²³⁹ decay, 300-450 keV 8=16049
 Ra²²⁶, and derivatives, low-energy obs. 8=16046
 Re¹⁸⁰, 2.5 min. decay 8=3885
 Rh⁹⁹ \rightarrow Ru⁹⁹ 8=978
 Rh¹⁰², 2 year, singles and coincidence spectra 8=20751
 S³⁴(p, γ)Cl³⁵, at 2079 keV, p γ -correlation 8=1063
 Sc⁴²(f, γ)³ 3 and 5 spin states obs., 1500 keV 8=15973
 Sm¹⁴⁵, bremsstrahlung-induced activity 8=986
 Sn¹²⁵ \rightarrow Sb¹²⁵ 8=3874
 Sn(Ar⁴⁰, xn), cpd. nuclei rel. to ground-band collective levels population, obs. 8=11953
 Ta¹⁸⁰ decay 8=1023
 Ta¹⁸², decay, sum coincidence studies 8=3884
 Te¹¹¹, recoil nuclei with 290 \pm 27 and 660 \pm 28 keV 8=11818
 Te^{119m} decay 8=3877
 Te(Ar⁴⁰, xn) cpd. nuclei rel. to ground-band collective levels population, obs. 8=11953
 Tm¹⁷² decay, spins and parities of Yb¹⁷² 8=11823
 of U fission products, short lived 8=7263
 U²³³, identification of 7 new lines 8=20760
 U²³⁵ thermal neutron fission, total γ energy release 8=7247
 V⁴⁸, β - γ circular polarization correl. meas. 8=7131
 Xe¹²³ decay, and energy level scheme 8=7138
 Y⁸⁹, isospin analogue resonance decay 8=11754
 Y⁸⁹(n, γ)Y⁹⁰, separation energy 8=7215
 Gamma-ray spectrometers
 See also Beta-ray spectrometers; X-ray spectrometers.
 Compton-effect, compensation 8=11448
 Compton, improved sensitivity by replacing NaI(Tl) scintillator by an organic one 8=6788
 Compton scatt., excitation of nuclear resonance fluoresc. 8=20666
 Compton, with 2 summing Ge(Li) detectors, 150-350 kV, reduction of tail 8=6789
 double crystal diffraction for high energy (n, γ) reactions 8=11442
 double-focusing magnetic pair spectrometer 8=6793
 gain and baseline discrepancy adjustment 8=11441
 high-resolution production by cooling 8=6811
 Hoogenboom method, apparatus with semicond. detector 8=16011
 low-level, NaI(Tl) crystal with quartz window, in 20 cm thick Fe room underground 8=6790
 Mössbauer, attenuation coeffs. of plastic and metal mounting materials 8=3579
 Mössbauer, constant velocity, automation technique 8=8210
 Mössbauer, MS10 8=693
 Mössbauer spectrometer 8=15722
 Mössbauer, time analyser for vel. precision meas. 8=20361
 neutron capture, excitation of nuclear resonance fluoresc. 8=20660
 n-capture, thermal, Ge(Li) 8=3576
 n radiative capture, anti-Compton 8=6785
 n radiative capture, high sensitivity 8=6783
 plastic scintillation, ASG-48, aerial, calibration 8=20364
 positron annihilation radiation meas. efficiency 8=17905
 semiconductor detectors and cooled pre-amplifier, X-ray range 8=698
 semiconductor, gain stabilization with digital system 8=11439
 semiconductor, noise, trapping and energy resolution 8=6791
 Ge(Li) annular detectors 8=6787
 Ge(Li), calibration, non-linearity of amplifier-analyzer system 8=11440
 Ge(Li) detector applications 8=15630
 Ge(Li) detectors, high resolution, fabrication and use 8=6782
 Ge(Li) detectors in parallel 8=6781
 Ge(Li), Compton, reduction of background by use of single crystal 8=697
 Ge(Li), determ. of full peak and 2-escape peak efficiencies 8=6784
 Ge(Li) photopeak analysis by computer programme 8=6792
 Ge, p-i-n, for nuclear decay 8=16010
 Ge(Li), 30 c.c., coaxial 8=6786

Gamma-ray spectrometers—contd

- Ge(Li), and NaI, 3-crystal high resolution 8=3844
 Ge(Li)-Na(Tl), high efficiency 8=20365
 H_2O , in the vicinity of nuclear power stations 8=4032
 Mn^{54} reference source, calibration 8=20750
 NaI scintillator, for geological logging 8=14528
 NaI(Tl) photopeak analysis by computer programme 8=6792
 NaI(Tl) 64-channel probe for 0.05-9.6 MeV 8=20363
 Zn^{65} reference source, calibration 8=20750

Gamma-rays

- See also Cosmic rays/photons.
 background, linear accelerator, reduction by beam shaping 8=15655
 beams, equipment for production 8=7118
 diffraction in crystal structure deter.ms. 8=17326
 field, near-surface atm., effect of rock and soil moisture 8=9795
 $\gamma + p \rightarrow \pi^+ + n$, in hydrogen 8=3626
 heating calculations, use of infinite medium spectra 8=7345
 image, conversion to visible image by solid scintillators 8=9587
 isotropic obs., rel. to cosmic blackbody theory 8=23485
 from n reactions on 14 elements, prompt γ rays and prod. processes, 14.7 MeV 8=7211
 in p bombarded spherical shell shield, dose rate 8=3568
 source, spent fuel elements, in irradi. plants 8=16163
 source up to 3.5 MeV for calibrating detectors 8=11428
 spectrum stabilizer, using 2 single channel analysers 8=20357
 from $\text{C}(n, n', \gamma)$ reaction, Monte Carlo calc. of unscatt. flux distrib. 8=7206
 Cs^{137} source in level control 8=1010
 Co^{60} cylindrical source, dose rates in radial direction at half-height of source, meas. 8=11434
 Co^{60} , source in level control 8=1010
 Co^{60} , specific constant 8=16029
 Cs^{137} , specific constant 8=16029
 Gd^{158} , Mössbauer effect meas. rel. to 79.5 keV transitions 8=3786
 I^{121} decay obs. 8=20752
 Pb^{211} radiation obs. 8=7149
 Po^{215} radiation obs. 8=7149
 Rn^{219} radiation obs. 8=7149
 Ru^{99} , M_1 - E_2 transition time-reversal invariance, Mössbauer obs. 8=7091

absorption

- See also Mössbauer effect.
 Mössbauer spectrometer mounting material criteria 8=3579
 Mössbauer spectroscopy, use of NGR in chemistry and solid state 8=692
 p photon-absorption sum rule applied to N, d, H^3 , He^3 8=3577
 steel, effect of tensile stresses 8=13483
 total mass absorpt. coeffs., by cryst. diffraction spectrometer 8=696
 Cu, effect of tensile stresses 8=13483
 Nd^{145} , recoilless nuclear resonance absorpt. rel. to energy level scheme 8=20724
 Zn-Al, spectrum distrib. compression effects 8=4999

angular distribution

- β - γ - γ correlation, CP violation in strong interactions 8=669
 e capture coeff. determ. 8=11798
 γ - γ correlation, effect of magnetic resonance 8=20761
 KX- γ directional correlations 8=20739
 nuclear structure studies with heavy ion bombard. 8=932
 particle range calc. for heavy ions 8=8756
 π -p charge exchange scattering at 96.6 MeV 8=6876
 rare-earth nuclei, $4^+ \rightarrow 2^+$ rotation 8=15938
 $\text{Cr}^{53}(\text{p}, \text{n})\text{Mn}^{53}$, 2, 3, 2, 4, 2.5 MeV 8=3926
 $\text{Cr}^{53}(\text{p}, \text{p}')\text{Cr}^{53}$ and $\text{Cr}^{53}(\text{p}, \text{n})\text{Mn}^{53}$, yields 8=7185
 Cs^{137} point source scattered by Al shields, determ. 8=16028
 $\text{Cu}^{93}(\text{p}, \text{n})\text{Zn}^{93}$, rel. to compound nucleus statistical model 8=1948
 $\text{Cu}^{65}(\alpha, \text{n})\text{Ga}^{68}$, rel. to compound nucleus statistical model 8=11948
 Eu^{154} , 1855-123 keV β - γ directional correl., energy depend. obs. 8=7142
 $\text{F}^{19}(\text{d}, \text{p}, \gamma)\text{F}^{20}$, 1.6 MeV rel. to reaction mechanism 8=16116
 Fe^{54} , after n scatt. branching ratios 8=3934
 Gd^{154} , rel. to M_1 - E_2 mixing, 693-123 keV transition obs. 8=15993
 Hg^{198} , $\gamma\gamma$ ang. correl. 8=11782
 Kr^{82} , $\gamma\gamma$ ang. correl. 8=11782
 $\text{Ni}^{60}(\alpha, \text{n})\text{Zn}^{63}$, rel. to compound nucleus statistical model 8=11948
 $\text{O}^{16}(\text{He}^3, \text{p})\text{F}^{18}$ for spin and parity of 1.131 MeV level of F^{18} 8=3800
 Pt^{192} , $\gamma\gamma$ ang. correl. 8=11782
 $\text{S}^{34}(\text{p}, \gamma)\text{CP}^5$, at 2079 keV, p, γ -correlation 8=1063
 Sm^{153} , β - γ ang. correl. obs. 8=16035
 Te^{122} , $\gamma\gamma$ ang. correl. 8=11782
 W^{182} , γ - γ angular correlation obs. 8=20728
 $\text{Zn}^{68}(\text{p}, \text{n})\text{Ga}^{68}$, rel. to compound nucleus statistical model 8=11948

Gamma-rays—contd**detection, measurement**

- See also Dosimetry; Gamma-ray spectrometers;
 Particle detectors; Radioactivity measurement.
 atmosphere, vertical intensity meas. 8=20639
 balloon-borne telescope, orientation system 8=19328
 calibration factors for low-energy γ -ray emitters 8=114
 calibration using Co^{60} source 8=11428
 camera, image intensifier system 8=15719
 contamination with natural radioactive materials 8=2035
 cosmic, high-energy meas. 8=19096
 crystal counter, correction for radial depend. in fast fission ratio meas. 8=20358
 Doppler-shift attenuation method for nuclear-lifetime meas. for low recoil vels. 8=7156
 dose from radioactive gas cloud, calc. 8=10448
 dose-rate, scattered 8=15718
 dosimeters calibration 8=11436
 dosimeter, personnel, with alarm 8=7346
 dosimetry with polyvinyl fluoride 8=6779
 energy determ. using digital computer programme 8=679
 energy determ. utilizing Q-value and transition consistency 8=3574
 film recording monitor using CsI(Tl) crystal 8=11444
 fission-product contamination of earth, spectra, aircraft meas. 8=9895
 4 π plastic scintillator detector with clinical applications 8=11304
 4 π gas counter, γ counting efficiency 8=605
 Geiger-Müller tube, efficiency rel. to incidence angle 8=6639
 geometric imaging props. of detectors 8=11437
 high energy, new Al spark chamber spectrometer 8=6685
 n- γ discriminating detector for n spectrometer 8=11627
 n- γ mixed, dose equiv. and quality factor, organic scintillator meas. 8=20561
 n- γ pulse-shape-discrimination in B loaded liq. scintillation detectors 8=20563
 nuclear lifetimes, coincidence technique for meas. 8=385
 photometer, single pulse reception, operational props. 8=3575
 polarization, linear, correls. of cascades 8=11433
 repetitive correction for finite resolving power of collimator in scintiscanning 8=20366
 scintillation dosimeter detector, energy depend. correction 8=15720
 shield for detectors 8=11438
 source activity by scintill. counter, corrections 8=3851
 spark chamber, magnetic core, suitable for satellites 8=6688
 spheroidal source, calc. of γ -dose on axis 8=3855
 thermonuclear explosion γ -glow 9 July 1962, riometer obs. validity 8=14636
 vacuum diode detector for high flux 8=15721
 C analysis in bulk materials, from n scatt. 8=18801
 CdTe, photopeak resolution 8=3578
 Co^{60} , appl. of Hoogenboom spectrometer 8=16011
 Co^{60} underwater source, flux density in air 8=1008
 CsI crystals, Na-activated, characteristics 8=6641
 Ge detector preamplifier, low noise, charge sensitive, for 8=6780
 Ge detectors for reactor meas. 8=1127
 Ge(Li) detectors, fabrication and appl. 8=15630
 Ge semiconductor detector, full registration efficiency 8=11429
 Ge(Li) coaxial detectors, current pulse generation 8=114
 Ge(Li) detectors and Compton effect 8=11435
 Ge(Li) detectors, cryostat systems 8=11443
 Ge(Li) detectors, high resolution, fabrication and use 8=6782
 Ge(Li), pulse height defects due to dead layer, correction 8=6777
 Kr-85 branching ratio 8=7133
 LiF, response to n- γ reactor fluxes 8=20899
 NaI-Tl, single cryst., with oxygen-containing impurities, response 8=18610
 Si(Li), cooled, linearity of charge conversion 8=6778
 $\text{Ta}^{181}(5/2^+ \rightarrow 7/2^+)$, circular polarization 8=991
 from $\text{Te}^{119\text{m}}$ decay, level structure of Sb^{119} obs. 8=7136

effects

- See also Nuclear reactions due to/photons.
 alkyl iodides, γ -irrad. at -196°C , ionic processes 8=1427
 N-allylmonomides of maleic and succinic acids, polymerization 8=23131
 anthracene, colour centres 8=17689
 dielectric liqs., energy to create ion pair 8=21723
 ethylene in solution, reactions in presence of O 8=14446
 frozen aq. solns., e.p.r. of trapped H atoms 8=18423
 fluorescent X-rays from γ -irradiated target, absolute yield meas. 8=23039
 glasses, aluminosilicate, thermoluminesc. spectrum 8=18
 glasses of $\text{Na}_2\text{O}-\text{TeO}_2$ system on e.p.r. spectrum at 77 and 295°K 8=9434
 graphite, energy spectra of electron calc. 8=20769
 n-hexane, elec. cond. obs. 8=21714
 n-hexane, theory of electrical conductivity 8=6628
 ice, solvated e spectrum obs. at 77°K 8=22989
 liquids, radiolysis at high press. 8=14444
 MOS diode on Si, Co^{60} γ -rays effect on surface state density and oxide charge density 8=22641

gamma-rays—contd
effects—contd

- noise pulses from photomultiplier tubes 8=3216
paraffin block (human body imitation) 8=615
phosphates, glassy and cryst., e. s. r. 8=22913
polymethylmethacrylate, trapped free radicals, e. s. r.
spectra obs. 8=4682
polypropylene, free radicals prod., e. s. r. obs. 8=7628
polytetrafluoroethylene, carbon-black filled 8=17700
scintillation in plastics 8=9656
water, e-photon cascade calc. 8=21722
TFE-HFP copolymers, dielectric props. 8=9202
Al, energy spectra of electron calc. 8=20769
Al₂O₃, with Cr/Mn impurity, thermal cond. meas. 8=1886
Au¹⁹⁸ impurity nucleus in metallic solid solutions,
isomeric shifts 8=1653
Ba silicate glasses, defects and absorpt. 8=13479
CaF₂:Mn dosimeters, temperature stability and
thermoluminescence during γ -irrad. 8=11314
GaAs, p-type, on elect. props. 8=18039
p-Ge, on microhardness 8=17810
HCl, gaseous, ion lifetimes 8=23164
K₂B₂O₄ glass, γ -irrad., induced absorption bands assoc.
with Tl⁺, Pb²⁺ or Bi³⁺ 8=5639
KCl, irradiated at room temp., defect production and
annihilation 8=8696
KNO₃, irrad. cryst., e. p. r. of NO₂ at 4°K 8=5537
LiF (TLD 100) dosimeters, temperature stability and
thermoluminescence during γ -irrad. 8=11314
Mo, polycrystalline, X-ray scattering 8=22253
Na acetate, trapping of CH₃CO₂[•] free radical 8=4242
NaBrO₃, prod. of paramag. centres 8=2372
NaCl, electron centres form. by Co⁶⁰- γ -irrad. 8=22235
NaPO₃, colour centres and thermoluminesc. 8=22234
P₂O₅, glassy and cryst., e. s. r. 8=22913
Se, hexagonal, effect on conductance, rel. to temp. and rad.
damage 8=18067
SeO₂(NH₄)₂, form. of paramag. centres 8=9305
Sn¹¹³ impurity nucleus in metallic solid solutions, isomeric
shifts 8=1653
SrCl₂, electron centres form. by Co⁶⁰- γ -irrad. 8=22235
TiCl₄, heptane solns., γ -radiolysis obs. 8=18747
TeO₂K₂, on e. s. r. spectrum 8=9444
TeO₂Na₂, on e. s. r. spectrum 8=9444
Zn, polycrystalline, X-ray scattering 8=22253
Zn-Al, spectrum distrib. compression effects 8=4999

internal conversion

- See also Beta-ray spectra/conversion electrons.
atomic screening effect 8=15946
e pair formation spectrometer 8=20668
K-coeffs. for M1 transitions in odd-mass nuclei,
anomalies 8=15945
Mössbauer effect, efficient geometry 8=691
Ag¹⁰², unsuccessful search in isomeric transition 8=7094
Ag^{106m}, 8.5d, decay, conversion coeffs. and multipolarity
assignments 8=979
Ba¹³³ decay, K, L, M coeffs. determ. 8=11820
Ba¹³³ \rightarrow Cs¹³³ decay, K coeff. obs. 8=16031
Cd¹¹⁷, ^{117m} \rightarrow In¹¹⁷, K-conversion coeff. obs. 8=15984
Ce¹³³, ^{133m} \rightarrow La¹³³ 8=20722
Ce¹³⁵ decay 8=20721
Ce¹³⁵ K-conversion coeffs. and γ -spectrum,
119-1469 keV 8=11763
Co⁵⁷, K shell coeffs. obs., 122 and 136.4 keV 8=3812
Cs¹³⁴, anomalous K-conversion coeff. of 124 keV
transition 8=15988
Eu¹⁴⁹ \rightarrow Sm¹⁴⁹, K coeff. 8=7143
Ga⁷² decay, K coeff. 8=16021
Gd¹⁴⁹ \rightarrow Eu¹⁴⁹, K coeff. 8=7143
Gd¹⁵⁴, E2 transition, anomalies 8=1020
In¹¹⁵, K-conversion coeff. 8=3822
Lu¹⁷² \rightarrow Yb¹⁷², multipolarities of K=3 rot. band
deduced 8=15996
Nb⁹⁰, K, L coeffs. 8=11813
Np²³⁹, in elec. field, e binding energy var. in Pu²³⁹ 8=4085
Pb²⁰⁷ 569.6 keV transition K-conversion coeff. 8=3842
Po²¹⁴, coeff. and multipole transitions 8=16046
Pt^{198m} decay 8=3837
Pu²⁴⁵ \rightarrow Am²⁴⁵ 8=11833
Ru¹⁰³ decay spectrum 8=11815
Sm¹⁵², E2 transition, anomalies 8=1020
Sn^{117m}, ^{119m}, of M4, M1 transitions to ground state 8=20717
Th¹⁸¹, ¹⁸², γ -transitions in Gd¹⁸¹, ¹⁸² 8=3882
Tb¹⁵⁵ \rightarrow Gd¹⁵⁵ decay, Nilsson model 8=988
Tb¹⁵⁶ decay \rightarrow Gd¹⁵⁶ 8=7144
Te^{131m}, decay, multipolarities of transitions 8=3878
Tm¹⁷⁰ β -Yb¹⁷⁰, 84.3 keV radiation, coeff. 8=16041

scattering

- See also Compton effect.
back-scatter meas. of soil density 8=23231
coherent, Rayleigh, nuclear Thomson and
Delbrück 8=20355
collimated source in hollow cavity 8=1009
Compton, excitation of nuclear resonance fluoresc. 8=20666
dose-rate 8=15718
double layer transition, theory 8=703
flux density from sources on reflector surfaces 8=1007
 $\gamma p \rightarrow \rho p$, 2π exchange model 8=3650
by graphite and cadmium shielding 8=1128

Gamma-rays—contd
scattering—contd

- in meas. of physical quantities 8=19345
Mössbauer effect, X-ray, efficient geometry 8=691
ore prospecting, effects of variable density 8=18819
steel, effect of tensile stresses 8=13483
transport eqn. in slab geometry 8=19478
water-differential albedo obs. 8=16844
Al, 40-411 keV, scatt. cross-section 8=1188
Al, differential albedo obs. 8=16844
Al, incoherent, 320, 411 and 662 keV 8=1037
Au¹⁹⁸, by air, soil and water 8=20356
C, incoherent, 320, 411 and 662 keV 8=1037
Ca⁴⁰, spin and lifetime assignments to 6.91,
6.95 MeV states 8=11743
Co⁶⁰, by air, soil and water 8=20356
Cs¹³⁷, by air, soil and water 8=20356
Cu, effect of tensile stresses 8=13483
Cu, incoherent, 320, 411 and 662 keV 8=1037
Fe, differential albedo obs. 8=16844
He⁺⁺ \rightarrow He⁺ + H⁺, e capture probability calc. 8=1192
In^{116m}, isomer activation 8=3821
Ir¹⁹¹ resonance fluorescence, Pt¹⁹¹ sources 8=993
Pb, differential albedo obs. 8=16844
Pb, incoherent scatt. cross-sections, 279-1330 keV 8=16058
Sn, incoherent, 320, 411 and 622 keV 8=1037

Gamow-Teller transitions. See Beta-decay theory; Nucleus/
energy levels.

Garnets

- See also Ferrites.
elastic constants and derivatives w. r. t. temp. and press.,
obs. 8=2037
ferrimagnetic res. and relax., effects of paramag.
impurities 8=2357
garnets: rare earth ions powders, electron relax.
study 8=18419
magneto-optical props., i. r. meas. 8=5643
rare earth Fe garnets, intrinsic coercive force near
compensation temp. (>77°K) 8=14005
rare earth Fe garnets, magnetostriction const. 8=2322
rare-earth, paramagnetic susceptibilities and antiferro-
transitions 8=9298
spinel, polycryst., temp. depend. of hysteresis
props. 8=14047
Al, mag. structure by n-diffr. 8=22865
Bi_{0.4}Ca_{2.6}Fe_{3.2}Ga_{0.5}V_{1.3}O₁₂, mag. props. and ferrimag.
resonance 8=18398
Bi_{0.5}Ca_{2.5}Fe_{3.75}V_{1.25}O₁₂, magnetoelastic inter-
action 8=22850
Bi_{0.24}Ca_{2.76}Fe_{2.26}V_{1.39}O₁₂, Faraday effect
mechanism 8=18508
Bi-Ca-V, resonance absorption of longit. acoustical
waves 8=18397
Dy, mag. structure by n-diffr. 8=22865
Er ferrite, dichroism and mag. anisotropy 8=18523
in MgSiO₃-CaSiO₃-Al₂O₃, garnet-pyroxene equilib. press.
depend. obs. 8=1676
Nd:Cr:YAG, sidelight fluorescence changes, due to laser-
ing at 1.06 μ 8=6473
NdGa garnet, antiferromag. ordering by n-diffr. at
0.31°K 8=22884
YAlFe, X-ray fluoresc. analysis 8=9761
YAl garnet: Ru³⁺, e. s. r. 8=18440
YIG crystal, ferrimag. reson., rel. to domain
structure 8=5513
YFe garnet: CuO, preparation and reson. props. 8=21968
YIG delay lines, magnetoelastic waves,
excitation 8=22398
YIG, magnetoelastic delay lines, ray-theory
analysis 8=22397
YFe garnet, reflectivity 8=5642
YIG : Si, doped, photomag. anneal 8=23022
YFe garnet single crystal, magnetoacoustic resonance
obs. 8=22891
YIG slab, magnetostatic surface waves 8=22862
YIG, spin and acoustic Bragg diffraction in longitudinal
magnetoelastic waves 8=18482
YFe interaction of microwave phonons with domain
walls 8=22087
YFe, nonlinear photon-magnon interaction under
parallel pumping 8=14056
YFe, resonance absorption of longit. acoustical
waves 8=18397
Y₃Fe₅InO₁₂ (In-substituted yttrium garnets), magneto-
crystalline anisotropy 8=9386
YGa garnet, reflectivity 8=5642
YGa garnet: Ru³⁺, e. s. r. 8=18440

Gas analysis. See Chemical analysis.

Gas-discharge tubes

- See also Counters; Ion sources.
cathode sputtering, variation with current 8=2019
characteristic E α of stratification, radius depend. 8=21220
circuits with flash lamps, current and voltage 8=4291
Crookes' tube, X-ray dosage 8=16405
electron back-scattering, cathode reflections 8=1331
light detector using metastable atoms 8=20059
light source, cathode noise expt. 8=15521
positive column, constricted, wall control 8=12406
water-cooled electrode, construction 8=21232

Gas-discharge tubes—contd

- Ar, electrodeless, e density cinematography 8=16398
- Ar, 10 GHz noise source 8=7664
- Cs diodes, electrode inhomogeneity influence 8=297
- Cs vapour thermionic diodes, ion current and Schottky effect 8=339
- D, constant-current power supply 8=19714
- H, constant-current power supply 8=19714
- He-Ne mixture, dia. and pressure effects on electron temp. 8=7676
- He, electrodeless, e density cinematography 8=16398
- Ne radial distribution of parameters in subnormal region 8=7668
- O₂, electrodeless, e density cinematography 8=16398

Gas flow. See Flow/gases.**Gases**

See also Kinetic theory/gases.

- absorption in turbulent liquid 8=12745
- acoustic wave generation by entropy discontinuities flowing past an area change 8=177
- advances in applied mechanics, book 8=16683
- air-CO₂ interfaces, plane shock refraction and expansion wave generation 8=4482
- air-CH₄ interfaces, plane shock refraction and expansion wave generation 8=4482
- air in tube, forced vibrations of finite amplitude 8=16705
- analyser, magneto-mechanical 8=5758
- analysis, optical-acoustic, selectivity and sensitivity on gas pressure 8=23192
- analyzer, quadrupole mass filter, rod mounting, simplified 8=7357
- 9, 10-anthraquinone, sensitized emission spectrum in visible region 8=4177
- arc-heated, enthalpy meas. 8=19672
- atmosphere constituents, number density determ. using laser beams 8=14585
- axisymmetric non-uniformities, multi-beam interferometry 8=21498
- bubble, aut propulsion by rocket effect, applications 8=7894
- bubble, imploding, rel. to trailing liquid microjet 8=12658
- compressed, Kerr effect for h.v. meas. 8=6564
- critical, sound attenuation 8=12688
- cyclohexane, in soln., rel. to solubility and entropy 8=4536
- detonation wave, collapsed cylindrical 8=7907
- diatomic, e interference study of molecular parameters 8=4115
- diatomic, macroscopic distribution of binuclear distance, rotating Morse oscillators 8=7499
- dielectric permeability calc. for resonance atoms 8=1481
- dilute, molec. interactions, statistical calc. 8=4466
- discharges, low-freq. noise 8=21226
- diverging detonation wave, motion 8=4461
- dust laden, electronic component of transfer props., calc. 8=1472
- dynamics problems, integral characts. method 8=21460
- expansion of cloud into a vacuum 8=4447
- flow rate-measurement by modified continuous-ionization method 8=12659
- fuels, combustion in fluidized beds 8=23119
- fugacity of nonpolar and quantum gas mixtures 8=16939
- gas-liquid mass transfer, effect of moving interface, theory 8=16710
- gas-particle mixtures, sound propag. and acoustic combustion instability 8=16704
- gravitating mass, homogeneous, Jeans' instability criterion, effect of grains 8=2793
- grey gas, absorbing, between heated plates, source functions for heat transfer 8=21507
- heating, by lasers, dynamic processes 8=7928
- heat transfer, absorption related to temperature distribution 8=230
- heat transfer, effect of sound 8=12680
- high press systems at low temp., compact elec. lead 8=3147
- highly rarefied, effect of gas-surface interaction on sound propagation 8=21519
- ideal, multiply ionized, Raizer's method of calc. degree of ionization, applicability 8=21257
- inert, interact. potential rel. to parameters of solid at 0°K 8=1468
- intermolecular interactions, thermodynamics 8=3002
- intermolecular potential, bound double molecules formation 8=12357
- interstellar, C¹²/C¹³ ratio, a lower limit 8=5919
- ionic movement under influence of electric fields 8=7705
- ionized mixture, composition and thermodynamic props. 8=12422
- ionized, partially, l.f. oscillations described by operation of plasma continuity eqns. 8=12541
- macroparameters near leading edge of plate in hypersonic flow, asymptotic values 8=16672
- mass, inhomogeneous, convective instability, model 8=2794
- mass of large volumes, determ. by direct weighing 8=7890
- methane, molec. dynamics, study by slow n. scatt. 8=16374
- mixture, axial transport in d. c. discharge 8=1333
- mixtures, intensity of rotation lines, modification theory by density effect 8=16244

Gases—contd

- molecular, resonance phenomena in kinetics 8=21493
 - monatomic, sound propagation 8=1474
 - multicomponent mixtures, viscosity, additional matrix elements for third approx. 8=12700
 - non-equilibrium boundary layer problems, finite-difference soln. 8=18662
 - nongray, diatomic, i. r. radiative heat transfer, theory 8=16693
 - nonisothermal nongray, radiation heat transfer 8=21506
 - non-polar, aqueous solutions, freezing 8=1618
 - nonpolar, Clausius-Mossotti function, effect of molec. interaction 8=12693
 - organic mixtures in air, optical-acoustic effect using cm e.m. waves 8=21520
 - photodissociation, orientation of transition moment, photolysis mapping 8=1307
 - photoelectric control for rotary power meas. 8=15549
 - polar, collision freqs. of thermal electrons 8=4471
 - polar, rotational relax. 8=7909
 - polar, second virial coefficient contribution of bound double mols. 8=7914
 - polyatomic, gyro-thermal effect in mag. field 8=12672
 - polytropic changes for gas-solid system 8=4472
 - pressure gauge, sensitive differential, for corrosive gas 8=4448
 - pressure temp. coeff. meas. apparatus 8=7922
 - purification by cataphoresis 8=2536
 - quantum gas, slow neutron scatt. 8=16685
 - quantum ideal gases, effective potential 8=19456
 - radiating, nonisothermal, general band model 8=7520
 - radiative transfer, differential approximation, modfn. 8=222
 - radiative transfer, non-grey, plane-parallel geom., approx. methods 8=6117
 - reaction kinetics, use of e.s.r. to study 8=14351
 - reactions, transition state and Arrhenius parameters 8=4465
 - relativistic, in magnetic field, energy-momentum tensor evaluation 8=15362
 - relativistic, non-relativistic bulk motion, e. m. effects and suprathermal waves 8=5925
 - relativistic, perfect, distrib. function in external force field 8=4338
 - residual, in e tube manufacture, mass spectrometry 8=18
 - resistance to relative motion 8=16686
 - Rice-Allnatt assumption in low-density limit 8=1464
 - second harmonic generation in homogeneous mag. field 8=12123
 - slightly ionized, continuum theory of electrostatic probes 8=16545
 - slightly rarefied, with shock wave, corrections to Crook's soln. for density, temp. and vel. of gas 8=16667
 - sound absorption, rel. to free energy associated with critical density fluctuations 8=16703
 - sound amplification, radiation induced, possibility 8=21516
 - spin-lattice relax. 8=12697
 - spin-lattice relaxation 8=21176
 - specific heat meas., capillary flow calorimeter 8=7921
 - spectra, continuous 8=4060
 - spectral line broadening theory, phase effects 8=1154
 - surface energies and equilb. forms of anisotropic phases 8=4464
 - temperature, high nozzle thermocouple meas. 8=7927
 - temperature meas. by spectral line reversal, effect of continuous absorber 8=16695
 - thermodynamics, calc., correl. of corresponding states law 8=16697
 - transport coeffs. in critical region 8=4490
 - transport coeffs. from inelastic collisions 8=7939
 - turbulent, energy dissipation by suspended particles 8=7
 - uniform gas, frequency-integrated radiation due to weak lines 8=12690
 - vapour-cavity form. in pipes, column separation, for liquid transients 8=16757
 - vel. distrib. near solid wall in non-uniformly heated gas 8=21494
 - vibration in reactor, meas. with acoustic transducer 8=20885
 - vibrational relax. of diatomic mols. 8=1218
 - water vapour attenuation of millimeter wavelength radiation 8=12689
 - weakly ionized, propag. of longit. ion waves 8=4398
 - SF₆, self. induced transparency using 10.6 μ laser radiation 8=1478
- Gegenschein.** See Zodiacal light.
- Geiger counters.** See Counters/Geiger.
- Gelatin**
- No entries
- Gels**
- crystal growth, large, method 8=21934
 - diffusion 8=1540
 - isotropic, low-angle light scatt. 8=16911
 - rubber + benzene mixtures, tracer diffusion 8=21641
 - silica, adsorbed H₂O, proton relax. 8=12932
 - silica, PbS crystal growth near ambient temperatures 8=1743
 - silica, surface meas., adsorption method 8=21742
 - silicates, microprobe analysis standards prep. 8=14496

Cells—contd

- surface, energy states and dynamics of Sn atoms 8=16912
 thoria, crystallite size obs. 8=12960
 viscometer-gelation timer 8=16810
 Cu₂Cl₂ crystals, growth from Cl⁻ ions from HCl
 soln. 8=8406
 CuCl-HCl, growth of clear CuCl crystals 8=8405
 Si, factors influencing growth of CuCl 8=21944

Geochemistry. See Earth/composition.

Geochronology. See Earth/age; Radioactive dating.

Geodesy

See also Gravity.

- day length, annual and semi-annual vars. rel. to geophysical
 obs. 8=14510
 earth's pole movements, free and forced amplitude, long
 period var. 8=9770
 equatorial curve from equilibrium position of synchronous
 satellite 8=2756
 gravitational pulsation, geological evidence for 8=2554
 gravity gradiometer computer model for simulated
 gradient contour mapping 8=5771
 oscills., spheroidal and torsional, Q values from decay of
 seismogram spectral amplitude 8=23205
 tidal forces of sun and moon, long period vars. 8=19241
 U.S. Navy Doppler system and accuracy 8=5766

Geoelectricity. See Earth/electricity.

Geomagnetism. See Earth/magnetic field.

Geometrical optics. See Optics/geometrical.

Geometry

- electromagnetic field, energy-impulse tensor
 treatment 8=3172
 Gauss hypergeometric function, unit circle, univalent
 conformal mapping 8=14926
 irrational surfaces of zero orders 8=14927
 of magnetrons, calculation of e. m. f. 8=15333
 perimetric coordinates 8=4045
 superficial discrete set of points in Euclidean
 space 8=6012

Geons. See Gravitation.

Geophysical prospecting

- aerial radiometry, directional detectors 8=18829
 California north coast ranges, upper mesozoic
 graywackes 8=2565
 e. m. prospecting for ore deposits, rel. to e. m. diffraction
 by conducting strip 8=23214
 e. m. wave diffraction by conducting half-plane, in
 layered medium 8=6385
 gravimetry in correctly posed problems, soln. by
 convolution-type integral eqns. 8=23199
 groundwater flow, radioactive tracer obs. 8=2568
 magnetometry, in correctly posed problems, soln. by
 convolution-type integral eqns. 8=23199
 metalliferous deposits, induced polarization field
 expts. 8=2561
 ores, variable density, selective γ -ray logging 8=18819
 rotatable field em prospecting system, anal. and model
 studies 8=14540
 by u. s. wave absorpt. in rocks, lab study by
 bending vib. method 8=22095
 NaI crystal scintillation gamma spectrometer in search
 for U deposits 8=14528

Geophysics

See also Atmosphere; Earth; Oceanography;
 Seismology.

- acoustical phenomena resulting from artificial sources,
 instrumental role in obs. 8=9804
 alluvium nuclear detonation, cavity press. and temp.,
 time history afterwards 8=14527
 Brazilian glauconites, K-Ar age meas. 8=18830
 colour indices of some earth surfaces 8=2816
 conference, Dallas 1967 8=14280
 continental drift and polar wandering, deductions from
 paleomag. Sierra Nevada obs. 8=14701
 core and mantle motions and variations of main geo-
 magnetic field 8=14554
 core, surface fluid motions from mag. obs. of 1885, 1912,
 1933 and 1960 8=5813
 cosmic ice residuum and astrobleme 8=2562
 earth's core, surface fluid motion rel. to secular mag.
 field changes 8=2724
 elastic half-space in mag. field, disturbances 8=10703
 elastic wave propagation rel. to identification of one-
 dimensional mechanics 8=10702
 electromagnetic induction in conductor bounded by inclined
 surface 8=18802
 fault propag. model, rel. to prod. of seismic shock 8=14536
 γ methods, classification system 8=23224
 geomagnetic dipole axis, vib. round geographic N pole
 in historic time 8=5812
 gravimetry, in correctly posed problems, soln. by
 convolution-type integral eqns. 8=23199
 Greenland ice cap, dielectric constant rel. to ice
 density 8=14565
 high pressure gas, sphere, expansion in porous
 medium 8=1439
 Hugoniot eqns. of state for 12 rocks from shock wave data,
 rel. to those derived from geophys. obs. 8=14558
 interior density, pressure and rigidity distrib. 8=18826

Geophysics—contd

- isostatic equilb. of crust, and viscosity of
 asthenosphere 8=14556
 isostatic equilb. disturbances, rel. to tectonics and
 internal processes 8=14555
 large-scale mantle convection rel. to thermal requirements
 for crustal processes 8=14521
 liquid flow, through porous media and packed
 beds 8=12739
 magnetometry, in correctly posed problems, soln. by
 convolution-type integral eqns. 8=23199
 magnetometry and gravimetry, soln. of convolution
 integral eqns. 8=23200
 magneto telluric two- and three-layer master
 curves 8=18827
 mantle convection and continental drift hypotheses,
 criticism 8=14518
 mantle, flow inferred from continental drift and low
 harmonics of geopot. 8=14551
 mantle, upper, low velocity zone temp. and density
 distributions, thermodynamic approach 8=14553
 mantle, upper, preferred mineral orientation by recrystal-
 under stress 8=14552
 mantle, viscosity and finite strength of transient water and
 ice loads 8=14548
 mantle, viscosity variation with depth 8=14549
 microtektites in deep-sea sediments, obs. 8=14568
 pyroclastic rocks, New Hampshire obs. 8=23228
 ridge, mid-Atlantic 22-23°N, and tectonic rises 8=23219
 rigidity of Earth, estimation from tidal studies 8=14546
 rocks, displacement field in horiz. layer of elastic and
 granular material 8=2567
 rotation period radio interferometric meas.,
 implications 8=18804
 Sahara basins, evolution of water isotopic comp. during
 evaporation 8=18832
 sand, "singing" phenomenon 8=23232
 scattering of telluric currents and signal extraction 8=14564
 soil pressure cell, effect of diaphragm flexibility on
 calibration 8=9803
 soil stratification, allowance for in compiling elect.
 cond. maps U.S.S.R. 8=23229
 statistical reduction of acoustic and mag. data 8=6092
 stress state in crust rel. to energy of tectonic processes
 ass. with upper mantle 8=14516
 tectonic processes, effect of gravity, model expts. 8=14512
 tektites, association with geomagnetic reversal 8=14567
 terrestrial heat flow distrib., consistent with mantle
 convection 8=14522
 thermal convection theory for mantle, problem of non-
 linearity of eqns. 8=14520
 tidal flow and mass transport in Humber estuary 8=5785
 tide damping, isostasy and mantle convection, rel. to
 creep 8=14559
 turbulence and boundary layers with geophysical appl.,
 conference, Kyoto, Japan 1966 8=7850
 viscosity of upper and lower mantle, from creep and solid
 state theory 8=14550
 viscosity of upper mantle, and postglacial uplift of
 Scandinavia 8=14547
 volcanic ashes, nonhomogeneous, from turbulent
 diffusion, distribution 8=23216
 Zuni Lineament, evidence from Pb isotope meas.,
 depth sounding and seismic data 8=5781
 Au, exogenous, different categories from Ag distrib.
 mode 8=14562
 NaAlSi₃O₈, isomorph of high pressure NaAlGeO₄, rel. to
 formation in earth's mantle 8=1678
 Pb isotopes, abundance ratios, interpretation, generalized
 model 8=16236
- Germanium**
- See also Semiconducting devices; Semiconducting
 materials/germanium.
 absorption edge, imperfections effect 8=5603
 absorption K-edge, proximity of X-ray interference 8=14218
 addition to 50 Ni Permalloy, isotropic and anisotropic,
 effect on mag. props. 8=22815
 atom displacement in collision cascade calcs. 8=8754
 atoms, electron-impact ionization cross-sections 8=12428
 atomic scattering factor, Pendellösung meas. 8=22025
 Auger recombination, indirect band-to-band 8=14221
 band structure calc. using LCAO approximation 8=8906
 coating effect on Sn and Ti films superconducting
 transition temp. 8=5214
 crystal window in double spectrometer, X-ray diffr.
 profile exam. with monochromatic radiation 8=22004
 cubic crystals, thermal expansion coeff., temp.
 depend. 8=8646
 diodes, high freq. noise and double injection, obs. 8=13854
 dislocation arrangements in foils after crystal-
 lization 8=1975
 dislocation investigation by Borrmann's method: appl. of
 asymmetric exposures 8=17655
 etching in HNO₃-HF-CH₃COOH 8=4791
 etching, vac. thermal 8=17217
 film, complex index and optical thickness from meas. of
 reflecting powers at oblique incidence 8=18530
 films, epitaxial growth in open iodide process 8=17131
 films, epitaxial, prep. by pyrolysis of hydrides 8=17130

Germanium—contd

- films, growth, from liq. films, structure obs. 8=1741
 films, recryst. by electron beam zone melting 8=17235
 films, thin, piezoelectricity, above fundamental energy gap 8=22986
 generation-recombination noise, 100°–350°K 8=22593
 group V diffusion, hot implantation behaviour, comp. with group III diffusion 8=22160
 group V diffusion, hot implantation behaviour, comp. with group III diffusion in Si 8=22160
 internal friction phenomena, screw and edge dislocation damping 8=22370
 irradiation, low-energy, by He⁺ and Xe⁺ 8=8772
 lattice energy rel. to elastic deform., electron distrib., internal strain 8=13576
 lattice theory of third order elastic consts. 8=13261
 liquid, interaction between O₂ and B in Ge 8=23104
 optical energy gap, pressure coeff. meas. 8=14220
 Pendellösung meas. 8=13262
 phonons stimulated emission by supersonic electrons, n-type, 4.2°K 8=5257
 photodiodes, shot-noise meas. at high freqs. 8=22706
 photoelastic constants, bond stretching and bending model 8=8830
 photoelectromagnetic receivers with optically polished thin elements, sensitivity and inertness 8=6275
 plasticity at room temp., obs. 8=22372
 positron annihilation meas. cf Se 8=5150
 p-type, bombardment-produced defects at low temps. 8=22170
 refining effect in vacuum melting of Fe-Ni alloy, rel. to mag. props. 8=22815
 reflection coeff. of I vapour from crystal surface etching vel. 8=8382
 reflectivity, low freq., in mag. field 8=22988
 refractive index in far i.r. 8=14219
 resistance thermometers, below 1°K 8=19665
 semiconductor detector, full registration efficiency for γ -rays 8=11429
 substrate with layer CdS elastic surface wave behaviour 8=8850
 surface contamination, detection and identification 8=1688
 surface stress in polished and clean (111) surfaces 8=8849
 thermal conductivity, lattice component, effect of impurities 8=1888
 thermal expansion from 2–40°K 8=4937
 thermoreflectance spectra in region of a critical point, calc. and obs. 8=14217
 undercooling 8=4649
 X-ray K-absorption spectrum 8=2423
 X-ray transmission, multiple Bormann effect 8=14222
 As in Ge, solid solution, supersaturated, decomposition mechanism 8=17005
 As and Sb impurities, excitation spectra, under uniaxial compression 8=13424
 Ge⁷³, Larmor freq. rel. to H² and K⁴¹ 8=5558
 Ge + MoO₃ in powder form., reaction mechanism 8=14365
¹H⁺, ²D⁺, ³He⁺ ions, channelling props., diffr. calc. 8=13485
 Li-doped, impurity vibrational modes rel. to i.r. absorpt. 8=9532
 P-doped, impurity vibrational modes rel. to i.r. absorpt. 8=9532

Germanium compounds

- fluoro- and hydroxyfluoro-compounds and thermal polymerization products, i.r. vibr. freqs. of Ge-O-Ge bond 8=4170
 GeD₄, vibr.-rot. spectrum 8=12187
 GeH₄ radical, struct. and Ge⁷³ coupling 8=12346
 GeH₃NCO, i.r. spectra and struct. 8=21074
 Ge:In, detector for pulsed far infrared laser radiation 8=9262
 Ge-O system, sticking coeff., orientation dependence 8=22154
 GeS_{1-x}, effect of defects on lattice thermal conductivity 8=1892
 GeS, gaseous, dissociation energies 8=7616
 GeSe_{0.75}Te_{0.25}, prep. and props. 8=2197
 Ge-Si alloys, heterojunctions, electron microprobe analysis 8=2216
 Ge-Si alloyed heterojunctions, elec. props. at interface region 8=2217
 GeSi alloy, meas. of reflectivity 8=2422
 Ge-Si alloys, ultrasonic attenuation 8=1853
 GeTe-SnTe alloys, $\alpha \rightarrow \beta$ transition, at high press. 8=17084

Getters. See Adsorption; Electron tubes; Vacuum technique.

Giant pulsations. See Earth/magnetic field; Magnetic storms.

Gibbs functions. See Thermodynamic properties.

Ginzburg-Landau theory. See Superconductivity.

Glaciers

- Kesselwandferner, Pb²¹⁰ and Sr⁹⁰ meas. on firn and ice samples 8=18831

Glass

- See also Optical materials; Vitreous state.
 advanced optical techniques, book 8=15489
 alkali aluminosilicate, ion-exchanged, effect of stress on durability 8=13525
 alkali borate, binary, u.v. absorpt. of Cr(VI) 8=18519
 alkali borate glasses, co-ord. equilibria of Ni(II) 8=21836

Glass—contd

- alkali silicate glasses, X-irrad., trapped hole centres 8=1998
 alkali silicate, validity of Nernst-Einstein eqn. 8=8354
 aluminate i.r., optical, mech. and thermal props. 8=22954
 aluminophosphate glasses, radiocolouration and luminescence kinetics 8=1996
 aluminosilicate, gamma-irradiated, thermoluminescence spectrum 8=18614
 blocks, fracture produced by impact 8=2055
 borate glasses, e.p.r. of Mn²⁺, 293–4°K 8=18408
 boric acid, dissolved aromatics direct and sensitized photo-oxidation 8=23160
 borosilicate, neutron transmission determ. of B content 8=23196
 BSC, annealing, effects of relax. times 8=4770
 breakdown and fracture, laser-induced 8=8851
 ceramic, from SiO₂-Li₂O-ZnO system, plastic deformation 8=17829
 chalcogenide, electrical properties 8=18028
 chalcogenide elements based, elec. cond. 8=22522
 chalcogenide, Hall mobilities 8=18027
 chalcogenide, Hall effect meas. method 8=13789
 chemical bonds, nature, det. by spectral char. of Mn 8=811
 contact with metal electrodes in vacuum, generation and dissipation of static charge 8=18159
 containing In, superconductor, flux jumping during magnetization 8=2163
 crack-branching, vel. meas. and stress effects 8=8815
 crack propagation and bifurcation vel. 8=22296
 crystal growth, contamination-nucleated, at bubble surfaces 8=21937
 CW laser at room temperature 8=19998
 damage and spectral emission during illum. by ruby laser light 8=14246
 degassing by 100–1000 eV bombardment 8=13945
 dielectric props. and losses, meas. at 40 Gc/s 8=22649
 diffusion processes in surface layer, rel. to distrib. of alkali ions 8=22146
 disks for X-ray fluoresc. anal., casting technique 8=2551
 electrification by friction with metals in a 3 × 10⁻⁷ torr vacuum 8=13872
 electron bombardment luminescence, viewing by optical microscopy 8=14296
 ethanol, naphthalene-d₈ biphotonic T→T transitions, obs. 8=23161
 fibres, drawing apparatus and tensile strength 8=5073
 fibres, length rel. to strength 8=1666
 fibre, passive core, Nd-doped cladding, laser action by total internal refl. 8=11073
 flint, refraction, mean reference indices calc. 8=20044
 fracture, conference, Boston, USA (1966) 8=13518
 gallate i.r., props. 8=22954
 Hertzian stress cracks 8=13540
 ion-bombardment-induced emission of gas 8=17173
 irrad. effect suppressed by high pressure synthesis 8=499
 irradiation resistance, h.p. H₂ synthesis 8=8353
 mass spectrometer, miniature, charact. spectra 8=16176
 metaphosphate, trapped Ag radicals 8=4990
 methyl-pentane, naphthalene-d₈ biphotonic T→T transitions, obs. 8=23161
 microporous, shrinkage and deformation under load at high temp. 8=17021
 molten, diffusion of Ne bubbles 8=4554
 oxides, four new, rapid quenching techniques 8=5087
 phosphate glass: Ag, radiophotoluminescent centres 8=14331
 phosphate, layers on SiO₂ films prevent Na contamination 8=18069
 phosphate, luminescence, with Mn as activator 8=2483
 photochromic, information storage capacity meas. by holography 8=6570
 photoluminescence, effect of heat treatment 8=2482
 plates, precise interferometry for thickness and refractive index variation 8=14223
 porous, adsorption of water vapour, increase in surface conductivity 8=4766
 porous, strength rel. to micromechanical stress concentrations 8=13577
 Pyrex, thermal props. 0.4–4°K in 0–90 kG fields 8=1752
 reflection light at large incidence, indicatrices with two maxima 8=5631
 resistance thermometers, self-heating 8=6219
 ring cracking by spherical indenters 8=17747
 selenide i.r., props. 8=22954
 semiconducting oxide and non-oxide, cond. mechanisms and struct. 8=22580
 silica, dielec. loss at low temp., OH⁻ conc. and irradiation effects 8=18172
 silica, thermal conductivity, measurement method 8=13396
 silicate, containing fluorides, nucleation and cryst. growth 8=8357
 silicate glasses, e.p.r. of Mn²⁺, 293–4°K 8=18408
 silicate, rare earth doped, Faraday rotation, freq. depend. 8=18531
 silicate, 6% Nd, multimode generation 8=2487
 silicate, on Si-steel, rel. to mag. props., obs. 8=22843
 soda, laser prod. photocond. rel. to dielec. breakdown 8=18239

Glass—contd

- soda-lime, with adsorped water, spreading of org. liquids 8=1520
solid-lime silicate, quantum efficiency of Nd^{3+} absorpt. and excitation spectra 8=5667
spheres, adhesion in water or mineral oil 7=8150
 β spodumene-silica in $\text{Li}_2\text{O}-\text{Al}_2\text{O}_3-\text{TiO}_2-\text{SiO}_2$ glass ceramic 8=1661
substrate, self-heated, for vacuum deposition of thin films 8=4736
superconductor-glass vacuum seals 8=21551
surface cleaning meas. by evolution of H with Na-ammonial solns. 8=21868
tempered, fracture, rel. to elastic strain energy and rate of crack extension 8=22373
thermal neutrons, effects 8=8771
thermostable org. glasses cont. P 8=13110
thin, transmission electron microscopy 8=21995-6
transition metal oxide, elec. cond. 8=22522
uran, fluorescence, quantum yield in anti-Stokes region 8=18640
vanadate, electronic conduction rel. to crystallinity 8=18091
Verdet constant, spectral dependence 8=2424
viscosity-temp. data in range 10^{12} to 10^{14} poises, approx. by fibre elongation 8=17725
Vycor, porous, film area hysteresis 8=13050
X-ray total reflection of films 8=5604
 Al_2O_3 -glass composite, effects of hot-pressing on chemical reaction 8=18671
As-S, origin of 800 cm^{-1} absorpt. 8=5584
As-S systems, dielectric properties 8=9193
 AsSe_3 , refractive index 8=14198
As-Se, thermal expansion 8=13382
 B_2O_3 glass, permanent densification by hydrostatic press. 8=22314
 B_2O_3 -PbO- Al_2O_3 spinodal decomposition structures, obs. 8=17268
Ba silicates, γ -ray effects 8=13479
Ba silicates, internal friction due to condensation 8=13537
 Ce^{3+} paramagnetic resonance in glassy phase 8=9436
Cs silicate, n.m.r. absorption, ionic conduction 8=9197
Fe dispersions in matrix, superparamagnetism 8=14013
Ga, e.s.r. study 8=18420
 He^4 superleak construction 8=15149
 $\text{K}_2\text{B}_2\text{O}_7$, γ -irrad., induced absorption bands assoc. with Ti^{4+} , Pb^{2+} or Bi^{3+} 8=5639
Li-silicate glass, second phase particle growth, diffusion controlled 8=21847
 $\text{Li}_2\text{O}-\text{B}_2\text{O}_3$ systems, fraction of four-co-ord. B atoms present 8=21915
 $\text{Li}_2\text{O}-\text{SiO}_2$ system, crystallization of Li disilicate 8=21953
 Mn^{2+} e.p.r. 8=5536
 $\text{MoO}_3-\text{P}_2\text{O}_5$, X-ray study of good formation 8=8356
Na aluminosilicate, Na self-diffusion rel. to elec. cond. 8=22158
Na borate, ht. of soln., density and refractive index changes under high pressure 8=1715
 $\text{Na}_2\text{B}_4\text{O}_7$, Eu activated, luminescence 8=23061
Na-Ca aluminosilicate, Na self-diffusion rel. to elec. cond. 8=22158
 $\text{Na}_2\text{O}-\text{B}_2\text{O}_3$ systems, fraction of four-co-ord. B atoms present 8=21915
 $\text{Na}_2\text{O}-\text{BaO}-\text{SiO}_2$ system, internal friction 8=22383
 $\text{Na}_2\text{O}-\text{GeO}_2-\text{B}_2\text{O}_3$ system, and melts, structure 8=21605
in $\text{Na}_2\text{O}-\text{TeO}_2$ system, γ -irradiation effect on e.p.r. spectrum at 77 and 295°K 8=9434
Nd doped laser, travelling-wave, features 8=3333
Nd-doped, stimulated emission cross-section, from free-running laser oscillator output 8=19979
Nd:glass laser, mode-locked, Eastman 9740 bleachable dye transmission obs. 8=11110
Nd glass, measurement cross-section stimulated emission 8=449
with Nd^{3+} ions, influence of composition on luminesc. characts. 8=18592
Nd laser, picosecond pulses, spontaneous appearance 8=439
Nd silicate glass laser, stimulated emission cross section, from fluorescence changes 8=14292
 Nd^{3+} doped, influence on Q-spoiled laser dynamics 8=11017
 Nd^{3+} laser glass, self-Q-switching by saturable absorpt. of colour centres 8=11107
 Nd^{3+} paramagnetic resonance in glassy phase 8=9436
 $\text{Nd}^{3+}-\text{Yb}^{3+}$ glass, laser emission at $1.06\text{ }\mu$ 8=11109
 $\text{Nd}^{3+}-\text{Yb}^{3+}$ laser glass, self-Q-switching by saturable absorpt. of colour centres 8=11107
with Pb oxide, volatilization of volatile constituent from melts 8=21775
 $\text{PbO}-\text{Al}_2\text{O}_3-\text{B}_2\text{O}_3-\text{SiO}_2$ system glasses, elec. props. temp. and comp. dependence 8=18170
 $\text{PbO}-\text{BaO}_3$ systems, fraction of four-co-ord. B atoms present 8=21915
 TiO_2 , enamel, opacification kinetics, X-ray diffr. meas. 8=17221
Ti silicate, n.m.r. absorption, ionic conduction 8=9197
Zn tellurite, formation, refractive index, optical transmission range 8=5644

Glass—metal seals

- alumina ceramics-Mb seals, bonding mechanism obs. 8=16743

Glass—metal seals—contd

- gold wire for ultrahigh vacuum, config. of unpolarized rotatable u.h.v. flanges with Au wire gasket 8=21549
high-vacuum h.v. apparatus 8=1498
quartz-metal sealed window, bakeable 8=16741-2
silicone resin sealant for i.r. vacuum windows 8=16739
Al film, vacuum deposition technique 8=17123
- Glow discharges.** See Discharges, electric/glows.
- Goks.** See Hypernuclei.
- Gold**
- cold-worked, recrystallization during α -irrad. 8=21943
collapsed tetrahedra and stacking fault energy 8=22216
colloidal in water, extinction light curves 8=4579
contacts, to n-Si surface, props. 8=18070
crystals, well-annealed, stress at which dislocations multiply 8=13545
diffused in Si, precipitates formation 8=17620
diffusion in Cu, detect. by deuteron elastic scatt. 8=8675
diffusion in SiO_2 8=13896
diffusion in Ti, obs. by radiotracer technique 8=22163
electrodeposits struct. and porosity rel. to Cu substrate surface prep. and undercoats, obs. 8=21981
electron back-scattering from Be-Au 2-layer target 8=3203
electroplating inside metal containers 8=14428
energy loss of fission fragments, range-energy relation 8=2021
energy loss by low-energy protons 8=13478
exogenous, study of categories from Ag mode of distrib. 8=14562
films, critical angles for channeling of H^+ , D^+ and He^+ ions 8=17704
film, electrical conductivity, island structure, on quartz glass and BaTiO_3 substrates 8=13709
film formation on NaCl, deposition rate and residual gas effects 8=1693
film, growth effected by ultrasonic vibrations, of substrate 8=4827
film growth on NaCl, high vacuum 8=21878
films, growth on NaCl, high vacuum, model 8=21879
films, light scattering, thickness and wavelength dependence between 2000–7000 Å 8=14199
films, meas. of secondary electron emission from exit side 8=2285
films, morphological changes following deposition 8=4743
films on MoS_2 , epitaxial growth under u.h. vacuum and defect structure 8=17125
films, recrystallization obs. in electron microscope 8=8314
film, reflectance and transmittance, anomalous skin and size effects 8=9498
films, thin, ohmic and thermoelectric props., –100 to $+100^\circ\text{C}$ in ultrahigh vacuum 8=22513
fluorescence corrections to X-ray absorption in a sphere 8=23037
foil, electron diffraction intensities, temp. dependence 8=8509
foil, n flux determ. by β , γ activity meas. 8=11620
foils, optical absorpt., and structure and surface characts. 8=18502
grain boundary diffusion in Cu 8=17568
heat capacity, temp. dependence, effect of crystal lattice defects 8=13368
heavy ion penetration along low index channels, effect of atomic thermal motion 8=2024
hemispherical reflectance, rel. to λ and surface roughness 8=2399
laser induced non-linear photoelectric effect in metals 8=22721
lattice fringes, electron microscope resolution 8=1783
in liquid Pb, thermodynamic props. 8=8043
microcrystals, uniform, obtained from hydrosols 8=1745
microdeformation measuring technique 8=22273
nucleation density on cleavage surface of NaCl 8=4742
nuclei on MoS_2 substrate, elastic strain nucleus size and misalignment orientation 8=8823
optical absorption band edge in film 8=5585
penetration distrib. of $^{133}\text{Xe}^+$ ions, effect of Au temp. 8=2023
photoelectric effect, non-linear, laser induced 8=2258
plastic stress relaxation rel. to stacking fault energy 8=13529
quenched and aged, structure 8=22185
quenched, slip channel formation and other defect behaviour on plastic deform. 8=17663
quenched, stacking fault tetrahedra as vacancy sinks 8=13443
quenching experiments 8=8824
radioactive colloids, Ag coated for radiotherapy 8=14893
shear strength in grossly deformed sample at high temps. 8=8833
single crystals, D^+ blocking 8=22241
single crystals, D^+ channeling model 8=22243
single crystals, D^+ transmission 8=22242
single crystal film, effects of ion bombardment on texture and structure 8=17124
small particles, conduction electron spin reson. 8=14093
sols, radioactive conc. determ. from spectrophotometric data 8=16910

Gold—contd

- sputtered films, due to negative O ions in O discharges 8=21877
- target for ion emission, bombard by Ar⁺ 8=6626
- thermal desorption of inert gas ions 8=9280
- thermal desorption of inert gases 8=17701
- thermoelectric power and elec. resist., high press. effects 8=13902
- thick films, optical constants, least squares method 8=2403
- thin films, Hall effect 8=2133
- twins formation during diffusion between films of Au and Pd 8=13127
- ultrasonic attenuation rel. to Fermi surface deformation 8=1851
- vacancy annealing, three different experiments 8=13421
- vacancy diffusion rate calc., Debye model 8=22172
- vacancy and divacancy behaviour from elec. resistance meas. on quenching and annealing 8=1945
- vapour press., from Knudsen effusion 8=12999
- wire seals for ultrahigh vacuum 8=21549
- X-ray microanalysis e backscatt. correction, obs. 8=14469
- X-ray prod. and e backscatt. rel. to microanalysis, obs. and calc. 8=18794
- X-ray total reflection of films 8=5604
- Au III, transition strengths between 5d⁶6s and 5d⁶6p configurations 8=4071
- Au¹⁹⁷, n. m. r., Knight shifts 8=2379
- Au¹⁹⁷, 10–80 MeV He⁺ ions, recoil range 8=13489
- Au¹⁹⁹ ion exchange removal from n irradi. Pt 8=23168
- Au–Ni spinodal, re-calc. 8=13245
- Au/Ni–Cr, contacts and conductive paths 8=8993
- Be–Au two-layer target, electron energy losses 8=22496
- inBiTe, electrotransport, 150 and 250 A/cm², ≤ 400°C 8=17564
- in Fe, magnetization saturation at 20°K 8=2324
- O¹⁶ ion beam energy loss 8=13477
- PbTe–Au pseudobinary section 8=17098
- S³² ion beam energy loss 8=13477
- Si–collodion–Au contacts, photocapacitive effects 8=22673

Gold compounds

- Au–Ag alloys, Ag¹⁰⁹ n. m. r., Knight shifts 8=2379
- AuAg alloy optical const., deform., recryst. and ordering effects, 276–1200 nm 8=22958
- Au–Ag–Cu natural alloys, e probe microanalysis obs. 8=14477
- AuAl₂, Fermi surface topology 8=5116
- Au–Ba alloys, work function 8=18245
- Au–C alloys, growth of spheroidal graphite crystals 8=13156
- Au₃Cd alloy, long-period ordered, X-ray diffraction study 8=13250
- Au–Cd alloys, quenched and aged, structure 8=22185
- Au–Cd binary system, point defect segregation at melting rel. to comp. 8=17624
- Au–Cd phase transformations, thermodyn. investigation 8=8263
- AuCu alloy optical const., deform., recryst. and ordering effects, 276–1200 nm 8=22958
- AuCu₂ alloy optical const., deform., recryst. and ordering effects, 276–1200 nm 8=22958
- Au₃Cu, shear modulus change during ordering 8=17769
- Au–Cu–Zn ternary alloys, phase relation and kinetics of transformations 8=13063
- Au–Fe solid soln., magnetic ordering rel. to electric hyperfine interactions 8=2289
- AuGa mol., emission in Ar atm. at 2100°C 8=16265
- Au–Hg alloys, liq., abs. thermoelec. power 8=12913
- Au₇₇Mg₂₃ phase, crystal structure 8=13251
- Au–Mg system, some phase structures 8=17043
- Au₂(Mn, Al)₂ alloys, coexistence of ferro. and antiferro. structures 8=9389
- β–AuMn, change to f. c. c. structure on cold working 8=17042
- AuMn, magnetic structure 8=22872
- Au₂Mn, magnetisation process up to 50 kOe at 4.2°K and up to 70°K at 80°K 8=9281
- AuMn, spin-disorder resist., anisotropic 8=14064
- Au–Mn–Al alloys, ferromag. order dependence on comp., n-diff. study 8=18387
- Au–Ni alloys, modulated structure formation, conc. and temp. dependence 8=17044
- AuPd alloy, localized states from permittivity obs. 8=13656
- Au–Pt alloys, annealed, defects rel. to X-ray diff. "tails" 8=17341
- Au–Pt system, X-ray meas. of chem. diffusion coeff. 8=1913
- Au–Si alloy, specific heat and enthalpy near eutectic composition 8=1548
- Au–Sn alloy, atom pair distrib., partial interference functions 8=4531
- AuTe₂, liq, Hall coeff. rel. to possible semicond. nature 8=12917
- Au–V alloys, dilute, mag. susceptibilities rel. to mag. moment quenching 8=2288
- Au–V alloys, thermoelectric power, resistivity near Kondo temp. 8=8992
- Au–V alloys, s-d interaction from elec. resistivity and mag. susceptibility meas. 8=13657
- Au₄V, sp. ht. meas. 1.5–60°K 8=4930

Gold compounds—contd

- Au–Zn alloys, long-period ordered, X-ray diffraction study 8=13250
- Au–Zn alloys, quenched and aged, structure 8=22185
- Au–Zn system, β' thermal stability 8=17037
- β'–AuZn, reflectance and other optical props. 8=2402
- Grain boundaries.** See Crystal imperfections; Crystal structure, microstructure.
- Gramophones.** See Sound reproduction.
- Granato–Lücke theory.** See Crystal imperfections/dislocations.
- Granular structure**
 - brass, grain size, dependence of hardness 8=8835
 - films, thin discontinuous, grain size distribution, conservative systems 8=13084
 - films, thin, grain size distrib., non-conservative systems 8=13085
 - grain boundary segregation, autoradiography 8=8738
 - grain boundary sliding, contribution to creep strain of polycrystal 8=8802
 - grain density, measuring methods, resolution limit 8=825
 - grain size distrib. by e microprobe 8=17260
 - heat transfer to contact plates, calc. 8=19629
 - impact cratering in granular materials 8=8253
 - layer of elastic and granular material, horizontal displacement 8=2567
 - moisture effect on tensile strength 8=22285
 - moving boundaries, solute profiles 8=8468
 - orientation depend. of grain size, X-ray meas. 8=4832
 - particle sizes and strains, determ. from three different diffraction parameters 8=22257
 - plasticity theory 8=8798
 - size distrib. in 1 μm range, by X-ray diff. 8=13151
 - statics of granular materials, theory 8=21829
 - steel, austenite grain size, high temp. microscope obs. 8=13157
 - steel, growth of secondary grains during annealing 8=172
 - steels, intergranular fracture 8=22222
 - tensile strength equation 8=22288
- Ag–base, solid solutions, impurity atoms in grain-boundary transition zones 8=17277
- Ag–5.64 wt. %Al alloys, grain boundary precipitation 8=17038
- Al, during extrusion recovery and recrystallization 8=48
- Al, sub-boundaries in single crystals grown from melt, direct observation 8=17678
- AlZn–Mg cast alloys, boundaries rel. to stress corrosion cracking 8=22312
- Be sheet rolled from ingots, grain boundary precipitation 8=17046
- BeO, grain growth during sintering, effects of SiC and MgO 8=22315
- C grains, production in discharge, light scatt. and interstellar matter 8=4296
- Fe, glass-doped, and orientation after annealing, model for doped W 8=17025
- Fe grains, production in discharge, light scatt. and interstellar matter 8=4296
- LiF, single crystals, X-ray studies on sub-grain boundaries by limited projection topography 8=13446
- MgO grain shape change during creep 8=13584
- MgO segregation of impurities to grain boundary 8=1345
- Pb, ball indentation tests 8=13602
- UO₂ swaged compacts, equiaxed grain growth under temp. grad. 8=8255
- W, thermochem. deposited, effect of F impurities on high temp. grain stability 8=17294
- Graphite**
 - adsorption of CO₂, anisotropy of polarizability 8=21900
 - adsorption, localized 8=8339
 - adsorption of various gases and vapours by fresh surface 8=8338
 - crystal impurity growth during diamond crystallization by catalyst-metal system 8=1737
 - deformation mechanism 8=5053
 - deformation props. and anomalous strength in nuclear grade A, 20–2200°C 8=8829
 - diffusion of fission products, Xe and I 8=12015
 - electrodes, bisulphate intercalates form. and elec. props. 8=18731
 - electrodes for spectroscopy, purification by electron beam heating 8=23187
 - escape behaviour of captured fission Xe, isothermal annealing 8=11975
 - Fermi surface pressure dependence 8=8926
 - foamed, shock compression 8=22316
 - gasification by pure CO₂, transient phenom. rel. to impurities 8=9678
 - Graphon, adsorpt. of isopropyl alcohol 8=1700
 - interstellar grains, adsorption 8=23572
 - interstellar matter, computed and observed extinction curves 8=10247
 - interstellar, role of impurities 8=10246
 - irradiated at 77°K, effect on phys. props. 8=8763
 - irradiation induced creep under constant stress 8=8828
 - magnetoresistance, linear, in the quantum limit 8=13711
 - monocrystalline, e. p. r. of free charge carriers, thermal variation of line width anisotropy 8=5524
 - n-irradiated, optical absorpt. 8=14202
 - neutron scattering law S(α, β), values at 1300°K and 1800°K 8=11898

graphite—contd

- neutron prod. dimens. changes rel. to bromination test 200°C 8=8764
- noble gas isotope anomalies, origin 8=9793
- optical absorption of pi-electrons 8=18511
- optical props., transverse and longitudinal 8=2407
- permeability for gaseous fission products 8=4950
- polycrystalline, brittle, form. and growth of cracks 8=22318
- polycrystalline, Youngs modulus, comment on effect of porosity and orientation 8=22319
- pyrolytic, dynamic mech. behaviour, rel. to reactor rad. dose 8=8827
- pyrolytic, electron momentum distrib. by Compton X-ray scattering 8=17907
- pyrolytic, formation and structure 8=13134
- pyrolytic hot-worked, shear compliance 8=5054
- pyrolytic, oxidation pitting comp. with vitreous C 8=8292
- pyrolytic, prep. for transmission electron microscopy 8=4835
- pyrolytic, two-stream instability, dispersion relations 8=8968
- quasi monocrystalline, thermal conductivity, effect of neutron irradiation 8=13389
- quasi monocrystalline, thermal conductivity, quantitative description 8=13390
- reactor, gasification with CO₂ and H₂O 8=2514
- rubbed over ceramics, for optical accentuation of fine pores 8=17019
- slabs, density meas. and isodensity curves 8=22317
- soldering to metals, by first electroplating with Cu 8=5998
- solubility of B, 1800–2500°C 8=17006
- spheroidal crystal growth in Fe-C, Ni-C, Co-C, Au-C and Fe-C-Si alloys 8=13156
- thermal vib. amps. of C atoms in lattice parallel to c-axis 8=22085
- thermoelectric and galvanomagnetic props. rel. to cryostat size and structure 8=5384
- FeCl₃-graphite cpd., electron microscopy 8=1972
- ICl doped, anelasticity, impurity-dope effects 8=13541
- K-graphite lamellar cpds., phase equilb. 8=4712
- Xe captured by nuclear recoil, escape behaviour 8=4017

Graphs

See also Nomograms.

- Chebyshev polynomials, fitting to equidistant points 8=14941
- geometric representation of indeterminacy reln. 8=550
- for perpendicular reflectivity and phase angle at boundary of two mats. 8=500

Gratings. See Diffraction gratings; X-ray diffraction.

Gravimeters. See Gravity.

Gravitation

See also Relativity.

- Aharonov-Bohm effect in flat space-time metric 8=6060
- Brans-Dicke theory and solar neutrino flux 8=14731
- Cauchy problem, symmetric tensors, covariant decomposition 8=6071
- change with time 8=6085
- charged particle in expanding universe 8=10600
- charged relativistic fluid in e.m. field, Larmor and Helmholtz theorems 8=16633
- classical field, interaction with quantized matter field 8=19430
- collapse, criticism of spherically symmetric models 8=23484
- collapse of large masses 8=19083
- collapse of massive star, evolution of ejected matter rel. to nucleosynthesis 8=14726
- collapse of a non-rotating, spherically symmetric star, optical appearance 8=19153
- collapse, oscill. model with pressure, gradient 8=14735
- collapse in red giants of non-degenerate He shell, energy release calc. 8=10128
- collapse, Schwarzschild soln. proved to be unique in its non-singular event horizon 8=10589
- collapse of supernova 8=10186
- collapse of supernovae 8=2790
- collective processes in limited systems, considering finiteness of parabolic velocity 8=19103
- cosmological models, homogeneous, with bounded potential 8=23477
- effects on interstellar gas motion in radiating star neighbourhood 8=23580
- e-gravitational field interaction, Dirac eqn. 8=708
- Einsteinian, centre-of-mass line 8=10593
- Einstein eqns. of field, difficulties in combining with quantum field theory 8=19414
- Einstein eqns., problem of evolution 8=6067
- Einstein free field and free Yang-Mills fields, conditional dynamic equivalence 8=6076
- Einstein general relativity eqns., solutions in presence of strong field 8=19415-16
- Einstein's gravitation theory, motion of extensive object 8=6086
- energy change with time using Poynting pseudo-vector 8=2946
- Eötvös expt., quasi-inertial principle instead of general covariance 8=14967
- experiments with cylindrical galaxy 8=10086
- experiments in universe, rel. to general relativity 8=80

Gravitation—contd

- extended theory, Mach's principle and rot. masses 8=6087
- field, degenerate caustic surfaces in Tolman's solution 8=6073
- field, elongation of a hanging meter bar 8=6002
- field energy functional, extremum under variation of metric field variables 8=14976
- field eqns. for ideal, rigid, rot. liq. 8=6088
- fields, higher dimensional spaces and symmetries from LCt linear pseudogroup 8=2948
- field of uniformly rotating axially symm. source 8=19420
- field of unspherical planet, particles eqns. of motion, from method of averaging 8=23660
- fluid, charged in e. m. field, relativistic, Hamilton-Jacobi eqn. 8=16634
- g absolute meas. 8=37
- general relativity and recent development 8=2956
- general relativity theory and expts. 8=10592
- general relativity, verification 8=6070
- graviton-spin-0 particle scatt., low-energy theorem 8=20283
- gravitons, prod. by two photons, mean density in universe 8=19422
- Hoyle-Narlikar conformal theory, generalization 8=10594
- ideal fluid, in Einstein space-time 8=10595
- instability in a compressible fluid cylinder 8=19084
- instability of stars and galaxies, conference Belgium 1966 8=14734
- inverse-square law, simple proof 8=10587
- Jacobi's ellipsoidal figures under influence of halo, stability 8=14725
- Kepler motion, relativistic spinor regularization 8=19418
- Kepler problem, formulation invariant with respect to SO₄, SO_{3,1} groups 8=14943
- Kerr metric and rotating masses 8=2950
- Klein-Gordon-Maxwell-Einstein field eqns. fine-structure constant and internal energy 8=19423
- Lagrangian struct. rel. to Einstein's eqns. violation by Mercury 8=10586
- linearized theory, canonical transformation rel. to quantization of general relativity 8=10597
- Mach principle, positive-definiteness of inertial mass and e. m. coupling 8=14980
- magnetic-gravitational analogy rel. to planet parameters perturbations 8=19417
- magnetic monopole analogue in gravitation theory 8=6078
- mass in radial motion, spherically symmetric metrics description 8=6072
- Newtonian, and relativistic, theories of collapse 8=10087
- Newtonian version of generalized theory 8=19426
- non-Einstein eqns. rel. to Einstein eqns. 8=82
- null fields, three-dim. formulation 8=2957
- one-body theories, Lorentz-invariant, classification and empirical tests 8=70
- particles, classical spin, self-forces and radiation losses 8=71
- particle wave function in weak field 8=2947
- persecution trajectories in central field, method of construction 8=19098
- perturbations, motion of artificial earth satellite, analytical expressions 8=14718
- planet, unspherical averaging of motion in field 8=10096
- planetary precession derived without use of Einstein's field eqns. 8=19421
- potential, spherical harmonics, perturbations of satellite orbits 8=14719
- pre-galactic collapse, H₂ formation 8=23483
- quantum theory, covariant, appl. to gravodynamics 8=3452
- quantum theory of general relativity and elementary particle structure 8=6081
- quantum theory, manifestly covariant 8=3451
- radiation, generator built and obs. 8=19419
- radiation scattering, asymptotic 8=2954
- reddening of galactic light 8=14804
- relativistic particle in gravitational and central fields, equivalent Newtonian pot. calc. method 8=6080
- relativistic theories, one-body problem 8=10584
- rotating masses 8=14975
- in Schwarzschild field, behaviour of moving clocks 8=6084
- singularity anticollapse in space filled with nonideal medium 8=19424
- in solar field, motion of variable mass particle 8=10093
- Soviet work, review covering 50 years 8=19425
- space filled with dustlike medium, simultaneous physical singularity 8=14978
- space times, empty, algebraically special on given world-line 8=14968
- spin-1/2 particles in field, theory 8=2959
- stars, line-blanketing effect 8=14769
- stellar model, liquid sphere, frequency spectrum 8=4504
- three bodies problem, near periodic soln. 8=19097
- Tolman solutions for geodesic motion 8=2952
- transitions, role of Bose statistics 8=14969
- Treder theory, non-singularity of cosmological models 8=10596
- 2-body system, gravitational radiation, scalar component 8=6079
- two bodies with variable masses, quadrature soln. 8=19409

Gravitation--contd

- unified field theory, geodesic principle 8=83
- unified quantum field theory 8=10606
- universe models density fluctuations and vibrs. normal modes 8=14732
- Vierbien field for nonlinear theory 8=19428
- waves, charact. features and calc. of propag. velocity 8=79
- waves, generation in optically closed systems 8=2949
- waves, generations and detection 8=10585
- waves, gravitational, generation and obs. 8=81
- waves, from quasars, binaries, primordial fireball, obs. 8=14959
- waves, transport of energy and momentum from rotating rod, linear approx. 8=14979
- waves, 2 spinning rods as source 8=19427

Gravitational collapse. See Gravitation.**Gravitational red shift. See Relativity/general.****Gravitons. See Gravitation.****Gravity**

See also Geophysical prospecting.

- acceleration determ., Poland, history 8=14515
- acceleration, meas. using laser-interferometer system 8=10487
- anomalies arising from horiz. cylinder type bodies, e. m. analog computation 8=18807
- Canada, 1963 to 1966, obs. 8=18806
- compensator for biophysical space studies 8=10446
- earth's field asymmetry rel. to satellite orbits perturbation 8=14716
- earth's field, determ. from satellite obs. 8=9769
- earth interior intensity distrib. 8=18826
- earth, thermal rel. to gravitational anomalies 8=2555
- effects in electrochemistry 8=14416
- effect on origin of geosynclines and orogens, model expt. 8=14512
- elastic waves perturbation rel. to \bar{S} and \bar{P} pulses and dispersion curves 8=3030
- electric fields induced near metals 8=5159
- on electrons, freely falling and metallic, force compared 8=704
- field, low degree, amplitude spectra 8=14513
- "g", absolute meas., review 8=38
- geopotential, odd zonal harmonics from satellite orbits 8=5770
- gradiometer computer model for simulated gradient contour mapping 8=5771
- gravimeter, superconducting 8=18805
- gravimetry, in correctly posed problems, soln. by convolution-type integral eqns. 8=23199
- longitude dependence of geopotential deduced from synchronous satellites 8=5769
- Love's number from satellite observations 8=5768
- moon craters, scaling, Ranger VIII obs. 8=23641
- pulsation, geological evidence for 8=2554
- residual, meaning rel. to Bouguer gravity and convolutions 8=14514
- and satellite orbits 8=5767
- sea and air meas. errors 8=23198
- Soviet work, review covering 50 years 8=19425
- stars HR 4533 and 4657, surface 8=23533
- Stokes and Vening Meinesz formulae integration, truncation errors 8=9768
- stratified atmos., acoustic and gravity-wave emission by turbulent motions 8=23270
- tidal var., spectral analysis 8=9817
- variable, heat transfer domains for fluids 8=16692
- wave propagation in atmosphere after nuclear explosion, effects 8=2583
- waves, instability 8=21450
- zero field, rotation induced heat transfer in liquids 8=4562

Grey atmosphere. See Radiative transfer; Stars/radiation.**Group theory**

- associative algebra for mass formulae 8=15688
- Bondi-Metzner generalized, reduction 8=14933
- causality group of Zeeman examined 8=3416
- classical, decomposition of tensors 8=2880
- classical dynamical systems, construction of symm. groups 8=2912
- conformal, example of Poincaré extension 8=10503
- conformal group on a space-time curve and associated Yang-Mills field 8=15679
- crystal lattice, magnetic symmetry groups, representation 8=5111
- crystals, normal vibrations, symmetry props. 8=17474
- crystals, normal vibrations, symmetry props. 8=17475
- deviation from symmetry, use of generalized perturbation theory 8=11259
- Dirac eqns., symmetry group props. 8=6593
- Ditkin subsets, finiteness proof 8=12
- double and space group representations, analogy 8=19363
- eigenfunction expansions for hyperboloids and cones 8=2889
- field theory, relativistic, exactness of symmetry 8=11280
- Galilei group, physical and nonphysical representations 8=6728
- Gamow-Teller matrix elements for super multiplet states, exact determ. 8=15930
- harmonic oscillator, $SU_{n,1}$ representation 8=3409
- Group theory--contd
 - holonomy, internal of solns. to Yang-Mills eqns. 8=10506
 - inhomogeneous Lorentz, manifest covariant representations 8=11274
 - interchange symmetry, molcs., crystals and excitons 8=4118
 - internal and space-time symmetry, double structure 8=2891
 - isometry groups with surface-orthogonal trajectories 8=2888
 - ladder-operators, self-adjoint, harmonic oscillator and (Dirac) Kepler problem appls. 8=11261
 - ladder operators, self-adjoint, n-dimens. orbital angular momentum appls. 8=11260
 - Landau theory of 2nd-order phase transitions, $\{\Gamma\}^3$ and $\{\Gamma\}^2$ for crystallographic point groups 8=17031
 - Lie algebras, deformation and contraction 8=6026
 - Lie algebra, deformation of subalgebra 8=10500
 - Lie algebra extensions of the Poincaré group 8=14
 - Lie algebra realization in classical mechanics 8=2913
 - Lie rel. to general mass formula for elementary particles 8=20266
 - Lorentz, complex unimodular, finite and rotation groups representation 8=19362
 - Lorentz group, inhomogeneous, nonzero mass components 8=2892
 - Lorentz, inhomogeneous, "canonical" representations 8=2893
 - Lorentz rel. to lepton field 8=11450
 - Lorentz, lightlike permutation lemma 8=6024
 - Lorentz proper G, continuous subgroups 8=2895
 - Lorentz, representation rel. to scatt. amplitude 8=15696
 - Lorentz, unitary and non-unitary representations 8=10501
 - Lorentz, unitary representation matrix elements 8=6023
 - Lorentz, unitary representations, rel. to particle dynamics 8=3507
 - magnetic monopole quantization applic. 8=20271
 - multipole interactions, derivation 8=15190
 - noninvariance groups in particle physics 8=3502
 - nuclear shell model as n-fermion system error in Hamiltonian matrix diagonalization 8=3761
 - O_{n+1} symm. in simple harmonic oscillator 8=10521
 - $O_{3,1}$ unitary representation from IO_4 8=3506
 - $O(3,1)$ representation and Regge daughter-poles 8=11413
 - $O(3,2)$ and $O(4,2)$, mass spectrum and mag. moment derivation 8=20265
 - $O(4,2)$ and appl. to meson decay rate 8=20414
 - $\hat{O}(n) \supset O(n-1) \supset \dots \supset O(2)$, lowering and raising operators and generator matrix elements 8=19361
 - orthogonal, lowering and raising operators, in chain $O(n) \supset O(n-1) \supset \dots$ 8=6028
 - $P \times SL(6, C)$, with infinite multiplets, predictions of model 8=579
 - particle in spherical potential 8=6732
 - Poincaré, "canonical" representations 8=2893
 - Poincaré group extension to internal symmetry group, non-physical 8=649
 - Poincaré group generators from soln. of Killing eqns. for 5D pseudosphere 8=3417
 - Poincaré, positive mass representations rel. to elem. particle interactions 8=15614
 - properties, rel. to Hamiltonian symmetries for symmetry violating states and collective motions 8=557
 - q. e. d., renormalization extension 8=20170
 - quantum mechanics, representations theory appls. 8=20137
 - R_3 , Lie algebra 8=11360
 - R_3 rotational group infinite-dimensional representation 8=6022
 - Regge-pole hypothesis, multiple, Toller analysis 8=6769
 - representations, analytically continuing, Gell-Mann formula 8=6027
 - rotation group, irregular representations, completeness 8=2886
 - $SL(n, C)$ Clebsch-Gordan coefficients 8=651
 - $SL_{2,c}$ decomposition into sums over unitary representations of SU_1 and $U_1 \wedge T_2$ 8=10502
 - $SL(2C)$ group, irreducible unitary representations 8=576
 - $SL(2C)$, unitary irreducible represent., decomposition, restricted to $SU(1,1)$ 8=6029
 - $SL_{2,c}$ unitary representations, transformation from O_3 to O_1 , recast as series of Γ functions 8=20264
 - $SO_0(4,2)$, symm. group for elementary particles 8=15682
 - $SO_0(p,q)$, decomposition of most degenerate representations, restricted to $SO_0(p,q-1)$ or $SO_0(p-1,q)$ 8=19360
 - SO_4 , $SO_{4,1}$ rel. to Kepler problem 8=14943
 - $SU(n)$ crossing matrices and meson-baryon scatt. 8=741
 - SU_n representation of harmonic oscillator 8=3409
 - SU_n symm. in simple harmonic oscillator 8=10521
 - $SU(p,1)$, irreducible representations, classification and characters 8=2894
 - $SU(2)$ and internal symmetry group b, embedding in larger group b 8=652
 - $SU(2) \otimes SU(2)$ symmetry of Kepler motion 8=653
 - $SU(2)$ and $SU(3)$, rel. between "outer" and "inner" multiplicity 8=3504
 - SU_3 anal. applied to possible octodecimet of axial-vector mesons, in quark picture 8=11556
 - $SU(3)$, commutation rules of generators, conversion to set of diff. eqns. 8=600
 - SU_3 as dynamical group of $H = \frac{1}{2} p^2 + V(r)$ 8=11265

Group theory—contd

- SU(3) chiral dynamics 8=15744
SU(3) irreducible representations, quasispin and multiplet structure 8=594
SU(3), irreducibility representations and Weyl formula 8=15
SU(3) multiplets explained by obs. parity doublets of baryons resonances 8=6981
SU₃, projection operators and Clebsch-Gordan coeffs. calc. 8=15680
SU(3) and Regge poles: classification and high-energy scatt. 8=15708
SU₃ symmetry for systems of 3 and 4 particles in 2s-1d shell 8=7042
SU(3), Weyl coefficients 8=2887
SU, Wigner coeffs. 8=2885
SU(6)_w-symmetry and peripheral hadron scatt. 8=6832
SU(6), SU(6)_w and SU(6, 6) 8=11366
SU(6) ⊗ SU(6) symm. rel. to algebra of spin currents 8=11272
SU₆, Clebsch-Gordan coefficients 8=15683
spectra of generators in irreducible unitary representations 8=14932
strong coupling group representations 8=6731
symmetrized tensor products, Clebsch-Gordan series 8=2890
symmetry groups in nuclear and particle physics 8=11361
symplectic, branching theorem 8=6025
tensors, Q₈ decomposition into its rotational subgroup 8=19355
2, 3, 4-particle systems with harmonic oscillator pot., group theory 8=11258
U(2, 2) algebra unitary representations and massless fields 8=15689
U(3) isoscalar factors, recursion relations 8=3420
U(6, 6) algebra in harmonic function space 8=14934
unitary symmetry, SU(3) 8=6722
Wigner coefficient. See Specific heat; Thermal expansion.
Wigner-Pohl effect. See Electroluminescence.
Wigner-Preston zones. See Crystal structure/microstructure.
Wigner effect. See Crystal electron states/plasma; Semiconducting materials; Semiconductors.
Zeeman effect
sun, thermal r.f. emission from active regions 8=23713
Zeeman ratio
alkali metals, precision determ. by atomic beam resonance technique 8=12089
measurement by differential perturbed angular correlation 8=7066
rigidity, eqn. of motion 8=4047
Dy¹⁶¹, from branching-ratio expt. 8=11772
H₂⁺, by selective photodissociation 8=12195
Hf^{176, 178, 180} precession obs. following Coulomb excitation by O¹⁶ and recoil into liquid Ga 8=15998
In¹¹⁷, g-factor of ³/₂⁺ 660 keV 8=3823
Ir^{191, 193}, g factors, for first excited states 8=3836
Np^{237, 239}, g-factor meas. by α-γ correl. 8=3846
Rb⁸⁵, g₁/g₂ meas. by atomic beam resonance method 8=20709
Rb^{85, 87}, g₁/g₂, optical pumping determ. 8=1173
Yb^{174, 176}, Mössbauer effect meas. for first excited states 8=3832
Zn⁶⁷, 184 keV state 8=7085
Zeeman effect
precession and nutation, simplification by vectors 8=10529
Schiff's, as test for Brans-Dicke scalar-tensor theory 8=14977
quartz sphere with superconducting Nb for satellite instrumentation and expts. 8=17984
vibrating, solid-state, new resonator 8=33

Hadrons

- β-decay Fermi part, radiative corrections 8=20409
hook 8=6830
bootstrap conditions in S-matrix theory, rôle of CDD zeros 8=15712
bootstrap and finite-energy sum rules 8=15711
bootstrap incompatibility with closure and locality 8=15710
bootstrap model of NN*π dynamics, e. m. perturbation effect 8=11486
classification rel. to weak and e. m. currents 8=731
cluster model using sakaton 8=20401
collisions, high energy, secondary particles, charge ratio and transverse momentum 8=11524
composite particle theory, construction of Hamiltonian 8=11487
Compton effect, J^p = 1⁻, 3/2⁺, sum rules 8=6901
current algebra and sum rules 8=15743
current dynamics, self-interacting charged meson model 8=20398
currents formulation of dynamics 8=20397
decay, weak, time-reversal invariance, K⁰ → μ⁺ν_e⁺e⁻ as test 8=789
decay with CP conservation and violation in the same interaction 8=6827
ΔI = 1/2 rule derived using chiral transformation 8=15752
e. m. current as part of neutral vector-meson fields 8=6899

Hadrons—contd

- e. m. interactions need not be CT invariant 8=20475
electromagnetic interactions, vector-dominance model tests 8=15751
electric and mag. polarizabilities, in quark model 8=6823
form factors and structure effects in vacuum polarization 8=588
form factors e. m., as infinitely composite particle rel. to bootstraps 8=11484
hadron-lepton neutral transitions, neutral current and limit of weak interaction theory 8=6829
interactions, 4-fermion, with ΔS=1, SU₃ symm. and RP invariance 8=20400
isomultiplet splittings of e. m. origin, quark model 8=6824
isovector e. m. current and ρ field, as in Yang-Mills theory 8=6831
lepton-hadron weak interactions and lepton octet 8=11449
leptonic decay, two-angle Cabibbo theory rel. to data anal. 8=6819
levels, assignment, evidence for O(4, 2) 8=15747
meson-baryon S-wave scatt. length calc., pseudo-scalar 8=20420
meson-baryon scatt., QQQ model 8=20418
magnetic moment relations using sidewise dispersion relations 8=3605
mass difference, e. m., superconvergence dispersion relation approach 8=11485
mass difference, model 8=20415
mass differences, rel. to weak vector currents 8=732
mass spectrum, asymptotic bootstrap approach 8=15746
meson-baryon systems, systematics of forces 8=6918
pion-hadron, elastic amplitude calc. 8=20451
pion-hadron scatt., strong-interaction sum rules, mass relations 8=20450
production at high energies, statistical characteristics 8=6821
quark model as deformable sphere 8=15673
quark model based on collinear group 8=728
quark model for elastic 90° 8=15754
quark model for interactions, breaking of SU(3) 8=20405
quark scattering model, additivity test from decay distrib. in double reson. prod. 8=11479
Regge branch-point exchange effect 8=20319
Regge poles and interaction total cross sections, universality and degeneration 8=15748
Regge pole hypothesis in amplitude with photons 8=15716
Regge-pole model with L-S coupling for PN → P⁺N, PN → VN 8=20318
Regge-quark scattering model 8=734
relativistic trion model 8=20396
reson. splitting and multiple poles 8=11483
scatt. in additive quark model, shadowing correction 8=6825
scatt. at high energy and arbitrary angle, quark model 8=15755
scattering, peripheral, [SU(6)]_w-symmetry 8=6832
scatt., similarities to multi-π prod. 8=20530
SU(3) chiral dynamics 8=15744
SU(3, 1) representation, mass spectrum 8=20258
SU(12) ⊗ SU(12) symm. and sum rules relating isovector states, mass relationship 8=15745
sub-hadronic system, mass term, in Lagrangian, chiral-type interactions 8=11481
sum rules and equal-time commutation relations for composite fields 8=15750
2-body reactions by Pomeranchukon exchange, spin parity rule 8=20317
2-body scatt., sakaton model 8=15753
Thirring model, 2D based on currents for hadron dynamics 8=20399
Haemoglobins. See Proteins.
Hafnium
deformation planes after dehydrogenation and hydride habit planes 8=8728
isotopic shift in spectrum, rel. to deform. of Hf¹⁷⁴ nucleus 8=20953
ore deposits in Republic of South Africa 8=9792
thermionic emission in Cs vapour, meas. by plasma-anode tech. 8=18264
Hf¹⁷² + Lu¹⁷², positrons, number, in decay 8=11824
Hafnium compounds
iodide, thermal conductivity and blackness 8=1890
oxides, u. v. transparency, temp. depend. and effect of Cl⁻ and NO₃⁻ 8=5605
HfC, Verneuil growth by arc melting 8=4799
HfCuSi single crystals. 8=4777
HfO₂, defect struct. and elec. cond. 8=13419
HfO₂, elec. cond., struct. defects, high temp. 8=9198
HfO₂ films e beam evaporation and dielec. props. 8=22652
HfO₂ films dielec. and resist. props., and resistors and capacitors characts. 8=22654
HfO₂-ZrO₂ system, phase equilibria 8=21863
HfSiO₄, synthesis and X-ray study, lattice parameters 8=8524
Half-lives. See Radioactivity/decay periods.
Hall effect
See also Semiconducting materials; Semiconductors.
analogue multiplier application 8=19374
anthracene, d.c. dark mobility obs. 8=22523

Hall effect—contd

- carbon, pyrolytic 8=5174
 compensated, multiband conductor, high field coeff. mag. field dependence 8=8920
 chalcogenide glasses, mobilities in vitreous and liq. states 8=18027
 current, influence of flow of conducting gas at high vel. 8=16653
 devices, and magnetoresistance, appls. and design 8=13839
 for e and hole mobility and density in cryst. phosphors meas. 8=8898
 ferromagnetic metals, spontaneous Hall and Nernst-Ettingshausen effect 8=9329
 in ferromagnetics, theory 8=22765
 glasses, chalcogenide, meas. method of temp. depend. 8=13789
 gyration device, design considerations rel. to use of only one neg. resistance element 8=19751
 influence on magnetogasdynamics flow round nose of blunt body 8=15378
 liquid alloys, Hall coeff. and resistivity meas. 8=16880
 liquids, chalcogenide, meas. method of temp. depend. 8=13789
 low-mobility samples at high temps., apparatus 8=8977
 magnetic induction and coercive force meas. 8=19738
 metals, high purity, for texture investigations 8=8454
 plasma, hydromagnetic, in collision damping theory 8=12486
 in polaron hopping conduction, theory 8=17998
 polaron model, Holstein, temp. variation 8=8954
 polaron, small, mobility from perturbation treatment of Kubo's formula 8=13678
 semiconductors with edge dislocation, effect of non-uniformity of density 8=13780
 n-type semiconductor, Hall mobility as function of impurity 8=5226
 semiconductors, many-valley, at high electric fields 8=22417
 semiconductors with non-uniform charged ion conc., theory 8=22421
 in semiconductor trace analysis 8=18757
 semiconductors, voltage, influence of skin effect 8=5232
 semimetals with equal numbers of electrons and holes, quantum theory 8=22416
 weak-field coefficient, new computation method for most band models 8=13645
 Ag, thin films 8=2133
 Ag-In liq. alloys, depend. on temp. and conc. 8=12923
 α -Ag₂S mixed conductor, coeff. meas. rel. to electronic props. 8=22500
 AgTe, liq., rel. to possible semicond. nature 8=12917
 Al, between 2.5° and 300°K 8=5170
 Al, high field coeff. from helicon resonances 8=5169
 Au, thin films 8=2133
 AuTe₂, liq., rel. to possible semicond. nature 8=12917
 Bi, effect of pressure 8=5173
 Bi films, temp. dependence 8=8995
 Bi, positive, explanation 8=8994
 Bi, 300-540°K 8=13710
 Bi_{1-x}Sb_x, (0 < x ≤ 0.15), at 77°K rel. to band structure 8=22518
 CdCr₂Se₄, ferromagnetic 8=2189
 CdS, photo Hall mobility at high electric field 8=2187
 CdS single crystal, elec. field and mobility 8=17860
 p-CdSb, coefficient anisotropy 8=13794
 n-CdSe, meas. and anal., and magnetoresistance effects 8=13796
 CdSe, p-type, meas. 8=5239
 CdSAs₂, rel. to temp., conduction band structure 8=8929
 CoO, paramagnetic, anomalous 8=17914
 Cr, at 4.2, 77 and 273°K, rel. to applied mag. field 8=8855
 Cr, at 4.2°K, 77°K and room temp., magnetic fields up to 147 kOe 8=9002
 Cr-Mo alloys, and sp. ht. meas., between 125-625°K rel. to comp. 8=4931
 Cr-SiO cermet films, coeff. and other elec. props. 8=8981
 Cr_{1-x}Te_x alloys, in paramagnetic state 8=9300
 Cu, thin films 8=2133
 α -Cu-Ag alloy, coeff. and resistivity, interpretation 8=13641
 p-Cu₂S, and thermoelectric power and elec. cond. 8=22585
 Cu-Sn alloy, rel. to bound state form. round Sn atoms 8=12917
 CuTe, liq., rel. to possible semicond. nature 8=12917
 FeCrAl alloys as ferromag. Hall probes 8=14011
 α -Fe₂O₃, paramagnetic, anomalous 8=17914
 GaAs, insulating, high-field photo-Hall effect 8=9105
 GaAs, Cu-diffused crystals, defect centres 8=1954
 GaAs, semiconducting, at high electric fields 8=22417
 GaAs, Sn doped meas. 8=2191
 GaAs:Zn polycrystalline films, obs. and theory 8=5255
 GaP crystals, coefficient, 4.2-300°K 8=9100
 GaP:S, coeff. meas. 4.2 to 400°K 8=13805
 GaP:Zn, coeff. meas., 4 to 300°K 8=13806
 GaSb 8=22587
 p-GaSb at 4.2°K, valence band studies, and by magnetoresistance 8=13803
 p-GaSb, Hall coeff. and conductivity, pressure dependence at diff. temps. 8=13804

Hall effect—contd

- GaSe, charge carrier mobility from elec. resistivity and Hall constants 8=5247
 p-Ge bolometer 8=6205
 n-Ge, effect of dislocations on galvanomag. props. 8=22592
 Ge, holes mobilities at 9.6 GHz between room and liquid He temp. 8=13836
 n-Ge, hot electron mobility, and magnetoresist. for elec. field along <100> direction 8=18052
 Ge, screw dislocations, optical effects 8=1979
 Ge-Si alloyed heterojunctions, coeff. and conductivity at interface region 8=2217
 GeTe liq. 8=16877
 HgTe, coeff. and magnetoresistance at 4.2 and 77°K rel. to carrier model 8=2200
 HgTe-ZnTe, coefficient, at low temperatures 8=13816
 InAs, quantum oscs. 8=13818
 p-InSb bolometer 8=6205
 InSb, coeff. and conductivity, high pressure dependence 8=13819
 n-InSb, Corbino conductivity 8=9114
 InSb, electron drift velocity and mobility calc. 8=9112
 p-InSb, Li-saturated, and resistivity, annealing effects 8=5270
 InSb, n- and p-type, saturation of drift velocity 8=2201
 InSb, microwave emission 8=5267
 InSb, quantum oscs. 8=13818
 p-InSb, 90% compensated, Hall const., 4.2-300°K 8=13822
 MoS(Se)₂, charge carrier mobility from elec. resistivity and Hall constants 8=5247
 Na_{0.33}V₂O₅, single cryst. 8=22601
 NbN, effect of N content variation 8=13702
 Ni films and conductivity dependence on O₂ adsorption 8=17936
 Ni-Cu alloys, rel. to electrical resistivities 8=9014
 NiO at high temps. 8=8977
 NiO, mobility at 1007°K 8=13827
 NiO, paramagnetic, anomalous 8=17914
 PbS films, rel. to space-charge layers on crystallite surfaces 8=5273
 Pb-Sn alloy polycrystalline vs impurity concentration obs. of two maxima 8=8803
 PbTe, anomalously high-mobility rel. to sample prep. 8=2138
 PbTe films, thin, and conductivity and resistivity 8=22603
 PbTe liq. 8=16877
 PbTe, p-type, mobility and thermoelectric power rel. to Na doping 8=5274
 Si, screw dislocations, optical effects 8=1979
 Si₃ ion implanted with Sb, Ga and As rel. to carrier conc. distrib. 8=18072
 Si:In, and photoconductivity and noise meas. rel. to electron and hole-capture coeff. 8=13915
 SiO₂, rel. to electron mobility determ. 8=9124
 SnO₂, rel. to electron scattering polar optical modes 8=22611
 SnTe films, thin, prep., resist. meas., Hall effect and cryst. props. 8=13096
 SnTe liq. 8=16877
 TaN, effect of N content variation 8=13702
 Te-Ge eutectic alloy 8=16877
 ThC₂, nonstoichiometric 8=2140
 Th_xY_y, (x = 1, 3; y = 1, 4), coeff. rel. to electronic props. 8=2139
 UO_{2-x} and U₃O₈, Hall coeff. rel. to carrier mobility investigation 8=18090
 WSe₂, charge carrier mobility from elec. resistivity and Hall constants 8=5247
 Zn-Ag, polycrystalline 8=17941
 Zn-Al, polycrystalline 8=17941
 Zn_xCd_{1-x}Sb, rel. to temp. and conc. of acceptors 8=2131
 Zn-Cu, polycrystalline 8=17941
 ZnO:(Ni, Co) crystals, liquid N₂ to room temp. 8=9132
 ZnS, e and hole mobility obs. 8=8898
 ZnS, photoexcit. assoc., rel. to recomb. mechanisms 8=9258
- Hall generators.** See Electricity/direct conversion; Semiconductor devices.
- Hall mobility.** See Semiconducting materials; Semiconductors.
- Halogens**
 crystals, intensities of i.r. -active lattice vibr. 8=22084
 molecules, dipole strengths as function of internuclear distance 8=21084
 solid, space groups dependence on electron density 8=17328
- Hamidashi effect.** See Ferroelectric materials; Ferroelectric phenomena.
- Hard-sphere gases.** See Quantum theory/many-particle systems; Statistical mechanics.
- Hardness**
 See also Abrasion; Work hardening.
 beam, rigid-plastic, strain-hardening rel. to permanent deformation 8=19402
 binary cpds., inorganic, rel. to point defects 8=8689
 brass, rel. to grain size 8=8835
 brass, 70-30, rel. to deformation texture development, pole figure 8=17777
 Brinell hardness, analytical interpret. rel. to common mech. props. 8=17748

Hardness—contd

- carbon steels, at 2 to 20°K, rel. to C content 8=8639
- diamond, abrasion and surface strains and damage 8=8826
- epoxy polymers, micropenetrator for surface characterisation 8=8876
- hardboard and nonmetallic materials, measurement of 8=13520
- lithium ferrites-chromites, effect on spontaneous magnetization 8=2341
- polycapromide, correl. with melting temp. and nature and cond. of filters 8=21914
- sapphire, single crystals, alloyed with Ti, increased hardness 8=17767
- sormite type alloys, influence of Nb conc. 8=5066
- steels, ausforming effect 8=13561
- steel EI-702, deformation and hardening temp. effect on mechanism of precipitation 8=17078
- steel, EI702, dispersional, investigation by tensile tests 8=8845
- AgCl single crystal, surface, effect of aqueous environment 8=4727
- Ag-Mg solid soln., Ag-rich, microhardness short-range order dependence 8=21819
- Al, annealed, commercially pure, rel. to strain ageing 8=5042
- Al-Cu-Mg alloy with 1%Fe and 1%Ni, age hardening rel. to intermetallic phases comp., obs. 8=14495
- Al-Mg alloys, effect of various ageing conditions and recovery 8=17765
- Al-Zn-Mg alloys, quenching rate rel. to age hardening 8=8817
- Al-Zn, lattice defects and aging phenomena 8=13536
- Al-Zn-Mg, lattice defects and aging phenomena 8=13536
- CaF₂, proton irradiated, change in microhardness, kinetics 8=22320
- CdSnAs₂ and CdGeAs₂, semiconducting, microhardness changes rel. to high-temp. modifications 8=21842
- Cu, rel. to deformation texture development, pole figure 8=17777
- Cu-Be-Al alloys, ageing characts. obs. 8=22335
- Fe alloys, and wear resist. influence of strengthening mode 8=8847
- FeCo, micro-, microstrain under deformation 8=13596
- Fe-Ni-C martensites, ferrous, change due to deform. 8=22352
- GaAs, microhardness temp. dependence, 20-800°C rel. to doping effects 8=17809
- p-Ge, microhardness on e-irradiation and X-ray irradiation 8=17810
- LiF, microhardness at 20, 60 and 115°C 8=17813
- Mg-9 wt.% Al alloy, age hardening mechanism and precip. process 8=13683
- Mn steel, effect of multiple $\gamma \rightleftharpoons (\epsilon, \epsilon')$ transformations 8=17785
- (Mn, Me)(S, Se)-type solid solutions, microhardness 8=4692
- NaCl:Mn, particle hardening 8=22381
- Nb, rel. to dissolved O₂-N₂ mixtures 8=9011
- Nb, rel. to precip. of nitride 8=8274
- Nb-Mo steel, high-strength, combined effect of Nb and Mo 8=22385
- NbN, microhardness, effect of N content variation 8=13702
- Nb-Zr alloy, rel. to precip. of nitride 8=8274
- Ni, polycrystalline, shock-hardening 8=13595
- Ni₂Co, micro-, microstrain under deformation 8=13596
- Ni₃Mn, micro-, microstrain under deformation 8=13596
- Pt-Ir alloy electrodeposits, obs. 8=23153
- β -Pu from α and γ parent phases, anomalies, 120-190°C 8=8860
- Pu-Ga alloys, microhardness 8=8859
- Si, microhardness temp. dependence, 20-800°C rel. to doping effects 8=17809
- Ta-Mo alloys, compared with pure Ta 8=8862
- Ta-Nb alloys, compared with pure Ta 8=8862
- Ta-N, microhardness, effect of N content variation 8=13702
- W, effect of non-metallic trace additions 8=17835
- W, effects of neutron irradiat. and subsequent annealing 8=2141
- Y₂O₃, inference of segregation of ThO₂ at grain boundaries 8=13444
- ZrO₂, Y₂O₃- and MgO- stabilized, microhardness rel. to stress relief mechanism 8=17839

Hardness, magnetic. See Magnetic properties of substances/ferromagnetic.

Harmonic analysis. See Acoustic analysis; Calculating apparatus; Fourier analysis.

Harmonic generation, optical. See Lasers; Optics.

Harmonic oscillators. See Quantum theory.

Hartree-Fock method. See Atoms/structure; Solids/structure.

Hearing

- See also Ear; Speech.
- acoustic stimulation aftereffects 8=6197
- aids, ear level, shadow and baffle effects of head 8=10733
- American English /s/ transitions as cues to adjacent stop consonants identity 8=201
- animal sonar in air 8=19620
- artificial mastoid for calibration of bone vibrators 8=6189
- attenuation provided by ear plugs, fingers, palms and tragi 8=213
- auditory threshold determ. with circumaural-earphone, reliability 8=3085

Hearing—contd

- aural difference tones and masking 8=15088
- beating of sound, and excitation pattern of hearer's cochlea 8=214
- binaural exposure on threshold shift, effect of two interaural phase conds. 8=3093
- binaural intelligibility gain and release from masking for speech, prediction 8=205
- bone conduction improvement when ear is covered rel. to unilateral hearing loss 8=19600
- cat, single unit activity of primary auditory vortex 8=19618-9
- clocks, monotonic and dichotically alternating, perceived rate 8=15083
- communication systems in schools for semi-deaf 8=10748
- complex tonal perception, residue rel. to fine basilar membrane displacements 8=209
- critical bands for tonal stimuli, intensity effect meas. by band limiting 8=15084
- damage criterion 8=19602
- damage-risk criteria from impulse noise 8=19611
- difference limen concept from viewpoint of information theory 8=15090
- directional information, improvement of ability with attention 8=19607
- discrimination of acoustic stimuli, prompting versus confirmation for training 8=3087
- discrimination, freq. and amplitude, prediction by modified energy detector 8=6196
- duration thresholds of click pitch and tone pitch, interpretation 8=6190
- eardrum impedance obs. 8=19601
- earphones, free-field frequency response determination 8=3050
- fatigue, role of subjects attitude 8=15089
- forward masking, freq. selectivity 8=3091
- free-field lab. for psycho-acoustic expt. 8=19584
- guinea pig, depend. of cochlear pot. on K⁺ in endolymph obs. 8=19616-7
- harmonic distortion produced by ear 8=19606
- harmonics, masking of 2000 Hz tone by 1000 Hz fundamental 8=217
- H-bond, in chloroform-triethylamine system 8=18649
- human perception, amplitude modulated noise 8=3094
- impulsive noise of 'toys', damage-risk criterion 8=3083
- interaural time delay for release of speech masking 8=3088
- jitter discrimination obs. 8=19609
- localization of source, proximity image effect in absence of distance-indicating clues 8=15091
- loudness, matching functions and equal sensation contours 8=215
- loudness, psychophysical scaling method validity 8=15085
- low-signal-probability tasks, human performance 8=3092
- man, thresholds underwater at 12 and 35 ft 8=6193
- masker level and sinusoidal signal detection 8=6194
- masking, additivity 8=211
- masking by subjectively diffuse sound fields, obs. 8=6192
- mechanistic aspects 8=210
- memory, importance obs. 8=19604
- minimal pitch, number of pulses needed 8=206
- MLD's rel. to angle between narrow band masker and tonal masker 8=15081
- monaural, masking level differences due to interaural intensive noise disparities 8=6198
- monaural, optimum receiver detection theory 8=19614
- monaural phase effects in signal det. 8=19615
- monkeys, successive auditory discrimination, acquisition 8=15092
- monaural minimum audible press. threshold, 1.5 to 100Hz obs. 8=10760
- narrow-band freq. contours, development 8=3090
- nerve fibres in cats, threshold rel. to stapes displacement 8=10761
- noise, acceptable exposure identification 8=208
- noise criterion curves, Beranek's revised version 8=19586
- periodic and jittered pulse patterns, perception of temporal gaps 8=15082
- perceived noisiness concepts, applic. 8=19612
- pitch of complex sounds, freq. dominant in perception 8=3086
- pitch of complex tones 8=212
- pitch perception obs. using noise bands 8=19610
- psychometric function generated by pure tones in noise, Marill's expression 8=15087
- rat, startle depend. on sensation level 8=19595
- repetition pitch mediated by temporal fine structure at dominant spectral regions 8=6191
- repetition pitch of periodic room reflections, threshold 8=3096
- selective, application of signal detection theory 8=216
- sequential dependencies in psychophysics testing for 8=15086
- signal detectability theory, receiver-operating characteristics determ. 8=19608
- sound range perception 8=19613
- speech discrimination and high-frequency hearing loss 8=19599

Hearing—contd

- speech intelligibility, effect of compressor action 8=207
 speech sound perception, dimensions 8=200
 syllable duration in oral and whispered reading, masking noise effect 8=15078
 talker identification from monosyllables in context 8=6188
 temporal gap perception within periodic auditory pulse patterns 8=6195
 temporary threshold shift with simultaneous auditory task obs. 8=19603
 tone pitch, duration threshold, and information transfer by short tonal signals 8=3095
 two-dimens. auditory stimuli, perceptual independ. and recognition 8=3089
 vertex pot. obs. rel. to acoustic input 8=19605
 visual and auditory sensory modalities, interaction 8=10449
 vowel quality and musical timbre as functions of spectrum envelope and fundamental freq. 8=15079
 vowels, Polish, formant freq. regions 8=6187

Heat

- See also Radiation/heat; Thermodynamics.
 exchangers, periodic, equations for determ. of coefficients 8=3100
 flow, general problem 8=6199
 generation during torsional oscillations of polymethylmethacrylate tubes 8=4946
 moving body appears cool? 8=219
 polymethylmethacrylate tube torsional oscillations rel. to ht. generation 8=4946
 principles, review 8=10764
 relaxation processes, analysis 8=19621
 solar energy receivers, cylindrical cavity, optimal dimensions 8=19676

Heat capacity. See Specific heat.**Heat conduction**

- See also Conductivity, thermal.
 applications of probability theory 8=10774
 approximate soln. by elec. networks 8=19646
 in atmosphere, upper, and ionosphere, cond. waves propag. 8=2614
 below 0.2°K 8=15131
 combination of thermal resistances at contact surface 8=235
 conjugated functions appl. to transient processes 8=19631
 diffusion equation, one dimensional, analytical solutions 8=3105
 diffusion equation, general solution 8=3102
 equation, solution using finite strip tech. 8=6209
 finite speed of propagation in all matter 8=239
 fluctuating, quadrupole network analogy 8=19645
 fluid, effect on gravity waves, internal, at critical level 8=7887
 gas, rarified, appl. of conventional eqn. for conductivity and boundary temp. jumps 8=12682
 granular sphere to contact plates, calc. 8=19629
 heat insulation coatings, with phase transitions, numerical solns. 8=237
 heated tube, steady state behaviour 8=10782
 hollow cylinders, periodically heated, lumped heat-transfer coeff. 8=19644
 internal sources, appl. of variation method 8=19647
 Laplace eqn. with mixed boundary conditions, soln. for special class 8=15107
 in layer with irradiated boundary 8=236
 measurement, appl. of solns. of eqns. for nonsteady state monotonic heating 8=10773
 metal surfaces at low temps 8=22130
 non-homogeneous body, particular problems 8=3104
 nonlinear, in solids, temp. dependence calc. 8=8653
 packing in packed bed of spheres, with fluid stream, determ. of heat transfer, dispersion and conductivity 8=13363
 random medium, temp. wave penetration 8=10772
 refractory materials, determination of heat resistance review 8=1894
 reversed, appl. to transient heat transfer determ. 8=19636
 solids, contact with weakly conducting interstitial medium 8=22128
 solid-liquid interface, supercooling criterion, thermal diffusion effect 8=1617
 steady state, effective boundary conditions 8=3103
 superconducting wire in composite conductor, int. thermal resistance rel. to min. propag. current 8=17993
 temperature field in cylindrical bodies with longit. fins, boundary problems 8=19648
 wall, effect on convection from a surface 8=6211

Heat exchange. See Heat transfer.**Heat flow.** See Convection; Heat conduction; Heat transfer.**Heat losses.** See Heat transfer.**Heat measurement.** See Calorimeters; Calorimetry.**Heat of adsorption**

- and immersion heat, thermodynamic relations and lateral interactions effects 8=17152
 krypton, on zeolite LiX 8=1713
 xenon, on zeolites LiX and NaX 8=1713
 He, by condensed gas layers 8=8329

Heat of combustion

- α -AlB₁₂ 8=2512
 AlB₂ 8=2512

Heat of crystallization. See Crystallization.**Heat of dissociation**

- steam, thermodynamic analysis 8=7917
 CH radical 8=7618
 OsAs₂ 8=12338
 OsSe₂ 8=12338
 PtAs₂ 8=12338
 RuSe₂ 8=12338
 SrS 8=16957

Heat of formation

- hydrocarbons, semiempirical SCF MO calc. 8=4199
 Ag-Mg solid soln., Ag-rich, short-range order dependence 8=21819
 α -AlB₁₂ 8=2512
 AlB₂ 8=2512
 AlH₃ 8=4928
 CdSe 8=16955
 CN 8=12433
 CN halides 8=12433
 H-bonding systems, by two methods 8=12156
 KBr-KI solid solns., free energy of form. and gap of solubility 8=16998
 KrF₂ 8=2519
 OsAs₂ 8=12338
 OsSe₂ 8=12338
 Pt oxides, gaseous 8=5716
 PtAs₂ 8=12338
 Rh-Hg phases, out of elements in normal state 8=8280
 RuSe₂ 8=12338
 Si₂Te₃ 8=9662
 TiF₃ from Ti/CaF₂ reaction at 1564-1699°K 8=1623
 U₂N₃, calc. from press. of decomposition from U₂N₃ to UN 8=9660
 ZnTe 8=16956
 W-O system, free-energy changes 8=14388

Heat of fusion

- latent, rel. to surface tension 8=16936
 parahydrogen, at up to 400 atmos. 8=16928
 polyethylene 8=8171
 1, 3, 5-tri- α -naphthylbenzene 8=4563
 Ar at high pressures and random close packing 8=8181
 KAlSi₃O₈ 8=21753
 K₂ZrCl₆ 8=8640
 Li₂HfCl₆ 8=8640
 Li₂ZrCl₆ 8=8640
 NaAlSi₃O₈ 8=21753
 Na₂ZrCl₆ 8=8640
 PuO₂, rel. to UO₂-PuO₂ phase diagram 8=8284
 UO₂, determ. 8=21750
 UO₂, rel. to UO₂-PuO₂ phase diagram 8=8284

Heat of mixing. See Heat of solution.**Heat of reaction**

- calorimeter, with Peltier cooling for operation at const. temp. 8=9677
 exothermic front in condensed medium (k-phase), theory of stationary propag. vel. 8=18660
 hydrogen ion solvation by H₂O molcs. in gas phase 8=18661

Heat of solution

- hydrocarbon liqs. in surfactants 8=8147
 solvation of ions 8=12807
 Ag-Au-Sn liq. alloys, of Ag and Au, at 723°K 8=21652
 Al in liquid Fe 8=16799
 Ar in H₂O-methanol system 8=12809
 CaF₂, enthalpies, Born model calculation 8=21650
 Cd(ClO₄)₂-HClO₄-H₂O saturated system 8=12847
 Cu in liquid Fe 8=16799
 Na borate glasses, and density and refractive index changes under high pressure 8=1715
 Na₂HPO₄ hydrates 8=17521
 Si in liquid Fe 8=16799
 Sn in liquid Na 8=21621

Heat of sublimation

- azo compounds 8=16958
 AlF₃ 8=12997
 CdSe 8=16955
 Ho 8=16950
 TiF₃, by mass spectrometry 8=1623
 ZnTe 8=16963

Heat of transformation

- azoxymethylcinnamic acid-dialkylester, liq. crysts. 8=4533
 binary eutectic system, solidification, heat-transfer analysis 8=21756
 cholesteryl capriate during transition from liquid crystal into isotropic-liquid and solid phases 8=16917
 condensation of solvent vapour into polymer solns., rel. to molec. weight determ. 8=18643
 freezing rate of semi-infinite slab, effect 8=16932
 lattice gas model, calc. 8=4638
 organic liquids, rel. to sound velocity 8=16829
 parazoxyanisole during transition from liquid crystal into isotropic-liquid and solid phases 8=16917
 regelation, theory 8=8165
 regelation, theory, supplementary note 8=8166

Heat of vaporization

- ethyl ketone, and vapour heat capacity 8=1471
 ethyl propyl ketone, and vapour heat capacity 8=1471
 latent, relation with sonic vel. rel. to Bridgman eqn. 8=12852

Heat of vaporization—contd

methyl isopropyl ketone, and vapour heat capacity 8=1471
methyl phenyl ether, and vapour heat capacity 8=1471
Ho 8=16950
Pt 8=5716

Heat of wetting. See Wetting.

Heat pumps. See Heat transfer.

Heat radiation. See Radiation/heat.

Heat transfer

See also Convection; Heat conduction; Radiation/heat; Radiative transfer.
across turbulent boundary layer from nonisothermal flat plates 8=15101
alkali metals, liquid, boundary resistivities 8=8049
argon plasma jet, heating of condensed powder particles 8=12574
in atmosphere, unstable, turbulent transport, obs. 8=23260
in atmospheric lower layers, two-dimens. model 8=23267
in axisymmetric boundary layer flow over circular cylinder 8=21565
below 0.2°K 8=15131
boiling, data at low heat flux 8=21773
boundary layer flows with large injection 8=21485
boundary-layer turbulence promoters, rel. to power reactor systems 8=21510
boundary values for uniform wall temp. in non-circular conduits 8=4429
circular pipe, turbulent heat transfer and temp. distrib. 8=232
coefficient determ. by dynamic characteristics 8=3100
in compressible laminar m. h. d. flow in flat duct 8=15364
compressible, turbulent, free jets exhausting into quiescent air 8=12652
conducting liquid in turbulent flow, effect of mag. field 8=10930
conductivity, nonsteady state, inverse problem soln. for monotonic heating of bodies 8=10773
conjugated functions appl. to transient processes 8=19631
convective in stabilized turbulent flow of liquid in tube at supercritical press. 8=1550
crossed-in-line tube bundles in nuclear reactors 8=7235
cylinder cooling on moving through fluid 8=227
di-ethyl ether, in nucleate boiling 8=16948
in dispersions, interrelationships with mass transfer 8=16904
distributed parameter nonadiabatic heat and mass transfer, thermal dynamics 8=12976
electroconductive media, theory 8=15105
energy pulse interaction with solid 8=12968
evaporation, nonadiabatic, from porous system, convection 8=8183
exchange, in m. h. d. flow stabilization, in plane channel 8=3240
flat plate, thermal cond. effect 8=22126
from flat plate, viscous and Joule heating effects 8=19630
in flow behind detonation, effect on transition to steady flow 8=15058
fluctuating, from a sphere at small Reynolds numbers 8=6207
fluid, from cylinder by acoustic streaming 8=3098
fluids, domains in variable gravity 8=16692
between fluid and hot porous medium 8=6206
fluids laminar and turbulent flow, variational and physical analysis 8=7870
fluids, non-Newtonian and turbulent 8=12647
fluid, turbulent boundary layer, global energy eqn. soln. 8=12611
fluidized beds, combustion of gaseous fuels 8=23119
in fluidized beds, externally heated and internally cooled 8=19640
fluidized bed, dense, with vibrating cylinder 8=8144
fluidized bed, interphase heat transfer, meas. method 8=8145
to fully developed liquid metal flow in tubes 8=21568
gases, absorbing-emitting, in free-convection flow at stagnation point 8=4454
gas coolant compared to liquid in nuclear reactor 8=20887
gases, effect of sound 8=12680
gas flow with droplet suspension 8=12663
gas-liquid interaction, intensification, survey 8=19637
gas with micron-size particles, props 8=21735
gas-solid mixt. in supersonic flow in convergent-divergent nozzle, obs. 8=16902
gas temps., rapidly varying in an unsteady flow, meas. 8=16694
granular material in fluidized bed 8=4628
heat pipes, capillarity-limited, operating characts. 8=6216
heated flat plate in high-Mach-number laminar stream, and mass transfer 8=19634
hollow cylinders, periodically heated, lumped heat-transfer coeff. 8=19644
from horizontal fine wire, effect of vibration 8=19649
hydrodynamic boundary layer, radial jet 8=12587
between incompressible fluid and a porous medium 8=16821
interfacial resistance in filmwise condensation of steam 8=16940
interfacial resistance in forced convective condensation in presence of noncondensable gas 8=16941

Heat transfer—contd

irradiated vapours with side spreading 8=231
laminar boundary layer with variable fluidity 8=10769
laminar compressible boundary layer 8=21491
laminar flow, effect of elec. and mag. fields 8=348
laminar forced convection in entrance region between parallel flat plates 8=21459
laminar free convection with moving interface 8=240
on large droplets in pure vapour, perturb. anal. of condensation control 8=16942
layer system of air, snow, sea ice and water 8=23226
linear response to arbitrary thermal perturbation 8=2969
in liquids, influence on corrosion, review 8=18667
liquid, laminar flow in circular tube 8=21656
liquid, laminar viscous film flow on a rotating disc 8=4522
liquid-liquid, effect of flow rate disturbances 8=8048
liquid metals, in channels with periodic boundary conditions 8=8051
to liquid metals flowing along a row of spheres 8=21660
liquid metals in smooth tubes, effect of thermal contact resistance 8=16824
liquids, plug-viscous, laminar flow 8=4566
liquid, rotating, in zero-gravity field 8=4562
to liquid in square ducts 8=12854
liquid, viscous, flowing in channel, asymptotic representation of temp. field 8=1546
magnetohydrodynamic flow at flat duct entrance 8=19809
Malkus' transition in thermal turbulence 8=19653
metal corrosion, test apparatus 8=18665
metal, liquid rot. in magnetic field 8=8054
metal, quenching in water at 100°C 8=8635
methane, h. p. boiling apparatus 8=16944
non Newtonian fluid with nonlinear heat conduction law 8=4424
nonlinear diffusion equations 8=10771
nonsteady state, exponential point meas. method 8=10781
nuclear reactors, coolant and fuel temp. calc. 8=7342
Nusselt numbers for fully developed flow in tube with exp. varying heat flux 8=19642
ocean, flow anomalies 8=18838
between packing in packed bed of spheres, and fluid streaming through it 8=13363
between parallel plates in transition regime, and density-distribution obs. 8=21505
from partially dissociated gas stream, effect of mass injection 8=21457
in phase-changes with time-depend. surface temp., approx. soln. appl. to Stefan problem 8=16913
from piezoelectric resonator, into surroundings, meas. of coeff. 8=1884
pipe flow, forced, free convection effect 8=16623
plasma generator, discharge chamber, in mag. field 8=7847
polymer, dilute solutions, in turbulent flow 8=7981
progress in, book 8=15104
propyl alcohol, subcooled boiling in tubes, rate study 8=21657
pulsating gas flow, particle motion 8=16696
radiant, in fibrous insulator 8=1883
radiation, in nonisothermal nongray gases 8=21506
radiation, semi-isotropic model 8=15103
radiation of spectrum lines 8=230
radiative, and emissivities of emitting volumes, relations between 8=3099
radiative, between parallel plates separated by non-isothermal medium with anisotropic scatt. 8=19625
radiative in fluids, optically dense, volumetric absorpt. effects 8=10674
radiative, between two narrow strips 8=221
reactor, thermionic, conversion, simulation apparatus 8=1134
Rosseland approximation appl. 8=19633
shock wave effect around blunt body 8=19538
in simulated boiling, on submerged heating surface rel. to bubble growth 8=16945
solar air heaters, rating parameters 8=228
solid-to-fluid, in fluidized systems 8=21470
solid in high-enthalpy gas flow, in stagnation region 8=22140
solidification of binary eutectic system, analysis 8=21756
solids, variable, transient temp. field 8=22127
source function soln. for radiative transfer through absorbing grey gas between heated plates 8=21507
sphere with air flow, obs. 8=19632
spheres, effect of fluid turbulence 8=17541
sphere heat transfer to air current 8=19635
from sphere, to turbulent streams 8=4434
superconductor, type I, transport by moving magnet 8=22544
steam temp. influence on corrosion 8=18666
system physical props. effects calc. 8=10770
thermal fluxmeter in shear flow, theory 8=19639
thermal-wave generator, cam equation 8=3101
thermoelectric pile to liquid flows past hot and cold junctions 8=4567
thin-film resistance thermal flux gauge 8=10768
three-fluid heat exchanger, NTU-effectiveness relns. 8=19643

Heat transfer—contd

- through dispersed system having irregular pore sizes comparative study 8=8142
- through semitransparent materials, radiation heater 8=19641
- transient natural convection, from vertical plate, leading edge effect 8=19652
- transient, reversed conduction methods appl. 8=19636
- for turbulent air flow in vertical square duct, temp. inner-law parameters 8=4456
- turbulent boundary layer problems, solutions 8=62C8
- turbulent liquid at supercritical pressure 8=8050
- in turbulent motion, in presence of transverse homogeneous mag. field 8=12742
- turbulent in non-Newtonian fluids 8=4565
- in turbulent skin friction, Preston tube meas. 8=12750
- turbulent, in tube with circumferentially varying thermal boundary conditions 8=19638
- turbulent, in viscoelastic liqs. 8=1510
- in verneuil crystal growth process 8=21936
- in vertical cylinder containing heat-generating liq., due to natural convection 8=7916
- vertical plate to power-law fluid 8=8052
- of viscoelastic fluids, in turbulent region 8=4426
- wall to turbulent fluid, hot-film sensor 8=16822
- water, acoustical effects on free convective transfer from horizontal wire 8=21663
- to water in channel formed by bundle of tubes or rods 8=12849
- water, local during viscogravitational flow in horizontal tube 8=12730
- in water, saturated pool boiling, effect of interfacial vibration 8=12985
- water, subcooled boiling in tubes, rate study 8=21657
- in Ar plasma laminar flow in entrance region of circular tube 8=16477
- CO₂, near critical point, forced convection 8=16915
- in H₂-air, free convection and binary diffusion 8=4491
- H₂O turbulent, flow in square duct, temp. distribution in wall, obs. 8=1545
- in He-air, free convection and binary diffusion 8=4491
- He, liquid, impulse 8=10798
- He II, body immersed in flow, exchange torques 8=3127
- He II filling narrow gap, heat exchange with solid body 8=6233
- He, supercritical, circulation systems 8=19690
- Hg turbulent flow in square duct, temp. distribution in wall, obs. 8=1545
- N₂, h.p. boiling apparatus 8=16944
- to NaK flowing through unbaffled rod bundles 8=21649
- Ni alloys, temp. effects on corrosion 8=15102
- UO₂/sheath, in irradiation of reactor 8=7339

Heat treatment

- alkaline beryls, structure dependence on tempering at 600-1200°C 8=17345
- annealing of defects in crystals, observation 8=1933
- anthracite, rel. to reduction of paramag. absorpt. 8=5441
- carbon, soft, structural defects 8=1955
- deformation, metallurgical problems 8=22277
- diamonds, natural, effect on luminescence 8=18596
- failure of materials subjected to thermal shock by cooling, statistical analysis 8=22295
- garnet, elastic constants and derivatives w. r. t. temp. and press., obs. 8=2037
- glass, BSC, annealing, relax. effects 8=4770
- glasses, commercial, rel. to photoluminescence 8=2482
- glass, four new oxides, rapid quenching techniques 8=5087
- glass, tempered, fracture, rel. to elastic strain energy and rate of crack extension 8=22373
- graphite electrodes for spectroscopy, by electron beam, for purification 8=23187
- iron, pure, annealing effect on internal friction temp. dependence 8=17791
- lanthanides, recrystallization and work-hardening characts. 8=5089
- martensite decomposition, effect of thermomechanical treatment during low-temp. tempering 8=21845
- martensite, tempered, precipitation of Fe carbides 8=17080
- metals, rel. to Bauschinger effect 8=5020
- metal sheets, by lasers, pulse frequency effect rel. to sheet thickness 8=2871
- metals, thermomechanical deformation 8=23777
- Nimonic 80A creep props. recovery by annealing, 600-750°C 8=5083
- Old Red Sandstone, effect on mag. props. 8=5821
- piezoelectric ceramics, reduction of stress sensitivity of permittivity 8=19555
- polyethylene, noncryst. regions, changes during annealing 8=17183
- steel, growth of secondary grains during annealing 8=17283
- steel, low-C, quench-ageing at 240°C after rapid annealing 8=17806
- steel, nodular graphite, effect on mechanical properties 8=8843
- steel, quenching in mag. fields, review 8=22343
- steels, strain ageing of martensite rel. to brittle fracture susceptibility 8=13573
- Ag, annealing in hydrogen rel. to water vapour bubble formation 8=22307
- Heat treatment—contd**
- Ag film, vapour-deposited, resistivity annealing temp. and thickness dependence 8=17925
- Al, in air and vacuum, form. of surface tops and pits 8=17117
- Al, degassed, form. of dislocation loops 8=1966
- Al, dislocation densities and configs. during slow heating and cooling 8=22198
- Al, electron-irradiated, stage III annealing study 8=13475
- Al, e-irradiated, stage II and III recovery temp. and impurity conc. dependence 8=1935-6
- Al, formation during slow heating and cooling 8=8723
- Al, quenched, yield stress rel. to aging temp. 8=13530
- Al sections, reinforcing with continuous steel wires 8=10459
- Al vacuum condensates, annealing effect on block structure charact. 8=4741
- Al₂O₃, sintering, activation enthalpy 8=13052
- As₂Se₃, vitreous, effects on electrical conductivity 8=8991
- Au quenching experiments 8=8824
- Au, vacancy and divacancy behaviour on quenching and annealing 8=1945
- AuAg alloy recryst. rel. to optical const., 276-1200 nm 8=22958
- AuCu alloy recryst. rel. to optical const., 276-1200 nm 8=22958
- AuCu₂ alloy recryst. rel. to optical const., 276-1200 nm 8=22958
- C composite sintered materials, firing duration, firing atm., forming process, effect on elec. resist. 8=2129
- C, in quenched steel, behaviour 8=22354
- CdS rel. to luminesc., absorpt. and refl. spectra, obs. 8=9606
- CdS, S₂ annealing pressure effect on resist. homogeneity 8=8980
- CdSe rel. to luminesc., absorpt. and refl. spectra, obs. 8=9606
- Co hexagonal single crystal, Young's modulus dependence on thermal expansion 8=22324
- CsI, isothermal annealing effect on dislocation density 8=17650
- Cu hot working, grain struct. prod., obs. 8=21984
- Cu, plastically deformed, annealing behaviour, effect of dispersed phases 8=17772
- Cu, quench hardening, study 8=22334
- Cu₂-Mg₂Fe₂O₄, quenching in high oxygen pressure furnace 8=2516
- Cu, quenched, vacancy annihilation kinetics 8=1946
- CuFeMnO₄, annealing of cubic and tetragonal crystals 8=17205
- Fe, annealing and plastic deform., rel. to X-ray diffraction line intensity 8=21989
- Fe crystals with 8-20 p.p.m. C, n-irradiated, yield stress and annealing expts. 8=17800
- Fe-Cu, Cu precip. and coagulation rel. to ferromag. props., obs. 8=22809
- Fe-Mn austenite, plastic deform. and annealing rel. to H permeability 8=17573
- p-GaAs, photoluminescence, effect with excess As pressure 8=23054
- GaAs, Zn-doped, effect on photoluminescence 8=2481
- Ge, effect of annealing on (111) surface stress 8=8849
- Ge, e-irradiated, annealing of Hall mobility changes 8=2196
- Ge, n-type, formation of acceptor centres, vacancies 8=4962
- InSb, diffusion effect rel. to disloc. density 8=1919
- p-InSb, Li-saturated, annealing effects on Hall coeff. and resistivity 8=5270
- K, deformation by thermal activation at low temps. 8=1957
- KCl, X-irradiated, α -centre production and thermal annealing 8=17685
- LiF, influence on luminescent properties 8=14322
- MgO aggregates, hot-pressing 8=17816
- Mg(OH)₂, reactive hot-pressing 8=5077
- Mn basic carbonate and magnesite containing ZnO, calc. 8=4698
- MnO, axially cooled or stressed, anisotropy from torque meas. 8=14072
- Mo permalloy, coercive force, neutron bombardment and annealing effect 8=18344
- Mo steel, quenched and tempered, orientation relationship between Mo₃C and matrix 8=17369
- NaCl, quenching rel. to dislocation structure on {100} faces 8=22207
- NaF, F-aggregate centres 8=17686
- NaI, isothermal annealing effect on dislocation density 8=17650
- NaI, in O rel. to capture centres luminesc., obs. 8=23060
- NaI: Tl, in O rel. to capture centres luminesc., obs. 8=23060
- NbN, quenching curves, critical data in magnetic fields 8=2165
- Ni, annealing, weakly deformed, recrystallization nucleation 8=8421
- Ni-base alloy 718, correl. with mech. props. 8=21827
- Ni films, electrolessly deposited e microscope study 8=17136
- Ni, thermo-mechanical, increase in creep strength 8=13601

Heat treatment—contd

- Ni_{0.5}Fe_{2.5}O₄, annealing temp. dependence of magneto-crystalline anisotropy 8=9385
 NiO, axially cooled or stressed, anisotropy from torque meas. 8=14072
 Pt, annealed, anelastic effect at low temps. 8=22211
 Pt, damage on annealing rel. to damage on e-irradiation at 90°K 8=1947
 Pt, refinement by annealing in air 8=4812
 Rh and Ir, hot working, poor ductility 8=22390
 S ion implanted with Sb, Ga and As, anneal characts. obs. 8=18072
 Se, crystal structure, and other props., effect of cooling to 100°K 8=1808
 Si, proton-irrad. damage isothermal annealing 22-158 MeV, 100-300°C 8=22605
 Si:Li, annealing rate, rel. to defect concentration 8=2067
 n-Si, n-irradiated, elec. props. rel. to defect structure and annealing 8=5283
 SiO thin-film capacitors 8=22676
 Si, P-doped, annealing of the Si-E centre 8=2209
 p-Si thermally quenched, effect on electrical properties 8=18084
 Sn vacuum condensates, annealing effect on block structure charact. 8=4741
 SiO₂-UO₂ vitroceraamics, irrad. induced vol. changes and annealing 8=8779
 W, annealing of n-irrad. damage, migration of point defects 8=17601
 W, annealing subsequent to neutron irrad., effects on elec. resist. and hardness 8=2141
 W wires, on secondary recrystallization, from electron optical meas. based on emission 8=1765
 Y, recrystallization and work-hardening characts. 8=5089
 ZrO₂-TiO₂ system, change of mineral composition 8=4721

alloys

- Alnico magnets, at temperatures below 1000°C 8=9361
 β -brass, effect on elec. resistivity 8=13714
 Magnox ZR-55, creep behaviour in 350-450°C range 8=5078
 metallic, crystalline structure changes at early stages of ageing and order-disordering 8=17036
 non-ferrous, thermomechanical deformation 8=23777
 steels, fatigue crack propagation obs. 8=5072
 steel, low-alloyed chrome, effect of tempering on Young's modulus 8=13560
 steel, low-carbon, sheets, rolling and annealing textures 8=17799
 steel, mechanical strength after tempering, effect of lower bainite 8=17805
 steel, mild strip, tensile strength rel. to quench rate 8=22365
 steel, Nb carbon-nitrides on dissolution, precip. and age hardening effects 8=1660
 steel sheet, rapid soaking effect on strength 8=22364
 steels solid soln. and precip. hardening and grain refining rel. to mech strength 8=22344
 steel, straining at elevated temp. and retempering, rel. to increase in yield strength 8=17782
 steel, temper brittleness, effects of alloying with Ni and Cr and adding Sb, P, Sn or As impurities 8=17797
 steel, temper brittleness rel. to structural imperfections 8=17626
 Udimet-500, -520 and -700, effect on stress-rupture props. and structural stability 8=13599
 Zircaloy-2, annealed in α and (α + β) regions, effect on H₂ terminal solubility 8=8250
 Al, cracking during welding 8=5047
 Al, microstruct. changes 8=21979
 Al, natural ageing effect prior to artificial ageing 8=17764
 Al-Cu-Cd alloys, deformation before and during ageing, effects on precip. 8=17039
 Al-Cu-Mg, effect on corrosion 8=8819
 Al-Mg alloy, ageing effect on structure 8=17004
 Al-Mg, various ageing regimes and recovery 8=17765
 Al-Zn-Mg alloys, conc. and dilute, quenching rate rel. to ageing 8=8817
 Al-Zn-Mg, effect on precipitation 8=13062
 AlM, (M = Mg, Ga, Ag), e-irradiated, stage II and III recovery temp. and impurity conc. dependence 8=1935-6
 C steels, austenite formation and tempering 8=13067
 CdS phase structure recovery to room press. at 77°K 8=1671
 Co based, f. c. c., ageing effects after deformation 8=17622
 16/13 CrNi steels, high temp. embrittlement after n irrad. 8=22362
 Cu-Be-Al, ageing characts. obs. 8=22335
 Cu-Be, Guinier-Preston zone formation, conc. and ageing dependence 8=17606
 Cu-Be, quenched and aged, vacancy role in solute clustering 8=17607
 Cu-2%Be, precip. and twins appearing on ageing 8=17625
 Cu-Mg alloys, variation of Cu₂Mg precipitation 8=4705
 Fe-Al, rel. to paracrystal detect. from X-ray powder patterns 8=17368
 Fe-Co-Ni-Cr, new ferromagnetic state during recrystallisation 8=9342

Heat treatment—contd**alloys—contd**

- Fe-Cr-Ni-Nb steel, recrystallization obs. 8=21950
 Fe-N alloys, tempering process 8=8840
 Fe-N, quenching, study of structures 8=8522
 Fe-Ni-Al-Ti, microstruct. and mech. props. 8=21987
 Fe-Ni-Ti alloy, structural changes during martensite ageing 8=17064
 Fe-Si, annealing effect on physical props. 8=23778
 GaSb, effect of annealing on (111) surface stress 8=8849
 InSb, effect of annealing on (111) surface stress 8=8849
 InSb vapor-deposited films, electrical resistivity 8=9008
 n-InSe crystals, thermal and i. r. quenching of photo-conductivity 8=18233
 Nb-Mo steel, strengthening effect of precipitates 8=22386
 Ni-base alloy, refractory-melt reactions in vacuum induction melting 8=9694
 Ni-bearing steels, ageing rel. to martensitic structure 8=1762
 NiAl, ordered b. c. c., supersaturation of vacancies on quenching 8=17611
 Ni-12.7 at.%Al, rolled, effect of coherent γ' (Ni₃Al) particles on annealing 8=13598
 Ni-Al₂O₃ alloys, annealing and creep meas. 8=22388
 Ni-Mo, quenched, deformation effects on transformation during annealing 8=17094
 Ni-SPAN-C alloy 902, vacuum remelt versus air-melt, rel. to elastic and fatigue props. 8=17822
 Pt-Rh, quenching expts. 8=13423
 Pu-0.85at%Ga, metastable δ -phase, effect of thermal cycling on transform. behaviour 8=8278
 Zn-Al, superplastic, effect on strain rate 8=5090
 Zr rich, effect of rolling temp. on texture developed 8=22399
 ZnTe, melt-grown, edge emission, annealing effects 8=5681
 Zr-2.5wt%Nb, annealed in α and (α + β) regions, effect on H₂ terminal solubility 8=8250

Heating

- carbon furnace i. r. source 8=15093
 distortion of semi-infinite solid due to uniform circular heat source on surface 8=22122
 ferrites, by ferromag. resonance 8=14082
 furnace, simple thyristor controller 8=15125
 gases by lasers, dynamic processes 8=7928
 gas flow, by arc, enthalpy meas. 8=19672
 hotplate corrosion, steam temp. influence 8=18666
 magnetron cathodes, surface-wave, ion bombardment 8=15334
 metals, by laser radiation pulse 8=3285
 radiation heater, electrically-powered, operation to 1200°C 8=19641
 relaxation solution of d.c. 3-wire network, effects of steady currents 8=281
 rotary kilns, charge flow rate, enthalpy depend. 8=22108
 solids, focused laser beam 8=15130
 system, for n.m.r. spectrometer 8=19912
 thermal gradient apparatus for Pu glovebox 8=7334
 Fe-Ni alloys, by ferromag. resonance 8=14082
 He, afterglow, microwave by standing wave 8=1340
 Ni powder, by ferromag. resonance 8=14082

Heaviside layer. See Ionosphere.**Heavy water.** See Water.**Height measurement.** See Length measurement.**Heisenberg model.** See Ferromagnetism; Statistical mechanics.**Helicity.** See Elementary particles; Field theory, quantum.**Helicons.** See Crystal electron states.**Helions.** See Alpha particles and helium nuclei; Alpha rays.**Heliotron.** See Plasma/devices.**Helium**

- absorpt. coeff., continuous 8=7387
 abundance in proto-Galaxy 8=14799
 abundance in sun 8=10381
 adsorption on Molecular Sieves 5A, 10X, and 13X, at 77.3°K and press. range 10² to 10⁻⁶ torr, effect of preadsorbed H₂O 8=21897
 adsorption on powders at room temp. 8=21899
 after glow, microwave heating by standing wave 8=1340
 alkali ions scatt. at He atoms 8=7464
 arc, pulsed, spectrographic meas. 8=21253
 atom, aligned, scatt. resonance fluorescence, depolarization 8=20982
 atomic collisions, autoionization 8=7714
 atom, correlation factors, effective range 8=20938
 atoms, determ. of excited state lifetimes by single-photon counting 8=7429
 atom, double ionization by 1-3 MeV p, using product of H-like orbitals 8=21280
 atom, dynamic polarizability of ground state, variational calc. 8=20945
 atom, elastic scatt. of zero-energy positrons 8=20995
 atoms, e capture by μ^+ , cross section calc. 8=7481
 atom, e excitation, rearrangement collision, spin flip effects 8=7445
 atoms, e excitation of 2¹P and 2³P states 8=7446
 atom, e scatt., long-range interaction, nonadiabatic contrib. 8=12092

Helium—contd

- atom, energy level calc. by variational perturbation method based on the principle of moments 8=20919
- atom, excitation, from metastable 2^3S He, cross-section 8=4055
- atom excitation by 100-400 eV electrons, cross sections rel. to Born approx. 8=16218
- atom, excitation by 0.15-1.0 MeV p and d impact 8=7384
- atoms excited states, adiabatic exchange approx. calc. 8=7434
- atoms, form factor and incoherent-scatt. function 8=12053
- atom, ground state from perturb. theory 8=7369
- atom, ground state, variational calc. of expected values 8=7386
- atom, Hartree-Fock energy, saddle-point character 8=7370
- atom, hyperpolarizability calc. 8=20942
- atoms, interaction energies calc. 8=4110
- atoms ionization by e impact, cross-section calc. 8=12084
- atoms, isoelectronic sequence multipole polarizabilities and shielding factors 8=16199
- atoms, large-angle electron-impact spectra 8=16224
- atoms, lower bounds to eigenvalues 8=11253
- atom, 0.15-1.0 MeV p and d impact, quadrupole and dipole transition theory compared to obs. 8=7385
- atom params. from wave functions with pole-eliminating correl. factors 8=16197
- atoms, S limit, energy surface in parameter space 8=16196
- atomic-stopping cross section in Al 8=2022
- atom, He⁺, charge exchange in atmospheric gases, 40-1500 eV 8=21275
- atom, He-p e capture excitation of 3s, 4s states of H 8=7462
- atom, He³⁺ single and double e-capture cross-sections obs. in He³⁺-He, 7.2-181 keV 8=21278
- atoms, He⁺-He collision, excitation and e capture probabilities calc. 8=7463
- atoms, He-He, Van der Waals interaction, self-consistent calc. 8=21002
- Atom He³⁺-N₂, 7.7-166 KeV, cross -sections for single and double e capture 8=21279
- atom, scatt. of charged particles, Bethe cross-section sum rule 8=12107
- autoionizing D states, character 8=12445
- autoionization, kinetic energy 8=12443
- in B star He λ 4771 strength in IC2391, 2602, Southern galactic cluster 8=2783
- beam on H₂ scatterer, total cross section meas. using high intensity nozzle beam source 8=7639
- bubbles, in Al-Li alloys, neutron irradi. 8=8456
- chemical reactions with D₂⁺ and H₂⁺ cross sections 8=14348
- in chromosphere, low temp. emission theory 8=10430
- conductivity, thermal, line-source transient-heat-transfer technique 8=16701
- collisions with inert gases, total scatt. cross-sections 8=7634
- content in subdwarf stars 8=5865
- cosmic rays, isotope production 8=20607
- cryostat, for use with torque magnetometer down to 4.2°K 8=15140
- cylindrical plasma, instability 8=1430
- discharge, electrodeless, cyclotron harmonic resonances 8=4274
- discharge, positive column, correlation functions 8=1405
- discharge, positive column at above critical field 8=16410
- dissolved in water, molec. diffusion coeffs. 8=12828
- effect on lifetime of CO₂ laser levels 8=420
- electric discharge positive column, electrons energy distrib. 8=7655
- e capture by H⁺ + He(1s²) → H(1s, 2s, 2p) + He⁺(1s) 8=7465
- electron impact cross sections 8=1347
- flow, rarified, molecular velocity distribution function Doppler obs. 8=16664
- glow discharge, fast electron energy decrease in neg. region 8=4288
- glow discharge in toroidal tube, expt. investigation 8=4286
- ground and metastable states, dipole props. 8=20980
- ion beam, 910 MeV, in thin absorbers, energy loss distrib. 8=13471
- ion, energy loss in passing through ZnS:Ag film 8=8758
- ion, recombination afterglow, differential level decay 8=21237
- ionization cross-section, electron impact 8=7700
- ionization cross-sections for 100-2000 eV electrons 8=12446
- ionization, electron and proton impact, classical model 8=12444
- ionization processes, double by γ and e impact 8=7715
- isoelectronic sequence, calc. of 1s² 1S-1sn¹P transitions 8=7388
- isoelectronic sequence, 1sn¹P and ³P states, wave functions calc. 8=7390
- isoelectronic sequence, 1S states eigenvalues calc. 8=7391
- isoelectronic sequence, ³S states eigenvalues and wave functions calc. 8=7392
- isoelectronic series, ground-state wavefunctions and energies 8=4067

Helium—contd

- isotope mixtures, thermal diffusion props. 8=1492
- laser, He-Ne mixture, pulse delay 8=3314
- mass spectrometer, applications 8=7359
- metastable atoms, Penning ionization of gases 8=21258
- molecular flow through capillary, interaction with tube wall 8=7893
- para- and ortho-, electron impact ionization, ratios of cross-sections 8=7431
- plasma, axial injection into mag. dipole field, obs. 8=16506
- plasma in coaxial accelerator 8=4337
- plasma, electron density meas. with regenerative laser amplifier dev. 8=11027
- pressure broadening of Hg resonance line 8=7403
- shell-burning stars, pulsational instability 8=5873
- spectra, excitation of 4F states 8=12054
- stars atmospheres 8=5891
- in star Groombridge 1830, abundance 8=23505
- stars, vibrational stability, non-constant opacity effects of 8=2788
- target nucleus, thermonuclear reaction rates 8=11976
- thermal conductivity meas. with hot-wire cell 8=6210
- third virial coeff., and for nonpolar mixtures 8=12677
- ³P-²P transition, polarization 8=7432
- ³P, ⁴S and ⁴D levels, lifetime obs., using positive ion Van de Graaff accelerator 8=16183
- triplet spectrum in expanding nebulae, capture-cascade intensities 8=19194
- triplet spectrum in expanding nebulae, self-absorption 8=19195
- ²S state, in planetary nebulae, depopulation rate 8=5913
- in Universe, abundance 8=10073
- viscosity, effect of organic vapour molecules, for determ. of mol. dims. 8=1485
- Wigner spin rule validity in He-He collision 8=21015
- H atom in 3s state prod. in collisions with H₂⁺, H₃⁺ 8=21191
- to H⁺ ratio, galactic rays of low energy, balloon obs. rel. to solar modulation possibility 8=2770
- H₂-He mixture, composition-depend. of thermal-diffusion factor 8=1493
- He-air system, free convection, heat transfer and diffusion 8=4491
- He-n-butane mixtures, second virial coeffs. determ. 8=12980
- He-n-butane system, phase and volumetric behaviour showing gas-gas equil. for low He conc. 8=12979
- He-methane solid-vapour equil., 55°-91°K, to 140 atm. 8=16953
- He I 4026 Å stellar line rel. to rotation and vel. 8=19121
- He II, 4686 Å line complex excited in atomic-beam light source, analysis 8=12052
- He II, interference of fine-structure levels 8=4066
- He II line, Lamb shift 8=1161
- He II, Stark broadening of 3203 Å line 8=7383
- He₂, ground-state potential 8=12200
- He₂, ground state, wavefunctions and potential curves 8=7526
- He³, atoms, radio-optical resonance, coherence 8=16219
- He³, nuclear (fund.) and electronic (excited) orientations 8=16226
- He³, optically oriented, magnetic resonance 8=20999
- He³, transverse optical pumping and detection of modulation resons. 8=16195
- He³, ⁴ and D, relative abundances, implications of Brans-Dicke theory 8=23478
- He⁴, density measurement near critical point to test $\beta(6+1) + \alpha^1 \geq 2$ 8=259
- He⁴, virial coefficient, 2nd, for exponential repulsion potential 8=12678
- He⁻, negative, lifetime obs. 8=20944
- He⁻, critical angles for channeling in thin Au films 8=17704
- He⁻, electron-impact excitation and auto-ionization 8=4091-2
- He⁻, low-energy irradi. of Ge crystals 8=8772
- He⁺ photoionization reactions with N₂ and O₂ 8=16444
- He₂⁺, potential curves for X² Σ ⁺ and ² Σ ⁺ states 8=12201
- He⁺ + H₂ and He⁺ + HD reactions 8=21277
- He²⁺, ground state calcs. 8=4130
- ³He²⁺ ions, prod. by r.f. ion source 8=10914
- ³He⁺ in Ge, channelling props., diff. calc. 8=13485
- He₂⁺, potential energy curves calc. 8=12149
- ³He²⁺, ⁴He⁺, in solar wind, Vela satellite meas. 8=23715
- He-Ar mixtures in jets, separation 8=21471
- He-CF₄ compressed mixtures, nonresonant absorpt. and dispersion 8=1486
- p + He → H(2p) + He⁺, cross-section 8=21009
- He³-HD mixture, thermal diffusion model 8=12705
- He⁴-HT mixture, thermal diffusion model 8=12705
- He-He interaction, SCF-MO approx. 8=21013
- He-Li⁺ interaction energy at small internuclear distances 8=21014
- He-Ne d.c. discharge, relation between electron temp. and conc., and discharge parameters 8=7666
- He-Ne discharge tube, dia. and pressure effects 8=7676
- He-Ne laser, with axial magnetic field, resonance dips in output 8=11065
- He-Ne laser, axial mode frequency and power, characteristics 8=19967

Helium—contd

- He-Ne laser, axial mode number from moving mirror experiments 8=11026
- He-Ne lasers, cold cathodes for 8=11067
- He-Ne laser for colour television display 8=11068
- He-Ne laser, c.w., 6328Å, modes 8=19971
- He-Ne laser, discharge modulation noise 8=6449
- He-Ne laser, ears on line profile of decay transitions 8=3316
- He-Ne laser, intensity fluctuations, correlation meas. 8=3315
- He-Ne laser, method for meas. of depend. of gain per pass on power inside cavity 8=19969
- He-Ne laser, mode-locked quieting 8=15466
- He-Ne laser and monochromatic incoherent light fog scattering, comparison 8=14615
- He-Ne laser, oscill. mode interactions, with spher. mirror resonator 8=427
- He-Ne laser, power enhancements with double pulse excitation, comments 8=11062
- He-Ne laser probability of $3s_2$ - $2p_4$ transition in Ne 8=3317
- He-Ne laser rough reflector, noise and operation at $\lambda = 3.39 \mu$ obs. 8=11064
- He-Ne laser, single-mode, single freq., stabilization of output 8=11060
- He-Ne laser, spatial coherence, expt. investig. 8=19968
- He-Ne laser, spatial coherence and mode structure 8=6447
- He-Ne laser, Stark effect produced frequency shifts 8=11058
- He-Ne laser 3.39 μ Ne line, modulation by electro-optic gases 8=426
- He-Ne laser wavelength increase due to Ar addition 8=11063
- He-Ne mixture excitation in d.c. discharge 8=4093
- He-Ne mixture, meas. of thermal-diffusion factors 8=1488
- He-Ne mixture optical pumping by He-Ne laser, Hanle and saturation effects obs. 8=20983
- He-Ne 6328Å laser, self-pulsating oscillator 8=11057
- He-42.5% Xe gas mixture scintillation props. 8=11301
- Ne-He laser, stationary regime and oscill. damping 8=15471
- Ne-He mixtures, integral Joule-Thomson effect 8=15139
- TiO₂ surface discharge, channel development 8=1330
- Xe-He couples in binary mixtures, translation spectra 8=7425
- in ZnO:Zn, ions energy losses obs. 8=18624
- accommodation coeff. in impact on Al, Ag, Au and Pt, 500-12 000 eV 8=12685
- gas, annihilation rate of positrons 8=20998
- atoms, superradiance at transitions terminating at metastable levels 8=20943
- gas bubbles in austenitic steel after n-irrad., rel. to B distrib. 8=13040
- discharge, h.f. electrodeless, e density cinematography 8=16398
- discharge, low-pressure, p.d. meas. 8=16415
- electron-impact ionization cross section 8=16446
- enthalpy calc. from Redlich-Kwong eqn. 8=16689
- excitation by fast protons and H atoms 8=7433
- excitation in hollow-cathode discharge balance eqns for 2^3S , and 2^3P levels 8=20981
- excitation by H^+ , D^+ , H_2^+ and H_3^+ 8=16217
- glow discharge, secondary electron energy distrib. 8=16409
- ions, atomic and mol., mobility, 195-665°K 8=16445
- low-pressure h.f. discharge, luminosity of 5875Å line 8=16416
- of normal atoms, diffusion coeff. of metastable He atoms 8=4494
- residual, in colour picture c.r.t., mass spectrometry 8=15324
- scattering ionization, short range forces 8=1364
- solution and diffusion in tridymite and cristobalite 8=8247
- in stellar evolution flash and thermally unstable shell form., calc. 8=19133
- test gas in ballistic compressor, thermodynamic conditions 8=1470
- thermal conductivity, hot-wire cell meas., 30°-100°C, 120-150 torr 8=16700
- viscosity, low-temp., high press. 8=4493
- Cs vapour thermal diffusion in mixture 8=21525
- He³, nucl. spin relax. by surface interactions suppression 8=1160
- gas, and He-Ar, He-Ne mixtures excited by α , scintillation mechanism 8=12202
- He-N₂ mixtures, viscosity, low-temp., high press. 8=4493
- He-Ne, cataphoresis in d.c. discharges 8=1334
- He-Ne laser, frequency standard 8=15467
- He-Ne laser, growth of oscillations 8=19964
- He-Ne laser intensity correl. near threshold, 6328Å and 3.39 μ 8=19970
- He-Ne laser, intra-cavity loss perturb. rel. to Faraday effects in glasses 8=11059
- He-Ne laser modulation by inactive cavity 8=19965
- He-Ne laser, optimum d.c. excitation 8=15470
- He-Ne laser, output intensity variation of, in a magnetic field 8=15468
- He-Ne laser, radiation divergence meas. 8=6448

Helium—contd**gas—contd**

- He-Ne laser, stimulation rel. to radiation noise obs. 8=19966
- He-Ne laser Zeeman resonances 8=15469
- N₂-He mixtures, diffusive separation obs. 8=19537

liquid

- See also Quantum theory/many-particle systems; Superfluidity.
- advances in low temp. physics, book V 8=19680
- boiling point, thermodynamic temp. scale 8=19689
- Brillouin scattering, stimulated 8=19691
- electric current supply by vapour-cooled leads 8=15195
- Feynman-Onsager vortex, classical theory 8=10807
- filling of storage dewar, control device 8=15147
- film, rotating, thickness rel. to superfluid component motion, obs. 8=10796
- heat transfer, impulse 8=10798
- hot-electron injection from tunnel junction, effective barrier 8=257
- Kapitza resistance of Ce ethylsulphate 8=19700
- λ point, elec. field suppression 8=15151
- light absorption and scattering by excess electrons 8=19687
- minimum propag. current of immersed supercond. wire 8=22541
- quantized circulation, evidence from torque on cylinder 8=10808
- Rice model rel. to spin diffusion, thermal cond. and viscosity 8=10800
- specific heat, re-evaluation of spin fluctuation contrib. 8=2995
- specific ht. and susceptibility, from lattice model of planar 'spins' 8=126
- supercritical, heat circulation systems 8=19690
- superfluid circulation in a porous medium 8=19698
- superfluid, closed-cycle refrigeration at 1.85°K 8=6224
- superfluid, flow through orifices, critical vel. and vortices form obs. 8=6234
- superfluid, intrinsic critical vel. near λ point 8=263
- superfluid, vortex lines 8=3124
- superfluid, wave function exam. 8=261
- superfluidity penetration into Zeolite micropores., obs. 8=10805
- superfluidity, phonons origin and rotor excits., collective coordinates theory 8=10799
- superfluid, rotating in annular channel 8=10809
- thin film, fermion model, specific heat, size effects 8=10656
- ultrasonics and superfluidity 8=10806
- viscosity, appl. to theory of nearly ferromag. Fermi liqs. 8=2994
- vortex ring formation by ions, evidence for peeling model 8=10797
- vorticity in flow through orifices 8=19699
- X rays, phonon and muonic 8=1211
- H II vaporization, limiting ht. current density for initiation at Pb surface 8=4660
- He I, temp. distrib. with height, meas. with Pb-Sn wire cryotron relax. oscillator 8=22571
- He II, back flow effect appl. to impurity atom among Bogoliubov quasiparticles 8=3122
- II, counterflow past a flat plate, anisotropy 8=19701
- He II near critical point, superfluid density obs. 8=19702
- He II filling narrow gap, heat exchange with solid body 8=6233
- He II, heat exchange torques on bodies immersed in flow 8=3127
- He II, ion velocity discontinuity at 1.1°K 8=19697
- He II, Kapitza conductance, depend. on Debye temp. of solid 8=10811
- He II, local gauge invariance and broken symmetry 8=3126
- He II in plane-parallel capillary, wave processes 8=3123
- He II quantized circulation around a fine wire obs. 1.2-1.9°K 8=19703
- He II quantized vortex lines threshold in rotating annulus, obs. 8=10810
- He II, rotating, interaction of quantized vortex and lines 8=10804
- II, rotating, superfluid velocity rel. to temp. 8=6231
- He II, rotating, wave propagation 8=262
- He II single, vortex and rotating vortex lattice, quantum theory 8=3125
- He II, specific heat, logarithmic singularity 8=15150
- He II, subcritical flow, press. obs. 8=19695
- He II, surface tension calc. 8=3128
- He³, dilute solution in liquid He⁴ rel. to elementary excitations, model 8=6229
- He³, collective treatment 8=19692
- He³, Fermi liquid theory rel. to specific heat and magnetic susceptibility 8=15020
- He³, Fermi model, flow along narrow channel, spin diffusion, thermal cond. calc. 8=15017
- He³, heat capacity and freezing curve 8=3118
- He³ solubility in He⁴ and dilute mixtures molar density, 1.25-0.025°K 8=6230
- He³ in superfluid He⁴, dilute mixtures 8=15152
- He³, transport coeffs., pressure depend., spin fluctuation theory 8=19693
- He³, vapour press. in mag. field, theory 8=15144

Helium—contd**liquid—contd**

- He^{3,4}, ground state energy calc. using Lennard-Jones pot. and de Boer-Michels parameters 8=10803
 He-3, 4, solid-liquid phase transition prediction 8=10813
 He³, Cr, and Fermi liquid quasiparticle self-energy 8=3117
 He³-He⁴ dilution refrigerator, rapid start-up 8=15145
 He³ in He⁴ dissolution refrigerator 8=19682
 He³-He⁴ mixture, heat capacity and freezing curve 8=3118
 He³-He⁴ mixture, thermal conduction due to phonons for $T \leq 0.6^\circ\text{K}$ 8=10801
 He³ in He⁴, osmotic pressure of dilute solutions 8=10795
 He³-He⁴ solutions, nuclear spin polarization enhancement 8=256
 He³-He⁴ solutions, thermodynamic properties at λ -transition, n. m. r., studies 8=10794
 He⁴, with He³ impurities, model of dilute fermion mixture in dense bose fluid 8=19688
 He⁴-3.9% He³, positive ion mobility, $T, -1.4^\circ\text{K}$ 8=15141
 He⁴, atomic collisions and Ramsauer-Townsend effect 8=1200
 He⁴ cryostat for 0.9°K 8=15146
 He⁴, energy spectrum of elementary excitations 8=3115
 He⁴ glass superleak construction 8=15149
 He⁴, lambda curve, meas. and empirical eqns. 8=3116
 He⁴, λ -transition, Patashinskii-Pokrovskii theory 8=255
 He⁴, molar volume, coeff. of thermal expansion obs., $1.25-4.2^\circ\text{K}$, $0.5-28\text{ atm}$ 8=10802
 He⁴, positive ion mobility, $T, -1.4^\circ\text{K}$ 8=15141
 He⁴, superfluid model, normal-mode anal. 8=15153
 He⁴ superfluid, with soln. of He³, model of fermion soln. in boson gas 8=6232
 He⁴, turbulently flowing, λ -point shift 8=19694

liquid, sound propagation

- absorption of sound below 0.6°K 8=6235
 second sound, laser beam scatt. photocounting method 8=11192
 second sound wave, observation by laser beam diffraction 8=6236
 He II attenuation of second sound during rotation 8=10812
 He II, rotating, first and second 8=262
 He II second sound visual obs. by Toepler method 8=264
 He³ soln. in He⁴, temp. and freq. dependence 8=15143
 He³, zero sound 8=3119
 He³, zero sound in magnetic field 8=3120
 He³-He⁴ mixture, attenuation due to He³ viscosity and phonon-He³ scatt. 8=10801
 He³-He⁴ mixtures, speed of second sound below 1°K 8=3129
 He³-He⁴ mixtures, zero sound existence 8=3121
 He⁴, sound vel. at 1 Mc/s in critical region 8=15142
 He⁴, 3-phonon mechanism incompatibility with obs. 8=258

solid

- b. c. c. crystals, phonon freq. calcs. and thermodynamic props. 8=1836
 EMS (Saunders) theory, anomalies 8=19704
 isotope mixtures, lattice thermal conductivity 8=1889
 lattice dynamics at 2.9°K and 125 atm. by n-scattering 8=1837
 thermal conductivity, h. c. p. single crystals 8=8659
 He³, exchange energy diffusion rate meas. 8=15156
 He³, melting curve calc. below 0.04°K 8=15158
 He³, nuclear magnetic relaxation $0.3-0.04^\circ\text{K}$ 8=3130
 He³, nuclear spin ordering evidence 8=6237
 He-3, 4, at 0°K , ground state energy rel. to density 8=10813
 He³-He⁴ mixtures, phase separation, theory 8=15157
 He⁴ crystals, hexagonal, birefringence 8=15155
 He⁴, and isotopic mixtures, thermal cond. at high densities 8=15154
 He⁴ phonon dispersion measurements on single crystals 8=10815
 He⁴ II-I transition under rot., higher than first order 8=10814

Helium compounds

- HeH²⁺, one-centre perturbation calc. 8=4138
 HeH⁺ $1s\sigma$ and $2p\pi$ states, approx. wave functions calc. 8=4153
 HeH⁺, the $3d\sigma$ state, approx. molec. wave function 8=1245

Hellmann-Feynman theorem. See Quantum theory.**High-pressure phenomena and effects**

- albite, elec. cond. 8=8978
 alkali aluminogermanates, transforms rel. to geochem. 8=8261
 alkali aluminosilicates, transforms rel. to geochem. 8=8261
 alloys, hydrostatic tension on solidification 8=21759
 apparatus for obtaining high static press., rel. to effect on solids 8=2873
 atoms, electron shell filling order 8=7364
 ball bearing, flanged-mounted, Weibull plot of contact fatigue data 8=17741
 basalt, elec. cond. 8=8978
 compressibility of metals, effect of electron structure 8=17724
 compression loads in controlled atmos., apparatus for meas. 8=5019
High-pressure phenomena and effects—contd
 conductance of aqueous solns., meas. cell, $1-3000\text{b}$ and $25-225^\circ\text{C}$ 8=14424
 cryostat for studies at $\sim 100\text{kbar}$ at liq. He temp. 8=3112
 crystal electronic spectra, theory 8=8914
 dead weight piston gauge for press. to 26 kbar 8=5999
 depolymerization, by ultrasound 8=4568
 differential thermal analysis technique 8=9684
 DPPH, absorpt. spectra 8=18579
 ferrocene, effect of press. on Mössbauer resonance 8=1652
 gases, compact elec. lead for use at low temp. 8=3147
 glass molten, viscosity high-temp., high-pressure viscometer obs. 8=8022
 glass, suppression of irradiat. effects 8=4996
 haloquinone complexes in polymer matrices, absorpt. spectra 8=14274
 n-hexane, dielec. const. 8=1582
 high-pressure chambers, to 19 kbar , working at liq. He temp. 8=10464
 hydrostatic to 60 kbar , technique 8=7971
 hydrostatic tension in solidifying materials 8=21758-9
 inductive coil tech. for meas., anal. of error sources outside apparatus 8=19342
 ionic crystals, changes in cryst. and electron struct. 8=4699
 low temp. closure and elect. leadthrough for high-pressure systems 8=23781
 magnetic materials, magnetization and anisotropy meas. 8=13952
 metals, changes in cryst. and electron struct. 8=4699
 metals, strain fields under omnidirectional uniform compression 8=17756
 minerals, hydrothermal synthesis, apparatus 8=23782
 nitrobenzene, dielectric props. 8=21713
 optical cell for absorpt. and luminescence studies up to 40 kbar and at 77°K 8=6502
 parahydrogen, fluid, eqn. of state 8=4525
 parahydrogen, solid, ht. of fusion and density at up to 400 atmos. 8=16928
 n-pentane, solidification at high press. 8=21747
 phenolphthalein and congeneric mol. crystals, plastic deformation effects 8=23033
 phlogopite, stability at high press. rel. to presence in Earth's mantle 8=23221
 piston-cylinder devices, friction pressure loss 8=14909
 pistons of press. booster, sealing with rubber ring 8=10465
 plastics, solid, hydrostatic creep, linear strain and recovery 8=22280
 polymer-diluent mixtures, melting 8=4642
 polymers, glass transition 8=8359
 polymers, influence on crystallinity 8=4774
 powders, preparation of samples for melting point determ. 8=8172
 radiolysis of liquids 8=14444
 reactions in solutions 8=14356
 semiconductors, changes in cryst. and electron struct. 8=4699
 shock-velocity-particle-velocity relationship in study of solids under pressure 8=8787
 silicate-water system, melting, hydrothermal curves 8=21752
 solids, mech. props. 8=8796
 solid-state physics research tool 8=10463
 static, demountable, low temp. seal 8=14910
 on stress/strain relns. of mats in mech. props. 8=13502
 surface press. generated by pistons on spherical and cylindrical baffles 8=6134
 ultrasonic press. gauge to 20 kbar for solid rods 8=19341
 vapour-liquid equilibria 8=16939
 vessel flush nozzles, stress analysis 8=10557
 AgI, ionic diffusion 8=1907
 Al, thermoelectric power and elec. resist. 8=13902
 Ar, heats of fusion and random close packing 8=8181
 Ar, shock compression, Thomas-Fermi-Dirac theory 8=16994
 Au, thermoelectric power and elec. resist. 8=13902
 B, polycryst., on thermopower and resist. at 25 to 300°C 8=18210
 B₂O₃ glass, permanent densification by hydrostatic press. 8=22314
 Ba I-II transition, pressure determ. with single-piston apparatus 8=4702
 C₂ClF₅-He mixtures, microwave absorption 8=7936
 Cr, spin density wave studies by n-diff., high pressure effects 8=22876
 CrO₂ reduction from CrO₃, under high press. and temp. 8=9674
 Fe ionic cpds., Mössbauer effect 8=4674
 FeO, synthesis of stoichiometric cpd. 8=13259
 FeS₂, effect of press. on Mössbauer resonance 8=1652
 p-GaSb, Hall coeff. and conductivity, pressure dependence at diff. temps. 8=13804
 H₂ cell, Raman emission at $8.84\mu\text{m}$ 8=15484
 He gas, viscosity 8=4493
 He-N₂ gas mixtures, viscosity 8=4493
 In, superconducting critical fields, up to 30 k atm 8=5212
 InSb, on Hall coeff. and conductivity 8=13819
 KCl solns., elec. cond. 8=12922
 KH₂PO₄, ferroelec., transition temps. shifts by hydrostatic press 8=18189

High-pressure phenomena and effects—contd

- K₂Fe(CN)₆, Mössbauer effect 8=4673
 K₄Fe(CN)₆, Mössbauer effect 8=4673
 K₄[Fe(CN)₆]₃, Mössbauer effect 8=4673
 LiBO₂, prep. of β and γ forms 8=8269
 LiF, effect of hydrostatic pressure on dislocation mobility 8=1976
 Li₂SO₄·H₂O, incongruent melting and polymorphism 8=12970
 MnP, Curie point and anisotropy energy decrease under hydrostatic pressure 8=2328
 MnT'O₃, (T' = Ho, Er, Tm, Yb, Lu), hexagonal, transform. to perovskite form 8=17089
 N₂ gas, viscosity 8=4493
 Na borate glasses, ht. of soln., density and refractive index changes up to 40 kbar 8=1715
 Nb, superconducting, influence on transition temp. 8=9060
 Ni, thermoelectric power 8=13902
 NiS, on mag. and elec. transition pt. 8=22885
 PbCrO₄, synthesis 8=23110
 Pt, thermoelectric power 8=13902
 Re, superconductivity, transition temp. var. 8=17972
 Re—Os alloys, superconductivity, transition temp. var. 8=17972
 Sn, superconducting critical fields, up to 30 k atm 8=5212
 Sn₂Te₂, about 840°C and 12.0 kb, liquid and two solid polymorphs. 8=1614
 Ta, superconducting, influence on transition temp. 8=9060
 Te, liquid, elec. cond. meas. 8=1588
 TiO₂, II modification at 40–120 kbar and 400–1500°C 8=17104
 V, superconducting, influence on transition temp. 8=9060
 Zn₂GeO₄, phase transformations 8=13075
 Zn₂SiO₄, phase transformations 8=13075

High-speed photography. See Cinematography; Photography/
high-speed.

High-temperature production and effects

- Alnico alloys, magnetization obs. 8=22813
 in cold gas 8=2274
 conductance of aqueous solns., meas. cell., 1–3000b and 25–225°C 8=14424
 laser beam, focused on solids, heating and evaporation effects 8=15130
 plasma, shock wave generation for nuclear fusion 8=7798
 polymeric and refractory heat shield materials, ablation obs. 8=1860
 on quartz spoon gauges 8=5990
 solar concentrators, use of polyurethane foam in construction 8=19677
 solar energy receivers, cylindrical cavity, optimal dimensions 8=19676
 solar furnace of polyethylene terephthalate film 8=19675
 solar stills, aerodynamic coeffs. rel. to leakage of steam-air mixture 8=19678
 solar still, effect of leakage on performance under thermal head 8=19679
 vacuum film solar concentrator, proposed long-focus type 8=19674
 Fe, alloys, levitation apparatus for phase equilibria 8=1669
 Fe—Al alloys, oxidation after storage 8=9666
 In, creep, pressure dependence 8=8852
 UC, oxidation behaviour obs. 8=23115
 UO₂·Dy₂O₃ dispersion, behaviour in steep temp. grad. 8=4694
 UO₂·Eu₂O₃ dispersion, behaviour in steep temp. grad. 8=4694
 UO₂·Sm₂O₃ dispersion, behaviour in steep temp. grad. 8=4694

High voltage production

- accelerators, linear, compressed gas insulation and other improvements 8=15652
 d. c. power supply of shielded design 8=15185
 d. c. power supplies, small, improvements 8=15186
 electrical feedthrough, compact 60 kV UHV, construction 8=3140
 for electron beam machine 8=15290
 1250 kW thyristor converter plant as power source for CERN-MeV synchrocyclotron 8=15663
 particle accelerators, principles 8=6689
 pulse rate generator exponential, associated with reactor 8=3144
 progress in nuclear physics, book IX 8=15627
 pulses, by three-electrode spark gap 8=7680
 ultrastable source to 10 kV, using capacitive feedback 8=3146
 Van de Graaff accelerator, 3 MV, square and sine wave modulation of beam 8=19713
 van de Graaff method, development and application 8=11341
 voltage meas. using Kerr effect 8=6564

History

- acceleration due to gravity, Poland, determ. 8=14515
 auroral exceptional periods 8=23336
 Burrau three-body problem, historical review and soln. 8=19100
 crystallography achievements in USSR, 1917–1967 8=2874
 earth, thermal 8=9772
 Ising–Lenz model solns. and appls., review 8=10612
 Kepler and Tycho on lunar theory 8=14821
 "non-mathematical theoretical physics" 8=10467
 origin of word "plasma" as applied to gaseous electronics 8=12457

History—contd

plasma, survey of concept 8=1375

Hodoscopes. See Cosmic rays/apparatus; Particle detectors.

Hole theory of liquids. See Liquids/theory.

Holes. See Crystal electron states; Semiconducting materials; Semiconductors.

Holmium

- absorption spectrum, 3mm microwave radn., mag. structures effects 8=14226
 deformation planes after dehydrogenation and hydride habit planes 8=8728
 microwave absorption phenomena at 9.44 and 35.3 Gc/s, 10–290°K 8=14269
 neutron diffraction study under high pressure, helical periodicity 8=14040
 vapour pressure 8=16950
 Ho-doped crystals, infrared quantum counter action of Ho³⁺ 8=18606
 Ho²⁺, e.p.r. of CaF₂, stress effects 8=14128

Holmium compounds

- holmium ethyl sulphate, far-infrared high resolution, spectroscopy on e.p.r. lines 8=14110
 HoAl₃, nuclear magnetic resonance 8=22920
 Ho₂C, mag. structure by n-diffr. 8=22865

Holography

- acoustic, with inclined planar reference 8=10744
 acoustic, recording technique 8=6176
 advanced optical techniques, book 8=15489
 aerodynamic flow visualization 8=6572
 antenna polar diagram, Fresnel zone field meas. 8=19900
 antennas and propagation conference, Ann Arbor 1967 8=15401
 birefringent beam splitter 8=3379
 bubble chamber track holograms 8=6567
 coherent optical systems, improvement of two-dimensional image quality 8=11132
 cylindrical, construction and appl. 8=11206
 diffuse object, noise-like structure 8=12127
 by division of amplitude 8=528
 double exposure interferometric, theory and expt. 8=20114
 double exposure, white-light interference-pattern reconstruction 8=15557
 dynamical X-ray diffraction theory application 8=530
 electron, ion and laser beams technology, conference, Berkeley, USA (1967) 8=15283
 film nonlinearities effects, extension 8=20112
 for filtering spatial frequencies in incoherent light 8=20111
 focused-image-hologram copying with white light 8=20121
 gas laser light sources 8=15559
 glass, photochromic, information storage capacity meas. 8=6570
 gratings, six types, response and efficiency 8=20122
 ground tests 8=521
 hologram aberrations, evaluation by ray tracing 8=11216
 holograms, binary Fraunhofer, computer generation and reconstruction 8=6576
 holograms, coded multiple exposure 8=20117
 holograms, construction with direct reference beams 8=3381
 hologram copying by Gabor holography, analysis 8=6575
 holograms with increased range coverage 8=11211
 holograms, inexpensive method 8=6569
 holograms, instant, prep. and characteristics 8=11208
 hologram, laser reconstruction of image 8=524
 hologram-Moire interferometry for transparent objects 8=522
 holograms, point, as optical elements 8=6568
 hologram, pulsed formation of diffusely reflecting systems 8=527
 holograms, quantity reproduction process 8=11209
 hologram reconstruction, influence of emulsion thickness and absorption 8=15556
 hologram, resolving power, calculation by Abbe and Airy methods 8=15561
 hologram rotation for image scanning 8=523
 holograms synthesized on cathode-ray tube 8=11207
 holograms, training bleach bath, variation of method 8=20119
 holographic fringes, stabilization by f. m. feed-back 8=20116
 holographic interferometry appl. to plasma meas. 8=7779
 holographic stereogram from sequential component photographs 8=15555
 holomicrography, image transformation during reconstruction 8=525
 image separation increase by total reflection 8=11210
 image systems, real and virtual 8=520
 interference, isophase surfaces 8=20113
 interferogram for conical flow studies, refined analysis 8=6565
 interferograms as image holograms 8=15554
 interferometer, 3-beam with single emulsion exposure 8=6541
 interferometric, ghost lines 8=3380
 introduction, undergraduate level 8=11213
 laser application, review 8=6479

Holography—contd

- lens, imaging analogy and formulae appls. 8=20105
 light sources, mutually coherent, interference paradox 8=6546
 light yield and signal/noise ratio 8=20108
 measurement of transfer function of an objective 8=15514
 microwave 8=20109
 microwave, and optical reconstruction 8=11214
 moving objects, using front-illum. of pulsed laser 8=11218
 multiple freq. wavefront recording 8=15558
 nonpseudoscopic real image from holograms, technique 8=6577
 phase objects, three-dimensional, scope and limitations 8=15560
 phase structures, interferometric meas. 8=15553
 photographic film non-linearities, effects 8=6574
 photographic material resolution limit 8=15552
 principles and practical requirements 8=20106
 progress in optics, book VI 8=15541
 pulsed laser holograms, resolution 8=20110
 pulsed, and microscopy, interferometry and dynamic recording appls. 8=20107
 recording on 3-dimens. media, theory and reconstruction 8=20120
 review of progress 8=11119
 sampled wavefront scatt. from laser illuminated object 8=20115
 spatial coherence, influence on holographic processes 8=11215
 spatial filters for image restoration and code translation 8=519
 techniques, limitations, theory 8=6566
 with total internally reflected light 8=3378
 two hologram-copying parameters, effect 8=11212
 ultrasonic, by electronic scanning of piezo-electric crystal 8=19580
 ultrasonic, recording technique 8=6176
 velocity meas. of steady fields 8=15562
 wavefront reconstruction by hologram transmitted on closed circuit television system 8=6573
 X-ray, Fresnel-zone lenses appls. 8=15591
 X-ray microscopy with Fourier-transform holograms, high resolution attainment 8=15592
 CaF_2 photochromic crystals, thick hologram storage 8=20118
 SrTiO_3 photochromic crystals, thick hologram storage 8=20118

Hot-atom chemistry. See Chemical analysis/radioactive; Nuclear reactions/chemical effects; Radiochemistry.

Hubble model. See Cosmology.

Hugoniot diagrams. See Equations of state.

Humidity

See also Atmosphere/humidity; Hygrometers; Moisture.

- air, effect on electric breakdown 8=12691
 control system for small chamber 8=16645
 distributed parameter nonadiabatic heat and mass transfer, thermal dynamics 8=12976
 hygrometer, frost point, sensing element with fast response 8=9838
 measurement by slowing down of high-speed neutrons 8=9839
 sound absorpt. in the atmosphere, pressure depend. obs. 8=23268
 Al alloy, rel. to surface bubble formation during fatigue 8=4729
 rel. to Pu oxidation rate in air 8=5717

Hydrodynamics

- See also Flow/liquids; Jets; Liquid oscillations; Liquid waves; Magnetohydrodynamics; Viscosity/liquids.
 aerosol particles in sound field under Oseen flow, interaction calc. 8=21731
 Boltzmann eqn., linear, soln. for flow over point source 8=7875
 boundary layer at a disc in transverse air flow 8=4449
 cavitation, gas diffusion, into void 8=4497
 circular Couette flow, problem of Taylor instability, suppression of effect of geometry 8=21425
 compressible fluid flow in wake of symmetrically positioned body 8=7862
 continuous medium, space and time dependent correlation fluctuations 8=6103
 critical mixtures, equations for nonlinear effects in shear viscosity 8=8163
 Crocco-Vazsonyi relativistic eqn. for ideal fluids 8=1442
 crystals, liquid, nematic type, linear theory 8=8007
 cylindrical shell containing flowing fluid 8=152
 differential equations, nonlinear, solution 8=12584
 elastico-viscous fluid, drag on oscill. sphere 8=21557
 electron gas, equations 8=131
 electron gas, non-uniform, relativistic, kinetic equations 8=132
 equations, microphysical derivation 8=12726
 explosive detonation, theory 8=6146
 flow, discontinuous one dimensional non-dissipative 8=15375
 flow, laminar incompressible viscous, nonlinear stability theory 8=12586
 flow in rotating and stratified fluids 8=21427

Hydrodynamics—contd

- fluidic amplifier, improved sensitivity 8=4427
 fluid flow through porous media, numerical simulation 8=12594
 fluid shear flow, turbulent, waveguide model 8=12598
 gas jet impinging on liq. surface 8=12728
 Hamilton-Jacobi eqn. for charged relativistic fluid in e. m. and gravit. fields 8=16634
 Hamilton's principle, Noether's theorems appl. 8=12583
 high pressure gas, sphere, expansion in porous medium 8=1439
 jet oscillation in the presence of a separator 8=16780
 laminar flow development in rectangular ducts 8=4451
 laminar source flow between 2 parallel co-axial discs rotating at different velocities 8=21426
 liquid-gas media dynamics under zero-gravity, surface effects 8=4506
 liquid sphere, influenced only by gravity, frequency spectrum 8=4504
 local potential of fluctuations, variational properties 8=1440
 MHD pipes, hydraulic resistance 8=15385
 motion of gas behind diverging detonation wave 8=4461
 Navier-Stokes eqns. for dissipation processes 8=7859
 Navier-Stokes equations, non-stationary, new finite-difference scheme 8=21558
 non-linear problems in fluid mechanics, Newton's approximation application 8=12721
 non-Newtonian fluids, natural convection flow, boundary layer equation solution 8=7857
 non-Newtonian fluid, rotational motion through annulus with porous walls 8=21433
 oscillations of viscoelastic fluids 8=7861
 particle aggregation, in sound field 8=6156
 particle movement in a viscous irregularly moving medium 8=7853
 perfect fluid, rotation of heavy smooth object 8=12729
 pipe flow, effect of vibrations rel. to laminar and turbulent transition regimes 8=1501
 pipeline flow of capsules, velocity and press. gradient 8=7972
 plasma, laser-produced in vacuum chamber, coding by expansion, obs. 8=4322
 Poiseuille flow in parallel channel, with variable fluid props. 8=21472
 Poiseuille flow, stability and incipient turbulence, study by difference method 8=12722
 polymer solutions, effects on quasi-elastic scattering 8=4542
 polymer solns., influence of intermol. interaction on viscosity and streaming birefringence 8=4505
 porous column dispersion, for small linear porosity var. of with distance 8=1441
 rotating liquid with free cylindrical surface, stability to small inviscid disturbances 8=1505
 rotating and stratified non-rotating fluids, analogous behaviour 8=1445
 shock waves in fluid with steady uniform flow 8=21447
 silicone oil heated under constant temp. air surface 8=1504
 similarity method using governing eqns., boundary condns. and dimensional analysis 8=16620
 sound wave absorption by forced alternating viscous fluid flow 8=3058
 sphere, charged, moving in polarizable liquid, Stoke's law correction 8=12723
 spherical waves, radiated in fluid, finite amplitude 8=19516
 stability, spectrum of operator 8=1443
 stellar, gaseous, mass, inhomogeneous, convective instability, model 8=2794
 Stokes resistance, translation and rotation, boundary effect 8=1444
 stratified fluid, spin-up 8=7855
 swimming, doubly infinite and flexible sheet 8=16752
 thin films, behaviour in transient state 8=16783
 Tietjens function, numerical evaluation 8=21420
 time-dependent motion due to cylinder moving in unbounded rotating or stratified fluid 8=7856
 trapezoidal models, lift and drag coefficients 8=7858
 two-phase flows in vertical tubes 8=21560
 underwater explosion, phase shift due to total internal reflection 8=19547
 underwater explosions, π/λ phase shift at caustics 8=19546
 variational principle for hydromagnetic flows 8=15374
 viscoelastic Maxwell fluids, contained between concentric spheres, motion 8=21421
 viscous flow in a tube, constant temp. 8=12734
 viscous fluid, initially prescribed surface normal velocity 8=7854
 water, corona discharge characts. 8=21250
 wave pattern, 2D, produced by disturbance moving in density stratified liquid 8=4514
 wedge in viscous fluid, impulsive motion 8=16619
 He II, rotating, interaction of quantized vortex and lines 8=10804
 He II, rotating, superfluid velocity rel. to temp. 8=6231
 He II, superfluid in rotating annular channel 8=10809

Hydrogen

See also Deuterium; Protons and antiprotons; Tritium.
 accommodation coeff. in impact on Al, Ag, Au and Pt, 500-12 000 eV 8=12685

Hydrogen—contd

adhesion coefficients at 4.2° and 20°K 8=7954
 adsorption with CO on Rh electrodes 8=18727
 adsorption on Ni surfaces, electron probe surface mass spectrometer obs. 8=21908
 adsorption on Ta ribbon, work function changes 8=9276
 auroral arc, Balmer α emission rel. to incident H flux obs. 8=2636
 beam-plasma systems, beam generated, interacting components 8=21289
 bond, nature of, and water structure 8=4529
 bonding in solns., n. m. r. obs. 8=16883
 bubble chamber, sealing of glass illuminators using pneumatic packing 8=15645
 bubble tech. for flow visualization and vel. of H₂O in clear tubes 8=16756
 chemisorption on Re 8=23126
 combination with D₂, gas torque effect on heated cylinder 8=1320
 crystal-structure changes during transitions in ortho- and para-states, X-ray exam. 8=13263
 desorbed from Ti anode, discharge 8=21227
 desorption from Ni polycrystals 8=17170
 diffusion in fused SiO₂; Tb, Eu 8=17585
 diffusion in α -Pd-H, study by n-scatt. 8=17581
 diffusion in Pd and Pd alloys, at 0° to 100°C 8=17582-3
 discharge lamp, constant-current power supply 8=19714
 discharge in spark channel, voltage drop, expansion rates etc. 8=12410
 dissolved in α -Zr, equilib. press. 8=8251
 dissolved in water, molec. diffusion coeffs. 8=12828
 electromigration in Fe 8=8677
 electron microscope investigation of condensed H₂ 8=8465
 electron transport coeff. 8=21521
 estimation, in solid and liquid samples, by neutron thermalisation 8=23197
 flames, chemiluminesc., effects of SO₂ 8=18693
 flame, O, H kinetic calc. 8=9699
 flash lamp pressure and voltage gradient effects 8=15522
 galaxy M33, H II, kinematical and physical data from interferometric obs. 8=23568
 gas, high pressure synthesis of glass rel. to suppression of irradiation effects 8=4996
 gas, Is diagram, 16°-100°K, up to 500 kg/cm² 8=7915
 gas, rotational relaxation, high temp. u. s. obs. 8=1251
 ground-state dissoc. energy, theory and expt. 8=16364
 heat transfer props. in reduced gravity 8=16692
 high-pressure cell, Raman emission at 8.84 μ m 8=15484
 high-pressure glass synthesis, irradiation desensitization 8=8353
 ignition, slot-injected in supersonic air stream 8=15112
 interstellar distribution, 21 cm obs. with 300 foot telescope 8=23565
 interstellar H II, r. f. line, emission enhancement by departures from thermal equil. 8=23567
 interstellar neutral regions, i. r. emission and m. h. d. shock waves 8=23566
 interstellar, formed by chemical-exchange reaction, upper limit on abundance 8=5926
 interstellar, radial motion within the Galaxy 8=10243
 intramolecular bridging bond, pot. 8=7497
 ionized partly, viscosity obs. 8=12701
 isotope mixtures, thermal diffusion props 8=1492
 jet, supersonic and dense, as charge exchange target 8=21451
 lamp, spectrum, 2500-1100 Å, intensity distrib. 8=4065
 laser action in electrical discharge containing H 8=12398
 lines, broadening by Stark effect 8=1159
 liquid-solid mixtures, quality determ. 8=15138
 liquid-solid rocket fuel mixture obs. 8=19067
 liquid, thin walled nuclear bombard. target, description 8=15838
 magnetic drift vel. and deflection coeff. for slow electrons 8=7712
 mixtures in He and Ne, striations in glow discharge 8=7657
 multiphoton ionization of atom 8=12440
 nebulae vels. $n_{105} \rightarrow n_{104}$ line intensity and width obs. 8=10233
 neutral, galactic, detection, and model profiles investigated 8=5934
 neutron activation analysis determ. 8=2553
 ohmic heating discharges, in C-stellarator, computer description 8=21407
 ortho, solid, self-consistent model, Pca2, ordering 8=17375
 orthohydrogen, solid, orientational ordering, h. c. p. molecular lattice 8=22026
 para, fluid, eqn. of state 8=4525
 para-H₂, solid, deformation curves at 4.2°K, mech. constants 8=5074
 parahydrogen, ht. of fusion and density at up to 400 atmos. 8=16928
 permeation rate in W, pressure, thickness and temp. dependence 8=4958
 permeation through Ni, kinetics 8=8682
 planetary nebulae model, ionization balance rel. to Lyman continuum problem 8=19190
 plasma of d. c. discharge positive column, cross wave of moving striations 8=4281

Hydrogen—contd

plasma, laser-produced, temp. and density meas. rel. to absorpt. at laser freq. 8=12514
 plasma, pulsed relaxation 8=4410
 plasma, in shock tube, elec. props. and Cu cold electrodes V-I characts. 8=21359
 profiles of H lines of peculiar stars α^2 CVn and γ Lyr, anal. 8=19146
 pumping speed-press. data, getter-ion pump 8=1495
 quark-atom lines in solar spectrum 8=6718
 quasi-molecular absorpt. in metal-deficient subdwarfs, calc., 0.2-0.45 μ 8=23528
 radiation belts, interaction with charged particles and subsequent Lyman α emission 8=18963
 reaction with O(D) 8=5744
 recombination lines 158 α in galactic H II regions 8=5930
 recombination system of H₂-O₂-gases in BER reactor 8=4014
 residual, effect on BaO cathode emission 8=18663
 residual, pressure obs. in picture c. r. t. 8=15325
 shock wave thickness 8=16646
 slush, liquid-level sensor, superconducting 8=16929
 solar Ly- α and - β line intensities rel. to emitting layers e temp. and density 8=10390
 solid and liquid, Raman spectra, intensity anomaly 8=9536
 solid H₂, n. m. r. data, correl. time for mol. rot. 8=14141
 solid, ortho, quadrupole-quadrupole interaction and λ transition 8=8267
 solid, pressure changes on phase transitions 8=4711
 solid, Raman effect intensity anomalies 8=6523
 solid, Raman spectra anomalies rel. to mol. vibrations 8=9535
 solid, statistical model applied to n. m. r. 8=22923
 solubility in hydride phase of Pd, V, Nb and Ta, isotherm 8=1924
 solubility in liq. Ag 8=21617
 solution in liq. Ar, translational absorpt. spectrum in far i. r. 8=12889
 solubility in solid Ni-Cu alloys 8=21826
 spectral-isotopic definition in high-sorption metals 8=9743
 stellar atmosphere, theoretical study 8=2773
 stellar clusters H₂ index rel. to distance moduli and distances, photo-elec. obs. 8=10207
 stellar, mixing by He-shell flashes, calc. 8=10145
 stimulated emission in beam laser, line shape and width obs. 8=421
 target nucleus, thermonuclear reaction rates 8=11976
 terminal solubility and partitioning in α -Zr, Zircaloy-2 and Zircaloy-4 8=8249
 terminal solubility in Zircaloy-2 and Zr-2.5wt%Nb, thermal diffusion obs. 8=8250
 third virial coeff., and for nonpolar mixtures 8=12677
 in variable star α Lupi, spectroscopic obs. 8=10182
 viscosity, effect of organic vapour molecules, for determ. of mol. dimens. 8=1485
 rel. to Ag surface struct., catalytic oxidation effects, obs. 8=18706
 D content, neutron spectrometry 8=9765
 in Fe, anomalous behaviour at low temps. 8=22182
 H-bond stretching freq., effect of bond strength 8=21141
 H α line in aurora, variation in width over 1 hour 8=14650
 H α emission in galaxy with 1967 supernova in NGC 3389 8=14781
 H γ , Stark broadening in plasma column 8=4063
 HD, liquid, n. m. r. proton transitions 8=8133
 H-e exchange scattering amplitudes 8=12090
 H-line Stark broadening functions 8=12051
 H-H system, 2nd virial coefficient for different electron states at 2000-6000°K 8=1469
 H I clouds, high velocity, search for interstellar Ca II and Na I lines near 8=5880
 o-H₂ prep. by preferential adsorption 8=17158
 H₂ sorption, Bayard-Alpert gauge modification 8=16732
 H β , Larmor freq. rel. to Ge¹³, and K⁴¹ 8=5558
 Mo tip, absorption, field emission study 8=21905
 in Na-K reactor coolants, effect on efficiency of coolant, corrosion act. and residual radioact. 8=7328
 Ne-H bubble chamber, cryogenic 8=20224
 Ni-Cr film sputtering control 8=8777
 Ni-Cu, effect of cathodic hydrogen loading on ferromag. resist. anomaly 8=14023
 in Pd-H, α -phase, diffusion, by small energy transfer neutron scattering 8=13411
 U, surface potential of H₂ 8=21909
 in ZnO:Zn, ions energy losses obs. 8=18624

ions

collision cross-sections determ. by ion cyclotron reson. 8=12442
 e partition function from screened Coulomb interactions 8=1157
 e-H compound states, 5 parameter wave function for lowest two 8=20997
 ions, 0.2-40 keV, deceleration in Ag foil 8=2020
 plasma, heating by large amp. ion cyclotron wave, efficiency 8=4332
 plasma, internal energy of free p and e, calc. 8=12469
 plasma in mirror machine cyclotron resonance and nonadiabatic trapping 8=21370

Hydrogen—contd
ions—contd

- solvation by H_2O mols. in gas phase, kinetics and thermodynamics 8=18661
- H II regions in anticentre region, electron temp. determ. by radio obs. 8=19199
- p-H collision, charge transfer, 1D model 8=20152
- H^+ , absorption coeff., from numerical soln. of Schrödinger eqn. 8=7382
- H^+ , hyperpolarizability calc. 8=20942
- H_1^+ , D_1^+ and T_1^+ ion injector, for charge-exchange generator 8=7713
- H^+ ion source, polarization increase 8=10915
- H^+ , photoabsorption coeff. in u.v., study of resonance near $n = 2$ level 8=7444
- H_2^+ source, duoplasmatron 8=15339
- H^+ -H collision, 2-60 keV ionization and e capture obs. 8=21007
- H^+ -H interaction pot. rel. to H_2 mol. 8=21075
- H_2^+ , Hartree-Fock and correl. energies 8=12197
- H^+ cation, in Antarctic atmosphere 8=23264
- H^+ , H_2^+ charge exchange in atmospheric gases, 40-1500 eV 8=21275
- H^+ , critical angles for channeling in thin Au films 8=17704
- $^1H^+$ in Ge, channelling props., diff. calc. 8=13485
- H^+ to H^+ charge exchange in K and Cs vapour 8=12441
- H^+ on Kr scattering, charge transfer 8=1203
- H^+ -rare gas collision, polarization of Lyman- α radiation 8=21004
- H^+ -H(1s) elastic and resonant exchange collisions, nuclear symmetry 8=12106
- $H^+ + N(O) \rightarrow H + N^+(O^+)$, classical calc. Bates-Mapleton theory 8=7461
- H_2^+ , accurate wavefunction, James function as approx. to Guillemin and Zener 8=1249
- H_2^+ chemical reactions with He, cross sections 8=14348
- H_2^+ , collision-induced excitation, angular dependence 8=1362
- H_2^+ , cross-sections for photo-dissociation 8=21188
- H_2^+ , electron collisions, proton production cross section meas. 8=7519
- H_2^+ , e-energy, linear eqn. computation method 8=1248
- H_2^+ , ground state, variational function 8=7518
- H_2^+ , improved Gaussian wavefunctions 8=21080
- H_2^+ , interaction energy 8=12370
- H_2^+ , one-centre perturbation calc. 8=4138
- H_2^+ , passage through $N_2 + He$ mixture, N_2^+ vibration and rotation 8=4156
- H_2^+ polarizability, longit. and transverse, variational calc. 8=1254
- H_2^+ , by proton collision, electron capture probability 8=1199
- H_2^+ , 2p σ state, variational function 8=21078
- H_2^+ , 3d δ_5 and 4f δ_5 states, approx. MO's 8=1244
- H_2^+ wave function and electronic terms for large H-H distances 8=1255
- H_2^+ , vibrational excitation effect on dissociation under e and p impact 8=21076
- H_2^+ , Zeeman sublevels, g-factor ratios, h.f.s. spectrum in 20 cm region 8=12195
- H_2^+ - H_2 , He, Ar, Ne, N_2 collisions, 20-120 keV, cross-section for prod. of H atom in 3s state 8=21191
- H_2^+ - H_2 , He, Ar, Ne collisions 100 KeV, cross-section for prod. of H atom in 3s state 8=21191
- $He^{2+} \rightarrow He^+ + H^+$, e capture probability calc. 8=1192
- ZnS:Ag film, energy loss in passing through 8=8758

neutral atoms

- α -particle capture of electrons in H_2 , collision process 8=12101
- atom in 1s state, e-impact ionization cross-section obs. 8=21273
- atomic beam, photoionization 8=21020
- atomic beam, prod. by thermal dissociation, dissociation temp. var. 8=7474
- atoms, collisions, excitation of fine-structure levels 8=1193
- atom, and Coulomb potential energy of two charges 8=7378
- atoms, discrete spectrum and radiodiapason obs. 8=7377
- atoms—fast H^+ and He^+ collision processes rel. to astrophysics 8=16230
- atomic interactions, hyperfine splitting of energy 8=12105
- atoms, line broadening, electron concentration meas. 8=4062
- atom position in $BaAl_2Si_2O_{10} \cdot 4H_2O$ 8=18456
- atomic-stopping cross section in Al 8=2022
- Balmer- α line excitation by electron impact, cross section and polarization meas. 8=20979
- Balmer series emission, auroral zones 8=18946
- beam detector, ZnO crystal, change in surface conductivity 8=7475
- coherent, elastic scatt. of photons 8=7379
- elastic resonance in electron scattering 8=16222
- e capture by μ^+ , cross section calc. using Born approx. 8=7481
- e and p scatt. simplified second Born approx. 8=20996
- e + H, collision, polarization of Lyman-alpha radiation produced 8=12096
- e^+ impact, formation of positronium 8=12095
- electron scattering, correlation method analysis 8=7441
- electron scattering, effect resonances on excitation 8=7443

Hydrogen—contd**neutral atoms—contd**

- electron scattering, excitation to $n = 2$ level, theory and expt. 8=7442
- electron scattering, low-energy, expansion approach 8=20994
- electron scattering, six-state close-coupling at low energy 8=7440
- e scattering theory using Hulthén, Kohn and Malik variational methods 8=7448
- e. s. r. transitions involving changes in spin states of up to 3 neighbouring protons 8=16227
- energy of interact. in ground-state, by Gaussian-type functions 8=1198
- $F = 1$ level of ground state, relax., appl. to H maser 8=12049
- frequency standard, comp. with Cs for average freq. and freq. stability 8=10483
- Gaussian wavefunctions, improved 8=21080
- Green function 8=4035
- ground state, differential polarizability 8=12048
- hydrated, bimolecular rate constants in aqueous solns. 8=2510
- hypervirial operators 8=3408
- interaction with radiation field, Coulomb-Green's function calc. 8=12047
- ionization by e impact, asymptotic form of wave function 8=16443
- ionization, by passage through hot-cathode discharge 8=21274
- ionization recombinations and wall effects 8=1363
- maser, dynamic behaviour near equilib. osc. level 8=19919
- model for diatomic mol. rel. to auto-ionization 8=21034
- one-centre perturbation calc. 8=4138
- oscillator strength sum rules, 2 1 -pole, recurrence formula derivation 8=7380
- photon elastic scattering, evaluation of Kramers-Heisenberg matrix element 8=16221
- photon scatt. analytic expression and numerical computation 8=1196
- polarized, for prod. of polarized e beam by spin exchange 8=15304
- polarized source, atomic conc. from H_2 dissociation in h.f. discharge 8=21018
- positronium formation from positron cross-section calc. 8=1195
- positronium formation in e^+ -H collisions, cross-section calc. 8=16223
- positrons, elastic scatt. 8=20995
- p e capture on He, Ar, Ne, N_2 , H_2 , O_2 with 3s, 4s states obs. 8=7462
- p-H collision, charge transfer, 1D model 8=20152
- p polarized beam scatt., 300-700 MeV, polarization parameter 8=6927
- quantum theory, applic. of factorization theory with absence of Inonu-Wigner contraction 8=20145
- quantum theory, insertion of barrier and change of symm. 8=11371
- radius, mean square, expectation value, variational method 8=20146
- reaction with acetaldehyde 8=18668
- reaction with F^- ions, formation of hydrated electrons 8=18679
- reaction with O_2 8=5743
- reactions with simple hydrocarbons, e. s. r. study 8=14376
- recombination with O_2 in shock tube 8=14367
- resonance scatt. of light and level crossings 8=4064
- spin exchange cross-section in H-H collisions 8=21008
- surface density in interstellar clouds 8=23574
- 3s state prod. in H_2^+ , H_2^+ collisions with H_2 , He, Ar, Ne, N_2 8=21191
- trapped in irradiated frozen aq. solns. 8=18423
- two, long-range interact., appl. of electrostatic Hellman-Feynman theorem 8=1197
- two-photon absorpt. calc. 8=16286
- W Centauri and 47 Tucanae clusters, limits to content 8=23555
- Zeeman effect, Lamb shift and quantum electrodynamics 8=1158
- $H\alpha$ line profiles of β Doradus rel. to atmos. 8=10133
- H-C collisions, excitation of fine-structure levels 8=1193
- H-H collisions, e transfer and ionization cross-sections 1.25-117 KeV 8=21276
- H-H, H- H_2 collisions, ionization and e capture obs. 8=21007
- H-H Van der Waals interaction, self-consistent calc. 8=21002
- H-O collisions, excitation of fine-structure levels 8=1193
- H(1s)- H^+ elastic and resonant exchange collisions, nuclear symmetry 8=12106
- $H(1s) + He^{2+} \rightarrow He^+(1s) + H^+$, back-coupling and distortion 8=7466
- H^0 or H^+ + H^+ fluxes, 1-10 keV, an energy independent detector 8=7381
- N_2 -H collisions, optical emission rel. to Aurora 8=12212
- NH_3 gas radiolysis, effect of scavengers 8=23162

neutral molecules

- Born inelastic differential cross-sections 8=12191
- coherently vibrating molecule static field effect 8=16283

Hydrogen—contd

neutral molecules—contd

- collective states analogy with nuclear orthostates 8=20653
 collisions with inert gases, total scatt. cross-sections 8=7634
 dipole polarizability, refractive index, Rayleigh and Raman scattering calcs. 8=7517
 dissociation in h.f. discharge of polarized atom source 8=21018
 dissociative attachment of e, vibrational resonances obs. 8=21182
 electron collisions, Lyman- α prod. 8=12050
 electron scatt., low-energy elastic 8=7516
 e impact excitation cross-sections and dissociation 8=1241
 excitation of c^3H_2 states by trapped-electron method 8=16281
 excited states, Weinstein calcs. 8=16254
 formation in pre-galactic clouds 8=23483
 Gaussian wavefunctions, improved 8=21080
 i.r. absorpt. bands, press. induced, anal. of profiles 8=12188
 in interstellar clouds, reduced estimate 8=23577
 ionization by fission fragments, pair production energy 8=1361
 molecules vibr.-rotational spectrum for e ground state, VKB calc. 8=1246
 ortho, in solid para- H_2 , crystal-field splitting by n.m.r. obs. 8=13010
 positron cross-section for rotational excitation 8=12168
 perturbation-variation calc. 8=21079
 predissociation, absorption spectral evidence 8=12189
 production, ethylene radiolysis, as dosimeter 8=614
 p annihilation in H_2 and D_2 , rates rel. to initial state 8=20537
 quenching of $Hg^*(^3P_1)$ atoms, phase-space theory 8=14436
 Raman effect, stimulated, meas. in terms of laser oscillator and amplifier theories 8=21081
 Rydberg states 8=1250
 solid, ortho molecular rot. at 0°K 8=8233
 two-photon absorpt. calc. 8=16286
 H-H⁺ interaction pot. using isotope effect in dissociative attachment 8=21075
 H- H_2 collision, 2-60 keV ionization and e capture obs. 8=21007
 H₂-air system, free convection, heat transfer and diffusion 8=4491
 H₂ arc lamp for high intensity u.v. 8=6518
 H₂-CO₂ gas mixtures, thermal conductivity 8=4473
 H₂-CO₂ mixture, meas. of thermal-diffusion factors 8=1488
 H₂ + D₂ homogeneous reaction 8=5697
 H₂, dense gas and liquid states, thermal conductivity calc. 8=4476
 H₂ e-impact ionization spectrum, long autoionizing lifetime of some states 8=21272
 (H₂, D₂) exchange reaction, vib. versus translational energy importance 8=4257
 H₂, H₂-p, Balmer emission radiation 8=12190
 (H₂, H₂) exchange reaction, vib. versus translational energy importance 8=4257
 H₂-H₂ system, self-consistent group calc. 8=12372-3
 H₂-He mixture, composition-depend. of thermal-diffusion factor 8=1493
 H₂-He, thermal conductivity, normal composition variation 8=7924
 (p, H₂, He) system, translation-rotation energy transfer calc. 8=12374
 H₂ + HeH⁺, energy hypersurface, MO calc. 8=16285
 H₂ + I₂ reaction kinetics 8=5706-7
 H₂ + I₂ reaction paradox 8=23105
 H₂ in liq. Ar, induced rot-translation spectra 8=1564
 o-H₂, solid, orientational ordering of mols. in c.c.p. lattice 8=1793
 H₂ mol, B² Σ_u^+ state, Rydberg-Klein-Rees curve 8=1227
 H₂-N₂ gas mixtures, thermal conductivity 8=4473
 H₂-Ne liquid-vapour phase equilib., 26°-42.5°K, 10-25 atm. 8=16937
 H₂-O₂ combination at 325°C, Cu epitaxial film catalyst changes obs. 8=8318
 H₂ + O₂, slow reaction rate, computer calc. 8=18678
 H₂, potential energy curves calc. 8=12149
 H₂-p e capture excitation of 3s, 4s states of H 8=7462
 H₂-T₂ mixtures, equilibria and reaction rates 8=14448
 H₃, ground state calcs., and potential-energy surfaces 8=4130
 H₃, potential-energy surface 8=12193
 H₃ rainfall input to North Pacific rel. to water mixing time calc. 8=23247
 H₃ system, single-centre expansions 8=12192
 H₂⁺ + H₂ → H₃⁺ + H, cross-section obs. 0.1 ≤ W ≤ 10 eV 8=21192
 H₂ geometrics and binding energies 8=12194
 HD in liq. Ar, induced rot.-translation spectra 8=1564
 α -Ti(H₂D₂) system, thermodynamic props. 8=21858
 Xe-H₂ couples in binary mixtures, translation spectra 8=7425

Hydrogen compounds

See also Ice; Steam; Water.

- heavy hydrides, rot. energy levels of 1/2 states 8=1220
 hydrides, diatomic, charge distrib. and binding 8=7496
 hydrides, diatomic, Platt's model 8=4151
 metal carbonyl hydrides, Platt's model 8=4152

Hydrogen compounds—contd

- BD₄-like, electric field gradient calc. using one-centre expansion wave function 8=7513
 DBR, infrared laser transitions 8=6476
 DCl, far i.r. microwave absorpt. spectra 8=7523
 DCl, infrared laser transitions 8=6476
 DF, chemical laser, during flash photolysis of UF₆ with D 8=424
 D₂O as buffer for vibr. relaxation of CO₂ meas. with sound absorpt. and vel. 8=21071
 D₂O ice, O¹⁷ n.m.r. 8=18470
 D₂O isotopic shifts in uranyl salt 8=5641
 D₂O lasers, gas, far i.r., construction and characts. 8=425
 D₂O, press. broadening obs. using CN maser 8=21073
 D₂O in solid N₂, i.r. absorpt. spectrum 8=22977
 D₂O in soln., absolute i.r. intensities rel. to meas. in gas phase 8=1561
 D₂O, at 77°K, γ -irrad., e.s.r. of OD radical 8=9439
 DOCl, i.r. spectrum, rot. const. and geometry of mol. 8=21083
 D₂S, harmonic freqs., empirical estimation 8=21072
 D₂Se, harmonic freqs., empirical estimation 8=21072
 Er-H₂ system, phase analysis by X-ray exam. 8=17058
 H-foreign gas Van der Waals complexes bound states 8=6523
 H₂⁺, excited states, Weinstein calcs. 8=16254
 H₂, para, rotational h.f.s. 8=16284
 H₂, calc. using 1s Gaussian basis functions 8=16282
 HBr, far i.r. microwave absorpt. spectra 8=7523
 HBr, ferroelect. in solid lowest temp. phase, obs. 8=13889
 HBr, gaseous, spin-lattice relax. 8=12697
 HBr, infrared laser transitions 8=6476
 HBr, solid film at 80°K, u.v. absorpt. rel. to intermol. interactions 8=18510
 HBr, in solid N₂, i.r. absorpt. 8=9554
 H₂C₂, spectra and approx. to excited states 8=1213
 HCF, spectra and approx. to excited states 8=1213
 HCN, CW submillimeter laser lines, absolute freq. meas. 8=422
 HCN, excited state, effects of quasi-linearity 8=1243
 HCN laser, 337 μ harmonics mixed with 190 μ and 180 μ for i.r. lasers 8=19950
 HCN and DCN, microwave and i.r. spectra 8=7522
 H₂CO, spectra and approx. to excited states 8=1213
 HCl dimers, far i.r. spectra 8=18532
 HCl, infrared laser transitions 8=6476
 HCl, far i.r. microwave absorpt. spectra 8=7523
 HCl, ferroelect. in solid lowest temp. phase, obs. 8=13889
 HCl, gaseous, γ -irrad., ion lifetimes 8=23164
 HCl, gaseous, spin-lattice relax. 8=12697
 HCl impurity in ice, dielec. dispersion obs. 8=18188
 HCl, i.r. spectra in inert-gas matrix 8=9537
 HCl laser, electrically pulsed 8=20007
 HCl, pressure effect on rot. and vibr. spectra 8=21077
 HCl, rot. line strengths, by Fourier transform. 8=1253
 HCl, in solid N₂, i.r. absorpt. 8=9554
 HCl, vapour corrosion of mild steel 8=23103
 HCl-HCN, concurrent ion-molecule reactions with D₂ and CD₄ 8=4312
 HCl.2H₂O, crystal structure and H bonding 8=8504
 HCl.2H₂O and HCl.3H₂O, structure rel. to proton hydration 8=17196
 HCl.3H₂O, crystal structure and H bonding 8=8505
 HClO₄.2H₂O, structure rel. to proton hydration 8=17196
 HCo(CO)₄, metal-H bond distance, anal. from n.m.r. 8=5559
 HD, autoionization process, calc. using H atom model 8=21034
 HD solid with H₂ impurity, high proton spin polarization 8=1639
 HD-D₂ system, thermal diffusion factor 8=1494
 HF, chemical laser, during flash photolysis of UF₆ with H 8=424
 HF, correlation energy and molec. props. 8=1252
 HF impurity in ice, dielec. dispersion obs. 8=18188
 HF, labelled with F¹⁸, use of etches in study of fluoride chemisorption on Si and SiO₂ surfaces 8=18697
 HF, laser emission from rotational transitions 8=423
 HF, rotational spectrum, frequencies and linewidths 8=12198
 HF, single-centre LCAO SCF calc. 8=7524
 H₂F₃, structure 8=2425
 HI, gaseous, spin-lattice relax. 8=12697
 HMn(CO)₅, metal-H bond distance, anal. from n.m.r. 8=5559
 HNCO, matrix-isolated photolysis, spectra of NCO 8=16369
 H₂NH₂PO₃ films, i.r. absorpt in polarized light, 400-4000 cm⁻¹ rel. to internal vibrations 8=14224
 HNO, spectra and approx. to excited states 8=1213
 HO₂ destruction on various surfaces 8=18704
 HO₂⁺, dissociation lifetime 8=5743
 HO₂, e.s.r. in Ar at 4.2°K 8=18424
 H₂O, Brillouin shifts, temp. dependence, hypersonic velocity and compressibility deduction 8=1502
 H₂O molecule, one-electron props. 8=4148
 H₂O, spin-rotation constant 8=1242
 H₂O in soln., absolute i.r. intensities rel. to meas. in gas phase 8=1561

Hydrogen compounds—contd

- H_2O_2 , chemiluminescent reactions with H_2O_2 and fluorescent compounds 8=18685
 H_2O_2 , decomposition thermodynamics and kinetics 8=1466
 H_2O_2 destruction on various surfaces 8=18704
 H_2O_2 impurity in ice, dielec. dispersion obs. 8=18188
 H_2O_2 , reactions with electronneg. subs. aryl oxalates and fluorescent cpds. chemiluminescence 8=18672
 $H_9O_4^+$ group in polystyrene sulphuric acid film, i.r. spectroscopic investigation 8=4150
 $HOCl$, i.r. spectrum, rot. consts. and geometry of mol. 8=21083
 HPF_3 , n. m. r., sign of coupling consts. 8=4232
 H_2S , effect on contact resistance of Ag and Ag-alloy contacts 8=22512
 H_2Se , harmonic freqs., empirical estimation 8=21072
 H_2Se , sum rule analysis of interacting (2,0,0) and (1,0,1) states 8=12199
 $HSiF_3$, n. m. r., sign of coupling consts. 8=4232
 O_2 in H_2O_2 -urea addition compound, single crystal, γ -irradiated at 77°K, e.s.r. 8=2373

Hydrogen ion concentration. See Electrochemistry

Hydromagnetics. See Magnetohydrodynamics.

Hydrometry. See Flowmeters.

Hydrophones. See Acoustic transducers; Oceanography.

Hydrostatics

- liquid level, magnetostrictive sensing 8=10872
 magnetohydrostatic bearing, circular step, squeezing effects 8=16751
 non-Newtonian liquid, boundary layer 8=12720
 oscillations of buoyant disk, gravity wave damping 8=16770
 pressure deform. of Al circular foils 8=5044
 pressure to 60 kbar, technique 8=7971

Hygiene. See Medical science.

Hvgrometers.

- frost point, sensing element with fast response 8=9838
 BaF_2 film element, storage stability 8=18856

Hyperfine structure. See Paramagnetic resonance and relaxation; Spectra.

Hyperfragments. See Hypernuclei.

Hypernuclei

- decay rel. to non-leptonic 4-fermion hadron interactions 8=20400
 double and $\Lambda\Lambda$ interaction 8=20735
 hyperfragment decay, π -p-r rel. to Λ nuclear pot. well depth 8=11795
 light, binding energy determ. 8=20734
 light hyperfragments, non-mesic to π^- mesic ratio calc. 8=7115
 of Λ n instability 8=20733
 π^- decays, final state interaction effects 8=16008
 production in Σ^- capture by emulsion nuclei, model for 8=7218
 resulting from K^- interacts., binding energies 8=11794
 s-shell, Λ -N pot. 8=16009
 spallation, prod. by 6 GeV/c K^- on heavy emulsion 8=3949
 $\Lambda Be^0 \rightarrow \alpha + \alpha + p + \pi^-$ energy distribution calc. 8=949
 $\Lambda\Lambda Be^{11}$, calc. for 2π and K ranges of ΛN interaction 8=3849
 $\Lambda\Lambda He^3$, effect ΛNN force on binding energy 8=950
 $H_\Lambda^+ \rightarrow He^4 + e^+ + \nu_e$ 8=11796
 $H_\Lambda^+ \rightarrow He^4 + \mu^- + \bar{\nu}_\mu$, possible checking of V-A theory 8=11796
 ΛHe , non-mesonic- π -mesic decay ratios, obs. of K^- stars in nuclear emulsion 8=20736
 ΛHe^4 , non-mesonic and total decay rates obs. from K^- stars in emulsion stacks 8=20736
 ΛHe^5 , effect ΛNN force on binding energy 8=950
 ΛHe^5 non-mesonic- π -mesic decay ratios, obs. of K^- stars in nuclear emulsion 8=20736
 $\Lambda\Lambda He^6$, pot. yielding and binding energy 8=3847
 ΛHe^6 pot. yielding and binding energy 8=3847
 ΛLi^6 , existence rel. to charge symm. violation in Λ -N interaction 8=11793
 $\Lambda Li^8 \rightarrow \pi^- + p + p + He^4$ obs. in nuclear emulsion 8=3848

Hyperons

- hyperfragments produced by 800 MeV/c K^- 8=20817
 Λ binding energy in nuclear matter 8=3766
 Λ binding energy in nuclear matter 8=15857
 Λ , NAK coupling constant determ. 8=6891
 $\Lambda\pi$ and NK composite model of Σ 8=11633
 Λ polarization in $\pi^- + p \rightarrow \Lambda + K^0$ at 1.03 GeV/c and 1.06 GeV/c 8=6971
 Λ pot. central depth from $K^- + He^4 \rightarrow \Lambda^0 + p + d + \pi^-$ 8=20417
 Ω as bound state of ΞK , test of bootstrap theory 8=6978
 Σ , composite model as bound state of $\Lambda\pi$ and NK 8=11633
 Σ , $N\Xi K$ coupling constant determ. 8=6891
 Σ in p-p and π -p collisions, charge ratio 8=11524
 Σ pot. central depth from $K^- + He^4 \rightarrow \Lambda^0 + p + d + \pi^-$ 8=20417
 Ξ , Ω as bound state of ΞK 8=6978

absorption

No entries

capture

No entries

decay

- cosmic γ spectrum, effect on 8=23489
 4-body semileptonic by Cabibbo current, PCAC and soft π hypothesis 8=3727

Hyperons—contd**decay—contd**

- Λ decay, meas. of time-reversal parameter 8=6972
 $\Lambda \rightarrow N\pi$, amplitude derived in superconductivity model with $SU(3) \times SU(3)$ 8=11501
 $\Lambda \rightarrow p + \pi^0$ β parameter rel. to T-invariance 8=6971
 Λ^0 lifetime using $K^- + p \rightarrow \Lambda^0 + \pi^+ + \pi^-$ 8=20572
 mesonic, nonleptonic, s and p-waves 8=3728
 nonleptonic, current algebra anomalies 8=3729
 nonleptonic, model of T violation 8=6820
 nonleptonic, quark model, parity violation and conservation explained 8=3726
 non-leptonic, radiative corrections estimation 8=6976
 non-leptonic, review 8=857
 non-leptonic, $\Delta T = 1/2$ rule 8=11630
 nonleptonic $SU(3)$ Chew-Low static and bootstrap models 8=11629
 $\Omega \rightarrow \Lambda K$, ratio with $\Omega \rightarrow \Xi\pi$ calc. 8=20576
 $\Omega \rightarrow \Xi\pi$, ratio with $\Omega \rightarrow \Lambda K$ calc. 8=20576
 $\Omega^- \rightarrow B(\frac{1}{2}^- \text{ or } \frac{3}{2}^-) + M(0^-)$ using current algebra 8=20576
 $\Omega^- \rightarrow \Lambda + K$, $\Xi + \Pi$ ratio prediction 8=3726
 $\Omega^- \rightarrow \Lambda K$ obs. 8=15803
 $\Omega^- \rightarrow \Xi^- + 2\pi^0$, comparable with $\Omega^- \rightarrow \Xi^- + \pi$ 8=6979
 $\Omega^- \rightarrow \Xi^0 \pi^-$, $\Xi^- \pi^0$, $\Delta I = 1/2$ rule, rel. to $\Omega \rightarrow \Lambda K'/\Xi\pi$ ratio 8=20576
 P-wave in vector meson-dominance models 8=11632
 radiational, weak, and quark model 8=20571
 $\Sigma \rightarrow \Lambda$, non Hermitian weak hadronic current 8=860
 $\Sigma^- \rightarrow \pi^-$, zero asymm. rel. to $\pi^- p \rightarrow \Sigma^- K^+$, 1170 MeV/c 8=20449
 $\Sigma^- \rightarrow n + \pi^-$, parameters 8=861
 Σ^+ , experimental limit on $\Delta S = -\Delta Q$ leptonic decays 8=11634
 $\Sigma^- \rightarrow n\mu^+ \nu$, possible violation of $\Delta S = \Delta Q$ 8=20575
 $\Sigma^+ \rightarrow n\pi^+$, purely p wave 8=3728
 $\Sigma^+ \rightarrow n + \pi^+$ S-wave theory using quark model of baryons 8=6975
 $\Sigma^+ \rightarrow p + e^+ + e^-$, CP conservation, possible tests 8=6914
 S-wave as test of octet dominance in weak, e. m. and strong interactions 8=3516
 $\Xi \rightarrow \Sigma^- + e^- + e^+$, CP conservation, possible tests 8=6914

decay observations

No entries

detection, measurement

No entries

effects

No entries

interaction

See also Hypernuclei.

- Λ - Λ and double hypernuclei 8=20735
 ΛN , nuclear, C violation and existence of Li^6 8=11793
 ΛN , 2π and K range, calc. from $\Lambda\Lambda Be^{11}$ hypernuclear event 8=3849
 Λ -N rel. to hypernuclear binding energy 8=20734
 Λ -N rel. to Λ nuclear pot.-well depth 8=11795
 Λ -nucleon stimulation, hyperfragments $A = 50$, calc. 8=15861
 ΛNN , 2π exchange force in nuclear matter 8=3766
 Λ -p, low energy 8=11631
 $\Lambda \Sigma$, low energy meson exchange plus hard core model 8=6977
 $\pi + \Lambda \rightarrow \pi + \Sigma$, simultaneous s-t analyticity 8=6740
 (Σ^-) possible bound state 8=863
 ΞN , low energy meson exchange plus hard core model 8=6977

magnetic moment

- Λ from consistency conditions for $\gamma + N \rightarrow \Lambda + K$ 8=20344
 Σ^0 , Σ^+ from consistency conditions for $\gamma + N \rightarrow \Sigma + K$ 8=20344

mass

- Ω and Ξ^0 , precision meas. 8=15862
 $\Sigma^+ + \Sigma^- 2\pi^0$ mass difference, e. m., superconvergence dispersion relation approach 8=11485
 Σ^+ , using range-energy relation in He bubble chamber obs. 8=862

production

- $\gamma p \rightarrow \Sigma^+ K^+$, Regge-pole calc. of cross-sections 8=3621
 $\gamma p \rightarrow \Lambda^+ K^+$, Regge-pole calc. of cross-sections 8=3621
 $K^+ p \rightarrow K^+ \Xi^0$, mass difference effect in Wali-Warnock model, violation of $SU(3)$ 8=3692
 $K^+ p \rightarrow \pi^+ \pi^- \Sigma^0$, 6 GeV/c, ang. corrs. rel. to spin parity of exchanged particles 8=798
 $K^- p \rightarrow \pi^- \Sigma^+$, Regge-pole model based on K^* , K^{**} exchange 8=15777
 $K^- p \rightarrow \Sigma^- \pi^+$, mass difference effect in Wali-Warnock model, violation of $SU(3)$ 8=3692
 $K^+ \Sigma^-$ in $\pi^- p$ reaction, Regge cut 8=3631
 Λ in $\gamma + N \rightarrow \Lambda + K$, consistency conditions for non-Born amplitudes 8=20344
 ΛK^0 backward peak in associated prod. at 5, 7 and 12 GeV/c 8=6973
 Λ in $K^- p \rightarrow \Lambda \eta$, 1.2-1.7 BeV/c 8=6888
 $\bar{\Lambda}$ (or Σ^+) in $K^+ p \rightarrow$, 7.3 GeV/c 8=858
 Λ in $\Omega^- \rightarrow \Lambda K$ 8=15803
 Λ , from $\pi^- p$, 1.5-4.2 BeV/c 8=6861
 ΛK^+ enhancement at 1.7 GeV, $\pi^- p \rightarrow \Lambda K^+ \pi^-$ at 6 GeV/c 8=3630
 Λ in $\pi^+ + p \rightarrow \Sigma^+ + K^+$, quark model for backward process 8=11480

Hyperons—contd

production—contd

- Λ/Σ ratio in $\bar{K}N$ interaction, current algebra calc. 8=15858
- Λ to Σ ratio quark model in $I = 1$ S-wave $\bar{K}N$ reaction 8=15860
- Λ^0 in $K^- + He^4 \rightarrow \Sigma + \text{nucleus} + \pi^- \rightarrow \Lambda^0 + p + d + \pi^-$, Λ^0, Σ -nuclear pots. similar 8=20417
- Λ^0 in $\pi^+ p \rightarrow K^0 \Sigma^0(\Lambda^0)$, Regge-pole model based on K^*, K^{**} exchange 8=15777
- $\bar{\Omega}$, not found in $K^+ p$, 9 GeV/c 8=865
- $\bar{\Omega}^+$ in 10 GeV/c $K^+ p$ 8=15803
- $pp \rightarrow YKN$, OBE model with approx. 8=20522
- $\pi^+ + n \rightarrow \Sigma^+ + K^0$, in polyethylene, 1 GeV/c, polarization 8=864
- $\pi^+ p \rightarrow K^+ \Sigma^+$, mass difference effect in Wali-Warnock model, violation of SU(3) 8=3692
- $\pi^+ + p \rightarrow \Sigma^+ + K^+$, in polyethylene, 1 GeV/c, polarization 8=864
- Σ as intermediate state in $K^- + He^4 \rightarrow \Lambda^0 + p + d + \pi^-$ 8=20417
- Σ from pn , 1.5-4.2 BeV/c 8=6861
- Σ - π final states near 1 BeV, partial wave analysis 8=20574
- Σ in $\gamma + N \rightarrow \Sigma + K$, consistency conditions for non-Born amplitudes 8=20344
- Σ in $\pi + \Lambda \rightarrow \pi + \Sigma$, simultaneous s-t analyticity 8=6740
- Σ^- in $\pi^- p \rightarrow \Sigma^- K^+$, 1170 MeV/c, cross-section obs., C independence confirmed 8=20449
- Σ^+ in $\pi^+ p \rightarrow K^+ \Sigma^+$, 3.23 GeV/c, ang. dist., Σ polarization 8=6852
- Σ^0 in $\pi^+ p \rightarrow K^0 \Sigma^0(\Lambda^0)$, Regge-pole model based on K^*, K^{**} exchange 8=15777
- Ξ intermediate hyperfragment in reaction K^- with emulsion nuclei 8=11912
- Ξ in 10 GeV/c $K^+ p$ 8=15803
- Ξ in $K^+ p$, 9 GeV/c 8=865
- obs. in πp interactions 1.5-4.2 BeV/c 8=6860
- Ξ in $\Omega^- \rightarrow \Xi^- + 2\pi^+$, comparable with $\Omega^- \rightarrow \Xi^- + \pi$ 8=6979
- Ξ in 10 GeV/c $K^+ p$ 8=15803
- $Y_1, pp \rightarrow YY$, absorpt. model, U(66) symm. 8=20524
- $Y_1^* + \pi^- \rightarrow \Sigma^+ \pi^+ \pi^-$, spin and parity of Y_1^* 8=6987

resonances

- Ξ^* obs. in πp interactions 1.5-4.2 BeV/c 8=6860

scattering

- ΛN , one-boson-exchange model, cross-section calc. 8=20573
- Λ -N, unitary symmetry and N-N scattering phase shifts 8=6974
- Λ -p from Λ -N pot. with hard core and Yukawa shape 8=16009
- Λ -p, 400-1300 MeV/c, obs. 8=859
- ΣN , one-boson-exchange model, cross-section calc. 8=20573

spin and parity

- Λ and Σ from K^+ -p dispersion relations 8=3730

Hypersonics. See Ultrasonics.

Hypertrons. See Hypernuclei: Tritons.

Hypervirial theorem. See Quantum theory.

Hypochromism. See Absorption/light; Polymers.

Hysteresis

- See also Dielectric phenomena; Dielectric properties of substances; Ferroelectric phenomena; Magnetization process.
- acoustic waves, combustion chamber with self-oscillatory system 8=243
- coercive force rel. to low freq. iron losses, domain wall eqn. 8=22777
- dynamic cycle, measurement 8=304
- elongated single-domain particles, magnetization reversal mechanisms 8=5453
- films, double layer of different chem. comp., mag. props. 8=9332
- of fractional phonons 8=22081
- LCR circuit, ferro-reson. at low freq. 50 Hz, potential difference-inductance curve 8=6242
- massive circuits, transient behaviour 8=10867
- Permalloy magnetic films, rotational, temp. depend. 8=22823
- in rheology, expt. obs. 8=63
- spinel ferrites and garnets, polycryst., temp-depend and stability 8=14047
- spinel ferrites, orientation superstructures and their effects 8=14046
- steel, SAE 1020, loop measurement during fatigue testing at 30 Hz 8=5069
- Vycor, porous, film area 8=13050
- BaTiO₃, ceramic, loss meas. 8=13881
- Cu-M (M = Cu, Mo, steel, constantan), contact cond.-normal loading curves 8=8986
- Fe powder dispersed in perspex, loops as function of Fe separation 8=5470
- FeCl₂, and metamag. phase transform. 8=9396
- Fe-Gd films, loops, by static method 8=9345
- FeNi films, electrodeposited, rel. to struct. 8=9347
- Fe-Rh alloys, in antiferro-ferromagnetic transforms., rel. lattice parameter changes 8=9395
- Fe-3%Si, grain-oriented, and eddy current losses rel. to domain wall motion, obs. 8=22842
- Fe-Si sheet, iron losses in alternating mag. fields, ≤ 24 kGauss 8=22804

Hysteresis—contd

- In single spheres, superconducting transition and size effects 8=17961
- MnMg-ferrite, square-loop, coercive force temp. depend 8=14051
- Mo permalloy, coercive force, neutron bombardment effect 8=18344
- Nb, superconductive, irreversible magnetisation obs. 8=2160
- Ni, magnetization temp. dependence 8=14025
- NiFe-SiO-Co multilayer, of magnetoresistance, rel. to stray field effects 8=14027
- Pb, superconductive, irreversible magnetisation obs. 8=2160
- PbZrO₃, new Curie point 8=13887
- Si-Fe thin tapes, dynamic phenomena 8=5483
- SiO₂ films, capacitance-voltage, deposited on n-type Si 8=4757
- Sn, superconductive, irreversible magnetisation obs. 8=2160

INDOR (internuclear double resonance). See Nuclear magnetic resonance and relaxation.

Ice

See also Glaciers; Snow.

- accreted, mechanical strength, effect of impurities 8=17739
- acoustic characts., under static press. 8=1854
- alkaline, irradi., e. p. r. of trapped electrons 8=2370
- amorphous \rightarrow hexagonal, enthalpy and ht. capacity changes 8=21846
- in Antarctica, variable load rel. to isostatic motions and crustal fracture 8=18823
- Arctic sea-ice, reverberation under 8=5788
- cavities, filled with air, vapor and brine, migration under temp. gradient 8=1991
- covering sea, tidal drift, vel. and direction 8=9799
- crystal growth of hollow tubes and needles of controlled size 8=8413
- crystal growth in H₂O or NaCl solns. by contact with evaporating butane, rates 8=13137
- crystalline, optical absorpt. spectra 8=18533
- dendritic solidification from aqueous solution, effect of freezing rate 8=8178
- dislocation structure and plastic deformation 8=4977
- doped with Mössbauer ions, phase transform. kinetics 8=13069
- γ -irradi., e. p. r. of trapped H atoms 8=18423
- γ -irradi., e. s. r. identification of OH radical and trapping site 8=9438
- γ -irradi., e. s. r. of OH radical 8=9439
- γ -irradiated, solvated e spectrum obs. at 77°K 8=22989
- growth from melt, preferred orientation 8=21924
- growth in supercooled aqueous solns., electrical effects 8=21762
- growth velocities in supercooled water and aq. sucrose solns. 8=17236
- heat transfer through four layer system of air, snow, sea ice and water 8=23226
- ice/water interface, electrostatic potentials 8=18723
- impure, dielec. dispersion obs., above -190°C 8=18188
- isotope fractionation factor at solid-vapour transformation 8=2503
- low frequency optical spectra, interpretation using crystal lattice model 8=13326
- metastable, superheated, in liquid-water inclusions in minerals under high neg. pressure 8=1609
- Mössbauer effect of ferrous ions 8=4675
- nucleation of different phases, selective using different org. nucleators 8=4805
- nuclei, atmospheric, sizes 8=2587
- persistent electric dipole moment obs. at -78°C 8=13890
- polycrystalline, flow at low stresses and small strains 8=22373
- radiation chem., pH depend. of reducing species 8=2540
- regelation, expt. using objects of different geometries and thermal props. 8=8167
- regelation expts. with wires 8=8168
- regelation, theory 8=8165
- regelation, theory supplementary note 8=8166
- spiral air bubbles, formation 8=4989
- square, residual entropy at low temp. 8=4945
- from supercooled H₂O, particles growth and struct., obs. 8=23274
- surface and interfacial science, symposium 8=21867
- thermoelectric effect on atmospheric electricity 8=14625
- vitreous, X-ray diffr. spectrum, comparison with water 8=8355
- D₂O ice, O¹⁷ n.m.r. 8=18470

Illumination

See also Brightness.

- interior lighting, evaluation by visual criteria 8=459
- luminous transfer in discrete spaces 8=458
- moon, table of relative intensity received on earth for any phase and altitude 8=5951
- parabolic cylinder, diffraction short wave asymptotic 8=508

Illumination—contd

SbSI, ferroelectric, causing polarization discontinuities 8-18192

Image convertors and amplifiers

for astronomical obs., two-chamber intensifier 8-11147
electron-optical, appl. to vacuum breakdown 8-16396
for high speed camera 8-20125
i.r. image convertor, for obs. of CO₂ laser radiation 8-19962
image processing by electron optical techniques 8-486
intensifier for γ -ray camera 8-15719
n intensifier tube, increased efficiency 8-6954
Lippmann effect, application in spectrography 8-3363
solid scintillators, for conversion of γ -ray image to visible image 8-9587
spectra recording, mass spectrographs 8-7356
television camera system, intensifier 8-15527
for X-rays, soft 8-17261
Ag-O-Cs photocathodes in convertor tubes, instability caused by residual Cs vapour 8-18275

Image orthicons. See Electron tubes.

Impact

See also Ballistics.

crater formation, momentum calcs. and modeling of impact processes 8-17742
deceleration of long rods after impact, hydrodynamic theory inc. for strength effects 8-19378
elastoplastic, on rigid targets, direct anal. of dynamic behaviour 8-17728
impact cratering in granular materials 8-8253
metal cylinder, penetration into massive target 8-10534
periodic motions of systems with impulsive interaction 8-10530
polyethylene, fragment shapes in hypervel. impact rel. to lunar surface struct. 8-13609
as shock-loading for solids, rel. to meas. of physical props. 8-17719
silicates, porous, fragment shapes in hypervel. impact rel. to lunar surface shock 8-13609
on viscoelastic half-space, boundary value solution 8-10575
Al alloy, short-transverse, effect of ingot quality 8-13531
Pb, ball indentation tests and grain structure 8-13602

Impedance, acoustic. See Acoustic impedance.

Imperfections in solids. See Alloys; Crystal imperfections; Solids/structure.

Impurities. See Crystal imperfections; Crystal/growth; Semiconducting materials.

Independent particle model. See Nucleus/models.

Indeterminacy

Heisenberg principle, geometric representation 8-550
measuring theory, postulate of proper values 8-20139
uncertainty principle, Einstein-Bohr ideal expt. 8-549
uncertainty principle, foundations 8-547
uncertainty reln. between phase and number of quanta 8-563

Indium

analysis, γ -activation method 8-14502
Auger effect, L and K from Sn¹¹³ capture decay 8-4099
band structure, Fermi surface, and Knight shift 8-22463
diffusion in Al 8-8671
electromigration of small amount in liq. Bi 8-12815
films, longitudinal magnetomorphoric effect 8-5430
films, superconducting transition temp. thickness dependence 8-9045
films with superconductive and ferromag. overlays, tunnelling 8-22549
film, transverse phonon generation by microwave excitation 8-4903
line-broadening collisions, cross-sections 8-12083
liquid, nuclear spin lattice relax. time, and elec. field grad. 8-12933
liquid, structural sensitivity of thermoelectric props. 8-16878
normal and superconducting, ultrasonic attenuation 8-13354
oxide film on surface, kinetics of growth 8-8322
photoemission and nearly-free-e model density of states 8-13718
in porous glass, superconductor, flux jumping during magnetization 8-2163
specific mag. susceptibility between 80° and 1850°K 8-5439
spectral line intensity, in Hg-In fluoresc. spectrum 8-4080
spheres, hysteresis in superconducting transition and size effects 8-17961
spheres, supercond. transition, superheating and super-cooling effects 8-13750
superconducting, critical fields, 0.1-4°K, pressure effect up to 30 k atm 8-5212
superconducting, spin-lattice relax. 8-18464
thermal expansion 20° to 2°K, length differences between normal and supercond. states 8-22124
type I superconductors intermediate state statics and dynamics 8-5204
ultrasonic waves, quasi-longitudinal, superconducting electronic attenuation 8-22103
X-ray reflections, diffuse, in order-disorder transition near melting pt. 8-8525

Indium—contd

in Ag, polycrystalline, diffusion as impurity 8-8670
in Ar, Kr and Xe solid films, absorption spectra 8-9541
In-In superconducting tunnel junctions, I-V characts. and 3-cm radiation emission 8-17981
in Si, implanted atoms location and lattice disorder, obs. 8-17414

Indium compounds

f.c.t. alloy, atomic relaxations 8-22375
suboxide, structure in gaseous phase by e-diff. 8-16290
(HgTe)_{1-x}In_xTe₃ alloys, single-crystals, optical energy gap 8-5608
In-40 at. % Pb, supercond., resist. and Hall angle, theory and obs. 8-2162
In-Al alloys, liq., charact. energy losses of 8 keV electrons 8-12791
InAs, avalanche breakdown theory 8-22599
InAs epitaxial film on GaAs, orientated growth 8-17132
InAs, e.s.r. at 4.2°K 8-9429
InAs n-type, Faraday rotation, interband and free-carrier 8-9540
InAs, growth and electrical props. 8-1749
InAs, i.r. laser and fast detector 8-11103
InAs, light absorpt. by free carriers, 300°K and 80°K obs. 8-18536
InAs, Knight shift calc. 8-18463
InAs, quantum oscs. in Hall effect and magneto-resistance 8-13818
InAs, photoelectromagnetic receivers with optically polished thin elements, sensitivity and inertness 8-6275
InAs, solubility and diffusion of Cu 8-17011
InAs, thermal expansion from 2-40°K 8-4937
InAs thin films, obtained by discrete evaporation, structure 8-8324
InAs thin films, optical props. 8-18535
InAs thin film transistor, fabrication and charact. 8-22635
InAsTe, chemical structure analysis 8-1760
In-Bi alloy foils, superconducting type-I, in mag. field, mixed state evidence 8-17962
In-Bi alloys, liq., charact. energy losses of 8 keV electrons 8-12791
In-Bi liq. alloys, n.m.r. of In¹¹⁵ and Bi²⁰⁹, rel. to InBi and In₂Bi groups in liq. state 8-12934
In-Bi molten alloys, free energy of mixing and elec. resistivity 8-12842
InBi, preparation and electrophysical properties 8-5268
In 1.5 at. % Bi, superconducting type II, ideal flux flow resistance 8-22547
In₂Bi, u.s. attenuation in pre-melting region 8-21751
In₂(MoO₄)₃, structural type 8-8526
In₂O₃ films, pyrolytically grown, voltage-current charac. 8-13873
In₂O₃, temp.-induced striations in flux crystallization 8-13449
InOF, preparation and properties 8-8414
InP, coherent emission, laser excitation 8-6470
n-InP, effect of As doping on electrical properties 8-9113
InPb type II superconductors, magnetostriction and magnetization 8-22548
InP-Cs-O, photoemission 8-22724
InS crystals, twinning and phase transformations on e-irradiation 8-17209
In₄S₃, photosensitivity, spectral distrib. 8-22695
In-Sb alloys, liq., meas. of electrotransport 8-12816
In-Sb molten alloys, free energy of mixing and elec. resistivity 8-12842
In-Sb-Ni, ternary alloy, the quasibinary section InSb-NiSb in 8-4691
InSe crystal, infrared absorption 8-5609
In₃Sn cryst. grown from Sn-In solder in electrotransport processes 8-8433
n-InSe crystals, photoconductivity, thermal and i. r. quenching 8-18233
InTiBO₉ (B=Nb, Ta, Sb), crystal structure and fluorescence 8-4879
In-Tl alloys, anomalous superconducting nucleation fields 8-13751
In-Tl alloys, Ginzburg-Landau parameters rel. to temp. 8-9046
In-Tl alloy, Ginzburg-Landau parameter changes under pressure 8-22550

indium antimonide
See also Semiconducting materials/indium antimonide.
avalanche breakdown theory 8-22599
Compton effect and thermal agitation in X-ray diffusion 8-13332
crystal, selective etching in HCl solns. of FeCl₃ 8-8383
epitaxy on single crystal substrate 8-17133
films, epitaxial growth, electron diffraction study 8-21884
films, vacuum deposited, crystallization by electron beam zone-melting process 8-13090
growth kinetics using temp.-gradient zone melting 8-21951
heat treatment effect rel. to disloc. density 8-1919
i. r. detectors, photoconductive, spark-machining 8-15096
i. r. lasers and fast detectors 8-11103
m.o.s. storage device for i. r. images 8-13863

Indium compounds—contd**indium antimonide—contd**

- nuclear spin-lattice relax. temp. dependence 8=9472
- photoconductivity, 10, 6 μ m wavelength 8=22696
- photoelectromagnetic receivers with optically polished thin elements, sensitivity and inertness 8=6275
- θ pinch effect in e-hole plasma, 250°K 8=13821
- plasma waves, X-ray scattering 8=5148
- polaron induced anomalies in interband magneto-absorpt., Coulomb effect 8=22818
- pulled p-n junctions, coherent radiation obs. 8=6471
- surface stress in polished and clean (111) surfaces 8=8849
- thermal expansion from 2-40°K 8=4937
- transport phenomena and microwave generation 8=9112
- X-ray scattering by transverse polarized phonons 8=8613
- In¹¹⁵, Sb^{121,123} nuclear spin-lattice relax. rates 8=9471
- InSb-oxide-metal structure, osc. tunnel conductance induced by L.O. phonons 8=13862
- InSb-GaSb solid solns., thermal cond. meas. 8=1891

Inductance

- complex μ meas. at microwaves 8=6399
- meas. by twin-T bridges at 10 MHz 8=303
- mutual, primary standard 8=283
- superinductors, props. and applications 8=17986
- thermometer 8=19667
- Mo, reluctance field dependence, 1. 8-35°K rel. to K ler law deviations 8=22750
- Se, forward biased p-n junctions 8=5314
- W, reluctance field dependence, 1. 8-35°K rel. to K ler law deviations 8=22750

Inert gases

- See also the individual gases.
- accommodation coeffs. on W and Mo 8=4734
- adsorption on Ar and Xe f. c. c. crystals, potential energy profiles 8=17159
- analysis, 90°-sector mass spectrometer 8=12033
- atomic excited levels, obs. by time analyser 8=20926
- breakdown by laser action, radiative equilb. theory 8=7937
- charge-transfer collisions, high energy, adiabatic hypothesis 8=21005
- charge transfer, Gryzinski procedure tested 8=12424
- collision cross-sections with 6s6d Hg atoms 8=1201
- collisions with Na atoms, depolarisation cross-section 8=7436
- crystals, laser generation of short wave-lengths (vac.u.v.) 8=18534
- crystals with trapped mols., rotation-translation coupling 8=8230
- depolarization of scattered e.m. waves 8=6387
- diffusion coeffs. of binary mixtures, as function of temp. and conc. 8=16719
- diffusion in KCl, KBr and KI at energies up to 85 keV 8=22156
- discharges, diffuse continua-emitting 8=4273
- electric discharges, modes of screw instability in positive column 8=12407
- electric discharge, stationary unstratified, simple models 8=7654
- glow discharges, moving striations at medium pressures 8=7657
- interaction potentials with inert gases 8=12104
- ionization by Fe atoms, ionization ratio meas. 8=1359
- ionization by p impact classical binary approx. calc. 8=12417
- ionization, mechanical damage to BaO cathode 8=18663
- ions, doubly charged, mobility in their own gases 8=7458
- ions, trapping energy on W surface 8=13081
- ion waves, stationary 8=1424
- lasers, activated U getter 8=15452
- liquefied, equilibrium vapour pressure data 8=21779
- molecule-noble gas atom collision ang. mom. reorientation cross-section 8=21524
- in nuclear reactor, fuel meltdown obs. 8=20902
- optical third-harmonic generation 8=1479
- recombination, energy partition between radiation and e collision 8=1355
- scintillators, fluorescence induced by α -particles 8=6643
- solid, compressibility 8=5075
- solid, elastic constants, contribution of a non-central force 8=22259
- solid matrices, spectra of trapped atoms 8=8227
- solids, thermal expansion coeff. calc. 8=1879
- thermal cond. of binary, ternary, and quaternary mixtures 8=21509
- thermal desorption from W and Au 8=17701
- transport through rubber membrane 8=1487
- viscosity, Sutherland-Wassiljeiva coeffs. of binary mixtures 8=7940
- in Au and W, thermal desorption of trapped ions 8=9280
- Cs-inert gas collisional J reorientation, e spin polarization determ. from D₂ pumping 8=1194
- D₂ collisions, total scatt. cross-sections 8=7634
- H₂ collisions, total scatt. cross-sections 8=7634
- He collisions, total scatt. cross-sections 8=7634
- O₂ field desorption from W, enhancement 8=17176
- in Te ore, isotope anal. 8=14455

Inflammability. See Combustion.**Information theory**

- See also Entropy; Random processes; Statistical analysis/applications.
- auditory system, difference limen 8=15090
- detection of incoherent finite acoustic signal using sensors in isotropic noise field 8=6159
- duration threshold, tone pitch, and information transfer by short tonal signals 8=3095
- entropy, theoretical relationship with thermodynamics 8=6104
- holography and interference information processing 8=531
- Marill's detection formula for pure tones in noise 8=15087
- measuring instrument, concept of information value 8=14913
- nuclear counting expts., data display 8=6631
- oscilloscope, intensity modulation effect on multi-parameter display 8=6238
- reactive optical information processing 8=532
- signal det. using Fresnel diffraction pattern 8=14935
- signal detectability application to acoustic receiver design 8=184
- signals, single-step compared with poly-step by noisy channel 8=10504
- speech, maximization of intelligibility over noisy channel for peak power limited transmitter 8=15080
- Infrared detectors.** See Bolometers; Radiation detectors.
- Infrared sources.** See Light sources; Radiation/heat.
- Infrared spectra.** See Spectra.
- Instruments**

- See also Laboratory apparatus and technique; Measurement; Recording; and under specific subjects, e.g. Astronomical instruments. Some specific instruments are listed separately, e.g. Spectrometers; Thermometers. Where no separate heading exist, entries describing instruments may be found included under the headings of the appropriate quantities or subjects.
- for atomic particle accelerators 8=20231
- dynamic elastic modulus at elevated temp. using a rapid heating technique 8=5005
- level gauge, using scatt. γ -rays 8=19345
- measuring, analysis of errors 8=14912
- measuring, information value and effectiveness 8=14913
- Insulating materials, acoustic.** See Noise abatement.
- Insulating materials, electrical.** See Dielectric properties of substances.
- Insulating materials, thermal.** See Conductivity, thermal.
- Integral equations**

- Chandrasekhar, solns. for neutron transport 8=3011
- for charge density in correlationless plasma with time-dependent background state 8=4344
- circular hole, tangential stresses 8=19391
- in classical fluid theory, hypernetted chain eqns., generalizations 8=101
- convolution eqns., for approx. soln. of eqns. of a second kind 8=23200
- excitation spectra, complete, by Heaviside expansion theorem 8=2881
- Fredholm, for electrostatic charge distrib. on cylindrical conductor 8=15189
- functional integration for incompressible fluid turbulence based on Hopf space-time formulation 8=12642
- impedance boundary scatt. e. m. waves 8=19872
- indentation of elastic sheet 8=2920
- pair correl. function of fluid, hard-sphere solns. 8=12579
- prolate spheroidal, asymptotic representations, testing 8=19357
- three-point functions, Neumann series soln. 8=20416
- Yvon-Born-Green eqn. for rigid spheres and disks, asymptotic modification 8=16616

Integrals

- See also Calculus.
- atomic, for correlated wavefunctions 8=7371
- atomic, two-particle, recursive evaluation 8=4056
- crystal fields, ion energy levels 8=1628
- in elementary particle scatt., soln. by extension to complex plane and determ. of singularities 8=20290
- exploding loop eqn., second integrals of simplified eqn. 8=6135
- four-centre molec., in quantum chem. 8=4136
- functional, for Smoluchowski eqn. of Brownian movement 8=10614
- Lipshits-Hankel incomplete, asymptotic methods 8=14929
- molecular, review of recent development in computation 8=16248
- molecular, two-centre 8=12159
- multidimensional, new method for evaluation 8=16247
- Robey's, first acoustic reactance for uniformly vibrating cylinder, evaluation 8=181
- turbulent dissipation, fluid 8=12628

Intensity measurement

- spectral-lines, revised tables below 2450  8=1152
- X-rays, from several cosmic sources, and spectra 8=5893

acoustics-

- infrasound spectra, rocket flight and take-off 8=197
- Interatomic forces, between bound atoms.** See Bonds; Molecules/internal mechanics; Solids.

Interatomic forces, between free atoms. See Collision processes.

Interface tension. See Surface tension.

Interference

- electron beams, polarization relationship 8=10894
- electron diffraction patterns, effect of incoherent scattering 8=3202
- laser radiation mixing, ruby and Nd 8=436
- X-ray, Ge absorption K-edge, proximity 8=14218

acoustic waves

No entries

electromagnetic waves

- microwave holograms and optical reconstruction 8=11214
- microwaves, flaw detection, erosion rate measurement 8=5032
- power spectrum modulation for unmodulated signal, 2800 MHz 8=19850
- radio, corona caused from EHV transmission lines, model 8=16422

light

- See also Optical films
- air layer, convecting, temp. gradient reversal obs. 8=4475
- coherent sources, equi-energy and equi-phase contours paradox 8=6546
- coupled cavity interferometry with He-Ne and CO₂ lasers, for plasma diagnosis 8=12522
- in double-pass interferometer with two imaginary plates, and obs. 8=504
- filter, narrow-band, u.v. region 8=6513
- filters, for i. r. spectral region 8=20064
- Fizeau fringes in reflection, wedge-angle depend. of half-width 8=20094
- holograms, double-exposed, white-light pattern reconstruction 8=15557
- hologram, laser reconstruction of image 8=524
- hologram rotation for image scanning 8=523
- holographic systems and images 8=520
- holography, information processing 8=531
- holography spatial filters for image restoration and code translation 8=519
- holomicrography, image transformation during reconstruction 8=525
- microscope, dry-mass determ. of biological substs., ext. of Pehland Hager theory to anisotropic systems 8=20098
- modulation in spectrometers by cam mechanisms 8=3361
- moiré fringes, apparatus and applications 8=20090
- Moiré fringe multiplication phenomena 8=11170
- Moiré fringes use for Fabry-Perot spectrometer wavelength scanning 8=6531
- Moiré patterns from superimposed Sorét-type plates, theory and photographs 8=11179
- multiple-beam in refl. light Fizeau fringes intensity distrib. rel. to geometry of interference layer 8=11177
- pattern in bands of equal inclination in a wedge-like interferometer 8=11178
- photon behaviour theory, modified field quantization 8=20096
- quantum theory of transient patterns 8=20097
- wave theory, corpuscular interpretation 8=15547
- waves of an interference field 8=20091
- Ag on Mo, moiré fringes 8=21977
- Ar I and II, wavelength meas. in region 5000–7000 Å 8=4070

Interference spectroscopy. See Spectroscopy.

Interferometers

- electron, low energy 8=330
- Fabry-Perot recording, for spectroscopy 8=15545
- field-sensitive, for quasi-coherent scatt. studies 8=11195
- lateral wavefront shearing with variable shear 8=11172
- microwave, for electron concentration in low density plasmas 8=7790
- multiple beam, for use with spherical wavefronts 8=11174
- polarization, Savart-polariscopes, astigmatism 8=514
- resonators, precisely confocal, for scanning 8=11173
- X-ray, combined Laue- and Bragg-case; a non-achromatic system 8=13229
- X-ray, design and application 8=13228

acoustic waves

No entries

electromagnetic waves

- Fabry-Perot resonator, microwave, plasma diagnostics 8=16542
- of 425 metres baseline, using 2 steerable radiotelescopes, operation at λ 21 cm 8=10441
- microwave, Fabry-Perot, design techniques 8=363
- microwave Fabry-Perot, design techniques 8=6379
- radio, 2800 Mc/s, multielement 8=2867
- radioastronomy, long base line technique 8=5978
- shock tube electron density meas. 8=159
- two-antenna, characts. for obs. along base line 8=6383

light

- actual Littrow and Wadsworth systems, deviation, scanning equation and spectral widths of slits 8=15531
- crossed interferometric-spectrographic method, study of physical processes 8=12523
- diffraction gratings, control of ruling 8=11180
- double-pass, for meas. of small path differences, and deform. of elastic bodies 8=20092
- Fabry-Pérot, active, charact. depend. on amplification and dispersion of active medium 8=20099
- Fabry-Pérot appl. to fast spectrometer 8=20076

Interferometers—contd

light—contd

- Fabry-Pérot etalon, flatness quality determ. using He-Ne laser 8=20093
- Fabry-Perot with mirrors deviating from parallelism, theory 8=11178
- Fabry-Perot with multilayer dielectric broad band surfaces 8=11167
- Fabry-Perot, for precise laser wavelength meas. 8=19992
- Fabry-Perot, press. controlled 8=501
- Fabry-Perot resonator, field distribution 8=3368
- Fabry-Perot spectrometer scanning using Moiré fringes system 8=6531
- Fabry-Perot spherical for giant pulse laser spectroscopy 8=6416
- Fizeau, surface-coated reference flats for testing aluminized surfaces 8=11171
- Fourier transform, sources of systematic error 8=1253
- gas lasers, axial mode number from moving mirror experiments 8=11026
- interferograms as image holograms 8=15554
- laser light source, aspects of fringe counting 8=11176
- laser streak, or holometer, optics rel. to relative beam displacement 8=6542
- lateral shearing, use for testing mirrors and lenses 8=20043
- LIN-1, for laboratory use 8=6545
- Lloyd's mirror for surface flatness testing 8=6547
- Mach-Zehnder for laser induced discharges 8=16403
- measuring film thickness 8=1692
- Michelson double-pass, interference in two imaginary plates theory and obs. 8=504
- Michelson, use to calibrate Fabry-Pérot photoelec. spectrometer 8=20077
- Moiré fringe technique for control of equipment 8=506
- optical flats absolute contours 8=11175
- polarization, for spectral modulation transfer functions of monochromators 8=488
- ruby laser, for fluid mechanics 8=16618
- scanning Fabry-Pérot etalon, for multimode operation of gas laser 8=20095
- series type, for refractive diagnosis of large-diameter θ -pinch 8=7788
- stellar amplitude, and obs. 8=19135
- for stellar temps. meas., intensity interferometer 8=19134
- strain meas. by moiré tech., mod. of profile projector 8=13501
- Tuyman-Green, multipass 8=6544
- u.v. region, teaching 8=6548
- wavefront shearing, inexpensive 8=505

Interferometry

- apparatus comprising a laser source for length meas. 8=6003
- double exposure holography, theory and expt. 8=20114
- Fourier spectroscopy, spectral recovery 8=15528
- holographic, fractional-fringe, appl. to plasma meas. 8=7779
- interference fringes, stabilization by f. m. feed-back 8=20116
- Lummer-Gerke plate, application in ruby laser 8=3328
- modification of phase-compensated corner cube for interferometry 8=502
- optical transducer, effect of air compression between plates 8=7892
- progress in optics, book V 8=15542
- shock waves in ionized Ar 8=4311
- for stress analysis, new method 8=46
- X-ray, early expts. and Bouse interferometer 8=15591
- X-ray, and moiré images of lattice planes 8=13228
- X-ray, thin film thickness meas. 8=8301
- CO₂ laser, oscillations and amplifiers dispersion meas. 8=11052

acoustic waves

No entries

electromagnetic waves

- earth rotation period precision meas., geophysical implications 8=18804
- earth rotation period, precise meas. 8=18833
- Jodrell Bank-Malvern baseline for 38 MHz radio-astronomy 8=10287
- plasma diagnostics using microwave Fabry-Perot resonator 8=16542
- radiotelescopes, phase link by magnetic recording and atomic clocks 8=10440
- Fe-3wt.% Si single crystals, X-ray fringes rel. to domain arrangements 8=22021

light

- acceleration of gravity meas. using laser-interferometer system 8=10487
- application to thermal expansion measurement 8=8647
- dry-mass determ. of biological substs., ext. of Pehland-Hager theory to optically anisotropic systems 8=20098
- Fabry-Perot etalon in focal plane of telescope 8=23563
- glass plates, small changes in thickness and refractive index 8=14223
- hologram, ghost lines 8=3380
- hologram-Moire, for transparent objects 8=522

Interferometry—contd**light—contd**

- holographic, for conical flow studies, refined analysis 8=6565
 - holographic 3-beam with single emulsion exposure 8=6541
 - holographic, in electrochem. 8=2528
 - holography, isophase surfaces 8=20113
 - holography, pulsed, appls. 8=20107
 - infrared photography with interf. microscope 8=20123
 - laser, Michelson for 6328Å use 8=6543
 - laser, vibrational displacement and mode shape determination, transducer face 8=6178
 - length measurement, lasers 8=7
 - low-angle holographic, use of Tri-X Pan film 8=6571
 - multi-beam, determ. of axisymmetric non-uniformities 8=21498
 - multiple-beam, resolution limits 8=15544
 - Perot-Fabry ring meas. for atomic spectral distrib. 8=15530
 - progress in optics, book VI 8=15541
 - refractive index meas. of molten alkali nitrates by wave-front-shearing interferometry 8=4583
 - shearing interferograms, semiautomatic method for interpretation 8=20043
 - shearing, wavefronts with rotational symm. 8=15546
 - shock wave profile, determ. 8=10717
 - spectroscopy, using modified line shape 8=11152
 - two-beam, signal and noise 8=503
 - two-wavelength, of laser-produced C plasma 8=21357
 - white, use of multilayer dielectric coatings 8=6540
 - Ar arc, current perturbed, electron density meas., laser technique 8=7694
 - Fe-N alloys, structure after quenching 8=8522
 - He-Ne laser, i. r. meas. of shock-tube plasma e density 8=16541
 - He-Ne laser, spatial coherence, expt. investig. by Mach-Zehnder 8=19968
 - He-Ne laser, spatial coherence, expt. investig. by Mach-Zehnder interferometer 8=19968
- intergalactic matter.** See Galaxies.
- intermetallic compounds.** See Alloys; Semiconducting materials and under the compounds and alloys of the individual metals.
- intermolecular forces.** See Molecules/intermolecular mechanics.
- internal conversion.** See Beta-ray spectra/conversion electrons; Gamma-rays/internal conversion.

Internal friction

- alkali halides, Peierls stress estimation 8=1968
- amplitude dependent rel. to dislocation pile-ups 8=13496
- anelasticity, plastic yielding of cylinder rel. to stress rate 8=22275
- α -brasses, and elastic props. 8=13552
- carbon steel, magnetoelastic scattering rel. to amplitude dependence 8=13565
- of dislocations rel. to optical properties of dielectrics 8=14165
- glasses, glass-ceramics, empirical determ. of background 8=22266
- inhomogeneities, parameters from anisotropic stage of cosmic ray bursts 8=23688
- iron, pure, temp. dependence, effect of annealing 8=17791
- magnetite, rel. to acoustic loss peak, electronic mech. 8=1852
- measurement at kHz frequencies, simplified bridge system 8=5007
- measurement by vibrator-controlled oscillator system 8=8785
- metals, b. c. c., diffusion coefficients meas. 8=17557
- metals, measuring and recording equipment, low frequencies 8=8784
- polyacronitrile drawn film, anisotropy of tan δ 8=17847
- power spectra and discontinuities, Mariner 4 obs. 8=23685
- reed pendulum apparatus with rapid data processing 8=13495
- reeds, vibrating granular, application to vitreous silica 8=13606
- relaxation time of atomic ordering effects 8=17717
- spectrum, power and solar proton and electron diffusion 8=23686
- spiral model, charged particle motion calc. 8=23689
- ultrasonic pulse attenuation meas. 8=17715
- Al, peak at room temp. 8=13532
- Al, rel. to elasto-plastic behaviour obs. 8=8848
- Al-0.25 wt.% Fe, in temp. range 200-400°C 8=5049
- Ba silicate glasses, effect of condensation 8=13537
- Cu-Ag (0.083 at. %) alloy at low frequencies 8=8784
- α -Fe (b. c. c.), impurity-induced peak (Snoek's peak), for torsional vibrs., anisotropy 8=13572
- Fe, rel. to elasto-plastic behaviour obs. 8=8848
- Fe, forces of moving dislocations 8=22206
- Fe, purified, amplitude-dependent, and induced modulus defect rel. to dislocation motion 8=13557
- Fe, H-charged, rel. to H interstitial-dislocation binding 8=4965
- Fe-Mn-N alloys, torsion pendulum obs. 8=8839
- Fe-3.5 at. % V alloy, forces of moving dislocations 8=22206
- Gd, torsional pendulum obs., magnetic damping effect 8=14020

Internal friction—contd

- Ge, screw and edge dislocation damping 8=22370
- KBr, rel. to dynamic characts. of dislocations 8=8730
- Mo, amplitude dependence rel. to dislocations mobility 8=22209
- Mo, due to interstitial atoms 8=17817
- Na₂O-BaO-SiO₂ glass system, peak shift rel. to Na replacement by Ba 8=22383
- Nb, amplitude dependence rel. to dislocations mobility 8=22209
- Nb, superconducting, mixed and normal states, variation 8=2063
- Pt, annealed, relax. effect of new peak at low temps. 8=22211
- Si, and elec. resist. on repeated alternating bending 8=17828
- Si-Fe, (b. c. c.), impurity-induced peak (Snoek's peak), for torsional vibrs., anisotropy 8=13572
- Zn, rel. to elasto-plastic behaviour obs. 8=8848
- W, rel. to temp. 8=1980

liquids. See Liquids; Viscosity/liquids.

Internal stresses. See Stresses, internal.

Internuclear double resonance (INDOR). See Nuclear magnetic resonance and relaxation.

Interplanetary magnetic fields

- connection with earth's polar cap lines, interpretations of riometer and satellite obs. Feb. 1965 8=905
- convection away from Sun at solar wind velocity, IMP 1 and 2 obs. and magnetosheath penetration 8=14861
- cosmic ray storm, February 1962, rel. to structure 8=2833
- filamentary, effect on solar flare structure obs. 8=10424
- geomagnetic activity index response, obs. 8=10052
- IMP-2 satellite obs. 8=2832
- Jupiter magnetospheric model 8=14836
- magnetized plasma, partial corotation 8=14834
- meteorites, stony, stony-iron and iron, deductions from thermoremanent magnetization obs. 8=19279
- and polar cap absorption separation into 2 types 8=10407
- polarity pattern, 28 Nov. 1964-1 Oct. 1965 8=14862
- scattering of cosmic particles 8=19086
- sector structure, 1962-66 variations 8=10371
- sector structure, solar source 8=2831
- solar origin and effects 8=10375
- solar stream mag. morphology rel. to geomag. storms 8=10053
- solar wind, review of relationship 8=2849
- variations rel. to earth's surface field, IMP 1 and terrestrial obs. 8=14860

Interplanetary matter

- asteroids, crossing earth's orbit as stone meteorite source 8=19249
- corona obs. rel. to magnetogasdynamical model for stars 8=23506
- cosmic particle scattering on random mag. field 8=19086
- elements diffusion in the Sun rel. to observed abundances 8=19285
- earth's bow shock, plasma and mag. field correlation obs. 8=23328
- earth's bow shock, solar wind plasma changes across, Vela 3 obs. 8=9908
- electrons, cislunar content asymmetry, radar obs. 8=2834
- electrons and protons, high energy, absence in vicinity of Venus from Mariner 2 obs. 8=23676
- features, large distance, rel. cosmic rays 8=10088
- meteorites, stony, stony-iron and iron, thermoremanent magnetization obs. rel. to interplanetary field 8=19279
- plasma density in solar neighbourhood, irregularities 8=19284
- plasma flow past non-magnetized bodies, lab. simulation 8=12475
- plasma, shock wave propag., brightness temp. obs. 8=10432
- properties from cosmic-ray var. data 8=19283
- secondary electron spectrum and intensity, IMP-A obs. rel. to atmospheric balloon obs. 8=7020
- shock waves in solar wind, Vela 3 obs. 8=23687
- solar cosmic ray diffusion rel. to sun distance 8=23722
- solar plasma flow outward, spherically symmetric, influence of polytropic heat source 8=19304
- structure of medium, small scale, scintillation obs. 8=10409
- zodiacal cloud, meteor model, rel. to brightness and polarization of zod. light 8=23341
- Fe fractionation in Solar System 8=10323

Interstellar matter

- absorption band at 4430Å, var. with galactic longitude 8=23534
- absorption band at 6180 Å, profile 8=10235
- atmosphere plane parallel, specific intensity behaviour at infinity 8=2774
- atomic medium with three energy levels, polychromatic scatt. of rad. 8=16186
- brightness temp. of clouds 8=23574
- collisional excitation of low-energy transitions by charged particles 8=10244
- conducting gas in strong mag. field, oscillatory convection 8=19308
- cooling processes rel. to H-O and H-C collisions 8=1193
- cosmic grains, theory of formation 8=19196
- cosmic ice residuum and astroleme 8=2562
- cosmic medium, inhomogeneous, motion of shock waves 8=10242

Interstellar matter--contd

- cosmic particle scattering on random mag. field 8=19086
 cosmic rays, effect on composition and energy spectra, calc. 8=11668
 density inhomogeneities, large scale, from microwave background obs. 8=10082
 e spectrum prod. by cosmic-ray collisions 8=19094
 equilibrium properties, at very high temp. and densities 8=19167
 fluid layer of finite thickness, self-gravitating, stability 8=10237
 galactic cosmic rays, chemical evolution in path 8=23430
 galactic secondary spectrum rel. to prod. and confinement in galaxy and halo 8=19198
 gas, absolute and convective instability 8=10261
 gas, gravitational effects on motion in radiating star neighbourhood 8=23580
 gas, C^{12}/C^{13} ratio, a lower limit 8=5919
 gas and dust heating and ionization by subcosmic rays and star form 8=10245
 gas-dust medium, m.h.d. 8=23579
 gas layer containing 2- or 3-level atoms, radiative transfer 8=16188
 gas layer, optically thick, X- and Y-functions in theory of multiple scatt. in spectral line 8=16187
 gas, relativistic, non-relativistic bulk motion, e.m. effects and suprathermal waves 8=5925
 gaseous mass, inhomogeneous, convective instability, model 8=2794
 graphite, computed and observed extinction curves 8=10247
 graphite grains adsorption 8=23572
 graphite grains, role of impurities 8=10246
 hydrogen atmosphere, structure determination 8=2773
 hydrogen, radial motion within the Galaxy 8=10243
 IC 410, electron densities from 4 cm obs. 8=23570
 impurities, interaction with e.m. waves 8=10238
 impurity-induced emission and absorpt. 8=23571
 ionization and heating by superthermal particles 8=23575
 Jeans' instability criterion, effect of grains 8=2793
 light scatt. theory, necessity of including non spherical particles 8=4206
 meteors in asteroid belt collision probability calc. 8=2818
 model atmospheres in theory of stellar classifications 8=2777
 neutrino distribution in space and maximum energies in cosmic rays 8=14796
 NGC 6611, 6523 and 7000, electron densities from 4 cm obs. with 85 foot scope 8=23570
 particle tracks near massive star, relativistic eqns. of motion 8=10110
 plasma interactions and cosmic rays, theories review 8=23578
 plasma with Coriolis force, wave propag. rel. to fragmentation 8=16515
 plasma, stratified, anisotropic, internal gravitational instability 8=10241
 plasma, turbulent, accel., scatt. and diffusion of charged particles calc. 8=7741
 plasma, v.l.f. and e.l.f. e.m. wave propagation 8=2674
 polarization of starlight, theory 8=5920
 proper motion, work of R.M. Petrie 8=10195
 relativistic gas, Fermi accn. by shocks, and radio spectra 8=10292
 shock waves effects on gas and dust densities 8=10239
 spiral arm, magnetic field and gas outflow association 8=10280
 stellar co-operative effects for the enhancement of dynamical friction 8=19108
 stellar system, one-dimensional, a variational principle 8=19209
 stellar wind, flow recombination shell between HI and H II 8=23576
 thermal radiation from, far i. r. sky survey 8=19197
 H spatial structure, 21 cm obs. with 300 foot telescope 8=23565
 HI regions, i.r. emission and m.h.d. shock waves 8=23566
 H II in M33, kinematical and physical data from interferometric obs. 8=23568
 H II regions in anticentre region, electron temp. determ. by radio obs. 8=19199
 H II regions, higher-order high-quantum H recombination lines 8=23569
 H II regions, interference photography 8=19200
 H II regions, obs. at 178 MHz, contour maps of brightness temp. 8=10240
 H II, stimulated emission of r.f. lines, enhancement by small departures from thermal equilb. 8=23567
 H₂ abundance, reduced estimate 8=23577
 H₂ formed by chemical-exchange reaction, upper limit on abundance 8=5926
 H₂ in Galactic corona, maser effect 8=5924
 H₂, maser action on 21 cm radiation 8=5923
 OH 18cm transition, calc. of Einstein A coefficient 8=10169
 OH, 18-cm transitions, Einstein A coeffs. 8=12351
 OH molecules, polarization theory of 18 cm lines 8=7543
 OH normal emission in dust clouds 8=23573

Interstellar matter--contd

- OH radical, radio absorpt. obs. 8=23581
 OH, CH and CN, collisional excitation by charged particles 8=10244
 Interstitials. See Crystal imperfections/interstitials.
 Iodine
 adsorption by atmos. particles 8=9892
 additive in Cs arc diode, effect on performance 8=15225
 atomic, new Rydberg absorpt. series and ionization pot. 8=1165
 charge transfer complexes with subs. pyridines, spectro-photometric obs., rel. to struct. and stability 8=4216
 compressibility, of solid 8=13578
 crystalline, insulator-metal transition from diatomic bond destruction under high pressure 8=2084
 diatomic mol., electron spin polarization meas. 8=1232
 dissociation and assoc. of gas at h.p. 8=23080
 ionization in supersonic Hg vapour jet, charge distrib. 8=7716
 ions I⁻ on Hg electrode, partial charge transfer react. 8=18722
 ions, registration in olivine and hypersthene crystals 8=11325
 liquid, elec. cond. of salt solns. 8=21719
 melting temp. under high pressure 8=4644
 molecular beam, laser-induced fluorescence 8=16288
 pure quadrupole reson. in tetraiodothallates 8=18477
 spectrochem. anal. in vac. u.v., quantitative 8=18788
 vapour, interactions with W surface 8=18699
 vapour, reflection coeff., from surface of single crystal Ge 8=8382
 in BiTeI, electrotransport, obs. 8=17564
 H₂+I₂ reaction paradox 8=23105
 I⁺, photodetachment probability for simultaneous two-quantum absorpt. 8=12437
 I(⁵P_{1/2}), excited, reaction with propane 8=5745
 I(⁵P_{3/2}), time resolved emission obs. 8=4079
 I²⁷ quadrupole spectrum in paramag. and antiferromag. U₃ 8=9469
 I²⁹ abundance in early solar system 8=23468
 I²¹, use in metals-iodine reaction study 8=23093
 I¹³¹, self-diffusion in CsI single crystals and polycrystalline samples 8=8674
 I-131 as tracer for groundwater flow obs. 8=2568
 I-I system, 2nd virial coefficient for different electron states at 2000-6000°K 8=1469
 I₂ beam, reaction kinetics with K and Cs atoms 8=1202
 I₂ crystals, intermediate triplet excitons props., theory 8=22479
 I₂, 5350 Å band, resolving power test 8=16289
 I₂, orientation of transition moment in photodissociation 8=1307
 I₂-Ar mixtures, vibr. relax. time meas. 8=7932
 I₂-He mixtures, vibr. relax. time meas. 8=7932
 I₂-CCl₄ solns., stimulated thermal Rayleigh scatt. obs. 8=8068
 I₂+H₂ reaction kinetics 8=5706-7
 Iodine compounds
 chemical shifts of inner levels, determ. by photo-emission 8=16971
 tetraiodothallates, pure quadrupole reson. of I 8=18477
 IBr, crystal structure refinement 8=22027
 ICl, impurity-dope in graphite, effect on anelasticity 8=13541
 IF₅, liq., Raman spectra and vib. assignment 8=1568
 IF₇, molec. struct. 8=21107
 Ion beams
 See also Ion optics; Mass spectrometers; Particle accelerators; Particle range; Sputtering.
 accelerators, high current target design 8=3231
 accelerator, h.f. with static mag. field gradient, obs. 8=21405
 chopper for spark source mass spectrography 8=18767
 collective interact. with plasma, and instability caused 8=16595
 constant diameter, focussed by uniform magnetic field, perturbations 8=15278
 deflection by current carrying plasma 8=6336
 d, polarized, prod. from T(d,n)He⁴ 8=11602
 electron, ion and laser beams technology, conference, Berkeley, USA (1967) 8=15283
 electronic integrator to control magnetic field 8=3597
 emittance in duoplasmatron source linked to single gap accelerator 8=20229
 energy losses on traversing crystal lattice channels 8=17695
 excited by thin foils, spectroscopic props. 8=6535
 extraction from gas discharges 8=342
 focusing, by mag. field, theory 8=10919
 heavy, penetration in Au, Al and W, effect of atomic thermal motion 8=2024
 injection for accelerator with multiple pulse width and intensity capability 8=15658
 injector for electrostatic generator 8=3150
 intense, production using magnetised plasma 8=15349
 intense, for thermonuclear expts. 8=16139
 ion-electron, emitted by a plane, neutralization 8=3225
 loss detector, ionization chamber 8=20227
 magnetic slit for momentum definition and beam separation 8=6700

Ion beams—contd

- micro-machining performance 8=6339
- multiple acceleration in electric field by charge exchange 8=630
- neutralization by supersonic gas jet 8=6335
- oscillations, beam-plasma interaction 8=12548
- path stabilizer, automatic 8=3224
- Penning discharge in vacuum, energy spectra 8=7648
- plasma density contour meas. using mol. ion beam breakup 8=7791
- polarized, depolarization due to magnetic focusing 8=10888
- for processing, and colour obs., apparatus 8=15351
- production by electron bombard. ion thruster 8=10917
- progress in nuclear techniques and instrumentation, book II 8=15648
- p in 4 MV accelerator, 1 mA current 8=15650
- p injection into centre of cyclotron 8=11342
- p polarized, prod. method in $2S_{1/2}$ state 8=11602
- pulsed, current converters for 8=629
- pulsed, submicrosecond, hot cathode source 8=3223
- reflection from crystal surface, rel. to surface micro-structure 8=13201
- spectral-line profiles for fast-ion-beam source 8=341
- spherically diverging current, neutralization and pot. behaviour of subsequent flow 8=15350
- unipolar, effect of resonant charge exchange collisions with neutral gas 8=7707
- Ar duoplasmatron, relative abundance of ions 8=7780
- Cs plasma, synthesized, electrostatic oscillation obs. 8=16584
- D⁺ prod. by charge exchange polarization obs. 8=15352
- D⁺ channeling in crystals, transparency model 8=22243
- D⁺, critical angles for channeling in thin Au films 8=17704
- D⁺ transmission through thin films 8=22242
- in Ge, $^1H^+$, $^2D^+$ and $^3He^{++}$, channelling props., diff. calc. 8=13485
- H from accelerator, bunched 8=10916
- H, from duoplasmatron source 8=3222
- H⁺, critical angles for channeling in thin Au films 8=17704
- He⁴⁺ prod. by charge exchange of He⁴⁺ from duo-plasmatron 8=15347
- He⁺, critical angles for channeling in thin Au films 8=17704
- $^3He^{2+}$, prod. by r.f. ion source 8=10914
- K, range distrib. in amorphous Al_2O_3 8=13476
- Kr, range distrib. in amorphous Al_2O_3 8=13476
- Na, range distrib. in amorphous Al_2O_3 8=13476
- O₂ from accelerator, bunched 8=10916
- Xe, range distrib. in amorphous Al_2O_3 8=13476
- Xe⁺ in O₂, monitoring of Xe⁺ $^{232}P_{3/2}$ conc. using charge transfer 8=12454
- $^{133}Xe^+$, penetration distrib. in Au, effect of target temp. 8=2023

effects

- density effect for the ionization loss of charged particles in solid media 8=8775
- detector plates, sensitivity vs. ion energy 8=16179
- discharges, low-pressure, r.f., time-averaged potentials, meas. using probe 8=21224
- glass, ion-bombardment-induced emission of gas 8=17173
- glow-discharge tubes, cathode sputtering variation 8=2019
- hypersthene crystals, registration of As and I ions 8=11325
- inert gases, re-emission from W and Au 8=17701
- ion-molecule reactions, mass spectrometry, pulsed-source method 8=10918
- ionization of molecules adsorbed to a surface by energetic ion bombardment 8=16435
- metal polycrystals, corrosion, angle of incidence 8=13522
- metallic surfaces, u.v. emission on K⁺ ion bombardment, analysis by spectral micrography 8=14299
- nuclear bombard., γ -ray emission, E2 and M1 transition calc. 8=932
- olivine crystals, registration of As and I ions 8=11325
- semiconductors, implantation techniques 8=18014
- Ag foil, deceleration of 0.2–40 keV H and D ions 8=2020
- Ag, Ar-ion bombardment, LEED study 8=22240
- Al range-energy curve of Po. At recoils 8=13473
- Al_2O_3 , of 2.5–10 keV Cs ions, sputtering 8=8760
- Al_2O_3 range-energy curve of Po. At recoils 8=13473
- Ar, paraboloid eroded by ion bombardment 8=13466
- Ar⁺ emission function for var. targets 8=6626
- Au single crystal film, structural and texture changes 8=17124
- Au-Cu alloy single crystal film, structural and texture changes 8=17124
- Au films, D⁺ blocking effects 8=22241
- C, stopping cross-section for ions with $21 \leq Z_1 \leq 39$ betw. 200–1500 KeV 8=13482
- C target thin, 2 MeV beam passing through, N spectrum obs. 8=20960
- CdS films, on elec. props. 8=13791
- CdTe thin films effect on resistance 8=5244
- Cr, deposition from low-energy source 8=19796
- Cu crystal, reflection of Cu and Ar ions for oblique incidence 8=8767
- Cu foils, agglomerates formation and density 8=13417
- Cu foils, defect clusters, type and configuration analysis 8=13416
- Cu single crystal film, structural and texture changes 8=17124

Ion beams—contd**effects—contd**

- GaSb, cleaned by ion bombard. effect on (111) surface stress 8=8849
- Ge, cleaned by ion bombard. effect on (111) surface stress 8=8849
- Ge, irradiation, low-energy, by He⁺ and Xe⁺ 8=8772
- p-Ge, on microhardness 8=17810
- He target excitation by H⁺, D⁺, H₂⁺ and H₃⁺ 8=16217
- He⁴, D, Fe⁵⁴ in M (M = V⁵¹, Zr⁹⁰, Au¹⁹⁷, Ni⁵⁸ or Li⁶), recoil range 8=13489
- He⁺ on Cu crystal, u.v. emission 8=2025
- InSb, cleaned by ion bombard. effect on (111) surface stress 8=8849
- (Mg, Fe), SiO₄, iron ion tracks 8=8768
- Mo, Auger electron yield on Ar⁺ and He⁺ bombardment 8=9279
- Ni films, thin, bombardment rel. to induced mag. anisotropy 8=22829
- NO₂⁻ production using NO₂ beam crossed with O⁻, O₂⁻, O₃⁻ and OH⁻ beams 8=1367
- O¹⁶ in Au, Ag, 10–30 MeV obs. discrepancy due to auto-ionization 8=13477
- S³² in Au, 19–40 MeV obs. discrepancy due to auto-ionization 8=13477
- Si, B-doped by ion bombardment, B distrib. profiles 8=18071
- Si, surface properties after irradiation with 50 keV nitrogen, boron and helium ions 8=18078
- Si, surface structure, temp. dependence 8=5278
- ZnO:Zn phosphor deterioration, heavy ion irradi., obs. 8=18623
- ZnO:Zn phosphor of H, He, N, Ar and Kr, deterioration depth obs. 8=18624
- ZnS:Ag, deterioration depth under prolonged heavy ions bombard. obs. 8=4998
- ZnS:Ag, made nonluminescent to det. ion energy loss 8=8758

Ion counters. See Counters.

Ion emission

- emission from and adsorpt. on a substrate surface in equilib. with ionized vapour 8=18263
- field-ion specimen tips, electron microscope exam. 8=18285
- on laser light interaction with conductors, semiconductors and dielectrics 8=18272
- solid solution alloys, field patterns, computer simulation 8=8453
- Ag target, Ar bombard, emission function var. 8=6626
- Al target, Ar bombard, emission function var. 8=6626
- Au target, Ar bombard, emission function var. 8=6626
- Be, multicharged rel. to laser intensity, and X-ray emission 8=13947
- Be target, Ar bombard, emission function var. 8=6626
- C, multicharged rel. to laser intensity, and X-ray emission 8=13947
- C target, Ar bombard, emission function var. 8=6626
- Cu target, Ar bombard, emission function var. 8=6626
- MgO surfaces, gas emission 8=2272
- Mo, multicharged rel. to laser intensity, and X-ray emission 8=13947
- Mo target, Ar bombard, emission function var. 8=6626
- U atoms from uranium oxide pellets 8=20859
- W, due to laser irradi., study of masses, energies and numbers of ions 8=13948

secondary

- alloys rel. to chemical analysis 8=18286
- magnetron anodes, cathode bombardment 8=15334
- review 8=2283
- Al alloys, mass spectroscopic investigation 8=18287
- Fe alloys, mass spectroscopic investigation 8=18287
- NaCl, of Cl⁻ on electron bombardment rel. to surface potential meas. 8=5425

thermionic

- from refractory compound surfaces, cesiated, rel. to stable, at 1500°. low work function surface 8=18262
- and surface ionization, stress depend. 8=13946
- thermionic conversion Specialists Conference San Diego USA October 1967 8=6273

Ion exchange. See Exchanges, chemical: Ions. electrolytic.

Ion microscopes

- field, atom-probe type with mass spectrometer 8=15353
- field, computer simulation for interstitial solid solutions 8=21817
- field-ion images from asymmetric specimens, streak contrast 8=8452
- field-ion micrograph interpretation of contrast from dislocation loops 8=17633
- field-ion, pumped by sputter-ion pumps, gas contamination 8=6338
- field-ion specimens, automatic electropolishing supervisor 8=17273
- field-ion specimen tips, electron microscope exam. 8=18285
- field microscopy, use of fibre optic window 8=6512
- field, preparation of tungsten specimens 8=15354
- field, single crystal tip pattern, approx. to collection of Fresnel zones 8=3230
- field, tip radius variation rel. to operation 8=343

Ion microscopes—contd

- field, W field evaporation end form 8=4735
 microprobe mass analyzer development 8=6340
 scanning, performance 8=6339
 ultra-high vacuum field, specimen transfer device 8=3229
 ultra-high vacuum metallic dismountable apparatus
 for obs. 8=15320

Ion mobility. See Ion velocity.**Ion optics**

- See also Alpha-ray spectrometers; Ion microscopes;
 Mass spectrometers; Particle optics.
 duoplasmatron ion source 8=15340
 electronic integrator to control magnetic field 8=3597
 electrostatic sector fields, image aberrations 8=19802
 field, rot. symm., 3D, quadrupole, trapping,
 trajectories 8=19799
 focusing, by mag. field, theory 8=10919
 magnetic spectrograph, split-pole 8=3228
 of mass spectrometers 8=20915
 quadrupole magnetic lens using ceramic magnets 8=3226
 quadrupole mass filter, resolution 8=3227
 quadrupole mass filter, rod mounting, simplified 8=7357
 retardation lens to improve abundance sensitivity of
 mass spectrometer 8=4040
 selectors, useful current calc. 8=19773
 synchrocyclotron, increasing of p beam current 8=3499
 trajectories in accelerating tube of neutron
 generator 8=3714
 trajectory meas. in magnetic field 8=3192
 transmission of a system, Monte Carlo calc. 8=19801

Ion pumps. See Vacuum pumps.**Ion sources**

- See also Ion emission/thermionic.
 accelerator, tandem, p and d 8=6694
 calutron, ionized spectrum, Doppler shift due to charge
 exchange 8=6334
 cyclotron, cold-cathode high intensity 8=15346
 duoplasmatron, comp. of H ion beam 8=3222
 duoplasmatron, expanded plane plasma front 8=15340
 duoplasmatron, with expansion cup 8=15341
 duoplasmatron, improvements 8=15661
 duoplasmatron linked to single gap accelerator, beam
 emittance 8=20229
 duoplasmatron prod. of He⁺ used to produce He⁺ by charge
 exchange with K 8=15871
 dynamag, with open cylindrical extractor 8=15344
 electron bombardment, for radioisotope
 implantation 8=15343
 films, thin, ion bombardment apparatus 8=17121
 heavv. highly stripped, HIPAC type source 8=19797
 high-vacuum, without focusing field 8=3221
 hot cathode for submicrosecond ion pulses 8=3222
 ionizer, e-bombard. weak field 8=19798
 magnetized plasma emitter, density and temp.
 meas. 8=1432
 magnetron anodes, occluded gas and vaporized
 material 8=15334
 magnetron cold cathode for ultrahigh vacuum residual
 gas analysis 8=4039
 mass spectrometer, cathode -temp. effects 8=16177
 Nier type, optimum conditions for electron beam 8=6332
 output calculation, from simple open source with longit.
 ionization 8=6333
 Penning discharge, high brightness 8=15345
 Penning ionization gauge as low pressure 8=15338
 Penning ionization gauge, characts. 8=10913
 Penning for tandem accelerators investigated 8=11338
 polarized targets and ion sources, conference, Saclay
 France (1966) 8=15629
 spectral-line profiles for fast-ion-beam source 8=341
 surface ionization applic. 8=15348
 Van de Graaff accelerator, polarized p and d 8=6692
 Cr, deposition, low-energy 8=19796
 Cs, improvement by Ta precoating 8=15342
 D⁺ polarized beam prod. by charge exchange for
 accelerators 8=15352
 H⁺ and D⁺, polarization increase 8=10915
 H₁⁺, from duoplasmatron, for charge-exchange
 generator 8=15339
 H₁⁺, D₁⁺ and T₁⁺ injector for charge-exchange
 generator 8=7713
 He⁺ beam prod. for Van de Graaff accelerator 8=15347
 He using Cs vapour exchange 8=15872
 He prod. from He⁺ by K charge exchange 8=15871
 He for Van de Graaff accelerator improved by K vapour
 exchange 8=6693
³He²⁺ r.f. prod. 8=10914
 O₂ with Xe beam to determ. relative charge transfer
 efficiencies of ²P_{3/2}, ²P_{1/2} of Xe⁺ 8=12454
 Re, thermal ionization sources, isotopic anal. 8=7479
 Ti anode, discharge in desorbed H₂ 8=21227

Ion velocity

- acceleration in electron beams, apparatus and
 meas. 8=15337
 in biological membranes, device to meas. V-I
 characts 8=5988
 carrier mobility estimation 8=4612
 drift with interconversion Tyndal drift-tube expt.
 interpretation 8=7704

Ion velocity—contd

- effect on efficiency of a continuous channel electron
 multiplier 8=6635
 electron diffusion in gases, time-of-flight meas. 8=7702
 in gases under influence of electric fields 8=7705
 liquid membrane and elect. props. 8=4560
 translational energy meas. with time-of-flight
 spectrometer 8=7703
 Cs silicate glass ionic conduction, n.m.r.
 absorption 8=9197
 HeII, discontinuity above 1.1°K 8=19697
 N ions in N drift vels. and reactions at 300°K,
 0.5-1 Torr in elec. field 8=7718
 Tl silicate glass ionic conduction, n.m.r.
 absorption 8=9197
 ZrO₂, cubic, influence of neutron irradiation on ionic
 mobility 8=5152

electrolytic

- See also Conductivity, electrical/liquids, electrolytic;
 Electrophoresis.
 No entries

Ionization

- See also Dissociation; Electrons/ionization.
 alkali metals, preferential contact, in magnetoplasma
 device, rel. to purification 8=4302
 alkynes, field-ion mass spectra obs. of eleven
 compounds 8=1372
 aniline, photoionization efficiency 8=7724
 aromatic amino-acids in frozen solns., photo-
 ionization 8=9650
 aromatic mols., probabilities correl. with geometric
 charge cross-sections 8=4318
 atom, Ar⁺ + Ar → Ar^{m+} + Arⁿ⁺ + (m + n - 1) e, final change
 states and discrete loss mechanism 8=4107
 atoms, by e impact, study using Coulomb wave
 approx. 8=7427
 atoms, electron impact cross-section, Bethe calc. 8=7700
 atoms by laser, photoelectron counting statistics,
 quantum theory 8=20987
 atoms, long-lived highly excited, by collisions 8=4303
 atoms, shell-struct. effects 8=7452
 atoms, in strong light field, quasiclassical
 approx 8=3411
 autoionization process rel. to energy loss by O, S ions in
 matter 8=13477
 autoionization, transition probability 8=6597
 β decay causing, imperfect overlap of orbital e wave
 functions 8=12419
 capture collisions between ions and polar mols. 8=7696
 charge exchange, double nonresonance, model 8=1353
 charge transfer, Gryzinski procedure tested 8=12424
 collision-induced, with Dempster mass spectro-
 meter 8=4309-10
 comets 8=2827
 concurrent ion-molecule reactions 8=4312
 degree of, effect on efficiency of a continuous channel
 electron multiplier 8=6635
 dimethyl sulfide, rate of base-catalyzed
 triation 8=4610
 electrojet equatorial Sq currents on individual quiet
 days, obs. 8=2641
 electron-impact cross-section, empirical
 formula 8=1351
 energy of H like impurity centres in
 semiconductors 8=13785
 energy levels of systems, lower bound, ΔE method 8=561
 flame, aerosol particle size analyser 8=16908
 impact in semiconductors, a fast high current pulse
 generator for 8=6249
 ion collection in Bayard-Alpert gauge, calc. 8=4306
 ions, multiple acceleration in electric field 8=630
 ionizer, e-bombard. for ion source 8=19798
 metastable transitions obs. in time-of-flight mass
 spectrometer 8=16438
 molecule, diatomic, H atom model applied to H₂ 8=21034
 molecule, photoionization cross-section calc. 8=21259
 multiple in heavy particle atomic collisions 8=7451
 non-equilibrium in low voltage arc. 8=21254
 nuclear emulsion, by π, p beams at relativistic vel. 8=15647
 nucleic acid components in frozen solns., photo-
 ionization 8=9650
 precursor to shock wave in e.m. tube, meas. 8=6137
 preferential assoc. of pos. charge with butadiene
 fragment in 4-vinylcyclohexene mass spectra 8=4320
 pressure gauge, e ionization of molecules, character-
 istics 8=4500
 resonant exchange collisions, with neutral gas, effect on
 unipolar beam 8=7707
 spark-gap-switch deionization det. 8=7679
 wave equations, asymptotic stability 8=7845
 Ag, electron-impact cross-sections 8=12428
 Ag⁺, electron-impact cross-sections 8=12429
 Ar²⁺ + Ar, reaction cross-sections 8=4310
 C⁴⁺ by e impact, cross-sections calc. 8=12435
 C⁵⁺ by e impact, cross-sections calc. 8=12435
 CF₃ free radical, photoionization 8=7724
 CH₃, by ion-molecule reactions, 8.10⁻⁶-10⁻³ mm Hg 8=4258
 CN halides, photoionization 8=12433
 C₂N₂, photoionization 8=12433

Ionization—contd

- CO by proton beam, cross-section, and charge transfer 8=1357
 $\text{CO}^+ + \text{CO}_2$, reaction cross-sections 8=4310
 $\text{CO}^{2+} + \text{CO}$, reaction cross-sections 8=4310-11
 Cs vapour, charge exchange H^+ to H^- 8=12441
 CuO_2 cryst. excitons photoionization, assoc. absorpt. coeff. calc. 8=9529
 Fe X-XVIII , autoionization rel. to rates and equil. 8=16442
 Ge, electron-impact cross-sections 8=12428
 H , neutral atoms, by passage through hot-cathode discharge 8=21274
 H^+ , photoionization in u.v., study of resonance near $n = 2$ level 8=7444
 H-H , 2-60 keV ionization and e capture obs. 8=21007
 H at. beam, photoionization 8=21020
 H atom in H-H collisions 1.25-117 KeV cross-section function of projectile quantum number 8=21276
 H , by e impact, asymptotic form of wave function 8=16443
 H in 1s state, e-impact ionization cross-section obs. 8=21273
 H-H , 2-60 keV ionization and e capture obs. 8=21007
 H-H , 2-60 keV ionization and e capture obs. 8=21007
 H^+ , H_2^+ in N_2 , O_2 , CO_2 , H_2O , charge exchange 40-1500 eV 8=21275
 H_2 , autoionization lifetime calc. using H atom model 8=21034
 H_2 , by CF^{252} fission fragments, energy per ion pair 8=1361
 H_2 e-impact obs, derivative spectrum rel. to photoionization, autoionization 8=21272
 HCl-HCN mixtures with D_2 and CD_4 8=4312
 HD autoionization lifetime calc. using H atom model 8=21034
 HF energy and core rearrangement 8=7701
 He atoms by e impact, cross-section calc. 8=12084
 He , double by fast p, 1-3 MeV using wave functions which are products of H -like orbitals 8=21280
 He , with simultaneous excitation by p, d impact, obs. compared with theory 8=7385
 He^+ , lifetime, photodetachment cross-section obs. 8=20944
 He -like atoms, 1'S state conservation prob. in β -decay 8=7426
 He^+ , below $n=3$ level, autoionization 8=4091
 He^+ , below $n=3$ level, autoionization 8=4092
 He^+ in N_2 , O_2 , CO_2 , H_2O , charge exchange 40-1500 eV 8=21275
 Kr atomic spectra, autoionization 8=20954
 K X-ray prod. following β scatt., Bethe-Born and Bang-Hansteen approx. 8=20930
 Li to Kr , atoms by β decay, probabilities calc. 8=4090
 N atomic beam, photoionization 8=21022
 N , atomic, enhancement at 100 km with natural incidence of auroral electrons 8=9929
 $\text{N} + \text{O} \rightarrow \text{NO}^+ + \text{e}$, ionization cross section calc. 8=4111
 N_2 -p collisions, 0.15-1.0 MeV, populations obs. 8=12213
 $\text{N}_2 + \text{N}_2$, reaction cross-sections 8=4310
 $\text{N}_2\text{O}^+ + \text{N}_2\text{O}$, reaction cross-sections 8=4310
 by NaCl , KCl solns. evaporation 8=4307
 Ni^{63} electron absorpt. detector 8=14505
 O atomic beam, photoionization 8=21021
 Pb , electron-impact cross-sections 8=12428
 Pm^{147} β decay, K ionization probability obs. 8=12419
 Sn , electron-impact cross-sections 8=12428
 Tc^{99} β decay, K ionization probability obs. 8=12419
 Xe atomic spectra, autoionization 8=20954
 $\text{Xe}^+ + \text{Xe} \rightarrow \text{Xe}^+ + \text{X}^+$, relative charge-transfer efficiencies of $^2\text{P}_{3/2}$, $^2\text{P}_{1/2}$ states 8=12454

gases

- See also Plasma.
 acetylene, cross-sections for 100-2000 eV electrons 8=12446
 acetylene, electronic energy levels 8=1371
 air, effect on discharging of insulators 8=15192
 air, high temp., r.f. rates meas. 8=16430
 air, ionization energy per ion pair formed by H^+ β particles 8=4315
 air, Joule heating by low-voltage d.c., 6700-7800°K and 10-20 atm. 8=12421
 air, by laser spark and resulting breakdown voltage 8=7670
 air, shock wave profiles 8=4460
 alkaline-earth metals, temperature in flames meas. 8=7946
 atoms by multiquantum absorpt. and laser coherence meas. 8=20986
 atoms, by p impact classical binary approx. calc. 8=12417
 benzene ion reactions with benzene 8=16452
 n-butane, photoionization 8=4319
 butane, probability by RPD mass spectrometry 8=21283
 in charged aerosol jets caused by aerodynamic discontinuities 8=4301
 chemi-ionization in upper atm., model 8=23307
 chloroethylene, ion-molecule reactions, study by ion cyclotron reson. spectroscopy 8=16453
 collisions, effects of excited particles 8=16373
 comet interaction with solar wind, laboratory simulation 8=23678
 conditional ionization in columnar contraction, neutral gas temp. var. effect 8=16431

Ionization—contd

gases—contd

- conductivity, electrical, approx. calc. 8=4487
 effect on discharge shape in dielectric-bounded cavity 8=7681
 electron collision cross section data, low energy bibliography 1925-1966 8=20990
 e impact of atoms and ions, Gell-Mann-Goldberger theory 8=12420
 electron impact cross sections, semi-empirical 8=1350
 by electron impact, single and double ionization, energy depend 8=21264
 electron temperature shock structure in partially ionized gas 8=4361
 electron transport coeffs., fifth and sixth approx 8=21260
 electron velocity distribution function, power series expansion 8=4300
 eqn. of state in Debye-Huckel approximation 8=10623
 ethane, photoionization 8=4319
 exploding wire discharge, precursor, rel. to gas, wire distance, press. and capacitor 8=16433
 flow over biased arbitrary bodies in side-wall of shock tube 8=10712
 fragmentation patterns, beam-modulation mass spectra 8=16439
 fusion, inertial-electrostatic confinement 8=1352
 helium, electron impact cross sections 8=1347
 hexafluoroethane, secondary ion-mol. reactions, ion cyclotron reson. 8=21284
 ideal, multiply ionized, Raizer's method of calc. degree applicability 8=21257
 ion collection from subsonic stream 8=21261
 ion-formation energy of charged particles 8=21262
 ion-molecule reactions, energy depend. 8=16432
 ion-molecule reactions, studied in corona discharges 8=12409
 ions in flow discharges, mass spectra 8=16429
 kinetic electron ejection from gas covered surfaces 8=16435
 laminar boundary layer, two temp. ionized gases 8=7900
 laser beam, <1 atm, e prod. by inverse bremsstrahlung, thin e-impact ionization 8=16434
 in magnetized plasma, and nonthermal particles 8=4351
 metallic plasma 8=4343
 methane, dissoci. attachment of electrons, isotope effects 8=16454
 methane, electronic energy levels 8=1373
 microwave meas. electron density and ionization time 8=12518
 mixture, composition and thermodynamic props. 8=12422
 mixture, slightly ionized, ion slip estimation 8=16436
 monatomic mixtures, transport props. 8=4304
 monatomic, by multi-photon absorption, ionization probability 8=7697
 multicomponent mixtures, electric conductivity max. rel. to thermodynamic parameters 7=1354
 noble-gas mixtures, by fission fragments, rel. to thermionic energy conversion 8=15215
 nonuniform electrical conduction in MHD channels 8=16437
 optical pot. in terms of self-energy of single particle Green's function 8=20992
 between parallel plates, field distortion, calc 8=21248
 partially, in elect. and magnetic field, e vel. distrib. calc. 8=12423
 Penning, by metastable He atoms 8=21258
 photo, in soft X-ray range, Z depend. in central pot. model, calc. 8=12418
 photoelectron spectrometer, single grid 8=16441
 photoionization, microwave plasma light source 8=3355
 plasma, collisional rel. to spectra 8=12470
 plasma generation, equilibrium and non-equilibrium states 8=288
 plasma, two-temp., inelastic losses and population of levels 8=12460
 prebreakdown spark discharge, channel parameters 8=7671
 propane ion reactions with mols. 8=14381
 propane, photoionization 8=4319
 radiolysis systems, ion lifetimes meas. 8=23163
 rare gases, ionic wave propagation excited by impulsion 8=12427
 shock wave investigation pipe 8=4305
 by short laser pulses, many-photon interact. 8=399
 solar corona, effect of doubly excited levels 8=2863
 stellar atmospheres, line-blanketing 8=14761
 Townsend coefficients, influence of photon absorption 8=7699
 Townsend-Huxley swarm techn., space charge effects 8=7698
 Ar, beam scattering, short range forces 8=1364
 Ar, behind shock front, ioniz. relaxation 8=1356
 Ar, caesium-reeded, tensor electrical conductivity, third Chapman-Enskog approx. 8=12432
 Ar, cross-sections for 100-2000 eV electrons 8=12446
 Ar, by evaporated Fe atoms, ionization ratio meas. 8=1359
 Ar, gamma and neutron irradiated, wall effect 8=1363
 Ar, to ground and excited states of Ar^+ , cross-sections 8=21267
 Ar, ionization energy per ion pair formed by H^+ β particles 8=4315
 Ar, near threshold by electron impact 8=7711

Ionization—contd**gases—contd**

- Ar, rate measurement by spectrograph 8=7709
 Ar, shock layer e density meas 8=21265
 Ar by shock wave, electron density and collision freq. microwave obs. 8=12431
 Ar, shock wave interferometry 8=4311
 Ar, structure of normal ionizing shock wave 8=21490
 Ar supersonic flow, by h.f. induction, electronic and ionic properties 8=21266
 Ar⁺, highly excited, autoionization prod. by electron impact 8=12430
 Bi₁ and Bi₂, electron-impact fragmentation 8=4239
 C, chemi-ionization on gaseous oxidation 8=5699
 CO, kinetic energies in time-of-flight mass spectrometer 8=7721
 CO₂, by electron impact, absolute cross section 8=21268
 CO₂, due to electron impact, curve shape 8=12434
 CO₂, by evaporated Fe atoms, ionization ratio meas. 8=1359
 CO₂, Franck-Condon factors calc. 8=21269
 CO₂, ionization energy per ion pair formed by H³ particles 8=4315
 CO₂, ions and fragments, sequential mass spectrometry 8=21270
 CS₂, ions and fragments sequential mass spectrometry 8=21270
 Cs, absolute values of cross-section close to threshold 8=12436
 Cs, by resonance irradi. by Cs vapour discharge 8=4362
 Cs, two-quantum photoionization rate 8=12437
 Cs vapour, decay microwave cavity studies 8=21271
 Cs₂⁺ form. by collision of two excited atoms 8=12438
 D, mag. drift vel. and deflection coeff. for slow electrons 8=7712
 D, temporal growth and secondary processes 8=12439
 D₂ autoionization, kinetic energy 8=12443
 H atom, multiphoton process 8=12440
 H, gamma and neutron irradiated, wall effect 8=1363
 H and other ions, collision cross-sections determ. by ion cyclotron reson. 8=12442
 H, mag. drift vel. and deflection coeff. for slow electrons 8=7712
 H₂⁺, collision-induced excitation, angular dependence 8=1362
 HCl, γ -irrad., ion lifetimes 8=23164
 H₂O, partial photoionization cross-sections by photoelectron spectra 8=1369
 H₂O vap., irradi., H⁺ solvation, kinetics and thermodynamics 8=18661
 He⁴⁺ beam prod. by charge exchange with K 8=15347
 He, autoionization by collisions 8=7714
 He, autoionizing D states, character 8=12445
 He autoionization, kinetic energy 8=12443
 He, beam scattering, short range forces 8=1364
 He, cross-sections for 100-2000 eV electrons 8=12446
 He, double by photon, e, atomic correl. effect 8=7715
 He, electron impact cross section 8=16446
 He, electron and proton impact, classical model 8=12444
 He, by evaporated Fe atoms, ionization ratio meas. 8=1359
 He⁺ + H₂ and He⁺ + HD reactions 8=21277
 He⁺ photoionization reactions with N₂ and O₂ 8=16444
 I, photo detachment probability due to two-quantum absorpt. 8=12437
 I₂, in supersonic Hg vapour jet, charge distrib. 8=7716
 K, electron-impact ionization, empirical calculations 8=12448
 K vapour, charge exchange H⁺ to H⁻ 8=12441
 K vapour, photoionization 8=12447
 Kr, beam scattering, short range forces 8=1364
 Kr, by evaporated Fe atoms, ionization ratio meas. 8=1359
 Li, electron-impact ionization, empirical calculations 8=12448
 Li, electron and proton impact, classical model 8=12444
 Li, photoionization cross section as function of wavelength 8=7717
 N, electron and proton impact, classical model 8=12444
 N₂ afterglow 8=21239
 N₂, by e collisions 8=16448
 N₂, electron impact cross sections 8=1348
 N₂, by evaporated Fe atoms, ionization ratio meas. 8=1359
 N₂, ionization energy per ion pair formed by H³ particles 8=4315
 N₂, kinetic energies in time-of-flight mass spectrometer 8=7721
 N₂, partial photoionization cross-sections by photoelectron spectra 8=1369
 N₂⁺, absolute electron impact excitation cross-section 8=7720
 NH₃, photoionization 8=4314
 N₂O, due to electron impact, curve shape 8=12434
 N₂O, photoionization 8=16449
 N₂O, photoionization coeff., 600-1000 Å 8=16447
 NO, kinetic energies in time-of-flight mass spectrometer 8=7721
 NO₂, photoionization 8=16449
 NO₂⁺ production by electron transfer from O⁺, O₂⁺, O₃⁺ and OH 8=1367
 NO₂, rate of electron attachment 8=12449

Ionization—contd**gases—contd**

- Na electron-impact ionization, empirical calculations 8=12448
 Na-like atoms, structure of ionization curves 8=21256
 Ne, beam scattering, short range forces 8=1364
 Ne, cross-sections for 100-2000 eV electrons 8=12446
 Ne, by evaporated Fe atoms, ionization ratio meas. 8=1359
 Ne, rate temp. dependence correction 8=12450
 Ne, e-temp. depend. of e-ion recombination 8=12351
 O, atomic, photoionization cross sections for $\lambda > 25\text{Å}$ 8=12452
 O₂, by e collisions, comparison with photoionization 8=16451
 O, electron and proton impact, classical model 8=12444
 O II, equilibrium population of states in plasma 8=7418
 O₂, electronically excited, photoionization 8=16450
 O₂, electron impact cross sections 8=1349
 O₂, by evaporated Fe atoms, ionization ratio meas. 8=1359
 O₂ by extreme u.v. radiation produced on O₂ dissociation by e-collisions 8=7722
 O₂, ionization energy per ion pair formed by H³ particles 8=4315
 O₂, partial photoionization cross-sections by photoelectron spectra 8=1369
 O₂, photoionization and dissociation meas. 8=12453
 O₂, secondary ionization coeffs. at press. up to atm. 8=4316
 O₂, thermal electron capture 8=7723
 SrI, 5s² 1S_g-4dnp, nf spectrum, analysis of autoionization resonance structure 8=20968
 TaO⁺, transition, in TaO electronic bands rot. anal. obs. in arc between Ta rods 8=1267

liquids

- acetic acid, ionization const. in propanol-H₂O mixtures 8=21720
 aqueous solutions, dissociation rate from ultrasonic relaxation study 8=18712
 carrier mobility estimation 8=4612
 energy to create ion pair in dielec. liqs. 8=21723
 hydrocarbons, energy to create ion pair 8=21723
 ionic recomb. rate, electrostatic model 8=4611
 nonpolar, by X- and γ -irrad., theory of separated ion pairs 8=2539
 LiNO₃ solns., ion assoc. 8=21715
 NaClO₄ solns., ion assoc. 8=21716

solids

- alkali halides, ion overlap meas. by strain polarization 8=23003
 anthracene, autoionization and exciton annihilation 8=17890
 in cold gas 8=2274
 colour centres, F⁺, photo-ionization theory 8=8740
 crystal fields, energy level integrals 8=1628
 semiconductors, radiative capture by impurities 8=5228
 Ag, K-ionization by relativistic electrons, theory 8=4994
 GaAs, due to high field domains and subsequent recombination processes 8=2192
 GaAs, impurity photoionization, quantum defect study 8=2207
 GaAs-GaP 50% alloy, impact, and charge transport 8=18038
 Ge, impurity photoionization, quantum defect study 8=2207
 Ge(Li), γ -ray detector current pulse generation 8=11430
 Hg-Mo system, mobility, work function 8=21903
 Hg-W system, mobility, work function 8=21903
 K-ionization by relativistic electron theory 8=4994
 Si detectors, measurement of effect within solid from which constructed 8=2212
 Si, impact, transition probability 8=13665
 Si, impurity photoionization, quantum defect study 8=2207
 Si surface barrier detection, pulse height defect 8=3465
 Sn, K-ionization by relativistic electrons, theory 8=4994

Ionization, atmosphere

- See also Atmosphere/radioactivity; Ionosphere.
 density profiles and e.m. wave propagation 8=9909
 EAS radio pulses due to slow electron movement in elect. field 8=15900
 F region, vertical displacements, apparent-vel. distribution rel. to geomag. latit. 8=23416
 in F₂, space-time distribution at high southern latits. 8=23421
 interaction with space vehicles, book 8=14706
 ionosphere, low-lying nocturnal N(h) profiles 8=23397
 meteors, possible cause of geomagnet. micropulsations, math. model 8=2734
 oxygen line excitation, and heating, by conjugate photoelectrons 8=18975
 photoelectrons, ionospheric, velocity distribution and Landau damping near 600 km 8=23362
 sporadic E layer, positive ion comp., Aerobee rocket obs. 8=14685
 by thermonuclear explosion γ -glow 9 July 1962, riometer obs. validity 8=14636
 topside, spread, Alouette 1 obs. 8=2714

Ionization, surface

- See also Electron emission, thermionic; Ion emission/thermionic; Work function.
 dyes, adsorbed, energy 8=5424

ionization, surface—contd

- ion source for various elements 8=15348
 magnetron anodes, occluded gas ions 8=15334
 Saha-Langmuir equation and application, modifications 8=13949
 substrate in equilib. with ionized vapour, adsorpt. on and emission from 8=18263
 and thermionic emission, stress depend. 8=13946
 Ba, on W surface, coeff. meas. 1800-2600°K 8=18288
 Cs plasma, in mag. confinement device 8=1415
 Cs thermionic converter, departure from Saha-Langmuir ionization reln. 8=15238
 Mo, positive and negative 8=13950
 Pt, of K, Rb, Cs and Tl atomic beams 8=12110
 W, of K, Rb, Cs and Tl atomic beams 8=12110
- ionization chambers**
 accelerator beam loss monitor, applic. 8=20227
 bremsstrahlung meas. with scintillation spectrometer 8=3582
 calibration factors for low-energy γ -ray emitters 8=11431
 calorimeter, simulation of operation 8=15635
 cavity, fabrication, low cost 8=6640
 for double pulse, for fission energy and mass distrib. obs. 8=1106
 environmental radiation, new obs. technique 8=20190
 fission chamber, employed for reactor n flux meas. 8=4026
 n-hexane, recombination after irradiation with γ -rays 8=6628
 human tissue equivalent response 8=606
 for leakage of bremsstrahlung energy from calorimeter absorber meas. 8=11447
 magnetron gauges, gas pressure conversion consts. 8=7958
 X-ray dosimetry 8=15595
 Ar, extreme u.v. absolute detectors, comparison with thermopile 8=11162
 C⁶⁰ absolute γ -activity obs. 8=20749

ionization gauges. See Vacuum gauges.

ionization potential

- acetylene 8=1371
 benzene, σ states 8=12257
 benzene, SCF calc. 8=7565
 chloroform under 120 atmospheres with dissolved O₂ and electron donors 8=7708
 contact charge transfer spectra for evaluation 8=7708
 diphenyls, 4-monosubstituted, rel. to absorpt. peak shift, obs. 8=4212
 1,4-distyrylbenzenes, 4-monosubstituted, rel. to absorpt. peak shift, obs. 8=4212
 N-heterocyclic mols., from charge-transfer absorpt. of complexes 8=12455
 hydrogenic atom, lowering effect and e partition energy 8=1157
 methane 8=1373
 pyridine positive ion, MO calc. 8=12294
 reaction rates dependence on I.P. 8=14357
 trans-stilbenes, 4-monosubstituted, rel. to absorpt. peak shift, obs. 8=4212
 terphenyls, 4-monosubstituted, rel. to absorpt. peak shift, obs. 8=4212
 Ar-C₂H₂ mixture, defect meas. 8=7710
 Be⁺, e affinity calc. by superposition of configurations 8=21281
 Br, atomic, rel. to new Rydberg series of absorpt. 8=1165
 CF₃ free radical 8=7724
 C₆H₆⁺ 8=21120
 C₆H₅F⁺ 8=21120
 CO, in time-of-flight mass spectrometer 8=7721
 CO, to CO₂²⁺, by sequential mass spectrometry 8=21270
 CS₂ to CS₂²⁺, by sequential mass spectrometry 8=21270
 Cl, atomic, rel. to new Rydberg series of absorpt. 8=1165
 F, atomic, rel. to new Rydberg series of absorpt. 8=1165
 I, atomic, rel. to new Rydberg series of absorpt. 8=1165
 K⁺, e affinity calc. by superposition of configuration 8=21281
 Li⁺, e affinity calc. by superposition of configuration 8=21281
 Mg⁺, e affinity calc. by superposition of configurations 8=21281
 N₂, in time-of-flight mass spectrometer 8=7721
 NH₃ 8=4314
 NO, in time-of-flight mass spectrometer 8=7721
 Na⁺, e affinity calc. by superposition of configuration 8=21281
 of Na atom clusters, up to 8 atoms, rel. to metallic props. 8=16231

ionized gases. See Ionization/gases; Plasma.

ionosondes. See Ionosphere measuring apparatus.

ionosphere

- See also Electromagnetic wave propagation/ionosphere.
 absorption of cosmic noise on 25 MHz, effect of solar eclipse of May 20, 1966 8=9979
 absorption, at low latitude, geomag. anomaly 8=23352
 absorption, solar cosmic rays, review 8=18997
 absorpt. var. rel. to solar protons 8=2687
 acoustic-gravity waves: model wave eqn. solved 8=2686
 activity, July-Sep. (1965) 8=19053
 activity, Oct-Dec (1965) 8=19054
 activity, Jan-March (1966) 8=19055

Ionosphere—contd

- antarctic, irregularities, seasonal maps at sunspot min. 8=9987
 auroral absorption of cosmic noise in conjugate high latit. regions 8=23335
 auroral absorption rel. to luminosity, narrow beam obs. 8=23338
 auroral absorption structure over 300 km and conjugate region correlation, obs. 8=18987
 auroral, elect. fields parallel to mag. field, expt. investigation 8=23354
 auroral electrojet circuit, closure soln. from magnetosphere meas. 8=9951
 auroral, electron density, r.f. capacity probe obs. 8=2666
 aurora electron precip., bremsstrahlung obs. 8=2635
 auroral, electron temp. and flux obs. indicating geomag. caused layer structure 8=9938
 aurora, proton, secondary ionization processes 8=14683
 auroral radar echoes rel. to particle precipitation satellite obs. 8=9942
 aurora radar echoes, wavelength dependence and aspect sensitivity 8=2637
 auroral zone, winter, total electron content and variations 8=9960
 auroral-zone X-ray events, pulsating, E-W movement balloon obs. 8=18943
 backscatter, h.f., synthesis assuming irregularity motion at constant height and speed 8=23401
 blackouts in polar cap and auroral zones rel. to solar wind activity, 1957-65 8=23363
 Canadian national report 8=14639
 composition and reactions 8=23361
 composition and temp. from topside sounder electron scale height data 8=2665
 cosmic noise absorption rel. to micropulsations of impulsive Pi subtype 8=2736
 coupling with outer magnetosphere, rel. to geomag. field topology 8=9910
 dissipation as limitation to magnetospheric convection 8=9918
 disturbances, travelling ray tracing simulation of h.f. radio obs. 8=23392
 disturbance due to SF₆ release near F2 peak, ray tracing synthesis of ionogram obs. 8=23383
 drifts, comparison of anal. methods 8=19000
 drift and diffusion, review 8=18999
 drifts over mag. equator, seasonal var. obs. 8=19016
 drifts, 3D, statistical determination 8=9990
 drifts, winter, during quiet-sun period 8=19004
 E and F1, sub-peak electron content diurnal asymmetries 8=10009
 E-W trough of low I_p, inference from Explorer 20 reception of Loran transmissions 8=2684
 electric currents induced by nonperiodic winds 8=23387
 electric field meas. 8=9913
 electrojet, equatorial, in India, prelim. results 8=18948
 electrojet, equatorial, model involving meridional currents 8=18949
 electrojet equatorial Sq currents, S. America IGY obs. 8=2640
 electromechanical wave propag. by refraction 8=19566
 electron beam attenuation at different levels 8=18972
 electron conc. diurnal vars. and temp. changes, 160-200 km 8=23355
 electron concentration profiles, prediction 8=23393
 electron concentration profiles during sunspot maximum and minimum 8=23357
 electron conc. and temp., sounding rocket obs. 8=23396
 electron content, abnormal increase, search for explanation 8=14665
 electron content, daily variation February-March and July-October 1964 from Sputnik obs. 8=5805
 e-content distrib. parameters 8=2659
 e-content, Early Bird meas. using Faraday effect 8=2662-3
 e-content, geographic var. 8=2664
 electron content and horizontal gradient by satellite signals above Haifa, Israel 8=14669
 electron content irregularities, satellite obs. 8=2668
 e-content meas. at Delhi from Faraday fading 8=2658
 e-content meas. by Syncom-3 with Faraday effect 8=2661
 electron content over Texas from Faraday rotation of radio waves from satellites 8=14663
 electron content over Texas from satellites obs. 8=5802
 e content, total, from Faraday fading of Explorer 22 signal 8=2660
 e-content, total, depend. on geomagnetic activity 8=2657
 electron density ang. distrib. in wake of satellite 8=14664
 electron density data, estimation of solar-flare spectra from 8=10425
 electron density, detm. by coherent frequency method 8=14670
 electron density, lunar tidal variations at fixed real heights 8=9962
 electron density, lunar tidal variations near magnetic equator 8=2656
 electron density perturbations, rocket obs. 8=9968
 electron density profiles, determination from ionograms, review 8=2699

Ionosphere—cont'd

electron density profiles, higher derivatives rel. to virtual-height slopes 8=2696
 electron-density profiles, ionograms, data extraction using computers 8=2702
 electron density profiles, ionogram real-height problem, computer formulation 8=2701
 electron density profiles, real-height determination from ionograms 8=2700
 e and ion accel. by mag. solitary waves 8=2620
 electron number densities, by wave interaction expt., limitations 8=14658
 electron precip. from outer radiation belt 8=23360
 electron temp. and ion density using sounding rockets obs. 8=2654
 electron total content latitude variation and refraction correction 8=9965
 electron total content, peak concentration and equivalent slab thickness variations 8=9966
 electrons, total no., and gradients, from Elektron signal obs. 8=18971
 equatorial anomaly, E. Asian zone of Pacific 8=19003
 equatorial anomaly peaks rel. to movement and shape of airglow arcs 8=23390
 equatorial, total electron content, latitude variation 8=9967
 Galactic radio noise attenuation, 25 and 21.3 MHz, Ahmedabad, 1957-64 8=14673
 heat conduction waves propag. 8=2614
 heating during storm by hydromagnetic waves 8=23386
 height, virtual, meas. errors using phase ionosonde 8=9992
 high-latitude, effect on u.l.f. e.m. radiations 8=9971
 hydromagnetic gradient waves 8=14674
 induced currents and sudden mag. storms, explanation 8=2729
 inhomogeneities, correlation analysis applicability 8=9993
 internal gravity wave propag. rel. thermal conditions 8=9994
 investigations, at NIRFI for 1957-1967 8=23369
 ion composition and recombination coeff. var. 8=9961
 ion-molecule reaction rates 8=18973
 ion temperature, Elektron 2 satellite obs., 4000-8000 km 8=14659
 ionization, low-lying nocturnal N(h) profiles 8=23397
 ionization-neutralization constants and dynamic processes 8=23391
 ionograms, multifreq., conversion to electron density profiles 8=2695
 ionograms, overlapping-polynomial analysis 8=2698
 ionograms, true heights at selected freq. by 10 point reduction method 8=2693
 irregularities caused by earthquake acoustic waves 8=23395
 irregularities, isolated, rocket studies 8=14679
 irregularities, large, changes in size and electron density obs. 8=9988
 irregularities, large scale, radio interferometer obs. 8=9986
 irregularities, large scale, spatially and temporally periodic disturbances 8=23385
 irregularity magnitudes, deduction from backscatter 8=23394
 irregularities, nocturnal radio star obs., 22-38 MHz, Puerto Rico 8=9989
 irregularities, sub-auroral, satellite scintillation transition obs. 8=18945
 Jupiter, decametric radiation, effect 8=2819
 local electron conc., determ. from Doppler dispersion meas. of satellite radio beacons 8=23358
 lower, electron concentration and collision freq. from rocket obs. 8=9963
 lower, electron content inhomogeneities 8=9964
 lower, electron density distrib. through impact and photoionization 8=18969
 lower regions, review 8=19011
 lower, wind profiles from rocketsonde parachutes 8=2681
 lunar tidal variations in equivalent slab thickness over Hawaii 8=9991
 rel. to magnetic storms, e conc. at 640 km 8=2667
 magnetodynamic turbulence at low mag. Reynolds number 8=19813
 meteor echoes during v. h. f. forward scattering, diurnal and seasonal vars. 8=19267
 model for e.m. wave propag., viscosity and thermal cond. effects 8=19903
 monotonic and nonmonotonic models, virtual height tables 8=2688
 morning ionospheric perturbations, relation with v.l.f. emissions 8=23318
 motion of low energy charged particles in geomagnetic field, perturbing forces effects 8=19052
 movements, real 90 km, v.l.f. cross spectrum meas. 8=14677
 neutral-positive ion reactions, laboratory rate coefficients 8=14662
 N(h) parameters, vars. during IGY and IQSY 8=18970
 night, negative ion conc. rel. to sub-e.l.f. var. of Earth's mag. field 8=14699
 nocturnal movement of disturbances, vertical 8=9995
 no-echo occurrences and absorption of cosmic radio noise 8=9980

Ionosphere—cont'd

no-echo occurrences using ionograms data 8=9999
 noise and geomag. micropulsations, review 8=18995
 outer region, to 2000 km, review 8=19018
 outer, transition to interplanetary medium 8=2689
 oxygen line excitation and heating, by conjugate photoelectrons 8=18975
 PCA midday recovery, Sept. 2, 1966, end-phase obs. 8=14661
 parameter calc., manual, using single polynomial analysis 8=2694
 phase perturbations, v.l.f., produced by solar protons February 5, (1965) 8=18990
 phase refractive indices, use on reducing $h'(f)$ waves to N(h) profiles 8=2697
 photoelectron heating efficiency 8=23359
 photoelectrons, 7-20 eV, velocity distribution and Landau damping near 600 km, radar scatt. obs. 8=23362
 plasma scale height, local, error minimization 8=2691
 polar caps, electric currents 8=23351
 polar, electron density and radio absorpt. during solar event, 1961 8=2655
 positive ion-neutral reactions, rate coeffs., laboratory meas. 8=14657
 precursor whistler generation, obs. 8=18895
 proton gyroresonance observed in incoherent scattering of e.m. waves 8=2669
 radar backscatter from vehicle wake 8=14676
 radar determination of electron content, effect of density fluctuations 8=5803-4
 radio aurora and electric current, two-stream plasma instability model 8=2638
 radio behaviour, indices, book 8=19005
 r.f. waveguide regions below F_2 layer maximum 8=14675
 radio pulse reflections received by E-W aerial, anomalous phase path variations 8=9978
 radio signals, incoherently scattered, and meas. electron conc. profiles 8=23398
 radio waves, group path-phase path relation 8=385
 riometer quiet day curve determination 8=9997
 rotating and stratified non-rotating fluids, analogous behaviour 8=1445
 S-current system and 10.7 cm radio noise flux, study of Schmidt's phenom. 8=18968
 satellite, electron-emitting, pot. build-up, theory 8=14710
 solar eclipse effects of May 30, 1965, obs. 8=9959
 SIDs and geomag. rel. to solar activity, review 8=18996
 solar radiation, and gravit. tides, contrib. to geomag. var., calc. 8=14678
 solar X-ray flare, effects 8=18967
 soundings, oblique, and ray tracing, nomenclature 8=2690
 statistical props., effect on radio absorption meas. 8=9973
 storms, review 8=19002
 sudden freq. deviations, rel. to solar flare X-radiation 8=9985
 temp. and density from ALO trail obs., 105-165 km 8=2613
 tides at 90 to 120 km from wind distribution obs. 8=18998
 topside, over the Americas, Alouette I obs. 8=2652
 topside, corpuscular radiation effects, ionogram obs. 8=2709
 topside, use of ionograms for electron distribution determ. 8=2704
 topside proton gyro-effects, Alouette 1 obs. 8=2685
 u.l.f. emission rel. disturbances, mag. activity and earth current var. 8=9974
 Venus, re-examination of porous model 8=14848
 vertical elec. soundings, methods of interpretation 8=19007
 v. h. f. aurora at sunspot maximum, echo movement obs. 8=9947
 v.l.f. amplitude perturbations, Antarctic, due to Starfish explosions July 9, 1962 8=23389
 v.l.f. hiss at very low L values, obs. 8=23353
 waves, period ~ 1 minute, due to nuclear explosions, obs. 8=23388
 wide band signal reception and inhomogeneities 8=23364
 winds, nocturnal variation from gun projectile luminous trail obs., Barbados 8=2683
 wind parameters, statistical meas. 8=19001
 wind system, middle and upper, derivation 8=9996
 H distribution, solar cycle and diurnal variations 8=2615
 H⁺ temp. determ. from proton whistlers 8=23356
 N₂ atomic, enhancement at 100 km with natural incidence of auroral electrons 8=9929
 N₂⁺ reaction with O₂, rate coeff., study by photo-ionization mass spectra tech. 8=14666
 N₂⁺, NO⁺ dissociative recombination rates 8=9961
 O⁺ concentration and temp., equatorial, Dec. 65, March-May 66, Jicamarca 8=18974
 O⁺ reaction with O₂ and N₂, rate coeff., study by photo-ionization mass spectra tech. 8=14666
 O⁺ + O₂ → O₃⁺ + O rate constants energy var., drift tube meas. 8=14667-8
 O₂⁺ dissociative recombination rate 8=9961
 O₂ reaction with N₂ and NO, rate coeff., study by photo-ionization mass spectra tech. 8=14666

D-region

disturbance by radio pulse, electron concentration var. estimation 8=10000

Ionosphere—contd

F-region—contd

- electron density distribution obs. 8=14681
- electron density distributions from propagation data 8=5808
- electron densities during IQSY's at 19°S, 35°N, 60°N and 69°N 8=10001
- equatorial, u. h. f. radar returns from 75 km 8=10002
- formation, effect of corpuscular streams and electron photo-detachment 8=14682
- height from analysis of N(z) profile 8=23403
- midlatitude, winter anomaly 8=19009-10
- upper atm. >40 keV e flux rel. to form, <100 km 8=14680

E-region

- current system rel. to equatorial anomaly 8=10008
- drift meas., comparison of similar fade and max. cross correl. methods 8=14684
- drift velocity, height var. obs. 8=23411
- Es, blanketing freq. and occurrence vars., latit. ± 600 8=2706
- E_s clouds, mid-latitudes, v.h.f. forward scattering obs. 8=10006
- foEs, dependence on absorption 8=19015
- E_s layer, disturbances, velocity and direction of propagation 8=23415
- E_s parameters fb, f and fo, physical significance from simultaneous rocket and ionosonde obs. 8=23414
- Es, range of semitransparency 8=23406
- f_oE, ratio of morning to afternoon values 8=23408
- Es stability coeff. calc., nomogram 8=23407
- electron and ion temps., by Thomson diffusion 8=23410
- F2 ionization drift rel. to current systems in dynamo region obs. 8=23420
- irregularity magnitude calc. 8=23394
- recombination coefficient and coronal contribution to ionosphere, solar eclipse obs. 8=19014
- recombination coefficient, effect of ion vibration level 8=23409
- resonance relaxation sounder for electron density 8=19012
- scattering propagation caused by field aligned irregularities on v. h. f. band, obs. 8=5809
- solar daily disturbance var., 1961-64 8=14687
- sporadic, auroral 'flat-type', rel. to mag. disturbance 8=10005
- sporadic cutoff freqs., long periodic vars. 8=23405
- sporadic, cut-off freq. var. 8=10007
- sporadic-E, correlation with meteor activity 8=10362
- sporadic E, form. in middle latitudes 8=23412
- sporadic rel. to mag. activity 8=10004
- sporadic and mag. activity 8=23404
- sporadic rel. to meteoric and magnetic activity 8=2707
- sporadic E layer, positive ion comp., Aerobee rocket obs. 8=14685
- sporadic E, prod. near geomagnetic pole 8=19013
- sporadic layers in temperate zone, formation allowing for neutral wind profile with descending phase vel. 8=23413
- sporadic, effect of wind on, formation time constants 8=2708
- sporadic, E, and wind struct. 8=14686
- wind structure and meteor influx from sporadic E blanketing freqs. obs. 8=2705
- wind velocity and diffusion coeff. at 96 km from artificial luminescent cloud obs. 8=10003
- OH(8, 3) band, OI 5577 Å line and continuum at 5775 Å, nocturnal, mid-latit., rocket obs. 8=2631

E-region

- conjugate regions, rectilinear model 8=10011
- densities and temps. at sunspot minima, 1964 8=14688
- disturbances, vertically moving and rel. structure 8=10013
- e. m. wave whispering gallery, expt. design 8=2716
- electron content, peak density height and characteristic thickness, synoptic obs. 8=2713
- electron density peak, seasonal, non-seasonal and semi annual var. 8=5810
- electron-ion gas distribution, vertical, with weak diffusion flux sources 8=10014
- electron temp. from cosmic noise absorption at 25 and 21.3 MHz 8=10015
- equatorial, F2, electron content anomaly, obs. 8=2719
- F1, solar daily disturbance var., 1961-64 8=14687
- F2, electron concentration rel. to 10 cm solar flux 8=23423
- F-2, electron loss rate, effect of high altitude nuclear explosion 8=14691
- F2, equatorial meridional winds and e. m. drifts 8=10020
- F2 equatorial night, max. rel. to electrodynamic drift 8=14690
- F2, field aligned layers, satellite signal Faraday rot. obs. 8=2715
- F2, height of peak at middle and high-latitudes, effect of atmospheric winds 8=10022
- F2, ionization space-time distribution at high southern latits. 8=23421
- h_pF2 latitudinal variations of (m-3000)F2 and statistical result 8=23422
- F-2 layer, changes in electron densities and heights due to nuclear explosions 1962 8=2721
- F2, low and mid latits., electron concentration diurnal obs. 8=2720

Ionosphere—contd

F-region—contd

- F2, noon electron density lunar tides 8=23424
- F2, obs. during 5 different storms 8=2718
- F2 peak, effect of meridional winds in neutral air 8=10019
- F2, response to upper atmospheric neutral temp. and geomag. activity changes, obs. 8=10018
- F2, summer-night in mid-latits., abnormal f_o diurnal vars. due to large electron conc. 8=23425
- F2, temp. from electron conc. profiles 8=10021
- F2 during 3 solar eclipses, obs. 8=2717
- geographic distribution of electrons, approx. 10 ev. 8=23417
- global morphology, structure and processes, review 8=19017
- IF2 index, system, based on this, for prediction of radiowave conditions 8=18991
- ionization spread, Alouette 1 obs. 8=2714
- ionization vertical displacements, apparent-vel. distribution rel. to geomag. latit. 8=23416
- irregularities, effects on radiowave propagation, book 8=18978
- midlatitude electron and ion temps. at sunspot minimum 8=14689
- nighttime ionic velocities obs. and recombination calc. 8=19020
- nocturnal behaviour and maintenance 8=19022
- nocturnal drifts over Thumba, obs. 8=19023
- polar at sunspot min., mean structure and storm-time changes, Alouette 1 data 8=19021
- profile parameters from routine world netwk. obs. 8=2711
- radio beam transmissions, effect on critical freq. and isoconcentration surfaces 8=19019
- radio reflection phenomena, high latitudes associated with atmospheric winds at certain universal times 9=10012
- spread, nocturnal, rel. to mag. activity at Kodaikanal 8=10010
- spread-F occurrence over half sunspot cycle 8=23419
- sunrise effect in summer, onset time and plasma temp. rise 8=23402
- topside, delay of remote-resonance ionogram traces, explanatory model 8=2712
- topside, m. f. conjugate echoes, Alouette II sounder obs. 8=18981
- during total solar eclipse, May 20, 1966, obs. from 6 African stations 8=2710
- travelling disturbance associated with nuclear detonations 8=10016-7
- travelling disturbance following low-altitude nuclear explosion, spatial model 8=23418
- v. l. f. wave normals, influence of horizontal e density gradients on direction 8=23367

Ionosphere measuring apparatus

- field height, mean, from fading of satellite transmissions 8=9998
- ionograms, precautions for identifying no-echo occurrences 8=9999
- panoramic vertical soundings data processing 8=2703
- phase ionosonde, virtual height meas. errors 8=9992
- probe, Faraday cup type assembly 8=23400
- probes, effect of plasma sheath, book 8=14706
- r. f. capacity probe 8=2666
- resonance relaxation sounder for electron density 8=19012
- riometer quiet day curve determination 8=9997
- satellites, for electron content over Texas 8=14663
- satellite plasma expt., laboratory simulation 8=2692
- sounding, multiple freq., scanning range 50 KHz to 15-20 MHz 8=19006
- sounding rockets, positive ion density and electron temp. at 140 km, 360 km and 1824 km 8=2654

Ions

- See also Atoms; Ion emission/thermionic; Molecules; Plasma.
- in air, density profiles in expanded shock tube flows 8=15050
- atomic, elastic and resonant exchange cross-sections 8=4104
- in chloroethylene, reactions with molecules, study by ion cyclotron reson. spectroscopy 8=16453
- collection in Bayard-Alpert gauge, calc. 8=4306
- in crystals, with incomplete shells, spectra calcs. rel. to structure parameters 8=13033
- in crystal, 3d⁺ configs. splitting by octahedral field 8=1654
- cycloparaffins, chem. ionization mass spectra 8=1374
- detector for fast scanning mass spectrometer 8=1141
- diffusion with var. elec. and mag. fields by violation of 3rd adiabatic invariant 8=7706
- dihydroanthracenes and their Li salts, ion-pair struct. from n. m. r. 8=7559
- 1, 1-dimethoxy-2, 4, 6-trinitro-benzene ion, structure 8=8572
- gauge based on storage in 3D rot. symm. quadrupole field 8=19799
- identification, and metastable transition meas., by semi-automated mass spectrometer 8=1138
- in ignited thermionic converter, generation mech. rel. to electron energy distrib. 8=15221
- inactive, induced optical activity 8=16214

Ions—contd

- inert gas in W surface, interaction energy rel. to trapping of 8=13081
 interactions, second-order three-body, with Gaussian wavefronts 8=7457
 ionospheric ion-molecule reaction rates 8=18973
 ion slip in slightly ionized gas mixture 8=16436
 d^{2+} ions in tetragonal cryst. fields, e.p.r. and optical spectra 8=21798
 ketones, aromatic, decomp. rel. to charge and radical sites 8=4308
 line broadening, influence of elastic collisions 8=12099
 in liquids, short-range non-Coulombic interactions rel. to thermodyn. and electrokinetic props. 8=21602
 in liquid He, vortex ring formation, evidence for peeling model 8=10797
 mass spectrometry, anomalous glow discharge 8=7658
 metal, promotion of atom-transfer oxidation-reduction reactions 8=14401
 movement in gases, under influence of electric fields 8=7705
 multiply-charged, appl. in gas laser 8=15449
 negative, config. rel. to neutral, obs. effects 8=4140
 negative, effect on double space-charge sheaths 8=16549
 negative, in late-type stars 8=10154
 nitrate in alkali halides, lattice vibration and i. r. absorption spectra 8=17471
 nonexistent molec. ions, detect. 8=16440
 organic, non-classical, 1,2-rearrangements, MO description 8=21057
 oxalate, i. r. and Raman spectra and symmtry 8=21154
 pair association constants and solvent composition 8=8009
 pair form. in liquid membranes, transport and elect. props. 8=4560
 plasma, hydromagnetic Larmor radius included in collision damping theory 8=12486
 positive, detection efficiency of a continuous channel electron multiplier 8=6635
 in radiolysis systems, lifetimes meas. 8=23163
 reacting system with drift, vel. calc. 8=7704
 relative equilibrium in rotating system of reference 8=7674
 removal from plasma, acoustic wave generation 8=12569
 S-state, dipole polarizabilities, bounds, from oscillator-strength sum rule 8=7373
 spectra, first transition ion impurities in solids 8=14171
 temp. and density in theta pinch plasma, laser scatt. expt. 8=16553
 transition metal, recent Japanese work 8=16992
 transport in redox reactions of living cell, rel. to separation of positive and negative charges 8=23762
 trapping in 3D rot. symm. field rel. to meas. spectrometer 8=19800
 tribromide, charge distrib. in different crystals. 8=5567
 X-ray scattering factors calc. from Hartree-Fock wave functions 8=16189
 Ar binary mixture glow discharge, mass analysis 8=7665
 in Ar, density profiles in expanded shock tube flows 8=15050
 Ar in ZnO:Zn, energy loss and phosphor deterioration depth obs. 8=18624
 Ar⁺ and Kr⁺, multielectron ionization in close collisions, with Ar and Kr atoms 8=21012
 Ar²⁺, identification from mass spectra 8=12056
 Ar₂⁺, identification from mass spectra 8=12056
 BO₂⁺ in alkali halides, vibr. spectrum and bonds, obs. 8=22946
 C⁴⁺ ionization by e impact, cross-sections calc. 8=12435
 C⁵⁺ ionization by e impact, cross-sections calc. 8=12435
 C₆H₆⁺, lowest electronic states 8=12257
 C₆H₆⁺, position of electronic states 8=21120
 C₆H₆F⁺, lowest electronic states 8=12257
 C₆H₆F⁺, position of electronic states 8=21120
 CO₃²⁻, electron absorpt. spectra 8=12793
 CO₃²⁻, CO₂, injected in alkali halides, i. r. absorption 8=5583
 Co²⁺ in KCoF₃, polarizabilities and dipole moments from i. r. studies 8=2426
 CS₂²⁻, electron absorpt. spectra 8=12793
 CSe₂²⁻, electron absorpt. spectra 8=12793
 from Cs thermionic converter, anal. of dominant species 8=15211
 D₂⁺ chemical reactions with He, cross sections 8=14348
 D₂⁺, kinetic energy of autoionization 8=12443
 D₃⁺, reaction with alkanes and alkenes, energy transfer and deactivation 8=1358
 Fe X-XVIII, autoionization rel. to ionization rates and equilib. 8=16442
 Fe³⁺ in Ca₂Fe₂Si₂O₁₂, 3d⁵ configs. splitting by cryst. field 8=1654
 Fe³⁺,³⁺, ground states, universal potential field calc. 8=20952
 Ga V, 3d⁹-3d⁸4p transition spectra 8=12082
 Gd³⁺, energy structure 8=2421
 Ge VI, 3d⁹-3d⁸4p transition spectra 8=12082
 H, decay in collisions with thermal electrons 8=1360
 H in ZnO:Zn, energy loss and phosphor deterioration depth obs. 8=18624
 H₁⁻, duoplasmatron source for charge-exchange generator 8=15339

Ions—contd

- (H₁⁻, D₁⁻, T₁⁻), gen. purpose injector for charge-exchange generator 8=7713
 H⁺, energy distrib. function when moving in H under influence of electric field 8=7705
 H₂⁺, accurate wavefunction, James function as approx. to Guillemin and Zener 8=1249
 H₂⁺ chemical reactions with He, cross sections 8=14348
 H₂⁺, cross-sections for photo-dissociation 8=21188
 H₂⁺, energy distrib. function when moving in H under influence of electric field 8=7705
 H₂⁺ polarizability, longit. and transverse, variational calc. 8=1254
 H₂⁺, props. of 3d₀ and 4f₀ states 8=1244
 H₂O₄ group in acid soln., i. r. spectroscopic investigation 8=4150
 He, atomic and mol. mobility, 195-665°K 8=16445
 He-like, Hartree-Fock equations for 1s2p, ³P and ¹P states, perturbation treatment 8=20921
 He II, interference of fine-structure levels 8=4066
 He II, 4 → 3 transition excited by d bombard. 8=7384
 He in ZnO:Zn, energy loss and phosphor deterioration depth obs. 8=18624
 He⁺, electron-impact excitation and auto-ionization 8=4092
 He⁺, kinetic energy of autoionization 8=12443
 He⁺, 2s state, close-coupling calc. of electron-impact excitation 8=4091
³He²⁺, ⁴He⁺, in solar wind, Vela satellite meas. 8=23715
 He⁺, positive ion mobility, T, -1.4°K 8=15141
 He⁴⁺, 3.9% He³, positive ion mobility, T, -1.4°K 8=15141
 Hg discharge, ion-acoustic waves, propagation and damping 8=4313
 K, charge composition, effect of target state 8=1365
 Kr in ZnO:Zn, energy loss and phosphor deterioration depth obs. 8=18624
 L³⁺, (L=Ce, Pr, Nd, Sm, Gd, Dy, Er and Yb), 4f electron radial wave functions 8=1168
 Li, charge composition, effect of target state 8=1365
 Li dihydroanthracene salts, structure of ion-pairs from electronic spectra 8=7558
 Mg²⁺ in KMgF₃, polarizabilities and dipole moments from Mn²⁺:CaZrO₃, paramag. reson. spectrum 8=14118
 Mn²⁺ in KMnF₃, polarizabilities and dipole moments from i. r. studies 8=2426
 Mo₇O₂₄ in a crystal of ammonium heptamolybdate tetrahydrate, structure 8=8234
 MoS₂²⁻ and WS₂²⁻, in aq. soln. electron absorption spectra 8=12792
 N II, Stark effect in multiplet lines 8=4084
 N II-V, lifetimes meas. by decay of optical radiation 8=7412
 N in ZnO:Zn, energy loss and phosphor deterioration depth obs. 8=18624
 NO₂, NO₃, injected in alkali halides, i. r. absorption 8=5583
 Na, charge composition, effect of target state 8=1365
 Nd³⁺ in rare-earth trichlorides, new satellite structure 8=12070
 Ne (IV and V), mean lines of some excited levels 8=4097
 Ni²⁺ in KNiF₃, polarizabilities and dipole moments from i. r. studies 8=2426
 O (III and IV), mean lines of some excited levels 8=4097
 O⁶⁺ in solar wind, Vela satellite meas. 8=23715
 O⁺, photodetachment cross-sections and polarization 8=4101
 O⁺ from fermalta anode, cathode poisoning 8=15330
 Pr³⁺, wave functions 8=7419
 RaA, capture on metal disk 8=1370
 Rb²⁺ in RbMnF₃, polarizabilities and dipole moments from i. r. studies 8=2426
 Tb³⁺ in phosphors, radiative transition probabilities 8=4683
 Ti (III), hexahydrated, electronic struct. 8=16995
 Ti³⁺ in SrTiO₃, electronic ground state structure 8=9445
 V²⁺ and Ni²⁺ superexchange interaction in MgO 8=9355
 V (III), hexahydrated, electronic struct. 8=16995
- recombination**
 in columns, theory 8=12425
 energy partition between radiation and e-collision 8=1355
 n-hexane, after irradiation with γ-rays 8=6628
 ionosphere, E region, effect of vibrational level 8=23409
 ionosphere, F-region, coeff. calc. from nighttime velocities obs. 8=19020
 irradiated dipolar systems 8=2541
 three-body process with general third body, low density limit to rate, state anal. 8=12426
 three-body recomb. rate 8=21263
 Ar, gamma and neutron irradiated 8=1363
 Cs, electron, at 6P and 5D levels, cross section obs. 8=12080
 Cs vapour, ionization decay, microwave cavity studies 8=21271
 H, gamma and neutron irradiated 8=1363
 H₂ + e → H⁺ + H⁻, reactions of decay 8=1360
 HCl, γ-irrad., ion lifetimes 8=23164
 He- lifetime obs. 8=20944
 He afterglow, differential level decay 8=21237
 He⁺⁺ → He⁺ + H⁺, e capture probability calc. 8=1192
 He³⁺, e-capture on N₂ target 7.7-166 MeV 8=21279

ns—contd

recombination—contd

- He³⁺ single and double e-capture cross-sections obs.
 in He ³⁺-He. 7.2-181 KeV 8=21278
 N₂⁺ e-ion, temp. depend. obs. 8=7719
 N₂⁺ + N₂, is N₂⁺ produced? 8=1366
 Ne, e-temp. depend. 8=12451
 Ne₂⁺ rate, obs. of temp., press. depend. 8=21282
 O₂ radiolysis, ion lifetimes meas. 8=23163
 Pb halides, gaseous, recomb. rates 8=4317
 Si surface barrier detection, pulse height defect 8=3465
 Tl halides, gaseous, recomb. rates 8=4317

scattering

- alkali ion scatt. at He atoms 8=7464
 double-scatt. effect on cross-section meas. 8=10893
 0.5-3 keV, by atoms and mols., cross-sections determ. 8=1139
 on nuclei, with mutual excitation, diffraction theory 8=1102
- ns, electrolytic
- See also Conductivity, electrical/liquids, electrolytic; Dissociation/electrolytic.
- acetate, oxidation by K₂S₂O₈, Ag catalysis 8=23094
 alkali halide crystals, impure, cation vacancy generation 8=9718
 anions, adsorpt. maxima 8=4760
 anions, change in chem. potential on transfer from protic to dipolar aprotic solvents 8=14418
 cations, adsorpt. maxima 8=4760
 cation hydration, charge-dipole model 8=9670
 cation off-centre displacements in octahedral environments 8=13172
 contact pairs, effect of ionic polarizability on equilib. const. 8=8118
 4,4'-dimethoxyazobenzene anion, e.s.r. 8=12303
 dissociation rate, computation from ultrasonic relaxation study 8=18712
 dipyrindyl mononegative ion and alkali metal ion biradical, e.s.r. and structure 8=4247
 durosemiquinone, ion-pair assoc. 8=1591
 exchange, use of Rumanian molecular sieves 8=18652
 macroions of rigid-sphere potentials, potential of average force 8=21203
 methylene blue, water induced dimerization, absorpt. spectrum obs. 8=8123
 methyl viologen cation, aq. and alcoholic solns., water induced dimerization, e.s.r. spectra obs. 8=8123
 γ-picoline-halogen complexes, ionization in polar solvents, i.r. spectra obs. 8=7592
 recombination rate, electrostatic model 8=4611
 solvation, thermodynamic functions 8=12807
 tetracyanoquinodimethane anion, aq. and alcoholic solns., water induced dimerization, e.s.r. spectra obs. 8=8123
 zeolites, synthetic, ion exchange theory 8=18651
 AlCl₃, p.m.r., determ. of coord. no. in aq. mixtures 8=16888
 Br⁻, passivity breakdown of stainless steel 8=23147
 Cl⁻, passivity breakdown of stainless steel 8=23147
 Co²⁺ ion hydration, n.m.r. 8=12937
 H⁺, competitive solvation in water-methanol vapour 8=14443
 ZnSO₄ soln. in H₂O-glycol, ion assoc. 8=8062

asers. See Lasers.

dium

- brittleness, on hot and cold working 8=22390
 films, ultra-thin, vacuum-deposited, structure from e-diffr. and microscopy 8=17292
 Schottky deviations for thermionic emission at 1500-2000°K 8=5415
 Al-coated, u.v. reflectivity calc. 8=14227
 with Cs film, adsorption and electron emission 8=9268
 Ir(III), spectra in fused LiCl-KCl 8=1567
 Ir¹⁹³, mag. fields in Ir-rare-earth cpds 8=1634
 Ir⁴⁺, substitution in spinel ferrites, spin wave line-width variations 8=5495
 on SiO₂, chemisorpt. of HCN, C₂N₂ and BrCN 8=23127
- dium compounds
- alloys, superconductivity, mag. susceptibility and sp. ht. 8=13752-3
 Mössbauer effect of Ir¹⁹³ 8=4679
 IrCl₆²⁻, electron transfer bands in crystals at 20°K 8=22992
 IrO₂, resistivity, temp. depend. 8=17939
 Ir₂Se₃, Rh₂Se₃ and Rh₂Se₃, octahedron pairs, crystal structure 8=1807

on

- absorption coeff. for AgKα radiation, meas. 8=2436
 abundance, problem of 8=2769
 abundance, in sun and meteorites 8=23682
 additions to Ti alloys, superconducting props., phase transformations 8=22563
 analysis, Cu determ. by at. absorpt. spectrometry 8=2545
 anodic behaviour in H₂SO₄ and alkaline solutions 8=14432
 armco, explosive formation, residual strains and hardening 8=13564
 armco, lattice parameters obs. 8=8521
 Armco, lower yield stress rel. to grain size 8=17798
 armco, strain-aged, tensile stress strain relations 8=17792
 armco, strain ageing, effect of preliminary deformation 8=17786
 atoms, ionization of various gases, ionization ratio meas. 8=1359

Iron—contd

- atom and ions, ground states, universal potential field calc. 8=20952
 atom, photoelectric cross-section for K-Mv subshells for X-rays 412-1332 keV 8=7438
 atomic scattering factor, absolute 8=8519
 b.c.c., critical values for Bloch wall types 8=9320
 b.c.c., density of states 8=22460
 b.c.c., screw dislocation core structure 8=4976
 b.c.c., O migration energy and solubility 8=22150
 caked powder ceramic, porosity and thermal conductivity 8=13388
 cast, austenitic, effect of Ce on struct. 8=21988
 compressibility, 4.2-300°K 8=5061
 corrosion rate rel. to impurities 8=18664
 corrosion in H₂SO₄, thiourea inhibition and K₂Cr₂O₇, NH₄CNS and KI effects 8=2518
 critical magnetic scattering of neutrons, spin correlation 8=2026
 crystals, having [100] and [110] axes, tensile deformation, -70°C to 250°C 8=13553
 Debye-Waller-factor and Mössbauer-thermal-shift meas. 8=8214
 deformation microcontours, during fatigue testing 8=2053
 dissolved in Zn, magnetic moment, revision of superconducting props. 8=9344
 distribution of additions during oxidation 8=1917
 elasto-plastic behaviour study of pure mono-crystalline sheets 8=8848
 electron irradi., anisotropy of defect production 8=8770
 electron irradiated, resistivity studies 8=5180
 electronic sp. ht. calc. by band model 8=4932
 etching, thermal in vacuum 8=17652
 fatigue damage from intergranular weakness 8=5060
 ferromagnetic lattice, hyperfine magnetic field on Sm¹⁵⁰ 8=2335
 ferromagnetic, maximum susceptibility 8=18338
 ferromagnetic powders, magnetic props., lattice parameters 8=14033
 films, electrolytically deposited, growth rate rel. to structure and ferromag. props. 8=13999
 fractionation in Solar System 8=10323
 frictional forces of moving dislocations 8=22206
 v-beam scatt., differential albedo obs. 8=16844
 glass-doped, granular structure, orientation, after annealing, model for doped tungsten 8=17025
 grains, production in discharge, light scatt. and interstellar matter 8=4296
 h.c.p., thermodynamic props. 8=13371
 hydrostatic tension on solidification 8=21758-9
 impurity ion in Pa, range of spin perturbation 8=1655
 ions, Fe X-XVIII, autoionization rel. to ionization rates and equilib. 8=16442
 ion, Fe XVII, electron impact, Coulomb-Born calc. 8=12081
 liquid, deoxidation with Al, rel. to form. of cloud group of oxide inclusions 8=22183
 liquid, heat of solution of Al, Cu and Si 8=16799
 liq.-silica deoxidation product growth and separation, collision model 8=18658
 magnetic atoms, phonon motion studied by polarized neutron scatt. 8=14012
 magnetic properties, Anderson-type localized moments, model 8=2314
 magnetic props. from meas. of critical diffusion of slow neutrons 8=22810
 magnetic scattering of neutrons, rel. to spin correlation function 8=2325
 magnet with superconducting coil 8=15263
 magnetocrystalline energy, electronic charge, Fermi surface 8=2089
 magneto-optical props., u.v., visible and i.r. 8=18550
 martensite, atomic displacements 8=4877
 mass ejection by laser pulse 8=8759
 α, mechanical change due to tension, compression and rolling 8=5067
 metallurgy, homogeneity and interface reactions 8=5704
 meteorites, Australian, comp. differences obs. 8=23684
 Mössbauer effect in ionic cpds. at high press. 8=4674
 Mössbauer effect study of state in AgCl single crystals 8=8215
 Mössbauer effect in K ferro- and ferricyanides 8=4673
 Mössbauer-thermal-shift and Debye-Waller-factor meas. 8=8214
 nebula NGC 6960, FeX 6374 Å line, obs. 8=10225
 neutron irradi., rel. to plastic deformation, stress-strain curves 8=22348-9
 oxidation in water vapour at 550°C, effect of cold work 8=23101
 particle size range for magnetostatic accretion 8=23632
 point defects recovery after low-temp. deform. 8=13418
 polycrystalline, coarse grained, defects under tensile deformation 8=1985
 polycrystalline, lower yield stress, temp. depend. 8=13562
 polycrystalline, two-pole magneto-optical Kerr effect, 6.5-20 μ 8=18526
 potentiostatic anodic dissolution under yielding conditions obs. 8=8793
 powder dispersed in perspex, magnetization process and Mössbauer effect 8=5470

Iron—contd

purified, amplitude-dependent internal friction and modulus defect 8-13557
 pure, annealing effect on internal friction temp. dependence 8-17791
 reproducible residual resistance measurement 8-5179
 resistivity as function of temp. and magnetization 8-13716
 rod, vibrating and heated, stress distribution 8-10688
 rolled, orientation analyses by means of quantitative pole figures 8-17282
 γ -phase, self-diffusion, effect of traces of Sn, Sb, Pb and Bi 8-1930
 in silicate materials, site populations, Mössbauer effect 8-8218
 in silicate matrix, superparamagnetism 8-14013
 single crystals, relaxation and yield 8-22340
 sintered, mag. props. and eddy current losses reduction, obs. 8-22807
 sintered, mag. props. rel. to porosity, obs. 8-22808
 solubility of Pu 8-13041
 solubility in TiO_2 , X-ray examination 8-13042
 stars HR 4533 and 4657, [Fe/H] abundance 8-23533
 steel, exoelectronic emission due to sliding friction, obs. 8-18254
 surface texture 8-8295
 technical, microstructure during fatigue tests 8-13566
 whiskers, ferromag., nucleation, theor. investigation 8-18335
 whiskers surface microstruct., scanning e microscope obs. 8-17281
 X-ray diffraction line intensity after plastic deform. and annealing 8-21989
 in Ag, liquid, diffusion 8-12836
 α -AlFeSi, 4 possible phases 8-13057
 containing Au, magnetization saturation at 20°K 8-2324
 Cr diffusion in experimental obs. in 950-1265°C range 8-4951
 on Cu, hot, pseudomorphic growth 8-21880
 in ϵ Cu-Zn phase, local moment formation 8-9340
 Fe I 6302.5 Å line contours in sunspots rel. to Zeeman splitting anomalies, obs. 8-10418
 Fe II, III, beam-foil excitation 8-12079
 Fe(III) ions, sublation studies by radioactive tracers 8-23075
 Fe XIII solar emission lines, photoelectric abundance meas. during eclipse 8-5965
 α -Fe (b. c. c.), anisotropy of impurity-induced internal friction peak (Snoek's peak), for torsional vibrs. 8-13572
 Fe crystals with 8-20 p. p. m. C, n-irradiated, yield stress rel. to radiation hardening 8-17800
 α -Fe crystals, D^+ transmission 8-22242
 α -Fe, diffusion of C 8-17572
 α -Fe, dilation by C 8-17615
 α -Fe, dislocation structure rel. to plastic deform. 8-4975
 α -Fe, phonon dispersion relation at room temp. 8-1835
 α -Fe, phonons and magnons, dispersion relations 8-13331
 α -Fe, precipitation of C, n-irrad. effect 8-17059
 α -Fe, solid solutions, mechanical props. 8-22350
 α -Fe, vacancies and interstitials, calcs. 8-22179
 Fe-whiskers, nucleation mag. field strength investigations 8-5467
 Fe, H-charged internal friction rel. to H interstitial-dislocation binding 8-4965
 Fe and Mg multilayered film structure, X-ray diffraction 8-1758
 γ -Fe, NbC solubility from C content analysis at temps. 950-1050°C 8-4535
 α -Fe, 3.28%Ni addition, effect on yield and fracture behaviour at low temps. 8-22346
 Fe-Ni phase diagram and α and γ solid solubilities, e micro-probe obs. 8-17034
 Fe-Mn, (M = Mn, Ni, Sb, Sn, W) systems α - γ equilib. 8-4709
 Fe/O relative abundances in solar corona 8-23748
 Fe-4.4%Si, direct observation of twin formation 8-13125
 Fe⁵⁴, 15-60 MeV Li⁶ ions, recoil range 8-13489
 Fe⁵⁵ radioactive isotope, use as source for X-ray structural anal. 8-13227
 Fe⁵⁶-Fe⁵⁷ mass difference, from mass-spectroscopic and reaction Q-value analysis 8-21017
 Fe⁵⁷, in dilute alloys of Fe, n.m.r. spectra 8-14140
 Fe⁵⁷ isomer shift, calibration 8-16988
 Fe⁵⁷ Mössbauer expts. at 1-0.08°K rel. to Co nuclear polarization in Fe 8-4676
 Fe⁵⁷ Mössbauer spectrum, variable-freq. u.s. spectrometer obs. 8-13021
 Fe⁵⁷ in Fe(OH)₂, Mössbauer effect at 90 and 4.2°K 8-13027
 Fe⁵⁹ diffusion in Pd, obs. 8-17579
 Fe⁵⁹, extraction from aqueous soln. using 1-phenyl-3-methyl-4-capryl-pyrazolone-5 8-18750
 Fe₃Mn₂O₄, cation distrib. determ. 8-17364
 α -Fe₂O₃ easy-axis critical fields and resonance involving Dzyaloshinsky interaction 8-22871
 Fe²⁺, cubic, magnetically induced electric field gradients, theory 8-21803
 Fe²⁺, Mössbauer spectrum in BaFeSi₄O₁₀ 8-13026
 Fe²⁺ in sphalerite, i.r. absorpt. spectra 8-18570
 Fe²⁺ in MgO, microwave phonon interaction 8-9450
 Fe²⁺ ion in MgO, thermal conductivity, mag. field depend. 8-13395

Iron—contd

Fe²⁺ in MgO u.p.r. temp. depend. 8-2367
 Fe³⁺ spin-lattice relax. in K₃Co(CN)₆ 8-10994
 Fe³⁺ in CaF₂, e.p.r. spectrum 8-9437
 Fe³⁺ in Ca₂Fe₂Si₂O₁₂, 3d⁵ configs. splitting by cryst. field 8-1654
 Fe³⁺ in KAlF₄, e.p.r. spectrum 8-9426
 Fe³⁺ in KTaO₃, e.p.r. 8-9425
 Fe³⁺ in K₃Co(CN)₆, e.p.r. spin-spin interaction temp., 3 cm, 1.8°K 8-18425
 Fe³⁺ in LiF, crystal field distortions, e.s.r. study 8-13005
 H in Fe, anomalous behaviour at low temps. 8-22182
 H₂, dissolved, electromigration 8-8677
 N impurity, spectrophotometric determ. 8-23178
 NH₃ adsorption catalyst, Mössbauer spectra 8-13108
 Ni diffusion, volume and grain-boundary 8-17571
 in Ni-Mn Nivalloy, effect on mag. permeability 8-22832
 O adsorption at (011) surface, low energy electron diffraction study 8-1701
 Sb impurity, internal nucl. mag. field 8-8198
 Sb²⁴ implanted, hyperfine mag. field 8-8199
 Si-Fe, [110], necking and fracture at 293 and 473°K 8-13607
 3% Si-Fe upper yield stress rel. to etch pitting experiments 8-5065
 V:Fe⁵⁷, Mössbauer effect, recoil-free fraction and Doppler shift meas., localized modes 8-13338

Iron alloys

See also Iron compounds; Steel.
 abrasive wear resistance, influence of strengthening mode 8-8847
 Alnico, high-temp. magnetization obs. 8-22813
 alnico permanent magnets magnetization, 550-800°C 8-22806
 Alnico, structure on formation at different ageing temps. (300-800°C) 8-17077
 analysis, Mn determ. by at. absorpt. spectrometry 8-2547
 austenite formation from spheroidized ferrite-carbide aggregate, kinetics 8-21844
 austenite in Fe-Ni alloys, effect of C on Curie pt. 8-18336
 dilute, charge screening 8-13661
 drop, liquid, voids formation 8-8257
 elinvar, influence of Cr on mag. props. 8-9348
 ferritine, superantiferromag, independence on Fe content and aq. dissolution 8-14068
 invar, Fe⁵⁷ Mossbauer spectrum, plastic deform. effects obs. 8-21811
 kovar, anode desorption efficiency, photoelec. meas. 8-17167
 liquid, oxide saturated, first-order interactions rel. to oxide solubilities 8-16797
 phase equilibria by leveitation melting apparatus 8-1669
 secondary ion emission 8-18287
 silicon, notched, fracture topology rel. to crack nucleation and growth 8-17793
 solid-solution strengthening 8-22341
 sormite type, influence of Nb on hardness and structure 8-5066
 Ticonal, structure on formation at different ageing temps. (300-800°C) 8-17077
 transition metal, magnetization values 8-22811
 low-Al, storage effect on oxidation at high temps. 8-9666
 Fe-Al, elastic stiffness coefficients, experimental results and thermodynamic analysis 8-5062
 Fe-Al, electron energy losses 8-17912
 FeAl alloys, kinetic order-disorder transform. by X-ray investigation 8-17076
 Fe-0.5-6%Al, mag. props. of doubly oriented sheets, obs. 8-22789
 Fe-Al, nature of K state 8-9005
 Fe-Al 40 oil quenched alloy, source of dislocations 8-13438
 Fe-Al, paracrystals from X-ray powder patterns rel. to comp. and annealing treatments 8-17368
 Fe-Al, stiffness coefficients, long range order effects 8-5063
 Fe-20 at. %Al, structure factor variations for electrons with accelerating voltage 8-13260
 Fe-Al, yield effect from elevated temp. constant strain-rate tests 8-13555
 Fe-Al₂O₃, dispersion strengthened, and hot extruded mechanical properties 8-8842
 Fe-Au-Cu, ordered G.P. zones 8-8461
 Fe-Be, ferromag. props. rel. to transfer of electron states 8-14018
 Fe-C austenite, quadrupole splitting of Mossbauer resonance, disappearance at elevated temps. 8-21808
 Fe-C, effect of noble metal additions on toughness 8-17795-6
 Fe-C, growth of spherical graphite crystals 8-13156
 Fe-C alloys, liq., diffusion of N. at 1600°C 8-16815
 Fe-C martensite, static atomic displacements by X-ray diffractions 8-4878
 Fe-C, structural transitions from density and emissive power meas. 8-1673
 Fe-C, thermodynamic of martensite transform. 8-17075
 Fe-C-Cr solns., liq., activity of C 8-21653
 Fe-C-Mn, induction melting under vacuum at 1600°C, evaporation of Mn 8-12993

Iron alloys—contd

- Fe-C-Ni-Mn, martensitic transformation, magnetic field effect 8=17079
- Fe-Co, ferromagnetic powders, magnetic props., lattice parameters 8=14033
- Fe-Co, fine particles, mag. props. 8=5471
- FeCo, grain boundary theory 8=17258
- Fe-Co, magnetic anisotropy 8=14019
- Fe-Co-Ni-Cr, new ferromagnetic state during recrystallisation 8=9342
- Fe-Cr, electrotransfer of components at 1150–1400°C 8=4952
- Fe-Cr, mechanism of lifting and cracking of protective Cr_2O_3 scale 8=23099
- Fe-Cr(0–53%), mechanical properties after ageing at 475°C 8=8841
- σ -FeCr, mech. props. rel. to atomic ordering and co-ordination 8=17030
- Fe-Cr of 25–95%Cr comp., oxidation at 1000° to 1300°C 8=18677
- Fe-28%Cr, early growth of oxide, rel. to environment 8=21882
- Fe-Cr phase transformation, 500°C 8=13068
- Fe-30%Cr, yielding and fracture 8=13558
- Fe-Cr X-ray fluorescence analysis 8=9750
- Fe-Cr, X-ray microanalysis rel. to fluoresc. and absorpt. corrections evaluation 8=14476
- FeCrAl as ferromag. Hall probes 8=14011
- Fe-Cr-Al, high-temp. corrosion by S 8=23102
- Fe-7.9Cr-1.1C, isothermal transforms. betw. 750 and 285°C 8=17068
- (Fe,Cr)Co, (Fe,Mn)Co, Fe(CoNi) with FeCo super-structures, neutron diffraction 8=1757
- Fe-Cr-N ternary system, microstructures and nitrides 8=4845
- Fe-Cr-N ternary system, structural diagrams and phase reactions 8=4846
- Fe-Cu, Cu precip. and coagulation rel. to ferromag. props., obs. 8=22809
- Fe-Cu, fracture obs. 8=22347
- Fe-Cu, induction melting under vacuum at 1600°C, evaporation of Cu 8=12993
- Fe-Cu mixed whiskers, strength, hardness and growth mechanism 8=17249
- Fe-C-Si, growth of spheroidal graphite crystals 8=13156
- Fe-Gd films, hysteresis loops, by static method 8=9345
- Fe-In system, liq. miscibility gap, no intermetallic cpds., and solubility 8=8160
- Fe-MgO, dispersion strengthened, and hot extruded mechanical properties 8=8842
- Fe-Mn austenite, effect of plastic deform. and annealing on H permeability 8=17573
- Fe-Mn, dilute, nearest neighbour antiferromag. exchange interaction energy of Mn 8=18383
- Fe-Mn, induction melting under vacuum at 1600°C, evaporation of Mn 8=12993
- Fe-Mn, paramagnetic susceptibility of martensitic phases 8=9304
- Fe-Mn-As system, first order ferrimag. to antiferromag. transition, temp. dependence 8=9376
- Fe-Mn-N, internal friction meas. 8=8839
- Fe-Mn-N, stress change effects on creep resistance 8=5064
- Fe-Mo alloys, Fe-rich, precip. reactions and solid solns. from Mössbauer spectra 8=4678
- Fe-N alloys, tempering process and quenched structure 8=8840
- Fe-N, thermodynamics of martensite transform. 8=17075
- Fe-N, martensite lattice meas. 8=8522
- Fe-Ni alloy, refining effect of Ge in vacuum melting rel. to mag. props. 8=22815
- Fe-Ni, annealed, vacancies rel. to X-ray diffr. "tails" 8=17341
- Fe-Ni base alloy: 9 at %Cu, microstructural and mechanical strength changes on ageing 8=1759
- Fe-Ni binary solns, interdiffusion coeff. conc. dependence, by X-ray analysis 8=17570
- Fe-Ni, evaporation characteristics 8=12719
- Fe-Ni films, electrodeposited, internal stresses rel. to deposition conditions 8=17653
- Fe-Ni, heating during ferromag. resonance 8=14082
- Fe-Ni(35 wt. %)-Cr(0–20 wt. %) alloys (in as-coldworked state), strain gauge factor in relation to electrical and magnetic properties 8=9006
- Fe-Ni, mag. thin film, evaporated with oblique incidence, structure 8=14017
- Fe-Ni, mag. and mech. anisotropies, by diffusion 8=22814
- Fe-50%Ni mag. props., metallic impurities effects, obs. 8=22825
- Fe-Ni, martensitic transformation, calorimetric study 8=17069
- Fe-Ni, n-irradiated, mag. props. 8=2326
- Fe-Ni, phase-hardened, condition for thermal stability 8=17066
- Fe-Ni, rapid heating effect during reverse martensite transform. on high temp. stability 8=17065
- Fe-Ni, sintered, mag. props. and eddy current losses reduction, obs. 8=22807
- Fe-Ni, surface relief rel. to supercond. transition 8=19686

Iron alloys—contd

- Fe-Ni thermal bimetal strip, ageing 8=22345
- Fe-Ni-Al-Ti, microstruct. and mech. props. 8=21987
- Fe-Ni-As constitution diagram, up to 50 wt. %As 8=17074
- Fe-26%Ni-0.4%C alloy, effect of prior plastic deformation of austenite on M_s 8=4710
- Fe-Ni-C martensites, ferrous, hardness change due to deformation 8=22352
- Fe-Ni-C, mech. props., effect of rapid re-austenitizing 8=17807
- Fe-Ni-Co-Al coercivity and energy increase by Ti and Si, Se or Te addition 8=22805
- Fe-Ni-Cr aged, dislocation structure and grain size effect on validity of Cottrell-Stokes law 8=8721
- Fe-Ni-Cr, ang. depend. of mag. phenomena in interacting particle chains 8=5429
- Fe-Ni-Cr, mag. props., ht. treatment, comp. and external field dependence 8=18337
- FeNi-FeNiMn films with ferro-antiferromagnetic coupling, study 8=9346
- Fe-Ni-Mo, sintered, mag. props. and eddy current losses reduction 8=22807
- Fe-Ni-Te, structural changes during martensite ageing 8=17064
- Fe-Ni-Ti, ageing during $\alpha \rightarrow \gamma$ martensitic transformation 8=17070
- Fe-Ni-Ti alloy of Invar type, Young modulus anomalies 8=17790
- Fe:Pd and Fe:Pt, giant moments theory 8=9302
- Fe(Pd,Pt_{1-x})₃ alloys, antiferro-ferro, transitions 8=5465
- Fe-Rh, structural defects, phase transformations crystal lattice parameters 8=9395
- Fe-Ru alloys, h.c.p., high electronic sp.ht. 8=13369
- Fe-Ru, h.c.p., thermodynamic props. 8=13371
- Fe-Si, annealing effect on physical props. 8=23778
- Fe-Si, chemical polishing 8=1687
- Fe-3%Si crystal, dislocation movement 8=17661
- Fe-3wt.% Si single crystals, X-ray interference fringes rel. to domain arrangements 8=22021
- Fe-Si, ferromagnetic after-effect by plastic deformation 8=5466
- Fe-Si, grain-oriented, domain wall mobilities rel. to alternating field freq., obs. 8=22841
- Fe-3%Si, grain-oriented, hysteresis and eddy current losses rel. to domain wall motion, obs. 8=22842
- Fe-Si, grain-oriented transformer sheet, magnetostriction 8=22839
- Fe-4.5%Si, growth obs. on Neumann bands by high-speed photography 8=4783
- Fe-Si, magnetic Zener relaxation, diffusion mechanism 8=9451
- Fe-Si, Mössbauer spectra near ϵ -phase 8=8242
- Fe-Si sheet, initial permeab. depend. on demag. freq. 8=5464
- Fe-Si sheet, iron losses in alternating mag. fields, ≤ 24 kGauss 8=22804
- Fe-Si, sintered, mag. props. and eddy current losses reduction, obs. 8=22807
- Fe-SiO₂, dispersion strengthened, and hot extruded mechanical properties 8=8842
- Fe-Sn, induction melting under vacuum at 1600°C, evaporation of Sn 8=12993
- Fe-Ta system, liquid and solid δ -phases 8=8161
- Fe-TaC, fracture obs. 8=22347
- Fe-3.5 at. %V, frictional forces of moving dislocations 8=22206
- Fe-V-C, anomalous Snoek peak 8=13559
- PbTe-Fe pseudobinary phase equilibria 8=17097
- S solubility at 1000°C, effect of Cr, Cu, Ni and V 8=17012
- Si-Fe, (b. c. c.), impurity-induced internal friction peak (Snoek's peak), for torsional vibrs., anisotropy 8=13572
- Si-Fe, dislocation structure and ductility, low-temp. creep effects 8=13571
- Si-Fe, intercrystalline fracture 8=13567
- Si-Fe thin tapes, dynamic hysteresis phenomena 8=5483

Iron compounds

- See also Ferrites; Iron alloys; Steel.
- alum, ammonium, n.m.r. obs. 8=2385
- borides, transfers of electronic states 8=5461
- botryogen, cryst. struct. 8=4876
- carbides, precipitation in tempered martensite 8=17080
- carbides, transfers of electronic states 8=5461
- ferrian ilmenites in basalts, electron probe 8=14703
- ferric oxides, hydrous, colloidal, mineralogical comp. 8=12954
- ferric oxyhydroxide, structure determ. by Mössbauer spectroscopy 8=17370
- ferrocene-tetracyanoethylene complex, cryst. struct. 8=1792
- ferrous ions in ice, Mössbauer effect 8=4675
- fluorotitanate complexes, F-F coupling consts. 8=4230
- goethite dehydration and haematite/magnetite formation rel. to c. c. p. orientations 8=4875
- hematite, natural, stress induced mag. anisotropy 8=22748
- hexaferrites, Al-Fe substitution by i.r. spectroscopy 8=16999
- ionic, Mössbauer effect, at high press. 8=4674

Iron compounds—contd

- iron(II)-bis(α -diimine) complexes Fe^{2+} Mossbauer spectra 8=8200
- iron oxide scale, hematite phase physico-chemical state 8=17201
- isomer shift of Fe nucleus 8=4681
- magnetite, acoustic loss peak, electronic mech. 8=1852
- magnetite film on Fe, formed by corrosion, crit. tensile fracture strains 8=21875
- magnetite, self-diffusion of O, 8=22151
- magnetite, thermal cycling, effect of compression 8=22798
- oxides, bond distances and angles, cryst. struct. 8=22022
- oxides (hematite, maghemite, magnetite), reduction processes below 400°C 8=5703
- oxyhydrates, bond distances and angles, cryst. struct. 8=22022
- phosphides, transfers of electronic states 8=5461
- tetracarbonyl (fumaric acid) iron racemate 8=1790
- titanomagnetites in basalts, electron probe 8=14703
- wüstite, hole mobility obs. 1000-1300°C 8=13697
- wüstite, Seebeck coeff. grain size and Mg doping dependence rel. to p to n transition 8=5387
- Fe-I-boracite, ferroelectric orthorhombic phase, optical study 8=22980
- Fe carbonyl toluene complex, crystal structure, by X-ray analysis 8=4874
- Fe(III) oxide, mobility evidence from Zn ferrite form. at 400°C 8=23117
- FeBr_2 , hyperfine structure at 78°K and 4°K, Mössbauer effect obs. 8=13025
- Fe_2C , Hägg iron carbide, lattice structure 8=17372
- $\text{FeCl}_2 \cdot 2\text{H}_2\text{O}$, antiferromag., magnetization process from exchange interactions 8=2349
- FeCl_2 , hyperfine structure at 78°K and 4°K, Mössbauer effect obs. 8=13025
- FeCl_2 , metamag. phase transform. and hysteresis 8=9396
- $\text{FeCl}_2 \cdot \text{Fe}^{3+}, \text{Mn}^{2+}$, impurity spin resonance at low temps. 8=14108
- $\text{FeCl}_3 \cdot 6\text{H}_2\text{O}$, cryst. structure 8=1791
- FeCl_3 -graphite cpd., electron microscopy 8=1972
- FeCl_3 , hyperfine structure at 4°K, Mössbauer effect obs. 8=13025
- FeCl_3 , monomeric, mol. structure from gas e-diff. exam. 8=16264
- $\text{Fe}(\text{CN})_6^{-3}$ aqueous con., cathodic reduction on ZnO 8=14423
- FeCO_3 , quadrupole Mössbauer doublets, vibrational anisotropy 8=16983
- FeCO_3 , Fe^{57} asymmetry of quadrupole splitting components 8=21806
- $\text{Fe}_3(\text{CO})_{12}$, C^{14}O isotope exchange reactions 8=2506
- FeCo, micro-strain and hardness under deformation 8=13596
- FeCr_2S_4 containing Fe^{2+} , Mössbauer spectra 8=8216
- FeCr_2S_4 , effective fields in Fe^{57} Mössbauer spectra 8=1647
- FeCr_2Se_4 , structural, electrical and thermal parameters rel. to d-orbital interactions 8=5391
- FeF_2 , spectrum, near i.r., mag. effects 8=18525
- FeF_2 , tetragonal antiferromagnet, scattering of light by one- and two-magnon excitations 8=18546
- FeF_3 , antiferromagnetic, Mossbauer spectra, interpret. of broadened and shifted lines 8=21807
- $\text{Fe}_{1-x}\text{Ga}_x\text{O}_3$, ferrimag. structure considerations 8=18360
- $\text{Fe}_{1-x}\text{Ga}_x\text{O}_3$, magneto-electric susceptibility versus temp. 8=5427
- FeGe hexagonal single crystal, magnetic torsion measurements 8=14069
- Fe_2 , hyperfine structure at 78°K and 4°K, Mössbauer effect obs. 8=13025
- FeIn_2S_4 containing Fe^{2+} , Mössbauer spectra 8=8216
- FeLiO_2 , Q_{11} (or β) phase, X-ray diff. results rel. to periodic antiphase model 8=17386
- Fe-Mn carbides, cell volume obs. 8=22019
- $\text{Fe}_2\text{Mn}_3\text{TO}_3$, (T = rare earth), structure and mag. props. rel. to x value (0 to 1) 8=22851
- Fe, MnWO_4 X-ray microanalysis, atomic number effect correction, obs. 8=14479
- $\text{Fe}_2(\text{MoO}_4)_3$, crystal structure refinement and formation 8=17374
- $\text{Fe}_2(\text{MoO}_4)_3$, structural type 8=8526
- Fe-N supersaturated solutions, n-irrad. rel. to nitride precipitation 8=17060
- Fe-N₂ solid solns., N₂ desorption kinetics 8=1704
- $\text{Fe}(\text{NCS})_2 \cdot 4\text{Py}$, Mössbauer effect probabilities 8=8213
- FeNeMo/SiO₂/Fe double layer magnetic film, hysteresis loops theory and experimental 8=5458
- $\text{Fe}(\text{NH}_4)_2(\text{SO}_4)_6 \cdot 6\text{H}_2\text{O}$, isothermal dissoln. and growth, mag. field effect 8=8411
- $\text{FeNH}_4(\text{SO}_4)_6 \cdot 12\text{H}_2\text{O}$, sp. ht. and mag. susceptibility calcs. at very low temps. 8=13370
- FeNi films, electrodeposited, mag. props. 8=9347
- $\text{Fe}(\text{NO}_3)_3 \cdot 9\text{H}_2\text{O}$ magnetic relaxation, Mössbauer spectra 8=2378
- $\alpha\text{-Fe}_2\text{O}_3$, antiferromag., spin waves and mag. exchange interacts. 8=18379
- FeO, high-pressure synthesis of stoichiometric cpd. 8=13259
- FeO, Néel temp., effect of hydrostatic pressure 8=9394
- FeO- Fe_2O_3 -ZrO₂-SiO₂ system, phase equilib. 8=17072
- Fe_2O_3 adsorption of poly(dimethyl siloxane) from CCl₄ and xylene solns. 8=8336
- Iron compounds—contd**
- $\alpha\text{-Fe}_2\text{O}_3$, antiferromag. resonance obs. 8=22892
- $\alpha\text{-Fe}_2\text{O}_3$ crystals, domain walls, n.m.r. obs. 8=5557
- $\alpha\text{-Fe}_2\text{O}_3$, ferromag. ultrafine particles, Mössbauer study of mag. props. 8=2318
- Fe_2O_3 , γ to α transformation, liquid N₂ temp. 8=13066
- Fe_2O_3 (hematite), magnetization and susceptibility rel. to temp. 8=5469
- $\delta\text{-Fe}_2\text{O}_3$ (hydrate), crystal structure 8=22023
- $\delta\text{-Fe}_2\text{O}_3$, mag. props., effect of struct. and chem. alterations 8=17627
- $\alpha\text{-Fe}_2\text{O}_3$, magnetisation process up to 80 kOe from 4.2-290°K, transitions and Morin point entropy change 8=9281
- $\alpha\text{-Fe}_2\text{O}_3$, Morin transition, surface effects 8=2323
- $\alpha\text{-Fe}_2\text{O}_3$, new type of antiferromagnetic resonance 8=2360
- $\alpha\text{-Fe}_2\text{O}_3$, paramagnetic, anomalous Hall effect 8=17914
- Fe_2O_3 powders, Mossbauer fraction rel. to packing 8=21805
- Fe_2O_3 powder, pH depend. of adsorp. of the anions VO_3^- , WO_3^- , MoO_4^{2-} and $\text{Cr}_2\text{O}_7^{2-}$ 8=8342
- Fe_2O_3 , superpar-, ferro- and antiferromag., Mössbauer effect 8=14016
- $\alpha\text{-Fe}_2\text{O}_3$, transition from antiferro. to weakly mag., from magnetization obs. 8=5503
- $\alpha\text{-Fe}_2\text{O}_3$ whiskers on Fe, morphology and growth 8=17250
- $\text{Fe}_2\text{O}_3\text{-Al}_2\text{O}_3$ solid solns., mag. susceptibility 8=13972
- $a(\text{Fe}_2\text{O}_3) + b(\text{Cr}_2\text{O}_3) + x_1(\text{NiO}) + x_2(\text{ZnO})$ ferrites, complex dielec. const. and mag. susceptibility 8=9371
- Fe_2O_4 crystals, growth by arc-transfer 8=4806
- Fe_2O_4 , diffraction of slow electrons at octahedral surface 8=8520
- Fe_3O_4 , fine grained, coercivity rel. to edge dislocations 8=9343
- Fe_3O_4 , hyperfine mag. fields rel. to sublattice magnetizations 8=21809
- Fe_3O_4 magnetite, weak reflections obs. in diff. pattern 8=22020
- Fe_3O_4 , order-disorder transition, constant entropy below transition 8=17067
- Fe_3O_4 spinel phase, methods for its characterization 8=5703
- $\text{Fe}(\text{OH})_2$, Fe^{57} Mössbauer effect at 90 and 4.2°K 8=13027
- $\text{Fe}(\text{OH})_3$ from degraded protein, superantiferromag. 8=14068
- $\text{Fe}(\text{OH})_3$ suspension, flow meas. by Br⁹² 8=21727
- $\alpha\text{-FeOOH}$ antiferro-paramag. transition temps., e. s. r. obs. 8=22879
- $\alpha\text{-FeOOH}$, mag. structure and hyperfine field 8=22878
- β - and $\delta\text{-FeOOH}$, susceptibility and magnetization 8=22747
- FePO_4 , calcinated, Mössbauer effect studies of magnetic ordering 8=8217
- $\text{Fe}_3(\text{PO}_4)_2 \cdot 8\text{H}_2\text{O}$, vivianite, mag. symmetry 8=5502
- $\text{Fe}_{0.88}\text{S}$, pyrrhotite, mag. structure from Fe^{57} resonance 8=16985
- FeS, troilite, mag. structure from Fe^{57} resonance 8=16985
- FeS_2 , effect of pressure on Mössbauer resonance 8=1652
- FeS_2 X-ray microanalysis, atomic number effect correction, obs. 8=14479
- Fe_2Se with NiAs structure, Mössbauer effect 8=16981
- Fe_2S_8 magnetisation process up to 90 kOe at 1.2°K, 201°K and room temperature 8=9281
- Fe_2Se_8 , magnetocryst. anisotropy const. 8=2321
- $\text{FeSiF}_6 \cdot 6\text{H}_2\text{O}$, Mössbauer spectra for hyperfine interactions 8=8220
- $\text{FeSiF}_6 \cdot 6\text{H}_2\text{O}$, pure and diluted crystals, ligand field behaviour and mag. susceptibility 8=18297
- Fe_2SiO_4 , hydrothermally synthesized, melting curve at press up to 40 kb 8=1615
- FeSn, antiferromag. with Néel temp. at 163°K, Mossbauer study 8=18339
- Fe_2Sn , ferromag., moments of Fe and Sn nuclei, Mossbauer study 8=18339
- FeSn, mag. structure from n diff. study 8=2320
- $\text{Fe}(\text{SO}_3\text{F})_3$, i. r. spectra and mag. props. 8=9562
- $\text{FeSO}_4 \cdot \text{H}_2\text{O}$, antiferromag. structure (spin order) 8=18380
- FeTiO_3 , mag. props., theoretical interpretation 8=9399
- FeTiO_3 , mag. resonance and susceptibility 8=9398
- FeV_2O_4 , lattice vibration, effect of deformation 8=8614
- (Mg, Fe) SiO_4 , iron ion tracks 8=8768
- Irradiation effects.** See Biological effects of radiations; Chemical effects of radiations; Physical effects of radiations.
- Ising lattice.** See Statistical mechanics.
- Ising model.** See Alloys; Ferromagnetism.
- Isomerism**
- See also Nuclear isomerism.
- acrylyl fluoride, rotational, i. r. and Raman spectra obs. 8=16311
- allyl halides, rotational 8=21111
- bromoacetone, rotational, in vapour, liq. and solid forms 8=1271
- dialkoxytetrahydropyrans, spin-spin coupling-models 8=12292
- 0,0-dimethyl phosphorochloridithioate, rotational ethyl nitrite, in gas, soln. and solid state, i. r. study 8=16329
- fluoroacetone, rotational, in vapour, liq. and solid forms 8=1271
- 2-fluoro- α -chloro- α , α -difluorotoluene 8=4227

Isomerism—contd

- 2-fluoro- α , α -dichloro- α -fluorotoluene 8=4227
 hexafluorobenzene, photochem. valence tautomerization, kinetics 8=2537
 methane, nuclear spin isomerization 8=18681
 methyl nitrite, in gas, soln. and solid state, i. r. study 8=16329
 methyldichlorotriphosphate, rotational isomers 8=4203
 phenylalanine rotamers, n. m. r. study 8=12289
 polymethylmethacrylate, rotational, in ester group 8=4220
 pyridocyanines, stereoisomerism 8=7596
 reversible isomerization in multilevel system 8=9680
 rotational, n. m. r. obs. 8=4226
 3,4,5-trimethoxyphenylglyoxal semidiones, rel. to e. s. r. meas. 8=12305
 CHBr₂-CFBr₂, rotational isomers, n. m. r. 8=4226
 C₃O₂-olefin mixtures, photolysis, product isomerization 8=5747
 Co complex, trans-dichloro(1,4,8,11-tetraazaundecane) cobalt (III) ion 8=7512
 Fe cpds. isomer shift of Fe nucleus 8=4681
 Sb¹²¹, Mössbauer effect in Sb isoelectronic cpds., chem. shifts 8=16987
 Sn(halide)₆⁻², Mössbauer line shift 8=8222
 Te(halide)₆⁻², Mössbauer line shift 8=8222

Isomerization. See Isomerism.

Isotope effects

- alcohols, deuterated, vapour press. 8=12995
 amines, deuterated, vapour press. 8=12995
 diffusion, interstitial, model 8=1901-2
 γ -u alloys, superconducting 8=2176
 gas mixtures, thermal diffusion props. 8=1492
 i. r. maser freqs., generated by isotopic substitution 8=10993
 K α , electronic shift in various isotopes 8=20671
 methane, dissociation, attachment of electrons 8=16454
 methanes, vapour press. 8=12994
 molecules, diatomic vibrations 8=12137
 naphthalene-d₈-naphthalene-h₈ mixed crystals, in triplet state, e. s. r. 8=18433
 shifts in deformed nuclei, rel. to vol. and surface vibs. 8=3781
 solids, isotope thermotransport effects theory 8=1904
 transition metal superconductor, rel. to dirtiness 8=5215
 uranyl salts, of D₂O, effect on spectra 8=5641
 vapour pressures, H-bond effects 8=4662
 vapour pressures of T₂O and D₂O 8=21780
 water, isotopic, e. m. f. of cells with alkali halides in soln. 8=4527
 water, var. of specific mass 8=7478
 Am, shift constants 8=16234
 C¹³ in decarboxylation of quinaldic acid 8=9697
 CO^{12,13}, laser, selective emission 8=19959
 Cd, elec. cond. 8=13712
 CeI, four natural isotopes, shift 8=21025
 D₂O in uranyl salts spectra 8=5641
 in H-H interaction pot. rel. to H₂ mol. 8=21075
 H₂O and D₂O, Debye temp. calc. 8=1544
 H¹, spectral shifts rel. to deform. of Hf¹⁷⁴ nucleus 8=20953
 KH₂(D₂)PO₄, rel. to conductivity 8=2130
 LiF, depleted of Li⁶, n thermoluminescence 8=20899
 LiF, shift of U-center local mode 8=13462
 NOF, vibr. spectra and force consts. 8=7539
 Na self-diffusion 8=17576
 NaH₂(SeO₄)₂ and NaD₂(SeO₄)₂, crystal symm. and nature of phase transitions 8=21849
 Pu, shift constants 8=16234
 Pu²³⁸⁻²⁴², arc spectrum, rel. shift 8=20965
 Th, shift constants 8=16234
 U, shift constants 8=16234
 α -U, superconducting transition temp., positive effect 8=22565
 Zn, rel. to superconducting transitions 8=9062
 Zn, self-diffusion, meas. rel. to vacancies and dislocations 8=4959

Isotope exchanges

- 1-iodo-2-4-dinitronaphthalene and KI¹³¹ acetone-H₂O, solvent effect 8=2504
 1-iodo-2-4-dinitrobenzene and KI¹³¹ in acetone-H₂O, solvent effect 8=2504
 in separation by multiple contact, analytical procedure of frontal process 8=23086
 thermal diffusion of gas mixtures in chem. equil. 8=9661
 B^{10,11} fractionation between BF₃ and additional cpds. 8=5698
 between BF₃ and liq. BF₃·dimethyl sulphide complexes 8=1569
 C¹⁴O in Fe₃(CO)₁₂ and Co₄(CO)₁₂ 8=2506
 in CO₂-NiO/Ni system, study of reaction with O¹⁸ labelling 8=9663
 [Co(C₂O₄)₃]³⁻-¹⁴C₂O₄²⁻ 8=21796
 [Cr(CNS)₆]³⁻-¹⁴CNS⁻ system 8=23087
 [Cr(C₂O₄)₃]³⁻-¹⁴C₂O₄²⁻ 8=21796
 H-D in non- α -helical polyamide 8=14349
 H₂ + D₂ homogeneous reaction 8=5697
 H₂O in atmosphere, liquid-vapour and solid-vapour below 0°C 8=2503
 H[Re₂O(CNS)₁₀]³⁻-¹⁴CNS⁻, kinetics 8=23089
 H₂-T₂ mixtures, equilibria and reaction rates 8=14448

Isotope exchanges—contd

- [Mo(CNS)₆]³⁻-¹⁴CNS⁻ system 8=23087
 N₂ equilibration on Mo 8=18655
 N^{14,14} + N₂^{15,15} = 2N₂^{14,15}, in shock tube 8=5696
 NH₃ system, deuterium disproportionation reactions 8=2505
 T, with toluene, self-induced 8=5695
 Ti(III)-Ti(I) in complexes, obs. 8=18653-4
 [V(CNS)₆]³⁻-¹⁴CNS⁻ system 8=23087
 [V(CN)₅NO]⁵⁻-¹⁴CN⁻, kinetics 8=23088
 [V(C₂O₄)₃]³⁻-¹⁴C₂O₄²⁻ 8=21796

Isotope separation

- See also Radiochemistry.
 calutron, ionized spectrum, Doppler shift due to charge exchange 8=6334
 calutron operating with 1-50 mg. of material 8=7480
 in dual-temp. systems with open circuits, conds. for separation 8=7477
 gases, thermal diffusion apparatus 8=16237
 Groningen e. m. separator, construction and use 8=21028
 magnetic prism, optical axis and correcting profile determ. 8=12114
 mass meter, signacon, resolution 8=21030
 by multiple contact, frontal process, analytical procedure 8=23086
 polar isotopic mols., by gas chromatography 8=9744
 real (mixing) cascade, dynamic behaviour, efficiency of separating element, distrib. of concs. in arb. range 8=21027
 real (mixing) cascade, theory for const. cut number and without losses 8=21026
 thermal-diffusion column, expt. test of theory 8=16715
 B complex, (CH₃)₂OBF₃, by exchange distillation, coeff. 8=18656
 Cf²⁴², from U²³⁵(C¹², 5n) 8=11834
 Co⁵⁸, extraction from aqueous soln using 1-phenyl-3-methyl-4-carpryl-pyrazolone-5 8=18750
 D₂-HT mixture, thermal diffusion 8=4495
 Fe⁵⁹, extraction from aqueous soln using 1-phenyl-3-methyl-4-carpryl-pyrazolone-5 8=18750
 Fm^{248,247,247m} from Pu²³⁹ bombardment 8=7239
 Mn⁵⁴, extraction from aqueous soln using 1-phenyl-3-methyl-4-carpryl-pyrazolone-5 8=18750
 N¹⁵, ion exchange electromigration method with superposition of a. c. on d. c. 8=12113
 Ne, processes in Hg diffusion column 8=1208
 Pu²³⁸O₂, depleted in O¹⁸ for radiation minimization 8=10443
 U, ion exchange reaction obs. 8=21029
 U²³⁵, ion exchange electromigration method with superposition of a. c. on d. c. 8=12113
 Xe, in telluriumbismuthite, Te¹³⁰ decay rate 8=1017

Isotope shifts. See Isotope effects; Spectra.

Isotopes

- inert gases anal. in Te ore 8=14455
 laser generation, frequency shift effect 8=416
 mass spectrometer for abundance ratio meas. 8=7355
 production by particle accelerators 8=6689
 radioactive, produced by 60 MeV p bombard. of Al, Fe, and Cu 8=1061
 ratio measurements, conference Japan 1966 8=16235
 Au^{177,178,179,182,183,185,187} prod. from Lu¹⁷⁵(O¹⁸, xn), Tm¹⁶⁹(Ne²⁰, xn), Yb^{168,170,174}(P¹⁹, xn) reactions 8=16045
 Au²⁰⁴, from Hg²⁰⁴(n, p)Au²⁰⁴, decay characteristics 8=11828
 B¹⁰ content, determ. 8=14456
 Ba, fission products of Cf²⁵² 8=20858
 Ca^{40,42,44,46,48}, energy level assignments from (t, p) 10-12 MeV 8=1094
 Cd¹⁰⁹ and Cd¹¹¹ n. m. r. frequency ratio between 8=16232
 Cd¹⁰⁹ and Cd¹¹¹ oriented by optical pumping, relaxation on silica walls 8=16233
 Cs, fission products of Cf²⁵² 8=20858
 Cs¹³⁷-Ba^{137m} generator 8=1207
 Er, n scatt. resonance parameters 8=1073
 Er¹⁷³, new radioactive 8=20756
 Fe⁵⁶-Fe⁵⁷ mass difference, from mass-spectroscopic and reaction Q-value analysis 8=21017
 He³ in He⁴ dissolution refrigerator 8=19682
 Hg, Holtsmark collisions 8=7468
 Hg, new isotopes prod. by Yb¹⁷⁰ + Ne²⁰, Sm¹⁴⁷ + Ar⁴⁰, Tm¹⁶⁹ + Ne²² reactions 8=7148
 Hg¹⁹⁹ and Hg²⁰¹, 6¹P₁ level hyperfine structures 8=7404
 Ho¹⁵⁴, new α -active isotope 8=3883
 LiF, with various Li isotope ratios, growth control using Stockbarger-Bridgman method 8=1742
 Nd, specific shift and deformation coefficient 8=21024
 Ni, ground state energy calc. 8=922
 Re¹⁸⁷, Os¹⁸⁷ terrestrial rel. to p charge time var. 8=15826
 Sn^{116,120,124}, charge density changes from 150 MeV electron elastic scatt. 8=1046
 Sn, neutron scattering amplitudes from powder patterns of SnO₂ 8=1809
 U^{233,235} fission, relative neutron yields, 0.08-1 MeV 8=7264
 Xe, fission products of Cf²⁵² 8=20858
 Z=102 synthesis by O^{16,18} + Pu²⁴² 8=1206
 103^{256,257} prod. by bombard. of Am²⁴³ with O¹⁸ 8=7151
 126³¹⁰ production possibility calc. 8=3972

detection

- See also Mass spectra; Radioactivity.
 abundance measurements, conference Japan 1966 8=16235

Isotopes—contd**detection—contd**

$\text{Ac}^{209,215}$ mass number assignment 8=20759
 Cs^{137} , Sr^{90} and Ce^{144} activity, in rain water, Sydney 8=14632
 H_2O , isotopic anal. of micro quantities 8=22151
 $\text{H}_2\text{O}-\text{D}_2\text{O}$ mixtures, comp. determ. by F^{19} n.m.r. 8=14454
 O_2 stable isotopes, microanal. by nuclear reactions 8=14453

relative abundances

See also Elements/relative abundances.
 anomalies, explanation by cosmic annihilation 8=7116
 graphite, noble gas anomalies, origin 8=9793
 ocean, U isotope deposition meas. 8=9813
 ratio meas. by peak matching in mass spectra 8=4112
 C^{14} , excess deposit after nuclear explosion, decay calc. 8=2610
 Er^{167} , after neutron capture, using mass spectrometer 8=11910
 H, in atmospheric precipitation 8=2503
 $\text{He}^{3,4}$, implications of Brans-Dicke theory 8=23478
 O and H, vars., firm core in W. Antarctica 8=14563
 O^{16} and O^{18} in minerals, liberation for mass spectrometry 8=12112
 Pb, common, abundance ratios, interpretation, generalized model 8=16236
 Re, by mass spectra from thermal ionization source 8=7479
 $\text{U}^{233}-\text{U}^{235}$ mixtures, radiometric anal. 8=4113

Jahn-Teller effect. See Molecules.

Jet stream. See Atmosphere/movements.

Jets

See also Sprays.

air/air, free, nozzle-fluid concentration field 8=4453
 air, cold axisymmetric, turbulent mixing with room temp. stagnant, obs. 8=16669
 air, impingement on liquid surface 8=12757
 air into compressible turbulent boundary layer, transformation 8=12665
 arc jet, thrust calc., mass flow rate 8=4421
 axisymmetric exhausting into quiescent atmos., length of supersonic core 8=16680
 axisymmetrical, and radial turbulent, appl. of boundary layer eqns. 8=19634
 capillary, oscills., infinite electric conductivity, in magnetic field 8=1518
 charged aerosol, ionization caused by aerodynamic discontinuities 8=4301
 circular jet along cylinder axis, electrostatic instability 8=12761
 compressible free, model for mixing with moving environment 8=16661
 compressible, turbulent, free jets, momentum and heat transfer 8=12652
 conducting, 2D, annihilation by transverse mag. field 8=352
 cylindrical, in immiscible liquid systems, Tomotika stability analysis 8=12760
 decay of axisymmetrical free flows with rotation 8=21463
 fluid, incompressible, three dimensional, turbulent, bulk properties 8=12585
 fluid, turbulent swirling, axial velocity and shear stress profiles 8=12626
 free and choked, with periodic structure, acoustic radiators 8=10722
 gas, diatomic, macroscopic radial distrib. rel. to vibrational temp. obs. 8=7499
 gas, impinging on liq. surface 8=12728
 gas from nozzle, plume geometry calc. 8=21453
 gas, rotating, generation of strong, travelling, transverse acoustic modes 8=15063
 hydromagnetic stationary 8=6359
 laminar, entrainment model 8=4437
 liquid, breakup rate and penetration in gas stream 8=16779
 liquid, high-pressure, pulsed, study by spark photography 8=16778
 liquid laminar, fluid mechanics 8=7989
 liquid, Landau thermal, temp. distrib. 8=16777
 liquid, micro, trailing an imploding gas bubble 8=12658
 M87 galaxy, radiation and props. 8=23592
 MHD, stability of 8=15367
 MHD, turbulent, incompressible 8=15377
 microcalorimeter for spatial distribution of particle energy 8=1457
 oscillation in the presence of a separator 8=16780
 parietal, spatial velocity correlations 8=7990
 penetration in basic O_2 furnace 8=10454
 phasograms with laser phase contrast system 8=7792
 plane, conducting liquid, propagation in mag. field and damping 8=19807
 plane laminar, eigensolutions 8=21424
 plane non-isothermal, turbulent mixing, velocity, temp. and pressure 8=4515
 plasma, coating of metallic materials 8=19337
 radial wall, turbulent, mass transfer from axial source 8=1451
 round, vortex evolution 8=21437
 rotating, acoustic energy density spectrum 8=19551

Jets—contd

smoke distribution, pulsed laser obs. 8=8152
 thin, injection into uniform stream 8=21445
 two-dimensional vertical, under gravity 8=21583
 viscous liquid, two-dimensional flow under gravity 8=21562
 wall-jet, laminar, over curved surface 8=21443
 Ar clusters in nozzle beams, dimer concs. 8=12379
 Ar, subsonic, electron densities, Langmuir probe 8=1409
 H, dense supersonic in high vacuum, in charge exchange target 8=21451
 Hg, turbulent, velocity profile in axial mag. field, obs. 8=7991
 He-Ar mixtures, separation 8=21471
 N_2 -He mixtures, diffusive separation obs. 8=19537
Jets, cosmic-ray. See Cosmic rays/showers and bursts.
Jogs. See Crystal imperfections/dislocations.
Johnsen-Rahbek effect. See Adhesion; Electrostatics.
Johnson noise. See Fluctuations/electrical.
Jordan-Thiry field. See Cosmology; Relativity/general.
Josephson tunnelling effect. See Superconductivity.
Joshi effect. See Discharges, electric/glows.
Joule-Thomson effect
 porous-plug expt. analysis, consistency in different reference frames 8=6061
 Ne-He mixture, integral effect 8=15139
Jupiter. See Planets.

K-capture. See Radioactivity/electron capture.

KDP. See Potassium compounds.

Kaons. See Mesons.

Keratin. See Proteins.

Kerr effect. See Electro-optical effects; Magneto-optical effects.

Kicksorters. See Counting circuits.

Kikuchi lines. See Electrons/scattering.

Kinematics

acceleration, referred to moving curvilinear coordinates 8=10531
 coupled oscillators and normal coordinates 8=10532
 equations of motion, computer formulation using tensor notation 8=19380
 Euler angles, helicity formalism for 4 identical particles 8=15912
 mechanisms with more than one degree of freedom,
 dynamic acceleration analysis 8=34
 nuclear reactions, simplified calc. 8=20766
 periodic motions of systems with impulsive interaction 8=10530
 potential flow, numerical solution for flux components 8=19365
 relativistic, of rigid rotor 8=11383

Kinetic theory

Boltzmann systems, spectrum and evoln. for soft potentials 8=1462
 boundary-value problem for Boltzmann eqn. 8=16687
 e.m. wave propag. through plasma in magnetic field 8=1392
 fluid diffusion, corrections 8=21416
 fluid transient Couette flow problem 8=21423
 m. h. d., wave correlations in uniformly turbulent weakly non-linear systems 8=4352
 Morse oscillator, one- and two-dimens, energy levels 8=1217
 photophoresis of particle in Knudsen gas 8=4629
 plasma, cylindrical column, model 8=16457
 plasma, Gibbs entropy calc. outside equilb. 8=4334
 plasma, inelastic processes 8=21303
 plasma, with inelastic processes 8=1379
 plasma, relativistic, momentum distribution after adiabatic compression 8=7731
 Poisson-Boltzmann eqn. rel. to internal energy of free p and e in H plasma 8=12469
 radiation fluctuation, detection 8=3010
 solar wind, two fluid model (electrons and protons) 8=23710
 stellar system, self-gravitating, with uniform rotation 8=23502

gases

See also Association/gases; Brownian movement; Collision processes; Diffusion in gases; Equations of state/gases; Joule-Thomson effect; Molecules/intermolecular mechanics.

Boltzmann's distrib. law, evaluation of exponent 8=19446
 Boltzmann equation, Chapman-Enskog method 8=134
 Boltzmann equation, linear and stationary solution 8=19474

diatomic, thermodynamic functions with molecules in Σ^3 state 8=1467
 dilute, correlation function when using Boltzmann and Fokker-type integrals 8=1463

Enskog-Chapman, appl. to thermal diffusion 8=21525
 exchange of energy between non-equipartition mixtures 8=16688
 fluctuation theory based on heirarchy eqn. 8=21501
 free-flight theory of mixtures 8=4467

free-molecule theory, applic. of Nocilla wall reflection model 8=21495
 hard-sphere, sequence of relaxation constants 8=133

Kinetic theory--contd**gases--contd**

inverse velocity space spectra and kinetic equations 8=10645

linearized collision operator, matrix elements 8=21499

loaded-sphere gases 8=4495

loaded sphere-smooth sphere mixture, thermal diffusion 8=12705

long-range attraction, kinetic equation 8=7908

Lorentz gas, non-analytic density behaviour of diffusion coeff. 8=16720

mixtures, equilibrium and nonequilibrium 8=118

mixtures, viscosity calc. 8=21522

molecular flow in long cylindrical tubes, soln. of Clausing's integral eqn. 8=21529

mols. vel. distrib. function near solid wall in non-uniformly heated gas 8=21494

Onsager relations, relativistic 8=21500

partially ionized 8=21497

plasma, multicomponent, Fokker-Planck eqn. 8=4327

plasma, partially ionized in time dependent mag. and e. m. fields 8=16466

polyatomic gases 8=16684

polyatomic, gyro-thermal effect in mag. field 8=12672

polyatomic relaxation and transfer eqns. 8=21502

polyatomic, transport processes, effect of varying elec. and mag. fields 8=1465

resistance to relative motion of gases 8=16686

Rice-Allnatt assumption in low-density limit 8=1464

scattering of short waves, eqns. 8=7911

shock wave density discontinuity, evolution governed by Boltzmann collision integral 8=7933

Stokes paradox 8=21496

thermal equil., approach through black-body radiation interaction 8=12673

transition state and Arrhenius parameters of reactions 8=4465

ultrasound propagation in mol. gas 8=4479

Van der Waals, fallacies 8=21503

van der Waals gas, Yang-Lee distrib. of zeros 8=12671

velocity distribution function, tail filling rate 8=7910

Ar on W surface, translation accommodation coeff. 8=17113

He⁴, virial coefficient, 2nd, for exponential repulsion potential 8=12678

N₂ on W surface, translation accommodation coeff. 8=17113

NH₃-H₂O-N₂-H₂ system, fugacities 8=12977

O₂ on W surface, translation accommodation coeff. 8=17113

liquids. See Liquids/theory.

link pairs. See Crystal imperfections/dislocations; Plastic deformation.

Markendall effect. See Diffusion in solids; Precipitation.

neutrons. See Electron tubes.

night shift. See Nuclear magnetic resonance and relaxation.

Nudsen number. See Flow; Hydrodynamics.

phon effect. See Crystal electron states; Crystals/lattice mechanics.

ramers-Kronig relations. See Dielectric phenomena; Optical properties of substances.

trypion

additive in Cs arc diode, effect on performance 8=15225

adsorption on zeolite LiX 8=1713

atom, influence of autoionization on spectra 8=20954

atom, spectral foreign gas broadening and shift due to Ne, Ar, He 8=20956

atoms, electron scatt., 40 keV 8=7447

atoms and ions, multielectron ionization in close collisions 8=21012

atoms and Rb, optically pumped, collisions, relax. correl. times 8=7472

condensation coeff. at 4.2°K 8=12981

excitation cross sections for some of the states of 4p²-5p configuration 8=20973

excitation functions of spectral lines by electron-atom collisions 8=4096

free-carrier drift-velocity studied in liquid and solid state 8=8119

gas, self-broadening and resonance oscillator strengths 8=20955

gas, spectral self-broadening and oscillator strengths 8=7416

ion, energy loss in passing through ZnS:As film 8=8758

ions, incident on polycrystalline targets rel. to sputtering coeff. 8=8766

ions, range distrib. in amorphous Al₂O₃ 8=13476

isotopic comp. with Xe, in B carbonaceous chondrites 8=19276

isotope mixtures, thermal diffusion props. 8=1492

liquid, sound velocity and law of corresponding states 8=1552

purification by directional freezing 8=4810

radioactive, luminescence due to atomic rearrangement, and inelastic collisions with electrons 8=7406

resonance lines, oscillator strength meas. 8=7449

scattering ionization, short range forces 8=1364

solid, compressibility 8=5075

solid, free carrier mobility 8=17863

solid at 0°K, parameters from interact. potential of gas 8=1468

solid, longitudinal sound velocity meas. at 4.2°K, 77°K and 90°K 8=17500

Krypton--contd

solid, phonons anharmonic effects 8=17481

solid, zero-point energy, effect of long-range 3-body forces 8=22083

solidified, vapour pressure, binding energy and mean vibration freq. 8=16960

superradiant transitions 8=7398

thermal conductivity, hot-wire cell meas., 30°-100°C, 120-150 torr 8=16700

thermal plasma, continuous emission spectrum 8=16207

trapped in diondrites, isotopic composition 8=19275

H⁺ on Kr scattering, charge transfer 8=1203

In-doped solid film, absorption spectra 8=9541

Kr₂, 2nd virial coeff. obs. 8=7913

Kr⁸³ in Br⁻ and BrO₃⁻ crystals, Mössbauer studies 8=8221

Kr⁸⁵, diffusion in multicomponent gaseous mixtures 8=1491

Kr-Ar binary mixture, spectra in vapour, liq. and solid states 8=7425

Kr-CO system, binary diffusion, unlike interactions 8=7943

Kr-NO system, binary diffusion, unlike interactions 8=7943

in ZnO:Zn, ions energy losses obs. 8=18624

Krypton compounds

KrF₂, absence of Fermi reson. 8=7528

KrF₂, ht. of formation 8=2519

KrF₂, identification and struct. by electron diffr. 8=17383

Kuhn-Thomas sum rule. See Molecules/electronic structure.

Kurie plots. See Beta-decay theory; Beta-ray spectra.

Kyropoulos method. See Crystals/growth.

LCAO calculations. See Molecules/electronic structure; Orbital calculation methods.

LS coupling. See Atoms; Spectra/atoms.

Laboratories

See also Acoustical laboratories.

electricity and magnetism unstructured, project type 8=15159

Frascati gas ionization, high-temp. plasma study 8=7798

modified open-ended, mechanics at general-physics level 8=10469

Naval Research (USA), optical studies 8=15490

Laboratory apparatus and technique

absorbing film containing pinholes, meas. of optical transmission 8=9483

acoustic drying of capillary-porous materials 8=19575

acoustic wave absorption in rocks, u.s. meas by bending vibration method 8=22095

airlock chamber for Siemens Elmiskop I 8=5993

alkali metal purification by preferential contact in magnetoplasma device 8=4302

alloys, preparing ball-shaped samples for mag. meas. 8=10859

alpha particle range, simple stand for determination 8=883

amplitude modulated, vibrations, mechanical demonstration apparatus 8=10679

automatic supervisor for electropolishing field-ion microscope specimens 8=17273

automatic temp. regulator for interval 10 to 150°K 8=15122

blender-reactor, jacketed 8=23091

calibrated leak prod. app., adapted for mats. with m. p. s. above room temp. 8=14907

carrier distillation, electrodes, apparatus for rapid prep. 8=14903

cathode-ray oscilloscopes, use in schools 8=10818

cell for adsorption study by i. r. spectrography 8=17157

cell for electrotransport meas. in liq. alloy systems 8=12816

ceramic, preparing ball-shaped samples for mag. meas. 8=10859

charged-particle detector expts. for students, using semi-cond. counter 8=609

cleaving device, in ultra-high vac. 8=21926

coating of fuel particles for 'Dragon' reactor expt. 8=7336

column for crystal purification with cyclic solids movement 8=17223

compression loads, meas. app. in controlled atmos. 8=5019

control device for filling liq. He storage dewars 8=15147

creep apparatus, for low temp. meas. 8=22256

cryogenic expt. for undergrad., mini-Dewar apparatus 8=254

crystal rotating head apparatus 8=8361

detection of conductor movement in homogeneous mag. field, possibility 8=10344

display of statistical data from nuclear expts. 8=6631

double cantilever beam specimens, use in determ. plane strain fracture toughness of metals 8=17721

dual-temp. system with open circuits, for isotope separation 8=7477

for efficiency meas. of cryogenically cooled pumping plane 8=7950

electricity and magnetism, project laboratory 8=15159

electron beam drilling of diamond dies 8=14906

electron beam zone refiner, conversion to r. f. heating 8=23774

Laboratory apparatus and technique—contd

electronic digital integrator 8=10817
 electronic furnace for electron beam smelting of rare metals 8=10457
 electropolishing of thin foils, for electron microscopy, specimen temperatures 8=4836
 embedding media for electron microscopy 8=6315
 field effect microscope, ultra-high vacuum metallic dismountable apparatus 8=15320
 films, thin, production and ion bombardment 8=17121
 flat discs for electropolishing, prod. by trepanning from bulk mat. 8=5996
 flaw detection and erosion rate meas. by microwave interferometry 8=5032
 foil, source supporting, e^+e^- annihilation 8=13693
 foils, simultaneous prep., by chemical thinning 8=8449
 Frascati Lab., plasma shock wave prod. 8=7798
 Fresnel zone plate generation 8=6551
 gas-tight thermobalance-load seal for corrosion studies 8=5991
 glass-fibre drawing apparatus 8=5073
 graphite soldering to metals, by first electroplating with Cu 8=5998
 high-pressure chambers, to 19 kbar, working at liq. He temp. 8=10464
 high-temperature electromagnetic stirrer 8=10455
 hydraulic feeding device for zonal melting of thin layers 8=8394
 hydrostatic weighing app. for meas. thermal expansion of polymorphic solids 8=17531
 image furnace for simulation of thermal effects of nuclear weapons 8=3986
 injector of T_1^+ , D_1^+ and H_1^+ ions for charge-exchange generator 8=7713
 instrument for digitizing continuous waveforms on paper or film 8=10816
 interferometer-LIN-1 8=6545
 interferometer, u.v. region, simple 8=6548
 internal friction and elastic modulus measurement at low frequencies 8=8784
 ion sublation using anionic and cationic collectors, radioactive tracer structures 8=23075
 isotope separation by thermal diffusion 8=16237
 Langmuir probe curve second derivative plotting devices, comparison 8=1335
 lens, determ. of longit. spherical aberration 8=470
 liquid drops, coalescence cell and bridge 8=12765
 liquid phase horiz. thermal diffusion column 8=12838
 for measuring liquid quantity 8=21575
 mechanics, demonstrations using electrical readout 8=10472
 metal chamber for meas. of elec. props. of organic semiconductors 8=9092
 metals, corrosion testing under heat transfer 8=18665
 microwave system, expt. and demonstration 8=6366
 miniaturized King furnace for absorpt. spectra of metal vapours 8=7393
 model expts. on gravity effect on tectonic processes 8=14512
 modified open-ended laboratory in mechanics at general-physics level 8=10469
 neutron diffraction installation on thermal column for meas. on liquid metals 8=8002
 neutrino expts. at CERN 8=15724
 new materials and processes in instrument manufacture, conference Eastbourne, 1965 8=2872
 nuclear phys. expt. based on $F^{19}(p,\alpha)O^{16}$, for senior students 8=1059
 nuclear structural engineering research facilities 8=4034
 parallel wire resistance wavemeters, dynamic testing 8=7986
 particle size comparator 8=5
 pen recorder for gas reaction kinetics 8=14353
 photometer for geology students 8=460
 polymeric mats., engineering, design problems and appls. 8=23773
 pore size distrib. meas. in solids, automatic control 8=17022
 profile projector modification for strain meas. by moiré tech. 8=13501
 radial grating dividing engine of high accuracy 8=11181
 real-time electro-optical signal processors, with coherent detection 8=6532
 recording Snoek spectra of metal wires at low freq. 8=8786
 reed pendulum for internal friction meas. 8=13495
 resonators, filled with TiO_2 dielec. discs, h. f. props. 8=19829
 rollers, at temps. between 42 and 300°K 8=19335
 rotating head, automatic, for single cryst. studies 8=8361
 sealing of glass illuminators of H bubble chamber, using pneumatic packing 8=15645
 sealing piston of pressure booster with rubber ring 8=10465
 seismology model, accuracy rel. to receiver-model coupling 8=14525
 ship performance measurement 8=5995
 shock-decating of eutectics 8=8170
 single channel recorder, device for conversion to multi-channel sequential recorder 8=6239

Laboratory apparatus and technique—contd

slitting thin foil, 25 μm , method 8=14904
 slotted disk velocity selector, construction by electric discharge machining 8=10453
 small high-press. gas vessel, for direct weighing of mass of large vol. 8=7890
 solar energy receivers, cylindrical cavity, optimal dimensions 8=19676
 solids under high press. 8=2873
 spectral lines, hyperfine structure obs. 8=7078
 static high-press., low-temp. seal 8=14910
 Stern-Gerlach app. for expt. on space quantization of atomic ang. momentum 8=1144
 surface contour meas. using gas laser probe 8=19339
 strain free polishing of accurate flats 8=5989
 targets, obtained by directed evaporation in high vacuum 8=23775
 Tremschaukel, four-tube all glass, new design 8=1488
 valve packing for cryogenic service 8=3139
 verneuil crystal growth, plasma heat transfer 8=21936
 vibrating quartz microbalance, transistorized temp. regulator 8=19671
 viscometer-gelation timer 8=16810
 water baths, const. temp., minimizing evaporation 8=16947
 water vapour counter for tritiated water analysis 8=9748
 X-ray microanalyser for industrial lab. 8=14492
 zone melting device, automatic 8=4800
 Al purification using fractional crystallization 8=4801
 Be polishing and etching by metallographic technique 8=4790
 Co(II)-Ni(II)-Mn(II)-V(V)-Mo(VI) chloride systems, extraction separation studies 8=23077
 Cu-base mats., oxidized, pickling in dilute H_2SO_4 , effect of u. s. vibs. 8=23780
 Cu wire, drawing process with lubricant under externally generated pressure 8=2052
 He³-He⁴ dilution refrigerator, rapid start-up 8=15145
 MO(VI) extraction with TBP, mechanism study by radioisotopes 8=23076
 Si, pellet bonding 8=22608
 Si polishing 8=10452
 W wire, recrystallized, sample prep. for transmission e-microscopy 8=17267
Lamb shift. See Spectra/atoms.
Lambda (λ) point. See Helium/liquid; Phase transformations.
Lamps. See Light sources.
Landé splitting factor. See Spectra; Zeeman effect.
Langmuir probes. See Discharges, electric; Plasma/measurement technique; Space vehicles/instrumentation.
Lanthanides. See Rare earth metals.
Lanthanons. See Rare earth metals.
Lanthanum
 film, superconducting, electron-tunneling meas. 8=9047
 oxidation kinetics, high temp. 8=18680
 position in periodic table rel. to densities of states in conduction band 8=8936
 La III, new spectra lines in 2000 to 12 000 Å region 8=12066
 La(Br_3 , Cl_3 , F_3), multiphonon orbit-lattice relaxation 8=133
Lanthanum compounds
 telluride phases, crystal chemistry 8=17202
 La aminoacetate mixed complex with salicylate in aqueous solution, fluorescence 8=21703
 La phosphate-vanadates, struct. and luminesc. 8=14330
 LaAlO₃:Cr³⁺, e. p. r. spectrum at room temp. 8=18426
 LaB₆ cathode modification for Bayard-Alpert gauge 8=16732
 LaB₆, powder suspension in N₂, m. h. d. generator working fluid 8=15199
 LaB₆, prep. and X-ray investigation 8=17384
 LaB₆, Cd⁺ sputtering coeff. determ. 8=17705
 LaBr₃, e. s. r. spectra of Gd³⁺ rel. to temp. 8=2369
 La-Ce alloy film, gapless superconductivity 8=5205
 La-Ce alloys, superconducting transition temp., paramagnetic impurity effect 8=9303
 La-Ce(Gd) alloys, Kondo effect in superconducting props. 8=5206
 LaCl₃ aq. soln., phenomenological coeffs. for elect. cond. and diffusion 8=12924
 LaCl₃, e. s. r. spectra of Gd³⁺ rel. to temp. 8=2369
 LaCl₃:Gd³⁺, energy levels and cryst. field 8=16975
 LaCO₃, p- and n-type, optical absorpt. by small polarons 8=2434
 LaF₃, gaseous, electronic states 8=7549
 LaF₃, condensation coeff. from thin film meas. 8=4655
 LaF₃:Nd³⁺, absorpt., luminesc. and generation spectra 8=3334
 LaF₃:Nd³⁺, stimulated emission, high-temp. effects 8=22960
 LaF₃:Nd³⁺, Yb³⁺, fluoresc. and energy transfer 8=14328
 La-Gd alloys, superconducting transition temp., paramagnetic impurity effect 8=9303
 (La, Gd)₂CoMnO₈ system, mag. interactions 8=9354
 LaH₂, sp. ht. 1.3-20°K 8=13373
 La-Lu alloy film, superconducting, electron-tunneling meas. 8=9047
 LaMg nitrate, Nd doped, proton spin-lattice relaxation 8=9462
 La₂Mg₃(NO₃)₁₂·24H₂O impurities, effect on proton dynamic polarization 8=14147

Lanthanum compounds—contd

- La₂Mg₃(NO₃)₁₂·24H₂O, ligand endor 8=22925
 La₂O₃—Al₂O₃ system, alumina-rich phase diagram 8=21746
 La₂S₃, gaseous, dissociation energies 8=7616
 La_{0.5}Sr_{0.5}CoO₃, magnetic props. near Curie point 8=18341
 La₂WO₆, prep., lattice constants and elec. resistivities 8=5709
 LaX₃, (X = Sn, Pb, Tl, In), with Cu₃Au structure, superconductivity 8=22551

Lasers

See also Light/coherence.

- acceleration of gravity meas. using laser-interferometer system 8=10487
 acoustic, mag. pumped paramag. salts appls. 8=15473
 advanced optical techniques, book 8=15489
 amplification coeff. meas. 8=19926
 amplitude noise and rate equations 8=11022
 appl. to gas determ. in metals 8=9747
 applications to metrology 8=6003
 applications, semi-popular review 8=401
 appl. to spectrometer scanning-function calibration 8=15539
 application to sound field spectral analysis 8=19552
 atmosphere, number density determ. of gas constituents 8=14585
 atmospheric propag., compared with nonlaser light 8=9867
 atmospheric scatter, mesosphere and above, obs. 8=9875
 atomic, multiquantum photoelec. effects as coherence meas. 8=20986
 atomic system, 2-level, statistics of 2-photon processes 8=20948
 beam effect on naphthalene, four-photon absorpt. 8=18517
 beam expansion in a turbulent medium 8=6428
 beams, intense, trapped filaments in liqs., props. 8=16832
 beam in liquids, self-trapping, obs. 8=21670
 beams in low-loss liqs, self-defocusing rel. to thermal convection and spherical aberration 8=15442
 beam modulation by Kerr cells 8=6488
 beam propagation through random medium 8=3251
 beam scanning using ultrasonic devices 8=15072
 beams, self-focused, for plasma meas. 8=16544
 beamwidth reduction, by optical antenna, radiometer check 8=20068
 calorimeter, C cone, pulse energy meas. 8=6223
 and chaotic superposed, intensity fluctuations obs. 8=20017
 cavity, reactive optical information processing 8=532
 chelates, rare-earth, in soln. 8=3338
 chloro-Al phthalocyanine, oscillation obs. 8=6475
 coherence props., quantum mechanical theory 8=19938
 coherence and quantum optics Conference, Rochester University, New York, June 1966 8=6484
 coherent field dynamics in first- and second-order processes 8=20034
 continuous-wave, appl. to electroretinography 8=11233
 continuously tunable radiation generation 8=15485
 coupling efficiency, optically pumped 8=413
 damage induced in glasses 8=8851
 damage to materials in high-power, review 8=403
 devices bibliography 8=11011
 diethylthiatricarbocyanine iodide and chloro-aluminium phthalocyanine, stimulated emission obs. 8=452
 direct reference beams for hologram construction 8=3381
 dust particles in cavity, propulsion and angular stabilization 8=6422
 dye, flashlamp excitation obs. 8=451
 dye laser, pumped by flash lamp 8=6477
 dye, longitudinally pumped, narrow-band continuously tunable 8=20006
 dye solution, wavelength dependent time development of intensity 8=20005
 effects on NaCl dislocation structure 8=17659
 elastic stress wave generation in pressure bar 8=6130
 electron, ion and laser beams technology, conference, Berkeley, USA (1967) 8=15283
 electron trapping in beam rel. to scatt. light freq. shift meas. 8=19821
 emission control devices, use of 45° X-cut ADP crystals. 8=6424
 emission, rel. to induced absorpt. effects 8=3287
 exact eqn. for distrib. function of macroscopic variables 8=3290
 experiments and explanations 8=19932
 field, N-mode photostatistics 8=412
 frequencies, dynamic behaviour 8=3296
 frequency spectrum, meas. with active Fabry-Pérot interferometer 8=20099
 frequency stabilization by induced fluorescence 8=16288
 frequency stabilization by nonlinear absorpt. in gas in resonator 8=15443
 filaments, self-trapped, type II superconductor model 8=9030
 fluctuating beams, anal. via photon counting statistics 8=6425
 fluids, filament formation, linearized theory 8=8067
 f.m., path-length-difference effects in photo mixing 8=19934
 focal evaporation, energy dependence 8=11007
 focused on nonlinear crystals., rel. to second harmonic generation 8=14166
 frequencies, dynamic behaviour, theoretical investigation 8=3297

Lasers—contd

- frequency fluctuations of field, photoelec. meas. by cross-correl. 8=11028
 frequency of radiation, increase by 3-photon process 8=408
 giant pulse spectroscopy, Fabry-Perot interferograms quasi-linear dispersion 8=6416
 giant pulse technique 8=6415
 for glass plates thickness and refractive index variation 8=14223
 gradient deflection of focused beams, spot distortion 8=11012
 harmonic freq. mixing of two different far i.r. lines up to 118 μ 8=19950
 harmonic generation with multiple-photon transitions in n.m.r. expts. 8=10984
 heating, gasdynamic processes 8=7928
 high power cavities, optimization of mirror transmissivity 8=6420
 high power, performance and limitations, review 8=10997
 hologram storage capacity of photochromic glass, meas. 8=6570
 illuminating NaCl and glass, characts. of emission rel. to damages 8=14246
 imaging of microwave acoustic beam, cross section in rutile by Bragg laser 8=6175
 impulse generation in stationary regime with mode trapping, limiting parameters 8=19946
 induced discharges, optical interferometry of 8=16403
 induced non-linear photoelectric effects in metals 8=22721
 inducing breakdown in gases, dynamics 8=1344
 incident on substances, optical absorpt. rel. to incident flux 8=12873
 information recovery from intracavity phase object 8=6578
 intense beams, interaction against single charged particles 8=19768
 intensity fluctuations at threshold, statistics 8=402
 intensity fluctuations, analogue and photon counting meas. 8=19970
 intensity noise theories rel. to photon counting distribts. 8=19939
 intensive single-freq. beam generation at second harmonic of f.m. laser 8=15444
 interaction with hypersound in laser cavity with Stokes feedback 8=11005
 interferometer, Michelson, for 6328Å use 8=6543
 interferometric determination of transducer face displacement and mode shape 8=6178
 internally scanned beam prod., with pulsed optical delay line in cavity 8=11008
 ionization of gases below 1 atm., inverse bremsstrahlung and e-impact processes 8=16434
 irradiancy, spectroscopic study of resulting plasma 8=12514
 in isotropic media, induction of elec. and mag. anisotropy 8=8106
 leuco-sapphire crystals, destruction by powerful radiation 8=2247
 light amplification, variable refractive index medium 8=400
 light frequency translation by moving grating 8=11189
 light mode and atoms, Fokker-Planck equation 8=19942
 light, modulation and demodulation 8=19933
 light source, props. of ions and electrons in plasma, expt. 8=16553
 light waves standing, obs. of deflection of 1.6 keV electrons 8=20378
 for linear velocity measurement 8=19936
 liquid, advantages and properties 8=20004
 liquids, molecular anisotropic, Rayleigh-Wing scatt. theory 8=8092
 liquid, new cavities with long capillary cells 8=11115
 liquid, organic, optimum pumping for homogeneity 8=11114
 in liquids, self-focusing, Raman and Brillouin scattering 8=4585
 in liquids, self-trapping filaments of light 8=4577
 magnetically pumped i.r., paramag. salts appls. 8=15473
 many element, mode selection props. 8=3301
 metal sheet heating, pulse frequency effect rel. to sheet thickness 8=2871
 4-methyl umbelliferone, aq. soln., stimulated emission at 454 m μ 8=6478
 microanalysis method using laser evaporation 8=14457
 mixing of emissions of Ruby and Nd, in non-linear crystal 8=14237
 mode competition by spatial hole-burning in saturable absorbers 8=11020
 mode-locked for reproducible optical second-harmonic generation 8=11024
 modes competition in laser with appl. external signal 8=411
 modes, coupled, correlation functions using thermodynamic Green's functions 8=6430
 modes, off resonance, instability 8=19947
 modulated light signal, amplification 8=19945
 modulation, ADP crystal props. 8=23002
 modulation by atmospheric turbulence 8=404
 multimode generation, during quasi-equilibrium disturbance in active medium 8=11014

Lasers—contd

- multi-mode generation rel. to spectral and spatial inhomogeneity 8=3300
- multimode generation in system with nonuniformly broadened luminesc. line 8=11004
- multimode, optical heterodyne applications 8=11030
- multimode, saturation of Ne for Landé factor meas. 8=1186
- in multiphoton absorpt. processes, stat. anal. rel. to source characts. 8=11165
- noble gas breakdown, radiative equilb. theory 8=7937
- noise, Fokker-Planck solution 8=11023
- noise and operation, quantum theory 8=19438
- noise in phase locking region, quantum mech. theory 8=3291
- noise, quantum Fokker-Planck soln. 8=19937
- nonlinear, for ultrashort light pulses 8=11145
- with nonresonance feedback, statistical props. of radiation 8=19943
- with non-resonant feedback due to scatt. 8=11003
- with nonuniformly broadened luminesc. line, spectral width and characts. 8=3289
- open resonator, diffraction losses 8=15447
- optical and magneto-optical rotation, light-intensity dependence from laser obs. 8=517
- optical parametric devices, quantum noise 8=15445
- optical parametric oscillation, theory and appl. to threshold cond. deriv. 8=11029
- optical pumping of materials 8=11010
- optical resonator with movable mirror, e.m. field 8=19944
- optical superheterodyne receiver, for communications expts. 8=6423
- oscillation disappearance with intense pumping 8=6413
- oscillator quantum noise, classical models 8=398
- oscills., stationary, diffusion effect 8=405
- oscillators, 3- and 4- level, output intensity fluctuations calc. 8=19940
- parametric amplification 8=6419
- passive Q-spoiling cells, intracavity Brillouin scatt. from CH₃OH solvent 8=16847
- 90° phase matching in KH₂PO₄, elec. field control for different freq. combinations 8=14234
- peak emission spin-orbit splitting rel. to g-factor and valence band of semiconductors 8=9094
- phase contrast system for plasma phasography 8=7792
- photomultiplier gate for stimulated-spontaneous light scattering discrim. 8=6331
- photon development of photographic grain 8=15563
- plasma heating, radiation spectra 8=16200
- plasma irradi., absorption rel. to magnetic field 8=1400
- plasma, laser-produced, u. v. emission spectra 8=7777
- plasma produced by non-Q-switched beam acting on target 8=21285
- plasma-producing in polythene films, formation mechanism 8=23034
- plasma, pulsed scatt. for calc. of e density 8=1401
- Pockels and travelling-wave modulators 8=20036
- polarization, non-linear macroscopic, calcs. using diagram method 8=406
- polystyrene soln., laser scatt. for verification of Brownian motion 8=1557
- potential as probes for study of structure of matter, with exponential amplifier 8=6421
- power stabilization by means of nonlinear absorption 8=3288
- progress in optics, book VI 8=15541
- propag. of spherical wave with Gaussian amplitude distrib. 8=20087
- pulsating conditions, theory 8=11009
- pulse energy meas., pyroelectric calorimeter 8=15128
- pulsed, induced retinal injury, melanin granules models 8=20130
- pulse irradi. of polypropylene, melting and recryst. or evap. 8=17710
- pulses, mode-locked, optical rectification 8=19931
- pulsed plasma, production and diagnostics 8=21353
- pulse reflection and transmission modes, laser rate equations 8=409
- pulsed source, high power and continuously tunable from 4820 to 5790 Å 8=11032
- pumping of ruby maser at 77°K 8=19920
- Q-spoiled, fluorescence of Nd³⁺ in glass, influence on dynamics 8=11017
- Q-switched, as light source in fluorescent photography of spray droplets 8=4636
- Q-switched, of variable pulse length, pulse duration reduction by nonlinear amplification 8=11002
- quantum mechanical calc. of photon number and amplitude fluctuation 8=11013
- quantum theory 8=19928
- quantum theory of optical behaviour 8=15441
- quantum theory of single mode operation 8=19453
- quantum theory, spectral profile 8=19929
- radar cross section, definition 8=19935
- radar selenodesy of moon 8=2813
- radar, target miss probability, atm. scintillation effects 8=9869
- radiation field, focused by optical systems with spherical aberration 8=10999

Lasers—contd

- radiation field, statistical props. by photon counting distrib. 8=10998
- radiation intensity and frequency fluctuations 8=6429
- radiation, linear and circular polarized, in optical third harmonic generation 8=11016
- radiation pulse heating of metals 8=3285
- radiation, resonance effect in field 8=20354
- Raman scattering, intense, pulsed mode, calc. 8=18488
- range finder, multipulse returns energy detect. statistics 8=6414
- rate eqns. for spontaneous emission, Lie-series soln. 8=10996
- ray focusing between concave mirrors of resonator 8=11025
- recordings detection, magneto-optic, high-density 8=14185
- regenerative amplifiers, theory, expt. and appls. 8=11027
- relativity, general, proposed test by lunar ranging 8=2953
- resonant elastic response of matter to intense light pulse, transient effects, bibliography 8=19925
- resonator, Fabry-Perot spherical mirror, utilization in spectral anal. 8=6432
- resonator, optical multicavity, use of laser mirror 8=15446
- review, materials, influence of reliability 8=10451
- rhodamine B dye, emission spectrum 8=21694
- rhodamine 6G and B, and mixtures, mode locking 8=20009
- ruby crystals, destruction by powerful radiation 8=22247
- ruby oscillator output phase vars. obs. 8=19991
- ruby, thermal effects in transparent crystals 8=4926
- scattering from gas particles, speckle pattern 8=3286
- scattering medium with negative resonance absorpt. 8=11021
- second sound effect on photostatistics 8=11192
- self-focusing of different polarizations in liqs, test of a. c. Kerr effect mechanism 8=12870
- self-focusing rel. to intensity depend. refractive index 8=11000
- self-focusing as a pulse sharpening mechanism 8=6433
- self-locked, large-signal effects 8=15448
- self-locking mode conditions 8=3302
- self-trapped filaments, study by second-harmonic-generation technique 8=11018
- self-trapped light filaments, rel. to stimulated Raman emission 8=11006
- short pulses, one- and many-photons interact. with matter 8=399
- spark discharge, surface, as light source for pumping 8=6412
- spark excitation of trace elements in powdered mats 8=23186
- spark region in air, electric breakdown 8=7670
- spark, spectroscopic investigation 8=3293
- spherical and ellipsoidal pumping chambers, optimum design 8=11019
- spin-rate sensor, two-mirror c.w. laser 8=6004
- statistical props. of light, quantized e.m. field model 8=19941
- steady-state, semiclassical and rate eqns., use for design 8=11001
- stimulated emission cross section from fluorescence changes 8=14292
- stimulated emission in selected compounds containing C, N and H or D 8=12398
- stimulated rad. from atoms during nonlinear interact. of transitions 8=417
- stimulated radiation of classical oscillators and h.f. electronics 8=3298
- stimulated Raman scatt., molec. mechanism 8=7487
- stimulated Raman scatt., quantum theory 8=3292
- streak interferometer, (or holometer), optics rel. to relative beam displacement 8=6542
- submillimeter wave, resonator modes 8=407
- super-luminescence field, correlation props. 8=19924
- surface discharge at end of active rod 8=19927
- surface interaction, production of high-energy molecules 8=18273
- theory, diagram method 8=6427
- rel. to transmission line noise theory, operation below oscill. threshold 8=19889
- 10.6 μ rad., photographic recording on thermoplastic resin film 8=6579
- tube, end windows set near Brewster angle, rel. to transmission 8=6426
- with tunable generation frequency, superior to two-quantum luminescence 8=19930
- tunable Raman laser, theory 8=11104
- ultrashort light pulse generation 8=3356
- ultrashort pulses, parametric amplification 8=11015
- wideband pulse compression using Brillouin scatt. in Bragg limit 8=10948
- Zeeman, theory 8=6417-18
- Al plasma produced, energy spectra 8=2122
- for CdS refractive index inhomogeneities and absorption saturation effects inducement 8=9515
- DBR, infrared transitions 8=6476
- DCI, infrared transitions 8=6476
- Eu, 3-diketon complexes, four-ligand, rel. to laser use 8=22978

Lasers—contd

- H₂, Raman effect, stimulated, meas. in terms of oscillators and amplifier theories 8=21081
 HBr, infrared transitions 8=6476
 HCl, infrared transitions 8=6476
 He-Xe plasma positive column, Xe-level population inversion 8=12405
 Hg⁺ hollow cathode, wide bore, fabrication 8=3294
 n-InSb, pumped by 10.6 μ CO₂ laser, tunable Raman laser 8=11104
 Nd³⁺/SeOCl₂ liquid, preparation 8=20008
 W irradiating, study of ion emission 8=13948

gaseous

- active medium gain value 8=3305
 activated U getter 8=15452
 amplifier, solution of wave equation in frequency domain 8=11040
 atmospheric absorpt. of 3.39 and 3.51 μ radiation expt. investigation 8=9880
 atomic or molec. beam, freq. stability theory 8=6438
 cavity with external mirrors, effect of windows 8=15451
 coherent properties demonstration 8=418
 confocal resonators, influence of optical defects 8=3313
 continuously operating with high radiation stability 8=11033
 cyanide, discharge, HCN mm absorption obs. 8=11055
 emitting power as function of resonator length and pumping 8=6437
 frequency changing method 8=19953
 frequency generation, isotopic frequency shift effect 8=416
 frequency of 118.6 μ m transition, freq. meas. 8=10482
 glass:Nd laser excitation of second harmonic generation in Cu₂Cl₂ 8=14213
 gyro, Langmuir flow effects 8=19952
 harmonics useful for freq. translation 8=6436
 infrared, annular output coupling 8=11038
 intensity fluctuations, theory and meas. 8=19951
 light source for hologram transmitted on television circuit, used for wavefront reconstruction 8=6573
 light sources for holography 8=15559
 in magnetic field, review 8=3306
 modes, axial and angular, phase and amplitude interactions 8=15456
 modes, axial, interaction of several waves travelling in both directions 8=15455
 mode generation during self-locking of modes 8=3303
 mode selector for, resonant prism, temperature-stabilized and tunable 8=11031
 multimode, excess photon noise in detected photocurrent 8=11039
 multimode operation, study with scanning Fabry-Pérot etalon 8=20095
 use of multiply-charged ions 8=15449
 negative ion, using mixture of oxygen and other atoms as working medium 8=19955
 oscillators, self-sustained, near threshold, noise exam. 8=6259
 parametric reson. rel. to nonlinear Zeeman effect, theory 8=6435
 perturbation theory, higher-order 8=6434
 photon distrib. in equil. and non-equilib. fields, obs. 8=19954
 power and collision broadening of transitions 8=414
 power output, broadening and shift of spectral lines, press. effects 8=11034
 processes surveyed 8=11041
 quantum theory 8=15454
 radiation, time dependent statistical props. 8=3304
 resonators, passive and active, polarization properties 8=19948
 resonators for producing single mode with optimum parameters, investigation 8=6431
 ring, counter-wave conds., polarization vector and stability 8=415
 with ring resonator, operational mode with stable travelling waves of different amplitudes 8=19949
 rocket propulsion particle velocity meas. 8=23457
 saturation and gain, information obtained from modulation expts. 8=11035
 spectrometer, Zeeman-tuned 8=490
 submillimetre c.w. construction and meas. 8=15450
 temperature compensation method 8=15453
 Zeeman, theory in presence of external static magnetic field 8=11036
 Zeeman type, monomode, polarization in mag. field 8=11037
 AgCl vapour, suggested 8=1235
 Ar, discharge ionization rate, spectrographic measurement 8=7709
 Ar for colour television display 8=11068
 Ar, high gain laser lines identification 8=7395
 Ar ion laser, c.w., resonance scatt. by Ar plasma 8=12513
 Ar ion, mode interactions 8=15458
 Ar ion, single frequency operation 8=6440
 Ar, long life construction 8=6439
 Ar, mode-locked quieting 8=15466
 Ar, multiwatt, experimental investigation 8=11146

Lasers—contd

gaseous—contd

- Ar, in thermionic hollow cathode discharge 8=15457
 Ar pulsed, inducing electron emission from W and Ta targets 8=18271
 Ar, pulsed, upper level population obs. 8=19956
 Ar, spectrum stable, magnetic field-tunable and linewidth determ. 8=11043
 Ar-ion, single-freq. operation at 5145 Å 8=19957
 Ar II, polarization in perturbed spontaneous emission spectrum 8=11042
 Ar', spectroscopic study of transition wave functions and probabilities 8=3307
 Ar', study of relevant characts. of Ar gas discharge 8=12402
 Ar-O₂ gas mixtures, mechanism for laser transitions 8=19975
 Ca, ionized vapour, pulsed, efficiency 8=11056
 CN, far i.r., characts. 8=11054
 CO, oscillation characteristics on electronic transitions 8=11069
 CO₂, amplifier gain characteristics at 10.6 μ 8=6445
 CO₂, amplifier, nonresonant multipass 8=6446
 CO₂ amplifiers, 10.6 μ gas flow effect on gain 8=11053
 CO₂, appl. with d.c. field to InAs, optical second-harmonic generation 8=5610
 CO₂, atmospheric absorpt. of radiation 8=6441
 CO₂ chem. laser possibility via excitation transfer from heated N₂ 8=16271
 CO₂, and coupled cavity interferometry for plasma diagnosis 8=12522
 CO₂ discharge, gain 8=19963
 CO₂, effect of tube structure on power and efficiency 8=11044
 CO₂, flux limits for continuous and Q-pulse gain for 10.6- μ line 8=19960
 CO₂, freq. of oscill., press. and current depend. shifts 8=15460
 CO₂, i.r. emission, effect of He or N₂ 8=12177
 CO₂, for i.r.-microwave double reson. 8=6402
 CO₂ laser excitation of second harmonic generation in Cu₂Cl₂ 8=14213
 CO₂ levels, lifetimes, effects of CO₂, He and N₂ 8=420
 CO₂, molecular, review 8=11049
 CO₂, obs. of radiation using i.r. image converter 8=19962
 CO₂, oscillations and amplifiers dispersion meas. by interferometric method 8=11052
 CO₂, output visual obs. by controlled incandescence 8=15463
 CO₂, photolysis of hydrocarbon gases 8=2538
 CO₂, plasma temperature meas. 8=15459
 CO₂, population inversion time 8=3309
 CO₂, power output increase, inexpensive 8=6444
 CO₂ radiation, second harmonic generation in α -HgS 8=5606
 CO₂, recovery time from pulse discharges 8=6443
 CO₂, review of development 8=11050
 CO₂, sealed-off, high output and long lifetime 8=11048
 CO₂, sealed tube, life expectancy rel. to form. and adsorpt. of CO and O₂ 8=15461
 CO₂, second harmonic generation in Se 8=6442
 CO₂, selective oscillation of P and R branches 8=11051
 CO₂ at 10.6 μ in SF₆ gas, self-induced transparency 8=1478
 CO₂, transitions near 10 μ , Lamb dip. obs. 8=15462
 CO₂, vibr. levels population calc. 8=15464
 CO₂, selective isotope emission 8=19959
 CO-N₂, modulation of optical cavity 8=19961
 CO₂-N₂, multipath cell for oscillator and amplifier 8=419
 CO₂-N₂-He, multikilowatt in modular form construction 8=11046
 CO₂-N₂-He, Q-switching, appls. and progress 8=11047
 CO₂-N₂-He, radiation prod. mechanism, effect of water vapour addition 8=11045
 CO₂-N₂-He, sealed, catalysed output using heated Pt wire 8=3308
 CS₂-N₂, interpretation and mechanism 8=19958
 CS₂-N₂, P-branch vibrational transition 8=3310
 Cu, atomic vapour, pulsed, efficiency 8=11056
 Cu vapour, pulsed 5106 Å, theoretical model 8=15465
 D₂O and H₂O, far i.r. oscillators, construction and characts. 8=425
 DF, chemical, during flash photolysis of UF₆ in presence of D 8=424
 H-beam, stimulated emission line shape and width obs. 8=421
 HCN, CW submillimeter lines, absolute freq. meas. 8=422
 HCN, 337 μ harmonics mixed with 190 μ and 180 μ for i.r. lasers 8=19950
 He-Ne, with axial mag. field, resonance dips in output 8=11065
 He-Ne, axial mode frequency and power, characteristics 8=19967
 He-Ne, axial mode number, from moving-mirror experiments 8=11026
 He-Ne, backscattered depolarized component rel. to multiple scatt. 8=19839
 He-Ne c.w., microcalorimeter 8=19673
 He-Ne, c.w. 6328 Å, modes 8=19971
 He-Ne, Fabry-Pérot etalon flatness quality determ. 8=20093

Lasers—cont'd

gaseous—cont'd

- He-Ne, cold cathodes for 8=11067
 He-Ne, collision processes 8=11061
 He-Ne for colour television display 8=11068
 He-Ne continuous wave, hazards to eye 8=14900
 He-Ne, and coupled cavity interferometry for plasma diagnosis 8=12522
 He-Ne, deflection by ultrasonic wave 8=6450
 He-Ne, discharge modulation noise 8=6449
 He-Ne, divergence meas., optimal conditions 8=6448
 He-Ne, double resonance spectroscopy in Ne 8=11066
 He-Ne, ears on line profile of decay transitions 8=3316
 He-Ne, growth of oscillations 8=19964
 He-Ne, i. r. interferometry of shock-tube plasma 8=16541
 He-Ne intensity correl. near threshold, 6328Å and 3.39μ 8=19970
 He-Ne, intra-cavity loss perturb. rel. to Faraday effects in glasses 8=11059
 He-Ne laser, intensity fluctuations, correlation meas. 8=3315
 He-Ne laser light source for light scatt. by He⁴ superfluid 8=8078
 He-Ne laser and monochromatic incoherent light fog scattered comparison 8=14615
 He-Ne, light absorption by air, experimental apparatus 8=7935
 He-Ne light source for Raman spectroscopy of powders 8=14175
 He-Ne, light source for velocity meas. 8=6489
 He-Ne, meas. method for depend. of gain per pass on power inside cavity 8=19969
 He-Ne mixture, pulse delay rel. to partial Ne pressure 8=3314
 He-Ne, mode-locked quieting 8=15466
 He-Ne, modulation by inactive cavity 8=19965
 He-Ne, optimum d. c. excitation 8=15470
 He-Ne, oscill. mode interaction, with spher. mirror resonator 8=427
 He-Ne, output intensity variation of, in a magnetic field 8=15468
 He-Ne, photoexcitation of GaAs p-n junction 8=9252
 He-Ne, plasma-optical effects at 0.63μ, 1.15μ and 3.39μ 8=3319
 He-Ne, plasma parameters meas. 8=3318
 He-Ne, power dependence on longitudinal magnetic field 8=3320
 He-Ne, power enhancements with double pulse excitation, comments 8=11062
 He-Ne, probability of 3s₂-2p₂ transition in Ne 8=3317
 He-Ne, properties, application: interference measurement of length 8=7
 He-Ne, radiation noise rel. to discharge stimulation 8=19966
 He-Ne, resonances due to Zeeman effect 8=15469
 He-Ne, rough reflector, noise and operation at λ = 3.39μ obs. 8=11064
 He-Ne for Rowland's ghosts, obs. 8=3372
 He-Ne single-mode, single freq., stabilization of output 8=11060
 He-Ne, spatial coherence, expt. investig. 8=19968
 He-Ne, spatial coherence and mode structure 8=6447
 He-Ne, spontaneous emission as wavelength standard 8=15467
 He-Ne, Stark effect produced frequency shifts 8=11058
 He-Ne, stationary regime and oscilln. damping 8=15471
 He-Ne, super radiant transition due to Ar addition 8=11063
 He-Ne 6328Å for contour measurements 8=19339
 He-Ne 6328 Å, self-pulsating oscillator 8=11057
 He-Ne, 3.39 μ Ne line, modulation by electro-optic gases 8=426
 HF, chemical, during flash photolysis of UF₆ in presence of H 8=424
 HF, emission from rotational transitions 8=423
 H₂O vapour, pulsed, single wavelength operation 8=3312
 H₂O vapour transition, 220μm, absolute freq. meas. 8=19972
 H₂O, Zeeman effects in 118.65μm transition 8=3311
 N₂, oscillation characteristics on electronic transitions 8=11069
 N₂ pulsed, four new lines 8=11070
 N₂ pulsed for planograms of smoke distribution in turbulent jets 8=8152
 N₂, pulsed, two-photon absorpt, in alkali halides 8=5578
 N₂, pulsed, theory 8=15472
 N₂ pulsed, u.v., Raman scatt. from atm. 8=23289
 N₂, as u. v. source with repetitive subnsec. kW pulses 8=20069
 N₂-CO₂, direct obs. of 10.6μm output beam patterns 8=19973
 Ne, i. r. Zeeman-tuned, for fine-structure anal. of absorpt. spectra 8=11160
 Ne, Zeeman type, polarization in mag. field 8=11037
 Ne-H, light vel. meas. 8=457
 Ne-He, self-oscillations, stability 8=19974
 Ne-O₂ gas mixtures, mechanism for laser transitions 8=19975
 NOCl, photodissociative chemical reversibility, solar excitation rates 8=3321

Lasers—cont'd

gaseous—cont'd

- OH, hyperfine polarization, rel. to OH cosmic rad. 8=23582
 Xe, i. r. Zeeman-tuned, for fine-structure anal. of absorpt. spectra 8=11160
 Xe, ionized, c. w. oscillation at 9697Å 8=6451
 Xe, microwave excited, new c. w. ion laser oscillation 8=6452

solid

- amplification of amplitude-modulated light signal 8=19977
 CW using vitreous substances, at room temp. 8=19998
 diodes, mag. field effect on spontaneous emission linewidth 8=19999
 efficiency of optical system with cathode luminescent pumping 8=6454
 emission in anisotropic Pérot-Fabry cavity 8=19981
 excitation cavities, geometry and continuous operation 8=19980
 exciton, quantum mechanical theory 8=6456
 external distributed resonator correction of angular divergence 8=3299
 glass fibre, passive core and Nd-doped cladding, osc. and amp. by total internal refl. 8=11073
 glass, Nd doped, Q switching with dyes 8=430
 glass: Nd, stimulated emission cross-section, from free-running oscillator output 8=19979
 glass: Nd, travelling-wave, features 8=3333
 increasing pump flux by immersion 8=433
 inert-gas crystals, laser generation of short wave-length (vac. u. v.) 8=18534
 infrared rangefinder 8=448
 injection, review of structural parameters 8=15476
 irradiated metal temp. from crater microscopy 8=8769
 junction, threshold current calc. 8=6467-8
 with large annular dispersion of light, spectral props. 8=431
 laser CW with Czochralski material, diffraction-limited emission 8=11083
 laser light on LiD and LiH target, plasma prod. 8=8774
 light polarization determ., apparatus 8=11074
 mode selection within active element 8=6455
 non-linear crystals, tuning for second harmonic 8=3322
 operation and properties, review 8=6453
 optical pumping by spherical reflector 8=11108
 oscillations, non-stationary, theory 8=19978
 photolysis apparatus, nsec range 8=9728
 pulse lamp supply for pumping, calc. 8=3323
 pulse output and mass ejection from metals 8=8759
 pumping cavities, machining assembly 8=23771
 Q-spoiled, passively, axial mode discrimination 8=3324
 quartz, stimulated Raman scattering from i. r.-active phonons 8=11112
 radiation dynamic eqns. 8=6457
 radiation, heating of plasma in magnetic field 8=7735
 ruby, alignment method, rapid and accurate 8=19988
 ruby, amplification of R₂ line in stimulated scattering system in CS₂ 8=9520
 ruby, appl. to biological microscope 8=6503
 ruby, axial emission modes, self-locking 8=11087
 ruby, beam divergence testing 8=15478
 ruby, cavity, for stimulated Brillouin scattering in methanol 8=4584
 ruby, change and stabilization of operating wave-length 8=19987
 ruby, continuous, power output and efficiency 8=437
 ruby, damage on semiconductor surfaces 8=2028
 ruby, effect of giant pulse irradiat. 8=3327
 ruby, effect of internal modes on operation 8=19986
 ruby, excitation of quartz, rel. to stimulated Mandel'shtam-Brillouin scattering 8=5632
 ruby, excitation of Raman spectra 8=9570
 ruby, expts. on phonon terminated laser amplification 8=14196
 ruby, Faraday Q-switch 8=435
 ruby, giant pulse, dynamics of generation field, spectrum and coherence 8=3329
 ruby, giant pulse, frequency drifts, inversion depend. 8=19984
 ruby, giant-pulse mode selection 8=15479
 ruby illumination, pulsed hologram formation 8=529
 ruby, induced changes in GaAs optical properties and carriers density 8=5633
 ruby, induced changes in Si optical properties and carriers density 8=5633
 ruby, interferometers for fluid mechanics 8=16618
 ruby-laser filaments, diffraction-coupling 8=19990
 ruby, with lens system, spectral characts. and radiation kinetics 8=19989
 ruby, light interaction with conductors, semiconductors and dielectrics 8=18272
 ruby, loss measurement, new method 8=11085
 ruby, losses of resonant cavity, meas. by comparison of R₁, R₂ thresholds 8=11080
 ruby, Lummer-Gerke plate application 8=3328
 ruby rel. to macroparticles accel. by radiation-reaction 8=10885
 ruby, mode competition caused by saturable absorbers 8=11020

- Lasers—contd**
solid—contd
- ruby, mode self-synchronization in broad spectrum giant pulse, obs. 8=11076
 - ruby and Nd, radiation mixing 8=436
 - ruby, nonlinear absorpt. by K_2 vapour 8=7527
 - ruby, nonlinear propag. in dielectrics 8=22931
 - ruby, non-Q-switched, picosecond substruct. of laser spikes 8=20002
 - ruby, with non-resonant feedback due to scatt. 8=11003
 - ruby, output spectra rel. to linewidth determ. mechanism in YAl garnet:Nd 8=11111
 - ruby, phonon breakdown theory 8=22952
 - ruby, picosecond pulses, spontaneous appearance 8=439
 - ruby, plasma scattered light, 12-channel Doppler-profile spectrophotometer 8=3357
 - ruby, precise wavelength meas. by Fabry-Perot interferometer 8=19992
 - ruby, production of single longitudinal mode 8=6459
 - ruby pulse laser, 50 Hz, emission 8=3326
 - ruby, pulsed, calorimetric meas. of output energy 8=11084
 - ruby, pulsed, pure transverse modes from special cavity 8=11086
 - ruby, pulses photography of plasma sheath 8=12526
 - ruby, pump power and efficiency calc. 8=3331
 - ruby, pumping of quartz rel. to quartz behaviour as Ramn oscillator 8=2453
 - ruby, Q-switched, energy losses 8=6458
 - ruby, Q-switched, feedback control, expt. and theory 8=11079
 - ruby, Q-switched, formation time and resonator loss, exp. 8=434
 - ruby, Q-switched, giant pulse generation by external signal 8=19983
 - ruby, Q-switched, hologram resolution 8=20110
 - ruby, Q-switched, for production of C plasma 8=21357
 - ruby, Q-switched, time resolved beam structure 8=11082
 - ruby, Q-switching using liq. Se mirror as a reflector 8=11078
 - ruby, quenching of one pulsed laser osc. by another rel. to coupled rate eqns. 8=11075
 - ruby, rad. field structure rel. to optical inhomogeneities in substance 8=3330
 - ruby, resonators, prism for state and plane of polarization preservation 8=438
 - ruby, rod distortion compensation rel. to brightness gain and mode control 8=11081
 - ruby, shock wave production using solid target, and plasmoid scattering 8=19534
 - ruby, simultaneous pulsing 8=15477
 - ruby, single-mode, characts. as laser radar transmitter 8=11077
 - ruby, single-pulse single mode, with diffractive beam divergence 8=19985
 - ruby, spike smoothing by optical filter 8=11141
 - ruby, stimulated Brillouin scatt. in quartz, optical heterodyne detection 8=14267
 - ruby, with tilted plates as discrimination, modes and generation kinetics 8=3332
 - ruby, tunable, repetitively pulsed, with solid etalon mode control 8=19993
 - ruby, for two-quantum photoionization rate of Cs and Γ 8=12437
 - ruby, use in generation of hypersound in MgO:Cr crystal 8=10727
 - ruby, variable freq. monochromatic source, for study of absorption specrum in pink ruby 8=18499
 - semiconductor, degenerate, emission props. rel. to band-tail spreading energy 8=13781
 - semiconductor, freq. modulation by u.s. waves 8=11093
 - semiconductor, interband magneto-optical, theory of e. m. modes and threshold conds. 8=11071
 - semiconductor, optical pumping rel. to saturable transmission by multiphoton absorpt. 8=9478
 - semiconductor, population and current noise 8=429
 - semiconductor, potential use, capabilities 8=9589
 - semiconductor, with radiating mirrors, using electron or laser beam exciting 8=11072
 - semiconductors, review 8=19982
 - semiconductor, theory considering saturation effects 8=15475
 - spectrum, with nonuniform pumping 8=15474
 - stimulated emission in conditions of reabsorption 8=3325
 - water-cooled pumping systems for continuous operation 8=432
- A¹¹B¹¹ semiconductor cpds., (A=Zn, Cd, Hg; B=S, Se, Te) 8=18023**
- CaF₂:Dy²⁺, giant pulse, with high repetition rate 8=11090
 - CaF₂:Er³⁺, stimulated emission at $\lambda_1 = 8456 \text{ \AA}$ and $\lambda_2 = 8548 \text{ \AA}$ 8=22963
 - CaF₂:Nd³⁺, new spectral line, oscillations from ions at noncubic sites 8=3335
 - CaF₂:Nd³⁺, stimulated emission, high-temp. effects 8=22960
 - CaF₂:Sm²⁺, from giant pulse ruby laser excitation 8=11089
 - CaF₂:Yb³⁺, new spectral line, oscillations from ions at noncubic sites 8=3335
 - CaWO₄ crystals, light loss, possible scattering contribution 8=19994
 - CaWO₄:Nd³⁺, quasicontinuous 8=440
- Lasers—contd**
solid—contd
- Cd, c. w. oscillation at 4416 Å obs. 8=6460
 - CdS laser transition at 90°K using two-photon excitation 8=11091
 - CdS(Se) semiconductor, free exciton annihilation 8=11088
 - CdS_{1-x}-CdSe_{1-x} crystals, temp. depend. of freq. 8=11092
 - CdS_{1-x}-CdSe_{1-x}, stimulated rad. during two-photon excitation 8=23049
 - Ga_{1-x}Al_xAs diodes, stimulated emission at 77°K 8=19997
 - GaAs 8=11095
 - GaAs, cw, linewidths meas. at 77°K 8=11094
 - GaAs, diode, c. w.-operated, junction temp., current depend. 8=442
 - GaAs diode, freq. modulation by u.s. waves 8=11093
 - GaAs diode, operating at room temp. 8=441
 - GaAs, diodes, continuous operation in liquid He 8=11101
 - GaAs diodes, lasing wavelength rel. to threshold current density and impurity conc. 8=15483
 - GaAs diodes, increased efficiency and output 8=428
 - GaAs diodes parameters, influence of junction structure 8=6464
 - GaAs, dislocation free, diode showing homogeneous neon-field pattern 8=11097
 - GaAs, dual type, quenching response 8=443
 - GaAs, electron beam excited, pulsed operation 8=6469
 - GaAs epitaxial p-n junctions, spontaneous and coherent light emission 8=6466
 - GaAs, injection, compensated p region, elec. and optical props. 8=15482
 - GaAs, injection, emission modulation and synchronization 8=15481
 - GaAs, injection, degradation characteristics, investigation 8=9140
 - GaAs injection, catastrophic degradation 8=6461
 - GaAs junction, e. m. cavity properties 8=19996
 - GaAs junction, operation on diamond heat sinks at 200°K 8=6465
 - GaAs junction, output spikes 8=11096
 - GaAs, light pulse synchronization 8=15480
 - GaAs, low threshold diodes 8=19995
 - GaAs for optical ranging system 8=14918
 - GaAs p-n junction laser, direct investigation method 8=445
 - GaAs, radiation pulsations, investigation 8=11098
 - GaAs semiconductor, optically pumped, av. power output 8=11102
 - GaAs, threshold current calc. 8=6467-8
 - GaAs, threshold current density temp. dependence 8=6463
 - GaAs, time characteristics 8=11099
 - GaAs:Sn, electron-beam pumped, quantum efficiency 8=11100
 - GaSb, diode, fine structure spectrum 8=444
 - GaSb, influence of doping on emission parameters 8=5313
 - GaSb, injection, emission in pulsed conditions 8=6462
 - Ge, stimulated laser emission 8=5664
 - Hg_{1-x}Cd_xTe, i. r. coherent emitter and fast detector 8=11103
 - InAs diode, prod. by liquid phase epitaxy low efficiency 8=11106
 - InAs, i. r. coherent emitter and fast detector 8=11103
 - InP, optical excitation of coherent emission 8=6470
 - InSb diodes at low temp., mag. field effect on spontaneous emission linewidth 8=19999
 - InSb, i. r. coherent emitter and fast detector 8=11103
 - InSb, mag. field depend. of mode spacing and total no. of modes 8=11105
 - InSb, pulled p-n junctions, coherent radiation obs. 8=6471
 - LaF₃:Nd³⁺, absorpt., luminesc. and generation spectra 8=3334
 - LaF₃:Nd³⁺, stimulated emission, high-temp. effects 8=22960
 - NaCaYF₆, Nd³⁺ activated 8=446
 - Nd, giant pulse generation 8=6472
 - Nd glass, measurement cross-section stimulated emission 8=449
 - Nd glass, with travelling wave 8=20000
 - Nd: glass amplifiers, gain saturation 8=447
 - Nd: glass, mode-locked, Eastman 9740 bleachable dye transmission obs. 8=11110
 - Nd: glass, picosecond pulses, spontaneous appearance 8=439
 - Nd: glass, picosecond substruct. of laser spikes 8=20002
 - Nd-glass, broadband, second harmonic generation 8=15486
 - Nd-glass, rad. spectra, spatial inhomogeneity 8=450
 - Nd, Q improvement by resonator deformation 8=3336
 - Nd, Q-switching by Pockels shutter 8=20001
 - Nd silicate glass, stimulated emission cross section obs. 8=14292
 - Nd, simultaneous pulsing 8=15477
 - Nd, spark propagation from weak lens 8=3337
 - Nd:Cr:YAG, sidelight fluorescence changes, due to laser ing at 1.06 μ 8=6473
 - Nd:Cr:YtAl garnet optical pumping by spherical reflector 8=11108
 - Nd³⁺/glass, generation of continuously tunable radiation source 8=364
 - Nd³⁺ glass, self-Q-switching by saturable absorpt. of colour centres 8=11107
 - Nd³⁺:glass, stimulated Raman emission in H₂ at 8.84 μ m 8=15484
 - Nd³⁺, high-repetition-rate Q-spoiled, in YAG, output characts. 8=15487

Lasers--contd
solid--contd

- Nd³⁺-Yb³⁺ glass, at 1.06 μ 8=11109
 Nd³⁺-Yb³⁺ glass, self-Q-switching by saturable absorpt. of colour centres 8=11107
 Ne in Fabry-Pérot cavity, light polarization obs. 8=19976
 YAG crystals, light loss, possible scattering contribution 8=19994
 YAl garnet:Nd, output spectra rel. to linewidth determ. mechanism 8=11111
 Y-Al garnet:Nd, five KHz repetition-rate pulsed, design 8=11113
 YAlG:Nd, repetitively Q-switched, continuously pumped operations 8=6474
 YAlG:Nd³⁺, transition cross-section and fluorescence branching ratio 8=20003
 ZnO semiconductor, free exciton annihilation 8=11088
 ZnTe, submillimetre-wave generation by optical difference-frequency mixing of ruby lines 8=18569

Latent heat

- See also Heat of adsorption, etc.; Thermodynamic properties.

No entries

Latent image. See Photographic process.

Lattice constants. See Crystal structure, atomic.

Lattice dynamics. See Crystals/lattice mechanics.

Lattice energy. See Bonds; Crystals; Solids.

Lattice gas. See Statistical mechanics.

Laves phases. See Alloys; Phase transformations/solid-state.

Lawrencium

No entries

Lawrencium compounds

No entries

Lead

- abundance in sun, spectrometry 8=23696
 atoms, electron-impact ionization cross-sections 8=12428
 ball indentation tests and grain structure 8=13602
 collective motions of atoms in liq. state, compared with polycryst. solid 8=12796
 creep, stress sensitivity at low stresses, article discussion 8=17825
 dislocation-electron interactions, normal and supercond. 8=17864
 effect of small amounts on self-diffusion of Fe in γ -phase 8=1930
 electron emission, secondary, for large incident angles of primary beam 8=5421
 explosive welding to steel 8=10456
 fatigue mechanism, 0.5-0.85 Tm°K 8=8806
 Fermi surface 8=5114
 films, self-supporting, 250-500Å thick, prep. 8=4751
 γ -beam scatt., differential albedo obs. 8=16844
 inhibitor, in Cu-Zn alloys, selective corrosion 8=23100
 isotopes, abundance ratios, interpretation, generalized model 8=16236
 isotope meas. in New Mexico, as evidence of Zuni Lineament 8=5781
 liquid, containing Ag, Au, or Pt, thermodynamic props. 8=8043
 liquid, n and X-ray scatt. expts. rel. to structure and props. 8=12794
 liquid, n scatt., classical fluid calc. 8=7851
 liquid, optical consts and dielec. const $\epsilon_1 + i\epsilon_2$ 8=12877
 molten, electronic band struct., density of states, and resistivity calc. 8=16789
 optical props., visible to i.r., room to He temp. meas. 8=14253
 phonon dispersion relations at 80 and 300°K 8=1839
 phonon-frequency distrib. and ht. capacity 8=1868
 phonons, relns between freq. and wave vector, rel. to dispersion relns. 8=17483
 phonon spectrum, energy shifts, observed by electron-tunneling 8=2085
 solid solutions, n.m.r. spin echoes, Knight shift 8=2387
 superconducting, energy gap and electron-phonon coupling strength press. depend. 8=22557
 superconducting, far i.r. absorpt. rel. to energy gaps 8=18555
 superconducting film, frequency conversion in 3 cm band 8=22558
 supercond. films tunnelling characts., size effects 700-3200Å 8=2172
 superconducting, flux line motion in current-carrying, direct detection 8=13758
 superconducting, microwave absorption in surface-sheath regime, depairing effect of mag. field 8=13760
 superconducting and normal, thermally induced He II vaporization threshold 8=4660
 superconducting, phonon spectrum change by lattice distortion 8=22559
 superconducting, point tunnelling 8=5211
 superconducting shell, attainment of zero mag. field 8=17990
 superconducting, surface nucleation and bulk superheating fields, 1.2°K-T_c 8=17968
 superconducting, surface nucleation field 8=17971
 superconducting, thermal forces on vortices 8=13761
 superconducting, tunnelling meas. of energy gap, high pressures 8=22554

Lead--contd

- superconductive defects rel. to structure of intermediate stage 8=22556
 superconductive, irreversible magnetisation obs. 8=2160
 thermal diffusivity meas. 8=1898
 thermal vibration spectra, experimental 8=8607
 two-band conduction model for resistivity, contradictions 8=2107
 Pb-Ag system, galvanic cell studies using PbO-SiO₂ melts 8=23150
 Pb-insulator-Al tunnel junctions, electron tunnelling 8=2180
 Pb-Pb superconducting tunnel junctions, I-V characts. and 3-cm characts. emission 8=17981
 Pb²⁺ impurities in soln. grown KCl crystals, distrib. 8=17238
 Pb²⁺ in K₂B₂O₄ glass, γ -irrad., induced absorption bands 8=5639
 Pb²¹⁰ in alpine glacier, meas. in firn and ice samples 8=18831
 Pb₂CuCrO₄(As, P)O₄OH, formacite, crystal structure 8=13284
 Sb¹²⁵ in crude Pb 8=14499

Lead compounds

- acetate, i. r. spectra and thermal decomp. 8=23095
 gases, electrical resistivity and gas purification 8=4488
 halides, gaseous ions, recomb. rates 8=4317
 neutron monochromator 8=854
 Pb stearate, crystal optimization for X-ray diffraction 8=14254
 Pb zirconate-titanate ceramics, depolarization at high strain rates 8=2243
 Pb-Bi alloy, liq., cavitation damage data for venturi and vibratory systems 8=16767
 Pb-Bi liquid alloy, heat conductance 8=16823
 Pb-Bi molten alloys, free energy of mixing and elec. resistivity 8=12842
 Pb-Bi, type II superconducting foils, critical current density 8=2173
 PbB₂O₇, interface temp. of crystallizing melt 8=21960
 PbBr, emission spectrum of molecule 8=7546
 PbBr₂:Mn luminesc. excit. and emission and absorpt. spectra 8=9622
 Pb²⁰⁷(CH₃)₄, indirect nuclear spin coupling 8=4233
 PbCl₂:Mn luminesc. excit. and emission and absorpt. spectra 8=9622
 PbCrO₃, high-pressure synthesis 8=23110
 2PbCO₃ anodization and PbO₂ struct. obs. 8=23148
 PbCrO₄ adsorption of poly(dimethyl siloxane) from CCl₄ and xylene solns. 8=8336
 PbF, emission spectrum 8=21099
 PbI₂ on different substrates, exciton spectrum 8=13675
 PbI₂, optical absorpt. and photoconduction in 0.52 μ region 8=2444
 Pb-In alloy type II superconducting tube, magnetic induction meas. on wall 8=5221
 Pb-30 at. %In, superconducting sheets, transport current distrib. obs. 8=9051
 Pb_{0.88}In_{0.12}, transitions during destruction of superconductivity 8=22567
 Pb. 0.4wt% Mg alloy, structural ageing process at room temp., X-ray study 8=22389
 α -PbN₆, solid-state photodecomp. 8=9724
 Pb(NO₃)₂, photo-annealing of chemical radiation damage 8=9732
 Pb(NbFe)_{1-x}O₃, study using Mössbauer effect of Fe⁵⁷ 8=1698
 PbO anodization and PbO₂ struct. obs. 8=23148
 Pb(OH)₂ anodization and PbO₂ struct. obs. 8=23148
 PbO layers, vapour-deposited, elec. behaviour 8=8941
 PbO, orthorhombic and tetragonal forms, conversion at low temp. 8=8276
 PbO, single crystal, yellow form, optical absorption coeffs. 8=5628
 PbO, yellow, photoconductivity, surface effect 8=22697
 PbO-Al₂O₃-B₂O₃-SiO system glasses, elec. props. temp. and comp. dependence 8=18170
 PbO-TiO₂-ZrO₂ system, phase equilib. 8=17099
 PbO₂ electrodeposits cryst. struct. rel. to electrolyte impurities 8=21919
 PbO₂ from PbSO₄, Pb₂O₃, 2PbCO₃, Pb(OH)₂ and PbO anodization, struct., obs. 8=23148
 PbO₂ layers, secondary electron emission 8=18284
 Pb₂O₄ anodization and PbO₂ struct. obs. 8=23148
 Pb-PbO-As₂O₃ system, slag-metal equilibria, phase diagrams 8=8277
 PbO-B₂O₃ glass system, fraction of four-co-ord. B atoms present 8=21915
 PbS chemical films, photovoltaic effect of const. current 8=18234
 PbS, crystal growth in silica gel near ambient temperatures 8=1743
 PbS, energy-band structures and electronic props., investigation 8=22465
 PbS films, Hall effect data rel. to space charge layers on crystallite surfaces 8=5273
 PbS, mobility temp. dependence 8=18062
 PbS, sulphation 8=9698
 PbS X-ray microanalysis, atomic number effect correction, obs. 8=14479
 PbS(Te), lattice dynamics 8=13337

Lead compounds—cont'd

- Pb-S-O system, equilib. relns., diagrammatic representation 8=16920
 PbSO₄ anodization and PbO₂ struct. obs. 8=23148
 PbSe, energy-band structures and electronic props., investigation 8=22465
 p-PbSe, free carrier Faraday rot. rel. to band struct. 8=2445
 PbSe, forbidden band width and temp. depend. 8=5272
 PbSe_(1-x)Te_x, comp. variations shown by chemical polishing 8=1689
 PbSe-SnSe, optical energy gap 8=5629
 PbSe-SnTe, optical energy gap 8=5629
 Pb-Sn alloys, composite growth from melt 8=4648
 Pb-Sn alloys, lamellar stability on solidification 8=4785
 Pb-Sn alloys, liq., meas. of electrotransport 8=12816
 Pb-Sn alloy polycrystalline, atomic block theory of hardening investigation 8=8803
 Pb-Sn eutectic, undercooling at solid/liq. interface 8=16933
 Pb-Sn, Na conc. at grain boundaries 8=8344
 Pb-Sn wire cryotron relax. oscillator, as thermometer for temp. distrib. with height in He-I 8=22571
 Pb_xSn_{1-x}Te alloys, lattice parameters, redeterm. 8=22037
 Pb_{0.63}Sn_{0.07}Te, energy gaps, thermal and optical 8=2446
 Pb_{0.85}Sn_{0.15}Te, energy gaps, thermal and optical 8=2446
 Pb_{0.95}Sr_{0.05}(Zr_{0.53}Ti_{0.47})O₃, u. s. velocity and Young's modulus 8=1856
 PbTe, anomalously high-mobility from Hall meas. rel. to sample prep. 8=2138
 PbTe compatibility with metals study 8=18686
 PbTe, diffusion coeff. of Na meas. by radio tracer technique 8=17580
 PbTe films, thin, resistivity, Hall mobility and cond. 8=22603
 PbTe, p-type, Hall mobility and thermoelectric power rel. to Na doping 8=5274
 p-PbTe heavily doped thermal conductivity betw. 80-400°K 8=8662
 PbTe, helicon-phonon coupling at 4.2°K 8=18063
 PbTe, p-type, oscillatory magnetostriction 8=13964
 PbTe, reflectivity, low freq., in mag. field 8=22988
 PbTe-Au pseudobinary section 8=17098
 PbTe-Fe pseudobinary section phase equilibria 8=17097
 PbTe:Na, acceptor centre model from Na:hole ratio determ. 8=2205
 PbTe-PbS, n-type, elec. props. temp. and pressure dependence 8=18061
 PbTe-PbS solid solns., i. r. transmission spectra rel. to forbidden band optical width 8=18554
 PbTe-Sb₂Te₃ alloy system, thermoelectric props. and phase relations 8=4716
 PbTe-Se_{1-x}, effect of defects on lattice thermal conductivity 8=1892
 PbTe-SnSe, optical energy gap 8=5629
 PbTe-SnTe, optical energy gap 8=5629
 PbTiO₃-PbZrO₃-PbMg_{0.5}W_{0.5}O₃ system, dielectric polarization and thermal expansion 8=5367
 Pb-Tl alloys, electron-phonon coupling and phonon spectra, electron tunnelling studies 8=22555
 Pb-Tl alloys, superplasticity during creep 8=13603
 Pb-Tl supercond. foils, type II, sheath irreversible magnetization obs. 8=17970
 Pb-Tl(In) alloys, order-disorder transform. from superconducting transition temp. meas. 8=1680
 Pb₂V₂O₇ (chervetite), crystal structure 8=13285
 PbZrO₃, coprecipitation meas. 8=1744
 PbZrO₃ elec. cond. near antiferroelec.-ferroelec. transition rel. to ageing and relax. polarization 8=2249
 PbZrO₃, l.f. dielectric study 8=5368
 PbZrO₃ polycrystals, temp. changes of polarization at phase transition 8=13888
 PbZrO₃, rel. to ferroelec. phase, current hysteresis loops obs. 8=13887
 Pb(Zr,Sn,Ti)O₃ ferroelectric ceramics, Nb-doped, elec. props. 8=2246
 Pb(Zr-Ti)O₃ ceramics, addition of Cr₂O₃ 8=13043
 Pb(Zr_{0.98}Ti_{0.02})O₃, shock-wave compression 8=13538
 Pd complex, bis-(Ni-isopropyl-3-ethylsalicylaldiminato) palladium, structure 8=8552
 Zn determ. by atomic absorpt. spectrometry 8=23184

Leak detection

- conference 8=21531
 gas or liq., calibrated leak prod. for mats. with m. p. s. above room temp. 8=14907
 nuclear fuel, e. s. precipitator 8=20909
 oil diffusion pump, e. microscopic monitoring of molecular seive 8=21535
 omegatron efficiency, comparison of oil-free and oil diffusion pumps 8=21538
 semiconductor devices, using Xe-133, radioactive 8=2211
 sensitivity increase by use of org. liq. tracer 8=7969
 He mass spectrometer application, practical considerations 8=7359

Leather. See Materials.**See model.** See Field theory, quantum.**Length measurement**

- See also Micrometry; Strain gauges; Thickness measurement.

Length measurement—cont'd

- dilatometers, Al₂O₃ and quartz specimen for testing 8=13381
 dilatometric, from mean strain curves of corundum, 0-900°C 8=6
 displacement meas. using guarded sphere as gauging electrode 8=10823
 fibres, length distrib. 8=13054
 interference, using lasers 8=7
 interferometric apparatus comprising a laser source 8=6003
 meter bar, elongation in gravitational field 8=6002
 optical ranging system using a laser 8=14918
 pneumatic testing, method of speeding 8=14917
 precision, using an electronic contact indicator 8=14916
 rangefinder, automatic, proposed 8=475
 spherical radii, superposable spherometer 8=20053
 standard quartz metre gauges 8=10475
 Cu, length change after e irradiation 8=22338
- Length standards.** See Standards.
- Lennard-Jones and Devonshire theory.** See Liquids/theory.
- Lennard-Jones potential.** See Kinetic theory; Molecules/intermolecular mechanics.
- Lenses**
- See also Electron lenses.
- aberrations, primary, two-lens system of Ramsden type 8=6493
 advanced optical techniques, book 8=15489
 apertometer, precision, for microscope objectives 8=6507
 birefringent, in optical system, path of extraordinary ray 8=15510
 centring, vacuum technique 8=6494
 contact, tightly fitting with plane mirror for retinal image stabilization 8=15575
 equiconvex, nonlinear oscillations on plane surface 8=19511
 535 mm, objective of coronagraph, investigation of 8=536
 and holographic imaging, analogy and lens formulae appls. 8=20105
 human, thin shell deformation analysis 8=15573
 image deflectors, achromatic 8=472
 interferogram testing 8=20043
 liquid for acoustic waves, focusing props. 8=19573
 longitudinal spherical aberration, determ. by simple tech. 8=470
 optical transfer function measurement 8=6491
 pancratic systems rel. to Seidel aberrations 8=471
 point holograms as lenses 8=6568
 progress in optics, book VI 8=15541
 quadrupolar multiplet, evaluation of acceptance angle 8=15500
 quality control by modulation transfer meas. 8=11129
 single and cemented, thickening 8=6492
 small lens null compensator, algebraic soln. 8=20046
 superresolution, and Abbe resolution limit 8=6505
 telescope objective, cemented, 5th order spherical aberration 8=3351
 theory, systematic approach to teaching 8=15502
 thick concentric single, use of characteristic functions in design 8=11130
 transfer factor, meas. by harmonic analyser 8=11131
 triplets, spherical aberration evaluation 8=15501
 X-ray, Fresnel-zone and appls. 8=15591
 Nd laser focusing, spark propagation 8=3337
- aspherical**
- aplanatic Fresnel system correction 8=20048
 correction of optical system aberrations 8=3347
 double Gauss, study of use of aspherics 8=11127
 surface calc. for aberration corrections 8=20042
- photographic**
- off-axis wave aberration and optical transfer function 8=15503
 picture quality, effects of lens flare 8=11224
- Leptons**
- See also Electrons; Mesons; Neutrinos and antineutrinos.
- antineutrino scatt. by electron, cross-section 8=6799
 charge conservation and $\nu \leftrightarrow \bar{\nu}$ expts. 8=15725
 data on properties, updating 8=15671
 decay, nonleptonic, surface terms connected with reduction formulae 8=3511
 e, μ , ν as independent states of a single lepton 8=11450
 electro-pair-production, trident expts. 8=3584
 interaction, ultraweak, CP-odd, $|\Delta S| = 1$, neutral lepton currents 8=3531
 lepton-lepton long-range force due to ν pair exchange unobservable 8=20273
 mass spectrum, wave eqn. in SU(3, 1) 8=20258
 masses, extremum relationship 8=3601
 model, photon and intermediate-boson gauge fields 8=11451
 N weak decay, PCAC hypothesis, pole-dominance version 8=3696
 and nucleons form factors and structure effects in vacuum polarization 8=588
 octet, weak interactions governed by current-parity selection rule 8=11449
 π leptonic decays with intermediate boson, e. m. corrections 8=6836
 polarization rel. to Furry's theorem in quantum electrodynamics 8=20176

Leptons—contd

- polarization in $\nu_1 + N \rightarrow N^* + 1$ and $\bar{\nu}_1 + N \rightarrow N^* + \bar{1}$ 8=3585
 production in $\nu_1 + N \rightarrow N^* + 1$, N^* polarization 8=3586
 ρ vector β -decay coupling, radiative correction 8=20374
 scatt., rel. to weak interaction theory 8=3418
 statistics effect examined in μ, e reactions in PbCu 8=20392
 strange, conservation in semileptonic interactions and
 absence of neutral currents 8=20368

Lie groups. See Group theory. For applications see Elementary particles; Field theory, quantum.

Ligands. See Bonds; Molecules.

Light

See also Diffraction; Interference, etc.; Doppler effect; Radiation.

- amplification, parametric, in nonlinear medium 8=6419
 in antiferromagnets, fluctuations and scattering in strong
 magnetic field 8=5498
 atmospheric propag., comparison of laser and
 nonlaser 8=9867
 beam in random medium, fluctuations 8=20089
 beam trajectories in media with refractive index
 inhomogeneities 8=371
 chopper, feedback-stabilized with continuously variable
 frequency 8=6509
 fluctuations correl. functions, 3-channel photoelec. counting
 obs. 8=20015
 Gaussian, intensity-fluctuation distribution 8=20019
 interaction with sound and applications 8=11120
 Lorentz group, Zeeman's lemma, light-like permuta-
 tions 8=6024
 macroparticles accel. by laser radiation 8=10885
 modulated or time-varying, dispersion anal. 8=6486
 modulation by K^{π} at ground-state, optical pumping 8=12085
 modulation, u. h. f., photomultiplier meas. 8=6487
 modulation by ultrasonic fields 8=20035
 optical beam waveguides, self-aligning 8=10965
 photoelectric detect statistics, communication channel
 model 8=20010
 photon count distrib., meas. rel. to field statistics 8=20014
 photon counting distrib., meas. and analysis 8=20351
 photon number and energy density, fluctuation
 formulae 8=20016
 photothermal effects in semiconductors 8=8650
 picosecond pulses, display and meas. via two-photon
 fluoresc. in liqs. 8=8071
 propagation in elec. and mag. anisotropic media 8=515
 propagation in inhomogeneous cosmologies, statistical
 effects 8=10078
 pulse meas. with photocells, accuracy 8=9245
 pulse self-steepening 8=6480
 pulses, spatial and temporal division 8=20021
 resonator, prism, mode eqn., soln. 8=20088
 scale of optical rad., development 8=11117
 self-focusing by Kerr effect and striction 8=3377
 signal $< 10^{-4}$ W detection methods 8=15495
 statistical props. meas., photodetect. e emission
 distrib. 8=15493
 thermal effect causes self-focusing of light beam 8=14170

coherence

See also Lasers.

- advanced optical techniques, book 8=15489
 annular and disc-like objects, diffraction images under
 partially coherent illumination 8=11188
 cascaded optical systems, transfer function 8=11133
 Cherenkov radiation, coherence effects 8=20027
 coherent scatt., expt. conditions for turbid media 8=11193
 crystals, KDP type, second harmonic generation 8=5569
 degree, from intensity correlation obs. 8=20028
 diffracted field of rectangular aperture with partially
 coherent illum., calc. 8=20101
 diffraction and focusing of apertures under partially
 coherent illumination 8=6559
 diffraction pattern depend. 8=20100
 equivalence theorem and diagonal representations 8=20025
 field dynamics in first- and second-order
 processes 8=20034
 field, rel. to photostatistics of N-mode laser
 field 8=412
 fluctuating beams, anal. via photon counting
 statistics 8=6425
 fourth-order function, classical formulation, props. and
 appls. 8=20032
 fourth-order functions meas. 8=20031
 harmonic generation in optically active medium, coupled-
 wave solution 8=455
 higher-order functions and degree of coherence 8=20033
 higher-order functions, propag. in lossy media 8=5570
 higher-order, normalized functions considering
 classical and quantized fields 8=20030
 holography and spatial filtering, applications 8=11119
 image of quasi-monochromatic source, meas. of mod. of
 degree of coherence 8=6483
 laser, mode-locked, for reproducible optical second-
 harmonic generation 8=11024
 lasers, quantum mechanical theory 8=19938
 in multiphoton absorpt. processes, stat. anal. rel. to source
 characts. 8=11165
 near focus of coherent beam, energy flow and Poynting
 vector 8=6499

Light—contd**coherence—contd**

- nonlinear medium, scatt. involving photon decay 8=6560
 optical imaging systems, significance of
 nonlinearity 8=11134
 optical mixing for converting near infrared to visible
 light 8=11118
 optical systems, improvement of two-dimensional image
 quality 8=11132
 partial, effect on phase-contrast microscopy 8=15515
 partial, two-point resolution 8=15508
 partially coherent illumination, transfer function to
 image ambiguity 8=3340
 phase problem, determ. of zeros 8=15491
 progress in optics, book VI 8=15541
 pulse generation, ultrashort duration 8=454
 rel. to quantum and classical theories equivalence, p-
 representation in twisted convolution formation 8=20026
 quantum operators, coherent states diagonal repre-
 sentation 8=19820
 scattering by spherical particles 8=11198
 self-focusing, instability in nonlinear medium 8=15540
 self-locking mode conditions in lasers 8=3302
 spatial, influence on holographic processes 8=11215
 spectra recombination from coherence meas., phase
 problem 8=20074
 of stable freq., prod. by atomic or molec. beam,
 theory 8=6438
 statistical props., freq. and phase determ. 8=20029
 systems, ultrasonic devices for scanning and
 processing 8=15072
 two-photon absorption, effects 8=6485
 InP, emission after laser excitation 8=6470
 He³, induced by r. f. field 8=16219
 K³⁹, intensity modulation of transmitted light 8=12085
- electromagnetic theory**
 correlation functions, normally ordered, for e. m. field,
 calc. by $Q(\beta)$ -function 8=20018
 in films, thin, reversibility of rays, generalized
 theorem 8=11169
 Gaussian beam in random medium, log amplitude and
 phase fluctuations 8=20089
 Maxwell's equations, three derivations 8=10934
 propagation in helicoidal nematic films 8=16837
 quantum operators, coherent states diagonal repre-
 sentation 8=19820
 radiation field characteristic states 8=19818
 radiation and matter interacting system, fluctua-
 tions 8=19819
 thermal effect in absorbing media 8=18487
 wave to geometrical optics, conditions for transition 8=15488
 wide angle systems focal region struct. 8=6558
- quantum theory.** See Photons; Quantum electrodynamics;
 Quantum theory.
- velocity.** See Velocity/light.
- Light guides.** See Optical instruments.
- Light modulation.** See Light; Optics.
- Light sources**
 See also Lasers; Monochromators; Photometry/light
 sources; Spectroscopy/light sources.
 advanced optical techniques, book 8=15489
 artificial, for simulating natural daylight and
 skylight 8=20070
 with atomic beam 8=12111
 coherent pulse generation, ultrashort duration 8=454
 collimated, in scattering medium, discrimination
 depth, obs. 8=3374
 electroluminescent panel, modulatable 8=6517
 freq.-modulated light generation 8=15492
 gas discharge tube, cathode noise expt. 8=15521
 gases, electroluminescence 8=484
 gas lasers for holography 8=15559
 incandescent, angular dependence of emissivity 8=15524
 lasers, Ar, multiwatt, experimental investigation 8=11146
 laser beamwidth reduction, by optical antenna, radio-
 meter check 8=20068
 laser, He-Ne, radiation divergence meas. 8=6448
 laser in interferometers, aspects of fringe
 counting 8=11176
 laser light, 3×10^{12} W/cm² onto LiD and LiH plasma
 prod. 8=8774
 laser, Q-switched, for fluorescent photography of spray
 droplets 8=4636
 laser radiation intensity and frequency fluctua-
 tions 8=6429
 laser, ruby, in microscope 8=6503
 light dist. analysis by Fourier transformation 8=11164
 microwave plasma, characts. 8=3355
 pulse lamp supply for laser pumping, calc. 8=3323
 requirements for holography 8=20106
 scattering medium with negative resonance
 absorpt. 8=11021
 spark discharge, surface, for laser pumping 8=6412
 spatial distrib. of emission coeff., in limit of small
 self-absorption 8=3354
 spectral irradiances, spectroradiometric
 determ. 8=462
 ultrashort pulses generation 8=11145

Light sources—contd

- ultrashort pulse generation with lasers 8=3356
- ultraviolet, natural and artificial, book 8=20012
- vacuum-u.v. for gas flash photolysis 8=14433
- volume, intensity definition 8=11158
- Ar resonance line, for u.v. photochemistry 8=18738
- D₂ flash lamps, pressure and voltage gradient effects 8=15522
- GaP miniature diode for nsec. pulses 8=15525
- H lamp, intensity distrib. in spectrum between 2500-1100Å 8=4065
- H₂ arc lamp, high intensity u.v., design 8=6518
- H₂ flash lamps, pressure and voltage gradient effects 8=15522
- He-Ne laser light source for light scatt. by He⁴ superfluid 8=8078
- He-Ne laser for velocity meas. 8=6489
- Hg arcs, effect of TII on temp. 8=485
- K lamp, line shape dependence on current 8=15523
- N₂ laser, as u.v. source with repetitive subnsec. kW pulses 8=20069
- ZnS electroluminescent lamp calibrated for use as standard 8=20067

Lighting. See Illumination.**Lightning**

- acoustic output from long spark 8=18889
- ball, laboratory, formation mechanism 8=18892
- characteristics of 7 discharges which have caused forest fires 8=18890
- core diameter of return stroke, determination from Al needle craters 8=23294
- corona currents and e.l.f. emissions 8=2598
- currents, e.l.f. and v.l.f. radio noise, amplitude statistics 8=2602
- damage recording and density evaluation 8=23292
- electricity distribution in thunderstorms, effect of particle interactions 8=18891
- interval between strokes and initiation of dart leaders 8=18888
- point discharge current rel. to p.d. and wind speed, lab. expt. 8=9884
- point discharge through small tree in artificial electric field 8=2599
- return stroke, current time-variation 8=18887
- thunderstorm, Monte San Salvatore obs. 8=23293
- v.l.f. sferic counting rates, Uppsala and Ankara 8=18893
- K changes, ground and intracloud discharges, audio spectra 8=9885
- K changes, v.l.f. characteristics 8=14627

Linear accelerators. See Particle accelerators/linear.**Linewidths.** See Spectral line breadth.**Liouville equation.** See Statistical mechanics.**Liquefaction, gases**

See also Low-temperature production.

- spinodal vs. p, T and use in comparing equations of state 8=1620
- Ar, self-diffusion in critical region 8=16716
- H, liq.-solid mixtures, quality determ. 8=15138

Liquid crystals

- 4'-n-alkoxy-3'-nitrodiphenyl-4-carboxylic acids, polymorphism 8=21614
- p-azoxyanisole, in mag. fields, X-ray structure investigations 8=4532
- azoxymethylcinnamic acid-dialkylester, calorimetry 8=4533
- cholesterine, structure by optical obs. 8=21612
- cholesteryl caprylate, heat of formation and critical size of centres 8=16918
- cholesteryl caprylate, heat of transformation during transition into isotropic-liquid and solid phases 8=16917
- cholesteryl mynstate mesophase polymorphism obs. 8=12802
- crystals of higher order, relation to other super-phases 8=8363
- glyceride aqueous systems, struct. of mesomorphic and micellar phases 8=12804
- helicoidal nematic films, e.m. wave propag. 8=16837
- magnetically oriented lyotropic phases 8=8008
- methyl iodide in liq. cryst. soln., n.m.r. 8=4234
- neat mesomorphic phase, struct. 8=16796
- nematic, mechanical equilibrium, linear theory 8=8007
- nematic, orientation fluctuations and Rayleigh scattering 8=16795
- n.m.r., chem. shift anisotropies 8=4624
- n.m.r., equivalence of nuclear spins 8=16892-3
- paraoxyanisole, heat of formation and critical size of centres 8=16918
- paraoxyanisole, heat of transformation during transition into isotropic-liquid and solid phases 8=16917
- polyethylene, supercooled liquid, nucleation rel. to temp. 8=1533
- poly-γ-benzyl-L-glutamate, orientation in mag. fields, n.m.r. study 8=8006
- relation of nematic to cholesteric mesophases 8=12803
- smectic trimorphism 8=21613
- structure and properties, review of data 8=1527
- s-trioxane in nematic solvent, n.m.r. 8=4618
- water model for Debye temp. calc. 8=1544

Liquid-drop model. See Nucleus/models.**Liquid flow.** See Flow/liquids.**Liquid helium.** See Helium/liquid.**Liquid oscillations**

- jet of infinite σ in uniform magnetic field 8=1518
- methyl isobutyl ketone, drops rising in H₂O and H₂O-sugar soln., vol. of continuous phase translated in water 8=21592
- relaxing, flow through tubes and porous beds 8=1513
- surfaces, air jet impingement 8=12757
- swimming sheet, doubly infinite and flexible 8=16752
- toluene-CCl₄ mixtures, drops rising in H₂O and H₂O-sugar soln., vol. of continuous phase translated in water 8=21592
- toluene, drops rising in H₂O and H₂O-sugar soln., vol. of continuous phase translated in water 8=21592
- He II, superfluid, solns. for rotation in annular channel 8=10809

Liquid waves

See also Acoustic waves.

- acoustic energy, backscattering, apparatus and method of analysis 8=6168
- compression waves, temporal and spatial autocorrelation functions 8=19623
- gravity, interactions 8=19
- gravity, internal, in density stratified medium 8=7984
- gravity, second-order radiation 8=21581
- instability in nonlinear dispersive systems 8=18
- internal, motion in ocean, perturbation technique appl. nonlinear eqns. 8=14577
- internal, propag. effects on underwater sound transmission 8=3051
- longitudinal, prod. by periodic press. in variable depth inhomogeneous fluid 8=9805
- m.h.d. gravity-capillary in conducting film 8=7987
- nonlinear interactions, application to generation by wind 8=20
- parallel wire resistance wavemeters, dynamic testing 8=7986
- pattern, 2D, produced by disturbance moving in density stratified liquid 8=4514
- production, experimental study 8=7985
- Rayleigh, in layer on anisotropic half-space 8=6132
- of ship in stratified ocean, surface and internal 8=9818
- special cases treated by Whitham theory 8=1517
- spherical, finite amplitude, calc. 8=19516
- swimming sheet, doubly infinite and flexible sheet 8=16752
- thermal density fluctuation, temporal and spatial autocorrelation functions 8=19623
- trapping along a discontinuity of depth in a rotating ocean 8=23234
- in viscous liq. in cylindrical conduit, symmetric modes of propag. 8=16773
- water, variational methods, applications of 8=1516
- He II, rotating 8=262

surface

See also Oceanography.

- capillary ripple, on monolayers 8=1514
- Cauchy-Poisson eqns., soln. by Fourier and Laplace transforms 8=16774
- Cauchy-Poisson problem with Navier-Stokes soln. 8=7983
- diffraction by a wedge, for time-periodic and concentrated elevation of vol. sources 8=9815
- film on plate contaminated, wind generated 8=12756
- at gas-liquid interface, effect on turbulent air flow 8=21464
- generation by shear flows 8=1515
- interaction, perturbation theory 8=12649
- Kelvin, corner diffraction 8=12758
- liquid sloshing in rigid cylindrical tank at simulated low gravity, expt. and theoretical studies 8=21580
- m.h.d., conducting liquid surrounded by compressible gas 8=3243
- ocean, excitation of atm. oscills. 8=9899
- ocean, generation and dissipation 8=18836
- progressive, partition of energy 8=12759
- sea, contamination effect on wind generation 8=14573
- sea, review 8=14572
- water, boundary between smooth surface and small waves, air flow over 8=1460
- wave impedance calc. rel. to viscosity 8=16775
- wind amplification 8=16776

Liquids

See also Association/liquids; Diffusion in liquids; Solutions.

- acoustic wave propagation, non-Newtonian viscous liquid 8=16830
- cavitation and streaming due to sound waves of finite amplitude 8=12753
- centrifuged, temp. distrib. 8=21654
- Cotton-Mouton effect, theory 8=12869
- cylinder withdrawal, gravity corrected theory for speed range extension 8=12762
- detonation during gap testing, shock initiation and wall interacts. 8=15057
- dispersion interact. energy as molar vol. /int. press. prod., rel. to H bonding energies 8=12779
- explosive, detonation initiation, effect of shape and material of container 8=10720
- explosive, detonation by shock wave 8=171
- finite-amplitude waves 8=12856

Liquids—contd

- free volume calc. 8=4561
 frequency broadening by short pulse 8=4574
 gas-liquid mass transfer, effect of moving interface, theory 8=16710
 heat transfer in laminar flow, plug-viscous 8=4566
 immiscible liq.-liq. system, agitated, drop size distrib. 8=12955
 jets, laminar, fluid mechanics 8=7989
 light scatt., multi-harmonic molec. 8=12872
 metals, optical meas. by ellipsometer 8=16836
 mixing, ultrasonically induced 8=21554
 nuclei polarization by optical pumping 8=13016
 optical self-focusing kinetics and channel instability 8=21668
 organic binary mixtures, volume changes 8=1528
 organic, heats of transformation rel. to sound velocity 8=16829
 piezo-optic coefficients by pulses u.s. light diffraction 8=8064
 second harmonic generation in homogeneous mag. field 8=12123
 simple, changes of state 8=17032
 spin-lattice relax. time equation 8=8131
 stimulated Raman scattering, spontaneous emission and mol. vibr. damping effects 8=4587
 structure and properties of liquids, conference Exeter England (1967) 8=16784
 supercooled, nucleation of freezing by cavitation 8=16934
 tangential disturbances, viscosity effect on instability 8=12618
 transient movement in pipes, problem of column separation 8=16757
 velocity of sound, determ. with u.s. interferometer-laser optical diffraction cell 8=8060
 vertically oscillating, terminal velocities of suspended spherical particles 8=7988
 viscoelastic, evaluation of theories 8=1535
 visco-elastic, isotropic turbulence, non-Newtonian effects in decay 8=12645
 viscous flow, unsteady temp. distrib. 8=7977
 H-bonded, shear compliance and free volume 8=1537
 K-NH₃ dilute soln., absence of vol. change on dilution at -34°C 8=1530
 Li, molten, supercooling due to crystallization of N₂ 8=12814
 Na-NH₃ dilute soln., absence of vol. change on dilution at -45°C 8=1530
- structure**
 acetone-chloroform system, n. m. r. study 8=2498
 alkali-metal halide aq. solns. 8=12800
 alkali metals, appl. of structure factor and pot. relation to elec. resistivities 8=12920
 alkanes, end-to-end distances, direct meas. via substituted atoms 8=1526
 alloys, atomic distrib. and electronic transport props. from X-ray diff. 8=12799
 alloys, correl. by X-ray and n diffraction 8=12795
 alloys, interatomic distances from X-ray diff. patterns 8=12784
 alloys, n. m. r. study of short-range atomic order 8=12934
 bromobenzene, molec. motion by n. m. r. 8=8132
 cholesterol liquid crystals 8=21612
 copolymer mols. in soln, peculiarities of conformation 8=16802
 electronic, bonding and short-range order effects 8=12902
 ethanol, at room temp., rel. to H bonding 8=1523
 glyceride aqueous systems, struct. of mesomorphic and micellar phases 8=12804
 iron-silica deoxidation product growth and separation, collection model 8=18658
 liquid crystals, statistical theory 8=1527
 metals, atomic distrib. connection with solid 8=12787
 metals, density of states and autocorrel. of independent electrons 8=12898
 metals, electronic structure 8=12899
 metals, electronic struct. as problem of multiple scatt. 8=12897
 metals, interatomic distances from X-ray diff. patterns 8=12784
 metal melts, double structure of spherical close packing and layer lattice 8=12786
 metals, neutron diffraction installation on thermal column in meas. 8=8002
 metals, rel. to pair pot., and structure rel. to phys. props. 8=12790
 metals, from positron annihilation, and ang. correl. of resulting γ rays 8=12896
 metals, rad. scatt. n and X-ray, rel. to macro- and microscopic props. 8=12794
 metals, reln. with interatomic potential 8=12781
 metals, Ziman pseudo-atom phase shifts calc. for monovalent ions 8=16882
 methane, molecular dynamics, translational and rot. 8=16374
 methane, proton spin-lattice relaxation 8=4617
 methanol, at room temp., rel. to H bonding 8=1523
 methylbenzenes, hindered rot., from neutron scatt. 8=17484
 nematic crystal, orientation fluctuations and Rayleigh scattering 8=16795

Liquids—contd**structure—contd**

- neutron scattering, inelastic, container for studies at high temps. 8=8001
 n scatt. Van Hone distrib. function, new approx. 8=12797
 ordering 8=21608
 orientation of polar mols. in non-polar solvents 8=21673
 pentanol, slow neutrons, quasi elastic scattering 8=8000
 phosphates, molten, rigid sphere model 8=7999
 polymer modifications u. s. induced, concentration dependence 8=21622
 polymethylacrylate and copolymers solns. bond networks rel. to rheological props., obs. 8=21552
 radial distribution function 8=12789
 significant theory applied to liquid O₂ 8=4528
 thiocetams, study of dimerization 8=4241
 triacetin, e distrib., X-ray scatt. obs. 8=16794
 1,3,5-trideuterobenzene, molec. motion by n. m. r. 8=8132
 water, influence of alkali halides 8=4527
 water-methanol system 8=12809
 water, molec. dia. from solubility and diffusion meas. 8=21606
 water, and nature of H₂ bond. 8=4529
 water, two-state model, Raman data 8=21690
 Ag-Sn alloys, partial interference and atomic distrib. functions 8=12801
 Al, h. f. waves study by n scatt., compared with solid 8=12796
 Ar collective motion, evidence from n scatt. 8=16793
 Ar, inelastic scattering of cold neutrons, at high temps. 8=16792
 Ar, quasielastic scattering of cold neutrons 8=1524
 Au-Sn alloy, atom pair distrib., partial interference functions 8=4531
 Bi, h. f. waves study by n scatt., compared with solid 8=12796
 Bi, spherical close packing and layer lattice structure 8=12786
 Bi, X-ray diffraction investigation 8=21610
 Cu₂Sn₅, partial structure factors 8=12788
 Ga, rel. to thermoelectric props. 8=16878
 Hg, electronic, from optical const. meas. 8=16846
 Hg-In alloys, electronic, from optical const. meas. 8=16846
 Hg-In₂, interf. functions, pair distrib. 8=8005
 H₂O, H bonds from thermodynamic functions, n scatt. meas. 8=1525
 H₂O¹⁸ and D₂O¹⁸, relax. parameters calc. 8=12780
 In, rel. to thermoelectric props. 8=16878
 In-Al alloys, from charact. energy losses of 8 keV electrons 8=12791
 In-Bi alloys, from charact. energy losses of 8 keV electrons 8=12791
 MoF₆, molec. motion from F¹⁹ relax. 8=12930
 Na, electronic, rel. to optical absorption 8=8111
 Na at 110° and 525°C 8=4530
 Na₂O·GeO₂·B₂O₃ system, glasses and melts, structure 8=21605
 Ni centres in molten LiCl-KCl 8=8087
 Ni centres in molten MgCl₂-KCl 8=8086
 O₂, significant structure theory appl. 8=4528
 Pb, h. f. waves study by n scatt., compared with solid 8=12796
 Rb, h. f. waves study by n scatt., compared with solid 8=12796
 Sn, h. f. waves study by n scatt., compared with solid 8=12796
 UF₆, molec. motion from F¹⁹ relax. 8=12930
 WF₆, molec. motion from F¹⁹ relax. 8=12930
- theory**
 See also Dielectric phenomena; Equations of state/liquids.
 alloys, reln. between pair pots. and radial distrib. functions of ions 8=16787
 atoms motion, veloc. self-correl. function, stochastic calc. 8=1522
 backflow effect appl. to impurity atom among Bogulivbov quasiparticles 8=3122
 binary mixtures, hard-sphere model 8=4539
 classical, dynamic form factor calc. 8=7851
 classical, theory of atomic self-motion 8=21603
 deoxidation product growth and separation, collision model 8=18658
 diborane, significant struct. calcs. 8=4526
 dielectric properties, criticism of Debye and Onsager theories 8=8102
 electrolytic solns., two-structure model 8=23142
 electronic struct., bonding and short-range order effects 8=12902
 electronic wave functions, generalized coherent-wave approx. 8=7998
 equilibrium vapour pressure, math. functions 8=21779
 excitons, nonreson. broadening of impurity spectra 8=4586
 Fermi liquid specific heat, particle-hole excits. rel. to quasiparticle self-energy 8=3117
 gravitational field eqns. for ideal, rigid, rot. liq. 8=6088
 hard-sphere model 8=1521
 hexane, behaviour of negative charge carriers 8=21717
 hydrazine, significant struct. calcs. 8=4526
 individual particle vel., oscillations of autocorrel. function 8=12727

- Liquids**—contd
theory—contd
 ion interactions, short-range non-Coulombic rel. to thermodyn. and electrokinetic props. 8=21602
 intermolecular attraction and repulsion 8=16371
 intermolecular interactions, thermodynamics 8=3002
 intermolecular potential 8=4524
 iron-silica deoxidation product growth and separation, collision model 8=18658
 itinerant oscillator model velocity autocorrelation function 8=12777
 magnetic resonance and relaxation, conference 8=22889
 metals, conduction-electron states, variational soln. 8=12903
 metals, density of states also in solid, from Knight shift data 8=12928
 metals, electronic struct. as problem of multiple scatt. 8=12897
 metals, liq. state theory and electron theory, correl. and meeting points 8=16786
 metals, model pseudo pot. from phonon freqs., for ion interacts. 8=16789
 metals, reln. between pair pots. and radial distrib. functions of ions 8=16787
 metals, reln. between structure and interatomic pot. 8=12781
 mixtures, extension of Widom model 8=12785
 molecular interactions 8=21601
 molecular state, from solid-liq. surface tension 8=12825
 nitrogen temporal stability of quiet metastable states 8=16788
 non-electrolyte solns., structural effects 8=16785
 Onsager theory of local field rel. to nonlinear refractive indices 8=12871
 perturbation theory and eqn. of state 8=12783
 photoluminescence concentration depolarization 8=1573
 polar, collective oscillations 8=21721
 polar, microwave to far infrared spectra, relaxation theories 8=8081
 precipitation deoxidation kinetics, collision model 8=18658
 Rice, for nearly ferromagnetic Fermi liquids and He^3 8=10800
 significant structure, applied to liquid O_2 8=4528
 significant struct., appl. to melting 8=12967
 solutions, scale-particle theory 8=4534
 temporal stability of quiet metastable states 8=16788
 transition metals, density of states of non-degenerate (s) band 8=12901
 turbulence, determining dynamical eqn. for 2-pt. correlation tensor 8=4438
 vibrational relax. of diatomic mols. 8=1218
 viscosity, volume, rel. to u. s. compression waves absorpt. and vel. 8=16804
 water, domain theory 8=4550
 Ar, shock compression, Thomas-Fermi-Dirac theory 8=16994
 He, collective coordinates theory 8=10799
 O_2 , significant structure theory appl. 8=4528
 Ra, parameters, "synchronised precipitation" 8=9736
- Lithium**
 absorpt. coeff., continuous 8=7387
 abundancies estimated in expanding hot universe 8=5840
 atom, e scatt., long-range interaction, nonadiabatic contrib. 8=12092
 atoms excited states, adiabatic exchange approx. calc. 8=7434
 atoms, ground-state energy, perturbation theory 8=16206
 atom ground-state levels excit. by slow electrons, cross sections obs. 8=7435
 atom and ions of isoelectronic sequence, wavefunctions calc., using effective potential 8=20958
 atoms, Kerr dispersion, theory 8=12068
 atoms, pseudopotentials 8=7409
 atom sequence, eigenvalues of $1s^2 2p^2 P$ states 8=20957
 colloidal, in n-irradiated LiF, e. p. r. meas. rel. to distrib. 8=9431
 diffusion in GaSb, and solubility 8=13409
 diffusive behaviour in temp. grad. and elec. potential grad. rel. to atomic mobility 8=22157
 electron-impact ionization, empirical calculations 8=12448
 electron momentum distrib. by Compton X-ray scattering 8=17907
 Fermi surface by positron annihilation 8=8937
 ferrite magnetostriction constants from ferromagnetic resonance 8=14045
 hyperfine coupling constants of $2p^2 P$ levels 8=7408
 ionization cross-section, electron impact 8=7700
 ionization, electron and proton impact, classical model 8=12444
 ionized gas, absorption and emission of radiation by photoionization and bremsstrahlung 8=7717
 ions, charge composition effect of target state 8=1365
 liquid, cavitation damage data for venturi and vibratory systems 8=16767
 liquid, density in range 400-1125°C 8=12813
 liquid, elec. resistivity, appl. of structure factor and pseudo pot. relation 8=12920
 mass spectrum of isotopes prod. in p- O^{16} reaction 8=20793
 molten, supercooling due to N_2 crystallization 8=12814
- Lithium**—contd
 photoconductivity calc. from Kubo-Greenwood formula 8=5393
 plasma, parameters and thermodynamic characteristics, calc. 8=12462
 spectra in inert-gas matrices 8=4082
 target nucleus, thermonuclear reaction rates 8=11976
 traces in refractory oxides, spectrograph. determ. using discharge tube 8=23189
 wires, explosion discharges initiated at the surface and inside the wire 8=4272
 X-ray Raman scatt. of Cu K α rad. 8=2396
 GaAs with Li complexes, local mode spectra 8=22982
 in Li methoxide-methanol ions coordination number and solvates comp. obs. 8=2497
 Li I, first-level lifetimes 8=7407
 Li $^+$ atom, hyperpolarizability calc. 8=20942
 Li $^+$, lower bounds to eigenvalues 8=11253
 Li 0 conc. and diffusion in neutron irradi. BeO 8=8672
 Li 7 spin-lattice relax. in aqueous alkali halide solns. 8=1593
 Li $_2$, simple alternant MO calc. for ground state 8=1257
 Li $^+$ -He, interaction energy at small internuclear distances 8=21014
 Li-NH $_3$ solns in metallic range, optical consts. 8=12884
 Na-Li liq. mixtures, near demixing temp., crit. opalescence 8=1558
 Si donor, ground state chemical splitting 8=1950
- Lithium compounds**
 alloys, solid and liquid, conduction spin-lattice relax. 8=9430
 ferrite, magnetostriction constants at -170 and +340°C, effect of ion ordering 8=9379
 ferrites, Young's modulus, temp. depend. 8=22378
 ternary intermetallic phases, crystal structure 8=22028
 zeolite LiX, adsorpt. of Xe and Kr, press. and temp. depend. 8=1713
 Li borate system, e. p. r. of Mn $^{2+}$ 8=5536
 Li disilicate, crystallization from Li $_2\text{O}$ -SiO $_2$ glasses 8=21953
 Li ferrite, FeLiO $_2$, Q_{11} (or β) phase, X-ray diffr. results rel. to periodic antiphase model 8=17386
 Li ferrite, self-decoration effect 8=1729
 Li ferrite, X-ray topography of defects 8=8708
 Li fluorophlogopite, 4-layer, new mica polytype 8=8531
 Li metaborate, "washing out" effect in mol. e-diffr. pattern 8=16266
 Li-silicate glass, second phase particle growth, diffusion controlled 8=21847
 α -Li $_3\text{AlF}_6$, crystal structure 8=17390
 LiAl(SiO $_3$) $_2$ (spodumene) natural crystals e. p. r. of Mn $^{++}$ 8=22908
 LiAl(SiO $_3$) $_2$ (spodumene), heated crystals, e. p. r. of Mn $^{++}$ 8=22909
 Li-B system, cpd, formation, crystal class identification 8=8244
 LiBH $_4$ and LiBD $_4$, n.m.r. 8=18465
 LiBO $_2$, β and γ high-press. forms 8=8269
 Li $_2\text{B}_4\text{O}_7$, maximum sensitivity to thermal neutrons in pocket size ionization chambers 8=851
 LiBaH $_3$, and deuterated cpd., n-diffr. study 8=17391
 Li $_2\text{Bi}$ films, prep. and props. 8=8325
 LiBr, photoabsorpt. near K-edge 8=18544
 Li-C system, cpd., formation, crystal class identification 8=8244
 Li $_2\text{CO}_3$ -Na $_2\text{CO}_3$, molten, electrochem. studies 8=5741
 LiCl, adiabatic elastic const., 300°-4.2°K, obs. 8=2058
 LiCl, alkali halides, F-band peak, Mollwo relation 8=17688
 LiCl aqueous solns., formation of pulse discharges 8=4608
 LiCl, electron struct. calc. of molec. props. 8=12206
 LiCl-KCl molten mixtures, absorpt. spectra of Ni centres 8=8087
 LiCl, photoabsorpt. near K-edge 8=18544
 Li ^7Cl and Li ^6Cl solns., proton relax. times 8=8139
 LiClO $_3$ in acetonitrile-dioxane, elec. cond. 8=8108
 LiClO $_3$ in methanol-dioxane, elec. cond. 8=8108
 LiClO $_3$ in H $_2\text{O}$ -dioxane, elec. cond. 8=8107
 Li-Co-ferrite-aluminates, thermostable waveguide valves in decimetre range 8=9377
 Li $_{0.5}\text{Cr}_{1.25}\text{Fe}_{1.25}\text{O}_4$, spontaneous magnetization rel. to compensation temp. 8=14049
 LiD target for laser light, plasma prod. 8=8774
 Li $_{0.5}\text{Fe}_{2.5-x}\text{Al}_x\text{O}_4$ ($0 < x < 1$), mag. moments and mol. field coeffs. 8=9378
 Li $_{0.5}\text{Fe}_{2.5}\text{O}_4$, thermal conductivity rel. to non-stoichiometric vacancies 8=8660
 Li $_2\text{GeO}_5$:Cr, fluorescence at 4.2-300°K 8=9619
 LiH colour centre form. dynamics obs. 8=8748
 LiH, floating spherical Gaussian orbital model calc. 8=12153
 LiH, n-irradiated, F-centre exchange interactions from optical and e.p.r. spectra 8=17684
 LiH plasma, line broadening by microfields 8=12515
 LiH, red-luminesc., study of centres 8=18608
 LiH target for laser light, plasma prod. 8=8774
 Li ^7H and Li ^7D , compressions to 40 kbar 8=13581
 LiH $_2$ (SeO $_3$) $_2$, fundamental absorpt. edge near ferroelectric phase transition pt. 8=9548
 Li $_2\text{HfCl}_6$, thermal props. 8=8640

Lithium compounds—contd

- LiI, photoabsorpt. near K-edge 8=18544
 (Li, K)₂(SO₄, WO₄) system, molten, elect. cond. up to 1100°C 8=8112
 LiLn(WO₄), crystals, hydrothermal synthesis, (Ln = Ce, Pr, Nd) 8=21954
 Li-Mg dilute alloy, liq., resistivity, theory and expt. 8=12919
 LiMnPO₄, spin-flopping 8=5506
 LiMSiO₄ and related sulphates, (M = Al with Ga and Ge substitution) 8=17013
 LiN₃, crystal structure 8=17387
 Li(NH₃)₄, ht. capacity, 2°-4°K 8=13374
 LiN₂H₂SO₄, -NH₃ group mol. reorientation 8=8235
 LiNO₃ molten, refr. index meas. by interferometry 8=4583
 LiNO₃, molten, water solubility 8=12806
 LiNO₃ solns., ion assoc. 8=21715
 LiNaSO₄, crystal structure 8=8530
 LiNbO₃ crystal for converting near i.r. to visible light by optical mixing 8=11118
 LiNbO₃, electro-optic effect 8=5619
 LiNbO₃, image conversion from 1.6 μ to visible 8=22998
 LiNbO₃, refractive index 20°-900°C 8=5620
 LiNbO₃, rel. to second harmonic generation of Nd-glass laser 8=15486
 LiNbO₃, second harmonic generation from short pulses 8=18495
 LiNbO₃, second-harmonic phase-matching temp., dependence on melt composition 8=22997
 LiNbO₃, shear-wave attenuation 8=2059
 LiNbO₃ single crystals, domain structure 8=13886
 Li₂NbO₃, mixing of ruby and Nd laser emissions 8=14237
 LiNbO₃, d.c. constant, temp. and optical freq. dependence 8=9547
 LiNbO₃, elastic and piezoelectric constants 8=9226
 LiNbO₃, single crystal, dielectric properties up to 9 GHz 8=9216
 LiNbO₃, spontaneous electro-optical effect 8=18543
 LiNbO₃:Cr³⁺, e.p.r. 8=18428
 LiNbO₃:Cr³⁺, propag. 10⁵ Mc/s hypersound, room and He temps. 8=8631
 LiNbO₃:Dy³⁺, e.p.r. 8=18428
 LiNbO₃:Er³⁺, e.p.r. 8=18428
 LiNbO₃:Nd³⁺, e.p.r. 8=18428
 LiNbO₃:Yb³⁺, Nd³⁺, Cr³⁺, e.s.r. and optical spectra 8=22999
 Li₂O-B₂O₃ glass system, fraction of four-co-ord. B atoms present 8=21915
 Li₂O.2B₂O₃, crystal structure refinement 8=17389
 Li₂O.nB₂O₃ (n = 1, 2), as neutron detector 8=6953
 Li₂O-SiO₂ solutions, activities 8=21620
 LiOH impurity in ice, dielec. dispersion obs. 8=18188
 LiOH-LiF-H₂O, molten, corrosion of metals 8=14368
 Li₂SO₄, high-temp. modification, conductivity, diffusion thermoelec-power and viscosity 8=17169
 Li₂SO₄ with Na₂SO₄ or CsSO₄, differential thermal anal. 8=8270
 Li₂S₂O₈.2H₂O cryst., dynamics of H₂O 8=8537
 Li₂S₂O₈.2H₂O, crystal structure rel. to H₂O dynamics 8=8538
 LiTaO₃, coeff. temp-dependence, 200-800°C and spontaneous polarization 8=18200
 LiTaO₃, elastic and piezoelectric constants 8=9226
 LiTaO₃, elastic and piezoelec. props. 8=8853
 LiTaO₃, pyroelectricity and spontaneous polarization 8=13895
 LiTaO₃, thermal expansion, room temp. to 850°C 8=13383
 LiTaO₃:Yb³⁺, Nd³⁺, Cr³⁺, e.s.r. and optical spectra 8=22999
 Li₂ZrCl₆, thermal props. 8=8640

lithium fluoride

- anisotropy of orientation of U fission fragment tracks 8=17706
 attenuation of sound waves along (110) axis, rel. to third-order elastic const. 8=4916
 condensation coeff. from thin film meas. 8=4655
 crystals, generalized surface wave propag. 8=1855
 crystals with various Li isotope ratios, growth control using Stockbarger-Bridgman method 8=1742
 diamagnetic molecular susceptibility calc. 8=12176
 dislocation mobility, effect of hydrostatic pressure 8=1976
 elastic constants, higher order, theoretical calcs. 8=17811
 elastic constants, theoretical detm. 8=17812
 elastic limit, optically determ., in temp. range 300-1.4°K 8=5076
 emissivity of film on Mo substrate, at 420°K and 605°K, at 20° and 0° 8=14236
 F centres, ENDOR 8=18465
 400 Bragg spot, unusual K-shape 8=17380
 gap modes 8=22180
 isotopic, shift of U-center local mode 8=13462
 lattice constant, effect of X-ray bomb. 8=2030
 luminescent properties, influence of thermal treatment 8=14322
 microhardness at 20, 60 and 115°C 8=17813
 M-centre luminesc. excit. spectra and transitions, obs. 8=8747
 M-centre, upper excited states 8=2010
 n-irradiated, colloidal Li e.p.r. meas. rel. to colloid distrib. 8=9431
 neutron-irradiated, F-centre exchange interactions from optical and e.p.r. spectra 8=17684

Lithium compounds—contd**lithium fluoride—contd**

- neutron-irradiated, paramag. centre due to atomic H³ formation 8=18427
 photoabsorpt. near K-edge 8=18544
 pile-irradiated crystals, study of metallic Li colloids 8=12947
 in plastic sachet dosimeter for surface and finger-tip dosimetry 8=20204
 polarization rel. to lattice imperfection prod. during shock wave plastic deformation 8=9225
 radiation defect formation 8=13487
 radiation heating in reactor 8=13488
 R-centre, linear Stark effect 8=1993
 single crystals, X-ray studies on sub-grain boundaries by limited projection topography 8=13446
 6955Å zero-phonon line, pseudo Stark and uniaxial stress splitting 8=18542
 sphere, extinction coeff. in X-ray exam. 8=17388
 strain amplitude independent dislocation damping, recovery 8=13582
 stresses, internal, obs. by X-ray diffraction in single crystal 8=5014
 surface morphology, after etching in Fe³⁺ soln. 8=1724
 thermal cond. obs., by cryostat, 0.05 → 2°K 8=22112
 in thermoluminescence dosimeter for radiobiological work 8=14890
 thermoluminescence fading characteristics 8=14295
 thermoluminescence fading after γ doses 10-10³ rad. 8=14321
 thermoluminescence, thermal activation energies 8=18609
 third-order elastic constant, obs. 8=13579
 V_K centre, ENDOR study of lattice distortion by dipole-dipole hyperfine const. 8=2009
 water vapour adsorption on cleavage surface 8=17166
 Li⁺ mol-ion in LiF, stability study 8=22181
 LiF:Fe³⁺ system, mag. resonance studies of crystal field distortions 8=13005
 LiF-U, radioluminescence, temp. dependence 8=14323
- Lithosphere.** See Earth.
- Loges (molecular bonds).** See Bonds; Molecules/electronic structure.
- Lorentz-Lorentz relation.** See Dielectric phenomena.
- Lorentz transformation.** See Relativity/special.
- Lorentz number.** See Conductivity, electrical/solids; Conductivity, thermal/solids.
- Loschmidt number (= Avogadro number).** See Constants.
- Loudness.** See Hearing; Intensity measurement, acoustics.
- Loudspeakers.** See Acoustic radiators.
- Love waves.** See Elastic waves; Seismic waves.
- Low-temperature phenomena**
 See also Helium/liquid; Helium/solid; Joule-Thomson effect; Superconducting materials and devices; Superconductivity; Superfluidity.
 advances in low temp. physics, book V 8=19680
 carbon, pyrolytic, Hall effect 8=5174
 cryogenic liqs, saturated, correl. for viscosities, thermal cond. and self-diffusivities 8=15132
 Fermi hard-sphere gas at zero-temp., eqn. of state distrib. function 8=10658
 gases, diatomic, thermal conductivity and viscosity in mag. field 8=7919
 heat transfer below 0.2°K 8=15131
 parahydrogen, solid, ht. of fusion and density at up to 400 atms. 8=16928
 plastics, glass-reinforced, high-strength prop. meas. at cryotemps. 8=17840
 polystyrenes, dielc. props. 8=5359
 polyethylene, ht. capacity 2.5-30°K 8=1875-6
 Pyrex glass, 0.4°-4°K in 0-90 kG fields 8=17525
 quartz, Debye temp. meas. ~1-4°K 8=4934
 quartz piezoelec. resonator at 2°K 8=18204
 research in USSR, obs. 8=19681
 second order transitions as critical phenomena of phase equilibrium 8=8260
 steel, stainless with high N content, tensile and creep props. 8=17784
 steels, stainless, irradiation effects on tensile and shear props. at cryotemps. 8=17763
 Ukraine, research development review 8=10791
 Al alloys, irradiation effects on tensile and shear props. at cryotemps. 8=17763
 C resistors, resistance and magnetoresistance 8=17929
 CdS, green-edge fluorescence, 4.2°K 8=2479
 CeCl₃, e. s. r. and susceptibility meas 8=14097
 Cs metal, ht. capacity, 2-4°K 8=13374
 Eu, ht. capacity 5°-300°K 8=17518
 Gd Cl₃.6H₂O heat capacity singularities below 1°K 8=22115
 Gd₂(SO₄)₃.8H₂O, heat capacity singularities below 1°K 8=22115
 He adsorption, by condensed gas layers 8=8329
 He II, absorption of sound below 0.6°K 8=6235
 K₂MoCl₆ specific heat rel. to mag. ordering 1.5-20°K 8=1872
 KNO₃, irrad. cryst., e.p.r. of NO₂ at 4°K 8=5537
 LaH₂, sp. ht. 1.3-20°K 8=13373
 Li(NH₃)₄, ht. capacity, 2-4°K 8=13374

Low-temperature phenomena--contd

- in MnCu, Mn⁵⁴, anomalous susceptibility 8=13962
 Mn(NH₄)₂(SO₄)₂·6H₂O, ht. capacity 1°-4°K in mag. fields 8=17520
 Na₂HPO₄ hydrates, entropy and disorder 8=17521
 Ni alloy, irradiation effects on tensile and shear props. at cryotemps. 8=17763
 Ni-Fe, permalloy, thin films, exchange anisotropy, 4.2°K 8=2333
 NiSiF₆·6H₂O, thermodynamic and mag. props. 8=8641
 Pd, magnetic moment data at 4.2°K, limits of exchange enhancement 8=13973
 Sb, crystal resist. in mag. field 8=9016
 Sr_{0.925} Ba_{0.075} TiO₃, heat capacity, 0.3 to 4°K 8=1877
 Te, p-band absorption at 4°K 8=8945
 Ti alloy, irradiation effects on tensile and shear props. at cryotemps. 8=17763
 US, ht. capacity and thermodynamic props. 8=22848
 V(CO)₆, e.s.r. spectrum at liq. He temps. 8=18438
 ZnS, Fe²⁺ i. r. luminescence spectra, 5 and 77°K 8=2491

Low-temperature production

- See also Joule-Thomson effect; Liquefaction/gases; Magnetic cooling.
 cascade processes, thermodynamic efficiency 8=10792
 closed cycle refrigerator, Claude cycle, 4.5°K 8=19683
 cryogenic liquids, differential density meas. 8=19347
 Dewar cooling vessel for molecular u. v. absorpt. spectra recording 8=22930
 4.2 to 0.3°K, using charcoal adsorpt. pumps for pumping liq He⁴ and He³ 8=15133
 1.85°K, closed-cycle refrigeration 8=6224
 solid cryogenics, A, CO, H₂, CH₄, Ne and N₂, review 8=19634
 specimen cooling stage for scanning electron microscope 8=6227
 He³-He⁴ dilution refrigerator, rapid start-up 8=15145
 He³ in He⁴ dissolution refrigerator 8=19682
 KCl:OH⁻ cooling to 0.36°K by adiabatic depolarization of OH⁻ 8=1874

Low-temperature technique

- β, γ-spectrometers, improved resolution with cooling 8=6811
 calorimeter for enthalpy meas. 8=15126
 calorimetry, use of pure Cu standard 8=15127
 charcoal adsorpt. pump in adiabatic vacuum calorimeter, for 4.2 to 300°K 8=17511
 cryogen storage, fluid heat transfer domains 8=16692
 cryogenic liquids, differential density meas. 8=19347
 cryogenic tank temp. meas. 8=19685
 cryogenic tensile assembly for testing combined nucl. radiation and cryotemp. effects 8=17763
 cryosorption props. of molecular sieves in ultra-high vacuum 8=12714
 cryostat sample holder, two degrees of freedom 8=18292
 electrical termination, use of quartz crystals 8=15137
 electroacoustic thermometry 8=19663
 evacuation of containers in liq. He, use of zeolites 8=4502
 filling of liq. He storage dewars, control monitor 8=15147
 GkZh-94 oil, use for acoustic contact at liq. He temp. 8=15136
 gases at high press., compact elec. lead 8=3147
 inexpensive app. for undergrad., for range 2°K-300°K 8=254
 Joule-Thomson refrigerator, for n diffraction at liq. N temp. 8=8501
 liquid H target, thin walled, description 8=15838
 liquid-level sensor, superconducting, for slush hydrogen use 8=16929
 microbalance, vacuum for 77.3°K operation 8=7965
 packing of valves 8=3139
 for plastics, glass-reinforced, high-strength prop. meas. 8=17840
 research in USSR, obs. 8=19681
 resistance thermometers, below 1°K 8=19665
 review, superconducting magnets 8=6225
 sapphire window mountings for low temp. spectroscopy 8=3362
 sealing of glass illuminators of H bubble chamber, using pneumatic packing 8=15645
 solid-state, appl. of superconducting electro-magnets 8=6281
 specimen cooling stage for scanning electron microscope 8=6227
 specimen holder for obs., and method of thinning specimen 8=6228
 thermal cond. determ. of semiconductor cylinders 8=3107
 thermal cond. meas. at liq. He temp., use of zeolites 8=3106
 torque meas. by superconducting torus 8=14924
 Ukraine, research development review 8=10791
 variable temp. liq. He optical stage, for metallographic studies of supercond. mats. 8=19686
 Al alloys, high strength with good weldability for cryogenic service 8=17762
 C resist. temp. meas., calibration 8=19682
 Cu calorimetric standard, atomic heat meas. 8=17517
 Ge(Li) γ-ray spectrometers cryostat systems 8=11443
 H₂ liq.-solid mixtures, quality determ. 8=15138
 H₂ liquid-solid mixture storage obs. 8=19067

Low-temperature technique--contd

- He Dewar fast precooling to N₂ temp. 8=3114
 He vapour cooling of current leads 8=15195
 Ne-H bubble chambers 8=20224
 Si, possible use in resistance thermometers 8=248

Lubrication

- See also Friction.
 bearings, full journal, turbulent and laminar flow 8=8810
 bearings, laminar and turbulent flow analysis 8=12733
 fluid inertia effects 8=21589
 lubrication and wear, conference, Plymouth, England (1967) 8=13521
 m.h.d. flow in step-type thrust bearing induced by rot. upper plate 8=351
 metalworking, role of surface energy of adhesion 8=5034
 thrust bearing, hydrostatic, MHD lubricated, effects of inertia 8=8809
 Cu wire, under externally generated pressure, drawing process 8=2052

Ludwig-Soret effect. See Diffusion in solids.**Luminescence**

- See also Electroluminescence; Luminescent devices; Thermoluminescence.
 alkali metal, emission spectra, influence of electrical field 8=1895
 band shape, complex molecules 8=1215
 benzene, N and Ar excit. in solid solns., obs. 8=13036
 benzyl radical fluoresc. in methylcyclohexane, cyclopentane and methylcyclopentane, 4°K 8=12342
 cathode, optical pumping in solid state laser 8=6454
 cathodoluminescent chemical analysis using electron microprobe 8=14493
 colour centres excit. and recomb. near fundamental absorpt. limit 8=9580
 cooperative, in solids 8=14298
 in crystals, determ. of 'colour' of short scintillations 8=14297
 energy-compensated spectrofluorometer, adjustment 8=15533
 energy transfer from triplet state in rigid solns. 8=9584
 rel. to exciton annihilation and bound complexes 8=9582
 fluorescent corrections to X-ray absorption in a sphere 8=23037
 fluorescence and phosphorescence spectrometry, sensitivity comparison, and with absorption 8=23180
 fluorescent source, quantum statistics of polarization 8=23036
 fluorescence in upper atmosphere 8=9926
 glass, silicate, 6% Nd broadening of individual center 8=2487
 Gudden-Pohl effect correl. with photoelectret state 8=5679
 high pressure cell for studies at 77°K 8=6502
 lasers in meas. of stimulated emission cross section 8=14292
 rel. to meteor trails luminosity, recomb. radiation 8=19263
 molecules, ππ* and nπ* states 8=12117
 moon, due to solar wind 8=19244
 nonuniformly broadened line system, theory of multimode laser generation 8=11004
 photoluminescence limit yield, thermodynamic calc. 8=12126
 in planetary nebulae, stratification 8=10215
 plasma slab, plasma yield from s- and p- polarized photon bombardment 8=8961
 population and r. f. coherence transfer by spontaneous emission 8=16220
 radiationless transition probabilities, weak solvent-solute interactions 8=16256
 resonance quenching as diffusion process 8=2471
 scintillators, due to X-ray pulses 8=9588
 solid scintillators, for conversion of γ-ray image to visible image 8=9587
 solid solutions, excitation transfer by multimolecular resonance 8=18590
 spectroradiometer-luminometer 8=492
 spectroradiometer-luminometer for quantum-yield studies 8=18589
 super-luminescence field, correlation props. 8=19924
 thermally stimulated conductivity, in photoexcited cryst. 8=1940
 the triplet state, conference Beirut Lebanon (1967) 8=16347
 two-quantum, use in laser 8=19930
 3C273, interplanetary scintillation 8=14807
 AIO clouds, chemiluminescent reaction 8=18872
 O+P(PH₃) reactions, chemiluminescence 8=23109
 Tb³⁺ activated phosphors, correlation of fluorescence with crystal and other properties 8=9581
 Ti, 4-valent cpds., with OH and O₂H radicals, chemiluminescence 8=2522
 U VI, dil. alkali soln., low temp. luminesc. spectrum 8=18618
 Yb, anticrossing signals from 6s²P₁ level 8=16211

gases

- air, shock wave front obs. 8=21483
 anthracene fluoresc. spectrum fine struct. and vibr. analysis, 23 000-28 000 cm⁻¹ 8=1274

Luminescence—contd**gases—contd**

- anthracene vapour, structured fluoresc. spectrum 8=21113
 anthracene vapour, vibr. effects in radiationless transitions 8=21114
 atoms resonance, forward-scatt. curves 8=20946
 atoms spontaneous emission under classical and quantum fields and collisions 8=20937
 electron excitation, for shock wave meas. 8=3033
 ethanol, spectrum vibrational analysis 8=7577
 hexafluoroacetone, fluoresc. lifetime and enhancement 8=12247
 metals in flames, detect. by atomic fluoresc. 8=14460
 methane-O₂ mixtures, vibr. energy transfer 8=21200
 NGC4151 galaxy, O III fluorescence 8=5937
 pyrene vapour, vibr. effects in radiationless transitions 8=21114
 Ar-air mixture, shock wave front obs. 8=21483
 Ar, shock wave front obs. 8=21483
 Ar-5%He, scintillation props. 8=11301
 H, resonance fluoresc. scatt. and level crossings 8=4064
 H₂ flames, chemiluminesc., effects of SO₂ 8=18693
 He excited by α , scintillation mechanism 8=12202
 He-42, 5% Xe, scintillation props. 8=11301
 He-Ar mixture excited by α , scintillation mechanism 8=12202
 He-Ne mixture excited by α , scintillation mechanism 8=12202
 Hg vapour, intensity-modulated fluorescence, stimulation in double reson. expt. 8=15492
 Hg-In fluoresc. spectrum, in line intensities 8=4080
 I₂, laser-induced fluoresc. in beam 8=16288
 K₂ vapour, resonance fluoresc. from nonlinear absorpt. of ruby laser light 8=7527
 Kr, radioactive, due to atomic rearrangement, and inelastic collisions with electrons 8=7406
 N₂, by fission fragments along entire track 8=7531
 Na I, atomic fluoresc., Doppler profiles 8=12069
 Na-Na collisions, energy transfer in sensitized fluorescence 8=16213
 NO₂ chemiluminescence, rad. from far wake of hypersonic spheres 8=21478
 OH from reaction H(P) with O₂ 8=14366
 P, K-shell fluorescence obs. 8=16208
 Xe, shock wave front obs. 8=21483

Liquids and solutions

- acetophenone in soln., lowest π, π^* triplet state 8=12892
 n-alkyl derivatives, $1 \rightarrow a_1$ transitions 8=12252
 3-aminophthalimide solution in frozen dioxane, fluorescence 8=5682
 2-aminopurine solns., quantum yield 8=4595
 aniline, $1 \rightarrow a_1$ transitions 8=12252
 anthracene in diethylaniline, charge-transfer complex 8=7560
 9-anthranaldehyde in alcohol and hexane solutions, singlet-triplet conversion 8=21693
 aromatic hydrocarbons, dipolar complexes in excitation 8=7553
 aromatic hydrocarbons in solns., mixed excimer fluoresc. 8=4593
 aromatic solns., excimer formation 8=8094
 aryl oxalates, electronegatively substituted, reactions with H₂O, and fluorescent compounds 8=18672
 p-biphenylaldehyde in alcohol and hexane solutions, singlet-triplet conversion 8=21693
 butyl-PBD, concentration effects 8=4594
 chemiluminescent reactions 8=1574
 chloroaluminum phthalocyanine, fast fluorescence meas. 8=18689
 chlorophyllide a and b, fluoresc. polarization spectra, 390-440 μ 8=21700
 cryptocyanine, fast fluorescence meas. 8=18689
 dibenzosuberone, phosphoresc. spectra 8=8096
 4,4'-dibrombenzophenone, phosphoresc. spectra 8=8096
 9,10-dimethyanthracene excimers fluoresc. quenching by anthracene and 9-bromoanthracene 8=1575
 dimethylaniline, α, β -unsaturated ketone derivatives in toluene 8=21702
 9,10-di-n-propylanthracene excimers fluoresc. quenching by anthracene and 9-bromoanthracene 8=1575
 eosin, fluorescence spectrum, effect of conc. 8=21701
 fluorescence polarization, effect of self-quenching 8=21698
 fluorescence, self-depolarization, "critical distances" in theories 8=21697
 fluorescence, self-depolarization, mathematico-physical models 8=21696
 hydroxide of hyamine 10-X, chemiluminescence in liquid scintillation counting 8=11305
 indole in polar solns., fluoresc., red shift and loss of vib. struct. rel. to exciplex 8=4591
 iso-propyl benzene, pure and in hexane, excimer fluoresc. 8=21699
 mixed excimer fluoresc., charge-transfer interaction 8=4593
 molten metals, sonoluminesc., temp. variation 8=12859
 naphthalene derivatives as donors in reson. energy transfer 8=18639
 α - β -naphthylaldehyde in alcohol and hexane solutions, singlet-triplet conversion 8=21693

Luminescence—contd**liquids and solutions—contd**

- n-nonane + p-xylene + CCl₄, quenching and decay 8=8097
 organic liquids, electron-impact excited 8=12893
 organic molecules de-exciting in rare earth chelates 8=16333
 organic mol. solns., two-photon fluoresc. excitation by picosec. pulses 8=4592
 organic supercooled melts, scintillation 8=8089
 oxalic anhydrides, reactions with H₂O₂ and fluorescent compounds 8=18685
 PBD, concentration effects 8=4594
 PPO + o-xilen, and butyl-borate, radioluminescent properties 8=1578
 phenanthrene in viscous cyclohexanol 8=12894
 phenylindole derivatives, scintillation of supercooled melts 8=8089
 photoluminescence band intensity distrib. rel. to excit. freq. 8=21695
 photoluminescence concentration depolarization 8=1573
 pinacyanol dye in alcohol, long wavelength bands 8=8091
 polycyclic monoazines, solvent effect 8=8095
 polystyrene in benzene, chemiluminesc., conc. effects obs. 8=23072
 proteins in soln., polarization, ang. correl. functions 8=16384
 pseudocyanine dye in alcohol, long wavelength bands 8=8091
 p-quaterphenyl derivatives, scintillation of supercooled melts 8=8089
 quinine sulphate solns., quantum yield 8=4595
 quenching and decay in multicomponent systems 8=8097
 rare-earth ions, energy transfer to H₂O 8=16870
 relative quenching factor, definition and use in correction terms 8=20195
 salicylate mixed complexes with La aminoacetate, aqueous, fluorescence 8=21703
 scintillation spectrometers, developments 8=6644
 sonoluminescence, timing of flash obs. 8=8093
 sprays, fluorescent photography using Q-switched laser light source 8=4636
 tetrachlorophthalic anhydride complexes, polarization of charge-transfer fluoresc. 8=1576
 tetracyanoethylene complexes, polarization of charge-transfer fluoresc. 8=1576
 s-trinitrobenzene complexes, polarization of charge-transfer fluoresc. 8=1576
 two-photon fluoresc. from 2 picosec light pulses of different freqs., as display of pulses 8=8071
 viscous solns., decay and energy transfer 8=12894
 xanthane rel. to mol. π, π^* and $\pi\pi^*$ levels location 8=1302
 xylenes, pure and in hexane, excimer fluoresc. 8=21699
 TL' ions in aqueous solns., intensity and quenching 8=21704
 UO₂(CO₃)₂, dil. soln., low temp. luminesc. spectrum 8=18618
 UO₂(NO₃)₂, dil. soln., low temp. luminesc. spectrum 8=18618
- solids, inorganic**
- alkali halides, cathodoluminesc., electron-probe meas. 8=1754
 alkali halide crystals with activating impurities, and colourability 8=17682
 alkali halides, F-centre, under hydrostatic pressure 8=9599
 alkali halides, fluoresc. from two-photon absorpt. with N₂ laser 8=5578
 alkali halides, inactivated, radioluminesc. and scintillation props. obs. 8=9592
 alkali halides, intrinsic recomb. rad. and triplet state of self-trapped exciton 8=2476
 alkali halide phosphors radioluminesc. and carrier motion rel. to F-centres, obs. 8=18594
 alkali halide phosphors radioluminesc. and storage props. obs. 8=9591
 alkali-halide phosphors, temp. depend. of X-ray luminesc. and optical flash 8=5653
 alkali halides, thermal quenching of O₂⁻ and S₂⁻ 8=2485
 alkaline earth metal double orthophosphates, Sn-activated 8=14309
 alkaline-earth pyrophosphates, Eu²⁺ activated 8=9628
 alloys, analysis by X-ray fluorescence 8=9750
 alumina, X-ray fluorescence, anodic layer analysis 8=18595
 aluminophosphate glasses, radiocolouration and luminescence kinetics 8=1996
 anthracene crystals, fluorescence and absorpt. spectra symmetry 8=18631
 anthracene, recombination luminescence in mag. field 8=18630
 apatites, stoichiometry 8=2477
 book, 1966 8=18593
 calcium fluoxytantalate: Eu³⁺, Sm³⁺, rel. to crystalline field parameters of ions 8=16973
 cathodoluminescence, electron-probe meas. 8=1754
 ceramic and glass materials, viewing by optical microscopy 8=14296
 diamond, rel. to Lave spike refls., obs. 8=22014
 diamonds, natural, effect of heat treatment and irradiation 8=18596
 dielectrics, exciton transitions in 2-photon stimulation 8=9583
 diffusion couples, fluoresc. effects obs. by X-ray microanalysis 8=17553
 F-centres for hole processes meas. 8=8888

Luminescence—contd

solids, inorganic—contd

fluorescent X-rays from γ -irradiated target, absolute yield meas. 8=23039
garnet, Ce activated, fluorescence 8=2474
glasses, photo, commercial, influence of heat treatment 8=2482
injection lasers, review of structural parameters 8=15476
lanthanide complexes, mixed, energy transfer 8=2433
metal-phthalocyanines, singlet-singlet transitions 8=18591
metallic surfaces, u.v. emission on K⁺ ion bombardment, analysis by spectral micrography 8=14299
perovskites:Eu³⁺, vibronic structure in spectra 8=14333
phosphate glass:Ag radiophotoluminescent centres 8=14331
phosphate glasses, with Mn as activator 8=2483
phosphors based on ZnS and ZnO, radical-recombination, quantum efficiency 8=23064
phosphors, Tb³⁺ activated, fluorescence 8=4683
porphyrin vanadyl complexes 8=5685
quartz, X-ray, as a function of irradiation time of exposure 8=13871
rare-earth ions in NaCl:Se crystals 8=14334
rare-earth oxides, Bi-activated 8=14304
rare-earth trivalent ions, energy transfer between 8=9594
rock salt, in ultra-strong electric fields 8=23059
ruby, cathodoluminesc., efficiency 8=18586
ruby, elec. field effect 8=2475
ruby, fluorescence pair lines temp. dependence 8=9597
ruby, fluoresc. rel. to energy transfer from Cr single ions to pairs 8=14302
ruby, light breakdown mechanism 8=23043
ruby monocrystals, X-ray effects 8=14301
ruby, quantum output, spectral depend. meas. 8=1995
semiconductors, intrinsic, exciton transitions in 2-photon stimulation 8=9583
silicate glass:Nd³⁺, fluoresc., quantum efficiency 8=5667
II-VI compounds photoluminesc. and equidistant band edge emission, 4.2°K 8=9590
two-valence electron systems, model potential rel. to excited impurity states 8=23035
uran glass, quantum yield in anti-Stokes region 8=18640
uranyl compounds, molecular vibr. manifestation 8=12235
X-ray emission yield dependence on diffraction conditions of electrons 8=13237
zircon, natural, obs. of two types of centres 8=9649
zirconium-silicates, radioluminescence 8=9624
ATiBO₆ (A=Lu, In, Sc, Cr, Ga or Al; B=Nb, Ta, or Sb), fluorescence and crystal structure 8=4879
AgBr(I) photographic films, influence of dyes 8=23042
AgBr pure and doped with AgI and CdBr₂, at 4.2°K edge spectra 8=23041
AgCl, electroluminescence, negative resist., and current-voltage characts. 8=17918
AgCl, at 4.2°K, edge spectra 8=23041
AlN:Cr photo-cathodo- and electroluminesc. and S and Zn impurity effects, obs. 8=9595
AlN:Eu photo-cathodo- and electroluminesc. and S and Zn impurity effects, obs. 8=9595
AlN:Mn photo-cathodo- and electroluminesc. and S and Zn impurity effects, obs. 8=9595
AlN:Sm photo-cathodo- and electroluminesc. and S and Zn impurity effects, obs. 8=9595
Al₂O₃ films, photoluminesc, spectral distrib. curves 8=9596
Al₂O₃:Rh 8=14300
Au sphere fluorescent corrections to X-ray absorption in a sphere 8=23037
BaClF:Sm²⁺, evidence of phonon annihilation from ³D₁ and ³D₂ fluorescence 8=9600
BaClF:Sm²⁺, temp. depend. 8=14332
BaF₂, additively coloured, phonon-assisted colour centre fluorescence 8=14306
BaO, Al₂O₃:Mn sensitized by Th and Ce 8=14303
BaS:Bi and electroluminesc. rel. to activator and BaSO₄ phase concs., obs. 8=9601
BaS:Cu and electroluminesc. rel. to activator and BaSO₄ phase concs., obs. 8=9601
BaS:Mn and electroluminesc. rel. to activator and BaSO₄ phase concs., obs. 8=9601
BaS:Mn phosphors in alternating and constant electric fields 8=23045
BaTiO₃:Eu²⁺, vibronic structure in spectra 8=14333
Bi in rare-earth oxides 8=14304
Bi³⁺-activated phosphors 8=23046
CaCO₃, X-ray luminesc., empirical decay law 8=14307
CaF₂, additively coloured, phonon-assisted colour centre fluorescence 8=14306
CaF₂(Eu) fluorescent response function to X and γ -rays 8=5665
CaF₂:Sm²⁺, temp. depend. 8=14332
CaF₂:Sm³⁺, tetragonal field, energy levels 8=13009
Ca₂, and scintillation props. 8=5654
CaO, Al₂O₃:Mn²⁺, sensitized by Th and Ce 8=14303
CaSO₄:Mn, X-ray, accumulation capacity 8=5655
CaSO₄:Sm²⁺ 8=23047
CaS, SrS phosphors excit. spectra obs. 8=9511
CaS, SrS:Ce:Sm i. r. flash stimulation rel. to trapping 8=9511
CaWO₄:Nd³⁺, fluoresc., quantum efficiency 8=5667
Cd, resonance fluorescence, modulation effects and lifetime meas. 8=9609

Luminescence—contd

solids, inorganic—contd

CdL₂ 8=5660
CdL₂(Eu) 8=5660
CdL₂(Pb) phosphoresc. and fluoresc. excit., e transitions 8=9605
CdS, alloyed with Au, recombination centre parameters in single crystals 8=14293
CdS, cathodoluminesc., electron-probe meas. 8=1754
CdS, cathodoluminescence temp. dependence 8=18597
CdS edge emission, doping, heat treatment and deform. effects, 4.2°K 8=9606
CdS, edge emission, peak shift with excitation intensity 8=2478
CdS, e microprobe obs. 8=14317
CdS, etched in KOH(NaOH) soln., light sensitization investigation 8=14294
CdS excit. by high photon densities, 4.2 and 77°K 8=9607
CdS, fluorescence, rel. to growth in improved furnace 8=1739
CdS, green-edge fluorescence, 4.2°K 8=2479
CdS, heat treatment and impurity effects rel. to centres nature, obs. 8=8741
CdS, i. r., and thermally stimulated currents 8=5661
CdS, photochemically sensitized and unsensitized, spectra 8=9603
CdS, and photoconduction induced by double photon absorpt. 8=14313
CdS, photoluminesc. efficiency 8=14312
CdS, photoluminescence spectrum, emission bands rel. to N₂ impurities 8=5657
CdS, pure crystals, submission to excitation of 50 keV electrons 8=14311
CdS, sensitizing recomb. centres, radiative capture yield of electrons 8=9602
CdS, two-photon excitation case 8=18599
CdS, with Te as isoelectronic trap, optical fluorescence and absorpt. 8=23048
CdS_x-CdSe_{1-x}, stimulated rad. during two-photon excitation 8=23049
CdSe, band-edge emission, excitation intensity effect 8=14316
CdSe edge emission, doping, heat treatment and deform. effects, 4.2°K 8=9606
CdSe, yield from radiative electron capture by sensitizing recombination centres 8=18598
CdSe-CdS mixed crystals at 4.2°K, photoluminescence 8=5656
Cd(S:Se) i. r. quenching rel. to band gap, 100-300°K 8=2261
Cd(S:Se) powder, cathodic luminescence 8=9604
Ce³⁺-activated phosphors 8=18600
CsBr:P radioluminesc. rel. to hole storage at centres, obs. 8=9625
Cs₂DyF₇ 8=21814
CsI(Na), fluorescent response function to X and γ -rays 8=5665
CsI(Na), single crystal, optical props. 8=2480
CsI(Tl), fluorescent response function to X and γ -rays 8=5665
CuBr, exciton spectra 8=23052
CuCl emission line lifetimes, positions and intensities, 4.2-300°K 8=9526
CuCl, exciton spectra 8=23052
CuCl, and weak absorpt., rel. to exciton complexes 8=9525
CuI, exciton spectra 8=23052
Cu₂O, non-linear dependence on photoexcitation intensity 8=18601
Dy³⁺ in tungstates and molybdates, u. v. excitation of fluoresc. 8=2473
Er³⁺, energy transfer in Na rare-earth tungstates 8=9610
Eu salts, fluoresc. lifetimes and multi-phonon deactivation, 4.2°, 77° and 300°K 8=14315
Eu³⁺ in garnet struct., hypersensitivity of ³D₀-⁷F₂ transition 8=18602
Eu³⁺ in tungstates and molybdates, u. v. excitation of fluoresc. 8=2473
EuAl borate, nonstoichiometry, X-ray fluoresc. 8=8410
EuF₃ 8=14214
Fe²⁺ in ZnS, i. r. spectra, 5 and 77°K 8=2491
GaAs, band-edge emission, excitation intensity effect 8=14316
GaAs diffused p-n junctions, longwave bands in luminescence spectra 8=5663
GaAs, epitaxially grown from Ga soln. 8=4829
GaAs, heavily doped with Te, S, Se and Sn, spectra at 77°K 8=18605
p-GaAs, photoluminescence, effect of heat treatment with excess As pressure 8=23054
GaAs, recombination processes following impact ionization by high field domains 8=2192
GaAs spherical recomb. diodes, use in optical pumping elements 8=23074
GaAs, stepwise excitation 8=23055
GaAs, Cu-diffused crystals, photoluminesc, failure to observe defect level 8=1954
n-GaAs radiative recombination 8=9612
p-GaAs, Zn doped, compensated, at 77, 194, 300°K 8=5662
GaAs, Zn-doped, rel. to heat treatment 8=2481
GaAs:Zn, photoluminescence, effect of As pressure 8=23053

Luminescence—contd

solids, inorganic—contd

- GaP p-n junctions, and microplasma obs. 8=5310
 Gd phosphate-vanadates 8=14330
 Ge, anisotropically deformed, under pinch conditions 8=18603
 Ge, emission by hot carriers 8=5664
 p-Ge, Ga doped and As compensated, rel. to impurity conc. 8=9613
 Ge:Zn, Sb-compensated, Zn-impurity conc. dependence 8=18604
 Hg-type activators, spectra genetic relationships and new phosphors prop. prediction 8=9593
 Ho-doped crystals, infrared quantum counter action of Ho^{3+} 8=18606
 K-Ba-SiO₂ glass: Nd³⁺, non-uniformly broadened band, half-width of separate centres and migration probability 8=14329
 KBr, e microprobe obs. 8=14317
 KBr-In, inner-centre luminescence, spectral-kinetic investigations 8=14319
 KBr-In photo- and thermostimulated, rel. to impurity C excits. delocalization mechanism 8=8903
 KBr:NO₃⁻, CO₃²⁻, SO₄²⁻, SeO₃²⁻ and Cu, centres nature, obs. 8=8745
 KBr:(Ni, Cu, In, Pb and Tl), roentgenoluminesc. and F-flash temp. depend. obs. 8=9626
 KBr:O₂, effect anharmonic vibrations on isotopic displacement 8=22937
 KBr:P radioluminesc. rel. to hole storage at centres, obs. 8=9625
 KBr:Sm²⁺, one-phonon sideband of 6890 Å transition at 7°K 8=9614
 KBr:Tl F-centres rel. to hole processes, obs. 8=8888
 KCl, e microprobe obs. 8=14317
 KCl:Ag, B-centre meas. 8=2006
 KCl(Ag), colouration, impurity centres produced 8=1994
 KCl-In, inner-centre luminescence, spectral-kinetic investigations 8=14319
 KCl:Na, F₁ centres 8=9615
 KCl:(Ni, Cu, In, Pb and Tl), roentgenoluminesc. and F-flash temp. depend. obs. 8=9626
 KCl:P radioluminesc. rel. to hole storage at centres, obs. 8=9625
 KCl:Pb phosphor, tetragonal symmetry 8=18607
 KCl:Tl, photostimulated, rel. to optical and thermal electron roles in recomb., 77-300°K 8=9617
 KI, e microprobe obs. 8=14317
 KI:In photo- and thermostimulated, rel. to impurity C excits. delocalization mechanism 8=8903
 KI and KI(In) self-luminesc. due to X-rays, decay 8=14318
 KI:(Ni, Cu, In, Pb and Tl), roentgenoluminesc. and F-flash temp. depend. obs. 8=9626
 KI:P radioluminesc. rel. to hole storage at centres, obs. 8=9625
 KI:Tl roentgenoluminesc., elec. field stimulation mechanism, obs. 8=9618
 KI:Tl roentgenoluminesc. and F-flash build-up obs. 8=9616
 KI:Tl⁺, at 77°K rel. to Tl⁺ clustering 8=23056
 KMgF₂:Ni²⁺, i. r. emission 8=18626
 KX: Cu⁺, (X = Br, Cl, I) lifetime of excited Cu⁺ 8=23057
 La phosphate-vanadates 8=14330
 LaF₃: Nd³⁺, absorpt., luminesc. and generation spectra 8=3334
 LaF₃:Nd³⁺, Yb³⁺, energy transfer 8=14328
 LiF, influence of thermal treatment 8=14322
 LiF, M-centre excit. spectra and transitions, obs. 8=8747
 LiF-U, radioluminescence, temp. dependence 8=14323
 Li₂Ge₂O₇:Cr, fluorescence at 4.2-300°K 8=9619
 LiH, study of red luminesc. centres 8=18608
 Lu phosphate-vanadates 8=14330
 MgF₂:V²⁺, i. r. fluorescence and phonon-terminated stimulated emission 8=2489
 MgGa₂, Mn activated, aluminium-substituted 8=14325
 MgO, fluorescence, "mirror" absorption 8=9620
 MgO:Co²⁺, near i. r. 8=23050
 3MgO.B₂O₃:Ge:Mn and cathodoluminesc. and excit. spectra rel. to mechanism 8=9621
 MgO:Ni²⁺, near i. r. 8=23050
 Mg₂TiO₄, emission spectra, temp. var. 8=2488
 MgTiO₃:Mn²⁺, at 77°K 8=14324
 (Mg, Tn)₂TiO₄, emission spectra, temp. var. 8=2488
 Mn²⁺ in hexa- and tetracoordinated cpds. 8=9551
 Mn alloys with Dy, Ho and Er, X-ray fluorescence analysis 8=2552
 MnF₂, pure and Eu³⁺, Co²⁺ doped, antiferromagnetic radiationless processes and afterglow kinetics 8=23058
 MnS 8=2484
 MnS/ZnS mixed crystals. 8=2484
 Na₂B₄O₇ glass, Eu activated, rel. to energy migration 8=23061
 NaBr:P radioluminesc. rel. to hole storage at centres, obs. 8=9625
 NaCl, e microprobe obs. 8=14317
 NaCl phosphors, X-ray luminescence, depend. on radiation time 8=18612
 NaCl(Ag), colouration, impurity centres produced 8=1994

Luminescence—contd

solids, inorganic—contd

- NaCl:Ag, electrophotoluminescence 8=2486
 NaCl:Eu, and excit. spectrum, rel. to centres structure, obs. 8=9623
 NaCl:(Ni, Cu, In, Pb and Tl), roentgenoluminesc. and F-flash temp. depend. obs. 8=9626
 NaI capture centres, i. r. excit., heat treatment in O effects, obs. 8=23060
 NaI(Tl), activator distrib. rel. to Cl⁻ ion addition 8=14327
 NaI: Tl capture centres, i. r. excit., heat treatment in O effects, obs. 8=23060
 NaI(Tl), fluorescent response function to X and γ-rays 8=5665
 NaI-Tl, photoluminesc. spectra, effect of X-irrad. and O-containing impurities 8=5666
 NaI(Tl), recomb. luminesc. at low temp. 8=18611
 NaI-Tl, single cryst., with oxygen-containing impurities, response 8=18610
 NaI, X-ray luminesc., effect of Cu impurity 8=23062
 NaMg[Cr(C₂O₄)₃].9H₂O 8=14247
 NaMgF₂:Ni²⁺, i. r. emission 8=18626
 Nd³⁺ ions, influence of glass comp. and activator conc. on quantum yield and quenching time 8=18592
 Nd silicate glass laser, stimulated emission cross section 8=14292
 Nd³⁺ in disordered matrices, structure of non-uniformly broadened luminesc. bands 8=14329
 Nd:Cr:YAG, sidelight fluorescence changes, due to laser at 1.06 μ 8=6473
 PbBr₂:Mn excit., emission and absorpt. spectra 8=9622
 PbCl₂:Mn excit., emission and absorpt. spectra 8=9622
 RbI:Tl, and formation of excitons 8=5131
 Sb₂O₃:Mn, impurities rel. to spectral props., brightness and temp. stability, obs. 8=18613
 Si, non-equilib. carrier recombination at high photo-excitation levels 8=18616
 Si, p-n junctions, mesoplasma, visible and i. r. 8=2218
 SiC, B and N doped 8=18615
 SiC crystals spectrum, deduction of energy spectrum of acceptor states 8=5668
 SiO₂:Tb, Eu, fused, and H diffusion 8=17585
 Sm²⁺ in host lattices, temp. depend. 8=14332
 SrF₂, additively coloured, phonon-assisted colour centre fluorescence 8=14306
 SrF₂:Sm²⁺, temp. depend. 8=14332
 (Sr, Mg)₂(PO₄)₂:Eu²⁺, Mn²⁺ phosphors, obs. 8=9629
 (Sr_{0.88}Mg_{0.11})₂(PO₄)₂:Eu yellow luminesc. and mechanism 8=9629
 SrO, photoluminescence, photoelectric emission and enhanced thermionic emission 8=23063
 SrTiO₃:Eu²⁺, Tb³⁺, Pr³⁺, vibronic structure in spectra 8=14333
 SrY₂O₇:Ce 8=18600
 Tb chelate phosphors, radiative quantum efficiencies, enhancement 8=18617
 Tb salts, fluoresc. lifetimes and multi-phonon deactivation, 4.2°, 77° and 300°K 8=14315
 Tb³⁺, energy transfer in Na rare-earth tungstates 8=9610
 Tb³⁺, energy transfer with Nd³⁺ 8=9594
 Tb³⁺ in tungstates and molybdates, u. v. excitation of fluoresc. 8=2473
 TiBr₃:Mn excit., emission and absorpt. spectra 8=9622
 TiCl₃:Mn excit., emission and absorpt. spectra 8=9622
 Tm³⁺, energy transfer in Na rare-earth tungstates 8=9610
 Y phosphate, vanadates 8=14330
 Y vanadate phosphors, particle size rel. to preparation 8=13048
 YAl garnet, Er, Tm and Ho doped 8=5669
 YAl garnet:Nd³⁺, fluoresc., quantum efficiency 8=5667
 YAlG:Nd³⁺, laser transition cross-section and fluorescence branching ratio 8=20003
 Y₃Al₂O₇:Ce 8=18600
 YVO₄:Bi 8=2490
 YVO₄(Dy or Sm) activated, const. quantum yield 8=5670
 YVO₄:Eu, Bi 8=2490
 ZnF₂:Ni²⁺, i. r. emission 8=18626
 ZnO, prepared by annealing in O₂, mechanism 8=5672
 ZnO, radical-recombination spectra, new bands attributed to surface centers 8=5673
 ZnO radicaloluminesc. and excit. mechanism, obs. 8=9635
 ZnO:Ni²⁺, i. r. emission 8=18626
 ZnO:Zn, heavy ion irrad. damage deterioration obs. 8=18623
 ZnO:Zn rel. to H, He, N, Ar and Kr ions energy losses and deterioration depth, obs. 8=18624
 ZnS cathodoluminescence spectra and bands lifetimes obs. 8=9646
 ZnS crystals, rel. to phase transforms on crushing 8=17106
 ZnS crystals, two-photon excitation of u. v. emission 8=9632
 ZnS, electroluminescence, influence of illumination 8=9630
 ZnS films, cathodoluminescence energy losses, rel. to photoluminesc. yield 8=9645
 ZnS, Cudden-Pohl effect correl. with photoelectret state 8=5679
 ZnS luminors, effect of Te on emission 8=14336
 ZnS phosphors rel. to carrier redistrib. among traps under i. r. irrad., obs. 8=9135

luminescence—contd

solids, inorganic—contd

- ZnS phosphors, cryoluminescence 8=14347
 ZnS phosphors, glow curve anal. rel. to traps 8=5675
 ZnS phosphors, mech. excited, behaviour of light emissions 8=9633
 ZnS phosphors, spectra, time constants of build-up and decay 8=5677
 ZnS phosphors, stimulated with i.r. wavelengths 8=5671
 ZnS, radical-recombination spectra, new bands attributed to surface centers 8=5673
 ZnS, reabsorption rel. to equilb. emission kinetics 8=9641
 ZnS, u. v., cryst. prep. conditions for optimum obs. 8=18629
 ZnS, u. v., under electron excitation 8=18619
 ZnS:Ag, red fluorescence of rapidly quenched phosphor 8=9648
 ZnS:Ag, use of radiation deterioration for meas. ion energy losses 8=8758
 ZnS-Ag single crystal, influence of i.r. radiation following α excitation 8=5674
 Zn-CdS graded band-gap semiconductor, spectra electric-field dependence 8=9134
 ZnS:CdS luminors, nonmonotonic var. 8=14337
 ZnS:Cl rel. to green and blue centres excit. 8=9642
 ZnS:Cu electroluminescence brightness non-additivity obs. 8=9636
 ZnS:Cu²⁺, filled trap distrib. rel. to duration of u. v. irradiation 8=18628
 ZnS:Cu photo- and electroluminescs., effects of grinding, obs. 8=9647
 ZnS(Cu), photoluminescent emissions, exptl. determ. of surface temps. 8=13082
 ZnS:Cu rel. to green and blue centres excit. 8=9642
 ZnS:Ho³⁺, and blue centres rel. to lattice-activator energy transfer, obs. 8=9643
 ZnS:Mn²⁺, decay time for tetrahedrally coordinated ions 8=14326
 ZnS:Ni²⁺, i. r. emission 8=18626
 ZnS, S³⁵ radioactive, photoluminescence spectrum, dark conductivity 8=5000
 Zn(S,Se)-Ag luminors, interaction of heated centres 8=14338
 ZnS:Sm³⁺, and blue centres rel. to lattice-activator energy transfer, obs. 8=9643
 ZnS:Tm, Tm luminesc. centres form rel. to Zn vacancies obs. 8=8434
 ZnSe crystals, hexagonal 8=9631
 ZnSe crystals, recombination centre parameters 8=18627
 ZnSe:Ni²⁺, i. r. emission 8=18626
 ZnTe, melt-grown, edge emission, annealing effects 8=5681
 ZnTe, photoluminescence spectra with anomalous temp. dependence 8=2492
 ZnTiO₄, emission spectra, temp. var. 8=2488
- solids, organic**
 acetophenone, lowest π, π^* triplet state 8=12892
 3-aminophthalimide solution in frozen dioxane, fluorescence 8=5682
 anthracene, delayed fluoresc. rel. to triplet-triplet interaction and triplet exciton diffusion, obs. 8=23066
 anthracene delayed fluoresc. decay time, 2-300 °K 8=23065
 anthracene excimers in rigid matrices at low temp. 8=14339
 anthracene, fluoresc. decay curve 8=18633
 anthracene, fluorescence intensity depend. after two-photon photocarrier generation 8=13918
 anthracene frozen in n-paraffin forms, fluorescence 8=23067
 anthracene, light output under influence of α -particles 8=2495
 anthracene and plastic scintillator, radiation damage by 4→10 keV electrons 8=23029
 anthracene, polarization of triplet factor group states 8=2494
 anthracene, quenching by mag. field, distinction of excitons 8=18632
 anthracene, u. v. irradiated, fluorescence and photo-conductivity rel. to carrier generation 8=2266
 aromatic amino-acids, frozen solns., delayed luminesc. 8=9650
 aromatic hydrocarbons, zero-field splitting of triplet states 8=4181
 benzaldehyde at 77°K, influence of solvent on time resolved phosphorescence 8=18635
 benzene, in cryst. matrices, and state of dispersion 8=9651
 benzene, phosphoresc. cryst., e. p. r. 8=14095
 benzyl, single crystals, and solid solns. in polystyrene 8=18634
 biphenyl in methylcyclohexane glass, gamma-irradiated, radiophotoluminescence 8=9652
 3-bromopyrene in ethanol, fluoresc. decay 8=21128
 charge-transfer complexes, triplet states 8=2493
 1-chloronaphthalene in ethanol, fluoresc. decay 8=21153
 chrysene-d₁₂ in plastics, γ -ray scintillation 8=9656
 coronene in CCl₄, phosphoresc. rel. to mol. deform. by lattice interactions, 77°K 8=1577

Luminescence—contd

solids, organic—contd

- coronene-d₁₂ in plastics, γ -ray scintillation 8=9656
 delayed, decay time study 8=9579
 durene, doped monocrys., mechanism 8=18637
 4-dimethylamino-4'-nitrodiphenyl in decalin, frozen solution 8=5684
 9,10-diphenylanthracene, intersystem crossing obs. 8=4207
 4,4'-diphenylstilbene in polymethyl methacrylate, solid soln., temp. effect on anisotropy 8=9654
 durene, single cryst., progressive fluoresc. and delayed induced luminesc. 8=18636
 energy transfer in irrad. crystals 8=23038
 halogenated benzenes, excimer phosphoresc. in organic glasses 8=9653
 halonaphthalenes in host crystals, three-dimens. polarization anal. 8=5683
 1-methylnaphthalene excimers in rigid matrices at low temp. 8=14339
 naphthacene in aggregates of anthracene in n-heptane, fluorescence 8=23067
 naphthalene derivatives as donors in reson. energy transfer 8=18639
 naphthalene in ethanol, fluoresc. decay 8=21153
 naphthalene solns. phosphoresc. and delayed fluoresc. rel. to triplet state obs. 8=23068
 naphthalene-d₈, triplet reabsorpt. and e. s. r. 8=9655
 naphthalene, phosphoresc., effect of impurity molecules 8=23069
 naphthalene in PMMA, triplet-triplet annihilation 8=2114
 naphthalene, polarization of triplet factor group states 8=2494
 2-(1-naphthyl)-5-phenyloxazol in polymethyl methacrylate, solid soln., temp. effect on anisotropy 8=9654
 nucleic acid components, frozen solns., delayed luminesc. 8=9650
 nucleotides 8=16334
 oxalyl chloride 8=2468
 perylene excimers in rigid matrices at low temp. 8=14339
 phenoxide ion in rigid-glass, polarization 8=14340
 phenanthrene-d₁₀, in solidified solvents, thermoluminesc. and delayed fluoresc., mech. 8=23070
 phenanthrene-d₁₀, triplet reabsorpt. and e. s. r. 8=9655
 phenazine, polarization of triplet factor group states 8=2494
 phthalimiden compounds, quantum yield in anti-Stokes region 8=18640
 plastic scintillator, light output under influence of α -particles 8=2495
 plastic scintillators for β -ray detect., complications rel. to absorpt. of contaminants 8=20386
 plastic scintillators, excited by Co⁶⁰ γ -rays 8=9656
 polarization of triplet factor group states 8=2494
 poly-2,2-propyl-bis-4-phenylcarbonate, chemiluminesc. obs. 8=23072
 polycyclic monoazines, solvent effect 8=8095
 polymers, polarized-fluorescence experiment, preferred orientation mathematics 8=1721
 polymethylmethacrylate, phosphoresc. of solute mols., quenching rel. to O₂ diffusion 8=8687
 polyphenyl benzenes, triplet states, zero-field splitting 8=12288
 polyphenyls in n-butanol glass, triplet lifetimes and T-T extinction coeff., obs. 8=23071
 polystyrene:anthracene:chloranil fluoresc. obs. 8=9261
 polystyrene, organic cpd. activated, chemiluminesc. obs. 8=23072
 polyvinylthalamide rel. to triplet-triplet energy transfer, 15000-40000 cm⁻¹ 8=12389
 pyrazine, in frozen aq. solvents 8=14342
 pyrazine, Zeeman splitting at 4.2°K 8=14341
 pyrene excimers in rigid matrices at low temp. 8=14339
 pyronine B, by excitation of S → T band 8=5686
 quinoxaline, optical detect. of e. s. r. transitions 8=14343
 rhodamine B, by excitation of S → T band 8=5686
 rigid solns., p-type delayed fluoresc. 8=14291
 scintillating plastic fibres, light-conduction characts. 8=9586
 stilbene crystals with anthracene impurities, quantum output as function of impurities 8=5687
 stilbene, light output under influence of α -particles 8=2495
 styrene scintillators radioluminesc. yield rel. to polymerization, obs. 8=14346
 p-terphenyl in plastics, γ -ray scintillation 8=9656
 tetramethylpyrazine rel. to triplet state struct., 4.2°K 8=22907
 1,1,4,4-tetraphenylbutadiene in polymethyl methacrylate, solid soln., temp. effect on anisotropy 8=9654
 4,4,4-trifluoro-3-hydroxy-3-trifluoromethylbutyrophenone 8=18638
 triphenylene in CCl₄, phosphoresc. rel. to mol. deform. by lattice interactions, 77°K 8=1577
 triphenylene-d₁₂, energy transfer with rhodamine B in rigid soln. 8=9584
 triphenylene, triplet reabsorpt. and e. s. r. 8=9655
 tryptaflavin in lucite, α -phosphoresc. and fluoresc. spectra shift rel. to O and pigment conc. 8=2496

Luminescence chambers

image intensifier application 8=608

Luminescent devices

See also Counters/scintillation.

cathodoluminescent detector for an electron microprobe 8=5689

cathodoluminescent, for distinguishing phase assemblages in reaction system MgO-MgSiO_3 8=18641

electron sensitive resist. 8=14345

fluorescence emission detector with 100 psec time resolution 8=5690

n, fast thermoluminescent 8=20564

n image intensifier tube 8=6954

phosphor screens, replaceable 8=5688

proton scintillator, energy dependence obs. 8=20536

scintillation transmitter resolution meas. by amp.

pulse analyzer, statistical error 8=3460

semiconductor, potential use, capabilities 8=9589

$\text{CaSO}_4(\text{Mn})$ thin film phosphors as thermoluminesc. dosimeters 8=11800

CdS acoustoelec. light scanner 8=5309

GaAs, electroluminescent diode, temp. depend. of recombination lifetimes 8=2222

GaAs spherical recomb. drodes, use as optical

pumping elements 8=23074

GaP:Ge p-n junctions, electroluminescence 8=23073

ZnS electrolumiphors, radiation-controlled enhancement 8=14344

ZnS:Cu phosphor condenser, characts. depend. on props. of crystal barrier layer 8=9657

Lumino(ph)ors. See Luminescence/solids, inorganic;

Luminescence/solids, organic; Luminescent devices.

Lutetium

X-ray L emission spectrum 8=9549

$\text{Lu}^{172} + \text{Hf}^{172}$, positrons, number, in decay 8=11824

Lu^{175} , nuclear dipole moment from hyperfine structure in III spectrum 8=4083

Lutetium compounds

Lu phosphate-vanadates, struct. and luminesc. 8=14330

LuTiBO_6 (B=Nb, Ta, Sb), crystal structure and fluorescence 8=4879

Luxemburg effect. See Electromagnetic wave propagation/ionosphere.

M-centres. See Colour centres.

M-regions. See Sun.

Mach number. See Aerodynamics; Shock waves; Supersonic flow.

Mach's principle. See Relativity.

Macromolecules. See also Molecules/configuration and dimensions, macromolecules; Polymers; Proteins.

antiferromagnetic spin structure in mols. with conjugate bonds 8=21208

aqueous solns, freezing 7=21761

biological, diffusion consts. from scatt. spectra 8=12381

biological one-electron or radical group transfer, e.s.r. study 8=12341

DNA with complexed carcinogen, elec. and optical props. 8=18093

DNA in soln., birefringence relax. 8=16849

DNA, intermolec. interaction energies, MO calc. 8=1318-19

DNA, triplet state 8=4263

macroions of rigid-sphere potentials, potential of average force 8=21203

n-alkane chains, polarizability anisotropy 8=16385

networks, viscoelasticity theory 8=21209

nongaussian chains, light scatt. 8=16386

polynucleotide helices, stability against torsional deform. 8=4268

polynucleotides, singlet energy transfer 8=16334

polynucleotides, synthetic, helix-coil transition 8=16387

ribonucleic acid derivatives, Raman spectra and molec. structure 8=7598

solutions, props. determ. by distillation 8=8018

in soln., X-ray scatt. 8=21205-6

volume effects by Monte-Carlo method 8=4261

Madelung constant. See Solids/structure.

Maggi-Righi-Leduc effect. See Magnetothermal effects.

Magnesium

in alloys, electrographic determ. 8=18762

atom, wavefunctions and oscillator strengths, semi-empirical calc. 8=20959

compression, plane-strain, anisotropy 8=17814

cold-worked, particle size and strain determ. by variance method 8=1761

crystal, electronic structure from optical

properties 8=14239

crystal interband absorpt., 82° and 295°K 8=18545

determination in picomole range by emission photometry 8=9757

Fermi surface from de Haas-van Alphen studies 8=2102-3

fused electrolyte, NaCl, KCl, CaCl_2 additives, elec. cond. and density obs. 8=23143

isoelectronic sequence, spectra, transition probabilities 8=7411

liquid, effective ion-ion potential 8=8237

liquid, wavenumber-dependence of elastic moduli 8=1499

Magnesium—contd

mass ejection by laser pulse 8=8759

muonic K series X-rays 8=1209

oxidation and diffusion removal in Al and Al-Mg alloys 8=18670

quark-atom lines in solar spectrum 8=6718

Rydberg states obs. from electron collision 8=20941

silico-thermal prod., isotopic studies 8=23776

solid solns. in Cu, precipitation of Cu_2Mg 8=4705

stacking fault energy calcs. using pseudopotentials 8=17673

Sun, Mg II resonance line, emission peaks 8=23744

twins, second-order (1011)-(1012) irrational habits 8=4784

vapour discharge, colour change 8=12393

in β -AgMg, stoichiometric, diffusion of Mg 8=17562

Er doped, e.s.r. 8=5531

Mg⁺ e affinity calc. by superposition of configurations 8=21281

Mg I, theoretical multiplet strengths 8=7410

Mg II, H and K lines in solar spectrum, rel. to chromosphere model 8=23707

Mg II reson. lines rel. to photosphere-chromosphere transition zone temp. distrib. 8=19319

Mg II solar line in lower chromosphere 8=2859

Mg⁺, ²F and ²G levels, polarization by outer electron 8=7411

Mg⁺, pseudopotentials 8=7409

Mg III and Mg IV, vacuum ultraviolet spectroscopy 8=1169

Mg²⁺, dipole polarizability from spectra 8=7414

in Ni, evaporation rel. to CO evolution 8=16745

Magnesium compounds

alloy, deform. by hydro-explosive loads 8=17815

alloy, magnetic properties 8=22755

alloys, Mg content, electrographic determ. 8=18762

aluminate spinels, defect structure and mech.

props. 8=22187

binary alloy, isothermal growth of Mn precipitates

in 8=4688

chrysotile asbestos, microfibrils and lattice parameters

from electron microscopy 8=1796

ferrites, Mössbauer power spectra in external mag. field 8=18342

ferrous ferrites, magnetically-induced ordering 8=22857

magnesia, hot-pressed, preferred orientation 8=8375

Magnox ZR-55, heat treated, creep behaviour in

350-450°C range 8=5078

photoelectrons created by soft X-rays, energy

spectra 8=18274

phthalocyanine, luminesc. singlet-singlet transitions 8=18591

vanadate, neutron diffr. determ. of O_2 parameters and degree of conversion 8=8534

Mg-9 wt. % Al alloy, age hardening mechanism and precip. process 8=13683

Mg-Al spinel, plastically deformed, slip parallel to {111} plane 8=17664

MgAl_2O_4 , crystal field theory rel. to optical transition variation with temp. 8=23000

MgAl_2O_4 fibres and platelets, growth and crystal chemistry 8=21956

MgAl_2O_4 , hot-pressed, microstructure and mech. props., quadratic multivariable analysis 8=21991

Mg-Ag, dilute alloy, temp. depend. of impurity resistance 8=5182

$\text{Mg}[\text{B}_3\text{O}_6(\text{OH})_6]_6\text{H}_2\text{O}$, crystal structure 8=13270

Mg-Cd alloys, Cd-rich, diamag. from mag.

susceptibility 8=5431

MgCd , order-disorder transformations obs. by electrical resistance and thermal investigation 8=8271

Mg_3Cd , antiphase boundaries, size, shape and orientation 8=17679

Mg_3Cd , critical resolved shear stress for slip, degree of order dependence 8=5079

Mg_3Cd , order-disorder transformations obs. by electrical resistance and thermal investigation 8=8271

MgCl_2 :Ag, γ -irradiated, e.p.r. and optical spectra 8=9419

MgCl_2 -KCl molten mixtures, absorpt. spectra of Ni centres 8=8086

Mg-Cr-Cu ferrites, mag. permeability tensor, influence of porosity 8=22852

$\text{MgCr}_{2-x}\text{Mn}_x\text{O}_4$, tetragonal distortion of Jahn-Teller type, study by X-ray and neutron diffr. 8=13269

MgCu_2 , Laves structures 8=13071

MgF_2 , F-treated, photocathodes, spectral characts. 8=18281

MgF_2 films, thin, charging with electrons of average energy 8=22505

MgF_2 films, thin, Molter electron emission 8=22732

MgF_2 , lattice dynamics and phonon dispersion relns. 8=13335

MgF_2 and Na_3AlF_6 and CaF_2 , i. r. antireflectant suitability 8=2435

MgF_2 , phonon-terminated stimulated emission and i. r. fluorescence 8=2489

MgF_2 , sintered, effect of additives on density and grain size 8=17026

Mg-Fe ferrites, magnetic diffusion after-effect 8=5491

Mg-Fe mixed hydroxides, and dehydration prods., microstruct. and pore struct., obs. 8=17023

(Mg, Fe)O, (magnesiowustite), oxidation depend. on temp., oxygen press., and crystal composition 8=23108

Magnesium compounds—contd

- MgFe₂O₄, thermal conductivity dependence on anion vacancies (produced by chem. reduction) 8=17543
 MgFe₂O₄, thermal conductivity rel. to non-stoichiometric vacancies 8=8660
 MgFe₂O₄:Sn, Mössbauer effect 8=16980
 MgGa₂, Mn activated, aluminium-substituted, luminescence 8=14325
 MgGa_{2-x}Mn_xO₄, tetragonal distortion of Jahn-Teller type, study by X-ray and neutron diffr. 8=13269
 Mg₂Ge, and selection rules for transitions and intervalley scattering 8=22437
 MgH, (A²Π-X²Σ⁺), oscill. strengths meas. 8=7530
 MgH, solar lines, centre-limb anal. in five photospheric models 8=23697
 Mg-In, energy of order-disorder transformation 8=13072
 Mg-Li, compression, plane-strain, anisotropy 8=17814
 Mg-Mn ferrite composition microinhomogeneities 8=21990
 Mg-Mn ferrites, magnetostriction and mag. anisotropy consts. 8=5492
 Mg-Mn ferrites, Mössbauer spectra in external mag. field 8=18342
 Mg_{0.4}Mn_{0.7}Fe_{1.9}O₄ mag. resonance spectra rel. to sintering temp. effects 8=2342
 Mg_{0.293}Mn_{0.636}Fe_{1.77}O₄:Sn, symmetry round Sn⁴⁺ from Mössbauer effect 8=16980
 MgMn₂O₄, cation migration at high temps 8=4955
 MgNi₂, Laves structures 8=13071
 Mg₂Ni, soft X-ray emission spectra 8=5624
 MgO, absolute structure factor meas. 8=17392
 MgO, addition up to 2% in BeO, rel. to rupture and grain growth props. 8=22315
 MgO, adsorpt. of nitro-cpds. rel. to electron donor props. on surface 8=8343
 MgO aggregates, hot-pressing 8=17816
 MgO, (B¹Σ⁺-X¹Σ⁺), oscill. strengths meas. 8=7530
 MgO bicrystals, transgranular cleavage fracture studies 8=8854
 MgO colour centre production, effect of atomic displacements 8=2011
 MgO containing Ni²⁺, e. s. r. line investigation from spin-phonon interactions 8=5532
 MgO crystallites, from thermal decomposition of Mg cpds., X-ray strain analysis 8=22379
 MgO crystals, Compton scatt. power 8=23012
 MgO, diffusion of Ba rel. to dislocation densities 8=4954
 MgO, doped, thermal conductivity, mag. field depend. 8=13395
 MgO, ductile whiskers, growth 8=13586
 MgO, electrical cond. at low temps. 8=22506
 MgO, grain shape change during creep 8=13584
 MgO, impurity distribution 8=13450
 MgO, Kikuchi band, line in middle, many-beam dynamical theory 8=13272
 MgO, Kikuchi patterns rel. to anomalous absorpt. 8=17362
 MgO, lattice expansion and density decrease rel. to n irr. 8=13249
 MgO, lattice vibration, surface modes 8=17482
 MgO matrix composites, Young's and shear moduli 8=13585
 MgO, mechanical props., high-press. data 8=19342
 MgO, "mirror" absorption, fluorescence 8=9620
 MgO, neutron or γ irradiated, O₂ chemisorption rel. to surface states 8=5724
 MgO, optical props. 8=9550
 MgO, powdered, mag. quenching, "anomalous", of three photon annihilations of positrons 8=17908
 MgO, primary step growth obs. by direct transmission microscopy 8=4789
 MgO, retention of OH 8=1703
 MgO, sintered, fast n-irr., effects on lattice, thermal cond., microstruct., density etc. 8=22245
 MgO, solubility in Al₂O₃ in H₂ atmos., temp. dependence 8=21818
 MgO, specific heat from 1.2 to 36°K and Debye θ 8=22116
 MgO-stabilized ZrO₂, stress relief mechanism 8=17839
 MgO substrate chemical interaction with Nb condensate 8=8326
 MgO surfaces, gas emission 8=2272
 MgO, whisker growth by vapour-liquid-solid mechanism 8=13144
 in MgO-Al₂O₃ system, phases in splat-quenched mets. 8=1677
 MgO-Al₂O₃-Cr₂O₃ system, coherent precip. 8=21848
 3MgO.B₂O₃:Ge:Mn cryst. growth and luminesc. mechanism 8=9621
 MgO:Co²⁺, anisotropy of spin-lattice relax. for Kramers doublets 8=9414
 MgO:Co²⁺, near i.r. fluoresc. and absorpt. 8=23050
 MgO:Cr, hypersound generation using ruby laser 8=10727
 MgO:Cu²⁺, paramagnetic reson. in ²E state, effect of linear Jahn-Teller coupling 8=18402
 MgO:Fe solid solutions, superparamagnetic magnesioferrite precipitate 8=1675
 MgO:Fe²⁺, microwave phonon-impurity ion interactions 8=9450
 MgO:Fe²⁺, Mössbauer effect, low temp. quadrupole splitting 8=13019
 MgO:Fe²⁺, spin lattice relaxation 8=9452

Magnesium compounds—contd

- MgO:Fe²⁺, u. p. r. temp. depend. 8=2367
 MgO-MgSiO₃ system, cathodoluminesc. study of reaction product distrib. 8=18641
 MgO:Mn²⁺, angular depend. of intensities of "forbidden" transitions 8=18430
 MgO:Mn²⁺ paramag. resonance transition probability temp. dependence 8=14113
 MgO:Mn²⁺, stress induced nuclear quadrupole splitting 8=22928
 MgO:Ni²⁺ absorption spectra line shift rel. to temp. 8=2442
 MgO:Ni²⁺, microwave phonon-impurity ion interactions 8=9450
 MgO:Ni²⁺, near i.r. fluoresc. and absorpt. 8=23050
 MgO:V²⁺, Ni²⁺, superexchange interaction between V²⁺ and Ni²⁺ 8=9355
 Mg(OH)₂, reactive hot-pressing 8=5077
 α-Mg₂P₂O₇, crystal structure 8=17367
 Mg-Pb, dilute alloy, temp. depend. of impurity resistance 8=5182
 MgSO₄ aqueous solution sound absorption and velocity, improved method 8=12858
 MgSO₄.7H₂O, epsomite, left form predominance during crystal growth 8=17241
 Mg₂Si, Renninger effect rel. to X-ray reflections 8=13271
 Mg₂Si, and selection rules for transitions and intervalley scattering 8=22437
 in MgSiO₃-CaSiO₃-Al₂O₃, garnet-pyroxene equilib. press. depend. obs. 8=1676
 Mg₂SiO₄ in earth's mantle, temp. and press. for reactions calc. 8=2556
 Mg₂SiO₄, forsterite, growth by flame fusion method 8=17242
 n-Mg₂Sn, piezoresistance at 80-300°K rel. to valence-band structure 8=2204
 Mg₂Sn, and selection rules for transitions and intervalley scattering 8=22437
 Mg-Th, compression, plane-strain, anisotropy 8=17814
 Mg-Th alloy, elastic constants 8=5080
 MgTiO₃, solubility in Al₂O₃ in H₂ atmos., temp. dependence 8=21818
 Mg(UO₂AsO₄).nH₂O, novacekite, e-diffr. meas. 8=17360
 Mg-Zn alloy, dendrite arm spacing and grain size, influence of coarsening 8=4849
 MgZn₂, plastic deformation, dynamic and creep tests 8=5081
 MgZn₂, Laves structures 8=13071
Magnetic amplifiers. See Amplifiers; Magnetic devices.
Magnetic anisotropy. See Magnetic properties of substances; Magnetization state.
Magnetic bays. See Earth/magnetic field, variations; Magnetic storms.
Magnetic bottles. See Magnetic fields; Plasma/confinement.
Magnetic cooling
 cryostat, demagnetization, for Mössbauer effect expts. 8=1642
Magnetic devices
 amplifier, appl. in millivoltage to current converter 8=10831
 amplifier, single-core, output-circuit transmittance 8=6282
 balanced mag. circuit, as memory element, anal. using theory of ratchet writing 8=19753
 character recognizer, sequential, using domain wall motion in Permalloy wire 8=10876
 coincident current store with ferrite core 8=14043
 combining Hall effect and magnetoresistance, design and charact. 8=13839
 Curie converter, thermomechanical 8=3167
 ferrite dev., superhigh freq. for operation in band 8.1-12.4 Gc 8=10939
 ferrite magnetostatic degenerated-type amplifier with resonator coupling 8=358
 ferrite magnetostatic degenerated-type amplifier with waveguide coupling 8=359
 ferromagnetic junction, magnetoresistance 8=18343
 field detector 8=6280
 film memories, multilayer processing techs. 8=19752
 film memory accessed by combined photon and electron beams, proposal 8=19754
 film memory and logic devices, appl. of domain tip propag. 8=13992
 film memory, written by focused light, thermal cycle-time and read bandwidth 8=10874
 gas analyser, magneto-mechanical 8=5758
 generator, without ferromagnetic core for MHD investigations 8=15356
 Hall-effect gyrators, geometrical design considerations rel. to use of only neg. resistance element 8=19751
 Kerr effect app. with polarization azimuth vibrator, for dynamic analog readout 8=19750
 liquid level sensor, magnetostrictive 8=10872
 magnetostrictive vibrators, limit of available mechanical output power 8=18322
 massive circuits, transient behaviour 8=10867
 metal tapes, moving, resulting mag. field distrib. and eddy-current energy losses 8=13957
 mirror, rel. to stochastic acceleration of charged particle 8=15271

Magnetic devices—contd

- parallel-to-serial converter, using domain wall motion in Permalloy films 8=10875
- permalloy films, memory performance and hysteresis in inhomogeneous magnetic field 8=2319
- Permalloy-SiO-Permalloy multilayer films, memory appls. 8=14035
- Permalloy wire dev., domain wall propag. and digital appls. 8=14034
- quadrupole magnetic lens using ceramic magnets 8=3226
- recording head, mag. field meas. using tapes of various coating thickness 8=19746
- recordings detection, magneto-optic, high-density 8=14185
- resonators, ferrite electro-mech. coupling coeff., mech. reson. freq., meas. accuracy 8=9368
- sensor, noise cancelling, for proton magnetometer meas. geomag. field near a.c. lines 8=302
- square cross-section coils, for prod. of uniform mag. fields 8=3162
- superconducting magnets, low-temp. technique, review 8=6225
- tapes of various coating thickness, for meas. of field geometry and strength of recording head 8=19746
- transducers, magnetostrictive, design 8=10873
- transducers, magnetostrictive, electro-mech. coupling coeff., mech. reson. freq., meas. accuracy 8=9368
- variometer, 3-component portable with resolution better than 1% 8=6278
- vibrating coil magnetometer for use below 0.3°K 8=15264
- wideband magneto-optic readout from rotating disc thin film 8=10871
- GdFe garnet wafer, magneto-optic memory element 8=19755

Magnetic domains. See Magnetization state/domains.

Magnetic field measurement

- alternating direction implicit method for grid of long lens spectrometer 8=6337
- betatron, transient, field distrib. 8=16563
- calibration, absolute, generated by small coil 8=10863
- current magnetometer with closed superconductor circuitry 8=15253
- direct plotting method 8=311
- earth's field, meas. from rockets, use of Rb and p magnetometers 8=14720
- electron guns for mapping and tuning 8=15289
- five-wire superconducting probe 8=22574
- fluxgate magnetometer probe, analytic model 8=10861
- Hall effect magnetometer, for small mag. fields 8=3162
- high field, by periodic size effect in Ga 8=3161
- Lorentz microscopy, wave-optical aspects 8=6279
- magnetograph for meas. of Zeeman effect in sun spectrum 8=14865
- magnetometer, fast response, using ferromag. resonance in thin films 8=19744
- magnetometer, transistorized with 10⁻⁴ accuracy 8=19914
- magnetometer, vibrating head, for meas. of transitions in high coercive force films 8=19745
- magnetometer, v.l.f. integrating vibrating sample 8=19743
- magnetometer, wide range, utilizing intensity modulation of transmitted light, optical pumping 8=12085
- meter for remanent rock magnetism 8=10058
- n.m.r., accuracy with strong field modulation 8=3282
- n.m.r. field discriminator 8=15433
- probe, gives audible signal for lab. demonstration 8=10822
- quartz variometer experience 8=23443
- recording head, using tapes of various coating thicknesses 8=19746
- sensitive variation indicator, based on Barkhausen effect 8=15257
- sensor, noise-cancelling, for proton magnetometer geomag. meas. near a.c. lines 8=302
- solar and stellar, review of methods 8=5963
- spinner magnetometer using mag. for shielding to reduce ambient mag. noise 8=14702
- of sweep for field of solenoidal supercond. magnet 8=10869
- torque magnetometer, for use to 4.2°K, design of cryostat 8=15140
- variometer, portable, 3-component with resolution better than 1% 8=6278
- weak field detector 8=6280
- weak fields, possibilities of meas. by optical orientation of atoms 8=20934
- Rb magnetometer using small vapour cells 8=19739

Magnetic fields

- See also Earth/magnetic field; Electromagnetic fields; Interplanetary magnetic fields; Sun/magnetism.
- accelerators, electron loading in tubes, suppression 8=15653
- amplitude modulation of e.m. waves 8=15391
- anomalies arising from horiz. cylinder type bodies, e.m. analog computation 8=18807
- anomalous, rock magnetization vector direction from statistical parameters 8=23449
- bottle for e spin-exchange collisions with H atoms 8=15304
- conducting sphere in alternating field, boundary values, transition from theory to actual values 8=19742
- confinement by ion-beam, geomag. appl. 8=1417
- cylindrical bar magnets, axial field at distance closer than magnet length, calc. 8=19749

Magnetic fields—contd

- cylindrically symmetric, in presence of freely moving particles 8=14966
- deflection, one-dimensional, production and analysis 8=1978
- dipolar, motion of mag. monopole 8=19031
- distributions in running metal tape, and eddy-current energy losses 8=13957
- entry into open shielding cylinders 8=10866
- ferromagnet, and elastic field around dislocation 8=18316
- finite parallel conductors, complex calc. 8=15256
- fluctuation stabilization, study by integration system using temp. variation 8=19740
- flux linkage of mag. thin film with rectangular coupling loop 8=22782
- force-free, relevant to dynamics of stellar shells 8=23509
- Galaxy, meas. method 8=14798
- high, effect on recombination through centres 8=22223
- high, production, field limitations in cylindrical flux compression experiments 8=10862
- high, prod. methods, review 8=306
- homogeneous, detection of conductor movement possibility 8=10344
- interaction with steady-state plasma 8=21286
- leakage, on ferromag. cryst., effect of mag. film 8=2313
- Lorentz microscopy, wave-optical aspects 8=6279
- magnetohydrostatic, application of variation principle 8=305
- magnetosphere and near space, IMP-2 results 8=2832
- modulated, stability of charged particle 8=3178
- multipole, spherical for use in plasma confinement 8=4393
- orbital accelerators, distortion by parasitic currents 8=635
- periodic, focusing and stability of intense electron beams 8=10895
- production, small uniform 8=3165
- pulsed, magnetoelastic waves 8=156
- pulsed, prod. by Si-controlled rectifier switching circuit 8=3164
- pulsed, prod. from electromagnets with variable-spaced helical windings 8=15260
- shaping, use of supercond. shields 8=13769
- slit for momentum definition and beam separation 8=6700
- solar prominences, quiescent, intensity obs. 8=10423
- solenoids, axially symmetrical and rectangular cross sectional, calc. 8=10865
- space anisotropy, soln. by linear sources 8=14936
- strong, of large volume, prod. 8=15255
- structure, analysis rel. to plasma confinement 8=19741
- sunspots field structure 8=2851
- superconducting films, surface parallel critical field, calc. 8=13727
- superconducting strips, flux motion 8=2152
- superconductors, type II, flux motion prod. voltages obs. 8=2149
- susceptibility meas, influence of field profile 8=15252
- synchrotron modifications, guide-field arrangements 8=636
- toroidal, drift of plasma ring 8=21367
- toroidal in stellar radiative zones, stability 8=23507
- transverse homogeneous, heat exchange in turbulent motion 8=12742
- uniform, prod. by system of four square coils 8=3162
- Venus, and Ashen light 8=5958
- waves at plasma-mag. field interface 8=21384
- weak, effect on electron spin echo 8=15429
- Al superconducting cylinders, periodicity in flux quantization expts., temp. depend. 8=22539
- Bi, high, magnetoresistance 8=5172
- Fe₃O₄, hyperfine, rel. to sublattice magnetizations 8=21809
- in Pb superconducting shell, attainment of zero field 8=17990
- Pt-Fe alloys, internal magnetic fields at Pt nuclei 8=2334

effects

- acoustoelectric gain in semiconductors 8=13345
- anthracene, photoconductivity, theory 8=22691
- antiferromagnetism, mol. field treatment 8=14062
- atoms, resonant freq. shifts rel. to electrostatic potentials 8=314
- axial torque on heated cylinder in rarefied gas 8=1320
- p-oxoanisole, nematic, X-ray structure investigations 8=4532
- on boundary layer in m.h.d. flow 8=10922
- crystal lattice, symmetry groups representation 8=5111
- deflection of electron beams, aberration 8=10897
- diffusion after-effects in high-amplitude fields 8=9322
- discrete charges in crossed elec. and mag. fields, rotating ring stability 8=6291
- domain wall velocity, numerical study 8=9321
- elastic wave propag. in conducting plate 8=10708
- electroconducting fluid flow between rough plates 8=8110
- electron beam compression 8=326
- electron beam deflection and spot distortion on target 8=6306
- electron scattering 8=3201
- electron transmission through aperture and R.P.D. technique 8=6312
- electronic conductors, electrons and lattice distribution functions 8=13635

Magnetic fields--contd
effects--contd

electrons, induced emission, moving in const., homogeneous field, exposed to e.m. waves 8=6805
 ferromagnetic single domains, isolated spherical, rotation under varying field and strain 8=13993
 fringing field, focus of spectrograph 8=10920
 gas flow, subsonic with crossed elect. field 8=16659
 gas, partially ionized, e vel. distrib. function 8=12423
 gases, polyatomic, viscosity at 290°K 8=1484
 graphite, linear magnetoresistance in the quantum limit 8=13711
 heat transfer from flat plate 8=19630
 on input transformers of measuring devices 8=10864
 ion beam focusing, theory 8=10919
 interactions in rotating molecule 8=12124
 jet, viscous, infinite σ perturbation effect 8=1518
 on Landau damping in Maxwellian plasma 8=7826
 laminar boundary flow, over dielec. disc 8=4507
 laminas in microtron, vertical focusing props. 8=3495
 light amplification, variable refractive index medium 8=400
 masers, gaseous optical, props. in weak axial fields 8=6410
 metal drop falling in viscous dielectric medium 8=7994
 metals, electron-nuclear relax. at low temps. 8=9449
 m.h.d. flow in expanding pipe 8=6354
 Mössbauer spectra in fluctuating environment 8=13017
 motion of low energy charged particles, perturbing forces effects 8=19052
 nuclear polarization determination by appl. to recoil nucleus stopped by foil 8=3955
 particle accelerator, 4 MV, reduction of e loading and X-ray intensity 8=15650
 Permalloy films, alternating mag. reversal 8=5474
 plasma compression 8=12535
 plasma, containment by closed configurations (toroidal) 8=1411
 plasma, cyclotron-resonance attenuation 8=7744
 plasma, high frequency, instability 8=12564
 plasma, potential surface wave propagation 8=7811
 plasma rarified, shock wave 8=12491
 quantizing, free electron absorpt. of ultrasonics 8=6165
 semiconductor diodes, minority carrier lifetime 8=13853
 semiconductor surface wave propag. and amplification in strong fields, theory 8=9090
 semiconductors, thermomagnetic coeffs. in strong fields, quantum oscs. 8=5426
 semiconductors, tunneling in crossed and parallel elec. and mag. fields 8=5227
 sols, birefringence 8=12878
 on spin density wave, one-band model 8=13980
 steel, quenching, review 8=22343
 stellarator mag. surface destruction by irregularities 8=16562
 superconducting foil, type I, in transverse mag. field, evidence for mixed state 8=17962
 on superconducting quantum interference device 8=17991
 superconductivity by proximity effect, breakdown field dependence 8=13733
 superconductor, type I, rel. to heat transport 8=22544
 superconductors, Ginzburg-Landau eqns. for arbitrary tangential fields, solution 8=9027
 superconductors, h.f. surface resistance, field dependence 8=9035
 superconductors, thin-film, rel. to far-infrared absorpt. 8=22938
 superconductors, type II, vortex structure motion in high field 8=9033
 thermocouples, theory 8=284
 viscosity of dilute diamag. gas 8=12703
 viscous flow under transverse magnetic field 8=6353
 Au₂Mn, magnetization in fields up to 50 kOe at 4.2°K and up to 70 kOe at 80°K 8=9281
 Bi, galvanomagnetic effects 8=8994
 Bi, quantum variation of Fermi level 8=17882
 Bi_{1-x}Cu_xMnO₂ solid solns., mag. props. in pulsed mag. field of 160kOe 8=18330
 CH₄ thermal cond., 290°K 8=4469
 CO thermal cond., 290°K 8=4469
 Ce ethylsulphate, thermal conductivity 8=13393
 Co films, rotating, galvanomagnetic effect 8=17931
 Cr-Ni steel, γ - α transform., pulsed field 8=17063
 EuS, magnetically ordered, rel. to internal field emission, obs. and model 8=5428
 EuSe, magnetically ordered, rel. to internal field emission, obs. and model 8=5428
 Fe, purified, induced oscillations rel. to amplitude-dependent internal friction and modulus defect 8=13557
 Fe-C-Ni-Mn alloys, martensitic transformation 8=17079
 Fe(NH₄)₂(SO₄)₂·6H₂O, isothermal dissoln. and growth 8=8411
 α -Fe₂O₃, magnetization in fields up to 80 kOe from 4.2-290°K 8=9281
 Fe₃S₈, magnetization in fields up to 90 kOe at 1.2°K, 201°K and room temperature 8=9281
 GaAs, absorption edge shift 8=9531
 n-GaAs, circularly polarized waves, doping rel. to optical absorpt. 8=22981

Magnetic fields--contd
effects--contd

Ge p-n junction at 77°K 8=18112
 n-Ge, on I-V characts. 8=13808
 Ge, photon-assisted magnetotunneling in parallel and crossed, elec. and mag. fields 8=5260
 He³ liquid, zero sound propagation 8=3120
 on He-Ne laser output 8=15468
 He-Ne laser, power output 8=3320
 He-Ne laser, resonance dips in output 8=11065
 In films, longitudinal magnetomorphic effects 8=5430
 InSb acoustic amplifiers, d.c. power dissipation reduction at max. gain 8=13355
 InSb laser, mode spectrum 8=11105
 InSb, n-type, microwave detection props. 8=2224
 InSb, polaron induced anomalies in interband magneto-absorpt., Coulomb effect 8=22818
 InSb, rel. to shallow donor levels 8=22462
 KAl(SO₄)₂·12H₂O, isothermal dissoln. and growth 8=8411
 KBr, electron transport props. in high fields at low temps. 8=2264
 KCl and KF, dichroism circular, of R₂ band 8=14235
 Mg ferrites, on Mössbauer spectra 8=18342
 Mg-Mn ferrites, on Mössbauer spectra 8=18342
 Mg-Mn ferrites, strong, impulse mag. reversal 8=9380
 MgO, doped, thermal conductivity, depend. 8=13395
 MgO, powdered, quenching, "anomalous", of three photon annihilations of positrons 8=17908
 Mn ferrites, on Mössbauer spectra 8=18342
 Mn_{2-x}Cr_xSb(x > 0.035), antiferromagnetic-ferromagnetic transition 8=9282
 MnHg magnetization in fields up to 100 kOe at dry ice temperature, room temperature and liquid air temperature 8=9281
 N₂ thermal cond., 290°K 8=4469
 NO thermal cond., 290°K 8=4469
 Nb, superconducting, u.s. attenuation depend. 8=17503
 Nb-25%Zr supercond. wires carrying a.c. 8=5208
 Ni, dynamic ΔE effect frequency dependence in weak mag. field 8=2065
 Ni(NiO) films, anisotropy in electrical resistance 8=5166
 Ni-Co alloys, uniaxial anisotropy by electron irradiation 8=5479
 O₂ thermal cond., 290°K 8=4469
 Pb, superconducting, depairing effect, microwave absorpt. in surface-sheath regime 8=13760
 Sm¹⁵⁰ in ferromagnetic lattices 8=2335
 Sn, superconducting films, thermal conductivity 8=22137

Magnetic films
 ageing problem, analytic solution 8=22784
 anisotropy field, low-freq. meas., appl. to automation 8=18325
 diagonalization procedure for Hamiltonian 8=5459
 domain structure in uniaxial thin films 8=14002
 double layer of different chem. comp., props. 8=9332
 double layer, separated by a dielectric, magnetic reversal quasi-statistical analysis 8=5458
 effect on leakage mag. field, on ferromag. cryst. 8=2313
 ferromagnetic, complex susceptibility 8=22786
 ferromagnetic, effect of superconducting screen on relative stability of Bloch and Neel walls 8=18327
 ferromagnetic, electrolytically deposited, growth rates and structure characts. 8=13999
 ferromagnetic, electron diffraction images from single and periodic domain structs. 8=22772
 ferromagnetic, ferromag. resonance, theory rel. to boundary conditions 8=18394
 ferromagnetic, inhomogeneity of magnetization calc. 8=2311
 ferromagnetic, magnetization inversion by Barkhausen-Cisman-Brion method, e.m. aspect 8=22781
 ferro, magnetization ripple theory 8=22785
 ferromagnetic, model including interactions between regions 8=14003
 ferromagnetic, resonance, due to hypersound in substrate 8=1841
 ferromag. resonance, use in fast response magnetometer 8=19744
 ferromagnetic, sputtered, controlled crystalline orientation rel. to coercive force 8=9333
 ferromagnetic, with surface anisotropy, spin-wave theory 8=5456
 ferromagnetic, susceptibility tensor under spin-wave resonance excitation 8=9330
 flux linkage of thin film with rectangular coupling loop 8=22782
 of high coercive force, meas. of mag. transitions with vib. head magnetometer 8=19745
 Lorentz microscopy, wave-optical aspects 8=6279
 magnetic structure and ferromagnetic resonance 8=22787
 magnetite on Fe, tensile fracture 8=21875
 magneto-optical transmission convertivity optimization 8=518
 memory accessed by combined photon and electron beams, proposal 8=19754
 memory devices, multilayer processing techs. 8=19752
 memory systems, written by focused light, thermal cycle-time and read bandwidth 8=10874
 multi-domain, demagnetising field rel. to ferromag. reson. condns. 8=22783

Magnetic films—contd

- with non-planar surfaces, determ. of magnetization and field distrib. 8=14000
- Permalloy, anisotropy, effect of defects caused by plastic deform. 8=14031
- permally, deposited on silicon grease over glass substrate, props. 8=2331
- permally deposition with varying degrees of anisotropy 8=21885
- permally, domain wall obs. by pulse technique 8=9364
- Permalloy, evaporated, influence of residual gases and metal bases on props. 8=5476
- Permalloy films hysteresis, effect of deposition conditions 8=14032
- permally, "flash-evaporated", standing spin-wave resonance 8=14083
- Permalloy, hysteresis, effect of deposition conditions 8=14032
- Permalloy, large-angle flux reversal meas., eddy-current-free 8=14030
- Permalloy, mag. reversal in alternating mag. field 8=5474
- permally, memory performance and hysteresis in inhomogeneous magnetic field 8=2319
- permally, r.f. reflecto-polarimetry 8=9409
- Permalloy, rotational hysteresis, temp. depend. 8=22823
- Permalloy-SiO-Permalloy multilayers, memory device appls. 8=14035
- Permalloy, worm motion of domain walls 8=14028
- polycrystalline, magnetization ripple wavelength 8=18326
- properties and applications 8=22780
- on silicon grease over glass substrate, hysteresis 8=2331
- spatial distribution of spontaneous magnetization, contribution 8=22779
- spin-wave resonance, nonuniform magnetization models in theory 8=14080
- stripe domains, electron mirror microscopy study 8=22778
- switching by non-coherent rot., propag. at high speed 8=18319
- tape recording, short-section scanner 8=15265
- tapes, storage capacity improvement through anisotropic props. 8=5457
- thin films, demagnetizing field problem 8=9331
- uniform rotation mode of flux reversal, analogue simulation 8=14001
- Co, electrolytically deposited, growth rates and structure characts. 8=13999
- Co foils, domain width depend. on thickness 8=22791
- Cr-Co successive layers, high coercive force, for storage in digital mag. recording 8=14009
- EuO, Faraday rot., mag. moment, susceptibility and squareness 8=13090
- Fe, electrolytically deposited, growth rates and structure characts. 8=13999
- FeNeMo/SiO/Fe double layer, hysteresis loops theory and experimental 8=5458
- FeNi, electrodeposited, static mag. props. 8=9347
- Fe-Ni alloy, thin, evaporated with oblique incidence, structure 8=14017
- FeNi-FeNiMn films with ferro-antiferromagnetic coupling, study 8=9346
- Ni, deposited on silicon grease over glass substrate, props. 8=2331
- Ni, electrodeposited, perp. anisotropy 8=14024
- Ni, electrolytically deposited, growth rates and structure characts. 8=13999
- Ni, galvanomagnetic effect obs. 8=5475
- Ni, ion bombardment rel. to induced mag. anisotropy 8=22829
- Ni, magnetostriction meas. and obs. 8=18347
- Ni-Fe double films, domain wall motion 8=2329
- Ni-Fe, dynamic energy losses during magnetization reversal 8=14029
- NiFe, mag. props. rel. to vacuum deposition press., 10^{-10} torr. 8=22822
- Ni-Fe, meas. of internal field; and wall pinning effects on domains 8=14026
- Ni-Fe memory elements, dispersion of anisotropy 8=14052
- Ni-Fe, permally, thin, exchange anisotropy, 4.2°K 8=2333
- Ni-Fe, thickness dependence of domain wall energy 8=18346
- Ni-Fe, thin, ferromagnetic resonance linewidth, rel. to temp. 8=2356
- Ni-Fe-Co, strain sensitivity rel. to Co content 8=18345
- Ni-Fe-Cr, mag. props. rel. to high speed computer storage use, obs. 8=22826
- Ni-Fe-Cr-Si alloy, 200-300 Å thick, galvanomagnetic effect 8=5478
- Ni-Fe-Cu, mag. props. rel. to high speed computer storage use, obs. 8=22826
- Ni-Fe-Mn, mag. props. rel. to high speed computer storage use, obs. 8=22826
- NiFe₂C₄ ferrite, single cryst., prep. and props. 8=18362
- NiFe₂O₄, thin, microstructure, ferrimagnetic props., electrical conductivity 8=2343
- Ni-Fe-Pd, mag. props. rel. to high speed computer storage use, obs. 8=22826
- NiFe-SiO-Co multilayer, stray-field coupled, magneto-resistance 8=14027
- Ni(NiO) ferromagnetic anisotropy effect on elect. resistance 8=5166

Magnetic flux. See Magnetic field measurement; Magnetic fields.**Magnetic hysteresis.** See Magnetization process.**Magnetic lenses.** See Electron lenses/magnetic; Ion optics.**Magnetic materials**

- alloys, ordered, effect of electrons of opposite spins on elec. resistivity 8=22432
- alloys, sp.ht.rel. to Kondo model 8=17510
- finished-product meas. technique 8=19737
- metals, electrons 8=22739
- paramagnetic, anomalous Hall effect 8=17914
- solid, symmetry projections for electronic states 8=18777
- Fe-Ni alloy, refining effect of Ge in vacuum melting rel. to mag. props. 8=22815

Magnetic measurement

- See also Magnetic field measurement. Entries describing measurement methods for specific magnetic quantities and effects may also be found listed under the various headings for the subjects concerned.
- on alloys, prep. of ball-shaped samples 8=10859
- apparatus for meas. of magnetoelectric effect between 1.8°K and 330°K 8=5427
- on ceramics, prep. of ball-shaped samples 8=10859
- coercive force, Hall-effect instruments 8=19738
- hysteresis, dynamic cycle 8=304
- induction, Hall-effect instruments 8=19738
- materials, ferromag., annular specimen sizing 8=19736
- materials, finished-product technique 8=19737
- pressurized materials, magnetization and anisotropy 8=13952
- reactor, Na cooled, flowmeter 8=7317
- susceptibilities, between 77° and 3000°K 8=10860
- susceptibility, Faraday method, influence of positioning errors 8=15252
- susceptibility, method for anisotropic materials 8=15251
- viscosity, effect of suspension mechanism 8=15254

Magnetic memories. See Calculating apparatus; Magnetic devices**Magnetic mirrors.** See Magnetic fields; Plasma/confinement.**Magnetic properties of substances**

- See also Magnetic films.
- AlNi A, coercive field strength, time- and temp.-depend. 8=5460
- Alnico-alloy, Ti-containing, and crystallization 8=8399
- breakdown and oscillatory magnetoresistance by Kubo formula 8=13954
- ceramics spinels and related structures 8=18291
- Conference on materials and their applications, London, 1967 8=9286
- crystals, exchange coupling, effect of multiplicity of mag. ions 8=22412
- crystals, orthorhombic, mol. susceptibilities and anisotropies, calc. errors 8=18290
- crystals, phonon process selection rules 8=13318
- Curie point, second order phase transitions, specific heat singularities 8=13365
- diffusion after-effects in high-amplitude fields 8=9322
- ethyleneimine, solvent and anisotropy effects in n.m.r. obs. 8=16895
- Fermi liqs., nearly ferromag., viscosity theory 8=2994
- field and domain structure, obs. with scanning electron microscope 8=13991
- finished products, meas. technique 8=19737
- graphite, galvanomagnetic of well oriented crystals 8=5384
- guanidine hexaquo V(III) sulphate 8=16995
- h. c. p. alloys of later 4d and 5d transition metal series, mag. susceptibilities 8=18296
- hematite, natural, stress induced anisotropy 8=22748
- hyperfine fields in crystals, with mag. ordering 8=1630
- ilmenite particles, beach sand, props. 8=23454
- interband breakdown conds, dynamics of conductivity electrons 8=5100
- isotropic media, anisotropy induced by intense laser beam 8=8106
- liquid crystals, review of data 8=1527
- magnetic impurity degenerate orbitals, Kondo and Anderson Hamiltonians 8=13008
- "Malcolloy", Co-Al, effects of Ni addition 8=13960
- metal impurity, ground state 8=8909
- metals and semimetals in liq. state, susceptibility meas. 8=12926
- metals, Kondo spin-compensated impurities, low temp. props. 8=8882
- metals, magneto-optical phenomena, quantum theory 8=13981
- metals, nearly ferromag., spin fluctuations, effect of band structure 8=2092
- metals, spin polarization of single mag. impurity 8=2132
- metals, spin susceptibility, dynamic, Fermi liquid theory 8=22447
- Mössbauer spectrum shift rel. to degree of spin-system ordering 8=22734
- noble transition elements and alloys, susceptibility, and superconductivity and sp.ht. 8=13752
- noble transition elements and alloys, susceptibility, and supercond. and sp.ht. 8=13753
- 1-aziridinepropionate, solvent and anisotropy effects in n.m.r. obs. 8=16895
- oscillatory free energy for nearly free electrons rel. to de Haas-van Alphen oscillations 8=2088

Magnetic properties of substances—contd

- plasma, resonantly sustained, behaviour at high h. f. power 8=21290
- polyatomic gases in mag. field, gyro-thermal effect 8=12672
- rare earth cobalt compounds with CaZn_5 structure, and crystallographic props. 8=22753
- rare earth-cobalt cpd., RCO_5 , Curie temp. dependence on comp. 8=18350
- rare-earth, Co (RCO_5) cpds. permanent mag. props., obs. 8=22743
- rare earth Fe garnets, intrinsic coercive force near compensation temp. ($>77^\circ\text{K}$) 8=14005
- rare-earth metals, heavy, ordering 8=22466
- rare earth metals, rel. to low temp. specific heat 8=17513
- rare-earths, theory of antisymmetric exchange 8=16972
- rocks, magnetization vector direction from statistical parameters of anomalous field 8=23449
- sample holder, two degrees of freedom 8=18292
- semiconductors, effect of mag. element impurities on resistivity 8=18016
- shielding efficiencies of cylindrical shells with axis parallel to field 8=22737
- spin array with two sublattices, exactly soluble model 8=6093
- steel, type 1H18N9T, austenitic, and influence of elastic and plastic deform. 8=9291
- structure determination from neutron diffraction data by spin density Patterson function 8=22735
- susceptibility, isothermal, lower bound 8=13958
- susceptibility, non-linear magnetization 8=2287
- tetraborides of Gd, Dy, Ho, Er and Tm, susceptibility rel. to temp. 8=5437
- transition-metal alloys, stiffness constant 8=9334
- transition-metal molybdates, and structure 8=13296
- transition metals, susceptibility in solid solns. 8=9283
- Zeeman spectroscopy, solid-state, crystallographic alignment 8=22936
- $\alpha\text{-Ag}_2\text{S}$ mixed conductor, susceptibility due to conduction electrons 8=22500
- Al, liquid, rare earth impurities, susceptibility and Knight shift changes 8=21724
- Au-Fe solid soln., magnetic ordering rel. to electric hyperfine interactions 8=2289
- Au-V alloys, dilute, susceptibilities rel. to mag. moment quenching 8=2288
- Au-V alloys, susceptibility and elec. resistivity temp. dependence rel. to s-d interaction 8=13657
- BaZnFe₂O₄, (ZnY) (ferroxplana) crystals 8=22744
- Be alloys, superconducting, magnetization meas. 8=17959
- Cr-Si alloys, Néel temp. 8=9001
- Cu, susceptibility and resist. studies of localized Fe moments 8=22796
- Cu-Fe alloys, high and low temp., effect of cold working 8=17934
- CuFeS₂, from Fe⁵⁷ Mössbauer spectrum 8=1649
- CuFe₂Mn₂O₄, tetragonal distortion 8=17205
- Cu(SO₄)₂ 8=9562
- Cu₂FeS₃, (cubanite) 8=14066
- Er, structure using Mössbauer effect 8=2291
- EuPd₃, hyperfine field studies by Mossbauer e.p.r. and n.m.r. 8=18334
- EuRh₂, hyperfine field studies by Mossbauer e.p.r. and n.m.r. 8=18334
- EuO₄, metamagnetism 8=22746
- Fe dissolved in Zn, magnetic moment, revision of superconducting props. 8=9344
- β - and δ -FeOOH, susceptibility and magnetization 8=22747
- Fe_{0.88}S, pyrrhotite, structure from Fe⁵⁷ resonance 8=16985
- FeS, troilite, structure from Fe⁵⁷ resonance 8=16985
- Fe(SO₄)₃ 8=9562
- FeSiF₆·6H₂O, pure and diluted crystals, susceptibility and ligand field behaviour 8=18297
- H, absorption spectrum, 3mm microwave radn., structures effects 8=14226
- Hg-In liq. alloy system, susceptibility up to 60 at. % In 8=12925
- K₃Cr₂(C₄O₃)·3H₂O, anomalous behaviour, between room and liq. O₂ temps. 8=18298
- K₂MoCl₃ mag. state from dynamic susceptibility, 4-14°K 8=2297
- K₂MoCl₃ mag. ordering from specific heat 1.5-20°K 8=1872
- (La, Gd)₂CoMnO₅ system, interactions 8=9354
- Li_{0.5}Cr_{1.25}Fe_{1.25}O₄, spontaneous magnetization rel. to compensation temp. 8=14049
- Mn nodules from dredged W. Pacific basalts 8=10055
- MnCu, anomalous low-temp. susceptibility 8=13962
- MnFe₂O₄, anisotropy constant change 8=5488
- Mn_{0.8}Zn_{0.2}Fe₂O₄, anisotropy constant change 8=5488
- Mo containing Co, susceptibility meas., Kondo temp. obs. 8=9009
- Mo, reluctance field dependence, 1.8-35°K rel. to K_{öler} law deviations 8=22750
- Nb, flux lines-dislocations interaction, 4.2°K 8=22210
- Nb, specific susceptibility rel. to dissolved O₂-N₂ mixtures 8=9011
- Ni-Cr₂O₃ system, thermomag. curves in low mag. field 8=9366

Magnetic properties of substances—contd

- Ni₃Ga, susceptibility, temp. dependence, density of states curve explanation 8=9359
- Ni₃Ge alloy, susceptibility in range $0 < T < 1000^\circ\text{C}$ 8=18299
- NiMn₂O₄ single crystals, Curie temp. and magnetization 8=21959
- Ni-Mn-Fe alloys, atomic mag. moment, conc depend. 8=9358
- NiSiF₆·6H₂O, moment, 0.05°-4.2°K 8=8641
- Pb-In alloy type II superconducting tube, magnetic induction meas. on wall 8=5221
- PdNi alloys, dilute, susceptibility and elec. resists., local exchange enhancement effects 8=13634
- Pr, rel. to crystalline field splitting and exchange interaction parameters 8=2292
- RCO₅, (R = rare earth metal), Curie temp. dependence on comp. 8=18350
- Rh and Ir, ductility, with hot and cold working 8=22390
- Sb, mag. resistance anisotropy, temp. depend. 8=5432
- Sc, anisotropy of susceptibility, rel. to electron charge density 8=13965
- Sc₂In phase, and pressure depend. of Curie point 8=17885
- TbCrO₃, mag. structure at 77, 4.2 and 3.05°K, by n-diffr. studies 8=5508
- TCO₃ (T=Y or rare earth), and crystallographic structure 8=13967
- Ti(III) chloride hexahydrate 8=16995
- Ti₂O₃, susceptibility rel. to temp., effective mass calculation 8=5120
- α -U, susceptibility 8=13966
- UC₂, 300-5°K, rel. to n diffr. exam. 8=1810
- V(III) chloride hexahydrate 8=16995
- VAu₄, susceptibility, atomic environment effect 8=9294
- W, reluctance field dependence, 1.8-35°K rel. to K_{öler} law deviations 8=22750
- Y, anisotropy of susceptibility, rel. to electron charge density 8=13965
- Y, susceptibility anomaly 8=18302
- Yb-Sb phases 8=22754
- YFe garnet, Al and Ga substituted, effects of heat treatment 8=14055
- ZnCr₂Se₄, interactions, spiral ground states 8=2296
- (Zr_{0.6}Nb_{0.4})Fe₂, Laves structure, mag. anomaly 8=2295
- antiferromagnetic**
- See also Antiferromagnetism.
- absorption of hypersound 8=8620
- canted, orthorhombic, domain-wall motion anal. 8=14059
- conduction electrons energy spectrum, near Curie point temp. 8=5099
- dipole radiation intensity and mag. moment oscillation freq. 8=18328
- easy-axis critical fields and resonance involving Dzyaloshinsky interaction 8=22871
- ferritine, superantiferromag., independence on Fe content and aq. dissolution 8=14068
- insulators, cumulant expansion of localized-electron model 8=14061
- ionic dielectrics, interact. between magnons and optical phonons 8=2231
- magneto-elastic waves, coupled 8=18368
- metal, superconductivity, proximity effect 8=5193
- nuclear magneto-acoustic resonance 8=22916
- perovskites, localized v. collective d electrons and Néel temps. 8=9391
- polyene chains, spin structure 8=21208
- rare earth chromates, and ferromag. transition 8=18388
- semiconducting, ferromag. domain 8=22866
- sternbergite (AgFe₂S₃?) 8=14066
- ultrasonic attenuation rel. to lattice and Heisenberg spin systems 8=9388
- unidimensional lattice, theory of bound states of spin waves 8=9315
- Al in Cr solid solution, obs. with concentration variation 8=14063
- AuMn, spin-disorder resist., anisotropic 8=14064
- AuMn, structure 8=22872
- Au₂(Mn, Al)₂ alloys, coexistence with ferromagnetic structures 8=9389
- B rich lattices 8=22870
- Ba_{1-x}Ca_xMnO₃ solid solns. 8=18330
- BeFeO₃, atomic and mag. structure from time-of-flight n-diffr. 8=17346
- Ca manganates, CaMnO₃, Ca₄Mn₂O₁₀, Ca₃Mn₂O₇ and Ca₂MnO₄ 8=9390
- Ca manganates, localized v. collective d electrons and Néel temps. 8=9391
- CaCr₂Fe_{2-x}O₄, structure rel. to that of CaFe₂O₄ 8=18371
- Ca₂Cr₂Fe_{2-x}O₈, structure rel. to that of Ca₂Fe₂O₈ 8=18371
- Ca₂Fe₂O₈, Néel temp. 8=5499
- CdCO₃, and crystal growth and e.p.r. study 8=18372
- CoCO₃, and resonance 8=18372
- CoO, excitations and crystal dynamics 8=22086
- CoO, Néel temp., effect of hydrostatic pressure 8=9394
- Cr alloys with Co and Ni, rel. to Co/Ni conc. 8=22875
- Cr alloys with d-transition group elements, n-scattering studies 8=18349
- Cr alloys, time-of-flight n-diffr. studies 8=18375
- Cr alloys, transport props. 8=18374
- Cr, band structure by Green's function 8=2348

Magnetic properties of substances—contd**antiferromagnetic—contd**

- Cr, energy gap rel. to i. r. reflectivity temp.-depend.
dip. 8=22874
- Cr itinerant antiferromagnetism, Néel temp. press. depend.
obs. 8=5500
- Cr, spin density wave studies by n-diffr., high pressure
effects 8=22876
- Cr, X-ray line splitting above and below Néel point 8=17358
- Cr-Fe alloys, Cr rich, ordering rel. to energy gap in band
structure 8=8931
- Cr-Fe alloys, dilute, rel. to Fe content 8=2347
- Cr₂BeO₄, spin-flopping 8=5506
- Cr₂O₃, acoustic spin waves, studied by neutron
scattering 8=14065
- Cr₂O₃, magneto-electric susceptibility versus temp. 8=5427
- Cr-Re alloys, dilute, rel. to Re conc. 8=18373
- Cr₂WO₆, mag. ordering and spin modes 8=22873
- CuCl₂·2D₂O, spin density distrib. 8=22877
- CuCl₂·2H₂O, dipolar mag. field at proton site 8=18378
- CuCl₂·2H₂O, mag. ordering by unpaired electron
interactions 8=18377
- CuCl₂·2H₂O, unpaired electrons, wave function 8=18376
- Cu-Fe alloy, existence of antiferromag. coupled bound
state 8=22519
- Cu(HCOO)₂·4H₂O, susceptibilities and crystal
fields 8=5501
- CuSO₄, e. s. r. at Néel point 8=2364
- Dy, probability distrib. functions 8=13994
- Dy single crystals, 4-300°K 8=14067
- ErGa garnet, transition at 0.8°K 8=9298
- Eu metal, and Fermi surface 8=22459
- EuZn₂, hyperfine field studies by Mossbauer e.p.r. and
n.m.r. 8=18334
- FeCl₂, metamag. phase transform. and hysteresis 8=9396
- FeCl₂:Fe³⁺, Mn²⁺, impurity spin resonance at low
temps. 8=14108
- FeCl₂·2H₂O, magnetization process from exchange
interaction study 8=2349
- FeF₂, near i. r. spectrum, effects 8=18525
- FeF₂, tetragonal, scattering of light by one- and two-
magnon excitations 8=18546
- FeF₃, Mossbauer spectra, interpret. of broadened and
shifted lines 8=21807
- FeGe hexagonal single crystal, magnetic torsion
measurements 8=14069
- Fe-Mn alloys, dilute, nearest neighbour exchange inter-
action energy of Mn 8=18383
- FeNi-FeNiMn films with ferro-antiferromagnetic
coupling, study 8=9346
- FeO, Néel temp., effect of hydrostatic pressure 8=9394
- Fe(OH)₃ from degraded protein, superantiferro-
mag. 8=14068
- α-FeOOH antiferro-paramag. transition temps., e. s. r.
obs. 8=22879
- α-FeOOH, mag. structure and hyperfine field 8=22878
- Fe(Pd,Pt)_{1-x}, alloys, transition to ferro- 8=5465
- FeSn, coupling of c-plane to adjacent c-plane, and mag.
unit cell 8=2320
- FeSn, Mossbauer study, Néel temp. at 163°K 8=18339
- FeSO₄·H₂O, mag. structure (spin order) 8=18380
- Fe₂O₃, Mössbauer effect, depend. on crystallite
size 8=14016
- α-Fe₂O₃ easy-axis critical fields and resonance involving
Dzyaloshinsky interaction 8=22871
- α-Fe₂O₃, spin waves and mag. exchange interacts. 8=18379
- α-Fe₂O₃, transition to weakly mag., obs. via
magnetization 8=5503
- Fe₃(PO₄)₂·8H₂O, vivianite, mag. symmetry 8=5502
- GdAlO₃, antiferromag. order, from optical absorption
studies 8=22880
- HgCr₂S₄, metamagnetism 8=18340
- HoAl garnet, transition at 0.8°K 8=9298
- KCuF₃, antiferromagnet, one-dimensional, formation in
perovskite structure 8=5504
- KCuF₃, n. m. r. of F¹⁹, shifts on a and c axes 8=5505
- KFeF₃, exchange and spin-orbit coupling 8=22881
- KMnF₃, critical mag.-scattering of neutrons 8=22882
- K₂MnF₄, crystal struct. and anisotropy 8=14070
- KNiF₃ and K₂NiF₄, comparative study 8=9397
- KNiF₃, optical absorpt., anomalous temp. depend. 8=22996
- LiMnPO₄, spin-flopping 8=5506
- MTiO₃, (M=Mn, Fe, Co and Ni), theoretical inter-
pretation 8=9399
- MTiO₃, (M=Mn, Fe, Co and Ni), susceptibility and
resonance meas. 8=9398
- Mn-based CuAu-I type alloys, mag. structures and phase
transformations 8=18381
- MnAu₂, spontaneous magnetostriiction 8=9400
- MnBr₂·4H₂O, n.m.r. studies 8=14148
- MnCO₃, and resonance 8=18372
- MnF₂, pure and Eu²⁺, Co²⁺ doped, spin ordering rel. to
luminescence 8=23058
- MnF₂, tetragonal, scattering of light by one- and two-
magnon excitations 8=18546
- Mn-Ni system, crystal and mag. structures rel. to phase
transformation 8=17088
- MnO, axially cooled or stressed, anisotropy from
torque meas. 8=14072

Magnetic properties of substances—contd**antiferromagnetic—contd**

- Mn-Pt, structures and exchange interactions 8=22883
- MnTe, semiconductor, optical meas. 80-375°K 8=5622
- MnUO₄, mag. structure and exchange interactions 8=18384
- Mn₂P, structure 8=22736
- Mn₂Pt, first-order mag. transformation, X-ray and
susceptibility study 8=18382
- Mo-Fe solid soln., above 300°C 8=22749
- Na₂Fe₂O₉, spin arrangement 8=8540
- Na₂Mn₂Si₂O₉, susceptibility temp. depend. below
100°K 8=9292
- NdGa garnet, ordering by n-diffr. at 0.31°K 8=22884
- NiMn alloy, ordered, rel. to antiphase boundaries and
order twins 8=17289
- NiO, axially cooled or stressed, anisotropy from
torque meas. 8=14072
- NiO, domain ordering rel. to rhombohedral
distortion 8=5507
- NiO, reduced, behaviour 8=14071
- NiO, ultrafine particles, Mössbauer study 8=2318
- α-O₂, rel. to crystal structure 8=17406
- ζ-Pd₂Mn₂, structure exam. by n-diffr. 8=18385
- Pr, rel. to crystalline field splitting and exchange
interaction parameters 8=2292
- PrC₂, structure determs. 8=18386
- Pt-Fe-Mn alloys, ordering dependence on comp., n-diffr.
exam. 8=18387
- Pu, α and β, possibility from transverse magneto-
resistivity meas. 8=2350
- RCrO₃, (R = rare earth), and ferromag. transition 8=18388
- RbMnF₃, near critical magnetic point, ultrasonic
attenuation and velocity 8=17504
- RbMnF₃, spin waves, nuclear and electronics, simultaneous
parallel pumping 8=14107
- RbMnF₃, F¹⁹ nuclear acoustic resonance 8=22922
- Rb₂MnF₄, crystal struct. and anisotropy 8=14070
- Tb, critical mag.-scattering of neutrons near transition
pt. 8=22882
- TbAl garnet, transition at 1.35°K 8=9298
- TbC₂, structure determs. 8=18386
- TbCrO₃, in mag. structure at 3.05°K by n-diffr. 8=5508
- TlMnF₃:Co, zero anisotropy Co conc. dependence 8=9401
- Tl₂O₃, dielec.-metal phase transition rel. to mag.
ordering 8=18389
- U cpds., Néel temp. and stability 8=5509
- UO₂, magnetic excitations 8=22888
- UO₂, magnetic point groups and selection rules 8=9402
- UP₂, mag. structure from n-diffr. study 8=22887
- VO, VO₂, dielec.-metal phase transition rel. to mag.
ordering 8=18389
- V₂O₅, dielec.-metal phase transition rel. to mag.
ordering 8=18389
- YCrO₃, and ferromag. transition 8=18388
- YFe_{0.8}Al_{0.1}O₃ crystal, at 602°K and ferromag. at
600°K 8=14074
- Y-Tb alloys, Néel point deviations 8=2299

diamagnetic

See also de Haas-van Alphen effects; Diamagnetism.

alkali halides, mag. susceptibility additivity 8=13959

2,3-dimethylnaphthalene, anisotropy rel. to mol. and
crystal structure study 8=18574

fluoroacetylene, molec. susceptibility 8=12246

organic crystals, anisotropies 8=18295

susceptibility, temp. dependence calc. 8=18294

Ag₂S, nonstoichiometric, meas. 8=9290

Ag₂Se, nonstoichiometric, meas. 8=9290

Be isoelectronic sequence, susceptibility calc. 8=12058

Bi: Sb, susceptibility max. and depend. on Sb
content 8=22745

Cu₂S, nonstoichiometric, meas. 8=9290

Cu₂Se, nonstoichiometric, meas. 8=9290

Mg-Cd alloys, Cd-rich, susceptibility 8=5431

Pd based double cyanide complexes obeying square
planar symmetry, mean susceptibility 8=22751

PbTe, p-type, oscillatory magnetostriiction 8=13964

α-SiC, mag. susceptibility and anisotropy, 90°K to
1000°K 8=18301

ferrimagnetic

See also Ferrimagnetism

ferrites, spinel, substitution of transition metals, linewidth
variations 8=5495

ionic dielectrics, interact. between magnons and optical
phonons 8=2231

lithium ferrites-chromites, effect hardening on
spontaneous magnetization 8=2341

nonlinear phenomena, simplified theory 8=5487

orthotitanate ferrite solid solns., xM₂TiO₄ (1-x)MFe₂O₄
(M = metal), spinel structure 8=18365

permeability tensor of ferrites, meas. of wire
components 8=14044

rare earth Ga garnets, mag. moments of rare earth
ions 8=2340

rare-earth-nickel alloys, (R₂Ni₄; R = rare earth
or Y) 8=18363

rare earth orthoferrites, spontaneous spin
reorientation 8=14048

tetragonal spinel lattices, Néel ionic migration law 8=8502

Magnetic properties of substances—contd**ferrimagnetic—contd**

- titanomagnetite, rel. to structure changes on oxidation 8=14054
 Al garnet, mag. structure by n-diffr. 8=22865
 $\text{BaCo}_2\text{Fe}_{12}\text{O}_{27}$, hexagonal, spin structure and anisotropy 8=22849
 $\text{BaFe}_{12}\text{O}_{19}$, complex permeability and mag. loss in cm. and mm.-wave range 8=5489
 $\text{BaFe}_{12}\text{O}_{19}$, polycrystalline samples, mag. dispersions 8=5490
 $\text{Ba}_2\text{Zn}_2\text{Fe}_{12}\text{O}_{22}$, Bloch wall structure determs. 8=5496
 $\text{BaFe}_{12}\text{O}_{19}$, hexagonal ferrite, magnetization temp. dependence 8=18358
 $\text{Bi}_{0.4}\text{Ca}_{2.6}\text{Fe}_{3.2}\text{Ga}_{0.5}\text{V}_{1.3}\text{O}_{12}$, and ferrimag. resonance 8=18398
 $\text{Bi}_{0.24}\text{Ca}_{2.76}\text{Fe}_{3.26}\text{V}_{1.39}\text{O}_{12}$, Faraday effect mechanism 8=18508
 CoCr_2O_4 , spinel, study by neutron diffr. 8=9374
 CuMn ferrites, saturation induction and coercive force Sc_2O_3 effects obs. 8=18359
 Dy garnet, mag. structure by n-diffr. 8=22865
 $\text{Fe}_1\text{Ga}_{1-x}\text{O}_3$, structure considerations 8=18360
 $\text{Fe}_{1.15}\text{Ga}_{0.85}\text{O}_3$, magneto-electric susceptibility versus temp. 8=5427
 $\text{Fe}_{1-x}\text{Mn}_x\text{TO}_3$ (T = rare earth), dependence on x value (0 to 1) 8=22851
 $\text{Ga}_{2-x}\text{Fe}_x\text{O}_3$ and related cpds., Mössbauer investigations 8=13028
 $\text{Ga}_{0.65}\text{Fe}_{1.15}\text{O}_3$ magnetically ordered crystal, electron resonance spectrum 8=14087
 Mg ferrites, Mössbauer spectra in external mag. fields 8=18342
 Mg ferrous ferrites, magnetically-induced ordering 8=22857
 Mg-Cr-Cu ferrites, permeability tensor, influence of porosity 8=22852
 Mg-Mn ferrites, mag. anisotropy consts. and magnetostriction 8=5492
 Mg-Mn ferrites, Mössbauer spectra in external mag. fields 8=18342
 Mn ferrite, spin waves, nuclear and electronic, simultaneous parallel pumping 8=14107
 Mn ferrites, Mössbauer spectra in external mag. fields 8=18342
 MnCr_2O_4 , spinel, study by neutron diffr. 8=9383
 MnZn ferrite, rel. to final firing cycle cooling conditions, obs. 8=22855
 Mn-Zn high permeability ferrites, dynamical magnetization curve 8=18361
 Ni ferrite, origin of $k\pi$ and mobile domain walls 8=5493
 Ni ferrous ferrites, magnetically-induced ordering 8=22857
 NiFe_2O_4 , thin films 8=2343
 $\text{Ni}_{0.5}\text{Fe}_{0.5}\text{O}_4$, crystalline anisotropy, effect of oxygen stoichiometry and annealing temp. 8=9385
 RbNiF_3 , circular dichroism and rot. of plane of polarization of light 8=18556
 RbNiF_3 , magnon sidebands in optical spectrum 8=23010
 RbNiF_3 transparent single crystal, properties near Curie point 8=14053
 $\text{Rb}(\text{Ni}_{1-x}\text{Co}_x)\text{F}_3$ transparent single crystal, properties near Curie point 8=14053
 $(\text{Sr}, \text{Ba})_2\text{Zn}_2\text{Fe}_{12}\text{O}_{22}(\text{Y})$ ferrite, spin ordering using neutron diffraction meas. 8=22858
 TmFeO_3 , spontaneous spin reorientation 8=14048
 TmFeO_3 , structure, variation with temp. 1.6°K–94°K 8=22859
 Y orthoferrite, mag. sublattice switching under mag. pulses 8=18366
 YFe garnet, nonlinear photon-magnon interaction under parallel pumping 8=14056
 YFe garnet, spheres and powders, determ. of Curie points 8=18367
 YFeGa garnet, spheres and powders, determ. of Curie points 8=18367
 $\text{Y}_3\text{Fe}_{5-x}\text{In}_x\text{O}_{12}$, magnetocrystalline anisotropy 8=9386
 YIG slab, magnetostatic surface waves 8=22862
 YIG, spin wave susceptibility saturation above instability threshold, Al and rare earth doping effects 8=22864
 YIG, substitution of rare earths, linewidth variations 8=5495
 $\text{Zn}_2\text{Y}(\text{Ba}_2\text{Zn}_2\text{Fe}_{12}\text{O}_{22})$ single crystals, Bloch wall structure determs. 8=5496
 ZrCr_2Se_4 , mag. structure by n-diffr. 8=22865

ferrimagnetic

- See also Ferromagnetic relaxation; Ferromagnetic resonance; Ferromagnetism; Magnetization process; Magnetization state.
 alloys, additives of electronic states 8=5446
 alloys, sp. ht. rel. to Kondo model 8=17510
 Alnico alloys, high-temp. obs. 8=22813
 Alnico alloys, interaction effects 8=14036
 Alnico 8, Mossbauer spectroscopy study of paramagnetic environment 8=5480
 Alnico, effect of heat treatment below 1000°C 8=9361
 alnico permanent magnets magnetization, 550–800°C 8=22806
 anisotropy rel. to magnetization energy 8=9325
 austenite in Fe-Ni alloys, effect of C on Curie pt. 8=18336
 Bloch walls, properties, application of statistical interpretation 8=13989
 conduction electrons energy spectrum, near Curie point temp 8=5099

Magnetic properties of substances—contd**ferromagnetic—contd**

- cubic lattices, Bloch wall orientations, relative energies 8=18312
 crystals, micromag. theory of magnetization processes 8=5452
 Curie converter, thermomechanical 8=3167
 dielectric, magnetization eqns. of motion and eqn. for temp. change 8=5451
 dipole radiation intensity and mag. moment oscillation freq. 8=18328
 dislocation, elastic and magnetic fields around 8=18316
 domain structures, two-phased, and superconductors, theory 8=13742
 elinvar alloys, influence of Cr 8=9348
 Fermi liquid, ferromagnetic spin fluctuation effect on susceptibility 8=15020
 ferrites, heating during ferromag. resonance. 8=14082
 ferroelectric, magnetization along axis of difficult magnetization 8=18318
 50 Ni Permalloy, iso- and anisotropic, effects of Ge addition 8=22815
 films, double layer of different chem. comp. 8=9332
 films, magnetization inversion by Barkhausen-Cisman-Brion method, e. m. aspect 8=22781
 films, magnetization ripple theory 8=22785
 film, model including interactions between regions 8=14003
 films, multi-domain, demagnetising field rel. to reson. condns. 8=22783
 films, on silicon grease, hysteresis, magnetization anisotropy 8=2331
 grains and relation between magnetic-viscosity 8=2754
 Hall effect, theory 8=22765
 Heisenberg, impurity spins, coupling 8=22771
 Heisenberg model, spin pair correlation 8=9316
 Heusler alloys: Cu_2MnAl and associated structures, studies 8=22794
 Heusler alloys: Cu, Mn, Al structure studies 8=22795
 impurities, non-mag., local magnetization calc. 8=13987
 junctions, magnetoresistance 8=18343
 lead, superconductive, irreversible magnetisation obs. 8=2160
 leakage mag. field in cryst. surface, effect of mag. film 8=2313
 longitudinal susceptibility in mats. with non-uniform saturation magnetization 8=9327
 magnetite, thermal cycling, effect of compression 8=22798
 magnetoacoustic excitation of rf. resons. and echoes. 8=17493
 magnetoelastic interactions for infinitely long prism, transformation 8=13997
 magnetostriction, circular magnetization calc. and method of meas. 8=13998
 magnon dispersion relns rel. to spin interacts, from n scatt. 8=22768
 measurement, annular specimen sizing 8=19736
 metals and alloys, diffusion 8=17560
 metals, anomaly in elec. resist. near T. 8=13985
 metals, n scatt. from spin-waves, and continuum spin-flip band 8=2315
 metals, nonlinear polarizability tensor 8=5473
 metals, simple. exchange and correlation instabilities 8=22788
 metals, spontaneous Hall and Nernst-Ettingshausen effect 8=9329
 meteorites, stony, stony-iron and iron, thermoremanent magnetization obs. rel. to interplanetary field 8=19279
 mixed mag. systems, neutron elastic diffuse scatt. 8=22766
 niobium, superconductive, irreversible magnetisation obs. 8=2160
 n. m. r. theory, low concs. of mag. nuclei 8=9456
 n. m. r. with automatic swept-freq. spin-echo spectrometer 8=9454
 non-uniform saturation magnetization, longit. susceptibility 8=9327
 non-uniform saturation magnetization, static magnetization 8=9326
 nuclear magneto-acoustic resonance 8=22916
 orthorhombic ferromagnetics, theory and calcs. 8=18306
 particles with high uniaxial anisotropy, critical size calc. 8=22773
 Permalloy, composite films, structure, resonance 8=9357
 permalloy, domain wall obs. by pulse technique 8=9364
 Permalloy evaporated films, influence of residual gases and evaporated metal bases 8=5476
 permalloy film on Cu, magnetization under circular alternating and longitudinal static fields 8=9335
 permalloy film, on silicon grease, hysteresis, magnetization anisotropy 8=2331
 permalloy films, memory performance and hysteresis in inhomogeneous magnetic field 8=2319
 Permalloy films, rotational hysteresis, temp. depend. 8=22823
 Permalloy, magnetic domains, electron diffraction obs. 8=22824
 Permalloy, susceptibility, maximum 8=18338
 permanent magnet materials temperature variation 8=18320
 phonon spectral density near Curie pt. 8=17468

Magnetic properties of substances—contd

- ferromagnetic—contd**
 polycrystalline, with hexagonal anisotropic crystal orientation, torque curve calcs. 8=5455
 powder, in nonmagnetic matrix 8=14004
 pressurized crystals, anisotropy meas. 8=13952
 rare-earth alloys, n-scattering studies 8=18349
 rare earth chromites, at low temps. 8=18388
 rare earth-cobalt cpd., RCO_5 , Curie temp. dependence on comp. 8=18350
 relaxation after effects due to structural point defects 8=18321
 relaxation by two-magnon scattering on dislocations 8=14078
 saturation magnetization, temp. depend., demagnetizing field technique 8=22834
 single domains, isolated spherical, rotation under varying mag. field and strain 8=13993
 static magnetization in mats. with non-uniform saturation magnetization 8=9326
 steel, change in coercive force during deformation 8=14015
 superparamagnetic magnesioferrite precipitate from MgO:Fe dilute solutions 8=1675
 susceptibility depend. on h. f. field at ferromag. resonance 8=2354
 switching behaviour 8=13996
 tin, superconductive, irreversible magnetisation obs. 8=2160
 transition metals, electron-magnon interaction 8=2300
 transition-metal monophosphides 8=22847
 transition metals, susceptibility spin-orbit coupling dependence 8=2332
 twisting, magnetic var. effect 8=2312
 unsaturated media, rotational susceptibility 8=13995
 Au-Mn-Al alloys, ordering dependence on comp., n-diff. exam. 8=18387
 $\text{Au}_2(\text{Mn}, \text{Al})_2$ alloys, coexistence with antiferromagnetic structure 8=9389
 B rich lattices 8=22870
 Bi-MnBi eutectic single crystal growth dependence 8=8402
 BiMn_2O_8 , mag. structure and ordering 8=22844
 $\text{Bi}_{1-x}\text{Cu}_x\text{MnO}_3$ solid solns., in pulsed mag. field of 160 kOe 8=18330
 CdCr_2Se_4 , magnetostriction constants, resonance linewidth, anisotropy constant and Curie temp. 8=2316
 $\text{CdCl}_2\text{:Cu}^{2+}$ layer, e. s. r. rel. to sign of exchange interaction 8=18416
 $\text{CdCr}_2\text{Se}_4\text{:Ag}$, mag. semiconductor, helicon-spin wave interaction 8=18329
 CdCr_2Se_4 , rel. to electrical transport props. 8=18031
 $(1-x)\text{CdCr}_2\text{S}_4-x\text{CdCr}_2\text{Se}_4$ system, and crystallographic props. 8=14006
 Co, critical scattering of neutrons above Curie point 8=2317
 Co crystals, anisotropy and temp. dependence 8=9336
 Co film on Cu, magnetization under circular alternating and longitudinal static fields 8=9335
 Co foils, domain width depend. on thickness 8=22791
 $\alpha\text{-Co}$, hexagonal cryst. magnon obs. 8=14008
 Co, magneto-caloric effects and sp. ht. near Curie temp. 8=9337
 Co mag. recording films and deposition, obs. 8=22790
 Co^{60} , n.m.r. in domains and spin lattice relaxation times 8=18331
 Co-Al alloy, 'Malcolloy', effect of V addition 8=22793
 Co-Al Malcolloy, effect of Mo addition 8=22792
 CoB systems transfers of electronic states 8=5461
 Co-Be alloy, rel. to transfer of electron states 8=14018
 CoCr_2S_4 , mag. structure determ. by n-diff. 8=18332
 CoMo alloys, coercive field, remanance, structure 8=5462
 Co-Ni mag. recording films and deposition, obs. 8=22790
 Co-P mag. recording films and deposition, obs. 8=22790
 Co-Pd alloys, Co^{59} and Pd^{105} n.m.r. studies 8=2381
 CoW alloys, coercive field, remanance, structure 8=5462
 Cr-Ge alloys, elect. resist. at 20-300°K, and Curie point 8=9338
 $\text{CuCl}_2 \cdot 2\text{H}_2\text{O}$, dipolar mag. field at proton site 8=18378
 $\text{CuCl}_2 \cdot 2\text{H}_2\text{O}$, mag. ordering by unpaired electron interactions 8=18377
 CuCrSe_4 , magnetic moment from neutron diff. expts. 8=1788
 CuCr_2Te_4 , Te^{125} Mössbauer effect study of hyperfine field 8=8223
 Cu-Mn-Al system, effect of quenching and ageing on mag. phases 8=14010
 Cu-Ni alloys, thermal expansion, rel. to ferromag. Curie point of Ni 8=17532
 Dy, dimensions of correlation range by neutron depolarization obs. 8=22797
 Dy, probability distrib. functions 8=13994
 Dy single crystals, 4-300°K 8=14067
 Dy, spiral-to-ferromag. transition 8=22799
 Dy, uniaxial mag. anisotropy 8=18333
 EuO films, from Faraday rot. and force balance meas. 8=13090
 EuO, susceptibility and mag. sp. ht., Padé approximant estimates 8=22861
 EuPd_2 , hyperfine field studies by Mossbauer e.p.r. and n.m.r. 8=18334

Magnetic properties of substances—contd

- ferromagnetic—contd**
 EuPt_2 , hyperfine field studies by Mossbauer e.p.r. and n.m.r. 8=18334
 EuS, magnetocrystalline anisotropy 8=9341
 EuS, susceptibility and mag. sp. ht., Padé approximant estimates 8=22861
 EuSe, moment measurements, showing transition to antiferromag. 8=22802
 EuSe, structure 8=22803
 Fe-based alloys, charge screening 8=13661
 Fe, cold neutron scattering, Van Hove theory 8=5468
 Fe, dilute Au, saturation magnetization 8=2324
 Fe, dispersions within silicate matrix, superparamagnetism 8=14013
 Fe, electronic sp. ht. calc. by band model 8=4932
 Fe, from meas. of critical diffusion of slow neutrons 8=22810
 Fe, mag. form factor of mag. atoms, from polarized n scatt. 8=14012
 $\alpha\text{-Fe}$, phonons and magnons, dispersion relations 8=13331
 Fe powder dispersed in perspex, domain structure 8=5470
 Fe, powders, lattice parameters 8=14033
 Fe, sintered, and eddy current losses reduction, obs. 8=22807
 Fe, sintered, magnetization curve and coercive force rel. to porosity, obs. 8=22808
 Fe, spin correlation function from mag. scattering of neutrons 8=2325
 Fe, susceptibility, maximum 8=18338
 Fe-whiskers, nucleation mag. field strength investigations 8=5467
 Fe-whiskers, nucleation, theor. investigation 8=18335
 Fe-0.5-6% Al doubly oriented sheet rel. to comp., thickness and prep., obs. 8=22789
 Fe, (Al, Ga, Si, Ge, Sn, Sb) impurities, magnetization distribution 8=9349
 FeB systems transfers of electronic states 8=5461
 Fe-Be alloy, rel. to transfer of electron states 8=14018
 Fe-Co, alloys anisotropy 8=14019
 Fe-Co alloy fine particles 8=5471
 Fe-Co alloy, powders, lattice parameters 8=14033
 FeCo superstructures in (Fe, Cr)Co, (Fe, Mn)Co and Fe(Co, Ni) alloys neutron diffraction 8=1757
 Fe-Co, Cu precip. and coagulation effects, obs. 8=22809
 Fe-Co-Ni-Cr, change during recrystallisation 8=9342
 FeCrAl alloys as Hall probes 8=14011
 Fe in c Cu-Zn phase, local moment formation 8=9340
 Fe-Ni alloy, n-irradiated 8=2326
 Fe-Ni alloys, anisotropy, by C diffusion 8=22814
 Fe-Ni alloys, heating during ferromag. resonance 8=14082
 FeNi films, electrodeposited 8=9347
 Fe-50%Ni, metallic impurities effects rel. to domain wall trapping and elements solid solubility, obs. 8=22825
 Fe-Ni, sintered, and eddy current losses reduction, obs. 8=22807
 Fe-Ni-Co-Al coercivity and energy increase by Ti and Si, Se or Te addition 8=22805
 Fe-Ni-Cr alloys, dependence on ht. treatment, comp. and external fields 8=18337
 FeNi-FeNiMn films with ferro-antiferromagnetic coupling, study 8=9346
 Fe-Ni-Mo, sintered, and eddy current losses reduction, obs. 8=22807
 Fe(Pd, Pt, ...), alloys, transition from antiferro- 8=5465
 Fe-Si alloys, after-effect by plastic deformation 8=5466
 Fe-Si sheet, initial permeab. depend. of demag. freq. 8=5464
 Fe-Si, sintered, and eddy current losses reduction, obs. 8=22807
 FeSn, coupling within a c-plane, and mag. unit cell 8=2320
 Fe_2O_3 , ferro. and superpara., Mössbauer effect depend on crystallite size 8=14016
 Fe_2O_3 (hematite), magnetization and susceptibility rel. to temp. 8=5469
 $\alpha\text{-Fe}_2\text{O}_3$, Morin spin-flip transition 8=2323
 $\alpha\text{-Fe}_2\text{O}_3$, ultrafine particles, Mössbauer study 8=2318
 $\delta\text{-Fe}_2\text{O}_3$, rel. to struct. and chem. alterations 8=17627
 Fe_3O_4 , fine grained, coercivity rel. to edge dislocations 8=9343
 Fe_3Sn , Mossbauer study, dirn. of moments of Fe and Sn nuclei 8=18339
 Fe_2Se_3 , magnetocryst. anisotropy const. 8=2321
 Ga-Fe system, room temp. moments 8=22817
 Gd, internal friction obs. rel. to field at max. susceptibility 8=14020
 Gd, neutron diffraction study 8=14021
 GdCl_3 , with dipolar interactions, magnon spectrum analysis 8=9353
 GdCl_3 , high-temp. expansion coeffs. calc. 8=9352
 Gd-Dy alloys, magnetocrystalline anisotropy 8=9350
 Gd-Tb alloys, magnetocrystalline anisotropy 8=9350
 Gd-Y alloys 8=5472
 HgCr_2S_4 , mag. structure and metamagnetism 8=18340
 Ho, helical periodicity, neutron diff. study under high pressure 8=14040
 Ho_2C , mag. structure by n-diff. 8=22865
 In films with superconductive and ferromag. overlays, tunneling 8=22549

Magnetic properties of substances—contd**ferromagnetic—contd**

- La_{0.5}Sr_{0.5}CoO₃, near Curie point 8=18341
 MgO:V²⁺, Ni²⁺, superexchange interaction between V²⁺ and Ni²⁺ 8=9355
 Mn²⁺, n.m.r. in domains and spin lattice relaxation times 8=18331
 MnB systems transfers of electronic states 8=5461
 MnCO₃, ferro. moment spatial distrib. using polarized neutrons 8=9356
 MnFe₂O₄ from silicate melts, superparamagnetism 8=14022
 MnP, Curie point and anisotropy energy decrease under hydrostatic pressure 8=2328
 Mn-Pt, structures and interactions 8=22883
 MnSb, existence region, and electrical props. 8=22820
 Mn₂Si₂C₂, below 152°K, rel. to non-stoichiometry 8=22819
 Mo-Fe solid soln., low Fe concs. below 300°C 8=22749
 Mo-y at. % Co alloys, y=1.65, 1.085, 0.535, 27-300°K 8=14007
 Na₂Mn₂Si₂O₇, ferromag. moment below 26°K, anisotropy of susceptibility 8=9292
 Ni alloys, and paramag. behaviour, saturation and susceptibility meas. 8=5477
 Ni, band structure and Fermi surface, study by de Haas-van Alphen effect 8=2106
 Ni cylindrical crystals, (100) axis, basic structure, investigations 8=14038
 Ni cylindrical crystals, (110) axis, closure-domain structure, investigations 8=14037
 Ni, de Haas van Alphen effect and electronic band structure 8=9360
 Ni, dynamic ΔE effect frequency dependence in weak mag. field 8=2065
 Ni, electronic sp. ht. calc. by band model 8=4932
 Ni eqn. of state near Curie temp. 8=2330
 Ni film, on silicon grease, hysteresis, magnetization anisotropy 8=2331
 Ni films, electrodeposited, perp. anisotropy 8=14024
 Ni films, thin, ion bombardment rel. to induced anisotropy 8=22829
 Ni, hot-electron scattering and rigid-band model 8=13940
 Ni, plastic deformation effects on 8=9363
 Ni powder, heating during ferromag. resonance 8=14082
 Ni, powders, lattice parameters 8=14033
 Ni, saturation magnetization, temp. depend., applic. of demagnetizing field technique 8=22834
 Ni single crystals, anisotropy 8=9362
 Ni single crystals, susceptibility rel. to dislocations 8=22830
 Ni, sintered, magnetization curve and coercive force rel. to porosity, obs. 8=22808
 Ni, susceptibility, maximum 8=18338
 Ni, susceptibility spin-orbit coupling dependence 8=2332
 Ni, temp. dependence of reversible and irreversible magnetization 8=14025
 Ni-Al alloys, hot-electron scattering and rigid-band model 8=13940
 Ni-Be alloy, rel. to transfer of electron states 8=14018
 Ni-Co alloys, uniaxial anisotropy by electron irradiation in mag. field 8=5479
 Ni-Cr₂O₃ system, superparamagnetism of Ni particles 8=9366
 NiCr₂S₄, and structure analogy to Cr₂S₄ 8=22833
 Ni-Cu, effect of cathodic hydrogen loading on ferromag. resist. anomaly 8=14023
 Ni-Cu (0-30.42%), longitudinal magnetoresistance up to 1100 Oe at 0°C 8=9013
 Ni-Fe double films, domain wall motion 8=2329
 Ni-Fe films, bias susceptibility meas., effects of wall pinning 8=14026
 Ni-Fe films rel. to vacuum deposition press., 10⁻⁶-10⁻⁹ torr. 8=22822
 Ni-Fe, mag. thin films, thickness dependence of domain wall energy 8=18346
 Ni-Fe, permalloy, thin films, exchange anisotropy, 4.2°K 8=2333
 Ni-Fe-Co film, strain sensitivity rel. to Co content 8=18345
 Ni-Fe-Cr films rel. to high speed computer storage use, obs. 8=22826
 Ni-Fe-Cr-Si alloy, 200-300Å films, galvanomagnetic effect 8=5478
 Ni-Fe-Cu films rel. to high speed computer storage use, obs. 8=22826
 Ni-Fe-Cu-Mo alloy, effect anisotropy on permeability 8=9365
 77 Ni-14 Fe-5 Cu-4 Mo wt. %, sheet thickness effects rel. to domain wall energy and anisotropy 8=22827
 Ni₃(Fe, Mn), analysis detection of long-range order 8=1763
 Ni-Fe-Mn films rel. to high speed computer storage use, obs. 8=22826
 Ni-Fe-Pd films rel. to high speed computer storage use, obs. 8=22826
 Ni₃Mn alloy, magnetic field at Mn⁵⁵ 9=1635
 Ni₃Mn, intermed. ordered, mag. field induced anisotropy 8=2327
 Ni-Mn Nimalloy, effect of Fe addition 8=22832
 Ni-Mn Nimalloy, permeability obs. 8=22831
 Ni-Mo-Fe for power line de-icing transformer core, obs. 8=22828

Magnetic properties of substances—contd**ferromagnetic—contd**

- Ni-Pd alloy system, coupling 8=22821
 Pd, susceptibility spin-orbit coupling dependence 8=2332
 Pd-Co alloys, (8.3 to 0.03 at. %Co), effective mag. field at Co⁶⁰ nuclei 8=5463
 Pd-Co alloys, ferromagnetic specific heat 8=8642
 Pd-Fe alloys, ferromagnetic specific heat 8=8642
 Pd:Fe spin polarization around local mag. impurity 8=18317
 Pd-Ni alloys, magnetic moment, rel. to hydrostatic pressure 8=9351
 PdNi alloys, thermoelectric power 8=13904
 Pt-Co alloys, coercivity and remanence obs. 8=22835
 Pt-Co alloys, high (BH)_{max}, criticism 8=22836
 PtCo magnet alloy rel. to prep. and purity, obs. 8=22837
 Pt-Fe alloys, internal magnetic field at Pt nuclei 8=2334
 PtFe magnet alloy, obs. 8=22837
 Pt₃Fe, mag. structure dependence on atomic ordering 8=18348
 [PtPd]Co Curie and order-disorder transform. temps. obs. 8=22837
 [PtPd]Fe Curie and order-disorder transform. temps. obs. 8=22837
 RbFeF₃, magneto-optical 8=2450
 RbNiF₃ structure crystals, magnetic ordering 8=5482
 RC₂, (R = rare earth metal), Curie temp. dependence on comp. 8=18350
 RCrO₃, (R = rare earth), at low temps. 8=18388
 RGe-Si system (R = Gd, Tb, Dy, Ho and Er), rel. to 5:4 stoichiometry 8=4779
 R_xM_{1-x}Al₂ (R=Gd, Tb, Er and M=Y, La, Th) cubic Laves phases, Curie temps. and magnetizations 8=14039
 Si-steel, silicate glass film effects, obs. 8=22843
 α-SiC, mag. susceptibility and anisotropy 8=18301
 Si-Fe, temp. dependence, influence of plastic deformation 8=14014
 Si-Fe thin tapes, dynamic hysteresis phenomena 8=5483
 Tb, exchange coupling 8=9367
 Tb, ferromag. to paramag. phase transition 8=18352
 Tb, helical periodicity, neutron diffr. study under high pressure 8=14040
 Tb, spin waves, dispersion reln. from inelastic n scatt. 8=18351
 Tb, spiral-to-ferromag. transition 8=22799
 Tb, uniaxial mag. anisotropy 8=18333
 U selenides, (except USe₂) 8=5440
 U sulphides, (except U₃S₄) 8=5440
 UFeO₄, meas. and neutron diffraction exam. 8=18353
 β-UH₃, magnetic contribution to specific heat 8=8644
 VFe, atomic spin values by polarized n-diffr. 8=18354
 YCrO₃, at low temps. 8=18388
 W-x at. % Co alloys, x=1.05, 0.87, 0.54, 27-300°K 8=14007
 YFe_{0.9}Al_{0.1}O₃ crystal, at 600°K and antiferromag. at 602°K 8=14074
 ZrSn₂, magnetic isotherms meas. c.f. band model 8=22764
 ZrZn₂, itinerant electron model, rel. to Curie temp. and magnetization 8=2336
 ZrZn₂ mag. moment rel. to impurity and intrinsic ferromag., <150 K 8=14041
- paramagnetic**
 See also Paramagnetic resonance and relaxation; Paramagnetism.
 adenosine triphosphate, susceptibility thermomagnetic obs., 80-380°K 8=13974
 adiabatic demagnetization, use of supercond. solenoid 8=5217
 alkali halide crysts., and optical birefringence 8=18501
 Alnico 8, Mössbauer spectroscopy study of environment 8=5480
 anthracite, absorption reduction by heating 8=5441
 dilute alloy, susceptibility, Green function calc. 8=9299
 Heisenberg system, neutron scattering 8=22758
 Heisenberg system, paramag. phase, spin-waves 8=22756
 liquid metals, spin-orbit coupling 8=13969
 methane, susceptibility and proton shielding 8=7584
 platinum metals (i.e. Ru, Rh, Pd, Pt, Ir, Os), specific mag. susceptibility 8=5439
 rare-earth garnets, susceptibilities meas. 0.6-4.2°K 8=9298
 rare-earth hexaborides 8=5438
 rare-earth-zinc intermetallic compounds, susceptibilities 8=2298
 spin diffusion in paramag. temp. range 8=9318
 taurine, susceptibility, e.p.r. 8=5540
 Würster's blue perchlorate, susceptibility and transition heat rel. to triplet excitons 8=22763
 Ag-Au alloys, Pauli spin susceptibility, electron states variation, electronic sp. ht. 8=13970
 Ce ethyl sulphate, Schottky anomaly and spin-phonon coupling 8=8636
 Ce ethyl sulphate, spin-phonon scatt. in mag. field rel. to thermal cond. 8=13393
 CeCl₃, susceptibility meas. 1.07-4.2°K 8=14097
 Co in Pd and Pt, giant moments, theory 8=9302
 Cr halides (CrBr₃ and CrF₃), exchange integrals by neutron scattering 8=13971
 Cr-Mn alloys susceptibility rel. to band struct., obs. 8=22759

Magnetic properties of substances—contd paramagnetic—contd

- Cr-Os alloys susceptibility rel. to band struct., obs. 8=22759
Cr-Ru alloys susceptibility rel. to band struct., obs. 8=22759
Cr_{1-x}Te_{1+x} alloys, Hall effects and susceptibilities 8=9300
Cr₂O₃-Al₂O₃ solid solns., susceptibility 8=13972
Cu solid solns., with Ti, V, Cr and Mn, localized moments 8=22760
Cu-Au alloys, α -phase, Pauli spin susceptibility, electron states variation, electronic sp. ht. 8=13970
Cu-Zn alloys with (Cr, Mn, Fe, Co) impurities 8=9339
Dy-Al-garnet, hyperfine splitting of lowest 2' state of Dy 8=9301
ErCl₃·6H₂O, hyperfine splitting of lowest 2' state of Er 8=9301
Eu chelates 8=9306
Fe in Pd and Pt, giant moments, theory 8=9302
Fe-Mn alloys, susceptibility of martensitic phases 8=9304
FeNH₄(SO₄)₂·12 H₂O, sp. ht. and susceptibility calcs. at very low temps. 8=13370
Fe₂O₃-Al₂O₃ solid solns., susceptibility 8=13972
 α -FeOOH antiferro-paramag. transition temp., e. s. r. obs. 8=22879
Ga-Fe system, moments, above room temp. 8=22817
K₃Fe(CN)₆, hyperfine structure of Mössbauer spectra 8=16986
K₂MoCl₃ magnetization rel. to mag. structure, 1-300°K 8=2297
La-Ce alloys, impurity effect on superconducting transition temp. 8=9303
La-Gd alloys, impurity effect on superconducting transition temp. 8=9303
La₂Mg₃(NO₃)₁₂·24H₂O impurities, effect on proton dynamic polarization 8=14147
MTiO₃, (M=Mn, Fe, Co and Ni), susceptibility and resonance meas. 8=9398
MTiO₃, (M=Mn, Fe, Co and Ni), theoretical interpretation 8=9399
Mn steel, susceptibility of martensitic phases 8=9304
Mn-Ni system, crystal and mag. structures rel. to phase transformation 8=17088
MnYb₂S₄, a spinel, and structural study 8=5436
Mo-Fe solid soln., below 300°C 8=22749
MoO₃ in TiO₂, solid solutions, susceptibility 8=13963
Mo-Re alloys susceptibility rel. to band struct., obs. 8=22759
NaBrO₃, γ -irrad., form. of paramag. centres 8=2372
Na₂Mn₂Si₂O₇, susceptibility and validity of Curie-Weiss law from 100-300°K 8=9292
Nb-Re alloys susceptibility rel. to band struct., obs. 8=22759
Nb₃Sn, normal-state, susceptibility temp. depend. rel. to Fermi level motion 8=5118
Nd ethyl sulphate, Faraday effect, mag. resonance saturation 8=14278
NH₄(Fe, Al)(SO₄)₂·12H₂O, Mossbauer-effect study of electronic relax. 8=21812
Ni, density of states from soft-X-ray analysis 8=8940
Ni₄/3Fe₂/3 coprecipitate, and structure 8=23078
Pd, magnetic moment data, limits of exchange enhancements, 4.2°K 8=13973
Pd-Ni alloys, s-electron-paramagnon scattering 8=9015
Pd-Ni alloys, specific heat, paramagnon mass enhancement theory 8=17524
Pd-Ni alloys, susceptibility enhancement and sp. ht. obs. 8=18300
PdNi alloys, thermoelectric power anomalies 8=13904
PrH₂ 8=22761
RbCoF₃, spin-density oscillation in space at T > 96°K, by n.m.r. meas. 8=18472
SeO₄(NH₄)₂, γ -irrad., form. of paramag. centres 8=9305
Si powders, paramagnetic centres 8=22762
Tb ferromag. to paramag. phase transition 8=18352
TiO₂·V⁴⁺, multiple electron-spin echoes by interaction with dielectric modes 8=22657
UP₂, P³¹ Knight shift meas. 8=5564
UP₂, P³¹ Knight shift temp. dependence 8=5563
U₃P₄, P³¹ Knight shift meas. 8=5564
USe₂, $\Theta_c < 0$, susceptibility 8=5440
U₃S₅, $\Theta_c < 0$, susceptibility 8=5440
USn₃, susceptibility and Sn¹¹⁹ n.m.r. rel. to interband mixing effects 8=18474
V₃Ga, normal-state, susceptibility temp. depend. rel. to Fermi level motion 8=5118
V₃Si, normal-state, susceptibility temp. depend. rel. to Fermi level motion 8=5118
Y crystals, susceptibility temp. dependence, 80-300°K 8=18303
Y-Tb alloys, susceptibility meas. and Curie constant analysis 8=2299
YbCl₃·6H₂O, hyperfine splitting of lowest 2' state of Yb 8=9301

transitions

- austenite in Fe-Ni alloys, effect of C on Curie pt. 8=18336
in ferromagnets, effect of non-mag. impurities 8=5444

Magnetic properties of substances—contd transitions—contd

- ilmenites, Curie point from thermomag. plot 8=18324
metallic surface, oscillations of impedance, quantum spectroscopy 8=2094
Ca₂Fe₂O₃, Néel temp. 8=5499
CoCl₂·6H₂O, antiferro-paramag. at low temps. 8=9392
CoCl₂·6H₂O, antiferro-paramag. transition rel. to Fisher's relation 8=9393
Cr Néel temp. press. depend. and itinerant antiferromagnetism, obs. 8=5500
Cu(HCOO)₂·4H₂O crystal, antiferromagnetic at 60°K, possibility 8=5501
DyFeO₃, antiferromag. ordering, at liq. He temps. 8=9375
EuPd₂, Curie temp. determ. and hyperfine field studies by Mossbauer e.p.r. and n.m.r. 8=18334
EuPt₂, Curie temp. determ. and hyperfine field studies by Mossbauer e.p.r. and n.m.r. 8=18334
EuZn₂, Néel temp. determ. and hyperfine field studies by Mossbauer e.p.r. and n.m.r. 8=18334
Fe-Mn-As system, first order ferrimag. to antiferromag., temp. dependence 8=9376
Fe-Ni(35 wt. %)-Cr(0-20 wt. %) alloys (in cold worked state) Curie temperature 8=9006
Fe-Rh alloys, antiferro-ferromagnetic, rel. lattice parameter changes 8=9395
 α -Fe₂O₃, antiferromagnetic-ferromagnetic with magnetic field and Morin point entropy change 8=9281
 α -Fe₂O₃, antiferro. to weakly mag., obs. by magnetization in pulsed fields 8=5503
FeCl₂, metamag., at 4.2°K and hysteresis 8=9396
Fe(Pd_{1-x})₃ alloys, antiferro-ferro, neutron-diffraction study 8=5465
Ga, near 1.7°K, absence, from sp. heat meas. 8=1871
M Mn₂N, (perovskite, M=metal), first order, and mag. struct. 8=22742
MnBr₂·4H₂O, antiferro-paramag. at low temps. 8=9392
Mn-Ni system, para-antiferromag., rel. to phase structure transforms. 8=17088
Mn-Pd alloys, structural and mag. props. rel. to compos. 8=4714
Mn_{2-x}Cr_xSb₂ (x > 0.035), antiferromagnetic-ferrimagnetic with magnetic field 8=9281
Mn₂GaC_{1-x}, antiferro-ferro, transition at 150°K, rel. to non-stoichiometry 8=22819
Mn₃Pt, first-order mag. transformation, X-ray and susceptibility study 8=18382
Ni ferro-paramag., photostimulated exoelectron emission obs. 8=2273
NiO antiferro-paramag., photostimulated exoelectron emission obs. 8=2273
NiO, Co⁵⁷-doped, in ultrafine particles rel. to Mössbauer spectra 8=4680
NiS, pressure dependence from elec. resistivity meas. 8=22885
Pd-Mn alloys, structural and mag. props. rel. to compos. 8=4714
RbCoF₃, T_N \approx 96°K from n.m.r. meas. 8=18472
RbNiF₃ structure crystals, ordering 8=5482
Tb, ferromag. to paramag., neutron diffraction study 8=18352
TbCu_{1-x}Zn_x alloys, antiferro-ferromag., on increasing Zn conc. 8=14073
TbFeO₃, antiferromag. ordering, at liq. He temps. 8=9375
US, ferromag. transition 8=22848
YFe₂Al₆O₃ crystal, antiferro-ferromag. over 602-600°K 8=14074
YFe garnet, Ga substituted, in spheres and powders, determ. of Curie points 8=18367
YFe garnet, in spheres and powders, determ. of Curie points 8=18367
Y-Tb alloys, Néel point deviations 8=2299
ZnWO₄·Mn, to antiferromag., e.p.r. obs., 4.2-77°K 8=5535

Magnetic resonance and relaxation

- See also Antiferromagnetic resonance; Ferrimagnetic resonance; Ferromagnetic relaxation; Ferromagnetic resonance; Nuclear magnetic resonance and relaxation; Paramagnetic resonance and relaxation.
ang. momentum meas. method at low fields 8=14075
echoes, radiative 8=3274
electromagnetic resonance with propag. effects, exact soln. 8=6403
excitation in var. effective field 8=10990
ferrite, uniaxial two-sublattice in a noncollinear phase, reson. freq. 8=5486
ferromagnetic, thin mag. film 8=22787
Gaussian and Lorentzian line shapes 8=19904
induced by modulated optical excitation, in rotating coord. system 8=4102
intermodulation in spin systems obeying Bloch's equations 8=10992
ion pairs, exchange coupled, and symm. props. 8=14076
line broadening, non-uniform, saturation 8=18390
lineshapes with exchange among many sites, rapid computation 8=3277
magnetic resonance and relaxation, conference 8=22889
metals, nonlinear quantum pseudo-resonance 8=1631
microwave resonance absorpt. modulation effect 8=15426

Magnetic resonance and relaxation—contd

- mol. beam, nuclear spin relaxation in spherical-top mols. 8=12119
 molecular generators, mag. tuning characteristics asymmetry 8=16362
 molecular relaxation and reorientation 8=16346
 multispin systems, relax. theory in presence of lattice and spin modulating mechanisms 8=9453
 naphthols, triplet state, rel. to electronic struct. 8=21152
 nitroxide polymers 8=4270
 parameters obs. with high mod. freq. radio-spectrometer 8=10980
 polycaprolactam p polarization by "solid effect". 3150-19 200 Oe and 1.65-4.2°K 8=13015
 polymers p polarization by "solid effect". 3150-19 200 Oe and 1.65-4.2°K 8=13015
 polymers, spin-lattice relax., side chains thermal motion obs. 8=22915
 polypeptides, helix-coil transition, proton mag. resonance obs. 8=21211
 quadrupolar spin system, acoustic free induction 8=5543
 relaxation, perturbation effects, theory 8=10982
 semiconductors, in higher harmonics generated by free carriers 8=5223
 semiconductors, spin-cyclotron-phonon resonance 8=2352
 solid, magnetically dilute, free-induction decay evaluation 8=14135
 spin generator, effect of radiation damping 8=15438
 spin-lattice, and electrostatic coupling, Racah operator equivs., calcs. 8=14129
 spin-lattice relax. rel. to lattice anharmonicity 8=4902
 spin-lattice relax. times at low temp., meas. apparatus 8=19913
 spin relaxation theory, book 8=18446
 spin transfer in different environments, magnetic resonance phenomena 8=10986
 the triplet state, conference Beirut Lebanon (1967) 8=16347
 $\text{BaF}_2:\text{Yb}^{3+}$, spin-lattice relax. 8=18444
 $\text{CaF}_2:\text{Yb}^{3+}$, spin-lattice relax. 8=18444
 $(\text{CF}_3)_2$, polymer, peroxide radicals spin-lattice relax., 14 and 4°K 8=2377
 $(\text{CF}_2\text{CFCFCl})_n$, polymer, peroxide radicals spin-lattice relax., 14 and 4°K 8=2377
 $(\text{CF}_3\text{CFH})_n$, polymer, peroxide radicals spin-lattice relax., 14 and 4°K 8=2377
 F in fluorobenzene, spin-lattice relax. rel. to spin-rot. coupling 8=1594
 $\text{Fe}(\text{NO}_3)_3 \cdot 9\text{H}_2\text{O}$, relaxation, Mössbauer spectra 8=2378
 Fe-Si, magnetic Zener relaxation, diffusion mechanism 8=9451
 2H-1,4-thiazines, spin-spin coupling obs. 8=21166
 He_3 , optically oriented 8=20999
 Hg vapour, induced by freq.-modulated light 8=15492
 KD_2PO_4 , deuteron spectrum due to intrabond jumping 8=9212
 $\text{K}_3\text{Co}(\text{CN})_6:\text{Fe}^{3+}$, spin-lattice relax. rel. to maser material 8=10994
 $\text{LiNH}_2\text{H}_2\text{SO}_4$, spin-lattice and proton, temp. dependence rel. to mol. reorientation 8=8235
 $\text{Mg}_{0.4}\text{Mn}_{0.6}\text{Fe}_{1-x}\text{O}_4$ rel. to sintering temp. effects 8=2342
 $\text{MgO}:\text{Fe}^{2+}$, spin lattice relaxation 8=9452
 MnCr_2O_4 , freq. 8=22890
 ND_3NO_3 polycrystals, spin-lattice relax. of p and d 8=14149
 $\text{NH}_4\text{Fe}(\text{SO}_4)_2 \cdot 12\text{H}_2\text{O}$, relaxation, Mössbauer spectra 8=2378
 NH_4NO_3 polycrystals, spin-lattice relax. of p and d 8=14149
 $\text{SrF}_2:\text{Yb}^{3+}$, spin-lattice relax. 8=18444
 YFe garnet, magnetoacoustic 8=22891
 $\text{ZnWO}_4:\text{Cr}^{3+}$, spin-lattice relax. rel. to maser material 8=10994
- Magnetic storms**
 activity rel. ionospheric u.l.f. emission 8=9974
 April 17-18, 1965, ground and satellite obs. 8=2730
 and auroral event, class II low latitude 25-6 May 1967 8=10054
 and aurora, night, at low and middle latits., obs. analysed 8=2752
 bays, negative, associated outward magnetotail plasma flows 8=18928
 bays as superposition of effects due to Hall current system and westward electrojet 8=19047
 causing low-altitude trapped electrons boundary collapse 8=14656
 and cosmic ray neutron intensity 8=7011
 cosmic ray nuclei Forbush decreases obs. 8=15910
 current system dynamics rel. to phase of Dst vars. 8=19045
 disturbances, solar flares and radio bursts, rel. 8=10397
 effects associated with magnetosphere tail 8=9912
 e-content, total, in ionosphere, effect 8=2657
 elementary disturbance on day side 8=18940
 and F2 layer obs. 8=2718
 frequency in arctic, obs. 8=10042
 initial phase, duration, IGY-IGC obs. from 59 stations 8=19044
 intensity rel. position oval aurora boundaries 8=9937
 rel. to ionosphere e conc. at 640 km 8=2667
 ionospheric parameter variations 8=9966

Magnetic storms—contd

- microstructure of solar-diurnal var., Pc1 , Pi2 + Pc1 and Pi1 8=19049
 moving plasma interaction with dipole mag. field, analogy 8=12465
 1957, 13 Sept., solar flare effects 8=9934
 polar activity and ring current growth 8=19056
 polar disturbances and current system, IGY winter obs. 8=23442
 polar sub-storm rel. to auroral sub-storm and radiation belt 8=19046
 polar substorms, appl. of flux tube flow eqn. 8=10029
 polar substorms and electrojet 8=18950
 polar substorm event on 18 April 1965, trapped particle accel. Explorer 26 obs. 8=23349
 polar, substorms, mag. aspects 8=14697
 polar substorms rel. to Van Allen radiation changes, Alouette 1 obs. 8=18966
 pp bursts, short term, as geomag. pulsations 8=10044
 review 8=19002
 and ring currents, proton and electron differential energy spectra from OGO 3 obs. 8=2646
 and solar stream mag. morphology 8=10053
 sudden commencement amplitude, Indian equatorial belt 8=10045
 sudden commencements rel. to cosmic ray anisotropy 8=11673
 sudden commencement duration, Electron 2 obs. interpretation 8=10043
 sudden commencement, explanation in terms of induced ionospheric currents 8=2729
 theory, review 8=19043
 and trapped radiation, adiabatic betatron acceleration 8=2645
- Magnetic traps.** See Plasma/confinement.
Magnetic wells. See Plasma/confinement.

Magnetism

- See also Antiferromagnetism; Diamagnetism; Earth/magnetic field; Ferrimagnetism; Ferromagnetism; Gyromagnetic effect; Magneto hydrodynamics; Paramagnetism; Rock magnetism; Stars/magnetism; Sun/magnetism.
 Anderson model of localized mag. moments, high temp. behaviour 8=9284
 Anderson model of localized mag. moments, integral eqn. 8=9285
 induction equations, use of SI units 8=3177
 interacting array of fine mag. particles, study with hysteretic mag. dipole model 8=22738
 itinerant-electron, band structure effects 8=9287
 magnetism 8=301
 monopoles, rotational invariance 8=20271
 project laboratory, advantages and disadvantages 8=15159
 review of physics 8=2286
 Shubnikov groups, three dimensional periodic mag. structure 8=8367
 superconductors, type II, pinning forces and hysteresis 8=22538
 susceptibility calc., dimensional anal. 8=15250
 susceptibility of four level quantum systems 8=391
 susceptibility of spin systems with several time dependent temps. 8=15009
 temp. coeffs., reversible, r. t. to 400°K, columnar permanent magnets 8=19748
- Magnetization process**
 See also Ferromagnetic relaxation.
 coercivity temp. depend., new expt. approach 8=14051
 crystals, micromagnetic theory 8=5452
 crystals, uniformly magnetized rectangular prismatic, demagnetizing fields 8=5454
 diffusion vector rel. to ang. momentum conservation principle 8=13953
 elongated single-domain particles, reversal mechanisms 8=5453
 ferrites, magnetic anisotropy constants, mag. saturation intensity dependence, temp. effects 8=2338
 ferrite, r. f., time variation when subject to spin wave instability 8=14079
 ferrites, square-loop polycrystalline, magnetization reversal by Bloch wall movement, model 8=18356
 ferrites, square-loop, reversal by domain wall movement, model 8=2337
 ferroelectric, along axis of difficult magnetization 8=18318
 ferromagnets, appl. of conventional Bloch wall models 8=9320
 ferromagnetic dielectric, eqns. of motion and eqn. for temp. change 8=5451
 ferromagnetic films, inversion by Barkhausen-Cisman-Brion method, e. m. aspect 8=22781
 ferromagnetic films, magnetization ripple theory 8=22785
 ferromagnetics, switching behaviour 8=13996
 fluctuations, local, micromagnetic treatment using Green's function 8=5450
 Heisenberg ferromagnetics, low-temp. expansion 8=13982
 Heisenberg ferromagnetics, magnetisation and susceptibility temp. dependence near Curie pt. 8=18308
 hysteresis, constitutive eqns. rel. to mag. field strength history 8=307

Magnetization process—contd

- lithium ferrites—chromites, spontaneous, effect hardening on temp. depend. 8=2341
- longitudinal susceptibility in mats. with non-uniform saturation magnetization 8=9327
- in magnetic films, demagnetizing fields 8=9331
- metal tapes, moving, resulting mag. field distrib. and eddy-current energy losses 8=13957
- paramagnetic salt, supercond. solenoid for adiabatic demagnetization 8=5217
- Permalloy films, large-angle flux reversal meas., eddy-current-free 8=14030
- permalloy film on Cu, magnetization under circular alternating and longitudinal static fields 8=9335
- rare earth orthoferrites, hysteresis loop study of temp. induced spin flop 8=14048
- rare earth Ga garnets, rel. to mag. moment of rare earth ions 8=2340
- saturation magnetization, temp. depend., demagnetizing field technique 8=22834
- static magnetization in mats. with non-uniform saturation magnetization 8=9326
- superconductors, type II, magnetization curves 8=2151
- susceptibility, measurement on anisotropic materials 8=15251
- switching by non-coherent rot., propag. at high speed 8=18319
- Au in Fe, saturation at 20°K 8=2324
- Au₂Mn, up to 50 kOe at 4.2°K and up to 70 kOe at 80°K 8=9281
- Co film on Cu, magnetization under circular alternating and longitudinal static fields 8=9335
- Cr/Co layered films, high coercive force, for storage medium in digital recording 8=14009
- CuFe alloy, magnetic field and temp. depend. 8=5178
- CuMn alloy, magnetic field and temp. depend. 8=5178
- Fe powder dispersed in perspex, anhysteretic curves 8=5470
- Fe-whiskers, nucleation mag. field strength investigations 8=5467
- FeCl₂·2H₂O, antiferromag., from exchange interaction study 8=2349
- α-Fe₂O₃, in pulsed fields to 140 kOe, rel. to antiferro. to weakly mag. transition 8=5503
- Fe₂S₈, up to 90 kOe at 1.2°K, 201°K and room temperature 8=9281
- Fe₂Se₃, rel. to magnetocryst. anisotropy const. 8=2321
- In in porous glass, superconductor, flux jumping 8=2163
- Li_{0.5}Cr_{1.25}Fe_{0.25}O₄, spontaneous, rel. to compensation temp. 8=14049
- Mg-Mn ferrites, impulse reversal in strong fields 8=9380
- MnHg, up to 100 kOe at dry ice temperature, room temperature and liquid air temperature 8=9281
- Mn(NH₄)₂(SO₄)₂·6H₂O, 1°-4°K 8=17520
- Mo-Fe solid soln., susceptibility 8=22749
- Nb, mag. flux lines—dislocations interaction, 4.2°K 8=22210
- Nb, superconducting, flux penetration and a. c. losses 8=5210
- Nb, superconducting, rel. to n-irradiation 8=2169
- Ni, dynamic ΔE effect frequency dependence in weak mag. field 8=2065
- Ni, reversible and irreversible temp. dependence 8=14025
- Ni saturation magnetization, temp. depend., applic. of demagnetizing field technique 8=22834
- Ni-Fe films, dynamic energy losses during magnetization reversal 8=14029
- NiFe₂O₄ ferrite obs. in 14-600°C 8=5494
- NiSiF₆·6H₂O, isothermal work, 0.05°-4.2°K 8=8641
- R_xM_{1-x}Al₂(R=Gd, Tb, Er and M=Y, La, Th) cubic Laves phases, and Curie temps. 8=14039
- Si-Fe, freq. depend. of mag. reversal mechanism 8=5484
- TmFeO₃, hysteresis loop study of temp. induced spin flop 8=14048
- YFe garnet, Al and Ga substituted, heat treatment effects 8=14055
- (Zr_{0.6}Nb_{0.4})Fe₂, Laves struct., anomalous behaviour 8=2295
- ZrZn₂, itinerant electron model of ferro-magnetism 8=2336

Magnetization state

- AlNi Al, magnetization coercive field strength, time- and temp.-depend. 8=5460
- Brillouin function and spontaneous magnetization table for J=1/2 to 7/2 and J=∞ 8=9328
- electron gas, polarized free, spin density oscillations 8=22482
- elementary, excitations in mag. crystal with strong crystalline field 8=22770
- ferrites, dilute solid solns., saturation, and Néel temp. 8=9369
- ferromagnetic materials subject to magnetostriction, calc. 8=13998
- ferromagnetic metal, particle contrib. and assoc. differential suscept. 8=22764
- film, anisotropy field, low-freq. meas., appl. to automation 8=18325
- films, ferromagnetic with surface anisotropy spin-wave theory 8=5456
- films, thin ferromagnetic, inhomogeneity calc. 8=2311

Magnetization state—contd

- films, thin, rel. to spatial distrib. of spontaneous mag. 8=22779
 - helicoidal structures, coupled e.m., plasma, and spin waves 8=18307
 - Ising ferromagnets, high-temp. absence of spontaneous magnetization 8=18304
 - localized mag. impurities, spin polarization 8=18317
 - Lorentz microscopy, wave-optical aspects rel. to domain and ripple problems 8=6279
 - magnetic films with non-planar surfaces, equilib. state 8=14000
 - magnetic tapes, storage capacity improvement through anisotropic props. 8=5457
 - microwave-induced change, approximations 8=13955
 - non-linear, susceptibility 8=2287
 - periodic magnetic structures and phase transitions 8=1399
 - polycrystalline films, ripple wavelength 8=18326
 - pressurized materials, meas. 8=13952
 - rare earth Fe garnets, intrinsic coercive force near compensation temp. (>77°K) 8=14005
 - rocks, igneous, remanent at low temp. 8=2755
 - Shubnikov groups, three dimensional periodic mag. structure 8=8367
 - spinel ferrites, orientation superstructures and their effects 8=14046
 - structure analysis, space group representation 8=13951
 - sublattices, mol. field soln. uniqueness 8=14042
 - superstructures in reciprocal space by n-diff. method 8=18293
 - 3-dimensional structures described by Shubnikov groups 8=13956
 - trivalent heavy rare-earth ions, anisotropy in high mag. fields 8=2293
 - BaFe₁₂O₁₉, complex permeability and mag. loss in cm. and mm.-wave range 8=5489
 - Co, transmission of polarized n 8=2031
 - Cu-Fe alloy, rel. to existence of antiferromag. coupled bound state 8=22519
 - Fe, resistivity, and rel. to temp. 8=13716
 - Fe-rich alloys, with various transition elements 8=22811
 - Fe-whiskers, nucleation mag. field strength investigations 8=5467
 - Fe, (Al, Ga, Si, Ge, Sn, Sb) impurities, magnetization distribution 8=9349
 - Fe-Ni-Cr alloys, ang. depend. of phenomena in interacting particle chains 8=5429
 - β- and δ-FeOOH, and mag. susceptibility 8=22747
 - Fe₂O₃ (hematite), rel. to temp. 8=5469
 - Fe₃O₄, hyperfine mag. fields rel. to sublattice magnetizations 8=21809
 - Gd-Y alloys, temp. depend., and props. 8=5472
 - I. Pb type II superconductor, and magnetostriction 8=22548
 - Li_{0.5}Fe_{2-x}Al_{0.5}O₄ (0<x<1), mag. moments and mol. field coeffs. 8=9378
 - Ni, transmission of polarized n 8=2031
 - Ni-Co alloys, uniaxial anisotropy 8=5479
 - NiMn₂O₄ single crystals. 8=21959
 - Ni₂Mn, intermed. ordered, mag. field induced anisotropy 8=2327
 - PrC₂, antiferromag. structure 8=18386
 - TbC₂, antiferromag. structure 8=18386
 - TmFeO₃, antiferromag. ordering, variation with temp., 1.6°K-94°K 8=22859
 - ZrZn₂, particle contrib. and assoc. differential suscept. 8=22764
- domains**
- antiferromagnets, canted, orthorhombic, domain-wall motion anal. 8=14059
 - Bloch-type, periodic structures 8=2310
 - Bloch walls in ferromag. b.c.c. crystals, variational calc. 8=2308
 - Bloch walls in ferromag. f.c.c. crystals, variational calc. 8=2309
 - Bloch walls, properties, application of statistical interpretation 8=13989
 - boundary energy, rel. to angle between magnetizations 8=22776
 - channeled tip propag., threshold, rel. to memory and logic devices 8=13992
 - electron diffraction images from single walls and periodic structs. 8=22772
 - ferrites, boundary shift resonance 8=5512
 - ferrites, magnetic walls, nucleation 8=2339
 - ferromagnetic film, effect of superconducting screen on relative stability of Bloch and Neel walls 8=18327
 - ferromagnetic particle with high uniaxial anisotropy 8=22773
 - ferromagnetic, single isolated spherical, rotation under varying mag. field and strain 8=13993
 - ferromagnetics and superconductors, structure, theory 8=13742
 - in films, demagnetizing field rel. to ferromag. reson. condns. 8=22783
 - films, double layer of different chem. comp., mag. props. 8=9332
 - films, thin uniaxial 8=14002
 - fixed and mobile in crystal with induced anisotropy, origin and consequences 8=5449

Magnetization state—contd

domains—contd

- iron losses, low freq., rel. to coercive force, wall eqn. 8=22777
- Kerr technique improved for domain obs. 8=9323
- observation, direct, by scanning e microscopy 8=18315
- 180°-wall energy due to magnetic-diffusion after-effects, calc. 8=9322
- particle, single, temp. depend. of props. 8=22775
- Permalloy, electron diffraction obs. 8=22824
- Permalloy films, mag. reversal in alternating mag. field 8=5474
- permalloy films, obs. by pulse technique 8=9364
- Permalloy films, worm motion of domain walls 8=14028
- Permalloy wire devices, domain wall propag. and digital appls. 8=14034
- review 8=18313
- semiconductors, negative differential cond., slowly propagating high-field 8=13777
- single-, elongated, particles, reversal mechanisms 8=5453
- stripe, electron mirror microscopy study 8=22778
- structure and mag. field obs. with scanning electron microscope 8=13991
- transition temp. of magnetization rel. to domain structure 8=9324
- walls, bulges and curvature under influence of applied easy axis field 8=18314
- wall velocity in applied magnetic field, numerical study 8=9321
- Weiss, mean susceptibility matrix calc. 8=13995
- Co foils, ferromagnetic domain width depend. on thickness 8=22791
- Fe particles, for magnetostatic accretion 8=23632
- Fe powder dispersed in perspex 8=5470
- Fe-50%Ni mag. props., metallic impurities effects rel. to wall trapping, obs. 8=22825
- Fe-3%Si, grain-oriented, hysteresis and eddy current losses rel. to wall motion, obs. 8=22842
- Fe-Si, grain-oriented, wall mobilities rel. to alternating field freq., obs. 8=22841
- Fe-Si sheet, rel. to mag. freq., and initial permeab. depend. 8=5464
- Fe-3wt.%Si single crystals, rel. to X-ray interference fringes 8=22021
- $\alpha\text{Fe}_2\text{O}_3$ crystals, n. m. r. obs. 8=5557
- Fe_3O_4 , fine grained, coercivity rel. to edge dislocations 8=9343
- Gd, internal friction, obs., torsional damping effect 8=14020
- HgCr_2S_4 , and metamagnetism 8=18340
- MnO, axially cooled or stressed, anisotropy from torque meas. 8=14072
- Ni, Bloch-wall-friction model, rel. to Rayleigh-region 8=5481
- Ni cylindrical crystals, (100) axis, ferromag. basic structure, investigations 8=14038
- Ni cylindrical crystals, (110) axis, closure-domain structure, investigations 8=14037
- Ni-Fe double films, domain wall motion 8=2329
- Ni-Fe films, wall pinning effects on bias susceptibility meas. 8=14026
- Ni-Fe, magnetic thin films, thickness dependence of wall energy 8=18346
- 77Ni-14Fe-5Cu-4Mo wt. %, wall surface energy rel. to mag. props. sheet thickness depend. 8=22827
- NiO, axially cooled or stressed, anisotropy from torque meas. 8=14072
- NiO, rhombohedral distortion, antiferromagnetic ordering 8=5507
- Si-steel, sample prep. for domain struct. meas. 8=22840
- Si-Fe, freq. depend. of mag. reversal mechanism 8=5484
- YFe garnet, configs. and cryst. defects effects, obs. 8=22863
- YIG crystal, ferrimag. reson., influence of structure 8=5513
- YFe interaction of microwave phonons with domain walls 8=22087
- Magnetoacoustic effects**
- ferroacoustic resonance, theory 8=4918
- ferro- and antiferromagnetics, nuclear magneto-acoustic resonance 8=22916
- ferromagnet, u.s. attenuation near transition temp., phonon interact. with spin system 8=18323
- Landau quantization near singular or saddle point 8=22439
- magnetic materials, excitation of rf resons. and echoes 8=17493
- magnetophonon resonance, influence of optical phonon heating 8=8622
- plasma excitation, non-linear by magnetoacoustic resonance 8=21333
- plasma oscills., ion heating 8=7824
- plasma waves, instability 8=21390
- resonance, double electron-nuclear, at local electron centres 8=8623
- resonance effects in metals in inclined mag. fields 8=1844
- sound attenuation near critical points 8=13344
- Al alloy, frequency and damping change, structural and impurity dependent 8=8624
- Al, u.s. shearwave attenuation and rot. in mag. field 8=17497

Magnetoacoustic effects—contd

- Bi, microwave phase velocity obs. 8=22097
- Bi, u.s. attenuation, amplitude of giant quantum oscs. 8=1848
- Bi and Bi alloys, magnetoacoustic attenuation, $\text{Fe}^{1,2-4,2}\text{K}$ 8=13659
- $\text{Fe}^{1,2-4,2}\text{K}$ in MgO , u. p. r. temp. depend. 8=2367
- Ga, Fermi surface study, by u.s. geometric reson. 8=8935
- InSb, rel. to acoustoelec. domain form. and amplifiers d.c. loss mag. fields effect 8=13355
- K, shear wave 8=22105
- Li donors in Si, acoustic paramagnetic resonance 8=9443
- $\alpha\text{-Mn}$, ultrasonic attenuation in vicinity of Néel point 8=17501
- NaCl , plastically deformed, acoustic n. m. r. 8=5561
- Ni-Co-Mn ferrites, shifting of u.s. vel. minima due to mag. polarization changes 8=8632
- YFe garnet single crystal, resonance obs. 8=22891
- Magnetocaloric effects.** See Magnetoenthal effects.
- Magnetocrystalline anisotropy.** See Magnetic properties of substances; Magnetization state.
- Magnetoelastic effects.** See Magnetomechanical effects.
- Magnetoelectric effects**
- See also Hall effect; Magnetoresistance.
- apparatus for meas. between 1.8°K and 330°K 8=5427
- $^{15}\text{S}_6$ atomic systems, susceptibility 8=4053
- hot-electron gas, galvanomagnetic and thermomagnetic size effects 8=19466
- linear motor, induced currents in secondary 8=15197
- metal microplasticity by strain effects on the a.c. resistance 8=5036
- Nernst-Ettingshausen effect rel. to magnetoresistance 8=9082
- semiconductor films, longit. oscs. rel. to thickness and field strength 8=9074
- semiconductors, nonlinear effects, in strong electric and magnetic fields, theory 8=5225
- submetallic films, longit. oscs. rel. to thickness and field strength 8=9074
- Bi, galvanomagnetic effects 8=8994
- Bi, Sn-doped, galvanomag. effects at low fields at 77°K rel. to doping 8=2186
- Co films, in rotating mag. field 8=17931
- Co films in rotating magnetic field, longitudinal and transverse effect obs. 8=5475
- HgTe-ZnTe system, determination 8=5263
- n-InSb, electrical cond. and magnetoresist. below 1°K 8=13820
- Nb, galvanomagnetic props. 8=22682
- Ni films in rotating magnetic field, longitudinal and transverse effect obs. 8=5475
- Sb, galvanomag. coeffs. temp. and pressure dependence 8=17938
- Se, magnetoconductivity, mobility and direction dependence 8=5275
- Magnetogasdynamics.** See Magneto hydrodynamics.
- Magneto hydrodynamic generators.** See Electricity/direct conversion; Magneto hydrodynamics.
- Magneto hydrodynamic waves.** See Magneto hydrodynamics; Plasma/magneto hydrodynamics; Plasma/oscillations.
- Magneto hydrodynamics**
- See also Plasma/magneto hydrodynamics.
- advances in applied mechanics, book 8=16683
- aerofoil problems in magneto aerodynamics 8=19804
- Alfvén waves, Cherenkov emission by moving force source 8=6343
- Alfvén wave growth, effect of rotation 8=3242
- annular channel flow 8=15371
- armature, sliding field and sodium vein, power transfer between 8=6265
- automodel motion involving variable conductivity 8=346
- boundary layer growth in non-conducting fluid on a magnetized circular cylinder 8=7872
- boundary layer problem 8=15359
- boundary layers, self-similar motion 8=3239
- channel characteristics, partition wall dislocation effect 8=15369
- charge interaction with space-perturbed magnetic field, asymptotic calculation 8=3232
- closed-cycle unit, nuclear reactor as heat source 8=10839
- coaxial channel with helical field, m. h. d. mode degeneration 8=6351
- compressible, boundary-value problems 8=3233
- compressible fluids, superposed, stability of rotating vortex sheet 8=6357
- compressible, laminar flow in flat duct, with heat transfer 8=15364
- conducting gas flow at high vel., effect of Hall currents 8=16653
- conducting gas in strong mag. field, convective instability for large temp. grad. 8=19308
- conference, Dallas 1967 8=12480
- converter, isothermic with electrodes in series 8=6270
- Crab nebula, synchrotron X-ray production in central mag. field 8=5918
- critical point, near, analysis of movement 8=15376
- cyclotron waves in moving cold plasmas, theory 8=16586
- devices using liquid metals 8=6263
- direct conversion with reactor heat source 8=295
- direct convertor, molten metal mixing, thermodynamics of cycles 8=294

Magnetohydrodynamics—contd

discontinuities in the presence of electric fields 8=15360
 drag in conducting fluid with aligned field, obs. 8=6349
 dragging motion of a liquid by plane walls 8=10926
 dynamos, nearly symm., Braginskii result true to second approx. 8=10097
 earth's core, surface fluid motion rel. to secular mag. field changes 8=2724
 earth's core, surface fluid velocity rel. to mag. field 8=5813
 earths mag. field, dynamo model 8=23427
 electric and m. h. d. currents in pipes 8=6347
 electroconducting fluid flow between rough plates 8=8110
 electrohydrodynamic waves in super-permeable media 8=10925
 electrolytic turbulent flow, temp. fluctuation meas. 8=356
 engines, rel. to electrical conductivity of ionized gases 8=4487
 engine with liquid Na 8=289
 equations, class of exact solns. 8=19808
 eqns., invariant soln. 8=6344
 ferromagnetic colloidal suspension, mag. field prod. rotation 8=16622
 field diffusion into moving conductor 8=3237
 flat channel flow, current and pot. distrib. 8=15366
 flow in cylindrical pipes with non-uniform mag. field 8=19810
 flow, discontinuous one dimensional non-dissipative 8=15375
 flow distortion by strong Hall effect and effect on power generation 8=15381
 flow in expanding pipe, magnetic field effect 8=6354
 flow, one dimensional, and Monge-Ampère eqn. 8=19812
 flow through a pipe, coefficients of resistance 8=16753
 flow in quasi-aligned fields 8=10924
 flow, quasi-unidimensional, stability of transverse oscillations 8=349
 flow, solution for small magnetic interaction 8=3236
 flow stabilization, heat exchange, in plane channel 8=3240
 flow, subsonic in crossed elect. and mag. fields 8=16659
 fluctuating boundary layer near magnetized plate 8=10922
 fluid, elec. cond., Hall effect for variable mag. field and high Reynolds numbers 8=16614
 fluid with finite conductivity, flow 8=10921
 fluid flow electrically conducting, incompressible near accelerated plate under transverse magnetic field 8=3241
 fluids, incompressible, exact solns. valid for all conductivities and viscosities 8=10928
 galactic proton plasma, anisotropic relativistic, transverse e. m. wave effect 8=5850
 gas conductor in aligned magnetic field with normal magnetogasdynamic shock 8=15375
 gas flows, temp. dependence of elect. conductivity 8=16491
 gas, longitudinal flow stability in crossed E and H fields 8=10923
 gas, partly ionized in mag. field, transport properties 8=10927
 gas, vorticity and current density behind shock wave in unsteady flows 8=6358
 generation, closed cycle, prospects for 8=292
 generation of elect. power, status report 8=15201
 generator boundary flow calc. 8=19725
 generators, combustion fired 8=291
 generators, critical survey 8=290
 generator, effects of electrode ends on flow 8=3155
 generator, elec. conductivity of high-void-fraction two-phase flow, expt. 8=15202-3
 generator, extreme value of voltage 8=6269
 generator, homopolar without ferromagnetic core 8=15356
 generator, induction type, fundamentals 8=6268
 generator, liquid metal, computer efficiency calc. 8=3156
 generators, liquid vein 8=6262
 generator, liquid vein, sliding field 8=6264
 generator, non-equilib. flow of conducting fluid in channel on sudden short-circuiting 8=6267
 generator, power, Li-Cs cycles, 1366°K 8=10837
 generator, pulse, explosively driven lumped-parameter (slug) model 8=10838
 generator, rectangular channel, 2-dimensional flow analysis 8=15209
 generators, review 8=19724
 generator, segmented-electrode, effective cond. 8=15200
 generators from superconducting magnets 8=3166
 generator with water-cooled electrodes, temp. distrib. in channel wall 8=19726
 generator, LaB₆ powder suspension in N₂ as working fluid 8=15199
 half-jet, compressible, inviscid stability 8=354
 heat transfer of flow at flat duct entrance 8=19809
 hydromagnetic energy conversion, thermodynamics of 8=345
 hydromagnetic oscillations of conducting incompressible fluid cylinder 8=19817
 hydrostatic thrust bearing, MHD lubricated, effects of inertia 8=8809
 incompressible flow, group props. of eqns. 8=15357
 induction generator, flat channel, linear, comparison of three analyses 8=15204
 induction machine, general equations of sliding magnetic field 8=15383

Magnetohydrodynamics—contd

interface of ferromag. with non-magnetizable fluid, instability 8=6355
 of interstellar gas-dust medium 8=23579
 ionosphere, hydromagnetic gradient waves 8=14674
 rel. to ionosphere, turbulence at low mag. Reynolds number 8=19813
 jet, flat, stability of 8=15367
 jet, stationary 8=6359
 jet, turbulent, incompressible 8=15377
 jet, 2D, annihilation by transverse mag. field 8=352
 laminar flow thro' conducting parallel porous walls 8=347
 laminar flow, heat exchange, effect of fields 8=348
 liquid, conducting and in turbulent flow, effect of mag. field on heat transfer 8=10930
 liquid, conducting, surrounded by compressible gas, surface waves 8=3243
 liquid conductor in magnetic field aligned with flow with magnetohydraulic jump 8=15375
 liquid phase, alkali metal appl. 8=15384
 liquid, stagnant conducting, flows induced by nonuniform m. h. d. pinch 8=10932
 liquid vein m. h. d. generators 8=15207
 liquid, viscous, flow in porous channel with transverse mag. field 8=15363
 liquid wave, gravity-capillary, in film, effect of transverse mag. field 8=7987
 mag. dipole, nonlinear inflation by plasma 8=10028
 mag. field deformation by conducting-fluid motion 8=6346
 magnetic field enhancement by conducting fluid 8=15380
 magnetogasdynamic accelerator and generator local characts., graphical display 8=15382
 magnetogasdynamic flow round nose of blunt body, influence of Hall effect 8=15378
 magnetohydrodynamic electrical power generation, conference, Salzburg, Austria (1966) 8=15355
 MHD generators, stability of plasma, voltage oscils. 8=15208
 MHD machines, liquid metal, efficiency 8=19727
 mercury in tube in longitudinal mag. field, turbulent flow 8=10933
 metal rotating in magnetic field, heat transfer 8=8054
 nonequilibrium, wave propag. three-dimens. 8=344
 nozzles with end effects 8=6348
 oblique shock waves, stability 8=16456
 pipes, hydraulic resistance 8=15385
 pipe, rough, rectangular, flow 8=15368
 piston, conducting, motion in mag. field 8=15361
 piston, expansion into compressible conducting fluid in mag. field 8=353
 plane jet propagation and damping 8=19807
 plasma column diffusion across uniform mag. field, kinetic theory 8=4341
 plasma model, physical interpretation 8=6342
 plasma stability, influence of initial density and temperature gradients 8=7844
 power generator with peg walls, effect of internal short-circuiting 8=3157
 power plant 8=19728
 proton motion in Alfvén wave field 8=9958
 pumps and flowmeters applications 8=6266
 rarefaction, reflection waves 8=15358
 relativistic, energy-momentum tensor evaluation 8=1536
 relativistic, props. of rays 8=6341
 remote measurement of speed, hydraulic circuit application 8=3235
 resonances, highly asymmetric, guided poloidal mode 8=3
 Reynolds number determ., magnetic 8=6352
 shock and current layer structure in mag. driven tubes 8=6140
 shocks in fluids, transition soln. 8=19805
 shock waves, low intensity, theory 8=6345
 sliding-field liquid-vein generator 8=15205
 in solar wind flowing round comets 8=19262
 spiral flow, over dielec. disc, laminar boundary layer 8=4507
 stars, ionized, thermomagnetic instability and thermodynamic waves 8=10109
 stations, large scale, open cycle, economics and thermal efficiency of 8=293
 steady rotating motions of cond. fluids over rotating disc, influence of general e. m. forces 8=19806
 steady-two-dimensional flow 8=3234
 stellar corona model 8=23506
 stellar mag. field with differential rotations in spherical fluid shell of infinite elect. conduct. 8=23508
 Stokes flow past a circular cylinder 8=15372
 supersonic flow, for blunt bodies 8=355
 T-layer formation processes 8=3244
 thermionic conversion transport processes, effect of mag. field 8=15246
 thin body in perpendicular fields 8=15373
 thin plate, lifting force 8=15365
 thrust bearing, step-type, lubrication flow induced by rot. upper plate 8=351
 turbulence, conservation theorem 8=15379
 turbulence decay, with small mag. Reynolds no. 8=3245
 turbulent flow friction coeff. in ducts 8=6356

Magnetohydrodynamics—contd

- turbulent structure hydromagnetic homogeneous, large scale 8=10929
- turbulence suppression by uniform magnetic field 8=10931
- tuyere, extremity effect of extending magnetic field 8=19816
- two-dimensional motion, finite Reynolds numbers 8=3238
- 2-phase liquid metal devices 8=19729
- unsteady channel flows, osc. characts. under Heaviside-type applied mag. fields 8=19814
- variational principle for hydromagnetic flows 8=15374
- viscous flows, reduction 8=6350
- viscous flow round a rotating sphere 8=15370
- viscous flow under transverse magnetic field 8=6353
- vorticity and current density generated behind a shock 8=19815
- waves, development behind ionizing shock wave 8=19811
- Hg induction pump, vel. distrib. 8=16727
- Na, liquid, Alfvén wave resonances 8=19803
- Na vein generator, power transfer to armature 8=15206

Magnetomechanical effects

- See also Gyromagnetic effect; Magnetostriction.
- antiferromagnet, gyromagnetic effect at low temps. 8=14058
- BVC-garnet, magnetoelastic interaction 8=22850
- carbon steel, magnetoelastic scattering rel. to amplitude dependence of internal friction 8=13565
- coil forces for uniform transverse field magnet, exact solution 8=19747
- cylinder, solid isotropic conducting, magnetoelastic vibrs. 8=13499
- elastic half-space, disturbances 8=10703
- on elastic waves in conducting plate 8=10708
- ferromagnets, var. in magnetic field due to twisting 8=2312
- magnetoelastic tension transducer 8=13504
- magnetoelastic waves in pulsed magnetic fields 8=156
- magnetoelastic wave scattering from surface of ferromagnetic medium 8=2301
- magnetostriction prod. by torsion, circular magnetization calc. 8=13998
- magnetostrictive vibrators, limit of available mechanical output power 8=18322
- prismatical bar, elastic deformation 8=10552
- Fe-Si(3%) sheet, oriented, dynamic magnetostriction under longit. and transverse stresses 8=22812
- Gd, internal friction, torsional pendulum obs. 8=14020
- Ni-ThO₂, magnetoelasticity rel. to damping capacity, 20-500°C 8=17821
- YIG delay lines, magnetoelastic waves, excitation 8=22398
- YIG, magnetoelastic delay lines, ray-theory analysis 8=22397
- YFe garnet, magnetoelastic wave propag. 8=22861

Magnetometers. See Magnetic field measurement.**Magneto-optical effects**

- See also Optical constants; Zeeman effect.
- apparatus for experimental study at low temp. 8=5576
- benzene, mag. circular dichroism 8=21123
- benzene mol. crystal, Faraday effect of lowest exciton states 8=9568
- chlorins, optically active, mag. circular dichroism 8=16317
- coronene, mag. circular dichroism 8=21123
- Cotton-Mouton effect in liquid, theory 8=12869
- Cotton-Mouton effect obs. in alkali metal gases 8=4485
- crystal, variable temp. for meas. 8=5592
- cubic crystals, method of determ. of refractive index 8=18565
- dynamic detector for analog readout, by adding polarization vibrator to Kerr apparatus 8=19750
- Faraday effect in exciton absorpt. region in strong mag. field 8=18491
- Faraday effect in gyrotropic layer 8=3376
- Faraday effect, rel. to Raman scatt. 8=5575
- Faraday, in solid state plasma (circular) waveguide 8=10968
- Faraday shutter for laser 8=435
- field, magnetic hyperfine, sign determ. by Mössbauer-Faraday effect 8=13007
- Franz-Keldysh effect, spectral broadening representation 8=17853
- garnets, meas. in infra-red 8=5643
- gases, diamagnetic, Cotton-Mouton birefringence 8=7934
- glasses, silicate, rare-earth doped, Faraday rotation, freq. depend. 8=18531
- glasses, Verdet constant of, spectral dependence 8=2424
- Kerr technique improved for mag. domain obs. 8=9323
- laser diode spontaneous emission linewidth, mag. field effect 8=19999
- laser, gas 8=3306
- light intensity-dependent changes rel. to observation by laser techniques 8=517
- magnetic film, rotating disc, wideband readout 8=10871
- magnetic films, longit. magneto-optical transmission conversivity optimization 8=518
- metals, ferromagnetic, quantum theory 8=13981
- nitrobenzene and liquids, Raman and Brillouin scattering 8=4580
- paramagnetic ions, spin-lattice relax. temp. meas. by Faraday rotation 8=22895

Magneto-optical effects—contd

- Raman spectra, directional intensity of Stokes and anti-Stokes lines 8=4122
- permalloy films, reflecto-polarimetry at ferromag. resonance 8=9409
- photoelectric control for rotary power meas. 8=15549
- photomagnetic susceptibility, pulse method of meas. 8=9282
- polarized photon scattering by Dirac particle 8=15713
- polymers, rotation and circular dichroism, theory 8=12384
- p-type semiconductors (Ge, GaAs, GaSb, InAs, ZnTe), Faraday rotation 8=14216
- rare gases, Faraday effect theory of excitons 8=5130
- recordings detection, high-density 8=14185
- semiconductors, direct-band, phonon-assisted magnetoabsorption 8=5222
- semiconductors, electron-lattice effect on free-carriers 8=8890
- semiconductors, hot-electron Faraday effect 8=22420
- semiconductors, interband absorption, optical phonons 8=18492
- semiconductors, intrinsic, polaron effects in interband absorpt. 8=18493
- semiconductors, magneto-absorption and rotary dispersion for electronic band parameters determination 8=9493
- spectral line profile determ. 8=4057
- spectrometer for absorpt. in pulsed fields at 4.2°K 8=11157
- triphenylene, mag. circular dichroism 8=21123
- Bi_{0.24}Ca_{0.76}Fe_{3.24}V_{1.38}O₁₂, Faraday effect mechanism 8=18508
- CaF₂ crystal, Nd³⁺ doped, rotatory dispersion curves using variable temp. cryostat 8=5592
- CaF₂, paramagnetic rare-earth activated, magneto-optic rotation 8=5590
- CaF₂:Ho³⁺, rotation of plane of polarized light 8=18512
- Co, u. v., visible and i. r. spectral ranges, props. 8=18550
- Cu₂O n = 1 line, Zeeman effect in pulsed fields, 4.2°K 8=11157
- EuO films, Faraday rotation, rel. to mag. props. 8=13090
- Fe, polycrystalline, two-pole Kerr effect, 6.5-20μ 8=18526
- Fe, u. v., visible and i. r. spectral ranges, props. 8=18550
- GaAs, interband absorpt. meas. at 2°K, 77°K and room temp. 8=22985
- GdFe garnet wafer for magneto-optic memory element 8=19755
- Ge, photomagnetic susceptibility, pulse method of meas. 8=9282
- Ge, shallow acceptor impurities, magneto-oscillatory excitation 8=22991
- n-HgSe, photomag. effects, magnetothermo-e. m. f. and magnetoresistance effects 8=5261
- InAs, i. r. Faraday effect 8=9539
- InAs, n-type Faraday rotation, interband and free-carrier 8=9540
- InSb, 10.6μ four-port circulator 8=9538
- InSb, shallow acceptor impurities, magneto-oscillatory excitation 8=22991
- KCl, Faraday rotation of Z, center 8=14229
- KCl, paramagnetic rare-earth activated, magneto-optic rotation 8=5590
- KNiF₃, antiferromagnetic, magnetic exchange dichroism 8=14257
- MnF₂, magnon sidebands, selection rules for coupling to excitons 8=14240
- MoS₂, thin anisotropic, crystals, delocalized excitons from magneto absorpt. study 8=13674
- Nd ethyl sulphate, Faraday effect, mag. resonance saturation 8=14278
- Nd³⁺ in CaF₂, rotatory power temp. var. 8=5576
- Ni, u. v., visible and i. r. spectral ranges, props. 8=18550
- p cpds., covalent bonds and mag. rot. 8=21098
- p-PbSe, i. r. free carrier Faraday rot. 8=2445
- RbCl, Z, centre circular dichroism 8=22224
- RbFeF₃, magnetic rotation, Cotton-Mouton effect and optical absorption 8=2450
- RbNiF₃, ferrimagnetic, circular dichroism and rot. of light polarization plane 8=18557
- RbNiF₃, ferrimagnetic, magnetic exchange dichroism 8=14257
- Si, i. r. Faraday effect 8=9539
- SrF₂, paramagnetic rare-earth activated, magneto-optic rotation 8=5590
- SrF₂:Tm²⁺, rotation of plane of polarized light 8=18512
- Te, magnetoabsorption meas. 8=23016
- YFe garnet, magnetoelastic wave propag. light diffraction study 8=22861
- YIG : Si doped, photomag. anneal 8=23022
- Y₃Fe₅·M₂O₁₂, (M = In, Sc, Al, Ga) Faraday rot. and i. r. modulator appls., 1.15 and 3.39μ 8=23021
- Y₃Fe₅O₁₂:Ho³⁺, Faraday effect obs. 8=14271

Magnetoresistance

- See also Magnetoelectric effects.
- current-field non-linear relations in Shubnikov-de Haas conditions 8=17923
- ferromagnetic junctions 8=18343
- graphite, linear in the quantum limit 8=13711
- metals, high purity, for texture investigations 8=8454

Magnetoresistance—contd

- metals, low temp., general theory 8=13644
 n-type semiconductors as function of impurity 8=5226
 narrow layer of open trajectories, rel. to mag. field and temp. depend. 8=5157
 Nernst-Ettingshausen effect relationship 8=9082
 oscillatory, and mag. breakdown by Kubo formula 8=13954
 Permalloy, and effect of 3d orbital degeneracies 8=13724
 semiconductors with edge dislocation, effect of non-uniformity of density 8=13780
 semiconductor films, longit. oscs. rel. to thickness and field strength 8=9074
 semiconductors, high-ohmic, meas. by capacitive method 8=5234
 semiconductors with non-uniform charged ion conc., theory 8=22421
 semiconductors, voltage ratio meas. appl. 8=10821
 Shubnikov-de Haas effect, additional oscillation due to $4\pi M = B - H_0$ 8=22446
 Shubnikov oscillations, resistance jumps, galvanomagnetic charact. 8=22445
 submetallic films, longit. oscs. rel. to thickness and field strength 8=9074
 transverse negative, in low-temp. inelastic scattering by optical phonons 8=8892
 Ag, longitudinal from 4.2 to 35°K, electron scattering effects 8=22511
 Ag single crystals, at 4.2°K 8=8997
 Al, mag. resist. var., 2.5° to 300°K 8=5170
 Al, plastically deformed 99.999% pure, and strain effects, 4.2°K and ≤ 175 kOe 8=17926
 Bi, effect of pressure 8=5173
 Bi, in high mag. field 8=5172
 Bi and Bi alloys, Shubnikov-de Haas effect, 1.2-4.2°K 8=13659
 Bi-Sb alloy, Shubnikov-de Haas effect vanishing under pressure 8=22514
 Bi-Sb, transformation of semiconductor into metal, obs. 8=22581
 Bi_{1-x}Sb_x, (0 < x < 0.15), coeff. meas. at 77°K rel. to band structure 8=22518
 C resistance thermometer, negative magneto-resistance 8=19666
 C resistors at low temp. 8=17929
 n-CdSe, and Hall effect meas. and anal. 8=13796
 CdSnAs₂, n-type, 77° and 300°K obs. 8=5241
 n-CdSnAs₂, in pulsed magnetic field, influence of spin 8=2290
 Co single crystals, up to 1000 Oe 8=8999
 Cu, and transverse effect, rel. to Fermi surface 8=13713
 Cu, longitudinal from 4.2 to 35°K, electron scattering effects 8=22511
 Cu single crystals, at 4.2°K 8=8997
 Cu-Cr alloys, obs. on quasibound state 8=17933
 Cu-Fe alloy, rel. to existence of antiferromag. coupled bound state 8=22519
 CuFe alloy, magnetic field and temp. depend. 8=5178
 CuMn alloy, magnetic field and temp. depend. 8=5178
 p-GaSb, at 4.2°K, valence band studies, and by Hall effect meas. 8=13803
 n-Ge, and hot electron Hall mobility for elec. field along <100> direction 8=18052
 n-Ge, piezomagnetoresistance for mixed scattering mechanism 8=18047
 n-Ge, Shubnikov-de Haas oscillations, 20-80°K 8=18044
 n-HgSe, magnetothermo-e. m. f. magnetoresistance and photomag. effects, meas. 8=5261
 HgSe, oscillatory, beat freq. rel. to inversion asymmetry 8=2100
 HgTe, and Hall coeff. at 4.2 and 77°K rel. to carrier model 8=2200
 In films, longitudinal magnetomorphic effects 8=5430
 InAs, transverse, quantum oscs. 8=13818
 InSb, Corbino, admixture and layer distrib. effects 8=5266
 InSb, n-type, and electrical resistivity, from 4.2°K to 0.1°K 8=5265
 InSb, transverse, quantum oscs. 8=13818
 Ni, low-temp. resistivity 8=17937
 Ni-Cu(0-30.42%) alloys, longitudinal in single crystals up to 1100 Oe at 0°K 8=9013
 Ni-Fe-Cr-Si alloy, 200-300 Å films, obs. 8=5478
 NiFe-SiO-Co multilayer, hysteresis loops rel. to stray-field coupling effects 8=14027
 Pu, α and β , transverse magnetoresistivity 8=2350
 Se, magnetoconductivity rel. to mobility mechanisms 8=18065
 Tl, field dependence up to 150 kG at low temps. 8=5433
 TlCl, transient, of holes 8=9020
- Magnetosphere.** See Atmosphere/upper; Earth/magnetic field.
- Magnetostriction**
 constants for ferrites from ferromagnetic resonance 8=14045
 ferrites, electro-mech. coupling coeff., mech. reson. freq., meas. accuracy 8=9368
 liq. level sensing, appln. 8=10872
 magnetite, anisotropy depend. on hydrostatic press 8=19065
 magnetite, reversible, at high temp. 8=23448

Magnetostriction—contd

- magnetoelastic interactions for infinitely long prism, transform of linear eqns. 8=13997
 meas. method in ferromagnetic materials 8=13998
 metals destruction in magnetostriction oscillator by cavitation and droplet impact 8=22306
 polar crystals, theory 8=22741
 prismatic bar, magnetoelasticity 8=10552
 rare earth Fe garnets, consts. λ_{111} and λ_{100} 8=2322
 transducers, magnetostrictive, design 8=10873
 vibrators, limit of available mechanical output power 8=18322
 Au₂Mn, up to 90 kOe at 0°K and 20°K 8=9281
 CdCr₂Se₄, by ferromag. resonance technique 8=2316
 Ce in YFe garnet 8=2344
 Fe-Ni(35 wt. %)-Cr(0-20 wt. %) alloys (in as-cold worked state), parallel and perpendicular to rolling direction 8=9006
 Fe-Si, grain-oriented transformer sheet 8=22839
 Fe-Si(3%) sheet, oriented, dynamic, under longit. and transverse stresses 8=22812
 InPb type II superconductor, and magnetization 8=22548
 Li ferrite, effect of ion ordering, constants at -170 and +340°K 8=9379
 Mg-Mn ferrites, and mag. anisotropy consts. 8=5492
 MnAu₂ antiferromagnet, spontaneous appearance 8=9400
 Ni films, meas. and obs. 8=18347
 NiFe₂O₄ ferrite obs. in 14-600°K 8=5494
 PbTe, p-type, oscillatory magnetostriction 8=13964
 Si-steel, silicate glass coated, film removal effects rel. to corrosion, obs. 8=22843
 Sm₂V₃-Fe₂O₁₂, anomalies, 4.2-100°K and ≤ 25 kOe 8=18364
 Tm₃Fe₂O₁₂, anomalies, 4.2-100°K and ≤ 25 kOe 8=18364
 Yb in YFe garnet 8=2344
- Magnetothermal effects**
 crystal, Ettingshausen and Nernst coeffs. depend. on magnetic field 8=13635
 ferrites, magnetic anisotropy constants, mag. saturation intensity dependence, temp. effects 8=2338
 ferrites, magnetic anneal relaxation, correlation with ferromagnetic relaxation 8=9407
 ferromagnetic metals, spontaneous Hall and Nernst-Ettingshausen effect 8=9329
 hot-electron gas, galvanomagnetic and thermomagnetic size effects 8=19466
 phonon drag effect contribution 8=5103
 semiconductors, coeffs., quantum oscs. in strong mag. field 8=5426
 semiconductors, phonon-drag Seebeck effect, quantum theory 8=9236
 in superconductors 8=9040
 thermocouple in mag. field 8=284
 thermoelectric semiconducting materials, measuring method 8=9288
 thermogalvanomagnetic phenomena, quantum theory 8=18208
 Bi, magneto-Seebeck effect 80°K, effect of surface recombination 8=18211
 Bi, Nernst effect, increase due to phonon dragging 8=22435
 Cd₂As₂, Righi-Leduc effect meas. 8=9289
 Co, and sp. ht. near Curie temp. 8=9337
 Co during the $e^- \gamma$ phase transition 8=13961
 Cu_{1-x}Mg_xFe₂O₄, on quenching in high oxygen pressure furnace 8=2516
 n-HgSe, magnetothermo-e. m. f., magnetoresistance and photomag. effects, meas. 8=5261
 In films, superconducting, Nernst effect 8=2174
 Mn(NH₄)₂(SO₄)₂·6H₂O, ht. capacity 1°-4°K in mag. fields 8=17520
 Nb, galvanomagnetic props. 8=22682
 Nb, superconducting, explanation 8=2167
 Nb, superconducting, thermal conductivity rel. to mag. hysteresis 8=2166
 n-Si, Nernst-Ettingshausen effects, longit. and transverse, 100-400°K 8=18075
 Sn films, superconducting, Nernst effect 8=2174
- Magnetrons.** See Electron tubes.
- Magnets**
 alnico-type for use > 550°K 8=22806
 bar, five pairs for compensating magnetic field gradients 8=3165
 cylindrical bar, empirical expression for axial field, at range closer than magnet length 8=19749
 electromagnet, double mushroom, design 8=10868
 electromagnets, high-field liq. Ne-cooled 8=15261
 electromagnets for particle accelerators 8=643
 electromagnets, pulsed field prod., helical windings with variable spacing 8=15260
 electromagnet for variable-delay vacuum valve 8=7955
 ferrites, design and performance in loud-speaker circuits 8=15258
 magnetics 8=301
 periodic permanent for electron beam focusing in mm. wave tubes 8=6308
 permanent, application in motors, separators and switching tubes 8=3154
 permanent, columnar, high-temp. stability 8=19748

Magnets—contd

- permanent, temperature dependence of magnetic properties 8=18320
- permanent, transforming mag. into mechanical energy 8=308
- quadrupole, misalignment tolerances 8=15277
- rare-earth Co(RCO₃) cpds. permanent magnets props., obs. 8=22743
- superconducting electromagnets, construction and use 8=6281
- superconducting, mag. field sweep 8=10869
- superconducting, as MHD generators 8=3166
- superconducting, stability of 8=5189
- superconductive, applications 8=10870
- technology, conference Oxford England (1967) 8=15259
- travelling wave maser magnets, use of supercond. shields in field shaping 8=13769
- uniform transverse field, coil forces, exact solution 8=19747
- Al-Ni-Co, permanent, effect of heat treatment below 1000° C 8=9361
- Fe, with superconducting coil 8=15263

Magnons. See Ferromagnetism.**Magnus effect. See Aerodynamics.****Majorana effect. See Magneto-optical effects.****Majorana forces. See Nuclear forces.****Malter effect. See Electron emission/secondary; Photo-multipliers.****Mandelstam representation. See Scattering, particles.****Manganese**

- absorption coeff. for Ag K α radiation, meas. 8=2436
- e.p.r. spectrum in alkali-chloride crystals, resolution by X-radiation 8=14117
- evaporation from Fe-Mn and Fe-C-Mn alloys at 1600°C under vacuum 8=12993
- ferrite magnetostriction constants from ferromagnetic resonance 8=14045
- ions, MnI hyperfine-broadened line profiles rel. to Arcturus spectrum 8=23527
- isothermal growth of precipitates in Mg binary alloy 8=4688
- liquid, vapour-pressure meas. 8=8185
- metals analysis, Mn determ. by at. absorpt. spectrometry 8=2547
- nodules from dredged W. Pacific basalts, mag. props. 8=10055
- solid solns. in Cu, mag. moments 8=22760
- spectral characteristics, rel. to chem. bonds in glasses 8=8194
- steel, martensitic transform., rel. to elec. resist. 8=17061
- sublimation kinetics in chambers with cryogenic surfaces, obs. 8=16959
- in BaS, luminescence 8=23045
- CaSO₄, of Mn²⁺ allowed and forbidden transitions in e.s.r. 8=14116
- in Fe-Mn alloy, dilute, nearest neighbour exchange interaction energy 8=18383
- Fe-Mn systems, α - γ equilib. 8=4709
- MgO lattice, as imperfection, h.f.s. of spectrum 8=14238
- α -Mn, atomic parameters, refinement 8=8532
- α -Mn, n.m.r. spectrum, quadrupole effects 8=18467
- α -Mn, non-centrosymmetric structure with Bijvoet differences 8=13273
- α -Mn, specific heat comparison with α -Pu 8=17512
- α -Mn, ultrasonic attenuation and elastic moduli between 4.2-300°K 8=17501
- Mn IV, vacuum spectrography and energy levels 8=12067
- Mn²⁺, e.p.r. in glasses and Li borate cpds. 8=5536
- Mn²⁺, e.p.r. in K₂SO₄ single cryst. 8=22910
- Mn²⁺ e.p.r. in LiAl(SiO₃)₂ heated crystals 8=22909
- Mn²⁺ e.p.r. in LiAl(SiO₃)₂ natural crystals 8=22908
- Mn²⁺, e.p.r. spectrum in CsCl and NH₄Cl, spin-Hamiltonian parameters 8=5534
- Mn²⁺, e.s.r. in BaCl₂·2H₂O 8=14115
- Mn²⁺ in fluorides, hyperfine coupling constants temp. dependence 8=18429
- Mn²⁺ impurity in ZnWO₄, e.p.r. spectra rel. to conc. and temp. 8=5535
- Mn²⁺ ion in MnCsCl₃·2H₂O, crystalline field parameters from absorpt. spectrum 8=8197
- Mn²⁺ solns., proton relax. and hyperfine coupling 8=8130
- Mn²⁺, spectra in hexa- and tetracoordinated cpds. 8=9551
- Mn²⁺:2(Ca₂Mg₅Si₈O₂₂(OH)₂), e.s.r. 8=18414
- Mn²⁺ in CaO and SrO, hyperfine coupling constant temp. dependence 8=8196
- Mn²⁺:CaZrO₃, paramag. resonance spectrum 8=14118
- Mn²⁺ in MgO, stress induced nuclear quadrupole splitting 8=22928
- Mn²⁺ in MgTiO₃ luminescence at 77°K 8=14324
- Mn²⁺:ZnS, luminescence decay time for tetrahedrally coordinated ions 8=14326
- Mn²⁺, extraction from aqueous soln. using 1-phenyl-3-methyl-4-capryl-pyrazolone-5 8=18750
- in PbCl₂, PbBr₂, TiCl and TiBr, luminescence 8=9622
- with Sn, bonds in organo-Sn cpds., Mössbauer obs. 8=4668
- in V₂O₅ crystals, e.s.r., 77°K 8=14114

Manganese compounds

- alloys with Dy, Ho and Er, X-ray fluorescence analysis 8=2552

Manganese compounds—contd

- dioxides, electrochem. props. and formula 8=18718
- ferrites, Mössbauer spectra in external mag. field 8=18342
- manganate-VI-permanganate redox electrode, mechanism 8=18724
- pyrosomalite, crystal structure 8=17393
- tetramethylammonium Mn(II) chloride, crystal structure 8=1795
- triphenyltin pentacarbonyl manganese, structure 8=8594
- Fe₃Mn₂·TO₃, (T = rare earth), structure and mag. props. rel. to x value (0 to 1) 8=22851
- M Mn₃N, (perovskites, M=metal), first order mag. transitions 8=22742
- Mg-Al alloy, sublimation kinetics in chambers with cryogenic surfaces, obs. 8=16959
- Mg-Mn ferrites, magnetostriction and mag. anisotropy consts. 8=5492
- MgTiO₃:Mn²⁺, luminescence at 77°K 8=14324
- Mn basic carbonate and magnesite containing ZnO, calc. 8=4698
- Mn complexes, inversion-vibr. levels and splitting 8=4121
- Mn complex, μ -hydrido- μ -diphenylphosphido-bis (tetracarbonyl-manganese), structure 8=1799
- Mn ferrites, elec. props. influence of Mn³⁺ clustering 8=13720
- Mn ferrite, intermed. phases in formation 8=17087
- Mn ferrite Maxwell-Wagner dielec. dispersion meas. 8=22647
- Mn ferrite, Mn rich, lattice parameter temp. dependence (293-4.5°K) rel. to comp. 8=17394
- Mn ferrite, spin waves, nuclear and electronic, simultaneous parallel pumping 8=14107
- Mn(II) perchlorates, water solns., u.s. velocity 8=12865
- MnAu₂ antiferromagnet, spontaneous magnetostriction 8=9400
- MnB, transfers of electronic states 8=5461
- MnBr₂·2H₂O, cryst. structure 8=1798
- MnBr₂·4H₂O, antiferro-paramagnetic transitions at low temps. 8=9392
- MnBr₂·4H₂O n.m.r. 8=14148
- MnCl₂·4H₂O e.p.r., thermal detect. obs. 8=14100
- MnCO₃, crystal growth, antiferromagnetism and resonance 8=18372
- MnCO₃, ferromagnetic moment spatial distrib. using polarized neutrons 8=9356
- MnCr₂O₄, mag. resonance freq. 8=22890
- MnCr₂O₄, spinel, mag. study by neutron diffr. 8=9383
- Mn_{2-x}Cr_xSb, antiferromagnetic-ferromagnetic transition 8=9281
- MnCsCl₃·2H₂O, crystalline field parameters for Mn²⁺ ion 8=8197
- MnCu, Mn²⁺ anomalous low-temp. susceptibility 8=13962
- MnF₂, antiferromagnetic, radiationless processed and afterglow kinetics 8=23058
- MnF₂, Co doped, magnon sidebands and local order 8=23001
- MnF₂, i.r. spectra due to lattice vibrations 8=14241
- MnF₂, phonon processes, selection rules 8=13318
- MnF₂, stressed magnon sidebands in absorpt. spectra 8=14240
- MnF₂, tetragonal antiferromagnet, scattering of light by one- and two-magnon excitations 8=18546
- MnF₂:Co²⁺, antiferromagnetic, radiationless processes and afterglow kinetics 8=23058
- MnF₂:Eu²⁺, antiferromagnetic, radiationless processes and afterglow kinetics 8=23058
- MnFe₂O₄:Sn, Mössbauer effect 8=16980
- Mn-Fe spinels, Mn-rich, Mn²⁺ clustering effect on ferromag. resonance linewidth 8=18396
- Mn₂Fe(CO)₁₄, crystal structure 8=8533
- MnFe₂O₄, cation distrib. in sample from aq. soln., by n-diffr. 8=13274
- Mn₂Fe₃O₄, dielec. loss peaks rel. to check of electron diffusion 8=14050
- Mn₃GaC_{1-x}, mag. props. and transitions rel. to non-stoichiometry 8=22819
- Mn(HCOO)₂·2H₂O, heat capacity between 1.4 and 20°K 8=13375
- MnHg, magnetic susceptibility, variation with temperature 8=9281
- (Mn, Me)(S, Se)-type synthetic cpds. and selenide-sulphide inclusions 8=4692
- MnMg-ferrite, square-loop, coercive force temp. depend. 8=14051
- Mn(Mg)SO₄·4H₂O:Mn²⁺, e.p.r. temp. dependence and spin-lattice relax. 8=9432
- MnMoO₄, crystal structure preliminary data 8=17395
- Mn(NH₄)₂(SO₄)₂·6H₂O, heat capacity, near critical point 8=13376
- Mn(NH₄)₂(SO₄)₂·6H₂O, ht. capacity 1°-4°K in mag. fields 8=17520
- Mn-Ni alloys, mag. structures and phase transformations 8=18381
- Mn-Ni system, phase transformations rel. to crystal and mag. structures 8=17088
- MnO, antiferromagnetic, u.s. attenuation 8=22106
- MnO, axially cooled or stressed, mag. anisotropy from torque meas. 8=14072

Manganese compounds—contd

- Mn-O, high-temp. phase diagram 8=16954
 Mn₂O₄ crystals, growth by arc-transfer 8=4806
 MnO₂, electrolytic, pore struct. and surface area, sorption obs. 8=21904
 MnO₂ films, prep. and props. 8=4750
 MnO₂, radiochem. separation by adsorpt. 8=9763
 MnO₄⁻, MO calc. of u.v. spectrum 8=12207
 MnO₄⁻, vibr. spectrum 8=21085
 MnO₂-Zn alkaline cell discharge curves and reactions, obs. 8=18717
 MnP, Curie point and anisotropy energy decrease under hydrostatic pressure 8=2328
 Mn₂P, magnetic structure 8=22736
 Mn-Pd alloys, mag. structures and phase transformations 8=18381
 Mn-Pd alloys, structural and mag. props. 8=4714
 Mn-Pt alloys, mag. structures and phase transformations 8=18381
 Mn-Pt, magn. structures and interactions 8=22883
 Mn₂Pt, first-order mag. transformation, X-ray and susceptibility study 8=18382
 α-MnS, conductivity rel. to optical reflectance and absorption props. 8=18057
 MnS, phosphoresc. 8=2484
 MnSb, existence region and mag. and elec. props. 8=22820
 Mn₂Sb₂O₆, prep., thermal stability, X-ray diffr. and reflection meas. 8=14363
 MnSe, K absorption spectra rel. to chemical bonding 8=14242
 MnSe-MnS system, phase relations 8=17014
 Mn₃Si₂C₂, mag. props. and transitions rel. to non-stoichiometry 8=22819
 MnSO₄ in water-glycol, elec. cond. 8=12921
 MnSO₄·4H₂O e. p. r., thermal detect. obs. 8=14100
 MnSO₄·(NH₄)₂SO₄·6H₂O, n. m. r. obs. 8=2385
 MnS/ZnS mixed crystals, phosphoresc. 8=2484
 MnT'O₃, (T' = Ho, Er, Tm, Yb, Lu), hexagonal, transform. to perovskite form under high press. 8=17089
 MnTe, antiferromag. semiconductor, optical meas. 80-375°K 8=5622
 MnTiO₃, mag. props., theoretical interpretation 8=9399
 MnTiO₃, mag. resonance and susceptibility 8=9398
 MnUO₄, antiferromag. structure 8=18384
 MnYb₂S₄, a spinel, mag. and structural study 8=5436
 Mn-Zn eutectics, shock-decanted, interface examination 8=8170
 MnZn ferrite, mag. props. rel. to final firing cycle cooling conditions and atm. equilib. maintenance, obs. 8=22855
 MnZn ferrite, monodisperse fractions, prepn. 8=9384
 Mn-Zn ferrite, oxidation rate and phase 8=9691
 MnZn ferrites, comp. rel. to stability and losses and prep. 8=22854
 Mn-Zn ferrites, dielectric props., influence of ultrasound 8=9370
 Mn-Zn ferrites, intermed. phases in formation 8=17087
 Mn-Zn high permeability ferrites, dynamical magnetization curve 8=18361

Manometers

- See also Vacuum gauges.
 glass bellows, for ultrahigh vacuum devices, 1-760 torr 8=7964
 manometric liquids, outgassing 8=4503
 mercury, avoiding parallax error when reading 8=10489
 micro-, 15 μ in. methylated spirits. limit 8=7891
 thermal conductivity, error in radiation limitation formula 8=21544

Many-particle systems. See Quantum theory/many-particle systems.**Markov processes.** See Statistical analysis.**Mars.** See Planets.**Masers**

- amplifiers, low-noise, basic characteristic meas. methods 8=396
 amplifying medium, polarization, and of cosmic OH radiation 8=19916
 atoms with angular momenta interaction with photons 8=19921
 cyclotron, resonator excitation near electron cyclotron freq. 8=395
 four-level system, susceptibility at saturation 8=393
 gaseous, optical, props. in weak axial mag. fields 8=6410
 in heterodyne radiation detector 8=6201
 i. r. freqs., generated by isotopic substitution 8=10993
 interstellar hydrogen, maser effect 8=5924
 materials, spin-lattice relaxation meas. 8=10994
 multi-cavity, theoretical transfer characts. 8=15440
 noise and operation quantum theory 8=19438
 optical, quantum theory of 8=15441
 pumping power minimization 8=19918
 push-pull, pumping power and Qm(l, max) 8=392
 reflex multi-cavity solid-state, bandwidth 8=19922
 ruby, C-band, with quarter-wave coupled transmission cavities 8=392
 ruby: Cr³⁺, L-band performance 8=15439
 ruby, laser pumping at 77°K 8=19920
 ruby, operating in 8 mm range 8=6411
 ruby, three-cavity, 21 cm. 8=19923
 solid state, amplifier, phase characteristics, saturation effects 8=394

Masers—contd

- two-resonator molecular generator with opposite beams, operation regimes study 8=19917
 X-ray scatt. expts. shortened by exposure 8=15408
 X-ray scatt. expts, shortening time of exposure 8=15409
 H, appl. of theory of relax. of F = 1 level of ground state 8=12049
 H, dynamic behaviour near equilib. osc., level 8=19919
 H, meas. of spin-exchange cross-section from oscill. characteristics 8=21008
 NH₃, amplifier, characteristics: theory, exp. 8=397
 NH₃ beam oscillator, modulation effects 8=10995
 OH mols. in interstellar space, masering action 8=5927
 optical. See Lasers; Optical pumping.

Mass spectra

- See also Chemical analysis/by mass spectrometry.
 acetaldehyde reaction with atomic H 8=18668
 aliphatic ketons, metastable ions 8=12238
 alkynes, field-ion, of eleven compounds 8=1372
 advances in atomic and molecular physics, book I and II 8=16171-2
 barbitol 8=20912
 barbitol, fragmentation patterns 8=12031
 benzene, by electron impact 8=16452
 benzoates 8=20912
 benzoic acids 8=20912
 1, 3-butadiene, photodissoc., primary processes 8=23155
 n-butane, photoionization 8=4319
 cycloparaffins, chem. ionization 8=1374
 digital recording method, and automatic reduction of data 8=1137
 ethane, photoionization 8=4319
 ethylamine and its deuterated analogs, dissociative mechanism 8=16326
 hydroxybenzoates 8=20912
 ions in flow discharges 8=16429
 ketones, aromatic, ion decomp. rel. to charge and radical sites 8=4308
 metastable ions, abundances variation 8=12237
 nonexistent molec. ions, detect. 8=16440
 organic mass spectrometry, lecture 8=12030
 phenylferrocenes, carbonyl-subst., ortho-effects in decomposition 8=4183
 proaporphine-type alkaloids and derivatives 8=12032
 propane, photoionization 8=4319
 pteridines 8=20912
 pulse shape calc. for quadrupole spectrometer 8=7362
 purines 8=20912
 pyrimidines 8=20912
 pyrones, metastable ions 8=12239
 γ-pyrones, monocyclic, fragmentation obs. 8=21023
 silazanes, expulsion of stable mols, etc. 8=1275
 salicylic acids 8=20912
 tetraethyl compounds, group IV elements 8=18766
 tetramethyl compounds, group IV elements 8=18766
 4-vinylcyclohexene, preferential ass. of pos. charge with butadiene fragment 8=4320
 Al alloys, investigation of secondary ion emission 8=1828
 AlF₃ 8=12997
 Al₂O₃ systems, photochemical effects 8=14441
 Ar, autoionization 8=12430
 Ar binary mixture glow discharge, fast channel ions 8=7665
 Ar clusters in nozzle beams, dimer concs. 8=12379
 Ar, mass 80 peak, identification in spectrum obtained with static operation 8=12056
 B isotope ratios prod. by p-O⁺ reactions 8=20792
 Be isotope ratios prod. by p-O⁺ reactions 8=20792
 Bi₂ and Bi₄ 8=4239
 C₂H₂ isomers, chem. ionization 8=9745
 (CH₃)₂N radical, ionization pot. and heat of form. obs. 8=4245
 CH₂OH radical, ionization pot. and heat of form. obs. 8=4245
 CN halides, photoionization 8=12433
 C₂N₂, photoionization 8=12433
 CO₂, ions and fragments, sequential mass spectrometry 8=21270
 CS₂, ions and fragments, sequential mass spectrometry 8=21270
 Cs⁺, abundance sensitivity improvement on low mass side 8=12029
 Fe alloys, investigation of secondary ion emission 8=1828
 Li isotope ratios prod. by p-O⁺ reactions 8=20792
 N₂, positive column of glow discharge 8=1341
 NH₄ClO₄, thermal decomp. 8=9693
 NO dimers 8=7637
 NaF + AlF₃ in saturated vapour mixture 8=9692
 Pt oxides 8=5716
 Re, isotopic anal. from thermal ionization source 8=7479
 ScF and ScF₂, high temp. 8=7617
 Si₂Te₃ 8=9662
 TiF₃, high-temp. sublimation 8=1623
 YF and YF₃, high temp. 8=7617

Mass spectrometers

- See also Ion optics.
 double-focusing, new version using plane condenser as energy analyser 8=7350
 double, with non-uniform magnetic field 8=7354

Mass spectrometers—contd

- dynamic quadrupole, pulse shape calc. 8=7362
- electrical r. f. field replaces mag. field 8=4042
- fast-response, temp. effects on ion source 8=16177
- fast scanning, ion detector 8=1141
- glass, miniature, charact. spectra 8=16176
- high-resolutions, ions 0.5-3 keV, angle and energy 8=1139
- high resolution, real-time data acquisition and processing 8=20916
- ion-detecting plates for mass spectrograph 8=16179
- ion microprobe mass analyzer development 8=6340
- ion optics 8=20915
- ion-sensitive plates, thin-film, construction 8=16178
- ion storage in 3D rot. symm. quadrupole field 8=19799
- ions trapped in 3D rot. symm. quadrupole field, current integration 8=19800
- LKB 9000 with gas chromatograph, testing and application results 8=7363
- loss of atomic O in relative concentration meas. at 120 km altitude 8=18920
- magnetic deflection type for atmosphere composition above 100 km obs. 8=9901
- magnetic, photorecording for 400 MeV/c spectra 8=11292
- magnetic prism, optical axis and correcting profile determ. 8=12114
- Mattauch-Herzog type with connected β -dependent image defects for able masses 8=4041
- 90°-sector type for gas analysis 8=12033
- 180°, fast scanning, small, description 8=7353
- polyphenols 8=1204
- quadrupole mass filter, rod mounting, amplified 8=7357
- quadrupole and omegatron, main parameters 8=7361
- r. f., 8, 16 and 24 stage instruments 8=7352
- refractive electron systems 8=16175
- semi-automated, rel. to ion identification, and metastable transition meas. 8=1138
- sensitivity improvement design using image converter 8=7356
- tandem double-focusing for n cross-sections 8=7355
- time-of-flight, blanking circuit for mag. electron multiplier 8=20913

accessories

- See also Ion sources.
- inlet leak 8=7358
- ion-sensitive emulsions, characts. 8=1140
- magnetic analysers, spherical aberration calculation 8=10898
- magnetron cold cathode ion source for ultrahigh vacuum residual gas analysis 8=4039
- omegatron efficiency, comparison of oil-free and oil diffusion pumps 8=21538
- photographic plates for ion detection, AgBr grain distrib. 8=7360
- retardation lens to improve abundance sensitivity 8=4040
- semiautomatic admission system of C-free stainless steel 8=7351
- synchronous operation by solid state circuit 8=20914
- tandem, retardation lens for improved abundance sensitivity 8=12029

applications

- See also Chemical analysis/by mass spectrometry.
- adsorption and cryst. nucleation 8=17155
- anomalous glow discharge, positive ions 8=7658
- beam-modulation, ionization fragmentation patterns 8=16439
- butane, ionization probability meas. RPD method 8=21283
- colour picture c. r. t., residual gas analysis 8=15324
- Dempster, collision-induced phenomena 8=4309-10
- electron tube manufacture, gas flow analysis 8=18770
- gas chromatography, interface separators 8=14506
- ion-current apportionment 8=4239
- ion-molecule reactions, pulsed-source meas. 8=10918
- isotope ratio meas. by peak matching 8=4112
- photocathode deposition, vapour detect. 8=21532
- photoionization, microwave plasma light source 8=3355
- silicone resins investigation 8=16740
- time-of-flight, meas. of translational energy of ions 8=7703
- time-of-flight, metastable transitions 8=16438
- weak intermolec. potentials, well-depth determ. 8=7636
- Ba, on W surface, ionization coeff. meas. 1800-2600 K 8=18288
- Cs ions from thermionic converter, analysis 8=15211
- He, leak detector 8=7359
- O^{16} and O^{18} relative abundances in minerals 8=12112
- UO_2 burnup determ. 8=7344

Mass standards. See Standards.**Mass transfer.** See Transport processes.**Master equation.** See Transport processes.**Materials**

- See also individual materials (if separately named) e.g. Ruby.
- bone, comparative deposition of radioisotopes 8=23766
- composites, with buckled microfibrils, effect on elasticity and initial strength 8=22289
- composite mats., high-strength, strengthening effects of fibres and particles 8=5026

Materials—contd

- composite, perfectly disordered, elastic moduli 8=13493
- elastic, thermodynamic props. 8=50
- embedding media for electron microscopy 8=6315
- fabrics in vapour, equilibrium moisture content 8=21765
- GET reactor, core change damaging effects 8=7270
- hardboard, hardness meas. 8=13520
- high temp. and determ. of thermal props. at 3500°C 8=4925
- influence of reliability, lasers 8=10451
- ionic, necessary conds for plastic deformation 8=13511
- metal-forming, cold rolling theories, validity 8=5033
- new, in instrument manufacture, conference Eastbourne, 1965 8=2872
- non-metallic, hardness meas. 8=13520
- refractory compounds, cesiated, work function for electron and ion emission 8=18262
- silicone resin sealant for i. r. vacuum windows 8=16739

Materials testing. See Mechanical strength.**Mathematical methods.** See Calculation; Statistical analysis.**Mathematics**

- angular-momentum operators, generation of matrix 8=10492
- averaging in non-linear mechanics 8=10494
- calculus of physical quantities, theory and application 8=10491
- collisions on air track, matrix description 8=14946
- contact transformations 8=10493
- control problems, optimal, gradient method 8=2883
- distributions, notation proposal 8=6011
- eigenvalues, perturbed, finiteness of 8=10497
- Green's function, bounds for first derivatives 8=10498
- harmonic analysis on Riemannian spaces 8=10496
- Jacobi identity condition for use of partial integration rel. to Gell-Mann current commutators 8=20291
- Lagrangian for non-conservative linear systems 8=10520
- Lie algebra, infinite-dimensional, tensor product of one-particle representations 8=6724
- magnetic resonance in presence of spin transfer, description 8=10986
- multiple scattering processes, singularities 8=10513
- nonlinear problems in physics, interactions of matter and fields 8=14930
- particle mechanics and geometry, constraints 8=10519
- potential flow, numerical solution for flux components 8=19365
- for scientists, book 8=6007
- spinors, generalized in complex n-space 8=6014
- systems analysis using thermodynamic and nonlinear circuit eqns. 8=26
- two variational methods, a comparison 8=19356
- Wiener-Hermite expansion, truncated, dynamic properties 8=12641

Matrices

- angular-momentum operators, generation of matrix 8=10492
- atomic elements involving interelectronic coordinates, ang. coeffs. 8=20925
- Coulomb elements, recursion relations 8=20144
- crystalline fields, calc. using Racah methods 8=13006
- density matrix elements in resonance production 8=11381
- Dirac γ in general relativity 8=11359
- Dirac, representation adaptable to free particle spinor 8=560
- fermion density, N representability 8=10657
- group-similar isometries 8=16
- Hamiltonian for n. m. r. spin coupling, digital computer calc. 8=19909
- inverse overlap matrix, cluster expansion 8=5096
- $(\lambda Px + \mu Py + \nu Pz)$ for asymmetric-top mols. 8=12142
- matrix elements of Racah operator equivalents 8=6598
- reduced density, for atoms and mols. 8=4037
- reduced density matrices, permutational symmetry 8=13
- reduced-width amplitude, exact distrib. 8=2908
- Ritz soln. in three-dimensional elasticity 8=19386
- rotation orthogonality and completeness 8=7062
- SU(p,1), irreducible representations, classification and characters 8=2894
- Szász's inequality, extension 8=88
- third order correction for energy 8=11257

Matrix-isolation methods. See Free radicals; Molecules.**Matteucci effect.** See Magnetoelectric effects; Magneto-mechanical effects.**Maxwell-Boltzmann distribution.** See Kinetic theory; Statistical mechanics.**Maxwell effect.** See Double refraction/flow.**Maxwell equations.** See Electromagnetism.**Measurement**

- See also Instruments; Recording; Standards; Units;
- Acoustical measurement; Dielectric measurement;
- Electrical measurement; Magnetic measurement;
- Mechanical measurement; Radioactivity measurement;
- Thermal measurement; X-ray measurement.
- Some specific quantities are listed separately, e.g. Calorimetry; Density measurement. Where no separate heading exists, measurement methods and instruments are included among the other entries under the heading of the appropriate quantity or subject.
- laser, infrared rangefinder 8=448
- macroscopic, interpretation by statistical mechanics 8=14911

Measurement—contd

- magnetostrictive ferrites, electro-mech. coupling coeff., mech. reson. freq., meas. accuracy 8=9368
- mass on conveyer belt, using scatt. γ -rays 8=19345
- quantum theory 8=544
- quantum theory of consistency problems 8=20138
- quantum theory of, and symbolic logic 8=20140
- randomly varying parameters 8=14913

errors

- See also Statistical analysis.
- entropy, r.m.s., and boundary values, a comparison 8=10474
- instruments, arising in manufacture, storage and use 8=14912
- manometers, mercury, avoiding parallax error when reading 8=10489
- negligibly small, rational quantization 8=4
- oscillator strengths, interpretation of stellar spectra 8=10159
- polarography, statistical errors 8=14508
- precision normalizing of measuring devices 8=14914
- in scattering patterns in the Fresnel region 8=6390
- searches, repeated, exact treatment of statistics 8=6679
- spectrum distortion due to discrete sampling, choice of readings interval 8=2875
- surveying, atm. refraction correction 8=23286
- temperature of solid bodies 8=10783
- trajectory estimation, sequential estimation of obs. error variances 8=19071
- upper atmospheric pressure, adsorption in gauges 8=5838
- Young's modulus, errors due to shear and rotatory inertia in flexural vibrations method 8=17712

Mechanical measurement

- Individual quantities and instruments are listed separately e.g., Length measurement, deformation, elec. meas. on double-rotating mechanism 8=13505
- friction, coeff. meas. methods 8=22302
- polycrystalline ferromagn., torque curve calcs. and theoretical agreement 8=5455

Mechanical properties of substances

- See also Individual properties, e.g. Abrasions; Elastic deformation; Mechanical strength; Plastic deformation; Slip; Wear; etc.

- albite and anorthosite, Hugoniot eqns. of state from shock wave and geophys. data 8=14558
- alloys, relax. due to changes in short-range order produced by stress 8=5009
- advances in applied mechanics, book IX 8=16747
- bearings with rolling contact, electron fractographs of spalls 8=17750
- brass rolled, texture representation by biaxial pole figures 8=17778
- brass, rolling texture development at room temp. and -196°C 8=22328
- brass, 70-30, texture development deformation dependence, pole figure 8=17777
- brittle-to-ductile transition, effect of pressure 8=13502
- bronzitites, diabase, durites and eclogites, Hugoniot eqns. of state from shock wave and geophys. data 8=14558
- cavitation damages in water to various metals 8=5035
- ceramics, basic mechanisms of deform. and fracture, survey 8=17726
- ceramics, laminated, rel. to residual stresses 8=17723
- clay mineral mixtures, high-temp. reactions, and ceramic props. 8=22323
- cylinder, hollow, changes in geometry during compression 8=10563
- dry modulus of rupture and drying shrinkage, response surface anal. 8=17737
- 18Ni(250) maraging steel influence of banding 8=8463
- flaw detection and erosion rate meas. by microwave interferometry 8=5032
- glasses, aluminate for i.r. use 8=22954
- granite and jadeite, Hugoniot eqns. of state from shock wave and geophys. data 8=14558
- granular materials, statics, theory 8=21829
- graphite, foamed, shock compression 8=22316
- graphite, pyrolytic, dynamic behaviour rel. to reactor rad. dose 8=8827
- H36XII steel, austenitic, strain ageing dynamic and static, effect 8=13569
- high-cycle fatigue, rotating principal stress axes in 8=5029
- high pressure effects 8=8796
- high-strain fatigue, conference, Cambridge, England (1966) 8=13490
- kaolinite-muscovite-quartz mixtures, pore-size distrib. and dimensional and wt. changes on refining 8=22323
- ionic structures, energetics of damage, stability and breakdown 8=17735
- linear dissipation model with Q almost freq. independ. 8=23204
- metal bond interfaces, diffusion-induced strains obs. 8=13506
- metals, effect of superimposed u.s. vibration on deformation 8=8795
- metals, fibre reinforced, fracture mechanics 8=8805
- metals, fracture toughness, plane strain, determ. using double cantilever beam specimen 8=17721
- metals, rel. to stacking faults 8=22305
- Mechanical properties of substances—contd
 - metal sheets, bore-expanding test, anal. by incremental theory of plasticity 8=22272
 - oligomers, reticulate crystalline nature from X-ray and thermomechanical tests 8=17192
 - particle sizes and strains, determ. from three different diffraction parameters 8=22257
 - plastics, under hydrostatic press., vol. decrease with time, creep and recovery 8=22280
 - plastic wave propagation in a bar 8=2928
 - plastics under tensile strain using a torsional pendulum obs. 8=8880
 - polyethylene, irradiated, at melting point 8=9201
 - polymers, anelastic effects, books 8=22658
 - polyurethanes, polyester- and polyether-based extensional 8=13623
 - pyrophyllite, high-press. data 8=19342
 - quartz rocks, hydrolytic weakening at high temp. and press. 8=14561
 - reinforced fibre, cyclic extension 8=19403
 - relaxation strength, direct measurement 8=13500
 - rod-drawing anal. of metals, use of work hardening and redundant work 8=22300
 - shell, truncated, conical, thin buckling under uniform static press. 8=19382
 - shock loading of nonlinearly elastic material 8=5008
 - solid-filled pistons, u.s. meas. of expansion rel. to internal press. 8=10580
 - steels, ausforming effect 8=13561
 - steel, austenitic, containing 4% Ti, ageing and zone formation study 8=17071
 - steel, mild, strip, tensile strength rel. to quench rate 8=22365
 - steel, nodular graphite, effect of heat treatment 8=8843
 - steel, notch-brittle fracture, torsional prestraining, influence on 8=13563
 - steel plates, proof stress props. 8=17802
 - steel sheet, effect of rapid heat treating 8=22364
 - theoretical and applied mechanics, conference, Haifa Israel (1967) 8=16750
 - thin gauge specimens, tensile testing, environmental chamber for 8=8792
 - thin walled shells, supported, pressurized, anal. of short endurance fatigue 8=17716
 - torsional vibrations of non-homogeneous spherical and cylindrical shells 8=19513
 - Udimet-500, -520 and -700, heat treatment and composition rel. to stress-rupture and structural stability 8=13599
 - "whisker" straining devices, two, for low temp. 8=22258
 - Zircalloy-2, cold rolled, age hardening and recovery, obs. 8=8872
 - AgCl, high-press. data 8=19342
 - αAgZn , relax. due to changes in short-range order produced by stress 8=5009
 - Al alloy, dynamic indentation, conical projectile, up to 550°C 8=17780
 - Al alloys, high strength with good weldability for cryogenic service 8=17762
 - Al alloy at short time elevated temp. 8=5048
 - Al alloy, short-transverse, effect of ingot quality 8=13531
 - Al rods, polycrystalline, texture changes rel. to mech. forming processes 8=22308
 - Al, rolled, texture representation by biaxial pole figures 8=17778
 - Al-5% Mg with small Ag additions, X-ray investigation of ageing 8=13528
 - Al-Si alloy, interaction between dislocations and precipitates 8=13431
 - Al-Zn-Mg, lattice defects and aging phenomena 8=13536
 - Bi, deformation and simultaneous elec. resistance meas. 8=5052
 - CoAl-Co eutectic 8=17770
 - Co alloys, low-temp. compilation from literature 8=17779
 - Cu, and crystallization, rel. to plastic deform. at low temps. 8=8403
 - Cu, dislocation structure effect 8=13550
 - Cu, dynamic indentation, conical projectile, up to 600°C 8=17780
 - Cu, low-temp. compilation from literature 8=17779
 - Cu rolled, texture representation by biaxial pole figures 8=17778
 - Cu, rolling texture development at room temp. and -196°C 8=22328
 - Cu, texture development deformation dependence, pole figure 8=17777
 - Cu_2O , plane stress effect on 4 exciton line series 8=22973
 - Fe alloys, containing Al_2O_3 , MgO and SiO_2 , dispersion strengthened and hot extruded 8=8842
 - $\alpha\text{-Fe}$, change due to tension, compression and rolling 8=5067
 - $\alpha\text{-Fe}$, solid solutions 8=22350
 - Fe-Cr(0-53%) alloys, aged at 475°C 8=8841
 - Fe-Ni alloys, anisotropy, by C diffusion 8=22814
 - Fe-Ni-Al-Ti alloy, after thermomech. treatment 8=21987
 - Fe-Ni-C alloy, effect of rapid re-austenitizing 8=17807
 - LiNO_3 , shear-wave attenuation 8=2059
 - Mg aluminate spinels, and defect structure 8=22187
 - MgAl_2O_4 , hot-pressed, rel. to microstructure, quadratic multivariable analysis 8=21991

Mechanical properties of substances—contd

- Mg-Mn-Zn ferrite, ageing mechanism 8=9381
- MgO, high-press. data 8=19342
- Mo, rel. to 8×10^{20} n/cm² dose 8=8856
- Mo, structure and low-temp. ductility, deform.-induced changes 8=13589
- NaCl, high-press. data 8=19342
- Nb-Mo steel, heat-treated, high strength, combined effect of Nb and Mo 8=22385
- Ni-base alloy 718, correl. with comp., microstruct. and heat treatment 8=21827
- Ni, electroformed, tensile strength and weldability at room and cryo-temps. 8=17823
- Ni-Co-Mo steels, precipitate reversion 8=17096
- Nb alloys for nuclear reactors 8=5082
- YH₃, stability of pressed pellets, expansion obs. 8=8871
- W, effect of fast n irradi. rel. to microstruct. changes 8=21998
- W-Re alloys, rel. to phases and struct. from H reduction of ReF₆ and WF₆ 8=17100
- Zr, cold rolled, age hardening and recovery, obs. 8=8872
- Zr-2.5wt.%Nb cold rolled, age hardening and recovery rel. to stress relax., obs. 8=8872

Mechanical strength

- See also Elasticity; Hardness.
- alloys, time and temp. depend., non-equilib. state 8=8811
- anisotropic cohesive medium, slope stability under instantaneous failure conditions 8=22284
- bending and buckling of frame system under its own weight 8=6042
- ceramics, meas. 8=22321
- composite high strength material design 8=5025
- composite mats., effects of fibres and particles 8=5023
- composites with buckled microfibrils 8=22289
- cylinders, orthotropically stiffened, elastic instability under torsion loading 8=19393
- dry modulus of rupture and drying shrinkage, response surface anal. 8=17737
- glass-ceramics, strengthening by application of compressive glazes 8=22322
- ice, accreted, effect of impurities 8=17739
- insulators, high-tension, ultrasonic pulse method for non-destructive testing 8=22286
- in long rods, effects in deceleration theory after impact 8=19378
- metals, time and temp. depend., non-equilib. state 8=8811
- polycrystalline metal whiskers rel. to high strength materials 8=21971
- polymer melts 8=16748-9
- rectangular beams, stress anal. of cracks and longit. shear and torsion and flexure 8=22297
- reinforcement of mag. transparent vacuum chamber by glass fibre laminate 8=16722
- rocks under confining press., rupture and elastic wave propag. and absorpt. 8=13515
- rod, inhomogeneous, internal stresses and loading capacity 8=10553
- sapphire, single crysts., alloyed with Ti, increased fracture strength 8=17767
- shallow shell equations; displacement, stress function and mixed solutions 8=48
- sheet, plate and multilayered adhesive-bonded panels, fracture toughness 8=17734
- steels, ausforming effect 8=13561
- steel, austenitic type 304, creep-rupture props, influence of N and other elements 8=17754
- steel, Cd plated, fatigue strength and delayed brittle failure 8=22361
- steels, CrMoV cast, load-time curves in breaking-strength meas. rel. to carbide precip. 8=17804
- steel, correlation of fatigue limit with stress-strain behaviour 8=17783
- steel, effect of lower bainite after tempering 8=17805
- steel, rel. to grain size and precip., hot working effects 8=22356
- steels, rel. to solid soln., precip. and work hardening and grain refining 8=22344
- steels, time-to-rupture tests, theory of occurring notch-brittleness 8=17753
- whitewaves, quartz-free, flexural strength rel. to elasticity mod. 8=17733
- Al alloys, natural ageing effect prior to artificial ageing 8=17764
- Al, strengthening rate in slow loading process 8=22311
- Al, stressed, thermally cycled, temp. after-effect 8=13534
- Al-Mg alloys, effect of various ageing conditions and recovery 8=17765
- Al₂O₃ grain, effect of environments on fracture strength 8=13526
- BeO, rupture props. rel. to SiC and MgO additions 8=22315
- Cd-Zn solder alloys, high-strength, props. 8=5056
- Cu-Fe mixed whiskers, high strength and hardening rate, and growth mechanism 8=17249
- Fe-base alloys, solid-soln. strengthening 8=22341
- Fe-Ni alloy, phase-hardened, condition for thermal stability 8=17066
- Fe-Ni alloy, rapid heating effect during reverse martensitic transform. on high temp. stability 8=17065

Mechanical strength—contd

- Fe-Ni-Ti, rel. to aging during transformation 8=17070
- MgAl₂O₄, hot-pressed, rel. to microstructure, quadratic multivariable analysis 8=21991
- Mn steel, effect of multiple $\gamma = (\epsilon, \epsilon')$ transformations 8=17785
- NaCl crystals under tension along body and face diagonals 8=13590
- Nb-Mo steel, heat treated, combined effect of Nb and Mo 8=22385
- Nb-Mo steel, strengthening effect of precipitates 8=22386
- Nb-W alloys, influence of carbide and boride additions 8=22384
- Nb-W-Ta alloys, influence of carbide and boride additions 8=22384
- Ti, textural, biaxial strengthening 8=5086
- U containing small alloying additions, creep strength 8=8868
- W, low temp. yield strength, effect of non-metallic trace additions 8=17835
- W single crystals, from elec. field required to break whiskers 8=2069
- WC cemented pistons, crushing 8=8870
- compressive**
- apparatus to meas. compression loads in controlled atmos. 8=5019
- crush strength apparatus with photocell detection 8=5022
- cylindrical shells, axisymmetric collapse under pressure 8=10554
- graphite, nuclear grade A, anomalous strength and deform. props. 20-2200°C 8=8829
- plastic, glass-reinforced, at cryotemps. 8=17840
- Portland cement, development, obs. 8=14362
- Ni:Al₂O₃, sintered, dependence on grain size 8=2048
- shear**
- dynamic and constant rate, comparison 8=22287
- graphite, pyrolytic hot-worked, compliance 8=5054
- plastic, glass-reinforced, at cryotemps. 8=17840
- steels, stainless, irradiated, at cryotemps. 8=17763
- Al alloys, irradiated, at cryotemps. 8=17763
- Al-Zn eutectoid alloy, superplasticity rel. to grain boundary shear 8=17766
- Ag, grossly deformed, at high pressures and temps. 8=8833
- Au, grossly deformed, at high pressures and temps. 8=8833
- CCl₄ solid, 187° to 247°K 8=22401
- Cu, grossly deformed, at high pressures and temps. 8=8833
- Fe-Ni base alloy: 9 at %Cu, changes on aging 8=1759
- Ni-Al₂O₃ alloys, rel. to creep 8=22388
- Ni alloy, irradiated, at cryotemps. 8=17763
- Ti alloy, irradiated, at cryotemps. 8=17763
- UO₂, calc. of temp. depend. modulus 8=13610
- tensile**
- alloys, structural, from strain hardening formula 8=22282
- glass fibres 8=5073
- glass fibres, rel. to length 8=1666
- glass, porous, effect of micromechanical stress concentrations 8=13577
- granular materials, effect of moisture 8=8804
- granular materials, equation 8=22288
- granular materials, rel. to moisture 8=22285
- HK-40 alloy, short-time props. to 2000°F 8=17755
- hastelloy X-280, thermomechanical effects 8=17288
- instability mechanism, effect of variation of Poisson's ratio 8=8799
- low C steel, to failure, effect of large torsional prestrains 8=22367
- lucite, and struct. disintegration, obs. 8=17843
- plastic, glass-reinforced, at cryotemps. 8=17840
- polycarbonate films, rel. to chem. struct. 8=22403
- stainless steel, type 310, short-time props. to 2000°F 8=17755
- steel, EI702, dispersional, hardening, investigation 8=8845
- steel, nodular graphite, heat treatment effect, 800-850°C 8=8843
- steel, stainless with high N content, at cryotemps. 8=17784
- steels, stainless, irradiated, at cryotemps. 8=17763
- steel, structural, fracture toughness, temp. and strain rate effects 8=5070
- styrene-polypropylene graft-copolymers, obs. 8=23139
- Teflon, and struct. disintegration, obs. 8=17843
- vinyl plastic, and struct. disintegration, obs. 8=17843
- Ag, effect of purity 8=8722
- Ag-Mg solid soln., Ag-rich, short-range order dependence 8=21819
- Ag-Mg solid solns., Ag-rich, long-range order dependence 8=21820
- Al alloys, irradiated, at cryotemps. 8=17763
- Al alloy, short-transverse, effect of ingot quality 8=13531
- Al alloys, wrought-, and ductility rel. to ingot structure 8=5046
- Al rods, polycrystalline, rel. to texture changes on different mech. forming 8=22308
- Al-Ag alloys, rel. to GP zones and stacking faults 8=8821
- α -Al₂O₃ crystal whiskers, testing 8=17248
- Al₂O₃ whiskers, rel. to surface area 8=5050
- B, "amorphous", contradiction of Weibull relationship 8=2050

Mechanical strength—contd**tensile—contd**

- CuZn(β -brass), hydrostatic extrusion effects obs. 8=5059
 Fe, crystalline, increase by step-wise low temp. creep 8=2054
 Fe-C alloys, effect of noble metal additions on toughness 8=17795-6
 Ni alloy, irradiated, at cryotemps. 8=17763
 Ni base alloy with improved oxidation resistance to 2200°F 8=22387
 Ni, crystalline, increase by step-wise low temp. creep 8=2054
 Ni, electroformed, at room and cryo-temps. 8=17823
 Pu/1 wt.% Ga alloy, rel. to plastic flow props. from -60 to 77°C 8=13604
 Ti alloy, irradiated, at cryotemps. 8=17763
 TiNi, hydrostatic extrusion effects obs. 8=5059

Mechanics

See also Dynamics.

- adiabatic pulsations and convective instability of gaseous masses 8=5857
 applied, convention, Cambridge, England (1966) 8=13490
 calculus, theory and application 8=10491
 centrifugal force, explanation via two problems 8=35
 classical, contact transformations 8=10493
 classical Poisson brackets, Lie algebra realization 8=2913
 Fock variables, rel. to group invariant formulation of Kepler problem 8=14943
 foundations of, book 8=10518
 kinetic foci of system for isoenergetic trajectories 8=6049
 laboratory demonstrations using electrical readout 8=10472
 linear discrete medium, equations of motion 8=30
 linear discrete medium, geometry 8=29
 man in boat, dynamical paradox 8=36
 motion of a triple rod in a Newtonian field 8=14947
 moving body appears cool? 8=219
 network models for systems dynamical behaviour study, theory 8=6038
 Newton's law, discussion 8=2917
 non-linear, averaging method 8=10494
 non-linear systems, phase plane 8=6046
 particle, holonomic constraints formulated in Riemannian space 8=10519
 quantum mechanics helps understand classical mechanics 8=545
 restricted three-body problem, props. of soln. of first-order variational eqns. 8=10094
 rotational movement of carriage meas. method 8=6001
 solid continua, equilibrium equations 8=6041
 stability of equilibrium, elastic body 8=6040
 three bodies problem, new periodic soln. 8=19097
 three body problem in space, regularization of singularities 8=10533
 3-body problem, 3 dimensional, dispersion of fragments 8=19102
 Van der Pol system, forced solutions 8=14945
 variational methods for model of continuous media in special relativity 8=2911

Mechanics of gases. See Aerodynamics.

Mechanics of liquids. See Hydrodynamics.

Medical science

See also Physiology; Radiation protection.

- antagonism in pharmaceuticals, study by structural analogy between vit. and antiv. K 8=23765
 appl. of e.s.r. meas. of animal tissues 8=14891
 biochemistry, soft X-ray microanalysis appls. 8=18795
 bone crystal surfaces, Mossbauer effect appl. to ion uptake mechanism study 8=14902
 dental apatites, carbonate effects on morphology 8=1720
 electroretinography, use of c.w. laser 8=11233
 γ ray beam prod. equipment 8=7118
 liquid crystals, applications 8=1527
 Au colloids, use in radiotherapy 8=14893
 Fe₂O₃ aerosol disperser, with long-time output stability 8=21738

Meissner effect. See Superconductivity.

Melting

See also Zone melting and refining.

- alkali halides, calc., Born treatment 8=12966
 alkali halides, slopes of curves 8=12969
 alkali halides under high pressure 8=1612
 computer calc. to locate transition 8=16923
 crystalline solids, electron-beam-induced shock wave 8=8757
 energy pulse interaction with solid, heat and mass transfer 8=12968
 glassy materials, unsteady film movement on melting surface, calc. using Lagrange's variables 8=16922
 mixtures, thermodynamics 8=4643
 polyethylene- α -chloronaphthalene, under press. 8=4642
 polymer-diluent mixtures under press. 8=4642
 polypropylene, under action of laser pulses 8=17710
 powders, preparation of sample for high pressure experiments 8=8172
 rubber, stark, partially melted 8=4771
 significant struct. theory 8=12967
 silicate-water system, h.p. hydrothermal curves 8=21752
 Stefan problem, appl. of approx. solns. to heat transfer in phase-changes 8=16913

Melting—contd

- volume jump rel. to solid volume at melting point 8=16924
 Ar discharge, anode fall determ. 8=16427
 Ar, melting curve to 30 kb, obs. 8=1610
 Ar, in theory of liquids 8=12967
 Au-Cd binary system, point defect segregation at melting rel. to comp. 8=17624
 CH₄, melting curve to 30 kb, obs. 8=1610
 CO₂, melting curve to 30 kb, obs. 8=1610
 Ca-Bi eutectic melt, displacement of inactive marks during diffusion 8=17565
 CsNiCl₂, effect on electronic spectra 8=9519
 Cs₃NiCl₂, effect on electronic spectra 8=9519
 CuSO₄-H₂O system, phase boundaries to 40 kilobars 8=4640
 Fe alloy drops, voids formation 8=8257
 Fe alloys at 1600°C under vacuum, rate of evaporation of Mn, Cu and Sn 8=12993
 Fe, alloys, levitation apparatus for phase equilibria 8=1669
 Fe₂SiO₄, hydrothermally synthesized, at press. up to 40 kb 8=1615
 He³, below 0.04°K, calc. of melting curve 8=15158
 He-3, 4 density prediction 8=10813
 In, Bi, u.s. attenuation in pre-melting region 8=21751
 K, invariance of photocurrent and work function 8=13939
 KAlSi₃O₈, enthalpy of fusion 8=21753
 KCl-NaCl, phase equilibrium diagram 8=8164
 Li₂SO₄-H₂O, incongruent, and polymorphism 8=12970
 MgO-Al₂O₃ system, phases in splat-quenched melts. 8=1677
 NaAlSi₃O₈, enthalpy of fusion 8=21753
 N₂, melting curve to 30 kb, obs. 8=1610
 NH₃, melting curve to 30 kb, obs. 8=1610
 Rb, invariance of photocurrent and work function 8=13939
 Si, zone melting, temperature field, theory 8=8427
 Sn₂Te₃, curve by thermal analysis between 5-40 kilobars 8=1614
 TiO₂, enamel, opacification kinetics, X-ray diffr. meas. 8=17221
 Zn, anal. for thermometric fixed point 8=4645
 ZrO₂-TiO₂ liquidus curve, specular reflection method in solar furnace 8=1608

Melting point

- actinide cpds., group IVA-VIA, with NaCl structures, and lattice constants 8=4867
 alkali halide crystals, calc. from thermal expansion 8=16970
 films, thin 8=1611
 metals, relation with coeff. of self-diffusion 8=12837
 polycapromide, rel. to hardness, density and spherulite size of polymer, and nature and conc. of filters 8=21914
 polyethylene, effect of crystallinity and mol. wt. 8=12971
 poly(vinylidene fluoride)-poly(vinyl fluoride) solid solns. rel. to comp. 8=8173
 preparation of sample for high pressure experiments 8=8173
 tin, particle size dependence 8=16925
 vinylidene fluoride-vinyl fluoride copolymers solid solns. rel. to comp. 8=8173
 Al₂O₃, environment effects 8=1613
 CF₃P(O)F₂ 8=21177
 Na₂AlF₆ (cryolite) 8=21754
 PuO₂, rel. to UO₂-PuO₂ solid-liquid phase diagram 8=8169
 UO₂, rel. to UO₂-PuO₂ solid-liquid phase diagram 8=8169

Membranes

- biological, device to meas. V-I characts due to ion flux through them 8=5988
 cation exchange, H₂O vapour diffusion 8=8040
 cellulose, ZnO₂⁺ diffusion and absorpt. 8=21645
 circular, on nonlinear elastic foundation, periodic oscs. 8=3016
 with epiclycloidal boundary shapes, vib. problem, appl. of eigenvalues 8=19510
 imperfect semipermeable, convective diffusion in stagnation flow, rel. to reverse osmosis 8=12841
 induced thermal stresses rel. to increase in fundamental freq. of rotating annuli 8=19503
 lipid, black, interface free energy 8=8038
 liquid, ion transport and elect. props. 8=4560
 polyethylene, permeation of liqs. rel. to temperature 8=1508
 rubber, ht. of transport of inert gases 8=1487
 shell, inelastic, with rotation symmetry, creeping at finite deformations 8=10571
 spinning, with two nodal diameters, soln. for nonlinear flexural, asymmetric waves 8=19498
 tensile instability at large deformations 8=13503
 thick, circular, symmetrical vib., effects of flexural stiffness, shear deform. and rot. inertia 8=19500
 toroidal shell, perturbation theory 8=10543
 transpiration of propane and ethane 8=12662
 Al circular foils, hydrostatic deform. 8=5044
 NaCl uptake by cellophane, rel. to ion exchange props., obs. 8=23084

Memory devices. See Calculating apparatus; Magnetic devices; Superconducting materials and devices.

Mendelevium

No entries

Mercury (planet). See Planets.

Mercury

- adsorbed layer nucleation onto W field emitter tips 8=1702

Mercury—contd

adsorption at Hg/methanol interphase 8=18721
 afterglow of vapour pulsed discharge 8=21238
 anisotropy of relaxation in 6^3P_2 level 8=7609
 atoms, electron scatt. angular distribution and spin polarization, influence of plural scatt. 8=16225
 atom, 6^3P_1 state depopulation, effect of N₂ and CO 8=7405
 atoms, $6s6d$ levels, collision cross-sections with inert gases 8=1201
 atom, $6s6d$ levels, lifetime, magnetic meas. 8=4095
 atoms, 7^3S_1 - 6^3P_1 - 6^3S_0 cascade correlation, and 6^3P_1 coherence time 8=4078
 atom, Stark effect obs. 8=20966
 atoms, temperature dependence of 1849 Å absorption in saturated vapour 8=1166
 atomic vapour, optical pumping, polarization effect 8=4088
 discharge, ion-acoustic waves, propagation and damping 8=4313
 freezing, invariance of photocurrent and work function 8=13939
 induction pump, vel. distrib. 8=16727
 isotopes, Holtsmark collisions 8=7468
 jet, turbulent, velocity profile in axial mag. field, obs. 8=7991
 liquid, cavitation damage data for venturi and vibratory systems 8=16767
 liquid, eqn. of state and elec. resistivity, rel. to temp. and press. 8=12900
 liquid, large amp. sound propag. 8=12859
 liquid, optical const. and dielec. const. $\epsilon_1 + i\epsilon_2$ 8=12877
 liquid, optical props. and Drude theory 8=12881
 liquid, press. depend. of resistivity, thermopower and phonon dispersion 8=16879
 molecular 4850 Å and 3350 Å bands, role of Hg 6^3P_0 atoms 8=21033
 optical const. of clean surface as function of temp. 8=4582
 plasma, ion acoustic waves phase vel. and ambipolar diffusion coeff. 10^{-3} torr 8=21377
 plasma, longit. waves second harmonic generation, 10^{-3} torr 8=21389
 solid, elec. resistance, low temperature variation meas. 8=5181
 superconducting, surface nucleation and bulk superheating fields, $1.2^\circ\text{K}-\text{T}_c$ 8=17968
 resonance line, pressure broadening by He 8=7403
 turbulent flow in square duct, temp. distribution in wall, obs. 8=1545
 turbulent flow in tube in longitudinal mag. field 8=10933
 vapour positive column zeroth order distrib. changes 8=7667
 3P_1 state, lifetime meas. by Hanle effect 8=1181
 $^3\text{P}_2$ metastable state, intensity heats in absorpt. due to coherent e excitation 8=4094
 6^3P_0 state rel. to molecular 4850 Å and 3350 Å band 8=21033
 6^3P_2 level, destruction of alignment 8=7469
 C_6H_4 impurity, absorption spectrum of Hg λ 2537 Å line 8=16287
 Hg⁺ cathode lasers, hollow cathode, wide bore, fabrication 8=3294
 Hg₂ excimers, kinetics of band emissions 8=12203
 Hg₂, trapped in inert gas matrices, spectra 8=8227
 Hg¹⁹⁸, 2537 Å line, H₂ and D₂ effects compared 8=7470
 Hg¹⁹⁸ 4356 Å line shape, intensity correl. obs. 8=20075
 Hg¹⁹⁸ double reson., Zeeman sublevel transitions shifts, obs. 8=21001
 Hg¹⁹⁹ and Hg²⁰¹, comparison of nuclear magnetic relaxation 8=7450
 Hg¹⁹⁹ and Hg²⁰¹, 6^1P_1 level hyperfine structures 8=7404
 Hg¹⁹⁹, hyperfine structure of the 2967 Å (6^3P_0 - 6^3D_1) and of 6^3D_1 level 8=16205
 Hg²⁰¹, hyperfine levels, population transfers 8=7467
 Hg($^3\text{P}_1$) atom reaction with gaseous paraffins 8=9688
 Hg*($^3\text{P}_1$) atoms, quenching by H₂, phase-space theory 8=14436
 Hg-In fluoresc. spectrum, In line intensities 8=4080

Mercury compounds
 EDTA chelates of Hg²⁺, comp. study by ultrasonic vel. meas. 8=23170
 Hg alloys, liq. with In, Tl and Na, abs. thermoelec. power 8=12913
 Hg-halogen-chalcogenides, single cryst. growth, by modified vapour phase method 8=21955
 Hg-Bi alloy, Knight shift 8=14142
 HgBr₂, spectrum in vacuum u.v. 8=12204
 Hg(CN)₂, 0.80 tetrahydrofuran, morphology and atomic structure 8=1794
 Hg-Cd alloy, Knight shift 8=14142
 Hg_{1-x}Cd_xTe, i.r. laser and fast detector 8=11103
 HgCr₂S₄, mag. structure and metamagnetism 8=18340
 HgI₂ crystal, polarisation vs field strength under light excitation 8=5373
 HgI₂, Raman spectra in molten state 8=21691
 HgI₂, trap levels rel. to photoelectret state 8=5372
 HgIBr, Raman spectra in molten state 8=21691
 HgICl, Raman spectra in molten state 8=21691
 Hg-In alloy, Knight shift 8=14142

Mercury compounds—contd

Hg-In alloys, liq., atomic distrib. and electronic transport 8=12799
 Hg-In alloys, liq., optical const. rel. to free-electron theory 8=16846
 Hg-In, interf. functions, pair distrib. electron transport 8=8005
 Hg-In liq. alloy system, mag. susceptibility up to 60% In conc. 8=12925
 Hg-Mo system, desorption, mobility, work function 8=21903
 Hg(OH)F, crystal structure 8=17376
 Hg-Pb alloy, Knight shift 8=14142
 HgS, linear electrooptic effect at 0.63 and 3.39 microns 8=14225
 α -HgS, second harmonic generation of laser radiation 8=5606
 HgS single crysts., growth by vapour phase method 8=21955
 HgS-HgSe solid solns., optical props. 8=5607
 Hg₃S₂Cl₂ single crysts., growth, by vapour phase method 8=21955
 Hg₃S₂Cl₂, structure confirmation and refinement 8=13264
 HgSO₄·1H₂O, proton magnetic resonance 8=9457
 HgSe, oscillatory magnetoresistance, inversion asymmetry splitting 8=2100
 n-HgSe, quantum oscills. of transport coeffs. 8=5261
 Hg-Sn system, superconducting transition temp. comp. dependence 8=17960
 HgTe, Hall coeff. and magnetoresistance at 4.2 and 77°K rel. to carrier model 8=2200
 HgTe, metal vacancies formation energies rel. to Te-Te covalent bonding 8=17608
 (HgTe)₃-In₂Te₃ alloys, single-crystals, optical energy gap 8=5608
 HgTe-ZnTe, Hall coefficient and conductivity at low temp. 8=13816
 Hg-Tl alloys, liq., atomic distrib. and electronic transport 8=12799
 Hg-W system, desorption, mobility, work function 8=21903
 HgX₂-TiX (X = I, Br, Cl) systems, cpds. formed 8=17085

Mesic atoms. See Atoms, mesic.
Mesic molecules. See Molecules, mesic.
Mesomorphic state. See Liquid crystals.
Meson field theory. See Field theory, quantum/meson field.
Mesons
 See also Atoms, mesic; Cosmic rays/mesons; Hyperons; Molecules, mesic; Pions.
 bound state, relativistic, symmetries of Bethe-Salpeter eqn. 8=3608
 charge-current commutators between states and vacuum 8=599
 data on properties, updating 8=15671
 decay mode, B + pseudoscalar meson, classification of particles 8=6766
 electric and mag. polarizabilities, in quark model 8=6823
 e^+ search for in $\pi^+ + d \rightarrow p_{sp} + p + \text{neutrals}$, 2.7 GeV/c 8=11488
 η -N coupling constant in $\pi^- + p \rightarrow n + \eta$, $\gamma + p \rightarrow p + \eta$ 8=20490
 hadron dynamics, self-interacting charged meson model 8=20398
 K in p-p and π -p high energy collisions, charge ratios 8=11524
 K₁ phenomenological summary 8=11545
 K-B coupling constants from K-N scatt. sum rules 8=20483
 \bar{K} , $\Delta\pi$ and $N\bar{K}$ composite model of Σ 8=11633
 K-N coupling constants from 2 sum rules for meson-N scatt. 8=20469
 $\bar{K} \Omega$ as bound state of ΞK 8=6978
 K_{π^4} vector form factor calc. 8=6906
 $K_S^0 \rightarrow \pi^+ \pi^-$ decay, CP violation 8=777
 K_S^0 , C, CP, CPT theory consequences 8=777
 low-energy theorems not involving Schwinger terms from divergence of vector currents 8=20495
 model, Singer's vector-dominance for η decay 8=20488
 meson-meson coupling in Fubini sum rule from K^+ decay 8=20474
 meson-N coupling constant calc. in non-linear spin theory 8=20288
 MMM rel. to BBM coupling constant from πN scatt. superconvergence relations 8=3640
 ninth pseudoscalar in broken SU_c(6) symmetry 8=15756
 nonets, mass-splitting calc. via quark-antiquark scatt. 8=677
 π^- beam, 370 MeV, in thin absorbers, energy loss distrib. 8=13471
 photon-meson coupling in Fubini sum rule from K^+ decay 8=20474
 polarization, η in $\pi^- + p \rightarrow \eta + n$, Regge-pole model 8=11519
 pseudoscalar, bootstraplike conditions from superconvergence 8=11497
 pseudoscalar, strong decay of $\frac{3}{2}^-$ baryon resonances 8=11635
 pseudoscalar in $Y_0^* \text{ BP}$ coupling from $K + N \rightarrow \Sigma + \pi$ 8=20580
 quantum theory scalar field with nonstatic source 8=11362
 quark-antiquark model, soln. of Bethe-Salpeter eqn. 8=15687

Mesons—contd

σ model for PCAC, improved 8=11489
strangeness zero, prod. in K⁺p final state at
6 GeV/c 8=3661
sources, strong coupling group model 8=20492
symmetries based on nonchiral SU(3) \otimes SU(3) 8=3609
vector interacting with spin- $\frac{1}{2}$ fermion field, derivation of
Regge trajectory 8=6770

absorption

π by nuclei, radiative, rel. to μ capture 8=20775

capture

See also Nuclear reactions due to mesons.

π^- in O and light nuclei 8=7221

decay

$A_1 \rightarrow \rho\pi$, current algebra and dispersion relation
analysis 8=811

$A_1 \rightarrow \rho + \pi$, current algebra calc. 8=11565

$A_1 \rightarrow \rho\pi$, decay constant anomaly, d-wave coupling
constant 8=6907

$A_1 \rightarrow \rho\pi$ S/D wave ratio determ. 8=11566

$A_2 \rightarrow KK$ obs. 8=6860

e^+, ω and ϕ lepton-pair decay rates relations 8=11562

$\eta \rightarrow \pi^0 e^+ e^-, \pi^0 \mu^+ \mu^-$ branching ratio calc. rel. to
C-conservation 8=20487

η rel. to form factor calc. for K_{rad} decay 8=3657

$\eta \rightarrow \gamma\gamma$, for η -pole contrib. to $K^+ \rightarrow \pi^+ \gamma\gamma$ 8=791

$\eta \rightarrow$ neutrals, $\pi^+ \pi^- \pi^0$ branching ratio, rel. to
 $K^+ p \rightarrow \Lambda \eta$ 8=6888

$\eta \rightarrow \pi^0 \gamma\gamma$ search in reaction $\pi^+ p \rightarrow \pi^+ p + 4\gamma$ 8=3670

$\eta \rightarrow e^+ + e^- + \gamma$, Dalitz agreement 8=3672

$\eta \rightarrow e^+ + e^- + \pi^0$, branching ratio 8=3672

$\eta \rightarrow \pi^0 e^+ e^-,$ C-conservation, vector-meson model, decay
width calc. 8=3674

$\eta^0 \rightarrow \pi^0 e^+ e^-$, unsuccessful search 8=804

$\eta \rightarrow 3\pi$, current algebra approach review 8=15808

$\eta_{3\pi}$, dynamical model, suppression of $3\pi^0$ mode 8=3673

$\eta \rightarrow 3\pi, \pi$ spectra 8=6885

$\Gamma(\eta \rightarrow 3\pi^0)/\Gamma(\eta \rightarrow 2\gamma)$ using 4π spark chamber obs. 8=11552

$\eta \rightarrow \pi^0 \pi^0 \pi^0, \pi^+ \pi^- \pi^0$, ratio obs., $T = 1$ sufficient 8=20485

$\eta \rightarrow \pi^+ \pi^- \pi^0 \gamma$ and $\eta \rightarrow \pi^0 \gamma\gamma$ branching ratio calc. 8=11551

$\eta \rightarrow \pi^+ \pi^- \pi^0 \gamma$ in terms of $\eta \rightarrow \pi^0 \gamma\gamma$ using CA and
PCAC 8=20488

$\eta \rightarrow \pi^+ + \pi^- + \pi^0 + \gamma$, search, rel. to $\eta \rightarrow \pi^+ + \pi^- + \pi^0$
mode 8=805

f^0 in $\pi p \rightarrow \pi^+ \pi^- n$ 8=6851

f^0 , in $\pi p \rightarrow \rho N^*$, ang. decay correl. with
 $\pi p \rightarrow f^0 N^*$ 8=11636

f^* , modes and spin and parity 8=809

405 multiplets, SU(6)_v invariant amplitudes 8=807

K, rel. to axial vector current consisting of pseudo-
scalar octet. 8=6743

K, and CP violation and $\Delta S = \Delta Q$ 8=11546

K_{e^+} and K_{e^-} rates 8=6881

K_{e^+} rate in calc. $\pi^+ \pi^-$ S-wave scatt. length 8=20466

K_{e^+} rate, form factor determination and η decay 8=3657

K_{e^+} vector form factor calc. by current algebra 8=6906

K, leptonic 8=797

K_{l3} , form factors, $f_+(t)$ "leakage" matrix element
contribution 8=15796

K_{l3} form factors q^2 var. 8=788

K_{l3} , form factors 8=6878

K_{l3} , $f_+(q^2)$ momentum dependence 8=15795

$K \rightarrow \mu + \nu, \pi \rightarrow \mu + \nu$, evaluation of a_K/a_π using SU(3)
algebra and PCAC 8=15798

$K \rightarrow \mu\nu$, superconductivity model with SU(3) \times SU(3)
symm. 8=11501

K, model of T violation, non-leptonic 8=6820

K, nonleptonic 8=15799

K, nonleptonic, $\Delta T = \frac{1}{2}$ amplitudes correlation 8=15800

$K \rightarrow 2\pi$, CP violation in current-current models 8=20467

$K \rightarrow \pi\pi$, phenomenological analysis in terms of isospin
amplitudes, CP violation 8=3652

$K \rightarrow 2\pi$ and $K \rightarrow \pi^+ \pi^0$, related probabilities 8=784

$K \rightarrow 2\pi\gamma$, matrix elements from radiative $\pi\pi$ scatt. using
unitarity 8=15793

$K \rightarrow \pi\pi e\nu$ 8=20422

$K \rightarrow 2\pi, 3\pi$ relation between modes 8=15752

$K_{\pi3}$, CP noninvariance and $|\Delta T| = \frac{1}{2}, \frac{3}{2}$ amplitudes
limits 8=6886

$K \rightarrow 3\pi$ rel. to $\eta \rightarrow 3\pi$ 8=15808

$K \rightarrow 3\pi, \pi$ spectra 8=6885

$K \rightarrow 3\pi$, with TCP or time reversal, $\Delta I = \frac{1}{2}$
rule 8=20471

$K \rightarrow 3\pi$, p-wave interaction calc. using Fadeev
formalism 8=11547

$K_A \rightarrow K^* \pi, F_K/F_\pi$ calc. using Weinberg sumrule 8=11568

$K_A \rightarrow K^* \pi, 95$ MeV, resonance width calc. from spectral
function sum rule 8=20261

$K_A \rightarrow \rho K, 97$ MeV, resonance width calc. from spectral
function sum rule 8=20261

$K \rightarrow K^* + \pi$ in $K^+ + p \rightarrow N + \pi + K^*$, diffraction
dissociation 8=15815

K^0 , CP-invariance breaking 8=11541

K^0 , CP violation and $\pi^+ \pi^-$ interference 8=778

K^0 , vector form factor, energy depend. 8=787

$K^0 \rightarrow \gamma + \gamma$, CP violation, interference effect theorem 8=3653

K^0 , total reflection TCP, or time reflection T 8=790

K^0 , leptonic, test of validity of $\Delta S = \Delta Q$ rule 8=792

$K_{\mu3}^0$ T-odd correl. and π e.m. form factor 8=6883

Mesons—contd

decay—contd

K^0 , nonorthogonality of states and CP nonconservation 8=783

$K^0, \bar{K}^0 \rightarrow \pi^+ \pi^-$ pair decay into neutral particles and CPT 8=15814

$K^0 \rightarrow \pi^+ + \pi^- + \gamma$ CP violation, interference effect
theorem 8=3653

$K^0 \rightarrow \pi^+ \pi^-$, long-lived decays, status of CP
invariance 8=779

$K^0 \rightarrow 2\pi$, determ. of $\text{Re}(A_2/A_0)$ 8=11544

$K^0 \rightarrow 2\pi$, TCP-invariance test 8=15792

K^0 , CP-violation and interference phenom. 8=6880

$K_L^0 \rightarrow \pi^0 e^+ e^-$ and CP nonconservation 8=20475

$K_L^0 \rightarrow \pi^+ + \mu^+ + \bar{\nu}(\nu), \Delta S = -\Delta Q$ amplitude determ. 8=11543

$K_L^0 \rightarrow \pi^+ + e^+ + \bar{\nu}(\nu), \Delta S = -\Delta Q$ amplitude determ. 8=11543

$K_L^0 \rightarrow \pi^+ + e^+ + \nu$, charge asymmetry 8=782

$K_L^0 \rightarrow \pi^+ \pi^-$, CP violation 8=777

$K_L \rightarrow 2\pi$, isotopic spin selection rules and CP
violation 8=780

$K_L \rightarrow 2\pi^+ + \gamma$, CP conservation effects 8=20472

$K^0 \rightarrow \pi^+ \pi^- \pi^0$, charge asymmetry 8=6884

K_S^0 , CP-violation and interference phenom. 8=6880

$K_S^0 \rightarrow \pi + \pi$, e.m. correction to meas. $\text{Re}(A_2/A_0)$ 8=785

$K_S \rightarrow 2\pi$ mode, as test of octet dominance in weak, e.m.
and strong interactions 8=3516

$K^0 \rightarrow 2\pi, SU_3$ -breaking effect and hyperon decay 8=3729

$K_L^0 \rightarrow \pi^+ \pi^- \pi^0$, CP conserving, Hamiltonian, estimate of
 $K_L^0 \rightarrow 3\pi/K_S^0 \rightarrow 3\pi$ 8=20470

K^0 CP noninvariance rel. to non-classical theory of mag.
monopoles 8=781

$K_2 \rightarrow 2\gamma, \pi^+ + \pi^- + \gamma$, branching ratio 8=3659

$K^0 \rightarrow \pi^+ + \mu^+ + \bar{\nu}, \mu^+ + e^+$, branching ratio 8=11569

$K_2^0 \rightarrow \pi^+ + l^+ + \nu$ and CP violation 8=15791

$K_2 \rightarrow \pi^+ \pi^-$, CP violation, energy depend. on branching
ratio 8=11569

$K_2 \rightarrow 3\pi$, CP conserving, Hamiltonian, estimate of
 $K_L^0 \rightarrow 3\pi/K_S^0 \rightarrow 3\pi$ 8=20470

$K^0 \rightarrow \pi^+ + \pi^- + \gamma$, rate calc. 8=3659

K_{e^+} decay rates and ratios obs. 8=20473

K_{e^+} , e⁺ momentum spectrum, branching ratio
obs. 8=20477

$K^+ \rightarrow e^+ + \pi + \nu$, pure vector coupling and form factor
structure 8=11542

$K^+ \rightarrow l^+ + \nu + \gamma, \pi^+ + l^+ + \nu + \gamma$, Fubini sum rule between
form factors, meson-meson couplings and photon-meson
couplings 8=20474

$K^+ \rightarrow \mu^+ \nu_e e^+$ as hadron weak decay time-reversal
invariance test 8=789

$K^+ \rightarrow \mu^+ + \nu + e^+ + e^-$, test for T invariance in μ
polarization meas. 8=20476

$K^+ \rightarrow \mu^+ \nu + e^+ + e^-$ as a test of time-reversal
invariance 8=20476

$K^+ \rightarrow \pi^+ \gamma\gamma$, use of η -pole approx. 8=791

$K^+ \rightarrow \pi^+ l^+$ obs., $K_{\text{e}^+}/K^+, K_{\mu3}/K^+$ ratios 8=20473

$K^+ \rightarrow \pi^+ \pi^0$, rel. to e.m. π^0 mixing 8=791

$K^+ \rightarrow \pi^+ \pi^0 \gamma, (\pi^+, \gamma)$ ang. distrib. obs. 8=3655

$K^{*0} \rightarrow \pi^+ \phi 1^-$, using weak Hamiltonian 8=20470

$K_{\text{e}^+}^+$, Dalitz plot, radiative corrections 8=3656

$K^*(1420)$, agreement with 2^+ , SU(3) nonet 8=813

K^* , radiative, e.m. structure 8=6911

$K^* \rightarrow K\pi, F_K/F_\pi$ calc. using Weinberg sum rule 8=11568

leptonic, SU(3) theory yielding unobserved modes 8=11490

μ on mass values maximization of ratio Γ/Q 8=3601

$\omega \rightarrow$ baryons, coupling constants calc. 8=3677

$\omega \rightarrow e^+ e^-$, following $\pi^+ + p \rightarrow \omega + n$ 8=808

ω_0 , leptonic, vector boson model 8=20497

Ω , lifetime estimation, from production by K^-
mesons 8=20498

189 multiplets, SU(6)_v, invariant amplitudes 8=807

in 189-plet of SU(6), mixing coeffs. of unitary
multiplets 8=20411

phenomenological analyses, lectures 8=20413

PCAC hypothesis, pole dominance version 8=3696

$\phi \rightarrow e^+ e^-$, following $\pi^+ + p \rightarrow \phi + n$ 8=808

$\phi \rightarrow KK$, calc. using asymptotic symmetry 8=3677

$\phi \rightarrow KK$ obs. 8=6860

pseudoscalar, SU(3) theory of 3-body leptonic mode 8=3610

radiative decay widths, calc. in static quark model 8=736

rates, calc. via relativistic quark model 8=735

rates in O(4, 2) and introduction of SU(3) 8=20414

$\rho, \rho N^*$, distrib. using statistical tensors 8=20505

$\rho \rightarrow e^+ e^-$, following $\pi^+ + p \rightarrow \rho^+ + n$ 8=808

$\rho \rightarrow \pi + \pi$ current algebra calc. 8=11565

$\rho \rightarrow 2\pi$, calc. of rate via relativistic quark model 8=735

$\rho \rightarrow 2\pi$, current algebra and dispersion relation
analysis 8=811

$\rho \rightarrow 4\pi$ rel. to equality of ρ complete and perturbative
propagators 8=15811

ρ_0 , leptonic, vector boson model 8=20497

ρ^0 in reaction $\pi p \rightarrow \pi^+ \pi^- p$ at 2.77 GeV/c 8=20503

$\rho^0 \rightarrow e^+ e^-$ and $\pi^+ \pi^-$, branching ratio, 600-900 MeV/c² 8=6908

ρ^0 in $\pi^+ + p \rightarrow \pi^+ + \pi^+ + n, 1.38-3.00$ GeV/c compared to
OPE model 8=3685

ρ^0 in $\pi p \rightarrow \pi^+ \pi^- n$ 8=6851

tensor and axial vector, using quark model 8=11557

$35\pi^{*1}$ in three octets 8=733

vector, electromagnetic, calc. using asymptotic
symmetry 8=3677

vector meson, orthodox quark model 8=6822

vector, radiative relations 8=6901

weak, problem of divergences in gauge-field algebra 8=737

Mesons—contd

decay—contd
X⁰ → 2γ, width rel. to mixing in η, X⁰ 8=20499
decay observations
η lifetime, Primakoff effect obs. 8=806
η⁰, neutral modes/charged modes branching ratio 8=15807
η⁰ partial decay rates 8=15807
η → π⁰γγ, 2γ, 3π⁰, detected in iron-plate spark chamber 8=3671
η → π⁰π⁰γ, Dalitz plot analysis 8=20486
(η⁰ → π⁰π⁰γ)/(η⁰ → π⁰π⁰π⁰) branching ratio 8=15807
η⁰ → 3π⁰, π⁰γγ, and γγ, branching ratios 8=15806
(η⁰ → 3π⁰)/(η⁰ → π⁰π⁰π⁰) partial decay rate 8=15807
K_L⁰ → π + e + ν, energy distrib. 8=15797
K_L⁰ → πμν, form factors and possible energy depend. 8=6879
K_L⁰ → π⁰π⁰π⁰ at 10.7 GeV/c, vector field effect rel. to CP invariance 8=6882
K_L⁰ → π⁰π⁰π⁰, anal. of π⁰ spectrum 8=6879
K_S⁰, muonic, charge asymmetry 8=793
K_S⁰, relative probabilities of various branches 8=3654
K⁺ → e⁺ + ν, branching ratio meas. 8=786
K⁺ → π⁺ + γ + γ, branching ratio meas. and limit on K⁺ → π⁺ + π⁰ 8=15794
K⁺ → π⁰π⁰μ⁺ν, μ⁺μ⁺π⁰ and e⁺e⁺π⁰, rate in detuerium bubble chamber 8=3658
detection measurement
pions, r. f. separated beam at the AGS 8=3491
K_L photoproduction method 8=11548
K_L 320 litres cylindrical detector, 70% efficiency 8=3669
r. f. separated beam at the AGS 8=3491
effects
N-N scatt. pot. meson coupling constants and masses 8=11583
ρ in π-π scatt. as sum rule, as input 8=3646
interactions
See also Nuclear reactions due to mesons.
A₂ exchange in meson-B scatt. 8=740
bootstrap calc. in qq channel 8=3607
lectures 8=20422
K, phenomenological fields and Lagrangians description 8=797
K*(890) exchange in meson-B scatt. 8=740
K**(1411) exchange in meson-B scatt. 8=740
K d → Σ⁰π⁰p, 815-, 915-, 1015- and 1115 MeV/c incident K⁺ momenta 8=20574
K⁺ d total cross section at 1.2 GeV/c, I = 0 peak rel. to K → K*(890) channel coupling 8=15804
K⁺ + He⁴ → Λ⁰ + π⁰ + p + d obs., impulse model fit, via intermediate Σ + nucleus + π⁰ state 8=20417
K+K → 2π extension of domain of validity of dispersion relations 8=6895
K⁺n 2, 3 GeV/c charge exchange and ρ⁺ Regge trajectory 8=3665
KN, current algebra calc. of Λ/Σ ratio 8=15858
KN, I = 1, S-wave reaction, quark model of Λ to Σ ratio 8=15860
KN → K*(890)N, 3 GeV/c, absorpt. model, π and vector meson exchange 8=6889
KN, multichannel phase-shift analysis from 0-555 MeV/c 8=3663
KN, multichannel phase-shift analysis from 0-550 MeV/c 8=3663
K̄ + N → Σ + π, use of dispersion relations and Regge trajectories to calc. Y₀* BP coupling 8=20580
KN, NAK and NΣK coupling constants determinations 8=3664
Kp, one π exchange 8=6847
K⁺p, 4.1, 5.5 GeV/c, K*(890), (1400) prod. 8=20509
K⁺p, at 4.6 and 5.0 BeV/c, evidence for A₁⁰ production 8=11567
K⁺p, 10 GeV/c, Ξ⁻, Ω⁻, antibaryon prod. 8=15803
K⁺p, high energy and ρ⁺ Regge trajectory 8=3665
K⁺p → K⁰Ξ⁰, mass difference effect in Wali-Warnock model, violation of SU(3) 8=3692
K⁺p → K⁰π⁰n, 6 GeV/c ang. correl. in final states 8=798
K⁺ + p → Λ + f* at 5.5 GeV/c, f* study 8=810
K⁺p → Λη, 1.2-1.7 BeV/c 8=6888
K⁺ + p → Λ + π⁺ + π⁰, 1.5 GeV/c beam, peripheral production 8=870
K⁺ + p → Λ⁰ + π⁺ + π⁰, Λ⁰ lifetime obs. 8=20572
K⁺ + p → N + π + K*, peripheral model, diffraction dissociation 8=15815
K⁺p → π⁰Σ⁺, Regge-pole model based on K*, K** exchange 8=15777
K⁺p → π⁰Σ⁺ rel. to analytic structure of Regge-cut amplitude 8=20319
K⁺p → Σ⁺π⁰, analysis in K⁺p c.m. energy range 1735 to 1845 MeV 8=20574
K⁺p → π⁰π⁰Σ⁰, 6 GeV/c, ang. correls. rel. to spin parity of exchanged particles 8=798
K⁺ + p → p → K⁺ + π⁺ + π⁰ + p at 5.5 BeV/c 8=15816
K⁺p → Σ⁰π⁰, mass difference effect in Wali-Warnock model, violation of SU(3) 8=3692
K⁺p → strangeness zero meson, 6 GeV/c 8=3661
K⁺p, total cross-sections, new structures interpreted as I = 1 res. 8=796
K⁺p → Y₁*(1385) + π (780-1220) MeV/c 8=800
K⁺p → Y₁* + π⁰, spin and parity of Y₁* 8=6987
K⁺-p, charge exchange, double Regge-pole analysis 8=799

Mesons—contd

interactions—contd
K⁺p at 4.97 GeV/c, K*(1660) evidence 8=6912
K⁺p, 5 GeV/c, baryon resonance production 8=869
K⁺p, (Kππ)⁺ resonant state below 1.4 GeV, at 4.97 GeV/c 8=6890
K⁺p → KπN, 735, 785 MeV/c, production possibility 8=3686
K⁺ + p → K⁰ + Δ⁺(1238), Regge-pole fit 8=3662
K⁺p, 9 GeV/c, Ξ⁻ production 8=865
K⁺p at 9 BeV/c, evidence K*(1250) production 8=814
Λ(or Σ⁰) in K⁺ + p →, 7.3 GeV/c 8=858
meson-baryon interactions in quark model, prod. cross-sections 8=20405
meson-baryon systems, systematics of forces 8=6918
ω + π → π + π amplitude and Regge trajectory bootstrap 8=11563
ω in φ-ω mixing and equality of Schwinger terms 8=11561
φ-ω mixing and equality of Schwinger terms 8=11561
p exchange in meson-B scatt. 8=740
p + K → p + K*, Mandelstam branch cuts rel. to scatt. and prod. amplitudes 8=11594
p + π → p + A₂, Mandelstam branch cuts rel. to scatt. and prod. amplitudes 8=11594
PN → P'N, VN Regge pole model 8=20318
pseudoscalar-baryon coupling from current divergences 8=6983
pseudoscalar, vector prod., Regge-pole model, parity effects 8=6902
pseudoscalar-vector, superconvergence relations, symms., mass spectra 8=11493
pseudoscalons, pair, quark model, spin-2 meson coupling 8=3612
ρ exchange in π-N scatt. 8=3637
ρ photoprod. cross-section calc. 8=20508
SU(2) × SU(2), chiral, method of phenomenological Lagrangians 8=6744
vector exchange as origin of nuclear repulsive core 8=20642
vector meson sum rules from current commutators 8=3525
vector-vector, superconvergence relations, symms., mass spectra 8=11493
magnetic moment
K* calc. from radiative decay 8=6911
mass
equal spacing rule from meson symmetries based on SU(3) ⊗ SU(3) 8=3609
field theory, vector, interacting with massless fermions 8=3678
field theoretical model prediction 8=3421
K_S⁰ obs. in CP violating decay 8=11569
K₁K₂⁰ mass spectrum, phenomenological interpretation 8=6913
K₁⁰-K₂⁰ difference 8=15801
K₁⁰-K₂⁰ mass difference from asymptotic chiral symmetry and superconvergence sum rules 8=795
K⁺-K⁰, e.m. mass difference 8=15802
K⁺-K⁰ difference, field theoretic model 8=20415
K⁺-K⁰ mass difference, wrong sign from Weinberg sum rules 8=3660
m₁²-m₂², divergences in gauge-field algebra 8=737
K*, from Reggeized bootstrap 8=6910
mass splitting in bootstrap model for even-parity resonances 8=20491
massless in asymptotic symm. approach to derivation of Weinberg sum rules 8=20260
meson-baryon scatt., response of decuplet to octet perturbations 8=3691
nonets, J^P = 1⁻ and 2⁺ from eigenvalue problem solved with SU₃ harmonics 8=11555
in non-linear spin theory 8=20288
Ω, estimation, from production by K⁻ mesons 8=20498
pseudoscalar mass difference, vector meson exchange model 8=20415
pseudoscalar octet, splitting and coupling constants 8=3565
pseudoscalar-vector meson interactions, spectra 8=11493
π and η, agreement value of κI 8=20416
quark model rel. to qq scatt. 8=11478
R agreement with quark model 8=3676
resonance, strangeness-carrying, from SU(3) × SU(3) spectral function sum rules 8=20493
ρ, e. m. effects 8=20251
ρ, in low-energy πN scatt. channels 8=765
ρ⁺, from reaction π⁰p → π⁰π⁰p at 2.77 GeV/c 8=20503
ρ⁺-ρ⁰ mass difference, e. m., superconvergence dispersion relation approach 8=11485
s wave bound states in quark model for Bethe-Salpeter eqn. 8=11476
scatt. crossing-symm. model, equality assumption of resonances 8=3613
σ, in low-energy πN scatt. channels 8=765
SU(2) × SU(2), chiral, method of phenomenological Lagrangians 8=6744
2-body bound problem of Dirac particles 8=11491
unified formula in quark model 8=738
U(3) invariant 4-fermion interaction 8=657
Weinberg's relation m₁ = √2 m_ρ derived in the framework of current algebra 8=20506
production
A₁ production in πp scatt., 2π exchange model 8=3650

Mesons—contd

production—contd

- A_1° in Kp, at 4.6 and 5.0 BeV/c 8=11567
 A_2 in $p + \pi \rightarrow p + A_2$, Mandelstam branch cuts rel. to amplitudes 8=11594
 A_2 in $\pi^- p \rightarrow \pi^- \pi^+ \pi^- p$, 8 GeV/c 8=20447
 A_2 production in πp scatt., 2 π exchange model 8=3650
 cosmic rays as high-energy source 8=7004
 $\Delta^-(1238)$ in $\pi^- p$, 5.5 GeV/c, multiple π prod. 8=3633
 $\Delta^+(1238)$ in $\pi^- p$, 5.5 GeV/c, multiple π prod. 8=3633
 e^+e^- collision, spin current 8=739
 electromagnetic processes and collisions 8=727
 η , ang. distrib. in $\pi^- + p \rightarrow \eta + n$, $T_s = 593$ -704 MeV 8=6853
 η in $\gamma + p \rightarrow p + \eta$, N pole and vector meson resonance below c.m. energy 1700 MeV 8=20490
 η in K $^-p \rightarrow \Lambda \eta$, 1.2-1.7 BeV/c 8=6888
 η in N* decay modes from $\pi^- + p \rightarrow \eta + N$ 8=11637
 η in $\pi^- + p \rightarrow \eta + n$, 561-1300 MeV, resonances and branching ratios 8=11520
 η , in $\pi^- + p \rightarrow n$, 670-805 MeV/c obs. 8=20489
 η in $\pi^- + p \rightarrow n + \eta$, N pole and resonances below c.m. energy 1700 MeV 8=20490
 η in $\pi^- p \rightarrow \eta n$, partial wave analysis in terms of Lorentz group 8=6856
 η in $\pi^- + p \rightarrow n + \eta$, phenomenological model 8=15758
 η in $\pi^- p \rightarrow \eta^0 n \rightarrow \pi^+ \pi^- \pi^0$ 8=15772
 η in $\pi^- p \rightarrow \pi^+ \pi^- \eta$, 3.2, 4.2 GeV/c obs. 8=20448
 η in $\pi^- + p \rightarrow \eta + \Delta^+(1238)$, cross-section and Δ^+ spin density 8=6855
 η^0 from $\gamma + p$, recoil p polarization 8=838
 η^0 in $\pi^- p \rightarrow \eta^0 n$, and ρ' Regge trajectory 8=3665
 f^0 in $\pi^- p \rightarrow \pi^+ \pi^- n$, 8 GeV/c 8=6851
 f^* in K ^-p interactions at 5.5 GeV/c 8=810
 g^0 in $\pi^- p \rightarrow \pi^+ \pi^- n$, 8 GeV/c 8=6851
 η photoproduction on p, 553-850 MeV analysis in second reson. region 8=6843
 $\gamma + p \rightarrow \eta + p$ amplitude, unitarity and S-matrix analysis 8=3569
 $\gamma p \rightarrow \Lambda^+ K^+$, Regge-pole calc. of cross-sections 8=3621
 $\gamma p \rightarrow \Sigma^+ K^+$, Regge-pole calc. of cross-sections 8=3621
 $\gamma p \rightarrow \rho p$, 2 π exchange model 8=3650
 K, photoform. on nucleons, and quark model 8=6842
 K in $\gamma + N \rightarrow \Sigma + K$, consistency conditions for non-Born amplitudes 8=20344
 K in $\pi^- p \rightarrow K^+ K^- n$, cross-section calc. 8=20442
 K factories, linear accelerators 8=15661
 K from π^- , 1.5-4.2 BeV/c 8=6861
 K in pp collisions, high energy π, k, p prod. cross-section depend on longitudinal and transverse momentum components 8=20478
 K in pp \rightarrow YKN, OBE model with approx. 8=20522
 K in $p + p \rightarrow$ hyperon + K + N, 6 BeV/c obs., N $^+$ prod. and decay to hyperon + K 8=20480
 KK in pp \rightarrow KK π , K $^*(891)$ prod., KK $J^P = 2^+$ resonance at 1280 MeV 8=6940
 K $\pi\pi$ mass enhancement between 1.1 to 1.4 BeV 8=815
 K $^-$ in $\pi^- p \rightarrow \Sigma^- K^+$, 1170 MeV/c, cross-section obs., C independence confirmed 8=20449
 K 0 in K $^+ + p \rightarrow K^0 + \Delta^+(1238)$ 8=3662
 K 0 in $\pi^- + p \rightarrow \Lambda + K^0$, $\Sigma^0 + K^0$, phenomenological model 8=15758
 K 0 K 0 , pp, 2.7 GeV/c, 2 meson final states 8=843
 K $^0\Lambda$ backward peak in associated prod. at 5, 7 and 12 GeV/c 8=6973
 ΛK^+ enhancement at 1.7 GeV, $\pi^- p \rightarrow \Lambda K^+ \pi^-$ at 6 GeV/c 8=3630
 K $^+$ photoprod., 3.4 and 5.0 GeV 8=6887
 K $^+$ photoprod. rel. to Y * , 4.0-6.1 BeV 8=15859
 K $^+$ in p-p collisions 2.5-3.0 GeV 8=20479
 K $^+$ in $\pi^- p \rightarrow K^+ \Sigma^+$, 3.23 GeV/c, ang. dist., Σ polarization 8=6852
 K $^+$ in $\pi^+ + p \rightarrow \Sigma^+ + K^+$, $\pi^- + p \rightarrow \Sigma^- + K^+$, phenomenological model 8=15758
 K $^+$ in $\pi^+ + p \rightarrow \Sigma^+ + K^+$, quark model for backward process 8=11480
 K $^+ K^-$, pp, 2.7 GeV/c, 2 meson final states 8=843
 K $^+ \Sigma^-$ in $\pi^- p$ reaction, Regge cut 8=3631
 K b in $\pi^+ p \rightarrow K^b \Sigma^b (\Lambda^b)$, Regge-pole model based on K * , K ** exchange 8=15777
 K $^+$, η , π^+ in cosmic ray collisions 8=20617
 K $^+$ photonuclear reactions, 16-18 GeV e acceleration, with metal targets 8=20768
 K * (890), (1500) prod. in Kp, 4.1, 5.5 GeV/c 8=20509
 K * in pseudoscalar-pseudoscalar scatt. 8=11559
 K * in KN \rightarrow K $^*(890)$ N, 3 GeV/c, absorpt. model, π and vector meson exchange 8=6889
 K * in $p + K \rightarrow p + K^*$, Mandelstam branch cuts rel. to amplitudes 8=11594
 K $^*(1250)$, in K $^+$ p interactions at 9 BeV/c 8=814
 Λ/Σ^0 photoproduction cross sections, ratio 8=15859
 NN \rightarrow KK, predictions 8=825
 NN \rightarrow MM, rel. to baryon exchange model of MN scatt. 8=825
 ω in $\pi^- p \rightarrow \omega n$, ϕn , 2.1 BeV/c, cross-section calc. 8=20442
 ω in $\pi N \rightarrow \omega \Delta$, Reggeization procedure 8=11412
 ω in $\pi^- p$, 5.5 GeV/c, multiple π prod. 8=3633
 ω in $\pi^- p \rightarrow \pi^+ \pi^- \pi^- \pi^0$, 3 GeV/c 8=20446
 ω^0 photoprod., OPE, diffraction contrib., polarization prediction 8=20502

Mesons—contd

production—contd

- Ω , by 6 GeV/c K $^-$ mesons 8=20498
 ϕ , high-energy diffraction photoproduction, expt. limit 8=20500
 $\phi \rightarrow$ KK obs. in πp interactions 1.5-4.2 BeV/c 8=6860
 ϕ in $\pi^- p \rightarrow \omega n$, ϕn , 2.1 BeV/c, cross-section calc. 8=20442
 ϕ in pseudoscalar-pseudoscalar scatt. 8=11559
 photo-, diffractionlike mechanism 8=20507
 photoproduction on nuclei, threshold 8=1034
 photoproduction, Regge-pole hypothesis 8=3611
 $\pi^+ p \rightarrow K^+ \Sigma^+$, mass difference effect in Wali-Warnock model, violation of SU(3) 8=3692
 from \bar{p} annihilation on N \rightarrow two mesons and higher symmetries 8=15839
 p-p collisions, synchrotron-radiation model 8=11492
 p-p interaction, 20 GeV, nuclear emulsion 8=831
 resonance in He $^4(\pi, M)$ He 4 , magnitude and phase of meson scatt. amp. 8=890
 resonances photoproduction on nuclei with zero spin and isospin 8=11558
 ρ in $A_1 \rightarrow \rho \pi$, decay constant anomaly, d-wave coupling constant 8=6907
 ρ in $A_1 \rightarrow \rho \pi$ S/D wave ratio determ. 8=11566
 ρ in e^+e^- colliding beams 8=812
 ρ in $\gamma \pi \rightarrow \rho \pi$, sum rules rel. to e.m. widths of ω , A_1 , A_2 8=11566
 ρ in NN \rightarrow NN ρ absorptive peripheral model 8=6920
 ρ , parametrization for resonant scatt. applic. to NN, $\pi\omega$ 8=3683
 ρ in πN collisions and rel. to conserved current 8=15813
 ρ in $\pi N \rightarrow \rho \pi N$, mass distrib. from Regge-pole exchange model 8=20440
 ρ in π -N scatt., semiclassical theory 8=20452
 ρ , in $\pi p \rightarrow \rho N^*$, ang. decay correl. with $\pi p \rightarrow \rho^0 N^*$ 8=11636
 ρ in pseudoscalar-pseudoscalar scatt. 8=11559
 ρ^- , in reaction $\pi^- p \rightarrow \pi^+ \pi^- p$ at 2.77 GeV/c 8=20503
 ρ^0 in $\gamma + p \rightarrow p + \rho^0$, 3.2-4.9 GeV 8=16057
 ρ^0 photoprod. on N, cross-section calc. 8=20508
 ρ^0 photoproduction in nuclei, cross-section 8=20767
 ρ^0 in $\gamma + A \rightarrow \pi^+ + \pi^-$ on $9 \leq A \leq 207$ nuclei, 4.35 and 6.02 GeV 8=7164
 ρ^0 in Al(γ, ρ^0)Al, 3.2-4.9 GeV 8=16057
 ρ^0 in C(γ, ρ^0)C, 3.2-4.9 GeV 8=16057
 ρ^0 , OPE calc., normalization for S-wave $\pi^+ \pi^-$ S-wave scatt. cross section 8=20439
 ρ^0 in $\pi^- p \rightarrow \pi^+ \pi^- \rho^0$, 3.2, 4.2 GeV/c obs. 8=20448
 ρ^0 prod. in $\pi^- p \rightarrow \pi^+ \pi^- \pi^+ p$, 8 GeV/c 8=20447
 ρ^0 in $\pi^+ p \rightarrow \rho^0 N^{*+} \rightarrow \pi^+ \pi^+ p$, peripheral models 8=11515
 vector, conspiracies and forward prod. 8=6898
 vector, double-Regge-pole model, appl. of SU(6) $_v$ symm. 8=3680
 vector in $\pi B \rightarrow V \Delta$, Regge-pole couplings 8=6903
 vector in pseudoscalar interactions, Regge pole model, parity effects 8=6902
 vector, Regge pole residues, kinematical singularities 8=11415
 vector and tensor by π exchange Reggeization 8=11499
 X 0 from π p cross sections obs. 8=20501
- resonances**
 A_1 , $m_A = \sqrt{2} m_\rho$ derived from current algebra 8=20605
 A_1 , e.m. width determ. from sum rules for $\gamma \pi \rightarrow \rho \pi$, $\rho \pi \rightarrow \rho \pi$ 8=11566
 A_1 in $\pi N \rightarrow \rho \pi N$, mass distrib. from Regge-pole exchange model 8=20440
 A_1 in $\pi^- p$ at 3.2, 4.2 GeV/c obs. 8=20448
 A_1 production in πp scatt., 2 π exchange model 8=3650
 $A_1 \rightarrow \rho + \pi$ current algebra calc. 8=11565
 $A_1 \rightarrow \rho \pi$, current algebra and dispersion relation analysis 8=811
 $A_1 \rightarrow \rho \pi$, current algebra and pole-dominance appls. 8=3684
 $A_1 \rightarrow \rho \pi$, decay constant anomaly, d-wave coupling constant 8=6907
 A_1° production in Kp interactions at 4.6 and 5.0 BeV/c 8=11567
 Re(A_2/A_1) in K $^0 \rightarrow \pi + \pi$ decay, e.m. correction to meas. 8=785
 A_2 , e.m. width determ. from sum rules for $\gamma \pi \rightarrow \rho \pi$, $\rho \pi \rightarrow \rho \pi$ 8=11566
 A_2 exchange in meson-B scatt. 8=740
 A_2 in $\pi^- p$ at 3.2, 4.2 GeV/c obs. 8=20448
 A_2 , from $\pi^- p$ at 3.25 GeV/c 8=6909
 A_2 exchange in $\pi^- p \rightarrow \eta n$, Regge-pole analysis 8=6856
 A_2 in $\pi^- p \rightarrow \pi^+ \pi^- \pi^+ p$, 8 GeV/c 8=20447
 A_2 - π scatt., superconvergence sum rules 8=20421
 A_2 -p vacuum trajectory branch cuts conspiracy in NN and NN charge exchange scatt. 8=11584
 A_2 prod. in $p + \pi \rightarrow p + A_2$, Mandelstam branch cuts rel. to amplitudes 8=11594
 A_2 production in πp scatt., 2 π exchange model 8=3650
 A_2 in $\pi^- p \rightarrow \pi^+ \pi^- \pi^-$, 3 GeV/c 8=20446
 A_2^+ prod. in pp annihilations, spin and parity 8=15810
 B in $\pi^- p$ at 3.2, 4.2 GeV/c 8=20448
 bootstraplike conditions from superconvergence 8=11497
 bootstrap model for even-parity 8=20491
 conference, Varenna, Italy July 1964 8=6745
 contribution to N form factors 8=820

Mesons—contd

resonances—contd

D, mass under asymptotic $SU(3) \otimes SU(3)$ 8=3682
 $\Delta^-(1238)$ in π^-p , 5.5 GeV/c, multiple π prod. 8=3633
 $\Delta^{*+}(1238)$ in π^+p , 5.5 GeV/c, multiple π prod. 8=3633
E, mass under asymptotic $SU(3) \otimes SU(3)$ 8=3682
 $e^+, \omega \rightarrow \phi$ lepton-pair decay rates relations 8=11562
 η , octet-singlet mixing, evidence from $X^0 \rightarrow 2\gamma$ 8=20499
 η^0 in $\pi^+p \rightarrow \eta^+n$, and ρ^+ Regge trajectory 8=3665
exchange model vector, rel. to mass difference of pseudoscalar mesons 8=20415
exchanges, Regge trajectories 8=11560
 I_0 , coupling in $\pi-\pi$ interaction 8=3612
 I^0 , in $\pi p \rightarrow \rho N^*$, ang. decay correl. with $\pi p \rightarrow \rho N^*$ 8=11636
 f^0 in $\pi^+p \rightarrow \pi^+\pi^+n$ 8=11522
 f^0 prod. in $\pi^+p \rightarrow \pi^+\pi^+n$, 8 GeV/c 8=6851
 f^* , decay modes and spin and parity 8=809
fireball hypothesis, obs. statistics 8=20622
 f^* production in K^+p interactions at 5.5 GeV/c 8=810
 g^+ prod. in $\pi^+p \rightarrow \pi^+\pi^+n$, 8 GeV/c 8=6851
 $I = 0$ enhancement of $\pi^+p \rightarrow \pi^+\pi^+n$, 3.1 36^{-1} GeV/c obs. 8=15773
 $J^1 = 1^+$ octodecimet, in quark picture 8=11556
 $J^2 = 2^+$ 8=20448
 $K\pi\pi$ mass enhancement between 1.1 to 1.4 BeV 8=815
 $K\pi\pi$ resonant state in K^+p reactions at 4.97 GeV/c 8=6912
 $K_1^0 K_1^0$ system for π^+p interaction at 5, 7 and 12 GeV/c 8=794
 $K^*(1400)$ and $K^*(1320)$ 8=11571
 $K^*(1400)$ and $K^*(1320)$ 8=11572
 $K^*(890)$ -K S-state channel coupling, K^+d structure in $I = 0$ 8=15804
 $K^*(1420)$, decay rates and 2^+ , $SU(3)$ nonet 8=813
 K^* and K_1 decays and F_K/F_π calc. using Weinberg sum rule 8=11568
 K^* radiative decay process 8=6911
 $K^*(1230)$, $K^*(1280)$, $K^*(1320)$, $K^*(1420)$ from $K^*(892)\pi$ decay mode 8=6890
 $K^*(890)$ exchange in meson-B scatt. 8=740
 K^* prod. in $KN \rightarrow K^*(890)N$, 3 GeV/c, absorpt. model, π and vector meson exchange 8=6889
 $K^*(890)$, (1400) prod. in K^+p , 4.1, 5.5 GeV/c 8=20509
 K^* in $K^+p \rightarrow N + \pi + K^*$, peripheral model, diffraction dissociation 8=15815
 $K^*(1660)$ in K^+p reactions at 4.97 GeV/c 8=6912
 $K^*(1250)$ production, in K^+p interactions at 9 BeV/c 8=814
 K^* prod. in π^+p , 1.5-4.2 BeV/c 8=6860
 K^* prod. in pseudoscalar-pseudoscalar scatt., bootstrap calc. with Schrodinger eqn. 8=11559
 K^* prod. in $p + K \rightarrow p + K^*$, Mandelstam branch cuts rel. to amplitudes 8=11594
 $K^*(891)$ prod. in $\bar{p}p \rightarrow KK\pi$ 8=6940
 K^* , Reggeized bootstrap 8=6910
 K^* , K^{**} exchange for Regge-pole model for π^+p , K^-p reactions 8=15777
 K^* and K^{**} Regge parameters determ. and $SU(3)$ symmetry breaking 8=20510
 $K^{**}(1411)$ exchange in meson-B scatt. 8=740
 K^{**} prod. and generalized Deck effect 8=15816
 K^{**} scatt. superconvergence sum rules 8=20421
lepton- p vector β -decay coupling, radiative correction and ρ e. m. mass splitting 8=20374
mass ratio of strangeness-carrying, from $SU(3) \times SU(3)$ spectral function sum rules 8=20493
meson resonance-N scatt., from π -He⁴ resonance prod. interaction 8=3736
 $N^*(2825) \rightarrow \rho + N^*(1236)$, cascade decay, theory 8=3734
 $N_{1/2}^*(1688)$, association with A_k^+ enhancement in $\pi^+p \rightarrow A_k^+\pi^-$ 8=3630
 $\omega \rightarrow$ baryons, coupling constants calc. 8=3677
 ω , e. m. width determ. from sum rules for $\gamma\pi \rightarrow \rho\pi$, $\rho\pi \rightarrow \rho\pi$ 8=11566
 ω -exchange, dips in contribution to $\pi N \rightarrow \rho N$ 8=11514
 ω in N-N scatt., Mandelstam representation 8=824
 ω in $\pi N \rightarrow w\Delta$, Reggeization procedure 8=11412
 ω in $\pi^+p \rightarrow \omega n$, ϕn , 2.1 BeV/c, cross-section calc. 8=20442
 $\omega + \pi \rightarrow \pi + \pi$ amplitude and Regge trajectory bootstrap 8=11563
 ω as pole of N isoscalar magnetic form factor 8=3694
 ω , in ϕ - ω mixing and equality of Schwinger terms 8=11561
 ω - ϕ mixing, models rel. to spectral-function sum rules 8=11562
 ω production, decrease in ρ exchange by Regge pole model 8=11560
 ω in Y-N scatt. 8=20573
 ω_8 , leptonic decay, vector boson model 8=20497
 ω (1238) in π^+p , 5.5 GeV/c, multiple π prod. 8=3633
 ω^+ , photoprod., polarization prediction 8=20502
 $\omega^+ \rightarrow \pi^+\gamma$ from π^-X e interactions, 9 GeV/c 8=6904
 ω^+ prod. in $\pi^+p \rightarrow p^+\pi^-\pi^0$, 3 GeV/c 8=20446
 Ω^- , production by 6GeV/c K^- mesons 8=20498
 $\phi \rightarrow KK$ decay, calc. using asymptotic symmetry 8=3677
 ϕ - ω mixing and equality of Schwinger terms 8=11561
 ϕ in $\pi^+p \rightarrow \omega n$, ϕn , 2.1 BeV/c, cross-section calc. 8=20442
 ϕ as pole of N isoscalar magnetic form factor 8=3694
 ϕ prod. in pseudoscalar-pseudoscalar scatt., bootstrap calc. with Schrodinger eqn. 8=11559
photoproduction on nuclei with zero spin and isospin 8=11558

Mesons—contd

resonances—contd

prod. in He⁴(π , M)He⁴, magnitude and phase of meson. scatt. amp. 8=890
 $\pi^+\gamma$, mass 1300 MeV, in $\pi^- + p$ reaction 8=3675
pseudoscalar scatt. crossing-symm. model 8=3613
quark model prediction 8=20404
R structure from $\pi^+ + p \rightarrow p + R^-$ 8=3676
Regge poles and NK superconvergence sum rules 8=3681
Regge trajectories passing through ρ and A_2 as models for boson resonances R, S, T, U 8=11411
 ρ bootstrap for $\pi\pi$ scatt., formulations 8=20462
 ρ rel. to chiral-equivalent Lagrangians 8=20262
 ρ coupling constant determ. using π e. m. form factor 8=15811
 ρ , decay distrib. using statistical tensors 8=20505
 ρ dominance and nucleon size 8=11580
 ρ production, e^+e^- colliding beams 8=812
 ρ exchange in meson-B scatt. 8=740
 ρ exchange in π - p scatt., corrections 8=6874
 ρ exchange in $\pi^- + p \rightarrow \eta + n$ 8=20433
 ρ in dipion photoprod. 8=20507
 ρ , second, decoupling in πN forward scatt. 8=15783
 ρ -like singularities in πN scatt. in complex J-plane 8=11530
 ρ mass/ π mass prediction from πN interaction 8=15771
 ρ $m_1 = \sqrt{2} m_\rho$ derived from current algebra 8=20506
 ρ , in N isoscalar magnetic form factor fit 8=3694
 ρ in N-N scatt., Mandelstam representation 8=824
 ρ prod. in $NN \rightarrow NN\rho$ absorptive peripheral model 8=6920
 ρN^* decay distrib. using statistical tensors 8=20505
 $\rho NN, \rho NN^*, \rho NN_{3/2}^*$ coupling from current algebra 8=11564
 ρ in OPE model for $\pi-\pi$ scatt. 8=15789
 ρ parameters in bootstrap $\pi-\pi$ scatt. 8=11536
 ρ , parametrization for resonant scatt. applic. to NN , $\pi\omega$ 8=3683
 ρ phenomenological Regge trajectory, 8=20504
 ρ photoprod. in $\gamma + A \rightarrow A + \pi^+ + \pi^-$ on $9 \leq A \leq 207$ nuclei, 4.35 and 6.02 GeV 8=7164
 ρ , prod. in πN collisions and rel. to conserved current 8=15813
 ρ -P vacuum trajectory branch cuts conspiracy in NN and NN charge exchange scatt. 8=11584
 ρ , in π prod. 8=20438
 ρ in πN high energy interactions, N/D effective-range theory 8=3554
 ρ in $\pi N \rightarrow \rho p N$, mass distrib. from Regge-pole exchange model 8=20440
 ρ , πN scatt. exchange contrib. 8=761
 ρ , in $\pi p \rightarrow \rho N^*$, ang. decay correl. with $\pi p \rightarrow f^0 N^*$ 8=11636
 ρ in $\pi-\pi$ scatt. as sum rule, as input 8=3646
 ρ in $\pi^-\pi^0$ scatt., Chew-Low method 8=768
 $\rho \rightarrow \pi + \pi$ current algebra calc. 8=11565
 $\rho \rightarrow 2\pi$, current algebra and dispersion relation analysis 8=811
 ρ prod. in pseudoscalar pseudoscalar scatt., bootstrap calc. with Schrodinger eqn. 8=11559
 ρ propagator, complete equal to perturbative since $\rho \rightarrow 4\pi$ is absent 8=15811
 ρ Regge trajectory, derivation and solution of integral eqn. 8=20412
 ρ^- in $\pi^+p \rightarrow \pi^-\pi^+p$ 8=11522
 ρ^- , production and decay, from reaction $\pi^+p \rightarrow \pi^-\pi^+p$ at 2.77 GeV/c 8=20503
 ρ^- in $C(\gamma, \rho^-)C$, 3.2-4.9 GeV 8=16057
 ρ^- in $Al(\gamma, \rho^-)Al$, 3.2-4.9 GeV 8=16057
 $\rho^- \rightarrow e^-e^+$ and $\pi^+\pi^-$, branching ratio, 600-900 MeV/c² 8=6908
 ρ^- in $\gamma + p \rightarrow p + \rho^-$, 3.2-4.9 GeV 8=16057
 ρ_0 , leptonic decay, vector boson model 8=20497
 ρ_0^+ , ω , and ϕ , photon coupling form factor 8=6905
 ρ^+ in photoprod. on N, cross-section calc. 8=20508
 ρ^+ photoproduction in nuclei, cross-section 8=20767
 ρ^+ , OPE calc., normalization for S-wave $\pi^+\pi^-$ S-wave scatt. cross-section 8=20439
 ρ^+ in $\pi^+ + p \rightarrow \pi^+ + \pi^+ + n$, 1.38-3.00 GeV/c compared to OPE model 8=3685
 ρ^+ prod. in $\pi^+p \rightarrow \pi^+\pi^+n$, 8 GeV/c 8=6851
 ρ^+ in $\pi^+p \rightarrow \pi^+\pi^+n$ 8=11522
 ρ^+ in $\pi^+p \rightarrow \pi^+\pi^+\pi^-$, 3 GeV/c 8=20446
 ρ^+ prod. in $\pi^+p \rightarrow \pi^+\pi^+\pi^+p$, 3 GeV/c 8=20447
 ρ^+ in $\pi^+p \rightarrow \rho^+N^{*++} \rightarrow \pi^+\pi^+\pi^+p$, peripheral models 8=11515
 ρ^+ trajectory in π - p charge-exchange scatt., Regge parameters 8=11538
 $\rho\Delta$ from πN interaction, π conspiracy consequences 8=6867
 $\rho\pi$, in $\pi^+\pi^-\pi^0$ system 8=15812
 σ , coupling constant to nucleons 8=11554
 σ , 700 MeV for π prod. 8=20438
 σ in Y-N scatt. 8=20573
sources, strong coupling group model 8=20492
 SU_3 harmonics as basis states 8=11555
tensor and axial vector, quark couplings and strong decays 8=11557
 $35^{1/2}$ in three octets, decay 8=733
 2^+ , partial conservation 8=11570
vector-baryon couplings from superconvergence relations 8=6900
vector, conspiracies and forward prod. 8=6898
vector-current spectral functions sum rules rel. to vector-meson dominance 8=3679
vector, radiative decay relations 8=6901

Mesons—contd

resonances—contd

- vector exchange as origin of nuclear repulsive core 8=20642
- vector gauge, as chiral partners in Yang-Mills theory 8=15809
- vector prod. in $\pi B \rightarrow V \Delta$, Regge-pole couplings 8=6903
- vector in $\gamma + p \rightarrow p + \eta$ 8=20490
- vector, and photoprod. 8=15669
- vector and tensor prod. by π exchange Reggeization 8=11499
- vector, interaction with massless spinors in 2 dimensions 8=15617
- V scatt. in $PV \rightarrow VV$, superconvergent sum rules 8=15759
- vector-meson field theory, coupling parameters, current algebra determ. 8=6899
- X^0 prod. from $X^0 \pi^+ p \rightarrow X^0 n$, cross sections obs. 8=20501
- $X^0 \rightarrow 2\gamma$, width rel. to mixing in η , X^0 8=20499
- z decaying to $\pi^+ \pi^-$, search in $\pi^+ + p \rightarrow \pi^+ + \pi^0 + p$ 8=11553
- Z_1 (1910), spin and parity from backward K^-p elastic scattering 8=6892

scattering

- A_2 - π superconvergence sum rules 8=20421
- on baryons, cross-sections, in $SU(3)$, asymptotic limits 8=742
- BM, MM, couplings in quark model, soln. to superconvergence relations 8=20404
- $He^4(\pi, M)He^4$, magnitude and phase of meson scatt. amp. 8=890
- K^+ , 240-300 MeV in emulsion, optical-model anal. 8=20482
- K - α , differential cross section, low-energy elastic 8=11549
- K - K , extension of domain of validity of dispersion relations 8=6895
- KK , extension of domain of validity of dispersion relations 8=6895
- K^+n , sum rule analysis 8=6896
- $K(\bar{K})$ - N , elastic, dispersion calc. compared with expt. 8=15830
- KN dispersion relations and coupling constants determ. 8=11550
- KN forward dispersion relation for $\Delta \bar{K}N$ coupling constant calc. 8=802
- K - N , phenomenological model of diffraction 8=6894
- KN , Regge secondary poles, cuts and conspiracies rel. to crossover and polarization 8=11529
- KN superconvergence sum rules and Regge pole parameters 8=3666
- KN superconvergence sum rules and vector meson Regge poles 8=3661
- K - N , s-wave absent with t-channel singularities, K - B coupling constants 8=20483
- K^+N , dispersion relations, $SU(3)$ invariance violation 8=6891
- $K\pi$ extension of domain of validity of dispersion relations 8=6895
- $K^{*-}\pi$, superconvergence sum rules 8=20421
- Kp , sum rule analysis 8=6896
- Kp superconvergent sum rule and Regge parameters 8=3667
- $K^- + p \rightarrow K^0 + n, \rho + R$ Regge-pole model determ. of parameters 8=6893
- $K^-p, \sim 1$ GeV/c, phenomenological model of diffraction 8=6894
- $K^-p \rightarrow K^+n, K^-p$, resonant partial wave amplitudes 8=6897
- K^-p elastic, s-wave interaction, 0 - 250 MeV/c 8=20481
- K^-p total and elastic cross sections at 2.66 GeV/c 8=801
- K^+p , backward elastic, as evidence for baryon exchange 8=803
- K^+p , backward elastic at 1-3.5 GeV/c 8=6892
- K^+p phase-shift analysis below 1500 MeV/c 8=20484
- K^+p , mass difference effect in Wali-Warnock model, violation of $SU(3)$ 8=3692
- $K^+p, l=1$ P-wave phase shifts from $N^*(1238)$ prod. 8=15805
- K^+p , test of PDDAC for A_1^{++} 8=3668
- K^+p , and parity of Δ and Σ 8=3730
- M - N factor from $\pi + d \rightarrow M + d$ 8=3736
- MN baryon exchange model rel. to $NN \rightarrow MM$ 8=825
- meson-B scatt. p-wave, low energy sum rules 8=6833
- meson-baryon, quark model 8=20418
- meson-baryon with Regge poles and $SU(3)$ symmetry 8=740
- meson-baryon, response of masses to perturbations in N/D model 8=3691
- meson-baryon, saturation of superconvergence relations 8=15818
- meson-baryon, $SU(n)$ crossing matrices 8=741
- meson-baryon s-wave scatt. length calc., pseudo-scalar 8=20420
- meson-baryon, test of a superconvergent relation 8=11494
- meson-N, amplitude determ., neutral scalar meson models 8=11496
- meson-N, amplitude expansion using Lorentz group representation 8=15696
- meson-N amplitude at high energy, Regge asymptotic behaviour 8=11495
- meson-N, quark model for mesons, Glauber formalism, correction to Johnson-Trieman relation 8=20419

Mesons—contd

scattering—contd

- meson-N, 2 sum rules and meson-N coupling constants 8=20469
- η - n as Regge pole in $\pi^- + p \rightarrow \eta + n$, phase shift calc. 8=20433
- ω - N , superconvergent sum rules 8=3553
- $\pi\omega, \rho$ parametrization 8=3683
- pseudoscalar meson-spin 2^+ meson, superconvergence sum rules 8=20421
- $PV \rightarrow VV$, superconvergent sum rules 8=15759
- pseudoscalar-pseudoscalar, to derive internal symmetries 8=3613
- pseudoscalar-pseudoscalar, with vector resonances, bootstrap calc. with Schrodinger eqn. 8=11559
- ρB rel. to baryon magnetic moment relations 8=6900
- ρ - π , sum rule rel. to e.m. widths of ω, A_1, A_2 8=11566
- ρ, π Regge-pole theory, constraint eqns. 8=20321
- $\rho\rho$ Regge-pole theory, constraint eqns. 8=20321
- $SU(6)_w$ symm. satisfied rel. to bootstrap model for meson resonances 8=20491
- vector meson-B scatt. lengths, symm. breaking and Ademollo-Gatto theorem 8=6916

spin and parity

- A_2 , from analysis of $\bar{p}p \rightarrow \pi\pi\pi\pi$ 8=15810
- A_2 in $\pi\pi \rightarrow p\pi^+\pi^-\pi^-, 3$ GeV/c 8=20446
- A_2 in $\pi\pi \rightarrow \pi^-\pi^+\pi^+p, 8$ GeV/c 8=20447
- chiral symmetry breaking 8=15757
- e^+e^- collision, spin current 8=739
- f^* , assignment from decay modes 8=809
- $K\pi 3$ decays, CP noninvariance 8=6886
- R^+ agreement with quark model 8=3676
- resonances in bootstrap model 8=20491
- ρ^+ prod. in $\pi^+p \rightarrow \pi^+\pi^-\pi^+p, 8$ GeV/c 8=20447
- Z_1 (1910) from backward K^-p elastic scattering 8=6892

Mesosphere. See Atmosphere

Metallo-organic compounds. See under appropriate metal compound headings

Metallurgy

- See also Zone melting and refining.
- analysis by ultra-soft X-rays 8=14474
- equilibrium partition between ferrite and cementite, temperature dependence 8=17279
- austenite, alloyed, C activity at 1000°C 8=17008
- austenite, grain coarsening temp. effects of Al and Nb 8=8462
- basic O_2 furnace, jet penetration, bath circulation 8=10454
- brass, rolling texture development at room temp. and -196°C 8=22328
- cast iron, austenitic, effect of Ce on struct. 8=21988
- cold rolling theories, validity 8=5033
- cold work and recovery, in h.c.p. metals, X-ray study 8=22283
- cutting at high velocities rel. to plastic deformation 8=19338
- deoxidation product growth and separation, collision model 8=18658
- dry milling, effect of oxidation, vacuum obs. 8=19334
- electron beam machining beam divergence and electron diffusion heating in boundary area 8=15285
- electron microscope, 500 kV, use and improvement of characts. 8=8500
- grinding at high velocities rel. to plastic deformation 8=19338
- heat deform., discussion from symposium 8=22277
- iron, homogeneity and interface reactions 8=5704
- ingot structure comp. dependence 8=16927
- laser heating, pulse frequency effect rel. to sheet thickness 8=2871
- lasers, pumping cavities, machining assembly 8=23771
- macrosegregation on solidification, and mold design effect 8=16930-1
- metal sulphide chlorination in ore roasting 8=5712
- metalworking, role of surface energy of adhesion 8=5034
- micro-notch prototype, spark machining 8=23772
- ores and slags, analysis with unipolar arc 8=1345
- precipitation deoxidation kinetics, collision model 8=18658
- sample prep. for electron microscopy, electrolytic techniques 8=17271
- sectioning metallic materials using spark-erosion 8=14905
- slags, dephosphorizing capacity effect of BaO and CaF₂ 8=9676
- specimens for electron microscopy, electrolytic polishing 8=17270
- steel, continuous casting, alternating e.m. fields 8=4847
- steel, decomposition process and inter-element effect by emission spectra analysis 8=14392
- steel, fatigue softening and hardening 8=22363
- steel, high-carbon, carbide formation mechanism during tempering 8=17073
- steel, homogeneity and interface reactions 8=5704
- steel, low-carbon, sheets, rolling and annealing textures 8=17799
- steel, mild, high speed impact extrusion 8=19340
- steel, mild strip, tensile strength rel. to quench rate 8=22365
- steel stainless, Cr-Ni, intercrystalline corrosion, theory 8=8460

Metallurgy—contd

- steels, ausforming effect 8=13561
 thermomechanical deformation 8=23777
 Udimet-500, -520 and -700, heat treatment and composition
 rel. to stress-rupture and structural stability 8=13599
 wustite reduction in CO, promoters 8=5702
 Al brazing sheet with improved corrosion
 behaviour 8=10462
 Al, cladding rel. to streak free sheets 8=10460
 Al cladding with stainless steel rel. to composite sheet
 prod. 8=10461
 Al, high speed impact extrusion 8=19340
 Al purification using fractional crystallization 8=4801
 Al purity by resistance meas. at He boiling temp. 8=9741
 Al rods, polycrystalline, texture changes rel. to mech.
 forming processes 8=22308
 Al sections and wires, reinforced with continuous steel
 wires 8=10459
 Al-4, 5% Cu, macrosegregation on solidification, and mold
 design effect 8=16930-1
 Al-Cu-Cd alloy, artificial ageing, resistivity change 8=13708
 Al-Zn-Mg alloys, quenching rate rel. to age
 hardening 8=8817
 Cu-base mats., oxidized, pickling in dilute H₂SO₄, effect of
 u. s. vibs. 8=23780
 Cu, high speed impact extrusion 8=19340
 Cu, O.F.H.C., furnace and foundry equipment 8=5997
 Cu, rolling texture development at room temp.
 and -196°C 8=22328
 α -Fe, dilation by C 8=17615
 Fe, glass-doped, granular structure and orientation after
 annealing, model for doped W 8=17025
 Fe-Ni thermal bimetal strip ageing 8=22345
 Fe oxides (hematite, maghemite, magnetite), reduction
 processes below 400°C 8=5703
 Ge-Si alloys, heterojunctions, electron microprobe
 analysis 8=2216
 Mg-Zn alloy, dendrite arm spacing and grain size,
 influence of coarsening 8=4849
 MnO, sintering Mn basic carbonate and magnesite
 containing ZnO, calc. 8=4698
 Mo alloys, anti-oxidation treatment 8=23779
 Nb alloys, anti-oxidation treatment 8=23779
 Ni-base superalloys, struct. and props. 8=4850
 Ni-12.7 at. % Al alloys, rolled, effect of coherent γ' (Ni₃Al)
 particles on annealing 8=13598
 Pb to steel, explosive welding 8=10456
 Ta alloys, anti-oxidation treatment 8=23779
 W alloys, anti-oxidation treatment 8=23779
 Zn, electric spark discharge machining, damage 8=1959

metals.

- See also Alloys; Semiconductors
 adsorption of active gases, bond strength and mean adsorpt.
 times 8=14399
 alloys, crystalline structure changes at early stages of
 ageing and order-disordering 8=17036
 alloys, structural characts. from solubility method 8=17001
 analysis for metal impurities by atomic absorpt.
 spectrophotometric method 8=2544
 antiferromagnetic, superconductivity, proximity
 effect 8=5193
 Rauschinger effect in quenched metals 8=5020
 b. c. c., c. p. h., and f. c. c., fracture 8=22290
 b. c. c., diffusion of interstitial impurities 8=17558
 b. c. c., diffusions coeffs. by internal friction meas. 8=17557
 b. c. c. and f. c. c., approx. dispersion relns. for
 vibrations 8=17467
 b. c. c., radiation effects rel. to prod. of imperfections
 and diffusion, review 8=17702
 b. c. c., vibrational freq. spectrum 8=17465
 body centered cubic, irradiation damage effect on rate
 controlling mechanism of slip 8=4987
 combustion, compact metallic materials 8=2524
 complexes, and amino acid derivatives, crystal
 structures 8=1814
 conductivity electron bound states with localized spins,
 formation 8=5168
 conductivity, thermal, 4, 2-273°K 8=22129
 conductors, electron and ion emission on laser light
 interaction 8=18272
 contact resistance, tarnishing effect of atmospheric
 pollutants 8=8988
 corrosion in acids, kinetics rel. to organic inhibitors
 specificity 8=2509
 corrosion with heat transfer, test apparatus 8=18665
 corrosion in steam, influence of temp. 8=18666
 creep, elevated temp., and high-strain fatigue, data
 correlation 8=2060
 crystal and electron struct., effect of high press. 8=4699
 crystallization on levitation in e. m. field 8=17222
 crystals, growth vel. rel. to supercooling, theory of
 expt. method 8=8419
 cubic, thermal expansion calc. from Morse function 8=17530
 Debye temp. rel. to energies of vacancies form. and
 diffusion 8=17509
 deformation, compressive, effect of u. s. vibration 8=8795
 detection of thin dielectric films on surface,
 apparatus 8=8299

Metals—contd

- diffusion kinetics description from computer
 programme 8=1906
 diffusivity rel. to electron-concentration concept 8=17559
 ductility and rupture of shells rel. to thickness and strain
 rate, obs. 8=5037
 e⁺ annihilation time spectra 8=13693
 e gas, e correls. 8=22483
 elastically anisotropic f. c. c., shear stresses and energies
 of $\frac{1}{2}$ {110}, {111} edge dislocations, new data 8=17640
 electric fields, gravitationally induced 8=5159
 electrodynamic force, time variation 8=19721
 electromagnetic waves, and interaction with u. s. waves,
 theory 8=22951
 electron density near chemisorbed atom or
 molecule 8=8908
 electron emitters, effect of surface micropatches on
 average thermionic consts. 8=18260
 electron-nuclear relax. at low temps. in strong mag.
 fields 8=9449
 electron states near boundaries 8=2113
 electron theory and liq. state theory, correl. and meeting
 points 8=16786
 electronic attenuation of sound, magnitude meas. 8=4919
 electronic configuration and orbital compressibility
 under shock-wave compression 8=8225
 electrons, gravitational force compared with freely
 falling electrons 8=704
 embrittlement prod. by (α , n) reaction 8=22237
 e. p. r. rel. to conducting props. 8=5515
 emitting electrons, current tangential to surface 8=5410
 evaporation, "flash", high vacuum device for rate
 metering 8=8186
 excitons rel. to infinite hole mass from optical
 conductivity 8=5129
 extraction from molten state, thermal regime 8=8175
 face-centred cubic, self-diffusion coeffs. allowing
 for divacancies 8=8681
 fatigue crack growth, dislocation model 8=17740
 fatigue crack propag., anal. 8=5038-9
 fatigue mechanism at elevated temperatures 8=8806
 f. c. c., elastically anisotropic, shear stresses of tilt
 boundaries of {111}, 1/2 {110} dislocations 8=22195
 f. c. c., formation and configurations of faulted
 dipoles 8=8716
 f. c. c. polycrystals, plastic deformation computer
 simulation and derived rolling texture 8=13512
 ferromagnetic, n scatt. from spin-waves, and continuum
 spin-flip band 8=2315
 ferromagnetic, nonlinear polarizability tensor 8=5473
 fibre reinforced, tensile properties 8=8805
 film, Fuchs geometry, size effect calcs. for elec.
 cond. 8=13631
 films, adsorbate binding state characterization 8=14398
 films, chemisorpt. of gases, evaluation of sticking
 probability without gas pressure meas. 8=14397
 films, epitaxial growth on NaCl and KCl in vacuum 8=13147
 films, growth, deposition parameters rel. to coalescence
 stage 8=21873
 films, temp. changes during vapour deposition 8=8304
 films, thin, props. at microwave freqs. 8=21874
 films, thin, transmission, reflection and absorpt. of
 electrons 8=22494
 flow and fracture 8=17736
 foil, scattered radiation at plasma frequency 8=8958
 foil, thin slitting method 8=14904
 fracture, conference, Boston, USA (1966) 8=13518
 fracture toughness, plane strain, determ. using double
 cantilever beam specimen 8=17721
 free-electron, impurity screening, preasymptotic
 form 8=8907
 halides, i. r. absorpt. freq. and charact. Debye temp. 8=14190
 h. c. p., deformation planes after dehydrogenation and
 hydride habit planes 8=8728
 h. c. p., phonon dispersion relations, calcs. 8=13329
 h. c. p., twinning process on {1012}, structural
 mechanism 8=13126
 heating by laser radiation pulse 8=3285
 helicoid instability of sound oscs. 8=5139
 hexagonal, stress fields due to dislocation pile-ups on
 anisotropic treatment 8=1963
 with impurities possessing spin, scatt. and exchange
 interact. of electrons 8=8899
 impurity microsegregation in liq. stream interaction with
 solidification front 8=17224
 intermetallic cpds. of CsCl structure, defect formation
 energies rel. to comp. and ordering 8=17623-4
 intermetallic compounds, press. effects on ductility 8=13535
 internal friction and elastic modulus recording
 equipment 8=8784
 interstitial-metal system, polyphase diffusion and phase
 boundary motion 8=17035
 ion losses on traversing crystal lattice channels 8=17695
 ions, promotion of atom-transfer oxidation-reduction
 reactions 8=14401
 Kondo spin-compensated impurities, low temp.
 props. 8=8882
 Kondon anomaly, cond. const. as $KT < \omega$ 8=13642

Metals—contd

- latent elastic strain energy due to residual stresses after plastic deform 8=22269
 lattice expansion and residual stress by X-ray goniometric methods 8=4862
 lattice stability rel. to highest density principle 8=17329
 lattice stability rel. to space-filling and coordination number 8=17330
 liquid, Born approx. of resistivity, X-ray testing, comments 8=12915
 liquid, conduction-electron states, variational soln. 8=12903
 liquid, density of states and autocorrel. of independent electrons 8=12898
 liquid drop falling in viscous dielectric medium with magnetic field 8=7994
 liquid, elastic moduli, wavenumber-dependent 8=1499
 liquid, elec. resistivity calc., failure of Born approx. 8=12914
 liquid, electronic struct. as problem of multiple scatt. 8=12897
 liquid, flowing along row of spheres, anal. of heat transfer 8=21660
 liquid, heat capacity 8=1549
 liquid, heat transfer, in channels with periodic boundary conditions 8=8051
 liquid, heat transfer to fully developed flow in tubes 8=21568
 liquid, interatomic distances from X-ray diff pattern peaks 8=12784
 liquid, mag. susceptibility meas. in Ar atmos. 8=12926
 liquid, mutual diffusion, absolute rate and corresponding states theories 8=21642
 liquid, optical meas. by ellipsometer 8=16836
 liquid-oxygen solutions, equilb. press. meas. by solid electrolytic cell 8=16951
 liquid, pair potential rel. to structural props. 8=12790
 liquid, paramag. spin-orbit coupling 8=13969
 liquid, polyvalent, absolute thermoelec. powers 8=16881
 liquid, rad. scatt. n and X-ray, rel. to macro- and microscopic props. 8=12794
 liquid, reln. between pair pots. and radial distrib. functions of ions 8=16787
 liquid, reln. between structure and interatomic potential 8=12781
 liquid, resistivity Born approx, reply to criticism on X-ray testing 8=12916
 liquid, review of electronic structure 8=12899
 liquid rotating in magnetic field, heat transfer 7=8054
 liquid, self-diffusion coeff. using Enskog dense-gas formulation 8=12837
 liquid, self diffusion, model using ion pair pot. and number density 8=12833
 liquid, in smooth tubes, heat transfer laws for turbulent flow 8=16824
 liquid and solid, connection between atomic distrib. 8=12787
 liquid and solid, Knight shift data interpret. rel. to density of states 8=12928
 liquid, sound velocity temp. coefficient var. with disorder processes 8=12857
 liquid, temp. depend. of self-diffusion 8=12831
 liquid, 2-phase m. h. d. applications 8=19729
 liquid, Ziman pseudo-atom phase shifts calc. for monovalent ions 8=16882
 liquids, MHD generators, computer efficiency calc. 8=3156
 localized impurity states 8=17921
 M-O-M sandwich, electroluminescence rel. to electron emission 8=9277
 magnetic, electrons 8=22739
 magnetic impurity in metal, ground state 8=8909
 magnetoresistivity, low temp. general theory 8=13644
 in magnetostriiction oscillator, destruction by cavitation and droplet impact 8=22306
 mass ejection by laser pulse 8=8759
 mechanical properties, stacking faults, effects 8=22305
 metal-dielectric-supercond. structure, electron tunneling in sound field 8=5219
 metal oxide, hypostoichiometric, partially ordered defects, statistical model 8=17600
 metal-SiO_x-CdSe (metal) contacts, photocurrent studies 8=2281
 metallic Mn perovskites, first order mag. transitions 8=22742
 metallides, isomorphous substitution of atoms in crystals 8=17195
 microplasticity, study by strain effects on the a.c. resistance 8=5036
 molten, double structure of spherical close packing and layer lattice 8=12786
 molten, vacuum induction furnace 8=16744
 with monomolecular semiconductor or dielectric layers, work function 8=9091
 nearly ferromag., band struct. and interatomic exchange effects on spin fluctuations 8=2092
 noble, effect on Fe-C alloys toughness 8=17795-6
 noble metals, dispersion energies and surface tensions 8=21791

Metals—contd

- with nonmagnetic impurities, freq. depend. of elect. cond. 8=17920
 nucleation on solidification, low freq. vibration effect 8=4796
 occluded gases, determ. by laser spectral method 8=9747
 optical second harmonic generation, nonlinear polarization vector calc. 8=18483
 oxidation, high temp., scales form. mechanism 8=5711
 oxidation mechanism, isotopic study 8=23092
 oxides, dehydration processes investigated by emanation methods 8=14369
 oxide film growth kinetics, model based on thermionic emission and ionic diffusion 8=5710
 oxides, i.r. absorpt. freq. and charact. Debye temp. 8=14190
 photoconductivity from Kubo-Greenwood formulae 8=5393
 photoconductivity rel. to self-consistent theory of optical transitions 8=5394
 photoelectric effect, vacuum u.v. 8=13934
 polycrystals, ionic corrosion, angle of incidence 8=13522
 positron mean lives, temp. depend. 8=2127
 positron momentum distrib. relax. 8=8973
 pure, liq., elec. cond. and other transport props. 8=12911
 quasi-particle excitation attenuation, ferrite temp. theory 8=2120
 rare, electronic furnace for electron beam smelting 8=10457
 repeated discontinuous yielding, mechanics 8=22274
 rod-drawing anals, use of work hardening and redundant work 8=22300
 semimetals and semiconductor insulating (excitonic) phase, anisotropy effect 8=9192
 in sheet form, anal. of bore-expanding test by incremental theory of plasticity 8=22272
 simple, relns. between lattice dynamics and liq. state props. 8=16789
 sputtering, comparison of laser beam and pulsed discharge effects 8=17698
 solid and liquid, angular correlation of positron annihilation 8=8974
 solid and liquid, positron annihilation 8=12896
 specific heat at high temp. diathermic calorimeter temp. depend. meas. 8=1864
 spin polarization of single mag. impurity, in ext. mag. field 8=2132
 strain fields under omnidirectional uniform compression 8=17756
 strength, time and temp. depend., non-equilib. state 8=8811
 stress-strain curves in work-hardening range, linearization 8=17722
 submetallic films, oscs. of conductivity, and mag. resistance 8=9074
 sulphides, chlorination in ore roasting 8=5712
 superconducting non-transition, band structure 8=17868
 surface exam. by u.v. emission on K⁺ bombardment analysed by spectral microscopy 8=14299
 surface films, influence on optical meas. 8=11168
 surface impedance changes on acoustic wave generation by r.f.e.m. radiation 8=180
 surface photoeffect, external 8=22720
 surface thermal resistance at low temps. 8=22130
 target, electron emission by Auger de-excitation of atoms by sputtering 8=5422
 tempered initial cooling in non-vaporizable liquid 8=8044
 texture study by magnetores. and Hall effect 8=8454
 thermal expansion: thermodynamic approach to anharmonicity of lattice vibrs. 8=17529
 thermodynamic props. and heat processes meas. in twin calorimeter 8=250
 thermoelectric power, high approximations 8=13901
 thermogalvanomagnetic phenomena, quantum theory 8=18208
 thin-film cathode drop meas. on vacuum arcs 8=7686
 trace characterization rel. to physical props. of materials 8=18755
 trivalent, molybdates and tungstates, structural type 8=8526
 ultrasonic shear waves in 8=17488
 ultrasonic wave generation 8=4920
 vapour absorpt. spectra, using modified King furnace 8=7393
 vapour phase deposition, applics. in electronics 8=13840
 wire, Snoek spectra at low freq., recording app. 8=8786
 work function anisotropy as meas. by field emission and thermionic techs. 8=18244
 work function, "volume" concept, discussion 8=18242
 Ag-M(M=Cd, Mg, In) alloys, one-phase, inhomogeneous concs., from Zener relax. 8=8239
 GaAs-metal ohmic contacts, thin multilayer 8=9145
 Si-metal contact characts. 8=18082
 Te, interband hole transitions 8=9018

theory

- See also Crystals; Electron gas; Plasma.
 alkali ions, pseudo-atom phase shifts 8=8910
 atoms, magnetic, in non-mag. host, ground state spin 8=16991
 cohesive and volume props., quantum-statistical ab initio calc. 8=4665

Metals—contd**theory—contd**

- conductivity, electrical 8=22508
 conductivity rel. to electron fluctuation pairing 8=17919
 containing impurities, energy spectrum 8=2077
 coupled cyclotron and spin waves 8=13682
 d-transition, formulae of Slater-Koster interpolation procedure 8=8885
 dielectric constant, exchange term 8=2137
 electrical conductivity due to isotopic disorder 8=13630
 electromag. surface waves on semiinfinite metals 8=14164
 electron giant oscillations, electron scatt. effect 8=5136
 electron plasma, sound-like waves, in quantized mag. field 8=17895
 electronic band structure, approx. calculation 8=13650
 electrostatic energy calc. by plane wave summation 8=8201
 evaporation, by powerful heat flux, pulse effect 8=8187
 films, thin, optical absorb. and photoelectric emission, vectorial selective surface effects 8=22950
 interband transitions due to Bragg reflection and pseudo-potentials 8=22442
 intermetallic cpds., bond length dependence on hybrid character of bond orbitals 8=13004
 localized spin and singlet bound state 8=8884
 magnetic moments nonlinear quantum pseudo-resonance 8=1631
 magnetoacoustic resonance effects in inclined mag. fields 8=1844
 metallic lattice, coefficients of accommodation and capture 8=8334
 Mössbauer effect, shift and intensity calc. 8=1643
 Nernst-Ettingshausen effect rel. to magnetoresistance 8=9082
 noble ions, pseudo-atom phase shifts 8=8910
 oscillatory size effects with arbitrary quasiparticle dispersion law 8=22441
 passivity, oxide-film form. and breakdown 8=9702
 phase diagrams and atomic interactions 8=13003
 plasmon satellite in soft X-ray spectra, theoretical interpretation 8=13680
 semimetals, m.h.d. waves, plasma-phonon 8=5135
 shock wave excitation by e. m. irrad. 8=6143
 simple, exchange and correlation mag. instabilities 8=22788
 sound absorpt., transport eqns. 8=17492
 spin susceptibility, dynamic, Fermi liquid theory 8=22447
 spin-wave dispersion in strong mag. field 8=9308
 superconducting characteristics, topological singularities of electron spectrum 8=22524
 transition to insulators 8=22451
 u.s. absorpt. in quantizing mag. field by free electrons, calc. 8=22093
 Ga₂-Fe₂O₃ and related cpds., Mössbauer investigations 8=13028
 Mg, electronic structure from optical properties 8=14239
 Pt/rare-earth alloys, conduction electron polarization 8=17857

Metamagnetism. See Antiferromagnetism; Ferromagnetism.**Meteorites**

- See also Meteors.
 Abee, enstatite chondrite, origin of 'excess' Ar³⁹ 8=19277
 Canyon Diablo, hexagonal diamond discovery and implication 8=10369
 chondrites, carbonaceous and disequib., isotopic composition of trapped Kr and Xe 8=19275
 chondrites, ordinary, total C content of 86 specimens 8=19272
 3 chondrites, carbonaceous, Xe and Kr isotopic composition 8=19276
 conference, U. K. research, Leicester, (1966) 8=19274
 cosmic ray radioactive particles distrib. in meteorites calc. 8=10367
 cosmic-ray tracks, very heavy, identification 8=20596
 fireball, 9 Dec. 1965, trajectory and orbit 8=19280
 fireball, 25 April 1966, Canadian obs. 8=19281
 fireball of 14 June 1967, trajectory 8=19282
 Goalpara, hexagonal diamond discovery and implication 8=10369
 Goose Lake, structure of typical fragments 8=10368
 Gosses Bluff astrobleme, shatter cone orientation 8=23680
 iron, Os in three specimens 8=14857
 lunar craters, meteoroidal impact hypothesis 8=14824
 Misteca and Carbo, inert gas compositions 8=10366
 Norton County achondrite, Rb⁸⁷-Sr⁸⁷ isochron and K⁴⁰-Ar⁴⁰ ages 8=19278
 orgueil carbonaceous, electron microscopy of biological structures 8=2830
 Orgueil, round-body structures, origin 8=23683
 parent bodies, origin of chondrules 8=14856
 radioactive nuclides in Peace River and Harleton chondrites, cosmic ray history deductions 8=14858
 St. Severin, chem. comp. 8=19273
 stone, asteroids crossing earth's orbit as source 8=19249
 stony, stony-iron and iron, interplanetary field from thermoremanent magnetization obs. 8=19279
 stony, surface, optical characteristics 8=2816
 surface, optical characteristics 8=2816
 tritium loss from iron meteorites by solar wind hydrogen 8=10370

Meteorites—contd

- Br in stony, analysis by thermal neutron activation 8=19271
 Fe abundance 8=23682
 Fe, Australian, comp. differences obs. 8=23684
 Fe ion tracks in olivine 8=8768
 Pu²⁴⁴ and P²³⁹ early abundances, obs. in achondrites, rel. to early solar system abundances 8=23468
 Xe fission and spallation, isotope ratios 8=14859
Meteoroids. See Meteorites.
Meteorological instruments
 See also Anemometers; Hygrometers; Ionosphere measuring apparatus.
 balloon-borne diffusing system, for i. r. rad. from 1 to 5 μ 8=9840
 dew-point instrument, minimizing effect of contamination on mirror 8=14581
 humidity meas., atmospheric, ceramic sensing device 8=18855
 radiosonde, rotation of fan and ascent of balloon 8=14580
Meteorology
 aerosol concentration and size distribution 8=18870
 astronomical observatory, influence on choosing site 8=14579
 atmosphere general circulation, computer model for global study 8=9822
 atmospheric radio refractivity, world atlas 8=18905
 canonical correlation and relation to discriminant analysis and multiple regression 8=23254
 characteristics correl. with outgoing rad. of "earth-atmos." system 8=9861
 computerized weather forecasting 8=18849
 data for southern hemisphere stratospheric circulation 8=2574
 frontogenesis, narrow zone, from field having only large-scale var., numerical expt. 8=18860
 high altitude fronts, theory 8=9830
 satellite, meas. of conds. via vertical vel. and stream function 8=10027
 solar cycle rel. to circulation 8=23253
 synoptic, abd boundary layer over oceans 8=14582
 temperatures, potential, formulae for different types 8=9823
 tropospheric propagation, radio-meteorological correlations over Bass Strait 8=18899
 weather analysis and predictions 8=18848
 weather correl. with Rn decay product conc. variation 8=5794
 O₃, oscillation, quasi-biennial, from monthly O₃ data 8=2581

Meteors

- See also Meteorites.
 activity, correlation with sporadic-E 8=10362
 in asteroid belt, collision probability, calcn. 8=2818
 asteroids, crossing earth's orbit as stone meteorite source 8=19249
 in atmosphere, fragmentation, deform. and ablation and luminous intensity 8=10364
 Canadian national report 8=14639
 comets rel. to shavers origin, Canada and N. Zealand radar obs. comparison 8=19265
 dust, effect on v.l.f. propag. 8=18992
 dust, upper atmosphere, detection from sounding rocket 8=18918
 Earth's orbit vicinity, part, distrib. rel. to extraterrest. telescope lifetime and radar echo obs. 8=10363
 rel. to formation of sporadic-E 8=2707
 Geminids, mag. effect due to passage through interplanetary space 8=2733
 geomagnetic micropulsations, possible cause, math. model 8=2734
 ionosphere, influx from sporadic E blanketing freqs. obs. 8=2705
 kinetic energy distrib. and rel. to radar obs. 8=10361
 luminous efficiency, laboratory measurement 8=14855
 lunar crater erosion 8=23643
 meteoroid environments in solar system, correl. rel. to mass conc. and 'perforation capability' 8=19269
 micro-, flux at 60 to 145 km, rocket obs. 8=2829
 radar echo duration as function of meteoroid mass 8=5960
 size, calc. from cosmic-ray-induced nuclear reactions 8=19266
 spectral lines identification by lab. dispersion standards 8=19270
 trail echoes during v. h. f. forward scattering, diurnal and seasonal vars. 8=19267
 trails luminous flux and ionisation powder 8=10365
 trails luminosity rel. to recomb. radiation 8=19263
 trails, molecular dissociation 8=19268
 Tunguska, energy density of explosion 8=23681
 visual observations recorder 8=19264
 visual over Waltair, November to January inclusive from 1961 to 1964 8=23679

Metrology. See Measurement; Mechanical measurement.**Mica**

- biotite, adsorpt. isotherms of alkyl ammonium ions in aqueous solns. 8=13106
 crystal as retardance meter 8=6510

Mica—contd

- electric dipoles on cleaved surfaces, LEED obs. 8=22650
- foil, e^+ annihilation fraction 8=13693
- polytype, Li fluorophlogopite 8=8531
- single crystals, D^+ transmission 8=22242
- superimposed layers subject to alternating field, elec. stress distrib. 8=9235
- tracks caused by electron showers 8=22246
- triclinic polytypes giving monoclinic diffraction patterns, symmetry enhancement phenomena 8=13290
- Ag film evaporation, W substrate nucleation 8=13087
- As ions registration in cryst. 8=11325
- Ions registration in cryst. 8=11325

Micelle systems. See Colloids.

Microanalysis. See Chemical analysis.

Microhardness. See Hardness.

Micrometeorites. See Meteorites.

Micrometry

- See also Interferometry; Strain gauges; Thickness measurement.
- photoelectric for meridian passage times 8=10104

Microphones

- See also Acoustic transducers.
- hearing aids, ear level, shadow and baffle effects of head 8=10733
- second-order gradient, random efficiency 8=183
- C contacts, resistance increase due to surface deterioration 8=19558

Microphotometers. See Densitometry.

Microprobe analysis. See Chemical analysis/X-ray.

Micropulsations. See Earth/magnetic field, variations; Magnetic storms.

Microscopes

- See also Electron microscopes; Ion microscopes.
- development during last 50 years, review 8=15516
- electron bombardment luminescence obs. 8=14296
- interference, dry-mass determ. of biological substs., ext. of Pehland-Hager theory to optically anisotropic systems 8=20098
- interference, two-beam Linnik, surface studies 8=13078
- laser, appl. to biology 8=6503
- objectives aperture meas., precision apertometer 8=6507
- X-ray projection, resolution and exposure time improvement 8=17263
- X-ray, soft, image intensifier 8=17261

Microscopy

- See also Electron microscopy.
- bright field image with partially coherent illumination, nonlinear transfer 8=15513
- bubble chamber exposures, electronic co-ordinate measurements 8=482
- dislocation loops from contrast in field-ion micrographs 8=17633
- extinction and area meas., integration method 8=20058
- field-ion images of hexagonal structures and superlattices, computer simulation 8=8494
- field ion images, interpretation 8=8493
- field-ion micrograph interpretation of contrast from dislocation loops 8=17633
- high-speed cinephotomicrography 8=11220
- holography, pulsed, appls. 8=20107
- holomicrography, image transformation during reconstruction 8=525
- microkymography, new method and apparatus 8=15566
- part. size distribn., photograph-projection comparator, nonautomatic, descr. 8=5
- phase contrast, direct obs. of conc. fluctuations in critical mixture 8=21616
- phase-contrast, partial coherence effects 8=15515
- silicon iron, notched, fracture topology from optical microscope obs. 8=17793
- steels, notched, fracture topology from optical microscope obs. 8=17793
- superresolution, and the Abbe resolution limit 8=6505
- trace analysis by electron and optical microscopy 8=17269
- tubes, thin-walled, non-absorbing, in living cells, conditions for visibility 8=6501
- ultrathin sections, Pb contrasting 8=19336
- X-ray hologram microscopy, high resolution attainment 8=15592
- X-ray image intensifier for soft X-rays 8=17261

Microstructure of crystals. See Crystal structure/microstructure; X-ray examination of materials/microstructure.

Microtomes. See Biological technique and instruments;

Laboratory apparatus and technique; Microscopy.

Microtrons. See Particle accelerators/orbital.

Microwave spectra. See Spectra.

Microwave spectrometers. See Spectrometers, radiofrequency.

Mie theory. See Scattering.

Milky Way. See Galaxies/the Galaxy.

Mineralogy. See Minerals.

Minerals

- See also Mica; Quartz; Ruby.
- asbestos, adsorpt. of gases 8=21898
- albite crystals in K^+ solns., hydrothermal Na-K "exchange" process 8=18648
- albite, elec. cond. at high press. and temp. 8=8978
- aluminous pyroxene peridotite and garnet peridotite, stability fields in upper mantle 8=9789

Minerals—contd

- Antarctic rocks, mag. props. rel. to mineralogy, methodology 8=10062
- apatite crystallites, carbonate effects on morphology during growth 8=1720
- apatites, luminesc. and stoichiometry 8=2477
- arsenolite epitaxial growth on fluorine rel. to temp. of As_2O_3 vapour and CaF_2 8=17252
- basalt, elec. cond. at high press. and temp. 8=8978
- basalts from Pacific, K-Ar ages and mag. props 8=19062
- basalts, submarine, self-reversal of remanent magnetism 8=19058
- beryl and beryl melts, thermal decomposition at high temps., press. depend. 8=18645
- beryl, i.r. spectra of foreign mols. 8=2400
- biotite, adsorpt. isotherms of alkyl ammonium ions in aqueous solns. 8=13106
- biotites, phengites and chlorites in schists, obs. on Al content 8=13055
- Brazilian glauconites, K-Ar age meas. 8=18830
- calcite, elastic compliances temp. dependence 273-90°K 8=5055
- calcite, motional effects in e. s. r. of CO_2 8=22899
- chalcophyrite, Mössbauer effect 8=16982
- chlorapatite, crystal structure 8=17352
- chlorospondiosite, e. s. r. and optical spectra of CrO_4^{2-} 8=14099
- cryolite melts, solubility of Al, comp. and temp. dependence 8=21618
- diamond hexagonal polymorph, "lonsdaleite", natural occurrence and crystal analysis 8=13121
- diopside in upper mantle, plastic deform. 8=14557
- diopside, radiative thermal cond. calc., rel. to planetary interiors 8=23654
- dolomite earthenware, cracking of applied glaze 8=2044
- epsonite, $MgSO_4 \cdot 7H_2O$, left form predominance during crystal growth 8=17241
- erionite and offretite, differentiation 8=13153
- ettringite, $3CaO \cdot Al_2O_3 \cdot 3CaSO_4 \cdot 32H_2O$, crystal structure and chemistry 8=13253
- eustatite in upper mantle, plastic deform. 8=14557
- feldspar, plagioclase, etching and replicating technique studied by electron microscopy 8=21930
- ferrian ilmenites in basalts, electron probe paleomag. analysis 8=14703
- fluorapatite, crystal structure 8=17352
- formacite, $Pb_2CuCrO_4(As, P)O_4OH$, crystal structure 8=13284
- fresnoite, $Ba_2TiSi_2O_{10}$, i.r. absorpt. spectra and X-ray powder data 8=18506
- galena, PbS, X-ray microanalysis, atomic no. effect corrections 8=14479
- galena, pitchblende and pyrite deposits, induced polarization field expts. 8=2561
- gibbsite in bauxites of Mas Rouge region, e-microscope exam. 8=17275
- gillespite, Fe^{2+} Mössbauer spectrum 8=13026
- goethites, structure determ. by Mössbauer spectroscopy 8=17370
- granite compression, microfracture events spatially located by S waves 8=23215
- granite and judeite, Hugoniot eqns. of state from shock wave and geophys. data 8=14558
- granodiorite shocked mechanically and by nuclear explosion, triaxial compression obs. 8=23212
- graphite, noble gas anomalies, origin 8=9793
- haradaite, $SrVS_4O_{10}$, crystal structure $SrVS_4O_{10}$, and Si-O bond lengths 8=17416
- hayne, polysynthetic structure 8=17348
- hydrothermal synthesis, apparatus 8=23782
- hydroxyapatite, crystal structure 8=17352
- ilmenites, Curie point from thermomag. plot 8=18324
- ilmenites, mag. props., theoretical interpretation 8=9399
- ilmenite particles, beach sand, mag. props. 8=23454
- ilmenite powders, mag. resonance and susceptibility 8=9398
- labradorite, supersatellite X-ray reflections 8=13255
- lamprophyllite, $(Ba, Sr, K)Na(Ti, Fe)TiSi_2(O, OH, F)_3$, structure determ. 8=17344
- lanthanide conc. ratios between pyroxene and garnet 8=5780
- lepidocrocite, structure determ. by Mössbauer spectroscopy 8=17370
- leucophanite, crystal structure 8=13252
- lonsdaleite, diamond hexagonal polymorph natural occurrence and crystal analysis 8=13121
- magnetite, Fe_3O_4 , weak reflections obs. in X-ray diffraction pattern 8=22020
- magnetite, magnetostriction and magnetocryst. anisotropy, depend. on hydrostatic press 8=19065
- magnetite, reversible magnetostriction 8=10063
- magnetite, reversible magnetostriction at high temp. 8=23448
- meliphanite, crystal structure 8=17351
- montmorillonite, Na and Li, adsorpt. of trimethylcarbonil, by i.r. spectra 8=1705
- murmanite-lomonosovite group, crystal chemistry 8=17198
- muscovite, superstructure when heated in vacuum 8=17285
- natrolite, $(Na_2(Al, Fe)_2Si_3O_{10} \cdot 2H_2O)$, e.p.r. of Fe^{2+} , at 4.2 and 293°K 8=18432

Minerals—contd

- neptunite, oxidation state of Fe, by Mössbauer effect 8=8369
- nordstrandite, $\text{Al}(\text{OH})_3$, structure determ. by X-ray powder analysis 8=17339
- obsidian, elastic props. by u.s. interferometry 8=17713
- oil, adhesion of glass spheres 8=8150
- oligoclase, radiative thermal cond. calc., rel. to planetary interiors 8=23654
- olivine, elec. cond. rel. to mantle cond. distrib. 8=23223
- olivine-spinel equilibria in Mg_2SiO_4 - Fe_2SiO_4 system, 43 to 96 kb at 800, 1000 and 1200°C 8=23218
- olurne in upper mantle, plastic deform. and glide 8=14557
- ores, variable density, selective γ -ray logging 8=18819
- pascoite, $\text{Ca}_3\text{V}_{10}\text{O}_{28} \cdot 17\text{H}_2\text{O}$, crystal structure 8=17350
- periclase, jadeite and spinel, thermal diffusivity from 300° to 1100°K at 1 atm 8=22131
- peridot, radiative thermal cond. calc., rel. to planetary interiors 8=23654
- phlogopite, stability at high press., possible presence in Earth's upper mantle 8=23221
- pigeonite, volcanic, Fe cation distrib. 8=9790
- pitchblende, purite and galena deposits, induced polarization field expts. 8=2561
- plagioclase feldspars, birefringence variation, rel. to age 8=14182
- potash feldspar, Al-Si order and Rb impurity effect 8=17618
- pyridine complexes formed with metallic halogenes, i. r. spectra 8=16860
- pyrites, FeS_2 , X-ray microanalysis, atomic no. effect corrections 8=14479
- pyrosmalite, crystal structure 8=17393
- pyrrhotite, $\text{Fe}_{0.88}\text{S}$, mag. structure from Fe^{57} resonance 8=16985
- quartz, high-low phase inversion, press. 6 to 35 kb, obs. 8=1681
- radioactive, aerial directional detectors 8=18829
- rinkite, features of crystal structure, rel. to analogous silicates 8=8543
- rock, moisture, effect on γ -field, in near-surface atm. 8=9795
- rock, moist, meas. dielect. constant and conductivity in lab. 8=13899
- rocks, creep, temp. and stress effects, rel. to isostasy and tide damping 8=14559
- rocks, phase transitions, under shock compression 8=9800
- rocks, rupture, and elastic wave propag. and absorpt. 8=13515
- rocks, thermal conductivity, rapid determ. by ring heat source probe 8=8654
- rutile, microwave acoustic beam, cross section imaging by Bragg laser diffraction 8=6175
- sandstones, fracture strength and mechanism 8=13517
- schists, Al content in biotites, phengites, chlorites 8=13055
- silica, quartz and olivine, thermal diffusivity from 300° to 1100°K at 1 atm 8=22131
- silicates, microprobe analysis standards prep. from gels 8=14496
- silicate powders, spectral reflectance classification into glasses, cryst.-acidic and basic-ultrabasic 8=14264
- sodalites, photochromic, e.s.r. 8=14120
- soil elect. cond. maps, U.S.S.R., allowance for stratification 8=23229
- spectrographic analysis, i. r. 8=9760
- sphalerite, ZnS, X-ray microanalysis, atomic no. effect corrections 8=14479
- spinel, prep. with ordered vacancies by exchange reactions 8=23082
- standard silicate rocks, chem. anal. techniques 8=9802
- sternbergite, Mössbauer spectra and mag. props. 8=14066
- stishovite, lattice parameters, effect of press. 8=22039
- syngenite, $\text{K}_2\text{Ca}(\text{SO}_4)_2 \cdot \text{H}_2\text{O}$, crystal structure 8=13268
- telluriumbismuthite, Xe extraction, Te^{130} decay rate 8=1017
- thortveitite, e. s. r. 8=9447
- titanomagnetites in basalts, electron probe 8=14703
- troilite, FeS, mag. structure from Fe^{57} resonance 8=16985
- ultrabasic rocks and nodules, anal. rel. to upper mantle comp. 8=5778
- umangite, Cu_2Se_3 , crystal structure 8=17366
- vivianite, $\text{Fe}_3(\text{PO}_4)_2 \cdot 8\text{H}_2\text{O}$, mag. symmetry 8=5502
- Wairakite, conversion of stilbite and Heulandite under very low water s.v.p. 8=2563
- wolframite, Fe, MnWO_4 , X-ray microanalysis, atomic no. effect corrections 8=14479
- wustite reduction in CO, promoters 8=5702
- xanthoconite, Ag_3AsS_3 , crystal structure 8=13248
- X-ray microanalysis errors 8=14485
- X-ray microanalysis, standards and correction methods 8=14480
- zeolites containing H_2O , ethane diffusion 8=8685
- zeolite, surface, energy states and dynamics of Sn atoms 8=16912
- zeolites, synthetic, Sr ion-exchange selectivity 8=23081
- zeolites, use for evacuation of containers in liq. He 8=4502
- zeolites, use in meas. of thermal cond. at liq. He temp. 8=3106

Minerals—contd

- Al-serpentine, hexagonal, crystal structure 8=17336
- $\text{Al}_2\text{Be}_2\text{Si}_4\text{O}_{18}$, crystochemical analysis and structure refinement 8=17338
- $\text{BaCa}_2\text{Al}_3(\text{Si}, \text{Al})_{12}\text{O}_{30} \cdot 2\text{H}_2\text{O}$, crystochemical analysis and structure refinement 8=17338
- Cr^{3+} diopside, absorpt. 10 000–20 000 cm^{-1} , 1.7–290°K 8=18520
- $\alpha\text{Fe}_2\text{O}_3$ crystals, domain walls, n. m. r. obs. 8=5557
- Fe_2SiO_4 , hydrothermally synthesized, melting curve at press. up to 40 kb 8=1615
- Hf, ore deposits in Republic of South Africa 8=9792
- KAlSi_3O_8 , polymorphic transform. at 120 kbar and 900°C 8=8268
- $\text{KC}_2(\text{Be}, \text{Al})_2\text{Si}_2\text{O}_{30} \cdot 0.8\text{H}_2\text{O}$, crystochemical analysis and structure refinement 8=17338
- Li fluorophlogopite, complex mica polytype 8=8531
- Mg_2SiO_4 reactions in mantle, required temp. and press. from thermal and compressibility data 8=2556
- Mn nodules from dredged W. Pacific basalts, mag. props. 8=10055
- $\text{NaAlSi}_3\text{O}_8$, isomorph of high pressure NaAlGeO_4 , rel. to formation in earth's mantle 8=1678
- O^{16} and O^{18} liberation for mass spectrometry 8=12112
- Zr and ore deposits in Republic of South Africa 8=9792
- Minor planets.** See Planets.
- Mirages.** See Atmospheric optics.
- Mirrors**
- See also Telescopes/astronomical.
- concave spherical, image form. for arb. angles of incidence and wide rays 8=469
- dew-point instrument, minimizing effect of contamination 8=14581
- electrostatic analysers, comparison with spherical deflectors 8=15309
- gimballed systems, matrix anal. 8=3348
- interferogram testing 8=20043
- laser resonator, diffraction losses 8=15447
- laser transmissivity optimization in high power cavities 8=6420
- for light pulse separation, spatial and temporal division 8=20021
- Mangin system, elimination of coma 8=20041
- point holograms as mirrors 8=6568
- reflectometer, single and normal incidence 8=6504
- spherical, apparatus involving repeated reflectors for air light absorption meas. 8=7935
- telescope in satellite, thermal deformations in mirror 8=480
- multilayer dielec., high reflectance 8=2461
- Mixing.** See Heat of solution; Solubility; Solutions.
- Moderation.** See Neutrons and antineutrons/moderation.
- Moderators.** See Nuclear reactors, fission/materials.
- Modulation of light.** See Light; Optical properties of substances; Optics.
- Moiré fringes.** See Interference/light.
- Moisture**
- See also Atmosphere/humidity; Humidity; Permeability, mechanical.
- atmospheric, condensation from tropical maritime air masses as freshwater source 8=18854
- colloids, absorpt., chemical potential 8=21730
- detection, beta-ray measurements efficiency 8=9842
- dew-point instrument, minimizing effect of contamination on mirror 8=14581
- fabrics in vapour, equilibrium content 8=21765
- granular materials, rel. to tensile strength 8=22285
- powder, adhesion to solid in temp. field 8=22303
- rock and soil, effect on γ -field, in near-surface atm. 8=9795
- steel effect on crack growth 8=5071
- wood, effect on ignition by radiation 8=15110
- Molar volume.** See Density.
- Molecular beams**
- See also Particle velocity, analysis.
- benzene, scatt. of K, Rb and Cs, compared with cyclohexane 8=1205
- for coherent light prod. of stable freq., theory 8=6438
- cyclohexane, scatt. of K, Rb and Cs, compared with benzene 8=1205
- differential cross-sections at thermal energies, trans-formations and averaging 8=21199
- focusing properties, rabi-type-state selector 8=1322
- force measurement microbalance 8=16380
- generator with opposite beams, optimal variant 8=7642
- ion gauge as species-discriminating detector 8=12380
- line quality, meas. 8=7485
- metastable and repulsive electronic states, time-of-flight determ. 8=4133
- modulated, scatt. from solid surfaces, anal. of 'lock-in' detection 8=1323
- 1 eV energies and above 8=7641
- refractory metal dioxides, geometries determ. 8=7550
- scattering of solid surfaces, quantum mech. calcs. 8=16378
- shock-tube produced, for O atoms at 3 eV 8=7640
- slotted disk velocity selector, construction by electric discharge machining 8=10453
- source, high intensity nozzle for total cross section obs. 8=7639

Molecular beams—contd

- time-of-flight velocity analysis 8=16379
 triple resonance h.f.s. spectroscopy 8=16279
 Ar clusters in nozzle beams, dimer concs. 8=12379
 Ar, at high intensity, condensation forming single crystals 8=16383
 Ar, reflection at Al surface, energy meas. from 100-7500 eV 8=16382
 Ar on W surface, translation accommodation coeff. 8=17113
 Au, vapour press. from Knudsen effusion 8=12999
 Br₂, reaction with K, Rb and Cs atoms, cross-sections 8=1202
 CO₂, at high intensity, condensation forming single crystals 8=16383
 Cs¹³³F¹⁹, h.f.s. meas. 8=16278-9
 He₂ in rarified flow, velocity distribution function Doppler obs. 8=16664
 I₂, laser-induced fluorescence 8=16288
 I₂, reaction with K and Cs atoms, cross-sections 8=1202
 K + HBr, DBr, crossed-beams, velocity and ang. distrib. of KBr 8=9689
 KBr, dipole moment meas. by elec. reson. 8=4154
 N₂ on W surface, translation accommodation coeff. 8=17113
 NH₃ gas, electron diffr., chem. bonding effect 8=6303
 NO, dimers obs. by mass spectra 8=7637
 O₂ on W surface, translation accommodation coeff. 8=17113
 Sb₂Se₃ film deposition, optical anisotropy 8=14259
 XeF₆, mag.-field deflection 8=16377

Molecular orbitals. See Molecules/electronic structure; Orbital calculation methods.

Molecular relaxation. See Molecules/relaxation.

Molecular spectra. See Spectra/inorganic molecules; Spectra/organic molecules and substances.

Molecular structure. See Molecules/configuration and dimensions.

Molecular weight

- cellulose acetates, from sedimentation in acetone, rel. to macromol. characts. 8=4262
 dioxolane polymer, rel. to conversion and temp. 8=18709
 DNA, from birefringence relax. 8=16849
 p-methacrybenzoic acid, polymerized in liq. cryst. state 8=18710
 polycapraamide, oriented, rel. to elastic modulus 8=22405
 polydimethylsiloxane elastomers, MWD changes rel. to octamethylcyclotetrasiloxane polymerization 8=14409
 polyethylene, effect on melting temp. 8=12971
 polyethylene, and ethylene polymerization chain transfer kinetics 8=23129
 polyethylene, vibro-mech. treatment effects, obs. 8=18253
 polymers, and non-Newtonian flow 8=16759
 polymethylmethacrylate, vibro-mech. treatment effects, obs. 8=18253
 polystyrene, rel. to dielec. props. 8=5360
 polystyrene, vibro-mech. treatment effects, obs. 8=18253
 polystyrene, and viscoelastic props. of solns. 8=8030
 polytrioxane rel. to preirrad. dose and temp., obs. 8=21210
 polyvinylacetate, rel. to dielec. props. 8=5360
 polyvinyl alcohol, vibro-mech. treatment effects, obs. 8=18253
 trioxane in soln, at polymerization, effect. of temp. and catalyst conc. 8=18708
 Se vapour 8=4659

Molecular weight determination

- by i.r. spectroscopy 8=9755
 proteins, by u.v. spectrophotometry of sample on sephadex column 8=18642
 thermoelectric method, by meas. of heat of condensation of solvent vapour into polymer solns. 8=18643

Molecules

See also Kinetic theory; Spectra.

- advances in atomic and molecular physics, book I and II 8=16171-2
 dipole, scatt. of e.m. waves, classical and quantum theory 8=7486
 homonuclear diatomic, electron scatt., theory 8=12371
 ionospheric ion-molecule reaction rates 8=18973
 Jahn-Teller coupling, linear, effect on paramag. resonance in ²E state 8=18402
 Jahn-Teller effect at lattice sites of D_{3d} symmetry 8=17308
 Jahn-Teller inclusion in linear Stark effect of R-centre 8=1992
 molecular spectroscopy, conference, Copenhagen Denmark (1965) 8=16239
 molecular structure and spectroscopy, conference Ohio USA (1966) 8=16238
 myoglobin in soln., X-ray scatt. 8=21206
 neutral, high energy, production by laser-surface interaction 8=18273
 neutron high energy scattering 8=1234
 orientation of fibres by polarized internal reflexion spectroscopy 8=16394
 polar, cross-sections for low-energy electron scatt. 8=1233
 in polybromoprene, motion, dielec. polarization obs. 8=22660
 in polychloroprene, motion, dielec. polarization obs. 8=22660

Molecules—contd

- positron, slow, scattering 8=12168
 propionate groups, retarded motion and phase transitions 8=8229
 PR separations prod. by prolate and oblate top mols. 8=12120
 rigid-body motion in mol. crystals 8=17311
 second harmonic generation in homogeneous mag. field 8=12123
 slow electrons, critical scattering 8=7638
 spectra exhibiting accidental resonances, numerical analysis 8=12116
 spectra, optical, Canadian N.R.C. apparatus and meas., review 8=7484
 spectral band, assuming gaussian line profile, calc. 8=7488
 stellar hot, spectroscopy trapped at 4°K 8=4116
 triplet, oriented in rigid-glass matrix, e.s.r. 8=9448
 He, scatt. of changed particles, total cross-section, Bethe cross-section sum rule 8=12107
- configuration and dimensions**
 See also Chemical structure; Crystal structure, atomic, complexes, crystal, analysis using N.Q.R. 8=22927
 Cartesian coords. calc. from internal molec. coords. 8=7500
 diatomic gas, by e interference examination 8=4115
 electron-diffr. determ. from high temp. vapour, rel. to excited vibrational populations 8=16245
 electron-mol. collisions, polarization meas. 8=1232
 gas diffraction data, least squares analysis 8=12165
 negative ions, config. rel. to neutral, obs. effects 8=4140
 macroscopic distrib. of binuclear distance, diatomic 8=7499
 modification by radioactive decay of constituent atom 8=12167
 nonbonded interaction influence on geometry and energy 8=12166
 from optical rotatory dispersion of transient species excited by flash photolysis 8=12258
 terminal atom position determ. by X-rays, rel. to charge distribution effect 8=1261
- configuration and dimensions, inorganic**
 boron oxide, "washing out" effect on mol. electron-diffr. pattern 8=16266
 intermetallic cpds., bond length dependence on hybrid character of bond orbitals 8=13004
 norbornene-2, 3-dicarboxylic acid mono-potassium salt dihydrate, and crystal structure 8=22052
 oxygen fluorides 8=4231
 refractory metal dioxides 8=7550
 silazanes, structure from mass spectra 8=1275
 Ag(I) complex, monothiosemicarbazidesilver(I)chloride crystal structure 8=22013
 AlCl₃, monomeric, by gas e-diffr. 8=16264
 As(SiH₃)₃, i.r. and Raman spectra obs. 8=4144
 BH₂, lowest bent state, effects of quasi-linearity 8=1243
 B₂O₃ planar cpds., B-O bond lengths, mol.-orbital treatment 8=16268
 CeO₂, molec. beam meas. 8=7550
 Co complex, trans-dichloro(1, 4, 8, 11-tetraazaundecane) cobalt (III) ion isomerism 8=7512
 Co(CN)₃³⁻ 8=4147
 Cu complex, N-salicylidene-glycinatoaquocopper(II) hemihydrate 8=8518
 CuF₆⁴⁻, absorpt. spectrum and struct. 8=16280
 CuI, internuclear distances, determ. from rot. consts. 8=1240
 DOCl, from i.r. spectra of ν, bands 8=21083
 F₂CN₂ 8=12816
 FeCl₃, monomeric, by gas e-diffr. 8=16264
 GaO, by gas e-diffr. analysis 8=16290
 GeH₃ radical 8=12346
 GeH₃NCO, from i.r. spectra 8=21074
 H₂⁺ 8=12194
 HBF₂ 8=21063
 H₂B₂O₃, cyclic. 8=12170
 H₂F₃⁺ 8=2425
 H₂O, lowest bent state, effects of quasi-linearity 8=1243
 HOCl, from i.r. spectra of ν, bands 8=21083
 H₂S₂ gaseous, electron diffr. study 8=21103
 HSiCl₃ 8=4169
 IF₇ 8=21107
 InO, by gas e-diffr. analysis 8=16290
 KrF₂, electron diffr. obs. 8=17383
 Li metaborate, "washing out" effect in mol. electron-diffr. pattern 8=16266
 M(CO)₆, (M=W, Mo), by gas electron-diffr. expts 8=12236
 MF₆, (M=U, W, Te, Mo), by gas electron-diffr. expts. 8=12236
 Mn complex, μ-hydrido-μ-diphenylphosphido-bis(tetracarbonyl-manganese) 8=1799
 MoCl₄-graphite, and crystal structure by single-crystal electron and X-ray diffr. 8=1797
 trans N₂F₂, geometry rel. to vib.-rot. bands 8=12218
 NH₂, lowest bent state, effects of quasi-linearity 8=1243
 N₂¹⁸O⁸, internuclear distances 8=21086

Molecules—contd

configuration and dimensions, inorganic—contd

- N_2O_3 8=7538
 NSCl, i.r. spectrum obs. 8=4161
 NSF, centrifugal distortion consts. 8=12219
 Ni complex, tetraethylammonium tetrachloronickelate, and crystal structure 8=8547
 OSO_4 , by gas electron-diffr. expts. 8=12236
 Pd complex, trans-dichlorobis(dimethyl sulphoxide)Pd(II), and crystal structure 8=1804
 Pt complex, cis- and trans-bis(dialkyl sulphide) dichloroplatinum (II) complexes, struct. and inversion mech. n.m.r. obs. 8=16355
 Pt complex, cis-bis(dibenzyl sulphide) dichloroplatinum(II), n.m.r. obs. 8=16356
 OH_3^+ , one-centre expansion SCF calc. 8=4202
 $Sb(SiH_3)_3$, i.r. and Raman spectra obs. 8=4144
 $SiDBr_3$ struct. from microwave spectrum 8=21105
 SiF_4 8=16301
 $SiHBr_3$ struct. from microwaves spectrum 8=21105
 SiO_2 , molec. beam meas. 8=7550
 SO_2 , gaseous, struct. by electron diffr. 8=21104
 SOF_4 , revision of struct. 8=21101
 Ti complex, diethoxytitanium dichloride, and crystal structure 8=17421
 TaO_2 , molec. beam meas. 8=7550
 ThO_2 , molec. beam meas. 8=7550
 TiO_2 , molec. beam meas. 8=7550
 UO_2 , molec. beam meas. 8=7550
 Va(III) complexes tris(salicylaldehydes) and tris(salicylaldimines) 8=16343
 VBr_4 , by gas-phase electron diffr. 8=16303
 VCl_4 , by gas-phase electron diffr. 8=16303
 XeF_6 8=21107
 $Zn[Co(CO)_4]_2$ 8=17431
 ZrO_2 , molec. beam meas. 8=7550
- configuration and dimensions, organic**
 acetoinenediol cyclophosphate 8=17438
 acetylene-diphenyl Ge addition cpd, and crystal structure 8=22046
 acetylene- GeI_4 addition cpd, and crystal structure 8=22046
 alkylbenzenes rel. to cryst. absorpt. spectra 8=5645
 p-aminobenzamide, and crystal structure 8=22075
 anthraquinone, 1,5-dihalo derivs. and crystal structure 8=22048
 aromatic, overcrowded, conformational analysis 8=21115
 L-ascorbic acid, and crystal structure 8=13303
 azidopurine from 6-hydrazinopurine + HNO_3 , and crystal structure 8=21117
 benzene rel. to cryst. absorpt. spectrum 8=5645
 benzoin in soln., optical rotatory dispersion of transient species 8=12258
 5,5'-biisoxazole, and crystal structure 8=22067
 biphenyl, phosphoresc. state 8=12288
 N-(p-bromophenyl) benzene sulphonamide, and intramolecular van der Waals interactions 8=1278
 2-bromo-1,1-diphenyl-prop-1-ene, crystal 8=4187
 p-bromobenzoyldimethylamine, X-ray obs. 8=21129
 p-bromobenzoylenimine rel. to ethyleneamide group struct., obs. 8=21129
 bromomalonaldehyde 8=21144
 bromomalonaldehyde anion 8=21144
 bromomexicanin E, and crystal structure 8=21151
 (3:1) bullvalene- $AgBF_4$ complex 8=4890
 ϵ -caprolactones, conformation 8=12879
 Δ^3 -cavene and oxide, from gas-electron-diff. meas. 8=21161
 chlorins, optically active 8=16317
 chloroform molec. complex with benzene 8=2464
 cyclic, asymmetry parameters from anal. of i.r. type A bands 8=1277
 cycloalkanes and alkylcycloalkanes semidiones, struct. and conformation, e.s.r. obs. 8=22898
 cyclobutadiene, πO calc. of stability and geometry 8=21131
 in crystals, rel. to π electron systems 8=13031
 determination of dimensions by effect of vapour mols. on viscosity of H and He 8=1485
 dialkoxytetrahydropyran isomers, spin-spin coupling models 8=12292
 diaminodiphenylsulphone and crystal structure 8=22075
 4,4'-dibromo-dibenzoyl peroxide, and crystal structure 8=17442
 4,4'-dichloro-dibenzoyl peroxide, and crystal structure 8=17442
 2,4-dichlorophenoxyacetic acid, steric distortions 8=2390
 difluorobenzenes 8=1285
 diketene, config. and ring deform. vibr. 8=4200
 2,6-dimethyl benzoic acid, and crystal structure 8=22049
 2,5-dimethyl-p-benzoquinone, and electron density 8=8573
 meso- α, α' -dimethylglutaric acid and crystal structure refinement 8=1819
 2,3-dimethylnaphthalene, and cryst. structure from i.r. spectra and diamag. anisotropy 8=18574
 2,2-dimethyl propane, C-C distance and covalent rad. of C atom 8=7586
 α, α' -dimethylsuccinic acids 8=22000
 ethylene, nonplanarity of first Rydberg state 8=21134
 formate ion, rel. to isoelectronic AB_2 mols. 8=1269

Molecules—contd

configuration and dimensions, organic—contd

- uran, $Hg(^3P_1)$ photosensitized, struct. of excited states 8=14434
 furane- α, α' -dicarboxylic acid and crystal structure 8=17448
 haloxine, new alkaloid, and crystal structure 8=17451
 hydrocarbons, effect of nonbonded interactions 8=12166
 magnesium hexa-antipyrine perchlorate, and crystal structure 8=8593
 malonaldehyde anion 8=21144
 trans N-methyl-N-benzylthioformamide, and crystal structure 8=22050
 methylcyclohexanes, C^{13} chemical shifts obs. 8=16359
 methyl formate, in benzene and CCl_4 solns. 8=12276
 methyl-1-indanones, ring geometry 8=12329
 C-methyl-B-pentaethyl-2-carbahehexaborane (9) 8=21119
 N-methyl-piperidine-3,4-semidione, struct. and conformation, e.s.r. obs. 8=22898
 methyl vinyl sulphide 8=12283
 methyldichlorothiophosphate, rotational isomers 8=4203
 methylisocyanate 8=12278
 methylisothiocyanate 8=12278
 methylthiocyanate 8=12278
 naphthalene, 1,4-diol and crystal structure 8=8586
 naphthodioxane, low-temp. n.m.r. spectrum meas. 8=12939
 1,3 oxathiolanes, 2-substituted, n.m.r. study of ring system 8=1595
 pentamethylenetetrazole-ICl complex 8=17453
 n-perfluorobutane, conformational energies 8=1324
 phenylhydrazine, X-ray diffr. obs. 8=22069
 phenanthroline, electron excitation spectra 8=4208
 o-phenylenediamines, orientation of amino groups 8=1295
 phosphine oxides, $R_1R_2R_3PO(R_{1-3}$ are different hydrocarbon radicals) 8=16345
 phosphoramidates and phosphoramidothioates, i.r. spectra obs. 8=7591
 α -pinene and oxide, from gas-electron-diff. meas. 8=21161
 polyethylene, short branches, quant. det. by γ radiolysis 8=16392
 polyphenoxyacetylene, by X-ray anal. and i.r. spectra 8=4266
 polyphenylacetylene, by X-ray anal. and i.r. spectra 8=4266
 pyridazine 8=12297
 quinaldic acid, dimer formation, H-bonding and crystal structure at low temps. 8=1825
 reserpine, and crystal structure 8=13310
 selenocyclopentane dibromide, and mol. structure 8=22068
 sulphanilamide polymorphs and hydrate, and crystal structure 8=22075
 sulphur cpds., determ. by ESCA (electron spectroscopy for chem. anal.) 8=21100
 1,2,5-selenadiazole 8=12298
 steric perturbation of C^{13} chem. shift 8=7605
 sydnone ring, geometry 8=12299
 terpenes, bicyclic, and oxide derivs., from gas-electron-diffr. meas. 8=21161
 tertiary butyl fluoride, meas. by electron diffr. in gas 8=7569
 7,7,8,8-tetracyanoquinodimethane-anthracene complex and crystal structure 8=17460
 2,2,6,6-tetramethylpiperidin-4-ol-1-oxide, radical rel. to crystal structure 8=16370
 trans-propyleneimine 8=12290
 tetracyanoethylene-naphthalene complex 8=8585
 tetraphenylporphyrin, triclinic 8=4896
 s-tetrazine, asymmetry parameters from anal. of i.r. type A bands 8=1277
 thienylphenyl-ketones and thioketones, steric effects, n.m.r. and electronic spectra obs. 8=4218
 toluene-dimethyl Si addition cpd, and crystal structure 8=22046
 p-toluidine, and crystal structure by X-ray and n-diffr. 8=22077
 s-trioxane in nematic solvent 8=4618
 triphenylphosphine, modified Mataga SCF calc. 8=4209
 vitamin K and antivitamin K, rel. to antagonism studies in pharmaceuticals 8=23765
 $[Al(CH_3)_3]_2 \cdot C_6H_6O_2$ 8=8568
 CCl_4 , molec. complex with benzene 8=2464
 $CF_3P(O)F_2$ 8=21177
 CH_2 , lowest bent state, effects of quasi-linearity 8=1243
 CH_3^+ , one-centre expansion SCF calc. 8=4202
 CH_3SiCl_3 8=4169
 $(Et_4N)_2Cu(C_2B_5H_{11})_2$ 8=13305
 $HCNO$ 8=12270
 Pb diethyl-dithiocarbamate, and crystal structure 8=17445
 Zn diethyl-dithiocarbamate, and crystal structure 8=17445
- configuration and dimensions, macromolecules**
 amylose triacetate I 8=17461
 anionic polymers, effect of impurities and initiation and transfer rate consts. on statistical character 8=12388
 coiled-coil, modified, Fourier transforms 8=7643
 copolyesters, formation, and degree of randomness by high resolution n.m.r. spectra 8=12387

Molecules—contd

configuration and dimensions, macromolecules—contd

- copolymers, dimens. in soln. 8=12811
 copolymers in soln., effect of interaction between unlike segments 8=4541
 nongaussian chains, light scatt. 8=16386
 oligomers, reticulate crystalline nature from X-ray and thermomechanical tests 8=17192
 polyamide, non- α -helical 8=14349
 trans-1,4-polybutadiene, random-coil configs., interpretation 8=16388
 poly-L- γ -benzyl glutamate in soln. 8=21705
 poly- ϵ -caprolactones, conformation 8=12880
 poly(ethylene oxide), config. 8=12390
 poly-DL-phenylalanine in soln. 8=21705
 trans-1,4-polyisoprene, random-coil configs., interpretation 8=16388
 poly-L-proline, config. in aq. soln. 8=12891
 polymers of 2,3-dimethylbutadiene-1,3, rel. to polymerization conditions. obs. 8=21212
 polymers, rel. to viscoelasticity 8=8869
 polymers, size distrib. changes on cross linking 8=12385-6
 polymethyl methacrylates, stereoregular, broad line n.m.r. obs. 8=18462
 polynucleotide helices, stability against torsional deform. 8=4268
 polynucleotides, synthetic, helix-coil transition 8=16387
 polypeptide chains, dipole moments rel. to config. 8=16389
 polypropylene, γ -irrad., free radicals e.s.r. obs. 8=7628
 polystyrene, adsorbed, conformation meas. 8=8350
 polytetrafluoroethylene, conformational energies 8=1324
 poly(tetramethylene oxide), config. 8=12390

dissociation

See also Heat of dissociation.

- 1,3-butadiene, photodissoc., primary processes 8=23155
 decay, quantum theory, WKB-method 8=12147
 diatomic gas, by e interference examination 8=4115
 diatomic, by inert Hurd bodies and recomb., stochastic theory 8=1308
 diatomic mols., kinetics 8=7615
 diatomic, thermal transfer of energy, shock wave appl. 8=6144
 diatomic, vibr. and rot. relax. effect 8=4123
 discharge-flow system, free radicals and atoms reactions in fast flow 8=9700
 equilibrium constant calc. as meas. of determining sums over states at high temps. 8=10634
 fragmentation pathways from metastable transition meas. by semi-automated mass spectrometer 8=1138
 hemoglobin, stat. mech. anal. rel. to association with O_2 8=1311
 meteor trails 8=19268
 methane, dissoc. attachment of electrons, isotope effects 8=16454
 paraffins by e irrad., probability for specific bond, calc. 8=4206
 pre dissociation, transition probability 8=6597
 rates and incubation times calc. 8=4238
 reversible termolec. reactions in multilevel system 8=9679
 3α in He, He-Ar, He-Ne gases bombard. by α rel. to scintillation mechanism 8=12202
 Br_2 , photodissoc., orientation of transition moment, photolysis mapping 8=1307
 CD, $C^2\Sigma^+$ decay rates and predissociation probability 8=21185
 CH, $C^2\Sigma^+$ decay rates and predissociation probability 8=21185
 CH_3OH and $(CH_3)_2N$ radicals, ionization pots. and heats of form. obs. 8=4245
 CO, incubation time 8=21184
 CO in solar photosphere-chromosphere transition zone 8=12337
 CO_2 , by electron impact, metastable CO prod. 8=4133
 CO_2^- ions, electron absorpt. spectra 8=12793
 CS_2^+ ions, electron absorpt. spectra 8=12793
 CSe_2^+ ions, electron absorpt. spectra 8=12793
 F_2O dissociation react. with Ar 8=12335
 H_2 , attachment of e rel. to H-H interaction pot. 8=21075
 H_2 by p, Balmer emission 8=12190
 H_2 , dissociative attachment of e, vibrational resonances obs. 8=21182
 H_2 e impact, as sum of first and second triplet cross-sections 8=1241
 H_2 , in h.f. discharge of polarized atom source 8=21018
 H_2 predissoc., absorption spectral evidence 8=12189
 H_2 , survival probability of e attachment 8=1310
 H_2^+ , cross-sections for photo-dissociation 8=21188
 H_2^+ , by electron collisions, proton production cross section meas. 8=7519
 H_2^+ by e and p impact, effect of vibrational excitation 8=21076
 H_2^+ , photo-, to determ. h. f. s. spectrum in 20 cm region 8=12195
 H_2^+ , H_3^+ in collisions with H , He, Ar, Ne N. 8=21191
 HO_2^+ , lifetime 8=5743
 I_2 , photodissoc., orientation of transition moment, photolysis mapping 8=1307

Molecules—contd

dissociation—contd

- N_2 , recomb. rates 8=1313
 N_2^+ , by e impact, 10-500 eV reaction energy, cross-section determ. 8=1312
 NH_3 , photodissoc. in vac. u. v. 8=16365
 NH_4Cl 8=12217
 N_2O , by electron impact, metastable N_2 prod. 8=4133
 $N_2O_4 \rightleftharpoons 2NO_2$, thermal conductivity and relaxation effects 8=7929
 NaI, atomic fluoresc. in photodissoc. 8=12069
 O_2 , continua from photoionization meas. 8=12453
 O_2^+ , by e impact, 10-500 eV reaction energy, cross-section determ. 8=1312

dissociation energies

- ethane, energy transfer 8=16363
 RLC, gaseous 8=4240
 AgMn 8=21183
 Bi_2 and Bi_4 8=4239
 $BiCl$ 8=1309
 C_2 , spectroscopic determ. from $^3\Pi$ terms 8=12336
 CsS 8=7616
 GeS 8=7616
 H_2 , ground-state, expt/theoretical discrepancy 8=16364
 LaS 8=7616
 PtC, gaseous 8=4240
 ScF, high-temp. stability 8=7617
 ScF_2 , high-temp. stability 8=7617
 ScS 8=7616
 SrS 8=16957
 TiF 8=1623
 UAu 8=16366
 YF, high-temp. stability 8=7617
 YF_2 , high-temp. stability 8=7617
 YS 8=7616

electronic structure

See also Bonds.

- approximate open-shell theory 8=4119
 asymmetric rotor, Stark effect in electronic spectra 8=21035
 axially symmetric, constants from ground-state combination differences, simultaneous analysis 8=16258
 charge on an atom, definitions 8=21053
 complexes, crystal, analysis using N. Q. R. 8=22927
 complexes, formation and Van der Waals forces, quantum theory 8=16249
 configuration interaction using open-shell functions 8=12028
 correlated polyelectronic wavefunction for soln. of Schrödinger eqn. 8=4129
 correlation effects in calc. of ordinary and rotatory intensities 8=12023
 correlation energy depend. upon bond angle 8=16252
 diatomic, adjustment of ab initio potential curves 8=12150
 diffraction studies, importance of small angle domain 8=12045
 e-energy, linear equation computation method 8=1248
 electron spectroscopic method for study 8=16180
 electron-vibrational transition probability, diatomic 8=1216
 electronic Raman effect and vibronic coupling 8=12129
 energy calc. by method of local moments 8=12025
 energy calcs. by modified local-energy method, reliability 8=1146
 energy variance function, and estimate of energy eigenvalues 8=4131
 excited states, semi-empirical calc., comb. of closed and open shell SCF LCAO MO methods 8=4134
 excited states, Weinstein calcs. 8=16254
 floating spherical Gaussian orbital model 8=12154
 floating spherical Gaussian orbital model 8=12153
 four-centre molec. integrals 8=4136
 Franck-Condon integrals, cancellation effects 8=21056
 free-electron energy levels for symmetric 3-dimens. frameworks 8=21059
 Hartree-Fock eqns. solns., stability conditions 8=16174
 Hartree-Fock-Rootham eqns., numerical solns. 8=7349
 heavy particle collision processes, adiabatic representation 8=4249
 homonuclear diatomic mols., $^1\Sigma_g^+ - ^1\Sigma_u^+$ dipole strengths 8=21051
 interactions between nearly degenerate electron configs. 8=16252
 lowest triplet-state energies, SCF-MO calcs. 8=16255
 many-electron wavefunctions, CF method 8=20911
 metastable and repulsive electronic states, moles. beam determ. 8=4133
 molecular extinction coefficients of the triplet-triplet transitions, kinetic method of meas. 8=16257
 multi-configuration self-consistent field theory 8=16261
 muonic S-states, bound, variational calc. 8=12392
 non-adiabatic transitions between bound states 8=21054
 orbital theory, chemical bonding and spectroscopy 8=16246
 one-centre electron repulsion integral, Pariser approx. 8=16253
 one-electron systems, one-centre perturbation calc. 8=4138

Molecules—contd

electronic structure—contd

- 1/2 states, Ω -type splitting, Λ -type splitting and intensities in 1/2-1/2 transitions 8=1220
 optimized-valence configs., general theory 8=4137
 oscillator strengths calc. from approx. wavefunctions 8=12161
 perturbation theory for exchange forces 8=12155
 π -electron approximation of conjugated linear chains, FE and LCAO MO models 8=16259
 π -electron Hamiltonian 8=12162
 π electron, MO's in LCAO 8=21049
 π -electron systems, Hartree-Fock perturbation theory 8=12158
 π -electron systems, interaction energies, MO calc. 8=1318-19
 polyatomic, wavefunctions, ab initio calc. 8=12151
 polyatomic, e eqn. of motion rel. to secondary light emission 8=1212
 quantum mechanics, noninvariance groups 8=1136
 quantum orbital calc. using convolution theorem 8=1228
 radiationless transition probabilities, weak solvent-solute interactions 8=16256
 reduced density matrices 8=4037
 repulsion theory of chemical bond 8=1229
 Rydberg states, model potentials 8=21058
 s-hybrid charact. of bonding orbitals 8=16251
 SCF theory, open-shell, coalescence conditions as constraints 8=16173
 Schrödinger eqn., evaluation of multidimens. integrals 8=16247
 σ -bonded mols., ground state calc. 8=4199
 σ - π coupling, generalized time-dependent Hartree theory 8=12163
 spin-interaction operators, matrix elements 8=1225
 stability, for molecule with a nearly degenerate electronic state, rel. to nuclei motion 8=21052
 stationary principle for discontinuous trial functions 8=12164
 two-centre penetration integrals 8=12159
 variational principle for phase of wavefunction 8=21055
 wave functions, continuum, construction method 8=21259
 wavefunctions, integral coalescence conditions 8=12026
 wavefunctions, single-center expansions, review 8=16260
 zero-differential-overlap theories 8=12164

electronic structure, inorganic

- azides, metallic, rel. to explosive props. 8=1259
 diatomic hydrides, charge distrib. and binding 8=7496
 halogens, dipole strenths as function of internuclear distance 8=21084
 nitrates, metallic, rel. to explosive props. 8=1259
 one- and two-electron-pair systems, spherical Gaussian orbital model calc. 8=12154
 perchlorates, metallic, rel. to explosive props. 8=1259
 transition metal complexes, by isotopic exchange 8=23087
 transition metal complexes, ligand exchange and e.s.r. linewidths 8=4616
 transition metal complexes, ligand substitution 8=14387
 transition-metal fluorides, MO calc. of 10 Dq 8=4667
 AlO, absorption spectrum, dissociation energy 8=12169
 Ar₂, ground state, single config. wavefunctions 8=7526
 AsH and AsD 8=21062
 AsO, potential curves of electronic states 8=1236
 B-N chains and rings, MO calc. 8=1237
 BD₄-like, electric field gradient calc. using one-centre expansion wave function 8=7513
 BF, diamag. susceptibilities LCAO-MO-SCF calc. 8=12176
 Be₂, potential curves, MO calc. 8=16267
 BeF, $^2\Sigma^+$ state and $^3\Pi$ levels, calcs. from Hartree-Fock equations 8=7503
 BeH₂, configuration-interaction calc. 8=16252
 BeH₂, Hartree-Fock limit 8=1238
 Br₂, $^3\Pi_{g,u}$ state, complete pot. energy curve 8=7511
 CH₄, correlation energy, from Gaussian basis SCF calcs. 8=1263
 CN group, effects of σ and π bonding on coordination 8=12181
 CO, diamag. susceptibilities LCAO-MO-SCF calc. 8=12176
 CS₂, laser action, P-branch vibrational transition 8=3310
 Cl₂, $^3\Pi_{g,u}$ state, complete pot. energy curve 8=7511
 ClH, ground-state props. calc. 8=7514
 Co(CN)₅³⁻ 8=4147
 CrO₃²⁻ in chlorospodiosite (Ca₂PO₄Cl) 8=14099
 Cs¹³³F¹⁹, h.f. s., molec. beam meas. 8=16278-9
 FH, ground-state props. calc. 8=7514
 H₂, accurate perturbation-variation calc. 8=21079
 H₂, Born inelastic differential cross-sections 8=12191
 H₂, calc. of Rydberg states 8=1250
 H₂, dipole polarizability calc. using variational methods 8=7517
 H₂, excited states, Weinstein calcs. 8=16254
 H₂, H atom model, autoionization processes 8=21034
 H₂, improved Gaussian wavefunctions 8=21080
 H₂, low-energy elastic electron scatt. calc. 8=7516
 H₂, one-centre perturbation calc. 8=4138
 H₂-H₂ system, self-consistent group calc. 8=12372-3
 H₂ + HeH⁺, energy hypersurface, MO calc. 8=16285
 H₂⁺, accurate wavefunction, James function as approx. to Guillemin and Zener 8=1249
 H₂⁺, excited states, Weinstein calcs. 8=16254
 H₂⁺, ground state, variational function 8=7518
 H₂⁺, improved Gaussian wavefunctions 8=21080
 H₂⁺, 3d σ and 4f σ states, props. 8=1244
 H₂⁺ wave function and electronic terms for large H-H distances 8=1255
 H₃⁺, Hartree-Fock and correl. energies 8=12197
 H₃, calcs. on ground state and potential-energy surfaces 8=4130
 H₃, potential-energy surface 8=12193
 H₃ system, single-centre expansions 8=12192
 H₃⁺, calc. using 1s Gaussian basis functions 8=16282
 H_n⁺ 8=12194
 H₂C₂, excited states, virtual-orbital approx, and spectra 8=1213
 HCF, excited states, virtual-orbital approx, and spectra 8=1213
 HCN, rel. to CW submillimeter laser lines, absolute freq. meas. 8=422
 HCN, excited state, effects of quasi-linearity 8=1243
 H₂CO, excited states, virtual-orbital approx, and spectra 8=1213
 HF, ground state correlation energy 8=1252
 HF, single-centre LCAO SCF calc. 8=7524
 H₂O, Compton profile, unified atoms method 8=1256
 H₂O, correlation energy, from Gaussian basis SCF calcs. 8=1263
 H₂O, laser oscillating at 118.65 μ m transition 8=3311
 H₂O, one-electron props. 8=4148
 HNO, excited states, virtual-orbital approx, and spectra 8=1213
 He²⁺, calcs. on ground state and potential-energy surfaces 8=4130
 He₂, ground-state potential 8=12200
 He₂, ground state, single config. wavefunctions 8=7526
 He₂⁺, potential curves for X² Σ_u^+ and $^2\Sigma_u^+$ states 8=12201
 HeH⁺, approx. wave function of 3d σ state 8=1245
 HeH²⁺, one-centre perturbation calc. 8=4138
 I₂, crystalline, insulator-metal transition from diatomic bond destruction under high pressure 8=2084
 IrCl₆²⁻ in cryst. at 20°K 8=22992
 K+NaCl=KCl+Na, electronic pot. energy surfaces 8=23106
 LaF, rotational analyses of a number of bands 8=7549
 Li₂, ground state, simple alternant MO calc. 8=1257
 LiCl, MO calc. of molec. props. 8=12206
 LiF, diamago susceptibilities LCAO-MO-SCF calc 8=12176
 LiH, floating spherical Gaussian orbital model calc. 8=12153
 MnF₂:Co doped, magnon sidebands and local order 8=23001
 MnO₄⁻, MO calc. of u.v. spectrum 8=12207
 N₂⁻, struct. of 2 eV resonance 8=12214
 N₂, model dipole spectrum consistent with oscillator strength sum rule 8=7533
 N₂⁺, ground and excited states 8=4158
 NCO, matrix-isolated free radical 8=16369
 NH, fine structure of $^3\Sigma^-$ and $^3\Pi$ states 8=7541
 NH₃ + HCl \rightleftharpoons NH₄Cl, charge transfer 8=5714
 NH₃, Compton profile, unified atoms method 8=1256
 NH₃, correlation energy, from Gaussian basis SCF calcs. 8=1263
 NH₃, excited states, virtual-orbital approx, and spectra 8=1213
 NH₃, one-electron props. 8=4148
 NH₃ pressure broadening theory 8=16294
 NH₃-He collision-induced quadrupole-type transitions 8=12216
 NH₄Cl, inner and outer complex 8=12217
 NO, hybridization of O atom effect on terminal atom position determ. by X-rays 8=1261
 NO₂⁻, ground state, minimal-basis-set LCAO-SCF-MO calc. 8=21096
 NO₂, its ions and dimer 8=4159
 NO₂⁺, configuration-interaction calc. 8=16252
 NOF, ground state, minimal-basis-set LCAO-SCF-MO calc. 8=21096
 NSCl, polarizability, i.r. spectra obs. 8=4161
 NaCl, MO calc. and molec. props. 8=21092
 NaCs, $^1\Sigma^+$ and $^3\Sigma^+$ potentials from total cross-section meas. 8=21091
 NaMg[Cr(C₂O₄)₂].9H₂O, vibronic spectra 8=14247
 Ne₂, ground state, single config. wavefunctions 8=7526
 O₂ 8=16297
 O₂, configuration interaction calc. 8=12028
 O₂ single and double transitions 8=1262
 O₃, ground state, minimal-basis-set LCAO-SCF-MO calc. 8=21096
 OF₂, ground state, minimal-basis-set LCAO-SCF-MO calc. 8=21096
 OH⁻, correlation energy, from Gaussian basis SCF calcs. 8=1263
 OH⁻($^2\Sigma^+$), Hartree-Fock wavefunctions and molec. props. 8=4165
 OH⁺, fine structure of $^3\Sigma^-$ and $^3\Pi$ states 8=7541

Molecules—contd

electronic structure, inorganic—contd

Molecules—contd

- electronic structure, inorganic—contd
 OH_2^+ , one-centre expansion SCF calc. 8=4202
 PH, fine structure of $^3\Sigma^-$ and $^3\Pi$ states 8=7541
 PO , $A^2\Sigma^-X^2\pi$ system, r-centroids and FC factors 8=1264
 PO , β -system subsystems anal. 8=12225
 PO radical, γ -system 8=12224
 PbF , emission spectrum 8=21099
 $[\text{PtCl}_2(\text{NH}_3)_4]^{2+}$ square planar complexes, MO calc. 8=4168
 Re(IV) thiocyanate complex, from radioisotopic exchange kinetics 8=23089
 RhC , $C^2\Sigma-X^2\Sigma$ band, Franck-Condon factors and r-centroids 8=7548
 SH^+ ($^2\Sigma^+$), Hartree-Fock wavefunctions and molec. props. 8=4165
 SH^+ , fine structure of $^3\Sigma^-$ and $^3\Pi$ states 8=7541
 S^{33}O_6 8=12353
 ScF , rotational analyses of a number of bands 8=7549
 Sn cpds., rel. to isomer shifts in Mössbauer spectra 8=12233
 Va(III) complexes tris(salicylaldehydes) and tris(salicylaldimines), electron delocalization properties, n.m.r. obs. 8=16343
 $[\text{V}(\text{CN})_5\text{NO}]^{2-}$, $^{14}\text{CN}^-$, by isotope exchange 8=23088
 XeF_8 8=16377
 XeF_6 , pseudo-Jahn-Teller effect evidence 8=7552
 YF , rotational analyses of a number of bands 8=7549
- electronic structure, organic**
 acetophenone, lowest π, π^* triplet state 8=12892
 3-acetyl-1, 4-dihydropyridine, SCF-CI calc. 8=16306
 acetylene, energy levels 8=1371
 acetylene, σ and π reorganization 8=12243
 acrolein, π -electrons, MO calc. 8=16310
 acrylamide, rel. to amide substitution 8=1272
 alkanes, sigma-bond transitions, expt. and theory 8=1273
 n-alkyl derivatives, $1 \rightarrow a_n$ transitions and spin-orbit coupling 8=12252
 amino acids, polarizability anisotropy 8=2462
 aminobutadiene, SCF-CI calc. 8=16306
 aminobutadienone, SCF-CI calc. 8=16306
 aminoethylene, SCF-CI calc. 8=16306
 aminoferrocene, MO calcs., charge self-consistent semiempirical 8=4197
 aminopurines, Pariser-Parr-Pople calc. 8=7594
 aminopyridines, π -electron distrib. and n.m.r. chem. shift 8=12296
 aniline $1 \rightarrow a$ transitions and spin-orbit coupling 8=12252
 9-anthranaldehyde in alcohol and hexane solutions, singlet-triplet conversion 8=21693
 aromatic hydrocarbons, Hückel coeffs. 8=12251
 aromatic hydrocarbons, π -electron polarizabilities 8=12254
 aromatic hydrocarbon-tetracyanoethylene complexes, self-consistent MO calc. 8=12253
 aromatic hydrocarbons, triplet-ground-state transitions 8=4180
 aromatic hydrocarbons, zero-field splitting of triplet states 8=4181
 aromatic, and ionization probabilities 8=4318
 aromatics, triplet-triplet absorpt. at 77°K 8=7561
 azacyclic aromatics, π -electronic spectrum model 8=7562
 azatetrabenzoporphins, porphin ring struct, polarization and absorpt. spectra obs 8=21116
 azines, CNDO SCF calcs. 8=16331
 azoalkanes, electron states 8=12255
 benzodioxins, u.v. and e.s.r. spectra calc. 8=7575
 benzene, and ionized states, SCF calc. 8=7565
 benzene, lower states, vibronic interaction 8=7564
 benzene, mag. circular dichroism data 8=21123
 benzene, molecular orbital pair correlations 8=4185
 benzene, orbital calc. 8=12256
 benzene, π -electron density distrib. and free-electron model 8=7563
 benzene, SCF-MO-CI theory, empirical params. choice 8=21127
 benzenes, substituted, proton chemical shifts and π -electron densities 8=12262
 p-biphenyl aldehyde in alcohol and hexane solutions, singlet-triplet conversion 8=21693
 3-bromopyrene, double intersystem crossing 8=21128
 charge-transfer complexes, triplet states 8=2493
 charge-transfer interactions, assignment of donor transitions 8=16332
 chloranil, absorption spectrum in near u.v. 8=21126
 chlorobenzenes, LCAO-CUV calc. 8=21124
 chloroferrocene, MO calcs., charge self-consistent semiempirical 8=4197
 1-chloronaphthalene, double intersystem-crossing 8=21153
 chlorotoluenes, LCAO-CUV calc. 8=21124
 cinoline vapour, $n \rightarrow \pi^*$ transitions 8=16318
 coronene, mag. circular dichroism data 8=21123
 coronene, π transitions, free-electron and MOLCAO calcs. 8=4139
 cyclic polyenes, π -electron model 8=16174
 cyclobutadiene, MO calc. of stability and geometry 8=21131
 cyclopropanes and cyclopropenes, strain energies, SCF MO calc. 8=4190

Molecules—contd

- electronic structure, organic—contd**
 decane, C-C and C-H bond electrons momentum distrib. rel. to β^+ annihilation 8=16324
 2,5(6)-dichloro-p-benzoquinone absorption spectrum in near u.v. 8=21126
 difluoromethylene, triplet-to-singlet conversion 8=1293
 α -diketones, excited state geometry from absorpt. spectra 8=1297
 dihydronicotinamides, SCF-CI calc. 8=16306
 dihydropyridines, SCF-CI calc. 8=16306
 dimethyl amides 8=21150
 dimethylaniline, α, β -unsaturated ketone derivatives in toluene 8=21702
 2,5-dimethyl-p-benzoquinone, electron density and structure 8=8573
 1,4-dioxane, from solvent shift obs. 8=16862
 dioxazines, electronic spectra, MO calc. 8=4205
 9,10-diphenylanthracene, Pariser-Parr method calc. 8=4207
 dipole moments and charge distrib. calc. by self-consistent MO theory 8=1230
 dipyrrolyl mononegative ion and alkali metal ion biradical, e.s.r. and structure 8=4247
 DNA, intermolec. interaction energies, MO calc. 8=1318-19
 DNA, triplet state 8=4263
 ethylene, LCAO-SCF calc. 8=21139
 ethylene, nonplanarity of first Rydberg state 8=21134
 ethylene, proton spin-spin coupling calc. 8=21136
 excited states and ions, changes in atomic orbitals, study by C in valence states 8=4135
 ferrocene, MO calcs., charge self-consistent semiempirical 8=4197
 fluoroacetylene, ground state 8=12246
 fluorobenzenes, CNDO/2 MO calc. 8=12261
 fluoronitrobenzenes, CNDO/2 MO calc. 8=12261
 formaldehyde, oscillator strength of singlet-triplet transition 8=16322
 formaldehyde, π -structure, rel. to Ohno's formula and constraining Koopman's theorem 8=1286
 α -germyl ketones, MO calc. 8=21159
 glyoxal, π -electrons, MO calc. 8=16310
 haemoglobin, quadrupole splittings and isomer shifts 8=16344
 halomethyl diazirines, analogies with n-diazirine, spectra obs. 8=12268
 heterocyclic, 77°K, triplet-triplet absorpt. 8=7554
 heterocyclic cpds. 8=21142
 heterocyclics, five-membered with C, N and O, CNDO SCF calcs. 8=16331
 heterocyclics, triplet-triplet absorpt. at 77°K 8=7561
 hexane, C-C and C-H bond electrons momentum distrib. rel. to β^+ annihilation 8=16324
 hydrocarbons, CNDO calcs. 8=16325
 hydrocarbons, saturated, perturbed orbital energies in radiolysis 8=18742
 hydrocarbons, semiempirical SCF MO calc. 8=4199
 8-hydroxy-1-methyl quinolinium hydroxide 8=1566
 iodine and substituted pyridines charge transfer complexes, spectrophotometric obs. 8=4216
 methane, energy levels 8=1373
 methylacetylene, methyl-triple bond interact. MO calc. anal. 8=1291
 methylene, triplet from photodecomp. of ketene 8=23157
 naphthalene, double intersystem-crossing 8=21153
 naphthalene ENDOR study of metastable triplet state 8=21169
 naphthols, triplet states, rel. to optical and mag. props. 8=21152
 α - β -naphthylaldehyde in alcohol and hexane solutions, singlet-triplet conversion 8=21693
 nickelocene, MO calcs., charge self-consistent semiempirical 8=4197
 non-alternant hydrocarbons, spin densities, UHFAA calc. 8=12348
 by n.m.r., anisotropic effects of carbonyl group 8=4225
 nucleotides, excited states, energy transfer 8=16334
 oxalyl chloride, triplet-singlet transition 8=2468
 perylene, π transitions, free-electron and MOLCAO calcs. 8=4139
 phenantholine, π electron density and proton signals in n.m.r. spectra 8=4236
 p-phenetidine vapour, near u.v. obs. spectrum 8=21157
 phenoxide ion, symmetry of lowest triplet state 8=14340
 phenylacetylene, singlet and triplet states, formed from total π -electron system 8=4210
 phthalocyanine, π MO calc. 8=4214
 π electron systems and mol. packing in crystals 8=13031
 π -electron systems, semi-empirical calc. 8=7575
 2-picoline exchange with dichlorobis (2-picoline) Co(II), n.m.r. obs. of ligand exchange 8=2501
 polycyclic monoazines, vibronic spin-orbit interactions 8=8095
 polyene, polarizability due to π -electrons 8=16390
 polynucleotides, singlet-energy transfer 8=16334
 polyphenyl benzenes, triplet states, zero-field splitting 8=12288

Molecules—contd

electronic structure, organic—contd

- polyphenyls, spin-spin interactions 8=2374
 polystyrene 8=14290
 porphyrins, π -electron conjugation 8=4215
 proton chemical shifts rel. to phys.-chem. quantities 8=7498
 purine, Pariser-Parr-Pople calc. 8=7594
 pyrazine, triplet states 8=14342
 2-pyrazolines, trisubstituted, spectra and analogues 8=12293
 pyrene, π transitions, free-electron and MOLCAO calcs. 8=4139
 pyrene, vibr. effects in radiationless transitions 8=21114
 pyridazine, 3700 Å transition 8=12297
 pyridine positive ion, all-electron SCF wave-functions 8=12294
 pyrrole, SCF-CI calc. 8=16306
 quantum absorption, study 8=4128
 radicals, hyperconjugation and spin delocalization 8=4172
 σ -radicals, comparison of calc. electron densities and e.p.r. coupling consts. 8=12347
 1,2-rearrangements, MO description of non-classical ion 8=21057
 α -silyl ketones, MO calc. 8=21159
 stilbene, triplet-triplet energy transfer and "phantom triplet" 8=21160
 sulphur cpds., by ESCA (electron spectroscopy for chem. anal.) 8=21100
 three-membered rings 8=12322
 p-tolunitrile, emission bands 8=21163
 triacetin, liq., e distrib. from X-ray scatt. obs. 8=16794
 α, α, α -trichlorotoluene 8=4219
 triphenylene, mag. circular dichroism data 8=21123
 triphenylene triplet dianion, Jahn-Teller instability 8=21170
 triphenylphosphine, modified Mataga SCF calc. 8=4209
 u. v. spectra, orbital energy level diagrams, limitations on use 8=1268
 unsaturated, triplet-state energies and spin densities, VB calc. 8=12240
 CD, $C^2\Sigma^+$ decay rates and predissociation probability 8=21185
 CH, $C^2\Sigma^+$ decay rates and predissociation probability 8=21185
 CH radical, relative oscillator strengths 8=7618
 CH_3^+ , one-centre expansion SCF calc. 8=4202
 C_2H_2 , equiv. orbitals. 8=21110
 C_2H_4 , equiv. orbitals 8=21110
 C_2H_6 , equiv. orbitals 8=21110
 $\text{C}_6\text{H}_6\text{F}^+$, lowest states 8=12257
 $\text{C}_6\text{H}_6\text{F}^+$, lowest states 8=21120
 C_6H_6^+ , lowest states 8=21120
 C_6H_6 , lowest states 8=12257
 CF_2 , from absorpt. spectrum at 2500 Å 8=4188
 CF_2 , triplet-to-singlet conversion 8=1293
 CF_4 , single-centre LCAO SCF calc. 8=7524
 Mg-azatetrabenzoporphyrins, porphyrin ring struct, polarization and absorpt, spectra obs. 8=21116

excitation

- acetylene, by proton collisions 8=1288
 alkali-metal halides, inner-electron spectra 8=7529
 aminoferrocene, energy assignment 8=4197
 amplifying medium, polarization 8=19916
 anthracene excimer fluoresc. in rigid matrices 8=14339
 aromatic amino-acids 8=9650
 aromatic hydrocarbons, dipolar nature of complexes 8=7553
 aromatic solns., excimer formation 8=8094
 aromatic at 77°K, triplet-triplet absorpt. 8=7554
 aromatics, molten, lifetime of excited states prod. charge carriers 8=12904
 benzenes, alkyl substituted, excimer fluoresc. 8=21699
 benzoin, flash photolysis, and optical rotatory dispersion of transients 8=12258
 chloroferrocene, energy assignment 8=4197
 3-bromopyrene, double intersystem-crossing 8=21128
 1-chloronaphthalene, double intersystem-crossing 8=21153
 cosmic OH radiation, polarization 8=19916
 dimers and complexes, electronic excitation binding 8=12241
 Einstein coeffs. in condensed medium 8=12118
 by electron scattering 8=21061
 electronic, organic, degradation in chelate solns. 8=16333
 ethane, vibr. excited, kinetics 8=18675
 ethane, by proton collisions 8=1288
 ethylene, by proton collisions 8=1288
 excimers in organic liqs. excited by electrons 8=12893
 excited states, semi-empirical calc., comb. of closed and open shell SCF LCAO MO methods 8=4134
 ferrocene, energy assignment 8=4197
 by flash photolysis, and optical rotatory dispersion of transients 8=12258
 fragmentation pathways from metastable transition meas. by semi-automated mass spectrometer 8=1138
 furan, $\text{Hg}(\text{P}_1)$ photosensitized, struct. of excited states 8=14434
 halogenated benzenes, excimer phosphoresc. in organic glasses 8=9653

Molecules—contd

excitation—contd

- heterocyclic, at 77°K, triplet-triplet absorpt. 8=7554
 homonuclear diatomic, electron scatt., theory 8=12371
 methane, by proton collisions 8=1288
 methylene triplet, from photodecomp. of ketene 8=23157
 ($n\pi^*$) and ($\pi\pi^*$) states spin-orbit interaction 8=1226
 naphthalene- d_8 biphotonic $T \rightarrow T$ transitions in ethanol and methyl-pentane glasses, obs. 8=23161
 naphthalene, double intersystem-crossing 8=21153
 nickelocene, energy assignment 8=4197
 non-reactive collisions, internal excitation 8=21193
 nucleic acid components 8=9650
 paraffins by e irradi., energy transfer to vibr. degrees of freedom 8=4206
 perylene excimer fluoresc. in rigid matrices 8=14339
 phenanthroline, electron excitation spectra 8=4208
 $\pi\pi^*$ and $n\pi^*$ states, luminescence 8=12117
 polyatomic, secondary light emission rel. to e eqn. of motion 8=1212
 polyatomic by unimolecular collision, activation mechanism 8=4260
 polyvinylphthalimide with impurity acceptors, triplet excitons and triplet-triplet energy transfer, 15 000-40 000 cm^{-1} 8=12389
 quinolines, oscillator strengths 8=4590
 rare-earth ions, electronic energy transfer to H_2O vibrations 8=16870
 resonance dipole interaction between 2 identical nuclei 8=21032
 rotational, by inelastic scatt. of atoms, sudden approx. calc. 8=12367
 rotational levels in two-temp. plasma 8=12460
 $\sigma-\pi$ coupling, generalized time-dependent Hartree theory 8=12163
 stilbene, triplet-triplet energy transfer and "phantom triplet" 8=21160
 stimulated Raman scatt., mechanism 8=7487
 translational-vibr. energy transfer, steric factor 8=4250
 triplet Rydberg states, pseudo-pot. theory 8=22479
 triplet state, energy transfer in rigid soln. 8=9584
 xanthane $\pi\pi^*$ and $n\pi^*$ levels location rel. to e-donor substituent and solvent, obs. 8=1302
 C, chemi-excitation on gaseous oxidation 8=5699
 C^{1-}H n. m. r. coupling consts. 8=4229
 C_2 , in hydrocarbon flames 8=7509
 CH , in hydrocarbon flames 8=7509
 CH_4 , ion formation by collision, $8.10^{-5}-10^{-3}$ mm Hg 8=4258
 CN, electronically in active N_2 flames, vibr. population 8=12179
 CO_2 , by electron impact, absolute cross section 8=21268
 CO_2 , by N_2 , emission spectrum obs. 8=21068
 CO_2 , by transfer from heated N_2 , rel. to chem. laser action 8=16271
 H_2 $\text{B}^2\Sigma_u^+$ state, Rydberg-Klein-Rees curve 8=1227
 H_2 and D_2 $\text{c}^3\Pi_u$ states, by trapped-electron method 8=16281
 H_2 by e impact, ground to first and second states, O and OR approx. 8=1241
 H_2 , Lyman- α prod. by electron collisions 8=12050
 H_2 solid, ortho, near 0°K, Holstein-Primakoff theory 8=8233
 H_2^+ , collision-induced, angular dependence 8=1362
 H_2^+ , electron collisions, proton production cross section meas. 8=7519
 H_2^+ by e and p impact, vibration effect on dissociation 8=21076
 H_2^+ , 2p σ state, variational function 8=21078
 H_2^+ , highly excited, production by H_2^+ and H_3^+ passing through Ne, H_2 , Na and Mg 8=21082
 Hg_2 excimers, kinetics of band emissions 8=12203
 N_2 , struct. of 2 eV resonance 8=12214
 N_2 , by microwave discharge, vibrational deactivation 8=12211
 $\text{N}_2(\text{A}^3\Sigma_u^-)$, kinetics in active nitrogen 8=7534
 N_2 , $\text{B}^3\Pi$ state, time estimates at 8000-9000°K 8=4155
 N_2 , by fast protons and H atoms 8=7433
 N_2 , by fission fragments along entire track 8=7531
 NH, $^3\Pi$ state fine structure, and $^3\Sigma^-$ 8=7541
 NO, by fast protons and H atoms 8=7433
 O_2 , emission spectrum 8=1262
 $\text{O}_2(^1\Delta_g)$ collisional-radiative reaction 8=12220
 OH, chemiluminescence by flame photometry, predissociation 8=12223
 OH radical, 18-cm transitions 8=12351
 OH $^+$, $^3\Pi$ state fine structure, and $^3\Sigma^-$ 8=7541
 PbBr, emission spectrum 8=7546
 PH, $^3\Pi$ state fine structure, and $^3\Sigma^-$ 8=7541
 RhC, $\text{C}^2\Sigma-X^2\Sigma$ band, Franck-Condon factors and r centroids 8=7548
 SH, $^3\Pi$ state fine structure, and $^3\Sigma^-$ 8=7541

intermolecular mechanics

- See also Association; Collision processes; Kinetic theory/gases; Liquids/structure; Liquids/theory; Solids/theory.
 acetone, potentials from viscosity obs. 30-200 °C 8=21523
 alcohols, solid, intra-molecular motion of OH, n. m. r. study 8=16989

Molecules—contd**intermolecular mechanics—contd**

- amplitude-density-functions method for scattering 8=12358
 asymmetric, atom scatt., classical theory 8=12368
 atom-diatomic mol. collision, compound state resonances 8=4255
 attraction and repulsion, appl. to theory of liquids 8=16371
 barium-ferrite magnets as "self-crystallizing" models 8=16375
 bimolecular reactions, velocity spectra 8=7635
 binary mixtures, excess thermodynamic functions 8=4423
 bound double molecules formation rel. to intermolecular potential 8=12357
 charge transfer in biological systems 8=14895
 chloroform, potentials from viscosity obs. 30-200°C 8=21523
 classical gas model, kinetic equation for long-range attraction 8=7908
 collision broadening of rot. absorpt. lines 8=12121
 collision broadening of spectral lines 8=21197
 collisions with solid wall, energy exchange 8=16381
 complexes, formation rel. to London's dispersion forces 8=16249
 correlation functions, linear mols. 8=4252
 diatomic gas, accommodation coeffs. 8=7629
 diatomic, Rydberg-Klein-Rees pot. curves uniqueness 8=1227
 dihalogenomethanes in CCl₄, methylene group valence vibr. bands rel. to weak intermol. interaction 8=1292
 e.s.r. line shapes of systems undergoing intermolec. exchange 8=12302
 energy transfer in polar mols., probability 8=12363
 ethyl alcohol, potentials from viscosity obs. 30-200°C 8=21523
 exchange interactions in different perturbation formalisms 8=12361
 exchange interacts, Schrödinger perturb. formalism 8=4256
 fluids mixtures, semiempirical theory 8=1436
 fluid, radial distrib. and direct correl. functions, square-well model 8=16613
 force constants, determ. for spherically symmetric potential functions 8=12362
 force, long range due to ν pair exchange 8=20273
 formulas for vibr. and rot. eigenvalues in Lennard-Jones 12-6 potential 8=21201
 gases, dilute, nonadditive molec. interactions 8=4466
 gases at high temp., rotational collisions 8=4478
 gases, polar rotational relax. 8=7909
 gaseous, correlation functions by Bloom-Oppenheim theory 8=1461
 hydrocarbons, nonbonded potential parameters calc. from cryst. 8=13002
 hyperfine interacts between electrons and systems of several nuclei 8=4253
 inelastic scattering, semiclassical theory 8=12364
 interaction force constants sign determ. 8=12369
 liquid phenomena, theory 8=21601
 liquids, exciton theory 8=4586
 liquids, intermolecular potential 8=4524
 low-energy "orbiting" collisions, semiclassical phase shifts 8=12366
 in methane, gaseous, translational and rot. motions, study by slow n scatt. 8=16374
 methane-O₂ mixtures, vibr. energy transfer 8=21200
 methyl alcohol, potentials from viscosity obs. 30-200°C 8=21523
 mixed solns., electronic transitions 8=8010
 naphthols, solid, intra-molecular motion of OH, n.m.r. study 8=16989
 nonpolar gases, effect on Clausius-Mossotti function 8=12693
 pairwise additive potentials, deviations 8=16376
 partial stress tensors in isothermal multicomponent systems 8=19448
 perturbation theory for interactions 8=7631
 perturbation theory in wave operator formalism 8=12359-60
 π -electron systems, interaction energies, MO calc. 8=1318-19
 polar, interaction energy representation 8=21194
 polyatomic, convex-core potential 8=16375
 polyatomic, in unimolecular reactions, activation mechanism and non-equilib. distrib. functions 8=4260
 polymer solns., influence of intermolecular hydrodynamic interaction on viscosity and streaming birefringence 8=4505
 potential between atom and diatomic mol. rel. to scatt. 8=4254
 potential energy functions, linear mols. 8=4251
 radiationless transition probabilities, weak solvent-solute interactions 8=16256
 resonances in elastic scatt. of atoms by diatomic mols. 8=21193
 rotation, hindered, van der Waals interaction 8=21202
 s.c.f. calcs. of large molecules, interaction with solvents, using imaginary particles, solvation 8=4127
 second virial coefficient of polar gases, contribution of bound double molecules 8=7914
 second virial coeffs. of unpol. mols. 8=12676

Molecules—contd**intermolecular mechanics—contd**

- spectroscopic study of dynamical and statistical features 8=4141
 spherically symmetrical, viscosity and potential 8=7630
 spin-lattice relax. in dilute gases 8=21176
 statistical mechanical behavior, hard sphere simulation 8=14981
 sudden approx. calc. for rot. excitation by atomic impact 8=12367
 thermodynamics of interactions 8=3002
 translational-vibr. energy transfer, steric factor 8=4250
 Van der Waals force const. calc., self-consistent 8=21002
 van der Waals forces, macroscopic, macroscopic derivation 8=4105
 van der Waals interactions, Casimir effect, temp. correction 8=12378
 vibrational energy transfer in collisions between diatomic mols. 8=21190
 vibrational relax. with Lennard-Jones potential 8=4259
 vibrational-translational energy transfer, molec. orientation effect 8=7632
 vibration-translation energy transfer probability calc. 8=21196
 vibrators and librators perturbed by collisions 8=100
 wave operator perturbation theory 8=12370
 weak interactions, new perturbation procedure 8=12103
 weak intermolec. potentials, well-depth determ. 8=7636
 CCl₄ rel. to vibr. transitions and gas and liquid spectra 8=16274
 CCl₄-CCl₄, intermolecular potential in benzene 8=4524
 CH₄, ion molecule reactions at pressure $8.10^{-8}-10^{-3}$ mm Hg 8=4258
 CO₂, D₂O vibr. relaxation of CO₂ obs. 8=21071
 (o-D₂, He) system, translation-rotation energy transfer calc. 8=12374
 D₂O⁺ + M → MD⁺ + OD (M = hydrocarbon) deuteron transfer 8=9671
 H, solid, quadrupole-quadrupole interaction, rel. to λ transition 8=8267
 H-He-H₂ systems, interaction potentials 8=12376
 H₂ B¹ Σ^+ state, Rydberg-Klein-Rees curve 8=1227
 H₂ and D₂ combinations, gas torque effect on heated cylinder 8=1320
 H₂-H₂ system, self-consistent group calc. 8=12372-3
 (p-H₂, He) system, translation-rotation energy transfer calc. 8=12374
 H₂⁺, interaction energy 8=12370
 N₂, vibr. relax. in shocked gas mixtures 8=21195
 N₂-CO₂ near-reson. vibr. energy transfer 8=12375
 NH₃-He collision-induced transitions between rot. levels 8=12216
 NO, cross-section for conversion of positronium atoms 8=7476
 O₂, cross-section for conversion of positronium atoms 8=7476
- internal mechanics**
 aliphatic complexes, energy levels and wavefunctions calc. 8=16312
 alkyl halides, effects of molec. motions on n.q.r. 8=2388
 XYZ type, mean-square vibration and shrinkage amplitudes 8=12135
 bond energy-force constant relationship 8=7493
 butatriene, force field, mean amplitudes of vibration, shrinkage effect and Coriolis coupling constants 8=16314
 coriolis coupling in ethylene-type 8=4195
 diatomic, ground-state reduced potential curves 8=12144
 diatomic, internuclear separation derivatives of energy 8=21048
 diatomic potential energy, scaled atoms-in-mol. theory 8=2149
 diatomic, testing and improving molec. const. 8=21065
 diatomic, transition probability from Hulbert-Hirschfelder potential 8=4117
 dimethylacetylene, normal modes, Coriolis coupling and centrifugal distortion 8=16330
 hydrides, diatomic, Platt's model 8=4151
 interchange symmetry concept 8=4118
 integral computations, review 8=16248
 long-range interatomic forces 8=12232
 metal carbonyl hydrides, Platt's model 8=4152
 methane, nuclear spin isomerization 8=18681
 methylsilylacetylene, normal modes, Coriolis coupling and centrifugal distortion 8=16330
 ($n\pi^*$) and ($\pi\pi^*$) states spin-orbit interaction 8=1226
 nitroanilines, singlet-singlet transition energy calc. 8=7557
 nitrophenols, singlet-singlet transition energy calc. 8=7557
 oscillations, r.m.s. displacement formulae 8=12134
 paraffins, e irrad., energy transfer to vibr. degrees of freedom 8=4206
 n-perfluorobutane, conformational energies 8=1324
 polymer, flexible, radius of gyration, probability distrib. 8=7644
 polytetrafluoroethylene, conformational energies 8=1324
 polyvinylphthalimide with impurity acceptors, triplet-triplet energy transfer and triplet excitons, $15000-40000\text{ cm}^{-1}$ 8=12389

Molecules—contd**internal mechanics**—contd

- quantum, solution of $\Delta U = f(M) + g(M)V(M)$ 8=7495
 quinols, solid, intra-molecular motion of OH, n.m.r. study 8=16989
 rare-earth chelates, exchange-reson. energy transfer overlap integrals calc. 8=1656
 stability for molecule with a nearly degenerate electronic state, rel. to nuclei motion 8=21052
 torsional energy levels and semiempirical potentials 8=12139
 vitamin K and antivitamin K, rel. to antagonism studies in pharmaceuticals 8=23765
 XY₂ type, centrifugal force constants, graphical representation 8=1222
 Ar₂, potential curves calc. 8=7526
 CCl₄, from Raman spectrum at 64°K 8=18576
 CHCl₃, from Raman spectrum at 64°K and -120°C 8=18576
 CH₂Cl₂, from Raman spectrum at 64°K 8=18576
 Cl₂, anomaly of ground-state reduced potential curve 8=16275
 GaH, $a^3\Pi_0^- \rightarrow X^1\Sigma^+$ transition 8=7515
 H vibr.-rotational spectrum, from Rydberg-Klein-Rees pot., VKB calc. 8=1246
 H₂, H-H interaction pot. using isotope effect in dissociative attachment 8=21075
 H₂, intramol. bridging bond, pot. 8=7497
 H₂, potential energy, scaled atoms-in-mol. theory 8=12149
 He-He, energies, quantum calc. 8=4110
 He₂, ground-state potential 8=12200
 He₂, potential curves calc. 8=7526
 He₂⁺, potential curves for X² Σ_u^+ and ² Σ_u^+ states 8=12201
 He₂²⁺, potential energy, scaled atoms-in-mol. theory 8=12149
 K-Ar, interatomic potential, χ^2 minimum method 8=12205
 Ne levels, population and depopulation, radiative lifetimes 8=1171
 Ne₂, potential curves calc. 8=7526
 NSF, force field 8=12219
 Pt complex, cis-bis(dibenzyl sulphide) dichloroplatinum(II), struct., inversion and AB chemical shifts, n.m.r. obs. 8=16356
 Pt complex, cis- and trans-bis(dialkyl sulphide) dichloroplatinum(II) complexes, struct. and inversion mech. n.m.r. obs. 8=16355
 SbCl₃, solid, from NQR temp dependence studies, 20-150°K 8=22929
 Se₂, long-range potential 8=12232
 SF₆, X-ray absorpt. 8=12229
 UF₆, mol. interaction pot. determ. 8=7944

moments

- aldehydes, dipole moments at 3 cm. 8=21108
 n-alkane chains, polarizability anisotropy 8=16385
 n-alkanes, polarizability anisotropies 8=12248
 n-butanol complexes in amine solns., dipole 8=12909
 chloroform-triethylamine complex, dipole 8=18649
 cholesterol derivatives, dipole 8=1279
 CNDO method calc. 8=12148
 diamond lattice, second order dipole moments 8=1629
 dichlorotoluenes, 2,4-, 2,6- and 3,4-, with benzene solvent, dipole moment 8=21121
 difluorobenzenes, dipole 8=1285
 diketene, dipole moments 8=4200
 dimethyl amides, dipole 8=21150
 dipole, determination using Stark effect 8=21037
 electric dipole, gas phase, selected values 8=21050
 f.c.c. lattices, second order dipole moments 8=1629
 fluoroacetylene, g value 8=12246
 fluorobenzenes, CNDO/2 MO calc. 8=12261
 fluoronitrobenzenes, CNDO/2 MO calc. 8=12261
 m-fluorotoluene, dipole moment 8=21164
 halogens, dipole strengths as function of internuclear distance 8=21084
 heterocyclics, dipole, MO calc. 8=12272
 n-hexane, dipole 8=1582
 homonuclear diatomic mols., ¹ $\Sigma_g^+ - ^1\Sigma_u^+$ dipole strengths 8=21051
 hydrocarbon radicals, e.p.r. spectroscopy meas. of g factor 8=12301
 indole, excited state dipole moment, calc. 8=21143
 ketones, dipole moments at 3 cm. 8=21108
 methyl formate, dipole, in benzene and CCl₄ solns. 8=12276
 4-methylpyridine, dipole moment 8=12295
 polarizability and hyperpolarizabilities, from Kerr effect 8=4578
 polarizability increase by induced deformation, new nonlinear effects 8=20910
 poly(ethylene oxide), dipole 8=12390
 poly(hexene-1 sulphone), dipole, from dielec. meas. in soln. 8=1584
 polymethylene chains, polarizability anisotropy 8=16385
 poly(2-methylpentene-1 sulphone), dipole, from dielec. meas. in soln. 8=1584
 polymethylpolysiloxanes, dipole 8=4597
 polypeptide chains, dipole moments rel. to config. 8=16389
 poly(tetramethylene oxide), dipole 8=12390
 propylene imine, dipole 8=12291
 trans-propyleneimine, dipole 8=12290

Molecules—contd**moments**—contd

- radial in diatomic, e interference rel. to structure parameters 8=4115
 1,2,5-selenadiazole, dipole 8=12298
 surface dipole moments of organic cpds. 8=13107
 transition metal ions, octahedral complexes, electric quadrupole transitions 8=16976
 tryptophan, excited state dipole moment, calc. 8=21143
 Al acetylacetonate, polarity and atomic polarization 8=16872
 BrO, dipole, from electron reson. 8=12345
 CH₃SiCl₃, dipole moment 8=4169
 CO(CO)₅NO, dipole 8=12185
 ClH, computed 8=7514
 ClO, dipole, from electron reson. 8=12345
 Cr acetylacetonate, polarity and atomic polarization 8=16872
 FH, computed 8=7514
 H₂⁺ polarizability, longit. and transverse, variational calc. 8=1254
 HBF₂, dipole 8=21063
 H₂B₂O₃, cyclic, dipole 8=12170
 HCN, mol. dipole moment 8=12270
 HCl, dipole 8=1253
 HCl, hexadecapole 8=8230
 H₂O, dipole moment matrix components 8=7521
 H₂O, in vapour laser 8=3311
 HSiCl₃, dipole moment 8=4169
 IF₇, elec. dipole 8=21107
 KBr, dipole, meas. by molec.-beam elec.-reson. 8=4154
 KCl:OH⁻, cooling to 0.36°K by adiabatic depolarization of OH⁻ 8=1874
 KF, dipole, meas. by molec.-beam elec.-reson. 8=4154
 N₂ 12.28 quadrupole transition, far u.v. absorpt. obs. 8=12208
 NH₃ and ND₃, dipole moment and polarizability differences 8=12215
 NSF, dipole 8=12219
 O¹⁶O¹⁶ molecule, e.p.r. spectrum and g factor 8=12309
 OH⁻ 8=4165
 SH⁻ 8=4165
 SH, dipole, from electron reson. 8=12345
 SO(Δ), dipole, from electron reson. 8=12345
 XeF₆, elec. dipole 8=21107
 Zr acetylacetonate, polarity and atomic polarization 8=16872
- nuclear coupling**
- aldehydes, modified Hückel MO calc. 8=12328
 aromatic hydrocarbons, hyperfine coupling 8=12251
 bromo-naphthalenes, n.m.r. meas. 8=7613
 β -bromopropionitrile, 2 rot. isomers, virial H-H couplings from n.m.r. solvent depend. 8=21158
 1,3-butadienes, π -electron contrib. 8=7604
 carbamylphosphonates, long-range P³¹-H¹ spin-spin coupling 8=16353
 cyclopropane derivatives, C-C coupling 8=12320
 detection of v. small spin coupling const. 8=6408
 1,3-difluoro-4,6-dinitrobenzene, solvent effects 8=21178
 p-dihalobenzenes, C¹³-H satellites 8=21174
 ethylene, proton spin-spin coupling calc. 8=21136
 2-fluoro- α -chloro- α , α -difluorotoluene, J^{FF} temp. depend. 8=4227
 2-fluoro- α , α -dichloro- α -fluorotoluene, J^{FF} temp. depend. 8=4227
 fluorobenzene, coupling const. 8=12326
 fluorobenzene, H-H and H-F couplings 8=12325
 fluorotitanate complexes, F-F coupling const. 8=4230
 fluorotoluene derivatives, signs of spin-spin coupling const. 8=16358
 group IV hydrides, geminal coupling const. 8=21175
 hydrocarbon C¹³-H coupling 8=7510
 hydrocarbons, modified Hückel MO calc. 8=12328
 indirect spin saturation 8=16350
 methane, proton spin-lattice relaxation, liq. and gas 8=4617
 methylfluorosilanes, F coupling const. 8=7608
 methylisocyanate, N¹⁴ quadrupole interaction 8=12278
 methylisothiocyanate, N¹⁴ quadrupole interaction 8=12278
 4-methyl pyridine, quadrupole coupling const. 8=12295
 methylsilane derivatives 8=16360
 methylthiocyanate, N¹⁴ quadrupole interaction 8=12278
 trans-propyleneimine, quadrupole coupling const. 8=12290
 pyridines, substituent effects on ring proton coupling 8=12332
 pyrrole, spin-spin coupling const. 8=21180
 1,2,5-selenadiazole, quadrupole coupling const. 8=12298
 spherical top, theory of hyperfine interactions 8=12119
 spin coupling const., finite perturbation theory 8=12160
 spin coupling const., v. small, detect. by resolution enhancement 8=10985
 spin-rotational interaction in non-rigid symmetric top in doublet state 8=4166
 stability, for molecule with a nearly degenerate electronic state, rel. to nuclei motion 8=21052
 tetramethyl compounds of gp. IV, indirect nuclear spin coupling 8=4233
 tetramethyl lead, C¹³ spin-spin coupling 8=12317
 trifluorocyclopropanes, F¹⁹ coupling const. 8=12321
 BrF₃, quadrupole coupling const. 8=16276

Molecules—contd**nuclear coupling—contd**

- C^{13} spin-spin coupling to group IV elements 8=12317
 C^{13} -H, variation of S charact. and excitation energy 8=4229
 $CFCl_3$, quadrupole coupling consts. 8=16315
 $CF_3P(O)F_2$, spin-spin coupling 8=21177
 $CHCl_3$, quadrupole coupling consts. 8=16315
 CH_3SiF_3 , sign of coupling consts. 8=4232
 CH_4 , spin-rotation interaction constants determ. by nuclear spin relax. meas. 8=7573
 ClF_3 , quadrupole coupling consts. 8=16276
 ClH , computed values 8=7514
 Co^{60} , quadrupole, in cobaltic complexes 8=22919
 $Cs^{133}F^{19}$, molec. beam meas. 8=16278-9
 D_2O ice, O^{17} quadrupole coupling consts. 8=18470
 F in hexafluoroethane 8=8134
 $F-F$ spin-spin coupling in perfluoro-o-xylene 8=16357
 FH , computed values 8=7514
 GeH_4 , Ge^{73} coupling 8=12346
 $2H-1,4$ -triazines, spin-spin coupling obs. 8=21166
 HBF_4 , quadrupole coupling consts. 8=21063
 $HCNO$, nuclear quadrupole coupling const. for N^{14}
 HPF_2 , sign of coupling consts. 8=4232
 $HSiF_3$, sign of coupling consts. 8=4232
 Hg dimethyl, signs of constants 8=7610
 NH_3 , signs of spin-spin coupling consts. 8=12330
 $NaCl$, MO calc. 8=21092
 PH_2 , 2A , 2B , transition mpl. consts. 8=4166
 SO_2 , Coriolis coupling consts. from Q-heads 8=21102
 $Se^{77}-H^1$, spin-spin coupling in 1,2,5-selenadiazole 8=12333

relaxation

See also Acoustic wave propagation; Dielectric phenomena; Liquids/theory; Nuclear magnetic resonance and relaxation; Paramagnetic resonance and relaxation.

- benzenes, microwave relaxation times 8=7599
n-decanol in non-polar solns., microwave relax. 8=21711
diatomic mols., rotational relax., theory 8=12365
diatomic, vibration and rotation, dissociation effect 8=4123
diatomic, vibr. relax. in gases and liqs. 8=1218
ethane, vibr. excited, kinetics 8=18675
gaseous, rel. to intermolecular forces, Bloom-Oppenheim theory 8=1461
gases at high temp., vibr. relax. 8=4478
gases, polar rotational relax. 8=7909
polymethylpolysiloxanes 8=4597
time-dependent reorientation probabilities 8=16346
vibrational, with Lennard-Jones potential 8=4259
vibrational states, times amplitude-freq. opticoacoustical meas. 8=7490
 $BrC(CH_3)_3$, dielec., in solid and liquid, 9GHz, 10 and 200kHz 8=18179
 Br_2CNO_2 , dielec., in solid and liquid, 9GHz, 10 and 200kHz 8=18179
 Cl_2 , vibrational 8=4259
 $ClC(CH_3)_3$, dielec., in solid and liquid, 9GHz, 10 and 200kHz 8=18179
 Cl_2CNO_2 , dielec., in solid and liquid, 9GHz, 10 and 200kHz 8=18179
 $ClSi(CH_3)_3$, dielec., in solid and liquid, 9GHz, 10 and 200kHz 8=18179
 CO , vibr. relax. in shock-wave and nozzle expansion-flow 8=16270
 CO_2 , relaxation in D_2O obs. by meas. sound absorpt. and vel. 8=21072
 CO_2 , vibr. in CO_2-D_2O mixture obs. by sound absorpt. and vel. meas. 8=21071
 CO_2 , vibrational 8=4146
 H_2O , adsorbed in oxide films on Si, dielectric relax. 8=1706
 N_2 , behind shock waves, electronic excitation 8=21087
 N_2 , mixed with CO_2 and N_2O , vibr. excited 8=12210
 N_2 , vibr. relax. in shocked gas mixtures 8=21195
 N_2 , vibr. relax. in shock tube, vac. u. v. absorpt. obs. 8=7532
 $NO-CH_4$ systems, vibr. relax. 8=21200

rotation

- acetonitrile- d_3 , in liq. 8=8140
acetonitrile, in soln., vibr. bandwidth obs. 8=21681
acetylene, rotational constants from i. r. spectra 8=16307
acrylyl fluoride, rot. isomerism, i. r. and Raman spectra obs. 8=16311
allene, two rotational lines 8=21112
amides, restricted rot. and aryl-N bonds, rel. to chem. shift nonequiv. of diastereotopic p 8=4175
ammonia, elec. dipole effect on refractive index 8=4162
asymmetric rotor in electronic spectra 8=21089
asymmetric tops, centrifugal-distortion coeffs. determ. 8=21043
asymmetric-top, matrix elements 8=12142
barriers determ. from low-temp. ht. capacity 8=1221
collision broadening of rot. absorpt. lines 8=12121
constants calc., computer programming 8=21044
contact transform., choice of S-operator 8=7494
correlation function in liquid from u. r. f. spectra 8=16855
delay potentials in single molecules 8=1223
diatomic gas, by e interference examination 8=4115

Molecules—contd**rotation—contd**

- diatomic gas, influence on thermal cond. 8=12681
diatomic mols., rotational relax., theory 8=12365
diatomic nongray gases, i. r. radiative heat transfer, theory 8=16693
diatomic potential curves, calc. of vibr.-rot. energy levels 8=12140
diatomic, relaxation, dissociation effect 8=4123
difluorobenzenes 8=1285
1,1-difluoro-1,2-dibromodichloroethane, spin-echo n. m. r. meas. 8=4622
diketene, rot. spectrum 8=4200
dimethylacetylene vibr. force field centrifugal distortion 8=16330
ethane, internal rot. barrier, free-electron treatment 8=4194
ethane, staggered and eclipsed, barrier to int. rotation 8=1281
ethyl alcohol, isotope derivatives, constants 8=21135
excitation, by inelastic scatt. of atoms, sudden approx. calc. 8=12367
formic acid, doubling energy 8=7525
formaldehyde doubling energy 8=7525
fluorotetrachloroethane, liquid 8=8137
formaldehyde, vibrational-rotational interactions for force field determ. 8=4198
m-fluorotoluene, hindrance pot. of internal rot. 8=21164
gases, polar rotational relax. 8=7909
halogenated ethanes, internal rot. barriers 8=12269
hexamethylbenzene, motions in solid 8=14143
hindered, role of van der Waals interaction 8=21202
internal, in asymmetric-asymmetric mols., theory for twofold pot. barriers 8=4125
magnetic-field interactions in rotating mol. 8=12124
methane, hindered, in solid and liq. 8=12994
methane, scattering curves rel. to interatomic distances 8=7572
methylbenzenes, hindered rot., from neutron scatt. 8=17484
N-methyl-N-benzylformamide, internal, determ. by n. m. r. and equilibration methods 8=4623
methylisocyanate, internal barrier 8=12278
methylisothiocyanate, internal barrier 8=12278
4-methylpyridine, hindrance pot. of internal rot. from microwave spectrum 8=12295
methylsilylacetylene vibr. force field centrifugal distortion 8=16330
methylthiocyanate, internal barrier 8=12278
methyl vinyl sulphide 8=12283
microwave and infrared transition spectra, determ. of vel. of light 8=11122
n scatt., interaction effect 8=21060
of 1/2 state energy levels, and 1/2-1/2 transitions 8=1220
partition function of Morse vibrating-rotator model of diatomic mol. 8=16240
phenylalanine rotamers, n. m. r. study 8=12289
poly(hexene-1 sulphone), rel. to dielec. relax. in soln. 8=1585
polymethine-merocyanine dyes, n. m. r. spectra solvent depend. and rot. inhibition 8=12929
polymethylmethacrylate, rotational isomerism in ester group 8=4220
poly(2-methylpentene-1 sulphone), rel. to dielec. relax. in soln. 8=1585
propylene imine 8=12291
trans-propyleneimine, internal barrier 8=12290
proteins, effect of internal rot. on ang. correl. functions 8=16384
quantum mechanics of optical activity 8=12138
quasi-linear, rotational constants 8=12136
resonances in axially symmetric mols., nomenclature 8=21045
spin-rotational interaction in non-rigid symmetric top in doublet state 8=4166
symmetric-top mols., vibr.-rot. interaction, theory 8=16241
torsional energy levels and semiempirical potentials 8=12139
transitions, identification using Stark effect 8=21037
trapped in inert-gas crystals., rotation-translation coupling 8=8230
o-trifluoromethyl group, hindered in e. s. r. of trifluoromethylnitrobenzene 8=4615
d,1-valine radical, hindered rotations, e. s. r. study 8=4248
-vibration energy levels of a tetrahedral molecule 8=16243
 XY_2 type, centrifugal force constants, graphical representation 8=1222
AsH and AsD 8=21062
 BF_4^- in NH_4BF_4 cryst. 8=5560
BaF, gaseous, $A^2\Pi$ and $B^2\Sigma^+$ states 8=7502
BiCl, spectrum analysis in 4220-4000Å region 8=7504
 $Br_2(^1\Sigma^+)$, improving consts. 8=21065
 CF_2 , absorpt. spectrum at 2500Å, subbands perpendicular 8=4188
 $CFCl_3$ 8=16315

Molecules—contd

rotation—contd

CH, C²Σ⁺ oscillator strength meas. and predissociation probability 8=21185
 CHCl₃ 8=16315
 CH₂, centrifugal distortion effects in spectra 8=21089
 CH₃CH₂CH₂OH rot. consts. and Q, Q⁺ branches transitions, 10-32 GHz 8=7593
 CH₂Br₂ gas, multiple relaxation sound absorption 8=1475
 CH₃CH₂O¹⁸H rot. consts. and Q branch transitions 18-33.5 GHz 8=1282
 CH₃CH₂OD rot. consts. and ³R, ³P branches transitions 18-33.5 GHz 8=1282
 H₃C-CR₂R₂ radical in acetyl-(d, l)-alanine, spin-lattice relax. time rel. to rot. quantiz. 8=22906
 CH₄, inelastic scattering of cold neutrons 8=12274
 CH₄, spin-rotation interaction constants determ. by nuclear spin relax. meas. 8=7573
 C₂T₂, analysis of ν₂ fundamental 8=12244
 CN⁻ in alkali halides, environmental perturbation 8=2405
 CO₂⁺, 2Π_g → 2Π_u transition 8=16277
 CaF₂, A-X and B-X band spectra 8=21069
 CuBr, C band system in region 3900-4600 Å 8=1239
 CuI, consts. rel. to equil. internuclear distances 8=1240
 D₂, relaxation, high temp. u.s. obs. 8=1251
 (o-D₂, He) system, translation-rotation energy transfer calc. 8=12374
 D₂O, interchange with vibration of CO₂ 8=21071
 D₂O, spin-rotation constants 8=1242
 DOCl, from i.r. spectra of ν₂ bands 8=21083
 GeD₃I 8=12187
 H₂ position cross-section for rotational excitation 8=12168
 H₂, relaxation, high temp. u.s. obs. 8=1251
 H₂ solid, correl. time form n.m.r. data 8=14141
 H₂, solid ortho, theory at 0°K 8=8233
 (p-H₂, He) system, translation-rotation energy transfer calc. 8=12374
 H₂ vibr.-rotational spectrum for e ground state, VKB calc. 8=1246
 H₂⁺, para, r.f. transitions for electron spin-molecule rotation interaction 8=16284
 HBF₄ 8=21063
 HBr, in solid N₂ 8=9554
 HCl, line strengths 8=1253
 HCl, pressure effect 8=21077
 HCl, in solid N₂ 8=9554
 HDO, spin-rotation constants 8=1242
 HF, laser action 8=423
 HF, spectrum, frequencies and linewidths 8=12198
 HOCl, from i.r. spectra of ν₂ bands 8=21083
 H₂O, spin-rotation constants 8=1242
 H₂O vapour, pure rot. spectrum 8=4149
 H₂Se, sum rule analysis of interacting (2, 0, 0) and (1, 0, 1) states 8=12199
 I₂, 5350 Å band, rot. anal. 8=16289
 MoF₆, liquid 8=12930
 N₂, positron cross-section for rotational excitation 8=12168
 N₂, relaxation, high temp. u.s. obs. 8=1251
 N₂⁺, band intensity distribution due to passage of H₂⁺ through N₂ + He mixture 8=4156
 NDF₂, centrifugal distortion constants 8=7542
 NF₃ 8=1260
 NF₃, centrifugal distortion constants from mm wave spectra 8=1258
 NH₃, centrifugal distortion effects in spectra 8=21089
 -NH₂ group, in LiN₂H₂SO₄ from spin-lattice and mag. resonance studies 8=8235
 NH₃, inelastic scattering of cold neutrons 8=12274
 NH₃-He collision-induced transitions between rot. levels 8=12216
 NH₄⁺, in NH₄BF₄ cryst. 8=5560
 NH₄⁺ in (NH₄)₂Cr₂O₇ 8=14250
 N₂H₄, internal, barrier from LCAO-MO-SCF wave-functions 8=1247
 NHF₂, centrifugal distortion constants 8=7542
 NH₂OH, internal, barrier from LCAO-MO-SCF wave-functions 8=1247
 (NH₄)₂SiF₆ cubic crystals, n.m.r. obs. 8=14154
 N₂O 8=21088
 N₂¹⁵O¹⁸ 8=21086
 NSF, centrifugal distortion consts. 8=12219
 O₂, relaxation, high temp. u.s. obs. 8=1251
 OF₂ 8=4164
 OH, oscillator strengths in 2Σ⁺-2Π band system 8=7544
 OH, vib.-rot. interact. and the transition moment 8=7545
 P₂⁺, rotational analysis of the (2, 3) band of a new transition 2Π → 2Π 8=16299
 PD⁺, emission bands 8=4167
 PH₂⁺, A⁺-2B, transition mol. constants. 8=4166
 PO, β-system subsystems anal. 8=12225
 RbCl:CN, rotational degrees of freedom rel. to thermal props. 8=22120
 SO₂, microwave absorpt. 8=16302
 SO₂, reorientation in soln., theory of vibr. spectra 8=16867
 TaO, gaseous, electronic bands rot. anal. 8=1267
 UF₆, liquid 8=12930
 WF₆, liquid 8=12930

vibration

acetamide, mean amplitudes using Wilson's FG matrix method 8=4174

Molecules—contd

vibration—contd

acetonitrile N-oxide, symmetry force consts. 8=16309
 acetonitrile, in soln., bandwidth obs. 8=21681
 acetyl bromide and CD₃COBr, i.r. and Raman spectra obs. 8=7555
 alkali-halide crystals, i.r. absorpt. spectra, impurity ions 8=14197
 α-aminoacid hydrochlorides 8=7556
 anthracene from fluoresc. spectrum fine structure, 23 000-28 000 cm⁻¹ 8=1274
 anthracene vibr. effects in radiationless transitions 8=21114
 autocorrelation functions for librations and vibrations with many degrees of freedom 8=16242
 XYZ type, mean-square amplitudes 8=12135
 azides, i.r. spectra, anomalous band splittings 8=21118
 azobenzene 8=4182
 benzene and derivatives, structure of ν(CH) bands, 300 and 80°K 8=12260
 benzene, interaction, lower electronic states 8=7564
 benzene spectra in solid solns., matrix effects rel. to vibr. freqs., 77°K 8=13037
 benzene, u.s. relaxation obs. 8=12687
 borazine and deuteroborazine 8=4145
 boron oxide, "washing out" effect in mol. electron-diffr. pattern 8=16266
 2-bromocyclobutanone 8=12266
 bromomalonaldehyde 8=21144
 bromomalonaldehyde anion 8=21144
 2-bromo-2,4,4-tridentrocyclobutanone 8=12266
 butatriene, mean amplitudes 8=16314
 butatriene, potential field and force constants calc. 8=12264
 caffeine salts 8=14277
 carbonyl group coupling in cyclic anhydrides and imides rel. to solvent effect on valence vibrations 8=16857
 carboxylic acids, H-bonded 8=7571
 p-chloro-phenol, OH stretching band struct. 8=4211
 chlorosilyl dialkylamines 8=1300
 complex mols., absorpt. band shape 8=1215
 contact transform., choice of S-operator 8=7494
 coupling of oscillators in liq. state 8=16854
 p-cresol, OH stretching band struct. 8=4211
 cyclobutane, freq. factor for rate const. 8=14364
 cyclohexane benzene, near u.v. absorption spectrum 8=16861
 cyclopentadiene 8=12267
 cyclopentene, i.r. spectrum 8=7590
 cyclopentene, ring puckering 8=16304
 cyclopropane, force consts. from i.r. and Raman spectra 8=1298
 deuterobenzenes, band structure obs. 8=21683
 diamond, valence force potentials for calc. cryst. vibrs. 8=16968
 diatomic gas, by e interference examination 8=4115
 diatomic isotope effects and JWKB method 8=12137
 diatomic nongray gases, i.r. radiative heat transfer, theory 8=16693
 diatomic potential curves, calc. of vibr.-rot. energy levels 8=12140
 diatomic, quantum mechanics 8=12141
 diatomic, relaxation, dissociation effect 8=4123
 dibenzenechromium iodide, C-H out-of-plane force consts. for ligand mols. 8=14276
 1,4-dibromonaphthalene, triplet states 8=2467
 dichloromethane, ¹³CH₂ valence vibrations in vapour and condensed phases 8=16328
 dihalogenomethanes in CCl₄, methylene group valence vibr. bands rel. to weak intermol. interaction 8=1292
 2,5-dihydrofuran, ring puckering 8=12271
 dihydrofuran, ring puckering 8=16304
 dihydrothiophene, ring puckering 8=16304
 diiodomethane, ¹³CH₂ valence vibrations in vapour and condensed phases 8=16328
 dimer, relative vib. of moiety and jumping freq. of excitation, rel. to energy levels 8=7491
 tetrakis-[dimethylamides] of group IV 8=1290
 2,5-dimethyl-p-benzoquinone 8=8573
 p-dithiane, 16 modes assigned from i.r. absorpt. 8=18575
 ditoluenechromium iodide, C-H out-of-plane force consts. for ligand mols. 8=14276
 dixanthogens, i.r. spectra, anomalous band splittings 8=21118
 electronic Raman effect and vibronic coupling 8=12129
 electron-vibrational transition probability 8=1216
 energy levels of one and two-dimens. anharmonic Morse oscillators 8=1217
 energy transfer in collisions between diatomic mols. 8=21190
 ethane, torsional vibrs, meas. of frequency 8=1284
 ethane, vibr. excited, kinetics 8=18675
 ethylenediamines 8=1283
 ethylgermane 8=1280
 ethylsilane 8=1280
 excited levels rel. to structure determ. by electron-diffr. in high temp. vapour 8=16245
 force constants, extremal props. 8=12143
 force consts. calc. by iterative procedure 8=21042
 formic acid, normal coordinate calc. 8=14279

Molecules—contd

vibration—contd
 p-fluoro-phenol, OH stretching band struct. 8=4211
 formaldehyde, vibrational-rotational interactions for force field determ. 8=4198
 frequencies, 54 molecules, data compilation 8=21036
 furan, u.s. relax. obs. 8=12687
 germanium fluoro- and hydroxyfluoro-compounds and thermal polymerization products, i.r. vibr. freq. of Ge-O-Ge bond 8=4170
 haloacetonitriles 8=16323
 halogenated ethanes 8=12269
 halogenides, mean-square oscillatory amplitudes, calc. 8=4124
 halogens cyanoacetylenes, force consts. 8=1270
 halogens, dipole strengths as function of internuclear distance 8=21084
 heteronuclear, diatomic, constants rel. to electronegativity and reduced mass 8=7492
 d¹ impurity systems, octahedrally coordinated, dynamic Jahn-Teller effect 8=16990
 interatomic distance of various mols., calc. 8=21046
 i.r. intensities, CNDO calc. 8=12148
 isothiocyanates, i.r. spectra, anomalous band splittings 8=21118
 isotropic spacial, autocorrelation functions 8=16242
 ketones, intermolecular forces 8=1287
 Lagrange eqns. with non-vanishing couplings appl. to dependent coords. 8=1219
 ligand-metal-halide complexes 8=1296
 liquid oscillation and spectrum near Rayleigh line 8=21678
 liquids, stimulated Raman scattering, and spontaneous emission, effects 8=4587
 malonaldehyde anion 8=21144
 mean-square oscillatory amplitudes, calc. 8=4124
 metal carbonyls 8=4189
 methane-O₂ mixtures, vibr. energy transfer 8=21200
 methyl bromide and methyl bromide-d₃ 8=12280
 methylgermane and deuterioisotopes, spectra calc. 8=21148
 methyl lithium monomer 8=12282
 methylphosphine, fundamentals and force consts. 8=1289
 methylsilane and deuterioisotopes, spectra calc. 8=21148
 methylsilyl dialkylamines 8=1300
 methylstannate and deuterioisotopes, spectra calc. 8=21148
 methyl vinyl sulphide 8=12283
 monohalogen diacetylenes 8=1270
 naphthalene at liquid He temp., i.r. spectrum, interpretation of fundamental vibrations 8=18577
 naphthols, vibronic transitions, dichroic spectra in PVA sheets obs. 8=14285
 n scatt., interaction effect 8=21060
 1,2,5-oxadiazole, complete assignment from i.r. and Raman spectra 8=16335
 1,3,4-oxadiazole 8=12285
 partition function of Morse vibrating-rotator model of diatomic mol. 8=16240
 pentachlorotoluene from crystals and solns. i.r. spectra obs. 8=9575
 pentadeuteropyridine, structure of vibration bands, i.r. spectra 8=7597
 pentaerythrite, mono, di and trihalogen derivatives, vibr. spectra 8=7576
 p-(perfluorovinyl)toluene copolymer with styrene, molec. motion 8=17191
 γ-picoline-halogen complexes, and comparison with pyridine analogues 8=7592
 phenol-d₃, complete assignment, and torsion 8=16336
 phenol, OH stretching band struct. 8=4211
 phenol vapour, extended assignments and band contour anal. 8=16337
 phosphoramidates and phosphoramidothioates, i.r. spectra obs. 8=7591
 polar diatomic mol. dissolved in nonpolar solvents, i.r. band shapes 8=12885
 polyatomic, anharmonic calc. 8=12133
 polyatomic, frequency calc. using perturbation method 8=4120
 polyatomic, r.m.s. displacement formulae 8=12134
 polyethylene chain, methylene wagging 8=4265
 polymer rod, effects in absorption spectrum 8=7645
 polymers and periodic molecules of finite length 8=21039
 pyrene, vibr. effects in radiationless transitions 8=21114
 pyridine, structure of vibration bands, i.r. spectra 8=7597
 pyridine, u.s. relaxation obs. 8=12687
 2-pyrrolidone, vibration spectra, 3500-250 cm⁻¹ 8=7595
 Raman, relaxation times 8=9485
 relaxation times, amplitude-freq. opticoacoustical meas. 8=7490
 resonances in axially symmetric mols., nomenclature 8=21045
 rigid-body motion rel. to triclinic coordinates 8=8231
 -rotation energy levels of a tetrahedral molecule 8=16243

Molecules—contd
vibration—contd

1,2,5-selenadiazole 8=16342
 spectra, by inelastic electron tunnelling 8=13633
 substituted and perturbed, frequencies and force constants, Green's function use 8=21041
 sum rule for frequencies 8=7489
 symmetric-top mols., vibr.-rot. interaction, theory 8=16241
 tetrachloro-p-xylene from crystals and solns. i.r. spectra obs. 8=9575
 2,3,5,6-tetrachlorotoluene from crystals and solns. i.r. spectra obs. 8=9575
 theobromine salts 8=12300
 thiazoles, monosubstituted, i.r. and Raman spectra obs. 8=4217
 triethylphosphine and related cpds. 8=21137
 thiophene, u.s. relaxation obs. 8=12687
 thiophosphoryl halides 8=16300
 thiophosphoryl halides, spectra 8=7547
 tin fluoro- and hydroxyfluoro-compounds and thermal polymerization products, i.r. vibr. freqs. of Sn-O-Sn bond 8=4170
 trigonal bipyramidal XY₅ molecular model, amplitudes 8=16298
 trimethylaluminium 8=16327
 trimethylene oxide, ring puckering 8=16304
 triphenylaluminium, rel. to i.r. spectrum 8=12287
 trans-uranyl ions, M-O bond force consts. in various media 8=21094
 uranyl salts, crystal spectra, D₂O isotopic shifts 8=5641
 vibrational-translational energy transfer, molec. orientation effect 8=7632
 vibrators and librators perturbed by collisions 8=100
 weakly distorted systems, inversion-vib. levels and splitting 8=4121
 X₂Y₆, bridged type, mean-square amplitude of vibration 8=4126
 XY₃ type mols. and ions, force consts. calc. 8=21047
 XY₂-type oxides, potential relations 8=21038
 XY₂-type with T_h symmetry, force consts. calc. 8=12145-6
 AgCl, optically pumped, level population 8=1235
 AlCl₃ ion, h.f. i.r. active l. vibr., correction 8=4142
 Al₂Cl₆, force field 8=4143
 Al₂Me₂Cl₂, force field 8=4143
 Al₂Me₃, force field 8=4143
 AmO₂⁺, M-O bond force consts. in various media 8=21094
 AsF₃, general force field 8=4157
 AsF₅, mean amplitudes 8=16298
 AsO, potential curves of electronic states 8=1236
 BF₃, force consts. calc. 8=21047
 Br₂(C₂H₅), improving consts. 8=21065
 BrHBr⁺ and BrDBr⁺ ions 8=12174
 CCl₄ transitions and gas and liquid spectra intensities rel. to intermol. interactions 8=16274
 CD₃CD₂Cl, torsional 8=4193
 CD₃, mono, di- and tri-substituted compounds, far i.r. torsional vibration spectra 8=4196
 CF₂ band system from absorpt. at 2500 Å 8=4188
 CF₃, mono, di- and tri-substituted compounds, far i.r. torsional vibration spectra 8=4196
 [(CF₃)₂CF]₂SF₂, i.r. spectra 8=16273
 CF₃SF₃, i.r. spectra 8=16273
 C-H bond strengths, student expt. 8=21109
 CH₃ radical, bending force consts. 8=7624
 CH₃, mono, di- and tri-substituted compounds, far i.r. torsional vibration spectra 8=4196
 CH₃Cl, Fermi and Coriolis resonances in the ν₄ band 8=16319
 (CH₃)₂POCl 8=12286
 (CH₃)₂PSBr 8=12286
 (CH₃)₂PSCl 8=12286
 [C₆H₅]₄As⁺[MoOBr₄]⁻, i.r. Mo-O stretching freq. 8=9552
 CN⁻ in alkali halides, environmental perturbation 8=2405
 CN, electronically excited in active N₂ flames, vibr. population 8=12179
 CO, vibr. relax. in shock-wave and nozzle expansion-flow 8=16270
 CO, vibration-rotation band centred at 6350 cm⁻¹ 8=7505
 CO₂, deactivation by collisions, in presence of Fermi resonance 8=1321
 CO₂ + N₂ mixture, relax. time meas. of ν₃ mode of CO₂ with spectrophone 8=7508
 CO₂, vibr. relax. times 8=4146
 CO₂⁺, ²Π_g → ²Π_g transition 8=16277
 CO₂⁺ ²Π_g → ²Π_g transition probabilities 8=21066
 CaDPO₄ and dihydrate, i.r. spectra obs. 8=5594
 CaHPO₄ and dihydrate, i.r. spectra obs. 8=5594
 ClO₄⁻ ions in alkali-halide lattices 8=22968-9-70
 ClO₄⁻ ions in alkali-halide lattices 8=22968-9-70
 Cu(II) formate in planar network struct. 8=2466
 D, solid, rel. to Raman spectra anomalies 8=9535
 D₂S, harmonic freqs., empirical estimation 8=21072
 D₂Se, harmonic freqs., empirical estimation 8=21072
 FCN, ν₁ and ν₂ vibration-rotation bands 8=12183
 FCN, microwave spectrum of excited states 8=12182
 GeD₃I 8=12187
 H-bond stretching freq., effect of bond strength 8=21141
 H, solid, rel. to Raman spectra anomalies 8=9535

Molecules—contd**vibration -contd**

- H vibr.-rotational spectrum for e ground state, VKB calc. 8=1246
H₂, coherently vibrating, static field effect 8=16283
H₂, dissociative attachment of e, vibrational resonances obs. 8=21182
H₂ e-impact ionization spectrum rel to vibrational thresholds. 8=21272
H₂⁺, effect on dissociation under e and p impact 8=21076
H₂, in electron collisions, rel. to proton production cross section 8=7519
H₂⁺, para, coupling coeffs. for states with v = 5 and v = 6 8=16284
HCN and DCN, l-type resonance doublets 8=7522
HCl dimers, H-bond stretching force const. 8=18532
HCl, in inert-gas matrix 8=9537
HCl, pressure effect 8=21077
HDO in H₂O 8=21690
H₂F₃⁻ 8=2425
(μHO), fundamental frequencies 8=21218
HOBr, force consts. 8=12175
HOCl, force consts. 8=12175
H₂O vapour, pulsed laser action due to vibration-rotation transitions 8=3312
H₂Se, harmonic freqs. and bending freq. 8=21702
H₂Se, sum rule analysis of interacting (2, 0, 0) and (1, 0, 1) states 8=12199
IF₅, assignment, from Raman spectra 8=1568
KCl:OH, i.r. absorpt. spectra rel. to temp. dependence of intensity of OH vibrations 8=18538
KrF₂, absence of Fermi reson. 8=7528
Li metaborate, "washing out" effect in mol. electron-diffr. pattern 8=16266
MnO₄⁻ 8=21085
MoS₄²⁻ 8=2438
N₂, excitation by microwave discharge, vibrational deactivation 8=12211
N₂, lifetime obs. using positive ion Van de Graaff accelerator 8=16183
N₂, mixed with CO₂ and N₂O, relax. 8=12210
N₂, model dipole spectrum consistent with oscillator strength sum rule 8=7533
N₂, vibr. relax. in shocked gas mixtures 8=21195
N₂, vibr. relax. in shock tube, vac. u. v. absorpt. obs. 8=7532
N₂⁺, band intensity distribution due to passage of H₂⁺ through N₂ + He mixture 8=4156
NCO, matrix-isolated free radical 8=16369
NF₃ 8=1260
NF₃, general force field 8=4157
NH₃, bending, solvent effect 8=21093
NO, integrated intensity of fundamental vib. band 8=7535
NO⁺ from N + O collisions, excitation 8=4111
N₂O 8=21088
N₂O, i.r. absorpt. bands rel. to isotopic mols. and crystal lattice vibrations 8=14251
N₂O + N₂ mixture, relax. time meas. of ν₃ mode of N₂O with spectrophone 8=7508
N₂O, relaxation times, spectrophone determ. 8=21090
N₂O, 00¹-10⁰ transition 8=7537
N₂O₃, force consts. 8=7538
NS, γ- and β-systems 8=16293
NSCl, force constants, i.r. spectrum obs. 8=4161
NaCl:OH, i.r. absorpt. spectra rel. to temp. dependence of intensity of OH vibrations 8=18538
NaMg[Cr(C₂O₄)₃].9H₂O, vibronic spectra 8=14247
NbCl₅ 8=14249
NpO₂²⁺, M-O bond force consts. in various media 8=21094
OCS, absorpt. spectrum analysis, 1350-1420 Å 8=16296
OH-stretching, in solid alcohols, bandwidth 8=8228
OH groups in phenol H complexes with benzene and ethers 8=4213
OH, oscillator strengths in 2Σ⁺-2Π band system 8=7544
OH, vib.-rot. interact. and the transition moment 8=7545
ONF, and N¹⁵ and O¹⁸ species, force consts. 8=7539
Os carbonyl halide cpds., solvent depend. stretching freqs. 8=16856
PCl₃, potential function 8=12226
PD⁺, emission bands 8=4167
PF₃, general force field 8=4157
PF₅, mean amplitudes 8=16298
PO₂, bending modes 8=21097
PuO₂²⁺, M-O bond force consts. in various media 8=21094
ReO₃Br, force consts. calc. 8=1265
ReO₃Cl, force consts. calc. 8=1265
ReO₃N²⁻, force consts. calc. 8=1265
S₈ 8=12227
S₈, mean square amplitudes 8=12228
S₂Cl₂, torsional 8=12231
SF₆Cl, mean amplitudes 8=12230
S-N cpds., bond stretching freqs. 8=1299
SO₂, force constants of S-O bond 8=21104
SO₂, liq. and solid, spectra 8=8088
SbCl₃, solid, from NQR temp. dependence studies, 20-150°K 8=22929
SiF₂, force consts. 8=16301
Sr₁₀(PO₄)₆(OH)₂, i.r. frequencies 8=12234
V:Fe⁵⁷:Mössbauer system, force-constant changes and localized modes 8=13338

Molecules—contd**vibration-contd**

- WS₄²⁻ 8=2438
XH₂ groups, sym. and antisym. frequencies, relationship between overtones 8=21040
X₃P. BH₃ type additive compounds, frequency and absorption of vibrations 8=16305
XeF₄, r.m.s. amplitudes calc. 8=21106
XeF₂, r.m.s. amplitudes calc. 8=21106
ZnCl, band head quantum formula 8=4171
- Molecules, mesic and muonic**
(μHO), possible formation and vibrational frequencies 8=21218
pμd wave function rel. to D(p, γ)He³ cross-section 8=11593
(p-μ-p) molecule ion, ground state 8=20657
S-states, bound, variational calc. 8=12392
- Mollier diagrams.** See Thermodynamic properties.
- Molybdenum**
attack by atomic O at high temp. 8=14370
Auger electron yield on Ar⁺ and He⁺ bombardment 8=9279
catalyst, N₂ isotope equilibration 8=18655
coating by plasma jet 8=19337
collector in thermionic converter with vapour deposited W emitter 8=15230
combined effect with Nb on mech. props. and hardness of Nb-Mo steel 8=22385
conductivity, thermal, meas. and analysis, 100-400°K 8=4943
containing Co, Kondo temp obs. 8=9009
creep, 950° to 1385°K, 3500 to 12 000 lb/in² stress 8=13588
crystal, approx. dispersion relations 8=17480
crystal surface structure exam. 8=21992
crystals with adsorbed O₂, surface exam. by LEED and work function studies 8=17165
crystals, deformation at slow rates of strain 8=13587
crystals, dislocation velocity-stress relations 8=17657
cyclotron resonance, corresponding effective masses 8=2126
diffusion in Al 8=1911
dislocations etch pitting single crystal 8=4978
dislocations mobility rel. to amplitude depend. of internal friction 8=22209
effect on Co-Al magnetic alloy 8=22792
electron field emission, anomalous total-energy distribution and electronic structure 8=5411
Fermi surface 8=17887
Fermi surface determ. r.f. size effect 8=22464
Fermi surface investigation by cyclotron resonance meas. at 1.6°K and 9.7 GHz 8=13664
film heteroepitaxial growth on insulating substances 8=17134
films, on W crystal, adsorption and electron emission 8=9269
fluorinated, adsorpt. of Cs, structure of adsorbed layer, and effect on thermionic conversion 8=17154
internal friction due to interstitial atoms 8=17817
laser induced emission of electrons, ions and X-rays 8=13947
lattice expansion, temp. dependence 28°-522°K 8=22125
Kα rad., prep. of Ross difference filters 8=2437
mechanical prop. rel. to 8 × 10²⁰ n/cm² dose 8=8856
micromosaic block size and misorientation in zone-melted crystals, impurity depend. 8=8470
neutron irradiated and annealed, vacancy and interstitial loop identification 8=17610
optical props., rel. to conduction band transitions 8=9553
polycrystalline, γ-irrad. and non-irrad. X-ray scattering 8=22253
polycrystalline target, sputtering coeff. rel. to incident angle of Ne, Ar and Kr ions 8=8766
recrystallized, impurity effects on strain hardening 8=22380
reluctance field dependence, 1.8-35°K rel. to Kübler law deviations 8=22750
secondary electron emission, H⁺ bombardment 8=5423
sorption of CO, physical and chemical processes from low energy electron interactions 8=18702
stress-rupture characteristics, high temp. 8=2061
structure and low-temp. ductility, deform.-induced changes 8=13589
superconducting, energy gap anisotropy, u.s. investigation 8=9048
superconducting single crystals with small residual resistance 2 × 10⁻⁴ Ω 8=5207
surface, accommodation coeffs. of inert gases 8=4734
surface ionization, positive and negative 8=13950
target for ion emission, bombard by Ar⁺ 8=6626
thermionic converter emitters, UO₂ filled, radiation tests 8=15241
thermionic emitters, UO₂-fueled, irrad. studies rel. to in-core converters 8=15226
tip, absorption of O₂, H₂ and N₂, field emission study 8=21905
tracer-diffusion studies 8=17575
low work function region in Cs and Cs-Ba vapours, rel. to pot. as collector in converters 8=15213
zone refined, removal of C and W rel. to residual resistivity 8=17935
C, solubility limit and diffusivity 8=17007

Molybdenum—contd

- Fe-Mo systems, α - γ equil. 8=4709
 MO(VI) extraction, with TBP, mechanism study
 by radioisotopes 8=23076
 Mo-alumina ceramic seals bonding mechanism,
 obs. 8=16743
 Mo-F-Cs system, electron-emission rel. to vapours
 present 8=18261
 with Sn, bonds in organo-Sn cpds., Mössbauer obs. 8=4668
 in UF_6 , determ. by atomic absorpt. spectroscopy 8=18776

Molybdenum compounds

- alloys, anti-oxidation metallurgy 8=23779
 alloys, stress-rupture characteristics, high temp. 8=2061
 cavitation damage resistance 8=5035
 tetrathiomolybdates, i.r. spectra 8=2438
 $[(C_2H_5)_4As][MoOBr_4]^-$, i.r. Mo-O stretching freq. 8=9552
 Ge + MoO_3 in powder form., reaction
 mechanism 8=14365
 Mo permalloy, coercive force, neutron bombardment
 effect 8=18344
 Mo-Al intermetallic resistor films, sheet resistivity and
 temp. coefficients of resistance 8=22520
 Mo_2B , superconductivity transition temp. and
 d-shell 8=2164
 Mo_2C , rhombic modifications and polymorphic
 transitions 8=8561
 $MoCl_5$ -graphite, structure, by single-crystal electron and
 X-ray diffr. 8=1797
 $[Mo(CNS)_6]^{3-}$, ^{14}CNS , isotopic exchange rel. to structure
 study 8=23087
 $Mo(CO)_6$, structure determ. by electron diffr. 8=12236
 MoF_6 , liq., molec. motion, F^{19} relax. 8=12930
 MoF_6 , spin-lattice relax. of F in intense r.f. field 8=14139
 MoF_6 , structure determ. by electron diffr. 8=12236
 Mo-Fe solid solns., mag. props. 8=22749
 Mo_2NiB_2 , crystal structure rel. to analogues 8=17396
 MoO_4^{2-} anion, pH depend. of adsorp. of Fe_2O_3 powder 8=8342
 Mo_2O_8 ion in a crystal of ammonium heptamolybdate
 tetrahydrate, structure 8=8234
 $MoO_3-P_2O_5-K_2O$ glass, X-ray diffr. study 8=8356
 $MoO_3-P_2O_5-Ag_2O$ glass, X-ray diffr. study 8=8356
 MoO_3 in TiO_2 , solid solutions, magnetic
 susceptibility 8=13963
 Mo-Re alloys paramag. susceptibility rel. to band
 struct., obs. 8=22759
 MoS_2 polytypes by e-diffr. 8=17397
 MoS_2 surfaces, detection of monatomic steps and
 vacancies 8=4730
 MoS_2 , thin anisotropic, crystals, delocalized excitons from
 magneto absorpt. study 8=13764
 MoS_2 , vacancy detect. by etch-decoration 8=4963
 Mo-Ti systems, b. c. c., binary interdiffusion 8=17577
 Mo(V) complexes, liquid solutions, Overhauser
 effect 8=21725
 $(Mo_xV_{1-x})_2O_5$, crystal structure 8=17425
 Mo-y at. % Co alloys, $y=1.65, 1.085, 0.535$, mag. props.,
 28-300°K 8=14007
 MoZr crystal surface texture exam. 8=21992

Monitoring. See Radiation monitoring.

Monochromators

- See also Filters, optical; Light sources; X-ray
 monochromators.
 actual Littrow and Wadsworth systems, deviation, scanning
 equation and spectral widths of slits 8=15531
 Czerny-Turner, lab. construction and
 demonstration 8=11154
 Ebert-type plane-grating, scanning, construction and
 characts. 8=3358
 electron beam, for atom excitation cross-section
 data 8=12077
 image illuminance distrib. with concave diffr. grating
 calc. 8=487
 neutron, using Al, PbGe, Cu crystals 8=854
 resonance, for absorpt. meas. in visible and u.v. 8=11155
 slit regulation and recording device 8=20080
 for space vehicles u.v. receivers spectral sensitivity
 determ., vacuum diffr. monochromator 8=11156
 spectral modulation transfer functions determ. 8=488
 spectroradiometer with automatic digital recording 8=6202
 u.v., extreme, off-plane Eagle mounting 8=6527
 volume source, radiation intensity definition 8=11158
 LiF for n spectrometry 8=3724

Monolayers. See Adsorbed layers.

Monomers. See Molecules.

Monomolecular layers. See Adsorbed layers.

Monte Carlo method. See Statistical analysis.

Moon

- albedo under solar wind action, reason for
 differences 8=19245
 Aristarchus crater, tidal influences 8=19239
 close-up views of ground, comments 8=5950
 colour, by photometric analysis 8=14825
 Copernicus H crater, and central peaks of Copernicus,
 Orbiter photos 8=23638
 crater, Alphonsos, geological struct. 8=19243
 crater depth statistics, meteoroidal impact hypo-
 thesis 8=14824
 crater erosion by meteor bombardment, math.
 model 8=23643

Moon—contd

- craters, gravity scaling, Ranger VIII obs. 8=23641
 craters, Ptolemaean, clustering and alignment obs. 8=10335
 craters, secondary, rel. to lunar relief form. 8=10328
 density of soil, simulation by vacuum sifted
 powders 8=10330
 domes, photometric study, rel. to height and
 brightness 8=23640
 earth-moon system astron. params. optical radar
 meas. 8=14827
 earth-moon system, corrected mass derived from motion
 of Eros, 1926-45 8=10340
 Earth-Moon system history, effect of tidal friction 8=23662
 earth-moon system, mass from Eros motion,
 1926-65 8=10341
 earth-moon system, solar perturb. of motion near
 collinear libration points 8=19070
 earth-moon system, Trojan manifold 8=19242
 eclipse, 25th June 1964, Czech photometry and atmospheric
 extinction 8=10326
 e.m. reflection from plane-layered model 8=23645
 emission spectra, 8-13 μ 8=23644
 Ephemeris time det. from lunar occultations 8=5952
 Ephemeris time corrections rel. to revised lunar
 theory 8=10485
 Ephemeris and Universal time difference by lunar photo-
 graphy 8=10486
 features, absolute co-ords., deriv. using stereoscopic
 method 8=23635
 geomagnetic variations 8=14696
 gravitational field from satellite orbits 8=5955
 history, thermal 8=2814
 illumination received, table of relative intensity for any
 phase and altitude 8=5951
 Kepler and Tycho on lunar theory 8=14821
 laser ranging for testing general relativity 8=2953
 luminescence due to solar wind 8=19244
 luminance, enhanced, from normal reflectivity and photo-
 luminesc. enhancement 8=23636
 lunar space communications, techniques 8=23652
 luni-solar daily variation of geomagnetic field at
 Tananarive 8=10040
 mag. field, Explorer 35 investigation 8=14819
 mag. field, intrinsic, Explorer 35 obs. 8=10333
 magnetosphere interaction 8=2815
 materials, method of obs. 8=10336
 moment of inertia, limited by internal structure
 model 8=23639
 neutron emission induced by cosmic rays 8=19240
 oblate, dynamical figure, explanation by nonisothermal
 state of interior 8=19247
 occultation observations for radio sources 8=10301
 occultation obs. of radio sources, two-dimensional
 brightness distrib. 8=5943
 orbit precession rel. to quadrupole moment of
 Sun 8=23691
 Orbiter photographic systems 8=23651
 origin of chondritic meteorites 8=14856
 origin, with Mars, as part of Earth 8=23657
 Ptolemaeus photography, comparison from space probes
 and ground observatories 8=2811
 pulse-height analyzer for charged-particle spectro-
 scopy on lunar surface 8=20214
 radar cross section, time average 8=2810
 radio emission at 25.0 and 30.2 cm by the "artificial
 moon" method 8=10327
 rel. to surface struct., silicates and polyethylene fragment
 shapes in hypervel. impact, obs. 8=13609
 rotation params. meas. from interplanetary
 stations 8=10339
 rough surface scatt., quasi-specular and multiple
 scatt. 8=15412
 selenodesy, laser-radar, operational theory 8=2813
 self-radiation obs. 8=5949
 shock wave, trailing 8=10332
 solar wind flow, effect on, Explorer 35 obs. 8=14828
 spacecraft explorations, review 8=5953
 spectra, differential 8-13 μ , obs. method 8=14822
 surface chemical analysis using scatt.- α particles
 aboard Surveyor V 8=23463
 surface composition and particle size from laboratory and
 lunar reflectance spectra 8=14820
 surface, depolarization of backscattered e.m.
 waves 8=19237
 surface disturbance by footpads of Surveyor 1, inferences
 from photographs and laboratory obs. 8=14818
 surface, inhomogeneous, e. m. wave backscatt. 8=19238
 surface lineaments displayed on Lunar Orbiter
 pictures 8=14823
 surface materials stimulation 8=14826
 surface morphology of Mare Cognitum, Ranger VII
 obs. 8=10329
 surface, optical characteristics 8=2816
 surface, porosity-polarization relationship 8=23646
 surface roughness rel. to emissivity and radio-
 brightness 8=10334
 surface roughness, rel. to thermal emission and
 shadowing 8=2809
 surface, space weathering by exposure to solar
 wind 8=19246

Moon — contd

- surface strength estimate from Orbiter II photo-graph 8=5948
- surface structure, granular, indicated by geometry of impact craters 8=23637
- theory, literal developments on Computer 8=23648
- theory, main problem, literal solution 8=23649
- thermal convection in mantle? comparison with Earth 8=14519
- thermoluminescence, obs. and theory 8=23650
- tidal effect on earth's pole movements 8=9770
- tidal forces, and sun, long period vars. 8=19241
- tidal influence on electron density in ionosphere 8=2656
- twilight colour theory 8=23647
- Tycho i.r. images on dark moon 8=2812
- unipolar generator, due to solar wind 8=23642
- variations in auroral zone 8=10331
- water on surface, evidence 8=23634

Morse potential. See Kinetic theory; Molecules/intermolecular mechanics.

Mosaic structure. See Crystal structure/microstructure.

Mössbauer effect

- See also Gamma-rays/absorption; nuclear excitation.
- analyzer, multichannel with automatic folding through forward backward operation 8=3787
- apparatus, transducer velocity generator 8=20360
- bell, amplitude-time distribution of partial tones 8=19572
- bone crystal surfaces, appl. ion uptake mechanism study 8=14902
- chalcopyrite effect 8=16982
- in crystal structure determs. 8=17326
- crystals with vacancies in the case of alocal vibrations, intensity calc. 8=8209
- ferrocene, effect of press. on resonance 8=1652
- ferrous ions in ice 8=4675
- ferric oxyhydroxide, in structure determ. 8=17370
- field, magnetic hyperfine, sign determ. by Mössbauer-Faraday effect 8=13007
- films, freq. spectrum 8=13024
- films, thin, rel. to spatial distrib. of spontaneous magnetization 8=22779
- garnet-type cpds., of Sn^{119} , rel. to Sn^{4+} coordination 8=17415
- goethites, in structure determ. 8=17370
- haemoglobin fluoride, low temp. spectrum, neighbour nucleus effects 8=21810
- haemoglobin, quadrupole splittings and isomer shifts 8=16344
- ice doped with Mössbauer ions, phase transform. kinetics 8=13069
- intensity sums, formulae for single crystals and polycrystals 8=8211
- lattice distortion effect on Debye-Waller factor rel. to Mössbauer studies 8=1779
- lepidocrocite, in structure determ. 8=17370
- line narrowing, quantum-mechanical model 8=1830
- linewidth calc. for various absorption thicknesses 8=15952
- metals, shift and intensity calc. 8=1643
- multicomponent systems complex, thermal shift, and Debye-Waller factor 8=13023
- polymers, doublet spectra obs. of line asymmetries 8=13022
- powders of small particles, rel. to packing 8=21805
- pressure depend. energy shift, using Debye integral 8=1641
- resonance detectors using conversion electrons, efficiency etc. 8=20673
- solid solutions in the case of alocal vibrations, intensity calc. 8=8209
- spectra in fluctuating environment, mag. field variation 8=13017
- spectra in fluctuating environment, randomly varying electric field gradients 8=13018
- spectra in presence of electron spin relaxation 8=1644
- spectrometer 8=15722
- spectrometer, constant-accel. drive 8=20362
- spectrometer, constant velocity, automation technique 8=8210
- spectrometer, MS10 8=693
- spectrometer, time analyser for vel. precision meas. 8=20361
- spectrometer, variable-freq. u.s. 8=13021
- spectroscopy, use of NGR in chemistry and solid state 8=692
- spectroscopy selection of mounting materials 8=3579
- spectrum intensity, mag. ions exchange interaction dependence 8=8208
- spectrum shift depending on degree of spin-system ordering 8=22734
- steel, stainless, rel. to plastic deform. 8=8219
- sternbergite, rel. to mag. props. 8=14066
- thin films, calc. of Debye-Waller factors 8=8207
- X-rays following internal conversion, new experimental method 8=691
- AgCl single crystals, state of iron study 8=8215
- Au-Fe solid soln., magnetic ordering rel. to electric hyperfine interactions 8=2289
- Co_2 , Sn and Ni_2 , Sn, quadrupole splitting 8=1645
- Cs^{133} , determ. of magnetic moment of first excited state 8=15987

Mössbauer effect—contd

- Cs^{133} , isomer shift of 81.0 keV γ -transition obs. 8=11762
- CuFe_2O_4 , spin relax. obs. 8=21804
- Cu_2FeS_3 (cubanite), rel. to mag. props. 8=14066
- Dy-Al-garnet hyperfine splitting of lowest 2^+ state of Dy 8=9301
- Dy^{161} in Dy^{3+} salts, hyperfine structure at 4.2°K 8=1646
- $\text{Dy}^{161,162}$, 75 and 81 keV states, magnetic and quadrupole moments determ. 8=3829
- Er, magnetic structure study 8=2291
- $\text{ErCl}_3 \cdot 6\text{H}_2\text{O}$ hyperfine splitting of lowest 2^+ state of Er 8=9301
- Eu^{151} in Eu-Yb, conduction-electron contribution to hyperfine field in Eu 8=1633
- Eu metal, 16^+ K anomaly 8=8212
- EuM_2 , (M=Pt, Pd, Zn, Rh), by mag. hyperfine Mössbauer studies 8=18334
- EuPd_3 , mag. hyperfine Mössbauer e.p.r. and n.m.r. studies 8=18334
- Fe ionic cpds., pressure effect 8=4674
- Fe, metallic, C impurity effects 8=20704
- Fe in silicate, site populations in amplitude, quantitative estimates 8=8218
- Fe, thermal-shift and Debye-Waller-factor meas. 8=8214
- Fe^{57} in chalcopyrite (CuFeS_2), resonant configuration 8=1649
- Fe^{57} in ferrites with compensation point 8=1648
- Fe^{57} in FeCr_2S_4 , effective field parameters 8=1647
- Fe^{57} in FeIn_2S_4 , sulpho-spinel, spectra 8=8216
- Fe^{57} in $\text{Fe}(\text{OH})_2$, at 90 and 4.2°K 8=13027
- Fe^{57} in $\text{FeSiF}_6 \cdot 6\text{H}_2\text{O}$, hyperfine interactions 8=8220
- Fe^{57} , in Fe-Si near ϵ -phase 8=8242
- Fe^{57} , meas. method with scatt. geometry 8=1651
- Fe^{57} , Mössbauer energy shift, Gruneisen parameter var. 8=1641
- Fe^{57} Mössbauer spectra of iron(II)-bis(α -diimine) complexes 8=8200
- Fe^{57} , in neptunite, oxidation state 8=8369
- Fe^{57} in $\text{Na}_2[\text{Fe}(\text{II})(\text{CN})_6]\text{NO}$, $2\text{H}_2\text{O}$, hyperfine interacts. and splitting 8=1650
- Fe powder dispersed in perspex spectra 8=5470
- Fe^{57} at 1-0.08°K, rel. to Co nuclear polarization in Fe 8=4676
- Fe^{57} in RbFeF_3 , effective field parameters 8=1647
- Fe^{2+} in square-planar environment, $\text{BaFeSi}_4\text{O}_{10}$ 8=13026
- Fe^{2+} in FeCr_2S_4 , sulpho-spinel, spectra 8=8216
- Fe^{57} , variable-freq. u.s. spectrometer obs. 8=13021
- Fe^{57} , in $\text{Y}_3\text{-Ca}_2\text{Fe}_{12}\text{-Sn}_2\text{O}_{12}$, obs. 8=4677
- FeBr_2 , rel. to hyperfine structure at 78°K and 4°K 8=13025
- Fe-C austenite, quadrupole splitting disappearance at elevated temps. 8=21808
- FeCl_3 , rel. to hyperfine structure at 4°K 8=13025
- FeCl_2 , rel. to hyperfine structure at 78°K and 4°K 8=13025
- FeCO_3 , Fe^{57} asymmetry of quadrupole splitting components 8=21806
- FeCO_3 , quadrupole doublets, vibrational anisotropy 8=16983
- FeF_3 , antiferromagnetic, interpretation of broadened and shifted lines 8=21807
- FeI_2 , rel. to hyperfine structure at 78°K and 4°K 8=13025
- Fe-Mo alloys, Fe-rich, precip. reactions and solid solns. from Mössbauer spectra 8=4678
- $\text{Fe}(\text{NCS})_2 \cdot 4\text{Py}$, probabilities for modifications 8=8213
- $\text{Fe}(\text{NO}_3)_3 \cdot 9\text{H}_2\text{O}$ magnetic relaxation 8=2378
- Fe-12 at. % Ni alloy, finely dispersed system, rel. to phase compositions 8=17280
- Fe-12 at. % Ni alloy, finely dispersed system, rel. to particle size and oxidation 8=17280
- Fe-Ni invar. Fe^{57} spectrum, plastic deform. effect obs. 8=21811
- $\alpha\text{-Fe}_2\text{O}_3$, ferromag. ultrafine particles 8=2318
- Fe_3O_4 , hyperfine mag. fields rel. to sublattice magnetizations 8=21809
- Fe_2O_3 powders, rel. to packing 8=21805
- Fe_2O_3 , superpara-, ferro- and antiferromag., depend. of crystallite size 8=14016
- FePO_4 , calcinated, study of magnetic ordering 8=8217
- FeS_2 , effect of press. on resonance 8=1652
- $\text{Fe}_{0.88}\text{S}$, pyrrhotite, mag. structure from Fe^{57} resonance 8=16985
- FeS, troilite, mag. structure from Fe^{57} resonance 8=16985
- Fe_{1-x}Se with NiAs structure, rel. to atomic structure 8=16981
- FeSn, study of antiferromag. characts. 8=18339
- Fe_3Sn , study of ferromag. characts. 8=18339
- $\text{Ca}_2\text{-Fe}_2\text{O}_4$ and related cpds. 8=13028
- Gd^{158} , obs. rel. to 79.5 keV gamma rays 8=3786
- H_2SnO_3 conversion to SnO_2 , kinetics obs. 8=14386
- $\text{Ir}^{191,193}$, g factors, for first excited states 8=3836
- Ir^{193} in Ir cpds. and salts 8=4679
- Ir^{193} in Ir-rare-earth cpds. 8=1634
- $\text{K}_2\text{Fe}(\text{CN})_6$, paramagnetic hyperfine structure 8=16986
- $\text{K}_2\text{Fe}(\text{CN})_6$, pressure effect 8=4673
- $\text{K}_4\text{Fe}(\text{CN})_6$, pressure effect 8=4673
- $\text{K}_4[\text{Fe}(\text{CN})_6]$, pressure effect 8=4673
- $\text{K}_4\text{Fe}(\text{CN})_6 \cdot 3\text{H}_2\text{O}$, ferroelectric phase transitions, test for lattice-dynamical model 8=22667
- KFeF_3 : Fe^{57} , isomer shift, calibration 8=16988

Mössbauer effect—contd

- Kr⁸³ in Br⁻ and BrO₃⁻ crystals 8=8221
 Kr⁸³, investigation using Rb⁸³ obtained from Sr⁸⁸(p;2p,4n) at 660 MeV 8=3817
 Kr^{83m} prep. by n irradiation of Se⁸² 8=3872
 Mg_{0.293}Mn_{0.696}Fe_{1.77}O₄:Sn, symmetry round Sn⁴⁺ 8=16980
 Mg ferrites, spectra in external mag. fields 8=18342
 MgFe₂O₄:Sn, symmetry round Sn⁴⁺ 8=16980
 Mg-Mn ferrites, spectra in external mag. fields 8=18342
 MgO:Fe²⁺, comparison with spin-lattice relaxation 8=9452
 MgO:Fe²⁺, low temp. quadrupole splitting 8=13019
 Mn ferrites, spectra in external mag. fields 8=18342
 Mn⁵⁴ in MnCu, anomalous low-temp. susceptibility 8=13962
 MnFe₂O₄:Sn, symmetry round Sn⁴⁺ 8=16980
 NH₃ adsorption on Fe catalyst, spectra 8=13108
 NH₄(Fe,Al)(SO₄)₂·12H₂O, study of electronic relax. 8=21812
 NH₄Fe(SO₄)₂·12H₂O magnetic relaxation 8=2378
 NiO, antiferromag. ultrafine particles 8=2318
 NiO, Co⁵⁷-doped, Fe⁵⁷ spectrum rel. to bulk and ultrafine particles 8=4680
 NpAl₂:Np²³⁷ rel. to nuclear moment ratios of Np²³⁷ 8=11790
 NpCl₄:Np²³⁷ rel. to nuclear moment ratios of Np²³⁷ 8=11790
 Pb(NbFe)_{1/2}O₃, study using Fe⁵⁷ 8=16984
 Pd-Fe alloy containing H, hyperfine fields and isomer shifts temp. dependence 8=13020
 Pt-Fe alloys, transition in Pt¹⁹⁵ 8=2334
 Ru⁹⁹ M₁-E₂ transition, time-reversal invariance obs. 8=7091
 Sb¹²¹, in Sb isoelectronic cpds., isomer chem. shifts 8=16987
 Sn bonds with Co, Mn, Mo and Re in organo-Sn cpds., obs. 8=4668
 Sn(halide)₂, isomeric chemical shift 8=8222
 Sn, isomer shifts rel. to electron struct. in cpds 8=12233
 Sn nuclei in Mn ferrites, mag. fields at nuclei investigations 8=9382
 Sn¹¹⁹ nuclei, impurity in semiconducting cpds., isomeric shifts 8=9086
 SnO₂ in glycerine/castor oil, line widening, temp. and viscosity dependence 8=1603
 Sr(TaFe)_{1/2}O₃, study using Fe⁵⁷ 8=16984
 SrTiO₃-1.15 Sr(TaFe)_{1/2}O₃ solid soln., study using Fe⁵⁷ 8=16984
 Te(halide)₂, isomeric chemical shift 8=8222
 Te¹²⁵ in CuCr₂Te₄, ferromag. spinel, mag. hyperfine structure study 8=8223
 Te¹²⁵ in Te(NO₃)₄, atomic structure study 8=4887
 Te¹²⁵ in TeO₂, atomic structure study 8=4887
 Te¹²⁵ in Te, atomic structure study 8=4887
 Tm, determ. of crystalline elec. field determ. 8=8203
 TmT₂ (T = transition element), cryst. elec. field splittings 8=16979
 V:Fe⁵⁷, recoil-free fraction and second-order Doppler shift meas., localized modes 8=13338
 W¹⁸³, 46.5 keV level, and lifetime 8=15999
 Yb^{174,176}, g_N meas. for first excited states 8=3832
 YbCl₃·6H₂O hyperfine splitting of lowest 2¹ state of Yb 8=9301

Multiple stars. See Stars.**Muonium**

- atomic, presence in chem. inert substances 8=6818
 behaviour in scintillating plastic 8=723
 chemical reactions 8=5713
 h.f. splitting as test for Q.E. 8=11285
 hyperfine struct. 8=15741
 triplet, behaviour obs. by precession in transverse mag. field 8=6818

Muons

- bremsstrahlung on collision with resting electron, theory 8=722
 magnetic moment anomaly in muonium as test for Q.E. 8=11285
 magnetic moment, intermediate vector boson contrib. 8=3602
 magnetic moment, using nth rank tensor of photon polarization 8=6815
 mass values maximization of ratio decay rate/Q-value 8=3601
 momentum, from $\pi^+ \rightarrow \mu^+ + \nu$, obs. ν_μ mass upper limit 8=6814
 e- μ e. m. difference from μ -p scatt. obs. 8=20395
 N- μ scatt. inequality 8=6923
 progress in nuclear physics, book IX 8=15627
 as e, statics obs. in μ trident prod. 8=20392

capture

- β decay theory anomalies 8=3862
 μ^- capture rate calc. for He³ using He³ charge form factor and vacuum polarization corrections 8=20393
 $\mu^- + p \rightarrow n + \nu_\mu$, muon capture rate 8=721
 by nuclei rel. to radiative π absorpt. 8=20775
 radiative, by free protons in hydrogen 8=6816
 in Ca⁴⁰, rate calc. in hole-particle model 8=3916
 He³, rate in channel $n + n + p + \nu$ 8=6817
 Li⁶, total rate assuming nuclear clustering 8=3915

decay

- electron spectrum and measurement methods 8=11472
 $\mu^- \rightarrow e^- + \nu_e + \nu_\mu$ as detector for reaction
 $\mu d + Y_2 \rightarrow \mu Y_2 + d$ 8=12115

Muons—contd**decay—contd**

- μ^- , helicity of e 8=3593
 $\mu^- \rightarrow e^-$, in 140 000 Oe field, e⁺ asymmetry 8=3618
 rel. depend. violation of special relativity 8=2935
 spectrum obs., parameters determ. 8=20394

detection, measurement

- cosmic ray flux at 8800 m. w. e. 8=3591
 cosmic rays ν induced and atmospheric, 7500 m. w. e. 8=3590
 lifetime, rel. depend., violation of special relativity 8=2935
 $p + \mu^- \rightarrow n + \nu_\mu$ prop. counter for capture rate meas. 8=3457
 p - μ discrimination by Owen-Batchelor method, theory of high-energy limit 8=6672
 telescope for μ reactions, rejection of stops 8=1048

interactions

- e capture by μ^+ from H and He atoms 8=7481
 μ^+ μ^- coupling to weak vector bosons 8=720
 $\mu^- + \text{He}^3 \rightarrow \text{H}^3 + \nu_\mu$, asymm. in recoil of H³ 8=15740
 trinucleon μ capture rate and S' state 8=20583

production

- B + $\bar{B} \rightarrow \mu + \nu$, with π as Regge particle 8=11502
 cosmic-ray, positive-to-negative charge ratio at sea-level 8=20606
 cosmic ray spectrum at sea-level 8=20605
 $K \rightarrow \mu + \nu, \pi \rightarrow \mu + \nu$, evaluation of a_K/a_π 8=15798
 μ tridents from 12 BeV μ reactions in Pb, rel. to statistics 8=20392
 $\mu^+ \mu^-$, from vector meson decay, boson model 8=20497
 ν -N interaction, with formation of μ , spin depend. 8=20370
 pair by cosmic ray μ on nuclei 8=15909
 $\pi \rightarrow \mu + \nu$, with π as Regge particle 8=11502
 $\pi \rightarrow \mu \nu$ superconductivity model with SU(3) \times SU(3) symm. 8=11501
 superconductivity model with SU(3) \times SU(3) symm. 8=11501

scattering

- high energy, in NaI(Tl), energy loss and straggling 8=8776
 μ -p, e-p comparison as test for Q.E. 8=11285
 μ -p, 1.5-6.0 BeV/c obs., e. m. e- μ difference calc. 8=20395
 nuclei, radiative background compared with electrons 8=11868

Music. See Acoustics/musical.**Musical instruments**

- brass wind instruments, optimum length of valve tubes 8=3069
 guitar string tone, harmonic analysis for different excitation methods 8=6172
 organ pipes, self excited vibrations 8=10749
 percussive, electronic tuning aid 8=6173
 pipe organ, sound absorpt. due to resonant vib. of pipe walls 8=3068
 sounds, Fourier integral analysis 8=192
 stiff strings, normal freq. meas. 8=6171
 stringed, analytical mechanics of bridged deformation 8=15070
 timbre as function of spectrum envelope and fundamental freq. 8=15079
 trumpet, trombone, tuba and French horn tones, attack transients and steady states, Fourier analysis 8=6170
 violins, acoustic parameters of wood 8=3070
 violin vibrato tones, quality 8=193

Navier-Stokes equations. See Flow; Hydrodynamics.**Nebulae**

See also Galaxies.

- Andromeda (M31), 11-cm radio obs. 8=10268
 Andromeda, radioemission obs. 8=14791
 Andromeda, RR Lyrae star projected on arm 8=10229
 Barnard Loop, structure from Gemini II photographs obs. 8=10222
 η Carinae spectrum polarization obs. 8=10228
 cluster of stars, unclassifiable, in large Magellanic cloud 8=14777
 Crab, circularly polarized radiation upper limit 8=10309
 Crab flux density and 77.5 Gc/s emission 8=10223
 Crab, high energy photons due to universal microwave field 8=14795
 Crab, plasma waves 8=14794
 Crab, polarised intensity distrib. at 1.55 cm 8=10284
 Crab, radioemission of longwave radio source, interpretation by coherent plasma mechanism 8=14813
 Crab radio emission sources, lunar occultation obs. 8=10224
 Crab, sky survey of cosmic X-rays and source spectra 8=10230
 Crab, synchrotron radiation and resultant thermal instability 8=5944
 Crab, synchrotron X-ray production 8=5918
 Crab, 3C273B, structure and mass envelope from radio wave scatt. 8=19176
 Crab, X-rays in 8-80 keV, search with sounding rocket 8=5916
 Crab, X-ray source, balloon obs. 8=19231
 Crab, X-rays, thermal 8=5941
 expanding, He triplet spectrum, capture-cascade intensities 8=19194

Nebulae—contd

- expanding, He triplet spectrum, self-absorption 8=19195
 extragalactic, Kant's theory 8=2828
 galactic H_{II} regions, radial velocities and kinematics 8=19208
 gaseous, H_2 recombination lines relative intensities 8=14793
 NGC 5189 position rel. to X-ray source CRUX 8=10214
 NGC 1976, 6618 and 6853, inertial motions 8=23563
 NGC 604, diffuse, in Triangulum galaxy M33, spectrophotometric studies 8=19193
 NGC 6960 spectrum, FeX 6374A line, obs. 8=10225
 NGC 6302, flux density and thermal spectrum 8=5911
 NGC 700, filaments H_2 line contours obs. 8=10232
 NGC 2440, emission-line intensities for excitation from [MgI] to OIV and [NeV] 8=10231
 Orion, fine structure of new class 8=14792
 Orion, high resolution obs. at 408 MHz 8=23564
 planetary, bolometric corrections for central stars 8=10220
 planetary, evolution of central stars 8=14790
 planetary, flux densities, at 10 cm wavelength 8=5911
 planetary, He 2s state, depopulation rate 8=5913
 planetary, high-latitude, new 8=5914
 planetary, intensities of emission lines 8=5910
 planetary, lifetime 8=19191
 planetary, Ly- α radiation density 8=5912
 planetary, model atmos. for central stars 8=10217
 planetary, obs. of radio emission at 3 microwave freqs. 8=10218
 planetary, IC418 and NGC6572, optical depths and electron temps., from r.f. spectra 8=23561
 planetary, origin mechanism 8=10221
 planetary, params. rel. to nucleus temp. 8=10219
 planetary, pure H plane-parallel models, rel. to Lyman continuum problem 8=19190
 planetary, radio emission at 408 MHz 8=5909
 planetary, Seaton's distance scale 8=23562
 planetary, stratification of luminesc. 8=10215
 planetary, temps. of central stars and u.v. spectrum 8=10216
 planetary, 35 central stars, effective temp. calc. 8=23560
 radio recombination lines and anomalous Balmer line intensities 8=5915
 reflection, illumination hypothesis 8=19192
 reflection, polarization and colour vars. rel. to distance from Meropa 8=10226
 Seyfert galaxy NGC 1068, nuclear motions 8=10227
 surrounding stars, temp. from continuity obs. 8=5896
 Taurus A (Crab), at 1420 MHz, r.f. occultation obs. 8=5917
 30 Doradus, Balmer-line isophotes and r.f. thermal flux rel. to radio flux obs. 8=10234
 $H_{n_{105}} \rightarrow n_{104}$ line intensity and width rel. to vels. obs. 8=10233
- Néel temperature.** See Magnetic properties of substances.
 Negatons. See Electrons.
 Negatrons. See Electrons.
 Nematic phase. See Liquid crystals.

Neodymium

- glass laser, travelling-wave mode 8=20000
 glass:Nd laser, travelling-wave, features 8=3333
 isotopes, specific shift and deformation coefficient 8=21024
 laser, continuously tunable, applications 8=15485
 laser, giant pulse generation 8=6472
 laser, Q-switching by Pockels shutter 8=20001
 laser, radiation mixing with ruby 8=436
 laser, simultaneous pulsing 8=15477
 H_2 definition, spectral-isotopic method 8=9743
 Nb-Ta-W alloys, creep strength, effects of metallic carbides and borides 8=22384
 Nd:Cr:YAG, sidelight fluorescence changes, due to laser at 1.06 μ 8=6473
 Nd: glass laser amplifiers, gain saturation 8=447
 Nd:glass laser, picosecond substruct. of laser spikes 8=20002
 Nd¹⁴³, ¹⁴⁵, neutron capture, γ -ray spectra 8=16032
 Nd³⁺-containing phases, e.p.r. rel. to molecular and structural props. 8=9436
 Nd³⁺ in disordered matrices, non-uniformly broadened luminesc. bands 8=14329
 Nd³⁺, energy transfer with Yb³⁺ in LaF₃ 8=14328
 Nd³⁺ in glass, CaWO₄ and YAl garnet, quantum efficiency 8=5667
 Nd³⁺:glass laser, stimulated Raman emission in H_2 at 8.84 μ m 8=15484
 Nd³⁺ in glass, influence on Q-spoiled laser dynamics 8=11017
 Nd³⁺, high-repetition-rate Q-spoiled, in YAG, lasers, output characts. 8=15487
 Nd³⁺ in CaF₂ and LaF₃, stimulated emission, high-temp. effects 8=22960
 Nd³⁺ in CaF₂, magnetic rotatory power temp. var. 8=5576
 Nd³⁺, in CaF₂, new laser line oscillations from ions at noncubic sites 8=3335
 Nd³⁺ ions, luminesc. characts., influence of glass composition and activator conc. 8=18592
 Nd³⁺ ions in rare-earth trichlorides, new satellite structure 8=12070
 Nd³⁺ in LiNbO₃, e.p.r. 8=18428

Neodymium—contd

- Nd³⁺/SeOCl₂ liquid laser, preparation 8=20008
 Nd³⁺, in silicate glass, Faraday rotation, freq. depend. 8=18531
- Neodymium compounds**
 glass laser, picosecond pulses, spontaneous appearance 8=439
 telluride phases, crystal chemistry 8=17202
 Nd glass, measurement cross-section stimulated emission 8=449
 Nd-glass laser, rad. spectra, spatial inhomogeneity 8=450
 Nd silicate glass laser, stimulated emission cross section 8=14292
 NdAlO₃, crystal structure, X-ray diffr. 8=8544
 NdBr₃, paramag., Br⁷⁹,⁸¹ quadrupole spectra 7=9469
 Nd³⁺:CaF₂, cubic e.p.r. spectrum 8=5539
 NdGa garnet, antiferromag. ordering by n-diffr. at 0.31 K 8=22884
- Neon**
 adsorption on Molecular Sieves 5A, 10X, and 13X, at 77.3 K and press. range 10² to 10⁻⁶ torr, effect of preadsorbed H₂O 8=21897
 afterglow, msec microwave pulses nonlinear interactions 8=21340
 atom, collision broadening and shift of Kr spectrum 8=20956
 atoms, electron scatt., 40 keV 8=7447
 atom, e scatt., long-range interaction, nonadiabatic contrib. 8=12092
 atom, Ne-p e capture excitation of 3s, 4s states of H 8=7462
 atoms, 2p levels, average lifetime 8=20963
 atomic interaction potential calc. 8=7456
 breakdown, secondary ionization mechanisms, theory 8=16419
 bulk mod. and Debye temp. at T=0°K, anharmonic contribs. 8=13594
 collision cross sections, elastic differential, meas. 8=4108
 collision with H₂⁺, H₃⁺, prod. of H atom in 3s state 8=21191
 conductivity, thermal, line-source transient-heat-transfer technique 8=16701
 crystals, lattice constants, thermal expansion and isothermal compressibility 8=1803
 diffusion in glass melt 8=4554
 discharge, hot-cathode, electron energy distribution in moving striations 8=12404
 discharge tubes, radial distribution of parameters in subnormal region 8=7668
 double resonance laser spectroscopy of excited states 8=11066
 electric discharge positive column, electrons energy distrib. 8=7655
 energy levels, radiative lifetimes, population mechanism 8=1171
 excitation cross sections for some of the states of 2p⁴-3p configuration 8=20973
 free-carrier drift-velocity studied in liquid and solid state 8=8119
 gas, He-Ne mixture excited by α , scintillation mechanism 8=12202
 gas, spectral self-broadening and oscillator strengths 8=7416
 glow discharge, secondary electron energy distrib. 8=16409
 glow discharge in toroidal tube, expt. investigation 8=4286
 i.r. Zeeman-tuned laser, for fine-structure anal. of absorpt. spectra 8=11160
 ionization cross-section, electron impact 8=7700
 ionization cross-sections for 100-2000 eV electrons 8=12446
 ionization rate temp. dependence correction 8=12450
 ions, incident on polycrystalline targets rel. to sputtering coeff. 8=8766
 isotope mixtures, thermal diffusion props. 8=1492
 isotope separation, in Hg diffusion column 8=1208
 Landé factors, meas. by saturation from laser 8=1186
 laser, He-Ne mixture, pulse delay 8=3314
 laser pumped microwave emission in excited states 8=12071
 laser, Zeeman type, polarization in mag. field 8=11037
 liquid, cooling of high-field electromagnets 8=15261
 liquid, isothermal compressibility and density to press. of 1000 atmos. 8=21555
 metastable atoms in glow discharge, conc. at low temp. 8=1368
 mol., recombination, e-ion, e-temp. depend. 8=12451
 molecular flow through capillary, interaction with tube wall 8=7893
 population transfer and alignment by spontaneous emission 8=20985
 refractive index, real part, calc. from Kramers-Kronig dispersion relation 8=16707
 scattering ionization, short range forces 8=1364
 self-consistent phonon theory, phonon spectrum and bulk thermodynamic props. 8=13336
 633 n.m. spectral line emitted by He³-Ne²⁰ discharge, effect of press. and mixture on profile 8=16295
 solid, free carrier mobility 8=17863

Neon—contd

- solid at 0°K, parameters from interact. potential of gas 8=1468
 solid, zero-point energy, effect of long-range 3-body forces 8=22083
 solution and diffusion in tridymite and cristobalite 8=8247
 thermal conductivity, hot-wire cell meas., 30°–100°C, 120–150 torr 8=16700
 thermal conductivity meas. with hot-wire cell 8=6210
 third virial coeff., and for nonpolar mixtures 8=12677
 thermal plasma, continuous emission spectrum 8=16207
 transition rates at levels excited by electron collision 8=20947
 X-ray, $\kappa\alpha$ satellites (non-diag. lines) intensity 8=1170
 He–Ne discharge tube, dia. and pressure effects 8=7676
 in He–Ne laser, collision excitation 8=11061
 He–Ne laser, ears on line profile of decay transitions 8=3316
 He:Ne laser, intensity fluctuations, correlation meas. 8=3315
 He–Ne laser, stationary regime and oscilln. damping 8=15471
 Ne(IV and V), mean lines of some excited levels 8=4097
 Ne-like ions, phys. props rel. to electronic config. for excited states 8=1148
 Ne₂, ground state, wavefunctions and potential curves 8=7526
 Ne₂, press and temp. depend of recombination rate. 8=21282 A
 Ne–Ar, cataphoresis in d. c. discharges 8=1334
 Ne–Ar system, electron density in plasma prod. by fission fragments 8=15215
 Ne–H bubble chamber, cryogenic 8=20224
 Ne–H₂ liquid-vapour phase equilib., 26°–42.5°K, 10–25 atm. 8=16937
 Ne–He laser, self-oscillations, stability 8=19974
 Ne–He mixtures, integral Joule-Thomson effect 8=15139
 Ne–He plasma, cross section for second kind collisions, meas. 8=21016
 p + Ne → H(2p) + Ne*, cross-section 8=21009
 Ne–O₂ gas lasers, mechanism of laser action 8=11975
 TiO₂ surface discharge, channel development 8=1330
 Xe–Ne couples in binary mixture, translation spectra 8=7425

Neon compounds

No entries

Neptunium

No entries

Neptunium compounds

- NpAl₂:Np²⁺, Mossbauer effect, nuclear moment ratios 8=11790
 NpCl₄:Np²⁺, Mossbauer effect, nuclear moment ratios 8=11790
 NpO₂²⁺, M–O bond force consts. in various media 8=21094

Nernst effect. See Magnetothermal effects.**Nernst–Ettingshausen effect.** See Magnetothermal effects.**Neumann algebra.** See Algebra; Elementary particles; Field theory, quantum.**Neutretos.** See Neutrinos and antineutrinos.**Neutrinos and antineutrinos**

See also Nuclear reactions due to/neutrinos.

- B + \bar{B} → μ + ν with π as Regge particle 8=11502
 CERN apparatus and expts. 8=15724
 CERN p synchrotron neutrino programme 8=3587
 conference, Varenna, Italy, June 1964 8=6747
 cosmic ray, μ production, 7500 m. w. e. 8=3590
 cosmic ray ν rate at 8800 m. w. e., meas. and obs. 8=3591
 energy losses due to neutrino processes in hot plasma 8=10137
 force, long range, between particles due to ν pair exchange 8=20273
 mass, finite and finite e. m. coupling with matter 8=14980
 μ capture reactions, Doppler effect rel. to γ - ν ang. correl. 8=16065
 $\mu^- + p \rightarrow n + \nu_\mu$, muon capture rate 8=721
 $n + \mu^- \rightarrow n + \nu_\mu$, prop. counter system for μ^- capture meas. 8=3457
 $n(p) \rightarrow p(n) + e^-(e^+) + \bar{\nu}(\nu)$, decay observations 8=6798
 ν_μ absorption by protons 8=20371
 ν_μ mass squared using range-energy relation in He bubble chamber obs. 8=862
 ν -N interaction, with formation of μ , spin depend. 8=20370
 $\bar{\nu}$, prompt, in n-induced fission of Pu^{239,241} 8=20851
 $\nu_1 + N \rightarrow N^* + l$, lepton polarization calc. 8=3585
 $\nu_1 + N \rightarrow N^* + l$, N* polarization 8=3586
 $\nu + n \rightarrow \mu^- + p$, ν elastic scatt. obs. 8=3589
 $\nu = \bar{\nu}$ expts, and lepton charge conservation 8=15725
 ν -p sum rule used to derive e-p scatt. inequality 8=6923
 orbital electron capture induced by $\bar{\nu}$ 8=1042
 pairs from hot stars 8=19130
 $\pi \rightarrow \mu + \nu$, mass limit 8=6839
 $\pi \rightarrow \mu + \nu$, with π as Regge particle 8=11502
 $\pi \rightarrow \mu \nu$ superconductivity model with SU(3) × SU(3) symm. 8=11501
 pulsed source reactivity meas. in reflected reactor 8=4009
 scattering by electron, cross-section 8=6799

Neutrinos and antineutrinos—contd

- scattering by nuclei, cross section rules from current commutation relations 8=16061
 solar, capture by Cl³⁷ atoms 8=23718
 solar flux, Brans-Dicke gravitation theory 8=14731
 solar ν , inverse β decay and elastic scatt. meas. 8=2848
 solar, use in search for $(\nu e)(\bar{\nu} e)$ scatt. 8=14871
 spectra, calc. of enhanced beam flux density produced by 70 GeV protons 8=20369
 in stars evolution, prod. in β processes rel. to matter density 8=10138
 superconductivity model with SU(3) × SU(3) symm. 8=11501
 transport operator in plane geometry 8=3993
 transport, relax. lengths props. in angle-space synthesis approx. 8=3716
 transport, solns. of Chandrasekhar eqns. 8=3011
 transport, thermalized populations kinetics in heterogeneous media 8=4000
 waves, source and use for graphite props. meas. 8=3719
 weak interactions theory testing by high energy ν interactions 8=3588
 white dwarfs, energy loss 8=10150
 B⁸ solar neutrino flux dependence on heavy element composition 8=5968
 B⁸ solar neutrino flux dependence on rate of the reaction He³(He³, 2p)He⁴ 8=5969

Neutron diffraction

guides, present state of development 8=15846

Neutron diffraction crystallography

See also Crystal structure, atomic.

- Bragg reflections used for monochromatization giving high resolution 8=13243
 computer-controlled single-crystal diffractometry, counting time optimization 8=13214
 error elimination from multiple reflection on four-circle diffractometer 8=17312
 indexing reflections on 3- or 4-circle diffractometers, graphical aid 8=17320
 at liquid N temp., use of Joule-Thomson refrigerator as cryostat 8=8501
 phase problem, soln. using anomalous scattering 8=13244
 specimen motion effects 8=21976
 systematic absences due to mag. scattering caused by symmetry elements 8=13242

Neutron diffraction examination of materials—contd

- alloys, liq. and amorphous, structure and correl. 8=12795
 β -brass, order-disorder transition 8=17051
 glycerol, molecular translational and rotational analysis 8=21609
 liquid metals, atomic motions compared with polycryst. solid 8=12796
 liquids at high pressures, container 8=8001
 liquids, molecular translational and rotational analysis 8=21609
 liquids, Van Hone distrib. function, new approx. 8=12797
 magnetic structure determ. by spin density Patterson function 8=22735
 magnetic superstructures in reciprocal space by n-diffr. method 8=18293
 metals, ferromag., inelastic scatt. from spin-waves, rel. to wave vector q 8=2315
 metals, liquid 8=8002
 metals, liq. scatt. data compared with X-ray scatts. 8=12794
 neutron radiography, divergent beam collimator 8=21975
 paramagnetic exchange broadening d scatt., temp. depend. 8=13968
 n-propanol, molecular translational and rotational analysis 8=21609
 Al in Cr solid solution, antiferromagnetism obs. 8=14063
 Ba_{2-x}Sr_xZn₂Fe₁₂O₂₂, quasi-spiral ordering, at 4, 2–400°K 8=9372
 Be, long-wavelength scatt. meas. of defect clusters induced by n-irrad. 8=22177
 CoCr₂O₄, spinel, mag. study 8=9374
 Cr, spin density wave studies under high pressure 8=22876
 Cu, recrystallization and cold-rolled textures 8=17278
 EuSe, magnetic structure 8=22803
 Fe, polarized n scatt., rel. to phonon motion of mag. atoms 8=14012
 FeSn, rel. to mag. structure 8=2320
 Gd, magnetic study 8=14021
 H solid, cross-section due to mol. libration waves 8=8267
 Ho, helical periodicity, under high pressure 8=14040
 KH₂PO₄, anomalous incoherent scattering of thermal neutrons in Laue-case 8=13267
 Ln₂O₂S₂ (Ln=rare-earth), crystalline structure 8=4883
 MgCr_{2-x}Mn_xO₄, tetragonal distortion of Jahn-Teller type 8=13269
 MgGa_{2-x}Mn_xO₄, tetragonal distortion of Jahn-Teller type 8=13269
 MnCr₂O₄, spinel, mag. study 8=9383
 Mn₂P, magnetic structure 8=22736
 O¹⁸, in enriched-¹⁸O₂ coherent scattering length 8=8553
 α -O₂, solid, structure obs. 8=4882
 SiO₂ vitreous, intensities calc. for random network model 8=8467

Neutron diffraction examination of materials—contd

- SnO₂, rel. to scattering amplitudes of seven Sn isotopes 8=1809
 (Sr, Ba), Zn₂Fe₁₂O₂₃ (Y) ferrite, spin ordering 8=22858
 Pd-Au-D system, α phase 8=17407
 Pd-Au-H system, α phase 8=17407
 Tb, ferromag. spin waves, dispersion reln. from n scatt. 8=18351
 Tb, helical periodicity, under high pressure 8=14040
 UC₂, 300-5°K, rel. to mag. props., phase change and cryst. struct. 8=1810
 UFeO₄, ferromagnetic, and magnetic measurements 8=18353
 UO₂, Debye-Waller factors, anharmonic temp. contribs. 8=13299
 VFe, atomic spin values by polarized n-diffr. 8=18354

Neutron sources. See Neutrons/production.

Neutron spectra

- from (α , n) reactions on medium and heavy nuclei 8=7232
 in crystalline moderators, flux values near discontinuities 8=7292
 epithermal, determ. by Cd difference method 8=20554
 fast-neutron, in Daphne reflector, experimental and calculated 8=12009
 flux energy depend., calc. from activation meas. 8=849
 in graphite, meas. near temp. discontinuity 8=12000
 in graphite, time-depend., rel. to comparison of different scatt. kernels 8=16147
 in moderator, heterogeneous theory of reflected lattices 8=4004
 n-d, deuteron breakup, 14.1 MeV 8=11643
 position depend. thermal spectra in U²³⁵ multiplying assembly 8=11999
 p reactions with nuclei 30-340 MeV, anomalies 8=1051
 reactor neutrons energy distrib., up to 20 MeV obs. 8=16146
 reactor, thermionic, flux density determ. 8=1116
 resolution corrections, by pulsed source time of flight technique 8=20566
 slow, determination from foil activations 8=846
 space dependent, in plain water-Fe-water shield layers, calc. 8=20879
 thermal energies from soln. of Corngold eqn. 8=3998
 thermal neutron leakage spectra investigation 8=11611
 thermalization, time dependent, Monte Carlo method 8=11981
 in VVR-S reactor, meas. by stationary and dynamic methods 8=7311
 in water, rel. to temp. and poison concentrates 8=7331
 in Be, thermalization analysis 8=7303
 from Be⁹(p, n)B⁹ reaction, high-resolution fast-n spectra 8=1056
 D(n, p)2n, at 14 MeV 8=3715
 in D₂O-moderated lattices, epithermal and thermal indices 8=20866
 in D₂O, time-depend. 8=6948
 U²³⁵ fission fragments 8=11967

Neutron spectrometers

- associated particle time-of-flight spectrometer, fast neutron scattering 8=11625
 cross-section and temp. meas. 8=7355
 defocusing, for MeV range 8=15856
 diffractometer, biaxial 8=20567
 emission, absorpt. and scatt. aspects 8=20565
 high resolution, for cold source of high flux reactor 8=6964
 n- γ discriminating detector 8=11627
 for nuclear level identification, from orb. momentum of incident n 8=7041
 1-15 MeV, measuring energy and direction 8=6969
 photomultiplier, satellite pulse effect 8=20569
 polarized chopper for producing bursts 8=20568
 p recoil scintillation, 10s of keV range 8=11628
 pulse height discriminator 8=3479
 resolution corrections, by pulsed source time of flight technique 8=20566
 resonance parameter determ., resolution 8=15840
 semiconductor, sandwich using Li⁶ and He³ reactions 8=6968
 single crystal, time-of-flight for use with reactor 8=3725
 supermonitor radio channel, dead time instability rel. accuracy 8=6955
 time-of-flight, computer analysis of resonances by S wave 8=856
 time-of-flight, correlation type, with magnetically pulsed polarized neutrons 8=11626
 He³ semiconductor sandwich, increased efficiency to 20 MeV 8=6967
 Li⁶, He³ types, for fast-neutron spectra in Daphne reflector 8=12009
 LiF monochromator, correction factors 8=3724

Neutrons and antineutrons

See also Cosmic rays/neutrons; Nucleons and antinucleons.

advances in nuclear science and technology, book III 8=17691

β -decay, quark shell model of baryons, finite mass correction 8=15819

beta decay, ratio C_A/C_V and time reversal invariance 8=845

Neutrons and antineutrons—contd

- in body bounded by vacuum, n-th order collision probabilities 8=7297
 Boltzmann eqn., time-depend., spectral props. in cylindrical geometry 8=20545
 branching processes in multiplying medium, statistical theory 8=1998
 coupling parameter, axial vector, p-n 8=20253
 decay of free n, ν correlation 8=3712
 decay of pulse in low temp. Be 8=20905
 delayed emission, quantitative analysis of fissile materials 8=12012
 density field in heterogeneous systems with pulsed source, meas. 8=20548
 elec. dipole moment calc. with new CP violation model 8=6828
 electric dipole moment, model 8=3713
 electric dipole moment rel. to CP violation 8=11607
 emission from lunar surface 8=19240
 fast-reactor cross sections, collapsing many-group to few-group 8=3997
 first-flight, in coupled reactor, effect on kinetic behaviour 8=16148
 flux density, cavity boundary conditions 8=11982
 half-life of free n, $T_{1/2} = 10.80 \pm 0.16$ min 8=6943
 leakage from 2-dimens. system, collision probability calc. 8=7296
 mass difference n-p, calc. 8=15825
 mass difference n-p, rainbow graph model calc. 8=11587
 mass difference p-n, field theoretic approach 8=11586
 mass difference p-n, in terms of p-e and n-e cross-sections 8=655
 mass difference p-n, rel. to bootstrap model of hadron dynamics 8=11486
 mass difference from p using Dashen-Frautschi method 8=20267
 mass from capture-gamma ray energy as student excise 8=6944
 Milne's problem for plane slab with constant source 8=3994
 multigroup transport eqns., convergence of source iteration tech. in soln. 8=11997
 multiplication in reactor, new concept for subcritical system with reflector 8=7275
 neutron gas in finite media, anal. of behaviour 8=7311
 n-wave propag. in moderating media, eigenfunction anal. 8=11986
 one-speed transport eqn., closure relns. for eigenfunctions 8=847
 prompt, in NORA reactor, decay const. meas. by interval distrib. tech. 8=4010
 prompt, in spherical-cavity reactor, time depend. kinetics of population 8=4003
 pulse decay in moderator, anal. 8=4007
 pulsed in slab geometry 8=20555
 pulsed n source, Cockcroft type, for thermal reactor phys. 8=7282
 radiation when moving in a magnetic field 8=6945
 reactor noise, threefold corrls. and third order moments 8=11984
 reactors, extrapolation distance, calc. 8=11979
 real and adjoint fluxes, bi-linear functionals, perturb. anal. 8=7294
 slowing down of rel. to humidity meas., high speed 8=9839
 source energy spectra and ang. distrib. by e bombard. of Pb, Bi, W and U 8=11867
 spatial distrib. in H₂O, from T(p, n)He³ source 8=11612
 star, and eqn. of state of nuclear matter 8=19166
 thermal-group constants in three-region lattices, calc. 8=11988
 thermal n flux distribution and flux trap effect in active core of UA-RR-1 reactor 8=20871
 transport, anisotropic scatt. representation in S_n codes 8=3999
 transport eqn. in 3-dimens., truncation of spherical harmonic expansion 8=11990
 transport, invariant imbedding theory 8=7307
 transport kernel, first-flight collision probab. calc. 8=20544
 transport, 1-dimens. critical slab problem with anisotropic scatt., soln. 8=20546
 transport operator in spherical assembly, fundamental mode 8=7302
 transport in plane geometry 8=20547
 transport theory, two-region problem 8=7305
 transport theory, two-region problem 8=7306
 transport, transforms. of variational problems 8=7308
 tunneling reactions 8=20765
 wave propag. in graphite, effects of Bragg cut-off 8=7285
 Cf²⁵² fission source, standard, construction and emission props. 8=6950
 H²(n, p), 14.1, 18, 21.5 MeV search for trineutron 8=11649
 Sb¹²⁴ delayed neutron precursor 8=3875

absorption

See also Nuclear excitation; Nuclear reactions due to neutrons.

Doppler resonance profiles, mathematical theory 8=848
 human body, influence on dose meas. 8=855

Neutrons and antineutrons—contd**absorption—contd**

- in multi-nuclide systems, intermed. resonance absorpt., one eqn. for calc. 8=15849
- pile oscillator for meas. 8=4033
- in solids, spectrum, series representation and temp. transforms, appls. 8=7310
- spectrometers, absorpt. aspects 8=20565
- Au foil, induced β, γ activity for flux meas. 8=11620
- B, thermal, cross-section 8=20808
- B,C coating prep. for antiradiation screens 8=20551
- Pu²⁴⁰, resonance escape probability, Monte Carlo calc. 8=16152

angular distribution

- Corngold eqn. soln., and resulting thermal-n spectra 8=3998
- emerging from plane surface in semi-infinite scatt. variational approach 8=11994
- $Kp \rightarrow K^* \pi^+ n$, 6 GeV/c ang. correl. in final states 8=798
- macroscopic flux distrib. in light water reactor, $1/2$ group model 8=20867
- monochromatization of beams giving high resolution by multiple Bragg reflection 8=13243
- pulsed source technique for synthesis 8=7273
- Ca⁴⁰ (n, α_0), 5.13 MeV, obs. 8=16095
- Ca⁴⁰ (n, α_0) reaction, curves $E_n = 2.90$ and 3.28 MeV 8=16094
- Cr⁵³ (p, n) Mn⁵³, 2.3, 2.4, 2.5 MeV 8=3926
- Li⁶ (Li⁸, n) C¹³, 4.1 MeV bombard., rel. to C¹¹ levels compound nucleus model 8=11950
- Si²⁸ (d, n) P²⁹, 3 MeV n- γ ang. correl. 8=16117
- W^{182, 184, 186}, states obs. 0.3-1.5 MeV 8=1074
- Y⁸⁹ (p, n) Zr⁸⁹, 5.503 MeV, low lying states obs. of Zr⁸⁹ 8=977

capture. See Nuclear reactions due to/neutrons.**detection, measurement**

- See also Dosimetry; Neutron spectrometers.
- absorpt. in reactor, pile oscillator 8=4033
- antineutron, 2-4 GeV/c from π following annihilation using scintillation counter 8=6970
- associated particle time-of-flight spectrometer, fast neutron scattering 8=11625
- borazine and borazorene derivatives scintillation counter 8=6963
- charged particle coincidence 8=3722
- cosmic ray monitors, lifetime within 8=15877
- counter, 0-14 MeV 8=850
- counting statistics, interval distrib. in reactor 8=7276
- cross-section meas. by bright line technique 8=7198
- cross-section meas., thermostat 8=11893
- (D, D) and (D, T) depth dose in tissue-equiv. phantom 8=15847
- detectors, adjacent, interaction, in water 8=6962
- digital techniques in meas. current from n detectors 8=6624
- distribution in long H₂ counter, by semiconductor detector 8=852
- dosimeter, thermoluminescent 8=20564
- efficiency meas. method 8=3722
- emission aspects of spectrometer 8=20565
- fast neutron radiometers, power sensitivity 8=20562
- flux by Au foil absorpt. 8=11620
- flux density from activated Au, correction of β -detectors 8=6966
- fluxes of incident epicalcium neutrons, calc. and expt. 8=7286
- foils for dosimetry, thermal neutrons 8=851
- GET reactor, core change effects 8=7270
- half-life of free n, $T_{1/2} = 10.80 \pm 0.16$ min 8=6943
- image intensifier tube, increased efficiency 8=6954
- low fluxes, use of "spinner" 8=20202
- meas. of activation correction of activation probe via Albedo concept 8=7299
- n counting system containing fission detection 8=4028
- n- γ discriminating detector for n spectrometer 8=11627
- n- γ mixed, dose equiv. and quality factor, organic scintillator meas 8=20561
- n- γ pulse-shape-discrimination in B loaded liq. scintillation detectors 8=20563
- neutron monitoring for radiological protection, conference Vienna, Austria (1966) 8=15852
- neutrons, 14 MeV, detection, nuclear reactions in cellulose nitrate 8=11619
- paraffin pile with Na(I)/Tl detector for KeV range 8=11624
- personal dosimetry, use of hair 8=11315
- photoneutrons, liq. scintillation detector 8=20560
- plastic scintillation for 10-70 MeV, efficiency determ. 8=11621
- polarimeter, α -particle avalanche counter 8=6952
- reactor flux, employing fission chamber, covering 10 decades 8=4026
- in reactor, spectrum deformation using threshold data 8=3456
- recoil p counter for flux 8=3720
- Rossi- α expt., point reactor theory 8=7300
- scatt. separated from capture and fission effects 8=3723
- scintillation detectors 8=6956
- scintillation detector with spherical moderators, energy response 8=11623

Neutrons and antineutrons—contd**detection, measurement—contd**

- scintillator, Gd loaded to measure (n, 2n) cross-sections 8=20558
 - scintillator, organic, with controlled γ -background 8=15853
 - scintillator, organic, efficiency determ. using accelerator 8=6961
 - scintillators, organic, fast neutron response 8=15855
 - secondary-dose equivalent 8=841
 - solid-state detectors, advantages 8=12021
 - source strength, via Mn bath tech., resonance scatt. self-shielding tech. 8=7208
 - space vehicle instrum. directional detector 8=6958
 - stilbene scintillation detector, instrumentation 8=6965
 - supermonitor radio channel, dead time instability rel. accuracy 8=6955
 - thermal, calibration 8=853
 - thermal, flux density standard, optimal geometry 8=20869
 - thermal flux, using glass beads with B¹⁰ 8=6951
 - time distrib. analysers, count-loss corrections 8=20559
 - time-of-flight, computer front end 8=6960
 - transport theory, an inverse problem and dynamic programming 8=11613
 - ultrasonic cavitation in water 8=3721
 - Au¹⁹⁷, differential flux density by resonance detectors 8=6957
 - B, method of B¹⁰ isotope determ. 8=14456
 - BF₃ counters, paraffin-moderators with counting nearly proportional to dose-rate 8=15854
 - He³ detector, high temp. 8=6959
 - La¹³⁹, differential flux density by resonance detectors 8=6957
 - Mn⁵⁵, differential flux density by resonance detectors 8=6957
 - Ra-Be (α , n) standard source, comparison of meas. 8=11618
 - Sm¹⁵², differential flux density by resonance detectors 8=6957
 - Sb-Be photoneutrons, energy estimate using meas. of γ -ray of Sb¹²⁴ 8=11622
 - W¹⁸⁶, differential flux density by resonance detectors 8=6957
- diffusion**
- across temperature discontinuity in cryst. moderators, graphite and Be 8=20872
 - in anisotropic media, measurement 8=11614
 - appl. to criticality in heterogeneous media 8=7272
 - in benzene, pulsed meas. at 20°C, transport mean free path 8=20549
 - Boltzmann equation, non-local, in absorbing disk geometry 8=6115
 - Corngold eqn. soln., and resulting thermal-n spectra 8=3998
 - density field in heterogeneous systems with pulsed source, meas. 8=20548
 - entropy prod. in non-absorbing moderator 8=15850
 - finite cylindrical medium, matrix factorization soln. 8=15024
 - graphite, decay of thermalized neutron fields 8=7288
 - in graphite, n-wave obs. 8=3719
 - Jacobi polynomial method for solving Boltzmann's transport eqn. 8=11983
 - in JEN-2 reactor, pulsed determ. of parameter $\alpha = \beta/1^*$ 8=20882
 - with modulated source, one dimensional system 8=11617
 - multigroup eqns., convergence of source iteration tech. in soln. 8=11997
 - multigroup theory, boundary perturbations 8=4001
 - operator-type perturbation method utilizing variational principles 8=11992
 - in plain water-iron-water shielding layers, multi-group calcs. 8=20878
 - in polyethylene, rectangular moderation assemblies 8=20550
 - in reactor core and reflector 8=11982
 - slab method, S_N calc. method 8=20874
 - space-time group diffusion eqns., soln. by time-discontinuous tech. 8=4002
 - temperature regular of samples 8=6218
 - transport eqn. for critical slab, perturbation theory 8=16143
 - transport equation soln., isotropic, for spherical-symmetric medium 8=16150
 - transport process, Boltzmann soln. by extrapolation 8=3003
 - transport theory, kinetics, mathematical foundations 8=15848
 - transport theory in one-dimensional geometries, integral 8=16151
 - two adjacent media, from point source 8=4005
 - two-group transport eqns. 8=11991
 - variational functionals for space-time neutronics 8=7287
 - in BeO assemblies of bucklings beyond (B²)*, crit. study of decay 8=16159
 - ZrH, parameters meas. 8=16161

effects

- See also Nuclear reactions due to/neutrons.
- activity of radioisotope in reactor, hybrid computer for calc. 8=4025
- austenitic steel, B distrib. from obs. of He gas bubbles 8=13040

Neutrons and antineutrons—contd**effects—contd**

delayed, effective fraction rel. to source strength in reactor 8=16145
 diamond, current glow processes, dosimetric capabilities 8=20205
 dosimetry, depend. on distance from neutron source 8=10444
 fast, irradiation of water, rel. to charged particle slowing down 8=644
 glass, optical, thermal, effects 8=8771
 graphite, dimens. changes rel. to bromination test 200°C 8=8764
 graphite, irradiated, optical absorpt. 8=14202
 graphite, quasi monocrystalline, thermal conductivity 8=13389
 graphite, thermoelectric and galvanomagnetic props. 8=5384
 metals, b.c.c., rel. to rate controlling mechanism of slip 8=4987
 pn-pn devices, narrow base, permanent damage 8=22642
 paraffin block (human body imitation) 8=615
 polymethylmethacrylate, effect on permittivity 8=18180
 pulsed neutron researches, multiplying and non-multiplying systems 8=12020
 silica glass, on dielec. loss at low temps. rel. to OH⁻ conc. 8=18172
 solid solutions, rel. to rate controlling mechanism of slip 8=4987
 steel, stainless, voids obs. 8=22251
 Al, damage and recovery rel. to defect doping effect 8=1953
 Al, low temp. irradi., electrical resistivity recovery 8=2134
 Al, stacking fault removal 8=17670
 Al-Li alloys, grain boundary migration and gas bubble growth 8=8456
 α -Al₂O₃, induced macroscopic growth along a and c axes 8=13132
 Al₂O₃, on lattice, density, length, energy, thermal cond. and microstruct. 8=22245
 Al₂O₃, lattice expansion and density decrease 8=13249
 Al₂O₃, 5×10^{21} fast neutrons cm⁻², damage 8=22244
 Al-Zn alloys, n-irradiation effect on Guinier-Preston zone formation 8=17274
 Al-10% Zn alloy, irradi., pre-precipitation rate at 78°K 8=21980
 Au foil, self shielding and self-absorption rel. to n flux meas. 8=11620
 Be, low temp., decay of neutron pulse 8=20905
 Be, low temp. irradi., electrical resistivity recovery 8=2134
 Be, n-irradiated, recovery meas. 27-77°K 8=22249
 BeO, decoration at high temps. of twin boundaries and dislocations 8=22199
 BeO irradi., determ. of Li⁶ conc. and diffusion 8=8672
 BeO, irradi. at high temp., dislocation loops 8=8761
 BeO, radiation damage, electron microscope investigation 8=22250
 16/13 CrNi steels, high-temp. embrittlement after irradi. 8=22362
 Cu crystal, slip band development 8=22212
 Cu, dislocation pinning 8=1974
 Cu, small dislocation loops, type 8=13437
 Cu₂O, absorpt. spectrum and photocond. 8=5597
 Cu₂O exciton absorpt. spectrum, obs. 8=9521
 α -Fe, rel. to C precipitation 8=17059
 Fe crystals with 8-20 p.p.m. C, n-irradiated, yield stress rel. to radiation hardening 8=17800
 Fe, plastic deformation, stress-strain curves 8=22348
 Fe, plastic deformation, work-hardening parameters 8=22349
 Fe-N supersaturated solutions, irradi. rel. to nitride precipitation 8=17060
 Fe-Ni alloy, on mag. props. 8=2326
 Ge diodes, irradiated, L-shaped current characteristics 8=22630
 n-Ge, Hall meas. during irradiation over 78-330°K 8=18042
 LiF crystals, radiation heating in reactor 8=13488
 LiF, rel. to F-centre exchange interactions from optical and e.p.r. spectra 8=17684
 LiF, formation of macrodefects and metallic Li colloids 8=12947
 LiF, n-irradiation, colloidal Li e. p. r. meas. rel. to colloid distrib. 8=9431
 LiF, paramag. centre due to atomic H² formation 8=18427
 MgO, on lattice, density, length, energy, thermal cond. and microstruct. 8=22245
 MgO, lattice expansion and density decrease 8=13249
 Mo, dose of 8×10^{20} neutrons/cm², mechanical properties 8=8856
 Mo, n-irradiated, vacancy and interstitial loop identification 8=17610
 Mo permalloy, coercive force, bombardment effect 8=18344
 Nb, superconducting, on magnetization behaviour and transition temp. 8=2169
 NiO effect on elect. props. 8=18058
 Pt, damage and recovery rel. to defect doping effect 8=1953
 Se, hexagonal, effect on conductance, rel. to temp. and rad. damage 8=18067

Neutrons and antineutrons—contd**effects—contd**

Si damage, as fast n counter 8=4030
 Si diodes, irradiated, L-shaped current characteristics 8=22630
 Si, irradiation damage, investigation by transmission electron microscopy 8=17707
 n-Si, elec. props. rel. to defect structure and annealing 8=5283
 Si, energy given to lattice by primary ions 8=2033
 n-Si, Hall meas. during irradiation over 78-330°K 8=18042
 Si, impurities testing by non destructive neutron activation method 8=18086
 Si, rel. to O₂ conc. effects 8=5279
 Si, containing O₂, thermal conductivity, irradi. effects at 80°K 8=8663
 Si, p-type, thermal neutron irradiation effects 8=18068
 W, elec. resist. and hardness 8=2141
 W, microstructure changes rel. to mech. props. 8=21998
 W, point defect damage, annealing phases and mechanism 8=17601
 ZrO₂, cubic, influence on ionic mobility 8=5152

interactions

D(n,p)2n, at 14 MeV, neutron spectra 8=3715
 K⁺ n 2.3 GeV/c change exchange and p⁺ Regge trajectory 8=3665
 Λ -neutron stimulation, hyperfragments A = 50, calc. 8=15861
 n + D \rightarrow p + 2n, counter telescope for energy and ang. distrib. 8=11646
 n-d, 14.1 MeV, coincidence meas. 8=11643
 n + He³ \rightarrow p + H² rel. to "elementary particle" model of nuclei 8=15873
 n-n low energy parameters in n-d scatt. 8=15841
 n-p capture theory 8=827
 n-p pairing interaction, charge-independent 8=3771
 np, 2-10 GeV, search for nucleon T = $\frac{1}{2}$ isobar 8=3699
 ν + n \rightarrow μ^- + p⁺, ν elastic scatt. obs. 8=3589
 π^+ n \rightarrow ω p, Regge-pole model with L-S coupling 8=20444
 π^+ + n \rightarrow $\Sigma\pi$ + K⁺, in polyethylene, 1 GeV/c, Σ polarization 8=864
 \bar{p} n \rightarrow \bar{N}^{*+} (1238)p, at 2.8 GeV/c, isobar and anti-isobar production 8=844
 \bar{p} + n \rightarrow 2 π^- + π^+ in D bubble chambers, (Γ^{π^0} =1-0)-3 pion state analysis 8=20436
 H³(n,d)2n, 15.1 MeV, n-n scatt. length deduced 8=20543
 Nd^{145,146}, capture, γ -ray spectra 8=16032
 U²³³ fragment energy by 430, 630 keV and 1.1 MeV neutrons 8=11974
 U²³⁵ fragment energy by 100, 260, 700 keV and 1.3 MeV neutrons 8=11974
 U²³⁵, spin depend. of n cross-section 8=20849

moderation

absorption resonance in aqueous MnSO₄ soln. calc. from slow down theory 8=7208
 cosmic ray monitors, lifetime within 8=15877
 in crystalline moderator, flux values near discontinuities 8=7292
 diphenyl decay const. pulse meas., time of flight effects 8=16149
 graphite, diffusion across temp. discontinuity 8=20872
 in graphite, slowing down time, influence of chem. binding effect 8=7330
 in graphite, spectra meas. near temp. discontinuity 8=12000
 graphite thermalization params., n-wave obs. 8=3719
 heating up in cryst. moderators of low-energy neutrons 8=7293
 in hydrogenous mixture, second spatial moment, effect of heavier nuclei 8=7312
 length, effect of empty channels 8=20894
 n-wave propag. in moderating media, eigenfunction anal. 8=11986
 in polyethylene rectangular assemblies 8=20550
 pulse decay, pseudoexponential 8=20553
 in RI heavy water reactor, study of cold moderator combs. 8=7315
 slowing down, multiple collision soln. 8=7304
 slowing down in nonmultiplying medium, approx. theory 8=3717
 slowing down theory in reactor, eigendistrib. for continuous energy variable 8=20876
 in solids, spectrum, series representation and temp. transforms. appls. 8=7310
 spatial dependence, in water 8=1129
 thermal, density fluctuations, application of slowing down kernels 8=16158
 thermalization initial value problem 8=11980
 thermalization, time dependent, Monte Carlo method 8=11981
 time decay constant in pulsed multiplying assemblies 8=1120
 time eigenvalues, secondary model 8=20552
 transport operator fundamental mode, manoenergetic pulse calc. 8=20877
 in Be assembly, decay of pulse, anal. via energy-depend. mean lifetimes 8=7332
 Be, diffusion across temp. discontinuity 8=20872
 D, age and fast effect 8=16160

Neutrons and antineutrons—contd**moderation—contd**

- D₂O, age and fast effect 8=16160
 D₂O lattices, RESCUE method for resonance escape probability calc. 8=20880
 in D₂-O moderated lattices, epithermal and thermal spectral indices 8=20866
 H₂O decay const. pulse meas., time of flight effects 8=16149
 PuBe source, scattering moderator effect 8=1121

polarization

- in ferromagnets 8=15843
 generator, formulae for T(d, n)He⁴, D(t, n)He⁴ 8=15844
 multiple scatt. and finite geometry effects 8=11610
 polarimeter, α -particle avalanche counter 8=6952
 spectrometer, spin-flip chopper 8=20568
 thermal beam refl. from magnetized mirrors 8=15842
 from B¹¹(p, n)C¹¹ reaction 8=7189
 C¹²(He³, n)O¹⁴, 2.24-3.70 MeV, DWBA analysis 8=3965
 C¹²(n, n)C¹² and C¹²(n, n')C¹², 15.85 MeV neutrons 8=7204
 Co, magnetized, transmission 8=2031
 Dy, dimensions of ferromag. correlation range by neutron depolarisation obs. 8=22797
 H²(d, n)H³, below 400 keV, polarization of n emission obs. 8=20582
 Ni, magnetized, transmission 8=2031
 N¹⁴(d, n)O¹⁵, 3.1-3.7 MeV, ang. momentum transfer 8=3956
 in N¹⁵(d, n₀)O¹⁶, ang. depend. of polarization and diff. cross section 8=7227
 U²³⁵, spin depend. of n cross-section 8=20849

production

- continuous—pumping D-T generator 8=11608
 delayed, in infinite slab, initial-value transport problem 8=20875
 deuteron bombardment of tritium targets 8=11290
 d-T reaction, yield from annihilation radiation 8=874
 DIDO source, intensity improvement by rethermalization 8=20556
 $\gamma p \rightarrow n\pi^+$, ang. depend. of cross-section 8=6841
 generator, acceleration tube, properties of 8=3714
 generator with high intensity of n flux 8=3718
 generator with short structure accelerating system 8=15851
 high flux densities in range 10¹⁶ cm⁻²s⁻¹, applications 8=11609
 $\mu^- + p \rightarrow n + \nu_\mu$, muon capture rate 8=721
 n⁰ from $\pi^- + C^{12}$, probability < 2.6 × 10⁻⁶ 8=11915
 photoproduction of antineutrons, photon energy 4.0 to 5.7 BeV 8=20570
 $\pi^- p \rightarrow \eta^0 n$ and charge exchange polarization 8=3665
 $\pi^- + p \rightarrow \pi^- + \pi^+ + n$, 1.38-3.00 GeV/c p⁰ formation and decay ang. dist. 8=3685
 $\pi^- p \rightarrow \pi^- \pi^+ n$, 8 GeV/c, 2421 events 8=6851
 $\pi^- p \rightarrow p\bar{p}n$, 8 GeV/c, obs. in bubble chamber 8=6857
 $p + \bar{p} \rightarrow n + \bar{n}$, charge-exchange, calc. using U(6, 6) and absorpt. model 8=829
 $p\bar{p} \rightarrow n\bar{n}$, Regge pole analysis, anomalies 8=6932
 proprietary accelerators 8=6689
 pulse neutron generator 8=12020
 reactor, energy distrib., up to 20 MeV obs. 8=16146
 $\Sigma^+ \rightarrow n + \pi^+$ S-wave theory using quark model of baryons 8=6975
 source calibration, radiation-fields similarity method 8=20538
 source to target geometry, computer soln. of activation eqn. 8=3854
 source using d-d reaction for cyclotron 8=6703
 source-width analysis in nuclear reactors 8=20873
 superbooster, physics 8=1118
 thermal, radiation meters calibration 8=853
 by thermonuclear reaction in 6-pinch plasma, laser scatt. obs. 8=1399
 by t+d with t in Zr or Ta, yield decrease diffusion mechanism theory 8=6921
 variational functionals for space-time neutronics 8=7287
 PuBe source, intensity, moderator effect 8=1121
 Pu²³⁸O₂, depleted in O¹⁸ for radiation minimization 8=10443
 T(p, n), He³, obs. 8=882
 U²³³ and U²³⁵ fission, relative yields, 0.08-1 MeV 8=7264
 U²³⁵, prompt n emission 8=20853

reflection

- Doppler-effect, by rotating crystal, condition for time focusing 8=15845
 Al crystal monochromator 8=854
 Cu crystal monochromator 8=854
 PbGe crystal monochromator 8=854

scattering

- anisotropic, in Boltzmann eqn. soln. 8=20541
 in antiferromagnets and fluctuations in strong magnetic field 8=5498
 charcoal, activated/adsorbed ethylene system, rel. to adsorbant mol. motions 8=21901
 continuum wave-functions, for determ. of spectroscopic factors, comment 8=15931
 cross-section meas. by bright line technique 8=7198
 crystal analysis, use of anomalous scattering 8=13244
 by defect in solids, mathematical formulation, long wavelength 8=22167
 defocusing spectrometer, for MeV range 8=15856

Neutrons and antineutrons—contd**scattering—contd**

- diffuse, time depend., and diffusion in crystalline solid solns. 8=8667
 double-differential slow-n data, corrections for multiple scatt. 8=11894
 elastic diffuse, from mixed mag. systems 8=22766
 elastic 14 MeV, analysis using Fraunhofer diffraction model 8=1071
 elastic, on nuclei of mean atomic weight 8=3932
 fast neutron, meas., particle spectrometer 8=11625
 ferromagnet, Heisenberg, with magnetic impurity, diffuse inelastic neutron cross section 8=9319
 flux, at plane black boundary, boundary condition 8=6947
 4 π technique for separating capture and fission effects 8=3723
 graphite, scattering law S(α , β), values at 1300°K and 1800°K 8=11898
 Hauser-Feshbach model in scatt. from V⁵¹, Mn⁵⁵, 1.0-3.1 MeV 8=15975
 heavy nuclei, imaginary part of optical pot. 8=7197
 Heisenberg system, paramagnetic 8=22758
 hydrogen in solid and liquid, estimation by samples by n thermalisation 8=23197
 Kⁿ, sum rule analysis 8=6896
 liquids, rel. to eigenfunctions for collective motion in simple classical fluids 8=21419
 liquids, form factor calc. in classical fluid 8=7851
 liquids at high pressures, container 8=8001
 liquid, simple, new approx. for Van Hove distrib. function 8=12797
 methane, liq, slow n scatt., allowing rot. relax. functions of order 3 and 4 8=12798
 methane, solid, rotational hindrance effect 8=13038
 methylbenzenes, hindered rot. determ. 8=17484
 Milne's problem for 2 adjacent spaces, solution 8=1119
 molecule, spherical-top, including rotation-vibration interaction 8=21060
 molecules, structure, at high energies 8=1234
 multiple and finite geometry effects in polarization expts. 8=11610
 multiple, calc. using combination of Monte Carlo and analytical methods 8=6946
 multiple, soln. to slowing down 8=7304
 multiple in target, theory including atomic recoil 8=20804
 n- α phase shifts, polarized, 25 and 28 MeV 8=6949
 n-d counter telescope for energy and ang. distrib. 8=11646
 n-d Fadeev eqns., sensitivity to n-n parameters 8=15841
 n-d, Hamada potential, variational calc. 8=885
 n-d, length calc. using N-N non-local separable pot. 8=11647
 n-d, length calc. using pair pot. 8=881
 n-d length, obs. anomaly rel. to 3N binding energy 8=11648
 n-n length from H³(n, d)2n, 15.1 MeV 8=20543
 nuclei, even-even, using square-well generalized optical model 8=16086
 nuclei, heavy, 6.24 MeV, optical model parameters obtained 8=16085
 nuclei, polarized, elastic cross sections at E = 4 MeV obs. 8=7203
 by a nucleus, time dependent wave packet behaviour 8=20803
 paramagnet, Ising 8=9297
 paramagnetism, theory 8=9296
 pentanol, quasi elastic 8=8000
 polarization parameter 300-700 MeV 8=6927
 in polyethylene, for Nelkin-kernel, cross-sections and thermal n spectra 8=20802
 by polymer solutions, elastic, effects of hydrodynamic interactions 8=4542
 quantum gas, slow neutrons 8=16685
 reactors, spectra, review 8=7269
 resonance parameter determ. 8=15840
 shadow bar to shield detector from source 8=7199
 slab method, S_n calc. method 8=20874
 spectrometers, scatt. aspects 8=20565
 in spherical geometry media, Boltzmann eqn. soln. 8=20542
 thermal anisotropic, Milne problem, variational approach 8=11994
 thermal cross sections, computer codes SCAT and SLAB 8=20540
 thiourea, l.f. modes determ. 8=13340
 rel. to transport calcs., anisotropy representation in S_n codes 8=3999
 transport eqn. in slab geometry 8=19478
 transport, 1-dimens. critical slab problem with anisotropic scatt., soln. 8=20546
 urea, l.f. modes determ. 8=13340
 Al, 1-4 MeV, optical model pot. 8=3935
 Ar, liquid cold-n scatt. at 94.4°K, analysis using computer molecular-dynamics expts. 8=21611
 Ar, liquid, evidence for collective motion 8=16793
 Ar, liquid, inelastic scattering of cold neutrons, at high temps. 8=16792
 Ar, liquid, quasielastic 8=1524
 Au¹⁹⁷, 0.13-1.5 MeV, levels assigned 8=11899
 Bi²⁰⁹ rel. to isospin dependence of optical pot. 8=7039

Neutrons and antineutrons—contd

scattering—contd

- C^{12} , ang. distrib. and differential cross sections, 14.1 MeV 8=7205
- $C^{12}(n,n)C^{12}$ and $C^{12}(n,n')C^{12}$, polarization of 15.85 MeV neutrons 8=7204
- $C^{12}(n,n',\gamma)C^{12}$, obs. and compared with DWBA 8=16088
- $C(n,n',\gamma)$ transport problem in graphite, Monte Carlo calc. of unscatt. γ -flux distrib. 8=7206
- C^{12} , 1-2 MeV, multiple scatt. and finite geometry effects 8=11610
- CH_4 , gaseous, inelastic scattering 8=12274
- Ca, 2-8 MeV cross-section component to optical model calc. 8=3933
- Co, critical magnetic 8=2317
- Co^{59} rel. to isospin dependence of optical pot. 8=7039
- Cr halides ($CrBr_3$ and CrF_3), paramag. phase, exchange integrals 8=13971
- Cr_2O_3 , acoustic spin waves, study 8=14065
- $Cu^{63,65}(n,n'\gamma)$, 0.7-1.4 MeV 8=7209
- Cu, polarization 8=7210
- D, inelastic, at 14 MeV, neutron spectra 8=3715
- Er isotopes, thermal and paramagnetic cross-sections 8=1073
- F^{19} , intermediate-structure resonances as particle-hole states 8=3931
- Fe, magnetic, spin correlation 8=2026
- Fe, 1-4 MeV, optical model pot. 8=3935
- Fe^{54} , 1.81-40 MeV, γ radiation ang. distrib. 8=3934
- Fe, rel. to spin correlation function 8=2325
- H_2O H bonds from thermodynamic functions, meas. 8=1525
- H_2O molecules, double differential cross section 8=20806
- He^4 , single crystals, phonon dispersion measurements 8=10815
- Ho^{165} , 35-750 eV, spin assignments of resonances 8=16101
- I^{127} , 60-900 keV spin assignments, discrepancy 8=7096
- K, 2-8 MeV cross-section component to optical model calc. 8=3933
- $K^{39,41}$, inelastic, levels and cross-sections obs. 8=20809
- KH_2PO_4 , anomalous incoherent, rel. to standing neutron wave production 8=13267
- $KMnF_3$, antiferromag.-scattering 8=22882
- Li^6 , 4.83, 5.74, 7.5 MeV, cross-section meas., 3-particle break-up obs. 8=11897
- Li^7 , 3.35, 4.83, 5.74, 7.5 MeV, cross-section meas., 3-particle break-up obs. 8=11897
- Mn^{55} , 1.0-3.1 MeV, levels, spin assignment 8=15975
- in $MnSO_4$ aqueous soln., resonance self-shielding correction, rel. to meas. of source strength 8=7208
- N optical potential, complex symmetry term 8=924
- NH_3 , gaseous, inelastic scattering 8=12274
- Ni, magnetic, spin correlation 8=2026
- O^{16} , structure of negative parity states 8=1069
- O^{16} , 2.2-4.2 MeV resonance-parameters obs. 8=1070
- O^{18} , in enriched- UO_2 coherent scatt. length 8=8553
- Pb, liquid, classical fluid calc. 8=7851
- Pb, polarization 8=7210
- $Pb^{208}(n,n)Pb^{208}$, fine structure 8=996
- PuBe source, intensity, moderator effect 8=1121
- Si, differential cross sections between 4 and 5.75 MeV 8=1072
- Sn, grey, phonon spectrum from inelastic scattering of cold neutrons 8=4905
- Ta, total cross-section by time-of-flight spectroscopy 8=7196
- Tb, antiferromag.-scattering near transition point 8=22882
- U^{238} , energy level obs. 8=16007
- U, polarization 8=7210
- V^{51} , 1.0-3.1 MeV, levels, spin assignment 8=15975
- $W^{182,184,186}$, states obs. 0.3-1.5 MeV 8=1074

scattering, proton-neutron

- n-n length from 14.1 MeV n-d interactions 8=11643
- np \rightarrow pn, one π exchange 8=6847
- np \rightarrow pn, pion-exchange, Regge-pole model 8=11516
- n-p, 3-10 GeV, cross-section obs. 8=20539
- pn \rightarrow np evidence for conspiracy of branch cuts in a.m. phone 8=11584
- pn \rightarrow np, Regge-pole analysis, anomalies 8=6932
- particle spectrometer efficiency, different neutron energies, meas. 8=11625
- polarization parameter 300-700 MeV 8=6927
- real part at 8 GeV, elastic 8=6929

Newtonian fluids. See Fluids.

Nickel

- adsorption of Ar, temp. dependence, 78-120°K 8=17168
- alloying with steel, effect on temper brittleness 8=17797
- anode desorption efficiency, photoelec. meas. 8=17167
- band structure and Fermi surface, study by de Haas-van Alphen effect 8=2106
- band theory and low energy electron diffraction 8=2105
- catalyst, effect of support in benzene hydrogenation to cyclohexane 8=9707
- catalytic effect on BaO cathode contamination by residual gases 8=18663
- centres in molten $LiCl-KCl$, absorpt. spectra 8=8087
- centres in molten $MgCl_2-KCl$, absorpt. spectra 8=8086
- chromatographic separation, complex formation and reflectance spectros. detect. 8=23176

Nickel—contd

- cold-worked, nucleation of recrystallization 8=8397
- collector in W-emitter thermionic converter, comparison with Nb 8=15228
- compressibility, 4.2-300°K 8=5061
- creep at 700°K rel. to deformation at 77 and 4.2°K 8=17824
- creep strength increase after thermo-mechanical treatment 8=13601
- critical magnetic scattering of neutrons, spin correlation 8=2026
- crystal, plastically deformed, ferromag. props. using micromag. phase theory 8=5452
- cylindrical crystals, (110) axis, closure-domain structure, investigations 8=14037
- cylindrical crystals, (100) axis, ferromag. basic structure, investigations 8=14038
- Debye temp., 0 to 300°K, sp. ht. anal. 8=13377
- deformation, intermittent, upper temp. limit and dislocation density 8=2064
- de Haas van Alphen effect and electronic band structure 8=9360
- density of states from soft-X-ray analysis 8=8940
- deposits, pseudomorphic, of Cr 8=21886
- diffusion in Fe, volume and grain-boundary 8=17571
- dislocations, effect on mag. susceptibility 8=22830
- dull electroplating salt, formulation 8=23152
- dynamic ΔE effect frequency dependence in weak mag. field 8=2065
- electrochemical behaviour in $In-H_2SO_4$, influence of alternating current 8=5739
- electrodeposition from $NiCl_2$ soln. by a. c., microstruct. obs. 8=22035
- electroformed, mech. props. at room and cryogenic props. 8=17823
- electronic sp. ht. calc. by band model 8=4932
- electrolytically deposited layers, lattice deformations and crystal orientation 8=1805
- energy loss of fission fragments, range-energy relation 8=2021
- equation of state near Curie temp., approx. 8=2330
- exoelectron emission, photostimulated, during ferromag. transition, obs. 8=2273
- f. c. c., critical values for Bloch wall types 8=9320
- ferromagnetic, hot-electron scattering and rigid-band model 8=13940
- ferromagnetic lattice, hyperfine magnetic field on Sm^{150} 8=2335
- ferromagnetic, maximum susceptibility 8=18338
- ferromagnetic powders, magnetic props., lattice parameters 8=14033
- ferromagnetic reson. linewidth anisotropy rel. to relax. process, 25.92 and 9.42 GHz 8=2355
- film, electrolessly deposited, e microscope study 8=17136
- film on silicon grease, magnetic props. 8=2331
- films, condensed polycrystalline, structure and substructure elements 8=17286
- films, electrodeposited, perp. anisotropy 8=14024
- films, electrolytically deposited, growth rate rel. to structure and ferromag. props. 8=13999
- films, magnetostriction, meas. and obs. 8=18347
- films, resistivity, after magnetically induced anisotropy 8=5166
- films, thin, ion bombardment rel. to induced mag. anisotropy 8=22829
- galvomag. effect obs. in thin film specimens 8=5475
- hemispherical reflectance, rel. to λ and surface roughness 8=2399
- hydrostatic tension on solidification 8=21758-9
- laser induced non-linear photoelectric effect in metals 8=22721
- low work function collector in thermionic converter, effect of W emitter evaporation on to surface 8=15245
- magnetic properties, Anderson-type localized moments, model 8=2314
- mag. props., plastic deformation effects 8=9363
- magnetic susceptibility spin-orbit coupling dependence 8=2332
- magnetized, polarized n transmission 8=2031
- magneto-optical props., u. v., visible and i. r. 8=18550
- {100}, clean, adsorption of CO 8=21906
- (110) surface, adsorpt. of CO 8=17169
- oxygen chemisorption and film growth 8=9703
- photoelectric effect, non-linear, laser induced 8=2258
- plastic stress relaxation rel. to stacking fault energy 8=13529
- polycrystalline, ferromag. resonance, variation between -100 and +400°C 8=5511
- polycrystalline, secondary electron emission, temp. depend, 100 to 600°C 8=13944
- polycrystalline, shock-hardening 8=13595
- polycrystalline target, sputtering coeff. rel. to incident angle of Ne, Ar and Kr ions 8=8766
- powder, heating during ferromag. resonance 8=14082
- Rayleigh-region, derivation based on Bloch-wall-friction model 8=5481
- reactions, diffusion-controlled, at cylindrical surfaces, kinetics 8=14372
- recrystallization during creep, models criticism 8=8857

Nickel—contd

- recrystallization nucleation of weakly deformed foils 8=8421
 recrystallization rel. to polygonization 8=4808
 resistivity, elec., low-temp. obs. 8=17937
 resistivity temp. coeff., divergence at Curie temp. 8=9012
 reversible and irreversible magnetization temp. dependence 8=14025
 ribbons exposed to water, low-energy electron bombardment 8=21907
 saturation magnetization, temp. depend., applic. of demagnetizing field technique 8=22834
 secondary electron emission, H⁺ bombardment 8=5423
 self-diffusion, Arrhenius plot analysis allowing for divacancies 8=8681
 single crystals, magnetic anisotropy 8=9362
 sintered, effective volume self-diffusion 8=1923
 sintered, mag. props. rel. to porosity, obs. 8=22808
 in S solns., NiS surface film growth kinetics and mechanisms, obs. 8=2525
 specific heat, anomalous, at low temps. 8=22118
 specific heat at high temp., meas. of temp. depend. 8=1864
 structural changes under supersonic air streams at 900°C 8=17290
 surface segregation of S, obs. by Auger electron emission 8=22730
 thermal diffusivity meas. 8=1898
 thermoelectric power, high press. effects 8=13902
 twin and grain boundaries free energy ratios, from e-micros. exam. 8=17287
 Au-Ni spinodal, re-calc. 8=13245
 CO evolution by vacuum heating 8=16745
 Cu-Ni diffusion pairs, pore migration during counter-current diffusion 8=17569
 Fe-Ni systems, α - γ equilib. 8=4709
 and GaAs surface barrier diodes, elec. props. 8=22629
 H₂ desorption from surface 8=17170
 H₂ permeation, kinetics 8=8682
 Ni(II), co-ord. equilibria in alkali borate glasses 8=21836
 Ni(II) ions, sublation studies, by radioactive tracers 8=23075
 Ni(III), oriented growth of Ni₃S₂, e-diff. study 8=17254
 Ni²⁺, near i.r. fluoresc. and absorpt. in MgO 8=23050
 Ni-bearing steels, structure of martensite during ageing 8=1762
 Ni-induced surface structure on Si(111), LEED 8=4732
 Ni:Al₂O₃, sintered, compressive strength grain size dependence 8=2048
 Ni-Fe magnetic film memory elements, dispersion of anisotropy 8=14052
 Ni_{1-x}Sn, Mössbauer effect 8=1645
 Ni²⁺ centres in solids, i. r. luminesc. emission 8=18626
 Ni²⁺ in CaF₂, e. p. r. spectrum 8=9437
 Ni²⁺ in MgO absorption spectra line shift rel. to temp. 8=2442
 Ni²⁺ in MgO, microwave phonon interaction 8=9450
 Ni²⁺ and V²⁺ superexchange interaction in MgO 8=9355
 Ni²⁺ in KMgF₃, acoustic p. r., propag. factor changes near reson. 8=22912
 Ni³⁺ in KTaO₃, e. p. r. 8=9425
 Ni⁶³, 2-21 MeV deuterons, recoil range 8=13489
 Sn^{113,123} diffusion mobility obs. 8=17579
 Sb impurity, internal nucl. mag. field 8=8198
 on SiO₂, chemisorpt. of HCN, C₂N₂ and BrCN 8=23127
 Td-nickel, twin and grain boundaries free energy ratios, from e-micros. exam. 8=17287

Nickel alloys

See also Nickel compounds.

- alloy 718, superalloy, metallurgy, correl. of mech. props. with comp., microstruct. and heat treatment 8=21827
 Alnico-alloy permanent magnets, Ti-containing, columnar crystallization investigations 8=8399
 Alnico alloys, interaction effects 8=14036
 Alnico 8, Mössbauer spectroscopy study of paramagnetic environment 8=5480
 Alnico magnets, heat treatment below 1000°C 8=9361
 creep, temp. cycling effects 8=2066
 fatigued at several temps., dislocation structure 8=4981
 γ' particles, growth, distrib. and shape 8=21993
 hastelloy X-280, microstructure and tensile props., thermomechanical effects 8=17288
 heat transfer and corrosion relations 8=15102
 high-strength, with improved oxidation resistance to 2200°F 8=22387
 Inconel, anode desorption efficiency, photoelec. meas. 8=17167
 Inconel, stress corrosion cracking 8=8844
 Inconel, twin and grain boundaries free energy ratios, from e-micros. exam. 8=17287
 irradiated, tensile and shear props. at cryotemps. 8=17763
 nichrome ribbon, convection rel. to heat flux 8=17548
 Nimonic 80A creep damage and recovery by annealing, 600-750°C 8=5083
 Permalloy, composite films, structure and magnetic props. 8=9357
 permalloy deposition with varying degrees of anisotropy 8=21885
 permalloy, domain wall obs. by pulse technique 8=9364
 Permalloy evaporated films, influence of residual gases and metal bases on props. 8=5476
 Permalloy, ferromagnetic, maximum susceptibility 8=18338
 permalloy films, "flash-evaporated", standing spin-wave resonance 8=14083
 Permalloy films hysteresis, effect of deposition conditions 8=14032
 Permalloy films, mag. anisotropy, effect of defects caused by plastic deform. 8=14031
 Permalloy films, mag. reversal in alternating mag. field 8=5474
 Permalloy films, meas. of large-angle flux reversal 8=14030
 permalloy films, memory performance and hysteresis in inhomogeneous magnetic field 8=2319
 permalloy film on silicon grease, magnetic props. 8=2331
 Permalloy films, worm motion of domain walls 8=14028
 permalloy layers on Cu, magnetization under circular alternating and longitudinal static fields 8=9335
 Permalloy, magnetic domains, electron diffraction obs. 8=22824
 Permalloy magnetic films, rotational hysteresis, temp. depend. 8=22823
 Permalloy, magnetoresistance and effect of 3d orbital degeneracies 8=13724
 Permalloy, possibility of electron-beam vaporization 8=8189
 permalloy, r. f. reflecto-polarimetry 8=9409
 Permalloy-SiO-Permalloy multilayers, memory device appls. 8=14035
 Permalloy wire devices, domain wall propag. and digital appls. 8=14034
 Permalloy wire, domain wall motion appl. in character recognizer 8=10876
 Permalloy wires, domain wall motion used in parallel-to-serial converter 8=10875
 Supermalloy, ferromag. resonance rel. to spin diffusion 8=9404
 superalloys, struct. and metallurgical props. 8=4850
 Udimet-500, -520 and -700, heat treatment and composition effect on stress-rupture props. and structural stability 8=13599
 Udimet 700, sigma phase 8=13158
 Cr, plastically deformed, resistance recovery 8=13722
 Cu, plastically deformed, resistance recovery 8=13722
 In-Sb-Ni, the quasibinary section InSb-NiSb in 8=4691
 K-effect 8=13723
 Ni-base, molten, reactivity in vacuum with refractories 8=9694
 Ni base superalloy, carbide phases, structure, composition 8=8246
 50 Ni Permalloy, isotropic and anisotropic, effect of Ge addition on mag. props. 8=22815
 Ni-Al, ferromagnetic, hot-electron scattering and rigid-band model 8=13940
 NiAl, ordered b. c. c., supersaturation of vacancies on quenching 8=17611
 Ni-Al₂O₃, dispersion-strengthened, annealing and creep 8=22388
 Ni-Be, ferromag. props. rel. to transfer of electron states 8=14018
 Ni-C, growth of spheroidal graphite crystals 8=13156
 Ni-Co alloys, orientation superstructures by electron irradiation in mag. field 8=5479
 Ni-Co binary solns., interdiffusion coeff. conc. dependence, by X-ray analysis 8=17570
 Ni-Co, deformed, positron annihilation 8=17909
 Ni-Co-Mn ferrites, shifting of u. s. vel. minima due to mag. polarization changes 8=8632
 Ni-Cr film sputtering, role of H₂ rel. to thickness control 8=8777
 Ni-Cr, creep-resistant, fracture behaviour 8=17803
 Ni₂Cr, short-range order parameters from n-diff. data 8=17291
 Ni-Cr solid solns., interdiffusion, conc. and temp. dependence 8=17578
 Ni-Cr, sputtering in Ar, comparison of film and target composition 8=22254
 Ni-Cu, effect of cathodic hydrogen loading on ferromag. resist. anomaly 8=14023
 Ni-20%Cu, electron penetration at moderate energies, meas. 8=17694
 Ni-Cu, Hall effect, rel. to electrical resistivities 8=9014
 Ni-Cu(0-30.42%), longitudinal magnetoresistance up to 1100 Oe at 0°C 8=9013
 Ni-Cu, Portevin-Le Chatelier effect, hydrogen level dependence 8=22331
 Ni-Cu, solid, H solubility 8=21826
 Ni-Cu solid solns., variation of thermoelectric power and resist. 8=5389
 Ni-Fe, compressibility from 4 to 50 kbar by impact tech. 8=11719
 Ni-Fe, deformed, positron annihilation 8=17909
 Ni-Fe double films, domain wall motion 8=2329
 Ni-Fe ferrite, crystal growth, using arc image furnace 8=8422
 Ni-Fe films, lattice contractions by electron diffraction 8=1806
 Ni-Fe films mag. props. rel. to vacuum deposition press., 10⁻⁶-10⁻⁹ torr. 8=22822

Nickel alloys—contd

- Ni-Fe, film thickness and composition determ. by X-ray fluorescence 8=9750
 Ni-Fe films, vacuum-deposited thickness meas. by elec. resistivity method 8=17135
 Ni-Fe films, wall pinning effects on bias susceptibility meas. 8=14026
 Ni-Fe, mag. thin films, thickness dependence of domain wall energy 8=18346
 Ni-Fe, permalloy, thin films, exchange anisotropy, 4.2°K 8=2333
 Ni₃Fe alloyed with Cr, Mo or W, solid solutions, effects of atomic ordering 8=4690
 Ni₃Fe, order-disorder transition, n-diff. exam. 8=17095
 Ni-Fe sintered relay core prod. 8=22808
 Ni-Fe thin films, dynamic energy losses during magnetization reversal 8=14029
 Ni-Fe thin films, ferromagnetic resonance linewidth, rel. to temp. 8=2356
 Ni-Fe-Co thin films, strain sensitivity rel. to Co content 8=18345
 Ni-Fe-Cr films mag. props. rel. to high speed computer storage use, obs. 8=22826
 Ni-Fe-Cr-Si, 200-300Å films, galvanomagnetic effect 8=5478
 Ni-Fe-Cr-Ti Bourdon tubes, vacuum versus air-melted, rel. to elastic and fatigue props. 8=17822
 Ni-Fe-Cu films mag. props. rel. to high speed computer storage use, obs. 8=22826
 Ni-Fe-Cu-Mo, effect anisotropy on magnetic props. 8=9365
 77 Ni-14 Fe-5 Cu-4 Mo wt. % mag. props., sheet thickness effects 8=22827
 Ni-Fe-Mn films mag. props. rel. to high speed computer storage use, obs. 8=22826
 Ni₃(Fe, Mn), Ni₃(Fe, Cr), Ni₃(Mn, Cr), (Ni, Co)₃Mn, (Ni, Co)₃Fe_{0.5}Mn_{0.5} n analysis of superstructure 8=1763
 Ni-Fe-Pd films mag. props. rel. to high speed computer storage use, obs. 8=22826
 NiFe-SiO-Co multilayer, magnetoresistance hysteresis rel. to stray field effects 8=14027
 Ni₂Ge alloy, susceptibility in range 0<T<1000° C 8=18299
 Ni₃Ge, resistivity and thermoelectric power in the range 77°K < T < 1300°K 8=18215
 Ni₃Mn alloy, magnetic field at Mn^{5s} 8=1635
 Ni₃Mn, mag. field induced anisotropy 8=2327
 Ni-Mn Nimalloy, effect of Fe addition 8=22832
 Ni-Mn Nimalloy, permeability obs. 8=22831
 Ni₃Mn ordered, dislocation structure and grain size effect on validity of Cottrell-Stokes law 8=8721
 Ni-Mn, n. m. r. meas. of Mn^{5s} atom 8=9465
 NiMn, tetragonal, order twins and antiphase boundaries 8=17289
 Ni-2.2 wt.%Be, ageing investigated by electron microscopy 8=17056
 Ni₃(MnCo) ordered dislocation structure and grain size effect on validity of Cottrell-Stokes law 8=8721
 Ni-Mn-Fe, atomic mag. moment, conc. depend. 8=9358
 Ni-Mn-Fe ordered, dislocation structure and grain size effect on validity of Cottrell-Stokes law 8=8721
 Ni-Mo, quenched, deformation effects on transformation during annealing 8=17094
 Ni-Mo-Fe core power line de-icing transformer core, obs. 8=22828
 NiPb formation by simultaneous evaporation of NiPb 821852
 Ni-Pd system, mag. coupling 8=22821
 Ni-Pt binary solns, interdiffusion coeff. conc. dependence, by X-ray analysis 8=17570
 Ni-Si, reflection coeff. and thermal e. m. f. 8=18551
 Ni₃Si with coherent, ordered, stressed precipitates, dislocation motion 8=1978
 Ni-ThO₂, dispersion hardening and damping capacity, 20-500°C 8=17821
 Ni-Ti martensite transformation, atomic structure changes 8=21851
 Ni-Ti, obs. on non-spherical distortions by diff. contrast 8=8688
 Ni-Zn alloys, soft X-ray emission spectra 8=5624
 Ni-ZnO-Fe₂O₃ ferro(ferri)mag. reson., heat prod. obs. 8=14100
 Ni-1%Cr, prestrain during creep 8=13600
 Ni-12.7 at.%Al, rolled, effect of coherent γ'(Ni₃Al) particles on annealing 8=13598
 Ni-60 at.%Co, deformed, thermal conductivity decrease rel. to dislocation density increase 8=8658
 Ni-20Cr-2ThO₂, creep and creep fracture 8=8858
 Rh alloys, ferro- and paramag. behaviour saturation and susceptibility meas. 8=5477
 V alloys ferro- and paramag. behaviour saturation and susceptibility meas. 8=5477

Nickel compounds

- See also Nickel alloys
 hydroxide electrochem. oxidation, γ NiOOH form., obs. 8=18716
 nickelous nitrate-water-magnesium oxide system, low-temp. cementation effects 8=14374
 (CH₃)₂N. NiCl₂, crystal structure 8=22076

Nickel compounds—contd

- Ni(II)bromides, absorption spectra at high temp. and pressure 8=1580
 Ni complex, bis(diethyldithiophosphato) nickel (II), structure 8=8548
 Ni(II) complex, bis-(N, N-di-n-propyldithiocarbamate), pseudo-homometric structure 8=22034
 Ni complex, bis-(N-isopropyl-3-ethylsallycaldiminato) nickel, structure 8=8551
 Ni complex, bis-(N-methylsallycaldiminato) nickel, orthorhombic form 8=8550
 Ni complex, bis-sallycaldoximato-nickel, bond lengths 8=8549
 Ni complex, bistrisphenylphosphine-ethylene nickel, crystal structure 8=13281
 Ni complex, tetraethylammonium tetrachloronickelate, crystal structure 8=8547
 Ni-ferrite-chromite, Mössbauer effect on Fe⁵⁷ 8=1649
 Ni ferrite, origin of $k\pi$ and mobile domain walls 8=5493
 Ni ferrous ferrites, magnetically-induced ordering 8=22857
 Ni hydride, reduction in electrical resistance during formation 8=5183
 Ni(II) perchlorates, water solns., u. s. velocity 8=12865
 NiAl, electrical resist., temp. and composition depend. 8=13721
 NiAl₂O₄, cations distrib. as function of equilibrium temp. 8=13282
 NiAl₂O₄, distribution of cations as function of equilibrium temp. 8=13282
 NiBr₂ crystals, surface-spikes, growth and impurities conc. 8=4807
 Ni(CO)₄, in CCl₄, CO stretching vibs. 8=1570
 Ni₄(CO)₆[P(C₂H₅CN)₃]₄, cryst. struct. with tetrahedral Ni cluster 8=8589
 Ni₃Co, micro-strain and hardness under deformation 8=13596
 Ni-Cr₂O₃ system, mag. props. and superparamagnetism of Ni particles 8=9366
 NiCr₂O₄, lattice vibration, effect of deformation 8=8614
 NiCr₃S₄, mag. structure, analogy with Cr₃S₄ 8=22833
 NiCr₂Se₄, structural, electrical and thermal parameters rel. to d-orbital interactions 8=5391
 Ni_{1/3}Fe_{2/3} coprecipitate, structure and mag. props. 8=23078
 Ni_{0.5}Fe_{0.5}O₄, crystalline anisotropy, effect of oxygen stoichiometry and annealing temp. 8=9385
 NiFe₂O₄, ferrite films, single cryst., prep. and props. 8=18362
 NiFe₂O₄, thin films, microstructure, ferrimagnetic props., electrical conductivity 8=2343
 NiGa, elec. resist., temp. and comp. depend. 8=13721
 Ni₂Ga, magnetic susceptibility, temp. dependence, density of states curve explanation 8=9359
 Ni₂GeO₄, cations distrib. as function of equilibrium temp. 8=13282
 Ni₂GeO₄, distribution of cations as function of equilibrium temp. 8=13282
 Ni-H system, lattice parameter H conc. dependence at -40° C 8=17404
 Ni₃Mn, micro-strain and hardness under deformation 8=13596
 NiMn₂O₄, single crystals, growth 8=21959
 Ni₄Mo ordered alloys, effect of symmetry on field ion images 8=4881
 Ni(NO₃)₂·4H₂O, crystal structure 8=17405
 NiO, absorpt. spectrum, fine structures 8=2441
 NiO, antiferromag. ultrafine particles, Mössbauer study of mag. props. 8=2318
 NiO, axially cooled or stressed, mag. anisotropy from torque meas. 8=14072
 NiO crystals, growth by arc-transfer 8=4806
 NiO crystals, structure study by LEED rel. to (100) face 8=8379
 NiO, dislocation etch pits, shape and size rel. to etching time 8=1977
 NiO electrodes hydration state and struct., obs. 8=23146
 NiO exoelectron emission, photostimulated, during antiferromag. transition, obs. 8=2273
 NiO ferrite, heating during ferromag. resonance 8=14082
 NiO, films, resistivity, after magnetically induced anisotropy 8=5166
 NiO, Hall effect at high temp. 8=8977
 NiO, neutron irradi. effect on elect. props. 8=18058
 NiO, paramagnetic, anomalous Hall effect 8=17914
 NiO, reduced, mag. behaviour 8=14071
 NiO, rhombohedral distortion, domain ordering 8=5507
 NiO, semiconducting, near and far i. r. absorpt. by small polarons 8=23008
 NiO, stoichiometry, thermodynamic and elec. props. 8=13826
 NiO, Co⁵⁷-doped, bulk and ultrafine particles, Mössbauer spectra 8=4680
 NiO/Ni-CO₂ system, isotopic exchange reaction between O¹⁶ and O¹⁸ 8=9663
 α-Ni₃P₂O₇, crystal structure 8=17367
 NiS film on Ni in S solns., growth kinetics and mechanisms, obs. 8=2525
 NiS, mag. and elec. transition pt. pressure dependence 8=22885
 Ni₃S₂, oriented growth on Ni(III), e-diff. study 8=17254

Nickel compounds—contd

- NiSiF₆·6H₂O, thermodynamic and mag. props., 0.35°-4.2°K 8=8641
 Ni₂SiO₄ (cubic nickel orthosilicate), synthesis from stoichiometric compound 8=21853
 Ni₃Sn, antiphase boundaries, size, shape and orientation 8=17679
 Ni₃TeO₈, crystal structure 8=4880
 NiTiO₃, mag. props., theoretical interpretation 8=9399
 NiTiO₃, mag. resonance and susceptibility 8=9398
 Ni-2ThO₂, dispersion-strengthened, fatigue behaviour on cycling 8=13597
 Ni₂Zn_{1-x} ferrites, doped with transition elements 8=22856

Night sky. See Airglow

Night glow. See Airglow.

Nilsson's model. See Nucleus/models.

Niobium

- additions to Ti alloys, superconducting props., phase transformations 8=22563
 anisotropic energy gap meas. by tunneling 8=17964
 collector in W-emitter thermionic converter, comparison with Ni 8=15228
 combined effect with Mo on mech. props. and hardness of Nb-Mo steel 8=22385
 crystals, dislocation structures, chemical and electro-etched, optical microscope obs. 8=22208
 deformed single crystals, mag. flux gradients, 4.2°K 8=22210
 diffusion studies 8=17575
 diffusion, summary of ORNL work 8=17593
 dislocations mobility rel. to amplitude depend. of internal friction 8=22209
 effect on grain coarsening temp. of austenite 8=8462
 electronic band struct. by modified OPW method 8=8939
 epitaxial film on MgO, rel. to substrate-condensate chemical interaction 8=8326
 films, for cryotron ground planes 8=2171
 foil, dislocation density and flow stress, effects of grain size 8=4980
 galvanomagnetic props. 8=22682
 hydride phase, solubility of H₂, isotherm 8=1924
 low work function region in Cs and Cs-Ba vapours 8=15213
 nitride precip., rel. to hardness and micro-structure 8=8274
 property changes by dissolved O₂-N₂ mixtures 8=9011
 in sormite type alloys, influence on hardness and structure 8=5066
 in stabilized stainless steels, spectrophotometric determ. 8=23179
 superconducting, anisotropic energy-gap meas. by tunnelling 8=22552
 superconducting, energy gap anisotropy by single crystal tunneling technique 7=5209
 superconducting, flux diffusion 8=9053
 superconducting, flux penetration and a.c. losses 8=5210
 superconducting, heat effects rel. to mag. processes 8=2167
 superconducting, helicon resonances near H₂ 8=9049
 superconductive, irreversible magnetisation obs. 8=2160
 superconducting, magnetocaloric effect, rel. to upper critical field 8=9052
 superconducting, mixed and normal states, internal friction and Young's modulus variation 8=2063
 superconducting mixed state, u.s. attenuation rel. to transverse mag. field 8=17502
 superconductor, nuclear relax. near upper crit. field 8=2170
 superconducting, resist. and Hall angle, theory and obs. 8=2162
 superconducting, thermal conductivity rel. to energy gap and mag. hysteresis 8=2166
 superconducting, u.s. attenuation 8=17503
 superconducting upper two critical fields ratio, temp. dependence 8=17963
 superconductivity under high pressure 8=9060
 surface exam. by field electron microscopy 8=13930
 surface superconductivity investigation 8=2157
 thermal conductivity, temp. dependence of temp. coefficient 8=13387
 Nb^{90m}, influence of chemical binding on half-life 8=16024
 O and C, effect on creep strength 8=13593
 O₂-Nb system at very low pressure, adsorption, absorption and degassing 8=4763

Niobium compounds

- alloys, anti-oxidation metallurgy 8=23779
 alloys, stability in nuclear reactors 8=5082
 cavitation damage resistance 8=5035
 niobates, single crystals, ferroelec., growth 8=21958
 stannide, superconducting coils with high Q's 8=17982
 CbBe₃, X-ray diffraction data 8=17426
 (C₂NH₅)[NbCl₄O], deviation from superposition structure 8=13279
 Nb₃(Al, Ge, Sn), solid solns., superconducting transition dependence on atomic ordering 8=17967
 NbB₂, specific heat 0.6-0.28°K 8=17522
 σ-2NbAl alloy, mech. props. rel. to atomic ordering and co-ordination 8=17030
 NbC precipitation, brittleness in steel 8=22358

Niobium compounds—contd

- NbC, solubility in 20%Cr-25%Ni stainless steel 8=4689
 NbC solubility in γ-Fe from C content analysis at temps. 950-1050°C 8=4535
 NbC, stoichiometric, enthalpy and specific heat in range 500 to 2400°K 8=13366
 NbCl₅, vibrational spectra 8=14249
 Nb-Cu composite, strong proximity effects: superconductivity 8=22553
 Nb-Fe alloys, structure 8=8272
 Nb-Hf, (-W), (-Mo) alloys, interstitial solid solubilities of O, N, C 8=17015
 Nb-Mo, alloys, Debye temp., Young's modulus, atomic bond strength 8=1626
 Nb-Mo alloy single crystals, plastic deformation, -196°C -250°C 8=17819
 Nb-Mo-C alloys, constitution 8=8275
 NbN, lattice dimensions, thermal and elect. cond., Hall coefficient, thermal e.m.f. and microhardness 8=13702
 NbN, prep. and superconductive props. 8=17966
 NbN, preparation and critical superconductive data 8=2165
 NbN, with Ti, preparation and superconductivity 8=2158
 NbN, with Zr, preparation and superconductivity 8=2158
 Nb-Ni-Al alloy, M phase structure determ. 8=17403
 NbO, precipitation from supersaturated solutions electron microscope examination 8=1679
 Nb-O solid solutions, CO equilibrium pressure 8=21825
 Nb₂O₅, high temp. and related phases exam. by e-microscopy and diffr. 8=22033
 α-Nb₂O₅, near-stoichiometric, diffusion of O₂ 8=1922
 Nb-Re alloys paramag. susceptibility rel. to band struct., obs. 8=22759
 NbS₂, specific heat 1.7-6.4°K 8=17522
 Nb₂S₃, crystal structure 8=22032
 Nb₃Sn, cubic → tetragonal martensitic transform., low temp. 8=8273
 Nb₃Sn Fermi level motion rel. to normal-state props. temp. depend. 8=5118
 Nb₃Sn, specific heat, temp. range 1-42°K in mag. fields up to 52.5 kG 8=17523
 Nb-Ta, alloys, Debye temp., Young's modulus, atomic bond strength 8=1626
 (Nb-Ta)N, prep. and superconductive props. 8=17966
 Nb-50 at. % Ta superconducting sheets, transport current distrib. obs. 8=9051
 Nb-Ti, alloys, Debye temp., Young's modulus, atomic bond strength 8=1626
 Nb-Ti alloy wires, superconducting, flux jumping 8=9050
 NbTi, superconducting large coils, performance 8=17994
 Nb-Ti systems, b.c.c., binary interdiffusion 8=17577
 (Nb-Ti)N, prep. and superconductive props. 8=17966
 Nb-Ti-Zr alloy, magnetic props. 8=13754
 Nb-Ti-Zr alloy solenoid at mag. field strength more than 75 kG 8=309
 Nb-Ti-Zr wire, transitions during destruction of superconductivity 8=22567
 Nb-V, alloys, Debye temp., Young's modulus, atomic bond strength 8=1626
 Nb-V systems, b.c.c., binary interdiffusion 8=17577
 Nb-W alloys, creep strength, effects of metallic carbides and borides 8=22384
 Nb-W, alloys, Debye temp., Young's modulus, atomic bond strength 8=1626
 Nb-Zr alloy, electron microscope investigation of structure 8=8245
 Nb-Zr alloy, nitride precip., rel. to hardness and microstructure 8=8274
 Nb-Zr alloy superconducting solenoid, flux jumping-patterns 8=2168
 (Nb-Zr)N, prep. and superconductive props. 8=17966
 Nb-Zr and Nb-Ti wire, in composite superconducting cable, critical current 8=13770
 Nb-25 at. % Zr, superconducting sheets, transport current distrib. obs. 8=9051
 Nb-25% Zr, superconducting large coils, performance 8=17994
 Nb-25% Zr supercond. wires carrying a.c. in mag. field 8=5208
 Nb 25% Zr wire, superconductivity, a.c. quenching 8=13755
 R₂O-M₂O₅ (R = rare earth, M = Nb, Ta or Pa), crystal structure 8=1802

Nitrogen

- accommodation coeff. in impact on Al, Ag, Au and Pt, 500-12000 eV 8=12685
 active, in flames, electronic excitation of CN 8=12179
 active kinetics of N₂(A³Σ_g⁺) 8=7534
 adhesion coefficients at 4.2° and 20°K 8=7954
 adsorption on Molecular Sieves 5A, 10X, and 13X, at 77.3°K and press. range 10² to 10⁻⁶ torr, effect of preadsorbed H₂O 8=21897
 adsorption on W films, sticking probability temp. dependence 8=14396
 adsorption on W, phase transforms caused by e-impact 8=21913
 adsorption on W, rel. to work function 8=1711
 afterglow, surface catalytic efficiency and decay of atomic N 8=21239

Nitrogen--contd

atmospheric, Raman scatt., N_2 u.v. laser obs. 8=23289
 atom, spectral absorption coeffs. compilation 8=12060
 atomic beam, photoionization 8=21022
 atoms, e loss in collisions with H^+ , He^+ 8=7461
 atoms, recomb. rates 8=1313
 atoms, spin-relax. effects in e.p.r. 8=12098
 aurora enhancement 8=9929
 aurora, second positive system, vibrational development 8=18944
 aurora, $\lambda 3914$ and $\lambda 4709$ N_2^+ , ratio of spectral intensity to $H\beta$ 8=23340
 beam-plasma systems, beam generated, interacting components 8=21289
 benzene luminesc. excit. in solid solns., obs. 8=13036
 bubbles in water, decay constants and pulsation frequencies determ. 8=21588
 cascade arcs, conductance decay after switch-off 8=7685
 collision cross sections from meas. on arc discharges 8=4294
 conductivity with LaB_6 powder suspension, m. h. d. generator working fluid 8=15199
 desorption kinetics, from Fe- N_2 solid solns. 8=1704
 diffusion of interdiffused O_2 and org. vapours 8=14452
 diffusion in liquid Fe-C alloys. at 1600°C 8=16815
 discharges, high-freq. unipolar, spectral diagnostics, 1 to 5 atm. press. 8=4290
 dissolved in Nb, with O_2 , effect on props. 8=9011
 effect of lifetime on CO_2 laser levels 8=420
 e-ion recombination, temp. depend. obs. 8=7719
 electric breakdown, wave shape effect 8=21246
 electron drift velocity obs. 8=12695
 electron microscope investigation of condensed N_2 8=8465
 enthalpy calc. from Redlich-Kwong eqn. 8=16689
 ethane mixture, Joule-Thomson coeff. prediction 8=12679
 excitation of CO_2 , emission spectrum 8=21068
 excitation by fission fragments along entire track 8=7531
 excited by microwave discharge, vibrational deactivation 8=12211
 gas, rotational relaxation, high temp. u. s. obs. 8=1251
 gas, thermomagnetic torque, temp. dependence 8=16712
 heated, excitation by transfer of CO_2 , rel. to chem. laser action 8=16271
 high-pressure boiling apparatus 8=16944
 ion, energy loss in passing through ZnS:Ag film 8=8758
 ionization cross-section, electron impact 8=7700
 ionization, electron and proton impact, classical model 8=12444
 ionization energy per ion pair formed by $H\beta$ particle 8=4315
 ionization, mechanical damage to BaO cathode 8=18663
 ionosphere, 100 to 280 km, distribution and lifetime of atoms 8=23308
 ions, molecular among neutral molecules, drift vels. and reactions 8=7718
 ions, II-V, lifetimes meas. by decay of optical radiation 8=7412
 in iron and steel, spectrophotometric determ. 8=23178
 isotope equilibration on Mo 8=18655
 isotope mixtures, thermal diffusion props. 8=1492
 laser action in electrical discharge containing N 8=12398
 laser-heated plasma radiation spectra 8=16200
 laser, u.v., Raman scatt. from atm. 8=23298
 laser, as u. v. source with repetitive subsec. kW pulses 8=20069
 liquid, equations of state 8=4543
 liquid, temporal stability of quiet metastable states 8=16788
 liquid, volume viscosity meas. via u. s. attenuation 8=1538
 melting curve to 30 kb, obs. 8=1610
 molecular, electron impact cross sections 8=1348
 molecular, ionization by e collisions 8=16448
 molecule, N_2 -p e capture excitation of 3s, 4s states of H 8=7462
 molecules excited by electron beam, rot. temp. obs. 8=16292
 molecules, ionization by scattering 8=1364
 in Na-K reactor coolants, effect on efficiency of coolant, corrosion activity and residual radioactivity 8=7328
 partial photoionization cross-sections, determ. by photoelectron spectra 8=1369
 phase change, dramatic demonstration 8=1607
 plasmas, electron velocity distrib., non-Maxwellian form. 8=16418
 plasma, excitation temps. from multiplet intensities 8=1376
 positron cross-section for rotational excitation 8=12168
 pressure over $UN_{2,1} + U_{1,1}$ system 8=18646
 pulsed molecular laser, theory 8=15472
 pumping speed-press. data, getter-ion pump 8=1495
 radiative transfer, for local thermodynamic equil. 8=7926
 relaxation behind shock waves, electronic excitation 8=21087
 residual, in colour picture c. r. t., mass spectrometry 8=15324
 residual, pressure obs. in picture c. r. t. 8=15325
 sorption isotherms on purified silica gel, rel. to modification of gel struct. 8=1663
 sorption in Ti films, sticking coeff. obs. 8=17175
 sound velocity 8=4484
 Stark effect on n.q.r. 8=7611

Nitrogen--contd

stars, Am, abundance 8=23514
 in steel, austenitic type 304, influence on creep-rupture props. 8=17754
 steel, mild, effect of content on dynamic strain-ageing 8=13554
 stream, laminar boundary with coolant mixture injected through porous surface 8=4459
 on Teflon 6, isotherms 8=13047
 translation accommodation coeff., on W surface 8=17113
 transport properties, single-component model 8=1438
 u. s. velocity and absorpt., 300°-1300°K 8=4478
 vibrational relax. in shock tube, vac. u. v. absorpt. obs. 8=7532
 vibrationally excited, relax. 8=12210
 viscosity, low-temp., high press. 8=4493
 X-ray microanalysis using network method analyser, obs. 8=14489
 in Cr alloys, determ. from nitride behaviour 8=9740
 D content, neutron spectrometry 8=9765
 H_2 - N_2 gas mixtures, thermal conductivity 8=4473
 in Li melt, supercooling due to N_2 crystallization 8=12814
 Mg-Fe mixed hydroxides adsorpt. and desorpt. rel. to pore struct., obs. 8=17023
 Mo tip, absorption, field emission study 8=21905
 N I and N II electrostatic interaction integrals using screened hydrogenic orbitals calc. 8=7394
 N II, Stark effect in multiplet lines 8=4084
 N + O \rightarrow NO $^+$ + e, ionization cross section calc. 8=4111
 N $^+$ reaction with O_2 in ionosphere, rate coeff. study 8=14666
 N_2^- , struct. of 2 eV resonance 8=12214
 N_2 , $B^3\Pi$ state, excitation time estimates at 8000°-9000°K 8=4155
 N_2 , collisions with p, H, optical emission rel. to Aurora 8=12212
 N_2 , collision with H_2^+ , H_3^+ , prod. of H atom in 3s state 8=21191
 N_2 discharge, prebreakdown Townsend discharge 8=7677
 N_2 discharge, release of secondary electrons by metastable N_2 and its quenching 8=7663
 N_2 , energy deposited in electron slowdown 8=2634
 N_2 gas, H^+ , H_2^+ , He^+ charge exchange, 40-1500 eV 8=21275
 N_2 ionization by Fe atoms, ionization ratio meas. 8=1359
 N_2 ions, appearance potential and kinetic energy 8=7721
 N_2 , large-angle electron-impact spectra 8=16224
 N_2 , laser oscillation characteristics on electronic transitions 8=11069
 N_2 , model dipole spectrum consistent with oscillator strength sum rule 8=7533
 N_2 , new Rydberg series 8=4160
 N_2 , positive column, mass spectrometric analysis 8=1341
 N_2 , pre-breakdown currents rel. to temp. at high pressure 8=16417
 N_2 , p 0.15-1.0 MeV collisions, ionization and excitation 8=12213
 N_2 pulsed laser, new lines 8=11070
 N_2 second positive system excited by impact with a metastable Ar atom 8=12209
 N_2 sorption and reaction with Bayard-Alpert gauge 8=16732
 N_2 , spectra on excitation by fast protons and H atoms 8=7433
 N_2 thermal cond., mag. field effects, 290°K 8=4469
 N_2 , thermal conductivity at 100-300°C, 1 atmosphere, obs. 8=4477
 N_2 , vibr. relax. in shocked gas mixtures 8=21195
 N_2 12.28 quadrupole transition, far u. v. absorpt. obs. 8=12208
 $N_2(A^3\Sigma_u^+)$, kinetics in active nitrogen 8=7534
 N_2 , vibrational levels, lifetime obs., using positive ion Van de Graaff accelerator 8=16183
 N_2 -Ar gas mixtures, thermal conductivity 8=4474
 N_2 -Ar mixtures, virial coeffs. from Burnett meas. 8=16691
 N_2 -CO $_2$ gas laser use of multipath cell 8=419
 N_2 + He mixture, passage of H_2^+ , N_2^+ rotation and vibration 8=4156
 $N_2^{14+14} + N_2^{15+15} \rightleftharpoons 2N_2^{14+15}$, in shock tube 8=5696
 N^{14} hyperfine splitting in e. s. r. of Cr(NH $_3$) $_6$ NO $^{2+}$ 8=1592
 N^{14} nuclei, n. q. r. study with modified Robinson spectrometer 8=3283
 N^{14} quadrupole coupling in CN free radical 8=1316
 N^{15} , enrichment by ion exchange electromigration method with superposition of a. c. on d. c. 8=12113
 N^{15} in solids, detect. by nuclear activation 8=14504
 N_2^+ , absolute electron impact excitation cross-section 8=7720
 N_2^+ , dissociation by e impact, 10-500 eV, cross-section 8=1312
 N_2^+ , ground and excited states 8=4158
 N_2^+ intensity distrib. among bands, obs. in atmosphere 8=18933
 N_2^+ , ionosphere, dissociative recombination rate 8=9961
 N_2^+ λ 3914 spectra, auroral luminosity spatial var. obs. 8=14649
 N_2^+ reaction with O_2 in ionosphere, rate coeff. study 8=14666
 N_2^+ , vibration and rotation, band intensity distribution 8=4156

Nitrogen—contd

- $N_2^+ + N_2$ reactions, is N_4 produced? 8=1366
 $N_2^+ + N_2$, reaction cross-sections 8=4310
 $N_2^+ + O_2 \rightarrow O_2^+ + N_2$, low-energy cross sections 8=16372
 N_2 -CO₂ 10.6 μ m laser, beam patterns 8=19973
 N_2 -He mixtures, diffusive separation obs. 8=19537
 NO, from W, desorption by electron impact 8=21912
 Ta + N_2 system, adsorpt.-absorpt. kinetics 8=18698
 W film, adsorption, sticking probabilities obs. 8=4761
 in ZnO:Zn, ions energy losses obs. 8=18624

Nitrogen compounds

- azides, explosive props. and electronic struct. 8=1259
 nitrates, explosive props. and electronic struct. 8=1259
 nitrides, extraction from Cr alloys 8=9740
 nitroso dimers, photodissociation on irradiation with u.v. light 8=9726
 trans N_2F_2 , vib.-rot. bands and molec. geometry 8=12218
 BrCN, chemisorpt. on Ni and Ir on SiO₂, i.r. spectroscopy 8=23127
 C_2N_2 , chemisorpt. on Ni and Ir on SiO₂, i.r. spectroscopy 8=23127
 Fe-Cr-N ternary system, microstructures and nitrides 8=4845
 HNO₃ aq. soln., phenomenological coeffs. for elect. cond. and diffusion 8=12924
 N oxides, reactivity with cellulose hydroxyl groups 8=5721
 HCN, chemisorpt. on Ni and Ir on SiO₂, i.r. spectroscopy 8=23127
 NCO, free radical, matrix-isolated spectra 8=16369
 NDF₂, centrifugal distortion constants 8=7542
 NF₃, centrifugal distortion consts, from mm wave spectrum 8=1258
 NF₃, general force field 8=4157
 NF₃, i.r. spectrum and molec. constants. 8=1260
 NF₃, new compound by fission-fragment radiolysis 8=9730
 NF₃, solution H in, spectral simultaneous transitions 8=21675
 NH, fine structure of $^3\Sigma^-$ and $^3\Pi$ states 8=7541
 NH⁺, emission band systems 8=16291
 NH₃, centrifugal distortion effects in spectra 8=21089
 NH₃, in lowest bent state, effects of quasi-linearity 8=1243
 N₂H₄, liq., significant struct. theory 8=4526
 N₂H₄, hydrazine, int. rot. barriers from LCAO-MO-SCF wave-functions 8=1247
 NHF₂, centrifugal distortion constants 8=7542
 NH₂OH, hydroxylamine, int. rot. barriers, from LCAO-MO-SCF wave-functions 8=1247
 NiO films, semicond. and insulating, prep. and thin-film triodes 8=22602
 NO, dimers obs. by mass spectra 8=7637
 NO, elec. field effect on n.m.r. 8=7612
 NO, far u.v. photolysis, N₂O yield 8=23159
 NO, fundamental vib. band, integrated intensity 8=7535
 NO, gas-phase electron reson., double quantum transitions 8=12308
 NO in solid Ne, Ar and Kr, absorpt. rel. to excited states, 2300-1100 Å 8=14243
 NO ions, appearance potential and kinetic energy 8=7721
 NO molecule, electric field effect on electron resonance, obs. of transitions 8=16349
 NO, reaction with perfluorodimethyl peroxide 8=14371
 NO, rotational lines at 150 GHz, a high-Q Fabry-Perot resonator 8=7536
 NO, solid, absorpt. rel. to mol. excited states, 2300-1100 Å 8=14243
 NO, spectra on excitation by fast protons and H atoms 8=7433
 NO thermal cond., mag. field effects, 290°K 8=4469
 NO, thermodynamic props., 200°-2000°K and at 1000 bar 8=7918
 NO at 100 to 280 km height, distribution and lifetime calc. 8=23308
 NO + Ar mixture, conversion of positronium atoms 8=7476
 NO⁺, ionosphere, dissociative recombination rate 8=9961
 NO⁺ from N + O collisions, ionization cross section calc. 8=4111
 NO₂⁻, ground state, minimal-basis-set LCAO-SCF-MO calc. 8=21096
 NO₂⁻, i.r. spectra in solid solns. 8=2439
 NO₂ ions in soln., shift of absorpt. bands 8=12890
 NO₂ production by electron transfer from O⁻, O₂⁻, O₃⁻ and OH⁻ 8=1367
 NO₂⁻, NO₃⁻ ions, injected in alkali halides, i.r. absorption 8=5583
 NO₂, attachment of gaseous electrons 8=12449
 NO₂, chemiluminescence, rad. from far wake of hypersonic spheres 8=21478
 NO₂, e.p.r. in irr. KNO₃ at 4°K 8=5537
 NO₂, its ions and dimer, electronic struct. 8=4159
 NO₂, photoionization 8=16449
 NO₂, thermal cond. 8=16699
 NO₂⁻, configuration-interaction calc. 8=16252
 NO₂ ions in soln., shift of absorpt. bands 8=12890
 NO₃, effect on transparency of Hf and Th oxide films 8=5605
 NO₃⁻ ions, role in thunderstorm electrification 8=23290
 N₂O-acetylene flame in emission anal. 8=18782

Nitrogen compounds—contd

- N₂O bubble in water, laminar flow obs. 8=21591
 N₂O, cryst. Raman spectra 8=9510
 N₂O, electron-impact dissoc. 8=4133
 N₂O, heat cond., extension of Saxena-Saksena-Gambhir theory 8=16702
 N₂O, ionization curves due to electron impact 8=12434
 N₂O, i.r. absorpt. bands rel. to isotopic mols. and crystal lattice vibrations 8=14251
 N₂O, near i.r. bands 8=21088
 N₂O, use in obtaining high stagnation-enthalpies in shock tunnels 8=16676
 N₂O, photochemistry, and vac. u.v. actinometry 8=14439
 N₂O, photoionization 8=16449
 N₂O, photoionization coeff., 600-1000 Å 8=16447
 N₂O, photolysis at 1470 Å 8=14438
 N₂O pure and in a matrix, absorption spectrum between 63 and 14°K 8=18552
 N₂O, vibrational state relaxation times, spectrophone determ. 8=21090
 N₂¹⁵O¹⁸, i.r. vibr. rot. bands 8=21086
 N₂O-CO mixture, study of overlapping absorpt. bands 8=7507
 N₂O-CO₂ mixtures, separation in thermal-diffusion column 8=7945
 N₂O + N₂ mixture, vib. relax. time of ν_3 mode of N₂O, meas. with spectrophone 8=7508
 N₂O⁺ + N₂O, reaction cross-sections 8=4310
 N₂O₃, i.r. spectra 8=7538
 N₂O₄ \rightleftharpoons 2N₂O₂, thermal conductivity and relaxation effects 8=7929
 2NOBr \rightleftharpoons 2NO + Br₂ system thermal conductivity in range 290-900°K 8=12684
 NOCl, photodissociative laser, chemical reversibility, solar excitation rates 8=3321
 NOF, ground state, minimal-basis-set LCAO-SCF-MO calc. 8=21096
 NOF, vibr. spectra and force consts. 8=7539
 γ NOOH electrochem. form. and props., obs. 8=18716
 NO(SO₃)₂⁻, aq. solution, dynamic proton polarization at 38 and 3400 gauss. obs. 8=1602
 NOSO₂Cl, crystal structure 8=3275
 NS, Frank-Condon factors for B² Π -X² Π transition 8=7540
 NS gaseous free radical, e.s.r. study 8=12340
 NS, spectra, γ - and β -systems 8=16293
 NSCl, i.r. spectrum and molecular props. 8=4161
 NSF, microwave spectrum and molec. consts. 8=12219
- ammonia**
 adsorption on Fe catalyst support, Mössbauer spectra 8=13108
 alkali metal-NH₃ solns., phase separation model 8=12808
 ammonia, refractive index, electric dipole rot. effect 8=4162
 beam maser oscillator, modulation effects 8=10995
 crystals, plastic deformation at liq. N₂ temps. 8=17820
 deuterium isotopic disproportionation equilibria 8=2505
 decomposition in glow discharge 8=18682
 electron diffr. by molecular beam 8=6303
 enthalpy calc. from Redlich-Kwong eqn. 8=16689
 gas, mol. refr. and Lorentz-Lorenz rel. 8=1477
 gas, radiolysis, effect of H and e scavengers 8=23162
 inelastic scattering of cold neutrons 8=12274
 ionization potentials 8=4314
 maser amplifier, characteristics 8=397
 melting curve to 30 kb, obs. 8=1610
 molecular pressure broadening theory 8=16294
 molecule, Compton profile, unified atoms method 8=1256
 molecule, one-electron props. 8=4148
 molecule, signs of nuclear spin-spin coupling consts. 8=12330
 photodissociation in vac. u.v. 8=16365
 radiolysis in gas-phase 8=18743-4
 solvent effect on bending vibr. 8=21093
 spectra, and virtual-orbital approx. to excited states 8=1213
 steel analysis, extraction-spectrophotometric determ. 8=2546
 supercritical, use for growing hexagonal Se crystals 8=8425
 SCF calcs, correlation energies and Hartree-Fock limits 8=1263
 K-NH₃ dilute soln., absence of vol. change on dilution at -34°K 8=1530
 Na-K-NH₃ solns., liq.-liq. phase separation 8=8014
 Na-NH₃ dilute soln., absence of vol. change on dilution at -45°K 8=1530
 Na-NH₃ solns., liq.-liq. phase separation 8=8013
 NH₃-methylamine gas mixtures, viscosity 8=4492
 NH₃-Ar, thermal cond., 39° to 199.6°K 8=4470
 N¹⁴H₃, resolution of central line, at J = 3, K = 3, $\Delta F = 0$ 8=4163
 NH₃-He collision-induced transitions between rot. levels 8=12216
 NH₃ + HCl \rightleftharpoons NH₄Cl charge transfer 8=5714
 NH₃-H₂O-N₂-H₂ system, vapour-liq. equil., fugacities and activation coeffs. 8=12977
 NH₃ and ND₃, dipole moment and polarizability differences 8=12215

Nitrogen compounds—contd**ammonia—contd**

NH_3 -Ne, thermal cond., 39° to 199.6°C 8=4470

NH_3 -He, thermal cond., 39° to 199.6°C 8=4470

NH_3 -Li metallic solns, optical consts. 8=12884

ammonium compounds

quaternary salts, in water-glycine mixtures, elec. cond. 8=8104

ND_4Br , deuteron quadrupole coupling consts. 8=14159

ND_4Br , deuteron quadrupole coupling const., theoretical calc. 8=14160

ND_4Br , spin-lattice relax. and phase transitions 8=4713

ND_4Br , ht. capacity 17°-300°K 8=22117

ND_4Cl , deuteron coupling consts., theoretical calc. 8=14160

ND_4Cl , deuteron quadrupole coupling consts. 8=14159

ND_4NO_3 , d.m.r. studies 8=18460

ND_4NO_3 , deuteron mag. resonance, from 100 to 403°K 8=14150

ND_4NO_3 polycrystals, spin-lattice relax. of p and d 8=14149

$(\text{ND}_4)_2\text{Cr}_2\text{O}_7$, phase transitions and i.r. spectra 8=23006

NH_4OHC , neutron diffr. study 8=8546

NH_4^+ cation, in Antarctic atmosphere 8=23264

$\text{NH}_4\text{Ag}_2\text{I}_5$, cryst. struct. rel. to ionic mobility 8=17379

NH_4BF_4 , n.m.r. and ion motions 8=5560

$\text{NH}_4\text{Br}:\text{Cu}^{2+}$, e.p.r. 8=14102

NH_4BrCl , crystal structure at 140°K 8=8545

NH_4CNS effect on Fe acid corrosion inhibition by thiourea 8=2518

NH_4Cl crystals, photoelastic constants, temp.

variation 8=2440

NH_4Cl , e.p.r. spectrum of Mn^{2+} , spin-Hamiltonian parameters 8=5534

NH_4Cl , e.s.r. studies of VO^{2+} 8=5542

NH_4Cl , harmonic scatt. and critical pt. correl. 8=23007

NH_4Cl , inner and outer complex in formation from

$\text{NH}_3 + \text{HCl}$ 8=12217

NH_4Cl optical harmonic generation near second-order phase transform., obs. 8=14245

NH_4Cl , ordering, anomalous changes in vol. 8=21850

NH_4Cl solutions, electrical effects during freezing 8=1587

NH_4Cl , transition $\text{II} \rightleftharpoons \text{III}$, energy and temp. meas. 8=17091

NH_4ClO_4 , solid, elec. cond. 8=2128

NH_4ClO_4 , thermal decomp., mass spectra 8=9693

$\text{NH}_4\text{Cl}(\text{ZnCl}_2) \cdot \text{H}_2\text{O}$, crystn. interphase equilb. 8=21933

$\text{NH}_4\text{CuTiF}_6 \cdot 4\text{H}_2\text{O}$, crystal structure 8=13280

NH_4F impurity in ice, dielec. dispersion obs. 8=18188

$\text{NH}_4(\text{Fe}, \text{Al})(\text{SO}_4)_2 \cdot 12\text{H}_2\text{O}$, paramagnetic, Mossbauer-

effect study of electronic relax. 8=21812

$\text{NH}_4\text{Fe}(\text{SO}_4)_2 \cdot 12\text{H}_2\text{O}$ magnetic relaxation, Mössbauer

spectra 8=2378

$(\text{NH}_4)_2\text{H}_2\text{PO}_4$, 45°X-cut, use in laser emission control

devices 8=6424

$\text{NH}_4\text{H}_2\text{PO}_4$ light modulation props. of crystals 8=23002

$\text{NH}_4\text{H}_2\text{PO}_4$ noncollinear parametric scatt. of

visible light 8=18489

$\text{NH}_4\text{H}_2\text{PO}_4$ photoelastic consts. 8=14244

NH_4I , modifications II and III, lattice parameters 8=17398

NH_4I , nuclear spin-lattice relax. for protons and I

nuclei 8=14151

NH_4NO_3 polycrystals, spin-lattice relax. of p and d 8=14149

NH_4OH impurity in ice, dielec. dispersion obs. 8=18188

NH_4OH solution, electrical effects during freezing 8=1587

NH_4SCN polycrystals, light scattering, diffuse, effect of

anisotropy 8=23004

$(\text{NH}_4)_2\text{Cr}_2\text{O}_7$, i.r. spectrum, low temp. 8=14250

$(\text{NH}_4)_2[\text{InCl}_4\text{H}_2\text{O}]$, nuclear quad. res. freqs. of Cl^{125} and In^{115}

rel. to temp. 8=2389

$(\text{NH}_4)_2\text{SO}_4$, ferroelec., deuteron spin-lattice relax.

time 8=2386

$(\text{NH}_4)_2\text{SO}_4$ and $(\text{ND}_4)_2\text{SO}_4$, phase transitions correl. with

i.r. spectra 8=23005

$(\text{NH}_4)_2\text{SiF}_6$ cryst., molec. motions from n.m.r. 8=14154

Nobelium

No entries

Nobelium compounds

No entries

Noble gases. See inert gases.**Noctilucent clouds.** See Atmosphere/upper; Clouds.**Noise**

additive, in quantum e.m. communication channel 8=19433

ambient sea noise in deep and shallow ocean, simultaneous

meas. 8=5787

atmospheric, v.l.f. bands 8=23291

electromagnetic, reduction method 8=15161

immunity of coded communication 8=19434

linear systems, noise temp. definition 8=19437

metal bolometers, impedance 8=224

signal-to-noise ratio, enhancement in hypersonic meas. by

time averaging 8=3075

signals, single-step compared with poly-step by noisy

channel 8=10504

water reactor, power noise spectra in l.f. region 8=7320

white noise plus signal, zero crossings calc. 8=10607

Ar laser, mode-locked quieting 8=15466

He-Ne laser, mode-locked quieting 8=15466

KH_2PO_4 optical parametric amplifier, quantum noise,

0.5-0.6 μ 8=16526

Noise—contd**acoustic**

aerodynamic generation 8=21479

amplitude modulated, human perception 8=3094

animal sonar in air 8=19620

bands used to establish pitch in hearing 8=19610

booth, lightweight, design and instruction 8=6184

cavitation, modelling parameters 8=19587

compressor radiation suppression rel. to rotor-stator

spacing and duct-mode directivity 8=15076

control by architectural acoustics, conference 8=3076

criterion curves, Beranek's revised version 8=19586

explosion bangs, subjective reaction of community,

obs. 8=10757

fans and compressors, radiation study 8=6183

gas flames, ultrasonic abatement 8=10779

hearing, masker level and sinusoidal signal

detection 8=6194

impulse, damage-risk criteria 8=19611

infrasound spectra, rocket flight and take off 8=196

jet aircraft during landing 8=19588

jitter discrimination obs. 8=19609

Marill's detection formula for pure tones 8=15087

masking level differences due to interaural intensive

disparities 8=6198

masking by subjectively diffuse sound fields, obs. 8=6192

mean level rel. to that deduced from noise energy

density 8=3078

perceived noisiness concepts, applic. 8=19612

signal detection, incoherent, using sensors in isotropic

noise field 8=6159

sonic bangs and explosions subjective estimation 8=15075

total exposure evaluation 8=19589

vibrating sonar dome, generalised field formulation

and loading 8=15062

waterfalls 8=3077

CdS crystal, S/n during u.s. amplification at

87 MHz 8=22098

electrical. See Cosmic radiation, radiofrequency;

Fluctuations/electrical; Sun/radiation, radiofrequency.

Noise abatement

See also Absorption/acoustic waves.

acceptable exposure identification 8=208

compressor radiation, rel. to rotor-stator spacing and

duct-mode directivity 8=15076

double walls, optimum parameters 8=3079

explosion bangs, subjective reaction of community,

obs. 8=10757

in fans and compressors 8=6183

insulation by double and single walls, calc. 8=10741

panels, multimode response to sonic booms, normal and

travelling 8=6123

sonic booms, building response 8=10758

Nomenclature and symbols

See also Units.

in oblique ionospheric soundings and ray tracing 8=2690

Nomograms

See also Graphs.

ionosphere, Es, stability coeff. calc. 8=23407

two reading time interval, optimal correspondence

choice rel. to meas. device 8=2875

satellite lifetime rel. to upper atm. density vars. 8=14711

for visibility of light sources against background

of uniform luminance 8=11230

Non-crystalline state. See Amorphous state; Vitreous state.**Non-Newtonian fluids.** See Fluids.**Novae**

See also Stars.

binary nature, relevant spectroscopic and photoelec. obs.,

and periods 8=14779

Chudze-Lovas (1967) supernova, spectrophotometry 8=5900

Cygnus loop supernova remnant obs. at 41, 195

and 430 MHz 8=5904

Delphini 1967, spectrum obs. 8=5899

Herculis 1960, spectrum 8=19174

multiple supernova interpretation of quasi-stellar

sources, and stellar coalescence 8=5947

Nova Herculis 1960, spectrum 3530-6560 Å 8=10187

nucleosynthesis in supernovae shock waves 8=5842

1967 supernova in NGC 3389, spectrum and H α emission

within galaxy 8=14781

pre-supernova models, rel. to C and O $_2$ burning stars,

evolution 8=5874

quasars novae and supernovae, identity of

mechanisms 8=23629

super-, 1966 Palomar search, obs. 8=14780

super, shock wave propagation 8=1390

supernova, gravitational collapse computation 8=10186

supernova hydrodynamics and nucleosynthesis 8=14726

supernova 1962A, type I in Coma 8=23550

supernova remnants CTA $_1$ and HB $_3$ struct. and spectral

indices, 81.5 and 178 MHz 8=10191

supernova SN 1966b in NGC 4688, photometric and

spectral obs. 8=10180

supernova, Type I, white dwarf as genitor by

explosion 8=23549

supernovae 8=23546

Novae—contd

- supernovae, emission spectrum rel. to structure and masses of envelopes 8=19176
- supernovae, rel. to galaxy class and abs. value distrib. 8=19223
- supernovae, gravitational collapse and neutrino imploding 8=2790
- supernovae and remnants 8=23545
- supernovae shells plasma turbulence state determ. 8=10185
- supernovae, Type I, rel. to white dwarfs 8=5903
- supernovae types I and II colour indices phase depend. 8=10184

Novoids. See Novae.

Nuclear acoustic resonance. See Absorption/acoustic waves, ultrasonic; Nuclear magnetic resonance and relaxation.

Nuclear alignment. See Nuclear orientation.

Nuclear bombardment targets

- bremsstrahlung, linear polarization 8=11446
- deuterated, Cu backed, characteristics 8=11291
- gas, high pressure, trap for removing impurities 8=20187
- methane, elastic e scatt, 250 MeV off C^{13} 8=3912
- polarized proton target for investigating low energy nucleon-nucleon interactions 8=822
- polarized targets and ion sources, conference, Saclay France (1966) 8=15629
- polyethylene, for π -n and π -p interactions, Σ production and polarization meas. 8=864
- p polarization determ. with Q-meter 8=11600
- reaction widths from yield curves, temperature and contaminant effects 8=959
- reactor, for thermal n capture, γ -ray spectro-meter 8=3576
- Ag, emission function, Ar^+ beam bombard. 8=6626
- Al, emission function, Ar^+ beam bombard. 8=6626
- Ar^{40} shot into Mo, Ta backings, distrib. studies 8=6625
- Au, emission function, Ar^+ beam bombard. 8=6626
- Au foil on C, O^{16} scatt., charge state fractions 11.5–37.3 MeV obs. 8=20839
- Be, emission function, Ar^+ beam bombard. 8=6626
- C, emission function, Ar^+ beam bombard. 8=6626
- C film backings for use in reaction studies 8=8316
- Cu, emission function, Ar^+ beam bombard. 8=6626
- ErT_3 , life under deuteron bombardment in accelerator 8=11290
- F compounds, additivity of stopping power 8=20188
- H, liq. target, thin walled, description 8=15838
- H, within Ne-H bubble chamber 8=6682
- Mo as backing material for noble gas targets 8=6625
- Mo, emission function, Ar^+ beam bombard. 8=6626
- Ne^{22} shot into Mo, Ta backings, distrib. studied 8=6625
- Si^{28} , from $P^{31}(p, \alpha_0)Si^{28}$ 8=963
- Ta as backing material for noble gas targets 8=6625
- $TiTi_4$, life under deuteron bombardment in accelerator 8=11290

Nuclear decay schemes. See Radioactivity/decay schemes.

Nuclear decay theory

See also Beta decay theory; Nucleus/theory.

- α -decay, charge of recoil atoms 8=16014
- α , highest penetrability of Coulomb barrier 8=3857
- α , reduced transfer amplitudes calc. using Rassey wave functions 8=3860

β -decay time-reversal invariance violation, RaE obs. 8=11829

β , Fermi matrix element, exact calc. using superfluid model 8=20653

effect on molecular configuration 8=12167

heavy emulsion nucleus, 24 GeV/c proton collisions 8=16076

induced capture of orbital electron, cross-section 8=1042

internal conversion, atomic screening effect 8=15946

nuclides far off the stability line, conference, Lysekil Sweden (1966) 8=15911

Schrödinger's eqn., modification test 8=3407

unstable particles and resonances, application of general wave function 8=20268

Z = 104–115 superheavy elements, lifetime predictions 8=7122

Eu^{156} , Fermi β transition 8=16036

$Ne^{19} \rightarrow F^{19} + e^+ + \nu$, e.m. simulation of T violation 8=3863

Nuclear emulsions. See Nuclear track emulsions.

Nuclear excitation

See also Mössbauer effect; Nucleus/energy levels.

analog states during quasi-elastic scattering 8=15936

Coulomb, of light and medium nuclei, at overbarrier energies 8=935

eqns. of motion, time-depend. eqns. 8=11705

functions, in nuclear reactions, peak counting method 8=20762

Gamow-Teller matrix elements for super multiplet states, exact determ. 8=15930

giant resonances in even, heavy nuclei, treated as coupling of collective modes, inelastic e scatt. calc. 8=20772

giant resonances interacting with surface vibrations, correl. 8=933

giant resonances, scatt. of plane-polarized photons 8=11856

by ion scatt., with mutual excitation, diffraction theory 8=1102

isobaric analog resonance in elastic p scattering, width calc. using Lane eqns. 8=11698

Nuclear excitation—contd

isobaric analogue resonances, optical potential theory 8=7046

isobaric analogue states in density matrix approach to superfluid model 8=20653

isobaric analogue states, transition induced in charge exchange reaction, formalism 8=11845

longitudinal correl. of excited states 8=3784

by n reactions, prompt γ rays from 14 target elements, 14.7 MeV 8=7211

radioactive isotopes produced by 60 MeV p bombard. of Al, Fe and Cu 8=1061

rare-earth even nuclei, by (d, p) reaction 8=3782

residual, following nuclear reaction, equilibrium 8=11700

resonance fluoresc., appl. of Compton-scattered γ -rays 8=20666

resonances, giant (LITW) from neutron total cross sections 8=1067

resonance reaction, cluster representation 8=11849

superheavy-ion reactions, Coulomb distortion and nuclear stiffness 8=11688

2^+ excitation in n-nucleus scatt. 8=16086

Al^{24} , energy of first analog states 8=16017

Al^{25} , isospin-forbidden analogue resonances 8=20691

Ar^{38} , analogue resonance of Cl^{38} from $Cl^{37}(p, \gamma)Ar^{38}$ 8=11737

$B^{10} 2^+$ resonance excited by $Li^7(He^3, \gamma)B^{10}$, 3.4 MeV 8=11943

$Be^8, 2^+$ 2.0 MeV state, in $d + B^{10} \rightarrow C^{12*} \rightarrow Be^{8*} + \alpha \rightarrow \alpha + \alpha + \alpha$ 8=16111

$Be^9(\gamma, n)Be^8$, core coupled to single particle states 8=3907

Bi^{209} analog states of Pb^{208} in 14–18 MeV p scatt. 8=11784

Bi^{209} in $Pb^{208}(He^3, d)Bi^{209}$, single proton strength in multiplet at 2.6 MeV 8=11787

C^{12} , giant resonance, interference between bremsstrahlung and nuclear γ radiation 8=6796

C^{12} , of 19.5 MeV level by inelastic e scatt. 8=1045

C^{12} , 25 MeV giant resonance formed by $d + B^{10}$, 0.4 MeV 8=16111

C^{12} and C^{13} , by inelastic electron scattering, 15.11 MeV levels 8=3791

Ca^{43} , proton hole states excitation by $K^{41}(He^3, p)Ca^{43}$ 8=11742

Cl^{32} , energy of first analog states 8=16017

Co^{59} , inverse reaction cross-section effect 8=3900

Cr^{52} isobaric analogue state in Mn^{52} obs. in $Cr^{52}(He^3, p)Mn^{52}$, 12 MeV 8=20703

Dy^{161} , Coulomb excitation, gyromagnetic ratios from branching ratio 8=11772

F^{20} analogue states from $F^{19}(d, n) 2.980$ MeV 8=20688

Fe^{56} analogue ground state identified in $Fe^{54}(He^3, p)Co^{56}$, 12 MeV 8=20706

Fe^{56} , isobaric analog resonances obs. in $Mn^{55}(p, \gamma)Fe^{56}$, $Mn^{55}(p, n)Fe^{56}$ 1.3–1.85 MeV 8=15977

$In^{115}(n, n')In^{115m}$, spatial distrib. in water of In resonance and neutrons 8=11612

In^{115} , 600 and 830 keV photoexcitation 8=20714

Kr^{78} in $Br^{78}(p, n)Kr^{78}$, half-life and g-factor meas. 8=11752

Li^5 resonance obs. in p- α scatt. 22–25 MeV 8=20532

Li^8 , search for T = $\frac{1}{2}$ states 8=11659

$Mg^{24, 26}(\alpha, \gamma)Si^{28, 30}$, giant dipole resonance 8=11944

N^{15} , isobaric analog states of O^{16} 8=15956

Na^{24} analogue states from $Na^{23}(d, n) 2.98$ MeV 8=20688

O^{15} , excited states with isobaric analogs in N^{15} 8=15956

O^{16} , giant resonance, interference between bremsstrahlung and nuclear γ radiation 8=6796

O^{16} , 27.6 MeV state, from $J^{\pi} = 3^{-}$, T = O, resonance in $C^{13}(He^3, \alpha)C^{12}$ 8=3795

O^{17} , 2.2–4.2 MeV n scatt. 8=1070

Os^{189} , Coulomb, reduced transition probabilities 8=3835

P^{28} , energy of first analog states 8=16017

P^{29} , isospin-forbidden analogue resonances 8=20691

Pb^{208} , analog resonance parameters from p scatt. 8=11881

Pb^{208} , excitation obs. from e scatt., 28–73 MeV 8=11785

Sc^{40} , energy of first analog states 8=16017

Si^{27} , first and second excited states in $Si^{28}(He^3, \alpha)Si^{27}$ 8=7082

$Si^{28}(\alpha, \gamma)Si^{32}$, 7–12 MeV, giant dipole resonance 8=11944

Si^{30} , isobaric analog of Al^{29} 8=3959

$Ti^{47, 48, 49}$, by bremsstrahlung, photoproton yields 8=7168

$Ti^{48}(p, p'\gamma)$, 4–6 MeV, ang. correl. compared with compound nucleus and direct reaction theories 8=11879

V^{48} , transition to ground state analogue Ti^{48} in $Ti^{46}(He^3, p)V^{48}$ 8=20702

Y^{90} , isospin analogue resonance decay 8=11754

$Y^{90}(p, n)Zr^{90}$, 3.6–5.8 MeV, $2^{-}, 3^{-}$ analogue state resonances 8=11889

Zr^{90} in $Y^{90}(He^3, d)Zr^{90}$, T_C single-proton single-proton hole states 8=3818

Nuclear explosions. See Explosions/nuclear.

Nuclear field theory. See Field theory, quantum.

Nuclear fission

See also Explosions/nuclear; Nuclear reactors, fission.

α emission accompanying fission, probability 8=3977

angular anisotropy in neutron fission of nuclei, quasiclassical relation 8=7254

energy, and mass distrib. using double pulse ionization chamber obs. 8=1106

energy gap increase using assumption G \propto magnitude of nuclear surface 8=11956

Nuclear fission—contd

- fast-fission effect in lattices with cluster elements, anal. 8=11962
 fragment charge distrib. as function of kinetic energy 8=11966
 fragment det. with Si surface barrier detector 8=3465
 in heavy ion reactions 8=20842
 kinetic part of Hamiltonian computed as quadratic form of time derivatives of nuclear surface 8=7241
 (n, γ) prod. of isomers, statistical model 8=20847
 xny reactions, spin-dep. treatment 8=1108
 photofission, up to 1600 MeV 8=7169
 rate meas. use of "spinner" 8=20202
 ratio meas., γ counter correction 8=20358
 scintillation tank for meas. ratio of capture and fission events 8=11958
 ternary, emission of light charged particles at moment of fission 8=20850
 ternary, by heavy ions, mechanism 8=1110
 track densities of internal and ext. surfaces, etched, comparison after n irradi. 8=20852
 Am, spontaneously fissioning, prod. by p reactions with Am 8=20843
 Am^{240, 242}, spontaneous, spin determination 8=1108
 Am^{241, 242m}, n-induced cross-sections meas. 8=20846
 Am²⁴², prod. by (n, γ), most probable spin values 8=20847
 Am^{242m}, spontaneous, obs. agree with "shape isomerism" 8=1107
 Am^{242m}, 14 msec spontaneously fissioning, spin value 8=7243
 Bi²⁰⁹, by Ar⁴⁰ ions, excitation function 8=1110
 Cf²⁵², on-line studies of mass-separated products 8=20858
 Fm^{246, 248}, spontaneous half lives, new nuclides Fm^{244, 245} identified 8=7242
 Np²³⁷, α emission accompanying probability 8=3977
 Np²³⁷ n fission yields, $131 \leq A \leq 135$ 8=20856
 Np²³⁷ n fission yields $141 \leq A \leq 153$ 8=20857
 Np²³⁷ n fission yield of Zr^{95, 97}, Mo⁹⁹ 8=20855
 Pu²³⁸, n-induced, cross-section obs. at 1.0, 1.5, 3.0 and 14.9 MeV 8=1109
 Pu²³⁹(d, pf), fragment ang. distrib. anisotropy 8=3983
 Pu^{239, 240, 241}, cross-sections relative to U²³⁵ 8=7252
 Pu²³⁹, energy depend. of n cross-section in range 0, 7-4 MeV 8=7251
 Pu²³⁹, n energy 14-90 eV, multilevel analysis 8=11961
 Pu²³⁹ neutron induced, properties of resonance levels 8=7258
 Pu²³⁹, by neutrons 8=7245
 Pu²³⁹ scintillation tank for meas. ratio of capture and fission events 8=11958
 Pu²³⁹, shielding effect of U²³⁸ on epi-cadmium fission 8=7246
 Pu^{239, 240, 242} photofission fragments, ang. distrib., and conservation of K quantum no. 8=11964
 Pu²⁴⁰ spontaneous fission half-life 8=7244
 Pu²⁴¹, fission and absorption g-factors 8=7250
 Pu²⁴², spontaneous, mass yield of I, isotopes rel. to Pu²⁴⁴ in early solar system 8=3978
 Ta, p-induced, 156 MeV, probability, fragment energy spectra 8=11965
 Th, rel. to creep 8=8866
 Th, induced by 15 MeV neutrons 8=3979
 Th²³², α emission accompanying probability 8=3977
 Th²³², neutron induced, integral and differential cross-sections near threshold 8=7257
 Th²³² photofission fragments, ang. distrib., and conservation of K quantum no. 8=11964
 U carbide-heavy water subcritical system 8=11957
 U, p-induced, 156 MeV, probability, fragment energy spectra 8=11965
 U²³⁵, n induced and capture cross-section meas., resonance analysis 8=20844
 U^{235, 238}, by monoenergetic neutrons, kinetic energies and fragment yields 8=7260
 U^{235, 238}, α emission accompanying probability 8=3977
 U²³⁸ photofission fragments, ang. distrib., and conservation of K quantum no. 8=11964

products

- activation detectors for fusion-n spectra, development and excitation meas. 8=11970
 α -particle emission from U^{235, 236, 238} induced by 2.5 and 14 MeV neutrons 8=7256
 angular distrib. anisotropy less than unity depend. on target deformation and spin 8=3983
 atmospheric explosions, interhemispheric transfer 8=23297
 ceramics, conference Harwell 1965 8=16168
 diffusion of gaseous products in graphite 8=4950
 fission-gas, recoil release from UO₂ 8=7266
 fragment detection efficiency in presence of intense α -rad., of spark counter 8=16134
 fragments, excitation of N₂ gas along entire track 8=7531
 fragment K. E. 8=16133
 fragment K. E. rel. to excitation of fissioning nucleus 8=16132
 fragments, multiple and plural scatt. 8=11969
 γ -ray spectra of earth contamination, aircraft meas. 8=9895

Nuclear fission—contd**products—contd**

- gases from n-irrad. UO₂-graphite pellets, γ -ray spectra 8=4016
 gas release from UO₂, activation energies in defect-trap model 8=3980
 ion prod. rate, space-depend., by fragments escaping from fuel plate 8=11968
 in kerosene degraded by HNO₃, removal with K₂Cr₂O₇ and H₂SO₄ soln. 8=20854
 lanthanides, chromatography 8=9739
 mass asymm. and probability of simultaneous α emission 8=3977
 mass and energy distrib. using parallel foils 8=20860
 migration and concentration along fuel rods rel. to burning up 8=16164
 $\bar{\nu}$ prompt, in n-induced fission of Pu^{239, 241} 8=20851
 $141 \leq A \leq 153$, from Np²³⁷ n fission 8=20857
 p, t, α fractional yield, U²³⁵ fission by slow and 14 MeV n 8=7262
 removal from degraded solvent by mixed ion exchange resins 8=5694
 short lived, from n-irrad. enriched U, γ -ray spectra 8=7263
 simulation in fast critical set-ups 8=11971
 Am²⁴² prompt, spectrum, prod. by d bombard. of Pu²⁴⁰ 8=16131
 Am^{242m}, spontaneous, spectrum, prod. in Pu²⁴²(d, 2n) Am^{242m} 8=16131
 Br⁸⁷ decay in atmosphere 8=2611
 Cd¹¹⁵ yield in U²³⁸ photofission, 5.3-6.5 MeV bremsstrahlung 8=16135
 Cf²⁵² fragments, transient responded Si surface barrier detectors rel. to plasma formed 8=20199
 Cf²⁵² fragments, K X-ray emission obs. 8=20850
 Cf²⁵², K X-ray yield rel. to odd-even effect 8=1113
 Fm^{244, 245}, new nuclides from Fm^{246, 248} fission 8=7242
 I, diffusion in graphite 8=12015
 I isotopes from Pu²⁴² spontaneous fission, rel. to Pu²⁴⁴ in early solar system 8=3978
 I^{131, 133, 135} from Np²³⁷ neutron fission 8=20856
 Mo⁹⁹ from Np²³⁷ n fission 8=20855
 Pd atoms, highly ionized, electron binding energies 8=1112
 Sm atoms, highly ionized, electron binding energies 8=1112
 Sr atoms, highly ionized, electron binding energies 8=1112
 Te¹³² from Np²³⁷ neutron fission 8=20856
 U atom emission from fissioning surface 8=3985
 U from irradi. of UO₂ pellets 8=20859
 U, by medium-energy p, isobaric yield distrib. 8=1111
 U^{235, 236} mean n yield 8=7264
 U^{235, 236} neutron yields, conversion from relative to absolute 8=7265
 from U^{235, 238}, γ -ray spectra at selected times after fission 8=3984
 U^{235, 238}, by monoenergetic neutrons, kinetic energies and fragment yields 8=7260
 U²³⁸, 14 MeV neutron induced instantaneous fission 8=7259
 UO₂ fuel, gas pressure calc. 8=7267
 UO₂-graphite mixture, fission gas (Xe and Kr) release during irradi. 8=4022
 Xe atoms, highly ionized, electron binding energies 8=1112
 Xe, captured in graphite, isothermal annealing and escape behaviour 8=11975
 Xe, diffusion in graphite 8=12015
 Xe, prod. by in-pile melting of irradi. UO₂(NO₃)₆·6H₂O 8=3982
 Xe, recoil prod. of U, diffusion in Ag 8=3981
 Xe¹³⁷⁻⁴² from Cf²⁵², decay props. 8=20858
 Zr^{95, 97} from Np²³⁷ n fission 8=20855
 Zr⁹⁷ from n + U²³⁵ fission at 14 MeV, fine structure obs. 8=7261

uranium

- ⁶²⁸ natural U cluster D₂O lattices obs. 8=20845
 electron beams, 1.5 and 3.0 GeV, product mass yields 8=11972
 emission of U from irradi. UO₂ pellets, due to superficial fissions 8=20859
 fragment tracks in LiF, anisotropy of orientation 8=17706
 induced by 15 MeV neutrons 8=3979
 meas. of U atom emission from surface 8=3985
 by medium-energy p, isobaric yield distrib. 8=1111
 n activation cross-section rel. to F¹⁹, Na²³, Mn⁵⁵, In¹¹⁵, Ho¹⁶⁵, Al²⁷ 8=3937
 p-induced, 156 MeV, probability, fragment energy spectra 8=11965
 short lived prods., γ -ray spectra 8=7263
 U²³⁵, by α particles 8=7245
 U²³⁵ fragment energy by 430, 630 keV and 1.1 MeV neutrons 8=11974
 U²³⁵, resonance parameters 8=11959
 U^{235, 236, 238, 239}, cross-sections relative to U²³⁵ 8=7252
 U^{235, 236} fragment mean kinetic energy, by 1.5 MeV neutrons 8=11973
 U^{235, 236}, neutron-induced, relative neutron yields of isotopes, 0.08-1 MeV 8=7264
 U^{235, 236} neutron yields, conversion from relative to absolute 8=7265

Nuclear fission—contd**uranium—contd**

- U^{235,236} scintillation tank for meas. ratio of capture and fission events 8=11958
 U^{235,236,238} induced by 2.5 and 14 MeV neutrons 8=7256
 U²³⁵, cross-section, ratio with U²³⁸ capture cross-section 8=20848
 U²³⁵ (C¹², 5n) Cf²⁴² 8=11834
 U²³⁵, cross-section at 30 and 64 keV 8=7253
 U²³⁵ (d, pf), fragment ang. distrib. anisotropy 8=3983
 U²³⁵ fragment energy by 100, 260, 700 keV and 1.3 MeV neutrons 8=11974
 U²³⁵ fragments, n emission rel. to mass 8=11967
 U²³⁵, γ -ray spectra due to products at selected times after fission 8=3984
 U²³⁶, n and diffusion widths rel. to compound nucleus spin 8=7255
 U²³⁵ n capture cross-section rel. to Na²³, Mn⁵⁵, In¹¹⁵ and Ho¹⁶⁵ 8=3943
 U²³⁵ neutron induced, properties of resonance levels 8=7258
 U²³⁵, prompt n emission from fragments 8=20853
 U²³⁵, p, t, α fractional yield, by slow and 14 MeV n 8=7262
 U²³⁵ quaternary fission by thermal neutrons, obs. 8=11963
 U²³⁵, resonance self-shielding of U²³⁸ 8=7246
 U²³⁵, spin-depend. of n cross-section 8=20849
 U²³⁵ thermal fission spectrum 8=16129
 U²³⁵ thermal neutron fission fragments charge division 8=11960
 U²³⁵, thermal neutron, total gamma energy release 8=7247
 U²³⁵, Zr⁹⁷ yield fine structure, E_a = 14 MeV 8=7261
 U^{235,238} capture and fission, Doppler effect obs. 8=7248
 U²³⁶ quaternary fission, total kinetic energy release obs. 8=11963
 U²³⁶, ternary fission with emission of particle with Z > 2 8=7249
 U²³⁸, angular distribution, n-induced, using solid-state track detector 8=16130
 U²³⁵, γ -ray spectra due to products at selected times after fission 8=3984
 U²³⁸, by Ne²² and Ar⁴⁰ ions, excitation function 8=1110
 U²³⁸ (n, f), mass, energy obs., range straggling data 8=20860
 U²³⁸, 14 MeV neutron induced instantaneous fission 8=7259
 U²³⁸ photofission, Cd¹¹⁵ yield, 5.3-6.5 MeV bremsstrahlung 8=16135
 UC rods, fast fission ratios meas. 8=16170

Nuclear fission reactors. See Nuclear reactors, fission.

Nuclear forces

See also Field theory, quantum/meson field.

- binding energy calc. using BHF model 8=3762
 binding energy from HF calc. for doubly even nuclei in s-d shell 8=7033
 binding energy rel. to π -nuclear scatt. 8=3948
 book, unified theory of nuclear models and forces 8=3760
 boson-exchange theory and N-N potential form 8=15916
 Brueckner theory of N-N wave functions tested in π absorpt. and 2N emission 8=20654
 central interactions, Wigner-Eckart theorem applied to SU₃ matrix elements 8=7037
 complex optical potentials, derivation 8=7038
 energy surface, force constant and mass parameter related to intrinsic structure 8=11707
 Fermi system, retarded interactions in meson theory 8=11693
 ground state props. of nuclear matter, A₁₁ approx. 8=15926
 Λ binding energy calc. 8=15857
 Λ binding energy and ANN potential 8=3766
 Λ -N pot. in s-shell hypernuclei 8=16009
 Λ^0 , Σ -nucleus pots. from K⁻ + He⁴ \rightarrow Σ + nucleus + $\pi^- \rightarrow$ Λ^0 + p + d + π^- 8=20417
 matter binding energy using 4N interactions 8=11695
 meson, vector exchange as origin of repulsive core 8=20642
 Mittelstaedt's definition of rearrangement energy extended 8=923
 n and p shell average field, N > 126, Z > 82 8=7035
 N optical potential, complex symmetry term from n scatt. data 8=924
 N, valence, effective interaction 8=11683
 N-N "free" potential and mass, 3-body force 8=7032
 N-N interaction, boson approx. 8=15917
 N-N interaction rel. to spin-orbit splitting 8=15947
 N-N, kuo-Brown, analysis for symm. 8=3759
 N-N potential to fit N-N scatt. data 8=3758
 N-N pot, Morse and vel. depend. investigated 8=11684
 N-N potential for odd parity spin triplet states, 320 MeV 8=3777
 optical pot. rel. to Al²⁷(He³, α) Al²⁶ 8=11945
 optical potential, (d, p) reactions, polarization effect 8=1087
 optical potential, form of imaginary part 8=3757
 potential, optical, isospin dependence investigated 8=7039
 optical pot., isospin term, (p, n) reactions 94 MeV 8=16070
 potential optical, for p scatt. 8=3917
 optical pot. rel. to polarized p scatt., ang. asymm. 8=11880
 potential, rel. to polarized p scatt, optical model 8=16067
- Nuclear forces—contd**
 optical pot. and p scatt. off F¹⁰ 8=7182
 optical pot., spin orbit interaction interference in 2N transfer reactions 8=11877
 optical potential in Te- α scatt. 8=1098
 pairing approx. appl. to spherical nuclei, separation energy calc. 8=3768
 pairing problem linearized approx. leading to ground and O⁺ states 8=11704
 parity-violating 8=15915
 4-particle T-matrix eqns. interacting via 2-body forces, rel. to nuclear matter 8=11695
 phenomenological approach justification 8=15918
 (p- μ -p)⁺, binding energy 8=20657
 p-n correlation effect on (π^+ , π^0) scatt. 8=3950
 pot. complex, replacement of single-particle by hole state rel. to quasi-free scatt. 8=16052
 potential, equivalent local 8=7034
 potential models, OPE, OBE, dispersion-theoretic, phenomenological 8=15919
 pot., spin-independent, s-state reaction-matrix calc., improved 8=11696
 proton hole states of odd parity in 2s-1d shell nuclei 8=20650
 Q-Q, effective N interaction calc. disagreement 8=11683
 realistic, core polarisation and quasiparticle theories of even Sn isotopes 8=15985
 repulsive interaction in atomic nucleus, strength 8=20643
 review of present knowledge, and suggested solution of uncertainties 8=11682
 shell-model potentials for heavy nuclei and stability of superheavy nuclei 8=11786
 soft core pot. fit for N-N and shell model of Ti⁵⁰ 8=11748
 soft and hard core pots. compared when they reproduce 2N scatt. 8=11691
 spherical nuclei, pairing approx., appl. to A > 20 8=3769
 star, neutron, zero temp., high density, soft core 8=19166
 tensor forces in residual interaction between particles 8=919
 tensor, Kuo-Brown interaction used in calc. collective O vibrations in 8 nuclei 8=11706
 tensor in shell model G-matrix interaction 8=7048
 Woods-Saxon pot. in calc. of e scatt. off light nuclei 8=7173
 Yale 2N pot. used in HF calc. 8=7033
 Yukawa pot., Regge trajectories for Schrödinger eqn. 8=11421
 Be¹⁰, binding energy, differentiating between p and n in h.f. approach 8=20677
 C¹⁰, binding energy, differentiating between p and n in h.f. approach 8=20677
 Ca isotopes, 3-body, contribution to binding energies 8=15970
 Ca, potential for n scatt. 2-8 MeV 8=3933
 Ca⁴⁰ BHF calc. of binding and single particle separation energy 8=3762
 Ca⁴⁰, HF calc. of binding energy using Tabakin potential 8=937
 F¹⁹, derivation of optical pot. from p capture, n scatt. 8=3931
 He³, effect ANN force on binding energy 8=950
 He³, Coulomb energy in non-local potential and binding energy diff. 8=11654
 He⁷ BHF calc. of binding and single particle separation energy 8=3762
 He⁴ binding energy rel. to α charge form factor calc. 8=11657
 He³, effect ANN force on binding energy 8=950
 He⁶ and He⁷, binding energy calc. 8=3847
 Hg²⁰⁰, n separation energy calc. 8=11911
 K, potential for n scatt. 2-8 MeV 8=3933
 N binding energy var. in shell model approx. and exact calc. 8=3764
 N pairing energy as a function of ang. momentum and total n number 8=3770
 O¹⁶ BHF calc. of binding and single particle separation energy 8=3762
 O¹⁶ binding energy calc. with Hamada-Johnston pot., corrections, anomalies 8=7074
 O¹⁶, HF calc. of binding energy using Tabakin
 O¹⁶, Q-Q and pairing rel. to lowest even-parity states 8=11727
 Pb²⁰⁸⁻²⁰⁹, particle-core coupling 8=16004
 Sn¹¹⁶, energy spectrum, and effective nuclear forces derived from realistic nucleon-nucleon potentials 8=20715
- Nuclear fusion**
 See also Explosions/nuclear; Nuclear reactors, fusion; Thermonuclear reactions.
 jets, dense, accel. to thermonuclear speeds by hypervelocity impact 8=16137
 plasma, confinement by mag. and e.m. fields 8=11977
 plasma, dense, implosion by hypervelocity macroparticle impact for controlled explosion 8=16601
 self-crowbar air gap, tests 8=12458
 D and T reactors, plasma compression study 8=7798
 Pt^{234,241}, n-induced, energy depend. of prompt γ 8=20851
- Nuclear induction.** See Nuclear magnetic resonance and relaxation.

Nuclear interactions. See Collision processes; Field theory, quantum/interactions; Elementary particles; Nuclear reactions; Scattering, particles.

Nuclear isomerism

- See also Nucleus/energy levels.
activation, by $\text{In}^{115\text{m}}$ γ -rays 8=3821
excitation by thermal n radiative capture 8=11703
fission, $\text{x}\gamma$ reactions, spin-dep. treatment 8=1108
 $\text{Ag}^{106\text{m}}$, γ -decay, energy levels of Pd^{106} 8=979
 $\text{Ag}^{106\text{e}}$, γ -decay, energy levels of Pd^{106} 8=979
 Ag^{109} , transition energy obs. 8=980
 Ag^{109} , transition meas. by reference to Ta^{182} decay 8=3820
 Am prod. by p reactions on Pu isotopes 8=20843
 $\text{Am}^{242\text{m}}$, 14 msec fissioning isomer, spin value 8=7243
 $\text{Am}^{242\text{m}}$, spontaneous fission 8=1107
 Au^{196} , impurity nucleus in metal solid solutions, shifts of γ radiation 8=1653
 Au^{199} , isomeric transition $\text{M}2 + 0.9\%$ $\text{E}3$ 8=994
 $\text{Br}^{82\text{m}}$ (I. T.) Br^{82} in liq. bromobenzene, chem. effects 8=18752
 Co^{58} , isomer ratios obs. for $\text{Co}^{58}(\gamma, n)\text{Co}^{58}$ and $\text{Ni}^{60}(\gamma, np)\text{Co}^{58}$ 8=20707
 Dy^{159} , γ -decay, $\text{E}1$ transitions 8=3828
 Fe^{57} isomer shift, calibration 8=16988
 $\text{F}^{130\text{m}}$, disintegration 8=7097
 $\text{In}^{194\text{m}}$, K X-ray and γ decay obs. 8=7147
 $\text{Ir}^{191\text{m}}$, isomeric state in reaction (γ, γ') 8=11781
 $\text{Lu}^{172, 173}$, γ -decay, $\text{E}1$ transition 8=3828
 $\text{Lu}^{176\text{e}}$ and half-lives 8=1022
 Na^{24} , γ -ray transition 8=3866
 Nb^{90} isomer, multipolarity deduced as $\text{M}2$ 8=20711
 $\text{Nb}^{99, 100}$, disintegration periods and energies 8=7089
 Np^{240} decay to Pu^{240} 1.131 MeV state 8=11791
 Pb^{205} , Bi^{205} γ -transitions to $13/2^+$ isomeric level 8=997
 Pu^{240} , 1.31 MeV state 8=11791
 $\text{Pt}^{195\text{m}}$, γ transitions, level decay 8=3837
 $\text{Rh}^{106\text{e}}$, γ -decay, energy levels of Pd^{106} 8=979
 Sn^{115} , 619 keV level, half-life of $1/2^+$ state 8=7095
 Sn^{119} impurity nucleus in metal solid solutions, shifts of γ radiation 8=1653
 Sr , isomer ratios from $\text{Sr}^{88}(\text{p}, \text{p}n)$ 8=11888
 $\text{Sr}^{87\text{m}}$, enrichment by recoil effect of $(n, 2n)$ reaction 8=7214
 $\text{Tb}^{158} \rightarrow \text{Dy}^{158}$, possible isomer of Tb^{158} 8=20755
 $\text{Te}^{127\text{m}}$ decay in $\text{Te}^{127\text{m}}(\text{OH})_2$ crystals, chem. effects 8=18751
 Tm^{165} , γ -decay, $\text{E}1$ transition 8=3828
 Tm^{170} , 4.1 μs isomeric state, strongly retarded $\text{E}1$ transitions 8=990
 W^{180} , γ -decay, $\text{E}1$ transition 8=3828
 Y , isomer ratios from $\text{Sr}^{88}(\text{p}, \text{xn})$ 8=11888
 $\text{Zn}^{69\text{m}}$, k conversion coeff. of 0.436 MeV transition 8=974

Nuclear magnetic resonance and relaxation

- See also Molecules/nuclear coupling.
acetone-chloroform system 8=2498
acetonitrile- d_3 , liq., anisotropic molec. rotation 8=8140
acetylene cpds., proton reson. spectra 8=21173
acoustic, ion crystal with trigonal symmetry 8=389
adsorbed mols. intermolecular relax. 8=8330
alcohols, solid, intra-molecular motion of OH group 8=16989
alkaline-earth fluorides, H -doped, polarization 8=8206
 n -alkyl fluorides 8=12315
alloys, spin echoes, Knight shift 8=2387
aminopyridines, chem. shift and π -electron distrib. 8=12296
aniline, in dilute soln. of CS_2 and CCl_4 , dependence on viscosity 8=126
autodyne, sensitivity regulation for linear response 8=3279
azines, additivity of p.m.r. solvent shifts 8=12931
1-aziridinepropionitrile, solvent and anisotropy effects 8=16895
azo-compounds decomp., tracing by n.m.r. spectroscopy 8=8127
benzenes, substituted, chem. shift of ring protons 8=12316
benzenes, unsymmetrical, ortho-disubstituted, shielding parameters 8=4625
 $\text{N-benzyl-N, 2, 4-6-tetramethylbenzamide}$, rate of internal rotation, equilibrium method calc. 8=12331
in binary liq. alloys of equi-valent metals, Knight shift charges rel. to comp. 8=12927
bromobenzene, molec. motion in liq. 8=8132
bromo-naphthalenes, chemical shifts meas. 8=7613
 β -bromopropionitrile, 2 rot. isomers, solvent depend. rel. to virial H-H couplings 8=21158
3-bromothiophene-2-aldehyde, double reson. 8=6408
1,3-butadienes, theory of π -electron coupling 8=7604
tri-tertiary butyl phenoxyl radical, double reson. 8=12312
butyl phthalate, spin-lattice relax. rel. to dielec. relax. and viscosity 8=9459
charcoal, surface heterogeneity meas. 8=8293
chemically induced dynamic nuclear polarization 8=7601
chemical reactions, n.m.r. spectra explanation 8=8128
chemical reactions, rapid, tracing by n.m.r. spectroscopy 8=8127
conduction band structure and electron effective mass from double resonance data 8=17874
copolyesters, degree of randomness by high resolution n.m.r. spectra 8=12387
crystals, single, holder for low temp. expt. 8=14130
crystals, single, rotating head apparatus 8=8361
- Nuclear magnetic resonance and relaxation—contd**
cyclopropane derivatives, C-C coupling 8=12320
cyclopropanes, substituted, C^{13} chem. shifts 8=1303
cis- and trans-bis(dialkyl sulphide) dichloroplatinum (II) complexes, struct. and inversion mech. 8=16355
diaziridin rings, methylene-group spectroscopy 8=12940
dibenzoylperoxide decomp., tracing by n.m.r. spectroscopy 8=8127
cis-bis(dibenzyl sulphide) dichloroplatinum(II), struct., inversion and AB chemical shifts obs. 8=16356
dibenzyl sulphoxide, comparison with cis-bis(dibenzyl sulphide) dichloroplatinum(II) 8=16356
di- p -chlorbenzoylperoxide decomp., tracing by n.m.r. spectroscopy 8=8127
2,4-dicyanopentanes 8=16884
dielectric solids, spin relax. and dynamic polarization rel. to electron spin-spin relax. 8=18443
1,1-difluoro-1,2-dibromodichloroethane, spin-echo 8=4622
1,3-difluoro-4,6-dimittrobenzene 8=21178
1,1-difluoroethylene in soln., nuclear spin relax. 8=16889
dihydroanthracenes and Li salts, rel. to structure of ion pairs 8=7559
dimethyl acetamide, solvent-solute interactions 8=12936
dimethyl amides 8=21150
 N,N -dimethylaniline and deuterated derivatives, p.m.r. 8=21179
dimethyl formamide, solvent-solute interactions 8=12936
dimethyl phthalates, in soln., high-resolution proton mag. res. 8=1601
dimethylsulfoxide, solid, methyl group movement 8=9466
dipolar broadening of fine-struct. lines 8=14131
dipole-dipole interact. of spin- $1/2$ nucleus with quadrupole-coupled nucleus 8=5559
double quantum transitions in systems with four protons 8=21172
double, using v . strong decoupling fields, AMX system 8=7603
energy level diagrams, alternative representation 8=19915
 Cu(II) in ethylenediamine-water solns. 8=4621
ethyleneimine, solvent and anisotropy effects 8=16895
ethyl iodide, in nematic phase 8=8135
ferrites of Cu , Mg , and Mn , of Fe 8=5554
of ferromagnetic alloys, automatic swept-freq. spin-echo spectrometer 8=9454
ferro- and antiferromagnetics, nuclear magneto-acoustic reson. 8=22916
ferromagnetics with low concs. of mag. nuclei, theory 8=9456
field discriminator 8=15433
fluorenylidine in diazofluorene crystals, spin densities from ENDOR 8=5555
fluorinated organotin cpds., n.m.r. spectra 8=12318
fluorobenzene 8=12326
fluorobenzene, H and F spectra 8=12325
fluorotetrachloroethane, liquid, internal rotation 8=8137
freon, of F , chemical shift press. depend. 8=12324
gases, spin-lattice relax. 8=21176
group IV hydrides, geminal coupling consts., from ENDOR meas. 8=21175
"growth effect" in n.m.r. for a weak directing field, theory 9=15432
 H -bonded complexes proton transfer meas. by F n.m.r. 8=12157
halogenophenanthrenes, spectra 8=9461
Heisenberg paramagnets, linewidths asymptotic behaviours near critical points 8=22757
hexafluorides of Mo , W and U , liquid, F^{19} relax. rel. to molec. motion 8=12930
hexafluoroethane, of F 8=8134
hexamethylbenzene, molec. motions 8=14143
high magnetic field meas. by periodic size effect in Ga 8=3161
high polymers, composition study 8=16886
in highly viscous liqs., theory 8=4619
hydrides of S , Se and Te , proton reson. gas and liq. phases 8=12327
hydrocarbons, saturated, theory of C^{13} chem. shifts 8=7606
indirect spin saturation 8=16350
intermodulation in spin systems obeying Bloch's equations 8=10992
isotropic chem. shifts, non-Curie behaviour 8=16351
Knight shift in tiny samples, electrostatic effect in superconductors 8=5194
ligand nuclei in distorted octahedral Co^{2+} systems, isotropic res. shifts 8=1597
line shapes and path averages 8=19910-11
liquid crystals, equivalence of nuclear spins 8=16892-3
liquid/liquid interfaces, molecular interactions and mobility 8=12778
liquids, spin-lattice relax. time 8=8131
magnetic insulators, spin-lattice relax. 8=18448
magnetic resonance and relaxation, conference 8=22889
magnetoacoustic, double electron-nuclear, at local electron centres 8=8623
magnetometer, transistorized with 10^{-4} accuracy 8=19914
malonic acids, intramolec. H-bonding 8=16894
many-photon transitions, ang. mom. det. 8=22904
metals, electron-nuclear relax. at low temps. in strong mag. fields 8=9449

Nuclear magnetic resonance and relaxation—contd

- metals, liq. and solid, interpret. of Knight shift data 8=12928
 methane, liquid, proton spin-lattice relaxation 8=4617
 methane, spin relaxation rel. to density and temp. 8=7938
 methanol, liq., effect of proton exchange on spin relax. 8=1596
 methyl 1-aziridinepropionate, solvent and anisotropy effects 8=16895
 N-methyl-N-benzylformamide, determ. of int. rot., compared with equilibration method 8=4623
 methylcyclohexanes, C¹³ chemical shifts 8=16359
 methylfluoresilanes, of F 8=7608
 methyl-1-indanones 8=12329
 methyl iodide, anisotropy of C chem. shift 8=4234
 methylsilane derivatives, p. m. r. 8=16360
 multiple-photon transition in low-field expt., with harmonic generation 8=10984
 naphthalene ENDOR study of metastable triplet state 8=21169
 naphthodioxane, low-temp. spectrum 8=12939
 naphthols, solid, intra-molecular motion of OH group 8=16989
 norbornene derivs, endo- and exo-, coupling consts. in n. m. r. spectra 8=1306
 nuclear signals in solids, pulse expts. 8=18447
 optically orientated spin system, magnetization equations 8=121
 organic mols., anisotropic effects of carbonyl group, rel. to struct. 8=4225
 oriented mols., chem. shift anisotropies 8=4624
 1, 3 oxathiolanes, 2-substituted, rel. to ring system and free energies 8=1595
 oxaziridin rings, methylene-group spectroscopy 8=12940
 oxygen fluorides, of F¹⁹ 8=4231
 oxygen, ⁸S° metastable state 8=1304
 paramagnetic impurities in viscous solns., dynamic polarization 8=8129
 paramagnetic ion nuclear relax. due to spin-phonon interaction 8=18450
 paramagnetic salts, obs. 8=2385
 phenantholiene, π electron density and proton signals in n. m. r. spectra 8=4236
 phenanthrene and alkyl derivatives, spectra 8=9460
 phenylalanine, rotamer study 8=12289
 2-picoline with dichlorobis (2-picoline) Co(II), study of ligand exchange 8=2501
 poly- γ -benzyl-L-glutamate, liquid crystal orientation in mag. fields 8=8006
 polybutadiene-active carbon black, -160° to 0°C, line shape 8=5550
 polybutadienes, stereoregular, -160° to 0°C, line shape 8=5550
 polyesters, unsaturated, hardened, determ. 8=5565
 polyethylene in soln. 8=16891
 polymers, high resolution 8=21216
 polymethine-merocyanine dyes spectra, solvent depend. and rot. inhibition 8=12929
 poly(methyl methacrylates) in soln. 8=16890
 polymethyl methacrylates, stereoregular, broad line obs. 8=18462
 polyoxymethylene system, in solid trioxane matrix, during polymerization 8=22921
 polystyrenes, of controlled molec. wt., as characterization 8=18473
 polyvinyl chloride linewidth dependence on correlation time distrib. 8=18471
 poly(vinyl formate), study of tacticity 8=16897
 poly-2-vinylpyridine 8=16391
 propionate groups, investigation of retarded motion and phase transitions 8=8229
 proteins, internal rot. and ang. correl. functions 8=16384
 proton bonded to quadrupolar nucleus, second moment 8=7602
 proton, double, spin-stabilized spectrometer 8=3281
 proton-electron double reson. in organic cpds. 8=12312
 pyridine in dilute soln. of CS₂ and CCl₄ dependence on viscosity 8=8126
 pyridines, solvent effects in p. m. r. 8=1600
 pyridines, substituent effects 8=12332
 pyrrole, N¹⁴ spin-lattice relax. 8=21180
 quinols, solid, intra-molecular motion of OH group 8=16989
 radical ions, in soln., hyperfine splitting constants 8=8136
 rare earth trifluorides, of F¹⁹ 8=5556
 r. f. hybrid tees 8=3280
 relaxation and correlation time, definition 8=18453
 review of applications 8=5545
 rotating single crystal, time-dependent Dyson expansion 8=14136
 rotational isomerism, limitations of method 8=4226
 salicylaldehyde soln., H bonding obs. 8=16883
 1, 2, 5-selenadiazole and its methyl derivative, p. m. r. 8=12333
 selenobenzanide, of N¹⁴, chemical shifts 8=7614
 semiconductors, organic, r. f. spectroscopy 8=14088
 solids, chemical shifts from n. m. r. resolution 8=4670
 solids, effect of elec.-field-gradient inhomogeneity on quadrupolar satellites 8=22917

Nuclear magnetic resonance and relaxation—contd

- solids, high-resolution resonance theory 8=18452
 solids, line shape with long spin-lattice relax. 8=14132
 solid, magnetically dilute, free-induction decay evaluation 8=14135
 solids, resolution of chemical shift, comments 8=18451
 solid, ultra-slow motion, relaxation study 8=5548
 solvent effects, molec. interactions theory 8=12935
 spin-coupling Hamiltonian, matrix elements calc. 8=19909
 spin-lattice and spin-spin in multi-level quadrupole systems 8=5547
 spin-lattice relax. in multilevel systems 8=12313
 spin-lattice relaxation via paramag. centres 8=18449
 spin relaxation theory, book 8=18446
 Stark effect, linear, rel. to effective field acting on electrons 8=14133
 succinimide-dimethyl sulphoxide, H-bonding 8=12334
 superconductors, particle-size effects, Knight shift 8=2351
 superconductors, type II, obs. and explanation 8=5196
 T₁ and T₂ measurement, spin echo attachment to single coil high-resolution n. m. r. spectrometer 8=10988
 TCNQ-complexes, semiconducting, Overhauser effect 8=5549
 temperature controller, -185 to +350°C 8=19907
 1, 1, 2, 2-tetrabromofluoroethane, medium effects 8=21181
 tetramethyldiphosphine, of C¹³, used in X spectra of X₂AA¹X¹ spin systems 8=4235
 thienylphenyl-ketones and -thioketones, spectra, steric effects obs. 8=4218
 thioamides, of N¹⁴, chemical shifts 8=7614
 three-membered rings, of F 8=12322
 transition impurities, non-magn. in Cu alloys, rel. to elec. field gradients 8=9458
 transition-metal monophosphides 8=22847
 trifluoroacetone, in proton donor solvents 8=16887
 trifluorocyclopropanes, chem. shifts and coupling consts. 8=12321
 2, 2, 2-trifluoroethanol as H bonding acid, freq. shifts rel. to bonds 8=16863
 1, 3, 5-trideuterobenzene, molec. motion in liq. 8=8132
 s-trioxane in nematic solvent 8=4618
 triptycene, effect of mag. anisotropy on proton shifts 8=1305
 vanadium (III) tris(salicylaldehydes) and tris(salicylaldehydes) complexes obs. 8=16343
 water of combination in solids 8=5546
 water, proton resonance appl. to rehydration monitoring 8=23770
 zeolites in liquid, proton relax. meas. 8=18454
 [Ag₂O₃]HF₂ clathrate, rel. to supercond. 8=17957
 Al, modulation and cross-relaxation effects on line shape 8=18455
 Al, pure, meas. of diffusion coefficient 8=4949
 AlCl₃, in aqueous binary solvent mixtures 8=8138
 AlCl₃, p. m. r. determ. of coord. no. in aq. mixtures 8=16888
 Al₂O₃·V³⁺, longit. relax. times by spin echo method 8=5541
 Au, Au¹⁹⁷ Knight shifts 8=2379
 Au-Ag alloy, Ag¹⁰⁹ Knight shifts 8=2379
 for B compounds, ferromagnetic, electronic configuration obs. 8=13658
 BaAl₂Si₂O₁₀·4H₂O, proton resonance and H atom position 8=18456
 C¹³ chem. shift, steric perturbation 8=7605
 C_xCS₂, Knight shift of C¹³³ rel. to comp. and temp. 8=2382
 CD₄, d. m. r. studies 8=18460
 CF₄ clathrate hydrates, of F¹⁹ 8=7607
 CF₄ gas, of F¹⁹ 8=21176
 CF₃P(O)F₂, F¹⁹ reson. 8=21177
 CHBr₂-CFBr₂, rotational isomers 8=4226
 (CH₂)₂O, linewidth as function of pressure 8=16354
 [(C₆H₅)₃PCH₃]₂ (TCNQ)₂, proton reson. 8=5551
 CaF₂, ENDOR study of F centre 8=9417
 CaF₂, of F²⁰, and β -radiation asymmetry 8=7128
 CaF₂, spin-lattice relax. via paramag. centres 8=18459
 CaF₂:Ce³⁺, Yb³⁺, doped at tetragonal sites, charge compensation 8=22918
 CaF₂:H, D, of F¹⁹, single crystal, nuclear polarization 8=1640
 Ca(NO₃)₂·4H₂O melts, p. m. r. 8=12938
 Cd, Knight shift anisotropy, reversal at low temps. 8=5552
 Cd¹⁰⁹ and Cd¹¹¹ frequency ratio between 8=16232
 Co⁶⁰, by resonant absorption destruction of nuclear orientation 8=18331
 Co²⁺ ion, hydration 8=12937
 Co(II) chelates in CDCl₃, isotropic res. shifts 8=1598
 Co(III) ethylenediamine complexes, p. m. r. 8=12319
 CoCl₂, in aqueous binary solvent mixtures 8=8138
 Co-Ni alloys, effective field at Co⁵⁹ using spin echo method 8=8195
 Co-Pd alloys, of Pd¹⁰⁵ and Co⁵⁹ 8=2381
 Cr(V) complexes, liquid solutions, Overhauser effect 8=21725
 Cr³⁺ trivalent ion hyperfine structure obs. 8=5553
 Cs¹³³ in metal, spin systems below 77°K 8=9463
 Cs silicate glass, ionic conduction 8=9197

Nuclear magnetic resonance and relaxation—contd

- Cu ferrite, of Cu 8=5554
 Cu-Mn alloys, of Cu⁶³, and spin-lattice relax. 8=9464
 Cu(NH₂)₄.SO₄.H₂O, proton n.m.r. at low temp. 8=2384
 Cu(NH₂)₄.SO₄.H₂O, proton resonance, 0.25-4.2°K 8=14138
 Cu-Pt alloy foils, quadrupole effects 8=2383
 CuSO₄.5D₂O, deuteron n.m.r. 8=18461
 Cu-Zr, supersaturated, decomposition study 8=8265
 D₂O ice, O¹⁷ n.m.r. 8=18470
 DyAl₃ 8=22920
 Er¹⁶⁰, ground-state spin using atomic beam magnetic resonance 8=11777
 α-ErAl₃ 8=22920
 EuM₂, (M=Pt, Pd, Zn, Rh), mag. props. by Mossbauer n.m.r. 8=18334
 EuPd₃, (M=Pt, Pd, Zn, Rh), mag. props. by Mossbauer n.m.r. 8=18334
 F, dynamic enhancement, effects of chem. environment 8=12323
 F, dynamic polarization in solns. of fluorocarbon free radicals 8=4627
 Fe dilute alloys, of Fe⁵⁷ 8=14140
 α-Fe₂O₃ crystals, domain walls 8=5557
 Ge⁷³, Larmor freq. rel. to H² and K⁴¹ 8=5558
 H², Larmor freq. rel. to Ge⁷³, and K⁴¹ 8=5558
 H₂, ortho, in solid para-H₂ crystal-field splitting 8=13010
 H₂, solid, 1.6-4.2°K, obs., shorter correlation time for mol. rot. 8=14141
 H₂, solid, statistical model 8=22923
 HBr, gaseous, spin-lattice relax. 8=12697
 HCl, gaseous, spin-lattice relax. 8=12697
 HD, liquid, proton transitions 8=8133
 HI, gaseous, spin-lattice relax. 8=12697
 H₂O, acidified, of O¹⁷, linewidth rel. to proton exchange 8=1599
 H₂O dynamics in Na₂S₂O₈.2D₂O, deuteron m. r. 8=8539
 H₂O dynamics in Na₂S₂O₈.2H₂O and Li₂S₂O₈.2H₂O crystals, H¹-n. m. r. spectra 8=8537
 H₂O¹⁷ liq. and vapour, O¹⁷ shifts 8=16896
 H₂O, proton-spin lattice relax. times, search for thermal anomalies 8=16885
 H₂O at silica gels, proton relax. 8=12932
 H₂O-D₂O mixtures, comp. determ. by F¹⁹ n.m.r. 8=14454
 He³ atoms, spin relax. suppression by surface interactions 8=1160
 He³, solid, meas. 0.3-0.04°K, attributed to single phonon process 8=3130
 He³-He⁴ solutions, thermodynamic properties at λ-transition, investigation 8=10794
 Hg, anisotropy of relaxation 8=7609
 Hg dimethyl, coupling constants 8=7610
 Hg¹⁹⁹ and Hg²⁰¹, comparison above 600°K 8=7450
 Hg-Bi alloy, Knight shift 8=14142
 Hg-Cd alloy, Knight shift 8=14142
 Hg-In alloy, Knight shift 8=14142
 Hg-Pb alloy, Knight shift 8=14142
 HgSO₄.1H₂O, proton magnetic resonance 8=9457
 HoAl₃ 8=22920
 I¹²⁷ in NaI, rel. to determ. of gradient elastic tensor 8=13014
 In, liq., spin lattice relax. time, and elec. field grad. 8=12933
 In, Knight shift, band structure and Fermi surface 8=22463
 In, superconducting, spin-lattice relax. 8=18464
 InAs, Knight shift calc. 8=18463
 In-Bi liq. alloys, of Bi²⁰⁹, influence of short range atomic order 8=12934
 In-Bi liq. alloys, of In¹¹⁵, influence of short range atomic order 8=12934
 InSb, Knight shift calc. 8=18463
 Ir, and dipole moments of ¹⁹¹Ir and ¹⁹³Ir 8=14144
 K⁴¹, Larmor freq. rel. to Ge⁷³, and H² 8=5558
 KBr single crystal, first-order quadrupole broadening 8=14146
 KCuF₄, of F¹⁹, shifts on a and c axes 8=5505
 K₂Fe(CN)₆.3H₂O, proton relax. 8=14145
 KH₂PO₄, of K³⁹, at 77°K (ferroelec. phase) 8=22924
 LaMg nitrate, Nd doped, proton spin-lattice relaxation 8=9462
 La₂Mg₃(NO₃)₁₂.24H₂O: Mn²⁺, ligand endor 8=22925
 La₂Mg₃(NO₃)₁₂.24H₂O, proton dynamic polarization, influence of paramag. impurities 8=14147
 Li⁷, in aqueous alkali halide solns., conc. depend. of spin-lattice relax. 8=1593
 LiBH₄ and LiBD₄ 8=18466
 Li⁶Cl and Li⁷Cl solns., proton relax. times 8=8139
 LiF, ENDOR study of V_K centre rel. to lattice distortion 8=2009
 LiF, F centres, ENDOR 8=18465
 LiF:Fe³⁺ system, crystal field distortions, study 8=13005
 Lu¹⁶⁹, ¹⁷⁰, ¹⁷¹, ground-state spin using atomic beam magnetic resonance 8=11777
 Mn⁵⁴ by resonant absorption destruction of nuclear orientation 8=18331
 Mn²⁺ solns., proton relax. and hyperfine coupling 8=8130
 α-Mn, quadrupole effects in spectrum 8=18467
 Mn ferrite, simultaneous parallel pumping of electron and nuclear spin waves 8=14107
 MnBr₂.4H₂O, antiferromagnetic, space groups 8=14148

Nuclear magnetic resonance and relaxation—contd

- MoF₆, of F, spin-lattice relax. in intense r.f. field 8=14139
 MoF₆, spin-lattice relax. of F in intense r.f. field 8=14139
 Mo(V) complexes, liquid solutions, Overhauser effect 8=21725
 ND₃, deuteron mag. reson., 100 to 403°K 8=14150
 ND₃NO₃, d.m.r. studies 8=18460
 (ND₃)₂SO₄, correl. with i. r. spectra 8=23005
 NH₄BF₄, BF₄⁻ and NH₄⁺ motions 8=5560
 NH₄Cl: Mn²⁺, spin-Hamiltonian parameters 8=5534
 NH₄I, spin-lattice relax. for protons and I nuclei 8=14151
 (NH₄)₂SO₄, ferroelec., deuteron spin-lattice relax. time 8=2386
 (NH₄)₂SiF₆, molec. motions 8=14154
 NO, effect of electric field 8=7612
 NO(SO₃)₂⁻, proton polarization in solution at 38 and 3400 gauss. obs. 8=1602
 Na²³, in aqueous alkali halide solns., conc. depend. of spin-lattice relax. 8=1593
 Na²³ in some ionic compounds, quadrupolar couplings 8=18469
 NaBD₄, d.m.r. studies 8=18460
 NaBr single crystal, first-order quadrupole broadening 8=14146
 NaBrO₃ cryst., anisotropic chem. shift of Br 8=18457
 NaCl, plastically deformed, acoustic n. m. r. 8=5561
 NaCl powders, of Na²³ 8=5562
 NaCl type crystals, endor of F-centres, in external electric fields 8=14137
 NaCl-type crystals, quadrupole splitting due to lattice distortion by impurities 8=9455
 NaCl:Ag⁺, double resonance investigation 8=18468
 NaClO₃, relax. of Na²³, thermally and acoustically induced transition probabilities 8=14152
 NaClO₄ aq. soln. with HCl, nucl. mag. relax. times 8=21726
 NaHCO₃, H and Na reson. 8=14153
 NaHg, Na₂Hg₂ and Na₂Hg₃, solid state Knight shift rel. to liquid state 8=22926
 NaHg, Na₂Hg₂ and Na₂Hg₃, Na²³ spectrum dependence on temp. and Hg content 8=22926
 Nb, supercond., relax. near H_c 8=2170
 Ni(II) chelates in COCl₂, isotropic res. shifts 8=1598
 Ni-Mn, of Mn⁵⁵, magnetic moment 8=9465
 P³¹ in soln. with radicals, Overhauser effect rel. to scalar interacts. 8=4626
 P₂F₄ 8=16361
 Pr₂(SO₄)₃.8H₂O, of Pr¹⁴¹, meas. 8=14155
 Pr¹³⁹ Knight shift, cond. electron polarization 8=17857
 Rb⁸⁷ in metal, spin systems below 77°K 8=9463
 RbCoF₃, rel. to spin density oscillation in space at T > 96°K 8=18472
 RbMnF₃, antiferromag., F¹⁹ acoustic reson. 8=22922
 RbMnF₃, simultaneous parallel pumping of electron and nuclear spin waves 8=14107
 SF₄ clathrate hydrates, of F¹⁹ 8=7607
 SiF₄ gas, of F¹⁹ 8=21176
 Si₃F₈, coupling consts. and chem. shifts of F¹⁹ and Si²⁹ rel. to SiF₄ 8=4237
 Sn, Knight shift oscillatory field dependence 8=5566
 TiCl₄, in aqueous binary solvent mixtures 8=8138
 TiFe_{1-x}Co_x alloys, ⁵⁹Co Knight shift and ⁵⁷Fe isomer shift 8=14156
 Tl, anisotropy 8=9467
 Tl silicate glass, ionic conduction 8=9197
 Tm¹⁶⁵, ground-state spin using atomic beam magnetic resonance 8=11777
 UP₂, of P³¹, in paramag. state, Knight shift temp. dependence 8=5563
 U₃P₄ and UP₂, of P³¹, in paramag. state, Knight shift meas. 8=5564
 USn₃, of Sn¹¹⁹ rel. to interband mixing effects 8=18474
 V, superconducting, local field mapping 8=2179
 V₃Au superconductor, atomic ordering 8=18475
 VO₂, of V⁵¹ rel. to crystalline field theory of V⁴⁺ ions in VO₂ 8=9411
 (Zn, Cu)K₂(SO₄)₂.6H₂O, dynamic polarization of protons, non-exponential behaviour 8=18476

measurement

- ABXY spectrum, methods of anal. 8=12314
 benzene, long transversal times, difficulty using spin-echo 8=2380
 cryostats, room temp. to 4.2°K 8=10793
 double, detect. of v. small spin coupling consts. 8=6408
 dynamic polarization, nuclei, exchange narrowing influence 8=22893
 field, accuracy with strong field modulation 8=3282
 heating system for spectrometer 8=19912
 high-resolution apparatus, performance tests 8=16352
 integrator, gated, solid state, for pulsed n.m.r. 8=14134
 liquid cryst. matrices for mols. 8=8008
 liquid, high-resolution apparatus, performance tests 8=16352
 molecules, high-resolution apparatus, performance tests 8=16352
 n. m. r. frequency sweep using voltage controlled oscillator 8=19908
 noisy signals, simple method for calibration 8=15434
 phase-lock circuit for 100 MHz spectrometer 8=15430

Nuclear magnetic resonance and relaxation—contd measurement—contd

- proton n.m.r. and free-electron cyclotron resonance freqs., ratio 8=10989
- spectrometers, advances in sensitivity and magnet technology 8=15431
- spectrometer, frequency swept, p stabilized 8=388
- spectrometer, variable freq. construction from commercial grid dip meter 8=10987
- spin coupling consts., v. small, detect. by resolution enhancement 8=10985
- spin-lattice relax., saturation-recovery method 8=12941
- theory 8=5546
- thermal-noise and voltage decrease across tuned circuit as n. m. r. meas. method 8=19906
- wide-band dispersion detector 8=15435

Nuclear matter. See Nucleus/theory; Quantum theory/many-particle systems.

Nuclear orientation

- β -ray asymm. meas. of stopped recoil nuclei 8=3955
- Coulomb excitation, reorientation effect 8=11841
- dynamic polarization, chem. induced 8=7601
- polarization effects in (d, p) stripping 8=1087
- polarization by interaction with e shells 8=944
- quadrupole interaction with axially symm. field as a method of determination 8=3775
- semiconductors, spin polarization by hot electron current 8=8204
- solids and liquids by optical pumping 8=13016
- 2^+ rot. state, reorientation effect in Coulomb excitation 8=15940
- Au nuclei on MoS_2 substrate, effect on elastic strain 8=8823
- Bi^{12} , recoil nucleus, meas. by magnetic field appl. to stopping plane 8=3955
- $\text{CaF}_2:\text{U}^{3+}$, F dynamic polarization of 45% 8=18458
- Co, in Fe from Fe^{57} Mössbauer expts. at 1-0.08°K 8=4676
- U^{156} , longitudinal polarization calc. from β spectrum shape factor 8=1019
- F^{19} , in CaF_2 single crystal, dynamical 8=1640
- F^{19} in H-doped alkaline-earth fluorides 8=8206
- HD solid with H_2 impurity, high proton spin polarization 8=1639
- He^3 in fund. state, for electronic orientation in excited states 8=16226
- He^3 , solid, spin ordering evidence 8=6237
- LaMg nitrate, Nd doped, dynamic polarisation 8=9462
- Mn^{54} in iron lattice, resonance absorption destruction for n.m.r. detection 8=18331
- MnCu , Mn^{54} anomalous low-temp. susceptibility 8=13962
- (Zn, Cu) $\text{K}_2(\text{SO}_4)_2 \cdot 6\text{H}_2\text{O}$, dynamic polarization non-exponential behaviour 8=18476

Nuclear photoeffect. See Gamma-rays/effects; Nuclear reactions due to photons; Photons/interactions.

Nuclear physics

- coincidence resolution improvement by energy-time correl. 8=6649
- current experiments at Desy 8=11349
- data analysis, mean rate 8=6633
- data collection using computer 8=19377
- digital computers in high-energy physics experiments 8=11350
- digital techniques in instrumentation 8=6624
- display of statistical data from expts. 8=6631
- experimental exact treatment of search statistics 8=6679
- experimental, instability and decoupling in semiconductor electronics 8=9142
- experimental, random trend removal in parity violation expts. 8=6630
- high-energy physics, conference Oiso Japan (1965) 8=11348
- level curves, automatic tracing 8=11289
- Lipari Summer School in theoretical Physics 1966 8=7028
- many-body theory, conference Oiso Japan (1965) 8=10641
- measurements, effects of random signal quantization 8=6260
- nuclear structure, conference Dacca Pakistan (1967) 8=15925
- nucleides far off the stability line, conference, Lysekil Sweden (1966) 8=15911
- photonic data index 8=19343
- prediction analysis applied to spectral peak separation 8=6632
- radiation, meas., point source assumption effect 8=11288
- review, 51st meeting of Italian Physical Society 8=7029
- spectra, increasing effective storage of a memory 8=19371
- spectroscopy, background suppression techniques, evaluation 8=3453
- stellar processes in laboratory experiments 8=15924
- superconducting electromagnets, appl. 8=6281
- symmetry groups in nuclear and particle physics 8=11361
- teaching, misconceptions 8=7027

Nuclear polarization. See Nuclear orientation.

Nuclear power. See Nuclear reactors, fission.

Nuclear quadrupole resonance

- alkyl halides, effects of molec. motions 8=2388
- p-bromoacetanilide, of Br^{79} , temp. var. and Zeeman effect 8=4228

Nuclear quadrupole resonance—contd

- coaxial bridge with helical line sample holders as detector 8=10991
 - correlation eqns., machine count program 8=3284
 - crystal molecular complexes, structure analysis 8=22927
 - 2,4-dichlorophenoxyacetic acid, Zeeman meas. 8=2390
 - hexachlorocyclopentadiene, two solid phases, Cl^{35} n.g.r. 8=8289
 - nonconducting crystals, spin relax. anomalies of impurity nuclei 8=9468
 - semiconductors, organic, r.f. spectroscopy 8=14088
 - solids, sensitive detection of interactions 8=18478
 - spectra, time-averaged, baseline slope elimination 8=6409
 - spectrometers, appl. of f.e.t.'s 8=15436
 - spectrometer, improved super-regenerative 8=15437
 - spin-1 nucleus, non-vanishing electric-field gradient, locus of magnetization vector 8=7067
 - Stark effect, linear, rel. to effective field acting on electrons 8=14133
 - tetraiodothallates, of I 8=18477
 - tribromide ions in different crystals. 8=5567
 - trichloroborazole, of Cl^{35} 8=6409
 - vanadates, of V^{51} , Na^{23} , quadrupole coupling constants 8=9474
 - III-V cpds., antishielding effects 8=14157
 - As_2Se_3 , of As^{75} , rel. to crystal structure refinement 8=17340
 - $\text{CaF}_2:\text{Eu}^{2+}$, stress induced quad. splitting using ENDOR tech. 8=22928
 - Cl^{35} , from charge-transfer complexes 8=14158
 - CN free radical, N^{14} coupling const. in ground and excited states 8=1316
 - CsI, antishielding factors of Cs ions, acoustic 8=9470
 - HCl^- ion, symmetrical, of Cl 8=5568
 - InSb, nuclear spin-lattice relax. temp. dependence 8=9472
 - InSb of $\text{Sb}^{121,123}$, In^{115} , nuclear spin-lattice relax rates 8=9471
 - $\text{MgO}:\text{Mn}^{2+}$, stress induced quad. splitting using ENDOR tech. 8=22928
 - N^{14} nuclei, modified Robinson type spectrometer 8=3283
 - N^{14} , Stark effect meas. 8=7611
 - ND_4Br , deuteron coupling consts. 8=14159
 - ND_4Br , deuteron coupling consts., theoretical calc. 8=14160
 - ND_4Cl , deuteron coupling consts. 8=14159
 - ND_4Cl , deuteron coupling consts., theoretical calc. 8=14160
 - $(\text{NH}_4)_2[\text{InCl}_4\text{H}_2\text{O}]$, freqs. of Cl^{35} and In^{115} rel. to temp. 8=2389
 - NaBrO_3 , of Br^{81} , at 150 MHz 8=10991
 - NaClO_3 , relax. of Na^{23} , ang. depend. of transition probabilities 8=14161
 - NaNO_2 , of N^{14} , ferroelectric phase 8=9473
 - NdBr_3 , paramag., of $\text{Br}^{79,81}$ 8=9469
 - RbI, antishielding factors of Rb ions, acoustic 8=9470
 - Sb Menshutkin complexes, electric field gradient, asymmetry parameter temp. depend. 8=21802
 - SbCl_3 , of $\text{Sb}^{121,123}$ and Cl^{35} , temp. dependence, 20-150°K rel. to mol. motions and intermol. forces 8=22929
 - $\text{SbCl}_4\text{CH}_3\text{CN}$, $\text{SbCl}_4\text{POCl}_3$, and SbCl_5 , of Sb , Cl 8=2391
 - U_3 , of F^{17} , in paramag. and antiferromag. crystal 8=9469
- Nuclear reactions**
- See also Chemical analysis/by nuclear reactions; Fallout; Nuclear bombardment targets; Nuclear excitation; Nuclear fission; Nuclear fusion; Nuclear spallation; Radioactivity; Thermonuclear reactions.
 - accelerator beam energy meas. by reaction on scatt. spectrum from multi-target 8=6691
 - Butler's stripping theory and single-particle strength sum rules 8=15937
 - cascade + evaporation in p prod. from 158 MeV p interactions with nuclei 8=20781
 - charge exchange including transitions to isobaric analogue states, theory 8=11845
 - coherent and incoherent particle production in nuclei, unstable particle cross-sections 8=20767
 - collective model applied to n radiative capture 8=11875
 - complex nuclei, single N transfer, cross-section 8=16127
 - compound nucleus, analysis of angular and range distrib. 8=1032
 - compound nucleus, recoil range as probe 8=1103
 - direct, semiclassical model, and predictions for backward peaking 8=7152
 - d-s shell, SU_3 reduction 8=7040
 - eigenfunction expansions, use of resonant states 8=16051
 - evaporation spectra analysis, charged particle emission 8=11699
 - exchange, evidence from ang. correl. function symm. angle at backward scatt. 8=11843
 - excited residual nucleus, equilibrium 8=11700
 - excitation functions, peak counting method 8=20762
 - excitation meas., rapid scanning by target self-changing 8=3897
 - exciton model, Griffin, precompound particle decay 8=1608
 - Fermi gas model for nuclear reactions not confirmed by 10^3 BeV cosmic ray obs. 8=20777
 - form factor calc. in stripping and pick-up 8=3902
 - heavy ions, nucleon tunneling through pot. barrier, analog of Josephson effect 8=3892
 - heavy and medium, conference 8=20640

Nuclear reactions—contd

- high-energy, with complex nuclei, mechanism 8=1028
high-energy stars in nuclear emulsions, frequency distrib. of heavy prongs 8=7160
indep. particle model, N-body scatt. theory 8=11850
inelastic, $T \geq 1$ GeV, energy and angular distribution of secondary particles 8=3518
inverse reaction cross-section investigated by $\text{Ni}^{62}(\text{p}, \alpha)\text{Co}^{59}$ and $\text{Fe}^{56}(\alpha, \text{p})\text{Co}^{59}$ 8=3900
K matrix theories rel. to transition operator T 8=3901
kinematics, simplified calc. 8=20766
knockout, DWBA analysis of $\text{Al}^{27}(\alpha, \text{d}_{0,1})\text{Si}^{29}$ 8=20837
Lippmann-Schwinger potential scatt. equation derivation from Bloch scatt. theory 8=3894
matrix calc, improved 3-body cluster corrls. applied to nuclear matter 8=11696
N transfer, orbital rearrangement energy large and different in different orbitals 8=16054
nucleon, computer, Monte Carlo simulation of intranuclear cascade, 380 MeV 8=20776
nucleon, Fermi gas model not confirmed by 10^8 BeV obs. 8=20777
neutron superbooster 8=1118
neutron tunneling reactions 8=20765
noble gas targets, electromagnetically separated, props. 8=6625
nucleons, distrib. and fraction of primary energy transferred to photons 8=16103
due to nucleons, optical model 8=1049
nuclides far off the stability line, conference, Lysekil Sweden (1966) 8=15911
optical potentials, complex, derivation 8=7038
optical potential, form of imaginary part 8=3757
particle range meas. using Coulomb excitation 8=8756
photoemulsion nuclei H^3 and He^3 (K.E. ~ 2 GeV) emission fluctuation mechanism 8=7159
pole, Butler in (d, p) reactions to calc. reduced widths 8=20818
polarization of production for separating direct and compound nucleus effects 8=1029
projection operator approach applied to decay of unstable systems 8=11262
R-matrix evaluation using projection operator 8=20764
R matrix theory in d- α 42 MeV 8=15868
rearrangement collisions, modified distorted-wave Born series 8=11838
resonance, cluster representations 8=11849
resonance, sum rule 8=1031
scatt. amplitude and cross-section, statistical props. using collision matrix 8=11839
scattering chamber of sliding cylinder type for cross-sect. meas. 8=7157
scattering, eigenfunction expansions, use of resonant states 8=16051
scatt. matrix S decomposed into direct interaction and compound nucleus parts, calc. of DI part. 8=7153
scattering, quasi-free, replacement of single-particle by hole state in complex pot. 8=16052
second-quantization formalism, yielding integral eqns. for n-body amplitudes 8=11853
shell model matrix elements, state depend. 8=926
 Σ^- capture by emulsion nuclei, hyperfragment prod. 8=7218
statistical model in n reaction on $\text{In}^{113,115}$ 8=11909
statistical, spectra of emitted particles, approx. suggested 8=3890
statistical theory, Si^{29} intermediate, evaluation of D_0 8=3899
in stellar surface layers, rel. to abundance anomalies 8=5870
stripping, DWBA, analysis of $\text{Al}(\alpha, \text{d}_{0,1})\text{Si}^{29}$ 8=20837
stripping, modified distorted-wave Born series 8=11838
stripping, trapping-state model 8=11920
studies 8=16050
superheavy-ion, Coulomb distortion and nuclear stiffness 8=11688
T violation effect on reciprocity relation 8=11851
theory, unified, overlapping resonances calc. 8=3889
time-reversal and detailed balance using DWBA theory 8=11847
three-body problem of neutron, proton and heavy nucleus 8=3888
three-body producing, coincidence meas. 8=3903
three-particle direct reaction amplitudes, mechanism identification 8=7155
transfer during collisions with cut-off diffraction model 8=7158
transfer, Feynman diagram technique 8=11852
2N transfer (pick-up), N pair corrl. effect 8=16053
2N transfer in n particle 2 j-shell model 8=15923
2s-1d shell nuclei, reduced width of levels, calc. using projected HF wave functions 8=11802
vacuum chamber for investigations 8=11846
wave functions for mixed reactions and Raich algebra of $\text{SU}(14)$ 8=3779
(a, by) and (a, by- γ), total and differential cross-sections 8=7154
A(x, yz)B, residual nuclei spin obs., polarized target 8=3898

Nuclear reactions—contd

- Ca^{40} , spectroscopic factors for pickup reactions in shell model, anomalies 8=11854
 $\text{Be}^9(\text{He}^6, \alpha)\text{Be}^{11}$, cross section 8=3964
 $(\text{NH}_4)_2[\text{OsCl}_6]$, use in expts concerning nucleus 8=16044
Ni isotopes, 2N transfer reactions 8=3814
chemical effects
See also Chemical effects of radiations/ionizing radiations.
cosmochemistry 8=23472
 $\text{Br}^{81}(\text{n}, \gamma)\text{Br}^{82\text{m}}$ in liq. bromobenzene 8=18752
 $\text{Br}^{82\text{m}}(\text{I. T.})\text{Br}^{82}$ in liq. bromobenzene 8=18752
 $\text{Te}^{127\text{m}} \rightarrow \text{Te}^{127}$ in $\text{Te}^{127}(\text{OH})_6$ crvsts. 8=18751
Nuclear reactions due to alpha-rays
 α -d, 1 MeV and the 2.19 MeV level of Li^6 8=20675
($\alpha, 2\alpha$) and reactions at medium-energy and alpha-clustering correlations in light nuclei 8=1055
($\alpha, 2\alpha$), 25 MeV, α -cluster model 8=11942
(α, n) reactions on medium to heavy nuclei, energy distrib. of emitted n 8=7232
nuclei about A = 60, 24.7 MeV, cross section by transmission method 8=7237
in stellar surface layers, rel. to abundance anomalies in peculiar A stars 8=5871
 $\text{Al}^{27}(\alpha, \text{d}_{0,1})\text{Si}^{29}$, 18.7 MeV DWBA, knockout and stripping models 8=20837
 $\text{Ar}^{36,38}(\alpha, \gamma)\text{Ca}^{40,42}$, 3-6 MeV, resonances 8=3967
 $\text{B}^{10}(\alpha, \text{p}_0)\text{C}^{13}$, excitation functions and p ang. distrib. 8=7236
 $\text{B}^{10,11}(\alpha, \text{d})\text{C}^{12,13}$, at ~ 25 MeV, ang. distrib. 8=1100
 $\text{Be}^9(\alpha, 2\alpha)$, reaction model with α cluster in nucleus 8=11942
 $\text{Be}^9(\alpha, \text{B}^8)\text{HF}$, H $^+$ unbound to particle emission 8=11659
 $\text{Be}^9(\alpha, \text{n})\text{C}^{12}$, stellar rates of 8=19131
 $\text{C}^{12}(\alpha, \text{Be}^9)\text{Be}^8$, O^6 8 particle-8 hole rotational band 8=7075
 $\text{C}^{12}(\alpha, 2\alpha)$, reaction model with α cluster in nucleus 8=11942
 $\text{C}^{12}(\alpha, \text{n})\text{O}^{15}$, T = $\frac{3}{2}$ states of F^{17} , calibration point 8=3799
 $\text{C}^{12}(\alpha, \text{p}_0)\text{N}^{15}$, excitation functions and p ang. distrib. 8=7236
 $\text{C}^{13}(\alpha, \text{n})\text{O}^{16}$, stellar rates of 8=19131
 $\text{Ca}^{40}(\alpha, \text{d})\text{Sc}^{42}$, at 24.7 MeV, d spectra 8=3968
 $\text{Cl}^{35}(\alpha, \text{p}_1)\text{Ar}^{38}$, lifetimes of states of Ar^{38} 8=11738
 $\text{Cl}^{35}(\alpha, \text{p}_1)$, 10.6 MeV and levels of Ar^{38} 8=3804
 $\text{Cu}^{65}(\alpha, \text{n})\text{Ga}^{68}$, gamma ray ang. distrib. 8=11948
 $\text{F}^{19}(\alpha, \text{n})\text{Na}^{22}$, polarization of γ de-excitation rel. to nuclear structure of Na^{22} 8=15961
 $\text{F}^{19}(\alpha, \text{n})\text{Na}^{22}$, 3.5-5.5 MeV for meas. of level lifetimes 8=11729
 $\text{F}^{19}(\alpha, \text{n})\text{Na}^{22}$, 4-7 MeV, γ -ray transitions 8=3801
 $\text{F}^{19}(\alpha, \text{n})\text{Na}^{22}$, 5.1 MeV and states of Na^{22} 8=20690
 $\text{Fe}^{54}(\alpha, \text{p})\text{Co}^{57}$, 10.5, 11 MeV for levels of Co^{57} 8=15978
 $\text{Fe}^{56}(\alpha, \text{p})\text{Co}^{59}$, inverse reaction cross-section to $\text{Ni}^{62}(\text{p}, \alpha)\text{Co}^{59}$ 8=3900
 He^4 and Li^4 products, excited states 8=15953
 $\text{Li}^6, ^7(\alpha, 2\alpha)$, reaction model with α cluster in nucleus 8=11942
 $\text{Li}^7(\alpha, \gamma)\text{Be}^{11}$ excited states of Be^{11} 9.5-11 MeV obs. 8=11721
 $\text{Li}^7(\alpha, \text{n})\text{B}^{10}$ for cross-section meas. in $\text{B}^{10}(\text{n}, \alpha)\text{Li}^7$ 8=11900
 $\text{Mg}^{20}(\alpha, \gamma)\text{Mg}^{24}$, 3-6 MeV, levels deduced for Mg^{24} 8=16121
 $\text{Mg}^{24}(\alpha, \gamma)\text{Si}^{28}$, 5.3-14.5 MeV, electric dipole transition obs. 8=11944
 $\text{Mg}^{24}(\alpha, \gamma)\text{Si}^{28}$, T = $\frac{3}{2}$ states of F^{17} , calibration point 8=3799
 $\text{Mg}^{26}(\alpha, \gamma)\text{Si}^{30}$, 4.0-13.5 MeV, electric dipole transition obs. 8=11944
 $\text{Mg}^{26}(\alpha, \text{p})\text{Al}^{29}$ and levels of Al^{29} 8=20693
 $\text{Ne}^{22}(\text{He}^6, \alpha)$, Ne^{21} Nilsson model validity test, near 3 MeV 8=7077
 $\text{Ni}^{60}(\alpha, \text{n})\text{Zn}^{63}$, gamma ray ang. distrib. 8=11948
 O^{16} , reaction model with α cluster in nucleus 8=11942
 $\text{O}^{16}(\alpha, \text{d})\text{F}^{18}$, two-nucleon transfer reaction, finite size effect 8=3952
 $\text{Os}^{192}(\alpha, \text{p})\text{Ir}^{195}$, levels and decay scheme 8=11827
 $\text{Pb}^{208}(\alpha, \text{t})\text{Bi}^{209}$, Bi^{209} single-p states rel. to $82 < 2 < 126$ shell 8=998
 $\text{Pt}^{194}(\alpha, 3\text{n})\text{Hg}^{195} \rightarrow \text{Au}^{195}$, stacked foil meas. 8=1066
 $\text{Si}^{28}(\alpha, \gamma)\text{S}^{32}$ 3.7-4.3 MeV, levels of S^{32} 8=963
 $\text{Si}^{28}(\alpha, \gamma)\text{S}^{32}$, 7-12 MeV, giant dipole resonance inhibited 8=11944
 $\text{Si}^{30}(\alpha, \text{p})\text{P}^{33}$ and levels of P^{33} 8=20693
 $\text{Ta}^{181}(\text{He}^6, 2\text{n})\text{Re}^{183}$, 19.8 MeV, levels of Re^{183} obs. 8=20729
 $\text{Tl}^{203, 205}(\alpha, \text{t})\text{Pb}^{204, 206}$, $\text{Pb}^{204, 206}$ transitions to ground and 2 $^+$ states obs. 8=20838
 $\text{Y}^{89}(\alpha, 3\text{n})\text{Nb}^{90\text{e}}$, $^{90\text{m}}$, cross-sections and isomeric ratios 8=1101
cosmic rays
See also Cosmic rays/effects and interactions.
Fermi gas model not confirmed by 10^8 BeV obs. 8=20777
graphite, electron shower energy spectra 8=16059
nucleons distrib. and fraction of primary energy transferred to photons 8=16103
 π -nuclei, distrib. and fraction of primary energy transferred to photons 8=16103
 π^0 prod. obs., high energy 8=20618
pions and protons, 100 to 1000 BeV energy, installation for study 8=15881

Nuclear reactions due to—contd**cosmic rays—contd**

- primary protons, inelastic cross-section with air nuclei 8=16075
 shower electrons in Cu, Fe, Al and graphite, calc. of integral spectra 8=16059
 Al, electron shower energy spectra 8=16059
 Cu, electron shower energy spectra 8=16059
 Fe, electron shower energy spectra 8=16059
 Pb nuclei, first interact, fraction of primary energy transferred to π^0 mesons 8=20841

deuterons

- d + nucleus interaction theory 8=11919
 (d, α), odd-odd nuclei, J, π , and T of unknown levels 8=16109
 (d, n), two nucleon transfer reaction, finite size effect, 8=3952
 (d, 2n) reactions with A ~ 100, half-life of Mo⁹³ 8=1014
 (d, p), analysis 8=16108
 (d, p) anomalous stripping, polarization and angular correl. selection roles 8=20821
 (d, p), J dependence for l = 1 N transfer 8=11922
 (d, p), extrapolation to Butler pole to determ. reduced widths 8=20818
 (d, p) leading to bound states in 1p shell, ang. distrib., DWBA and shell-model calc. 8=11921
 (d, p) reactions, j-dependence for 2p neutron transfer 8=20819
 (d, p) reaction in 1p shell, DWBA and shell model analyses compared 8=11921
 (d, p), two-nucleon transfer reaction, finite size effect 8=3952
 even rare-earth nuclei, (d, p) excitation of γ vibrational states 8=3782
 isotopic invariance, violation 8=1088
 in living tissue, observed in emulsion 8=3891
 on nickel foil, study of Co^{58m} \rightarrow Co^{58g} gamma decay 8=1011
 polarization effects in (d, p) reactions 8=1087
 recoil-charged from 14.5 MeV n, average cross-section 8=16072
 stripping, analysis avoiding objections to DWBA 8=16106
 stripping reaction, analysis of outgoing proton polarization 8=16107
 stripping reactions on deformed nuclei 8=7224
 stripping with spin-orbital distortion, angular distrib., polarization effects meas. 8=20820
 trapping-state model for stripping 8=11920
 Ag¹⁰⁶(d, 2n)Cd¹⁰⁹, at 21 MeV, yield 8=1014
 Al²⁷(d, α)Mg²⁵, excitation cross section rel. to Mg²⁵ rotational partitions 8=20828
 Al²⁷(d, n)Si²⁸, isobaric analogue states 8=7080
 Ar^{90, 92, 94, 96}(d, He³)Y^{89, 91, 93, 95}, 34.4 MeV, residual $\frac{1}{2}^-$ ground state in Y and shell model 8=20830
 Au, d disintegration ang. distrib. of p, n, rel. to Coulomb and nuclear forces 8=11934
 B¹⁰(d, $\alpha\alpha$) α , 0.6, 0.9, 1.45, 1.9 MeV, sequential process obs. 8=11718
 B¹⁰(d, 2 α) α , sequential decay via C¹², Be⁸ 8=16111
 B¹⁰(d, 3 α), 270 keV 8=1090
 B¹⁰(d, d₁)Be⁸ 8=16112
 B¹¹(d, n)C¹², 6 MeV, levels of C¹² 8=7073
 B¹¹(d, p)B¹², 1.70, 3.13 MeV, spin assignments to levels of B¹² 8=20679
 B¹¹(d, p)B¹², polarization of B¹² meas. by β -decay in stopping foil 8=3955
 B¹¹(d, p₁)B¹² rel. to γ decay of excited states of B¹² 8=20678
 Ba¹³⁸(d, p), 12 MeV, optical model parameters 8=1096
 C, d disintegration ang. distrib. of p, n, rel. to Coulomb and nuclear forces 8=11934
 C¹²(d, He³)B¹¹, two-step mechanism, 28-50 MeV 8=20825
 C¹²(d, He³)B¹¹, 52 MeV, energy and ang. distrib. of He³ 8=7228
 C¹²(d, np)C¹², 5.4 and 6.0 MeV, n-p ang. and energy correl. 8=7225
 C¹²(d, p)C¹³, 2.8 MeV, trapping-state model 8=11920
 C¹²(d, p)C¹³, 3.09 MeV to test determ. of reduced widths from Butler pole 8=20818
 C¹³(d, p)C¹⁴, 4-6 MeV, obs., optical model and DWBA analysis 8=16113
 Ca⁴⁰(d, α)K³⁸, 9.2 MeV, ang. distrib. of α 8=7230
 Ca⁴⁰(d, n)Sc⁴¹, 5-6.5 MeV, using optical model parameters from d scatt. 8=16118
 Ca⁴⁰(d, p)Ca⁴¹, applic. of general (d, p) theory 8=16108
 Ca⁴⁰(d, p)Ca⁴¹, 5-6.5 MeV using optical model parameters from d scatt. 8=16118
 Cd¹¹⁴, (d, p), 12 MeV, high resolution studies 8=11933
 Ce¹⁴⁰, (d, p), 12 MeV, optical model parameters 8=1096
 Ce¹⁴⁰(d, p)Ce¹⁴¹ (g. s. f_{7/2}), anomaly rel. to charge exchange effects 8=11755
 Cl³⁵(d, 2 α)Si²⁹, 9-12 MeV, double evaporation 8=11927
 Cl³⁵(d, 2p)S³⁵, 14.5 MeV, single and double evaporation 8=11926
 Cl³⁷(d, He³)S³⁶, positive parity S³⁶ levels obs. 8=20696
 Cr⁵⁰(d, α)V⁴⁸, 7 MeV, level obs. on V⁴⁸, in terms of shell model 8=20702
 Cr⁵⁴(d, p)Cr⁵⁵ at 12 and 6.8 MeV 8=11928
 Cu, d disintegration ang. distrib. of p, n, rel. to Coulomb and nuclear forces 8=11934
 Cu⁶⁵(d, p)Cu⁶⁶, anomalous γ -rad. 8=3960
 F¹⁹(d, α)O¹⁷, 0.9-4.25 MeV, 2l = 1 rule obs. 8=16115

Nuclear reactions due to—contd**deuterons—contd**

- F¹⁹(d, α)O¹⁷, 20.9 MeV, obs., evidence for n-p pair pickup 8=20827
 F¹⁹(d, Li⁶(Be⁹))N¹³(C¹²), 7.5-13.0 MeV DWBA and α -particle pick-up fits 8=3957
 F¹⁹(d, n)Ne¹⁰, 2.98 MeV analog state of F²⁰ 8=20688
 F¹⁹(d, p₁)F²⁰, 1.6 MeV, γ -p ang. correl. rel. to interaction mechanism 8=16116
 Fe⁵⁴(d, α)Mn⁵², 7 MeV and the levels of Mn⁵² 8=20703
 Fe⁵⁶(d, p)Fe⁵⁷, Q-value evaluation of the atomic masses of Fe^{56, 57} 8=21017
 Gd^{70, 72}(d, p), Gd^{71, 73} levels obs. 8=7087
 Gd^{155, 157, 159} in (d, p) and (d, t) reactions, transitions between spherical and deformed potentials 8=11770
 Ge(d, α)Ga⁶⁸, \leq 14.1 MeV excitation function meas. and compared to Peaslee theory 8=11930
 Ge(d, 2n)As⁷⁰, \leq 14.1 MeV excitation function meas. and compared to Peaslee theory 8=11930
 Ge(d, n)As⁷¹, \leq 14.1 MeV excitation function meas. and compared to Peaslee theory 8=11930
 Ge⁷⁰(d, p)Ge⁷¹, \leq 14.1 MeV excitation function meas. and compared to Peaslee theory 8=11930
 Ge⁷⁰(d, p)Ge⁷¹, 7.5 MeV 8=11931
 (d, He³), low binding energy of p-shell protons calc. 8=10650
 In¹¹⁵, (d, p), 12 MeV, high resolution studies 8=11933
 K⁴¹(d, α)Ar³⁹, 7.5 MeV bombarding energy, Ar³⁹ energy levels 8=20699
 Li⁷(d, n) α , 180 keV, sequential decay model 8=7226
 Li⁷(d, n)2 α , 2 MeV, coincidence meas. 8=3903
 Li⁷(d, n)Be⁸, n detection with organic scintillators 8=6963
 Mg²⁴(d, n)Al²⁵, 1.38-2.8 MeV, n group analysis 8=11923
 Mg²⁴ + d \rightleftharpoons Mg²⁵ + p test of time-reversal invariance 8=11924
 Mo⁹²(d, np)Mo⁹², analog states of Mo⁹³ 8=1095
 Mo^{92, 94}(d, p)Mo^{93, 95} (g. s. d_{5/2}), anomaly rel. to charge exchange effects 8=11755
 Mo⁹⁷(d, p)Mo⁹⁸, 10-12 MeV rel. to states of Mo⁹⁸ 8=11756
 N¹⁴(d, α)C¹², 28.5 MeV meas. 8=3962
 N¹⁴(d, α)C¹², E_d = 2.3-5.8 MeV, angular distributions obs. 8=16114
 N¹⁴(d, α)C^{12*}, E_d = 2.3-5.8 MeV, angular distributions obs. 8=16114
 N¹⁴(d, He³)C¹³, 52 MeV, energy and ang. distrib. of He³ 8=7228
 N¹⁴(d, n)O¹⁵, 3.1-3.7 MeV, n polarization 8=3956
 N¹⁴(d, t)N¹³, 52 MeV, energy and ang. distrib. of tritons 8=7228
 N¹⁵(d, α)C¹³, 20.9 MeV obs. 8=20827
 N¹⁵(d, n)O¹⁶, 6 MeV, levels of O¹⁶ 8=7073
 N¹⁵(d, n₀)O¹⁶, rel. to ang. depend. of n polarization 8=7227
 Na²³(d, n)Mg²⁴, 2.98 MeV analog state of Na²⁴ 8=20688
 Nb⁹³(d, 2n)Mo⁹³, at 21 MeV, yield 8=1014
 Nd^{142, 144, 146}, (d, p), 12 MeV, optical model parameters 8=1096
 Nd¹⁵⁰(d, p)Nd¹⁵¹, levels of Nd¹⁵¹ 8=11767
 Ne²⁰(d, p)Ne²¹, high resolution detector 8=6663
 Ne²¹(d, α)F¹⁸, high resolution detector 8=6663
 Ne²²(d, t)Ne²¹(d, He³)F²¹, to determ. mass in T = $\frac{3}{2}$ state 8=20656
 Ni⁵⁸(d, α)Co⁵⁶, 7 MeV and level structure of Co⁵⁶ 8=20706
 Ni⁶⁰(d, p)Ni⁶¹, 197 levels below 7.051 MeV 8=3815
 Pb(d, p) isobaric spin forbidden effects 8=20800
 Pb²⁰⁶(d, p)Pb²⁰⁷, 3.62 and 4.29 MeV states particle configurations obs. 8=3840
 Pb²⁰⁷(d, p₀)Pb²⁰⁸ at 10 MeV, proton-gamma coincidences 8=11935
 Pb²⁰⁷(d, t)Pb²⁰⁶, 21.6 MeV, levels of Pb²⁰⁶ 8=20730
 Pb²⁰⁸(d, p₁), Pb²⁰⁹ particle-vibration coupling expt. evidence 8=3841
 Pd¹¹⁰(d, p)Pd¹¹¹ level obs. 8=7087
 Pt¹⁹⁵(d, 2n)Au¹⁹⁵, stacked foil meas. 8=1066
 Pu²⁴⁰(d, f), prompt fission spectrum of Am²⁴² 8=16131
 Pu²⁴²(d, 2n)Am^{242m}, fission spectrum 8=16131
 Rb⁸⁵(d, 2n)Sr⁸⁵, at 21 MeV, yield 8=1014
 Rh, d disintegration ang. distrib. of p, n, rel. to Coulomb and nuclear forces 8=11934
 S^{32, 34}(d, He³)P^{31, 33} and levels of P^{31, 33} 8=20693
 Si²⁸(d, α)Al²⁶, 6.98-11.06 MeV excitation functions for levels of Al²⁶, isospin selection rule 8=20829
 Si²⁸(d, He³)Al²⁷, 34.4 MeV and levels of Al²⁷ 8=20692
 Si²⁸(d, n)P²⁹, 3 MeV, n- γ ang. correls., states of P²⁹ 8=16117
 Si²⁸(d, p)Si²⁹, modified distorted-wave Born series 8=11838
 Si²⁸(d, p)Si²⁹, non commutative correction terms 8=1091
 Si²⁸(d, p)Si²⁹, orthogonality of initial and final wave functions 8=1092
 Si²⁸(d, p)Si²⁹ to test determ. of reduced widths from Butler pole 8=20818
 Si³⁰(d, He³)Al²⁹ and levels of Al²⁹ 8=20693
 Si³⁰(d, t)Si²⁹, n configuration of Si³⁰ 8=3959
 Si³⁰(d, p)Si³¹, 7.10 MeV, spectroscopic factors, DWBA calc. 8=11925
 Sm^{147, 149}, (d, t) and (d, p) reactions, 12 MeV 8=987
 Sr⁸⁸(d, p)Sr⁸⁹, 7.0 MeV, levels of Sr⁸⁹ 8=11932
 Tb¹⁵⁹(d, 2n)Dy¹⁵⁸, effective cross sections E_d = 6-26.9 MeV 8=16119
 Tb¹⁵⁹(d, 4n)Dy¹⁵⁷, effective cross sections E_d = 6-26.9 MeV 8=16119

Nuclear reactions due to—contd
Deuterons—contd

- Tb¹⁵⁹(d, p)Tb¹⁶⁰, effective cross sections
 $E_d = 6-26.9$ MeV 8=16119
 Te(d, n, 2n)Te^{131, 130}, ≤ 14.1 MeV excitation function meas. and compared to Peaslee theory 8=11930
 Te¹²⁸(d, p)Te¹²⁹, 7.5 MeV, 87 levels of Te¹²⁹ 8=3961
 Te¹³⁰(d, p)Te¹³¹, 7.5 MeV, Te¹³¹ energy levels 8=984
 Te¹³⁰(d, p)Te¹³¹, ≤ 14.1 MeV excitation function meas. and compared to Peaslee theory 8=11930
 Th¹⁰³(d, 2n)Pd¹⁰³, at 21 MeV, yield 8=1014
 Ti(d, p), improved agreement with new pot. 8=20823
 Zn^{64, 66, 68, 70}(d, p), 10 MeV, spectroscopic factors 8=11929
 Zr(d, 2n)Nb⁹⁸, ≤ 14.1 MeV excitation function meas. and compared to Peaslee theory 8=11930
 Zr(d, 3n)Nb⁹⁸, ≤ 14.1 MeV excitation function meas. and compared to Peaslee theory 8=11930
 Zr⁹⁰(d, 2n)Nb^{90m}, influence of chemical binding on half-life of Nb^{90m} 8=16024
 Zr^{92, 94}(d, p)Zr^{93, 95}(g.s. d_{5/2}), anomaly rel. to charge exchange effects 8=11755
 Zr⁹⁴(d, p)Zr⁹⁵(S_{1/2}), anomaly rel. to charge exchange effects 8=11755
 Zr⁹⁶(d, n)Nb⁹⁷, ≤ 14.1 MeV excitation function meas. and compared to Peaslee theory 8=11930
 Zr⁹⁶(d, p)Zr⁹⁷, ≤ 14.1 MeV excitation function meas. and compared to Peaslee theory 8=11930

electrons

- capture rel. to KX ray- γ direction correl. 8=20739
 (e, e'p), rel. to low-lying shells obs. 8=20659
 e⁻ + Be⁷ effect on solar ν flux 8=10405
 Bi(e, n), study of n energy spectra and ang. distrib. 8=11867
 C¹²(e, ep)B¹¹, Born approx. and DWIA calc. compared 8=7175
 Cu, positron spectrum obs., 31.5 MeV 8=20392
 K⁴⁰, K capture 8=7176
 Lu¹⁷⁴ isomers, electron capture disintegration energies 8=11776
 Ni⁵⁶ and Ni⁵⁷, electron capture ratio using dicylopentadienyl nickel 8=3914
 O¹⁶, O⁺ state monopole excitation at 6.056 MeV 8=3798
 Pb(e, n), study of n energy spectra and ang. distrib. 8=11867
 U(e, n), study of n energy spectra and ang. distrib. 8=11867
 U, natural, fission product yields using 1.5 and 3.0 GeV electrons 8=11972
 W(e, n), study of n energy spectra and ang. distrib. 8=11867

gamma-rays. See Nuclear reactions due to/photons.

heavy ions. See Nuclear reactions due to nuclei of Z > 2.

helium-3

- (He³, p γ) total and differential cross sections 8=7154
 (He³, d), modifications due to t, T interactions 8=11938
 (He³, n), study of level schemes of Si²⁸, S³⁰, A³⁴, and Ti⁴² 8=20694
 T = $\frac{3}{2}$, from F¹⁹(He³, n) obs. 8=20689
 Ag, 29 MeV, total cross section compared with optical and geom. models 8=11937
 Al, 29 MeV, total cross section compared with optical and geom. models 8=11937
 Al²⁷(He³, α)Al²⁸, 10 MeV, excited states of Al²⁶ 8=11945
 Al²⁷(He³, d)Si²⁸, 37.7 MeV rel. to level structure of Si²⁸ 8=15963
 B¹⁰(He³, p)C¹² (1⁺, 12.71 MeV) + p \rightarrow 3 α + p 8=1006
 Be⁹(He³, α)Be⁸ (16.92) \rightarrow α + α , ang. correl. obs., Be⁸ 16.82 assigned J π = O⁺ 8=20834
 Be⁹(He³, p γ)B¹¹, 3, 4 MeV and levels of B¹¹ 8=20681
 B¹⁰(He³, He³)B⁷, for study of B⁷ ground state 8=11720
 B¹⁰(He³, α , p α)B⁹, Be⁸ and levels of B⁹ rel. to mirror props. of Be⁹, B⁹ 8=20676
 B¹¹(He³, α)B¹⁰, 15, 16 MeV, states of B¹⁰ 8=951
 C¹²(He³, $\alpha\gamma$)C¹¹, $\alpha\gamma$ correls. C¹¹ energy levels 8=953
 C¹²(He³, $\alpha\gamma$)C¹¹, 4-12 MeV and levels of C¹¹ 8=20681
 C¹²(He³, p γ)N¹⁴, 8.92 MeV, levels of N¹⁴, p, γ -decay widths 8=11724
 C¹²(He³, p γ)N¹⁴, p γ correls., N¹⁴ energy levels 8=953
 C¹³(He³, α)C¹², differential cross section, resonance J π = 3⁻, T = O, corres. to 27.6 MeV state in O¹⁶ 8=3795
 C¹³(He³, n)O¹⁴, 2.24-3.70 MeV, polarization of n 8=3965
 C¹⁴(He³, p)N¹⁶, study of T = 2 states in N¹⁶ 8=20683
 Ca⁴²(He³, d)Sc⁴³, energy levels obs., 16.5 MeV 8=7084
 Co⁵⁹(He³, d)Ni⁶⁰, 37.7 MeV, optical pot. fit, level structure of Ni⁶⁰ 8=15981
 Co⁵⁹(He³, p)Ni⁶¹, 11.65 MeV, structure of Ni⁶¹ 8=15980
 Cr⁵⁰(He³, p)Mn⁵², 12 MeV and the levels of Mn⁵² 8=20703
 Cr⁵²(He³, d)Mn⁵³, 10, 11, 12 MeV and levels of Mn⁵³ 8=3808
 Cu, 29 MeV, total cross section compared with optical and geom. models 8=11937
 Cu^{63, 65}(He³, d)Zn^{64, 66}, 18 MeV, levels of Zn^{64, 66} 8=3970
 F¹⁹(He³, B¹⁰)C¹², 7.5-13.0 MeV DWBA and α -particle pick-up fits 8=3957
 F¹⁹(He³, n)Na²¹, T = $\frac{3}{2}$, Na²¹ levels obs. 8=20689
 Fe, 29 MeV, total cross section compared with optical and geom. models 8=11937
 Fe⁵⁴(He³, d)Co⁵⁵, 10, 11, 12 MeV and levels of Co⁵⁵ 8=3808
 Fe⁵⁴(He³, p)Co⁵⁶, 12 MeV and level structure of Co⁵⁶ 8=20706
 Ge, activation meas. of oxygen conc. 8=18083

Nuclear reactions due to—contd

helium-3—contd

- K³⁹(He³, d)Ca⁴⁰, 14 MeV, nuclear transitions Gillet-Sanderson predictions anomaly 8=15971
 K³⁹(He³, p)Ca⁴¹, 13 MeV, Ca⁴¹ even-parity states 8=966
 K⁴¹(He³, p)Ca⁴³ at 13.0 MeV, proton hole states in Ca⁴³ 8=11742
 Li⁶(He³, d, γ)Be⁷, 8, 10, 14, 18 MeV cross-sections meas. for ground and first excited states using optical parameters from Li⁶-He³, Li⁷-d scatt. 8=20833
 Li⁶(He³, n)B⁶, 4-5.7 MeV and cluster structures of Li⁶ and B⁶ 8=1099
 Li⁷(He³, γ)B¹⁰, 3-6 MeV, strong resonance obs. 8=11943
 Li⁷(He³, p)Be⁹, 1.25 MeV and levels of Be⁹ 8=20676
 Mg, 29 MeV, total cross section compared with optical and geom. models 8=11937
 Mg²¹(He³, He³) reaction to determ. mass in T = $\frac{3}{2}$ state 8=20656
 Mg²⁴(He³, $\alpha\gamma$)Mg²³, 9.00 MeV and levels of Mg²³ 8=11730
 Mg²⁵(He³, α)Mg²⁶, 4-6 MeV, excitation functions obs., statistical fluctuation analysis 8=20836
 Mg²⁵(He³, d)Al²⁶, 12 MeV states of Al²⁶ obs. 8=16122
 Mg²⁵(He³, d)Al²⁶, unified model 8=16122
 Mg²⁶(He³, α)Mg²⁵, statistical fluctuation analysis 8=20836
 Mg^{26, 26}(He³, α), 5.5 MeV, finite value of spin cut-off parameter 8=16123
 N¹⁴(He³, α)N¹³, 13.9 MeV, levels of N¹³ 8=20835
 N¹⁵(He³, n)F¹⁷, lowest T = $\frac{3}{2}$ states of F¹⁷ 8=3799
 Ne²⁰(He³, n)Mg²², e⁺ decay, branching 8=3866
 Ne²⁰(He³, p γ)Na²², 6.56 MeV, γ -ray branching 8=3801
 Ne²²(He³, d)Na²³, 10, 12 MeV, levels of Na²³ 8=3802
 Ni, 29 MeV, total cross section compared with optical and geom. models 8=11937
 Ni⁵⁸(He³, p)Cu⁶⁰, 13.0 MeV, Cu⁶⁰ level scheme 8=11946
 Ni⁶²(He³, d)Cu⁶³, 11.0 MeV, levels of Cu⁶³ 8=11947
 O¹⁶(He³, p γ)F¹⁸ for determination of spin of 1.131 MeV level of F¹⁸ 8=3800
 Pb²⁰⁸(He³, d)Bi²⁰⁹, Bi²⁰⁹ single proton strengths in multiplet at 2.6 MeV 8=11787
 S³²(He³, α)S³¹, 7.6 MeV, α -ray ang. distrib. meas. 8=3966
 Si, activation meas. of oxygen conc. 8=18083
 Si²⁸(He³, α)Si²⁷, first and second excited states of Si²⁷ 8=7082
 Si²⁸(He³, $\alpha\gamma$)Si²⁷ and energy levels of Si²⁷ 8=3803
 Si³⁰(He³, α)Si²⁹, n configuration of Si³⁰ 8=3959
 Sn^{116, 118, 120}(He³, d) 8=3971
 Ti^{46, 48, 50}(He³, d) at 10 MeV 8=969
 Ti⁴⁶(He³, p)V⁴⁸, 12 MeV, obs. of levels in V⁴⁸, angular momentum transfer in shell model calc. 8=20702
 Ti⁴⁸(He³, d)V⁴⁹, 17 MeV levels obs. up to 8.7 MeV 8=20701
 Ti⁴⁸(He³, d)V⁴⁹, 18 MeV, level structure of V⁴⁹ 8=11750
 Ti⁵⁰(He³, d)V⁵¹, 10, 11, 12 MeV and levels of V⁵¹ 8=3808
 Y⁸⁹(He³, d)Zr⁹⁰, T_c single-proton single-proton hole states in Zr⁹⁰ 8=3818

mesons

- See also Cosmic rays/effects and interactions.
 K⁻, binding energies of resulting hypernuclei 8=11794
 K⁻, hyperfragments produced by 800 MeV/c 8=20817
 K⁻ stars in emulsion stacks for determ. of mesic-to-non-mesic decay ratios of He hyperfragments 8=20736
 K⁻ with emulsion nuclei, existence of intermediate Ξ hyperfragment 8=11912
 π absorpt. by nucleon pairs in nuclei and their consequent emission 8=16102
 π charge-exchange scatt. (π^+ , π^-) sum rules, p-n correlation effect 8=3950
 π cross-section rel. to ν for PCAC hypothesis 8=11862
 π -emulsion nuclei, star prod. 8=1084
 π + light nucleus $\rightarrow \gamma$ + light nucleus, by PCAC generalization of Kroll-Ruderman theorem 8=7217
 π , nuclear structure from 2 N emission 8=1086
 π -nuclei, distrib. and fraction of primary energy transferred to photons 8=16103
 π probes of nuclear structure 8=7052
 (π^- , N) interacts., momentum spectra of secondary p and π 8=1085
 π^- absorpt. 2N emission obs. and compared to theory 8=11913
 π^- + polyethylene, π^+ prod. at 0°, 2-6 BeV/c 8=16104
 (π^+ , 2p), on freon nuclei, at 40-80 MeV 8=1028
 π^+ -nuclei in emulsion, double charge exchange total cross sections, 40-176 MeV 8=7216
 spallation hypernuclei, by 6 GeV/c K⁻ on heavy emulsion 8=3949
 Ar, K⁺, Λ^0 (Σ^0) prod. cross sections, 120 MeV 8=11917
 Be(π^-), π^+ prod. at 0°, 2-6 BeV/c 8=16104
 C¹², π probes of structure 8=7052
 C¹², π^- absorpt., calc. of W(pn \rightarrow nn)/W(pp \rightarrow pn), test of Brueckner theory 8=20654
 C(π^-), π^+ prod. at 0°, 2-6 BeV/c 8=16104
 C¹²(π^- , n⁴)B⁸ 8=11915
 C¹²(π^- , He³n)Li⁸ + n, reaction probability (2-10) $\times 10^{-4}$ 8=11916
 C¹²(π^- , π^-)C¹¹, cross-section calc. including momentum depend. transfer factors 8=16105
 Cu, K⁺, (Σ^0) prod. cross sections, 120 MeV 8=11917
 Cu(π^-), π^+ prod. at 0°, 2-6 BeV/c 8=16104

Nuclear reactions due to—contd

mesons—contd

- He⁸ production from π^- , K⁻ interactions with emulsion nuclei 8=892
 Li⁸, π^- capture rel. to nucleon clusters 8=11865
 Li⁸, rate-meas. on radiative pion capture 8=16066
 N¹⁴(π^- , Li⁸)Li⁸ 8=11916
 O and light nuclei, π^- capture 8=7221
 O¹⁶, π change-exchange scatt., cross-section calc. 8=3950
 O¹⁶, π probes of structure 8=7052
 O¹⁶ radiative π -capture rates rel. to giant resons. 8=955
 O¹⁶(π^- , Be⁷n)Li⁸, reaction suppressed 8=11916
 Pb, K⁻, π^0 prod. cross sections, 120 MeV 8=11917
 Pb(π^-) π^+ prod. at 0°, 2-6 BeV/c 8=16104
 Xe, π^- , $\omega^0 \rightarrow \pi^0\gamma$ obs., 9 GeV/c beam 8=6904

muons

- asymm. of recoil nuclei 8=15740
 capture, ν and γ -quanta correl. 8=7177
 electron pair production in medium and low Z elements 8=7178
 μ pair prod. by cosmic ray μ 8=15909
 μ^- capture, Siegent's theorem 8=11871
 nuclei, capture rel. to radiative π absorpt. 8=20775
 ν - γ ang. correl. det. from Doppler broadening of γ 8=16065
 ν and γ directions correl. formula 8=11870
 nuclei capture, total probability relativistic effect var. 8=11869
 p spectra, CVC theory anomaly 8=11872
 telescope for μ reactions, rejection of stops 8=1048
 B¹⁰ capture, ν and γ -quanta correl. 8=7177
 B¹⁰, correlation of capture 8=11870
 B¹¹ \rightarrow B¹¹ capture rate rel. to inversion of shell model states in Be¹¹ 8=11873
 Ca⁴⁰, capture rate calc. in hole-particle model 8=3916
 F(ν), corrections to Fermi gas model for finite nuclear size 8=20648
 Li⁸, rate-meas. on capture 8=16066
 Li⁸, total capture rate assuming nuclear clustering 8=3915
 N¹⁴ capture, ν and γ -quanta correl. 8=7177
 N¹⁴, correlation of capture 8=11870
 O¹⁶ \rightarrow N¹⁶, pseudoscalar coupling effects 8=11873
 Pb, μ trident prod. obs., 12 BeV, rel. to μ statistics 8=20392

neutrinos

- Cl³⁷ solar ν capture rate and low energy nuclear cross-sections 8=23718
 PCAC hypothesis tested rel. to π cross-section 8=11862
 pion production threshold, current algebra calc. 8=751

neutrons

- See also Nuclear fission.
 activation cross-sections for fast n, comments on calc. from 0.5 to 2 MeV 8=7201
 capture data at stellar temps. 8=5872
 capture, radiative, spectrometer 8=6785
 cellulose nitrate target, fast neutron detection 8=11619
 complex nuclei, single N transfer, cross-section 8=16127
 cross-section meas., thermostat 8=11893
 cross sections, total, and giant resonances 8=1067
 deuterium capture, cross-section 8=6988
 Doppler-broadening of resonances, note on temp.-invariance of integrals 8=7202
 fission isomer prod. by (n, γ) reactions 8=20847
 in foils irradiated in reactor beam, rig for meas. of emitted disintegrating nuclei 8=4031
 γ rays, prompt, from 14 target elements and prod. processes, 14.7 MeV 8=7211
 graphite, scattering law S(α, β), values at 1300°K and 1800°K 8=11898
 inelastic scattering of 14 MeV neutrons by light nuclei 8=16050
 (n, α) activation energy for various nuclei, 13.7-14.67 MeV 8=20805
 (n, γ) in Ba¹³⁸, La¹³⁹, Pr¹⁴¹, 14.0 MeV, rel. to statistical model 8=11896
 (n, γ), β spectrometer for conversion electrons 8=11470
 (n, n, γ), (np, γ) total and differential cross sections 8=7154
 ($n, 2n$) activation energy for various nuclei, 13.7-14.67 MeV 8=20805
 ($n, 2n$) in Ba¹³⁸, Ce¹⁴⁰, Pr¹⁴¹, Nd¹⁴², Sm¹⁴⁴ 14.0 MeV, rel. to statistical model 8=11896
 ($n, 2n$), cross-section at 14 MeV, shell effect search 8=11895
 (n, p) activation energy for various nuclei, 13.7-14.67 MeV 8=20805
 (n, p), exciton model, precompound decay particles 8=16087
 (n, p) and (n, α) cross-sections at 14.8 MeV 8=1081
 (n, p) in Ba¹³⁸, La¹³⁹, Ce¹⁴⁰, Pr¹⁴¹, Nd¹⁴² 14.0 MeV rel. to statistical model 8=11896
 optical model 8=1049
 primary energy obs. 8=11874
 radiative capture, collective model including spin-orbit interaction 8=11875
 radiative capture cross-sections for 28 nuclei for 3 MeV/n 8=7200
 radiative capture, thermal, isomeric state excitation 8=11703
 resonance energies by time-of-flight methods, obs. correl. 8=3930
 scintillation tank for meas. ratio of capture and fission events 8=11958
 stars, rel. to heavy element synthesis 8=10143
 stellar synthesis of heavy elements 8=10140
 synthesis of heavy nuclei by n capture at high density 8=1068
 A(n, γ), γ -ray spectrometer meas. 8=3576
 Al²⁷(n, α)Na²⁴, cross-section fluctuation around 14 MeV 8=1077
 Al²⁷(n, α)Na²⁴, 6.1-19.4 MeV, activation cross-section rel. to U²³⁵ fission 8=3937
 Al²⁷(n, p) activation cross-section meas. 8=20810
 Am²⁴¹(n, γ)Am^{242m}, 14 ms spontaneously fissioning isomer obs. 8=1107
 Am²⁴¹(n, γ)Am²⁴², study of Am²⁴² 8=11792
 As⁷⁵(n, γ)As⁷⁶, levels of As⁷⁶ 8=20811
 As⁷⁵(n, d)Ge⁷⁴, 14.4 MeV, levels of Ge⁷⁴ compared to shell model 8=7212
 As(n, p), (n, α) cross-sections at 14.8 MeV 8=1081
 As, total cross-section, 3 to 5 MeV 8=11904
 Au, rel. to flux meas, corrections for 4 π - γ coincidence meas. 8=6966
 B in Si, determ. by irradiating with thermal neutrons 8=5765
 B, thermal absorption cross-section 8=20808
 B¹⁰(n, α)Li⁷, branching ratio and Q-value 8=20807
 B¹⁰(n, α)Li⁷, thermalized n distrib. obs. 8=852
 B¹⁰(n, α)Li⁷, 30-500 keV, cross-section from inverse reaction 8=11900
 B¹⁰, radiative capture, high sensitivity spectrometers 8=6783
 B¹¹(n, p)Be¹¹, cross-section of 7.1±2 mb 8=16072
 Ba¹³⁸(n, γ) isomeric cross sections ratio 8=16100
 Be⁹(n, α)He³ \rightarrow Li⁶, determ. of conc. and diffusion 8=8672
 Be⁹($n, 2n$)2He⁴, effective cross-section determ. 8=16089
 Bi, ($n, 2n$) effective cross-sections, meas. by Fermi-water-tank method 8=3944
 Br(n, p), (n, α) cross-sections at 14.8 MeV 8=1081
 Br⁸¹(n, γ)Br^{82m} in liq. bromobenzene, chem. effects 8=18752
 C¹², (n, α) in liquid scintill. α -p discrimination 8=1075
 C¹²(n, d)B¹² 14.5-22 MeV, excitation function for ground state 8=16090
 C¹², α , radiative capture, high sensitivity spectrometers 8=6783
 Ca isotopes activation cross-section meas. 8=20810
 Ca, total cross-section 8=7207
 Ca⁴⁰(n, α_0) ang. distrib. curves, E_a = 2.90 and 3.28 MeV 8=16094
 Ca⁴⁰(n, α_0), 5.13 MeV, ang. distrib. 8=16095
 Ca⁴⁰, (n, d) and (n, p) at 14.4 MeV 8=16096
 Ca⁴⁰(n, d)K³⁹, 14.4 MeV, levels of K³⁹ compared to shell model 8=7212
 Cd¹¹³ total cross-section 0.025-1 eV and 0.181 eV reson. params. 8=3941
 Cl³⁵(n, d)S³⁴, DWBA and spectroscopic factors, shell and collective models 8=1078
 Cl³⁵(n, d)S³⁴, 14.4 MeV, levels of S³⁴ compared to shell model 8=7212
 Cl³⁵(n, γ)Cl³⁶, crystal γ spectrometer meas. 8=11442
 Cl³⁵(n, γ)Cl³⁶, γ - γ directional correlation 8=20697
 Cl³⁵(n, γ)Cl³⁶, 2 new levels of Cl³⁶ 8=20811
 Cl³⁷, radiative capture at 0.15-1.4 MeV 8=16093
 Cr, total cross-sections, 3 to 5 MeV 8=11904
 Cu, natural, cross-section, 0.0001 eV to 15 MeV 8=11906
 Cu^{63,65}, cross-section, 0.0001 eV to 15 MeV 8=11906
 Cu⁶³(n, α)Co⁶⁰, excitation functions 8=3938
 Cu⁶³($n, 2n$)Cu⁶⁴, cross section fluctuation around 14 MeV 8=1077
 Er¹⁶⁶(n, γ)Er¹⁶⁷, thermal n-capture 8=1083
 Er¹⁶⁷, thermal neutron cross section meas. 8=11910
 F¹⁹($n, 2n$)F¹⁸, cross-section fluctuation around 14 MeV 8=1077
 F¹⁹($n, 2n$)F¹⁸, 12.7-19.4 MeV, activation cross-section rel. to U²³⁵ fission 8=3937
 Fe⁵⁴(n, γ), γ -ray spectrometer meas. 8=3576
 Fe⁵⁶, thermal-capture, γ circular polarization obs. 8=11905
 Fe⁵⁷(n, γ)Fe⁵⁸, thermal n-capture γ -ray spectrum 8=1080
 Ge, thermal capture, gamma ray spectra 8=3810
 Ge^{70,74,76}, isomeric ratios for thermal capture 8=16099
 He³ spectrometer using reaction 8=6968
 H^{17,178}(n, γ) isomeric cross sections ratio 8=16100
 Hg¹⁹⁹(n, γ)Hg²⁰⁰ γ radiation and excited states of Hg²⁰⁰ 8=11911
 Hg²⁰²(n, p)Au²⁰² half-life, β end-point energy 8=11828
 Hg²⁰⁴(n, p)Au²⁰⁴, decay of Au²⁰⁴ and lifetime 8=11828
 Ho¹⁶⁵(n, γ)Ho¹⁶⁶ cross-section rel. to U²³⁵ fission 8=3943
 Ho¹⁶⁵(n, γ), 2.5-10⁵ eV, spin assignments of Ho¹⁶⁶ resonances 8=16101
 Ho¹⁶⁵($n, 2n$)Ho^{164m}, 12.7-19.4 MeV, activation cross-section rel. to U²³⁵ fission 8=3937
 In¹¹³(n, γ)In^{114m, s}, activation energies, activation cross-section meas. 8=11909
 In¹¹³(n, n')In^{113m}, activation energies, activation cross-section meas. 8=11909

Nuclear reactions due to—contd

neutrons—contd

Nuclear reactions due to—contd

neutrons—contd

- $\text{In}^{113}(\text{n}, 2\text{n})\text{In}^{112}$, cross-section for isomer prod, spin distrib. parameter 8=20814
 $\text{In}^{115}(\text{n}, \gamma)\text{In}^{116\text{m}, 116\text{s}}$, activation energies, activation cross-section meas. 8=11909
 $\text{In}^{115}(\text{n}, \gamma)\text{In}^{116\text{m}}$ cross-section rel. to U^{235} fission 8=3943
 $\text{In}^{115}(\text{n}, \text{n}')\text{In}^{115\text{m}}$, activation energies, activation cross-section meas. 8=11909
 $\text{In}^{115}(\text{n}, \text{n}')\text{In}^{115\text{m}}$, 1-19.4 MeV, activation cross-section rel. to U^{235} fission 8=3937
 $\text{In}^{115}(\text{n}, 2\text{n})\text{In}^{114}$ cross-section for isomer prod, spin distrib. parameter 8=20814
 $\text{In}^{115}(\text{n}, 2\text{n})\text{In}^{114\text{m}}$, 12.7-19.4 MeV, activation cross-section rel. to U^{235} fission 8=3937
 Ir , thermal capture, gamma ray spectra 8=3810
 Ir^{193} , radiative capture at 0.15-3.2 MeV 8=16093
 K isotopes activation cross-section meas. 8=20810
 K , total cross-section 8=7207
 $\text{K}^{39}(\text{n}, \text{d})\text{Ar}^{38}$, 14.4 MeV, levels of Ar^{38} compared to shell model 8=7212
 $\text{K}^{39}(\text{n}, \text{p}\gamma)$ levels of K^{39} 8=20809
 K^{41} , reson. activation integral determ. 8=11808
 $\text{Li}^6(\text{n}, \alpha)\text{H}^3$, and $\text{O}^{16}(\text{t}, \text{n})\text{F}^{18}$, in nuclear reactor 8=4024
 $\text{Li}^6(\text{n}, \alpha)\text{H}^3$, Q-value 8=20807
 Li^6 , radiative capture, high sensitivity spectrometers 8=6783
 Li^6 , spectrometer using reaction 8=6968
 Mn , thermal capture, gamma ray spectra 8=3810
 Mn , 200 keV, resonance parameters 8=3809
 Mn^{55} , reson. activation integral determ. 8=11808
 $\text{Mn}^{55}(\text{n}, \gamma)\text{Mn}^{56}$ cross-section rel. to U^{235} fission 8=3943
 $\text{Mn}^{55}(\text{n}, 2\text{n})\text{Mn}^{54}$, 12.7-19.4 MeV, activation cross-section rel. to U^{235} fission 8=3937
 Mo , n cross-section obs, resonance energies and level widths 8=20813
 Mo , 10-25 keV radiative capture, resonances and cross-section obs. 8=3939
 $\text{Mo}^{92, 100}(\text{n}, [2\text{n}, \alpha])$, 14.1 MeV activation cross-sections 8=3940
 $\text{Mo}^{96, 97, 98}(\text{n}, \text{p})$, 14.0 MeV activation cross-sections 8=3940
 N^{14} , radiative capture, high sensitivity spectrometers 8=6783
 N^{14} , (n, d) and (n, t) at 14.4 MeV 8=16091
 $\text{N}^{14}(\text{n}, \text{d})\text{C}^{13}$, 14.4 MeV, levels of C^{13} compared to shell model 8=7212
 $\text{N}^{14}(\text{n}, 2\alpha)\text{Li}^7$, 14.1 and 15.7 MeV 8=1076
 $\text{Na}^{23}(\text{n}, \gamma)\text{Na}^{24}$ cross-section rel. to U^{235} fission 8=3943
 $\text{Na}^{23}(\text{n}, 2\text{n})\text{Na}^{22}$, 12.7-19.4 MeV, activation cross-section rel. to U^{235} fission 8=3937
 $\text{Ne}^{22}(\text{n}, \gamma)\text{Ne}^{23}$, unsuccessful search for 2.285, 2.405, 2.870 MeV levels of Ne^{23} 8=11806
 $\text{Ni}^{60}(\text{n}, \text{p})\text{Co}^{60}$, excitation functions 8=3938
 $\text{Ni}^{64}(\text{n}, \alpha)\text{Fe}^{61}$, Fe^{61} - Co^{61} decay schemes 8=3869
 $\text{O}^{16}(\text{n}, \alpha)\text{C}^{13}$, 14.1 MeV 8=11901
 $\text{O}^{16}(\text{n}, \alpha)\text{C}^{13}$, 14.1 MeV, ang. dist. of α -particles and levels in C^{13} 8=3936
 $\text{P}^{31}(\text{n}, \gamma)\text{P}^{32}$, obs. of 64 transitions, and reduced widths 8=11902
 Pa^{233} , n-capture resonance integral meas. 8=3946
 $\text{Pb}^{208}(\text{n}, \gamma)$, collective mechanism 8=11875
 Pd^{108} , total cross-section 0.005 to 10 eV, and resonance at 2.97 eV 8=11908
 $\text{Pd}^{110}(\text{n}, 2\text{n})\text{Pd}^{109}$ at 14.7 MeV, isomeric cross section ratio 8=1082
 Pr , n cross-section obs, resonance energies and level widths 8=20813
 Pu^{238} , fission cross-section obs. at 1.0, 1.5, 3.0 and 14.9 MeV 8=1109
 Pu^{238} , total and absorption cross sections 8=7335
 Pu^{238} scintillation tank for meas. ratio of capture and fission events 8=11958
 Pu^{240} , resonance escape probability, Monte Carlo calc. 8=16152
 $\text{Rb}^{85}(\text{n}, \gamma)$ isomeric cross sections ratio 8=16100
 Rb^{87} , radiative capture at 0.15-1.4 MeV 8=16093
 Re^{178} , thermal n capture, conversion e spectrum of Re^{188} 8=11780
 $\text{S}^{34}(\text{n}, \gamma)\text{S}^{35}$, effective cross-section 8=16092
 Sb , n cross-section obs, resonance energies and level widths 8=20813
 $\text{Se}(\text{n}, \text{p}), (\text{n}, \alpha)$ cross-sections at 14.8 MeV 8=1081
 Se^{74} , thermal activation cross-section 8=20812
 $\text{Se}^{76, 78, 80, 82}$, isomeric ratios for thermal capture 8=16099
 Se^{82} , n bombard. for $\text{Kr}^{83\text{m}}$ prep. 8=3872
 Sr^{84} , isomeric ratios for thermal capture 8=16099
 $\text{Sr}^{84, 86}(\text{n}, \gamma)$ isomeric cross sections ratio 8=16100
 $\text{Sr}(\text{n}, 2\text{n})$, rel. to enrichment of $\text{Sr}^{87\text{m}}$ by recoil effect 8=7214
 $\text{Sn}^{118, 120, 124}$ resonances following capture spin and parity of determ. of various levels 8=20716
 Ta , total cross-section by time-of-flight spectrometry 8=7196
 Te , n cross-section obs, resonance energies and level widths 8=20813
 Th^{228} , total cross-section for 1.9 and 7.5 eV resonances 8=3945

Nuclear reactions due to—contd

neutrons—contd

- Ti^{48} , thermal n capture, γ - γ coincidence and ang. correl. 8=11903
 Ti^{50} , fast radiative capture cross-section, 180-2600 keV 8=16097
 $\text{Ti}^{205}(\text{n}, \alpha)\text{Au}^{202}$ half-life, β end-point energy 8=11828
 U^{232} , total n cross-section from 0.01 to 10000 eV 8=3947
 $\text{U}^{233, 235}$ scintillation tank for meas. ratio of capture and fission events 8=11958
 U^{235} , particle yields, slow and 14 MeV n 8=7262
 U^{235} quaternary fission by thermal neutrons, obs. 8=11963
 U^{238} capture rates, absolute determ. 8=7348
 U^{238} capture and U^{235} fission, ratio of cross-sections 8=20848
 $\text{U}^{238}(\text{n}, \gamma)$, at high temp. and different n energies, Doppler effect 8=20815
 V , 200 keV, resonance parameters 8=3809
 V^{51} , fast radiative capture cross-section, 180-2600 keV 8=16097
 V^{51} , reson. activation integral determ. 8=11808
 $\text{V}^{51}(\text{n}, \gamma)\text{V}^{52}$, study of γ -rad. and decay scheme 8=1079
 $\text{W}^{186}(\text{n}, \text{p})\text{Ta}^{186}$, β - and γ -spectrometry 8=16043
 $\text{Xe}^{54}(\text{n}, \alpha)\text{Te}^{52}$, 12.5-18.0 MeV, Xe-He mixture as target and monitor 8=3942
 $\text{Y}^{89}(\text{n}, \gamma)\text{Y}^{90}$, separation of n energy 8=7215
 YH_3 pellet targets for (n, 2n), fabrication 8=8871
 $\text{Yb}^{176}(\text{n}, \alpha)\text{Er}^{173}$, new radioactive isotope prod. 8=20756
 $\text{Zn}^{64, 67}$, thermal-capture, γ circular polarization obs. 8=11905
 $\text{Zn}^{67}(\text{n}, \gamma)\text{Zn}^{68}$, γ -ray spectrum obs. 8=7213
 $\text{Zn}^{68, 70}$, isomeric ratios for thermal capture 8=16099
 $\text{Zr}^{90, 92, 94, 96}$, 2-60 keV, resonance structure 8=11907
 ZrH , slow capture cross section 8=16161
- nuclei of $Z > 2$**
 See also Ions/scattering.
 complex nuclei subbarrier scatt., interference effect 8=16125
 Coulomb excitation of light and medium nuclei 8=935
 fission in heavy ion reactions 8=20842
 fission, ternary, mechanism 8=1110
 heavy ion bombard, γ -ray emission, determ. of magnitude and phase of E2, M1 transitions 8=932
 inelastic scattering, accompanied by excitation of collective states 8=11949
 meteors, size calc. from reaction obs. on meteorites 8=19266
 nucleus-nucleus, by heavy cosmic ray primaries, multiply-charged fragments 8=16126
 $62 \leq Z \leq 74$, recoil implanted in polarized Fe-, Co- and Ni-environment, hyperfine fields 8=13034
 transfer, heavy ion, with identical initial and final states 8=16124
 Al, Po, At, range energy curve 8=13473
 Al_2O_3 , Po, At, range energy curve 8=13473
 $\text{Am}^{243}(\text{O}^{18}, 4-5\text{n})103^{256, 257}$ 8=7151
 $\text{Ar}^{40} + \text{Au}$, α particle distrib. and spectra 8=11955
 $\text{Ar}^{40} + \text{Th}$, α particle distrib. and spectra 8=11955
 $\text{B}^{10}(\text{F}^{18}, \text{F}^{18})\text{B}^{11}$, 10.5-76.5 MeV, n transfer reaction rate rel. to p transfer 8=20840
 $\text{B}^{10}(\text{F}^{18}, \text{O}^{18})\text{C}^{11}$ p transfer rel. to n transfer rate 8=20840
 $\text{Be}^8(\text{Li}^7, \text{p})\text{C}^{15}$, lifetime of first excited state of C^{15} obs. 8=20680
 $\text{Be}^8(\text{N}^{14}, \text{N}^{14})$, 30 MeV lifetime of mirror states of N^{15} and O^{15} 8=3793
 $\text{Bi}^{209}(\text{O}^{18}, \text{X})\text{Y}$, 76-163 MeV recoil products for bombard. of Al foils 8=11952
 $\text{C}^{12}(\text{Li}^7, \text{d})\text{O}^{17}$, 3.3, 3.5, 3.7 MeV 8=3975
 $\text{C}^{12}(\text{Li}^7, \text{p})\text{O}^{18}$, 3.3, 3.5, 3.7 MeV 8=3975
 $\text{C}^{12}(\text{Li}^7, \text{t})\text{O}^{17}$, 3.3, 3.5, 3.7 MeV 8=3975
 $\text{C}^{12}(\text{O}^{18}, \alpha)\text{Mg}^{24}$, cross-section fluctuations 24.3-27.7 MeV 8=1105
 $\text{C}^{12}(\text{O}^{18}, \alpha)\text{Mg}^{24}$, 19, 31, 42, 49 MeV, ang. dist. fluctuations 8=1104
 $\text{C}^{12, 13}(\text{B}^{11}, \text{B}^{10})$, 115.9 MeV, reaction spectra, mechanism 8=11951
 Cf^{252} , from $\text{U}^{235}(\text{C}^{12}, 5\text{n})$ 8=11834
 $\text{Cf}^{251}(\text{Ni}^{62}, \text{xn})$ rel. to production of 126^{310} 8=3972
 $\text{H}^2[\text{N}^{14}, \text{O}^{15}(\text{N}^{15})]$, 30 MeV lifetime of mirror states of N^{15} and O^{15} 8=3793
 Li^6 , elastic scatt. on C^{12} at 20 MeV 8=7238
 $\text{Li}^6(\text{Li}^6, \text{n})\text{C}^{11}$, 4.1 MeV n distrib. obs. for all levels except ground state 8=11950
 $\text{Li}^6(\text{Li}^6, \text{p})\text{B}^{11}$, p ang. distrib. compared with n ang. distrib. in $\text{Li}^6(\text{Li}^6, \text{n})\text{C}^{11}$ 8=11950
 $\text{Li}^7(\text{O}^{18}, \gamma)\text{Li}^{23}$ radiative capture, resonance structure obs. 8=3974
 $\text{N}^{14}(\text{N}^{14}, \text{N}^{14})\text{N}^{15}$ virtual Coulomb excitation in nucleon transfer 8=3976
 $\text{N}^{14, 15}(\text{B}^{11}, \text{B}^{10})$, 115.9 MeV, reaction spectra, mechanism 8=11951
 $\text{Nd}^{144}(\text{C}^{12}, 7\text{n})\text{D}^{149}$, recoil range distrib. 8=1103
 $\text{Ne}^{20}(\text{B}^{11}, \text{B}^{10})$, 115.9 MeV, reaction spectra, mechanism 8=11951
 $\text{Ne}^{22} + \text{Au}$, α particle distrib. and spectra 8=11955
 $\text{Ne}^{22} + \text{Th}$, α particle distrib. and spectra 8=11955

Nuclear reactions due to—contd**nuclei of $Z > 2$ —contd**

- $O^{16}(B^{11}, B^{10})115.9$ MeV, reaction spectra, mechanism 8=11951
 $O^{16}(Li^7, t)Ne^{20}$, excitation of rotational states 8=16128
 $O^{16,18} + P^{32}$, $Z=102$ isotope production 8=1206
 $Pa^{231}(Br^{79}, s^4xn)$, rel. to production of 126^{310} 8=3972
 $Pb^{208}(O^{16}, X)Y$, 123, 163 MeV, recoil products for bombard. of Al foils 8=11952
 $Pd^{102} + C^{12}$, Te^{111} delayed proton emitter in $Pd^{102} + C^{12}$ reaction obs. 8=7137
 $Pu^{239} + C^{12}$, $Fm^{240,247}$ prod. 8=7239
 $Sm^{147} + Ar^{40}$ radioactive isotope prod. 8=7148
 $Sn(Ar^{40}, xn)$, cpd. nucleus ground-band collective levels population, γ -rays obs. 8=11953
 $Te(Ar^{40}, xn)$, cpd. nucleus ground-band collective levels population, γ -rays obs. 8=11953
 $Tm^{169} + Ne^{22}$ radioactive isotope prod. 8=7148
 $U^{238}(O^{18}, xn)$ rel. to production of 126^{310} 8=3972
 $Y^{170} + Ne^{20}$, radioactive isotope prod. 8=7148

photons

- bremsstrahlung irradi. of water, and secondary reaction $O^{18}(p, n)F^{18}$ 8=16081
 cross-section det. by statistical method 8=1033
 fission of nuclei, up to 1600 MeV 8=7169
 (γ, n) reactions, $N \approx 56$, ang. distrib. of 75 MeV neutrons 8=11857
 meson production threshold 8=1034
 meson resons. prod. on nuclei with zero spin and isospin 8=11558
 photodisintegration, theory using Franz-Stech classification e. m. multipoles 8=16056
 photodisintegration of three-particle nuclei and Majorana exchange forces 8=7162
 photofission fragments, ang. distrib., and conservation of K quantum no. 8=11964
 photoneutron liq. detector, cross section meas. 8=20560
 photonuclear cross sections rel. to low-lying shells obs. 8=20659
 π^+, K^+, p^+, e^+ prod., 16-18 GeV electron accelerator on metal targets 8=20768
 rare earth elements, photoactivation anal. with 20 MeV bremsstrahlung 8=7161
 ρ meson production on nuclei, 2.8-4.5 GeV/c 8=7164
 20 MeV bremsstrahlung, γ -ray spectra study of activation products 8=7163
 $Al^{27} \rightarrow Na^{24}$, yield, 100-1250 MeV 8=1036
 $B^{11}(\gamma, \pi^+)Be^{11}$, obs. rel. to independent particle model 8=1035
 $B^{11}(\gamma, \pi^-)C^{11}$, obs. rel. to independent particle model 8=1035
 $Be^8(\gamma, n)Be^8$, model with single-particle states coupled to core rotations 8=3907
 $Be^9(\gamma, n)Be^8$, photoneutron cross-section 8=3906
 Be^9 from core-plus-n model of $Be^9(\gamma, n)Be^8$ 8=3908
 $C(\gamma, p)$, and angular distrib. and absorption up to 170 MeV 8=11859
 $C^{12} \rightarrow C^{11}$, yield, 100-1670 MeV 8=1036
 $Co^{59}(\gamma, n)Co^{58}$, isomer ratio obs, spin cutoff parameter calc. 8=20707
 Cu^{60} , photoneutrons energy spectra time of flight obs. 8=7165
 $F^{19}(\gamma, n)$, absolute cross-section, rel. to nuclear shape 8=7167
 $Fe, (\gamma, Tn)$ cross-sections, behaviour 8=3909
 $Fe^{56}(\gamma, n)Fe^{55}$, levels of Fe^{56} 8=3811
 H liquid, π^+ photoproduction 8=15763
 He^3, H^3 photodisintegration, Cabibbo-Radicati sum rule appls. 8=695
 $I^{12m}(\gamma, xn)$, $x = 1-M$, ≤ 830 MeV, cross-sect. obs., photomeson threshold anomaly 8=11861
 $I^{127}(\gamma, xn)$ yields, redetermination 8=20770
 $Nb(\gamma, \alpha)$, α -emission energy obs. 8=1041
 $Ni^{60}(\gamma, np)Co^{58}$, isomer ratio obs, spin cutoff parameter calc. 8=20707
 $O^{16}(\gamma, \rho)O^{16}$ for partial scatt. amplitude, determ. 8=11858
 $O^{16}(\gamma, \chi)N^{13}$, cross-section and $C^{12}(\gamma, t)$ yield 8=1039
 $O^{16}(\gamma, \chi)C^{12}$, cross-section and $C^{12}(\gamma, t)$ yield 8=1039
 $O^{16}(\gamma, p)$ and (γ, n) , resonance widths 8=1038
 O^{16} photodisintegration 8=7166
 O^{16} photoneutrons energy spectra time of flight obs. 8=7165
 P^{31} , photoneutrons energy spectra time of flight obs. 8=7165
 $Pr^{141}(\gamma, n)Pr^{140}$, cross-section calc. from e^+ decay of Pr^{140} 8=16060
 $S^{32}(\gamma, n)S^{31}$, 20-32 MeV, large dipole strength above 22 MeV 8=11860
 $Se, (\gamma, Tn)$ cross-sections, behaviour 8=3909
 $Si^{28} \rightarrow Na^{24}$, yield, 300-1250 MeV 8=1036
 U , attenuation cross section from 10-300 keV meas. 8=7170
 U^{238} photofission, Cd^{115} yield, 5.3-6.5 MeV bremsstrahlung 8=16135
 $Y^{89}(\gamma, n + \gamma, pn)$, $(\gamma, 2n)$ up to 30 MeV 8=1040
 $Zr^{90,91,92,94}(\gamma, n + \gamma, pn)$, $(\gamma, 2n)$ up to 30 MeV 8=1040
 $Zr^{90}(\gamma, p)$ isobaric analogue states in eigenchannel theory 8=3819

Nuclear reactions due to—contd**photons—contd**

$Zr^{94}(\gamma, 3n)$ up to 30 MeV 8=1040

protons

- deuteron production by 1-BeV protons 8=3735
 heavy emulsion nucleus, complete disintegration, 24 GeV/c proton 8=16076
 interactions of protons with tritium 8=16050
 of momentum 24 BeV/c, energy and angular characts. 8=16074
 nuclear emulsion nuclei disintegration and d emission, 9 GeV 8=15867
 nuclear emulsions, 24 and 27 GeV/c 8=7181
 nuclei, light, at 660 MeV, He^3 production 8=16071
 optical model 8=1049
 (p, n) , extinction of optical parameter data 8=1096
 (p, n) , 94 MeV, isobaric analogue states, isospin term in optical pot. 8=16070
 $(p, p\alpha)$ reactions at medium-energy and alpha-clustering correlations in light nuclei 8=1055
 $(p, p'\gamma)$, $(p, n\gamma)$ total and differential cross sections 8=7154
 p and n secondary spectra, 30-340 MeV, anomalies 8=1051
 p prod. on various nuclei, 158 MeV cross-section obs. 8=20781
 photographic emulsion in pulsed mag. field, obs. 8=16073
 primary energy obs. 8=11874
 radiative capture, collective model including spin-orbit interaction 8=11875
 radioactive isotopes produced from Al, Fe, Cu 8=1061
 recoil-charged from 14.5 MeV n , average cross-section 8=16072
 in stellar surface layers, rel. to abundance anomalies in peculiar A stars 8=5871
 $Ag, 1, 2, 3$ GeV, star prod., light fragment, α and Li^8 emission cross-sections obs. 8=11891
 Ag, Li^8 production, 660 MeV 8=7194
 $Ag, 200-400$ MeV, p, n knockout, Metropolis cascade model 8=11890
 $Ag, 200-400$ MeV, Pa, Ag spallation 8=11892
 $Ag, 3$ and 29 GeV, prod. of 60 radionuclides, cross-sections 8=20799
 $Al^{27}(p, \gamma)Si^{28}$, Q-value meas. of γ -ray energy 8=3574
 $Al^{27}(p, \gamma)Si^{28}$, resonant widths 8=959
 $Al^{27}(p, 2p)Mg^{26}$, deformation of Al^{27} 8=11884
 $Ar^{40}, 3, 5, 6, 0$ MeV, levels of K^{41} 8=964
 $Ar^{40,36}(p, d)Ar^{39,35}$, 27.5 MeV, levels of $Ar^{39,35}$ 8=11887
 Au , spallation, Pt^{188} γ -ray study 8=1024
 B , formation by spallation 8=3922
 $B^{10}(p, \gamma)C^{11}$, analog state to B^{11} 8=11721
 $B^{10,11}(p, d)B^{9,10}$ 33.6 MeV, difficulties with pick-up and stripping 8=20788
 $B^{11}(p, \alpha)2\alpha$, 2.65 MeV, coincidence meas. 8=3903
 $B^{11}(p, 2\alpha)He^4$, 163 keV, ang. distrib. 8=7190
 $B^{11}(p, n)C^{11}$, rel. to polarization of neutrons 8=7189
 $Ba, 730$ MeV p , spallation yield of Xe 8=20797
 Ba^{138} , rel. to isobaric analog resonances and particle-hole states 8=985
 Be , formation by spallation 8=3922
 $Be^{8,9}(p, d)$ at 33.6 MeV compared with DWBA analysis, isotopic spin mixing 8=3923
 $Be^8(p, n)B^8$, fast n -spectra 8=1056
 $Be^8(p, d)Be^8$, leading to d singlet state 8=20787
 $Be^8(p, d)Be^8$, rel. to detect. of singlet deuteron d 8=871
 $Be^8(p, d)$, 100 MeV, spin depend. models compared 8=7188
 $Br, 1, 2, 3$ GeV, star prod., light fragment, α and Li^8 emission cross-sections obs. 8=11891
 $Br^{79}(p, n)Kr^{79}$, Kr^{79} excited state, half-life and g-factor meas. 8=11752
 C , cross-sections for p energies 10^{10} - 10^{12} eV, meas. by satellite Proton 1 8=16080
 C , spallation, formation ratios of Li, Be and B 8=3922
 $C^{12}(p, d)$, 100 MeV, spin depend. models compared 8=7188
 $C^{12}(p, n)N^{12}$, 18.9-50 MeV variation of cross-section leading to ground state of N^{12} 8=16079
 $C^{12}(p, pn)C^{11}$, 385 MeV, cross-section obs. 8=20789
 $C^{12}(p, p'\gamma)$, 23 MeV, first excited state 8=954
 $C^{12}(p, pn)C^{11}$, 7500 MeV, activation meas. suitable for dosimetry 8=11603
 $C^{12}(p, pn)C^{11}$, from threshold to 85 MeV obs. 8=20790
 $C^{12}(p, 2p)$, cross-section and diffraction effect 8=3925
 $C^{12}(p, t)C^{10}$, $L = 0.2$ ang. distrib. shapes energy var., 20-54 MeV 7=1060
 $C^{13}(p, \gamma)N^{14}$, meas. of van de Graaff beam energy spread 8=20228
 $C^{13}(p, He^3)$, 49.6 MeV rel. to 2N transfer theory 8=11877
 $C^{13}(p, He^3)$, 2N transfer theory, inclusion of spin-depend. forces 8=11877
 $Ca^{42}(p, \alpha)K^{39}$, 10.6-11.1 MeV, spins and mixing ratios of levels of K^{39} 8=15967
 $Ca^{48}(p, n)Sc^{48}$, obs. for Sc^{49} analogue resonance 8=15972
 $Cd(p, n)$, 8-14 MeV, cross-section obs. 8=7193
 $Cd(p, 2n)$, 8-14 MeV, cross-section obs. 8=7193
 Cd^{114} , isobaric analog resonances, 7-10 MeV comparison with p scatt. 8=983
 $C^{137}(p, \gamma)Ar^{38}$, 1.0-1.8 MeV, levels of Ar^{38} 8=11737
 $Cr(p, n)$, 8-14 MeV, cross-section obs. 8=7193
 $Cr(p, 2n)$, 8-14 MeV, cross-section obs. 8=7193

Nuclear reactions due to—contd

protons—contd

- Cr⁵³(p,n)Mn⁵³, 2, 3, 2, 4, 2, 5 MeV, ang. correl. meas. 8=3926
- Cu⁶³(p,n)Zn⁶³, gamma ray ang. distrib. 8=11948
- Cu⁶⁵(p,p')Ni⁶⁵ cross-section calc. including momentum depend. transfer factors 8=16105
- Dy¹⁵⁶(p,xn), prod. of Ho isotopes 8=3883
- Er¹⁶⁶(p,2n)Tm¹⁶⁵, 5–17.5 MeV, isomeric levels and decay 8=3828
- F¹⁹, p capture, intermediate structure resonances as particle-hole states 8=3931
- F¹⁹(p,α)O¹⁶, expt. for senior students 8=1059
- He⁸ production from p \bar{p} reactions with emulsion nuclei 8=892
- In, 200–400 MeV, Pa, Ag spallation 8=11892
- In, 200–400 MeV, p, n knockout, Metropolis cascade model 8=11890
- K³⁹(p,(t,He³)K³⁷(Ar³⁷), 45 MeV, T = ½ levels mass determ. 8=20656
- K⁴¹(p,α)Ar³⁸, E_p=1400–1750 keV 8=16082
- K⁴¹(p,α)Ar³⁸, excitation functions and angular distributions 8=16083
- K⁴¹(p,γ)Ca⁴², E_p=1400–1750 keV 8=16082
- K⁴¹(p,n)Ca⁴¹, E_p=1400–1750 keV 8=16082
- Li, formation by spallation 8=3922
- Li⁶(p,pα)H², 9–10 MeV, sequential decay and knock-out obs. 8=7187
- Li⁶(p,pd)He⁴, 9–10 MeV sequential decay and knock-out obs. 8=7187
- Li⁶(p,p)He³H³, quasi-elastic, scatt. 156 MeV 8=16078
- Li⁶(p,2p)He⁵ rel. to α-d cluster structure of Li⁶ 8=11717
- Li⁶(p,2p) rel. to nucleon clusters 8=11865
- Li⁶,⁷(p,d) at 33.6 MeV, compared with DWBA analysis, n pickup indicated 8=3923
- Li⁷(p,α)He⁴, polarization effects, α-particle asymmetry as function reaction angle 8=11882
- Li⁷(p,d), 100 MeV, spin depend. models compared 8=7188
- Li⁷(p,n)Be⁷ (431 keV), total cross section and effective interaction 8=3924
- Li⁷(p,p')Li⁷ (478 keV), total cross section and effective interaction 8=3924
- Li⁷(p,t,He³)Li⁵, He⁸ search for analog states of H⁸ 8=11659
- Mg²⁴(p,α)Na²⁰, Na²⁰ prod. method 8=3865
- Mg²⁴(p,t)Mg²², excited states 8=11883
- Mg²⁵+p → 2 Mg²⁴+d, test of time-reversal invariance 8=11924
- Mg²⁶(p,γ), Al²⁷ resonant state decay, pγγ correl. of γ-rays, E = 10.480 MeV 8=7079
- Mg²⁶(p,t)Mg²⁴, L = 0.2 ang. distrib. shapes energy var. 20–54 MeV 8=1060
- Mn⁵⁵(p,γ)Fe⁵⁶[Fe⁵⁶], 1, 3–1.85 MeV 8=15977
- Mn⁵⁵(p,n)Fe⁵⁵, 510 and 680 keV levels of Fe⁵⁵ rot. obs. 8=3927
- Mo (p,n), 8–14 MeV, cross-section obs. 8=7193
- Mo (p,2n), 8–14 MeV, cross-section obs. 8=7193
- N, spallation, formation ratios of Li, Be and B 8=3922
- N¹⁴(p,He³)C¹³, 43.7 MeV C¹³ transitions spin and parity assignments 8=20791
- N¹⁵(p,n)O¹⁵, check on photodisintegration of O¹⁶ 8=1038
- N¹⁵(p,t), 43.7 MeV, rel. to 2N transfer theory 8=11877
- N¹⁵(p,t), 2N transfer theory, inclusion of spin-depend. forces 8=11877
- N¹⁵(p,t)N¹⁵, 43.7 MeV, N¹⁵ transitions, spin and parity assignments 8=20791
- N¹⁵(p,t(He³))N¹³, C¹³, DWBA approx. 8=20791
- Na²³(p,t)Na²¹, 42 MeV, lowest T = ¾ level in Na²¹, mass determ. 8=20656
- Ne, spallation, formation ratios of Li, Be and B 8=3922
- Ni⁵⁸(p,p')Ni⁵⁸ level anomalies rel. to shell model 8=3928
- Ni⁵⁸(p,pn)Ni⁵⁷, 370 MeV cross-section anomaly explained by nuclear skin thickness 8=20796
- Ni⁶²(p,α)Co⁵⁹, inverse reaction cross section to Fe⁵⁶(α,p)Co⁵⁹ 8=3900
- O, spallation, formation ratios of Li, Be and B 8=3922
- O¹⁶, 130, 550, 19 GeV, prod. of Li, Be, B isotopes, meas. of ratios 8=20792
- O¹⁶(p,d), 100 MeV, spin depend. models compared 8=7188
- O¹⁶(p,p)O¹⁶, lowest states of F¹⁷ 8=3799
- O¹⁶(p,α)N¹⁵, cross-section meas. apparatus 8=3897
- O¹⁶(p,n)F¹⁸, secondary reaction in bremsstrahlung irradi. of water 8=16081
- P³¹(p,α)Si²⁸ fluctuation analysis, no evidence of direct interaction or doorway states 8=11886
- P³¹(p,α_s), Si²⁸, for Si²⁸ target 8=963
- Pb (p,d), isobaric spin forbidden effects 8=20800
- Pb²⁰⁸(p,γ), collective mechanism 8=11875
- Pb²⁰⁸(p,t)Pb²⁰⁶, Pb²⁰⁶ excited levels obs. 8=3839
- Pd¹⁰²(p,2n)Ag¹⁰¹, decay of Ag¹⁰¹ 8=1015
- Pd¹⁰²(p,3n)Ag¹⁰⁰, possible reaction 8=1016
- Pd¹⁰²(p,4n)Ag⁹⁸, half-life of Ag¹⁰⁹ 8=1016
- Pt¹⁹⁶(p,2n)Au¹⁹⁵, stacked foil meas. 8=1066
- Pu isotopes, cross-sections for prod. of Am, ground state and self-fissioning isomers 8=20843
- Rb⁸⁷(p,n)Sr⁸⁷, 4, 1–5.8 MeV, Rb⁸⁸–Sr⁸⁸ isobaric analogue reson. 8=16084
- Rb⁸⁷(p,n)Sr^{87m}, compound nucleus—cross sections far below Coulomb barrier 8=1064

Nuclear reactions due to—contd

protons—contd

- Ru⁹⁹(p,n)Rh⁹⁹, γ-ray decay 8=978
- S³⁴(p,γ)Cl³⁵, ang. distrib., resonances 8=11736
- S³⁴(p,γ)Cl³⁵, Cl³⁵ analog states of S³⁵ 8=11735
- S³⁴(p,γ)Cl³⁵, at 2079 keV, pγγ-correlation 8=1063
- Sc (p,n), 8–14 MeV, cross-section obs. 8=7193
- Sc (p,2n), 8–14 MeV, cross-section obs. 8=7193
- Se^{78,80,82}(p,n)Br^{78,80,82}, 3, 6–5.8 MeV, isobaric analogue resonances, Se⁷⁹–Br⁷⁹ 8=16084
- Se⁸¹–Br⁸¹, Se⁸³–Br⁸³ 8=16084
- Si²⁸(p,d)Si²⁷, 27.6 MeV, spectroscopic factors 8=11885
- Si²⁹(p,γ)P³⁰ at energies 1460–1860 keV 8=7192
- Si³⁰(p,γ)P³¹, 0, 5–2.3 MeV, levels of P³¹ 8=11733
- Si³⁰(p,γ)P³¹, excited states of P³¹ 8=961
- Si³⁰(p,γ)P³¹, source of γ rays for resonant absorpt. by P³¹, level parameters 8=15965
- Sr, 730 MeV p, spallation yield of Kr 8=20797
- Sr⁸⁸(p,γ)Y⁸⁸, decay of analogue resonance 8=11754
- Sr⁸⁸(p,xn), isomer ratios 8=11888
- Sr⁸⁸(p,2p,4n) at 660 MeV, giving Kr⁸³ Mössbauer source 8=3817
- Sr⁸⁸(p,p3n), isomer ratios 8=11888
- Ta¹⁸¹(p,2n)W¹⁸⁰, 5–17.5 MeV, isomeric levels and decay 8=3828
- Tb¹⁵⁹(p,n)Dy¹⁵⁹, 5–17.5 MeV, isomeric levels and decay 8=3828
- Th, Li⁸ prod., 660 MeV 8=7194
- Ti^{47,48,49}, photoproton yield 8=7168
- V⁵¹(p,n)Cr⁵¹, cross-section, rel. to channelling effects 8=20795
- W and Si crystals, channelling behaviour in 2–30 MeV 8=11954
- W (p,n), 8–14 MeV, cross-section obs. 8=7193
- W (p,2n), 8–14 MeV, cross-section obs. 8=7193
- Y⁸⁹(p,γ)Zr⁹⁰, evidence for isobaric splitting of giant resonance 8=11753
- Y⁸⁹(p,γ)Zr⁹⁰, 11, 9–13.5 MeV, dipole resonances of Zr⁹⁰ 8=976
- Y⁸⁹(p,n)Zr⁸⁹, 3, 6–5.8 MeV, optical model parameters, Zr⁸⁹ states 8=11889
- Y⁸⁹(p,n)Zr⁸⁹, 5, 503 MeV, low-lying states of Zr⁸⁹ 8=977
- Yb¹⁷³(p,n)Lu¹⁷³, 5–17.5 MeV, isomeric levels and decay 8=3828
- Yb¹⁷³(p,2n)Lu¹⁷², 5–17.5 MeV, isomeric levels and decay 8=3828
- Zn⁶⁸(p,n)Ga⁶⁸, gamma ray ang. distrib. 8=11948
- Zr⁹¹(p,d)Zr⁹⁰, charge exchange 8=20798
- Zr⁹⁶(p,d), 19, 4 MeV, ang. dist. compound to DWBA calc. 8=3929

tritons

- (t,n_γ), (t,p_γ) total and differential cross sections 8=7154
- (t,p), stripping with two nucleon transfer 8=7223
- Bi²⁰⁹(t,α)Pb²⁰⁸, 13 MeV, levels of Pb²⁰⁸ deduced 8=11936
- Ca^{40,42,44,46,48}(t,p), 10–12 MeV isotope transitions 8=1094
- Ca^{40,44}(t,p)Ca^{42,46}, 7.5 MeV, levels and spin assignments of Ca^{42,46} 8=11741
- Ca^{46,48}(t,p)Ca^{48,50} absolute cross sections rel. to f_{γ2} neutron shell closure at N = 28 8=1093
- Ca⁴⁸(t,p)Ca⁵⁰, low lying states of Ca⁵⁰ 8=7083
- Cr⁵⁰(t,α)V⁴⁹, 13 MeV, level structure of V⁴⁹ 8=11750
- Mg²⁶(t,p)Mg²⁸, total cross-section 8=11807
- O¹⁶(t,n)F¹⁸, rel. to prod. of F¹⁸, after n irradi. of LiOH 8=4024
- O¹⁶(t,p)O¹⁸, shell-model amplitudes and relative phases for J = 0⁺, 2⁺ states of O¹⁸ calc. 8=20826
- Pb²⁰⁴(t,p)Pb²⁰⁶, Pb²⁰⁶ excited levels obs. 8=3839
- Si²⁸(t,p)Si³⁰, sign of interaction matrix element 8=3958

X-rays. See Nuclear reactions due to/photons.

Nuclear reactors, fission

- boiler, dynamic analysis 8=16140
- boundary layer turbulence promoters, improved heat transfer 8=21510
- control rods in multiregion reactor cores, worth evaluation by diffusion codes 8=4012
- control rods., studies on effectiveness 8=7321
- critical expts., organic-moderated assemblies 8=7316
- Dancoff corrections for square and hexagonal rod lattices 8=4006
- DIDO source, n intensity improvement by rethermalization 8=20556
- Doppler-broadened functions, calc. 8=11616
- Doppler effect, maximum 8=11615
- epithermal absorpt. by control rods, black-white model for calc. 8=12008
- fast, large, Na-cooled reactors, dynamic anal. stability and safety factors 8=20862
- fast reactor, reactivity effects in empty channels 8=12006
- foils irradi. in reactor beam, rig for meas. of emitted disintegrating nuclei 8=4031
- gamma rays heating calc. 8=7345
- γ-ray meas. with Ge detectors 8=1127
- GETR, core change effects on neutron spectra 8=7270
- heat source for m. h. d. generator 8=10839
- high-temperature type, gas cooled, fuel cycles 8=20906
- intrinsic thermocouples, transient response 8=10786
- JEN-2, pulsed determ. of parameter, α=β/1* 8=20882

Nuclear reactors, fission—contd

- kinetic behaviour in reactor with two loosely coupled cores, rel. to first-flight neutrons 8=16148
 leak-rate testings on containment vessels, calc. methods and results 8=20907
 light water type, macroscopic flux distrib., single $1\frac{1}{2}$ group model 8=20867
 Milne problem with anisotropic scatt., applic. of variational principle 8=11994
 n branching processes, statistical theory 8=11998
 neutron density fluctuations, application of slowing down kernels 8=16158
 neutron diffusion in non-absorbing moderator 8=15850
 neutron flux-densities and its appl. 8=11609
 n flux meas., correction for depression caused by probe introduction 8=7299
 n flux monitoring by N^{16} content in cooling water from $O^{16}(n,p)N^{16}$ reaction 8=7338
 neutron noise anal. in heterogeneous systems, infinite lattice and detector perturb. 8=11985
 n spectra in plain water-Fe-water shield layers, space-depend. calcs. 8=20879
 n spectrometer, LiF crystal 8=3724
 neutron spectrum deformation analysis using threshold detector data 8=3456
 neutron spectra, review 8=7269
 NORA reactor, prompt n decay const., meas. by interval distrib. tech. 8=4010
 pebble bed reactor, neutron flux density 8=11982
 plain water-Fe-water shielding layers, multigroup-diffusion calcs. 8=20878
 pulsed neutron source, thermal, design 8=7282
 radiation field in shields, from meas. at limited mono-directional beam 8=20908
 RI, heavy water, study of 18 cold moderator combinations 8=7315
 reflected reactor, pulsed source reactivity meas. 8=4009
 researches, pulsed neutron method 8=12020
 rocket engines, gaseous-core, nuclear analysis 8=5823
 Rossi- α experiment 8=4027
 space flight, thermionic convertor reactor 8=1122
 steady-state and pulsed, appl. as research instruments 8=7319
 structural engineering research facilities 8=4034
 subcritical assemblies, n-wave propag., eigenfunction anal. 8=11986
 thermal n flux distribution and flux trap effect in active core of UA-RR-1 reactor 8=20871
 thermal-n flux, effects of moderator temp. grads. 8=11996
 thermionic converter for space flight, temp. distrib. 8=1117
 thermionic converter for space flight, parameters 8=1123
 in-core thermionic converters, irradi. studies in UO_2 -fueled Mo emitters 8=15226
 thermionic, for space craft power supply 8=1115
 thermionic, for space flight, with radiation cooling, review 8=1114
 track detectors, solid-state 8=12021
 TRIGA Mk. II, radial neutron temp. distrib. 8=12007
 TRIGA reactors, stochastic fluctuations in power pulses 8=12004
 TRIGA type, delayed-n fraction-n lifetime ratio, meas. from noise anal. 8=12005
 water shields containing ducts, behaviour of thermal n by source-separation techs. 8=12022
 water type, power noise spectra in l.f. region 8=7320
 Windscale AGR, G-(C) values for grade A and other graphites 8=16154
 Al, fragments, energy loss rel. to range 8=2021
 Ag, fragments, energy loss rel. to range 8=2021
 Au, fragments, energy loss rel. to range 8=2021
 Be assembly, anal. of n pulse decay via energy-depend. mean lifetimes 8=7332
 BeO assemblies, pulsed, decay constants 8=7313
 with D_2O -moderated lattices, n spectral indices, thermal and epithermal 8=20866
 F^{18} prod. from n-irrad. of LiOH, in reactions $Li^6(n,\alpha)H^3$ and $O^{16}(t,n)F^{18}$ 8=4024
 Ni, fragments, energy loss rel. to range 8=2021
 U^{235} multiplying assembly, position depend. thermal n spectra 8=11999
 U^{238} capture rates, absolute determ. 87348
 U- H_2O subcritical assembly, meas. of Cd ratio 8=7314
 U-Pd, fragments, energy loss rel. to range 8=2021
 UO_2 /sheath heat transfer 8=7339
 Xe spatial oscillations linear analysis 8=7333

materials

- alkali metals, liquid, heat transfer efficiency 8=8049
 coolants, CO_2 , He, H_2O compared 8=20888
 coolant, gas and liquid compared 8=20887
 deuterium, thermal neutron capture, cross-section 8=6988
 extraction of NO_2 , U and fission prods. with tri-n-octyl-amine, temp. effects 8=5708
 fast reactor, irradiated fuel meltdown 8=20902
 fuel, acoustical thermometer 8=4018
 fuel burning up rel. to fission prod. migration 8=16164
 fuel burnout, pool boiling, nonhydrodynamic aspects 8=7343
 fuel elements, integral superheat 8=7337
 fuel elements with liquid metal coolants, temperature fields 8=7329

Nuclear reactors, fission—contd materials—contd

- fuel element temperature calculation methods 8=7277
 fuel element with variable axial mechanical stress of canning tube, simulator 8=20896
 fuel particle coated, influence of creep 8=20900
 fuel particle coating for 'Dragon' expt. 8=7336
 fuel particles, spherical, of carbides or mixed carbides, from solutions of metal salts 8=16166
 fuel pin temp. meas. by thermocouple 8=4029
 fuel rod in narrow annular coolant channel, stability against thermal buckling 8=12011
 gas cooled, fuel cluster, coolant flow resistance 8=1131
 gas with micron sized particles for heat transfer, behaviour 8=21735
 grain boundary gas bubbles, equilib. conditions 8=1986-9
 graphite, anal. of escape behaviour of Xe captured by nuclear recoil 8=4017
 graphite and cadmium shielding for γ -rays 8=1128
 graphite, diffusion of fission products Xe and I 8=12015
 graphite, Grade A, deform. props. 20-2200°C 8=8829
 graphite moderator, neutron diffusion across temp. discontinuity 8=20872
 graphite, n slowing down time, influence of chem. binding effect 8=7330
 graphite, optical absorpt. rel. to n-irradiation effects 8=14202
 graphite scatt. kernels, comparison via time depend. n spectra 8=16147
 graphites in Windscale AGR, G-value for radiolytic oxidation 8=16154
 heavy water level meas. telemeter 8=1135
 hydrogenated terphenyls as coolants, effects of e-irrad. 8=14445
 neutron moderation length, effect of empty channels 8=208
 nuclear science and technology for ceramists, conference, Washington USA (1966) 8=16167
 pin clusters and rod lattices, collision probabilities 8=7298
 polystyrene, cold neutron cross-section 8=7271
 polyethylene, cold neutron cross-section 8=7271
 rare gas diffusion eqns. following irradiation 8=13404
 rod cluster fuel elements, reson. integrals, initial conversion ratios 8=4023
 spent fuel elements as γ sources in irradi. plants 8=16163
 spent fuel, selective sampling for core burnup and conversion ratio determ. 8=20901
 water, neutron thermalization meas. 8=7331
 Zircalloy-2 corrosion in LiOH solns. rel. to pressure tubes hydriding 8=5719
 Al, γ -ray spectra obs. 8=7345
 Al-Dy-U system, use of Dy as burnable poison 8=13060
 Al-Li alloys, neutron irradi., grain boundary migration and gas bubble growth 8=8456
 Be low temp. moderator, decay of neutron pulse 8=20905
 Be moderator, neutron diffusion across temp. discontinuity 8=20872
 Be reflected, Zr moderated, parameters for thermionic conversion 8=299
 BeO assemblies of bucklings, decay of thermal neutron population 8=16159
 BeO dispersion fuels, fission fragment and β ray damage, X-ray study 8=12018
 D_2 age and fast effect 8=16160
 D_2O age and fast effect 8=16160
 D_2O viscosity at pressures 1-1200 kg/cm², 4-100°C 8=16806
 Dy_2O_3 dispersion in UO_2 , behaviour in steep temp. grad. 8=4694
 Eu_2O_3 dispersion in UO_2 , behaviour in steep temp. grad. 8=4694
 Fe, γ -ray spectra obs. 8=7345
 Hf, ore deposits in Republic of South Africa 8=9792
 K, natural convective boiling 8=12013
 Na ejection from reactor cooling channels 8=16162
 Na, natural convective boiling 8=12013
 Na, study of aerosol prod. by burning, rel. to safety 8=12950
 Na-K eutectic liquid metal alloy reactor coolants, role of impurity admixtures 8=7328
 NaK, flowing through unbaffled rod bundles, heat transfer to 8=21649
 Nb alloys, mechanical and thermal props. 8=5082
 Pb, γ -ray spectra obs. 8=7345
 Pu compounds, undermoderated, criticality 8=20897
 Pu glovebox, thermal gradient apparatus 87334
 Pu isotopes, effect on Doppler coeff. 8=7340
 Pu, study of aerosol prod. by burning, rel. to safety 8=12950
 Pu/1 wt.% Ga alloy, rel. to plastic flow props. from -60 to 77°C 8=13604
 Pu-Al alloy fuel, depleted, atom ratios and effective cross-section ratios 8=12016
 Pu-Be, n emission growth rel. to presence of Pu^{241} 8=16169
 Pu(N and S) fuels, chem. aspects 8=12017
 Pu/U, graphite moderated using lattice code WIMS 8=1133
 Pu^{238} , neutron total and absorption cross sections 8=7335
 Pu^{238} , separation and preparation from n irradiated Np^{237} target 8=20903

Nuclear reactors, fission--contd**materials--contd**

- Pu²³⁹, capture to fission ratios meas. 8=1132
 SiO₂-UO₂ vitroceraamics, irradi. induced vol. changes and annealing 8=8779
 Sm₂O₃ dispersion in UO₂, behaviour in steep temp. grad. 8=4694
 ThO₂ based fuels, vib. compacted sol-gel-derived, props. and prospect 8=20895
 ThO₂-UO₂, in-reactor microstructure for thermal simulation 8=1130
 U enrichment in fuel problems 8=20889
 U enrichment by gaseous diffusion 8=20890
 U enrichment technology in Japan 8=20891
 U, graphite moderated using lattice code WIMS 8=1133
 (U/Al) fuel alloys, use of Sm as burnable poison 8=13059
 U-M alloys, (M=Fe, Al and Si), irradiated, phase comp. changes rel. to resistivity meas. 8=8283
 U(N, P and S) fuels, chem. aspects 8=12017
 U²³⁵, ²³⁸ capture and fission, Doppler effect obs. 8=7248
 U²³⁵, new production techniques 8=20892
 U²³⁵, prompt n emission 8=20853
 U²³⁵ thermal neutron fission, total γ energy release 8=7247
 U²³⁷, enriched, prod. and specific activity 8=16165
 U²³⁸ shielding effect on epi-cadmium fissions in U²³⁵ and Pu²³⁹ 8=7246
 U^{VI} extraction by methyl propyl ketone 8=20898
 UC rods, fast fission ratios meas. 8=16170
 UC rod, temp. coeff. of resonance integral 8=12019
 UC¹⁴, C¹⁴ determ. 8=12014
 U_L, α self irradiation 8=17105
 UO₂, burnup, mass spectrometric determ. 8=7344
 UO₂, fission-gas release, activation energies in defect-trap model 8=3980
 UO₂ fuelled cores moderated by H₂O, material buckling and reaction rates 8=20904
 UO₂, irradi., microstruct. 8=8469
 UO₂, in-reactor microstructure from thermal simulation 8=1130
 UO₂ pellets, irradiation obs. 8=20883
 UO₂ powder compacted fuel, effective thermal cond. in simulated conds. 8=13398
 UO₂, calc. of temp. depend. shear modulus 8=13610
 UO₂, U ions diffusion, lattice and grain boundary, 1900-2150°C 8=13414
 UO₂-graphite mixture, fission gas (Xe and Kr) release during irradi. 8=4022
 UO₂-graphite pellets, n-irradi., γ -ray spectra of fission gases 8=4016
 UO₂ swaged compacts, equiaxed grain growth under temp. grad. 8=8255
 UO₂-SiO₂ vitroceraamics, thermal cond. 8=8664
 UO₂-stainless steel cermet, irradi. behaviour of particles to 4-10% burn-up 8=20893
 UO₂-ZrO₂-CaO fuel system, out-of-pile thermal tests 8=17527
 U-Pt fuel plate, spatial average ion prod. rate by escaping fission fragments 8=11968
 U₂Si, prep. from UCl₄, as first step in prep. of U₂Si 8=23114
 U₂Si, promising fuel for water-cooled reactors 8=4019
 U-Th mixtures, quantitative analysis by delayed n emission 8=12012
 Zr, ore deposits in Republic of South Africa 8=9792
 Zr for pressure tube technology 8=4020
 ZrH, diffusion parameters and capture cross section 8=16161

operation

- activity of radioisotope after n bombard., hybrid computer calc. 8=4025
 circumferential control plates, anal. of mutual interact. 8=16155
 computer programme for time optimal control 8=4015
 control systems, optimization, by Wiener's theory 8=7327
 cooling channels ejection of Na 8=16162
 cooling systems, hydraulic design calc. 8=16156
 criticality detector, n-sensitive 8=7324
 crossed-in-line tube bundles, heat transfer and pressure drop 8=7325
 Daphne reflector, fast-neutron spectra, experimental and calculated 8=12009
 digital techniques in instrumentation 8=6624
 direct conversion heat source 8=295
 E Fermi, pressurized water, power exhalation 8=1126
 FR2 optimisation of efficiency, second core of UO₂ 8=4013
 fast critical experiments and their analysis, Conference, Argonne National Laboratory, Oct. 1966 8=7240
 flowmeter, magnetic for Na-cooled 8=7317
 γ , n field dosimetry 8=11313
 Garigliano, core performance and safety margins at increased output 8=1124
 gas as heat transport medium, Conference, London, March 1967 8=7326
 generator, pulse rate 8=3144
 heat transfer to thermionic converter, simulation apparatus 8=1134
 Latina, core reactivity build up, expt. determ. 8=1125

Nuclear reactors, fission--contd**operation--contd**

- n counting system containing fission detection 8=4028
 n flux meas. channel detection 8=4026
 n spectrometer for polyethylene-beryllium cooled moderator 8=3725
 neutron slowing-down times in water 8=1129
 point, Xe- and temp.-controlled, rel. to asymptotic stability 8=16157
 pressure tube technology, use of Zr 8=4020
 recombination system of H₂-O₂-gases in BER reactor 8=4014
 stability analysis, sampled-data controlled system 8=7322
 stability analysis, sampled-data controlled system 8=7323
 stresses, acoustically induced, meas. with piezoelectric strain gauges 8=20884
 thermal gradient apparatus for Pu glovebox 8=7334
 thermionic, Ar-filled, thermionic converter 8=298
 thermionic for space flight, criticality and n flux density 8=1116
 vibr. of high pressure gases, piezo-electric transducers for meas., temp. limitation 8=20885
 vibr. problems in commissioning Dungeness power plant 8=20886
 N¹⁶ power control system 8=4011
 PuBe n source, scattering moderator effect 8=1121
- theory**
- asymptotic stability of coupled reactor 8=20865
 Boltzmann eqn. in plane geometry with linear-anisotropic scatt. funct. 8=135
 burnout, alternative forms for correls. 8=12003
 collision probabilities for finite cylinders and cuboids 8=11993
 collision probabilities, first-flight, in pin clusters and rod lattices 8=7298
 collision probability code, Minos program 8=7295
 coolant and fuel element temp., calc. from convection and radiation 8=7342
 critical system, perturbation formula for changes in freq. ratios of processes 8=16144
 critical systems, reactivity integral theorem 8=16153
 criticality in heterogeneous media 8=7272
 cross- and autospectral density obs. 8=16141
 cylindrical reactors, boundary value problems in p- ρ geometry 8=3989
 design, nuclear calc. 8=3987
 dynamic parameter estimation 8=11989
 eigendistributions in slowing down theory, with continuous energy variable 8=20876
 Enrico Fermi PWR, theoretical and experimental transients 8=20881
 fast, collapsing many-group n cross-sections to few-group cross-sections 8=3997
 fast critical experiments and their analysis, Conference, Argonne National Laboratory, Oct. 1966 8=7240
 fast system, power build-up rel. to core isotope comp. and fuel management 8=20863
 finite moderator, iterative method of multipole source-sink calc. 8=4021
 fuel elements with liquid metal coolants, temperature fields 8=7329
 fuel element temperature calculation methods 8=7277
 generalized albedo method, applications 8=15023
 Green's funct. with boundary conds. containing non-normal directional derivs. 8=6017
 heterogeneous, two-zone, compact, anal. method for calc. 8=7279
 hot-channel factors, for "flat" power reactors 8=7280
 kinetics according to P₁-approximation 8=3990
 kinetics eqn, two-point approx. for coupled reactors 8=7268
 Lie series application 8=7309
 long-term change of basic parameters 8=12001
 low power, sinusoidal anal. by WKB approx. 8=7289
 low temperature, design and operation 8=7283
 Milne's problem for 2 adjacent spaces, solution 8=1119
 model for estimation of states and parameters 8=3988
 monoenergetic neutrons, extrapolation distance, calc. 8=11979
 Monte Carlo analysis of reactor systems 8=7291
 multigroup diffusion theory, boundary perturbations 8=4001
 multigroup n transport eqns., convergence of source iteration tech. in soln. 8=11997
 multi-region, multi-group reactors, Fortran IV programme 8=16142
 natural mode approximation applied to space-time problems 8=7290
 neutron counting statistics, interval distrib. 8=7276
 neutrons, delayed, effective fraction rel. to source strength 8=16145
 neutron flux, at plane black boundary, boundary conditions 8=6947
 neutron leakage from 2-dimens. system, collision probability calc. 8=7296
 neutrons, low-energy, heating up in cryst. moderators 8=7293
 neutron multiplication, new concept for subcritical system with reflector 8=7275

Nuclear reactors, fission—contd
theory—contd

- neutron path length probability calc. 8=15011
- neutron pulse decay in moderator, anal. via simple model 8=4007
- neutron scatt. in media with spherical geometry, Boltzmann eqn. soln. 8=20542
- neutron scattering multiple, calc. using combination of Monte Carlo and analytical methods 8=6946
- neutron slowing down, multiple collision soln. 8=7304
- neutron space-time group diffusion eqns., soln by time-discontinuous techn. 8=4002
- neutron spectra in D_2O , time-dependent 8=6948
- n source width, perturbation method analysis 8=20873
- neutron streaming, pulsed-source technique 8=7273
- neutron thermalization, in Be, analysis 8=7303
- neutron thermalization, initial value problem 8=11980
- neutrons, thermalized, population kinetics in heterogeneous media 8=4000
- neutron transport eqns., two-group 8=11991
- neutron transport, invariant imbedding method 8=7307
- neutron transport operator in spherical assembly, fundamental mode 8=7302
- n transport operator fundamental mode calc. 8=20877
- neutron transport in plane geometry 8=20547
- neutron transport equation, time behaviour and ergodic theory of semigroups 8=3992
- neutron transport, two-region problem 8=7306
- neutron transport, two-region problem 8=7305
- neutron transport, variational problems, transforms. 8=7308
- noise-equivalent source 8=3991
- noise, threefold correls. and third order moments 8=11984
- noise in zero-power reactor, equiv. source 8=3995
- nonlinear reactor dynamics 8=11987
- particle sources, anisotropic, path-length formalism 8=7284
- plane-parallel core, analysis of equations 8=7278
- point reactors kinetics eqns. soln. by analytic continuation 8=4008
- pulsed, n pulse half-width calc. 8=3996
- reactor group cross sections calc. 8=20864
- real and adjoint n fluxes, bi-linear functionals, perturb. anal. 8=7294
- reflected lattice of moderator, heterogeneous theory of n spectrum 8=4004
- reflected slab, reactor kinetics 8=20870
- Rossi- α expt., point reactor theory 8=7300
- slow neutron spectra determination from foil activations 8=846
- spherical-cavity, prompt n population, time depend. kinetics 8=4003
- stability domains, in point reactor dynamics 8=7301
- thermal-group constants in three-region lattices, calc. 8=11988
- thermoelastic dynamics, pulse reactor 8=7281
- time decay, constant in pulsed multiplying assemblies 8=1120
- wave propag. in graphite, effects of Bragg cut-off 8=7285
- D_2O lattices, RESCUE method for resonance escape probability calc. 8=20880
- Na-cooled fast reactor kinetics 8=12002
- Pu^{240} , neutron resonance escape probability, Monte Carlo calc. 8=16152
- U lattices, H_2O moderated, microparameters, δ^{25} , δ^{28} , ρ^{28} , semi-emp. formulas 8=7274
- UO_2 lattices, H_2O moderated, microparameters δ^{25} , δ^{28} , ρ^{28} , semi-emp. formulas 8=7274

Nuclear reactors, fusion

- burn-out under transient condition, film flow model prediction 8=20861
- engineering and economics 8=16138
- leakage, magnetic bottles 8=7318
- plasma, sputtered atom impurities, search with neutrons 8=16600
- two group diffusion code with burnup, MAGOG, 3-d 8=20868

Nuclear relaxation. See Nuclear magnetic resonance and relaxation.**Nuclear-solid interactions.** See Mössbauer effect; Solids.**Nuclear spallation**

- complex nuclei, mechanism 8=1028
- hypernuclei prod. by 6 GeV/c K⁻ on heavy emulsion 8=3949
- Ag, induced by 1, 2, 3 GeV p obs. 8=11891
- Ag, p 200-400 MeV, Pa, Ag prod. 8=11892
- Br, induced by 1, 2, 3 GeV p obs. 8=11891
- C^{12} , by 70-200 MeV protons 8=1058
- In, p 200-400 MeV, Pa, Ag prod. 8=11892
- Ni^{58} (p, pn) Ni^{57} , 370 MeV cross-section anomaly explained by nuclear skin thickness 8=20796
- O^{16} , by 70-200 MeV protons 8=1058

Nuclear track emulsions

- antiproton scattering 8=1050
- chamber for about 10^{13} eV particle interactions 8=627
- cosmic ray stars in photographic emulsion at high altitude 8=15882
- dosimetry use of small β rad. doses 8=1001
- hole diameter meas. for particle energy 8=11293

Nuclear track emulsions—contd

- ionization loss at relativistic vel. by π , p beams 8=15647
 - K⁻ interaction, Ξ intermediate hyperfragment production 8=11912
 - latent image, erasure by pulsed elec. field 8=11330
 - n-p interaction 20 GeV, multiple meson production 8=831
 - Ag nuclei interaction with 9 GeV protons, d emission obs. 8=15867
- Nucleation.** See Clouds; Crystallization; Freezing.
- Nucleic acids.** See Macromolecules.
- Nucleons and antinucleons**
- See also Neutrons and antineutrons; Protons and antiprotons.
 - β -decay in presence of strong interactions, e.m. corrections 8=11581
 - boson-N coupling parameters from N-N scatt. potential 8=3700
 - Compton effect amplitude sum rules 8=6942
 - coupling constant e.m. isobar-N 8=15864
 - coupling constant, η -N in $\pi^- + p \rightarrow n + \eta$, $\gamma + p \rightarrow p + \eta$ 8=20490
 - decay, leptonic, weak, pole-dominance version of PCAC hypothesis 8=3696
 - distribution in nuclei by finite Fermi system theory 8=7036
 - e.m. form factor, Regge-pole model 8=3693
 - e.m. form factors and γNN^* (1238) coupling constant 8=3733
 - e.m. isovector form factor from π - π scatt. 8=11578
 - e.m. mass splitting rel. to n-p mass difference 8=11587
 - form factors, analytic continuation 8=820
 - form factors dominated by $N^*(1400)$ resonance, tested by calc. of $g_{\gamma NN}/g_{\gamma NN}$ 8=20515
 - form factor, e.m. asymptotic behaviour examined with superconvergent sum rules and $SU(6)_v$ 8=20514
 - form factor e. m. form special mixing scheme for $U(3) \otimes U(3)$ algebra 8=20253
 - form factor, magnetic, isoscalar, fitted with poles 8=3694
 - $g_{\gamma NN}/g_{\gamma NN}$ calc. rel. to domination of N form factors by $N^*(1400)$ 8=20515
 - internucleon forces and n-d scatt. length 8=11648
 - isobar decay, effect of cosmic γ spectrum 8=23489
 - isoscalar form factor from $O(4, 2)$ dynamics 8=6919
 - K-N coupling constants from 2 sum rules for meson-N scatt. 8=20469
 - $\Lambda\pi$ and $N\bar{K}$ composite model of Σ 8=11633
 - and leptons form factors and structure effects in vacuum polarization 8=588
 - magnetic moment, isovector anomalous, sum rule 8=3698
 - meson-N coupling constant calc. in non-linear spin theory 8=20288
 - N_σ Regge exchanges rel. to π^+p backward elastic scatt. 8=15778
 - $N \rightarrow N^*(1238) + (\text{virtual } \gamma)$, M1 form factor, asymptotic behaviour 8=20514
 - $N \rightarrow \pi + N$ form factor rel. to self-consistency theory and bootstrap dynamics 8=3703
 - $NN^*\pi$ dynamics, bootstrap model, e. m. perturbation effect 8=11486
 - N^*pNN , pNN^* , pNN^*_s coupling from current algebra 8=11564
 - $N^*N\gamma$ (1238) coupling constant current algebra calc. 8=3733
 - optical potential in nucleus from n scatt., 25 and 96 MeV 8=924
 - photo-absorpt. sum rule 8=3577
 - π -N coupling constant from N-N scatt., anomalies 8=20519
 - π N coupling constant related to that for πNN^* 8=11554
 - pole in $\pi^- + p \rightarrow n + \eta$, $\gamma + p \rightarrow p + \eta$ 8=20490
 - prod. in $pp \rightarrow YKN$, OBE model with approx. 8=20522
 - quark model, form factor derivation 8=3695
 - Regge-pole couplings, field theory model 8=20326
 - saturation of axial change commutators 8=3520
 - scalar, two, rel. to scatt. and infinite dimensional Lie algebra 8=658
 - σ meson coupling constant calc. 8=11554
 - size and ρ -meson dominance 8=11580
 - sum rule $N-N^*$ and $N^*\pi$ photoprod. 8=11504
 - sum rule, saturation assumption 8=819
 - $T = \frac{1}{2}$ isobar, search for in np interactions 8=3699
 - trajectory with D-wave π N resonance 8=20328
 - transfer reactions, single, between complex nuclei 8=16127
 - 2N nuclear emission process following π^- interaction 8=11913
 - trineutron, S' state, relative probability from charge form factors and μ capture rate 8=20583
 - 3N system, wave function determ. 8=20589
 - 3N wave-function, evidence from μ capture rate by He^3 8=20393
 - trineutron wave-function partial differential eqns. 8=880
- interactions**
- e-N, meson field model of excitation 8=3697
 - eN $\rightarrow eN$ amplitude reconstruction from expt. data 8=6803
 - $\gamma + N \rightarrow \Lambda + K$, consistency conditions for non-Born amplitudes 8=20344
 - $\gamma + N \rightarrow \pi + N$ 8=11507
 - $\gamma N \rightarrow \pi N$, test for conspiracy 8=6775

Nucleons and antinucleons—contd**interactions—contd**

- $\gamma N \rightarrow \pi N^*$, threshold cross-section calc. from current algebra 8=11504
 $\gamma + N \rightarrow \pi^+ + N, N^* + \pi$, varying γ polarization as test for Regge cuts 8=20331
 $\gamma + N \rightarrow \Sigma + K$, consistency conditions for non-Born amplitudes 8=20344
 $K\bar{N}$, current algebra calc. of Λ/Σ ratio 8=15858
 $KN \rightarrow K^*(890)N$, 3 GeV/c, absorpt. model, π and vector meson exchange 8=6889
 KN , multichannel phase-shift analysis from 0-555 MeV/c 8=3663
 $\bar{K} + N \rightarrow \Sigma + \pi$, use of dispersion relations and Regge trajectories to calc. Y_0^* BP coupling 8=20580
 Λ -N rel. to hypernuclear binding energy 8=20734
 Λ -N rel. to Λ nuclear pot.-well depth 8=11795
 ΔN , nuclear, C violation and existence of ${}_{\Lambda}Li^0$ 8=11793
 ΛN , 2 π and K range, calc. from ${}_{\Lambda\Lambda}Be^{11}$ hypernuclear events 8=3649
 ν -N interaction, with formation of μ , spin depend. 8=20370
 $\nu_1 + N \rightarrow N^* + l, N^*$ polarization 8=3586
n-d scatt. length using pot. with several variables 8=881
N-neutral pseudoscalar mesons, sum rule in perturbation theory 8=821
N pair correl. effect on 2 N transfer (pick-up) nuclear reactions 8=16053
NAK and NEK coupling constants determination 8=3664
N-N pot. determ. for nuclear forces 8=11684
 $N^*(2825) \rightarrow \rho + N^*(1236)$, cascade decay, theory 8=3734
nuclear, Kuo-Brown, analysis generation of states of O^{18} and F^{18} 8=3759
nucleus, pair absorpt. of pion and emission 8=16102
nucleus, π -N, rel. to nuclear structure 8=1086
particle-hole in nucleus, disagreement with Q-Q force 8=11683
with photons, to form K and π mesons 8=6842
 $PN \rightarrow P^*N$, VN Regge pole model 8=20318
 π electroproduction as function of momentum transfer 8=6840
 π photoproduction at high energy, O(4) symm. 8=3627
 π photoproduction, pole terms in fixed angle approach 8=3622
 πN channel, P_{11} resonance model 8=11513
 πN charge exchange, applic. of finite energy sum rules for Regge analysis 8=20296
 π -N collisions, multiple π production constraint 8=3619
 $\pi N \rightarrow \rho \Delta$ conspiracy consequences 8=6867
 πN , N/D formula for calc. of Regge trajectory 8=3554
 πN isobar prod. cause of TY anomaly in OPE model of $\pi N \rightarrow \pi \pi N$, 1-10 GeV 8=15770
 $\pi N \rightarrow Ne^+e^-$ amplitude reconstruction from expt. data 8=6803
 $\pi N \rightarrow \pi N^*$, below 1 GeV, ang. distribution using Legendre series 8=6849
 $\pi N \rightarrow \pi N^*$, N^* resonance 8=6849
 $\pi N \rightarrow \pi \pi N$ 1-10 GeV, OPE model, Treiman-Yang angle anomaly due to πN isobars 8=15770
 $\pi N \rightarrow \pi \rho N$, mass distrib. from Regge-pole exchange model 8=20440
 $SU(2) \times SU(2)$, chiral, method of phenomenological Lagrangians 8=6744
triton binding energy using pot. with several variables 8=881
 ΞN , low energy meson exchange plus hard core model 8=6977

interactions, nucleon—nucleon

- boson approx., s and d, in nuclear matter 8=15917
conference, Florida (USA) 1967 8=20516
excited baryons, search 8=20517
low energy, polarized proton target for investigation use 8=822
n-d scatt. length from N-N separable pot. 8=11647
 $NN \rightarrow KK$, predictions 8=825
 $NN \rightarrow MM$, rel. to baryon exchange model of MN scatt. 8=825
 $NN \rightarrow NN_0$ absorptive peripheral model 8=6920
 $NN \rightarrow \pi\pi$ predicted from πN scatt. 8=825
nuclear forces, free-potential, 3-body force inclusion 8=7032
nuclear rearrangement energy 8=923
 π exchange contribution to weak parity violating N-N potential, calc. 8=6922
potential form rel. to nuclear forces 8=15916
potential theory from p-p bremsstrahlung 8=833
separable potential 8=823
three nucleon system, inverse power parameter, perturbation theory appl. 8=11579
t binding energy from N-N separable pot. 8=11647

scattering

- baryon resonance-N from p-He⁴ and B prod. interaction 8=3736
Compton, new low-energy theorems 8=20521
Compton scatt., low-energy with π photoprod., use of $\pi\pi$ phase shift 8=20345
electron scatt., e.m. form factors 8=6941
e-N, inelastic, review of kinematics and sum rules, inequalities 8=20377

Nucleons and antinucleons—contd**scattering—contd**

- e-N inequality 8=6923
 η -n as Regge pole in $\pi^- + p \rightarrow \eta + n$, phase shift calc. 8=20433
Glauber formalism, correction to Johnson-Trieman relation 8=20419
He⁴, high energy scatt. and N-N correlation 8=891
meson-N, amplitude determ., neutral scalar meson models 8=11496
meson-N, amplitude expansion using Lorentz group representation 8=15696
meson-N amplitude at high energy, Regge asymptotic behaviour 8=11495
meson resonance—N from π -He⁴ and meson resonance prod. interaction 8=3736
on mesons, cross-sections, in $SU(3)$, asymptotic limits 8=742
n-d, second quantization formalism appl. 8=11853
n-d, soln. of Fadeev eqns. 8=11403
nuclear, polarization to separate direct and compound nucleus effects 8=1029
KN dispersion relations and coupling constants determ. 8=11550
KN forward dispersion relation for ΛKN coupling constant calc. 8=802
K-N, s-wave absent with t-channel singularities, K-B coupling constants 8=20483
KN superconvergence sum rules and vector meson Regge poles 8=3681
KN superconvergence sum rules and Regge pole parameters 8=3666
K⁺N, dispersion relations, $SU(3)$ invariance violation 8=6891
 ΛN , one-boson-exchange model, cross-section calc. 8=20573
MN baryon exchange model rel. to $NN \rightarrow MM$ 8=825
M-N factor from $\pi + d \rightarrow M + d$ 8=3736
meson-N, 2 sum rules and meson-N coupling constants 8=20469
 μ -N inequality 8=6923
NN phase shifts from Fadeev theory of $NN\pi$ system 8=6925
N-N potential to suit nuclear binding energy 8=3758
 $N\pi$ superconvergence relations for all values of momentum transfer 8=20455
 $NN\pi$ system, Fadeev theory Lovelace approx., phase shifts for N-N scatt. 8=6925
N-nucleus, exchange and Pauli principle effect 8=7179
 ω -N, superconvergent sum rules 8=3553
particle-N cross-sections from π prod. by p on nuclei 8=20778
 πN AW and spin-flip sum rules derived from dispersion relations without current algebra 8=11531
 πN amplitudes, static crossing matrix soln. 8=11533
 πN charge-exchange amplitude in terms of homogeneous Lorentz group 8=766
 πN charge exchange, sum rule for ρ -like singularities in complex J-plane 8=11530
 π -N, differential cross section, charge exchange and high-energy dynamics 8=15786
 πN dispersion sum rules, high energy 8=763
 πN fermion, N and Δ trajectories 8=20328
 πN form factor type contributions to s and p waves 8=765
 π -N, high energy behaviour and Regge pole model 8=6868
 πN interference model description, 2-6 GeV/c 8=11526
 πN integral eqn. reduced to Tarmarkin form, removal of singularity 8=20314
 πN , isospin effects, triangular CI diagram 8=762
 πN , Lagrangians, unified treatment 8=11535
 π -N, multi-GeV, spin-flip parameter determ. 8=11534
 πN , N/D approach, coupling constants 8=761
 πN below 1.6 GeV, elastic, phase-shift analysis 8=20458
 πN , 1-5 BeV/c Regge pole-plus-resonance model, modifications 8=20456
 πN p-wave, low energy by PCAC and CCR 8=11527-8
 πN p-wave low-energy sum rules derived 8=6833
 π -N partial-wave amplitudes, Regge-pole model 8=15784
 π -N phase shift of P_{33} state, CDD pole approach 8=20453
 π -N, phase shift parametrization based on generalized dispersion relation 8=20430
(π , K)-N, phenomenological model of diffraction 8=6894
 πN , π production amplitude, constraints 8=3636
 πN polarization effects 8=15785
 πN pot., generalized computed from known phase shifts for P_{33}, P_{11}, D_{13} partial waves 8=20454
 πN for prediction of $NN \rightarrow \pi\pi$ 8=825
 πN Regge exchange amplitudes rel. to resonance spectrum 8=764
 πN Regge-pole theory, constraint eqns. 8=20321
 π -N resonances, contrib. to helicity amplitude of $\pi\pi \rightarrow NN$ 8=11517
 πN , Roper resonance, magnetic moment relations using dispersion relations 8=3605
 πN , s-wave, low energy, semiphenomenological calc. 8=3641
 π -N, semiclassical theory with ρ, N^{**} prod. 8=20452
 πN sum rules from superconvergence relations 8=3635
 πN superconvergence relations correcting BBM and MMM coupling constant 8=3640
 πN superconvergent sum rules and existence of resonances 8=6866

Nucleons and antinucleons—contd**scattering—contd**

- polarization parameter for N-N, 300-700 MeV 8=6927
- Σ N, one-boson-exchange model, cross-section calc. 8=20573
- 3N-e for charge density function calc. for He^3 8=20393
- scattering, nucleon-nucleon**
 - amplitude expansion using Lorentz group representation 8=15696
 - angular momentum dependent potentials 8=20520
 - KN, Regge secondary poles, cuts and conspiracies rel. to crossover and polarization 8=11529
 - low-energy experiments, use of polarized proton target 8=6924
 - nuclear repulsive core pots., hard and soft compared 8=11691
 - N-N backward, superconvergence relations 8=3702
 - N-N pot. determ. for nuclear forces 8=11684
 - NN, ρ parametrization 8=3683
 - one boson exchange potential 8=3700
 - overlap functions from O_3 to O_{3c} for unitary representations of SL_{2c} as series of Γ functions 8=20264
 - phase-parameter fits up to 350 MeV rel. to π -N coupling constant 8=20519
 - phase shift analysis, 210 MeV, unique soln. obtained 8=20518
 - phase shifts, study of Λ -N weak-interaction 8=6974
 - polarization parameter, 300-700 MeV 8=6927
 - pot. determ. from dynamical singularities of partial-wave amplitudes 8=11397
 - pot., hard or soft core 8=11582
 - pot. which is superposition of meson exchange pole terms 8=11583
 - quark model due to Schiff 8=6826
 - Regge cuts rel. to spin-dependence 8=3701
 - Regge-pole theory, constraint eqns. 8=20321
 - regression planning and discriminating expts. 8=6926
 - 2- π contrib. to low energy, using Mandelstam representation 8=824
 - 3- π -exchange contrib. 8=15824

antinucleons

No entries

Nucleus

See also Elements/origin; Hypernuclei; Radioactivity; Scattering, particles.

- binding energy per nuclear, teaching misconceptions 8=7027
- charge distrib. effect on Fermi function calc. 8=7126
- charge distrib. studied by e scatt. and X-radiation from muonic atoms 8=7069
- charge distrib., suggested halo-effect, p change some distance from nucleus 8=20672
- charge, effective, in light nuclei 8=11711
- compound from $\text{Rb}^{87}(\text{p}, \text{n})\text{Sr}^{87\text{m}}$ cross sections far below Coulomb barrier 8=1064
- current algebra sum rule for light nuclei, possible test 8=3756
- cut-off potential restoration by nuclear-Coulomb scatt. phases 8=3896
- dynamics rel. to X-ray spectrum of muonic atoms 8=20655
- gravitational forces, teaching misconceptions 8=7027
- heavy and medium, conference 8=20640
- internal conversion, finite nuclear size effects 8=7061
- Levinson's theorem, validity for superimposed Yukawa and Coulomb repulsion potentials 8=938
- Lipari Summer School in theoretical Physics 1966 8=7028
- masses of 21 isospin quartet (F^{21} , Ne^{21} , Na^{21} , Mg^{21}) and Ar^{37} , K^{37} , Ca^{37} in $\frac{3}{2}$ levels 8=20656
- matter, reaction matrix calc. with 3-body cluster corrls. applied 8=11696
- nuclear matter, α -particle model 8=11650
- pair energies for spherical and deformed nuclei $100 < A < 256$ calc. 8=11702
- polarization, higher order core processes and effective interactions 8=7070
- p content, e scatt., charge density, magic numbers, Born-approx. modification 8=15950
- proton probe, high-energy 8=11604
- quadrupole-deformed, separation of surface and vol. vibs. 8=3781
- spherical to nonspherical phase transform, theory 8=3776
- structure and high-energy physics, conference Israel 1967 8=15672
- structure from high energy probes 8=7052
- structure and research 8=15924
- structure from two-nucleon phase shifts calc. 8=11681
- surface, moments Y_{λ} , evidence from HF calc. 8=7033
- surface properties rel. to π prod. in p scatt. 8=20778
- surface, time derivatives of parameters used in fission Hamiltonian 8=7241
- Thomas-Fermi realistic approach, finite 8=15914
- weak nucleon-nucleon forces, possible test for existence 8=939
- Am^{242} , study through $\text{Am}^{241}(\text{n}, \gamma)$ reaction 8=11792
- B^7 , ground state, mass and width, by reaction $\text{B}^{10}(\text{He}^3, \text{He}^4)\text{B}^7$ 8=11720
- Be^8 ground state search using $\text{He}^3(\text{He}^3, \text{n})$ at 18.0-26.0 MeV 8=3790

Nucleus—contd

- Ca^{49} , ground-state analogue 8=15969
- F^{19} , surface, var. of absorpt. pot. energy for p scatt. fit 8=7182
- $\text{He}^3 + \text{H}^3$ current algebra sum rule, possible test 8=3756
- Hg in Fe, internal field 8=16002
- Li^6 ground state wave function α -d cluster model 8=15954
- Na^{20} , mass excess 8=20745
- Sc^{49} , ground-state isobaric analogue resonance from $\text{Ca}^{48}(\text{p}, \text{n})$ obs. 8=15972
- Si^{28} ground state and density dependent forces 8=7081
- Sm^{145} data rel. to Eu^{145} radiation 8=16037
- Ta^{181} , g-factor measurement by differential perturbed angular correlation 8=7066
- electric moment**
 - See also Molecules/nuclear coupling.
 - asymmetric-rotor model for deformed even nuclei 8=999
 - atomic shielding factors 8=1155
 - odd A-nuclei quadrupole moments rel. to unpaired particle contrib., to deform., $153 \leq A \leq 191$ 8=927
 - quadrupole charge and quad.-quad. interaction const., calc. 8=942
 - quadrupolar spin-1, locus of magnetization vector calc. 8=7067
 - quadrupole effect on atomic hyperfine spectrum through induced e quadrupole moment 8=7402
 - quadrupole, of even-Z nuclei, optical spectroscopy meas. 8=7068
 - quadrupole of excited states, corrections in Coulomb excitation 8=15940
 - quadrupole interaction with axially symm. field, symmetry test 8=3775
 - quadrupole, mean field influence on nuclear deformation 8=7059
 - quadrupole, static, of projected deformed states 8=15935
 - quadrupole, static, of vibr. even nuclei and odd nuclei coupling scheme 8=11710
 - 2 $^+$ phonon quadrupole moment, rel. to odd-mass nuclear struct. 8=20670
 - $\text{Ca}^{40, 42, 44, 46, 48}$, 31 MeV α scatt., new octupole states 8=3807
 - Cu^{63} , quadrupole in $(3d)^{10}4p^2\text{P}_{3/2}$, polarization corrections 8=12061
 - $\text{Cs}^{131, 132}$ quadrupole moments, h.f. s. spectroscopy 8=20719
 - Dy^{161} , 75 keV state, quadrupole determ. 8=3829
 - Er^{162} intrinsic quadrupole from ErI and ErII line isotopic shift obs. 8=3830
 - Fe^{56} , dipole absorpt. function for γ -rays 8=3811
 - Fe^{57} in $\text{FeSiF}_6 \cdot 6\text{H}_2\text{O}$, from quadrupole splitting of Mössbauer spectra 8=8220
 - Fe^{2+} , cubic, quadrupole interaction rel. to mag. ordering 8=21803
 - $\text{Li}^{6, 7}$, 100-600 MeV e elastic scatt., quadrupole fit 8=1047
 - Li^7 , quadrupole, h.f. calc. 8=3789
 - Lu^{172} , quadrupole of the $\text{K}^{\pi}-\text{O}^{\pi}$ state 8=3834
 - Na^{23} in vanadates, quadrupole coupling constants 8=9474
 - Ni even isotopes, 2 $^+$ level 8=3824
 - Np^{237} ratio between 59.54 keV level and ground state 8=11790
 - $\text{Sm}^{150, 152}$, quadrupole, mean field influence on nuclear deformation 8=7059
 - Sn even isotopes, 2 $^+$ level 8=3824
 - Tm^{170} , Q_0 for K = 1 band from d scatt. 8=7106
 - V^{51} quadrupole moment and effective E2 transition moments 8=968
 - V^{51} in vanadates, quadrupole coupling constants 8=9474
- energy levels**
 - See also Radioactivity/decay schemes.
 - A = 4, structure 8=15874
 - from (α, n) reactions, level density parameters from n spectra 8=7232
 - analog states from B^{11} induced single N transfer reactions on $\text{C}^{12, 13}$, $\text{N}^{14, 15}$, O^{16} , Ne^{20} 8=11951
 - β -radiative, radiation asymmetry and n.m.r. 8=7128
 - β -transitions, second forbidden contrib. 8=1005
 - collective vibration and of nucleons, effective interaction and change, exact calc. 8=11683
 - Coulomb scatt., Rutherford, effect 8=11841
 - Davydov model, non-adiabaticity of β -vibrations in rare-earth even-even nuclei 8=947
 - decay processes, soluble model 8=3413
 - deformation of odd-A nuclei, unpaired particle contrib., $153 \leq A \leq 191$ 8=927
 - deformed gapless supercond. due to Coriolis force 8=928
 - deformed nuclei, rotational states by cranking model 8=11685
 - deformed nuclei, stripping reactions 8=7224
 - density for A = 24, 28 as a function of isospin and total angular momentum 8=20658
 - density in light nuclei, correction to Lang-Le Couteur formula 8=20662
 - density from nuclear evaporation data, spin effect 8=11695
 - dipole resonance, influence of spin-orbit splitting 8=7053
 - dipole resonance splitting rel. to 2p-2h states 8=929
 - doubly-even nucleides, unified model description 8=3788
 - d-s shell states, SU_3 , SU_6 selection rules 8=7050

Nucleus—contd

energy levels—contd

- E1 in deformed nuclei, anomalous and density matrix form of superfluid model 8=20653
 E1 and M1 transitions probability rel. to spins 8=11697
 E2 and M1 transitions in odd-A nuclei, from γ -ray emission 8=932
 electroexcitation, extension of Helm model 8=3773
 e.m., symmetry tests, use of ang. correl. from applied and internal fields 8=3775
 e.m. transition rate upper bounds calc. method 8=3774
 even-even, E2 transition probabilities in rotation-vibration model 8=15939
 even-even, half-life and systematics of E_2 transitions 8=7043
 even-even nuclei, $I^\pi = 1^-$ 8=15991
 even-even nuclei, rotational states 8=7056
 excited 2^+ states, static quadrupole moments 8=15935
 excitation spectra calc. for A=6, 18, 42, simple interaction model 8=11689
 Fermi transitions, matrix element calc. by treating Coulomb pot. accurately 8=3780
 forbidden states in d-induced reactions 8=1088
 4^+ rotational states, mag. moments 8=15938
 g-factor meas. of short-lived states, sum-coincidence method 8=20669
 γ -transitions, K-forbidden, absolute probabilities 8=20667
 γ -ray transition meas. utilizing Q-values 8=3574
 γ -vibrational states of even rare-earth nuclei, (d, p) excitation 8=3782
 giant resonances, collective model 8=7044
 half life using delayed coincidence meas. 8=7060
 HF calc., N-N potential to fit N-N scatt. data 8=3758
 heated, radiational transitions into rotational and basic states 8=7057
 identification from orbital momentum of incident n in n spectrometer 8=7041
 isobaric analog resonances external mixing 8=7045
 isobaric analogue resonances, optical potential theory 8=7046
 isobaric analogue states in heavy nuclei, quasiparticle theory 8=3778
 isobaric analogue states in various 94 MeV (p, n) reactions 8=16070
 isomeric, by thermal n radiative capture 8=11703
 intermediate and heavy nuclei, level densities in free gas model 8=7051
 j-levels charge-independent pairing interaction 8=3771
 lifetimes by γ transition probabilities E_0 , M_1 and E_2 8=936
 lifetime meas. with pulsing system for particle beams 8=7058
 lifetime meas. by resonance fluoresc., appl. of Compton-scatt. γ -rays 8=20666
 lifetime meas. technique using 2 converters 8=3859
 light, excited states from e scatt., using Woods-Saxon pot. 8=7173
 line width meas., resolution 1 in 10^6 8=20660
 Liperi Summer School in theoretical Physics 1966 8=7028
 M1 transitions lifetimes from analogous β -decays 8=11731
 M1 transitions in odd-mass nuclei, K-conversion coeffs. anomalies 8=15945
 mirror pair investigated 8=20676
 multipole, e-scatt. cross-section calc. using FORTRAN IV 8=20773
 multiple splitting rel. to SU_3 reduction of d-s shell interactions 8=7040
 nuclear level density parameters, ~ 8 and ~ 20 MeV, comp. 8=15928
 non-radiative internal processes following β -decay obs. 8=3861
 nucleon continua, effect on inelastic e-scattering form factors 8=16062
 nucleon-phonon interaction effects, calc. 8=3763
 $O^+ \rightarrow O^+$ superallowed transitions polar vector β -decay coupling constant calc. 8=7126
 octupole deformations, softness in pear-shaped oscill. model 8=3772
 odd-p nucleides, unified model description 8=3788
 odd spherical, low-lying state calc. using pairing aprox. 8=3769
 one-particle levels with $N_{\text{max}} \pm 1$ nucleons calc. 8=11701
 particle-hole excitations, Tamm-Dancoff and RPA eqns. 8=15932
 pair energies for spherical and deformed nuclei $100 < A < 256$ calc. 8=11702
 pairing problem, linearized approx. leading to ground and O^+ states 8=11704
 perturbation of statistical props. if Hamiltonian is not invariant under time reversal 8=15933-4
 pionic 3d-2p transitions 8=15944
 polarization effects rel. to X-ray spectrum of muonic atoms 8=20655
 proton hole states of odd parity in 2s-1d shell nuclei 8=20650
 quadrupole-octupole interaction rel. to two phonon states 8=15927

Nucleus—contd

energy levels—contd

- quasi- β and quasi- γ bands proposed between vibr. and rot. 8=3784
 from radioactive γ transitions 8=16019
 random phase approx. eqn., higher-order corrections 8=15932
 random-phase-approximation calcs., schematic interactions 8=934
 rare earth rotational spectra and Y_{40} and Y_{60} shape component determ. 8=11713
 rare-earth metals, single-particle and vibrational states 8=15992
 resonances, overlapping, unified theory of nuclear reactions appl. 8=3889
 resonant states used as basis for eigenfunction expansion of reaction and scatt. amplitudes 8=16051
 resonance structure in $Li^{17}(O^{16}, \gamma)Na^{23}$ radiative capture 8=3974
 rotational bands by collective variable method 8=11708
 rotational bands, $K=1/2$ states, energetics 8=15942
 rotational, deviation from $I(I+1)$ law 8=20664
 rotational in even-even nuclei, phenomenological analysis 8=948
 rotation, Villars formalism 8=15941
 $(1s)^4(1p)^{14}$, G matrix interaction, levels predicted 8=7048
 Schrödinger equation with Woods-Saxon potential, solution 8=7055
 shape characteristic var. rel. to mean field 8=7059
 shell, low-lying from photonuclear cross sections obs. 8=20659
 shell-model potentials for heavy nuclei and stability of superheavy nuclei 8=11786
 shell model, 2-particle approx. for light nuclei 8=930
 shell model var. with approx. and exact calc. 8=3764
 shell structure study by quasi free electron scattering 8=1043
 single-n reson. by time-of-flight methods, obs. correl. 8=3930
 single-particle replaced by hole state, rel. to quasi-free scatt. 8=16052
 single-particle strength sum rules and Butler's stripping theory 8=15937
 $SU(3)$ classification of wave functions, shell model, N^π structure discussed 8=931
 SU_3 Clebsch-Gordan coefficients for coupling of single particle to general state 8=15929
 SU_3 symmetry for systems of 3 and 4 particles in 2s-1d shell 8=7042
 spectra of odd-odd nuclei 8=7047
 spectra of odd-odd nuclei 8=20665
 spectroscopic factors for discrete states, comment 8=15931
 spherical and deformed nuclei, collective states contrib. to optical potential 8=11687
 spin-orbit splitting in spherical H-F theory 8=15947
 stationary and time-dependent, general variational eqns. 8=11705
 structure from 2N emission following π bombard. 8=1086
 $T = 3/2$ of 7 nuclei, mass determ. by reaction 8=20656
 $T = 3/2$, from $F^{19}(He^3, n)$ obs. 8=20689
 Tamm-Dancoff eqn. higher-order corrections 8=15932
 transition densities of dipole excitations in nuclei with $N > Z$ 8=7088
 2^+ excitation in n-nucleus scatt. 8=16086
 2^+ rot. state in doubly even, reorientation effect due to Coulomb excitation 8=15940
 vibrational, β -band, asymmetric rotor model 8=946
 vibrational, in closed-shell nuclei, breathing mode calc. 8=3783
 vibrations, collective HF eqns. with adiabatic approx. model 8=11707
 vibrational, medium heavy nuclei, Tam-Dancoff theories 8=20663
 vibrational model, anomaly in low-lying levels of Hg^{200} 8=11911
 vibration, O^+ , collective calc. in 8 nuclei, particle-hole model 8=11706
 virtual Coulomb excitation in nucleon transfer 8=3976
 Wigner supermultiplet theory, SU_4 , satisfied for A = 40-254 8=20661
 Z = 11 - 21, compilation of data 8=7054
 Z = 56-78, E2 transitions by internal conversion, M/L, N + O/M ratios 8=7140
 $40 \leq A \leq 48$, $1f_{7/2}^1$, $1f_{7/2}^{1,2}$, $1d_{3/2}^1$ configurations, shell model calc., M2 retardation factors 8=7049
 A^{34} , (He^3, n) reaction study 8=20694
 Ag odd mass isotopes, spectra anomaly rel. to 2^+ phonon quadrupole moment 8=20670
 Ag^{102} , isomeric transition, unsuccessful search for internal conversion 8=7094
 Ag^{109} , isomer, transition energy obs. 8=980
 Ag^{109} from $Pd^{109\beta}$ $\rightarrow Ag^{109}$ decay lifetimes, branching ratios, spin and parity assignments 8=16026
 Ag^{110m} , γ -radiation 8=982
 Al^{28} , excitation in $Si^{28}(d, \alpha)Al^{28}$ 6.98-11.06 MeV 8=20829
 Al^{28} , 1.059 MeV, M1 transition to 0.229 MeV, deduced from β decay of $Si^{28} \rightarrow Al^{28}$ 8=11731

Nucleus—contd

energy levels—contd

- Al²⁶ from Mg²⁶(He³, d)Al²⁶, 12 MeV obs. 8=16122
 Al²⁷, B(E2)₁ value 8=935
 Al²⁷(p, γ) 0.7-1.5 MeV, resonances 8=958
 Al²⁷ resonant state decay, pγγ correl. of γ-rays, E = 10.480 MeV 8=7079
 Al²⁷ deduced from Al²⁷(He³, α)Al²⁶, 10 MeV 8=11945
 Al²⁷ information from Al²⁷(p, 2p)Mg²⁶ 8=11884
 Al²⁷, l = 2 excitations, unreported levels from p scatt., 17.5 MeV 8=20786
 Al²⁷ reson., Mg²⁶(p, p)Mg²⁶ obs., 1-2 MeV 8=957
 Al²⁷ from Si²⁸(d, He³)Al²⁷, 34.4 MeV 8=20692
 Al²⁹ from Si²⁸(d, He³)Al²⁹, Mg²⁶(α, p)Al²⁹ 8=20693
 Am^{242m}, 14 msec spontaneously fissioning, spin value 8=7243
 Am²⁴⁵ following Pu²⁴⁵ decay 8=11833
 Ar^{35,39} from Ar^{36,40}(p, d)Ar^{35,39}, 27.5 MeV 8=11887
 Ar³⁸, 4.88 and 5.36 MeV, from Cl³⁵(α, pγ) reactions at 10.6 MeV 8=3804
 Ar³⁸ from K³⁹(n, d)Ar³⁸, 14.4 MeV 8=7212
 Ar³⁸, lifetimes obs. Ca⁴⁰ analogies 8=11738
 Ar³⁸, 23 bound states from Cl³⁷(p, γ)Ar³⁸, 1.0-1.8 MeV, J → J M1 transitions 8=11737
 Ar^{38,40}, deformed excited states 8=15966
 Ar³⁹, from K⁴¹(d, α)Ar³⁹, 7.5 MeV bombarding energy 8=20699
 Ar³⁹, nuclear spin and magnetic moment, spectroscopic measurement 8=11739
 As⁷⁵, multipolarities, spins and parities from 3.5-8.1 MeV α and 36-38 O¹⁶ scatt. 8=3816
 As⁷⁶ de-excitation in As⁷⁶(n, γ)As⁷⁶ 8=20811
 Au, rel. to shell and unified models 8=3833
 Au III, transition strengths between 5d⁹6s and 5d⁹6p configurations 8=4071
 Au¹⁹⁶, half life of 85 keV level 8=20747
 Au¹⁹⁷ from 0.15-1.5 MeV n scatt. 8=11899
 Au¹⁹⁹, props. of high levels 8=7112
 Au¹⁹⁹ from Pt¹⁹⁹ decay 8=994
 B⁸ cluster structure from Li⁶(He³, n)B⁸ 4-5.7 MeV 8=1099
 B⁸, second state excitation energy 8=11720
 B⁹, (p, d) reaction 33.6 MeV, p ang. dist. and DWBA analysis 8=3923
 B⁹ from B¹⁰(He³, α)B⁹, 2.49-3.74 MeV rel. to mirror props. of B⁹ and Be⁹ 8=20676
 Be^{9,10} from B^{10,11}(p, d)B^{9,10}, 33.6 MeV optical model 8=20788
 B¹⁰, lifetime of 1.74 MeV state rel. to C¹⁰ β-decay obs. 8=16015
 B¹⁰, lifetimes mes. by Doppler shift of γ-rays 8=11719
 B¹⁰, 2⁺, 3.59 MeV resonance excited in Li⁷(He³, γ)B¹⁰ 8=11943
 B¹⁰, from B¹¹(He³, α)B¹⁰, 15, 16 MeV new states 8=951
 B¹¹, 5.03, 6.81 MeV levels, spin assignments, transitions due to Be⁹(He³, pγ)B¹¹, 3.4 MeV 8=20681
 B¹¹ from Li⁷(α, γ)B¹¹, e.m. transitions 8=11721
 B¹², branching ratios in γ-decay 8=20678
 B¹², 0.95, 1.67, 2.62 MeV, spin assignments from γ-γ correl. meas. 8=20679
 Ba isotopes, vibrational and rot. spectra 8=15989
 Ba¹³⁰, partial scheme 8=20720
 Ba^{132,134} from La^{132,134} decay 8=20720
 Ba¹³⁴ from Cs¹³⁴ decay 8=7139
 Ba¹³⁴ populated by Cs¹³⁴ decay 8=7099
 Ba¹³⁶, Cs¹³⁶ γ-spectrum obs. 8=11761
 Ba¹³⁷, multipolarity of 661.59 keV transition 8=7100
 Ba¹³⁸, neutron particle-hole states 8=985
 Be ground state width from α-α scatt. 8=3738
 Be⁶ from H³-H³, H³-He³, He³-He³ scatt. 8=11656
 Be⁷ from He³-He⁴ and He³-H³ scatt. 8=7001
 Be⁷, second state excitation energy 8=11720
 Be⁷, spectroscopic factors ratio from Li⁶(He³, d_{0,1})Be⁷, 8, 10, 12, 14, 16 MeV 8=20833
 Be⁸, ground state energy and lifetime from α-α scatt. 8=7072
 Be⁸ from B¹⁰(d, α)α, 0.6, 0.9, 1.45, 1.9 MeV 8=11718
 Be⁸* decay in B¹¹(p, 2α)He⁴, 163 keV 8=7190
 Be⁹ from core-pulse-n model of Be⁹(γ, n)Be⁸ 8=3908
 Be⁹ from d scatt. and Li⁷(He³, p)Be⁹ rel. to mirror props. of B⁹ and Be⁹ 8=20676
 Be⁹, rel. to photoneutron cross-section 8=3906
 Be¹¹, shell model states, inversion and μ capture rate B¹¹ → Be¹¹ 8=11873
 Bi²⁰⁸ spectra 8=7047
 Bi²⁰⁹, $\rho_{n/2}$ analogue resonance proton decay 8=7113
 Bi²⁰⁹, Schrödinger equation with Woods-Saxon potential, solution 8=7055
 Bi²⁰⁹ single-p states rel. to 82 < 2 < 126 shell from Pb²⁰⁸(α, t)Bi²⁰⁹ 8=998
 Bi²⁰⁹ in Pb²⁰⁸(He³, d)Bi²⁰⁹, single proton strength in multiplet at 2.5 MeV 8=11787
 Bi²¹⁰, rel. to tensor pairing forces 8=919
 Bi²¹¹ from Pb²¹¹ decay, 16 γ-rays obs., and daughter products 8=7150
 Br⁸³ from Se⁸³ β, γ-decay 8=3871
 C¹¹ from αγ corrs. in C¹²(He³, αγ)C¹¹ 8=953
 C¹¹ excited states below 8.43 MeV, spin and transitions from C¹²(He³, αγ)C¹¹, 4-12 MeV 8=20681

Nucleus—contd

energy levels—contd

- C¹¹ obs. in Li⁶(Li⁶, n)C¹¹ at 4.1 MeV 8=11950
 C¹², first excited state from e scatt. 8=952
 C¹², first 2⁺ state from (p, p') reaction, at 23 MeV, Doppler broadening anomaly 8=954
 C¹², low-lying, inelastic 1 GeV p scatt. 8=3918
 C¹², magnetic dipole state and giant resonance levels excited by e scatt. 8=7173
 C¹²(1⁺, 12.71 MeV) state, breakup into three α-particles 8=1006
 C¹², 19.5 MeV, excitation by inelastic e scatt. 8=1045
 C¹², calc. using Nilsson wave functions 8=3792
 C¹², photon scatt. from dipole state 8=3905
 C¹², radiative widths, giant dipole resonance after 100-200 MeV e scatt. 8=16063
 C¹² excited states in B¹⁰(He³, p)C¹² → α + Be⁸ 8=20676
 C¹², from B¹¹(d, n)C¹², 6 MeV, transitions to 9 states 8=7073
 C¹³, first excited state, lifetime 8=15955
 C¹³, 3.09 MeV state, radiative width 8=11723
 C¹³ transitions from N¹⁴(p, He³)C¹³, 43.7 MeV 8=20791
 C¹³ resonances obs. in C¹²(n, p)B¹², 14.5-22 MeV 8=16090
 C¹³ from N¹⁴(n, d)C¹³, 14.4 MeV 8=7212
 C¹³ from O¹⁶(n, α)C¹³, 14.1 MeV 8=3936
 C¹³, from O¹⁶(n, α)C¹³, 14.1 MeV 8=11901
 C¹³, lifetime of first excited state obs. in Be⁹ Be⁹(Li⁷, p)C¹³ 8=20680
 Ca isotopes, assignments from (t, p), 10-12 MeV 8=1094
 Ca⁴⁰, β parameter for 26 MeV d scatt. 8=7229
 Ca⁴⁰, breathing mode calc. breakdown 8=3783
 Ca⁴⁰ continuum struct. S¹⁻ matrix 1p-1h shell model calc. 11-28 MeV 8=965
 Ca⁴⁰, first O⁺ states 4 particle-4 hole excitations in Tamm-Dancoff sense 8=15958
 Ca⁴⁰ lifetime analogies with Ar³⁸ 8=11738
 Ca⁴⁰, lifetimes obs. 8=11744
 Ca⁴⁰, particle-hole states in SU₃ scheme 8=11745
 Ca⁴⁰, 6.91, 6.95 MeV, γ-scatt. rel. to spin, lifetime assignments 8=11743
 Ca⁴⁰, spectroscopic factors from pickup reactions rel. to shell model 8=11854
 Ca⁴⁰ states from 31 MeV α-scatt. 8=11746
 Ca⁴⁰, from K³⁹(He³, d)Ca⁴⁰ excitation, 12, 14 and 16 MeV 8=15971
 Ca^{40,42}, resonances from Ar^{36,38}(α, γ) 3-6 MeV 8=3967
 Ca^{40,42}, 44, 48, 31 MeV α scatt., new multipole states, spin-parity assignments 8=3807
 Ca⁴¹, even-parity states from K³⁹(He³, p)Ca⁴¹, 13 MeV 8=966
 Ca⁴², low-lying levels, transition probability discrepancy 8=3806
 Ca^{42,46} from Ca^{40,40}(t, p), 7.5 MeV 8=11741
 Ca⁴³, proton hole states excitation by K⁴¹(He³, p)Ca⁴³ 8=11742
 Ca⁴⁴ from Sc^{44m} decay 8=3868
 Ca⁴⁷, shell model calc. using Hamada-Johnston pot. 8=20700
 Ca⁵⁰ from Ca⁴⁸(t, p)Ca⁵⁰, low lying states obs. compared to shell model calc. 8=7083
 Cd even isotope spectra, drawbacks of conventional interpretation 8=20713
 Cd¹¹⁰, energies and intensities of γ transitions 8=7135
 Cd¹¹¹, half-life of 246 keV state and B(E2) values from Ag¹¹¹ decay and α-scatt. 8=20712
 Cd¹¹³ 0.181 reson. params. obs. 8=3941
 Cd¹¹⁴, collective states, excited by inelastic scatt. of 55 MeV p 8=15983
 Cd¹¹⁴, resonances, p scatt., elastic and inelastic compared, 7-10 MeV 8=983
 Cd¹¹⁴, vibrational states, Tam-Dancoff theory 8=20663
 Ce¹³⁶, isomeric, half-life 8=3826
 Ce¹³⁶ from Pr¹³⁶ decay 8=7141
 Ce¹⁴⁰, identification of 1⁺ neutron particle-hole state from Ce¹⁴⁰(p, p')Ce¹⁴⁰ reactions 8=20723
 Ce¹⁴¹, f_{7/2} ground state anomaly, rel. to charge exchange effects 8=11755
 Cf²⁴⁹ from Fm²⁵³ decay 8=11836
 Cf²⁵¹, 227 keV state, half-life meas. 8=11835
 Cl³⁵ analog states of S³⁵, spin, parity and e.m. decay 8=11735
 Cl³⁵, lifetime of 3.163 MeV state 8=20698
 Cl³⁵, resonances from S³⁴(p, γ)Cl³⁵ 8=11736
 Cl³⁶, γ-γ directional correlation in Cl³⁶(n, γ)Cl³⁶ 8=20697
 Cl³⁶ 2 new levels in Cl³⁶(n, γ)Cl³⁶ 8=20811
 Cl³⁷ from S³⁷ β-decay 8=16018
 Co⁵⁵ from Fe⁵⁴(He³, d)Co⁵⁵, 10, 11, 12 MeV 8=3808
 Co⁵⁶, internal conversion coeff. and γ-ray angular distribution 8=15974
 Co⁵⁶ from Fe⁵⁴(He³, p)Co⁵⁶, 12 MeV and Ni⁵⁸(d, α)Co⁵⁶, 7 MeV 8=20706
 Co⁵⁷ from Fe⁵⁴(α, p)Co⁵⁷, 10.5 and 11 MeV 8=15978
 Co⁵⁹ from Fe⁵⁹ decay 8=15979
 Co⁶⁰ by 36 MeV O¹⁶ scatt., transition probabilities, spins 8=3813
 Co⁶⁰, decay obs. 8=11809
 Cr^{50,52,54} spectroscopic factors for (He³, α) at 18 MeV 8=3969
 Cr⁵², excited states, populated in decay of Mn⁵² and V⁵² 8=15976

Nucleus—contd

energy levels—contd

- Cr⁵², polarized p scatt. transitions 8=11880
 Cs¹³¹, anomalous K-conversion coeff. of 124 keV transition 8=15988
 Cs¹³³, 81 keV γ -transition, isomer shifts 8=11762
 Cs¹³³, first excited state, magnetic moment determ. by Mössbauer effect 8=15987
 Cs¹³³ from Ba¹³³ decay 8=11820
 Cs¹³³ from Ba¹³³ decay γ transition probabilities and branching ratios 8=16031
 Cu⁵⁹, from p scatt. 3-6 MeV 8=973
 Cu⁵⁹, shell description of lowest states 8=972
 Cu⁶⁰ in Ni⁵⁸(He³, p)Cu⁶⁰, and isobaric analogue of Ni⁶⁰ in Cu⁶⁰ 8=11946
 Cu⁶³(n, n') cross sections for 668 and 961 keV states 8=7209
 Cu⁶³, polarized p scatt. transitions 8=11880
 Cu⁶³ from Ni⁶²(He³, d)Cu⁶³ at 11.0 MeV 8=11947
 Cu⁶³ from Zn⁶³, decay, revised scheme 8=1012
 Cu⁶⁵, (n, n') cross sections for 764 and 1114 keV state 8=7209
 Cu⁶⁶, anomalous radiation widths following n capture 8=3960
 D^{150, 158} deform. parameters and elec. quadrupole transitions 8=20953
 Dy principal harmonic oscillator shell mixing 8=7086
 Dy^{150, 158}, half-lives and moments of inertia 8=20726
 Dy¹⁵⁸, lifetime of 2', transitions 8=20755
 Dy¹⁶⁰, half-lives of 2' states 8=11771
 Dy¹⁶¹, gyromagnetic ratios from branching-ratio expts. 8=11772
 Dy^{161, 162}, 75 and 81 keV, moments, spin, Mössbauer effect 8=3829
 Dy¹⁶², half life of 1148 keV level 8=20747
 Dy¹⁶⁵ conversion electron and transition multipolarities 8=989
 Dy¹⁶⁵, ground state h.f.s. 8=11773
 Er isotopes, levels from n scatt. 8=1073
 Er principal harmonic oscillator shell mixing 8=7086
 Er¹⁶² deform. parameters and elec. quadrupole transitions 8=20953
 Er^{162, 164, 166, 168, 170} 12 MeV d scatt., E2, E3 transition widths 8=11774
 Er¹⁶⁴, half life of 90 keV level 8=20747
 Er¹⁶⁵ from Tm¹⁶⁵ e-capture decay 8=20757
 Er^{166, 168}, half-lives of 2', 4' rot. states 8=11771
 Er¹⁶⁷, γ -ray spectra following thermal n capture 8=1083
 Eu¹⁴⁹ from Gd¹⁴⁹ \rightarrow Eu¹⁴⁹ 8=7143
 Eu^{153, 155}, E1 transition life times, possible dipole contrib. 8=3827
 Eu^{153, 155}, half life of $\frac{5}{2}^-(532)$ transic state obs. 8=7103
 Eu¹⁵⁵, transition probability, $5/2^-[532] \rightarrow 3/2^-[411]$ 8=15994
 Eu¹⁵⁵ from Sm¹⁵⁵ decay 8=7105
 F¹¹, 1 = 2 excitations and transition strengths from 17.5 MeV p scatt. 8=20786
 F¹⁷, lowest two T = $\frac{3}{2}$ states 8=3799
 F¹⁸ from core correl. effect on motion of outer N 8=3767
 F¹⁸, generation from Kuo-Brown N-N force 8=3759
 F¹⁸ shell-model calc. using Tabakin calc. 8=11728
 F^{18, 19, 20} shell model calc. 1' state anomaly 8=11726
 F¹⁹, deformation parameters from (γ , n) reactions 8=7167
 F¹⁹, intermediate-structure resonances for p capture, n scatt. 8=3931
 F¹⁹ rotational, p scatt. excitation 8=7182
 Fe⁵³, M_{zz} shell calcs. 8=970
 Fe⁵⁴, n scatt. multipole mixing ratio for M1, E2 transitions 8=3934
 Fe⁵⁴, 2-, 3-, polarized proton scatt. asymm. 8=3920
 Fe^{54, 56}, polarized p scatt. transitions 8=11880
 Fe⁵⁵ from Mn⁵⁵(p, n) γ Fe⁵⁵, 1.8-3.5 MeV 8=3927
 Fe⁵⁶, β parameter for 26 MeV d scatt. 8=7229
 Fe⁵⁶ from photoneutron cross-sections 8=3811
 Fe⁵⁶, precession of 0.847 MeV level 8=20705
 Fe⁵⁷, γ branching ratio following thermal n capture 8=11905
 Fe⁵⁸, γ -ray trans from Fe⁵⁷(n, γ)Fe⁵⁸ 8=1080
 Fr²²¹, γ transitions studied by α - γ coincidences 8=3845
 Ga⁶⁸, internal conversion coeff. and γ -ray angular distribution 8=15974
 Gd¹⁵¹ level population and ft value calc. 8=7145
 Gd^{151, 152}, from Tb^{151, 152} decay 8=3882
 Gd¹⁵², half-life and moment of inertia 8=20726
 Gd¹⁵⁴, β - and γ -vibrational bands 8=16034
 Gd¹⁵⁴ β - and γ -vibr. bands E₂ transitions and mixing params., obs. 8=11768
 Gd¹⁵⁴, E2 transitions, internal conversion 8=1020
 Gd¹⁵⁴, half-lives of 2' states 8=11771
 Gd¹⁵⁴ 2+ β vibr. decay, M1-E2 mixing, 693-123 keV transition obs. 8=15993
 Gd^{156, 157, 159} in (d, p) and (d, t) reactions, transitions between spherical and deformed potentials 8=11770
 Gd¹⁵⁵, 86.5 and 105.3 keV states, spins and attenuation coeffs. 8=20725
 Gd¹⁵⁶ from Eu^{152, 154, 156, 158} decay 8=11821
 Gd¹⁵⁵, obtained from β^- decay of Eu¹⁵⁶ 8=11769
 Gd¹⁵⁵ from Tb¹⁵⁵ decay 8=988

Nucleus—contd

energy levels—contd

- Gd¹⁵⁶ 1049 keV O⁺ state identification from Eu¹⁵⁶ decay 8=16036
 Gd¹⁵⁶ from Tb¹⁵⁶ decay, dipole-quadrupole mixtures 8=7144
 Gd^{156, 158}, half-lives of 2', 4' rot. states 8=11771
 Gd¹⁵⁸, lifetime of 2', transitions 8=20755
 Gd¹⁵⁸ in metal and halides, Mössbauer meas. rel. to 79.5 keV γ -transitions 8=3786
 Ge, from gamma ray spectra by neutron capture 8=3810
 Ge principal harmonic oscillator shell mixing 8=7086
 Ge⁷¹ from Ge⁷⁰(d, p)Ge⁷¹ at 7.5 MeV 8=11931
 Ge^{71, 73} from Ge^{70, 72}(d, p) 8=7087
 Ge⁷², excited states structure using Ga⁷² decay obs. 8=11751
 Ge⁷² from Ga⁷² decay 8=16021
 Ge⁷², 2' assignment 8=1013
 Ge⁷⁴ from As⁷³(n, d)Ge⁷⁴, 14.4 MeV 8=7212
 He, in planetary nebulae, 2S state depopulation rate 8=5913
 He³, T = $\frac{1}{2}$ states from p-H² scatt. 8=3739
 He³ search for excited states in reaction $^3\text{He}(p, p')^3\text{He}^*$ 8=11653
 He³, p-d final states, 5, 5-12.0 MeV rot. obs. in p reactions on Li⁶, 9-10 MeV 8=7187
 He⁴, odd-parity calc. 8=887
 He⁴ rel. to particle hole interaction 8=7003
 He⁴, product of nuclear reaction, excited states obs. 8=15953
 He⁶ estimated 8=3847
 He⁶ from H²-H², H²-He³, He³-He³ scatt. 8=11656
 Hf^{172, 174, 178}, half-lives and moments of inertia 8=20726
 Hf¹⁷⁴, deform. parameters and elec. quadrupole transitions 8=20953
 Hg¹⁹⁸, E2/M1 mixing ratio for 2'-2' transition 8=975
 Hg¹⁹⁸, first excited state, g-factor 8=16002
 Hg¹⁹⁸, 675 keV transition, E2/M1 mixing ratio from ang. correl. meas., $\gamma\gamma$ cascade 8=11782
 Hg^{198, 200, 202}, 2p holes and vibrating core model 8=3838
 Hg²⁰⁰ from Hg¹⁹⁹(n, γ)Hg²⁰⁰, vibrational model anomaly 8=11911
 Ho^{161, 163} isomeric, half-life 8=3826
 Ho^{165, 166}, resonances induced by n scatt., 35-750 eV and capture, 2.5-10⁵ eV, spin assignments 8=16101
 I^{125, 127} lifetimes, M1, E2 transition probabilities 8=11760
 I¹²⁷, n scatt., 60-900 keV, spin assignments, discrepancy 8=7096
 I^{130m}, disintegration of and transition from I^{130m} 8=7097
 I¹³¹, parity assignments from internal conversion decay of Te^{131m} 8=3878
 In^{112, 114}, prod. in In^{113, 115}(n, 2n)In^{112, 114} 8=20814
 In¹¹⁵, from β^- decay of Cd^{115m, 6} 8=3822
 In¹¹⁵, lifetimes of 579, 829 and 864 keV states 8=981
 In¹¹⁵, 600 and 830 keV photoexcitation 8=20714
 In¹¹⁷, g-factor of $\frac{3}{2}^+$ 660 keV 8=3823
 In¹¹⁷ from Cd^{117, 117m} decay, rot. band and multiplet identified 8=15984
 In¹⁹⁴ from In^{194m} decay 8=7147
 Ir, from gamma ray spectra by neutron capture 8=3810
 Ir, rel. to shell and unified models 8=3833
 Ir¹⁸⁸, from Au spallation 8=1024
 Ir¹⁹¹, resonance fluorescence with Pt¹⁹¹ source, level determ. 8=993
 Ir^{191, 193}, g factors, for first excited states 8=3836
 Ir¹⁹³ from Os¹⁹³ decay 8=11826
 Ir^{195, 195m}, γ -transitions from α bombard of Os¹⁹² 8=11827
 K³⁷, 2750 KeV level spin and branching 8=3805
 K³⁹, spins and mixing ratios from Ca⁴²(p, α)K³⁹, p-K³⁹ scatt. 8=15967
 K³⁹ from Ca⁴⁰(n, d)K³⁹, 14.4 MeV 8=7212
 K^{39, 41} from inelastic n scatt. and (n, p γ) reactions 8=20809
 K⁴⁰, mean lifetime of 1.64 MeV level 8=15968
 K⁴⁰ spectra 8=7047
 K⁴¹ from p reactions on Ar⁴⁰, 3.5 and 6.0 MeV 8=964
 K⁴⁷, shell model calc. using Hamada-Johnston pot. 8=20700
 Kr⁷⁹ excited state in Br⁷⁹(p, n)Kr⁷⁹, half-life and g-factor meas. 8=11752
 Kr⁸², E2/M1 mixing ratio for 2'-2' transition 8=975
 Kr⁸², 698 keV transition, E2/M1 mixing ratio from ang. correl. meas., $\gamma\gamma$ cascade 8=11782
 La¹³², from disint. of Ce¹³² 8=7101
 La¹³² scheme 8=20720
 La¹³³ from β -decay of Ce^{133, 133m} 8=20722
 La¹³³, deformed levels mean life 8=15990
 La¹³⁶ from Ce¹³⁶ decay, conversion e and γ spectra 8=20721
 Li⁴, product of nuclear reaction, excited states, obs. 8=15953
 Li⁵ resonance obs. in H²(He³, γ)Li⁵, 2-5.5 MeV 8=20581
 Li⁵ ground state obs. in p reactions on Li⁶, 9-10 MeV 8=7187
 Li⁶, odd parity P level, existence using d + α scattering phase shifts 8=15869
 Li⁶, 2.184 MeV state obs. 3.56 MeV not obs. in n scatt. 8=11897
 Li⁶ from H²-H², H²-He³, He³-He³ scatt. 8=11656
 Li⁶, 2.19 MeV (J = 3⁺, T = 0), studied in d-He⁴ collisions 8=20675

Nucleus—cont'd

energy levels—cont'd

- Li⁶, 3.56 MeV level, 60–130 MeV e scatt. 8=11716
 Li^{6,7}, from 50 MeV p scatt. up to 17 MeV level 8=7071
 Li^{6,7}, (p, d) reaction 33.6 MeV, p ang. dist. and DWBA analysis 8=3923
 Li⁷, h.f. calc. 8=3789
 Li⁷, search for 5.5 MeV level 8=20674
 Li⁷, second state excitation energy 8=11720
 Li⁷, branching ratio to ground and first excited state from B¹⁰(n, α)Li⁷ 8=11900
 Li⁷ from He³-He⁴ and He³-He³ scatt. 8=11001
 Li⁷, from n scatt. 8=11897
 Li⁸, cluster structure from Li⁶(He³, n)B⁸
 Lu, rel. to shell and unified models 8=3833
 Lu^{169, 171, 173, 175}, E1 and E3 transition probabilities 8=11778
 Lu¹⁷¹, 71.2 keV state period obs. 8=7107
 Lu¹⁷², lifetimes 8=3834
 Lu¹⁷⁴ isomers in electron capture disintegration 8=11776
 Lu¹⁷⁵, parity admixture obs. from polarization asymm. of γ-rays 8=15997
 Lu^{176, m} decay, half-lives 8=1022
 Mg²⁴, branching and mixing ratios from Mg²⁴(He³, αγ)Mg²³ 9.00 MeV 8=11730
 Mg²⁴, photon scatt. from dipole state 8=3905
 Mg²⁴ predicted from appl. of Wigner-Eckart theorem to central interactions 8=7037
 Mg²⁴, 6 excited states from inelastic p scatt., 49.5 MeV 8=3919
 Mg²⁴ from Na²³(d, n), 2.98 MeV, analog state with T = 1 8=20688
 Mg²⁴ from Na²³(p, γ), 0.7–1.5 MeV 8=958
 Mg²⁴ deduced from Ne²⁰(α, γ)Mg²⁴ 3–6 MeV 8=16121
 Mg²⁴, transitions in 42 MeV α-scatt., 3° indicated 8=11939
 Mg²⁴, excited states in Mg²⁴(p, t)Mg²² reaction 8=11883
 Mg^{24, 26}, β parameter for 26 MeV d scatt. 8=7229
 Mg²⁶ from Mg²⁶(He³, α)Mg²⁵, 4–6 MeV 8=20836
 Mg²⁶, second excited state lifetime 8=11731
 Mn, from gamma ray spectra by neutron capture 8=3810
 Mn, n scatt., deviation from Porter-Thomas distrib. 8=3809
 Mn⁵² from Cr⁵⁰(He³, p)Mn⁵² and Fe⁵⁴(d, α)Mn⁵² obs. 8=20703
 Mn⁵³ from Cr⁵²(He³, d)Mn⁵³, 10, 11, 12 MeV 8=3808
 Mn⁵⁵, from n scatt., 1.0–3.1 MeV, dominant M1 transitions 8=15975
 Mo, n resonance spectroscopy 8=20813
 Mo⁹³ analog states from Mo⁹²(d, np)Mo⁹² 8=1095
 Mo^{93, 95}, d_{5/2} ground state anomaly, rel. to charge exchange effects 8=11755
 Mo⁹⁷ from Nb⁹⁷ decay 8=16023
 Mo⁹⁸, monopole 0⁺ transition, 735 KeV 8=7090
 Mo⁹⁸ from Mo⁹⁷(d, p)Mo⁹⁸, 10–12 MeV 8=11756
 N¹³ resonances obs. in C¹²(p, n)N¹², 18.9–50 MeV 8=16079
 N¹³ in N¹⁴(He³, α)N¹³, 13.9 MeV 8=10835
 N¹³ transitions from N¹⁵(p, t)N¹³, 43.7 MeV 8=20791
 N¹⁴ from core correl. effect on motion of outer N 8=3767
 N¹⁴ from αγ correls. in C¹²(He³, pγ)N¹⁴ 8=953
 N¹⁴, 8.49, 8.96, 9.17 MeV levels from C¹²(He³, pγ)N¹⁴ at 8.92 MeV 8=11724
 N¹⁵, 6.32 MeV level, ground state e.m. widths 8=20684
 N¹⁵, lifetime of mirror states from N¹⁴ bombard. of H² and Be⁹ 8=3793
 N¹⁵, isobaric analog states of O¹⁵ 8=15956
 N¹⁶, T = 2 states, by C¹⁴(He³, p)N¹⁶ 8=20683
 Na²², lifetimes of 3 levels meas. by Doppler shift in C₂F₈ 8=11729
 Na²², from F¹⁹(α, nγ)Na²², and Ne²⁰(He³, pγ)Na²², reactions 8=3801
 Na²², 1.528, 0.891 MeV states, spin assignments, lifetimes using F¹⁹(α, nγ)Na²² 8=20690
 Na²² from β⁺ decay of Mg²² 8=3866
 Na²³, B(E2)₁ value 8=935
 Na²³, unreported levels from 17.5 MeV p scatt. 8=20786
 Na²³(p, γ) 0.7–1.5 MeV, resonances 8=958
 Na²³, rotational model of low-lying states 8=956
 Na²³ rotational from Ne²²(He³, d)Na²³, 10, 12 MeV 8=3802
 Na²⁴ upper limit for lifetime of second excited state 8=11732
 Nb⁹⁰ from Mo⁹⁰ decay, multipolarities of transitions 8=20711
 Nb⁹⁷ from Zr⁹⁷ decay 8=16022
 Nd⁴¹ obs. 8=7102
 Nd⁴¹ isomeric, half-life 8=3826
 Nd⁴³, p, f, h wave states spin assigned from p scatt. off Nd¹⁴² 8=7195
 Nd⁴³, Schrödinger equation with Woods-Saxon potential, solution 8=7055
 Nd⁴⁴, above 1.78 MeV, from Pm¹⁴⁴ decay, scintillation spectroscopy 8=16033
 Nd⁴⁴ deduced from Pr¹⁴⁴ decay 8=11765
 Nd⁴⁵, recoilless resonance absorpt. rel. to scheme 8=20724
 Nd¹⁵¹ from Nd¹⁵⁰(d, p)Nd¹⁵¹, ground-state Q value, levels assigned 8=11767
 Ne²⁰, Hartree-Fock calc. validity before angular momentum projection 8=15960
 Ne²⁰, O⁺ state calc. using adiabatic model for collective vibrations 8=11707

Nucleus—cont'd

energy levels—cont'd

- Ne²⁰ 4.97 MeV 2- and 7.02 MeV 4-, weak γ decay obs. 8=15959
 Ne²⁰, pairing effects in Hartree Fock wave function 8=7076
 Ne²⁰, rotational states from O¹⁶(Li⁷, t) reaction 8=16128
 Ne²⁰, shell model calc. of rot spectrum 8=11726
 Ne²⁰ from F¹⁹(d, n) 2.98 MeV, analog state with T = 1 8=20688
 Ne²⁰ from Na²⁰ decay 8=20745
 Ne²⁰, from β-decay of Na²⁰ 8=3865
 Ne²³, following Ne²²(n, γ), unsuccessful search for 2.285, 2.405, 2.870 MeV levels 8=11806
 Ni even isotopes, quasiparticle calc., E2 transition strengths 8=3824
 Ni isotopes, M1 and E2 using admixture of one and 3-particle states 8=971
 Ni isotopes shell model matrix elements 8=3814
 Ni⁵⁸, β parameter for 26 MeV d scatt. 8=7229
 Ni⁵⁸, E2 transition anomalies from Ni⁵⁸(p, p') 8=3928
 Ni^{58, 60}, 2⁺, 3⁻, polarized proton scatt. asymm. 8=3920
 Ni^{58, 60, 62}, radiative transition probabilities and radii 8=3913
 Ni^{58, 60, 62, 64}, polarized p scatt. transitions 8=11880
 Ni⁶⁰, 16 states from Co⁵⁹(He³, d)Ni⁶⁰ Co⁵⁹-He³ scatt., and p-Ni⁶⁰ scatt. 8=15981
 Ni⁶¹ structure from Co⁵⁹(He³, p)Ni⁶¹, 11.65 MeV 8=15980
 Ni⁶¹, from p scatt. d scatt. and (d, p) reactions 8=3815
 Np^{237, 239}, g-factor meas. by α-γ correl. 8=3846
 Np²³⁹ from U²³⁹ decay 8=11832
 O¹⁵, excited states with isobaric analogs in N¹⁵ 8=15956
 O¹⁵, multipole mixing ratios, high retardation of E1 8=11725
 O¹⁵ lifetime of mirror states from N¹⁴ bombard. of H² 8=3793
 O¹⁶, branching ratio meas. on 6.92, 7.12 MeV states 8=3797
 O¹⁶, elec. monopole and quadrupole excitations 8=20685
 O¹⁶, e. m. transition rates, corrections due to ground-state correls. 8=15957
 O¹⁶, even parity states, pairing-plus-quadrupole model 8=11727
 O¹⁶, 4-particle-4 hole correls. using Eichler-Marumori 2-step method 8=15958
 O¹⁶, 19.08 MeV level, form factor, spin and parity 8=3794
 O¹⁶, O⁺ state monopole excitation at 6.056 MeV 8=3798
 O¹⁶, octupole excitation, e scatt., Woods-Saxon pot. 8=7173
 O¹⁶ odd parity states, Fermi liq. theory 8=20686
 O¹⁶, resonances from (γ, p) and (γ, n) reactions 8=1038
 O¹⁶, rot. structure evidence 8=3796
 O¹⁶, 8 particle-8 hole rotational band in α + C¹² → Be⁸ + Be⁸ 8=7075
 O¹⁶, spectroscopy from F¹⁹(p, α)O¹⁶ reaction, for senior students 8=1059
 O¹⁶, from N¹⁵(d, n)O¹⁶, 6 MeV transitions to 5 states 8=7073
 O¹⁶ from n scatt. resonances 8=1069
 O¹⁶ giant multipole reson. and radiative π-capture rates 8=955
 O¹⁶, low-lying, inelastic 1 GeV p scatt. 8=3918
 O¹⁷, using (O¹⁶) harmonic oscillator function with free N-N pot., spin orbit separation calc. 8=20687
 O¹⁷, resonance parameters from 2.2–4.2 MeV n scatt. 8=1070
 O¹⁷, 5 lowest states obs. after F¹⁹(d, α)O¹⁷ 0.9–4.25 MeV 8=16115
 O¹⁸ from core correl. effect on motion of outer N 8=3767
 O¹⁸, generation from Kuo-Brown N-N force 8=3759
 O¹⁸, J = 0⁺, 2⁺ states, shell model amplitudes and relative phases 8=20826
 O¹⁸ shell-model calc. using Tabakin calc. 8=11728
 O^{18, 19, 20}, shell model calc. 8=11726
 Os^{182m}, rotational transitions 8=16001
 P²⁹ from n-γ ang. correl. in Si²⁸(d, n)P²⁹, 3 MeV 8=16117
 P³⁰ from Si²⁹(p, γ) decay property obs. 8=7192
 P³¹, l = 3 transitions, unreported levels in 17.5 MeV p scatt. 8=20786
 P³¹ 2187 keV reson. parity and width rel. to Si³¹ analogue, p scatt. obs. 8=960
 P³¹, 3.13 MeV state, width determ. by γ scatt. 8=11734
 P³¹ from S³²(d, He³)P³¹ 8=20693
 P³¹ from Si³⁰(p, γ)P³¹, branching ratios and parity assignments 8=961
 P³¹ from Si³⁰(p, γ)P³¹, 0.5–2.3 MeV, branching ratios, resonances and bound states 8=11733
 P³¹, resonant absorpt. of γ-ray from Si³⁰(p, γ)P³¹, level parameters 8=15965
 P³², lifetime of first excited state 8=11732
 P³³ from S³⁴(d, He³)P³³, Si³⁰(α, p)P³³ 8=20693
 Pb, proton shell-model potentials 8=11786
 Pb^{204, 206}, transitions obs. after Tl^{203, 208}(α, t)Pb^{204, 206} 8=20838
 Pb²⁰⁵, Bi²⁰⁵ γ-transitions to 13/2⁺ isomeric level 8=997
 Pb²⁰⁶ in Pb²⁰⁴(t, p)Pb²⁰⁶ and Pb²⁰⁸(p, t)Pb²⁰⁶ 8=3839
 Pb²⁰⁶, structure from Pb²⁰⁷(d, t)Pb²⁰⁶ 8=20730
 Pb^{206, 207, 208}, e.m. transition widths equal 8=11785
 Pb²⁰⁶⁻²⁰⁸, particle-core coupling 8=16004
 Pb²⁰⁷, fine structure of doorway state 8=996
 Pb²⁰⁷ 569.6 keV transition K-conversion coeff. 8=3842

Nucleus—contd

energy levels—contd
Pb²⁰⁷, 3.62 and 4.29 MeV states particle configuration obs. 8=3840
Pb²⁰⁸, breathing mode calc.breakdown 8=3783
Pb²⁰⁸, excited states at 5.28 and 5.96 MeV, J^π = 1⁻ 8=11935
Pb²⁰⁸, n particle hole structure from p scatt. 8=11784
Pb²⁰⁸, particle-hole structure of excited states 8=11881
Pb²⁰⁸, spin vibrational 1⁺, Tamm-Dancoff and random phase approx. calc. 8=16003
Pb²⁰⁸ transitions as in Pb^{204,206,207}, Bi²⁰⁹ from α-particle scatt. 8=995
Pb²⁰⁸ from Bi²⁰⁹(t, α)Pb²⁰⁸, 13 MeV 8=11936
Pb²⁰⁹, quantitative studies of nuclear structure through isobaric analogue resonances 8=11783
Pb²⁰⁹, from Pb²⁰⁸(d, pγ), particle-vibration coupling expt. evidence 8=3841
Pd⁹⁹, from decay of Ag⁹⁹ 8=1016
Pd¹⁰¹ from Ag¹⁰¹ decay 8=1015
Pd¹⁰⁵, Ag¹⁰⁵ e capture decay 8=3873
Pd¹⁰⁶, E2/M1 mixing ratio for 2⁺-2⁺ transition 8=975
Pd¹⁰⁶ from Ag^{106m} decay 8=7092
Pd¹⁰⁶ from decay of Ag^{106m}, 8 day 8=7134
Pd¹⁰⁶, from decay of 8, 5d Ag^{106m}, 24 min. Ag^{106s} and 30 sec Rh^{106s} 8=979
Pd¹¹⁰, energy gap, Hartree-Fock and Hartree-Fock-Bogolyubov approaches 8=7093
Pd¹¹¹ from Pd¹¹⁰(d, p) 8=7087
Pm¹⁴³, resonance deduced from 12 MeV p scatt. 8=7195
Pm¹⁴⁷, from Nd¹⁴⁷ decay 8=3881
Pm¹⁵¹, half life of 5/6 (532) transic state obs. 8=7103
Po²¹⁴, 10 new γ-rays 8=3844
Po²¹⁴, scheme from Bi²¹⁴ γ-spectral data 8=16006
Pr n resonance spectroscopy, 15 level widths 8=20813
Pr¹⁴¹, scheme obs. 8=7102
Pr¹⁴¹, 145 keV, lifetime meas., E2 transition rate 8=11759
Pr¹⁴³ from Ce¹⁴³ decay, spin assignments 8=11764
Pt^{184m}, rotational transitions 8=16001
Pt¹⁹¹, γ-ray transitions 8=993
Pt¹⁹², E2/M1 mixing ratio for 2⁺-2⁺ transition 8=975
Pt¹⁹², 296 keV transition, E2/M1 mixing ratio from ang. correl.meas., γγ cascade 8=11782
Pt¹⁹³, excited state at 1.64 keV 8=7111
Pt^{195m}, γ transitions 8=3837
Pt¹⁹⁶, 356 keV, g-factor 8=16002
Pt^{197m} and Pt¹⁹⁷ decays 8=7110
Pu²³⁹, n induced fission 14-90 keV 8=11961
Ra²²⁶, scheme 8=16005
Rb⁸⁴, half life of 250 keV level 8=20747
Rh⁸⁸-Sr⁸⁸, pair from Rb⁸⁷(p, n)Sr⁸⁷, 4.6-6.2 MeV 8=16084
Re, rel. to shell and unified models 8=3833
Re¹⁸³ from Ta¹⁸¹(He⁴, 2n)Re¹⁸³, 19.8 MeV 8=20729
Re^{185,187}, vibrational from α and d scatt. 8=3954
Re^{185,187}, γ-vibrational states 8=16000
Re¹⁸⁷, 686 keV, meas. technique 8=3859
Re¹⁸⁸, conversion e spectrum following thermal n capture 8=11780
Re¹⁸⁸ isomer, magnetic properties of K = 1 rotational band 8=7109
Ru⁹⁹ from Rh⁹⁹ γ-decay 8=978
Ru⁹⁹ M₁-E₂ transition time-reversal invariance, Mössbauer obs. 8=7091
S³⁰, (He⁴, n) reaction study 8=20694
S³² from Si²⁸(α, γ)S³², 3.7-4.3 MeV 8=963
S³³-Ca⁴¹, 1f_{7/2} and 2p_{3/2} states, single-particle description 8=962
S³⁴ from U³⁸(n, d)S³⁴, 14.4 MeV 8=7212
Sb, n resonance spectroscopy, 15 level widths 8=20813
Sb¹¹⁷ from Te¹¹⁷ decay 8=3876
Sb^{117,119,121}, location of 1^{1/2} state from (He³, d) on Sn^{118,119,120} 8=3971
Sb¹¹⁹, from Te^{119m} decay obs. 8=7136
Sb¹¹⁹, spin assignments from Te^{119m} decay 8=3877
Sb^{123,125} from Sn^{123,125} decay 8=11817
Sb¹²⁵ from Sn¹²⁵ γ-decay 8=16027
Sc⁴², deformed excited states 8=15966
Sc⁴²(f_{7/2})² 3 and 3 spin states obs., 1500 keV 8=15973
Sc⁴², from Ca⁴⁰(α, d) at 24.7 MeV 8=3968
Sc⁴³ 472 keV state mean lifetime obs. 8=967
Sc⁴³ from Ca⁴²(He³, d) at 16.5 MeV 8=7084
Se⁷⁹-Br⁷⁹ pair from Se⁷⁸(p, n)Br⁷⁸, 4.4-5.7 MeV 8=16084
Se⁸¹-Br⁸¹ pair from Se⁸⁰(p, n)Br⁸⁰ 3.6-5.7 MeV 8=16084
Se⁸³-Br⁸³ pair from Se⁸²(p, n)Br⁸² 4.1-5.8 MeV 8=16084
Si²⁸, (He³, n) reaction study 8=20694
Si²⁷, low-lying, spin assignments, transitions 8=3803
Si²⁷, single particle states from p scatt. and (p, d) at 27.6 MeV 8=11885
Si²⁷, first and second excited states in Si²⁸(He³, α)Si²⁷ 8=7082
Si²⁸, isobaric analogue states from Al²⁷(d, n)Si²⁸ 8=7080
Si²⁸ structure from Al²⁷(He³, d)Si²⁸ and Al²⁷-He³ scatt., 37.7 MeV 8=15963
Si²⁸ from Al²⁷(p, γ), 0.7-1.5 MeV 8=958
Si²⁸ from Al²⁷(p, γ)Si²⁸, resonant widths 8=959
Si²⁸, photon scatt. from dipole state 8=3905
Si²⁸, 2⁺, 3⁻, polarized proton scatt. asymm. 8=3920
Si²⁸, 5 excited states from 21.2 MeV p scatt. 8=15964
Si²⁸, Villars formalism for nuclear rotation, applic. 8=15941

Nucleus—contd

energy levels—contd
Si²⁸ compound nucleus, statistical theory of reactions 8=3899
Si³⁰, 3786 keV excited state, positive parity 8=20695
Si³⁰, transition from n pickup reactions 8=3959
Si³¹ from Si³⁰(d, p)Si³¹ 8=11925
Sm^{140,150,152,154}, E2, E3 transitions from inelastic d scatt. 8=20824
Sm¹⁴³, redetermination from γ-ray spectra 8=986
Sm^{147,149}, from d scatt. and (d, t) reactions 8=987
Sm^{148,152,154}, E2, E3 transition widths from inelastic α-scatt. 8=20824
Sm¹⁴⁹ from Eu¹⁴⁹ → Sm¹⁴⁹ 8=7143
Sm¹⁵² β- and γ-vibr. bands E₂ transitions and mixing params., obs. 8=11768
Sm¹⁵², β- and γ-vibrational bands 8=16034
Sm¹⁵², E2 transitions, internal conversion 8=1020
Sm¹⁵², half-lives of 2⁺ states 8=11771
Sm¹⁵², 122 keV, 2⁺ rotational state mag. moment 8=7104
Sn even isotopes, quasiparticle calc., E2 transition strengths 8=3824
Sn¹¹⁵, half-life of 7/2⁺ state of 619 keV isomeric level 8=7095
Sn¹¹⁶, energy spectrum, and effective nuclear forces derived from realistic nucleon-nucleon potentials 8=20715
Sn^{116,120,124}, by inelastic electron scattering at 150 MeV 8=11757
Sn^{117m,119m}, internal-conversion studies of M4, M1 transitions 8=20717
Sn^{118,120}, half-life of first 4⁺ state and 5⁻ state 8=11758
Sn^{118,120,124} from n capture resonances 8=20716
Sr⁸⁸, levels, spin and parity obs. by inelastic 65-70 MeV e scatt., width of E2 8=20710
Sr⁸⁸, from Sr⁸⁸(d, p)Sr⁸⁸, 7.0 MeV 8=11932
Sr⁸⁹ from p scatt. of Sr⁸⁸, 5-8.7 MeV 15 isobaric analog states 8=15982
Ta, rel. to shell and unified models 8=3833
Ta¹⁷⁹ isomer, negative search for high spin three-quasi-particle 8=7108
Ta¹⁸¹, parity admixture obs. from polarization asymm. of γ-rays 8=15997
Ta¹⁸², 16.3 min, study by Ge(Li) detector and e-e coincidence spectrometer 8=20727
Tb^{155,157,159}, transition probability, 5/2⁺[532] → 3/2⁺[411] 8=15994
Tb^{155,157,159,161}, E1 transition life times, possible dipole contrib. 8=3827
Tc⁹⁹, half life of 920 keV level 8=20747
Te, even isotope spectra, drawbacks of conventional interpretation 8=20713
Te isotopes, α-particle scatt. to one- and two-phonon states 8=1098
Te resonance spectroscopy, 15 level widths 8=20813
Te⁵², energy level density parameter from Xe⁵⁴(n, α)Te⁵², 12.5-18.0 MeV 8=3942
Te^{118,120,122,124,126}, half-lives and level schemes 8=20718
Te¹²¹, partial scheme from P¹²¹ decay obs. 8=20752
Te¹²², E2/M1 mixing ratio for 2⁺-2⁺ transition 8=975
Te¹²², 686 keV transition, E2/M1 mixing ratio from ang. correl.meas., γγ cascade 8=11782
Te¹²³, 145 keV, lifetime meas., E2 transition rate 8=11759
Te¹²⁴, g-factor of 603 KeV state obs. 8=20669
Te¹²⁵, half-life of first excited state from Sb¹²⁵, P¹²⁵ decay 8=15986
Te¹²⁹ from Te¹²⁸(d, p)Te¹²⁹, 7.5 MeV 8=3961
Te¹³¹, from Te¹³⁰(d, p)Te¹³¹, 7.5 MeV 8=984
Th²²⁸, asymmetric-rotor model 8=999
Ti⁴², (He³, n) reaction study 8=20694
Ti⁴⁸, mixing and branching ratios following p scatt. 8=11747
Ti^{48,50}, polarized p scatt. transitions 8=11880
Ti⁴⁹, cascades following Ti⁴⁸ thermal n capture 8=11903
Ti⁹⁰, B(E2)† value 8=935
Tl²⁰³, parity admixture obs. from polarization asymm. of γ-rays 8=15997
Tl²⁰⁸, rel. to tensor pairing forces 8=919
Tl²⁰⁸ spectra 8=7047
Tm¹⁷⁰, from d scatt. rot. states, B(E2) values 8=7106
Tm¹⁷⁰, 4.1 μs isomeric state, strongly retarded E1 transitions 8=990
Tm¹⁷¹ energy spectrum from Er¹⁷¹ → Tm¹⁷¹ 8=11775
Tm¹⁷², 0-forbidden transition, level lifetimes 8=15995
U²³³, absolute M1 and E2 transition probabilities 8=20731
U²³⁶, from P²³⁹, rotational parameters for 5 rotational bands 8=11789
U²³⁸, n- and d-scatt. obs. 8=16007
V n scatt., deviation from Porter-Thomas distrib. 8=3809
V^{47,49}, internal conversion coeff. and γ-ray angular distribution 8=15974
V^{47,49,51} from (He³, d) reactions on Ti^{46,48,50} at 10 MeV 8=969
V⁴⁸ from Ti⁴⁶(He³, p)V⁴⁸, 12 MeV 8=20702
V⁴⁹, structure from Cr⁵⁰(t, α), 13 MeV, and Ti⁴⁸(He³, d), 18 MeV 8=11750
V⁴⁹, p excitation in Ti⁴⁸(He³, d)V⁴⁹, 17 MeV, transitions obs. 8=20701
V⁶¹, B(E2)† value 8=935
V⁶¹ quadrupole moment and effective E2 transition moments 8=968

Nucleus—contd

energy levels—contd

- V^{51} reson. integral 8=16098
 V^{51} , from n scatt., 1.0-3.1 MeV, dominant E2 transitions 8=15975
 V^{51} from $Ti^{50}(He^3, d)V^{51}$, 10, 11, 12 MeV 8=3808
 V^{52} , study from $V^{51}(n, \gamma)V^{52}$ reaction 8=1079
 W^{180} from Re^{180} 2.5 min. decay 8=3885
 W^{182} , γ - γ angular correlation obs. 8=20728
 $W^{182, 184, 186}$ from n scatt., 0.3-1.5 MeV 8=1074
 W^{183} , retarded transitions, RPC model 8=992
 W^{186} , low level scheme 8=16043
 Xe^{123} decay, gamma ray and conversion electron spectra 8=7138
 Xe^{128} from I^{128} , Cs^{128} γ decay, no $O^+-2^+-4^+$ triplet obs. 8=3825
 Y , ground state $1/2^-$ from $Zr^{90, 92, 94, 96}(d, He^3)$ $Y^{89, 91, 93, 95}$ 8=20830
 Y^{89} from (p, p') reaction at 14.71 MeV 8=1054
 Y^{89} , giant resonance parameters from photon interactions 8=1040
 Y^{89} , obs. in inelastic 65-70 MeV e scatt. B(E2) of low-lying quadrupole states 8=20710
 Y^{89} , 0.908 MeV from 61.2 MeV p scatt. 8=1053
 Y^{90} , energy diagram 8=7215
 Yb^{172} , spins and parities of rot. bands 8=11823
 Yb^{172} , K=3 rot. band, multipolarities from Lu^{172} decay 8=15996
 Yb^{176} , 8.2n decay 8=3831
 Zn , β parameter for 4 26 MeV d scatt. 8=7229
 $Zn^{63, 65}$, internal conversion coeff. and γ -ray angular distribution 8=15974
 $Zn^{64, 66}$ from $Cu^{63, 65}(He^3, d)Zn^{64, 66}$, 18 MeV 8=3970
 $Zn^{64, 66, 68, 70}$ 50 MeV p scatt., optical analysis 8=7186
 $Zn^{64, 66, 68, 70}$ spectroscopic factors up to 3.5 MeV from 10 MeV (d, p) reaction 8=11929
 Zn^{67} , 184 keV transition, E2/M1 mixing parameter, half-life 8=7085
 Zn^{68} from $Zn^{67}(n, \gamma)$, γ -ray spectrum obs. 7=7213
 Zn^{69m} , 0.436 MeV, k conversion coeff. 8=974
 Zr , shell model p admixture in ground states 8=20830
 Zr^{89} from $Y^{89}(p, n)Zr^{89}$, low lying states obs. 8=977
 Zr^{89} , from $Y^{89}(p, n)Zr^{89}$, 3.6-5.8 MeV 8=11889
 Zr^{90} , dipole resonances from $Y^{89}(p, \gamma)Zr^{90}$ 11.9-13.5 MeV 8=976
 Zr^{90} giant resonance isobaric splitting, evidence from $Y^{89}(p, \gamma_n)$ 8=11753
 Zr^{90} isobaric analogue states in eigenchannel theory 8=3819
 $Zr^{90, 91, 92, 94}$, giant resonance parameters from photon interactions 8=1040
 $Zr^{90, 92, 94, 96}$, resonance structure, s-wave strength function, 2-60 keV 8=11907
 Zr^{91} , Schrödinger equation with Woods-Saxon potential, solution 8=7055
 $Zr^{93, 95}$, $d_{5/2}$ ground state anomaly, rel. to charge exchange effects 8=11755
 Zr^{96} , p elastic and inelastic scatt., spectroscopic factors 8=3929

excitation. See Nuclear excitation.

magnetic moment

- See also Gyromagnetic ratio; Molecules/nuclear coupling; Nuclear magnetic resonance and relaxation.
 atomic shielding factors 8=1155
 dipole interaction with external and internal fields, symm. test for e.m. transitions 8=3775
 e.m. of nuclear states, Tam-Dancoff theory for vibr. nuclei 8=20663
 e scatt. asymm. function as a means of meas. 8=3910
 4+ rotational states 8=15938
 "heated" nuclei, calc. 8=7065
 simple interaction model, calc. for A=6, 18, 42 8=11689
 spin-orbit correction, perturbation theory 8=941
 transition densities of dipole excitations in nuclei with $N > Z$ 8=7088
 Ar^{39} , measurement by spectroscopic techniques 8=11739
 Br^{209} , connection calc. with Hamada-Johnston potential 8=3843
 C^{12} , attenuated magnetic dipole and quadrupole transitions 8=11722
 Cs^{133} of first excited state by Mössbauer effect 8=15987
 Cs^{138} , and spin, at beam investigation 8=7098
 $Dy^{161, 162}$, 75 and 81 keV states 8=3829
 Hg^{199} radius meas. using optical method 8=7078
 In^{117} , g-factor of $3/2^+$ 660 keV 8=3823
 Ir , n.m.r. and dipole moments of $^{191, 193}Ir$ 8=14144
 Na^{23} radius meas. using optical method 8=7078
 Ni isotopes, model mixing 1- and 3-quasiparticle states 8=971
 Np^{237} ratio between 59.54 keV level and ground state 8=11790
 O^{16} , attenuated magnetic dipole and quadrupole transitions 8=11722
 Rb^{85} , g_1/g_2 meas. by atomic beam resonance method 8=20709
 Rb^{88} determ. from spin, hyperfine electronic structure 8=20708
 Si^{29} , connection calc. with Hamada-Johnston potential 8=3843
 Sm^{182} , 122 keV, 2⁺ rotational state 8=7104

Nucleus—contd

magnetic resonance. See Nuclear magnetic resonance and relaxation.

models

- adiabatic using HF eqns. for collective vibrations of deformed nuclei 8=11707
 asymmetric-rotor applic. to Th^{228} 8=999
 asymmetric rotor, rel. to rotational states in even-even nuclei 8=948
 breathing mode calc., breakdown for Ca^{40} , Pb^{208} 8=3783
 cascade-evaporation rel. to formation of radioactive nuclides in Ag from p bombard, 3 and 29 GeV 8=20799
 cascade evaporation rel. to U and Ta, 156 MeV p-induced fission 8=11965
 Clebsch-Gordan coeffs. and projection operators for SU₃ 8=15680
 collective, book 8=3760
 collective for $Be^8(Li^7, p)C^{15}$, lifetime of excited state of C^{15} 8=20680
 collective for $Cl^{35}(n, d)S^{34}$ 8=1078
 collective, giant resonances, dipole vibrations 8=7044
 collective interaction from deforming complete optical pot. for p scatt. asymm. 8=3920
 compound for $Mn^{55}(p, n\gamma)Fe^{55}$, 1.8-3.5 MeV 8=3927
 compound nucleus for (Li^7, p) , (Li^7, d) , (Li^7, t) on C^{12} at 3.5 MeV 8=3975
 cranking, rel. to nuclear rotation parameters 8=940
 cranking, rotational states of deformed nuclei 8=11685
 cranking, self-consistent, charge radii calc. 8=15921
 Davydov, non-adiabaticity of β -vibrations in rare-earth even-even nuclei 8=947
 Davydov-Chaban, validity of centrifugal stretching 8=16001
 de-Shalits core excitation and levels of Au^{199} 8=994
 diffraction, with surface absorption 8=11842
 drop, inertial deformation 8=20652
 elementary particle, test in $n + He^3 \rightarrow p + H_2^+$ 8=15873
 Elliot SU₃ shell for particle-hole states of Ca^{40} 8=11745
 Fermi gas, calc. of matrix elements for transitions 8=3780
 Fermi gas, finite size corrections rel. to the function $F(\nu)$ 8=20648
 Fermi liquid, Migdal's, density matrix approach 8=20653
 Fermi liquid theory rel. to O^{16} odd parity state 8=20686
 finite system, effective field eqn. 8=920
 harmonic oscill. core with superimposed N-N interactions in O^{17} 8=20687
 Helm's for electroexcitation of levels, extension 8=3773
 hydrodynamic, density distrib., influence of nonlinear surface vibrs. 8=11686
 impulse, for He^4 radius meas. 8=20590
 independent particle in π photoproduction reactions on B^{11} 8=1035
 isobaric analogue states in heavy nuclei, quasiparticle theory 8=3778
 liquid drop rel. to effective masses for fission 8=7241
 liquid-drop, for studying Coulomb distortion in superheavy-ion reactions 8=11688
 liquid drop rel. to U and Ta, 156 MeV p-induced fission 8=11965
 liquid drop, vibrating, incompressible, irrotational 8=11785
 n particles moving in 2 j-shells interacting via pairing force 8=15923
 Nilsson, of nuclear deformation 8=16005
 Nilsson, appl. to odd-mass rare-earth vibrational states 8=15992
 Nilsson in E1 transition of Eu and Tb isotopes, anomalies 8=3827
 Nilsson and the isomeric decay of Dy^{150} , Tm^{185} , $Lu^{172, 173}$ and W^{180} 8=3828
 Nilsson, and g-factors of $Np^{237, 239}$ 8=3846
 nucleon-phonon interaction model, energy spectra calc. 8=3763
 odd mass, near A ~ 190, systematics of shell and unified models 8=3833
 optical for $\alpha + S^{32}$ scatt., 10-17.5 MeV 8=20832
 optical analysis of π -nucleus scatt. 8=3948
 optical rel. to $Bi^{20, 11}(p, d)B^{9, 10}$ 8=20788
 optical, book 8=3760
 optical for $C^{15}(d, p)C^{14}$, 4-6 MeV compared to DWBA analysis 8=16113
 optical rel. to $Co^{59}(He^3, d)Ni^{60}$ and $Co^{59}-He^3$ scatt. 8=15981
 optical in d scatt. and stripping reactions on Ca^{40} 8=16118
 optical for d elastic scatt. from $Ti^{47, 48, 49, 50}$ 8=20823
 optical for d- Li^6 and He^3-Li^6 scatt. 8=20833
 optical for 50 MeV p scatt. from $Zn^{64, 66, 68, 70}$ 8=7186
 optical and geom., for total cross sections for He^3 8=11937
 optical rel. to $Mg^{24}(d, n)Al^{25}$, 1.38-2.8 MeV 8=11923
 optical for n scatt. from Fe, Al, 1-4 MeV 8=3935
 optical for n scatt. off heavy nuclei, 6-24 MeV 8=16085
 optical and Nilsson for $Ne^{22}(He^3, d)Na^{23}$, 10, 12 MeV 8=3802
 optical, nuclear reactions due to nucleons 8=1049
 optical, parameters for α -particles, influence of expt. errors 8=11941
 optical parameters for low energy α scattering 8=16120
 optical, parameters for polarized p scatt. 8=16067
 optical parameters from p elastic scatt., 3 GeV/c 8=20780
 optical, parameters from p, and d-induced reactions 8=109
 optical rel. to polarized p scatt., ang. asymm. 8=11880

Nucleus—contd**models—contd**

- optical potentials, complex, derivation 8=7038
 optical potential in DWBA calc. of direct interaction part of scatt. S matrix 8=7153
 optical potential of deuteron, link-cluster expansion 8=6991
 optical potential, form of imaginary part 8=3757
 optical potential for isobaric analogue resonance theory 8=7046
 optical pot., isospin dependent term investigated by n, p scatt. off Co⁶⁰, Bi²⁰⁹ 8=7039
 optical potential for neutron scattering on heavy nuclei 8=7197
 optical potential, N, complex symmetry term from n scatt. data 8=924
 optical potential relationship for spherical and deformed nuclei 8=11687
 optical potential, spin-spin interaction during quasi-elastic scattering 8=15936
 optical potential in Te- α scatt. 8=1098
 optical for p elastic scatt. 8=3917
 optical for p scatt. off Mg²⁴ 49.5 MeV 8=3919
 optical rel. to reaction cross-section for α -particles on nuclei of about A = 60 8=7237
 optical, real part of potential for proton diff. elastic scattering 8=11876
 optical, square-well, generalized for n-nucleus scatt. 8=16086
 pairing corrls. in even-even nuclei, ground-state energy calc. 8=922
 particle-hole in collective O⁻ vibration calc. in 8 nuclei 8=11706
 particle hole treatment of corrl. between resonances and surface vibrs. 8=933
 potential, deformed spin-dependent 8=20779
 p holes coupled to vibrating core for energy levels of Hg^{198, 200, 202} 8=3838
 quantal, of double even rotating in plane, energy depend. of ang. momentum 8=11708
 quasiboson approx. rel. to even-parity states of O¹⁶ 8=11727
 quasi-particle excitation, gapless super-conductivity 8=928
 quasi-particle, phenomenological test 8=925
 random phase approx. generalized to include ground state corrls. 8=15920
 rotational anomalies in transitions props. of Si²⁷ 8=3803
 rotational, applic. to low-lying states of Na²³ 8=956
 rotation vibration interaction rel. to E2 transition probabilities in even-even nuclei 8=15939
 rotation-vibration rel. to rotational states in even-even nuclei 8=948
 rotor, asymmetric, +ve parity level of β -vibration bands description 8=946
 schematic interactions for complex problems 8=934
 shell amplitude and relative phase calc. in O¹⁸ (t, p) O¹⁸ 8=20826
 shell, approx. and exact. solns. compared, var. in potential and radius 8=3764
 shell, Be¹¹, evidence from μ capture rate in B¹¹ \rightarrow Be¹¹ 8=11873
 shell, book 8=3760
 shell, bound to error in diagonalization of Hamiltonian 8=3761
 shell, Ca⁴⁰, anomalies revealed by pickup reactions 8=11854
 shell for C¹³ (n, d) S³⁴ 8=1078
 shell, for crossover to E2 transitions in Ni⁵⁸ 8=3928
 shell calc. of d-s states, SU₆, SU₃ selection rules 8=7050
 shell for (d, n) reactions on B¹¹ and N¹⁵, 6 MeV 8=7073
 shell, DWBA approach to nuclear reactions 8=7153
 shell effect in (n, 2n) reactions at 14 MeV 8=11895
 shell, extended, equations-of-motion method 8=15922
 shell calc. for F¹⁸, O¹⁸ 8=11728
 shell, G matrix fit in 1p shell 8=7048
 shell rel. to γ transitions in B¹¹, anomaly 8=11721
 shell rel. to γ transition of 8.96 and 8.49 MeV levels of N¹⁴ from C¹² (He³, p γ) N¹⁴ 8=11724
 shell for ground state configurations in Zr rel. to Zr^{90, 92, 94, 96} (d, He³) Y^{89, 91, 93, 95} 8=20830
 shell and ground state wave function of Te¹²⁸ 8=3961
 shell and (He³, d) reactions on Ti⁵⁰, Cr⁵² and Fe⁵⁴ 8=3808
 shell, hexadecapole equilibrium distortions 8=20645
 shell, invariant field operator formalism 8=3765
 shell rel. to levels of Al²⁷ from Si²⁸ (d, He³) Al²⁷, 34.4 MeV 8=20692
 shell, low-lying from photonuclear cross sections obs. 8=20659
 shell, low-lying states of Ca⁵⁰ compared to obs. of Ca⁴⁸ (t, p) Ca⁵⁰ 8=7083
 shell, matrix element calc. 8=926
 shell, matrix elements statistics 8=20646
 shell calc. of 1f_{7/2}, 1f_{5/2}, 1d_{5/2}⁻¹, configurations for 40 \leq A \leq 48 8=7049
 shell-model potentials for heavy nuclei and stability of superheavy nuclei 8=11786
 shell model calc. of props. of O^{18, 19, 20}, F^{18, 19, 20}, Ne²⁰ 8=11726

Nucleus—contd**models—contd**

- shell for (n, d) reactions on N¹⁴, C¹³, K³⁹, Ca⁴⁰, As⁷⁵ 8=7212
 shell rel. to N⁹⁰ decay 8=18113
 shell for Ni isotope matrix elements 8=3814
 shell, rel. to Ni⁹⁰-p scatt. form factors 8=15981
 shells, use of outer in phenomenological calc. of quasi-particle model 8=925
 shell for p capture and n scatt. off F¹⁹ 8=3931
 shell, s-d, intrinsic matrix element calc. 8=20651
 shell, separation energy calc. for spherical nuclei 8=3768
 shell, sign of interaction matrix element from Si²⁸ (t, p) Si³⁰ 8=3958
 shell, single particle, realistic N-N pot. BHF calc. of states 8=3762
 shell, SU₃ Clebsch-Gordan coefficients for coupling of single particle to general state 8=15929
 shell, Spicer's 1p-1h calc. for photoneutron cross-section of S³², compared to expt. 8=11860
 shell calc. of structure of Ca⁴⁷, K⁴⁷ using Hamada-Johnston pot. 8=20700
 shell for structure of Pb²⁰⁸ from Pb²⁰⁷ (d, t) Pb²⁰⁸ 8=20730
 shell, Ti⁵⁰ with soft core pot. between nucleons 8=11748
 shell, 2-body interaction matrix elements, calc. from scatt. phase shifts 8=20647
 shell model, 2-particle approx. for light nuclei 8=930
 shell calc. of V⁴⁸ levels in Ti⁴⁸ (He³, p) V⁴⁸ 8=20702
 simple interaction, calc. of excitation, β -decay lifetimes, e.m. moments for A=6, 18, 42 8=11689
 simple shell, core polarization and scatt. of 155 MeV p 8=15951
 single-particle states coupled to core rotations in photonuclear reactions 8=3907
 skin thickness effect in anomalous cross-section for Ni⁵⁸ (p, pn) Ni⁵⁷ 8=20796
 spherical nuclei structure 8=20644
 spherical with pairing-plus-quadrupole-force in levels of P^{25, 127} 8=11760
 statistical in inelastic p scatt. by Mg²⁶, 8.3-14 MeV 8=16077
 statistical in (n, γ) prod. of fissioning isoers 8=20847
 statistical rel. to n reaction on N = 82 isotones 8=11896
 superfluid, rel. to nuclear rotation parameters 8=940
 Thomas-Fermi using theory of nuclear matter, density eqn. developed 8=20649
 unified and e.m. transitions of odd-p and doubly-even nucleides 8=3788
 vibr. and rot., new β and γ bands 8=3784
 weak-coupling states of Y⁸⁹ excited by inelastic e scatt. 8=20710
 Cu⁵⁹, shell description of lowest states 8=972
 Fe⁵⁴, α scattering expt. data and optical model parameters 8=16120
 Ga⁶⁹, compound statistical model and ang. distrib. of γ rays in (α , n) and (p, n) reactions 8=11948
 Li⁶, α -d cluster structure rel. to results of Li⁶ (p, 2p) He³ 8=11717
 Li⁶, shell, harmonic oscillator parameter for p and s-shell N 8=11716
 Ne²¹, states near 3 MeV 8=7077
 Ni isotopes, superposition of 1 and 3 quasi-particle states 8=971
 Ni⁶⁰, α scattering expt. data and optical model parameters 8=16120
 Pb, proton shell-model potentials 8=11786
 Ps isotope for configuration mixing extended to s-d shell and non-degenerate case 8=20774
 Ti⁵⁰ with soft core pot. between nucleons 8=11748
 Zn⁶³, compound statistical model and ang. distrib. of γ rays in (α , n) and (p, n) reactions 8=11948
 Zn⁶⁶, α scattering expt. data and optical model parameters 8=16120
 Zn⁶⁸, α scattering expt. data and optical model parameters 8=16120
- size**
 A=12-124, radius, surface thickness from α -scatt. 8=15949
 β -decay, ft value, effect 8=7125
 charge radii of light nuclei from muonic 2p-1s transition energies 8=3785
 charge radius var. in isotopes from electronic K α , line shift 8=20671
 deformation parameter, location of new quasi bands between vibr. and rot. states 8=3784
 e scatt. study 8=7069
 ice, atmospheric 8=2587
 Fermi gas model, finite size correction effects 8=20648
 finite, effect on internal conversion 8=7061
 hexadecapole equilibrium distortions 8=20645
 muonic atom X-radiation study 8=7069
 π -nucleus scatt., optical model analysis 8=3948
 radius, change on addition of protons 8=945
 radius meas. using optical method 8=7078
 r. m. s. radius, with z protons 8=15950
 rare earth, Y₈₀ and Y₆₀ shape component determ. 8=11713
 shell model var. with approx. and exact calc. 8=3764
 shell struct., trapezoidal and modified Gaussian density 8=11712
 Y₄ moments, behaviour from aligned wave functions 8=11714
 Be⁴⁰, r. m. s. calc. of p, n radii 8=20677

Nucleus — contd

size — contd

- Bi²⁰⁹, charge distrib., possible p halo from muonic X-rays 8=20672
 C¹², r. m. s. calc. of p, n radii 8=20677
 C¹³, charge radius from 250 MeV e scatt. in methane 8=3912
 Ca⁴⁰, shell model, BHF calc. 8=3762
 Er isotopes, radius parameters from n scatt. 8=1073
 He³ perturbation calc. of Coulomb energy and e. m. radius 8=3740
 He⁴, radius meas., use of impulse model 8=20590
 He⁴ shell model, BHF calc. 8=3762
 K⁴⁰, A⁴⁰, mass difference determ. from Q value of various reactions 8=11740
 La¹³⁹ radius, e scatt. at 225 ± 0.7 MeV obs. 8=11866
 Li^{6,7}, 100-600 MeV e elastic scatt., r. m. s. radius determ. 8=1047
 Mg²⁴, equilibrium shape, restoration of axial symmetry by pairing correlations 8=15962
 O^{16,18}, radii 8=943
 O¹⁶, shell model, BHF calc. 8=3762
 W¹⁸³, large inertial parameter for high-lying bands 8=992
 Yb even-even isotopes, moment of inertia anomaly 8=3832

spin and parity

- See also Gyromagnetic ratio; Molecules/nuclear coupling.
 angular correl. coeff. with transitory formations betw. dipole-quadrupole mixtures 8=7063
 ang. momentum dependence of off-shell amplitudes 8=3895
 asymmetric-rotor applic. for negative parity levels in deformed nuclei 8=999
 compound nucleus, γ -ray emission ang. dist. effect 8=932
 (d, p) reaction in 1p shell, ang. distrib. calc., J-depend. effects 8=11921
 dipole resonance, influence of spin-orbit splitting 8=7053
 g-factor meas. of short-lived states, sum-coincidence method 8=20669
 heavy nuclei, rotation theory using cranking model and superfluid matter 8=940
 isospin for A = 24, 28 in nuclear level density calc. 8=20658
 isospin dependence of optical pot. 8=7039
 isospin hindered transitions, second-order contrib. 8=1005
 isospin mixing in d induced reactions 8=1088
 isospin term in nuclear pot. for (p, n) reactions, 94 MeV 8=16070
 J π = O $^-$ states calc. for 8 nuclei 8=11706
 level density spin depend. in evaporation analysis 8=11699
 moment of inertia, HF calc. for doubly nuclei 8=7033
 moment of inertia, Inglis formula generalization 8=11708
 nuclear e. m. transitions, role of applied field and ang. correl. instead of polarization 8=3775
 odd-odd nuclei, moments of inertia 8=15948
 odd triplet states, N-N potential 8=3777
 n pairing energy as a function 8=3770
 quadrupole-octupole interaction rel. to two phonon states 8=15927
 residual, A(x, yz)B produced, polarized target 8=3898
 rotation matrices, orthogonality and completeness 8=7062
 spin-orbital potential, large momentum 8=7064
 spin-orbit splitting in spherical H-F theory 8=15947
 spin-quadrupole interaction rel. to β -decay ratio to O $^+$ and ground states 8=11801
 spin-spin interaction in optical potential during quasi-elastic scattering 8=15936
 T = % of 7 nuclei, mass determ. by reaction 8=20656
 2I + 1 rule obs. in F¹⁹(d, α)O¹⁷, 0.9-4.25 MeV 8=16115
 2s-1d shell, moment of inertia calc. method 8=11709
 violation of parity, and time reversal, possible tests 8=939
 Ag¹⁰², spin 2 state by magnetic resonance technique obs. 8=7094
 Ag¹⁰⁹ from Pd^{109g} → Ag^{109g}, anomalies 8=16026
 Al²⁶, isospin selection rule in Si²⁸(d, α)Al²⁶ 6.98-11.06 MeV 8=20829
 Al²⁶ level assignments from Mg²⁵(He³, d)Al²⁶, 12 MeV obs. 8=16122
 Al²⁷, assignments from Si²⁸(d, He³)Al²⁷, 34.4 MeV 8=20692
 Al²⁹ in Si³⁰(d, He³)Al²⁹ 8=20693
 Am²⁴² prod. by (n, γ) 8=20847
 Am²⁴⁵ following Pu²⁴⁵ decay 8=11833
 Ar³⁸ assignments from Cl³⁷(p, γ)Ar³⁸, 1.0-1.8 MeV 8=11737
 Ar³⁸, 4.88 and 5.36 MeV, from Cl³⁵(α , p γ) reactions at 10.6 MeV 8=3804
 Ar³⁸, spin measurement by spectroscopic techniques 8=11739
 As⁷⁵ levels from α and O¹⁶ scatt. 8=3816
 Au¹⁹⁷ from 0.15-1.5 MeV n scatt. 8=11899
 Au¹⁹⁹ from Pt¹⁹⁹ decay 8=994
 Au¹⁹⁹ obs. 8=7112
 B⁹ levels from B¹⁰(p, d)B⁹, 33.6 MeV 8=20788
 B¹⁰, 2 $^-$ state from Li⁷(He³, γ)B¹⁰, 3-6 MeV 8=11943
 B¹¹ level assignments in Be⁹(He³, p γ)B¹¹, 3, 4 MeV 8=20681
 B¹¹ from Li⁷(α , γ)B¹¹, of 9.87, 10.26, 1062 MeV states 8=11721
 B¹², 0.95, 1.67, 2.62 MeV, spin assignments from γ - γ correl. meas. 8=20679
 Be⁷ from He³-He⁴ and He³-H³ scatt. 8=7001
 Be⁸, isotopic spin mixing in high excited states from (p, d) reaction 8=3923
 Be⁸, 16.82 level, J π = O $^+$ in Be⁹(He³, α)Be⁸ → α + α 8=20834
 C¹¹ from α γ correls. in C¹²(He³, α γ)C¹¹ 8=953
 C¹¹ level assignments after C¹²(He³, α γ)C¹¹, 4-12 MeV 8=20681
 C¹², from B¹¹(d, n)C¹², 6 MeV, spectroscopic factors 8=7073
 C¹² levels from inelastic 100-200 MeV e scatt. 8=16063
 C¹², 19.4 MeV level, 2 $^-$ assignment from e scatt. 8=20682
 C¹³ assignments from 52 MeV d bombard. of N¹⁴ 8=7228
 C¹³ assignments from N¹⁴(p, He³)C¹³, 47.3 MeV 8=20791
 Ca isotopes, assignments from (t, p), 10-12 MeV 8=1094
 Ca⁴⁰(d, α)K³⁸, isospin mixing in compound nucleus 8=7230
 Ca⁴⁰, 1 $^-$ assignment from 31 MeV α -scatt. 8=11746
 Ca⁴⁰, 6.91, 6.95 MeV, γ -scatt. rel. to spin, lifetime assignments 8=11743
 Ca⁴⁰, spin of 5.21 MeV state, parities of 5.25 MeV triplet 8=11744
 Ca^{40,42,44,48}, 31 MeV α scatt., new multipole states, spin-parity assignments 8=3807
 Ca^{42,46} from Ca^{40,40}(t, p), 7.5 MeV 8=11741
 Ca⁴⁷, low level of positive parity states, spectroscopic factors calc. 8=20700
 Ca⁵⁰ from Ca⁴⁸(t, p)Ca⁵⁰, low lying states obs. compared to shell model calc. 8=7083
 Ce¹³⁸, level assignments from Pr¹³⁹ decay 8=7141
 Ce¹⁴⁰ levels from Fm²⁵³ decay 8=11836
 Cl³⁵ analog states of S³⁵ from S³⁴(p, γ)Cl³⁵ 8=11735
 Cl³⁵, 8.385 MeV level 8=1063
 Cl³⁵ from S³⁴(p, γ)Cl³⁵, level assignments 8=11736
 Cl³⁷, level from β decay of S³⁷ 8=16018
 Co⁵⁶, from internal conversion coeff. and γ -ray angular distribution 8=15974
 Co⁵⁷, 1.22, 1.68 MeV levels from Fe⁵⁴(α , p)Co⁵⁷, 10.5 and 11 MeV 8=15978
 Co⁵⁸ spin cutoff parameter calc. from isomer ratios 8=20707
 Co⁵⁹, scatt. levels, from O¹⁶, d scatt. 8=3813
 Cs¹³⁸, and mag. moment, at beam investigation 8=7098
 Dy¹⁶¹, 75 keV level, by Mossbauer effect 8=3829
 Er¹⁶⁰, ground-state spin using atomic beam magnetic resonance 8=11777
 Eu¹⁵⁵ levels from Sm¹⁵⁵ decay 8=7105
 Eu¹⁵⁶, isobaric spin impurity calc. 8=1019
 F¹⁸, 1.131 MeV level, from O¹⁶(He³, p γ) 8=3800
 F¹⁹(d, α)O¹⁷, 0.9-4.25 MeV obs. of 2I + 1 rule 8=16115
 Ga⁶⁸, from internal conversion coeff. and γ -ray angular distribution 8=15974
 Gd¹⁵⁵, 86.5 and 105.3 keV states, and attenuation coeffs. 8=20725
 Ge⁷¹ from Ge⁷⁰(d, p)Ge⁷¹ at 7.5 MeV 8=11931
 Ge⁷², from Ga⁷² decay 8=1013
 Ge⁷² from Ga⁷² decay 8=16021
 He³-He⁴ solutions, polarization enhancement 8=256
 He⁴, calc. of odd-parity states 8=887
 Hf¹⁷⁸, 3 I = 0 states, positive parity obs. 8=11766
 Ho^{165,166}, resonances induced by n scatt., 35-750 eV and capture, 2.5-10⁵ eV 8=16101
 I¹²⁷, 60-900 keV n scatt., level spin 8=7096
 I^{130m}, isomeric transition and disintegration, levels 8=7097
 I¹³¹, parity assignments from internal conversion decay of Te^{131m} 8=3878
 K³⁷, 2750 KeV level, established as $\frac{5}{2}^+$ 8=3805
 K³⁹ de-excitation following Ca⁴²(p, α)K³⁹ and p scatt. 8=15967
 K^{39,41} level assignments from inelastic n scatt. and (n, p γ) reactions 8=20809
 K⁴⁰, J π = O $^+$, for 1.64 MeV level 8=15968
 K⁴¹ from p induced reactions 8=964
 K⁴⁷, ground state $\frac{1}{2}^+$ instead of $\frac{3}{2}^+$ in other K isotopes 8=20700
 Kr⁸², 1821 keV 8=11782
 La¹³³ from β -decay of Ce^{133,133m}, β -deformation 8=20722
 La¹³⁵ level assignments from Ce¹³⁵ decay 8=20721
 Li⁵ level $\frac{3}{2}^+$ deduced in H²(He³, γ)Li⁵ 2-5.5 MeV 8=20581
 Li⁵, $\frac{3}{2}^+$ state obs. in p- α scatt. 22-25 MeV 8=20532
 Li⁶ from d- α scatt., 3-14 MeV 8=11651
 Li⁷ from He³-He⁴ and He³-H³ scatt. 8=7001
 Li⁷(p, n)Be⁷ (431 keV), spin-flip and isospin-flip 8=3924
 Li⁷(p, p')Li⁷ (478 keV), spin-flip and isospin-flip 8=3924
 Lu^{169,170,171}, ground-state spin using atomic beam magnetic resonance 8=11777
 Lu¹⁷⁵ level, parity admixture obs. from polarization asymm. of γ -rays 8=15997
 Mg²³, level assignments from Mg²⁴(He³, α γ)Mg²³ 9.00 MeV 8=11730
 Mg²⁴, level assignments deduced from Ne²⁰(α , γ)Mg²⁴ 3-6 MeV 8=16121
 Mg^{24,26}(α , γ)Si^{28,30}, isospin allowed giant dipole resonance 8=11944
 Mn, 200 keV n scatt., resonance levels 8=3809
 Mn⁵⁵ assignments from n scatt., 1-3.1 MeV 8=15975
 N¹³ assignments from N¹⁵(p, t)N¹³, 43.7 MeV 8=20791

Nucleus—cont'd

spin and parity—cont'd

N¹⁴ from $\alpha\gamma$ correls. in C¹²(He³, p γ)N¹⁴ 8=953

N¹⁴, 8.86 MeV level from C¹²(He³, p γ)N¹⁴ at 8.92 MeV 8=11724

Na²², J = 5(or 3) for 1.528 MeV state, J = 4 for 0.891 MeV state 8=20690

Na²², from linear polarization meas. on γ de-excitation 8=15961

Na²² from Ne²⁰(He³, p γ)Na²², 6.56 MeV 8=3801

Nd¹⁴¹ obs. 8=7102

Nd¹⁴³, p, f, h-wave states from 12 MeV p scatt. off Nd¹⁴² 8=7195

Nd¹⁴⁴ deduced from Pr¹⁴⁴ decay 8=11765

Nd¹⁴⁴, 2.86 MeV, spin zero obs., positive parity 8=11766

Nd¹⁵¹ from Nd¹⁵⁰(d, p)Nd¹⁵¹, band mixing 8=11767

Ni⁵⁸(p, p' γ) levels, parity determ. 8=3928

O¹⁶, level assignments, multipole mixing ratios obs. 8=11725

O¹⁶, J π = 2+ and 4+ at 6.92 and 10.36 MeV, rot. structure 8=3796

O¹⁶, 19.08 MeV level, J π = 2 $^-$ from e scatt. 8=3794

O¹⁶, n scatt. negative parity states 8=1069

O¹⁶ from N¹⁵(d, n)O¹⁶, 6 MeV spectroscopic factors 8=7073

O¹⁶ odd parity states, Fermi liq. theory 8=20686

O¹⁷, J = 5/2 and J = 3/2, level separation calc. 8=20687

O¹⁷, 2, 2.4-2 MeV n scatt. 8=1070

P³¹ from Si³⁰(p, γ)P³¹ 8=961

P³³ in S³⁴(d, He³)P³³ 8=20693

Pb²⁰⁸, excitation obs. from e scatt., 28-73 MeV 8=11785

Pb²⁰⁸ levels from Bi²⁰⁹(t, α)Pb²⁰⁸, 13 MeV 8=11936

Pd¹⁰⁶ level assignments from Ag^{106m} decay 8=7092

Pm¹⁴⁷, from Nd¹⁴⁷ decay 8=3881

Pr, spin of compound nucleus in n resonance spectroscopy 8=20813

Pr¹⁴³, from Ce¹⁴³ β decay, 8 levels 8=11764

Pu²³⁹, α emission in fission, ang. momentum effect 8=3977

Rb⁸⁸, in S γ electronic ground state nucleus² 8=20708

Re¹⁸³ from Ta¹⁸¹(He⁴, 2n γ)Re¹⁸³, 19.8 MeV 8=20729

Re¹⁸⁶ deduced from thermal n capture by Re¹⁸⁷ 8=11780

Rh¹⁰², 2 year, rel. to γ -ray spectra 8=20751

Ru⁹⁹ from Rh⁹⁹ γ -decay 8=978

Ru¹⁰³, assignments from internal conversion β -spectrum 8=11815

S³² from Si²⁸(α , γ)S³², 3.7-4.3 MeV 8=963

S³⁶, positive parity, from Cl³⁷(d, He³) 8=20696

S³⁷, ground state 8=16018

Sb^{117, 119, 121}, low-lying levels 8=3971

Sb¹¹⁹, spin assignments from Te^{119m} decay 8=3877

Si²⁷ levels from Si²⁸(He³, $\alpha\gamma$)Si²⁷ 8=3803

Si²⁸(α , γ)S²⁸, 7-12 MeV, isospin allowed giant dipole resonance 8=11944

Si²⁸ levels from AP²⁷(He³, d)Si²⁸, 37.7 MeV 8=15963

Si³⁰, 3786 keV excited state, positive parity 8=20695

Si³⁰, transition from n pickup reactions 8=3959

Si^{118, 120, 124} from n capture resonances 8=20716

Sr⁸⁸ level obs. from inelastic 65-70 MeV e scatt. 8=20710

Sr⁸⁹ from p scatt. of Sr⁸⁸, 5-8.7 MeV 8=15982

Ta¹⁸¹, circular polarization of 482 keV γ transition obs. 8=11779

Ta¹⁸¹, e. m. transitions, symm. props. 8=3775

Ta¹⁸¹, parity admixture obs. from polarization asymm. of γ -rays 8=15997

Te isotopes, α -particle scatt. to one- and two-phonon states 8=1098

Te¹²⁸(d, p)Te¹²⁹, orbital ang. momentum for transferred n 8=3961

Ti⁴⁶ assignments from p scatt. 8=11747

Ti⁴⁹ assignments following Ti⁴⁸ thermal n capture 8=11903

Ti²⁰³, parity admixture obs. from polarization asymm. of γ -rays 8=15997

Tm¹⁶⁵, ground-state spin using atomic beam magnetic resonance 8=11777

Tm¹⁷⁰, from d scatt., 5.5 and 12 MeV 8=7106

Tm¹⁷¹ assignments from Er¹⁷¹ \rightarrow Tm¹⁷¹ 8=11775

U²³⁸, spin depend. of n cross-section 8=20849

V, 200 keV n scatt., resonance levels 8=3809

V^{47, 49}, from internal conversion coeff. and γ -ray angular distribution 8=15974

V^{47, 49, 51} from (He³, d) reactions on Ti^{46, 48, 50} at 10 MeV 8=969

V⁴⁸, isospin impurity deduced from β - γ circular polarization correl. 8=7131

V⁴⁸, 305 keV state, parity determ. from γ polarization meas. 8=11749

V⁵¹ assignments from n scatt., 1-3.1 MeV 8=15975

W¹⁸⁰ from Re¹⁸⁰ 2.5 min. decay 8=3885

W⁹⁰ level obs. from inelastic 65-70 MeV e scatt. 8=20710

Yb¹⁷² levels, rot. and vib. bands 8=11823

Zn^{63, 65}, from internal conversion coeff. and γ -ray angular distribution 8=15974

Zn^{64, 66} from Cu^{63, 65}(He³, d)Zn^{64, 66}, 18 MeV 8=3970

Zn^{64, 66, 68, 70} spectroscopic factors up to 3.5 MeV from 10 MeV (d, p) reaction 8=11929

Zn^{68, 66} from γ polarization meas. following thermal n capture 8=11905

Zn^{69m}, 0.436 MeV level 8=974

Nucleus—cont'd

theory

See also Nuclear forces.

algebra, invariant operator, applied to shell model harmonic potential 8=3765

Austern-Blair modification, deformation parameters 8=3963

boson approx. and antisymmetry 8=7030

Brueckner, calc. of π absorpt. rates in C¹² with 2N emission 8=20654

core correl. effect on motion of 2 outer N 8=3767

core polarization and scatt. of 155-MeV p 8=15951

diffraction theory of ion scatt. with mutual excitation 8=1102

DWBA analysis tested in (He³, α) on Cr^{50, 52, 54} at 18 MeV 8=3969

DWBA stripping rel. to Si²⁸(d, n)P²⁹, 3 MeV 8=16117

Eichler-Marumori 2-step method for 4 particle-4 hole states 8=15958

Fermi gas model, statistical description rel. to level density as a function of isospin 8=20658

field average, of n and p shells with N > 126 and Z > 82 8=7035

field eqn., effective, in finite system 8=920

4 identical particles, Euler angles, helicity formation 8=15912

generator-coordinate method and random phase approx. 8=20641

ground state props. of nuclear matter, Λ_{11} approx. 8=15926

group-symmetry breaking Hamiltonian operator 8=7031

HF and stability condition for stationary HF soln. 8=11705

Hauser-Feshbach for excitation functions in n scatt. off I¹²⁷ 8=7096

Majorana exchange forces and photodisintegration of three-particle nuclei 8=7162

many-body problem, linked-cluster expansions 8=11694

matrix element calc., intrinsic in s-d shell 8=20651

neutron shell, closed, near N = 50, parameter var. with n number and atomic weight 8=1040

Nilsson wave function for energy level calc. of C¹² 8=3792

nuclear matter, Brueckner-Goldstone theory 8=11692

nuclear matter, 3-body problem and Brueckner-Goldstone series convergence 8=11690

by nuclei, diffraction scatt. separation of variables 8=1030

nuclides far off the stability line, conference, Lysekil Sweden (1966) 8=15911

nucleon distribution in nuclei by finite Fermi system theory 8=7036

nucleon emission in electron scatt. 8=11864

oscill. well, pear shaped, wave functions for O¹⁶, Ne²⁰ and Mg²⁴ 8=3772

pairing correls. in even-even nuclei, ground-state energy calc. 8=922

PCAC hypothesis tested in ν cross-sections 8=11862

π radiative absorpt. rel. to μ capture 8=20775

potential, equivalent local 8=7034

potential scattering, non-relativistic, effect of CDD poles on long range pot. behaviour 8=6751

quadrupole charge and quad.-quad. interaction const., calc. 8=942

random phase approx, calc. of spin-vibrational 1 $^+$ states of Pb²⁰⁸ 8=16003

random phase approx. generalized to include ground state correls. 8=15920

schematic interactions for complex problems 8=934

shell, extended, equations-of-motion method 8=15922

spectral, eigenfunction expansions for hyperboloids and cones 8=2889

Wigner-Eckart theorem applied to central interactions 8=7037

SU(2) and SU(3), rel. between "outer" and "inner" multiplicity 8=3504

SU₃ Clebsch-Gordan coefficients for coupling of single particle to general state 8=15929

SU₄, Wigner model rel. to binding energy of Be¹⁰, p and n parts 8=20677

Tamm-Dancoff calc. of spin-vibrational 1 $^+$ states of Pb²⁰⁸ 8=16003

Tam-Dancoff for vibr. spherical nuclei with unfilled shells of n and p 8=20663

time reversal invariance of Hamiltonian tested in variation of n, radiation widths and energy level spacings 8=15933-4

transfer reactions, two-nucleon, finite size effects, calc. 8=3952

2, 3, 4-particle systems with harmonic oscillator pot., group theory 8=11258

wave functions for mixed reactions and Raich algebra of SU(14) 8=3779

Wigner supermultiplet theory, SU₄ satisfied for A = 40-254 8=20661

Bi²⁰⁸, density functions S₀ and S₁ and intermediate structure, 0-70 keV 8=7114

Ca isotopes, 3-body forces, contribution to binding energies 8=15970

He³ perturbation calc. of Coulomb energy and e. m. radius 8=3740

Li⁶, magnetic and charge form factors rel. to Hartree-Fock calc. 8=11715

Nucleus—contd**theory—contd**

- Mg²⁴, equilibrium shape, restoration of axial symmetry by pairing correlations 8=15962
 Ne²⁰, Hartree-Fock calc. validity before angular momentum projection 8=15960
 Sn, even isotopes, core polarisation and quasiparticle theories, realistic forces 8=15985

Oceanography

See also Liquid waves; Seawater.

- acoustics, nonlinear, underwater transmission 8=6164
 acoustic signal reflection from sea bed, time and Doppler frequency characteristics 8=19566
 air-sea interface, wave generation, review 8=14572
 ambient sea noise in deep and shallow water, rel. to windspeed, correl. 8=5787
 Atlantic north-east, rates of secular variations 8=10031
 Atlantic undercurrent, equatorial, origin deduced from temp., salinity and O₂ obs. 8=14569
 Caribbean waters, deep, Ra, C and O distrib. rel. to renewal time 8=5783
 Chukchi sea, N. E., marine magnetometer obs. 8=19034
 current and temp. gradients down to 4500 m at 12°N, 27°W 8=23239
 currents, bottom topography and variable wind stress effects 8=2571
 deuterium content as water mass parameter 8=23238
 earth tide studies rel. to mech. props. of upper mantle 8=14546
 Ekman spiral in western Mediterranean, obs. 8=18841
 e. m. field components rel. to floor topography 8=18846
 explosions in N. Pacific, location and enumeration 8=23245
 Fiji plateau, topography rel. to heat flow 8=23233
 gravity waves, interactions 8=19
 ground deform. due to tidal loads, rel. to mantles elastic props. 8=14545
 heat exchange on surface, and precipitation-evaporation balance 8=9814
 heat flow and free air gravity anomalies 8=18838
 heat flow, low values 8=18837
 heat transfer through four layer system of water, sea ice, snow and air 8=23226
 "Indo-Pacific" mid-ocean ridge, mag. profiles 8=23438
 internal wave motion, perturbation technique appl. nonlinear eqns. 8=14577
 latent heat exchange with atmos. in low latitudes 8=9828
 l. f. sound attenuation coeffs. in deep ocean 8=5786
 longshore current velocity, theory and data, review 8=18847
 marine geology, application of acoustics and ultrasonics 8=23248
 motions, large-scale, eddy diffusion and viscosity coeffs. 8=23237
 noise signals, cross correlation 8=3059
 North Atlantic, fallout of Sr⁹⁰ on surface, and water exchange processes 8=9816
 ocean bottom l. f. press. vars. during hurricane, obs. 8=14603
 Pacific basalts, deduction of mag. anomaly lineation pattern of floor 8=19062
 Pacific, N. E., and Bering, analysis of river discharge obs. 8=14576
 pacific, 20-Hz signals, biological origin 8=23246
 radar sea return, Doppler shift dependence on waves 8=23240
 radioisotope sediment tracing, digital computer processing of data 8=18835
 reflection of collimated light, time-average evaluation 8=18840
 reverberation under Arctic sea-ice 8=5788
 rotating basin of parabolic depth profile, horizontal transport 8=18839
 San Diego Trough, acoustic reverberation, spatial and spectral dependence 8=9819
 sea currents detect. by satellite, i. r. obs. 8=9855
 sea currents, dynamics of non-periodic, USSR studies review 8=9811
 shallow water, bottom friction layer 8=9812
 ship waves in stratified ocean, surface and internal 8=9818
 sonar detection in the present of interference 8=23241
 sonar, optimum waveform for 8=23249
 sonar, volume reverberation tests as function of pulse lengths and sweep rates 8=23242
 sound fluctuations and random inhomogeneities 8=3054
 sound, refl. and scatt., ocean bottom 8=2572
 sound signals scattered from bottom, time fluctuation characteristics calc. 8=23244
 sound transmissions, surface/bottom reflected in divergent channel 8=18844
 spherical waves, cavitation and induced nonlinear losses 8=9820
 spray droplets as function of wind speed and height (< 1.2 m) 8=23243

Oceanography—contd

- spreading of ocean floor, steady state model 8=9821
 surface layer, organized convection due to slicks and wave radiation 8=14571
 surface temp. meas. using airborne i. r. thermometer 8=2570
 surface, time varying, scattering of monochromatic acoustic plane wave 8=6167
 surface waves diffraction by a wedge 8=9815
 surface waves spatial-freq. struct. by correl. polarization 8=9808
 surface waves wind prod., spectrum recorder and 0.01-5.5 Hz obs. 8=9807
 swells, law of logarithmic distrib. 8=5784
 temperature meas. by airborne i. r. radiometer 8=18845
 third-order tides, calc. from spectral anal. of gravimetric obs. 8=18842
 tidal currents, turbulent mixing 8=14574
 tidal drift of floating ice, vel. and direction 8=9799
 tidal flow and mass transport in Humber estuary 8=5785
 tidal forces of sun and moon, long period vars. 8=19241
 tidal var. in force of gravity, spectral analysis 8=9817
 underwater acoustics applications, book 8=10751
 underwater explosions, $\pi/2$ phase shift at caustics 8=19546
 underwater explosion, phase shift due to total internal reflection 8=19547
 underwater sound transmission, effect of internal water wave propag. 8=3051
 upper sea layer, boundary flow, organic dye obs. 8=14570
 wave trapping along a discontinuity of depth in a rotating ocean 8=23234
 waves, generation, dissipation and prediction 8=18836
 wave generation, surface contamination effect 8=14573
 waves, longit., prod. by periodic press. rel. to surface and interface disturbances 8=9805
 waves, progressive, air interface, aerodynamic press. distribution, laboratory 8=5791
 waves, random, statistical props. 8=14575
 waves, wind amplification 8=16776
 wind-driven currents vel. components spectra and wind energy transfer process 8=9810
 wind-driven homogeneous ocean, transient Rossby waves, numerical study 8=23235
 wind-driven waves spectra and statistics, theory 8=9809
 Al²⁶ in sediment, atmospheric origin 8=23236
 CaCO₃ aragonitic oolites, solubility in sea water pressure coeff. obs. 8=8012
 H³, rainfall input to North Pacific rel. to water mixing time calc. 8=23247
 U isotope deposition meas. 8=9813
Octet theory. See Elementary particles; Field theory, quantum.
Omegatrons. See Leak detection; Mass spectrometers; Vacuum technique.
Onsager relations. See Statistical mechanics; Thermodynamics.
Optical activity. See Optical rotation.
Optical constants
 See also under individual headings, e.g. Absorption/light; Reflectivity.
 ADP, photoelastic consts. 8=14244
 calcite, in region of fund. freq. 8=9512
 crystals, and electro-optical effects, rel. to anisotropy 8=9495
 extinction coeff., collimated and diffuse fluxes of light, reln. between 8=3375
 eye spectral sensitivity, visual task effect 8=3390
 pigments in white emulsion paint, rel. to colour strength and shade 8=9574
 polyethylene, black, 4-50 μ 8=14289
 reflection and refraction coeffs., polarization angle rel. to impedance matching 8=3256
 refractive index and extinction coeff. determ., effect of meas. error 8=15517
 solids, determ. from weakly absorbing layers 8=18486
 superconducting lens, aperture and chromatic aberration 8=19791
 thin films, non-normal incidence meas. methods 8=14167
 white tin films, analysis over 0.1 to 27.5 eV energy region 8=2456
 Ag, thick films, least squares method 8=2403
 Au thick films, least squares method 8=2403
 AuAg alloy, deform., recryst. and ordering effects, 276-1200 nm 8=22958
 AuCu alloy, deform., recryst. and ordering effects, 276-1200 nm 8=22958
 AuCu₃ alloy, deform., recryst. and ordering effects, 276-1200 nm 8=22958
 Bi, liq. and dielec. const. $\epsilon_1 + i\epsilon_2$ 8=12877
 BrO₃Na monocrystals, and effect of cooling on spectrum 8=18509
 Cd, liq., and dielec. const. $\epsilon_1 + i\epsilon_2$ 8=12877
 Hg, clean surface, as function of temp. 8=4582
 Hg, liq., and dielec. consts. $\epsilon_1 + i\epsilon_2$ 8=12877
 Hg, liq., non-agreement with free-electron theory 8=16846
 Hg-In alloys, liq., rel. to free-electron theory 8=16846
 KBr in the far i. r. 8=5613
 KCl, absorpt., and reflectivity spectra rel. to exciton states 8=14230
 Mg crystal, electronic structure from optical properties 8=14239

Optical constants—contd

- MgO, from reflectance data rel. to electron energy losses 8=9550
 NaClO₃, and reflecting power, cooling effects 8=9555
 Pb, liq., and dielec. const. $\epsilon + i\epsilon_2$ 8=12877
 PbO, single crystal, yellow form, absorption coeffs. 8=5628
 δ -Pu, at 5461 Å 8=23009
 Sn films, in u.v. reflecting power, and dielectric constants deduced 8=5638
 p-SnTe, visible and i.r. obs. 8=18562
 Ti₂O₃ layers, between 0.2 and 4.5 μ m rel. to electronic carrier props. 8=23017

Optical dispersion. See Dispersion, optical.

Optical fibres. See Optical systems.

Optical films

- See also Filters, optical.
 advanced optical techniques, book 8=15489
 progress in optics, book V 8=15542
 reversibility of rays, generalized theorem 8=11169
 surface, influence on metal meas. 8=11168
 Ag, 0.4-1 μ range, reflection and transmission coeffs. 8=5580
 Ag, non-linear reflection on laser-radiation 8=18497
 Ag-Cr, 0.4-1 μ range, reflection and transmission coeffs. 8=5580
 Cr₂O₃, reactively evaporated, transmission characts. 8=9517
 Cr, 0.4-1 μ range, reflection and transmission coeffs. 8=5580
 Ge, complex index and optical thickness from meas. of reflecting powers at oblique incidence 8=18530
 Hf oxides, transparency in u.v., temp. depend. and effect of Cl⁻ and NO₃⁻ 8=5605

Optical filters. See Filters, optical.

Optical images

- See also Aberrations, optical; Resolving power, optics.
 advanced optical techniques, book 8=15489
 bright field, with partially coherent illumination, nonlinear transfer 8=15513
 Brocken observation, quantitative 8=11166
 from concave spherical mirror, form. for wide beams of rays and arbitrary incidence 8=469
 deflectors, achromatic 8=472
 of diffuse object, noise-like structure in holograms 8=11217
 distorted images, linear least-squares filtering 8=483
 electroluminescence Gudden-Pohl effect appln. for recording, storage and reproduction 8=6496
 evaluation techniques, accuracy test procedure 8=20051
 focus of coherent beam, behaviour of Poynting vector and energy flow 8=6499
 formation using systems with resolving power enhanced in one direction 8=20049
 Fourier transform use 8=11136
 holograms, appl. to bubble chambers 8=6567
 holograms, binary Fraunhofer, computer generation and reconstruction 8=6576
 holograms, construction with direct reference beams 8=3381
 holograms, cylindrical 8=11206
 holograms, inexpensive method 8=6569
 holographic interferometry, 3-beam with single emulsion exposure 8=6541
 hologram copying by Gabor holography and spurious images, theory 8=6575
 holography, photographic film nonlinearities effects 8=6574
 holograms, point, as optical elements 8=6568
 holography, principles and film requirements 8=20106
 holography with pulsed laser of front-illum. moving objects 8=11218
 hologram storage capacity of photochromic glass, meas. 8=6570
 holograms synthesized on cathode-ray tube 8=11207
 holograms, tanning bleach bath, variation of method 8=20119
 holographs, techniques and limitations 8=6566
 holograms, using total internally reflected light 8=3378
 interference patterns from double-exposed holograms, white-light reconstruction 8=15557
 laser intracavity processing of phase object and information recovery 8=6578
 laser, reconstruction from acoustical hologram 8=524
 lasers, holographic application, review 8=6479
 light dist. analysis by Fourier transformation 8=11164
 low-angle holograms using Tri-X Pan film 8=6571
 many discrete elements of area, limitations on obs. system 8=6498
 nonpseudoscopic real image from holograms, technique 8=6577
 object-image relns., demons. with flexible mirror 8=476
 optimum image plane position, in system with chromatic aberration 8=477
 out-of-focus images, props. and uses 8=475
 processing (max. likelihood) after propag. through turbulent atmosphere 8=23288
 of quasi-monochromatic source, meas. of degree of coherence 8=6483

Optical images—contd

- reactive information processing 8=531
 resolution and correlation by transfer function 8=11138
 restoration after random-media degradation 8=15507
 restoration, atmospherically degraded 8=473
 restoration and code translation, holographic production of spatial filters 8=519
 rod, partially submerged in water, "shadow-sausage effect", rel. to surface tension 8=6495
 scanning by rotation of hologram 8=523
 size analyser for 350 μ m diameters 8=14915
 spectrometers with concave diffr. gratings, luminance distrib. calc. 8=487
 transfer function with partially coherent illumination 8=3340
 velocity sensing with moving reticle scanners 8=6497
 wavefront reconstruction by hologram transmitted on television circuit 8=6573

Optical instrument testing

- lenses, quality control meas. apparatus 8=11129
 ruby laser, beam divergence 8=15478
 telescope, Queen Elizabeth II 8=10101

Optical instruments

- Some instruments are listed separately, e.g.
 Refractometers.
 advanced optical techniques, book 8=15489
 air light absorption, spherical mirrors apparatus involving repeated reflection 8=7935
 apertometer, precision, for microscope objectives 8=6507
 astronomical, for annular eclipse 20 May 1966 obs. 8=19288
 binoculars, compact streamlined, use of erecting prism systems 8=15509
 cornea, for measuring contour 8=20129
 detector using metastable atoms 8=20059
 dew-point instrument, minimizing effect of contamination on mirror 8=14581
 dielectrics, transparent, damage due to laser light 8=8755
 ellipsometer for liquid metals 8=16836
 end windows of laser tube, set near Brewster angle, rel. to transmission 8=6426
 focused collimator, resolution calc. 8=11139
 four part quartz plate in phase difference meas. 8=15512
 Fresnel zone plates, variable patterns 8=507
 high pressure cell for absorpt. and luminescence studies at 77°K 8=6502
 lasers, thin film monitor, industrial applications 8=6479
 for Laue pattern direct interpretation 8=8496
 light beam, meas. of small displacements, and optical ranging, novel method 8=20056
 light chopper, feedback-stabilized with continuously variable frequency 8=6509
 light scanner, solid-state acoustoelec. 8=5309
 mica cryst. retardance meter 8=6510
 Moiré fringe technique, appl. 8=506
 part. size distribn., photograph-projection comparator, nonautomatic, descr. 8=5
 plummet, using cells of liq. prisms, with apex angle varying as tilt 8=3350
 progress in optics, book V 8=15542
 progress in optics, book VI 8=15541
 rangefinder, automatic, proposed 8=475
 ranging system using a high power laser 8=14918
 reflectometer, single mirror, normal incidence 8=6504
 reflectometers, elimination of errors 8=15517
 resonator, single longitudinal mode Michelson-type, auxiliary-mirror curvature determ. 8=6519
 resonators, Fabry-Perot, for vibr. meas., quantum effects 8=10683
 rotation dispersion and circular dichroism meas. 8=20061
 simplified coherent optical correlator 8=20055
 size analyser for 350 μ m particles and images 8=14915
 superposable spherometer 8=20053
 thermal cond. meas. of molten NaNO₃ and KNO₃, plane source technique 8=21658
 time-to-amplitude converter, photoelectric correlation measurements 8=15496
 for transfer function meas. 8=11137
 transfer function, rel. to the autocorrelation function of the complex luminous amplitude 8=15514
 transverse surface velocity meas. 8=15518
 triplets, spherical aberration evaluation 8=15501
 use in teaching, geometrical optics, Fourier optics and wave theory 8=15502
- Optical materials**
 See also Filters, optical.
 focusing by quartz crystals 8=14261
 glass, i.r. gallate, transmission props. 8=22954
 glasses, i.r. aluminate, optical, mech. and thermal props. 8=22954
 glasses, i.r. selenide, transmission props. 8=22954
 i.r. refractive index, thermal change 8=479
 mat surfaces, i.r. reflectance 8=18485
 refractive index meas., near ultraviolet to middle infra red 8=478
 surface-coated reference flats, for testing aluminised surfaces in Fizeau interferometer 8=11171
 transmittance from 0.17 μ to 3.0 μ , studied 8=11140
 Al₂O₃ powders, reflection and polarization properties 8=14266

Optical materials—contd

- CsBr and CsI i.r. windows, polishing 8=495
 $K_{0.6}Li_{0.4}NbO_3$, stable nonlinear 8=5618
 SiC powders, reflection and polarization properties 8=14266
 SiC/ Al_2O_3 powder mixtures, reflection and polarization properties 8=14266
- Optical model.** See Nucleus/models.
- Optical properties of substances**
 See also Optical constants; Optical materials.
 absorption, electronic edge in strongly anisotropic substs. 8=9482
 acetone, Ar laser beam thermal defocusing obs. 8=16845
 alcohol, Ar laser beam thermal defocusing obs. 8=16845
 alkali halides, ion overlap meas. by strain polarization ability 8=23003
 alkali metal niobates with filled tetragonal W-bronze like structs., nonlinear appls. 8=22959
 n-alkanes, anisotropies, mol. calc. 8=12248
 alloys, reflecting surface preparation 8=14163
 anthracene and plastic scintillator, radiation damage by 4 → 10 keV electrons 8=23029
 anthracene, two-photon photocarrier generation 8=13918
 benzene and derivatives, structure of $\nu(CH)$ vibration bands, 300 and 80 °K 8=12260
 bulk, determ. using internal reflection meas. 8=22934
 cholesteric liq. crystals, rotatory power 8=12876
 colour indices of some cosmic and earth surfaces 8=2816
 Cotton-Mouton effect obs. in alkali metal gases 8=4485
 crystal class C_{6v} , waveguide, generation of second harmonic 8=5577
 crystal excitation by absorption and scatt. expts. 8=5095
 crystal impurity atoms, vibrational and optical props. from morphic effects 8=4966
 crystals, KDP type, second harmonic generation 8=5569
 crystals, non-linear optics, adiabatic approx. 8=18481
 crystals, uniaxial, electro-optical effects 8=18494
 DNA with complexed carcinogen 8=18093
 dielectric, multilayer coatings, for white light interferometry 8=6540
 dielectrics, internal friction of dislocations rel. to optical props. 8=14165
 dye solns., kinetics of photodichroism 8=8070
 dielectrics, nonlinear propag. of laser beam 8=22931
 electromag. surface waves on semiinfinite metals 8=14164
 filaments trapped in liquids in intense laser beams 8=16832
 garnet, Ce-activated 8=2474
 gas, laser beam filaments, Raman scatt., electrostriction and Kerr effect theory 8=8067
 gases, inert, third-harmonic generation 8=1479
 gases, magnetic birefringence 8=7934
 gases, organic mixtures in air, optical-acoustic effect using cm e.m. waves 8=21520
 gases, Raman active vibrations, relaxation 8=9485
 glass, gallate, for i.r. use 8=22954
 glass, rough, reflection at large incidence, indicatrices with two maxima 8=5631
 glasses, selenide, for i.r. use 8=22954
 graphite, transverse and longitudinal 8=2407
 hexafluoroacetone sesquihydrate, third harmonic generation anomalous dispersion 8=8072
 insulators, absorpt. calc. from exciton resonances 8=8947
 liquid crystals, review of data 8=1527
 liquid, laser beam filaments, Raman scatt., electrostriction and Kerr effect theory 8=8067
 liquid surface, scattering of light rel. to capillary waves on surface 8=16852
 liquids, anisotropic, mol. scatt. 8=1555
 liquids, Brillouin scatt., spatial correlation of density functions 8=12875
 liquids, laser beam self-trapping obs. 8=21670
 liquids, nonlinear refractive index, mol. orientation effect 8=12871
 liquids, Rayleigh-Wing scatt. of laser beam polarization effect 8=8092
 liquids, refractive index increase, due to mechanisms sensitive to energy density 8=8066
 liquids, self-focusing kinetics and channel instability 8=21668
 liquids, self-focusing of light of different polarizations, expt. to test a. c. Kerr effect mech. 8=12870
 liquids, self-trapped filaments of laser light, theory 8=4577
 liquids, stimulated Rayleigh scattering obs. 8=12874
 liquids, stimulated thermal Rayleigh scatt., theory 8=6561
 lossy media, propag. of higher-order coherence functions 8=5570
 metal surfaces, rough, plasma resonant radiation 8=9488
 mat surfaces, i.r. reflectance 8=18485
 metals, liquid, ellipsometry 8=16836
 metals, pseudopotential Fourier components determ. from opt. meas. 8=22442
 metals, second harmonic generation, nonlinear polarization vector calc. 8=18483
 methanol, multiple stimulated Brillouin scattering 8=4584
 4-methyl umbelliferone, aq. soln., stimulated emission at 454 m μ 8=6478
 mixing of waves of different polarization by non-linear crystal 8=14237
 molecular crystals, e.m. wave dispersion 8=18479

Optical properties of substances—contd

- molecular crystals, scatt. of e.m. waves 8=18480
 molecular extinction coefficients of the triplet-triplet transitions, kinetic method of meas. 8=16257
 nitrobenzene- CCl_4 mixts. stimulated Rayleigh scatt., obs. 8=16843
 nitrobenzene, Rayleigh line wing, four photon interaction obs. 8=21667
 nonlinear crystals., second harmonic generation by focused laser beams 8=14166
 organic liquids, light intensity in wing of Rayleigh line rel. to vibrating molecule model 8=16851
 organic liquid quenches of light pulse in GM counter 8=11297
 organic liquids, stimulated scatt. in Rayleigh line wing, obs. 8=16842
 paraelectric-resonance transitions, linewidths 8=14187
 perovskite oxides in paraelectric and ferroelectric phases, optical props. 8=18504
 piezo-optic coefficients by pulsed u.s. light diffraction, 24 liquids obs. 8=8064
 plasma excitation in e. m. shock tube 8=1337
 plasma, generalized approximation for e. m. wave scatt. 8=16534
 polyacetylene, use in understanding electronic structure 8=9576
 polymer solutions, activity 8=8065
 polymethine dyes, liquid solutions, stimulated light radiation 8=16848
 polymethylphenylsiloxane chains, anisotropy 8=12391
 polyvinyl chloride films, rheo-optical properties 8=2076
 pulse shape functions rel. to absorption and loss coefficients 8=2394
 quartz, bent crystals for X-ray focusing 8=14261
 quinoline-ethyl alcohol mixts. stimulated Rayleigh scatt., obs. 8=16843
 Raman scatt. by polarization waves in crystals 8=9485
 ruby, optical phonon breakdown theory 8=22952
 second harmonic generation from short pulses 8=18495
 semiconductors with nonparabolic nonspherical energy surfaces, mixing of two freqs. 8=5571
 sodalites, photochromic, e.s.r. 8=14120
 solids, fundamental spectra, review 8=9475
 sols, birefringence, electric and magnetic field effects 8=12878
 III-V compounds, second order optical susceptibility 8=18484
 transition metal cpds. rel. to crystal field calc. 8=4669
 transparent media, anisotropic, Brewster angle generalization 8=22947
 uniform gas, frequency-integrated radiation due to weak lines 8=12690
 Vavilov-Cherenkov radiation by charged ring motion in transparent uniaxial crystal 8=21148
 Vavilov-Cherenkov radiation by motion of charged ring in transparent crystal 8=22949
 water, Ar laser beam thermal defocusing obs. 8=16845
 O-xylol, Rayleigh line wing, four photon interaction obs. 8=21667
 A^{IVBVI} semiconducting cpds., (A=Zn, Cd, Hg; B=S, Se, Te) 8=18023
 ADP, crystal modulation of laser light 8=23002
 Ag, bilinear polarizability calc. 8=18498
 Ag colloidal solutions in water, extinction coefficients 8=4579
 Ag, 0.4-1 μ range, reflection and transmission coeffs. 8=5580
 Ag-Cr, 0.4-1 μ range, reflection and transmission coeffs. 8=5580
 AlSb, second order optical susceptibility calc. 8=18495
 AlN semiconductors 8=2185
 Ar, crystalline, optical regions rel. to growth parameters 8=2238
 Au colloidal solutions in water, extinction coefficients 8=4579
 BP, second order optical susceptibility calc. 8=18496
 Ba₂NaNb₂O₁₀, nonlinear coeffs. 8=9508
 BaTiO₃, ferroelectric, soft modes, and acoustic modes, mixing 8=22665
 BaTiO₃, optical phonon, i. r.-active, directional dispersions at room temp. 8=17478
 BaTiO₃, temp. dependence of l.f. transverse optic lattice vibration 8=17479
 CaCO₃, phase-matched 4-freq. mixing obs. 8=14203
 CaF₂:Nd³⁺, effect of rare earth ion on Nd³⁺ optical centres 8=5593
 CaF₂:Nd³⁺, stimulated emission, high-temp. effects 8=22960
 CdF₂:R, semiconducting, e.s.r. and i.r. studies 8=22901
 CaF₂:Sm²⁺ crystals, spectrum 8=9513
 CaI₂, excitation max. 8=5654
 CdCl₂:Ag, γ -irradiated, absorption bands 8=9419
 CdF₂, transmission and refraction 8=8409
 CdS, excitons lines, emission intensity var. rel. to u.v. laser beam excitation intensity, 4.2 °K 8=22964
 CdS, two-photon absorpt. obs. 8=18516
 CdSe, stoichiometric, in thin film, and structural and elec. props. 8=17127
 CdSe(S), rel. to electronic structure 8=8928
 CdTe, pressed, far i.r. props. 8=18518

Optical properties of substances—contd

Cd_{1-x}Zn_xS, mixed single crystals, optical quenching effect on photoconductivity 8=18227
 CeO₂, single crystal growth 8=1740
 Co, rel. to reflectance data 8=22975
 Cr, 0.4–1- μ range, reflection and transmission coeffs. 8=5580
 CsI(Na), scintillation single crystal 8=2480
 Eu chelates, u.v. irradiat., optical emission losses, study of causes 8=18571
 Fe–I–boracite, ferroelectric orthorhombic phase, study 8=22980
 GaAs injection lasers with compensated p-type region and elec. props. 8=15482
 GaAs, laser induced changes 8=5633
 GaAs, second order optical susceptibility calc. 8=18496
 GaAs, two-photon absorpt. obs. 8=18516
 GaF, second order optical susceptibility calc. 8=18496
 GaSb, Faraday rotation and spectral emittance 8=22587
 GaSe, generation of second optical harmonic 8=5600
 Ge, energy gap, pressure coeff. meas. 8=14220
 Ge film, complex index and optical thickness from meas. of reflecting powers at oblique incidence 8=18530
 Ge, photon emission from indirect band-to-band Auger recombination 8=14221
 Ge, screw dislocations, Hall effects 8=1979
 Ge, thermoreflectance spectra in region of a critical point, calc. and obs. 8=14217
 He liquid second sound, laser beam scatt. photostatistics 8=11192
 HF oxides, transparency in u.v., temp. depend. 8=5605
 Hg, liquid, and Drude theory 8=12881
 α -HgS, second harmonic generation 8=5606
 HgS–HgSe solid solns. 8=5607
 I₂–CCl₄ solns., stimulated thermal Rayleigh scatt. obs. 8=8068
 In film, e.m. radiation from surface excited by micro-wave phonons 8=4903
 InAs, light absorpt. by free carriers, 300 °K and 80 °K obs. 8=18536
 InAs, second-harmonic generation by laser interact. with drifting carriers 8=5610
 InAs, second order optical susceptibility calc. 8=18496
 InAs thin films 8=18535
 InP, coherent emission after laser excitation 8=6470
 InP, second order optical susceptibility calc. 8=18496
 InSb, second order optical susceptibility calc. 8=18496
 InSb, two-photon absorpt. obs. 8=18516
 KF, thin layers, u.v. 8=9546
 K(Ta–Nb) crystals 8=9199
 LaF₃:Nd³⁺, stimulated emission, high-temp. effects 8=22960
 LiNbO₃ crystal for converting near i.r. to visible light by optical mixing 8=11118
 LiNbO₃, image conversion from 1.6 μ to visible 8=22998
 Li₂NbO₃, mixing of ruby and Nd laser emissions 8=14237
 LiNbO₃, second harmonic generation from short pulses 8=18495
 LiNbO₃, second-harmonic phase-matching temp., dependence on melt composition 8=22997
 LiNbO₃: Yb³⁺, Nd³⁺, Cr³⁺, and e.s.r. spectra 8=22999
 Li–NH₃ metallic solns., ϵ_1 and ϵ_2 consts. 8=12884
 LiTaO₃, Yb³⁺, Nd³⁺, Cr³⁺, and e.s.r. spectra 8=22999
 MgCl₂:Ag, γ -irradiated, absorption bands 8=9419
 MnF₂, Co doped, magnon sidebands and local order 8=23001
 Mo, rel. to conduction band transitions 8=9553
 Na–Li liq. mixtures, near demixing temp., crit. opalescence 8=1558
 NH₄Cl, harmonic generation and critical pt. correl. 8=23007
 NH₄Cl, harmonic generation near second-order phase transform. obs. 8=14245
 Pb, visible to i.r., room to He temp. meas. 8=14253
 PbSe–SnSe, optical energy gap 8=5629
 PbSe–SnTe, optical energy gap 8=5629
 PbTe–SnSe, optical energy gap 8=5629
 PbTe–SnTe, optical energy gap 8=5629
 Sb₂Se₃ films, anisotropy 8=14259
 SbSi, optical principal axes 8=2448
 SF₆ gas, self-induced transparency using 10.6 μ laser radiation 8=1478
 Si, laser induced changes 8=5633
 Si, screw dislocations, Hall effects 8=1979
 Si, three-photon stepwise absorption 8=5635
 SiC, band edge absorption 8=9122
 SiC crystals, energy spectrum of acceptor states 8=5668
 SiC, vapour-deposited films 8=17137
 Sn films, in u.v., reflecting power, optical and dielectric consts. 8=5638
 SnTe, rel. to electronic band structure 8=8943
 SnTe, visible and i.r. obs. 8=18562
 Sr_{1-x}Ba_xNbO₃, uniaxial negative character 8=21966
 Te, non-linear props. 8=18563
 Th oxides, transparency in u.v., temp. depend. 8=5605
 ThO₂, single crystal growth 8=1740
 VO₂, change in constants, for radiant self-stabilization of temp. 8=23019
 V₂O₅ single crystals 8=23020
 ZnS crystals in X band travelling-wave light-intensity modulator 8=23025

Optical properties of substances—contd

ZnS, rel. to electronic structure 8=8928
 ZnTe, submillimetre-wave generation by difference-frequency mixing of ruby laser lines 8=18569

Optical pumping
 alkali atoms reson. states lifetimes, inert gases and vapour press. effects 8=20976
 alkali metal vapours, relaxation pulse study 8=12086
 alkali vapour, with buffer gas, rate eqns. 8=20978
 alkali vapour, polarization modification of light beam 8=4088
 cathode luminescent in solid state laser, efficiency 8=6454
 of chloro-aluminium phthalocyanine and diethylthiatricarbo-cyanine iodide by ruby laser, spectra comparison and interpretation 8=452
 dye, flashlamp excitation obs. 8=451
 dye laser by flash lamp 8=6477
 glass, silicate, 7% Nd, multimode generation, luminescence broadening 8=2487
 laser active materials, study 8=11010
 laser, coupling efficiency 8=413
 laser, use of surface spark discharge 8=6412
 lasers, optimum design of spherical and ellipsoidal chambers 8=11019
 lasers, solid, cavity geometry and continuous operation 8=19980
 lasers, threshold of oscillation 8=6413
 masers, power minimization 8=19918
 masers, push-pull, four level quantum systems 8=392
 nonuniform, solid state laser, spectrum 8=15474
 operator formalism, absorption of monochromatic light 8=1180
 organic laser, optimal homogeneity 8=11114
 parametric oscillator, theory and appl. to threshold cond. deriv. 8=11029
 plasma, density fluctuations due to monochromatic pumping, theory 8=12546
 progress in optics, book V 8=15542
 quartz, by ruby laser, behaviour as Raman oscillator rel. to mode pulling 8=2453
 ruby laser, power and efficiency calc. 8=3331
 ruby maser, by laser at 77°K 8=19920
 ruby, non-radiative relax. time between ⁴T_{1,2} and ²E states 8=9503
 semiconductor laser, rel. to saturable transmission by multiphoton absorpt. 8=9478
 solids and liquids for nuclei polarization 8=13016
 spherical reflector 8=11108
 water-cooled systems for continuous operation of lasers 8=432
 AgCl vapour, vibr. energy level population 8=1235
 CaF₂:Sm²⁺ laser, pumped by giant pulse ruby laser 8=11089
 Cd¹⁰⁹ and Cd¹¹¹ oriented by, relaxation on silica walls 8=16233
 Cs–inert gases, collisional J reorientation within the sublevels, with D₂ pumping 8=1194
 GaAs spherical recomb. drodes as pumping element characts. 8=23074
 HCN, CW submillimeter laser lines, absolute freq. meas. 8=422
 He atom, aligned, scatt. of resonance fluorescence depolarization 8=20982
 He³, r.f. field resonance 8=16219
 He³, transverse optical pumping and detection of modulation resons. 8=16195
 He–Ne mixture by He–Ne laser, Hanle and saturation effects obs. 8=20983
 Hg vapour, polarization modification of light beam 8=4088
 InSb Raman laser, by a 10.6 μ CO₂ laser, rel. to tuning 8=11104
 K³⁹, intensity modulation of transmitted light 8=12085
 Na and inert-gas atoms collision, depolarization cross-section 8=7436
 Nd glass, measurement cross-section stimulated emission 8=449
 Ne, laser pumped microwave emission in excited states 8=12071
 Rb magnetometer 8=19739
 Rb, relax. in collisions with Kr atoms, correl. times 8=7472
 YAlG:Nd laser, repetitively Q-switched 8=6474
 ZnS crystals, u.v. emission excitation 8=9632

Optical quantum generators. See Lasers.

Optical rotation
 See also Magneto-optical effects; Optical constants; Polarimeters; Polarized light.
 amides, molec. theory 8=12250
 amoebic ectoplasm and endoplasmic flow differentiation 8=2869
 benzil cryst., dispersion, compared with absorpt. and circular-dichroism spectra 8=2463
 cholesteric liq. crystals, rotatory power 8=12876
 crystals, microscopic rel. to macroscopic optical analogies 8=14181
 dispersion study of transient species excited by flash photolysis 8=12258

Optical rotation—contd

- ϵ -caprolactones, rel. to molec. conformation 8=12879
- Faraday effect, one band effective-mass approx. for Bloch electrons 8=13654
- Faraday, in ionized media and semiconductors 8=22948
- gyrotropic layer, transmission and reflection 8=3376
- harmonic generation in optically active medium, coupled-wave solution 8=455
- hexahelicene 8=12883
- light intensity-dependent changes rel. to observation by laser techniques 8=517
- microwaves, demonstration by macroscopic models 8=375
- molecular, anisotropy in transparent media 8=516
- photoelectric control for rotary power meas. 8=15549
- poly- ϵ -caprolactones, rel. to molec. conformation 8=12880
- polymer solutions, optical activity 8=8065
- starlight, effect of interstellar matter 8=5920
- Ag films, ellipsometric meas. 8=11201
- AgGaS₂, non-enantiomorphous crystal, obs. of rotation 8=14191
- CaF₂, paramagnetic rare-earth activated, magnetooptic rotation 8=5590
- KCl, paramagnetic rare-earth activated, magnetooptic rotation 8=5590
- K₂S₂O₈, rotatory dispersion interpretation 8=18539
- NaCl(Br)O₃, rotatory dispersion in visible and u.v. regions 8=5623
- SrF₂, paramagnetic rare-earth activated, magnetooptic rotation 8=5590

Optical systems

- See also Aberrations, optical; Lenses; Optical images; Optical instruments; Optical materials; Resolving power, optics.
- aberrations, correction by aspherical lenses 8=3347
- aplanatic Fresnel, sine condition generalization 8=20048
- aspherometer for rotational surface meas. 8=15511
- birefringent lenses, path of extraordinary ray 8=15510
- cascaded, system transfer function 8=11133
- cemented, localized var. of two paraxial ray paths 8=20047
- Cherenkov light, focusing system 8=6511
- as chopper, scanning interferometer spectrometer use 8=6528
- with chromatic aberration, optimum image plane position 8=477
- coherent, improvement of two-dimensional image quality 8=11132
- cylinder, parabolic illuminated, short wave asymptotics of diffraction 8=508
- data processing techniques, review 8=15506
- diffraction phenomena introduced by optical relay 8=15505
- dispersion of modulated or time-varying light 8=6486
- duct, curved with circularly refl. walls, transmittance props. 8=6508
- elliptical annular aperture, transfer function 8=11191
- erecting prism systems, use in compact binoculars 8=15509
- fiber, laryngoscopic technique 8=14892
- fibre optics in field ion microscopy 8=6512
- fibres, passive and lasing, coupling and coherence effects 8=20062
- fibres, wavelength multiplexing 8=15519
- gimballed mirrors and prisms, matrix anal. 8=3348
- glass fibre, passive core, Nd-doped cladding, laser action by total internal refl. 8=11073
- Hartmann test, Fortran programme for reduction of data 8=20050
- Hauser's formula for modulation transfer function, small aberrations 8=15504
- image evaluation techniques, accuracy test procedure 8=20051
- image formation using systems with resolving power enhanced in one direction 8=20049
- images of many discrete elements of area, limitations on design 8=6498
- imaging, significance of nonlinearity in image evaluation 8=11134
- infrared, for radiometry of semiconducting devices 8=22618
- invariance theorems for computations in 8=15500
- laser range finder, multipulse returns energy detection statistics 8=6414
- light beam, meas. of small displacements, and optical ranging, novel method 8=20056
- Mangin mirror, elimination of coma 8=20041
- monochromator, non-symmetrical with plane diffraction grating, aberrations 8=3345
- multipass-cell, noncentred, astigmatism 8=6490
- part. size distribn., photograph-projection comparator, nonautomatic, descr. 8=5
- with resolving power exceeding the classical limit 8=474
- of revolution, modulation transfer function calc. 8=11135
- Sorét-type plates, superposition to produce Moiré patterns, theory and photographs 8=11179
- spatial filters for character recognition, storage capacity 8=6514
- with spherical aberration, field amp. of focused laser beam 8=10999
- superresolving, and the Abbe resolution limit 8=6505
- surveillance, atmospheric turbulence effects 8=14598

Optical systems—contd

- telecentric, props. 8=3349
 - thick concentric single lens in media of constraint μ , use of characteristic functions in design 8=11130
 - transfer function meas. instrument 8=11137
 - transfer function with partially coherent illumination 8=3340
 - transverse surface velocity meas. 8=15518
 - two-lens, Ramsden type, primary aberrations 8=6493
 - variable-focal-length mirror, for object-image relns., demons. 8=476
 - vignetted pupil shape, approx. by ellipse 8=20052
- Optics**
- See also Aberrations, optical; Atmospheric optics; Lenses; Mirrors, etc.; Optical images.
 - advanced optical techniques, book 8=15489
 - in Canada, research programmes review 8=6481
 - channel symmetry and nonlinear transfer 8=6482
 - coherence and quantum optics Conference, Rochester University, New York, June 1966 8=6484
 - diffraction and mm waves optics, French-Canadian research review 8=6558
 - flats, determ. of absolute contours 8=11175
 - geometrical, Fourier and wave theory, teaching, systematic approach 8=15502
 - gravitational waves, generation, by e.m. field 8=81
 - harmonic generation with multiple-photon transitions in n.m.r. expts. 8=10984
 - Hartmann test, Fortran programme for reduction of data 8=20050
 - hexafluoroacetone sesquihydrate, third harmonic generation by anomalous dispersion 8=8072
 - in information processing 8=20020
 - invariant properties rel. to acceptance angle of a quadrupolar multiplet 8=15500
 - laser and chaotic light superposed, intensity fluctuations, obs. 8=20017
 - laser, mode-locked, for reproducible optical second-harmonic generation 8=11024
 - laser pulses, mode-locked, optical rectification 8=19931
 - light pulses, spatial and temporal division 8=20021
 - modulation, ADP crystal props. 8=23002
 - Naval Research Lab. (USA) studies 8=15490
 - nonlinear crystals, second harmonic generation by focused laser beams 8=14166
 - nonlinear, problems, adiabatic approximations 8=18481
 - optical mixing for converting near infrared to visible light 8=11118
 - photoelectron distrib., quantum statistics 8=20013
 - progress in optics, book V 8=15542
 - progress in optics, book VI 8=15541
 - rel. to quantum and classical theories equivalence, p-representation in twisted convolution formation 8=2002
 - quantum, detector field-source coupling 8=20022
 - quantum, equivalence theorem and diagonal representations 8=20025
 - quantum, philosophy and appls., review 8=20024
 - quantum, representation of operators 8=11425
 - quantum statistics of nonlinear interaction with medium 8=20023
 - scan of convergent light and generalized gradient deflector 8=453
 - second harmonic generation in nonlinear optical waveguide 8=5577
 - Soviet optics and spectroscopy during past 50 years 8=11116
 - three-wave mixing in wedge-shaped cells 8=3341
 - X-rays and microanalysis, Conference, Orsay, France, Sept. 1965 8=8441
 - KH₂PO₄ cryst. in 1-bromonaphthalene, refl. second-harmonic intensity obs. 8=5611
 - NaClO₃ cryst. in 1-bromonaphthalene, refl. second-harmonic intensity obs. 8=5611
- geometrical**
- advanced optical techniques, book 8=15489
 - aplanatic Fresnel system correction 8=20048
 - bright field image with partially coherent illumination, nonlinear transfer 8=15513
 - corrective aspherical surface calc. 8=20042
 - cube-corner prism, optimum incident-ray direction 8=3346
 - diffraction theory in inhomogeneous media, transition functions 8=20102
 - electromagnetic resonators, freq. calc. 8=11125
 - general relativity theory, transition from wave to geometrical optics 8=6083
 - gradient deflection of focused laser beams, spot distortion 8=11012
 - hologram aberrations, evaluation by ray tracing 8=11216
 - Lambert scatt. from cone and paraboloid of revolution 8=20103
 - prism, optical, as reflecting prism, conditions 8=3344
 - radar cross section, computerized approach 8=20040
 - reflection in 2-mirror systems, theorem 8=11126
 - scattering of particles in random force field 8=14940
 - sign conventions for mirror and lens formulae 8=467
 - transition from wave theory, conditions 8=15488
 - validity in turbulent atm. 8=18877
 - vignetted pupil shape, approx. by ellipse 8=20052
 - wave propagating in inhomogeneous media 8=6374

Orbital calculation methods

- approximate open-shell theory of molec. spectra 8=4119
- atom irradiated with wide-band coherent light 8=1143
- atomic and molecular, uniform localization 8=1147
- atomic orbital expansion on basis of Slater type functions 8=12075
- atoms and ions, second-order three-body interactions, with Gaussian wavefronts 8=7457
- benzene, SCF-MO-CI theory, empirical params. choice 8=21127
- CNDO method, for i.r. intensities 8=12148
- chemical bonding and spectroscopy 8=16246
- chemisorption, MO model 8=18695
- configuration interaction in MO theory 8=12152
- configuration interaction using open-shell functions 8=12028
- coronene, MOLCAO and free-electron appl. to π transitions 8=4139
- correlation effects in calc. of ordinary and rotatory intensities 8=12023
- floating spherical Gaussian orbital model 8=12153-4
- (d+s)ⁿ configurations, three-particle operators 8=4036
- four-centre molec. integrals 8=4136
- Hartree-Fock problem, multiple solns. 8=20933
- HF eqns, modification involving Slater $\rho^{1/3}$ term 8=1149
- Hückel calc. of electron densities for σ -radicals 8=12347
- hydrocarbons, generalized free-electron molecular orbital 8=12284
- hydrogen atom, quantum-mechanical treatment without complicated mathematics 8=12046
- integer-n Slater-type, by Fourier-transform convolution theorem 8=1228
- linear variation methods 8=556
- methane, solid, phase transition calcs. 8=17110
- perturbation theory for exchange forces 8=12155
- perylene, MOLCAO and free-electron appl. to π transitions 8=4139
- 1,2-rearrangements, MO description of non-classical ion 8=21057
- radial wave functions, atomic, new method for calc. 8=20931
- Slater determinant for electron wave function 8=18376
- π -electron approximation of conjugated linear chains, FE and LCAO MO models 8=16259
- pyrene, MOLCAO and free-electron appl. to π transitions 8=4139
- scaled atoms-in-mols. theory 8=12149
- s.c.f. calc. of large molecules include interaction with solvents 8=4127
- SCF theory, open-shell, coalescence conditions as constraints 8=16173
- single-centre expansions with Slater-type orbitals 8=12192
- Slater determinants, projection 8=12027
- spin-interaction operators, matrix elements 8=1225
- transition energies, perturbation calc. 8=12024
- trichalcogenocarbonate ions, HMO calc. 8=12793
- two-centre problem in quantum mechanics, numerical soln. 8=566
- two-centre moment integral, general formulation 8=16185
- WKB approx. for radial problems, 2nd and 3rd order correction terms 8=12039
- BD₄-like, electric field gradient calc. using one-centre expansion wave function 8=7513
- BF, diamag. susceptibilities LCAO-MO-SCF calc. 8=12176
- B₂O, planar cpds., rel. to B-O bond lengths 8=16268
- BeF₂, ² Σ^+ state and ² Π levels, calcs. from Hartree-Fock equations 8=7503
- CO, diamag. susceptibilities LCAO-MO-SCF calc. 8=12176
- He atom wave function product of H-like orbitals in p double ionization 8=21280
- He-He interaction, SCF-MO approx. 8=21013
- HeH⁺ 1s σ and 2p π states, approx. wave functions calc. 8=4153
- Li and ions of isoelectronic sequence, wavefunctions calc., using effective potential 8=20958
- LiF, diamag. susceptibilities LCAO-MO-SCF calc. 8=12176
- Na and ions of isoelectronic sequence, wavefunctions calc., using effective potential 8=20958

Orbitals. See Molecules/electronic structure.

Order-disorder transformations. See Phase transformations/solid-state.

Ordered structure. See Crystal structure; Solids/structure.

Organic compounds

See also Free radicals; Macromolecules; Plastics; Polymers; Waxes.

- acacia catechuic acid, scattering of light during neutralisation 8=8075
- acenaphthene, far i.r. absorption 8=23028
- acenaphthene monocrystals, determ. of elastic consts. by two methods 8=5092
- acenaphthene, Raman bands, broadening and freq. variation as function of temp. 8=5649

Organic compounds—contd

- acetaldehyde adsorption on Y₂O₃ and decomp. mechanism, i.r. obs. 8=4768
- acetaldehyde pyrolysis, acetone formation 8=9683
- acetaldehyde, reaction with atomic H 8=18668
- acetamide, vibration spectra and thermodynamic props. 8=4174
- acetate-alcohol binary mixtures, u.s. absorption 8=4571
- acetate ion, oxidation by K₂S₂O₈, Ag catalysis 8=23094
- acetates, rare earth, Pb and Cu, i.r. spectra and thermal decomp. 8=23095
- acetic acid, dissoc. consts. 8=4605
- acetic acid, ionization const. in propanol-H₂O mixtures 8=21720
- acetic acid-water, vapour-liquid equilb. 8=12974
- acetic and stearic acids, adsorption by Graphon and Spheron 6 8=8340
- acetoinediol cyclophosphate, cryst. and molec. struct. 8=17438
- acetone, Ar laser beam thermal defocusing obs. 8=16845
- acetone, diffusion into chloroform, mechanism 8=12834
- acetone, intermolecular potential and viscosity, 30-200°C 8=21523
- acetone, photo-oxidation, methyl hydroperoxide prod. 8=14437
- acetonitrile, in soln., vibr. bandwidth obs. 8=21681
- acetonitrile-d₃, liq., n.m.r., anisotropic molec. rot. 8=8140
- acetonitrile N-oxide, i.r. spectrum and symmetry force consts. 8=16309
- acetophenone in CHCl₃ shape intensities of i.r. absorpt. bands 8=8080
- acetophenone in chloroform, i.r. absorpt, co-band width and intensity at 1682 cm⁻¹ 8=4588
- acetophenone, lowest π, π^* triplet state 8=12892
- acetoxime crystals, production from benzine soln., props. 8=8396
- acetyl bromide and CD₃COBr, i.r. and Raman spectra, vibr. assignment 8=7555
- 3-acetyl-1,4-dihydropyridine, SCF-CI calc. 8=16306
- 4-acetyl-2'-fluorobiphenyl, crystal structure 8=17444
- acetylene cpds., proton reson. spectra 8=21173
- acetylene-diphenyl Ge addition cpd, crystal and mol. structure 8=22046
- acetylene-GeI₂ addition cpd, crystal and mol. structure 8=22046
- acetylene, heated, emission spectrum 4000-4160 cm⁻¹ 8=16308
- acetylene, ionization cross-sections for 100-2000 eV electrons 8=12446
- acetylene, ionization and electronic energy levels 8=1371
- acetylene, reaction with O, upper atm. 8=23307
- acetylene, rotational constants from i.r. spectra 8=16307
- acetylene, σ and π electron reorganization 8=12243
- acetylene, thermal cond. 8=16699
- acetylene, tritium-substituted, i.r. absorp. spectrum and ν_3 fundamental 8=12244
- acridine, e. s. r. of mononegative ion 8=21167
- acrolein, π -electron struct., MO calc. 8=16310
- acrylamide, electronic structure 8=1272
- acrylic acid, vinylchloride copolymerization relative reactivities obs. 8=23136
- acrylic layers for Zn alloys atmospheric corrosion prevention 8=14389
- acrylonitrile, sigma-type complex with metal chlorides 8=2527
- acrylyl fluoride, i.r. and Raman spectra and rot. isomerism 8=16311
- adenosine triphosphate, mag. susceptibility thermomagnetic obs., 80-380°K 8=13974
- adenosine triphosphate, synthesis in redox reactions of living cell rel. to separation of positive and negative charges 8=23762
- adipimide, anionic, polymerization triacetamide activated 8=9708
- agar agar, complex permitt., microwave meas. 8=22659
- alanine, α and β , comparison of dielec. increments and relax. wavelengths 8=8098
- β -alanine, elec. resistance meas. 8=19707
- alcohol-acetate binary mixtures, u.s. absorption 8=4571
- alcohol, Ar laser beam thermal defocusing obs. 8=16845
- alcohols, deuterated, vapour press. 8=12995
- alcohols, gas chromatograms and i.r. spectra 8=9759
- alcohols interaction with SO₂ 8=18688
- alcohols, solid, intra-molecular motion of OH, n.m.r. study 8=16989
- alcohols, tertiary, association consts. from dielec. consts. 8=12908
- aldehydes, dipole moments at 3 cm. 8=21108
- aldehydes, gas chromatograms and i.r. spectra 8=9759
- aldehydes, nuclear spin coupling consts., MO calc. 8=12328
- aleuritic acids (erythro and threo), powder diffraction data 8=22047
- aliphatic alcohols, domain theory of dielec. const. 8=4550
- aliphatic aldehydes and ketones, adsorpt. on SiO₂, i.r. study 8=8346
- aliphatic complexes, energy levels and wavefunctions calc. 8=16312

Organic compounds—contd

- aliphatic ketones, mass spectra, metastable ions 8=12238
 n-alkane derivative isomers with OH groups and
 n-heptane, phase equilibria 8=16949
 n-alkane mixtures, congruence principle appl. to
 viscosity 8=8024
 n-alkanes, binary mixtures, thermodynamic props. 8=16791
 n-alkanes, electronic spectra 8=12249
 n-alkanes, eqn. of state correl. with chain length 8=16790
 alkanes, liq., end-to-end distances, direct meas. vice
 substituted atoms 8=1526
 n-alkanes, polarizability anisotropies 8=12248
 alkanes, reactions with D_2^+ ions, energy transfer 8=1358
 alkanes, sigma-bond electronic transitions 8=1273
 alkenes, reactions with D_2^+ ions, energy transfer 8=1358
 4'-n-alkoxy-3'-nitrodiphenyl-4-carboxylic acids,
 liq. crystals, polymorphism 8=21614
 alkyl ammonium ions in aqueous solns., adsorpt. isotherms
 on biotite 8=13106
 alkylbenzenes mol. config. rel. to cryst. absorpt.
 spectrum 8=5645
 alkylbenzenesulphonate-octanol-water systems, phase
 behaviour 8=8159
 alkyl chlorides, gas chromatograms and i.r. spectra 8=9759
 n-alkyl derivatives, phosphoresc. and spin-orbit
 coupling 8=12252
 n-alkyl fluorides, n.m.r. 8=12315
 alkyl halides, effects of molec. motions on n.q.r. 8=2388
 alkyl iodides, γ -irrad. at -196°C , ionic processes 8=14275
 alkyl radicals, chem. activated, competitive
 decomp. 8=14359
 alkynes, field-ion mass spectra of eleven
 compounds 8=1372
 allene, two rotational lines 8=21112
 allyl halides, vibr. spectra 8=21111
 N-allylmonoamides of maleic and succinic acids,
 radiation polymerization 8=23131
 alstoveninemethiodide, single crystal X-ray study 8=17439
 alternant hydrocarbons, atomic orbital changes rel. to
 valence states of C 8=4135
 amides, liq. photolysis, e.s.r. 8=14435
 amides, spectra, theory 8=12250
 amides, subs., chem. shift nonequiv. of diastereotopic p
 rel. to rot. round aryl-N bonds 8=4175
 amines, deuterated, vapour press. 8=12995
 amines, effect on rubber soln. viscosity 8=21625
 amines, primary aliphatic, i.r. absorption spectra 8=16313
 amino acid anal., sensitive linear flowing-stream
 photometer 8=5762
 amino acids derivatives and metal complexes, crystal
 structures 8=1814
 α -aminoacid hydrochlorides, i.r. spectra 8=7556
 amino acids, polarizability anisotropy from refractive
 indices 8=2462
 aminoacids, temp. coeff. of piezoelec. resonance
 freq. 8=9224
 p-aminobenzamide, crystal structure 8=22075
 p-aminobenzoic acid, crystal structure 8=8570
 α -p-aminobenzoic acid, crystal structure 8=17443
 aminobutadiene, SCF-CI calc. 8=16306
 aminobutadienone, SCF-CI calc. 8=16306
 aminoethylene, SCF-CI calc. 8=16306
 aminoferrocene, MO calcs. and excitation energies 8=4197
 3-aminophthalimide solution in frozen dioxane,
 fluorescence 8=5682
 2-aminopurine, fluoresc. quantum yield 8=4595
 aminopurines, electronic spectra 8=7594
 aminopyridines, π -electron distrib. and n.m.r. chem.
 shift 8=12296
 ammonium acetate structure, rel. to H bonding 8=8503
 amyl stearate, crystal structure 8=22057
 amylose, asymm. interaction with DL-mandelic acid
 and DL-ethyl mandelate 8=18696
 5 α -androstan-3,17-dione(ANDR), crystal packing
 calculation 8=13311
 aniline, in dilute solns. of CS_2 and CCl_4 , dependence of
 nuclear relaxation times on viscosity 8=8126
 aniline, phosphoresc. and spin-orbit coupling 8=12252
 aniline, photoionization efficiency 8=7724
 aniline solution in benzene, CCl_4 and chlorobenzene,
 vap. press. and excess free energies 8=8056
 anilines, disubstituted, dielectric constant and loss in r.f.
 region 8=5357
 anthracene and plastic scintillator, radiation damage
 by $4 \rightarrow 10$ keV electrons 8=23029
 anthracene, autoionization and exciton
 annihilation 8=17890
 anthracene, carrier formation from excitons and charge
 transport 8=17858
 anthracene, charge carrier generation with polarized
 light 8=2268
 anthracene crystals., morphology, planes, twinning,
 etching 8=8381
 anthracene, d.c. dark Hall mobility obs. 8=22523
 anthracene in diethylaniline, luminescence 8=7560
 anthracene derivatives, absorption and emission
 displacement due to dispersion interaction 8=4176
 anthracene, dislocations 8=17648
 anthracene, elastic constants 8=5093

Organic compounds—contd

- anthracene, excimer fluoresc. in rigid matrices 8=14339
 anthracene, exciton theory, band theory and photo-
 conductivity meas. 8=13671
 anthracene crystals, fluorescence and absorpt. spectra
 symmetry 8=18631
 anthracene crystals, delayed fluoresc. decay time,
 2-300°K 8=23065
 anthracene crystals, e states rel. to carrier prod. 8=22434
 anthracene, delayed fluoresc. rel. to triplet-triplet inter-
 action and triplet exciton diffusion, obs. 8=23066
 anthracene, far i.r. absorption 8=23028
 anthracene, fluoresc. decay curve 8=18633
 anthracene fluoresc. spectrum fine struct. and vibr.
 analysis, 23 000-28 000 cm^{-1} 8=1274
 anthracene frozen in n-paraffin forms,
 fluorescence 8=23067
 anthracene, γ -irrad., colour centres 8=17689
 anthracene, Hall and drift mobilities of carriers 8=18178
 anthracene, luminesc. quenching by mag. field, distinction
 of excitons 8=18632
 anthracene, molecule, photo-ionization cross-section
 calc. 8=21259
 anthracene, radiation damage to optical absorption
 props. 8=9565
 anthracene, recombination luminescence in mag.
 field 8=18630
 anthracene, reflection spectra near exciton excitation
 low temp anomaly 8=23030
 anthracene, 9,10-dimethylantracene excimers fluoresc.
 quenching 8=1575
 anthracene-oxygen complex stabilization constants from
 solubility in compressed O_2 8=2499
 anthracene, photocond. depend. on temp., and carrier
 generation 8=2269
 anthracene, photoconductivity, mag. field effects,
 theory 8=22691
 anthracene, polarization of triplet factor group
 states 8=2494
 anthracene, pulsed photoconductivity rel. to carrier
 decay 8=2267
 anthracene scintillator, light output under influence
 of α -particles 8=2495
 anthracene, singlet-exciton collisions 8=17891
 anthracene, space-charge-limited crystal
 currents 8=17859
 anthracene, triplet exciton dynamics, spectroscopic
 approach 8=13672
 anthracene, triplet-triplet absorption under Shpol'ski's
 condition 8=21147
 anthracene, two-photon photocarrier generation 8=13918
 anthracene, u.v. irradiated, fluorescence and photo-
 conductivity rel. to carrier generation 8=2266
 anthracene, vapour- and melt-grown crystals., purity and
 perfection 8=21942
 anthracene vapour, structured fluoresc. spectrum 8=21113
 anthracene, vibr. effects in radiationless
 transitions 8=21114
 anthracite, reduction of paramag. absorption by
 heating 8=5441
 anthraquinone, 1,5-dihalo derivs., crystal and mol.
 structure 8=22048
 9-anthranilaldehyde in alcohol and hexane solutions,
 singlet-triplet conversion 8=21693
 9,10-anthraquinone, sensitized emission spectrum in
 visible region 8=4177
 aromatic and condensed ring, polyvinylchloride plastici-
 zation obs. 8=23141
 aromatic amino-acids, delayed luminesc. 8=9650
 aromatic compounds, triplet-triplet absorption under
 Shpol'ski's condition 8=21147
 aromatic crystals, photoconductivity 8=5403
 aromatic hydrocarbon-tetracyanoethylene complexes,
 self-consistent MO calc. 8=12253
 aromatic hydrocarbons, Hückel coeffs. 8=12251
 aromatic hydrocarbons, oriented, e.s.r. multiplet
 struct. 8=2363
 aromatic hydrocarbons, π -electron polarizabilities 8=12254
 aromatic hydrocarbons, pyrolysis, e.s.r. 8=2513
 aromatic hydrocarbons, radiation and photochem. induced
 tritium substitution 8=23166
 aromatic hydrocarbons in solns., mixed excimer
 fluoresc. 8=4593
 aromatic hydrocarbons, triplet-ground-state
 transitions 8=4180
 aromatic hydrocarbons, zero-field splitting of triplet
 states 8=4181
 aromatic, ionization probabilities correl. with geometric
 charge cross-sections 8=4318
 aromatic, molecular crystals, electronic plates 8=13671
 aromatic mols, overcrowded, conformational
 analysis 8=21115
 aromatic phosphors, intensity measurements in vacuum
 u.v. region 8=11159
 aromatic solns., excimer formation 8=8094
 aromatic, triplet-triplet absorpt. at 77°K 8=7561
 aromatics absorpt. spectra rel. to conjugated π -bonds
 obs. 8=4178
 aromatics in boric acid glasses, direct and sensitized
 photo-oxidation 8=23160

Organic compounds—contd

aromatics, cryst. triplet excitons props., theory 8=22479
 aromatics, molten, lifetime of excited states prod. charge carriers 8=12904
 aromatics, transient absorpt. bands 8=4179
 aryl oxalates, electronegatively substituted, reactions with H_2O_2 and fluorescent compounds, chemiluminescence 8=18672
 L-ascorbic acid, crystal and mol. structure 8=13303
 aspirins, substituted, rate of hydrolysis rel. to intra-molec. catalysis 8=5727
 auramine perchlorate, crystal structure, correl. with refl. spectroscopic obs. 8=13302
 azaretrabenzoporins, polarization and absorpt. spectra rel. to porphyrin ring e struct., obs 8=21116
 azides, i.r. spectra, anomalous band splittings 8=21118
 azidopurine from 6-hydrizinopurine + HNO_3 , and structure 8=21117
 azines, CNDO SCF calcs. 8=16331
 azacyclic aromatics, electronic structure 8=7562
 azaindoles, electronic spectra, oscillator strengths meas. 8=7580
 azines, additivity of p.m.r. solvent shifts 8=12931
 1-aziridinepropionitrile, solvent and anisotropy effects in n.m.r. obs. 8=16895
 azoalkanes, electron states 8=12255
 azobenzene, vibr. spectra, continuous bands 8=4182
 azo-compounds decomp. tracing by n.m.r. spectroscopy 8=8127
 azo cpds., vapour press. and ht. of sublimation 8=16958
 azomerocyanines optical absorpt. in elect. field rel. to Kerr effect 8=4573
 p-azoxyanisole, nematic, in mag. fields, X-ray structure investigations 8=4532
 azoxymethylcinnamic acid-dialkylester liq. crystals, calorimetry 8=4533
 barbitol, fragmentation patterns by mass spectrometry 8=12031
 barbitol, mass spectrum obs. 8=20912
 benzaldehyde at 77°K, influence of solvent on time resolved phosphorescence 8=18635
 1,2-benzanthracene, triplet-triplet absorption under Shpol'ski's condition 8=21147
 benzodioxins, u.v. and e.s.r. spectra calc. 8=7575
 benzene, absolute Raman scatt. cross section, 992 cm^{-1} line 8=16858
 benzene, adsorbed on silica gel, change in dielec. behaviour on gel purification 8=1663
 benzene, Brillouin shifts, temp. dependence, hypersonic velocity and compressibility deduction 8=1502
 benzene in compressed O_2 , 3300 Å transition 8=12259
 benzene-cyclohexane, vapour-liquid equilibrium data 8=4653
 benzene and derivatives, structure of $\nu(CH)$ vibration bands, 300 and 80°K 8=12260
 benzene derivs. liq., l.f. Raman lines 8=1563
 benzene-dioxan crystallized mixture, i.r. absorption spectrum at 80°K 8=18572
 benzene, electronic struct. 8=12256
 benzene, emission from liq. excited by electrons 8=12893
 benzene, freezing, under press., differential thermal analysis 8=9684
 benzene, gas chromatograms and i.r. spectra 8=9759
 benzene, gas, scatt. of K, Rb and Cs, compared with cyclohexane 8=1205
 benzene hydrogenation to cyclohexane, effect of support on Ni catalyst 8=9707
 benzene, induced Raman scatt. intensity rel. to sample length 8=8076
 benzene ion reactions with benzene 8=16452
 benzene, and ionized states, SCF calc. 8=7565
 benzene-isobutanol vapour-liquid equilibrium data 8=4653
 benzene, large-angle electron-impact spectra 8=16224
 benzene, liq., Cotton-Mouton effect 8=12869
 benzene, liquid and crystalline state, sub-millimeter wave spectra 8=7568
 benzene, liq., electrode effect on current transport 8=8116
 benzene, liq., hot-electron injection from tunnel junction, effective barrier 8=257
 benzene, liq., l.f. Raman lines 8=1563
 benzene, long transversal n.m.r. relaxation time 8=2380
 benzene, luminesc. in cryst. matrices 8=9651
 benzene, mag. circular dichroism 8=21123
 benzene on Mg-Fe mixed hydroxides, adsorpt., obs. 8=17023
 benzene mol. config. rel. to cryst. absorpt. spectrum 8=5645
 benzene, molecular orbital pair correlations 8=4185
 benzene mol., SCF-MO-CI theory, empirical params. choice 8=21127
 benzene mols. crystal, exciton states, Faraday effect and spin-orbit interaction calc. 8=9568
 benzene, N and Ar excit. luminesc. in solid solns., obs. 8=13036
 benzene, 992 cm^{-1} spectral line, Raman scatt., rel. to solvent and conc. 8=21672
 benzene, overtones of combination scattering 8=1559

Organic compounds—contd

benzene-oxygen complex stabilization constants from solubility in compressed O_2 8=2499
 benzene, phosphoresc. cryst. e.p.r. 8=14095
 benzene, π -electron density distrib. and free-electron model 8=7563
 benzene, pressure separation from H_2O system 8=8180
 benzene radical anion, electron exchange with neutral benzene 8=5692
 benzene, σ ionization potentials 8=12257
 benzene in solid solns., matrix effects on spectra and state of dispersion, 77°K 8=13037
 benzene, sorption into drawn and undrawn poly-ethylene 8=8349
 benzene, stimulated Raman effect, cyclic temp. depend 8=21125
 benzene sulphonyl chlorides, parasubstituted, crystal growth and structure 8=13133
 benzene, u.v. absorpt. spectra 8=7567
 benzene, vibr. exciton spectrum 8=9567
 benzene, vibronic interaction, lower electronic states 8=7564
 benzene-in-water emulsions, particle size and distrib. 8=12953
 benzene-water, interfacial tension 8=12827
 benzene, X-ray absorpt. spectra 8=12277
 benzenes, microwave relaxation times 8=7599
 benzenes, paradisubstituted, far i.r. absorption 8=7566
 benzenes, Raman scatt. cross-sections 8=12130
 benzenes, substituted, p.m.r. chem. shifts 8=12316
 benzenes, substituted, proton chemical shifts and π -electron densities 8=12262
 benzene, u.s. velocity, absorption and relaxation obs. 8=12687
 benzenes, unsymmetrical, ortho-disubstituted, n.m.r. 8=4625
 benzil cryst., optical rotatory dispersion, molec. origin 8=2463
 benzoates, mass spectrum obs. 8=20912
 benzoic acids, mass spectrum obs. 8=20912
 benzoin, optical rotatory dispersion of transient species 8=12258
 benzole, methyl alcohol diffusion, mechanism 8=12834
 benzonitrile, freezing and polymerization, under press., differential thermal analysis 8=9684
 benzophenone, absorpt. spectrum, by flash photolysis 8=4184
 benzophenone and derivatives, triplet-triplet absorpt. spectra 8=12263
 benzophenone, far i.r. absorption 8=23028
 benzophenone, u.v. flash photolysis, e.s.r. study of free radicals prod. 8=12339
 benzophenone, viscous liq., wing of Rayleigh line obs. 8=21671
 benzophenones, polarized absorpt. spectra 8=9566
 p-benzosemiquinone, reson. absorpt. in Zeeman region 8=16348
 benzo-thiopyrone, crystal structure 8=22051
 benzotropones, reactivity indices 8=18673
 o-benzoyl benzoic acid, space group 8=17441
 benzyl, lumines. of single cryst. and solid solns. in polystyrene 8=18634
 benzyl radical fluoresc. in methylcyclohexane, cyclopentane and methylcyclopentane, 4°K 8=12342
 benzyl radicals fluoresc. spectra in solid solns. and vibr. analysis 8=13032
 4-benzoyloxyphenol, packing relationship 8=17440
 N-benzyl-N, 2, 4, 6-tetramethylbenzamide, n.m.r. line shapes 8=12331
 2-(benzylthio) imidazoline hydrochloride, structure 8=8582
 2-(benzylthio) tetrahydropyrimidine hydrochloride, structure 8=8582
 benzimidazolone derivatives, spectra 8=4186
 5, 5'-biisoxazole crystal and mol. structure 8=22067
 p-biphenylaldehyde in alcohol and hexane solutions, singlet-triplet conversion 8=21693
 biphenyl derivs. of group IV b, u.v. spectra anal. by heteroatom model 8=8090
 2, 2'-biphenyldisulphide, crystal structure 8=22071
 biphenyl, far i.r. absorption 8=23028
 biphenyl in methylcyclohexane glass, radiophoto-luminescence 8=9652
 bis-[2-chlorobenzene-(1-azo-1')-naphthol-2'] Cu(III) e.p.r. rel. to e delocalization in azo groups 290 and 77°K 8=8122
 cis- and trans-bis(dialkyl sulphide) dichloroplatinum (II) complexes, struct. and inversion mech. n.m.r. obs. 8=16355
 bis-[2, 6-dichlorobenzene-(1-azo-1')-naphthol-2'] Cu(II) e.p.r. rel. to e delocalization in azo groups 290 and 77°K 8=8122
 p-bis(dimethylhydroxysilyl) benzene, cryst. struct. 8=22065
 bis(triphenylacetic) oxalic anhydride, chemiluminescent reactions with H_2O_2 and fluorescent cpds. 8=18685
 borazine and derivatives, as slow neutron scintillators 8=6963
 p-bromoacetanilide, Br 79 n.q.r., temp. var. and Zeeman effect 8=4228

Organic compounds—contd

- bromoacetone, rotational isomerism in all states 8=1271
 p-bromoanisole, i. r. absorpt. spectrum obs. 8=21682
 9, bromoanthracene, 9,10-dimethylanthracene excimers fluoresc. quenching 8=1575
 bromobenzene, molec. motion in liq. by n.m.r. 8=8132
 p-bromobenzoyldimethylamine mol. struct., obs. 8=21129
 p-bromobenzoylenimine mol. config. rel. to ethyleneamide group struct, obs. 8=21129
 2-bromocyclobutanone, vibr. spectra 8=12266
 2-bromo-1,1-diphenyl-prop-1-ene, crystal and molecular structure 8=4187
 bromomalonalddehyde anion, i. r. spectra 8=21144
 bromomalonalddehyde, i. r. spectra 8=21144
 bromomethyl diazine, electronic absorpt. spectra 8=12268
 bromomexicanin E. crystal and mol. structure 8=21151
 bromo-naphthalenes, n.m.r. meas. 8=7613
 N-(p-bromophenyl) benzene sulphonamide mol. structure and intramolecular interactions 8=1278
 β -bromopropionitrile, 2 rot. isomers, virial H-H couplings from n. m. r. solvent depend. 8=21158
 3-bromopyrene, double intersystem-crossing 8=21128
 3-bromothiophene-2-aldehyde n.m. double-r. 8=6408
 2-bromo-2,4,4-trideuterocyclobutanone, vibr. spectra 8=12266
 (3:1) bullvalene-AgBF₄ complex, cryst. and molec. structure 8=4890
 butadiene polymerization catalysis by π -crotyl NiII and -NiCl rel. to structs., obs. 7=8576
 1,3-butadiene, photodissoc., primary processes 8=23155
 1,3-butadienes, n.m.r., theory 8=7604
 butane, evaporating in H₂O or NaCl solns., rel. to ice cryst. growth 8=13137
 butane gas, sorption and diffusion in synthetic Na mordenite 8=13109
 n-butane-He system, phase and volumetric behaviour showing gas-gas equil. for low He conc. 8=12979
 n-butane-He mixtures, second virial coeffs. determ. 8=12980
 butane, ionization probability, mass spectrometry 8=21283
 n-butane, photoionization 8=4319
 1,3 butanediol, shear rigidity and free volume 8=1537
 n-butanol complexes in amine solns., dipole moments 8=12909
 butatriene, force field, mean amplitudes of vibration, shrinkage effect and Coriolis coupling constants 8=16314
 butatriene, vibrational force constants, amplitude of thermal motion and polarizabilities calc. 8=12264
 butyl alcohol, stimulated and thermal Mandel'shtam Brillouin scattering and dispersion of sound 8=21665
 butyl alcohol-water mixtures, hypersonic meas. 8=4572
 tertiary butyl fluoride gas, mol. struct. meas. 8=7569
 butyl PBD, fluoresc., concentration effects 8=4594
 butyl phthalate, spin-lattice relax. rel. to dielec. relax. and viscosity 8=9459
 caffeine salts, i. r. spectra 8=14277
 canthaxanthin, crystal structure 8=22053
 ϵ -caprolactones, optical rotation and molec. conformation 8=12879
 carbamylphosphonates, long-range P³¹-H¹ spin-spin coupling 8=16353
 carbon tetrachloride, Raman spectrum, difference bands 8=7570
 carbonium ion yield in radiolysis of liq. hydrocarbon-alcohol mixtures 8=5756
 carbonyl acids in perethers, spectrochem. determ. 8=2549
 carbonyl cpds., reversible hydration study, limitations of u. v. spectroscopy 8=9682
 carbonyl group coupling in cyclic anhydrides and imides rel. to solvent effect on valence vibrations 8=16857
 carboxylic acid C₂₀, persistent electric dipole moment obs. at -78°C 8=13890
 carboxylic acids, H-bonded, i. r. spectra 8=7571
 Δ^3 -carene and oxide, mol. structure from gas-e-diff. meas. 8=21161
 β carotene, all-trans optical, spectroscopic and elec. props. obs. 8=2465
 carotenoids, photocond. 8=18240
 catalase, crystal structure 8=8575
 cellophane membrane NaCl uptake rel. to ion exchange props., obs. 8=23084
 cellulose acetates, macromol. characts. from speed sedimentation in acetone 8=4262
 cellulose hydroxyl groups, reactivity to N oxides in presence of P₂O₅ 8=5721
 cellulose triacetate films, amorphous and cryst., transition temps. 8=4724
 cellulose, ZnO₂ diffusion and absorpt. in membranes 8=21645
 cetylpyridinium bromide, ion sublation studies by radioactive tracers 8=23075
 chelated amino acids, p exchange and mutarotation via carbanion intermeds. 8=5691
 chloranil, absorption spectrum in near u.v. 8=21126
 p-chloranil, space-charge limited currents meas. 8=9137
 chlorins, optically active, mag. circular dichroism 8=16317
 chloro-aluminium phthalocyanine and diethylthiatricarbo-cyanine iodide, stimulated emission obs. 8=452

Organic compounds—contd

- chloroaluminum phthalocyanine, fast fluorescence meas. 8=16869
 chloro-Al phthalocyanine, new laser oscillations 8=6475
 chlorobenzenes in CS₂ soln., i. r. intensity meas. of C-H out-of-plane vib. bands 8=21684
 chlorobenzenes, LCAO-CUV calc. 8=21124
 chloro-diphenyl-sulphone-urethanes, i. r. absorpt. spectra 8=9571
 chloroethylene, ion-molecule reactions in, study by ion cyclotron reson. spectroscopy 8=16453
 chloroferrocene, MO calcs., and excitation energies 8=4197
 chloroform, acetone diffusion, mechanism 8=12834
 chloroform, intermolecular potential and viscosity, 30-200°C 8=21523
 chloroform molec. complex with benzene, i. r. spectra 8=2464
 chloroform, near i. r. spectra, using high resolution grating spectrometer 8=20078
 chloroform, in nonpolar solvent, intensity meas. of i. r. band 8=21680
 chloroform-triethylamine system, equil. and H-bond formation 8=18649
 chloroform, ν_8 bands, gas and liq. 8=12265
 chloromethyl diazine, electronic absorpt. spectra 8=12268
 chloromethyl thiocyanate, i. r. spectrum 8=4201
 p-chloro-phenol, OH stretching band struct. 8=4211
 chlorophyllide a and b fluoresc. polarization and absorpt., spectra, 390-440 μ 8=21700
 3-chloropyridine, near u. v. absorption spectrum 8=21130
 chlorosilyl dialkylamines, vibr. spectra 8=1300
 chlorotoluenes, LCAO-CUV calc. 8=21124
 α -chloro-6-valerolactam, crystal structure 8=8597
 chlorpromazine, crystal structure 8=8592
 cholestric liq. crystals, optical rotatory power 8=12876
 cholesterol liquid crystals, structure by optical obs. 8=21612
 cholesterol derivatives, dipole moments 8=1279
 cholesteryl-caprinate, heat of transformation 8=16917
 cholesteryl caprinate, liquid crystals, heat of formation and critical size of centres 8=16918
 cholesteryl mynstate liquid cryst. mesophase polymorphism, obs. 8=12802
 chrysene-d₁₂, plastic scintillators 8=9656
 cinnoaline vapour, electronic spectrum 8=16318
 complexes formed by H-bonding, i. r. spectra 8=12242
 configuration interaction, improving convergence 8=16267
 copper formate tetrahydrate, cell doubling at antiferro-electric phase transition 8=9222
 copper phthalocyanine, e. s. r. 8=9441
 coronene in CCl₄, phosphoresc. rel. to mol. deform. by lattice interactions, 77°K 8=1577
 coronene-d₁₂, plastic scintillators 8=9656
 coronene, excited singlet state, nsec absorpt. 8=9728
 coronene, mag. circular dichroism 8=21123
 coronene, π transitions, free-electron and MOLCAO calcs. 8=4139
 corrosion inhibitors for metals in acids, specificity rel. to reaction kinetics 8=2509
 p-cresol, OH stretching band struct. 8=4211
 π -crotyl NiX, (X=Cl, I), structure rel. to butadiene polymerization catalysis, obs. 8=8576
 cryptocyanine, fast fluorescence meas. 8=16869
 cryptopine, C₂₁H₂₃O₂N, crystal structure 8=22055
 crystal chemistry, studies in USSR 8=8368
 crystals as adsorbents for gas-solid chromatography 8=18763
 crystals, diimag. anisotropies 8=18295
 crystals, oscillation spectrum and charact. temp. from thermodynamic props. 8=17470
 crystals, thermodynamic props. from structure 8=13360
 cyanethylacetylcellulose dielec. relax. rel. to acetate and cyanethyl groups motion, -160-200°C 8=22662
 cyclic moles, anal. of i. r. type A bands rel. to asymmetry 8=1277
 cyclic paraffins, molecular structure interatomic distances, chain folding 8=1827
 cyclic polyenes, π -electron model 8=16174
 cycloalkanes and alkylcycloalkanes semidiones, struct. and conformation, e. s. r. obs. 8=22898
 cyclobutadiene, MO calc. of stability and geometry 8=21131
 cyclobutane, freq. factor for rate const. 8=14364
 cyclobutane photolysis, energy distrib. in reaction products 8=5753
 cyclobutane photolysis, mechanism rel. to curved Stern-Volmer plot 8=5752
 cyclohexadiene-1,4 (and 1,3), X-ray absorpt. spectra 8=12277
 cyclohexane as α dosimeter 8=20592
 cyclohexane-aniline, critical binary fluids, spectral width temp. and angular dependence 8=21778
 cyclohexane-benzene mixtures, irradiated, charge transfer 8=9731
 cyclohexane benzene, near u. v. absorption spectrum 8=16861
 cyclohexane, gas, scatt. of K, Rb and Cs, compared with benzene 8=1205
 cyclohexane-isobutanol vapour-liquid equilibrium data 8=4653
 cyclohexane, liq., hot-electron injection from tunnel junction, effective barrier 8=257

Organic compounds—contd

- cyclohexane on Mg-Fe mixed hydroxides, adsorpt. and desorpt., obs. 8=17023
- cyclohexane, overtones of combination scattering 8=1559
- cyclohexane, X-ray absorpt. spectra 8=12277
- cyclohexane-2,2,4-trimethyl pentane mixture, H_2 yield on radiolysis 8=18748
- cyclo octatetraene anion radical, e.s.r., ion pairing effects 8=4614
- cycloparaffins, chem. ionization mass spectra 8=1374
- cyclopentadiene, i.r. and Raman spectra 8=12267
- cyclopentadiene nickel nitrosyl, laser-excited, Raman spectrum 8=21155
- cyclo-pentane-hexane and -heptane, translational diffusion in CCl_4 , expt. and theory 8=16814
- cyclopentene, i.r. absorpt. spectrum 8=7590
- cyclopentene, i.r. spectra and ring puckering 8=16304
- cyclopropane derivatives, C-C coupling 8=12320
- cyclopropane, gas and liq. i.r. and Raman spectra 8=1298
- cyclopropane, solubility in polyethylene 8=17188
- cyclopropanes and cyclopropenes, strain energies, SCF MO calc. 8=4190
- cyclopropanes, substituted, C^{13} chem. shifts 8=1303
- cyclopropylcarbanyl cations, equilibrating 8=5693
- p-cymene, oxidation with t-butyl chromate 8=9687
- L-cysteine hydrochloride monohydrate, Patterson sharpening function $[\sum Z_j / \sum f^2 - 1]$ 8=8577
- deca-trans-3, trans-7-dienedioic acid 8=8578
- decane, C-C and C-H bond electrons momentum distrib. rel. to β^+ annihilation 8=16324
- n-decane-water, interfacial tension 8=12827
- n-decanol in non-polar solns., microwave relax. 8=21711
- 15,15'-dehydrocanthaxanthin, crystal structure 8=22053
- depsides, lichen, i.r. and u.v. spectra 8=4191
- depsidones, lichen, i.r. and u.v. spectra 8=4191
- deuterobenzenes, vibr. band structure 8=21683
- deuteriochlorobenzenes, o-, m- and p-, i.r. and Raman spectra 8=7574
- deuterotoluenes, o-, m- and p-, i.r. and Raman spectra 8=7574
- diacetylene- H_2 , d_2 , absorpt. spectrum in vacuum u.v. to 1000 Å 8=12245
- dialkoxytetrahydropyrans, spin-spin coupling-models 8=12292
- diaminodiphenylsulphone, crystal structure 8=22075
- 2,3 diazabicyclo[2.2.1]hept-2-ene, photolysis products, distrib. of excess vib. energy 8=5751
- diaziridin rings, methylene-group n.m.r. spectroscopy 8=12940
- diazopropyne photolysis, C_3 and C_3H_2 radicals absorpt. spectra obs. 8=16368
- dibenzenechromium iodide, i.r. spectra and C-H out-of-plane force consts. 8=14276
- dibenzofuran, e.s.r. study of reactions of radical anion formed by e addition 8=14350
- dibenzosuberone, absorpt., phosphoresc. and polarization spectra 8=8096
- dibenzoylperoxide decomp. tracing by n.m.r. spectroscopy 8=8127
- 1,4-dibenzylxybenzene, packing relationship 8=17440
- cis-bis(dibenzyl sulphide) dichloroplatinum(II), struct., inversion and AB chemical shifts, n.m.r. obs. 8=16356
- dibenzyl sulphoxide, n.m.r. obs., comparison with cis-bis(dibenzyl sulphide) dichloroplatinum(II) 8=16356
- dibromoacetone, i.r. spectra 8=12281
- 4,4'-dibromobenzophenone, absorpt. phosphoresc. and polarization spectra 8=8096
- 4,4'-dibromo-dibenzoyl peroxide, crystal and mol. structure 8=17442
- 1,4-dibromonaphthalene, triplet states 8=2467
- 2,3-dibromo-1,4-naphthoquinone, crystal structure 8=8588
- di-tertiary-butyl nitroxide solns., spin exchange 8=8121
- dicalcium strontium propionate, $Ca_2Sr(C_2H_5CO_2)_6$, dielectric critical slowing down 8=2248
- dicalcium strontium propionate, $Ca_2Sr(C_2H_5CO_2)_6$, structure in ferroelectric phase 8=4892
- dicalcium strontium propionate, $Ca_2Sr(C_2H_5CO_2)_6$, structure in paraelectric phase 8=4891
- m-dicarbene, e.p.r. of quintet ground states 8=4221
- dicarboxylic acids, structure determ. from appl. of close-packing principle 8=22056
- 2,4(5)-dichloroaniline, near u.v. absorption spectrum in vapour phase 8=21132
- 2,5(6)-dichloro-p-benzoquinone, absorption spectrum in near u.v. 8=21126
- 4,4'-dichloro-dibenzoyl peroxide, crystal and mol. structure 8=17442
- di-p-chlorobenzoylperoxide decomp. tracing by n.m.r. spectroscopy 8=8127
- dichlorodifluoromethane, solution H in, spectral simultaneous transitions 8=21675
- dichloroethane, overtones of combination scattering 8=1559
- trans-dichloroethylene adsorbed on silica gel, laser Raman spectra 8=23031
- dichloromethane, CH_2 valence vibrations in vapour and condensed phases 8=16328
- 2,4-dichlorophenoxyacetic acid, n.q.r. 8=2390
- dichloro 1-2 propane, i.r. dispersion 8=8074

Organic compounds—contd

- dichlorotoluenes, 2,4-, 2,6- and 3,4 molecules with benzene solvent, dipole moment 8=21121
- 9-dicyanomethylene-2,4,7-trinitrofluorene crystal structure 8=8580
- 2,4-dicyanopentanes, high-resolution n.m.r. 8=16884
- dicyclopentadienyl nickel, electron capture ratio of Ni^{56} and Ni^{57} 8=3914
- di-ethyl ether, heat transfer in nucleate boiling 8=16948
- diethyl ether, thermal conductivity rel. to temp. 8=7925
- diethyl ethers, catalytic decomp. on W films 8=14404
- diethyl phthalate, ht. capacity, cryst., glass and liq. 8=1870
- diethyl sulphide-urea cpds., X-irrad., e.s.r. of $R\dot{C}HSR'$ type free radicals 8=1314
- diethylthiatricarbocyanine iodide and chloro-aluminium phthalocyanine stimulated emission obs. 8=452
- difluorobenzenes, microwave spectra 8=1285
- 1,1-difluoro-1,2-dibromodichloroethane, spin-echo n.m.r. and internal rot. 8=4622
- 1,3-difluoro-4,6-dinitrobenzene, n.m.r. 8=21178
- 1,1-difluoroethylene in soln., nuclear spin relax. 8=16889
- difluoromethylene, triplet-to-singlet conversion 8=1293
- 2,6 difluoropyridine, i.r. and Raman spectra 8=16341
- p-dihalobenzenes, C^{13} -H satellite spectra 8=21174
- dihalogenomethanes in CCl_4 , methylene group valence vibr. bands rel. to weak intermol. interaction 8=1292
- di-n-hexyl sulphide-urea, X-irrad., e.s.r. of $R\dot{C}HSR'$ type free radicals 8=1314
- dihydroanthracenes and their Li salts, n.m.r. rel. to ion-pair structure 8=7559
- dihydrofuran, i.r. spectra and ring puckering 8=16304
- 2,5-dihydrofuran, ring puckering 8=12271
- dihydronicotinamides, SCF-CI calc. 8=16306
- dihydropyridines, SCF-CI calc. 8=16306
- dihydrothiophene, i.r. spectra and ring puckering 8=16304
- dihydroxydurene cation radical, e.s.r. spectrum 8=1589
- dihydroxyethylalkylamine oxide micellar solns., potentiometric studies 8=8158
- diiodomethane, CH_2 valence vibrations in vapour and condensed phases 8=16328
- di-iodo-L-tyrosine dihydrate, crystal structure 8=1826
- diisopropylcyclohexane, heat loss to turbulent flow 8=8050
- 2,6 di-isopropyl phenol, elec. field induced spectral shifts in vib. lines 8=1572
- diketene, rot. spectrum, config., dipole moment and ring deform. vibr. 8=4200
- α -diketones, emission spectra and excited state geometry 8=1297
- 4,4'-dimethoxyazobenzene anion, e.s.r. 8=12303
- p-dimethoxybenzene, near u.v. absorption and emission spectra 8=21133
- dimethoxydurene cation radical, e.s.r. spectrum 8=1589
- 1,1-dimethoxy-2,4,6-trinitro-benzene ion, structure 8=8572
- dimethyl acetamide, n.m.r., solvent-solute interactions 8=12936
- dimethylacetylene mols. normal modes, Coriolis coupling and centrifugal distortion 8=16330
- dimethylacetylene, vib. spectrum, theory necessary for anal. 8=1294
- dimethylalkylamine oxide micellar solns., potentiometric studies 8=8158
- 4-dimethylamino-4'-nitrodiphenyl in decalin, frozen solution, luminescence 8=5684
- N-N-dimethylaniline and deuterated derivatives, p.m.r. 8=21179
- dimethylaniline, α,β -unsaturated ketone derivatives in toluene electronic absorption and luminescence spectra 8=21702
- N,N-dimethylaniline cation radicals, hyperfine splitting, substituent effects 8=4620
- 9,10-dimethyanthracene excimers fluoresc. quenching by anthracene and 9-bromoanthracene 8=1575
- 2,6-dimethylbenzoic acid, crystal structure 8=8571
- 2,6-dimethyl benzoic acid, crystal structure rel. to mol. distortion effects 8=22049
- 2,5-dimethyl-p-benzoquinone, structure and electron density 8=8573
- 2,6-dimethylbenzosemiquinone, monoprotonated, e.s.r. solvent depend. 8=8125
- 4,4-dimethylcyclohexenone radical anion, e.p.r. 8=12304
- 1,2-dimethylcyclopropane, cis- and trans-, vibration spectra, calc. and interpretation 8=7587
- dimethyl formamide, n.m.r., solvent-solute interactions 8=12936
- meso- α,α' -dimethylglutaric acid, molecular and crystal structure refinement 8=1819
- 2,3-dimethylnaphthalene, mol. and cryst. structure from i.r. spectra and diamag. anisotropy 8=18574
- 2,3-dimethyl-naphthalene in n-hexane rigid matrix at 77°K, absorpt. and emission spectra 8=14286
- 1,2- and 2,3-dimethylnaphthalene, triplet-triplet absorption under Shpol'ski's condition 8=21147
- 2,3-dimethyl-1,4-naphthoquinone crystal structure 8=8587
- 2,5-dimethyl-1,3,4-oxadiazole, i.r. spectrum 8=12285
- 0,0-dimethyl phosphorochloridodithioate, i.r. and Raman spectra 8=21146

Organic compounds—contd

- dimethyl phthalates, in soln., high-resolution proton mag. res. 8=1601
- 2,2-dimethyl propane, C-C distance and covalent rad. of C atom 8=7586
- dimethylsilylamine, cryst. struct. and penta co-ord. Si 8=4894
- α, α' -dimethylsuccinic acids, microstructure and molecular structure obs. 8=22000
- dimethyl sulfoxide, base-catalysed tritiation and ionization 8=4610
- dimethylsulfoxide, solid, n. m. r. study of methyl group movement 8=9466
- m-dinitrene, e. p. r. of quintet ground states 8=4221
- p-dinitroanisole radical anion, hyperfine coupling consts. of N^4 , solvent depend. 8=8124
- p-nitrobenzene alkali-metal salts, e.s.r. 8=8120
- p-nitrobenzene radical anion, hyperfine coupling consts. of N^4 , solvent depend. 8=8124
- dioctylphthalate aerosol, particle conc., by turbidity meas. 8=8153
- 1,4-dioxane, solvent shift obs. and structure 8=16862
- dioxazines, electronic spectra, MO calc. 8=4205
- 1,1-diphenylacetylene, e.s.r. study of reactions of radical anion formed by e addition 8=14350
- 9,10-diphenylanthracene, electronic structure and luminescence 8=4207
- 1,2-diphenyl benzene, solidification kinetics into under-cooled melt 8=8401
- 1,1,-diphenyl-2-bromo-prop(1)ene, crystal structure 8=22058
- diphenyl, crystal growth in constant electric field 8=21949
- diphenyl- α, α' -dipyridyl system, constitution diagram 8=4725
- diphenylboron halides, thermodynamic properties 8=1863
- 1,1-diphenylethylene, e.s.r. study of reactions of radical anion formed by e addition 8=14350
- diphenyl-picryl-hydrazyl, Faraday effect at 8.78 GHz 8=7600
- diphenyl, n. m. r. line shape 8=14132
- diphenyls, 4-monosubstituted, absorpt. spectra rel. to ionization pot. and conjugated π -bonds, obs. 8=4212
- 4,4'-diphenylstilbene in polymethyl methacrylate, solid soln. fluoresc. 8=9654
- 9,10-di-n-propylanthracene excimers fluoresc. quenching by anthracene and 9-bromoanthracene 8=1575
- di-n-propyl ethers, catalytic decomp. on W films 8=14404
- dipyridyl mononegative ion and alkali metal ion biradical, e.s.r. and structure 8=4247
- 1,4-distyrylbenzenes, 4-monosubstituted, absorpt. spectra rel. to ionization pot. and conjugated π -bonds, obs. 8=4212
- p-dithiane, i.r. absorpt. 15° and 300°K 8=18575
- dithiono-4-oxo-1,3-thiazane, unit cell and space group 8=4898
- ditoluenechromium iodide, i.r. spectra and C-H out-of-plane force consts. 8=14276
- 1,1,-di-para-tolyl-2-bromoethylene, crystal structure 8=22058
- dioxanthogens i.r. spectra, anomalous band splittings 8=21118
- DNA with complexed carcinogen, elec. and optical props. 8=18093
- n-dodecylaminum hydrochloride, ion sublation studies, by radioactive tracers 8=23075
- dodecylthiuronium chloride, ion sublation studies by radioactive tracers 8=23075
- DPPH, paramagnetic resonance at low fields 8=14122
- DPPH stable free radical, cryst. structure 8=1317
- durene, doped crystals, luminesc. mechanism 8=18637
- durene, far i.r. absorption 8=23028
- durene, irradi. cryst., e.p.r. of free radicals 8=5528
- durene, single cryst., progressive fluoresc. and delayed induced luminesc. 8=18636
- durene-tetracyanobenzene complex, e.s.r. of charge-transfer triplet state 8=12306
- durosemiquinone, e.s.r. in 1,2-dimethoxyethane 8=1591
- dye laser flashlamp excitation 8=451
- dye solns, two-photon absorpt., geometrical model and meas. 8=16834
- dyes, adsorbed, ionization energy 8=5424
- dyes, photocond., localized model 8=13920
- dyes, photocond., thermal activation energy 8=13919
- dyes, sorption dynamics 8=17149
- dye-like mol. induced optical activity, free-electron model 8=12382
- dyestuffs, elec. energy storage 8=18176
- EDTA chelates of Cd^{2+} and Hg^{2+} , comp. study by ultrasonic vel. meas. 8=23170
- elastomer viscoelastic props., tensile test obs. 8=22400
- electrolyte-water-phenol system 8=18714
- eosin, fluorescence spectrum, effect of conc. 8=21701
- epoxy, cold hardened, plasticized and filled, elec. cond. rel. to elec. field strength 8=22498
- epoxy resin, polymerization, interpretation of elect. resistivity meas. 8=18707
- esters, gas chromatograms and i.r. spectra 8=9759
- esters interaction with SO_2 8=18688
- esters, long-chain, crystal structure 8=22057

Organic compounds—contd

- estrone-related cpds., lattice constants 8=8579
- ethane, diffusion in zeolites containing H_2O 8=8685
- ethane, dissociation kinetics 8=16363
- ethane gas, sorption and diffusion in synthetic Na mordenite 8=13109
- ethane, i.r. spectrum, high resolution 8=490
- ethane, internal rot. barrier, free-electron treatment 8=4194
- ethane molecule, freq. of torsional vib., meas. 8=1284
- ethane, photoionization 8=4319
- ethane-1,1,1-d₃, Raman spectrum and rot. consts. obs. 8=16321
- ethane, solid films, far u.v. spectra 8=14283
- ethane, staggered and eclipsed, barrier to int. rotation 8=1281
- ethane, transpiration through membrane 8=12662
- ethane, vibr. excited, kinetics 8=18675
- ethanol adsorption on Y_2O_3 and decomp., mechanism, i.r. obs. 8=4768
- ethanol, at room temp., liq. structure and bonding 8=1523
- ethanol, crit. supersaturation for homogeneous nucleation from vapour 8=1621
- ethanol, evaporation into O_2 and CO_2 , effect of interface motion on mass transfer 8=16711
- ethanol- H_2O mixtures, cond. with electrolytes in soln. 8=4604-5
- ethyl acrylate polymerization by a.f. elec. field, obs. 8=9709
- ethyl alcohol, intermolecular potential and viscosity, 30-200°C 8=21523
- ethyl alcohol microwave spectra in region 13-50 kMc/sec obs. 8=4192
- ethyl alcohol, molecule, microwave spectrum 8=21135
- ethyl alcohol-water mixture, thermal diffusion meas. of separation 8=12838
- ethylamine and its deuterated analogs, dissociative mechanism by mass spectra 8=16326
- ethylamine molecule, microwave spectra 8=7578
- ethyl benzene, liq. and in hexane, excimer fluoresc. 8=21699
- ethyl caproate, in nonpolar solvent, intensity meas. of i.r. band 8=21680
- ethyl chloride, absorption of microwaves 8=7579
- ethylether, evaporation into He and CO_2 , effect of interface motion on mass transfer 8=16711
- ethyl ether, stimulated Brillouin scatt., quasi-steady state 8=21687
- ethyl ether, X-ray scatt. meas. 8=8077
- ethylgermane, vibr. spectra 8=1280
- ethyl iodide, electron spin polarization meas. 8=1232
- ethyl iodide, gas-phase photolysis, hot radical reactions 8=5749
- ethyl iodide, n.m.r. in nematic phase 8=8135
- ethyl ketone, vapour heat capacity and heat of vapourization 8=1471
- DL-ethyl mandelate, asymm. interaction with amylose 8=18696
- 2-ethyl naphthalene, emission from liq. excited by electrons 8=12893
- ethyl nitrite, gas, soln. and solid, i.r. spectra and rot. isomerism 8=16329
- ethyl propyl ketone, vapour heat capacity and heat of vapourization 8=1471
- ethyl-1-thio- α -D-glucopyranoside crystal structure 8=8581
- ethylene adsorbed on activated charcoal, mol. motions from n-scattering studies 8=21901
- ethylene adsorption on Y_2O_3 and decomp. mechanism, i.r. obs. 8=4768
- ethylene catalytic oxidation rel. to Ag surface struct., chemisorpt. obs. 8=18706
- ethylene, chem. overshoot in shock pyrolysis 8=9690
- ethylene-chlorhydride-water system, pressure effects 8=16938
- ethylenediamines, intramolec. H-bonds 8=1283
- ethylenimine, dipole moments meas. by benzene solvent method 8=1583
- ethylenimine, solvent and anisotropy effects in n. m. r. obs. 8=16895
- ethylene, large-angle electron-impact spectra 8=16224
- ethylene, LCAO-SCF calc. 8=21139
- ethylene, nonplanarity of first Rydberg state 8=21134
- ethylene, oxidation and pyrolysis in shock waves 8=18676
- ethylene oxide- H_2O clathrates, thermal and composition expansion 8=17447
- ethylene polymerization on CrO_3 , chain transfer reactions, obs. 8=23129
- ethylene, proton spin-spin coupling calc. 8=21136
- ethylene, radiolysis, H_2 production as dosimeter 8=614
- ethylene, Raman spectra and electrooptical parameters compared with trichloroethylene 8=21138
- ethylene in solution, reactions in presence of O 8=14446
- ethylene-type mols., coriolis coupling coeffs. 8=4195
- ethylidene-NN-diacetamide crystals, atomic structure obs. 8=1817
- ethylsilane, vibr. spectra 8=1280
- excitons in mol. crystals, meas. and obs. 8=8952

Organic compounds — contd

- ferrocene, effect of pressure on Mössbauer resonance 8=1652
 ferrocene, MO calcs., and excitation energies 8=4197
 ferrocene-tetracyanoethylene complex, cryst. struct. 8=1792
 ferrocenylbenzene, ortho-substituted mass spectral decomposition 8=4183
 fluorenylidene in diazofluorene crystals, spin densities from ENDOR 8=5555
 fluoroacetone, rotational isomerism in all states 8=1271
 fluoroacetylene, ground-state electron struct. 8=12246
 fluorobenzaldehydes, emission spectra 8=21122
 fluorobenzene, F spin lattice-relax. 8=1594
 fluorobenzene, H-H and H-F couplings 8=12325
 fluorobenzene, n.m.r. and coupling consts. 8=12326
 fluorobenzenes, CNDO/2 MO calc. 8=12261
 2-fluoro- α -chloro- α , α difluorotoluene, J^{FF} temp. depend. 8=4227
 2-fluoro- α , α -dichloro- α -fluorotoluene, J^{FF} temp. depend. 8=4227
 fluoronitrobenzenes, CNDO/2 MO calc. 8=12261
 fluoro-olefines on oriented polymer fibres, radiation graft-copolymerization 8=23138
 p-fluoro-phenol, OH stretching band struct. 8=4211
 fluorotetrachloroethane, liquid, internal rotation 8=8137
 fluorotitanate complexes, F-F coupling consts. 8=4230
 fluorotoluene derivatives, signs of spin-spin coupling consts. 8=16358
 m-fluorotoluene, microwave spectrum, rot. and dipole moment 8=21164
 formaldehyde, doubling energy of molecules 8=7525
 formaldehyde, K-type doubling lines in h.f. spectra 8=21140
 formaldehyde, oscillator strength of singlet-triplet transition 8=16322
 formaldehyde, π -electronic struct, test of Ohno's formula and constraining Koopman's theorem 8=1286
 formaldehyde, vibrational-rotational interactions for force field determ. 8=4198
 formate ion, reln. between geometry and isoelectronic AB, mols. 8=1269
 formic acid adsorbed on ZnO, i.r. spectra 8=18705
 formic acid, catalytic dehydration over Al_2O_3 and SiO_2 gel 8=9701
 formic acid, cryst., i.r. spectra 8=14279
 formic acid, doubling energy of molecules 8=7525
 formic acid, etching of NaCl crystals 8=17658
 formic acid, K-type doubling lines in h.f. spectra 8=21140
 Freon 113 horiz. strip, transition and film boiling, heat flux and surface temp. fluctuations 8=12986
 freon-113, i.r. dispersion 8=8074
 fuchsin red prod. anomalous dispersion for phase-matched third harmonic generation in hexafluoroacetone sesquihydrate 8=8072
 furan, cryst., i.r. absorpt. spectra at liq. N_2 temp. 8=14280
 furan, $Hg(^3P_1)$ photosensitized, struct. of excited states 8=14434
 furan, u.s. velocity, absorpt. and relax. obs. 8=12687
 furane- α , α' -dicarboxylic acid, crystal and mol. structure 8=17448
 galactital, crystal structure 8=22059
 gas-liquid chromatography, sample injection port 8=14450
 gases, mixtures in air, optical-acoustic effect using cm e.m. waves 8=21520
 α -germyl ketones, electronic spectra 8=21159
 glyceride aqueous systems, struct. of mesomorphic and micellar phases 8=12804
 glycerine, liquid, Brillouin scatt., 23-90°C, background due to relaxation 8=21689
 glycerol, n scatt. rel. to molecular diffusion 8=21609
 glycerol, shear rigidity and free volume 8=1537
 glycerol and water mixture, acoustic absorpt. rel. to macromolecule formation 8=8057
 glycine, kinetics of γ -radiolysis 8=5757
 glycine silver nitrate, i.r. absorption spectrum 8=5646
 glycine, thermal cond. obs. at 60° and 82°C 8=22135
 glycol sulphate, pyroelectric props. 8=13894
 α -glycylglycine, crystal structure 8=13307
 glyoxal, π -electron struct., MO calc. 8=16310
 gramicidin C, iodohydrate, crystallographic investigation 8=4893
 guanidinium $Al_2(SO_4)_3 \cdot 6H_2O$, cryst. struct. 8=17449
 guanidinium aluminium sulphate, $6H_2O$, structure refinement 8=17450
 guanidinium $Al_2(SO_4)_3 \cdot 6H_2O$, ferroelec. moment 8=18195
 guanidinium $Cr_2(SO_4)_3 \cdot 6H_2O$, cryst. struct. 8=17449
 guanidinium $Cr_2(SO_4)_3 \cdot 6H_2O$, ferroelec. moment 8=18195
 hemoglobin, association with O_2 , statistical mech. anal. 8=1311
 haemoglobin, quadrupole splittings and isomer shifts 8=16344
 haloacetonitriles, i.r. and Raman spectra 8=16323
 halogenated benzenes, excimer phosphoresc. in organic glasses 8=9653
 halogenated ethanes, i.r. spectra and internal rot. barriers 8=12269

Organic compounds — contd

- halogeno cyanoacetylenes, force consts. 8=1270
 halogenophenanthrenes, n.m.r. spectra 8=9461
 halonaphthalenes, phosphoresc. in host crystals 8=5683
 haloquinone complexes in polymer matrices, absorpt. spectra at high press. 8=14274
 haloxine, new alkaloid crystal and mol. structure 8=17451
 heterocyclic, triplet-triplet absorpt. at 77°K 8=7561
 heterocyclic cpds., u.v. spectra 8=21142
 N-heterocyclic-iodine complexes, assignment of donor transitions 8=16332
 heterocyclics, dipole moments, MO calc. 8=12272
 heterocyclics, five-membered with C, N and O, CNDO SCF calcs. 8=16331
 N-heterocyclics, ionization potentials 8=12455
 heterocyclics, transient absorpt. bands 8=4179
 hexachlorocyclopentadiene, two solid phases, C_{15}^s n.q.r. 8=8289
 hexachloroethane, far i.r. fundamentals, discussion of freqs. 8=16320
 hexafluoroacetone, fluoresc. in gas phase 8=12247
 hexafluoroacetone, photolysis in Hg vapour, primary process 8=23154
 hexafluoroacetone sesquihydrate, phase-matched third harmonic generation by fuchsin red prod. anomalous dispersion 8=8072
 hexafluorobenzene, photochem. valence tautomerization, kinetics and mech. 8=2537
 hexafluoroethane, F coupling 8=8134
 hexafluoroethane, secondary ion-mol. reactions, ion cyclotron reson. 8=21284
 hexahelicene, optical rot. and circular dichroism 8=12883
 hexamethylbenzene, molec. motions, n.m.r. 8=14143
 hexamethyldisiloxane polymerization on Al surface, in glow discharge 8=5731
 hexamethylphosphotriamide, i.r. dispersion 8=8074
 hexane, behaviour of negative charge carriers 8=21717
 hexane, C-C and C-H bond electrons momentum distrib. rel. to β^+ annihilation 8=16324
 hexane, crit. supersaturation for homogeneous nucleation from vapour 8=1621
 n-hexane, dielec. const. as function of temp. and press. 8=1582
 n-hexane, elec. cond., u.v. and γ radiation effects 8=21714
 n-hexane-nitrobenzene syst., diffusion in crit. separation region 8=21644
 n-hexane, oxidative adsorpt. on Pt electrodes 8=5737
 n-hexane stimulated Brillouin scatt., quasi-steady state 8=21687
 n-hexane, theory of elec. cond. after irradiation by γ -rays 8=6628
 hexatrienes, substituted, HMO calc. of electronic spectra 8=12273
 holmium ethyl sulphate, far-infrared high resolution spectroscopy on e.p.r. lines 8=14110
 hydrazines electrochem. oxidation, hydrazyls form., e.p.r. obs. 8=5722
 hydrocarbons, adsorpt. and oxidation on Pt electrodes 8=9714
 hydrocarbons, CNDO calcs. 8=16325
 hydrocarbons, effect of nonbonded interactions on geometry and energy 8=12166
 hydrocarbons, flames, excited CH and C_2 8=7509
 hydrocarbons, free-radical doped, proton polarization 8=4672
 hydrocarbon gases, photolysis by CO, laser 8=2538
 hydrocarbons, generalized free-electron molecular orbital 8=12284
 hydrocarbons, liq., energy to create ion pair 8=21723
 hydrocarbon liqs., interaction with surfactants 8=8147
 hydrocarbons, liq., thermal props. from similarity theory 8=21646
 hydrocarbon mols., C^{13} -H coupling 8=7510
 hydrocarbons, nonbonded potential parameters calc. from cryst. 8=13002
 hydrocarbons, nuclear spin coupling consts., MO calc. 8=12328
 hydrocarbons, saturated, theory of C^{13} chem. shifts 8=7606
 hydrocarbons, saturated, perturbed orbital energies in radiolysis 8=18742
 hydrocarbons, semiempirical SCF MO calc. 8=4199
 hydrocarbons, simple, reactions with free O and H atoms, e.s.r. study 8=14376
 hydrocarbons, unsaturated, ion-molecule reactions 8=9671
 hydrochinalines, spectral parameters of K and B bands 8=21677
 8-hydroxy-1-methyl quinolinium hydroxide soln. in chloroform, light absorption 8=1566
 hydroxybenzoates, mass spectrum obs. 8=20912
 imidazole, microwave spectra and struct. 8=21162
 imide, liq. photolysis, e.s.r. 8=14435
 2-imino-4-thiazolidinone 5-acetic acid unit cell and space group 8=4898
 indene polyassociates, conjugated, photoelectric emission 8=13938
 indole, electronic spectra, oscillator strengths meas. 8=7580
 indole, excited state dipole moment, calc. 8=21143
 indole in polar solns., red shift in fluoresc. rel. to exciplex state 8=4591

Organic compounds — contd

- indolene in CCl_4 , shape intensities of i.r. absorpt. bands 8=8080
 1-iodo-2-4-dinitrobenzene isotope exchange with KI^{131} in acetone- H_2O , solvent effect 8=2504
 1-iodo-2-4-dinitronaphthalene isotope exchange with KI^{131} in acetone- H_2O , solvent effect 8=2504
 α -iodododecanoic acid methyl ester, crystal structure 8=22057
 β -iodophenylacetylene, polymerization and props. of polymers obtained 8=23130
 isobutane, gas-phase photolysis and radiolysis 8=23158
 isobutyric acid- H_2O system near crit. mixing pt., correl. effect in conc. fluctuations 8=12882
 isopropyl alcohol, adsorpt. on Graphon 8=1700
 isopropyl iodide form. by $\text{C}_2\text{H}_6 + \text{I}_2$ irradiation with visible light 8=5745
 isothiazole, microwave spectra and struct. 8=21162
 isothiocyanates, anomalous band splittings 8=21118
 kerosene, degraded by HNO_3 , removal of fission prods. with $\text{K}_2\text{Cr}_2\text{O}_7$ and H_2SO_4 soln. 8=20854
 ketene-benzene mixture, photochem. and reactions of methylene radicals 8=5748
 ketene, microwave, Zeeman effect of rotational transitions 8=7581
 ketene, photochem. and reactions of methylene radicals 8=5748
 ketene, photodecomp. as source of triplet methylene 8=23157
 ketones, alcoholized, vapour phase, $\nu_{\text{C=O}}$ frequency 8=7582
 ketones, aromatic, ion decomp., influence of charge and radical sites 8=4308
 ketones, dipole moments at 3 cm. 8=21108
 ketones, gas chromatograms and i.r. spectra 8=9759
 ketones interaction with SO_2 8=18688
 ketones, intermolecular forces 8=1287
 latex particles, high-speed beam 8=12952
 lauryl aldehyde, oxidation by u.s. radiation 8=9735
 L-leucine hydrobromide, crystal structure 8=8583
 D-leucyl glycine hydrobromide, min. function Fourier integral approach to crystal structure 8=22061
 liquid binary mixtures, volume changes 8=1528
 liquid mixtures, eutectic forming, normal freezing and constitutional subcooling 8=12973
 liquid quenches of light pulse in GM counter, properties 8=11297
 liquids, heats of transformation rel. to sound velocity 8=16829
 liquids, l.f. Raman lines 8=1563
 lupolen, X-ray scatt., small-angle 8=14282
 magnesium hexa-antipyrine perchlorate, crystal and mol. structure 8=8593
 malonaldehyde anion, i.r. spectra 8=21144
 malonic acids, n.m.r. and intramolec. H-bonding 8=16894
 DL-mandelic acid, asymm. interaction with amylose 8=18696
 D-mannitol, α - and β -forms, crystal structures 8=22062
 mass spectrometry, lecture 8=12030
 Meisenheimer salts, crystal structure 8=22058
 metal carbonyls, i.r. spectra 8=4189
 methacrylic acid, vinylchloride copolymerization, relative reactivities obs. 8=23136
 methacrylonitrile, sigma-type complex with metal chlorides 8=2527
 p-methacryloxybenzoic acid, kinetics of polymerization in soln. 8=14410
 methane- Ar-H_2 system, unsteady diffusion 8=12712
 methane, chem. overshoot in shock pyrolysis 8=9690
 methane, dissoc. attachment of electrons, isotope effects 8=16454
 methane gas, sorption and diffusion in synthetic Na mordenite 8=13109
 methane, gas, liq. and solid, molecular dynamics, study by slow n. scatt. 8=16374
 methane, h.p. boiling apparatus 8=16944
 methane, ionization and electronic energy levels 8=1373
 methane, ion molecule reactions at pressure 8.10^{-4} – 10^{-3} mm Hg 8=4258
 methane, i.r. spectrum, high resolution 8=490
 methane, liquid, proton spin-lattice relaxation 8=4617
 methane, liq. slow n. scatt., with rot. relax. functions of order 3 and 4 8=12798
 methane, magnetic susceptibility calc. 8=7584
 methane, melting curve to 30 kb, obs. 8=1610
 methane, nuclear spin isomerization 8=18681
 methane, nuclear spin relaxation rel. to density and temp. 8=7938
 methane- O_2 mixtures, vibr. energy transfer 8=21200
 methane, photolysis in Ar and N_2 matrices, i.r. spectrum of CH_3 8=18737
 methane-propane mixtures, viscosities and densities at low temp., high press. 8=12819
 methane, residual, effect on BaO cathode emission 8=18663
 methane, rotating mol., scattering curves rel. to interatomic distances 8=7572
 methane, SCF calcs, correlation energies and Hartree-Fock limits 8=1263
 methane, solid films, far u.v. spectra 8=14283
 methane, solid, phase transition calcs. using James-Keenan model 8=17110

Organic compounds—contd

- methane, solid, slow neutron scatt. 8=13038
 methane, sorption in Ba films 8=17160
 methane, sorption in methane in picture c. r. t., effect of silicate binder residues 8=15325
 methane, spin-rotation interaction constants determ. by nuclear spin relax. meas. 8=7573
 methane-tetrafluoromethane system, PVT relations 8=7912
 methane-water vapour mixture, acoustic vel. dispersion and Napier time 8=4481
 methane, X-ray absorpt. spectra 8=12277
 methanes, isotopic, vapour press. and hindered rot. 8=12994
 methanol, adsorpt. by silica gel for surface meas. 8=21742
 methanol, adsorpt. of vapour on AgI 8=8337
 methanol adsorption on Y_2O_3 and decomp. mechanism, i.r. obs. 8=4768
 methanol, crit. supersaturation for homogeneous nucleation from vapour 8=1621
 methanol/Hg interphase, adsorption 8=18721
 methanol, liq., nuclear spin relax, effect of proton exchange 8=1596
 methanol, multiple stimulated Brillouin scattering 7=4584
 methanol, at room temp., liq. structure and bonding 8=1523
 methanol, X-irrad., u.v. photolysis at 77°K 8=5750
 3-methoxy- β , 19-cyclo-5, 10-secoandrosta-1(10), 2-4-trien-17 β -ol p-bromobenzoate, structure 8=22063
 p-methoxyphenol, near u. v. absorpt. spectrum 8=21156
 methyl acetate and stearate, adsorption by Graphon and Spheron 6 8=8340
 methylacetylene, methyl-triple bond interact. MO calc. anal. 8=1291
 methyl alcohol, diffusion into benzole, mechanism 8=12834
 methyl alcohol, intermolecular potential and viscosity, 30–200°C 8=21523
 methyl alcohol, overtones of combination scattering 8=1559
 methylamine- NH_3 gas mixtures, viscosity 8=4492
 methyl 1-aziridinepropionate, solvent and anisotropy effects in n.m.r. obs. 8=16895
 trans N-methyl-N-benzilthioformamide crystal and mol. structure 8=22050
 methylbenzenes, hindered rot., from neutron scat. 8=17484
 N-methyl-N-benzylformamide, int. rot., determ. by n.m.r. and equilibration methods 8=4623
 methyl bromide, microwave spectrum 8=12280
 2-methylbutane, condensed-phase photolysis and radiolysis 8=18739
 methyl chloride, microwave spectrum in excited vibr. states 8=21149
 methylcyclohexanes, C^{13} magnetic resonance, chemical shifts 8=16359
 methylchlorotriphosphate, rotational isomers 8=4203
 1-methyl-1, 4-dihydronicotinamide, dimeric acid product, crystal structure 8=1822
 methylethoxy silanes, integrated intensity of i.r. spectra 8=7551
 methylethyl ketone, chain propag. and breaking 8=7623
 methylethyl ketone, oxidation reactions 8=7623
 methylfluorosilanes, F n.m.r. 8=7608
 methyl formate, config. in soln. 8=12276
 methylgermane and deuterioisotopes, vibration spectra calc. 8=21148
 methyl-1-indanones, n.m.r., ring geometry 8=12329
 methyl iodide, anisotropy of C chem. shift 8=4234
 methyl iodide, i.r. dispersion 8=8079
 methyl iodide, photolysis in organic matrices 8=23156
 methyl isobutyl ketone, drops rising in H_2O and H_2O -sugar soln., vol. of continuous phase translated in water 8=2159
 methyl isobutyl ketone-salt water emulsion, drop size distrib. rel. to mixing and coalescence 8=12956
 methylisocyanate, microwave spectrum and molec. consts. 8=12278
 methyl isopropyl ketone, vapour heat capacity and heat of vapourization 8=1471
 methylisothiocyanate, microwave spectrum and molec. consts. 8=12278
 methyl lithium monomer, i.r. spectrum 8=12282
 methyl β -maltopyranoside crystal structure 8=8584
 methyl mercaptan, far i.r. spectrum from 15 to 45cm^{-1} 8=21145
 methyl methacrylate, sigma-type complex with metal chlorides 8=2527
 methylmethoxysiloxane polymerization on Al surface, in glow discharge 8=5731
 methyl methoxysilanes, films on base, i.r. structure study 8=4738
 1-methylnaphthalene, excimer fluoresc. in rigid matrices 8=14339
 β -methyl-naphthalene i.r. spectra and conductivity in polycrystalline, dissolved and melted state 8=16866
 2-methyl-1, 4-naphthoquinone vapour, near u. v. spectrum 8=7585
 methyl nitrite, gas, soln. and solid, i.r. spectra and rot. isomerism 8=16329
 methyl oxocarbonium ion, Friedel-Crafts acylation intermediate, crystal structure 8=22064

Organic compounds—contd

- C-methyl-B-pentaethyl-2-carbahexaborane (9)
mol. struct. 8=21119
- 3-methylpentanal, direct and sensitized photolysis 8=9725
- methyl phenyl ether, vapour heat capacity and heat of vapourization 8=1471
- methylphosphine, vibr. spectra and force consts. 8=1289
- N-methyl-piperidine-3, 4-semidione, struct. and conformation, e. s. r. obs. 8=22898
- 4-methyl pyridine, microwave spectrum 8 to 37 GHz 8=12295
- methylsilane derivatives, p. m. r. 8=16360
- methylsilane and deuterioisotopes, vibration spectra calc. 8=21148
- methylsilylacetylene mols. normal modes, Coriolis coupling and centrifugal distortion 8=16330
- methylsilyl dialkylamines, vibr. spectra 8=1300
- methylstannate and deuterioisotopes, vibration spectra calc. 8=21148
- methylthiocyanate, microwave spectrum and molec. consts. 8=12278
- methyltrichlorosilane, H reduction on C substrates, SiC growth 8=21963
- methyltrichlorosilane, thermal-decomp. and texture of SiC formed 8=21994
- 4-methyl umbelliferone, aq. soln., stimulated emission at 454 m μ 8=6478
- methyl vinyl sulphide, microwave spectrum 8=12283
- methyl viologen cation, aq. and alcoholic solns., e. s. r. spectra, rel. to water induced dimerization 8=8123
- methylene blue, absorpt. spectrum, depend. on solvent, dye conc. and solutes conc., rel. to water induced dimerization 8=8123
- methylene bromide, solid, i. r. spectra 8=14284
- methylene chloride, solid, i. r. spectra 8=14284
- methylene chloride, sorption into drawn and undrawn polyethylene 8=8349
- methylene iodide, solid, i. r. spectra 8=14284
- methylene radicals in photochem. of ketene 8=5748
- methylene triplet, from photodecomp. of ketene 8=23157
- molecular complexes exhibiting polarization bonding 8=8585
- molecular-crystals, structural class and subclass determ. 8=21917
- molecular dimens., determ. by effect of vapour mols. on viscosity of H and He 8=1485
- molecular interaction with superconductors 8=9668
- molecules spectra in solid solns. and vibr. analysis 8=13032
- monobromoacetonitrile, i. r. vib. spectra, and Raman spectra 8=12281
- monochlorobenzene, u. v. absorpt. 8=7567
- monodeuteromethane, 2 ν_4 band resonance 8=7583
- monoglycine nitrate, i. r. absorption spectrum 8=5646
- monohalogen diacetylenes, i. r. spectra 8=1270
- multi-configuration self-consistent field theory 8=16261
- myoglobin in soln., effects of solvent on X-ray scatt. 8=21206
- naphthacene in aggregates of anthracene in n-heptane fluorescence 8=23067
- naphthalene at liquid He temp., i. r. spectrum, interpretation of fundamental vibrations 8=18577
- naphthalene, crystal attenuated total refl. spectrum 8=9569
- naphthalene, cryst., impurity mols effect on phosphoresc. 8=23069
- naphthalene derivatives as donors in reson. energy transfer 8=18639
- naphthalene-d₈ in ethanol and methylpentane glasses, biphotonic T \rightarrow T transitions, obs. 8=23161
- naphthalene-d₈-naphthalene-h₈ mixed crystals, in triplet state, e. s. r. 8=18433
- naphthalene-d₈, triplet state, e. s. r. and phosphoresc. 8=9655
- naphthalene-1, 4-diol, crystal and mol. structure 8=8586
- naphthalene, effect of ultrasound on zone melting 8=13139
- naphthalene ENDOR study of metastable triplet state 8=21169
- naphthalene, expansion tensor meas., 78-323°K 8=17533
- naphthalene, far i. r. absorption 8=23028
- naphthalene, four-photon absorpt. from laser beam 8=18517
- naphthalene, i. r. spectra and conductivity in polycrystalline, dissolved and melted state 8=16866
- naphthalene-h₈ mol. pairs e. s. r. in naphthalene-d₈, exchange energy and optical spin polarisation, obs. 8=22911
- naphthalene-oxygen complex stabilization constants from solubility in compressed O₂ 8=2499
- naphthalene in PMMA, triplet-triplet annihilation 8=2114
- naphthalene, polarization of triplet factor group states 8=2494
- naphthalene, polycrystalline, self-diffusion 8=4960
- naphthalene, Raman spectrum 8=14174
- naphthalene, sublimation in air flow, calc. 8=21784
- naphthalenes, substituted, zero-field splitting meas. 8=9435
- naphthodioxane, low-temp. n. m. r. spectrum meas. 8=12939
- naphthols, dichroic spectra in PVA sheets, rel. to vibronic transitions 8=14285
- naphthols, solid, intra-molecular motion of OH, n. m. r. study 8=16989
- naphthols, triplet state, optical and mag. props. rel. to electronic structure 8=21152

Organic compounds—contd

- 1, 4-naphthoquinone, visible emission spectrum in vapour phase 8=7589
- α - β -naphthylaldehyde in alcohol and hexane solutions, singlet-triplet conversion 8=21693
- 2-(1-naphthyl)-5-phenyloxazol in polymethyl methacrylate, solid soln., fluoresc. 8=9654
- neopentane-D exchange, effects of desorption, diffusion and surface exchange 8=23083
- nickelocene, MO calcs., and excitation energies 8=4197
- nitriles interaction with SO₂ 8=18688
- nitrilotriacetic acid, crystal structure 8=1815
- nitroanilines, singlet-singlet transition energy calc. 8=7557
- nitrobenzene alkali-metal salts, e. s. r. 8=8120
- nitrobenzene-CCl₄ mixts. stimulated Rayleigh scatt., obs. 8=16843
- nitrobenzene, decay of free radical in alkali 8=21187
- nitrobenzene, dielec. permittivity, laser prod. vars. obs. 8=21712
- nitrobenzene, 1345 cm⁻¹ spectral line, Raman scatt., rel. to solvent and conc. 8=21672
- nitrobenzene, Rayleigh line wing, four photon interaction obs. 8=21667
- nitrobenzene, stimulated Raman and Brillouin scattering 8=4580
- nitro-cpds. adsorbed on MgO surface, rel. to electron donor props. 8=8343
- p-nitro-p'-dimethylaminoazobenzene, cryst., in KBr, Raman spectra 8=9570
- nitroglycerine, low velocity detonation, mechanism 8=21582
- nitroglycerine, shock initiation of detonation 8=6148
- nitrosobenzene, electrochem. oxidation in organic media, e. s. r. 8=14426
- non-alternant hydrocarbons, spin densities, UHF/AA calc. 8=12348
- n-nonane + p-xylene + CCl₄, luminesc. quenching and decay 8=8097
- norbornene derivs, endo- and exo-, coupling consts. in n. m. r. spectra 8=1306
- norbornene-2, 3-dicarboxylic acid mono-potassium salt dihydrate, structure 8=22052
- nucleic acid components, delayed luminesc. 8=9650
- nucleotides, excited states, energy transfer 8=16334
- octahydroanthracene crystals, impurities rel. to polymorphic transitions 8=17109
- octamethylcyclotetrasiloxane polymerization, MWD change of polydimethyldisiloxane elastomers 8=14409
- octyl stearate, crystal structure 8=22057
- oil, mean adsorpt. time obs. 8=17156
- oil, mineral, prebreakdown luminosity waves 8=4598
- oil molecules, mean adsorpt. time obs. 8=17156
- oils, diffusion pump, secondary electron emission 8=13942
- 1, 2-rearrangements, MO description of non-classical ion 8=21057
- organotin cpds., fluorinated, n. m. r. spectra 8=12318
- organotin-Sn cpds., Sn bonds with Co, Mn, Mo and Re, Mössbauer obs. 8=4668
- L-ornithine hydrochloride, crystal structure 8=8591
- oxyacetylene flame, in air or N₂, temp. determ. from rot.-vib. spectrum of OH 8=18692
- 1, 2, 4-oxadiazole, microwave spectra and struct. 8=21162
- 1, 2, 4, oxadiazole and methyl derivatives, i. r. spectra obs. 8=4204
- 1, 3, 4-oxadiazole, i. r. spectrum 8=12285
- 1, 2, 5-oxadiazole, vapour and liq. spectra rel. to vib. assignments 8=16335
- oxalate, NH₄(C₂O₄)₂·H₂O, crystal structure 8=8590
- oxalate ion, i. r. and Raman spectra and symmetry 8=21154
- oxalic anhydrides, reactions with H₂O₂ and fluorescent compounds, chemiluminescence 8=18685
- oxalyl chloride, triplet-singlet transition 8=2468
- d-oxamide, vibr. spectrum 4000-400 cm⁻¹ obs. 8=23032
- oxamide, vibr. spectrum 4000-400 cm⁻¹ obs. 8=23032
- 1, 3 oxathiodanes, 2-substituted, n. m. r. rel. to ring system and free energies 8=1595
- oxaziridin rings, methylene-group n. m. r. spectroscopy 8=12940
- paraffin with NaI(Tl) detector for KeV n 8=11624
- n-paraffins, crystallization kinetics of binary mixtures 8=1733
- paraffins, gaseous, reaction with Hg(P₁) atoms 8=9688
- paraffins, long-chain, intermolec. vibrations 8=13341
- paraffins mols., e. irr. rad., energy transfer to vibr. degrees of freedom 8=4206
- n-paraffins, sound vel. and adiabatic compressibility 8=21517
- paraoxyanisole, heat of transformation 8=16917
- paraoxyanisole, liquid crystals, heat of formation and critical size of centres 8=16918
- PBD, fluoresc., concentration effects 8=4594
- pentachlorotoluene i. r. spectrum and vibr. assignments, obs. 8=9575
- pentadeuteropyridine, i. r. spectra, structure of vibration bands 8=7597
- pentaerythrite, mono, di and trihalogen derivatives, vibr. spectra 8=7576
- pentamethylenetetrazole-1Cl complex, cryst. and molec. struct. 8=17453

Organic compounds—contd

- pentane-air mixtures, effect of vessel size and turbulence on explosion press. 8=6147
- pentane, enthalpy calc. from Redlich-Kwong eqn. 8=16689
- n-pentane, solidification at high press. 8=21747
- n-pentane, sorption into drawn and undrawn polyethylene 8=8349
- pentanol, slow neutrons, quasi elastic scattering 8=8000
- perethers, carbonyl acid determ. 8=2549
- perfluoro-aza-propene, $\text{CF}_3\text{N}=\text{CH}_2$, u.v. absorpt. band of NCF_2 radical 8=7626
- n-perfluorobutane, conformational energies 8=1324
- perfluorodimethyl peroxide, reaction with NO 8=14371
- perfluoropropene, reaction with O atoms 8=14377
- perfluoro-o-xylene, F-F spin-spin coupling 8=16357
- perylene, excimer fluoresc. in rigid matrices 8=14339
- perylene, π transitions, free-electron and MOLCAO calcs. 8=4139
- phenanthroline, π electron density and proton signals in n.m.r. spectra 8=4236
- phenanthrene, cryst. spectrum 8=5648
- phenanthrene- d_{10} in solidified solvents, thermoluminesc. and delayed fluoresc., mech. 8=23070
- phenanthrene- d_{10} , triplet state, e.s.r. and phosphoresc. 8=9655
- phenanthrene, far i.r. absorption 8=23028
- phenanthrene, fluoresc. in viscous soln. 8=12894
- phenanthrene heat capacity anomaly obs. 8=13378
- phenanthrene i.r. spectra and conductivity in polycrystalline, dissolved and melted state 8=16866
- phenanthrene, n.m.r. spectra 8=9460
- phenanthroline, electron excitation spectra 8=4208
- 1,10-phenanthroline-mercury (I) nitrate, cryst. struct. 8=17454
- phenazine, polarization of triplet factor group states 8=2494
- p-phenetidine vapour, near u.v. abs. spectrum 8=21157
- phenol-aqueous sodium salicylate- α -methyl naphthalene, solubility and equilib. data 8=4641
- phenol, 2750 Å band system, extended vib. assignments, and band contour anal. 8=16337
- phenol- d_6 , vibrational spectrum and torsion 8=16336
- phenol H complexes with benzene and ethers, spectra 8=4213
- phenol, H-bonding with N,N-dimethylacetamide 8=1571
- phenol, OH stretching band struct. 8=4211
- phenol, polymeric forms, H-bond stretching freq. 8=21141
- phenols, association constns. from dielec. constns. 8=12908
- phenols, substituted, in benzene soln., e.s.r. study of oxidation 8=14378
- phenolphthalein and congeneric mol. crystals, plastic deformation effects at high pressure 8=23033
- phenanthroline, crystal structure refinement 8=22070
- phenoxide ion, phosphoresc. and symmetry of lowest triplet state 8=14340
- phenylacetylene, singlet and triplet electronic states 8=4210
- phenylalanine rotamers, n.m.r. study 8=12289
- phenylboron dihalides, thermodynamic properties 8=1863
- phenylhydrazine, crystal and mol. structure 8=22069
- phenylindole derivatives, scintillation of supercooled melts 8=8089
- phenyl phosphine, migration polymerization with di-isocyanates 8=14411
- o-phenylenediamine, intramolec. H-bonds 8=1295
- phosphine oxides, $\text{R}_1\text{R}_2\text{R}_3\text{PO}$ (R_{1-3} are different hydrocarbon radicals), prep. and config. 8=16345
- phosphoramidates and phosphoramidothioates, i.r. spectra and structure 8=7591
- photoconductivity and photopot. rel. to solar cell use 8=9260
- phthalimiden compounds, fluorescence, quantum yield in anti-Stokes region 8=18640
- phthalocyanine blue adsorption of poly(dimethyl siloxane) from CCl_4 and xylene solns. 8=8336
- phthalocyanine lanthanides, acid adducts, absorption spectra 8=4589
- phthalocyanine, π MO calc. 8=4214
- γ -picoline-halogen complexes, i.r. spectra 8=7592
- picolinium tetrabromobismuthate, cryst. struct. 8=8574
- picolinium, tetraiodobismuthate, cryst. struct. 8=8574
- pinacanol due in alcohol, absorption and luminescence bands 8=8091
- α -pinene and oxide, mol. structure from gas-e-diff. meas. 8=21161
- piperazine, u.v. irradi., rel. to thermostability increase of polyamides 8=17182
- piperidinium picrates in chlorobenzene containing ligands tetrahydrofuran and triphenylphosphine, elec. cond. rel. to cation-oxide ligand complexes stability 8=16338
- piperine, supercooled, dipole polarization relax. time obs. 8=21710
- polar cpds., adsorpt. on Cr 8=13107
- polycyclic monoazines, vibronic spin-orbit interactions 8=8095
- polycyclic, monolayer, isotherms rel. to mol. struct., obs. 8=17178

Organic compounds—contd

- polynuclear hydrocarbons, heating for e.s.r. spectra 8=1230
- porphyrin vanadyl complexes, luminesc. 8=5685
- porphyrins, π -electron conjugation 8=4215
- PPO + o-xilen, and butyl-borate, radioluminescent properties 8=1578
- proaporphine-type alkaloids, mass spectra 8=12032
- procaine in scala tympani cochlear pot. changes 8=19617
- promazine, crystal structure 8=8592
- propane gas, sorption and diffusion in synthetic Na mordenite 8=13109
- propane ion reactions with mols. 8=14381
- propane, i.r. spectrum, high resolution 8=490
- propane- O_2 - N_2 mixtures, detonation velocity 8=172
- propane, oxidative adsorpt. on Pt 8=2534
- propane, photoionization 8=4319
- propane, pyrolysis in shock tube for temp. range 830 to 1180°C 8=14380
- propane, solid films, far u.v. spectra 8=14283
- propane, transpiration through membrane 8=12662
- propanol- H_2O mixtures, cond. with HCl in soln. 8=4607
- propanol- H_2O mixtures, cond. with NaCl in soln. 8=4606
- n-propanol, n scatt. rel. to molecular diffusion 8=21609
- 1 propanol, shear rigidity and free volume 8=1537
- n-propanol soln. of bromoform, thermal diffusion coeff. by heterodyning light 8=4553
- propionate groups, retarded motion and phase transitions 8=8229
- propionic acid, u.s. absorpt. 8=12860
- propyl alcohol, subcooled boiling in tube, heat-transfer rate 8=21657
- propylene, hydrogenolysis 8=14379
- propylene imine, microwave spectrum 8=12291
- trans-propyleneimine, microwave spectra and molec. constns. 8=12290
- propylene polymerization, catalysis with α - TiCl_3 - $\text{Al}(\text{C}_2\text{H}_5)_3$ - H_2O 8=5730
- protopine, $\text{C}_{20}\text{H}_{19}\text{O}_2\text{N}_3$, crystal structure 8=22072
- pseudocyanine dye in alcohol, absorption and luminescence bands 8=8091
- pterines, mass spectrum obs. 8=20912
- pure liquids, new correlation for surface tension 8=12824
- purine, electronic spectra 8=7594
- purines, mass spectrum obs. 8=20912
- pyrazine, phosphoresc. 8=14342
- pyrazine, Zeeman splitting of phosphoresc. at 4.2°K 8=14341
- 2-pyrazolines, trisubstituted, spectra and structural analogues 8=12293
- pyrene, excimer fluoresc. in rigid matrices 8=14339
- pyrene, π transitions, free-electron and MOLCAO calcs. 8=4139
- pyrene-tetracyanoethylene complex, crystal structure refinement 8=22073
- pyrene, vibr. effects in radiationless transitions 8=21114
- pyridazine, singlet-triplet transitions 8=9573
- pyridazine, 3700 Å transition and geometric parameters 8=12297
- pyridine-2-aldehyde-2-quinolyldiazine complexing reagent spray for Ni, Co, Cu analysis 8=23176
- pyridine complexes, far i.r. spectra 8=1296
- pyridine, in dilute solns. of CS_2 and CCl_4 , dependence of nuclear relaxation times on viscosity 8=8126
- pyridine, hydrogenated, e.s.r. 8=12310
- pyridine, i.r. spectra, structure of vibration bands 8=7597
- pyridine positive ion, all-electron SCF wavefunctions 8=12294
- pyridine, pulse radiolysis 8=18746
- pyridine, Raman scatt. cross-sections 8=12130
- pyridine and related N-heterocyclics, e.s.r. of radical anions 8=21171
- pyridine, substituted, charge transfer complexes with iodine, rel. to structure and stability 8=4216
- 3-pyridinesulphonic acid and salts, i.r. spectra 8=16339
- pyridines, electrophilic substitutions 8=18687
- pyridines, solvent effects in p.m.r. 8=1600
- pyridines, substituent effects on ring proton coupling 8=12332
- pyridine, u.s. velocity, absorption and relaxation obs. 8=12687
- pyridocyanines, electron spectra and modelling 8=7596
- pyrimidine, i.r. spectra, liq. N temp. meas. 8=9572
- pyrimidines, mass spectrum obs. 8=20912
- pyrones, mass spectra, metastable ions 8=12239
- γ -pyrones, monocyclic, mass spectral fragmentation 8=21023
- pyronine B, luminesc. 8=5686
- pyrrole, cryst., i.r. absorpt. spectra at liq. N_2 temp. 8=14280
- pyrrole, SCF-CI calc. 8=16306
- pyrrole, spin-spin coupling and spin-lattice relax. 8=21180
- 2-pyrrolidone, vibration spectra, 3500-250 cm^{-1} 8=7595
- p-quaterphenyl derivatives scintillation of supercooled melts 8=8089
- p-quaterphenyl, photoelec. props. of polycryst. layers, obs. 8=22703
- p-quaterphenyl polycrystals, thermally stimulated currents 8=13906

Organic compounds—contd

- quinaldic acid, crystal structure, dimer formation and H-bonding at low temps. 8=1825
- quinaldic acid, decarboxylation, isotope effects 8=9697
- quinaldic acid, Remlinger effect 8=17457
- quinhydrone, monoclinic, crystal structure refinement 8=22070
- quinine sulphate, fluoresc. quantum yield 8=4595
- quinoline-ethyl alcohol mixts. stimulated Rayleigh scatt., obs. 8=16843
- quinols, solid, intra-molecular motion of OH, n. m. r. study 8=16989
- quinoxaline, optical detect. of e. s. r. transitions 8=14343
- radicals, hyperconjugation and spin delocalization 8=4172
- radicals spectra in solid solns. and vibr. analysis 8=13032
- rare-earth chelates, exchange-reson. energy transfer overlap integrals calc. 8=1656
- refamycins B and Y, crystal structure by X-ray analysis 8=22074
- reserpine, crystal structure and mol. configuration 8=13310
- resin, mica-resin superimposed layers subject to alternating field, elec. stress distrib. 8=9235
- retusamine, α' -bromo-D-camphor-trans- π -sulphonate monohydrate crystal structure 8=1816
- rhodamine B dye lasers, emission 8=21694
- rhodamine B, luminesc. 8=5686
- rhodamine B, use in obs. sea upper boundary layer flow 8=14570
- rhodamine 6G and B, and mixtures, laser, mode locking 8=20009
- ribonucleic acid derivatives, Raman spectra and molec. structure 8=7598
- ring cpds., non-aromatic, conformation 8=8597
- rubrene, chemiluminescent reaction with H_2O_2 and bis(2,4-dinitrophenyl) oxalate 8=18672
- salicylaldehyde soln., H bonding, n. m. r. obs. 8=16883
- salicylate mixed complexes with La aminoacetate, aqueous, fluorescence 8=21703
- salicylic acid adsorpt. on portland cement component hydration products 8=21902
- salicylic acids, mass spectrum obs. 8=20912
- salol, viscous liq., wing of Rayleigh line obs. 8=21671
- scattering, stimulated, in Rayleigh line wing in liquids, obs. 8=16842
- 1,2,5-selenadiazole and its methyl derivative, p. m. r. 8=12333
- 1,2,5-selenadiazole, i. r. and Raman spectra 8=16342
- 1,2,5-selenadiazole, microwave spectrum 8=12298
- selenobenzanide, N^4 chemical shifts 8=7614
- selenocyclopentane dibromide, crystal and mol. structure 8=22068
- selenocystine-selenocysteine, polarography 8=18760
- semiconductors, r. f. spectroscopy, review 8=14088
- semiquinones in alcoholic soln., hyperfine interactions 8=7627
- semiquinones, e. s. r. in solid state 8=5521
- silazanes, mass spectra 8=1275
- α -silyl ketones, electronic spectra 8=21159
- solutions, two-photon fluoresc. excitation 8=4592
- spiropentane, vibration spectra calc. and interpretation 8=7588
- stearic acid aerosol, particle conc., by turbidity meas. 8=8153
- stilbene crystals with anthracene impurities, luminescence 8=5687
- stilbene, scintillation counter for n-detection 8=6965
- stilbene scintillator, light output under influence of α -particles 8=2495
- stilbene, triplet-triplet energy transfer and "phantom triplet" 8=21160
- trans-stilbenes, 4-monosubstituted, absorpt. spectra rel. to ionization pot. and conjugated π -bonds, obs. 8=4212
- styrene grafting to polypropylene films and copolymers tensile strength, obs. 8=23139
- styrene, n. scatt. before and after reactor irradi., showing prod. of cross-bindings 8=16969
- styrene scintillators radioluminesc. yield rel. to polymerization, obs. 8=14346
- succinimide-dimethyl sulphoxide, n. m. r. and H-bond 8=12334
- sucrose crystal, dislocations 8=4983
- sucrose soln., aq., supercooled, ice growth velocities 8=17236
- sulphanilamide monohydrate, three dimensional structure refinement 8=17458
- sulphanilamide polymorphs and hydrate, crystal structure 8=22075
- surface tension, binary liq. mixtures, theory 8=12826
- sydnones, molec. geometry of bonding 8=12299
- taurine, e. p. r., paramagnetic susceptibility 8=5540
- TCNQ derivatives of cyanine dyes, supercond. 8=17977
- tedrodotoxin in scala tympani, cochlear pot. changes 8=19617
- Teflon 6, immersion heats in hydrocarbons 8=13361
- terpenes, bicyclic, and oxide derivs., mol. structure from gas-e-diff. meas. 8=21161
- p-terphenyl, plastic scintillators 8=9656
- terphenyls, 4-monosubstituted, absorpt. spectra rel. to ionization pot. and conjugated π -bonds, obs. 8=4212

Organic compounds—contd

- 1,1,2,2-tetrabromofluoroethane, medium effects on n. m. r. and thermodynamic props. 8=21181
- tetrabutylammonium perchlorate soln., elec. cond. meas. 8=8105
- tetracene dimer, association const, absorpt. and emission spectra 8=1301
- 1,2,4,5-tetrachlorobenzene, in nonpolar solvent, intensity meas. of i. r. band 8=21680
- tetrachloroethylene Raman spectra and electrooptical parameters compared with trichloroethylene 8=21138
- tetrachloroethylene, sorption into drawn and undrawn polyethylene 8=8349
- tetrachlorophthalic anhydride complex, polarization of charge-transfer fluoresc. 8=1576
- 2,3,5,6-tetrachlorotoluene i. r. spectrum and vibr. assignments, obs. 8=9575
- tetrachloro-p-xylene i. r. spectrum and vibr. assignments, obs. 8=9575
- tetracyanoethylene complexes, polarization of charge-transfer fluoresc. 8=1576
- tetracyanoethylene, kinetics of free-radical formation 8=9686
- tetracyanoethylene-naphthalene complex, structure 8=8585
- tetracyanoquinodimethane anion, aq. and alcoholic solns., e. s. r. spectra, rel. to water induced dimerization 8=8123
- 7,7,8,8-tetracyanoquinodimethane-anthracene complex, crystal and mol. structure 8=17460
- tetradecanol, persistent electric dipole moment obs. at $-78^\circ C$ 8=13890
- tetraethylammonium perchlorate soln., elec. cond. meas. 8=8105
- tetraethylammonium triiodide, two modifications crystal structure 8=1818
- tetraethyl compounds, group IV elements, mass spectra 8=18766
- tetrafluoro-borate laser, narrow-band continuously tunable, longit. pumped 8=20006
- tetrafluoroethylene-hexafluoropropylene copolymers, γ -irrad. effects on permittivity and loss 8=9202
- tetrafluoromethane, solution H in, spectral simultaneous transitions 8=21675
- tetrahydrofuran, i. r. dispersion 8=8074
- tetrakis-[dimethylamides] of group IV, vibr. spectra 8=1290
- tetramethyl lead, C^{13} spin-spin coupling 8=12317
- tetramethylammonium fluoride tetrahydrate, crystal structure 8=1821
- tetramethyl compounds of gp. IV, indirect nuclear spin coupling 8=4233
- tetramethyl compounds, group IV elements, mass spectra 8=18766
- 2,2,6,6-tetramethylpiperidin-4-ol-1-oxide, radical structure 8=16370
- tetramethylpyrazine e. p. r. and luminesc. 77 and $4.2^\circ K$ 8=22907
- 1,3,7,9-tetramethyluric acid: 3,4-benzpyrene, 2:1 mol. complex, crystal structure 8=1823
- 1,1,4,4-tetraphenylbutadiene in polymethyl methacrylate, solid soln., fluoresc. 8=9654
- tetraphenylhydrazine, photodissoc., diphenyl-amino radical dimer prod. 8=7625
- tetraphenylporphin and Ag tetraphenylporphin, solid solution 8=1658
- tetraphenylporphyrin, cryst. and molec. struct. 8=4896
- s-tetrazine, anal. of i. r. type A bands rel. to asymmetry 8=1277
- tebromine salts, i. r. spectra 8=12300
- thiazoles, monosubstituted, i. r. and Raman spectra, vibr. and coupling 8=4217
- thienylphenyl-ketones and -thioketones, n. m. r. and electronic spectra, steric effects obs. 8=4218
- thioamides, N^4 chemical shifts 8=7614
- thiobutylolactam, dimerization, values of ΔH° , ΔG° and ΔS° 8=4241
- thiocaprolactam, dimerization, values of ΔH° , ΔG° and ΔS° 8=4241
- thiophene, cryst., i. r. absorpt. spectra at liq. H_2 temp. 8=14280
- thiophenes, reactivity theory 8=5720
- thiourea, ferroelec., i. f. modes from neutron scatt. 8=13340
- thiourea inhibition of Fe corrosion in H_2SO_4 ; $K_2Cr_2O_7$, NH_4CNS and KI effects 8=2518
- thiourea, lattice vibr. freq. and intensities calc. 8=13339
- thiovalerolactam, dimerization, values of ΔH° , ΔG° and ΔS° 8=4241
- thioxanthone anion radicals, e. p. r. and coupling consts. 8=4613
- thioxanthone sulfone anion radicals, e. p. r. and coupling consts. 8=4613
- TMPD-chloranil crystals, X-ray, e. s. r., elec. cond., u. v. and visible meas. 8=8595
- tobacco mosaic virus, polydisperse sample, distrib. of lengths 8=8073
- tolane-dimethyl Si addition cpd, crystal and mol. structure 8=22046
- toluene, Brillouin shifts, temp. dependence, hypersonic velocity and compressibility deduction 8=1502

Organic compounds—contd

- toluene- CCl_4 mixtures, drops rising in H_2O and H_2O -sugar soln., vol. of continuous phase translated in water 8=21592
 toluene, drops rising in H_2O and H_2O -sugar soln., vol. of continuous phase translated in water 8=21592
 toluene, emission from liq. excited by electrons 8=12893
 toluene, glow discharge prod. polymer films comp., spectra and elec. props. obs. 8=21894
 toluene, hydrogenolysis 8=14379
 toluene, Raman scatt. cross-sections 8=12130
 toluene, self-induced isotopic exchange of T 8=5695
 toluene, sound absorption and velocity, improved method 8=12858
 p-toluidine, crystal and mol. structure by X-ray and n-diffr. 8=22077
 p-toluidine, Raman bands, broadening and freq. variation as function of temp. 8=5649
 p-tolunitrile, emission bands 8=21163
 transition metal complexes, undergoing ligand exchange, e.s.r. linewidth 8=4616
 triacetate films, proportioning electron beam 8=10890
 triacetin, liq., e distrib. from X-ray scatt. obs. 8=16794
 triacetin, viscous liq., wing of Rayleigh line obs. 8=21671
 2H-1,4-triazines, spin-spin coupling obs. 8=21166
 2,4,6-tribromoaniline, crystal structure 8=8569
 tri-tertiary butyl phenoxyl radical, proton-electron double reson. 8=12312
 2,4,6-trichloroaniline, crystal structure 8=8569
 trichloroborazole, Cl^{35} n.q.r. spectra 8=6409
 trichloroethylene, Raman spectra, absolute intensities and depolarizations 8=21138
 3,4,5-trichlorotetracyclod 4.4.0.0³-90⁴-8] decan-Z-one, crystal structure 8=17446
 α, α, α -trichlorotoluene, vac. u. v. absorpt. spectrum 8=4219
 tricyclohexylboron, thermodynamic properties 8=1863
 1,3,5-trideutero benzene, molec. motion in liq. by n.m.r. 8=8132
 triethylamine-water syst., diffusion in crit. separation region 8=21644
 triethylborane, in upper atm., BO_2 emission spectrum 8=23330
 triethylphosphine, vibr. spectra 8=21137
 trifluoroacetone, n. m. r. and i. r. spectra in proton donor solvents 8=16887
 trifluorocyclopropanes, F^{19} coupling consts. and chem. shifts 8=12321
 2,2,2-trifluoroethanol, H bonding acid, i. r. and n. m. r. spectra rel. to bonds 8=16863
 4,4,4-trifluoro-3-hydroxy-3-trifluoromethylbutyrophenone, phosphoresc. 8=18638
 trifluoromethyl nitrobenzene radical anions in acetonitrile e.s.r. 8=4615
 2,4,6-trifluoropyrimidine, i. r. and Raman spectra 8=16340
 triglycerides, long-chain, cryst. growth rates and kinetics 8=8412
 triglycine fluoroberyllate, dielectric props. under hydrostatic press. 8=9221
 triglycine fluoroberyllate, ferroelec., e.p.r. study of Cu^{2+} ion 8=14105
 triglycine selenate, crystalline, transition from ferroelectric to paraelectric at high press. 8=8288
 triglycine sulphate crystals, pyroelectric effect, by dynamic method 8=18198
 triglycine sulphate, deuterated, electro-optical effects 8=5647
 triglycine sulphate, elec. resistance meas. 8=19707
 triglycine sulphate, kinetics of γ -radiolysis 8=5757
 triglycine sulphate, temp. coeff. of piezoelec. resonance freq. 8=9224
 triglycine sulphate, u.s. relaxation near ferroelec. transition 8=1858
 3,4,5-trimethoxyphenylglyoxal semidiones, e.s.r. spectra 8=12305
 trimethylaluminum, cryst. struct. 8=4895
 trimethylaluminum, vibrations 8=16327
 trimethylplatinum (IV) iodide and its misrepresentation as hexamethyldiplatinum 8=13308
 trimethylplatinum (IV) iodide and methylsodium reaction product identification 8=14382
 trimethylsulphonium cnds., i. r. vib. spectra 8=16864
 trimethylsulphoxonium cnds., i. r. vib. spectra 8=16864
 trimethylene oxide, i. r. spectra and ring puckering 8=16304
 s-trinitrobenzene complex with anthracene, polarization of charge-transfer fluoresc. 8=1576
 2,4,6-trinitrophenetole, crystal structure 8=13309
 tri-n-octylamine, temp. effect on extraction of NO_3 , U and fission products 8=5708
 trioxane, crystal structure determ. at -170°C 8=22066
 trioxane in benzene soln, cationic polymerization in presence of SnCl_4 , effect of temp. regime 8=23134
 trioxane in soln, molec. weight as function of conversion to polymer, temp. depend. 8=18708
 s-trioxane in nematic solvent, n. m. r. 8=4618
 trioxan, n.m.r. line shape 8=14132
 trioxane polymerization in soln., reaction order and kinetics 8=14407
 trioxane, pre-irrad., polymerization kinetics, 30-64°C 8=23133

Organic compounds—contd

- trioxane, solid, SnCl_4 initiated cationic polymerization, kinetics, obs. 8=23132
 triphenylaluminum, i. r. spectrum between 4000 and 300 cm^{-1} 8=12287
 triphenylboron, thermodynamic properties 8=1863
 triphenylphosphate aerosol, particle conc., by turbidity meas. 8=8153
 triphenyl phosphine complexes, far i. r. spectra 8=1296
 triphenylphosphine, modified Mataga SCF calc. 8=4209
 triphenyltin pentacarbonyl manganese, structure 8=8594
 triphenylene in CCl_4 , phosphoresc. rel. to mol. deform. by lattice interactions, 77°K 8=1577
 triphenylene- d_{12} , energy transfer with rhodamine B in rigid soln. 8=9584
 triphenylene, e. s. r. of negative ions in soln. 8=21170
 triphenylene, mag. circular dichroism 8=21123
 triphenylene, triplet state, e. s. r. and phosphoresc. 8=9655
 triphenylenethyllanionium-tetracyanoquinodimethan single crystals, optical absorption 8=14287
 triptycene, p. m. r., effect of mag. anisotropy 8=1305
 triscyclooctatetraen-ditanium crystal structure 8=13304
 tris(hydroxymethyl)aminomethane and HCl , heat of reaction 8=9677
 trispyridinecupriacetate, crystal structure 8=17456
 trithiane, polymerization to polythiomethylene due to radiation 8=17184
 tryptaflavin in lucite, α -phosphoresc. and fluoresc. spectra 8=2496
 tryptophan, excited state dipole moment, calc. 8=21143
 unsaturated, triplet-state energies and spin densities, VB calc. 8=12240
 uracil, crystal structure 8=8596
 uranyl cpds., luminescence spectra, intramolec. vibrations manifestation 8=12235
 urea aq. soln., dielec. dispersion 350-3600 MHz 8=8103
 urea, i. f. modes from neutron scatt 8=13340
 urea, mixed aqueous solns., v. p. meas. 8=12996
 d,l-valine radical, hindered rotations, e. s. r. study 8=4248
 vanadium (III) tris(salicylaldehydes) and tris(salicylaldehydes) complexes, n. m. r. obs., synthesis and stereochemistry 8=16343
 vinylchloride copolymerization with acrylic and methacrylic acids, relative reactivities obs. 8=23136
 vinyl cpds., pulse radiolysis and free radicals 8=18745
 vinyl monomers, liquid, polymerization by a. f. elec. field, obs. 8=9709
 vinylacetate, polymerization initiation efficiency and temp. depend. 8=14413
 4-vinylcyclohexene, mass spectra, preferential ass. of pos. charge with butadiene fragment 8=4320
 4-vinylpyridine, kinetics of polymerization 8=5728
 vinylene carbonate in aqueous soln., initiation of polymerization 8=5729
 vitamin K and antivitamin K, rel. to antagonism studies in pharmacetics 8=23765
 Wurster's blue perchlorate, cryst. reflect. spectra 8=14288
 Wurster's blue perchlorate, susceptibility rel. to triplet excitons 8=22763
 xanthane mols. $\pi\pi^*$ and $n\pi^*$ levels location, absorpt. and luminesc. obs. 8=1302
 xanthilium salt reagents, dissoc. consts. 8=18713
 xanthine oxidase, mech. of action, e. s. r. study 8=14406
 xylene, hydrogenolysis 8=14379
 p-xylene + CCl_4 + n-nonane, luminesc. quenching and decay 8=8097
 xylenes, Raman scatt. cross-sections 8=12130
 O-xylol, Rayleigh line wing, four photon interaction obs. 8=21667
 xylyl radicals fluoresc. spectra in cryst. xylenes, vibr. analysis obs. 8=12356
 Al acetylacetonate in benzene solution, electrical polarization and microwave absorption 8=12905
 Al acetylacetonate, polarity and atomic polarization 8=16872
 Al phthalocyanines, absorpt. spectra in soln. 8=21688
 $[\text{Al}(\text{CH}_3)_2\text{C}_6\text{H}_4\text{O}_2]$, cryst. and molec. struct. 8=8568
 $\text{Al}_2\text{Me}_2\text{Cl}_2$, force field and thermodynamics 8=4143
 Al_2Me_2 , force field and thermodynamics 8=4143
 BF_3 , dimethyl sulphide complexes, B^{10} and B^{11} , i. r. and Raman spectra 8=1569
 $\text{BrC}(\text{CH}_3)_3$ mols. dielec. relax. in solid and liquid, 9GHz, 10 and 200kHz 8=18179
 CCl_4 free radical, electronic and vib. spectra 8=1315
 CCl_3 radicals, photochemical production 8=12343
 CCl_4 adsorbed on silica gel, laser Raman spectra 8=23031
 CCl_4 , Brillouin shifts, temp. dependence, hypersonic velocity and compressibility deduction 8=1502
 CCl_4 + cyclohexane system, flow-cell meas. of Soret coeff. 8=1542
 CCl_4 , dissolved coronene and triphenylene mols. deform., phosphoresc. obs., 77°K 8=1577
 CCl_4 , liquid and crystalline state, sub-millimeter wave spectra 8=7568
 CCl_4 molec. complex with benzene, i. r. spectra 8=2464
 CCl_4 mols. vibr. transitions and gas and liquid spectra rel. to intermol. interactions 8=16274

Organic compounds—contd

- CCl₄, overtones of combination scattering 8=1559
 CCl₄, Raman spectrum at 64°K 8=18576
 CCl₄, 71°C, spectrum of scatt. microwave radiation 8=21686
 CCl₄, thermal cond. temp. depend. rel. to radiative transfer 8=12853
 CCl₄ solid, shear strength from 187° to 247°K 8=22401
 CCl₄ soln. of SO₂, absolute i. r. intensities meas. and calcs. 8=1560
 CCl₄, translational diffusion of cyclo-pentane, -hexane and -heptane, expt. and theory 8=16814
 CCl₄ + p-xylene + n-nonane, luminesc. quenching and decay 8=8097
 CCl₄-CCl₄, intermolecular potential in benzene 8=4524
 CD, C²Σ⁺ decay rates and predissociation probability 8=21185
 CD₃, mono, di- and tri-substituted compounds, far i. r. torsional vibration spectra 8=4196
 CD₃CD₂Cl, far i. r. spectrum 8=4193
 CD₄, d.m.r. studies 8=18460
 CD₄ mol., nuclear hyperfine interaction theory 8=12119
 CD₄, vibration spectra, anharmonic calc. 8=12133
 CFCl₃, microwave spectrum, h. f. s. 8=16315
 CF₂, absorpt. spectrum and rot. structure analysed 8=4188
 CF₂, triplet-to-singlet conversion 8=1293
 CF₂N₂, mol. struct. 8=12186
 CF₂(OF)₂, i. r. spectrum 8=12279
 CF₃, mono, di- and tri-substituted compounds, far i. r. torsional vibration spectra 8=4196
 CF₃, radiation grafting to polypropylene, polyethylene-terephthalate and polycapromide fibres rel. to adhesion props., obs. 8=22410
 [(CF₃)₂CF]₂CF₂, i. r. spectra 8=16273
 CF₃I, photolysis in matrices at 4.2°K, e. s. r. 8=14440
 CF₃OF, low-temp. photolysis, e. s. r. 8=9727
 CF₃OOFCF₃, low-temp. photolysis, e. s. r. 8=9727
 CF₃P(O)F₂, prep., props., n. m. r. and i. r. spectra 8=21177
 CF₃SF₃, i. r. spectra 8=16273
 CF₄, clathrate hydrate, F¹⁹ mag. reson. absorpt. 8=7607
 CF₄, liquid, sound vel. meas. 8=12868
 CF₄, radiative lifetimes of u. v. emission systems 8=7501
 CF₄, single-centre LCAO SCF calc. 8=7524
 CF₄, spin-lattice relax. gaseous 8=21176
 CF₄-He, compressed mixtures, nonresonant absorpt. and dispersion 8=1486
 CH, absorption and emission spectroscopy, in low-press. oxyacetylene flames 8=21189
 CH, electronically excited in hydrocarbon flames 8=7509
 CH(A²Δ-X²Π) line profiles in solar spectrum 8=10389
 CH, C²Σ⁺ decay rates and predissociation probability 8=21185
 CHBr₂-CFBr₂, rotational isomers, n. m. r. 8=4226
 CHClF₂, gas, F n. m. r. press. dependent chemical shifts 8=12324
 CHCl₃, microwave spectrum, h. f. s. 8=16315
 CHCl₃, Raman spectrum at 64°K and -120°C 8=18576
 CHD₃, ground state molec. consts. 8=12275
 C-H-N-O explosives, calc. of detonation props. 8=23122
 CH₂, centrifugal distortion effects in spectra 8=21089
 CH₂, in lowest bent state, effects of quasi-linearity 8=1243
 CH₂Br₂, gaseous, sound absorption by multiple relaxation 8=1475
 CH₂Cl₂, Raman spectrum at 64°K 8=18576
 CH₂Cl₂ soln. of SO₂, absolute i. r. intensities meas. and calcs. 8=1560
 CH₂Cl₂, thermodynamic props., to 750°K and 200 atm. 8=16819
 CH₃, mono, di- and tri-substituted compounds, far i. r. torsional vibration spectra 8=4196
 CH₃, one-centre expansion SCF calc. 8=4202
 CH₃Br, vibration-rotation band near 6000 cm⁻¹ 8=16859
 (CH₃)₂CCl mols. dielec. relax. in solid and liquid, 9GHz and 200kHz 8=18179
 (CH₃)₂CCl, γ irradi. at 77°K, C(CH₃)₃ radical struct., e. p. r. obs. 8=12349
 (CH₃)₂CCl₂, γ irradi. at 77°K, C(CH₃)₂CCl radical struct., e. p. r. obs. 8=12349
 CH₃CH₂CH₂OH mol. rot. consts. and Q^a, Q^b branches transitions, 10-32 GHz 8=7593
 CH₃CH₂OD mol. rot. consts. and ^aR, ^bP branches transitions, 18-33.5 GHz 8=1282
 CH₃CH₂O¹⁸H mol. rot. consts. and ^aQ branch transitions, 18-33.5 GHz 8=1282
 CH₃CN soln. of SO₂, absolute i. r. intensities meas. and calcs. 8=1560
 CH₃CO₂⁻ free radical trapped in γ-irrad. Na acetate, e. s. r. 8=4242
 CH₃. CR₂ radical in X-irradiated acetyl-(d,l)-alanine, spin-lattice relax. time 8=22906
 CH₃Cl, Fermi and Coriolis resonances in the ν₄ band 8=16319
 (CH₃)₂N. NiCl₂, crystal structure 8=22076
 (CH₃NH₂)₂CuCl₂, e. s. r. and optical spectra 8=14104
 (CH₃)₂O, n. m. r. linewidth as function of pressure 8=16354
 CH₃OH-H₂O solns., sp. ht. using calorimeter with adiabatic shell 8=21647
 (CH₃)₂POCl, i. r. and Raman spectra 8=12286

Organic compounds—contd

- (CH₃)₂PSBr, i. r. and Raman spectra 8=12286
 (CH₃)₂PSCl, i. r. and Raman spectra 8=12286
 (CH₃)₂SiCl, γ irradi. at 77°K, CH₂(CH₃)₂SiCl radical struct., e. p. r. obs. 8=12349
 CH₃SiF₃, n. m. r., sign of coupling consts. 8=4232
 CH₄, equilibrium vapour pressure data 8=21779
 CH₄, inelastic scattering of cold neutrons 8=12274
 CH₄, Jupiter, 3ν₃ band image tube obs. 8=14839
 CH₄ mol., nuclear hyperfine interaction theory 8=12119
 CH₄, Raman intensities and depolarizations 8=12131
 CH₄, spin-rotation interaction constants determ. by nuclear spin relax. meas. 8=7573
 CH₄ thermal cond., mag. field effects, 290°K 8=4469
 CH₄, vibration spectra, anharmonic calc. 8=12133
 CH₄-CF₄ dense mixtures, thermal conductivity 8=21511
 CS₂, adsorbed on silica gel, laser Raman spectra 8=23031
 CS₂, overtones of combination scattering 8=1559
 CT₄, vibration spectra, anharmonic calc. 8=12133
 C₂, absorption and emission spectroscopy, in low-press. oxyacetylene flames 8=21189
 C₂ClF₂-He mixtures, microwave absorption and dispersion 8=7936
 C₂H₂, equiv. orbitals 8=21110
 C₂H₂ reaction with H- and O-atoms, e. s. r. investigation 8=2511
 2C₂H₂+SO₂ mixture, continuous combustion in annular channel, rot. rate of luminesc. heads 8=23121
 C₂T₂, i. r. absorpt. spectrum and ν₃ fundamental 8=12244
 C₂H₄, equilibrium vapour pressure data 8=21779
 C₂H₄, equiv. orbitals 8=21110
 C₂H₆, equiv. orbitals 8=21110
 [(C₂H₅)₄N]₂Cu(C₂B₃H₁₁)₂, cryst. struct. 8=13305
 [(C₂H₅)₄NH₄]₂Pt(CN)₄(X=1 to 3) crystal structure, atomic 8=13306
 C₃H₂ radical absorpt. spectrum, diazopropyne photolysis obs. 8=16368
 (nC₄H₉)₂NBr, non centrosymmetric, morphology 8=22054
 C₃H₅N₂O₂. HCl, crystal and molecular struct. 8=17452
 (C₅NH₅)[NbCl₄O], deviation from superposition structure 8=13279
 C₆H₅CH=NC₆H₄CH₃ solns. and powder vibr. assignments, 400-3200 cm⁻¹ 8=1562
 C₆H₅CH=NC₆H₅ crystals and solns. spectra, vibr. assignments, 400-3200 cm⁻¹ 8=1562
 C₆H₅CH=NC₆H₂ crystals and solns. spectra, vibr. assignments, 400-3200 cm⁻¹ 8=1562
 C₆H₅F⁺, lowest electronic states 8=12257
 C₆H₅F⁺, position of electronic states 8=21120
 C₆H₅OD anharmonicity variation effect on frequency perturbations ν(OH) and ν(OD) 8=16316
 C₆H₅OH anharmonicity variation effect on frequency perturbations ν(OH) and ν(OD) 8=16316
 [(C₆H₅)₂PCH₃]₂(TCNQ)₂, proton n. m. r. 8=5551
 C₆H₆⁺, lowest electronic states 8=12257
 C₆H₆⁺, position of electronic states 8=21120
 C₈H₈ isomers, chem. ionization mass spectra 8=9745
 C₁₀H₁₂N₂O₈, condensation product of diaminosuccinic acid and pyruvic acid, X-ray studies 8=17437
 Ca dicarboxylates(malonate to sebacate), i. r. spectra and thermal decomp. 8=23095
 Ce ethylsulphate, spin-bath relaxation, Kapitza resistance 8=19700
 Ce ethyl sulphate, thermal cond., mag. field effect rel. to spin-phonon scatt. 8=13393
 Co complexes, inversion-vibr. levels and splitting 8=4121
 Co complex ions, specific activity values obtained by Sziland-Chalmers react., interpret. 8=18749
 Co(II) chelate complexes, in soln., isotropic nuclear res. shifts 8=1598
 Co²⁺ octahedral systems, theory of nuclear resonance shifts 8=1597
 Cr acetylacetonate, polarity and atomic polarization 8=16872
 Cr oxalate, ²E-⁴A₂ emission spectra, rel. to Cr³⁺ conc., and vibronic struct. 8=18578
 Cs ethylate-ethyl picrate complex, crystal structure 8=22058
 Cs methoxide-methanol solvates comp. and Cs ions coordination number obs. 8=2497
 Cu(II) complex ions in ethylenediamine-water solns., n. m. r. and e. p. r. 8=4621
 Cu(II) formate, normal vibrs. 8=2466
 Cu formate tetrahydrate, sp. ht. and entropy at anti-ferroelectric transition pt. 8=8638
 Cu-phthalocyanines cryst. growth from vap. phase 8=21946
 Eu chelates, mag. props. 8=9306
 Eu chelates, three-ligand β-diketones, under u. v. irradi., absence of stimulated emission 8=18571
 Fe(III) porphyrins, zero-field splitting determ. by far i. r. spectra 8=2469
 HCNO, microwave spectrum, struct. and l-type doublet 8=12270
 He-methane solid-vapour equil., 55°-91°K, to 140 atm. 8=16953
 Hg dimethyl, coupling constants, signs 8=7610
 K ethylate-ethyl picrate complex, crystal structure 8=22058

Organic compounds—contd

- K methoxide-methanol solvates comp. and K ions coordination number obs. 8=2497
- KH di-p-hydroxybenzoate hydrate, crystal structure 8=22060
- La (III) oxalate decahydrates, structures 8=8529
- Li methoxide-methanol solvates comp. and Li ions coordination number obs. 8=2497
- Li salts of dihydroanthracenes, electronic spectra rel. to ion-pair structure 8=7558
- LiBr (Cl), $2\text{NH}_3 \cdot \text{CH}_3 \cdot \text{CH}_2 \cdot \text{NH}_2$, ethylene diamine addition cpds. crystal structure 8=1820
- Mg-azatetraphenylporphyrins, polarization and absorpt, spectra rel. to porphyrin ring e struct., obs 8=21116
- Mn complexes, inversion-vibr. levels and splitting 8=4121
- Mn^{2+} in hexa- and tetracoordinated cpds., spectra 8=9551
- $\text{Mn}(\text{HCOO})_2 \cdot 2\text{H}_2\text{O}$, heat capacity between 1.4 and 20°K 8=13375
- Na acetate, γ -irrad., e. s. r. of trapped free radical $\text{CH}_3\text{CO}_2^\cdot$ 8=4242
- Na cyclopentadiene, u.v. photolysis 8=5754
- Na methoxide-methanol solvates comp. and Na ions coordination number obs. 8=2497
- Na tetradecyl sulphate, ion sublation studies, by radioactive tracers 8=23075
- Na tetraphenylborate in aqueous soln., photolysis products 8=5746
- Nd ethyl sulphate, crystal field parameters from ground state splitting of paramagnetic 8=18445
- Nd ethyl sulphate, mag. resonance saturation of Faraday effect, and spin-lattice relax. 8=14278
- NH_4 quaternary salts, in water-glycine mixtures, elec. cond. 8=8104
- Ni(II) chelate complexes, in soln., isotropic nuclear res. shifts 8=1598
- Ni(II) complexes of glycine peptides in aqueous soln., form. 8=9664
- $\text{Ni}_2(\text{CO})_8[\text{P}(\text{C}_2\text{H}_5\text{CN})_3]_4$, cryst. struct. with tetrahedral Ni cluster 8=8589
- Os carbonyl halide complexes, solvent effect in i. r. 8=16856
- P^{31} in soln. with radicals, nuclear-electron Overhauser effect, rel. to scalar interact. 8=4626
- Pb diethyl-dithiocarbamate, crystal structure 8=17445
- Rb methoxide-methanol solvates comp. and Rb ions coordination number obs. 8=2497
- S-N cpds., bond stretching freqs. 8=1299
- $\text{SbCl}_5 \cdot \text{CH}_3\text{CN}$, n. q. r. 8=2391
- Sr tartrate tetrahydrate, gel-grown, X-ray study 8=17459
- $\text{UO}_2[\text{S}_2\text{CN}(\text{C}_2\text{H}_5)_2]_2 \cdot [\text{H}_2\text{N}(\text{C}_2\text{H}_5)_2]$, monoclinic crystal structure 8=4899
- Zn diethyl-dithiocarbamate, crystal structure 8=17445
- Zn 2, 2-lquinoline mols., oriented in rigid-glass matrix, e. s. r. 8=9448
- Zr acetylacetonate, polarity and atomic polarization 8=16872

Orthicons. See Electron tubes.

Oscillations

- See also Electromagnetic oscillations; Liquid oscillations; Piezoelectric oscillations; Vibrations.
- beam oscills. anal., duality relations 8=15037
- bending of three-layer beam with various end constraints 8=10698
- bilinear hysteretic system, response to random excitation, time averaged statistics 8=19483
- of bubble, gas-filled in fluid, nonlinear 8=4520
- of circular membrane on nonlinear elastic foundation, periodic oscs. 8=3016
- classical fluids, h. f. linear response to Brownian oscillators 8=4446
- cylinders of gas, compressible, polytropic subject to stellar gravit. 8=5859
- cylinder, suppression of vortices and turbulence in wake, expt. 8=12666
- elastic systems, theory, book 8=15030
- elect. forced, nonlinear capacitor in series with inductor 8=19710
- fluid, bubble of different acoustic props. 8=21585
- fluid, flow, forced, behind vibrating cylinder 8=12609
- fluid, multi-layered rotating, normal modes 8=1452
- forced, of enclosed rigidly rot. inviscid fluid 8=7884
- gas flow, cylinder near-wake and separation point 8=12654
- gas, Rijke thermoacoustic, literature review 8=21515
- gas, Sondhauss thermoacoustic, literature review 8=21514
- gas sphere, high pressure, porous medium, theory of expansion 8=1439
- hydromagnetic, of conducting incompressible fluid cylinder 8=19817
- laser self-pulsating oscillator 8=11057
- linear and adiabatic of homogeneous sphere 8=146
- liquid-vapour interface of cavity in rot. cylindrical tank 8=16772
- magnetodynamic natural, in anisotropic ferrite crystals 8=5485
- mass flow, in modified Moore variometer configuration 8=4445

Oscillations—contd

- mechanical vibrators for adjustable l.f. compact oscillator 8=19495
- nonlinear, of spherically bounded solid on plane surface 8=19511
- non-stationary, in solid-state laser, theory 8=19978
- polymethylmethacrylate tubes, torsional, rel. to ht. generation 8=4946
- power flow between 2 groups of coupled oscillators 8=19482
- quantum in semimetals in strong magnetic fields 8=5235
- quartz, stimulated Raman oscillator behaviour, mode pulling 8=2453
- quasiphonon velocity, energy fluctuations in simple classical fluids 8=21419
- resonance, 3-axial ellipsoid containing non-central mass 8=10522
- third-order eqns., critical Lyapunov case, stability 8=6120
- torsional in rigid disc on surface of elastic half-space 8=10689
- Van der Pol system, forced solutions 8=14945
- Ga, quantum, of velocity of sound 8=13351
- Ge: Au double injection diodes, N- and S-type negative resist. and relax. oscs. 8=22628
- p-Ge:Ga, in impurity photoconductivity spectra 8=13912
- He shell-burning stars, pulsational instability 8=5873
- in He-Ne laser, growth 8=19964
- Sn, internal field, rel. to Knight shift 8=5566
- ZnO , acoustoelectric, 1-5 GHz range 8=22613
- Oscillator effect.** See Semiconductor.
- Oscillators.** See Semiconducting devices.
- Oscillographs.** See Electrical measurement.
- Oseen method.** See Flow; Hydrodynamics.
- Osmium**
- abundance in igneous and metamorphic rocks, relative to Re 8=18825
- in iron meteorites, three specimens 8=14857
- specific mag. susceptibility between 80° and 1850°K 8=5439
- Osmium compounds**
- thiocyanate, spectrophotometry 8=9752
- OsAs_2 , decomp. press. and enthalpy of formation 8=12338
- $\text{Os}(\text{CO})_X$, (X = halogen), solvent effects in i. r. 8=16856
- OsO_4 structure determ. by electron diffr. 8=12236
- OsS_2 , cryst. struct. 8=8556
- OsSe_2 , decomp. press. and enthalpy of formation 8=12338
- OsTe_2 , cryst. struct. 8=8556
- Osmosis**
- fixed-charge ionic systems, electro-osmotic contrib. to total cond. 8=8037
- polyelectrolyte solns., meas. during phase separation 8=16817
- polyelectrolyte solns., press. from e. m. f. meas. 8=16818
- polystyrene solns., osmotic pressures 8=8019
- polymer solutions, second virial coeff. calc. using lattice model 8=8039
- reverse, convective diffusion in stagnation flow with imperfect semipermeable interface 8=12841
- solutions, negative pressure of solvent 8=12840
- He^3 in He^4 , osmotic pressure of dilute solutions 8=10795
- ZnO_2 diffusion and absorpt. in cellulose membranes 8=21645
- Overhauser effect.** See Nuclear magnetic resonance and relaxation.
- Oxidation**
- acetate ion, by $\text{K}_2\text{S}_2\text{O}_8$, Ag catalysis 8=23094
- acetone, photo-oxidation, methyl hydroperoxide prod. 8=14437
- alloys, high temp., scales form. mechanism 8=5711
- aromatics in boric acid glass, direct and sensitized photo-oxidation 8=23160
- basic O_2 furnace, jet penetration, bath circulation 8=10454
- carbon, gaseous, chemi-ionization and excitation 8=5699
- catalytic, catalyst valence transitions energy rel. to oxidised subst. ionization pot. 8=2526
- p-cymene with t-butyl chromate 8=9687
- deoxidation product growth and separation, collision model 8=18658
- ethylene, catalytic, rel. to Ag surface struct., chemisorpt. obs. 8=18706
- ethylene, in shock waves 8=18676
- n-hexane on Pt electrodes 8=5737
- hydrazines, electrochem., hydrazyl radicals form., e. p. r. obs. 8=5722
- hydrocarbons, on Pt electrodes 8=9714
- iron, liq.-silica deoxidation product growth and separation, collision model 8=18658
- metals and alloys, mechanism, isotopic study 8=23092
- metal crystal, kinetics, model based on thermionic emission and ionic diffusion 8=5710
- metals, high temp., scales form. mechanism 8=5711
- metal ion promoted atom-transfer oxidation-reduction reactions 8=14401
- metals in metal vapour-CO-CO₂-neutral gas system 8=8182
- metal surfaces, chemisorption and film growth 8=9703
- metal surfaces, passivity theory 8=9702
- nitrosobenzene, electrochem., in organic media, e. s. r. 8=14426
- oxide powder reduction by gases, micromechanism from O_2 pressure change meas. 8=18683

Oxidation—contd

oxygen-peroxide electrode, exchange current 8=9695
 precipitation deoxidation kinetics, collision model 8=18658
 rare-earth ions, trivalent, in fluorite-type crystals,
 radiochemical reduction giving divalent centres 8=18740
 rutile, partial reduction rel. to defect nature from e.p.r.
 study 8=18436
 semiconductors, thermal oxidation, impurity
 redistrib. 8=18015
 silane, controlled, for deposition of SiO₂ films 8=13095
 solids, induced by u.s. radiation 8=9735
 steel, 18Cr-8Ni, thin film identification by electron
 microscopy 8=8319
 substituted phenols, in benzene soln., e.s.r.
 study 8=14378
 transition metal cpds. with concurrent shrinkage 8=4936
 wustite reduction in CO, promoters 8=5702
 zinc film evaporated 8=1691
 Al, anodic oxidation in presence of hydrated oxide 8=18729
 Al, controlled, in radio-freq. excited glow discharge 8=8310
 Al, effect on electron emission 8=9270
 Al film, effect on photocurrent 8=18221
 Al films in low-pressure O₂ atmosphere 8=18669
 Al, oxidation and removal by diffusion of Mg 8=18670
 Al reoxidation in electrolysis 8=23151
 Al, work function changes during and following 8=5407
 Al-Mg alloys, oxidation and removal by diffusion of
 Mg 8=18670
 B₁₂H₁₂²⁻, electrochem. controlled in acetonitrile 8=5732
 C, vitreous, and pyrolytic graphite, comp. of pitting 8=8292
 CO, catalytic, rel. to Ag surface struct., chemisorpt.
 obs. 8=18706
 CO preadsorbed on Pd film, induction period 8=5700
 CaF₂·Eu³⁺, radiochemical reduction giving Eu²⁺
 centres 8=18740
 Cr surface, rel. to Cr₂O₃ epitaxial growth 8=4828
 Cr-Ni stainless steel, intercrystalline, theory 8=8460
 Cu, vacuum deposited films, rel. to temp. 8=18674
 Cu_{1-x}Mg_xFe₂O₄, oxygen content on quenching in high
 oxygen pressure furnace 8=2516
 Er, thin films, electron microscope study 8=5701
 Fe, distribution of additions 8=1917
 Fe, liq., deoxidation by Al, rel. to form. of cloud group
 of inclusions 8=22183
 Fe, in water vapour at 550°C, effect of cold work 8=23101
 Fe-Al alloys, effect of storage 8=9666
 Fe-Cr alloy, after lifting and breaking Cr₂O₃ protective
 scales 8=23099
 Fe-Cr alloys of 25-95%Cr comp., at 1000° to
 1300°C 8=18677
 Fe-28%Cr alloy, form. and stability of oxide nuclei, and
 structure of film 8=21882
 Fe-12 at.%Ni alloy, finely dispersed system, effect on
 phase comp. 8=17280
 H, catalytic, rel. to Ag surface structure., chemisorpt.
 obs. 8=18706
 La metal, high temp. 8=18680
 Mg, reduction processes in silico-thermal prod., radioactive
 tracer study 8=23776
 (Mg, Fe)O₂ (magnesiowustite), depend. on temp., oxygen
 press., and crystal composition 8=23108
 MgFe₂O₄, and reduction effects on thermal
 conductivity 8=17543
 Mo alloys, anti-oxidation metallurgy 8=23779
 Mo, attack at high temp. by atomic O 8=14370
 Nb alloys, anti-oxidation metallurgy 8=23779
 Ni-base alloy, oxidation resistance to 2200°F 8=22387
 Ni hydroxide, electrochem., γ NiOOH form.,
 obs. 8=18716
 Ni, kinetics of diffusion-controlled reactions at
 cylindrical surfaces 8=14372
 Ni-base alloys molten, during vacuum induction melting
 by refractory-reduction 8=9694
 2PbCO₃ anodization and PbO₂ struct. obs. 8=23148
 PbO anodization and PbO₂ struct. obs. 8=23148
 Pb(OH)₂ anodization and PbO₂ struct. obs. 8=23148
 PbSO₄ anodization and PbO₂ struct. obs. 8=23148
 Pb₃O₄ anodization and PbO₂ struct. obs. 8=23148
 Pt, gaseous oxides 8=5716
 Pt, oxidative adsorpt. of propane 8=2534
 Pu in air rates 8=5717
 Si, high-temp., Al impurity redistrib. and depletion depth,
 obs. 8=22606
 Si, thermal, by wet O₂ stream 8=18689
 SiO₂, effect of dissolved O₂ on C-V characts. 8=5284
 Si-SiO₂ interface, thermal oxidation, effect of Na
 impurity 8=14384
 Sn electrodes in alkaline solns above pH9, mech. of
 passivation processes 8=18733
 SO₂ solns., effect of ullage 8=23111
 Ta alloys, anti-oxidation metallurgy 8=23779
 Ta, controlled, in radio-freq. excited glow discharge 8=8310
 U, protection given by UAl₃ coating 8=21892
 UC, high-temp. behaviour obs. 8=23115
 U-Ti alloys in CO₂ at 450°C 8=5718
 V-Ga alloys, anodic, and phase anal. 8=8286
 W alloys, anti-oxidation metallurgy 8=23779
 W, attack at high temp. by atomic O 8=14370

Oxidation — contd

ZnFe₂O₄, and reduction effects on thermal
 conductivity 8=17543
 Zr, low-press. 8=14391
 Zr-Nb alloy 8=14390

Oxide cathodes. See Cathodes/oxide.

Oxygen

adsorbed on Mo crystals, surface exam. by LEED and
 work function studies 8=17165
 adsorption on impure ZnO, i.r. absorpt. studies 8=4769
 adsorption on Ta ribbon, work function changes 8=9276
 absorption oscill. strengths of O I lines in vac.
 u.v. 8=7417
 association with hemoglobin, statistical mech.
 anal. 8=1311
 Atlantic undercurrent, equatorial, obs. 8=14569
 atmosphere, gas constituent number density determ. using
 laser beams 8=14585
 atmospheric, calc. of radiowave absorpt. coeff. 8=9888
 atmospheric, Raman scatt., N₂ u.v. laser obs. 8=23289
 atom, spectral absorption coeffs. compilation 8=12060
 atoms, reaction with Cl₂ 8=9696
 atomic beam, photoionization 8=21021
 atomic at 120 km altitude, mass spectrometric
 meas. 8=18920
 atomic spectra, vac. u.v., metastable states 8=12072
 atoms, in b.c.c. Fe, migration energy and
 solubility 8=22150
 atoms, e loss in collisions with H⁺ 8=7461
 atoms, H-O, collisions excitation of fine structure
 levels 8=1193
 atoms, interaction with inert gases 8=12104
 atoms, reaction with CO in shock wave tube 8=1342
 atoms, reaction kinetics with SO₂ 8=5715
 aurora, λ 5577 and λ 6300 O I, ratio of spectral intensity
 to Hβ 8=23340
 burning stars, evolution, and pre-supernova
 models 8=5874
 chemisorbed on Al films, stability and work function
 changes 8=5726
 chemisorption on carbon 8=5725
 combustion of single drops of liq. fuel, influence of O₂
 content of ambient gas, rel. to drop size 8=19657
 concentration effects in n-irradiated silicon 8=5279
 D content, neutron spectrometry 8=9765
 desorption, electron-stimulated, from W surface,
 mechanism 8=17177
 diffusion in α-Nb₂O₅, near-stoichiometric 8=1922
 diffusion in polymethylmethacrylate, meas. by quenching
 of phosphorescence 8=8687
 discharge, h.f. electrodeless, e density cinemato-
 graphy 8=16398
 discharge, r.f., dark-sheath form, mechanism 8=12399
 dissociation in elec. discharge and resulting ionization
 process 8=7722
 dissolved in Nb, with N₂, effect on props. 8=9011
 effect on creep strength on niobium at 800-1200°C over
 stress range 1500-5000 lb/in² 8=13593
 electron microscope investigation of condensed O₂ 8=8465
 e.s.r., O₁₆⁻¹⁸, O₁₇⁻¹⁸, O₁₈⁻¹⁶ 8=4222-3
 forbidden ¹D₂→³P₁ transitions obs. 8=1182
 free atoms, reactions with simple hydrocarbons, e.s.r.
 study 8=14376
 gas, low temp. flame, O, H or O, CO 8=9699
 gas, rotational relaxation, high temp. u.s. obs. 8=1251
 gettering rate obs. in colour picture c.r.t. 8=15324
 heat transfer props. in reduced gravity 8=16692
 interaction with B in Ge melt 8=23104
 interdiffusion with org. vapours and diffusion
 into N₂ 8=14452
 ionization coeffs., secondary, at press. up to atm. 8=4316
 ionization cross-section, electron impact 8=7700
 ionization, electron and proton impact, classical
 model 8=12444
 ionization energy per ion pair formed by H³β
 particle 8=4315
 ionosphere, line excitation rel. to heating 8=18975
 isotope chem. of ancient charts rel. to Precambrian
 ocean 8=5779
 isotope mixtures, thermal diffusion props. 8=1492
 isotope ratio in snow and firn at South Pole, rel. to air
 temp. 8=23227
 ions in solar wind, Vela satellite meas. 8=23715
 in liquid Na, solubility data 8=16798
 liquid, significant structure theory, application 8=4528
 molecular, electron impact cross sections 8=1349
 molecular, ionization by e collisions 8=16451
 molecules in mesosphere, temp. determ. from microwave
 spectra 8=23258
 molecules, O₂-p e capture excitation of 3s, 4s states
 of H 8=7462
 molecules, single and double electronic
 transitions 8=1262
 mol., used as ion source with Xe beams 8=12454
 molecular, mm. wave permeability, lower atm. 8=18906
 negative ions in O discharge, sputtering of Au
 films 8=21877
 neutral, solar lines, obs. rel. to temp. distrib., profile
 damping and abundance in photosphere 8=23704

Oxygen—contd

- in oxides of heavy elements, X-ray microanalysis 8=14475
 oxygen-acetylene flame temp. meas. by molecular spectroscopy 8=3109
 oxyhydrogen mixtures detonation waves, induction zone obs. at low initial pressures 8=170
 parameters of manganese vanadate, and degree of conversion, neutron diff. determ. 8=8534
 partial photoionization cross-sections, determ. by photoelectron spectra 8=1369
 permeation rate in W, pressure, thickness and temp. dependence 8=4958
 photoionization cross sections for $\lambda > 25\text{\AA}$, atomic 8=12452
 polarization effects in elastic e scatt., and photo-detachment from O^- 8=4101
 pumping speed-press. data, getter-ion pump 8=1495
 radiolysis, ion lifetimes meas. 8=23163
 reaction with acetylene, upper atm. 8=23307
 recombination system of $\text{H}_2\text{-O}_2$ -gases in BER reactor 8=4014
 scattering of K, atomic differential spin-exchange scattering 8=12109
 solid, abs. spectra of α, β, γ forms, $3400\text{-}42000\text{ cm}^{-1}$ 8=5625
 solid, α, n -diff. study of structure 8=4882
 solid, transform. characts. and thermal expansion 8=4938
 solubility and activity coeff. in liq. Cu-Co alloys 8=8011
 sorption on (111) face of W crystal, mechanism and kinetics 8=8348
 sorption on W surface, rel. to work function charges 8=4767
 stable isotopes, microanal. by nuclear reactions 8=14453
 stars, Am, abundance 8=23514
 stratosphere molecules, microwave emission spectra 8=23256
 translation accommodation coeff., on W surface 8=17113
 u. s. velocity and absorpt., $300^\circ\text{-}1300^\circ\text{K}$ 8=4478
 X-ray microanalysis using network method analyser, obs. 8=14489
 in Al, radioactivation anal. 8=5764
 Ar- O_2 gas mixtures, mechanism of laser action 8=11975
 BaO cathode emission, residual gas effects 8=18663
 in Cs 8=15224
 $\text{H}_2 + \text{O}_2$, slow reaction rate, computer calcs. 8=18678
 and H_2O , mixture of vapours, sound absorption obs. 8=1476
 Mo tip, absorption, field emission study 8=21905
 in Ge, activation meas. by He^3 bombard. 8=18083
 $\text{N} + \text{O} \rightarrow \text{NO}^+ + \text{e}$, ionization cross section calc. 8=4111
 in Na-K reactor coolants, effect on efficiency of coolant, corrosion activity and residual radioactivity 8=7328
 Ne- O_2 gas mixtures, mechanism of laser action 8=11975
 in Ni, diffusion rel. to CO evolution 8=16745
 $\alpha\text{-O}_2$, light absorpt., bands at 4.2°K , effect of 170 kOe mag. field 8=5626
 $\alpha\text{-O}_2$, solid, absorpt. line splitting in strong mag. field 8=14252
 $\text{O}(\text{D})$ reaction with H_2 8=5744
 $\text{O}(\text{D})$ deactivation 8=4098
 O/Fe relative abundances in solar corona 8=23748
 O-O system, 2nd virial coefficient for different electron states at 2000-6000 K 8=1469
 [OI] 5577 \AA and 6300 \AA in night airglow, rocket obs. 8=18935
 [OI] λ 5577 and λ 6300 spectra auroral luminosity spatial var. obs. 8=14649
 OI forbidden lines in sunspot spectrum obs. 8=14880
 O II electrostatic interaction integrals using screened hydrogenic orbitals calc. 8=7394
 O II, equilibrium population of states in plasma 8=7418
 O III, radio galaxies emission rel. to fine struct. const. time var., obs. 8=14727
 O(III and IV), mean lines of some excited levels 8=4097
 O IV lines in vacuum u. v. 8=20964
 O VIII in solar corona, L_α and L_β lines intensity ratio calc. 8=10434
 O, O_2 , energy deposited in electron slowdown 8=2634
 O+P(PH_3) reactions, stoichiometry and chemiluminescence 8=23109
 $\text{O}^{16}\text{O}^{16}$ molecule, e. p. r. spectrum 8=12309
 O^{16} and O^{18} relative abundances in minerals, mass spectrometry 8=12112
 O^{17} in acidified H_2O , n. m. r. linewidth rel. to proton exchange 8=1599
 O^{18} , in enriched- UO_2 coherent neutron scattering length 8=8553
 $\text{O}^+ + \text{O}_2 \rightarrow \text{O}_2^+ + \text{O}$ rate constants energy var., drift tube meas. 8=14667-8
 O^+ , cathode poisoning from feralma anode 8=15330
 O^+ concentration, equatorial ionosphere obs. 8=18974
 O^+ reaction with O_2 and N_2 in ionosphere, rate coeff. study 8=14666
 $\text{O}^+ + \text{N}_2 \rightarrow \text{NO}^+ + \text{N}$ rate constants energy var., drift tube meas. 8=14667-8
 O_2^- in alkali halides, thermal quenching of luminescence 8=2485
 O_2 e. s. r. in H_2O_2 -urea addition compound, γ -irradiated at 77°K 8=2373
 O_2^- in KI, reorientation at $1.5\text{-}4.2^\circ\text{K}$ 8=13123
 $\alpha\text{-O}_2$, crystal structure rel. to mag. props. 8=17406
 O_2 absorption line equivalent width rel. to atmospheric temp. 8=2577

Oxygen—contd

- O_2 , configuration interaction calc. 8=12028
 O_2 , electronically excited, photoionization 8=16450
 O_2 , electronic structure 8=16297
 O_2 ionization by Fe atoms, ionization ratio meas. 8=1359
 O_2 , photoionization and dissociation continua 8=12453
 O_2 thermal cond., mag. field effects, 290°K 8=4469
 O_2 , thermal electron capture 8=7723
 O_2 , H^+ , H_2^+ , He^+ charge exchange, 40-1500 eV 8=21275
 O_2 -Ar gas mixtures, thermal conductivity 8=4474
 $\text{O}_2 + \text{Ar}$ mixture, conversion of positronium atoms 8=7476
 O_2 -Nb system at very low pressure, adsorption, absorption and degasing 8=4763
 O_2 and $\text{O}_2\text{-N}_2$ mixtures, e density decay rates, microwave meas. of temp. depend 8=21240-1
 $\text{O}_2(\Delta_g)$ collisional-radiative reaction 8=12220
 O_2^{16} molecules, millimetre transfer radiation, influence of Earth's mag. field 8=23284
 O_2^+ ionosphere, dissociative recombination rate 8=9961
 O_2^+ reaction with N_2 and NO in ionosphere, rate coeff. study 8=14666
 O_2^+ dissociation by e impact, 10-500 eV, cross-section 8=1312
 on PuO_2 , adsorption, sites and sintering effects, obs. 8=8345
 in Si, activation meas. by He^3 bombard. 8=18083
 Si oxidation by wet stream 8=18689
 in UO_2 , self-diffusion 8=23113
 from W, desorption by electron impact 8=21912

Oxygen compounds

- hydroxyl normal emission in interstellar dust clouds 8=23573
 metal oxide, hypostoichiometric, partially ordered defects, statistical model 8=17600
 metal oxides, X-ray spectroscopic investigation of chem. bonding 8=9499
 oxides of heavy elements, O X-ray microanalysis 8=14475
 oxide matrices, trace element determ. by mass spectrometry 8=18769
 oxide powder reduction by gases, micromechanism from O_2 pressure change meas. 8=18683
 oxygen fluorides, F^{19} n. m. r. 8=4231
 pyrochlores, crystal chemistry 8=13117
 OCS absorpt. spectrum and vibr. analysis, 1350-1420 \AA 8=16296
 OCS cryst., i. r. intensity of librational mode 8=14201
 OCS pyrolysis in shock tube with quadrupole mass filter 8=14361
 OD, OH, transition $\text{B}^2\Sigma^+ \rightarrow \text{A}^2\Sigma^+$, high resolution obs. 8=21095
 OF_2 , ground state, minimal-basis-set LCAO-SCF-MO calc. 8=21096
 OF_2 , spectrum, Fermi diad 8=4164
 OH^- ions rel. to activator solubility in NaCl:Ni , KCl:T and KCl:Pb obs. 8=21824
 $\text{OH}^-(\Sigma^+)$, Hartree-Fock wavefunctions and molec. props. 8=4165
 OH^- in KCl, adiabatic depolarization rel. to crystal cooling to 0.36°K 8=1874
 OH^- , SCF calcs, correlation energies and Hartree-Fock limits 8=1263
 OH, absorption and emission spectroscopy, in low-press. oxyacetylene flames 8=21189
 $\text{OH}(8,3)$ band, OI 5577 \AA line, night airglow, mid-latit. rocket obs. 8=2631
 OH 18 cm lines, cosmic, polarization theory from maser studies 8=7543
 OH 18 cm cosmic rad., anomalous elec. polarization 8=23582
 OH, emission spectrum 8=12222
 OH emission bands in nightglow photometric obs. 8=9928
 OH galactic, radio emission, brightness and temporal variation 8=10253
 OH, luminesc., from $\text{H}(\text{P}) + \text{O}$, reaction 8=14366
 OH, microwave spectrum, low-field Zeeman effect 8=4246
 OH mols. in interstellar space, maser action mechanism 8=5927
 OH, oscillator strengths in $^2\Sigma^+ \rightarrow ^2\Pi$ band system 8=7544
 OH, predissociation in chemiluminescence spectrum 8=12223
 OH radical, interstellar radio absorpt. 8=23581
 OH radical and trapping site in γ -irrad. ice, e. s. r. identification 8=9438
 OH, reaction with itself and with CO 8=18684
 OH reaction with oximes, e. p. r. 8=14394
 OH retention on MgO 8=1703
 OH rotational temps. and intensities in nightglow 8=14647
 OH stretching band struct. in phenol and substituted phenols 8=4211
 OH, vib.-rot. interact. and the transition moment 8=7545
 OH, vib.-rot. spectrum from oxyacetylene burning in air or N_2 , rel. to flame temp. 8=18692
 OH $^+$, fine structure of $^3\Sigma^+$ and $^3\Pi$ states 8=7541
 OH_3^+ , one-centre expansion SCF calc. 8=4202

Ozone

- Antartica (90°S), monthly variations 8=9897
 atmospheric concentration, S. Africa, up to 45 km 8=14588

- Ozone**—contd
 atmospheric, eclipse effect, u.v. obs. 8=9871
 atmosphere, 8mm absorption and emission 8=18934
 atmospheric from satellite meas. 8=2576
 eclipse effect in sun spectrum 8=23692
 heating and radiative equilibrium in stratosphere 8=2579
 mesosphere during solar eclipse, rocketsonde obs. 8=18852
 molecule, ground state, MO calc. 8=21096
 oscillation, quasi-biennial, from meteorological data 8=2581
 reaction with H and OH 8=5744
 spectra, 9.6 μ absorbance band, empirical formulas 8=12221
 tropospheric and stratospheric distribution, obs. 8=18853
 troposphere and stratosphere, soundings over N and central America 8=18851
 $O_2(a^1\Delta_g) + O_3 \rightarrow 2O_2 + O$, reaction rate 8=16450
- pH**. See Electrochemistry.
- p-n junctions**. See Semiconducting devices/p-n junctions.
- P-V-T relations**. See Equations of state.
- Pair creation**. See Electron pairs; and under individual particles, e.g. Mesons.
- Palaeomagnetism**. See Rock magnetism.
- Palladium**
 adsorption of CO , i.r. spectra 8=4764
 diffusion in Al 8=8671
 electronic states density from X-ray spectroscopy of alloys 8=17884
 films, obliquely deposited, struct., effect of atom mobility 8=8296
 film, preadsorbed CO oxidation, induction period 8=5700
 gravimetric determ., appl. of tetrazoline-5-thiones 8=14188
 hydride phase, solubility of H_2 , isotherm 8=1924
 lattice vibrations, 16% accuracy in freqs 8=22080
 Lorentz number from 2.5-19°K 8=5184
 magnetic moment data, limits of exchange enhancements, 4.2°K 8=13973
 magnetic susceptibility spin-orbit coupling dependence 8=2332
 photoexcited electrons, discrete energy loss by plasmon excitation 8=2279
 specific mag. susceptibility, temp. depend. above melting point 8=5439
 twins formation during diffusion between films of Au and Pd 8=13127
 D diffusion at 0° to 100°C 8=17582-3
 Fe⁵⁹ diffusion mobility obs. 8=17579
 H diffusion at 0° to 100°C 8=17582-3
 H_2 definition, spectral-isotopic method 8=9743
 Pd(II), spectra in fused LiCl-KCl 8=1567
 Pd:Fe spin polarization around local mag. impurity 8=18317
- Palladium compounds**
 alloys, thermoelec. power meas. 2-120°K 8=18216
 Pd based double cyanide complexes, mean diamagnetic susceptibility 8=22751
 Pd complex, trans-dichlorobis(dimethyl sulphoxide)Pd(II), mol. and crystal structure 8=1804
 Pd-Ag, H and D diffusion at 0° to 100°C 8=17582-3
 Pd-Au-D system, α phase, neutron diffraction 8=17407
 Pd-Au-H system, α phase, neutron diffraction 8=17407
 Pd-Ba alloy, work function 8=18245
 Pd-Co alloys, (8.3 to 0.03 at. %Co), effective mag. field at Co⁶⁰ nuclei 8=5463
 Pd-Co alloys, ferromagnetic specific heat 8=8642
 Pd-Fe alloy containing H, hyperfine fields and isomer shifts temp. dependence by Mössbauer effect 8=13020
 Pd-Fe alloys, ferromagnetic specific heat 8=8642
 α -Pd-H, diffusion of H, study by n. scatt. 8=17581
 Pd-H, α -phase, diffusion of H, by small energy transfer neutron scattering 8=13411
 β -PdIn, reflectance and other optical props 8=2402
 Pd-Mn alloys, structural and mag. props. 8=4714
 ζ -Pd₃Mn, antiferromag. structure 8=18385
 Pd-Ni alloys, magnetic moment, rel. to hydrostatic pressure 8=9351
 Pd-Ni alloys, s-electron-paramagnon scattering 8=9015
 Pd-Ni alloys, specific heat, paramagnon mass enhancement theory 8=17524
 Pd-Ni alloys, paramag. susceptibility and sp. ht. 8=18300
 PdNi alloys, dilute, elec. resist., local exchange enhancement effects 8=13634
 PdNi alloys, thermoelectric power anomalies 8=13904
 Pd-Sn, H and D diffusion at 0° to 80°C 8=17583
- Paper**
 fibre comp. determ. by i.r. absorpt. 8=14462-3
 insulation, elec. discharge, d.c. detection and meas. 8=21242
- Paramagnetic resonance and relaxation**
 See also Lasers; Masers.
 acoustic wave induced, dispersion in paramagnetic crystals 8=5516
 acridine mononegative ion 8=21167
 alkaline ices, irradi., relax. of trapped electrons 8=2370
 alkali earth oxides, e.s.r. of F centres 8=13456
 alkali-halides: Cu 8=22897
- Paramagnetic resonance and relaxation**—contd
 alkali silicate glasses, e.p.r. study of trapped hole centres 8=1998
 animal tissues, e.s.r. spectroscopy, and possible medical appls. 8=14891
 anthracene, γ -irrad., colour centres 8=17689
 aromatic hydrocarbons, during pyrolysis 8=2513
 aromatic hydrocarbons, oriented, multiple struct. 8=2363
 benzodioxins, calc. 8=7575
 benzene, phosphoresc. cryst. 8=14095
 bis-[2,6-dichlorobenzene-(1-azo-1')-naphthol-2'] Cu(II), rel. to e delocalization in azo groups 8=8122
 p-benzosemiquinone, reson. absorpt. in Zeeman region 8=16348
 borate glasses, of Mn²⁺, 293-4°K 8=18408
 calcite, motional effects in e.s.r. of CO_2 8=22899
 bis-[2-chlorobenzene-(1-azo-1')-naphthol-2'] Cu(III), rel. to e delocalization in azo groups 290 and 77°K 8=8122
 chalcogenide glasses (Ti₂SeAs₂Se₃/Ti₂SAs₂, Ti₂TeAs₂Te₃), of Mn²⁺ in, hyperfine structure 8=5533
 chlorospodosite (Ca₂PO₄Cl): CrO₃⁻ 8=14099
 complexes of biomols. with radiosensitizers, e.p.r. meas. of spin-transfer 8=10450
 conduction electrons, in conducting solids 8=5515
 copper phthalocyanine, e.s.r. 8=9441
 crystal field parameter determ. from mol. effective change 8=18445
 cupric complexes, F¹⁹ hyperfine splittings 8=21168
 cyclo octatetraene anion radical, e.s.r., ion pairing effects 8=4614
 d^{3,7} ions in tetragonal cryst. fields 8=21798
 DPPH, r.f. field depend. 8=14122
 DPPH, sidebands from many photon transitions obs. 8=22904
 m-dicarbene cpds, e.p.r. of quintet ground states 8=4221
 dielectric solids, spin-spin relax. rel. to nuclear spin relax. and dynamic polarization 8=18443
 diethyl sulphide-urea cpds, X-irrad., e.s.r. of RCHSR' type free radicals 8=1314
 dihydroxydurene, cation radical, e.s.r. spectrum 8=1589
 N,N-dimethylaniline cation radicals, hyperfine splitting, substituent effects 8=4620
 2,6-dimethylbenzosemiquinone, monoprotonated, e.s.r. solvent depend. 8=8125
 4,4-dimethylcyclohexenone radical anion 8=12304
 4,4'-dimethoxyazobenzene radical anion 8=12303
 dimethoxydurene, cation radical, e.s.r. spectrum 8=1589
 m-dinitrene cpds, e.p.r. of quintet ground states 8=4221
 di-n-hexyl sulphide-urea, X-irrad., e.s.r. of RCHSR' type free radicals 8=1314
 dinitrobenzene alkali-metal salts 8=8120
 dinitrobenzene anion radicals, dynamic freq. shifts 8=4244
 p-dinitrobenzene radical anions, solvent depend. of N¹⁴ hyperfine coupling 8=8124
 diphenyl-amino radical dimer 8=7625
 diphenyl-picryl-hydrazyl, Faraday effect at 8.78 GHz 8=7600
 dipyrityl mononegative ion and alkali metal ion biradical, e.s.r. and structure 8=4247
 di-tertiary-butyl nitroxide solns., spin exchange 8=8121
 durene, irradi. cryst., free radicals 8=5528
 durene-tetracyanobenzene complex, charge transfer triplet state 8=12306
 durosemiquinone in 1,2-dimethoxyethane 8=1591
 dynamic proton polarization, model using spin-spin interaction 8=2361
²E state, effect of linear Jahn-Teller coupling 8=18402
 effect on γ - γ angular correl. 8=20761
 e.s.r. spectra at liq. He temp. cryostat to study effects of light 8=15135
 electron spin echo, effect of weak mag. field 8=15429
 exchange narrowing influence on nuclei dynamic polarization 8=22893
 ferrites: Fe²⁺ powders, electron relax. study 8=18419
 fluorides: Mn²⁺, hyperfine coupling constants temp. dependence 8=18429
 field modulation, microwave cavity 8=15427
 four-level system, susceptibility at saturation 8=393
 fluorenylidene in diazofluorene crystals, spin densities from ENDOR 8=5555
 free radicals of biological interest, e.s.r. study 8=12341
 free radicals in polymerization, and polymer oxidation, e.s.r. study 8=14414
 free radicals in soln., saturation in e.s.r. spectra 8=3278
 garnets: rare earth ions powders, electron relax. study 8=18419
 gaseous atom reactions, e.s.r. study 8=14376
 gaseous free radicals, results and anal. of spectra rel. to structure 8=12340
 gas phase, double quantum transitions 8=12308
 gases, reaction kinetics by e.s.r. 8=14351
 glass, irradi. effect, suppressed by synthesis render high press. H 8=4996
 glasses and Li borate cpds., of Mn²⁺ in 8=5536
 glasses of Na₂O-TeO₂ system, γ -irradiation effects 8=9434
 graphite, monocrystalline, free charge carriers, thermal variation of line width anisotropy 8=5524

Paramagnetic resonance and relaxation—contd

- group IV hydrides, geminal coupling consts., from ENDOR meas. 8=21175
 Heisenberg paramagnets, linewidths asymptotic behaviours near critical points 8=22757
 helicon relaxation 8=17901
 hydrocarbon radicals, e.p.r. spectroscopy meas. of g factor 8=12301
 hyperfine interacts. from perturbed angular corrls. 8=18401
 ice, γ -irrad., e. s. r. identification of OH radical and trapping site 8=9438
 ice, γ -irrad., e. s. r. of OH radical 8=9439
 intermodulation in spin systems obeying Bloch's equations 8=10992
 laser, acoustic, mag. pumped paramag. salts appls. 8=15473
 laser, gas, rel. to non-linear Zeeman effect theory 8=6435
 laser, i. r., mag. pumped paramag. salts appls. 8=15473
 line moments in systems with dominant exchange interaction 8=18403
 line profile parameters dependence on external elec. fields 8=18399
 lineshapes with exchange among many sites, rapid computation 8=3277
 line shapes of systems undergoing intermolec. exchange 8=12302
 linewidth calc. by methods of moments 8=14086
 magnetic resonance and relaxation, conference 8=22889
 magnetoacoustic, double electron-nuclear, at local electron centres 8=8623
 many photon transitions, ang. mom. det. 8=22904
 many-quantum transitions in rotating reference frame 8=18400
 metals, electron-nuclear relax. at low temps. in strong mag. fields 8=9449
 methanol, X-irrad., u.v. photolysis at 77°K 8=5750
 met-myoglobin, single cryst. 8=9433
 methyl viologen cation, aq. and alcoholic solns., e.s.r. spectra, rel. to water induced dimerization 8=8123
 molecules, matrix-trapped at 4°K 8=4116
 Mössbauer spectra in presence of electron spin relaxation 8=1644
 myoglobin azide, single cryst. 8=9433
 naphthalene- d_8 -naphthalene- h_8 mixed crysts. in triplet state 8=18433
 naphthalene- d_8 of naphthalene- h_8 mol. pairs, exchange energy and optical spin polarisation, obs. 8=22911
 naphthalene- d_8 , triplet state and phosphoresc. 8=9655
 naphthalene ENDOR study of metastable triplet state 8=21169
 naphthalenes, substituted, zero-field splitting meas. 8=9435
 natrolite, (Na_2 (Al, Fe) Si_3O_{10} , $2H_2O$), of Fe^{3+} , at 4.2 and 293°K 8=18432
 (nd)² ions in rutile-type crystals, crystalline field theory explanation 8=9411
 p-nitroanisole radical anions, solvent depend. of N^{14} hyperfine coupling 8=8124
 nitrobenzene alkali-metal salts 8=8120
 nitrosobenzene, electrochem. oxidation in organic media 8=14426
 nitroxide polymers 8=4270
 nonlinear response, formal theory 8=2989
 nonmetallic crystals, impurity centres, lineshape theory 8=14085
 nonoriented solids, weak fine struct. components 8=14098
 nuclear ultrasonic fast passage 8=10983
 organic glasses, γ -irrad., e. s. r. of trapped electrons 8=9729
 paraelectric-resonance transitions, linewidths 8=14187
 phenols, substituted, in benzene soln., e. s. r. study of oxidation 8=14378
 phenanthrene- d_{10} , triplet state and phosphoresc. 8=9655
 phosphates glassy and cryst., γ -irrad. 8=22913
 plant tissues and isolated chloroplasts, photoinduced changes in Mn^{2+} content 8=23763
 poly(glycol methacrylate), X-irrad. 8=18422
 polymethylmethacrylate, γ -irrad., trapped free radicals, e. s. r. spectra obs. 8=4682
 poly(methyl methacrylate), X-irrad. 8=18422
 polynuclear hydrocarbons, spectra 8=12307
 polyphenyls, spin-spin interactions 8=2374
 polyphenylacetylene, crystalline, and struct. obs. 8=8600
 polypropylene, free radicals 8=12352
 polypropylene, free radicals prod. on γ -irrad., e. s. r. obs. 8=7628
 powders, free radicals in simple chamber 8=7619
 proteins, internal rot. and ang. corrl. functions 8=16384
 pyridine, hydrogenated 8=12310
 pyridine and related N-heterocyclics, radical anions 8=21171
 quinoxaline, optical detect. of e. s. r. transitions 8=14343
 radical anion reactions formed by e addition to unsaturated mols. 8=14350
 relaxation, phonon superheating, model 8=5518
 Rochelle salt: Cu^{2+} ferrocyclic, e.p.r. Stark effect obs. 8=14101
 Rochelle salt: Cu^{2+} , influence through external elec. field 8=14111

Paramagnetic resonance and relaxation—contd

- rochelle salt, γ -irrad., e. s. r., analysis of centre No. 2 8=9442
 ruby: Cr^{3+} , second-harmonic generation, microwave 8=22896
 ruby crystal in liquid He, spin echo behaviour 8=14091
 ruby, microwave absorpt. spectra 8=14089
 ruby, spin lattice relax. times at He temp, Cr^{3+} conc. and temp. depend. 8=14092
 ruby, spin-lattice relaxation time at room temp., determ. 8=5523
 ruby, spin-lattice relax. time meas. 8=9416
 rutile analysis rel. to trace characterization 8=18771
 rutile, partially reduced, at 77°K rel. to defect nature 8=18436
 sapphire, Fe^{3+} -doped, u. s.-induced changes in spectra 8=18407
 sapphire, spin-lattice relax. time meas. 8=9416
 saturation and double-reson. effects, coherence 8=3278
 scalar relax., Bloch eqns. and memory effects 8=15428
 semiconductors with magnetic impurities, spin-lattice relaxation of conduction electrons, theory 8=5519
 semiconductors, organic, r. f. spectroscopy 8=14088
 semidiones of cycloalkanes, alkylcycloalkanes and N-methylpiperidine, struct. and conformation, e. s. r. obs. 8=22898
 semiquinones in alcoholic soln., hyperfine interactions 8=7627
 semiquinones, in solid state, hindered motion 8=5521
 σ -radicals, comparison of calc. electron densities and e.p.r. coupling consts. 8=12347
 silicate glasses, of Mn^{2+} , 293-4°K 8=18408
 sodalites, photochromic 8=14120
 spin-lattice relax. for Kramers doublets, dynamical spin Hamiltonian and anisotropy 8=9413-14
 spin-lattice relaxation of paramagnetic ions in ionic crystals 8=9415
 spin-phonon coupling in conc. salts and effect on thermal cond. 8=18405
 spin relaxation theory, book 8=18446
 spin-spin relax. with strong coupling in strong external field 8=5520
 spin systems, irreversibility, free induction decay and spin diffusion 8=22894
 symmetrical lines contracted by exchange interaction, evaluation 8=6407
 taurine, paramagnetic susceptibility 8=5540
 tetrafluoroethylene-hexafluoropropylene copolymers, photo-induced and thermal radical conversions 8=1326
 tetrafluoroethylene-hexafluoropropylene copolymers, γ -irrad., e. s. r. of radicals formed 8=1325
 tetracyanoethylene, kinetics of free-radical formation 8=9686
 tetracyanoquinodimethane anion, aq. and alcoholic solns., e. s. r. spectra, rel. to water induced dimerization 8=8123
 tetramethylpyrazine rel. to triplet state struct., 77°K 8=22907
 thioxanthone anion radicals, e.p.r. and coupling consts. 8=4613
 thioxanthone sulfone anion radicals, e.p.r. and coupling consts. 8=4613
 thortveitite, (Y, Sc) Si_2O_7 8=9447
 TMPD-chloranil crysts. 8=8595
 triphenylene, negative ions in soln. 8=21170
 transition metal ion complex in soln., undergoing ligand exchange, e. s. r. spectra 8=4616
 traveling wave helices in e.s.r. spectrometers, characts. 8=3276
 trifluoromethylnitrobenzene radical anions in acetonitrile 8=4615
 triglycine fluoroberyllate, ferroelec., of Cu^{2+} ion 8=14105
 3,4,5-trimethoxyphenylglyoxal semidiones 8=12305
 triphenylene, triplet state and phosphoresc. 8=9655
 triplet mols. oriented in rigid-glass matrix 8=9448
 triradical in soln. 8=12350
 ultrasound absorpt. rel. to spin-lattice relax., quantum theory appl. 8=17487
 d,l-valine, hindered rotation study 8=4248
 xanthine oxidase, e. s. r. study of mechanism of action 8=14406
 Ag in irrad. metaphosphate glass 8=4990
 AgBr:Se, studies of $Se_2^{\cdot-}$ centres 8=13464
 AgCl: Ag^{2+} , Ag^{2+} detection by e. s. r. 8=14090
 AgCl:Se, studies of $Se_2^{\cdot-}$ centres 8=13464
 Al, conduction e. s. r., g-factors range and breakdown 8=5522
 Al silicates, irradiated 8=23044
 $Al_2O_3:Cr^{3+}$, electron and acoustical, in elec. field, profiles 8=18406
 $Al_2O_3:V^{3+}$, longit. relax. times by spin echo method 8=5541
 $AlSiO_4F_2$, e.p.r. of Fe^{3+} , hyperfine structure 8=2368
 $AlSiO_4F_2:Fe^{3+}$, fine structure 8=9412
 Au, small particles, conduction electrons 8=14093
 Ba(ClO_3) $_2 \cdot H_2O$ and Ba(ClO_3) $_2 \cdot D_2O$, irradiated with X-rays 8=18409
 Ba(ClO_3) $_2 \cdot H_2O$, X-irradiated, spectral changes in u.v. irradiation 8=18410
 BaF $_2:Mn^{2+}$, hyperfine coupling constants temp. dependence 8=18429

Paramagnetic resonance and relaxation—contd

BaTiO₃, cubic and tetragonal phases, of Eu²⁺ 8=14094
 BaTiO₃, reduced, e. s. r. interpret. at Ti³⁺ resonance 8=2375
 BaCl₂·2H₂O:Mn²⁺ 8=14115
 Ba₂Cu(H₂COO)₆·4H₂O:Cu²⁺, e.s.r. study 8=14103
 BaF₂: Eu²⁺, at 77-964°K 8=9424
 BrO, gas-phase double quantum transitions 8=12308
 BrO, gas-phase electron reson. 8=12345
 C, e. s. r., effect of halogens 8=18411
 C(CH₃)₃ in (CH₃)₂CCl₂, radical struct. obs. 8=12349
 C(CH₃)₂CCl in (CH₃)₂CCl₂, radical struct. obs. 8=12349
 CF₃I, photolysis in matrices at 4.2°K 8=14440
 CF₃OF, photolysis at low temp. 8=9727
 CF₃OOCF₃, photolysis at low temp. 8=9727
 C₂H₂ reaction with H- and O-atoms, e. s. r. investigation 8=2511
 C₂H₅ cyclic radicals, total splitting parameters 8=4243
 CH₂(CH₃)₂SiCl in (CH₃)₂SiCl₂, radical struct. obs. 8=12349
 CH₃CO₂⁻ trapped in γ-irrad. Na acetate, e. s. r. 8=4242
 (CH₃NH₂)₂CuCl₂ 8=14104
 CaCO₃, X-irrad., radical formation 8=5105
 CaF₂ containing Mn²⁺, OH⁻ and oxygen 8=2371
 CaF₂, ENDOR study of F centre 8=9417
 CaF₂: Cu²⁺ rel. to impurity-ion siting 8=9422
 CaF₂: Eu²⁺, at 77-964°K 8=9424
 CaF₂:Eu²⁺, stress induced quad. splitting using ENDOR tech. 8=22928
 CaF₂: Fe³⁺ 8=9437
 CaF₂, of Ho²⁺, stress effects 8=14128
 CaF₂:Mn²⁺, hyperfine coupling constants temp. dependence 8=18429
 CaF₂: Nd³⁺ cubic 8=5539
 CaF₂: N³⁺ 8=9437
 CaF₂: Ti³⁺ 8=9422
 CaF₂:Ti³⁺ and optical spectrum 8=14126
 CaF₂:Yb³⁺, rel. to polarization effects in cubic cryst. field 8=21800
 CaF₂: Yb³⁺ spin-lattice relax for Kramers doublets 8=9414
 2(Ca₂Mg₆Si₆O₃₂(OH)₂)·fMn²⁺, e.s.r. 8=18414
 CaMoO₄: Er³⁺, spectra at 4.2 and 10°K 8=18412
 CaO e.s.r. of F centres 8=13456
 CaSO₄, of Mn²⁺ allowed and forbidden transitions 8=14116
 CaWO₄:Ce, charge-compensated sites 8=9418
 CaWO₄:Nd³⁺, uniaxial pressure effect meas. 8=14121
 CaWO₄:Tb³⁺ spin-lattice relaxation time obs. 8=22914
 CaWO₄:Yb³⁺, charge compensation effect of Na⁺ on symmetry of Yb³⁺ by e. p. r. study 8=18413
 CaZrO₃:Mn²⁺, hyperfine transitions, obs. 8=14118
 CdCl₂:Ag, γ-irradiated, spectra 8=9419
 CdCl₂:Cu²⁺ layer, exchange coupled pairs spectrum 8=18416
 CdCl₂:Mn²⁺, study 8=22902
 CdCO₃:Co, rel. to antiferromag. props. 8=18372
 CdF₂:R, semiconducting, and i. r. studies 8=22901
 CdS, rel. to surface centres 8=18415
 CdS:Au, of photosensitive carriers 8=2362
 CdSe powder, surface investigation 8=8294
 CdS:Ti²⁺ single crystals 8=22900
 CdTe:Mn²⁺ cubic crystals, obs. 8=14119
 Ce³⁺ cpds in various solvents at 4.2°K rel. to mol. and phase props. 8=9436
 Ce ethylsulphate, spin-bath relaxation, Kapitza resistance 8=19700
 CeCl₃, relax. 1. 07°-4. 2°K 8=14097
 CeCl₃·7H₂O, spin-lattice and cross relaxation, 1. 1 to 4. 2°K 8=14096
 CeO₂: Er³⁺, at 3, 9. 4 and 36 Gc betw. 1. 5-77°K 8=5530
 ClO, gas-phase double quantum transitions 8=12308
 ClO, gas-phase electron reson. 8=12345
 CoCO₃, rel. to antiferromag. props. 8=18372
 Cr³⁺ trivalent ion hyperfine structure obs. 8=5553
 Cr(I) bistoluene complex, e. s. r. spectra 8=12311
 Cr³⁺ alum, weak fine struct. components 8=14098
 Cr³⁺ in alum lattice, relaxation behaviour 8=22903
 Cr(NH₃)₆NO²⁺ ion in soln., e. s. r. and N hyperfine splitting 8=1592
 CrO₂K₂, γ and n irradiated, e. s. r. 8=18417
 CrO₂(NH₄)₂, γ and n irradiated, e. s. r. 8=18417
 CsAl(SO₄)₂·12H₂O:Ti³⁺, single crystal obs. 8=18418
 CsCl: Mn²⁺, spin-Hamiltonian parameters 8=5534
 Cu in BeO 8=2366
 Cu(II) in ethylenediamine-water solns., e. p. r. 8=4621
 Cu(NH₃)₄SO₄·H₂O, exchange and "10/3 effect" 8=2365
 Cu(NH₃)₂Br₂·2H₂O 8=9423
 Cu²⁺ rhombic e. s. r. spectra, angular dependence of applied mag. field 8=5526
 CuCl₂·2H₂O, thermal detect., obs. 8=14100
 CuSO₄, anhydrous cryst. 8=2364
 CuSO₄·5H₂O, thermal detect., obs. 8=14100
 D₂O, at 77°K, γ-irrad., e. s. r. of OD radical 8=9439
 EuM₂, (M=Pt, Pd, Zn, Rh), mag. props. by Mossbauer e. p. r. 8=18334
 Fe-group ions, spectrum calcs. allowing for electron-phonon interaction 8=9410
 FeCl₂:Fe³⁺, Mn²⁺ at low temps. rel. to impurity nature and exchange coupling 8=14108

Paramagnetic resonance and relaxation—contd

α-FeOOH antiferro-paramag. ferromag. transition temps., obs. 8=22879
 Ga glasses 8=18420
 GaAs, of shallow Cd acceptors, at 77°K 8=18421
 Ga_{0.85}Fe_{0.15}O₃ magnetically ordered crystal in presence of external electric field 8=14087
 Ge, acoustic-donor spin resonance rel. to attenuation coeff. determ. 8=22096
 H, atomic, changes in spin states of up to 3 neighbouring protons 8=16227
 H atoms trapped in irrad. frozen aq. solns. 8=18423
 H₃C-CR₂R₂ radical in X-irradiated acetyl-(d, l)-alanine, effect of rotational quantization 8=22906
 HO₂ in Ar at 4. 2°K 8=18424
 H₂O at silica gels, proton-paramag. impurity interaction 8=12932
 H₂O₂-area addition compound, single crystal, γ-irradiated at 77°K, of O₂ 8=2373
 Ho ethyl sulphate, far-infrared high resolution spectroscopy with laser 8=14110
 InAs, e. s. r. at 4. 2°K 8=9429
 KAlF₄: Fe³⁺ 8=9426
 KCl:Ag, colour centres assoc. rel. to relax. process 8=8743
 KCl: Eu²⁺ 8=5529
 KCl:Mn²⁺, X-ray irradiated, superhyperfine structure 8=14117
 KCl:Pb²⁺, Tl⁺ and Ag⁺, resonance due to electrons in conduction band 8=14112
 KCl:RbCl crystals, of Q₁ colour centre 8=22905
 K₂Co(CN)₆:Fe³⁺, spin-spin interaction temp., 3 cm, 1. 8°K 8=18425
 K₂Cr(CN)₆, spin-phonon transition probabilities, meas. 8=5544
 K₂CuFe(CN)₆, tetragonal, and i. r. spectra, rel. to X-ray analysis 8=13265
 KH₂PO₄, ferroelec. domain switching by irradiation damage 8=18184
 KH₂PO₄, paraelectric, proton dynamics 8=9214
 KMgF₃:Ni²⁺, acoustic, propag. factor changes near reson. 8=22912
 K₂NiFe(CN)₆, cubic, and i. r. spectra, rel. to X-ray analysis 8=13265
 K₂SO₄:Mn²⁺, single cryst. 8=22910
 KTaO₃: Fe³⁺ 8=9425
 KTaO₃: Ni³⁺ 8=9425
 LaAlO₃:Cr³⁺, spectrum at room temp. 8=18426
 LaBr₃, e. s. r. spectra of Gd³⁺ rel. to temp. 8=2369
 LaCl₃, e. s. r. spectra of Gd³⁺ rel. to temp. 8=2369
 Li donors in Si, acoustic 8=9443
 Li solid and liquid alloys, conduction spin-lattice relax. time 8=9430
 LiAl(SiO₃)₂ (spodumene) natural crystals e. p. r. of Mn²⁺ 8=22908-9
 LiF, rel. to F-centre exchange interactions 8=17684
 LiF, ENDOR study of V_K centre rel. to lattice distortion 8=2009
 LiF, n-irrad., of Li, rel. to colloidal Li distrib. 8=9431
 LiF, n-irradiated, centre due to atomic H³ 8=18427
 LiF:Fe³⁺ system, crystal field distortions, e. s. r. study 8=13005
 LiH, rel. to F-centre exchange interactions 8=17684
 LiNbO₃:Cr³⁺, e. p. r. 8=18428
 LiNbO₃:Dy³⁺, e. p. r. 8=18428
 LiNbO₃:Er³⁺, e. p. r. 8=18428
 LiNbO₃:Nd³⁺, e. p. r. 8=18428
 LiNbO₃: Yb³⁺, Nd³⁺, Cr³⁺, and optical spectra 8=22999
 LiTaO₃: Yb³⁺, Nd³⁺, Cr³⁺, and optical spectra 8=22999
 MTiO₃, (M=Mn, Fe, Co and Ni), meas. 8=9398
 MgCl₂:Ag, γ-irradiated, spectra 8=9419
 Mg: Er, linewidth anisotropy 8=5531
 MgO: Co²⁺, spin-lattice relax. for Kramers doublets 8=9414
 MgO: Fe²⁺, microwave phonon interaction 8=9450
 MgO: Fe²⁺, ultrasonic, temp. depend. 8=2367
 MgO:Mn²⁺, angular depend. of intensities of "forbidden" transitions 8=18430
 MgO:Mn²⁺, stress induced quad. splitting using ENDOR tech. 8=22928
 MgO:Mn²⁺, transition probability temp. dependence 8=14113
 MgO: Ni²⁺, line investigation from spin-phonon interactions 8=5532
 MgO: Ni²⁺, microwave phonon interaction 8=9450
 Mn ferrite, simultaneous parallel pumping of electron and nuclear spin waves 8=14107
 MnCl₂·4H₂O, thermal detect., obs. 8=14100
 Mn(Mg)SO₄·4H₂O, of Mn²⁺, temp. dependence and spin-lattice relax. 8=9432
 MnSO₄·4H₂O, thermal detect., obs. 8=14100
 N, gaseous atoms, spin-relax. effects 8=12098
 ND₂Br, spin-lattice relax. and phase transitions 8=4713
 NH₄Br:Cu²⁺ 8=14102
 NH₄Cl: VO²⁺ 8=5542
 NH₄H₂PO₄, antiferroelectric, nuclear and electron studies 8=22671
 NO, gas-phase double quantum transitions 8=12308

Paramagnetic resonance and relaxation—contd

- NO molecule, electric field effect, obs. of transitions 8=16349
 NO₂ in irradi. KNO₃ at 4°K 8=5537
 NO₂ radical, interpretation 8=7621
 NaBrO₃, γ -irradi., asymmetric e. s. r. spectrum due to paramag. centres 8=2372
 NaCl:Ag, colour centres assoc., rel. to relax. process 8=8743
 NaCl:Mn²⁺, hyperfine interaction, influence of lattice defects 8=18431
 NaNO₃, X-irradi., radical formation 8=5105
 NaSbF₆, X-irradi. cryst. 8=5538
 Nd ethylsulphate, for determ. of crystal field parameters 8=18445
 Nd ethyl sulphate, saturation of Faraday effect and spin lattice relax. 8=14278
 Nd³⁺ cpds in various solvents at 4.2°K rel. to mol. and phase props. 8=9436
 O atom reaction with SO₂, e. s. r. study 8=5715
 O₂(¹ Δ) collisional-radiative reaction 8=12220
 O + D₂ → OD + D reaction, e. s. r. detect. 8=14375
 OH reaction with oximes, free radical inter-mediate 8=14394
 O¹⁶O¹⁸ molecule, e. p. r. spectrum 8=12309
 O¹⁸-O¹⁷, O¹⁷-O¹⁸, O¹⁸-O¹⁸ 8=4222-3
 PF₄, electron spin resonance spectrum and second-order hyperfine effects 8=4224
 P₂O₅, glassy and cryst., γ -irradi. 8=22913
 Pr(NO₃)₃.6H₂O:Gd³⁺ spectrum, obs. 8=14109
 RbMnF₃, simultaneous parallel pumping of electron and nuclear spin waves 8=14107
 Ru, in solid Ar matrix, X-band and optical absorpt. spectra 8=18558
 SH, gas-phase electron reson. 8=12345
 SO, gas-phase double quantum transitions 8=12308
 SO(¹ Δ), gas-phase electron reson. 8=12345
 SSe⁻ in alkali iodide crystals. 8=14123
 S³³O¹⁸, gas phase 8=12353
 Se₂⁻ in alkali iodide crystals. 8=14123
 Si, acoustic-donor spin resonance rel. to attenuation coeff. determ. 8=22096
 Si:P, e-irradiated, spin-lattice relax. rel. to defect production 8=18434
 SiC, electron states study 8=9122
 Si²⁹Cl₃, hyperfine coupling const. rel. to struct., obs. 8=12349
 SmCl₃.6H₂O: Gd³⁺ single crystal 8=9427
 Sm(NO₃)₃.6H₂O:Gd³⁺ 8=18345
 SrCl₂ crystals., reaction intermediate with F₂ 8=14124
 SrF₂, F-centres obs. 8=2014
 SrF₂: Eu²⁺, at 77-964°K 8=9424
 SrF₂: V²⁺ 8=9446
 SrMoO₄: Er³⁺, spectra at 4.2 and 10°K 8=18412
 SrTiO₃, of Fe³⁺, axial spectrum, study at mm. wavelengths 8=14106
 SrTiO₃: Ti³⁺, electronic structure 8=9445
 TeO₄K₂, γ -irradi., e. s. r. spectra 8=9444
 TeO₄Na₂, γ -irradi., e. s. r. spectra 8=9444
 ThO₂, of Yb³⁺, stress effects 8=14128
 Ti, 4-valent, cpds. with OH and O₂H radicals, e. s. r. 8=2522
 TiCl₃ + H₂O₂ reaction 8=2521
 Ti₂O₃, e. s. r. at 77°K rel. to semiconductor-metal transition 8=14125
 TmN, excited state, crystal field, exchange effects 8=2376
 UF₆M (M = Li, Na, Cs, K, NH₄, Rb, Ag, Tl), absorption 8=14127
 UO₂, spin-lattice interaction, ground-state and spin-wave excitations 8=18437
 V(CO)₆, e. s. r. spectrum at liq. He temps. 8=18438
 V(O)₂ bisaromatic complexes, e. s. r. spectra 8=12311
 V₂O₅:Cr, spectral line explanations 8=9421
 V₂O₅:Mn crystals., 77°K 8=14144
 Y(Al, Cr)₃(BO₃)₃, of Cr³⁺ at room temp. 8=18439
 YFe garnet:CuO, and preparation 8=21968
 YGa garnet:Ru³⁺ and YAl garnet:Ru³⁺, data 8=18440
 YVO₄: Gd³⁺ 8=9428
 Zn 2,2-liquoline, oriented in rigid-glass matrix 8=9448
 Zn(NH₄)₂(SO₄)₂.6H₂O: Co²⁺ forbidden hyperfine spectra 8=9420
 ZnS:Cr⁺, photo-induced, decay obs. 77°-325°K 8=18441
 ZnTe: Cr⁺, photo-excited paramag. reson. 8=5525
 ZnTe: Pb³⁺, photo-induced res. at 77°K 8=9440
 ZnWO₄: (Cr³⁺, Li⁺), electric broadening of lines 8=18442
 ZnWO₄:Cr³⁺, theory 8=14085
 ZnWO₄: Cu²⁺, 8=5527
 ZnWO₄: Mn²⁺ rel. to conc. and temp. 8=5535

measurement

- ang. momentum method at low fields 8=14122
 computer of average transients, for rapidly changing spectra 8=6405
 cryostats, room temp. to 4.2°K 8=10793
 instrumentation, 100 kHz amplifiers, signal and power 8=6406
 positioning of samples in microwave cavities at low temp. 8=5517
 sensitivity, dependence on cavity resonator geometry 8=387
 spin-lattice relax. temp., meas. by optical Faraday rot. 8=22895

Paramagnetic resonance and relaxation — contd
measurement — contd

- thermal-noise and voltage decrease across tuned circuit as e. p. r. meas. method 8=19906
 by thermocouple for substs. with broad absorpt. lines, obs. 8=1590
 ultrasonic, continuous wave microwave spectrometer 8=19905

Paramagnetism

- See also Magnetic properties of substances/paramagnetic.
 Brillouin function calc. for J=1/2 to 7/2 and J=∞ 8=9328
 exchange broadening of mag. n-scatt. cross-sections, temp. depend. 8=13968
 Heisenberg paramagnets, u.s. attenuation, NMR and ESR linewidths asymptotic behaviours 8=22757
 Ising system, neutron scattering 8=9297
 neutron scattering theory 8=9296
 Pauli susceptibility, effect of spin-flip processes 8=13969
 spin-phonon coupling and Schottky anomaly in cerium ethyl sulphate 8=8636
 in superconductors, high-field, effect on upper critical fields 8=17950
 thermodynamics of cyclic processes in system of particles with spin $\frac{1}{2}$ 8=17506

Parametric amplifiers. See Amplifiers.

Parent. See Nucleus; Radioactivity.

Parity

- See also under individual particles, e.g. Mesons/spin and parity.
 baryons, quark model wave functions 8=3687
 C violation rel. to existence of Λ , Li⁶ 8=11793
 C-violating e pair photoprod. and q. e. d. 8=20390
 chiral-invariant π -N Lagrange functions in field theory 8=6614
 CP conservation and violation in same interaction, hadronic decay 8=6827
 CP conservation in K₁⁰ → $\pi^+\pi^-\pi^0$ 8=20470
 CP invariance in K₁⁰ decay at 10.7 GeV/c 8=6882
 CP nonconservation and K₁⁰ decay 8=20475
 CP violation and n electric dipole moment 8=11607
 CP violation by interference effects in K⁰ decay 8=3653
 CP violation model used to calc. n elec. dipole moment 8=6828
 CPT invariance test in pp scatt. 8=3711
 CPT, nondynamical test, specific reactions 8=20335
 CPT=Θ transformation of particle states and internal symms. 8=11370
 PCT transformation rel. to scatt. amplitude expansion 8=15696
 TCP-invariance in K⁰ → 2 π decay, test 8=15792
 TCP, time reversal in K → 3 π 8=20471
 ΔS = ΔQ violation in Σ⁺ decay 8=20575
 doubling avoided local field theory with infinite Lorentz group representation 8=6609
 fermion-antifermion system, bound state solns. with wrong parity 8=3603
 G-parity rel. to relationship between $\pi^0 \rightarrow 2\gamma$, $\pi^+ + e^- + \nu + \gamma$ 8=11500
 hyperon decay, nonleptonic, P violating models 8=11629
 hyperon decay, quark model violation explained 8=3726
 I = 0 enhancement of $\pi^+\pi^-p \rightarrow \pi^+\pi^0n$, 3.1 36¹ GeV/c obs. 8=15773
 K decay, total reflection TCP, or time reflection T 8=790
 K → $\pi\pi$, CP violation, phenomenological analysis 8=3652
 K₂⁰ → $\pi^+\pi^-$, CP violation, energy depend. on branching ratio 8=11569
 pseudoscalar-vector meson interactions, higher symms. 8=11493
 PT, nondynamical test, specific reactions 8=20335
 Regge pole model for vector meson prod. 8=6902
 symm. breakdown, spontaneous, correspondence 8=3425
 symm. postulate of quantum mechanics, proof without spatial connectivity in ID 8=6602
 symmetry problems rel. to SU(2) ⊗ SU(2) 8=653
 SU(3) invariance violated in KN scatt. 8=6891
 SU(3) and O(4), connection rel. to symms. 8=11371
 T invariance and $\pi\pi$ scatt. length 8=20465
 T invariance test in K decay 8=20476
 T invariance tested in Mg²⁵ + p ↔ Mg²⁴ + d 8=11924
 T violation effect on nuclear reactions, theory 8=11851
 T violation and invariance in K → 2 $\pi\gamma$, matrix element calc. 8=15793
 2-body reactions by Pomeranchukon exchange, spin parity rule 8=20317

Particle accelerators

- See also Ion beams.
 with acceleration focusing, phase oscs. rel. to transverse stability 8=11337
 activation, timing and control system 8=11799
 beam emittance in duoplasmatron source linked to single gap accelerator 8=20229
 beam energy meas. by reaction on scatt. spectrum from multi-target 8=6691
 beam h.f. structure analyser, impulse operation 8=11332
 beam loss detector using ionization chamber 8=20227
 beam pulse shape meas. 8=628
 beams, time analysis coincidence circuit 8=622

Particle accelerators—contd

- book, general discussion 8=11353
 bunched ion beams, O₂ and H 8=10916
 coaxial cable delay lines, delay time meas.
 method 8=6395
 dense jet, to thermonuclear speeds by hypervelocity
 impact 8=16137
 double-gap optimum focusing, theory 8=15651
 dynamitron, use of plexiglass and cinch rod method of
 tube support 8=20233
 electromagnets, construction 8=643
 electron loading in tubes, suppression 8=15653
 electron, 1 MeV for e microscope 8=15319
 e, prod. of polarized beam through magnetic bottle 8=15304
 electron, Tomsk Polytechnic design and
 performance 8=15667
 electrostatic, principles and appl. 8=6689
 for e spectrometer, $\pi\sqrt{2}$ 8=20387
 exciting circuit of r.f. amplifier driving the
 cavities 8=11334
 n generator with turbomolecular pumping 8=15851
 high-energy neutral particles, source 8=11333
 high energy particle separation by a progressive e.m.
 wave 8=15649
 instrumentation 8=20231
 ion, highly stripped heavy, HIPAC type 8=19797
 ions, multiple acceleration in electric field by charge
 exchange 8=630
 magnet technology, conference Oxford England
 (1967) 8=15259
 microbeam collimator 8=3487
 microtron, race-track, orbit stabilization 8=6708
 multiple accel. system, for electrodynamic particle
 separator 8=11336
 neutron counters suitable for radiation monitoring 8=15854
 neutron generator, acceleration tube, properties
 of 8=3714
 no-load current requirements 8=20232
 Penning ion source, molecular ions explained 8=11338
 positive ion, 4 MV, reduction of electron loading and X-ray
 intensity 8=15650
 production of new super-elements, design
 limitations 8=15913
 progress in nuclear techniques and instrumentation,
 book II 8=15648
 pulsed beam, zero-crossing discriminator for time-of-
 arrival 8=6675
 pulsed ion beams, current convertors, general
 discussion 8=629
 pulsed-time-to-pulse height converter 8=20210
 pumping tube, differential 8=15654
 radioactive dust and aerosol in neighbourhood 8=6690
 storage dev., obs. of coherent radial-phase oscs. for
 opposed beams 8=11335
 synchrophasotron, spark chambers with magneto-
 strictive readout 8=3486
 tandem, Lamb-shift polarized ion source 8=6694
- linear**
 beam injection with multiple pulse width and intensity
 capability 8=15658
 bremsstrahlung beam, reproducibility, pneumatic
 transfer system 8=6695
 of charge carriers, in alternating crossed e.m.
 fields 8=318
 Cockcroft-Walton, low-energy, Rutherford scattering
 meas. 8=7191
 column, high gradient, with good optics 8=15657
 current pulse stability, effect of microwaves 8=6697
 design advances, sources and columns 8=15661
 detector, dead time correction method 8=3489
 electron, radial beam shaping 8=15655
 e, radial motion 8=633
 electron gun design with radiantly heated or e bombarded
 cathode, Stanford 8=15659
 h.f. quadrupole focusing, proton beam limitations 8=632
 high voltage technology, new developments 8=15652
 iris cavity, transient response 8=6696
 klystrons for Stanford center 8=3488
 magnetic slit for momentum definition and beam
 separation 8=6700
 multi-section electron, asymptotic theory of beam
 break-up 8=20230
 organic scintillators n efficiency obs. 8=6961
 proton, redesign of injector 8=15656
 p beam, energy resolving apparatus 8=840
 for radiotherapy, safety aspects 8=5985
 review 8=631
 Sasbatchewan laboratory, electron-scattering
 facility 8=7171
 standing wave tanks, coupled resonator model 8=6698
 superconductor appl., 3 cm. resonator 8=6362
 superconducting, design, advantages and costs 8=17984
 tandem, d. c., techniques for use with elements of high
 atomic number 8=15660
 van de Graaff, development and application 8=11341
 van de Graaff, energy resoln. improvement 8=20234
 Van de Graaff improved He ion current using K vapour
 exchange 8=6693

Particle accelerators—contd

- linear—contd**
 van de Graaff, pulsed, beam energy spread 8=20228
 van de Graaff, 2 MeV, meas. and control of beam
 energy 8=11340
 Van de Graaff, nuclear reaction excitation meas.
 method 8=3897
 Van de Graaff, polarized p and d source 8=6692
 Van de Graaff, 3 MV, square and sine wave modulation of
 beam 8=19713
 van de Graaff type, undergraduate construction and
 operation 8=11339
- orbital**
 X-ray spectra in 2-6 MeV range 8=6699
 acceleration by travelling wave, influence of load
 current 8=3493
 beams, longitudinal stability criteria 8=3492
 betatron, low pulse rate or single radiation pulses 8=20240
 betatron, 35 MeV, medical, electron beam instability and
 isodose asymmetry 8=6710
 betatron resonances in electron accels, app. and method
 of study 8=11346
 betatron, resonant radial oscill. of electrons at
 5 and 15 MeV 8=20239
 CERN p synchrotron neutrino programme 8=3587
 coherent oscills., stability criterion 8=638
 coherent transverse beam stabilization 8=634
 colliding particle beams 8=639
 depolarization, resonance of Dirac particles 8=20236
 e beam between parallel metallic surfaces, bunching effect
 calc. in storage rings 8=15670
 e ring phasotron, description 8=3498
 electron storage ring, thin and superthin targets,
 calc. 8=6711
 e synchrotron, 4 GeV, description 8=3497
 electron synchrotron, NINA (National Institute Northern
 Accelerator), 4 GeV, review 8=642
 electrons, 30 MeV microtron resonator 8=3496
 IKO synchrocyclotron, r.f. system for rapid p-d
 switching 8=637
 magnetic field distortion by parasitic inter-lamination
 currents 8=635
 microtron, bunched electron beam injection 8=3494
 microtron, method of increasing beam current 8=6706
 microtron, racetrack, design, 400-600 MeV 8=6707
 microtron, vertical focusing props. of mag.
 laminas 8=3495
 NINA 4 GeV electron accelerator 8=11345
 phase space volume determination 8=15666
 prop. counter system to meas. μ^+ rate capture in
 $p + \mu^- \rightarrow n + \nu_\mu$ 8=3457
 plasma betatron, guide field construction 8=16563
 p beam, high intensity production 8=839
 p phasotron r.f. system model, accel. voltage amplitude
 programming 8=20241
 protons, low energy beam, apparatus for control and
 exit in air 8=6936
 r.f. separated beam at the AGS 8=3491
 review of improvements 8=15662
 ring resonator system excited by unreflected
 wave 8=6705
 sand as a side shield 8=3490
 6 GeV electron accelerator at Yerevan 8=11344
 storage-ring, bypass design 8=20245
 storage rings, Orsay 8=641
 storage rings, vector mesons and photoprod. 8=15669
 synchrotron accel. system design at Tomsk Polytechnic
 Institute 8=11343
 synchrotron and betatron oscills., damping 8=640
 synchrotron, damping of betatron oscills. 8=20244
 synchrotron, positron storage and production of colliding
 electron-positron beams 8=20243
 synchrotron, radial betatron oscill. freq. meas. 8=20235
 synchrotron radiation, review 8=15664
 synchrotron, guide-field arrangements for
 modifications 8=636
 synchrotron, max. polarisation of radiation 8=11456
 synchrotron, teaching misconceptions 8=7027
 synchrotron, 300 GeV, design and realization 8=15665
 synchrotron, 300 GeV, research programme 8=15666
 synchrotrons, double-period waveguide delay
 system 8=6702
 synchrotrons waveguide, rod accelerating systems,
 electrodynamics of 8=6712
 synchrotrons, waveguide wall deform. effects 8=15418
- orbital, cyclotrons**
 beam modulating system for pulsed beam 8=6713
 beam structure analysing circuit 8=617
 computers, on-line, application 8=6704
 construction and use, conference (Krakow, 1966) 8=6701
 detuning, theoretical and numerical investigation
 of diagnostic procedures 8=20237
 electron synchrotron, magnetic guide field 8=6709
 ion injection into the centre 8=11342
 n source using d-d reaction 8=6703
 p beam current, increase by additional electrostatic
 focussing 8=3499
 p, isochronous, separated turn, for prod. 200-1000 MeV
 current 8=20242

orbital, cyclotrons—contd

- magnetic field meas., ADI method 8=6337
 multi- ω -type, design rel. to users requirements 8=20238
 synchrocyclotron, CERN-MeV, 1250 kW thyristor convertor plant as power source 8=15663
 synchrocyclotron, proton beam depolarization 8=3710
 teaching misconceptions 8=7027
 use of mag. field to create electric drive for meas. device 8=11347
 He₄⁺ ions, accel., on third harmonic of fundamental freq. 8=6714

Particle detectors

- See also Bubble chambers; Cloud chambers; Counters; Ionization chambers; Nuclear track emulsions; Particle track visualization.
 activation detectors for fission-n spectra, development and excitation meas. 8=11970
 activation, for dosimetry meas. with high energy p 8=11603
 α counting efficiency, depend. on energy, source thickness and instrument constant 8=20591
 angular correl., automatic equipment 8=602
 annual review of nuclear science, book XV 8=15628
 ($\beta^+\gamma^+$) coincidence method, investig. of positron emitting nuclides 8=20743
 channel electron multiplier 8=11312
 coincidence resolution improvement by energy-time correl. 8=6649
 dead time correction, rel. to linear accelerators 8=3489
 developments and applications, review 8=3454
 dielectric for charge determ. of heavy cosmic ray particles 8=20598
 dielectric plastic track using rate of chemical etching 8=11331
 discrimination, ΔE , E telescope, improvements 8=6634
 high temp., survey of solid state materials 8=6652
 ionization calorimeter, simulation of operation 8=15635
 mean-rate analysis for multiparameter data, PDP8 analyser 8=20182
 n-charged particle coincidences 8=3722
 neutron, interaction in water 8=6962
 nuclear spectroscopy, small computer for time-saving analysis 8=6636
 photoelectrons, single detection 8=11463
 position determ., theory 8=6637
 position sensitive made by ion implantation in Si 8=20196
 pulsed ion beams, current converters, general discussion 8=629
 resonance detectors for Mössbauer expts. 8=20673
 review 8=603
 scattering chamber of sliding cylinder type 8=7157
 semiconductor, simple lightspot scanner application 8=3464
 source-detector solid angle, integral calc. 8=20184
 spinner using the sensitivity of centrifugically stressed liquid to radiation 8=20202
 threshold, data interpretation using Taylor developed polynomial method 8=3456
 Ar liquid, activation, for Cl^{40m} obs. 8=20203
 Li-drifted Si, photoresponse with simple light spot scanner 8=3464
 Ne²⁰(d, α)F¹⁸, high resolution det. 8=6663
 Ne²⁰(d, p)Ne²¹, high resolution det. 8=6663
 Si, B and P implantations, X-Y sensitive 8=3466

Particle focusing. See Particle optics.

Particle optics

See also Electron optics; Ion optics.

- beam, nuclear, time analysis circuits 8=622
 beam spreading by space charge 8=6295
 beam waveguides and cavities, gaussian brackets 8=321
 beams, constant diameter, focussed by uniform mag. field, perturbations 8=15278
 charged ellipsoid, potentials 8=3186
 collimator, microbeam, restricts charged particles for a few microns in radial extent 8=3487
 depolarization of Dirac particles in high energy synchrotron 8=20236
 electrode system design, soln. of Cauchy problem 8=15275
 electron beams, magnetically deflected, coma-dominated aberration 8=333
 electrostatic lens, cylindrical three electrode, field analysis 8=19778
 electrostatic lenses, cylindrical, telescopic 8=3205
 elliptical beam spread due to space charge 8=19779
 elliptical beam of finite immitance, spread due to space charge 8=19780
 linear accelerators, focusing 8=632
 magnetic analyzer with homogeneous field 8=11294
 mag. field, exponentially time dependent, directionally constant 8=15273
 magnetic field with gradient, oblique incidence 8=23343
 magnetic field meas. at grid of spectrometer, ADI method 8=6337
 magnetic prism, optical axis and correcting profile determ. 8=12114
 in magnetic spectrometers, appl. of Fermat's princ. 8=6629
 microanalysers appls. 8=14464
 modulated beams, dynamic stabilization by negative mass effect 8=3187

Particle optics—contd

- motion in time-dependent e. m. fields 8=15274
 plasma mirror trap, individual lifetimes obs. 8=16558
 polarized particles, depolarizing effect of magnetic focusing 8=10888
 p beam, energy resolution from Van de Graff accelerator 8=840
 proton beam in synchrocyclotron, depolarization 8=3710
 quadrupole lens aberrations, necessary coeffs. 8=3189
 quadrupole magnet systems, misalignment tolerances 8=15277
 quadrupole multiplet, angular acceptance 8=19775
 quadrupole multiplet, angular acceptance calc. 8=6296
 quadrupole multiplet series, aberrations 8=3185
 quadrupole multiplet, theory 8=19774
 radial focusing with transaxial electrostatic fields 8=15276
 scattered particle beams intensity fluctuations and corrls. meas. 8=19776
 scattering in block of matter 8=3190
 scattering at edge of plate 8=19777
 scattering by plane 8=3188
 selectors, useful current calc. 8=19773
 spiral mag. field, calc. 8=23689
 synchrocyclotrons, improved focusing techniques 8=15662
 Al crystals for neutron monochromating 8=854
 Cu crystals for neutron monochromating 8=854
 PbGe crystals for neutron monochromating 8=854

Particle range

- atoms, in solids, and energy loss 8=13469
 compound nucleus, analysis of angular and range distrib. 8=1032
 Coulomb energy and ang. correl. method 8=8756
 crystals, protons, fast, channeling and blocking 8=2016
 electrons, in Be-Au 2-layer target 8=3203
 fission fragment range-energy meas. 8=20860
 heavy, charged, in thin absorbers, energy loss fluctuations 8=13471
 protons, 0.8 to 2.0 MeV, in Si and Ge 8=13468
 protons stopping power on gold 8=13478
 Ar ions, 500 KeV to 2 MeV, in Be and C 8=13481
 Cu, W ions, 0.8 MeV, calc. using Coulomb excitation and ang. correl. 8=8756
 Dy ions, range distribution, production in compound nucleus reactions 8=1103
 K₂ ions, 40-1000 KeV, in amorphous Al₂O₃ 8=13476
 Kr ions, 40-1000 KeV, in amorphous Al₂O₃ 8=13476
 Kr ions, 500 KeV to 2 MeV, in Be, C and Al 8=13481
 M (M = V⁵¹, Zr⁹⁰, Au¹⁹⁷, Ni⁵⁸, Fe⁵⁴), ion recoil range 8=13489
 Na ions, 40-1000 KeV, in amorphous Al₂O₃ 8=13476
 Si, stopping power for p, d, t, α 8=8778
 Th²³², range distrib., production in compound nucleus reactions 8=1103
 Xe ions, 40-1000 KeV, in amorphous Al₂O₃ 8=13476
 Xe ions, 500 KeV to 2 MeV, in Be, C and Al 8=13481

Particle size

- See also Surface measurement.
 aerosols distribution determ. 8=4635
 aerosol, flame ionization-pulse analyser 8=16908
 analysis, methods survey 8=10477
 amine oxide micelles, and struct. 8=8158
 Armco iron, grain size rel. to lower stress yield 8=17798
 atmosphere, spectrum, calc., by small-angle scatt. pattern 8=23251
 rel. to capillary wave amplitude in ultrasonic atomizer 8=21734
 carbon blacks prod. from coals, X-ray study of structure 8=8351
 coagulation, by Brownian motion, distrib. 8=8148
 comparator, distrib., photograph-projection nonautomatic 8=5
 grain size distrib. in 1 μ m range, by X-ray diffr. 8=13151
 latex high-speed beam 8=12952
 lattice spacing dependence 8=17301
 mica, effect on lattice spacing 8=17301
 on-line analyzer 8=13045
 optical analyser for 350 μ m diameters 8=14915
 packed particles, degree of mixedness and bulk density 8=17017
 polymer latexes, size distrib. from light scatt. 8=16900
 powder grains, X-ray fluoresc. spectroscopy determ. 8=21830
 powders, ultrasonic dispersal method of meas. 8=13046
 powders, X-ray absorpt. determ. 8=17018
 precipitation particles, and charges, in free atm., meas. 8=23279
 spherulites in polymers, via polarized light scatt., effect of polydispersity 8=8358
 sprays, determ. from fluorescent photography using Q-switched laser light source 8=4636
 superconductor, granular, size effect 8=17955
 suspensions, from relax. of transient elec. birefringence 8=16899
 thoria sols, meas. by scatt. 8=12958
 tin, effect on melting point 8=16925
 wustite, and Mg doping dependence of Seebeck coeff. rel. to p to n transition 8=5387

Particle size—contd

- Al nuclei on MoS₂ substrate, effect on elastic strain 8=8823
- Au films, rel. to recrystallization obs. in electron microscope 8=8314
- CoFe₂O₄, coprecipitated, distribution 8=4843
- Dy₂O₃ dispersion in UO₂, behaviour in steep temp. grad. 8=4694
- Eu₂O₃ dispersion in UO₂, behaviour in steep temp. grad. 8=4694
- Fe, limits for magnetostatic accretion in solar system 8=23632
- Fe-whiskers, rel. to nucleation mag. field strength investigations 8=5467
- Fe-12at. %Ni alloy, finely dispersed system, effect on phase comp. 8=17280
- H₂ solid-liquid mixture obs. 8=19067
- H₂SO₄ aerosols, distrib., by light scatt. 8=12951
- Li-silicate glass, of second phase particles, distrib. 8=21847
- Mg, cold-worked, and strain determ. by variance method 8=1761
- MgF₂, sintered, effect of additives on density and grain size 8=17026
- MnFe₂O₄, effect on mag. props. 8=14022
- NaCl, elec. conductivity depend., obs. 8=17913
- NaCl, rel. to fracture strength 8=22382
- Nb foil, effects on dislocation density and flow stress 8=4980
- Ni:Al₂O₃ sintered, compressive strength grain size dependence 8=2048
- NiO, Co⁵⁷-doped, effect on Mössbauer spectra rel. to magnetization state temp. dependence 8=4680
- Sm₂O₃ dispersion in UO₂, behaviour in steep temp. grad. 8=4694
- in UO₂ powders, and shape, rel. to sintering props. 8=21834
- Y vanadate phosphors, rel. to preparation 8=13048

Particle spectrometers

- See also Alpha-ray spectrometers, etc.
- beam structure analysing circuit 8=617
- clipping problems, circuit for solution 8=6671
- cosmic rays, primary, nuclear charge obs. 8=15878
- current-pulse use with semiconductor detectors 8=610
- electrostatic analyser with high energy resolution in (p, γ) reactions on Na²³ and Al²⁷ 8=958
- energy meas. in track detectors by hole diameter 8=11293
- long magnetic lens, alternating direction implicit method of magnetic field meas. 8=6337
- magnetic analyzer with homogeneous field 8=11294
- magnetic, appl. of Fermat's princ. to trajectories 8=6629
- magnetic, 60° double focusing, design construction and performance 8=6627
- magnetic spectrographs, semi-popular review 8=604
- magnetic spectrograph, split-pole, ion optics 8=3228
- nuclear beam, high energy, high frequency, impulse operation 8=11332
- photoproduction in GeV range 8=6776
- preamplifier allowing use of 10-stage photo-multiplier 8=3474
- pulse generator and rectifier circuit 8=15632
- pulse-height analyzer for charged-particle spectroscopy on lunar surface 8=20214
- scintillation, system for instantaneous plotting of output 8=15636
- semiconductor oxygen conc., activation spectrometry 8=18083
- for solar X-ray spectrum, proportional counters 8=23709
- spectrograph, focus, effect of fringing field 8=10920
- Ge 2 detector telescope for separation of p and heavier particles 8=6654
- Ge(Li) detectors, fabrication and appl. 8=15630
- NaI crystal scintillation, bremsstrahlung meas. 8=3582

Particle track visualization

- See also Bubble chambers; Cloud chambers; Luminescence chambers; Nuclear track emulsions; Spark chambers.
- analogue computer method 8=6680
- bubble chambers, appl. of holography 8=6567
- computer controlled precision film scanner 8=3481
- dielectric plastic particle detector using rate of chemical etching 8=11331
- emulsion chamber for about 10¹³eV particle interactions 8=627
- film scanner cathode ray, computer directed 8=3482
- plastic detectors for light nuclei 8=20220
- plastics, cosmic ray nuclei 8=3741
- solid-state detectors for reactor expts. 8=12021
- streamer chambers, discharge mechanisms obs. 8=11326
- streamer tracks, ang. depend. of brightness 8=20226
- telecentric system 8=3349
- AgCl crystals, α-track decoration technique 8=15644
- As ions in olivine and hypersthene crystals. 8=11325
- I ions in olivine and hypersthene crystals. 8=11325

Particle tracks

- See also Particle range.
- bubble chamber exposures, electronic co-ordinate measurements 8=482

Particle tracks—contd

- fission fragments, excitation of N₂ gas along entire track 8=7531
- fission track densities, etched in int. and ext. surfaces, comparison after n irradi. 8=20852
- "hammer"; having no associated β particle 8=20221
- latent image in nuclear emulsions, pulsed-field erasure 8=11330
- in meteorites, cosmic-ray intensity obs. 8=20599
- in meteorites, heavy cosmic-rays, identification 8=20596
- mica, caused by e showers 8=22246
- momentum and direction, multiple scatt. effect 8=6683
- photographs in track chambers, calc. of kinematic parameters 8=11323
- spark chamber, multiwire, magnetostructure delay line 8=625
- spark chamber, wire, cylindrical, strategy for recognizing straight tracks 8=11329
- three-dimensional pictures, accuracy rel. to camera characts. 8=11324
- AgCl crystals, recording technique 8=15644

Particle velocity analysis

- See also Alpha-ray spectrometers; Beta-ray spectrometers; Ion velocity; Mass spectrometers; Particle range.
- atomic and mol. beams, time-of-flight method 8=16379
- cylindrical mirrors and spherical deflectors, comparison 8=15309
- fission fragment meas. using sandwiched acetylcelluloid foils 8=20860
- in single crystal, energy-loss distrib. calc. 8=20186
- spherical deflectors and cylindrical mirrors, comparison 8=15309
- rocket propulsion, laser-Doppler meas. 8=23457
- time-of-flight obs., large-area isochronous scintillation counters 8=15631

Particles. See Elementary particles; Particle range;

Scattering, particles; and under individual particles, e.g. Protons and antiprotons.

Paschen-Back effect. See Spectra.

Patterson diagrams. See X-ray crystallography/calculation methods.

Peierls-Nabarro force. See Crystal imperfections/dislocations; Internal friction.

Peltier effect. See Thermoelectricity.

Pendellösung fringes. See X-ray crystallography.

Pendulums

- bifilar, dynamics 8=6043
- inverted, stabilized, small oscillations 8=10527
- period meas., electronic system, ± 600 ns. 8=10481
- period meas. using phototransistor output triggering oscilloscope 8=10479
- properties of conjugate axes 8=2914
- reed, apparatus for internal friction meas. 8=13495
- spring suspensions 8=32
- stability with oscillating suspension 8=14944
- temp. control, electronic system 8=10480
- torsion, for automatic elastic moduli meas. 8=5006
- torsion, internal friction meas. in alloys 8=8839
- torsional for plastic materials under tensile strain 8=8880
- truncated ring, equivalence 8=10528
- vibrating solid friction, high frequency behaviour 8=3023

Periodic system

- See also Elements.
- atomic props., analysis 8=20918
- electronshell filling order, pressure effects 8=7364

Permalloy. See Iron alloys; Nickel alloys.

Permeability, magnetic. See magnetic properties of substances; Magnetization process.

Permeability, mechanical

- See also Diffusion in solids.
- inert gases through rubber membrane 8=1487
- liquids, through polyethylene membrane temp. effects 8=1508
- transpiration of propane and ethane 8=12662
- Fe-Mn austenite, H, effect of plastic deform. and annealing 8=17573
- Ni, kinetics of H₂ permeation 8=8682
- W, of H₂ and O₂, rates pressure, thickness and temp. dependence 8=4958

Permittivity. See Dielectric properties of substances.

Perturbation theory. See Field theory, quantum; Quantum theory.

Phase-contrast microscopy. See Microscopy.

Phase diagrams. See Phase equilibrium; Phase transformations.

Phase equilibrium

- See also Solubility; Solutions.
- acetic acid-water system, vapour-liquid 8=12974
- alkali metal-NH₃ solns., model 8=12808
- n-alkane derivative isomers with OH groups and n-heptane mixtures 8=16949
- alloys, finely dispersed two-phase, recrystn. behaviour 8=8395
- austenite, alloyed, C activity at 1000°C 8=17008
- benzene-cyclohexane, vapour-liquid equilibrium data 8=4653
- benzene-H₂O system, pressure effect 8=8180
- benzene-isobutanol, vapour-liquid equilib. data 8=4653

Phase equilibrium—contd

binary systems, conc., central X-ray diffusion, theory 8=13197
 coexistence curve for liquid and gas near critical point 8=21769
 cooperative phenomena in triangular lattice 8=89
 crystals of higher order, relation to other super-phases 8=8363
 crystal surface curvature, thermodynamic anal. 8=8377
 cyclohexane-isobutanol, vapour-liquid equilib. data 8=4653
 diphenyl- α , α' -dipyridyl system, constitution diagram 8=4725
 ethylene-chlorhydrine-water system, pressure effects 8=16938
 form of finite crystals, surface energy 8=21866
 garnet-pyroxene in MgSiO_3 - CaSiO_3 - Al_2O_3 , press. depend. obs. 8=1676
 ice phases, selective nucleation using different org. nucleators 8=4805
 ice, superheated, metastable, in liq.-water inclusions under high neg. pressure 8=1609
 ice/water interface, electrostatic potentials 8=18723
 iron alloys saturated with oxides, liquid, first-order interactions rel. to oxide solubilities 8=16797
 iron oxide scale, hematite phase physico-chemical state 8=17201
 lanthanide distrib. between pyroxene and garnet 8=5780
 Laves structure formation rel. to MgM_2 , ($\text{M} = \text{Cu}, \text{Zn}, \text{Ni}$) 8=13071
 levitation melting apparatus 8=1669
 liquid-gas supercritical region, C_1 and C_2 extrema calc. from phenomenological theory 8=12978
 liquid-vapour phase diagram, student expt. 8=21768
 liquids, quaternary systems 8=1529
 metal-interstitial systems, phase boundary motion and polyphase diffusion 8=17035
 molten salts, ternary mixtures 8=21648
 mullite, stability from CoO - Al_2O_3 - SiO_2 equilibrium 8=9669
 oscillations round steady state in systems of chem. reactions 8=2500
 phase diagram determ. by e probe microanalysis 8=17034
 phenol-aqueous sodium salicylate- α -methyl naphthalene, solubility and equilib. data 8=4641
 polyamides, increase in thermostability, based on piperazine after u. v. irradiat. 8=17182
 polymer fibres, supermolec. order, study by polarized light scatt. 8=18581
 semiconductor alloys, $\text{A}_x\text{I}^{\text{VI}}\text{B}_{1-x}\text{I}^{\text{III}}\text{C}_3^{\text{VI}}$ ($\text{A} = \text{Cu}, \text{Ag}; \text{C} = \text{Te}, \text{Se}; \text{B} = \text{In}$), equilib. diagrams and structure 8=8266
 steel, temp. determ. by mag. meas. 8=17062
 surface phase theory, experimental test 8=21530
 vapour-liquid, at high press. 8=16939
 vapour pressure of simple liquids 8=21779
 Zircaloy-2, annealed in α and $(\alpha+\beta)$ regions, H_2 terminal solubility 8=8250
 Ag-Cu-Sn system, electronic phases rel. to chemical displacements 8=17002
 AgI-Ag₂S, phase distrib. 8=21838
 Al distrib. in schistic biotites, phengites and chlorites 8=13055
 Al₁₅-type phases, binary, containing transition elements, atomic ordering 8=17419
 in Al-Dy-U system, rel. to use of Dy as burnable poison in (U/Al) nuclear fuel 8=13060
 Al-Fe-Si alloy, Al-rich, phases 8=13058
 α -AlFeSi, four possible phases 8=13057
 Al-U-Sm system, rel. to use of Sm as burnable poison in Al-U fuels 8=13059
 Al₂WO₃ bronzes, struct. evolution with temp., phase stability 8=17048
 Ar, adsorbed in equilibrium with gas in ultrahigh vacuum, obs. 8=21530
 Au₇₇Mg₂₃ phase, crystal structure 8=13251
 Au-Mg system, some phase structures 8=17043
 Bi-O system, new tetragonal phase, crystal structure 8=17347
 B₂O₃-SiO₂ system, metastable immiscibility 8=21748
 Bi-Tl-Te systems, in Te-rich regions 8=4703
 Ca phosphate, stoichiometry 8=13135
 CaAl_2O_4 - CaAl_2O_6 - $\text{Ca}_2\text{Al}_2\text{SiO}_7$ - MgAl_2O_4 , liquidus relations in quaternary subsystem 8=21763
 Ca₂WO₃ bronzes, struct. evolution with temp., phase stability 8=17048
 CdS, thin films, structure and phase composition 8=4746
 Cd-Se system 8=16955
 Cr-Fe-C-N alloys, 18% Cr, constitutional diagrams 8=21822
 Cu-InAs system 8=17011
 CuO-"FeO"-SiO₂ solid solutions, activity-composition relns. 8=17009
 CuSO₄-H₂O system, phase boundaries to 40 kilobars 8=4640
 of Cu-Te system in thin layers, electron-diff. obs. 8=17057
 Cu-Zn system 8=13546
 Fe alloy, levitation melting apparatus 8=1669
 Fe-C alloys, diags. from density and emissive power meas. 8=1673

Phase equilibrium—contd

Fe-In binary system, no intermetallic cpds. 8=8160
 Fe-M, ($\text{M} = \text{Mn}, \text{Ni}, \text{Sb}, \text{Sn}, \text{W}$) systems α - γ equilib. 8=4709
 Fe-Ni phase diagram, e probe microanalysis obs. 8=17034
 Fe-Ni-As constitution diagram, up to 50 wt.%As 8=17074
 FeO-Fe₂O₃-ZrO₂-SiO₂ system 8=17072
 Fe-Ta system, liquid and solid δ -phases 8=8161
 GaAs vaporization at 900-1200°K and vapour pressures 8=4664
 Ga-As-M ($\text{M} = \text{Au}, \text{Ag}, \text{Cu}$), ternary liquidus-solidus diags. 8=4639
 Ga-As-Zn system, vapour pressure on liquidus lines 8=21764
 Ga-Fe system, and comp. and struct., obs. 8=21749
 Ga-P-Te system 8=17082
 H₂ liquid-solid mixture storage obs. 8=19067
 H₂ terminal solubility and partitioning in α -Zr, Zircaloy-2 and Zircaloy-4 8=8249
 He-methane solid-vapour system, 55°-91°K, to 140 atm. 8=16953
 HgX₂-TLX, ($\text{X} = \text{I}, \text{Br}, \text{Cl}$) systems, cpds. formed 8=17085
 InSb-NiSb, eutectiferous type of constitution 8=4691
 K-graphite system lamellar cpds 8=4712
 KBr-KI system, thermal analysis 8=17092
 KCl-NaCl, solid-liquid 8=8164
 K₂O-SiO₂ solutions, activities 8=21620
 K₂V₂O₈ system, new phases of narrow homogeneity range, cryst. features 8=17086
 La telluride system, isostructural phases, crystal chemistry 8=17202
 La₂O₃-Al₂O₃ system, alumina-rich phase diagram 8=21740
 LiMSiO₄, ($\text{M} = \text{Al}$ with Ga and Ge substitution), with SiO₂ and GeO₂ 8=17013
 Li₂O-SiO₂ solutions, activities 8=21620
 MgM₂, ($\text{M} = \text{Cu}, \text{Zn}, \text{Ni}$), Laves structure formation 8=13071
 MgO-Al₂O₃ system, phases in splat-quenched melts 8=1677
 MgO-Al₂O₃-Cr₂O₃ system, rel. to coherent precip. 8=21848
 MgO-MgSiO₃ system, reaction product distrib. from cathodoluminesc. device 8=18641
 Mn-O, high-temp. diagram 8=16954
 MnSe-MnS system 8=17014
 Mn-Zn ferrite, phase diagram determined from cation diffusion coefficient 8=9691
 NH₃-H₂O-N₂-H₂ system, high press. vapour-liq. equilib. 8=12977
 NaCl-KCl system, thermal analysis 8=17092
 Na-K-NH₃ solns. 8=8014
 Na-NH₃ solns., with added NaBr and NaN₃ 8=8013
 Na₂O-SiO₂ solutions, activities 8=21620
 Nb-Fe alloys, diagram 8=8272
 Nb-Mo-C alloys, solid solubility, phase diagram, constitution 8=8275
 Nb-Ni-Al alloy, M phase structure determ. 8=17403
 Nd telluride system, isostructural phases, crystal chemistry 8=17202
 Ne-H₂ liquid-vapour system, 26°-42.5°K, 10-25 atm. 8=16937
 Pb-PbO-As₂O₃ system, slag-metal 8=8277
 PbO-TiO₂-ZrO₂ system 8=17099
 Pb-S-O system, equilib. relns., diagrammatic representation 8=16920
 PbTe-Au pseudobinary section 8=17098
 PbTe-Fe pseudobinary section, diag. 8=17097
 Pr telluride system, isostructural phases, crystal chemistry 8=17202
 in Pu-Th system 8=21854
 Pu-Zr phase diagram, obs. 8=8279
 Rh-Hg system, phase diagram 0-500°C 8=8280
 Se phase identification in V₂VI_{3+x} alloys 8=17102
 Sn-Te, about 840°C and 12.0 kb, liquid and two solid polymorphs. 8=1614
 Ta-O system, new phases, e-diff. study 8=17101
 Te phase identification in V₂VI_{3+x} alloys 8=17102
 Ti-Al-Co alloys, and microstructure rel. to Ti-rich corner 8=4851
 Ti-3 wt.%Fe alloy, quenched from β -sphere, study of martensites 8=21859
 TiFe₂, atomic arrangement in homogeneity range of Laves phase 8=1813
 α -Ti/H₂(D₂) system, thermodynamic props. 8=21858
 ϵ -Ti-N, high-temp. stability 8=21857
 in UAl₃ coatings on U, protection against U oxidation 8=21892
 U-C system, phase diagrams 8=21860
 in UC-Fe-Cr system, compatibility relationships 8=21861
 in UC-Fe-Ni, compatibility relationships 8=21861
 UN_(x) + U₍₁₎ + N_(g) system, N equil. pressure and UN thermodynamic props. 8=18646
 in U-Ni-C system, compatibility relationships 8=21861
 U-O system, non-stoichiometric oxides 8=21788
 U-O system, phase diagrams 8=21860
 U-O-C system, phase diagrams 8=21860
 UO₂-PuO₂ system, ideality, heats of fusion obs. 8=8284
 UO₂-PuO₂ system, solid-liquid phase diagram 8=8169
 U-UH₃ phase diagram \leq 150 atm and 860°C 8=8190
 V-Fe-Si alloy, D phase structure determ. 8=17403
 V-Ga alloys, anal. rel. to anodic oxidation 8=8286

Phase equilibrium—contd

- W-Mo-UC phase diagrams and ternary peritectics, obs. 8=9710
 Y_2O_3 - Al_2O_3 system, liquidus curve meas. 8=16921
 Y_2O_3 - ZrO_2 , cubic phase stabilization at low temps. 8=8287
 Zn-Te system 8=16956
 $ZrFe_2$, atomic arrangement in homogeneity range of Laves phase 8=1813
 Zr-H-C system, ZrC_{xH_y} cpd. formation and structure analysis 8=17433
 Zr-H-N system, ZrN_{xH_y} cpd. formation and structure analysis 8=17433
 ZrM_2 - H_2 systems, (M = Cr, V, Mo), betw. 0° and 900°C 8=4723
 Zr-2.5wt%Nb, annealed in α and ($\alpha+\beta$) regions, H_2 terminal solubility 8=8250
 ZrO_2 - HfO_2 system, by metallograpy, X-ray diffr. and microprobe analysis 8=21863

Phase meters. See Electrical measurement.

Phase transformations

- alloys, above solidus temp., fracture and deform. rel. to liquid content 8=22304
 anatase-rutile, enthalpy obs. 8=13074
 beryl and beryl melts, thermal decomposition at high temps., press. depend. 8=18645
 b.c.c. to σ -phase, atomic mechanism 8=17030
 Bose gas, quantum theory of second kind 8=10651
 calorimeter obs. 8=6221
 cholesterol mynstate liquid cryst. mesophase polymorphism, obs. 8=12802
 coexistence curve for liquid and gas near critical point 8=21769
 composite growth from melts 8=4647
 correlation function near critical point, thermodynamic behaviour 8=16914
 critical binary fluids, spectral width temp. and angular dependence 8=21778
 critical points, density fluctuations and Yang-Lee theory 8=10620
 at critical point, dynamical props. from generalized scaling laws 8=2346
 critical point thermodynamics, fundamental problems 8=12962
 cyclohexane-aniline, critical binary fluids, spectral width temp. and angular dependence 8=21778
 Curie point, dynamical susceptibility in Ising model 8=14985
 earth, phase boundary motion rel. to pressure, calc. 8=23201
 ethanol, critical supersaturation for homogeneous nucleation 8=1621
 eutectic systems, three-component, triple and binary points 8=12961
 gas, critical, sound attenuation 8=12688
 hard sphere fluid 8=12578
 heat insulation coatings, heat cond. eqns., numerical solns. 8=237
 heat transfer problems for time-depend. surface temp., approx. soln. appl. to Stefan problem 8=16913
 hexane, critical supersaturation for homogeneous nucleation 8=1621
 Ising model, second order 8=14986
 kinetic phase transitions 8=21743
 lattice gas model, props. of coexistent phases 8=4638
 liquid-crystal transition of quantum system at T = 0 8=119
 liquid-gas supercritical region, C_1 and C_2 extrema calc. from phenomenological theory 8=12978
 liquids and solids, simple, changes of state 8=17032
 liquid-vapour, anal. of change using irreversible thermodynamics 8=21766
 metals, supercooled, dynamic nucleation 8=21760
 metastable, state-area principle 8=12963
 methanol, critical supersaturation for homogeneous nucleation 8=1621
 near critical point, deceleration, thermodynamics 8=8162
 one-dimensional systems with hard cores, absence of transitions 8=19455
 n-pentane, solidification at high press. 8=21747
 points of second kind, theory of light scatt. 8=9489
 polynucleotides, synthetic, helix-coil transition 8=16387
 polypeptides, helix-coil transition, proton mag. resonance obs. 8=21211
 Portland cement clinker, Ca_3SiO_5 and Ca_2SiO_5 phases, high-temp. microscopic investigations 8=21841
 propionate groups, and retarded motion 8=8229
 regelation, expt. using objects of different geometries and thermal props. 8=8167
 regelation expts. with wires 8=8168
 regelation, theory 8=8165
 regelation, theory, supplementary note 8=8166
 second kind, hypothesis of correlation similarity in theory 8=19449
 sound waves coupled to infinities in transport coeffs. 8=10669
 square-well fluid 8=12581
 stars, eqns. of state for equilibrium 8=5861
 steam, thermodynamic props., near critical point 8=7920
 surface tension near crit. pt., quasichem. approx. 8=21635

Phase transformations—contd

- vapour to liquid, surface resistance 8=12975
 water, critical supersaturation for homogeneous nucleation 8=1621
 Al-Cu alloys, dendrite arm spacing rel. to coarsening effect 8=4820
 Al_2O_3 vapour-deposited, 300-1200°C 8=13061
 Au-Cd binary system, point defect segregation at melting rel. to comp. 8=17624
 Bi, Sn and Te doped, solid and liq. phase boundary, Peltier coeff. 8=9238
 CO_2 near critical point, admixture density distrib. 8=21744
 Fe-Cr-N ternary system, point defect segregation at melting rel. to comp. 8=17624
 Bi, Sn and Te doped, solid and liq. phase boundary, Peltier coeff. 8=9238
 CO_2 near critical point, admixture density distrib. 8=21744
 Fe-Cr-N ternary system, point defect segregation at melting rel. to comp. 8=17624
 Ga-Fe system, and comp. and struct. obs. 8=21749
 GaS, thermal stability 8=21786
 Ge undercooling 8=4649
 H, liq.-solid mixtures, quality determ. 8=15138
 He-3, 4, solid liquid density prediction 8=10813
 He-n-butane system, P-V-T-x relns. showing gas-gas equilib. 8=12979
 He⁴, liquid, λ -transition, Patashinskii-Pokrovskii theory 8=255
 He⁴, turbulently flowing, λ -point shift 8=19694
 K vapor, supersaturation and condensation shocks 8=12982
 $K_4Fe(CN)_6 \cdot 3H_2O$, ferroelectric, Mössbauer test for lattice-dynamical model 8=22667
 Mn-Zn eutectics, shock-decanted, interface examination 8=8170
 N_2 adsorbed on W, caused by e-impact 8=21913
 N_2 , liq. solid, dramatic demons. 8=1607
 $NaH_2(SeO_3)_2$ and $Na_2(SeO_3)_2$, order-disorder, isotope effects in crystal symm. and nature 8=21849
 Ni_2SiO_4 (cubic nickel orthosilicate), synthesis from stoichiometric compound 8=21853
 Pb-Sn alloys, composite growth from melt 8=4648
 Pb-Sn eutectic, interphase boundary energy 8=16933
 in Pu-Th system, peritectic at 596°C and eutectoid at 582°C 8=21854
 SF_6 - CO_2 , critical binary fluids, spectral width temp. and angular dependence 8=21778
 W-Mo-UC ternary peritectics and phase diagrams, obs. 8=9710
 ZrO_2 - TiO_2 liquidus curve, specular reflection method in solar furnace 8=1608
- solid-state**
- alkali aluminogermanates, at high press., rel. to geochem. 8=8261
 alkali aluminosilicates, at high press., rel. to geochem. 8=8261
 Alni A, magnetization coercive field strength, time- and temp.-depend. 8=5460
 Alnico, structure on formation at different ageing temps. (300-800°C) 8=17077
 anatase formation at high temps. 8=1684
 antiferromagnetism in a mag. field, mol. field treatment 8=14062
 austenite formation from spheroidized ferrite-carbide aggregate, kinetics 8=21844
 austenitic steel, sigma phase precip., from thin-foil transformation studies 8=1674
 binary cpds., kinetic, in crystallization, computer model 8=4794
 boehmite to γ - Al_2O_3 , rel. to anodic oxidation of Al in presence of hydrated oxide 8=18729
 β -brass, martensitic transform., deformation effects 8=21843
 β -brass, order-disorder transition, study by n diffraction 8=17051
 cellulose triacetate films, amorphous and cryst., transition temps. 8=4724
 Conference, Rennes, April 1965 8=8259
 copper formate tetrahydrate, antiferroelectric, cell doubling 8=9222
 freezing rate, effect of heat evolution, semi-infinite slab 8=16932
 glass, four new oxide phases, rapid quenching techniques 8=5087
 goethite dehydration and haematite/magnetite formation rel. to c.c.p. orientations 8=4875
 hexachlorocyclopentadiene, two phases 8=8289
 and holomorphy, scaling law for mag. systems 8=22740
 ice, amorphous \rightarrow hexagonal, enthalpy and ht. capacity changes 8=21846
 ice doped with Mössbauer ions, cubic to hex. 8=13069
 isothermal, time-dependent theory of interface stability 8=1667
 ionic crystals, under high static pressures, review 8=4699
 lattice parameters change around interface, meas. 8=8489
 magnetic films, ageing, analytic solution 8=22784
 magnetic structures, periodic 8=13990
 martensite-austenite, habit planes, with the aid of Kossel diagrams 8=4853
 metallic alloys, order-disorder and ageing, crystalline structure changes in early stages 8=17036
 metal bond interfaces, diffusion-induced strains variation during ageing 8=13506
 metals, under high static pressures, review 8=4699

Phase transformations—contd

solid-state—contd

- methane, transition calcs. using James-Keenan model 8=17110
 model I-D lattice 8=2965
 Mössbauer spectrometry, extension of range 8=20362
 multiphase diffusion couples, lattice transform. at interface on supercooling 8=17552
 nucleation theory of reactions 8=23090
 octahydroanthracene crystals, polymorphic transitions, impurities influence 8=17109
 ordering of ternary b. c. c. alloys having three types of sites, theory 8=17033
 perovskite structure, second-order phase, symmetry change theory 8=22663
 perovskite-type crystals, distorted, rel. to lattice dynamics of atomic displacive transitions 8=17332
 polyalkyl methacrylates, multiple transitions 8=21864
 polymethylmethacrylate, temp. depend. of conformation transitions and dipole moment 8=17111
 polyurethanes, linear, kinetics of glass form. in amorphous and cryst. state 8=22110
 PVC, effect of u. v. irradiation on glass transition temp. 8=17181
 quartz, α - β assoc. lattice modes from Raman scatt. -196-615°C 8=1682
 quartz, high-low inversion, press. 6 to 35 kb, obs. 8=1681
 quasi-binary crystals of continuously variable comp., order-disorder kinetic model 8=4701
 rare earth oxides, X-ray and spectrographic investigations 8=4722
 rocks, under shock compression 8=9800
 rubbers, study by radio-thermoluminesc. 8=13077
 second order rel. to Husimi-Templey model in ferromagnetism 8=13977
 second-order, Landau theory, $[\Gamma]^3$ and $[\Gamma]^2$ for crystallographic point groups 8=17031
 second order, specific heat, singularity using complex temperature plane 8=13365
 second-order, thermodynamic discontinuities 8=1668
 second order transitions as critical phenomena of phase equilibrium 8=8260
 semiconductors, under high static pressures, review 8=4699
 spinodal decomposition in multicomponent system, thermodynamic conditions 8=4700
 spinodal decomp., Institute of Metals lecture 1967 8=21835
 H36XII steel, austenitic, strain ageing dynamic and static. 8=13569
 steel, austenitic, containing 4% Ti, ageing and zone formation study 8=17071
 steel, carbide transformations during creep 8=17081
 steel EI-702, deformation and hardening temp. effect on mechanism of precipitation 8=17078
 steel, equilibrium partition between ferrite and cementite, temperature dependence 8=17279
 steel, high-carbon, carbide formation mechanism during tempering 8=17073
 steel, high strength, dynamic strain ageing 8=17782
 steels, low alloy, effect of martensite on kinetics of bainite formation 8=4708
 steel, quenching in mag. fields, review 8=22343
 steels, stainless, precip.-hardening rel. to retained austenite, X-ray meas. 8=4848
 strain ageing rel. to stress-assisted diffusion to dislocations 8=4969
 strain contrast on electron microscope images due to new phase 8=1773
 styrene graft-copolymer to butadienestyrene rubber, thermal ageing struct. changes 8=17112
 thermoluminescence of inorganic cpds during transitions 8=23040
 thiourea, ferroelec. 8=13340
 Ticonal, structure on formation at different ageing temps. (300-800°C) 8=17077
 transition metals, phase diagrams 8=13003
 Wurster's blue perchlorate 8=14288
 wustite, p to n transition rel. to Seebeck coeff. grain size and Mg doping dependence 8=5387
 X-ray and electron diffuse scattering by lattice particles in new phase 8=1773
 Zircalloy-2, cold rolled, age hardening and recovery, obs. 8=8872
 Al alloys, ageing, natural, effect on subsequent artificial ageing 8=17764
 Al garnet, phase change with symmetry enhancement as function of magnetic field 8=21839
 Al, rolling and recrystallization texture orientation relationships 8=1755
 Ag-5.64 wt. % Al alloys, grain boundary precipitation 8=17038
 Ag-Au-Zn system, $\beta' \rightarrow \xi$, temp. dependence 8=17037
 Ag-Cu-Zn alloys, low-temp. martensitic 8=13056
 Al-Cu-Mg alloys, atomic diffusion within lattice on ageing 8=17041
 AlF₃, anhydrous cryst., high temp. 8=4929
 Al-Mg alloys, various ageing regimes and recovery 8=17765
 Al-Mg alloy, deformation and ageing effect on structure 8=17004

Phase transformations—contd

solid-state—contd

- Ag-Mg alloys, order-disorder transition in range 17-16 at. % Mg 8=21820
 Al-Zn-Mg alloys, quenching rate rel. to age hardening 8=8817
 AlZn, ageing rel. to metastable α' phase appearance and stability 8=8262
 Au films, morphological changes following deposition 8=4743
 Au-Cd, thermodyn. investigation 8=8263
 Au₂Cu, shear modulus change during ordering 8=17769
 Au-Cu-Zn ternary alloys, phase relation and kinetics 8=13063
 β -AuMn, change to f. c. c. structure on cold working 8=17042
 Au-Ni alloys, modulated structure formation, conc. and temp. dependence 8=17044
 Au-Zn system, $\beta' \rightarrow \xi$, temp. dependence 8=17037
 Ar-F₂ phase diagram 8=1670
 Ba I-II transition, pressure determ. with single-piston apparatus 8=4702
 BaCO₃, aragonite/disordered rhombohedral polymorphic transition 8=21840
 BaTa₂O₆, polymorphism 8=4780
 BaTiO₃-Cr₂O₃ systems, rel. to changes in ferroelectric props. 8=17045
 Bi on 2-4°K, superconducting modification 8=2155
 in Bi₂O₃-WO₃ and Bi₂O₃-MoO₃ system, comp. and crystal structure determ. 8=17047
 Bi-Sn, intermetallic phase, superconducting props. 8=2156
 C steels, austenite form. and tempering under high rate heating 8=13067
 Ca hydrosilicate, in presence of gypsum and Al₂O₃ rel. to cement setting 8=1738
 CaF₂:Nd³⁺, 'ageing' by stimulated rad. conds. 8=8765
 CaF₂:YF₃:Nd³⁺, 'ageing' by stimulated rad. conds. 8=8765
 CdS, recovery of rocksalt structure to room press. at 77°K 8=1671
 CdSnAs₂ and CdGeAs₂, high-temp. modifications 8=21842
 Ce-Ni-Si system, ternary cpd. formation. comp. and structures 8=17200
 Ce₃S₄, γ -phase stabilization with additives 8=8264
 Co, f. c. c.-h. c. p. martensitic, thermodynamics 8=17049
 Co films, changes, thickness depend. 8=17050
 Cr-Ni steel, γ - α transform., pulsed mag. field effect 8=17063
 CsCl at 470°C, transition energy determination 8=1672
 Cu, plastically deformed, annealing behaviour, effect of dispersed phases 8=17772
 Cu-Al-Mn alloys, study of surface relief effects, rel. to supercond. transition 8=19686
 Cu₂Au, shear modulus change during ordering 8=17769
 Cu-2 wt. % Be, ageing investigated by electron microscopy 8=17056
 Cu-Be, X-ray and electron diffuse scattering by lattice particles in new phase 8=1773
 Cu:Cu-12.5 wt. % Al multiphase diffusion couples, lattice transform. on supercooling 8=17552
 Cu formate tetrahydrate, sp. ht. and entropy at antiferroelectric transition pt. 8=8638
 Cu-Mn-Al system, effect of quenching and ageing on mag. phases 8=14010
 Cu-Sn alloys, structural changes on natural ageing 8=17052
 Cu-Sn alloys, structures of metastable states during eutectoid transform. 8=17055
 Cu-Te system in thin films, and structure 8=17054
 β_1 Cu-Zn, martensite, after repeated thermal cycling 8=17053
 β_1 Cu-Zn, martensitic transformation temps. from elec. resistivity meas. 8=4704
 Cu-Zn-Si β -phase alloy, inhomogeneity effect on martensite transform. 8=4707
 Cu-Zr, supersaturated solid soln., n. m. r. study of decomposition 8=8265
 D₂, rel. to pressure changes 8=4711
 Dy garnet, phase change with symmetry enhancement as function of magnetic field 8=21839
 Er-H₂ system, by X-ray analysis 8=17058
 Fe, α to γ point, thermal etching in vacuum 8=17652
 Fe(III) oxide, cubic-trigonal, mobility evidence from Zn ferrite form. at 470°C 8=23117
 FeAl alloys, kinetic order-disorder transform. by X-ray investigation 8=17076
 Fe-C alloys, from density and emissive power meas. 8=1673
 Fe-C and Fe-N system, thermodynamics of martensite transform. 8=17075
 Fe-C-Ni-Mn alloys, martensitic magnetic field effect 8=17079
 Fe-Co-Ni-Cr, new ferromagnetic state during recrystallisation 8=9342
 Fe-Cr, 500°C 8=13068
 Fe-7.9 Cr-1.1 C alloy, isothermal transforms. betw. 750 and 285°C 8=17068
 Fe-30%Cr, yield and fracture stress, before and after ageing 8=13558
 Fe-Ni alloy, martensitic transformation, calorimetric study 8=17069

Phase transformations—contd

solid-state—contd

- Fe-Ni alloy, phase-hardened, condition for thermal stability 8=17066
- Fe-Ni alloy, rapid heating effect during reverse martensitic transform. on high temp. stability 8=17065
- Fe-Ni alloys, study of surface relief effects, rel. to supercond. transition 8=19686
- Fe-26%Ni-0.4% C alloy, effect of prior plastic deformation of austenite on M_s 8=4710
- Fe-Ni base alloy: 9 at %Cu, microstructural changes on ageing 8=1759
- Fe-Ni-Ti alloys, $\alpha \rightarrow \gamma$ martensitic 8=17070
- Fe-Ni-Ti alloy, structural changes during martensite ageing 8=17064
- Fe_2O_3 , $\gamma \rightarrow \alpha$, liquid N_2 temp. 8=13066
- Fe_3O_4 , order-disorder transition, constant entropy below transition 8=17067
- α -FeOOH antiferro-paramag., e. s. r. obs. 8=22879
- Fe-Rh alloys, crystal lattice parameters, structural defects 8=9395
- Ge, metallic modification formation under shock compression 8=17083
- GeTe-SnTe alloys $\alpha = \beta$ transition, at high press. 8=17084
- H and D, crystal-structure changes in ortho- and para-states, X-ray exam. 8=13263
- H, λ , due to quadrupole-quadrupole interaction between mols. 8=8267
- H_2 , ortho, mol. rot. excitation near absolute zero 8=8233
- H_2 , rel. to pressure changes 8=4711
- H_2 solid, fcc and hcp, electron microscope investigation 8=8465
- He^4 , hexagonal-b. c. c., birefringence obs. 8=15155
- He^4 II-I, under rot., higher than first order 8=10814
- In, diffuse X-ray reflections in order-disorder transition near melting pt. 8=8525
- InS crystals, on e-irradiation, and twinning 8=17209
- K and NaCl solid solns., decomp. mechanism from X-ray scattering studies 8=13070
- $KAlSi_3O_8$, polymorphic transform. at 120 kbar and 900°C 8=8268
- KBr, under dynamic compression due to shock loading 8=22376
- KCl, compressed by shock waves 8=17029
- KCl, under dynamic compression due to shock loading 8=22376
- KD_2PO_4 , dynamic disorder due to deuteron intrabond jumping at ferroelectric transition 8=9212
- KD_2PO_4 , order-disorder ferroelectric, transition studies, calorimetric investigations 8=22668
- KH_2PO_4 , high temp., isotope effect 8=9213
- KH_2PO_4 -type crystals, ferroelectric phase transition dynamics 8=9215
- K_3MoCl_6 mag. ordering from specific heat 1.5-20°K 8=1872
- K_3MoCl_6 mag. state, dynamic susceptibility obs., 4-14°K 8=2297
- $1K_2O-26Li_2O-73SiO_2$ (mol. %) glass, second-phase particle growth, diffusion controlled 8=21847
- $K_2SO_4:Mn^{2+}$ 8=22910
- K_2ZrCl_6 8=8640
- $LiBO_2$, β and γ high-pressure forms 8=8269
- Li_2SO_4 with Na_2SO_4 , Rb_2SO_4 or $CsSO_4$, differential thermal anal. 8=8270
- Mg-9 wt. % Al alloy, age hardening mechanism and precip. process 8=13583
- $MgCd_3$, Mg_3Cd kinetics of ordering and disordering 8=8271
- $MgCr_{2-x}Mn_xC_4$, $MgGa_{2-x}Mn_xO_4$ tetragonal distortion of Jahn-Teller type study X-ray and neutron diffr. 8=13269
- Mg-In, order-disorder, energy 8=13072
- $Mg_2SiO_4-Fe_2SiO_4$ system, olivine-spinel solid soln. equilibria, 43 to 96 kb at 800, 1000 and 2010°C 8=23218
- Mn ferrite, (and mixed with Zn), Mössbauer study of intermed. phases in formation 8=17087
- Mn. effect of multiple $\gamma = (\epsilon, \epsilon')$ transformations on strength and structure 8=17785
- Mn steel, on heat treatment rel. to crystal structures 8=17090
- Mn steel, martensitic, rel. to elec. resist. 8=17061
- Mn-Ni system, rel. to crystal and mag. structures 8=17088
- Mn-Pd alloys, structural and mag. props. rel. to compos. 8=4714
- $MnT'O_3$, ($T' = Ho, Er, Tm, Yb, Lu$), hexagonal, transform. to perovskite under high press. 8=17089
- ND_4Br , ht. capacity data 8=22117
- ND_4Br , low-temp. 8=4713
- $(ND_4)_2Cr_2O_7$, correl. with i. r. spectra 8=23006
- NH_4Cl , harmonic scatt. and critical pt. correl. 8=23007
- NH_4Cl , ordering, anomalous changes in vol. 8=21850
- NH_4Cl , II \rightleftharpoons III transition, energy and temp. meas. 8=17091
- $(NH_4)_2Cr_2O_7$, low temp. 8=14250
- NH_4I , modifications II and III, lattice parameters 8=17398
- $(NH_4)_2SO_4$, correl. with i. r. spectra 8=23005
- Na, martensitic rel. to shear wave temp. dependence 8=1838
- $NaAlGeO_4$, high pressure formation and crystal structure 8=1678

Phase transformations—contd

solid-state—contd

- NaCl compressed by shock waves 8=17029
- NaCl, pressure-induced 8=17093
- $NaH_3(SeO_3)_2$, ferroelectric, second, meas. 8=2245
- NaN_3 , crystal structures of α and β forms 8=17387
- Na_2ZrCl_6 8=8640
- $Nb_3(Al, Ge, Sn)$ solid solns., rel. to superconducting transitions 8=17967
- Nb_3Sn , cubic \rightarrow tetragonal martensitic, low temp. 8=8273
- Ni-2.2 wt. % Be, ageing investigated by electron microscopy 8=17056
- Ni_3Fe , order-disorder transition, n-diffr. exam. 8=17095
- Ni-H system, lattice parameter H conc. dependence at -40°C 8=17404
- Ni-Mo alloys, quenched, deformation effects during annealing 8=17094
- NiPb formation by simultaneous evaporation of Ni and Pb 8=21852
- Ni-Ti martensite, rel. to detailed atomic movements 8=21851
- O_2 , abs. spectra of α, β, γ forms, 34 000-42 000 cm^{-1} 8=5625
- O_2 solid, α, β and amorphous, electron microscope investigation 8=8465
- O_2 solid, characts. and thermal expansion 8=4938
- PbO, orthorhombic and tetragonal forms, conversion at low temps. 8=8276
- Pb. 0.4 wt. % Mg alloy, structural ageing process at room temp., X-ray study 8=22389
- Pd-Mn alloys, structural and mag. props. rel. to compos. 8=4714
- Pb-PbO- As_2O_3 system, slag-metal equilibria, phase diagrams 8=8277
- PbTe-Sb $_2$ Te $_3$ alloy system, thermoelectric props. and phase relations 8=4716
- Pb-Tl(In) alloys, order-disorder from superconducting transition temp. meas. 8=1680
- PbZrO $_3$ ageing rel. to elec. cond. near antiferroelec.-ferroelec. transition 8=2249
- [PtPd]Co [PtPd]Fe order-disorder transform. temp. obs. 8=22837
- Pu-0.85 at. % Ga, metastable δ -phase, effect of thermal cycling on transform. behaviour 8=8278
- PuZr peritectoid reaction and PuZr $_2$ form., obs. 8=8279
- PbZrO $_3$ polycrystals, temp. changes of polarization 8=13888
- R-Ni-Si, (R=rare-earth), system, ternary cpd. formation, comp. and structures 8=17200
- Sb, shock-induced 8=4715
- $SbCl_5$ 8=2391
- SbSI, photosensitive 8=2159
- Se, growth of hexagonal from orthorhombic by polymorphic transition 8=8426
- Si, metallic modification formation under shock compression 8=17083
- Sm_2O_3 verification of existence by nondestructive analysis 8=9738
- Sn, $\beta \rightarrow \alpha$ 8=21856
- Sn alloys, dilute, microsegregation nodes and cellular solidification substructures 8=16919
- SnO-SiO $_2$ glasses, crystallization and decomposition 8=21965
- SnTe-Bi $_2$ Te $_3$ alloy system, thermoelectric props. and phase relations 8=4716
- SrCO $_3$, aragonite/disordered rhombohedral polymorphic transition 8=21840
- SrZrO $_3$, at 700-1170°C, X-ray investigations 8=8281
- Ta-O, X-ray and electron diffuse scattering by lattice particles in new phase 8=1773
- Ti alloys, Fe and Nb additions 8=22563
- TiGaLiO $_4$, structure of ordered phase on annealing at 600°C 8=17423
- ϵ -Ti $_3$ N, high-temp. stability 8=21857
- Ti-22 at. % Nb alloy, ω phase precip. rel. to superconducting critical transport currents 8=4718
- Ti-O system, $\beta \rightarrow \alpha$, bainitic 8=17103
- TiO $_2$ II modification at 40-120 kbar and 400-1500°C 8=17104
- TiO $_2$, under shock-wave compression, from X-ray studies 8=1685
- TiI, and compressibility and thermal expansion 8=1683
- U-Cr alloys, martensite nucleation and growth in β - α transform., temp. dependence 8=4717
- UL $_6$, α self irradiation effects obs. 8=17105
- U-M alloys, (M=Fe, Al and Si), irradiated, phase comp. changes rel. to resistivity meas. 8=8283
- U-1.5 wt. % Mo structures rel. to cooling rate from γ phase, obs. 8=8285
- UC $_2$, 300-5°K, by n diffr. exam. 8=1810
- U $_2$ N $_3$, heat of form. calc. from press. of decomposition 8=9660
- UO $_2$, spin lattice interaction, first-order transition theory 8=22886
- UO $_2$ -ZrO $_2$ -CaO nuclear fuel system, stability over cycling tests 8=17527
- U $_2$ Ru $_3$, formation in peritectoid transform and crystal structure 8=22043
- in U-UH $_3$ and phase diagram \leq 150 atm and 860°C 8=8190
- V-H alloy, at low temps. rel. to anomalous props. of V 8=5186
- V-V $_3$ Si system 8=9061

Phase transformations—contd**solid-state—contd**

- V, H-charged, rel. to ductility drop 8=5088
 VO₂ 8=4719
 VO₂, 68°C, use in high-speed solid-state thermal switches 8=22616
 V₃Si, cubic → tetragonal martensitic, low temp. 8=8273
 V₃Si type compounds, tetragonal modifications 8=4888
 W-O system, intermediate phases on reduction by gases, O₂ conc. cell method 8=18683
 β-W, V₃Si type tetragonal modifications 8=4888
 Y₂O₃-Al₂O₃ system, formation of compounds 8=4720
 Zn ferrite, (and mixed with Mn), Mössbauer study of intermed. phases in formation 8=17087
 Zn₂GeO₄ at high pressures 8=13075
 ZnS crystals, on crushing rel. to luminescent props. 8=17106
 ZnS, hex. to cubic, Cu-induced 8=17107
 Zn₂SiO₄ at high pressures 8=13075
 Zr, cold rolled, age hardening and recovery, obs. 8=8872
 Zr rich alloys, effect of rolling temp. on texture developed 8=22399
 Zr-2.5wt. % Nb cold rolled, age hardening and recovery, rel. to stress relax. obs. 8=8872
 ZrO₂, superplasticity during monoclinic → tetragonal transform. 8=5091
 ZrO₂-CeO₂ mixtures, high-temp. 8=22614
 ZrO₂-HfO₂ system, monoclinic-tetragonal inversion 8=21863
 ZrO₂-MgO solid solns. 8=13076
 ZrO₂-TiO₂ system, change of mineral composition by heat treatment 8=4721
 ZrO₂-TiO₂ system, X-ray obs. 8=17108
 ZrO₂, X-ray and spectrographic investigations 8=4722

Phase transitions. See Phase transformations.

Phonographs. See Sound reproduction.

Phonon bottleneck. See Crystals; lattice mechanics.

Phonon drag. See Crystal electron states; Crystals; lattice mechanics.

Phonon-electron interactions. See Crystal electron states; Crystals; lattice mechanics.

Phonons. See Crystals; lattice mechanics.

Phosphorescence. See Luminescence.

Phosphors. See Luminescence; Luminescent devices.

Phosphorus

- atom, K-shell fluorescence obs. 8=16208
 diffusion in Si, appl. of dynamical theory of X-ray scattering 8=13412
 diffusion in Si, dislocation motion rel. to coefficient, enhancement by vacancy generation 8=1925-6
 impurity addition to steel, effect on temper brittleness 8=17797
 inhibitor, in Cu-Zn alloys, selective corrosion 8=23100
 isolation diffusion in Si, integrated circuits 8=1929
 red, energy levels from X-ray spectroscopy data 8=9559
 sulphides, i. r. spectra, dispersed in AgCl 8=18553
 sp²d config., 3d-radial functions 8=1172
 P³⁺ in UP₂ U₃P₄, in paramag. state, Knight shift temp. dependence and meas. 8=5563-4
 P₂, rotational analysis of the (2, 3) band of a new transition ²II → ²II 8=16299
 P IV, spectra, transition probabilities 8=7411
 αP₄, supercooled, solid/liq. interface temps. 8=21755
 P+O reaction, stoichiometry and chemi-luminescence 8=23109

Phosphorus compounds

- alkali phosphates, glassy and cryst., γ-irrad., e. s. r. 8=22913
 covalent bonds, mag, rot, and partial ionic charact. 8=21098
 phosphates, molten, rigid sphere model 8=7999
 pyrophosphates, divalent metal, far i. r. spectra 8=21097
 X-ray fluoresc. line shift 8=2443
 P III and V systems, nuclear-electron Overhauser effect, rel. to scalar interacts. 8=4626
 PCl₃, potential function 8=12226
 PD, emission spectra, vibrational and rotational 8=4167
 PF₃, general force field 8=4157
 PF₄, electron spin resonance spectrum and second-order hyperfine effects 8=4224
 PF₅, mean amplitudes of vibration 8=16298
 P₂F₄, n. m. r. 8=16361
 PH, fine structure of ³Σ⁺ and ³II states 8=7541
 PH₂, ²A₁-²B₁ transition mol. const., spin-rotational interaction 8=4166
 PH₃ adsorption on Si(111) surface, low energy electron diffraction study 8=4765
 PH₃+O reaction, stoichiometry and chemi-luminescence 8=23109
 P₂N₅Cl₂Br, i. r. dichroism 8=5627
 PO, A²Σ⁺-X²π system, r-centroids and FC factors 8=1264
 PO radical, β-systems subsystem analysis, electronic struct. 8=12224-5
 P₂O₅, glassy and cryst., γ-irrad., e. s. r. 8=22913
 P₄S₁₀, 273°K to 720°K, thermodyn. props. 8=4933

Photochemistry

- See also Photographic process.
 acetone, photo-oxidation, methyl hydroperoxide prod. 8=14437
 acid amides, liq. photolysis, e. s. r. 8=14435

Photochemistry—contd

- annual review of nuclear science, book XV 8=15628
 aromatics in boric acid glass, direct and sensitized photo-oxidation 8=23160
 aromatic hydrocarbons, induced tritium substitution 8=23166
 benzophenone, flash photolysis absorpt. spectrum 8=4184
 p-benzoquinone, dimers of anions in soln. 8=21186
 1,3-butadiene, photodissoc., primary processes 8=23155
 cyclobutane photolysis, energy distrib. in reaction products effects of curved Stern-Volmer plots 8=5752-3
 2,3 diazabicyclo[2.2.1]hept-2-ene, photolysis products, distrib. of excess vib. energy 8=5751
 diazopropene photolysis, C₃ and C₂H₂ radicals absorpt. spectra obs. 8=16368
 ethyl iodide, gas-phase photolysis, hot radical reactions 8=5749
 flash excitation reactions, obs. with modulated optical null spectrophotometer 8=3359
 flash photolysis, gas phase, vacuum-u. v. light source 8=14433
 flash photolysis and optical rotatory dispersion of transient species 8=12258
 furan, Hg(²P₁) photosensitized, struct. of excited states 8=14434
 hexafluoroacetone, photolysis in Hg vapour, primary process 8=23154
 hexafluorobenzene, photoisomerization, kinetics and mech. 8=2537
 hydrocarbon gases, photolysis by CO₂ laser 8=2538
 imide, liq. photolysis, e. s. r. 8=14435
 isobutane, gas-phase photolysis 8=23158
 isopropyl iodide form. by C₃H₈ + I₂ photolysis 8=5745
 ketene-benzene mixture, reaction of methylene radicals 8=5748
 ketene, Hg-sensitized decomp. as source of triplet methylene 8=23157
 ketene, reaction of methylene radicals 8=5748
 laser, continuously tunable, applications 8=15485
 laser photolysis in nsec range 8=9728
 mechanistic determ. rel. to curved Stern-Volmer plots 8=5752
 methane, photolysis in Ar and N₂ matrices, i. r. spectrum of CH₃ 8=18737
 2-methylbutane, condensed-phase photolysis 8=18739
 methyl iodide, photolysis in organic matrices 8=23156
 3-methylpentanal, direct and sensitized photolysis 8=9725
 naphthalene-d₈ in ethanol and methyl-pentane glasses, biphotonic T → T transitions, obs. 8=23161
 nitroso dimers, photodissociation on irradiation with u. v. light 8=9726
 photolysis mapping of orientation of transition moment in gas photodissociation 8=1307
 tetraphenylhydrazine, photodissoc., diphenyl-amino radical dimer prod. 8=7625
 u. v. flash photolysis, e. s. r. spectrometer for study of short-lived free radicals produced 8=12339
 vacuum u. v., Ar resonance light source 8=18378
 Wüster's salts, dimers of cations in soln. 8=21186
 xylenes, cryst., photolysis for xylol radicals fluoresc. obs. 8=12356
 Al₂O₃ systems, surface effects 8=14441
 CCl₄ radicals production 8=12343
 CF₃I, photolysis in matrices at 4.2°K, e. s. r. 8=14440
 CF₃OF, low-temp. photolysis 8=9727
 CF₃OOFCF₃, low-temp. photolysis 8=9727
 C₂O₂-olefin mixtures, photolysis, product isomerization 8=5747
 CIOO radical, matrix i. r. spectra 8=12344
 DF laser action in flash photolysis of UF₆ in presence of D 8=424
 H reaction with O₂, dissociation of HO₂* 8=5743
 HF laser action in flash photolysis of UF₆ in presence of H 8=424
 HNCO, matrix-isolated photolysis, spectra of NCO 8=16369
 Hg*(³P₁) atoms, quenching by H₂, phase-space theory 8=14436
 Hg(³P₁) atom reaction with gaseous paraffins 8=9688
 N₃CN photolysis with Cl₂ to prod. free radical CCl₂ 8=1315
 NH₃, photodissoc. in vac. u. v. 8=16365
 NO, far u. v. photolysis, N₂O yield 8=23159
 Na cyclopentadiene, u. v. photolysis 8=5754
 Na tetraphenylborate in aqueous soln., photolysis products 8=5746
 N₂O, photolysis at 1470 Å and for vac. u. v. actinometer 8=14438-9
 O₂ photolysis at 1470 Å 8=4098
 O₃-H₂ mixtures, photolysis 8=5744
 α-PbN₃, solid-state decomp. 8=9724
 Rh, photoinjection into liq. hydrocarbons 8=8113
 SbH₃, flash photolysis, SbH radical 8=12354
 ZnSe interface with electrolyte 8=13837

Photoconductivity

- all-trans β carotene crystals, obs. and theory 8=2465
 anthracene, charge carrier generation with polarized light 8=2268
 anthracene crystals, pulsed, in the 250-400 nm region 8=2267

Photoconductivity—contd

anthracene, mag. field effect, theory 8=22691
 anthracene, photocurrent intensity depend. after two-photon photocarrier generation 8=13918
 anthracene, temp. depend., and carrier generation 8=2269
 anthracene, u. v. irradiated, rel. to fluorescence and carrier generation 8=2266
 aromatic crystals, exciton and conduction band 8=5403
 avalanche-photodiode frequency response 8=2257
 carotenoids 8=18240
 cell resistance as meas. of photographic granularity 8=6581
 diamonds, particle-counting, spectra, model 8=5395
 dyes, localized model 8=13920
 homogeneous photoconductors, slow high field domains 8=5392
 i. r. detectors, generation-recomb. noise limited detectivities 8=22708-9
 lifetime-gradient photovoltages meas. in photoconductors 8=9246
 metals, calc. from Kubo-Greenwood formulae 8=5393
 metals, electronic optical transitions, self-consistent theory 8=5394
 metals, rel. to excitons 8=5129
 model photodetectors, image characteristics 8=9263
 molten aromatics, lifetime of excited states 8=12904
 organic dyes, thermal activation energy 8=13919
 organic materials rel. to solar cell use 8=9260
 photoelectret regime, thermally stimulated currents rel. to traps and inner polarization 8=5372
 photon counting with photoconductors 8=15717
 photoresistors, appl. to voltage-controlled attenuators 8=15181
 photoresistors, neg. and pos., electron beam exposure and polymerizing threshold 8=22236
 polyethylene, high density 8=13921
 polystyrene:anthracene:chloranil and excit. spectrum obs. 8=9261
 quartz, cryst., and fused, laser prod. by multiphoton excit. rel. to dielec. breakdown 8=18239
 semiconductors, differential spectral sensitivity 8=2220
 semiconductor, limited bipolar, in crossed elec. and mag. fields 8=22687
 semiconductors, negative photocond. instability and polarization induction 8=18218
 semiconductors, photoelectron diffusion in mag. field rel. to spectral singularities 8=13909
 soda glass, laser prod. by multiphoton excit. rel. to dielec. breakdown 8=18239
 solids, processes and analyt. expressions 8=13908
 spherical semiconductor photocell using lateral photoeffect 8=22705
 thermally stimulated cond. for single trap in presence of deeper traps 8=1940
 Ag₃AsS₃ properties 8=18220
 AgBr, charge compensation of trapped holes 8=22688
 Al₂O₃, single crystal and sintered, γ photoconductivity 8=18222
 BaTiO₃, hole transit time temp. dependence 8=18223
 Bi₁₂GeO₂₀, photo-induced changes in optical polarization 8=2404
 Bi-Se layers, vitreous, as near-infrared photo-detectors 8=22704
 CdS cell, as integrating radiation detector 8=5404
 CdS, double injection, current kinetics 8=22692
 CdS, effect of optical radiations and water vapour on trapping spectrum 8=5396
 CdS, field distrib. and current saturation meas. by electro-optic effect 8=9250
 CdS, h.f. current oscillations on multiple band illumination 8=5397
 CdS, impurity, stationary lux-ampere characts. 8=22693
 CdS layers, field effect freq. and temp. dependence 8=18228
 CdS, at low temps. 8=9248
 CdS, and luminescence induced by double photon absorpt. 8=14313
 CdS, optical quenching spectrum temp. dependence 8=9249
 CdS polycrystalline, microwave and d.c., spectral distribution 8=5400
 CdS, response and interpret. rel. to donor and acceptor levels 8=14312
 CdS, ruby laser excited 8=22690
 CdS, thermally stimulated currents and i. r. luminescence 8=5661
 CdS: Au, photosensitive carrier e. s. r. 8=2362
 CdS-CdSe films, thermal quenching 8=5399
 Cd(SSe), sintered, decay, rel. to temp. 8=2262
 Cd(S:Se), spectral distrib. rel. to band gap, 100 and 300°K 8=2261
 CdSe crystals, at high injection levels (on laser excitation) 8=18224
 CdSe layers, current saturation and negative resist. 8=18229
 CdSe polycrystalline, microwave and d.c., spectral distribution 8=5400
 CdSe, sintered, control of props. 8=18231
 CdSe, spectra dependence on light intensity over 0.55-0.75 μ 8=18226
 CdSe, as target in vidicon 8=3215

Photoconductivity—contd

CdSe whiskers, photoinjected space-charge-limited currents 8=18230
 CdSe:Mn, rel. to Mn deep donor level 8=2259
 n-CdTe, rel. to surface recombination velocity determ. 8=18225
 p-CdTe, thermally stimulated currents and trap levels 8=2260
 Cd_{1-x}Zn_xS, mixed single crystals, rel. to comp. and defect nature 8=18227
 Cr³⁺ in ZnTe, rel. to paramag. reson. 8=5525
 CsBr crystals with F⁻ and M-centres, wavelength and temp. dependence 8=22694
 CuCl spectrum rel. to optical absorpt. and excitons, 4°K 8=9251
 Cu₂O, neutron-irrad., and absorpt. 8=5597
 Cu₂-Te-CdTe photoconverter, efficiency 8=6276
 Cu and Zn complexes, tetraphenylporphine and tetraphenylchlorine 8=9117
 GaAs, intrinsic and extrinsic, rel. to carrier recomb. 8=2194
 GaAs:Cr 8=2263
 GaAs:Cr, semi-insulating, and i. r. quenching 8=18232
 GaP crystals, very high-ohmic, anomalous response 8=18241
 Ge, magneto-photocond., 300°-200°K, fields up to 22.3 kG 8=9109
 p-Ge:Ga, nature of oscs. in impurity spectra 8=13912
 Ge:In, detector for pulsed far infrared laser radiation 8=9262
 (HgTe)_{1-x}In_xTe₃ alloys, single-crystals, and optical energy gap 8=5608
 In₂S₃, photosensitivity, spectral distrib. 8=22695
 InSb films, slow photoconduction 8=9254
 InSb, spark machining for i. r. detectors 8=15096
 InSb, 10.6 μ m wavelength 8=22696
 n-InSe crystals, thermal and i. r. quenching 8=18233
 K, calc. from Kubo-Greenwood formula 8=5393
 KBr, elec. and mag. field dependence at low temps. rel. to F-centres 8=2264
 KBr:In rel. to impurity C excit. delocalization mechanism 8=8903
 KCl:Ag, B-centre meas. 8=2006
 KI:In rel. to impurity C excit. delocalization mechanism 8=8903
 Li, calc. from Kubo-Greenwood formula 8=5393
 Li₃Bi films, prep. and props. 8=8325
 Na, calc. from Kubo-Greenwood formula 8=5393
 Na, liquid, optical absorpt. and electronic structure 8=8111
 PbI₂, rel. to absorption edge at 0.525 μ 8=2444
 PbO, yellow, surface effect 8=22697
 PbS films, Hall effect due to space-charge layers on crystallite surfaces 8=5273
 RnI, intrinsic, in 5.5-6.5 eV range 8=5401
 Sb₂S₃, recomb. centres and trap levels, obs. 8=22698
 Se, amorphous layers activated by Hg, obs. 8=13914
 Se, effect of cooling to 100°K 8=1808
 Se films, anomalous, activated by Hg 8=9256
 Se, hexagonal, meas. during cooling from 300°K to 4.2°K 8=18238
 Se, photosensitivity spectrum dependence on crystallinity and oxygen impurities 8=18237
 Se, polycrystalline, hexagonal, local (conduction) levels, X-ray-induced 8=18236
 Se, trigonal, thermally stimulated currents after u. v. irradiation 8=22683
 Si doped with B, Al, Ga, P, As or Sb, extrinsic i. r. 8=9257
 Si photocells, rectifying props., effect of accelerated electron irradiation 8=22699
 Si:In, electron and hole-capture coeff. at low temps. 8=13915
 Si:Zn, slow rise photoresponse 8=5402
 ZnIn₂S₄ monocrystals, voltage-controlled negative differential resist. 8=13917
 ZnS, changes, during luminescence excited by alternating field 8=22701
 β -ZnS film, spectral distrib. of X-ray cond. 8=17143
 ZnS, optical quenching spectrum temp. dependence 8=9249
 ZnS phosphors, photoimpedance, a. c. field freq. and excitation intensity dependence 8=14335
 ZnS, and photovoltage meas. rel. to minority carriers 8=22700
 ZnS, spectra rel. to recomb. mechanisms, conduc. and lumines. changes 8=9258-9
Photodisintegration. See Deuterons/photodisintegration; Nuclear reactions due to photons.
Photodissociation. See Photochemistry.
Photoeffect, nuclear. See Gamma-rays/effects; Nuclear reactions due to photons; Photons/interactions.
Photoelasticity
 See also Double refraction/mechanical.
 anvil, high pressure, stress analysis by 8=2038
 correlation measurements of optical field with time-to-amplitude converter 8=15496
 criteria of materials for acoustic light modulators and scanners 8=9496
 diamond and diamond-type crystals, bond bending and stretching model for constants 8=8830
 diamond-like crystals, rel. to electrostriction and first-order Raman effect 8=9486

Photoelasticity — contd

- elastic waves, longit. and transverse, laser excit. thresholds 8=17831
- elastically restrained plate, analysis of thermal stresses 8=2926
- quartz, elastic waves, longit. and transverse, laser excit. thresholds 8=17831
- quartz, rel. to light amplification and hypersound generation 8=2451
- quartz, rel. to stimulated Brillouin scatt. 8=5634
- quartz, suitability for acoustic light modulators and scanners 8=9496
- r.f. stress analysis of opaque bodies 8=22267
- stress analysis, review of theory and exptl. details 8=5015
- strip, apertured, stress concentration, photoelastic study 8=55
- styrene network copolymers with dimethacrylate or ethyleneglycole, effect of crosslinking 8=22395
- GaAs, GaP, suitability for acoustic light modulators and scanners 8=9496
- Ge, bond bending and stretching model for const. 8=8830
- NH₄Cl crystals, temp. variation, obs. 8=2440
- NH₄H₂PO₄ photoelastic const. 8=14244
- Si, bond bending and stretching model for const. 8=8830

Photoelectrets. See Electrets; Photography.

Photoelectric cells. See Photoconductivity; Photoelectricity; Photovoltaic effects.

Photoelectric effect, atomic. See Atoms.

Photoelectric emission. See Electron emission/photoelectric.

Photoelectricity

- See also Electron emission/photoelectric; Photoconductivity; Photovoltaic effects.
- absorption from x-ray scattering producing fluorescence 8=23037
- memory circuits, optico-elec., static params. theory and obs. 8=6039
- metals, vacuum u.v. 8=13934
- micrometer for meridian passage times 8=10104
- p-n junction detectors, self-filtering with narrow spectral responses 8=9158
- photocathodes, current-limiting protective circuit 8=13923
- photocathode technique for anode desorption efficiency meas. 8=17167
- photocell detection unit for crush strength apparatus 8=5022
- photocells for light pulse meas., accuracy 8=9245
- photodetector signal: noise ratio rel. to electro-optic filter modulation voltage vars. 8=2270
- photodiodes, Schottky, carrier generation and spectral response, model 8=9264
- semiconductor converter with single-line scanning, theory 8=22707
- semiconductors, graded-band-gap, photo-excitation by anti-Stokes mechanism 8=9266
- semiconductors, photothermoelectric and thermally stimulated thermoelectric effects 8=22678
- semiconductors, quantum efficiency and impact ionization 8=13907
- solar cells for UK 3 satellite 8=19734
- u.v. sensitive photoemitters 8=13922
- ultraviolet refl. spectra, photoelec. method 8=15532
- visualization of quasilongitudinal and quasitransverse elastic waves 8=8788
- zero crossing timing, accurate, tunnel diode circuit 8=3142
- Ag, laser induced non-linear effect 8=2258
- Ag, laser-induced non-linear photoelectric effect 8=22721
- Al film, irradi. with polarized light, effect of oxidation 8=18221
- Al-Al₂O₃-Al sandwich, emission studies 8=13858
- Al-Al₂O₃-Al thin film structures, electrode props. rel. to photocurrent direction 8=22689
- Al-Al₂O₃-metal structures, int. effect, attenuation length 8=13910
- Au, laser induced non-linear effect 8=2258
- Au, laser-induced non-linear photoelectric effect 8=22721
- Au-GaAs Schottky barriers, photoresponse 8=13931
- CdS, etched in KOH(NaOH) soln., light sensitization investigation 8=14294
- CdS, photothermoelec. effects 8=22681
- CdS sintered photoelements with p-n-hetero-transitions 8=22710
- CdS thin film solar cell 8=19735
- CdSe, thin non-stoichiometric films, and elec. props. 8=13795
- CdTe thin film solar cell 8=19735
- GaAs thin film solar cell 8=19735
- n-GaAs-Al Schottky barriers, photoelectric barrier energy dependence on electric field 8=13924
- n-GaAs-Au surface barrier diode application to photocapacitors 8=13925
- GaAs-Cs-O photoemission 8=22718
- GaAs-Ga(AsP)heterojunctions, photocurrent, forward current injection modulation 8=13844
- (GaIn)As-GaAs heterojunctions, photocurrent, forward current injection modulation 8=13844
- GaP diffused single crystal layers p-n junction, properties 8=5406

Photoelectricity — contd

- GaP miniature diode for nsec. pulses 8=15525
- Hg, photocurrent and work function, melting 8=13939
- n-InSb, quantum oscillations 8=13913
- K, photocurrent and work function, melting 8=13939
- Ni, laser induced non-linear effect 8=2258
- Ni, laser-induced non-linear photoelectric effect 8=22721
- Rb, photocurrent and work function, melting 8=13939
- Rh, photoinjection into liq. hydrocarbons 8=8113
- Sb₂S₃, amorphous films, photo-e.m.f. meas. 8=9255
- Se electrophotographic layers, discharge kinetics 8=2265
- Si photo-detector, integrated circuit, with internal amplification 8=18235

Photoelectromagnetic effects

- optically polished semicond. elements, i.r. sensitivity and speed of response 8=6203
- semiconductors with light-heated electrons, theory 8=18219
- semiconductors rel. to photoelectron diffusion in strong mag. field 8=13909
- n-CdTe, rel. to surface recombination velocity determ. 8=18225
- CdTe-HgTe heterostructures 8=13911
- Ge, Dember photovoltage in n- and p-type, obs. 8=9253
- Si, Dember photovoltage in n- and p-type, obs. 8=9253
- Si, energy band structure dependence 8=13916

Photofission. See Nuclear fission.

Photographic light sources. See Light sources; Photography.

Photographic materials

- See also Nuclear track emulsions.
- emulsions, limitations on holography 8=6566
- glass, photochromic, information storage capacity meas. by holography 8=6570
- grain development by laser photons 8=15563
- granularity meas. using photocond. cells 8=6581
- holography, film nonlinearities effects 8=6574
- ion-sensitive, for mass spectroscopy 8=1140
- plates for mass spectrometers, AgBr grain distrib. 8=7360
- polaroid projection film, use in strobocameras 8=534
- requirements for holography 8=20106
- thermoplastic resin film, for recording 10.6 μ laser rad. 8=6579
- Tri-X Pan film, use in low-angle holographic interferometry 8=6571
- xerographic, electrostatic voltmeter used in conjunction with sample illumination 8=3133
- AgBr(I) film, influence of dyes on luminesc. 8=23042

sensitivity

- films, Kodak photoresisting, rel. to electron probes spot size and current density distrib. obs. 8=331
- ion-detecting plates for mass spectrograph 8=16179
- resolution limits of materials in holography 8=15552
- Rontgen film, spectral sensitivity 8=535
- sensitizer dyes, adsorbed, ionization energy 8=5424
- X-ray film, quantitative calibration, 5 keV-1.3 MeV 8=15565
- AgBr plates, ion-sensitive, for mass spectrograph 8=16178

Photographic process

- See also Photochemistry.
- electrostatic latent image transfer 8=6580
- photopolymerization appl. 8=23140
- AgBr, effect of Cd and Cu ions 8=533

development

- catalytic action of centres of development, mechanism 8=20124
- diffusion transfer film, grain structure 8=11222
- diffusion transfer film, image structure 8=11223

Photography

- See also Cameras; Cinematography; Lenses/photo-graphic; Radiography.
- astronomical photographs, spatial filtering theory 8=10108
- brightness detector, accuracy and stability 8=11225
- corneagrams, instrument for measuring contour of cornea 8=20129
- dispersion of differences in transparency due to granulation, obs. 8=15564
- electrophotography, use in meas. width of sensitive region of Ge p-i-n detectors 8=9152
- Ephemeris and Universal time difference by lunar photography 8=10486
- evaporographic image quality 8=11219
- exposure determination, incident light method 8=11221
- galaxy central region 8=2796
- hologram, interferometric, ghost lines in spectra from nonlinearity in exposure 8=3380
- infrared, with interf. microscope 8=20123
- integral, limitation of resolution 8=15568
- Kodak I-Z plates, modified hypersensitization procedure 8=494
- Lunar Orbiter system, dual lens 8=23651
- microkymography, new method and apparatus 8=15566
- phase structures, interferometric meas. 8=15553
- for planetary space science, analogue and digital data processes 8=10065
- planets, resolution limitations, atm. turbulence 8=14835
- sharp images making with X-rays, apparatus 8=6582
- spark chamber cathode ray film scanner, computer directed 8=3482
- spectral images, faint, electronic enhancement 8=6583
- Wilson cloud chamber, Polaroid-Land camera appl. 8=20222

Photography—contd

xerography, electrostatic voltmeter used in conjunction with sample illumination 8=3133

applications

astronomical, device for spatial filtering 8=14744
calibration curves, stars spectra 8=2785
comet Iyeka-Seki (1965), history 8=19258
computer controlled film scanner, particle tracks 8=3481
detectors, air to ground viewing, meas. of contrast and range 8=20126
detectors, radiation absolute meas. 8=537
elec. arcs formation in rectifier valves and switches, obs. by image converter camera 8=20125
electrodeless discharge, high-speed cinematography 8=16398
fluorescent, spray droplets, with Q-switched laser as light source 8=4636
fracture of metals, obs. 8=22293
fracture tests, recording 8=6584
 γ , X-ray monitor using CsI(Tl) crystal 8=11444
holographic stereogram from sequential component photographs 8=15555
3-d images, computer-generated subjects, recording and reconstruction by Lippmann's method 8=20127
laser beams, orientation of crystal for second harmonic 8=3322
magnetic spectrometer for recording 400 MeV/c spectra 8=11292
particle behaviour during electrostatic precipitation 8=10836
spark electrode erosion obs. 8=16423
spark type, for study of pulsed high-pressure jets 8=16778
ultracentrifugation, simultaneous automatic sequence and photo control system 8=4631
Weissenberg photographs, giving rectified representations of reciprocal lattice 8=4864
C arc electrode particle trajectory 8=16428
Si photocell for recorders spot-brightness control 8=2271

colour

multistage, integrity preservation 8=15569
photomicrography, of biological objects, app. using image intensifier 8=11226

high-speed

cinemicrophotography 8=11220
exposure methods extended to X-ray 8=15567
image converter camera, operation and applications 8=20125
microplasma production at solid surface by laser beam 8=21353
C arc electrode particle trajectory 8=16428

Photoionization. See Ionization.

Photolysis. See Photochemistry.

Photomagnetic effects. See Photoelectromagnetic effects.

Photomagnetolectric effects. See Photoelectromagnetic effects.

Photometers

See also Spectrophotometers.

actinometer for vac. u.v., using N_2O 8=14439
field of view, broadening by irregular surface refraction in u.v. 8=463
for geology students 8=460
linear flowing-stream type, for amino acid analysers 8=5762
single beam, supplement to compensate for light turbulence fluctuations 8=3343
single pulse reception, operational props. 8=3575
2, correl. in arbitrary field rel. to quantum field theory 8=6623
 K^* intensity modulation of transmitted light utilized 8=12085

Photometry

See also Brightness; Densitometry; Illumination; Spectrophotometry.

astronomical, effect of temp. changes on glass-filters 8=10103
for astronomical faint objects with small-diaphragm 8=23498
brightness detector, accuracy and stability 8=11225
correlation measurements of optical field with time-to-amplitude converter 8=15496
detectors, elimination of lumen from responsivity calibration 8=464
equivalent luminance of a colour, obs. 8=15499
flame, atomic absorpt. chemical analysis, accessories 8=18777
flame, pulverizer attachment 8=20085
fluctuations correl. functions, 3-channel photoelec. counting obs. 8=20015
flux, feeble luminous, detection using photomultiplier detector 8=20038
laser beam, photostatistics second sound scatt. effect 8=11192
laser intensity fluctuations, analogue and photon counting meas. 8=19970
light statistical props. meas., photodetect e emission distrib. 8=15493
photoelectric, correlation function factorization 8=20037
photoelectric detect statistics, communication channel model 8=20010

Photometry—contd

photoelectric control for rotary power meas. 8=15549
photon count distrib. rel. to light field statistics 8=20014
photon counting distrib., meas. and analysis 8=20351
photon count statistics in verification of Brownian motion 8=1557
precessing torques, rel. to shadow-boundary displacement 8=3342
rotating convex surfaces, flux density var. meas. 8=15497
three colour, of galaxies in Stephan's Quintet, obs. 8=5938
units, inappropriate use 8=461

light sources

No entries

Photomultipliers

after pulses due to ions between cathode and first dynode 8=5418
ageing and rejuvenation 8=15335
blanking circuit for mag. electron multiplier in time-of-flight mass spectrometer 8=20913
cathode poisoning 8=3220
channel electron multiplier for radiation detect. 8=11312
channel, life tests in high vacuum 8=15336
cooling effects, undesirable 8=3219
feeble luminous flux detection 8=20038
gain control system, automatic for use in presence of radiation 8=6324
gating method, for stimulated-spontaneous light scattering discrim. 8=6331
laser illum., photocurrent power spectrum and statistics 8=19951
light emission, causes 8=6327
light u, h. f. modulation meas. 8=6487
noise factor and photocathode quantum efficiency 8=10905
noise pulses from, effect of high energy radiations 8=3216
open structure, performance in 1100-250 Å region 8=6325
open type multiplier, poss. reason for appearance of 'false' pulses 8=6329
particle spectrometers, preamplifier for use with 8=3474
performance monitor 8=19794
as photon counter in photometry of very faint light sources 8=10904
for photon counting 8=15717
p-e, p- μ discrimination by Owen-Batchelor method, theory of high energy limit 8=6672
pulse shaping, nanosecond pulse integrator 8=15643
radiation intensity, measurements in vacuum u.v. region 8=11159
satellite pulses, effect (γ -n) spectroscopy 8=20569
shock resistant for scintillation counters in severe environment 8=6328
spectral depend. of quantum fields, 75-300 Å, for 9 photocathodes 8=19795
time resolution, new technique of pulse processing 8=6665
time resolution optimized with fast discriminator 8=6330
time resolution studies, optimization for scintillation counters 8=3218
time spread behaviour, optimum conditions 8=6323
time-spread meas. for different models 8=6326
timing props. of scintillation photomultiplier system 8=3459
u.v. response extension by liq. phosphor cell 8=340
zero crossing timing, accurate, tunnel diode circuit 8=3142
RCA 7265, single electron response 8=3217

Photons

See also Cosmic rays; photons; Gamma-rays; Nuclear reactions due to; photons; X-rays.
absorpt. by atoms, laser and thermal light, relative probability 8=20975
absorption, two-photon, rel. to light coherence 8=6485
angular distrib., from positron annihilation in Se-Te alloys 8=13692
charge on 2 eV γ , determ. 8=11455
cross correl. in atomic coupled bimodal system 8=12102
counters, stimulated emission, statistics 8=20183
counting distrib. rel. to statistics of laser or Gaussian rad. field 8=10998
counting distrib., meas. and analysis 8=20351
counting, using photomultipliers 8=15717
counting with photomultiplier, for very faint light sources 8=10904
counting with spectrofluorimeter, and reversible precounter 8=3573
counting statistics, rel. to anal. of light beam fluctuations 8=6425
creation and annihilation operators rel. to quantum optics 8=11425
decay in light scatt. in nonlinear medium 8=6560
detection of light scattered by extremely small aerosol particles 8=21740
diffraction, wave theory, corpuscular interpretation 8=15547
echoes, multiple and stimulated, theory 8=20340
e.m. fields coherence props. rel. to counting statistics 8=20352
e-beam scatt., emission 8=711

Photons—contd

- e-photon cascades in Pb plates, meas. in scintillator 8=6804
- energy density range 10^{17} - 10^{25} ergs.cm⁻³, by exponential laser amplification 8=6421
- form factor, coupling to 1^- mesons 8=6905
- $g_{\gamma NN}/g_{\pi NN}$ calc. rel. to domination of N form factors by $N^*(1400)$ 8=20515
- interference, wave theory, corpuscular interpretation 8=15547
- laser counting distrib. rel. to intensity noise theories 8=19939
- laser field, 3-photon effect on frequency 8=408
- laser light, development of photographic grain 8=15563
- in light fields, equil. and non-equil., distrib. obs. 8=19954
- light field statistics from photon count distrib., meas. 8=20014
- light statistical props. meas., photodetect. e emission distrib. 8=15493
- Low soft-photon theorem rel. to unpolarized, nonradiative cross section 8=15714
- in masers, interaction with atoms with angular momenta 8=19921
- mass increase in Schwinger models, solns. 8=11286
- model photodetectors, image characteristics 8=9263
- multi-photon absorption, probability 8=104
- multiphoton processes, resonance case, double photon contrib. 8=20011
- noise, excess, in multimode lasers 8=11039
- noise in lasers 8=11023
- pair production and annihilation, quantum electrodynamics 8=11445
- photoelectron distrib. rel. to probab. density 8=20016
- photon-meson coupling in Fubini sum rule from K^+ decay 8=20474
- photostatistics of laser beam, second sound effect 8=11192
- processes, low energy theorems, amplitudes 8=20341
- propagators, covariant and vertex functions for any spin 8=20336
- quantum statistics of fields, coherent-state techniques appls. 8=19450
- reflection, wave theory, corpuscular interpretation 8=15547
- self-energy graph, asymptotic behaviour 8=20170
- shot noise in lasers 8=11022
- spin-phonon interaction, ultrasonic waves in paramagnetic crystal 8=5516
- stability in absence of external field, proof for zero rest mass parts 8=6773
- stability in absence of mag. field, reply to criticism 8=6774
- statistics, rel. N-mode laser field 8=412
- 2 detectors, in photon field, correl. of output and quantum theory 8=6623
- two-photon process, theory using density matrix formalism 8=3339
- two-photon processes in 2-level atomic system, field statistics 8=20948
- wave function renormalization constant, divergence in quantum electrodynamics 8=6620
- Co⁶⁰ emission, exposure meas. 8=11427
- H scatt., analytic expression and numerical computation 8=1196
- MgO, powdered, mag. quenching, "anomalous", of three photon annihilations of positrons 8=17908

interactions

- coalescence in uniform e.m. field, quantum electrodynamics 8=590
- cross-section det. by statistical method 8=1033
- d disintegration, meson exchange contribution 8=872
- d photodisintegration theory 8=16056
- d photo-disintegration, 170-450 MeV p polarization obs. 8=20533
- e-pair photoprod. and test for q. e. d. 8=20390
- e.m. S-matrix theory formulation and dressed amplitudes 8=20343
- with field and intense e.m. wave, rel. to e^-e^+ pair prod. 8=717
- form factors, canonical 8=3512
- $\gamma + d$, at 285-345 MeV, π^0 prod., multiple scatt. correction 8=3620
- $\gamma + \text{He}^3 \rightarrow d + p$, with Cabibbo-Radicati sum rule 8=6999
- $\gamma + \text{He}^4 \rightarrow \rho^0 + \text{He}^4$, determ. of particle scattering amplitudes 8=11858
- H³, photodisintegration cross-section calc., normalization anomaly 8=11655
- K_L photoproduction method 8=11548
- $K^-p \rightarrow \Lambda\eta$, 1.2-1.7 BeV/c 8=6888
- $\gamma + N \rightarrow \Lambda + K$, consistency conditions for non-Born amplitudes 8=20344
- $\gamma + N \rightarrow N + \pi$ 8=11507
- $\gamma N \rightarrow \pi N$, test for conspiracy 8=6775
- $\gamma N \rightarrow \pi N^*$, threshold cross-section calc. from current algebra 8=11504
- $\gamma^+ N \rightarrow \pi^0 + N$, varying γ polarization as Regge cut test 8=20331
- $\gamma + N \rightarrow \Sigma + K$, consistency conditions for non-Born amplitudes 8=20344
- $\gamma p \rightarrow N^*$, missing mass determ. of excitation function of N_{15}^* (1688) 8=11638

Photons—contd**interactions—contd**

- $\gamma p \rightarrow n\pi^+$ at large angle, differential cross section, 260, 290, 320 MeV 8=752
- $\gamma p \rightarrow \Lambda K^+$ Regge-pole calc. of cross-sections 8=3621
- $\gamma + p \rightarrow \eta + p$ amplitude, unitarity and S-matrix analysis 8=3569
- $\gamma\pi \rightarrow \rho\pi$, sum rules rel. to e.m. widths of ω , A_1 , A_2 8=11566
- $\gamma + p \rightarrow N^* + \pi^+$, up to 6 BeV 8=6986
- $\gamma + p \rightarrow n + \pi^+$, ang. depend. of cross-section rel. to π^+ prod. 8=6841
- $\gamma + p \rightarrow n + \pi^+$, Regge pole model 8=20425
- $\gamma + p \rightarrow p + \eta$, N pole and vector meson resonance below c.m. energy 1700 MeV 8=20490
- $\gamma + p \rightarrow p + \pi^0$, angular distribution, E_0 , M_{1-} , M_{1-} calc. 8=6845
- $\gamma + p \rightarrow p + \pi^0$, differential cross section, E_γ =4-5.8 GeV 8=20426
- $\gamma + p \rightarrow p + \eta^0$, recoil p polarization 8=838
- $\gamma + p \rightarrow p + \rho^0$, 3.2-4.9 GeV 8=16057
- $\gamma + p \rightarrow \pi + N^*(1238)$, test of e.m. C noninvariance 8=694
- $\gamma + p \rightarrow \pi + N_{33}^*$ and current algebra 8=6985
- $\gamma + p \rightarrow \pi^+ + n$, GeV region absorption correction, choice of parameters 8=15764
- $\gamma + p \rightarrow \pi^+p$ in backward direction 8=15762
- $\gamma + p \rightarrow K^+ + (\Lambda^0, Z^0)$ at 3.4 and 5.0 GeV 8=6887
- $\gamma p \rightarrow \pi^+n$, pion-exchange, Regge-pole model 8=11516
- $\gamma p \rightarrow \pi^+n$ Regge-pole calc. of cross-sections 8=3621
- $\gamma p \rightarrow \Sigma^+ K^0$ Regge-pole calc. of cross-sections 8=3621
- $\gamma p \rightarrow \pi^+$, rel. to energy-depend. of recoil-p polarization 8=835
- $\gamma p \rightarrow \pi^+p$ Regge-pole calc. of cross-sections 8=3621
- $\gamma + p \rightarrow p + \pi^0$, 163-234 MeV, ang. dist. of π^0 8=750
- graviton prod. cross-section 8=19422
- high-energy diffraction photoproduction, of ϕ , expt. limit 8=20500
- isobar, $T = J = \frac{1}{2}$ production, soln. of dispersion relations 8=3732
- Λ/Σ^0 photoproduction cross sections, ratio 8=15859
- meson photoproduction, Regge-pole assumptions 8=3611
- meson photoproduction on nuclei, threshold 8=1034
- muon anomalous mag. moment contrib. 8=6815
- on nucleons, to form K and π mesons 8=6842
- ω^0 photoprod., OPE, diffraction contribs., polarization prediction 8=20502
- photopion production below 500 MeV 8=11509
- photoprod. at high energy, absorpt. derived using Regge amplitude 8=20342
- photoprod. on spin-1/2 target, superconvergence relations and current algebra identities 8=20376
- photoprod. of strange particles, PCAC and current algebra study 8=20344
- photoprod. of spinless particle, non-existence of poles 8=20249
- photoprod. rel. to isovector form factor 8=15864
- $p + \gamma \rightarrow p + \pi$, Mandelstam branch cuts rel. to scatt. and prod. amplitudes 8=11594
- π pair, dipion mass spectrum obs. 8=20507
- π pairs, charged, prod. from hydrogen, up to 1500 MeV energies 8=6844
- π photoproduction and electroprod., dispersion relation theory 8=11508
- π photoproduction at high energy, O(4) symm. 8=3627
- π photoproduction on N, pole terms in fixed angle approach 8=3622
- π photoproduction on p ang. distrib. parameters 8=11511
- π photoproduction on p, 553-850 MeV analysis in second reson. region 8=6843
- π photoprod. Regge pole residues, kinematical singularities 8=11415
- π photoproduction, violation of Knoll-Ruderman limit 8=6743
- π^0 photoproduction from deuterium, test of symmetry in e.m. current 8=670
- π^0 photoproduction, w and B exchange at low energy 8=11510
- π^+ photoprod., $1 < E_\gamma < 3$ GeV, simple isobar ansatz in fixed-t dispersion relations 8=20437
- π^+ photoprod. forward peak obs. 8=6846
- π^+ photoproduction, finite energy sum rules, parity doublet conspiracy 8=20423
- π^+ photoproduction, 300-600 MeV at small angles 8=3624
- π^+ , π^0 and K^+ photoproduction 8=15766
- π prod. 220-380 MeV near $P_{33}\pi N$ resonance 8=11506
- $\pi^+p \rightarrow \pi^+n$, $\pi^+\pi^+p$, rel. to phase shifts in $\pi\pi$ scatt. 8=6870
- ρ^0 photoprod. cross-section calc. on N 8=20508
- single pion photoproduction near threshold 8=20424
- spectrometer magnetic, for photoproduction reactions 8=6776
- two-photon absorpt. processes, model calcs. 8=16286
- three-particle nuclei disintegration cross section 8=11652
- vector meson prod., storage rings 8=15669
- Ag, $\eta \rightarrow \gamma\gamma$ decay obs. 8=806
- $\gamma + \text{He}^3 \rightarrow \pi^+ + \text{H}^3$, using PCAC and current algebra 8=15765
- $\gamma + \text{He}^4 \rightarrow \text{H}^3 + n + \pi^+$, impulse approximation 8=888
- $\text{H}^3(\gamma, n)d$, $\text{H}^3(\gamma, p)^3\text{He}$, $\text{H}^3(\gamma, 2n)p$, cross sections and ang. distrib. 8=11432
- H liquid single- π^+ prod. 5-16 GeV 8=15763

- Photons—contd**
interactions—contd
 H^3 , two- and three-body disinteg. cross section calc. 8=15870
 He^+ , photodetachment cross-section 8=20944
 He^3 , diffusion cloud chamber for investigation 8=7000
 He^3 , two- and three-body disinteg. cross section calc. 8=15870
 $He^4(\gamma, p)H^3$, 50 MeV, cross-section 8=889
 He^4 , photodisintegration, calc. using Levinger-Bethe sum rules and vel. depend. pot. 8=11658
 $Pb, \eta \rightarrow \gamma\gamma$ decay obs. 8=806
 Sb -Be photoneutrons, energy estimate using meas. of γ -ray of Sb^{24} 8=11622
 $Zn, \eta \rightarrow \gamma\gamma$ decay obs. 8=806
- polarization**
bremsstrahlung prod. from e bombard. of crystal 8=13465
Bremsstrahlung, thin-target linear polarization 8=11446
Compton scatt. off spin- $\frac{1}{2}$ particle with charge and anomalous magnetic moment 8=20348
meas. from e pair production 8=3572
meson photoproduction, Regge-pole assumptions 8=3611
n-th rank tensor, appl. to photon-photon interaction 8=6815
parity admixture determ. in nuclear energy levels 8=15997
photoprod. reactions on N, with π prod., test for Regge cuts by varying γ polarization 8=20331
- scattering**
atomic fluids, light, three-photon 8=4044
Compton, in intense fields, freq. shift 8=20349
Compton, off spin- $\frac{1}{2}$ particle with charge and anomalous magnetic moment 8=20348
Compton scatt. off spin-0, $-\frac{1}{2}$ particles, sum rules 8=20350
Compton, second harmonics, spectral profile 8=11426
Compton subtraction constants in sum 8=20347
diffusing in plane layer 8=3567
by electrons, rel. to Friedmann cosmology 8=23465
e, moving in a radiation field 8=20346
 $\gamma + C \rightarrow C + e^+ + e^-$, phase and magnitude of virtual Compton scattering 8=3904
 γd , sum rules for forward scatt. 8=6992
 γN , interaction constants of σ, f, η and X^0 calc. 8=6741
 $\gamma + Pb \rightarrow Pb + e^+ + e^-$, phase and magnitude of virtual Compton scattering 8=3904
 $\gamma\pi$, interaction constants of σ, f, η and X^0 calc. 8=6741
 $\gamma-\pi$, threshold vector dominance hypothesis and Compton scatt. of isovector photon 8=6864
giant resonances, dynamic collective model, sum rule 8=11856
Klein-Nishina formula, Legendre polynomial expansion 8=3370
large-angle Compton effect, double logarithmic approximation 8=15715
nuclear, amplitude separation into Thomson and Rayleigh terms 8=11855
nuclear, general case of all elect. and mag. multipoles 8=16055
optical, three-photon, in isotropic medium, general theory 8=3373
polarized, by Dirac particle 8=15713
Regge pole hypothesis in amplitude 8=15716
resonance Compton, on electrons, in field of intense laser ray 8=20354
resonant elastic response of matter to intense light pulse, transient effects, bibliography 8=19925
- Ag**, incoherent, e-binding effect, Thomas-Fermi model 8=17703
 $Al(\gamma, \rho^0)Al$, 3.2-4.9 GeV 8=16057
 $Al(\gamma, \pi^+\pi^-)Al$, 3.2-4.9 GeV 8=16057
Bi, incoherent, e-binding effect, Thomas-Fermi model 8=17703
 $C(\gamma, \pi^+\pi^-)C$, 3.2-4.9 GeV 8=16057
 $C(\gamma, \rho^0)C$, 3.2-4.9 GeV 8=16057
 C^{12} , giant magnetic dipole state, analog states 8=3905
H atom, elastic, evaluation of Kramers-Heisenberg matrix element 8=16221
 Mg^{24} , giant magnetic dipole state, analog states 8=3905
N, Compton, new low-energy theorems 8=20521
N Compton scatt., low-energy with π photoprod., use of $\pi\pi$ phase shift 8=20345
 P^{31} , to excite 3.13 MeV state, level width determ. 8=11734
Pt, incoherent, e-binding effect, Thomas-Fermi model 8=17703
 Si^{28} , giant magnetic dipole state, analog states 8=3905
- Photonuclear reactions.** See Nuclear reactions due to/photons.
- Photophoresis**
kinetic theory, particle in Knudsen gas 8=4629
- Photoproduction.** See Gamma-rays/effects; Nuclear reactions due to/photons; Photons/interactions.
- Photoresistors.** See Photoconductivity; Semiconducting devices.
- Photosphere.** See Sun.
- Photovoltaic effects—contd**
p-n junctions, drift time of photogenerated carriers 8=5318
p-quarterphenyl polycryst. layers rel. to electrodes and temp., obs. 8=22703
of r conversion of heat radiation into electricity, efficiency 8=15249
semiconducting thin layers, high voltage 8=9247
semiconductor solar cells multistage, selection of optimum combination of materials 8=6277
semiconductors, lifetime-gradient photovoltage, large signal theory 8=9253
solar cells, distributed model 8=9265
 $Al-Al_2O_3$ -Au tunnel structures, interface trapping 8=5381
 $Al-CaWO_4$ -Au tunnel structures, interface trapping 8=5381
CdS film solar cell, mechanism obs. 8=10847
CdS- Co_2S solar cell, mobile impurity ions model 8=10846
CdTe p-n junctions, excitation spectra 8=5405
CdTe, wedge-shaped films, rel. to incident angle of illum. 8=5398
CdTe-HgTe heterostructures, and photoelectromagnetic effect 8=13991
 Cu_2S -CdS p-n heterojunction, photovoltaic response 8=13843
GaAs p-n junction, max. photo-e.m.f. on laser excitation 8=9252
GaAs, wedge-shaped films, rel. to incident angle of illum. 8=5398
GaP-GaAs, n-p heterojunctions, photo e.m.f. spectral dependence 8=5311
Ge, lifetime-gradient photovoltage in n- and p-type, obs. 8=9253
PbS chemical films, effect of const. current 8=18234
Si cell for photographic recorders spot-brightness control 8=2271
Si-collodion-Au contacts, photocapacitive response 8=22673
Si-collodion-Au contacts, photocapacitive response 8=22673
Si, lifetime-gradient photovoltage in n- and p-type, obs. 8=9253
Si p or n solar cell characts. rel. to distributed model 8=9265
ZnS, negative differential photovoltages 8=22702
- Physical chemistry**
copolymers in dilute solution, recent aspects 8=8020
gases, monatomic and diatomic mixture, channel flow in chemical and thermodynamic non-equilibrium 8=7903
ion sublation using anionic and cationic collectors, radioactive tracer structures 8=23075
 $Co(II)-Ni(II)-Mn(II)-V(V)-Mo(VI)$ chloride systems, extraction separation studies 8=23077
F n.m.r., press., dependent chemical shifts in freon gases 8=12324
 $MO(VI)$ extraction with TBP, mechanism study by radioisotopes 8=23076
NbN preparation by gaseous diffusion 8=2165
NbN with Zr and Ti, preparation and superconductivity 8=2158
- Physical effects of radiations**
See also under individual radiations, e.g. Neutrons and antineutrons/effects.
advances in nuclear science and technology, book III 8=17691
alkali halides, formation of radiation defects 8=13487
 α particle damage to metals at high temperatures 8=22237
anomalous absorpt. and propag. when incident beam is Bragg diffracted 8=17362
anthracene, damage to optical absorption props. 8=9565
beryllia-based fuels with dispersions of (U, Th) O_2 , irradiation effects 8=22248
channeling phenomena, location of shoulders using Monte Carlo computer program 8=17690
crystals, transparent, thermal effects of laser beam 8=4926
damage displacement cascade, rel. to scattering law 8=22239
diamond as particle-counters 8=6647
dielectrics, transparent, damage due to laser light 8=8755
electrical insulation, breakdown under radioactive radiation 8=9190
energy loss of channelling particle, theoretical study 8=17697
f.c.c. metals, recovery kinetics, interstitial model 8=2015
fission track densities, etched in int. and ext. surfaces, comparison after n irradi. 8=20852
focused collision sequence generation, inverse-square potential calcs. 8=17696
glass, desensitization by h.p. H $_2$ synthesis 8=8353
glass, spectral characts. of emission, and damage, due to laser beam 8=14246
glass, suppression after high pressure H treatment 8=4996
grain boundary gas bubbles, equilib. conditions 8=1986-9
graphite, irradi., at 77°K 8=8763
graphite, irradi. induced creep under constant stress 8=8828

Physical effects of radiations—contd

- graphite, n prod. dimens. changes rel. to bromination test 200°C 8=8764
- graphite, pyrolytic, on dynamic mech. behaviour 8=8827
- laser beam, metal atom ejection compared with pulsed discharge 8=17698
- laser, damage to materials review 8=403
- laser focal evaporation, energy dependence 8=11007
- laser-surface interaction, production of high-energy molecules 8=18273
- leuco-sapphire crystals, destruction by powerful laser radiation, mechanism 8=22247
- magnetic resonances induced by mod. light in rotating co-ord. system 8=4102
- metals, b.c.c., rel. to production of imperfections, and diffusion 8=17702
- metal-insulator-semiconductor devices, survey 8=9171
- m. o. s. devices, charact. degradation 8=18138
- metallized plastic films, increased cond. 8=5153
- n-hexane, elec. cond., u. v. and γ radiation 8=21714
- nuclear science and technology for ceramists, conference, Washington USA (1966) 8=16167
- nuclear and space radiation effects, conference 8=22578
- organic crystals, energy transfer 8=23038
- ozone discharge and associated Joshi effect, external radns. rel. to leakage time constant 8=21222
- photoeffect internal in crystal lattice with atomic centres 8=8739
- photopolymerization, appl. to photography 8=23140
- polyacrylonitrile, density changes rel. to atomic-pile-irrad. 8=17709
- polyethylene, cross-bindings prod. by reactor irrad., showed by n scatt. 8=16969
- polyethylene, irradiated, at melting point 8=9201
- poly(glycol methacrylate), e. s. r. 8=18422
- poly(methyl methacrylate), e. s. r. 8=18422
- polypropylene films and blocks, melting and recryst. or evap. due to laser pulse irrad. 8=17710
- polytetrafluoroethylene, carbon-black filled 8=17700
- polythene film, laser-produced formation mechanism 8=23034
- PVC, effect of u. v. irrad. on glass transition temp. 8=17181
- quartz, X-ray irradiated, influence on permittivity, luminescence and thermoluminescence 8=13871
- radiation research, space radiation biology, conference, Berkley USA (1965) 8=23456
- refraction and reflection of resonance radiation through crystal 8=8752
- resonance rad. from Cs discharge, prod. of Cs plasma 8=4362
- resonant elastic response of matter to intense light pulse, transient effects, bibliography 8=19925
- rubber, cross-bindings prod. by reactor irrad., showed by n scatt. 8=16969
- ruby crystals, destruction by powerful laser radiation, mechanism 8=22247
- semiconductor devices, nuclear radiation damage estimation by equivalent circuits 8=13838
- semiconductor surfaces, damage by ruby laser 8=2028
- solid targets, laser induced emission of electrons, ions and X-rays 8=13947
- steels, stainless, irradiation effects on tensile and shear props. at cryotemps. 8=17763
- styrene, cross-bindings prod. by reactor irrad., showed by n scatt. 8=16969
- TFE-HFP copolymers, γ -irrad., dielectric props. 8=9202
- trioxane polymerization rate, 30-64°C 8=23133
- trithiane, polymerization 8=17184
- A_2B_3 type crystals, illumination effect on u. s. absorption 8=4915
- Ag, fission fragments energy loss rel. to range 8=2021
- Al-1 at. %Zn, electron irradiation hardening 8=8822
- Al alloys, irradiation effects on tensile and shear props. at cryotemps. 8=17763
- Al, atomic-stopping cross sections for H^+ and He^+ 8=2022
- Al and AlM, (M = Mg, Ga, Ag), e-irradiated, stage II and III recovery temp. and impurity conc. dependence 8=1935-6
- Al, fission fragments energy loss rel. to range 8=2021
- Al_2O_3 , 5×10^{21} fast neutrons cm^{-2} , damage 8=22244
- Au, fission fragments energy loss rel. to range 8=2021
- Ba silicate glasses, γ -ray induced defects 8=13479
- Ba(ClO_3) $_2$.H $_2$ O, X-irradiated, e. p. r. spectral changes in u. v. irradiation 8=18410
- BeO dispersion fuels, X-ray study of fission fragment damage 8=12018
- BeO, n-irradiated, electron microscope examination of damage 8=22250
- C, laser-induced 'blow-off' plasma, density and temp. 8=12467
- CaF $_2$.Nd $^{3+}$, 'ageing' and photoreduction to Nd $^{2+}$ by stimulated rad. conds. 8=8765
- CaF $_2$ -YF $_3$.Nd $^{3+}$, 'ageing' and photoreduction to Nd $^{2+}$ by stimulated rad. conds. 8=8765
- Cu, e irradiation, length change 8=22338
- Fe, critical magnetic scattering of neutrons, spin correlation 8=2026
- n-InSe crystals, thermal and i. r. quenching of photo-conductivity 8=18233

Physical effects of radiations—contd

- KH $_2$ PO $_4$, ferroelec. domain switching 8=18184
- KH $_2$ PO $_4$, fission fragment irrad., structural changes 8=8773
- LiD target for laser light, plasma prod. 8=8774
- LiF, anisotropy of orientation of U fission fragment tracks 8=17706
- LiF crystals, radiation heating in reactor 8=13488
- LiF, formation of macrodefects and metallic Li colloids 8=12947
- LiF, formation of radiation defects 8=13487
- LiH target for laser light, plasma prod. 8=8774
- NaCl, illumination effects on dislocation mobility 8=4979
- NaCl, spectral characts. of emission, and damage, due to laser beam 8=14246
- Ni alloy, irradiation effects on tensile and shear props. at cryotemps. 8=17763
- Ni, critical magnetic scattering of neutrons, spin correlation 8=2026
- Ni, fission fragments energy loss rel. to range 8=2021
- Pt, damage on e-irradiation at 90°K rel. to built-in annealing damage 8=1947
- Si, energy given to lattice by primary ions 8=2033
- Si:Li, radiation defects, effect on annealing rate 8=2067
- Si photoconverters, irradiation stability 8=2226
- SiO $_2$ -UO $_2$ vitroceraamics, irrad induced vol. changes and annealing 8=8779
- Te, fission-fragment irradiation effect on low-angle subgrain boundaries 8=8737
- Ti alloy, irradiation effects on tensile and shear props. at cryotemps. 8=17763
- U-Pd, fission fragments energy loss rel. to range 8=2021
- W, ion emission due to laser irrad., masses, energies and numbers 8=13948
- ZnO, damage 8=22255
- ZnO single crystal, γ -irradiated, defect structure 8=22168
- ZnS, electroluminesc. enhancement 8=14344
- ZnS, radioactive S 35 incorporation, photoluminescence spectra, dark conductivity 8=5000

Physics

See also Biographies; Books; Conferences; History; Nuclear physics; Teaching.

- NSF-supported secondary institutes in Physics 8=1
- "non-mathematical" theory, historical review 8=10467
- solid-state, in USSR, review 8=16964

Physics fundamentals

See also Cosmology; Elementary particles; Field theory, classical; Field theory, quantum; Indeterminacy; Mechanics; Parity; Probability; Quantum theory; Relativity; Thermodynamics; Units.

causality group of Zeeman examined 8=3416

charge, time-invariance, evidence 8=15690

e/m measurement, modification of experiment 8=10471

negative absolute temperatures 8=10642

Noether equations and conservation laws 8=6032

Rayleigh waves, conservation of energy 8=10707

square of charge, time-invariance, evidence 8=15691

Physiology

See also Biological technique and instruments; Blood; Hearing; Vision.

- electrophysiological meas., amplifier, high input impedance 8=5983
- lateral nervous interaction, Mach band brightness distrib. 8=15578
- microelectrode puller, pneumatically operated, for electrophysiology 8=23768
- retinal injury, pulsed laser induced, melanin granules models 8=20130
- X-ray pulmonary densitometry, physical aspects 8=14898

Piezoelectric oscillations

- aminoacids, temp. coeff. of resonance freq. 8=9224
- dielectric with piezoelectric film surface, surface wave amplification, ultra and hypersonic 8=13897
- excitation of elastic and e.m. waves, freq. and size resons. 8=10710
- quartz, frequency-controlled, temp. compensated 8=2252
- quartz plates, flexural and shear vibrations, thickness-twist overtones 8=15045
- self-excited prod. by current in separate semicond. layer 8=9223
- semiconductors, propagation and amplification 8=9088
- transducer, for wave velocity meas. in shock tubes 8=9230
- transversal waves in thin contactless piezoelectric layer of body 8=10711

Piezoelectricity

See also Electrostriction; Piezoresistance.

acetoxime crystal, (CH $_3$) $_2$ C:NOH, from benzine soln., props. 8=8396

ceramics, stress sensitivity of permittivity reduced by heat treatment 8=19555

class 3m crystals, constants meas. 8=9226

crystals, charge carrier motion, kinetic power theorem 8=22672

crystals, fields of dislocations and of linear charges 8=5376

current instabilities in crystals 8=5374

data handling system for sonic spark chamber 8=3484

dielectric, elastic, constants from lattice theory calcs. 8=13177

Piezoelectricity-contd

- elastic deform. of piezoelec. disc with inhomogeneous rigid inclusion 8=10542
 ferroelectrics, acoustic and polarization waves interaction, elastic consts. 8=18182
 linear eqns. of state, first and second order effects 8=2250
 phonon-electron interaction, rel. to nonlinear phonon damping 8=2079
 piezoelectric ceramics, sensitivity to high stress perpendicular to polar axis obs. 8=19556
 piezoelectrics, ultrasound generation under Gunn effect 8=22100
 piezo-optic coefficients by pulsed u.s. light diffraction, 24 liquids obs. 8=8064
 polaron, motion at zero temp. 8=13677
 polaron, strong coupling limit 8=8955
 quartz, elec. conductivity in a.c. field, 10^8 - 10^9 Hz, 20-700°C 8=18197
 quartz, rel. to microwave rectification 8=9227
 quartz resonator at 2°K 8=18204
 quartz thermometer, high-sensitivity 8=6220
 Raman-active vibrations and internal-strain rel. to elasticity and piezoelectricity 8=5013
 rectangular retaining wall, with pressure of loose material, piezoelectric analogue of elastic problems 8=6054
 resonator, meas. of heat transfer coeff. into surroundings 8=1884
 semiconducting crystals, transient acousto-elec. phenomena 8=13346
 semiconductors, acoustic amplification, critical electron drift velocity 8=19571
 semiconductors, acoustoelectric domain formation during thermal noise amplification 8=18001
 semiconductors, non-linearity of elec. props. during u. s. wave propag. in a. c. field 8=18022
 semiconductors, I-V characteristic under sound amplification conditions 8=18021
 semiconductors, stimulated Brillouin scattering 8=17495
 strain gauges for determ. of stress caused by acoustic excitations in nuclear structure 8=20884
 stress, static and dynamic, apparatus for combined application 8=5018
 transducer for meas. of vibr. of high pressure gases in reactor 8=20885
 transducer, with prescribed input, electrical response 8=15064
 ultrasonic holography by electronic scanning of piezo-electric crystal 8=19580
 in III-V cpds., rel. to phenomenological analysis of piezoelectric effect 8=13893
 Ba(NO₃)₂·H₂O, single crystal., meas. of coeff. in range 80-3000°K 8=5051
 CdS, polarons, cyclotron resonance theory 8=9220
 GaP, interband piezo absorpt. 8=18529
 Ge, piezothermal e.m.f., anisotropy 8=5390
 KBr, KCl and LiF polarization rel. to lattice imperfection prod. during shock wave plastic deformation 8=9225
 LiTaO₃ single cryst. 8=8853
 PbTiO₃-PbZrO₃-PbMg_{0.5}W_{0.5}O₃ domain orientation processes 8=5367
 Pb(Zr-Ti)O₃ ceramics, addition of Cr₂O₃ 8=13043
 Si, piezothermal e.m.f., anisotropy 8=5390
 Te, piezoresistance coefficient 8=5376
 ZnO, rel. to microwave rectification 8=9227

Piezoresistance

- See also Piezoelectricity.
 measurement in semiconductors 8=268
 BaTiO₃ semiconductors 8=9095
 n-Ge, piezomagneto-resistance for mixed scattering mechanism 8=18047
 n-Mg₂Sn at 80-300°K rel. to valence-band structure 8=2204
 n-SiC, α -phase, constants rel. to uniaxial deformation 8=18073

Piles, nuclear fission. See Nuclear reactors, fission.**Pinch effect.** See Discharges, electric; Plasma/confinement; Semiconducting materials.**Pions**

- Adler-Weisberger relation, π dominance implication 8=11424
 beam, meas. with filmless spark chamber system 8=3486
 charge radius determ. from $e^+ + e^- \rightarrow \pi^+ + \pi^-$ 8=15761
 Cherenkov counter, Pb glass for det. 8=6877
 composite, Goldberger-Treiman relation, bootstrap theory 8=3617
 cosmic ray attenuation length 8=899
 detection in H₂O with Si(Li) counter 8=7347
 e. m. form factor calc. 8=3615
 e. m. form factor determ., independence of $\pi\pi$ phase shift 8=15811
 e. m. form factor, from $\pi^+ \rightarrow \alpha$ scatt. 24 MeV 8=3616
 e. m. mass difference between charged and neutral 8=747
 e. m. mass difference, $\mu_{\pi^+} - \mu_{\pi^0}$ 8=749
 e. m. mass difference sum rule 8=748
 e. m. mass difference from Weinberg sum rules, corrections 8=3521
 e. m. mass, from source theory of gauge fields 8=20158

Pions-contd

- exchange theory, applied to various reactions 8=6847
 form factors calc., and violation of isotopic invariance 8=3614
 form factor fit in time-like region of Omnes-Mushkelishvili soln., $\pi-\pi$ P-wave dynamics 8=20435
 form factor from $e + p \rightarrow e + n + \pi^+$ 8=6834
 four-pion coupling const., sum rule resulting from current algebra 8=743
 $G_{\pi NN}$ in $G_{\pi NN}/G_{\pi NN}$ calc. rel. to domination of N form factors by $N^*(1400)$ 8=20515
 ionization loss at relativistic vels. in nuclear emulsions 8=15647
 $\Lambda\pi$ and $N\bar{K}$ composite model of Σ 8=11633
 mass determ. from 4f-3d transition in pionic Ca and Ti 8=6839
 $m_{\pi^+}^2 - m_{\pi^0}^2$ e. m. mass difference, divergences in gauge-field algebra 8=737
 mass, e. m. effects 8=20251
 mass smallness rel. to strong interaction 8=15760
 N-N scatt., 2π exchange contrib. 8=824
 NN $\pi\pi$ dynamics, bootstrap model, e. m. perturbation effect 8=11486
 OPE contrib. to ω^0 photoprod. 8=20502
 OPE model of $\gamma + p \rightarrow \pi^+ + n$ GeV region, absorpt. correction 8=15764
 OPE model for nuclear pot. 8=15919
 OPE model for $\pi N \rightarrow \pi\pi N$, 1-10 GeV, Treiman-Yang anomaly due to πN isobar prod. 8=15770
 OPE model for $\pi-\pi$ scatt., J = 1, I = 1 partial wave 8=15789
 OPE model in pp interactions, 10 GeV/c 8=11591
 parity doublet conspiracy, from finite energy sum rules in π^+ photoproduction 8=20423
 πN coupling constant related to that for πNN^* 8=11554
 pion field $\pi(x)$, identification with operators $\pi(x, \eta)$ 8=11498
 π^0 spectrum anal. in $K_L^0 \rightarrow \pi^+ \pi^- \pi^0$ decay 8=6879
 $\pi^+ - \pi^-$ mass difference, calc. on basis of isospin current algebra 8=6838
 $\pi^+ - \pi^0$ mass difference, field theoretic model 8=20415
 $\pi^+ - \pi^0$ mass difference, e. m., superconvergence dispersion relation approach 8=11485
 $\pi^+ \pi^-$ interference in K^0 decay CP violation 8=778
 Regge particle rel. to $\pi \rightarrow \mu + \nu$ and $B + \bar{B} \rightarrow \mu + \nu$ 8=11502
 secondary particles in (π^-, N) reactions, momentum spectra 8=1085
 3- π -exchange contrib. to N-N scatt. 8=15824
 vertex functions obeying SU(2) \otimes SU(2), calc. 8=744
- decay**
 β , Lagrangian approach to current algebra 8=20251
 leptonic, rel. to axial vector current consisting of pseudoscalar octet. 8=6743
 $\pi\beta$ with intermediate boson, e. m. corrections rel. to current algebra 8=6836
 $\pi \rightarrow l \nu \gamma$ structure-depend. axial-vector form factor, low energy theorem 8=6837
 $\pi \rightarrow \mu + \nu$, $K \rightarrow \mu + \nu$ evaluation of a_K/a_π using SU(3) algebra and PCAC 8=15798
 $\pi^- \rightarrow e^- + \bar{\nu} + \gamma$, in static quark model 8=746
 $\pi^0 \rightarrow 2\gamma$, $\pi^+ \rightarrow e^+ + \nu + \gamma$, relation 8=11500
 $\pi^0 \rightarrow 3\gamma$, C violating, upper limit on rate 8=745
 $\pi^+ \rightarrow \mu^+ \rightarrow e^+$, in 140,000 Oe field, e^+ asymmetry 8=3618
 $\pi^+ \rightarrow \mu^+ \rightarrow e^+$ and e spectrum in interstellar medium 8=19094
 $\pi^+ \rightarrow \pi^0 + e^+ + \nu$, rate obs., branching ratio 8=11503
 $\pi-\mu$ disintegration anisotropy based on 1062 π^+ data 8=6835
 $\pi\mu$ with intermediate boson, e. m. corrections rel. to current algebra 8=6836
 $\pi \rightarrow \mu\nu$ superconductivity model with SU(3) \times SU(3) symm. 8=11501
 $\pi \rightarrow \mu + \nu$, with π as Regge particle 8=11502
 $\pi \rightarrow \mu + \nu$, ν mass limit 8=6839
 $\pi^+ \rightarrow \mu^+ + \nu$, μ momentum and ν_μ mass upper limit 8=6814
- interactions**
 d photodisintegration exchange contribution 8=872
 $\gamma\pi \rightarrow \rho\pi$, sum rules rel. to e. m. widths of ω , A_1 , A_2 8=11566
 by nuclei, radiative absorpt., rel. to μ capture 8=20775
 $\omega + \pi \rightarrow \pi + \pi$ amplitude and Regge trajectory bootstrap 8=11563
 $\pi B \rightarrow V\Delta$, Regge-pole couplings 8=6903
 $\pi + d \rightarrow M + d$, and M-N scatt. factor 8=3736
 $\pi^+ + d \rightarrow p_\pi + p + \text{neutrals}$, 2.7 GeV/c search for e^+ 8=11488
 $\pi^0\gamma$ resonances, search for in $\pi^- + p$ reaction 8=3675
 π^- -He₃ π^+ yield obs. 8=7220
 $\pi^- + \text{He}^4$, inelastic at 140 MeV, excited and multineutron final states 8=6848
 $\pi + \text{He}^4 \rightarrow M + \text{He}^4$, M-N scatt. factor 8=3736
 $\pi + \text{He}^4 \rightarrow M + \text{He}^4$, magnitude and phase of meson scatt. amp. 8=890
 $\pi + \Lambda \rightarrow \pi + \Sigma$, simultaneous s-t analyticity 8=6740
 $\pi^+ + n \rightarrow \Sigma^+ + K^+$, in polyethylene, 1 GeV/c, Σ polarization 8=864
 $\pi^+ n \rightarrow \omega p$, Regge-pole model with L-S coupling 8=20444
 $\pi-N$ coupling constant from N-N scatt., anomalies 8=20519

Pions—contd**interactions—contd**

- $\pi\pi$ phase shift analysis 600-1000 MeV 8=757-8
 pion pair prod. by 12, 18 GeV/c π , OPE analysis 8=20439
 $\pi^+p \rightarrow K^+\Sigma^+$, mass difference effect in Wali-Warnock model, violation of SU(3) 8=3692
 π^- , stars in nuclear emulsions, multiple scattering measurements 8=1084
 p-p, bremsstrahlung production, exchange 8=830
 SU(2) \times SU(2), chiral, method of phenomenological Lagrangians 8=6744
- interactions, pion-nucleon**
 charge ratios and transverse momentum in high energy collisions 8=11524
 dispersion relation analysis, and peripheral model, lectures 8=20427
 exchange reactions, Regge-pole models 8=11516
 N/D formula for calc. of Regge trajectory 8=3554
 nucleus, π -N, rel. to nuclear structure 8=1086
 peripheral models, applied to $\pi^+p \rightarrow \rho^+N^{*++} \rightarrow \pi^+\pi^+\pi^+p$ 8=11515
 π -N collisions, multiple π production constraint 8=3619
 $\pi N \rightarrow Ne^+$ amplitude reconstruction from expt. data 8=6803
 $\pi N \rightarrow \omega \Delta$, Reggeization procedure 8=11412
 $\pi N \rightarrow \pi N^*$, below 1 GeV, ang. distribution using Legendre series 8=6849
 $\pi N \rightarrow \pi\pi N$ 1-10 GeV, OPE model, Treiman-Yang angle anomaly due to πN isobars 8=15770
 $\pi N \rightarrow \eta p N$, mass distrib. from Regge-pole exchange model 8=20440
 $\pi N \rightarrow \rho \Delta$ conspiracy consequences 8=6867
 $\pi N \rightarrow \rho N$, dips in ω -exchange contribution 8=11514
 pionic atoms, effects of strong interactions and finite nuclear charge radius 8=7482
 P_{11} resonance model 8=11513
 protons, recoil, transverse momentum and four-momentum transfer, cosmic ray obs. 8=11589
 ρ prod. and rel. to conserved current 8=15813
 S- and P-wave lengths, relation between vector and pseudoscalar coupling constants 8=15771
- interactions, pion-pion**
 dispersion relation analysis, and peripheral model, lectures 8=20427
 f_0 coupling, emission into S and D waves 8=3612
 πN scatt. contrib. 8=3637
 $\pi\pi \rightarrow NN$, contrib. from π -N resonance to helicity amplitude 8=11517
 $\pi^+p \rightarrow \pi^+\pi^+n$, rel. to $\pi\pi$ interaction 8=6850
 p-p scatt., longest range interaction is OPE mechanism 8=834
 P-wave dynamics, π form factor probe 8=20435
 Wolf phase shifts, and g_s/g_v ratio from Adler $\pi\pi$ sum rule 8=754
- interactions, pion-proton**
 four-momentum transfer distrib., high energy and high multiplicity 8=6862
 π^- , charge exchange on bound H nuclei, theory 8=3628
 πp at 650 MeV, elastic and charge exchange cross-sections 8=6854
 π exchange theory 8=6847
 $\pi p \rightarrow \rho N^*$, ρN^* , ang. correls. in decay 8=11636
 π^+p , A_2 -meson spin and parity and decay obs., 3.25 GeV/c 8=6909
 $\pi^+ + p \rightarrow n + \eta$ N pole and resonances below c.m. energy 1700 MeV 8=20490
 $\pi^+ + p \rightarrow \eta + n$, 561-1300 MeV partial wave analysis, S, P, D, F waves 8=11520
 $\pi^+p \rightarrow \eta n$, partial wave analysis in terms of Lorentz group 8=6856
 $\pi^+p \rightarrow \Lambda k^+\pi^-$ at 6 GeV/c, Λk^+ enhancement at 1.7 GeV 8=3630
 $\pi^+p \rightarrow \Lambda K^0, \Sigma^+ K^0, \Sigma^- K^+$, 1.5-4.2 BeV/c 8=6861
 $\pi^+ + p \rightarrow n + \eta, \Sigma^- + K^+, \Lambda + K^0, \Sigma^0 + K^0$, phenomenological model 8=15758
 $\pi^+p \rightarrow \eta^+ n$ and charge exchange polarization, ρ' Regge trajectory 8=3665
 $\pi^+p \rightarrow \eta n$, polarization meas., 3.2 and 5 GeV/c 8=15776
 $\pi^+ + p \rightarrow \eta + n$, Regge pole model of polarization 8=11519
 $\pi^+ + p \rightarrow \eta + n$, 670-805 MeV/c obs. 8=20489
 $\pi^+ + p \rightarrow \eta + n$, $T_x = 593$ -704 MeV, calc. of ang. distrib. of η 8=6853
 $\pi^+ + p \rightarrow \eta + N$, N^* resonant states and $N\pi, N\eta$ decay modes 8=11637
 $\pi^+p, K_1^0 K_1^0$ system resonance, 5, 7 and 12 GeV/c 8=794
 $\pi^+ + p \rightarrow K^+ + \Lambda^0/\Sigma^0$ at 4 GeV/c, forward and backward peak 8=3648
 $\pi^+p \rightarrow K^+\Sigma^-$ rel. to analytic structure of Regge-cut amplitude 8=20319
 $\pi^+p \rightarrow K^+\Sigma^-$, Regge cut 8=3631
 $\pi^+ + p \rightarrow n + X_{\gamma\gamma\gamma}$, X resonance identification 8=6858
 $\pi^+ + p \rightarrow \nu^0 + n$, 4.0 GeV/c vector meson decay to e pair 8=808
 $\pi^+p \rightarrow \omega n$, ϕn , 2.1 BeV/c cross-section calc. 8=20442
 πp at 650 MeV, cross-section, for single and multi pion prod. obs. 8=6854
 πp , 4.16 GeV/c scatt., π prod. and charge exchange 8=11522
 π^+p , 5.5 GeV/c, multiple π prod. 8=3633
 π^+p at 10 GeV, secondary π transverse momentum distrib., thermodynamic approx. 8=3625

Pions—contd**interactions, pion-proton—contd**

- π^+p , multiple π production, simple systematic behaviour, 25 GeV/c 8=15767
 $\pi^+p \rightarrow \pi^+n$ rel. to analysis of π -N scatt., 1-10 GeV/c 8=3639
 $\pi^+p \rightarrow \pi^+n$ cross section from π^+p scatt. obs. 8=15778
 $\pi^+p \rightarrow \pi^+n$, polarization meas., 2.0 and 5 GeV/c 8=15776
 $\pi^+p \rightarrow \pi^+n$, Regge pole branch points obs. method 8=3629
 $\pi^+p \rightarrow \pi^+n, \eta n$, Regge-pole model with L-S coupling 8=20444
 $\pi^+p \rightarrow \pi^+\pi^+$, inconsistency of Ferrari-Sellers form factor for π - π scatt. 8=3649
 $\pi^+p \rightarrow \pi^+\pi^0p$ rel. to $\pi^+\pi^0$ scatt. 8=768
 $\pi^+p \rightarrow \pi^+\pi^0p$, 2.77 GeV/c for $\pi^+\pi^0$ scatt. 8=770
 $\pi^+p \rightarrow \pi^+\pi^+n$, 8 GeV/c, 2421 events 8=6851
 $\pi^+p \rightarrow \pi^+\pi^+n$, rel. to $\pi\pi$ interaction 8=6850
 $\pi^+ + p \rightarrow \pi^+ + \pi^+ + n$, $\pi\pi$ phase shift analysis 8=757
 $\pi^+p \rightarrow \pi^+\pi^+n, \pi^+\pi^-p$, rel. to phase shifts in $\pi\pi$ scatt. 8=6870
 $\pi^+ + p \rightarrow \pi^+ + \pi^+ + n$ and $\pi^+ + p \rightarrow \pi^+ + \pi^0 + p$, $\pi\pi$ phase-shift analysis from 600-1000 MeV 8=758
 $\pi^+p \rightarrow \pi^+\pi^+n$, 870 MeV π^+ momentum spectrum obs. cross-section of π^+n deduced 8=20445
 $\pi^+p \rightarrow \pi^+\pi^+n$, 3.1.36¹ GeV/c, I=0 enhancement obs. 8=15773
 $\pi^+ + p \rightarrow \pi^+ + \pi^+ + n$, 1.38-3.00 GeV/c ρ^0 formation and decay ang. dist. 8=3685
 $\pi^+ + p \rightarrow p + \pi^+ + \pi^+$, 3.2-4.9 GeV 8=16057
 $\pi^+ + p \rightarrow \pi^+ + \pi^+, \pi^+ + \pi^+ + n$, 7.0 and 25 BeV 8=15768
 $\pi^+p \rightarrow \pi^+\pi^+p$ at 2.77 GeV/c, ρ^- meson production and decay 8=20503
 π^+p , 720 MeV, cross-section for ($\pi^+\pi^0$), ($\pi^+\pi^+n$), (2 π prod.), ($\eta\pi^0$) obs. 8=15772
 π^+p , 3 GeV/c $\rightarrow \pi^+\pi^+\pi^-p$, prod. of $N^{*++}(1238), \rho^0$ and A_2^- 8=20446
 π^+p , 3.2, 4.2 GeV/c obs. of multipion prod., $\pi\pi^+\pi^-\pi^-$, $\pi\pi^+\pi^0\pi^-\pi^-$, $\pi\pi^+\pi^+\pi^-\pi^-$ 8=20448
 $\pi^+p \rightarrow \pi^+\pi^-\pi^+p$, 8 GeV/c, meson and baryon resonance prod. 8=20447
 $\pi^+p \rightarrow \pi^+p n$, 8 GeV/c, obs. in bubble chamber 8=6857
 $\pi^+ + p \rightarrow p + R^+$, structure of R^+ 8=3676
 $\pi^+ + p \rightarrow p + X^-$ at 1.8 GeV/c, δ^- (960 MeV) resonance search 8=756
 $\pi^+p \rightarrow \Sigma^- K^+$, 1170 MeV/c, cross-section obs., C independence confirmed 8=20449
 π^+p , secret for $\pi^0\gamma$ resonances 8=3675
 π^+p , strange particle prod., 1.5-4.2 BeV/c 8=6860
 $\pi^+p \rightarrow X^0 n$, cross sections obs. 8=20501
 $\pi^+ \rightarrow N^*(225) \rightarrow \rho + N^*(1236)$, cascade decay theory 8=3734
 π^+p , at 8 GeV/c, 6-prong interactions, cross-sections 8=3632
 π^+p , 8 GeV/c, resonances obs. 8=20428
 π^+p , elastic, through 90° and Δ_2 Regge trajectory in S-channel 8=20460
 $\pi^+ + p \rightarrow \eta + \Delta^{*+}(1238)$, cross-section and Δ^{*+} spin density 8=6855
 π^+p , inelastic interactions at 8 GeV/c, van Hove's overlap function obs. 8=11521
 $\pi^+ + p \rightarrow N_{238}^+ + \pi^0$, 0.5-1.46 GeV, ang. distrib. of π^0 8=15780
 π^+p , 900 MeV π prod. through N_{33}^+ isobar 8=11523
 $\pi^+p \rightarrow N^{*++}\rho^0$, shrinkage effects and one-pion exchange 8=20429
 $\pi^+p \rightarrow N^{*++}\rho^0, N^{*++}\omega^0$ or $N^{*++}\eta^0$, cross-sections and ang. distrib. 8=755
 $\pi^+p \rightarrow \pi^+p + 4\gamma$, search for decay $\eta \rightarrow \pi^0\gamma\gamma$ 8=3670
 $\pi^+p \rightarrow \pi^+n$, $N\pi\pi$ decay mode of $\Delta(1920)$ and $\Delta(2420)$, possible evidence 8=15774
 $\pi^+ + p \rightarrow \pi^+ + \pi^0 + p$, 968 MeV/c search for scalar meson decaying to $\pi^+\pi^0$ 8=11553
 $\pi^+ + p \rightarrow \pi^+ + p + \pi^0$, < 1070 MeV, ang. distrib. 8=15779
 $\pi^+p \rightarrow \pi^+\pi^+p, \pi^+\pi^-n$, below 1 BeV 8=6859
 $\pi^+ + p \rightarrow \Sigma^+ + K^+$, in polyethylene, 2 GeV/c, Σ polarization 8=864
 $\pi^+ + p \rightarrow \Sigma^+ + K^+$, phenomenological model 8=15758
 $\pi^+ + p \rightarrow \Sigma^+ + K^+$, quark model for backward process 8=11480
 $\pi^+p \rightarrow K^+\Sigma^+$, 3.23 GeV/c, ang. dist., Σ polarization 8=6852
 $\pi^+p \rightarrow K^+\Sigma^0(\Lambda^0)$, Regge-pole model based on K^*, K^{**} exchange 8=15777
 $\pi^+p, I = \frac{1}{2} N^*(1400)$ prod. at 6 GeV/c 8=15775
 π^+p , total cross section from 8-29 BeV/c obs. 8=774
 p transfer distrib. obs., Regge-pole exchange model suggested 8=20441
 radiative capture as symm. test for e.m. current 8=670
- production**
 $A_1 \rightarrow \rho + \pi$ current algebra calc. 8=11565
 $A_1 \rightarrow \rho\pi$, current algebra and pole-dominance appls. 8=3684
 $A_1 \rightarrow \rho\pi$, decay constant anomaly, d-wave coupling constant 8=6907
 $A_1 \rightarrow \rho\pi$ S/D wave ratio determ. 8=11566
 charged pairs, photoproduction from hydrogen, up to 1500 MeV γ energies 8=6844
 $e^+e^- \rightarrow \pi^+\pi^-$, 775 MeV 8=15738
 $e^+ + e^- \rightarrow \pi^+ + \pi^-$ rel. to π e.m. structure and p-wave phase shift in π - π scatt. 8=15761
 $e^+ + p \rightarrow e^+ + n + \pi^+$, π form factor meas. 8=6834
 electroprod. on N, as function of momentum transfer 8=6840

Pions—contd

production—contd

electroprod. on p obs., single and multiple 8=11505
 $\eta_{3\pi}$ decay, suppression of $3\pi^0$ mode 8=3673
 $\eta \rightarrow 3\pi$, current algebra approach, review 8=15808
 $\eta \rightarrow$ neutrals, $\pi^+\pi^-\pi^0$ branching ratio, rel. to $K^-\rho \rightarrow \Lambda\eta$ 8=6888
 $\eta \rightarrow \pi^+\pi^-\pi^0\gamma$ in terms of $\eta \rightarrow \pi^0\gamma\gamma$ using CA and PCAC 8=20488
 $\eta \rightarrow \pi^0\pi^+\pi^-$, $\pi^+\pi^-\pi^0$, ratio obs., T = 1 sufficient 8=20485
 $\eta \rightarrow \pi^0 e^+ e^-$, C-conservation, vector-meson model, decay width calc. 8=3674
 $\eta^0 \rightarrow \pi^0 e^+ e^-$, unsuccessful search 8=804
 $\gamma + A$ reactions on $9 \leq A \leq 207$ nuclei, 4.35 and 6.02 GeV $\pi^+\pi^-$ pair prod. 8=7164
 $\gamma + H$ at 5-16 GeV single π^+ prod. 8=15763
 $\gamma H, \pi^+$ photoprod. 8=3626
 $\gamma + He^3 \rightarrow \pi^+ + H^3$, using PCAC and current algebra 8=15765
 $\gamma N \rightarrow \pi N$, test for conspiracy 8=6775
 $\gamma N \rightarrow \pi N^*$, threshold cross-section calc. from current algebra 8=11504
 $\gamma + N \rightarrow \pi^0 + N, N^* + \pi$, varying γ polarization as test for Regge cuts 8=20331
 γp reaction, π^+ prod., Regge-pole calc. of cross-sections 8=3621
 γp , of π^+ , Regge pole model 8=20425
 $\gamma + p \rightarrow \pi^+ + n$, GeV region, absorpt. correction, πN parameters 8=15764
in $\gamma p \rightarrow n\pi^+$ interact., ang. depend. of cross-section 8=6841
in $\gamma p \rightarrow \pi N^*(1238)$, test of e.m. C noninvariance 8=694
 $\gamma + p \rightarrow N^* + \pi^+$, up to 6 BeV 8=6986
 $\gamma + p \rightarrow p + \pi^0$, 163-234 MeV, ang. dist. of π^0 8=750
hypernuclear decay final state interactions 8=16008
 $K+K \rightarrow 2\pi$ extension of domain of validity of dispersion relations 8=6895
 $K \rightarrow \pi\pi$, CP violation, phenomenological analysis 8=3652
 $K \rightarrow 3\pi$, p-wave interaction calc. using Fadeev formalism 8=11547
 $K_1^0 \rightarrow 2\pi$, SU_3 -breaking effect and hyperon decay 8=3729
 $K_2^0 \rightarrow \pi^+ + \pi^-$, calc.. 8=3659
 $K_2^0 \rightarrow \pi^+\pi^-$, CP violation, energy depend. on branching ratio 8=11569
 $K^0 \rightarrow \pi^+ + \pi^- + \gamma$ CP violation, interference effect theorem 8=3653
 $K^+ \rightarrow \pi^+\pi^0$, rel. to e.m. $\pi^0\eta$ mixing 8=791
 $K^+ \rightarrow \pi^+\pi^0\gamma$ (π^+, γ) ang. distrib. obs. 8=3655
 $K^+ \rightarrow \pi^+\gamma\gamma$, use of η -pole approx. 8=791
 $K^+ p \rightarrow K^* \pi^+ n$, 6 GeV/c ang. correl. in final states 8=798
 $K^+ + p \rightarrow N + \pi + K^*$, peripheral model, diffraction dissociation 8=15815
 $K^+ p \rightarrow \Sigma^- \pi^+$, mass difference effect in Wali-Warnock model, violation of $SU(3)$ 8=3692
 $K^+ p \rightarrow \pi^+ \Sigma^+$, Regge-pole model based on K^*, K^{**} exchange 8=15777
 $K^+ p \rightarrow \pi^+ \pi^- \Sigma^0$, 6 GeV/c, ang. correls. rel. to spin parity of exchanged particles 8=798
 K^* radiative decay 8=6911
 $\Lambda \rightarrow N\pi$, amplitude derived in superconductivity model with $SU(3) \times SU(3)$ 8=11501
matrix element calc. for multiple emission 8=15769
multiple, in 25 GeV/c πp collision 8=15767
multi- π and hadron elastic scatt. 8=20530
neutrino nuclear reactions, thresh. 8=751
nuclear reactions due to 600 MeV p, surface prop. sensitivity 8=20778
by N, virtual photoprod., dispersion sum rules in static model 8=20457
 $NN \rightarrow \pi\pi$ predicted from πN scatt. 8=825
 N^* decay modes from $\pi^+ + p \rightarrow \eta + N$ 8=11637
 $\omega + \pi \rightarrow \pi + \pi$ amplitude and Regge trajectory bootstrap 8=11563
 $\Omega^- \rightarrow \Xi^- + 2\pi^0$, comparable with $\Omega^- \rightarrow \Xi^- + \pi$ 8=6979
 π^+ photoproduction, finite energy sum rules, parity doublet conspiracy 8=20423
 π^+ photoprod. forward peak obs. 8=6846
 π^+ photoproduction, 300-600 MeV at small angles 8=3624
 $\pi^+\gamma p$ reactions, π^+ at large angle, differential cross sections, 260, 290, 320 MeV 8=752
 π^+ photoprod., $1 < E_\gamma < 3$ GeV, simple isobar ansatz in fixed-t dispersion relations 8=20437
 π^+ , zero-degree, by π^- incident on nuclei, 2-6 BeV/c 8=16104
 πp , 900 MeV, through N_{33}^+ isobar obs., ρ -exchange model compared 8=11523
 $\pi^+ p \rightarrow \rho^0 N^{*++} \rightarrow \pi^+ \pi^+ \pi^- p$, peripheral models 8=11515
 $p + \gamma \rightarrow p + \pi$, Mandelstam branch cuts rel. to amplitudes 8=11594
 $\tilde{p}n \rightarrow \pi^+ \pi^- \pi$ in D bubble chamber, 3-pion state analysis 8=20436
 $p\bar{p}$ annihilation, 12 decay modes calc. 8=11605
 $p\bar{p} \rightarrow KK\pi, K^*(891)$ prod., $K\bar{K} J^P = 2^+$ resonance at 1280 MeV 8=6940
 $p\bar{p} \rightarrow \pi^+ \pi^-$, 2.7 GeV/c, 2 meson final states 8=843
p-p collisions, high energy π, k, \bar{p} prod. cross-section depend on longitudinal and transverse momentum components 8=20478
 $pp \rightarrow pn\pi^+$, 10 GeV/c and OPE model 8=11591
 $p + p \rightarrow \pi^+ + d$, 6 GeV/c cross-section meas. 8=20525

Pions—contd

production—contd

$\rho \rightarrow \pi + \pi$ current algebra calc. 8=11565
 $\rho^0 \rightarrow \pi^+\pi^-$, e^+e^- branching ratio, 600-900 MeV/c² 8=6908
 $\Sigma^+ \rightarrow n\pi^+$, purely p wave 8=3728
 $\Sigma^+ \rightarrow n + \pi^+$ S-wave theory using quark model of baryons 8=6975
soft- π emission, current algebra calc., avoidance of kinematic zeros 8=20468
sum rules, additive quark model 8=11512
 $Y_1^* + \pi^- \rightarrow \Sigma^+ \pi^+ \pi^- \pi^-$, spin and parity of Y_1^* 8=6987
 $Al(\gamma, \pi^+ \pi^-)Al$, 3.2-4.9 GeV 8=16057
 $Bi^{11}(\gamma, \pi^+)Bi^{11}$, obs. rel. to independent particle model 8=1035
 $Bi^{11}(\gamma, \pi^-)C^{11}$, obs. rel. to independent particle model 8=1035
 $C(\gamma, \pi^+ \pi^-)C$, 3.2-4.9 GeV 8=16057
pairs, by 12, 18 GeV/c π , OPE model analysis 8=20439
phenomenological analysis 500-700 MeV, in partial waves and isobars 8=20438
photoprod., theorem obtained 8=20341
photoproduction and electroproduction, dispersion relation theory 8=11508
photopion production below 500 MeV 8=11509
photo, electroproduction, evaluation of multipoles, low energy region 8=753
photoproduction, O(4) symm. in presence of unequal masses 8=3627
photoprod. of $\pi^+\pi^0, K^+$ 8=15766
photo, Regge pole residues, kinematical singularities 8=11415
photoproduction single, near threshold 8=20424
photoproduction, violation of Knoll-Ruderman limit 8=6743
photoproduction from deuterium, test of symmetry in e.m. current 8=670
photopions from nucleons 8=11507
photoprod. in Compton effect on N, use of $\pi\pi$ scatt. models 8=20345
photoproduction on N, pole terms in fixed angle approach 8=3622
photoformation on nucleons, and quark model 8=6842
photonuclear reactions, 16-18 GeV e acceleration, with metal targets 8=20768
photoproduction on p, ang. distrib. parameters 8=11511
photoproduction on p 220-380 MeV near $P_{33}\pi N$ resonance 8=11506
photoproduction on p, 553-850 MeV analysis in second reson. region 8=6843
photographic emulsion in pulsed mag. field, obs. 8=16073
 π -N collisions, multiple π production constraint 8=3619
 πN scatt, constraints on production amplitude pions 8=3636
 $\pi^- p$, 720 MeV, 2π prod. cross-section 8=15772
 $\pi^- p \rightarrow \pi^- \pi n$, 720 MeV cross-section obs. 8=15772
 $\pi^- p \rightarrow \pi^- \pi^+ n$, rel. to $\pi\pi$ interaction 8=6850
 $\pi^- p \rightarrow \pi^+ \pi^- n$, 3.1 36^1 GeV/c, I = 0 enhancement obs. 8=15773
 $\pi^- p \rightarrow \pi^+ \pi^- p$, $\pi^+ \pi^- p$, rel. to phase shifts in $\pi\pi$ scatt. 8=6870
 $\pi^- p$, 3.2, 4.2 GeV/c obs. of multipion prod., $p\pi^+\pi^-\pi^-$, $p\pi^+\pi^0\pi^-\pi^-$, $n\pi^+\pi^-\pi^-\pi^-$ 8=20448
 $\pi^- p \rightarrow \pi^+ p\pi^+$, inconsistency of Ferrari-Sellers form factor for $\pi-\pi$ scatt. 8=3649
 $\pi^- p$, 5.5 GeV/c, multiple π prod. 8=3633
in $\pi^- + p$ at 10 GeV, transverse momentum distrib., thermodynamic approx. 8=3625
 π^0 backward photoproduction 8=15762
 π^0 , by $\gamma + d$, at 285-345 MeV, multiple scatt. correction 8=3620
 π^0 , from $\gamma + p$, angular distribution E_{0+}, M_{1+}, M_{1-} calc. 8=6845
 π^0 from $\gamma + p$, differential cross section, $E_\gamma = 4-5$, 8 GeV 8=20426
 π^0 , by γp interact., energy-depend. of recoil-p polarization 8=835
 π^0 , in γp reaction Regge-pole calc. of cross-sections 8=3621
 π^0 in high energy nuclear interactions due to cosmic rays obs. 8=20618
 π^0 ang. distrib. in $\pi^+ + p \rightarrow N_{133}^+ + \pi^0$ 8=15780
 π^0 in $\pi^+ + p \rightarrow \pi^+ + p + \pi^0$, up to 1070 MeV 8=15779
 π^0 , multiple, emission cross-section in arbitrary scatt. processes 8=3623
 π^0 photoproduction ω and B exchange at low energy 8=11510
 $\pi^0\pi^0$ and $n\pi^+n$ from $\pi^- + p$ reaction at 7.0 and 25 BeV 8=15768
 $\pi^0\pi^+ p$, from $\pi^- p$, 720 MeV cross-section obs. 8=15772
scattering
 $A_2-\pi$ superconvergence sum rules 8=20421
Chew-Low eqns., soln. props. 8=6863
Compton scatt. low-energy theorem and sum rule 8=760
 π^+ , Coulomb and nuclear, contrib. to error formulae in bubble chamber analysis 8=6681
 $\gamma-\pi$, threshold vector dominance hypothesis and Compton scatt. of isovector photon 8=6864
 $K^*-\pi$ superconvergence sum rules 8=20421
nucleus, density parameters and π rms change radius 8=3948

Pions—contd

scattering—contd

- $\pi^+ - \alpha$, 24 MeV, π e.m. form factor 8=3616
- π -B, superconvergence relations, sum rules 8=3635
- π d scatt., fully covariant theory 8=6865
- π -d, coupling const. derived 8=759
- pion-hadron, elastic amplitude calc. 8=20451
- pion-hadron, strong-interaction sum rules, mass relations 8=20450
- π K extension of domain of validity of dispersion relations 8=6895
- πN^* , superconvergent sum rules 8=3634
- π -nucleus, elastic scatt. anal. 8=20816
- $\pi\omega, \rho$ parametrization 8=3683
- πN^* Regge-pole theory, constraint eqns. 8=20321
- $\pi\rho$ Regge-pole theory, constraint eqns. 8=20321
- Reggeization of exchange in prod. processes 8=11499
- $\rho - \pi$, sum rule rel. to e.m. widths of ω, A_1, A_2 8=11566
- Be^0 forward dispersion relations, appl. 8=7219
- $C\pi^+$, elastic scatt. anal. 8=20816
- C^{12} forward dispersion relations, appl. 8=7219
- H, He, Li^3 , C, O and Pb total and reaction cross-sections 8=1052
- scattering, pion-nucleon**
 - AW and spin-flip sum rules derived from dispersion relations without current algebra 8=11531
 - amplitude calc. to second order in energy using PCAC and commutation rels. 8=11532
 - amplitudes, static crossing matrix soln. 8=11533
 - charge-exchange amplitude in terms of homogeneous Lorentz group 8=766
 - charge exchange, applic. of finite energy sum rules for Regge analysis 8=20296
 - charge exchange, sum rule for ρ -like singularities in complex J-plane 8=11530
 - differential cross section, charge exchange and high-energy dynamics 8=15786
 - diffraction, model phenomenological model of diffraction 8=6894
 - dispersion relation for phase shift generalized to include S-matrix effects, partial waves described 8=20430
 - dispersion sum rules, for elastic scatt., static model 8=20457
 - dispersion sum rules, high energy 8=763
 - dispersion sum rules rel. to scatt. amplitude, ≤ 70 GeV 8=15787
 - fermion, N and Δ trajectories 8=20328
 - form factor type contributions to s and p waves 8=765
 - forward, decoupling of second ρ 8=15783
 - high energy behaviour and Regge pole model 8=6868
 - integral eqn. reduced to Tarmarkin form, removal of singularity 8=20314
 - interference model description, 2-6 GeV/c 8=11526
 - isospin effects, triangular CI diagram 8=762
 - Lagrangians, unified treatment 8=11535
 - low energy by PCAC and CCR, (3, 3) reson. contrib. 8=3637
 - nuclear, π charge-exchange scatt. rel. to p-n correlation 8=3950
 - multi-GeV, spin-flip parameter determ. 8=11534
 - NN $\rightarrow \pi\pi$, ang. dist. prediction 8=825
 - NN π system, Fadeev theory Lovelace approx., phase shifts for N-N scatt. 8=6925
 - N/D approach, coupling constants 8=761
 - 1-10 GeV/c, analysis using $\pi^+ - p$ scatt. and $\pi^- \pi^+ - p \rightarrow \pi^+ n$ 8=3639
 - p-wave, low energy by PCAC and CCR 8=11527-8
 - p-wave low energy sum rules derived 8=6833
 - partial-wave amplitudes, Regge-pole model 8=15784
 - phase shift analysis rel. to N^* 8=15866
 - phase shift of P_{33} state, CDD pole approach 8=20453
 - phase-shift analysis below 1.6 GeV for elastic 8=20458
 - phase shifts, W plane partial-wave dispersion relations calc. 8=6869
 - π production amplitude, constraints 8=3636
 - polarization effects 8=15785
 - pot., generalized computed from known phase shifts for P_{33}, P_{11}, D_{13} partial waves 8=20454
 - Regge exchange amplitudes rel. to resonance spectrum 8=764
 - Regge pole-plus-resonance model, modifications 8=20456
 - Regge-pole theory, constraint eqns. 8=20321
 - Regge secondary poles, cuts and conspiracies rel. to crossover and polarization 8=11529
 - Regge trajectories, polarization and charge exchange at high energy 8=3638
 - resonances, contrib. to helicity amplitude of $\pi\pi \rightarrow NN$ 8=11517
 - Roper resonance, magnetic moment relations using dispersion relations 8=3605
 - S-wave, low energy, semiphenomenological calc. 8=3641
 - semiclassical theory with ρ, N^{**} prod. 8=20452
 - spin flip amplitude limitation, elastic 8=20431
 - sum rules from superconvergence relations 8=3635
 - superconvergence relations correcting BBM and MMM coupling constant 8=3640
 - superconvergence relations for all values of momentum transfer 8=20455
 - superconvergent sum rules and existence of resonances 8=6866

Pions—contd

scattering, pion-nucleon—contd

- triangular inequalities become equalities 8=762
- scattering, pion-pion**
 - absolute upper bounds derived 8=3644
 - in chiral symm-breaking term of Lagrangian 8=20262
 - current algebra and dispersion relation approach 8=20463
 - Ferrari-Sellers form factor for πN vertex, inconsistency in $\pi^- + p \rightarrow \pi^- + p + \pi^0$ 8=3649
 - forward, dispersion relns., consistency with Wolf $\pi - \pi$ phase shifts 8=769
 - higher partial waves, resonance solutions 8=3642
 - lecture 8=20422
 - length calc. by current algebra 8=3645
 - lengths, using forward dispersion relations for amplitudes 8=15788
 - length, $I=2$, s-wave obtained 8=20446
 - lengths, phase shift analysis current algebra, dispersion relations 8=15782
 - length, S-wave, low energy using $K_{\pi 4}$ decay 8=20466
 - length, $T=2$, prediction of repulsive interaction 8=20465
 - lengths, numerical bounds, rel. to dispersion relation 8=20434
 - low-energy models 8=767
 - low-energy, short-range repulsion, calc. 8=3539
 - modulus of amplitude fixes amplitude, proof of axiomatic field theory 8=6872
 - N Compton scatt. analysis 8=20345
 - N e.m. form factor effect 8=11578
 - OPE model, description of $J=1, I=1$, partial wave 8=15789
 - p-wave calc. sum rule which suppresses S-wave and high-energy behaviour 8=3646
 - p wave phase shift from $e^+ + e^- \rightarrow \pi^+ + \pi^-$ 8=15761
 - Padé approx. calc. 8=11537
 - partial amplitudes representation and neutral model solution 8=6871
 - phase-shift, solution 8=11518
 - $\pi^+ \pi^0$, Chew-Low method from $\pi^+ p \rightarrow \pi^+ \pi^+ p$ 8=768
 - $\pi^+ \pi^0$ data from $\pi^+ p \rightarrow \pi^+ \pi^+ p$ at 2.77 GeV/c using Chew Low method 8=770
 - $\pi^0 \pi^0 \rightarrow \pi^0 \pi^0$, location of unique minimum of S-wave amplitude 8=20464
 - $\pi^0 - \pi^0$, lower bound for scatt. length 8=20179
 - radiative for calc. of matrix elements in $K \rightarrow 2\pi\gamma$ 8=15793
 - ρ bootstrap formulation 8=20462
 - ρ bootstrap parameters calc. 8=11536
 - S-wave length, $I=0$, possible existence of vacuum trajectory 8=15697
 - s-wave lengths, unitarity corrections to current algebra calc. 8=11525
 - S wave phase shifts from $\pi^+ p \rightarrow \pi^+ \pi^+ n, \pi^0 \pi^+ p$, 4.16 GeV/c 8=6870
 - S-wave phase shift at low energy 8=15781
 - S-wave, rel. to pion pair prod. by 12, 18 GeV/c π 8=20439
 - sum rule for scatt. length from AFRF assumption 8=3643
- scattering, pion-proton**
 - amplitude calc. from dispersion relations, of unknown parameters 8=20300
 - backward cone, conditions for existence of equal amplitude points 8=20432
 - elastic, dispersion calc. compared with expt. 8=15830
 - elastic at high energy, appl. of impact parameter development 8=11539
 - multi- π prod., similarities 8=20530
 - N isovector anomalous mag. moment, contrib. to sum rule 8=3698
 - overlap function analysis 8=6874
 - phase shift analysis for 9 possible new N^* 8=15865
 - $\pi p \rightarrow A_1(A_2)p, 2\pi$ exchange model 8=3650
 - $\pi^+ + p \rightarrow p^+ + \pi^+ + \pi^+, 3.2-4.9$ GeV 8=16057
 - $\pi^+ p$ amplitude, real part, in Coulomb interference region at 3.48 and 6.13 GeV/c 8=15790
 - $\pi^+ p$, backward elastic, ang. distrib., 3.3 GeV/c 8=771
 - $\pi^+ p$, backward, modified Regge representation 8=3651
 - $\pi^- - p$, charge exchange at 96.6 MeV, γ ray ang. distrib. meas. 8=6876
 - $\pi^- p$ charge exchange, real-to-imaginary ratio of amplitudes not a proof of Regge theory 8=20459
 - $\pi^- p$ at 180°, cross-section meas., N resonance evidence 8=11540
 - $\pi^- p$, 875-1579 MeV/c, p polarized obs. of resonances 8=20443
 - $\pi^- p \rightarrow \eta n$ asymptotic cross sections from separability and unitarity 8=772
 - $\pi^- + p \rightarrow \eta + n, J=1/2^-$ scatt. length and phase shift calc. 8=20433
 - $\pi^- p$ near 180° in 4-7 GeV/c π^- beam 8=6873
 - $\pi^- p \rightarrow \pi^+ n$ asymptotic cross sections from separability and unitarity 8=772
 - $\pi^- p \rightarrow \pi^+ \pi^+ p$ at 2.77 GeV/c, $\pi^+ \pi^-$ data, Chew-Low method 8=770
 - $\pi^- p \rightarrow \pi^+ \pi^- p$ data at 2.77 GeV/c rel. to $\pi^+ \pi^-$ cross-section 8=768
 - $\pi^- p$, 720 MeV cross-section obs. 8=15772
 - $\pi^+ p$, backward elastic, ang. distrib., 2.85 and 3.3 GeV/c 8=771
 - $\pi^+ p$, backward elastic, multiplate spark chamber for meas. 8=775

Pions—contd

scattering-pion—proton—contd

- π^+p , mass difference effect in Wali-Warnock model, violation of SU(3) 8=3692
- $\pi^+ - p$ at 97.1 MeV, differential cross section and phase shifts meas. 8=6875
- π^+p , Adler Weisberger, sum rule, S-wave πN lengths 8=773
- π^+p backward elastic rel. to N_α and Δ_δ Regge exchanges, $\pi^+p \rightarrow \pi^+n$ cross section calc. 8=15778
- π^+p polarization, analysis, high energies 8=776
- π^+p rel. to analysis of π^-N scatt., 1-10 GeV/c 8=3639
- Regge-pole model at small momentum transfer 8=20461
- review, high energies, new results 8=3647
- ρ' trajectory in charge exchange, Regge parameter evaluation and cut 8=11538

Pitch detection. See Acoustical measurement; Hearing.

Plages. See Sun.

Planetary nebulae. See Nebulae; Stars.

Planets

See also Solar system.

- angular-momentum density-mass diagram, inclusion of asteroids 8=23656
- angular momentum densities of planet-satellite systems (inc. asteroids, excepting Venus, Mercury, Mars, Neptune) 8=23655
- asteroids, surface, space weathering by exposure to solar wind 8=19246
- atmospheres, energy loss function for electrons and protons 8=23658
- atmospheres phenomena rel. to atomic collision processes 8=14832
- atmospheres, vertical stratification, observations from artificial satellites 8=14833
- earth-moon mass from Eros motion, 1926-65 8=10341
- earth-moon system, corrected mass derived from motion of Eros, 1926-45 8=10340
- Earth-Moon system history, effect of tidal friction 8=23662
- earth-moon system, Trojan manifold 8=19242
- formation, by accretion of planetisimals, statistical problems 8=19248
- general theory, application of von Ziepel method 8=10338
- global radiation at., emerging from a Rayleigh-scattering atmosphere 8=14831
- induced solar tidal force, relation with solar activity cycle 8=23731
- interior radiative thermal cond. 8=23654
- interplanetary space, importance and theory of elec. fields 8=9914
- Jupiter, apparent changes in rotation rate, from decameter radio obs. 8=23663
- Jupiter, atmosphere dynamics, appl. of baroclinic stability theory 8=19251
- Jupiter atmosphere, structure, composition 8=5956
- Jupiter brightness temp. and 77.5 Gc/s emission 8=10223
- Jupiter, CH_4 $3\nu_3$ band, image tube obs. 8=14839
- Jupiter, decametric bursts, wide bandwidth obs. 8=23666
- Jupiter, decametric radiation, ionospheric effect 8=2819
- Jupiter, decametric radiation, sub-msec. obs. 8=23665
- Jupiter, decametric radioemission 8=10346
- Jupiter, decametric radioemission dependence on Galilean satellites 8=10347
- Jupiter, decametric radio emission, dep. on position of satellites 8=14837
- Jupiter, hard X-ray fluxes, upper limits 8=23670
- Jupiter, internal structure and energy emission, model 8=10349
- Jupiter magnetospheric model 8=14836
- Jupiter's magnetosphere, particle acceleration due to elect. field generation 8=18930
- Jupiter, occultation of satellites I and II in Jan. and Feb. 1967 8=10348
- Jupiter, 18 MHz continuum emission obs. 8=23664
- Jupiter, presence of a new satellite 8=14840
- Jupiter, radio emission, influence of satellite Io 8=19250
- Jupiter radio emission stimulation by Io 8=10345
- Jupiter, radio rotation period 8=23667
- Jupiter, rotation period 8=14841
- Jupiter, S-bursts, long-baseline interferometry 8=23668
- Jupiter, upper atmosphere model to explain methane abundance 8=14838
- magnetic activity rel. to Pi2 micropulsations 8=10050
- magnetic field origin 8=10127
- Mars, aphelic apparition 1967 8=19252
- Mars, apparition obs. of 1965 8=10350
- Mars, atmosphere density, radar astronomical observation 8=19326
- Mars, atmosphere, laminar convective heating 8=2823
- Mars, atmosphere, progress of dark waves and friction layer 8=14842
- Mars, changes rel. to solar activity 8=5971
- Mars, hard X-ray fluxes, upper limits 8=23670
- Mars, low-resolution photometric map 8=14843
- Mars, mass ratio to Sun from Mariner IV and NASA deep space stations 8=23671
- Mars, model for upper atmosphere 8=10351
- Mars, optical model of atmos. 8=19254

Planets—contd

- Mars, origin of chondritic meteorites 8=14856
- Mars, possibility that it originated, with the Moon, from earth 8=23657
- Mars, press. of atm. at surface 8=19253
- Mars, radiative heating and equilib. in atmos., approx. calc. 8=14844
- Mars, surface elevation differences 8=23669
- Mars, secular changes and dark-area regeneration 8=2820
- Mars, surface pressures in maria deserts 8=2821
- Mars, thermal convection in mantle? comparison with Earth 8=14519
- Martian relief, ground based obs. during coming opposition 8=2822
- Mercury atmosphere search rel. to 1.049 μ CO_2 band obs. 8=10352
- Mercury, axial rotations determ. by radar 8=23672
- Mercury, insolation and surface temps. rel. to rot.-orbit period coupling 8=2824
- Mercury microwave phase effect 8=10353
- Mercury, motion rel. to gravitational Lagrangian struct. 8=10586
- Mercury perihelion precession and solar oblateness 8=2838
- Mercury, perihelion precession, verification of relativity 8=6070
- Mercury, rotation rate, radar astronomical observation 8=19326
- Mercury, rotational velocity 8=14845
- Mercury, surface brightness of photometric equator 8=19255
- minor, obs. with 15 in. wide-field astrographic camera 8=23661
- minor, photographic magnitudes 8=23659
- Neptune, internal structures 8=19256
- Neptune, 3.12 cm radio obs. 8=14830
- perihelion advances, rel. to solar core rot. and oblateness 8=23694
- photography, atm. turbulence limitations 8=14835
- planetary precession derived without use of Einstein's field eqns. 8=19421
- relativity, general, effects on planet parameter using magnetic-gravitational analogy 8=19417
- retrograde in solar system, loss due to tidal forces 8=23653
- rotation params. meas. from interplanetary stations 8=10339
- rotation, solar wind effect 8=10337
- rotational velocity and axial inclination from radiation to orbiting satellite 8=2817
- Saturn, new satellite during 1966 apparition 8=10354
- Saturn, presence of a new satellite 8=14840
- solar thermal flux refl. calc., geometrical model 8=14829
- spectra, differential 8-13 μ , obs. method 8=14822
- surface compositional trends, possibility of silicate rock powder reflection spectra as guide 8=14264
- system formation from stellar rotational behaviour 8=5853
- terrestrial, composition via mean atomic weight 8=5954
- 2-body system, gravitational radiation, scalar component 8=6079
- unspherical, particle motion in gravitational field, appl. of method of averaging 8=23660
- Uranus, internal structures 8=19256
- Uranus, presence of a new satellite 8=14840
- Uranus, 3.12 cm radio obs. 8=14830
- Venus, Ashen light and magnetic field 8=5958
- Venus, atmosphere above clouds, non-gray equilib. temp. distrib. 8=10357
- Venus atmosphere, dust insulation model, surface temp. 8=10356
- Venus, atmospheric evolution 8=2826
- Venus atm. light scatt. props. rel. to CO_2 bands intensities 8=14846
- Venus, axial rotations determ. by radar 8=23672
- Venus cloud composition 8=19257
- Venus, effects of volcanic effluents on observation in the atm 8=23673
- Venus enhanced, r.f. reflectivity areas obs. 8=10355
- Venus, hard X-ray fluxes, upper limits 8=23670
- Venus, ionosphere, re-examination of porous model 8=14848
- Venus, Mariner 2 microwave obs., anal. in hot-surface context 8=5957
- Venus, microwave emission, electrical discharge model 8=5959
- Venus radio brightness temp. distrib., 1.9 and 1.35 cm 8=14847
- Venus, rotation rate, radar astronomical observation 8=19326
- Venus, rotational velocity 8=14845
- Venus, scale height of scatt. centre 8=14849
- Venus, 6-cm observations and microwave spectrum 8=2825
- Venus, structure of lower atmosphere 8=23674
- Venus, surface, life possibilities 8=23675
- Venus vicinity, absence of high energy electrons and protons, Mariner 2 obs. 8=23676

Plasma

- See also Discharges, electric; Electrons; Ions; Space charge; Thermonuclear reactions.
- accelerated, current density from progressive waves 8=7743

Plasma—contd

acceleration, velocity limitation, theory 8=1381
 air containing electrophilic gases, microwave meas. behind shock waves 8=7754
 air permittivity and conductivity variations with freq. and electron density 8=4346
 alkali-halogen, drift wave excitation, collisionless limit 8=16577
 alkali, temp. meas. by spectral line reversal, effect of absorbing dimer 8=16695
 in alternating electric field, changes due to perp. magnetic field 8=16490
 anisotropic electron, linearised Vlasov equation solutions 8=7732
 anisotropic, relax. due to collisions of two kinds of particles 8=4323
 arcs, coaxial and nonsteady, in fully developed flow 8=7689
 argon permittivity and conductivity variations with freq. and electron density 8=4346
 Astron E layer, self-consistent, with spread in energy and angular momentum 8=12463
 atom distrib. function of excitation level 8=7730
 beam-plasma discharge, steady state condition 8=21294
 beam-plasma systems, beam generated, interacting components 8=21289
 beam system, two-stream interactions, suppression by a. c. fields 8=16507
 Cerenkov heating in radially non-uniform cylinder 8=16485
 cold, in Knudsen discharge, hot-cathode low-voltage 8=12414
 collisional rate for ions 8=12470
 columns, cylindrical, kinetic model 8=16457
 column, pseudo-sound wave excitation by electron beam 8=16570
 comet interaction with solar wind, laboratory simulation 8=23678
 conductivity, determination by r.f. probe 8=1382
 conductivity rel. to emissivity and absorpt. coeff. 8=4347
 conference, Dallas 1967 8=12480
 correlation functions and pressure for nonisothermal case 8=7733
 correlationless with time-dependent background state, charge density, calc. 8=4344
 Coulomb interactions, Green's functions 8=7739
 current carrying, charged particle beam deflection 8=6336
 current-convective instability of electron beam 8=21292
 current patterns, nonequilibrium, effect of convection 8=16486
 cyclotron-resonance attenuation in mag. fields 8=7744
 cylinder, thermal radiation resonances 8=16476
 dense and hot, production 8=7725
 dense, implosion by hypervelocity macroparticle impact for controlled thermonuclear explosion 8=16601
 dense, low temp., thermodynamics 8=21304
 dense, study by double floating probe method 8=21302
 density gradient effect on energy transfer to and from magnetoacoustic wave 8=16514
 dielectric-compressible plasma interface boundary condits. 8=4325
 dielectric-plasma interface, boundary conditions 8=7727
 dielectronic recombination, influence of radiation fields 8=23750
 diffusion in multipoles 8=21318
 dipole mag. field interaction with moving plasma with geophysical appl. 8=12465
 discharge column in magnetic field, low-pressure, steady-state theory 8=4283
 in discharge, d. c., electron temp. gradient effect on space-charge field 8=4278
 dispersion function, two-pole approx. 8=16475
 duoplasmatron ion source with plane plasma boundary 8=15340
 effect on small tuned dipoles 8=6398
 electrical cond., particle impenetrability 8=7745
 electrical conductivity in strong mag. field 8=21321
 elec. microfield at neutral and charged points, calc. 8=12479
 electrodeless discharge, fast e population conditions 8=21229
 electrodynamics on space and time dependent fields, guiding centre approximation in lowest order 8=3191
 e.m. waves negative absorpt. at e cyclotron reson. 8=12502
 e, extremely hot due to e beams 8=21306
 electron beam injection, prod. temp. distrib. and oscillations 8=21287
 electron beam-plasma interaction with transverse modulation 8=4368
 electron cyclotron harmonics, non-linear generation with current instability 8=16573
 electron densities of afterglow plasmas, determ. from Langmuir probe characts. 8=21355
 electron density and temp. using self-focused laser beams 8=16544
 electron distribution function with excitation collisions 8=4329

Plasma—contd

electron drift motion, collision effects 8=1380
 electron and ion streams, warm interpenetrating, non-linear interaction 8=7752
 electron heating, anomalous, during adiabatic compression 8=12471
 electron temp. and density in He coaxial accelerator 8=4337
 electron transport coeffs., fifth and sixth approx. 8=21260
 electron transport theory, and electron-ion collisions, rel. to thermionic converters 8=15235
 emissivity and absorpt. coeff. calc. 8=4347
 energy losses due to neutrino processes 8=10137
 equivalent circuit 8=7746
 excitation process in e.m. shock tubes 8=1337
 films, plasma reson. transmission of p-polarized u.v. light 8=12516
 flow in electric shock tube, pressure, trajectory and density profiles from spectrographic obs. 8=16510
 flow past unmagnetized obstacles, rel. to simulation of satellites in magnetosphere 8=12475
 flows and shocks, collision free, magnetic obstacle effects, wind tunnel obs. 8=16513
 fluctuations, nonlinear, correl. functions with Coulomb interact. 8=16458
 fluid eqns., singularities and relation to anomalous diffusion 8=21310
 free energy, second virial coeff. contribution at high temp. 8=12468
 free-streaming and spatial Landau damping 8=21291
 gas discharge, electron distrib. function 8=1328
 Gibbs entropy calc. outside equilb. 8=4334
 gyrotropic, bounded, new multipolar mode 8=21347
 Harris' quasi linear eqns., modification 8=12459
 heating by large amp. ion cyclotron wave, efficiency 8=4332
 heating by laser radiation in magnetic field 8=7735
 heating, turbulent in mirror, by current 8=4333
 high-density Z-pinch, ArII lines, Stark broadening parameters 8=20949
 high-frequency, discharge, energy transfer from e.m. field 8=16397
 high-pressure, radiation from 8=16533
 high-temp., dispersion relation 8=16471
 high temperature, in thermodynamic equilibrium, quantum theory 8=16468
 historical survey of concept 8=1375
 homogeneous, electron distrib. function under the effect of a frequency modulated electric field 8=16526
 hot-electron, shell-structure form., plasma prod. and e heating obs. 8=4335
 ignition, at second harmonic of e cyclotron freq. 8=21305
 incoherent scatt. spectrum, unequal e and ion temps. 8=16483
 inhomogeneities, motion and diffusion eqns. 8=12478
 inhomogeneous, current density, 2nd harmonic and sum and difference freq. components 8=12481
 inhomogeneous, imperfectly Lorentzian, Boltzmann equation solution 8=16464
 inhomogeneous, imperfectly Lorentzian, electron distribution function 8=16480
 inhomogeneous, warm, gradient coupling 8=16473
 interaction between ion-acoustic waves, transverse waves and plasma oscillations 8=16569
 interplanetary, shock wave propag., brightness temp. obs. 8=10432
 ion acoustic wave, nonlinear, evolution in Vlasov plasma 8=16463
 ion density and elect. field perturbations caused by acoustic-wave pulse in weakly ionized gas 8=21324
 of ions and drifted electrons, kinetic eqn. 8=4324
 ion spectrum, shifts due to e impact, semiempirical formulas 8=12511
 ionic waves, interaction with beam of charged particles 8=7822
 ion waves, longitudinal, propag. near and above ion plasma freq. 8=21297
 jet, coating of metallic materials 8=19337
 jets, dense, accel. to thermonuclear speeds by hypervelocity impact 8=16137
 kinetic equations for distrib. function 8=21303
 kinetic eqns. with inelastic processes 8=1379
 kinetic equation, various expressions 8=21314
 kinetics, partially ionized in time dependent mag. and e. m. fields 8=16466
 kinetic theory, Compton effect in astrophysics for intense radiation 8=21296
 lasers, gaseous in magnetic field 8=3306
 laser-heated, radiation spectra 8=16200
 laser irradi., absorption rel. to magnetic field 8=1400
 laser-produced in monatomic gases 8=7697
 laser-produced in polythene films, formation mechanics 8=23034
 laser-produced, in vacuum chamber, characteristics 8=4322
 laser-produced, vacuum u.v. emission spectra 8=7777
 longitudinal wave echoes, temporal and spatial 8=16571
 longitudinal waves, multiple echoes 8=16572
 losses, in toroidal mag. field 8=21235
 low-voltage arc, e beam disintegration 8=16425

- Plasma**—contd
- magnetic-sound shock waves, destruction at high Mach nos. 8=1388
 - magnetically stabilized, non-linear effects 8=16560
 - magnetized cold, potential distribution 8=7747
 - magnetized stream, lift/drag ratio on plate 8=21317
 - magneto-active, effective dielec. const. tensor and Green's function 8=16492
 - magneto-active, synchrotron radiation 8=4363
 - magneto-fluid and plasma dynamics, conference New York USA (1965) 8=16459
 - magnetogasdynamics shock propag. in, radiation effects 8=7755
 - magnetoplasmadynamic generator, analysis in uniform state 8=10840
 - magnetoplasmas, inhomogeneous warm, wave eqns. 8=12466
 - Maxwell electron distrib. functions, isotropic corrections, and rate of energy exchange 8=16470
 - metallic, elect. conduction and condensation 8=4343
 - micro, expansion rel. to Doppler effect 8=16465
 - multicomponent, Fokker-Planck eqn. 8=4327
 - multi-ion, elect. conductivity rel. temp. calc. 8=4345
 - negative glow, hollow cathode effect, princ. characts. 8=7660
 - neutral, spatial-distrib. of electrons and ions 8=16467
 - noble-gas mixtures, electron density prod. by fission fragment, rel. to thermionic conversion 8=15215
 - nonequilibrium, electron concentration and temp. profiles, obs. 8=12490
 - non-equilibrium processes, statistics of, book 8=16472
 - non-linear effects under the influence of an oscillating electric field 8=16480
 - nonstationary motions anal., via collisionless capture of electrons 8=7740
 - nonuniform, longitudinal wave propag. into, through sheath, Vlasov eqn. soln. 8=12488
 - one-dimensional, elec. field exact correlation function 8=21295
 - origin of word as applied to gaseous electronics 8=12457
 - oxygen, forbidden $D_1 \rightarrow P_{1,2}$ transitions 8=1182
 - particle diagnostics, review 8=7726
 - partly ionized, sound propag., $\lambda \gg$ m.f.p. neutral particles 8=7795
 - permittivity and conductivity variations with freq. and electron density 8=4346
 - plasmoid propag. at high press. 8=4340
 - population distribution of energy states, low temp. 8=12461
 - population of levels and inelastic losses in two temp. weakly ionized plasma 8=12460
 - positive column, i.f. impedance, theory 8=7659
 - positive column, kinetic model of Tonks-Datner resonances 8=4282
 - production by non-Q-switched laser beam acting on target 8=21285
 - quantum mechanics, divergence of neighbouring states 8=1378
 - quantum, test particle theory 8=10644
 - quantum ($Z=1$), e-e bremsstrahlung radiation 8=3581
 - quenching by electronegative gases, effect of detachment processes, comments 8=21319
 - quenching by electronegative gases, effect of detachment processes, reply to comments 8=21320
 - radiation processes, kinetic equations, magnetised 8=7775
 - radiation, pulse-stimulated at gyro-harmonics 8=12509
 - radiation rel. to thermodynamic structure, new integral eqn. 8=5887
 - radiation in thermal equilibrium, anomalous behaviour of O II 8=7418
 - rarefaction waves when bearing large currents 8=7753
 - rare gas, decaying, partition of recombination energy 8=1355
 - rare gases, ionic wave propagation excited by impulsion 8=12427
 - reflection coeff., complex, for finite width boundary 8=16535
 - in reflex discharge, hollow cathode, rot. vane freq. 8=7662
 - relativistic, heating by stochastic fields, theory 8=16479
 - relativistic, kinetic eqns. from covariant Debye-Hückel law 8=4338
 - relativistic, momentum distribution after adiabatic compression 8=7731
 - relativistic scalar, equilibrium props., hydrodynamical eqns. 8=21298
 - resonances of the magnetosphere, axially symmetric modes obs. 8=9922
 - resonantly sustained, mag. behaviour at high h.f. power 8=21290
 - review of plasma physics, book I 8=16460
 - reviews of plasma physics, book II 8=16461
 - reviews of plasma physics, book IV 8=16462
 - rotating, limiting velocity comments 8=21315
 - rotating, limiting velocity, reply to comments 8=21316
 - runaway electrons, quasilinear theory 8=1377
 - second sound, laser beam scatt. photostatistics 8=11192
 - seeded, drift velocities and thermal flux vectors in elect. and mag. fields 8=16488
 - seeded, nonequilibrium props. radiation effect 8=16484
- Plasma**—contd
- semilimited linear layer, focusing props., case of inner source 8=21351
 - sheathing of charged body, book 8=14706
 - sheath coating on infinite cylinder, e.m. waves scattering 8=6389
 - shock formation in Q-device 8=21325
 - shock-heated, microwave meas. of temp. 8=4360
 - in shock tube, electrically driven, nature 8=4359
 - shock tube, elect. current 8=16509
 - shock tube electron density meas. 8=159
 - in shock tube with parallel conductors, shape and vel. rel. to press. 8=1387
 - shock waves, anomalous electron heating obs. 8=1386
 - shock wave, bimodal distribution soln. 8=16511-2
 - shock waves, improved prod. by modified T-tube 8=161
 - shock wave profile measured by laser light scattering 8=7751
 - shock wave propagation at high densities 8=1390
 - single pulsed, by short circuiting current of plasma gun 8=4420
 - skin slab, properties in microwave gas discharge 8=12394
 - solar ejected, magnetosphere interaction, lab. analog 8=2622
 - solar, outward flow, spherically symmetric, influence of polytropic heat source 8=19304
 - spectra, continuous 8=4060
 - spectra, Stark-broadening and line shapes calc. 8=1402
 - spectral time broadening, e correls. in relaxation theory 8=21350
 - spectroscopy, vacuum u.v. and soft X-rays 8=12512
 - stable magnetic, collisional transverse diffusion 8=21312
 - Stark effect in h.f. stochastic fields, linewidths rel. to main parameters 8=7778
 - stationary in mag. and pot. fields, density and particle distribts. 8=12464
 - statistical mathematics for estimating parameters 8=7728
 - statistical mechanics, hierarchy of eqns. and correl. functions 8=16478
 - steady-state, interaction with mag. field 8=21286
 - stochastic approach to theory of fluctuations 8=21293
 - stochastic heating expt. in mag. mirror 8=4336
 - stochastic magnetic pumping 8=4321
 - stratified isotropic, electroacoustic wave propag. coupled eqns. 8=16508
 - striations, moving, in strong h.f. field, obs. 8=4280
 - theory, book 8=16455
 - thermal, control and use as environments for high temp. chem. reactions 8=21410
 - thermal, turbulent diffusion expts. 8=21313
 - thermionic converter, electron-transport phenomena 8=16487
 - thermionic converters, I-V curve, plasma effect 8=2277
 - thermodynamics of dense plasma 8=7736
 - thermodynamic props. rel. to radiation 8=5887
 - thermonuclear reaction in θ -pinch, n yield and laser scatt obs. 8=1399
 - thermonuclear, sputtered atom impurities, search with neutrons 8=16600
 - theta pinch, temp. and density of ions and electrons, laser scatt. expt. 8=16553
 - 3-component, in thermionic converter transport eqns by tech. of irreversible thermodynamics 8=15234
 - toroidal, possible stationary motion 8=4339
 - transfer phenomena in rarefied plasma in toroidal trap 8=4342
 - transport coeffs. from inelastic collisions 8=7939
 - transport phenomena, appl. Fokker-Planck eqn. 8=4328
 - transport in r.f. discharges, anomalous 8=16401
 - travelling-wave field in strophoton, interact. with electrons 8=10911
 - turbulent, accel., scatt. and diffusion of charged particles calc. 8=7741
 - turbulent, collision theory 8=7738
 - turbulent, Coulomb collisions calc. 8=16474
 - turbulent heating in current nonisothermal plasma 8=1383
 - two-component, equilibrium correlation functions 8=21307
 - two-fluid, jump conditions 8=4358
 - two-fluid plasma equations, singularities, and their relation to boundary conditions 8=4330
 - two-fluid plasma eqns., singularities and relation to boundary conditions, comments 8=21299
 - two-fluid plasma eqns., singularities and relation to boundary conditions, reply to comments 8=21300
 - two temp., dielect. constant analysis 8=7742
 - unstable sac, randomization at constriction in discharge column 8=1338
 - variable density discharge obs. 8=16406
 - viscosity in strong mag. field influencing particle collisions 8=16482
 - Vlasov eqn. with collision terms and external mag. fields, operator soln. 8=16469
 - Vlasov eqn, relativistic covariant form, derivation 8=4326
 - waves, nonlinear, in plasma pierced by quasi-neutral charged particle beam 8=1391

Plasma—contd

- waves, trapped electroacoustic, fast randomization of electron gas 8=16580
 weakly turbulent, local determ. of wave-particle interaction 8=21309
 Ar arc, Stark broadening of Ar I lines 8=12057
 Ar containing alkali metal additions, elect. conductivity 8=12482
 Ar downstream flow in uniform guide field structure probe obs. 8=12472
 Ar, flowing, specific energy and electric field for intense stable discharge 8=16402
 Ar, laminar flow heat transfer in entrance region of circular tube 8=16477
 Ar, microwave induced for spectrochem. anal. of metals 8=18785
 Ar, partially ionized, supersonic source flow expansion into vacuum 8=16658
 Ar, partially ionized, viscosity and thermal conductivity 8=7734
 Ar, thermal plasma, continuous emission spectrum 8=16207
 Ar-Cs and Ar-K in pulsed discharge with ionization confined to impurity atoms, props. 8=1346
 Ba, ion density, rel. obs. of resonance radiation scattering 8=4331
 C, laser induced 'blow-off' plasma, density and temp. 8=12467
 CO₂-N₂, i.r. emission spectra 8=12510
 CO⁺, cometary, prod. and flow under influence of solar wind 8=14854
 Cs, diffusion coeff. of ions, and reflection coeff. from plasma boundary, meas. 8=12473
 Cs, effective electron-Cs heavy particle momentum transfer collision freq. 8=12476
 Cs, electron current flow under influence of d.c. fields and plasma grads. 8=12477
 Cs, migration of ions and electrons in elec. field, conc. and temp. grad. 8=15212
 Cs, particle losses due to charge exchange 8=21288
 Cs, prod. by resonance rad. from Cs discharge, and parameters 8=4362
 Cs, vapour, physical props. 8=12474
 D, e and ion temps., laser incoherent scatt. obs. 8=21354
 D, homogeneous high-density, profiles of D _{α} line 8=16194
 H, e temp. and density, laser incoherent scatt. obs. 8=21354
 H, heating by large amp. ion cyclotron wave, efficiency 8=4332
 H, laser-produced, temp. and density meas. rel. to absorpt. at laser freq. 8=12514
 H, post shock 8=16646
 H, thermodynamic functions calc. for free p and e 8=12469
 H₂, positive column, cross wave of moving striations 8=4281
 H _{α} , Stark broadening of line profiles 8=4063
 He discharge with hot cathode, behaviour in alternating electric field 8=16489
 He discharge, mag. field stabilised, press. built-up 8=7691
 He in theta pinch discharge, electron densities and temp., spectroscopic meas. 8=21349
 He-Cs and He-K in pulsed discharge with ionization confined to impurity atoms, props. 8=1346
 in He-Ne d.c. discharge, relation between electron temp. and conc., and discharge parameters 8=7666
 He-Xe, population inversion in positive column 8=12405
 Hg discharge, ion-acoustic wave propagation 8=4313
 Hg vapour positive column zeroth order distrib. changes 8=7667
 K foils, reson. emission excited by light 8=7776
 Kr, thermal plasma, continuous emission spectrum 8=16207
 Li line broadening in LiH plasma by microfields 8=12515
 Li, parameters and thermodynamic characteristics, calc. 8=12462
 LiD and LiH target for laser light, energetic plasma prod. 8=8774
 Mg films, reson. transmission of p-polarized u.v. light 8=12516
 N, excitation temps. from multiplet intensities 8=1376
 Na gas discharge, line excitation rel. to cascade transitions 8=20962
 NaK seeded, in elec. field, temp. meas. 8=21308
 Ne, thermal plasma, continuous emission spectrum 8=16207
 Ne-He, cross section for second kind collisions, meas. 8=21016
 SF₆, electrical conductivity, 2400-9000°K 8=7737
 Xe, thermal plasma, continuous emission spectrum 8=16207

confinement

- in adiabatic trap with 'min. B', ion-cyclotron instability 8=4387
 air, θ -pinch effect use in electrodeless shock tube 8=6136
 bottle, use of field from ring-shaped coils 8=21372
 coaxial electrode gun, plasmoid field requirement 8=16609
 collisionless, boundary conditions 8=21363
 collisionless, equilibria config. 8=12538
 collisionless sheath, with transverse flow 8=21362
 compression by a mag. field 8=12535
 density contour meas. using mol. ion beam break-up 8=7791

Plasma—contd**confinement—contd**

- drift of plasma ring in toroidal mag. field 8=21367
 double space-charge sheaths, negative-ion effects 8=16549
 guide field for plasma betatron 8=16563
 injection of, in a closed magnetic configuration 8=16554
 instabilities hindering thermonuclear reaction control 8=12561
 instability, negative mass, with B_z field 8=16566
 inverse pinch discharge, current sheet dynamics 8=12534
 ion beam confinement of magnet field, geomag. appl. 8=1417
 magnetic bottles, leakage 8=7318
 magnetic bottle, superconducting 8=16555
 magnetic, drift-dissipative oscills. 8=7805
 magnetic and e.m. methods for controlled nuclear fusion 8=11977
 mag. field, rotating, integrodifferential eqn. for each mode of deformation 8=16565
 magnetic fields, structural analysis 8=19741
 magnetic field, toroidal, theory 8=1411
 magnetic mirror trap, asymmetric, motion of charges 8=7806
 magnetic mirror trap, charged particle lifetimes, obs. 8=16558
 magnetic mirror trap, heating by current 8=4285
 magnetic mirror trap rel. to electron cyclotron instability 8=7837
 mag. quadrupole field, ballooning instability 8=12537
 magnetic trap, non-adiabatic, particle motion, integral eqn. soln. 8=16557
 magnetic trap for "Sirius" stellarator 8=16556
 mirror magnetic field, charge exchange loss 8=21374
 multipole mag. field, spherical, as mag. trap 8=4393
 particle motion in e.m. field 8=19764
 Pascal mag. device, surface ionization of Cs 8=1415
 pinch solns., one-dimensional static 8=7802
 pinch, ultra-fast thetatron, obs. 8=7803
 reflection by linearly increasing magnetic field 8=7804
 relaxation time, appl. of var. principle 8=7797
 reviews of plasma physics, book II 8=16461
 ring-current configurations, possibilities as fusion device 8=21373
 sheaths at the electrodes of a plasma diode 8=296
 sheath, e, reflection of electrostatic waves 8=12532
 sheath, ion extraction in presence of secondary e 8=4389
 sheath, microwave diagnostics 8=21364
 sheaths, plane collisionless, between field-modified emitting electrodes and thermally ionized plasmas, e.g. Ce 8=21365
 sheet, pinch, finite-resistivity stabilities 8=1413
 single pulsed plasma, by short circuiting current of plasma gun 8=4420
 spire, tetrahedral, mag. field inside, obs. 8=16561
 stellarator field, toroidal, single particle motion 8=12536
 stellarator mag. surface destruction by mag. field irregularities 8=16562
 stellarator, trapping efficiency of non-adiabatic injection 8=7848
 stellarators, toroidal, trajectories of magnetic field lines 8=4388
 stochastic heating expt. in mag. mirror 8=4336
 symmetrical magnetohydrostatic fields, variation principle 8=305
 θ -pinch, collisional rate coeff. for C ions 8=12470
 θ -pinch compression for shock wave study 8=7798
 theta-pinch density distrib. meas., bremsstrahlung method 8=12525
 theta pinch dynamic stabilization 8=7801
 theta pinch, effect of welding joint in discharge tube 8=21369
 θ pinch, factors determining beta 8=16551
 theta-pinch, high and low pressure, measurement of β , n, T, 8=4391
 θ -pinch, large diameter, refractive diagnosis with series interferometer 8=7788
 θ pinch, low energy, mass pickup coefficient obs. 8=12533
 θ pinch, low energy, resistive instabilities, obs. 8=16552
 θ -pinch parameter meas., azimuthal magnetic field 8=7799
 theta-pinch profiles, adiabatic time development 8=4392
 theta pinch with sharp boundary, stability 8=4390
 theta pinch, slow, and stabilization effect 8=7800
 in slow theta pinch, axial behaviour 8=21368
 theta pinch, temp. and density of ions and electrons, laser scatt. expt. 8=16553
 θ pinch, travelling periodic bumpy, instabilities 8=16550
 in toroid geometry, cond. for flute instability 8=7796
 toroidal column, equilibrium in d.c. and h.f. mag. fields 8=16559
 toroidal discharges without axial magnetic field reproducibility conditions 8=1414
 toroidal magnetic trap with zero rot. 8=1416
 toroidal pulsed discharge in crossed fields 8=21371
 toroidal scheme, magnetohydrostatic equilibrium 8=16548
 toroidal systems, trapped particles, effect of static, radial elect. fields on stability 8=16564
 toroidal traps, antisymmetric, with arbitrary mag. axis 8=21366

Plasma—contd

confinement—contd

- toroidal trap, rarefied, transfer phenomena 8=4342
 z-pinch discharges, press. -depend. transition
 behaviour 8=4275
 H ion, in mirror machine, cyclotron resonance and non-
 adiabatic trapping 8=21370
 He, slow theta pinch, axial behaviour and end loss 8=1412
 InSb, e-hole plasma, 250°K, θ pinch effect 8=13821

devices

- alkali metal purification in magnetoplasma device
 using preferential contact ionization 8=4302
 antenna in nuclear environment 8=4422
 arc air heater for re-entry simulation 8=21408-9
 arc jet, thrust calc., mass flow rate 8=4421
 betatron, negative-mass instability, obs. 8=21393
 Circe plasma injected in Pleiade u.h.f. cavity, obs.
 compared with theory 8=21405
 coaxial accelerator, energy ang. distrib. obs. 8=16610
 coaxial electrode gun, plasmoid obs. 8=16609
 diode, stationary regimes 8=296
 duoplasmatron, comp. of H ion beam 8=3222
 duoplasmatron source, energy-spread parameters 8=16608
 flames, induction-coupled, in air and Ar, spectroscopic
 obs. 8=21411
 generator, discharge chamber, heat transfer meas. in
 mag. field 8=7847
 generator, with vortex stabilization, rotation of electrode
 segments of arc 8=16607
 gun, short circuiting current for single pulsed plasma
 production 8=4420
 gun-terrella, model expts. on solar wind-magnetosphere
 interact., scaling 8=14643
 gun with Ti electrodes, used for filling 50 litre mag
 trap 8=12568
 Hall current, acceleration process 8=12483
 h. f. source for emission spectrometry 8=20086
 hydromagnetic coaxial accelerator, production of dense
 plasma focus discharge 8=21221
 instability, nonlinear, in beam systems, calc. 8=12563
 ion beam, intense, production using magnetized
 plasma 8=15349
 ion beam source, density and temp. meas. 8=1432
 ion removal, excitation of ambipolar acoustic
 waves 8=12569
 J×B device, current distrib. in non-equilib. state 8=7849
 jet generator, nozzle electrodes 8=21412
 jet, u.h.f. diagnostics 8=1435
 jets, temp. meas. techniques 8=12572
 light sources 8=484
 magnetoplasmadynamics accelerator, phenomena in
 cathode region 8=7652
 microwave amplifier, electron beam interaction 8=12570
 MPD arcs, current and potential distrib., effect of
 electrode geometry 8=16495
 neutralizer for ion beams 8=6335
 Pascal, mag. confinement, surface ionization of Cs 8=1415
 plasmatron, a.c., 6 electrode, for temp. 2000-4000°K
 and press. 1-3 atmospheres 8=1434
 plasmatron jet, electrodynamic structure rel. to
 nozzle geometry 8=12573
 plasmatron jet, heating of condensed powder particles,
 calc. 8=12574
 plasmatron, vacuum gas-dynamic unit for studying
 operation 8=12531
 probe, electrostatic for artificial satellite 8=2764
 propulsion, ion-electron beams emitted by a plane,
 neutralization 8=3225
 Q, shock formation 8=21325
 rotating plasma expt., analysis 8=21404
 sources, optical density and degree of inhomogeneity from
 spectral distribution 8=7728
 stellarator field, toroidal, single particle motion 8=12536
 stellarator, non-adiabatic injection 8=7848
 C-stellarator ohmic heating discharges in H, computer
 description 8=21407
 stellarator, "Sirus", magnetic trap assembly 8=16556
 stellarator, stability with anisotropic pressure 8=7832
 stellarator, stochastic destruction of magnetic
 surface 8=1428
 stellarator, strong negative- v torus 8=21406
 stellarators, toroidal, trajectories of magnetic field
 lines 8=4388
 stellarator, toroidal and 1=3, plasma
 equilibrium 8=7846
 supersonic jet, structure and formation mechanism 8=16611
 symmetrical column equil. at high pressures 8=7833
 thermionic convertor, classification of operating
 regimes 8=3159
 thermionic convertor, transport equations 8=3158
 thermonuclear reactors, engineering and economics 8=16138
 thetatron discharge, microwave excitation and
 propag. 8=16523
 thruster, calorimetric probe to determine energy 8=4382
 TM-3, neutral atom density distrib. 8=1433
 torches, as source of thermal plasmas 8=21410
 torch, thermal r. f., energy-transfer mechanism and
 typical operating characts. 8=16612

Plasma—contd

devices—contd

- 2-phase m. h. d., liquid metal 8=19729
 verneuil plasma torch for crystal growth, heat
 transfer 8=21936
 waveguide, nonlinear coupling of slow and fast
 waves 8=4401
 Ar duoplasmatron, relative abundance of ions 8=7780
 Ar, h.f. torch, power developed at atmos
 press 8=21236
 Ar-H₂ jet, radial temperature distribution,
 determination 8=12571
 Ba source, fully ionized 8=4419
 for B₄C coating prep. for antiradiation screens 8=20551
 H supersonic jet in high vacuum, as charge exchange
 target 8=21451
 He accelerator, coaxial, electron temp. and
 density 8=4337
 Hg arc tube producing large volume of plasma 8=16606
electromagnetic wave propagation
 acceleration with microwaves near cyclotron
 resonance 8=4373
 adiabatic transformation of e. m. wave spectrum 8=21339
 Alfvén waves, for mag. field parallel to gravitational
 field 8=7771
 along unmagnetized column, for various guide
 structures 8=19885
 amplification, by charged particle beam for transient
 radiation at media boundary 8=12494
 amplitude modulation by a. c. magnetic fields 8=15391
 anisotropic, homogeneous, distortion of pulse
 carrier 8=16525
 antenna, current distrib. propag. const. and radiation
 resist. 8=16528
 antennas and propagation conference, Ann
 Arbor 1967 8=15401
 aperture field model for plane wave 8=16519
 in beam-plasma systems 8=7765
 beams-plasma interaction 8=21329
 beam shape in focal region of microwave lens,
 calc. 8=21356
 beat frequencies and harmonic generation 8=7758
 between antennas, effects of refr. and absorpt. 8=7783
 boundary layer on slender entry vehicles 8=14709
 bounded, collisionless absorption and emission 8=7770
 bounded plasma, nonlinear theory 8=12496
 bremsstrahlung, relativistic correction and electron-ion
 spectrum and energy loss rate in relativistic
 limit 8=21343-4
 Buchsbaum-Hasegawa wave excitation in low-temp.
 plasma cylinder 8=21337
 cold, motion in magnetic field with h. f. e. m.
 wave 8=21322
 collision-induced instabilities near electron cyclotron
 harmonics 8=7841
 collisionless, along applied mag. field 8=4372
 compressible, wave excitation and equivalence
 relations 8=4374
 conference, I.E.E.E., New York, 1967 8=1398
 Coriolis force, Hall current and self-gravitation
 effects 8=16515
 coupling due to inhomogeneous region 8=16518
 cyclotron harmonic emission along mag. field 8=21327
 cyclotron harmonic radiation from plasmas,
 theory 8=21328
 cyclotron instability in hot electron plasma with double-
 humped velocity distrib. 8=21398
 in cylindrical plasma with mag. field 8=7768
 demodulation, nonlinear, of an amplitude-modulated
 wave 8=1395
 diffraction by structure 8=4371
 dipole resonance of column, nonlinear effects 8=7763
 dispersion in hot inhomogeneous slab 8=4365
 Doppler shift, theory 8=12499
 drift wave with finite amplitude 8=7772
 edge condition and "intrinsic loss" in uniaxial
 plasma 8=16530
 effect on symmetric waves in a rectangular
 helix 8=6396
 electrostatic ion cyclotron waves, exptl. study 8=12500
 enhanced microwave emission due to irrad. by intense
 microwave 8=1396
 in external elec. field, fluctuations and scatt. of e. m.
 waves 8=4369
 Faraday rotation in semiconductors and ionosphere 8=22948
 guided waves, transformation theory 8=378
 gyromag. or synchrotron radiation, relativistic,
 amplification dependence on polarization 8=21345
 gyrotropic, bounded, new multipolar mode 8=21347
 half-bounded, e. m. fluctuations inc. surface waves 8=4377
 helix in plasma, symmetric wave behaviour 8=7766
 hydrodynamic solitary waves, nonlinear 8=7756
 imbedded in moving dielec. medium, governing eqns. for
 e. m. fields and waves 8=12507
 impedance meas. of quarter wave monopole,
 isotropic 8=19897
 inhomogeneous, asymptotic solution of waves 8=7774
 inhomogeneous with longit. mag. field, asymptotic
 solns. 8=21330

Plasma—contd

electromagnetic wave propagation—contd

- inhomogeneous magnetoactive medium, e. m. wave amplification by charged particle flow for transient radiation 8=21348
- in inhomogeneous warm magnetoplasmas, first-order coupled diff. eqns. 8=16532
- interaction, longitudinal and transverse waves 8=16524
- interaction of plasma waves 8=4364
- ion-acoustic wave excitation 8=7815
- ionizing shock, moving, interaction with transverse wave 8=12504
- klystron operation from wave coupling on beam modulation by low freq. 8=1397
- Landau damping and entropy 8=12505
- lateral wave on symmetrical Epstein transition 8=19840
- longitudinal, excitation at diffuse reflection of electrons from surface 8=12498
- magnetic field \parallel to plasma boundaries 8=1392
- magnetized column, radiation from dipole 8=7762
- magnetized, non-uniform, e. m. freq. near 2nd electron cyclotron harmonic 8=4367
- magneto-, warm, whistler mode propag., effect of longitudinal elect. field 8=19008
- magnetoacoustic resonance for non-linear excitation in cold plasma 8=21333
- in magnetoactive, one-component, unbounded plasma, anisotropic press. 8=7773
- magnetoplasma, a. m. wave, non-linear demodulation, theory 8=16521
- magnetoplasma, cold slab, radiative modes of e. m. oscillns. 8=16527
- magnetoplasmas, inhomogeneous wave, eqns. 8=12466
- magneto-plasmas, warm slightly ionized, interact. of e. m. fields 8=16517
- metal foils with rough surfaces 8=8958
- microwave nonlinear high-power coupling to electroacoustic resonances 8=12506
- microwave scattering by turbulence, numerical expt. 8=16516
- microwaves through turbulence, anomalous transmission 8=7759
- non-linear cross modulation due to time-dependent electron density 8=21334
- oblique incidence on plasma layer 8=21331
- oblique wave in drifting isotropic warm plasma 8=21323
- partially-filled waveguide, non-linear coupling dispersion eqns. 8=10958-9
- plane field perpendicular to plasma layer, independence 8=12508
- plasma layer in mag. field, kinetic theory 8=12497
- propag. refl. and absorpt. of e. m. waves 8=1392
- r.f. sources in ionized medium, behaviour 8=12495
- radiation by test particle in helical motion along mag. field 8=12501
- radiation characts. of linear resonant antenna, comments and reply 8=12492-3
- radiation from charge moving in magneto-active plasma with l. f. oscillations 8=21385
- radiation from plasma, photon bremsstrahlung calc. for e gas 8=12503
- radiation from warm plasma, freq. near electron cyclotron resonance second harmonic 8=21336
- radiation loss of finite dipole in moving plasma 8=7764
- radiation shown by antenna with dielectric sheath before surrounding plasma layer 8=10978
- reflection and transmission from magnetized nonuniform slab 8=21342
- refraction and focusing of spherical waves in parabolic layer 8=7761
- refractive index, relativistic, for drifting magnetoionic plasma 8=18977
- rarified, of thetatron discharge, microwave excited due to instability 8=16523
- resonant layer, absorption at oblique incidence 8=4376
- resonance phenom. in reflection and transmission from magneto-plasma column 8=1394
- scattering by collinear plasma waves 8=7757
- scattering by dielect. const. fluctuation 8=21338
- scattering in free-electron atmosphere 8=15028
- scattering, generalized physical optics approximation 8=16534
- scattering from immersed conducting cylinder 8=16529
- scattering by inhomogeneous spheres, collisionless approximation 8=4366
- slab, isotropic and incompressible, excitation by parallel plate guide with one plate truncated 8=21335
- space charge waves in electron beam 8=7767
- short antenna impedance, quasi-static approximation 8=15423
- shock tube, reflection by moving plasma 8=16531
- in stratified magnetoplasma, using energy propagation 8=23368
- surface microwaves along column 8=12456
- TE waves in collisionless sheet, dispersion relations and stability 8=21346
- transient oscillations excited by small antenna 8=21332
- transmission cross sections of infinite slit, excited by H-polarized plane wave 8=15395

Plasma—contd

electromagnetic wave propagation—contd

- transverse waves in magnetized laboratory plasma 8=21341
 - turbulent heating, intensity of e. m. rad. and noise 8=4370
 - turbulence, microwave investigation 8=7760
 - turbulent, skin layer, anomalous thickness obs. 8=7769
 - u. h. f., radiated rel. to instability mechanism 8=16520
 - warm, dipole impedance, effect of induced acoustic sources 8=4386
 - warm plasma loaded waveguides, surface waves 8=16522
 - waveguide, nonlinear coupling of slow and fast waves 8=4401
 - wave guide partially filled with plasma in infinite axial mag. field 8=3266
 - waveguide, solid-state, circular, and Faraday effect 8=10968
 - waveguide, stratified, study of orthogonal natural or eigen waves 8=10960
 - Ar afterglow, msec microwave pulses nonlinear interactions 8=21340
 - Ar, resonance scatt. of c.w Ar ion laser light 8=12513
 - Cs, ion-acoustic wave, non-linear Landau damping 8=4375
 - Ne afterglow, msec microwave pulses nonlinear interactions 8=21340
 - Xe afterglow, msec microwave pulses nonlinear interactions 8=21340
- magnetohydrodynamics**
- acceleration by self-induced mag. field 8=1327
 - acoustic mode, dipole magnetization field 8=1393
 - Alfvén waves, large-amplitude, nonlinear effects in propagation 8=21376
 - anisotropic, discontinuities, transition solns. 8=4353
 - atmosphere, upper, long period geomag. micropulsations explanation 8=2731
 - bounded beam-plasma system, axially symmetric oscills. 8=16568
 - boundary between stream and cavity with plane dipole, effect of external mag. field 8=16496
 - charge interaction with space-perturbed magnetic field, asymptotic calculation 8=3232
 - cold, electrostatic waves, nonlinear interaction of three 8=4355
 - cold, l. f. non-electrostatic waves in field excited by ion beam, instabilities 8=4348
 - cold, motion in magnetic field with h. f. e. m. wave 8=21322
 - collision damping including Hall current and Larmor radius 8=12486
 - collisionless, transverse wave propag. along applied field 8=4372
 - collisionless, viscosity, in weakly turbulent mag. field 8=18929
 - depolarization currents in curved magnetic field 8=16500
 - diffusion across mag. field, effect of boundary conditions for metal and glass cylinders 8=16502
 - diffusion and rot. in conducting container of finite length 8=4349
 - diffusion, transverse, across uniform mag. field, kinetic theory 8=4341
 - electron beam, gyrating, interaction with cold plasma 8=16501
 - electron current, stability 8=7836
 - electron density, redistribution by microwave field 8=7729
 - electron mode coupling in finite field 8=7840
 - energy conversion principles, by collision and gyration 8=288
 - energy exchanges for various excitation modes 8=7749
 - equations, study of instability 8=12556
 - equilibrium flow accompanying compression 8=16493
 - exosphere conc. by sounding 8=23314
 - Ferraro-Rosenbluth problem, computer expt. 8=1384
 - flows, temp. dependence of elect. conductivity 8=16491
 - flute growth, large amplitude stabilization 8=4350
 - generator boundary flow calc. 8=19725
 - generator, linear, analysis in uniform state 8=10840
 - gravitating rarified plasma, axially symmetric motion 8=21301
 - half-jet, compressible, inviscid stability 8=354
 - Hall current device, acceleration process 8=12483
 - heating by fast wave, rel. resistivity and damping 8=12484
 - horizontal strata, m. h. d. wave propag. 8=7748
 - hydrodynamic solitary waves, nonlinear, propagation 8=7756
 - instabilities, parametric, production by pumping wave of high implitude 8=12485
 - instability, transverse drift l. f., rel. to auroral bombardment 8=4356
 - localized modes in multipole configurations 8=16498
 - magnetized, space-charge effects by nonthermal ions 8=4351
 - MPD arcs, current and potential distribs, effect of electrode geometry 8=16495
 - magnetoplasma dynamics accelerator, phenomena in cathode region 8=7652
 - model, physical interpretation 8=6342
 - motion of oppositely charged particles 8=16497

- Plasma—contd**
magnetohydrodynamics—contd
 moving through transverse field, 2D time independent solns. 8=4354
 non-equilibrium and enhanced mixing at a plasma-fitted interface 8=5841
 nonequilibrium props. of seeded plasma, radiation effect 8=16484
 nonuniform electrical conduction in MHD channels 8=16437
 non-uniform, e. m. propag., freq. near 2nd electron cyclotron harmonic 8=4367
 oblique m. h. d. shock waves, stability 8=16456
 oblique wave propagation in drifting isotropic warm plasma 8=21323
 pinch solns., one-dimensional static 8=7802
 plane parallel flow, influence of viscosity anisotropy 8=16494
 plasmoid, laser-produced, expansion against mag. field 8=16505
 poloidal resonances of plasma magnetized by dipole field 8=18925
 positive column, l.p., in transverse mag. field 8=7661
 quantum mechanics of nonlinear phenomena in strong mag. field 8=16503
 reacting medium, effect of ionization and recombination 8=4357
 reviews of plasma physics, book II 8=16461
 shock, propag. perpendicular to mag. field, one parameter family of profiles 8=12489
 single electron motion, superphase velocity and wave excitation 8=12487
 spatial dispersion and Landau damping 8=1385
 stability in magnetic traps, theory 8=7843
 stratified anisotropic, gravitational internal instability 8=10241
 supersonic flow, investigation technique 8=7793
 theta pinch with sharp boundary, stability 8=4390
 toroidal confinement scheme magnetohydrostatic equilibrium 8=16548
 turbulent flow correl. with Langmuir probe current fluctuation 8=1406
 upper atmosphere, toroidal resonance, math. viability 8=2723
 warm, streaming, and a confined mag. field, boundary layer between 8=7750
 wave correlations, uniformly turbulent weakly nonlinear systems 8=4352
 waves, longitudinal excitation near electron-cyclotron harmonics in axial mag. field 8=16581
 wave modes behind normal ionizing shock waves 8=19535
 wave propag., dispersion relations and damping rel. to transport coeffs. 8=16499
 waves quasilinear transform. and nonlinear interactions 8=12552
 waves and theory of stability, book 8=16455
 wave, transverse, interaction with moving ionizing shock 8=12504
 Ar₂ gas-ionizing shock fronts, hydromagnetic, non-equilibrium structure 8=16504
 He, axial injection into mag. dipole field, obs. 8=16506
- measurement technique**
 arc jet temperatures, spectroscopy and calorimetry 8=12572
 beam shape in focal region of microwave lens, calc. 8=21356
 density contour meas. using mol. ion beam break-up 8=7791
 density distribution, Mach-Zender interferometric analysis 8=7786
 density distrib. in θ -pinch, bremsstrahlung method 8=12525
 density, spectroscopic, spectral line intensity and broadening 8=16538
 detector-characteristic method at intermediate pressures 8=12517
 diagnosis by coupled cavity interferometry with He-Ne and CO₂ lasers 8=12522
 diagnostics in microwave cavities using whistler resonance temp. effect 8=3272
 diagnostics, spectral line contour self-reversal 8=12521
 diamagnetism, using external coil near conducting wall 8=16543
 discharge model, relative abundance of ions 8=7780
 discharges, r. f., high voltage, current meas. 8=4277
 electron concentration by broadened hydrogen lines 8=4062
 electron conc., crossed interferometric-spectrographic method 8=12523
 electron concentration by 4mm microwave interferometer, low-density 8=7790
 electron conc., homodyne phase meter 8=7785
 electron density using complex reflection coeff., plasma boundary errors 8=16535
 electron density, microwave free-space method 8=16537
 electron-hole decay rate, double-pulse variable-decay circuit 8=15177
 electron temp. and density, methods 8=7799
 electron temp. due to shock waves 8=21326
 electron temps. and densities from transient He-like ion line emission 8=21358
- Plasma—contd**
measurement technique—contd
 Fabry-Perot resonator, microwave, electron density, collision freq. and Q change 8=16542
 Faraday cup for solar plasma 8=1403
 fluctuating, electron distrib. function meas. by Langmuir probes 8=4385
 fractional-fringe holographic interferometry 8=7779
 induction method, parameters, theory reviewed 8=4380
 ionospheric probe, resonance relaxation sounder 8=19012
 isotherms, visualization by seeding 8=7781
 Langmuir probe characts., determ. of e densities in afterglow plasmas, comp. of methods 8=21355
 Langmuir probe description 8=4382
 Langmuir probe, microwave, diagnostic techniques, comparison 8=1409
 Langmuir probes, exptl. investigation 8=7794
 Langmuir probes, modulated, spurious second harmonics 8=1410
 Langmuir probes, theory applic. to saturated-ion-current density, anomaly explanation 8=12529
 laser beams, self-focused for electron density and temperature 8=16544
 laser light incoherent scatt. 8=21354
 magnetoplasma dielectric in resonant cavity, absorpt. spectrum 8=21352
 magnetoplasma, resonance rectification effects 8=1407
 mass pickup in low energy θ pinch and obs. 8=12533
 microwave diagnostics 8=4379
 microwave diagnostics of plasma sheath 8=21364
 microwave diagnostic systems at 8, 4 and 2mm, ceramic window for 8=7789
 microwave, electron density and ionization time 8=12518
 modified-Langmuir-probe analysis, comp. with computer solns. of electrostatic probes 8=21360
 multiplexer for multifrequency microwave sounding 8=12524
 optical interferometry of laser induced discharges 8=16403
 orbit analyzer probes, for plasma temp. 8=12530
 pilot tube for supersonic flow investigation 8=7793
 probe, double with h. f. multistep pulse voltage 8=4384
 probe, electron charact. in magnetized plasma 8=16547
 probe, electrostatics for electrodeless r. f. plasma 8=21361
 probes, electrostatic, for lightly ionized gas, continuum theory 8=16545
 probes, mag., calibration by separate r. f. elect. and mag. field generation 8=4381
 probe, optical, laser phase contrast system for phasography 8=7792
 probe, structure, downstream flow in uniform guide field 8=12472
 e probe for supersonic flow investigation 8=7793
 pulsed, lasers, production and diagnostics 8=21353
 pulsed pressure causing electrode cleavage near axis 8=1336
 resonance probe effect near ion plasma frequency 8=4383
 resonance and r. f. impedance probes, freq. characts. in mag. field 8=1408
 sheath, ruby laser pulse photography 8=12526
 shock tubes, e density by i. r. laser interferometry 8=16541
 spectrophotometer, electron-temp. isotherms meas. using scattered laser light 8=3357
 spectroscopic, exptl. device for high temps. 8=16539
 spectroscopic, high-temp. preliminary expts. 8=16540
 speed of streams, application of correlation method 8=12519
 spherical resonance probe behaviour in mag. field 8=16546
 superconducting electromagnets, appl. 8=6281
 temperatures, discharges for CO₂ lasers 8=15459
 temperature, spectroscopic, spectral line intensity and broadening 8=16538
 temperature, from Stark-effect shift and broadening of spectrum lines 8=7787
 θ -pinch, large diameter, refractive diagnosis with series interferometer 8=7788
 toroidal resonator for elec. cond., elec. field config. 8=16536
 transmission coeff. between antennas, effects of refr. and absorpt. 8=7783
 turbulence, microwave investigation 8=7760
 two-probe detector-characteristic method 8=12528
 u. v. detector, e channel multiplier 8=6506
 vacuum gas-dynamic unit using arc heater, for studying plasmatron operation 8=12531
 warm, dipole impedance, effect of induced acoustic sources 8=4386
 waveguide discrimination method 8=12520
 waveguide method of determining electric characteristics behind shock front 8=1389
 X-ray spectroscopy, 15-150 Å 8=22945
 Ar, moving striations, electron temp. var. display 8=16407
 C, laser-produced, two-wavelength interferometry 8=21357
 Cs arc, use of Mo probe 8=7782
 Cs, diagnosis by spectra interpretation, molec. effects 8=12527
 Cs diode, pot. and particle energies, meas. by simultaneous obs. of ion and electron energy spectra 8=15210
 Cu cold electrodes in moving H plasma, V-I characts. 8=21359

Plasma—contd

measurement technique—contd

- Cu, exploding wire, temp. determ. 8=7784
- D, diagnosis using neutrons from d-d reactions 8=1404
- He₂ discharge, positive column, correlator for 10-200 kHz signals 8=1405
- He-Ne laser, use of Mo probe 8=3318

oscillations

- acoustic mode damping of hydromagnetic plasma 8=12486
- acoustic in turbulent plasma, existence of second sound 8=12560
- Alfvén waves, Cherenkov emission by moving force source 8=6343
- Alfvén waves in finite conductivity plasma 8=12545
- Alfvén wave propag., for mag. field parallel to gravitational field 8=7771
- Alfvén waves, guided propag., appl. to magnetosphere 8=23327
- Alfvén waves, large-amplitude, nonlinear effects in propagation 8=21376
- Alfvén waves in solar wind 8=23719
- axially symmetric, in bounded beam-plasma system 8=16568
- beam-plasma interaction, ion excitation 8=12548
- beam-plasma system, h.f. and l.f. interactions 8=12539
- cold two-fluid, propag. of point disturbance along mag. field 8=16582
- collision-free waves, collective damping interpret. as simple energy exchange phenom. 8=21311
- with Coulomb interact., soln. for nonlinear fluctuations 8=16458
- cyclotron, ion and e, excit. by charged particle beams 8=12540
- cyclotron waves in moving cold plasmas, theory 8=16586
- density fluctuations due to monochromatic pumping, theory 8=12546
- density variation, conducting boundary, electron plasma wave 8=1420
- detonation waves measurement using double probe 8=4384
- dipolar resonance in waveguide 8=12456
- drift-dissipative, spectrum from eikonal eqn. 8=7805
- drift wave instability in column, correlation study 8=12553
- drift waves, meas. of resulting enhanced plasma losses 8=4400
- e, hot, due to e beam 8=21306
- echo experiment and theory 8=16585
- in electric field 8=7817
- electron cyclotron harmonics, non-linear generation with current instability 8=16573
- at electron cyclotron reson., e.m. waves negative absorpt. 8=12502
- electron discharge, pot. and density distrib. 8=1329
- electronic movement at low temp., solution of equations 8=7845
- electrostatic oscs., longit., higher order approx. in theory 8=16583
- electrostatic waves, absorption by plasma electrons 8=21382
- electrostatic waves, reflection at an electron sheath 8=12532
- excitation, four-plasmon parametric, theory and expt. 8=4399
- excitation non-linear, by magnetoacoustic resonance 8=21333
- excitation by phased electron beam 8=7813
- flute instability, gravitational analogy 8=7829
- flute, stability effect of incoherent precession 8=12567
- flute, of tenuous plasma, effect of elect. field 8=21378
- generation with relativistic electron beam 8=7818
- half-bounded, e. m. fluctuations inc. surface waves 8=4377
- helical waves in magnetoactive plasma, scatt. and transform. 8=21379
- high frequency, with large B, rel. to anisotropy of vel. distrib. function 8=12564
- h. f. waves, longit., generated by high current electron beam 8=21387
- hydrodynamic solitary waves, nonlinear, propagation 8=7756
- hydromagnetic waves damping rel. to stochastic electron heating 8=7821
- inhomogeneous, quasilinear wave transformation 8=12544
- interaction with ion-acoustic and transverse waves 8=16569
- interaction, longitudinal and transverse waves 8=16524
- ion-acoustic, excitation in strong field 8=7808
- ion acoustic waves, damping by Coulomb collisions rel. e and ion temp. 8=12550
- ion-acoustic waves, effect of electron temp. var. 8=16574
- ion-acoustic waves, e. m. excitation 8=7815
- ion-acoustic waves, propagation in bounded plasma 8=16575
- ion-acoustic waves, turbulence effects 8=12559
- ion cyclotron harmonics, angular spectrum 8=7820
- ion plasma oscillations, propagation, rel. to geometry 8=1422
- ion waves, collisionless plasma 8=16576
- ion waves in inert gases 8=1424
- ion waves, interaction with charged particle beam 8=7822
- ion-waves, parametric excitation 8=7807

Plasma—contd

oscillations—contd

- isotropic electron, Landau waves, expt. verification 8=7827
- isotropic, homogeneous plasma, supra-luminous waves and power spectrum 8=21380
- Landau damping, expt. confirmation, inherent errors 8=16587
- Landau damping, external mag. field effects 8=7826
- Landau damping in Maxwellian plasma as $t \rightarrow 0$ 8=21375
- Langmuir wave freq. correction, turbulent 8=7823
- laser probe scatt. for calc. of e density 8=1401
- longitudinal, in bounded one-dimens. nonuniform plasma 8=21386
- longitudinal, coupling to l. f. ion-sound wave 8=16579
- longitudinal, excitation across plasma column with axial mag. field 8=16581
- l. f. excited, radiation from moving charge 8=21385
- l. f. partially ionized gas, described by operation of plasma continuity eqns. 8=12541
- magnetoacoustic, instability in low pressure plasmas 8=21390
- magnetoacoustic, ion heating 8=7824
- magnetoplasmas, warm, resonance-rectification effects 8=7825
- mixing, non-linear, with velocity dependent collisions 8=16578
- modulated beam interactions, charge density distrib. 8=1418
- moving plasma in shock tube, electrically-driven, nature 8=4359
- near-steady transition waves 8=16481
- non-linear ion-cyclotron, theory 8=7812
- nonlinear, in magnetoactive plasma 8=12551
- nonlinear in uniform mag. field, soln. of Vlasov-Maxwell eqns. 8=16567
- nonlocal reflection in inhomogeneous media 8=21383
- overstable modes, resistive, in current-carrying column, obs. 8=12542
- parametric build-up in high freq. elect. field 8=21388
- parametric excitation due to density grad. 8=1421
- parametric res. and nonlinearity, from field modulation 8=4396
- potential surface waves, mag. field effects 8=7811
- in presence of Langmuir wave, ion osc. propag. in opposite direction 8=4397
- quasi-static ion cyclotron waves 8=4395
- quasi-stationary, amplification by electron beam 8=7816
- random in turbulence, effect of collisions 8=7738
- relativistic Vlasov-Maxwell eqns. initial value soln. 8=21381
- resonance of particles and Alfvén waves 8=7814
- resonance waves formed by interact. with e. m. waves 8=1394
- rotating cylinder pulsations at zero temp. gradient 8=20401
- second-harmonic cyclotron resonance, electron temp. and density var. 8=1419
- shock wave prop. along magnetic field 8=12491
- spatial ion-wave echo obs. 8=16588
- stratification wave, determ. from transient wave 8=141
- surface, dispersion by Al surfaces 8=12547
- surface waves, excitation by linear mag. currents 8=7810
- surface waves along magnetized column, symmetric modes 8=12549
- and temp. distrib., electron beam injection prod. 8=21287
- transconductance due to Landau waves, theory 8=7828
- transverse wave instabilities in plasma with axially symmetrical velocity distrib. 8=12554
- turbulence, Coulomb collisions calc. 8=16474
- turbulent, interaction of ion-acoustic waves 8=7809
- wave energy, transform. from energy accumulated in active medium 8=4402
- wave excitation by external currents 8=4394
- wave interaction, nonlinear, beam instability 8=16598
- wave propagation, models 8=12543
- waves in inhomogeneous warm magnetoplasmas, first-order coupled diff.-eqns. 8=16532
- waves at plasma-mag. field interface 8=21384
- waves, nonlinear, in plasma pierced by quasi-neutral charged particle beam 8=1391
- waves quasilinear transform. and nonlinear interactions 8=12552
- waves, small- and large-amplitude, collisionless damping obs. 8=4403
- waves, steady-state decay instability 8=4405
- waves, in weak turbulence, nonlinear interaction and ion sound 8=1423
- weakly ionized gases, propag. of longit. ion waves 8=4398
- weakly turbulent 8=4404
- Cs ion beam, synthesized, electrostatic oscillation obs. 8=16584
- Cs, thermal, in Q device, noncorrelation with magnetic cross-field transport 8=7819
- Hg, ion acoustic waves dispersion relation and phase vel., 10^{-3} torr 8=21377
- Hg, longit. waves second harmonic generation, 10^{-3} torr 8=21389

stability

- alkali halogen, drift waves in collisionless limit 8=16577

- Plasma—contd**
stability—contd
- anisotropic pressure in helical mag. field 8=7832
 - ballooning in mag. quadrupole confining field 8=12537
 - beam instability of current 8=7837
 - beam instability, nonlinear wave interaction 8=16598
 - beta in θ pinch, determining factors 8=16551
 - cold, l. f. non-electrostatic waves in field excited by ion beam 8=4348
 - cold, multiperiodic h. f. field rel. to two-stream instability 8=21402
 - collision-induced instabilities near electron cyclotron harmonics 8=7841
 - collisionless compression, with anomalous friction, numerical investigation 8=21399
 - collisionless plasmas in cylindrical geometry, and equilibrium 8=21397
 - column equil. with helical symmetry 8=7833
 - column, flute, kinetic and hydrodynamic drift-beam instabilities 8=7835
 - current-convective and overheat instability, conductions 8=12556
 - cyclotron instabilities in two-component electron plasma 8=4409
 - cyclotron instability in hot electron plasma with double-humped velocity distrib. 8=21398
 - cyclotron instability, two-streaming 8=4414
 - dense, confined by rot. mag. field 8=16565
 - density gradient drift instability, mag. shear effect 8=12555
 - density-gradient instabilities, stabilization by dispersion of curvature drift velocity 8=12565
 - in dipole magnetic field, laboratory meas. 8=16594
 - discharge, linear, beam instability, heating 8=4285
 - dispersion relations for transverse waves due to spatially uniform elect. field varying sinusoidally with time 8=12557
 - disturbed zone near electron emitting surface 8=7842
 - drift-cyclotron instability, effect of magnetic curvature 8=4413
 - drift-dissipative instability 8=7805
 - drift instabilities in general mag. field configurations 8=21394
 - drift-temperature instability, dependence on initial density and temperature gradients 8=7844
 - drift wave instability in column, correlation study 8=12553
 - electron current in strong mag. field 8=7836
 - electronic movement at low temp., solution of equations 8=7845
 - end stabilization effect in slow theta pinch 8=7800
 - energy principle, for l. f. interchanges 8=16605
 - energy spread introduction by high energy neutral injection 8=16603
 - experimental evidence and evaluation of instabilities 8=12566
 - finite gyro-radius equation for flute instability 8=1427
 - firehose effect, persistence in highly relativistic collisionless plasma 8=21403
 - flute instability, conds. in toroid geometry 8=7796
 - flute instability, gravitational analogy 8=7829
 - flute oscillations of tenuous plasma effect of elect. field 8=21378
 - gravitating plasmas with mag. field and rot., 2-stream instability 8=19085
 - heated, non-uniformly, electron temp. instabilities 8=7838
 - rel. to helical wave fluctuations, magnetoactive plasma 8=21379
 - high frequency with applied longitudinal magnetic induction 8=12564
 - hollow column, helical instability 8=4407
 - hydromagnetic theory, two dimensional slab models 8=4415
 - incoherent precession, effect on flute oscils. 8=12567
 - instability caused by collective interact. of ion beams, and 'slipping' beams 8=16595
 - instabilities, h. f., in electron beam generated plasma 8=16604
 - instabilities, h. f. field influence 8=16597
 - instabilities hindering thermonuclear reaction control 8=12561
 - instability, ion-acoustic, excitation by e. m. waves 8=7815
 - instabilities leading to anomalous diffusion, explanation of onset 8=21310
 - instability of magneto-acoustic waves in low pressure plasma 8=21390
 - instabilities, micro, collisionless regime, configurations with periodic mag. curvature 8=16602
 - instabilities, "most dangerous", in mag. field 8=1431
 - instability, negative mass, with B_0 field 8=16566
 - instability, nonlinear, in beam systems, calc. 8=12563
 - instabilities, resistive in low energy θ pinch, obs. 8=16552
 - instability, two-stream, asymptotic state 8=16589
 - instability and turbulence 8=4412
 - ion-acoustic excitation 8=1429
 - ion-cyclotron instability in adiabatic trap with 'min. B' 8=4387
 - ion-cyclotron instability, threshold density meas. 8=7834
 - with isotropic distrib. functions in stationary mag. field 8=16596
- Plasma—contd**
stability—contd
- Kelvin-Helmholtz instability, effect of finite ion harmonic radius 8=21400
 - localized modes in multipole configurations 8=16498
 - low-band electron modes, coupling with space charge modes of electron beam 8=7840
 - magnetic surfaces in toroidal trap 8=1411
 - magnetic traps, magnetohydrodynamic theory 8=7843
 - magneto-plasma, production of parametric instability by pumping wave 8=12485
 - MHD flute growth, large amplitude stabilization 8=4350
 - MHD generators, and voltage oscils. 8=15208
 - MHD half-jet, compressible, inviscid 8=354
 - MHD and micro-instabilities, book 8=16455
 - mixed with cold neutral particles, stability of tangential discontinuity in vel. 8=1425
 - modulated beam interactions, parametric resonance 7=1418
 - moving through transverse mag. field, 2D time independent solns. 8=4354
 - negative-mass instability in plasma betatron, obs. 8=21393
 - nonlinear cross-field instability, structure of plasma turbulence 8=21395
 - nonlinear effects 8=4418
 - non-uniform, in d. c. elect. and mag. fields, kinetics 8=16591
 - overstable modes, resistive, in current-carrying column, obs. 8=12542
 - parametric excitation of upper and lower hybrid modes 8=12562
 - pressure anisotropy from mag. bremsstrahlung 8=16593
 - pulse effect, convective and absolute instabilities 8=19476
 - quasi-electrostatic, and shear stabilization 8=4408
 - in quasi-homogeneous mag. field 8=21391
 - quasi-linear theory of aperiodic instabilities 8=7831
 - recombination, population of hydrogen levels 8=4410
 - resonant resistive instability and hot electron production 8=1426
 - Runaway critical field, variational calc. 8=16590
 - saturation of beam-plasma instabilities due to flattening of beam distribution function 8=21396
 - sheet pinch, finite-resistivity stabilities 8=1413
 - single-humped distrib., applic. to e plasma wave 8=21392
 - skin-layer, collisional 8=7830
 - stellarator, stochastic destruction of magnetic surface 8=1428
 - stratified anisotropic with mag. field, gravitational internal 8=10241
 - stream penetrating inhomogeneous medium, convective instability 8=12558
 - theta pinch dynamic stabilization 8=7801
 - theta pinch with sharp boundary 8=4390
 - θ pinch, travelling periodic bumpy, instabilities 8=16550
 - toroidal column, equilibrium in d. c. and h. f. mag. fields 8=16559
 - toroidal configs, theory of hydromagnetic stability 8=4406
 - toroidal magnetic trap, condition 8=1416
 - toroidal systems, trapped particles, effect of statics, radial elect. fields 8=16564
 - transverse drift l. f., rel. to auroral bombardment 8=4356
 - transverse wave instabilities in plasma with axially symmetrical velocity distrib. 8=12554
 - trapped particle instabilities in toroidal systems, influence of static, radial, electric fields 8=4416
 - turbulent, existence of second sound 8=12560
 - turbulent stationary state theory 8=12559
 - unstable plasma theory in the ring approximation 8=16592
 - Vlasov eqn. integration in a reduced phase space 8=10499
 - Vlasov's equation, nonlinear, for "water-bag" model 8=4417
 - waves, steady-state decay instability 8=4405
 - weakly ionized, drift dissipative instability in crossed fields 8=4411
 - weak turbulence, entropy definition 8=7839
 - weakly turbulent 8=4404
 - He, cylindrical transport eqns. 8=1430
 - Na, stabilization by random electric field 8=16599
- Plasma diagnostics.** See Plasma/measurement technique
- Plasma diodes.** See Electricity/direct conversion; Electron tubes; Plasma/devices.
- Plasma guns.** See Plasma/devices.
- Plasma in solids.** See Crystal electron states/plasma; Electron gas; Semiconductors; Solids.
- Plasma jets.** See Plasma/devices.
- Plasma sheath.** See Plasma/confinement.
- Plasma thermocouples.** See Electricity/direct conversion; Plasma/devices.
- Plasma torches.** See Plasma/devices.
- Plasma waves.** See Plasma/oscillations.
- Plasmoids.** See Plasma.
- Plasmons.** See Crystal electron states/plasma.
- Plastic deformation**
 See also Slip.
 alloy, ordering, rel. to dislocations and antiphase boundaries 8=17634
 in anelasticity, yielding of cylinder rel. to stress rate 8=22275

Plastic deformation—contd

- asymmetrical bending of beams 8=10558
 b.c.c. metal, crystallographic study of yield condition 8=17727
 beams, iterative procedure 8=8797
 β -, brass, effect on martensitic transformation 8=21843
 block, indented by opposed narrow punches, deformation analysis, theoretical 8=10562
 bombs, tubular, behaviour, and modes of fracture 8=22292
 in composite bar, wave propag. at elastic-plastic interface 8=19394
 curved panels, buckling, edge restraint effect 8=19401
 cylindrical shells, axisymmetric collapse under pressure 8=10554
 ductile fracture with rotation, influence of inclusions and stress-state 8=17729
 f.c.c. alloy polycrystals, computer simulation and derived rolling texture 8=13512
 f.c.c. metal polycrystals, computer simulation and derived rolling texture 8=13512
 glass-ceramic from SiO_2 - Li_2O - ZnO system 8=17829
 high pressure effects 8=8796
 ice, and dislocation structure 8=4977
 ionic mats, necessary conds 8=13511
 iron, armco, strain-aged, rel. to tensile stress strain relations 8=17792
 limiting load theory, punching of a plate 8=13510
 in mechanism of excessive grain growth during recrystallization 8=17259
 rel. to metals destruction by cavitation and droplet impact in magnetostriction oscillator 8=22306
 metals, latent elastic strain energy due to residual stresses 8=22269
 metals, on cutting and grinding at high velocities 8=19338
 microdeformation of solids, measuring technique 8=22273
 mild steel beams, dynamically and statically tested, energy absorption 8=13574
 Permalloy, ferromagnetic, rel. to maximum mag. susceptibility 8=18338
 Permalloy films, effect of defects on mag. anisotropy 8=14031
 phenolphthalein and congeneric mol. crystals, effect on props. 8=23033
 polymers, theory 8=17844
 polystyrene, glassy, bands 8=22411
 pure non-cubic crystals, increase with temperature cycling 8=22276
 rectangular plates, stability, perturbation method 8=59
 shells, inelastic, membrane, with rotation symmetry, creeping at finite deformations 8=10571
 steel by dynamic compression and plasticine, Na use as models, 1000°C 8=13556
 steel, mild, yield stress rel. to strain 8=22368
 steel, stainless rel. to magnitude of Mössbauer effect 8=8219
 steel, type 1H18N9T, austenitic, mag. qualities, and influence of elastic deform. 8=9291
 zone length in moving brittle crack path direction, theory 8=57
 Ag crystals, plane strain compression 8=17662
 Al block, indented by opposed steel punches, deformation, theoretical and actual, comparison 8=10562
 Al, grain boundary sliding, constant-stress shear test 8=22220
 Al, grain boundary sliding, isothermal sheartest 8=22221
 Al, lattice distortion, e microprobe-Kossel obs. 8=21978
 Al, microdeformation measuring technique 8=22273
 Al, rel. to elasto-plastic behaviour obs. 8=8848
 Al, thin wall circular cylinders, buckling at 500°F 8=17757
 Al-2% Mg alloy, dislocation network knitting on stress-induced climb 8=17644
 Al-Mg alloy, effect on structure 8=17004
 Al-Zn eutectoid alloy, superplasticity rel. to grain boundary shear 8=17766
 Au, microdeformation measuring technique 8=22273
 Au, quenched, slip channel formation and other defects 8=17663
 Au, vacancy introduction at 4.2°K 8=13421
 BaF_2 , colorability enhancement 8=22228
 BeO polycrystals, high temp. dislocation 8=13539
 CaF_2 , colorability enhancement 8=22228
 CaO , colorability enhancement 8=22229
 Cd, dislocations and slip planes 8=8725
 Co hexagonal single crystal surface due to friction against sapphire ball 8=17771
 Cu, annealing behaviour, effect of dispersed phases 8=17772
 Cu crystals with dispersed Co/ SiO_2 phases, and dislocation distrib. 8=4974
 Cu, electron irradiated, yield stress increase 8=17773
 Cu, microdeformation measuring technique 8=22273
 Cu, rel. to recrystallization and mech. props., at low temp. 8=8403
 Cu, role of dislocation rearrangement in elastic mod. recovery 8=22337
 Cu_2O , by motion of a {100} dislocations on {100} glide planes 8=22327
 Fe, and annealing, rel. to X-ray diffraction line intensity 8=21989

Plastic deformation—contd

- Fe, coarse grained polycrystalline, under tensile stress 8=1985
 Fe crystals with 8-20 p.p.m. C, n-irradiated, yield stress rel. to radiation hardening 8=17800
 Fe crystals, having [100] and [110] axes, -70°C to 250°C 8=13553
 Fe, ferromagnetic, rel. to maximum mag. susceptibility 8=18338
 Fe, neutron irradi., stress-strain curves 8=22348
 Fe, neutron irradi., work-hardening parameters 8=22349
 α -Fe, rel. to dislocation structure 8=4975
 Fe, rel. to elasto-plastic behaviour obs. 8=8848
 Fe single crystals, yield props. 8=22340
 Fe-Mn austenite, and annealing rel. to H permeability 8=17573
 α -Fe, 3.28% Ni addition, effect on yield and fracture behaviour at low temps. 8=22346
 Fe-26% Ni-0.4% C alloy, austenite deformation effect on M_s 8=4710
 Fe-Ni invar, rel. to Fe^{57} Mossbauer spectrum, obs. 8=21811
 Fe-Si alloys, ferromagnet after-effect 8=5466
 Ge point contact diode, etch pits 8=5326
 in Mg-Al spinel, rel. to slip parallel to {111} plane 8=17664
 MgO whiskers, ductility obs. 8=13586
 MgZn_2 , dynamic and creep tests 8=5081
 NH_3 crystals, at liq. N₂ temps. 8=17820
 NaCl crystals, pure and doped, by indentation, rel. to pot. differences 8=16978
 NaCl, photostimulated exo-emission from F-centre crystals 8=5409
 NaCl, rel. to acoustic n.m.r. 8=5561
 NaCl, slip lines, electron microscopic study 8=22213
 Nb-Mo alloy single crystals, comp., temp. and orientation dependence 8=17819
 Ni alloys, resistance recovery 8=13722
 Ni, ferromagnetic, rel. to maximum mag. susceptibility 8=18338
 Ni-Co, rel. to positron annihilation 8=17909
 Ni-Fe, rel. to positron annihilation 8=17909
 Ni-Mo alloys, quenched, effects on transformation during annealing 8=17094
 Pu, electrorefined, and concurrent recrystallization, 24-115°C 8=21961
 Si, in brittle fracture region 8=5084
 Si, internal friction and elec. resist. on repeated alternating bending 8=17828
 Si-Fe, influence on temp. dependence of magnetic properties 8=14014
 Si-Fe, [110], necking and fracture at 293 and 473°K 8=13607
 SrF_2 , colorability enhancement 8=22228
 SrO , colorability enhancement 8=22229
 U-C alloys, around UC comp., die-forming and texture of extruded rods 8=22396
 Zn, dislocations and slip planes 8=8725
 Zn, rel. to elasto-plastic behaviour obs. 8=8848
 Zn-Al alloy, superplastic, effect of stress, temp. and heat-treatment 8=5090
 ZrO_2 , Y_2O_3 - and MgO- stabilized, in stress relief mechanism 8=17839
- Plastic flow**
 See also Rheology.
 advances in applied mechanics, book IX 8=16747
 in anelasticity, yielding of cylinder rel. to stress rate 8=22275
 Armco iron, lower yield stress rel. to grain size 8=17798
 cohesionless bulk solid, gravity flow in converging conical channel 8=13514
 ice, polycrystalline, at low stresses and small strains 8=22373
 martensite, flow stress rel. to temp. and strain rate 8=22351
 metal, deformations and probability of fracture 8=17736
 nylon, dislocation motion interpretation 8=2074
 plate, thin flat, and fracture under uniform stress 8=13513
 steel cylinders, tensile stress and natural strain 8=22353
 steel, stabilized sheet 8=8836-7
 velocity depend. on elastic interact. between dislocation loops 8=8720
 Zircaloy-2 tubing, ductility, effect of hydride 8=13615
 Be ductility rel. to prestraining, 50, 100 and 200°C 8=8825
 Cu, u.s. work hardened 8=22336
 CuZn (β brass), hydrostatic extrusion effects obs. 8=5059
 Fe-Al alloys, yield effect from elevated temp. constant strain-rate tests 8=13555
 Ge, at room-temp., obs. 8=22372
 KCl crystal dependence of dislocation density on compressive force obs. 8=8731
 NaCl crystal dependence of dislocation density on compressive force obs. 8=8731
 Nb foil, tensile stress, and dislocation density, effects of grain size 8=4980
 Pu1 wt. % Ga alloy, at -60, 30 and 77°C 8=13604
 Si-Fe alloy, dislocation structure and ductility, low-temp. creep effects 8=13571

Plastic flow—contd

- Te, dislocation theory 8=4984
 TiNi, hydrostatic extrusion effects obs. 8=5059
 Zn, basal slip, Al impurity effects 8=17836

Plasticity

See also Viscoelasticity.

- advances in applied mechanics, book IX 8=16747
 anodic oxide films, ductility 8=2047
 bending, asymmetrical, of beams 8=10558
 combined loadings, classification 8=10561
 coupled thermoplasticity, continuity at wave fronts 8=10577
 cylinder, hollow, changes in geometry during compression 8=10563
 cylindrical wafers, under compression plates, press. and stress distrib. anal. 8=19394
 deformable surface, theory, simple force multi-poles 8=2918
 disc edge, stress distrib. 8=2927
 elastic-plastic analysis, numerical methods 8=19400
 elastic-plastic continua, eigenmodal deform., crit. conds. and character 8=19399
 elasto-plastic crack behaviour under longit. shear 8=13519
 elastoplastic stress waves, cylindrical and spherical, soln. by unified direct anal. 8=14952
 flush nozzles in pressure vessels, stress analysis 8=10557
 general variational theorem 8=10559
 glass-reinforced, high-strength prop. meas. at cryotemps. 8=17840
 granular substances, theory 8=8798
 graphite, nuclear grade A, and deform. props. 20-2200°C 8=8829
 inequality conditions, obs. 7=58
 intermetallic compounds, press. effects on ductility 8=13535
 limiting load theory, punching of a plate 8=13510
 metal, micro-, study by strain effects on the a.c. resistance 8=5036
 metal sheets, incremental theory for anal. of bore-expanding test 8=22272
 metal shells ductility and rupture rel. to strain rate and thickness obs. 8=5037
 plane elastic-plastic waves of 1-dimens. strain, propag. anal. 8=19522
 plane-strain problem with two yield conditions 8=2041
 quartzite, precursor decay for cylindrical and spherical flow 8=13605
 reinforced fibre, cyclic extension 8=19403
 resonance of shock wave, longitudinal, in elastic-plastic bar 8=15052
 shells, cylindrical under piecewise pressure, ring forces and moments, and energy losses 8=41
 steel structures, application of theory to limit design 8=8846
 tensile instability, effect of variation of Poisson's ratio 8=8799
 stress-strain relations in elastoplasticity 8=8790
 Al alloys, wrought-, ductility and strength rel. to ingot structure 8=5046
 Al-Ag alloys, rel. to GP zones and stacking faults 8=8821
 Al-Zn eutectoid alloy, superplasticity rel. to grain boundary shear 8=17766
 CCl₄ solid, shear strength from 187° to 247°K 8=22401
 σ -FeCr alloy, ductility rel. to atomic ordering and co-ordination 8=17030
 Ge, at room-temp., obs. 8=22372
 Mo, structure and low-temp. ductility, deform.-induced changes 8=13589
 σ -2NbAl, ductility rel. to atomic ordering and co-ordination 8=17030
 Pb-Tl alloys, superplasticity during creep 8=13603
 β -Pu, superplasticity 8=17826
 V, ductility-brittle transition rel. to terminal H solubility 8=5088
 ZrO₂, super-, during monoclinic \rightleftharpoons tetragonal transform. 8=5091

Plastics

See also Polymers.

- cellulose nitrate and acetate, stress/strain isothermal curves 8=22406
 creep under hydrostatic press, linear strain and recovery 8=22280
 epoxy composites, filled and porous, Young's modulus obs. 8=13620
 fibre glasses, thermal expansion, unsteady regime meas. method 8=8645
 glass reinforced, adiabatic shock curve at pressures up to 130 thousand atm. 8=22409
 glassy thermoplastics, stress/strain isothermal curves 8=22406
 plates, fibre-glass-reinforced, crack extension, appl. of fracture mech. 8=22294
 plexiglass as material for accelerator tube 8=20233
 polyethylene, relation between adhesion and wettability 8=8879
 polyurethane, compression modes, obs. 8=22271
 polyurethane foam, under small deformations, elastic characts. 8=22261
 polyvinylchloride, conformation changes from i.r. spectra and dielec. losses 8=8360

Plastics—contd

- polyvinylchloride plasticization by aromatic and condensed ring cpds., obs. 8=23141
 PVC, stress/strain isothermal curves 8=22406
 β -ray spectrometer, 2-20 MeV 8=20388
 scintillation counter for n det., 10-70 MeV 8=11621
 scintillating fibres, light-conducting characts. 8=9586
 scintillator, light output under influence of α -particles 8=2495
 scintillating, muonium, behaviour in 8=723
 specialised applications in electronic and other industries 8=13876
 thermal mass thickness variation at elevated temperature, electron microscope examination 8=17186
 track detectors for light nuclei 8=20220
 triacetylcellulose films, thermomech. curves of elongation at const. strength, rel. to plastifier content 8=22407
 vinyl, tensile strength and struct. disintegration, obs. 8=17843

Platinum

- annealed, anelastic effect at low temps. 8=22211
 annealing damage, effect on further e-irradiation damage at 90°K 8=1947
 anodic oxidation in LiCl-KCl 8=5738
 atom, e-binding energy effect on incoherent γ scatt. 8=17703
 cyclotron effective mass, anisotropy and mass enhancement 8=22487
 deuteron-irradiation, damage and recovery 8=8697
 electrodes, adsorpt. and oxidation of hydrocarbons 8=9714
 electrodes, oxidative adsorpt. of n-hexane 8=5737
 electrodes, oxidative adsorpt. of propane 8=2534
 epitaxial growth, by sublimation in vacuum 8=4752
 Fermi surface determ. from de Haas-van Alphen effect 8=22752
 film, electrical conductivity, island structure, on quartz glass and BaTiO₃ substrates 8=13709
 films, obliquely deposited, struct., effect of atom mobility 8=8296
 heated wire, catalysed CO₂-N₂-He laser system 8=3308
 hemispherical reflectance, rel. to λ and surface roughness 8=2399
 in liquid Pb, thermodynamic props. 8=8043
 microcrystals, uniform, obtained from hydrosols 8=1745
 n-irradiation damage and recovery rel. to defect doping effect 8=1953
 n.m.r. spin echoes, Knight shift 8=2387
 refinement by annealing in air 8=4812
 resistance bridge thermostat for $\pm 25\mu^\circ\text{C}$ 8=15123
 resistivity, elect., and thermal conductivity, 373 to 1373°K, obs. 8=22521
 specific heat meas. from 1.4-100°K 8=22119
 specific mag. susceptibility between 80° and 1850°K 8=5439
 thermoelectric power, high press. effects 8=13902
 two-band conduction model for resistivity, contradictions 8=2107
 vacancies, divacancies and self-diffusion from quenching and recovery expts. 8=17612
 Au¹⁹⁹ ion exchange removal from n irradi. Pt 8=23168
 Co sorption 8=18701
 Pt(II), spectra in fused LiCl-KCl 8=1567
 Pt-Ir alloys electrodeposition and deposits hardness and stress obs. 8=23153

Platinum compounds

- alloys, thermoelec. power meas. 2-120°K 8=18216
 oxides, gaseous, thermodynamic data 8=5716
 rare-earth alloys, conduction electron polarization 8=17857
 PtAs₃, decomp. press. and enthalpy of formation 8=12338
 Pt-Ba alloy, work function 8=18245
 PtC, gaseous, dissociation energy 8=4240
 [PtCl₂(NH₃)_{4-n}]²⁻ⁿ complexes electronic struct., MO calc. 8=4168
 Pt-Co alloys, coercivity and remanence obs. 8=22835
 Pt-Co alloys, high (BH)_{max}, criticism 8=22836
 PtCo mag. props. rel. to prep. and purity, obs. 8=22837
 PtCo ordered alloys, effect of symmetry on field ion images 8=4881
 Pt₃-Co alloy, ordered, field-ion microscope study 8=1764
 Pt-Fe alloys, internal magnetic fields at Pt nuclei 8=2334
 PtFe mag. props., obs. 8=22837
 Pt₃Fe, mag. structure dependence on atomic ordering 8=18348
 Pt-Fe natural alloys, e probe microanalysis obs. 8=14477
 Pt-Fe-Mn alloys, antiferromag. order dependence on comp., n-diff. study 8=18387
 [PtPd]Co Curie and order-disorder transform. temps., obs. 8=22837
 [PtPd]Fe Curie and order-disorder transform. temps., obs. 8=22837
 Pt-Rh alloy, quenching expts. 8=13423

Pleochroism

- all-trans β carotene crystals, dichroism obs. 8=2465
 benzene, mag. circular dichroism 8=21123
 benzil cryst., circular-dichroism, compared with absorpt. and rotatory dispersion 8=2463
 chlorins, optically active, mag. circular dichroism 8=16317
 coronene, mag. circular dichroism 8=21123
 crystals, i.r. dichroism meas. by attenuated total refl. 8=18490

Pleochroism—contd

- dye solns., photodichroism, wavelength dependence 8=8070
 hexahelicene, circular dichroism 8=12883
 infrared dichroic polarization textures 8=11204
 linear dichroism in the u.v. meas. 8=6563
 naphthols, dichroic spectra in PVA sheets, rel. to vibronic transitions 8=14285
 nylon fibres dichroic ratios for molecular orientation 8=16394
 polyenes, prep. of films for dichroism meas. 8=18580
 polymers, i.r. dichroism meas. by attenuated total refl. 8=18490
 polymers, mag. circular dichroism, theory 8=12384
 triphenylene, mag. circular dichroism 8=21123
 Er ferrite-garnet, dichroism and mag. anisotropy 8=18523
 $P_3N_3Cl_6Br$, i.r. dichroism 8=5627
 PrF_3 , i.r. dichroism and absorption 8=9560
 $RbCl$, circular dichroism of K band 8=14256
 $RbCl$, Z_2 centre circular dichroism 8=22224
 $RbNiF_3$, ferrimagnetic, mag. circular dichroism and rot. of light polarization plane 8=18557

Plexiglas. See Plastics.

Plutonium

- α and β , transverse magnetoresistivity 8=2350
 α phase foils, electron microscope study 8=21887
 aerosol produced by burning, characts. rel. to reactor safety 8=12950
 α -Pu, specific heat comparison with α -Mn 8=17512
 β -Pu hardness anomalies rel. to α and γ parent phases, 120-190°C 8=8860
 β -Pu, superplasticity 8=17826
 containing sample preparation for electron probe microanalysis 8=4831
 δ -phase, optical consts. at 5461 Å 8=23009
 electrorefined, recrystallization and concurrent plastic deformation, 24-115°C 8=21961
 glovebox, thermal gradient apparatus 8=7334
 isotope shift constants 8=16234
 isotopes, effect on reactor Doppler coeff. 8=7340
 oxidation rate in air, 8=5717
 solubility in Fe 8=13041
 X-ray emission spectra, 8 to 75 Å 8=14255
 Pu^{244} abundance in early solar system 8=23468
 $Pu^{238-242}$, arc spectrum, rel. isotopic shift 8=20965

Plutonium compounds

- Pu-Ga alloy (3 at. %) alloy, α -phase precipitation in δ phase due to cold working 8=21855
 Pu-Ga alloys, microhardness 8=8859
 Pu/1 wt. % Ga alloy, plastic flow at -60, 30 and 77°C 8=13604
 Pu-0.85at% Ga, metastable δ -phase, effect of thermal cycling on transform. behaviour 8=8278
 PuO_2 adsorption of O, sites and sintering effects, obs. 8=8345
 PuO_2 , m. p., rel. to UO_2 - PuO_2 solid-liquid phase diagram 8=8169
 PuO_2^{2+} , M-O bond force consts. in various media 8=21094
 Pu-Th system, phase diagrams, peritectic and eutectoid of transform S 8=21854
 Pu_2Zn_{29} , crystal structure 8=17409
 PuZr peritectoid reaction, 615°C 8=8279
 Pu-Zr phase diagram, obs. 8=8279
 PuZr, synthesis from Pu and Zr, obs. 8=8279

Pockels effect. See Electro-optical effects.

Point defects. See Crystal imperfections.

Point groups. See Crystal structure, atomic.

Poiseuille flow. See Flow; Hydrodynamics.

Poisson ratio. See Elastic constants.

Polar cap absorption. See Electromagnetic wave propagation/ionosphere.

Polar cap glow. See Airglow.

Polarimeters

- Compton improved sensitivity by replacing NaI(Tl) scintillator by an organic one 8=6788
 ellipsometer, following, computer-operated for film growth monitoring 8=6562
 laser light apparatus for determ. polarization 8=11074
 n from reactions by α avalanche gas counter method 8=6952
 photoelectric control for rotary power meas. 8=15549
 photoelectric, two-cell, using rotatable achromatic half-wave plate, astronomical 8=10106
 polariscope, Savart-type, astigmatism when used as polarization interferometer 8=514
 reflection ellipsometer, use with permalloy films 8=9409
 for starlight, interstellar effect meas. 8=23541
 CdS soleil i. r. compensator 8=15550

Polarized light

- See also Double refraction; Optical rotation; Photoelasticity; Polarimeters.
 alkali vapour, optically pumped, modification 8=4088
 anthracene, generation of charge carriers 8=2268
 atmospheric depolarization by turbulent inhomogeneities 8=14619
 circularly and linearly polarized beams, self-focusing mech. in liqs. 8=12870
 comet Ikeya-Seki, tail polarization obs. 8=10358
 depolarization from backscattering 8=19839

Polarized light—contd

- dibenzosuberone, polarisation of $S_1(n\pi) \leftarrow S_0$ transition 8=8096
 comet Ikeya-Seki (1965) head and tail, 3890-5875 Å 8=10360
 dielectric rough-surface reflection 8=11200
 by elec. and mag. anisotropic media 8=515
 electromagnetic waves, angle rel. to impedance matching, small-reflection wall application 8=3256
 ellipsometric meas., quick response 8=11201
 ellipticity of light scatt. by atmos. air, rel. to haze aerosol microstruct. 8=9877
 far u. v., Te crystal reflectivity obs. 8=15551
 fluorescence polarization, effect of self-quenching 8=21698
 fluorescence, self-depolarization, "critical distances" in theories 8=21697
 fluorescence, self-depolarization, mathematico-physical models 8=21696
 fluorescent source, quantum statistics of polarization 8=23036
 4,4'-dibromobenzophenone, polarisation of $S_1(n\pi) \leftarrow S_0$ transition 8=8096
 four part quartz plate in phase difference meas. 8=15512
 graphite, transverse and longitudinal optical props. 8=2407
 helicoidal nematic films 8=16837
 infrared dichroic polarization textures 8=11204
 interference-polarization filters with transmission-band shift 8=11203
 interferometer, for spectral modulation transfer functions of monochromators 8=488
 laser, Pérot-Fabry cavity obs. 8=19976
 lasers, solid, apparatus for determ. 8=11074
 liquids, Rayleigh-Wing scatt., analysis showing increased gain 8=8092
 mica cryst. retardance meter 8=6510
 phase functions for light scatt. from atmos. surface layer 8=9876
 polymer fibre scatt. rel. to supermolec. order 8=18581
 polymers, preferred orientation, polarized-fluorescence experiment, mathematics 8=1721
 porosity-polarization relationship applicable to lunar surface 8=23646
 quasars, circular polarization, detectability 8=23631
 radial field distributions in a self-focusing light beam 8=11202
 scattering by Dirac particle 8=15713
 sky, obs. and object contrast improvement 8=18875
 starlight, interstellar polarization meas. 8=23541
 stars, most within 200 parsecs, obs. in galactic plane and direction of galactic poles 8=23521
 transparent media, anisotropic, Brewster angle generalization 8=22947
 Al_2O_3 powder reflection and polarization 8=14266
 Ba, emitted on slow electron bombardment, and excited levels lifetime 8=21019
 in $Bi_{12}GeO_{20}$, photo-induced static changes 8=2404
 CdSnAs₂, absorption at 295°K 8=22966
 CN laser, far i. r. 8=11054
 n-GaAs in mag. field, circularly polarized, waves, doping rel. to optical absorpt. 8=22981
 Hg, liquid, Drude theory and optical props. 8=12881
 Hg vapour, optically pumped, modification 8=4088
 OH, 18 cm cosmic rad., anomalous elec. polarization 8=23582
 $RbNiF_3$, ferrimagnetic, rotation of plane of polarization and mag. circular dichroism 8=18557
 SbSI, light polarization near ferroelec. phase transition 8=18559
 SiC powder reflection and polarization 8=14266
Polarography. See Chemical analysis/electrochemical.
Polarons. See Crystal electron states/polarons.
Polishing. See Surface texture.
Polonium
 beam, range energy in Al, Al_2O_3 8=13473
 critical surface tension 8=21869
 $Po^{208, 209, 210}$ beam, recoil prod., for bombard. of Al foil 8=11952
Polonium compounds
 No entries
Polyelectrolytes. See Electrochemistry; Polymers; Solutions.
Polymerization
 adipimide, anionic, triacetamide activated 8=9708
 alkylacrylates copolymers with methacrylamide, coalescence rel. to particle and film struct. 8=17189
 anionic polymers, effect of impurities and initiation and transfer rate consts. on statistical character 8=12388
 benzonitrile, under press., differential thermal analysis 8=9684
 β -iodophenylacetylene, synthesis and props. 8=23130
 butadiene, π -crotyl NiI and -NiCl, catalyst props., rel. to structs., obs. 8=8576
 bis(2-carballyloxyalkyl)phenylphosphanes, oxides and sulphides, for thermostable glasses 8=13110
 copolyesters, formation, and degree of randomness by high resolution n.m.r. spectra 8=12387
 copolymerization, cationic, mechanism and copolymer comp. 8=23135
 dioxolane in mass, equilib. conc., molec. weight rel. to temp. 8=18709

Polymerization—contd

- emulsion, kinetics 8=14415
 ethyl acrylate by a.f. elec. field, obs. 8=9709
 ethylene on CrO_2 , chain transfer kinetics and polyethylene mol. weight, obs. 8=23129
 epoxy resin, interpretation of elect. resistivity meas. 8=18707
 fluoro-olefines on oriented polymer fibres, radiation graft-copolymerization 8=23138
 glass-forming systems, radiation-induced 8=18711
 graft-copolymers of polydimethylvinylsiloxanes with polar vinyl monomers, synthesis and struct. 8=23137
 hexamethyldisiloxane on Al surface, in glow discharge 8=5731
 kinetics at low conversions, study by polarographic maxima 8=5728
 liquid phase, of monomers, e.s.r. study of free radicals concerned 8=14414
 p-methacrylbenzoic acid in liq. cryst. state, rate and molec. weight 8=18710
 p-methacryloxybenzoic acid in liq. state 8=14410
 methylmethoxysiloxane on Al surface, in glow discharge 8=5731
 octamethylcyclotetrasiloxane, study by MWD change of polydimethylsiloxane elastomers 8=14409
 organic adsorbed layers on metal films 8=2251
 phenyl phosphine, migration type with di-isocyanates 8=14411
 photopolymerization photography 8=23140
 polar monomers, sigma type complexes with metal chlorides 8=2527
 polycapraamide fibres, CF_3 radiation grafting rel. to adhesion props., obs. 8=22410
 polycarbonates, P containing, synthesis 8=14412
 polyethyleneterephthalate fibres, CF_3 radiation grafting rel. to adhesion props., obs. 8=22410
 polypropylene fibres, CF_3 radiation grafting rel. to adhesion props., obs. 8=22410
 polypyromellitimide kinetics i.r. spectra study 8=14408
 polytrioxane mol. weight rel. to preirrad. dose and temp., obs. 8=21210
 poly(vinyl chloride), tacticity, by i.r. spectroscopy 8=21217
 propylene, kinetics with catalytic system $\alpha\text{-TiCl}_3\text{-Al}(\text{C}_2\text{H}_5)_3\text{-H}_2\text{O}$ 8=5730
 semiconductors, polymeric, new, synthesis 8=5286
 statistics of substitution polymers 8=18659
 styrene grafting to polypropylene stabilized and unstabilized films, obs. 8=23139
 trioxane, in benzene soln, yield and molec. weight depend. on temp. regime 8=23134
 trioxane, pre-irrad., kinetics, 30-64°C 8=23133
 trioxane, solid, SnCl_4 initiated cationic polymerization, kinetics obs. 8=23132
 trioxane in soln., kinetics and reaction order 8=14407
 trioxane in soln, molec. weight rel. to temp. and catalyst conc. 8=18708
 trithiane, radiation induced formation of polythiomethylene 8=17184
 vinylacetate, initiation efficiency and temp. depend. 8=1413
 vinylchloride copolymerization with acrylic and methacrylic acids, relative reactivities obs. 8=23136
 vinyl monomers, liquid, by a.f. elec. field, obs. 8=9709
 4-vinyl-pyridine, reactivity 8=5728
 vinylene carbonate, in aqueous soln, with O_2 , initiation 8=5729
 N-allylmonoamides of maleic and succinic acids, in solid state by Co^{60} γ -rays 8=23131

Polymers

- See also Plastics.
 additives to water, effect on turbulent shear flow 8=16764
 adhesion to porous substrates, joint form. and strength 8=17751
 adhesion, wettability data 8=17841
 n-alkanes, eqn. of state correl. with chain length 8=16790
 alkylacrylates copolymers with methacrylamide, latex particles and films, struct. rel. to coalesc. 8=17189
 amylose triacetate I, cryst. struct. 8=17461
 anelastic and dielectric effects, book 8=22658
 anionic, effect of impurities and initiation and transfer rate consts. on statistical character 8=12388
 band theory, relevance to conduction and optical studies 8=17872
 biaxially oriented, triangular orientation function plot rel. to spherical harmonic expansion coeffs. 8=17462
 birefringence dispersion in amorphous, oriented polymers 8=9578
 from bis(2-carballyloxyalkyl)phenylphosphane oxides and sulphides as thermostable glass 8=13110
 cellulose acetates, characts. from speed sedimentation in acetone 8=4262
 cellulose fibres, surface structure, effect of ionic etching 8=13083
 cellulose nitrate and acetate, stress/strain isothermal curves 8=22406
 cellulose nitrate, α -ray spectrometer target 8=11293
 cellulose nitrate target, fast neutron detection from nuclear reactions 8=11619
 chain mol., rotary diffusion const. 8=16816

Polymers—contd

- chain twisting, effective barrier to reorientation 8=1716
 chains, distrib. function of distances between ends, volume effects in swelling 8=21215
 copolyesters, formation, and degree of randomness by high resolution n.m.r. spectra 8=12387
 copolymer comp. and cationic copolymerization mechanism 8=23135
 copolymers in dilute solution, physical chemistry, recent aspects 8=8020
 copolymers in soln., effect of interaction between unlike segments 8=4541
 copolymers in soln. molec. dimens. 8=12811
 cross-linked, under tension 8=17845
 crosslinked, viscoelasticity theory 8=8873
 crystalline, polyamellar habits 8=1766
 crystalline, unoriented, creep mechanisms 8=13619
 crystalline, u.s. propag. 8=1859
 crystallization of chain-folded crystals 8=1734
 crystallization, ciliation and fractionation 8=8390
 crystallization kinetics, a modified equation 8=8424
 crystals, fold surface packing from moiré patterns 8=17299
 de-oxyribonucleic acid, u.v. spectra of dichroic films, meas. 8=6563
 depolymerization, u.s., at elevated static press. 8=4568
 dichroism, i.r., meas. by attenuated total refl. 8=18490
 dilute solns., flow through curved pipes 8=21570
 dilute solution, Pitot-tube and hot film obs. 8=7981
 of 2, 3-dimethylbutadiene-1, 3, mol. struct. rel. to polymerization conditions, obs. 8=21212
 elasticity, statistical mechanics 8=8875
 electrical conduction properties, conference, Pasadena USA (1966) 8=13701
 as engineering mats., background to reln. between struct. and mech. props. 8=23773
 epoxy composites, porous, strain-rate dependence of elastic modulus 8=13621
 epoxy, micropenetrator for surface characterisation 8=8876
 epoxydimethyl siloxane, orientation birefringence temp. dependence rel. to structure 8=9577
 equilibrium distrib. between soln. and small voids 8=16801
 etch-resisting, cross-linking by electron beam, rel. to integrated cct. prod. 8=15279
 ethylene-butene-1 copolymers, crystalline structure 8=8598
 ethylene/propylene copolymers, orientation birefringence temp. dependence rel. to structure 8=9577
 ethylene-trifluoropropylene copolymer, microstruct. study by i.r. spectra 8=17298
 ethylene/vinyl acetate copolymers, orientation birefringence temp. dependence rel. to structure 8=9577
 fibres, low angle polarized light scatt. rel. to supermolec. order 8=18581
 fibres, X-ray small-angle scatt., review 8=8438
 film, trapping of electrostatic changes in surfaces 8=13891
 films on base, structure, i.r. spectra study 8=4738
 flexible, radius of gyration, probability distrib. 8=7644
 fracture, conference, Boston, USA (1966) 8=13518
 glass transition, pressure effects 8=8359
 glassy thermoplastics, stress/strain isothermal curves 8=22406
 Grüneisen number 8=1866
 guar gum in tap water, aging and degradation from Pitot tube obs. 8=12744
 heat shield material ablation obs. 8=1860
 high, crystalline regions, lattice strains, along and across fibre axis 8=8877
 high resolution n.m.r. spectroscopy 8=16886
 homo- and graft co-, in soln., intrinsic viscosity and free energy 8=1536
 hydrocarbon chains, effective masses estimation 8=17873
 hydroxyethyl cellulose aqueous soln, non-Newtonian, drag coeff. on falling sphere 8=12724
 latexes, size distrib. from light scatt. 8=16900
 linear chain, theory of expansion in solvent 8=4264
 linear chains, excluded-vol. effects, differential eqns. 8=12383
 linear, in aqueous solutions, in the turbulence vortices 8=12946
 lucite, Cherenkov time resolution function obs. 8=5690
 lucite, tensile strength and struct. disintegration, obs. 8=17843
 magnetic optical rot. and mag. circular dichroism, theory 8=12384
 Makrolon films stress cracking and crystallization obs. 8=8473
 melting, with diluents, under press. 8=4642
 melts, flow-induced crystallization, fibre nuclei formation mechanism 8=1532
 melts, strength and elasticity 8=16748-9
 methylmethacrylate copolymers with methacrylic acid, ht. capacities, 25-190°C 8=1579
 methylmethacrylate copolymers with styrene and p-chlorostyrene, dielec. relax. 8=12906
 methylmethacrylate-methylacrylate copolymers, dielectric relaxation 8=5358
 for microstructure exam. by X-ray diffr., crystallite randomization nondestructive methods 8=8440
 microstructure in ultrathin sections 8=17297

Polymers—contd

- molecular size distrib. changes on cross linking 8=12385-6
 molecular weight determ. from heat of condensation of solvent vapour into polymer solns. 8=18643
 Mössbauer-effect doublet spectra, line asymmetries and anisotropic lattice dynamics 8=13022
 Mylar films, electrical conduction in high fields 8=13877
 nitroso dimers, photodissociation on irradiation with u.v. light 8=9726
 nitroxide, prep. and mag. resonance 8=4270
 n. m. r., high resolution 8=21216
 non-Newtonian flow, rel. to molec. wt. 8=16759
 nylon, adsorpt. of polyethers at soln. solid interface 8=1709
 nylon fibres molecular orientation by polarized internal reflexion spectroscopy 8=16394
 nylon, plastic flow rates, dislocation motion interpretation 8=2074
 nylon 66, static electrification 8=5356
 nylon thread temp., i. r. pyrometer meas. 8=17187
 oligomers, reticulate crystalline nature from X-ray and thermomechanical tests 8=17192
 oxidation of high polymers, e.s.r. study of free radicals concerned 8=14414
 PDMS solns., form effect, conc. depend. 8=12895
 p-(perfluorovinyl)-toluene co- with styrene, molecular motion 8=17191
 phenol-formaldehyde, i. r. spectra during thermal treatment 8=4269
 plastic deformation, theory 8=17844
 p polarization by "solid effect", 3150-19 200 Oe and 1.65-4.2°K 8=13015
 in polyacene solid solns., energy transfer, 1965-66 bibliography 8=14162
 polyacetylene, study of optical properties 8=9576
 polyacrylamide in tap water, aging and degradation from Pitot tube obs. 8=12744
 polyacrylonitrile, atomic-pile-irradiated, density changes 8=17709
 polyacronitrile drawn film, anisotropy of mech. tan δ 8=17847
 polyacrylonitrile, pyrolytic products, analysis by mass spectrometry 8=23174
 polyalkylacrylates, crystallization rel. to lengths of side branches 8=21941
 polyalkyl methacrylates, dielectric props. 8=9203
 polyalkyl methacrylates, multiple transitions 8=21864
 polyamide, non- α -helical, H-D exchange 8=14349
 polyamides, increase in thermostability 8=17182
 polybenzoxazoles with O and S in chains, film synthesis 8=4772
 poly- γ -benzyl-DL-glutamate, dielectric props. rel. to mol. motion 8=2241
 poly-L- γ -benzyl glutamate, dielec. absorpt. in soln. 8=21705
 poly- γ -benzyl-L-glutamate, liquid crystal orientation in mag. fields 8=8006
 polybromoprene dielec. polarization rel. to mol. motion, obs. 8=22660
 polybutadiene-active C black, n. m. r. line widths 8=5550
 trans-1,4-polybutadiene, random-coil configs., interpretation 8=16388
 trans-1,4-polyisoprene, random-coil configs., interpretation 8=16388
 1.4 trans-polybutadiene, structure by i.r. polarized spectra obs. 8=4773
 polybutadienes, stereoregular, n. m. r. line widths 8=5550
 polybutylmethacrylate viscoelasticity freq. depend., obs. 8=22404
 polycaproamide, elastic modulus, molec. theory 8=22405
 polycaproamide fibres adhesion and wetting, CF₃ radiation grafting effects, obs. 8=22410
 polycaproamide fibres, fluoro-olefines radiation graft-copolymerization 8=23138
 polycaproamide, melting temp. rel. to nature and dispersity of filters, hardness, density and spherulite size of polymer 8=21914
 polycaprolactam, type II, p polarization by "solid effect", 3150-19 200 Oe and 1.65-4.2°K 8=13015
 polycarbonate, elec. conductivity under electron irradiation 8=9204
 polycarbonate films, BaTiO₃ and organic cpds. loaded, dielec. props. 8=22661
 polycarbonate films, deformation rel. to chem. structure 8=22403
 polycarbonates, phosphonated, synthesis of transparent films 8=14412
 polychloroprene dielec. polarization rel. to mol. motion, obs. 8=22660
 polydimethyldiphenyl siloxanes, copolymer, in soln., peculiarities of conformation 8=16802
 polydimethyldisiloxane elastomers, MWD changes rel. to octamethylcyclotetrasiloxane polymerization 8=14409
 poly(dimethyl siloxane) adsorption on solids from CCl₄ and xylene solns. 8=8336
 polydimethylvinylsiloxanes with polar vinyl monomers, graft-copolymers, struct. and synthesis 8=23137
 polydioxolane, i. r. spectra, cryst. and molec. vibs. 8=18584
 polydisperse solns., sedimentation equilb. 8=1531
 polyelectrolyte solns., osmotic coeffs. meas. during phase separation 8=16817

Polymers—contd

- polyelectrolyte solns., osmotic press. from e.m.f. meas. 8=16818
 polyelectrolyte solns., u.s. vibr. potentials 8=8061
 polyelectrolytes in salt solns., excluded vol. effect 8=12810
 polyelectrolytes, 2nd virial coeff. 8=4540
 polyene chain, antiferromagnetic spin structure in mols. with conjugate bonds 8=21208
 polyene, polarizability due to π -electrons 8=16390
 polyenes, prep. of films for dichroism meas. 8=18580
 poly- ϵ -caprolactones, optical rotation and molec. conformation 8=12880
 polyester foil, e⁺ annihilation fraction 8=13693
 polyester resins, water damage 8=13622
 polyesters, unsaturated, hardened, n.m.r. determ. 8=5565
 polymeric materials, engineering appls., design problems 8=23773
 polymethyl methacrylate in Aroclor, viscosity 8=8023
 polymethylmethacrylate graft copolymers viscosity solutions 8=8027
 polystyrene in Aroclor, viscosity 8=8023
 polystyrene graft copolymers, viscosity of solns. 8=8027
 polyetherdioxes, surface tension and parachor 8=4552
 polyethers, adsorpt. on carbon soln.-solid interface 8=1708
 polyethers, adsorpt. on nylon at soln.-solid interface 8=1709
 polyethers, adsorpt. on SiO₂ soln.-solid interface 8=1707
 polyethylene, adhesion and wettability 8=8874
 polyethylene, black, optical constants, 4-50 μ 8=14289
 polyethylene chain, methylene wagging 8=4265
 polyethylene, cold neutron cross-section 8=7271
 polyethylene, cryst., intermolec. vibrations 8=13341
 polyethylene, crystalline regions, lattice strains, along and across fibre axis 8=8877
 polyethylene, crystallinity degree, X-ray and density obs. 8=8472
 polyethylene, deformation, dislocation mechanism 8=2072
 polyethylene, derived elastic modulus 8=8608
 polyethylene, dielec. degradation by partial discharge 8=21214
 polyethylene, draw and undrawn, sorption of organic vapours 8=8349
 polyethylene, dynamic birefringence 8=18582
 polyethylene, elec. conductivity under electron irradiation 8=9204
 polyethylene, electron irradi. and not irradi., i. r. absorpt. spectrum, 150-310°K, 700-2100 cm⁻¹ 8=21165
 polyethylene, e emission and mol. wt. vars. in vibro-mech. treatment, obs. 8=18253
 polyethylene electron microscopy below 20°K 8=13159
 polyethylene ethyl and methyl branched copolymers, crystallization 8=17233
 polyethylene, filled, effect of substrate chem. nature on adhesion 8=13617
 polyethylene film, I-doped, current oscillations at high field strengths 8=8985
 polyethylene films, I-doped, elec. conductivity meas. 8=8984
 polyethylene films, oriented, structure and low angle X-ray scatt. 8=17144
 polyethylene, fold-surface struct. 8=17214
 polyethylene, fragment shapes in hypervel. impact rel. to lunar surface struct. 8=13609
 polyethylene, ht. capacity 2.5°-30°K 8=1875-6
 polyethylene, heat of fusion 8=8171
 polyethylene, high-density, creep behaviour 8=22408
 polyethylene, high density, photoconduction 8=13921
 polyethylene, irradi., etching with fuming HNO₃ 8=17216
 polyethylene, irradiated, properties at melting point 8=9201
 polyethylene membrane, temp. effects on permeation of liqs. 8=1508
 polyethylene melt, steady flow elasticity 8=12735
 polyethylene, melting temp., effect of crystallinity and mol. wt. 8=12971
 polyethylene, molecular structure, chain folding, inter-atomic distances 8=1827
 polyethylene mol. wt. and ethylene polymerization chain transfer reactions, obs. 8=23129
 polyethylene, n scatt. before and after reactor irradi., showing prod. of cross-bindings 8=16969
 polyethylene, noncryst. regions, changes during annealing 8=17183
 polyethylene obtained by xylene-stream method for electron microscopy 8=4852
 polyethylene, orientation birefringence temp. dependence rel. to structure 8=9577
 polyethylene, for π - π and π -p interactions, Σ production and polarization meas. 8=864
 polyethylene, point defects, molecular mechanics 8=1938
 polyethylene, regulation of degree of crystallinity 8=21932
 polyethylene, relation between adhesion and wettability 8=8879
 polyethylene, relax. X-ray diffr. obs. 8=21213

Polymers—contd

- polyethylene, short branches, quant. det. by γ radiolysis 8=16392
- polyethylene, slow n scatt. and thermal n spectra, using Nelkin-kernel 8=20802
- polyethylene, solubility of cyclopropane 8=17188
- polyethylene in soln., n. m. r. 8=16891
- polyethylene, supercooled liquid, nucleation rel. to temp. 8=1533
- polyethylene, surface struct. of single crystals. 8=17215
- polyethylene in tap water, aging and degradation from Pitot tube obs. 8=12744
- polyethylene targets for accelerators, characteristics 8=11291
- polyethylene, time-depend. birefringence 8=18583
- polyethylene- α -chloronaphthalene, melting under press. 8=4642
- polyethylene oxide aqueous soln, non-Newtonian, drag coeff. on falling sphere 8=12724
- poly(ethylene oxide), config. 8=12390
- polyethylene oxide solns., five, turbulent pips flow 8=4510
- polyethyleneterephthalate, determ. of crystalline fraction content, by i. r. spectra 8=17190
- polyethyleneterephthalate fibres adhesion and wetting, CF₃ radiation grafting effects, obs. 8=22410
- polyethyleneterephthalate fibres, fluoro-olefines radiation graft-copolymerization 8=23138
- polyethylene terephthalate film solar furnace 8=19675
- polyethylene terephthalate, rel. to space-charge effects 8=9185
- polyethylenimine, spectrophotometric analysis via Cu chelate 8=16393
- poly(glycol methacrylate), X-irrad., e. s. r. 8=18422
- poly(hexene-1 sulphone), dielectric relax. in soln. 8=1585
- poly(hexene-1 sulphone), dipole moment from dielec. meas. in soln. 8=1584
- polyisobutene viscoelasticity freq. depend., obs. 8=22404
- polyisobutylene in petrol, u. s. induced structural modifications, concentration dependence 8=21622
- poly-L-lysine, u. v. spectra of dichroic films, meas. 8=6563
- polymethacrolein reduction with LiAlH₄ and polymethanol prep., obs. 8=23107
- poly-p-methacrylbenzoic acid, struc. rel. to mesomorphic phase 8=18710
- polymethacrylic acid in alcohol-water mixtures 8=12822
- polymethacrylic acid solns., sedimentation and diffusion 8=12817
- polymethine dyes, liquid solutions, stimulated light radiation 8=16848
- polymethine dyes, Q-switching of laser 8=430
- polymethine-merocyanine dyes, n. m. r. spectra solvent depend. and rot. inhibition 8=12929
- polymethylacrylate and copolymers, solns. rheology rel. to bond networks, obs. 8=21552
- poly-3-methyl-butene-1, isostatic, single crystals. growth and structure, obs. 8=8599
- polymethyl methacrylate, cycle dependent fracture 8=2073
- polymethylmethacrylate, effect of impulse γ -neutrons on permittivity 8=18180
- polymethylmethacrylate, e emission and mol. wt. vars. in vibro-mech. treatment, obs. 8=18253
- polymethylmethacrylate, γ -irrad., trapped free radicals, e. s. r. spectra obs. 8=4682
- poly(methyl methacrylates) in soln., n. m. r. 8=16890
- poly(methyl methacrylate) in θ solvents, negative thixotropy 8=16758
- poly(methylmethacrylate), interface tension, tacticity determ. 8=4551
- polymethylmethacrylate, O₂ diffusion, meas. by quenching of phosphorescence 8=8687
- polymethylmethacrylate, rotational isomerism in ester group 8=4220
- poly(methyl methacrylate), stereoblock, low-temp. dielec. absorpt. 8=18175
- polymethyl methacrylates, stereoregular, broad line n. m. r. obs. 8=18462
- polymethylmethacrylate, temp. depend. of conformation transitions and dipole moment 8=17111
- polymethylmethacrylate tube torsional oscillations rel. to ht. generation 8=4946
- poly(methyl methacrylate), X-irrad., e. s. r. 8=18422
- poly(2-methylpentene-1 sulphone), dielectric relax. in soln. 8=1585
- poly(2-methylpentene-1 sulphone), dipole moment from dielec. meas. in soln. 8=1584
- polymethylphenylsiloxanes, optical anisotropy 8=12391
- polymethylpolysiloxanes, liq., dipole moment, dielec. relax. 8=4597
- poly(α -methylstyrene), in soln., viscosity and sedimentation 8=12823
- poly- α -methylstyrene, i. r. spectra in soln. 8=21692
- poly- α -methylstyrene, monodisperse, tensile creep behaviour 8=5094
- poly- α -methylstyrene, sedimentation, Johnston-Ogston effect 8=21729
- polymethylene chains, longitudinal acoustic vibrs. 8=8608
- polymethylene chains, polarizability anisotropy 8=16385

Polymers—contd

- polyoxymethylene, epitaxy and molec. struct. 8=17255
- polyoximethylenes, high molec. weight, form. using variation of temp. regime 8=23134
- polyoxymethylene system in solid trioxane matrix n. m. r. during polymerization 8=22921
- polypentene-1, polymorphism 8=17463
- polyphenols, mass spectrometry 8=1204
- polyphenoxyacetylene, structure and conjugated bonds 8=4266
- polyphenylacetylene, crystallinity, struct. and e. s. r., obs. 8=8600
- polyphenylacetylene, structure and conjugated bonds 8=4266
- poly-DL-phenylalanine, dielec. absorpt. in soln. 8=21705
- polyphenyl benzenes, triplet states, zero-field splitting 8=12288
- polyphenyl diffusion pump fluid film thickness continuous meas. 8=7949
- polyphenyl ester fluid, use in oil-vapour pump 8=7952
- polyphenyl ether, in unrefrigerated diffusion pumps for vacuum of 10⁻⁹ torr 8=7953
- polyphenyls in n-butanol glass, triplet lifetimes and T-T extinction coeff., obs. 8=23071
- polyphenyls, spin-spin interactions 8=2374
- poly-L-proline, i. r. spectra in aq. soln. 8=12891
- poly-2,2-propyl-bis-4-phenylcarbonate chemiluminesc. obs. 8=23072
- polypropylene fibres adhesion and wetting, CF₃ radiation grafting effects, obs. 8=22410
- polypropylene fibres, fluoro-olefines radiation graft-copolymerization 8=23138
- polypropylene, films and blocks, action of laser impuses, melting and recryst. or evaporation 8=17710
- polypropylene, free radicals, e. s. r. spectra 8=12352
- polypropylene, γ -irrad., free radicals e. s. r. obs. 8=7628
- polypropylene, styrene grafting to films and copolymer tensile strength, obs. 8=23139
- polypropyleneoxide, isothermal crystallization, calorimetric study of kinetics 8=4811
- polypyromellitimide, kinetics of formation, i. r. spectra study 8=14408
- polysiloxane-polyether block copolymers, equilib. surface tensions 8=8155
- polystyrene, activated, and in benzene soln. chemiluminesc. obs. 8=23072
- polystyrene, adsorbed, conformation meas. 8=8350
- polystyrene:anthracene:chloranil photocond. and fluoresc. obs. 8=9261
- polystyrene in benzene solns., flow birefringence 8=12732
- polystyrene in chlorinated biphenyl solns., dynamic mech. props. 8=12818
- polystyrene, cold neutron cross-section 8=7271
- polystyrene, conc. solns. viscosity, dependence on molecular weight and concentration 8=8026
- polystyrenes, of controlled molec. wt., characterization by n. m. r. 8=18473
- polystyrene, dielec. props. rel. to molec. weight 8=5360
- polystyrene di-n-butyl phthalate solns., u. s. meas. of shear impedance 8=4547
- polystyrene, e emission and mol. wt. vars. in vibro-mech. treatment, obs. 8=18253
- polystyrene, effect of crosslinking on photoelasticity 8=22395
- polystyrene, glassy, plastic deform. bands 8=22411
- polystyrene latex particles, aqueous suspensions, atomization 8=8154
- polystyrene matrix, dielec. meas. on polar solutes 8=9205
- polystyrene, oriented, birefringence dispersion 8=9578
- polystyrene soln., conc. fluctuations near critical temp. 8=21616
- polystyrene solns., excluded-volume effect 8=8019
- polystyrene soln., laser scatt., for verification of Brownian motion 8=1557
- polystyrene solns., viscoelastic props., mol. wt. depend. 8=8030
- polystyrene+solvent system, diffusion anomalies 8=12829
- polystyrene, vac. u. v. absorpt. spectrum 8=14290
- polystyrene viscoelasticity 8=8878
- polystyrenes, dielec. props., v. low temp. 8=5359
- polysulfone films, BaTiO₃ and organic cpds. loaded, dielec. props. 8=22661
- polysulphinimide, elec. props. 8=9138
- polysulphinimide, elec. props. 8=22615
- polytetrafluoroethylene, carbon-black filled, effects of γ -irrad. 8=17700
- polytetrafluoroethylene, conformational energies 8=1324
- polytetrafluoroethylene, fibril structure 8=1665
- PTFE, thermal cond. 8=17544
- polytetramethyl-p-silphenylenesiloxane, cryst. struct. 8=22065
- poly(tetramethylene oxide), config. 8=12390
- poly(tetramethylene oxide), dielec. meas. during crystallization 8=17240
- polythene film, laser-produced plasma formation mechanics 8=23034
- polythene-metal contact in vacuum, generation and dissipation of static charge 8=18159
- polythiomethylene, from trithiane by radiation 8=17184

Polymers—contd

- polytrioxane mol. weight rel. to preirrad. dose and temp., obs. 8=21210
- polyurethane coats, effect of Al bed on density of network in surface layer 8=17145
- polyurethane, compression modes, obs. 8=22271
- polyurethane elastomer, triaxial fracture in tensile field 8=2075
- polyurethane foam form., surface elasticity 8=8156
- polyurethane foam plastic under small deformations, elastic characts. 8=22261
- polyurethane foam, use in construction of faceted solar concentrators 8=19677
- polyurethane, layers for Zn alloys atmospheric corrosion prevention 8=14389
- polyurethanes, linear, temp. depend of heat capacity 8=22110
- polyurethanes, polyester- and polyether-based, extensional mech. props. 8=13623
- poly(vinyl acetate), conc. solns. viscosity, dependence on molecular weight and concentration 8=8026
- polyvinylacetate, dielec. props. rel. to molec. weight 8=5360
- polyvinyl alcohol, e emission and mol. wt. vars. in vibro-mech. treatment, obs. 8=18253
- polyvinyl alcohol film crystallization, i.r. study 8=13101
- polyvinyl alcohol film dichroic i.r. polarizers 8=11204
- polyvinyl alcohol films dyed in solutions of iodine in iodides and bromides, absorption spectra 8=5650
- polyvinyl alcohol, intrinsic viscosity in aq. salt solns. 8=21634
- 1, 2, 3% polyvinyl alcohol laminar-turbulent transition, obs. 8=4512
- polyvinyl alcohol, pyrolytic products, analysis by mass spectrometry 8=23175
- polyvinyl alcohol, sheets, dichroic spectra, naphthols vibronic transitions obs. 8=14285
- polyvinylchloride, conformation changes on plasticizing 8=8360
- polyvinylchloride, crystallinity degree determ. by X-ray analysis 8=1717
- polyvinyl chloride films, rheo-optical properties 8=2076
- PVC, effect of u. v. irradi. on glass transition temp. 8=17181
- polyvinylchloride, ht. capacity and sp. ht. values from studies at 60-300°K 8=1547
- polyvinylchloride, influence of high pressure on crystallinity 8=4774
- polyvinyl chloride, mechanism of Andrade creep 8=13624
- polyvinyl chloride, n.m.r. linewidth dependence on correlation time distrib. 8=18471
- polyvinylchloride plasticization by aromatic and condensed ring cpds., obs. 8=23141
- PVC, pyrolytic products, analysis by mass spectrometry 8=23175
- PVC single crystals of low mol. wt. 8=17300
- PVC solns., light scatt. 8=16850
- PVC, stress/strain isothermal curves 8=22406
- poly(vinyl chloride), tacticity, by i. r. spectroscopy 8=21217
- polyvinyl ethers, crystallization rel. to lengths of side branches 8=21941
- poly(vinyl formate), n. m. r. study of tacticity 8=16897
- polyvinylphthalimide with impurity acceptors, triplet-triplet energy transfer and triplet excitons, 15000-40 000 cm⁻¹ 8=12389
- poly-2-vinylpyridine, n. m. r. 8=16391
- polyvinyltoluene, solid solns. with phosphors, solubility and diffusivity of CO₂ 8=20386
- polyvinylidenechloride, ht. capacity, entropy and free energy studies, 60-300°K 8=1547
- polyvinylidene chloride, pyrolytic products, analysis by mass spectrometry 8=23174
- poly(vinylidene fluoride)-poly(vinyl fluoride) solid solns. melting point rel. to comp. 8=8173
- poly-p-xylene films, molecular orientation, cell dimensions 8=1828
- preferred orientation, polarized-fluorescence experiment, mathematics 8=1721
- reinforced, spiral fracture characteristics 8=2043
- relaxation times, from birefringence relax. 8=16849
- scanning electron microscope examination, sample preparation technique 8=17180
- semiconductors, new, synthesis and properties 8=5286
- silicones, # 200 series, ultrasonic absorption in range 30-350 MHz and -30° to +30°C, rel. to viscosity 8=8063
- solutions, critical opalescence 8=21669
- solutions, drag-reducing effects in turbulent flow past cylinders 8=16754
- solutions, flow in pipes, drag reduction 8=1511
- solutions, influence of intermolecular hydrodynamic interaction on viscosity and streaming birefringence 8=4505
- solutions, intrinsic viscosity determ. from meas. at a single point 8=16808
- solutions, intrinsic viscosity rel. to sedimentation 8=12823
- solutions, kinetics of solvent evaporation at film formation 8=12972
- solutions, optical activity 8=8065

Polymers—contd

- solutions, polynomial expansion of log relative viscosity 8=16805
- solutions, quasi-elastic scattering, effects of hydrodynamic interactions 8=4542
- solution, second osmotic virial coeff. calc. using lattice model 8=8039
- solutions, 2nd virial coeff., cryometric determ. 8=8017
- solutions, turbulent shear flow 8=12743
- solutions, u.v. refractive indices 8=8350
- solutions, viscosity, concentration var., compression of chains 8=4545
- solutions, viscosity, Newtonian 8=8025
- solutions, viscosity theory tests 8=8029
- solutions viscous flow, conc. depend. of activation energy 8=16807
- spherulite polydispersity rel. to low angle scatt. of polarized light 8=8358
- spin-lattice relax., side chains thermal motion obs. 8=22915
- statistics of substitution 8=18659
- styrene graft-copolymer to butadienestyrene rubber, thermal ageing struct. changes 8=17112
- styrene network copolymers with dimethacrylate or ethyleneglycole, cross linking effect on photoelasticity 8=22395
- styrene scintillators polymerization rel. radioluminesc. yield, obs. 8=14346
- Teflon films, electrical conduction in high fields 8=13877
- Teflon friction on steel, adhesion component modification by e irradi., obs. 8=17842
- teflon, I and AgCl, melting and pyrolysis, high pressure 8=4644
- Teflon 6, surface area and particle struct. 8=13047
- Teflon, tensile strength and struct. disintegration, obs. 8=17843
- tetrafluoroethylene-hexafluoropropylene copolymers, γ -irrad. effects on permittivity and loss 8=9202
- tetrafluoroethylene-hexafluoropropylene copolymers, γ -irrad., radical conversions 8=1326
- tetrafluoroethylene-hexafluoropropylene copolymers, γ -irrad., e. s. r. of radicals formed 8=1325
- tetrahedral lattice, self-avoiding walks 8=1768
- toluene glow discharge prod. films, comp., spectra and elec. props. obs. 8=21894
- triacylcellulose films, plastified, thermomech. curves of elongation at const. strength 8=22407
- ultimately uniaxially oriented, molec. theory of elasticity 8=22405
- vibrational effects in absorption spectrum of rod 8=7645
- vibrational spectra theory 8=21039
- vinylchloride, ht. capacity, entropy and free studies, 60-300 K 8=1547
- vinylchloride with vinylidenechloride copolymers, crystallinity degree 8=1717
- vinyl plastic, tensile strength and struct. disintegration, obs. 8=17843
- vinylidene fluoride-vinyl fluoride copolymers solid solns. melting point rel. to comp. 8=8173
- viscoelastic behaviour, meas. method based on Volterra operator 8=13616
- viscoelastic behaviour and structure 8=8869
- viscoelastic relax., Isakovich-Chaban theory 8=16771
- viscoelasticity and rheology, temp. dependence 8=2071
- viscose fibres, fluoro-olefines radiation graft-copolymerization 8=23138
- wettability rel. to melts heterogeneous nucleation, substrate effects 8=8298
- X-ray meas., small-angle method 8=17185
- C fibres reinforced, friction and wear 8=13618
- (CF₂)_n, peroxide radicals spin-lattice relax., 14 and 4°K 8=2377
- (CF₂CFH), peroxide radicals spin-lattice relax., 14 and 4°K 8=2377
- (CF₂CFCl), peroxide radicals spin-lattice relax., 14 and 4°K 8=2377
- S chains, rotational isomeric state models 8=21207
- S, relaxation mechanisms 8=4267
- Se chains, rotational isomeric state models 8=21207

Polymorphism

See also Crystal structure.

- 4'-n-alkoxy-3'-nitrodiphenyl-4-carboxylic acids, liq. crystals, modifications 8=21614
- anatase formation at high temps. 8=1684
- cholesteryl mynstate liquid cryst. mesophase struct. obs. 8=12802
- crystals of higher order, relation to other superphases 8=8363
- diamond, "lonsdaleite", hexagonal form, natural occurrence and crystal analysis 8=13121
- fresnoite, Ba₂TiSi₂O₈, isomorphism with pyrogermanate 8=18506
- isomorphism of cryst. pair from statistical analysis of normalized Bijvoet differences 8=22007
- isomorphous replacements 8=13120
- liquid crystals, smectic trimorphism 8=21613
- mica complex polytype, Li fluorophlogopite 8=8531
- polypentene-1 8=17463
- tetraethylammonium triiodide, two modifications crystal structure 8=1818

Polymorphism—contd

- BaTa₂O₆, orthorhombic, tetragonal and hexagonal forms prep. 8=4780
 Ca₂SiO₄ and solid solutions 8=13064
 CaYb₂O₄, Ca ferrite isomorph, crystal structure 8=4870
 CdI₂, two new polytypes crystal structure 8=1786
 CdTe films, from multiple refl. studies 8=1694
 GaP films, vacuum deposited 8=21883
 Ir₂Se₃, Rh₂S₃ and Rh₂Se₃, octahedron pairs 8=1807
 KAlSi₃O₈, transform, at 120 kbar and 900°C 8=8268
 LiMSiO₄ and related sulphates, (M = Al with Ga and Ge substitution) 8=17013
 Li₂SO₄, H₂O, high-pressure, and incongruent melting 8=12970
 Mo₂C, rhombic modifications and polymorphic transitions 8=8561
 NaAlSiO₄, isomorph of high pressure NaAlGeO₄, rel. to formation in earth's mantle 8=1678
 PbO, at low temps. 8=8276
 Rh₂S₃, Rh₂Se₃ and Ir₂Se₃, octahedron pairs 8=1807
 SiC, X-ray topographic obs. of polytypes 8=13115
 TiI, and compressibility and thermal expansion 8=1683
 TiO₂ II modification at 40-120 kbar and 400-1500°C 8=17104
 W₂C, rhombic modifications rel. to annealing temp. 8=8561
 YAl₃, two forms, crystal structures 8=1811
 YTaO₄, M¹-phase of fergusonite, lattice structure 8=8562
 ZnS, polytype families 8=8564
 ZnS polytypes 8=8563
 ZnS polytypes of family 24L-72R, unit cell and Zhdanov symbols 8=17194
 ZrO₂ and rare-earth oxides, X-ray and spectrographic investigations 8=4722

Polynomials. See Algebra; Functions.**Polytypism.** See Polymorphism.**Pomeranchuk rule.** See Scattering, particles.**Population inversion.** See Lasers; Masers; Optical pumping.**Porosity.** See Porous materials.**Porous materials**

- See also Permeability, mechanical; Surface measurement.
 carbon blacks prod. from coals, X-ray study of structure 8=8351
 carbon black, study of domain structure 8=8352
 ceramics, optical accentuation of fine pores 8=17019
 convection currents, critical temp. gradient 8=10776
 equilibrium distrib. between polymer soln. and voids 8=16801
 ferrite, firing temp. and pore volume 8=8256
 flow of suspensions 8=12738
 flow of viscoelastic fluids 8=1446
 flow of viscoelastic fluids 8=21573
 fluid flow through, numerical simulation 8=12594
 gas bubble collisional coalescence in solids 8=4695
 gas flow and diffusion eqns. 8=21467
 glass, strength, micromechanical stress effect 8=13577
 glasses, shrinkage and deformation under load at high temp. 8=17021
 graphite, pyrolytic, formation and structure 8=13134
 heat transfer to fluid 8=6206
 hydrodynamic mixing of flowing fluids 8=12596
 irradiated, pores, dislocation loops and coalescence 8=17632
 kaolinite-muscovite-quartz mixtures, pore-size distrib. and dimensional and wt. changes on refining 8=22323
 liquid-filled, elastic wave transmission 8=13497
 permittivity and conductivity at cell level 8=18149
 plasticity and rupture conditions 8=8798
 pore size distrib. meas. in solids, automatic control 8=17022
 pore struct. meas. without shape assumptions 8=17020
 pore volume, equation 8=13049
 porosity meas. in non-conducting mats. by microwave interferometry 8=5032
 sand column drainage, capillary conductivity law 8=16762
 silica gel, modification of struct. on purification 8=1663
 sorption-diffusion 8=17147-9
 surface pores, distrib. determ. by He adsorpt. 8=21899
 tensile strength, effect of moisture 8=8804
 Vycor, film area hysteresis 8=13050
 X-ray scatt., small-angle 8=4696
 Au electrodeposits porosity, Cu substrate surface prep. and undercoats effects, obs. 8=21981
 B₂C, low porosity effect on elastic props. 8=22313
 BaTiO₃, firing temp. and pore volume 8=8256
 Cl₂ porous electrodes, high current density, impurity effects 8=18730
 Fe alloy drops, voids formation 8=8257
 Fe powder, thermal conductivity 8=13388
 Fe, sintered, mag. props. rel. to porosity, obs. 8=22808
 He II superfluid flow through 8=19698
 Mg-Cr-Cu ferrites, mag. permeability tensor, influence of porosity 8=22852
 Mg-Fe mixed hydroxides and dehydration prods., pore struct., desorption obs. 8=17023
 MnO₂, electrolytic, pore struct. and area, obs. 8=21904
 Ni, sintered, mag. props. rel. to porosity, obs. 8=22808
 UO₂, porosity effect on thermal conductivity 8=13397
 ZrO₂-CeO₂ mixtures, porosity, high temp. 8=22614
Porter-LeChatelier effect. See Stress/strain relations.

Positive column. See Discharges, electric.**Positive ray sources.** See Ion sources.**Positive rays.** See Chemical analysis/by mass spectrometry; Ion beams.**Positons.** See Positrons.**Positronium**

- annihilation, and Compton wavelength of electron 8=15739
 atom conversion on O₂ and NO mols. 8=7476
 atoms and mols. of chem. cpds., crystal colour centres as models 8=13451
 e⁻-H collisions, cross-section calc. 8=16223
 e⁻-H scatt., formation, soln. improvements by including polarizability 8=1195
 energy approx. computation, upper bounds to error 8=681
 formation and decay 8=6812
 formation, by e⁺ + H 8=12095
 h.f. splitting as test for Q.E. 8=11285

Positrons

- See also Electron pairs; and Electrons, which include both negative and positive electrons when the differences between them are of no special significance.
 annihilation in pure Fermi gas, ladder-graph approx. 8=22492
 annihilation, single-quantum, higher-shell contributions and polarization correlations 8=22491
 annihilation in solids, efficiency of crystal spectrometers 8=17905
 backscattering by various targets 8=1044
 (β⁺γ⁺) coincidence method, investig. of positron emitting nuclides 8=20743
 chemical compounds, crystal colour centres as models of positronium atoms and mols. 8=13451
 complex bound systems in crystals 8=6812
 in cosmic rays, evidence for secondary origin 8=19093
 emission from radioactive atoms in crystal, spacial dependence, wave mechanical treatment 8=17910
 emitters, disintegration rate meas. 8=11848
 e⁻-p backward scattering, ratio R = σ(e⁺ + p)/σ(e⁻ + p) meas. 8=15733
 e⁺-p scatt., 800, 1200 MeV, cross-section obs., energy meas., ratio to e-p cross-section calc. 8=20383
 lifetime in water, liq. and solid state, temp. depend. 8=16871
 in metals, temp. depend. of mean lives 8=2127
 scattering by proton, differential cross section, comparison with e⁻-p scattering 8=3600
 slow, scattering by mols. 8=12168
 spectrum in 31.5 MeV e tridents in Cu 8=20392
 in stars evolution, ν radiation from β⁺ capture 8=10138
 storage, and e⁻e⁺ colliding beams in alternating magnetic field storage rings at 280 MeV 8=20243
 zero-energy, scatt. by H and He atoms 8=20995
 Ag¹⁰¹ decay scheme 8=1015
 + H, positronium formation 8=12095
 H-e⁺ scatt., positronium formation calc. 8=1195
 in Hf¹⁷² + Lu¹⁷² decay, number 8=11824
 MgO, powdered, mag. quenching, "anomalous", of three photon annihilations 8=17908
 Ni-Co, deformed, annihilation 8=17909
 Ni-Fe, deformed, annihilation 8=17909

Potassium

- atom, ²F level, polarization by outer electron 8=7413
 atom, ⁴P_{1/2}, selection rules for transitions from collisions with inert gases 8=12064
 atomic absorption cross section, 580 Å to 1000 Å, experimental values 8=12065
 atomic beam, scatt. by benzene and cyclohexane beams, comp. 8=1205
 atomic beam, surface ionization on Pt and W 8=12110
 atoms, excitation by low energy electrons, absolute cross sections 8=12087
 atoms, pseudopotentials 8=7409
 atoms, reaction with Br₂ and I₂ molec. beams, kinetics 8=1202
 atoms, stimulated emission from 4P_{3/2,1/2} - 4S_{1/2} 8=20984
 conduction electrons, u.s. attenuation 8=22104
 crystal, approx. dispersion relations 8=17480
 deformation by thermal activation at low temps. 8=1957
 desorption from emitter of field emission microscope 8=3211
 electron-impact ionization, empirical calculations 8=12448
 electron scatt. differential spin-exchange cross section and differential cross section, 0.5 eV 8=12097
 elastic moduli and pressure derivs. at absolute zero 8=17818
 feldspar content of upper mesozoic graywackes California north 8=2565
 film condensation of saturated vapour 8=21770
 films, optical absorption 8=5612
 flares on astron. spectrograms, real or artificial? 8=14753
 foils, plasma reson. emission excited by light 8=7776
 helicon waves, nonlocal damping 8=17904
 ions, charge composition effect of target state 8=1365
 ions K⁺ on Hg electrode, partial charge transfer react. 8=18722
 ions, range distrib. in amorphous Al₂O₃ 8=13476
 lamp, line shape dependence on current 8=15523
 light modulation by K³⁹ at ground-state, optical pumping 8=12085
 liquid, effective ion-ion potential 8=8237

Potassium--contd

- liquid, elec. resistivity, appl. of structure factor and pseudo pot. relation 8=12920
 liquid, wavenumber-dependence of elastic moduli 8=1499
 magnetoacoustic effect, shear wave 8=22105
 melting, invariance of photocurrent and work function 8=13939
 molten, electronic band struct., density of states, and resistivity calc. 8=16789
 one-electron energy levels, for extended Thomas-Fermi-Dirac pot. 8=1167
 photoconductivity calc. from Kubo-Greenwood formula 8=5393
 photoionization of vapour 8=12447
 plasma, elect. conduction and condensation obs. 8=4343
 radioactive, abundance in crystalline shield rocks 8=9794
 scattering from O_2 , atomic differential spin-exchange scattering 8=12109
 size effect, r.f., line shapes for surface reactance and resist. derivatives 8=13719
 spectroscopy r.f. reson. lamp for kgauss fields use 8=6536
 sputtering ratio, differential, (energy spectrum) meas. for incident Ar and Xe ions 8=2029
 surface impedance near cyclotron edge for helicons 8=13686
 vapor, supersaturation and condensation shocks 8=12982
 vapour, charge exchange H^+ to H^- 8=12441
 vapour exchange to improve He ion source for accelerator 8=6693
 K absorption spectra in MnSe rel. to chemical bonding 8=14242
 in K methoxide-methanol ions coordination number and solvates comp. obs. 8=2497
 K⁻ e affinity calc. by superposition of configurations 8=21281
 K⁺ cochlear microphonic depend. on conc. in endolymph 8=19616-7
 K⁺, dipole polarizability from spectra 8=7414
 K₂ vapour, nonlinear absorpt. of ruby laser light, and resonance fluoresc. 8=7527
 K⁴¹, Larmor freq. rel. to Ge⁷³, and H² 8=5558
 K-Ar, interatomic potential, χ^2 minimum method 8=12205
 K-graphite lamellar cpds., phase equilib. 8=4712
 K-NH₃ dilute solns., absence of vol. change on dilution at -34°C 8=1530
 K+NaCl=KCl+Na, electronic pot. energy surfaces 8=23106
 Na, K radioactive ion separation, spacers in electrophoresis 8=5742
 Na²² impurity, diffusion 8=8680

Potassium compounds

- alum, chrome, n. m. r. obs. 8=2385
 halides, phonon scattering by monatomic impurities 8=4904
 transition metal halides, Raman and i. r. spectra 8=9542
 KAgI₃, cryst. struct. rel. to ionic mobility 8=17379
 KAlF₆·Fe³⁺, e. p. r. spectrum 8=9426
 KAl(SO₄)₂·12H₂O, isothermal dissoln. and growth, mag. field effect 8=8411
 KAlSi₃O₈, enthalpy of fusion 8=21753
 KAlSi₃O₈, polymorphic transform. at 120 kbar and 900°C 8=8268
 K₂B₂O₄ glass, γ -irrad., induced absorption bands assoc. with Tl⁺, Pb²⁺ or Bi³⁺ 8=5639
 KCN, elec. cond. of single cryst. 8=5352
 K₂CO₃, i. r. cryst. spectra 8=18556
 2K₂CO₃·3H₂O, cryst. struct. 8=8528
 KCa₂(Be, Al)₂Si₂O₁₀·0.8H₂O, crystochemical analysis and structure refinement 8=17338
 KCa₄H₁₆Si₄O₂₆ (apophyllite) crystals, etch pits rot. on basal cleavages 8=8384
 K₂Ca(SO₄)₂·H₂O, syngenite, crystal structure 8=13268
 KClO₃, effect of X-irrad., new absorpt. bands in i. r. region 8=22993
 KClO₃, X-ray irrad., colour centres 8=22233
 K₃Co(CN)₆·Fe³⁺, e. p. r. spin-spin interaction temp., 3 cm. 1.8°K 8=18425
 K₃Co(CN)₆·Fe³⁺ spin-lattice relax. rel. to maser material 8=10994
 KCoF₃, thermal and thermodynamic props., 80°-300°K 8=17519
 K₃Cr(CN)₆, spin-phonon transition probabilities, meas. 8=5544
 K₃Cr₂(C₄O₃)₂·3H₂O, anomalous mag. behaviour, between room and liq. O₂ temps. 8=18298
 K₂Cr₂O₇, effect on Fe acid corrosion inhibition by thiourea 8=2518
 K₂Cu(CN)₄, crystal structure and refinement 8=17361
 KCuF₃, antiferromagnet, F¹⁹ n. m. r. shifts on a and c axes 8=5505
 KCuF₃, antiferromagnet, one-dimensional, formation in perovskite structure 8=5504
 K₂CuFe(CN)₆, tetragonal, X-ray analysis, i. r. and e. s. r. spectra 8=13265
 KDF₂, i. r. absorpt. study of lattice vibrations 8=5617
 K₂PO₄, dynamic props. due to deuteron intrabond jumping 8=9212
 K₂PO₄, ferroelectric props. pressure dependence 8=5366
 K₂PO₄, mag. susceptibility thermomagnetic obs., 80-380°K 8=13974

Potassium compounds--contd

- KD₂PO₄, spec. heat and permittivity 8=1873
 KF, alkali halides, F-band peak, Mollwo relation 8=17688
 KF, dichroism, mag. circular, of R₂ band 8=14235
 KF, dipole moment 8=4154
 KF, elastic constants meas. from 300-4.2°K 8=2056
 KF, monocrystals, slow electron diffraction 8=8527
 KF, thin layers, u. v. optical props. 8=9546
 KF-SnF₂-H₂O system 8=4781
 K₂Fe(CN)₆, heat capacity below 1°K, meas. 8=13372
 K₂Fe(CN)₆, Mössbauer effect at high press. 8=4673
 K₂Fe(CN)₆, Mössbauer effect at high press. 8=4673
 K₂Fe(CN)₆·3H₂O, dielectric dispersion 8=9211
 K₂Fe(CN)₆·3H₂O, ferroelectric phase transition, Mössbauer test for lattice-dynamical model 8=22667
 K₂Fe(CN)₆·3H₂O, proton relax. and translational diffusion 8=14145
 K₂[Fe(CN)₆], Mössbauer effect at high press. 8=4673
 KFeF₃, exchange and spin-orbit coupling 8=22881
 KFeF₃:Fe²⁺, isomer shift, calibration 8=16988
 KHCO₃·2H₂O, i. r. cryst. spectra 8=18556
 KH₂(D₂)PO₄, conductivity rel. to isotope effect 8=2130
 KHf₂ and KDF₂, elec. cond. of crystals. 8=13704
 KHf₂, i. r. absorpt. study of lattice vibrations 8=5617
 KH₂F₃, i. r. spectra 8=2425
 KH₂PO₄, anisotropic crystal, analysis of stimulated Raman effects 8=9543
 KH₂PO₄, anomalous incoherent scattering of thermal neutrons in Laue-case 8=13267
 KH₂PO₄ cryst. in 1-bromonaphthalene, refl. second-harmonic intensity obs. 8=5611
 KH₂PO₄ crystal growth in static system, pH effects 8=17239
 KH₂PO₄, dielectric const. just above transition temp., freq. and temp. depend. 8=22666
 KH₂PO₄, ferroelec. domain switching by irradiation damage 8=18184
 KH₂PO₄, ferroelec., transition temps. shifts by hydrostatic press. 8=18189
 KH₂PO₄ films, i. r. absorption spectrum, internal vibrations 8=9545
 KH₂PO₄, mag. susceptibility thermomagnetic obs., 80-380°K 8=13974
 KH₂PO₄ n. m. r. of K³⁹ at 77°K (ferroelectric phase) 8=22924
 KH₂PO₄ optical parametric amplifier, quantum noise, 0.5-0.6 μ m 8=15526
 KH₂PO₄, paraelectric, proton dynamics 8=9214
 KH₂PO₄, 90° phase matching, elec. field control to alter birefringence 8=14234
 KH₂PO₄, phase transition, high temp., isotope effect 8=9213
 KH₂PO₄, reactor and fission fragment irrad., structural changes 8=8773
 KH₂PO₄, rel. to second harmonic generation of Nd-glass laser 8=15486
 KH₂PO₄-type crystals, ferroelectric phase transitions, dynamics 8=9215
 KH₃(SeO₃)₂, fundamental absorpt. edge near ferroelectric phase transition pt. 8=9548
 KI, alkali halides, F-band peak, Mollwo relation 8=17688
 KI aqueous solution, possible applications as dosimeter 8=6664
 KI cathodoluminescence, e microprobe obs. 8=14317
 KI, containing H₂O, solubility, diffusion absorpt. spectrum 8=4953
 KI, crystals, bremsstrahlung absorpt. 8=6795
 KI, diffusion of inert gases at energies up to 85 keV and release behaviour 8=22156
 KI effect on Fe acid corrosion inhibition by thiourea 8=2518
 KI, F¹ centre formation quenching 8=8744
 KI, Hartree-Fock multiplet strengths 8=4081
 KI:Cu⁺, lifetime of excited Cu⁺ 8=23057
 KI:In luminesc. and elec. cond. thermostimulated rel. to impurity C excites delocalization mechanism 8=8903
 KI(In) self-luminesc. due to X-rays, decay 8=14318
 KI intrinsic electroluminesc. and excit., 77°K and 5 × 10⁴ V/cm 8=14320
 KI monocrystals, photoelectric emission 8=18280
 KI:(Ni, Cu, In, Pb and Tl), roentgenoluminesc. and F-flash temp. depend. obs. 8=9626
 KI:P radioluminesc. rel. to hole storage at centres, obs. 8=9625
 KI, pure and doped, transmission and reflection spectra, low temps. 8=18540
 KI, reflection, 5-25 eV rel. to band level transitions 8=22995
 KI, reorientation of O₂, 1.5-4.2°K 8=13123
 KI, second order Raman scattering spectrum, exptl. study 8=5615
 KI self-luminesc. due to X-rays, decay 8=14318
 KI: Tl⁺, absorpt. and emission at 77°K rel. to Tl⁺ clustering 8=23056
 KI:Tl⁺, B band symmetry assignment 8=5616
 KI with Tl impurities, growth using vacuum furnace 8=17237
 KI, Tl⁺ and In⁺ activated F-centre form. spectrum rel. to mechanisms, 5-21.2 eV 8=2008
 KI:Tl roentgenoluminesc., elec. field stimulation mechanism, obs. 8=9618

Potassium compounds—contd

- KI: Tl roentgenoluminesc. and F-flash build-up obs. 8=9616
 KI: Tl, Zeeman effect of A absorption bands 8=9504
 KI, van-der-Waals dipole-dipole coeffs. 8=1625
 KI-NaI, (-RbI), (-KCl) solid solns., absorpt. edge temp. dependence, 80-100°K 8=22994
 K-Li_{1/2}Li_{1/2}M_{1/2} and quasi-stationary states 8=2432
 K₃Li₂Nb₅O₁₅, electro-optic and nonlinear optic characts. 8=22959
 K₂Li₂NbO₃ single crysts., growth 8=21952
 K₂Li₂NbO₃, stable nonlinear optical material 8=5618
 KMF₃, (M = Mg, Mn, Co, Ni), i.r. reflectance spectra rel. to lattice vibrations 8=2426
 KMF₃ (M = Mg, Mn, Co, Ni, Zn, Mg/Ni), i.r. transmission spectra rel. to multiphonon processes 8=2427
 KMgF₃, i.r. spectra and lattice vib. anal. 8=2428
 KMgF₃:Ni²⁺, acoustic p. r., propag. factor changes near reson. 8=22912
 KMgF₃:Ni²⁺, i.r. luminesc. emission 8=18626
 KMnCl₃, prep. and crystallographic props. 8=13138
 KMnCl₃·2H₂O, crystal structure 8=17411
 K₂MnF₄, antiferromagnetic anisotropy 8=14070
 KMnF₃, critical antiferromag.-scattering of neutrons 8=22882
 KMnO₃, Raman spectra 8=21085
 K₃MoCl₆ specific heat rel. to mag. ordering, 1.5-20°K 8=1872
 K₂MoO_xF_y·H₂O (x=1, 2, 3; y=5, 4); crystal structure 8=17381
 KNO₃ containing KNO₃ impurity, analysis by i. r. and Raman spectra of solns. 8=23177
 KNO₃, dynamic compression by explosive impact loading 8=22377
 KNO₃, elec. resistivity rel. to other props including transforms and thermodynamic charact. 8=18191
 KNO₃, irradi. cryst., e. p. r. of NO₂ at 4°K 8=5537
 KNO₃, molten, optical determ. of thermal cond. 8=21658
 KNO₃, molten, refr. index meas. by interferometry 8=4583
 KNO₃ and other nitrates, molten mixtures, u.v. absorption 8=8085
 KNO₃, Raman spectrum 8=14174
 (K, Na)(Ba, Cl) solid soln., constitutional supercooling, convection cells 8=8417
 K-Na alloys, density 0 to 300°C 8=21624
 KNbO₃ crystals, ferroelectric, absorpt. edge temp. dependence 8=2430
 KNbO₃, hydrothermal synthesis of crystals, 2-3 mm in size 8=8418
 KNbO₃-AgNbO₃, system, elec., X-ray and thermal expansion studies 8=21823
 KNiF₃, antiferromagnetic, magnetic exchange dichroism 8=14257
 KNiF₃, antiferromagnetic, optical absorpt., anomalous temp. depend. 8=22996
 KNiF₃, i. r. spectra and lattice vib. anal. 8=2428
 KNiF₃ and K₂NiF₆, comparative study of mag. props. 8=9397
 K₂NiFe(CN)₆, cubic, X-ray analysis, i. r. and e. s. r. spectra 8=13265
 KOH impurity in ice, dielec. dispersion obs. 8=18188
 K₂O-SiO₂ solutions, activities 8=21620
 K₂O-SrO-SiO₂ system, diffusion, effective binary coeff. 8=22155
 K₂PtCl₆ lattice images with electron microscope 8=8500
 K₂SO₄:Mn²⁺, e. p. r. in single cryst. 8=22910
 K₂S₂O₈, rotatory, dispersion, interpretation 8=18539
 K₂S₂O₈, oxidation of acetate ion, Ag catalysis 8=23094
 KSO₃F, i. r. spectra and mag. props. 8=9562
 KSO₃NH₂, crystal structure by neutron diffr. meas. 8=4897
 K₂Sr₂Nb₅O₁₅, ferroelec. and electro-optic props. 8=5365
 KTa_{0.65}Nb_{0.35}O₃ electrooptical effects obs. in 8=14232
 KTa_{0.65}Nb_{0.35}O₃ paraelectric and ferroelectric phases, optical props. 8=18504
 KTa_{0.5}Nb_{0.5}O₃, elec. resistivity comp. dependence and effect of Sn doping 8=22503
 KTaO₃, Fe³⁺ and Ni³⁺ e. p. r. spectra 8=9425
 KTaO₃, hydrothermal synthesis of crystals, up to 1 mm in size 8=8418
 KTaO₃, paraelectric and ferroelectric phases, optical props. 8=18504
 KTaO₃, u.s. velocity meas. between 2-300°K 8=22088
 KTh₂(PO₄)₃, crystal structure 8=17382
 K(UO₂AsO₄)₃H₂O, abernathyite, e-diffr. meas. 8=17360
 K₂V₂O₆, new phases of narrow homogeneity range, crystallog. features 8=17086
 KZnF₃, i. r. spectra and lattice vib. anal. 8=2428
 K₂ZrCl₆, thermal props. 8=8640
 (Li, K)₂(SO₄, WO₄) system, molten, elect. cond. up to 1100°C 8=8112
 Na-K-NH₃ solns., liq.-liq. phase separation 8=8014

potassium bromide

- acoustic phonons, first and zero sound, elastic const. variation 8=13357
 cathodoluminescence, e microprobe obs. 8=14317
 colour centre studies by pulsed irradiation 8=13460
 from crossed-beam reactions K + HBr 8=9689
 crystals, bremsstrahlung absorpt. 8=6795
 crystals, impure, cation vacancy generation during electrolysis 8=9718

Potassium compounds—contd**potassium bromide—contd**

- diffusion of inert gases at energies up to 85 keV and release behaviour 8=22156
 dipole moment 8=4154
 dislocations, dynamic characts. by internal friction method 8=8730
 dislocation mobilities, temp. depend. 8=8729
 dynamic compression, shock wave propag. and phase transforms. 8=22376
 e emission, photostimulated, by F-centres, mechanisms, obs. 8=9278
 electron transport props. in high fields at low temps. 8=2264
 F-band absorption, u. s. strain modulation 8=22232
 F-band peak, Mollwo relation 8=17688
 F-centre form. spectrum rel. to mechanisms, in Tl⁺, In⁺ activated, 5-21.2 eV 8=2008
 F-centres, thermal stability 8=8750
 H centre aggregates 8=2005
 i. r. spectra rel. to complexes formed when doped with Ca²⁺ or Ba²⁺ with NOC⁻ 8=14233
 n.m.r. and quadrupole effects 8=14146
 optical constants in far i. r. 8=5613
 2-photon transitions to exciton states, oscillator strengths 8=8953
 polarization rel. to lattice imperfection prod. during shock wave plastic deformation 8=9225
 polaron cyclotron resonance 8=2124
 Raman scattering in polarized light, second order 8=14231
 self diffusion entropy and enthalpy from elec. cond. 8=8679
 structure factors, and electron distrib. in K and Br ions 8=17861
 U-centre local mode absorption 8=1831
 V-bonds, effect of stress, obs. 8=2000
 vacancy conc. changes during electrolytic coloration at 460-670°C 8=17609
 van-der-Waals dipole-dipole coeffs. 8=1625
 volume expansion, X-irrad. induced, by relaxs. at Frenkel defects 8=13486
 water vapour adsorption on cleavage surface 8=17166
 Ca doped, growth of optical absorpt. bands by X-irrad. 8=2429
 H₂O mols., solubility, diffusion absorpt. spectrum 8=4953
 KBr:Ca, conductance and capacitance distortion at low freq. 50 and 330°C obs. 8=5154
 KBr-In, inner-centre luminescence, spectral-kinetic investigations 8=14319
 KBr:In luminesc. and elec. cond. thermostimulated rel. to impurity C excites. delocalization mechanism 8=8903
 KBr:KCl solid soln(64:36), diffuse scatt. rel. to ion shift in lattice 8=17378
 KBr-KI system, thermodynamic studies 8=17092
 KBr:Li⁺, impurity displacement calcs. 8=8243
 KBr:NO₃, CO₃²⁻, SO₄²⁻, SeO₃²⁻ and Cu, centres nature, obs. 8=8745
 KBr:O₂, effect anharmonic vibrations on isotopic displacement of luminescence 8=22937
 KBr:OH, i. r. absorpt. spectra rel. to temp. dependence of intensity of OH vibrations 8=18538
 KBr:P radioluminesc. rel. to hole storage at centres, obs. 8=9625
 KBr:Pb, Zeeman effect of A absorption bands 8=9504
 KBr:Sm²⁺, one-phonon sideband of 6890Å transition at 7°K 8=9614
 KBr:Tl e emission, photostimulated, by F-centres, mechanisms, obs. 8=9278
 KBr:Tl F-centres luminesc. rel. to hole processes, obs. 8=8888
 KBr:Tl, Zeeman effect of A absorption bands 8=9504
 KBr-KI solid solns., free energy of formation, and gap of solubility 8=16998
 and KCl, mixed, Raman scattering 8=18541
 KCl(Br) foils, P-polarized light absorption at plasma resonance freq. 8=2123
 KCl: Br lifetime of excited Cu⁺ 8=23057
 KCl-KBr diffusion pairs, pore migration during counter-current diffusion 8=17569
 KCl-KBr solid solns, optical absorpt. 8=2431
 KCl-KBr solid solns., reflection, 5-25 eV rel. to band level transitions 8=22995
 NaBr-KBr solid solutions, fundamental absorption 8=18549
 Ni, Cu, In, Pb and Tl activated, roentgenoluminesc. and F-flash temp. depend. obs. 8=9626

potassium chloride

- absorption, in i. r., induced by monovalent impurities 8=9544
 aqueous solns., elec. cond. under high press. 8=12922
 Bragg spots origin 8=17380
 cathodoluminescence, e microprobe obs. 8=14317
 colour centre in crystal with blocking electrode 8=22230
 colour centre in crystal with blocking electrode, photoelectric polarization 8=22231
 conductivity, electrical, kinetics of radiational change 8=22501
 crystals, bremsstrahlung absorpt. 8=6795
 crystals, deformed, absorpt. of ultrasound by dislocations, rel. to freq. 8=8630

Potassium compounds—contd**potassium chloride—contd**

- crystal growth from aq. soln., effect of PbCl_2 8=8415-16
 crystals, impure, cation vacancy generation during electrolysis 8=9718
 dichroism, mag. circular, of R_2 band 8=14235
 diffusion of inert gases at energies up to 85 keV and release behaviour 8=22156
 dipole-lattice relaxation times for OH^- dipoles 8=8202
 dislocation density and plastic flow stress obs. in crystal 8=8731
 doped with Pb^+ , Ti^+ and Ag^+ , electron spin resonance obs. 8=14112
 doped and pretreated, diffusion of Ti^+ 8=13410
 dynamic compression, shock wave propag. and phase transforms. 8=22376
 elastic constants, higher order, theoretical calcs. 8=17811
 electric breakdown, directional, single crystals 8=18167
 electrolyte solns., self-thermal diffusion 8=21640
 e emission, photostimulated, by F-centres, mechanisms, obs. 8=9278
 electronic states of M_1 -centres 8=2003
 F-band absorption, u. s. strain modulation 8=22232
 F-band peak, Mollwo relation 8=17688
 F-centre, double electron-nuclear magnetoacoustic reson. 8=8623
 F-centre form. spectrum rel. to mechanisms, in Ti^+ , In^+ activated, 5-21.2 eV 8=2008
 F-centre half-width and effective lattice freq. calcs. 8=4993
 F centres, thermal stability 8=8750
 γ -irradiated at room temp., defect production and annihilation 8=8696
 heat of soln. meas. 8=9677
 impurity in ice, dielec. dispersion obs. 8=18188
 i.r. spectra rel. to complexes formed when doped with Ca^{2+} or Ba^{2+} with NCO^- 8=14233
 metal film epitaxial growth on KCl substrates 8=13147
 monocrystals, slow electron diffraction patterns 8=8527
 photoelectric emission 8=18280
 polarization rel. to lattice imperfection prod. during shock wave plastic deformation 8=9225
 powder, energy absorption during compression 8=13592
 pressed disc prep., reactions of Na_2CO_3 8=14373
 Raman scattering in pure and doped crystals 8=5614
 reflectivity spectra and absorpt. constant rel. to exciton states 8=14230
 solid soln. with NaCl , decomp. mechanism by X-ray scattering studies 8=13070
 solution grown crystals, distrib. of Pb^{2+} impurities 8=17238
 specific heat obs., by cryostat, 0.05 \rightarrow 2°K 8=22112
 third-order elastic constant, obs. 8=13579
 transformation of OH centres into U centres by electrolytic decoloration 8=13458
 transmission dynode, secondary electron emission, Polya statistics 8=5420
 tunneling states of OH^- 8=2101
 van-der-Waals dipole-dipole coeffs. 8=1625
 volume expansion, X-irrad. induced, by relaxs. at Frenkel defects 8=13486
 water vapour adsorption on cleavage surface 8=17166
 X-irradiated, α -centre production and thermal annealing 8=17685
 Z center, Faraday rotation 8=14229
 Ag and Pb activated, Cl_2^- centres conc. temp. depend., e.p.r. obs. 8=8742
 Ag, Pb and Tl activated, Cl_2^- centres conc. temp. depend., e.p.r. obs. 8=8742
 $\text{Ar}^{39,41}$ diffusion and trapping, n irradiated 8=1920
 Ca-doped, thermal conductivity, 20-90°C, influenced by segregation processes 8=13394
 H_2O mols., solubility, diffusion absorpt. spectrum 8=4953
 and KBr, mixed, Raman scattering 8=18541
 KCl:Ag, Ag colour centres form. rel. to point defects, obs. 8=8746
 KCl:Ag (from AgI), optical absorpt. of impurity rel. to E-band models 8=14228
 KCl:Ag, B-centre, luminescence and photocond. 8=2006
 KCl(Ag), colouration, impurity centres produced 8=1994
 KCl:Ag colour centres e.p.r. absorpt. rel. to relax. process 8=8743
 KCl:Ag:OH, Ag colour centres form. rel. to point defects, obs. 8=8746
 KCl:Ag:Sr, Ag colour centres form. rel. to point defects, obs. 8=8746
 KCl:Be $^+$, substituent behaviour from ionic thermocurrent spectra 8=8702
 KCl(Br) foils, P-polarized light absorption at plasma resonance freq. 8=2123
 KCl: Cu^+ , lifetime of excited Cu^+ 8=23057
 KCl:Eu $^{2+}$, e.p.r. 8=5529
 KCl, excited F centre lifetime below 100°K 8=2004
 KCl:KBr solid soln., (36:64), diffuse scatt. rel. to ion shift in lattice 8=17378
 KCl:Li $^+$, impurity displacement calcs. 8=8243
 KCl:Mn $^{2+}$ e.p.r. spectrum, resolution obtained by X-radiation 8=14117
 KCl:Na, luminescence of F, centers 8=9615
 KCl:OH $^-$, cooling to 0.36°K by adiabatic depolarization of OH^- 8=1874

Potassium compounds—contd**potassium chloride—contd**

- KCl:OH, i.r. absorpt. spectra rel. to temp. dependence of intensity of OH vibrations 8=18538
 KCl, paramagnetic rare-earth activated, magneto-optic rotation 8=5590
 KCl:P radioluminesc. rel. to hole storage at centres, obs. 8=9625
 KCl:Pb phosphor, tetragonal symmetry 8=18607
 KCl:Pb, Zeeman effect of A absorption bands 8=9504
 KCl:RbCl crystals, Q_1 colour centre e. s. r. study 8=22905
 KCl:Sr, F- Z_2 colour centre conversion, thermal equil. 8=2007
 KCl:Tl e emission, photostimulated, by F-centres, mechanisms, obs. 8=9278
 KCl:Tl, induced local 3p states on Cl^- ions nearest Ti^+ , calc. 8=8930
 KCl:Tl photostimulated luminesc. rel. to optical and thermal electrons roles in recomb., 77-300°K 8=9617
 KCl, U_2 -centre, electronic structure rel. to correlation effects 8=13459
 KCl(ZnCl_2)- H_2O , crystn. interphase equil. 8=21933
 KCl-In, inner-centre luminescence, spectral-kinetic investigations 8=14319
 KCl-KBr diffusion pairs, pore migration during counter-current diffusion 8=17569
 KCl-KBr, Kirkendall and Frenkel effect 8=8676
 KCl-KBr solid solns, optical absorpt. 8=2431
 KCl-KBr solid solns., reflection, 5-25 eV rel. to band level transitions 8=22995
 KCl-NaCl phase equilibrium diagram 8=8164
 in Mg fused electrolyte, elec. cond. and density obs. 8=23143
 Ni, Cu, In, Pb and Tl activated, roentgenoluminesc. and F-flash temp. depend. obs. 8=9626
 Pb activator solubility, OH $^-$ ions effects, obs. 8=21824
 Tl activator solubility, OH $^-$ ions effects, obs. 8=21824
Potential energy, gaseous molecules. See Molecules/intermolecular mechanics.
Potential energy, single molecules. See Molecules/internal mechanics; Molecules/vibration.
Potentiometers. See Electrical measurement.
Powder diffraction cameras. See X-ray crystallography/apparatus.
Powder metallurgy. See Metallurgy; Sintering.
Powders
 See also Granular structure; Particle size; Sintering; Surface measurement.
 adsorption of He at room temp. 8=21899
 bulk density of packed particles, rel. to degree of mixedness 8=17017
 carbon blacks prod. from coals, X-ray study of structure 8=8351
 compacts, relation between press. and density. 8=1662
 compresses, i.r. reflection spectra rel. to single crystal spectra 8=14169
 corundum macroparticles accel. by laser radiation 8=10885
 diffusion of rare gases following recoil labelling from adsorbed Ra^{226} 8=13404
 dust explosion prevention 8=18694
 dust particles, behaviour during electrostatic precipitation, a photographic study 8=10836
 dust particles in laser cavity, propulsion and angular stabilization 8=6422
 evaporation completeness, insufflation method 8=21781
 ferrites:Fe $^{3+}$, electron relax. study 8=18419
 fluidized bed, mean and variance of local particle conc., rel. to non-uniformity 8=21462
 with free radicals, production and e.s.r. study in simple chamber 8=7619
 garnets:rare earth ions, electron relax. study 8=18419
 grain size determ. from X-ray absorpt. 8=17018
 grain size determ., by X-ray fluoresc. spectroscopy 8=21830
 granular material in fluidized bed, heat transfer 8=4628
 insulating, thermal cond. and diffusivity meas. 8=8651
 metal macroparticles accel. by laser radiation 8=10885
 moist, adhesion to solid in temp. field 8=22303
 oxide, reduction by gases, micromechanism from O_2 pressure change meas. 8=18683
 packed, with fluids, permittivity 8=22648
 pore volume, equation 8=13049
 preparation of sample for high pressure experiments 8=8172
 Raman spectra, excitation by He-Ne laser 8=14175
 Raman spectroscopy, using oblique illumination 8=3360
 separation of impurities, by conical electric field 8=3149
 shock waves in a dusty medium 8=167
 of small particles, Mossbauer fraction rel. to packing 8=21805
 steel, stainless, sintering rel. to strain effects 8=4693
 Teflon 6, surface area and particle struct. 8=13047
 ultrasonic dispersal for particle size meas. 8=13046
 X-ray fluoresc. anal., casting in glass disks 8=2551
 zirconium carbide, diffusion of Xe 133 , activation energy rel. to struct. 8=8686
 α -AlFeSi, 4 possible phases 8=13057

Powders—contd

- CdTe:Mn²⁺ e.p.r., forbidden transitions 8=14119
 Cu, X-ray study 8=4844
 Fe dispersed in perspex, magnetization process and Mössbauer effect 8=5470
 Fe porosity and thermal conductivity 8=13388
 Fe, X-ray diffraction line intensity after plastic deform. and annealing 8=21989
 Fe-Co, mag. props. 8=5471
 δ -Fe₂O₃, mag. props., effect of struct. and chem. alterations 8=17627
 Fe₂O₃, Mossbauer fraction rel. to packing 8=21805
 Fe₂O₃, pH depend. of adsorpt. of the anions VO₃⁻, WO₄⁻, MoO₄²⁻ and Cr₂O₇²⁻ 8=8342
 GdF₃, Gd³⁺ reflection spectrum 8=2421
 Gd₂O₃, Gd³⁺ reflection spectrum 8=2421
 Ge dust, elec. charge, effect of crushing period 8=13813
 Ge dust, elec. charge, effect of crystal lattice defects 8=13812
 KCl, energy absorption during compression 8=13592
 LaB₆ suspension in N₂ as m. h. d. generator working fluid 8=15199
 NaCl, energy absorption during compression 8=13592
 NaCl-KCl mixtures, energy absorption during compression 8=13592
 NaCl, Na²³ n.m.r. 8=5562
 Si, paramagnetic centres 8=22762
 TiCl₃·α, X-ray diffraction spectra 8=22041
 UO₂, sintering behaviour rel. to particle size and shape 8=21834
 UO₂ swaged compacts, equiaxed grain growth under temp. grad. 8=8255
 ZnO, elec. cond. effect of O₂ adsorption 8=22612

Praseodymium

- atoms, Lα_{1,2} lines meas. 8=7420
 magnetism rel. to crystalline field splitting and exchange interactions 8=2292
 H₂ definition, spectral-isotopic method 8=9743
 Pr³⁺ in SrTiO₃ vibronic structure in luminescence spectra 8=14333
 Pr³⁺, wave functions 8=7419

Praseodymium compounds

- telluride phases, crystal chemistry 8=17202
 PrC₂, antiferromag. structure 8=18386
 PrCl₃, cryst. field, exchange charge effects 8=13011
 PrF₃, i.r. absorption and dichroism 8=9560
 Pr₂Fe₁₇, crystal structure refinement 8=17408
 PrH₃, mag. props. and cryst. struct. 8=22761
 Pr(NO₃)₃·6H₂O:Gd³⁺ e.p.r. spectrum obs. 8=14109
 Pr₂(SO₄)₃·8H₂O, Pr¹⁴¹ n.m.r. meas. 8=14155

Precipitation

- See also Atmosphere/precipitation.
 austenitic steel of sigma phase from thin-foil transmission studies 8=1674
 deoxidation product growth and separation, collision model 8=18658
 grain-boundary, growth kinetics 8=13445
 iron, liq.-silica deoxidation product growth and separation, collision model 8=18658
 martensite decomposition effect of thermomechanical treatment during low-temp. tempering 8=21845
 microanalysis in alloys by e-microscopy and energy analysis 8=17276
 spinodal decomp., Institute of Metals lecture 1967 8=21835
 steels, CrMoV cast, carbide, rel. to load-time curves in breaking-strength meas. 8=17804
 EI-702 steel, effect of deformation and hardening temp. 8=17078
 steel rel. to mech. strength, hot working effects 8=22356
 steel, of Nb carbon-nitrides, their dissolution and age hardening effects 8=1660
 systems, colloid stability 8=12949
 in thin foils, electron microscope images 8=13152
 Ag-5.64 wt. %Al alloys, grain boundary 8=17038
 Ag-Cu alloys, age hardenable, electron microscope study 8=21837
 Al-4wt. %Cu alloy, precip. phase microanalysis by e-microscopy and energy analysis 8=17276
 Al-Cu-Ag alloys, nucleation of precipitates 8=17040
 Al-Cu-Cd alloys, rel. to deformation before and during ageing 8=17039
 Al-Mg-Zn alloys, and defects rel. to ductility 8=17646
 Al-10 %Zn alloy, n-irrad., pre-precipitation rate at 78°K 8=21980
 Al-Zn-Mg alloys, pre-ageing and quenching effects 8=13062
 Be sheet rolled from ingots, grain boundary 8=17046
 Co alloys, f.c.c., of C and Mo atom segregation on ageing 8=17622
 Co mag. recording films deposition and props., obs. 8=22790
 Co-Cr alloy with W, Ta or Nb; precip. hardening rel. to cpd. structure 8=17621
 Co-8Cr-Ta, on hardening at 700°C 8=17621
 Co-M alloys (M = Cr, Fe, Ni, Cr-Ni), structural defects and precip. 8=17621
 Co-Ni mag. recording films deposition and props., obs. 8=22790
 Co-P mag. recording films deposition and props., obs. 8=22790

Precipitation—contd

- CrC at stainless steel grain boundaries, e probe obs. 8=17677
 Cu-2%Be alloy, and twinning on ageing 8=17625
 Cu-Be-Ag alloys, nucleation of precipitates 8=17040
 Cu-Mg from solid solns. of Mg in Cu 8=4705
 Cu-Ti alloys, direct obs. 8=13065
 Cu-Zn alloys, rel. to decomposition of β' 8=4706
 Cu-Zr, supersaturated, n.m.r. study 8=8265
 Fe carbides, in tempered martensite 8=17080
 α-Fe, of C, n-irrad. effects 8=17059
 in Fe-Cu, of Cu rel. to ferromag. props., obs. 8=22809
 Fe-Mo alloys, Fe-rich, and solid solns. from Mössbauer spectra and Young's modulus 8=4678
 Fe-N supersaturated solutions, of nitrides rel. to n-irrad. 8=17060
 GaAs, Zn-diffused 8=17617
 Li disilicate, cryst., from Li₂O-SiO₂ glasses 8=21953
 Mg-9 wt. %Al alloy, and age hardening mechanism 8=13583
 MgO:Fe solid solutions, superparamagnetic magnesioferrite 8=1675
 MgO-Al₂O₃-Cr₂O₃ system, coherency 8=21848
 Mn in Mg binary alloy, isothermal growth 8=4688
 NaCl, Cd doped, aggregation of divalent impurities 8=13425
 Nb, of nitride by equilibrating in N₂ atmos. 8=8274
 NbC in steel, brittleness 8=22358
 in Nb-Mo steel, heat-treated strengthening effect and mechanism 8=22386
 NbO, from supersaturated solutions electron microscope examination 8=1679
 Nb-Zr alloy, of nitride by equilibrating in N₂ atmos. 8=8274
 Ni-Co-Mo steels, reversion 8=17096
 Pu-Ga (3 at%) alloy, cold working and α-phase precipitation in δ-phase 8=21855
 Ra synchronised, solid-liquid phase 8=9737
 Ra, synchronised, technique, solid-liquid phase 8=9736
 Si containing oxygen, X-ray diffr. obs. at 1000, 1150 and 1300°C 8=13073
 Si, Au-diffused 8=17620
 Ta-Cr solid soln., precip. of TaCr₂, cellular from 1200-1450°C 8=8282
 TiC, B-doped, of TiB₂ rel. to defect structure 8=4967
 Ti-22 at. %Nb alloy, ω phase precip. rel. to superconducting critical transport currents 8=4718
 US crystals 8=21862
 V, of hydride phase rel. to ductility 8=5088

Pressure

- See also Atmospheric pressure and density; High-pressure phenomena and effects; Radiation pressure; Vapour pressure.
 drop across packed beds, for two-phase cocurrent flow, correls. 8=12651
 earth, interior distrib. 8=18826
 effect on spark discharge cavity configuration in oil 8=21249
 gases, modification due to formation of bound double molecules 8=12357
 Mössbauer effect depend., energy shift 8=1641
 random continuous field, representation by discrete set of point excitations 8=19509
 surface distribns. on sharp cones in rarified hypersonic flow 8=16681
 on surface, generated by pistons on spherical and cylindrical baffles 8=6134
 viscosity of water, effect 8=8021
 Al circular foils, hydrostatic deform. 8=5044
 He-n-butane system, P-V-T-x phase relns., showing gas-gas equilib. for low He conc. 8=12979
 He-Ne mixture, partial rel. to laser pulse delay 8=3314

Pressure measurement

- See also Manometers; Vacuum gauges; Vapour pressure measurement.
 acoustic radiator, circular plates, nearfield distribution calc. 8=6152
 barometer with digital output 8=9832-3
 Bayard-Alpert gauges, ion current anomalies 8=16734
 corrosive gases, sensitive differential gauge 8=4448
 dead weight piston gauge for press. to 26 kbar 8=5999
 gas, from atmos. to 10⁻⁴ mm Hg, sonic gauge design 8=7889
 gases, temp. coeff. meas. apparatus 8=7922
 hydrostatic to 60 kbar, technique 8=7971
 impulsive, strain-gauge transducer performance 8=14925
 internal in solid-filled pistons, by u.s. meas. of expansion 8=10580
 liquid metal-oxygen solns., by solid electrolytic cell 8=16951
 loss in high pressure cylinders, unsymmetrical friction 8=14909
 micro-manometer, modified Chattock 8=7891
 Penning gauge used as low pressure ion source 8=15338
 quartz spoon gauges, at elevated temps. 8=5990
 shock, in kbar range 8=6149
 soil pressure cell, effect of diaphragm flexibility on calibration 8=9803
 transducers systems, flush mounted, as spatial and spectral filters for turbulent boundary 8=10731
 ultrasonic gauge to 20 kbar for solid rods 8=19341

Pressure measurement—contd

- by n-Ge, with adsorbed gas, due to conductivity hydrostatic pressure dependence 8=18045
- He II flow, subcritical 8=19695

Prisms, optical

- actual Littrow and Wadsworth systems, deviation, scanning equation and spectral widths of slits 8=15531
- Cervit R, modification of Danjon astrolabe 8=10105
- cube-corner, optimum incident-ray direction 8=3346
- erecting systems, use in compact binoculars 8=15509
- gimbaled systems, matrix anal. 8=3348
- monocrystalline, angles meas. 8=11124
- as reflecting prism, conditions 8=3344

Probability

- See also Random processes; Statistical analysis.
- applications to heat conduction problems 8=10774
- cryopumps, molecules, return 8=7954
- energy distribution among particles, "negative temperature" concept 8=10642
- multi-photon processes 8=104
- path length in systems with variable number of particles 8=15011
- radiative atomic transitions, retarded pot. calc. 8=16212
- statistical, Boltzmann-Gibbs, redefinition 9=14992

Procopiu effect. See Films/solid; Magnetoelectric effects; Magnetomechanical effects.**Programming.** See Calculating apparatus/digital computer programmes.**Projectiles.** See Ballistics.**Projectors, optical**

- No entries

Promethium

- No entries

Promethium compounds

- No entries

Prominences, solar. See Sun/prominences.**Propagation.** See Acoustic wave propagation; Electromagnetic wave propagation.**Propagators.** See Field theory, quantum; Quantum electro-dynamics.**Proportional counters.** See Counters/proportional.**Prospecting.** See Geophysical prospecting.**Protactinium**

- coiled-coil, modified Fourier transforms 8=7643
- Fe impurity atom, range of spin perturbation 8=1655
- Pa²³¹ dating of Quaternary samples 8=9797
- Pa(V) ions, sublation studies, by radioactive tracers 8=23075

Protactinium compounds

- PaCl₅, structure and stoichiometry 8=13283
- PaOCl₂, crystal structure 8=22036
- R₂O₃-M₂O₃, (R = rare earth, M = Nb, Ta or Pa), crystal structure 8=1802

Proteins

- amino acid content in atmospheric precipitation 8=2589
- angular correl. functions, effect of internal rot. 8=16384
- crystallography, rapid meas. of large nos. of reflections by precession photography 8=17455
- films, myosin monolayers structure 8=2870
- haemoglobin, quadrupole splittings and isomer shifts 8=16344
- haemoglobin fluoride, low temp. Mossbauer spectrum, neighbour nucleus effects 8=21810
- lysozyme enzymatic props., crystallographic study 8=23128
- met-myoglobin, e. s. r. 8=9433
- molecular wt. determ. by u. v. spectrophotometry of sample on sephadex column 8=18642
- myoglobin azide, e. s. r. 8=9433
- polypeptide chains, dipole moments rel. to config. 8=16389
- polypeptide helix-coil transition under external force 8=21204
- polypeptides, helix-coil transition, proton mag. resonance obs. 8=21211

Proton magnetic resonance. See Nuclear magnetic resonance and relaxation.**Proton spectra**

- μ^- stars in emulsion, rel. to CVC theory 8=11872
- nuclear pair emission after π interaction 8=11913
- p reactions with nuclei 30-340 MeV, anomalies 8=1051
- rocket meas., and precip. and ang. distrib., also electrons 8=5798
- Cr⁵⁴(d, p)Cr⁵⁵, intensity $E_d = 6.8$ MeV to $E_a = 12.0$ MeV 8=11928
- He⁴(γ , p)H³, 50 MeV, cross-section 8=889

Protonium. See Protons and antiprotons.**Protonosphere.** See Atmosphere/upper.**Protons and antiprotons**

- See also Cosmic rays/protons; Nuclear reactions due to/protons; Nucleons and antinucleons.
- abundance upper limit in low energy galactic cosmic radiation 8=14730
- annihilations at rest 8=11601
- annihilation on N into two mesons and higher symmetries 8=15839
- auroral precipitation 8=18946
- beam, app. for production from Van de Graff accelerator 8=840

Protons and antiprotons—contd

- beam, emittance in duoplasmatron source linked to single gap accelerator 8=20229
- charge time var. from Re¹⁸⁷, Os¹⁸⁷ terrestrial, occurrence 8=15826
- coupling parameter, axial vector, p-n 8=20253
- $e \sim p$ charge difference, cosmological consequence 8=23480
- electric dipole moment, sensitive test for existence 8=11588
- excited state 8=11585
- form factor found to be equal to that of π 8=6834
- linear accelerators for, improvements 8=15656
- low-energy, precipitation at high-latitudes, satellite meas. 8=9954
- magnetosphere and tail, Explorer 33 flux obs. 8=23324
- mass difference from n using Dashen-Frautschi method 8=20267
- mass difference n-p, rainbow graph model calc. 8=11587
- mass difference p-n, rel. to bootstrap model of hadron dynamics 8=11486
- mass difference p-n, field theoretic approach 8=11586
- minimum size in nonrelativistic theory, from hyperfine structure 8=826
- as nuclear probe, high-energy 8=11604
- n-p pairing interaction, charge-independent 8=3771
- plasma, interaction of proton and electron plasma waves 8=4364
- p-e charge inequality determ. 8=11455
- proton-neutron mass difference calc. 8=15825
- p-n mass difference in terms of p-e and n-e cross-sections 8=655
- redox reactions of living cell, separation of positive and negative charges 8=23762
- reflection and emission from crystals, wave/particle duality 8=2018
- secondary particles in (π^- , N) reactions, momentum spectra 8=1085
- 70 GeV beam, ν flux spectra prod. 8=20369
- 730 and 45 MeV beams in thin absorbers, energy loss distrib. 8=13471
- storage rings, damping oscils. 8=640
- structure effect on pot. for p-e interactions 8=11590
- synchrocyclotron beam, increase by electrostatic focussing 8=3499

absorption

- photon-absorpt., sum rule applied to N, d, H³, He³ 8=3577
- statistical atomic model, evaluation of swift p stopping 8=20534
- in water, slowing down, n-irrad. 8=644

angular distribution

- aurora, rocket meas., and electrons, also precip. and spectra 8=5798
- Λ -p 400-1300 MeV/c scatt. 8=859
- p-d scatt., rel. to T = $\frac{1}{2}$ state of He³ 8=3739
- p-p scatt. semi-empirical formulae 8=11595
- from B¹⁰(α , p_n)C¹³, rel. to reaction mechanism 8=7236
- from C¹²(α , p_n)N¹⁵, rel. to reaction mechanism 8=7236
- C¹²(He³, p_n)N¹⁴, p_n corrs., N¹⁴ energy levels 8=953
- C¹³(α , p_n), 10.6 MeV and levels of Ar³⁸ 8=3804
- F¹⁹(d, p_n)F²⁰, 1.6 MeV rel. to reaction mechanism 8=16116
- Fe⁵⁴, asymm. scatt. from 2⁺, 3⁻ levels 8=3920
- He³(d, p)He⁴ 8=7002
- Li⁶(Li⁶, p)B¹¹, rel. to n ang. distrib. in Li⁶(Li⁶, n)C¹¹, 4.1 MeV 8=11950
- Na²² energy levels from Ne²⁰(He³, p_n)Na²², 6.56 MeV 8=3801
- Ni^{58,60}, asymm. scatt. from 2⁺, 3⁻ levels 8=3920
- Ni⁵⁸(p, p'_n), levels and transition anomalies 8=3928
- Si²⁸, asymm. scatt. from 2⁺, 3⁻ levels 8=3920
- Si²⁸ p scatt., symm. rel. to isobaric analog states of Si²⁹ 8=15982
- Te¹³⁰(d, p)Te¹³¹, 7.5 MeV, Te¹³¹ energy levels 8=984

detection, measurement

- antiproton, from π following annihilation using scintillation counter 8=6970
- chamber for simultaneous ang. correlations 8=20793
- channel multiplier for space research 8=5799
- coincidence circuit for simultaneous ang. correlations 8=20794
- liquid scintil. for α -p discrimination 8=1075
- p-d discriminator, surface barrier detector 8=6937
- p-e, discrimination by Owen-Batchelor method, theory of high-energy limit 8=6672
- p- μ discrimination by Owen-Batchelor method, theory of high-energy limit 8=6672
- r. f. separated beam at the AGS 8=3491
- recoil dose from DD and DT neutrons, LET distrib. 8=15837
- satellite instrumentation for auroral studies 8=5837
- scintillator output, energy dependence obs. 8=20536
- spark chamber sonic, obs. 8=3484
- spectrometer, e-insensitive for upper atmosphere 8=6938
- secondary-dose equivalent 8=841
- surface barrier detector for spectroscopy 8=6939
- thin metal foil apparatus, 25 μ m slit prod. 8=14904
- Ge total absorption, for 100 MeV proton scattering 8=7180
- Ge 2 detector telescope for separation of p and heavier particles 8=6654
- Si, Ge detectors, nuclear reaction effect 8=20535

Protons and antiprotons—contd

angular distribution—contd
ZnO crystal, change in surface conductivity 8=7475
effects
alkali halide crystals, conductivity, elec., kinetics of
radiational change 8=22501
crystals, reversibility and Rutherford scatt. 8=2016
hydrocarbons, free-radical doped, polarization 8=4672
hydrogen collision, electron capture probability 8=1199
ionization loss at relativistic vels. in nuclear
emulsions 8=15647
reflection and emission from crystals, wave/particle
duality 8=2018
solar cell performance of 400 keV irradi., integral covers
testing 8=10854
sporadic E, prod. near geomagnetic pole 8=19013
Al crystals, X-ray production, orientation effects 8=4995
Au, energy loss by low-energy protons 8=13478
CaF₂, irradiated, change in microhardness,
kinetics 8=22320
Cu crystal, u.v. emission 8=2025
Cu crystals, X-ray production, orientation effects 8=4995
Cu, irradiated, platelets of interstitial atoms rel. to
dislocation loops 8=22202
Ge, range-energy determ. 8=13468
K surface (100) electron emission under bombard-
ment 8=18249
Si, irradi. damage isothermal annealing, 22-158 MeV,
100-300°C 8=22605
Si, paramag. centres produced along range 8=8704
Si, range-energy determ. 8=13468
Si wafers, orientation, by proton channelling 8=8376
Si:B, radiation sensitivity, obs. 8=17414
W crystals, X-ray production, orientation effects 8=4995
W, scatt. intensity and channeling 8=4997
Y(C₂H₅SO₄)₃:Nd, dynamic polarization 8=2035

interactions

See also Nuclear reactions due to/protons.
e + p → e' + π⁺ + n obs. 8=11505
γ dose rate in p bombarded spherical shell shield 8=3568
γ + p → η + p amplitude, unitarity and S-matrix
analysis 8=3569
γp → Λ⁺K⁺ Regge-pole calc. of cross-sections 8=3621
γp → N*, missing mass determ. of excitation function of
N₂⁺ (1688) 8=11638
γ + p → N* + π⁺, up to 6 BeV 8=6986
γp → nπ⁺ at large angle, differential cross section,
260, 290, 320 MeV 8=752
γp → nπ⁺, ang. depend. of cross-section 8=6841
γ + p → π + N*(1238), test of e.m. C noninvariance 8=694
γp → π⁰p Regge-pole calc. of cross-sections 8=3621
γ + p → π⁺ + n, GeV region, absorpt. correction, πN
parameters 8=15764
γp → π⁺n Regge-pole calc. of cross-sections 8=3621
γ + p → p + η, N pole and vector meson resonance
below c.m. energy 1700 MeV 8=20490
γ + p → p + η⁺, recoil p polarization 8=838
γ + p → p + π⁺, 163-234 MeV, ang. dist. of π⁰ 8=750
γp → Σ⁺K⁺ Regge-pole calc. of cross-sections 8=3621
K⁺p, 4.1, 5.5 GeV/c, K* (890), (1400) prod. 8=20509
K⁺p, 10 GeV/c, Ξ⁺, Ω⁺, antibaryon prod. 8=15803
K⁺p, high energy and ρ' Regge trajectory 8=3665
K⁺p, total cross-sections, new structures 8=796
K⁺p → K*⁺π⁺n, 6 GeV/c ang. correl. in final states 8=798
K⁺p → K⁰Ξ⁺, mass difference effect in Wali-Warnock
model, violation of SU(3) 8=3692
K⁺ + p → Λ + f* at 5.5 GeV/c, f* study 8=810
K⁺ + p → Λ + π⁺ + π⁺, 1.5 GeV/c beam, peripheral
production 8=870
K⁺ + p → N + π + K*, peripheral model, diffraction
dissociation 8=15815
K⁺ + p → p → K⁺ + π⁺ + π⁺ + p at 5.5 BeV/c 8=15816
K⁺p → π⁺π⁺Σ⁰, 6 GeV/c, ang. correls. rel. to spin parity
of exchanged particles 8=798
K⁺p → π⁺Σ⁺ rel. to analytic structure of Regge-cut
amplitude 8=20319
K⁺p → π⁺Σ⁺, Regge-pole model based on K*, K**
exchange 8=15777
K⁺p → Σ⁺π⁺, mass difference effect in Wali-Warnock
model, violation of SU(3) 8=3692
K⁺p → Σ⁺π⁺, analysis in K⁺ p c.m. energy range 1735
to 1845 MeV 8=20574
K⁺p → Y^{*}(1385) + π (780-1220) MeV/c 8=800
K⁺p → Y^{*}₁ + π⁺, spin and parity of Y^{*}₁ 8=6987
Kp, one π exchange 8=6847
K⁺p, 5 GeV/c, baryon resonance production 8=869
K⁺p, 9 GeV/c, Ξ⁺ production 8=865
K⁺p, charge exchange, double Regge-pole analysis 8=799
K⁺p → K⁺nN, 735, 785 MeV/c, production possibility 8=3686
K⁺ + p → K⁰ + Δ⁺⁺ (1238) Regge pole fit 8=3662
Λ-p, low energy 8=11631
Λ-proton stimulation, hyperfragments A = 50,
calc. 8=15861
μ⁻ + p → n + ν_μ, muon capture rate 8=721
N*(1236) production, by polarized γ-quanta 8=868
n-p capture theory 8=827
p-d, low-energy, resonance charge exchange meas. 8=828
pd, at about 2 GeV/c, final state pπ⁺π⁻ 8=15827

Protons and antiprotons—contd

interactions—contd
p + d → B + d and B-N scatt. factor 8=3736
p-e, quasi pot., using two-time Green functions, p structure
effect 8=11590
p + γ → p + π, Mandelstam branch cuts rel. to scatt. and
prod. amplitudes 8=11594
p + He⁴ → B + He⁴, B-N scatt. factor 8=3736
p + K → p + K*, Mandelstam branch cuts rel. to scatt. and
prod. amplitudes 8=11594
p + μ⁻ → n + ν_μ, prop. counter to meas. μ⁻ capture
rate 8=3457
p̄ + n → 2π⁻ + π⁺ in D bubble chamber, (I⁰_π⁺=1-0) 3-pion
state analysis 8=20436
p̄n → N*⁻ (1238)p, at 2.8 GeV/c, isobar and anti-isobar
production 8=844
p-p collisions, high energy π, k, p̄ prod. cross-section
depend on longitudinal and transverse momentum
components 8=20478
p-π high energy collisions, charge ratios of π,
K and Σ 8=11524
p + π → p + A₂, Mandelstam branch cuts rel. to scatt. and
prod. amplitudes 8=11594
p̄ annihilation in H₂ and D₂, rates rel. to initial
state 8=20537
p̄p → YȲ, absorpt. model, U(66) symm. 8=20524
π charged pair photoproduction, up to 1500 MeV γ
energies 8=6844
π exchange theory 8=6847
π photoproduction, ang. distrib. parameters 8=11511
π photoproduction 220-380 MeV near P₃₃πN
resonance 8=11506
π photoproduction on p, 553-850 MeV analysis in second
reson. region 8=6843
π-p, four-momentum transfer distrib., high energy and
high multiplicity 8=6862
πp radiative capture as symm. test for e.m.
current 8=670
π-p transfer distrib. obs., Regge-pole exchange model
suggested 8=20441
π + p → p + π⁺ + π⁺, 3.2-4.9 GeV 8=16057
πp → ρN*, f₀N*, ang. correls. in decay 8=11636
π p, 1.5-4.2 BeV/c, strange particle prod. 8=6860
π⁻p, 5.5 GeV/c, multiple π prod. 8=3633
π⁻p, 3 GeV/c → pπ⁺π⁻π⁻, prod. of N*⁺⁺(1238),
ρ⁰ and A₂⁻ 8=20446
π⁻p, 3.2, 4.2 GeV/c obs. of multipion prod., pπ⁺π⁻π⁻,
pπ⁺π⁰π⁻π⁻, nπ⁺π⁺π⁻π⁻ 8=20448
π-p, 4.16 GeV/c scatt, π prod. and charge
exchange 8=11522
π⁻p at 650 MeV, cross-section, for single and multi pion
prod. obs. 8=6854
π⁻p, 720 MeV, cross-section for (π⁻pπ⁰), (π⁻π⁺n),
(2π prod.) (η⁺n) obs. 8=15772
π⁻p → ηn, partial wave analysis in terms of Lorentz
group 8=6856
π⁻p → ηn, polarization meas., 3.2 and 5 GeV/c 8=15776
π⁻ + p → η + n, Regge pole model of polarization 8=11519
π⁻ + p → η + n, 561-1300 MeV partial wave analysis,
S, P, D, F waves 8=11520
π⁻ + p → η + n, 670-805 MeV/c obs. 8=20489
π⁻ + p → η + n, T₁ = 593-704 MeV, calc. of ang. distrib.
of η 8=6853
π⁻ + p → η + N, N* resonant states and Nπ, Nη decay
modes 8=11637
π⁻p → η⁺n and charge exchange polarization, ρ' Regge
trajectory 8=3665
π⁻p, K₁K₂ system resonance, 5, 7 and 12 GeV/c 8=794
π⁻p → K⁺Σ⁺, Regge cut 8=3631
π⁻p → K⁺Σ⁺ rel. to analytic structure of Regge-cut
amplitude 8=20319
π⁻p → ΛK⁺, Σ⁰K⁺, Σ⁺K⁺, 1.5-4.2 BeV/c 8=6861
π⁻p → Λk⁺π⁺ at 6 GeV/c, Λk⁺ enhancement
at 1.7 GeV 8=3630
π⁻ + p → n + η N pole and resonances below c.m.
energy 1700 MeV 8=20490
π⁻ + p → n + η, Σ⁻ + K⁺, Λ + K⁰, Σ⁰ + K⁰, phenomenological
model 8=15758
π⁻ + p → n + X_{γγ}, X resonance identification 8=6858
π⁻p → ωn, φn, 2.1 BeV/c, cross-section calc. 8=20442
π⁻p → ppn, 8 GeV/c, obs. in bubble chamber 8=6857
π⁻ + p → p + R⁺, structure of R⁺ 8=3676
π⁻ + p → p + X⁺ at 1.8 GeV/c, δ⁻ (960 MeV) resonance
search 8=756
π⁻p → π⁻pπ⁰, inconsistency of Ferrari-Sellers form factor
for π-π scatt. 8=3649
π⁻p → π⁻π⁰p rel. to π⁻π⁰ scatt. 8=768
π⁻p → π⁻π⁰p, 2.77 GeV/c for π⁻π⁰ scatt. 8=770
π⁻ + p → π⁻ + π⁺ + n, 1.38-3.00 GeV/c ρ⁰ formation and
decay ang. dist. 8=3685
π⁻p → π⁻π⁺n, 8 GeV/c, 2421 events 8=6851
π⁻p → π⁻π⁺n, rel. to ππ interaction 8=6850
π⁻p → π⁺n, ηn, Regge-pole model with L-S
coupling 8=20444
π⁻p → π⁰n, Regge pole branch points obs. method 8=3629
π⁻p → π⁺π⁻n, 3.1 36⁻¹ GeV/c, I = 0 enhancement
obs. 8=15773
π⁻p → π⁺π⁻n, 870 MeV, π⁺ momentum spectrum obs.
cross-section of π⁺n deduced 8=20445

Protons and antiprotons—contd**interactions—contd**

- $\pi^+p \rightarrow \Sigma^- K^+$, 1170 MeV/c, cross-section obs., C independence confirmed 8=20449
- $\pi^- + p \rightarrow \nu^0 + n$, 4.0 GeV/c vector meson decay to e pair 8=808
- $\pi^+p, I = \frac{1}{2} N^*(1400)$ prod. at 6 GeV/c 8=15775
- $\pi^+p \rightarrow K^0 \Sigma^0(\Lambda^0)$, Regge-pole model based on K^* , K^{**} exchange 8=15777
- π^+p , 8 GeV/c, resonances obs. 8=20428
- π^+p , at 8 GeV/c, 6-prong interactions, cross-sections 8=3632
- π^+p , 900 MeV π prod., through N_{33}^* isobar 8=11523
- $\pi^+ + p \rightarrow \eta + \Delta^+(1238)$, cross-section and Δ^+ spin density 8=6855
- $\pi^+p \rightarrow K^+ \Sigma^+$, 3.23 GeV/c, ang. dist. Σ polarization 8=6852
- $\pi^+ + p \rightarrow N_{33}^* + \pi^0$, 0.5-1.46 GeV, ang. distrib. of π^0 8=15780
- $\pi^+p \rightarrow N^{*++}\rho^0$, shrinkage effects and one-pion exchange 8=20429
- $\pi^+p \rightarrow \rho^0 N^{*++} \rightarrow \pi^+\pi^-p$, peripheral models 8=11515
- $\pi^+p \rightarrow \pi^+\pi^0p, \pi^+\pi^-n$, below 1 BeV 8=6859
- $\pi^+ + p \rightarrow \pi^+ + \pi^0 + p$, 968 MeV/c search for scalar meson decaying to $\pi^+\pi^-$ 8=11553
- $\pi^+ + p \rightarrow \pi^+ + p + \pi^0$, < 1070 MeV, ang. distrib. 8=15779
- $\pi^+ + p \rightarrow \Sigma^+ + K^+$, in polyethylene, 1 GeV/c, Σ polarization 8=864
- $\pi^+ + p \rightarrow \Sigma^+ + K^+$, phenomenological model 8=15758
- $\pi^+ + p \rightarrow \Sigma^+ + K^+$, quark model for backward process 8=11480
- S8, channelling, anomalous energy losses, 1.5 MeV 8=17708
- H²(p, 2p)n, 9 and 10.5 MeV 8=875
- He⁴(p, B)He⁴, magnitude and phase of baryon scatt. amp. 8=890
- T(p, n), He³, obs. 8=882
- interactions, proton-proton**
- annihilation, statistical unitary-symmetry theory 8=3527
- bremstrahlung production cross-section 8=830
- collision, 24 GeV, transverse momentum of pions and protons 8=11524
- K^+ prod. 2.5-3.0 GeV, disagreement with phase-space, OPE model 8=20479
- mesons prod. synchrotron-radiation model 8=11492
- meson production, 20 GeV, in nuclear emulsion 8=831
- $p\bar{p}$ annihilation, pionic decay modes calc. 8=11605
- $p + \bar{p} \rightarrow B^* + \bar{B}^*$, absorpt. model 8=20526
- $p + p \rightarrow d + \delta^+$, search for resonance δ^+ , 960 MeV 8=6982
- $p + p \rightarrow d + \pi^+$, 1-3 BeV, cross-sections obs. 8=20523
- $p + p \rightarrow$ hyperon + K + N, 6 BeV/c obs., N^+ prod. and decay to hyperon + K 8=20480
- $p\bar{p} \rightarrow KK\pi, K^*(891)$ prod., $K\bar{K} J^P = 2^-$ resonance at 1280 MeV 8=6940
- $p\bar{p} \rightarrow p\pi\pi^+$, 10 GeV/c and OPE model 8=11591
- $p\bar{p} \rightarrow N^{*++}(1238)n$, at 2.8 GeV/c, isobar and anti-isobar production 8=844
- $p\bar{p} \rightarrow N^*N^*$, pion-exchange, Regge-pole model 8=11516
- $p + p \rightarrow p + N^*$, 6-30 BeV obs. 8=15828
- $p\bar{p} \rightarrow pN^* P_{11}$ resonance, mass shift in compound structure model 8=11592
- $p + p \rightarrow p + p$, Mandelstam branch cuts, rel. to scatt. and prod. amplitudes 8=11594
- $p + p \rightarrow \pi^+ + d$, 5 GeV/c cross-section meas. 8=20525
- $p\bar{p} \rightarrow YKN$, OBE model, with approx. 8=20522
- magnetic moment**
- quark shell model of baryons, finite mass correction 8=15819
- polarization**
- beam prod. method in $2S_{1/2}$ state 8=11602
- elastic scattering, interaction of differential cross section and polarization 8=16069
- d photodisintegration, 170-450 MeV obs. 8=20533
- (d, p) stripping reaction, theoretical analysis 8=16107
- $\gamma + p \rightarrow \eta + p$ amplitude, unitarity and S-matrix analysis 8=3569
- $\gamma + p \rightarrow p + \eta^0$, recoil p polarization 8=838
- p- α scatt., 22-25 MeV obs. 8=20532
- p- α , 6-11 MeV, p polarization obs. 7=837
- p-d elastic scatt., 11.6 MeV 8=11644
- p-d scatt. obs., 21.7 MeV 8=878
- p-d scatt., 1.5-11.5 MeV, phase-shift analysis 8=877
- (p, p) data at 19.7 MeV, phase shift analysis 8=3705
- in p-p scatt., asymmetry rel. to spin-orbit interaction, 9.6-19.7 MeV 8=836
- p-p scatt., 144, 1, 140.7 MeV, obs. 8=15832
- pp scatt., 500-1200 MeV 8=11598
- in polycaprolactam by "solid effect", 3150-19 200 Oe and 1.65-4.2°K 8=13015
- in polymers by "solid effect", 3150-19 200 Oe and 1.65-4.2°K 8=13015
- Q-meter circuit for meas. 8=11600
- recoil-p in π^0 photoprod., energy depend. 8=835
- synchrocyclotron beam depolarization 8=3710
- tandem beam, depolarization effects during charge exchange 8=1057
- target for low-energy N-N scatt. 8=6924
- in Al elastic scatt. at 6.6 and 7.4 MeV 8=7183
- Cr⁵², scatt. induced transitions, ang. asymm. 8=11880
- in Cu elastic scatt. at 6.6 and 7.4 MeV 8=7183

Protons and antiprotons—contd**polarization—contd**

- Cu⁶³, scatt. induced transitions, ang. asymm. 8=11880
- D(d, p)T, 8 energies, 2.1-14.1 MeV, p polarization obs. 8=11642
- Fe^{54,56}, scatt. induced transitions, ang. asymm. 8=11880
- He³(d, p)He⁴ 8=7002
- in Mg elastic scatt. at 6.6 and 7.4 MeV 8=7183
- Nd¹⁴², 12 MeV p scatt. 8=7195
- Ni^{58,60,62,64}, scatt. induced transitions, ang. asymm. 8=11880
- in O elastic scatt., meas. 8=20782
- O¹⁶, scatt., 24.5-39.7 MeV resonance effects on ang. distrib. 8=20785
- Ti^{48,50}, scatt. induced transitions, ang. asymm. 8=11880
- in Zn elastic scatt. at 6.6 and 7.4 MeV 8=7183
- production**
- beam, high intensity, production by charge exchange injection 8=839
- cosmic rays as high-energy source 8=7004
- fluxes, quasi-isotopic, 1-10 keV generation technique 8=3704
- $\gamma + p \rightarrow p + \pi^+$, angular distribution E_{0+}, M_{1-}, M_{1-} calc. 8=6845
- ion source for tandem accelerator 8=6694
- low energy beam, apparatus for control and exit in air 8=6936
- photonicuclear reactions, 16-18 GeV e acceleration, with metal targets 8=20768
- photoproduction of antiprotons, photon energy 4.0 to 5.7 BeV 8=20570
- π -N interactions, recoil p transverse momentum and four-momentum transfer, cosmic ray obs. 8=11589
- source for Van de Graaff accelerator 8=6692
- D(d, p)T, 8 energies, 2.1-14.1 MeV, p polarization obs. 8=11642
- H₂-electron collisions, cross section meas. 8=7519
- He³ + $\gamma \rightarrow d + p$, with Cabibbo-Radicati sum rule 8=6999
- He⁴(γ , p)H³, 50 MeV, cross-section 8=889
- scattering**
- antiprotons, by nuclei of ionographic emulsions 8=1050
- atom, ionization, characteristic K X-ray prod., approx. 8=20930
- Coulomb and nuclear, contrib. to error formulae in bubble chamber analysis 8=6681
- crystals, reversibility and Rutherford scatt. 8=2016
- cross sections, $\gamma p \rightarrow N^{*++}\pi^-$ linearly polarized γ -quanta 8=868
- elastic, interaction of differential cross section and polarization 8=16069
- elastic, isobaric analog resonance width calc. using Lane eqns. 8=11698
- elastic, optical model, rel part of potential 8=11876
- elastic, spin-orbit effects in optical-model anal. 8=879
- e-p cross-section data up to 1.1 GeV 8=11459
- e-p in equality derived from v-p backward scatt. sum rule 8=6923
- e-p high-momentum-transfer obs. 8=15731
- e-p N₃₃^{*}(1688), missing mass determ. of excitation function 8=11638
- e-p resonances, isobaric electrical excitation 8=713
- e⁺-p, differential cross section comparison with e⁻p scattering 8=3600
- e⁺-p, 800, 1200 MeV, cross-section obs., energy meas., ratio to e-p cross-section calc. 8=20383
- inelastic, and deformed spin-dependent optical potential 8=20779
- isobaric analogue resonances, optical potential theory 8=7046
- Kp superconvergent sum rule and Regge parameters 8=3667
- K⁺p total and elastic cross sections at 2.66 GeV/c 8=801
- K⁺p, ~ 1 GeV/c, phenomenological model of diffraction 8=6894
- K⁺p \rightarrow K⁺n, K⁺p, resonant partial wave amplitudes 8=6897
- K⁺ + p \rightarrow K⁺ + n, p + R Regge-pole model determ. of parameters 8=6893
- K⁺p, and parity of Λ and Σ 8=3730
- K⁺p, backward elastic, as evidence for baryon exchange 8=803
- K⁺p, backward elastic at 1-3.5 GeV/c 8=6892
- K⁺p, I = 1 P-wave phase shifts from N^{*}(1238) prod. 8=15805
- K⁺p, mass difference effect in Wali-Warnock model, violation of SU(3) 8=3692
- K⁺p phase-shift analysis below 1500 MeV/c 8=20484
- K⁺p, test of PDDAC for A₁⁺ 8=3668
- Λ -p from Λ -N pot. with hard core and Yukawa shape 8=16009
- Λ -p, 400-1300 MeV/c, obs. 8=859
- large angle, elastic, contrib. of statistical scatt. 8=15836
- μ -p, e-p comparison as test for Q.E. 8=11285
- μ -p, 1.5-6.0 BeV/c, obs., e. m. e- μ difference calc. 8=20395
- N isovector anomalous mag. moment, contrib. to sum rule 8=3698
- np \rightarrow pn, one π exchange 8=6847
- n-p, 3-10 GeV, cross-section obs. 8=20539

Protons and antiprotons—contd

scattering—contd

- nuclear optical potential change 8=3917
 nuclei, inelastic light, computer program for excitation function 8=16068
 155 MeV, inelastic, core polarization effects 8=15951
 optical model for polarized, new parameters 8=16067
 π prod. and nuclear surface props. 8=20778
 $\pi p \rightarrow A_1(A_2)p$, 2π exchange model 8=3650
 π -p amplitude calc. from dispersion relations, of unknown parameters 8=20300
 π -p, backward cone, conditions for existence of equal amplitude points 8=20432
 πp , overlap function analysis 8=6874
 πp , Regge-pole model at small momentum transfer 8=20461
 $\pi p, \rho'$ trajectory in charge exchange, Regge parameter evaluation and cut 8=11538
 π -p, similarities to multi- π prod. 8=20530
 π p amplitude, real part, in Coulomb interference region at 3.48 and 6.13 GeV/c 8=15790
 π -p at 180°, cross-section meas., N resonance evidence 8=11540
 π -p at 650 MeV, elastic and charge exchange cross-sections 8=6854
 π^- p, 720 MeV cross-section obs. 8=15772
 π^- p, 875-1579 MeV/c, p polarized obs. of resonances 8=20443
 π^- p, backward, modified Regge representation 8=3651
 π p charge exchange, real-to-imaginary ratio of amplitudes not a proof of Regge theory 8=20459
 π^- p near 180° in 4-7 GeV/c π^- beam 8=6873
 π^- p $\rightarrow \eta n$ asymptotic cross sections from separability and unitarity 8=772
 $\pi^- + p \rightarrow \eta + n$, J=1/2- scatt. length and phase shift calc. 8=20433
 $\pi^- + p \rightarrow K^0 + \Lambda^0/\Sigma^0$ at 4 GeV/c, forward and backward peak 8=3648
 π^- p $\rightarrow \pi^0 n$ asymptotic cross sections from separability and unitarity 8=772
 $\pi^+ p$ backward elastic, ang. distrib., 2.85 and 3.3 GeV/c 8=771
 $\pi^+ p$, total cross section from 8-29 BeV/c obs. 8=774
 $\pi^+ p$, mass difference effect in Wali-Warnock model, violation of SU(3) 8=3692
 polarization parameter in pn, 300-700 MeV 8=6927
 \bar{p} small-angle elastic scatt., 3 GeV/c, optical model 8=20780
 p- α , 6-11 MeV, p polarization obs. 8=837
 p- α , 22-25 MeV, Li⁵ resonance obs. 8=20532
 p-d, 17.1 MeV, elastic, cross-section obs. 15°-165° 8=20529
 p-n, elastic, real part at 8 GeV 8=6929
 pn \rightarrow np evidence for conspiracy of branch cuts in a.m. phone 8=11584
 pn \rightarrow np, Regge-pole analysis, anomalies 8=6932
 pp, general features 8=20530
 p-p polarization asymmetry rel. to spin-orbit interaction, 9.6-19.7 MeV 8=836
 $\bar{p}p$, Regge-pole model at small momentum transfer 8=20461
 pp, tests for symm. invariance 8=3711
 pp $\rightarrow N^*p$, 2π exchange contrib. 8=3650
 p-X, use of storage rings 8=842
 small-angle inelastic, obs. technique 8=20527
 spectrometer, Ge total absorption, for energy resolution at 100 MeV 8=7180
 spin correl. parameter obs. 8=11596
 v-p sum rule used to derive e-p scatt. in equality 8=6923
 Al, elastic at 6.6 and 7.4 MeV, polarization 8=7183
 Al²⁷(6.21 < E_p < 6.74 MeV) six resonances 8=11878
 Al²⁷, 17.5 MeV, from low-lying and excited levels, weak-coupling model fit 8=20786
 Ar⁴⁰, 3.5, 6.0 MeV, levels of K⁴¹ 8=964
 Au¹⁹⁷(p, p)Au¹⁹⁷, Rutherford scatt. at low energy 8=7191
 B¹¹(p, p)B¹¹, Rutherford scatt. at low energy 8=7191
 Ba¹³⁸ 8.6-12 MeV, optical model parameters 8=1096
 Be⁹, optical model parameters for Li^{6,7} (p, d) at 33.6 MeV 8=3923
 Bi, 5 MeV, yield depend. on orientation of crystal and beam 8=20801
 Bi²⁰⁹ rel. to isospin dependence of optical pot. 8=7039
 C, 1 GeV cross-sect. obs., π cross-sect. 8=1052
 C¹², assymmetric obs. rel. to degree of polarization of beam 8=1057
 C¹², inelastic, 1 GeV, from low-lying levels 8=3918
 C¹²(p, p)C¹², Rutherford scatt. at low energy 8=7191
 Ca⁴⁸(p, p)Ca⁴⁸, Ca⁴⁹ ground-state analogue 8=15969
 Cd¹¹⁴, collective states, excited by inelastic scatt. of 55 MeV p 8=15983
 Cd¹¹⁴, isobaric analog, 7-10 MeV levels compared with inelastic scatt. 8=983
 Ce¹⁴⁰ 8.6-12 MeV, optical model parameters 8=1096
 Ce¹⁴⁰(p, p' γ)Ce¹⁴⁰, identification of 1⁺ neutron particle-hole state in Ce¹⁴⁰ 8=20723
 Co⁶⁰ rel. to isospin dependence of optical pot. 8=7039
 Cr⁵², 16.5 MeV polarized, ang. asymm. optical model fits unsatisfactory 8=11880

Protons and antiprotons—contd

scattering—contd

- Cr⁵², 18.6 MeV polarized, ang. asymm. optical model fits unsatisfactory 8=11880
 Cu, elastic at 6.6 and 7.4 MeV, polarization 8=7183
 Cu⁶³, 18.6 MeV polarized, ang. asymm. optical model fits unsatisfactory 8=11880
 D(p, p)D, polarization and phase shift at 3.00 MeV 8=6993
 F¹⁹, 4.26, 5.96, 6.87 MeV, ACC approx. analysis 8=7182
 F¹⁹, 17.5 MeV, from low-lying and excited levels, strong coupling model fit 8=20786
 Fe⁵⁴, polarized, asymm. from 2⁺, 3⁻ levels 8=3920
 Fe^{54,56}, 18.6 MeV polarized, ang. asymm. optical model fits unsatisfactory 8=11880
 Ge, atomic displacement density by Coulomb scatt. 8=1062
 H atoms, simplified second Born approx. 8=20996
 H 3s and 4s state, cross-sections obs. from impact on He, Ar, Ne, N₂, H₂, O₂ 8=7462
 H²-p, 6.7-7.5, 10.3-11.3 MeV, T = 1/2 state of He³ 8=3739
 He atom, excitation of n¹S, n¹P, n¹D states 8=7384
 He, double ionization by fast 1-3 MeV 8=21280
 He, 1 GeV cross-sect. obs., π cross-sect. 8=1052
 p-He³, low energy, spin-dependent interaction theory 8=832
³He(p, p')He*, search for excited states 8=11653
 K³⁹, 7.12-8.51 MeV rel. to mixing ratios and spins 8=15967
 Li⁶, 1 GeV cross-sect. obs., π cross-sect. 8=1052
 Li^{6,7}, 50 MeV 8=7071
 Li^{6,7}, optical model parameters for Li^{6,7} (p, d) at 33.6 MeV 8=3923
 Li⁶(p, p)He³H³, quasi-elastic, 156 MeV 8=16078
 Mg, elastic at 7.6 and 7.4 MeV, polarization 8=7183
 Mg²⁴, 49.5 MeV, elastic and inelastic 8=3919
 Mg²⁴ rel. to Al²⁵ isospin-forbidden analogue resonances 8=20691
 Mg²⁵, 17.5 MeV from low-lying and excited levels, strong coupling model fit 8=20786
 Mg²⁶, inelastic, 8.3-24 MeV, cross-sections in statistical model 8=16077
 Mg²⁶(p, p)Mg²⁶, Al²⁷ resons. 1-2 MeV 8=957
 Mg²⁶(p, p')Mg²⁶, 6.46 MeV, spectrum obs. 8=20793
 N₂-p, collisions, optical emission rel. to Aurora 8=12212
 Na²³, 17.5 MeV from low-lying and excited levels, strong coupling model fit 8=20786
 Nd¹⁴², polarization meas. 8=7195
 Nd^{142,144,146}, 8.6-12 MeV, optical model parameters 8=1096
 Ni⁵⁸, scatt., 3-6 MeV, levels of Cu⁵⁹ 8=973
 Ni⁵⁸(p, p)Ni⁵⁸, Rutherford scatt. at low energy 8=7191
 Ni^{58,62,64}, 18.6 MeV polarized, ang. asymm. optical model fits unsatisfactory 8=11880
 Ni⁶⁰-p, 17.9 MeV, shell model form factors 8=15981
 Ni^{60,62}, 16.5 MeV polarized, ang. asymm. optical model fits unsatisfactory 8=11880
 Ni⁶¹, compound nucleus, levels of Ni⁶¹ below 4.0 MeV 8=3815
 O¹⁶, inelastic, 1 GeV, from low-lying levels 8=3918
 O¹⁶(2⁺, 8.88 MeV) inelastic p scatt. exciting non-normal parity state 8=20783
 O¹⁶, 23.4-46.1 MeV, elastic cross-section and resonances obs. 8=20784
 O¹⁶, 24.5-39.7 MeV, polarized, resonance effects on ang. distrib. 8=20785
 by O, elastic, meas. of p polarization 8=20782
 O, 1 GeV cross-sect. obs., π cross-sect. 8=1052
 P³¹, 17.5 MeV, from low-lying and excited levels, weak-coupling model fit 8=20786
 Pb, 1 GeV cross-sect. obs. π cross-sect. 8=1052
 Pb²⁰⁸, excitation function, isobaric analogs obs. 8=11881
 Pb²⁰⁸, 14-18 MeV into isobaric analog states in Bi²⁰⁹ 8=11784
 Pb²⁰⁸(p, p'), angular distrib. to 18 states in Pb²⁰⁸, total widths calc. 8=7113
 S³²(1⁺, 4.70 MeV) inelastic p scatt. exciting non-normal parity state 8=20783
 Si²⁸, polarized, asymm. from 2⁺, 3⁻ levels 8=3920
 Si²⁸(p, p')Si²⁸, 21.2 MeV rel. to 5 excited levels 8=15964
 Si²⁸ rel. to P²⁹ isospin-forbidden analogue resonances 8=20691
 Si²⁸(3⁺, 6.27 MeV) inelastic p scatt. exciting non-normal parity state 8=20783
 Si²⁸, 27.6 MeV, optical model analysis 8=11885
 Si³⁰(p, p)Si³⁰, P³¹ 2187 keV reson. parity and width obs. 8=960
 Si, atomic displacement density by Coulomb scatt. 8=1062
 Si crystals, 2 MeV, directional effects 8=2034
 Sm¹⁴⁴ 8.6-12 MeV, optical model parameters 8=1096
 Sm¹⁵², 6.05 MeV Rutherford correction due to excited levels calc. 8=11841
 Sn even isotopes, 2⁺ cross section, 16 MeV 8=1065
 Sr⁸⁶ 5-8.7 MeV rel. to isobaric analog states of Sr⁸⁹ 8=15982
 Ti⁴⁶, 6.5-6.8 MeV, transitions and spin assignments 8=11747
 Ti⁴⁸, 4-6 MeV, γ -p ang. correl, p spin flip obs. 8=11879
 Ti^{48,50}, 18.6 MeV polarized, ang. asymm. optical model fits unsatisfactory 8=11880
 W, intensity rel. to channeling 8=4997

Protons and antiprotons—contd**scattering—contd**

$W^{56,60}$, polarized, asymm. from 2^+ , 3^- levels 8=3920

$Y^{89}(p, p')$ at 14.71 MeV rel. to excited nuclear levels 8=1054

Y^{89} , 18.9 MeV, from first excited state, DW calc. 8=3921

Y^{89} , 61.2 MeV, excitation of 0.908 MeV level 8=1053

Zn, elastic at 6.6 and 7.4 MeV, polarization 8=7183

$Zn^{64,66,68,70}$ 50 MeV, optical analysis 8=7186

Zn^{90} , 19.4 MeV, ang. dist. compound to DWBA calc. 8=3929

scattering, proton-deuteron

cross-section obs., 1-2 BeV 8=11645

cross-section and polarization meas. at 150 MeV 8=6930

$D(p, \gamma)He^3$, cross-section from pud wave function 8=11593

$d(p, n)p$, $E_n = 9$ MeV 8=6989

elastic, large-angle, cross-sections, 0.75-2 GeV 8=3709

d polarization obs., 21.7 MeV 8=878

phase-shift analysis, 1.5-11.5 MeV 8=877

p polarization obs., 11.6 MeV 8=11644

scattering, proton-neutron. See Neutrons and antineutrons/scattering, proton-neutron.**scattering, proton-proton**

amplitude, real part at 3 GeV 8=3708

ang. distrib. at high energy, semi-empirical

formulae 8=11595

bremsstrahlung cross-section calc. 8=833

bremsstrahlung, theory 8=6928

cross-section curve not smooth, implications 8=11599

cross sect., 1 GeV obs. rel. to π cross sect. 8=1052

cross-section obs. at 52.34 MeV 8=15833-4

cross-section and polarization obs., 144.1,

140.7 MeV 8=15832

cylindrical wire spark chamber 8=11329

elastic, dispersion calc. compared with expt. 8=15830

elastic, at large momentum transfers 8=15831

elastic, plot of high energy data using particle

identity 8=3706

elastic, small-angle differential and total cross

sections, 8-26 BeV/c 8=6935

50 MeV, reanalysis of data removing anomaly 8=15835

high-energy, large angle, complex potential

models 8=6933

high-energy large-momentum-transfer collisions 8=15829

high energy, phenomenological analysis 8=3707

large angle as test for minimal interaction

hypothesis 8=11597

N_1^2 (1688), excitation function, missing mass

determ. 8=11638

phase-shift analysis of polarization data at

19.7 MeV 8=3705

π exchange theory 8=6847

\bar{p} - p elastic, small-angle differential, cross section,

12 BeV/c 8=6935

$p + \bar{p} \rightarrow n + \bar{n}$, charge-exchange, calc. using U(6, 6) and

absorpt. model 8=829

$p\bar{p} \rightarrow n\bar{n}$, Regge pole analysis, anomalies 8=6932

polarization parameter, 300-700 MeV 8=6927

polarization and spin correl. parameters obs.

500-1200 MeV 8=11598

pole, 4S_0 p - p , spin-2, Regge recurrence, possible

existence 8=20531

R parameter and phase shift analysis at 605 MeV

meas. 8=6934

Regge-pole model at small momentum transfer 8=20461

Regge theory of high-energy, with large momentum

transfer 8=20329

3 parameters at 9.69 MeV, OPE mechanism 8=834

time reversal invariance, test at 430 MeV 8=20528

U(θ) asymmetry, elastic at 635 MeV 8=6931

Ar^{40} , inelastic, mechanism 8=7184

Ti^{48} , inelastic, mechanism 8=7184

antiprotons

annihilation radius of 3 GeV/c antiprotons 8=11606

K in pp collisions, high energy π , k , \bar{p} prod. cross-section

depend on longitudinal and transverse momentum

components 8=20478

photoproduction, photon energy 4.0 to 5.7 BeV 8=20570

$\pi^+p \rightarrow p\bar{p}n$, 8 GeV/c, obs. in bubble chamber 8=6857

\bar{p} annihilation in H_2 and D_2 , rates rel. to initial s

state 8=20537

$\bar{p} + n \rightarrow 2\pi^- + \pi^+$ in D bubble chamber, ($I^3J^P=1-0$) 3-pion

state analysis 8=20436

$p\bar{p}$ annihilation, pionic decay modes calc. 8=11605

$pp \rightarrow KK\pi$, $K^*(891)$ prod., $KK J^P = 2^-$ resonance at

1280 MeV 8=6940

$p\bar{p} \rightarrow n\bar{n}$ evidence for conspiracy of branch cuts in a.m.

phone 8=11584

$p\bar{p} \rightarrow n\bar{n}$, Regge pole analysis, anomalies 8=6932

pp scatt. tests for symm. invariance 8=3711

pp , 2.7 GeV/c, 2 meson final states 8=843

scattering by nuclei of ionographic emulsions 8=1050

Pulse generators. See Circuits.**Pulse-height analysers. See Counting circuits.****Pumps**

See also Vacuum pumps.

circulation, demountable, glass, 0.8 to 8 l/min 8=7901

gas sampling, non-reactive 8=4452

induction, Hg vel. distrib. 8=16727

Pumps—contd

pumping tube, differential for electrostatic

accelerators 8=15654

Toepler automatic, for gases meas. system 8=14442

Purkinje effect. See Vision.**Pyroelectricity**

comparison of mats, rel. to i.v. radiation detector 8=18199

effect, i.r. detectors, performance 8=5378

glycolic sulphate, metastable polarization, dynamic

study 8=13894

laser calorimeter 8=15128

pyroelectric radiation receivers, large area

characts. 8=15100

triglycine sulphate crystals, coeff. meas. by dynamic

method 8=18198

$Ba(NO_3)_2 \cdot H_2O$, single crystal, meas. of coeff. in range

80-3000°K 8=5051

$BaTiO_3$, use for meas. of low-field switching 8=9209

$LiTaO_3$, coeff. temp. dependence, 200-800°C and spontaneous

polarization 8=18200

$LiTaO_3$, spontaneous polarization, estimate 8=13895

Sb_2S_3 crystals, effect 8=9229

$SbSeI$ crystals, pyrocurrent props. 8=9228

Pyrolysis. See Chemical reactions.**Pyrometers**

double-beam modulated for colour temp. meas. 8=20039

infrared, for nylon thread temp. meas. 8=17187

infrared, optical negative feedback type 8=15099

optical, calibration from $Pt/Pt_{10}Rh_{10}$ thermo-

couple 8=19670

photographic pyrometry 8=10784

spectral ratio, with semiconductor photo-electric

elements 8=245

Quadrupole moments, molecular. See Molecules/moments.**Quadrupole moments, nuclear. See Nucleus/electric moment.****Quanticule theory (of chemical binding). See Bonds.****Quantization. See Field theory, quantum/quantization; Quantum theory/quantization.****Quantum chemistry**

electron-transfer reactions, transition-state

parameter 8=9675

energy calc. by method of local moments 8=12025

four-centre molec. integrals 8=4136

Hartree-Fock eqns. solns., stability conditions 8=16174

perturbation theory, 2nd-order energy sum, upper and

lower bounds 8=6592

Quantum counters. See Photons; Radiation detectors.**Quantum electrodynamics**

See also Electrodynamics; Electromagnetism.

Aharonov-Bohm effect, gravitational analogue 8=6060

Aharonov-Bohm and Mercereau effects, classical

analogue 8=585

antisymmetrical field quantization and functional

integration 8=3436

asymptotic condition and covariant gauges 8=6618

blackbody radiation, spectral correls. relativistic

treatment 8=23479

charged particle, self-interaction corrections, non-

relativistic 8=20174

charged particles in mag. field 8=11445

conserved currents and Ward identity renormalization

of 8=587

covariant quantization of e. m. field in Landau

gauge 8=3435

current commutation relations and conical form

factors 8=3512

Dirac electron theory, central potential scatt. 8=6801-2

Dirac equation for electron-nucleus processes in light

nuclei, approx. scatt. soln. 8=11863

dispersion relations, calc. of traces 8=3439

electron interaction with intense e.m. wave 8=19761

electron propagator, relativistically invariant positively

definite spectral representation 8=6807

electrons, quantum-relativistic concepts 8=6800

electron wave function in e. m. field 8=6290

e.m. field in Landau gauge, canonical formation 8=3434

e pair photoprod. as possible test, corrections at high

energy 8=20390

equal-time current commutators, calc. 8=20164

Feynman rules in statistical mechanics 8=120

four-potentials, Heisenberg picture for strong Lorentz

cond. 8=589

fundamental length of the order of 10^{-90} - 10^{-96} cm 8=20171

Furry's theorem applic. to lepton polarization 8=20176

gauge invariance, apparent contradiction 8=11284

gauge problem due to 4-vector potential 8=3446

Green function and mobility in random potential,

calc. 8=11461

group renormalization, extension 8=21070

hadrons form factors and structure effects in vacuum

polarization 8=588

infrared divergence in S-matrix theory avoided by use

of 'dressed' amplitudes 8=20343

Kapitza-Dirac effect in strong radiation field 8=714

Quantum electrodynamics—contd

- Lagrangian, rel. to boundary conditions governing small-distance behaviour 8=15619
- light wave train, adiabatic compression 8=10884
- non-local effects, comparison with classical theory 8=10883
- one-speed transport eqn., closure relns. for eigenfunctions 8=847
- paraxial motion in const. spatially modulated mag. field 8=19759
- particle in nonlocal potential, interaction with e. m. field 8=3440
- perturbation expansion of Schwinger-Dyson eqns. 8=20177
- photon coalescence in uniform e.m. field 8=590
- photon field coherent states and gauge invariance 8=3437
- positronium formation in e^+H , cross-section calc. 8=16223
- radiative corrections to e^+e^- beam collisions 8=591
- radiative corrections in renormalization 8=3441-2
- relativistic charge radiation in a plane wave e.m. field 8=10881
- relativistic electrons in mag. and weak electrostatic field, effect of radiation 8=6292
- S-matrix formulation, gauge dependence of propagators 8=20175
- S-matrix theory third-order vertex part of single electron line 8=20385
- and semiclassical theory, optics expts. as tests 8=20173
- spin $\frac{1}{2}$ particles, relativistic plane motion 8=6619
- strong interactions and nonlocality 8=15618
- symmetry breaking distinctions 8=3438
- Schwinger model, current and gauge transformations props. 8=12286
- Schwinger's 2D model, radiation gauge formulation 8=3678
- test by e-e scatt. 8=11458
- test μ -p, e-p scatt. or hyperfine splitting of positronium or of muonium 8=11285
- 2-component fermion theory, simplification of algebraic structure 8=3433
- two-dimensional-model theory solution 8=3443
- two-fermion, infinite renormalizations elimination 8=15620
- 2-particle scatt., double-log. asymptotics 8=592
- vacuum polarization, divergence of reciprocal of renormalization constant and finiteness 8=6620
- zero mass quanta and i. r. problem, coherence appls. 8=20172
- Z_3 , divergent part, higher-order contributions 8=586
- H Lamb shift, and from Zeeman spectrum theory 8=1158

Quantum electronics. See Lasers; Masers; Optics; Photons.**Quantum field theory.** See Field theory, quantum.**Quantum generators.** See Masers.**Quantum mechanics.** See Quantum theory.**Quantum statistics.** See Statistical mechanics.**Quantum theory**

See also Electron theory; Field theory, quantum; Elementary particles.

- alkali metal, as basis of nonlinear continuum theory 8=17711
- anharmonic oscillators, energy levels, WKB calc. 8=564
- atomic polarizability calc. for e systems with several open shells 8=1142
- Born approximation in scattering improvement 8=15611
- bound state, intrinsic size as a function of mass 8=20270
- Brownian movement 8=6094
- coherent states, She and Heffner theorem 8=2974
- coherent state time development 8=2975
- Compton scatt., intensity effect 8=20349
- complex angular momenta and inverse scatt. 8=15610
- consistency problem in theory of measurement 8=20138
- contour integral method for stationary and nonstationary problems 8=15606
- crystal construction, possible use of quantum mechanics 8=21790
- degenerate time-independent perturbation theory 8=548
- diamagnetic susceptibility calc. and temp. dependence 8=18294
- duality of hypervirial and conservation theorems 8=15015
- dynamical information from expt. higher symmetries using H atom and harmonic oscillator 8=11266
- dynamical symms. in nonrelativistic systems commuting integrals of motion 8=11246
- dynamical systems, quantum-mechanization 8=20135
- eigenvalues, perturbed, finiteness of 8=10497
- e. m. mode mixing in non-linear media, statistics 8=19822
- electron interaction with intense photon beam 8=20372
- exclusion of hidden variables, comment on refutation 8=15597-8
- factorization theory and Inonu-Wigner contraction applied to H atom, harmonic oscillator and constant pot. 8=20145
- ferroelectrics, order-disorder, statistical perturbation theory, Zeroth approximation 8=9191
- film, metallic, thin, perp. elec. conductivity 8=22510
- finite translations in solid-state physics 8=13648
- flux quantization and dimensionality 8=19461
- Fokker-Planck solution for laser noise 8=11023
- forced harmonic oscillator, wave-interference effects 8=3410
- fundamentals of quantum mechanics, book 8=6589

Quantum theory—contd

- harmonic oscillator and (Dirac) Kepler problem, self-adjoint ladder operators appl. 8=11261
- harmonic oscillator and H atom insertion of barrier and symm. relation 8=11371
- harmonic oscillator, number of quanta and creation and annihilation operators 8=563
- hidden variables, reply to comments 8=15599
- Hilbert space structure, theorems 8=3394-5
- Inonu-Wigner contraction, and factorization theory 8=20145
- K^0 , C, CP, CPT theory consequences 8=777
- $K_L^0 \rightarrow \pi^+ \pi^-$ decay, CP violation 8=777
- kinetic equations, derivation 8=552
- Lagrangians for fields satisfying wave and Klein-Gordon eqns. 8=572
- lasers, calc. of photon number and amplitude fluctuation 8=11013
- laser coherence props. 8=19938
- laser, gas 8=15454
- lasers, gaseous, higher-order perturbation theory 8=6434
- laser noise, quantum Fokker-Planck soln. 8=19937
- laser operation, quantum mechanics 8=19928
- lattice cell vol. depend. in calc. of two-point function in quantum mech. 8=4856
- Lorentz proper G_2 , continuous subgroups 8=2895
- lower bounds to eigenvalues, extension of Gay's eqn. 8=20143
- matrix elements of Racah operator equivalents 8=6598
- matrix mechanics, third order energy correction 8=11257
- measurement and symbolic logic 8=20140
- measurement problems 8=544
- measuring theory, postulate of proper values 8=20139
- mechanics, fundamental, book 8=20133
- mechanics, group representations theory appls. 8=20137
- mechanics, mathematical theory of linear operators 8=15596
- mechanics, principles, elementary outline 8=20134
- metals u.s. absorpt. in mag. field by free electrons, calc. 8=22093
- methods for applications in chemistry, book 8=11247
- model, one-dimensional, of interacting electrons, flux quantization 8=19460
- model states, symmetry violating, collective motions 8=557
- molecular beams scatt. at solid surfaces, quantum mech. calcs. 8=16378
- molecular quantum mechanics, noninvariance groups 8=1136
- molecules, spin-interaction operators, matrix elements 8=1225
- noise in lasers 8=11022
- nonanalytic perturbations 8=3412
- optical coherence, p-representation in twisted convolution formation 8=20026
- optical interference transient patterns 8=20097
- optical maser, spectral profile 8=19929
- optics, equivalence theorem and diagonal representations 8=20025
- optics, nonlinear interaction with medium, statistics 8=20023
- optics, philosophy and appls., review 8=20024
- optics, photoelectron distrib. 8=20013
- orbital angular momentum, n-dimens., self-adjoint ladder operators appl. 8=11260
- orthodox interpretation, alternative calc. procedure 8=6601
- oscillators, coupled with classical harmonic driving force, soln. of eqns. 8=20149
- perturbation method for calc. vibrational frequency of polyatomic molecule 8=4120
- perturbation methods and perturbation-variation generalisations 8=546
- perturbation theory, classical, applied to atomic excitation 8=7460
- perturbation theory for exchange forces 8=4043
- perturbation theory, 2nd-order energy sum, upper and lower bounds 8=6592
- perturbation theory in wave-operator formalism for inter-molec. interactions 8=7631
- phase space distrib. function, new 8=11245
- plasma, nonlinear phenomena in strong mag. field 8=16503
- plasmas, high temperature, investigated 8=16468
- point quantum-mech. systems, spectral reps. for two-point functions 8=569
- potential barrier, invariant imbedding soln. 8=20148
- ψ not determ. by probability densities in time and space, but by probability density and current 8=20141
- quantum mechanical model of Mössbauer line narrowing 8=1830
- quantum-mechanical time operator 8=11255
- quantum mechanics helps understand classical mechanics 8=545
- quantum statistics, classical statistics as limiting case 8=2968
- quasi-harmonic oscillators, self-excited, fluctuation anal. 8=6370
- radiation and matter interacting system, fluctuations 8=19819
- reflection and emission from crystals, wave mechanical description, wave/particle duality 8=2018
- relativistic, proper-time formulation 8=20136

Quantum theory—contd

- resonators, optical Fabry-Perot, sensitivity 8=10683
- rings, nearly superconducting, coherence and quantization 8=22542
- rotating single crystal, time-dependent Dyson expansion 8=14136
- scattering amplitudes in perturbation theory 8=6605
- semiconductors in mag. field, phonon-drag Seebeck effect 8=9236
- semimetals with equal numbers of electrons and holes, Hall effect 8=22416
- signal detection, statistical mechanics 8=10945
- spin-Hamiltonian parameters, sign determination 8=15601
- statistical mechanics and thermodynamics, conference Copenhagen Denmark (1966) 8=15007
- statistics of multiple-mode, superposed coherent and chaotic radiation 8=2984
- stimulated Raman scatt. 8=3292
- strong interactions and nonlocality 8=15618
- Sturm-Liouville equation, one dimensional upper bounds to eigenvalues 8=2882
- and symm. breakdown, a classical approach 8=20257
- symm. postulate of quantum mechanics, proof without spatial connectivity in ID 8=6602
- theoretical physics, conference Providence USA (1966) 8=20246
- three-body interactions in solids 8=8238
- transformation, point, achieved by isometric transformations in Hilbert space 8=559
- transition probability approximation 8=6597
- transport coeffs. collisional transfer contribs. 8=19475
- 2-level system coupled to harmonic oscillators, kinetic equations 8=11263
- 2,3,4-particle systems with harmonic oscillator pot., group theory 8=11258
- two-particles interacting in infinite square well, mechanics 8=3403
- Wien displacement law and rad. fluctuations 8=14997
- He⁴, 2nd virial coefficient, first quantum correction 8=12678

application methods

- amplitude-density-functions method for scattering 8=12358
- anharmonic oscillator, eigen values and eigen solutions
- anharmonic oscillator, equation of motion, exact soln. 8=15608
- anharmonic oscillator, uniformly valid asymptotic approx. 8=15607
- atomic and molecular interactions, weak, new perturbation procedure 8=12103
- barrier penetration, nonstationary problem, quasiclassical approx. 8=3411
- cosmology using quantum models 8=10084
- decay processes, soluble decay model 8=3413
- decay, sequential of unstable system using projector-operator algebra 8=11262
- deviation from symmetry, use of generalized perturbation theory 8=11259
- diatomic potential curves, calc. of vibr.-rot. energy levels 8=12140
- diatomic rigid molecule and harmonic oscillator 8=12141
- DWBA in shell model approach to nuclear reactions 8=7153
- e-e. m. wave scatt. 8=15409
- energy eigenvalues, WKB method 8=3396
- energy-moment methods 8=3397
- excited states, Weinstein calcs. 8=16254
- exciton laser, mechanical theory 8=6456
- expectation values for physical quantities other than energy, variational approach 8=20146
- Feynman baskets to quantum theory of gravity 8=3451
- Feynman diagrams, Cayley eqns. equiv. to Landau 8=3448
- Feynman diagrams, simplification of trace calc. 8=3439
- formalism in perturbation methods 8=6599
- Green functions in atomic and molec. calc. 8=4035
- harmonic oscillator, driven, time-dependent P-distribution 8=562
- harmonic oscillator, SU_{1,1} representation 8=3409
- Hartree-Fock expectation values for phys. props. 8=4038
- Hartree-Fock perturbation, appl. to π -electron systems 8=12158
- high energy approx., second order 8=20147
- hypervirial operators in perturbation theory 8=3408
- many-boson problem, operators of zero-momentum states considered as q-number quantities 8=10652
- many-electron wavefunctions, GF method 8=20911
- molecular mechanics, integral technique for solving $\Delta U = f(M) + g(M)V(M)$ 8=7495
- molecule decay, WKB-method 8=12147
- molecules, optical activity 8=12138
- n-particle system, Schrodinger eigen-numbers 8=668
- optics, quantum, representation of operators 8=11425
- paramagnetic crystals, u.s. absorpt. rel to spin-lattice relax. 8=17487
- perturbation expansion, appl. to two-photon absorpt. 8=16286
- perturbation formalisms for exchange interactions 8=12361
- perturbation theory for intermolec. interactions 8=12359-60
- perturbation theory for retarded Green's function of crystal phonons with anharmonicity 8=17469

Quantum theory—contd**application methods—contd**

- perturbation theory, time-dependent, new place factor 8=6603
 - quasi-spin to matrix elements of Coulomb interaction 8=21011
 - rectangular plates, stability, perturbation method 8=59
 - scatt. from diffuse edge potentials energy eigenvalues 8=3414
 - scattering, one-dimensional, edge effects 8=6606
 - self-consistent field theory, spin-free 8=20917
 - Slater approx. X-ray atomic scatt. factors of Al 8=8506
 - Slater determinants, projection 8=12027
 - to statistical wave system in randomly fluctuating medium 8=2986
 - SU₃ as dynamical group of $H = \frac{1}{2}p^2 + V(r)$ 8=11265
 - transition energies, perturbation calc. 8=12024
 - transitions, many-quantum, in rotating reference frame, in conduction-e.s.r. 8=18400
 - three-body problem in one-dimens. 8=558
 - two-centre problem, numerical soln. 8=566
 - 2 non-relativistic spinless particles 8=11264
 - variation principles for lower bounds by means of density matrices 8=10647
 - variational method for calc. of dynamic polarizability of He atom 8=20945
 - variational perturbation method based on the principle of moments 8=20919
 - variational principle for phase of wavefunction 8=21055
 - water waves, variational methods 8=1516
 - waves, Whitham theory, special cases 8=1517
 - WKB approx. for radial problems, 2nd and 3rd order correction terms 8=12039
- many-particle systems**
- See also Bosons; Fermions; Helium/liquid; Statistical mechanics; Superconductivity; Superfluidity.
 - atoms in coupled radiation field, correlations 8=19458
 - Boltzmann-Gibbs statistical probability, redefinition 8=14992
 - Bose gas, phase transformations of second kind 8=10651
 - canonical statistics, temp. depend. near phase transition 8=97
 - canonical transformations for susceptibility determ. 8=3295
 - charged particles, ground-state energy, absence of exclusion principle implication 8=15013
 - charged particles at high temp., statistical mechanics 8=10630
 - coherent states, evolution of Gaussian distrib. 8=20149
 - collisions, angular momentum eigenstates, review 8=122
 - collisions, application of unitarity 8=123
 - correlation function for noninteracting system 8=2987
 - decay theory 8=659
 - dynamical systems, quantum-mechanization 8=20135
 - e gas, high density, slowly varying, correl. energy calc. 8=10659
 - electron-impurity interactions, h.f. elec. cond., elec. 8=2999
 - electron-impurity interactions, master eqns. 8=2998
 - electron-impurity interactions, one-particle evolution eqns. 8=2997
 - energy approx. computation, upper bounds to error 8=681
 - Fermi system with direct interaction, retarded temp. Green's functions, perturbation theory 8=15021
 - fermions interacting finite system, continuous energy spectrum 8=128
 - Fermions, meson theory of nuclear matter 8=11693
 - fermions, non-relativistic, 2-particle Green's function spectral functions 8=2996
 - fluorescent source, quantum statistics of polarization 8=23036
 - 4 identical particles, Euler angles, helicity formation 8=15912
 - 4N interactions nuclear matter binding energy 8=11695
 - free particles, Green function 8=19457
 - generalized density operators for identical particles 8=19454
 - ground state energy, lower bound using density matrices 8=10647
 - Hamiltonian, covariant, with interactions, classical, canonical formalism 8=19441
 - hard-sphere gas, collisional relax. eigenvalues 8=3000
 - harmonic oscillators, infinitely many, with linear interaction 8=10638
 - harmonic oscillators, infinitely many, uncoupled 8=10637
 - Hartree-Fock-Slater method, many-state extension 8=10640
 - heavy particle collisions, exchange matrix elements, evaluation 8=12100
 - Heisenberg ferromagnet 8=9317
 - inequalities and variational methods in classical statistical mechanics 8=14993
 - infinite, macroscopic evolution systems 8=2967
 - interacting with field, eigenvalue eqn. for excitation momenta 8=10643
 - inverse velocity space spectra and kinetic equations 8=10645

Quantum theory—contd

many-particle systems—contd

- Ising model lower bound to free energy with small external field at low temp. 8=10647
 Ising spin correl. function, calc. 8=14987
 kinetic eqns., Green function method, causality principle 8=14990
 kinetic and relaxation processes 8=10650
 Kondo scattering problem, ground state 8=5098
 Langevin eqn. of Mori and Kubo derived from theory of stochastic processes 8=10616
 lattices, harmonic, motion of heavy impurity 8=19440
 linear discrete medium, eqns. of motion 8=30
 linear discrete medium, geometry 8=29
 liquid-crystal transition of quantum system at $T = 0$ 8=119
 lower bounds for binding energies 8=6107
 many boson system in coherent states and superfluidity 8=19696
 many-e., HF scheme, new formulation of time-depend. perturbation theory 8=6603
 matter and radiation, equilibrium props., anomalies 8=2990
 metals and solid solns., cohesive and volume props., ab initio calc. 8=4665
 molecules, simple, sums over states at high temp. 8=10634
 N-fermion model, analysis of 2- and 4-point functions 8=15014
 N-particles system bound state approx. solution 8=11579
 N two level systems interacting with single mode, quantized radiation field 8=2970
 nuclear many-body problem, linked-cluster expansions 8=11694
 nuclear matter, binding energy calc. 8=823
 nuclear matter, Brueckner-Goldstone theory 8=11692
 nuclear matter, 3-body problem and Brueckner-Goldstone series convergence 8=11690
 nuclear shell model, group classification of many body interactions 8=3761
 nuclear spin in magnetic field, "negative absolute temperature" concept 8=10642
 one-dimensional interaction, repulsive delta-function problem 8=15010
 one-dimensional systems with hard cores, absence of phase transitions 8=19455
 oscillators coupled, quantum statistics 8=2981
 point quantum-mech. systems, spectral reps. for two-point functions 8=569
 polarized media, ang. momentum laws 8=10636
 polarized media, relativistic energy-momentum tensor 8=10635
 quantum ideal gases, effective potential 8=19456
 quantum plasma, test-particle theory 8=10644
 quantum statistics of system with Coulomb interaction 8=2988
 quasiparticles and contracted description 8=10639
 radiation transport in scatt. media, eqn. deduction 8=3012
 repulsive δ interaction problem in one dimension 8=10648
 scattering theory of N non-relativistic particles 8=10649
 Schrodinger equation, eigen-numbers 8=668
 spin dipole, properties 8=10622
 spin systems, statistical mechanics 8=15006
 spontaneous emission from a system of 2 level atoms interacting with relaxation mechanism 8=20971
 stationary, orthogonality of excited states 8=14995
 statistical mechanics, equilibrium states 8=10627
 statistical mechanics, equil. states, factor type 8=6101
 superconductors, macroscopic quantum phenomena 8=3124
 superfluid systems elementary approach, for understanding simple models 8=15148
 superfluid vortices 8=3125
 3-body problems, 3 families of integrals 8=10646
 three-particle distribution function of extended uniform system 8=115
 three particle, Faddeev's theory 8=6604
 uniform N-particle system, necessary conds. for radial distrib. functions 8=124
 Wigner function, kinetic eqns., Green function method 8=14991
 Wigner method 8=2977
 He, liquid, collective coordinates theory 8=10799
 He, superfluid, vortex lines 8=3124
 KCl, U_2 -centre, electronic structure rel. to correlation effects 8=13459

quantization

- See also Field theory, quantum/quantization.
 energy levels of systems, lower bound, ΔE method 8=561
 geometrical, applns. 8=6600
 Heisenberg type particle eqn. field, according to Fermi statistics 8=3419
 Kirchhoff-Planck radiation law 8=10762
 lattice vibrations, Green's and wave functions 8=8606
 quantized matter field, interaction with classical gravitational field 8=19430
 relativity, general theory, canonical transformation in gravitation theory 8=10597
 superconductors, and thermodynamic fluctuations 8=17987
 thermogalvanomagnetic phenomena 8=18208
 topological properties of theory 8=20154

Quantum theory—contd

quantization—contd

- Al superconducting cylinders, mag. field periodicity in flux expts., temp. depend. 8=22539

wave equations

- approximation by class-C potentials 8=553
 atom irradiated with wide-band coherent light 8=1143
 Bargmann-Wigner eqns. for spin $>1/2$ 8=3401
 Broglie fusion theory and the double solution theory, review 8=551
 Brownian movement of particle within wave 8=91
 Clebsch-Gordon, derivation of coeffs. rel. to nuclear energy levels 8=11704
 collapse time for hidden variable theory 8=15600
 Coulomb matrix elements, recursion relations 8=20144
 Dirac eqn., Drukarev transformation 8=15603
 Dirac matrices, representation adaptable to free particle spinor 8=560
 Dirac, symmetry group props. 8=6593
 discontinuous wavefunctions, variation principle 8=11248
 distributions, notation proposal 8=6011
 eigenvalues, degenerate, introduction 8=3404
 electron transmission through periodic pile 8=3406
 energy eigenvalues, WKB method 8=3396
 equations of motion, non-linearity, asymptotic behaviour and renormalization, connections 8=6595
 error bounds for expectation values 8=554
 fundamentals of quantum mechanics, book 8=6589
 Klein-Gordon eqn. for spinors 8=15621
 K-G, plane wave solution generalization 8=11256
 Klein-Gordon, time-depend., quasi-stationary solns., new method 8=11249
 linear variation methods 8=556
 Maxwell's equations, group theoretical derivation 8=10935
 molecular, energy variance function, and estimate of energy eigenvalues 8=4131
 molecular Schrödinger eqn., correlated polyelectronic wavefunction 8=4129
 phase shifts, Brysk approx. 8=3400
 phase shifts for inverse-power force field 8=20142
 pionic atoms, rel. to strong interactions and finite nuclear charge radius effects 8=7482
 plasma, classical and two-component short distance divergence 8=1378
 radiative transfer in multiple scattering 8=137
 real spinor fields, in modified Dirac theory 8=705
 relativistic, eigenvalue specifies spin 8=3399
 S-wave nonlocal potentials, scatt. soln. 8=15622
 Schrödinger for α -d cluster model of Li^8 8=15954
 Schrödinger, applic. to expansion approach to scatt. 8=672
 Schrödinger, applic. to scattering 8=20285
 Schrodinger in bootstrap calc. 8=11559
 Schrödinger eqn., appl. of displacement and collective variables method 8=3402
 Schrödinger eqn., lower bounds to eigenvalues 8=15605
 Schrodinger equation in imaginary time, integration 8=6590-1
 Schrödinger equation, two-parameter Hamiltonians 8=11250
 Schrödinger, generalized, valid for velocity dependent forces 8=15602
 Schrödinger, lower bounds to eigenvalues, excited states 8=11252-3
 Schrödinger, modification from Coulomb potential between two particles 8=3407
 Schrödinger, molec., evaluation of multidimens. integrals 8=16247
 Schrodinger, numerical solutions, accurate and stable 8=6594
 Schrödinger, new aspect of calc. of energy spectrum 8=3398
 Schrodinger, for n-particle system, scatt. of particle from bound system 8=668
 Schrödinger's perturbational-variational soln. 8=3405
 Schrodinger, radial, perturbation theory for discrete spectrum 8=555
 Schrödinger, Regge trajectories with Yukawa pot. 8=11421
 Schrödinger solns., unique continuation theorem 8=11251
 Schrödinger, spectral function, asymptotic behaviour 8=15604
 Schrödinger's, time-dependent, MacLachlan's variational principle examined 8=11254
 Schrödinger, time-depend., quasi-stationary solns., new method 8=11249
 Schrödinger with Woods-Saxon potential, approximate solution 8=7055
 single-particle Schrodinger eqn., rel. to positive energy bound states 8=2985
 spin $1/2$ particles, relativistic plane motion 8=6619
 spinors, interaction with vector mesons in 2 dimensions 8=15617
 statistics, applied to Schrodinger and Heisenberg force 8=2982
 stimulated Raman scattering in liqs., spontaneous emission and mol. vibr. damping effects 8=4587
 unified, for elementary particles, rel. to mass-spin depend. 8=11373-4
 unstable particles and resonances, application of general function 8=20268

Quantum theory—contd

wave equations—contd

- "vactal" representation, physical meaning 8=6596
- wave function, many electron, natural expansion 8=20920
- for zero rest-mass particles 8=11354
- H⁺, absorption coeff., numerical soln. for two-electron at. systems 8=7382
- He atom params. from wave functions with pole-eliminating correl. factors 8=16197
- L³⁺, (L=Ce, Pr, Nd, Sm, Gd, Dy, Er and Yb), 4f electron radial wave functions 8=1168
- Xe III, ground state Slater integrals 8=4087

Quarks

- antiquarks in baryon model 8=817
- atoms in solar spectrum 8=6718
- in baryon model 8=817
- baryon model, field-theoretic restriction 8=15817
- baryon nuclear shell model, finite mass effect 8=15819
- baryon resonance decay model 8=15821
- baryon resonances, symm. model, mass formula derivation 8=6980
- B-B scatt. model 8=11577
- baryons, model with three-body interaction forces 8=11573
- baryonic states model 8=3688
- Bethe-Salpeter eqn. accurate numerical soln. with Yakawa kernel 8=11476
- boson, meson resonances and SU₃ analysis applied to quark picture 8=11556
- in cosmic rays, negative evidence 8=11474
- cosmic ray search for charges $\geq \frac{2}{3}e$ 8=15742
- diquark, tightly bound state of two quarks in baryon model 8=20511
- elastic scatt. model 8=725
- "elementary particles", nonrelativistic model 8=6822
- experimental search in matter 8=11475
- fermion-antifermion system using Bethe-Salpeter eqn. 8=3603
- fermion interactions, strong-coupling quark-model SU(3) invariance limit, mass formula 8=20276
- galactic production, search 8=3604
- $\gamma + N \rightarrow \pi, K$, model 8=6842
- hadron elec. and mag. polarizabilities model 8=6823
- hadron-hadron scatt., λ -nonstrange and qq scatt. 8=6825
- hadron interactions model, prod. cross-sections, SU(3) breaking 8=20405
- hadron model as deformable sphere, fractional change avoided 8=15673
- hadrons as many-sakaton systems 8=20401
- hadron scatt., high energy, with factorizability assumption 8=15755
- hadron scatt. model for elastic 90° 8=15754
- hyperon decay model, nonleptonic 8=3726
- hyperon non-leptonic S-wave decay 8=6975
- Lagrangian model, mass term, chiral-type interactions 8=11481
- Λ to Σ ratio in $I = 1$ S-wave $\bar{K}N$ reaction 8=15860
- meson-baryon scatt. model assuming tighter meson structure 8=20418
- meson decay rate model 8=736
- meson-N scatt. model, Glauber formalism, correction to Johnson-Trieman relation 8=20419
- mesons as $q-q$ bound states, soln. of Bethe-Salpeter eqn. 8=15687
- mesons, tensor and axial vector, strong decay 8=11557
- model for BM, MM scatt., soln. to superconvergence relations 8=20404
- model and Lagrangian field theory of self-generating interactions 8=20161
- model for elementary particle and hyperon radiational weak decay 8=20571
- model rel. to $K_1^0 K_1^0$ mass spectrum 8=6913
- model rel. to $\pi^- + p \rightarrow n + \gamma, \gamma + p \rightarrow p + \eta$ 8=20490
- multipion production processes, establishment of sum rules 8=11512
- n- and p-quark mass difference explained on e. m. basis rel. to hadron isomultiplet splittings 8=6824
- nucleon model 8=3695
- $\pi^+ + p \rightarrow \Sigma^+ + K^+$, quark model for backward process 8=11480
- population in Fe spheroid determ. 8=11455
- production cross-section 8=726
- quark-antiquark channel, bootstrap calc. for meson solns. 8=3607
- quark-antiquark scatt. and meson nonet mass formulae 8=677
- quasiquarks rel. to fibre bundle C(N) cross sections 8=20407
- sakaton model for 2-body hadron scatt. 8=15753
- search for, in cosmic rays at sea level 8=20402
- search for fractionally charged particles 12 GeV e on Cu 8=20403
- scattering, additivity test from decay distrib. in double reson. prod. 8=11479
- scatt. invariant under group transformation 8=6763
- qq scatt., superconvergence relations 8=11478
- scattering and weak interaction model 8=724
- Schiff model extended to scatt. 8=6826
- search, geophysical, chemical, in cosmic rays and accelerators 8=11477

Quarks—contd

- solar photosphere, search for quark-atom spectra 8=23727
- strong and weak interactions, present problems, conference Erice Italy (1966) 8=15695
- substructure for mesonic and baryonic states, lecture 8=20408
- three-quark interactions 8=3606
- three-quark system, binding with complex charge 8=11473
- with unit and fractional charges in region $m_\pi > m_p$, search in cosmic rays 8=15888
- vector meson decay model 8=6822

Quartz

- alloyed with C, anomalous auto-electron emission 8=22712
- AT-cut plates with partial electrodes, thickness-shear vibrations 8=19501
- attenuation of 3GHz sound waves from 4 to 40°K 8=17490
- Brillouin scattering, stimulated, temp. dependence 8=14265
- conductivity, elec. in a.c. field, 10³-10⁷Hz, 20-700°C 8=18197
- crystal conductivities, appl. in low-temp. elec. termination 8=15137
- crystals, focusing of X-rays 8=14261
- crystal window in double spectrometer, X-ray diffr. profile exam. with monochromatic radiation 8=22004
- crystalline, laser prod. photocond. rel. to dielec. breakdown 8=18239
- crystallization from dil. solns. at low temps. 8=4816
- Debye temp. meas. $\sim 1-4^\circ K$ 8=4934
- discharge bulb, in atomic tritium experiments 8=4276
- dispersion spectrum, anomalous, due to Si-K absorption 8=18560
- elastic waves, longit. and transverse, laser excit. thresholds 8=17831
- film, spark discharge along surface 8=7682
- frequency-controlled oscillators, temp. compensation 8=2252
- fused, laser prod. photocond. rel. to dielec. breakdown 8=18239
- fused, stimulated Mandel'shtam-Brillouin scattering, depend. on excitation intensity 8=5632
- at high press. and temp., hydrolytic weakening 8=14561
- impurities on annealed semiconductor surfaces 8=9087
- light scatt. by u.s. surface waves 8=5636
- natural and cultured, distinction between rhombohedral faces 8=4731
- optical inhomogeneities, screw dislocations 8=4982
- piezoelectric, microwave rectification 8=9227
- phase inversion, high-low, press. 6 to 35 kb, obs. 8=1681
- photoelastic amp. of light, and hypersound generation by stimulated Brillouin scatt. 8=2451
- photoelastic props. rel. to use as acoustic light modulators and scanners 8=9496
- piezoelectric coeff. from 2.6 to 25 kbar, meas. by impact tech. 8=17719
- piezoquartz, surface waves 8=17832
- plates, flexural and shear vibrations, thickness-twist overtones 8=15045
- polished surface X-ray diffr. microscopy 8=17599
- α , isotropic sound velocity, temp. and press. derivative 8=22089
- α - β transition assoc. lattice modes from Raman scatt. -196-615°C 8=1682
- α -quartz, combination scatt., freq. depend. 8=18561
- α -quartz, integrated intensities, expt. test of general formula 8=13480
- quartz-kaolin-microdine reactions during firing, i.r. studies 8=1690
- α -quartz, polariton spectrum 8=2115
- α -quartz, structure factor ratios by Pendellösung method 8=13291
- quartzite, elastic precursor decay for cylindrical and spherical flow 8=13605
- Raman oscillator, stimulated behaviour rel. to mode pulling 8=2453
- reaction in water soln., 400-500°C, 1 kb, molecularity obs. 8=2520
- refractive index in far i.r. 8=14219
- resonator, $Q=120 \times 10^6$ at 2°K 8=18204
- spoon gauges, at elevated temps. 8=5990
- standard metre gauges 8=10475
- stimulated Brillouin scatt., depend. on temp. and photoelastic props. 8=5634
- stimulated Brillouin scatt. of ruby laser light, optical heterodyne detection 8=14267
- stimulated Raman scattering from i.r.-active phonons 8=11112
- synthetic, artificial twinning during plate sawing 8=17210
- thermal expansion 8=13381
- thermal expansion, mean curves 8=17534
- thermometer, high sensitivity rel. to piezoelectric effect 8=6220
- vibrating, microbalance, transistorized temp. regulator 8=19671
- X-cut plates, Rayleigh surface wave vel. 8=155
- X-ray emission spectrum, photon-counting obs. 8=2454
- X-ray irradiation effect on permittivity, luminescence and thermoluminescence 8=13871
- X, Y and Z cut, elastic shock compression obs. 8=13608
- Au coated fibres in high pressure proportional counters 8=11298

Quartz resonators. See Acoustic transducers; Piezoelectric oscillations; Resonators.

Quasars

See also Cosmic radiations, radiofrequency; Cosmology; Galaxies; Stars.
absorption lines 8=23621
brightness-Doppler shift correlation, explanation of absence 8=23625
coherent plasma radioemission 8=14813
continuum radiation, simplification of synchrotron-radiation hypothesis 8=23626
emission-line variability, evidence for origin 8=23627
gravitation radiation, obs. proposed through scintillation effect 8=14959
gravitational radiation, vibr. and rot. modes 8=10313
interferometer baselines obs. up to 3074 km 8=10315
inverse Compton radiation, rel. to γ -rays, spectrum and X-ray background 8=23619
lagging-core model 8=10314
light and r.f. radiation, circular polarization 8=23631
light, fluctuations, evidence for fragmentation model 8=19235
luminosity functions and space distrib. 8=19232
magnetic field and energy rel. to origin, l.f. spectra and redshift obs. 8=23613
novae and supernovae, identity of mechanism 8=23629
[O II] transitions, forbidden, emission theory 8=23620
oscillations, general relativity exact solutions 8=19429
and radio galaxies contrasted 8=5945
radio, quasi stellar sources as galactic condensations 8=14808
radio sources, spatial distribution 8=14814
redshift absolute magnitude rel. to Universe models 8=10317
red-shift brightness relation 8=10320-1
red-shift effect caused by distance, log N-log S curve for 70 objects 8=14815
red-shift, gravitational and cosmological 8=10318
red shift and large energy emission 8=2805
space distribution 8=23630
spectra, 2974 Å emission line identification 8=19234
spectral energy distrib. rel. to red shift 8=19233
stellar coalescence and multiple supernova interpretation 8=5947
3C 147, a distance limit 8=5946
3C 191, absorption line spectrum model 8=14817
3C 273, 3C 279, 3C 446 and 3C 454. 3, variations in 1.96 cm flux density 8=2804
3C446 et al., angular meas. 8=23623
3C446, optical variations 8=14816
3C446, optical var. obs. and model 8=23624
U, B, V-data and redshifts and cosmological models 8=2768
variable radiation in magnetodynamic model 8=10312
variable, relativistically expanding synchrotron model 8=10316
variability of elementary charge and quasistellar objects 8=23628
visual identification evidence 8=23622
Quasi-particles. See Excitons, Magnons, Phonons, Polarons, etc.
Quenching, optical. See Luminescence.
Quenching, thermal. See Heat treatment.

RS coupling. See Atoms; Spectra/atoms.

Racah coefficients. See Quantum theory.

Radiation

See also Acoustic radiators; Bremsstrahlung; Cherenkov radiation; Electromagnetic waves; Electrons/radiation; Emissivity; Radiative transfer; Stars/radiation; Sun/radiation; Sunlight.
atomic, spectral line breadth, effect 8=7372
black-body, autocorrelation functions 8=19824
black-body and stochastic fields correl. props., relativistic theory 8=19823
black body, temporal and spatial autocorrelation functions 8=19623
Boltzmann eqn. with cut-off pots. 8=3005
charge moving in anisotropic medium 8=6360
derivatives of functions, pseudo-radiation conditions 8=381
diffusion from a cavity, moments method description 8=19622
diffusion, photons in plane layer, number of scatterings 8=3567
effects on magnetogasdynamics shock propag. in a plasma 8=7755
electromagnetic, experimental introduction 8=10936
e.m. wave, due to dipole over moving dielectric medium 8=383
Fermi particles in crossed fields 8=6739
gravitational, high frequency generator 8=19419
i. r., carbon furnace source 8=15093
ionizing, dose equivalent 8=20741
Kirchhoff-Planck law, quantization 8=10762
matter and radiation, equilibrium props., anomalies 8=2990
and matter interacting system, fluctuations 8=19819
millimeter wavelength, attenuation by gaseous water vapour 8=12689
mode mixing in non-linear media, quantum statistics 8=19822

Radiation—contd

optical, development of scale 8=11117
optical, effect on CdS trapping spectrum 8=5396
rel. to photon counting statistics, e.m. fields coherence props., dynamical calc. 8=20352
propagation in a resonance medium 8=21000
quadrupole spin echo, amplitude calc. 8=370
quantum electrodynamics, 6th order correction, method of calc. 8=3441-2
relativistic charge, in a plane e.m. field 8=10881
space, measurement of 8=10066
transition probability for multi-photon process with resonance 8=20011
ultraviolet, sources and material props., book 8=20012
Ba plasma, resonance, scattering obs. rel. ion density 8=4331
Ge:In detector pulsed far infrared laser radiation 8=9262

heat
atmospheric surface layer, meas. 8=23261
blackbody, dispersive, intensity fluctuations meas. by photon detector 8=6200
black-body, source for calibration of net pyrradiometer 8=15097
cavities, cylindrical, nr. black body, emissivity calculation 8=220
diffusion from a cavity, description by moments method 8=229
earth rel. to atmosphere available pot. energy generation, obs. 8=23262
elec. non conductor, monochromatic directional distrib. rel. to surface roughness and λ 8=22138
energy fluxes, calculations of 8=15095
energy transfer in spectrum lines 8=230
gray gas, absorbing, between heated plates, source functions for heat transfer 8=21507
gray gas layer by thermal radiation, unsteady energy transfer 8=7923
heat transfer between two narrow strips 8=221
ignition of wood 8=15110
infrared, principles and applications 8=10765
interstellar matter, far i. r. sky survey 8=19197
Jeans' number appl. to anisotropic absorber 8=10763
penetration curve determination for temp. distrib. 8=19660
Rosseland approximation appl. 8=19633
solar, refl. by planet, geometrical model for calc. 8=14829
thermal conductivity manometer, error in common formula 8=21544
thermal-wave generator, cam equation 8=3101
transfer limits, opaque and transparent case, and rad. and conduction predominant case 8=19624
uneven periodic surface, theory 8=15094
GaAs, infrared on absorpt. of ultrasonic waves 8=13352
Ti, increase from microrough surface compared with polished one 8=22139

Radiation belts. See Atmosphere/radiation belts.
Radiation chemistry. See Chemical effects of radiations/ionizing radiations; Radiochemistry.
Radiation damage. See Physical effects of radiations.
Radiation detectors
 See also Bolometers; Photometry; Radioactivity measurement.
biothermal radiometer 8=6204
channel electron multiplier 8=11312
direct obs. of i. r. laser beam patterns 8=19973
directional, for aerial radiometry of ores 8=18829
extreme u. v., detection by retarding potential analyzers 8=20060
far infrar-red, Josephson effect, spectral response curves - and characts. 8=17979
heterodyne for 0.337 mm using maser source 8=6201
i. r., condenser-microphone type, freq. response for interrupted rad. 8=3097
i. r., development trends, review 8=15098
i. r. photocond. materials, generation-recomb. noise 8=22709
i. r. photocond., noise limited detectivities 8=22708
i. r., possible use of optically polished semicond. photo-e.m. elements 8=6203
infrared radiometer for structural stress meas. 8=8794
i. r. (3 to 15 microns), fast InAs, InSb and Hg_{1-x}Cd_xTe detectors 8=11103
for light signals < 10⁻⁴W, methods 8=15495
net pyrradiometer, long wave radiation source for calibration 8=15097
p-n junction detectors, self-filtering with narrow spectral responses 8=9158
photographic, i. r. and visible 8=537
pyroelectric i. r., comparison of various mats. 8=18199
pyroelectric, large-area receiver, description and zonal sensitivity 8=15100
quantum, and emitters, spectral characterization, clarification 8=20054
quantum, stimulated emission, statistics 8=20183
radiometer signal compensation 8=3271
radiometer, thermolec. circular foil type, peculiarities in stationary regime 8=19626
satellite cosmic-ray counter data 8=19089
spectroradiometer with automatic digital recording 8=6202
thermistor flake arrays, optically immersed in Ge and Si lenses, for the i. r. 8=9143

Radiation detectors—contd

- thin-film resistance thermal flux gauge 8=10768
 ultraviolet, book 8=20012
 ultraviolet, sodium salicylate appl. 8=15494
 u.v., with e channel multiplier 8=6506
 X-ray, point-anode proportional counters 8=14497
 InSb infrared, spark machining process 8=15096
 InSb m.o.s., infrared image storage 8=13863
 Si doped with B, Al, Ga, P, As or Sb, for 10.6- μ from CO₂ laser 8=9257
 Si, in rel. to earth reflectivity 8=18834

Radiation effects. See Biological effects of radiations; Chemical effects of radiations; Physical effects of radiations.

Radiation monitoring

- See also Dosimetry.
 accelerator neighbourhood, radioactive dust 8=6690
 criticality detector, n-sensitive 8=7324
 electrostatic precipitator for fuel leakage 8=20909
 environmental, new ionization technique for obs. 8=20190
 image furnace for simulation of thermal effects of nuclear weapons 8=3986
 kinetic theory for fluctuating source 8=3010
 leak-rate testings on containment vessels, calc. methods and results 8=20907
 linear accelerators, for safe radiotherapy 8=5985
 n counter, semi-conductor, using crystal damage 8=4030
 neutrons, dose equivalent monitor, portable 8=20557
 n flux in reactor, by N⁶ content in cooling water from O¹⁶(n, p)N¹⁶ reaction 8=7338
 radioactive waste, from U.K.A.E.A. establishments, 1966 8=20738
 thermal-neutron radiation meters, calibration 8=853
 thermionic converters with UO₂-filled emitters 8=15241
 thin foils in reactor beam, rig for meas. of emitted disintegrating nuclei 8=4031
 Co⁶⁰ photon emission, exposure meas. 8=11427
 H₂O, in the vicinity of nuclear power stations 8=4032
 LiF, response to n+ γ reactor fluxes 8=20899

Radiation pressure

- See also Acoustic streaming.
 acoustic, on small rigid sphere in fluid 8=6151
 solar, perturbation of earth satellite orbits 8=23462
 waveguides and e. m. resonator walls 8=19879

Radiation protection

- See also Radiation monitoring.
 ceramic elect. insulators in thermal neutron flux 8=12010
 dose rate calc. for γ rays from spent fuel rods 8=16163
 γ dose rate in p bombarded spherical shell shield 8=3568
 γ -ray source cavity design 8=1009
 graphite and cadmium shielding for γ -rays 8=1128
 health and safety in U.K.A.E.A., 1966, research and development work 8=19329
 radiotherapy, safety aspects of linear accelerators 8=5985
 sand as side shield for accelerator 8=3490
 shield for γ -ray spectrometry 8=11438
 urinary U determ., simplified method 8=23181
 water shields containing ducts, behaviour of thermal n by source-separation techs. 8=12022
 X-ray generator, remote operation 8=15585
 X-ray powder diffractometer safety shutter 8=15594
 B₄C coatings for antiradiation screens, prep. by plasma method 8=20551
 Cs¹³⁷- γ rays, diff. energy and angle spectra in water and air 8=11819

Radiative transfer

- black-body, interaction with gas, approach to thermal equilib. 8=12673
 through clouds by spherical harmonics method 8=18866
 dispersive medium between non-black walls 8=15106
 Doppler lines for nonisothermal paths, total radiances and equiv. widths 8=10676
 electron-scattering atmosphere, Case's method applied to Milne problem 8=15028
 entropy production, size 8=6118
 flame in cylindrical chamber, effect of recirculation on temp. field 8=15114
 fluctuation meas. theory 8=3010
 fluids, optically dense, volumetric absorpt. rel. to Rosseland approx. 8=10674
 gases, diatomic nongray, infrared, vibr.-rot. theory 8=16693
 in gas, differential approximation, modification 8=222
 in gas layer containing 2- or 3-level atoms, rel. to spectral lines 8=16188
 gas, non-grey, plane-parallel geom., approx. methods 8=6117
 heat, absorbing and anisotropically scattering medium 8=10675
 heat and emissivities of emitting volumes, relations between 8=3099
 heat, in fibrous insulator 8=1883
 heat transfer limits, opaque and transparent case, and rad. and conduction predominant case 8=19624
 interaction of 2 infinite plates, unsteady state 8=10766
 model atmosphere construction, in radiative and thermodynamic equilibrium 8=2777

Radiative transfer—contd

- Monte Carlo method calcs., nonlinear and frequency-dependent 8=6119
 multiple scattering by statistical model 8=137
 nongray gases, differential formulations 8=139
 non-stationary diffusion of rad. in non-uniform stationary medium 8=19481
 organic liquids rel. to thermal cond. temp. depend., obs. 8=12853
 between parallel plates separated by nonisothermal medium 8=19625
 polarized radiation in slightly anisotropic medium 8=6375
 radiation-driven acoustic waves in confined gas 8=4483
 in relativistic medium 8=15029
 Rosseland radiative mean opacity, calc. 8=11163
 with reflection from atmos. boundaries 8=9862
 resonance-radiation transfer theory, H-functions 8=6116
 semi-isotropic model for heat-transfer, rel. to boundary and blackbody intensities 8=15103
 shock layer, radiation coupled, upstream absorpt. effects 8=19545
 solid heated by high temp. source, conductivity calc. 8=13386
 solution of transfer equation in Lyman continuum 8=10124
 source function soln. for heat transfer through absorbing grey gas between heated plates 8=21507
 spectra, regular band, absorptance calc. 8=12125
 spectral line formation, integration of equation by Riccati method 8=3009
 specific intensity, behaviour at infinity in plane parallel atmosphere 8=2774
 spherical shell of absorbing-emitting grey medium 8=10677
 suspensions, with wall, zonal calc. 8=8143
 transport eqn. with anisotropic scatt. 8=138
 uniform gas, frequency-integrated radiation due to weak lines 8=12690
 CCl₄ rel. to thermal cond. temp. depend., obs. 8=12853
 N, uniform, for local thermodynamic equil. 8=7926
- Radiators.** See Acoustic transducers; Electromagnetic waves/radiators.
- Radicals.** See Free radicals.
- Radioactive dating**
 carbon dating, influence of changes of Earth's magnetic field 8=9796
 cosmogenic nuclides in Peace River and Harleton chondrites, cosmic ray history deductions 8=14858
 Kesselwandferner glacier, Pt²¹⁰ and Sr⁹⁰ meas. in firn and ice samples 8=18831
 Norton County achondrite, Rb⁸⁷-Sr⁸⁷ isochron, and K⁴⁰-Ar⁴⁰ ages 8=19278
 nuclear debris, fresh, by activity-ratio determ. 8=7119
 Quaternary samples, use of Th²³⁰ and Pa²³¹ 8=9797
 scintillation liquid radio carbon count 8=9798
 C¹⁴, 42 samples 8=2566
 C¹⁴ in tree rings, rel. to sunspot cycle and Tunguska meteor 8=23225
 K-Ar ages of basalts dredged from E and W Pacific 8=19062
 K-Ar meas. on Brazilian glauconites 8=18830
 Te ore, by isotope anal. of inert gases 8=14455
- Radioactive tracers**
 absorption obs. for Sn self-diffusion 8=22161
 for diffusion in solids, effect of lattice defects conc. 8=22141
 gas flow appl. for particle residence time 8=21454
 ion sublation studies 8=23075
 rubber + benzene mixtures, tracer diffusion 8=21641
 in sediments and silt, digital computer data processing 8=18835
 in semiconductor research, appl. of autoradiography 8=18019
 in trace characterization, symposium 8=18797
 Br⁸², for Fe(OH)₃ suspension flow meas. 8=21727
 Cd-CdCl₂ soln., physico-chemical props. study 8=21615
 Co(II)-Ni(II)-Mn(II)-V(V)-Mo(VI) chloride systems, extraction separation studies 8=23077
 F¹⁹ in HF etches, rel. to fluoride chemisorption in Si and SiO₂ surfaces 8=18697
 HTO, suitability for atmospheric boundary layer mass transfer obs. 8=14594
 H-3, I-131, for groundwater flow obs. 8=2568
 I¹³¹, for metals-iodine reaction kinetics 8=23093
 I¹³¹, suitability for atmospheric boundary layer mass transfer obs. 8=14594
 In^{113m}, generator method 8=14449
 Mg, silico-thermal prod., mechanism 8=23776
 MO(VI) extraction, with 100% TBP mechanism study 8=23076
 N¹⁵ in solids detec. by activation 8=14504
 Na in SiO₂ films, rel. to Na contamination obs. 8=18069
 Na²², cosmic ray prod., meas. for atm. exchange studies 8=18857
 Ra, in Ra-Ba mixed crysts., crystn. study 8=21962
 S³⁵ and O¹⁸, in metals and alloys oxidation study 8=23092
 W¹⁸⁵, in tungstate soln. aggregation study 8=21607
 Xe¹³³, diffusion in zirconium carbide, activation energy, rel. to struct. 8=8686

Radioactivity

See also Alpha-, Beta-, Gamma-rays; Atmosphere/radioactivity; Beta-decay theory; Chemical analysis, radioactive; Chemical effects of radiations/ionizing radiations; Fallout; Geophysical prospecting; Nuclear decay theory; Nuclear bombardment targets; Nuclear excitation; Nuclear reactions; Radiochemistry.

activation by accelerator bombard., timing and control system 8=11799

α -ray counting, determination of Avogadro's number 8=7483

Auger effect, charging recoil atoms from α -decay 8=16014

β -decay and non-radiative internal processes 8=3861

β -emitting isotopes, counting doubly labelled quenched samples 8=23171

β - γ directional correlation in retarded allowed β -transitions, higher order effects 8=11803

β - γ angular correlation, rel. to CP violation 8=669

coating contamination, diffusion model 8=7341

crystalline shield rocks, abundance of elements, Th, U and K 8=9794

emitters, disintegration rate meas. 8=11848

environmental, National Nuclear Research Centre, Pelindaba, S. A., 1966 8=18908

fallout, from French 1966 Pacific tests 8=18907

Fierz term, and new data on ϵ/β^+ ratio in forbidden transitions 8=1002

fission-product contamination of earth, spectra, aircraft meas. 8=9895

γ -field, near-surface atm., effect of rock and soil moisture 8=9795

γ methods in geophysics, classification system 8=23224

γ -ray dose distributions in phantom exposed to fallout and simulated fallout 8=23301

natural materials, data improvement since U fission discovery, review 8=7123

nuclear transformations in nature 8=7116

nuclides far off the stability line, conference, Lysekil Sweden (1966) 8=15911

nuclides, 60, prod. by irradiation of Ag with 3 and 29 GeV p, isobaric charge distrib., mass-yield curves 8=20799

positron emitting nuclides, use of (β^+ γ) coincidence method 8=20743

products from 20 MeV bremsstrahlung irradiation, γ -ray study of activities 8=7163

radiation asymmetry and n. m. r. of β -radiative nuclei 8=7128

sources, alkali-metal and alkaline-earth prod. by α bombard. of rare gases 8=7121

spherical nuclei to nonspherical, phase transform, theory 8=3776

of upper mesozoic graywackes, north coast ranges of California 8=2565

Ac²²⁵ α decay 8=16048

Ac²²⁸ separation and purification in Ra²²⁸ solns. by solvent extraction method 8=16047

Al²⁷ resonant state decay, $\gamma\gamma$ correl. of γ -rays, E = 10.480 MeV 8=7079

Am²⁴¹ α decay, charge of recoil atoms 8=20742

At²¹⁰ β -decay and non-radiative internal processes 8=3861

Au^{177,178,179,181,183,185,187} α -decay energy, half-life 8=16045

Au^{179,180,183,185} α -decay energies and lifetimes 8=7148

Au¹⁹⁸ γ rays scatt. by air, soil and water, distrib. obs. 8=20356

B¹² ground state in β -decay in C¹²(n, p)B¹², 14.5-22 MeV 8=16090

Ba isotopes from Cf²⁵² fission obs. 8=20858

Ba, spallation yield of Xe after 730 MeV p irradiation 8=20797

Bi²¹⁴ γ spectrum, Po²¹⁴ level scheme 8=16006

C¹²(1⁺, 12.71 MeV) \rightarrow 3 α , breakup anal. 8=1006

Ca⁴⁸, double decay and conservation of leptons 8=7129

Cf²⁵² fission n source, standard, construction and emission props. 8=6950

Cl³⁶ \rightarrow S³⁶, β -decay shape factor 8=1004

Co⁶⁰ absolute γ -activity monitors 8=20749

Co⁶⁰, γ back scattering density 8=1007

Co⁶⁰, γ intensity distrib. 8=1009

Co⁶⁰, γ rays scatt. by air, soil and water, distrib. obs. 8=20356

Co⁶⁰, specific γ -ray constant 8=16029

Co⁶⁸, decay 8=11809

Cs⁵³(p, p' γ)Cr⁵³ and Cr⁵³(p, n γ)Mn⁵³, γ -yields 8=7185

Cs isotopes from Cf²⁵² fission obs. 8=20858

Cs¹³⁷, γ back scattering density 8=1007

Cs¹³⁷ γ rays scatt. by air, soil and water, distrib. obs. 8=20356

Cs¹³⁷, isolation with Cu ferrocyanide-anion exchange resin 8=3879

Cs¹³⁷ point source γ energy and angular distrib. obs. 8=16028

Cs¹³⁷, specific γ -ray constant 8=16029

Er¹⁶⁹ \rightarrow Tm¹⁶⁹ disint., conversion electron spectrum 8=16039

Eu¹⁵² decay, longitudinal polarization of β -rays 8=20754

Eu¹⁵⁴, 1855-123 keV β - γ directional correl., energy depend. obs. 8=7142

Radioactivity—contd

Eu¹⁵⁵ \rightarrow Gd¹⁵⁵, investigation by iron free magnetic β spectrometer 8=11769

Fm²⁵¹ \rightarrow Cf²⁴⁷ transition energy using γ - α coincidence obs. 8=1027

Ga⁷² decay rel. to Ge⁷² level structure obs. 8=11751

Ge⁷⁶ \rightarrow Se⁷⁶ + 2e⁻, lepton non-conservation search 8=3870

H⁵ unbound to particle emission 8=11659

He-like atomic nuclei β -decay rel. to 1S state conservation prob. 8=7426

Hg^{179,180,182}, α -decay energies and lifetimes 8=7148

Ho¹⁶² \rightarrow Dy¹⁶², β -decay calc. of spin-quadrupole force effect 8=11801

I^{130m} disintegration to I¹³⁰ level 8=7097

K⁴¹, reson. activation integral determ. 8=11808

Kr⁸⁵, at. excitation following β decay in solid 8=8226

Mg²⁸, production 8=11807

Mn⁵⁴ γ -spectrometric source calibration 8=20750

Mn⁵⁴ \rightarrow Cr⁵⁴, upper limit to positron decay 8=7132

Mn⁵⁵, reson. activation integral determ. 8=11808

N¹⁶ β -decay and non-radiative internal processes 8=3861

(NH₄)₂OsCl₆, use in expts. concerning nucleus 8=16044

Nb¹⁰⁰, activity obs. 8=3940

Ni⁶³, β -emitter, meas. and β -self-absorpt. as metallic Ni 8=16020

Np²³⁷, γ -spectrum obtained with Ge-Li detector 8=20732

Np²³⁹ electron binding energy determ. in different chemical states 8=4065

Np²⁴⁰ decay to Pu²⁴⁰ 1.131 MeV state 8=11791

O and H isotope vars., firm core in W. Antarctica 8=14563

P³⁰ 5.5 MeV level, property obs. 8=7192

P³², inner bremsstrahlung obs. 8=11811

Pb²¹¹, γ -ray obs. 8=7149

Pm¹⁴⁷, β decay, K ionization probability obs. 8=12419

Po²¹⁵, γ -ray obs. 8=7149

Pr¹⁴⁰, e⁻ decay, rel. to photoneutron cross-section of Pr¹⁴¹ 8=16060

Pt^{176,177,178,180}, α -decay energies and lifetimes 8=7148

Pu²³⁹ decay, 300-450 keV γ -radiation 8=16049

Ra²²⁶ and derivatives low energy γ radiation 8=16046

Rb⁸¹ impurity in Ir^{196,195m}, confusion in decay scheme 8=11827

Rn²¹⁹, γ -ray obs. 8=7149

Rn²²⁰ exhalation and prods. in atmosphere 8=9893

Ru¹⁰⁶ in Black Sea seaweeds, identification and separation 8=9734

Sb³⁴ delayed neutron precursor, half-life 11.3 sec. 8=3875

Sr^{87m}, enrichment by recoil effect of (n, 2n) reaction 8=7214

Sr, spallation yield of Kr after 730 MeV p irradiation 8=20797

Ta¹⁷⁸-Ha¹⁷⁸, β -decay calc. of spin-quadrupole force effect 8=11801

Tc⁹⁹, β decay, K ionization probability obs. 8=12419

Te¹¹¹ delayed proton emitter in Pd¹⁰² + C¹² reaction 8=7137

Te¹¹¹, identification by daughter products of proton decay 8=11818

Tl²⁰⁴, continuous β -spectrum and K Auger-line spectrum 8=1026

Tm¹⁶⁴-Er¹⁶⁴, β -decay calc. of spin-quadrupole force effect 8=11801

U²³³ α -ray spectra 8=11830

U²³³, γ -spectrum from decay, identification of 7 new lines 8=20760

V⁵¹, reson. activation integral determ. 8=11808

V⁵¹ reson. integral 8=16098

Xe isotopes, prod. by in-pile melting of irradiated UO₂(NO₃)₂·6H₂O 8=3982

Xe in meteorites, fission and spallation, isotope ratios 8=14859

Xe-133, in leak test method, for semicond. devices 8=2211

Xe¹³⁷⁻¹⁴² from Cf²⁵² fission obs. 8=20858

Y⁹⁰ β -decay and non-radiative internal processes 8=3861

Y⁹⁰, inner bremsstrahlung obs. 8=11811

Zn⁶⁵ γ -spectrometric source calibration 8=20750

dating. See Radioactive dating.

decay periods

deformed nuclei, even-even, systematics of E₂ transitions 8=7043

energy levels, particle beam pulsing system obs. 8=7058

ft values for 0⁺-0⁺ transitions calc., suggested change of definition 8=7125

isomers, by In^{116m} activation 8=3821

nuclear excited states using delayed coincidence at Studsvik 8=7060

103^{266,267}, half-lives obs. 8=7151

tables for residual activity 8=7124

Ac^{209,215} obs. 8=20759

Ag⁹⁹ \rightarrow Pd⁹⁹ 8=1016

Ag¹⁰¹ \rightarrow Pd¹⁰¹ positron spectrum 8=1015

Ag¹⁰⁰, possibility 8=1016

Al, isotope produced by 60 MeV p bombard. 8=1061

Al²⁴, ground state mass, T_{1/2}=0 analog state 8=16017

Al^{26m}, β -decay calc. 8=7126

Ar³⁸, lifetimes obs. Ca⁴⁰ analogies 8=11738

Au^{177,178,179,181,183,185,187} 8=16045

Radioactivity—contd

decay periods—contd

Au¹⁹³ internal conversion spectrum rel. to Pt¹⁹³ level at 1.64 keV 8=7111
 Au¹⁹⁸, obs. 8=7130
 Au²⁰², from n reactions on Hg²⁰² and Tl²⁰⁵ 8=11828
 Au²⁰⁴, prod. by Hg²⁰⁴(n, p)Au²⁰⁴ 8=11828
 Ba¹³³ → Cs¹³³ 8=11820
 C¹⁰, β-decay calc. 8=7126
 C¹³, first excited state 8=15955
 C¹³, 3.09 MeV state, mean life 8=11723
 Ca⁴⁰ lifetime analogies with Ar³⁸ 8=11738
 Cd¹⁰⁹ → Ag^{109m}, obs. for 220 days 8=11816
 Ce¹³⁰, isomeric levels, 10.5 MeV p-bombard. 8=3826
 Ce¹⁴³ → Pr¹⁴³, β decay lifetimes 8=11764
 Ce¹⁴⁴, obs. 8=7130
 Cl³², ground state mass, T_z=O analog state 8=16017
 Cl³⁴, β-decay calc. 8=7126
 Co⁵⁴, β-decay calc. 8=7126
 Cu, isotope produced by 60 MeV p bombard. 8=1061
 Dy¹⁶⁰, half-lives of 2⁺ states 8=11771
 Er^{166,168}, half-lives of 2⁺, 4⁺ rot. states 8=11771
 Er¹⁷³ 8=20756
 Eu^{153,156}, half life of $\frac{1}{2}$ (532) transic state obs. 8=7103
 Fe, isotope produced by 60 MeV p bombard. 8=1061
 Fm^{244,245}, new nuclides 8=7242
 Fm²⁵², two α-particle groups obs. 8=1027
 Gd¹⁵⁴, half-lives of 2⁺ states 8=11771
 Gd^{156,158}, half-lives of 2⁺, 4⁺ rot. states 8=11771
 Hf¹⁷² → Lu¹⁷² 8=3834
 Hg¹⁹⁴ → Au¹⁹⁴, L e-capture 8=1025
 Ho^{161,163}, isomeric levels, 10.5 MeV p-bombard. 8=3826
 I¹²⁵, obs. 8=7130
 In¹¹⁵, 597, 829 and 864 keV states 8=981
 Ir^{191m}, isomeric state in reaction (γ, γ') 8=11781
 K⁴² obs. 8=16025
 Kr-85, γ-ray branching 8=7133
 Lu¹⁷¹, 71.2 keV level obs. 8=7107
 Lu^{170g,m} and decay schemes 8=1022
 Lu¹⁷⁶, γ-ray spectra 8=1023
 Mg^{23,27}, β-γ decay 8=16016
 Mn⁵⁰, β-decay calc. 8=7126
 Mn⁵⁶, obs. 8=7130
 Mo⁹³, from yields of (d, 2n) reactions 8=1014
 Mo⁹⁹, half-life determ. 8=11814
 N¹⁵, lifetime of mirror states from N¹⁴ bombard. of H² and Be⁹ 8=3793
 Na²⁰ 8=20745
 Na²² energy level obs. in C₂F₆ 8=11729
 Nb^{90m}, influence of chemical binding on half-life 8=16024
 Nb⁹⁵, obs. 8=7130
 Nb^{99,100}, short-period isomers 8=7089
 Nd¹⁴¹ isomeric levels, 10.5 MeV p-bombard. 8=3826
 Ne¹⁸, β-γ decay 8=16016
 O¹⁴, β-decay calc. 8=7126
 O¹⁵ lifetime of mirror states from N¹⁴ bombard. of H² 8=3793
 Os^{186,188} first excited 2⁺ level obs. 8=7109
 P³² first excited state 8=11732
 Pb²⁰⁹ levels obs. 8=3841
 Pd⁹⁹, daughter of Ag⁹⁹ 8=1016
 Pd⁹⁹ daughter of Ag⁹⁹ 8=1016
 Pm¹⁵¹, half life of $\frac{1}{2}$ (532) transic state obs. 8=7103
 Pr¹⁴⁴ 8=11765
 Pr¹⁴⁴, obs. 8=7130
 Pu/Xe and I/Xe concordant intervals of achondrites 8=23468
 Re¹⁸⁸ isomer obs. 8=7109
 Rh¹⁰², 2 year and γ-ray spectra 8=20751
 Rn^{210,211,212} 8=11952
 Sc⁴⁰, ground state mass, T_z=O analog state 8=16017
 Sc⁴², β-decay calc. 8=7126
 Sc⁴³ 472 keV state mean lifetime obs. 8=967
 Si²⁸, β-γ decay 8=16016
 Sm¹⁴³, redetermination from γ-ray spectra 8=986
 Sm¹⁵², half-lives of 2⁺ states 8=11771
 Sn¹¹⁵, 619 keV level, $\frac{1}{2}$ state 8=7095
 Sn^{118,120} 4⁺ and 5⁺ states obs. 8=11758
 Ta¹⁷⁰, using a time-amplitude convertor 8=16042
 Ta¹⁷⁰, rel. to negative search for high spin three-quasiparticle isomer 8=7108
 Ta¹⁸⁰, γ-ray spectra 8=1023
 Ta¹⁸², 16.3 min, study by Ge(Li) detector and e-e coincidence spectrometer 8=20727
 Te^{128,130}, double β-decay 8=1017
 Tl²⁰⁸, half-life, accurate value 8=20758
 Tm¹⁷⁰, 4.1 μs isomeric state, strongly retarded E1 transitions 8=990
 Tm¹⁷⁰, Nilsson model for β-decay 8=1021
 Tm¹⁷⁰ → Yb¹⁷⁰, β-decay lifetime, anomaly in forbidden transitions 8=11822
 Tm¹⁷² Ω-forbidden transition levels 8=15995
 U²³³, absolute M1 and E2 transition probabilities 8=20731
 Vn⁴⁶, β-decay calc. 8=7126
 W¹⁸³, 46.5 keV level 8=15999
 Y⁸⁷ isomer, β decay 8=11812
 Y⁹⁰, obs. 8=7130
 Yb¹⁶³ → Tm¹⁶³ obs. 8=7146
 Z = 104-115 superheavy elements, lifetime predictions 8=7122

Radioactivity—contd

decay schemes

103^{266,267}, α-decay 8=7151
 γ-transitions of 10 nuclei 8=16019
 Ac^{209,215} obs. 8=20759
 Ag⁹⁹ → Pd⁹⁹ 8=1016
 Ag¹⁰⁰, possible obs. 8=1016
 Ag¹⁰¹, γ-trans, positon decay 8=1015
 Ag¹⁰², γ-rays 8=7094
 Ag^{106m}, 8 day, 45 γ-rays 8=7134
 Ag^{106m,r}, γ-decay, energy levels of Pd¹⁰⁶ 8=979
 Ag^{106m} → Pd¹⁰⁶, γ-spectrum 8=7092
 Ag^{110m}, disint. and γ-transitions 8=7135
 Ag¹¹¹ → Cd¹¹¹, new transitions, B(E2) values, energy level lifetimes 8=20712
 Al²⁴, ground state mass, T_z=O analog state 8=16017
 Am²⁴¹, γ-spectrum 8=3846
 Au¹⁹⁹, β-transitions, shape and longitudinal polarization meas. 8=20753
 Au²⁰², β endpoint energy, γ-decay, half-life 8=11828
 Au²⁰⁴, βγ 8=11828
 Ba¹³³, γ Cs¹³³, K conversion coeffs. obs. 8=16031
 Ba¹³³ → Cs¹³³, e. m. transitions, conversion coeffs. determ. 8=11820
 Ba¹³³, γ and X-rays, calibration standard for Ge(Li) detectors 8=6655
 Bi²⁰⁵ → Pb²⁰⁵ γ-transitions 8=997
 Br⁸⁷, in atmosphere 8=2611
 C¹⁰ → B¹⁰, β-decay obs. rel. to anomaly in 1.74 MeV state of B¹⁰ 8=16015
 Cd¹⁰⁹, for meas. of isomeric transition of Ag¹⁰⁹ 8=3820
 Cd^{117,117m} → In¹¹⁷ for levels of In¹¹⁷ 8=15984
 Ce¹⁴¹, β-transitions, shape and longitudinal polarization meas. 8=20753
 Ce^{133,133m} → La¹³³, β-decay, levels of La¹³³ 8=20722
 Ce¹³⁵ → La¹³⁵ 8=20721
 Ce¹⁴³ → Pr¹⁴³, β decay lifetimes 8=11764
 Cf²⁵¹ → Cm²⁴⁷, α, γ 8=11835
 Cl³², ground state mass, T_z=O analog state 8=16017
 Cl³⁵, from S³⁴(p, γ) 8=1063
 Co⁵⁶ → Fe⁵⁶, for calibrating γ-ray detectors up to 35 MeV 8=11428
 Co⁶⁰, for level control 8=1010
 Cr⁴⁶ → V⁴⁶, polarization of 305 keV radiation 8=11749
 Cs¹²⁸, γ-decay rel. to existence of O⁺-2⁺-4⁺ vibrational triplet in Xe¹²⁰ 8=3825
 Cs¹³⁴ → Ba¹³⁴ 8=7139
 Cs¹³⁴ → Ba¹³⁴, β-spectrum 8=16030
 Cs¹³⁴ → Ba¹³⁴, levels obs. 8=7099
 Cs¹³⁶ γ-spectrum obs. 8=11761
 Cs¹³⁷, for level control 8=1010
 Er¹⁷¹ → Tm¹⁷¹, β decay 8=11775
 Er¹⁷³, new isotope 8=20756
 Eu¹⁴⁵, radiation obs. 8=16037
 Eu¹⁴⁹ → Sm¹⁴⁹, γ-ray spectra, K-shell internal conversion coeff. 8=7143
 Eu^{152,154,155,156} γ-intensities 8=11821
 Eu^{152,154}, E2 transitions of Sm¹⁵² and Gd¹⁵⁴ internal conversion 7=1020
 Eu^{152,154}, rel. to Sm¹⁵², Gd¹⁵⁴, β- and γ-vibrational bands obs. 8=16034
 Eu^{152,154} → Gd^{152,154}, first forbidden β-transitions relative intensity of K-components 8=11822
 Fe⁵⁹ → Co⁵⁹ 8=15979
 Fe⁶¹, γ- and β-spectra, Fe⁶¹-Co⁶¹ 8=3869
 Fm²⁵³ → Cf²⁴⁹, α, γ and e spectra 8=11836
 Ga⁷², β-γ circular-polarization parameter 8=1013
 Ga⁷² → Ge⁷², new γ-rays 8=16021
 Gd¹⁴⁹ → Eu¹⁴⁹ → Sm¹⁴⁹, γ-ray spectra, K-shell internal conversion coeff. 8=7143
 Hf¹⁷² + Lu¹⁷², positrons, number 8=11824
 Hg¹⁹⁴ → Au¹⁹⁴, e-capture 8=1025
 Ho^{152,153}, α-decay energies and half-lives 8=3883
 Ho¹⁵⁴, α, half-life, new isotope 8=3883
 Ho¹⁵⁵, α, unsuccessful search 8=3883
 I¹²¹, γ obs. 8=20752
 I¹²⁵ → Te¹²⁵, half-life of first excited state of Te¹²⁵ 8=15986
 P²⁸ γ-decay rel. to existence of O⁺-2⁺-4⁺ vibrational triplet in Xe¹²⁰ 8=3825
 In^{194m}, K X-ray and γ decay obs. 8=7147
 I^{195,195m}, γ-decay scheme disentangled from Rb⁸¹ 8=11827
 La^{132,134} → Ba^{132,134} 8=20720
 Lu¹⁷² → Yb¹⁷² γ, K=3 rot. band of Yb¹⁷², multipolarities deduced 8=15996
 Lu¹⁷⁶, lifetime 8=1023
 Lu^{176g,m} half-lives 8=1022
 Mg^{23,27}, β-γ branching ratios, lifetimes 8=16016
 Mg²², positron, branching ratios 8=3866
 Mn⁵² → Cr⁵², excited states populated in decay 8=15976
 Mo⁹⁰ → Nb⁹⁰, obs. 8=20711
 Na²⁰, β, γ-decay spectra 8=20745
 Na²⁰ → Ne²⁰, β decay meas. by delayed α emission 8=3865
 Na²² positron spectrum, statistical shape obs. 8=20746
 Nb⁹⁰, end-point energy of e⁺, internal-conversion spectrum 8=11813
 Nb⁹⁷ → Mo⁹⁷ 8=16023
 Nd¹⁴⁷ → Pm¹⁴⁷, γ-ray spectrum 8=3881
 Ne¹⁸, β-γ branching ratios, lifetimes 8=16016

Radioactivity—contd**decay schemes—contd**

Ne²³, following Ne²²(n, γ), unsuccessful search for 2.285, 2.405, 2.870 MeV levels 8=11806
 Os¹⁹¹, harder γ -rays 8=3886
 Os¹⁹³ \rightarrow Ir¹⁹³, levels of Ir¹⁹³ 8=11826
 P²⁸, ground state mass, T_x=O analog state 8=16017
 Pb²¹¹ \rightarrow Bi²¹¹ 8=7150
 Pd¹⁰¹, γ -trans, positron decay 8=1015
 Pd¹⁰⁹ \rightarrow Ag¹⁰⁹, excited states of Ag¹⁰⁹ 8=16026
 Pm¹⁴⁴, Nd¹⁴⁴ energy levels above 1.78 MeV 8=16033
 Pr¹³⁹ \rightarrow Ce¹³⁹, γ -rays, e⁻ capture and e⁺ decay 8=7141
 Pr¹⁴⁴ \rightarrow Nd¹⁴⁴, γ -ray schemes 8=11765
 Pt¹⁹⁸, from Au spallation 8=1024
 Pt¹⁹⁹ \rightarrow Au¹⁹⁹ 8=994
 Pu²³⁹ \rightarrow U²³⁵ 8=11789
 Pu²⁴⁵ \rightarrow Am²⁴⁵, β -spectrum, conversion spectrum 8=11833
 Re¹⁸⁰, 2.5 min. 40 γ rays and levels of W¹⁸⁰ 8=3885
 Re^{186,9}, Nilsson model for β -decay 8=1021
 Rh⁹⁹, γ -ray decay 8=978
 Rh¹⁰², 2 year and γ -ray spectra 8=20751
 Rh¹⁰⁶, γ -decay energy levels of Pd¹⁰⁶ 8=979
 Ru¹⁰³, e internal conversion 8=11815
 S³⁷ \rightarrow Cl³⁷ β -decay 8=16018
 Sb¹²⁵ \rightarrow Te¹²⁵, half-life of first excited state of Te¹²⁵ 8=15986
 Sc⁴⁰, ground state mass, T_x=O analog state 8=16017
 Sc^{44m} \rightarrow Ca⁴⁴ 8=3868
 Se⁸³ \rightarrow Br⁸³, β , γ 8=3871
 Si²⁶, β - γ branching ratios, lifetimes 8=16016
 Sm¹⁵³, β - γ ang. correl. obs. 8=16035
 Sm¹⁵⁵ \rightarrow Eu¹⁵⁵, β and γ decay 8=7105
 Sn^{117m, 119m}, internal-conversion studies of M4, M1 transitions 8=20717
 Sn^{123, 125m} \rightarrow Sb^{123, 125} 8=11817
 Sn¹²⁵ \rightarrow Sb¹²⁵, γ -spectra 8=16027
 Sn¹²⁵ \rightarrow Sb¹²⁵, new γ -rays, branching 8=3874
 Ta¹⁸⁰, e-capture search 8=1023
 Ta¹⁸² for meas. of isomeric transition of Ag¹⁰⁹ 8=3820
 Ta¹⁸², 16.3 min, study by Ge(Li) detector and e-e coincidence spectrometer 8=20727
 Ta¹⁸² \rightarrow W¹⁸² 8=11825
 Ta¹⁸⁶ 8=16043
 Tb¹⁵¹-Gd¹⁵¹, by γ -spectrum and γ -coincidence spectra 8=7145
 Tb^{151, 152}, new γ -transitions 8=3882
 Tb¹⁵⁵ \rightarrow Gd¹⁵⁵, internal conversion e spectrum 8=100 keV 8=988
 Tb¹⁵⁵ \rightarrow Gd¹⁵⁵, internal conversion e spectrum 8=600 keV 8=988
 Tb¹⁵⁶ \rightarrow Gd¹⁵⁶, γ -decay, internal conversion coefficients 8=7144
 Tb¹⁵⁸ \rightarrow Dy¹⁵⁸ new level and γ transitions 8=20755
 Tb¹⁶⁰ \rightarrow Dy¹⁶⁰, first forbidden β -transitions relative intensity of K-components 8=11822
 Te¹¹⁷ \rightarrow Sb¹¹⁷, β , γ decay 8=3876
 Te^{119m} gamma and conversion electron spectra obs. transitions 8=7136
 Te^{119m} \rightarrow Sb¹¹⁹, γ -ray cascades 8=3877
 Te^{131m}, decay, multiplicities of transitions 8=3878
 Tl²⁰⁷, γ -ray spectrum 8=7150
 Tm¹⁶⁵ \rightarrow Er¹⁶⁵, by e-capture 8=20757
 Tm¹⁷⁰, β -decay, first-forbidden, conserved vector current theory 8=16040
 Tm¹⁷⁰, Nilsson model for β -decay 8=1021
 Tm¹⁷⁰ \rightarrow Yb¹⁷⁰ β -decay, forbidden transitions, anomaly in in K-mixture calc. 8=11822
 Tm¹⁷² \rightarrow Yb¹⁷², γ transitions 8=11823
 U^{234m}, γ -spectrometry 8=11831
 U²³⁸, γ -spectrum 8=11832
 V⁴⁸, β - γ circular polarization correl. meas. 8=7131
 V⁵² \rightarrow Cr⁵², excited states populated in decay 8=15976
 Xe¹²³, half-life 2.08 h 8=7138
 Xe^{125, 127} \rightarrow I^{125, 127} 8=11760
 Y⁸⁷ isomer, β decay 8=11812
 Z = 56-78 M/L, N + O/ M ratio in internal conversion E2 transitions 8=7140
 Zn⁶⁵ \rightarrow Cu⁶⁵, new γ -rays 8=1012
 Zr⁹⁷ \rightarrow Nb⁹⁷ 8=16022

electron capture

induced capture of orbital electron, cross-section 8=1042
 internal conversion cascade γ , accurate determ. 8=11798
 in stars evolution and ν prod. rel. to matter density 8=10138
 Ag¹⁰⁵, P_L/P_K for transitions to 1088 and 344 keV levels of Pd¹⁰⁵ 8=3873
 Ar³⁷, M/L ratio, for calc. of K _{α} fraction in K-series of Cl 8=20748
 Ba¹³³ 8=11820
 Ba¹³³ \rightarrow Cs¹³³ 8=16031
 Hf¹⁷⁸, Lu, K Auger spectrum 8=1187
 Hg¹⁹⁴ \rightarrow Au¹⁹⁴, half-life 8=1025
 Ho¹⁵³, α -e capture ratio 8=3883
 K⁴⁰, energy from various reactions 8=11740
 K⁴⁰, specific activity of K capture 8=7176
 KX- γ directional correlations 8=20739
 Lu¹⁷⁴ isomers, disint. energies 8=11776
 Na²², evidence of orbital electron exchange 8=20746
 Ni⁵⁶ and Ni⁵⁷, meas. of P_L/P_K using dicyclopentadienyl nickel 8=3914

Radioactivity—contd**electron capture—contd**

Pr¹³⁹ decay, spin and parity assignments to Ce¹³⁹ levels 8=7141
 Rb⁸⁶, $\lambda_{E.C.}/\lambda_{\beta}$ -branching ratio obs. 8=11810
 Sn¹¹³, L and K Auger effect spectra of In¹¹³ 8=4099
 Ta¹⁸⁰, search 8=1023
 Tm¹⁶⁵ \rightarrow Er¹⁶⁵ obs. 8=20757
 Tm¹⁷⁰ \rightarrow Yb¹⁷⁰, 84.3 keV γ conversion coeff. 8=16041
protection. See Radiation protection.
Radioactivity measurement
 See also Dosimetry; Radiation monitoring; and the specific radiation, e.g. Gamma rays.
 autoradiography, quantitative, emulsion density-sample activity characts. obs. 8=23764
 β -emitter weak, automatic compensation for liquid scintillation counters 8=20740
 β - γ emitters, standardization using low-efficiency detectors 8=11797
 β -ray spectra, backscattering deformation, experimental corrections 8=3850
 Doppler, shift attenuation method for low recoil vels. 8=7156
 γ cascade from e capture, from ang. correl. meas. 8=11798
 γ -ray dose from gas cloud, calc. 8=10448
 fallout, from French 1966 Pacific tests 8=18907
 inert gases, radioactive, precision determ. 8=3864
 nuclear radiation 8=601
 source-to-detector solid angle calc. 8=1000
 source-detector solid angle, integral calc. 8=20184
 source to target geometry, computer soln. of activation eqn. 8=3854
 spheroidal source, calc. of γ -dose on axis 8=3855
 tritium liquid scintillation counter 8=3856
 C¹⁴ containing substs., precision determ. in gas phase 8=3864
 C¹⁴, low level β activity, apparatus 8=3852
 Cs¹³⁷, isolation with Cu ferrocyanide-anion exchange resin 8=3879
 H³ containing substs., precision determ. in gas phase 8=3864
 H³, low level β activity, apparatus 8=3852
 K⁴² in aqueous media, det. 8=3867
 Nb⁹³, irradiated α -emission energy 8=1041
 Ne²⁰ β -decay by delayed α emission 8=3865
 Pm¹⁴⁴, Nd¹⁴⁴ energy levels above 1.78 MeV scintillation spectroscopy 8=16033
 Te¹³⁰, double β -decay, by Xe analysis in mineral 8=1017
apparatus
 See also Particle detectors.
 activation of specimens in bremsstrahlung bundles 8=7117
 β emitter standardization, proportional counter 8=16012
 e spectrometer, background signals 8=11467
 4 π gas counter, γ counting efficiency 8=605
 heart, γ -scanning to separate blood flow and muscle 8=5981
 hybrid computer for calc. of radioisotope activity after n flux bombard. in reactor 8=4025
 neutron monitoring for radiological protection, conference Vienna, Austria (1966) 8=15852
 point source assumption effect 8=11288
 portable radiation survey instruments, regulated d.c.-d.c. converter for low standby current 8=3455
 proportional counter, gas for low level β emitters 8=3852
 scintillation camera, autofluoroscope, data processing for 8=5982
 scintill. counter for γ sources, corrections 8=3851
 solid state detectors, suppression of interference pulses by anti-coincidence tech. 8=6650
 source mounts, increasing cond. of metallized plastic films 8=5153
 spark counter for α -activity meas. 8=7120
 tritium low energy β -rays, evacuation of scintill. probe 8=3853
 ultra-stable, for exact meas. 8=20737
 C¹⁴, low energy β -rays, evacuation of scintill. probe 8=3853
 H₂ counter, effect of Cd thickness on response 8=852
 Si detectors, simple laboratory applications 8=11311

Radioastronomy

See also Cosmic radiations, radiofrequency; Sun/ radiation, radiofrequency.
 accurate positions of 210 radio sources 8=23617
 activity during eclipse, 20 May 1966, obs. 8=19301
 Andromeda nebula (M31), 11-cm obs. 8=10268
 antennas and receivers, book 8=19005
 antennas array of 36 with resolutions of 1, 3, 9 and 27 seconds of arc at 11 cms 8=10442
 atmospheric opacity and source brightness obs. 8=2595
 auroral absorpt., apparent poleward expansion 8=18988
 centimetre-wave, atm. noise fluctuations 8=18894
 converter, wideband of waveguide type 8=23757
 cosmic background temperature, 9.24 mm 8=14728
 cosmic noise, night-time var. with solar activity 8=10283
 cosmic radio emission, frequency spectrum, 10-207 MHz, high galactic latitudes 8=23612
 decimetre waves, atmos. radiation temp., for 0.5-10° elevations 8=18896

Radioastronomy—contd

- extra galactic sources 8=23606
 extra galactic sources, spectroscopic obs. 8=23607
 fan-beam scans inversion 8=5979
 flux density obs. at 153 MHz 8=19228
 Fornax A source structure 8=23601
 galactic emission, Compton effect calculations 8=3571
 galaxies, normal, radiation at 8 cm flux densities and angular dimensions obs. 8=10266
 galaxies, normal spiral, radio radiation at 430 and 611 MHz 8=5933
 galaxies, normal spiral, r. f. spectra, flux densities of radio sources 8=5935
 hydrogen, interstellar distribution, 21 cm obs. with 300 foot telescope 8=23565
 interferometer measurements with 910⁶ wavelength baseline 8=10286
 interferometer, 2800 Mc/s, multielement 8=2867
 interferometer using 2 steerable paraboloids, of 425 metres baseline, operation at λ 21 cm 8=10441
 interferometry, long base line, using tape recorders 8=5978
 Jupiter, decametric emission, satellite Io effect 8=19250
 Jupiter, decametric radiation, ionospheric effect 8=2819
 Jupiter, decametric radiation, sub-msec. obs. 8=23665
 Jupiter, decametric radioemission 8=10346
 large array 8=23761
 lunar occultation obs. of radio sources, two-dimensional brightness distrib. 8=5943
 lunar radio emission at 25.0 and 30.2 cm by the "artificial moon" method 8=10327
 at Mackenzie University, Brazil 8=23756
 magnetic tape recording, short-section scanner 8=15265
 at N. Copernicus University, Poland 8=23755
 NGC 6611, 6523 and 7000, electron densities from 4 cm obs. with 85 foot scope 8=23570
 pencil-beam radio telescope, survey of emission at 178 MHz 8=19225
 phase-coherent interferometry without r. f. link 8=10440
 planetary rotations, radar determ. 8=23672
 polarization, linear, of 950 MHz emission 8=14806
 quasars 3C 273, 3C 279, 3C 446 and 3C 454.3, variations in 1.96 cm flux density 8=2804
 quasars 8=2805
 radio sources between declinations +27° and -30°, identification 8=23615
 31 radio sources between 40 and 130 MHz, obs. 8=23616
 radiointerferometer of the Haute-Provence observatory, description 8=14889
 radiometer for meas. cosmic background radiation 8=2866
 radiotelescope of the Nauca station, the pointing device 8=5980
 scintillations, em. wave propag. 8=386
 scintillation meas. with interferometer system 8=2865
 scintillation study of Cassiopeia A 8=2801
 solar bursts, type III, obs. by automatic interplanetary station "Venus-2" 8=10396
 solar eclipse 20 May 1966 obs. 8=19287
 sources, 9.55mm, flux density obs. 8=23599
 sources, 38 MHz, interferometric obs. 8=10287
 sources, 458 with declination in range +18° to +20° at 750 and 1410 MHz, pencil beam survey 8=23605
 Sun, apparatus for 239 MHz obs. 8=19300
 survey of southern sky at 85 MHz 8=10257
 3C273, interplanetary scintillation 8=14807
 telescope, 150 ft at Algonquin Park 8=23760
 telescope, 140 ft precision at Greenbank 8=23759
 tropospheric radio absorption meas. 8=5792
 in USA, Dicke panel recommendations 8=23758
 Venus ionosphere, re-examination of porous model 8=14848
 zenith temp. at wavelength 3.2 cm 8=23754
 H, atomic, discrete spectrum and radiodiapason obs. 8=7377
 IC 410, electron densities from 4 cm obs. 8=23570
Radiocarbon dating. See Radioactive dating.

Radiochemistry

- See also Chemical analysis/radioactive; Chemical effects of radiations/ionizing radiations; Radioactive tracers.
 balance, remote controlled for weighing in high radiation environment 8=6005
 hot-atom reactions, energy dependence 8=14447
 polyethylene, short branches, quant. det. by γ radiolysis 8=16392
 separation by adsorpt. on MnO₂ 8=9763
 Au¹⁹⁹ removal from n irradiat. Pt by ion exchange 8=23168
 Co⁵⁸, carrier-free extraction using 1-phenyl-3-methyl-4-capryl-pyrazolone-5 8=18750
 Cs¹³⁷, isolation with Cu ferrocyanide-anion exchange resin 8=3879
 Cs¹³⁷, Sr⁹⁰ and Ce¹⁴⁴ activity, in rain water, Sydney, analyses 8=14632
 F¹⁸ prod. from n-irrad. of LiOH, Li⁶ (n, α) H³ and O¹⁸ (l, n) F¹⁸ 8=4024
 Fe⁵⁹, carrier-free extraction using 1-phenyl-3-methyl-4-capryl-pyrazolone-5 8=18750
 H₂-T₂ mixtures, equilibria and reaction rates 8=14448

Radiochemistry—contd

- In^{113m}, generator method 8=14449
 Kr^{83m} preparation by n bombard. of Se⁸² 8=3872
 Mn⁵⁴, carrier-free extraction using 1-phenyl-3-methyl-4-capryl-pyrazolone-5 8=18750
 Ru¹⁰⁶ in Black Sea seaweeds, identification and separation 8=9734
Radiography
 See also Luminescent devices; X-ray tubes.
 autoradiography, quantitative, emulsion density-sample activity characts. obs. 8=23764
 neutron, divergent beam collimator 8=21975
 semiconductor research, autoradiography appl. to tracer studies 8=18019
 X-ray film, quantitative calibration, 5 keV-1.3 MeV 8=1556
 X-ray pulmonary densitometry, physical aspects 8=14898
 X-ray tube power supply voltage fluctuation effects 8=11243
 Al and Al-Au alloy, solid-liq. interface 8=4646
 Sn, recrystallization, autoradiography 8=13142
Radiolysis. See Chemical effects of radiations/ionizing radiations.
Radiometer gauges. See Vacuum gauges.
Radiosondes. See Meteorological instruments.
Radiosources. See Cosmic radiations, radiofrequency.
Radiostars. See Cosmic radiations, radiofrequency; Stars.
Radiotelescopes. See Radioastronomy.
Radiowave propagation. See Electromagnetic wave propagation.
Radiowave spectra. See Nuclear magnetic resonance and relaxation; Paramagnetic resonance and relaxation; Spectra.
Radium
 distribution, Ba-Ra chromate mixed crystals 8=9736
 tracer, in Ra-Ba mixed crystals, crystn. study 8=21962
 vapour absorpt. spectra using modified King furnace 8=7393
 RaA, charged atoms, capture on metal disk 8=1370
Radium compounds
 No entries
Radium emanation. See Radon.
Radon
 in atmosphere, exhalation changes rel. to conc. and conc. of decay products 8=9891
 Rn^{210, 211, 212} beam, recoil prod., for bombard. of Al foil 8=11952
 Rn²²⁰ exhalation and prods. in atmosphere 8=9893
 Rn²²² in atm. over Atlantic, Antarctic and Paris 8=14635
Rain
 See also Condensation; Snow.
 amino acid content obs. 8=2589
 atmospheric aerosol particles removal by drops 8=23275
 electric charge on drops in warm clouds over Hawaii 8=9858
 electrical conductivity of water in cloud over Hawaii 8=9857
 rel. to precipitation near earth's surface, microstruct. at 500-1000 m, radar obs. 8=9854
 Cs¹³⁷, Sr⁹⁰ and Ce¹⁴⁴ activity, Sydney 8=14632
 H³ input to North Pacific rel. to water mixing time calc. 8=23247
Raman spectra
 See also Luminescence.
 cryostat for crystals. 8=22941
 crystal powder spectra, absolute intensity meas. 8=14174
 crystalline powders, oblique illumination apparatus 8=3360
 diamond-like crystals, first-order effect rel. to electrostriction and photoelasticity 8=9486
 dielectrics, mag. ordered, two-magnon scattering 8=9487
 dielectrics, magnetically ordered, rel. to Faraday effect 8=5575
 directional intensity of Stokes and anti-Stokes lines 8=4122
 electronic Raman effect and vibronic coupling 8=12129
 fluids, laser beam filament formation, linearized theory 8=8067
 gases, rot. and rot.-vibr., obs. 8=6523
 infrared absorpt. and Raman scatt. calc. 8=14176
 insulators, lattice Raman scattering theory 8=2397
 liquids, stimulated, effects of spontaneous emission and mol. vibr. damping 8=4587
 liquids, stimulated scattering, self-focusing 8=4585
 laser line widths obs. 8=6523
 molecules, diatomic, pressure broadening obs. 8=6523
 plasma, laser beam scatt. 8=1401
 powders, He-Ne laser excitation 8=14175
 pulsed mode intense scattering, calc. 8=18488
 resonance effect, connection with absorpt. freq. 8=9484
 and Rayleigh scatt. by molecules in bounded medium 8=21031
 review, expt. and theory since 1962 8=12128
 review of Soviet work 8=12132
 ruby, R, R¹ and B absorpt. linewidth and phonon-induced relaxations 8=14194
 scattering by polarization waves 8=9485
 stimulated, quantum theory 8=3292
 stimulated scatt., molec. mechanism 8=7487
 stimulated, study by second-harmonic-generation technique 8=11018
 totally symmetrical lines, depolarization factor, near resonance 8=16250

Raman spectra—contd

- vibrational frequencies, 54 molecules, data compilation 8=21036
- inorganic substances**
- calcite, stimulated 8=5591
- quartz α - β transition assoc. lattice modes from Raman scatt. -196-315°C 8=1682
- quartz, stimulated scattering under optical pumping rel. to mode pulling theory 8=2453
- sapphire, with Ar⁺ laser source rel. to vib. of cryst. 8=2401
- stimulated emission without resonant cavity 8=12127
- transition metal anions in crystalline phase 8=9542
- water, in concentrated ionic solns. 8=1565
- AgMnO₄ 8=21085
- AlP, and infrared active modes 8=18500
- As(SiH₃)₃, rel. to struct. 8=4144
- B, X-ray scatt. of Cu K α rad. 8=2396
- BaTiO₃ overdamped vibr. made from 30 ft mode line-shape obs. 8=5586
- Be, X-ray scatt. of Cu K α rad. 8=2396
- BeO excited by 6328Å line of a He-Ne laser 8=18507
- Br absorbed on silica gel, laser obs. 8=23031
- BrHBr⁺ and BrDBr⁺ ions 8=12174
- C, X-ray scatt. of Cu K α rad. 8=2396
- CO₂, cryst. 8=9510
- CS₂ adsorbed on silica gel, laser obs. 8=23031
- CsBr, and i.r. absorption spectrum at second order, interpretation 8=5595
- CsMnO₄ 8=21085
- D, solid, anomalous intensities rel. to mol. vibrational motion and coupling 8=9535
- GaAs, scattering by coupled optical-phonon-plasmon modes 8=22984
- GaP, and i.r. spectra near optic phonon modes, dielectric dispersion 8=14215
- H₂ cell, stimulated emission at 8.84 μ m by Nd³⁺:glass laser 8=15484
- H₂, Q(1) line stimulated by laser wave in presence of static field 8=16283
- H₂, Raman scattering cross section calc. 8=7517
- H, solid, anomalous intensities rel. to mol. vibrational motion and coupling 8=9535
- H, solid, intensity anomalies 8=6523
- H₂, solid and liquid, intensity anomaly 8=9536
- H₂, stimulated effect meas. in terms of laser oscillator and amplifier theories 8=21081
- HDO in H₂O 8=21690
- HgI₂, molten state 8=21691
- HgIBr, molten state 8=21691
- HgICl, molten state 8=21691
- IF₃, rel. to vib. assignment, and Fermi resonance 8=1568
- K vapour, stimulated emission from Raman scattering from 4P_{3/2} level 8=20984
- KBr, second order scattering in polarized light 8=14231
- KBr and KCl, mixed, scattering 8=18541
- KCl, pure and doped, scattering 8=5614
- KH₂PO₄, anisotropic crystal, analysis of stimulated Raman effects 8=9543
- KI, second order, exptl. study 8=5615
- KMnO₄ 8=21085
- K_nMⁿX₆ (Mⁿ = Au, Pt, Pd; X = Cl, Br), solid and soln. comparison 8=14189
- K_nMⁿX₆ (Mⁿ = Au, Pt, Pd; X = Cl, Br), solid and soln. comparison 8=14189
- KNO₃ containing KNO₂ impurity, analysis 8=23177
- KNO₃ 1050 cm⁻¹ line, absolute scatt. coeff. determ. 8=14174
- KrF₂, absence of Fermi reson. 8=7528
- KSO₃F 8=9562
- Li, X-ray scatt. of Cu K α rad. 8=2396
- MgF₂, scattering and i.r. absorpt., selection rules 8=5621
- N₂ in atm., scatt. obs. 8=23289
- N₂O, cryst. 8=9510
- NaCl, polarized light study 8=18547
- NbCl₅ cryst. 8=14249
- O₂ in atm., scatt. obs. 8=23289
- S₂Cl₂ 8=12231
- S₈ 8=12227
- Sb(SiH₃)₃, rel. to struct. 8=4144
- SnTiO₃, electric-field-induced, optical-phonon freq. 8=5370
- TiCl₄, difference bands 8=7570
- Zn(NO₃)₂·xH₂O, molten 8=16868

organic substances

- acenaphthene, broadening and freq. variation as function of temp. 8=5649
- acrylyl fluoride, rel. to rot. isomerism 8=16311
- allyl halides 8=21111
- benzene, absolute scatt. cross section of 992 cm⁻¹ line 8=16858
- benzene derivs, liq., l.f. lines, effects of temp. solvents, etc. 8=1563
- benzene, liq., l.f. lines, effects of temp., solvents, etc. 8=1563
- benzene, 992 cm⁻¹ line, rel. to solvent and conc. 8=21672
- benzene, stimulated Raman effect, cyclic temp. depend 8=21125
- 2-bromocyclobutanone 8=12266
- 2-bromo-2,4,4-tridenterocyclobutanone 8=12266

Raman spectra—contd**organic substances**—contd

- carbon tetrachloride, difference bands 8=7570
- chlorosilyl dialkylamines 8=1300
- cloud seeding, results in Australia 8=23280
- cyclopentadiene 8=12267
- cyclopentadiene nickel nitrosyl, laser-excited 8=21155
- cyclopropane, liq. rel. to fundamentals and force consts. 8=1298
- deuterotoluenes, o-, m- and p- 8=7574
- deuteriochlorobenzenes, o-, m- and p- 8=7574
- trans-dichloroethylene adsorbed on silica gel, laser obs. 8=23031
- 2,6 difluoropyridine, liq. 8=16341
- 0,0-dimethyl phosphorochlorodithioate 8=21146
- ethane-1,1,1-d₃, rot. consts. obs. 8=16321
- ethylene, Raman spectra and electrooptical parameters compared with trichloroethylene 8=21138
- haloacetoneitriles 8=16323
- halogenated ethanes 8=12269
- intensities and depolarizations calc. 8=12131
- methylsilyl dialkylamines 8=1300
- monobromoacetoneitrile 8=12281
- naphthalene 1383cm⁻¹ line, absolute scatt. coeff. determ. 8=14174
- nitrobenzene and liquids, quenching with picosecond pulse excitation 8=4580
- nitrobenzene, 1345 cm⁻¹ line, rel. to solvent and conc. 8=21672
- p-nitro-p'-dimethylaminoazobenzene, cryst., in KBr, ruby laser excitation 8=9570
- 1,2,5-oxadiazole, liq., rel. to complete vib. assignment 8=16335
- oxalate free ion, D_{2d} symmetry and freq. assignment 8=21154
- polymethylene chains, longitudinal acoustic vibrs. 8=8608
- 2-pyrrolidone, vibration spectra, 3500-250 cm⁻¹ 8=7595
- ribonucleic acid derivatives, and molec. structure 8=7598
- scattering cross-sections calc. 8=12130
- 1,2,5-selenadiazole 8=16342
- tetrachloroethylene Raman spectra and electrooptical parameters compared with trichloroethylene 8=21138
- thiazoles, monosubstituted, vibrs. and coupling 8=4217
- p-toluidine, broadening and freq. variation as function of temp. 8=5649
- trichloroethylene, absolute intensities, depolarizations and electrooptical parameters 8=21138
- triethylphosphine and related cpds. 8=21137
- 2,4,6-trifluoropyrimidine, liq. and vapour 8=16340
- trimethylaluminium 8=16327
- BF₃:dimethyl sulphide complex, liq. 8=1569
- CCl₄ adsorbed on silica gel, laser obs. 8=23031
- CCl₄, 64°K 8=18576
- CD₂COBr 8=7555
- CHCl₃, 64°K and -120°C 8=18576
- CH₂Cl₂, 64°K 8=18576
- (CH₂)₂S, scattering spectra in liquid phase 8=18573
- (CH₂)₂POCl 8=12286
- (CH₂)₂PSBr 8=12286
- (CH₂)₂PSCl 8=12286
- Ramsauer effect.** See Electron beams; Electrons/absorption; Particle range.
- Random functions.** See Random processes.
- Random processes**
- See also Brownian movement; Fluctuations; Statistical analysis.
- branching-diffusion, no absorbing boundaries 8=85
- disordered lattices, 3D, spectral gaps 8=10609
- fluctuation-dissipation theorem, steady-state 8=10608
- Gaussian light, intensity-fluctuation distribution 8=20019
- geoaoustic and geomag. data, statistical reduction methods 8=6092
- lattice, self-energy expressed as a continued fraction 8=10613
- linear systems, noise temp. definition 8=19437
- non-stationary, ejections of 8=84
- nuclear reactor noise, equivalent source 8=3991
- in nuclear reactor, zero-power, noise-equiv. source 8=3995
- observed-likelihood-ratation criterion, steps for estimation 8=2961
- photoemission, random-walk models 8=22719
- Rayleigh waves, scattering, at elastic body random boundary 8=10700
- scattering of particles in random force field 8=14940
- self-avoiding walks, statistical thermodynamics 8=14984
- stationary, probability error and entropy 8=2962
- stationary, real normal, energy spectrum estimation 8=14982
- statistical mechanics and thermodynamics, conference Copenhagen Denmark (1966) 8=15007
- Stochastic, control, recent approaches 8=19436
- stochastic, in linear configurations with transition probab. independ. of components' states 8=6089-90
- system with random Hamiltonian, evolution 8=19435
- walk in presence of absorbing barriers 8=86
- H theorem of Boltzmann and Brownian motion 8=16905
- Range of particles.** See Particle range.

Rare earth metals

- See also the individual metals.
 aluminium binary systems, arrangement 8=13286
 analysis via photoactivation with 20 MeV
 bremsstrahlung 8=7161
 antisymmetric exchange theory 8=16972
 compressibility, 8 metals subjected to high press., effect
 of electron structure 8=17724
 desorption from W surface 8=17171
 elastic moduli and Debye temps. of polycryst. metals,
 4.2 and 300°K 8=2057
 electron interaction 8=22838
 fergusonite system, crystal chemistry 8=8515
 fission products, chromatography 8=9739
 of h. c. p. and Sm structures, stability and axial
 ratios 8=4866
 hyperfine interactions, calorimetry 8=17514
 inverse-phase chromatography with phosphoric-acid
 treated paper 8=18765
 ion luminescence in NaCl:Se crystals 8=14334
 ions, electric multipole interactions 8=16977
 ions, electronic energy transfer to H₂O vibrations 8=16870
 ions, paramagnetic, in crystals, magneto-optic
 rotation 8=5590
 ions, Re³⁺, in fluoride crystals, molar absorpt.
 coeff. 8=23011
 lanthanides in fields of cubic symmetry, composite fⁿD
 configurations theory 8=21799
 lanthanides (IV), free ion 4f levels 8=21814
 lanthanides, recrystallization and work hardening
 characts. 8=5089
 magnetic ordering and electronic properties 8=22466
 in Scheelites, cryst. field rel. to tetragonal centres
 optical and e. p. r. spectra 8=1637
 specific heat, 3 to 25°K, rel. to mag. props. 8=17513
 spin interaction, from magnon dispersion curves 8=22768
 trivalent ions, energy transfer between, in inorganic
 solids 8=9594
 trivalent ions in fluorite type crystal, radiochemical
 reduction giving divalent centres 8=18740
 X-ray emission spectra, self-absorpt. effects 8=2447
 in Al, liquid, mag. susceptibility and Knight shift
 changes 8=21724
 La³⁺, (L=Ce, Pr, Nd, Sm, Gd, Dy, Er and Yb), 4f electron
 radial wave functions 8=1168

Rare earth compounds

- See also the compounds of the individual metals;
 Ferrites.
 acetates, i. r. spectra and thermal decomp. 8=23095
 alloys, n-mag.-scattering 8=18349
 aluminides, RAl₃, (R=rare earth metal), closest-packing
 superstructure 8=17410
 chelate solns. as acceptors of e-de-excitation of organic
 molecules 8=16333
 chelates in soln., laser action 8=3338
 chromites, antiferro- and ferromag. props. 8=18388
 cobaltides, Curie temp. dependence on comp. and
 structure 8=18350
 crystal field parameters from ground state splitting of
 paramagnetic 8=18445
 dicarbide formation when diffusing in graphite 8=4950
 garnets, paramagnetic susceptibilities and antiferro.
 transitions 8=9298
 germanides, R₂Ge₃, 13 new cpds., structures 8=8554
 intermetallic compounds, paramagnetic
 susceptibilities 8=2298
 lanthanide complexes, mixed, energy transfer 8=2433
 lanthanide-gallium cpds., crystal structures 8=1812
 lanthanide phthalocyanines, acid adducts, absorption
 spectra 8=4589
 lanthanide (III) oxalate decahydrates, structures 8=8529
 oxides, non-stoichiometric, semiconducting props. 8=9118
 oxides, Bi-activated, luminesc. 8=14304
 oxides, X-ray and spectrographic investigations of phase
 transitions and polymorphism 8=4722
 rare-earth Al borates, nonstoichiometry 8=8410
 rare-earth Co (RCO₅) cpds. permanent mag. props.,
 obs. 8=22743
 rare-earth chelates, exchange-reson. energy transfer
 overlap integrals calc. 8=1656
 rare-earth hexaborides, magnetic properties 8=5438
 rare earth Fe garnets, intrinsic coercive force near
 compensation temp. (>77°K) 8=14005
 rare earth Fe garnets, magnetostriction constns. 8=2322
 rare-earth-manganese cpds., prep. by amalgam process
 and structures 8=17203
 rare-earth sesquioxides, crystal growth by Verneuil
 method, and optimum conditions 8=4813
 scatts, ion-pair spectra 8=9497
 sesquioxides, crystal growth by Verneuil method;
 radiation effects and optimum conditions 8=4813
 sesquisulphide crystals, electronic struct. 8=9119
 silicides, R₂Si₃ and R₃Si₂, new cpds., structures 8=8554
 sulphate hydrates, crystallographic data 8=17385
 tetraborides, of Gd, Dy, Ho, Er and Tm, magnetic suscep-
 tibility rel. to temp. 8=5437
 trichlorides, cryst. fields 8=13011
 trifluorides, n. m. r. of F¹⁹ 8=5556

Rare-earth compounds—contd

- trivalent heavy rare-earth ions, magnetization anisotropy
 in high mag. fields 8=2293
 Co compounds with CaZn₂ structure, mag. and
 crystallographic props. 8=22753
 Ir-rare-earth, mag. fields at Ir¹⁹³ 8=1634
 Ln₂O₃S₂, crystalline structure 8=4883
 Nd³⁺ ions in rare-earth trichlorides, new satellite
 structure 8=12070
 Pt alloys, conduction electron polarization 8=17857
 R-Ni-Si, (R=rare earth), system, ternary cpd. formation,
 comp. and structures 8=17200
 RAl, (R = rare earth), structures rel. to DyAl and CeAl
 structures 8=1789
 RAl₃, (R=rare-earth metal), closest-packing super-
 structures 8=17410
 RCrO₃, antiferro- and ferromag. props. 8=18388
 RCO₃, mag. props. and crystallographic structure 8=13967
 RCO₃, Curie temp. dependence on comp. and
 structure 8=18350
 RGe-Si system, (R = Gd, Tb, Dy, Ho and Er), 5:4 stoichio-
 metry and mag. props. 8=4779
 R₂M_{1-x}Al₂ (R=Gd, Tb, Er and M=Y, La, Th) cubic Laves
 phases, Curie temps. and magnetizations 8=14039
 R₂Ni, alloys, (R = rare earth), mag. props. 8=18363
 R₃Ni, cryst. structure 8=13247
 R₂O₃-M₂O₃, (R = rare earth, M = Nb, Ta or Pa), crystal
 structure 8=1802
 in YFe garnet rel. to spin wave susceptibility saturation
 above instability threshold, obs. 8=22864
 in YIG, spin wave linewidth variations 8=5495

Rare gases. See Inert gases.**Rayleigh scattering.** See Scattering/light.**Rayleigh waves.** See Elastic waves; Seismic waves.**Reaction kinetics**

- See also Catalysis; Chemical reactions; Exchanges,
 chemical; Explosions.
 acetaldehyde pyrolysis, acetone formation 8=9683
 acetaldehyde with atomic H, mass spectra 8=18668
 acetate ion oxidation by K₂S₂O₈, Ag catalysis 8=23094
 austenite, alloyed, C activity at 1000°C 8=17008
 bimolecular rate constant, table for e, H and OH in
 aqueous solns. 8=2510
 catalytic heterogeneous, forward and reverse rate constns.,
 dynamic method of calc. 8=14403
 chemical relaxation methods for study 8=14352
 chemisorption, molec.-orbital model 8=18695
 cyclobutane, freq. factor for rate const. 8=14364
 deoxidation product growth and separation, collision
 model 8=18658
 dielectric relax. due to rate processes 8=9673
 diffusion-controlled processes 8=4555
 diffusion-controlled reactions, temp. effects 8=18657
 dissociation of diatomic mols. 8=7615
 dissociation field effect relax. apparatus, square wave,
 for rapid reaction rate obs. 8=9665
 electron affinity or ionization potential, dependence 8=14357
 electron-transfer reactions, transition-state
 parameter 8=9675
 ethane, vibrationally excited 8=18675
 ethylene, oxidation and pyrolysis in shock
 waves 8=18676
 ethylene polymerization on CrO₂, chain transfer,
 obs. 8=23129
 flame, low temp. O with H or CO 8=9699
 fluoro-olefines on oriented polymer fibres, radiation
 graft-copolymerization 8=23138
 free-radical formation in tetracyanoethylene 8=9686
 gas production, pen recorder 8=14353
 gases, e. s. r. study 8=14351
 gases, non-equilib. boundary-layer problems, finite-
 difference soln. 8=18662
 hydrated electron, bimolec. recomb. 8=5705
 hydrogen ion solvation by H₂O mols. in gas phase,
 equilibrium constns. 8=18661
 hydrogenolyses of propane, toluene and xylene 8=14379
 ion-molecule reactions, energy depend. 8=16432
 ion-polar mols., capture collisions 8=7696
 iron alloys saturated with oxides, liquid, first-order
 interactions rel. to oxide solubilities 8=16797
 iron, liq.-silica deoxidation product growth and separation,
 collision model 8=18658
 isopropyl iodide form. by C₃H₈ + I₂ irradiation with
 visible light 8=5745
 light scatt. as probe of fast reactions 8=9681
 metal corrosion in acids rel. to organic inhibitors
 specificity 8=2509
 metal crystal oxide film growth, model based on thermionic
 emission and ionic diffusion 8=5710
 metal sulphide chlorination in ore roasting 8=5712
 metal surfaces, passivity theory 8=9702
 metals-iodine, use of I₂ 8=23093
 p-methacryloxybenzoic acid, kinetics of polymerization
 in soln. 8=14410
 oscillations round steady state in systems far from
 equilib. 8=2500
 oxy-halogen radical systems 8=23125
 perfluoropropene, reaction with O atoms 8=14377

Reaction kinetics—contd

- polar mols. with no activation energy 8=2507
- polymerization at low conversions, study via polarographic maxima 8=5728
- polymers, statistics of substitution 8=18659
- polypyromellitimide formation, i.r. spectra study 8=14408
- precipitation deoxidation, collision model 8=18658
- propionic acid, u.s. absorpt. 8=12860
- propylene, hydrogenolysis 8=14379
- quinaldic acid, decarboxylation, isotope effects 8=9697
- rate consts., cross sections, D₂O-M system reactions (M = H-carbon) 8=9671
- rates of reactions of radical anions, e.s.r. meas. 8=14350
- reversible isomerization in multilevel system 8=9680
- reversible termolec. reactions in multilevel system 8=9679
- solid state reactions, nucleation theory 8=23090
- in solutions under pressure 8=14356
- solvent effects in n.m.r., collision complexes 8=12935
- stainless steel corrosion in CO₂ and CO₂-CO, C behaviour 8=2515
- steel, anodic dissolution and corrosion potential 8=9723
- thermal gravimetric apparatus, sample 8=9658
- thermobar, strain gauge, continuously recording 8=9659
- time-correlation-functions for nonlinear rate consts. 8=6113
- toluene, hydrogenolysis 8=14379
- transition metal complexes, ligand substitution 8=14387
- trioxane in soln., polymerization in soln. 8=14407
- trioxane, pre-irrad., polymerization, 30-64°C 8=23133
- trioxane, solid, SnCl₄ initiated cationic polymerization, obs. 8=23132
- unimolecular, competitive decomp. in chem. activated systems 8=14359
- xylene, hydrogenolysis 8=14379
- Al + Cl reaction, from 500 to 650°F 8=14358
- Br₂, with K, Rb and Cs atoms 8=1202
- CH₄-O₂ mixtures, combustion products, thermodynamic equilibrium calc. 8=14393
- CaO, water vapour effect on sintering kinetics, 921-1123°C 8=21833
- Fe oxides (hematite, maghemite, magnetite, reduction processes below 400°C 8=5703
- Fe-Cr alloys of 25-95%Cr comp., oxidation at 1000-1300°C 8=18677
- in Ge melt, interaction between O₂ and B 8=23104
- H₂ + HeH⁺, energy hypersurface, MO calc. 8=16285
- H₂ + I₂, interpretation ambiguities 8=5706-7
- H₂ + I₂ reaction paradox 8=23105
- H + O₂ recomb. in shock tube 8=14367
- H₂ + O₂, slow rate and second limit, computer calc. 8=18678
- H₂O desorption in from TiO₂, 25-100°C 8=18703
- H₂O destruction on surfaces 8=18704
- H[ReO(CNS)₁₀]₁₀³⁻ → ⁴CNS⁻, radioisotopic exchange 8=23089
- H₂SnO₃ conversion to SnO₂, Mössbauer obs. 8=14386
- H₂-T₂ mixtures 8=14448
- He⁺ photoionization reactions with N₂ and O₂ 8=16444
- I₂, with K and Cs atoms 8=1202
- K + HBr, DBr, crossed-beams, velocity and ang. distrib. of KBr 8=9689
- La metal high-temp. oxidation 8=18680
- N atoms, recomb. rate 8=1313
- N₂¹⁴⁻¹⁴ + N₂¹⁵⁻¹⁵ → 2N₂¹⁴⁻¹⁵, in shock tube 8=5696
- NH₃, decomp. in glow discharge 8=18682
- NH₃ + HCl → NH₄Cl, charge transfer 8=5714
- NO with perfluorodimethyl peroxide 8=14371
- Ni, diffusion-controlled, at cylindrical surfaces 8=14372
- NiO in O₂, stoichiometry 8=13826
- NiS film growth on Ni in S solns., obs. 8=2525
- O atoms and SO₂, e.s.r. study 8=5715
- O atoms with Cl₂ 8=9696
- O + COS → CO + SO, vel. const. determ. 8=9672
- O + D₂ → OD + D, using e.s.r. detect. 8=14375
- O(¹D) with H₂ 8=5744
- O + H₂ → OH + H, vel. const. determ. 8=9667
- O + O₂ + M → O₃M, rate constant measurements 8=2508
- O₂(a¹Δg) + O₃ → 2O₂ + O, reaction rate 8=16450
- O₂(¹Δg) collisional-radiative reaction 8=12220
- O₂-Nb system, at very low pressure, adsorption, absorption and degassing 8=4763
- O₃ reaction with H and OH 8=5744
- OCS pyrolysis in shock tube with quadrupole mass filter 8=14361
- OH with itself and with CO 8=18684
- PbS, sulphation 8=9698
- SiO₂ film deposited from SiCl₄-water vapour reaction 8=21889
- UO₂ dissoln. in acid media 8=18691
- UO₂, lattice defects rel. to thermochem. and non-stoichiometry 8=23113
- [V(CN)₅NO]⁵⁻ → ¹⁴CN⁻, isotope exchange 8=23088
- Zn corrosion in CO₂ solns., rel. to predominance diagrams 8=2523

Reactors. See Nuclear reactors, fission; Nuclear reactors, fusion.

Re(h) binder effect. See Mechanical strength; Surface phenomena.

Recombination. See Ions, recombination; Semiconductors.

Recombination radiation. See Luminescence.

Recording

- See also Sound recording.
 - gas production kinetics, pen recorder 8=14353
 - magnetic tape, appl. to radiotelescope interferometry 8=10440
 - magnetic tape, short-section scanner 8=15265
 - ratios, simple method using existing recorders 8=6037
 - superconductor critical current curves 8=13738
 - X-Y recorder, time mark generating circuit 8=15176
- Rectifiers**
- See also Electron tubes; Semiconducting devices.
 - quartz, piezoelectric, for microwave energies 8=9227
 - semiconducting, and other power devices, review 8=18094
 - thyristors for power frequencies above 400 Hz, rating and applications 8=13849
 - Al-Al₂O₃-metal diodes, negative resistance obs. 8=5377
 - BaTiO₃, silver-ceramic, junction manufacture 8=18125
 - Si controlled, for generation of rectangular current pulses 8=15178
 - psn-Si, switching processes, doping conc. effect at strong doping 8=5320
 - psn, switching processes, doping conc. effect 8=5319
 - Si-controlled circuits for prod. pulsed mag. field 8=3164
 - ZnO, piezoelectric, for microwave energies 8=9227

Recrystallization (metals). See Heat treatment.

Red giants. See Stars.

Red shifts. See Astronomical spectra; Cosmology; Relativity/general.

Reflectance. See Reflectivity.

Reflection

- See also Neutrons/reflection; X-ray reflection.
 - elastic waves in cylindrical wedge 8=10706
 - electrons at zero energy, from Ag surface, coeff. 8=6301-2
 - internal total as cause of π₂ phase shift in refractive media 8=19547
 - MHD waves 8=15358
 - GdF₃ powders spectrum 8=2421
 - Gd₂O₃ powders, spectrum 8=2421
 - p-HgTe, i.r. in region of plasma minimum 8=5262
 - Se films, polycrystalline and single crystal, in electron diffraction pattern 8=4753
 - Tm and Tm₂O₃, total reflection of 8.4 keV γ-radiation of Tm¹⁶⁹ 8=23018
- acoustic waves**
- See also Echo; Reverberation.
 - bass, dimensioning of loudspeaker casings using equivalent electric circuits 8=10730
 - coefficient of discontinuous changes of cross-section in tubes with air flow, expt. 8=19565
 - elastic, plane, at boundary between viscoelastic media 8=6129
 - focusing system, double mirror, analysis 8=19576
 - from ionized medium, current boundary layer prod. 8=6378
 - masking levels in concert halls 8=19594
 - nonstationary, from arbitrary inhomogeneous half-space at fixed angle 8=15067
 - ocean bottom, review 8=2572
 - rough boundary time and frequency characteristics 8=19566
 - shock waves, conical, apparatus and expts. 8=10718
 - split beam sound-field, WKB-type approx. 8=19567
 - CO₂, normal shock, with vibrational relaxation 8=1455

acoustic waves, ultrasonic

- Lamb and Rayleigh waves, from plate end sections, rectangular 8=3060
 - radar system 8=3072
- electromagnetic waves**
- bremsstrahlung, from single crystal, spectro-metry 8=6794
 - coefficient for layered media (ionosphere model) 8=18980
 - complex permeability and permittivity, meas. of at microwaves 8=6399
 - creeping wave excit. by mode conversion of critically incident ray 8=19826
 - cylindrical passive oscillator 8=3179
 - dielectric medium moving at relativistic speed, Brewster angle 8=6377
 - dielectric, moving perpendicular to incident plane 8=10947
 - dielectric plate, moving, and transmission 8=369
 - dielectrics, periodic pile, nodes of standing waves 8=19837
 - dispersive Epstein layer, pulse response 8=19841
 - elementary particle behaviour 8=20279
 - ellipsoid of revolution, ideally conducting, plane 8=367
 - gyrotropic layer, Faraday effect 8=3376
 - interface between moving media 8=19842
 - from ionized medium, current boundary layer prod. 8=6378
 - ionospheric coefficient, e.l.f. 8=18993
 - lateral wave on symmetrical Epstein transition 8=19840
 - magnetosphere, He ion effects 8=9921
 - moon, plane layered model 8=23645
 - from moving media, energy relations 8=368
 - plane, incident on stratified medium 8=18979
 - polarization angle rel. to impedance matching 8=3256
 - quadrupole spin echo, amplitude calc. 8=370
 - radar cross section, computerized geometrical optics approach 8=20040
 - radiation beats and rotating systems 8=15396

Reflection—contd

electromagnetic waves—contd

- spherical reflectors, feeds 8=19894
 transhorizon tropospheric propagation, book 8=14630
 and transmission by moving dielectric slab, parallel polarization 8=19836
 2 dimensionally inhomogeneous medium, general theory 8=10951
 undulating surface, character of signals 8=18989
 Venus enhanced, r.f. reflectivity areas obs. 8=10355
 wax-film on painted surface, determ. of thickness and roughness 8=2470
 X-rays incident on periodic pile of absorbing layers 8=3255
 AuCu₃, X-ray rel. to atomic characteristic temp. 8=13029
 Ge, low-freq. reflectivity in mag. field 8=22988
 NaClO₃, spectrum and constants, cooling effects 8=9555
 PbTe, low-freq. reflectivity in mag. field 8=22988

light

- See also Mirrors; Optical films.
 at boundary of two absorbing mats., phase angle, graphical representation 8=500
 Brocken observation, quantitative 8=11166
 coefficient at lowest exciton level calc. from polariton model 8=22480
 crystals, birefringent, internal and external faces 8=14184
 dielectric rough-surface, polarization properties 8=11200
 earth-moon system astron. params. optical radar meas. 8=14827
 glass, rough at large incidence, indicatrices with two maxima 8=5631
 gyrotropic layer, Faraday effect 8=3376
 internal, rel. to bulk optical props. 8=22934
 invariant properties rel. to acceptance angle of a quadrupolar multiplet 8=15500
 laser radar target miss probability, atm. scintillation effects 8=9869
 light impulse, in scatt. from semi-infinite layer 8=9878
 mat surfaces, i.r. reflectance 8=18485
 by molecular excitons, form of bands 8=5127
 multilayer dielectric broad band surfaces 8=11167
 multiple, between two mirrors in rel. motion, expression for Doppler freq. shift 8=15543
 nebula, luminosity gradient calc. 8=19192
 ocean surface, time-average evaluation 8=18840
 prism resonator, mode eqn., soln. 8=20088
 reststrahl, anomalous structure from slight surface roughness 8=5572
 retro-reflection by diffusing surfaces 8=468
 rotating convex surfaces, flux density var. meas. 8=15497
 scattering media, spectral line profiles near resonance 8=509
 total internally, use in holography 8=3378
 two-mirror system, theorem 8=11126
 u.v. attenuated total, for meas. conformation of adsorbed polymers 8=8350
 ultraviolet, book 8=20012
 ultraviolet refl. spectra, photoelec. method 8=15532
 wave theory, corpuscular interpretation 8=15547
 Ag film, 0.4-1 μ range 8=5580
 Ag films, non-linear effects on laser-radiation 8=18497
 Ag-Cr film, 0.4-1 μ range 8=5580
 Al₂O₃ powders, and polarization properties 8=14266
 BiI₃ spectrum doublet structure rel. to spin-orbit interaction, 1-5 eV 8=9509
 BrO₃Na monocrystals, effect of cooling on spectrum 8=18509
 CaF₂, MgF₂, Na₃AlF₆, thin films, i. r. antireflectant suitability 8=2435
 Ca₃Sb₂O₇ (x = 1, 2, 3; y = 4, 5, 6), spectra 8=14363
 CdSb₂O₄, spectra 8=14363
 CdSe, and absorption spectra in i.r. at low temps. 8=23026
 Cr film, 0.4-1 μ range 8=5580
 GaAs, electroreflection meas. 8=2422
 GaAs, laser induced changes 8=5633
 CdO, u. v., influence of lattice vibrations 8=9514
 CdS, doping, heat treatment and deform. effects, 4.2°K 8=9606
 CdSe, doping, heat treatment and deform. effects, 4.2°K 8=9606
 Cu₂O spectrum rel. to band struct., obs. 8=9524
 KCl-KBr solid solns., 5 and 25 eV rel. to band level transitions 8=22995
 by KH₂PO₄ cryst. in 1-bromonaphthalene, refl. second-harmonic intensity obs. 8=5611
 KI, 5-25 eV rel. to band level transitions 8=22995
 MnSb₂O₄, spectra 8=14363
 MnTe, antiferromag. semiconductor, and transmission, 80-375°K 8=5622
 Na-Li liq. mixtures, crit. opalescence 8=1558
 by NaClO₃ cryst. in 1-bromonaphthalene, refl. second-harmonic intensity obs. 8=5611
 Ni-Si alloys, coeff., and thermal e. m. f. 8=18551
 SbI₃ spectrum doublet structure rel. to spin-orbit interaction, 1-5 eV 8=9509
 Si, laser induced changes 8=5633
 SiC powders, and polarization properties 8=14266

Reflection—contd

light—contd

- SiC/Al₂O₃ powders, and polarization properties 8=14266
 SnO₂, rel. to electron scattering polar optical modes 8=22611
 Sr₂Sb₂O₇ (x = 1, 2; y = 4, 5), spectra 8=14363
 V₂O₅, diffuse reflection spectra 8=18564
 ZnSe, and absorption spectra in i.r. at low temps. 8=23026
 ZnTe, and absorption spectra in i.r. at low temps. 8=23026
 ZrO₂, monoclinic, diffuse reflectance characts. as function of purity 8=18568

Reflectivity

- See also Diffusion/light; Optical constants; Optical films.
 earth, in rel. to Si det. response 8=18834
 electroreflectance near anisotropic interband edges in cubic crystals 8=14186
 exact meas. method, also for changes 8=2422
 graphite, temp.-modulated reflectance meas. rel. to critical points in band structure 8=14200
 measurement accuracy, reflectometer design 8=15517
 metameric object colours, spectral intersections 8=15498
 mirrors, multilayer dielec., high reflectance 8=2461
 modulated, at oblique incidence for analysing band structure 8=14168
 noble metal films, and transmittance, anomalous skin and size effects 8=9498
 perpendicular, and phase angle at boundary of two mats., graphical representation 8=500
 powders, compressed and single crystal, i.r. spectra comparison 8=14169
 reflectometer, single mirror, normal incidence 8=6504
 semiconductor surface, parameters from electroreflectance study 8=5230
 semiconductors, reflectance in i. r. region 8=22933
 semiconductors, var., in i. r. absorpt. 8=9479
 silicate rock powders, classification into glasses, crystalline acidic and basic-ultrabasic 8=14264
 single-layer coating rel. to substrate absorpt. 8=6539
 spectra, lunar and laboratory, and inferences about Moon's surface 8=14820
 Ag incident polarized laser beam 8=18498
 Ag, infrared reflectance rel. to anomalous skin effect theory 8=14192
 Al, hemispherical reflectance rel. to λ and surface roughness 8=2399
 Ar mol. beam reflection at Al surface, energy meas. from 100-7500 eV 8=16382
 Au films, and transmittance, anomalous skin and size effects 8=9498
 Au, hemispherical reflectance rel. to λ and surface roughness 8=2399
 β' -AuZn, Kramers-Kronig anal. rel. to interband transitions 8=2402
 Ba₂Sr_{1-x}F_{2+x}, far i. r. spectra rel. to vibration model 8=9507
 BaTiO₃, application of small polaron problem 8=5587
 BaTiO₃, i. r., rel. to d.c. conductivities, small polaron theory 8=18505
 Bi film, band structure determ. 8=13859
 Bi₂(Te, Se)₃ system, rel. to effective mass of conduction electrons 8=2096
 CdS, and wavelength, rel. to longitudinal optical phonon-plasmon coupling 8=14206
 Cr, i. r., temp.-depend. dip rel. to antiferromag. energy gap 8=22874
 Cu films, and transmittance, anomalous skin and size effects 8=9498
 β' -CuZn, Kramers-Kronig anal. rel. to interband transitions 8=2402
 GaAs, i. r. spectral, rel. to free carriers 8=2418
 Ga_{1-x}In_xAs alloys, electroreflectance rel. to band structure 8=2419
 Ge, low-freq., in mag. field 8=22988
 n-Ge, i. r. spectral, rel. to free carriers 8=2418
 Ge, thermoreflectance spectra in region of a critical point, calc. and obs. 8=14217
 GeSi alloy 8=2422
 Ir, u. v. effect of Al coating, calc. 8=14227
 KCl, spectra and absorpt. constant rel. to exciton states 8=14230
 KI, far i. r., liq. He, liq. H₂ and room temp. 8=18540
 KMF₃ (M = Mg, Mn, Co, Ni), i. r. reflectance spectra rel. to lattice vibrations 8=2426
 LaCoO₃, i. r., rel. to d.c. conductivities, small polaron theory 8=18505
 MgO, meas. rel. to electron energy losses 8=9550
 α -MnS, rel. to elec. conductivity 8=18057
 Ni, hemispherical reflectance rel. to λ and surface roughness 8=2399
 β' -PbIn, Kramers-Kronig anal. rel. to interband transitions 8=2402
 PbTe, low-freq. in mag. field 8=22988
 Pt, hemispherical reflectance rel. to λ and surface roughness 8=2399
 RbMnF₃, i. r. reflectance spectra rel. to lattice vibrations 8=2426
 ReO₃ metal, absolute meas. in range 0.1-22 eV, dielectric const., interband transitions 8=14258

Reflectivity—contd

- Sb film, band structure determ. 8=13859
- Se, i. r. spectra 8=8615
- SnTe, i. r. rel. to free carrier dispersion theory 8=2457
- Sr, Ba_{1-x}F₂, far i. r. spectra rel. to vibration model 8=9507
- SrTiO₃, i. r., rel. to d.c. conductivities, small polaron theory 8=18505
- Te crystals, far u. v. obs. 8=15551
- YFe garnet 8=5642
- YGa garnet 8=5642
- ZnO, electroreflectance rel. to gas adsorption 8=9564

Refraction

- electron beam in intense e. m. wave 8=19761

acoustic waves

- See also Dispersion/acoustic.
- air-CH₄, plane shock, expansion wave generation 8=4482
- air-CO₂, plane shock, expansion wave generation 8=4482
- wind and temp. effects on anomalous propagation in atmosphere 8=9898

acoustic waves, ultrasonic

- No entries

electromagnetic waves

- See also Electromagnetic wave propagation.
- beam trajectories in media with refractive index inhomogeneities 8=371
- interface between moving media 8=19842
- in isotropic inhomogeneous medium 8=15398
- lower atm., mm. waves, permeability of O₂ 8=18906
- microwaves, solid-state refractometer 8=15397
- in plasma, drifting magnetoionic, relativistic expression for index 8=18977
- plasma, effect on inter-antenna transmission coeff. 8=7783
- polarization angle rel. to impedance matching 8=3256
- ray tracing study with satellites 8=2672
- spherical, incident on parabolic plasma layer 8=7761
- transhorizon tropospheric propagation, book 8=14630

light

- See also Double refraction.
- acetone, Ar laser beam thermal defocusing obs. 8=16845
- alcohol, Ar laser beam thermal defocusing obs. 8=16845
- atmosphere, corrections in surveying 8=23286
- beam divergence variation across plane interfaces 8=11128
- crystals, birefringent, internal and external faces 8=14184
- laser beam thermal defocusing theory 8=16845
- liquids, nonlinear indices, mol. orientation effect 8=12871
- spherical surface, in system of birefringent lenses 8=15510
- u. v., irregular surface refraction 8=463
- water, Ar laser beam thermal defocusing obs. 8=16845
- NH₃ mol., var. with gas density 8=1477

Refractive index

- ammonia, electric dipole rot. effect 8=4162
- beam trajectories, inhomogeneity effect 8=371
- liquids, increase, due to mechanisms sensitive to energy density 8=8066
- liquid lens for acoustic waves, optimum value 8=19573
- quartz, in far i. r. 8=14219
- uniaxial absorbing crystal, complex indices 8=5579
- in whistler resonance, temp. dependence rel. to plasma diagnostics 8=3272
- white tin films, analysis over 0.1 to 27.5 eV energy region 8=2456
- CaCO₃, absorbing crystal, complex indices 8=5579
- CdS, laser induced inhomogeneities 8=9515
- Ge, in far i. r. 8=14219
- Si, in far i. r. 8=14219

light

- See also Dispersion, optical; Double refraction; Optical constants.
- alkali halides, anisotropic strain polarization, rel. to ion overlap 8=23003
- alkali nitrates and thiocyanates, fused 8=1556
- all-trans β carotene crystals, obs. 8=2465
- amino acids, anisotropy and bond polarizability 8=2462
- atmosphere, amplitude distrib. of differences, Deam refractometer obs. 8=2596
- atmospheric, gradient meas. 8=9870
- calcite, variation with pressure to 7 kbar 8=22961
- flint glasses, mean reference indices calc. 8=20044
- fluids, rel. to dielectric constant and thermodynamic props. 8=16615
- gases, Fabry-Perot spectrometry 8=6520
- glass plates, small changes with precise interferometry 8=14223
- glasses, aluminate for i. r. use 8=22954
- liquids, non-linear, approx. for molecular redistrib. 8=4575
- liquids, non-linear, freq. shifts from Kerr effect 8=8083
- of magneto-optically active media, method of determ. 8=18565
- optical materials, i. r., thermal change 8=479
- polymer solns., u. v. 8=8350
- reflectometer error elimination 8=15517
- thin transparent films, and thickness meas. 8=8300
- time-dependent, effect on wave train propag. 8=10884
- 2,3-dimethylnaphthalene, rel. to mol. and crystal structure study 8=18574
- variable, amplification 8=400
- Ar plasma, meas. 8=4378

Refractive index—contd**light**—contd

- Ar, real part calc. from Kramers-Kronig dispersion relation 8=16707
- AsSe₃ glass 8=14198
- CdS, determ. from interference max. on transmission curve 8=2409
- Cr₂O₃, reactively evaporated and transmission characts. 8=9517
- CsNO₃ molten, meas. by interferometry 8=4583
- Cu₃TaSe₄, and other optical props. 8=8408
- n-Ge anisotropy in electric field 8=9533
- KNO₃ molten, meas. by interferometry 8=4583
- K₂S₂O₈, dispersion, interpretation 8=18539
- LiNbO₃, 20-900°C 8=5620
- LiNO₃ molten, meas. by interferometry 8=4583
- Na borate glasses, and ht. of soln. and density changes under high pressure 8=1715
- NaNO₃ molten, meas. by interferometry 8=4583
- Ne, real part calc. from Kramers-Kronig dispersion relation 8=16707
- RbNO₃ molten, meas. by interferometry 8=4583
- SbSi, rel. to temp. and wavelength 8=2448
- SiO₂ film, rel. to temp. of deposition 8=21889
- SnTe, visible and i. r. obs. 8=18562
- Sr_{1-x}Ba_xNb₂O₆, ferroelec. crystals. 8=21966
- Sr_{1-x}Ba_xNb₂O₆ (x = 0.25, 0.50, 0.75), temp. and wavelength depend. 8=14268
- YFe garnet, determ. using thin plane-parallel disc. 8=18565
- Zn tellurite glass, optical transmission range, i. r. spectra 8=5644

Refractive index measurement

- alkali nitrates, molten, by wave-front-shearing interferometry 8=4583
- microwaves, solid-state refractometer 8=15397
- optical materials, i. r., thermal change 8=479
- optical materials, near ultraviolet to middle infra red 8=478
- organic laser, fluctuations, schlieren method 8=11114

Refractometers

- differential interference type for liquids 8=20057
- microwave, solid-state 8=15397

Refractories. See High-temperature production and effects.**Refrigerators.** See Low-temperature production.**Regge poles.** See Scattering, particles.**Relativity**

- aberration of light from binary stars 8=14788
- arbitrary space-time world, formulation of quantum field theory 8=3423
- blackbody radiation, spectral correl. relativistic treatment 8=23479
- Boltzmann eqn., collision-free, soln. in certain external fields 8=65
- Galilean invariance of self-induced strong interactions of elementary particles 8=20277
- causality group of Zeeman examined 8=3416
- charge radiation in a plane wave e. m. field 8=10881
- Cherenkov radiation, relativistic changed particle passing through classical changed oscills. 8=3583
- classical, and thermodynamics, consistency of Joule-Thomson porous-plug expt. anal. 8=6061
- conservation of energy law, invariant form 8=3431
- cosmological models with non-zero cosmological constant 8=19080
- Crocco-Vazsonyi eqn. of ideal fluid hydrodynamics 8=1442
- curved space time, Machian principle classification 8=6064
- Doppler and Einstein freq. shifts in Schwarzschild space 8=10590
- extended bodies, energy of, relativistic transformation 8=6063
- fluid, charged in e. m. and gravit. fields, Hamilton-Jacobi eqn. 8=16634
- hydrodynamics, wave propagation in relativistic fluid 8=7888
- Kepler motion, relativistic spinor regularization 8=19418
- Killing eqns. of 5D pseudosphere, soln. generators of Poincaré group 8=3417
- kinematics of free spin particle 8=11382
- kinematics of rigid rotor 8=11383
- light-like permutations in Lorentz group, Zeeman's lemma 8=6024
- magnetohydrodynamics, props. of rays 8=6341
- space-time fluctuations as propagator of elementary particles 8=15677-8
- spin particle in outer Maxwell field, kinematics 8=11384
- statistical mechanics, hierarchies for reduced densities 8=2966
- thermodynamic appl. 8=6062
- thermodynamics, conservation of energy 8=3001
- thermodynamics transformation formulas for temp. and heat 8=19444
- K-G eqn., solution generalization 8=11256

general

- See also Cosmology; Gravitation.
- bouncing spheres problem, analysis 8=6075
- Brans-Dicke scalar-tensor theory, Schiff's gyroscope test 8=14977

Relativity—contd**general—contd**

- Brans-Dicke theory, correction to planetary motion derived 8=19421
- class D space containing an electromagnetic field 8=14971
- class D space containing anisotropy group G₂ 8=14972
- class III spaces, solutions of Maxwell-Einstein equations 8=14973
- conservation laws, superenergy 8=2946
- curvature tensor of null-hypersurface 8=2958
- Clifford algebras, generalization 8=10604
- convective instability, Schwarzschild's criterion 8=10591
- cylindrically symmetric mag. field in presence of freely moving particles 8=14966
- Einstein eqns., gravitational wave solns. with strong gravit. fields 8=19415-16
- Einstein eqns., problem of evolution 8=6067
- Einstein's equation solutions, global theorem of uniqueness 8=14974
- Einstein eqns., spherically symmetric solns. 8=6072
- Einstein equations, solution for case of static axial symmetry 8=2939
- Einstein equations with flat spacelike hypersurfaces, solutions 8=19081
- Einstein field equations, Kerr-Nut solution of 8=75
- Einstein's field eqns., static, axisymmetric, interior solns. 8=6077
- Einstein-Maxwell fields construction 8=2944
- electromagnetic null field in form of spherical radiation 8=3175
- e.m. fields produced by rot. bodies, proposed tests 8=3174
- equations integration, collapse of supernova 8=10186
- equivalent Newtonian pot. for same orbit, calc. method 8=6080
- "equivalent" potential near a force center 8=6068
- experiments on gravitation significance 8=80
- fluid vortices, relativistic theory 8=7878
- Fock's hypothesis, disagreement with red shift 8=2955
- Fresnel's eqn. derivation 8=6082
- global connectivity by timelike geodesics 8=2943
- gravitation, one-body theories, Lorentz-invariant, classification and empirical tests 8=70
- gravitation, singularity anti-collapse in space filled with nonideal medium 8=19424
- gravitation, symmetric tensors, covariant decomposition 8=6071
- gravitation, theories, one-body problem 8=10584
- gravitation, theory and expts. 8=10592
- gravitational field, geodesic motion using Tolman solutions 8=2952
- gravitational fields, higher dimensional spaces and symmetries 8=2948
- gravitational free fields and free Yang-Mills fields, conditional dynamic equivalence 8=6076
- gravitational Lagrangian struct. rel. to Einstein's eqns. violation by Mercury 8=10586
- gravitational radiation scattering 8=2954
- gravitational self-forces and radiation losses of classical spin particles 8=71
- gravitational transitions, role of Bose statistics 8=14969
- gravitational waves, transport of energy and momentum from rotating rod, linear approx. 8=14979
- hypersurfaces, null, treatment by Ricci rotation 8=2951
- internal Schwarzschild field, geodesic motion within 8=72
- interpretation and verification 8=6070
- Kerr metric and rotating masses 8=2950
- Klein-Gordon-Maxwell-Einstein field eqns. fine-structure constant and internal energy 8=19423
- Lagrangian densities, scalar and vector fields in space X₄ 8=73
- Lorentz principle application, nearly straight system of reference 8=2945
- Lorentz transform, ambiguity rel. to high order terms 8=74
- Mach's principle, enforcement and space closure at infinity 8=76
- and Mach's principle rel. to origins of space-time and inertia 8=10598
- magnetic-gravitational analogy rel. to planet parameters perturbations 8=19417
- moving dielectric resonator, relativistic frequency shift 8=3248
- Newtonian version of generalized theory of gravity 8=19426
- and oblate sun 8=10599
- oscillating spheres, uniform density, non-uniform press., exact interior solns. 8=19429
- particle wave function in weak gravitational field as test 8=2947
- physical singularity, degenerate caustic surfaces in Tolman's solution 8=6073
- pressure-free matter dynamics 8=2941
- problem 8=77
- quantization, rel. to canonical transformation generated in linear gravitation theory 8=10597
- quantum theory and metrical disturbance rel. to elementary particle structure 8=6081
- quasi-inertial frame used for gravitational fields 8=14967

Relativity—contd**general—contd**

- recent development, rel. to gravitation 8=2956
- redshift and Einstein-Bohr expt. for uncertainty principle 8=549
- rel. to elementary particle masses, interaction of fields with negative self-energy contribs. 8=647
- relativistic fluid sphere, Schwarzschild internal solution 8=2937
- relativistic free multipole field, theory 8=11279
- Riemann space, covariant method of infinitesimal translations 8=6069
- Riemannian manifolds, spacelike hypersurfaces 8=10588
- rotating-body, macroscopic, eqn. of motion 8=2938
- Schwarzschild metric, high order frequency shift 8=14970
- space-times, another proof of Lichnerowicz' theorem 8=10601
- space-times, spherically symmetric, Petrov's classification 8=78
- in Schwarzschild field, behaviour of moving clocks 8=6084
- Schwarzschild's instability criterion, influence of mag. field 8=10072
- Schwarzschild's soln. uniqueness of nonsingular infinite-red-shift surface 8=10589
- space-times with ideal-fluid gravitation 8=10595
- spin-angular momentum, field theory 8=10602
- spinor fields as distortions of space-time 8=2942
- static scalar and elec. fields in Einsteins theory 8=2940
- test proposed through laser ranging to Moon 8=2953
- thermodynamics, ambiguity of pressure concept 8=6102
- 2-body system, gravitational radiation, scalar component 8=6079
- two- or three-body motion problem 8=6074
- universe, Gödel-type, filled with charged-incoherent matter 8=2767
- wave optics to geometric optics transition 8=6083
- weakened vacuum field equations 8=10603

special

- composition of velocities, alternative theory 8=19410
- Ehrenfest's paradox of rotating disc 8=14961
- Einstein's theory, proof, implications 8=19413
- equations of state of matter, condition satisfying relativistic principles 8=6065-6
- experimental basis from high energy physics 8=69
- fluid charged in e. m. and gravitational fields, Larmor and Helmholtz theorems 8=16633
- Lorentz-Einstein metric and length contraction 8=68
- Lorentz group, theory 8=16
- Lorentz transformations, unimodular matrices homomorphism 8=2934
- Lorentz transformations, vector 8=14960
- mass-energy relation, atomic masses of Fe⁵⁶, Fe⁵⁷ and the Q value for Fe⁵⁶(d, p)Fe⁵⁷ 8=21017
- mechanics, Hamiltonian formulation 8=19442
- Michelson-Morley experiment, classical explanation 8=2933
- μ lifetime depend. as violation 8=2935
- multipole moments specifying extended bodies 8=14962
- Poincaré and Einstein's theory, discussion 8=10582
- rotatory motion of observer with respect to inertial observer 8=2936
- temperature, $T=T_{em}/\beta$, does a moving body appear cool 8=14964-5
- Thomas precession formula, derived by multiplying Lorentz transforms 8=67
- time dilatation, comment and reply 8=14963
- transformations between inertial systems, necessity of linearity 8=66
- "twin paradox", analysis 8=10583
- variational methods for model of continuous media 8=2911
- validity of theory, argument against 8=19411
- validity of theory, argument for 8=19412
- without postulate of constancy of light 8=10581

unified field theories

- geodesic principle, validity for charged matter 8=83
- gravitation combined with quantum field theory, gauge problem 8=19414
- gravitational field theory 8=10606
- Maxwell-Einstein eqns., spherically symmetric soln. 8=10605
- new geometry using GL(4,C) 8=2960
- positive-definiteness of inertial mass, nonpositive-definiteness of e. m. coupling 8=14980
- Vierbiën field for nonlinear theory 8=19428

Relaxation

- See also Acoustic wave propagation; Dielectric phenomena; Elastic relaxation; Ferroelectric phenomena; Ferromagnetic relaxation; Molecules/relaxation; Nuclear magnetic resonance and relaxation; Paramagnetic resonance and relaxation.
- anisotropic, orientation of atoms in presence of electron alignment interaction 8=7374
- beams, thin, elastic, large amplitude oscillations 8=145
- chemical, in reaction kinetics exam. 8=14352
- dielectric behaviour at low freq. anomalous charging and discharging currents 8=13866
- dielectric, in copolymers 8=5358
- dielectric solids, effects, meas. by ionic thermocurrents method 8=5346

Relaxation—contd

- electron avalanches statistics, influence of energy distrib. 8=4289
 - energy, of heated-electron distribution, role of two-phonon processes 8=8893
 - equations and renormalisation, derivation 8=14988
 - ferromagnetic, due to point defects 8=18321
 - glycerine, Brillouin scatt., background 23-90°C 8=21689
 - harmonic oscillator systems, simple 8=15005
 - in internal friction problems 8=17717
 - liquid, and inelastic Brillouin scattering from density fluctuations 8=16840
 - nets, conformal mapping method 8=19352
 - nitrate melts, binary mixtures of $\text{Ca}(\text{NO}_3)_2$ and MNO_3 ($\text{M} = \text{Na, Cs, Rb, K}$), supercooled, relax. processes 8=1586
 - nonadiabatic transitions in solids 8=13039
 - polyethylene, X-ray diffraction obs. 8=21213
 - shell, circular, thick walled, radial oscillations, analysis 8=144
 - shock waves magnetically generated 8=15054
 - shock waves rel. to dissociated free stream 8=10715
 - spin in Ising model, sum rule for times 8=14985
 - thermal, single processes, analysis method 8=19621
 - C steel wire, for concrete, stress relax. obs. 8=17789
 - CaFe_2O_4 , spin relax. from Mossbauer study 8=21804
 - $\text{CoO}:\text{Li}$, ($\text{Li}^+-\text{Co}^{2+}$) dipole relax. losses rel. to free hole movement 8=18165
 - Fe single crystals, pre-yield 8=22340
 - $\text{N}_2\text{O}_4 \rightleftharpoons 2\text{NO}_2$ system, effects in thermal conductivity 8=7929
 - NaCl structure, elect. and mechanical modes, allowing for 1st and 2nd neighbour vacancies 8=22174
 - PbZrO_3 polarization rel. to elec. cond. near antiferroelec.-ferroelec. transition 8=2249
 - Pt, annealed, anelastic effect at low temps. 8=22211
- Remanence.** See Magnetization state.
- Renner effect.** See Molecules.
- Replica techniques.** See Electron microscopy.
- Reproduction.** See Sound reproduction.
- Resistance, electrical**
- See also Conduction, electrical; Conductivity, electrical; Contact resistance; Magnetoresistance; Piezoresistance.
 - absolute determination by Campbell's method 8=282
 - β -alanine, meas. with electrometric apparatus 8=19707
 - between superconductors, low joint, meas. via closed loop system 8=2182
 - gas/liquid flow through absorpt. column 8=12737
 - metal microplasticity, study by strain effects on a.c. resistance 8=5036
 - rocks, saturated, changes due to fracture and frictional sliding, obs. 8=23222
 - semiconductor, wander error in four probe meas. 8=22577
 - standard resistors, effect of power dissipation on performance 8=10825
 - surface, r.f., computation using skin effect theory 8=19720
 - triglycine sulphate, meas. with electrometric apparatus 8=19707
 - Al, sintered (SAP) and normal 8=13707
 - Bi, simultaneous meas. with deformation 8=5052
 - C, for low-temp. meas., calibration 8=19682
 - Cd, very pure, temp. variation below 3.7°K meas. with supercond. bolometer 8=22573
 - Cr, near Néel point 8=5177
 - Cr alloys, antiferromagnetic, transport props. 8=18374
 - CuFe alloy, Kondo, magnetic field dependence 8=5178
 - CuMn alloy, Kondo, magnetic field dependence 8=5178
 - ϵ Cu-Zn phase, dissolved Fe, low-temp. minimum 8=9340
 - Gd-Yt alloy, spin-disorder meas., and exchange coupling calc. 8=9007
 - Ge, change with time when thermal environment changed, at liq. He temp. 8=15119
 - Mg-Ag alloys, dilute, temp. depend. of impurity resistance 8=5182
 - Mg-Pb alloys, dilute, temp. depend. of impurity resistance 8=5182
 - Ni hydride, reduction during formation 8=5183
 - Ni-Cu, effect of cathodic hydrogen loading on ferromag. resist. anomaly 8=14023
 - Ni(NiO) films, magnetized to induced anisotropy 8=5166
 - Pt and thermal conductivity, 373 to 1373°K. obs. 8=22521
 - Tl, pure, temp. depend. and dimension effect at liq. He temp. 8=5185
 - β -US-, single crystal 8=4818

Resistance thermometers. See Thermometers/resistance.**Resistivity.** See Conductivity, electrical.**Resolving power, optics**

See also Optical instrument testing.

- atomic absorpt. flame photometry, improvements 8=18777
- "condenser-objective" for microscope up to 700 kV and spherical aberration 8=19790
- electron microscope, emission, spherical aberration and limit of resolution 8=10902
- focused collimator 8=11139
- hologram, calculation by Abbe and Airy methods 8=15561
- holography, influence of spatial coherence 8=11215
- Integral photography, limitations 8=15568
- multiple-beam interferometry, limits 8=15544

Resolving power, optics — contd

- planetary photography, atm. turbulence effects 8=14835
- spectrometers, 5350 Å band of I_2 as test 8=16289
- spectrometers with concave diffr. gratings, calc. 8=487
- superconducting e lens, calc. 8=19791
- systems with resolving power exceeding the classical limit 8=474
- telescope, effect of sensitivity curve of the eye 8=481
- two-point, partial coherence 8=15508
- vision, square-wave grating patterns 8=15576

Resonance, elementary particles. See Baryons/resonances; Hyperons/resonances; Mesons/resonances.**Resonance, magnetic.** See Magnetic resonance and relaxation.**Resonance spectra.** See Spectra.**Resonators**

- cavity, for dielec. const. meas. at 32 GHz, 4.2°-300°K 8=18150
 - coupled model for standing wave accelerator tank 8=6698
 - in cyclotron maser mag. field, excitation near cyclotron freq. 8=395
 - cylindrical, with losses, criteria rel. to length 8=6367
 - electromagnetic, dielectric prism between mirrors 8=6361
 - electromagnetic, freq. calc. by geometrical optics 8=11125
 - electromagnetic, radiation pressure 8=19879
 - electron, of non-split anode, magnetron, quality factor 8=15326
 - Fabry-Perot, for scatt. cross-section determ. 8=19861
 - Fabry-Perot, high Q, for NO absorption meas. at 150 GHz 8=7536
 - h.f. props. when filled with TiO_2 dielec. discs 8=19829
 - klystron, effect of space charge 8=19827
 - laser, diffraction losses 8=15447
 - laser, Fabry-Perot spherical mirror, utilization in spectral anal. 8=6432
 - laser, single mode, with optimum parameters, investigation of various types 8=6431
 - microtron, for 30 MeV electrons 8=3496
 - microwave cavity for e. s. r. field modulation 8=15427
 - microwave cavities, high-Q, application of superconductors in construction 8=15388
 - microwave, rotating cavity for u. s. meas. 8=15071
 - mode suppression, non-axial 8=410
 - molecular generators, mag. tuning characteristics asymmetry 8=16362
 - moving dielectric, relativistic frequency shift 8=3248
 - open dielectric, whispering-gallery modes 8=6364
 - optical, Fabry-Perot, quantum effects on meas. of small vibrs. 8=10683
 - optical multicavity use of laser mirror 8=15446
 - optical, with movable mirror, e.m. field 8=19944
 - plasma waveguide short circuiting 8=4401
 - quartz, 1MHz, Q=120 × 10⁶ at 2°K 8=18204
 - ring in accelerating systems 8=6705
 - rings and discs, uniform, radial and torsional vibrations 8=10693
 - rings, discs, and rods, arbitrary profile, resonant freqs., modes and stress distributions 8=10694
 - superconducting cylindrical iris for 3 cm waves 8=6362
 - travelling-wave, resonance field effect on double radiation 8=10942
 - Nd laser, thermal deformation for Q improvement 8=3336
- acoustic.** See Acoustic resonators.
- electromagnetic.** See Electromagnetic oscillations.

Reverberation

See also Architectural acoustics; Echo.

- absorption in room, meas. by steady-state and decay rate methods 8=191
- acoustic in San Diego Trough, spatial and spectral dependence 8=9819
- in buildings, quality obs. 8=19590
- hall, speech distortion obs. 8=19592
- monopole in chamber, acoustic power radiation calc. 8=178
- room, boundary conditions effect on sound field 8=6182
- and similar first-order scattered fields, statistical model construction 8=3043-4
- sonar tests 8=23242
- spectral meas., anechoic, in reverb. environment 8=6180
- Stadthalle Göttingen, model, obs. 8=10756

Reviews

- air-sea interface, wave generation 8=14572
- astronomical telescopes of future 8=5851
- atomic vibrations in solids, basic theory 8=22082
- atmosphere, upper, auroral and airglow research at Saskatchewan University 8=9925
- atmosphere, upper, main concepts and classification 8=18911
- atmosphere, upper, neutral motions review 8=18921
- atoms, in solids, energy loss and range 8=13469
- aurora, optical 8=18937
- aurora, radio 8=18938
- auroral and geomag. storms, theory 8=19043
- beta decay theory 8=1003
- breakdown electric, p-n junctions, effect of imperfections on 8=9150
- Brogie fusion theory and the double solution theory 8=551

Reviews—contd

ceramics, mechanical props. 8=17726
 condensation theories 8=21782
 conservation laws 8=3430
 convection in fluid cell heated from below, finite amplitude 8=6215
 cooling with solid cryogenics 8=19684
 corona-caused radio interference from EHV transmission lines 8=16422
 corrosion in liquids, influence of heat transfer 8=18667
 cosmic rays, solar wind and magnetosphere, spacecraft obs. 8=23717
 CP symmetry 8=11282
 crystal symmetry, theories and applications 8=8364
 cyclotrons 8=15662
 e.m. wave propag., inhomogeneous medium 8=18983
 earth's surface elec. conductivity 8=9791
 electric discharge, positive low pressure column with low electron density 8=7654
 electron diffraction study of atomic surface structure 8=22012
 electrochemical potentials and work function 8=9715
 electron synchrotron, NINA (National Institute Northern Accelerator), 4 GeV 8=642
 electronic devices and instruments 8=5292
 electronic structure of liquid metals 8=12899
 electrons in solids 8=8881
 electrosorption of neutral substs. 8=9716
 e.m. wave propag., homogeneous medium 8=18982
 e-N inelastic scatt., kinematics and sum rules 8=20377
 $\eta \rightarrow 3\pi$ 8=15808
 evaporation theories 8=21782
 fibres, synthetic, X-ray small-angle scatt. 8=8438
 films formation conditions of natural and atomic structure, USSR review 8=8309
 flow, laminar incompressible viscous, nonlinear stability theory 8=12586
 flow, laminar to turbulent, transition, incompressible fluid obs. 8=12608
 fluid, sporadic turbulence 8=12621
 fluid turbulent boundary layer structure 8=12607
 "g", absolute meas. 8=38
 gas, Rijke thermoacoustic oscills. 8=21515
 gas, Sondhauss thermoacoustic oscills. in pipe with one end closed 8=21514
 General Relativity 8=2956
 geomag. and ionospheric storms 8=19002
 geomag. micropulsations and ionospheric noise 8=18995
 Graham's laws of diffusion and effusion 8=12707
 gravitation and cosmology 8=80
 gravitation, Soviet work, covering 50 years 8=19425
 heat, temp. and internal energy 8=10764
 helicon waves in solids 8=8965
 Hertzian resonances, optical methods 8=20929
 high magnetic fields, prod. 8=306
 high temp. detectors, semiconductor 8=6652
 high temp. materials and determ. of thermal props. at 3500°C 8=4925
 hyperon non-leptonic decay 8=857
 i. r. detectors, development 8=15098
 infrared spectroscopy and current appls. 8=11149
 injection laser, structural parameters 8=15476
 ionic dissociation and cond. in liq. phase 8=4603
 ionosphere, lower regions 8=19011
 ionosphere, outer region to 2000 km 8=19018
 ionospheric absorption of solar cosmic rays 8=18997
 ionospheric drift and diffusion 8=18999
 ionospheric electron density profiles, determination from ionograms 8=2699
 ionospheric F-region 8=19017
 laser applications, semi-popular review 8=401
 laser damage in materials 8=403
 lasers, gaseous, in magnetic field 8=3306
 lasers, giant pulse technique 8=6415
 lasers, high power 8=10997
 lasers, solid state 8=6453
 liquid crystals, structure and properties 8=1527
 liquid far i. r. spectra 8=12886
 liquid films stability in annular 2-phase and falling film flow, literature survey 8=12774
 liquid scintillation counting quenching correction methods 8=11805
 liquid vein MHD 8=6262-6
 low temperature devices and techniques 8=6225
 low-temperature physics, research development in Ukraine 8=10791
 lunar exploration, spacecraft 8=5953
 m. h. d. elect. power generation 8=15201
 m. h. d. generators 8=19724
 m. h. d. generators, combustion fired 8=291
 m. h. d. generators, survey 8=290
 m. h. d. nuclear gas-turbine cycle 8=10839
 m. h. d. stations, open cycle, thermal efficiency and economics 8=293
 m. p. d. power generation, closed cycle, prospects 8=292
 magnetic domains 8=18313
 magnetic materials, physics 8=2286
 magnetic-spectrographs, semi-popular review 8=604

Reviews—contd

materials and components 8=10451
 metal-insulator-semiconductor devices, radiation effects 8=9171
 metal sample prep. for electron microscopy 8=17271
 microelectronics 8=18097
 microscope, development during last 50 years 8=15516
 molecular electronic wavefunctions, single-center expansions 8=16260
 molecular integral, review of recent development in computation 8=16248
 Mössbauer spectroscopy 8=692
 multiparticle collisions, angular momentum eigenstates 8=122
 natural radioactivity data improvement since U fission discovery 8=7123
 neutron spectra in nuclear reactors 8=7269
 non-leptonic decay by current algebra 8=3511
 "non-mathematical physics", history 8=10467
 nuclear forces 8=11682
 nuclear instruments 8=3454
 nuclear mag. reson., applications 8=5545
 nuclear Physics, 51st meeting of Italian Physical Society 8=7029
 nuclear power units, thermionic, for space vehicles 8=1114
 optical data processing techniques 8=15506
 optical instruments, lasers as light source, holography 8=6479
 optical space research, 1946-66 8=19066
 optical spectra of solids 8=9475
 optics in French-Canada 8=6558
 optics at Naval Research Lab. (USA) 8=15490
 optics research in Canada 8=6481
 organic mols., proton chemical shifts 8=7498
 oscillatory viscous flows, evaluation of literature within developed self-consistent theory 8=21556
 particle accelerators, linear 8=631
 particle detectors 8=603
 physiological optics, survey of current state 8=6587
 pion-proton scattering at high energies 8=3647
 plasma and gas light sources 8=484
 plasma, hot, particle diagnostics 8=7726
 plasma physics, book I 8=16460
 plasma physics, book II 8=16461
 plasma physics, book IV 8=16462
 positron decay 8=6812
 pressure effects on ionic crystals, semiconductors and metals 8=4699
 quantum optics philosophy and appls. 8=20024
 radiosources 8=2803
 Raman spectra, expt. and theory since 1962 8=12128
 Raman spectra investigation in Soviet Union 8=12132
 refractory materials, determination of heat resistance 8=1894
 satellites, artificial, orbit determination 8=5836
 satellite tracking methods 8=5834
 scintillations, radio star and satellite 8=386
 sea currents dynamics, USSR studies 8=9811
 secondary ion emission 8=2283
 semiconductor breakdown mechanism, review 8=18009
 semiconductor counters 8=20197
 semiconductor hot carrier effects, review 8=18008
 semiconductor lasers 8=19982
 semiconductor power devices 8=18094
 semiconductor theory, Soviet contributions 8=18000
 semiconductors, organic paramag., nuclear quadrupole and mag. resonances and relax. obs. 8=14088
 shock waves generated by mag. press., and associated relaxation 8=15054
 SIDs and geomag. effects, rel. to solar activity 8=18996
 silicates, structural anal. and their crystal chemistry 8=8466
 solar optical radiation, and upper atmospheric processes 8=18910
 solar radiation and rel. to geomag. activity 8=19303
 solar radio bursts 8=2845
 solar system environment, planetary and interplanetary 8=23633
 solar wind and interplanetary magnetic field 8=2849
 solar X-radiation, soft and vacuum u. v. in USSR 8=14867
 solid-state physics in USSR 8=16964
 sophisticated plastics for specialised applications in electronic and other industries 8=13876
 sound, refl. and scatt., ocean bottom 8=2572
 Soviet optics and spectroscopy during past 50 years 8=11116
 spark chambers, wire 8=626
 spectra, continuous of atomic gases and plasma 8=4060
 spectroscopy, optical of mols., Canadian N. R. C. apparatus and meas. 8=7484
 spectroscopy research at Toronto University 8=6523
 stabilization of multichannel data acquisition systems 8=11319
 stars, contact binary of W Ursae Majoris type, structure and evolution 8=14783
 superconvergence and e. m. mass differences calc. 8=11372
 synchrotron radiation 8=710
 synchrotron radiation 8=15664

Reviews—contd

- thermoelectric power generation 8=19733
 turbulence, incompressible fluids, Kraichnan's theory 8=12625
 vacuum technique progress rel. to electron physics 8=5994
 II-VI compounds band struct. obs. and calcs. 8=8911
 A¹¹B^{VI} semiconducting cpds., (A=Zn, Cd, Hg; B=S, Se, Te), prep., props. and uses 8=18023
 A¹¹B^V semiconducting cpds., prep., props. and uses 8=18024
 CO₂ lasers development 8=11050
 CO₂ molecular lasers 8=11049
 HII reddening anomaly, explanations 8=14797
 Rh and Ir brittleness 8=22390
 Si, deep-level impurities, review of props. 8=22607
 Si film on insulators, epitaxy 8=8328

Reynolds number. See Flow; Hydrodynamics.

Rhenium

- abundance in igneous and metamorphic rocks, relative to Os 8=18825
 cesiated, evaluation of thermionic emitter surfaces, rel. to conversion 8=18269
 deposition by H reduction of ReF₆, strength, struct. and props. 8=17100
 electroetched surface in variable-parameter diode, output characts. 8=19793
 isotopic anal. from thermal ionization source 8=7479
 low work function region in Cs and Cs-Ba vapours, rel. to pot. as collector in converters 8=15213
 polycrystalline and 3 orientations, bare work functions 8=18247
 superconducting isotope effect 8=17973
 superconductivity, transition temp., h.p. dependence 8=17972
 thermal and elec. resistivities from 2°K to 20°K 8=17546
 thermal expansion, X-ray diffraction determination 8=13384
 thermionic emitter cesiated surface evaluation 8=22717
 H chemisorption 8=23126
 Re thermionic converters, prototype, performance rel. to variable spaced test diodes 8=15219
 Re⁴⁺, substitution in spinel ferrites, spin wave linewidth variations 8=5495
 with Sn, bonds in organo-Sn cpds., Mössbauer obs. 8=4668

Rhenium compounds

- H[Re₂O(CNS)₁₀]₉- -14CNS-, radioisotopic exchange kinetics 8=23089
 ReAl₃, structure refinement 8=8555
 Re-Nb alloy surface, work function rel. to H₂O vapour contamination 8=13927
 ReO₃, metal, optical props. in range 0.1-22 eV 8=14258
 ReO₃Br, force consts. calc. 8=1265
 ReO₃Cl, force consts. calc. 8=1265
 ReO₃N²⁻, force consts. calc. 8=1265
 Re-Os alloys, transition temp., h.p. dependence 8=17972

Rheology

- See also Plasticity; Viscoelasticity.
 Bingham plastic, settling of spherical particles 8=21553
 bodies, elastic/visco-plastic, compressible, plane strain condition 8=10573
 deformation, controllable, of incompressible simple materials 8=13509
 of Earth's material, rel. to seismic regime 8=14537
 granular substances, plasticity and rupture conditions 8=8798
 hysteresis expts. 8=63
 hysteresis experiments for thixotropic materials, near max. flow resistance 8=7860
 liquid crystals, theory 8=1527
 non-linear problems in fluid mechanics, Newton's approximation application 8=12721
 non-Newtonian flow in porous media 8=7979
 polyethylene melt, steady flow elasticity 8=12735
 polymer solns., rheopectic charges in shear stress 8=8023
 polymers in aqueous solutions, reduction in turbulent skin friction 8=12946
 polymers, rel. to structure and viscoelasticity 8=8869
 polymers, and viscoelasticity, temp. dependence 8=2071
 polymethylacrylate and copolymers solns. rel. to band networks, obs. 8=21552
 Reiner-Rivlin type fluids, rotating flows over rotating discs 8=21561
 shells, inelastic, membrane, with rotation symmetry, creeping at finite deformations 8=10571
 tube, long, cylindrical, under internal pressure and axial tension, elastic/visco-plastic flow 8=10574
 Li₂SO₄, high-temp. modification 8=18169

Rhodium

- brittleness, on hot and cold working 8=22390
 de Haas-van Alphen effect and Fermi surface 8=13643
 electrodes, adsorpt. of CO 8=18726
 electrodes, adsorpt. of CO + H 8=18727
 photoinjection into liq. hydrocarbons 8=8113
 specific mag. susceptibility between 80° and 1850°K 8=5439
 Rh(III), spectra in fused LiCl-KCl 8=1567

Rhodium compounds

- Rh-Ba alloys, work function 8=18245
 RhC, C²⁻-X²⁺ band, Franck-Condon factors and r centroids 8=7548
 RhC, gaseous, dissociation energy 8=4240

Rhodium compounds—contd

- Rh₄(CO)₁₂ twinned, cryst. struct. 8=17412
 Rh-Hg system, phase diagram and heat of form. of cpds. 8=8280
 Rh₂S₃, Rh₂Se₃ and Ir₂Se₃, octahedron pairs, crystal structure 8=1807
 Rh₂S₃, crystal structure 8=17413
Riemann-Cristoffel tensors. See Relativity; Tensors.
Righi-Leduc effect. See Magnetothermal effects.
Ring currents. See Atmosphere; Ionosphere.
Rimeters. See Ionosphere measuring apparatus.
Rochelle salt
 dielectric permittivity and permeability 8=5371
 e.p.r., ferroelec. Stark effect in Cu²⁺ doped, obs. 8=14101
 e.s.r., γ -irrad., analysis of centre No. 2 8=9442
 Rochelle salt:Cu²⁺ e.s.r. spectrum influence through external elec. field 8=14111
 ultrasonic relaxation near ferroelec. transition 8=1858
 X-ray extinction rules and radiation damage effect 8=13266

Rock magnetism

- aero-magnetic obs., Dixie Valley, Nevada and Basin-Range structure 8=23450
 anisotropy, by translation inductometer 8=23451
 Antarctic, mag. props. rel. to mineralogy, methodology 8=10062
 archeomag. obs. suggesting dipole field wobbling over last 2000 years 8=10034
 Atlantic and Pacific cores, stratigraphy of reversals 8=23452
 basalts, dredged, self-reversal of remanent magnetism 8=19058
 basalts dredged from W and E Pacific, and K-Ar ages 8=19062
 Bloomsberg formation, Appalachians, paleomag. obs. 8=14704
 carboniferous glacial varves from C. Africa 8=19060
 contacts, baked, and dykes for tertiary geomag. field determ. 8=2725
 ferrian ilmenites and titanomagnetites, optically homogeneous in basalts, electron probe microanalysis 8=14703
 ferromagnetics grains properties and relation between magnetic-viscosity 8=2754
 Hurley Creek formation, New Brunswick, magnetization stability 8=19059
 igneous, remanent magnetization at low temp. 8=2755
 ilmenite particles, beach sand, props. 8=23454
 late paleozoic 8=14700
 magnetite, magnetostriction and magnetocryst. anisotropy, depend. on hydrostatic press 8=19065
 magnetite, reversible magnetostriction at high temp. 8=23448
 magnetite, reversible magnetostriction rel. microseismic oscills. 8=10063
 magnetization vector direction from statistical parameters of anomalous field 8=23449
 meter, for remanent mag. 8=10058
 microtektites in deep-sea sediments, obs. 8=14568
 Miocene lavas, S. E. Oregon, evidence of geomagnetic polarity transition 8=19057
 Old Red Sandstone, effect of heat treatment on mag. props. 8=5821
 paleo field intensities determ. and mechanisms responsible for non-ideal behaviour in Thellier's method 8=10061
 palaeomagnetism of the Atlantic island Fernando Noronha 8=10060
 palaeomagnetism of carboniferous glacial varves from C. Africa 8=19060
 palaeomagnetism of Kamthi sandstones, upper Permian age, from Godavary, India 8=19063
 palaeomagnetism of Ntonya ring structure, Malawi 8=19061
 palaeomagnetism of Steens mountain, S. E. Oregon and age of geomag. polarity transition 8=19064
 palaeomagnetism self-reversal and field reversal 8=10059
 Permian zhyolites in Corsica, obs. 8=10056
 Permo-Carboniferous, rel. to past dipole moments 8=23453
 plutonic mesozoic, Sierra Nevada, rel. to polar wandering and continental drift 8=14701
 sandstones, Kanthi, upper Permian age, from Godavary, India 8=19063
 spinner magnetometer using mag. shielding to reduce ambient mag. noise 8=14702
 Steens mountain, S. E. Oregon, geomag. polarity transition from reversed to normal 8=19064
 strata, superimposed, remanent magnetization directions from adjacent horizons, serial correlation 8=14705
 tektites, association with geomagnetic reversal 8=14567
 tertiary lavas from Greenland, remanent magnetization reversed to Earth's field 8=5819
 Tirupati sandstones from Godavary Valley, India, n. m. r. study 8=5820
 triassic Manicouagan group, lower, Quebec, obs. 8=2753
 viscosity, effect of exchange anisotropy 8=10057
 Mn nodules from dredged W. Pacific basalts 8=10055
 Ni, plastic deformation effects on mag. props. 8=9363

Rockets

- Aerobee, for obs. of sporadic E positive ion comp. 8=14685

Rockets—contd

- Aerobee-150, for study u. v. radiation from early-type stars 8=10170
 arc jet, thrust calc., mass flow rate 8=4421
 constant accn. flows, appl. to high-speed guns and launchers 8=16668
 electron density perturbations in ionosphere 8=9968
 electron multiplier for study of low energy auroral electron 8=10903
 heat transfer, liquid in zero-gravity field 8=4562
 infrasound spectra, flight and take-off, meas.: report 8=196
 n director, directional 8=6958
 nuclear engine, gaseous-core, nuclear analysis of 8=5823
 propulsion, ion-electron beams emitted by a plane, neutralization 8=3225
 propulsion particle velocity, laser-Doppler meas. 8=23457
 proton aurora meas., precip., spectra and ang. distribs., also electrons 8=5798
 reactor, thermionic as power supply 8=1115
 triethylborane injection in upper atmosphere, obs. of yellow-green luminosity 8=9904
 AIO trails, obs. to determ. temp. and density of upper atmosphere 8=2613
 H₂ fuel storage, liquid-solid mixture obs. 8=19067

Rotating bodies

- See also Angular velocity measurement; Centrifuges; Earth/rotation; Gyroscopes.
 cylinders, thick, steady motion under mech. and thermal loading 8=6047-8
 discs, rough, torque due to friction 8=6044
 double rot., connection of elec. meas. devices 8=13505
 gravitation, extended theory, Mach's principle and rot. masses 8=6087
 gravitation of 8=14975
 liquids, heat transfer in zero-gravity field 8=4562
 macroscopic, eqn. of motion rel. to general relativity 8=2938
 non-central mass within ellipsoid resonance oscills. 8=10522
 nonlinear system, critical resonance 8=14944
 relativity, special, with respect to inertial observer 8=2936
 sphere, boundary layer flow, numerical solution 8=7871
 sphere, parallel to plane wall, motion under influence of streaming flow 8=7866
 sphere, parallel to plane wall, motion through quiescent fluid 8=7865
 spin-rate sensor, two-mirror c.w. laser 8=6004
 stars, ang. momenta and braking systems, rel. to planetary systems formation 8=5853
 stars, exchange of stabilities, onset of convective Lagrangian displacements 8=5856
 transducer for rotational displacement using light sensitive resistors 8=6000
 He II flow transitions in 5 rotating annuli at 1.4°K 8=10812
 He II-I transition, higher than second order 8=10814

Rotation, molecular. See Molecules/rotation.

Rotatory power, dispersion. See Optical rotation.

Rubber

- chloroprene, optically obs. supermolecular structures, morphology 8=13112
 circular sheet, with hole and axially symmetric stretching, stress conc. 8=22263
 elastomer viscoelastic props. tensile test obs. 8=22400
 elastomers, stress/strain relations in multiaxial deformations 8=5010
 latex spheres in H₂O, coherent and incoherent light scatt. rel. to Mie theory 8=20104
 membrane, ht. of transport of inert gases 8=1487
 natural, n scatt. before and after reactor irradi., showing prod. of cross-bindings 8=16969
 polyurethane elastomer, triaxial fracture in tensile field 8=2075
 rubber + benzene mixtures, tracer diffusion 8=21641
 solution in amines, viscosity obs. 8=21625
 stark, partially melted, recryst. and melting 8=4771
 static and dynamic props. using a torsional pendulum, C black filled 8=8880
 transition temps. and composition, study by radio-thermoluminesc. 8=13077
 vulcanizates, diffusion of liqs. 8=1932

Rubidium

- atom, calc. of lifetime of first excited states from obs. of Hanle effect 8=7422
 atom, collisional depolarization of doublets 8=7471
 atoms, excitation by low energy electrons, absolute cross sections 8=12087
 atoms, 5²P_{3/2} state, level crossing expt. 8=1174
 atom, h.f.s. of 7²P_{1/2} state 8=7421
 atoms, optically pumped, collisions with Kr atoms, relax. correl. times 8=7472
 atoms, pseudopotentials 8=7409
 atom, reaction with Br₂ molec. beam, kinetics 8=1202
 atom, stark effect obs. 8=20966
 atomic beam, scatt. by benzene and cyclohexane beams, comp. 8=1205
 atomic beam, surface ionization on Pt and W 8=12110

Rubidium—contd

- collective motions of atoms in liq. state, compared with polycryst. solid 8=12796
 elastic moduli and pressure derivs. at absolute zero 8=17818
 electron-impact ionization, empirical calculations 8=12448
 ions, antishielding factors, by nucl. acoustic quadrupole reson. in RbI 8=9470
 liquid, density in range 50-800°C 8=12813
 liquid, elec. resistivity, appl. of structure factor and pseudo pot. relation 8=12920
 liquid, wavenumber-dependence of elastic moduli 8=1499
 melting, invariance of photocurrent and work function 8=13939
 nuclear spin relax. below 77°K 8=9463
 optical pumping magnetometer 8=19739
 vapour-deposited crystal growth rate 8=13140
 in Ar, solid, optical and X-band e.s.r. spectra 8=18558
 ions Rb⁺ on Hg electrode, partial charge transfer react. 8=18722
 in Rb methoxide-methanol ions coordination number and solvates comp. obs. 8=2497
 Rb^{85,87} g_L g_T optical pumping determ. 8=1173

Rubidium compounds

- F-band absorption, u. s. strain modulation 8=22232
 (Li, Rb)₂SO₄, differential thermal anal. 8=8270
 RbAg₄I₃, cryst. struct. rel. to ionic mobility 8=17379
 RbBr, alkali halides, F-band peak, Mollwo relation 8=17688
 RbCl, adiabatic elastic const. 300°-4.2°K, obs. 8=2058
 RbCl, alkali halides, F-band peak, Mollwo relation 8=17688
 RbCl, circular dichroism of K band 8=14256
 RbCl:CN, thermal props., rel. to rot. degrees of freedom of mols. 8=22120
 RbCl, F-band absorption, u. s. strain modulation 8=22232
 RbCl, Z₁ centre circular dichroism 8=22224
 Rb₂CO₃, i. r. cryst. spectra 8=18556
 RbCoF₃, spin-density oscillation in space at T > 96°K, by n.m.r. meas. 8=18472
 RbFeF₃, effective fields in Fe⁵⁷ Mössbauer spectra 8=1647
 RbFeF₃, magneto-optical properties 8=2450
 RbHCO₃, 2H₂O, i. r. cryst. spectra 8=18556
 RbHCO₃, RbDCCO₃, i. r. cryst. spectra 8=18556
 RbI, alkali halides, F-band peak, Mollwo relation 8=17688
 RbI, elastic constants temp. dependence 8=13591
 RbI, intrinsic photoconductivity 8=5401
 RbI, nucl. acoustic quadrupole reson., antishielding factors of Rb ions 8=9470
 RbI:TL, luminesc. and exciton formation 8=5131
 RbMnCl₃, prep. and crystallographic props. 8=13138
 β RbMnCl₃, 2H₂O, crystal structure 8=17411
 RbMnF₃, absorpt. spectrum 8=2449
 RbMnF₃, i. r. reflectance spectra rel. to lattice vibrations 8=2426
 RbMnF₃, near critical magnetic point, ultrasonic attenuation and velocity 8=17504
 RbMnF₃, spin waves, nuclear and electronic, simultaneous parallel pumping 8=14107
 Rb₂MnF₄, antiferromagnetic anisotropy 8=14070
 RbMnF₃, F¹⁹ nuclear acoustic resonance 8=22922
 Rb(Ni_{1-x}Co_x)F₃, new transparent ferrimagnet single crystal 8=14053
 RbNiF₃, ferrimagnetic, circular dichroism and rot. of plane of polarization of light 8=18557
 RbNiF₃, ferrimagnetic, magnetic exchange dichroism 8=14257
 RbNiF₃, magnon sidebands in optical spectrum 8=23010
 RbNiF₃, new transparent ferrimagnet single crystal 8=14053
 RbNiF₃ structure crystals, magnetic ordering 8=5482
 RbNO₃, molten, refr. index meas. by interferometry 8=4583

Ruby

- absorption linediths, R, R¹ and B, and phonon-induced relaxations 8=14194
 cathodoluminescence, efficiency 8=18586
 colour centres, luminescence meas. 8=1995
 destruction by powerful laser radiation, mechanism 8=22247
 dislocations observation by X-ray topography 8=13434
 electron spin echo behaviour 8=14091
 energy transfer from single Cr ions to closely coupled ion pairs 8=14302
 fluorescence pair lines temp. dependence 8=9597
 γ photoconductivity 8=18222
 growth by floating zone tech., with resistance heating 8=21939
 laser alignment method, rapid and accurate 8=19988
 laser, axial emission modes, self-locking 8=11087
 laser beam divergence testing 8=15478
 laser beam, nonlinear propag. in dielectrics 8=22931
 laser, change and stabilization of operating wavelength 8=19987
 lasers, continuous, power output and efficiency 8=437
 laser, damage on semiconductor surfaces 8=2028
 laser, effect of giant pulse irradi. 8=3327
 laser, effect of internal modes on operation 8=19986
 laser, giant pulse, inversion depend. freq. drifts 8=19984
 lasers, giant-pulse mode selection 8=15479
 laser interferometers for fluid mechanics 8=16618
 laser, with lens system, spectral characts. and radiation kinetics 8=19989
 laser light, plasma scattered, 12-channel Doppler-profile spectrophotometer 8=3357

- ruby**-contd
lasers, loss measurement, new method 8=11085
laser losses of resonant cavity, meas. by R_1, R_2 threshold comparison 8=11080
laser, Lummer-Gerke plate appl. 8=3328
laser, mode self-synchronization in broad spectrum giant pulse 8=11076
laser, non-Q-switched, picosecond substruct. of laser spikes 8=20002
laser oscillator output phase vars. obs. 8=19991
laser, output spectra rel. to mech. of linewidth determ. in YAl garnet:Nd laser 8=11111
laser, picosecond pulses, spontaneous appearance 8=439
laser, pulsed, calorimetric meas. of output energy 8=11084
laser, pulsed, pure transverse modes from special cavity 8=11086
laser, pump power and efficiency calc. 8=3331
laser, Q-switched, energy losses 8=6458
laser, Q-switched, feedback control, expt. and theory 8=11079
laser, Q-switched, formation time and resonator loss, exp. 8=434
laser, Q-switched, giant pulse generation by external signal 8=19983
laser, Q-switched, hologram resolution 8=20110
laser, Q-switched, time resolved beam structure 8=11082
laser, Q-switching using liq. Se mirror as a reflector 8=11078
laser, quenching of one pulsed laser osc. by another, rel. to coupled rate eqns. 8=11075
laser, rad. field structure rel. to optical inhomogeneities in substance 8=3330
laser radar transmitter, single-mode, characts. 8=11077
laser, radiation mixing with Nd 8=436
laser resonators, prism for state and plane of polarization preservation 8=438
laser, rod distortion compensation rel. to brightness gain and mode control 8=11081
laser, with non-resonant feedback due to scatt. 8=11003
laser, simultaneous pulsing 8=15477
laser, single longitudinal mode production 8=6459
laser, single-pulse single mode, with diffractive beam divergence 8=19985
laser, with tilted plates as discriminator, modes and generation kinetics 8=3332
laser, tunable, repetitively pulsed, with solid etalon mode control 8=19993
laser, WC with Czochralski material, diffraction-limited emission 8=11083
light breakdown induced by ruby laser beam mechanism 8=23043
linear Stark effect in U band 8=9501
luminescence spectrum, effect of elec. field 8=2475
maser, C-band, with quarter-wave coupled transmission cavities 8=392
maser, operating in 8 mm range 8=6411
maser, pumping by laser at 77°K 8=19920
maser, three-cavity, 21 cm. 8=19923
microwave resonance absorpt. spectra 8=14089
monocrystals, X-ray luminescence 8=14301
non-radiative relax. time between $^4T_{1,2}$ and 2E states 8=9503
optical phonon breakdown theory 8=22952
optically pumped, absorpt. and emission props., rel. to transitions 8=14196
pink, nonlinear absorption of coherent resonance radiation 8=18499
pulse laser, 50 Hz, emission 8=3326
spin lattice relax. times at He temp, Cr³⁺ conc. and temp. depend. 8=14092
spin-lattice relaxation time at room temp., determ. 8=5523
spin-lattice relax. time meas. 8=9416
Cr³⁺-doped, L-band maser appl. 8=15439
Cr³⁺ resonant two-level spin system, microwave second harmonic generation 8=22896
Po, At range-energy studies 8=13473
Russell-Saunders coupling. See Atoms; Spectra/atoms.
Ruthenium
low work function region in Cs and Cs-Ba vapours, rel. to pot. as collector in converters 8=15213
specific mag. susceptibility between 80° and 1850°K 8=5439
in Ag, liquid, diffusion 8=12836
Ru⁴⁺, substitution in spinel ferrites, wpin wave linewidth variations 8=5495
Ruthenium compounds
RuO₂, resistivity, temp. depend. 8=17939
RuS₂, cryst. struct. 8=8556
RuSe₂, decomp. press. and enthalpy of formation 8=12338
RuTe₂, cryst. struct. 8=8556
Rutile. See Titanium compounds.
- SC (sudden commencement).** See Magnetic storms.
S-matrix theory
See also Dispersion relations.
amplitude-density-functions method 8=12358
auto-interactions, invariance of standard 8=3432
bootstrap conditions, rôle of CDD zeros 8=15712
- S-matrix theory**-contd
causal, properties of cluster expansion 8=577
causality implying analyticity 8=20307
compositeness criteria of particles 8=6764
construction without accompanying pole in non-physical sheet 8=20309
Couture-Newton formalism, relativistic extension 8=15702
CTP invariance in theory of local observables 8=583
decay processes, soluble decay model 8=3413
dispersion relations, n-pole problems, N/D soln. 8=3552
eigenphases and crossing branch points, relation 8=11404
e.m. interactions involving photons, using dressed amplitudes 8=20343
elementary particle interactions 8=683
with extra Coulomb interact., analyticity for complex ang. momenta 8=15703
Feynman rules in statistical mechanics 8=120
 $\gamma + p \rightarrow \eta + p$ amplitude, unitarity and S-matrix analysis 8=3569
gravity, quantum theory, applic. 8=3451
high-isospin system, strong-coupling model 8=6762
interacting infinite fields, invalidity of assumptions 8=11271
Landau singularities, absence from the physical sheet 8=3549
on mass shell elements only, causality cond. 8=582
M-functions, reduced type defined 8=15625
M matrix transformation, 6 parameters, associated functions 8=6765
 πN scatt., generalized to include S-matrix effects, partial-wave analysis 8=20430
q. e. d., gauge dependence of propagators 8=20175
quantum electrodynamics, gauge problem 8=3446
quantum electrodynamics, third-order vertex part of single electron line 8=20385
scatt., high rank, transforming 8=6763
scatt. relativistic, applic. of coupled inhomogeneous Lorentz group 8=20289
scattering with energy losses, covariance matrix 8=20308
uniqueness, expt. tests 8=11405
unitarity and the relationship between spin and statistics 8=20163
unitarity cond. and non-compact symmetry groups 8=578
unitarity in covariant gauge quantum electrodynamics 8=3435
wave-packet formulation, semiclassical approx. time-depend. 8=20153
H²(He³, γ)Li⁶ reaction, 2-5, 5 MeV, analysis of excitation curve 8=20581
- SU₂ group theory.** See Elementary particles; Field theory, quantum/interactions, strong; Group theory.
Safety precautions. See Radiation protection.
Sakata model. See Elementary particles.
Samarium
Sm²⁺, fluoresc. in host lattices 8=14332
Sm¹⁵⁰ in ferromagnetic lattices, hyperfine magnetic field 8=2335
Sm²⁺, in CaSO₄ luminescence 8=23047
in ThO₂, spectrometric determ. 8=18787
in YVO₄, rel. to const. quantum yield 8=5670
Samarium compounds
SmCl₃·6H₂O single crystals, e. s. r. of Gd³⁺ 8=9427
Sm(NO₃)₃·6H₂O:Gd³⁺, e. s. r. 8=18435
Sm₂Y_{3-x}Fe₃O₁₂, magnetostriction anomalies, 4.2-100°K and ≤ 25 kOe 8=18364
Sampling. See Statistical analysis.
Sand
acoustical propagation parameters 8=22107
desert, "singing" phenomenon 8=23232
effect on elec. cond. of ferrites 8=13715
particle accelerator side shield 8=3490
with kaolinite, water saturated sediment, acoustic props. at 4-600 kHz, obs. 8=1857
- Satellites, artificial**
accelerations at high altitude rel. to air density 8=5832
Alouette I obs. of topside ionosphere 8=2652
Alouette 1, polar topside ionosphere, mean structure and storm-time change at sunspot min. 8=19021
Alouette II, outer radiation belt high-latitude boundary, local time asymmetries 8=18955
Alouette II topside-sounder data, m.f. conjugate echoes 8=18981
Alouette 2, Van Allen radiation changes rel. to polar substorms 8=18966
antenna resonance at proton gyrofrequency 8=6400
for astronomical seeing verification 8=14746
atmosphere, upper, density from orbital decay 8=5796
atmosphere, upper, density variations at 280 km from air drag 8=5797
ATS 1, local-time particle asymmetries, obs. 8=9916
auroral precipitation event, Injun 3 and simultaneous balloon obs. 8=6957
Beacon Explorer-C, ionospheric electron content irregularity, obs. 8=2668
bow shock compression, IMP 2 and OGO 1 simultaneous obs. 8=23329
Cosmos 49, analytical representation of mag. field according to obs. 8=19029

Satellites, artificial—contd

- Cosmos-49 mag. field obs. rel. to computed values 8=10030
 Doppler shift data accuracy rel. to ionospheric refraction 8=23371
 drag, obs. geomag. and upper atm. density var. 8=14695
 Early Bird, meas. of e content using Faraday effect 8=2662-3
 earth, near dynamical theory 8=10064
 earth's potential field meas. 8=9769
 in earth's field, stabilization with soft mag. alloys 8=5824
 eclipse times in circular and elliptic orbits 8=14712
 electrostatic probe, theory 8=2764
 for electron content in ionosphere over Texas 8=14663
 electron-emitting, in ionosphere, pot. build-up, theory 8=14710
 electrons trapped in low L shell, 1962-1965 obs. 8=2644
 Elektron 1 and 2, outer radiation belt electron energy spectra 8=18953
 Elektrons 1 and 3, signal obs., ionospheric deductions from 8=18971
 Elektron 2, mag. field obs. at 3-7R 8=19033
 e.m. wave propag., satellite-to-satellite 8=2716
 equatorial, synchronous, equilibrium position rel. to curve of earth's equator 8=2756
 equatorial, 24 hour orbit, resonance phenomena 8=19074
 Explorer 9 drag data rel. to geomagnetic activity 8=5816
 Explorer 12, magnetometer obs. of earth bow shock 8=2619
 Explorer 22, meas. of total e content 8=2658
 Explorer 35 obs. of lunar mag. field 8=10333
 geomagnetic tail, IMP 3 rel. to Lunik 10 obs. 8=23315
 geopotential, odd zonal harmonics from satellite orbits 8=5770
 gravitational perturbations, analytical expressions, automation of deduction 8=14718
 gravity gradient rod temp. distrib. 8=23461
 Hitch-hiker I, for study of energetic electrons in radiation belts 8=2651
 horizon data units, infrared, errors 8=2763
 IMP-2, magnetosphere and near space, meas. of magnet. field, results 8=2832
 IMP 2 plasmopause obs. 8=9917
 Injun 3 and Alouette 1, proton whistlers, dispersion characteristics 8=18958
 Injun 4, geomagnetically trapped α -particles 8=18961
 laboratory simulation of plasma expt. 8=2692
 with large-eccentricity orbits, estimates of lifetime and developments 8=14717
 Love's number determination for Earth 8=5768
 Luna 9 and Luna 10 obs., near Moon 8=5831
 Mariner 4 Doppler tracking data for Sun-Mars mass ratio 8=23671
 Mariner 4 interplanetary mag. field obs. 8=23685
 minimum distance from observer, timing digital device 8=19069
 NRL 1965-93A obs. of eclipse 8=19289
 OGO-A mag. field obs., 4 to 24.5 R_E 8=10024
 ORBIS, e.m. wave propag. expt. 8=2670
 orbital drag coeffs., rel. to atmos. density, computer estimation 8=2612
 orbital motion in earth's shadow 8=2761
 orbits analysis for upper atmos. rotational speed 8=18922
 orbits, cylindrical coordinate systems 8=2757
 orbit determination from Minitrack obs. 8=5833
 orbit determination, survey 8=5836
 orbits rel. to Earth's gravitational field 8=5767
 orbits rel. to gravitational field of Moon 8=5955
 orbit, oscillating transfer, of earth satellite 8=14715
 orbit perturbation by solar radiation pressure 8=23462
 orbit prediction 8=5835
 orbits perturbation by earth's gravit. field asymmetry 8=14716
 orbits, perturbations from spherical harmonics of gravitational potential 8=14719
 OSO-B2, airglow obs. 8=23332
 Pioneer 7 obs. of geomag. tail at 10³ earth radii 8=2748
 Proton 1 and 2, inner radiation belt proton component in Brazilian magnetic anomaly 8=18954
 'proton-2', investigation of nuclear component of primary cosmic rays 8=15893
 radiation belt, inner, electron flux and spectra obs. following Starfish test 8=9953
 resonance with longitude-dependent gravity 8=19073
 S-66, signals from above Haifa, Israel for ionospheric electron content 8=14669
 scintillation, seasonal var. 8=2673
 sea currents, jet streams and noctilucent clouds detect. by i.r. obs. 8=9855
 solar illum. period in circular and elliptic orbits 8=14713
 stream function reln. with vertical vel. rel. to inverse meteorology problems 8=10027
 synchronous, rel. to longitude dependence of geopotential 8=5769
 Syncom-3, meas. of ionospheric e-content 8=2661
 Telstar 1, stat. anal. and modeling of high-energy proton data 8=9955
 terrestrial radiation 7-26 μ , statistical characts. from Cosmos obs. 8=23283
 Tiros VII albedo obs. 8=23285

Satellites, artificial—contd

- Tiros VII, lower stratosphere circulation from temp. obs. 8=18858
 tracking by kinetheodolites 8=5828
 tracking methods, review 8=5834
 tracking by radar, Royal Radar Establishment, Malvern 8=5829
 tracking by radio, at Winkfield 8=5830
 tracking using Schmidt cameras 8=5827
 tracking by Smithsonian Astrophysical Observatory from I. G. Y. photographic stations 8=5826
 transmission fading, means of determining meas field height 8=9998
 and twilight layer noctilucent cloud detection 8=2626
 UK 3, solar cell system 8=19734
 upper atmosphere, deny, from drag meas. 8=14640
 in upper atmosphere, lifetime rel. to density vars., nomogram 8=14711
 upper atmosphere properties, determination 8=5795
 for upper atmosphere rotational speed obs. 8=14642
 Vela, SCNA obs., and X-ray flares 8=2653
 Vela, solar wind ion composition meas. 8=23715
 Vela 3 obs. of solar wind shock waves 8=23687
 visibility latitudes prediction 8=19068
 visual appearance and stellar magnitudes from UK 8=14714
 visual obs. in Finland, January to December 1966 8=5825
 O₂ in earth's atm. microwave spectrum obs. to obtain vertical sense 8=2762
 for O₃, atmospheric, estimation 8=2576
- Scalars.** See Circuits; Counting circuits.
- Scandium**
 band structure, density of states and Fermi surface by cellular method 8=8942
 magnetic susceptibility, anisotropy rel. to electron charge density 8=13965
 Sc III, Hartree-Fock multiplet strengths 8=4081
- Scandium compounds**
 ScF₃, gaseous, electronic states 8=7549
 ScF₃, high-temp. stability 8=7617
 ScF₃, high-temp. stability 8=7617
 Sc₂O₃ rel. to CuMn ferrites mag. props., obs. 8=18359
 Sc₂O₃:Er³⁺ absorption and emission spectra 8=14260
 ScS, gaseous, dissociation energies 8=7616
 ScTiBO₆ (B=Nb, Ta, Sb), crystal structure and fluorescence 8=4879
- Scattering**
 amplitude at high energy, lower bounds to absorptive part 8=11385
 amplitude rel. to new amplitude for charge-conjugating a lepton line 8=20176
 amplitudes in perturbation quantum theory 8=6605
 anisotropic, radiative heat transfer between parallel plates separated by nonisothermal medium 8=19625
 atoms, from continuous media 8=2017
 atom-molecule, quenching of glory undulations 8=7633
 Born approximation in theory, improvement 8=15611
 Brillouin, in damage to materials in lasers 8=403
 cross section, classical differential, calc. 8=6033
 current amplitudes single, non-Regge terms 8=3561
 diffuse edge potentials, Breit-Wigner formula deduced 8=3414
 elastic waves, freq. depend. of amplitudes 8=3027
 e.m. rel. to reconstruction of canonical field theories 8=11275
 Feynman amplitudes, majorization in high-energy limit 8=6754
 field, neutral, scalar, without pairing symmetry 8=20410
 gravitational radiation 8=2954
 gravitational rel. to reconstruction of canonical field theories 8=11275
 Haag-Ruelle asymptotic states, uniqueness 8=15623
 incoherent waves from point source in random medium 8=19366
 inverse, connection with complex ang. momenta 8=15610
 inverse scatt. problem at fixed energy, general method 8=567
 JWKB phase shifts, efficient computation 8=10514
 Laplace transforms, analytic continuation by asympt. series 8=2905
 light source, negative resonance absorpt. 8=11021
 low-energy by singular potentials 8=3415
 methane, rotating mol., curves rel. to interatomic distances 8=7572
 molecules, inelastic, semiclassical theory 8=12364
 multiple processes, singularities 8=10513
 one-dimensional, edge effects 8=6606
 phase shifts, use of upper bound eigenvalue technique of Sturm-Liouville equation 8=2882
 plane compressional step wave by circular obstacle in elastic medium, using Kirchhoff's integral eqn. 8=19523
 polychromatic, in 1-dimens. medium of atoms with 3 energy levels 8=16186
 pot., rel. to d binding energy 8=11641
 potential of wave packets rel. to a proper-time formulation of relativistic quantum mechanics 8=20136
 quartz, stimulated Raman from i.r.-active phonons 8=11112
 radiation, isotropic in finite homogeneous 2D atmosphere 8=2906
 resonance, one-pole approx. to S-matrix description 8=11404

Scattering—contd

- S-wave nonlocal potentials, soln. 8=15622
 scalar sound field, radiative transfer 8=137
 semiclassical approx. for elastic scatt. and eigenvalues 8=20151
 short waves in gas, eqns. 8=7911
 telluric currents, and signal extraction 8=14564
 time delay, application of quantal operator 8=11255
 time-dependent and invariant imbedding 8=2907
 variation procedure for multichannel processes 8=20150
 wave-packet formulation, semiclassical approx. time-depend. 8=20153
 weak, rel. to reconstruction of canonical field theories 8=11275

acoustic waves

- aperture in rigid screen, l.f. 8=10745
 cylinder, elastic 8=15069
 elastic tube, semi-infinite, in moving medium 8=3062
 first-order scattered fields, statistical model construction 8=3043-4
 flexural waves, by point obstacles system 8=3063
 hard surface of arbitrary shape, transient, retarded pot. technique 8=19568
 inhomogeneous medium, effect on scatt. by uneven surface 8=3065
 narrowband signal, by statistically rough surface, correlation 8=3064
 ocean bottom, review 8=2572
 from ocean bottom, time fluctuation characteristics calc. 8=23244
 by penetrable sphere with statistically irregular surface 8=3061
 plane monochromatic, by time varying sea surface 8=6167
 semiconductors, piezoelectric, stimulated Brillouin scattering. 8=17495
 simulation of audience using rows of spheres, experimental results 8=15068
 turbulent media, statistical properties, book 8=10735
 water waves, backscattering energy from, apparatus and method of analysis 8=6168

acoustic waves, ultrasonic

- butyl alcohol, stimulated and thermal Mandel'shtam Brillouin scattering 8=21665

electromagnetic waves

- from absorbing spheres, calc. of Mie cross-sections 8=6386
 antiferromagnetics, fluctuations and scatt., theory 8=5497
 area with Gaussian-distributed random irregularities 8=10956
 axially-symmetric E-wave in waveguide with impedance changing along length 8=19881
 backscattering from dielectric cylinders, geometrical optics method 8=19867
 backscatt. by prolate spheroid conductor 8=19876
 from body, homogeneous and finite conductivity, integral eqns. 8=15407
 by collinear plasma waves 8=7757
 Compton effect on neutral fermions 8=675
 computer soln. of 3-d. problems 8=19858
 cross polarized, from random surface 8=19857
 cross section determ. by Fabry-Perot resonator 8=19861
 curved irregular waveguide, near cut-off freq. 8=19878
 cylindrical passive oscillator 8=3179
 by cylinder, source directivity rel. to pattern 8=15405
 depolarization by compressed inert gas 8=6387
 dipole field, by two spheres 8=15404
 by dipole molecules, classical and quantum theory 8=7486
 from edges, finite, geometrical diff. theory, calc. 8=19859
 e-e. m. wave, non-relativistic quantum field theory 8=15409
 by electrons, classical theory, frequency mixing 8=15408
 by electrons, free, classical theory, frequency mixing 8=15408
 electrons, free, intensity dependent freq. shift 8=19866
 elementary particle behaviour 8=20279
 far field at low frequencies 8=19871
 by free electrons in stellar atmosphere 8=15028
 Fresnel region, errors in meas. of scatt. pattern 8=6390
 by hemisphere 8=3259
 h.f., multiple in random continuum 8=3260
 hollow conducting cylinders, re-radiation 8=19865
 impedance boundary, integral eqn. 8=19872
 infinite cylinder coated with a plasma sheath 8=6389
 infinite strip, absorbing, with arbitrary face impedances 8=6388
 insulators, lattice Raman scattering theory 8=2397
 inverse problem, plane waves by a sphere 8=19863
 ionosphere, "turbidity" and geophysical influences 8=2682
 irregular medium, probability distrib. of field 8=376
 lunar surface, depolarization of backscatter 8=19237
 lunar surface, inhomogeneous, intensity calc. of backscatter field 8=19238
 metal foil roughness rel. to scattered radiation at plasma frequency 8=8958
 molecular crystals, excitation spectrum and polarization theory 8=18480
 moving cylinder in free space 8=10957
 by moving electrons, quantum theory 8=6290

Scattering—contd

electromagnetic waves—contd

- from moving layer in transmission line 8=19869
 multi-element reflector, statistical matrix of scatt. 8=19432
 multiple, by two spheres, multipole expansion 8=19874
 near to far field, l.f. continuation 8=19870
 by perturbed surface formed by semiconducting bodies 8=22943
 plane, infinite perfectly conducting, from a half-loop 8=6391
 by plasma, generalized physical optics approximation 8=16534
 plasma spheres, inhomogeneous, collisionless approximation 8=4366
 plasma, warm, from immersed conducting cylinder 8=16529
 quartz, stimulated Raman, under optical pumping rel. to mode pulling theory 8=2453
 radar signals, backscattered, meas. 8=19864
 radiation from charge moving in magneto-active plasma with l.f. oscillations 8=21385
 resonance scatt. from absorbing spheres 8=511
 rough-surface, phase distrib. 8=19873
 Rytov solution, multiple-scattering interpretation 8=18884
 sea surface, rough, frequency shift 8=10955
 from sharp-edged smooth bodies, anal. 8=19868
 specular, geometrical diff. theory modification 8=19860
 spheres, propag. through an assembly, relations between diffusion multiple theories 8=22
 by spheres, two, using translational additional theorem 8=15406
 strip current approx. by Fresnel integrals 8=19862
 surface, rough and finitely conducting, comment and reply 8=15410-11
 turbulent media, statistical properties, book 8=10735
 water, γ -beam scatt., differential albedo obs. 8=16844
 wave depolarization by rough surface, appl. to earth and moon expt. 8=15412
 by waveguide bifurcation and aperture, ray-optical calc. 8=19882
 wire loop scatt. patterns 8=19895
 Al, γ -beam scatt., differential albedo obs. 8=16844
 CCl₄, 71°C, spectrum of scatt. microwave radiation 8=21686
 C₂ClF₅-He mixtures 8=7936
 Fe, γ -beam scatt., differential albedo obs. 8=16844
 Pb, γ -beam scatt., differential albedo obs. 8=16844

light

- See also Diffusion, light; Raman spectra.
 acacia catechuic acid, during neutralisation 8=8075
 ADP, noncollinear parametric scatt. 8=18489
 by aerosol particles, photon detection 8=21740
 by air, ellipticity of polarization, rel. to atmos. aerosol microstruct. 8=9877
 by atmospheric surface layer, polarization phase functions 8=9876
 atoms reson. fluoresc., forward-scatt. curves 8=20946
 atoms, reson. fluoresc. modulation coherency matrix calc. 8=20974
 benzene, induced Raman in parallel beam, intensity rel. to sample length 8=8076
 benzophenone, viscous liq., wing of Rayleigh line obs. 8=21671
 Bragg scatt. by u. s. waves, rel. to pulse compression 8=8617
 Brillouin, for crystals in hydrodynamic region 8=14177
 Brillouin, intracavity scatt. from CH₃OH solvent in passive Q-spoiling cells 8=16847
 Brillouin, laser obs. 8=6523
 Brillouin, spatial correlation of density functions 8=12875
 Brillouin, spectrum determination, systematic errors 8=16833
 bubbles, in bubble chamber 8=16835
 chemically reacting system 8=9681
 coherent, by spherical particles 8=11198
 coherent, expt. conditions for obs. in turbid media 8=11193
 collimated beams, applicability of Bugar law for fog and smoke 8=510
 collimated beams in turbid media, attenuation 8=11194
 collimated source in scattering medium, discrimination depth, obs. 8=3374
 by colloid solns., transient elec., rot. diffusion const. determ. 8=8073
 colloidal, for turbulence study 8=4440
 concentric spheres, efficiency factors 8=512
 diamond-like crystals, first-order Raman effect rel. to electrostriction and photoelasticity 8=9486
 dielectrics, mag. ordered, two-magnon Raman scattering 8=9487
 by Dirac particle 8=15713
 electrons, rel. to freq. shift meas., e trapping in laser beam 8=19821
 electrons, reflection of 1.6 keV e by laser pulses obs. 8=20378
 ethyl ether Brillouin, stimulated, quasi-steady-state 8=21687
 extinction coeff., collimated and diffuse fluxes, reln. between 8=3375
 fog scattered, comparison with laser 8=14615
 Fresnel region, errors in meas. of scatt. pattern 8=6390

Scattering—contd

light—contd

- gels, ionotropic, low-angle scatt. 8=16911
 glycerine, liquid, Brillouin 23-90°C, background due to relaxation 8=21689
 n-hexane Brillouin, stimulated, quasi-steady state 8=21687
 haze, small-grained, characteristics 8=18882
 holographic arrangement, for samples of scatt. wavefront 8=20115
 inelastic by liquid surface rel. to thermal excitation of capillary waves 8=16853
 interstellar matter, non-spherical particles 8=4296
 isobutyric acid-H₂O system near crit. mixing pt., correl. effect in conc. fluctuations 8=12882
 isotropic solids, and freq. shifting of light reflected from acoustic surface waves 8=9490
 Lambert, from cone and paraboloid of revolution, geometrical optics approx. 8=20103
 laser atmospheric backscatter, Raman component, obs. 8=23263
 laser beam in gas, speckle pattern from particles 8=3286
 laser beam from second sound, photostatistics 8=11192
 laser radiation, by atmosphere 8=18878
 latex spheres in H₂O of coherent and incoherent light rel. to Mie theory 8=20104
 liquid amplifier, stimulated Brillouin scatt., phonon lifetimes meas. 8=21666
 liquids, anisotropic, dipole moment effect 8=1555
 liquid, Brillouin, inelastic, from density fluctuations, and relaxation 8=16840
 liquids, Brillouin, laser stimulated, self-focusing 8=4585
 liquids, depolarized Rayleigh scattering anomaly under pulsed laser excitation 8=16841
 liquids, freq. broadening shifts 8=8083
 liquid, heterodyning as a means of meas. thermal diffusion coeff. 8=4553
 liquids, meas. for calc. of acoustic props. 8=8059
 liquids, multi-harmonic molec. scatt. 8=12872
 liquids, stimulated Rayleigh, Brillouin and Raman 8=12874
 in liquids, stimulated thermal Rayleigh scatt., theory 8=6561
 liquid surface, rel. to capillary waves on surface 8=16852
 liquids, viscoelastic obs. 8=16839
 macromolecules in soln., diffusion consts. 8=12381
 macromolecules, nongaussian 8=16386
 multiply forward-scattered, brightness 8=18885
 near phase transition points of second kind, theory 8=9489
 nematic crystal, rel. to orientation correlations 8=16795
 nitrobenzene, Brillouin with picosecond pulse 8=4580
 nitrobenzene-CCl₄ mixts. stimulated Rayleigh scatt., obs. 8=16843
 nitrobenzene, Rayleigh line wing, four photon interaction obs. 8=21667
 nonlinear medium, new kind involving photon decay 8=6560
 organic liquids, intensity in wing of Rayleigh line rel. to vibrating molecule model 8=16851
 organic liquids, stimulated scatt. in Rayleigh line wing, obs. 8=16842
 particle density distrib., from spectral and angular data 8=18881
 plasma density fluctuations induced by monochromatic pumping 8=12546
 polymer fibres, polarized light scatt. low angle, rel. to supermolec. order 8=18581
 polymer latexes, size distrib. determ. 8=16900
 polymer solutions, critical opalescence 8=21669
 polymer solns., dilute 8=8023
 polymers, polydispersity of spherulites effect on low-angle scatt. of polarized light 8=8358
 polystyrene soln., laser scatt. for verification of Brownian motion 8=1557
 progress in optics, book VI 8=15541
 PVC solns. 8=16850
 quartz, fused, stimulated Mandel'shtam-Brillouin, depend. on excitation intensity 8=5632
 quartz, stimulated Brillouin, rel. to hypersound generation 8=2451
 quartz, stimulated Brillouin scatt., depend. on temp. and photoelasticity 8=5634
 in quartz, stimulated Brillouin scatt. of ruby laser, optical heterodyne detection 8=14267
 quartz, stimulated Brillouin, temp. dependence 8=14265
 quartz, by u.s. surface waves 8=5636
 quasi-coherent studies, field sensitive spectrometer 8=11195
 quinoline-ethyl alcohol mixts. stimulated Rayleigh scatt., obs. 8=16843
 Raman, crystal lattice dynamics 8=14176
 Rayleigh in anisotropic medium, birefringence meas. 8=11197
 Rayleigh, in stellar atmospheres, rigorous calc. 8=5921
 Rayleigh line wing stimulated scattering, four-photon interaction obs. 8=21667
 Rayleigh-Wing of laser beams in liquids, theory 8=8092
 by relativistic (non-linear) oscillator 8=11199
 resonance scatt. from absorbing spheres 8=511
 resonant elastic response of matter to intense light pulse, transient effects, bibliography 8=19925
 salol, viscous liq., wing of Rayleigh line obs. 8=21671

Scattering—contd

light—contd

- scattering media, spectral line profiles near resonance 8=509
 seawater, Mueller phase matrix 8=18843
 from semi-infinite media, light impulse reflection 8=9878
 solutions, activity coeffs. calc. from Brillouin scatt. 8=4576
 spectra of thermal and molecular, stimulated 8=11196
 spectroscopy, principles and methods for scatt. media 8=11151
 by spherulites, ringed, patterns rel. to deform. 8=9491
 stimulated Brillouin scatt. with Stokes feedback, theory 8=11005
 stimulated thermal, rel. to Raman effects 8=15548
 surface thermal ripplon obs. 8=16838
 three-photon, by atomic fluids 8=4044
 three-photon, in isotropic medium, general theory 8=3373
 triacetin, viscous liq., wing of Rayleigh line obs. 8=21671
 by turbid medium with highly directive scatt., of narrow light beam 8=11161
 by turbulence, vel. field meas. from scatt. light spectrum fine struct. 8=12749
 Venus atm. rel. to CO₂ bands in intensities 8=14846
 wideband pulse compression via Brillouin scatt. in Bragg limit 8=10948
 Ar ion laser, resonance scatt. by Ar plasma 8=12513
 Au films, thickness and wavelength dependence between 2000-7000 Å 8=14199
 C particles, computation: results discussed 8=513
 CO₂, Brillouin scatt. in critical temp. region, obs. 8=16708
 CS₂, Brillouin, stimulated, quasi-steady state 8=21687
 CS₂, induced combination scatt. and self-focusing 8=4581
 CS₂, stimulated spectrum, amplification of ruby-laser radiation line R₂ 8=9520
 CaWO₄ laser crystals, possible loss contribution 8=19994
 D plasma e and ion temps., laser incoherent scatt. obs. 8=21354
 FeF₂, tetragonal antiferromagnet, magnon excitation, one- and two- 8=18546
 n-GaAs, Raman scatt. by mixed plasmon-phonon modes, polarization and intensity obs. 8=5599
 H, atomic, coherent elastic 8=7379
 H plasma e temp. and density, laser incoherent scatt. obs. 8=21354
 by H₂ resonance scatt. and level crossings 8=4064
 H₂SO₄ aerosols study 8=12951
 He atoms at resonance, aligned, depolarization 8=20982
 He liquid, by excess electrons 8=19687
 He, liquid, stimulated Brillouin scattering 8=19691
 He⁺ superfluid, scatt. of laser light 8=8078
 I₂-CCl₄ solns., stimulated thermal Rayleigh scatt. obs. 8=8068
 InAs, by plasmons and Landau levels of electron gas 8=22990
 KBr, second order Raman scattering in polarized light 8=14231
 MgF₂, Raman, selection rules 8=5621
 MgO crystals, Compton scatt. power 8=23012
 MnF₂, tetragonal antiferromagnet, magnon excitation, one- and two- 8=18546
 NH₄Cl, harmonic scatt. and critical pt. correl. 8=23007
 NH₄Cl near second-order phase transform., harmonic generation obs. 8=14245
 NH₄SCN polycrystals, diffuse, effect of anisotropy 8=23004
 O-xylol, Rayleigh line wing, four photon interaction obs. 8=21667
 Si crystals, Compton scatt. power 8=23012
 YAl garnet, laser crystals, possible loss contribution 8=19994
 Y(OH)₃ polycrystals, diffuse, effect of anisotropy 8=23004
 X-rays. See X-ray scattering.
- Scattering, particles**
 See also Collision processes; Field theory, quantum/interactions; Elementary particles; Nuclear forces; Nuclear reactions; Particle range; Particle tracks; S-matrix theory; and under individual particles, e.g. Alpha-rays.
 accelerator beam energy meas. on scatt. 8=6691
 amplitude analyticity for particles described by not strictly-local fields 8=20295
 amplitude calc. nonrelativistic, applic. of Schrödinger eqn., coupled energy extended into physical region 8=20285
 amplitude determ. from dispersion relations, of unknown parameters 8=20300
 amplitude determ. from nuclear photoproduction 8=11858
 amplitude, expansion in functions interpolating Legendre polynomials 8=685
 amplitude expansion using Lorentz group representation 8=15696
 amplitude multichannel, calc. with and without coupling effects 8=11401
 amplitudes, relativistic, and asymptotic theorems, integral representations 8=11398
 amplitudes, theory of analytical structure 8=19476
 ang. depend. at high energy of cross-section 8=20297
 ang. distrib. of particles, distortion by medium 8=11844
 antiparticles, high-energy relations for oscillating scatt. amplitudes 8=11400
 Bethe-Salpeter amplitudes, normalization methods 8=3540

Scattering, particles—contd

- Bethe-Salpeter amplitudes rel. to crossing symmetry 8=20282
- Bethe-Salpeter eqn., soln. below threshold, scatt. amplitude extended to physical region 8=20281
- in block of matter 8=3190
- bootstrap, crossing-symm. model of nearly degenerate vector meson octet 8=3565
- bootstrap and S-matrix perturbation theories 8=11367
- bootstrap calc. using Schrödinger eqn. 8=11559
- bound system, Schrödinger eigen-numbers 8=668
- branch-point contributions in complex momentum plane 8=20319
- branch-points, ang. momentum, sum rules and features 8=3541
- channels, low-lying, effect of hidden channels 8=15706
- Chew-Low eqns., deduction, and origin of cut-off function in static models 8=3537
- classical in a force field which is a random function of time 8=14940
- complex nuclei, inelastic, accompanied by excitation of collective states 8=11949
- composite system, nonrelativistic, high-energy collision 8=15012
- cosmic, on random mag. field 8=19086
- by Coulomb field, modified 8=674
- from Coulomb-like pots, generalized Lippman-Schwinger eqns. 8=680
- Coulomb-nuclear S-matrix, analyticity for complex ang. momenta 8=15703
- Coulomb phase shifts, algebraic calc. 8=20280
- Couture-Newton formalism, relativistic extension 8=15702
- diffraction model with surface absorption 8=11842
- diffraction theory of ion scatt. with mutual excitation 8=1102
- Dirac, high-energy, multiple scattering 8=679
- disordered system of scatt. centres, energy spectrum and fluctuations 8=3538
- dispersion relations and magnetic moments of hadrons 8=3605
- at edge of plate, normal incidence, ang. distrib. 8=19777
- elastic, asymptotic, and real rel. to imaginary parts 8=2904
- elastic, proposals for experiments 8=11837
- elastic, with spin relations between helicity amplitudes 8=20298
- electrodynamics, 2-particle, double-log. asymptotics 8=592
- by e.m. field, stochastic 8=10880
- energy approx. computation, upper bounds to error 8=681
- energy dependence of cross-section near 3-body reaction threshold 8=3547
- exchange reaction evidence from ang. correl. function symm. angle at backward scatt. 8=11843
- expansion approach, within Schrödinger eqn. applic. 8=672
- Fadeev eqns. rel. to n-d scatt. and n-n low energy parameters 8=15841
- Fadeev eqns., soln. by quasi-particle method of Weinberg 8=11403
- finite-energy sum rules for bootstrap calc. 8=15711
- fission fragments on Au, Ag and Formvar foils 8=11969
- form factors in local field theory with infinite Lorentz group representation 8=6609
- 4 body correls. rel. to 4 particle-4 hole excitations in closed-shell nuclei 8=15958
- gravitational, covariant theory of gravity 8=3452
- graviton-spin-0 particle scatt., low-energy theorem 8=20283
- groups, noninvariant 8=3502
- hadron-hadron, quark model 8=6825
- hadrons, Regge-quark model 8=734
- hadrons, using composite particle theory 8=11487
- Hamiltonian for unstable particle, hermitian and non-hermitian 8=15626
- harmonic oscill., 3-D, e. m. field coupling, scatt. amplitude heirarchy 8=3427
- helicity amplitude, absorption corrections, simplified procedure 8=6759
- helicity formalism, conspiracy and superconvergence props. 8=11406
- high energy, appl. of quark model 8=724
- high energy, implications of quark model 8=730
- impact-parameter representation and group contraction 8=15698
- inelastic differential cross sections high energy behaviour 8=3532
- infinite dimensional symmetry schemes in Fok space 8=658
- integral eqns., soln. by extension to complex plane and determ. of singularities 8=20290
- invariant amplitudes, Reggeization using dispersion relations 8=11418
- invariant under groups $O(n)$, $S_p(n)$, $SU(n)$, $n \geq 1$, total cross-section positive 8=6763
- inverse one-dimensional, finite-range solns. 8=11394
- Landau singularities, absence from the physical sheet 8=3549
- length as function of complex ang. momentum 8=15697

Scattering, particles—contd

- Levinson's theorem applic., non-equivalence of one-channel and multichannel N/D eqns. 8=20312
- Lippman-Schwinger, potential scatt. equation derivation from Bloch scatt. theory 8=3894
- low-energy, short-range repulsion, calc. 8=3539
- Mandelstam representation, moment conditions for double spectral functions 8=3543
- Mandelstam type diagrams, asymptotic behaviour, taking spins into account 8=3536
- many-channel, finite, structure of the unitary S-matrix 8=684
- matrix elements, with $(A + a)$ and $(1 + 2 + 3)$ open channels 8=6761
- minimum interaction hypothesis tested in p-p scatt. 8=11597
- multiple, from metal block 8=20286
- multiple, positive- α Landau surfaces 8=15701
- N-body problem, set of integral eqns. 8=11850
- N/D eqns., appl. of Padé approximants 8=15704
- N/D eqns. Padé pole approx. 8=20315
- N/D equations, S-wave, domain of self-damping interactions 8=6767
- N/D model of weak amplitudes 8=15705
- N/D multichannel amplitude, discrepancy with single channel N and D procedure 8=11407
- N/D problems, soln. without simultaneous eqns. 8=20316
- in non-linear spin theory 8=20288
- non-relativistic, by centrally symm. pot., Brysk approx. of phase shifts 8=3400
- nonrelativistic square diagram, amplitude 8=20284
- nuclear, Bethe's formula for Coulomb interference 8=3893
- nuclear-Coulomb scatt. phases, restoration of cut-off nuclear potential 8=3896
- nuclear, polarization to separate direct and compound nucleus effects 8=1029
- nuclear, projection operator applied to calc. of R-matrix 8=20764
- nuclear scatt. amplitude and cross-section, statistical props. using collision matrix 8=11839
- nuclear, small angle, contribution to bubble chamber analysis 8=6681
- by nuclei, diffraction scatt. separation of variables 8=1030
- Q_{31} partial wave expansion, recurrence relation, 2-particle 8=15699
- off-shell dynamics relativistic, new covariant integral eqns. 8=20293
- one-channel elastic scatt., partial wave soln. and CDD-poles 8=6755
- one-channel problem, soln. via integral eqns. of Jost function formalism 8=6757
- operator, theorems for existence 8=673
- optical potential relationship for spherical and deformed nuclei 8=11687
- oscills. allowed in asymptotic region, whole amplitude does not oscillate 8=20299
- overlap function analysis applied to $\pi\pi$ 8=6874
- overlap functions from O_3 to $O_{2,1}$ for unitary representations of $SL_{2,C}$ as series of Γ functions 8=20264
- partial-wave amplitude derived from cluster property of Wightman functions, Greenberg-Low bound 8=20294
- partial wave amplitude perturbation comparison of off-shell and Dashen-Frautschi methods 8=20292
- partial-wave amplitudes, asymptotic behaviour with vel. depend. pot. 8=20302
- partial-wave amplitudes for vel. depend. pot., analyticity props. in energy and ang. mom. variables 8=20301
- partial wave dispersion relations, number of subtractions 8=15700
- particle range meas. using Coulomb excitation 8=8756
- phase shift formula in pot. scatt. 8=20287
- phase shifts calc. from Bethe-Salpeter eqn. 8=571
- by plane 8=3188
- Poincaré and Lorentz invariant expansions of relative amplitudes 8=11396
- poles complex double in propagator and spectral condition 8=11408
- Pomeranchon, is it fixed pole 8=689
- Pomeranchuk trajectory: actuality or mirage? 8=11423
- pomeranchon as self-reproducing singularity, colliding poles mechanism 8=20330
- pot. determ. from dynamical singularities of partial-wave amplitudes 8=11397
- potential, non-relativistic, effect of CDD poles on long range pot. behaviour 8=6751
- quark model due to Schiff 8=6826
- quark model, elastic scatt. 8=725
- quasi-elastic, analog states excitation and spin-spin interaction in optical potential 8=15986
- radiation damage displacement cascade, rel. to law 8=22239
- Regge amplitudes cancelled by daughter trajectories, Toller poles from residue factorization 8=3555
- Regge analysis for spinless particle scatt., extended to lower energies 8=6771
- Regge analysis, finite energy sum rules 8=20296
- Regge analysis of non-forward $N\pi$ superconvergence relations 8=20455

Scattering, particles—contd

- Regge branch-point exchange effect 8=20319
 Regge cuts and absorptive corrections 8=20326
 Regge cuts in ang. mom. plane, photoprod. as test 8=20331
 Regge cuts with superconvergence relations 8=11417
 Regge cuts, rel. to vanishing total cross sections and constant diffraction peaks 8=15709
 Regge daughter trajectory for boson resonances 8=3557
 Regge "daughter" trajectories model depend. 8=11419
 Regge daughter trajectories, operator formalism 8=3563
 Regge-like poles in impact parameter plane 8=11416
 Regge model, multiple Pomeranchuk exchange, violation of unitarity 8=15707
 Regge pole hypothesis, multiple, Toller variables and group theory 8=6769
 Regge pole decomposition of Lorentz poles 8=15696
 Regge-pole model, ghost-eliminating 8=20332
 Regge pole and SU(3) theories, high-energy 8=15708
 Regge poles, classification necessarily Lie Algebra of Lorentz group SL(2, C) 8=20325
 Regge-poles, 0(3, 1) conspiracy, high energy, equal mass. 8=20322
 Regge poles, using generalized algebra of currents 8=3558
 Regge poles, Van Hove model generalized to study unequal mass daughter trajectories 8=20323
 Regge representations for amplitude rel. to pots. 8=11409
 Regge residue function, $\beta(s)$, decrease with $\alpha(s)$ as $s \rightarrow \infty$ 8=11420
 Regge theory of high-energy, with large momentum transfer 8=20329
 Regge trajectories and the Bethe-Salpeter eqn. 8=3559
 Regge trajectories, construction of Green's function 8=687
 Regge trajectories, infinitely rising, kinematic constraints 8=11422
 Regge trajectories, universality of slopes 8=3562
 Regge trajectory formulation of dynamics, with unitarity, and narrow-resonance approx. 8=20324
 Regge-trajectory slopes, props. without assuming 4-particle unitarity eqn. 8=20320
 Reggeization, general scheme and classification of Regge poles 8=20321
 Reggeization of helicity amplitudes 8=11414
 reggeon diagram tech. for branch point anal. in ang. momenta complex plane 8=3556
 relativistic S-matrix, use of complex inhomogeneous Lorentz group 8=20289
 relativistic of spin-zero particles 8=15609
 renormalized coupling consts., and inversion problem 8=6610
 renormalized meson theories, test of existence of stationary singularity 8=20168
 rot. state, 2^+ in doubly even nuclei, corrections to reorientation effect 8=15940
 Rutherford, excited level effect on cross-section 8=11841
 saturation a good approx. to sum rules? 8=3513
 scatt. amplitude, power behaviour and Cerulus-Martin lower bound 8=3544
 scattered particle beams intensity fluctuations and corrls. meas. 8=19776
 S-matrix, causality implying analyticity 8=20307
 S-matrix, construction without accompanying pole in non-physical sheet 8=20309
 S-matrix, reduced, definition of elements 8=6765
 S-wave, off Yukawa potential, expansion approach 8=672
 off-shell partial wave amplitudes, ang. momentum effect 8=3895
 soft particle production model, change invariance and group transformation props. 8=3534
 spin- $\frac{1}{2}$ -spin 0, Austern-Blair theory, cross-section and polarization derived 8=11840
 spinless, O(4) amplitudes of Freedman-Wang symm. props. for Sommerfeld-Watson transformation 8=6771
 spinless off arbitrary spin, relations among superconvergence conditions 8=6758
 spin-one, polarization effects 8=6752
 strong and weak interactions, present problems, conference Erice Italy (1966) 8=15695
 strongly interacting particles, amplitude at vanishing field coupling const. 8=3533
 storage rings, use for p-X scatt. 8=842
 SL(2C), unitary irreducible represent., decomposition, restricted to SU(1, 1) 8=6029
 SU(3), Weyl coefficients 8=2887
 sum rules with divergent integrals from general treatment of current algebra 8=3535
 superconvergence 8=11399
 superconvergence sum rules algebraic struct., rel. to mass formulae 8=656
 superconvergence sum rules and current algebra 8=3564
 superconvergent sum rules from generalization of chiral symm. 8=20310
 superconvergent sum rule, model for saturation using Regge pole theory 8=6756
 superconvergent sum rules, Regge pole contrib. 8=3553
 symm. breaking in vector meson-B scatt. lengths 8=6916
 symmetries of scatt. including mass-splitting 8=676
 systems involving low-dimensional representations of high-rank Lie groups, stability 8=6762

Scattering, particles—contd

- theory and propagation functions 8=6753
 3-body, Amado model, amplitude continued in complex ang. mom. 8=20306
 3-body, approx. from Lovelace-Faddeev eqns. 8=20305
 3-body DWBA, integral eqn. derived, modification 8=11838
 3-body, unitary modifications of impulse approx. 8=682
 3-body, Faddeev's theory, iteration method 8=3545
 3-particle model, Lovelace approx. 8=3546
 3-particle, spinless, Yukawa potential, amplitudes given by Fredholm series 8=3548
 3 point particles, max. number of binary collisions interacting through zero-range forces 8=20304
 time delay, definition, stationary approach 8=678
 time-dependent, theory for singular potentials 8=20303
 Toller poles as sum of constraints for Regge amplitude residue factorization 8=3555
 Toller's 2-body amplitude, covariant inclusion of spin 8=11402
 trajectories with energy losses in matter, covariance matrix 8=20308
 2 different fermions, polarization quantities and cross sections 8=20380
 2-particle amplitude, matrix element of Lorentz group, expansion 8=3542
 2-particle-to-2 particle, kinematics for Regge crossing 8=6760
 unitarity rel. to multiparticle prod. reactions 8=20275
 As⁷⁶, 36-38 MeV O¹⁶, multipolarities, spins and parities of levels 8=3816
 Au foil on C, of O¹⁶ 8=20839
 CDD pole rel. to π N scatt. 8=20453
 Co⁵⁹ of O¹⁶ ions, 36 MeV, spin and lifetimes of levels 8=3813
 H-He-H₂ systems, interaction potentials 8=12376
 In¹¹⁵ (O¹⁶, O¹⁶, γ), 35 MeV, deduced levels 8=3822
 O¹⁶, ¹⁷, ¹⁸- + C¹², elastic, ang. distrib. and radius parameter 8=3973
 Sc₂In phase, magnetization meas. and press. depend. of Curie point 8=17885
 Si and SiO₂ films, re-emission coeffs. in r.f. and d.c. sputtering 8=2032
 Sm¹⁵², 50 MeV O ion, Rutherford correction due to excited levels calc. 8=11841
 in W and Si crystals in 2-30 MeV rel. to channelling behaviour 8=11954
Schizons. See Elementary particles; Field theory, quantum/interactions, weak.
Schlieren systems
 No entries
Schottky defects. See Crystal imperfections/vacancies.
Schottky effect (noise). See Electron tubes; Fluctuations/electrical; Semiconducting devices.
Schrödinger equation. See Quantum theory/wave equations.
Schwarzschild space. See Cosmology; Gravitation; Relativity/general.
Scintillation. See Luminescence.
Scintillation chambers. See Luminescence chambers.
Scintillation counters. See Counters/scintillation.
Seals, glass-metal. See Glass-metal seals.
Seawater
 absorption and scattering coeffs., from light coeffs. of extinction 8=3375
 in Caribbean basins, deep, renewal time from Ra, C and O distrib. 8=5783
 currents detect. by satellite i.r. obs. 8=9855
 currents vel. components spectra and wind energy transfer process 8=9810
 light scatt., Mueller phase matrix 8=18843
 radiation scattering from surface, frequency shift 8=10955
 radioactive contamination from atmosphere 8=9806
 spectral attenuation coeffs., relative 8=12888
 spectral brightness coeffs., atmospheric extinction and absorpt. 8=9872
 surface, dynamical and thermal interaction with atm. 8=9829
 surface scattering of h.f. radio waves 8=18976
 surface wave interaction theory 8=12649
 temperature meas. by airborne i.r. radiometer 8=18845
 tidal flow and mass transport in Humber estuary 8=5785
 in AgCl-Mg battery electrolytes, elec. cond. 8=16875
 CaCO₃ aragonitic oolites, solubility pressure coeff. obs. 8=8012
 Cs¹³⁷ conc., determ. by adsorpt. on Cu ferrocyanide-anion exchange resin 8=3879
 Ru¹⁰⁶ in Black Sea seaweeds, identification and separation 8=9734
Second sound. See Helium/liquid, sound propagation.
Secondary electron emission. See Electron emission/secondary.
Sedimentation
 Bingham plastic, settling of spherical particles 8=21553
 cellulose acetates in acetone, rel. to macromol.
 Johnston-Ogston effect 8=21729
 lamella thickening, theoretical analysis 8=21728
 polydisperse solns., equilb. 8=1531
 polymer solns., rel. to intrinsic viscosity 8=12823
 polymethacrylic acid solns. 8=12817

Sedimentation—contdAl²⁶ in ocean, atmospheric origin 8=23236

Ra trace element distribution coefficients 8=9737

Seebeck effect. See Thermoelectricity.**Seidel theory.** See Aberrations, optical.**Seignette salt.** See Rochelle salt.**Seignettelectric materials.** See Ferroelectric materials.**Seismic waves**

See also Seismology.

absorbing medium, depend. on charge weight 8=9784

diffracted S, obs. 8=23202

excitation of atm. oscills. 8=9899

from explosions, nuclear, P travel times obs. 8=2557

in friable medium, propag., elastic model and microseismic zoning appls. 8=157

gravitational perturbation rel. to \bar{S} and \bar{P} pulses and dispersion curves 8=3030

isostatic equilibrium in earth's crust, theory 8=9782

line sources polar and azimuthal radiation patterns 8=3032

longitudinal wave propag. vel., correl. with rock density 8=18816

longitudinal-wave spectra meas. from earth-
quakes 8=9777

Love waves, propag. in anisotropic medium with

hexagonal symmetry 8=23206

Love waves, theoretical dispersion tables for wedge
propag. 8=9775

magnetite deposit, seismomagnetic effects 8=10032

micro, nature and location of source 8=5773

microseisms rel. to microbaroms 8=9773

orientation of principal stresses in earthquake foci,
Mediterranean—Asian belt 8=9779P/Rayleigh, conversion coefficients at a stress free
wedge 8=14534

P waves, angle of incidence 8=9774

P waves, long period, for earthquake fault parameter
determination 8=18814P waves in upper mantle, velocity profile down to
750 km 8=18810

P and S, velocity by pulse transmission method 8=14542

phase vels. of Rayleigh waves in Finland, originating at
5 Green earthquakes 8=23208phase-velocity dispersion in real absorbing
media 8=23209

polar ice sheet as heterogeneous wave guide, obs. 8=18811

in porous solid, liquid-filled 8=13497

propagation and detection, conference Cambridge
1966 8=18809

Rayleigh, apparent initial phase of point source 8=18812

Rayleigh, conservation of energy 8=10707

Rayleigh-Love second modes, coupled 8=2558

Rayleigh-Love, velocity depend. on Earth's crust 8=9776

reflection and refr. coeffs. of thin-layered media 8=158

refracted-wave travel-time curves rel. to vert. and
horiz. vel. grads. for discrete obs. 8=23210S travel times and J-B deviations analysis, distance
28°–82° 8=2560Somigliana's theory rectification, and Rayleigh's
equation 8=3028surface wave due to explosion in air, detonation power
and height, verification of theory 8=23211

torsional vibrations of earth, tables of derivs. 8=9783

transmission in system of corrugated layers 8=13498

velocity of vibr. on earth's surface in body waves 8=9778

Seismology

See also Geophysical prospecting; Seismic waves.

alluvium nuclear detonation, cavity press. and temp.
time history afterwards 8=14527

anelastic Earth, torsional oscs. 8=14533

attenuation of seismic body waves in mantle 8=14531

azimuthal variation in source term of longshot 8=5772

Canada, national report, 1963–66 8=14526

chart signals in presence of noise, visual detection
sensitivity 8=18818

compressional wave vel. in fluid-saturated particles

aggregates, appl. to exploring and oil prod. 8=22270

core convection and continental drift 8=23217

crystal transfer functions, truncated, and structure
determ. 8=2559damping of S waves, absorptions for different
periods 8=14535damping props. of mantle, for unified viscosity and
viscoelasticity theory 8=14538discrete obs., refracted-wave travel-time curves rel.
to vert. and horiz. vel. grads. 8=23210

earth's crust, Far Eastern transition zone, 1963–4 8=9780

earth crust movements meas., e.m. waves atm. refr.
effects correction 8=2605earth's crust, velocity parameters from reflected-wave
travel times 8=9786

earthquake fault parameters from long period

P waves 8=18814

earthquakes and faulting, rel. to triaxial stress systems
effect on rock fracture 8=13516earthquakes, shallow, time sequence using layered half-
space model 8=14530

earthquake, and upper atm. acoustic-gravity waves 8=14641

Seismology — contdelastic wave propag. and absorpt. in rocks under
confining press. 8=13515elastico-viscous medium, model, rel. to influence of
rheological props. 8=14537

energy released by dipslip faults in upper mantle 8=18820

fault propag. model, rel. to prod. of seismic shock 8=14536

frequency charact. of channel, correction 8=9781

granodiorite shocked mechanically and by nuclear
explosion, triaxial compression obs. 8=23212

Hugoniot eqns. of state for 12 rocks from shock wave

data, rel. to those derived from geophys. obs. 8=14558

ionospheric irregularities, acoustic waves ascribed to
earthquake 8=23395

joint epicentre determination 8=9785

longitudinal wave propag. vel., correl. with rock
density 8=18816major fault zones, seismic moment and slip rate
calc. 8=18813

mantle-core transition zone, wave velocity 8=9788

mantle, flow inferred from continental drift and low
harmonics of geopot. 8=14551mantle, upper, anomalous structures suggested by Tonga-
Kermadec obs. 8=2564marine geology, application of acoustics and
ultrasonics 8=23248microseismic oscills. rel. reversible magnetostriction in
magnetite 8=10063

model accuracy rel. to receiver-model coupling 8=14525

optical processing, filtering and interpretation of
data 8=14529oscills. of earth, spheroidal and torsional, Q values from
decay of spectral amplitude 8=23205

P waves in upper mantle, velocity profile down to

750 km 8=18810

P and S travel time anomalies, interpret. 8=5774

phase vels. of Rayleigh waves in Finland, originating at

5 Greek earthquakes 8=23208

resistivity prospecting, appl. of reciprocity
theorem 8=14541rock compression, microfracturing and inelastic
deformation obs. 8=23203rotatable field e. m. prospecting system, anal. and
model studies 8=14540

salt dome nuclear explosion, deep reflection obs. 8=18815

scattering of long wavelength plane elastic waves,
theory 8=22262

seismic attenuation in earth rel. to thermal grad. 8=14539

seismic wave attenuation in Earth's mantle, rel. to
anelasticity 8=14543

shock motion, structure-foundation interaction 8=3034

shock spectrum of interaction between superstructure
and non-rigid foundation 8=19543signal stacking on emulsion layer, and recordings of
variable density 8=23207spheroidal free oscs. of earth, freq. and modes from
1964 Alaska quake 8=14532surface wave arrival at Eskdalemuir array, generated
by scatt. of initial P wave 8=5775surface wave data, compatibility with Q and body wave
travel times 8=5777tectonic processes, model expts. of effect of
gravity 8=14512as test of convection hypothesis by anisotropy of
vel. 8=14524theory and applications, conference Cambridge
1966 8=18809transition of earthquake activity between seismic
regions 8=5776travel times of P waves from nuclear explosions in
central Pacific 8=23213volcanic ashes, nonhomogeneous, from turbulent
diffusion, distribution 8=23216Willmore Mk II seismometer, e. m. calibration
coil 8=18817**Selenium**atoms, ($p^4 \leftrightarrow p^3s$) excited-state wavefunctions and
oscillator strengths 8=16209amorphous, atomic radial distrib. function rel. to quenching
from different melt temps. 8=1714amorphous layers and single crystals, photo-emission
studies 8=22725

band structure, relativistic KKR-calcs. 8=22468

Bijvoet differences in the non-centrosymmetric
structure 8=13273

compressibility and structure 8=17827

conductivity during n and γ -irrad., rel. to temp. and rad.
damage 8=18067

critical surface tension 8=21869

cyclooctaselenium, entropy changes in formation 8=21207

crystal growth, monoclinic 8=4814

crystal structure, and other props., effect of cooling to
100°K 8=1808crystal structure refinement of α -monoclinic and hexa-
gonal modifications 8=13288

electrophotographic layers, discharge kinetics 8=2265

etch pits 8=1990

films, photoconductivity, anomalous, activated by Hg 8=9256

Selenium—contd

- films, polycrystalline and single crystal, extra reflections in electron diff. pattern 8=4753
- films, viscoelastic properties, obs. 8=21888
- films, vitreous, space-charge-limited currents and high elec. field effect 8=13828
- granite compression, microfracture events spatially located by S waves 8=23215
- hexagonal, photoconductance meas. during cooling from 300° to 4.2°K 8=18238
- hexagonal, single crystal growth from supercritical NH_3 8=8425
- high-purity, elec. conductivity rel. to Na and O_2 impurity admixture 8=5276
- hydrides, proton reson. 8=12327
- laser irradiation, second harmonic generation 8=6442
- lattice vibrational properties, i. r. spectra rel. to reflectivity and transmission 8=8615
- liquid mirror as reflector in ruby laser, rel. to Q-switching 8=11078
- magnetoconductivity, mobility and direction dependence 8=5275
- magnetoconductivity rel. to mobility mechanism 8=18065
- molten, sound velocity and compressibility 8=12866
- phase detection in $\text{V}_5\text{V}_{13}\text{xx}$ alloys, by etching 8=17102
- photoconductivity of amorphous layers activated by Hg 8=13914
- photosensitivity spectrum dependence on crystallinity and oxygen impurities 8=18237
- polycrystalline, hexagonal, local (conduction) levels, X-ray-induced 8=18236
- polymorphic transition from orthorhombic to hexagonal 8=8426
- positron annihilation meas. 8=5150
- production in u. s. field 8=21967
- rectifiers, prebreakdown region, I-V fluctuations 8=2225
- selenide i. r. glasses, props. 8=22954
- semiconductors band structure Green's function method 8=8913
- trigonal, thermally stimulated currents after u. v. irradiation 8=22683
- vapour, thermodynamic props. 8=4659
- vitreous, electronic processes in photo-crystallization 8=22471
- Se_2^- , e. s. r. in alkali iodide crystals. 8=14123
- Se_2 , long-range potential 8=12232

Selenium compounds

- (Mn, Me)(S, Se)-type synthetic cpds. and selenide-sulphide inclusions 8=4692
- Se-Te alloys, positron annihilation, photon ang. distrib. 8=13692

- SeO gaseous free radical, e. s. r. study 8=12340
- $\text{SeO}_4(\text{NH}_4)_2$, paramag. centres from γ -irrad. 8=9305

Self-diffusion. See Diffusion in gases, in liquids, in solids.

Semiconducting devices

See also Counters/semiconductor; Lasers; Masers.

- analogue Hall-effect amplifier multiplier 8=19374
- bolometer, for i. r. 8=226
- bulk oscillator, convective instability of solid state plasma 8=18098
- bulk-microwave oscillators, hot e relax. times in two-valley semiconductors 8=22422
- characteristics, meas. by fine focussed electron beam 8=22575
- conference, Dallas 1967 8=12480
- Conference on meas. and test methods, Budapest 1967 8=9144
- dielectric, electronics, review 8=18203
- electron beam probing 8=18026
- electronic components conference, Jackson USA, 1967 8=6244
- γ -ray spectrometer, noise and trapping 8=6791
- Gunn effect diodes, and other electronic devices, review 8=5292
- Gunn-effect oscillators 8=5295
- Gunn effect oscillator, freq. modulation by mag. tuning, 9, 300 and 10, 900 MHz 8=361
- Gunn effect oscillator, l. f. analog 8=5290
- Gunn effect oscillators, frequency modulation 8=5289
- Gunn effect oscillator, negative resistance type, analysis 8=13845
- Gunn-effect oscillators, non-uniform field effects 8=18124
- Gunn oscillator, one electrode split 8=5293
- Gunn oscillators in parallel in transmission line, current waveform 8=22643
- Gunn oscillators, pulsed, injection priming 8=5294
- Gunn oscillator, X-band, performance rel. to temp. 8=5296
- Hall effect, with magnetoresistance, design and appls. 8=13839
- at high injection levels, theory 8=22617
- infrared radiometry 8=22618
- integrated circuit fabrication, rel. to precision of photo etching techs. 8=18096
- integrator, gated, for pulsed n. m. r. 8=14134
- internal structural defects, testing by electrical methods 8=18100
- lasers, population and current noise 8=429
- lasers, review 8=19982

Semiconducting devices—contd

- leak test method, using radioactive Xe-133 8=2211
- metal-intrinsic semiconductor junction, self-consistent free electron model 8=2112
- metal-to- BaTiO_{3-x} , contact, elec. conduction temp. dependence 8=22623
- metal-oxide-Si, Au-doped, C-V props. 8=13896
- M-SiO₂-Si, m. i. s. system, tunneling props. 8=5340
- metals, vapour phase deposition, appls. in electronics 8=13840
- microelectronics, review 8=18097
- microwave impedance, dynamic behaviour 8=5288
- metal-anodic oxide-Si structures, frequency response 8=18143
- m. i. s. systems, tunneling, expt. with M-SiO₂-Si 8=5340
- m. i. s. systems, tunneling theory 8=5341
- m. i. s. tunnel junctions, conductance extrema 8=22620
- m. o. s. capacitors, inversion layer behaviour at low temp. 8=9178
- m. o. s. capacitor, minority carrier lifetime from transient response 8=9177
- m. o. s. charact. degradation by radiation 8=18138
- m. o. s., currents controlled by surface space charge 8=5343
- m. o. s., principles and elec. characts. 8=18145
- m. o. s. structure, built in voltage and charge distrib. of oxide layer 8=18141
- m. o. s. structures, complex capacity interpretation as function of freq. temp. and potential difference 8=18142
- m. o. s. structure, rel. to localized surface charges 8=22640
- m. o. s. structure, oxide layer surface states 8=2228
- m. o. s. structures, radiation induced space-charge buildup in SiO₂ layers 8=9181
- nuclear and space radiation effects, conference 8=22578
- nuclear electronics, instability and decoupling 8=9142
- nuclear particle detectors photoresponse with simple light spot scanner 8=3464
- nuclear radiation counters, charge fluctuations 8=612
- nuclear radiation damage, estimation by equivalent circuit 8=13838
- p-n junction detectors, self-filtering with narrow spectral responses 8=9158
- pnpn, narrow base, neutron radiation damage 8=22642
- photoelectric converter with single-line scanning, theory 8=22707
- photoresponse using a simple light spot scanner 8=3464
- power devices, review 8=18094
- solar cells, distributed model 8=9265
- solar cell props., integral covers effects, obs. 8=10854
- surface barrier detectors, pulse, shapes obs. and compared with theory 8=9141
- surface effects of radiation 8=18101
- surface phenomena by light spot scanning method 8=18099
- surface properties, measurement methods 8=18147
- technology and physics including m. o. s. devices, book 8=5287
- thermistor flake arrays, optically immersed in Ge and Si lenses, for i. r. detection 8=9143
- thermistors for calorimetry, resist. rel. to temp. and immersion depth, obs. 8=3110
- thermistors, as circuit elements in low-freq. circuits 8=22619
- thermistors, temp. charact. matching 8=18095
- thin film techniques, development and application 8=13841
- thyristors for power frequencies above 400 Hz, rating and applications 8=13849
- transmission and scattering parameters measurement of 8=9139
- 'varitherm', a three terminal thermistor with third lead as control electrode 8=5306
- waveguide with semiconducting wall, propag. 8=19877
- Al-Al₂O₃-Al film, current instabilities 8=18201
- Al-SiO₂-Si-Al structure, surface states in SiO₂ 8=2228
- BaTiO_{3-x}, -to-metal contact, elec. conduction temp. dependence 8=22623
- BaTiO_{3-x}-metal, surface barrier heights determ. 8=9184
- CdS acoustoelec. light scanner 8=5309
- CdS crystal amplifier 8=5337
- CdS film solar cell, mechanism obs. 8=10847
- CdS layer on dielectric, ultrasonic Love wave amplification 8=4921
- CdS solar cell deployable rigid-frame array, performance obs. 8=10845
- CdS solar cells environmental thermal cycling test obs. 8=10848
- CdS solar cells, thin film on Cu and plastic, characts. and stability 8=10855
- CdS, thin crystals, capacitance changes under d. c. bias 8=9195
- CdS-Co₂S solar cell, mobile impurity ions model 8=10846
- CdS(Se) lasers, free exciton annihilation 8=11088
- CdTc solar cells, spectral response and integrated array fabrication 8=10856
- CdTc solar cells, 28 V module and roll-up array 8=10857
- GaAs, contact alloys investigated, fabrication and ohmic props. 8=5291
- GaAs, Gunn, design for c. w. operation, rel. to temp. 8=5297

Semiconducting devices—contd

- GaAs, Gunn-effect oscillators, parameters rel. to frequency 8=5300
 GaAs, Gunn oscillators, electrical performance 8=5299
 GaAs, Gunn oscillators, high peak power 8=5298
 GaAs, Gunn oscillators, microwave amplification 8=5302
 GaAs, Gunn oscillators, n-type, inhomogeneity effects 8=362
 GaAs i. r.-sensitive, made by Cr diffusion 8=18126
 GaAs junction laser, operation on diamond heat sinks at 200°K 8=6465
 GaAs laser, excited by electron beam, pulsed operation 8=6469
 GaAs laser, optically pumped, av. power output 8=11102
 GaAs-metal contacts, thin multilayer 8=9145
 GaAs, ohmic contacts, simple technique 8=13846
 GaAs oscillators, microwave circuit characteristics 8=5301
 GaAs solar cells, thin film on Mo and Al, fabrication and props. 8=10853
 GaP-GaAs, n-p heterojunctions, photo-effects 8=5311
 GaP-Ge heterojunctions, prep., structure and props. 8=18111
 Ge oscillator, excitation threshold, injection level influence 8=9182
 Ge oscillators, current oscillations, cause 8=9183
 Ge-GaAs n-n heterojunctions, barrier heights pressure dependence 8=22624
 Ge(Li) detector for γ -spectrometer with cooled pre-amplifier 8=698
 Ge(Li) detectors, review of properties and applications in gamma spectrometry 8=11443
 Ge-Si alloyed heterojunctions, conductivity and Hall coeff. at interface region 8=2217
 Ge-Si, heterojunctions, electron microprobe analysis 8=2216
 Hg_{1-x}Cd_xTe, i. r. lasers and fast detectors 8=11103
 InAs diode laser, epitaxy prod., characts. 8=11106
 InAs, i. r. lasers and fast detectors 8=11103
 InSb, i. r. lasers and fast detectors 8=11103
 InSb m.o.s. struct., i. r. image detect. and storage 8=13863
 InSb, n-type, microwave detector, influence of mag. field and impurities 8=2224
 InSb-oxide-metal structure, osc. tunnel conductance induced by L.O. phonons 8=13862
 Mg-SiO₂-Si, m.o.s. structure, Fowler-Nordheim tunnelling and energy band structure 8=2229
 Pt: CdTe solar cell prep. by sputtering 8=10856
 Se rectifiers, prebreakdown region, I-V fluctuations 8=2225
 Si anodic oxide, B-doped, growth mechanism 8=14422
 Si, avalanche oscillators, uniaxial stress effects 8=5303
 Si detectors, charge collection, α and β particles 8=2212
 Si, heteroepitaxial films on sapphire, space-charge limited currents 8=2213
 Si, integrated circuits, isolation diffusion of P 8=1929
 Si-metal, Schottky barriers rel. to mode of preparation 8=18116
 Si, microwave spectrometer, Stark modulated 8=3275
 Si, m. o. s. capacitor, minority carrier lifetime, from transient response 8=9179
 Si p or n solar cell characts. rel. to distributed model 8=9265
 Si solar cell characts, thickness and temp. depend. rel. to power-weight param., obs. 8=10850
 Si solar cell deployable rigid-frame array, performance obs. 8=10845
 Si solar cell, integrated high-voltage 8=10852
 Si solar cells, dendritic and refr. back, prod. by implantation 8=10849
 Si solar cells for 0.4 and 0.2 AU from sm use 8=10851
 n-Si surface, Au contacts, props. 8=18070
 Si thyristors and other power devices, review 8=18094
 Si-Au potential barriers prep. by local sputtering 8=9166
 SiO₂ films, characts. rel. to m. o. s. devices 8=18148
 SiO₂ isolation struts. for integrated circuits, fabrication 8=21964
 VO₂ high-speed solid-state thermal switches 8=22616
 ZnO laser, free exciton annihilation 8=11088

diodes

- avalanche-transit, microwave uses 8=2221
 capacitance measurement at h.f. and v.h.f., reverse biased 8=13850
 ceramic titanate rectifying barriers 8=18125
 with chalcogenide glass between metallic electrodes, I-V characts. 8=18118
 charge storage, characteristics and application to u. h. f. fast pulse generator 8=18122
 ferrite, waveguide applications 8=22626
 frequency conversion using diffusion capacity 8=18120
 Gunn diode, non-ohmic contact formation by liq. epitaxy 8=5321
 Gunn effect, rel. to microwave devices 8=9159
 Gunn, small signal impedance behaviour 8=5322
 lasers, emission props. rel. to band-tail spreading energy 8=13781
 long, negative resistance mechanism 8=18117
 m.i.s., (m=Al, l=chalcogenide glass, s=In, Sn or Ag), I-V characts. 8=18118
 m. o. s., instabilities of clean structure 8=22636
 m. o. s., on Si, effects of Co⁶⁰ γ -rad. on surface state density and oxide charge density 8=22641

Semiconducting devices—contd**diodes—contd**

- microwave harmonic generators and detectors 8=19830
 photo, differential spectral sensitivity 8=2220
 Schottky photodiodes, carrier generation and spectral response, model 8=9264
 space-charge-limited, thermal noise 8=18132
 space-charge-limited, transit-time effects 8=18119
 space charge noise, suppression and amp. rel. to no. of traps 8=5380
 surface-barrier, on SiC, fabrication and properties 8=22625
 thin-film heterojunction, fabrication process, props. 8=13861
 Al-Al₂O₃-Al thin film, noise meas. 8=13851
 Au-CdS-In, elec. props. rel. to CdS electroluminesc. excit., obs. 8=9608
 Au-GaAs Schottky barriers, thermionic emission 8=13931
 Au/CdS/Te, d.c. and a.c. behaviour of CdS film 8=13852
 Fe(Li) γ -ray detectors 8=15630
 GaAs, Gunn, high-field dipole domains in, steady-state and transient charact. 8=18121
 GaAs, electroluminescent, fabrication 8=5323
 GaAs, electroluminescent, temp. depend. of recombination lifetimes 8=2222
 GaAs, electroluminesc., with thermoelec. cooling, efficiency 8=22684
 GaAs, Gunn type, ageing effects 8=22627
 GaAs injection devices (tunnel diodes, electroluminescent diodes, injection lasers), degradation 8=9140
 GaAs injection laser, lasing wavelength rel. to threshold current and impurities 8=15483
 GaAs injection lasers with compensated p-type region, elec. and optical props. 8=15482
 GaAs, laser, increased efficiency and output 8=428
 GaAs, reverse-biased, light emission position and waveform 8=9160
 GaAs, spherical recomb. diodes, shift luminesc. band and use in optical pumping 8=23074
 n-GaAs-Al Schottky barriers, photoelectric barrier energy dependence on electric field 8=13924
 n-GaAs-Au surface barrier diode application to photocapacitors 8=13925
 GaAs:Si Gunn diode, non-ohmic contact formation by liq. epitaxy 8=5321
 GaAs, X-band Gunn, epitaxial layer selection 8=5246
 GaP, green electroluminescence at room temp. 8=9161
 GaSb, laser diode, spectrum fine structure 8=444
 Ge, backward, curvature coefficient 8=5327
 Ge, double injection and high freq. noise, obs. 8=13854
 Ge, Frenkel effect 8=18129
 Ge, gamma detector, low noise preamplifier for 8=6780
 n-Ge, inverse current surface recombination velocity dependence 8=9162
 Ge, microwave-oscillator, admittance measurements 8=2223
 Ge, minority carrier lifetime, mag. field effect 8=13853
 Ge, neutron irradiated, L-shaped current characteristic 8=22630
 Ge n-i-p, as detector for γ -radiation from Bi²¹⁴ 8=11788
 Ge, negative differential resistance during injection of minority carriers 8=5325
 Ge photodiodes, shot-noise meas. at high freqs. 8=22706
 Ge, p-i-n and p-n-i-n, avalanche breakdown voltage evaluation 8=13855
 Ge, point contact, etch pits due to plastic deform. 8=5326
 Ge, reverse current and lifetime of minority carriers, anisotropic press. 8=9163
 Ge, reverse static characts. in pre-breakdown region, theory 8=18128
 Ge, thermal breakdown rel. to temp. dependence of forbidden zone width 8=18127
 Ge with deep levels, impedance and transient processes 8=5324
 Ge: Au double injection, N- and S-type negative resistances and relax. oscs. 8=22628
 Ge(Li) in multiple arrays for spectrometry 8=6656
 Mo-Si epitaxial Schottky, reverse characteristics 8=13857
 Ni and GaAs surface barrier, elec. props. 8=22629
 Si alloy, dynamic resistance and static capacitance 8=18131
 Si, avalanche breakdown 8=18123
 Si, avalanche, microwave 8=5329
 Si diodes, Au doped, for companders 8=9165
 Si, Frenkel effect 8=18129
 Si grown epitaxially on sapphire, charact. 8=18130
 Si, high conduction characteristics 8=2219
 Si, hyper-abrupt variable-capacitance 8=9156
 Si, minority carrier lifetime, mag. field effect 8=13853
 Si, neutron irradiated, L-shaped current characteristic 8=22630
 Si, p-i-n and p-n-i-n, avalanche breakdown voltage evaluation 8=13855
 Si p-i-n, Co-doped, current oscillation 8=2227
 Si p-i-n gold-doped, negative resist. region in characts. 8=9164
 Si, prod. by electron beam mask-forming 8=15279
 Si, variable capacitance, low-temp. epitaxial growth 8=13856
 Si, zener, breakdown, between avalanche and field emission 8=5328
 SiC, electroluminescent, props. 8=9627
 Si-SiO₂-Au, relaxation of conductance 8=9180

Semiconducting devices—contd**p-n junctions**

- α -particle detector for counter response measurement 8=852
- acoustic domains, generation of electroluminescent light 8=18587
- boundary tension, moment of distrib. of alternating component 8=18103
- boundary tension oscills. 8=9149
- breakdown electric, effect of imperfections on 8=9150
- capacitance of junction with deep donor impurities, theory 8=18102
- capacitance rel. to applied voltage, effect of doping 8=18106
- characteristics, to determ. onset temp. for intrinsic conduction in semiconductors 8=9147
- characteristics, effect of hydrostatic pressure, band gap variation 8=5304
- currents, forward and reverse, sensitivity to small deformations 8=13842
- depletion layer capacitance 8=5307
- depth meas. by spherical drilling 8=5305
- e.m. radiation, single quanta, detection and measurement 8=382
- impact ionization at high freqs. 8=18104
- impurity electroluminescence, kinetics 8=18588
- injection lasers, review of structural parameters 8=15476
- lasers, threshold current calc. 8=6467-8
- linear gradient, with short carrier diffusion length, theory 8=18107
- linearly graded, mathematical theory 8=9146
- microplasma characteriograph 8=2214
- n-p reverse biased, effect of deep impurities on capacitance 8=18115
- planar dielec. waveguides, field excitation 8=10969
- photogenerated carriers, drift time obs. 8=5318
- planar diffused profiles, electron microscope investigation 8=2215
- spherical photocell, using lateral photoeffect 8=22705
- randomly graded, hole-electron pairs regeneration-recombination formula 8=13632
- rectifiers and other power devices, review 8=18094
- reverse-biased, effect of avalanche multiplication on elec. props. 8=18105
- reverse characts., influence of undepleted carriers 8=22622
- thermopile, stationary temp. field calc. 8=22685
- thin layers, nature of high voltage photo-e.m.f. 8=9247
- thyristors, high conduction characteristics 8=2219
- transport eqns., numerical steady-state one-dimens. soln. 8=9148
- tunnel-diode, capacity modulation by harmonic signal 8=9157
- AlAs-GaAs heterojunction, alloyed, preparation and electrical properties 8=5308
- CdTe, photovoltaic effect, excitation spectra of 8=5405
- CdTe-HgTe heterostructures, photovoltaic response and photoelectromagnetic effect 8=13911
- Cu₂S-CdS heterojunction, photovoltaic response 8=13843
- Ga_{1-x}Al_xAs crystals, high voltage, characts. 8=9151
- GaAs diffused junctions, luminescence spectra 8=5663
- GaAs, epitaxial, spontaneous and coherent light emission 8=6466
- GaAs laser diodes, influence of junction structure on parameters 8=6464
- GaAs lasers, direct investigation method 8=445
- GaAs, max. photo-e.m.f. on laser excitation 8=9252
- GaAs p-i-n, formed by solid-to-solid diffusion 8=18110
- GaAs-Ga(AsP), photocurrent, forward current injection modulation 8=13844
- GaAs-Ge heterojunctions, prep. by iodine process 8=5312
- GaAs(P), Zn conc. gradient near junction 8=8678
- (GaIn)As-GaAs, photocurrent, forward current injection modulation 8=13844
- GaP diffused single crystal layers, photoelectric properties 8=5406
- GaP, microplasma and light emission 8=5310
- GaP:Ge, electroluminescence 8=23073
- GaSb, influence of doping on electrical properties and laser emission parameters 8=5313
- Ge, magnetic field effect at 77°K 8=18112
- Ge p-i-n detectors, width of sensitive region, meas. with electrophotography 8=9152
- p-InAs, properties 8=9153
- InAs, possibility of drifted junctions using Cu 8=17011
- InAs-GaAs heterojunctions, prep. by iodine process 8=5312
- InAs(Sb)(P), Zn conc. gradient near junction 8=8678
- InSb, coherent radiation obs. 8=6471
- InSb p⁻n, in forward bias, charact. 8=18113
- p- π -n Si structures, double injection regime, IV charac. 8=22621
- Se, forward biased, inductive properties 8=5314
- Si, I-V characts. in avalanche breakdown region 8=18114
- Si alloyed, Zener and avalanche breakdown, distinguishing criteria and temp. effects 8=9155
- Si alloys, Zener and avalanche breakdown, reverse characteristics, analysis 8=9154
- Si, anisotropic stress effects on V-I and noise characteristics 8=13847

Semiconducting devices—contd**p-n junctions—contd**

- Si, B and P implantations, particle detector X-Y sensitive 8=3466
- Si detector, fast n, using crystal damage 8=4030
- Si, detectors operating 77°K-150°C 8=6660
- Si, diffused, breakdown voltage 8=5317
- Si diffused junctions, reactive properties in region of high injection levels 8=13848
- Si flexode, prep. and switching props. 8=5315
- Si, large area, by epitaxial growth technique 8=5316
- Si, large area, high voltage, destructive reverse breakdown 8=18109
- Si, mesoplasma, visible and i. r. radiation 8=2218
- Si photoc converters, irradiation stability 8=2226
- Si:In, n-p reverse biased, effect of deep impurities on capacitance 8=18115
- SiC, sublimation epitaxy, p-i-n type structure 8=9122
- Si₃N₄ over SiO₂ as seal, H₃PO₄ etching 8=17218
- Si-P, prep. and elec. props. 8=18108
- transistors**
- double diffused, physical model 8=18134
- f.e.t., app. to n.q.r. spectrometers 8=15436
- f.e.t., bibliography 8=9169
- f.e.t., insulated, as electrometer 8=5336
- f.e.t., junction noise calcs. of meas. values 8=5334
- f.e.t. operational amplifiers, use as fast electrometers
- f.e.t., thin-film fabrication process, props. 8=13861
- f.e.t., i.g., different modes of operation 8=22637
- f.e.t., Ge, for preamplifier 8=3473
- h.f., fabrication, use of double photoresist. technique 8=18136
- m.i.s., radiation effects, survey 8=9171
- m.o.s., application requirements 8=18144
- m.o.s., charact. dependence on substrate resistivity 8=18137
- m.o.s., effective mobility theory 8=22433
- m.o.s., generation-recombination noise theory 8=9174
- m.o.s., p-channel enhancement, h.f. properties 8=18146
- m.o.s., and Si planar in logarithmic amplifiers for space instrumentation 8=5342
- m.o.s. structures, C-V plots, rapid evaluation 8=9173
- m.o.s., surface properties 8=18147
- m.o.s., surface states, l.f. noise 8=9176
- m.o.s., switching characts, and relns of turn-on switching time with circuit 8=18139
- m.o.s., thermal noise, theory accounting for substrate doping 8=9170
- m. o. s. t. IC, three types of basic configs., design princs. 8=18140
- m.o.s. f.e.t., static and dynamic behaviour, with inclusion of saturation region, analysis 8=22639
- planar, current gain, effect of carrier recombination outside active base zone 8=22632
- plane transistor with circular geometry, input impedance identification 8=5338
- p-n-p-n, minority carrier lifetime in floating region 8=22634
- stability, p-n-p devices 8=22633
- thin film, thermal limitations 8=9168
- thin film, trap effects 8=5335
- Al₂O₃-Si i.g.f.e.t. 8=22638
- CdS thin film 8=18135
- GaAs, field-effect 8=9167
- Ge, p-n-p, structure study, hole injection 8=5339
- HfO₂ film gate insulators in MOS transistors 8=22654
- InAs thin film, fabrication and charact. 8=22635
- InSb thin film- 8=18135
- NiO thin-film triode 8=22602
- NiO-TiO₂ thin-film triode 8=22602
- Si, npn, effect of fields on diffusion, overcoming "push out" effect 8=22145
- SiO₂, vacuum deposited insulating layer, instability in field effect transistors 8=9175
- tunnel diodes**
- discrimination, theory of switching properties 8=5332
- flipflops in 500 MHz ring counter 8=3469
- hot-electron injection into He liq., benzene and cyclohexane 8=257
- relaxation oscill. circuit, variable frequency 8=5330
- transducers, miniature electromechanical, function and mats. 8=5333
- tunneling anomalies, zero-bias, temp., voltage and mag. field depend. 8=13860
- vibration spectra molecular, by inelastic electron tunnelling 8=13633
- voltage threshold discriminator, charge sensitivity 8=5331
- zero crossing timing, accurate, circuit 8=3142
- Al-Al₂O₃-Al sandwich, photoemission studies 8=13858
- Bi junctions, conductance maxima rel. to band structure 8=13859
- Bi tunnel junction, semimetal-insulator, phonon-assisted tunnelling 8=22455
- GaAs p-n junctions, alloying temp. rel. to characts. 8=22631
- GaAs, degradation characteristics, investigation 8=9140
- GaSb(As), excess current studies 8=18133
- Ge, curvature coefficient 8=5327
- Ge, from degenerate epitaxial films produced by modified iodide method 8=8321
- Sb junctions, conductance maxima rel. to band structure 8=13859

Semiconducting materials

- See also Magnetoelectric effects, Photoconductivity; Photovoltaic effects.
- absorption of charge carriers and Beers law 8=5102
- alloys, $A_2C^{VI}-B_2^{III}C_3^{VI}$ (A=Cu, Ag; B=In; C=Te, Se), equilib. diagrams and structure 8=8266
- chalcogen group, liquid and solid phase, thermal conductivity 8=12850
- chalcogenic glasses and liquids, Hall effect meas., temp. depend. 8=13789
- chalcogenide glasses, electrical props. 8=18028
- chalcogenide glasses, Hall mobilities in vitreous and liq. states 8=18027
- characteristics, meas. by fine focussed electron beam 8=22575
- DNA with complexed carcinogen, elec. cond. 8=18093
- electron beam probing 8=18026
- etching in $HNO_3-HF-CH_3COOH$ 8=4791
- g-factor and valence band spin-orbit splitting, laser induced, determ. 8=9094
- glasses, oxide and non-oxide, cond. mechanisms 8=22580
- Hall effect at high temp., low-mobility samples, apparatus 8=8977
- hole processes in phosphors, F-centres luminesc. meas. 8=8888
- impurity redistrib. during thermal oxidation 8=18015
- ion implantation techniques 8=18014
- micro-inhomogeneities, investigation 8=18013
- Nernst-Ettingshausen effect, measuring method 8=9288
- new, for electronics 8=18025
- nuclear and space radiation effects, conference 8=22578
- optical second-harmonic generation by CO_2 laser interact. with drifting carriers 8=5610
- organic, r.f. spectroscopy, review 8=14088
- p-chloranil, space-charge limited currents meas. 8=9137
- p-type (Ge, GaAs, GaSb, InAs, ZnTe), Faraday rotation 8=14216
- plasma, Faraday and Voigt effects 8=22948
- polymers, new, synthesis and properties 8=5286
- polysulphinimide, elec. props. 8=9138
- polysulphinimide, elec. props. 8=22615
- quantum oscillations in strong magnetic fields 8=5235
- randomly doped, hole-electron pairs regeneration-recombination formula 8=13632
- rare-earth oxides, non-stoichiometric, conductivity and hopping model 8=9118
- rare-earth sesquihydride crystals, elec. props. 8=9119
- resistivity meas., volume, surface and contact 8=18020
- review, influence of reliability, laser applications 8=10451
- solar cells multistage, selection of optimum combination of materials 8=6277
- thermal conductivity, temp. dependence meas. 8=17539
- thermogalvanomagnetic phenomena, quantum theory 8=18208
- III-V compounds, second order optical susceptibility 8=18484
- trace analysis using Hall effect 8=18757
- vanadate glasses, electronic conduction rel. to crystallinity 8=18091
- vitreous, bandgap variation, resistivity and photo-sensitivity 8=22579
- waveguide loading, e. m. wave propagation 8=19833
- II-IV compounds with wurtzite structure, intrinsic absorpt. edge rel. to exciton creation 8=5224
- $A^{IV}B^{VI}$ cpds., (A=Zn, Cd, Hg; B=S, Se, Te), prep., props. and uses 8=18023
- $A^{III}B^V$ cpds., prep., props. and uses, review 8=18024
- AlN, electrical and optical properties 8=2185
- Al_2O_3 , Cs activated, low work function films, props. 8=17999
- As, vitreous, polarizability 8=9505
- Ba-Bi titanate (IV), ceramic, Fe^{3+} doped, model and props. 8=5236
- $BaTiO_3$, conductivity rel. to optical props., small polaron theory 8=18505
- $BaTiO_3$ doped with Sb_2O_3 , surface states 8=13790
- $BaTiO_3$, piezoresistance effect 8=9095
- n- $BaTiO_3$, single domain ferroelectric, optical absorpt. 26-130°C 8=9506
- BeSeI, dielec. const. and elec. conductivity meas. -200 to +50°C 8=18193
- Bi and Bi alloys, band structure from quantum oscillatory phenomena, 1.2-4.2°K 8=13659
- Bi, Shubnikov-de Haas effect meas. at 15 kbar 8=5237
- Bi, Sn-doped, galvanomag. effects at low fields at 77°K rel. to doping 8=2186
- Bi-Sb alloys, electron energy spectrum meas. 8=5104
- Bi-Sb, transformation of semiconductor into metal, obs. using magnetoresistance 8=22581
- BiSI, dielec. const. and elec. conductivity meas. -200 to +50°C 8=18193
- $Bi_2Te_3-Bi_2Se_3$ alloys, n-type, thermoelectric props. 8=9237
- $Bi_2(Te, Se)_3$ system, reflectivity rel. to effective mass of conduction electrons 8=2096
- $Bi_{12}GeO_{20}$, photo-induced changes in optical polarization 8=2404
- C(diamond), lattice potential, mean internal, using Thomas-Fermi-Dirac model 8=13833
- Cd oxide, controlled resistors 8=18034

Semiconducting materials—contd

- $CdCr_2Se_4$, transport properties rel. to ferro-magnetism 8=18031
- $CdCr_2Se_4$, transport properties rel. to ferro-magnetism 8=18031
- $CdCr_2Se_4$:Ag, helicon-spin wave interaction 8=18329
- $Cd_{0.25}Hg_{0.75}Te$ alloy, n-type, determ. of lifetime and recombination mechanism 8=5238
- $Cd_3P_2-Cd_3As_2$ solid. soln. system 8=22582
- $Cd_{1-x}Zn_xAs_2$, thermal and elec. cond. and thermoelec. power 8=5385
- CdF_2 , carrier mobility 8=18029
- CdF_2 crystal activated by rare earth ions 8=5658
- CdF_2 :R, e. s. r. and i. r. studies 8=22901
- CdS acoustoelectric effect 3- and 4-phonon processes obs. 8=1850
- CdS, chemical sensibilization 8=22584
- CdS, conductivity, thermally stimulated, influence of electric field 8=9239
- CdS, current saturation on non-ohmic behaviour 8=13793
- CdS, domains due to electron-phonon coupling, characts. appl. 8=5240
- CdS, edge emission, peak shift with excitation intensity 8=2478
- CdS film in diode, d.c. and a.c. behaviour 8=13852
- CdS, first and second current saturation, build-up time 8=2188
- CdS, photo Hall mobility at high electric field 8=2187
- CdS, photoluminescence spectrum, emission bands rel. to N_2 impurities 8=5657
- CdS, piezoelec., elec. field distrib. determ. by optical probe 8=18033
- CdS in strong electric field, elect. cond. 8=18030
- CdS, surface and volume conductance, kinetics comparison 8=18032
- CdS, temp. dependence of mobility for u. s. amplification rel. to electron trapping 8=2081
- CdS thin films, elec. props. changes on O_2 adsorpt. and ion bombardment 8=13791
- CdS, two-photon absorpt. obs. 8=18516
- CdS, Cu-diffused insulating layers, elec. behaviour 8=13792
- CdS-SiO₂ film system, heat-stimulated currents, and 'quenched' cond. 8=9096
- CdSb, alloyed with Au, acceptor level depth 8=22456
- CdSb, doping experiments 8=13698
- p-CdSb, Hall coefficient anisotropy 8=13794
- CdSb, Te donor level energy position 8=9097
- CdSb, thermoelec. conversion efficiency rel. to transport coeffs. 8=2254
- CdSe, band-edge emission, excitation intensity effect 8=14316
- CdSe, Hall effect meas. 8=5239
- n-CdSe, Hall effect meas. and anal., magnetoresistance effects 8=13796
- CdSe, luminescent yield from radiative electron capture by sensitizing recombination centres 8=18598
- CdSe, thin non-stoichiometric films, elec. and photoelectric props. 8=13795
- $CdSnAs_2$ and $CdGeAs_2$ compound, high-temp. modifications, microhardness, elec. props. and thermal cond. changes 8=21842
- CdTe, film, wedge-shaped, photo-voltages rel. to incident angle of illumination 8=5398
- n-CdTe, Gunn effect 8=5242
- CdTe, Gunn effect and impact ionization, influence of ionized impurity scatt. 8=22583
- CdTe, Gunn effect, rel. to current instabilities 8=5243
- n-CdTe:In, free carrier absorpt. 8=22967
- CdTe, metal vacancies formation energies rel. to Te-Te covalent bonding 8=17608
- p-CdTe, thermostimulated currents and trap levels 8=2260
- CdTe thin films, ion bombardment effect on resistance 8=5244
- $CdTiS_2$, electronic props. and crystal parameters 8=17354
- CoO, elec. meas. rel. to hopping model 8=18060
- CoO, i. r. absorpt., 0.5-700 μm , by small polarons 8=23008
- CoO-Li doped, elec. meas. rel. to hopping and narrow-band conduction 8=18059
- CoSi, scattering mechanism and band structure 8=2098
- Cs-GaAs interface, Schottky barrier height obs. 8=13797
- Cs_3Sb , time depend. of absorpt. and photoemission 8=13937
- Cu oxide, controlled resistors 8=18034
- Cu phthalocyanine films, thin, trap distrib. 8=22586
- CuBr, lattice potential, mean internal, using Thomas-Fermi-Dirac model 8=13833
- Cu_3P monocrystals, props. and prep. 8=21948
- p- Cu_2S , thermoelectric power, elec. cond. and Hall effect 8=22585
- CuX , (X=Cl, Br and I), band structures 8=2190
- Fe-Cu ferrites, mixed conduction mechanisms from resistivity and Seebeck meas. 8=18035
- $\alpha-Fe_2O_3$, elec. meas. rel. to hopping model 8=18060
- Ga(As, P), thermal expansion coeffs. from -62 to 200°C 8=1880
- Ga, r.f. size effect, temp. and freq. dependence 8=9099
- Ga_{1-x}In_x-As alloys, optical energy gap variation 8=18040
- GaP, electroluminescence and elec. props, effect of two zone melting prep. techniques 8=9611

Semiconducting materials—contd

- GaP epitaxial layers with high mobility 8=9101
 GaP, Hall coefficient and conductivity, 4.2-300°K 8=9100
 GaP, hot-electron-phonon interactions 8=5245
 GaP, thermal expansion coeffs. from -62 to 200°C 8=1880
 GaP, uniaxially stressed, optical transmission and absorpt. rel. to energy levels 8=18529
 GaP-GaAs, n-p heterojunctions, photo-effects 8=5311
 GaP: Ni, absorption spectrum 8=22983
 GaP:S, electrical properties 8=13805
 GaP:Zn, electrical properties 8=13806
 GaSb, diffusion and solubility of Li 8=13409
 n-GaSb, electron mobility carrier conc. dependence at 77°K 8=2195
 GaSb, Faraday rotation, spectral emittance and Hall effect 8=22587
 p-GaSb, Hall coeff. and conductivity, pressure dependence at diff. temps. 8=13804
 n-GaSb, Shubnikov-de Haas oscs., beating effects 8=9102
 GaSb, thermal expansion from 2-40°K 8=4937
 GaSb-InSb alloys, thermal and elec. props. at high temps. rel. to comp. 8=4944
 GaSe, band gap rel. to second optical harmonic generation 8=5600
 GaSe, charge carrier mobility from elec. resistivity and Hall constants 8=5247
 GeSe_{0.75}Te_{0.25}, prep. and props. 8=2197
 GeTe liquid, Hall effect meas. 8=16877
 n-HgSe, quantum oscs. of transport coeffs. 8=5261
 HgSe, oscillatory magnetoresistance, inversion asymmetry splitting 8=2100
 HgTe, Hall coeff. and magnetoresistance at 4.2 and 77°K rel. to carrier model 8=2200
 p-HgTe, i.r. reflection in region of plasma minimum 8=5262
 n-HgTe, magnetoplasma reflection at 296 and 85°K 8=13815
 HgTe, metal vacancies formation energies rel. to Te-Te covalent bonding 8=17608
 HgTe-ZnTe, Hall coefficient and conductivity at low temp. 8=13816
 HgTe-ZnTe system, electrical properties 8=5263
 InAs, avalanche breakdown theory 8=22599
 InAs diode laser, epitaxy prod., characts. 8=11106
 InAs, epitaxial, preparation and properties 8=1749
 InAs, infra-red Faraday effect 8=9539
 InAs, Knight shift calc. 8=18463
 InAs, light absorpt. by free carriers, 300°K and 80°K obs. 8=18536
 InAs, light scattering by plasmons and Landau levels of electron gas 8=22990
 InAs n-type, Faraday rotation, interband and free-carrier 8=9540
 InAs, photo-emission rel. to surface props. and interband transitions 8=5417
 InAs, surface inversion layer props. in elec. quantum limit 8=5231
 InAs, thermal expansion from 2-40°K 8=4937
 InAs thin films, obtained by discrete evaporation, structure 8=8324
 InAs thin films, optical props. 8=18535
 InBi, preparation and electrophysical properties 8=5268
 InOF, temp. independent conductor 8=8414
 n-InP, effect of As doping on electrical properties 8=9113
 n-InSb, polar, hot electron mobility 8=22430
 InSb, quantum efficiency and overlap integrals 8=5264
 n-InSe crystals, thermal and i.r. quenching of photo-conductivity 8=18233
 KCl:Ti, induced local 3p states on Cl⁻ ions nearest Ti⁺, calc. 8=8930
 LaCoO₃, p- and n-type, optical absorpt. by small polarons 8=2434
 LaCoO₃, conductivity rel. to optical props., small polaron theory 8=18505
 n-Mg₂Sn, piezoresistance at 80-300°K rel. to valence-band structure 8=2204
 α-MnS, conductivity rel. to optical reflectance and absorption props. 8=18057
 MnTe, p-type, antiferromag., optical meas. 80-375°K 8=5622
 MoS(Se)₂, charge carrier mobility from elec. resistivity and Hall constants 8=5247
 Nb stannide coils, Q-factors, in 20-35 MHz range 8=17982
 NiO, elec. meas. rel. to hopping model 8=18060
 NiO films prep. and thin-film triodes 8=22602
 NiO, Hall effect at high temp. 8=8977
 NiO, Hall mobility at 1007°K 8=13827
 NiO, i.r. absorpt., 0.5-700 μm, by small polarons 8=23008
 NiO, stoichiometry and elec. props. 8=13826
 NiO-Li doped, elec. meas. rel. to hopping and narrow-band conduction 8=18059
 PbS, mobility temp. dependence 8=18062
 PbSe, forbidden band width and temp. dependence 8=5272
 p-PbSe, hole mass and valence band, from free carrier Faraday rot. 8=2445
 Pb_{0.85}Sn_{0.15}Te, thermal and optical energy gaps 8=2446
 Pb_{0.95}Sn_{0.05}Te, thermal and optical energy gaps 8=2446
 p-PbTe, doped, interband interactions of light and heavy holes rel. to Lorenz number 8=9116

Semiconducting materials—contd

- PbTe films, elec. characts. and vacuum evaporation 8=8327
 PbTe films, thin, resistivity, Hall mobility and conductivity 8=22603
 p-PbTe heavily doped thermal conductivity betw. 80-400°K 8=8662
 PbTe liquid, Hall effect meas. 8=16877
 PbTe, p-type, Hall mobility and thermoelectric power rel. to Na doping 8=5274
 PbTe, helicon-phonon coupling at 4.2°K 8=18063
 PbTe, stimulated emission of phonons by electrons, obs. 8=9115
 PbTe:Na, acceptor centre model from Na:hole ratio determ. 8=2205
 PbTe-PbS solid solution, n-type, conductivity temp. and pressure dependence 8=18061
 S, orthorhombic, electron hopping transport and orbital overlap 8=18064
 Sb₂S₃, anomalies in temp. depends. of dielectric properties 8=9217
 Sb₂S₃ and SbSI, anomalous dispersion of permittivity and reson. absorpt. of microwaves 8=9218
 SbSeI, dielec. const. and elec. conductivity meas., -200 to +50°C 8=18193
 SbSI, ferroelectric, fund. absorpt. edge profile 8=9120
 SbSI, photo-induced microwave response obs. 8=5630
 SbSI, photosensitive phase transition 8=2159
 SbSI(Br), dielec. const. and elec. conductivity meas., -200 to +50°C 8=18193
 Se, amorphous, conductivity rel. to optical absorpt. props. 8=18066
 Se, effect of cooling to 100°K on elec. props. 8=1808
 Se films, vitreous, space-charge-limited currents and high elec. field effect 8=13828
 Se, hexagonal, photoconductance meas. during cooling from 300° to 4.2°K 8=18238
 Se, high-purity, hole conductivity rel. to Na and O₂ impurity admixture 8=5276
 Se, magnetoconductivity rel. to mobility mechanism 8=18065
 Se, vitreous, electron and hole drift mobilities, temp. depend. 8=13639
 n-SiC, α-phase, piezoresistance constants 8=18073
 SiC, hole mobility and interband transitions 8=9122
 SiC, p-type and n-type, field-effect mobilities 8=13835
 SiO₂-C structure, anomalous auto-electron emission 8=22712
 SiO₂, effect of dissolved O₂ on C-V characts. 8=5284
 SiO₂ films on Si, electron beam effects and etching rate 8=22609
 SiO₂ films on Si, pinhole locating by electrograph method 8=1698
 SiO₂ films, thermally grown, electronic conduction mechanism 8=18076
 SiO₂ layers, dielec. breakdown 8=18080
 SiO₂-openings, diffusion induced dislocations, arrangement, rel. to transistor simulation 8=8733
 SiO₂-Si system, interface states, influence of heat treatments on oxide charge 8=13834
 α-Sn, lattice potential, mean internal, using Thomas-Fermi-Dirac model 8=13833
 SnO₂, electron scattering polar optical modes 8=22611
 SnTe liquid, Hall effect meas. 8=16877
 SrTiO₃, conductivity rel. to optical props., small polaron theory 8=18505
 SrTiO₃, superconducting semiconductor films and whiskers, transition temps. 8=9056
 SrTiO₃, superconducting transition temp. 8=9055
 TCNQ-complexes, Overhauser effect 8=5549
 Te, amorphous, conductivity rel. to optical absorpt. props. 8=18066
 Te, interband hole transitions 8=9018
 Te-Ge eutectic alloys, Hall effect meas. 8=16877
 Te-Sb eutectic alloys, Hall effect meas. 8=16877
 Ti₂O₃, e.s.r. at 77°K rel. to semiconductor-metal transition 8=14125
 TiO₂ layers, electronic props. from optical meas. 8=23017
 TiSe, thermal conductivity 8=17547
 UO₂, conductivity, electrical 8=18089
 UO_{2-x} and U₃O_{8-x}, carrier mobility investigation 8=18090
 WS₂, single crystal, thermistor characts. 8=18092
 WSe₂, charge carrier mobility from elec. resistivity and Hall constants 8=5247
 Zn-CdS, graded band-gap, luminescent spectra, electric-field dependence 8=9134
 Zn,Cd_{1-x}Sb, thermoelec. conversion efficiency rel. to transport coeffs. 8=2254
 Zn₃In₂S₈, crystal structure 8=8567
 ZnO, acousto-electric oscillations, 1-5 GHz range 8=22613
 ZnO, cathodic reduction of aqueous Fe(CN)₆³⁻ 8=14423
 ZnO, polycryst. containing 3% Bi₂O₃, doped, semiconducting and semi-insulating props. 8=18205
 ZnO powder, cond. effect of O₂ adsorption 8=22612
 ZnO rel. to radicaloluminesc. excit., sorption-recomb. processes 8=9635
 ZnO:(Ni, Co) crystals, Hall effect and conductivity, liquid N₂ to room temp. 8=9132

Semiconducting materials—contd

β -ZnS film, activation energy of current carriers 8=17143
ZnS, hexagonal, elastic stiffness conductivity dependence, corrections 8=17838
ZnS phosphors, carrier redistrib. among traps under i.r. irradi., obs. 8=9135
ZnS phosphors, photoimpedance, a. c. field freq. and excitation intensity dependence 8=14335
ZnS photocond. and Hall effect rel. to recomb. mechanisms 8=9258
ZnS:Cu conductivity rel. to electrolumesc., obs. 8=9133
ZnSb and ZnSb-CdSb mixed crystals, doping experiments 8=13698
ZnSe, electron mobility rel. to prep. by direct fusion 8=2210
n-ZnSe, Gunn effect 8=9136
ZnSe, hexagonal crystals, luminesc. 8=9631
ZnSe interface with electrolyte, chem. and elec. props. 8=13837
ZnSe, lattice potential, mean internal, using Thomas-Fermi-Dirac model 8=13833
ZnTe films, electroabsorpt. rel. to determ. of reduced effective mass 8=18566
ZnTe, i.r. transmission and reflection spectra 8=2460
ZnTe, metal vacancies formation energies rel. to Te-Te covalent bonding 8=17608
ZnTe:Pb, photo-induced paramag. resonance at 77°K 8=9440
ZrO₂-CeO₂ mixtures, high-temp. cond. 8=22614

gallium arsenide

abrupt junctions, formed by solid-to-solid diffusion 8=18110
absorption edge, influence of magnetic field 8=9531
appl. to field-effect transistors 8=9167
band-edge emission, excitation intensity effect 8=14316
defect centres produced by Cu diffusion 8=1954
density-of-state effective mass 8=5256
diodes, electroluminescent, temp. depend. of recombination lifetimes 8=2222
diode, i. r.-sensitive, made by Cr diffusion 8=18126
dislocation free, laser diode showing homogeneous near-field pattern 8=11097
electric field at 80°K using Pockels electro-optic effect 8=2193
electroluminescent diodes, fabrication 8=5323
energy band pinch effect 8=13662
epitaxially grown from Ga soln., elec. props. 8=4829
Fermi level, influence of volume dope 8=8934
field effect at low temperatures 8=13798
film, wedge-shaped, photo-voltages rel. to incident angle of illumination 8=5398
Gunn devices, design for c. w. operation, rel. to temp. 8=5297
Gunn diodes, layer selection for X-band 8=5246
Gunn effect, electron-transfer mechanism, domain propagation 8=9077
Gunn-effect, long samples 8=5252
Gunn effect, negative mobility model for oscillator analysis 8=9098
Gunn-effect oscillations in biconical cavity 8=5300
Gunn effect oscillator, negative resistance type, analysis 8=13845
Gunn oscillators, epitaxial, high peak power 8=5298
Gunn oscillations in epitaxial layers, u. h. f. 8=18036
Gunn oscillators, electrical performance 8=5299
Gunn oscillators, microwave amplification 8=5302
Hall effect at high electric field 8=22417
high electric field domain behaviour 8=9103
high-field dipole domains in, steady-state and transient charact. 8=18121
high-mobility, grown by liquid-phase epitaxy 8=22589
injection laser, output spikes 8=11096
impurity photoionization, quantum defect study 8=2207
laser diode, freq. modulation by u. s. waves 9=11093
laser diode operating at room temp. 8=441
laser, dual type, quenching response 8=443
laser, injection, compensated p region, elec. and optical props. 8=15482
laser, injection, emission modulation and synchronization 8=15481
laser, injection, lasing wavelength rel. to threshold current density and impurity conc. 8=15483
laser, light pulse synchronization 8=15480
laser for optical ranging system 8=14918
laser, optically pumped, av. power output 8=11102
laser radiation pulsations, investigation 8=11098
laser, time characts. 8=11099
lasers 8=11095
lasers, continuous operation in liquid He 8=11101
lasers, cw, linewidths meas. at 77°K 8=11094
lattice potential, mean internal, using Thomas-Fermi-Dirac model 8=13833
lattice Raman scattering theory 8=2397
luminescence spectra at 77°K rel. to doping with Te, S, Se, Sn 8=18605
microhardness and dislocation structure temp. dependence, rel. to doping effects 8=17809
microwave amplification 8=5251
microwave dielec. const., resonance behaviour 8=13799-802
negative conductance in zero ion density limit 8=5250

Semiconducting materials—contd

gallium arsenide—contd

negative magnetoresistance, causes from published dates 8=5258
n-type crack formation at high pressures 8=22369
n-type, current-field strength characts., microwave technique 8=5249
n-type, in mag. field, circularly polarized waves, doping rel. to optical absorpt. 8=22981
n-type, negative differential conductivity when electrons are heated by strong microwave pulses 8=5253
n-type, obs. of multiple high-field domains with point-contact probe 8=22588
n-type radiative recombination 8=9612
n-type, S, Se, Te-doped, i. r. absorpt. spectra 8=18528
ohmic contacts, simple technique 8=13846
optical properties and carriers density, laser induced changes 8=5633
oscillators, microwave circuit characteristics 8=5301
paramagnetic resonance of shallow Cd acceptors, at 77°K 8=18421
piezoelectric, ultrasound generation under Gunn effect 8=22100
p-type, effect of γ -radiation on elect. props. 8=18039
p-type, photoluminescence, effect of heat treatment
p-type, valence band studies by magnetoresistance and Hall effect meas. at 4.2°K 8=13803
p-type, Zn-doped, compensated, photoluminescence at 77, 194, 300°K 8=5662
p-n junction characteristics, effect of hydrostatic pressure 8=5304
p-n junctions, epitaxial, spontaneous and coherent light emission 8=6466
recombination of current carriers 8=2194
recombination processes following impact ionization by high field domains 8=2192
reflectivity, i. r. spectral, rel. to free carriers 8=2418
second order optical susceptibility calc. 8=18496
surface prep. for epitaxial deposition 8=9104
thermal expansion coeffs. from -62 to 200°C 8=1880
thermal expansion from 2-40°K 8=4937
thin multilayer GaAs-metal ohmic contact 8=9145
traveling domains, electric field profile 8=5254
tunnel-diode p-n junctions, alloying temp. rel. to characts. 8=22631
two-photon absorption obs. 8=18516
ultrasonic absorpt., infrared radiation effect 8=13352
AlAs-GaAs alloyed heterojunctions, preparation and electrical properties 8=5308
Cs-GaAs interface, Schottky barrier height obs. 8=13797
GaAs:Cr, photoconductivity 8=2263
GaAs:Cr, semi-insulating, photoconductivity and i. r. quenching 8=18232
GaAs-GaP alloys, electronic mobility comp. dependence 8=18037
GaAs-GaP 50% alloy, impact ionization and charge transport 8=18038
GaAs:Ge, acceptor behaviour 8=13807
GaAs:Sn laser, electron-beam pumped, quantum efficiency 8=11100
Ga_{1-x}In_xAs alloys, electroluminescence rel. to band structure 8=2419
with Li complexes, local mode spectra 8=22982
LSA operation, bulk samples 8=5248
and Ni surface barrier diodes, elec. props. 8=22629
Sn doped, resistivity and Hall effect meas. 8=2191
Zn doped, Zn diffusion coeff. Fermi level dependence 8=1918
Zn polycrystalline films, electrical resistance and Hall effect obs. 8=5255
Zn-doped, photoluminescence, heat treatment effects 8=2481

germanium

acceptor impurities, magneto-oscillatory excitation 8=22991
amorphous, conductivity rel. to optical absorpt. props. 8=18066
amorphous, electronic struct. and i. r. absorpt. bands 8=22987
Auger recombination, indirect band-to-band 8=14221
amorphous, short-range order, rectification, cond., Hall effect etc. 8=22597
bolometer using Hall effect 8=6205
carrier lifetime determ. through self-associated cyclotron resonance 8=13831
complex band structure and real energy-lines 8=9125
compressive uniaxial stress, effect on high field domains 8=18051
conduction electron g-tensor from k-p theory 8=9110
conductivity, electrical, microwave freqs., rel. to impurity deformed, cyclotron resonance due to edge-type dislocations 8=9106
diodes, minority carrier lifetime, mag. field effect 8=13853
diodes, neutron irradiated, L-shaped current characteristic 8=22630
dislocations, optical effects, Hall effect 8=1979
dislocations, overlap phenomena of space-change cylinders 8=17656
dust electrification, effect of crushing period 8=13813

Semiconducting materials—contd**germanium—contd**

- dust electrification effect of crystal lattice defects 8=13812
- γ -ray coaxial detector current pulse generation 8=11430
- electrolyte electroreflectance technique, line shape of spectra 8=2199
- electron-irradiated, annealing of Hall mobility changes 8=2196
- electroreflectance spectra and band structure, at int. pts. in interband transitions 8=13663
- exciton lines, obs. with optical wavelength wobbles 8=5573
- Fano factor, 77°K 8=2198
- field emitters, Fowler-Nordheim plots 8=5412
- films on Al_2O_3 by vacuum deposition, elec. props. 8=4749
- films, charge-carrier mobility 8=9107
- film crystallization by zone melting 8=8320
- films, degenerate epitaxial, production by iodide method, rel. to tunnel diodes 8=8321
- films, polycrystalline, acceptor and scattering centre natures 8=18046
- films, produced by vacuum deposition 8=8309
- films, transition to metallic conduction at high exciton concs. 8=18048
- Hall mobilities of holes at 9.6 GHz between room and liquid He temp. 8=13836
- impurity photoionization, quantum defect study 8=2207
- interband electro-optical props., electroabsorption 8=22595
- interband electro-optical props., electro-reflectance 8=22596
- interstitial Cu impurity, irradiated, obs. 8=2027
- k.p. expansions, approx. symmetry relations 8=22461
- lattice dislocations rel. to structure of kinks and steps 8=8727
- lattice potential, mean internal, using Thomas-Fermi-Dirac model 8=13833
- luminescence emitted by hot carriers 8=5664
- luminescence under pinch conditions 8=18603
- magneto-photocond., 300°-200°K, fields up to 22.3 kG 8=9109
- metallic etching rel. to facet forming planes 8=1728
- microwave-oscillator diodes, admittance meas. 8=2223
- motion of molten metal drops on surfaces under action of electric current 8=5259
- near-intrinsic, avalanche breakdown effects 8=9127
- negative magnetoresistance, causes from published dates 8=5258
- n-type, with adsorbed gas, conductivity hydrostatic pressure dependence 8=18045
- n-type, breakdown on photoinjection of carriers rel. to impact ionization of excitons 8=18050
- n-type, bulk neg. differential cond. and travelling domains 8=13810
- n-type dislocations effects on electrical properties 8=18053
- n-type, electron hole plasma, helical density waves and oscillator effect, theory 8=17903
- n-type, galvanomagnetic props., effect of dislocations 8=22592
- n-type, Hall meas. during n-irradiation over 78-330°K 8=18042
- n-type, hot electron Hall mobility and magnetoresist. for elec. field along <100> direction 8=18052
- n-type, i.r. spectral reflectivity rel. to free carriers 8=2418
- n-type lattice mobility at low temps. 8=8902
- n-type, low-temp. transport processes 8=18043
- n-type, mag. field effects on I-V charact. 8=13808
- n-type, oscillatory phenomena at 77°K 8=9108
- n-type, piezomagnetoresistance for mixed scattering mechanism 8=18047
- n-type, quenching rel. to form of vacancies 8=4962
- n-type refractive index anisotropy in elec. field 8=9533
- n-type, Shubnikov-de Haas oscillations, 20-80°K 8=18044
- n-type, subthreshold electron damage 8=22252
- n-type, surface recombination changes due to edge dislocations 8=22591
- n-type, small field d.c. conduction in presence of large microwave field 8=13811
- optical absorption edge, electron irradi. 8=9534
- optical energy gap, pressure coeff. meas. 8=14220
- oxygen conc., activation meas. by He^3 bombard. 8=18083
- p-type, bombardment-produced defects at low temps. 8=22170
- p-type, e-irradiated, angular dependence of radiation-induced conductivity 8=18041
- p-type, microhardness on e-irradiation and γ -ray irradiation 8=17810
- p-type, Ga doped and As compensated, interimpurity radiative recomb. 8=9613
- p-n-p transistors, structure study, hole injection 8=5339
- photodiodes, shot-noise meas. at high freqs. 8=22706
- photoexcited carriers, observed trapping parameters, rel. to Hall number anomalies 8=13637
- photomagnetic susceptibility, pulse method of meas. 8=9282
- photon-assisted magnetotunnelling in parallel and crossed elec. and mag. fields 8=5260
- photothermal effect, experimental study 8=8650

Semiconducting materials—contd**germanium—contd**

- photovoltages, Dember and lifetime-gradient, in n- and p-type 8=9253
 - piezothermal e.m.f., anisotropy 8=5390
 - pinch effect and breakdown in pure material 8=8956
 - protons, 0.8 to 2.0 MeV, range-energy determ. 8=13468
 - pure, field effect kinetics on surface 8=22598
 - recombination process in space-charge region 8=18049
 - reflection coeff. of I vapour from surface, etching vel. 8=8382
 - resistance meas. under shock-wave loading 8=17719
 - resistance, negative differential, during injection of minority carriers 8=5325
 - resistance thermometer, thermal time consts. at liq. He temp. 8=15119
 - surface recombination, generation process 8=22610
 - surface states on clean surfaces, study of origin 8=13814
 - thermal conductivity, lattice component, effect of impurities 8=1888
 - thermal expansion from 2-40°K 8=4937
 - thin films, Seebeck coefficient, Hall mobility 8=2255
 - tubes, preparation by pulling from melt 8=9111
 - tunnel and backward diodes, curvature coefficient 8=5327
 - ultrasonic attenuation, low temp. 8=8629
 - velocity field charact. of electrons 8=22590
 - with warped energy surfaces, low field transport props., theory 8=18055
 - X-ray stress topography, rel. to film-crystal interface stresses 8=22371
 - X-ray total reflection of films 8=5604
 - Al diffusion 8=13406
 - As doped, electrical breakdown at 4.2°K 8=13809
 - B diffusion 8=13406
 - As doped-resistor, as resistance thermometers for range 2.1 to 5.0°K 8=247
 - Ga-doped p-type, impurity photoconductivity spectra, nature of oscs. 8=13912
 - Ge-electrolyte interfaces, surface recombination obs. 8=18054
 - Ge(Li) detector for γ -spectrometer with cooled pre-amplifier 8=698
 - Hg-doped, dielectric relax. phenomena 8=2230
 - Li doped, coaxial radiation detectors, electron-hole collection time 8=20391
 - Li drift rate determ. 8=22594
 - Zn-doped, Sb-compensated, luminescence rel. to Zn impurity conc. 8=18604
- indium antimonide**
- absorption of charge carriers and Beers law 8=5102
 - acceptor impurities, magneto-oscillatory excitation 8=22991
 - acoustoelectric domains form. and amplifiers d.c. loss, mag. fields effects 8=13355
 - acoustoelectric oscillations in presence of magnetic field, field-dependent period 8=4923
 - alloy films, electrical resistivity 8=9008
 - avalanche breakdown theory 8=22599
 - bolometer using Hall effect 8=6205
 - Corbino magnetoresistivity, admixture and layer distrib. effects 8=5266
 - crystal, selective etching in HCl solns. of FeCl_3 8=8383
 - donor levels, shallow, in mag. field 8=22462
 - electron-TO- and electron-LO-phonon interactions from donor spectrum in magnetic field 8=13817
 - films, slow photoconduction 8=9254
 - free carrier rotation for 10.6μ circulation 8=9538
 - Hall coeff. and conductivity, high pressure dependence 8=13819
 - heat treatment effect rel. to disloc. density 8=1919
 - helicon wave propag. 8=5141
 - holes, effective mass by i.r. reflection states 8=5269
 - hot electron polar scattering 8=13638
 - impact ionization using a fast high current pulse generator 8=6249
 - interband magnetoabsorption polaron induced anomalies, Coulomb effect 8=22818
 - ionization waves in plasma, predictions of theory 8=18056
 - Knight shift calc. 8=18463
 - Landau levels, electron-hole pair effects 8=5113
 - lasers, mag. field depend. of mode spacing and total no. of modes 8=11105
 - laser, Raman tunable type, pumped with CO_2 laser 8=11104
 - lattice potential, mean internal, using Thomas-Fermi-Dirac model 8=13833
 - m.o.s. infrared image detect. and storage 8=13863
 - metallic etching rel. to facet forming planes 8=1728
 - microwave emission, Hall effect 8=5267
 - microwave power coupling to helicon mode 8=13825
 - n-type, absorpt. in 0.2-4 mm. range at 4.2°K 8=18537
 - n-type, acoustoelectrically oscillating, microwave emission at 77°K 8=13823
 - n type at 77°K, acoustoelectric effect in crossed electric and magnetic fields 8=13356
 - n-type, electrical cond. and magnetoresist. below 1°K 8=13820
 - n-type, electron mobility at intermediate and high fields 8=18005

Semiconducting materials—contd**indium antimonide—contd**

- n-type, electron shielding rel. to impurities 8=2202
- n-type, Hall coefficient, Corbino conductivity 8=9114
- n-type, hot carrier double injection process 8=2203
- n-type, influence of impurities on microwave detection props. 8=2224
- n-type, magnetic-field-free electron-hole, and gigahertz radiation 8=8969
- n-type, microwave emission during plasma formation 8=22600
- n, relaxation oscillations and responsivity obs. in far i.r. 8=13824
- n-type, resistance anomaly at very low temps. 8=5265
- n- and p-type, current instability under crossed electric and magnetic fields 8=2201
- p'-n junction in forward bias, charact. 8=18113
- p-type, lifetime of nonequilibrium carriers, influence of illumination on 8=5271
- p-type, Li-saturated, annealing effects on Hall coeff. and resistivity 8=5270
- p-type, 90% compensated, Hall const., cond. coeff. and energy levels, 4.2-300°K 8=13822
- plasma waves, x-ray scattering 8=5148
- quantum oscs. in Hall effect and magnetoresistance 8=13818
- quantum oscillations in photoelec. coeffs. in n-type 8=13913
- recombination through centres, effect of high mag. field 8=22223
- second order optical susceptibility calc. 8=18496
- thermal expansion from 2-40°K 8=4937
- θ pinch effect in e-hole plasma, 250°K 8=13821
- thin films by electron beam re-crystallization, electrical props. 8=8323
- transport phenomena and microwave generation 8=9112
- two-photon absorption obs. 8=18516
- X-ray scattering by transverse polarized phonons 8=8613

silicon

- absorption rel. to bound excitons 8=5132
- acceptor states from Group III impurities (B, Al, Ga and In), spectra 8=5285
- amorphous, conductivity rel. to optical absorpt. props. 8=18066
- amorphous, electronic struct. and i.r. absorpt. bands 8=22987
- amorphous, short-range order, rectification, and cond., Hall effect etc. 8=22597
- avalanche diodes, microwave 8=5329
- avalanche oscillators, uniaxial stress effects 8=5303
- carrier lifetime determ. through self-associated cyclotron resonance 8=13831
- carrier recombination, non-equilib., at high photo-excitation levels 8=18616
- channeling-effect in α -particle detection 8=3467
- complex band structure and real energy-lines 8=9125
- conductivity, electrical, microwave freqs., rel. to impurity conc. and temp. 8=13829
- deep-level impurities, rel. to i.r. absorpt., impurity interacts, and interact. with lattice defects 8=22607
- diffused diodes in Si grown epitaxially on sapphire, charact. 8=18130
- diffusion of Li, Na and K experimental results cf. Weiser theory 8=8683
- diodes, minority carrier lifetime, mag. field effect 8=13853
- diodes, neutron irradiated, L-shaped current characteristic 8=22630
- dislocations, optical effects, Hall effect 8=1979
- electron-beam heated, stress investigation, triangular macrodefect, X-ray and i.r. studies 8=1862
- electron Hall effect 8=9124
- electron-phonon interaction in ionized impurity-pairs 8=9128
- epitaxial wafer, slip and bowing control by etching technique 8=8385
- evaluation by frozen drop method 8=14509
- exciton lines, obs. with optical wavelength wobbles 8=5573
- extrinsic, doped with Group III and V elements, carrier thermalization 8=18010
- films, epitaxial on α -alumina, carrier conc. and mobility 8=9121
- films, heteroepitaxial on sapphire, space-charge limited currents 8=2213
- films on insulators, epitaxial growth 8=8328
- hole-optical-phonon interaction, degenerate p-type, in tunneling obs. 8=18088
- hot carrier drift velocity theory 8=9130
- impact ionization, transition probability 8=13665
- impurity compensation degree, determ. 8=18085
- impurity photoionization, quantum defect study 8=2207
- impurity redistrib. during thermal oxidation 8=18015
- impurities testing by non destructive neutron activation method 8=18086
- infra-red Faraday effect 8=9539
- internal friction and elec. resist. on repeated alternating bending 8=17828
- ion-bombarded, surface structure, temp. dependence 8=5278
- isolation diffusion of P, integrated circuits 8=1929
- lattice potential, mean internal, using Thomas-Fermi-Dirac model 8=13833

Semiconducting materials—contd**silicon—contd**

- localized state energies rel. to neutral divacancy 8=9123
- metal-anodic oxide-Si structures, frequency response 8=18143
- metal impurities determ. by spectrochemical analysis 8=18081
- m.o.s. capacitor, minority carrier lifetime 8=9179
- microhardness and dislocation structure temp. dependence, rel. to doping effects 8=17809
- motion of molten metal drops on surfaces under action of electric current 8=5259
- near-intrinsic, avalanche breakdown effects 8=9127
- n-irradiated, effect of O₂ concentration 8=5279
- n-metal, Schottky barriers rel. to mode of preparation 8=18116
- n-type, Hall meas. during n-irradiation over 78-330°K 8=18042
- n-type, e-irradiated, elec. props. rel. to impurity and irradiation-temp. dependence 8=5282
- n-type, n-irradiated, elec. props. rel. to defect structure and annealing 8=5283
- n-type, Nernst-Ettingshausen effects, longit. and transverse 100-400°K 8=18075
- n-type permittivity and conductivity of microwave freq. 8=5277
- n-type, uniform-field hot-electron effect theory 8=9129
- n-type, warm electron coefficient, meas. with microwave cavity TM₀₂₀ 8=18087
- optical properties and carriers density, laser induced changes 8=5633
- oxidized surface, MOS avalanche and tunnelling effects 8=2206
- oxygen conc., activation meas. by He³ bombard. 8=18083
- paramagnetic centres 8=22762
- pellet bonding, for large pellets, using vibration 8=22608
- photocells, rectifying props., effect of accelerated electron irradiation 8=22699
- photo excited carriers, observed trapping parameters, rel. to Hall number anomalies 8=13637
- photovoltages, Dember and lifetime-gradient, in n- and p-type 8=9253
- piezothermal e.m.f., anisotropy 8=5390
- p-n junctions, anisotropic stress effects 8=13847
- p-n junction characteristics, effect of hydrostatic pressure 8=5304
- p-n junctions, diffused, breakdown voltage 8=5317
- p-n junctions, diffused, reactive properties in region of high injection levels 8=13848
- p, thermally quenched, effect on electrical properties 8=18084
- p-type, B-doped, impurity conduction, effect of uniaxial compression 8=9131
- p-type, hole velocity depend. on elec. field and hole density 8=13832
- p-type, space-charge-limited, transient behaviour 8=5280
- p-type, thermal neutron irradiation effects 8=18068
- proton irradi. damage isothermal annealing, 22-158 MeV, 100-300°C 8=22605
- protons, 0.8 to 2.0 MeV, range-energy determ. 8=13468
- polishing of, methods 8=10452
- rectifier, for generation of rectangular current pulses 8=15178
- radiation detectors, theory and simple laboratory applications 8=11311
- in resistance thermometers, possible use at liq. He temp. 8=248
- on sapphire, chemical-vapour deposition, electron microscopy obs. 8=4826
- s.c.r. circuit for prod. pulsed mag. fields 8=3164
- single crystals growth on cleaved planes, faults investigation 8=17244
- solid state microwave spectrometer, Stark modulated 8=3275
- surface diffusion of Li, electron mirror microscope obs. 8=22159
- surface electronic states, from field effect kinetics study 8=22472
- surface inversion layer props. in elec. quantum limit 8=5231
- surface properties after irradiation with 500 keV nitrogen, boron and helium ions 8=18078
- surface recombination, generation process 8=22610
- surface, shallow donors ground and optically excit. states calc. 8=9126
- thermal expansion from 2-40°K 8=4937
- vacuum deposition on corundum 8=5281
- X-ray stress topography, rel. to film-crystal interface stresses 8=22371
- zener diode, breakdown, between avalanche and field emission 8=5328
- Al impurity redistrib. in oxidation and depletion depth, obs. 8=22606
- As ion implanted, carrier conc. and distrib., Hall effect obs. 8=18072
- Au-Si contact props, potential barrier and work function 8=18077
- B acceptor states, effects of ext. and int. elec. fields 8=2208

Semiconducting materials—contd**silicon**—contd

- B-doped, absorption line broadening 8=2452
- B-doped, deformed in elec. fields, hole relax. times at low temps. 8=18074
- B-doped by ion bombardment, B distrib. profiles 8=18071
- B-doped, temp. depend. of half-widths of internal absorpt. lines 8=14263
- BN as a diffusion source for Si 8=8684
- Co doped, p-i-n structure, current oscillations 8=2227
- Ga ion implanted, carrier conc. and distrib., Hall effect obs. 8=18072
- Li-donor ground state, chemical splitting 8=1950
- Li doped, e irradi. prod. defects and annealing at 20°C, 1 MeV 8=22604
- P-doped, annealing of the Si-E centre 8=2209
- Sb ion implanted, carrier conc. and distrib., Hall effect obs. 8=18072
- n-Si: Au, electrical props. 8=13830
- Si-metal contact characts. 8=18082
- Si: In, electron and hole-capture coeff. at low temps. 8=13915
- Si: P, As, X-ray investigation of impurities distrib. 8=18079
- Si, and Si-SiO₂ interface in MOS dev, influences of SiO₂ struct. and characts. 8=18148
- Si-SiO₂ structure, fixed charge at interface, and built-in voltage in SiO₂ 8=18141
- n-Si surface, Au contacts, props. 8=18070
- Si: Zn, slow rise photoresponse 8=5402

Semiconductors

- acoustoelectric amplification and negative differential cond. rel. to traps 8=1843
- acoustoelectric effect theory 8=17494
- acoustoelectric gain, magnetic field effect 8=13345
- adhesion, electronic theory 8=2046
- alkali metal doping, in small quantities, by electrolysis of fused salt 8=18017
- amorphous, charge transport mechanisms 8=18006
- anisotropic, electron density fluctuations, nonlinear excitation by e.m. radiation 8=13772
- annealed surfaces, influence of quartz impurities 8=9087
- antiferromagnetic crystal, magnetic polaron suggested 8=9068
- antiferromagnet, ferromagnetic domains 8=22866
- band structure Green's function method 8=8913
- breakdown mechanism, review 8=18009
- carrier conc. instability prod. by hot e diffusion 8=13773
- carrier mobility, influence of screened electron-phonon interact. 8=9075
- carrier temp., electric field depend. 8=8900
- characteristics, meas. by fine focussed electron beam 8=22575
- compensated, carrier scattering at liq. He temps. 8=18003
- compensated, electron mobility rel. to ionized impurity scattering 8=9080-1
- complex permittivity variations meas. 8=265
- conduction, intrinsic, onset temp., from p-n junction characts. 8=9147
- coupled cyclotron and spin waves 8=13682
- crystal and electron struct., effect of high press. 8=4699
- current instability in the case of weak surface recombination, theory 8=18011
- current oscills, growth rate calc. 8=13774
- degenerate, band-tail spreading energy meas. from emission of laser diodes 8=13781
- dense electron-hole gas 8=8959
- density distrib. and lifetime of injected plasma 8=9069
- differentiation of lattice defect types 8=9067
- diffusion layers, elec. characts. 8=22418
- direct-band, phonon-assisted magnetoabsorption 8=5222
- domains, elec., in sample with neg. differential resistance 8=17997
- doping, repeated diffusion, concentration distributions formation 8=1899
- double injection regime, effects of diffusion and thermal generation 8=22419
- drift mobility experiments rel. to trapping effects 8=8896
- e.m. wave excitation by electron beam, quasilinear theory 8=5151
- e.m. wave propag., electron temp. not unique function of incident field amp. 8=9084
- electronic band parameters determination from optical and magneto-optical properties 8=9493
- electron exchange eqns., between surface and vol. zones 8=22431
- electron-hole gas density, Green function method 8=8889
- electron-hole pairs yield and Fano factor calc. from van Roosbroeck statistical model 8=2183
- electron-hole plasma decay meas. by double-pulse variable-delay circuit 8=1E177
- electron-hole plasma, i.f. waves excitation 8=13683
- electron and ion emission on laser light interaction 8=18272
- electron irradi. effects, design of β -spectrograph for meas. 8=11466
- electron-lattice interaction effect on free-carrier magneto-optics 8=8890
- e.p.r. rel. to conducting props. 8=5515
- Semiconductors**—contd
 - electrical processes, phase space analysis in lower than 3 dimension subspaces 8=13776
 - elemental, hot-carrier microwave conductivity 8=13779
 - energy level displacement by interactions 8=5109
 - excitation of electron-phonon density fluctuations, nonlinear mechanism 8=9070
 - exciton condensate form., and optical absorpt. 8=5128
 - exciton superfluidity 8=22476
 - excitons, multielectron theory 8=22478
 - extrinsic, carrier thermalization, recombination mechanism 8=18010
 - Faraday effect, hot-electron 8=22420
 - films, effective density of electron states per unit volume 8=22448
 - films, oscs. of conductivity, and mag. resistance 8=9074
 - films, thin, electron-phonon interactions at low temps. 8=22428
 - films, thin, transmission, reflection and absorpt. of electrons 8=22494
 - Franz-Keldysh effect 8=5227
 - galvanomagnetic effects, nonlinear, in strong electric and magnetic fields, theory 8=5225
 - generators of e.m. oscillations, conditions for sustained oscillations 8=8957
 - graded-band-gap, electronic transport 8=9083
 - Gunn domain stability 8=17996
 - Gunn effect, domain field distrib. for inhomogeneous doping 8=13783
 - Gunn effect, electron-transfer mechanism, domain propagation 8=9077
 - Gunn effect, negative mobility model for oscillator analysis 8=9098
 - Gunn effect, qualitative explanation 8=9076
 - Gunn oscillators in parallel in transmission line, current waveform 8=22643
 - Hall effect, magnetoresist. and mobility in semiconds. with non-uniform charged ion conc. 8=22421
 - Hall voltage, influence of skin effect 8=5232
 - helicoid instability of sound oscs. 8=5139
 - high-ohmic, magnetoresistance meas. by capacitive method 8=5234
 - high-resistance, device for investigating weak pulse currents 8=22576
 - H like impurity centres, ionisation energy 8=13785
 - hot carrier effects, review 8=18008
 - hot-electron diffusion theory for space-charge-limited current flow 8=9129
 - hot electrons, photomagnetic effect, theory 8=18219
 - impurity distrib., apparatus 8=2184
 - impurity redistribution for out-diffusion 8=5229
 - insulating (excitonic) phase, anisotropy effects 8=9192
 - insulating phase in presence of normal impurities, excitonic props. 8=8951
 - intrinsic, pinch effect and its mag. field dependence 8=9072
 - ionization waves in plasma theory 8=18056
 - ion losses on traversing crystal lattice channels 8=17695
 - i.r. absorpt., by reflectivity var. 8=9479
 - kinetic phenomena, effect of non-uniformity of edge dislocation density 8=13780
 - Landau damping and phonon, plasmon and photon wave dispersions 8=9093
 - lasers, excited by electron or laser beam, with radiating mirrors 8=11072
 - lasers, interband magneto-optical, theory of e.m. modes and threshold conds. 8=11071
 - lifetime of high density plasma, obs. 8=13685
 - 1/f noise at surfaces, theory 8=13787
 - luminescence, exciton transitions in 2-photon stimulation 8=9583
 - magnetic resonances in higher harmonics generated by free carriers 8=5223
 - magnetoconcentrational Suhl effect, excitation threshold and oscillator frequency 8=13778
 - magneto-optical absorption, interband, optical phonons 8=18492
 - magneto-optic interband absorpt., phonon effects 8=18493
 - magnetoresistance, voltage ratio meas. appl. 8=10821
 - many-valley, Hall effect at high electric field 8=22417
 - metal-semiconductor contact props, potential barrier and work function 8=18077
 - metal-semiconductor contact of small area, voltage-current characts., within diffusion theory 8=9089
 - β -methyl-naphthalene, i.r. spectra and conductivity in polycrystalline, dissolved and melted state 8=16866
 - monomolecular layers on metals, effect on metal work function 8=9091
 - multilayer, ultrasound amplification by carrier drift 8=17855
 - multiphoton absorpt. rel. to saturable transmission 8=9478
 - naphthalene, i.r. spectra and conductivity in polycrystalline, dissolved and melted state 8=16866
 - negative bulk differential conductivity, stationary state 8=13782
 - negative differential conductivity, slowly propagating high-field domains 8=13777
 - n-type, impurity effect on transport props. 8=5226
 - Nernst-Ettingshausen effect rel. to magnetoresistance 8=9082

Semiconductors—contd

- non-homogeneous, excess current carriers distrib. eqns. 8=18007
- non-linear props. governed by electron-phonon interactions 8=18004
- nonparabolic nonspherical energy surfaces, optical freq. mixing due to free carriers 8=5571
- nuclear spins polarization by hot electron current 8=8204
- organic, metal chamber for elec. measurements 8=9092
- perturbed surface formed by semiconducting bodies, scattering of e. m. radiation 8=22943
- phenanthrene, i. r. spectra and conductivity in polycrystalline, dissolved and melted state 8=16866
- phonon-drag Seebeck effect in mag. field, quantum theory 8=9236
- phosphors, Hall effect for e and hole mobility meas. 8=8898
- photoconductivity, in crossed elec. and mag. fields of limited bipolar semicond. 8=22687
- photoconductivity, negative, instability and polarization induction 8=18218
- photoelectron diffusion in mag. field rel. to current and photoelectromag. effect anomalies 8=13909
- photoexcitation by anti-Stokes mechanism in graded band-gap type 8=9266
- photon-assisted magneto tunneling in crossed and parallel elec. and mag. fields 8=8650
- photothermal effect, study 8=8650
- photothermoelectric and thermally stimulated thermoelectric effects, rel. to photoelectronic anal. techniques 8=22678
- photovoltage, lifetime-gradient assoc., large signal theory 8=9253
- piezoelectric, acoustic amplification, critical electron drift velocity 8=19571
- piezoelectric, acoustic wave propagation 8=22094
- piezoelectric, acoustoelec. domain formation during thermal noise amplification 8=18001
- piezo-electric crystals, transient acousto-elec. phenomena 8=13346
- piezoelectric, elastic wave propagation and amplification 8=9088
- piezoelectric, non-linearity of elec. props. during u. s. wave propag. in a. c. field 8=18022
- piezoelectric, I-V characteristic under sound amplification conditions 8=18021
- piezoelectric, stimulated Brillouin scattering 8=17495
- piezoresistance, meas. 8=268
- plasma, collision induced instability 8=8964
- plate, flexural waves, theory of instability 8=17496
- polar, electron mobility at intermediate and high fields 8=18005
- polar, electron temp. approx. 8=13775
- polar, hot electron mobility 8=22430
- polar, mobility and temp. of electrons or holes 8=17856
- polar, optical phonon scatt. of charge carriers 8=13628
- polarons, bound, ground-state energy 8=5133
- probe conductivity meas., sample thickness dependence 8=9073
- propagation of e. m. waves, amplitude modulation by a. c. mag. fields 8=15391
- quantum efficiency and impact ionization 8=13907
- radiative capture by impurities 8=5228
- recombination process in space-charge region 8=18049
- reflectance in i. r. region 8=22933
- research problems, appl. of autoradiography to tracer studies 8=18019
- resistivity, effect of mag. element impurities 8=18016
- resistivity, four-probe meas., probe wander error 8=22577
- saturation effects rel. to laser theory, combination of 4 relax. times 8=15475
- semimetals with equal numbers of electrons and holes, quantum theory of Hall effect 8=22416
- semimetals, m. h. d. waves, plasma-phonon 8=5135
- solar cells multistage, selection of optimum combination of materials 8=6277
- space charge conduction, review 8=18002
- spin-cyclotron-phonon resonance 8=2352
- spin-lattice relaxation of conduction electrons in a quantizing magnetic field, theory 8=5519
- stabilizer of small d. c. currents 8=15183
- static electrical inhomogeneity stability in sample with neg. differential resistance 8=17997
- with stoichiometric vacancies, crystalline, chemical and thermal props. 8=17197
- surfaces, damage by ruby laser 8=2028
- surface e. m. wave propag. and amplification in strong mag. fields, theory 8=9090
- surface free conductivity, thickness and external field dependence 8=18018
- surface inversion layer props. in elec. quantum limit 8=5231
- surface parameters, determ. from electrorreflectance studies 8=5230
- surface, space-charge layer, electrostatic energy and external charge distrib. 8=13788
- surface space-charge layers, elec. cond., theory 8=5233
- ternary inorganic, composition predictions 8=9071
- theory, Soviet contributions, review 8=18000

Semiconductors—contd

- thermal cond. determ. of cylinders in He bath 8=3107
 - thermally stimulated conductivity, carrier liberation process 8=9079
 - thermoelectric power, absolute, rel. to impurity and chem. pot. in degenerate semicond. 8=18207
 - thermoelectric power in strong elec. field 8=18209
 - thermomagnetic coeffs. in strong mag. fields, quantum oscs. 8=5426
 - III-V compounds, second order optical susceptibility calc. 8=18496
 - with traps, acoustoelectric effects and sound amplification, theory 8=9078
 - trap level concentration determ. using thermostimulated conductance 8=18012
 - travelling domains, velocity and current determination 8=9085
 - tunneling in crossed and parallel elec. and mag. fields 8=5227
 - two-band model in intense photon field 8=17867
 - 2-photon transitions to exciton states, oscillator strengths 8=8953
 - two-valley, hot e relax. times, effect on bulk-microwave oscillators 8=22422
 - ultrasonic electro-acoustical attenuation theory 8=1845
 - voltage rectification rel. to surface states 8=13786
 - voltage stabilizers, stabilization coefficient of 8=15184
 - with InSb-type valence band, statistics 8=22449
 - zero bias anomalies due to paramagnetic impurities, theory 8=13784
 - Ba-Bi titanate (IV), ceramic, Fe³⁺ doped, model and props. 8=5236
 - Cu and Zn complexes, tetraphenylporphine and tetraphenylchlorine as photosemiconductors 8=9117
 - CuFeS₂, Mössbauer spectrum 8=1649
 - Si-Li drifted detectors, monoenergetic electron backscattering obs. 8=11464
 - Sn¹¹⁹ nuclei, impurity, isomeric shift 8=9086
- Semi-insulating materials (high-resistivity semiconductors).**
See Semiconducting materials.
- Semimetals.** See Metals; Semiconductors.
- Series**
- Fourier, absolute convergence theorems 8=11
 - Legendre polynomial expansion for Klein-Nishina formula 8=3570
 - Lie, appl. to reactor theory 8=7309
- Sferics.** See Atmospheric.
- Shadow universe.** See Cosmology; Elementary particles.
- Shear strength.** See Mechanical strength/shear.
- Shell model.** See Nucleus/models.
- Shielding.** See Radiation protection.
- Shock tubes**
- air, θ -pinch effect, use in electrodeless tube 8=6136
 - arc-driven and pressure-driven, comparison 8=19527
 - detonation initiation of liquid explosives, effect of shape and material of tubes 8=10720
 - diaphragm opening-time effect on shock trajectory 8=164
 - electrically driven, nature of moving plasma 8=4359
 - electromagnetic, h. f. mag. press. wave generation and associated relaxation 8=15054
 - e. m. precursor ionization meas. with double probe 8=6137
 - e. m. wave reflection by moving plasma 8=16531
 - electron density, interferometric determ. 8=159
 - expanding flows behind incident waves, probe studies 8=15049
 - explosive shutter for flash spectrography 8=15047
 - flow pattern near diaphragm during opening process 8=10713
 - magnetic annular arc-driven 8=19528
 - magnetic driving current rel. to load var. 8=19529
 - magnetically driven, press. meas. 8=15048
 - mag. driven, shock and current layer structure 8=6140
 - for molecular beam for O atoms at 3 eV 8=7640
 - with parallel conductors, discharge plasma shape and vel. rel. to press. 8=1387
 - piston movement, optical and mag. oscilloscopy 8=163
 - plasma e density meas. by i. r. laser interferometry 8=16541
 - plasma excitation of air, optical props. 8=1337
 - plasma, fast moving, elect. current 8=16509
 - plasma flow, pressure, trajectory and density profiles from spectrographic obs. 8=16510
 - production of uniform shocks by detonation 8=160
 - semi-infinite flat plate, in compressible laminar boundary layer for impulsive motion 8=15046
 - side-wall electrostatic probes, local electrical characteristics and resistance 8=10712
 - simultaneous ultrasonic and line reversal temp. determination 8=4463
 - T-tube, modified, for improved shock wave prod. 8=161
 - tunnels, use of N₂O for obtaining high stagnation enthalpies 8=16676
 - wave propagation between tube end and container 8=162
 - wave velocity meas. by piezoelectric transducer 8=9230
 - Venturi, ultrasonic shock waves emitted by cavitation 8=19530
 - CO, shock-heated, incubation time in dissociation 8=21184
 - H in shock tube, elec. props. and Cu cold electrodes V-I characts. 8=21359

Shock waves

See also Detonation; Explosions; Supersonic flow.
 adiabats, discontinuous, rel. to nonuniformity of compressions 8=165
 in air, front luminance temp. obs. 8=21483
 auroral infrasonic radiation, model 8=19533
 Burger's equation, Lagrangian-history statistical theory 8=19536
 chemico-physical processes 8=6144
 collisionless, destruction of sharp transition due to high β effect 8=10714
 conical, refl., apparatus and expts. 8=10718
 coupling of longitudinal oscilns. to l.f. ion-sound waves 8=16579
 crystalline solids, induced by electron beam 8=8757
 density distrib. across low wave, interferometric obs. 8=10717
 detached shock, non-adiabatic temp. distrib. behind rel. to radiative coupling coeff. 8=15053
 diaphragms, opening-time effect on trajectory in tube 8=164
 diaphragm rupture, acoustics of generated shock waves 8=15051
 diffraction and reflection 8=16656
 diffraction in fluid by supersonic wedge 8=21492
 diffraction by wedge, corner conditions 8=10716
 diffusive separation obs. 8=19537
 discontinuity in density, evolution governed by Boltzmann collision integral 8=7933
 distortion of wavefront, amplitude calc. 8=166
 dusty medium, eqn. of state, thermodynamic parameters 8=167
 earth's bow, plasma and mag. field correl. obs. 8=23328
 earth's bow shock obs. with Explorer 12 magnetometer 8=2619
 in elastic nonconductors, amplitude, rel. to extrinsic body sources and heat supply 8=19517
 electroacoustic in isotropic stratified plasma, coupled eqns. of propagation 8=16508
 electron temperature shock structure in partially ionized gas 8=4361
 exploding loop eqn., second integrals 8=6135
 of explosion, propag. in generalized Roche model 8=15060
 flow properties distrib. behind spherical detonation wave 8=15061
 formation in Q-device 8=21325
 gas, collapsed cylindrical detonation wave 8=7907
 in gas normal reflection with vibrational relaxation 8=1455
 in gases, effect on critical flow 8=7898
 gas flow, Navier-Stokes equations for short waves 8=7895
 gas, rigid sphere molecules, velocity distribution function by using model and computer 8=6139
 generated by rupture of diaphragms in tube, acoustics 8=15051
 growth and decay of discontinuities in fluids with internal state variables 8=3036
 h. f., magnetic press. generation, and associated relaxation 8=15054
 hypersonic viscous shock layer of blunt body, effects of surface mass transfer 8=3035
 imploding shocks, non-uniform self-propag. nature 8=15059
 interaction with an area change, solution 8=19531
 intersections, analysis by vector polar method 8=19526
 ionized gases, pipe for investigation 8=4305
 ionizing, inducing m. h. d. waves 8=19811
 laser radiation production using solid target, and plasmoid scattering 8=19534
 leading shock in 2-dimens. secondary fluid injection into supersonic stream 8=16678
 longitudinal, resonance, in elastic-plastic bar 8=15052
 magnetoaerodynamic flow, supersonic, blunt body, theory 8=355
 magnetogasdynamics propag. in a plasma, radiation effects 8=7755
 m. h. d., in fluids, transition soln. 8=19805
 m. h. d., low intensity, theory 8=6345
 m. h. d. wave modes behind normal ionizing shock waves 8=19535
 magnetosphere attached, 2nd standing 8=2624
 metals, excitation by e. m. irradiation 8=6143
 moon, effect of solar wind 8=23642
 motion along converging or diverging ducts 8=15056
 motion in inhomogeneous cosmic medium 8=10242
 multiple, detect. with ionization gauge circuit 8=3041
 Newtonian hypersonic theory 8=19539
 neutron stars and supernovae, propagation 8=1390
 nitroglycerine, low velocity detonation mechanism 8=21582
 non-equilibrium flow, formation 8=6141
 oblique m. h. d. waves, stability 8=16456
 oblique, with complete condensation 8=19541
 parameters, while outflowing from a nozzle 8=16663
 phasograms with laser phase contrast system 8=7792
 planar, propag. in lossless nonlinear mag. medium 8=19832
 plane, reflected normally from perturbed flat walls, stability study 8=19532
 plasma, alkali halogen, drift wave excitation 8=16577
 plasma, anomalous electron heating obs. 8=1386
 plasma bearing large currents, rarefaction waves 8=7753

Shock waves—contd

plasma, bimodal distribution soln. 8=16511-2
 plasma, collisionless, magnetic obstacle effects, wind tunnel obs. 8=16513
 plasma flow in elect. shock tube, pressure, trajectory and density profiles from spectrographic obs. 8=16510
 plasma, nonequilibrium, electron concentration and temp. profiles, obs. 8=12490
 plasma, nonuniform, longitudinal wave propag. into, through sheath, Vlasov eqn. soln. 8=12488
 plasma, profile measured by laser light scattering 8=7751
 plasma, propag. perpendicular to mag. field, one parameter family of profiles 8=12489
 plasma, rarified, prop. along magnetic field 8=12491
 in plasma, two-fluid, jump conditions 8=4358
 plastic, glass reinforced, adiabatic curve at pressures up to 130 thousand atm. 8=22409
 pressure meas. in kbar range 8=6149
 pressure perturbation calc. 8=166
 production of uniform shocks by detonation 8=160
 propagation in degenerate gases 8=19544
 propagation in plasma for nuclear fusion 8=7798
 radiation coupled shock layer including upstream absorpt. effects 8=19545
 rebounding, detonation, trajectory; analytical determination 8=169
 reflected, exothermic reactions 8=23120
 reflection coeff. of disturbance wave 8=3037
 reflection at rigid wall in presence of boundary layer 8=6138
 relaxation phenomena, effect of free stream dissociation and vibrational excitation 8=10715
 rigid unloading, closed solution 8=3038
 semi-infinite flat plate, in compressible laminar boundary layer for impulsive motion 8=15046
 in slightly rarified gas, middle Mach number, corrections to Crook's soln. for gas parameters 8=16667
 spherical, decay 8=10719
 structure and current sheet in mag. driven tubes 8=6140
 structure, from fluorescence meas. 8=3033
 structure, gaskinetic investigation 8=19542
 sudden compressions, effect on turbulent boundary layer 8=15055
 surface press. from pistons on spherical and cylindrical baffles 8=6134
 thermal in disks, statistical analysis 8=22295
 ultrasonic, emitted by cavitation in Venturi tubes 8=19530
 underwater explosion, phase shift due to total internal reflection 8=19547
 underwater explosions, $\pi/2$ phase shift at caustics 8=19546
 viscous hypersonic layers in gases, soln. of eqns. in presence of chem. reactions 8=16671
 viscous, liquids, layer thickness 8=168
 weak, structure on reflection from wall, Navier-Stokes eqn. 8=21448
 wire, elec. explosion, specific energy distrib. investigation 8=6142
 wire explosion discharge effects 8=4272
 in Ar-air mixture, front luminance temp. obs. 8=21483
 Ar, explosively generated, radiation 8=1480
 in Ar, front luminance temp. obs. 8=21483
 Ar₂ gas-ionizing shock fronts, hydromagnetic, non-equilibrium structure 8=16504
 Ar, ionizational relax. behind shock front 8=1356
 Ar, ionized, interferometry 8=4311
 Ar, shock layer e density meas. 8=21265
 in Ar, structure of normal ionizing wave 8=21490
 Cu, by electron beam pulses 8=13484
 D-T gas mixture, propagation of thermonuclear detonation wave 8=21482
 H, thickness rel. to velocity 8=16646
 K vapor, supersaturation and condensation shocks 8=12982
 N₂, relaxation, electronic excitation 8=21087
 in Xe, front luminance temp. obs. 8=21483

effects
 advances in applied mechanics, book 8=16683
 air, ion density profiles 8=4460
 air, ion density profiles in expanded shock tube flows 8=15050
 air plasma containing electrophilic gases, microwave meas. 8=7754
 conductor shape changes during "wire explosions" 8=6150
 detonation waves, interaction against flow of stoichiometric mixture of H-O gases, meas. 8=10721
 dielectric, e. m. f. production 8=5344
 rel. to earthquakes, structure-foundation interaction 8=3034
 ethylene, oxidation and pyrolysis 8=18676
 explosive liquids, cavitative detonation 8=171
 in fluid with steady uniform flow, dynamical treatment 8=21447
 gas, self-similar motions 8=4462
 geomagnetic disturbance due to atmospheric explosion 8=2746
 on heat transfer around blunt body 8=19538
 interstellar gas and dust densities 8=10239
 ion density and elect. field perturbations caused by acoustic-wave pulse in weakly ionized gas 8=21324
 ionized air, heating with low voltage d.c. discharge to 6700-7800°K and 10-20 atm. 8=12421

Shock waves—contd
effects—contd

- ionizing, moving, interaction with transverse e.m. or m.h.d. wave 8=12504
- liquid detonation initiation during gap testing, rel. to wall interacts. 8=15057
- magnetogasdynamic, vorticity and current density behind in unsteady flows 8=6358
- metals, on electronic configuration and orbital compressibility 8=8225
- nitroglycerine, initiation of detonation 8=6148
- nucleosynthesis in supernovae 8=5842
- panels, multimode response to sonic booms, normal and travelling 8=6123
- in plasma, anisotropic, transition solns. 8=4353
- plasma behind front, electric characteristics waveguide meas. 8=1389
- plasma, destruction of magnetic sound at high Mach nos. 8=1388
- plasma, e temp. meas. 8=21326
- in plasma, microwave meas. of temp. 8=4360
- plasma, non-linear mixing with velocity dependent collisions 8=16578
- quartz, X, Y and Z cut, elastic compression obs. 8=13608
- quartzite, elastic precursor decay for cylindrical and spherical flow 8=13605
- relativistic gas, Fermi accn and radio spectra 8=10292
- reviews of plasma physics, book IV 8=16462
- rocks, phase transitions 8=9800
- shock tube, precursor ionization meas. with double probe 8=6137
- shock spectrum of interaction between superstructure and non-rigid foundation 8=19543
- shock-velocity-particle-velocity relationship in study of solids under pressure 8=8787
- solids, phys. props., meas. 8=17719
- sonic booms, building response 8=10758
- sound generation interaction 8=188
- in star, pulsating, on atmospheric density distribution 8=5869
- steel, 0.04% C, residual strains due to single pulse compression stress wave 8=17787
- vorticity and current density in a magneto fluid 8=19815
- Al, attenuation 8=8814
- Ar, ion density profiles in expanded shock tube flows 8=15050
- Ar ionization, electron density and collision freq., microwave obs. 8=12431
- Ar, shock compression, Thomas-Fermi-Dirac theory 8=16994
- BaTiO₃ ceramics, recovery after depoling under shock loading 8=2243
- BaTiO₃, shock compression 8=13538
- CO₂, vibr. relax. 8=4146
- CO, vibr. relax., spectrophotometry 8=16270
- Ge, metallic modification formation under shock compression 8=17083
- H + O₂ recomb. rate in shock tube 8=14367
- KBr, dynamic compression and phase transitions 8=22376
- KBr polarization rel. to lattice imperfection prod. during shock wave plastic deformation 8=9225
- KCl, dynamic compression and phase transitions 8=22376
- KCl, polarization rel. to lattice imperfection prod. during shock wave plastic deformation 8=9225
- LiF, polarization rel. to lattice imperfection prod. during shock wave plastic deformation 8=9225
- N₂¹⁴⁻¹⁴ + N₂¹⁵⁻¹⁵ = 2N₂¹⁴⁻¹⁵ reaction in single-pulse shock tube 8=5696
- N₂, vibr. relax. in gas mixtures 8=21195
- N₂, vibr. relax. in shock tube 8=7532
- NaCl, polarization under shock load, obs. 8=5353
- O + CO, shock-heated system, radiation 8=1342
- OCS pyrolysis in shock tube with quadrupole mass filter 8=14361
- Pb zirconate-titanate ceramics, recovery after depoling under shock loading 8=2243
- Pb(Zr_{0.96}Ti_{0.04})O₃, shock compression 8=13538
- Sb, phase transition induction 8=4715
- Si, metallic modification formation under shock compression 8=17083
- TiO₂, phase transforms. under compression, from X-ray studies 8=1685

Shot noise. See Fluctuations/electrical.**Showers.** See Cosmic rays/showers and bursts.**Shubnikov-de Haas effect.** See Magnetoresistance.**Silicon**

- See also Semiconducting devices; Semiconducting materials/silicon.
- absorption rel. to bound excitons 8=5132
- anodic oxide growth behaviour 8=14422
- autophotoluminescence energy rel. to e distrib. 8=22726
- band structure calc. using LCAO approximation 8=8906
- bonding, covalent, X-ray diffr. meas. 8=4869
- Brillouin zone symm. props. obs. by e⁺ annihilation 8=13690
- channelling of MeV projectiles 8=11954
- colloid-Au contacts, photocapacitive effects 8=22673
- containing Li donors, acoustic paramagnetic resonance 8=9443

Silicon—contd

- crystal growth by Czochralski method 8=13141
- crystal window in double spectrometer, X-ray diffr. profile exam. with monochromatic radiation 8=22004
- crystals, Compton scatt. power 8=23012
- crystals, density by hydrostatic weighing, precision obs. 8=14920
- crystal growth, Czochralski, radial solute segregation 8=4815
- cubic crystals, thermal expansion coeff., temp. depend. 8=8646
- deposition and etching through windows in SiO₂ 8=17245
- diffusion of B, dislocation motion rel. to coefficient 8=1925
- diffusion of B, lattice contractions. contrast reversal in reflection topography 8=1927-8
- diffusion of P, dislocation motion rel. to coefficient 8=1925
- diffusion of P, enhancement by vacancy generation 8=1926
- dislocation motion under e-bombardment during e-microscope investigations 8=17660
- distorted crystals, X-ray topography 8=13198
- doped with B, Al, Ga, P, As or Sb, extrinsic i.r. photoconductivity 8=9257
- e-drift, hot, e-phonon scatt. 8=22438
- effective mass, intrinsic concentration 8=5119
- elastic constants between 25 and 300°C from u.s. wave velocity 8=17830
- electron-beam heated, stress investigation, triangular macrodefect, X-ray and i.r. studies 8=1862
- electron energy loss probability, retardation effects 8=22497
- electron scattering, anomalous, coeffs. determ. 8=13289
- energy given to lattice by primary ions 8=2033
- epitaxial growth, effect of surface perturbations 8=17256
- epitaxial layers, "hillock" formation 8=17619
- epitaxial layers, stacking faults, cause and cure 8=8736
- etching in aq. h. f. solns. 8=17219
- etching conditions, SiO₂ and Si₃N₄ elimination, epitaxial growth 8=13128
- etching in HNO₃-HF-CH₃COOH 8=4791
- etching, in H₂O-amine-complexing agent 8=4792
- etching, vac. thermal 8=17217
- faults, extrinsic, climb 8=22217
- film on Ni substrate, total reflection of X-rays of different wavelengths 8=22038
- films, amorphous, structure 8=13092
- films, epitaxial, prep. by pyrolysis of hydrides 8=17130
- films, etch rates in H₃PO₄, influence of H₂O content 8=17218
- films, evaporated, quantitative determ. by radioisotope analysis following n-activation 8=4756
- films grown on W substrate 8=4758
- films, prep. by rheotaxial method 8=4739
- fluoride chemisorption on surfaces, use of F¹⁹ in HF etches 8=18697
- galactic source 3C 191, Si:C ratios 8=14810
- group III diffusion, hot implantation behaviour, comp. with group V diffusion in Ge 8=22160
- homoepitaxial, vacuum deposition, low temp. 8=1697
- impurity diffusion anomaly 8=13427
- impurity spectrochemical analysis 8=18771
- junctions, large area p-n type, by epitaxial growth technique 8=5316
- p-n junctions, mesoplasma, visible and i. r. radiation 8=2218
- lattice theory of third order elastic consts. 8=13261
- lattice, vibr. freq. spectrum 8=8616
- metal-oxide-Si structures, Au-doped, C-V curves 8=13896
- muonic K series X-rays 8=1209
- n-irradiation damage, investigation by transmission electron microscopy 8=17707
- npn transistor, effect of fields on diffusion, overcoming "push out" effect 8=22145
- n-type, anodic passivity in NaOH rel. to cryst. orientation 8=2533
- nuclear methods of boron determ. 8=5765
- (111) surface, low energy electron diffraction study of PH₃ adsorption 8=4765
- optical three-photon stepwise absorption 8=5635
- oxidation by wet O₂ stream 8=18689
- paramagnetic centres produced along proton range 8=8704
- permittivity calculation 8=5354
- photocells, rectifying props., effect of accelerated electron irradiation 8=22699
- photoelastic constants, bond stretching and bending model 8=8830
- photoelectromagnetic effect, energy band structure dependence 8=13916
- for photographic recorders spot-brightness control, photocell 8=2271
- plastic deform. in brittle fracture region 8=5084
- positron annihilation meas. in Se 8=5150
- proton scatt. by monocryst., directional effects 8=2034
- protons, channelling, anomalous energy losses, E_p = 1.5 MeV 8=17708
- refractive index in far i.r. 8=14219
- site transfer in GaAs 8=17574
- solar cell characts, thickness and temp. depend. rel. to power-weight param., obs. 8=10850

Silicon—contd

- solar cell deployable rigid-frame array, performance obs. 8=10845
- solar cell, p or n, characts. rel. to distributed model 8=9265
- solar cell, integrated high-voltage 8=10852
- solar cells, dendritic and refr. back, prod. by implantation 8=10849
- solar cells for 0.4 and 0.2 AU from sun, use 8=10851
- sputtered films, r.f. and d.c., re-emission coeffs. 8=2032
- in steel, spectrochem. determ., line interferences due to Cr, V and Mo 8=23190
- stopping for p, d, t, α 8=8778
- surface contamination, detection and identification 8=1688
- surface exoemission of mechanically treated n- and p-type samples 8=18255
- surface properties rel. to u.v. illumination 8=8297
- surface states from charges in oxide coating 8=22469
- surfaces, solid, elec. decoration, new method 8=8380
- thermal conductivity, elec. resistivity and Seebeck coeff. from 100 to 1300°K 8=22136
- thermal conductivity, neutron irradiat. effects at 80°K 8=8663
- thermal expansion from 2-40°K 8=4937
- wafers, orientation, by proton channelling 8=8476
- web dendrite, stacking faults, contrast in X-ray topographs 8=1983
- X-ray emission spectrum obs., valence bonds 8=2454
- zone melting, temperature field, theory 8=8427
- Au-diffused, precipitates formation 8=17620
- B doped, p radiation sensitivity, obs. 8=17414
- B (or P) diffused, appl. of dynamical theory of X-ray scattering 8=13412
- in Fe liquid, heat of solution 8=16799
- Ga and Bi impurities photoexcit. lines anomalous broadening rel. to optical phonons, obs. 8=5601
- on Ge(111) surfaces, epitaxial films struct., LEED obs., 870°K 8=17140
- Ni-induced surface structure on (111), LEED study 8=4732
- Si-Au potential barriers prep. by local sputtering 8=9166
- Si:B, "internal" impurity spectrum, conc. depend. 8=13426
- Si:B, Li mobility and drifted n-i-p⁺ counters prep. and characts., obs. 8=20200
- Si I lines, shift by Van der Waals interact. with Ar atoms 8=7423
- Si II λ 4128 and λ 4130Å in model atmospheres and B stars 8=19163
- Si II, stellar, superposition of configuration applied to a series of states 8=19158
- Si III, spectra, transition probabilities 8=7411
- Si III, theoretical multiplet strengths 8=7410
- on Si(311) surfaces, epitaxial films struct., LEED obs., 870°K 8=17140
- Si:Ga, Li mobility and drifted n-i-p⁺ counters prep. and characts., obs. 8=20200
- Si:Li, radiation defects, effect on annealing rate 8=2067
- Si:P, e-irradiated, spin-lattice relax. rel. to defect production 8=18434
- Si:Sb, melt-grown, tetrahedral defects 8=1958
- Si-SiO₂ interface, thermal oxidation, effect of Na impurity 8=14384
- Si-WSi₂-Si, epitaxial struct. 8=17257
- Si:X (X=Sb, Ga, As, In and Xe), implanted atoms location, lattice disorder and radiation sensitivity, obs. 8=17414
- YIG: Si doped, photomag. anneal 8=23022

Silicon compounds

- See also Quartz.
- alkali silicate melts, bubble formation, wet atmosphere effect 8=7996
- carbides, formation by chemical vapour deposition 8=23112
- cristobalite, solution and diffusion of He and Ne 8=8247
- erionite and offretite, differentiation 8=13153
- garnet, Ce activated, fluorescence 8=2474
- hydrides decomp. in r.f. glow discharge rel. to films deposition 8=21872
- metal-SiO₂-CdSe (metal contacts, photocurrent studies 8=2281
- methylethoxy silanes, integrated intensity of i.r. spectra 8=7551
- olivine crystals, registration of As and I ions 8=11325
- quartz and silica, thermal diffusivity from 300° to 1100°K at 1 atm 8=22131
- sesquiteroxide, formula and ht. of formation 8=9662
- silica gel, factors influencing growth of CuCl 8=21944
- silica gel, modification of struct. on purification 8=1663
- silica gel, surface meas., absorption method 8=21742
- silica gels, adsorbed H₂O, proton relax. 8=12932
- silica gels, surface, energy states and dynamics of Sn atoms 8=16912
- silica glass, dielec. loss at low temps., OH⁻ conc. and irradiation effects. 8=18172
- silica, physisorpt. of Ar at low temps., process and mean adsorpt. time 8=17172
- silicate glasses, e.p.r. of Mn²⁺, 293-4°K 8=18408
- silicate glass, validity of Nernst-Einstein eqn. 8=8354
- silicate materials containing Fe, site populations, Mössbauer effect 8=8218
- silicate melts, Newtonian flow, viscosity eqn. and bond rearrangement 8=21628

Silicon compounds—contd

- silicates, microprobe analysis standards prep. from gels 8=14496
- silicates, porous, fragment shapes in hypervel. impact rel. to lunar surface struct. 8=13609
- silicate rocks at high press. and temp., hydrolytic weakening 8=14561
- silicates, structural anal. and their crystal chemistry, review 8=8466
- silicone oil, cellular convection obs. 8=6213
- silicones, #200 series, ultrasonic absorption in range 30-350 MHz and -30° to +30°C, rel. to viscosity 8=8063
- trichlorosilane, evaluation for prep. of electronic grade Si 8=14509
- tridymite, solution and diffusion of He and Ne 8=8247
- α -AgCd alloys, specific heat from 1 to 4°K 8=8637
- AgBr micro-crystals, growth rates and defect formation 8=8698
- α -AgPb alloys, specific heat from 1 to 4°K 8=8637
- α -AlFeSi, 4 possible phases 8=13057
- CH₃SiCl₃, r.f. spectrum, structure and dipole moment 8=4169
- Fe-Si sheet, initial permeab. depend. on demag. freq. 8=5464
- HSiCl₃, r.f. spectrum, structure and dipole moment 8=4169
- PbO-Al₂O₃-B₂O₃-SiO₂ system glasses, elec. props. temp. and comp. dependence 8=18170
- Si²⁹(CH₃)₄, indirect nuclear spin coupling 8=4233
- Si₃F₈, n.m.r. study, coupling consts. and chem. shifts of F¹⁹ and Si²⁹ rel. to SiF₄ 8=4237
- SiC, addition up to 15% in BeO, rel. to rupture and grain growth props. 8=22315
- SiC, B and N doped, luminescence efficiency 8=18615
- β -SiC, cryst. growth from soln. 8=17246
- SiC crystals, deduction of energy spectrum of acceptor states 8=5668
- SiC, delayed fracture and creep 8=22391
- α -SiC on diamond, directed crystallization 8=8428
- SiC diodes, electroluminescent, props. 8=9627
- SiC, fibrous single cryst., i.r. spectrum 8=2455
- SiC films deposition in r.f. glow discharge 8=21872
- SiC, growth single crystal films on Si 8=1748
- SiC, hole mobility and interband transitions 8=9122
- α -SiC, magnetic studies 8=18301
- SiC, polarity of structure 8=21999
- SiC, polycrystalline, creep 8=22393
- SiC polytypes, infrared absorption 8=23013
- SiC powders, reflection and polarization properties 8=14266
- SiC, pyrolytic, texture 8=21994
- SiC, vapour-deposited films, phys. props. 8=17137
- SiC, vapour-liq.-solid and melt growth 8=21963
- β -SiC whiskers, elastic modulus 8=22392
- SiC whisker and field emission 8=9273
- SiC X-ray emission spectrum obs., valence bonds 8=2454
- SiC, X-ray topographic obs. of polytypes 8=13115
- SiC/Al₂O₃ powders, reflection and polarization properties 8=14266
- SiCl₄, use in epitaxial growth of GaAs 8=13146
- SiDBr₃, microwave spectrum and struct. 8=21105
- SiF₄, radiative lifetimes of u.v. emission systems 8=7501
- Si²⁹Cl₃, radical struct. and hyperfine coupling const., e.p.r. obs. 8=12349
- SiCl₄ reaction with water vapour, SiO₂ film deposition 8=21889
- Si-Fe alloys, elec. resist. at 800-1700°C 8=9017
- Si-Fe, dislocation structure changes during creep 8=8734
- Si-Fe, freq. depend. of mag. reversal mechanism 8=5484
- SiF₄, gaseous, spin-lattice relax. 8=21176
- Si₂, i.r. spectrum and molec. props. 8=16301
- Si-Fe, temp. dependence of magnetic properties, influence of plastic deformation 8=14014
- Si-Fe thin tapes, dynamic hysteresis phenomena 8=5483
- Si-Ge alloy thermoelec. props. and generator modules 8=19732
- SiH₄ decomp. in r.f. glow discharge rel. to films deposition 8=21872
- SiH₄, spectrum 8=12355
- SiHBr₃, microwave spectrum and struct. 8=21105
- SIN films deposited on metal-coated substrates, dielectric properties 8=13870
- SiN films deposition in r.f. glow discharge 8=21872
- Si₃N₄, deposited on GaAs, i.r. absorpt. 8=14262
- Si₃N₄, elimination, Si substrate, etching conditions 8=13128
- Si₃N₄ films, amorphous structure dependence on deposition parameters 8=17179
- Si₃N₄ films, etch rates in H₂PO₄, influence of H₂O content, and use of SiO₂ mask 8=17218
- Si₂N₄ film, thermal expansion coefficient 8=4939
- Si₃N₄ films, fabrication and characts. 8=21891
- Si₃N₄ films on Ge to mask Al and B diffusion 8=13406
- Si₃N₄ films, prod. by reactive sputtering 8=17139
- Si₃N₄, reactively sputtered, evidence of excess Si 8=21890
- Si₃N₄, vapour deposition on GaAs, by SiCl₄-NH₃-N₂ system 8=13094
- SiO₂, adsorpt. of aliphatic aldehydes and ketones, i.r. study 8=8346
- SiO₂, adsorpt. of polyethers at soln.-solid interface 8=1707

Silicon compounds—contd

SiO capacitors, rel. to impurities in vapour source 8=18202
 SiO₂, conduction in films by Pool-Frenkel eqn. 8=13705
 SiO₂, diffusion of Au 8=13896
 SiO₂, effect of dissolved O₂ on C-V characts. 8=5284
 SiO₂, effect on elec. cond. of ferrites 8=13715
 SiO₂, electron Hall effect 8=9124
 SiO₂, elimination, Si substrate, etching conditions 8=13128
 SiO₂, epitaxial systems, vapour deposition 8=13148
 SiO₂, film deposition from SiCl₄-water vapour reaction 8=21889
 SiO₂, film growth in microwave discharge 8=4755
 SiO₂ film on Si, thickness (< 900 Å) meas. with reflection tech. 8=13093
 SiO₂ films, borax diffusion 8=4957
 SiO₂ films, Na contamination, and diffusion and drift of tracer Na 8=18069
 SiO₂ films deposited on n-type Si 8=4757
 SiO₂ films, deposition from silane 8=13095
 SiO₂ films, effects on Si and Si-SiO₂ interfaces in MOS devices 8=18148
 SiO₂ films, etch rates in H₃PO₄, influence of H₂O content, and use as mask for etching Si₃N₄ 8=17218
 SiO₂ films on Ge to mask Al and B diffusion 8=13406
 SiO₂, films, MOS capacitors, noncrystalline structure, electronic conduction 8=9234
 SiO₂, films, proton and Na transport 8=9172
 SiO₂ films, pyrolytically grown, voltage-current charac. 8=13873
 SiO₂ films on Si, electron beam effects and etching rate 8=22609
 SiO₂ isolation strcuts. for integrated circuits, fabrication 8=21964
 SiO₂ layers, dielec. breakdown. 8=18080
 SiO₂ layers in MOS structures, radiation induced space charge buildup 8=9181
 SiO₂ films, thermally grown, electronic conduction mechanism 8=18076
 SiO₂, fine patterns, 2 μ wide, obtained by photo-etching 8=18096
 SiO₂, molec. geometry 8=7550
 SiO₂, in MOS struct., built-in voltage and charge distrib. 8=18141
 SiO₂ sputtered films, r.f. and d.c., re-emission coeffs. 8=2032
 SiO₂, sputtering in Ar, r.f. dielectric system with non-grounded electrodes 8=17138
 SiO₂, surface states, study using Al-SiO₂-Si-Al structure 8=2228
 SiO₂ surfaces, fluoride chemisorption, use of F¹⁹ in HF etches 8=18697
 SiO thin film capacitors, heating effects 8=9233
 SiO, thin-film capacitor props. 8=22676
 SiO₂, vacuum deposited insulating layer, instability 8=9175
 SiO₂, vitreous, acoustic shear wave propag. characts. obs. 8=13358
 SiO₂ vitreous films, i.r. absorpt. 8=5637
 SiO₂, vitreous, rel. to internal friction in vibrating granular reeds 8=13606
 SiO₂, vitreous, structure and correl. by X-ray and n diffraction 8=12795
 SiO₂, vitreous, X-ray and neutron diffracted intensities analysis 8=8467
 SiO films, evaporated, forming process variables 8=4754
 SiO, thin-film capacitors, a.c. electrical breakdown 8=2253
 SiO₂-B₂O₃, metastable immiscibility 8=21748
 SiO₂-C structure, anomalous auto-electron emission 8=22712
 Si-O tetrahedral distances in aluminosilicate framework structures 8=21795
 SiO₂-Si₃N₄ films on Si, optical thickness obs. 8=1699
 SiO-Ta₂O₅ dielectric thin film capacitors, prep. and props. 8=9232
 SiO₂:Tb, Eu, fused, fluoresc. and H diffusion 8=17585
 SiO₂-UO₂ vitroc ceramics, rad. induced volume changes and annealing 8=8779
 SiO₂-UO₂ vitroc ceramics, thermal cond. 8=8664

Silver

analysis, γ-activation method 8=14502
 anomalous-skin-effect theory, in i.r., verification 8=14192
 atom, e-binding energy effect on incoherent γ scatt. 8=17703
 atoms, electron-impact ionization cross-sections 8=12428-9
 atomic impurity in KCl, optical absorpt. rel. to E-band models 8=14228
 catalysis of acetate ion oxidation by K₂S₂O₈ 8=23094
 catalyst, exo-emission, chem. stimulation 8=22711
 cementation on Cu in perchloric acid and alkaline cyanide solns., kinetics 8=14427
 contacts, effect of H₂S contamination on contact resistance 8=22512
 crystal containing alumina, self-diffusion 8=1909
 crystal, thermal oscillations frequency, temp. variation 8=17476

Silver—contd

crystals, orientation stability under plane compression 8=17662
 crystals, well-annealed, stress at which dislocations multiply 8=13545
 deceleration of 0.2-40 keV H and D ions in foil 8=2020
 diffusion in AgCl under pressure 8=1910
 diffusion in Al 8=8671
 diffusion in Al 8=22147
 diffusion in Tl, obs. by radiotracer technique 8=22163
 diffusion of Xe from recoil fission of U 8=3981
 dislocation (Bordoni) relaxation 8=22197
 dislocation density and strength, effect of purity 8=8722
 electrical erosion, obs. 8=22342
 electromigration of small amount in liq. Bi 8=12815
 energy loss of fission fragments, range-energy relation 8=2021
 ethylene catalytic oxidation rel. to surface struct., chemisorpt. obs. 8=18706
 film, 0.6 μ thick, filtered electron diffraction obs. 8=8455
 film, optical constants, ellipsometric meas. 8=11201
 film, reflection and transmission coeffs. in 0.4-1 μ range 8=5580
 film, vapour-deposited, resistivity annealing temp. and thickness dependence 8=17925
 films on mica, W substrate nucleation 8=13087
 films, non-linear reflection on laser-radiation 8=18497
 foils, optical absorpt., structure and surface characts. 8=18502
 grain boundary diffusion in Cu 8=17568
 heat capacity, temp. dependence, effect of crystal lattice defects 8=13368
 hydrogen embrittlement 8=22307
 intense rad. prod. by electrons at grazing angles, interpret. via surface waves 8=3181
 laser induced non-linear photoelectric effect in metals 8=22721
 liquid, diffusion of Ru, Fe and Co 8=12836
 liquid, metal solute diffusion, theory 8=12832
 in liquid Pb, thermodynamic props. 8=8043
 liquid, solubility of H 8=21617
 magnetoresistance coeff. at 4.2°K 8=8997
 magnetoresistance, longitudinal from 4.2 to 35°K, electron scattering effects 8=22511
 mode of distrib. rel. to categories of exogenous Au 8=14562
 nucleation on NaCl 8=8188
 optical polarizability and dielectric constant, calc. 8=18498
 photoelectric effect, non-linear, laser induced 8=2258
 photoexcited electrons, discrete energy loss by plasmon excitation 8=2279
 polycrystalline, diffusion of In impurities 8=8670
 polycrystalline, Sb volume and grain-boundary diffusion 8=17563
 polycrystalline target, sputtering coeff. rel. to incident angle of Ne, Ar and Kr ions 8=8766
 secondary electron emission from self-supporting films 8=2284
 shear strength in grossly deformed sample at high temps. 8=8833
 single crystals, D⁺ transmission 8=22242
 solutions in water, extinction light curves 8=4579
 sulphiding by H₂S, effect of surface Fe 8=23096
 surface reflection of zero-energy electrons 8=6301-2
 target for ion emission, bombard by Ar⁺ 8=6626
 thick films, optical constants, least squares method 8=2403
 thin films, Hall effect 8=2133
 trace analysis, spectrochemical 8=18773
 ultrasonic attenuation rel. to Fermi surface deformation 8=1851
 vacancy diffusion rate calc., Debye model 8=22172
 wires, electric explosion, temp. variation during first stage 8=1622
 Ag¹¹⁰, diffusion in Bi, dependence on crystallographic direction 8=13407
 Ag¹¹⁰, diffusion coeff. in Sn 8=22162
 Ag⁺ doped alkali halide, B-centre 8=17681
 Ag(III) face, exam. by LEED rel. to secondary emission 8=17212
 Ag-Al solid soln., Debye temp. and lattice vibrations 8=1867
 in AgMg, silver-rich, diffusion, re-examination 8=17561
 in β-AgMg, stoichiometric, diffusion of Ag 8=17562
 Ar-ion bombardment, LEED study 8=22240
 in BiTe, electrotransport, 150 and 250 A/cm², < 400°C 8=17564
 CO catalytic oxidation rel. to surface struct., chemisorpt. obs. 8=18706
 H catalytic oxidation rel. to surface struct., chemisorpt. obs. 8=18706
 K-ionization by relativistic electron theory 8=4994
 on Mo, moiré fringes, dynamical effects 8=21977
 O⁶ ion beam energy loss 8=13477
 Pb-Ag system, galvanic cell studies using PbO-SiO₂ melts 8=23150

Silver compounds

alloy, effect of H₂S contamination on contact resistance 8=22512

Silver compounds—contd

- alloys, thermopowers interpret. rel. to resistivity and band structure 8=18213
 halides, e.s.r. studies of different $\text{Se}_{2-}^{\cdot-}$ centres 8=13464
 halides, optical absorb. spectra of $\text{T}_{2g} \rightarrow \text{E}_g$ transitions of Ti^{3+} and Fe^{2+} , Jahn-Teller effect 8=14193
 sternbergite, antiferromag. ordering, and Mössbauer spectra 8=14066
 van-der-Waals dipole-dipole coeffs. 8=1625
 Ag alloys, dilute, stacking-fault energy from extended node meas. 8=17669
 Ag-rich solid solutions, solubility limits 8=8240
 Ag(I) complex, monothiosemicarbazidesilver(I)chloride, crystal and mol. structure 8=22013
 Ag-5.64 wt. %Al alloys, grain boundary precipitation 8=17038
 Ag_2AsS_3 , photoconductivity 8=18220
 Ag-Au alloys, charging and mag. susceptibility, electron states variation, electronic sp. ht. 8=13970
 Ag-Au alloys, tracer diffusion coeff. rel. to activity-coeff. and vacancy flow effect 8=4948
 Ag-Au-Sn liq. alloys, thermodynamic props. of Ag and Au, at 723°K 8=21652
 Ag-Au-Zn system, β' thermal stability 8=17037
 Ag-Bi molten alloys with segregation tendencies, densities 8=12812
 AgBr, charge compensation of trapped holes 8=22688
 AgBr, line edge luminescence at 4.2°K 8=23041
 AgBr plates, ion-sensitive, for mass spectrograph 8=16178
 AgBr(I) photographic films, influence of dyes on luminesc. 8=23042
 AgBr:AgI:CdBr₂, line-edge luminescence at 4.2°K 8=23041
 Ag-Cd alloy, elec. erosion, obs. 8=22342
 AgCdO, sintered and internal oxidized, elec. erosion, obs. 8=22342
 AgCl absorpt. edge, polaron states 8=22955
 AgCl crystals, α -particle track recording 8=15644
 AgCl, electron distrib. from structure factors 8=17334
 AgCl, line edge luminescence at 4.2°K 8=23041
 AgCl, as an embedding medium for i.r. spectroscopy 8=18553
 AgCl, mechanical props., high-pressure data 8=19342
 AgCl, negative resist., electroluminescence and current-voltage characts. 8=17918
 AgCl, state of Fe impurity ions 8=1657
 $\text{Ag}[\text{C}_6\text{H}_5\text{N}_3\text{ClO}_4]$, structure by X-ray diffraction 8=17333
 Ag-Cr film, reflection and transmission coeffs. in 0.4-1 μ range 8=5580
 Ag-Cu alloys, age hardenable, precip. 8=21837
 Ag-Cu, liquid, oxygen solubility 8=16800
 Ag-Cu-Zn alloys, low-temp. martensitic transformation 8=13056
 ζ -Ag-Ga alloys, lattice spacings on addition of Cd 8=17335
 AgI, state of Fe impurity ions 8=1657
 Ag-In alloys, liq., Hall coeff., resistivity and electron states 8=12923
 AgI-Ag₂S, phase distrib. 8=21838
 AgIn mol., u.v. absorpt. bands, system A, vibrational analysis 8=16262
 Ag-In-Ge(Zn) contacts for GaAs semiconducting devices 8=5291
 Ag-M(M=Cd, Mg, In) alloys, one-phase, inhomogeneous concs., from Zener relax. 8=8239
 AgMg, silver-rich, Ag diffusion, re-examination 8=17561
 Ag-Mg solid soln., Ag-rich, short range order effects 8=21819
 Ag-Mg solid solns., Ag-rich, long-range order dependence 8=21820
 β -AgMg, stoichiometric, simultaneous diffusion of Ag and Mg 8=17562
 AgMn, dissoc. energy 8=21183
 AgMnO₄, Raman spectra 8=21085
 Ag-Ni alloys, f.c.c. stacking and twin faults 8=4988
 AgNO₃-alkali nitrates, molten ternary mixtures, thermodynamics 8=21648
 $[\text{Ag}_2\text{O}_9]^{2-} \cdot \text{HF}_2^-$ clathrate, n.m.r. and supercond. 8=17957
 Ag-Pb molten alloys with segregation tendencies, densities 8=12812
 Ag-Sn alloys, liq. atomic distrib. and electronic transport 8=12799
 Ag-Sn liq. alloys, atomic distrib. functions 8=12801
 Ag₂Al, elastic constants meas. 77-700°K 8=5040
 Ag₂O₃, formation for catalysis 8=9706
 Ag₂S_{1+x}, melt, elec. conductivity and thermoelec. power dependence on S vapour pressure 8=16876
 α -Ag₂S, mixed conductor: electronic and ionic conduction props. 8=22500
 Ag₂S, nonstoichiometric, mag. props. meas. 8=9290
 Ag₂Se, nonstoichiometric, mag. props. meas. 8=9290
 Ag₂Se-In₂Se₃, constitution diagrams, structure 8=8266
 Ag₂Te-In₂Te₃, constitution diagrams, structure 8=8266
 Ag₃AsS₃, xanthoconite, crystal structure 8=13248
 AgBr, effect of Cd and Cu ions on photography 8=533
 AgBr grain distrib. in photographic plates for mass-spectrometers 8=7360
 AgBr, microcrystals, effect of solvolysis on growth of faces 8=4786

Silver compounds—contd

- AgBr, migration of photoexcited holes, obs. 8=1908
 AgBr, polaron internal states detection using piezo-optical transmission 8=13679
 AgCl dislocation etching 8=1965
 AgCl, elastic constants, 4.2 to 300°K 8=5041
 AgCl, optically pumped vapour, vibr. energy level population 8=1235
 AgCl single crystals, state of iron, Mössbauer study 8=8215
 AgCl single crystal, surface hardening while in contact with aqueous environment 8=4727
 AgCl, teflon and I, melting temp. under high pressure 8=4644
 AgCl, ultrasonic field effect on conductivity 8=2237
 AgCl, Ag diffusion under pressure 8=1910
 AgCl:Ag²⁺, Ag²⁺ detection by e.s.r. 8=14090
 AgCl + CdCl₂, state of impurity ions 8=1657
 AgI, adsorpt. of methanol vapour 8=8337
 AgI, ionic diffusion under high pressure gradient 8=1907
 AgI smoke used in cloud seeding, hygroscopicity and chemical composition 8=1605
 AgI.KNO₃ nuclei, water vapour adsorption obs. 8=8335
 AgPd alloy, localized states from permittivity obs. 8=13656
 AgTe, liq. Hall coeff. rel. to possible semicond. nature 8=12917
 Ag-Zn alloys, deformed, stacking faults and twin-fault probability 8=17668
 Ag, Zn alloys, ϵ -phase, Zn thermodynamic activity dependence on density of states 8=22109
 α -AgZn, Zener relax. 8=5009
 AgZnSn, liq. alloys, activity coeffs. 8=8016
 GaAgS₂, non-enantiomorphous crystal optical activity obs. 8=14191
Sinanoğlu's theory. See Atoms/structure.
Sintering
 metals, diffusion, surface, vol. and grain boundary 8=21832
 steel, stainless, powder, strain effects 8=4693
 thoria gel, crystallite size distribution 8=12960
 wires, by surface diffusion, theory 8=13051
 Al₂O₃, activation enthalpy 8=13052
 Al₂O₃, kinetics, data correlation 8=8258
 Al₂O₃, kinetics, resonant freq. meas. 8=17027
 As-S-Se system partially vitreous, flow mechanism 8=13053
 BaTiO₃, high purity, meas. of impurity content, crystallinity and particle size 8=17024
 Bi₂Te₃ alloys sintered, orientation 8=21922
 C composite materials sintered, effect of heat treatment on electrical resistivity 8=2129
 C composite sintered materials, elec. resistivity, temp. depend. 8=22502
 CaO, water vapour effect on kinetics, 920-1123°C 8=21833
 CdSe, control of photocond. props. 8=18231
 Dy₂O₃, kinetics, data correlation 8=8258
 Dy₂O₃, kinetics, resonant freq. meas. 8=17027
 Er₂O₃, kinetics, data correlation 8=8258
 Er₂O₃, kinetics, resonant freq. meas. 8=17027
 Fe, mag. props. rel. to porosity and high densities prod. 8=22808
 GaSb-GaAs alloy, pressure-sintered, densification and thermoelectric props. 8=4697
 MgF₂, effect of additives on density and grain size 8=17026
 Mg_{0.9}Mn_{0.1}Fe_{0.9}O₄, effect on mag. spectra 8=2342
 Mn basic carbonate and magnesite containing ZnO, calc. 8=4698
 Ni, effective volume self-diffusion 8=1923
 Ni, mag. props. rel. to porosity and high densities prod. 8=22808
 Ni-Fe relay core prod. 8=22808
 PuO₂ rel. to O adsorption, obs. 8=8345
 UO₂ powders, rel. to particle size and shape 8=21834
 Y₂O₃, inhibition of grain growth by addition of ThO₂ 8=13444
 Y₂O₃, kinetics, data correlation 8=8258
 Y₂O₃, kinetics, resonant freq. meas. 8=17027
Skin effect
 anomalous in layer lattices 8=5115
 anomalous theory, computation of r.f. surface impedance 8=19720
 corrections in immittance standards using air-dielec. coaxial lines 8=10964
 discharge, electrode, analysis using semi-bounded plasma model 8=21219
 electromagnets, effect on pulsed field prod. 8=15260
 a. c. current distribution in cylindrical conductor with elliptical section 8=15194
 Ag, anomalous theory, in i.r., verification 8=14192
 K, anomalous, rel. to surface impedance near cyclotron edge for helicons 8=13686
Sky brightness
 See also Airglow; Twilight.
 Balmer alpha in night sky, May-Nov. 1965 obs. 8=14620
 conditions of sky, Cerro Tololo Observatory, predictions for 1968 8=14621
 electrons, Van allen, by e.m. transverse waves travelling along mag. field 8=18965
 horizon, spectral radiance obs. 8=18874
 India, blue luminance distribution 8=9864

Sky brightness—contd

- northern sky, contour maps, radio emission survey at 178 MHz 8=19225
- observations rel. to atmos. transparency 8=18886
- polarization, obs. and object contrast improvement 8=18875
- scattered radiation at small angles, intensity aerosol spectrum 8=18880
- sky temp., apparent, at mm wavelengths 8=2593
- in solar eclipse July 20, 1963, seven colours, from air-borne photometer obs. 8=2629

Sliderules

No entries

Slip

- coagulation, by Brownian motion, correction 8=8148
- metals, b.c.c., rate controlling mechanism rel. to neutron-irradiation damage 8=4987
- parallel bands, edge type, interaction 8=17732
- plate, thin flat, under uniform stress in one direction 8=13513
- solid solutions, rate controlling mechanism rel. to neutron-irradiation damage 8=4987
- Al single crystals, dynamic deformation 8=22310
- Au, quenched, channel formation on plastic deformation 8=17663
- Be single crystals, directions in deformed specimens 8=1969
- Cu crystal, band development on n-irradiation 8=22212
- Cu, cyclic deform., and crack form. and propag., obs. 8=22330
- Cu, fatigued at low strain amplitude, surface lines and interior planes 8=17774
- β' -CuZn alloys, binary and ternary, cross slip 8=8634
- Fe crystals, [100] and [110] axes, -70°C to 250°C 8=13553
- Fe, fatigue damage from intergranular weakness 8=5060
- α -Fe, 3.28%Ni addition, effect on behaviour 8=22346
- Mg-9 wt.% Al alloy, in age hardening mechanism 8=13583
- Mg-Al spinel, plastically deformed, parallel to {111} plane 8=17664
- Mg,Cd, critical resolved shear stress needed rel. to degree of order 8=5079
- NaCl, plastically deformed, lines, electron microscopic study 8=22213
- Nb-Mo alloy single crystals, rel. to plastic deformation, -196°C -250°C 8=17819
- Si, and bowing, control by etching technique 8=8385
- 3% Si-Fe, upper yield stress rel. to etch pitting experiments 8=5065
- Ti, non-basal vector identification 8=17665
- Ti-Al alloys, non-basal vector identification 8=17665
- U, α and β mono- and poly-crysts., creep mechanisms 8=8867
- US single crystals, transmission electron microscopy obs. 8=17834
- Zn, basal, Al impurity effects 8=17836
- Zn, second-order pyramidal slip on {1213} {1212} system 8=22214
- Zr-H alloys, rel. to H conc. 8=13613
- Zr-O alloy crystals, rate-controlling mechanism at $77-473^\circ\text{K}$ 8=13614

Smectic phase. See Liquid crystals.

Smokes. See Aerosols.

Snoek effect. See Crystal imperfections/interstitials; Elastic relaxation.

Snow

- atmospheric aerosol particles removal by crystals 8=23275
- heat transfer through four layer system of air, snow, sea ice and water 8=23226
- in South Pole region, O isotope ratio rel. to air temp. 8=23227

Sodium

- aerosol produced by burning, characts. rel. to reactor safety 8=12950
- alkali metal impurities (K^{84} and Rb^{86}), diffusion 8=8680
- atmosphere, upper 8=18916-7
- in atmosphere, upper, daytime distrib. and origin, 92.4 km 8=2616
- atmosphere, upper, distribution 8=9903
- atmosphere, upper, meteoric origin 8=9902
- atomic absorption and emission enhancement by alcohol, flame photometric obs. 8=20961
- atom, e scatt., long-range interaction, nonadiabatic contrib. 8=12092
- atoms, excitation by low energy electrons, absolute cross sections 8=12087
- atom, ^2F level, polarization by outer electron 8=7413
- atom and ions of isoelectronic sequence, wavefunctions calc., using effective potential 8=20958
- atoms, gas discharge plasma, line excitation rel. to cascade transitions 8=20962
- atoms, Kerr dispersion, theory 8=12068
- atoms, pseudopotentials 8=7409
- atom, resonance fluorescence quenching in inert gases 8=1185
- atoms scatt. from polyat. gases, quenching of glory undulations 8=7633
- atomic spectra in fluoresc. of NaI 8=12069

Sodium—contd

- clusters of atoms prod. by vapour flow through orifice, ionization pots. 8=16231
- Na D lines in comet 1965f near perihelion passage 8=14852
- D-lines in night airglow using rocket obs. 8=18935
- D-lines in solar spectrum, profile anal. assuming pure absorpt. 8=10383
- D-lines in solar spectrum, profiles rel. to coherent and non-coherent scatt. 8=23708
- diffusion in NaCl-NaBr system, self-diffusion coefficient 8=13402
- diffusion in PbTe, coeff. meas. by radio tracer technique 8=17580
- elastic moduli and pressure derivs. at absolute zero 8=17818
- electron-impact ionization, empirical calculations 8=12448
- electron-self-energy, phonon contrib., numerical calc. rel. to temp. 8=17862
- excited atoms, depolarization cross-section in inert-gas collision 8=7436
- helicon waves, nonlocal damping 8=17904
- ions, charge composition, effect of target state 8=1365
- ions, range distrib. in amorphous Al_2O_3 8=13476
- isoelectronic sequence, dipole polarizabilities and shielding factors 8=7415
- lattice dynamics, quasi-harmonic calcs. 8=1838
- liquid, Alfvén wave resonances 8=19803
- liquid, conducting, with aligned mag. field, drag obs. 8=6349
- liquid, density of states and autocorrel. of independent electrons 8=12898
- liquid, effect on creep and stress-rupture props of austenitic steel 8=22359
- liquid, effective ion-ion potential 8=8237
- liquid, elec. resistivity, appl. of structure factor and pseudo pot. relation 8=12920
- liquid, electronic structure and optical absorpt. 8=8111
- liquid in m.h.d. engine 8=289
- liquid, oxygen solubility data 8=16798
- liquid, solubility of Sn 8=21621
- liquid, structure rel. to pair pot., and effect on phys. props. 8=12790
- liquid vein m. h. d. generator, power transfer to armature 8=15206
- liquid, wavenumber-dependence of elastic moduli 8=1499
- molten, electronic band struct., density of states, and resistivity calc. 8=16789
- photoconductivity calc. from Kubo-Greenwood formula 8=5393
- plasma stabilization by random electric field 8=16599
- positron enhancement factor 8=8975
- scattering from Cs, atomic differential spin-exchange scattering 8=12109
- self-diffusion, isotope effect 8=17576
- self-diffusion in Na silicate liquids 8=8036
- solar D-line rel. to solar atmosphere min. temp. calc. 8=10388
- as steel plastic deform. props. at 1000°C model, obs. 8=13556
- structure at 110° and 525°C 8=4530
- trace impurity determ. by atomic absorpt. spectrometry 8=14459
- Zeeman effect, longitudinal inverse and magneto-optical meas. of line profile 8=4057
- Na, K radioactive ion separation, spacers in electrophoresis 8=5742
- Na I stellar lines near HI clouds, search for 8=5880
- Na^+ e affinity calc. by superposition of configuration 8=21281
- Na^+ , cochlear microphonic pot depend. on 8=19616-7
- Na^+ , dipole polarizability from spectra 8=7414
- Na^{22} , cosmic ray prod., meas. for atm. exchange studies 8=18857
- Na^{22} in KCl solns., self-thermal diffusion 8=21640
- Na^{23} n. m. r. spectrum in NaHg , Na_2Hg_2 and Na_4Hg_2 , Knight shift in solid and liquid state 8=22926
- Na^{23} in NaCl powders, n. m. r. 8=5562
- Na^{23} in some ionic compounds, n. m. r. study of quadrupolar couplings 8=18469
- Na^{23} spin-lattice relax. in aqueous alkali halide solns. 8=1593
- Na^{23} in vanadates, quadrupole coupling constants 8=9474
- in Na methoxide-methanol ions coordination number and solvates comp. obs. 8=2497
- Na-K seeded plasma in elec. field, temp. meas. 8=21308
- Na-Li liq. mixtures, critical opalescence 8=1558
- Na-Na collisions, energy transfer in sensitized fluorescence 8=16213
- $\text{Na}-\text{NH}_3$ dilute solns., absence of vol. change on dilution at -45°C 8=1530
- Pb-Sn, Na conc. at grain boundaries 8=8344
- in SiO_2 films, contamination, and diffusion and drift of tracer Na 8=18069

Sodium compounds

- borax diffusion in SiO_2 films 8=4957
- kernite, crystal structure by X-ray diffraction 8=8542
- natrolite, $(\text{Na}_4(\text{Al}, \text{Fe})_2\text{Si}_3\text{O}_{10}, 2\text{H}_2\text{O})$, e.p.r. of Fe^{3+} , at 4.2 and 293°K 8=18432
- salts, K-doped, n irradiated, $\text{Ar}^{39,41}$ diffusion and trapping 8=1920

Sodium compounds—contd

- sodalites, photochromic, e.s.r. 8=14120
zeolite NaX, adsorpt. of Xe, press. and temp. depend. 8=1713
K-Na alloys, density 0 to 300°C 8=21624
 Li_2CO_3 - Na_2CO_3 , molten, electrochem. studies 8=5741
(Li, K) $_2\text{SO}_4$, differential thermal anal. 8=8270
Na mordenite, synthetic, sorption and diffusion coeffs. of C_1 to C_4 paraffin hydrocarbon gases 8=13109
Na rare-earth tungstates, energy transfer of Er^{3+} , Tb^{3+} and Tm^{3+} 8=9610
Na silicate liquids, self-diffusion of Na 8=8036
Na tetraborate, $\text{Na}_2\text{O} \cdot 4\text{B}_2\text{O}_3$, crystal struct. 8=8541
 Na_3AlF_6 (cryolite), melting point 8=21754
 Na_3AlF_6 , and MgF_2 and CaF_2 , i. r. antireflectant suitability 8=2435
 NaAlGeO_4 , high pressure form. and crystal structure 8=1678
 $\text{NaAlSi}_3\text{O}_8$, enthalpy of fusion 8=21753
 NaAlSiO_4 , isomorph of high pressure NaAlGeO_4 , rel. to formation in earth's mantle 8=1678
 NaBD_4 , d.m.r. studies 8=18460
 $\text{Na}_2\text{B}_4\text{O}_7 \cdot 10\text{H}_2\text{O}$, borax, diffusion in SiO_2 films 8=4957
 $\text{Na}_2\text{B}_4\text{O}_7$, glass, Eu activated, luminescence 8=23061
NaBr, alkali halides, F-band peak, Mollwo relation 8=17688
NaBr single crystal, n. m. r. and quadrupole effects 8=14146
NaBr, water vapour adsorption on cleavage surface 8=17166
NaBr-KBr solid solutions, fundamental absorption 8=18549
 NaBrO_3 cryst., anisotropic chem. shift of Br 8=18457
 NaBrO_3 , γ -irrad., e. s. r. of paramag. centres 8=2372
 NaBrO_3 , nuclear quadrupole res. of Br^{81} 8=10991
NaBr:P radioluminesc. rel. to hole storage at centres, obs. 8=9625
 Na_2CO_3 , reactions during prep. of KCl pressed discs 8=14373
 $\text{Na}_2\text{Ca}_2\text{Si}_2\text{O}_9$, X-ray powder data 8=22030
 NaCaYF_6 , Nd^{3+} activated laser 8=446
 $\text{Na}_2\text{CdSi}_2\text{O}_6$ lattice struct., obs. 8=22031
 $\text{NaCl}(\text{Br})\text{O}_3$, rotatory dispersion in visible and u. v. regions 8=5623
NaCl-KCl system, thermodynamic studies 8=17092
 NaClO_3 cryst. in 1-bromonaphthalene, refl. second-harmonic intensity obs. 8=5611
 NaClO_3 , cryst. growth rate, rel. to supersaturation 8=21940
 NaClO_3 , n. m. r. of Na^{23} , thermally and acoustically induced transition probabilities 8=14152
 NaClO_3 , quadrupole relax. of Na^{23} , ang. depend. of transition probabilities 8=14161
 NaClO_3 , reflection spectrum, cooling effects 8=9555
 NaClO_3 , X-ray irradiated crystals, optical absorption 8=18548
 NaClO_4 aq. soln. with HCl, nucl. mag. relax. times 8=21726
 NaClO_4 solns., ion assoc. 8=21716
 NaCs , $^1\Sigma^+$ and $^2\Sigma^+$ potentials from total cross-section meas. 8=21091
 $\text{NaD}_2(\text{SeO}_3)_2$, ferroelec., growth 8=8420
NaF, alkali halides, F-band peak Mollwo relation 8=17688
NaF, assoc. with AlF_3 in saturated vapour 8=9692
NaF, F-aggregate centres 8=17686
NaF, ionic crystal, elastic constants, calc. 8=2062
NaF, thermoluminesc., thermal activation energies 8=18609
NaF, universal etch 8=1730
 $\text{Na}_2[\text{Fe}(\text{II})(\text{CN})_5 \cdot \text{NO}] \cdot 2\text{H}_2\text{O}$, Mössbauer absorpt. of Fe^{57} 8=1650
 $\text{Na}_2[\text{Fe}(\text{CN})_5 \cdot \text{NO}] \cdot 2\text{H}_2\text{O}$, i. r. spectrum in polarized light between 400-700 cm^{-1} 8=14248
 $\text{Na}_2\text{Fe}_2\text{O}_9$, prep., crystal structure and mag. props. 8=8540
 $\text{Na}_4\text{Ge}_2\text{Si}_2\text{O}_{15}(\text{OH})_2$, crystal structure 8=17402
 NaHCO_3 , H and Na n. m. r. 8=14153
 NaHF_2 , i. r. absorpt. study of lattice vibrations 8=5617
 $\text{NaH}_3(\text{SeO}_3)_2$, ferroelec., growth 8=8420
 $\text{Na}_2\text{HfSiO}_6$, phys. and luminesc. props. 8=9624
 Na_2HPO_4 hydrates, entropy and disorder at low temp. 8=17521
 $\text{NaH}_3(\text{SeO}_3)_2$ and $\text{NaD}_3(\text{SeO}_3)_2$, phase transitions, isotope effects in crystal symm. and nature 8=21849
 $\text{NaH}_3(\text{SeO}_3)_2$, second ferroelec. phase transition 8=2245
 $\text{NaH}_3(\text{SeO}_3)_2$, fundamental absorpt. edge near ferroelectric phase transition pt. 8=9548
NaI, absorption, in i. r., induced by monovalent impurities 8=9544
NaI, alkali halides, F-band peak, Mollwo relation 8=17688
NaI, atomic fluoresc. in photodissoc. 8=12069
NaI capture centres luminesc., heat treatment in O effects, obs. 8=23060
NaI, elastic constants temp. dependence 8=13591
NaI, elastic tensor of gradient elec. field induced by uniaxial stress, n. m. r. obs. 8=13014
NaI, i. r. vibrational absorption by U-centres 8=9557
NaI, isothermal annealing effect on dislocation density 8=17650
NaI, X-ray luminesc., effect of Cu impurity 8=23062
NaI: Tl capture centres luminesc., heat treatment in O effects, obs. 8=23060
NaI(Tl) crystal growth, effect of Cl^- ions 8=14327
NaI(Tl), fluorescent response function 8=5665
NaI(Tl), high-energy muon absorpt. energy loss and straggling 8=8776
NaI(Tl) phosphor, recomb. luminesc. 8=18611

Sodium compounds—contd

- NaI-Tl, photoluminesc. spectra, effect of X-irrad. and O-containing impurities 8=5666
NaI-Tl, single cryst., with oxygen-containing impurities, photoluminesc. and gamma ray response 8=18610
NaI(Tl) 64-channel γ -spectrometer probe, 0.05-9.6 MeV 8=20363
NaK, flowing through unbaffled rod bundles, heat transfer to 8=21649
NaK liq. alloys, ordering and excess entropies and energies 8=12843
NaK liq., structure and correl. by X-ray and n diffraction 8=12795
Na-K-NH₃ solns., liq.-liq. phase separation 8=8014
 $\text{NaMg}[\text{Cr}(\text{C}_2\text{O}_4)_2] \cdot 9\text{H}_2\text{O}$, vibronic spectra 8=14247
 $\text{NaMgF}_3 \cdot \text{Ni}^{2+}$ i. r. luminesc. emission 8=18626
 NaMnCl_2 , prep. and crystallographic props. 8=13138
 $\text{Na}_2\text{Mn}_2\text{Si}_2\text{O}_7$, mag. susceptibility between 1.7 and 300°K 8=9292
 NaN_3 , crystal structures of α and β forms on phase transform. 8=17387
Na-NH₃ solns., liq.-liq. phase separation 8=8013
Na-NH₃ solns., reactions with contaminants on surface of glass 8=21868
 NaNO_2 , dipole interaction and electronic polarizabilities 8=22655
 NaNO_2 , ferroelectric phase, n. q. r. 8=9473
 NaNO_2 , inhibition of steel corrosion by NaCl solns., 20°C 8=2517
 NaNO_2 molten, optical determ. of thermal cond. 8=21658
 NaNO_2 , molten, solvent props. 8=4538
 NaNO_2 , absorpt. spectra from 450-5700 cm^{-1} 8=9556
 NaNO_2 cryst. growth and dislocations, obs. 8=21957
 NaNO_2 , elec. resistivity rel. to other props including transforms and thermodynamic charac. 8=18191
 NaNO_2 , fused, complex permittivity 8=8101
 NaNO_2 molten, refr. index meas. by interferometry 8=4583
 NaNO_2 , permittivity, dielec. loss and d. c. conductivity, temp. depend. 8=2239
 NaNO_2 , X-irrad., electron-hole trapping 8=5105
 NaNiF_3 , i. r. spectra and lattice vib. anal. 8=2428
 $\text{Na}_2\text{O}-\text{B}_2\text{O}_3$ glass system, fraction of four-co-ord. B atoms present 8=21915
 $\text{Na}_2\text{O}-\text{BaO}-\text{SiO}_2$ glass system, internal friction 8=22383
 $\text{Na}_2\text{O} \cdot \text{GeO}_2 \cdot \text{B}_2\text{O}_3$ system, glasses and melts, structure 8=21605
 $\text{Na}_2\text{O}-\text{SiO}_2$ solutions, activities 8=21620
NaOH impurity in ice, dielec. dispersion obs. 8=18188
NaOH soln. with additives, rel. to stress-corrosion cracking of mild steel 8=22366
 NaPO_3 , colour centres and thermoluminesc. due to γ -irrad. 8=22234
 $\text{Na}_3\text{P}_2\text{O}_7 \cdot 10\text{H}_2\text{O}$, improved dimensions 8=17400
 $\text{Na}_2\text{S}_2\text{O}_8 \cdot 2\text{D}_2\text{O}$ cryst. dynamics of D_2O 8=8539
 $\text{Na}_2\text{S}_2\text{O}_8 \cdot 2\text{H}_2\text{O}$ cryst. dynamics of H_2O 8=8537
 $\text{Na}_2\text{S}_2\text{O}_8 \cdot 2\text{H}_2\text{O}$ crystal structure rel. to H_2O dynamics 8=8538
 NaSbF_6 , e. s. r. of X-irrad. cryst. 8=5538
 Na_2SiO_3 , improved dimensions 8=17400
 α - $\text{Na}_2\text{Si}_2\text{O}_6$ crystal structure 8=13278
 $\text{Na}_2\text{Si}_3\text{O}_8$, crystal structure 8=1801
 $\text{NaTi}_2\text{Al}_3\text{O}_{12}$, crystal structure 8=1800
 $\text{Na}_2\text{Ti}_2\text{O}_{15}$, crystal structure 8=22029
 Na_2Ti , crystal structure rel. to Ti-Ti bonding 8=17399
 Na_2Ti , structure and bonding model 8=8536
 $\text{Na}_{0.33}\text{V}_2\text{O}_6$, elec. props. 8=22601
 $\text{Na}_2\text{ZnSiO}_4$, crystal structure 8=17401
 Na_2ZrCl_6 , thermal props. 8=8640
 $\text{Na}_7\text{Zr}_6\text{F}_{31}$, crystal structure 8=13276
 $\text{Na}_w\text{Zr}_x\text{Si}_y\text{O}_z$ ($w = 2, 4; x = 1, 2; y = 1, 2, 3; z = 5, 7, 12$), phys. and luminesc. props. 8=9624
- sodium chloride**
aqueous solution, phenomenological coeffs. for elect. cond. and diffusion 8=12924
cathodoluminescence, e microprobe obs. 8=14317
cellophane membrane uptake rel. to ion exchange props., obs. 8=23084
condensational growth of soln. drops on nuclei 8=9853
conductivity, elec., var. with particle size and temp., obs. 8=17913
crystal etching by formic acid 8=17658
crystals under tension, theoretical strength 8=13590
damage and spectral emission during illum. by ruby laser light 8=14246
diffusion of Cd^{2+} in single cryst. 8=4956
dislocation density and plastic flow stress obs. in crystal 8=8731
dislocation mobility, photoexcitation 8=4979
dislocation structure on light impulse exposure 8=17569
dislocation structure on {100} faces in quenched crystals. 8=22207
elastic constants, higher order, theoretical calcs. 8=17811
electrolyte solns., self-thermal diffusion 8=21640
electron centres form. by $\text{Co}^{60}\gamma$ -irrad. 8=22235
e emission, photostimulated, by F-centres, mechanisms, obs. 8=9278
electronic struct. and molec. props. 8=21092
etch-pit morphology changes on cleavage faces due to water 8=1731

Sodium compounds—contd**sodium chloride—contd**

- exo-electron emission, photostimulated, from F-centre crystals 8=5409
- F-band absorption, u. s. strain modulation 8=22232
- F-band peak, Mollwo relation 8=17688
- F-centre first-stage colouring, X-ray induced 8=2012
- F-centre half-width and effective lattice freq. calcs. 8=4993
- F centres, thermal stability 8=8750
- fracture strength, particle size effect 8=22382
- growth of Au films, high vacuum, model 8=21879
- heat capacity, 0–25°C 8=6221
- hole motion in a mag. field, theory 8=22436
- luminescence, X-ray, depend. on radiation time 8=18612
- mechanical props., high-pressure data 8=19342
- metal film epitaxial growth on NaCl substrates 8=13147
- monocrystals, slow electron diffraction patterns 8=8527
- nucleation density of Au on cleavage surface 8=4742
- nuclear quadrupole interactions, sensitive detection 8=18478
- (100) face, epitaxial growth of Pt 8=4752
- (100) surface study by LEED 8=17116
- phase transformation, pressure-induced 8=17093
- plastically deformed, acoustic n.m.r. 8=5561
- plastically deformed, slip lines, electron microscopic study 8=22213
- polarization under shock load, obs. 8=5353
- powder, energy absorption during compression 8=13592
- powder, Na²³ n.m.r. 8=5562
- propanol-H₂O mixtures, with NaCl in soln. 8=4606
- pure and doped crystals, pot. differences due to plastic deform., temp. dependence 8=16978
- Raman spectrum, polarized light study 8=18547
- resonant phonon scattering 8=8661
- rock salt, luminescence, in ultra-strong electric fields 8=23059
- solid soln. with KCl, decomp. mechanism by X-ray scattering studies 8=13070
- solution, aqueous, Cu anodic behaviour 8=2532
- solutions at 25°C, density using temp. sensitive magnetic float densimeter 8=4544
- steel corrosion by solns., NaNO₂ inhibition, 20°C 8=2517
- structure factors and Debye-Waller factors at 300, 202 and 70°K 8=8535
- surface potential meas. by Cl⁻ emission on electron bombardment 8=5425
- thermal diffusion of strontium ions, Soret effect obs. 8=1921
- thermoelectric power of single crystals 8=2256
- thermoluminescence, thermal activation energies 8=18609
- third-order elastic constant, obs. 8=13579
- 2% aqueous solns., ice cryst. growth by butane evaporation subcooling 8=13137
- valence band, three-centre corrections 8=2104
- water vapour adsorption on cleavage surface 8=17166
- X-ray reflection intensities, thermal diffuse scattering contribs. 8=13277
- X-ray structure amplitudes, statistical exam. 8=4885
- Ag-doped, electrophotoluminescence 8=2486
- Ag and Pb activated, Cl₂⁻ centres conc. temp. depend., e.p.r. obs. 8=8742
- Au films growth, high vacuum 8=21878
- Ca-doped dielectric properties 8=22656
- Cd doped, aggregation of divalent impurities 8=13425
- Cl₂⁻ centres conc. temp. depend., e.p.r. obs. 8=8742
- Cu ions in crystal, optical absorption 8=18521
- in Mg fused electrolyte, elec. cond. and density obs. 8=23143
- Mn-doped, particle hardening 8=22381
- NaCl(Ag), colouration, impurity centres produced 8=1994
- NaCl:Ag colour centres e.p.r. absorpt. rel. to relax. process 8=8743
- NaCl:Ag F-centres thermal stability rel. to dislocations, microspectrophotometry obs. 8=8749
- NaCl:Ag⁺, nuclear magnetic double reson. investigation 8=18468
- NaCl:Ag phosphors, photo-excited F-colour centres, microdefect interactions 8=2013
- NaCl:Ag, Sr phosphors, F centre thermal ionization mechanism 8=17687
- NaCl:Be⁺, substituent behaviour from ionic thermocurrent spectra 8=8702
- NaCl:CaCl₂ + NaOH crystal, dielectric loss maxima and conductivity 8=5164
- NaCl, Co, dielectric props., 90–200°C, 30 c/s–100 kc/s 8=13869
- NaCl:Eu luminesc., excit. and absorpt. spectra rel. to luminesc. centres, obs. 8=9623
- NaCl-KCl phase equilibrium diagram 8=8164
- NaCl-NaBr system, Na isotope diffusion, self-diffusion coefficient 8=13402
- NaCl:Mn, ratio of concentrations of nnn to nn complexes at low temp. 8=13420
- NaCl:Mn²⁺ e.p.r. spectrum, resolution obtained by X-radiation 8=14117
- NaCl:OH, i.r. absorpt. spectra rel. to temp. dependence of intensity of OH vibrations 8=18538
- NaCl-Sr(Ba)Cl₂, ionic conductivity, rel. to assoc. enthalpies of Sr and Ba 8=5165

Sodium compounds—contd**sodium chloride—contd**

- NaCl(ZnCl₂)-H₂O, crystn. interphase equilib. 8=21933
- Ni activator solubility, OH⁻ ions effects, obs. 8=21824
- Ni, Cu, In, Pb and Tl activated, roentgenoluminesc. and F-flash temp. depend. obs. 8=9626
- with Sr, Cd, Ag, Ca and Tl impurities, F-centres stability rel. to cryst. defects 8=8751
- Sofar. See Sound ranging.
- Sogicons. See Semiconducting devices.
- Soil
- density meas. by γ -ray back-scatter 8=23231
- moisture, effect on γ -field, in near-surface atm. 8=9795
- plasticity, rupture conditions 8=8798
- shock waves, rigid unloading, high press. approx. 8=3038
- slope stability under instantaneous failure conditions rel. to anisotropic cohesion 8=22284
- Solar activity.** See Sun; Sunspots.
- Solar batteries.** See Electricity/direct conversion.
- Solar cells.** See Electricity/direct conversion; Semiconducting devices.
- Solar constant.** See Sunlight.
- Solar corona.** See Sun/corona.
- Solar corpuscular streams.** See Sun/radiation, corpuscular.
- Solar eclipses.** See Sun/eclipses.
- Solar flares.** See Sun/flares.
- Solar furnaces.** See Heating; High temperature production and effects.
- Solar noise.** See Sun/radiation, radiofrequency.
- Solar prominences.** See Sun/prominences.
- Solar system**
- See also Planets, etc.
- cosmogony, and origin of deuterium 8=19236
- early history, meteorite data 8=23493
- environment, planetary and interplanetary, review 8=23633
- existence of Pu²⁴⁴ in early history 8=3978
- exploration, by unmanned vehicles 8=2807
- global radiation emerging from a Rayleigh-scattering atmosphere 8=14831
- inertial frame of ref. 8=14739
- meteoroid environments, correl. rel. to 'mass conc.' and 'perforation capability' 8=19269
- nongravitational forces and resonances, and origin of Kirkwood gaps 8=10322
- planetary and interplanetary environments 8=10324
- planetary bodies ang. momentum density-mass diagram, inclusion of asteroids 8=23656
- planet-satellite systems, ang. momentum densities 8=23655
- retrograde satellites and possible past planets, loss due to tidal forces 8=23653
- Sun-Earth-Moon-artificial satellite system, equations of motion 8=2808
- Fe fractionation 8=10323
- Fe, magnetostatic accretion, particle size range 8=23632
- Li, Be, B spallation formation from CNOE 8=3922
- Pu²⁴⁴ and P²³⁹ early abundances 8=23468
- Solar wind.** See Sun/radiation, corpuscular.
- Solid solutions**
- See also Alloys; and under Compounds of the individual elements. Solid solutions such as Au-Cu., Au-Cu-Zn are indexed under compounds of the first named element, i.e. "Gold compounds" in these examples.
- alloys, field ion emission patterns, computer simulation 8=8453
- benzene-Ar, luminesc. excit. obs. 8=13036
- benzene in hydrocarbon matrices, state of dispersion 8=9651
- benzene-N, luminesc. excit. obs. 8=13036
- benzene state of dispersion in solvents and matrix effects on spectra, 77°K 8=13037
- benzyl radicals fluoresc. spectra in solid solns., obs. 8=13032
- β -brass-type superstructure, stoichiometric cpd segregation on antiphase boundaries 8=16997
- binary, metallic, Debye temp. and thermal lattice vibs., rel. to local order 8=1867
- binary systems, diffusion coeff. conc. and temp. dependence 8=17554
- concentration parameters rel. to cation distrib. in multisublattice 8=4775
- crystalline, diffusion theory and time evolution X-ray and thermal neutron scattering 8=8667
- 4-dimethylamino-4'-nitrodiphenyl in decalin, luminescence 8=5684
- dislocation structure and grain size effect on validity of Cottrell-Stokes law 8=8721
- garnets, rel. to cation distrib. in multisublattice 8=4775
- hexaferrites, Al-Fe substitution by i.r. spectroscopy 8=16999
- interstitial, field-ion microscopy, computer simulation 8=21817
- irradiation damage effect on rate controlling mechanism of slip 8=4987
- luminescent, excitation transfer by multimolecular resonance 8=18590
- metallic, cohesive and volume props., quantum-statistical ab initio calc. 8=4665

Solid solutions—contd

- metals, impurity nuclei isomeric shifts of γ radiation 8=1653
 Mössbauer effect intensity calc. in case of alocal vibrations 8=8209
 olivine-spinel equilibria in Mg_2SiO_4 - Fe_2SiO_4 system, 43 to 96 kb at 800, 1000 and 1200 °C 8=23218
 organic mols. and radicals spectra in solid solns. 8=13032
 polyacene, energy transfer, 1965-66 bibliography 8=14162
 poly(vinylidene fluoride)-poly(vinyl fluoride) melting point rel. to comp. 8=8173
 resistivity dependence on short range order 8=17915
 spinels, rel. to cation distrib. in multisublattice 8=4775
 spins, nuclear or ionic, indirect interaction derivation from ground state energies 8=17897
 β spodumene-silica in Li_2O - Al_2O_3 - TiO_2 - SiO_2 glass ceramic 8=1661
 supercooling, constitutional, in presence of convection cells 8=8417
 tetraphenylporphin and Ag tetraphenylporphin 8=1658
 thermal eqn. of state 8=8634
 thermodynamic and elastic props. from exam. of diffuse background scattering of X-rays 8=13359
 tin-molten BiCl_3 , study of reaction 8=17000
 transition metals, mag. susceptibility 8=9283
 vinylidene fluoride-vinyl fluoride copolymers melting point rel. to comp. 8=8173
 Ag-base, impurity atoms in grain-boundary transition zones 8=17277
 Ag-rich, solubility limits 8=8240
 Ag-Cu-Sn system, electronic phases rel. to chemical displacements 8=17002
 Ag-M(M=Cd, Mg, In) alloys, one-phase, inhomogeneous concs., from Zener relax. 8=8239
 Ag-Mg solid solns., Ag-rich long range order effects 8=21820
 Ag-Mg, Ag-rich, short-range order effects 8=21819
 Al in Cr, antiferromagnetism obs. 8=14063
 α - Al_2O_3 - Cr_2O_3 , crystalline parameters 8=8241
 As in Ge, super saturated, decomposition mechanism 8=17005
 $\text{Ba}(\text{BrO}_3)_2$ - BaBr_2 , during thermal decomposition of $\text{Ba}(\text{BrO}_3)_2$ 8=21816
 BiFeO_3 with $\text{Pb}(\text{Ti}, \text{Zr})\text{O}_3$, dielectric props. at high temp. and freq. 8=13885
 Bi_2Te_3 - In_2Te_3 , thermal and microscope analysis 8=21828
 Bi_2Te_3 - PbTe alloys, thermoelect. props. 8=22680
 Ca_2SiO_5 , polymorphism 8=13064
 Cd_3P_2 - Cd_3As_2 system, semiconducting props. 8=22582
 $\text{Cd}(\text{S};\text{Se})$ photocond. spectral distrib. and band gap, 100 and 300°K 7=2261
 Co-Ni-Al-Cu-Ti-Fe alloys, structure 8=17010
 Co-Pt, interdiffusion coeff. conc. dependence from X-ray analysis 8=17570
 Cr_2O_3 - Al_2O_3 , mag. susceptibility 8=13972
 $\text{CsF}:\text{Na}^+$, impurity displacement calcs. 8=8243
 Cu_3Au , thermodynamic characts. determ. from short-range order parameters 8=16996
 Cu-Si dislocation motion, nature of obstacles 8=22200
 Cu-Zn alloy, latent energy of deformation 8=13551
 CuO - FeO - SiO_2 in contact with metallic iron, activity-composition relns. 8=17009
 Fe-base alloys, rel. to strengthening 8=22341
 α -Fe, mechanical props. 8=22350
 Fe-Mo alloys, Fe-rich, and precip. reactions from Mössbauer spectra and Young's modulus 8=4678
 Fe-N_2 , N_2 desorption kinetics 8=1704
 Fe-Ni, interdiffusion coeff. conc. dependence from X-ray analysis 8=17570
 Fe_2O_3 - Al_2O_3 , mag. susceptibility 8=13972
 In-Ti f.c.t. alloy, atomic relaxations 8=22375
 K and NaCl, decomp. mechanism from X-ray scattering studies 8=13070
 $\text{KCl}(\text{Br}):\text{Li}^+$, impurity displacement calcs. 8=8243
 KCl-KBr , optical absorpt. 8=2431
 KCl-KBr system, elec. props. 8=22504
 KI-NaI , ($-\text{RbI}$), ($-\text{KCl}$) solid solns., absorpt. edge temp. dependence, 80-100°K 8=22994
 LiMSiO_4 and related sulphates, (M = Al with Ga and Ge substitution) 8=17013
 Mg in Cu, mode of precipitation of Cu_2Mg 8=4705
 (Mn, Me)(S, Se)-type synthetic cpds. and selenide-sulphide inclusions 8=4692
 MnSe-MnS phase relations 8=17014
 Mo-Fe, mag. props. 8=22749
 MoO_3 in TiO_2 , magnetic susceptibility 8=13963
 NaBr-KBr , fundamental absorption 8=18549
 $\text{Nb}_3(\text{Al}, \text{Ge}, \text{Sn})$, superconducting transition dependence on atomic ordering 8=17967
 Nb-Hf , ($-\text{W}$), ($-\text{Mo}$) alloys, interstitial solubilities of O, N, C 8=17015
 Nb-O , in CO equilibrium pressure 8=21825
 Ni-Co , interdiffusion coeff. conc. dependence from X-ray analysis 8=17570
 Ni-Cr , inter diffusion, conc. and temp. dependence 8=17578
 Ni-Cu , thermoelectric power and resist. rel. to temp. and Cu% 8=5389

Solid solutions—contd

- Ni_3Fe alloys with Cr, Mo or W effects of atomic ordering 8=4690
 Ni-Pt, interdiffusion coeff. conc. dependence from X-ray analysis 8=17570
 O in Nb, precipitation from supersaturated solutions
 electron microscope examination 8=1679
 PbTe-PbS i.r. transmission spectra rel. to forbidden band optical width 8=18554
 PbTe-PbS , n-type, elec. props. temp. and pressure dependence 8=18061
 $\text{Pb}(\text{Zr-Ti})\text{O}_3$ ceramics, addition of Cr_2O_3 8=13043
 Sb_2Se_3 - In_2Se_3 , thermal and microscope analysis 8=21828
 Sb_2Te_3 - In_2Te_3 , thermal and microscope analysis 8=21828
 Si in V, solubility to 1200 °C 8=9061
 SrTiO_3 -1,15 Sr ($\text{TaFe}_{1/2}\text{O}_3$), study using Mössbauer effect of Fe^{57} 8=16984
 Ta-O-C , CO solubility and equilib. press., 1700-2000°K 8=21787
 Tb-Y alloys, crystal struct., 77-300°K 8=22040
 Ti, V, Cr and Mn, in Cu, mag. moments 8=22760
 $\langle \text{U}, \text{H} \rangle$ comp. and thermodynamic props. ≤ 150 atm and 860°K 8=8190
 UO_2 - PuO_2 , heats of fusion obs. 8=8284
 UO_{2+x} - LaO_{2+x} at 1100° to 1400 °C, equilib. oxygen pressures 8=13044
 UO_{2+x} - YO_{2+x} urania-yttria at 1100° to 1400°K equilibrium oxygen pressures 8=13044
 α -Zr-D, thermodynamic props. 8=8252
 α -Zr-H, equilib. press. of H 8=8251
 ZrO_2 -MgO system, phase relations 8=13076
 ZrO_2 - TiO_2 system, phase X-ray obs. 8=17108
- Solidification.** See Freezing.
- Solids**
- See also Crystals; Films/solid; Metals; Plastics; Powders; Semiconductors; Vitreous state.
 electron spectroscopic method for study 8=16180
 gravity flow in converging conical channel 8=13514
 high pressure as tool for solid-state research 8=10463
 nonlinear props. 8=4684
 nuclei polarization by optical pumping 8=13016
 physical props., apparatus for study under high pressure 8=2873
 positron annihilation 8=17906
 second sound dispersion and damping 8=4910
 simple, changes of state 8=17032
 ultra-slow motion, magnetic relaxation nuclear 8=5548
- structure**
- See also Crystal structures; Electron diffraction examination of materials; Electron microscope examination of materials; Granular structure; Neutron diffraction examination of materials; X-ray examination of materials.
 alkali metals, ionic crystals, cohesion with noble gas atoms 8=8193
 Alnico, effect of heat treatment below 1000°K 8=9361
 borate glasses, fraction of four-co-ordinated B atoms present 8=21915
 brass, surface contour meas. using laser probe 8=19339
 carbides, stoichiometry and bonding rel. to carbon κ and metal emission bands 8=2406
 carbon black, study of domain structure 8=8352
 clay, surface contour meas. using laser probe 8=19339
 coherent cube-shaped particle, strain field 8=21797
 conference, Moscow, July 1966 8=8362
 glass, BSC, annealing, relax. effects 8=4770
 ingots, comp. dependence 8=16927
 ion removal from square lattices 8=21791
 metal alloys, from solubility method 8=17001
 plaster, surface contour meas. using laser probe 8=19339
 propionate groups, retarded motion and phase transitions 8=8229
 rubber, chloroprene, supermolec. structures, morphology 8=13112
 silica gel, modification of struct. on purification 8=1663
 6-12 gas-atom-solid atom pairwise model rel. to gas-solid interaction 8=8332
 steels, equilibrium partition between ferrite and cementite, temperature dependence 8=17279
 Al, effective ion-ion potential 8=8237
 Al-base alloys, unidirectionally solidified eutectic, structure 8=4685
 Al- Al_3Ca alloy, unidirectionally solidified eutectic, structure 8=4685
 Al- Al_3Ce alloy, unidirectionally solidified eutectic, structure 8=4685
 Al- Al_3Y alloy, unidirectionally solidified eutectic, structure 8=4685
 α - Al_2O_3 , containing oxygen ion, electronic quadrupole polarizability 8=8232
 Au-Cu-Zn ternary alloys, phase relation and kinetics of transformations 8=13063
 B_2O_3 planar cpds., B-O bond lengths, mol.-orbital treatment 8=16268
 Ca sulphaluminate hydrates, expansion characts. 8=21831
 Cr-Fe-C-N alloys, 18%Cr, constitutional diagrams 8=21822
 Dy^{161} in Dy^{3+} salts, hyperfine structure at 4.2°K 8=1646

- Solids—contd**
structure—contd
 Fe-Al, nature of K state 8=9005
 Fe-N alloys, quenched, and tempering process 8=8840
 K, effective ion-ion potential 8=8237
 KD_2PO_4 , deuteron intrabond jumping and dynamical effects 8=9212
 Mg, effective ion-ion potential 8=8237
 Mg-Zn alloy, dendrite arm spacing and grain size, influence of coarsening 8=4849
 Na, effective ion-ion potential 8=8237
 Nb-Zr alloy, electron microscope investigation 8=8245
 $Ni_{1.3}Fe_{2.3}$ coprecipitate, and mag. props. 8=23078
 Sm_2O_3 , verification of existence by nondestructive analysis 8=9738
- theory**
 AB binary alloys, triplet probabilities rel. to pair correlations 8=9313
 adiabatic potential of complex system, calc. using perturbation theory 8=13626
 alkali halide crystals, box model 8=1627
 alloys, electron cell model 8=21815
 amorphous, exciton theory 8=13669
 atoms, magnetic, in non-mag. host metal, ground state spin 8=16991
 band effective masses for nineteen elements 8=13651
 band structure principles and pseudopot. 8=8912
 crystal construction, possible use of quantum mechanics 8=21790
 cyclotron echo signal 8=5149
 electronic conductors, magnetic effects, theory 8=13635
 electronic correlation 8=2093
 electro-optical effects and e transitions rel. to cryst. anisotropy 8=9495
 finite translations in solid-state physics 8=13648
 Gaussian effective-electron model, three- and four-atom exchange interactions, perturbation theory 8=21793
 hard-sphere solid, pair distrib. functions 8=6091
 interatomic forces, moderately long-range and meas. 8=16993
 intermolecular interactions, thermodynamics 8=3002
 inverse overlap matrix, cluster expansion 8=5096
 ion transport, under conditions including large elec. fields 8=21813
 ion $3d^5$ configs. splitting by octahedral intracryst. field 8=1654
 ionic crystals, polarization theories 8=9186
 ionic, polarization capacitance, comments 8=22509
 metal to insulator transitions 8=22451
 methane, slow neutron scatt., rotational hindrance effect 8=13038
 micro, geometric and kinematic properties 8=6105
 nonadiabatic transitions 8=13039
 non-conductors band struct. calc. from spectra 8=8915
 nuclear and electron spin polarization by hot electrons 8=1638
 partition function for cryst. 8=17507
 rare-earth chelates, exchange-reson. energy transfer overlap integrals calc. 8=1656
 rigid disks at high density 8=15003
 semiconductors band structure, Green's function method 8=8913
 statistical model, appl. to metals and solid solns. 8=4665
 surface elastic waves, excitation by transient surface heating, piezoelectric and nonpiezoelectric 8=17720
 II-VI compounds, band structure obs. and calcs., review 8=8911
 vibration of loaded elastic continuum 8=23
 X-ray spectra rel. to atomic energy levels and excitons 8=9492
 Ar, shock compression, Thomas-Fermi-Dirac theory 8=16994
 KCl crystals, electric dipole-lattice relaxation times for OH^- dipoles 8=8202
- Solions.** See Acoustic transducers.
- Sols**
 See also Colloids; Sedimentation.
 birefringence due to electric or magnetic fields 8=12878
 ferromagnetic, mag. field prod. rotation 8=16622
 thoria, particle size meas. by scatt. 8=12958
 Au, colloidal radioactive conc. determ. from spectrophotometric data 8=16910
 $ZnS: CdS$, Cu phosphor-silicic acid, adhesion to glass, obs. 8=8157
- Solubility**
 See also Phase equilibrium.
 cristobalite, solution and trapping of He and Ne 8=8247
 cryolite melts, of Al, comp. and temp. dependence 8=21618
 cyclohexane, gases in solution, rel. to entropy 8=4536
 cyclopropane in polyethylene 8=17188
 diffusion in sphere, and diffusivity with error anal., calcs. 8=16813
 gas bubbles dissolving in liquid 8=12763
 iron alloys saturated with oxides, liquid, of oxide rel. to first-order interactions 8=16797
 method for determining structural charact. of metal alloys 8=17001
 oxygen, compressed, of anthracene, benzene and naphthalene rel. to complex stabilization 8=2499
- Solubility—contd**
 phenol-aqueous sodium salicylate- α -methyl naphthalene, solubility and equilb. data 8=4641
 polyvinyltoluene + phosphors, solid solns, solubility of CO_2 8=20386
 steel, dissolution of Nb carbon-nitrides and their precip. and age hardening effect 8=1660
 tridymite, solution and trapping of He and Ne 8=8247
 Ag, liq. of H 8=21617
 Ag-rich, solid solutions, limits 8=8240
 AgCl in water rel. to liquid structure 8=21608
 Al_2O_3 , of MgO ; TiO_2 and $MgTiO_3$, in H_2 atmos., temp. dependence 8=21818
 Ar, in H_2O -methanol system 8=12809
 B, in graphite, 1800-2500°C 8=17006
 CO_2 : molten salts, influence on current efficiency in Al electrolysis 8=12805
 $CaCO_3$ aragonitic oolites in sea water, pressure coeff. obs. 8=8012
 Cd in $CdCl_2$, radiometric method 8=21615
 Cr_2O_3 , in $Pb(Zr-Ti)O_3$, limit 8=13043
 Cu in InAs 8=17011
 Cu-Co liq. alloys, solubility and activity coeff. of O 8=8011
 Fe alloys, of S at 1000°C, Cr, Cu, Ni, V effect 8=17012
 γ -Fe, of Nb from C content analysis at temps. 950-1050°C 8=4535
 Fe in TiO_2 , X-ray examination 8=13042
 in Fe-50%Ni of metallic impurities rel. to mag. props., obs. 8=22825
 in Fe-Ni system, α and γ solid solubilities rel. to phase diagram, e microprobe obs. 8=17034
 GaSb, of Li, and diffusion 8=13409
 H in U and $\langle U, H \rangle$ solid soln. comp., ≤ 150 atm and 860°C 8=8190
 H_2 in α -Zr, Zircaloy-2 and Zircaloy-4, terminal solubility and partitioning 8=8249
 H_2 , in Zircaloy-2 and Zr-2.5wt.%Nb, thermal diffusion obs. 8=8250
 He³ in He⁴, and 0°K limiting solubility, 1.25-0.025°K 8=6230
 In in Fe 8=8160
 KBr-KI solid solns., large gap at room temp. from free energy of formation data 8=16998
 KCl of Pb activator, OH^- ions effects, obs. 8=21824
 KCl of Tl activator, OH^- ions effects, obs. 8=21824
 KX, (X = Cl, Br, I), of H_2O mols, mechanism 8=4953
 $LiNO_3$ molten, water solubility at 230-280° up to 30 torr 8=12806
 $LiNO_3 + NaNO_3$ (or $+ KNO_3$) molten, water solubility at 230-280°, up to 30 torr 8=12806
 M hydrides, M = Pd, V, Nb and Ta, of H_2 solubility isotherm in hydride phase 8=1924
 Mo, of C, limit, and diffusivity 8=17007
 NaCl of Ni activator, OH^- ions effects, obs. 8=21824
 $NaNO_3$, molten, solvent props. 8=4538
 NbC in 20%Cr-25%Ni stainless steel 8=4689
 Nb-Hf, (-W), (-Mo) alloys, interstitial solid solubilities of O, N, C 8=17015
 Nb-Mo-C alloys, solid, phase diagram, constitution 8=8275
 Ni-Cu alloys, solid, of H 8=21826
 O atoms, in b.c.c. Fe, rel. to temp. 8=22150
 O in liquid Ag-Cu alloys 8=16800
 O in Na, data analysis 8=16798
 PbTe-Fe pseudobinary section of Fe in PbTe and PbTe in Fe 8=17097
 Pu in Fe 8=13041
 Sn in liquid Na 8=21621
 in Ta-O-C solid solns. of CO , 1700-2000°C 8=21787
 U cpds, solid-solubility relationships 8=8248
 V, of H, rel. to ductility drop 8=5088
- Solution energy.** See Heat of solution.
- Solutions**
 See also Heat of solution; Liquids; Solid solutions.
 absorption on solids from non-ideal solns. 8=8331
 activity coeffs. calc. from Brillouin scatt. 8=4576
 activity coeffs., meas. by gas chromatography 8=5760
 alkali halides in aq. soln., influence on struct. of water 8=4527
 alkali metal- NH_3 , phase separation model 8=12808
 alkali nitrates- $AgNO_3$, molten ternary systems, thermodynamics 8=21648
 n-alkanes, binary mixtures, thermodynamic props. 8=16791
 n-alkane mixtures, congruence principle appl. to viscosity 8=8024
 anions, change in chem. potential on transfer from protic to dipolar aprotic solvents 8=14418
 aqueous, dissociation computation from ultrasonic relaxation study 8=18712
 aqueous electrolytic, sound velocity at 1160 Hz rel. to molar conc. 8=16828
 aqueous, frozen, electron hole pairs 8=8950
 aqueous, of macromolecules, freezing 8=21761
 aqueous, non-polar gases, freezing 8=1618
 aqueous, of strong electrolytes, far i. r. absorpt. spectra 8=21679
 bimolecular rate constants for reaction of e, H and OH 8=2510
 binary mixtures elec. cond. rel. to dielec. const. 8=4609

Solutions—contd

bromides, aq. solns., partition coeffs. by thermal diffusion 8=4559
 n-butanol complexes in amine solns., dipole moments 8=12909
 butyl alcohol-water mixtures, hypersonic meas. 8=4572
 competitive solvation of H^+ in water-methanol vapour 8=14443
 concentration meas. using reactance meter 8=5733
 copolymers, effect of interaction between unlike segments 8=4541
 copolymer, molec. dims. 8=12811
 critical mixture, conc. fluctuations, direct visual obs. 8=21616
 d.c. transport coeffs., effect of non-Brownian motion 8=21718
 dielectric properties, criticism of Debye and Onsager theories 8=8102
 di-tertiary-butyl nitroxide solns., spin exchange 8=8121
 dye, laser, wavelength dependent time development of intensity 8=20005
 EDTA chelates of Cd^{2+} and Hg^{2+} , comp. study by ultrasonic vel. meas. 8=23170
 electrolytes in alcohols, dielec. relax. 8=8100
 electrolytes, intermediate conc., statistical theory 8=14417
 electrolytes, n-component, isothermal vector transport 8=8046
 electrolyte, self-thermal diffusion 8=21640
 electrolytes, Zwanzig theory of dielec. friction 8=8099
 electrolytic, two-structure model 8=23142
 eosin, fluorescence spectrum, effect of conc. 8=21701
 ethanol- H_2O , with electrolytes in soln., cond. 8=4604-5
 gases in liq., density difference up to 1 part in 10^8 meas. 8=16803
 graft copolymers, viscosity 8=8027
 guar gum in tap water, aging and degradation from Pitot tube obs. 8=12744
 heat of soln. calorimeter with Peltier cooling for operation at const. temp. 8=9677
 iodine in iodides and bromides, effect on absorption spectra of polyvinyl alcohol films 8=5650
 ion-exchange equilibria in mixed solvents 8=18647
 ion interactions, short-range non-Coulombic rel. to thermodyn. and electrokinetic props. 8=21602
 isobutyric acid- H_2O system near crit. mixing pt., correl. effect in conc. fluctuations 8=12882
 liquid-liquid mixtures, ordering 8=21608
 liquid metal-oxygen, solid electrolytic cell for measuring equilib. press. 8=16951
 liquid mixtures, extension of Widom model 8=12785
 liquid scintillation counting, new efficient solutes with high solubility 8=15637
 macromolecular, props. determ. by distillation 8=8018
 macromolecules in soln., effects of solvent on X-ray scatt. 8=21205-6
 metals, molten, in m.h.d. convertor, thermodynamics of cycles 8=294
 methylene blue, water induced dimerization, absorpt. spectrum obs. 8=8123
 methyl viologen cation, aq. and alcoholic solns., e.s.r. spectra, rel. to water induced dimerization 8=8123
 mixed, intermol. electronic transitions 8=8010
 molten salts containing water, quasi-lattice model of hydration 8=8015
 molten salts, ternary systems, thermodynamics 8=21648
 myoglobin effects of solvent on X-ray scatt. 8=21206
 non-electrolyte, structural effects 8=16785
 n.m.r. solvent effects, molec. interactions 8=12935
 of organic mols., two-photon fluoresc. excitation 8=4592
 photoelectric control for rotary power meas. 8=15549
 photoluminescence band intensity distrib. rel. to excit. freq. 8=21695
 polar, proton shielding, role of reaction field 8=12782
 polyacrylamide in tap water, aging and degradation from Pitot tube obs. 8=12744
 polydisperse, sedimentation equilib. 8=1531
 polyelectrolytes, osmotic coeffs. meas. during phase separation 8=16817
 polyelectrolytes, osmotic press. from e.m.f. meas. 8=16818
 polyelectrolytes in salt solns., excluded vol. effect 8=12810
 polyelectrolytes, 2nd virial coeff. 8=4540
 polyelectrolytes, thermodynamics of potentiometric titration 8=5736
 polyelectrolytes, u.s. vibr. potentials 8=8061
 polyethylene in soln., n.m.r. 8=16891
 polyethylene in tap water, aging and degradation from Pitot tube obs. 8=12744
 polymer, conc., viscosity dependence on molecular weight and concentration 8=8026
 polymer, critical opalescence 8=21669
 polymeric, diffusion for solutes of low molecular weight 8=1540
 polymer, effect on resistance of circular cylinder in turbulent flow 8=16754
 polymer, equilib. distrib. between soln. and small voids 8=16801
 polymers, flow in pipes, drag reduction 8=1511
 polymers, flow through curved pipes 8=21570

Solutions—contd

polymer, intrinsic viscosity rel. to sedimentation 8=12823
 polymer, Newtonian viscosity 8=8025
 polymers, optical activity 8=8065
 polymer, quasi-elastic scattering, effects of hydrodynamic interactions 8=4542
 polymers, second osmotic virial coeff. calc. using lattice model 8=8039
 polymer, 2nd virial coeff., cryometric determ. 8=8017
 polymers, solvent evaporation kinetics at film formation 8=12972
 polymer, theory of expansion of linear chain 8=4264
 polymer, viscosity theory tests 8=8029
 polymer, viscous flow, conc. depend. of activation energy 8=16807
 polymethacrylic acid in alcohol-water mixtures 8=12822
 polymethine dyes, liquid solutions, stimulated light radiation 8=16848
 poly(methyl methacrylates) in soln., n.m.r. 8=16890
 polystyrene in chlorinated biphenyl solns., dynamic mech. props. 8=12818
 polystyrene solns., excluded-volume effect 8=8019
 polystyrene, viscoelastic props., mol. wt. depend. 8=8030
 propanol- H_2O mixtures, cond. with HCl in soln. 8=4607
 propanol- H_2O mixtures, cond. with NaCl in soln. 8=4606
 PVC solns., light scatt. 8=16850
 quaternary systems, equilibria 8=1529
 rare earth chelate for de-excitation meas. of organic molecules 8=16333
 reactions in, under pressure 8=14356
 rhodamine 6G and B, and mixtures, laser, mode locking 8=20009
 rubber, in amines, viscosity obs. 8=21625
 scaled-particle theory 8=4534
 second virial coeff., cryometric determ. 8=8017
 solvent composition and ion pair association constants 8=8009
 solvent effects in u.v. spectra 8=1571
 strong electrolytes, polarization contribs. to thermodynamic props. 8=4599
 tetracyanoquinodimethane anion, aq. and alcoholic solns., e.s.r. spectra, rel. to water induced dimerization 8=8123
 uranyl nitrate, organic soln., complexing, i.r. spectrum study 8=21619
 urea and inorganic salts, v.p. meas. 8=12996
 volume change on mixing simple liqs., corresponding states calc. 8=4537
 $AlCl_3$, p.m.r. determ. of coord. no. in aq. mixtures 8=16888
 B_2O_3 - SiO_2 system, metastable immiscibility 8=21748
 Bi-Sn eutectic alloys, of type 304 stainless steel, dissolution kinetics, convective-diffusion study 8=4558
 CH_3OH - H_2O , sp. ht. using calorimeter with adiabatic shell 8=21647
 $CaCO_3$ in H_2O , equilib. and zeta pot. rel. to surface charge zero point, obs. 8=16903
 Co^{2+} ion hydration, n.m.r. 8=12937
 H_2O , molec. dia. from solubility meas. 8=21606
 I_2 molten salt solns., elec. cond. 8=21719
 KCl, aq. solns., elec. cond. under high press. 8=12922
 K_2O - SiO_2 , activities 8=21620
 $LiClO_4$ in acetonitrile-dioxane, solvent-solute interaction 8=8108
 $LiClO_4$ in H_2O -dioxane, solvent-solute interaction 8=8107
 $LiClO_4$ in methanol-dioxane, solvent-solute interaction 8=8108
 Li_2O - SiO_2 , activities 8=21620
 $MnSO_4$ in water-glycol, elec. cond., viscosity effect 8=12921
 NH_3 , solvent effect on bending vibr. 8=21093
 NaCl aqueous, Cu anodic behaviour 8=2532
 Na-K- NH_3 solns., liq.-liq. phase separation 8=8014
 Na-NH₃ solns., liq.-liq. phase separation 8=8013
 Na_2O - SiO_2 , activities 8=21620
 Ni(II) complexes of glycine peptides in aqueous soln., form. 8=9664
 Pt, liquid, dilute, containing Ag, Au or Pt, thermodynamic properties 8=8043
 SO_2 , oxidation, effect of ullage 8=23111
 Sonar. See Sound ranging.
 Sonic boom. See Aerodynamics; Shock waves/effects.
 Sonoluminescence. See Luminescence/liquids and solutions.
 Soret effect. See Diffusion in liquids, thermal.
 Sorption
 See also Adsorption.
 carbon, chemisorption of O_2 8=5725
 chemisorbed species in catalytic reaction, dynamic treatment 8=9701
 chemisorption, meas. apparatus 8=5723
 chemisorption, molec.-orbital model 8=18695
 chemisorption, surface mobility parameter 8=14400
 chemisorption and physisorption, conference, Rome, March 1967 8=8333
 cubic lattices, of gas atoms, interaction potentials rel. to 6-12 pairwise model 8=8332
 desorbed molecules, angular distrib. in physisorpt. processes 8=17146
 desorption, activation energy distrib., mathematical exam. 8=21896
 desorption from graphite of Xe captured by nuclear recoil 8=4017

Sorption—contd

- diffusion-controlled, in heterogeneous systems 8=17147-9
 dye molecules 8=17149
 electrosorption of neutral substs. 8=9716
 emulsion polymerization, free radical desorpt. and readsorpt., rel. to kinetics 8=14415
 gases, Bayard-Alpert gauge modification 8=16732
 glass, desorption of O_2 by electron bombardment 8=13945
 inconel, anode, desorption efficiency meas. 8=17167
 kovar, anode, desorption efficiency meas. 8=17167
 laminar, flow instability due to film of adsorption 8=7974
 liquid phase adsorpt. fractionation in fixed beds, anal. 8=17151
 mechanism model 8=4450
 metals, of active gases, bond strength and mean adsorpt. times 8=14399
 metals, desorption of multiple additives, rel. to thermionic converters 8=17154
 metal, electron density near chemisorbed atom or molecule 8=8908
 metal films, adsorbate binding state characterization 8=14398
 metal films of gases, evaluation of sticking probability without gas pressure meas. 8=14397
 metal surfaces, oxygen chemisorption 8=9703
 methane in picture c. r. t., effect of silicate binder residues 8=15325
 neopentane-D exchange, desorption effects 8=23083
 organic cpds. and superconductors, interaction 8=9668
 Penning pumps, influence of pre-evacuation cycle 8=16725
 polyethylene, drawn and undrawn, of organic vapours 8=8349
 pre-exponential factor of desorption, energy variation due to localized vibration mode 8=17153
 semiconductor chemisorption, test for no. of atoms 8=13786
 silica, of Ar, low temp. physisorpt. process and mean adsorpt. time 8=17172
 silica gel, of benzene, change in dielec. behaviour of benzene on gel purification 8=1663
 silica gel, purified, of nitrogen, rel. to modification of gel struct. 8=1663
 steel, stainless, anode, desorption efficiency meas. 8=17167
 steel surfaces, stainless, electron-induced desorption of gas 8=17164
 surface active monolayers on H_2O substrate, reduction in gas desorption 8=12830
 surface reactions exam. by simultaneous X-ray emission and electron diff. 8=8290
 thermal desorpt. of inert gases from W and Au 8=17701
 transition metals with adsorbed CO, entropy changes on desorption 8=17174
 in vacuum gauges, Bayard-Alpert-Redhead, e desorption effects 8=7960
 Ag chemisorpt. props. rel. to surface struct., catalytic oxidation effects, obs. 8=18706
 Al surfaces, (111), (100), (110), atomically clean, chemisorpt. of O_2 8=4728
 Au, thermal desorption of inert gas ions 8=9280
 Ba films, of methane 8=17160
 Ba film, of O_2 in colour picture c. r. t. 8=15324
 CO adsorbed on transition metals, entropy changes on desorption 8=17174
 CO, chemisorbed on Pt-Aerosil surfaces, i. r. spectra 8=9704
 CaO, neutron or γ irradiated, chemi- of O_2 , rel. to surface paramag. centres 8=5724
 H, chemisorption on Re 8=23126
 H_2 , definition in metals 8=9743
 H_2 desorbed from Ti anode, discharge 8=21227
 H_2 desorption from Ni polycrystals 8=17170
 Ir on SiO_2 , chemisorpt. of HCN, C_2N_2 and BrCN, i. r. spectroscopy 8=23127
 Kr, desorption spectrum, rel. to He⁺ bombardment on glass (with trapped Kr) 8=17173
 Mg-Fe mixed hydroxides, cyclohexane desorpt. rel. to pore struct. 8=17023
 Mg-Fe mixed hydroxides, N desorpt. rel. to pore struct. 8=17023
 MgO, neutron or γ irradiated, chemi- of O_2 , rel. to surface paramag. centres 8=5724
 MnO_2 , electrolytic, of N, O, Ar and Ne, rel. to pore struct. and area 8=21904
 Mo, of CO, physical and chemical processes from study of low energy electron interactions 8=18702
 N_2 desorption kinetics, from Fe- N_2 solid solns. 8=1704
 Na mordenite, synthetic, sorption of methane, ethane, propane and butane 8=13109
 Ni, anode, desorption efficiency meas. 8=17167
 Ni polycrystals, desorption of H_2 8=17170
 Ni on SiO_2 , chemisorpt. of HCN, C_2N_2 and BrCN, i. r. spectroscopy 8=23127
 O_2 -Nb system at very low pressure, ad-, ab- and degassing 8=4763
 O_2 from W, field desorption, inert-gas enhancement 8=17176
 O from W surface, electron-stimulated desorption, mechanism 8=17177
 Pt, of CO rel. to binding states 8=18701

Sorption—contd

- Si and SiO_2 surfaces, fluoride chemisorption obs. by F^{19} in HF etches 8=18697
 SrO, neutron or γ irradiated, chemi- of O_2 , rel. to surface paramag. centres 8=5724
 Ta + N_2 system, adsorpt.-absorpt. kinetics 8=18698
 Ti, of N_2 , sticking coeff. obs. 8=17175
 TiO_2 , H_2O desorpt. kinetics, 25-100°C 8=18703
 W cathode, carbon adsorbed, field desorption effect 8=2276
 W crystal, of O_2 , mechanism and kinetics 8=8348
 W, desorption of CO, by electron impact 8=21911
 W, desorption of CO, NO and O by electron impact 8=21912
 W films of N_2 , sticking probability temp. dependence 8=14396
 W film, sorption and interact. of H_2O vapour, rel. to catalytic activity 8=14405
 W single crystals, chemisorption of diatomic molecules, work function studies. 8=18700
 W surface, desorption of rare earth elements 8=17171
 W surface, O_2 sorption, study by mass-spectra 8=4767
 W, of Th, desorption by high energy electrons 8=1712
 W, thermal desorption of inert gas ions 8=9280
 ZnO crystals, effect oxygen chemisorption on electrical conductivity 8=5160
 ZnO_2 , in cellulose membranes 8=21645
 ZnO, of formic acid, i. r. spectra 8=18705
 ZnO rel. to radicaloluminesc. excit., sorption-recomb. processes 8=9635
 Sound. See Acoustics.
 Sound field. See Acoustic radiators; Acoustics; Intensity measurement/acoustics.
 Sound ranging
 animal sonar in air 8=19620
 human perception of source distance 8=19613
 sonar detection in the presence of interference 8=23241
 sonar, optimum waveform for 8=23249
 Sonar signal processing, time and frequency characteristics 8=19566
 sonar, volume reverberation tests as function of pulse lengths and sweep rates 8=23242
 subjective localization, proximity image effect in absence of distance-indicating clues 8=15091
 ultrasonic position sensing devices in air 8=19579
 underwater, theory, book 8=10751
 shallow water propag. loss at sonar freqs. 8=1554
 Sound recording
 reverberation room acoustics, effect of boundary conditions 8=6182
 Sound reproduction
 See also Acoustic radiators; Acoustic transducers; Sound recording.
 magnetic circuit of a loudspeaker 8=15258
 via flames 8=10750
 Space charge
 anisotropic electron plasma, linearised Vlasov equation solutions 8=7732
 anthracene crystals, limited currents, temp. dependence 8=17859
 anthracene, hole injection from electrolyte and space-charge-limited current 8=18177
 atmospheric, guarded double field meter 8=15163
 coaxial resonator, effects in gas discharge 8=7647
 coaxial waveguide, effect in gas discharge, rel. to spark voltage 8=7646
 conduction in solids with introduced carriers 8=5158
 cross-field electron guns, effect on shot noise 8=19781
 crossed-field distributed-emission amplifier, effects in computer simulation 8=19712
 diodes, solid state S. C. limited, transit-time effects 8=18119
 double plasma sheaths, negative-ion effects 8=16549
 effects on resonant-electron discharge 8=16399
 effects in Townsend-Huxley swarm techn. 8=7698
 e. m. wave interaction 8=6297
 electron beams, mag. focused, conds. for compensation 8=6300
 electron gun design, computer soln. of eqns. 8=15284
 electrons in a magnetron lens, lifetimes meas. 8=6319
 electron transmission through thin films 8=13470
 ellipsoid, potentials and image effects 8=3186
 elliptical beam of finite emittance, spread 8=19780
 elliptical beam spread 8=19779
 field in d. c. discharge, electron temp. gradient effect 8=4278
 field of electron beams, reduction factor 8=322
 field emission, influence on potential barrier 8=9271
 ion and e selectors, useful current limitations 8=19773
 klystron, effect on resonator parameters 8=19827
 liquids, distribution after passage through a filter 8=12910
 in magnetized plasma, nonthermal ion effects 8=4351
 magnetron diode, radial oscillations 8=15332
 magnetron, effect of e. m. field fluctuation 8=338
 magnetrons, applicability of adiabatic theory 8=15331
 in magnetrons, cylindrical, effect on cut-off field 8=19828
 magnetrons, effect on operation 8=15333
 m. o. s. structures, currents controlled by surface-space charge 8=5343

Space charge—contd

- minority carriers, effects on mobility, diffusion and recombination 8=22429
- monocurrent similarly charged particles, theory 8=19767
- motion in vacuum, arc initiation 8=7688
- neutral plasma, spatial distrib. of electrons and ions 8=16467
- neutralization in Gabor-type auxiliary discharge converter, cost 8=15239
- in oxide cathodes 8=18259
- particle beam spreading effect 8=6295
- in Penning cell, potential in presence of, calc. 8=3212
- plasma, correlationless, with time-dependent background state 8=4344
- polyethylene terephthalate, e-irradiated, effects 8=9185
- radial electron beam, wave parameters 8=15291
- semiconductors, anisotropic, electron density fluctuations, nonlinear excitation by e.m. radn. 8=13772
- semiconductor surface layers, elec. cond., theory 8=5233
- in semiconductor surface layer, electrostatic energy and external charge distrib. 8=13788
- waves in electron beam, propagation 8=7767
- waves in electron beams, decay 8=6299
- KCl, current, electron dark, space-charge-limited 8=18168

Space groups. See Crystal structure, atomic.

Space research

- See also Atmosphere.
- astronautics and aviation Conference, Israel 1966 8=5822
- cosmic ray meas., review 8=5849
- cryogen storage, fluid heat transfer domains 8=16692
- Explorer 12, magnetometer obs. of earth bow shock 8=2619
- extra terrestrial observational astronomy, advantages 8=14721
- Gemini II photographs obs. of Barnard Loop nebulae structure 8=10222
- genetic investigations in space 8=14901
- gravitational compensator for biophysical studies 8=10446
- IMP-2, magnetosphere and near space, meas. of magnet. field, results 8=2832
- interplanetary mag. field, convection away from Sun and magnetosheath penetration, IMP 1 and 2 obs. 8=14861
- interplanetary mag. field power spectra and discontinuities, Mariner 4 obs. 8=23685
- lunar surface disturbance by Surveyor 1 footpads, inference from photographs and laboratory obs. 8=14818
- lunar surface roughness rel. to thermal emission and shadowing 8=2809
- mhd supersonic flow, for blunt bodies 8=355
- magnetosphere and tail, proton flux Explorer 33 obs. 8=23324
- moon, Explorer 35 investigation of mag. field 8=14819
- Moon surface strength estimate from Orbiter II photograph 8=5948
- nuclear and space radiation effects, conference 8=22578
- optical, 20 year review 8=19066
- plasma arc air heater for re-entry simulation 8=21408-9
- radiation, measurement of 8=10066
- re-entry plasma stability near photoemission surface 8=7842
- slender entry vehicles, communication through plasma boundary layers 8=14709
- solar flare, X-ray, July 7, 1966, Explorer 33 GM tube obs. 8=14882
- solar system environment, planetary and interplanetary, review 8=23633
- solar wind shock waves, Vela 3 obs. 8=23687
- solar wind thermal anisotropies, Vela 3 and IMP3 obs. 8=10406
- spacecraft power system, conference, Florida USA 1967 8=9243
- spectrum, u.v., of solar corona rel. to spectroscopy of highly ionized atoms 8=16192
- Van Allen belts, outer, pitch angle diffusion of relativistic electrons, Hitch-hiker I obs. 8=2650

Space vehicles

- See also Rockets; Satellites, artificial.
- aerodynamic manoeuvre of gliding vehicle 8=14708
- Apollo near-wake temp., Reynolds number depend. 8=23459
- correction manoeuvres in interplanet. flight, theory 8=2758
- drag coeffs. for cones, supersonic 8=23460
- at earth's atm. re-entry, thermal state and optimum trajectory 8=14707
- Gemini, optical environment 8=23455
- interaction with ionized atmosphere, book 8=14706
- interplanetary probe, orbit correction 8=19072
- interplanetary trajectories correction, by radial heliocentric velocity impulses 8=2760
- interplanetary trajectories correction, systems requirements 8=2759
- ionosphere, radar backscatter from wake 8=14676
- lunar exploration, review 8=5953
- motion near Earth-Moon collinear libration points, effect of solar perturb. 8=19070
- pitch-damping at hypersonic speeds 8=23458
- Ranger VIII, moon crater, gravity scaling obs. 8=23641
- trajectory estimation, sequential estimation of obs. error variances 8=19071

Space vehicles—contd

- velocity requirements for solar system exploration 8=2807
- instrumentation**
- amplifiers logarithmic, MOS and Si planar transistors for 8=5342
 - auroral particles, channel multiplier 8=5799
 - cosmic-ray intensity meas. 8=19090
 - cosmic rays, OGO data system 8=5847
 - cosmic X-rays counters and electronic systems for obs. 8=5848
 - detector for H^0 or $H^+ + H^+$ fluxes, energy-independent, 1-10 KeV 8=7381
 - discriminator, pulse, zero-crossing 8=6674
 - e energy meas. for auroral studies 8=5837
 - γ -ray telescope, balloon-borne, orientation 8=19328
 - horizon data units, infrared, errors 8=2763
 - magnetron ionization gauges, press. conversion const. 8=16733
 - monochromator for u.v. receivers calibration 8=11156
 - neutron detector, directional 8=6958
 - nuclear magnetometers, Rb and p, for earth's field meas. 8=14720
 - nuclear power plant, thermionic converter 8=1122
 - nuclear power units, thermionic, with radiation cooling, review 8=1114
 - photography planetary, analogue and digital data processes 8=10065
 - Pioneer, Si solar cells for near-sun use 8=10851
 - for planets rot. params. meas. from interplanetary stations, phototelevision 8=10339
 - pressure gauges, airstream adsorption errors 8=5838
 - p energy meas. for auroral studies 8=5837
 - p spectrometer, e-insensitive 8=6938
 - quartz sphere with superconducting Nb for satellite instrumentation and expts. 8=17984
 - radiation meas. data handling system 8=10067
 - r.f. sources in ionized medium, behaviour 8=12495
 - reactor, with thermionic converter, parameters 8=1123
 - reactor, thermionic, criticality and n flux density 8=1116
 - reactor, thermionic as power supply 8=1115
 - reactor, thermionic, temp. distrib. 8=1117
 - satellites, artificial, electrostatic probe theory 8=2764
 - solar cells, calc. of optimum grid 8=3160
 - solar cell systems for UK 3 8=19734
 - solar energy, system of acquisition 8=10858
 - spark chamber, digitized 8=6687
 - spark chamber, magnetic core, for satellites 8=6688
 - Surveyor V, Si detector for chemical analysis of lunar surface 8=23463
 - telescope in satellite, thermal deformations in mirror 8=480
 - CdS solar cell deployable rigid-frame array, performance obs. 8=10845
 - CdTe solar cell roll-up array 8=10857
 - H^0 or $H^+ + H^+$ fluxes, 1-10 keV, an energy independent detector 8=7381
 - Si horizon sensors, in rel. to earth reflectivity 8=18834
 - Si solar cell deployable rigid-frame array, performance obs. 8=10845
- Spallation.** See Nuclear spallation.
- Spark chambers**
- data handling system with piezo-electric microphones 8=3484
 - decision-making, for scatt. preselection 8=20225
 - discharge mechanism, image converter obs. 8=11326
 - electronic system, modular 8=6686
 - emulsion for 15 GeV cosmic ray photon det. 8=20594
 - filmless system with on-line computer 8=3486
 - film scanner, cathode ray, computer directed 8=3482
 - magnetic core, suitable for satellites 8=6688
 - with magnetostrictive line recording of track co-ords. and angles 8=11327
 - magnetostrictive, thin-wire, large dimension 8=6684
 - multiplate, and 'curtain-discharge' chambers, simplified systems 8=624
 - multiplate, for meas. of elastic π^+ backward scatt. 8=775
 - multiwire monitor and readout system by magnetostrictive delay line 8=625
 - piezoelectric readout device, matching and backing problems 8=3485
 - space research 8=6687
 - spark gap, triggered 8=623
 - streamer, ionization from particle track brightness meas. 8=15646
 - streamer tracks, ang. depend. of brightness 8=20226
 - vidicon tubes for automatic recording 8=3483
 - wire, cylindrical, for p-p scatt. 8=11329
 - wire, semi-popular review 8=626
 - Al, thin foil chamber, descrip. 8=6685
 - He, for α det. with alcohol vapour lowest pressure for spark 8=11328
- Spark counters.** See Counters/spark.
- Sparks, electric**
- See also Breakdown, electric; Lightning.
 - air, by focused laser beam, development 8=4292
 - air and water vapor mixtures 8=12412
 - between parallel plates, field distortion, calc. 8=21248

Sparks, electric—contd

- discharge in oil, electrode cavity configuration rel. to pressure 8=21249
 discharge shape in dielectric-bounded cavity 8=7681
 discharge, surface, as light source for laser pumping 8=6412
 electrode erosion photography 8=16423
 light source for atomic absorpt. anal., time resolved 8=18783
 machining device for metal sectioning 8=14905
 machining of micro-notch prototype 8=23772
 preionized gas gap, study 8=7671
 quartz films, discharge along surface 8=7682
 spark-gap-switch, de-ionization detection with exploding wire 8=7679
 spectrochemical anal. of steel, sample condition 8=2548
 steel emission analysis, decomp. and inter-element effects 8=14392
 three-electrode gap, switching characs. 8=7680
 triggered, for spark chambers 8=623
 switching using parallel bank of spark gaps, performance 8=273
 underwater, energy balance and sound radiation 8=12863
 BaTiO₃, films, discharge along surface 8=7682
 CaTiO₃, films, discharge along surface 8=7682
 H₂, high-current spark channels, voltage drop, expansion rates etc. 8=12410
 He-alcohol chamber, lowest pressure for α det. 8=11328
 from Nd laser beam, weakly focused 8=3337
 TiO₂ films, discharge along surface 8=7682

Specific heat

- See also Thermodynamic properties.
 adsorbates, isotherm analysis 8=13102
 at critical point, lattice gas model 8=4638
 ferromagnetic metals, rel. to anomaly in elec. resist. near T_c 8=13985
 gases meas., capillary flow calorimeter 8=7921
 Grüneisen parameters of some II-VI compounds 8=17537
 heat-resistant materials, meas. device under cooling conditions 8=251
 inequality rel. to expectation value of variable which varies rapidly with temp. 8=6099-6100
 Ising model, distrib. of roots of partition function in complex temp. plane 8=19443
 liquid-gas supercritical region, C₁ and C₂ extrema calc. from phenomenological theory 8=12978
 magnetic alloys, dilute, low temp. props. 8=18289
 metals, Debye temp. rel. to energies of vacancies form. and diffusion 8=17509
 metal halides and oxides, i.r. absorpt. freq. and charact. Debye temp. 8=14190
 porcelain, rel. to structure 8=1893
 solid solns., anomalies 8=8634
 thin film, specific heat, size effects in fermion model 8=10656
 Cu, low-temp. calorimetric standard 8=15127
 CuK₂(SO₄)₂·6H₂O, heat capacity below 1°K, meas. 8=13372
 D, polycrystalline, Debye temp. calc. from sound velocity meas. at 2 and 16°K. 8=17499
 KCl:OH⁻, below 4°K 8=1874
 K₂Fe(CN)₆, heat capacity below 1°K, meas. 8=13372
 Li plasma, calc. 8=12462
 LiCl, Debye temp. meas. 8=2058
 Mn(HCOO)₂·2H₂O, heat capacity between 1.4 and 20°K 8=13375
 Mn(NH₄)₂(SO₄)₂·6H₂O, heat capacity, near critical point 8=13376
 Pd:Ni alloys, correl. with paramag. susceptibility enhancement 8=18300
 RbCl, Debye temp. meas. 8=2058
 Sr_{0.925}Ba_{0.075}TiO₃, heat capacity, 0.3 to 4°K 8=1877
 TaC, heat content valves, entropy 8=8643
 TiNi, heat capacity 8=4935
 TlBr, Debye temp. obs. 8=2068
 β -UH₃, ht. capacities from 1 to 4-23°K 8=8644
 WC, heat content valves, entropy 8=8643

gases

- ethyl ketone, ethyl propyl ketone, methyl isopropyl ketone, methyl phenyl ether, vapour heat capacity and heat of vapourization 8=1471
 Cr measurement, influence of small volume changes 8=21508
 Xe, heat capacity in critical region, obs. 8=21513

liquids

- condensed substance, rel. to sound velocity 8=1551
 diethyl phthalate 8=1870
 Fermi liqs., nearly ferromag., re-evaluation of spin fluctuation contrib. 8=2995
 metals, heat capacity 8=1549
 1,3,5-tri- α -naphthylbenzene 8=4563
 Au-Si alloy, near eutectic composition 8=1548
 CH₃OH-H₂O solutions, using calorimeter with adiabatic shell 8=21647
 He II, logarithmic singularity 8=15150
 He³, Cr, and Fermi liquid quasiparticle self-energy 8=3117
 He³ meas. 8=3118
 He³-He⁴ mixture, interpolation between isotopes 8=3118

Specific heat—contd**liquids—contd**

- K₂ZrCl₆ 8=8640
 Li₂HfCl₆ 8=8640
 Li₂ZrCl₆ 8=8640
 Na₂ZrCl₆ 8=8640
 P₄S₁₀, heat capacity, 560°K to 720°K 8=4933

solids

- absorbent-adsorbate systems, heat capacity and length changes, simultaneous obs. using new calorimeter 8=6221
 antiferromagnets in strong mag. fields, spin sp. ht., theory 8=18369
 carbon steels, at 2 to 20°K 8=8639
 cryostat meas., 0.05 \rightarrow 2°K 8=22112
 diamond-like, ht. capacities from chain hetero-dynamism 8=17515
 Debye temp., vacancy formation and migration energy dependence 8=1865
 diethyl phthalate, cryst. and glass 8=1870
 electrical conductors from 25 to 900°C by pulse calorimetry 8=4927
 ferromagnet, dilute, critical behaviour 8=9307
 heat capacity meas. in adiabatic vacuum calorimeter, use of charcoal adsorpt. pump 8=17511
 Heisenberg ferromagnet, semi-infinite, surface effects 8=2303
 ice, amorphous and hexagonal 8=21846
 Kapitza conductance, depend. on Debye temp. of solid, exptl. evidence 8=10811
 magnetic alloys, dil., calcs. 8=13367
 magnetic alloys, rel. to Kondo model 8=17510
 metals, at high temp., meas. of temp. depend. 8=1864
 noble transition elements and alloys, electronic, and supercond. and mag. susceptibility 8=13753
 noble transition elements and alloys, and superconductivity and mag. susceptibility 8=13752
 non-cubic solids, heat capacities 8=22111
 organic, calc. of barriers to internal rotation 8=1221
 phenanthrene heat capacity anomaly obs. 8=13378
 from phonon freq. meas. calcs. 8=22113
 polyethylene, ht. capacity 2.5°-30°K 8=1875-6
 polymeric, Grüneisen number 8=1866
 polyurethanes, linear, temp. depend. of heat capacity 8=22110
 Pyrex glass, 0.4°-4°K in 0-90 kG fields 8=17525
 quartz, Debye temp. meas. \sim 1-4°K 8=4934
 rare earths, hyperfine interaction meas. 8=17514
 rare earth metals, 3 to 25°K, rel. to mag. props. 8=17513
 rare-earth, polycryst., Debye temps. and elastic moduli, 4.2 and 300°K 8=2057
 singularity in second order phase transitions using complex temp. plane 8=13365
 solid solns., binary metallic, Debye temp. calc. 8=1867
 superconductors with strong electron-phonon interaction 8=17508
 superconductors, transition point calc. 8=13745
 superconductors, two-dimensional 8=17522
 1,3,5-tri- α -naphthylbenzene, glassy and cryst. 8=4563
 wave statistics, applied to Debye's theory, and Schrodinger eqn., Heisenberg force 8=2982
 Ag, heat capacity, temp. dependence, effect of crystal lattice defects 8=13368
 Ag₂Al, Debye temp. calc. from elastic constant meas., 77-700°K 8=5040
 Ag-Au alloys, electronic, mag. susceptibility, electron states variation 8=13970
 α -AgCd alloys, from 1 to 4°K 8=8637
 α -AgPb alloys, from 1 to 4°K 8=8637
 Al, heat capacity between 2.7 and 20°K 8=22114
 Al, heat capacity and phonon-frequency distrib. 8=1868
 AlF₃, anhydrous cryst., high temp. 8=4929
 Ar, at T=0°K, anharmonic parameters of Debye charact. temp. 8=13594
 Au, heat capacity, temp. dependence, effect of crystal lattice defects 8=13368
 AuCu₃, rel. to atomic characteristic temp. 8=13029
 Au₄V, 1.5-60°K 8=4930
 CdS, elastic const. and Debye temp. calc. at 0°K 8=13542
 Ce ethyl sulphate, Schottky anomaly and spin-phonon coupling 8=8636
 Co, near Curie temp., from magneto-caloric effects 8=9337
 CoCr₂O₄, in 80-273°K range 8=17516
 Cr-Mo alloys, and Hall effect meas., between 125-625°K rel. to comp. 8=4931
 Cs metal, ht. capacity, 2°-4°K 8=13374
 CsCl, and dispersion curves, using shell model 8=8610
 Cu, Debye temp. calcs. from X-ray transmission temp. dependence (77-377°K) 8=14210
 Cu, for low-temp. calorimetry, atomic heat meas. 8=17517
 Cu formate tetrahydrate, anomalies at antiferroelectric transition pt. 8=8638
 Cu, heat capacity, temp. dependence, effect of crystal lattice defects 8=13368
 Cu-Au alloys, α -phase, electronic, mag. susceptibility, electron states variation 8=13970
 Cu-Ni alloys, anomalous, at low temps 8=22118
 Cu₂O, Debye temp. calc. from elastic constants 8=1869

Specific heat—contd

solids—contd

- Eu, ht. capacity 5°-300°K 8=17518
 Fe, electronic sp. ht. calc. by band model 8=4932
 FeNH₄(SO₄)₂·12H₂O, and mag. susceptibility calcs. at very low temps. 8=13370
 Fe-Ru alloys, h.c.p., rel. to electronic states density 8=13369
 Ga, near 1.7°K, no anomaly, rel. to absence of mag. transition 8=1871
 GdCl₃·6H₂O heat capacity singularities below 1°K 8=22115
 Gd₂(SO₄)₃·8H₂O heat capacity singularities below 1°K 8=22115
 KCl, 0.05 → 2°K, cryostat obs. 8=22112
 KCoF₄, heat capacity, 80°-300°K 8=17519
 KD₂PO₄, near Curie point (-70°K) 8=1873
 KF, Debye temp. and lattice energy calc. from elastic constants meas. 8=2056
 K₂MoCl₆ rel. to mag. ordering, 1.5-20°K 8=1872
 K₂ZrCl₆ 8=8640
 LaH₂, 1.3-20°K 8=13373
 Li₂HfCl₆ 8=8640
 Li(NH₂)₂, ht. capacity, 2°-4°K 8=13374
 Li₂ZrCl₆ 8=8640
 Mg-In alloys, rel. to ordered and disordered transformation energy 8=13072
 MgO, from 1.2 to 36°K, and Debye θ as function of temp. 8=22116
 α -Mn, comparison with α -Pu 8=17512
 Mn(NH₄)₂(SO₄)₂·6H₂O, 1°-4°K in mag. fields 8=17520
 ND₂Br, ht. capacity 17°-300°K 8=22117
 NaCl, 0- -25°K, heat capacity new calorimeter 8=6221
 Na₂HPO₄ hydrates, molar ht. capacity 8=17521
 Na₂ZrCl₆ 8=8640
 NbB₂, 0.6-2.8°K 8=17522
 NbC, stoichiometric, 500 to 2400°K 8=13366
 Nb-Mo alloys, Debye temp., Young's modulus, atomic bond strength 8=1626
 NbS₂, 1.7-6.4°K 8=17522
 Nb₂Sn, temp. range 1.42°K in mag. fields up to 52.5 kG 8=17523
 Nb-Ta, Nb-Ti, Nb-V, Nb-W alloys, Debye temp., Young's modulus, atomic bond strength 8=1626
 Ne crystals, caloric Debye charact. temp. and thermal Grüneisen parameter 8=1803
 Ne, at T=0°K, anharmonic parameters of Debye charact. temp. 8=13594
 Ni, anomalous, at low temps. 8=22118
 Ni, Debye temp., 0 to 300°K 8=13377
 Ni, electronic sp. ht. calc. by band model 8=4932
 Ni, at high temp. meas. of temp. depend. 8=1864
 Ni₃Mn alloy, 0.3 to 1.5°K 8=1635
 NiSiF₆·6H₂O, heat capacity below 0 35°K 8=8641
 P₂S₅, heat capacity, 273°K to 560°K 8=4933
 Pb, heat capacity and phonon-frequency distrib. 8=1868
 Pd-Co alloys, ferromagnetic 8=8642
 Pd-Fe alloys, ferromagnetic 8=8642
 Pd-Ni alloys, paramagnon mass enhancement theory 8=17524
 Pt, meas from 1.4-100°K 8=22119
 α -Pu, comparison with α -Mn 8=17512
 RbCl:Cn, and thermal cond., rel. to rot. degrees of freedom of mols. 8=22120
 Th cpds., refractory, charact. temp. meas. 8=13379
 Ti, near phase transition point, 1000 to 1300°K 8=17526
 TiO₂ (rutile), vac. reduced, below 4.5°K, rel. to impurity band model 8=13380
 Ti-Rh superconducting alloys 8=9058
 UO₂-ZrO₂-CaO, nuclear fuel, out-of-pile tests 8=17527
 US, ht. capacity 1.5°-350°K 8=22848
 W, in 1600-2900°K range 8=17528
 W-Re alloy, VR-20, in 1600-2900°K range 8=17528
 YH₂, charact. temp. from resistivity meas. 1000-1200°K 8=17942
 Zn, pure 8=22121
 Zn-Mn alloys 8=22121
 ZrC, stoichiometric, 500 to 2400°K 8=13366
 ZrH_{1.89-1.99}, charact. temp. from resistivity meas. 1000-1200°K 8=17942
 ZrO, and enthalpy in temp. range 100-2500°K 8=1878

Spectra

- See also Absorption/light; Astronomical spectra; Atmospheric spectra; Colour; Mass spectra; Raman spectra; Spectrochemical analysis; Spectroscopy; Stark effect; X-ray spectra; Zeeman effect.
 absorptance and radiative transfer by regular band 8=12125
 absorption band shape, complex molecules 8=1215
 complex mols, shape of continuous absorpt. bands 8=1214
 crystals, impurity, isotopic composition effect on electronic-vibration lines 8=22937
 deconvolution for exponential, Gaussian and Cauchy slit functions 8=6521
 diatomic polar mols. in liq. non-polar solvents, orientation 8=21673
 Einstein coeffs. for emission and absorpt. of mol., rel. to characts. in condensed media 8=22932
 emission, alkali metal, influence of electrical field 8=1895

Spectra—contd

- emission line distribution in d.c. arcs 8=7684
 energy spectrum representation and interpretation 8=94
 flames, absorption line profiles, Zeeman scanning 8=12044
 frequency-contrast characts, calc. by Hopkins method 8=20045
 gas layer, optically thick, X- and Y-functions in theory of multiple scatt. in spectral line 8=16187
 glass miniature mass spectrometer, charact. 8=16176
 high pressure modification of cryst. electronic spectra 8=8914
 inert gases, diffuse continua-emitting discharges 8=4273
 i. r. absorpt. bands, intensity meas. by Ramsay's direct integration method 8=21680
 infrared for Al-Fe substitution in hexaferrites 8=16999
 ions with incomplete shells in crystals, rel. to structure parameters 8=13033
 laser-heated plasma radiation 8=16200
 laser spark 8=3293
 light, profile from intensity correlation obs. 8=20028
 liquids, coupling of oscillators 8=16854
 liquids, far infrared, survey 8=12886
 liquids, frequency broadening by short pulse 8=4574
 liquids, freq. broadening in self-focused light 8=8083
 liquid molecules near the Rayleigh line, distribution 8=21678
 liquids, polar microwave to far infrared spectra, relaxation theories 8=8081
 luminescence rel. to exciton annihilation and bound complexes 8=9582
 β -methyl naphthalene in polycrystalline, dissolved and melted state in 750-3500 cm⁻¹ 8=16866
 mixed cryst., absorpt., deep-trap impurities effects 8=17865
 molecular, approximate open shell theory 8=4119
 molecular band, assuming gaussian line profile, calc. 8=7488
 molecular generator, line quality meas. 8=7485
 molecular systems and generalized response function 8=4141
 molecules, axially symmetric, nomenclature of rot. and vib. resonances 8=21045
 molecules, diatomic, electron-vibrational transition probability 8=1216
 molecules, discrete perturbation, quasi-classical soln. 8=12147
 molecules exhibiting accidental resonances, numerical analysis 8=12116
 molecules, Franck-Condon integrals, cancellation effects 8=21056
 molecules f-valves by hook method, theory and use 8=6525
 molecules, microwave and i. r., rel. to torsional energy levels and semiempirical potentials 8=12139
 molecules, PR separations prod. by prolate and oblate top mols. 8=12120
 molecules, rotational absorpt. lines, collision broadening 8=1224
 molecule vibrational relax. in gases and liquid 8=1218
 muonic mols., S-states, bound, variational calc. 8=12392
 naphthalene in polycrystalline, dissolved and melted state in 750-3500 cm⁻¹ 8=16866
 nonisothermal gases 8=12122
 odd-odd nuclei 8=20665
 optical cell, null press., for liquids at elevated temp. and press. 8=21676
 oxygen-acetylene flame temp. meas. by molecular spectroscopy 8=3109
 phenanthrene in polycrystalline, dissolved and melted state in 750-3500 cm⁻¹ 8=16866
 plasma, laser-produced, vacuum u. v. emission spectra 8=7777
 plasma, statistical mathematics for estimating parameters 8=7728
 polar liqs., Hertzian spectra of binary mixtures 8=8082
 polyatomic mols. secondary light emission rel. to e. eqn. of motion 8=1212
 quartz-kaolin-microdine reactions during firing, i. r. studies 8=18690
 quasars, absorpt. lines 8=23621
 radiationless transition probabilities, weak solvent-solute interactions 8=16256
 reflectance, lunar and laboratory, and inferences about Moon's surface 8=14820
 rotation lines in gaseous mixtures, modification theory by density effect 8=16244
 volatile solns., under press., up to 300°C, optical cell 8=8084
 Al plasma, energy spectra of ions 8=2122
 ALP, infrared and Raman active modes 8=18500
 Ar II laser, polarization in perturbed spontaneous emission spectrum 8=11042
 CO₂-N₂ plasma, i. r. emission 8=12510
 Cu and Zn complexes, tetraphenylporphine and tetraphenylchlorine, absorpt. 8=9117
 H-foreign gas Van der Waals complexes bound states 8=6523

Spectra—contd

- Hg vapour + C_6H_4 impurity, absorption of $Hg\lambda$ 2537 Å line 8=16287
 K lamp, line shape dependence on current 8=15523
 atoms
 See also Atoms/excitation; Atoms/structure.
 air, high-temp., continuum and atomic line rad. 8=16198
 alkali-metal, fine-structure transitions in adiabatic collisions 8=4106
 alkali metals 2P fine structure transitions in adiabatic collisions, calc. 8=1162
 arcs, free-burning, oscill. strengths, systematic errors 8=7683
 cascade transitions with stimulated emission, freq.-correl. effects 8=12043
 correlation effects in complex spectra 8=7411
 density matrix kinetic equation 8=21000
 doublet-term inversion, non-central electrostatic corrections 8=4054
 effective potential calc. 8=12038
 e.m. field effect, decay theory, projector-operator approach 8=11262
 emission and Raman scattering lines 8=7376
 energy levels, perturbation by e.m. wave 8=7375
 excited state lifetimes by e impact, using single-photon counting 8=7429
 fine structure constant, exact reduced mass correction 8=4114
 fluorescence efficiencies in hot gas 8=4059
 f-valves by hook method, theory and use 8=6525
 gases, continuous 8=4060
 Hertzian resonances, optical methods, review and bibliography 8=20929
 highly ionized, rel. to space research observations 8=16192
 Hanle effect obs. in Rb^{87} 8=7422
 high degrees of ionization produced by vacuum u.v. source 8=7399
 hyperfine line structure, expt. apparatus for nuclear radius meas. 8=7078
 hyperfine structure, e quadrupole moment induced by nuclear quadrupole moment, effect 8=7402
 hyperfine structure, rel. to min. size of p and e in nonrelativistic theory 8=826
 Lamb shift, rel. to self-interaction corrections in q. e. d. 8=20174
 line intensities revised tables below 2450 Å 8=1152
 line profile meas., magneto-optical 8=4057
 L_1 - L_{II} level separation, effect of finite nuclear size 8=20927
 Lyman α from radiation belts due to interaction with charged particles 8=18963
 magnetic hyperfine anomaly, nonrelativistic derivation 8=12042
 many-electron, fine-structure splitting, use of Hartree-Fock functions 8=20923
 metal vapours, absorption, in modified miniaturized King furnace 8=7393
 multipole radiation, exploding-wire technique 8=20939
 oxygen, S^0 metastable state 8=1304
 pionic $2p$ - $1s$ transitions Ge counter obs. 8=1179
 plane isothermal gas-layer, radiative transfer in spectral lines 8=16188
 plasma, CV, OVII, collisional rate coeffs. deduced 8=12470
 plasma, line shifts due to e impact, semiempirical formulas 8=12511
 plasmas, Stark-broadening and line shapes calc. 8=1402
 pressure-broadened, quantum oscillations in line shape 8=20932
 pressure shift of excited states, when embedded in gas medium 8=4052
 quark-atoms in spectrum of sun 8=6718
 reabsorption line, Fermi calc. 8=7366
 resonance fluoresc., forward-scatt. curves 8=20946
 spectral line broadening, effect of collisions 8=1153
 spontaneous emission under classical and quantum fields and collisions 8=20937
 spontaneous emission from a system of 2 level atoms interacting with relaxation mechanism 8=20971
 stellar atmospheres, line-blanketing 8=14761
 trapped in inert gas matrices, molecular features 8=8227
 reabsorption method for concentration of line with complex structure 8=4051
 spontaneous emission, line shape for imperfect mixing of degenerate levels 8=4049
 stimulated rad. during interact. of cascade transitions 8=417
 term splitting in interaction of identical atoms in different states 8=4055
 X-radiation, characteristic, polarization following ionization of inner electron 8=12041
 X-ray emission, bonds effects 8=16191
 X-ray satellites and excitation states belonging to same inner vacancy 8=16216
 X-ray satellites, new screening doublets 8=16193
 X-ray, screening doublet formation, extended study 8=20922
 Al II, theoretical multiplet strengths 8=7410
 Al II, transition probabilities 8=7411
 Al II, III, beam-foil excitation 8=12079
 Al III, vacuum u.v. obs. 8=16202
 Al IV, V, VI from 125-315 Å, relative intensities, spectra response of detectors 8=15494

Spectra—contd

- atoms—contd
 Al^{III} and Al^{III} produced by 17-18 kV spark 8=7399
 Ar, abs. coeffs. in thermal plasmas 8=16207
 Ar, arc, rel. to temp. meas. 8=4297
 Ar, explosively generated shock waves 8=1480
 Ar, isotopic displacements of i.r. laser lines 8=7397
 Ar laser lines, high gain, identification 8=7395
 Ar, L_1 shell, Coster-Kronig and Auger spectrum 8=7396
 Ar, self-broadening and oscillator strengths 8=7416
 Ar, transition probabilities in intermediate coupling 8=12055
 Ar I in arc plasma, Stark broadening 8=12057
 Ar I, mean lives of some 4p levels 8=4069
 Ar I and II, interferometric meas. in region 5000-7000 Å 8=4070
 Ar II capillary arc discharge, mag. field effect on inversion population 8=7692
 Ar II lines, Stark broadening parameters, obs. 8=20949
 Ar II, stationary arc discharge, population inversion in 4s and 4p states 8=7693
 Ar⁺ laser, study rel. to transition wave functions and probabilities 8=3307
 Ar, Kr and Xe, superradiant transitions 8=7398
 Au III, transition strengths between $5d^66s$ and $5d^86p$ configurations 8=4071
 Ba II isotope shifts and mag. h. f. s., 4.934 Å 8=16204
 Be to F, Rydberg orbitals, Slater-Condon parameters 8=12059
 Be hyperfine structure, e quadrupole moment induced by nuclear quadrupole moment, effect 8=7402
 Bi I, $^2D_{3/2}$ and $^2P_{1/2}$ levels hyperfine structure, $6p^3$ ground configuration 8=4072
 Br, new Rydberg series of absorpt. in 600-1500 Å region 8=1165
 C, absorption coeffs. compilation 8=12060
 C using resonance lamp 8=15538
 C^v and C^{VI} produced by 6 kV spark 8=7399
 Ca, pionic, rel. to π mass 8=6839
 Ca II, spatial extent in twilight, airborne obs. 8=9868
 Ca IX, transition probabilities 8=7411
 Ca²⁺, dipole polarizability evaluation 8=7414
 Cd $5^2P_{0,1,2}$ levels lifetimes and transitions, obs. 8=1183
 Cd, Stark effect obs. in $5s5^2P_1$ state 8=20966
 Cl, K-series, K_α line calc. from M/L e capture ratio of Ar³⁷ 8=20748
 Cl, new Rydberg series of absorpt. in 600-1500 Å region 8=1165
 Cm³⁺, low-lying levels 8=4074
 Cs in Cs-Ar low-pressure discharges 8=7401
 Cs freq. standard, comp. with H 8=10483
 Cs, interpretation rel. to plasma diagnosis and molec. effects 8=12527
 Cs, Stark effect obs. in $7^2P_{3/2}$ state 8=20966
 Cu hyperfine structure, e quadrupole moment induced by nuclear quadrupole moment, effect 8=7402
 Cu, λ 3247.5 Å-resonance line profile from hollow-cathode source, by interferometry 8=3365
 Cu⁶³ in $(3d^{10}4p^2P_{3/2})$, h. f. s. constants, rel. to polarization corrections 8=12061
 D, using broadening of D_β line, expt. 8=16194
 Es, sensitive spark lines 8=12063
 F, new Rydberg series of absorpt. in 600-1500 Å region 8=1165
 Fe²⁺ in sphalerite, i.r. absorpt. 8=18570
 Fe³⁺ in $Ca_2Fe_2Si_2O_{12}$, $3d^5$ configs. splitting by cryst. field 8=1654
 Fe II, III, beam-foil excitation 8=12079
 Fe^{XVI} produced by 6 kV spark 8=7399
 Fe^{XVIII} produced by 17-18 kV spark 8=7399
 Ga V in vacuum u.v. 8=12082
 Gd I, Zeeman, rel. to g-values of levels 8=4077
 Gd II, Zeeman, rel. to g values of levels 8=4076
 Ge VI in vacuum u.v. 8=12082
 H, auroral arc, Balmer α emission rel. to incident H flux obs. 8=2636
 H, Balmer- α line excitations by electron impact, cross section and polarization meas. 8=20979
 H discrete spectrum and radiadiapason obs. 8=7377
 H freq. standard, comp. with Cs 8=10483
 H, Lamb shift calc. from precise theory of Zeeman effect 8=1158
 H, line broadening, electron concentration meas. 8=4062
 H, lines, broadening by Stark effect 8=1159
 H-line Stark broadening functions 8=12051
 H, Lyman- α line, spectral broadening in a plasma 8=21350
 H, Lyman- α prod. by electron collisions on H_2 8=12050
 H, N_2 -H collisions rel. to aurora 8=12212
 H, resonance scatt. of light and level crossings 8=4064
 H stimulated emission in beam laser, line shape and width obs. 8=421
 H, 2500-1100 Å, intensity distrib. 8=4065
 He, balance eqns for 2^3S , and 2^3P levels in hollow-cathode discharge 8=20981
 He, continuous absorpt. coeff. 8=7387
 He coupling width anomaly, linear extrapolation of Lorentz width to zero 8=20955
 He, excitation of 4F states 8=12054

Spectra—contd

atoms—contd

- He, excited by fast protons and H atoms 8=7433
 He, ground and metastable states, dipole props. 8=20980
 He, large-angle electron-impact 8=16224
 He II, 4686 Å line complex excited in atomic-beam light source, analysis 8=12052
 He II, interference of fine-structure levels 8=4066
 He II, Lamb shift 8=1161
 He³, optical orientation of 2³S₁ state 8=16219
 He, recombination afterglow, differential level decay 8=21237
 He, superradiance at transitions terminating at metastable levels 8=20943
 Hf, isotopic shifts of 20 spectral lines, rel. to deformation of Hf¹⁷⁴ 8=20953
 Hg, 7³S₁—6³P₁—6¹S₀ cascade correlation, and 6³P₁ coherence time 8=4078
 Hg, Stark effect obs. in 6s6p³P₁ state 8=20966
 Hg, temperature dependence of 1849 Å absorption in saturated vapour 8=1166
 Hg¹⁹⁸ double reson., linewidth narrowing and Zeeman sublevel transition and shifts obs. 8=21001
 Hg¹⁹⁸ 4358 Å line shape, intensity correl. obs. 8=20075
 Hg¹⁹⁹, hyperfine structure of the 2967 Å (6³P₀—6³D₁) and of 6³D₁ level 8=16205
 Hg¹⁹⁹ and Hg²⁰¹, 7³S₁ level, hyperfine structure 8=1184
 Hg¹⁹⁹ and Hg²⁰¹, 6¹P₁ level hyperfine structures 8=7404
 Hg²⁰¹, hyperfine levels, population transfers 8=7467
 Hg, metastable state, coherent excitation by e, rel. to resonance absorpt. 8=4094
 Hg, in pulsed discharge, afterglow, rel. to delayed emission 8=21238
 Hg, resonance line, press. broadening by He 8=7403
 I, new Rydberg series of absorpt. in 600–1500 Å region 8=1165
 I(5²P_{1/2}), time resolved emission obs. 8=4079
 In line intensities, in Hg–In fluoresc. spectrum 8=4080
 K, 580 Å to 1000 Å, atomic absorption cross section, experimental values 8=12065
 K, in 4²P_{1/2} state, collisional mixing with inert gases obs. 8=12064
 K-series dipole elec. transitions 8=7367
 K vapour, stimulated emission from 4P_{3/2 1/2}—4S_{1/2} 8=20984
 Kα, X-ray shift in various isotopes 8=20671
 K⁺, dipole polarizability evaluation 8=7414
 Kr, abs. coeffs. in thermal plasmas 8=16207
 Kr, autoionization influence 8=20954
 Kr, collision broadening and shift due to Ne, Ar He 8=20956
 Kr, excitation functions of 33 lines by electron-atom collisions 8=4096
 Kr gas self-broadening and resonance oscillator strength 8=20955
 Kr, resonance lines, oscillator strength meas. 8=7449
 Kr, self-broadening and oscillator strengths 8=7416
 Kr–Ar couple, and form of "satellite" bands 8=7425
 La III, new spectra lines in 2000 to 12000 Å region 8=12066
 Li, continuous absorpt. coeff. 8=7387
 Li, in inert-gas matrices 8=4082
 Li hyperfine structure, e quadrupole moment induced by nuclear quadrupole moment, effect 8=7402
 Li sequence, eigenvalues of 1s²2p²P states 8=20957
 Li, 2p²P levels, hyperfine coupling constants 8=7408
 Li I, first-level lifetimes 8=7407
 Lu III, hyperfine structure, nuclear dipole moment 8=4083
 Mg isoelectronic sequence, transition probabilities 8=7411
 Mg²⁺, dipole polarizability evaluation 8=7414
 Mg I, theoretical multiplet strengths 8=7410
 Mg III and Mg IV, vacuum ultraviolet spectroscopy 8=1169
 Mn IV, vacuum spectroscopy and energy levels 8=12067
 N, absorption coeffs. compilation 8=12060
 N, radiative transfer, for local thermodynamic equil. 8=7926
 N II, Stark effect in multiplet lines 8=4084
 N II–V, lifetimes meas. by decay of optical radiation 8=7412
 NII, NIII and NIV emitted by ion beam passing through C target 8=20960
 Na absorption and emission enhancement by alcohol, flame photometric obs. 8=20961
 Na, Doppler profiles in atomic fluoresc. of Na I 8=12069
 Na⁺, dipole polarizability evaluation 8=7414
 Na gas discharge plasma, line excitation rel. to cascade transitions 8=20962
 Nd³⁺ ions in rare-earth trichlorides, high-resolution, low-temp. absorption spectra 8=12070
 Nd, isotope shift 8=21024
 Ne, abs. coeffs. in thermal plasmas 8=16207
 Ne coupling width anomaly, linear extrapolation of Lorentz width to zero 8=20955
 Ne, double resonance laser spectroscopy of excited states 8=11066
 Ne, Landé factors meas. by saturation from laser 8=1186
 Ne, microwave emission in excited states, when laser pumped 8=12071
 Ne-self-broadening and oscillator strengths 8=7416
 Ne, transition between levels, electron induced 8=20947

Spectra—contd

atoms—contd

- O, absorption coeffs. compilation 8=12060
 O₂ in Ar cascade arc, absorpt. oscill. strengths of O I lines in vac. u.v. 8=7417
 O, ¹D₂—³P_{1/2} forbidden transition origin 8=1182
 O I(¹D₂) and O I(³S₁) metastable states, vac. u.v. 8=12072
 OI, 5577 and 6300 Å, auroral, ratio of intensity to H₃ 8=23340
 [OI] λ 5577 and λ 6300, auroral luminosity spatial var. obs. 8=14649
 O II, equilibrium population of states in plasma 8=7418
 O IV lines in vacuum u.v. 8=20964
 O VIII in solar corona, L_α and L_β lines intensity ratio calc. 8=10434
 P IV, transition probabilities 8=7411
 Pr hyperfine structure, e quadrupole moment induced by nuclear quadrupole moment, effect 8=7402
 Pr, L_{α1,2} meas. 8=7420
 Pu²³⁸⁻²⁴², arc, rel. isotopic shift 8=20965
 Rb photon emission following β-decay in solid 8=8226
 Rb, Stark effect obs. in 6p²P_{3/2} state 8=20966
 Rb⁸⁵, 5²P_{3/2} state, level crossing expt. 8=1174
 Rb⁸⁷ Hanle effect obs., calc. of lifetime of first excited states 8=7422
 Si I lines, width and shift by Van der Waals interact. with Ar atoms 8=7423
 Si III, theoretical multiplet strengths 8=7410
 Si III, transition probabilities 8=7411
 SnI forbidden lines, obs. 8=1175
 Sr, absorption, u.v. extension of arc spectra 8=20967
 Sri, 5s² ¹S₀—4dnp, nf spectrum, analysis of autoionization resonance structure 8=20968
 Tb I, neutral, levels with extreme J 8=12073
 Th, 1–2.5 μ emission 8=12074
 Ti, pionic, rel. to π mass 8=6839
 TiI resonance lines, absolute oscillator strengths 8=1176
 TI, oscillator strengths for np → ms_{1/2} and np → md transitions 8=4086
 TI, superradiance at transitions terminating at metastable levels 8=20943
 Tm hyperfine structure, e quadrupole moment induced by nuclear quadrupole moment, effect 8=7402
 W, transition probabilities, 9 lines, 4700–5300 Å 8=20969
 Xe, abs. coeffs. in thermal plasmas 8=16207
 Xe, autoionization influence 8=20954
 Xe 1469, 6 Å line perturbation by Ar, He, H₂ and H₂ compressed gases 8=16201
 Xe¹²⁹, hyperfine structure of i.r. laser lines 8=16210
 Xe–A couples (A = He, Ne, Ar, H₂), and form of "satellite" bands 8=7425
 Yb, anticrossing signals from 6s¹P₁ level 8=16211
- inorganic molecules**
 See also Molecules.
 air, high-temp., continuum and atomic line rad. 8=16198
 gases, absorption function of overlapping spectral lines 8=498
 germanium fluoro- and hydroxyfluoro-compounds and thermal polymerization products, i.r. vibr. freqs. of Ge–O–Ge bond 8=4170
 tin fluoro- and hydroxyfluoro-compounds and thermal polymerization products, i.r. vibr. freqs. of Sn–O–Sn bond 8=4170
 van der Waal molecules, trapped in inert gas matrices 8=8227
 AlO, absorption, dissociation energy 8=12169
 CCl₄ vibr. transitions rel. to intermol. interactions 8=16274
 CO₂, trapped in inert gas matrices 8=8227
 D, Lamb shift calc. from Zeeman spectrum precise theory 8=1158
 FCN, microwave, excited vibrational states 8=12182
 H, N₂–H collisions rel. to Aurora 8=12212
 Hg₂, trapped in inert gas matrices 8=8227
 HgBr₂, in vacuum u.v. 8=12204
 KI, containing H₂O mols. 8=4953
 N₂⁺ intensity distrib. among bands, obs. in atmosphere 8=18933
 N₂⁺ λ 3914, auroral luminosity spatial var. obs. 8=14649
 N₂–p collisions rel. to Aurora 8=12212
 N₂O solid, pure and in a matrix, absorption spectrum between 63 and 14°K 8=18552
 Ne²⁰, 633 n.m., He³–Ne²⁰ discharge, effect of press. and mixture on profile 8=16295
 O + CO, emission in shock-heated system 8=1342
 Zn, optically pumped, collision broadening obs. 8=6523
- inorganic molecules, diatomic**
 alkali-metal halides, inner-electron excitation 8=7529
 Condon loci, primary and subsidiary, geometry 8=1231
 Raman spectra pressure broadening obs. 8=6523
 transition probability from Hulbert–Hirschfelder potential 8=4117
 AgIn, u.v. absorpt. bands, system A, vibrational analysis 8=16262
 AlO, new ²Σ⁺–²Σ⁺ band, Franck-Condon factors 8=16263
 AsH and AsD, A, ³Π₁–³Σ⁺ band systems 8=21062
 AuGa, in Ar atm. at 2100°K 8=16265
 BO₂⁺ ion in alkali halides, vibr. bands obs. 8=22946
 BeF, discharge, emission in vacuum u.v. 8=21064

Spectra—contd

inorganic molecules, diatomic—contd

- BiCl, rotational analysis in 4220-4000 Å region 8=7504
 BiO, magnetic interactions in Hund's case 8=12172
 BiO, rotational structure absorption bands 8=12171
 Br₂, continuum and line absorption, 6328 Å, half-width meas. 8=12173
 C₂, absorption and emission spectroscopy, in low-press. oxyacetylene flames 8=21189
 C₂, dissociation energy determ. 8=12336
 C₂, electronically excited in hydrocarbon flames 8=7509
 CN, assuming gaussian line profile, calc. 8=7488
 CN bands, red system, electronic transition strength 8=12180
 CO, adsorbed on Pd, i.r. 8=4764
 CO, chemisorbed on Pt-Aerosil surfaces 8=9704
 CO, fundamental band at high temp., spectral absorpt. coeff. 8=21067
 CO, 3ν band, strengths, widths and shapes 8=16269
 CaF, A-X and B-X level systems 8=21069
 CdI, 3586 to 3495 Å C-system band, representation by vibr. quantum eqn. 8=21070
 CuBr, rel. to rot. structure of C band system 8=1239
 H vibr.-rotational spectrum for e ground state, generalized VKB calc. 8=1246
 H₂, Balmer emission following p collisions 8=12190
 H₂, predissoc., weak absorpt. lines 8=12189
 H₂, press. induced i.r. bands, anal. of profiles 8=12188
 H₂, Rayleigh and Raman scattering cross section calcs. 8=7517
 H₂, para, rotational h.f. s. and vibrational coupling coeffs. 8=16284
 HCl, pressure effect 8=21077
 HCl, rot. line strengths, by Fourier transform. 8=1253
 HF, rotational spectrum, frequencies and linewidths 8=12198
 Hg₂ excimers, kinetics of band emissions 8=12203
 Hg, 4850 Å and 3350 Å bands, role of Hg⁶³P, atoms 8=21033
 I₂, 5350 Å band, resolving power test 8=16289
 K₂ vapour, nonlinear absorpt. of ruby laser light, and resonance fluoresc. 8=7527
 LaF, gaseous, electronic states 8=7549
 MgH, (A²Π-X²Σ⁺), oscill. strengths meas. 8=7530
 MgO, (B²Σ⁺-X²Σ⁺), oscill. strengths meas. 8=7530
 MgO, colour centre production, effect of atomic displacements 8=2011
 N₂ absorpt., 12.28 eV quadrupole transition obs. 8=12208
 N₂, often p collision at 0.15-1.0 MeV and secondary e collisions 8=12213
 N₂, on excitation by fast protons and H atoms 8=7433
 N₂, excited by electron beam, rot. temp. obs. 8=16292
 N₂, large-angle electron-impact 8=16224
 N₂, model dipole spectrum consistent with oscillator strength sum rule 8=7533
 N₂, new Rydberg series 8=4160
 N₂ second positive system excited by impact with a metastable Ar atom 8=12209
 N₂⁺, 3914 and 4709 Å, auroral, ratio of intensity to H_β 8=23340
 NH⁺, emission band systems 8=16291
 NO, on excitation by fast protons and H atoms 8=7433
 NO, integrated intensity of fundamental vib. band 8=7535
 NO in solid Ne, Ar and Kr rel. to excited states, 2300-1100 Å 8=14243
 NS, Franck-Condon factors for B²Π-X²Π transition 8=7540
 NS, vibr. bands, γ- and β-systems 8=16293
 O₂ (b²Σ⁺) emission 8=4098
 O₂, electronic structure 8=16297
 O₂, excited emission 8=1262
 O₂ microwave emission, stratosphere 8=23256
 OD, transition B²Σ⁺-A²Σ⁺, high resolution obs. 8=21095
 OH, absorption and emission spectroscopy, in low-press. oxyacetylene flames 8=21189
 OH, chemiluminescence by flame photometry, predissociation 8=12223
 OH cosmic 18 cm lines, anomalous polarization theory 8=7543
 OH, emission band systems 8=12222
 OH galactic, radio emission, brightness and temporal variation 8=10253
 OH in NI cloud, excitation temp. of 18-cm line 8=10299
 OH, oscillator strengths in 2Σ⁺-Π band system 8=7544
 OH-stretching, vibration in solid alcohols, band-width 8=8228
 OH, transition B²Σ⁺-A²Σ⁺, high resolution obs. 8=21095
 OH, transition moment and vib.-rot. interact. 8=7545
 OH, vib.-rot. from oxyacetylene flame in air or N₂ rel. to flame temp. 8=18692
 P₂⁺, rotational analysis of the (2, 3) band of a new transition 2Π → 2Π 8=16299
 PD⁺, emission, vibrational and rotational structure 8=4167
 PO, β-system subsystems anal. 8=12225
 PbBr emission 8=7546
 PbF, emission 8=21099
 RhC, C²Σ⁺-X²Σ⁺ band, Franck-Condon factors and r centroids 8=7548
 SbH and SbD radicals, absorpt. 8=12354
 ScF, gaseous, electronic states 8=7549

Spectra—contd

inorganic molecules, diatomic—contd

- SrF emission bands and C²π-X³Σ vibr. consts. obs. 8=1266
 TaO, gaseous, electronic bands rot. anal. 8=1267
 YF, gaseous, electronic states 8=7549
 ZnCl, emission, visible region 8=4171
 inorganic molecules, diatomic, radiofrequency
 See also Nuclear magnetic resonance and relaxation; Paramagnetic resonance and relaxation.
 Cs¹³³F¹⁹, h.f. s., molec. beam meas. 8=16278-9
 H⁺, Zeeman sublevels, g-factor ratios 8=12195
 HBr, far i.r. microwave, rot. lines 8=7523
 HCl, DCl, far i.r. microwave, rot. lines 8=7523
 NO, rotational lines at 150 GHz, a high-Q Fabry-Perot resonator 8=7536
 OH radical, low-field Zeeman effect 8=4246
 inorganic molecules, polyatomic
 ammonia, pure rotation band absorpt. rel. to refractive index of ammonia 8=4162
 borazine and deuteroborazine, i.r. 8=4145
 contact transform., choice of S-operator 8=7494
 Franck-Condon factors calc. 8=21269
 lanthanide complexes, mixed, energy transfer 8=2433
 pyrophosphates, divalent metal, far i.r. 8=21097
 thiophosphoryl halides, vibration 8=7547
 3α decay, as cause of scintillation in He, He-Ar, He-Ne bombard. with α 8=12202
 trans N₂F₂, vib.-rot. bands and molec. geometry 8=12218
 AlCl₃ ion, h.f. i.r. active f₂ vibr., correction 8=4142
 AlF₃, i.r. 8=12997
 As(SiH₃)₃, i.r., rel. to struct. 8=4144
 BF₃, radiative lifetimes of u.v. emission systems 8=7501
 BrDBr⁺ and BrHBr⁺, i.r. 8=12174
 C₃ radical, absorpt., diazopropyne photolysis obs. 8=16368
 CCl, free radical, electronic and vib. 8=1315
 [(C₆H₅)₃As]⁺[MoOBr₄]⁻, i.r. Mo-O stretching freq. 8=9552
 CO-N₂O mixture, study of overlapping absorpt. bands 8=7507
 CO₂, band emissivities, evaluation 8=16272
 CO₂, excited by N₂, emission obs. 8=21068
 CO₂, i. r. emission from low vib.-rot. levels in discharge 8=12177
 CO₂, relative intensities, 160°-280°K calc. 8=7506
 CO₂, 10.4 μ band, strength and half-width 8=12178
 CO₂, 2Π_g → 2Π_u transition 8=16277
 CO₂, 2Π_g → 2Π_u vibrational transition probabilities 8=21066
 C₃O₂ flames in reactions with O atoms and active N 8=14360
 CS₂, ν₃ bands 8=12265
 Cl₂ radical, i.r. 8=7620
 ClOO, i.r., in matrix 8=12344
 CuF₆⁴⁻, absorpt. spectrum and struct. 8=16280
 D₂O, press. broadening obs. using CN maser 8=21073
 D₂O in solid N₂, i.r. absorpt. 8=22977
 D₂O in soln., absolute i. r. intensities rel. to meas. in gas phase 8=1561
 DOCl, i.r. spectra of ν, bands, rel. to rot. consts. and geometry 8=21083
 GeD₃, i.r. 8=12187
 GeH₃NCO, i.r. 8=21074
 H₂C₂, rel. to virtual-orbital approx. to excited states 8=1213
 HCF, rel. to virtual-orbital approx. to excited states 8=1213
 HCN and DCN, l-type resonance doublets 8=7522
 H₂CO, rel. to virtual-orbital approx. to excited states 8=1213
 HCl dimers in solid solns., far i.r. 8=18532
 HNO, rel. to virtual-orbital approx. to excited states 8=1213
 H₂O, band emissivities, evaluation 8=16272
 H₂O, 2.7 μ bands radiant emission, compared with general band model 8=7520
 H₂O in soln., absolute i. r. intensities rel. to meas. in gas phase 8=1561
 H₂O vapour, pure rot. spectrum 8=4149
 H₃O⁺ group in acid soln., i.r. spectroscopic investigation 8=4150
 HOBr, i. r., in matrix 8=12175
 HOCl, i. r., in matrix 8=12175
 HOCl, i.r. spectra of ν, bands, rel. to rot. consts. and geometry 8=21083
 HeH⁺ 1σ and 2π states, approx. wave functions calc. 8=4153
 ICN, i. r. 8=12184
 KrF₂, i. r. 8=7528
 MnO₄⁻, MO calc. of u.v. spectrum 8=12207
 NF₃, i. r. 8=1260
 NF₃, mm wave, rel. to centrifugal distortion consts. 8=1258
 NH₃, centrifugal distortion and electron spin coupling effects 8=21089
 NH₃, rel. to virtual-orbital approx. to excited states 8=1213
 N¹⁴H₃, resolution of central line, at J = 3, K = 3, ΔF = 0 8=4163
 N₂O₃, i. r. 8=7538
 N₂¹⁵O¹⁸, i. r. vibr. rot. bands 8=21086

Spectra—contd

inorganic molecules, polyatomic—contd

- N_2O , near i.r. 8=21088
 N_2O , vibrational state relaxation times, spectrophone determ. 8=21090
 $NSCl$, i.r., and molecular props. 8=4161
 O_3 , 9.6 μ absorptance band, empirical formulas 8=12221
 OCS , absorpt. and vibr. analysis, 1350-1420 \AA 8=16296
 OF_2 , Fermi diad 8=4164
 ONF , and N^{15} and O^{18} species, i.r. vibr. 8=7539
 S_2 , i.r. 8=12227
 S_2Cl_2 , i.r. 8=12231
 SF_6 , i.r., high resolution 8=490
 SO_2 in CCl_4 , CH_2Cl_2 , CH_3CN , absolute i.r. intensities meas. and calcs. 8=1560
 SO_2OH groups in polymer foils, i.r. continuum absorpt. extinction 8=17028
 SO_3 , Q-heads of ir. bands rel to Coriolis coupling consts. 8=21102
 $SPFBr_2$, and $SPFCI_2$, i.r. 8=16300
 $Sb(SiH_3)_3$, i.r., rel. to struct. 8=4144
 SiF_4 , i.r. 8=16301
 SiF_4 , radiative lifetimes of u.v. emission systems 8=7501
 SiH_4 8=12355
 $Sr_{10}(PO_4)_6(OH)_2$, i.r. frequencies 8=12234

inorganic molecules, polyatomic, radiofrequency

- See also Nuclear magnetic resonance and relaxation;
 Paramagnetic resonance and relaxation.
 $H_2B_2O_3$, cyclic. 8=12170
 HBF_4 8=21063
 HCN and DCN , l -type resonance doublets 8=7522
 NSF 8=12219
 $SuDBr_3$, from 28 to 40 GHz 8=21105
 $SiHBr_3$, from 28 to 40 GHz 8=21105

inorganic liquids and solutions

- aqueous solns. of strong electrolytes, far i.r. absorpt. 8=21679
 azides, metallic, in soln. 8=1259
 Brillouin light spectrum determination, systematic errors 8=16833
 critical binary mixtures, spectral width temp. and angular dependence 8=21778
 hydrated electron, temp. effect 8=5705
 hydrated electrons in $H + F^-$ reaction 8=18679
 infrared absorpt., cell for low temp. use 8=8069
 infrared absorption band intensity rel. to additional bandwidth parameters 8=4588
 line anal. using Gaussian and Lorentzian convolution tech. 8=15529
 mm-wave Fourier transform technique 8=21674
 nitrates, metallic, in soln. 8=1259
 nitrates, molten mixtures, u.v. absorption 8=8085
 perchlorates, metallic, in soln. 8=1259
 polar diatomic mol. dissolved in nonpolar solvents, i.r. band shapes 8=12885
 ultra radiofrequency rel. to correlation function for molecular rotation 8=16855
 CO_2 , Brillouin scatt. in critical temp. region, obs. 8=16708
 CO_2 , near i.r., temp. effects 8=21685
 CO_3^{2-} ions, electron absorpt. 8=12793
 CS_2 Brillouin, stimulated, quasi-steady state 8=21687
 CS_2 , liquid and crystalline, sub-millimeter region 8=7568
 CS_2 , ν_3 bands 8=12265
 CS_2^{2-} ions, electron absorpt. 8=12793
 CSe_2^{2-} ions, electron absorpt. 8=12793
 $Cr(ONO)_3(H_2O)_3 \cdot 1.5 KNO_3$, formation and struct. in crystalline state and in soln. 8=9518
 $CsNiCl_4$, molten, near m.p. 8=9519
 Cs_2NiCl_6 , molten, near m.p. 8=9519
 D_2 dissolved in liquefied inert gases 8=12887
 D_2 in liq. Ar, induced rotation-translation spectra 8=1564
 H in solution in liq. Ar, translational absorpt. in far i.r. 8=12889
 H_2 in liq. Ar, induced rotation-translation spectra 8=1564
 HD in liq. Ar, induced rotation-translation spectra 8=1564
 $HSiCl_3$, 8 to 40 Gc rot. spectrum 8=4169
 $Ir(III)$ ions in fused $LiCl-KCl$ 8=1567
 KNO_3 containing KNO_2 impurity, analysis by i.r. spectra of solns. 8=23177
 $Kr-Ar$ binary mixture, at 135°K 8=7425
 MoS_4^{2-} in aq. soln. electron absorption 8=12792
 $NbCl_5$ in soln., far i.r. 8=14249
 NF_3 , solution H in, simultaneous transitions 8=21675
 NO_2^- ions in soln., shift of $n \rightarrow \pi^*$ bands 8=12890
 NO_3^- ions in soln., shift of $n \rightarrow \pi^*$ bands 8=12890
 Ni centres in molten $LiCl-KCl$ 8=8087
 Ni centres in molten $MgCl_2-KCl$ 8=8086
 $Ni(CO)_4$ in CCl_4 , corrections for CO stretching vibs. 8=1570
 $Pd(II)$ ions in fused $LiCl-KCl$ 8=1567
 $Pt(II)$ ions in fused $LiCl-KCl$ 8=1567
 $Rh(III)$ ions in fused $LiCl-KCl$ 8=1567
 SF_6 , solution H in, simultaneous transitions 8=21675
 SF_6-CO_2 critical binary mixtures, spectral with temp. and angular dependence 8=21778
 SO_2 , microwave absorpt. 8=16302
 SO_2 , and solid, vibrational 8=8088
 SO_2 soln., vibr. bandwidth, reorientation theory 8=16867
 Tl^+ ions in aqueous soln., absorpt. characts. 8=21704

Spectra—contd

inorganic liquids and solutions—contd

- WS_4^{2-} in aq. soln., electron absorpt. 8=12792
 $Zn(NO_3)_2 \cdot xH_2O$, molten 8=16868
- inorganic solids**
 alkali-halide crystals, i.r. absorpt., local vibs. of mol. impurity ions 8=14197
 alkali halides, i.r. absorpt. of U-centres, sidebands 8=4991-2
 alkali halides with injected molecular ions 8=5583
 alkali halides, two-photon theory using two-band model 9=22935
 alkali metal halides, comparison with absorpt. formula 8=8947
 azides, metallic 8=1259
 beryl, i.r. spectra of foreign mols. 8=2400
 carbides, carbon κ and metal emission bands rel. to bonding 8=2406
 $d^{2,7}$ ions in tetragonal cryst. fields 8=21798
 diamond, zero-phonon 415 $m\mu$ line temp. dependence 8=5589
 first transition ion impurities in solids 8=14171
 fluorite type crystals, rare-earth ion doped, molar absorpt. coeff. 8=23011
 fresnoite, $Ba_2TiSi_2O_8$, i.r. absorpt., rel. to isomorphous $Ba_2TiGe_2O_8$ 8=18506
 glass, emission characts. due to laser beam illum. 8=14246
 glass, irradi. effect suppressed by H high pressure synthesis 8=4996
 ice, crystalline, optical absorpt. 8=18533
 ice, γ -irradiated, solvated e obs. at 77°K 8=22989
 ice, low frequency optical spectra, interpretation using crystal lattice model 8=13326
 mixed crystals, persistence and amalgamation types of intrinsic spectra 8=22452
 nitrate ions in alkali halides, lattice vibrations and i.r. absorption spectra 8=17471
 nitrates, metallic 8=1259
 oxides in graphite electrodes thermochemical reactions, rel. to spectral line intensity 8=14385
 paramagnetic crystals, absorpt. and emission by impurity centres 8=5574
 perchlorates, metallic 8=1259
 powders, compressed and single crystal, i.r. reflection comparison 8=14169
 quartz, anomalous dispersion due to Si-K absorption 8=18560
 α -quartz, combination scatt., freq. depend. 8=18561
 rare-earth salts, ion-pair 8=9497
 rare-earth sesquisulphide single crystals. 8=9119
 rel. to band struct. semi-empirical calc. in non-cond. solids 8=8915
 ruby, absorption meas. 8=1995
 ruby, optically excited, absorpt. and emission props. 8=14196
 ruby, pink, nonlinear absorption of coherent resonance radiation 8=18499
 semiconductors, i.r. absorption 8=9493
 sphalerite: Fe^{2+} , i.r. absorpt. of Fe^{2+} 8=18570
 steel, analysis of decomposition process and inter-element effect 8=14392
 tetrathiomolybdates, i.r. 8=2438
 tetrathiotungstates, i.r. 8=2438
 transition metal anions, i.r. and Raman 8=9542
 transition metal complexes with tetrazoline-5-thiones 8=14188
 Tuttons salt, line anal. using convolution tech. 8=15529
 uranyl salts, D_2O isotopic shifts 8=5641
 Al, X -ray K-satellites and K-absorption 8=2398
 $Al_2O_3 \cdot V^{3+}$, absorption lines, Zeeman effect up to 79 kOe at 4.2°K and intensities 1.3-20.3°K 8=9500
 $AlSb$, Te and Se donors, photoexcitation 8=22953
 $Ba, 0.3-4.0$ eV range, and band structure 8=5598
 $BaF_2 \cdot Gd^{3+}$, Stark splitting and centre of gravity of $^6P_{7/2}$ and $^6P_{5/2}$ 8=23015
 $BaTiO_3$ with Fe and Co impurities, transmission props rel. to elec. props 8=18187
 $Ba_2TiSi_2O_8$, fresnoite, i.r. absorpt., rel. to isomorphous $Ba_2TiGe_2O_8$ 8=18506
 Bi in Si , photoexcit. lines, anomalous broadening rel. to optical phonons 8=5601
 BiI_3 refl., doublet structure rel. to spin-orbit interaction, 1-5 eV 8=9509
 Br_2 , solid film at 80°K, u.v. absorpt. rel. to intermol. interactions 8=18510
 $[C_6H_5)_4As][MoOBr_4]^-$, i.r. $Mo-O$ stretching freq. 8=9552
 CN^- in alkali halides, environmental perturbation 8=2405
 CO_2 , near i.r., temp. effects 8=21685
 CS_2 , crystalline and liq. in sub-millimeter region 8=7568
 $CaDPO_4$ and dihydrate i.r. 8=5594
 $CaF_2:Nd^{3+}$, effect of rare earth on Nd^{3+} optical centre 8=5593
 $CaF_2:Ti^{3+}$, optical, Jahn-Teller splitting 8=14126
 $CaF_2:Yb^{3+}$, rel. to polarization effects in cubic cryst. field 8=21800
 $Ca_3Fe_2Si_2O_{12}$, F^{3-} 3d e configs. splitting by cryst. field 8=1654
 $CaHPO_4$ and dihydrate, i.r. 8=5594
 CaS , SrS phosphors absorpt. excit. and i.r. flash stimulation 8=9511
 $Ca(SO_3F)_2$, i.r. 8=9562
 $Ca_xSb_2O_7$ ($x = 1, 2, 3; y = 4, 5, 6$), reflection 8=14363

Spectra—contd

inorganic solids—contd

- CaWO₄:Nd activated, role of Nd in reduction coloration 8=22962
 CaWO₄:Yb³⁺, absorpt. and Zeeman effect 8=14205
 CdCl₂:Ag, γ -irradiated, absorption bands 8=9419
 CdL₂, absorpt. bands 8=5660
 CdI₂ (Eu), absorpt. bands 8=5660
 CdS luminesc., absorpt. and refl. rel. to doping, heat treatment and deform., 4.2°K 8=9606
 CdS luminesc. excit. by high photon densities, 4.2 and 77°K 8=9607
 CdS, splitting of exciton lines by uniaxial stress 8=14273
 CdSb₂O₄, reflection 8=14363
 CdSe, band-edge emission; excitation intensity effect 8=14316
 CdSe luminesc., absorpt. and refl. rel. to doping, heat treatment and deform., 4.2°K 8=9606
 CdSe, splitting of exciton lines by uniaxial stress 8=14273
 CdTe, absorption edge, imperfections effect 8=5603
 CdTe, far i.r., 30cm⁻¹ to 4000cm⁻¹ 8=14207
 CdTe, i.r. absorpt. 8=14208
 ClO₃⁻ ions in alkali-halides, i.r. 8=22968-9-70
 ClO₄⁻ ions in alkali-halides, i.r. 8=22968-9-70
 CoF₂, optical 8=22974
 CoBr₂, absorption, high temp. and pressure 8=1580
 CoCl₂:MCl (M=Rb, K, Na, Li), symmetry changes rel. to CoCl₂ conc. 8=9516
 CoCl₂, absorption, high temp. and pressure 8=1580
 CoO, semiconducting, near and far i.r. absorpt. by small polarons 8=23008
 Cr, L-emission, fine structure 8=14270
 Cr³⁺ diopside, absorpt. 10 000–20 000 cm⁻¹, 1, 7–290°K 8=18520
 Cr(CO)₆ halogen and pseudohalogen derivs., i.r. 8=14209
 CrO₄²⁻ in chloroaspidosite (Ca₃PO₄Cl) 8=14099
 CrO₂Cl₂, cryst. at 1.7°K, electronic absorpt. 8=22971
 Cr(ONO)₃(H₂O)₅ 1.5 KNO₂, formation and struct. in crystalline state and in soln. 8=9518
 CsBr, Raman and i.r. spectra at second order, interpretation 8=5595
 Cs₂DyF₇, i.r. absorpt. 8=21814
 CsHCO₃, CsDCO₃, i.r. 8=18556
 CsNiCl₂, effect of melting 8=9519
 Cs₂NiCl₂, effect of melting 8=9519
 Cu, thin films, absorpt. 8=5596
 Cu₂O rel. to band struct., absorpt. and refl. obs. 8=9524
 Cu₂O exciton absorpt., uniaxial press. and n irrad. effects obs. 8=9521
 Cu₂O rel. to exciton-phonon interactions, n=1 line profile, 4.2–112°K 8=9527
 Cu₂O, 4 exciton line series, effect of plane stress 8=22973
 Cu₂O, neutron-irrad., absorpt. and photoconductivity 8=5597
 CuCl absorpt. and photocond. rel. to excitons, 4°K 8=9251
 CuCl crystals, two-photon absorption 8=2412
 CuCl emission line lifetimes, positions and intensities, 4.2–300°K 8=9526
 CuCl exciton absorpt., 4.2°K 8=9523
 CuCl exciton states rel. to absorpt. spectrum oscils. 8=8932
 CuCl luminesc. and weak absorpt. rel. to exciton complexes 8=9525
 CuI layers, absorpt. and reflect. at liq. N₂ temp., rel. to nature of substrate 8=9528
 Cu(SO₃F)₂, i.r. 8=9562
 D₂O in solid N₂, i.r. absorpt. 8=22977
 Dy, M_{IV} and M_V absorpt. lines and edges 8=5602
 Dy₂O₃ single cryst. 8=18522
 Er ferrite-garnet, absorption, dichroism and mag. anisotropy 8=18523
 Eu, 0.3–4.0 eV range, and band structure 8=5598
 EuAl borate, nonstoichiometry 8=8410
 EuF₃, absorpt. 8=14214
 EuO, u.v. reflect. 8=18524
 Eu₂O₃, u.v. reflect. 8=18524
 FeF₂, near i.r., mag. effects 8=18525
 Fe(SO₃F)₃, i.r. 8=9562
 Ga in Si, photoexcit. lines, anomalous broadening rel. to optical phonons 8=5601
 GaAs, band-edge emission, excitation intensity effect 8=14316
 GaAs diffused p-n junctions, luminescence spectra 8=5663
 GaAs, with Li complexes, local mode 8=22982
 n-GaAs:S, Se, Te, i.r. absorpt. 8=18528
 GaSb, laser diode, fine structure 8=444
 Gd, M_{IV} and M_V absorpt. lines and edges 8=5602
 GdF₃ powder, Gd³⁺ energy structure obs. 8=2421
 Gd₂O₃ powder, Gd³⁺ energy structure obs. 8=2421
 Gd₂O₃, u.v. reflect 8=18524
 Ge, absorption edge, imperfections effect 8=5603
 Ge, absorpt. rel. to photon-assisted magnetotunnelling in elec. and mag. fields 8=5260
 Ge, electroreflectance, line shape 8=2199
 Ge, exciton lines, obs. with optical wavelength wobbles 8=5573
 Ge, thermorelectance in region of a critical point, calc. and obs. 8=14217
 H halides trapped in inert-gas crystals, theory 8=8230
 HBr in solid N₂, i.r. absorpt. 8=9554

Spectra—contd

inorganic solids—contd

- HBr, solid film at 80°K, u.v. absorpt. rel. to intermol. interactions 8=18510
 HCl dimers in solid solns., far i.r. 8=18532
 HCl in inert-gas matrix, i.r. 8=9537
 HCl in solid N₂, i.r. absorpt. 8=9554
 H₂NH₂PO₃ films, i.r. absorpt. in polarized light, 400–4000 cm⁻¹ rel. to internal vibrations 8=14224
 In-doped, Ar, Kr and Xe films, absorption and auto-ionizing levels of In 8=9541
 n-InSb, absorpt. in 0.2–4 mm. range at 4.2°K 8=18537
 InSe crystal, infrared absorption, transition energy and radiative recombination lifetime 8=5609
 IrCl₆²⁻ in cryst. at 20°K 8=22922
 KBr, doped with Ca²⁺ or Ba²⁺ with NCO⁻, i.r. rel. to complexes formed 8=14233
 KBr in the far i.r. 8=5613
 KBr:OH, i.r. absorpt., rel. to temp. dependence of intensity of OH⁻ vibrations 8=18538
 KCl, doped with Ca²⁺ or Ba²⁺ with NCO⁻, i.r. rel. to complexes formed 8=14233
 KCl:OH, i.r. absorpt., rel. to temp. dependence of intensity of OH⁻ vibrations 8=18538
 KCl:Pb absorpt., OH⁻ ions effects rel. to activator solubility, obs. 8=21824
 KCl:Ti absorpt., OH⁻ ions effects rel. to activator solubility obs. 8=21824
 K₂CO₃, i.r. 8=18556
 KBr, containing H₂O mols. 8=4953
 KCl, containing H₂O mols. 8=4953
 K₂CuFe(CN)₆, tetragonal, i.r. and e.s.r., rel. to X-ray analysis 8=13265
 KHCO₃·2H₂O, i.r. 8=18556
 KH₂F₃, i.r., and struct. of H₂F₃⁻ ion 8=2425
 KH₂PO₄ films, i.r. absorption, internal vibrations 8=9545
 KI, pure and doped, transmission and reflection, low temps. 8=18540
 KI: TI⁺, absorpt. and emission at 77°K rel. to TI⁺ clustering 8=23056
 KMF₃ (M = Mg, Mn, Co, Ni), i.r. reflectance rel. to lattice vibrations 8=2426
 KMF₃ (M = Mg, Mn, Co, Ni, Zn, Mg/Ni), i.r. transmission rel. to multiphonon processes 8=2427
 KMGf₃, i.r. transmission, rel. to lattice vib. anal. 8=2428
 KNiF₃, i.r. transmission, rel. to lattice vib. anal. 8=2428
 K₂NiFe(CN)₆, cubic, i.r. and e.s.r., rel. to X-ray analysis 8=13265
 Kr–Ar binary mixture at 77°K and 1600 bar 8=7425
 KSO₃F, i.r. 8=9562
 KZnF₃, i.r. transmission, rel. to lattice vib. anal. 8=2428
 LaCl₃:Gd³⁺ 8=16975
 LiF, 6955Å zero-phonon line, pseudo Stark and uniaxial stress splitting 8=18542
 MgAl₂O₄, optical transitions rel. to temp., Ni²⁺ and Cr³⁺ dopants 8=23000
 MgCl₂:Ag, γ -irradiated, absorption bands 8=9419
 MgO, absorption and emission, fluorescence 8=9620
 MgO:Co²⁺, near i.r. absorpt. 8=23050
 MgO with Mn impurity, h.f.s. 8=14238
 MgO:Ni²⁺, near i.r. absorpt. 8=23050
 MnF₂, i.r., due to lattice vibrations 8=14241
 MnF₂, uniaxially stressed, exciton magnon sidebands 8=14240
 MnO₂ films, i.r. 8=4750
 MnS 8=2484
 α -MnS, reflectance and absorpt. rel. to elec. conductivity 8=18057
 MnS/ZnS mixed crystals. 8=2484
 MnSb₂O₄, reflection 8=14363
 (NH₄)₂Cr₂O₇, i.r., low-temp. 8=14250
 (ND₄)₂Cr₂O₇, low temp. i.r. 8=23006
 (NH₄)₂SO₄ and (ND₄)₂SO₄, low-temp. i.r. 8=23005
 NO absorpt. rel. to mol. excited states, 2300–1100Å 8=14243
 NO₂⁻ in solid solns., i.r. 8=2439
 N₂O, i.r. absorpt. bands rel. to isotopic mols. and crystal lattice vibrations 8=14251
 N₂O pure and in a matrix, between 63 and 14°K 8=18552
 NaCl, emission characts. due to laser beam illum. 8=14246
 NaCl:Eu luminesc., excit. and absorpt. rel. to luminesc. centres, obs. 8=9623
 NaCl:Ni absorpt., OH⁻ ions effects rel. to activator solubility, obs. 8=21824
 NaCl:OH, i.r. absorpt., rel. to temp. dependence of intensity of OH⁻ vibrations 8=18538
 NaClO₃ crystals, u.v. and i.r., X-ray induced 8=18548
 Na₂[Fe(CN)₅NO]·2H₂O, i.r., rel. to assignment of bands 8=14248
 NaMg[Cr(C₂O₄)₃]·9H₂O, polarized absorpt. 8=14247
 NaNiF₃, i.r. transmission, rel. to lattice vib. anal. 8=2428
 NaNO₃, absorpt. spectra from 450–5700cm⁻¹ 8=9556
 NbCl₅, far i.r. 8=14249
 Nd glass, measurement cross-section stimulated emission 8=449
 Ni²⁺ in MgO, absorption, line shift rel. to temp. 8=2442
 NiBr₂, absorption, high temp. and pressure 8=1580
 NiO, absorpt., fine structures 8=2441

Spectra—contd

inorganic solids—contd

- NiO, semiconducting, near and far i.r. absorpt. by small polarons 8=23008
 α -O, absorpt, bands at 4.2°K, effect of 170 kOe mag. field 8=5626
 α -O, absorpt. line splitting in strong mag. field 8=14252
 O_2 , α , β , γ forms, 34000-42000 cm^{-1} 8=5625
 OCS cryst., i.r. intensity of librational mode 8=14201
 P sulphides, dispersed in AgCl 8=18553
 PbBr₂:Mn luminesc. excit. and emission and absorpt. 8=9622
 PbCl₂:Mn luminesc. excit. and emission and absorpt. 8=9622
 PbTe-PbS solid solns., i.r. transmission, rel. to forbidden band optical width 8=18554
 Rb₂CO₃, i.r. 8=18556
 RbHCO₃.2H₂O, i.r. 8=18556
 RbHCO₃, RbDCO₃, i.r. 8=18556
 RbMnF₃ 8=2449
 RbMnF₃, i.r. reflectance rel. to lattice vibrations 8=2426
 RbNiF₃, magnon sidebands in visible and i.r. absorpt. region 8=23010
 Ru, in solid Ar matrix, optical absorpt. and X-band e. s. r. 8=18558
 SbI₃ refl., doublet structure rel. to spin-orbit interaction, 1-5 eV 8=9509
 SbSI, microwave response, photo-induced, obs. 8=5630
 Sc₂O₃:Er³⁺, absorpt. and emission 8=14260
 Se, i.r. rel. to reflectivity and transmission 8=8615
 Si, exciton lines, obs. with optical wavelength wobbles 8=5573
 Si:B, "internal" impurity spectrum, conc. depend. 8=13426
 Si, B-doped, internal absorpt. lines half-widths, temp. depend. 8=14263
 Si, B(Al, Ga and In)-doped, rel. to acceptor states 8=5285
 SiC crystals, deduction of energy spectrum of acceptor states 8=5668
 SiC, fibrous single cryst., i.r. 8=2455
 SiC polytypes, infrared absorption 8=23013
 Si₃N₄, deposited on GaAs, i.r. absorpt. 8=14262
 SO₂, and liqs., vibrational 8=8088
 SnO₂, thin films, u.v. absorption edge 8=2458
 SrF₂, F-centres obs. 8=2014
 SrF₂:Gd³⁺, Stark splitting and centre of gravity of ⁶P_{7/2} and ⁶P_{5/2} 8=23015
 Sr,Sb₂O₇ (x = 1, 2; y = 4, 5), reflection 8=14363
 TlBr:Mn luminesc. excit. and emission and absorpt. 8=9622
 TlCl:Mn luminesc. excit. and emission and absorpt. 8=9622
 TlI crystal, CsI stabilized, transmission in 30-65 μ region 8=5640
 V, L-emission, fine structure 8=14270
 V₂O₅, diffuse reflection spectra 8=18564
 Yb, M_{IV} and M_V absorpt. lines and edges 8=5602
 YGa garnet, Er³⁺ optical obs. intensities and quantum counter action 8=22979
 Zn.K β _{2,3} band fine structure 8=23027
 ZnO, impure, with adsorbed O₂, i.r. absorpt. studies 8=4769
 ZnO single crystal, transmission spectrum, rel. to exciton absorpt. and exciton-phonon complexes 8=14272
 ZnO, splitting of exciton lines by uniaxial stress 8=14273
 ZnO:Cu²⁺, absorption band obs. 8=14211
 ZnO:Ni(Co), lattice-vibration effects 8=9563
 ZnS phosphors, luminescence and electroluminescence, time constants 8=5677
 ZnS-phosphor, vibrational structure in stimulation spectrum 8=2459
 ZnS, Fe²⁺ i.r. luminescence, 5 and 77°K 8=2491
 ZnS;S²⁻, photoluminescence, dark conductivity 8=5000
 ZnS, Se_{1-x}, infrared reflection, transmission and Raman, LO and TO phonons 8=4909
 Zn(SO₄F)₂, i.r. 8=9562
 Zn tellurite glass, i.r., optical transmission range 8=5644
 ZnTe, i.r. transmission and reflection 8=2460
 ZrO₂, monoclinic, diffuse reflectance characts. as function of purity 8=18568

inorganic solids, radiofrequency

- See also Nuclear magnetic resonance and relaxation;
 Paramagnetic resonance and relaxation.
 Dy, microwave absorption phenomena at 9.44 and 35.3 Gc/s, 10-290°K 8=14269
 Er, microwave absorption phenomena at 9.44 and 35.3 Gc/s, 10-290°K 8=14269
 Ho, microwave absorption phenomena at 9.44 and 35.3 Gc/s, 10-290°K 8=14269
 LiAl(SiO₃)₂ (spodumene) heated crystals, e p r of Mn²⁺ 8=22909
 LiAl(SiO₃)₂ (spodumene) natural crystals, e p r of Mn²⁺ 8=22908
 Tb, microwave absorption phenomena at 9.44 and 35.3 Gc/s, 10-290°K 8=14269
organic molecules and substances
 See also Molecules.
 acetamide, vibration and potential energy constants 8=4174
 acetonitrile, in soln., vibration bandwidth 8=21681

Spectra—contd

organic molecules and substances—contd

- acetophenone in chloroform, co-band width and intensity at 1682 cm^{-1} 8=4588
 acetylene, excitation by proton collisions 8=1288
 alcohols, bandwidth of OH stretching vibration 8=8228
 n-alkanes, far u.v. 8=12249
 alkyl benzenes crystals, absorpt. rel. to mol. config. 8=5645
 alkyl iodides, γ -irrad. at -196°C 8=14275
 allene, two rotational lines 8=21112
 amides, theory 8=12250
 aminopurines, electronic spectra calc. 8=7594
 anthracene crystals, absorpt. and fluorescence spectra symmetry 8=18631
 anthracene derivatives, displacement due to dispersion interaction 8=4176
 anthracene in diethylaniline, luminescence 8=7560
 anthracene, γ -irrad., colour centres 8=17689
 anthracene, reflection, near exciton excitation low temp anomaly 8=23030
 anthracene, triplet-triplet absorption under Shpol'ski's condition 8=21147
 anthracene vapour, fluoresc. fine struct. and vibr. analysis, 23 000-28 000 cm^{-1} 8=1274
 9-anthranaldehyde in alcohol and hexane solutions, singlet-triplet conversion 8=21693
 9,10-anthraquinone, sensitized emission in visible region 8=4177
 aromatics absorpt. rel. to conjugated π -bonds, obs. 8=4178
 aromatic compounds, triplet-triplet absorption under Shpol'ski's condition 8=21147
 aromatic hydrocarbons, luminescence 8=7553
 aromatic mols., triplet-triplet absorpt. at 77°K 8=7561
 aromatic, 77°K, triplet-triplet absorpt. 8=7554
 aromatics, transient absorpt. 5000-8800 Å 8=4179
 azaindole, electronic, oscillator strengths meas. 8=7580
 azatetrabenzoporphins, polarization and absorpt. rel. to porphyrin ring e struct. 8=21116
 azoalkanes, electron states 8=12255
 azobenzene, continuous bands 8=4182
 1,2-benzanthracene, triplet-triplet absorption under Shpol'ski's condition 8=21147
 benzodioxins, u.v., P-method calc. 8=7575
 benzene crystals, absorpt. rel. to mol. config. 8=5645
 benzene in compressed O₂, 3300 Å transition 8=12259
 benzene and derivatives, structure of ν (CH) vibration bands, 300 and 80°K 8=12260
 benzene, large-angle electron-impact 8=16224
 benzene, liquid and crystalline state, sub-millimeter region 8=7568
 benzene luminesc., N and Ar excit. in solid solns., obs. 8=13036
 benzene in solid solns., matrix effects rel. to intramol. vibrs. and lattice vibrs. coupling, 77°K 8=13037
 benzene, u.v. absorpt. 8=7567
 benzil cryst., optical rotatory dispersion, circular dichroism and absorpt. 8=2463
 benzophenone and derivatives, triplet-triplet absorpt. 8=12263
 benzophenone, flash photolysis absorpt. 8=4184
 benzophenones, polarized absorpt. 8=9566
 p-benzoquinone anion dimers in soln. 8=21186
 benzyl radical fluoresc. in methylcyclohexane, cyclopentane and methylcyclopentane, 4°K 8=12342
 benzyl radicals fluoresc. in solid solns., vibr. analysis 8=13032
 p-biphenylaldehyde in alcohol and hexane solutions, singlet-triplet conversion 8=21693
 biphenyl derivs of group IV b, u.v. spectra anal. by heteroatom model 8=8090
 bromomethyldiazirine, electronic absorpt. spectra 8=12268
 carbonyl group coupling in cyclic anhydrides and imides rel. to solvent effect on valence vibrations 8=16857
 chloranil, absorption in near u.v. 8=21126
 chlorins, optically active 8=16317
 chloro-aluminium phthalocyanine and diethylthiatricarbo-cyanine iodide pumped by ruby laser, comparison expt. and interpretation 8=452
 chloroethylene, ion-molecule reactions in, study by ion cyclotron reson. spectroscopy 8=16453
 chloroform, gas and liq., ν_h bands 8=12265
 chloromethyldiazirine, electronic absorpt. spectra 8=12268
 α -chloronaphthalene two-photon absorpt. 8=16865
 chlorophyllide a and b fluoresc. polarization and absorpt., 390-440 μ 8=21700
 3-chloropyridine, near u.v. absorption 8=21130
 cinnoline vapour, rel. to electronic spectrum 8=16318
 coronene, excited singlet state, nsec absorpt. 8=9728
 coronene in CCl₄, phosphoresc. rel. to mol. deform. by lattice interactions, 77°K 8=1577
 coronene, π transitions, free-electron and MOLCAO calcs. 8=4139
 critical binary mixtures, spectral width temp. and angular dependence 8=21778
 cyclohexane-aniline critical binary mixtures, spectral width temp. and angular dependence 8=21778
 cyclohexane benzene, near u.v. absorption 8=16861
 de-excitation in rare-earth chelate solns. 8=16333
 deuterobenzenes, vibr. band structure 8=21683

Spectra—contd**organic molecules and substances—contd**

- diacetylene- h_2 , - d_2 , absorption, in vacuum u.v. to 1000 Å 8=12245
- diatomic, Franck-Condon factors rel. to mol. constant var. 8=4173
- dibenzosuberone, absorpt. phosphoresc. and polarization spectra 8=8096
- 4,4'-dibromobenzophenone, absorpt., phosphoresc. and polarization spectra 8=8096
- 1,4-dibromonaphthalene, triplet states 8=2467
- 2,4(5)-dichloroaniline, near u.v. in vapour phase 8=21132
- 2,5(6)-dichloro-p-benzoquinone, absorption in near u.v. 8=21126
- dichloromethane, $^n\text{CH}_2$ valence vibrations in vapour and condensed phases 8=16328
- diethylthiatricarbocyanine iodide and chloro-aluminium phthalocyanine pumped by ruby laser, comparison expt. and interpretation 8=452
- dihalogenomethanes in CCl_4 , methylene group valence vibr. bands rel. to weak intermol. interaction 8=1292
- diiodomethane, $^n\text{CH}_2$ valence vibrations in vapour and condensed phases 8=16328
- 2,6-di-isopropyl phenol, OH vib. absorpt. line, elec. field induced shift 8=1572
- α -diketones, emission and absorpt., rel. to excited state geometry 8=1297
- p-dimethoxybenzene, near u.v. absorption and emission 8=21133
- dimethylacetylene, vib., theory necessary for anal. 8=1294
- dimethylaniline, α,β -unsaturated ketone derivatives in toluene, electronic absorption 8=21702
- 1,2-dimethylcyclopropane, cis- and trans-, vibration, calc. and interpretation 8=7587
- 2,3-dimethyl-naphthalene in n-hexane rigid matrix at 77°K, absorpt. and emission 8=14286
- 1,2- and 2,3-dimethylnaphthalene, triplet-triplet absorption under Shpol'ski's condition 8=21147
- 1,4-dioxane, solvent shift obs. rel. to structure 8=16862
- dioxazines, electronic spectra, MO calc. 8=4205
- diphenyls, 4-monosubstituted, absorpt. rel. to ionization pot. and conjugated π -bonds, obs. 8=4212
- DPPH, high press., low temp. effects 8=18579
- 1,4-distyrylbenzenes, 4-monosubstituted, absorpt. rel. to ionization pot. and conjugated π -bonds, obs. 8=4212
- dye laser flashlamp excitation obs. 8=451
- ethane, excitation by proton collisions 8=1288
- ethane-1,1,1- d_3 , Raman spectrum and rot. consts. obs. 8=16321
- ethane, solid films, far u.v. 8=14283
- ethanal, luminescence vibrational analysis 8=7577
- ethylamine and its deuterated analogs, dissociative mechanism by mass spectra 8=16326
- ethylamine molecule, microwave 8=7578
- ethyl chloride, absorption of microwaves 8=7579
- ethyl ether Brillouin, stimulated quasi-steady state 8=21687
- ethylene, excitation by proton collisions 8=1288
- ethylene, large-angle electron-impact 8=16224
- fluorobenzaldehydes, emission obs. 8=21122
- formate ion in various states, rel. to isoelectronic AB, mols. 8=1269
- α -germyl ketones, electronic spectra 8=21159
- glycerine, liquid, Brillouin scatt., 23-90°C 8=21689
- halogenophenanthrenes, n.m.r. obs. 8=9461
- haloquinone complexes in polymer matrices, at high press. 8=14274
- N-heterocyclic complexes, ionization potential determ. 8=12455
- heterocyclic cpds., u.v. 8=21142
- heterocyclics, transient absorpt. 5000-8800 Å 8=4179
- heterocyclic, at 77°K, triplet-triplet absorpt. 8=7554
- heterocyclic mols., triplet-triplet absorpt. at 77°K 8=7561
- n-hexane Brillouin, stimulated, quasi-steady state 8=21687
- hexatrienes, substituted, HMO calc. of electronic spectra 8=12273
- hydrochinolines, spectral parameters of K and B bands 8=21677
- 8-hydroxy-1-methyl quinolinium hydroxide anhydro-soln. in chloroform 8=1566
- indole, electronic, oscillator strengths meas. 8=7580
- iodine and substituted pyridines charge transfer complexes, rel. to structure and stability 8=4216
- ketones, alcoholized, vapour phase, $\nu_{\text{C=O}}$ frequency 8=7582
- liquids, intensity in wing of Rayleigh line rel. to vibrating molecule model 8=16851
- liquids, mm-wave Fourier transform technique 8=21674
- liquids, overtones of combination scattering 8=1559
- macromolecules, scattering in soln. 8=12381
- metal-phthalocyanines, luminesc. singlet-singlet transitions 8=18591
- methane, excitation by proton collisions 8=1288
- methane, solid films, far u.v. 8=14283
- p-methoxyphenol, near u.v. absorpt. obs. 8=21156
- 2-methyl-1,4-naphthoquinone vapour, in near u.v. 8=7585
- methylene blue, absorpt., depend. on solvent, dye conc. and solutes conc., rel. to water induced dimerization 8=8123

Spectra—contd**organic molecules and substances—contd**

- monochlorobenzene, u.v. absorpt. 8=7567
- naphthalene crystal, attenuated total refl. 8=9569
- naphthols, dichroic spectra in PVA sheets, rel. to vibronic transitions 8=14285
- naphthols, triplet state, rel. to electronic structure 8=21152
- naphthalene solid solns., phosphoresc. and delayed fluoresc. rel. to triplet state, obs. 8=23068
- α - β -naphthylaldehyde in alcohol and hexane solutions, singlet-triplet conversion 8=21693
- nucleotides 8=16334
- 1,4-naphthoquinone, visible emission in vapour phase 8=7589
- α - β -naphthylaldehyde in alcohol and hexane solutions, singlet-triplet conversion 8=21693
- oxalyl chloride 8=2468
- pentachlorotoluene, crystals and solns., and vibr. assignments, i.r. obs. 8=9575
- pentaerythrite, mono, di and trihalogen derivatives, vibr. spectra 8=7576
- perfluoro-aza-propene, $\text{CF}_3\text{N}=\text{CH}_2$, u.v. absorpt. band of NCF_2 radical 8=7626
- perylene, π transitions, free-electron and MOLCAO calcs. 8=4139
- phenanthrene, cryst. 8=5648
- phenanthrene, n.m.r. obs. 8=9460
- p-phenetidine vapour, near u.v. abs. 8=21157
- phenol and N,N-dimethylacetamide, solvent effects on H-bonding 8=1571
- phenol, 2750 Å band system, extended vib. assignments, and band contour anal. 8=16337
- phenylacetylene, singlet and triplet electronic states 8=4210
- phthalocyanine lanthanides, acid adducts, absorption 8=4589
- pinacyanol dye in alcohol, long wavelength bands 8=8091
- polyacene solid solns., energy transfer bibliography 8=14162
- polynuclear hydrocarbons, e.s.r. 8=12307
- polystyrene, vac. u.v. absorpt. 8=14290
- polyvinyl alcohol films dyed in solutions of iodine in iodides and bromides, absorption in 220-1000 nm range 8=5650
- propane, solid films, far u.v. 8=14283
- pseudocyanine dye in alcohol, long wavelength bands 8=8091
- purine, electronic spectra calc. 8=7594
- 2-pyrazolines, trisubstituted, structural analogues 8=12293
- pyrene, π transitions, free-electron and MOLCAO calcs. 8=4139
- pyridazine, singlet-triplet transitions 8=9573
- pyridocyanines, stereoisomerism 8=7596
- 2-pyrrolidone, vibration spectra, 3500-250 cm^{-1} 8=7595
- rhodamine B dye lasers, emission 8=21694
- α -silyl ketones, electronic spectra 8=21159
- solids, non-cond., rel. to band struct. semi-empirical calc. 8=8915
- solid solns. of mols. and radicals, and vibr. analysis 8=13032
- spiropentane, vibration calc. and interpretation 8=7588
- trans-stilbenes, 4-monosubstituted, absorpt. rel. to ionization pot. and conjugated π -bonds, obs. 8=4212
- stilbene, triplet-triplet energy transfer and "phantom triplet" 8=21160
- terphenyls, 4-monosubstituted, absorpt. rel. to ionization pot. and conjugated π -bonds, obs. 8=4212
- 2,3,5,6-tetrachlorotoluene crystals and solns., and vibr. assignments, i.r. obs. 8=9575
- tetrachloro-p-xylene crystals and solns., and vibr. assignments, i.r. obs. 8=9575
- tetramethylpyrazine emission rel. to triplet state struct., 4.2°K 8=22907
- thienylphenyl-ketones and -thioketones, electronic, steric effects obs. 8=4218
- p-tolunitrile, emission bands 8=21163
- α,α,α -trichlorotoluene, vac. u.v. absorpt. 8=4219
- 3,4,5-trimethoxyphenylglyoxal semidiones, e.s.r. measurements 8=12305
- triphenylene in CCl_4 , phosphoresc. rel. to mol. deform. by lattice interactions, 77°K 8=1577
- triphenylphosphine, modified Mataga SCF calc. 8=4209
- TMPD-chloranil crystals, u.v. and visible meas. 8=8595
- u.v. absorption spectra cooling device for recording 8=22930
- u.v., orbital energy level diagrams, limitations on use 8=1268
- Wurster's blue perchlorate, cryst. reflect. 8=14288
- Wurster's cation dimers in soln. 8=21186
- xanthane $\pi\pi^*$ and $n\pi^*$ levels location, absorpt. and luminesc. obs. 8=1302
- xyl radicals fluoresc. in cryst. xylenes, vibr. analysis obs. 8=12356
- Al phthalocyanines, absorpt. spectra in soln. 8=21688
- CCl_4 , liquid and crystalline state, sub-millimeter region 8=7568
- CCl_4 soln. of SO_2 , absolute i.r. intensities meas. and calcs. 8=1560
- CCl_4 , 71°C, spectrum of scatt. microwave radiation 8=21686
- CCl_4 vibr. intensities rel. to intermol. interactions 8=16274

Spectra—contd

organic molecules and substances—contd

- CCl₂F₂, solution H in, simultaneous transitions 8=21675
 CD₄ nuclear hyperfine interactions 8=12119
 CD₄, vibration, anharmonic calc. method 8=12133
 CF₂, absorpt. at 2500 Å, and rot. structure 8=4188
 CF₄, radiative lifetimes of u.v. emission systems 8=7501
 CF₄, solution H in, simultaneous transitions 8=21675
 [(CF₃)₂CF]₂SO₂, i.r. vibration 8=16273
 CH, absorption and emission spectroscopy, in low-press. oxyacetylene flames 8=21189
 CH, electronically excited in hydrocarbon flames 8=7509
 CH radical, electronic absorpt. bands 8=7618
 CH₂, centrifugal distortion and electron spin coupling effects 8=21089
 CH₄, nuclear hyperfine interactions 8=12119
 CH₄, vibration, anharmonic calc. method 8=12133
 CHD₃, ground state molec. consts. 8=12275
 CH₃Br, vibration-rotation band near 6000 cm⁻¹ 8=16859
 CH₃Cl₂ soln. of SO₂, absolute i. r. intensities meas. and calcs. 8=1560
 CH₃Cl, Fermi and Coriolis resonances in the ν₄ band 8=16319
 CH₃CN soln. of SO₂, absolute i. r. intensities meas. and calcs. 8=1560
 (CH₃NH₂)₂CuCl₂ 8=14104
 C₃H₂ radical, absorpt., diazopropyne photolysis obs. 8=16368
 C₆H₅OD anharmonicity variation effect on frequency perturbations ν(OH) and ν(OD) 8=16316
 C₆H₅OH anharmonicity variation effect on frequency perturbations ν(OH) and ν(OD) 8=16316
 CN, Franck-Condon factors rel. to mol. constant var. 8=4173
 CT₄, vibration, anharmonic calc. method 8=12133
 C₂T₂, i.r. absorption spectrum 8=12244
 Cr oxalate, ²E-⁴A₂ emission, rel. to Cr³⁺ conc. 8=18578
 Eu, β-diketon complexes, for laser use 8=22978
 Eu chelates, u. v. irrad., optical emission losses, study of causes 8=18571
 Li dihydroanthracene salts, electronic rel. to ion-pair structure 8=7558
 Mg-azatetrabenzoporphins, polarization and absorpt. rel. to porphin ring e struct. 8=21116
 Mn²⁺ in hexa- and tetracoordinated cpds. 8=9551
 X₃P. BH₃ type additive compounds, frequency and absorption of vibrations 8=16305

organic molecules and substances, infrared

- acenaphthene, single crystal absorpt. 8=23028
 acetates, rare earth, Pb and Cu, rel. to thermal decomp. 8=23095
 acetonitrile N-oxide, and symmetry force consts. 8=16309
 acetophenone in CHCl₃, shape intensities of i.r. absorpt. bands 8=8080
 acetyl bromide and CD₃COBr 8=7555
 acetylene, heated emission 4000-4160 cm⁻¹ 8=16308
 acetylene, rotational constants 8=16307
 acrylyl fluoride, rel. to rot. isomerism 8=16311
 Allyl halides 8=21111
 amines, primary aliphatic, absorption spectra 8=16313
 α-aminoacid hydrochlorides 8=7556
 anthracene, single crystal absorpt. 8=23028
 azides, anomalous band splittings 8=21118
 azines, absorpt. of ν_{C-N} band 8=1276
 benzene-dioxan crystallized mixture at 80°K 8=18572
 benzene, vibr. excitation spectrum 8=9567
 benzenes, paradisubstituted, far i. r. absorption 8=7566
 benzophenone, single crystal absorpt. 8=23028
 benzimidazolone derivatives 8=4186
 biphenyl, single crystal absorpt. 8=23028
 bromoacetone, rel. to rotational isomerism 8=1271
 p-bromoanisole, 400-4600 cm⁻¹ obs. 8=21682
 2-bromocyclobutanone 8=12266
 bromomalonaldehyde 8=21144
 bromomalonaldehyde anion 8=21144
 2-bromo-2,4,4-tridentercyclobutanone 8=12266
 caffeine salts 8=14277
 carboxylic acids, H-bonded 8=7571
 all-trans β-carotene, crystals, absorpt. 8=2465
 all-trans β-carotene, cryst. and free mol. electronic absorpt. 8=2465
 chlor-diphenyl-sulphone-urethanes, 9 cpds., absorpt., rel. to struct. 8=9571
 chlorobenzenes in CS₂ soln., i. r. intensity meas. of C-H out-of-plane vib. bands 8=21684
 chloroform, molec. complex with benzene 8=2464
 chloroform, in nonpolar solvents, intensity meas. of 1216 cm⁻¹ band 8=21680
 chloroform-triethylamine system 8=18649
 chloroform, using high resolution grating spectrometer 8=20078
 chloromethyl thiocyanate 8=4201
 p-chloro-phenol, OH stretching band struct. 8=4211
 chlorosilyl dialkylamines 8=1300
 complexes formed by H-bonding 8=12242
 p-cresol, OH stretching band struct. 8=4211
 cyclic mols, anal. of type A bands rel. to asymmetry parameters 8=1277

Spectra—contd

organic molecules and substances, infrared—contd

- cyclopentadiene 8=12267
 cyclopentene, ring puckering 8=16304
 cyclopentene, vibration, phases I and II 8=7590
 cyclopropane, gas and partially deuterated, rel. to force consts. 8=1298
 depsides, lichen, and u.v. 8=4191
 depsidones, lichen, and u.v. 8=4191
 deuteriochlorobenzenes, o-, m- and p- 8=7574
 deuterotoluenes, o-, m- and p- 8=7574
 dibenzenechromium iodide, band assignments and force consts. 8=14276
 dibromoacetonitrile 8=12281
 2,6 difluoropyridine, vapour and liq. 8=16341
 2,5-dihydrofuran 8=12271
 2,3-dihydrofuran, ring puckering 8=16304
 2,5-dihydrofuran, ring puckering 8=16304
 2,3-dihydrothiophene, ring puckering 8=16304
 2,5-dihydrothiophene, ring puckering 8=16304
 diimines, absorpt. of ν_{C=N} band 8=1276
 2,5-dimethyl-1,3,4-oxadiazole 8=12285
 2,3-dimethylnaphthalene, rel. to mol. and crystal structure study 8=18574
 0,0-dimethyl phosphorochloridothioate 8=21146
 p-dithiane, absorpt. 15° and 300°K 8=18575
 p-dithiane in CS₂, absorpt. 15° and 300°K 8=18575
 ditluenechromium iodide, band assignments and force consts. 8=14276
 dixanthogens, anomalous band splittings 8=21118
 durene, single crystal absorpt. 8=23028
 ethane, high resolution 8=490
 ethyl caproate, in nonpolar solvents, intensity meas. of 1737 cm⁻¹ band 8=21680
 ethyl nitrite, gas, soln. and solid, rel. to isomerism 8=16329
 ethylene-trifluoropropylene copolymer, rel. to microstruct. 8=17298
 ethylenediamines 8=1283
 ethylgermane 8=1280
 ethylsilane 8=1280
 fluoroacetone, rel. to rotational isomerism 8=1271
 p-fluoro-phenol, OH stretching band struct. 8=4211
 formic acid adsorbed on ZnO 8=18705
 formic acid, cryst. 8=14279
 frequency shifts, correl. with gas chromatographic retentions 8=9759
 furan, cryst., absorpt. at liq. N₂ temp. 8=14280
 glycine silver nitrate and monoglycine nitrate, absorption obs. 8=5646
 haloacetonitriles, far i. r. 8=16323
 halogenated ethanes 8=12269
 halogens cyanoacetylenes 8=1270
 hexachloroethane, far i. r. fundamentals, discussion of freqs. 8=16320
 indolene in CCl₄, shape intensities of i. r. absorpt. bands 8=8080
 isothiazole, microwave obs. and struct. 8=21162
 isothiocyanates, anomalous band splittings 8=21118
 ketones, intermolecular forces 8=1287
 ligand-metal-halide complexes, far i. r. 8=1296
 malonaldehyde anion 8=21144
 metal carbonyls 8=4189
 methane, high resolution 8=490
 methylethoxy silanes, integrated intensity 8=7551
 methyl iodide, fundamental bands 8=8079
 methyl lithium monomer in solid Ar 8=12282
 methyl mercaptan, from 15 to 45 cm⁻¹ 8=21145
 methyl methoxysilanes on base, structure study 8=4738
 methyl nitrite, gas, soln. and solid, rel. to isomerism 8=16329
 methylphosphine 8=1289
 methylsilyl dialkylamines 8=1300
 methylene bromide, solid 8=14284
 methylene chloride, solid 8=14284
 methylene iodide, solid 8=14284
 monobromoacetonitrile 8=12281
 monodeuteriomethane, 2ν₄ band resonance 8=7583
 monohalogen diacetylenes 8=1270
 naphthalene at liquid He temp., interpretation of fundamental vibrations 8=18577
 naphthalene, single crystal absorpt. 8=23028
 organic uranyl nitrate solution, complexing study 8=21619
 1,2,4-oxadiazole and methyl derivatives 8=4204
 1,3,4-oxadiazole 8=12285
 1,2,5-oxadiazole, vapour and liq. absorpt., rel. to vib. assignment 8=16335
 oxalate free ion, D_{2d} symmetry and freq. assignment 8=21154
 oxamide, 4000-400 cm⁻¹ obs. 8=23032
 d-oxamide, 4000-400 cm⁻¹ obs. 8=23032
 paraffins, long-chain 8=13341
 o-phenylenediamine 8=1295
 pentadeuteropyridine, structure of vibration bands 8=7597
 phenanthrene, single crystal absorpt. 8=23028
 phenol-d₄, vib. and torsional i. r. freqs. 8=16336
 phenol-formaldehyde, polymer, during thermal treatment 8=4269

Spectra—contd

organic molecules and substances, infrared—contd

- phenol H complexes with benzene and ethers 8=4213
 phenol, OH stretching band struct. 8=4211
 phenol, polymeric forms, H-bond stretching freq. 8=21141
 phosphoramidates and phosphoramidothioates and struct. 8=7591
 γ -picoline-halogen complexes 8=7592
 1,4 trans-polybutadiene, structure 8=4773
 polydioxolane, rel. to chain vibs. and molec. struct. 8=18584
 polyethylene, cryst. 8=13341
 polyethylene, electron irradi. and not irradi., 150-310°K, 700-2100 cm^{-1} 8=21165
 polyethyleneterephthalate, for determ. of crystalline fraction content 8=17190
 poly- α -methylstyrene in soln. 8=21692
 poly-L-proline, in aq. soln. 8=12891
 poly(vinyl chloride), tacticity study 8=21217
 polyvinylphthalimide absorpt. and luminesc. rel. to triplet-triplet energy transfer, 15000-40000 cm^{-1} 8=12389
 polymers on base, structure study 8=4738
 polymethylmethacrylate, rotational isomerism in ester group, absorption study 8=4220
 polypentene-1, polymorphs 8=17463
 propane, high resolution 8=490
 pyridine complexes, far i. r. 8=1296
 pyridine, structure of vibration bands 8=7597
 pyrimidine, liq. N temp. meas. 8=9572
 pyridine complexes formed with metallic halogenes 8=16860
 3-pyridinesulphonic acid and salts 8=16339
 pyrrole, cryst., absorpt. at liq. N, temp. 8=14280
 rotational rel. to vel. of light 8=11122
 1,2,5-selenadiazole 8=16342
 shape intensities of i. r. absorpt. bands, liquid phase 8=8080
 1,3,4,5-tetrachlorobenzene, in nonpolar solvents, intensity meas. of 878 cm^{-1} band 8=21680
 tetrakis-[dimethylamides] of group IV 8=1290
 s-tetrazine, type-A bands anal. rel. to asymmetry parameters 8=1277
 theobromine salts 8=12300
 thiazoles, monosubstituted, vibs. and coupling 8=4217
 thiophene, cryst., absorpt. at liq. N, temp. 8=14280
 toluene glow discharge prod. polymer films, obs. 8=21894
 triethylphosphine and related cpds 8=21137
 trifluoroacetone, in proton donor solvents 8=16867
 2,2,2-trifluoroethanol as H bonding acid, freq. shifts rel. to bonds 8=16863
 2,4,6-trifluoropyrimidine, liq. and vapour 8=16340
 trimethylaluminium 8=16327
 trimethylsulphonium cpds., and freq. assignments 8=16864
 trimethylsulphoxonium cpds., and freq. assignments 8=16864
 trimethylene oxide, ring puckering 8=16304
 triphenylaluminium, rel. to vibs 8=12287
 triphenyl phosphine complexes, far i. r. 8=1296
 BF_3 :dimethyl sulphide complex, liq. 8=1569
 Ca dicarboxylates (malonate to sebacate), rel. to thermal decomp. 8=23095
 CCl_4 , molec. complex with benzene 8=2464
 CD_3 , mono, di- and tri-substituted compounds, far i. r. torsional vibration spectra 8=4196
 $\text{CD}_3\text{CD}_2\text{Cl}$, far i. r. torsional vibr. 8=4193
 $\text{CF}_3(\text{OF})_2$ 8=12279
 CF_3 , mono, di- and tri-substituted compounds, far i. r. torsional vibration spectra 8=4196
 $\text{CF}_3\text{P}(\text{O})\text{F}_2$ 8=21177
 CH_3 , mono, di- and tri-substituted compounds, far i. r. torsional vibration spectra 8=4196
 CH_3 , in photolysis of methane 8=18737
 CH_3 radical in solid Ar 8=7624
 $(\text{CH}_3)_2\text{POCl}$ 8=12286
 $(\text{CH}_3)_2\text{PSBr}$ 8=12286
 $(\text{CH}_3)_2\text{PSCl}$ 8=12286
 $(\text{CH}_3)_2\text{S}$, absorption spectra (4000-400 cm^{-1}) at 10°K 8=18573
 $\text{C}_6\text{H}_5\text{CH}=\text{NC}_6\text{H}_5$ crystals and solns., vibr. assignments, 400-3200 cm^{-1} 8=1562
 $\text{C}_6\text{H}_5\text{CH}=\text{NC}_6\text{H}_5$ crystals and solns., vibr. assignments, 400-3200 cm^{-1} 8=1562
 $\text{C}_6\text{H}_5\text{CH}=\text{NC}_6\text{H}_5$ solns. and powder, vibr. assignments, 400-3200 cm^{-1} 8=1562
 Cu(II) formate in planar network struct. 8=2466
 Fe(III) porphyrins, rel. to zero-field splitting 8=2469
 Os carbonyl halide complexes, solvent effects on stretching and vib. modes 8=16856
 S-N cpds., bond stretching freqs. 8=1299
- organic molecules and substances, radiofrequency**
 See also Nuclear magnetic resonance and relaxation;
 Paramagnetic resonance and relaxation.
 difluorobenzenes 8=1285
 ethyl alcohol from 9-50 GHz, application of Watson formula 8=21135
 ethyl alcohol, spectra in region 13-50 kMc/sec. obs. 8=4192
 m-fluorotoluene 8=21164
 formaldehyde, HCHO, K-type doubling lines 8=21140
 formic acid, HCOOH, K-type doubling lines 8=21140
 imidazole, microwave obs. and struct. 8=21162

Spectra—contd

organic molecules and substances, radiofrequency—contd

- methyl bromide and methyl bromide- d_3 8=12280
 methyl chloride, in excited vibr. states 8=21149
 methylisocyanate 8=12278
 methylisothiocyanate 8=12278
 4-methylpyridine, 8 to 37 GHz 8=12295
 methylthiocyanate 8=12278
 methyl vinyl sulphide 8=12283
 1,2,4-oxadiazole, microwave obs. and struct. 8=21162
 propylene imine 8=12291
 trans-propyleneimine 8=12290
 quinolines, oscillation strengths 8=4590
 rotational rel. to vel. of light 8=11122
 1,2,5-selenadiazole 8=12298
 CFCl_3 , h.f.s. 8=16315
 CHCl_3 , h.f.s. 8=16315
 $\text{CH}_3\text{CH}_2\text{CH}_2\text{OH}$ rot. const. and Q^p , Q^c branches transitions, 10-32 GHz 8=7593
 $\text{CH}_3\text{CH}_2\text{OD}$ rot. const. and pR , bP branches transitions 18-33.5 GHz 8=1282
 $\text{CH}_3\text{CH}_2\text{O}^{18}\text{H}$ rot. const. and bQ branch transitions 18-33.5 GHz 8=1282
 CH_3SiCl_3 , 8 to 40 Gc rot. spectrum 8=4169
 HCN, l-type doublets 8=12270
- Spectral line breadth**
 See also Doppler effect; Stark effect; Zeeman effect.
 atomic, weak collisions, intense fields, effects 8=7372
 atoms, press. broadened, quantum oscillations 8=20932
 broadening of spontaneously emitted, in presence of laser beam 8=12040
 broadening theory, phase effects 8=1154
 chloroform, gas and liq., ν_3 bands 8=12265
 collision broadening 8=21197
 collision broadening, quantum theory, rel. to mech. of negative absorption 8=2395
 complex mols, shape of continuous absorpt. bands 8=1214
 Doppler broadening, effect of collisions 8=1153
 electron collisions, semi-classical broadening calculations 8=7459
 gas laser, Doppler and impact broadening, and press. effects 8=11034
 gas layer, containing 2- or 3-level atoms, rel. to radiative transfer 8=16188
 Gaussian and Lorentzian line shapes 8=19904
 hydrogenic atom, fall in intensity and e partition energy 8=1157
 liquids, exciton theory 8=4586
 liquids, frequency broadening by short pulse 8=4574
 liquids, i. r. absorpt., coupling of oscillators 8=16854
 magneto-optical meas. of line profiles 8=4057
 plasma, e corrls. in relaxation theory 8=21350
 plasma, theory 8=16538
 polar diatomic mol. dissolved in nonpolar solvents, i. r. band shapes 8=12885
 rotational absorpt. lines, microwave, collision broadening 8=1224
 ruby, microwave absorpt. spectra 8=14089
 slit function effects, atomic lines 8=20082
 stars 09-B5, H γ and HeI lines 8=10157
 symmetric-top mols., self-broadening of rot. lines 8=12121
 Al in anode zone of vacuum pulse discharge, broadening 8=16203
 Ar arc plasma, Stark broadening of Ar I lines 8=12057
 Ar, self-broadening and oscillator strengths 8=7416
 ArII lines, Stark broadening parameters, obs. 8=20949
 CO, 3 ν band 8=16269
 CO $_2$, liq. and solid, press. broadening 8=21685
 CO $_2$, 00 0 -10 0 transition, gas perturbation 8=7537
 CS $_2$, gas and liq., ν_3 bands 8=12265
 D, using broadening of D $_A$ line, expt. 8=16194
 D $_2$ O, press. broadening obs. using CN maser 8=21073
 Ga atoms, line-broadening collisions 8=12083
 H atoms, broadening theory 8=4062
 H, broadening by Stark effect 8=1159
 H $_{\alpha}$ line in aurora, variation in width over 1 hour 8=14650
 H $_{\alpha}$, $\nu_{\alpha\beta}$ Stark broadening in plasma column 8=4063
 H-line Stark broadening functions 8=12051
 H stimulated emission in beam laser 8=421
 HBr, far i. r. microwave, shape and collision effects 8=7523
 HCl, DCl, far i. r. microwave, shape and collision effects 8=7523
 Hg 198 , 2537Å line, D $_2$ and H $_2$ effects compared 8=7470
 Hg, resonance line, press. broadening by He 8=7403
 Hg vapour + C $_6$ H $_4$ impurity, absorption spectrum of Hg λ 2537Å line 8=16287
 In atoms, line-broadening collisions 8=12083
 Kr, collision broadening and shift due to Ne, Ar, He 8=20956
 Kr, self-broadening obs. 8=20955
 Kr, self-broadening and oscillator strengths 8=7416
 Li line broadening by microfields in LiH plasma 8=12515
 Nd glass laser, travelling-wave mode 8=20000
 Ne, self-broadening and oscillator strengths 8=7416
 Si I, shift by Van der Waals interact. with Ar atoms 8=7423
 S II linewidths, inelastic e collision contributions 8=20991

Spectral line breadth—contd

- Si, B-doped, absorpt. line broadening 8=2452
 Si, B-doped, half-widths of internal absorpt. lines, temp. depend. 8=14263

Spectrochemical analysis

- absorption, fluorescence and phosphorescence spectrometry, sensitivity comparison 8=23180
 alloys, X-ray fluorescence 8=9750
 amino acids, sensitive linear flowing-stream photometer 8=5762
 arc source, for emission anal. of solns. 8=23185
 atomic absorpt., evaluation as source 8=23183
 atomic absorpt. flame photometry, instrument developments 8=18777
 atomic absorpt. and fluoresc. in graphite cell, comparison 8=18775
 atomic absorpt. method, high temp. flames 8=14458
 atomic absorpt., multi-elements, using time-resolved spark 8=18783
 atomic absorpt., selection of wavelengths 8=18774
 atomic absorpt. using bandpass filter 8=489
 atomic fluorescence flame photometry, at. fluorescence intensity rel. to at. conc. 8=2543
 atoms, fluoresc. flame, quantum efficiency 8=4059
 carbonyl acids in perethers, determ. 8=2549
 d.c. arc, thermochemical reactions of oxides in graphite electrodes 8=14385
 detector for gas chromatography, spectral-emission type 8=18764
 2,4-dicyanopentanes, high-resolution n.m.r. 8=16884
 emission, use of N_2O -acetylene flame 8=18782
 flame, absorpt.-emission intensity ratio 8=18778
 flame, atomic fluorescence, absorption, emission sensitivity 8=2542
 flame, optimizing instrument parameters 8=18779
 flame spectroscopy, analytical applications, bibliography 1800-1966 8=23182
 free radicals, direct i. r. spectrometry 8=16367
 gamma-resonance Mossbauer spectra, use in chemistry and solid state 8=692
 gas chromatographic retentions, correl. with i. r. freq. shifts 8=9759
 gas mixtures, i. r. technique 8=9758
 gases, optical-acoustic, selectivity and sensitivity on gas pressure 8=23192
 h. f. plasma source, for emission of solns. and powders 8=20086
 hollow-cathode lamp for atomic absorpt. 8=497
 hollow cathode lamp for atomic fluoresc. flame 8=18781
 internal reflection, rel. to bulk optical props. 8=22934
 laser materials, trace analysis 8=18773
 laser microanal. by atomic absorpt. 8=14457
 marine waters, of trace elements 8=18773
 maser materials, trace analysis 8=18773
 metals in flames by atomic fluoresc., optimum conditions 8=14460
 metals in metal, atomic absorpt. spectrophotometric method 8=2544
 microwave induced Ar plasmas for metal excitation 8=18785
 minerals, i. r. spectrography 8=9760
 paper, fibre comp. by i. r. absorpt. 8=14462-3
 polyethylenimine, via Cu chelate, by spectrophotometry 8=16393
 rotation dispersion and circular dichroism meas., instruments 8=20061
 standard specimens, metrological prep. 8=18784
 steel, Cu determ. by at. absorpt. spectrometry 8=2545
 steel, Mn determ. by at. absorpt. spectrometry 8=2547
 steel, NH_3 extraction-spectrophotometric determ. 8=2546
 steel, oxygen content, by d. c. carbon arc 8=9751
 steel, sample condition in spark region 8=2548
 steel, by spark emission, decomp. and inter-element effects 8=14392
 steel, of V trace quantities 8=18773
 symposium on trace characterization 8=18773
 trace characterization-chemical and physical, symposium NBS, USA, Oct. 1966 8=8437
 trace characterization by different methods 8=18773
 trace characterization, flame, emission and X-ray techniques 8=18789
 trace characterization, techniques 8=18771
 trace characterization, techniques review 8=18772
 trace characterization, techniques survey 8=18790
 trace elements homogeneously distrib. in powders, laser-spark excitation 8=23186
 Ag in sub-mg. quantities 8=18773
 Al alloys, estimation of Zn 8=23184
 Al and alloy, Cu determ. by at. absorpt. spectrometry 8=2545
 Al alloy, Mn determ. by at. absorpt. spectrometry 8=2547
 Al metals and alloys, Fe content, from absorption at 2483 Å 8=9756
 B in low-alloy steel, vacuum spectrometric determ. 8=23188
 Bi, atomic-absorpt. characts., using turbulent-flow total-consumption burner 8=18780
 Ca, picomole range, emission 8=9757
 CdS_xSe_{1-x} , concs. of components from birefringence 8=5763

Spectrochemical analysis—contd

- Co complex detect. by reflectance spectros. after thin-layer chromatographic separation 8=23176
 Cu alloys, estimation of Zn 8=23184
 Cu complex detect. by reflectance spectros. after thin-layer chromatographic separation 8=23176
 Dy in ThO_2 , direct determ. 8=18787
 Eu in ThO_2 , direct determ. 8=18787
 Gd in ThO_2 , direct determ. 8=18787
 Hg(II) in aq. KI, spectrophotometry 8=9753
 I_2 , vac. u. v., hollow cathode light source, quant. anal. 8=18788
 KCl pressed disc prep., reactions of Na_2CO_3 8=14373
 KNO_3 containing KNO_2 impurity, analysis by i. r. and Raman spectra of solns. 8=23177
 Li traces in refractory oxides, using hollow-cathode discharge tube 8=23189
 Mg, picomole range, emission 8=9757
 Mo determ. in UF_6 by atomic absorpt. 8=18776
 N in iron and steel, spectrophotometry 8=23178
 Na, trace impurity determ. by atomic absorpt. 8=14459
 Nb in stabilized stainless steels, spectrophotometric determ. 8=23179
 Ni complex detect. by reflectance spectros. after thin-layer chromatographic separation 8=23176
 Os, thiocyanate spectrophotometry 8=9752
 Pb alloys, estimation of Zn 8=23184
 Si impurity analysis 8=18771
 Si, metal impurities determ. 8=18081
 Si in steel, line interferences due to Cr, V and Mo 8=23190
 Sm in ThO_2 , direct determ. 8=18787
 Ta thin films, impurities determ. 8=18786
 Ta in B, U, Zr, spectrophotometry 8=9749
 U, estimation in carnotite ores by spark technique 8=14461
 U, urinary, method for radiation analysis 8=23181
 Zn, high-purity, comparison of fine optical spectrographic methods 8=23191

Spectrometers

- See also Mass spectrometers; Monochromators; Particle spectrometers; Spectrophotometers; X-ray spectrometers.
 astronomical multi-slit spectrograph 8=23498
 bremsstrahlung, use of single-crystal refl. 8=6794
 cam mechanisms for interference modulation 8=3361
 echelle spectrometer-spectrograph for astronomical use 8=14740
 Fabry-Perot photoelec., obs. deconvolution, least-squares method 8=6524
 Fabry-Pérot photoelec. type, spectrum calibration using Michelson interferometer 8=20077
 Fabry-Perot, scanning using Moiré fringes system 8=6531
 field-sensitive, for quasi-coherent scatt. studies 8=11195
 grating type, for rapid scanning over wide spectral range, design and capabilities 8=20079
 high resolution grating, for near i. r., construction 8=20078
 high resolution grating spectrometer, for four-pass operation in near i. r. 8=6529
 interferometer spectrometer, scanning, use as optical chopper 8=6528
 i. r. high resolution, using Zeeman-tuned laser 8=490
 liquid-scintillation types, developments 8=6644
 for magneto-absorpt. in pulsed fields at 4.2°K 8=11157
 neutrons, very slow, high resolution for cold source of high flux reactor 8=6964
 new methods of instrumental spectroscopy, colloquium 8=20071
 nuclear quadrupole resonance, f. e. t. appl. 8=15436
 optical system for time and space resolution 8=20076
 resolving power test, 5350 Å band of I_2 8=16289
 spectrographs image illuminance distrib. with concave diff. grating, calc. 8=487
 spectroradiometer-luminometer, for luminescence spectral distributions: descr., applic. 8=492
 slit function effects, atomic lines 8=20082
 time-of-flight, appl. to neutron cross-section meas. 8=7196
 u. v. reflection spectrum using photoelec. method 8=15532
accessories
 bandpass filter for atomic absorpt. 8=489
 Barnes ES-100 Educational, absorpt. of four filters 8=491
 cassette, for simultaneous recording of several lines 8=20084
 cooling vessel for molecular u. v. absorpt. recording 8=22930
 data reduction, computer programme 8=15534
 for diffraction gratings blazed to high orders, predispersion order sorter 8=6534
 Fabry-Perot recording interferometer 8=15545
 Fourier transform spectrograph using Lippmann effect 8=3363
 infrared absorption cell for liquids at low temps. 8=8069
 Kodak I-Z plates, modified hypersensitization procedure 8=494
 laser source for scanning-function calibration 8=15539
 multichannel spectral recording instrument 8=20083
 near i. r., for diffuse reflectance 8=496
 n.m.r., spin echo attachment, single coil 8=10988
 optical cell, null press., for liquids at elevated temp. and press. 8=21676
 Raman, oblique illumination 8=3360
 real-time electro-optical analyzers, with coherent detection 8=6532

Spectrometers—contd**accessories—contd**

- for reflectance, bidirectional, dual beam device with top illum. and $\pm 45^\circ$ sample tilting 8=6533
- shock-tube flash spectrography, explosive shutter 8=15047
- sliding shutter, e. m. induction drive 8=15535
- solar, large Echelle grating 8=10385
- white surface reference standards, U.S.S.R. specimens 8=466

CsBr and CsI i.r. windows, polishing 8=495

Spectrometers, radiofrequency

- See also Nuclear magnetic resonance and relaxation measurement; Paramagnetic resonance and relaxation measurement.
- automatic swept-freq. spin-echo, for n. m. r. in ferromag. mats. 8=9454
- coaxial bridge with helical line sample holder, for nuclear quadrupole res. 8=10991
- e. s. r., for short-lived free radicals prod. by u. v. flash photolysis 8=12339
- fluctuations spectrum analyser, statistical props. 8=10981
- with high modulation freq. for mag. resonance parameters 8=10980
- hybrid tees for n. m. r. 8=3280
- i. r.-microwave double reson., using CO₂ laser 8=6402
- mm spectroscopes, klystron-oscillator power supply 8=15425
- microwave, construction of helices, design criteria 8=3276
- microwave, continuous wave, for u. p. r. 8=19905
- microwave, solid state, Stark modulated 8=3275
- modified Robinson type, for n. q. r. of N¹⁴ nuclei 8=3283
- n. m. r. frequency sweep using voltage controlled oscillator 8=19908
- n. m. r., heating system 8=19912
- n. m. r. 100 MHz, phase-lock circuit 8=15430
- n. m. r. p stabilised 8=388
- n. m. r. sensitivity and magnet technology, advances 8=15431
- n. m. r., spin-stabilization for double proton rdsonance 8=3281
- n. m. r., variable freq., construction from commercial grid dip meter 8=10987
- n. q. r., improved super-regenerative instrument 8=15437
- resonator, high Q, for NO absorption meas. at 150 GHz 8=7536
- for spin-lattice relax. times, meas. 8=19913
- system for meas. frequencies up to 345 GHz 8=6401

Spectrophotometers

- a. c. for low intensity signals, dark noise discrimination 8=20081
- actual Littrow and Wadsworth systems, deviation, scanning equation and spectral widths of slits 8=15531
- energy-compensated spectrofluorometer, adjustment 8=15533
- laboratory performance assessment 8=11153
- modulated optical null type, for flash excitation reactions 8=3359
- 12-channel Doppler-profile, plasma scattered laser light 8=3357
- ultraviolet, sodium salicylate appl 8=15494
- vibrating-reed, conversion to modulation system 8=15536

Spectrophotometry

- atomic line, spectral distrib. from Perot-Fabry meas. 8=15530
- chromic (III) cpds., stability study 8=23079
- Chudze-Lovas (1967) supernova, spectrophotometry 8=5900
- diffusion pump fluid film thickness meas. 8=16728
- γ Cen, visual binary system 8=10200
- ocean, for atm. absorpt. coeffs. 8=9872
- polyethylenimine, analysis via Cu chelate 8=16393
- polyphenyl diffusion pump fluid film thickness, continuous meas. 8=7949
- protein mol. wt. determ. 8=18642
- radiation intensity, measurements in vacuum u. v. region by aromatic phosphors 8=11159
- solar corona, 5303 and 6374 Å lines, charts of equal luminosity 8=19323
- solar, high resolution, appl. of rapid spectral scanning 8=10386
- spectral irradiances determ. 8=462
- CO, low concentrations in air, determ. 8=14589
- KNO₃ and other nitrates, molten mixtures, u. v. absorption 8=8085
- N in iron and steel, determ. 8=23178
- Os determ. from thiocyanate 8=9752
- Ta, spectrochemical determ. in metals 8=9749

Spectroscopy

- See also Spectra; Spectrometers; Spectrophotometry.
- in acoustics, optics and radiophysics using a modulation method 8=6404
- advanced optical techniques, book 8=15489
- atmosphere, upper, Saskatchewan University research, review 8=9925
- atomic absorpt., atomization of solid samples, use of solid fuel 8=11150
- atomic absorpt. for thermodynamic meas 8=16962
- atoms, highly ionized, rel. to space research observations 8=16192

Spectroscopy—contd

- carbonyl cpds., u. v. study of reversible hydration, limitations 8=9682
- carrier distillation, electrodes, apparatus for rapid prep. 8=14903
- computer processing of spectrograms for absolute intensities 8=493
- derivative, to filter unwanted contents in source spectrum 8=20073
- electron-excited Auger electrons for material analysis 8=22729
- exploding wires, time-resolved 8=15537
- Fabry-Perot photoelec. obs. deconvolution, least-squares method 8=6524
- Fourier, spectral recovery from interferogram 8=15528
- Fourier transform, masks in optically formed spatial filters, storage capacity 8=6514
- Fourier transform, sources of systematic error 8=1253
- Fourier transform, for unequal number of input and output points 8=6522
- gamma-resonance Mossbauer use, in chemistry and solid state 8=692
- high-resolution, Fabry-Perot developments 8=6520
- hook method for f-valves, theory and use 8=6525
- i. r., adsorbed species on solids, cell 8=6530
- i. r., AgCl as an embedding medium 8=18553
- i. r. band envelopes, math. functions to fit 8=6526
- i. r., review and current applications 8=11149
- interferometric, using modified line shape 8=11152
- internal reflection, for meas. conformation of adsorbed polymers 8=8350
- internal reflection, rel. to bulk optical props. 8=22934
- laser photolysis in nsec range 8=9728
- lasers, giant pulse, Fabry-Perot interferograms quasi-linear dispersion 8=6416
- line anal. using Gaussian and Lorentzian convolution tech. 8=15529
- low temp., sapphire window mountings 8=3362
- molecular 8=16246
- molecular beam triple reson. for h. f. s. 8=16279
- molecular, liq. cryst. matrices 8=8008
- molecular spectroscopy, conference, Copenhagen Denmark (1965) 8=16239
- molecules, optical, Canadian N. R. C. apparatus and meas., review 8=7484
- molecular structure and spectroscopy, conference Ohio USA (1966) 8=16238
- molecular wt. determ., by i. r. 8=9755
- new methods of instrumental spectroscopy, colloquium 8=20071
- nuclear improvement of peak to background ratio 8=3453
- nuclear quadrupole moments of even-Z isotopes optical meas. 8=7068
- optical illumination, coherent, phase-modulated, spectrum broadening 8=20072
- photographic images, faint, electronic enhancement 8=6583
- plasma, high-temp. exptl. device 8=16539
- plasma, high-temp. preliminary expts. 8=16540
- plasma jet, seeded, photography of isotherms 8=7781
- plasma jet temp. meas. techniques 8=12572
- plasma, vacuum u. v. and soft X-rays 8=12512
- polarized internal reflexion for molecular orientation of fibres 8=16394
- scattering media, physical principles and methods 8=11151
- spectra reconstruction from coherence meas., phase problem 8=20074
- stellar spectra, automatic data reduction 8=23540
- theoretical, symposium (Yerevan, 1966) 8=11148
- Toronto University research programmes review 8=6523
- Zeeman, solid state, crystallographic alignment 8=22936
- Hg¹⁹⁸ 4358 Å line shape, intensity correl. obs. 8=20075
- He plasma in theta pinch discharge, electron densities and temp. meas. 8=21349

Light sources

- arc, low-temp., for emission anal. of solns. 8=23185
- flames, evaluation for atomic absorpt. 8=23183
- graphite electrodes, purification by electron beam heating 8=23187
- h. f. plasma, for emission of solns. and powders 8=20086
- hollow-cathode, high intensity, λ 3247.5 Å -copper resonance line profile by interferometry 8=3365
- hollow-cathode lamp for atomic absorpt. 8=497
- hollow cathode lamp for atomic fluoresc. flame 8=18781
- ionic beam source, electronically excited by thin foil, characts. 8=6535
- laser, continuously tunable, applications 8=15485
- lasers for spectrometer scanning-function calibration 8=15539
- microwave induced Ar plasmas for metal excitation 8=18785
- modulator for hollow cathode lamps 8=15536
- Nernst glower, control circuitry 8=3364
- ruby laser, tunable, repetitively pulsed, with solid etalon mode control 8=19993
- spark, time-resolved, for atomic absorpt. anal. 8=18783
- vacuum u. v., low voltage, high capacitance and very low inductance spark source 8=7399
- volume, intensity definition 8=11158

Spectroscopy—contd**light sources**—contd

- C arc, electrode particle trajectory photography 8=16428
- C resonance lamp 8=15538
- He-Ne laser for Raman excitation of powders 8=14175
- K r.f. resonance lamp for Zeeman scanning in kgauss fields 8=6536
- Ne laser, i.r. Zeeman-tuned, for absorpt. line fine-structure anal. 8=11160
- Xe laser, i.r. Zeeman-tuned, for absorpt. line fine-structure anal. 8=11160

Spectroscopy, radiofrequency

- See also Nuclear magnetic resonance and relaxation; Paramagnetic resonance and relaxation; Spectrometers, radiofrequency.
- magnetic resonance, many photon transitions, obs. 8=22904
- magnetosphere, He ion effect 8=9921
- microwave resonance absorpt., modulation effect 8=15426
- mm-wave Fourier transform, for liquids 8=21674
- using modulation method 8=6404
- semiconductors, organic, review 8=14088
- separator beam at the AGS 8=3491

Speech

- See also Hearing.
- American English /s/ transitions as cues to adjacent stop consonants identity 8=201
- articulation score meas. in reverberating conditions using a correlation method 8=15077
- automatic recognition, time-invariant measure of contour similarity 8=19597
- discrimination, consonant-vowel-consonant words, statistical theory 8=19599
- distortion in reverberating hall 8=19592
- filter, linear, giving max. intelligibility over noisy channel for peak power limited transmitter 8=15080
- identification of talkers from monosyllables in context 8=6188
- information transfer by short tonal signals and tone pitch duration threshold 8=3095
- intelligibility, effect of compressor action 8=207
- intelligibility gain, binaural, and release from masking, prediction 8=205
- laryngoscopic technique using fiber optics 8=14892
- listening, selective, application of signal detection theory 8=216
- periodic and jittered pulse patterns, perception of temporal gaps 8=15082
- recognition of spoken digits in real time, sequential system 8=3084
- release of masking through interaural time delay 8=3088
- rhyming minimal contrasts, diagnostic articulation test 8=3080
- sound perception, dimensions 8=200
- syllable duration in oral and whispered reading, masking noise effect 8=15078
- synthesis, machine aided format determination 8=204
- vocal freq., perceptual study 8=19596
- voiceprints, automatic system recognition 8=19598
- vowels, Polish, formant freq. regions 8=6187
- vowel quality as function of spectrum envelope and fundamental freq. 8=15079
- vowel recognition, formant transitions effect 8=202
- waveform instantaneous amplitude, asymmetries in the cumulative probability distributions 8=203

Spherical aberration. See Aberrations, optical.**Spicules.** See Sun, prominences.**Spin.** See Elementary particles; Hyperons/spin and parity; Mesons' spin and parity; Nucleus/spin and parity; Rotating bodies.**Spin echo.** See Nuclear magnetic resonance and relaxation.**Spin-lattice relaxation.** See Crystals/lattice mechanics; Magnetic resonance and relaxation.**Spin waves.** See Ferromagnetism/spin-wave theory.**Spinors.** See Quantum theory, wave equations.**Spions (pions with spin).** See Pions.**Spirality.** See Elementary particles; Field theory, quantum.**Sporadic-E.** See Ionosphere/E-region.**Sprays**

- See also Aerosols; Drops; Jets.
- combustion of liq. fuel, comparison with single drops 8=19657
- evaporation in air, continuum model 8=8184
- liquid, droplet size distribution 8=4635

Spurions. See Elementary particles.**Sputtering**

- alkali halides, and colour centres, induced by slow electron bombardment, formation theory 8=13472
- e.m. field, crossed, effect 8=7651
- films, resistive temp. and pressure var. 8=8303
- focused collision sequence generation, inverse-square potential calcs. 8=17696
- glow-discharge tube cathodes, variation with current 8=2019
- magnetron anodes, cathode heating by ion bombardment 8=15334
- metal carbides, with Cd⁺ ions up to 500 eV energy, coeffs. 8=8762
- metals, comparison of laser beam and pulsed discharge effects 8=17698

Sputtering—contd

- metallic target, electron emission by Auger de-excitation of atoms 8=5422
- plasma, thermonuclear, search for impurity atoms using neutrons 8=16600
- spark discharge in oil, cavity configuration rel. to pressure 8=21249
- transition metal nitrides and borides, by Cd⁺ ions, coeff. determ. 8=17705
- travelling-wave tubes, pumping, auxiliary electrode 8=15287
- triode, new discharge arrangement, high current in 10⁻⁴ torr range 8=7653
- Ag, polycrystalline target, coeff. rel. to incident angle of Ne, Ar and Kr ions 8=8766
- Al, distribution of sputtered atoms by electron microprobe 8=21876
- Al₂O₃, by Cs ions, surface oxide film 8=8760
- Ar films, due to negative O ions in O discharge 8=21877
- Cu polycrystalline target, coeff. rel. to incident angle of Ne, Ar and Kr ions 8=8766
- K, differential sputtering ratio (energy spectrum) meas. for incident Ar and Xe ions 8=2029
- LaB₆, by Cd⁺ ions, coeff. determ. 8=17705
- MnO₂ films, prep. and props. 8=4750
- Mo, polycrystalline target, coeff. rel. to incident angle of Ne, Ar and Kr ions 8=8766
- Ni polycrystalline target, coeff. rel. to incident angle of Ne, Ar and Kr ions 8=8766
- Ni-Cr alloys, in Ar, comparison of film and target composition 8=22254
- Ni-Cr films, use of H₂ for thickness control 8=8777
- NiFe₂O₄ ferrite films, single cryst., prep. 8=18362
- Si and SiO₂ films, r.f. and d.c., rel. to re-emission coeffs. 8=2032
- Si₃N₄ films prod. 8=17139
- Si₃N₄ films reactively sputtered, evidence of excess Si 8=21890
- SiO₂, in Ar, r.f. dielectric system with non-grounded electrodes 8=17138
- Ta₂O₅ film capacitors preparation 8=13097
- Ti by positive ions of N₂, O₂ and Ar 3-9 keV 8=8780
- W films, and condensed on NaCl, structure rel. to temp. 8=4759

Stacking faults. See Crystal imperfections.**Standards**

- See also Constants; Units.
- air-dielectric coaxial-lines for immittance, skin-effect corrections 8=10964
- calorimetric, pure Cu for low temp. 8=15127
- e.m.f. rel. to a.c. Josephson effect 8=17989
- frequency multiplier, phase-locked 8=2877
- masses, precision for torsion balances 8=19349
- ohm 8=19708
- optical radiation scale development 8=11117
- primary, mutual inductance 8=283
- resistance, absolute determination by Campbell's method 8=282
- quartz metre gauges, interferometric meas. 8=10475
- reference data, concept for properties of substances 8=10473
- thermal n flux density, optimal geometry 8=20869
- time, mean atomic scales accuracy 8=10484
- 2.5 MHz frequency, design 8=19351
- voltage, electrostatic method for absolute meas. 8=10824
- wavelength, Al III vacuum u.v. 8=16202
- wavelength, use of spontaneous emission from He-Ne laser 8=15467
- white surfaces for colorimetry and spectrophotometry 8=466
- X130 standard attenuator, for super high freq. transmission systems 8=15415
- Cs, errors in reproducing frequency 8=15160
- H and Cs freq. standards, intercomp. of average freq. and freq. stability 8=10483
- Mn⁵⁴ γ -spectrometric source calibration 8=20750
- Ra-Be(α , n) neutron source, comparison of meas. 8=11618
- Zn⁶⁵ γ -spectrometric source calibration 8=20750

Stark effect

- electronic spectrum of asymmetric rotor 8=21035
- gas-phase electron reson. of free radicals 8=12345
- molecular crystals 8=22940
- n.m.r. and n.q.r., rel. to effective field acting on electrons 8=14133
- in plasma, with h.f. stochastic fields, linewidths rel. to main characts. 8=7778
- plasmas spectral line shapes calc. 8=1402
- quadratic, computation of 39 const. for 8 elements 8=20935
- quadratic shift in plasma temperature meas. 8=7787
- R-centre, inclusion of Jahn-Teller, spin-orbit and internal stress interaction 8=1992
- Rochelle salt:Cu²⁺ ferroelec. e.p.r. Stark effect obs. 8=14101
- rotational transitions identification and dipole moment detm. 8=21037
- ruby, linear, in U absorpt. band 8=9501
- waveguide for 258 GHz modulator 8=6365
- Al in anode zone of vacuum pulse discharge, line broadening and displacement 8=16203
- ArII lines, broadening parameters, obs. 8=20949

Stark effect—contd

- BaF₂:Gd³⁺, Stark splitting and centre of gravity of ⁶P_{3/2} and ⁶P_{1/2} 8=23015
 CaF₂:Gd³⁺, thermoluminescence, splittings of ⁶P_{7/2} and ⁶P_{5/2} levels 8=14310
 Cd obs. in 5s5p ³P₁ state 8=20966
 Cs obs. in 7p ²P_{3/2} state 8=20966
 D, using broadening of D₂ line, expt. 8=16194
 H, contribution of polarizabilities 8=12048
 H lines, broadening 8=1159
 H-line broadening functions 8=12051
 H_α, γ, _δ, broadening of line profiles in plasma column 8=4063
 He II, broadening of 3203Å line 8=7383
 He-Ne laser, frequency shifts produced by 8=11058
 Hg obs. in 6s6p ³P₁ state 8=20966
 LiF, 6955Å zero-phonon line, pseudo Stark splitting 8=18542
 LiF, R-centre 8=1993
 N II, multiplet lines 8=4084
 Rb obs. in 6p ²P_{3/2} state 8=20966
 Si, B acceptor lines, effects of ext. and int. elec. fields 8=2208
 SrF₂:Gd³⁺, Stark splitting and centre of gravity of ⁶P_{7/2} and ⁶P_{5/2} 8=23015

Stars

- See also Nebulae; Novae; Sun.
 ADS 8804 and ADS 16417, eclipses probability 8=10198
 adiabatic pulsations and convective instability of gaseous masses 8=5857
 associations in Cen, statistical obs. 8=10264
 atmosphere, outside local thermodynamic equilibrium 8=2773
 atmosphere, plane parallel, specific intensity behaviour at infinity 8=2774
 atmosphere, Rayleigh scattering problems, rigorous calcs. 8=5921
 atmospheres for early type, statistical equilibrium model, Lyman continuum formation 8=10124
 BD +68°278 triple system, parallax, proper and orbital motion 8=10114
 BL Telescopii evolution and secondary body nature 8=10204
 β Canis Majoris, non-radial oscillations, effect of differential rotation 8=5901
 β Cephei pulsating variables 8=10188
 β 208AB, ADS 6914 and HD 73752 orbits 8=19106
 binary, aberration of light 8=14788
 binaries, obs. of gravitational radiation by photon counters in space 8=14959
 binarity of HD 3950, obs. 8=10209
 binary, scalar component of gravitational radiation 8=6079
 binarity of Z And and components nature 8=10201
 binaries, spectroscopic, masses and inclinations calc. 8=19183
 bright, micrometer meas. of companions 8=10210
 CQ Cephei, eclipsing-binary, variability of envelope 8=19145
 calibration of correl. between abs. magnitude and K line width, use of small parallaxes 8=19110
 central, of planetary nebulae, model atmos. 8=10217
 Cephei, photoelectric search 8=2786
 Cepheids, classical, evidence for overtone pulsations 8=10193
 cepheids, composite period-luminosity relation at mean and max. light 8=19179
 cepheids S Mus and β Dor, temps. from H_α profiles and pulsation modes obs. 8=10181
 cepheid U Sgr vel., radius and light vars. obs. 8=10192
 Ci 18, 2354 binary, parallax and orbital motion obs. 8=23557
 χ Draconis effective temp., abundance of metals and microturbulent vel. obs. 8=2791
 in clusters and assoc., O and B stars luminosity depend. interstellar reddening rel. to system age 8=10167
 clusters globular, apparent visual magnitudes of brightest stars 8=19180
 clusters and multiple stars, work of R. M. Petrie 8=10195
 cluster NGC 6834, distance and colour excess 8=10196
 clusters, open, distance moduli and distances from photo-electric H_β index obs. 8=10207
 clusters, open, intrinsic diameters of 8 Trumpler classes 8=14785
 cluster, unclassifiable, in large Magellanic cloud 8=14777
 coalescence, and multiple supernova interpretation of quasi-stellar sources 8=5947
 colour, 33 dye-transfer photograph in blue and i. r. light 8=10165
 convention of Italian Astronomical Society, Catania Italv (1966) 8=19111
 convective cores, criterion for occurrence 8=10142
 rel. to cosmological models, clusters and universe ages 8=19076
 DA, colours and space motions 8=10174
 dK and dM type, radial velocities 8=10115
 δ Cephei variable type, adiabatic pulsations of models, rel. to mixing path lengths 8=19173
 δ Cephei, convection-pulsation interaction 8=10126
 δ Ceti, period since 1900 8=19127

Stars—contd

- Delta Sonti, relative phases of light and radial velocity variations 8=10178
 dense, thermal equilibrium and characteristic time for thermal propagation 8=2776
 distance to star associated with Scorpio XR-1 8=23503
 distribution of neighbours 8=14747
 distribution in space 8=14814
 dynamical friction enhancement of travelling massive particle by stellar co-operative effects 8=19108
 dwarfs, G and K, energy distribution at red wave-lengths 8=5894
 dwarf in near group galaxy 8=19218
 dwarfs, red, convective, Kr 60 A and B, vibr. stability calc. 8=19123
 dwarf, white, pulsation after mass loss during development 8=19177
 early-type, effective temp. and bolometric corrections 8=19151
 eclipses in visual binary systems 8=10198
 eclipsing binary solutions, approximating functions 8=23556
 eclipsing systems, interpret. as inverse problem of the photometry classic and half-classic models 8=19188
 energy losses due to neutrino processes in hot plasma 8=10137
 epochs of minimum, determ. 8=23559
 ε Eridani and GMB 1830 convective model atmospheres compared 8=10125
 550 and B, Milky Way field in Scorpius, K line and λ4430 absorption band 8=19201
 53 Cam, light and magnetic variations rel. to wavelengths 8=19155
 44i Bootis B, VW Cephei and W Ursae Majoris radial-velocity curves 8=19187
 dynamics in a discrete phase space 8=19107
 field stars system, dynamics of test star 8=10211
 flare star, Butlers, comment rel. to ape of stellar aggregate 8=14770
 formation, interstellar matter heating and ionization by subcosmic rays 8=10245
 4C radio sources optical indentifications 8=10305
 47 Tucanae cluster diameter and ellipticity obs. 8=10208
 fundamental processes imitation and study in laboratory experiments 8=15924
 G- and -K star atmospheres, departures from LTE 8=5864
 gaseous mass, inhomogeneous, convective instability, model 8=2794
 globular clusters, blue end of horiz. branch 8=10212
 globular clusters, differential rot. 8=5908
 globular cluster in centre of Galaxy 8=5929
 GMB 1830 and ε Eridani convective model atmospheres compared 8=10125
 gravitation collapse, evolution of ejected matter rel. to nucleosynthesis 8=14726
 Hyades cluster, distance modulus 8=10202
 Hyades cluster distance modulus parallax 8=10194
 Hyades cluster, distance modulus and stellar models 8=10203
 HD 107904, radial vel. and photometric meas. 8=14774
 HD 140283 subdwarf, model-atmosphere abundance analysis 8=19125
 HD 19445 subdwarf, model-atmosphere abundance analysis 8=19125
 HD217050, spectral study 8=2784
 HD 30353, H- poor, visual magnitude and effective temp. 8=5881
 He, atmospheres 8=5891
 He shell-burning, pulsational instability 8=5873
 Hertzler, i. r. spectral classification 8=5892
 He, vibrational stability, non-constant opacity effects of 8=2788
 in intergalactic arms, formation 8=10260
 interstellar polarization, wavelength depend. 8=10173
 Jeans' instability criterion, effect of grains 8=2793
 λ Bootis, temp. and gravity 8=5885
 Leo II system obs. 8=14784
 LTE models for atmosphere 8=14750
 M giants, early, classification by photometry of 7050 Å TiO bands 8=14768
 M31 five new variables 8=23548
 Magellanic Clouds, obs. rel. to massive stars evolution 8=10274
 magnetic, α²CvN and modified solar model 8=19117
 magnetic, equilibrium, magnetostatic models 8=19116
 magnitude, directly from in-focus images, method 8=5852
 main sequence, mass-radius, mass-luminosity, empirical relations 8=14771
 main-sequence upper-part, effective-temp. and bolometric correction scales 8=14772
 massive, non radial oscillations 8=10190
 massive, particle-tracks, relativistic eqns. of motion 8=10110
 metallic-line, temp. and gravity from struct. models and spectra 8=19136
 Mira variables, analysis of motions 8=10189
 μ Orionis, spectroscopic binary, obs. 8=14789
 NGC 7006 remote globular cluster, anomalous colour magnitude diagram 8=5906

Stars—contd

neutron, shock wave propagation 8=1390
 new C star at South Galactic Pole 8=14755
 new variables, around globular clusters NGC6304, 6638 and 7099 (M30) obs. 8=19182
 non-rotating, spherically symmetric, optical appearance when gravitationally collapsing 8=19153
 ν pairs prod., hot 8=19130
 OB in I Puppis and Norma, radial vels. rel. to galactic struct., obs. 8=23594
 OB stars, distrib. in Southern Milky Way 8=10111
 one-zone pulsation model with proper boundary conditions 8=14751
 orbits, non-linear coupling of two harmonic oscillations 8=14738
 observations, direct elimination of sky background 8=23542
 oscillations, adiabatic, freq. distrib. and non-radial oscils. reson. excit. rel. to struct. 8=10183
 oscillations, radial, toroidal mag. field effects in polytrope $n=3$ 8=10129
 oscillating spheres, exact solns. in gen. relativity 8=19429
 parallaxes and proper motions of 6 nearby stars 8=10113
 parallaxes, 21 stars, from plates taken with McCormick 26-in. refractor 8=23501
 periodic magnetic variables, orientation of magnetic axes, statistical investigation 8=5902
 with phase transition, eqns. of state for equilibrium 8=5661
 Pleiades region, proper motions for 125 M stars 8=23500
 polytropes, uniformly rotating, perturbation theory 8=10116
 population I, velocity distribution and orbits in spiral galaxies 8=5932
 protostar, collapsing, dynamical calc. for different initial condns. 8=14752
 pulsating, periodic shock wave effects on atmospheric density distribution 8=5869
 R lunis Majoris system, Tu Monocerotis 8=14782
 RR Lyrae, eclipsing system, photometric elements, absolute dimensions and masses 8=19189
 RR Lyrae stars, pulsation 8=14778
 RR Lyrae variable, projected on Andromeda nebula 8=10229
 RRLyr variable type, adiabatic pulsations of models, rel. to mixing path lengths 8=19173
 radial pulsation, coupled with convection 8=14775
 radial velocities of fourteen stars between 8 and 12 mpg 8=10164
 radio, in declination range + 18° to + 20°, freq. 750 and 1410 MHz, pencil beam survey 8=23605
 radiostars, existence? 8=2799
 random motion in phase space 8=19109
 red giants, gravitational collapse of non-degenerate He shell, energy release calc. 8=10128
 red giants, limiting temp. and dynamic instability 8=19178
 red giant, Tc synthesis mechanism 8=2779
 red giant, Tc⁹⁹, disintegration probability 8=2780
 relaxation time in an infinite uniform stellar medium 8=19112
 rotating, exchange of stabilities, onset of convective Lagrangian displacements 8=5856
 rotating, line intensities calc. rel. to gravity darkening and other effects 8=19121
 rotating, pseudo-radial pulsations and stability 8=19120
 rotation stability differential, in radiative zones 8=5854
 rotational velocities and braking systems, rel. to planetary systems formation 8=5853
 rotational vels. obs. with spectracon, stars in Praesepe and Hyades clusters 8=19105
 s-process nucleosynthesis in thermal relaxation cycles 8=10144
 Scorpio-Centaurus assoc. distance moduli and distances from photo-electric H. index obs. 8=10207
 Scorpius X-ray source, model 8=10310
 Sco X-1 X-ray source, brightness variations 8=10289
 self-gravitating stellar system with uniform rotation, kinetic theory 8=23502
 self-gravitating system, one-dimensional sheet model, thermalization effects 8=5858
 73 Draconis, magnetic, spectrum, and radial velocity var. 8=10179
 solar type, non-gray model atmosphere 8=2775
 solar-type, rotation dependence on age 8=5855
 stellar clusters, dist. of vel. 8=14800
 stellar systems, statistical mechanics of violent relaxation 8=10273
 Stock 13, cluster of early-type stars 8=23515
 supergiants, F- and G-type, temps. from H α profiles, obs. 8=10181
 supernova, remnants, coherent plasma radio-emission 8=14813
 symbiotic, hot components, temp. from nebulae continuity obs. 8=5896
 thermodynamic waves and thermomagnetic instability in ionized objects 8=10109
 3C273, photographic obs. 8=10175
 276 stars in NGC6067 region, magnitudes and colours 8=19142
 UBVRi meas. applied to calculation of wideband sensor magnitudes 8=14762

Stars—contd

variability, short period, Coma cluster δ -Scuti type 8=23552
 variable α Lupi, H outflow and vel. amplitude, spectroscopic obs. 8=10182
 variable β Cen vel. vars. and spectrum, rel. to nature, obs. 8=10182
 variable Carinae brightness vars. 1963–67, UBVRi obs. 8=23544
 variable in direction SCOX-1, photometry 8=5897
 variable HD 170682, Be characts. development rel. to magnitude vars., obs. 8=23547
 variables, long-period, UBVR photoelec. obs. 8=19175
 variables in NGC 2403 galaxy 8=23593
 variables, new, in nearby galactic clusters and assoc. 8=2787
 variable SZ Lyr, period and light and colour curves vars., obs. 8=19170
 variables, short-period, photoelectric obs. 8=5898
 vibrating neutron stars, time variation of characts. 8=14773
 W Centauri and 47 Tucanae clusters, limits to neutral H content 8=23555
 white dwarfs energy content and cooling rate 8=10134
 wind, recombination shell between H I and H II 8=23576
 Wolf-Rayet stars, masses, presence of severe anomalies 8=14748
 X-ray Sco XR-1 and assoc. optical source, binary model 8=10177
 ζ tan (HD 37202), pulsation of the envelope 8=19169
 Be, temp. from nebulae continuity obs. 8=5896
 Be, three new stars HD87543, HD 91269 and HD109857 8=19139
 β CrB, abundances of elements, and atmos. turbulence and excitation 8=19159
 H mixing by He-shell flashes, calc. 8=10145
 He white dwarf, evolutionary sequence 8=10147
 O₂ and C burning, and pre-supernova models, evolution 8=5874
composition
 See also Elements/origin.
 A- and B-types binaries, He abundance 8=10130
 Am, five, oxygen and nitrogen abundances 8=23514
 Ap, overabundances of Si, Cr, Mn, Sr and Eu, binary theory 8=5867
 binaries, A- and B-type, He abundance 8=10130
 binary peculiar A star HR4072, chem. comp. 8=10199
 carbon, H C N:O equilibrated abundances calc. 8=10141
 chemical, influence on position of main sequence in Hertzsprung-Russell diagrams 8=14772
 density gradient inversion in convection zone 8=2778
 early-type, effective temp. and bolometric corrections 8=19151
 F and G main-sequence, Li/Be ratio 8=19152
 5 nonvariable C stars, H deficient, abundance analyses 8=10118
 G dwarfs, [Fe/H] ratio and u.v. excess 8=10155
 γ ser, metal abundance ratio determ. 8=5868
 Groombridge 1830 He content 8=23505
 heavy elements, synthesis by neutron capture 8=10140
 heavy elements synthesis, n radiational capture 8=10143
 HD 122563, abundances of iron-peak elements, from u.v. spectra 8=5862
 HD 30353, H-poor, abundances of light elements 8=5882
 HR 1105, Zr isotope ratios 8=14759
 HR 4533, surface gravity, temp. and [Fe/H] abundance 8=23533
 HR 4657, surface gravity, temp. and [Fe/H] abundance 8=23533
 K-type, curve-of-growth analyses 8=2782
 main-sequence, minimum mass calc. 8=19119
 neutron capture data at stellar temps. 8=5872
 OB supergiants in Orion, mass loss 8=5866
 Of, occurrence in H II regions and clusters rel. to O type 8=23512
 planetary nebulae, central stars 8=14790
 Pleiads, Li abundances 8=5863
 RU Cam, spectral obs. 8=19172
 red giants, Tc disintegration probability 8=2780
 s-process abundances obs. 8=10144
 subdwarfs, He content 8=5865
 supergiants, HD 96248 and HD 14443, N-deficiency 8=5889
 surface layers, abundance anomalies produced by nuclear reactions 8=5870-1
 τ Bootis, metal abundances 8=5860
 Tc synthesis, at different steps of stellar evolution 8=2779
 thermonuclear reaction of heavy ions 8=10151
 Ursa Major clusters, Li abundances 8=5863
 yellow supergiants, fine analysis of two, preliminary results 8=5878
 ζ Lyr A, from visible spectra by method of model atmospheres 8=23514
 H mixing by He-shell flashes, calc. 8=10145
 He, surface abundance in B stars 8=10136
evolution
 binaries, contact, W Ursae Majoris type, review 8=14783
 binaries, models approximating possible remnants after mass loss 8=19126
 binary systems, appl. of Iben's theory 8=19127

Stars—contd

— evolution — contd

- conference, Brussels, 1964 8=23510
- early and main sequence 8=10148
- formation 8=23511
- of galactic clusters 8=14787
- in galaxies, from gas with Population I composition 8=19132
- instability of gravity waves 8=21450
- low mass 8=10149
- mass loss effects 8=10146
- models with isothermal cores, secular stability 8=19129
- ν radiation from β processes rel. to matter density 8=10138
- Nova Delphini 1967 8=19148
- pre-main sequence, models, criticism 8=23513
- stellar rates of the C¹³(a, n)O¹⁶ and Be⁹(a, n)C¹² reactions 8=19131
- supermassive, stabilized by large-scaled motions 8=10139
- supernova and remnants 8=23545
- white dwarfs, ions crystallization and effect on rate of cooling 8=10152
- white dwarfs, radiation loss mechanisms, critical temp. for nuclear reactions 8=10150
- by He consumption in core, rel. to horiz. branch in globular cluster 8=10212
- He flash and thermal pulses of 1.3 solar mass star. calc. 8=19133
- Si burning, nucleosynthesis, model 8=16136

magnetism

- See also Sun/magnetism.
- α^2 CVn, cross-over effect 8=2781
- 53 Cam, light and magnetic variations rel. to wavelength 8=19155
- force-free mag. fields 8=23509
- HD 32633, variations obs. by UVB photometric and Zeeman spectroscopy 8=19154
- HD98088 cross-over effect 8=2781
- magnetic field, review of literature 8=5963
- radio sources field strengths, l.f. spectra obs. 8=23613
- turbulent motion as origin 8=10127
- variable magnetic stars, Babcock theory 8=2789
- variations due to precession 8=19114
- variation not in entire volume, possible obs. effect. 8=19115

radiation

- See also Cosmic radiations, radiofrequency; Sun radiation.
- β Centauri et al., brightness obs. 8=19164
- β Lyrae polarization, variability interpretation 8=5877
- bolometric corrections scale standardization 8=19149
- Cassiopeia A, polarised intensity distrib. at 1.55 cm 8=10284
- centrals of planetary nebulae, 35, effective temp. calc. 8=23560
- Cepheids, period-luminosity-color relations 8=23554
- continuous energy distribution, 1350–10 000 Å, effect of rot. 8=23520
- Cygnus A, polarised intensity distrib. at 1.55 cm 8=10284
- Cygnus, sky survey of cosmic X-rays 8=10230
- Cygnus XR-1, X-ray flux, twofold increase at high energy 8=19162
- diffusion, source excitation power from spectral line profile 8=5895
- dwarfs, solar type, u.v. excess and DM, residuals 8=14760
- early type, far u.v. 8=10170
- faint Pleiades, confirmation of membership 8=19186
- flares, rel. to solar 8=2857
- free electron scattering in stellar atmosphere 8=15028
- galactic, abundance of anti-protons 8=14730
- globular cluster M13, luminosity function 8=10213
- gravitational, by binaries, obs. 8=14959
- gravitationally collapsing, non-rotating, spherically symmetric star 8=19153
- interstellar polarization meas. 8=23541
- light polarization vars., meas. programme proposal 8=23532
- neutron, model for mag. and rot. energy release 8=23543
- NLM Cygnus i.r. polarization rel. to nature 8=23529
- optical research, 20 year review 8=19066
- planetary nebulae, Ly- α density 8=5912
- polarization by interstellar matter, theory 8=5920
- polarization, intrinsic, rapidly rot. early types 8=23518
- polarization obs. in galactic plane and direction of galactic poles, 308 stars mostly within 200 parsecs 8=23521
- radio sources, non-thermal, thermal X-rays 8=5941
- radio-sources, two-dimensional brightness distrib. from lunar occultation obs. 8=5943
- SCO XR-1 photometric monitoring 8=10153
- 73 Draconis, magnetic, spectrum, and radial velocity var. 8=10179
- synchrotron, resultant thermal instability in surrounding medium 8=5944
- T Tauri type, i.r. excesses 8=23525
- 3C273, harmonic analysis of light variation 8=23537
- 3C273, interplanetary scintillation 8=14807
- transfer in relativistic medium 8=15029
- U Her, photoelectric obs. 8=19171
- variable P Cyg, tight curve eclipsing W UMa props. obs. 8=23551

Stars—contd

radiation—contd

- X-ray source in vicinity of the constellation Crux 8=10291
 - X-ray emission and stellar accretion 8=10310
 - H II regions, higher-order high-quantum H recombination lines 8=23569
 - H II, stimulated emission of r.f. lines, enhancement by small departures from thermal equilib. 8=23567
- spectra
- A star 73 Draconis, spectrum variations 8=5879
 - A stars, peculiar, u.v. spectra 8=14766
 - Algol rel. to component bodies nature, 6700–11000 Å 8=10205
 - α^2 CVn, profiles of H lines, anal. 8=19146
 - analysis, special device for reading diagram coordinates 8=14763
 - Ap, A- and B-type normal, continuous energy distrib. 8=10168
 - Ap stars, Balmer discontinuities rel. to temp. grads. and model atmos. 8=19161
 - OO Aquilae, light variation and orbital elements 8=23524
 - Arcturus, Mn I and VI hyperfine-broadened profiles rel. to obs. 8=23527
 - Arcturus, K2 giant, curve-of-growth anal. 8=19160
 - atmosphere, line-blanketed, statistical procedure 8=19150
 - Zeta Aurigae, photoelectric observations and chromosphere K-line during 1963–64 eclipse 8=14764–5
 - binary β Per K(Ca II) linewidth rel. to eclipse phases, obs. 8=10197
 - binary 47 Audromedae, study of 8=2792
 - and binarity of HD 3950, obs. 8=10209
 - BL telescopii rel. to evolution and secondary body nature 8=10204
 - blanketing in high-gravity stars 8=14769
 - blue identified as 4C radio sources 8=5940
 - BVR system, 44 standard stars obs. 8=23539
 - RU Cam, quantitative analysis 8=19172
 - Z Cam, during light plaus. 8=10158
 - β Canis Majoris, period-colour-luminosity relation 8=5888
 - Cas A, 5.8–25 Mc/s 8=10304
 - Cen XR-2, X-ray emission 8=5883
 - γ Cen, spectrophotometric obs. 8=10200
 - RR Centauri, improved orbital soln. of photoelectric obs. 8=23553
 - central stars of planetary nebulae, u.v. spectrum and temp. 8=10216
 - Cepheids, classification, numerical methods application 8=2785
 - VV Cephei in the photographic infrared 8=5876
 - Cepheids, reddening line on U-B/B-V diagram 8=23535
 - cepheids S Mus and β Dor, H α profiles rel. to temp. obs. 8=10181
 - μ Cephei, wavelength dependence of polarization 8=23516
 - class B5 to M2 absolute energy distrib. obs. 8=10160
 - classification and photometry, high proper motion 8=23536
 - classifications, theory, model atmospheres 8=2777
 - clusters NGC6242, NGC6268, Tr24, 3 colour photometry 8=19181
 - Crux regions, photometric standard sequences 250 stars 8=19205
 - Cyg A, 5.8–25 Mc/s 8=10304
 - CH Cygni, emission lines in u.v. 3140–3500 Å 8=23517
 - 41 Cyg, F-stars, rel. to atmos. parameters, comparison with the sun 8=19137
 - P Cyg, ionization temp. in atmos., Balmer decrement, and chem. comp. 8=19147
 - Cygnus sky survey of source spectra 8=10230
 - DB, peculiar, colours and space motions 8=10174
 - β Doradus cepheid, H α line profiles rel. to atmos. 8=10133
 - χ Draconis effective temp., abundance of metals and microturbulent vel. obs. 8=2791
 - dwarfs, G and K, energy distribution at red wavelengths 8=5894
 - dwarf, late K and early M charac. for stars in the Hyades 8=19157
 - early-type, far u.v. spectroscopy and photometry using Aerobee-150 rocket 8=10170
 - element abundance, microturbulence vel. in atmos. etc. 8=19159
 - F and G main-sequence, Li/Be ratio 8=19152
 - 4C sources in declination 40°–44°, 38, 178, 610–5 and 1417 Mc/s 8=10297
 - G dwarfs, u.v. excess and [Fe/H] ratio 8=10155
 - G and K dwarfs, scanner obs. 8=14758
 - G stars, CO, CH, C₂ and CN band intensities 8=10171
 - Of group, variations obs. 8=19140
 - HD 32633, light variations obs. by UVB photometric and Zeeman spectroscopy 8=19154
 - HD 37202, speed from He I λ 4026 line 8=19169
 - HD 11844–5, classification 8=14756
 - HD 151804 and 152408, 4430 Å absorpt. vars., obs. 8=23530
 - HD217050 star, study from 8 high dispersion spectra 8=2784
 - ν Her, F-stars, rel. to atmos. parameters, comparison with the sun 8=19137
 - Hetzler, i.r. classification 8=5892

Stars—contd

spectra—contd

- hot molecules, trapped at 4°K 8=4116
hydrogen emission lines of three new Be stars 8=19139
interferometer 8=19134-5
interstellar absorpt. at 4430 Å, var. with galactic longitude 8=23534
interstellar absorption band at 6180 Å, profile 8=10235
K, CO, CH, C₂ and CN band intensities 8=10171
K flares, astronomical or match flame origin? 8=14753
K giants, variable chromospheric activity, obs. 8=14754
late-type, emission component of Ca_{II} K-line 8=19156
late-type, negative ions 8=10154
line formation in inhomogeneous atmospheres, soln. of 3D Eddington approx. 8=23519
line formation in stellar atmosphere 8=14761
SZ Lyncis, photoelect. obs. 8=23526
γ Lyr, profiles of H lines, anal. 8=19146
RR Lyrae stars, three-colour photometry 8=5875
Magellanic cloud, small, colour-magnitude array for core region 8=10163
magnetic variables, two-cell photoelectric polarimeter, obs. 8=19168
metallic-line, multicolour UBVRI observations 8=10166
metallic-line stars, continuum energy distrib. anal. 8=19138
metallic-line, and temp. and gravity, obs. 8=19136
Milky Way field in Circinus (SA195), V magnitudes and B-V and U-B colours 8=19202
Milne-Eddington curve, modifications allowing for depth 8=5886
V372 monocerotis S star, peculiar spectrum, obs. 8=5884
Morgan-Keenan system, slit spectrograms of 185 bright stars 8=10156
nebula NGC 6960, FeX 6374 Å line, obs. 8=10225
NGC 2451, three-colour photometric results 8=5905
NGC 362 cluster, colour-magnitude diagram 8=10206
276 stars in NGC 6067 neighbourhood, colours and magnitude 8=19142
nova Delphini 1967, obs. 8=5899
Nova Delphini 1967 8=19148
Nova Herculis 1960 8=19174
Nova Herculis 1960, 3530-6560 Å 8=10187
O and B, early-type line profiles rapid time vars., obs. 8=23531
opacity, source of in u.v. continuum 8=2775
α Orionis cluster, classification 8=14786
paradoxes ascribed to erroneous oscillator strengths 8=10159
Pasch discontinuity, theoretical importance 8=23538
photoelectric polarization measurements on faint objects, detection principle 8=19143
Pleiades, absolute energy distribution in 14 bright stars 8=10172
polarization of starlight, possible variations 8=19144
Praesepe cluster, colours and magnitudes, effect of rotation 8=23523
proper-motion, colours and space motions 8=10174
Puppis, three regions, 78 stars, magnitudes and colours 8=19204
VV Pup, U Gem and UX UMa, peculiarities, explanation 8=5907
quasars, emission-line variability 8=23627
quasars redshift-absolute magnitude correl. rel. to Universe models 8=10317
quasars, 2974 Å emission line identification 8=19234
quasistellar, intensity distribution in 1000 Å ≤ λ ≤ 7200 Å and colour index 8=2806
radial-velocity curves, 44i Bootis B, VW Cephei and W Ursae Majoris 8=19187
radiation rel. to thermodynamic structure, plasma radio recombination lines and anomalous Balmer line intensities 8=5915
red-shift due to interstellar photon collisions 8=5922
red star in Vela, large colour index 8=19141
resonance lines, weak, effect of axial rotation on equivalent widths 8=10176
Sco X-1, additional photometry of nearby stars 8=10162
Sirius B, high dispersion spectrum 8=14767
spectral types of fourteen stars between 8 and 12 mpg 8=10164
spectrograms, automatic data reduction 8=23540
Stock 13, cluster of early-type stars, five-colour photometry 8=23515
subdwarfs, He content 8=5865
subdwarfs, metal-deficient, quasi-H₂ absorpt. calc., 0.2-0.45 μ 8=23528
supergiants, F- and G-type, Hα profiles rel. to temp., obs. 8=10181
supergiants, HD 96248 and HD 14443, N-deficiency 8=5889
63 Tau, continuum energy distrib. anal. 8=19138
u.v., subtractive dispersion spectrographs for 8=10319
universe, Friedman and steady-state models from Q.S.S. data 8=2768
χ Ursae Majoris, spectra compared with 37 Coma Berenices 8=2782
15 UMa, continuum energy distrib. anal. 8=19138
variable α Lupi, H outflow and vel. amplitude obs. 8=10182

Stars—contd

spectra—contd

- variable β Cen, linewidth and vel. vars. rel. to nature, obs. 8=10182
variable HD 170682, Be characts. development rel. to magnitude vars., obs. 8=23547
white dwarfs, colours and space motions 8=10174
yellow supergiants, fine analysis of two, preliminary results 8=5878
X-ray intensities and spectra from several sources 8=5893
AlO, new ²Σ⁺-X²Σ⁺ band, Franck-Condon factors 8=16263
Am, five, near i.r. 8=23514
B, He λ4771 strength, in IC2391, 2602, Southern galactic cluster 8=2783
Be stars, classification 8=10161
Be, southern, photometric data 8=19165
carbon star identification, Scutum region 8=14757
C stars, temp. determ. and Franck-Condon factors for CN mols. 8=4173
Ca II lines, Scorpio XR-1, distance estimation 8=23503
Ca II and Na I interstellar lines near HI clouds, search for 8=5880
Ca II, photometric index of K-line strength, independent of atmos. extinction and interstellar reddening effects 8=23522
H_α contours in NGC 700 filaments, obs. 8=10232
H_β index in open clusters rel. to distance moduli and distances, photo-elec. obs. 8=10207
H_γ and He I lines 8=10157
H II reddening anomaly, review of explanations 8=14797
He, as a function of hydrogen abundance 8=5891
He I 4026 Å line for stellar rotation velocity 8=19121
Si II λ4128 and λ4130 Å in model atmospheres and B stars 8=19163
Si II, superposition of configuration applied to a series of states 8=19158
- structure
angular vel. distrib., massive stars 8=19122
atmosphere, line-blanketed statistical procedure 8=19150
atmosphere models, discrete optical depths 8=10119
atmosphere models, soln. of transfer eqns. subject to constraint of radiative equil. 8=10135
atmospheres, plane parallel, specific intensity behaviour at infinity 8=2774
atmospheres, radiative equilibrium line-blanketing 8=14761
atmospheric Rayleigh scatt. problems, calc. 8=5921
atmosphere theory 8=2773
BV267 single-line eclipsing binary 8=19184
binaries, contact, W Ursae Majoris stars with unequal components at zero age 8=23558
binaries, contact, W Ursae Majoris type, review 8=14783
binary systems, close, effect of jet in envelope of one 8=5907
carbon, H:C:N:O equilibrated abundances calc. 8=10141
cephheids rel. to freq. of reson. exit. non-radial oscils. 8=10183
cephheid variables, models, nonlinear calc. 8=14776
cephheids, radii determ. by Wesselink's method 8=10117
δ Ceti, period since 1900 8=19127
cool stars, outer atmosphere 8=10120
curves of growth, transfer eqn. modification by electron scattering 8=14749
V477 Cyg binary system, from photoelec. obs. 8=19185
cylinders, compressible, polytropic, oscils. 8=5859
density gradient inversion in convection zone 8=2778
differential rotation models, instability 8=10377
dwarfs, cold, chromospheres 8=19113
dwarfs, red, convective, Kr60A and B, calc. 8=19123
early-type, model atmospheres, departures from LTE in H and He 8=10132
finite amplitude convection theory 8=10122
u Her system, from photoelec. obs. 8=19171
HD 140283 subdwarf, model-atmosphere abundance analysis 8=19125
HD 19445 subdwarf, model-atmosphere abundance analysis 8=19125
interface location, coord. stretching method 8=19367
line-blanketing, high gravity effect 8=14769
liquid sphere, influenced only by gravity, frequency spectrum 8=4504
mag. field with differential rotations in spherical fluid shell of infinite elect. conduct. 8=23508
mag. fields, toroidal in radiative zones, stability 8=23507
magnetogasdynamical model of corona 8=23506
mass loss gross effects on evolution 8=10146
mass-radius-temperature relationship 8=19118
metallic-line, photosphere struct. and turbulence, models 8=19136
neutron, soft repulsive core among baryons, mass and radius 8=19166
one-zone pulsation model with proper boundary conditions 8=14751
photosphere in B to K spectral stars, deviation of H and H⁺ from LTE 8=10131
polytropes in magnetostatic equil. 8=19124
pre-main sequence, models, criticism 8=23513
pulsations, adiabatic, and convective instability of gaseous masses 8=10121

Stars—contd

structure—contd

- radial pulsation, coupled with convection 8=14775
- quasars, consequences of gravitational collapse theory 8=10087
- red giants H burning shell, calc. 8=10128
- rotating main-sequence model construction 8=10112
- rotating, radial pulsation eigenfrequencies 8=23504
- rotating, slow and relativistic, equations for equilibrium calc. 8=10123
- γ Ser, microturbulent vel., var. with depth 8=5868
- shock wave propag. in degenerate gases 8=19544

Stars (nuclear). See Particle track visualization.

Statistical analysis

See also Measurement/errors; Probability; Random processes.

- adaptive system, effect of random perturbations 8=10516
- collision probabilities for finite cylinders and cuboids 8=11993
- degenerate time-independent perturbation theory 8=548
- energy spectrum representation and interpretation 8=94
- experimental data, with equal and nonequal spacing 8=27
- fluctuation in dispersion formulae 8=10517
- Gaussian light, intensity-fluctuation distribution 8=20019
- inverse velocity space spectra and kinetic equations 8=10645
- lattice, determ. of critical behaviour from series expansion 8=14983
- in liquids, atoms motion, stochastic calc. of veloc. self-correl. function 7=1522
- Monte Carlo calc. of e penetration, and X-ray prod. in solid targets 8=18792
- Monte Carlo method, time depend. neutron thermalization 8=11981
- observed-likelihood-ratio criterion, steps for estimation 8=2961
- plasma parameters estimation 8=7728
- random processes, non-stationary, ejections of 8=84
- reduced-width amplitude, exact distrib. 8=2908
- reverberation and similar first-order scattered fields, statistical model construction 8=3043-4
- stability of motion of oscillatory system with one degree of freedom 8=10515
- stochastic processes in linear configurations with transition probab. independ. of components' states 8=6089-90
- Stokes paradox in kinetic theory of gases 8=21496
- system with random Hamiltonian, evolution 8=19435
- wave statistics, Schrodinger eqn. Heisenberg force, line spectra selection rule and Debye's theory 8=2982
- $o\text{-H}_2$, solid, self-consistent model, Pca2, ordering 8=17375

applications

See also Counters/statistical analysis.

- acoustic transmissivity density distribution function for two layer system with random parameter 8=19564
- atmospheric boundary layer, Eulerian rel. to Lagrangian correlation coeffs. 8=14593
- atmospheric motion, governing equations and spectra, transports in freq., wave-number space 8=23269
- atoms embedded in electron gas, statistical model calcs. 8=22486
- bilinear hysteretic system, response to random excitation, time averaged statistics 8=19483
- canonical correlation and relation to discriminant analysis and multiple regression 8=23254
- cloud droplet growth by hydrodynamic capture 8=18869
- coded communication, noise immunity 8=19434
- convergence and invariance questions for point systems in R, under random motion 8=19353
- crystal growth from soln., error anal. of rate determ. 8=8393
- electrolyte theory, intermediate conc. 8=14417
- electron avalanches, influence of relax. of energy distrib. 8=4289
- electron beam in crossed fields 8=15301
- Fermi gas, one-dimensional case, impulse-distribution ("sharpness") 8=129
- ferroelectrics, order-disorder, perturbation theory, Zeroth approximation 8=9191
- fission xy reactions, spin-dep. treatment 8=1108
- fluctuations spectrum analyser, errors 8=10981
- fluid, Eulerian rel. to Lagrangian statistics 8=12582
- fluid, high order time correlations in field and rel. to Gaussian probability distributions 8=12623
- fluid turbulence, small-scale, cascade process of sequential breakdown 8=12636
- fluorite-related systems, rel. to gross anion sub-stoichiometry 8=22175
- gaussian brackets to beam waveguides and cavities 8=321
- geomagnetic field 8=5814
- hard disks in isothermal-isobaric ensemble, Monte Carlo calc. 8=19467
- imperfection-sensitivity in elastic post-buckling 8=19396
- ionized gas, eqn. of state in Debye-Huckel approximation 8=10623
- ionospheric drifts, 3D, calc. 8=9990
- ionospheric inhomogeneities, correlation analysis applicability 8=9993
- Ising paramagnet, neutron scattering 8=9297

Statistical analysis—contd

applications—contd

- Laplace eqn., soln. of boundary Dirichlet problem 8=19369
- laser field, N-mode, photostatistics 8=412
- laser rad. intensity fluctuations at threshold 8=402
- laser radiation, nonresonance feedback, statistical props. 8=19943
- laser radiation, time dependent props. 8=3304
- laser range finder, multipulse returns energy detection 8=6414
- lattice, distributive, subadditive functions 8=88
- lattice gas, analyticity problems 8=87
- lattice, harmonic, two-dimensional, stability 8=2963
- lattice points, mutually visible, some theorems 8=90
- least-squares curve fitting tech., appl. to thermodynamics 8=19451
- liquid crystal structure, theory 8=1527
- many-body problem, classical, solution using Lie series 8=116
- molecules, simple, at high temp., sums over states 8=10634
- Monte Carlo methods applied to EAS 8=11667
- multi-element reflector, statistical matrix of scatt. 8=19432
- nuclear scatt. amplitude using statistical collision matrix 8=11839
- optical data channel, atm scintillation effects 8=9869
- orientation of magnetic axes in the periodic magnetic stars 8=5902
- paleomag. remanent magnetization directions, adjacent horizons, serial correlation 8=14705
- photodetection, communication channel model 8=20010
- plasma, low temp., population distribution of energy states 8=12461
- plasma, non-equilibrium processes, book 8=16472
- polymer, flexible, radius of gyration, probability distrib. 8=7644
- polymer solutions, second osmotic virial coeff. calc. using lattice model 8=8039
- precipitation, studies on local, national and continental scales 8=18865
- pulse-height analysers, statistics of digital stabilizers 8=20215
- pulse signal behind layer with random irregularities, shape and statistical characts. 8=19431
- quantum e.m. communication channel with additive noise 8=19433
- radiative transfer, Monte Carlo method 8=6119
- reduction of geoaoustic and geomag. data 8=6092
- scattering, isotropic, of radiation in finite homogeneous 2D atmosphere 8=2906
- sea surface waves, random 8=14575
- searches, repeated, exact treatment of statistics 8=6679
- secondary electron yields from targets, Polya statistics 8=5420
- shell model of nucleus, matrix elements statistics 8=20646
- shock waves, Burger's equation, Lagrangian-history statistical theory 8=19536
- solar granulation photometry obs. 8=19307
- stability conds., almost sure, for parametrically excited random vib. system 8=19499
- stellar associations in Cen 8=10264
- stellar atmosphere line-blanketed model 8=19150
- stellar system, self-gravitating, with uniform rotation, kinetic theory 8=23502
- stochastic approach to theory of fluctuations in plasma 8=21293
- trajectory estimation problem, sequential estimation of obs. error variances 8=19071
- transport coeffs., using autocorrel. functions 8=3006
- theoretical growth rate versus rel. supersat. curve, using least squares method 8=13130
- three-body recomb. of ions with general third body, low density limit to rate 8=12426
- N two level systems interacting with single mode, quantized radiation field 8=2970
- ultracentrifuge sedimentation during period of const. accn. 8=19379
- viscoelasticity of textile fibres 8=17846
- wave propagation and turbulent media, book 8=10735
- white noise pus signal, zero crossings calc. 8=10607
- $\text{C}^{12}(\text{O}^{18}, \alpha)/\text{Mg}^{24}$, cross-section fluctuations 24. 3-27. 7 MeV and ang. distrib. 8=1104-5
- Ge, lattice energy rel. to elastic deform., electron distrib., elastic conds. 8=13576
- H_2 , solid, model rel. to n. m. r. 8=22923
- He^3 , liq., collective treatment 8=19692

Statistical mechanics

- See also Bosons; Fermions; Quantum theory/many-particle systems.
- absence of ordering in certain classical systems 8=2979
- algebra, von Neumann, types rel. to extremal invariant states 8=6013
- asymptotic equivalence of canonical and pressure ensemble 8=111
- Boltzmann's distrib. law, evaluation of exponent 8=19446
- Boltzmann eqn. with cut-off pots. 8=3005
- Boltzmann equation, linear and stationary solution 8=19474

Statistical mechanics—contd

Boltzmann equation, nonlinear and nonlinear, for gas between two parallel plates 8=19470
 Boltzmann gas, nonequilibrium, logarithmic density behaviour 8=2980
 Boltzmann-Gibbs probability, redefinition 8=14992
 Boltzmann's theory of irreversibility and velocity inversion 8=95
 Bose-Einstein condensation criterion and canonical commut. relns. represent. 8=6108
 Bose gas, 3-body correl. function with hard-sphere interaction 8=2993
 canonical partition function, classical limit 8=10621
 chemical potential, appl. to problems 8=105
 classical, "canonical" representations of the inhomogeneous Lorentz group 8=2893
 classical, canonical statistics, temp. depend. near phase transition 8=97
 classical, inequalities and variational methods 8=14993
 classical, linear closure approx. 8=19445
 classical, mean entropy of states 8=10628
 classical, relativistic, Hamiltonian formulation without interactions 8=19442
 coherent states, She and Heffner theorem 8=2974
 cooperative phenomena in triangular lattice 8=89
 crystals, partition function 8=17507
 dense hard-sphere gas, propag. of density disturbances 8=10660
 diffusion coeff. of Lorentz gas 8=136
 disordered lattices, 3D, spectral gaps 8=10609
 distribution functions, integral equations for 8=10619
 entropy, indefinability for Hamiltonian system 8=2971
 equilibrium, cluster development by quantum field theory 8=10626
 excitons, Frenkel, by Bose operators 8=5122
 Fermi hard-sphere gas at zero-temp., eqn. of state, distrib. function 8=10658
 Fermi system with direct interaction, retarded temp. Green's functions, perturbation theory 8=15021
 Feynman rules 8=120
 fluctuation theory of irreversible processes 8=10624
 fluid, classical with Lennard-Jones pot., correlation function 8=12576
 fluid surface layer distant from boundary surface 8=99
 fluorescent source, polarization, quantum theory 8=23036
 galaxies, elliptical, collisionless relax. 8=10273
 gas, critical density fluctuations free energy calc., rel. to sound absorption 8=16703
 gas mixtures macroscopic theory from Boltzmann equation 8=118
 gas thermodynamic props. at transition 8=19459
 gases, dilute, nonadditive molec. interactions 8=4466
 Green's functions and double-time distrib. 8=15000
 Gyarmati principle and canonical equations 8=10633
 Hamiltonian, covariant, with interactions, classical, canonical formalism 8=19441
 Hamiltonian time-reversal-noninvariant term detect. from energy-level spacings 8=10625
 hard disks in isothermal-isobaric ensemble, Monte Carlo calc. 8=19467
 hard sphere fluid, phase transition 8=12578
 hard-sphere gas, collisional relax. eigenvalues 8=3000
 hard sphere gas, sequence of relaxation constants 8=133
 hard-sphere solid, pair distrib. functions 8=6091
 harmonic, stationary nonequil. Gibbsian ensemble 8=4901
 Heisenberg ferromagnet, spin pair correlations 8=9316
 infinite system state descriptions 8=14999
 interacting particles, partition function with singularities 8=98
 irreversible evolution of dynamic systems 8=2972
 Ising chain, computation of Green functions 8=10610
 Ising-Lenz model solns. and appls., review 8=10612
 Ising model, chain dynamics 8=10611
 Ising model, distrib. of roots of partition function in complex temp. plane 8=19443
 Ising model, Kawaski modification, generalized to two master eqns. 8=10669
 Ising model, Onsager's results using Green's function 8=2964
 Ising model near T_c , second order phase transitions 8=14986
 Ising model, time-independ., kinetic eqns. developed 8=14985
 Ising problem for lattice with substitutional and interstitial impurities 8=1951
 Ising spin correl. function, calc. 8=14987
 kinetic equations and Lorentz transformation 8=15002
 kinetic equations, transformation properties 8=14996
 kinetic equations, unified formulation 8=15001
 kinetic gas theory, relativistic Onsager relations 8=21500
 kinetic phase transitions 8=21743
 laser light props., quantized e.m. field model 8=19941
 lattice gas, honeycomb, exact finite method 8=10661
 lattice gas models, low temp. phase separation 8=19439
 lattice model of planar 'spins' for Bose fluid 8=126
 lattice points, mutually visible, some theorems 8=90
 linear molecules, correl. functions 8=4252
 linear molecules, potential energy functions 8=4251
 linear response theory, quasi-static processes 8=114

Statistical mechanics—contd

linearized collision operator, matrix elements 8=21499
 Liouville equation, solution in infinite limit 8=106
 local potential, variational method, appl. to plasma stability 8=16590
 macroions of rigid-sphere potentials, potential of average force 8=21203
 macroscopic measurement, theory 8=14911
 mag. susceptibility of spin systems with several time dependent temps. 8=15009
 molecular stress tensors in isothermal multicomponent systems 8=19448
 many-body theory, conference Oiso Japan (1965) 8=10641
 many-particle systems, path length probabilities 8=15011
 master eqn., generalized, without time convolution 8=103
 matter and radiation, equilibrium props., anomalies 8=2990
 'memory' props. of g master eqns. 8=102
 micro-materials, thermoelasticity 8=2931
 micro-solid theory geometric and kinematic properties 8=6105
 model I-D lattice, phase transitions 8=2965
 molecules, hard sphere simulation of behavior 8=14981
 mols. vel. distrib. function near solid wall in non-uniformly heated gas 8=21494
 molten salts containing water, quasi-lattice model 8=8015
 of multi-mode radiation from atomic ensemble 8=19452
 noise sources harmonic oscillator and atomic quantum theory 8=19438
 noninteracting particle in thermal equilibrium, < E ⁷ state occupation numbers calc. 8=6096
 nonlinear mats. with internal state variables, thermodynamics 8=112
 nonlinear response, formal theory 8=2989
 occupation-number and functional formalisms, equivalence 8=10629
 one-dimensional systems, binary correl. functions, Bogolyubov and config. integral method comparison 8=14998
 Onsager relation, generalization for high order symmetries and their invariance 8=96
 oscill. systems, coupled, quantum statistics 8=2981
 Percus-Yevick approximation 8=15004
 phase transitional in I-D model lattice 8=2965
 phase transitions of second kind, hypothesis of correlation similarity in theory 8=19449
 physical clusters and critical phenomena 8=4654
 plasma, hierarchy of eqns. and correl. functions 8=16478
 plasma, two-component, equilibrium correlation functions 8=21307
 polarized system relativistic dynamics 8=10631
 polymer chain, expansion in solvent 8=4264
 polymerized material, elasticity 8=8875
 probability density, partial differential eqn. 8=19447
 quantum, coherent-state techniques appls. 8=19450
 quantum correlation function for noninteracting particle system 8=2987
 quantum distribution functions, temp. dependence 8=10618
 quantum, equilibrium states 8=10627
 quantum, equil. states, factor type 8=6101
 quantum gas, slow neutron scatt. 8=16685
 quantum, of high-temp. charged particles 8=10630
 quantum ideal gases, effective potential 8=19456
 quantum spin systems, thermodynamic limit 8=15006
 quantum statistics, classical statistics as limiting case 8=2968
 quantum statistics of many-particle system with Coulomb interaction 8=2988
 quantum stat., method of displacement and collective variables 8=10617
 quantum, stochastic forces and lasers appls. 8=19453
 quantum systems, fluctuations, Gibbs method calc. 8=6095
 quantum, Wigner method 8=2977
 quasiparticles and contracted description 8=10639
 radiation field interacting with photodetector 8=20037
 radiation fluctuation obs., quantum theory 8=3010
 relativistic, formalisms 8=6106
 relativistic, hierarchies for reduced densities 8=2966
 of relativistic magnetic anomaly 8=2973
 relaxation of harmonic oscillator systems, simple 8=15005
 random walks, self-avoid, thermodynamics 8=14984
 rigid disks at high density 8=15003
 signal detection, quantum theory 8=10945
 specific heat inequality 8=6099-6100
 spin array with two sublattices, mag. props. 8=6093
 spin-one operators, Wick theorem 8=20181
 statistical mechanics and thermodynamics, conference Copenhagen Denmark (1966) 8=15007
 superfluid, many boson system, coherent states 8=19696
 surface tension near crit. pt., quasichem. approx. 8=21635
 symmetries, spontaneously broken, state decomposition 8=6010
 tetrahedral lattice, self-avoiding walks 8=1768
 theoretical physics, conference Providence USA (1966) 8=20246
 thermodynamic evolution criterion of Glansdorff and Prigogine, derivation 8=6097
 thermodynamic Green's functions, zero-freq. behaviour 8=113

Statistical mechanics—contd

- thin film, specific heat, size effects 8=10656
- time-correlation-functions for nonlinear chem. rate const. 8=6113
- with topological constraints 8=14994
- transport coeffs., time-correlation-function 8=6112
- two-phonon energy relaxation 8=8893
- unifying principle for equations of motion 8=2976
- vibrators and librators perturbed by collisions 8=100
- of weakly interact. system, entropy and temp. 8=107
- Wien displacement law and rad. fluctuations 8=14997
- zero-point kinetic energy of relativistic fermion gases 8=15018
- He, collective coordinates theory 8=10799
- M hydride phase, $M = \text{Pd, V, Nb, Ta}$, solubility of H_2 , isotherm 8=1924

Statistical thermodynamics. See Statistical mechanics.**Steady-state theory.** See Cosmology.**Steam**

- dissociation, thermodynamic analysis 8=7917
- filmwise condensation, rel. to existence of interfacial heat transfer resistance 8=16940
- laminar film condensation on vertical plate, effect of variable phys. props. 8=21771
- steam-air mixture leakage from solar still, rel. to aerodynamic coeffs. 8=19678
- temperature influence on metal corrosion 8=18666
- thermal conductivity at 140–180°C, 1 atmosphere, obs. 8=4477
- thermodynamic properties, near critical point 8=7920

Steel

- analysis, Cu determ. by at. absorpt. spectrometry 8=2545
- analysis, Mn determ. by at. absorpt. spectrometry 8=2547
- analysis, NH_3 extraction-spectrophotometric determ. 8=2546
- analysis, spectrochemical, sample condition in spark region 8=2548
- Armco, work hardening rel. to dislocations 8=5067
- ausforming, some experiments 8=13561
- austenite, alloyed, C activity at 1000°C 8=17008
- austenite grain size, high temp. microscope obs. 8=13157
- austenite, retained in precip. hardening of stainless steel, X-ray meas. 8=4848
- austenite retention, X-ray diffr. determ. 8=22355
- austenitic, containing 4% Ti, ageing and zone formation study 8=17071
- austenitic, corrosion pot. and anodic dissolution 8=9723
- austenitic, creep and stress-rupture props. liquid Na effects 8=22359
- austenitic, distrib. of B inferred from He gas bubble obs. after n-irrad. 8=13040
- austenitic, passivity breakdown by halide ions 8=23147
- austenitic sigma phase precip. from thin foil transmission studies 8=1674
- austenitic stainless foil, formation of dislocation loops 8=17654
- austenitic stainless, in different fatigue stages, dislocation structure 8=22205
- austenitic, stress corrosion cracking 8=8844
- austenitic, structural changes during creep 8=17284
- austenitic type 304, influence of N and other elements on creep-rupture props. 8=17754
- brittleness due to NbC precip. 8=22358
- carbide transformations during creep 8=17081
- carbon steel, internal friction, magnetoelastic scattering rel. to amplitude dependence 8=13565
- carbon steels, specific heat and hardness at He temps. 8=8639
- carbon, wire stress relax. obs. 8=17789
- cast slabs, solidification, heat transfer model 8=8179
- coercive force changes during deformation 8=14015
- continuous casting, alternating e. m. fields 8=4847
- continuous wires reinforcing Al sections and wires 8=10459
- corrosion, by H_2O , solid-state diffusion of O_2 8=22151
- corrosion in NaCl solns., inhibition by NaNO_2 , 20°C 8=2517
- corrosion rate as function of minor element content 8=18664
- creep-resistant, fracture behaviour 8=17803
- cylinders, plastic flow stress in rel. to natural strain 8=22353
- decomposition process and inter-element effect by emission spectra analysis 8=14392
- EI-702, deformation and hardening temp. effect on mechanism of precipitation 8=17078
- EI702, deformation mechanism, metallographical investigation 8=13570
- EI 702, investigation of dispersional hardening, by tensile tests 8=8845
- equilibrium partition between ferrite and cementite, temperature dependence 8=17279
- exoelectronic emission due to sliding friction, obs. 8=18254
- explosive welding to Pb 8=10456
- fatigue softening and hardening 8=22363
- fatigue under triaxial stresses, influence of principal stress, apparatus design 8=5068
- γ -ray absorpt. and scatt., stress effects 8=13483
- growth of secondary grains during annealing 8=17283
- H36XII, austenitic, strain ageing 8=13569
- high-C, α - and κ' -martensite, lattice structure 8=17373
- high-carbon, carbide formation mechanism during tempering 8=17073
- high strength, dynamic strain ageing 8=17782
- laser irradiation temp. determ. by microscopy 8=8769
- low-alloy, vacuum spectrometric determ. of B 8=23188
- low-alloyed chrome, Young's modulus, change on tempering 8=13560
- low alloy, effect of martensite on kinetics of bainite formation 7=4708
- low-alloy, heat treated, fatigue crack propagation obs. 8=5072
- low C, Cr diffusion in, experimental obs. in 950–1265°C range 8=4951
- low C, large torsional prestrains rel. to subsequent failure in tension 8=22367
- low-C, quench-ageing at 240°C after rapid annealing 8=17806
- low-carbon, sheets, rolling and annealing textures 8=17799
- low and medium strength, correlation of fatigue limit with stress-strain behaviour 8=17783
- manufacture, homogeneity and interface reactions 8=5704
- maraging, 15 and 18% Ni, influence of small cold deformation preceding ageing, discussion 8=17801
- martensite carbon strength rel. to thermally activated deformation 8=22351
- martensite decomposition, effect of thermomechanical treatment during low-temp. tempering 8=21845
- martensite, strain ageing, rel. to brittle fracture susceptibility 8=13573
- martensite, tempered, precipitation of Fe carbides 8=17080
- mechanical strength after tempering, effect of lower bainite 8=17805
- mechanical strength, grain size and precip., hot working effects 8=22356
- mechanical strength rel. to solid soln., precip. and work hardening and grain refining 8=22344
- medium-strength, fracture toughness 8=17808
- mild, alternating stress for crack propagation, tensile mean stress dependence 8=8838
- mild, beams, testing, energy absorption under conditions of gross deformation 8=13574
- mild, dynamic strain-ageing, effect of N content 8=13554
- mild, HCl vapour corrosion 8=23103
- mild, high speed impact extrusion 8=19340
- mild, stress-corrosion cracking in NaOH solns. with various additions 8=22366
- mild strip, tensile strength rel. to quench rate 8=22365
- mild, yield stress rel. to strain 8=22368
- Murnaghan's n constants by ultrasonic waves 8=13568
- nodular graphite, effect of heat treatment on mechanical properties 8=8843
- notch-brittle fracture, torsional prestraining, influence on 8=13563
- notch-brittleness occurring during time-to-rupture tests, theory 8=17753
- notched, fracture topology rel. to crack nucleation and growth 8=17793
- oxygen content, spectrographic content d.c. carbon arc method 8=9751
- phase equilib. temp., magnetic meas. 8=17062
- plastic deform. by compression and plasticine, Na use as models, 1000°C 8=13556
- plastic flow in stabilized sheet 8=8836-7
- plates, proof stress props. 8=17802
- quenched, behaviour of C 8=22354
- quenching in mag. fields, review 8=22343
- recrystallization, observation using thermoelectronic emission-type electron microscope 8=337
- SAE 4340, thin sheets under loading, slow crack growth, effect of moisture 8=5071
- SAE 1020, hysteresis loop measurement during fatigue testing at 30 Hz 8=5069
- sheet, rapid heat treatment effect on strength 8=22364
- sheets, annealed low-carbon and cold-rolled, orientation distrib. function of crystallites 8=21923
- stainless, anode desorption efficiency, photoelec. meas. 8=17167
- stainless, C content, e beam analyser obs. 8=15588
- stainless, CrC precipitation at grain boundaries, e probe obs. 8=17677
- stainless, cavitation damage resistance 8=5035
- stainless, corrosion in CO_2 and CO_2 -CO, C behaviour 8=2515
- stainless, electron-induced desorption of gas from surfaces 8=17164
- stainless, outgassing reduction in ultra-high vacuum 8=7947
- stainless, inclusion counting by e probe micro-analyser 8=17616
- stainless, irradiated, tensile and shear props. at cryotemps. 8=17763
- stainless, n-irradiated, voids obs. 8=22251
- stainless, plastic deform. rel. to magnitude of Mössbauer effect 8=8219

Steel—contd

- stainless, powder, loose sintering rel. to strain effects 8=4693
- stainless, secondary electron emission, H⁺ bombardment 8=5423
- stainless, 301 and 310, crack propag. under low cyclic load rates 8=17746
- stainless, type 304, dissolution in Bi-Sn eutectic alloy, kinetics 8=4558
- stainless, type 310, short-time tensile and long-time creep-rupture props. 8=17755
- stainless with high N content, tensile and creep props. at cryotemps. 8=17784
- steels, carbon, volume fraction analysis, X-ray diffraction 8=8464
- structural, fracture toughness, effect of temp. and strain rate 8=5070
- structural imperfections rel. to temper brittleness
 - reversibility 8=17626
- structures, limit design rel. to plasticity theory 8=8846
- surface composition vars., e probe obs. 8=14494
- surface segregation of S, Cr and Sb obs. by Auger electron emission 8=22730
- surface stacking faults after mechanical working, e-microscopy obs. 8=17675
- surface texture 8=8295
- temper brittleness, effects of alloying with Ni and Cr and adding Sb, P, Sn or As impurities 8=17797
- type 1H18N9T, austenitic, mag. qualities, influence of elastic and plastic deform. 8=9291
- X-ray fluorescence analysis 8=9750
- 0.04% C, residual strains due to single pulse compression stress wave 8=17787
- C, fatigue crack propagation, effect of atmosphere 8=17794
- C-steel, hardened, Young's modulus rel. to carbide transforms., $\leq 400^\circ\text{C}$ 8=22360
- C steels, austenite form. and tempering under high rate heating 8=13067
- Cd plated, fatigue and delayed brittle failure 8=22361
- CrMoV cast, load-time curves in breaking-strength meas. rel. to carbide precip. 8=17804
- Cr-Ni, deformation behaviour 8=5085
- 18% Cr, 9% Ni, 73% Fe, cladding of Al rel. to composite sheet prod. 8=10461
- Cr-Ni, γ - α transform., pulsed mag. field effect 8=17063
- Cr-Ni stainless, intercrystalline corrosion, theory 8=8460
- 20% Cr-25% Ni stainless, NbC solubility 8=4689
- Cr-Ni steels, electrochem. behaviour rel. to vacuum melt purifying 8=9713
- 18Cr-8Ni, thin oxide film identification by electron microscopy 8=8319
- Fe-C, atomic displacements from X-ray diff. meas. 8=17371
- Fe-1.82% C, {110} twins in bcc martensite 8=21925
- Fe-Cr-Ni-Nb, recrystallization obs. 8=21950
- Fe-Ni-Si-C, deformation characts. rel. to martensite ageing 8=22357
- H₂ adsorpt. in plating from Cd-TiO₂ baths 8=17163
- Mn, effect of multiple $\gamma = (\epsilon, \epsilon')$ transformations on strength and structure 8=17785
- Mn, martensitic transform., rel. to elec. resist. 8=17061
- Mn steel, paramagnetic susceptibility of martensitic phases 8=9304
- Mn steel, phase and structural changes on heat treatment 8=17090
- Mo, orientation relationship and coherency between Mo₂C and ferrite matrix 8=17369
- N impurity, spectrophotometric determ. 8=23178
- Nb carbon nitrides dissolution, precip. and age hardening effect 8=1660
- Nb in stabilized stainless, spectrophotometric determ. 8=23179
- Nb-Mo steel, heat-treated, with 80 kg/mm² strength level, combined effect of Nb and Mo on mech. props. 8=22385
- Nb-Mo steel, heat-treated, strengthening effect of precipitates 8=22386
- Ni-bearing, structure of martensite during ageing 8=1762
- 18Ni(250) maraging, banding of structure, effect on mechanical props. 8=8463
- Ni-Co-Mo, precipitate reversion 8=17096
- Ni-Cr-Mo and Ni-Cr-Mo-V, intergranular fracture 8=22222
- NiCrWTi, recrystallization diagrams and results 8=8423
- Si determ. by spectrochem. anal., line interferences due to Cr, V and Mo 8=23190
- Si-, for domain struct. meas., sample prep. 8=22840
- Si-, silicate glass coated, magnetostriction rel. to corrosion in film removal, obs. 8=22843
- V trace analysis, spectrochemical 8=18773

Stellar atmospheres. See Stars.**Stellar clusters.** See Stars.**Stellar composition.** See Stars/composition.**Stellar motion.** See Celestial mechanics; Stars.**Stellar structure.** See Stars/structure.**Stellarator.** See Plasma/devices.**Stereoisomerism.** See Isomerism.**Stereophonic sound.** See Acoustics.**Stereoscopy**

- frame of reference in asymmetric convergence of eyes 8=11227

Stimulated emission. See Lasers; Luminescence; Masers.**Stimulated Raman scattering.** See Lasers; Raman spectra; Scattering/light.**Stochastic processes.** See Probability; Random processes; Statistical analysis.**Stokes flow.** See Flow; Hydrodynamics.**Stokes law, fluids.** See Flow; Viscosity.**Stokes law, optical.** See Luminescence.**Stokes lines.** See Luminescence; Raman spectra; Spectra.**Stopping power.** See Particle range.**Storms.** See Atmosphere/movements; Magnetic storms; Thunderstorms.**Strain effects.** See Deformation; Elastic deformation; Plastic deformation.**Strain gauges**

- aligning and bonding, simple device for small cylindrical specimens 8=5001
- deformation measurements, advantages of analogue computer treatment 8=10476
- impulsive pressure transducer performance 8=14925
- inductive differential gauge, highly sensitive and with elec. zero adjustment 8=8791
- magnetoelastic tension transducer 8=13504
- moiré fringe extensometers 8=13507
- piezoelectric for determ. of stresses caused by acoustic excitations in nuclear structure 8=20884
- scales, parameters 8=10478
- for thermobalance, continuously recording weight changes 8=9659

Strain hardening. See Work hardening.**Strange particles**

- electro and photo-prod. in the framework of current algebra and PCAC 8=20344
- non-strange, weak interactions 8=11392
- π^+p , 1.5-4.2 BeV/c, prod. 8=6860
- progress in nuclear physics, book IX 8=15627

Strangeness. See Elementary particles; Field theory, quantum.**Stratosphere.** See Atmosphere.**Streamers.** See Discharges, electric.**Strength.** See Electric strength; Mechanical strength.**Stress analysis**

- See also Bending; Photoelasticity; Strain gauges; Torsion.
- aeolotropic elliptic plate, compressed along major axis 8=47
- anvil, high pressure, by photoelasticity 8=2038
- Bingham plastic, settling of spherical particles 8=21553
- bridge deformation in stringed instruments 8=15070
- circular block, anisotropic compressible, finite 8=6052
- circular hole, tangential stresses 8=19391
- circular ring disc, eccentric 8=6051
- circular sheet, with hole and axially symmetric stretching, stress conc. 8=22263
- closed cylindrical shell with doubly periodic holes system 8=19398
- composites, reinforced, fibre-matrix interaction forces calc. 8=22268
- computer, analogue, stress-strain diagrams 8=2919
- crack, penny-shaped, application to diffraction of plane longitudinal wave 8=2924
- of cracked rectangular beams, soln. of mixed boundary-value problems 8=22297
- creep tests, on helical spring specimens 8=5021
- cylindrical shells, axisymmetric collapse under pressure 8=10554
- cylindrical shell in elastic casing, stress and displacement fields 8=10538
- deformation of microinhomogeneous bodies 8=42
- disc edge subject to plastic strain 8=2927
- elastic half-space, stresses 8=14958
- elastic material, theorem 8=50
- elastic-plastic, numerical methods 8=19400
- flush nozzles in pressure vessels 8=10557
- fuel element with variable axial mechanical stress of canning tube, simulator 8=20896
- infinite strip, inclusion problem 8=19383
- intensity factors for penny-shaped cracks in infinite solid 8=22298
- interaction of parallel elastic cracks 8=17743
- interaction of parallel slip bands 8=17732
- interferometric method, new 8=46
- lattice-type discs, edge effect 8=6050
- optical strain testing, review of theory and exptl. details 8=5015
- plates with stiffened perforations, effective elastic modulus and stress concs. calc. 8=10546
- photoelastic, birefringence automatic meas. 8=11205
- photoelastic, r. f. for opaque bodies 8=22267
- Poisson's ratio in resonance calcs. for longitudinal vibrations of tapered rods 8=19484
- rectangular plates, stability, perturbation method with biaxially compressed forces 8=59
- rectangular retaining wall, with pressure of loose material, piezoelectric analogue of elastic problems 8=6054

Stress analysis—contd

- rod, vibrating and heated nonuniformly but symmetrically 8=10688
- rotating principal stress axes in high-cycle fatigue 8=5029
- semi-circular edge cracks, stress intensity, factor, for axial, bending and thermal loads 8=22299
- semi-infinite plate with circular inclusion 8=10551
- shell, axisymmetric cylindrical, effects of anisotropy 8=19388
- shell, shallow spherical, bending 8=2925
- shallow shell equations 8=48
- shell, conical weakened by a circular hole 8=43
- shell, cylindrical around elliptical hole 8=44
- short specimen, from long cylinder, residual stresses, theory and expt. 8=14949-50
- solids, by polarised u. s. frequency method 8=2039
- steel fatigue, under triaxial stresses, new apparatus 8=5068
- stretching and spin tensors of surface and linear material elements 8=40
- strip, apertured, photoelastic study 8=55
- at surfaces of 2 cavities in elastic-medium, thermoelastic anal. 8=19407
- thermal, in composite solid cylinder, book 8=19408
- thermal, in an elastically restrained plate, by photoelasticity 8=2926
- thermal in plate with transversely isotropic material 8=2930
- thermoelastic, energy-derived difference eqns. 8=19406
- thin circular plates, symmetrical bending 8=10555
- thin elastic disk, numerical determ. of stress field 8=6059
- thin strip material, approximate 8=5011
- Ge, X-ray stress topography, rel. to thin films on crystal 8=22371
- Si, X-ray stress topography, rel. to thin films on crystal 8=22371

Stress effects

- alloys, hydrostatic tension on solidification 8=21759
- alloys, mechanical relax. due to changes in short range order from stress 8=5009
- alloys, rel. to strength, time and temp. depend., non-equilib. state 8=8811
- α -brass stress corrosion cracking 8=8844
- cutting rocks and similar brittle materials 8=5012
- on cutting rocks and similar brittle materials 8=5012
- cyclic-loaded structure, numerical anal. of crack propag. 8=17745
- cylindrical wafers, between compression plates, anal. of press. distrib. 8=19394
- cylinders, orthotropically stiffened, elastic instability under torsion loading 8=19393
- dislocations, flexible rel. to internal and external stresses 8=1961
- electrode kinetics of stressed wires, cell for study 8=8793
- elastic disturbance, longit. propag., in thin inhomogeneous elastic rod 8=2921
- in fatigue crack propag. in plates under extension and bending, effect of mean stress 8=17758
- f. c. c. crystals, dislocation dissociation width dependence on dislocation velocity 8=17638
- glass, alkali alumino-silicate, ion exchanged surfaces durability 8=13525
- glass, crack-branching, vel. meas. 8=8815
- glass, on cracks 8=13540
- glass, porous, micromechanical stress concentrations, effect on strength 8=13577
- grain boundaries, growth of pores rel. to tensile stresses 8=17676
- graphite, creep induction during irradiat. 8=8828
- hematite, natural, induced mag. anisotropy 8=22748
- hydrostatic tension in solidifying alloys 8=21759
- hydrostatic tension in solidifying materials 8=27158
- Inconel stress corrosion cracking 8=8844
- p-n junctions, sensitivity to small deformations 8=13842
- low C steel, large torsional prestrains rel. to subsequent failure in tension 8=22367
- Makrolon films stress cracking obs. 8=8473
- metals, a. c. resistance-strain dependence rel. to microplasticity determ. 8=5036
- metals, b. c. c., c. p. h., and f. c. c., rel. to fracture 8=22290
- metals, rel. to strength, time and temp. depend., non-equilib. state 8=8811
- metals, strain-hardening in rod-drawing, use of mean yield stress in anal. 8=22300
- multiaxial, probability of fracture in metals 8=17736
- Permalloy, ferromagnetic, external, rel. to maximum mag. susceptibility 8=18338
- piezoelectric ceramics, sensitivity to high stress perpendicular to polar axis obs. 8=19556
- piezoelectric ceramics, stress sensitivity of permittivity reduced by heat treatment 8=19555
- polyalkyl methacrylates, dielectric absorption 8=9203
- polyseptide helix-coil transition under external force 8=21204
- polyurethane elastomer, rel. to triaxial fracture in tensile field 8=2075
- polyvinyl chloride films, rheo-optical properties, changes in birefringence 8=2076

Stress effects—contd

- powder, loose sintering rel. to strain effects 8=4693
- pulse loading, unloading boundary 8=19385
- quartzite, elastic precursor decay for cylindrical and spherical flow 8=13605
- rotating annuli, induced thermal membrane stresses rel. to increase in natural freqs. 8=19503
- shallow trusses and arches, nonlinear creep buckling 8=22278
- shell, truncated conical, thin, buckling under uniform static press. 8=19382
- steel, austenitic, stress corrosion cracking 8=8844
- steel, high strength, dynamic strain ageing 8=17782
- steel, mild, dynamic strain-ageing, effect of N content 8=13554
- steel, on γ -ray absorpt. and scatt. 8=13483
- steel, 0.04% C, residual strains due to single pulse compression stress wave 8=17787
- steels, structural, brittle fracture susceptibility, effect of strain ageing of martensite 8=13573
- strain hardening influence on loading and unloading biwaves in elastic-visco-plastic body 8=17718
- surface ionization and thermionic emission, depend. 8=13946
- thermoelasticity and elastic constants of stressed materials 8=2036
- Zircaloy-2 tubing, biaxial 8=13615
- Ag crystals, well-annealed, stress at which dislocations multiply 8=13545
- Ag, rel. to dislocation (Bordoni) relaxation 8=22197
- α -AgZn, mechanical relax. due to changes in short range order from stress 8=5009
- Al alloys, stress corrosion cracks at cutting planes 8=8818
- Al, annealed, commercially pure, strain ageing 8=5042
- Al, slow loading, rate of strengthening 8=22311
- Al-Cu-Mg alloy corrosion pot. 8=8819
- Al-2%Mg alloy, dislocation network knitting on stress-induced climb 8=17644
- Al_2O_3 (sapphire), crack-branching, vel. meas. 8=8815
- Au crystals, well-annealed, stress at which dislocations multiply 8=13545
- BaTiO₃ ceramics, depolarization at high strain rates 8=2243
- BeO, on cracks 8=13540
- CaF_2 , e. p. r. of Ho^{2+} 8=14128
- CdS, splitting of exciton lines 8=14273
- CdSe, splitting of exciton lines 8=14273
- Cu, cavitation damage, by magnetostrictive vibratory method 8=22339
- Cu crystals, well-annealed, stress at which dislocations multiply 8=13545
- Cu, cyclic, defect concentrations at room temp., resist. studies 8=17604
- Cu, explosively deformed, rel. to dislocation density and distrib. 8=17651
- Cu, on γ -ray absorpt. and scatt. 8=13483
- Cu single crystals in stressed condition, dislocation arrangement, electron microscope obs. 8=22201
- Cu_2O exciton spectrum of uniaxial press., obs. 8=9521
- Fe-Mn-N alloys, rel. to creep resistance 8=5064
- Fe, polycrystalline, lower yield stress, temp. depend. 8=13562
- Fe-Si(3%) sheet, oriented, dynamic magnetostriction and mech. strain 8=22812
- n-Ge, compressive uniaxial stress, effect on high field domains 8=18051
- Ge, As and Sb impurities, stress-induced splitting of spectral lines 8=13424
- KBr crystals, and temp. depend. of dislocation mobilities 8=8729
- KBr, V-bonds, effect of stress, obs. 8=2000
- KNO₃, dynamic compression by explosive impact loading 8=22377
- LiF, strain amplitude independent dislocation damping, recovery 8=13582
- Mg₂Cd, critical resolved shear stress for slip, degree of order dependence 8=5079
- MnF₂, magnon sidebands, selection rules for coupling to excitons 8=14240
- MnO, axially cooled or stressed, anisotropy from torque meas. 8=14072
- Mo and alloys, rupture characteristics 8=2061
- Mo crystals, dislocation velocity-stress relations 8=17657
- NaI, elastic tensor of gradient elec. field induced by uniaxial stress, n. m. r. obs. 8=13014
- Nb foil, dislocation density and flow stress, effects of grain size 8=4980
- NiO, axially cooled or stressed, anisotropy from torque meas. 8=14072
- Pb, creep, stress sensitivity at low stresses, article discussion 8=17825
- Pb zirconate-titanate ceramics, depolarization at high strain rates 8=2243
- p-Si, B-doped, uniaxial compression, effect on impurity conduction 8=9131
- Si, avalanche oscillators 8=5303
- Si p-n junctions, noise and V-I characteristics 8=13847
- SiC, polycrystalline, rel. to creep 8=22393

Stress effects—contd

- SrTiO₃ supercond. transition temp., ≤ 1.5 kbar 8=2175
 ThO₂, e.p.r. of Yb³⁺ 8=14128
 Ti alloy in non-electrolyte, corrosion cracking susceptibility 8=8863
 Ti hydrides, disaligning by plastic straining 8=4782
 Zn, deformation at high strain rates in hardening process 8=17837
 Zn single crystals, wave-induced cleavage 8=21927
 Zn-Al, γ -ray spectrum distrib. compression effects 8=4999
 ZnO, splitting of exciton lines 8=14273
- Stress measurement.** See Strain gauges.
- Stress/strain relations**
 See also Elastic constants.
 Armco iron, lower yield stress rel. to grain size 8=17798
 beams, rigid-plastic, effects of strain-hardening and strain-rate sensitivity on permanent deform. 8=19402
 cellulose nitrate and acetate, isothermal curves, model 8=22406
 curves, under variable stresses 8=14955
 dislocation stress field and solute atom strain in lattice rel. to strain ageing 8=4969
 elastomers, in multiaxial deformations 8=5010
 in elastoplasticity, incremental 8=8790
 glassy thermoplastics, isothermal curves, model 8=22406
 graphite, deformation mechanism, cracking 8=5053
 ice, polycrystalline, flow at low stresses and small strains 8=22373
 iron, armco, tensile, after strain ageing 8=17792
 metals, elevated temp. creep and high-strain fatigue, data correlation 8=2060
 metals, strain fields under omnidirectional uniform compression 8=17756
 metals, in work hardening range, linearized curves 8=17722
 milk, coagulating, shear logarithmic eqn. 8=22402
 non-linear in thin plates, rel. to bending, comments and reply 8=22264-5
 nonlinear material, bending of thin plates 8=10548
 para-H₂, solid, deformation curves at 4.2°K, mech. constants 8=5074
 pressure effect a brittle-ductile transition 8=13502
 pressurized shell, effect on creep near sealed opening 8=10560
 PVC, isothermal curves, model 8=22406
 steel, austenitic effect of liquid Na on stress rupture props. 8=22359
 steel, correlation with fatigue limit 8=17783
 steel cylinders, plastic flow stress in rel. to natural strain 8=22353
 steel in dynamic compression and plasticine, Na use as models, 1000°C 8=13556
 steel, mild, yield characts. for cold rolling 8=22368
 strain meas. by moiré tech., modification of profile projector 8=13501
 strain tensor, relation between cpnents, applied to bars 8=19397
 Al-1 at.% Zn, electron irradiation hardening 8=8822
 Al, during extrusion recovery and recrystallization 8=4841
 Al flow stress, effect of specimen diameter 8=8820
 Al single crystals, high strain rates 8=22310
 Al, zone-refined, curves for shear deformation along slip direction 8=17761
 Al-Mg alloys, Portevin-le Chatelier effect, rel. to comp. and testing temp. 8=22309
 Au nuclei on MoS₂ substrate, strain nucleus size and misalignment dependence 8=8823
 Be rel. to mechanical eqn. of state obs. 8=8825
 Cu crystals with dispersed Co/SiO₂ phase on plastic deformation 8=4974
 Fe, armco, strain ageing, effect of preliminary deformation 8=17786
 Fe crystals, under tensile deformation, -70°C to 250°C 8=13553
 Fe, neutron irradi., plastic deformation 8=22348
 Fe-Al alloys, yield effect from elevated temp. constant strain-rate tests 8=13555
 Fe-Ni-Ti alloy of Invar type, Young modulus anomalies 8=17790
 Mg-Li alloy, plane-strain compression, anisotropy 8=17814
 Mg, plane-strain compression, anisotropy 8=17814
 Mg-Th alloy, plane-strain compression, anisotropy 8=17814
 Mo crystals, deformation at slow rates of strain 8=13587
 Mo crystals, dislocation velocity-stress relations 8=17657
 Ni-Cu alloys, Portevin-Le Chatelier effect, hydrogen level dependence 8=22331
 Zn-Al, alloy, superplastic, effect of stress, temp. and heat-treatment 8=5090
 Zn, basal slip, Al impurity effects 8=17836
 ZrO₂, Y₂O₃- and MgO- stabilized, rel. to stress relief mechanism 8=17839

Stresses, internal

- alkaline metals, strain critical systems 8=13524
 alloys, shear stress increase due to coherent precipitates 8=5017
 anisotropic half-space, Boussinesq problems 8=10540

Stresses, internal—contd

- body, elastic, with hexagonal lattice technical micro-structure 8=10544
 ceramics, laminated, residual stresses at interfaces, rel. to mech. props. 8=17723
 composites, reinforced, fibre-matrix interaction forces calc. 8=22268
 crystalline materials, obs. by means of X-ray diffraction 8=5014
 crystal, static and dynamic uniaxial stress apparatus 8=5018
 dislocations, flexible rel. to internal and external stresses 8=1961
 distribution in composites with planar interfaces 8=5016
 distribution in elastic thin strip material 8=5011
 f. c. c. metals, elastically anisotropic, shear stresses of tilt boundaries of $\{111\}$, $1/2 \{110\}$ dislocations 8=22195
 field, periodic, thermally activated dislocation motion 8=8711
 graphite, deformation mechanism, localized cracking, interlayer slip 8=5053
 lattice strain and Raman-active vibrations rel. to elasticity and piezoelectricity 8=5013
 meas. with i.r. radiometer 8=8794
 metals, elastically anisotropic f. c. c., shear, and energies of $1/2 \{110\}$, $\{111\}$ edge dislocations, new data 8=17640
 metals, hexagonal, due to dislocation pile-ups on anisotropic treatment 8=1963
 metals, plastically deformed, residual stresses and latent elastic strain energy 8=22269
 metals, residual and lattice expansion by X-ray goniometric methods 8=4862
 metals, strain fields under omnidirectional uniform compression 8=17756
 molecular crystal strain tensors, temp. dependence 8=13508
 pressure in solid-filled pistons, u.s. meas. of expansion 8=10580
 rod, inhomogeneous curved, loading capacity 8=10553
 in rubber vulcanizates on diffusion of liqs. 8=1932
 short specimen, from long cylinder, residual stresses, theory and expt. 8=14949-50
 solid, mobility of dislocations 8=8715
 strain accumulation, second-order, at ultrasonic freq. 8=13527
 stress-assisted diffusion to dislocations and strain ageing 8=4969
 thermal, distrib. in sandwich plate with rigid core 8=2040
 thermoelastic, on edge of semi-infinite strip of aetotropic material, with 2 infinitely long sides insulated 8=19405
 toroidal shell, perturbation theory 8=10543
 in twin-induced fracture 8=5028
 Al, plastic relaxation rel. to stacking fault energy 8=13529
 Au, plastic relaxation rel. to stacking fault energy 8=13529
 Cr electrodeposits rel. to epitaxy, obs. 8=22325
 Cu, cyclic strain dispersal rel. to fatigue life improvement obs. 8=5031
 Cu, films, creep, elastic lattice strains 8=13548
 Cu, plastic relaxation rel. to stacking fault energy 8=13529
 Cu-Ni-Co alloys, critical shearing stress temp. dependence 8=1971
 Cu, polycrystalline, flow stress, meas. 8=9004
 Fe-Ni films, electro-deposited, rel. to deposition conditions 8=17653
 GaSb, effect of ion bombardment, annealing and polishing on (111) surface stress 8=8849
 Ge, effect of ion bombardment, annealing and polishing on (111) surface stress 8=8849
 Ge, lattice energy rel. to elastic deform., electron distrib., elastic const. 8=13576
 InSb, effect of ion bombardment, annealing and polishing on (111) surface stress 8=8849
 KCl and KF, dichroism, mag. circular, of R₂ band 8=14235
 LiF crystals obs. by means of X-ray diffraction, MoK α 8=5014
 Mg, cold-worked, strain and particle size determ. by variance method 8=1761
 MgO crystallite, from thermal decomposition of Mg cpds., X-ray analysis 8=22379
 Ni:Al₂O₃, sintered, flow stresses and dislocation movement resistance 8=2048
 Ni layers, electrolytically deposited, rel. to deposition inhibitor effect 8=1805
 Ni, plastic relaxation rel. to stacking fault energy 8=13529
 Pt-Ir alloys electrodeposits, obs. 8=23153
 ZrO₂, Y₂O₃- and MgO- stabilized, stress relief mechanism 8=17839
 Zr-2.5wt.% Nb, cold rolled, relax rel. to aging and recovery, obs. 8=8872
- Striations.** See Discharges, electric.
- Stripping reactions.** See Nuclear reactions.
- Stroboscopes**
 light chopper, feedback-stabilized with continuously variable frequency 8=6509

Strong interactions. See Field theory, quantum/interactions, strong.

Strontium

- films, thin, optical absorpt. between 0.5 and 5.5 eV 8=23014
 g_{1-} values of lowest 3P_1 states 8=7424
 ion-exchange selectivity in some synthetic zeolites 8=23061
 lifetime of $5s5p^3P_1$ state 8=7437
 Rydberg states obs. from electron collision 8=20941
 thermal diffusion of ions in NaCl cryst., Soret effect obs. 8=1921
 vapour, absorption spectrum, u. v. extension of arc spectra 8=20967
 Sr^{90} , activity, in rain water, Sydney 8=14632
 Sr^{90} in alpine glacier, meas. in fern and ice samples 8=18831
 Sr^{90} , global budget, implications of changes 8=14634
 SrI , $5s^2\ ^1S_0$ -4dnp, nf spectrum, analysis of autoionization resonance structure 8=20968

Strontium compounds

- $Sr_xBa_{1-x}Nb_2O_6$ ($x = 0.25, 0.50, 0.75$), refractive indices, temp. and wavelength depend. 8=14268
 $Sr_{1-x}Ba_xNb_2O_6$, cryst. growth and props. 8=21966
 $Sr_{0.925}Ba_{0.075}TiO_3$, heat capacity, 0.3 to 4°K 8=1877
 $(Sr, Ba)_2Zn_2Fe_{1-x}O_{22}(Y)$ ferrite, spin ordering using neutron diffraction meas. 8=22858
 $Sr(IO_{3/2})_x \cdot xH_2O$ ($x=3, 4; x=1, 6; x=4, 7$), structure 8=8558
 $SrCa_{1-x}F_2$, far i. r. reflectivity spectra 8=9507
 $SrCl_2$ cryst., e. s. r. of reaction intermediate with F_2 8=14124
 $SrCl_2$, electron centres form. by Co^{60} - γ -irrad. 8=22235
 $SrCl_2$, pure and $Y^{3+}(Na^+)$ doped, ionic conduction and diffusion mechanisms 8=8983
 $SrCO_3$, aragonite/disordered rhombohedral polymorphic transition 8=21840
 SrF_2 , colorability enhancement by plastic deformation 8=22228
 SrO , colorability enhancement after plastic deformation 8=22229
 SrF emission spectrum and $C^{2+}\pi-X^2\Sigma$ vibr. consts. obs. 8=1266
 SrF_2 additively coloured, phonon-assisted colour centre fluorescence 8=14306
 SrF_2 , lattice theory, elastic consts., dielectric const. 8=13178
 SrF_2 , paramagnetic rare-earth activated, magnetooptic rotation 8=5590
 $SrF_2:Eu^{2+}$, e. p. r. spectrum at 77-964°K 8=9424
 SrF_2 , F-centres, e. s. r. and optical data 8=2014
 SrF_2 , Gd^{3+} impurity centres, temp. effects 8=8703
 $SrF_2:Gd^{3+}$, Stark splitting and centre of gravity of $^6P_{7/2}$ and $^6P_{5/2}$ 8=23015
 $SrF_2:H,D$, polarization 8=8206
 $SrF_2:Sc^{2+}$, paramagnetic reson. in 2E state, effect of linear Jahn-Teller coupling 8=18402
 $SrF_2:Sm^{2+}$, fluoresc. 8=14332
 $SrF_2:Tm^{2+}$, magneto-optical rot. 8=18512
 $SrF_2:V^{2+}$, e. p. r. study 8=9446
 SrF_2 , X-ray coloured, absorbs. by colour centres, temp. dependence 8=17683
 $SrF_2:Yb^{3+}$, spin-lattice relax. 8=18444
 $SrGe$, crystal structure 8=8557
 $SrK_2(PO_3)_4$, cryst. struct., and features of P_4O_{12} rings 8=13293
 $(Sr, Mg)_3(PO_4)_2:Eu^{2+}:Mn^{2+}$ phosphors, luminesc. obs. 8=9629
 $(Sr_{0.88}Mg_{0.11})_3(PO_4)_2:Eu$ yellow luminesc. and mechanism 8=9629
 $SrMoO_4:Er^{3+}$, e. p. r. spectra at 4.2 and 10°K 8=18412
 $Sr(N_3)_2$, crystal structure refinement 8=17387
 $Sr_2NaNb_3O_{15}$, electro-optic and nonlinear optic characts. 8=22959
 SrO , defect structure studies 8=22171
 SrO , neutron or γ irradiated, O_2 chemisorption rel. to surface states 8=5724
 SrO , photoluminescence, photoelectric emission and enhanced thermionic emission 8=23063
 $SrO:Mn^{2+}$ impurity ion hyperfine coupling constant temp. dependence 8=8196
 $\alpha-Sr_2P_2O_7$, cryst. struct. atomic 8=13292
 $Sr_2P_2O_7:Eu^{2+}$ activated, luminesc. 8=9628
 $Sr_{10}(PO_4)_6(OH)_2$, i. r. frequencies 8=12234
 SrS , sublimation and dissociation energy 8=16957
 $Sr_2Sb_2O_7$ ($x = 1, 2; y = 4, 5$), prep. and props. 8=14363
 $SrSn$, crystal structure 8=8557
 $Sr(TaFe)_{1/2}O_3$, study using Mössbauer effect of Fe^{57} 8=16984
 $SrTiO_3$, optical-phonon freq., electric field dependence 8=5370
 $SrTiO_3$, phonon lifetime, at low temps. 8=4908
 $SrTiO_3$, photochromic crystals, thick hologram storage 8=20118
 $SrTiO_3$, reduced, u. s. propagation at low temps. 8=17505
 $SrTiO_3$, second-order renormalization and phase stability 8=9219
 $SrTiO_3$, semiconducting, superconducting transition temp. 8=9055
 $SrTiO_3$ supercond. transition temp., stress effects at ≤ 1.5 kbar 8=2175

Strontium compounds—contd

- $SrTiO_3$, superconducting semiconductor films and whiskers, transition temps. 8=9056
 $SrTiO_3:Eu^{3+}, Tb^{3+}, Pr^{3+}$, vibronic structure in luminescence spectra 8=14333
 $SrTiO_3$, of Fe^{3+} axial spectrum, paramag. reson. study at mm wavelengths 8=14106
 $SrTiO_3-1.15 Sr(TaFe)_{1/2}O_3$, solid soln., study using Mössbauer effect of Fe^{57} solid soln. 8=16984
 $SrTiO_3:Ti^{3+}$ electronic ground state structure 8=9445
 $SrVSi_2O_7$, haradaite, crystal structure $SrVSi_2O_7$, and $Si-O$ bond lengths 8=17416
 $SrWO_4$, low work function collector for thermionic converter 8=18266
 $SrY_2O_4:Ce$, phosphoresc. 8=18600
 $SrZrO_3$, phase transitions, at 700-1170°C, X-ray investigations 8=8281

Structure factors. See Crystal structure, atomic; X-ray crystallography.

Structure of matter. See Crystal structure; Liquids/structure; Solids/structure.

Sublimation

- See also Heat of sublimation; Vaporization.
 asymptotic solution 8=21783
 energy pulse interaction with solid, heat and mass transfer 8=12968
 rarefied multicomponent gas flow over subliming wall, boundary conditions 8=4663
 thin plate in gas flow, conc. and templ. eqns. 8=21784
 Ar, solidified, vapour pressure, binding energy and mean vibration freq. 8=16960
 CeC_2 , mass spectra-Knudsen cell determ. 8=21785
 Cu-phthalocyanines cryst. growth from vap. phase 8=21946
 Kr, solidified, vapour pressure, binding energy and mean vibration freq. 8=16960
 Mg, kinetics in chambers with cryogenic surfaces, obs. 8=16959
 Mg-Al alloy, kinetics in chambers with cryogenic surfaces, obs. 8=16959
 SrS 8=16957
 TiF_3 , pressures from mass spectra 8=1623
 Xe, solidified, vapour pressure, binding energy and mean vibration freq. 8=16960
 ZnTe 8=16956

Sudden commencement. See Magnetic storms.

Suhl effect. See Hall effect; Semiconductors.

Sulphur

- critical surface tension 8=21869
 cyclooctasulphur, entropy changes in formation 8=21207
 Fraunhofer spectrum, forbidden lines 8=19295
 molten, sound velocity and compressibility 8=12866
 molten, ultrasonic velocity 8=12867
 muonic K series X-rays 8=1209
 orthorhombic, electron hopping transport and orbital overlap 8=18064
 orthorhombic, hole and electron traps 8=8904
 orthorhombic, transient space-charge perturbed currents 8=18171
 polymeric, relax. mechanisms 8=4267
 self-diffusion in ZnS 8=1931
 solubility in iron alloys at 1000°C, effect of Cr, Cu, Ni and V 8=17012
 thermodynamic props. of vap., meas. 200-400°C 8=21512
 thiophosphoryl halides, vibration spectra 8=7547
 vapour pressure above Ag_2S_{11} , melt, rel. to elec. conductivity and thermoelec. power 8=16876
 S II, inelastic e scatt. collision contribution to linewidths 8=20991
 S_2^- in alkali halides, thermal quenching of luminescence 8=2485
 S_6 , vibrations and thermodynamic props. 8=12227
 S_8 molecule, mean square amplitudes of vibration 8=12228
 SF_6 , clathrate hydrate, F^{19} mag. reson. absorpt. 8=7607
 SH^+ , fine structure of $^3\Sigma^-$ and $^3\Pi$ states 8=7541
 SI forbidden lines in sunspot spectrum obs. 8=14880
 SO_2 , liq. and solid, vibrational spectra 8=8088
 SO_2 , thermal conductivity rel. to temp. 8=7925

Sulphur compounds

- alum, methylammonium chromium, crystal structure 8=22017
 hydrides, proton reson. 8=12327
 structure determ. by ESCA (electron spectroscopy for chem. anal.) 8=21100
 sulphide phosphors, freq. depend of shape of light pulse 8=5676
 sulphosalts, crystal chemistry 8=17204
 H_2SO_4 aerosols, light scatt. studies 8=12951
 H_2S_2 gaseous, struct. study by electron diff. 8=21103
 (Mn, Me)(S, Se)-type synthetic cpds. and selenide-sulphide inclusions 8=4692
 S_2Cl_2 , i. r. and Raman spectra 8=12231
 SF_6Cl molecule, amplitudes of vibration, shrinkage effect and Coriolis constants 8=12230
 SF_6-CO_2 , critical binary fluids, spectral width temp. and angular dependence 8=21778
 SF_6 , creep discharge over solid dielectrics 8=16420
 SF_6 , degradation in electrical equipment 8=14383
 SF_6 , discharge voltage, comparison with air 8=16421

Sulphur compounds—contd

- SF_6 , effect on combination coeff. of ions in γ -irrad.
 HCl gas 8=23164
 SF_6 , i.r. spectrum, high resolution 8=490
 SF_6 , solution H in, spectral simultaneous transitions 8=21675
 SF_6 , X-ray absorpt. 8=12229
 SH , dipole moment, from gas-phase electron reson. 8=12345
 $\text{SH}^+(\Sigma^+)$, Hartree-Fock wavefunctions and molec. props. 8=4165
 $\text{S}_4\text{N}_4\text{H}_4$, crystal structure by neutron diff. meas. 8=4884
 SO_3^- anion, in Antarctic atmosphere 8=23264
 $\text{S}_2\text{O}_6^{2-}$ anion, in Antarctic atmosphere 8=23264
 SO_2 asymmetric mol., microwave absorpt. 8=16302
 SO_3 , Coriolis coupling consts. from Q-heads 8=21102
 $\text{SO}(\Delta)$, dipole moment, from gas-phase electron reson. 8=12345
 SO gaseous free radical, e.s.r. study 8=12340
 SO_2 gaseous, struct. by electron diff. 8=21104
 SO , gas-phase electron reson., double quantum transitions 8=12308
 $\text{S}^{33}\text{O}^{16}$, gas-phase electron reson. spectrum 8=12353
 SO_2 hydrate, solid, l.f. vib. spectra of H_2O mols. 8=1840
 S_2O_8 , improved dimensions 8=17400
 SO_2 in CCl_4 , CH_2Cl_2 , CH_3CN , absolute i. r. intensities meas. and calcs. 8=1560
 SO_2 , reaction kinetics with O atoms 8=5715
 SO_2 soln., mol. reorientation theory of vibr. spectra 8=16867
 SO_2 solns., oxidation, effect of ullage 8=23111
 SO_2 , with ketones, nitriles, esters or alcohols, u.v. absorpt. spectra 8=18688
 SOF_4 , molec. struct. 8=21101
 SO_2OH groups in polymer foils, i.r. continuum absorpt. extinction 8=17028
 SPFBr_2 , i. r. spectra 8=16300
 SPFCl_2 , i. r. spectra 8=16300
 SSe^- , e.s.r. in alkali iodide crystals. 8=14123

Sun

- See also Sunspots.
 active M-regions props. rel. to quasistationary plasma emission 8=19311
 activity centres, creation, influence of solar movement towards apex 8=23735
 activity coinciding with changes in Mars 8=5971
 activity correl. with red aurora, 1946-1951 8=9930
 activity cycle, relation with solar tidal force induced by planets 8=23731
 activity, evolution and structure obs. 8=19286
 activity, July-Sep. (1965) 8=19053
 activity, Oct-Dec (1965) 8=19054
 activity, Jan-March (1966) 8=19055
 activity, minimum, rel. to cosmic ray radial density gradient and rigidity 8=5970
 activity rel. aurora frequency, obs. 8=9933
 activity, review chart 8=10417
 air heaters, rating parameters 8=228
 arch-filament systems in young bipolar spot groups 8=19310
 rel. to astronomical seeing verification by isophote of vertical satellite 8=14746
 centre-to-limb brightening in far i. r., obs. compared with theoretical predictions 8=23753
 chromosphere, Bilderberg continuum atmos. model 8=23730
 chromosphere, Ca II H and K core profiles near solar max. 8=10382
 chromosphere-corona transition zone, transport processes rel. to heavy ion abundances 8=19320
 chromosphere, heating, above a sunspot 8=5975
 chromosphere, lower, Ca II and Mg II lines 8=2859
 chromosphere model rel. to emission cores and profiles of H and K lines of Mg II and Ca II 8=23707
 chromosphere, relative abundances of O, Mg, Cr, Mn, Fe and Ni 8=23742
 chromosphere, solar r.f. radiation scatt. on turbulence rel. to temp. inversion at 6 mm 8=10404
 chromosphere, 300-sec. type oscillation, explanation 8=23743
 chromosphere, u.v. emission spectrum 8=10428
 convection region, lower thermal boundary layer 8=10380
 correlation of solar activity with geomagnetic drift 8=2750
 cosmic ray cycle effect in IGY 8=3754
 cosmic rays, intergalactic, modulation theory 8=2771
 cosmic ray nuclei generation rel. to intensity vars. (1964-65) 8=11680
 cosmic ray modulation effect 8=10086
 differential rotation models, instability 8=10377
 disk flattening, atmospheric, obs. 8=2597
 east limb passage of active region, July 7-10, 1959 8=10416
 elements diffusion in, rel. to observed abundances 8=19285
 granulation, colour, due to atm. dispersion 8=23725
 granulation, improvement of images distorted by atmospheric turbulence 8=23728
 granulation, statistical analysis of photometry obs. 8=19307
 horizontal wind field in atmos., comments on Plaskett's spectroscopic anal. 8=10378
 hydromagnetic waves, propagation through solar convective zone 8=10376

Sun—contd

- intensity profile near solar limits in far i. r. and m. m. regions 8=23700
 intensity for range $0.02 < \tau_0 < 10$, improved photospheric temp. model 8=23729
 limb darkening in range $4500 \text{ \AA} < \lambda < 2500 \text{ \AA}$, failure and modification of Bilderberg continuum atmos. 8=23752
 limb darkening obs. between 1800 and 2900 \AA , rel. to opacity of photosphere 8=23751
 luni-solar daily variation of geomagnetic field at Tananarive 8=10040
 model, for magnetic stars 8=19117
 modulation of cosmic rays, neutron monitor and direct space obs., 1958-65 8=11677
 modulation of galactic cosmic rays 8=10419
 modulation of galactic electrons and protons obs. 8=11679
 motion of emitter and receiver in Sun field, freq. shift 8=14970
 oblate, and relativity 8=10599
 oblateness and perihelion precession of Mercury 8=2838
 oblateness, core rot. rel. to planetary perihelion advances 8=23694
 oblateness, defence of Roxburgh's theory 8=23695
 oblateness obs. rel. to mag. stress 8=23693
 oblateness, quadrupole moment rel. to precession of Moon's orbit 8=23691
 observatory, Hawaii 8=10374
 outer atmosphere, struct. 8=10120
 perturbative effect on motion near collinear Earth-Moon libration points 8=19070
 photosphere, Bilderberg continuum atmos. model 8=23730
 photosphere, $\text{C}^{12}/\text{C}^{13}$ ratio 8=23726
 photosphere-chromosphere transition zone temp. distrib. from MgII and CaII reson. lines 8=19319
 photosphere, CO molecules, vibration and kinetic temp. 8=10412
 photosphere, curves of growth and rough analysis 8=14879
 photosphere, simplified model of temp. distrib., deriv. of emergent continuous spectrum 8=23745
 photosphere and sunspots, vel. and mag. fields, high resolution meas. 8=23724
 photosphere, x, T, P, ρ , K model 8=19306
 photospheric model, test by centre-to-limb anal. of O lines 8=23704
 photospheric temp. model, $0.02 < \tau_0 < 10$ range, for continuum intensity 8=23729
 plage, Ca, of post-limb event of March 2 1966 8=10427
 plage, X-ray emission model 8=10394
 reflection, very distant, Radcliffe Observatory, S.A. 8=19291
 research, Rome 8=10373
 rotation, differential and meridional currents using hydrodynamic equations of motion calc. 8=10372
 rotation, differential, and oblateness 8=2837
 solar-terrestrial physics, The Inter-Union Symposium Belgrade, 1966 8=10325
 solar wind, Alfvén waves 8=23719
 solar wind and interplanetary magnetic field 8=2849
 solar windows, effects of line blanketing rel. to high flux prediction to violet of 4500 \AA 8=23701
 stratified atmos., acoustic and gravity wave emission by turbulence 8=23270
 Sun-Mars mass ratio from Mariner IV and NASA deep space stations 8=23671
 supergranulation, mag. field accumulation 8=19292
 temperature min. rel. to u. v. spectrum interpret. in Bilderberg model 8=23703
 tidal forces, and moon, long period vars. 8=19241
 torque, solar wind induced, calc. 8=14873
 velocity rel. to cosmic microwave background anisotropy 8=23609
 $\text{C}^{12}/\text{C}^{13}$, atmospheric abundance ratio from spectral meas. 8=10429
 CO mols. dissociation in photosphere-chromosphere transition zone 8=12337
 CO mols. energy transfer to photosphere particles rel. to spectrum 8=12377
 Fe abundance 8=23682
 $\text{H}\alpha$ double-limb controversy, resolution 8=23746
 He abundance in 8=10381
 He in chromosphere, low temp. emission theory 8=10430
 Pb abundance, spectrometry 8=23696
- corona**
- above active regions, extreme u. v. rel. to r.f. 8=10431
 asymmetry, explanation of cosmic-ray variations 8=3755
 barrier and cosmic ray modulation effect 8=10088
 coronagraph, 535 mm objective lens 8=536
 coronagraph 5303 and 6374 \AA lines 8=19323
 chromosphere-corona transition zone, transport processes rel. to heavy ion abundances 8=19320
 condensations and noise storm centres, 408 and 169 MHz 8=19325
 dielectronic recombination, influence of radiation fields 8=23750
 dome formation around prominence, obs. 8=2864
 at eclipse of 20 May 1966 8=10437
 electron accel., source of type IV flare 8=14884
 electron streams in outer region rel. to type III and V radio bursts 8=10399
 electron temp. in outer region "Venus-2" obs. 8=10396

Sun—contd**corona—contd**

- emission data, Jul.-Sep. 1966 8=2836
- heat transfer, possible role of oscillatory convection 8=19308
- historical survey and book review 8=14886
- inner, temp. for each rotation during last sunspot cycle 8=14885
- ionization formula, effect of doubly excited levels 8=2863
- line profiles, temp. variation effects 8=23698
- line spectra at eclipse of 1952, anal. 8=10436
- optical research, 20 year review 8=19066
- outer, and interplanetary plasma, radio scatt. rel. to plasma irregularities 8=19284
- polar plumes, rel. to polar surface features 8=23747
- Razin effect, determ. of mag. field at one solar radius 8=23749
- relative abundances, from u.v. spectrum 8=5976-7
- rel. to solar wind origin, expansion, microscopic model 8=14876
- spectra, continuous and Fraunhofer obs. 8=19322
- spectrum during total eclipse of Nov. 1966 8=2862
- spectrum, u.v., rel. to spectroscopy of highly ionized atoms 8=16192
- spectrum, visible emission lines, excitation and electron density 8=10439
- spicule diffusion, obs. and model 8=10433
- structure and brightness distrib., 12 Nov. 1966 eclipse obs. 8=19321
- temperature, from intensity gradients meas. during total eclipse of May 30th, 1965 8=10435
- temperature rel. to dielectronic recomb. 8=10438
- transition region with chromosphere, spicules origin 8=2860
- u.v. emission spectrum 8=10428
- upper, rarefied plasma, turbulent structure and brightness temperature of radio emission 8=10432
- waves, solitary, calc. of structure 8=1391
- X-ray flare, 9.5-200 Å 8=14866
- O/Fe relative abundances 8=23748
- O VIII L_{α} and L_{β} lines intensity ratio as temperature function, calc. 8=10434

eclipses

- annular, 20 May 1966, optical instruments and obs. 8=19288
- annular, 20 May 1966, photoelectric obs. 8=19290
- annular, 20 May 1966, satellite obs. 8=19289
- convention of Italian Astronomical Society, Catania Italy (1966) 8=19111
- corona, spectrum, Nov. 1966 8=2862
- corona struct. and brightness distrib., 12 Nov. (1966) 8=19321
- ionospheric cosmic noise absorption, effect on, May 20, 1966 8=9979
- ionospheric E region recombination coefficient and coronal contribution to ionization, eclipse obs. 8=19014
- ionospheric effects, May 30, 1965, obs. 8=9959
- and ionosphere topside obs. 8=2717
- noise storm occultation 8=2843
- 1965 May 30, day airglow, λ 3914 Å and λ 6300 Å 8=2628
- 1966, May 20, corona obs. 8=10437
- 1966, May 20, limb-darkening, instrumentation and results 8=2861
- May 20, 1966, radiation at 19 Gc/s 8=10402
- November 12th, 1966, airborne spectrographic obs. 8=5962
- ozone-eclipse effect 8=23692
- partial, 20 May 1966, r.f. activity obs. 8=19301
- photoelectric meas. rel. to iron abundance 8=5965
- radiotelescope 20 May 1966 obs. 8=19287
- total, May 20, 1966, F-region obs. from 6 African stations 8=2710
- total, 12 Nov. 1966, effect on v.l.f. long path transmission 8=23374
- total, July 20, 1963, sky brightness in 7 colours from airborne photometer obs. 8=2629
- total, Nov. 1966, measurements performed with 4.28 cm radio polarimeter 8=14868

flares

- association rate with surges 8=10421
- association with type II bursts 8=19316
- bipolar flux tube model 8=5972
- in CMP region, rel. to mag. fields, 20 Sept. 1963 8=23736
- coronal X-ray and chromospheric optical, 9.5-200 Å 8=14866
- corpuscular effects, obs. through sudden increases in longwave field intensity 8=19314
- cosmic ray variation with solar activity 8=20634
- "disparitions brusques", phenomenological model, obs. 8=10422
- effect on altitudes of main isobaric surfaces in N. hemisphere 8=18923
- emission data, Jul.-Sep. 1966 8=2836
- energetic X-rays obs. by satellite, correlation with solar radio and energetic particle emission 8=14883
- energy, rel. to stability of force-free mag. fields 8=23737
- energy transport and cosmic rays 8=2857
- hydromagnetic resonance in hypothesis of temporary choking of energy flux to corona 8=19317

Sun—contd**flares—contd**

- importance 2, H α line study 8=2856
- ionospheric effects 8=18967
- loop-prominence event, model based on condensation theory 8=5973
- photometric meas. and classification 8=19315
- plasma blob ejections and radio bursts 8=10397
- plasma flow generated by, 3D structure 8=23740
- plasma interaction with magnetosphere, lab. analog 8=2622
- and polar cap absorption separation into 2 types 8=10407
- post-limb event of March 2 1966 8=10427
- proton, longitude distrib. over one century 8=10426
- radio burst flux density associated with proton events, 1966, obs. 8=10403
- radio bursts, type III and type V rel. to electron streams in outer corona 8=10399
- radio events, flare-associated, homology 8=10398
- spectral characteristics from ionosphere electron density data 8=10425
- structure, effect of filamentary interplanetary field obs. 8=10424
- tropospheric responses to chromospheric flares, search 8=23257
- type IV source, electron accel. in corona 8=14884
- X-radiations rel. to ionospheric sudden freq. deviations 8=9985
- X-ray and sudden cosmic noise absorpt. 8=2653
- X rays, 80 keV to 1 MeV, OGO 3 obs. and nonthermal bremsstrahlung hypothesis 8=23739
- X-ray, July 7, 1966, Explorer 33 GM tube obs. 8=14882
- 1957, 13 Sept., effects on aurora 8=9934
- Na D₂ line, brightening obs. 8=2858

magnetism

- Babcock theory and variability of magnetic stars 8=2789
- in CMP region, rel. to flares, 20 Sept. 1963 8=23736
- field at one solar radius, from Razin effect in solar corona 8=23749
- field, computations based on model 8=14864
- field, interaction with solar wind, calc. 8=14878
- field, origin and interplanetary effects 8=10375
- fields, small-scale, and "invisible sunspots" 8=2854
- galactic ray modulation possibility rel. to H⁺/He balloon obs. 1961-65 8=2770
- longitudinal field config. on both sides of dark chromospheric filaments 8=19318
- magnetic cycle, models 8=19309
- magnetic field, review of literature 8=5963
- oscillations of magnetic fields with simultaneous record of radial velocities at λ 5250 Å 6103 Å 8=10379
- spiral field, model charged particle motion calc. 8=23689
- stress rel. to obliteness obs. 8=23693
- sunspots, and Fe I 6302, 5 Å line contours, rel. to Zeeman splitting anomalies, obs. 8=10418
- sunspots, rel. to development 8=10415
- sunspots, magnetic field structure 8=2851
- sunspots, small and young, fields meas. 8=2853
- supergranules, growth of mag. fields around boundaries 8=19292

prominences

- dark chromospheric filaments, longit. mag. field config. on both sides 8=19318
- dome formation in corona, obs. 8=2864
- emission data, Jul.-Sep. 1966 8=2836
- flare-loop, model based on condensation theory 8=5973
- homogeneity, using monochromatic light photographs 8=2855
- magnetic field, He I 5876 Å line meas. 8=23738
- quiescent, mag. field intensities, obs. 8=10423
- H α filament, against chromosphere at limb, obs. 8=23741

radiation

- See also Sunlight.
- activity, cyclic var. of cosmic rays 8=20632
- activity minima correl. with cosmic ray intensity sudden change 8=20638
- albedo, earth, July 1963-June 1964 8=23285
- cosmic, ionospheric absorption, review 8=18997
- earth satellite orbit perturbation 8=23462
- e.m. flux incident on atmosphere, numerical calc. 8=2840
- energetic X-rays obs. by satellite, correlation with solar radio and energetic particle emission 8=14883
- ionospheric and geomag. effects, sudden, review 8=18996
- light from edge of solar disc, fluctuations rel. to atmos. turbulence 8=14623
- in magnetosphere rel. to geomag. micropulsations 8=10046
- optical research, 20 year review 8=19066
- optical, role in upper atmospheric processes, review 8=18910
- photons, 2.22 MeV from n, p capture, limit to flux obs. 8=23720
- planet refl. of thermal flux calc., geometrical model 8=14829
- relative spectral intensities, estimation of altitude of upper boundary of clouds 8=14833
- soft X-ray spectrum, proportional counter spectrometer 8=23709
- total eclipse Nov. 1966, measurements performed with 4.28 cm radio polarimeter 8=14868
- ultraviolet, book 8=20012

Sun—cont'd

radiation—cont'd

- X from flare, 80 keV to 1 MeV, OGO 3 obs. and nonthermal bremsstrahlung hypothesis 8=23739
 X, from flares, rel. to ionospheric sudden freq. deviations 8=9985
 X-radiation, soft and vacuum u.v. review, USSR 8=14867
 X-ray absorption rel. to 140-160 km atmosphere density changes, obs. 8=9900
 X-rays below 20 Å, Explorer 30 obs. 8=2841
 X-ray burst, hard, 1963 obs. 8=10393
 X-ray bursts, hard 8=10392
 X-ray emission from coronal region 8=14887
 X-ray meas. with space probes 8=2842
 X, rel. to field strength of 164 kHz received signal 8=5807
 He emission in chromosphere, low temp. theory 8=10430

radiation, corpuscular

- acceleration by geomag. neutral sheet 8=2618
 active M-regions quasi-stationary emission 8=19311
 cosmic, diffusion coeff. rel. to sun distance 8=23722
 cosmic, low energy cut-off dependence on latitude in geomag. field 8=897
 cosmic ray variation on earth, effect 8=911
 cosmic rays, effect on electron density and radio absorpt. in ionosphere 8=2655
 rel. to cosmic rays, primary, ionizing capacity increases, heavy nuclei accel. obs. 8=11663
 cosmic ray injection into magnetosphere 8=23721
 cosmic ray variations, diurnal and semidiurnal, seasonal changes 8=916
 cosmic rays, wind, protons and electrons propag. obs., review 8=23717
 diurnal anisotropy, variability of yearly means, obs. 8=2749
 earth's bow shock, plasma and mag. field correlation obs. 8=23328
 effect on moon, unipolar generator and shock wave 8=23642
 electrons > 40 keV and protons > 500 keV 8=2850
 electrons and protons, high energy, absence in vicinity of Venus from Mariner 2 obs. 8=23676
 energetic X-rays obs. by satellite, correlation with solar radio and energetic particle emission 8=14883
 energy of cosmic-ray particles in solar wind, rel. to distrib. in solar system 8=14872
 and geomag. activity, rel. to, review 8=19303
 high energy particles in new cycle, neutron monitor obs. 8=23723
 increase of January 28, 1967, neutron multiplicity obs. 8=915
 intensity variation with time, interplanetary diffusion model correction 8=2847
 ion wind, Vela 2 and 3 obs. 8=10410
 ionosphere, D-region, effect on formation 8=14682
 ionosphere topside, effect on, from ionogram obs. 8=2709
 ionospheric v.l.f. phase perturbations produced by protons, February 5, (1965) 8=18990
 luminescence of moon, obs. 8=19244
 magnetosphere, effect on, calc. by Euler potential method 8=2722
 neutrinos, capture by Cl^{37} atoms 8=23718
 neutrinos, interact. with electrons 8=14871
 neutrino flux, Brans-Dicke gravitation theory 8=14731
 ν flux rel. to Be^7 K-capture 8=10405
 ν , inverse β decay and elastic scatt. meas. 8=2848
 plasma changes across bow shock of earth, Vela 3 obs. 8=9908
 plasma flow generated by flares, 3D structure 8=23740
 plasma outward flow, spherically symmetric, influence of polytropic heat source 8=19304
 primary cosmic ray heavy nuclei cyclic modulation, Texas, March 1962, balloon obs. 8=3744
 production of Forbush decreases, Sept.-Oct. 1962 8=20633
 proton cosmic rays, low energy, cutoff diurnal vars. and pitch angle distributions 8=20631
 protons and electrons, diffusion and interplanetary mag. field power spectrum 8=23686
 proton precip. over polar caps, obs. of nonuniformity Feb. 1965, lat. 68° to 82°S 8=905
 secondary neutron flux after November 15, 1960 event, Atlas ballistic flight obs. 8=2623
 solar wind distortion of geomag. field rel. to models, $3\frac{1}{2}$ -13 earth radii 8=2751
 solar wind flowing round comets, m. h. d. effects 8=19262
 solar wind, intergalactic cosmic rays modulation theory 8=2771
 solar wind-magnetosphere interact., scaling for model plasma gun-terrella expts. 8=14643
 in solar wind, motion 8=19261
 rel. to solar wind origin, corona expansion, model 8=14876
 solar wind outside magnetosphere, ion spectrum rel. to geomag. vars. Venus 3 obs. 8=14875
 solar wind, Venus 3 and Pioneer 6 obs. comparison 8=14877
 spare flux obs. rel. to predictions on basis of balloon ionization chamber obs. 8=11666
 stream of fast particles, spectra of plasma and e. m. waves induced by stream instability 8=19305
 streams, magnetic morphology rel. to geomag. storms 8=10053

Sun—cont'd

radiation, corpuscular—cont'd

- p streams and var. in ionospheric absorpt. 8=2687
 27 day cosmic ray cycle, quasi spiral variation with solar activity 8=912
 wind and troposphere temp. field 8=18850
 wind, double shock wave structure 8=10411
 wind effect on planetary rotation 8=10337
 wind, effect of rotation 8=10408
 wind excitation of magnetosphere 8=9923
 wind, February-July 1966, obs. 8=10409
 wind flow, effect of Moon, Explorer 35 obs. 8=14828
 wind, $^3\text{He}^2+$, $^4\text{He}^+$, and O^8 species ions, meas. using Vela satellite 8=23715
 wind, interaction with solar mag. field 8=14878
 wind, interplanetary shock waves, Vela 3 obs. 8=23687
 wind, Parker's theory 8=19304
 wind, props. and magnetosphere interaction rel. to interstellar plasma theories 8=23578
 wind rel. to ionospheric blackout, polar cap and auroral zones, 1957-65 8=23363
 wind rel. to magnetosphere electron response during April 17-18, 1965 storm 8=23321
 wind, solar, props., from 11-year cosmic ray cycle 8=14874
 wind, thermal anisotropies, Vela 3 and IMP3 obs. 8=10406
 wind, two fluid model (electrons and protons) 8=23716
 B^8 solar neutrino flux dependence on heavy element composition 8=5968
 B^8 solar neutrino flux dependence on rate of the reaction $\text{He}^3(\text{He}^3, 2\text{p})\text{He}^4$ 8=5969

radiation, radiofrequency

- activity during eclipse, 20 May 1966, obs. 8=19301
 brightness temp. meas. near 1 cm wavelength 8=23714
 bursts, flux density associated with proton events, 1966, obs. 8=10403
 bursts, meter, longitude distrib. over one century 8=10426
 bursts showing freq. splitting, below 60 MHz 8=10401
 burst, spectrum in region 46 to 540 MHz 8=2844
 bursts, type II, Doppler shift suggested for splitting 8=10395
 bursts, type II rel. IV 8=10397
 burst, type II rel. to flare 8=19316
 bursts, type III 8=14870
 bursts, type III, interpret. where streams of fast particles are 8=19305
 bursts, type III, obs. by automatic interplanetary station 'Venus-2' 8=10396
 bursts, type III, starting freqs., daily variation 8=19299
 bursts, type III and type V rel. to electron streams in outer corona 8=10399
 cm, from spot groups sources, mag. field effect 8=10400
 comet 1965f "sun-grazing" effect, Oct 21 obs. 8=2846
 corona noise storms and condensations, 408 and 169 MHz 8=19325
 correlation with cosmic ray diurnal var. type IV burst 8=19298
 effective centre co-ords, determ. with interferometer 8=6383
 emission data, Jul-Sep. 1966 8=2836
 energetic X-rays obs. by satellite, correlation with solar radio and energetic particle emission 8=14883
 flare-associated events, homology 8=10398
 microwave obs., rel. to sudden cosmic noise absorpt. 8=23710
 in millimetric wave range 8=19297
 mm and submm diapasone of waves, meas., app., conditions and results 8=19302
 noise storm occultation during eclipse 8=2843
 radio behaviour, indices, book 8=19005
 review of recent activity 8=10417
 scattering on chromosphere turbulence rel. to temp. inversion at 6 mm 8=10404
 solar cycle var. of 1 GHz emission 8=5967
 solar eclipse 20 May 1966 obs. 8=19287
 solar radio spectrograph, 30-300 MHz 8=14869
 spectrographs and radiometer for 239 MHz 8=19300
 spectrum change of active region rel. to covering by solar limb 8=19296
 spectrum, S-component, millimetre wavelengths 8=23711
 10 cm rel. to F2 electron concentration 8=23423
 theory of bursts 8=2845
 thermal gyromag. emission from active regions 8=23713
 type I bursts, wavelength dependence of bandwidth and duration 8=23712
 5.65 mm, absorpt. by terrestrial atm. 8=5789
 19 Gc/s during eclipse of May 20, 1966 8=10402

spectra

- See also Sun/corona; Sun/flares; Sun/prominences.
 brightness temp. meas. near freqs. of 20 GHz 8=23714
 centre-limb anal. of C_2 , CH, CN, CO and MgH lines, rel. to photospheric inhomogeneities 8=23697
 chromosphere and corona, line profiles, temp. var. effects 8=23698
 chromosphere, H line intensity decrease 8=5974
 continuous, deriv. from simplified temp. distrib. model of photosphere 8=23745
 corona, above active regions, extreme u.v. rel. to r.f. 8=10431

Sun—contd

spectra—contd

- corona, continuous and Fraunhofer obs. 8=19322
 corona, u. v., rel. to spectroscopy of highly ionized atoms 8=16192
 corona, visible emission lines, excitation and electron density 8=10439
 coronal line spectra at eclipse of 1952, anal. 8=10436
 disk near 6708 Å obs. 8=5964
 eclipse, November 12th, 1966, airborne spectrographic obs. of Ca II, H- and K-lines 8=5962
 Evershed effect as wave phenomenon 8=10413
 far u. v., flux and limb darkening, obs. compared with Utrecht and Bilderberg modes 8=23703
 flares, chromospheric optical and coronal X-ray, 9.5-200 Å 8=14866
 high resolution spectrophotometry, used rapid scanning 8=10386
 i. r. Fraunhofer lines, source functions in cores rel. to atmos. models 8=23705
 infrared, forbidden NI lines 8=10384
 intensity profile near solar limits in far i. r. and m. m. regions 8=23700
 limb darkening in range 4500 Å < λ < 2500 Å, failure and modification of Bilderberg continuum atmos. 8=23752
 limb darkening obs. between 1800 and 2900 Å, rel. to opacity of photosphere 8=23751
 at limb, relative intensities of CI lines in EUV spectrum 8=19324
 line profiles, generalized theory for solar case 8=10387
 magnetograph for Zeeman effect meas. 8=14865
 ozone region, eclipse effect 8=23692
 photoelectric meas. rel. to iron abundance, during eclipse 8=5965
 photosphere, Ca II forbidden line identification 8=19293
 photosphere, search for quark-atom spectra 8=23727
 quark-atom lines, identifiability 8=6718
 spectrometer, large Echelle grating 8=10385
 spots, line contours and intensities, effect of image spreading 8=23699
 u. v. emission of chromosphere and corona 8=10428
 u. v. spectrum, continuous, and Balmer jump 8=23702
 X-ray, absolute intensities near min. activity 8=10391
 X-ray images at solar minimum 8=10394
 5577 and 6300 Å regions using a prism grating spectrometer 8=5966
 C^{12}/C^{13} ratio in solar photosphere 8=23726
 $CH(A^2\Delta-X^2\Pi)$ lines near 4300 Å, profiles 8=10389
 CI lines, rel. to f-value of $A^2\Delta-X^2\Pi$ transition of Ch 8=10389
 CO lines, in region of 2.3 μ , interpret. rel. to no. of mols. 8=19294
 Ca, ionized, mean and core profiles of H and K lines 8=23706
 Ca II lines in lower chromosphere 8=2859
 Ca II, profiles of H and K lines, emission cores and optically thick chromosphere 8=23707
 Ca II reson. lines rel. to photosphere-chromosphere transition zone temp. distrib. 8=19319
 Ca II resonance line, emission peaks 8=23744
 Ca II H and K lines, profiles of the cores in 1957 and early 1965, near solar minimum 8=10382
 H Ly- α and - β line intensities rel. to emitting layers e temp. and density 8=10390
 Mg II lines in lower chromosphere 8=2859
 Mg II, profiles of H and K lines, emission cores and optically thick chromosphere 8=23707
 Mg II reson. lines rel. to photosphere-chromosphere transition zone temp. distrib. 8=19319
 Mg II resonance line, emission peaks 8=23744
 Na D-lines, atmosphere min. temp. calc. 8=10388
 Na D-lines, profile anal. assuming pure absorpt. 8=10383
 Na D-lines, profiles rel. to coherent and non-coherent scatt. 8=23708
 Na D₂ line, brightening obs. 8=2858
 O lines, rel. to temp. distrib., vel. field, profile damping and O abundance in photosphere 8=23704
 S, neutral, forbidden lines in Fraunhofer spectrum 8=19295

Sunlight

See also Sky brightness.

- angle of arrival of light waves, fluctuations due to atmos. turbulence 8=14623
 long-wave back radiation formulae, cloud factor 8=2590-1
 Rayleigh scattering in atmosphere, as function of altitude 8=18873
 rel. to circumterrestrial motion of dust, light pressure 8=10342
 scattered radiation at small angles, intensity, aerosol spectrum 8=18880

Sunspots

- activity, auroral frequency during minimum 8=9941
 activity and F2 electron density peak, seasonal, non-seasonal under semi annual var. 8=5810
 activity rel. earth's pole movements 8=9770
 arch-filament systems in interspot region of young bipolar groups 8=19310
 areas of groups, given in Greenwich and Pulkovo catalogues, comparison 8=19312
 bipolar groups, role of twisting in evolution 8=23734

Sunspots—contd

- corpuscular heating effect, Explorer 6 obs. 8=18915
 and cosmic rays, solar cycle modulation of heavy primary nucleu, Texas, March 1962 balloon obs. 8=3744
 chromosphere, heating, above a sunspot 8=5975
 cycle rel. to Earth's atmospheric circulation 8=23253
 cycles, forthcoming, time of rise probable values 8=10420
 cycle rel. to Pi2 geomag. pulsations, 1956 to 1966 obs. 8=23447
 electrical conductivity gradients, proposed 8=2852
 electron conc. profiles during maximum and minimum 8=23357
 emission data, Jul.-Sep. 1966 8=2836
 "invisible", rel. to small-scale mag. fields 8=2854
 longitude distribution over eight cycles 8=10426
 magnetic field, area, struct. and motion rel. to development 8=10415
 magnetic fields meas. in small and young spots 8=2853
 magnetic field strength, time variation from origin to disappearance 8=19313
 magnetic field structure 8=2851
 Mt. Wilson No. 11730, curves of growth and rough analysis 8=14879
 number series, existence of 29 day period, 1940-64 8=10414
 number and spread-F occurrence 8=23419
 r. f. radiation associated with groups, mag. field effect 8=10400
 relative number, in solar cycle 19, autocorrel. 8=23733
 review of recent activity 8=10417
 spectra, line contours and intensities, effect of image spreading 8=23699
 structure, new model 8=23732
 velocity, and mag. fields, high resolution meas. 8=23724
 Wilson effect 8=14881
 zodiacal light, effect on brightness and polarization of 8=23690
 Fe I 6302.5 Å line contours, mag. fields and Evershed vels. rel. to Zeeman splitting anomalies, obs. 8=10418
 OI forbidden lines in spectrum obs. 8=14880
 SI forbidden lines in spectrum obs. 8=14880
- Superconducting materials and devices**
 See also Magnets.
 advances in low temp. physics, book V 8=19680
 advances in superconducting magnets at Brookhaven National Laboratory 8=310
 amplifiers, parametric, for d. c. voltage meas. 8=15166
 bolometer current modulator, in meas. amplifier for d. c. voltage 8=22573
 circuitry in current magnetometer 8=15253
 coils as energy storage elements in pulsed system operations 8=13766
 contacts, specific heat 8=13745
 critical current curves, continuous recording 8=13738
 critical currents, meas. with self-balancing current regulator 8=9039
 cryotron, crossed-film type, meas. of switching speed 8=17978
 cryotron relax. oscillator as thermometer 8=22571
 cryotrons, method for direct determ. of phase characts. 8=17980
 d. c. transformers and flux flow 8=17985
 disc, type II superconductor, in mixed state, flux-flow resistivity 8=9037
 domain structures, two-phased, and ferromagnetics, theory 8=13742
 dynamic lamellar struct., intermediate state 8=9038
 e. m. fields produced by rot. bodies, proposed test 8=3174
 electromagnets, construction and use 8=6281
 electromagnets, high-field liq. Ne-cooled 8=15261
 electron lens, magnetic, optical characteristics 8=6311
 electron lens, optical constants calc. 8=19791
 film ring as transformer secondary, modulated flux flow 8=17992
 five-wire field probe 8=22574
 foils, flicker noise explanation 8=5220
 γ -u alloys, isotope effects 8=2176
 gravimeter 8=18805
 in gyroscope construction for satellite instrumentation and expts. 8=17984
 hydrides with A-15 structure, superconductivity 8=9059
 inductance temp., mag. field and current dependence and appl. in devices 8=17986
 interference devices in mag. fields above 2000 gauss, operation 8=17991
 interstitial cpds., rel. to $T_c > 15^\circ\text{K}$ studies 8=17965
 Josephson (AC) effect rel. to standards of electromotive force 8=17989
 Josephson effect far infrared-red detectors, spectral response curves and characts. 8=17979
 Josephson junction coupled to resonant cavity, analog-computer studies 8=9064
 Josephson junction as a switching device 8=17983
 Josephson junctions, a. c. effect and microwave emission 8=13763
 Josephson junctions, interference phenom. 8=13762
 Josephson junctions, Meissner effect and vortex penetration 8=9066
 Josephson junctions, point-contact, structures for high-freq. props. meas. 8=13764

Superconducting materials and devices—contd

- Josephson junctions, vortex structure and critical currents 8=9065
- Josephson radiation from point contact, contribution of thermal noise to line-width 8=2181
- lead coated quartz cylinder, hollow, dynamics of magnetization in parallel field 8=13771
- linear accelerator, design, advantages and cost 8=17984
- liquid-level sensor, for slush hydrogen use 8=16929
- low joint resistance bet. superconds, meas. via closed loop system 8=2182
- magnets, applications 8=10870
- magnetic bottle, design and construction 8=16555
- magnets, high field prod., review 8=306
- magnets, low-temp. technique, review 8=6225
- magnets as MHD generators 8=3166
- magnet technology, conference Oxford England (1967) 8=15259
- microbridges, observed depression of T_c , anomalous critical-current behaviour 8=9036
- microwave mixing with weakly coupled superconductors 8=15386
- noble transition elements and alloys, and mag. susceptibility and electronic sp. ht. 8=13753
- noble transition elements and alloys, and mag. susceptibility and sp. ht., exptl. study 8=13752
- non-transition metals, band structure 8=17868
- non-transition metals, transition temp. pressure dependence 8=17956
- oscillator-detector 8=15172
- oxide, tunnelling theory 8=2153
- paramagnetic salt, solenoid for adiabatic demagnetization 8=5217
- parametric amplifier, for meas. of small d.c. voltages 8=3135
- point contacts, mechanism for control of characts. 8=5218
- point tunnelling, new method 8=5211
- quantization and thermodynamic fluctuations 8=17987
- quantum generation and phonon detection 8=17954
- quantum interference device for small voltage meas. 8=15165
- relaxation absorption of e.m. waves 8=9022
- resonator, cylindrical iris, for 3 cm waves 8=6362
- resonators, 30 MHz, for oscillators 8=13767
- rings, weakly connected, thermodynamical anal. of magnetization 8=13768
- roller bearings for flux pump with only frictional losses 8=15196
- shields, for travelling wave maser, mag. field shaping 8=13769
- solenoids, critical state exam. 8=15262
- solenoidal magnet, mag. field sweep 8=10869
- strips, magnetic flux motion 8=2152
- superconductor-glass vacuum seals 8=21551
- superconductor-metal-superconductor junctions, current 8=13765
- thermal props. rel. to strong electron-phonon interaction 8=17508
- thermodynamic effects 8=9040
- for thermometry with 10^{-3} K resolution 8=15117
- thin thread, resistance at near critical currents 8=22540
- torus for low-temp. torque meas. 8=14924
- transition metal, isotope effect rel. to dirtiness 8=5215
- tunnel junctions, current fluctuations 8=17988
- type II alloys, thin plates, Meissner effect 8=9034
- type II, critical surface current 8=13740
- type II, flux jumps 8=13741
- wire, in composite conductor, internal thermal resistance effect on min. prop. current 8=17993
- wires and magnets, transition to normal state 8=5189
- [Ag₂O₃]·HF₂ clathrate, n.m.r. 8=17957
- Ag-Sn superimposed films, proximity effect examination 8=9044
- Al, critical field as function of press. and temp. above 0.3°K 8=13746
- Al, 10^{-9} Ω joints to, by ultrasonic soldering 8=17995
- Al thin-film cylinder, temp. depend. of mag. field periodicity 8=22539
- Al, transition temp. calcs. 8=5201
- Al, transition temp. change due to 3d transitional impurities 8=9041
- Al-Al₂O₃-Al tunnel junctions, temp. dependence of energy gap 8=17958
- Al-Al₂O₃-Pb-M, (M = Ni, Fe and Pt), gapless props. induced by proximity effect 8=9042
- AlSb, metallic 8=9043
- B rich lattices 8=22870
- Be alloys, magnetization meas. 8=17959
- Bi, amorphous, strong-coupling superconductivity and phonon structure 8=5202
- Bi, 2-4°K on surface, tunnel effect investigation 8=2155
- C-W-Re alloy 8=22566
- Cd-Bi solder junctns, thermal transport near 0.1°K 8=5203
- Cr-Pb-PbO-Pb-Cr, gapless props. induced by proximity effect 8=9042
- Cu-Al-Mn alloys, transition and surface relief effects 8=19686

Superconducting materials and devices—contd

- CuRh₂S₄ with spinel structure, transition temperature obs. at 4.35°K 8=13749
- CuRh₂Se₄ with spinel structure, transition temperature obs. at 3.50°K 8=13749
- Fe magnet 8=15263
- Fe-Ni alloys, transition and surface relief effects 8=19686
- Fe-Sn superimposed films, proximity effect examination 8=9044
- Ga, boundary scattering rel. to critical temp. shifting 8=1374
- Ga crystal, energy gap and anisotropy meas. by tunneling effect, 0.36-1.1°K 8=22546
- Ga, pure, transition width 8=13748
- Hg, surface nucleation and bulk superheating fields, 1.2°K-T_c 8=17968
- Hg-Sn system, transition temp. comp. dependence 8=17960
- In, critical fields, 0.1-4°K, pressure effect up to 30 k atm 8=5212
- In, films, Nernst effect 8=2174
- In films, transition temp. thickness dependence 8=9045
- In films with superconductive and ferromag. overlays, tunnelling 8=22549
- In-40at.% Pb, resist. and Hall angle, flux pinning model and obs. 8=2162
- In in porous glass, flux jumping during magnetization 8=2163
- In, length differences between normal and supercond. states 8=22124
- In 1.5 at.% Bi, type II, ideal flux flow resistance 8=22547
- In single spheres, hysteresis near T_c , and size effects 8=17961
- In spheres, superheating and supercooling in normal to supercond. transition 8=13750
- In, spin-lattice relax., energy-gap broadening 8=18464
- In, ultrasonic attenuation 8=13354
- In-Bi alloy foils, superconducting type-I, in mag. field, mixed state evidence 8=17962
- In-In tunnel junctions, I-V characts. and 3-cm radiation emission 8=17981
- InPb type II, magnetostriction and magnetization 8=22548
- In-Tl alloy, Ginzburg-Landau parameter changes under pressure 8=22550
- In-Tl alloys, anomalous nucleation fields 8=13751
- In-Tl alloys, Ginzburg-Landau parameters rel. to temp. 8=9046
- Ir alloys, and mag. susceptibility and sp. ht., exptl. study 8=13752
- La films, electron-tunneling meas. 8=9047
- La-Ce alloy film, gapless, deviations from theory 8=5205
- La-Ce(Gd) alloys, Kondo effect in T_c and H_{c2} 8=5206
- La-Lu films, electron-tunneling meas. 8=9047
- LaX₃, (X = Sn, Pb, Ti, In), with Cu₂Au structure 8=22551
- Mo, energy gap anisotropy, u.s. investigation 8=9048
- Mo single crystals, pure with small residual resistance 2×10^{-5} Ω 8=5207
- Mo₂B, d-shell effect on transition temp. 8=2164
- Nb (and Nb alloys) wires, a.c. induced voltages 8=13757
- Nb crystal, anisotropic energy gap meas. by tunneling 8=17964
- Nb, energy gap anisotropy by single crystal tunneling technique 8=5209
- Nb, energy-gap, anisotropic, meas. by tunnelling 8=22552
- Nb films, for cryotron ground planes 8=2171
- Nb, flux diffusion 8=9053
- Nb, flux penetration and a.c. losses 8=5210
- Nb, heat effects rel. to mag. processes 8=2167
- Nb, helicon resonances near H_{c2} 8=9049
- Nb, internal friction and Young's modulus variation 8=2063
- Nb, irreversible magnetisation obs. 8=2160
- Nb, magnetocaloric effect, rel. to upper critical field 8=9052
- Nb, mixed state, u.s. attenuation rel. to transverse mag field 8=17502
- Nb, n-irradiation effects on magnetization behaviour and transition temp. 8=2169
- Nb, nuclear relax. near H_{c2} 8=2170
- Nb, resist. and Hall angle, flux pinning model, and surface layer effects, obs. 8=2162
- Nb, surface investigation 8=2157
- Nb, thermal conductivity rel. to energy gap and mag. hysteresis 8=2166
- Nb, transition temp. under high pressure 8=9060
- Nb, upper two critical fields ratio, temp. dependence 8=17963
- Nb, u.s. wave attenuation, temp. and mag. field depend. 8=17503
- Nb₃(Al, Ge, Sn) solid solns., transition temp. dependence on atomic ordering 8=17967
- NbB₂, specific heat 9.6-2.8°K 8=17522
- NbC-NbN-based alloys, pseudoquaternary, rel. to T_c > 15°K studies 8=17965
- Nb-Cu composite, strong proximity effects 8=22553
- NbN-based alloys, pseudobinary and -ternary, rel. to T_c > 15°K studies 8=17965
- NbN, critical fields and currents 8=2165
- NbN, critical temp., lattice parameter, N content 8=17966
- NbN with Zr and Ti, preparation and behaviour 8=2158

Superconducting materials and devices—contd

Nb-Nb oxide-Nb diode for microwave mixing 8=15386
 NbS₂, specific heat 1.7-6.4 K 8=17522
 Nb₃Sn-based ribbon, stabilized, prep. by diffusion process 8=13756
 Nb₃Sn Fermi level motion rel. to normal-state props. temp. depend 8=5118
 Nb-50 at. %Ta, sheets and cold-rolled and annealed foils, transport current distrib. obs. 8=9051
 (Nb-Ta)N_x, critical temp., lattice parameter, N content 8=17966
 NbTi, copper-coated, large coils, performances 8=17994
 (Nb-Ti)N_x, critical temp., lattice parameter, N content 8=17966
 Nb-Ti wires, flux jumping 8=9050
 Nb-Ti-Zr alloy, magnetic props. 8=13754
 Nb-Ti-Zr alloy solenoid at mag. field strength more than 75kG 8=309
 Nb-Ti-Zr wire, transitions during destruction of superconductivity 8=22567
 Nb-Zr alloy closed solenoid, flux jumping-patterns 8=2168
 Nb-25%Zr, copper-coated, large coils, performances 8=17994
 (Nb-Zr)N_x, critical temp., lattice parameter, N content 8=17966
 Nb-25 at. %Zr, sheets, transport current distrib. obs. 8=9051
 Nb 25%Zr wire, a.c. quenching 8=13755
 Nb-25%Zr wires carrying a.c. in mag. field 8=5208
 Nb-Zr/Ti cable, critical current 8=13770
 Ni-Sn alloy under pressure, transition temp. and stability interval 8=2156
 Pb, defects rel. to structure of intermediate stage 8=22556
 Pb, energy gap and electron-phonon coupling strength press. depend. 8=22557
 Pb, far i.r. absorpt. rel. to crit. energy gaps 8=18555
 Pb film, frequency conversion in 3 cm band 8=22558
 Pb films, thermal forces on vortices 8=13761
 Pb films, thin, far i.r. absorption 8=13759
 Pb, flux line motion in current-carrying, direct detection 8=13758
 Pb Josephson tunnel junctions, V-A characts. fine structure 8=9063
 Sn Josephson tunnel junctions, V-A characts. fine structure 8=9063
 Pb, in high-Q microwave cavities, application in construction 8=15388
 Pb, microwave absorpt. in surface-sheath regime, depairing effect of mag. field 8=13760
 Pb, phonon spectrum change by lattice distortion, tunnel effect method 8=22559
 Pb, point tunnelling 8=5211
 Pb shell, attainment of zero mag. field 8=17990
 Pb, surface nucleation field H_{c3} 8=17971
 Pb, surface nucleation and bulk superheating fields, 1 K-T 8=17968
 Pb, thermally induced H II vaporization threshold 8=4660
 Pb tunnelling characts., size effects in 700-3200 Å films 8=2172
 Pb, tunnelling meas. of energy gap, high pressures 8=22554
 Pb, type I, asymmetric critical currents 8=17969
 Pb-insulator-Al tunnel junctions, electron tunnelling 8=2180
 Pb-Ag superimposed films, proximity effect examination 8=9044
 Pb-Bi, type II critical current density rel. to surface 8=2173
 Pb-Fe superimposed films, proximity effect examination 8=9044
 Pb-In alloy, type II tube, magnetic induction meas. on wall 8=5221
 Pb_{0.99}In_{0.17}, transitions during destruction of superconductivity 8=22567
 Pb-Pb tunnel junctions, I-V characts. and 3-cm radiation emission 8=17981
 Pb-Tl alloys, electron-phonon coupling and phonon spectra, electron tunnelling studies 8=22555
 Pb-Tl type II foils, sheath irreversible magnetization obs. 8=17970
 Pb-Tl(In) alloys, order-disorder transform. from superconducting transition temp. meas. 8=1680
 Pb-30 at. %In, sheets and cold-rolled foils, transport current distrib. obs. 8=9051
 Re, isotope effect 8=17973
 Re, transition temp., h.p. dependence 8=17972
 Re-Os alloys, transition temp., h.p. dependence 8=17972
 Re-W-C alloy 8=22566
 Sn, critical fields, 0.1-4 K, pressure effect up to 30k atm 8=5212
 Sn, doped, us. attenuation studies 8=22572
 Sn film, nonlinear effect at about 10 GHz 8=22562
 Sn films and bulk Nb, microwave-photon assisted tunnelling 8=17975
 Sn films, Ge coating effect on transition temp. 8=5214
 Sn films in mag. field, thermal cond. 8=22137
 Sn, films, Nernst effect 8=2174
 Sn, in high-Q microwave cavities, application in construction 8=15388

Superconducting materials and devices—contd

Sn point contact electrode for microwave generation and detection 8=22570
 Sn, pure and Cd-doped, energy-gap effect on thermal conductivity 8=4942
 Sn, pure, superheating in cylindrical samples 8=22564
 Sn, quantum phase fluctuations at onset of long-range phase coherence 8=22561
 Sn, resistance jump at superconducting to intermediate transition rel. to London model 8=17974
 Sn, surface impedance, mag. field dependence, anomalies 8=9054
 Sn, transition temp. and resistance temp. depend., undergrad. expt. 8=254
 Sn, u.s. absorpt. by electrons near transition pt. 8=4924
 Sn, u.s. absorpt. at various amplitudes 8=5213
 Sn whiskers, intrinsic thermodynamic fluctuations from depressions of supercurrent and T_c 8=22560
 Sn-In, solder junctions, thermal transport near 0.1 K 8=5203
 Sn-In type II foils, sheath irreversible magnetization obs. 8=17970
 Sn-Pb Josephson junctions, radiation threshold absorption, mag. field depend. 8=22569
 Sn-Pb, solder junctions, thermal transport near 0.1 K 8=5203
 Sn-Pb tunnel junctions, I-V characts. and 3-cm radiation emission 8=17981
 Sn-SnO₂-Sn tunnel junction, d.c. Josephson current mag. field depend. and self-screening 8=22568
 SrTiO₃, anomalous behaviour of transition temp. rel. to electron density 8=9057
 SrTiO₃, superconducting semiconductor films and whiskers, transition temps. 8=9056
 SrTiO₃, transition temp., stress effects at ≤1.5 kbar 8=2175
 Ta, transition temp. under high pressure 8=9060
 TCNQ derivatives of cyanine dyes 8=17977
 Te films, Ge coating effect on transition temp. 8=5214
 Ti alloys, Fe and Nb additions, props., phase transformations 8=22563
 Ti-Rh alloys, specific heat and transition temp. meas. 8=9058
 Ti-22 at. %Nb alloy, critical transport currents on ω phase precip. 8=4718
 α-U, superconducting transition temp., positive isotope effect 8=22565
 V, local field mapping by n. m. r. 8=2179
 V, transition temp. under high pressure 8=9060
 V₃Al superconductivity, Si contamination effects 8=17976
 V₃Au, atomic ordering props. 8=18475
 V₃Ga Fermi level motion rel. to normal-state susceptibility temp. depend. 8=5118
 V₃In superconductivity, Si contamination effects 8=17976
 VN-based alloys, pseudobinary, rel. to T_c > 15 K studies 8=17965
 V₃Si Fermi level motion rel. to normal-state susceptibility temp. depend. 8=5118
 V₃Si type, properties by expt. 8=2178
 V-V₃Si, transition temp. and homogeneity regions 8=9061
 V₃X type compounds, strong-coupling 8=2177
 W₂B, d-shell effect on transition temp. 8=2164
 W-Re-C alloy 8=22566
 Zn^{64, 66, 68}, transition temp. isotopic mass dependence 8=9062
 Zr + 4%Nb, transitions during destruction of superconductivity 8=22567

Superconductivity

See also Quantum theory/many-particle systems.
 advances in low temp. physics, book V 8=19680
 alloys, non-mag. with transition-metal impurities, thermodynamic and transport props. 8=9025
 alloys, worked, critical current density rel. to dislocation distrib. 8=9029
 anisotropic, u.s. attenuation in ql < 1 limit 8=22090
 antiferromagnetic metal, proximity effect 8=5193
 bound states in superconductor with mag. impurity 8=9023
 charged systems, 1- and 2-dimensional 8=17944
 clean films, surface parallel critical field, calc. 8=13727
 clean thin films, characts. in strong parallel mag. fields 8=5188
 condensed Fermi system, phase transitions 8=19463
 conference, Työbä, Sweden 1966 8=8191
 crystal lattice study, theory 8=22534
 dangerous diagrams compensation principle, derivation 8=5191
 electromagnetic current with impurity scattering derived 8=2146
 electronic mechanism, pairing criterion 8=17943
 electrostatic effect in tiny samples, BCS Hamiltonian modification 8=5194
 energy gap eqn., linearized, boundary conditions 8=13726
 Fermi-systems with P-pairing, theory 8=9026
 Feynman-Onsager vortex, classical theory 8=10807
 film energy gap dependence on mag. field 8=22529
 film, thin, mag. field depend. of far-infrared absorption 8=22938
 film, thin, in mag. field, nonlocal and nonlinear effects theory, specular reflection 8=22530
 film with current flowing, energy gap and critical current 8=22528

Superconductivity—contd

films, superimposed, proximity effects 8=9044
 films, thick, far-infrared absorption spectra 8=22939
 flux quantization 8=3124
 gapless 8=13728
 gapless, expts. 8=13744
 gapless, induced by metallic contact, I-V curves
 interpret. 8=13739
 Ginzburg-Landau eqns. for arbitrary tangential mag.
 fields, solution 8=9027
 granular, characteristic parameters 8=22532
 granular superconductor, size effect 8=17955
 high-field, paramagnetism effect on upper critical
 fields 8=17950
 impossibility in partially finite geometries 8=127
 impurity (nonmagnetic) effect on electronic states where
 bands overlap 8=2147
 inner bands incomplete, expts. 8=17951
 intermediate state, thermal cond. 8=8652
 intermediate state, ultrasound absorpt. coeff. 8=4914
 interstitial cpds., rel. to T_c > 15°K studies 8=17965
 Josephson barriers, vortex lines 8=2143
 Josephson current, magnetic field dependence 8=2144
 Josephson effect analog in nuclear reactions with heavy
 ions 8=3892
 Josephson effect, radiation line width 8=17945
 Josephson junctions, free energy 8=2154
 Josephson radiation effects, analog-computer
 studies 8=9064
 Josephson tunnelling, research in USSR 8=19681
 Joulean dissipation in hard tubes and cylinders 8=5187
 lead, irreversible magnetisation obs. 8=2160
 London eqns., extension 8=13731
 low temp. resistivity meas., eddy current method,
 contactless, 1-10000 nΩ cm range 8=5162
 many-body theory, conference Oiso Japan (1965) 8=10641
 metal-dielectric-supercond. structure, electron tunneling
 in sound field 8=5219
 metals, characteristics, topological singularities of
 electron spectrum 8=22524
 metals, Kondo spin-compensated impurities, low temp.
 props. 8=8882
 molecular interaction with organic cpds. 8=9668
 n.m.r., particle-size effects, Knight shift 8=2351
 nuclear matter, vanishing of energy gap of quasi-particle
 in presence of Coriolis force 8=928
 ordinary and gapless, effect of phonon-bogolon processes
 on infinite cond. 8=13730
 organic supercond. model 8=17977
 plane films, critical currents rel. to thickness and bulk
 characts. 8=13729
 proximity-effect-induced, breakdown field
 dependence 8=13733
 quenching kinetics, effect of heat release 8=10798
 relaxation, e.m. wave absorpt. 8=9022
 rings, nearly superconducting, coherence and
 quantization 8=22542
 simple experiments 8=13743
 strong-coupled, transition temp. 8=22531
 superconducting channels, narrow, intrinsic resistive
 transition 8=9024
 superconductors, double point contact pot. 8=13732
 superconductors, temp. dependent interactions, effect on
 corresponding states law 8=9028
 superconductors, type II, magnetization curves 8=2151
 superconductors, type II, obs. and explanation 8=5196
 superfluid Fermi system, dynamics 8=130
 surface resistance, h.f., mag. field dependence 8=9035
 surface sheath, inhomogeneous distrib. of transport
 current 8=22543
 surface supercond., high temp. 8=17964
 theory and recent developments 8=9021
 thermodynamic behaviour in multiple pair-breaking
 regimes 8=22526
 thermoelectric effect 8=22679
 third critical field for massive supercond. with supercond.
 film on surface 8=5192
 tin, irreversible magnetisation obs. 8=2160
 transition temp. pressure dependence 8=17956
 tunnelling barrier, boundary condition on order
 parameter 8=22533
 two-band, mixed state near lower critical field 8=17952
 two-zone alloys, longitudinal u.s. absorpt. theory 8=22535
 type I, asymmetric critical currents 8=17969
 type I, entropy transport, mechanical 8=22545
 type I, heat transport by moving magnet 8=22544
 type I, metastable surface sheath below bulk critical
 field, obs. 8=5195
 type I, microwave absorption by surface states 8=2142
 type I, overheating critical field 8=22536
 type II, Abrikosov fluxoid, props. 8=13737
 type II alloys, thin plates, Meissner effect 8=9034
 type II, clean, perturbation expansions, convergence 8=5199
 type II, as Corbino Discs, critical currents and flux flow
 voltage meas. 8=9031
 type II, critical surface current 8=13740
 type II, degradation effects in high-field, pulse
 meas. 8=17953

type II, enhancement of Meissner effect by heat
 pulse 8=5198
 type II, flux flow state, apparent negative thermal
 conductivity 8=2148
 type II, flux jumps 8=13741
 type-II, flux transport noise 8=17949
 type II, lattice defects of flux lines 8=13734
 type II, linear I-V characts. under conditions of flux
 flow 8=22537
 type II, mixed state structure and vortex motion with
 transport current 8=2150
 type II model of self-trapped laser filaments 8=9030
 type-II, modified London model 8=17948
 type II, pinning forces and hysteresis 8=22538
 type-II, quantum theory of vortices 8=5200
 type II sheets, flux motion prod. voltages obs. 8=2149
 type II, thermal losses under a.c. conditions 8=5197
 type II, thermodynamics 8=13735
 type-II, thermodynamics of volume and press
 effects 8=17947
 type II, thermodynamic fluctuations of order parameter
 near upper critical field 8=9032
 type II, ultrasonic attenuation, anisotropy 8=22091
 type II, upper critical field and thermodynamic props.,
 two-band model 8=13736
 type II, vortex structure motion in high mag. field 8=9033
 type II wire, nonideal, a.c. quench phenomenon 8=13755
 wire in liq. He, minimum propag. current 8=22541
 A₂B type, intermetallic compounds, band structure 8=5216
 BCS model, critique of Bogoliubov-Haag
 treatment 8=22527
 BCS solutions at critical point 8=22525
 BCS theory, off-diagonal long-range order 8=2145
 BCS theory of superconductivity, Freidrichs-Berezin
 transformation reformulation 8=5190
 Cd-Bi eutectic solder, transition temp. 8=2161
 Fe dissolved in Zn, revision of props. rel. to magnetic
 moments 8=9344
 Ga, pure, transition width 8=13748
 In, type I, intermediate state statics and dynamics 8=5204
 In, ultrasonic waves, quasi-longitudinal,
 attenuation 8=22103
 La-Ce alloys, transition temp., paramagnetic impurity
 effect 8=9303
 La-Gd alloys, transition temp., paramagnetic impurity
 effect 8=9303
 Sn, type I, intermediate state statics and dynamics 8=5204
 Sr_{0.925}Ba_{0.075}TiO₃, heat capacity transition at
 0.5°K 8=1877
 SrTiO₃, semiconducting, transition temp. 8=9055
 Ti₃AuH, A-15 structure 8=9059

Supercooling

criteria for solid-liquid interface stability, thermal
 diffusion effect 8=1617
 ice crystals, in supercooled water, ultrasound
 effects 8=22102
 metallic crystals, rel. to growth vel., theory of
 expt. method 8=8419
 metals, rel. to dynamic nucleation 8=21760
 multiphase diffusion couples, lattice transform. at interface
 on supercooling 8=17552
 nitrate melts, binary mixtures of Ca(NO₃)₂ and
 MnO₃ (M = Na, Cs, Rb, K), relax. processes 8=1586
 organic supercooled melts, scintillation 8=8089
 sucrose soln., aq. and water, rel. to ice growth
 velocities 8=17236
 water and aq. sucrose solns., rel. to ice growth
 velocities 8=17236
 water, to -50°C, u.s. velocity rel. to precrystallization
 theory 8=13353
 Bi, growth of large crystals from melt 8=17227
 Cu: Cu-12.5 wt.%Al multiphase diffusion couples, lattice
 transform. on supercooling 8=17552
 (K, Na)(Ba, Cl) solid soln., constitutional supercooling,
 convection cells 8=8417
 αP₄, solid/liq. interface temps. 8=21755

Superexchange. See Antiferromagnetism.**Superfluidity**

See also Helium/liquid; Quantum theory/many-particle
 systems.
 adiabatic flow through capillaries 8=260
 advances in low temp. physics, book V 8=19680
 Bose system, Green's functions 8=10653-4
 dilute mixture of fermions in dense Bose fluid, possibility
 of superfluid rel. to He³ in He⁴ 8=19688
 Fermi gas, dynamics at finite temp. 8=130
 Fermi systems, low-density at zero temp. 8=15019
 intrinsic critical velocity near λ point 8=263
 many-body formalism, introduction 8=15148
 quantized circulation in liquid He, torque on
 cylinder 8=10808
 quasi averages in interact. Bose and Fermi systems, in
 partially finite geometries 8=127
 statistical mechanics of many boson system in terms of
 coherent states 8=19696
 He, closed-cycle refrigeration at 1.85°K 8=6224
 He film, rotating, thickness rel. to superfluid component
 motion, obs. 8=10796

Superfluidity — contd

- He flow through orifices, critical vel. and vortices form. obs. 8=6234
 He liquid 8=10806
 He, liquid, collective coordinates theory 8=10799
 He liquid, λ point suppression by elec. field 8=15151
 He, penetration into Zeolite microparcs., obs. 8=10805
 He, wave function exam. 8=261
 He II circulation in a porous medium 8=19698
 He II filling narrow gap, heat exchange with solid body 8=6233
 He II, liquid, counterflow past a flat plate, anisotropy 8=19701
 He II, local gauge invariance and broken symmetry 8=3126
 He II near critical point, density obs. 8=19702
 He II in plane-parallel capillary, wave processes 8=3123
 He II quantized circulation around a fine wire obs. 1.2°-1.9°K 8=19703
 He II rotating annulus, quantized vortex lines threshold obs. 8=10810
 He II rotating in annular channel, radial distrib. of vortex lines 8=10809
 He II, single cortex and rotating vortex lattic, quant. theory 8=3125
 He II, specific heat, logarithmic singularity 8=15150
 He II, subcritical flow, pressure obs. 8=19695
 He³ in superfluid He⁴, dilute mixtures 8=15152
 He⁴ glass superleak construction 8=15149
 He⁴, normal-mode anal. 8=15153
 He⁴, scatt. of laser light 8=8078
 He⁴, soln. of He³, model of fermion soln. in boson gas 8=6232
 He⁴, turbulently flowing, λ -point shift 8=19694

Superlattice structure. See alloys; Crystal structure, atomic; Solid solutions.

Supernovae. See Novae.

Superparamagnetism. See Ferromagnetism.

Supersonic flow

See also Shock waves.

- air stream, ignition of slot-injected H₂ 8=15112
 Chaplygin's equation near the vacuum line, solutions approximating 8=7905
 circular cylinders, flow field in far wake 8=16674
 of entropy layers, linearized perturb., and vorticity induced by shock waves 8=16652
 gas macroparameters near leading edge of plate in hypersonic flow, asymptotic values 8=16672
 gas, real, over solid of revolution, perturbations damping 8=21480
 gases, internal heat generation 8=1458
 high stagnation enthalpies in shock tunnels, use of N₂O 8=16676
 hypersonic viscous shock layer of blunt body, effects of surface mass transfer 8=3035
 leading shock from jet injection into 2-dimens. supersonic stream 8=16678
 magnetoaerodynamic, blunt body, theory 8=355
 nozzles, electrical potential development 8=1456
 plate vibration, parametric, self-excited, in supersonic flow 8=10685
 radiation coupled shock layer including upstream absorpt. effects 8=19545
 sharp cones in rarified hypersonic flow, surface pressure distrib. 8=16681
 shock wave Mach wave refl. coeff. 8=3037
 shock wave motion along converging or diverging ducts 8=15056
 tangential slot injection of gas into external stream, associated flow field 8=16675
 transverse-curvature parameter in hypersonic flow regime, required form 8=16682
 Ar ionized by h.f. induction, electronic and ionic properties 8=21266
 Ar, partially ionized, source-flow expansion into vacuum 8=16658
 NO₂, chemiluminescent radiation from far wake of hypersonic flow 8=21478

Supersonics. See Ultrasonics.

Surface diffusion. See Diffusion in liquids; Diffusion in solids; Surface phenomena.

Surface energy

- adhesion, role in metalworking 8=5034
 crystal, ang. depend., and thermodynamic classification of surface 8=8377
 cubic crystals, as function of orientation, calc. 8=21865
 deformable, theory, simple force multipoles 8=2918
 equilibrium form of finite crystals 8=21866
 gases, and equilib. forms of anisotropic phases 8=4464
 Inconel 600, twin and grain boundaries free energy ratios, from e-micros. exam. 8=17287
 lipid membranes, interface free energy 8=8038
 molecular forces at solid surface 8=21637
 NaCl, potential meas. by CF⁺ emission on electron bombardment 8=5425
 Ni, twin and grain boundaries free energy ratios, from e-micros. exam. 8=17287
 Po, allotropes, critical surface tension 8=21869
 S, allotropes, critical surface tension 8=21869

Surface energy—contd

- Se, allotropes, critical surface tension 8=21869
 Sn atoms on silica gels and zeolite, states and dynamics 8=16912
 TD-nickel, twin and grain boundaries free energy ratios, from e-micros. exam. 8=17287
 Te, allotropes, critical surface tension 8=21869
 U, potential of H₂ 8=21909
 W, (112) and (100) oriented crystal surfaces, potentials of CO 8=21910

Surface ionization. See Ionization, surface.

Surface measurement

See also Area measurement.

- aluminized surface, testing in Fizeau interferometer using coated reference flat 8=11171
 aspherical, optical systems 8=15511
 charcoal, n. m. r. and adsorpt. methods 8=8293
 diamond, strains and damage due to abrasion 8=8826
 elasticity constants of contacting solid bodies 8=56
 electron diffraction, pseudo-superstructures and low energy multiple scattering 8=1752
 electroplated, interferometric exam. 8=9722
 epoxy polymers, micropenetrator for surface characterisation 8=8876
 interferometric flatness testing, Lloyd's mirror appls. 8=6547
 metals, influence of optical films 8=11168
 microstructure of crystals, by reflection of atom and ion beams 8=13201
 polymers, scanning electron microscope, prep. technique for examination 8=17180
 pores, without shape assumptions 8=17020
 porous materials, pore volume eqn. 8=13049
 silica gel, adsorption method 8=21742
 Teflon 6, area meas. 8=13047
 temperature by i. r. television 8=15118
 two-beam Linnik interference microscope study 8=13078
 AgCl single crystal, surface hardening while in contact with aqueous environment 8=4727
 Mg-Fe mixed hydroxides and dehydration prods., absorpt. obs. 8=17023
 MnO₂, electrolytic, area and pore struct., sorption obs. 8=21904

Surface phenomena

See also Adsorption; Capillarity; Catalysis; Electron emission; Films; Ionization, surface; Liquid waves/surface. Sorption.

- adhesion, electronic theory 8=2046
 amine oxide micelles, potentials 8=8158
 analysis by simultaneous X-ray emission and electron diffr. 8=8290
 brass, dezincification before anodic dissoln, in NaOH 8=18732
 contamination meas. by evolution of H in reactions with Na-NH₃ solns. at -78°C 8=21868
 dielectrics, pulsed breakdown in non-uniform field 8=9189
 dielectrics, pulsed breakdown in uniform field 8=9188
 diffuse, retro-reflection 8=468
 discharge with ring-type electrodes 8=12397
 dislocation loops in thick plate rel. to sinusoidal surface temp. cycling 8=17630
 elastic waves, excitation by transient surface heating, piezoelectric and nonpiezoelectric 8=17720
 electrical contacts, corrosion degradation obs. 8=8987
 electrical contacts, tarnishing studies 8=8988
 emulsions, stabilized, barrier to coalescence model 8=12957
 films, epitaxial, role of surfaces in nucleation 8=1735
 films, thin metal, optical absorb. and photoelectric emission, vectorial selective effects 8=22950
 fracture-surface energies, double cantilever method, critical analysis 8=22291
 gas flow through microporous media, transport mechanisms 8=4450
 gas-solid collisions, study by 'lock-in' detect. of modulated molec. beams 8=1323
 in glass, bubble surfaces, contamination-nucleated crystal growth 8=21937
 Heisenberg ferromagnet, semi-infinite, surface effect on sp. ht. and spin deviation 8=2303
 ice, conference 8=21867
 insulator, electric breakdown in vacuum 8=7673
 insulator/semiconductor interfacial magnetoplasma wave instability 8=2116
 laser beam scattering, comparison with gas particles 8=3286
 liquid, films, cavitation destruction in sound field, at elevated static press., photographic obs. 8=12775
 liquid/liquid interfaces, molecular interactions and mobility by NMR spectroscopy 8=12778
 liquid, thermal excitation of capillary waves by scattering of coherent light 8=16853
 liquids, thermal ripplon scatt. of light 8=16838
 liquids, surface layer thermodynamics 8=8047
 metal foil roughness rel. to scattered radiation at plasma frequency 8=8958
 metal-gas, e emission, Thomas-Fermi-Dirac model of quantum mechanical contrib. 8=5414
 metals, oxygen chemisorption and film growth 8=9703

Surface phenomena—contd

- metal surface impedance changes on acoustic wave generation by r.f. e.m. radiation 8=180
 metallic, u.v. emission on K⁺ bombardment analysed by spectral microscopy 8=14299
 multiphase couples, interface comps., motion and lattice transformations 8=17552
 phase equilibrium between adsorbed and free Ar in ultra-high vacuum obs. 8=21530
 polymeric and refractory heat shield materials, ablation obs. 8=1860
 polymers wettability rel. to melts heterogeneous nucleation, substrate effects 8=8298
 quartz, natural and cultured, distinction between rhombohedral faces 8=4731
 radiative props., effect of scatter 8=1686
 roughness rel. to anomalous resistral structure, model 8=5572
 sapphire, critical surface tension 8=13080
 semiconductor properties, meas. methods 8=18147
 semiconductor voltage rectification effect 8=13786
 semiconductors, e. m. wave propag. and amplification in strong mag. fields, theory 8=9090
 semiconductors, 1/f noise theory 8=13787
 shock wave production using laser beam on solid target 8=19534
 soda-lime glass with adsorped water spreading of org. liqs. 8=1520
 solid-liquid interface, supercooling criterion, thermal diffusion effect 8=1617
 steel, 18Cr-8Ni, oxide film identification by electron microscopy 8=8319
 structure and reactions, meas. by low and high energy electron diffraction apparatus 8=4834
 superconducting sheath, inhomogeneous distrib. of transport current 8=22543
 superconductivity, high temp. 8=17946
 semiconductor devices, by light spot scanning method 8=18099
 superconductor surface reactance properties using superconducting oscillators 8=13767
 superconductor, type II, critical current 8=13740
 superconductors, surface resistance, h.f., mag. field dependence 8=9035
 thermionic conversion Specialists Conference San Diego USA October 1967 8=6273
 Ag foils, contamination and roughness rel. to optical absorpt. 8=18502
 Ag, reflection of zero-energy electrons 8=6301-2
 Ag, sulphiding by H₂S, effect of surface Fe 8=23096
 AgCl single crystal, surface hardening, effect of aqueous environment 8=4727
 Al alloy, bubble formation during fatigue, rel. to humidity 8=4729
 Al, effect on electron emission of abrasion in air, O₂, N₂ and H₂O vap. 8=9270
 Al, (111), (100) and (110), atomically clean, prep. and props. 8=4728
 Al and Al₂O₃, dispersion of surface plasma oscillns. 8=12547
 Ar impact on Al, Ag, Au and Pt, accommodation coeffs., 500-12 000 eV 8=12685
 Au foils, contamination and roughness rel. to optical absorpt. 8=18502
 Bi, condensed, 2-4°K, superconducting props. 8=2155
 C contacts in microphones, deterioration leading to resistance increase 8=19558
 CaF₂:GdF₃, surface-layer dielec. relax. 8=18163
 CdS layered system on Ge, elastic wave behaviour 8=8850
 CdS, surface and volume conductance, kinetics comparison 8=18032
 CdSe powder, investigation by e.p.r. method 8=8294
 CdTe-HgTe, mass transfer by evaporation-diffusion 8=8673
 Cu: Cu-12.5 wt.%Al multiphase couple, interface comps., motion and lattice transformations 8=17552
 Fe-Cr alloys of 25-95%Cr comp., oxidation at 1000-1300°C, scaling kinetics 8=18677
 GaAs Fermi level, influence of volume dope 8=8934
 Ge, contamination, detection and identification 8=1688
 Ge-electrolyte interfaces, recombination obs. 8=18054
 n-Ge, recombination changes due to edge dislocations 8=22591
 Ge, recombination, generation process 8=22610
 H impact on Al, Ag, Au and Pt, accommodation coeffs., 500-12 000 eV 8=12685
 H₂O, destruction on various surfaces 8=18704
 He impact on Al, Ag, Au and Pt, accommodation coeffs., 500-12 000 eV 8=12685
 Hg-Mo system, diffusion 8=21903
 Hg-W system, diffusion 8=21903
 K, impedance near cyclotron edge for helicons 8=13686
 K, size effect, r.f., line shapes for surface reactance and resist. derivatives 8=13719
 MgF₂ films, thin, charging with electrons of average energy 8=22505
 MgO, gas emission 8=2272
 Mn-Zn eutectics, shock-decanted, interface examination 8=8170

Surface phenomena—contd

- Mo, accommodation coeffs. of inert gases 8=4734
 Mo, rel. to O₂ interaction, from surface exam. by LEED and work function studies 8=17165
 MOS transistors, surface states, i.f. noise 8=9176
 MoS₂, detection of monatomic steps and vacancies 8=4730
 N impact on Al, Ag, Au and Pt, accommodation coeffs., 500-12 000 eV 8=12685
 NaCl(100) surface, low energy electron diffraction study 8=17116
 Nb, superconductivity investigation 8=2157
 Ni, adsorption of H₂, electron probe surface mass spectrometer obs. 8=21908
 NiS film on Ni in S solns., growth kinetics and mechanisms, obs. 8=2525
 Pb, superconducting, microwave absorpt. in surface-sheath regime, depairing effect of mag. field 8=13760
 PbBrO₃, interface temp. of crystallizing melt 8=21960
 PbO, yellow, photoconductivity, effect 8=22697
 Si, changes due to u.v. illumination 8=8297
 Si, contamination, detection and identification 8=1688
 Si, recombination, generation process 8=22610
 TiO₂ electric discharge channels 8=1330
 V₂O₅(101) surface structure transitions, e-induced in LEED expt. 8=4733
 W, accommodation coeffs. of inert gases 8=4734
 W, field evaporation end form in field ion microscope 8=4735
 W, interactions of I₂ vapour 8=18699
 W, tip radius in ion microscope 8=343
 W, translation accommodation coeffs. of Ar, O₂, N₂ 8=17113
 W, trapping energy calc. for inert gas ions 8=13081
 W, (110), atomic perfection rel. to field emission 8=2275
 ZnS(Cu), temps., exptl. determ. by photoluminescent emissions 8=13082

Surface tension

- See also Capillarity.
 adhesion, wetted spheres 8=8150
 benzene-water, interfacial, effect of temp. and press. 8=12827
 binary liq. mixtures, organic cpds., theory 8=12826
 and cellular convection in semi-infinite liquid layer 8=1503
 copolymers 8=17841
 cylinder withdrawal, gravity corrected theory for speed range extension 8=12762
 n-decane-water, interfacial, effect of temp. and press. 8=12827
 interfacial forces at plane surface of solids 8=21637
 interfacial, of polar mixtures 8=16811
 interfacial, of ternary random mixtures, lattice models 8=21639
 liquid drops subject to electrical forces 8=16782
 liquid mixtures 8=21636
 near phase transition, quasichem. approx. 8=21635
 noble metals, correl. with dispersion energies 8=21792
 organic liquid spreading on soda-lime glass rel. to adsorped water effects 8=1520
 organic liquids, pure, new correlation 8=12824
 phosphates, molten, rigid sphere model 8=7999
 physical-cluster theory of condensation 8=4654
 polyetherdioxols, meas. and theory, and parachor 8=4552
 poly(methylmethacrylate), interface, tacticity determ. 8=4551
 polysiloxane-polyether block copolymers, equilb. 8=8155
 polysiloxane-polyether block copolymer solns., dynamic 8=8156
 related to latent heat of fusion 8=16936
 sapphire, wet by liq. metals 8=13080
 solid-liquid, rel. to nature of liq. state 8=12825
 Teflon 6, in hydrocarbons, contact angle data 8=13361
 tin, solid-liquid interface meas. 8=16925
 tube, horizontal, effect on flow during emptying 8=16626
 variation, inducing fluid motion 8=21422
 water, rel. to "shadow-sausage effect" of illuminated, partially submerged rod 8=6495
 Bl₃, under its own vapour and contact angle on W 8=12998
 H₂O and D₂O, domain theory 8=4550
 H₂O liq.-vapour interface potential, molec. theory 8=12196
 He II liquid, calc. using Gross-Pitaevski model 8=3128
 Xe, liq. and energy, in temp. range 189°-280°K 8=1539

Surface tension measurement

- vertical plate method 8=8031
 viscous liquids, pendent drop method 8=21638
 Fe alloy liquid drop preparation 8=8257

Surface texture

- apophyllite, a-face structures 8=17220
 atomic, slow electron diffraction, a review 8=22012
 boundary layer turbulence promoters, improved heat transfer rel. to power reactor systems 8=21510
 brass, contour measurement using laser probe 8=19339
 carbon blacks, graphitized, Xe adsorpt. obs. 8=17162
 cellulose fibres, effect of ionic etching on structure 8=13083
 clay, contour measurement using laser probe 8=19339
 crystals grown from molten salts, growth spirals obs. 8=4838
 electroplated, interferometric exam. 8=9722

Surface texture—contd

- electropolishing for field-ion microscope specimens, automatic supervisor 8=17273
 electropolishing, prod. of flat discs required 8=5996
 electropolishing of thin foils for electron microscopy, specimen temperatures 8=4836
 field-ion images from asymmetric specimens, rel. to streak contrast 8=8452
 interferometric flatness testing, Lloyd's mirror appls. 8=6547
 low energy electron diffraction, sensitivity rel. to surface perfection 8=4726
 metal emitters, effect of micropatches on average thermionic consts. 8=18260
 metal polycrystals, ionic corrosion 8=13522
 micro-roughness of tyres, rel. to adhesion to wet road, and viscous hydroplaning 8=17752
 oriented crystals prep., lapping machine attachment 8=21918
 plaster, contour measurement using laser probe 8=19339
 polyethylene single crysts. 8=17215
 quartz, polished, X-ray diffr. microscopy 8=17599
 roughness determ. for wax-polished painted surface 8=2470
 roughness of electric noncond. rel. to directional distrib. of emitted thermal rad. 8=22138
 steel 8=8295
 steps, resolution and contrast, meas. with electron microscope 8=13079
 strain free polishing of accurate flats 8=5989
 structure of surfaces, conference, Nov, 1966, Durham, North Carolina 8=17115
 substrate roughness effect on work function of evaporated films 8=9267
 topography characterization with scanning electron microscope 8=17114
 two-beam Linnik interference microscope study 8=13078
 AgI, finely divided 8=8337
 Al alloys, preconditioning for electroplating, electron microscopy 8=8291
 Al, cold rolled 8=21938
 Al, electropolished, form. of tops and pits during heating in air and vacuum 8=17117
 Al film, rel. to hemispherical reflectance 8=2399
 Al, microrough compared with polished, for increase of thermal rad. 8=22139
 AlZn-Mg cast alloys, influence on stress corrosion cracking 8=22312
 Au film, rel. to hemispherical reflectance 8=2399
 C, vitreous and pyrolytic graphite, comp. of oxidation pitting 8=8292
 CsBr and CsI i.r. windows, polishing 8=495
 Cu-Al-Mn alloys, surface relief effects rel. to supercond. transition 8=19686
 Fe 8=8295
 Fe-Cr alloy, Cr₂O₃ protective scales, mechanism of breakthrough 8=23099
 Fe-Ni alloys, surface relief effects rel. to supercond. transition 8=19686
 Fe-Si alloys, chemical polishing 8=1687
 GaSb, effect of ion bombardment, annealing and polishing on (111) surface stress 8=8849
 Ge, effect of ion bombardment, annealing and polishing on (111) surface stress 8=8849
 Ge, thermally etched 8=17217
 InSb, effect of ion bombardment, annealing and polishing on (111) surface stress 8=8849
 LiF, structure, props. after annealing 8=8378
 Mo crystals, electron microscope exam. 8=21992
 MoZr crystals, electron microscope exam. 8=21992
 NaCl(100) surface, study with LEED 8=17116
 Nb, exam. by field electron microscopy 8=13930
 Ni film, rel. to hemispherical reflectance 8=2399
 NiBr₂ crysts. surface-spikes, growth and impurities conc. 8=4807
 PbSe_{0.9}Te_{0.1}, comp. variations shown by chemical polishing 8=1689
 Pt film, rel. to hemispherical reflectance 8=2399
 Si epitaxial growth, effect of perturbations 8=17256
 Si, ion-bombarded, temp. dependence 8=5278
 SiO₂ films on Si, pinhole locating by electrophograph method 8=1698
 Si, polishing methods 8=10452
 Si, solid, elec. decoration, new method 8=8380
 Si, thermally etched 8=17217
 Ti, microrough compared with polished, for increase of thermal rad. 8=22139
 V₂O₅, LED study 8=21870

Surveys. See Reviews.**Suspensions**

- See also Aerosols; Sedimentation; Sols.
 aluminosilicate catalyser in sludge, concentration by recording permittivity 8=15167
 Bingham plastic, settling of spherical particles 8=21553
 birefringence, transient elec., particle size determ. 8=16899
 clay, forced-flow electrophoretic filtration, elec. field effects 8=16898
 dioctylphthalate aerosol, particle conc., by turbidity meas. 8=8153

Suspensions—contd

- and drilling muds, in tubes, laminar and transitional flow 8=8151
 extremum principles for slow viscous flow, application to 8=1449
 flow in porous media 8=12738
 flows, particle migrations in 8=8146
 gas with micron-size solid particles, heat conduction 8=21735
 lamella thickening, theoretical analysis 8=21728
 latex spheres in water, monodispersed, light transmission meas. 8=4632
 milk, light absorpt. var. with beam dia. 8=6537
 ordered aggregates of rigid spheres, disks and rods in plane Couette flow 8=12944
 polystyrene latex particles, aqueous, atomization 8=8154
 radiant heat transfer with wall, zonal calc. 8=8143
 sheared, wall migration of fluid drops 8=7995
 stearic acid aerosol, particle conc., by turbidity meas. 8=8153
 triphenylphosphate aerosol, particle conc., by turbidity meas. 8=8153
 ultracentrifugation, simultaneous automatic sequence and photo control system 8=4631
 viscosity, concentrated solid spheres 8=8149
 Fe(OH)₃, flow meas. by Br⁹² 8=21727
 LaB₆ powder in N₂, m. h. d. generator working fluid 8=15199
 SnO₂ in glycerine/castor oil, Mössbauer line widening, temp. and viscosity dependence 8=1603
Suzuki atmospheres. See Crystals imperfections/dislocations.
Switching time, ferroelectric. See Ferroelectric materials; Ferroelectric phenomena.
Switching time, ferromagnetic. See Ferromagnetism; Magnetic properties of substances/ferromagnetic.
Symbols. See Nomenclature and symbols.
Symposia. See Conferences.
Synchrocyclotrons. See Particle accelerators/orbital, cyclotrons.
Synchrotron radiation. See Electrons/radiation
Synchrotrons. See Particle accelerators/orbital.
Szillard-Chalmers reactions. See Radiochemistry.

Tables, mathematical

- conversion relations for isotropic ceramic elasticity formulations 8=8783
 Green's functions for b.c.c. lattices 8=4859
 Laguerre polynomials, roots and weight factors 8=19370
 Love waves, theoretical dispersion tables for wedge propag. 8=9775
 radioactive and other exponential decay 8=7124
 Hermite polynomials, roots and weight factors 8=19370

Tables, physical. See Collections of physical data.**Tachometers.** See Angular velocity measurement.**Tandel.** See Dielectric devices.**Tantalum**

- anodic oxidation in LiCl-KCl 8=5738
 anodization, gas-phase 8=14420
 diffusion of C, investigation over wide temp. range 8=17586
 diffusion, summary of ORNL work 8=17593
 electron emission, laser induced, using pulsed Ar laser 8=18271
 film deposited by sputtering in crossed e.m. field 8=7651
 films, impurities, spectrochem. anal. 8=18786
 films, ultra-thin, vacuum-deposited, structure from e-diffr. and microscopy 8=17292
 hardness and deformation effect of Nb and Mo additions 8=8862
 hydride phase, solubility of H₂, isotherm 8=1924
 in metals, spectrochemical determ. 8=9749
 oxidation, controlled, in radio-frequency-excited glow discharge 8=8310
 recrystallized, impurity effects on strain hardening 8=22380
 secondary electron emission, H⁺ bombardment 8=5423
 superconductivity under high pressure 8=9060
 thermal conductivity, temp. dependence of temp. coefficient 8=13387
 work function changes on Cs, O₂ and H₂ adsorpt. on Ta ribbon 8=9276
 Ta¹⁷⁶, decay periods, using a time-amplitude converter 8=16042
 Ta¹⁸¹(5/2⁺ → 7/2⁺), circular polarization of γ-radiation 8=991
 Ta + N₂ system, adsorpt.-absorpt. kinetics 8=18698

Tantalum compounds

- alloys, anti-oxidation metallurgy 8=23779
 cavitation damage resistance 8=5035
 R₂O₃-M₂O₅, (R = rare earth, M = Nb, Ta or Pa), crystal structure 8=1802
 TaC, in Fe alloy, fracture obs. 8=22347
 TaC_x, thermal expansion, effect of stoichiometry 8=1881
 TaC, heat content valves, entropy specific heat 8=8643
 TaC, Verneuil growth by arc melting 8=4799
 TaC_{0.99}, elastic constant determ. 8=8861

Tantalum compounds—contd

- TaCl₅F, crystal structure 8=17418
 TaCr₂ precipitation from Ta-Cr solid soln. 8=8282
 TaN, lattice dimensions, thermal and electrical conductivity, Hall coefficient, thermal e.m.f. and microhardness obs. 8=13702
 Ta₂O₅ films e beam evaporation and dielec. props. 8=22652
 TaO, gaseous, electronic bands rot. anal. 8=1267
 Ta-O, lattice particle X-ray and electron scattering on new phase form. 8=1773
 TaO₂, molec. geometry 8=7550
 Ta-O system, new phases, e-diffr. study 8=17101
 TaO_{2-x} in thin films, e-diffr. exam. 8=17417
 Ta₂O₅, thin film prep. by anodizing and sputtering 8=13097
 Ta₂O₅, thin insulating film, effective mass meas. 8=8944
 Ta-O-C solids solns., CO solubility and equilib. press., 1700-2000°C 8=21787
 Ta₂O₅-SiO₂ dielectric thin film capacitors, prep. and props. 8=9232

Targets. See Nuclear bombardment targets.

Teaching

- crystal geometry, introductory course 8=1767
 electricity and magnetism project laboratory 8=15159
 electromagnetic theory, junior college course 8=19757
 holography, introduction 8=11213
 lens theory, systematic approach 8=15502
 meson decays, lectures 8=20413
 meson-meson interactions, lectures 8=20422
 modified open-ended laboratory in mechanics at general-physics level 8=10469
 nuclear physics, misconceptions 8=7027
 π -N interactions, lectures 8=20427
 programmes in education, American Institute of Physics 8=10468
 quark substructure for mesonic and baryonic states, lecture 8=20408
 solid state physics in USSR higher educational institutions 8=16965
 spinodal decomp., Institute of Metals lecture 1967 8=21835

demonstrations

- alpha particle range, simple stand for determination 8=883
 amplitude modulated, vibrations, mechanical demonstration apparatus 8=10679
 beats and Lissajous figures, demonstration using turntable oscillators 8=10680
 crystal models 8=10470
 crystallography, of Ewald construction 8=13204
 diffusion experiment, simple, quantitative 8=12709
 dynamics, apparatus 8=10525
 eigenvalues, degenerate, introduction 8=3404
 electric and magnetic field probes, audible signal demons. 8=10822
 electrolytic solutions, thermodynamics using molten salt 8=2529
 e/m measurement, modification of experiment 8=10471
 F-centre diffusion, lecture demonstration 8=13452
 films on acoustics and wave motion 8=19548
 gas laser, coherent properties 8=418
 geometrical optics sign convention 8=467
 holograms, instant, prep. and characteristics 8=11208
 liquid-vapour phase diagram, student expt. 8=21768
 mechanical vibration and resonance, combination of 8=142
 mechanics, using electrical readout 8=10472
 microwave system, expt. and demonstration 8=6366
 monochromator, Czerny-Turner, construction 8=11154
 neutron mass, from capture-gamma ray energy 8=6944
 n. m. r., acetone-chloroform system 8=2498
 object-image relns. of mirrors, and 3-dimens. Lissajous figures 8=476
 optical rotation of microwaves, by macroscopic models 8=375
 radiation, e. m., experimental introduction 8=10936
 statistical mechanical behavior, hard sphere simulation 8=14981
 thermodynamics 8=2983
 Van de Graaff type accelerator, undergraduate construction and operation 8=11339
 vibrations of circular membrane, resonant response 8=10691
 wave machine, dispersion, reflection and eigenfrequencies 8=10937
 wave motion, using air-suspended discs connected by light springs 8=10678
 wave theory by phasors 8=3013
 C-H bond strengths, student expt. 8=21109
 Cs¹³⁷-Ba^{137m} isotope generator 8=1207
 Hg, vapour, diffusion through rare gas 8=12711
 N₂ phase change 8=1607

Technetium

- disintegration probability in red giants 8=2780
 synthesis mechanism in different stages of stellar evolution 8=2779

Technetium compounds

- TcAl₃, structure refinement 8=8555

Tektites. See Meteorites.

Telescopes

- objective, cemented, 5th order spherical aberration 8=3351

Telescopes—contd

- resolving power, effect of eye sensitivity curve 8=481
 in satellite, thermal deformations in mirror 8=480
 X-ray mirror 8=15591

astronomical

See also Radioastronomy

- dome slit, microthermal vars. rel. to image quality, obs. 8=14741
 drive, clock-controlled 8=2772
 10 MHz, large array-type 8=19327
 optical, faint objective-prism spectra and diffr. patterns meas. 8=23498
 Queen Elizabeth II, optics design and testing 8=10101
 radiotelescope of the Naucay station, the pointing device 8=5980
 review of future requirements 8=5851

Tellurium

- atomic structure using Mössbauer effect 8=4887
 band structure calc. using LCAO approximation 8=8906
 band structure, relativistic KKR-calcs. 8=22468
 critical surface tension 8=21869
 crystal, multiple diffraction of X-rays 8=8559
 crystal, u. s. wave absorpt. meas. and dislocation loop length calcs. 8=8619
 cyclotron resonance, effective masses and diamagnetic resonances 8=22490
 dislocations, theory and plastic behaviour 8=4984
 films, vac.-evaporated, forbidden reflexes in e-diffr. 8=17141
 interband hole transitions 8=9018
 isoelectronic trap in CdS, optical fluorescence and absorpt. 8=23048
 isomorphous, non-centrosymmetric structure with Bijvoet differences 8=13273
 liquid, elec. cond., high pressure meas. 8=1588
 magnetoabsorption meas. 8=23016
 molten, ultrasonic velocity 8=12867
 non-linear optical props. 8=18563
 ore from Boliden, dating by isotope anal. of inert gases 8=14455
 p-band absorption at 4°K 8=8945
 phase detection in V₂VL₂ alloys, by etching 8=17102
 piezoresistance coefficient 8=5376
 semiconductors band structure Green's function method 8=8913
 single crystals, far u.v. reflectivity 8=15551
 subgrain boundaries, low-angle 8=8737
 thermal vibration spectra, experimental 8=8607
 in Bi, distribution coeff. and donor valency 8=22517
 ZnS luminescence, effect 8=14336

Tellurium compounds

- hydrides, proton reson. 8=12327
 telluriumbismuthite, Xe extraction, Te¹³⁰ decay rate 8=1017
 p-HgTe, i.r. reflection in region of plasma minimum 8=5262
 HgTe-ZnTe system, electrical properties 8=5263
 La telluride phases, crystal chemistry 8=17202
 Nd telluride phases, crystal chemistry 8=17202
 PbTe-Sb₂Te₃ alloy system, thermoelectric props. and phase relations 8=4716
 Pr telluride phases, crystal chemistry 8=17202
 SnTe-Bi₂Te₃ alloy system, thermoelectric props. and phase relations 8=4716
 Te(halide)₂, Mössbauer line, isomeric chemical shift 8=8222
 TeF₆, structure determ. by electron diffr. 8=12236
 Te(NO₃)₄, atomic structure using Mössbauer effect 8=4887
 TeO₂, atomic structure using Mössbauer effect 8=4887
 TeO₄K₂, γ -irrad., e. s. r. spectra 8=9444
 TeO₄Na₂, γ -irrad., e. s. r. spectra 8=9444
 Te-Se alloy, laser second harmonic generation 8=6442
 Te_{1-x}Se_x alloys, liq., elec. cond. and thermoelec. power 8=12918

Temperature control. See Cryostats; Thermostats.

Temperature

- See also High-temperature production and effects;
 Low-temperature production.
 auroral electrons, possible estimation from r.f. capacity probe obs. 8=2666
 automatic regulator for meas. in interval 10 to 150°K 8=15122
 control, pendulum apparatus, electronic system 8=10480
 furnace, simple thyristor controller 8=15125
 liquid, unsteady distrib. in viscous flow 8=7977
 negative, concept 8=10642
 plasma, multi-ion, rel. to elect. conductivity, calc. 8=4345
 potential in meteorology, formulae for different types 8=9823
 principles, review 8=10764
 radiant self-stabilization, by change in optical constants of VO₂ 8=23019
 relativistic thermodynamics, definition 8=10785
 surface, nonsteady state, exponential point meas. method 8=10781
 thermostatic water bath with $\pm 70\mu^\circ\text{C}$ stability 8=15124
 uniform field, stability props. 8=19661
 Ag wires, electric explosion, temp. variation during first stage 8=1622

Temperature—contd

- Ar discharge neutral gas, medium press. 8=16408
 Cu wires, electric explosion, temp. variation during first stage 8=16222
 He boiling, thermodynamic scale 8=19689
 Pt resistance thermostat for $\pm 25\mu^\circ\text{C}$ 8=15123

Temperature distribution

- bar with surface temp. oscillations 8=15115
 behind detached shock, non-adiabatic, in power series of radiative coupling coeff. 8=15053
 bundle of rods, during heat exchange, forming channel through which water flows 8=12849
 channel wall of m. h. d. generator with water-cooled electrodes 8=19726
 circular pipe, turbulent heat transfer and temp. distrib. 8=232
 in conductor with temp.-depend. conductance 8=3151
 in cylindrical bodies with longit. fins, rel. to heat conduction and boundary problems 8=19648
 electron-microscope specimens, calc. 8=1861
 flame in cylindrical chamber, recirculation effect 8=15114
 furnace wall, temp. dependent conductivity 8=19659
 heat equation, general solution 8=3102
 heat equation, one-dimensional, new solutions for spheres, cylinders and slabs 8=3105
 heat insulation coatings, with phase transitions, numerical solns. 8=237
 heated tube, steady state behaviour 8=10782
 hollow cylinder, low Fourier numbers 8=15116
 infrared heating, penetration curve determ. 8=19660
 jet, liquid, Landau thermal 8=16777
 laminar flow at high shear stresses 8=4508
 liquid, centrifuged 8=21654
 near Apollo wake, Reynolds number depend. 8=23459
 non Newtonian fluid with nonlinear heat conduction law 8=4424
 satellite gravity gradient rods 8=23461
 solid circular cylinder, axisymmetric field calc. 8=19658
 solid, one dimensional, transformation for calc. 8=13386
 solids and gas along height of a fluidized bed 8=4628
 surface, by i. r. television 8=15118
 in thin plate with convection losses, heated by moving discrete source 8=3111
 3-layer colloidal body 8=4633
 transient, in spherical region subjected to variable surface heat flux 8=19662
 unsteady, infinite regions of arbitrary geometry 8=6199
 unsteady, viscous flow 8=7977

Temperature measurement

- See also Pyrometers; Thermocouples; Thermometers.
 elec. meas. on double-rotating mechanism 8=13505
 electroacoustic, for low temps. 8=19663
 chromel-alumel thermocouples for small difference meas. 8=15121
 chromic potassium (methylamine) alums, temp. scales from nuclear orientation 8=8205
 differential thermal analysis, at high press. 8=9684
 fixed points, 232° – 661°C , gas thermometry 8=244
 gas-phases, by spectral line reversal, effect of continuous absorber 8=16695
 of gas, rapidly varying in an unsteady flow 8=16694
 iron and steel, laser irradi. temp. 8=8769
 moving body appears cool? 8=219
 neutron diffusion expts. samples, regulation 8=6218
 nylon thread, by i. r. pyrometer 8=17187
 oxide cathode, surface temp. meas. during pulsed emission 8=9275
 photographic pyrometry 8=10784
 in plasma, from quadratic Stark effect shift, and spectral line broadening 8=7787
 plasma, NaK seeded, in elec. field 8=21308
 pyrometer, optical, calibration from Pt/Pt₉₀Rh₁₀ thermocouple 8=19670
 reactor fuel, acoustical thermometer 8=4018
 rotating system, a contactless method 8=10780
 sea, i. r. radiometry problems 8=18845
 semicond. devs., i. r. meas. 8=22618
 solid bodies, errors 8=10783
 steel, phase equilib., mag. method 8=17062
 by superconducting device, with 10^{-3}K resolution 8=15117
 surface, by i. r. television 8=15118
 thermistors resist. rel. to temp. and immersion depth, obs. 8=3110
 thermocouple, nozzle, for high-temp. gases 8=7927
 thermocouples, resistance detectors, thermistors, comparison 8=10788
 virtual air, use of ultrasonic resonance thermometer 8=246
 C resistance, low-temp., calibration 8=19682

spectral methods

- double-beam modulated pyrometer 8=20039
 on oxygen-acetylene flames 8=3109
 oxyacetylene flame, in air or N₂, from vib.-rot. spectrum of OH 8=18692
 plasma, discharges for CO, lasers 8=15459
 plasma, rel. to line intensity and broadening 8=16538
 sea surface, using airborne i. r. thermometer 8=2570
 spectroradiometer with automatic digital recording 8=6202
 N₂ excited by electron beam, obs. 8=16292

Tensile strength. See Mechanical strength/tensile.**Tensors**

- decomposition of classical groups 8=2880
 elastic, anisotropic, decomposition for given crystal symmetries 8=17714
 electromagnetism, Green's function, singularities 8=19758
 energy-ang. momentum, polarized media 8=10636
 energy-impulse, geometry of electromagnetic field 8=3172
 energy-momentum, polarized media 8=10635
 energy tensor for null, source-free e.m. field 8=315
 group theory, symmetrized tensor products, Clebsch-Gordan series 8=2890
 ideal gas mixtures, diffusion, calc. 8=16718
 impulse-energy of e.m. field 8=3170
 Maxwell, for energy in e.m. field 8=3171
 irreducible of O₃, decomposition into its rotation subgroup D² 8=19355
 product of one-particle representations of an infinite-dimensional Lie algebra 8=6724
 quasi-spin, use of creation and destruction operators 8=918
 stretching and spin of surface and linear material elements 8=40
 symmetric, covariant decomposition for Cauchy problem 8=6071

Terbium

- antiferromagnetic, critical mag.-scattering of neutrons 8=22882
 exchange interactions and spin-wave spectrum 8=22846
 ferromagnetic to paramag. phase transition, neutron diffraction study 8=18352
 ferromagnetic spin waves, dispersion reln. from inelastic n. scatt. 8=18351
 magnetoelastic effects and mag. props. 8=22799
 microwave absorption phenomena at 9.44 and 35.3 Gc/s, 10–290°K 8=14269
 neutron diffraction study under high pressure, helical periodicity 8=14040
 in phosphors, fluorescence and radiative transition probabilities 8=4683
 spin-wave spectrum, temp.-dependent crystal field effects 8=22845
 uniaxial mag. anisotropy 8=18333
 Tb¹, spectrum, levels with extreme J 8=12073
 Tb³⁺ activated phosphors, correlation of fluorescence with crystal and other properties 8=9581
 Tb³⁺ in CaWO₄, spin-lattice relaxation time obs. 8=22914
 Tb³⁺, energy transfer in Na rare-earth tungstates 8=9610
 Tb³⁺, energy transfer with Nd³⁺ in inorganic solids 8=9594
 Tb³⁺ in SrTiO₃, vibronic structure in luminescence spectra 8=14333
 Tb³⁺ in tungstates and molybdates, u. v. excitation of fluoresc. 8=2473
 TbCrO₃, mag. structure at 77, 4.2 and 3.95°K, by n-diff. studies 8=5508
 TbCu_{1-x}Zn_x alloys, antiferro-ferromag. transition, on increasing Zn conc. 8=14073

Terbium compounds

- chelate phosphors, radiative quantum efficiencies, enhancement 8=18617
 salts, hydrated, fluoresc. lifetimes and multi-phonon deactivation, 4.2°, 77° and 300°K 8=14315
 TbC₂, antiferromag. structure 8=18386
 TbFeO₃, orthoferrite, transition to antiferromagnetism at liq. He temps. 8=9375

- Tb-Y alloys, crystal struct., 77–300°K 8=22040

Terrestrial electricity. See Earth/electricity**Terrestrial heat.** See Earth/heat.**Terrestrial magnetism.** See Earth/magnetic field; Magnetic storms.**Tetraneutrons.** See Neutrons.**Thallium**

- atomic beam, surface ionization on Pt and W 8=12110
 atoms, oscillator strengths for np, \rightarrow ms_{1/2} and np, \rightarrow md transitions 8=4086
 atoms, superradiance at transitions terminating at metastable levels 8=20943
 cyclotron resonance 8=8972
 depolarization in noble gas-atom collision 8=7473
 diffusion of Au and Ag in, obs. by radiotracer technique 8=22163
 films, Ge coating effect on transition temp. 8=5214
 magnetoresistance field dependence up to 150 kG at low temps. 8=5433
 n. m. r., anisotropy 8=9467
 pure, elec. resistance α to 5°K, dimension effect and temp. depend. 8=5185
 sensitizer for BaO. Al₂O₃:Mn emissions 8=14303
 vapour absorpt. spectra using modified King furnace 8=7393
 TI' clustering in KI from absorpt and emission spectra at 77°K 8=23056
 TI' ion, hydrated, luminesc. intensity and spectral characts. 8=21704
 TI' in K₂B₂O₄ glass, γ -irrad., induced absorption bands 8=5639

Thallium—contd

- Ti(III)-Ti(I) isotope exchange in complexes 8=18653-4
- Thallium compounds**
- halides, dielectric consts., temp. and press. depend. 8=13874
- halides, gaseous ions, recomb. rates 8=4317
- tetraiodothallates, pure quadrupole reson. of I 8=18477
- HgX₂-TlX, (X = I, Br, Cl) system, cpds. formed 8=17085
- TlBr, anisotropy of diamag. susceptibility 8=9295
- TlBr, elastic consts. and thermal expansion 8=17833
- TlBr, temp. and pr. dependence, obs. 8=2068
- TlBr:Mn luminesc. excit. and emission and absorpt. spectra 8=9622
- TlCl, cyclotron resonance obs. 8=8971
- TlCl, ionic conduction and thermal disorder 8=9200
- TlCl molten, self diffusion of Tl⁺ 8=21643
- TlCl, transient magnetoresistance of holes 8=9020
- TlCl, two photon absorption, angular dependence 8=9561
- TlCl:Mn luminesc. excit. and emission and absorpt. spectra 8=9622
- TlF, anisotropy of diamag. susceptibility 8=9295
- TlMnF₃:Co, antiferromag. zero anisotropy Co conc. dependence 8=9401
- Tl₂O₃, optical meas. rel. to semiconducting props. 8=23017
- Tl₂SA₂, paramag. reson. spectrum of Mn²⁺, hyperfine structure with g-factor ~ 4.3 8=5533
- TlSe single crystal growth in u.s. field 8=21967
- TlSe, thermal conductivity 8=17547
- Tl₂SeAs₂Se₃, paramag. reson. spectrum of Mn²⁺, hyperfine structure with g-factor ~ 4.3 8=5533
- Tl₂Te, rhombohedral, crystal structure by e-diffr. 8=17424
- Tl₂TeAs₂Te₃, paramag. reson. spectrum of Mn²⁺, hyperfine structure with g-factor ~ 4.3 8=5533
- TII crystal, CsI stabilized, transmission in 30-65 μ region 8=5640
- TII, effect on temp. of Hg arc 8=485
- TII, polymorphism, compressibility and thermal expansion 8=1683
- Thermal conductivity.** See Conductivity, thermal.
- Thermal decomposition.** See Chemical reactions.
- Thermal diffusion.** See Diffusion in gases/thermal; Diffusion in liquids/thermal.
- Thermal diffusion columns.** See Diffusion in gases/thermal; Isotope separation.
- Thermal diffusivity.** See Conductivity, thermal; Heat conduction.
- Thermal expansion**
- alkali halide crystals, m.p. calc. 8=16970
- alkali halides, at low temps. 8=22123
- alkali halides with CsCl structure, low temp. coeffs., and related thermodynamic props. 8=8648
- n-alkanes, rel. to chain length 8=16790
- condensed substances, coefficient rel. to sound velocity 8=1551
- corundum, mean curves 8=17534
- cubic metals, calc. from Morse function 8=17530
- earth, at high press., eqns. of state 8=18808
- ethylene oxide-H₂O clathrates 8=17447
- fibre glasses, unsteady regime meas. method 8=8645
- fuel rod in narrow annular coolant channel, stability against thermal buckling 8=12011
- gas-solid system, polytropic changes 8=4472
- glass, microporous, shrinkage rates rel. to heating 8=17021
- glasses, aluminate for i.r. use 8=22954
- Grüneisen parameters of some II-VI compounds 8=17537
- liquids, similarity theory and dimensional analysis 8=21646
- metals, thermodynamic approach to anharmonicity of lattice vibrs. 8=17529
- methyl ammonium aluminium sulphate dodecahydrate, interferometric method 8=8647
- naphthalene, tensor meas., 78-323°K 8=17533
- organic crystals, rel. to derivation of oscillation spectrum and charact. temp. 8=17470
- polyalkyl methacrylates, rel. to multiple transitions 8=21864
- polymeric solids, Grüneisen number 8=1866
- polymorphic solids, study by hydrostatic weighing 8=17531
- pure non-cubic crystals, causing plastic deformation rel. to temperature cycling 8=22276
- quartz for testing relative dilatometers 8=13381
- quartz mean curves 8=17534
- rare gas solids, expansion coeff. calc. 8=1879
- solid solns., coeff. incr. due to heavy component 8=8634
- stresses in composite solid cylinder, book 8=19408
- surface distortion of semi-infinite solid due to uniform circular heat source 8=22122
- transition metal cpds., shrinkage with concurrent reduction 8=4936
- unsteady regime meas. method 8=8645
- Al₂O₃ for testing relative dilatometers 8=13381
- As-Se glasses 8=13382
- Ba(NO₃)₂·H₂O, single crystal, coeff. meas. 80-3000°K 8=5051
- CaCO₃, (calcite), and precision lattice parameters 8=22015
- Co hexagonal single crystal, Young's modulus dependence 8=22324
- Cu cubic crystals, coeff., temp. depend. 8=8646
- Cu-Ni alloys, rel. to ferromag. Curie point of Ni 8=17532
- Fe-(9.75-11.66%)Al alloys, nature of K-state 8=9005
- Fe-Ni bimetal strip components, ageing effects 8=22345

Thermal expansion—contd

- GaAs, coeffs. from -62 to 200°C 8=1880
- Ga(As, P), coeffs. from -62 to 200°C 8=1880
- GaAs(Sb), from 2-40°K 8=4937
- GaP, coeffs. from -62 to 200°C 8=1880
- Ge cubic crystals, coeff., temp. depend. 8=8646
- Ge, from 2-40°K 8=4937
- He⁴, liquid, 1.25-4.2°K, 0.5-28 atm 8=10802
- In, 20 to 2°K, length differences between normal and supercond. states 8=22124
- InAs(Sb), from 2-40°K 8=4937
- KNbO₃-AgNbO₃ system, and elec. and X-ray studies 8=21823
- LiTaO₃, a₁₁ and c₁₁ axes, room temp. to 850°C 8=13383
- α-Mn, and structure study 8=8532
- Mo lattice, temp. dependence 28°-522°C 8=22125
- Ne crystals, volume coeff. and isothermal compressibility 8=1803
- O₂ solid, β and γ phase coeffs. and transform. characts. 8=4938
- Re, X-ray diffraction determination 8=13384
- Si cubic crystals, coeff., temp. depend. 8=8646
- Si, from 2-40°K 8=4937
- Si₃N₄ film, pyrolytically deposited, meas. 8=4939
- TaC_x, stoichiometric effect 7=1881
- α-Ti, anisotropic by X-ray method 8=17535
- TlBr, and elastic consts., from acoustic wave vel. 8=17833
- TlBr, 78°-673°K meas. 8=2068
- TII, polymorphism, compressibility and thermal expansion 8=1683
- TiO₂, single cryst., 100°-700°K 8=17536
- VO₂ tetragonal phase, from lattice meas. at 78-415°C 8=13385
- ZrO₂-CeO₂ mixtures, high temp. 8=22614
- Thermal measurement**
- See also Calorimeters; Calorimetry; Conductivity, thermal/measurement; Temperature measurement; Vapour pressure measurement. Entries describing measurement methods for specific thermal quantities and effects may also be found listed under the various headings for the subjects concerned.
- conductivity and capacity, appl. of solns. of eqns. for non-steady state monotonic heating 8=10773
- fluxes and surface temp., nonsteady state, exponential point method 8=10781
- fluxmeter in shear flow for local heat transfer rates, theory 8=19639
- hot film sensor for turbulent fluid 8=16822
- U₁, α self irradiation effects obs. 8=17105
- Thermal radiation.** See Radiation/heat.
- Thermal spikes.** See Crystal imperfections; Physical effects of radiations.
- Thermal transformations.** See Boiling; Condensation; Freezing; Heat of transformation; Melting; Phase transformations; Sublimation; Vaporization.
- Thermionic emission.** See Electron emission/thermionic; Ion emission/thermionic; Ionization, surface.
- Thermionic generators.** See Electricity/direct conversion; Electron tubes.
- Thermionic tubes.** See Electron tubes.
- Thermistors.** See Semiconducting devices.
- Thermochemistry.** See Heat of reaction, etc.
- Thermocouples**
- advances and applications 8=10787
- appl. to electrolyte boundary recording 8=5734
- chromel-alumel, for small difference meas. 8=15121
- comparison with resistance and thermistor temp meas. 8=10788
- extreme u.v. absolute detectors, comparison with Ar ionization chamber 8=11162
- gas-filled thermopiles, responsivity 8=15120
- intrinsic, transient response theory and meas. 8=10786
- junction form, and environmental effects 8=10789
- in magnetic field, theory 8=284
- nozzle, for high temp. gases 8=7927
- reactor fuel temp. meas., selection of materials 8=4029
- sapphire rod thermosensor 8=19668
- thermopile, semiconductor, stationary temp. field calc. 8=22685
- Cu-constantan thin film, thermopower 8=22686
- Cu, evaluation for cryogenic meas. 8=19685
- PbTe compatibility with metals study 8=18686
- Pt/Pt₉₀Rh₁₀, optical pyrometer calibration 8=19670
- SnTe compatibility with metals study 8=18686
- Thermodynamic properties**
- See also Critical constants, thermal; Entropy; Heat of reaction; Latent heat.
- acetamide, ideal gas calc. using rotator and harmonic approx. 8=4174
- alkali halides with CsCl structure, and low temp. thermal expansion coeffs. 8=8648
- n-alkanes, binary mixtures 8=16791
- aniline solution in benzene, CCl₄ and chlorobenzene, vap. press. and excess free energies 8=8056
- antiferromagnets in strong mag. fields, theory 8=18369
- atomic absorpt. spectroscopy measuring technique 8=16962
- austenite, alloyed, C activity at 1000° C 8=17008

Thermodynamic properties—contd

butatriene 8=16314
 correlation function near critical point 8=16914
 crystal, Helmholtz free energy, anharmonic contributions 8=8601
 crystals, high press. effects, theory 8=8914
 crystal lattices, ideal and with point defect, harmonic approx. calc. 8=13362
 dielectrics, elastic, thermodynamic pots. at finite deforms. 8=10541
 diethyl phthalate, cryst., glass, liq. 8=1870
 diphenylboron halides, thermodynamic properties 8=1863
 elastic material, no. of parameters 8=50
 enthalpy, charge in rotary kilns, depend on flow rate 8=22108
 enthalpy meas. at low temp. using conduction calorimeter 8=15126
 enthalpy and thermal pot. rel. to Hamilton-Jacobi eqn. for charged relativistic fluid 8=16634
 excess functions, temp. depend. 8=10667
 ferromagnet, dilute, depend. on magnetic atom conc. 8=9307
 fluid mixtures, excess functions 8=4423
 fluid at supercritical temps. 8=12575
 fluids, enthalpies at elevated press. and low temps. 8=21600
 fluids, rel. to refractive index and dielectric constant 8=16615
 force on a dislocation 8=17641
 gas mixtures, strongly ionized, and composition 8=12422
 gases, multi-atomic, temp. dependence formulae derived 8=12674
 haloacetonitriles 8=16323
 heat transfer between an incompressible fluid and a porous medium 8=16821
 Heisenberg ferromagnet, semi-infinite, surface effects 8=2303
 Helmholtz free energy, lower bound calc. using density matrices 8=10647
 high-enthalpy gas flow, stagnation point heat transfer of a solid 8=22140
 holomorphy and phase transitions, scaling law for mag. systems 8=22740
 hydrogen ion solvation by H₂O mols. in gas phase 8=18661
 ice, amorphous → hexagonal, enthalpy changes 8=21846
 ice, square, residual entropy at low temp. 8=4945
 Inconel 600, twin and grain boundaries free energy ratios, from e-micros. exam. 8=17287
 inorganic substances, vacancy formation enthalpy calcs. 8=22176
 Ising model near T_c, second order phase transitions 8=14986
 liquid alloys, activity coeffs. 8=8016
 liquid alloys, effect of electronic and structural parameters 8=12845
 liquid binary alloys, expt. and theory of mixing 8=12844
 liquid binary alloys, model for anal. of enthalpies and entropies of mixing 8=12846
 liquid, convective heat transfer during stabilized turbulent flow in tube at supercritical press. 8=1550
 liquid crystals, review of data 8=1527
 liquids, density meas. as function of temp. with temp. sensitive magnetic float densimetry 8=4544
 liquids, free volume calc., and new parameter $\delta = (3C_v - 1)/2$ 8=4561
 liquid, rotation-induced heat transfer in zero-gravity field 8=4562
 liquids, surface layer, estimate of thickness 8=8047
 magnetization vector diffusion rel. to ang. momentum conservation principle 8=13953
 materials high temp. and determ. of thermal props. at 3500°C 8=4925
 measurement by atomic absorpt. spectroscopy 8=16962
 methylmethacrylate copolymers with methacrylic acid, ht. capacities, 25-190°C 8=1579
 molten salts, ternary mixtures 8=21648
 non-ideal gas, relativistic, from electron gas kinetic eqn. 8=132
 non-vaporizable liquid, initial cooling of tempered metal 8=8044
 organic crystals, from structure 8=13360
 organic crystals, rel. to derivation of oscillation spectrum and charact. temp. 8=17470
 1,2,5-oxadiazole, from i. r. and Raman spectra 8=16335
 oxygen in urania-yttria and urania-lanthana solid solutions 8=13044
 paramagnetic specimen with particles of spin ½, cyclic processes 8=17506
 pentane, enthalpy calc. from Redlich-Kwong eqn. 8=16689
 perfect f. c. c. cryst. lattice, characts. in harmonic approx. 8=4854
 phenylboron dihalides, thermodynamic properties 8=1863
 polar crystals, eqn. of state, linear model 8=13013
 polymers, homo- and graft co-, in soln., intrinsic viscosity and free energy 8=1536
 polyvinylidenechloride, ht. capacity, entropy and free energy studies, 60-300°K 8=1547
 polyvinylchloride, ht. capacity and sp. ht. values from studies at 60-300°K 8=1547

Thermodynamic properties—contd

salt, molten concentration cells, association constants 8=2529
 semiconductors with stoichiometric vacancies 8=17197
 of solid solns., from exam. of diffuse background scattering of X-rays 8=13359
 solids, at contact, temp. field in neighbourhood 8=13364
 solids, diathermance at high radiator temp., obs. 8=1896
 solids, emissivity, integral, 100 to 1100°C, modified calorimetric method 8=13400
 solids, heat resistant, thermal diffusivity, theory 8=13405
 solvation of ions 8=12807
 steam, dissociating 8=7917
 steam, near critical point 8=7920
 superconducting rings, weakly connected, anal. of magnetization 8=13768
 superconductors, fluctuations and quantization 8=17987
 superconductors, in multiple pair-breaking regimes 8=22526
 superconductors, type II, fluctuations of order parameter near upper critical field 8=9032
 superconductors, type II, rel. to volume and press. effects 8=17947
 Teflon 6, immersion heats in hydrocarbons 8=13361
 1,1,2,2-tetrabromofluoroethane, medium effects 8=21181
 thermal props., similarity calc. 8=21646
 thermophysical properties, phenomenological relation 8=16698
 transition metal cpds. rel. to cryst. field calc. 8=4669
 tricyclohexylboron, thermodynamic properties 8=1863
 triphenylboron, thermodynamic properties 8=1863
 US, 1.5°-350°C 8=22848
 vinylchloride, ht. capacity, entropy and free energy studies, 60-300°K 8=1547
 water and aqueous solutions, discontinuities 8=8045
 water at high pressure from ultrasonic propag. meas. 8=21623
 water channel formed by bundle of rods or tubes, heat transfer to 8=12849
 water, Debye temp. calc. from model 8=1544
 Al₂Cl₆, calcs. for ideal gaseous state 8=4143
 AlF₃, anhydrous cryst., enthalpy 273°-1173°K 8=4929
 Al-Fe alloys, Al activity at 1315°C 8=21651
 AlH₃ 8=4928
 Al₂Me₆, calcs. for ideal gaseous state 8=4143
 Al₂Me₂Cl₄, calcs. for ideal gaseous state 8=4143
 Al₂O₃, sintering, activation enthalpy 8=13052
 Ag-Au-Sn liq. alloys, enthalpy interaction coeffs. of Ag and Au, at 723°K 8=21652
 Ag-Bi molten alloys, (segregation system) densities 8=12812
 Ag-Mg solid solns., Ag-rich, long-range order dependence 8=21820
 Ag-Mg solid soln., Ag-rich, short-range order dependence 8=21819
 Ag-Pb molten alloys, (segregation system), densities 8=12812
 AgZnSn, liq. alloys, activity coeffs. 8=8016
 Ar, liquid, calc. 8=8041
 Ar, liquid, C, and C_v calc. using geometric theory 8=8042
 Ar, test gas in ballistic compressor 8=1470
 Au-Cd phase transformations, thermodyn. investigation 8=8263
 Au-Si alloy, enthalpy, specific heat, near eutectic composition 8=1548
 BH₃ 8=7624
 Be₃N₂ vaporization, enthalpy and enthalpy of activation, vapour pressure and evap. coeff. 8=1624
 CH₃ radical 8=7624
 CH₂Cl₂ to 750°K and 200 atm. 8=16819
 CaCl₂-NaCl-H₂O systems, enthalpy 8=12848
 CaF₂ soln. enthalpy 8=21650
 CaO, rel. to water vapour effect on sintering kinetics, 920-1123°C 8=21833
 Cd(ClO₄)₂-HClO₄-H₂O system, saturated solution 8=12847
 Cd-Sb, molten, free energies of mixing 8=12842
 Co, of f. c. c.-h. c. p. martensitic transformations 8=17049
 CoO-Al₂O₃-SiO₂, free energy of reaction of formation of mullite 8=9669
 Cr measurement, influence of small volume changes 8=21508
 Cu, solid, thermal diffusivity meas. 8=1898
 Cu₃Au solid solutions, determ. from short-range order parameters 8=16996
 Cu-Co liq. alloys with dissolved oxygen 8=8011
 Fe, h. c. p., sp. ht., vapour press., lattice stability 8=13371
 Fe-C and Fe-N systems, martensite transformations 8=17075
 Fe-C-Cr solns., liq., activity of C 8=21653
 Fe-Ru alloys, h. c. p., sp. ht., vapour press., lattice stability 8=13371
 GaAs vaporization at 900-1200°K enthalpies from vapour pressure meas. 8=4664
 H₂, thermodyn. activity in α -Zr, Zircaloy-2 and Zircaloy-4 8=8249
 H₂, solid, ortho, near 0°K 8=8233
 H₂O rel. to liquid structure and H bonds, n scatt. meas. 8=1525
 H₂O¹⁸ and D₂O¹⁸, relax. parameters calc. 8=12780
 He, b. c. c. crystals, and phonon freq. calcs. 8=1836

Thermodynamic properties - contd

- He, enthalpy calc. from Redlich-Kwong eqn. 8=16689
 He liquid, quantized circulation, evidence from torque on cylinder 8=10808
 He, test gas in ballistic compressor 8=1470
 He II, lowest state of free energy obtained during rotation 8=10812
 He³-He⁴ solutions, at λ -transition, n.m.r. studies 8=10794
 He⁴ liquid 1.25-4.2°K, 0.5-28 atm 8=10802
 Hg, liq., press. depend. of phonon dispersion 8=16879
 In-Bi, molten, free energies of mixing 8=12842
 In-Sb, molten, free energies of mixing 8=12842
 K-graphite system lamellar cpds. 8=4712
 K, natural convective boiling 8=12013
 KAlSi₃O₈, enthalpy of fusion 8=21753
 KBr, of inert-gas diffusion and release behaviour 8=22156
 KBr self-diffusion, activation entropy and enthalpy from elec. cond. 8=8679
 KCl, of inert-gas diffusion and release behaviour 8=22156
 KI, of inert-gas diffusion and release behaviour 8=22156
 KCOF₃, 80°-300°K 8=17519
 K₂ZrCl₆, from 25°C to above m.p. 8=8640
 Li plasma, composition, enthalpy, specific heats, apparent molecular weights and velocity of sound 8=12462
 Li₂HfCl₆, from 25°C to above m.p. 8=8640
 Li₂ZrCl₆, from 25°C to above m.p. 8=8640
 N₂, enthalpy calc. from Redlich-Kwong eqn. 8=16689
 N₂-hydrocarbon mixtures, enthalpy calc. from Redlich-Kwong eqn. 8=16689
 NH₃, enthalpy calc. from Redlich-Kwong eqn. 8=16689
 NO, 200°-2000°K and at 1000 bar 8=7918
 NSCl, molar thermodyn. functions, i.r. spectra obs. 8=4161
 Na, natural convective boiling 8=12013
 NaAlSiO₃, enthalpy of fusion 8=21753
 NaK liq. alloys, excess entropies and Gibbs energies and ordering 8=12843
 Na₂ZrCl₆, from 25°C to above m.p. 8=8640
 Nb, conductivity, temp. coefficient dependence on temp. 8=13387
 NbC, stoichiometric, 500 to 2400°K 8=13366
 NbCl₅, calc. from spectra 8=14249
 Ni, solid, thermal diffusivity meas. 8=1898
 Ni, twin and grain boundaries free energy ratios, from e-micros. exam. 8=17287
 NiO, stoichiometry 8=13826
 NiSiF₆·6H₂O, thermodynamic temp. below 0.35°K 8=8641
 Pb, liquid, containing Ag, Au or Pt 8=8043
 Pb, solid, thermal diffusivity meas. 8=1898
 Pb-Ag system, galvanic cell studies using PbO-SiO₂ melts 8=23150
 Pb-Bi, molten, free energies of mixing 8=12842
 P₄S₁₀, 273°K to 720°K 8=4933
 Rh-Hg system phases 8=8280
 S₈ 8=12227
 S vapour, meas. 200-400°C 8=21512
 Se vapour 8=4659
 SiF₄, calc. from i.r. spectrum 8=16301
 Sn-Bi, molten, free energies of mixing 8=12842
 TD-nickel, twin and grain boundaries free energy ratios, from e-micros. exam. 8=17287
 Ta, conductivity, temp. coefficient dependence on temp. 8=13387
 TaC, heat content values, entropy, specific heat 8=8643
 α -Ti/H₂(D₂) system, thermodynamic props. 8=21858
 UH_{3-x} solid soln. rel. to comp. and temp. 8=8190
 <U, H> solid soln. rel. to comp. and temp. 8=8190
 UN, and equil. N pressures over UN_(s) + U_(l) system 8=18646
 UO₂, solid, thermal diffusivity meas. 8=1898
 WC, heat content values, entropy, specific heat 8=8643
 Zn in ϵ -phase Ag-Zn alloys, activity dependence on density of states of conduction electrons 8=22109
 Zn sulphides, standard free energy of formation 8=9712
 ZrC, stoichiometric, 500 to 2400°K 8=13366
 α -Zr-H and α -Zr-D solid solns. 8=8252

Thermodynamics

- See also Atmosphere/thermodynamics; Entropy;
 Equations of state; Statistical mechanics.
 analogy for transport processes 8=6098
 averages, <A, A'>, bounds 8=2978
 Boltzmann's H theorem, standardization of terms 8=10665
 Bose gas mean critical point 8=19459
 Carathéodory system, flow in absolute temp. treatment 8=93
 cascade production of low temp. 8=10792
 Clausius-Clapeyron eqn., derivation 8=10668
 critical point, liq.-vapour systems 8=16916
 Curie theorem, short proof 8=19468
 dense plasma 8=21304
 diffusion coeffs., solid-fluid mixture 8=19480
 dilution, heat of, derivation 8=110
 electron diamagnetism, case of inhomogeneous mag. moment 8=17896
 electron gas, state with broken geometrical symmetry, existence 8=19465
 entropy increase, principle 8=108
 entropy and temp. in equil. stat. mech. 8=107

Thermodynamics-contd

- evolution criterion of Glansdorff and Prigogine, statistical derivation 8=6097
 expansion, adiabatic, of mixture of two phases 8=10662
 fluctuations in continuous medium, space time dependent 8=6103
 fluid, classical with Lennard-Jones pot., correlation function 8=12576
 γ , comment on determination 8=10664
 gas flow into vacuum with exponential boundary temp. 8=4458
 gas mixture in field of bulk forces, equil. 8=6111
 gas-solid system, polytropic changes 8=4472
 gases and mixtures, props. calc., correl. of corresponding states law 8=16697
 Gibbs-Duhem relation, useful consequence 8=15008
 Green's functions, zero-freq. behaviour 8=113
 Gyarmati principle and canonical equations 8=10633
 hard-driven system, exact methods, application to dynamic relaxation phenomena 8=19469
 heat, temperature and internal energy, review 8=10764
 Heisenberg ferromagnet 8=13984
 of intermolecular interactions 8=3002
 irreversible, for anal. of liquid/vapour phase charge 8=21766
 irreversible, of hydromagnetic energy conversion 8=345
 Ising-Lenz model solns. and appls., review 8=10612
 Joule-Thomson porous plug expt. analysis rel. to classical relativity 8=6061
 kinetic gas theory, relativistic Onsager relations 8=21500
 least-squares curve fitting tech., problem and appls. 8=19451
 linear response to arbitrary thermal perturbation 8=2969
 metal surfaces, passivity theory 8=9702
 of nonlinear mats. with internal state variables 8=112
 Onsager relation, generalization for high order symmetries and their invariance 8=96
 phase transformations, density fluctuation at critical points, Yang and Lee theory 8=10620
 plasma, dense, electron-ion reflection 8=7736
 potential temperatures, formulae for different types 8=9823
 quantum distribution functions, temp. dependence 8=10618
 reciprocal relations, higher order 8=109
 relativistic, ambiguity of pressure concept 8=6102
 relativistic, form of second law 8=6062
 relativistic, reversible and irreversible processes in a fluid 8=10632
 relativistic, temperature definition 8=10785
 relativistic, thermodynamics conservation of energy 8=3001
 relativistic, transformation formulas for temp. and heat 8=19444
 scaling laws generalization to dynamical props. near critical point 8=2346
 second-order transitions, solid-state 8=1668
 stars, while dwarfs energy content and cooling rate 8=10134
 statistical mechanics and thermodynamics, conference Copenhagen Denmark (1966) 8=15007
 superconductors, type II 8=13735
 temperature and special relativity, $T=T_m/\beta$ 8=14964-5
 thermoelectric systems, single stage 8=10844
 teaching suggestions 8=2983
 Ar solution in water-methanol system 8=12809
 GaP-Cl₂-H₂ system, vapour transport in open tube, thermodynamics 8=12699
 He boiling point, temp. scale 8=19689
- applications
 adsorption isotherms, analysis 8=13102
 betatron acceleration of trapped radiation by geomag. storm, adiabatic 8=2645
 cosmology, instabilities in expanding universe 8=10080
 critical point, fundamental problems 8=12962
 crystal surface classification, and ang. depend. of free surface energy 8=8377
 earth's upper mantle, low velocity zone, density and temp. distributions 8=14553
 electrolyte solns., isothermal vector transport 8=8046
 ferromagnetic, ideal, using diagram technique 8=5442
 flow, slow viscous, extremum principles for and application to suspensions 8=1449
 fluid with deforming microstructure, governing eqns. 8=12577
 gas mixtures, diffusion with internal degrees of freedom 8=21528
 gases, equilibrium, approach through black-body radiation interaction 8=12673
 heterogeneous flow systems, 2nd law 8=12595
 homogeneous nucleation theory 8=23278
 m.h.d. convertor, molten metal mixing cycle 8=294
 melting and crystallization of mixtures 8=4643
 particle motion in dipole field, mag. moment adiabatic invariant 8=2649
 phase transformations, deceleration near crit. point 8=8162
 photoluminescence, limit yield 8=12126
 plasma, relativistic, momentum distribution after adiabatic compression 8=7731

Thermodynamics—contd**applications—contd**

- shock adiabats, discontinuous 8=165
- spinodal decomposition in multicomponent system, thermodynamic conditions 8=4700
- systems analysis using thermodynamic and nonlinear circuit eqns. 8=26
- CH₄-O₂ mixtures, combustion products, equilibrium calc. 8=14393
- H₂O₂ decomposition 8=1466
- He II, rotating, superfluid velocity rel. to temp. 8=6231
- Zn corrosion in CO₂ solns., rel. to predominance diagrams 8=2523

Thermoelasticity

- acceleration waves in elastic material of finite thermal, and infinite elect. conductivity 8=15042
- appl. to i.r. radiometric stress meas. 8=8794
- asymmetric, variational (Reissner), potential energy, complementary work theorems 8=64
- coupled thermoelasticity, continuity at wave fronts 8=10577
- critical states of instability and spectrum of isentropic bending-torsion vibrations 8=14957
- elastic half-space, stresses 8=14958
- generalized dynamical theory using heat transport equation 8=10578
- Helmholtz and Green theorems 8=2932
- linear, hyperstresses 8=10579
- medium with 2 spherical cavities, axisymmetric anal. 8=19407
- micro-materials, equations derived 8=2931
- stress analysis of composite cylinder, book 8=19408
- stress analysis, energy-derived difference eqns. 8=19406
- stress distrib. in sandwich plate with rigid core 8=2040
- stressed materials, and elastic constants comparison 8=2036
- stresses on edge of semi-infinite strip of anisotropic material, with 2 infinitely long sides insulated 8=19405
- stresses in plate with transversely isotropic material 8=2930
- triacetylcellulose, plastified, thermomech. curves of elongation at const. strength 8=22407
- waves, non-coupled, particular soln. of nonhomogeneous fundamental set of eqns. 8=10576

Thermoelectric conversion. See Electricity/direct conversion.

Thermoelectricity

See also Thermocouples.

- alkali metals, solid and liquid, thermopower pressure depend. 8=9010
- aqueous bromide solns. 8=4557
- carriers, hot, effect analyzed as Bernoulli effect 8=13629
- circular foil radiometer, peculiarities in stationary regime 8=19626
- dielectric solids, ionic thermocurrents rel. to meas. relax. effects. 8=5346
- eddy currents in anisotropic plates 8=5386
- electrolyte thermocells, flowing, gravity effect 8=14416
- graphite, props. of well oriented crystals 8=5384
- heat pump optimization 8=18217
- heat transfer from a pile to liquid flows past hot and cold junctions 8=4567
- ice, effect on atmospheric electricity 8=14625
- liquid alloys, absolute power rel. to temp. and comp. 8=12913
- liquid metals, polyvalent, absolute thermoelec. power 8=16881
- low-temp. behaviour, research in USSR 8=19681
- metals, thermoelectric power, higher approximations 8=13901
- molten salts, possibility for use in thermoelectric generation 8=22677
- Nernst-Ettingshausen effect rel. to magnetoresistance 8=9082
- power generation, review 8=19733
- p-quaterphenyl polycrystals, thermally stimulated currents 8=13906
- rare-earth sesquisulphide crystals. 8=9119
- semiconductor, degenerate, absolute power rel. to impurity and chem. pot. 8=18207
- semicond., photothermoelec. and thermally stimulated effects, rel. to photoelectronic anal. technique 8=22678
- semiconductor, power in strong elec. field 8=18209
- semiconductors in mag. field, phonon-drag Seebeck effect, quantum theory 8=9236
- semiconductors, organic, power meas. in metal chamber 8=9092
- semiconductors, thermoelectric power in strong transverse field 8=9236
- single stage systems, thermodynamics 8=10844
- superconductors, thermoelectric effect 8=22679
- thermionic conversion specialist conference 8=19731
- thermoelements, for semicond. device cooling, new appl. 8=22684
- thermogalvanomagnetic phenomena, quantum theory 8=18208
- thermopile, semiconductor, stationary temp. field calc. 8=22685
- trace characterization in metals by thermopower meas. 8=18757

Thermoelectricity—contd

- wüstite, Seebeck coeff. rel. to p to n transition, grain size and Mg doping dependence 8=5387
- Ag alloys, thermopowers interpret. rel. to resistivity and band structure 8=18213
- Al, power, high press. effects, and elec. resist. 8=13902
- Al, pure, thermopower meas. rel. to electronic diffusion and phonon drag contributions 8=5382
- Ag₂S_{1+x} melt, thermoelec. power dependence on S vapour pressure above melt 8=16876
- α-Ag₂S mixed conductor, thermoelectric power meas. rel. to electronic props. 8=22500
- Au films, thin, and ohmic props., -100 to +100°C in ultrahigh vacuum 8=22513
- Au, power, high press. effects, and elec. resist. 8=13902
- Au-Hg alloys, liq., abs. power rel. to temp. and comp. 8=12913
- Au-V alloys, thermoelectric power, near Kondo temp. 8=8992
- B, polycryst., thermopower and resist. temp. and press. effects 8=18210
- Bi, e. m. f. increase due to phonon dragging 8=22435
- Bi, magneto-Seebeck effect 80°K, effect of surface recombination 8=18211
- Bi, thin films, power and elec. resist. 8=5383
- Bi, 300-540°K 8=13710
- Bi, Sn and Te doped, solid and liq. phase boundary, Peltier coeff. 8=9238
- Bi₂Se₃-Bi₂Te₃, props. of cryst. and pressed powder 8=18212
- Bi₂Te₃ alloys sintered, Seebeck coeff. 8=21922
- Bi₂Te₃-Bi₂Se₃ alloys, n type, properties 8=9237
- Bi₂Te₃-PbTe alloys, thermoelect. power, low temp. 8=22680
- CdCr₂Se₄, ferromagnetic, Seebeck effect 8=2189
- Cd-In alloys, liq., abs. power rel. to temp. and comp. 8=12913
- CoO:Li, Seebeck-effect, thermogravimetric effect, high temps. 8=1956
- CdS, conductivity, thermally stimulated, influence of electric field 8=9239
- CdS, photothermoelec. effects 8=22681
- CdS-SiO₂ film devices, "frozen" cond. and thermo-stimulated currents 8=5388
- CdSb, conversion efficiency 8=2254
- CdSb, eddy currents in single crystals. 8=5386
- CdSb, investigation 8=13698
- Cd_{3-x}Zn_xAs₂, 80°-400°K, meas. 8=5385
- Cd_{1-x}Zn_xS, mixed single crystals, rel. to comp. and defect nature 8=18227
- CoO, paramagnetic, Seebeck coeff. and anomalous Hall effect 8=17914
- Cr alloys, antiferromagnetic, power 8=18374
- Cr-Fe alloys, Cr rich, Seebeck coeff. and antiferromag. ordering rel. to energy changes 8=8931
- Cr selenides, power, and elec. and thermal cond., lattice parameters 8=13703
- Cu alloy, dilute, phonon-drag power 8=18214
- Cu alloys, thermopowers interpret. rel. to resistivity and band structure 8=18213
- Cu, 99.999% pure, Seebeck coeff., 78-400°K 8=22134
- Cu, thin films, thermopower size-effect for determination of electronic structure 8=13903
- p-Cu₂S, power, elec. cond. and Hall effect 8=22585
- FeCr₂Se₄, thermoelectric power, rel. to d-orbital interaction clarification 8=5391
- Fe-Cu ferrites mixed conduction mechanisms from resistivity and Seebeck meas. 8=18035
- α-Fe₂O₃, paramagnetic, Seebeck coeff. and anomalous Hall effect 8=17914
- Ga liquid, structural sensitivity 8=16878
- GaSb-GaAs alloy, pressure-sintered, densification and thermoelectric props. 8=4697
- GaSb-InSb alloys, Seebeck coeff. at high temps. rel. to comp. and impurity doping 8=4944
- Ge, piezothermal, e. m. f. anisotropy 8=5390
- Ge, thin films, Seebeck coefficient 8=2255
- Hg alloys with In, Tl and Na, liq., abs. powers 8=12913
- In liquid, structural sensitivity 8=16878
- Li₂SO₄, power of high-temp. modification 8=18169
- Mn ferrites, Seebeck voltage and elec. cond., influence of Mn²⁺ clustering 8=13720
- Na_{0.33}V₂O₆, single cryst. 8=22601
- NaCl single crystals. 8=2256
- Ni, high press. effects, and elec. resist. 8=13902
- NiCr₂Se₄, thermoelectric power, rel. to d-orbital interaction clarification 8=5391
- Ni-Cu solid solns., and resist. rel. to temp. and Cu % 8=5389
- Ni₃Ge alloy, thermoelectric power in range 77°K < T < 1300°K 8=18215
- NiO, neutron irradiation effect on Seebeck coeff. 8=18058
- NiO, paramagnetic, Seebeck coeff. and anomalous Hall effect 8=17914
- Ni-Si alloys, thermal e. m. f. and reflection coeff. 8=18551
- PbSe, rel. to forbidden band width 8=5272
- p-PbTe, Hall mobility and thermoelectric power rel. to Na doping 8=5274
- PbTe-PbS solid solution, n-type, power temp. and pressure dependence 8=18061

Thermoelectricity—contd

- PbTe-Sb₂Te₃ alloy system, props., and phase relations 8=4716
- Pd alloys, thermoelec. power meas. 2-120°K 8=18216
- PdNi alloys, power anomalies 8=13904
- Pt alloys, thermoelec. power meas. 2-120°K 8=18216
- Pt, high press. effects, and elec. resist. 8=13902
- Sb, Seebeck coefficient and Fermi surface 8=22467
- Se, trigonal, thermally stimulated currents after u.v. irradiation 8=22683
- Si, piezothermal e.m.f., anisotropy 8=5390
- Si, Seebeck coeff. from 100 to 1300°K 8=22136
- Si-Ge alloy props. and generator modules prep. 8=19732
- SnTe, properties, effect of small Sn substitutions by Nd 8=13905
- SnTe-Bi₂Te₃ alloy system, props., and phase relations 8=4716
- Te_{1-x}Se_x alloys, liq., 0<X<0.5, power rel. to electron states 8=12918
- ThC₂, nonstoichiometric, power 8=2140
- ThN_x, (x = 1, 3; y = 1, 4), thermoelectric power rel. to electronic props. 8=2139
- UO₂, thermal cond. and Seebeck coeff. obs. 8=8665
- VCr₂Se₄, thermoelectric power, rel. to d-orbital interaction, clarification 8=5391
- Zn-Bi alloys, solid and liq. thermo-e.m.f. 8=9240
- Zn_{1-x}Cd_xSb, conversion efficiency 8=2254
- Zn_{1-x}Cd_xSb, power rel. to conc. of acceptors and temp. 8=2131
- ZrO₂ between O₂ electrodes, thermoelec. power 8=9241
- ZnSb and ZnSb-CdSb mixed crystals, investigation 8=13698

Thermoluminescence

- alkali halides, inactivated, and radioluminesc., obs. 8=9592
- alumina, γ -irrad. pure, and magnesia-doped 8=5652
- aluminophosphate glasses, radiocolouration and luminescence kinetics 8=1996
- apparatus, controlled heater 8=18585
- boric acid glass, solvated electrons rel. to aromatics photo-oxidation 8=23160
- glasses, aluminosilicate, gamma-irradiated, spectrum 8=18614
- inorganic cpds. during phase transitions 8=23040
- moon, obs. and theory 8=23650
- phenanthrene-d₁₀ in solidified solvents 8=23070
- quartz, influence of X-ray irradiation 8=13871
- radio, electronic instrument for research 8=9585
- rubber, study of transition temps. by radio-thermoluminesc. 8=13077
- Al silicates, irradiated 8=23044
- CaF₂ rel. to calcination and X-ray dosage, obs. 8=14305
- CaF₂:Gd³⁺, Stark splittings of ⁶P_{7/2} and ⁶P_{5/2} levels 8=14310
- CaO, unirradiated 8=14308
- Ca(OH)₂, unirradiated 8=14308
- CdI₂, curves, use of computer anal. 8=5659
- LiF dosimeter for radiobiological work 8=14890
- LiF, fading after γ doses 10-10³ rad. 8=14321
- LiF, fading characteristics and appl. dosimetry 8=14295
- LiF, response to n γ reactor fluxes 8=20899
- LiF, thermal activation energies 8=18609
- NaCl, thermal activation energies 8=18609
- NaCl:Ag, Sr phosphors rel. to F centre destruction 8=17687
- NaF, thermal activation energies 8=18609
- NaI, capture centres, heat treatment in O effects, obs. 8=23060
- NaI(Tl), after X-ray excitation at low temp., recomb. luminesc. 8=18611
- NaI: Tl capture centres heat treatment in O effects, obs. 8=23060
- NaPO₃, γ irradiation effect 8=22234
- ZnS+Cu, Cl, luminance and complex dielectric constant, comparison 8=13875
- SiC crystals, deduction of energy spectrum of acceptor states 8=5668
- ZnTe, melt-grown, flash-like 8=5680

Thermomagnetic effects. See Magnetothermal effects.**Thermometers**

- See also Pyrometers; Thermocouples.
- acoustical for reactor fuel 8=4018
- cryotron relaxation oscillator, possibility 8=22571
- gas, at high temp. 8=244
- gas pressure temp. coeff. meas. 8=7922
- inductance 8=19667
- low temp., use of Josephson line-width from point contact 8=2181
- quartz, high sensitivity rel. to piezoelectric effect 8=6220
- solid acoustic thermometer 8=19664
- ultrasonic resonance, for virtual air temp. meas. 8=246
- resistance
- photogalvanometric precision instrument 8=19669
- self-heating, determination 8=6219
- C, negative magnetoresistance 8=19666
- Ge, below 1°K 8=19665
- Ge, thermal time consts. at liq. He temp. 8=15119
- Ge, As-doped, for temp. range 2.1 to 5°K 8=247
- Pt bridge thermostat for $\pm 25\mu^\circ\text{C}$ 8=15123
- Pt, evaluation for cryogenic meas. 8=19685
- Si, possibility for use at liq. He temps. 8=248

Thermonuclear devices. See Plasma/devices.**Thermonuclear reactions**

- See also Elements/origin; Nuclear fusion.
- beam systems for 8=16139
- capture data at stellar temps. 8=5872
- control, problems of plasma instabilities 8=12561
- fusion device, possibilities of ring-current configurations 8=21373
- fusion, origin of elements 8=23471
- fusion reactor leakage problem 8=7318
- heavy elements synthesis in stars, n radiational capture 8=10143
- heavy ions in stellar interiors 8=10151
- heavy particle disintegration at high temperatures 8=11978
- neutrinos, supernovae explosions 8=2790
- in plasma θ -pinch, n yield and laser scatt. obs. 8=1399
- s-process nucleosynthesis in thermal relaxation cycles 8=10144
- stellar, H mixing by He-shell flashes, calc. 8=10145
- stellar synthesis of heavy elements 8=10140
- white dwarfs, critical temp. 8=10150
- B and Be, in information in expanding hot universe 8=5840
- Be as target nucleus, reaction rates 8=11976
- Be⁹(a, n)C¹², stellar rates of 8=19131
- C¹³(a, n)O¹⁶, stellar rates of 8=19131
- D-T gas mixture, propagation of thermonuclear detonation wave 8=21482
- H and He, as target nucleus, reaction rates 8=11976
- He shell-burning stars, rel. to pulsational instability 8=5873
- Li in formation in expanding hot universe 8=5840
- Li as target nucleus, reaction rates 8=11976
- Si burning, nucleosynthesis, model 8=16136
- Tc⁹⁹ disintegration probability in red giants 8=2780
- Tc synthesis, at different steps of stellar evolution 8=2779

Thermopiles. See Thermocouples.**Thermostats**

- See also Cryostats.
- continuously adjustable, for temp. range 0 to 250°C 8=249
- controlled heater for thermoluminescence expts. 8=18585
- temp. controller for n.m.r., -185 to +350°C 8=19907
- transistorized regulator for vib. quartz micro-balance 8=19671
- water bath with $\pm 70\mu^\circ\text{C}$ stability 8=15124
- Pt resistance bridge circuit for $\pm 25\mu^\circ\text{C}$ 8=15123

Theta pinch. See Plasma/confinement.**Thickness measurement**

- See also Particle size.
- diffusion pump fluid film, spectrophotometry 8=16728
- for film growth monitoring, computer-operated following ellipsometer 8=6562
- films, metallic, Leonard and Ramey (conductivity and Hall voltage meas.) method anal. 8=17119
- films, solid, X-ray meas. 8=14482
- films, thin, piezoelectric crystal-type instrument 8=21871
- film, thin X-ray interferometry 8=8301
- films, transparent, by interferometry 8=1692
- films, transparent thin (10-600 nm), simple non-destructive interferometric method 8=8302
- gauge, using scatt. γ -rays and Geiger-Muller counter 8=19345
- glass plates, small changes with precise interferometry 8=14223
- lathe section, capacitor method, applic. to diffusion studies 8=19346
- liquid surface layer, thermodynamics 8=8047
- plasma, turbulent, skin layer by h. f. probe 8=7769
- thin dielectric films 8=1690
- of thin transparent films, method 8=8300
- wax film on painted surface by reflectance 8=2470
- Al films, osc. quartz cryst. type monitor 8=17118
- Al₂O₃, films, by tunnel emission and capacitance 8=8312
- Ni-Fe films, vacuum-deposited, by elec. resistivity method 8=17135
- SiO₂ films on Si, < 900 Å, meas. with reflection tech. 8=13093
- SiO₂-Si₃N₄ thin film, optical 8=1699

Thirring model. See Elementary particles; Field theory, quantum.**Thixotropy**

- hysteresis experiments near max. flow resistance 8=7860
- polymer solns., shear stress charges 8=8023
- poly(methyl methacrylate) in θ solvents 8=16758

Thomas-Fermi method. See Atoms/structure.**Thomson effect. See Thermoelectricity.****Thorium**

- in atmosphere, exhalation changes rel. to conc. and conc. of decay products 8=9891
- creep, during fission 8=8866
- desorption from W by high energy electrons 8=1712
- Fermi surface from de Haas-van Alphen studies 8=2294
- isotope shift constants 8=16234
- radioactive, abundance in crystalline shield rocks 8=9794
- spectrum, 1-2.5 μ emission 8=12074
- thermionic emission in Cs vapour meas. by plasma-anode tech. 8=18264
- tracer-level diffusion in pyrolytic C, rel. to structure 8=1915

Thorium—contd

- Th²³⁰ dating of Quaternary samples 8=9797
 Th(IV) ions, sublation studies, by radioactive tracers 8=23075
 U/Th ratios, upper mesozoic graywackes, California north 8=2565

Thorium compounds

- oxides, u. v. transparency, temp. depend. and effect of Cl⁻ and NO₃⁻ 8=5605
 phosphides, prep. 8=23116
 refractory, charact. temps. and entropies, meas. 8=13379
 thorium gel, crystallite size obs. 8=12960
 Th(IV), sulphosalicyclic acid chelates of, u. s. velocity and adiabatic compressibility lowering 8=8633
 ThC₂, nonstoichiometric, electrical properties 8=2140
 ThCu₂Si₂ single crystals. 8=4777
 Th_xN_{3-y}, (x = 1, 3; y = 1, 4), elec. props. rel. to electronic states 8=2139
 ThO₂, addition to Y₂O₃, inhibition of grain growth during sintering 8=13444
 ThO₂, determ. of Dy, Eu, Gd, Sm impurities 8=18787
 ThO₂, e.p.r. of Yb³⁺, stress effects 8=14128
 ThO₂, molec. geometry 8=7550
 ThO₂ single crystal growth for laser and optical components 8=1740
 ThO₂-Mo cermet, cathodes thermoemission constants at high temp. 8=13932
 Th-Pu system, phase diagrams, peritectic and eutectoid of transform S 8=21854

Thulium

- crystalline elec. field determ. by Mössbauer effect 8=8203
 total reflection of 8.4 keV γ -radiation of Tm¹⁶⁹ 8=23018
 Tm³, energy transfer in Na rare-earth tungstates 8=9610

Thulium compounds

- TmFeO₃, antiferromag. ordering, variation with temp., 1.6°K-94°K 8=22859
 TmFeO₃, hysteresis loop study of temp. induced spin flop 8=14048
 Tm₂Fe₂O₁₂, magnetostriction anomalies, 4.2-100°K and < 25 K Oe 8=18364
 TmN, crystal field, exchange effects, e.p.r. study 8=2376
 Tm₂O₃, total reflection of 8.4 keV γ -radiation of Tm¹⁶⁹ 8=23018
 TmT₂ (T = transition element), Mössbauer effect determ. of cryst. electric field splittings 8=16979

Thunderstorms

See also Lightning.

- acoustic spectrum, dominant 200 Hz peak 8=18909
 charge generation and separation, model requirements 8=2586
 discharges, ground and intracloud, K changes, audio spectra 8=9885
 electricity distribution, effect of particle interactions 8=18891
 frequency and velocity obs. 8=23292
 ice growth in supercooled aqueous solns., electrical effects (lab.) 8=21762
 lightning, Monte San Salvatore obs. 8=23293
 non-disruptive electric currents, theory 8=2585
 radio noise effects, book 8=19005
 NO₃⁻ ions in precipitation, electrification role 8=23290

Thyratrons. See Gas-discharge tubes.**Tides.** See Atmosphere/movements; Ionosphere; Oceanography.**Time interval measurement**

- chromatographs, electronic method 8=14451
 differences in range milli- to picosecs, appl. to electronics of oscilloscope 8=3138
 meteoroid masses frequency distrib. rel. to freq. distrib. of radar echo duration 8=5960
 microcatalytic reactors, electronic method 8=14451
 microwave beam pulsing system of nuclear energy level lifetimes 8=7058
 pendulum apparatus, electronic temperature control system 8=10480
 pendulum period, electronic system, \pm 600 ns. 8=10481
 pendulum period, using phototransistor output triggering oscilloscope 8=10479
 phase locked pulsed oscillator method 8=14922
 photomultiplier pulse processing 8=6665
 pulse interval meas. 8=6666
 signals reception at l.f., receiver 8=8
 two readings, optimal correspondence choice rel. to meas. device 8=2875

Time measurement

- atomic clock, annual variation 8=19350
 atomic freq. standard, appl. to radiotelescope interferometry 8=10440
 atomic scales, accuracy of standards 8=10484
 bridge oscillator freq. stabilization 8=3145
 Conference on definition, realization and use of time and frequency London 1967 8=10
 Ephemeris time corrections rel. to revised lunar theory 8=10485
 Ephemeris and Universal time difference by lunar photography 8=10486
 frequencies up to 345 GHz 8=6401
 frequency, design of 2.5 MHz standard 8=19351

Time measurement—contd

- frequency multiplier, phase-locked 8=2877
 frequency of 118.6 μ m water-vapour laser transition 8=10482
 frequency standard servo-system 8=9
 meridian passages, photoelectric micrometer 8=10104
 photomultiplier, resolution improved with fast discriminator 8=6330
 satellite, minimum distance from observer, digital device 8=19069
 scintill. photomultiplier system 8=3459
 synchrotron, radial betatron oscill. freq. 8=20235
 transmission time for e. m. waves along coaxial cables 8=6395
 tuning-fork escapement regulator, optimization of design parameters 8=14921

Tin

- atmosphere, H Ly- α and - β emitting layers e temp. and density from line intensities 8=10390
 atoms, electron-impact ionization cross-sections 8=12428
 atom, photoelectric cross-section for K-Mv subshells for X-rays 412-1332 keV 8=7438
 atoms, on silica gels and zeolite, states and dynamics 8=16912
 $\beta \rightarrow \alpha$ transformation 8=21856
 brittle rupture during contact melting with multi-component eutectics 8=8832
 collective motions of atoms in liq. state, compared with polycryst. solid 8=12796
 crystals growth by Webb-dendrite method 8=4824
 cyclotron resonance at 9.5 Gc/s obs. in (010), (110) and (001) planes, in inclined mag. field 8=22489
 e-diffraction reflection anomalies in low-pressure condensation explained 8=13154
 diffusion coeff. of Ag¹¹⁰ 8=22162
 doped, superconductivity, us. attenuation studies 8=22572
 effect of small amounts on self-diffusion of Fe in γ -phase 8=1930
 electrodeposited, whisker growth 8=17251
 electrodes in alkaline solns., passivation by oxidation studies 8=18733
 electronic struct. in cpds. rel. to Mössbauer spectra 8=12233
 evaporation from Fe-Sn alloys at 1600°C under vacuum 8=12993
 films, Ge coating effect on transition temp. 8=5214
 films, obliquely deposited, struct., effect of atom mobility 8=8296
 films, in u. v., reflecting power, optical consts. and dielectric consts. deduced 8=5638
 freezing pt, as fixed pt. 8=244
 grey, phonon spectrum from inelastic scattering of cold neutrons 8=4905
 impurity addition to steel, effect on temper brittleness 8=17797
 isotope neutron scattering amplitudes from powder patterns of SnO₂ 8=1809
 K-ionization by relativistic electron theory 8=4994
 Knight shift oscillatory field dependence 8=5566
 liquid, metal solute diffusion, theory 8=12832
 mass ejection by laser pulse 8=8759
 melting point, particle size dependence 8=16925
 nuclei in Mn ferrite, mag. field at nuclei, Mössbauer effect studies 8=9382
 in organo-Sn cpds., bonds with Co, Mn, Mo and Re, Mössbauer obs. 8=4668
 polycrystalline films, influence of annealing on block structure charact. 8=4741
 pure and Cd-doped, thermal conductivity, effect of superconducting energy-gap 8=4942
 recrystallization, autoradiography 8=13142
 resistance temp. depend. and supercond. transition temp., undergrad. meas. 8=254
 self-diffusion, radioactive tracer absorpt. obs. 8=22161
 solubility in liquid Na 8=21621
 superconducting, critical fields, 0.1-4°K, pressure effect up to 30 k atm 8=5212
 superconducting film and bulk Nb, microwave-photon assisted tunnelling 8=17975
 superconducting film, nonlinear effect at about 10 GHz 8=22562
 superconducting point contact electrode for microwave generation and detection 8=22570
 superconducting, quantum phase fluctuations at onset of long-range phase coherence 8=22561
 superconducting resistance jump at superconducting to intermediate transition rel. to London model 8=17973
 superconducting, superheating in cylindrical samples 8=22564
 superconducting, surface impedance, mag. field dependence, anomalies 8=9054
 superconducting, u. s. absorpt. 8=5213
 superconducting whisker, intrinsic thermodynamic fluctuations from depressions of supercurrent and T. 8=22560
 superconductive, irreversible magnetisation obs. 8=2160
 type I superconductors intermediate state statics and dynamics 8=5204

Tin—contd

- u. s. absorption, longitudinal, by electrons, near supercond. transition 8=4924
- whiskers and filamentary growths on film due to d.c. 8=13145
- white tin films, optical data analysis over 0.1 to 27.5 eV energy region 8=2456
- Fe-Sn systems, α - γ equilib. 8=4709
- in GaAs, resistivity, Hall effect and lattice parameter meas. 8=2191
- β -Sn, crystal dynamics at 110°K 8=4907
- Sn crystals grown from Pb-Sn solder, in electrotransport processes 8=8433
- β -Sn, group-theoretical vibrational analysis 8=4906
- Sn^{113,129} diffusion in Ni, obs. 8=17579
- Sn¹¹⁹ nuclei, impurity in semiconducting cpds., isomeric shift 8=9086
- Sn¹¹⁹ in USn₃, n.m.r. rel. to interband mixing effects 8=18474
- Sn-Pb Josephson junctions, radiation threshold absorption, mag. field depend. 8=22569
- Sn-Pb superconducting tunnel junctions, I-V characts. and 3-cm characts. emission 8=17981
- Sn-Pb and Sn-In solder joints, thermal transport near 0.1°K 8=5203

Tin compounds

- alloys, dilute, microsegregation nodes and cellular solidification substructures 8=16919
- electronic struct. rel. to Mössbauer spectra 8=12233
- fluorinated organotin cpds., n.m.r. spectra 8=12318
- fluoro- and hydroxyfluoro-compounds and thermal polymerization products, i.r. vibr. freqs. of Sn-O-Sn bond 8=4170
- oxide films, electron emission from high resist. regions 8=22713
- triphenyltin pentacarbonyl manganese, structure 8=8594
- H₂SnO₃ conversion to SnO₂, kinetics, Mössbauer obs. 8=14386
- KF-SnF₂-H₂O system 8=4781
- with O, S, Se and Te, chem. shifts of the K_α X-ray line 8=9558
- Sn(halide)₂, Mössbauer line, isomeric chemical shift 8=8222
- Sn-molten BiCl₃ solutions, study of reaction 8=17000
- Sn¹¹⁹(CH₃)₄, indirect nuclear spin coupling 8=4233
- Sn-Bi alloys, dendrite morphology 8=4825
- Sn-Bi molten alloys, free energy of mixing and elec. resistivity 8=12842
- SnCl₄, polymerized with methyl methacrylate, methacrylonitrile and acrylonitrile 8=2527
- SnI mols. spectrum forbidden lines, obs. 8=1175
- Sn-In supercond. foils, type II, sheath irreversible magnetization obs. 8=17970
- SnO₂, electrical conductivity 8=5167
- SnO₂, electron scattering polar optical modes 8=22611
- SnO₂ in glycerine/castor oil, Mössbauer line widening, temp. and viscosity dependence 8=1603
- SnO₂- γ layers, secondary electron emission 8=18284
- SnO₂, neutron powder patterns rel. to scattering amplitudes of seven Sn isotopes 8=1809
- SnO₂, thin films, u.v. absorption edge spectrum 8=2458
- SnO-SiO₂ glasses, crystallization and decomposition 8=21965
- Sn-Pb, X-ray fluorescence analysis 8=9750
- Sn-Sb alloy, X-ray fluorescence analysis 8=9750
- Sn-Sb, moving boundaries, solute profile 8=8468
- Sn-SnO₂-Sn supercond. tunnel junction, d.c. Josephson current mag. field depend. and self-screening 8=22568
- SnTe compatibility with metals study 8=18686
- SnTe, electronic band structure, optical props. 8=8943
- SnTe films, thin, prep., resist. meas., Hall effect and cryst. props. 8=13096
- SnTe, i.r. reflectivity rel. to free carrier dispersion theory 8=2457
- SnTe, lattice dynamics 8=13337
- SnTe, melting curve by thermal analysis between 5-40 kilobars 8=1614
- SnTe, optical props. 8=18562
- SnTe, thermoelectric props., effect of small Sn substitutions by Nd 8=13905
- SnTe-Bi₂Te₃ alloy system, thermoelectric props. and phase relations 8=4716

Titanium

- absorption coeff. for Ag K α radiation, meas. 8=2436
- anode of ion source, discharge in desorbed H₂ 8=21227
- atom, pionic, 4f-3d transition rel. to π mass 8=6839
- band structure, density of states and Fermi surface by cellular method 8=8942
- deformation mechanisms, low-temp. 8=8864-5
- diffusion of C, investigation over wide temp. range 8=17586
- diffusion of metallic impurities 8=17596
- diffusion of Ti-44 and V-48 8=17587
- film deposited by sputtering in crossed e.m. field 8=7651
- getter pump, evacuation of t. w. t. 8=16731
- with microrough or dispersed surface, increase of thermal rad. compared with polished surface 8=22139
- resistivity in thickness range 75-350 Å 8=9019

Titanium—contd

- slip vector, non-basal, identification 8=17665
 - solid solns. in Cu, mag. moments 8=22760
 - specific heat near phase transition point, 1000 to 1300°K 8=17526
 - sputtering by positive ions of N₂, O₂ and Ar 3-9 keV 8=8780
 - textural, biaxial strengthening 8=5086
 - thermionic emission in Cs vapour meas. by plasma-anode tech. 8=18264
 - X-ray emission bands fine struct. rel. to e band struct. obs. 8=18527
 - B-Ti, diffusion mechanism 8=17594
 - CaF₂:Ti²⁺, impurity ion e. p. r. spectrum 8=9422
 - CdS:Ti²⁺, e. p. r. 8=22900
 - H₂ definition, spectral-isotopic method 8=9743
 - N₂ sorption, sticking coeff. obs. 8=17175
 - α -Ti, anisotropic thermal expansion by X-ray method 8=17535
 - β -Ti, diffusion behaviour from thermo and electrotransport meas. 8=17589
 - β -Ti, impurity diffusion summary 8=17588
 - Ti I spectral resonance lines, absolute oscillator strength 8=1176
 - Ti(III) hexahydrated ions, electronic struct. 8=16995
 - Ti²⁺ e. s. r. in CsAl(SO₄)₂·12H₂O single crystals 8=18418
 - Ti³⁺ in CaF₂, optical and e.s.r. spectra 8=14126
 - Ti³⁺ in SrTiO₃, electronic ground state structure 8=9445
 - α -Ti/H₂(D₂) system, thermodynamic props. 8=21858
- Titanium compounds**
- alloy, irradiated, tensile and shear props. at cryotemps. 8=17763
 - alloy in non-electrolyte, stress corrosion cracking susceptibility 8=8863
 - alloys, Fe and Nb additions, superconducting props., phase transformations 8=22563
 - alloy, VT15, solution-treated and aged, structural features 8=17293
 - anatase formation at high temps. 8=1684
 - anatase, permittivity rel. to that of rutile 8=18173
 - carbides, formation by chemical vapour deposition 8=23112
 - hydrides, disaligning by plastic straining 8=4782
 - K- and L-spectra 8=14281
 - quadrivalent Ti compounds with OH and O₂H radicals, e. s. r. and chemiluminescence 8=2522
 - rutile, adsorpt. at solid-liq. interface from binary soln. 8=1710
 - rutile, electronic mobility at high pressures 8=2087
 - rutile, partially reduced, e.p.r. studies at 77°K 8=18436
 - rutile, polaron theory of carrier props. 8=17894
 - titanates, Mg activated, luminescence model 8=2488
 - titanomagnetites in basalts, electron probe 8=14703
 - titanomagnetite structure rel. to magnetic props. on oxidation 8=14054
 - triscyclooctatetraen-dititanium crystal structure 8=13304
 - Ti complex, diethoxytitanium dichloride, crystal and mol. structure 8=17421
 - Ti complex, di(tetraethylammonium) tetrachloroxotitanate (IV) crystal structure 8=17422
 - Ti-Al alloys, dilute, hydride formation in thin foils 8=17016
 - Ti-Al alloys, slip vector, non-basal, identification 8=17665
 - Ti-Al-Co alloys, microstructure, rel. to Ti-rich corner 8=4851
 - Ti-6Al-4V alloy, stress-corrosion cracking in methanol 8=22394
 - Ti₃AuH₃, A-15 structure, superconductivity 8=9059
 - Ti-Be oxide, energy absorber of superhigh-freq. vibs. 8=10458
 - TiC, B-doped, TiB precip. rel. to defect structure 8=4967
 - TiC, fibrous, preparation by high-temp., vapour-phase process 8=14908
 - TiCl₃ + H₂O₂ reaction, e.s.r. 8=2521
 - TiCl₃ α , X-ray diffraction microstructure meas. 8=22041
 - TiCl₄, in binary solvent mixtures, n.m.r. 8=8138
 - TiCl₄-heptane solns., γ -radiolysis obs. 8=18747
 - TiCl₄, polymerized with methyl methacrylate, methacrylonitrile and acrylonitrile 8=2527
 - TiCl₄, Raman spectrum, difference bands 8=7570
 - TiF, dissociation energy 8=1623
 - TiF₂, ht. of formation 8=1623
 - TiF₃, sublimation pressures 8=1623
 - Ti-3 wt.%Fe alloy, quenched from β -phase, study of martensites 8=21859
 - TiFe₂, atomic arrangement in homogeneity range of Laves phase 8=1813
 - TiFe₂-Co₂ alloys, hyperfine fields and electronic structure 8=14156
 - Ti-Fe-Si system, R(M, X)₂ and RMX₂ cpds., crystal structure 8=17435
 - TiGaLiO₄, structure of ordered phase on annealing at 600°C 8=17423
 - Ti(HPO₄)₂·H₂O synthetic ion exchanger, crystal structure and exchange behaviour 8=13295
 - Ti-Mg oxide, energy absorber of superhigh-freq. vibs. 8=10458
 - ϵ -TiN, high-temp. stability 8=21857
 - Ti-22 at. %Nb alloy, ω phase precip. rel. to superconducting critical transport currents 8=4718

Titanium compounds—contd

- TiNi, heat capacity 8=4935
 TiNi mechanical props., hydrostatic extrusion effects obs. 8=5059
 Ti-O system, $\beta \rightarrow \alpha$ bainitic transformation 8=17103
 TiO 7050 Å band, photometric classification of early M giant stars 8=14768
 TiO₂, adsorption of CO, i.r. spectroscopy 8=8347
 TiO₂, adsorption of poly(dimethyl siloxane) from CCl₄ and xylene solns. 8=8336
 TiO₂, dielec. discs, in resonator, h.f. props. 8=19829
 TiO₂, effect of H₂O and NH₄Cl traces on ϵ^1 and ϵ^{11} 8=18174
 TiO₂, enamel, opacification kinetics, X-ray diffr meas. 8=17221
 TiO₂, enthalpy of anatase-rutile transformation 8=13074
 TiO₂ films, with large ionic space charge, conduction process 8=2233
 TiO₂ films, spark discharge along surface 8=7682
 TiO₂ growth by chem. transport with TeCl₄ 8=8429
 TiO₂, H₂O desorption kinetics, 25-100°C 8=18703
 TiO₂, molec. geometry 8=7550
 TiO₂, phase transforms. under shock-wave compression, from X-ray studies 8=1685
 TiO_{2-x}, (reduced rutile), dielec. relaxation processes at 1.2 to 50°K 8=5355
 TiO₂ (rutile), vac. reduced, sp. ht. below 4.5°K, rel. to impurity band model 8=13380
 TiO₂, solubility in Al₂O₃ in H₂ atmos., temp. dependence 8=21818
 TiO₂, solubility of iron, X-ray examination 8=13042
 TiO₂, thermal expansion, 100°-700°K 8=17536
 TiO₂:V⁴⁺, multiple electron-spin echoes 8=22657
 Ti₂O₃, dielec.-metal phase transition rel. to mag. ordering 8=18389
 Ti₂O₃, e.s.r. at 77°K rel. to semiconductor-metal transition 8=14125
 Ti₂O₃, growth of single crystals from melt 8=4817
 Ti₂O, ordered, structure determ. by e-microscopy 8=17420
 Ti₂O₃, effective mass, magnetic susceptibility rel. to temp. 8=5120
 Ti-Rh alloys, specific heat and superconducting transition temp. 8=9058
 ZrO₂-TiO₂ system, change of mineral composition by heat treatment 8=4721

Torquemeters. See Mechanical measurement.

Torsion

- See also Elastic constants; Stress analysis.
 balance, precision standard masses 8=19349
 ferromagnets, var. in magnetic field effect 8=2312
 hollow notched round bar, stress-intensity factor 8=5024
 intermetallic compounds, press. effects on ductility 8=13535
 low-temp. calibration, torque meas. 8=14924
 magnetic resonance meas. method 8=14075
 magnetostriction in ferromagnetic materials, circular magnetization calc. 8=13998
 oscillating in rigid disc on surface of elastic half-space 8=10689
 pendulum for automatic elastic moduli meas. 8=5006
 polymethylmethacrylate tube torsional oscillations rel. to ht. generation 8=4946
 viscoelastic conical rod 8=14956
 Gd internal friction obs., magnetic damping effect 8=14020

Total cross-sections. See under individual particles, no sub-heading.

Townsend coefficient. See Ionization/gases.

Tracers

- See also Radioactive tracers; Radiochemistry.
 anions and cations, adsorpt. on metal surface 8=4760
 radioactive, for study of chem. reactions in stationary droplets 8=14355

Transducers. See Acoustic transducers.

Transformations. See Phase transformations.

Transformations, mathematical

- canonical in gravitation theory rel. to quantization in general relativity 8=10597
 canonical and involutory, variational problems, transport theory 8=7308
 channel symmetry and nonlinear transfer 8=6482
 conformal, numerical calc. 8=19352
 contact 8=10493
 coordinate, Coriolis and other fictitious accelerations, derivation 8=10531
 Euler angles, helicity formalism for 4 identical particles 8=15912
 Fourier, appl. to optical images 8=11136
 Fourier appl. to Perot-Fabry spectrophotometry 8=15530
 Fourier and Laplace soln. of Cauchy-Poisson surface waves 8=16774
 Fourier, modified algorithm for unequal number of input and output points 8=6522
 infinitesimal, law of Yang-Mills field associated to the conformal group 8=15679
 invariant, rel. to noninvariant solns. of eqns for mono-energetic nonrelativistic particle beams 8=15270
 Laplace transforms, analytic continuation by asympt. series 8=2905
 Lorentz, 4-dimensional, note 8=14928

Transformations, mathematical—contd

- Lorentz, and motion of charges in electromagnetic field 8=15269
 Lorentz, vector, derivation 8=14960
 Noether equations and conservation laws 8=6032
 non-linear into equivalent linear systems 8=19359
 O₃ → O₁ for unitary representations of SL_{2,C} as a series of Γ functions 8=20264
 in quantum theory point, rel. to isometric transformations in Hilbert space 8=559
 Schrödinger equation, two-parameter Hamiltonians 8=11250
 SL_{2,C} decomposition into sums over unitary representations of SU₁ and U₁ A T₂ 8=10502
 spinors, generalized in complex n-space 8=6014
 Stieltjes, asymptotic behaviour 8=6015

Transistors. See Semiconducting devices/transistors.

Transition metals

- atoms, wave functions, limited-basis-set SCF in ground state 8=12075
 b.c.c., density of states, isochromat spectroscopic invest. 8=17876
 b.c.c., diffusion, theoretical critique 8=17590
 compressibility, 5 metals, subjected to high press., effect of electron structure 8=17724
 conductivity dependence on atomic wt. 8=17924
 electron binding energies 8=8976
 electron emission in Cs and F vapours, quantum chem. model 8=18261
 ion, recent Japanese work 8=16992
 liquid, density of states of narrow nondegenerate (s) band 8=12901
 Lorenz number, ideal, and itinerant electron correlation 8=8905
 magnetic susceptibility spin-orbit coupling dependence 8=2332
 noble elements and alloys, superconductivity, mag. susceptibility and sp. ht. 8=13752
 noble elements and alloys, supercond., mag. susceptibility and sp. ht. 8=13753
 phase diagrams and bond theory 8=13003
 solid solns., mag. susceptibility 8=9283
 in spinel ferrites, spin wave linewidth variations 8=5495
 superconductors, isotope effect rel. to dirtiness 8=5215
 d-transition, formulae of Slater-Koster interpolation procedure 8=8885
 valency structure for 5th and 6th periods 8=16967
 with CO adsorbed, entropy changes on desorption 8=17174
 Co(II)-Ni(II)-Mn(II)-V(V)-Mo(VI) chloride system, extraction separation, radioisotope study 8=23077
 in Cu, dilute alloys, effect on thermal cond. 8=22133
 in Fe-rich alloys, magnetization values 8=22811
 Pt-group, electron emission in Cs vapour at T_g=414°K 8=18265

Transition metal compounds

- alloys, electronic structure 8=22444
 A15-type phase, binary, atomic ordering 8=17419
 borides, Cd⁺ sputtering coeff. determ. 817705
 broad band versus d-level semiconductors 8=17886
 carbides, carbon κ and metal emission bands rel. to bonding 8=2406
 carbides, sputtering with Cd⁺ ions, 100-500 eV energies, coeffs. 8=8762
 chalcogenides of formula MM₃X₄, M(M¹) = trans. metal, X = S, Se, Te, structure 8=13294
 complexes, octahedral, electric quadrupole transitions 8=16976
 complexes with tetrazoline-4-thiones, i.r. spectra 8=14188
 complexes, theory of ligand substitution 8=14387
 crystal fields, thermodynamic and optical calcs. discrepancy correction 8=4669
 fluorides, MO calc. of 10 Dq 8=4667
 h.c.p. alloys of later 4d and 5d series, electronic structure from mag. susceptibilities 8=18296
 molybdates, structure and props. 8=13296
 monophosphides, mag. susceptibility and n.m.r. 8=22847
 nitrides, Cd⁺ sputtering coeff. determ. 8=17705
 oxalato complexes, C¹⁴ radioisotopic exchange 8=21796
 oxide glasses elec. cond. 8=22522
 oxides, shrinkage with concurrent reduction, obs. 8=4936
 thionibates, MNb₃S₄, with berthierite structure 8=8560
 [Me(CNS)₆]⁻³, struct., by isotopic exchange 8=23087

Transmission

- Co, magnetized of polarized n 8=2031
 Cu, of X-rays, temp. dependence, (Borrmann effect) from 77-377°K 8=14210
 Ge, of X-rays, multiple Borrmann effect 8=14222
 Ni, magnetized of polarized n 8=2031

acoustic waves

- See also Acoustic wave propagation.
 absorption resonance line, width and shift dependence on temp. 8=13342
 along $\langle 110 \rangle$ axis of cryst, third-order elastic consts. rel. to thermal attenuation 8=4916
 apertures, discrepancies 8=6162
 apertures, negligible thickness 8=6163
 aperture in rigid screen, i.f. 8=10745
 channel, divergent, surface/bottom reflected 8=18844

Transmission—contd

acoustic waves—contd

- circular apertures in thin panel 8=19561
 duct with nonlinear wall impedance, attenuation 8=15066
 finite amplitude, dynamics of propagation in free space 8=10736
 loss expt., room absorption meas. by steady-state and decay rate methods 8=191
 loss meas. using vibr. transducers 8=10754
 l.f. attenuation coeffs. in ocean, analytic description 8=5786
 Luneberg fluid lens, acoustic field 8=19562
 magnetite, acoustic loss peak, electronic mech. 8=1852
 metals, helicoid instability of sound oscs. 8=5139
 molecular, in perpendicular stationary and varying fields 8=21493
 panels, double, loss calc. allowing for absorption by cavity walls 8=10740
 physical acoustics, principles and methods; application to quantum and solid state physics, book IV A 8=17486
 in plasma, partly ionized, $\lambda \gg m.f.p.$ neutral particles 8=7795
 semiconductors, helicoid instability of sound oscs. 8=5139
 sound field in metal-dielec.-supercond. structure, rel. to electron tunneling 8=5219
 split beam sound-field, WKB-type approx. 8=19567
 transmittivity density distribution function for two layer system with random parameter 8=19564
 underwater, nonlinear 8=6164
 underwater sound-pulse distortion by converging lens 8=4570
 underwater, theory, book 8=10751
 water, acoustical effects on free convective transfer from horizontal wire 8=21663
- acoustic waves, ultrasonic**
 ferromagnet, attenuation near transition temp., phonon interact. with spin system 8=18323
 in non-conducting solids, low-temp. attenuation of 3 GHz waves 8=17490
 quartz, attenuation of 3 GHz waves, from 4 to 40°K 8=17490
 shallow water propag. loss at sonar freqs. 8=1554
 standing waves in anisotropic media, diffraction of e.m. waves 8=10952
 Al, attenuation and rotation of u.s. shearwaves in mag. field 8=17497
 Bi, amplitude of giant quantum oscs. 8=1848
 In₂Bi, pre-melting, 10 MHz pulse-echo obs. 8=21751
 N₂, liquid, rel. to meas. of volume viscosity 8=1538
 ZnO, attenuation of 3 GHz waves, from 4 to 40°K 8=17490
- electromagnetic waves.** See Electromagnetic wave propagation.
- light**
 See also Absorption/light; Filters, optical.
 absorbing film containing pinholes, meas. with laser system 8=9483
 in atmosphere, intensity fluctuations rel. to varying turbulence 8=14618
 coefficient at lowest exciton level calc. from polariton model 8=22480
 duct, curved with circularly refl. walls 8=6508
 far i.r. LWP filters, low temp transmittance 8=20066
 glasses, aluminate for i.r. use 8=22954
 gyrotropic layer, Faraday effect 8=3376
 Irtran 2, 4 and 6, total hemispherical emittance at low temps. 8=18467
 liquids, display of picosec. pulses via two-photon fluoresc. 8=8071
 narrow beam, in turbid media with highly directive scatt. 8=11161
 noble metal films, and reflectance, anomalous skin and size effects 8=9498
 optical materials, 0.17–3.0 μ 8=11140
 optical superheterodyne receiver, for communications expts. 8=6423
 optical wave packet kinetics in lens-like medium 8=3366
 optically thick layers 8=6538
 plastic scintillating fibres, light-conducting characts. 8=9586
 polymethine dyes, spectra 8=430
 Rosseland radiative mean opacity, calc. 8=11163
 scattering media, spectral line profiles near resonance 8=509
 spherical wave with Gaussian amplitude distrib. 8=20087
 suspensions of latex spheres in water, monodispersed, efficiency factor K meas. 8=4632
 through windows set near Brewster angle, rel. to laser tubes 8=6426
 ultraviolet, book 8=20012
 water vapour, attenuation of m.m. wavelength rad. 8=9865
 Ag film, 0.4–1 μ range 8=5580
 Ag-Cr film, 0.4–1 μ range 8=5580
 Au films, and reflectance, anomalous skin and size effects 8=9498
 BaTiO₃ with Fe and Co impurities, transmission props 8=18187
 Bi film, band structure determ. 8=13859
 CS₂, self-focusing and induced combination scatt. 8=4581
 CdS, interference max. on curve rel. to refractive index 8=2409

Transmission—contd

light—contd

- Cr film, 0.4–1 μ range 8=5580
 Cr₂O₃, reactively evaporated characts. and refractive index 8=9517
 Cu films, and reflectance, anomalous skin and size effects 8=9498
 Cu film on Si, in spectral region from 1.5–7 μ 8=14212
 Cu films, thin, and absorpt. in spectral region between 0.6 and 4 μ 8=22972
 Cu₃TaSe₄, and other optical props. 8=8408
 H₂NH₂PO₃ films in polarized light, 400–4000 cm⁻¹ rel. to internal vibrations 8=14224
 KI, pure and doped, spectra at low temps. 8=18540
 KMF₃ (M = Mg, Mn, Co, Ni, Zn, Mg/Ni), i.r. spectra rel. to multiphonon processes 8=2427
 Mg films, plasma reson. of p-polarized u.v. 8=12516
 MnTe, antiferromag. semiconductor, and reflection, 80–375°K 8=5622
 PbTe-PbS solid solns., i.r. spectra rel. to forbidden band optical width 8=18554
 Sb film, band structure determ. 8=13859
 Se, i.r. spectra 8=8615
 TlI, CsI stabilized, in 30–65 μ region 8=5640
 Zn tellurite glass range, i.r. spectra 8=5644
- Transmission lines, r.f.** See Electromagnetic wave propagation/ guided waves.
- Transparency**
 See also Optical constants; Transmission/light.
 in dielectrics, damage due to laser light 8=8755
 effect of multiquantum resonance 8=499
 Irtran 2, 4 and 6, total hemispherical emittance at low temps. 8=18467
 Rosseland radiative mean opacity, calc. 8=11163
 Hf oxides, u.v., temp. depend. and effect of Cl⁻ and NO₃⁻ 8=5605
 Th oxides, u.v., temp. depend. and effect of Cl⁻ and NO₃⁻ 8=5605
- Transport processes**
 See also Diffusion; Kinetic theory; Liquids/theory; Radiative transfer; Solids/theory; Statistical mechanics.
 active many-layer media, integral characteristics 8=8033
 atmosphere, lower, heat, water vapour and momentum 8=14583
 atmosphere, water vapour turbulent transfer at different stability conds. 8=14611
 atmospheric boundary layer, mass transfer from radio-active tracer obs. 8=14594
 atmospheric boundary layer, momentum rel. heat vertical transfer 8=14584
 atmospheric ground layer, turbulent t transfer for quasi-homogeneous flows 8=14610
 Boltzmann equation, Chapman-Enskog method 8=134
 Boltzmann eqn. for electrons interacting with acoustic waves in strong elec. fields 8=13343
 Boltzmann eqn., linear, approx. by Fokker-Planck eqn. 8=3004
 Boltzmann eqn., linear, soln. for flow over point source 8=7875
 Boltzmann equation, linear and stationary solution 8=19474
 Boltzmann equation, linear and nonlinear, for gas between two parallel plates 8=19470
 Boltzmann equation for neutrons in absorbing disk geometry 8=6115
 Boltzmann eqn. in plane geometry with linear-anisotropic scatt. funct. 8=135
 Boltzmann eqns. solns. with anisotropic scatt. 8=20541
 Boltzmann eqn., soln. by extrapolation 8=3003
 Boltzmann eqn. soln. for neutron scatt. in spherical geometry media 8=20542
 Boltzmann's eqn., solving by Jacobi polynomial method 8=11983
 Boltzmann systems, spectrum and evoln. for soft potentials 8=1462
 Boltzmann's theory of irreversibility and velocity inversion 8=95
 Brownian motion in quantum fluid 8=92
 bubbles, gas, meas. of interphase mass transfer at high Reynolds number 8=12764
 classical fluids, h.f. linear response to Brownian oscillators 8=4446
 contaminants in atmospheric turbulent boundary with unstable stratification 8=14608
 cross-section determ. from meas. on arc discharges 8=4294
 cryogenic liqs, saturated, correl. for viscosities, thermal cond. and self-diffusivities 8=15132
 diffusion of radiation from a cavity, moments method description 8=19622
 in dispersions, interrelationships with heat transfer 8=16904
 distributed parameter nonadiabatic heat and mass transfer, thermal dynamics 8=12976
 drop velocity in mixture of gases 8=1482
 electroluminescence, mathematical description by a system of equations 8=5651
 electrolyte solns., isothermal vector, in n-component systems 8=8046

Transport processes--contd

- e in solids, theory for strong field 8=2078
 energy pulse interaction with solid 8=12968
 energy transport, turbulent spectra, Kraichman-Spiege approx. 8=21442
 ethanol, evaporation into O_2 and CO_2 , effect of moving interface 8=16711
 ethylether, evaporation into He and CO_2 , effect of moving interface 8=16711
 evaporation from unsaturated surface using Dalton-type eqn. and energy balance 8=21777
 Fermi-gases, interacting 8=10655
 finite cylindrical medium, matrix factorization soln. 8=15024
 fluid of high thermal diffusivity, convective instability in heated layers 8=16639
 fluid, incompressible, transport equations 8=7879
 fluids, mass transfer in rectangular cavities 8=12600
 fluid, single component, new eqn. 8=1438
 fluid, turbulent energy transfer in universal equilibrium range 8=16643
 fluid, turbulent radial wall jet, mass transfer from axial source 8=1451
 fluid, turbulent separated flow in rectangular cavity 8=12610
 free fermions, generalized Boltzmann eqn. 8=15674
 gas, axial, in d.c. discharges in mixture gases 8=1333
 gases in critical region 8=4490
 gases, cross sections and angular distribution 8=1483
 gases, electron transport, effect of inelastic collisions 8=7939
 gas, interphase mass transfer coeffs. for insoluble monolayer on water 8=12830
 gas-liquid interaction, intensification, survey 8=19637
 gas-liquid mass transfer, effect of moving interface, theory 8=16710
 gas, partly ionized in mag. field, transport property eqns. 8=10927
 gases, polyatomic, effect of varying elec. and mag. fields 8=1465
 gas, turbulent boundary, streamwise wall curvature effect 8=12656
 generalized albedo method 8=15023
 generalized eqn., using quantum-mech. Green's function 8=19472-3
 heat and mass transfer in moving media, soln. of parabolic boundary layer eqns. 8=19634
 heat and mass transfer, turbulent boundary layer problems, solutions 8=6208
 heat radiation in absorbing and anisotropically scattering medium 8=10675
 inert gases through rubber membrane 8=1487
 inverse problem, theory 8=11613
 ion slip in slightly ionized gas mixture 8=16436
 Laplace eqn., soln with transport through cylindrical constrictions 8=10670
 laser, Fokker-Planck eqn. for atoms and light mode 8=19942
 laser noise, Fokker-Planck solution 8=11023
 laser noise, quantum Fokker-Planck soln. 8=19937
 linearized collision operator, matrix elements 8=21499
 liquid, conducting and in turbulent flow, effect of mag. field on heat transfer 8=10930
 liquid, convective heat transfer during stabilized turbulent flow in tube at supercritical press. 8=1550
 liquid phase adsorpt. fractionation in fixed beds, anal. 8=17151
 liquids, vel. autocorrelation function, calc. in itinerant oscillator model 8=12777
 local potential of fluctuations, in hydrodynamics, variational properties 8=1440
 longitudinal waves, phase velocity and damping in viscous fluid 8=1534
 macroscopic evolution systems, quantum mechanics 8=2967
 mass, by evaporation-diffusion between solids 8=8673
 mass and heat transfer, physical props. effects calc. 8=10770
 mass transfer between falling liq. film, and vertical surface, diffusion-controlled electrolytic tech. 8=21598
 mass transfer between single drop and a continuous phase 8=21594
 mass transfer between spherical particle and ambient medium under high temp. mixed convection 8=1473
 mass transfer effect on hypersonic viscous shock layer of blunt body 8=3035
 mass transfer, electroconductive media 8=15105
 mass transfer in laminar free convection with moving interface 8=240
 mass transfer in solid-liquid system 8=4630
 mass transfer to ,ear of sphere in Stokes flow 8=21563
 mass transport, vacancy mechanism 8=4947
 master equations, exact and asymptotic 8=19471
 master-eqn. model near critical point 8=10669
 master eqn. of Pauli and equilibrium between matter and radiation 8=2990
 master eqns. with and without time convolution 8=19477
 medium, response to a pulse disturbance, instabilities, convective, absolute 8=19476
 membranes, liquid, and elect. props. 8=4560

Transport processes--contd

- memory effects and autocorrel. function of dynamic variable 8=2007
 Milne's problem for 2 adjacent spaces, solution 8=1119
 mols. vel. distrib. function near solid wall in non-uniformly heated gas 8=21494
 monatomic ionized mixtures 8=4304
 in multicompartment assembly, reconsidered generalized B-G-K collision model 8=19479
 neutrons, in infinite slab, initial-value problem 8=20875
 neutrons, perturbation eqn. for critical slab 8=16143
 neutrons in reactor, ergodic theory of semigroups 8=3992
 neutrons, time-depend. Boltzmann eqn., cylindrical geometry soln. 8=20545
 nonlinear response, formal theory 8=2989
 ocean, heat flow and free air gravity anomalies 8=18838
 one-speed transport eqn., closure relns. for eigenfunctions 8=847
 plasma, appl. Fokker-Planck eqn. 8=4328
 plasma, Cerenkov heating in radially non-uniform cylinder 8=16485
 plasmas, electron transport, effect of inelastic collisions 8=7939
 plasma, with inelastic processes 8=1379
 plasma, rarefied, in toroidal trap 8=4342
 plasma, seeded, drift velocities and thermal flux vectors in elect. and mag. fields 8=16488
 plasma, various expressions for kinetic equation 8=21314
 polar-gas mixtures 8=4492
 polyatomic gases, molec. theory 8=16684
 in primordial fireball 8=14729
 quantum theory, collisional transfer contribs. 8=19475
 radiation fluctuation, kinetic theory of obs. 8=3010
 radiation heat transfer in nonisothermal nongray gases 8=21506
 radiation transport in scatt. media, eqn. deduction 8=3012
 radiative trans. eqn. with anisotropic scatt. 8=138
 rarified gas, heat transfer, appl. of conventional eqn. for conductivity and boundary temp. jumps 8=12682
 reformulation using autocorrel. functions 8=3006
 resonance phenomena in kinetics of molecular gases 8=21493
 scattering, anisotropic in energy depend. transport 8=19478
 Schwinger's variational principle for calc. transport coefficients 8=17916
 semiconductors in double injection regime, effects of diffusion and thermal generation 8=22419
 solutions, effect of non-Brownian motion 8=21718
 from spheres, prediction of macroscopic thermal and material transport 8=4434
 spherically symmetrical molecules, viscosity and intermolecular potential 8=7630
 in thermionic conversion, appl. Monte Carlo method 8=15246
 thermodynamic analogy 8=6098
 thermoionic convertor, general equations 8=3158
 time-correlation-function for coeffs. 8=6112
 time-correlation-function expressions 8=6113
 transport eqn. in 3-dimens., truncation of spherical harmonic expansion 8=11990
 turbulent, in free turbulent flows, effects of intermittency 8=16766
 viscoelastic fluids, turbulent heat transfer characts. 8=4426
 viscous momentum transfer effect 8=21736
 Al, thin film, electro-transport, direct obs. 8=17927
 Bi, liq., electromigration of small amounts of Ag, Cd, In and Sb 8=12815
 D, electron transport coeff. 8=21521
 GaP- Cl_2 - H_2 system, vapour transport in open tube, thermodynamics 8=12699
 Ge, n-type, low-temp. semiconductor obs. 8=18043
 Ge surfaces, motion of metal drops on, under action of electric current 8=5259
 H, electron transport coeff. 8=21521
 H_2O turbulent flow in square duct, heat transfer and wall temp. distribution obs. 8=1545
 Hg turbulent flow in square duct, heat transfer and wall temp. distribution obs. 8=1545
 n-HgSe, quantum oscillations of coeffs. 8=5261
 In-Sb liq. alloys, cell for electrotransport meas. 8=12816
 N_2 gas, thermomagnetic torque, temp. dependence 8=16712
 Pb-Sn liq. alloys, cell for electrotransport meas. 8=12816
 Si surfaces, motion of metal drops on, under action of electric current 8=5259
 SiO_2 films, role of proton and Na transport 8=9172
Trapped free radicals. See Free radicals.
Traps. See Crystal electron states; Crystal imperfections; Semiconductors.
Travelling wave tubes. See Electron tubes.
Triboelectric emission. See Electron emission.
Triboelectricity
 crystals rubbing with metals, nature of changes acquired 8=18158
 metals sliding on glass in a 3×10^{-7} torr vacuum 8=13872
 solid surfaces, mechanisms of charging 8=18156
 static charge, dissipation and generation on dielectrics in vacuum 8=18159

Triboluminescence. See Luminescence.

Trions (He^3, H^3). See Alpha-particles and helium nuclei; Tritons.

Triple point. See Critical constants, thermal.

Tritium

atomic, quartz contained discharge 8=4276
bremsstrahlung irradi., nuclear photoeffect 8=11432
hot-atom reactions, energy dependence 8=14447
isotopic exchange with toluene 8=5695
loss from iron meteorites by solar wind hydrogen 8=10370
radioactivity meas. with evacuated scintill. probe 8=3853
as tracer for groundwater flow obs. 8=2568
tritiated, scintill. probe for monitoring 8=3737
tritiated water analysis, water vapour counter 8=9748
 H_2 - T_2 mixtures, equilibria and reaction rates 8=14448
T-D gas mixture, propagation of thermonuclear detonation wave 8=21482

Tritium compounds. See Hydrogen compounds.

Tritons

See also Nuclear reactions due to tritons.

binding energy calc. using N-N non-local separable pot. 8=11647
binding energy calc. using pair potential 8=881
binding energy rel. to n-d scatt. length 8=11648
d-T reaction, n yield 8=874
Fadeev calc. of binding energy, T matrix perturbation theory 8=20584
ground state props. with Hamada potential 8=885
 $\bar{\mu} + \text{He}^3 \rightarrow \text{H}^3 + \nu$, asymm. in recoil of H^3 8=15740
 $\frac{3}{2}\text{n}$ particle instability 8=20733
photodisintegration, Cabibbo-Radicati sum rule appls. 8=695
photodisintegration cross-section calc., normalization anomaly 8=11655
photodisintegration cross section obs. 8=11652
photodisintegration, two- and three-body cross section calc. 8=15870
 $\pi^+ + t \rightarrow \gamma + \text{He}^3$ by PCAC generalization of Kroll-Ruderman theorem 8=7217
p photo-absorpt. sum rule 8=3577
d+t prod. of n with t in Zr or Ta, yield decrease diffusion mechanism theory 8=6921
radial wave-function partial differential eqns. 8=880
radius, mean square, expectation value, variational method 8=20146
trinucleon μ capture rate and S' state 8=20583
wave function, S and D state component calc. 8=6995
D(d, p)T, 8 energies, 2.1-14.1 MeV, p polarization obs. 8=11642
D(t, n)He⁴, as polarized n generator 8=15844
H³ charge form factors and charge distrib. calc. 8=886
H³(γ , n)d, H³(γ , p)2n, H³(γ , 2n)p, cross sections and ang. distribs. 8=11432
H³(n, d)2n, 15.1 MeV, n-n scatt. length deduced 8=20543
H³(n, p), 14.1, 18, 21.5 MeV search for trineutron 8=11649
H³-H³ scatt., using 2-body pot. calc. compared to expt. 8=11656
He³-H³ scatt. rel. to levels of Li⁷ and Be⁷ 8=7001
T(d, n)He⁴, as polarized n generator 8=15844
T(d, n)He⁴ rel. to polarized d beam prod. 8=11602
T(p, n), He³, obs. 8=882

Troposphere. See Atmosphere.

Tungsten

adsorbed Ce, Ba, e emission, Thomas-Fermi-Dirac theory 8=5414
adsorption of CO, on surface partly covered with O 8=4762
adsorption of Hg on field emitter tips, nucleation obs. 8=1702
adsorption of N₂, N₂ phase transforms caused by e-impact 8=21913
adsorption of N₂, rel. to work function 8=1711
adsorption of O₂, equilb. surface conc., sticking probability and work function charges 8=4767
adsorption of U, study by field emission work function of U film 8=22715
annealing of n-irrad. damage, migration of single vacancies 8=17601
anodic oxidation in LiCl-KCl 8=5738
atom, transition probabilities, 9 lines, 4700-5300Å 8=20969
attack by atomic O at high temp. 8=14370
catalyst for decomposition of diethyl and di-n-propyl ethers 8=14404
cathode, carbon adsorbed high temp. field emission, effect of oxygen and air 8=2276
cesiated, evaluation of thermionic emitter surfaces, rel. to conversion 8=18269
channelling of MeV projectiles 8=11954
chemisorption of diatomic molecules on single crystals, work function studies. 8=18700
coating by plasma jet 8=19337
conductivity, thermal, meas. and analysis, 100-400°K 8=4943
crystal faces, work function of Xe 8=18252
crystal, with Mo film, adsorption and electron emission 8=9269
crystal, single, mechanical strength from elec. field required to break whiskers 8=2069
crystal, sorption of O₂ on (111) face, mechanism and kinetics 8=8348

Tungsten—contd

cyclotron resonance meas. 8=13688
desorption, of CO by electron impact 8=21911
desorption of CO, NO and O by electron impact 8=21912
desorption, electron-stimulated, of O from surface, mechanism 8=17177
desorption of rare earth elements from surface 8=17171
desorption of Th by high energy electrons 8=1712
diffusion of C, investigation over wide temp. range 8=17586
dislocation pinning, internal friction rel. to temp. 8=1980
doped, annealed, evidence for voids 8=17613
doped, model from annealed glass-doped Fe 8=17025
elec. resist. and hardness, effects of neutron irradi. and subsequent annealing 8=2141
electron emission, laser induced, using pulsed Ar laser 8=18271
electron field emission, anomalous total-energy distribution and electronic structure 8=5411
electron field emission from (110) surface rel. to atomic perfection 8=2275
emission processes in Cs-additive systems, correl. 8=15214
emissivity, spectral in visible and i.r. range 8=1897
emitter in thermionic converter, effect of evaporation on to Ni collector 8=15245
emitter thermionic converter, performance with CsF additive 8=15244
Fermi surface 8=17887
field-emitted electron distrib. and work function 8=5413
film, adsorpt. of N₂, sticking probability temp. dependence 8=14396
film, interact. with and adsorpt. of H₂O vapour, rel. to catalytic activity 8=14405
films, sputtered and condensed on cleaved NaCl, structure rel. to temp. 8=4759
heavy ion penetration along low index channels, effect of atomic thermal motion 8=2024
ion emission due to laser irradi., masses, energies and numbers 8=13948
micromosaic block size and misorientation in zone-melted crystals, impurity depend. 8=8470
microstructure, thermochemically deposited sheet deformation studies 8=8471
n irradi., changes in mech. props. rel. to changes in microstruct. 8=21998
with non-metallic traces, effects on yield strength ductile-brittle transition, hardness and microstruct. 8=17835
nucleation of mica substrate for Ag film evaporation 8=13087
(112) and (100) oriented crystal surfaces, surface potentials of CO 8=21910
(100) surface, electron emission under proton bombardment 8=18249
permeation rates of O₂ and H₂, pressure, thickness and temp. dependence 8=4958
phonon drag effects below 2.6°K 8=5106
polycrystalline, U coated, photoelectric work function 8=5408
polycrystals, adsorpt. of CO 8=17169
proton scatt. and channeling 8=4997
recrystallized, impurity effects on strain hardening 8=22380
reluctance field dependence, 1.8-35°K rel. to K_{öler} law deviations 8=22750
ribbons exposed to water, low-energy electron bombardment 8=21907
specific heat in 1600-2900°K range 8=17528
specimen preparation for field-ion microscope 8=15354
stacking faults, electron micr. obs. 8=1984
substrate for growth of Si films 8=4758
surface, accommodation coeffs. of inert gases 8=4734
surface Ba ionization coeff. meas. 1800-2600°K 8=18288
surface interactions with I₂ vapour 8=18699
surface, translation accommodation of Ar, O₂ and N₂ mols. 8=17113
surface, trapping energy calc. for inert gas ions 8=13081
thermal desorption of inert gas ions 8=9280
thermal desorption of inert gases 8=17701
thermionic electron emission saturated, in Cs vapour 8=18268
thermionic emitter cesiated surface evaluation 8=22717
two-band conduction model for resistivity, contradictions 8=2107
vacancies and interstitials, calcs. 8=22179
vapour deposited emitter in thermionic converter with Mo collector 8=15230
vapour deposited from WCl₆, work function rel. to preferred orientation and surface treatment 8=18248
wire, recrystallized, prep. for transmission e-microscopy 8=17267
wires, secondary recrystallization, from electron optical meas. based on emission 8=1765
wire, Young's and shear moduli meas. 8=5003
work function differences between (110), (211), (100) and (111) planes 8=18244
work function distrib. when chem. vapour deposited, rel. to patch effect 8=18250
work function, effect of Cs additives 8=18251
work function of (100) surface 8=13928

Tungsten—contd

- work function of surface, influence of CsF adsorption 8=18270
- X-rays, L_{α} , film targets direct and fluoresc. components 8=14179
- X-ray production on p-bombardment 8=4995
- Fe-W systems, α - γ equilib. 8=4709
- from H reduction of WF_6 , effect of F impurities on high temp. grain stability 8=17294
- N_2 adsorption on film, sticking probabilities obs. 8=4761
- β -W, V_5Si type tetragonal modifications 8=4888
- W^{185} , in tungstate soln. aggregation study 8=21607
- W^{185} radioisotope distribution and stratospheric transport processes 8=23300

Tungsten compounds

- alloys, anti-oxidation metallurgy 8=23779
- tetrathiotungstates, i.r. spectra 8=2438
- tungstate soln. aggregation study, by W^{185} 8=21607
- tungstates, ($ZnWO_4$ -type), Cr^{3+} third crystal-field constant meas. 8=16974
- W oxide bronzes, struct. evolution with temp., phase stability 8=17048
- W_2B , superconductivity transition temp. and d-shell 8=2164
- WC, heat content valves, entropy, specific heat 8=8643
- WC pistons, cemented, crushing strength 8=8870
- WC, strain and crystallite size, compressed at high pressure 8=13612
- W_2C , rhombic modifications rel. to annealing temp. 8=8561
- $W(CO)_6$, structure determ. by electron-diffr. 8=12236
- W-x at.% Co alloys, x=1.05, 0.87, 0.54, mag. props., 27.300°K 8=14007
- WF_6 , liq., molec. motion, F^{19} relax. 8=12930
- WF_6 , structure determ. by electron-diffr. 8=12236
- W- La_2O_3 system alloys, thermoemission obs. 8=22716
- W-Mo-UC phase diagrams and ternary peritectics, obs. 8=9710
- W-O system, free-energies of formation changes 8=14388
- W-O system, intermediate phases on reduction by gases, O_2 conc. cell method 8=18683
- WO_3 , Pt-activated, films, as gas detector 8=13098
- WO_3^{2-} anion, pH depend. of adsorpt. of Fe_2O_3 powder 8=8342
- WO_4^{2-} ion in HCl, polarography 8=18736
- W-Re alloys, deposition by H reduction of WF_6 and ReF_6 , struct. and props. 8=17100
- W-Re alloy, VR 20, sp. ht. in 1600-2900°K range 8=17528
- W-Re alloys, work function of (100) surface 8=13928
- W-Re-C, superconductivity 8=22566
- WS_2 , single crystal, thermistor characts. 8=18092

Tuning forks. See Vibrating bodies.**Tunnel diodes. See Semiconducting devices/tunnel diodes.****Turbidimetry. See Chemical analysis.****Turbidity. See Scattering/light; Suspensions.****Turbulence**

See also Cavitation; Flow; Vortices.

- air/air free jet, nozzle-fluid concentration field 8=4453
- air flow, low-speed, study of skewed boundary layers 8=21475
- air flow through concentric annuli, experimental study 8=12650
- air, mixing of cold jet with room temp. stagnant, obs. 8=16669
- air-pentane mixtures, effect on explosion press. 8=6147
- air, thermal convection between horizontal plates, velocity and temp. obs. 8=12686
- apparent shear stress between concentric rotating cylinders 8=21444
- atmosphere, boundary over sea, stress and spectra hot-wire obs. 8=18859
- atmosphere, handover of vertical fluxes of momentum, heat, etc. from small to large scale 8=14578
- atmosphere, modulation of laser beam 8=404
- atmosphere, upper, energy balance 8=23311-2
- atmosphere, validity of ray optical calc. 8=18877
- atmosphere, vertical component at 300 and 1200 m 8=14612
- atmosphere, vertical velocity component vars., 430 m tower obs. 8=14613
- atmosphere, water vapour transfer at different stability conds. 8=14611
- atmosphere waves instability rel. to clear-air turbulence 8=23265
- atmospheric boundary layer 8=14595
- atmospheric boundary layer, joint probability density functions 8=14592
- atmospheric boundary layer over land and sea 8=14596
- in atmospheric boundary layer over oceans, large scale, importance in synoptic meteorology 8=14582
- atmospheric boundary layer, transfer coeff. heat rel. momentum 8=14584
- atmospheric ground layer, transfer for quasi-homogeneous flows 8=14610
- in axisymmetrical free flows, with rotation, decay of vel. 8=21463
- boundary layer, compressible, kinematic eddy analysis 8=21489
- boundary layer flow of Newtonian liq. in smooth annuli 8=16765
- and boundary layers with geophysical appl., conference, Kyoto, Japan 1966 8=7850

Turbulence—contd

- boundary layer, inactive motion and press. fluctuations 8=4436
- boundary layer, initial, rel. to transition point Reynold's critical number 8=12597
- boundary layer promoters, improved heat transfer rel. to power reactor systems 8=21510
- boundary layer, structure 8=7876
- boundary layer, transducer systems as spatial and spectral filters for press. field 8=10731
- boundary layers, turbulent with air injection, transformation 8=12665
- Burger's nonlinear diffusion eqn., viscous and non-steady solns. 8=4439
- cellular convection, finite amplitude stability rel. to extremum principle 8=6212
- circular pipe, turbulent heat transfer and temp. distrib. 8=232
- compressible free jet, momentum and heat transfer 8=12652
- conduction-convection critical transition time 8=16692
- convection from plane isothermal sheet 8=241
- diffusion, convectionless, above small evaporating water surface 8=14638
- dispersion, incompressible fluid, using Lagrangian diffusion eqn. 8=12634
- eddy viscosity of turbulent equilib. layers 8=16640
- energy equation rel. to boundary-layer development 8=7980
- fine-grained isotropic turbulence, visco-elastic character 8=4441
- flames, diffusion, thermal equil. meas. 8=7946
- flow, non-Newtonian fluids, heat transfer coefficients and friction factors 8=4565
- fluid, boundary layer, large eddies and correlation obs. 8=12615
- fluid, boundary layer, low-drag, induced by suction through slots 8=12667
- fluid boundary layer, structure, review 8=12607
- fluid boundary layer, 3D, with wall heat transfer 8=12611
- fluid, boundary, velocity fluctuations in and beyond viscous sublayer 8=12646
- fluids, confined, velocity profiles 8=7877
- fluid, convective cellular motion, Benard, Rayleigh number intervals 8=6213
- fluid, convective instability in heated layers 8=16639
- fluid, cylinder-wake, large eddy structure 8=12627
- fluid, development in boundary layer build-up between concentric rot. cylinders 8=12633
- fluid diffusion, local concentration fluctuations, variance 8=12631
- fluid, displacement variance, conservation and moment of moment eqns. 8=12629
- fluid, dissipation integral 8=12628
- fluid, eddy rel. to mean states, Eulerian vector 8=12630
- fluid, effect on heat transfer from spheres 8=17541
- fluid, elasticoviscous non-Newtonian, friction factors and velocity profiles in flow 8=12746
- fluid, energy transfer in universal equilibrium range 8=16643
- fluid flow, longitudinal dispersion by combination of convection and lateral spreading 8=12622
- fluid, free boundary layer, statistical behaviour 8=12617
- fluid, free stream, interaction with laminar boundary layer 8=12614
- fluid heat from below, Rayleigh convection cells of arbitrary wave numbers, 2D, evolution 8=10775
- fluid, high order time correlations in field and rel. to Gaussian probability distributions 8=12623
- fluids, homogeneous, statistical props. large eddies 8=16636
- fluids, hot-film sensor for heat transfer 8=16822
- fluid, incompressible, evolution of single-time moments of velocity field 8=16642
- fluid, incompressible, functional integration based on Hopf space-time formulation 8=12642
- fluid, incompressible, shear flow between parallel walls, statistical theory 8=12748
- fluid, incompressible, transport eqns. 8=7879
- fluid, instability nonlinear plane Couette flow 8=12591
- fluid layer, thermal, in forced convection 8=12638
- fluid, nonlinear instability development in laminar boundary layer 8=12613
- fluid, rotating, layer amplitude Benard convection 8=12616
- fluid, separated flows in rectangular cavity, transport processes 8=12610
- fluid, shear flow, energy spectrum eqn. 8=12599
- fluid shear flow, space-time correlation obs. interpretation 8=12605
- fluid shear flow, waveguide model 8=12598
- fluid, small-scale, cascade process of sequential breakdown of eddies and probability distributions 8=12636
- fluid, spiral, digital obs. 8=12640
- fluid, sporadic, review 8=12621
- fluids, stratified, stably and unstably, velocity and temp. fields 8=12624
- fluid, swirling jet, axial velocity and shear stress profiles 8=12626
- fluid, transition of separated boundary layer, wakes of cylinders, obs. 8=12620
- fluid unevenly heated from below, nonlinear model 8=16637

Turbulence—cont'd

- fluid, velocity defect law, surface roughness effect 8=12612
- fluid, visco-elastic, non-Newtonian effects in decay 8=12645
- fluid, viscosity associated with transfer of mean square vorticity across energy spectrum 8=12635
- fluid, wall, secondary currents 8=12639
- in free flows, effects of intermittency on turbulent transport processes 8=16766
- free turbulent shear, layer, approx. theory for development 8=21474
- gas boundary layers, intensity obs. 8=16673
- gas, boundary layer streamwise wall curvature effect 8=12656
- gas, cylinder near-wake velocity fluctuations, obs. 8=12654
- gases, energy dissipation by suspended particles 8=7897
- gas flow sound field freq. spectrum, laser appl. 8=19552
- gas, hot-wire meas., nonlinearity effects downstream of grid 8=12664
- gas, one-particle dispersion rel. to velocity distribution 8=16721
- in gas-particle flow, two-phase eqns. considering turbulent fluctuations of particle cloud 8=16660
- gas, suppression of turbulence behind oscill. cylinder, expt. 8=12666
- gas, transition and instability in Ekman boundary layer 8=12657
- gas, transition from laminar flow, small parameter method 8=12655
- gases, weakly ionized, correl. with Langmuir probe current fluctuation 8=1406
- guar gum in tap water, aging and degradation from Pitot tube obs. 8=12744
- heat exchange, in presence of transverse homogeneous magnetic field 8=12742
- heat flow in viscoelastic liqs. 8=1510
- homogeneous, in mag. field, decay, with small mag. Reynolds no. 8=3245
- hydromagnetic, conservation theorem 8=15379
- hydromagnetic homogeneous, large scale structure 8=10929
- incipient in Poiseuille flow, numerical finite-difference simulation 8=12722
- incompressible fluid, determining dynamical eqn. for 2-pt. correlation tensor 8=4438
- incompressible fluids, Kraichnan's theory, review 8=12625
- incompressible fluid, tangential disturbances, viscosity effect on instability 8=12618
- inertial energy transfer in isotropic turbulence, diffusion approximation 8=4444
- rel. to ionosphere, magnetodynamic turbulence at low mag. Reynolds number 8=19813
- isotropic homogeneous, decay of passive scalar fluctuations 8=21439
- isotropic, spectrum 8=16644
- laminar Poiseuille flow, slightly supercritical, disturbance evolution 8=1450
- light scatter study using colloidal particles 8=4440
- liquid, boundary layer on smooth wall, structure obs. 8=12741
- liquid, boundary layer transition, hydrogen bubble obs. 8=12740
- liquid, conducting, Lorentz force effects 8=16763
- liquid flow, transition in wake of cylinder 8=12752
- liquids, gas absorpt. 8=12745
- liquids, heat loss at supercritical pressure 8=8050
- liquid, swimming sheet problems 8=16752
- liquids, vel. field meas. from scatt. light spectrum fine struct. 8=12749
- liquid, viscous, breakdown of flow in Hale-Shaw cell with large wall separation 8=16760
- locally isotropic, veloc. and temp. derivatives cross-correl. moment 8=14604
- in lubrication of journal bearings 8=8810
- MHD friction coeff. in ducts 8=6356
- MHD jet, incompressible 8=15377
- mercury flow in tube in longitudinal mag. field 8=10933
- momentum defect superposition, wind-tunnel obs. 8=21481
- motions of differing scales 8=4443
- near solid wall, electrochemical flow obs. 8=12747
- negative eddy cond. and viscosity, production in presence of buoyancy and shear 8=21441
- nitromethane-acetone detonating solns., wave front turbulence 8=6145
- non-Newtonian fluids, flow through round tubes 8=16638
- non-Newtonian fluids, heat transfer 8=12647
- particle deposition on vertical surfaces 8=16909
- photometer light beams fluctuations, compensatory system 8=3343
- in pipe flow, numerical soln. of diffusion of injected dye 8=21576
- planetary atmospheres, photographic limitations 8=14835
- plasma, anomalous transmission of microwaves 8=7759
- plasma, collision effects on oscills. 8=7738
- plasma, due to nonlinear cross-field instability 8=21395
- plasma, ion-acoustic wave interaction 8=7809
- plasma, Langmuir wave freq. correction 8=7823

Turbulence—cont'd

- plasma, microwave investigation 8=7760
- plasma, microwave scattering, numerical expt. 8=16516
- plasma, nonisothermal, heating 8=1383
- plasma waves, nonlinear interaction and ion sound 8=1423
- plumes and wakes, entraining 8=4437
- polyacrylamide and polyethylene in tap water, aging and degradation from Pitot tube obs. 8=12744
- polymer additives in water, effect on turbulent shear flow 8=16764
- polymers in aqueous solutions in the turbulence vortices 8=12946
- polymer, dilute solutions, Pitot tube and hot film obs. 8=7981
- polymer solns., flow in pipe 8=4510
- polymer solns. in pipes, drag reduction 8=1511
- polymer solutions, shear flow 8=12743
- 1, 2, 3% polyvinyl alcohol laminar-turbulent transition, obs. 8=4512
- round spheres, macroscopic thermal and material transport 8=4434
- shock waves, Burger's equation, Lagrangian-history statistical theory 8=19536
- skin friction meas. with heat transfer 8=12750
- small-scale structure, simple model 8=21438
- spectra, from Kraichnan-Spiegel approx. 8=21442
- supersonic flow with heat sources through deformable cylindrical shell 8=16649
- suppression by uniform magnetic field 8=10931
- Taylor-vortex flow, perturbation instability 8=12643
- thermal, Malkus' transition 8=19653
- thermodynamically nonequilib. fluid, restraints on spectrum and energy of motion 8=16641
- troposphere, aerodynamic-acoustic theory 8=9905
- two-dimensional, diffusion approx. 8=21440
- two-dimensional, inertial ranges 8=4442
- viscoelastic fluids, heat-transfer characts. 8=4426
- viscoelastic fluid, linear instability of a plane-parallel Couette flow 8=7869
- vortex breakdown, 'conjugate-flow' theory 8=4513
- wakes, two dimensional, self preserving 8=7880
- water, pipe flow effect of vibrations rel. to laminar and turbulent transition regimes 8=1501
- Wiener-Hermite expansion, truncated, dynamic properties 8=12641
- He⁴, flow, λ -point shift 8=19694
- Hg jet, velocity profile in axial mag. field obs. 8=7991

Turbulent flow. See Flow.**Twilight**

- See also Atmospheric spectra; Zodiacal light.
- airglow, far u. v., rocket photometry obs. 8=9927
- atmospheric transparency vars., u. v. obs. 8=9871
- moon, Alpengluhn colour theory 8=23647
- Ca II H and K lines, spatial extent, airborne obs. 8=9868

Twinning. See Crystals, twinning.**Twistors. See Calculating apparatus; Magnetic devices.****Ultracentrifuges. See Centrifuges.****Ultrasonics**

- See also separate headings, e.g. Absorption.
- atomizer, particle size-capillary wave amplitude relation 8=21734
- Bragg scatt. of light by u. s. waves, rel. to pulse compression 8=8617
- bubble mass transfer, effect of streaming 8=21584
- cardiac valves and muscle, motion detection 8=2868
- cavitation bubbles, pulsations in wave 8=12862
- cavitation, gas diffusion, into void 8=4497
- depolymerization, at elevated static press. 8=4568
- detection of crack extension 8=8807
- on detection in water by cavitation 8=3721
- devices for coherent optical systems 8=15072
- diagnostic scan within body, localisation employing Doppler shift 8=15074
- diffraction of e. m. waves in anisotropic media 8=10952
- dissociation of aqueous solutions, computation from relaxation study 8=18712
- eye's interior structure, visualization 8=19581
- field effect in a cavitating liquid, parametric effects 8=21664
- forbidden frequency bands in laminated media 8=6166
- frequency modulation of semicond. lasers 8=11093
- gas flame audible noise abatement 8=10779
- graphite, stress wave packet, attenuation effect on freq. content 8=8626
- harmful effects in medical diagnosis 8=5986
- holography, by electronic scanning of piezoelectric crystal 8=19580
- holography, recording technique 8=6176
- hypersonic meas., signal-to-noise ratio enhancement by time averaging 8=3075
- insulators, high-tension, pulse method for non-destructive testing 8=22286
- interaction of hypersound with light in laser cavity with Stokes feedback 8=11005
- light diffraction in a medium, ultrasonic field effect 8=11190

Ultrasonics—contd

- liquids, mixing effect 8=21554
- location in gases, technical apl. 8=3072
- liquid crystals, irradiation effects 8=1527
- at liquid He temp., use of GkZn-94 oil for acoustic contact 8=15136
- liquids, light diffraction and modulation 8=20035
- liquids, viscosity meas. with transducer 8=8028
- marine geology, application 8=23248
- meas. of dynamic shear impedance of low viscosity liqs. 8=4547
- microwave cavity resonator, rotating 8=15071
- naphthalene, effect of ultrasound on zone melting 8=13139
- nuclear fast passage 8=10983
- obsidian elastic props. interferometry studies 8=17713
- and optical diffraction spectra, rel. to vel. of sound in liqs. 8=8060
- piezo-optic coefficients by pulsed u.s. light diffraction, 24 liquids obs. 8=8064
- plasma jet, u.h.f. diagnostics 8=1435
- powder dispersal for particle size meas. 8=13046
- pressure gauge to 20 kbar for solid rods 8=19341
- propagation and absorpt. in quantizing mag. field 8=6165
- pulse attenuation meas. for internal friction 8=17715
- pulse-echo apparatus for v. h. f. 8=15073
- pulse-echo detector, variable width gate 8=3073
- quartz, light scatt. by u. s. surface waves 8=5636
- resonance thermometer for virtual air temp. meas. 8=246
- rings, discs and rods, arbitrary profile, vibrations 8=10694
- surface wave amplitude from diffraction pattern of interacting light beam 8=6553
- surface waves, strain and velocity meas. 8=3025
- systems analysis, piezotransducer equivalent circuits 8=196
- vibration effects on crystallisation 8=3071
- water specific volume at high press. from propag. meas. 8=21623
- work hardening f.c.c. metals and alloys 8=22336
- CdS crystal, transverse wave amplification at 87 MHz 8=22098
- CdS crystal vibrations, diffr. of light 8=18514
- Cu-base mats., pickling in dilute H₂SO₄, appl. of u. s. vibs. rel. to rates 8=23780
- He-Ne laser, deflection of beam 8=6450
- He-Ne laser light modulation for velocity meas. 8=6489
- Se and TlSe production 8=21967
- ZnO and ZnS crystal vibrations, diffr. of light 8=18514

Ultraviolet detectors. See Radiation detectors.

Ultraviolet sources. See Light sources

Umklapp process. See Crystals/lattice mechanics.

Uncertainty. See Indeterminacy; Probability.

Undor. See Electron theory; Field theory, quantum.

Unified field theory. See Relativity/unified field theories.

Unimolecular layers. See Adsorbed layers.

Units

- See also Constants; Dimensions; Nomenclature and symbols.
- dosimetry of ionizing radiation 8=613
- light, inappropriate use 8=461
- physical quantities, dimension and orientation, rel. to units system 8=19344
- SI system in magnetic induction equations 8=3177

Upper atmosphere. See Atmosphere/upper; Ionosphere.

Uranium.

- See also Nuclear fission/uranium.
- activated, getter for rare gas lasers 8=15452
- addition to Sb embrittled brass, malleablizing effect 8=22326
- adsorbed film on W, study by field emission work function 8=22715
- atom, photoelectric cross-section for K-Mv subshells for X-rays 412-1332 keV 8=7438
- calutron enrichment of mg. amounts of material 8=7480
- creep mechanisms of α and β mono- and poly-crysts. 8=8867
- deposition from ocean 8=9813
- diffusion, lattice and grain boundary, of U ions in UO₂, 1900-2150°C 8=13414
- films, photoelectron attenuation lengths 8=22727
- films on polycrystalline W, photoelectric work function 8=5408
- film, vac.-deposited on W, props. in u. h. vac. and H₂ 8=17142
- isotopes, ion exchange separation obs. 8=21029
- isotope shift constants 8=16234
- pig-skin surface contamination by U 8=5987
- radioactive, abundance in crystalline shield rocks 8=9794
- spectrographic estimation in carnotite ores by spark technique 8=14461
- surface potential of H₂ 8=21909
- trace element determ. by mass spectrometry 8=18769
- urinary, determ. for radiation protection 8=23181
- H solubility in, \leq 150 atm and 860°C 8=8190
- Ta content, spectrochemical determ. 8=9749
- Th/U ratios, upper mesozoic graywackes, California north 8=2565
- γ -U, diffusion mechanism 8=17594

Uranium—contd

- α -U, magnetic susceptibility 8=13966
 - α -U, superconducting transition temp., positive isotope effect 8=22565
 - γ -U, tracer-diffusion 8=17591
 - U²³⁵, enrichment by ion exchange electromigration method with superposition of a. c. on d. c. 8=12113
 - U²³³-U²³⁵ mixtures, radiometric isotope abundance anal. 8=4113
 - U₍₁₎ + UN_(s) system, equilib. pressure of N and thermo-dynamic props. 8=18646
 - U VI, dil. alkali soln., low temp. luminesc. spectrum 8=18618
 - U(VI) ions, sublation studies, by radioactive tracers 8=23075
- Uranium compounds**
- alloys with small additions of Mo, V, Zr, Cr, Al and Ti, creep strength 8=8868
 - antiferromagnetic, Néel temp., stability 8=5509
 - electron states, systematics 8=17852
 - phosphides, prep. 8=23116
 - pitchblende-containing deposits, induced polarization field expts. 8=2561
 - salts, crystal spectra, D₂O isotopic shifts 8=5641
 - solid-solubility relationships 8=8248
 - uranyl nitrate, organic soln., complexing, i.r. spectrum study 8=21619
 - U carbide-heavy water subcritical system, reactivity 8=11957
 - U selenides, mag. props. either ferro or paramag 8=5440
 - U sulphides, mag. props. either ferro or paramag. 8=5440
 - UAl₃ coatings on U, phase struct. and protection against U oxidation 8=21892
 - UAu, dissociation energy 8=16366
 - U-C alloys, around UC comp., high-temp creep and hot extrusion 8=22396
 - U-C system phase diagrams 8=21860
 - UC, high-temp. oxidation obs. 8=23115
 - UC₂, n. diffr. exam. rel. to mag. props., cryst. struct. and phase change 8=1810
 - UC rod, temp. coeff. of resonance integral 8=12019
 - UC, self-diffusion parameters, appl. to activated processes 8=22164
 - UC-Fe-Cr system, phase equilib. and compatibility relns. 8=21861
 - UC-Fe-Ni system, phase equilib. and compatibility relns. 8=21861
 - UC-ZrC, W clad, vacuum emission stability, effect of temp. to 2473°K 8=18267
 - U-Cr alloys, martensite nucleation and growth in β - α transform., temp. dependence 8=4717
 - UF₃, atomic structure from n diffraction 8=13297
 - U₂F₆, body-centred, cryst. structure 8=13298
 - UF₆, determ. of Mo by atomic absorpt. spectroscopy 8=18776
 - UF₆, gaseous, thermal diffusion factor and mol. interaction pot. 8=7944
 - UF₆, liq., molec. motion, F¹⁹ relax. 8=12930
 - UF₆, structure determ. by electron-diffr. 8=12236
 - UF₆M (M=Li, Na, Cs, K, NH₄, Rb, Ag, Tl), paramag. reson. absorpt. 8=14127
 - UFeO₄, magnetic meas. and neutron diffraction exam. 8=18353
 - < U, H > solid soln. thermodynamic props. and comp. \leq 150 atm and 860°C 8=8190
 - β -UH₃, ht. capacities from 1.4-23°K 8=8644
 - UH₃, thermodynamic props. and comp. \leq 150 atm and 860°C 8=8190
 - U₃, paramag. and antiferromag. states, P²⁷ quadrupole spectrum 8=9469
 - U₄, phase transition rel. to α irradi. obs. 8=17105
 - U-M alloys, (M=Fe, Al and Si), irradiated, phase comp. changes rel. to resistivity meas. 8=8283
 - U-1.5wt% Mo struct. transforms. rel. to cooling rate from γ phase, obs. 8=8285
 - UN, diffusion of N 8=14504
 - U₂N₃, calc. of heat of formation 8=9660
 - UN-ThN pseudobinary system, lattice parameters 8=22044
 - UN_(s) + U₍₁₎ system, equilib. pressure of N and thermo-dynamic props. 8=18646
 - U-Nb-Zr alloy, anal. by X-ray absorpt. edge technique 8=18792
 - U-Ni-C system, phase equilib. and compatibility relns. 8=21861
 - U-O system, non-stoichiometric oxides 8=21788
 - U-O system phase diagrams 8=21860
 - UO₂, antiferromagnetic phase transition, magnetic point groups and selection rules 8=9402
 - UO₂ burnup, mass spectrometric determ. 8=7344
 - UO₂, calc. of temp. depend. shear modulus 8=13610
 - UO₂ columnar grain microstructure 8=21997
 - UO₂, conductivity, electrical 8=18089
 - UO₂, Debye-Waller factors, anharmonic temp. contrbs. 8=13299
 - UO₂ dissoln. in acid media 8=18691
 - UO₂:Dy₂O₃, dispersions, behaviour in steep temp. grad. 8=4694
 - UO₂, enthalpy of fusion determ. 8=21750
 - UO₂:Eu₂O₃, dispersions, behaviour in steep temp. grad. 8=4694

Uranium compounds—contd

- UO_2 -fueled Mo emitters, irradi. studies rel. to in-core converters 8=15226
 UO_2 , irradi., microstruct. 8=8469
 UO_{2+x} lattice defects rel. to chem. props. and O self-diffusion 8=23113
 UO_2 , magnetic excitations 8=22888
 UO_2 , molec. geometry 8=7550
 UO_2 , porosity effect on thermal conductivity 8=13397
 UO_2 powder compacted fuel, effective thermal cond. and structural change 8=13398
 UO_2 powders, sintering behaviour rel. to particle size and shape 8=21834
 UO_2 , reactor fuel, material buckling and reaction rates 8=20904
 UO_2 as second core in FR2 reactor, efficiency 8=4013
 UO_2 , with small amounts of yttria or lanthana, equilibrium oxygen pressure over solid solns. 8=13044
 $\text{UO}_2\text{:Sm}_2\text{O}_3$, dispersions, behaviour in steep temp. grad. 8=4694
 UO_2 , spin lattice interaction, first-order phase transition theory 8=22886
 UO_2 , spin-lattice interaction, ground-state and spin-wave excitations 8=18437
 UO_2 , surface self-diffusion meas. 8=13413
 UO_2 swaged compacts, equiaxed grain growth under temp. grad. 8=8255
 UO_2 , thermal cond., depend. on temp. and temp. gradient 8=8665
 UO_2 , thermal diffusivity meas. 8=1898
 UO_2 thermionic emitter-filling, radiation tests 8=15241
 UO_2 , U ions diffusion, lattice and grain boundary, 1900–2150°C 8=13414
 UO_{2+x} and U_3O_{8-x} , carrier mobility investigation 8=18090
 UO_2 , W clad, vacuum emission stability, effect of temp. to 2473°K 8=18267
U–O–C system phase diagram 8=21860
 $\text{UO}_2(\text{CO}_2)_2$, dil. soln., low temp. luminesc. spectrum 8=18618
 UO_2Cl_2 and hydrates, crystal structures 8=22042
 $\text{UO}_2(\text{NO}_3)_2$, dil. soln., low temp. luminesc. spectrum 8=18618
 UO_2 – PuO_2 phase diagram, ideality, heats of fusion obs. 8=8284
 UO_2 – PuO_2 system, solid-liquid phase diagram, and UO_2 m. p. 8=8169
 UO_2 – SiO_2 vitroceraamics, rad. induced volume changes and annealing 8=8779
 UO_2 – SiO_2 vitroceraamics, thermal cond. 8=8664
 UO_2 – ZrO_2 – CaO fuel system, out-of-pile thermal props. 8=17527
 UP_2 , antiferromag. structure from n-diffr. study 8=22887
 UP_2 , paramag. P^{31} Knight shift temp. dependence 8=5563
 UP_2 and U_3P_4 paramag., P^{31} Knight shift meas. 8=5564
U–Pd energy loss of fission fragments, range-energy relation 8=2021
 U_2Ru_3 , formation and crystal structure determ. 8=22043
US crystals, precipitation phenomena 8=21862
US, ferromag. transition, thermodynamic props. 1.5°–350°K 8=22848
 U_3S_5 , paramag. with $\Theta < 0$, susceptibility 8=5440
 US_2 , prep. from UCl_4 by reaction with Al and H_2S 8=23114
US single crystals, slip behaviour 8=17834
 $\beta\text{-US}_2$, single crystal, prep. and elec. resist. 8=4818
 USe_2 , paramag. with $\Theta_p < 0$, susceptibility 8=5440
 USn_3 , Sn^{119} n.m.r. rel. to interband mixing effects 8=18474
U–Ti alloys, oxidation in CO_2 at 450°C 8=5718
U– UH_3 phase diagram ≤ 150 atm and 860°C 8=8190
Urey–Bradley forces. See Molecules/internal mechanics.

V-centres. See Colour centres

V-particles. See Hyperons; Mesons

Vacancies. See Crystal imperfections/vacancies

Vacancy breakdown. See Diffusion in solids

Vacuum apparatus

See also Glass–metal seals.

- alkali metal vapour and residual gas obs. 8=21532
 arc discharge, thin-film cathode drop meas. 8=7686
 bell-jar system, rapid cycling 8=7970
 chamber, nuclear reactions, investigations 8=11846
 chamber strengthening by glass fibre laminate 8=16722
 differentially-pumped u. h. v. system, bakeable to 900°C press. $< 10^{-10}$ torr. 8=21548
 dual-expansion nozzle for use in vapour pump 8=21533
 electron diffraction crystallograph for epitaxial growth 8=8527
 feedthrough for small conductor 8=4501
 "flash" evaporation device for metering a variety of metals 8=8186
 gold wire seals for ultrahigh vacuum 8=21549
 high-speed rotating seal 8=21546
 h.v. conductor seal 8=1498
 international symposium, Rome, March 1967 8=6317
 joint, decomposable, with In sealing 8=7968
 manometer, glass bellows, for ultrahigh vacuum devices, 1–760 torr 8=7964
 microbalance for 77.3°K operation 8=7965
 moving mechanisms by mag. pull in ultrahigh vacuum chambers 8=7967

Vacuum apparatus—contd

- plastic pipelines, jointing technique 8=1497
 probe, simple, movable 8=21547
 quartz-metal sealed window, bakeable 8=16741–2
 rapid cycling system 8=16724
 residual gases in UHV systems, pressure eqns. 8=7948
 residual gases in ultrahigh vac. systems, press. eqns. 8=16723
 silicone resins, mass spectrometry 8=16740
 thermal manipulators for ultrahigh vacuum 8=21550
 toroidal vacuum chambers from high purity ceramics for high temperature plasma investigations 8=7963
 tubing connector for UHV systems 8=7966
 2-pump system, theoretical analysis of factors affecting pressure 8=21537
 ultra-high, metallic dismountable, for electron microscope obs. 8=15320
 Hg pumped u. h. v. small glass system without isolation valve 8=21534
 Ti–Be and Ti–Mg oxide energy absorbers for superhigh-freq. vibs. 8=10458

Vacuum gauges

- Bayard-Alpert, anomalous ion currents 8=16734
 Bayard-Alpert ionization gauge, modulation characts. from grid and caps 8=12718
 Bayard-Alpert, modification for gas sorption reduction 8=16732
 Bayard-Alpert–Redhead, e desorption effects and reduction 8=7960
 calibration, reference-transfer method 8=16737
 calibration, reference-transfer method, by press. ratio of gas flow in two conductances 8=7961
 CK-5702 pentode for pressure measurement 8=21540
 conference 8=21531
 hot cathode magnetron, calibration 8=21542
 hot-cathode magnetron ionization gauge, comp. calibration with cold-cathode inverted gauge 8=7959
 ionization, appl. to vapour detect. in photocathode deposition 8=21532
 ionization, comparison of static and dynamic calibration 8=21541
 ionization gauge, 50 μ torr–5 torr 8=16738
 ionization, initial ion-energy distrib. meas. of very low press. 8=7962
 ionization, pressure sensitivity 8=21543
 ionization, as species-discriminating detector for molec. beams 8=12380
 magnetron ionization gauge, press. conversion consts. 8=7958
 magnetron ionization gauges, press. conversion consts. 8=16733
 McLeod, capillary depression 8=12717
 McLeod, compression capillary sealing, improved method 8=16736
 McLeod, condensable gases 8=21545
 McLeod, extension of range from 10^{-10} to 10^{-2} torr 8=4499
 McLeod, with multiple compression device 8=4498
 McLeod, with multiple compression device 8=12716
 molecular flow in long cylindrical tubes, soln. of Clausing's integral eqn. 8=21529
 orbitron, e trajectories, and ion current characteristics 8=4500
 Penning discharge, cathode particle currents 8=7648
 suspended disc 8=16735

Vacuum polarization. See Quantum electrodynamics.

Vacuum pumps

- automatic e.m. valve with variable delay 8=7955
 baffle, for reducing stray currents in sputter-ion pump vacuum chambers 8=21539
 charcoal adsorpt. pump in adiabatic vacuum calorimeter, for 4.2 to 300°K 8=17511
 conference 8=21531
 cryogenically cooled plane, efficiency meas., expt. apparatus and techs. 8=7950
 cryogenically cooled plane, factors affecting efficiency 8=16729
 cryopump, design and performance 8=15134
 cryopumps, return probability of molecules 8=7954
 cryopump for ultrahigh vacuum 8=7951
 cryosorption, performance for two types of molecular sieve 8=12714
 diffusion, fluid film thickness meas. 8=16728
 diffusion pumps using polyphenyl ether, unrefrigerated, for 10^{-9} torr 8=7953
 diffusion pumps, polyphenyl fluid film thickness, spectrophotometer for continuous meas. 8=7949
 getter-ion, electrostatic, design 8=1496
 getter-ion, electrostatic, performance 8=1495
 getter-type, walls constructed from getter material 8=21536
 ion-sorption, cold-cathode, operation and performance 8=7956
 oil diffusion, back-streaming fluid analysis 8=9746
 oils, secondary electron emission 8=13942
 omegatron efficiency, comparison of oil-free and oil diffusion pumps 8=21538
 Penning system, influence of pre-evacuation cycle 8=16725
 speed meas., from mol. gas flow in cylindrical tube 8=1453
 speed measurements, high vacuum 8=7957

Vacuum pumps—contd

- sputter-ion, in field-ion microscope, gas contamination 8=6338
- test header arrangement, correction using impact pressure transducer 8=16730
- 2-pump system, theoretical analysis of factors affecting pressure 8=21537
- ultrahigh, isolation from oil, e microscopic obs. of molecular sieves, use of optical baffle 8=21535
- vapour pump, improvement using dual-expansion nozzle at elevated temp. 8=21533
- N-1S-2 oil-vapour pump, use of polyphenyl ester 8=7952
- Ti getter, evacuation of t.w.t. 8=16731
- Zr-Al getter cartridge for u. h. v. systems 8=16726

Vacuum technique

- activated U getter for rare gas lasers 8=15452
- bell-jar system, rapid cycling 8=7970
- channel multiplier, life tests in ultra-high vacuum 8=15336
- chemisorption and physisorption, Conference, Rome, March 1967 8=8333
- cleaving device, in ultra-high vac. 8=21926
- conference 8=21531
- contact resistance in vacuum 8=19628
- dry milling, effect of oxidation 8=19334
- electron tube manufacture, gas analysis by mass spectrometry 8=18770
- film deposition, nucleation and initial growth 8=17120
- gas inlet system for press. of 10^{-4} to 10^{-7} torr 8=12715
- gas pulses, measurements in 1 torr range 8=21540
- getter pump, walls constructed from getter material 8=21536
- glass surface cleaning meas. by evolution of H with Na-ammonial solns. 8=21868
- infrared windows, bakeable, sealing 8=16739
- ionization gauges, choice of grid material 8=16734
- jointing of plastic pipelines 8=1497
- manometric liquids, outgassing 8=4503
- metals, molten, induction furnace 8=16744
- method not using oil pump 8=7956
- molecular sieves, adsorpt. capacities for N_2 , He, Ne and air, effect of preadsorbed water 8=21897
- molecular sieve for oil diffusion pump, use of optical baffle 8=21535
- moving mechanisms by mag. pull in ultrahigh vacuum chambers 8=7967
- progress, rel. to electron physics, review 8=5994
- residual gases in UHV systems, pressure eqns. 8=7948
- stainless-steel outgassing reduction in ultra-high vacuum 8=7947
- superconductor-glass vacuum seals 8=21551
- 3-temp. zone technique, GaP film deposition 8=21883
- ultra-high, low and high energy electron diffraction apparatus 8=4834
- u. h. v. in small glass systems, tech. for Hg pumped systems without isolation valve 8=21534
- vacuum metallurgy conference New York USA (1966) 8=16746
- zeolites, use for evacuation of containers in liq. He 8=4502
- Al film deposition on glass 8=17123
- Al_2O_3 films e beam evaporation 8=22652
- Ar, adsorbed in equilibrium with gas in ultrahigh vacuum, obs. 8=21530
- Fe-Ni alloys, evaporation characteristics 8=12719
- H, chemisorption on Re 8=23126
- HfO₂ films e beam evaporation 8=22652
- InSb alloy films, evaporation 8=9008
- KI with Tl impurities, growth using vacuum furnace 8=17237
- Ni-base alloy, refractory-melt reactions in vacuum induction melting 8=9694
- Ni, elimination of CO 8=16745
- PbTe semicond. films evaporation 8=8327
- Si deposition on corundum 8=5281
- Ta₂O₅ films e beam evaporation 8=22652
- Ti films, N₂ sorption, sticking coeff. obs. 8=17175
- ZrO₂ films e beam evaporation 8=22652

Vacuum tubes. See Electron tubes.**Valence bands.** See Crystal electron states.**Valency**

- X-ray spectroscopy meas., 15-150 Å 8=22945

Valves, thermionic. See Electron tubes**Vanadium**

- addition to 'Malcolloy', a Co-Al alloy, effect on mag. props. 8=22793
- anomalous properties rel. to H₂ content 8=5186
- Compton effect and thermal agitation 8=13300
- diffusion, summary of ORNL work 8=17593
- diffusion of V-48 and Ti-44 in Ti 8=17587
- ductility rel. to terminal solubility of H 8=5088
- hydride phase, solubility of H₂, isotherm 8=1924
- ions, VI hyperfine-broadened line profiles rel. to Arcturus spectrum 8=23527
- L-emission spectra, fine structure 8=14270
- N interstitials, calcs. 8=22179
- solid solns. in Cu, mag. moments 8=22760
- superconducting local field mapping, n. m. r. studies 8=2179

Vanadium—contd

- superconductivity under high pressure 8=9060
- H₂ definition, spectral-isotopic method 8=9743
- V:Fe⁵⁷, Mössbauer effect, recoil-free fraction and Doppler shift meas., localized modes 8=13338
- V²⁺ in MgF₂, phonon-terminated stimulated emission and i. r. fluorescence 8=2489
- V²⁺ and Ni²⁺ superexchange interaction in MgO 8=9355
- V²⁺ in SrF₂, e. p. r. study 8=9446
- V³⁺ ions in Al₂O₃ (corundum), longit. relax. times by spin echo method 8=5541
- V⁴⁸, self-diffusion 8=17592
- V⁵¹, 10-80 MeV He⁴ ions, recoil range 8=13489
- V⁵¹ in vanadates, quadrupole coupling constants 8=9474
- V(III) hexahydrated ions, electronic struct. 8=16995
- X-ray emission bands fine struct. rel. to e band struct., obs. 8=18527

Vanadium compounds

- vanadates, V⁵¹ and Na²³ quadrupole coupling constants 8=9474
- vanadites, cryst. growth and elec. transport props. 8=4819
- vanadium (III) tris(salicylaldehydes) and tris(salicylaldehyde) complexes, n. m. r. obs., synthesis and stereochemistry 8=16343
- V complex, di(tetraethylammonium) tetrachloroxovanadate (IV) crystal structure 8=17422
- V₃Al superconductivity, Si contamination effects 8=17976
- VAlu₃, magnetic props., atomic environment effect 8=9294
- V₃Au superconductor, atomic ordering 8=18475
- VBr₄, structure determ. by gas-phase e-diffr. 8=16303
- [V(CN)₆]³⁻—¹⁴CN⁻, isotope exchange kinetics 8=23088
- [V(CNS)₆]³⁻—¹⁴CNS⁻, isotopic exchange rel. to structure study 8=23087
- [V(C₂O₄)₃]³⁻—¹⁴C₂O₄²⁻, radiosotopic exchange 8=21796
- V(CO)₆, e. s. r. spectrum at liq. He temps. 8=18438
- VC₁₄, structure determ. by gas-phase e-diffr. 8=16303
- VCr₂Se₄, structural, electrical and thermal parameters rel. to d-orbital interactions 8=5391
- VFe, atomic spin values by polarized n-diffr. 8=18354
- V-Fe-Si alloy, D phase structure determ. 8=17403
- V-Ga alloys, anodic oxidation rel. to phase anal. 8=8286
- V₃Ga Fermi level motion rel. to normal-state susceptibility temp. depend. 8=5118
- V-H alloys: V anomalous properties rel. to H₂ content 8=5186
- V₃In superconductivity, Si contamination effects 8=17976
- V₂MoO₈, crystal structure 8=17425
- VN, atomic state, by absolute meas. of X-ray scattering factors 8=13030
- VN, electronic state from X-ray diffr. intensity meas. 8=22414
- V(O) bisaromatic complexes, e. s. r. spectra 8=12311
- VO phthalocyanine, luminesc. singlet-singlet transitions 8=18591
- VO²⁺ in NH₄Cl, e. s. r. studies 8=5542
- VO, VO₂, V₂O₃ dielec. -metal phase transition rel. to VO₂, change in optical constants, for radiant self-stabilization of temp. 8=23019
- VO₂, domain structure and twinning in low temp. monoclinic phase 8=4889
- VO₂ high-speed solid-state thermal switches 8=22616
- VO₂, phase transformation 8=4719
- VO₂ tetragonal phase, thermal expansion from lattice meas. at 78-415°C 8=13385
- VO₂, V⁵¹ n. m. r. spectra, rel. to crystalline field theory of V⁴⁺ ions in VO₂ 8=9411
- VO₃ anion, pH depend. of adsorpt. on Fe₂O₃ powder 8=8342
- V₂O₅:Cr, e. s. r. spectra 8=9421
- V₂O₅, diffuse reflection spectra 8=18564
- V₂O₅, LEED study of surface 8=21870
- V₂O₅:Mn crystals, e. s. r., 77°K 8=14114
- V₂O₅ single crystals, optical props. 8=23020
- V₂O₅ (010) surface structure transitions, e-induced in LEED expt. 8=4733
- V₃Si, cubic → tetragonal martensitic transform., low temp. 8=8273
- V₃Si Fermi level motion rel. to normal-state susceptibility temp. depend. 8=5118
- V₃Si, superconducting props. 8=2178
- V₃Si, superconductivity, band structure 8=5216
- V₃Si type crystals, tetragonal modifications 8=4888
- V₃Si type in cubic phase, elastic const., temp. depend. explanation 8=13611
- V-V₃Si, supercond. transition temp. and homogeneity regions 8=9061
- V₃X type, strong-coupling superconductivity 8=2177

Van Allen radiation. See Atmosphere/radiation belts.**Van de Graaff generators.** See High voltage production; Particle accelerators/linear.**van der Waals forces.** See Atoms; Kinetic theory; Molecules/intermolecular mechanics; solids.**Vaporization**

- See also Boiling; Condensation; Distillation; Evaporation; Heat of vaporization; Vapour pressure.
- adiabatic, regularities of metastable states 8=4661
- diffusion limited, crit. supersaturation approx. for enhancement by condensation 8=4658

Vaporization—contd

- effusion oven, vapour-solid interactions 8=7899
 energy pulse interaction with solid, heat and mass transfer 8=12968
 Permalloy, by electron-beams, without appreciable fractionation 8=8189
 powders, evaporation completeness, insufflation method 8=21781
 spinodal vs. p, T and use in comparing equations of state 8=1620
 strain gauge thermobalance continuously recording 8=9659
 supercritical region, C_c and C_p extrema calc. from phenomenological theory 8=12978
 vapour bubble-growth calc., importance of non-equilib. region at bubble wall 8=21767
 water in contact with wall, application to quenching 8=8635
 water, light and heavy, effect of inorganic salts 8=21774
 Be_3N_2 , vapour pressure, enthalpy, evaporation coeff. and enthalpy of activation 8=1624
 H_2 -Ne liquid-vapour phase equilib., 26°-42.5°K, 10-25 atm. 8=16937
 He II, initiation at Pb surface, limiting ht. current density 8=4660
 Pb-glass melts, volatilization of volatile constituent from surface 8=21775
 Se, thermodynamics 8=4659

Vapour density. See Density/gases.

Vapour pressure

- See also Humidity; Vaporization.
 alcohols, deuterated 8=12995
 n-alkane derivative isomers with OH groups and n-heptane mixtures 8=16949
 amines, deuterated 8=12995
 aniline solns. in benzene, CCl_4 and chlorobenzene, 25-50°C 8=8056
 azo compounds 8=16958
 equilibrium, math. functions for simple liquids 8=21779
 ferromagnetic crystal, dependence on spin ordering 8=16961
 methanes, isotopic 8=12994
 solids, from laser irradiation heating and evaporation effects 8=15130
 solutions, osmotic explanation 8=12840
 surfactant-hydrocarbon liq. solns. 8=8147
 water, H-isotope effect 8=4662
 Ar, solidified, and binding energy and mean vibration freq. 8=16960
 Au, from Knudsen effusion 8=12999
 Be_3N_2 vaporization, and enthalpy, evaporation coeff. and enthalpy of activation 8=1624
 BiI_3 , solid, rel. to nucleation studies by vapour deposition 8=12998
 $CF_3P(O)F_2$ 8=21177
 $Cd(ClO_4)_2 \cdot HClO_4 \cdot H_2O$ saturated system 8=12847
 GaAs, at 900-1200°K rel. to phase equilibria 8=4664
 Ga-As-Zn system, on liquidus lines 8=21764
 GaS, as function of temp., and thermal stability 8=21786
 Gd_2O_3 , from 2350° to 2590°K 8=21789
 H-isotope effect 8=4662
 H_2O over 11 desiccants, 90°C 8=5717
 He^3 , liq. in high mag. field, theory 8=15144
 Ho, solid and liq. 8=16950
 Kr, solidified, and binding energy and mean vibration freq. 8=16960
 Mn liquid, ΔH calc. using Third Law 8=8185
 N, over $UN_{(s)} + U_{(l)}$ system 8=18646
 S above Ag_2S_{1-x} melt, rel. to elec. conductivity and thermoelec. power 8=16876
 Se 8=4659
 SrS, partial press. of vapour species 8=16957
 T_2O and D_2O 8=21780
 Ta-O-C solid solns., CO equil. press. rel. to comp., 1700-2000°C 8=21787
 U-O non-stoichiometric oxides, equil. oxygen partial pressures 8=21788
 Xe, solidified, and binding energy and mean vibration freq. 8=16960
 ZnTe, torsion meas. 8=16963

Vapour pressure measurement

- by atomic absorpt. spectroscopy rel. to thermodynamic meas. 8=16962
 ebulliometric determ., improved boilers 8=16952
 liquid alloys, by torsion-effusion, activity coeffs. determ. 8=8016
 torsion-effusion apparatus, angular deflection recording, automated 8=4637
 urea and inorganic salt solns. 8=12996
 K-graphite system, gravimetric Knudsen effusion method 8=4712
 Mn liquid, using high-temp. torsion-effusion apparatus 8=8185

Variable stars. See Stars.

Variational calculus. See Mathematics.

Variational method. See Quantum theory/application methods.

Vavilov-Cherenkov radiation. See Cherenkov radiation.

Vectons (vector mesons). See Mesons.

Vectors

- gyroscopes, precession and nutation, simplification 8=10529

Vectors—contd

- SU_2 subgroup passage to new base vectors labelled by non-compact subgroups 8=10502
 spatial density rel. to potential theory 8=2897
 spinors, generalized in complex n-space 8=6014
 vector pot. expansion for spherical wave 8=15403
 wave intersections, analysis by vector polar method 8=19526

Velocity

- in composite rods, asymptotic phase vels. of axisymmetric waves 8=3014
 composition, alternative to special relativity theory 8=19410
 compressional waves in fluid-saturated aggregate of particles 8=22270
 gas flow, profile and slip coefficient calc. 8=16647
 optical images, sensing with moving reticle scanners 8=6497
 Pitot tube and hot film obs. in dilute polymer solution 8=7981
 terminal, spherical particles in oscillating liquid 8=7988
 H_2O flowing in clear plastic tube, meas. by H bubble tech. 8=16756

acoustic waves

- See also Dispersion, acoustic; Helium/liquid, sound propagation; Shock waves.
 in condensed substances, rel. to heat capacity and expansion coefficient 8=1551
 crystals, rel. to lattice dissociation energy 8=4911
 in electrolytic aqueous solutions at 1160 Hz rel. to molar conc. 8=16828
 Fermi hard sphere gas at zero temp. 8=10658
 ice, under static press. 8=1854
 inert-gas liquids 8=1552
 kaolinite and kaolinite-sand, water saturated, 4-600 kHz obs. 8=1857
 liquids, calc. from optical scatt. meas. 8=8059
 in liquids, determ. with u.s. interferometer-laser optical diffraction cell. 8=8060
 liquid metals, var. temp. coefficient with disorder processes 8=12857
 liquids, normal, calc. using correlative distribution functions 8=21661
 ocean, random inhomogeneities, sound fluctuations 8=3054
 organic liquids, rel. to heat of transformation 8=16829
 n-paraffins, and adiabatic compressibility 8=21517
 physical acoustics, principles and methods: application to quantum and solid state physics, book IV A 8=17486
 plane longit. waves in bar, vel. gains for free free mode-resonator case 8=3057
 quartz, α , temp. and pass-derivatives 8=22089
 rock, P and S, by pulse transmission method 8=14542
 solids, non-isotropic, second sound 8=4910
 solids, Poisson's ratio between 0.1 and 0.5 8=189
 CF_4 , liquid, interferometric meas. 8=12868
 CO_2 - D_2O mixture, rel. to vibr. relaxation of CO_2 8=21071
 CaO , rel. to Birch's law 8=13349
 D, polycrystalline, at 2 and 16°K rel. to elastic props. determ. 8=17499
 in Ge, under shock compression 8=17083
 He^3 soln. in He^4 , temp. and freq. dependence 8=15143
 Kr, solid, meas. at 4.2°K, 77°K and 90°K. 8=17500
 α -Mn, longitudinal and transverse, betw. 4.2-300°K 8=17501
 in N_2 8=4484
 S and Se, molten 8=12866
 in Si, under shock compression 8=17083

acoustic waves, ultrasonic

- See also Dispersion, acoustic/ultrasonic.
 benzene and furan vapours obs. 8=12687
 butyl alcohol-water mixtures, hypersonic 8=4572
 crystals of general symmetry, rel. to determ. of elastic constants 8=8782
 EDTA chelates of Cd^{2+} and Hg^{2+} , comp. study 8=23170
 ferroelectrics, near phase transition rel. to long range dipole-dipole effects 8=18181
 gases at high temp., rot. collision and vibr. relax. determ. 8=4478
 liquids, temp. variation 8=8058
 in molten metals 8=12859
 phase, pulse-echo-overlap method incorporating diffraction phase corrections 8=6177
 pyridine and thiophene vapours obs. 8=12687
 resonance reverberation method, 10 to 300 kc/s 8=12858
 Rochelle salt, u.s. relaxation near ferroelec. transition 8=1858
 in solids, total-reflection method, expt. evaluation of accuracy 8=4912
 triglycine sulphate, u.s. relaxation near ferroelec. transition 8=1858

- water, at up to 10⁷ gcm⁻², 80°C 8=16831
 water, supercooled down to -50°C, precrystallization theory 8=13353

- Al-Fe alloys, 12.42-12.8% Al, effect of magnetic polarization and temperature 8=13348
 Cd, molten, phase path interference method 8=12867
 Cd(II), sulphosalicyclic acid chelates of 8=8633

Velocity—contd**acoustic waves, ultrasonic**—contd

- Co(II) perchlorates, water solns., 25°C 8=12865
- CO₂, 300°-1300°K 8=4478
- Cu(II) perchlorates, water solns., 25°C 8=12865
- Ga, quantum oscs. 8=13351
- He⁴ at 1 Mc/s in critical region 8=15142
- KTaO₃, meas. between 2-300°K 8=22088
- LiTaO₃, single cryst. 8=8853
- Mn(II) perchlorates, water solns., 25°C 8=12865
- N₂, 300°-1300°K 8=4478
- Ni(II) perchlorates, water solns., 25°C 8=12865
- Ni-Co-Mn ferrites, shifting of minima due to mag. polarization changes 8=8632
- O₂, 300°-1300°K 8=4478
- Pb_{0.95} Sr_{0.05} (Zr_{0.53} Th_{0.47})O₃ 8=1856
- RbMnF₃, near magnetic critical point 8=17504
- S, molten, phase path interference method 8=12867
- Si, for determ. of elastic constants between 25 and 300°C 8=17830
- Th(IV) sulphosalicylic acid chelates of 8=8633
- Tl, molten, phase path interference method 8=12867
- Zn, molten, phase path interference method 8=12867
- Zn(II) perchlorates, water solns., 25°C 8=12865

light

- constancy 8=456
- particles faster than light, effect precedes cause 8=3500

Velocity analysis, particles. See Particle velocity analysis.**Velocity measurement**

- See also Angular velocity measurement; Stroboscopes.
- bullets, paper screen method 8=10488
- laser Doppler velocimeter, flow-velocity fluctuation obs. 8=21574
- by laser, linear vel. 8=19936
- magnetohydrodynamic, remote, by hydraulic circuit 8=3235
- rocket propulsion particles, laser-Doppler meas. 8=23457
- steady fields, holographic method 8=15562
- transverse surface, optical method 8=15518
- ultrasonic surface waves 8=3025
- viscoelastic fluids, restrictions on probes 8=12603
- waves in shock tubes, by piezoelectric transducer 8=9230

acoustic waves

- CdS, depend. on elec. cond., 5, 8, 14, 30 Mc/s 8=1849

acoustic waves, ultrasonic

- No entries

light

- Michelson determ., errors 8=11121
- Michelson-Morley experiment, classical explanation 8=2933
- molecules, linear, infrared and microwave rot. spectra used 8=11122
- He-Ne laser source 8=6489
- Ne-H laser 8=457

Venus. See Planets.**Verdet constant.** See Magneto-optical effects.**Verneuil process.** See Crystals/growth.**Vertex functions.** See Elementary particles; Field theory, quantum; Functions.**Vibrating bodies**

- See also Crystals/lattice mechanics; Elastic waves; Pendulums; Piezoelectric oscillations.
- annular duct, boundary elements, flutter, gas flow induced 8=15038
- articulated joints linking beams and plates, vibr. isolation 8=10684
- beam eqn., damped cantilever, transform soln. 8=6127
- beams, tapered, transverse vibs., gen. hypergeometric function solns. 8=19487
- beams, thin cantilever, air and internal damping forces 8=19486
- beams, thin, elastic, large amplitude oscillations 8=145
- circular cylindrical shell closed at one end by elastic plate, natural freqs. and mode shapes 8=15034
- circular plate supported by a concentric ring of arbitrary radius 8=147
- circular plate, weights or bar on outer boundary 8=15039
- circular plates, torsional vibs. 8=19490
- complex systems, 'statistical energy anal.' for multi-modal random vibs. 8=19504
- composition bar, soft and hard sections, plastic wave propag. at elastic-plastic interface 8=19395
- cylinder, solid, isotropic, in acoustic medium 8=3020
- cylindrical shell containing flowing fluid 8=152
- cylindrical shell, orthotropic finite, dynamic response to arbitrary press. field 8=19508
- cylindrical shells, thin orthogonally stiffened, boundary conditions effect on flexural vibs. 8=149
- cylinder, thin-walled, circumferential wave reflection at slit 8=6133
- cylindrical shell, long mobility obs. 8=6121
- cylindrical, wind-induced lateral vibs., statistical soln. 8=3022
- dielectric cylinders, between reflecting planes vibrations 8=10699
- double-beam system, elastically connected, damped response to cyclic moving load 8=151
- double-plate system, elastically connected, resonance conditions with cyclic load 8=143
- elastic plates, thin, rib-stiffened carrying concentrated masses 8=19496
- fibres, electrostatically driven in vibroscope, polarizing voltage effect on frequency 8=6124
- finitely deformable structures, natural vibs. 8=15031
- flat plate, response to acoustic excitation in a gas 8=20884
- flexible liq. filled cylinder, rel. to press. distrib. and bubble formation 8=16781
- floating plate, loaded 8=6126
- with harmonic excitation, use of mass as perturbation parameter 8=19505
- homogeneous sphere, radial oscs. 8=146
- horizontal fine wire, effect of vibration on heat transfer 8=19649
- hysteretic structures, multidegree-of-freedom, random vib. 8=3017
- liquid sphere, influenced only by gravity, frequency spectrum 8=4504
- mechanical impedance, driving point, new method of meas. 8=19502
- mechanical oscillators, thermally excited 8=10697
- membrane, circular, resonant response demonstration 8=10691
- membrane, general solns. 8=10695
- nonlinear damped oscillations, elliptic functions 8=6122
- oscillators, adjustable i.f., compact 8=19495
- panels, multimode response to sonic booms, normal and travelling 8=6123
- paraboloidal bar, longitudinal vib. 8=19512
- plate, damping of transverse normal modes 8=19492
- plates, elastic, large deflexion analysis 8=10687
- plate, finite, forced vibr. in plane of supersonic flow 8=10686
- plates, flexurally, radiation statement, by damping 8=3019
- plate in narrow channel, flow-induced vibs. 8=19497
- plate, in supersonic flow, parametric self-excited vibration 8=10685
- plates of complicated shape, fundamental freq. calc. by complex variable theory 8=154
- plates on elastic foundations 8=10549
- plates, upper and lower bounds for freq. 8=15036
- quartz plates, flexural and shear, anharmonic thickness-twist overtones 8=15045
- reactor structural damage due to vibr. of high pressure gas 8=20885
- rectangular AT-cut quartz plates, with partial electrodes 8=19501
- rings and discs, uniform, radial and torsional vibs. 8=10693
- rings, discs, and rods, arbitrary profile, resonant freqs., modes and stress distributions 8=10694
- rod, heated nonuniformly, but symmetrically, stress distribution 8=10688
- rod, tapered, longitudinal vibrations, Poisson's ratio not necessary 8=19484
- rod with variable cross section, forced, combination of reduction and successive approx. methods 8=19506
- rotating annuli, increase in natural freqs. by induced thermal membrane stresses 8=19503
- rotor, nonlinear flexural-torsional 8=3021
- sandwich, and homogeneous spherical shells, axisymmetric obs. inc. effect of thickness-shear deform. 8=19488
- shell, circular, thick walled, radial oscillations, analysis 8=144
- shell of revolution, symmetrical vibrations 8=10690
- shells, fluid filled spherical and spheroidal 8=6125
- shells of revolution free vibs., ring finite element analysis extension 8=10696
- simple beam with tuned viscoelastic dampers, response and damping 8=3018
- spherical caps., approx. solns. for freqs. of axisymmetric vibs. 8=19489
- spherical caps, torsional vibs. 8=19490
- in spinning membrane, soln. for nonlinear, flexural, asymmetric waves 8=19498
- stringed instruments, analysis of bridge behaviour 8=15070
- "summed and differential harmonic" oscillation in non linear vibratory systems, multiple-degrees of freedom 8=3024
- thick membranes, effects of flexural stiffness, shear deform. and rot. inertia 8=19500
- two-dimensional regions with irreg. boundaries, construction of eigenfunctions 8=19510
- 2-layered plates, flexural and extensional vib., theory 8=148
- two-mass vibrator-hammer, contribution to theory 8=10524
- wall, nonuniform, sound radiation 8=3049
- wave machine, dispersion, reflection and eigenfrequencies 8=10937

Vibration, molecular. See Molecules/vibration**Vibrations**

- See also Acoustics; Damping; Oscillations; Vibrating bodies; Waves.
- acoustic in high pressure gases in a reactor, meas. with piezoelectric transducer 8=20885

Vibrations—contd

- air in tube, forced and finite amplitude 8=16705
 amplitude modulated, mechanical demonstration apparatus 8=10679
 bar, uniform straight, and effects on lateral freqs. 8=150
 centrosymmetric cubic cryst. model, normal-mode rel. to elastic const. 8=5002
 of circular cylindrical shell closed at one end by elastic plate, natural freqs. and mode shapes 8=15034
 circular plate, weights or bar on outer boundary 8=15039
 control by architectural acoustics, conference 8=3076
 cylinder, solid isotropic conducting, magneto-elastic 8=13499
 in cylindrical shell, long, mobility obs. 8=6121
 cylindrical shells, sandwich, nonaxially symmetric 8=19507
 damping structure, viscoelastic material armoured with rigid sheath 8=19494
 elastic bodies, axially symmetric, stationary dynamic problems within range of very short waves 8=10537
 elliptic plates, free, large amplitude 8=6045
 of flexible liq. filled cylinder, rel. to press. distrib. and bubble formation 8=16781
 flexural, perfectly conducting solid circular in presence of uniform mag. field 8=15032
 with harmonic excitation, use of mass as perturbation parameter 8=19505
 linear, complementary variational principles 8=10692
 linear systems, response to stochastic impulses, non-stationary 8=6128
 loaded elastic continuum 8=23
 longitudinal, of paraboloidal bar 8=19512
 mechanical, use of vibrators in adjustable l.f. oscillators 8=19495
 metals on solidification, rel. to nucleation 8=4796
 metals, supercooled, rel. to dynamic nucleation 8=21760
 motion of body over tangentially vibr. surface allowing for friction 8=19493
 natural, of simple elastic structures, effect of initial finite deformation 8=15031
 organ pipes, self excited 8=10749
 of orthotropic stiffened plates and grillages, analysis 8=49
 parametrically excited random vib. system, almost sure stability conds. 8=19499
 particle restrained by two springs 8=10681
 plate, flexural waves, oblique incidence on slender obstacle 8=19521
 plate, infinite, driven by point source, near sound field 8=10725
 in plate in narrow channel, flow-induced 8=19497
 plate in plane supersonic flow, nonstationary parametric and self excited 8=15033
 plates, thin elastic, under random loading, and sound radiation 8=10729
 pressure field, random continuous, representation by discrete set of point excitations 8=19509
 random, of multidegree-of-freedom hysteretic structures 8=3017
 rigid disk on isotropic elastic plate calc. 8=3015
 sandwich, spherical caps with clamped edges, nat. freqs. inc. effect of thickness-shear deform 8=19488
 shells with variable curvatures, harmonics 8=19387
 solid friction, high frequency behaviour 8=3023
 of spherical caps, approx. solns. for freqs. of axisymmetric vibs. 8=19489
 springs connecting air-suspended discs, wave motion demonstration 8=10678
 superhigh-freq., (Ti-Mg) and (Ti-Be) oxide energy absorbers 8=10458
 thickness-shear in AT-cut quartz plates with partial electrodes 8=19501
 torsional in rigid disc on surface of elastic half-space 8=10689
 torsional, of spherical caps and circular plates 8=19490
 transverse of a moving thin rod 8=19485
 two-dimensional regions with irreg. boundaries, construction of eigenfunctions 8=19510
 2-layered plates, flexural and extensional, theory 8=148
 universe models, normal modes and stability 8=14732
 vibrators and librators perturbed by collisions 8=100
 wave machine, dispersion, reflection and eigen-frequencies 8=10937
 α -Fe, (b. c. c.), torsional, impurity-induced internal friction peak (Snoek's peak), anisotropy 8=13572
 MnHg, atomic thermal vibrations amplitudes at 298°K 8=8236
 Si-Fe, (b. c. c.), torsional, impurity-induced internal friction peak (Snoek's peak), anisotropy 8=13572
 Zn crystals, rel. to growth 8=8430

excitation

- eye, by humming, strobe vision effect 8=20128
 fibres, electrostatically driven in vibroscope, polarizing voltage effect on frequency 8=6124
 friction-induced, critical velocity theory 8=10682
 thermal, of mechanical oscillators 8=10697
 Al plates of constant cross section, high order Lamb waves 8=19491

measurement

See also Seismology.

Vibrations—contd**measurement—contd**

- mechanical, combination and mechanical resonance 8=142
 oscillators, minimum detectable disturbance, meas. by optical resonator 8=10683
 strings, stiff, normal frequencies, device 8=6171
Vibronic states. See Molecules/electronic structure; Molecules/vibration
Vidicons. See Electron tubes.
Virial coefficients. See Equations of state.
Virtuons (virtual phonons). See Crystals/lattice mechanics.
Viscoelasticity
 See also Plasticity.
 advances in applied mechanics, book IX 8=16747
 beams, stress waves propag. and reflection 8=14954
 biwaves, loading and unloading in elastic-visco-plastic body, strain hardening effect on propag. 8=17718
 circular plates, effect of random temperature distributions 8=10572
 contact problem in linear theory 8=10575
 crack propagation 8=2045
 dislocation losses in strain field 8=16617
 displacement in infinite slab due to transient twisting forces on surface of cylindrical cavity 8=19404
 dynamic shear, in model materials, thermistor analog study 8=62
 Earth model, elastic and viscoelastic behaviour 8=14948
 elastic-viscoplastic semi-infinite body, loading and unloading biwaves, numerical analysis 8=10565
 elastic-viscoplastic semi-infinite body, propag. of loading and unloading biwaves 8=10564
 elastic-visco-plastic semi-space, plane biwaves 8=10569
 elastic-visco-plastic waves, longitudinal, in finite bar, resonance 8=10568
 elastomer, tensile test and linear props, obs. 8=22400
 flow of fluids through porous media 8=21573
 fluid Couette flow, linear instability 8=7869
 fluid, decay of isotropic turbulence, non-Newtonian effects 8=12645
 fluid flow through porous media 8=1446
 of fluid, plane Poiseuille flow, effect on hydrodynamic stability 8=16632
 fluids, restrictions on velocity probes 8=12603
 fluids, turbulent heat-transfer characts. 8=4426
 linear fluids, Maxwell type, flow near osc. or accelerating plate 8=21559
 liquid film motion under gravity 8=12736
 liquids, Brillouin scattering obs. 8=16839
 liquids, linear, steady, two-dimens. flow 8=12725
 liquids, turbulent heat flow 8=1510
 macromolecular networks 8=21209
 materials, calc. of acceleration waves 8=10570
 nonlinear, generalized creep function and inversion 8=61
 nonlinear, generalized superposition principle 8=60
 nonlinear, stress/deformation relation 8=2929
 polybutylmethacrylate shear pliability freq. depend., obs. 8=22404
 polyisobutene shear pliability freq. depend., obs. 8=22404
 polymer melts 8=16748-9
 polymeric bodies, meas. method based on Volterra operator 8=13616
 polymers, crosslinked, theory 8=8873
 polymers, and rheology, temp. dependence 8=2071
 polymers, and structure 8=8869
 polystyrene 8=8878
 polystyrene in chlorinated biphenyl solns., 40 MHz 8=12818
 polystyrene solns., mol. wt. depend. 8=8030
 relaxation, Isakovitch-Chaban theory 8=16771
 shear waves in finite strain at surface of a half-space 8=15035
 spherical wave, propag. and reflection in viscoelast. medium, closed form soln. 8=10567
 static and dynamic props. using a torsional pendulum 8=8880
 stress waves, plane, produced by moving load in elastic plastic medium 8=10566
 textile fibres 8=17846
 theories, experimental evaluation 8=1535
 torsion of conical rod 8=14956
 turbulence, fine-grained, isotropic, visco-elastic character 8=4441
 waves in viscoelastic media 8=10709
 S, polymeric, relax. mechanisms 8=4267
 Se films, evaporated, properties, obs. 8=21888

Viscometers

- double cone, for non-Newtonian liquids, theory 8=12821
 for glass-forming oxides melts, high temp. and press. 8=8022
 pressurized capillary for liquids 8=21633
 radioactive, sinking ball principle 8=21631
 rotating Cartesian-diver 8=4548
 single rotating cylinder for plastic laminar flow 8=21632

Viscoplasticity. See Plasticity**Viscosity**

- aerosol separation, viscous momentum transfer effect 8=21736
 butyl phthalate, compared with dielec. and spin-lattice nuclear relax. 8=9459

Viscosity—contd

- critical mixtures, nonlinear effects in shear viscosity 8=8163
- dislocation losses in strain field 8=16617
- equilibrium layers, turbulent, eddy viscosity 8=16640
- in Fermi liqs., nearly ferromag. 8=2994
- fluid, effect on gravity waves, internal, at critical level 8=7887
- fluid, single-component, new eqn. 8=1438
- fluid, turbulent, associated with transfer of mean square vorticity across energy spectrum 8=12635
- glasses, in range 10^{12} to 10^{14} poises, viscosity-temp. data, fibre elongation approx. 8=17725
- laminar flow around semi-infinite obstacle 8=7864
- at liquid-gas critical point 8=21745
- MHD, due to rotating sphere 8=15370
- MHD turbulent flow friction coeff. in ducts 8=6356
- negative, production in presence of buoyancy and shear 8=21441
- oceanic and atm. motions, large-scale 8=23237
- polymer solutions, concentration var., compression of chains 8=4545
- polymer solns., time-depend. charges 8=8023
- polymers, homo- and graft co-, in soln., intrinsic viscosity and free energy 8=1536
- Reynolds number determ., magnetic 8=6352
- spherically symmetrical molecules 8=7630
- suspension of solid spheres, concentrated 8=8149
- viscous shear motion, finite propag. speed 8=239
- water, surface boiling in vertical tube, local fluid friction 8=12989

gases

- acetone, 30-200°C, for intermolecular potential information 8=21523
- boundary layer, compressible, kinematic eddy analysis 8=21489
- chloroform, 30-200°C, for intermolecular potential information 8=21523
- in critical region 8=4490
- diamagnetic mixtures, Senftleben-Beenakker mag. field dependence 8=21524
- diatomic, low-temp. in stationary mag. field 8=7919
- in diffuser, resultant force on sphere due to press. and shear forces 8=16717
- dilute, diamagnetic gas in external mag. field 8=12703
- ethyl alcohol, 30-200°C, for intermolecular potential information 8=21523
- flow behind detonation, friction effects on transition to steady flow 8=15058
- helium, effect of organic vapour molecules, for determ. of molec. dims. 8=1485
- hydrogen, effect of organic vapour molecules, for determ. of molec. dims. 8=1485
- induced drag of elliptically loaded lifting line in exponentially sheared flow in vertical dirn. 8=16677
- inert, binary mixtures, Sutherland-Wassiljeiva coeffs. 8=7940
- ionized, anisotropy effect on plane parallel flow in coplanar mag. field 8=16494
- ionosphere, model for e.m. wave propag. effects 8=19903
- methyl alcohol, 30-200°C, for intermolecular potential information 8=21523
- mixtures, calc. from potential parameters 8=21522
- molecular, in perpendicular stationary and varying fields 8=21493
- multicomponent mixts., Chapman-Cowling third order bracket integrals 8=16713
- multicomponent mixtures, additional matrix elements for third approx. 8=12700
- plasma, in strong mag. field influencing particle collisions 8=16482
- polyatomic, mag. fields effects, 290°K 8=1484
- Rayleigh instability theory 8=4546
- stagnation point laminar boundary layers and shock layer eqns., soln. in presence of chem. reactions 8=16671
- Ar plasmas, partially ionized 8=7734
- Cs vapour, in temp. range 1000°K to 2400°K, meas. by transpiration method 8=16714
- Cs vapour, from 800 to 2000°K, meas. by transpiration tech. 8=12702
- H₂, partly ionized, calc. 8=12701
- He, low-temp., high press. 8=4493
- He-N₂ mixtures, low-temp., high press. 8=4493
- N₂, low-temp., high press. 8=4493
- NH₃-methylamine mixtures 8=4492

liquids

- See also Lubrication; Superfluidity.
- acoustic wave propagation, non-Newtonian viscous liquid 8=16830
- alcohol-water mixtures and structure of water 8=4549
- n-alkane mixtures, congruence principle 8=8024
- aniline in CS₂ and CCl₄ solution, effect on nuclear relax. time 8=8126
- cellulose derivatives solns., Newtonian 8=8025
- cyrogenic liqs, correl. with thermal cond. and self-diffusivity 8=15132
- dynamic shear impedance for low visc., meas. at u.s. freqs. 8=4547
- elastic solid permeated with non-Newtonian fluid 8=19381

Viscosity—contd**liquids—contd**

- elastico-viscous fluid, drag on oscill. sphere 8=21557
- flow in circular pipe with absorbing walls 8=21630
- flow in rectangular open channel 8=7975
- flow in a tube at const. temp. 8=12734
- flow, numerical method of soln. 8=21626
- glass-forming oxides, molten, high-temp., high-pressure viscometer obs. 8=8022
- jet of infinite σ in magnetic field, oscills. 8=1518
- high, theory rel. features of n.m.r. 8=4619
- hydrocarbons, thermal props. from similarity theory 8=21646
- hydroxyethyl cellulose aqueous soln, drag coeff. on falling spheres 8=12724
- intrinsic, determ. from meas. of one value of relative viscosity 8=16809
- methane-propane mixtures, at low temp. and high press. 8=12819
- Navier-Stokes soln. for surface waves 8=7983
- nitrate melts, binary mixtures of Ca(NO₃)₂ and MnO₃ (M = Na, Cs, Rb, K), supercooled, rel. to relax. processes 8=1586
- non-Newtonian, theory of double cone viscometer 8=12821
- phosphates, molten, rigid sphere model 8=7999
- plastic laminar flow, automatic viscometer 8=21632
- polyelectrolytes in salt solns., excluded vol. effect 8=12810
- polyethylene oxide aqueous soln, drag coeff. on falling spheres 8=12724
- polymer solutions, theory tests 8=8029
- polymer solns., drag-reducing effects in turbulent flow past cylinders 8=16754
- polymer solns., flow, conc. depend. of activation energy 8=16807
- polymer solns., influence of intermolecular hydrodynamic interaction, and streaming birefringence 8=4505
- polymer solns., intrinsic, determ. from meas. at a single point 8=16808
- polymer solns., Newtonian 8=8025
- polymer solns., polynomial expansion of log relative viscosity 8=16805
- polymer solns., rel. to sedimentation coeff. 8=12823
- polymers, and non-Newtonian flow 8=16759
- polymethacrylic acid in alcohol-water solution 8=12822
- polymethacrylic acid solns., intrinsic 8=12817
- polystyrene and poly(methyl methacrylate) graft copolymer solns. 8=8027
- polystyrene conc. solns. dependence on molecular weight and concentration 8=8026
- polystyrene in chlorinated biphenyl solns., 40 MHz 8=12818
- polystyrene solns., mol. wt. depend. 8=8030
- poly(vinyl acetate) conc. solns. dependence on molecular weight and concentration 8=8026
- polyvinyl alcohol in aq. salt solns. 8=21634
- propanol-H₂O mixtures, with NaCl in soln. 8=4606
- pyridine in CS₂ and CCl₄ solution, effect on nuclear relax. time 8=8126
- radioactive viscometer, calibration and accuracy on silicone oil sample 8=21631
- Rayleigh instability theory 8=4546
- rubber soln., effect of amines 8=21625
- shock wave propagation 8=168
- silicate melts, Newtonian flow and bond rearrangement 8=21628
- sphere rolling in closed-end fluid-filled tube, incompressible fluid drag force 8=21629
- surface wave impedance calc. 8=16775
- ultrasonic transducer meas. 8=8028
- viscometer-gelation timer 8=16810
- volume, rel. to u.s. compression waves absorpt. and vel., theory 8=16804
- water, pressure to up 230 Kg/cm² and temp. 12.5-108°C 8=8021
- water, 25°-150°C 8=21633
- wave propag., symmetric modes, in cylindrical rigid and elastic conduits 8=16773
- Ar, shear viscosity coeffs., elec. meas., 0-200 Kg/cm² and 86-146°K 8=12820
- B₂O₃, molten high-temp. high-pressure viscometer obs. 8=8022
- D₂O at pressures 1-1200 kg/cm², 4-100°C 8=26806
- H-bonded, shear compliance and free volume 8=1537
- He³, pressure dependence, spin-fluctuation theory 8=19693
- He³ spin rel. to Rice theory of nearly ferromagnetic Fermi liquids 8=10800
- He³ in He³-He⁴ mixture, attenuation of sound propag. 8=10801
- MnSO₄ in water-glycol, effect on elec. cond. 8=12921
- N₂, volume visc. from u.s. attenuation meas. 8=1538
- Na-K alloys, K:49, 51 and 74% at 300°C 8=21627
- S, polymeric, relax. mechanism 8=4267

Visibility. See Atmospheric optics.**Vision**

- See also Colour vision; Eye; Stereoscopia.
- acuity, effect of oriented adapting patterns 8=15577
- asymmetric convergence of eyes, stereoscopic frame of reference 8=11227

Vision—contd

- binocular brightness summation, underlying processes 8=11236
- binocular rivalry, disappearance of patterns 8=11234
- brightness perception in complex fields 8=540
- early dark adaptation rel. to wavelength and pre-adapting level 8=3385
- electroretinogram, dependence on point of pupil entry 8=3386
- electroretinography, use of c.w. laser 8=11233
- entoptic effect following strong illumination 8=538
- eye, and looking through binoculars 8=3383-4
- flicker effect on eye movements 8=15574
- frequency-contrast characts. calc. by Hopkins method 8=20045
- frequency doubling 8=539
- human lens, thin shell deformation analysis 3=15573
- humming, eye vibration strobe effect 8=20128
- light sources, against background of uniform luminance, visibility 8=11230
- lighting and quantitative parameters of visual tasks 8=11232
- luminance difference between temporally separated flashes 8=3388
- Mach band brightness distrib., lateral nervous interaction 8=15578
- ocular and occipital responses, variation with stimulus patterns 8=11229
- photopic, mesopic and scotopic 8=11231
- physiological optics, survey of current state 8=6587
- resolution of square-wave grating patterns 8=15576
- retinal image stabilization with plane mirror on tightly fitting contact lens 8=15575
- retina structure model rel. to Stiles-Crawford effect 8=15570
- spontaneous saccadic eye movements, resulting visual threshold changes 8=11228
- subjective brightness of very-short-persistence television display 8=541
- thresholds, in-phase and out-of-phase, comparison 8=3387
- turtle retinas, isolated, directional sensitivity 8=3391
- units of light, visual effects 8=461
- visual evaluation of interior lighting 8=459
- visual potential, modification by monochromatic backgrounds 8=11235
- X-radiation response of human eye 8=6585

Vitreous state

- See also Glass
- diethyl phthalate, ht. capacity 8=1870
- dry modulus of rupture and drying shrinkage, response surface anal. 8=17737
- glass-forming systems, radiation-induced solid-state polymerization 8=18711
- ice, diff. spectrum, comparison with water 8=8355
- polymers, glass transition, press. effects 8=8359
- relaxation, Adam-Gibbs model 8=4563
- semiconductors glasses polarizability 8=9505
- As-Se alloys, introduction of Cu atoms 8=13111
- As₂Se₃, heat treatment effect on electrical conductivity 8=8991
- As-S-Se partially vitreous system, sintering obs. 8=13053
- C, oxidation pitting comp. with pyrolytic graphite 8=8292
- Se, atomic radial distrib. function rel. to quenching from different melt temps. 8=1714
- SiO₂ films, i. r. absorpt. 8=5637

Vlasov equation. See Plasma.**Vocoders.** See Speech.**Voigt effect.** See Magneto-optical effects.**Volta effect.** See Contact potential.**Volume measurement**

- organic binary liq. mixtures, volume changes 8=1528
- α -Fe, dilation by C 8=17615
- K-NH₃ dilute soln., absence of vol. change on dilution at -34°C 8=1530
- Na-NH₃ dilute soln., absence of vol. change on dilution at -45°C 8=1530
- SiO₂-UO₂ vitroceraamics, irradi. induced vol. changes and annealing 8=8779

Vortices

- See also Cavitation; Turbulence.
- atmosphere, Ekman spiral instability suppl. to boundary layer 8=14601
- atmospheric boundary layer, alternating and horizontally rolling with axes in mean flow direction 8=14600
- bath-tub vortex, generalized theory inc. secondary flow and initial ang. vel. 8=21578
- breakdown, 'conjugate-flow' theory 8=4513
- core, laminar diffusion flame, flow field and swirling motion 8=15111
- eddies, shear flow, deductions from space-time correlation obs. 8=12605
- in flow fields due to curved shock waves, rel. to perturb. of entropy layers 8=16652
- fluid, charged, relativistic in e. m. and gravitational fields, Helmholtz eqn. 8=16633
- fluid, curved flow, rate of change of vorticity components 8=12619
- fluid, cylinder-wake, large structure 8=12627

Vortices—contd

- fluid, eddy rel. to mean states, Eulerian vector 8=12630
- fluid, large, in homogeneous turbulence statistical props. 8=16636
- fluid, rot. stratified, second circulation generation 8=12637
- fluid, surface-distribution integral eqn. used to solve flow through orifice 8=16625
- fluid, turbulent boundary layer, and correlation obs. 8=12615
- fluid, turbulent displacement variance, conservation and moment of moment eqns. 8=12629
- fluid, wakes of cylinders, transition to turbulence of separated boundary layer, obs. 8=12620
- forced and periodic breakdown of confined vortex rotating in opposite direction 8=21469
- free-stream effects on parameter of flow in region of separated zones 8=12644
- gas, generation of free, factors affecting 8=7904
- gas, suppression of shedding behind oscill. cylinder, expt. 8=12666
- inviscid flow past delta wing, field near centre of rolled-up sheet 8=1459
- in jets, evolution 8=21437
- linear polymers in the turbulence vortices 8=12946
- liquid, boundary layer transition, hydrogen bubble obs. 8=12740
- liquid, shedding in wake of cylinder 8=12752
- liquid, translating cavity, equilibrium and stability 8=7982
- magneto fluid, generated by a shock 8=19815
- magnetogasdynamic shock wave, region behind 8=6358
- relativistic theory 8=7878
- shock-front interaction, rel. to sound generation 8=188
- superconductor, analogy of self-trapped filaments of laser light in liquids 8=4577
- Taylor flow, perturbation instability 8=12643
- Taylor, obs. in eccentric cylinders 8=21577
- wakes behind two-dimens. air bubbles 8=12767
- water, Karman, in wake of rot. cylinder, obs. 8=12751
- in He, superfluid, flowing through orifices, form. and critical vel. obs. 8=6234
- He II rotating annulus, quantized vortex lines threshold obs. 8=10810
- He II, rotating, interaction of quantized vortex and lines 8=10804
- He II, rotating, wave propagation 8=262
- He II, superfluid in rotating annular channel 8=10809
- He II, vorticity in flow through orifices 8=19699

WKB method. See Quantum theory
Water

- See also Ice; Seawater; Steam.
- acidified, proton exchange rel. to O¹⁷ n. m. r. linewidth 8=1599
- acoustical effects on free convective transfer from horizontal wire 8=21663
- adhesion of glass spheres 8=8150
- adsorbed, interactions of electrons 8=21907
- adsorption on Al, effect on electron emission 8=9270
- air-water vapour mixtures, third virial coeff. 8=4468
- alcohol mixtures, viscosity and structure 8=4549
- atmosphere, gas constituent number density determ. using laser beams 8=14585
- in atmosphere ground layer, vapour 183-31 GHz absorpt. line shape, obs. 8=23295
- in atmosphere, unstable, vapour turbulent transport obs. 8=23260
- Brillouin shifts, temp. dependence, hypersonic velocity and compressibility deduction 8=1502
- burnout, forced convection boiling 8=4657
- capillary at liquid surface, thermal excitation by scattering of coherent light 8=16853
- cation hydration, charge-dipole model 8=9670
- cavitation damage data for venturi and vibratory systems 8=16767
- cavitation damage to metals 8=5035
- in channel, formed by bundle of rods or tubes, heat transfer to 8=12849
- Cherenkov time resolution function obs. 8=5690
- combined in solids, n. m. r. 8=5546
- in concrete, diffusion, between 50 and 95°C, further comments 8=22148
- 'condensation' or mass accommodation coeff. 8=16940
- convection, penetrative, with lower boundary at 0°C and upper at above 4°C 8=16825
- corona, impulsive, elect. and hydrodynamic characts. 8=21250
- Debye temp. calc., quasi-crystalline model 8=1544
- deep, wave instability of periodic trains 8=18
- diffusion of vapour into CaO, effect on sintering kinetics, 920-123°C 8=21833
- n dosimetry by ultrasonic cavitation 8=3721
- drops, distortion and disintegration in elect. fields 8=21595
- drops free falling in elect. field, mass loss and distortion 8=21586
- drops in vertical wind tunnel, collision, coalescence and breakup obs. 8=1519

- Water**—contd
- droplets, charged evaporating, supported by elect. field, instability lab. obs. 8=7992
 - dynamics in $\text{Na}_2\text{S}_2\text{O}_8$, $2\text{H}_2\text{O}$ and $\text{Li}_2\text{S}_2\text{O}_8$, $2\text{H}_2\text{O}$, from structure studies 8=8538
 - dynamics in $\text{Na}_2\text{S}_2\text{O}_8$, $2\text{H}_2\text{O}$ and $\text{Li}_2\text{S}_2\text{O}_8$, $2\text{H}_2\text{O}$ crystals, H^+ -n. m. r. spectra and struct. 8=8537
 - electric breakdown, dimensional and similarity analysis 8=8114
 - electric charge on drops ejected by bursting air bubbles at surface 8=8117
 - e-photon cascade induced by e (0, 1-20 GeV) and photons (0, 0.1-20 GeV) at normal incidence 8=21722
 - flow in wake of rot. cylinder, obs. 8=12751
 - flow, viscogravitational, in horizontal tube 8=12730
 - flowing in clear plastic tube, vel. meas. by H bubble tech. 8=16756
 - flowing past fixed CO_2 bubble, interphase mass transfer 8=12764
 - γ -beam scatt., differential albedo obs. 8=16844
 - glycerol and water mixture, acoustic absorpt. rel. to macromolecule formation 8=8057
 - hailstones, liquid water content 8=23276
 - heat transfer through four layer system of air, snow, sea ice and water 8=23226
 - heavy and light Fricke dosimeter solns. ferric ion yield after 14.6 MeV n and $\text{Co}^{60}\gamma$ bombard. 8=9733
 - heavy, level meas. telemeter for reactor 8=1135
 - heavy water dynamics in $\text{Na}_2\text{S}_2\text{O}_8$, $2\text{D}_2\text{O}$ cryst. 8=8539
 - homogeneous nucleation from vapour, critical super-saturation 8=1621
 - hydrogen ion solvation in gas phase, kinetics and thermodynamics 8=18661
 - ice V, crystal structure 8=17377
 - ice/water interface, electrostatic potentials 8=18723
 - inclusions with metastable superheated ice under high neg. pressure within minerals 8=1609
 - induced cracks in cured polyester resins 8=13622
 - in ionic concentrated solns, Raman spectra 8=1565
 - isotopic anal. of micro quantities 8=22151
 - isotopic var. of specific mass 8=7478
 - laminar flow round CO_2 and N_2O bubbles, obs. 8=21591
 - lasers, gas, far i.r. construction and characts. 8=425
 - light and heavy, volatility, effect of inorganic salts 8=21774
 - liquid-vapour interface potential, molec. theory 8=12196
 - methane-water vapour mixture, vib. Napier relax. time 8=4481
 - mixture, in vertical pipes, hydrodynamics 8=21560
 - moderator for reactor, UO_2 fuel, material buckling and reaction rates 8=20904
 - molecular dia. from solubility and diffusion meas. 8=21606
 - molecular diffusion coeffs. of dissolved H and He 8=12828
 - molecular dipole moment, matrix components 8=7521
 - molecule, Compton profile, unified atoms method 8=1256
 - molecule in lowest bent state, effects of quasi-linearity 8=1243
 - molecules adsorbed in oxide films on Si, dielectric relax. 8=1706
 - on Moon surface, evidence 8=23634
 - muonic molecule, ($\mu\text{H}_2\text{O}$) possible formation and vibrational frequencies 8=21218
 - neutron thermalization, rel. to poison concentrates 8=7331
 - permittivity, 1.2 to 1.6 mm 8=21707
 - permittivity meas. at 8.6 mm from 1°-60°C 8=16873
 - polarity-reversal electrolytic purification, optimum reversal time 8=18734
 - with polymer additives, effect on turbulent shear flow 8=16764
 - pool boiling, effect of subcooling on wall superheat 8=21772
 - proton-spin lattice relax. times, n. m. r. search for thermal anomalies 8=16885
 - radiolysis with 10% ethanol, yield of solvated electrons 8=23167
 - rehydration monitoring, appl. of n. m. r. 8=23770
 - Sahara basins, evolution of isotopic comp. during evaporation 8=18832
 - saturated pool boiling heat transfer, effect of interfacial vibration 8=12985
 - shallow, u. s. propag. loss at sonar freqs. 8=1554
 - at silica gels, proton relax. 8=12932
 - solubility of AgCl in, rel. to liquid structure 8=21608
 - sound amplification, parametric, with uniformly distributed bubbles 8=12864
 - sound propagation model 8=3055
 - specific volume at high press., u. s. meas. 8=21623
 - spectral attenuation coeffs., relative 8=12888
 - spin-rotation constant 8=1242
 - steam-borne drops, collision behaviour 8=21593
 - structure, influence of alkali halides 8=4527
 - structure and H bonds from thermodynamic functions, n. scatt. meas. 8=1525
 - structure, and nature of H_2 bond. 8=4529
 - structure, role in interpretation of colloid stability 8=12948
 - subcooled boiling in tube, heat-transfer rate 8=21657
 - supercooled, ice growth velocities 8=17236
 - supercooled to -50°C, u. s. velocity rel. to precrystallization theory 8=13353
- Water**—contd
- surface boiling in vertical tube, local fluid friction 8=12989
 - thermal properties discontinuities 8=8045
 - thermostatic bath with $\pm 70^\circ\text{C}$ stability 8=15124
 - tritiated, analysis, water vapour counter 8=9748
 - trace analysis, spectrochemical 8=18773
 - tritiated, scintill. probe for monitoring 8=3737
 - turbulent flow in square duct, temp. distribution in wall, obs. 8=1545
 - two-state model, Raman data 8=21690
 - ultrasonic mixing obs. 8=21554
 - vapour, adsorption on cleavage surface of alkali halides 8=17166
 - vapour, adsorpt. on Re-Nb alloy, study by work function behaviour 8=13927
 - vapour, atmospheric, i. r. absorption over slant path 8=18879
 - vapour, attenuation of m. m. wavelength rad. 8=9865
 - vapour, band emissivities, evaluation 8=16272
 - vapour- CO_2 mixtures, ultrasonic absorption obs. 8=7931
 - vapour diffusion, in cation exchange membranes 8=8040
 - vapour, effect on BaO cathode emission 8=18663
 - vapour, effect on CdS trapping spectrum 8=5396
 - vapour, effect on radiation from CO_2 - N_2 -He laser 8=11045
 - vapour, H^+ , H_2^+ , He^+ charge exchange, 40-1500 eV 8=21275
 - vapour, interact. and absorpt. with W films, rel. to catalytic activity 8=14405
 - vapour laser, 118.6 μm transition, freq. meas. 8=10482
 - vapour laser transition, 220 μm , absolute freq. meas. 8=19972
 - vapour laser, Zeeman effects in 118.65 μm transition 8=3311
 - vapour, mm wavelength radiation attenuation 8=12689
 - vapour and O_2 , mixture, sound absorption obs. 8=1476
 - vapour, partial photoionization cross-sections, determ. by photoelectron spectra 8=1369
 - vapour pressure, H-bond effect 8=4662
 - vapour pressure over 11 desiccants, 90°C 8=5717
 - vapour, pulsed laser action due to vibration-rotation transitions 8=3312
 - vapour, pure rot., spectrum 8=4149
 - vapour, sparkover in mixtures with air 8=12412
 - vapor, stratosphere, absorption spectra obs. 8=14587
 - vapour turbulent transfer, atmosphere, at different stability conds. 8=14611
 - vapour, 2.7 μm bands radiant emission, compared with general band model 8=7520
 - u. s. velocity at up to 10^7 g cm^{-2} , 80°C 8=16831
 - viscosity of liquid 25°-150°C 8=21633
 - viscosity pressure up to 230 Kg/cm^2 and temp. 12.5-108°C 8=8021
 - wavemeter, parallel wire resistance, dynamic testing 8=7986
 - water-ethyl alcohol mixture, thermal diffusion meas. of separation 8=12838
 - waves, small, acoustic energy, backscattering, apparatus and method of analysis 8=6168
 - waves, variational methods 8=1516
 - X-ray scattering 8=8077
 - Ar laser beam thermal defocusing obs. 8=16845
 - C^{14} content obs. 8=2566
 - D_2O , viscosity at pressures 1-1200 kg/cm^2 , 4-100°C 8=26806
 - H isotope composition in atmospheric precipitation fractionation 8=2503
 - H_2O molecule, SCF calcs, correlation energies and Hartree-Fock limits 8=1263
 - H_2O mols. in solid SO_2 hydrate, l. f. vib. spectra 8=1840
 - H_2O and D_2O , domain theory of surface tension 8=4550
 - H_2O - D_2O mixtures, comp. determ. by F^{19} n. m. r. 8=14454
 - H_2O^{18} and D_2O^{18} , relax. parameters calc. 8=12780
 - H_2O^{17} , O^{17} n. m. r. shifts 8=16896
 - KX, (X = Cl, Br, I), solubility and diffusion of H_2O mols. 8=4953
 - N bubbles, decay constants and pulsation frequencies determ. 8=21588
 - T_2O and D_2O , vapour pressures 8=21780
 - from TiO_2 , desorption rate, 25-100°C 8=18703
 - Y_2O_3 , adsorption, i. r. spectroscopy obs. 8=4768
- Wave equations, quantum theory.** See Quantum theory/wave equations.
- Wave functions.** See Quantum theory/wave equations.
- Wave mechanics.** See Quantum theory.
- Wavefront-reconstruction imaging.** See Diffraction/light; Optical images.
- Waveguides.** See Electromagnetic wave propagation/guided waves.
- Waves**
- See also Acoustic waves; Elastic waves; Electromagnetic waves; Liquid waves; Magnetohydrodynamics; Seismic waves; Shock waves.
 - acceleration, in elastic nonconductors, amplitude, rel. to extrinsic body sources and heat supply 8=19517
 - acceleration type in elastic material of finite thermal, and infinite elect. conductivity 8=15042
 - adiabatic invariant for propagation, discussion 8=21
 - aggregate of particles, fluid-saturated, compressional wave vel. 8=22270

Waves—contd

- autocorrelation calculations for periodic functions 8=14938
- axial shear waves, radial propag. in nonhomogeneous elastic media 8=3026
- axisymmetric, in long composite rods, asymptotic phase vels. 8=3014
- beats and Lissajous figures, demonstration using turntable oscillators 8=10680
- circumferential in cylinder, thin-walled, reflection at slit 8=6133
- collapsed cylindrical detonation in gases 8=7907
- correlation group method in random medium 8=2903
- damped, frequency modulation theory 8=2902
- detonation, converging in medium with var. initial density 8=3039
- detonation, motion of gas behind 8=4461
- dispersion curve parameters, determ. from transient wave 8=141
- electrostatic in cold magnetized plasma, nonlinear interaction of three 8=4355
- flexural, in semiconductor plate, theory of instability 8=17496
- fluid, internal gravity at critical level, viscosity and heat conduction effects 8=7887
- fluid, internal gravity, propag. with shear flow and rotation 8=7885
- fluid, internal oscillatory, stability 8=7882
- fluid, nonlinear resonant, stability criteria 8=7886
- fluid, viscous, Tsunami problem 8=12648
- free-surface waves, interaction with viscous wakes 8=21449
- gravity, instability 8=21450
- gravity, interactions 8=19
- gravity in upper atmosphere, interactions 8=23310
- gravitational 2 spinning rods as source 8=19427
- Helmholtz equation, Bremmer series convergence 8=14939
- interface waves at bonded interface, existence rel. to bond stiffness and wavelength 8=19524
- internal gravity, ionosphere, propag. rel. thermal conditions 8=9994
- intersections, analysis by vector polar method 8=19526
- Korteweg-de Vries eqn., asymptotic soln. 8=2901
- Korteweg-de Vries equation, solution 8=2900
- in linear elastic bars, rectangular, dispersion of longit. or extensional waves 8=19515
- liquid, production, experimental study 8=7985
- longitudinal, excitation across plasma column with axial mag. field 8=16581
- Lorentz group, inhomogeneous, nonzero mass components 8=2892
- machine, dispersion, reflection and eigen-frequencies 8=10937
- m. h. d., propagation in horizontally stratified media 8=7748
- motion demonstration using air-suspended discs connected by light springs 8=10678
- nonlinear dispersive, asymptotic interaction 8=10511
- nonlinear envelope propag. 8=10512
- nonlinear interactions 8=20
- periodic, instability of 8=18
- plasma, ion waves, longit., propag. near and above ion plasma freq. 8=21297
- propagation in inhomogeneous media 8=6374
- propagation in plasma, models 8=12543
- propagation in relativistic fluid 8=7888
- propagation, inverse problems 8=10702
- propagation through a stratified medium 8=13497
- pressure in atmosphere after nuclear explosion 8=2583
- quantum in semimetals in strong magnetic fields 8=5235
- in randomly fluctuating medium, quantum theory techniques application 8=2986
- refractive medium, $\pi/2$ phase shift 8=19546
- refractive medium $\pi/2$ phase shift due to total internal reflection 8=19547
- scattering from point source in random medium 8=19366
- soliton, description using Korteweg-de Vries 8=2900
- spherical finite amplitude, fluid or elastic medium, calc. 8=19516
- spin density, existence theorem for 3D e gas 8=15022
- in spinning membrane, soln. for nonlinear, flexural, asymmetric waves 8=19498
- stationary, method of averaging 8=140
- Stokes' transformation in non-uniform medium 8=2899
- teaching films 8=19548
- theory, teching by phasors 8=3013
- transversal, surface, in thin contactless piezoelectric layer of body 8=10711
- two-dimensional propagation, lacunas 8=10510
- in viscoelastic media 8=10709
- in vortex breakdown, 'conjugate-flow' theory 8=4513
- variational methods 8=1516
- Whitham theory, applications 8=1517

Waxes

- film on painted surface, thickness and roughness determ. 8=2470
- paraffin, persistent electric dipole moment obs. at -78°C 8=13890
- shellac, electret surface charge obs. 8=13892

Weak interactions. See Field theory, quantum/interactions. weak.

Wear

- ablation of cones, obs. 8=22301
- lubrication and wear, conference, Plymouth, England (1967) 8=13521
- polymers reinforced with C fibres 8=13618
- steel, rel. to carbide diffusion 8=17788
- Cu contacts rel. to arc current 8=12415
- Cu, erosion by liq. droplets 8=22333
- Fe alloys, resistance, influence of strengthening mode 8=8847

Weather. See Meteorology.

Weighing. See Balances; Mechanical measurement.

Weissenberg cameras. See Cameras; X-ray crystallography/apparatus

Wentzel-Kramers-Brillouin method. See Quantum theory.

Wertheim effect. See Magnetomechanical effects.

Wetting

See also Capillarity.

- elastomers, rel. to adhesion 8=17841
- glass spheres adhesion, in water or mineral oil 8=8150
- group VI a elements, critical surface tension 8=21869
- organic liquid spreading on soda-lime glass rel. to adsorped water effects 8=1520
- polycapromide fibres, CF_3 radiation grafting effects, obs. 8=22410
- polyethyleneterephthalate fibres, CF_3 radiation grafting effects, obs. 8=22410
- polyethylene, relation between adhesion and wettability 8=8879
- polymers by glycerol rel. to melts heterogeneous nucleation, substrate effects 8=8298
- polypropylene fibres, CF_3 radiation grafting effects, obs. 8=22410

Whiskers. See Crystals/whiskers

Whistlers. See Atmospherics; Ionosphere

White dwarfs. See Stars.

Wiedemann effect. See Magnetomechanical effects; Magnetostriction.

Wiedemann-Franz Law. See Conductivity, electrical/solids; Conductivity, thermal/solids

Wien effect. See Conductivity, electrical/liquids, electrolytic.

Wigner coefficients. See Quantum theory

Wigner effect. See Physical effects of radiations

Wilson cloud chambers. See Cloud Chambers.

Wind

- atmospheric boundary layer profiles, approx. soln. 8=23273
- atmospheric, effect on F2-peak height at middle and high latitudes 8=10022
- atmospheric free oscillations rel. to mean wind 8=9844
- distribution in turbulent planetary boundary, appl. similarity analysis 8=16620
- diurnal osc. over eastern Hawaii 8=9849
- effects on d.c. corona discharge 8=12411
- F region, high latitudes, produced by press. gradients, associated radio reflection phenomena 8=10012
- Fort Greely in Alaska, light chaff obs. mesosphere 8=18863
- hurricane, ocean bottom l. f. press. vars., obs. 8=14603
- ionosphere, 90 to 120 km 8=18998
- ionospheric meridional, production of asymmetric F2 electron density distribution about equator 8=10020
- ionosphere, parameter meas. by statistical method 8=19001
- ionospheric, rel. to sporadic E layers 8=14686
- neutral meridional, effect on F2 peak 8=10019
- ocean waves generation, dissipation and prediction 8=18836
- over water with progressive waves, aerodynamic press. distribution 8=5791
- profiles, vegetation roughness effect 8=14605
- rel. to atmosphere acoustic-gravity waves propag. and grand-press. 8=23303
- sea currents vel. components spectra and wind energy transfer process 8=9810
- sea spray droplets as function of speed and height ($< 1.2\text{ m}$) 8=23243
- slope wind time vars. rel. to relief, model 8=9851
- speed and stress meas., effects of buoy motion 8=23272
- speed components in temp. stratified atmosphere, spectral structure 8=14607
- stratospheric, over Panama, obs. 8=14606
- structure, effect on infrasound generated by nuclear explosion 8=23304
- thermosphere, diurnal vel. oscill., new anal. 8=14602
- tropospheric field above low-level jet, diurnal oscillations 8=23271
- variable, stress effects on ocean currents 8=2571
- velocity field at unstable stratification, l. f. spectra 8=9850
- vertical component turbulence, 300 and 1200 m 8=14612
- vertical velocity component, turbulent vars., 430 m tower obs. 8=14613
- water waves, interaction with 8=16776
- waves prod., theory 8=9809
- zonal, and jet streams 8=18862

Wolfram. See Tungsten.

Wood

- acoustic parameters, unseasoned and aged 8=3070
- balsa plates, crack extension, appl. of fracture mech. 8=22294

- Wood**—contd
 conifer, X-ray diffraction patterns, analysis 8=17464
 ignition by radiation 8=15110
- Work function**
 See also Electron emission.
 conductors, electron work function from thermodynamic anal. of electron gas 8=18243
 electrochemical electrodes 8=9715
 films, evaporated, substrate roughness dependence 8=9267
 metals, anisotropy as meas. by field emission and thermionic techs. 8=18244
 metals with monomolecular semiconductor or dielectric layers 8=9091
 metal-semiconductor contact 8=18077
 metals, "volume" concept, discussion 8=18242
 refractory compounds, cesiated, electron and ion, search for stable, low function at 1500°K 8=18262
 Al, changes, during and following low press. oxidation 8=5407
 Al, chemisorption of O₂, rel. to stability 8=5726
 Al₂O₃, Cs activated, semicond. low work function, film, props. 8=17999
 Au-Ba alloys 8=18245
 Au-Si contact 8=18077
 Ba-M alloys (M=Pt, Pd, Rh, Au) 8=18245
 Cs electrodes, effect of vapour pressure 8=18246
 Cs on W crystal faces 8=13926
 Hg, room temp. and m. p. obs. 8=13939
 K, room temp. and m. p. obs. 8=13939
 Li film on W and Re faces, effect of film thickness and substrate orientation 8=18256
 Mo crystals with adsorbed O₂, surface exam. by LEED and work function studies 8=17165
 Mo films on W crystal, and adsorption 8=9269
 Mo, low region in Cs and Cs-Ba vapours, rel. to pot. as collectors in converters 8=15213
 Nb, low region in Cs and Cs-Ba vapours, rel. to pot. as collectors in converters 8=15213
 Ni, low, in thermionic converter, effect of evaporated W emitter mat. on surface 8=15245
 Pd-Ba alloys 8=18245
 Pt-Ba alloys 8=18245
 Rb, room temp. and m. p. obs. 8=13939
 Re, low region in Cs and Cs-Ba vapours, rel. to pot. as collectors in converters 8=15213
 Re, polycryst. and 3 orientations, bare work functions 8=18247
 Re-Nb alloy surface, rel. to H₂O vapour contamination 8=13927
 Rh-Ba alloys 8=18245
 Ru, low region in Cs and Cs-Ba vapours, rel. to pot. as collectors in converters 8=15213
 Ta ribbon, changes on adsorpt. of Cs, O₂ and H₂ 8=9276
 U film, vac. -deposited on W, in u. h. vac. and in H₂ 8=17142
 U monolayer film on polycrystalline W, photoelectric 8=5408
 W/adsorbed N₂, changes on e-impact rel. to N₂ phase transformations 8=21913
 W, chem. vapour deposited, distrib. rel. to 'patch effect' 8=18250
 W, effect of Cs additives 8=18251
 W, and field emitted electron distrib. and effects of Zr-O coating 8=5413
 W single crystals, chemisorption of diatomic molecules, studies. 8=18700
 W surface, influence of CsF adsorption 8=18270
 W, vapour-deposited, effect of preferred cryst. orientation and surface treatment 8=18248
 W, rel. to adsorption of N₂ 8=1711
 W and W-Re alloys, (100) surface 8=13928
 Xe, on W crystal faces 8=18252
- Work hardening**
 See also Cold working; Surface texture.
 alloys, structural, tensile, exponential relation 8=22282
 atomic block theory, existence of extremums on property impurity curves 8=8803
 f.c.c. metals and alloys, u.s. 8=22336
 H36XII steel, austenitic, effect on mechanical properties 8=13569
 h. c. p. metals and alloys, X-ray study 8=22283
 lanthanides, characteristics 8=5089
 metal sheets, strain-hardening, bore-expanding test anal. 8=22272
 metals, in rod-drawing anal., use of mean yield stress, and redundant work 8=22300
 metals, linearized stress-strain curves 8=17722
 steel Armco, rel. to dislocations 8=5067
 steel, cyclic fatigue softening and hardening 8=22363
 steel, rel. to surface defect obs. 8=17675
 steels, mech. strength effects 8=22344
 Al, rel. to surface defect obs. 8=17675
 Al-4%Cu, rel. to deformational instability 8=8816
 Al, rolling and recrystallization texture orientation relationships 8=1755
 Al single crystals, dynamic deformation 8=22310
 Cu-Be-Al alloys, ageing characts. obs. 8=22335
 CuZn(ϵ brass) strain hardening hydrostatic extrusion effects obs. 8=5059
 Fe, neutron irradi., plastic deformation, parameters 8=22349
- Work hardening**—contd
 Fe-Cr(0-53%) characteristic 8=8841
 Fe-Ni-Si-C steel, rel. to martensite ageing 8=22357
 Mo, recrystallized, temp. dependence 8=22380
 Mo-Fe solid soln., 500°C, mag. props. 8=22749
 Ta, recrystallized, temp. dependence 8=22380
 TiNi strain hardening hydrostatic extrusion effects obs. 8=5059
 W, recrystallized, temp. dependence 8=22380
 Y, characteristics 8=5089
 Zn, deformation at high strain rates 8=17837
- X-ray absorption**
 See also X-ray spectra/absorption.
 coefficients, anomalous, distortion correction 8=13206
 for electron probe microanalysis, absorpt. correction tables 8=14470
 electron probe microanalysis, corrections computer calc. 8=14478
 graphite slabs, rel. to meas. of isodensity curves 8=22317
 homogeneous beam, h.v.l. determinations, geometrical considerations 8=11242
 in microanalysis, absorpt. effects, computer calc. 8=14473
 Mössbauer spectrometer mounting material criteria 8=3579
 powder grain size determ. 8=17018
 total mass absorpt. coeffs. 8=696
 in Weissenberg methods, correction 8=8487
 Cu, transmission temp. dependence (Borrmann effect) from 77-377°K 8=14210
 Fe, Ag K α radiation, coeff. meas. 8=2436
 Fe-Cr alloys microanalysis, absorpt. corrections evaluation 8=14476
 Mn, Ag K α radiation, coeff. meas. 8=2436
 Ti, Ag K α radiation, coeff. meas. 8=2436
- X-ray analysis.** See Chemical analysis/X-ray; Crystal structure, atomic; X-ray crystallography
- X-ray astronomy.** See Astronomy and astrophysics.
- X-ray characteristic temperature.** See specific heat.
- X-ray crystallography**
 For results of structure analysis see Crystal structure, atomic.
 absorption coefficients, anomalous, distortion correction 8=13206
 binary systems, conc., central diffusion characts., theory 8=13197
 curved crystallite cluster, intensity curvature dependence 8=22005
 defects detect. by pseudo-Kossel lines, obs. 8=17598
 diffraction, divergent-beam, geometry rel. to Kossel patterns 8=17317
 diffraction, effect of anomalous scatterers 8=13150
 diffuse scattering by lattice particles in new phase on phase transformations 8=1773
 diffuse scattering in reciprocal space 8=13205
 Ewald construction demonstration in teaching 8=13204
 extended internal defects, effect on Debye-Waller factor 8=1779
 film shrinkage effect on lattice parameter determination by X-ray diffraction 8=13219
 imaging linear defects in 'spectral' position 8=4968
 imperfect crystals, fundamental eqns. of dynamic scattering theory 8=13196
 integrated intensities of real crystals, expt. tests of general formula 8=13480
 intensities, relative and absolute scales 8=22006
 lattice spacings, particle size effect rel. to Lave interference function 8=17301
 Laue case, secondary extinction correction 8=8486
 Pendellösung fringes in Darwin reflection 8=1772
 Pendellösung fringes, plane and spherical wave, direct obs. 8=22001
 scattering effects due to temp. gradients, thermal oscillation effects 8=17314
 surface lattice distortion rel. to Debye-Waller factors 8=1780
 transmission, anomalous, rel. to atomic thermal vibrations 8=13222
 wave fields in three beam case 8=4861
- apparatus**
 See also X-ray monochromators; X-ray spectrometers.
 bond crystal sphere grinder, modifications 8=4830
 cylinders, absorpt. corrections 8=1774
 diffractometer with Eulerian cradle, accurate alignment procedures 8=4865
 diffractometer for single crystals, automatic equi-inclination 8=8495
 Ewald sphere in aligning crystal pairs to produce moiré fringes 8=13225
 focusing diffraction instrument, aberrations, second-order theory 8=22009
 focusing monochromator for single crystal work 8=13226
 goniometer for X-ray diffraction analysis 8=22010
 interferometers, design and application 8=13228
 Kossel line camera for e probe microanalyser 8=17323
 Kratky small-angle camera, high -temp. sample cell 8=8003
 Laue back refl. method, puncture collimator 8=17322

X-ray crystallography — contd

apparatus — contd

- Laue pattern interpretation, optical instrument 8=8496
- mass absorption coefficient measuring device 8=1751
- metal film orientation rel. to X-ray production efficiency 8=13221
- powder camera, bulk specimen holder 8=17264
- projection microscope, resolution and exposure time improvement 8=17263
- Seemann-Bohlin diffractometer aberrations and intensities rel. to conventional diffractometers 8=1776
- Seemann-Bohlin diffractometry instrumentation 8=1775
- Weissenberg camera, orientation correction 8=17208
- Weissenberg photographs, giving rectified representations of reciprocal lattice 8=4864

calculation apparatus

- diffractograph interpretation using computers 8=1770

calculation methods

- analysis based on inadequate data 8=8480
- bond length corrections using 'riding' model 8=16966
- Bijvoet differences, normalized, from cryst. pair, statistical distrib. 8=22007
- Bragg contours, Kikuchi lines, simple construction for indexing 8=8478
- cell dimensions, least squares refinement using I.C.T. Fortran programme 8=8483
- centrosymmetric crystals, using anomalous scatt. 8=13218
- convolution in direct and reciprocal space, new relationships 8=13192
- convolution mol. method appl. to AlB_{10} crystal structure 8=17337
- convolution-molecule method, use extension 8=13183
- diffracton intensities, statistical distrib. 8=13193
- diffuse scattering functions of disordered crystals from Q functions 8=13186
- diffuse scattering in reciprocal space, representation 8=13205
- diffuse scattering region, construction by graphical method 8=17315
- distorted small crystals, Debye-Scherrer lines Fourier coeffs. 8=17313
- distribution rule of factors for non-uniform atomic distrib. 8=13180
- error elimination from multiple reflection on four-circle diffractometer 8=17312
- Fourier integral for solving structures 8=13188
- Fourier map atomic peak heights and corresponding Patterson functions, tables 8=1771
- heavy atoms in structures, determ. by systems of linear structure factor eqns. 8=13181
- hexagonal crystals, computer programme for calc. of constants 8=4860
- indexing reflections on 3- or 4-circle diffractometers, graphical aid 8=17320
- Kossel lines, rel. to crystal orientation and lattice parameters 8=21920
- Kossel patterns interpretation using Miller indices and reciprocal lattice 8=17316
- Laue pattern interpretation, optical instrument 8=8496
- likelihood ratio method for precise lattice parameter det. 8=8479
- line profile approx. 8=13220
- line-profile parameters, statistical variance rel. to intensity location and dispersion meas. 8=8485
- noncentrosymmetric, partial structure information combined with tangent formula 8=17319
- non-crystallography symmetry problem, linear analysis 8=8475
- orientation textures of three orthogonal sections represented using triangular grid 8=8372
- Patterson function deconvolution 8=13194
- Patterson function with atoms in special and particular positions 8=13187
- Patterson sharpening function $[\sum Z_j / \sum f]^2 - 1$, appl. to L-cyrtell hydrochloride monohydrate 8=8577
- Patterson synthesis modification 8=13191
- phase angle of structure factors by anomalous dispersion 8=8484
- phase correction method for solving partially known structures 8=13215
- phase correction using distorted electron-density functions 8=13185
- phase determination based on larger structure phases 8=13184
- phase-determining techniques in solving complex structures 8=13114
- powder data, data derivation 8=13200
- propagation in perfect and nearly perfect crystals, calc. using Takagi's theory 8=13212
- R factors for constant-count-per-reflection expts. 8=8491
- reciprocal lattice dimensions from meas. angular co-ordinates 8=17320
- scaling photographs, 2 methods compared 8=17321
- sign determ. by method of systems of linear structure-factor eqns. 8=13190

X-ray crystallography — contd

calculation methods — contd

- Silverman-Obata sum rule appl. to ionic radial deformations 8=8224
 - space group representation, irreducible, operational projection 8=17305
 - structure refinement and linear programming 8=8482
 - structure refinement by minimum residual analysis 8=1824
 - tetragonal crystals, computer programme for calc. of constants 8=4860
 - Weissenberg diags., equi-inclination, accurate correction procedure 8=8488
 - Wilson plots and normalized structure factors, evaluation, allowance for thermal anisotropy 8=8481
- structures.** See Crystal structure, atomic.
- technique**
- aligning crystals from Lave photographs using vector analysis 8=22003
 - constant-count-per-reflection, R factors 8=8491
 - Fraunhofer diffraction, validity of Babinet's principle 8=22008
 - interplanar distance precision determination in divergent beam, new technique 8=17318
 - moiré fringes 8=13203
 - Pendellösung fringe interferometry 8=8490
 - precision photography for the rapid meas. of large nos. of reflection intensities from proteins 8=17455
 - scanning type diffr. microscopy 8=13224
 - setting single crystals by rotation photographs 8=21916
 - Weissenberg methods, absorption correction 8=8487
 - Fe^{55} radioactive isotope for structural analysis 8=13227

X-ray diffraction

- See also X-ray crystallography; X-ray scattering.
- atomic deformations from data 8=13182
 - use of "balanced filters", elim. of fluoresc. rad., thickness required, and difficulties 8=6588
 - Bijvoet differences in non-centrosymmetric structure of elements, rel. to temp. effects 8=13273
 - Bragg reflections used for monochromatization giving high resolution 8=13243
 - calcite window in double spectrometer, profiles exam. with monochromatic radiation 8=22004
 - computer-controlled single-crystal diffractometry, counting time optimization 8=13214
 - counting loss correction, influence of line profile 8=11244
 - crystal line materials, obs. of internal stresses 8=5014
 - crystal orienting device 8=17207
 - crystallite size-with-depth-variation, line broadening effect 8=4833
 - crystallography, effect of anomalous scatterers 8=13150
 - crystallography, geometry of divergent-beam diffr. rel. to Kossel patterns 8=17317
 - curved crystallite cluster, intensity curvature dependence 8=22005
 - diffractometer with Eulerian cradle, accurate alignment procedures 8=4865
 - diffractometer for single crystals, automatic equi-inclination 8=8495
 - disordered, one-dimensionally, close-packed structures, theory 8=8476
 - distorted crystal, theory 8=13217
 - distorted small crystals, Debye-Scherrer lines Fourier coeffs. 8=17313
 - dynamical theory appl. to Si with diffused B (and P) 8=13412
 - edge dislocation contrast exam. 8=13207
 - electronic structures of atoms and mols., importance of small angle domains in study 8=12045
 - Ewald sphere in aligning crystal pairs to produce moiré fringes 8=13225
 - film shrinkage effect on lattice parameter determination by X-ray diffraction 8=13219
 - focusing instrument, aberrations, second-order theory 8=22009
 - Fresnel-zone lenses and appls. 8=15591
 - germanium window in double spectrometer, profiles exam. with monochromatic radiation 8=22004
 - grating, concave, use for light elements microanalysis 8=14491
 - hologram microscopy, high resolution attainment 8=15592
 - holography, application of Lloyd's mirror 8=529
 - ideal crystals, patterns with Pendellösung fringes of equal inclination 8=13213
 - indexing reflections on 3- or 4-circle diffractometers, graphical aid 8=17320
 - intensities, statistical distrib. 8=13193
 - interferometers, design and application 8=13228
 - line profile approx. 8=13220
 - line-profile parameters, statistical variance rel. to intensity location and dispersion meas. 8=8485
 - moiré fringes 8=13203
 - monochromator system for obtaining an extremely parallel beam by successive asymmetric diffrs. 8=13209
 - multiple Bragg-reflection diffractometry 8=13189
 - non-crystalline mats., pattern evaluation 8=8439
 - ordered alloy containing antiphase domains 8=4863
 - Pendellösung fringes in Darwin reflection 8=1772
 - Pendellösung fringes in Darwin reflection 8=13211
 - Pendellösung fringes of equal inclination in ideal crystals 8=13213

X-ray diffraction—contd

- phase analysis, mass absorption coefficient measuring device 8=1751
- phase angle of structure factors by anomalous dispersion 8=8484
- photograph interpretation using computers 8=1770
- powder diffractometer, operator protection shutter 8=15594
- powder patterns, 80 inorganic substances 8=17327
- quartz window in double spectrometer, profiles exam. with monochromatic radiation 8=22004
- R factors for constant-count-per-reflection expts. 8=8491
- reflection topography contrast reversal, lattice contractions 8=1927-8
- scanning method, new technique 8=13224
- scattering corrections for Z=10-98 8=4886
- Seemann-Bohlin instrumentation 8=1775
- Seemann-Bohlin diffractometer aberrations and intensities rel. to conventional diffractometers 8=1776
- silicon window in double spectrometer, profiles exam. with monochromatic radiation 8=22004
- stacking fault images 8=13442
- structure refinement and linear programming 8=8482
- 3-strong-ray case rel. to crystal of absorbing finite atoms 8=13175
- topography, for trace characterization and point defect location 8=17602
- topographic meas. without supplementary apparatus 8=20132
- triclinic mica polytypes giving monoclinic patterns, symmetry enhancement phenomena 8=13290
- vacuum attachment to diffractometer for studying thin films during deposition 8=8307
- windows in double spectrometer, profiles exam. with monochromatic radiation 8=22004

X-ray diffractometers. See X-ray crystallography/apparatus.**X-ray examination of materials**

- See also Chemical analysis/X-ray; Radiography.
- aleuritic acids (erythro and threo), powder diffraction data 8=22047
- alloys, long period ordered, obs. 8=13250
- bacteria flagella, surface structure 8=23769
- binary systems, conc., central diffusion characts., theory 8=13197
- busbars, location of elec. discharging cavities 8=21245
- crystalline, internal stresses meas. by X-ray diffraction 8=5014
- diamond covalent bonding 8=4869
- diamond, Lave spikes, i. r. absorpt. and impurity N location, obs. 8=22014
- fibres, synthetic, small-angle scatt., review 8=8438
- iron oxide scale, hematite phase physico-chemical state 8=17201
- isotactic polyvinyl tert. butyl ether, lattice strains, along and across fibre axis 8=8877
- metals, goniometric methods for lattice expansion and residual stress 8=4862
- metals, trivalent, molybdates and tungstates, structural type 8=8526
- non-crystalline, diffraction pattern evaluation 8=8439
- polyacrylonitrile, atomic-pile-irradiated, density changes 8=17709
- polyethylene cryst. surface, low-angle 8=17215
- polyethylene, lattice strains, along and across fibre axis 8=8877
- polyethylene, relaxation obs. 8=21213
- polymers, high, crystalline regions, lattice strains, along and across fibre axis 8=8877
- quartz polished surface 8=17599
- Rochelle salt, extinction rules and radiation damage effects 8=13266
- single crystals, explosive deformation 8=17029
- solids, scattering, small angle, for Kratky camera, high temp. sample cell. 8=8003
- steel, austenite retention determ. 8=22355
- thin films, Debye-Waller factors calc. from Mössbauer effect 8=8207
- topography of large cryst. areas, apparatus 8=17262
- trace characterization-chemical and physical, symposium NBS, USA, Oct. 1966 8=8437
- transition metals, K α lines, chemical shifts 8=16967
- vitreous ice, diff. spectrum, comparison with water 8=8355
- wood, conifer, X-ray diffraction patterns, analysis 8=17464
- Al in Cr solid solution, antiferromagnetism obs. 8=14063
- Al-Y, phase analysis and crystal structure studies 8=22045
- Au₃Cd, long-period ordered alloys, obs. 8=13250
- Au-Pt alloys, diff. "tails" rel. to defects 8=17341
- Au-Pt system, meas. of chem. diffusion coeff. 8=1913
- Au-Zn, long-period ordered alloys, obs. 8=13250
- C₁₀H₁₂N₂O₈, condensation product of diaminosuccinic acid and pyruvic acid 8=17437
- Ca aluminate hydrates, lamellar, crystal structures 8=8511
- Ca₂SiO₄ and solid solns., polymorphism 8=13064
- Cu crystals, nearly perfect, intensities in anomalous transmission, theory and expt. 8=4873
- Cu-Be-Al alloys, ageing characts. obs. 8=22335

X-ray examination of materials contd

- Cu-Mn alloys, interdiffusion kinetics 8=22149
- Fe, absorpt. coeff. for AgK α radiation, meas. 8=2436
- Fe, line intensity after plastic deform. and annealing 8=21989
- FeAl alloys, kinetic order-disorder transform. 8=17076
- Fe-C martensite, static atomic displacements from Bragg reflections 8=4878
- Fe-Ni alloys, diff. "tails" rel. to vacancies 8=17341
- Fe₃O₄, magnetite, weak reflections obs. in diff. pattern 8=22020
- GdBr₃ ($\kappa=4, 6$), thermal stability and emission characts. 8=17384
- Ge, atomic scattering factor, Pendellösung meas. 8=22025
- Ge, stress topography rel. to thin films on crystal 8=22371
- H and D, crystal-structure changes during transitions in ortho- and para-states 8=13263
- KNbO₃-AgNbO₃ system, and elec. and thermal expansion studies 8=21823
- LaB₆, and prep. 8=17384
- Li ferrite, topography of defects 8=8708
- LiF crystals, obs. of internal stresses with MoK α 8=5014
- LiF sphere, extinction coeff. 8=17388
- MgGa₂Mn₂O₄, tetragonal distortion of Jahn-Teller type 8=13269
- MgO crystallites, from thermal decomposition of Mg cpxs., strain analysis 8=22370
- Mn, absorpt. coeff. for Ag K α radiation, meas. 8=2436
- Mo film heteroepitaxially grown on insulating substances, cryst. relationships 8=17134
- Mo, polycrystalline, γ -irrad. and non-irrad. 8=22253
- PbO, orthorhombic and tetragonal forms, conversion at low temps. 8=8276
- Re, thermal expansion determination 8=13384
- Si containing oxygen, precip. processes and dislocation effects 8=13073
- Si covalent bonding 8=4869
- Si, stress topography rel. to thin films on crystal 8=22371
- SiC, topographic obs. of polytypes 8=13115
- SiO₂ vitreous, intensities calc. for random network model 8=4467
- Si:P, As, impurities distrib. 8=18079
- Te crystal, explanation of lines not theoretically predicted 8=8559
- Ti, absorpt. coeff. for AgK α radiation meas. 8=2436
- VN, electronic state from diff. intensity meas. 8=22414
- WC, strain and crystallite size, compressed at high pressure 8=13612
- YB₃ ($\kappa=4, 6, 12$), thermal stability and emission characts. 8=17384
- Zn, polycrystalline, γ -irrad. and non-irrad. 8=22253
- ZrO₂, phase transitions and polymorphism 8=4722

liquids

- alkali-metal halide aq. solns. 8=12800
- alloys, atomic distrib. and electronic transport props. 8=12799
- alloys, diff. pattern peaks rel. to interatomic distances 8=12784
- alloys, structure and correl. 8=12795
- p-azoxyanisole, nematic, in mag. field, structure investigations 8=4532
- metals, diff. pattern peaks rel. to interatomic distances 8=12784
- metals, scatt. data compared with n scatt. 8=12794
- monatomic, termination effect of isolated peak 8=8004
- scattering, small angle, Kratky camera, high temp. sample cell 8=8003
- triacetin, c distrib. function from scatt. obs. 8=16704
- Ag-Sn liq. alloys, atomic distrib. functions 8=12801
- Bi, diffraction investigation 8=21610
- Hg-In, interf. functions, pair distrib. 8=8005

microstructure

- See also Crystal structure/microstructure.
- biaxial pole figure representation of textures of rolled metals and alloys 8=17778
- brass, rolled, texture representation by biaxial pole figures 8=17778
- brass, deformation texture development, pole figure 8=17777
- combined X-ray microanalyzer and electron microscope, illuminating system 8=8442
- crystallography, effect of anomalous scattering 8=13150
- grain size distrib. in μ m range, by X-ray diff. 8=13151
- grain size, orientation depend. 8=4632
- h. c. p. metals and alloys, cold work and recovery 8=22283
- microanalysis and X-ray optics Conference, Orsay, France, Sept. 1965 8=8441
- paracrystalline substances, scattering intensities, normalization and absorption correction 8=1750
- polymers, crystallite randomization, nondestructive methods 8=8440
- polymers, small-angle method 8=17185
- powder camera, Philips, bulk specimen holder 8=17264
- powder grain size, absorption obs. 8=17018
- powder grain size determ., by fluorescent spectroscopy 8=21830

X-ray examination of materials—contd**microstructure—contd**

- ruby, dislocations 8=13434
- size-with-depth-variation, line broadening effect 8=4833
- steel, austenite retention, diffraction, determ. 8=22355
- Al, annealed, helices and large loops in prismatic dislocations 8=17647
- Al, rolled, texture representation by biaxial pole figures 8=17778
- Al-5% Mg with small Ag additions, ageing 8=13528
- C fibres, high modulus 8=8457-8
- Cu, cubic texture formation during recrystallisation 8=4809
- Cu, deformation texture development, pole figure 8=17777
- Cu, rolled, texture representation by biaxial pole figures 8=17778
- Cu-Zn alloys, rolling textures, -196° to 275°C 8=21985
- Fe, rolled, orientation analyses by means of quantitative pole figures 8=17282
- Fe-3wt. % Si single crystals, interference fringes rel. to domain arrangements 8=22021
- LiF single crystals, sub-grain boundaries by limited projection topography 8=13446
- Pb-0.4 wt. % Mg alloy, ageing process and G. P. zone formation 8=22389
- TiCl₃α, crystal constants and powder spectrum 8=22041
- Zn-Al alloy, superplastic, effect of stress, temp. and heat-treatment 8=5090

molecular structure

- alstoveninemethiodide, single crystal, prelim. study 8=17439
- biological systems, complemented by electron microscopy 8=14897
- catalase, crystal structure 8=8575
- mesomorphic phase 8=16796
- rinkite, features of crystal structure, rel. to analogous silicates 8=8543
- TMPD-chloranil crystals 8=8595
- wood, conifer, X-ray diffraction patterns, analysis 8=17464
- C₅H₁₂N₂O₂. HCl, using CuKα radiation 8=17452
- KCl, Bragg spots 8=17380
- LiF, 400 Bragg spot, unusual K-shape 8=17380

X-ray fluorescence. See Luminescence; X-ray spectra/emission.

X-ray measurement

See also Dosimetry.

- counting system for electron-probe microanalyzers, non-linearity corrections 8=4837
- dosage from Crookes' tube 8=16405
- dosimetry, using ionization chambers 8=15595
- energy analysis, apparatus 8=15582
- film recording monitor using CsI(Tl) crystal 8=11444
- Mössbauer effect, efficient geometry 8=691
- NaI(Tl) thin scintill. layers 8=3580

X-ray microscopes. See Microscopes.

X-ray monochromators

- approximately focusing, aberrations and diffraction intensity calc. 8=15593
- crystal diffractors giving high resolution by multiple Bragg reflection 8=13243
- crystal system for obtaining an extremely parallel beam by successive asymmetric diffractions. 8=13209
- by reflection, total, high freqs. suppression 8=15590

X-ray photoeffect. See Electron emission/photoelectric.

X-ray reflection

- glass 8=5604
- Laue crystal orientation method, puncture collimator 8=17322
- mirror telescope and Yoneda effect 8=15591
- periodic pile of absorbing layers, e. m. theory 8=3255
- quinadic acid, Renninger effect 8=17457
- Rochelle salt, extinction rules and radiation damage effects 8=13266
- ultrasoft X-ray wavelength identification by critical angle of total reflection 8=3392
- Au films 8=5604
- Ge, atomic scattering factor, Bragg reflections 8=22025
- Ge films 8=5604
- Si film on Ni substrate, total refl. of different wavelengths 8=22038

X-ray scattering

See also Compton effect; X-ray diffraction.

- alkali halides, from deformable ions 8=13330
- anomalous, in struct. anal. of centrosymmetric crystals. 8=13218
- atoms, He-Lw, factors calc. from Hartree-Fock wave functions 8=16189
- collimating slit width effect correction 8=15589
- Compton, rel. to electron momentum distrib. 8=17907
- corrections for Z=10-98 8=4886
- in crystals due to temp. gradients, thermal oscillation effects 8=17314
- defective crystals, kinematic theory 8=13223
- diffuse, time depend., and diffusion in crystalline solid solns. 8=8667
- dispersion corrections in factors 8=13195
- dynamical theory appl. to Si with diffused B (and P) 8=13412
- dynamical theory, role of lattice vibrations 8=13313
- ethyl ether, interference functions 8=8077
- expts., shortening of exposure time by simultaneous maser exposure 8=15408-9

X-ray scattering—contd

- fibres, synthetic, small-angle scatt., review 8=8438
- intensity distrib. of (hk) interferences in lattices with preferred orientation 8=13216
- ions, factors calc. from Hartree-Fock wave functions 8=16189
- by lattice particles in new phase on phase transformations 8=1773
- Laue case, secondary extinction correction 8=8486
- by lupolen platelets, small-angle 8=14282
- macromolecules in soln., effects of solvent 8=21205-6
- methane, rotating mol., curves rel. to interatomic distances 8=7572
- myoglobin in soln., effects of solvent 8=21206
- polyethylene films, oriented, low angle patterns and structure 8=17144
- rel. to photoelectric absorption producing fluorescence 8=23037
- scattering amplitude phase meas. from intensity fluctuations 8=19776
- Silverman-Obata sum rule appl. to crystals. 8=8224
- small-angle, porous solids, Porod's law 8=4696
- solid solns., exam. of diffuse background to measure thermodynamic and elastic props. 8=13359
- water, interference functions 8=8077
- Al, atomic scatt. factors, Slater approx. 8=8506
- Al polycrystals, temp. depend. of thermal diffuse scattering 8=5581
- Al, X-ray atomic scatt. factors, Slater approx. 8=8506
- for Ag crystal determ. of frequencies of thermal oscillations at 77, 293 and 580°K 8=17476
- C, glassy, small-angle, rel. to pore structure and conc. 8=21983
- Cu, polycrystals, temp. depend. of thermal diffuse scattering 8=5581
- Fe, absolute atomic scatt. factor 8=8519
- InSb, Compton effect and thermal agitation in X-ray diffusion 8=13332
- InSb, by transverse oscillations 8=8613
- K and NaCl solid solns., rel. to decomp. mechanism studies 8=13070
- Te crystal, evidence for lines not theoretically predicted 8=8559
- V, Compton effect and thermal agitation 8=13300

X-ray spectra

See also Atmospheric spectra; Chemical analysis/X-ray.

- atom, K, prod. following p scatt., Bethe-Born and Bang-Hansteen approx. 8=20930
- celestial, polarization 8=2802
- cosmic sources, and intensity meas. 8=5893
- helium, liquid pionic and muonic 8=1211
- high energy, from Cygnus XR-1 and others 8=5890
- K_{β2,5} band fine structure 8=23027
- L_{1-L11} level separation, effect of finite nuclear size 8=20927
- linear accelerators in 2-6 MeV range 8=6699
- linear unfolding methods and optimization 8=14180
- metals, plasmon satellite in soft spectra, theoretical interpretation 8=13680
- Mössbauer scatt., internal conversion of e, efficient geometry 8=691
- oxides of metals, chem. bonding investigation 8=9499
- polarization following ionization of inner electron 8=12041
- satellites and excitation states, belonging to same inner vacancy, relative prod. probabilities 8=16216
- satellites, new screening doublets 8=16193
- solar, absolute intensities near min. activity 8=10391
- solar, design of proportional counter spectrometer for meas. 8=23709
- solids, rel. to atomic energy levels and excitons 8=9492
- vitreous ice, diffraction, comparison with water 8=8355
- Al crystals, p beam interaction 250-1560 keV, orientation effect 8=4995
- B in its cpds. 8=18503
- B, Raman scatt. of Cu Kα rad. 8=2396
- Be, Raman scatt. of Cu Kα rad. 8=2396
- C, Raman scatt. of Cu Kα rad. 8=2396
- Ca, muonic K series 8=1209
- Cf²⁵² primary fission products rel. to odd-even effect 8=1113
- Cu crystals, p beam interaction 250-1560 keV, orientation effect 8=4995
- Li, Raman scatt. of Cu Kα rad. 8=2396
- Mg, muonic K series 8=1209
- Mo, Kα rad., prep. of Ross difference filters 8=2437
- Ne, Kα satellites (non-diag. lines) intensity 8=1170
- P, red, rel. to energy structure investigations 8=9559
- Pd alloyed with Rh and Ag, soft X-ray isochromats rel. to Pd density of states 8=17884
- Pb stearate, optimization for X-ray diffraction 8=14254
- S, muonic K series 8=1209
- Si, muonic K series 8=1209
- Sn cpds with O, S, Se and Te, chem shifts of the K_{α1} line 8=9558
- Ti cpds., K- and L-spectra 8=14281
- W crystals, p beam interaction 250-1560 keV, orientation effect 8=4995
- Yb⁷⁰ L spectrum 8=23023
- absorption
 - hydrocarbons, gaseous 8=12277

X-ray spectra—contd**absorption—contd**

- K-series dipole elec. transitions 8=7367
 mass absorpt. coeffs., obs. 8=14178
 rare earth elements, M_{IV} and M_{V} , rel. to effects in emission spectra 8=2447
 solids, Kronig-Hayasi, Kostarev et al. theories differences 8=2392
 Al and K-absorption, fine structures 8=2398
 Al, $L_{II, III}$ region, structure 8=22956
 Al_2O_3 , anodized and crystalline, $L_{II, III}$ region, structure 8=22956
 As, chemical effects in K abs. 8=22957
 Cd, K edge, variations rel. to beam direction 8=2408
 Cl in alkali-chlorides, K-absorption secondary structure 8=2410
 Cu, compared with isochromat at 8 kV 8=2414
 Cu, isochromats at Cu $K\alpha$ wavelength 8=2416
 Cu, polarised K-absorption, (100), (110) and (111) comparison 8=2413
 CuCl rel. to distrib. of states, Cu L absorpt. obs. 8=9522
 Cu_2O , isochromat structure 8=2415
 Cu_2O rel. to distrib. of states, Cu L absorpt. obs. 8=9522
 CuO , isochromat structure 8=2415
 CuO rel. to distrib. of states, Cu L absorpt. obs. 8=9522
 Ga in GaAs and GaP, K-absorption 8=2420
 Ge, interference passing near K-edge 8=14218
 Ge, K-absorption, fine structure 8=2423
 KCl, K- $L_{II, III}$, $M_{II, III}$, and quasi-stationary states 8=2432
 MnSe, K absorption spectra rel. to chemical bonding 8=14242
 SF₆, mechanism 8=12229
 Yb⁰, M_V , M_{IV} and M_{III} abs. edges 8=23024

emission

- atoms, bonds effects 8=16191
 fluorescent X-rays from γ -irradiated target, absolute yield meas. 8=23039
 rare earth elements, soft M_α and M_β , self absorpt. effects 8=2447
 screening doublet formation, extended study 8=20922
 solar radiation from coronal region 8=14887
 surface, and simultaneous refl. electron diffr. meas. 8=8290
 Al, solid, liquid and vapour states 8=9502
 Al, $K\alpha$ doublet obs. in metal and oxide 8=5582
 Al, X-ray K-satellites 8=2398
 Al-Cu alloys 8=9502
 Al-Fe alloys, disordered and ordered, at 40-90 eV 8=5624
 Al-Mn alloys 8=9502
 Co, K and L bands fine struct. rel. to e band struct. obs. 8=18527
 Cu K_α fluoresc. and direct components, films and solid targets 8=14179
 CuCl, Cu_2O and CuO , rel. to distrib. of states, Cu L emission obs. 8=9522
 Lu, L spectrum 8=9549
 Mg₂Ni, at 40-90 eV 8=5624
 Ni, soft-X-ray analysis rel. to density of states determ. 8=8940
 Ni-Zn alloys, at 40-90 eV 8=5624
 O^{1s, 1s}, muonic, nuclear radii determ. 8=943
 P cpds., fluoresc. line shift 8=2443
 Pu, 8 to 75 Å 8=14255
 Si, and cpds., photon-counting spectrograph, obs. compared to photographic and theory 8=2454
 W L_α fluoresc. and direct components, film targets 8=14179

X-ray spectrometers

- See also Gamma-ray spectrometers; X-ray crystallography/apparatus.
 automatic analysis of samples 8=543
 energy disperser using Si lithium drifted detector 8=23195
 monochromator system for obtaining an extremely parallel beam by successive asymmetric diffrs. 8=13209
 multi-grating for soft X-rays 8=15590
 2-beam, characteristics 8=542
 vacuum, with X-ray analyser, construction e use 8=15588

X-ray spectroscopy

- See also X-ray crystallography; X-ray diffraction.
 automatic high-speed continuous analysis of wet and dry processes 8=2550
 instruments and appls., 15-150 Å 8=22945
 microanalysis by X-ray fluoresc. meas. 8=14487
 plasma, radiation meas. 8=12512

X-ray tubes

- focus, intensity distrib. and dimensions meas. 8=15584
 FXR discharge, electron temp. in column and accelerating voltage 8=3393
 microfocus unit, with telefocus electron beams one-step reducing technique 8=15583
 power supply, high voltage waveform, radiographic effects 8=11243
 safety system for personnel, remote operation 8=15585
 soft X-ray, power enhancement 8=15590

X-rays

- See also Gamma-rays.
 Centaurus XR-2, variability obs. 8=23598

X-rays—contd

- Crab nebula, synchrotron production 8=5918
 8-80 keV from Large Magellanic Cloud and Crab Nebula, search with sounding rocket 8=5916
 emission from Be, C and Mo under laser irr., accompanying ion emission 8=13947
 focusing by quartz crystals 8=14261
 γ -spectrometer meas., Ge(Li) detector, cooled pre-amplifier 8=698
 homogeneous beam, h.v.l. determinations, geometrical considerations 8=11242
 KX- γ directional correlations 8=20739
 thermal from non-thermal radio sources 8=5941
 ScoXR-1 and assoc. optical source, binary model 8=10177
 sharp images, photographic, apparatus 8=6582
 solar, rel. to field strength of 164 kHz received signal 8=5807
 in solids, prod. depth distrib., calc. from e absorpt. obs. 8=17693
 visual response of human eye 8=6585
 in Al target, charact. radiation depth distrib., Mg tracer obs. 8=15587
 in Cu microanalyser target, K_α depth distrib. obs. 8=15586

effects

- See also Nuclear reactions due to photons.
 alkali halide crystals, conductivity, elec., kinetics of radiational change 8=22501
 alkali halides, energy spectra of emitted photoelectrons 8=18274
 alkali silicate glasses, form. of trapped hole centres 8=1998
 aluminophosphate glasses, on radiocolouration and luminescence kinetics 8=1996
 bremsstrahlung spectra on thick anodes, absolute meas. rel. to atomic number 8=699
 on electron micrography rel. to crystal orientation 8=17266
 film response, quantitative calibration, 5 keV-1.3 MeV 8=15565
 film, spectral sensitivity 8=535
 metaphosphate glass, Ag activated 8=4990
 quartz, on permittivity, luminescence and thermoluminescence 8=13871
 rel. to photoelectric absorption producing ruby monocrystals, luminescence 8=14301
 scintillators, obs. of luminescence 8=9588
 Ba(ClO₃)₂·H₂O, X-irradiated, e.p.r. spectral changes in u.v. irradiation 8=18410
 BaF₂, X-ray coloured, absorpt. by colour centres, temp. dependence 8=17683
 CaCO₃ cryst., radical formation 8=5105
 CaF₂ thermoluminesc. and thermostimulated emission, obs. 8=14305
 CaF₂(Eu) fluorescent response function 8=5665
 CaF₂, F-centre prod. 8=1999
 CaF₂, X-ray coloured, absorpt. by colour centres, temp. dependence 8=17683
 CsI(Na) fluorescent response function 8=5665
 CsI(Tl) fluorescent response function 8=5665
 CuSO₄, crystal growth with and without irr. 8=21947
 Ge, multiple Bormann effect in transmission 8=14222
 KBr, vol. expansion, irr.-induced, by relax. at Frenkel defects 8=13486
 KBr, Ca doped, growth of optical absorption bands 8=2429
 KCl, α -centre production and thermal annealing 8=17685
 KCl, vol. expansion, irr.-induced, by relax. at Frenkel defects 8=13486
 KClO₃, new absorpt. bands in near and far i. r. regions 8=22993
 KI and KI(In) self-luminesc., decay 8=14318
 LiF, change in lattice constant 8=2030
 Mg cpds., energy spectra of emitted photoelectrons 8=18274
 NaCl, F-centre first-stage formation 8=2012
 NaCl:Mn²⁺, e. p. r. resolution obtained by X-radiation 8=14117
 NaI(Tl), fluorescent response function 8=5665
 NaI-Tl, on photoluminesc. spectra 8=5666
 NaNO₃ cryst., radical formation 8=5105
 NaSbF₆, e. s. r. of irr. cryst. 8=5538
 Se, polycrystalline, hexagonal, local (conduction) levels, X-ray-induced 8=18236
 SrF₂, X-ray coloured, absorpt. by colour centres, temp. dependence 8=17683

protection. See Radiation protection.**Xenon**

- additive in Cs arc diode, effect on performance 8=15225
 adsorption on zeolites LiX and NaX, press. and temp. depend. 8=1713
 afterglow, msec microwave pulses nonlinear interactions 8=21340
 atom, influence of autoionization on spectra 8=20954
 atoms, electron scatt., 40 keV 8=7447
 captured in graphite by nuclear recoil, escape behaviour 8=4017
 on carbon blacks, graphitized, adsorption, obs. 8=17162
 condensation coeff. at 4.2°K 8=12981
 extraction from telluriumbismuthite, Te¹³⁰ decay rate 8=1017

Xenon—contd

- f. c. c. crystal, adsorpt. of inert gases, potential energy profiles 8=17159
 free-carrier drift-velocity studied in liquid and solid state 8=8119
 heat capacity in critical region, obs. 8=21513
 high-pressure arc, device for stabilizing radiant output 8=12416
 i.r. Zeeman-tuned laser, for fine-structure anal. of absorpt. spectra 8=11160
 ions, range distrib. in amorphous Al_2O_3 8=13476
 ion, relative charge transfer efficiencies of $^{20}\text{P}_{3/2}$, $^{21}\text{P}_{1/2}$ determ. 8=12454
 ionization efficiency obs. 8=21283
 ionized, c. w. laser oscillation at 9697 Å 8=6451
 isotope mixtures, thermal diffusion props. 8=1492
 liquid, sound velocity and law of corresponding states 8=1552
 liquid, surface tension and energy, 189°–286°K 8=1539
 microwave excited, new c. w. ion laser oscillation 8=6452
 radioactive, prod. by in-pile melting of irradi. $\text{UO}_2(\text{NO}_3)_2 \cdot 6\text{H}_2\text{O}$ 8=3982
 recoil fission prod. of U, diffusion in Ag 8=3981
 shock wave front, luminance temp. obs. 8=21483
 solid, band structure, deform. potential and exciton states 8=2108
 solid, free carrier mobility 8=17863
 solid at 0°K, parameters from interact. potential of gas 8=1468
 solid, zero-point energy, effect of long-range 3-body forces 8=22083
 solidified, vapour pressure, binding energy and mean vibration freq. 8=16960
 spectral line, 1469.6 Å, perturbation by Ar, He, N_2 and H_2 compressed gases 8=16201
 superradiant transitions 8=7398
 thermal conductivity, hot-wire cell meas., 30°–100°C, 120–150 torr 8=16700
 thermal plasma, continuous emission spectrum 8=16207
 work function on W crystal faces 8=18252
 Ar-Xe, He-Xe, H_2 -Xe, Ne-Xe couples, translation spectra 8=7425
 In-doped solid film, absorption spectra 8=9541
 in Si, implanted atoms location and lattice disorder, obs. 8=17414
 TiO_2 surface discharge, channel development 8=1330
 XeI, Hartree-Fock wavefunctions 8=1177
 XeII, Hartree-Fock wavefunctions 8=1177
 XeIII($5p^4$, 3P) HF calc. of ground state wave functions 8=1178
 Xe III, ground state Slater integrals 8=4087
 Xe^{129} , hyperfine structure of i. r. laser lines 8=16210
 Xe^{133} , diffusion in multicomponent gaseous mixtures 8=1491
 Xe^{133} diffusion in zirconium carbide, activation energy, rel. to struct. 8=8686
 Xe-133, radioactive, in leak test method, for semicond. devices 8=2211
 $^{133}\text{Xe}^+$ ions, penetration distrib. in Au, effect of target temp. 8=2023
 Xe^+ , low-energy irradi. of Ge crystals 8=8772
 Xe + D_2 collisions, compound state resonances 8=4255
 Xe + H_2 collisions, compound state resonances 8=4255

Xenon compounds

- XeF_2 , r.m.s. amplitudes of vibr., calc. 8=21106
 XeF_4 , r.m.s. amplitudes of vibr., calc. 8=21106
 XeF_6 , molec. beam, mag.-field deflection 8=16377
 XeF_6 , molec. struct. 8=21107
 XeF_6 , pseudo-Jahn-Teller effect evidence 8=7552
 XeF_6 , symmetry, electron diff. obs. 8=17383

Xerography. See Photography.**Y-particles.** See Hyperons resonances.**Yield.** See Elastic limit; Plastic deformation; Plastic flow.**Young's modulus.** See Elastic constants.**Ytterbium**

- anticrossing signals from $6s^2P_1$ level 8=16211
 M_V and M_V absorpt. lines and edges 8=5602
 Yb^{3+} , energy transfer with Nd^{3+} in LaF_3 8=14328
 Yb^{3+} , e.p.r. in ThO_2 , stress effects 8=14128
 Yb^{3+} in BaF_2 , SrF_2 , CaF_2 , spin-lattice relaxation 8=18444
 Yb^{3+} in CaF_2 , anisotropy of spin-lattice relax. for Kramers doublets 8=9414
 Yb^{3+} in CaF_2 , new laser line oscillations from ions at noncubic sites 8=3335
 Yb^{70} , L spectrum 8=23023
 Yb^{70} , M X-ray absorption 8=23024
 in YFe garnet, magnetostriction 8=2344

Ytterbium compounds

- $\text{YbCl}_3 \cdot 6\text{H}_2\text{O}$, hyperfine splitting of lowest 2^+ state of Yb 8=9301
 Yb-Sb phases, magnetic and electrical properties 8=22754
 Yb_2Sb_2 , crystal structure 8=17430

Yttrium

- band structure, density of states and Fermi surface by cellular method 8=8942

Yttrium—contd

- crystals, mag. susceptibility temp. dependence, 80–300°K 8=18303
 deformation planes after dehydrogenation and hydride habit planes 8=8728
 de Haas-van Alphen effect 8=5434
 ferrite magnetostriction constants from ferromagnetic resonance 8=14045
 magnetic susceptibility anomaly 8=18302
 magnetic susceptibility, anisotropy rel. to electron charge density 8=13965
 recrystallization and work hardening characts. 8=5089
 sulphate hydrates, crystallographic data 8=17385
 vacuum distillation, for low gas content 8=4652
 H_2 definition, spectral-isotopic method 8=9743
 Y^{91} deposition in bone, obs. 8=23766
- Yttrium compounds**
- Nd:Cr:YAG, sidelight fluorescence changes, due to laser ing at 1.06 μ 8=6473
 $\text{TCO}_2(\text{T}=\text{Y})$, mag. props. and crystallographic structure 8=13967
 Y orthoferrite, mag. sublattice switching under mag. pulses 8=18366
 Y phosphate-vanadates, struct. and luminesc. 8=14330
 Y vanadate phosphors, particle size rel. to preparation 8=13048
 YAl garnet, foils, simultaneous prep. 8=8449
 YAl garnet:Nd laser, output spectra and linewidth determ. mechanisms 8=11111
 Y-Al garnet:Nd laser, five KHz repetition-rate pulsed, design 8=11113
 Y Al garnet: Nd laser repetitively Q-switched continuously pumped operations 8=6474
 YAl garnet:Nd $^{3+}$, laser transition cross-section and fluorescence branching ratio 8=20003
 YAl garnet laser crystals, light loss, possible scattering contribution 8=19994
 YAl garnet, quantum efficiency of Nd $^{3+}$ absorpt. and excitation spectra 8=5667
 YAl garnets, Er, Tm and Ho doped, luminesc. and stimulated rad. 8=5669
 YAl garnet:Ru $^{3+}$, e.s.r. 8=18440
 YAl_2 , two polymorphic forms, crystal structure 8=1811
 $\text{Y}(\text{Al}, \text{Cr})_3(\text{BO}_3)_4$, e.p.r. of Cr^{3+} at room temp. 8=18439
 YAlFe garnet, X-ray fluoresc. analysis 8=9761
 YAlO_3 , crystal structure, X-ray diff. 8=8544
 $\text{Y}_3\text{Al}_2\text{O}_{12}$, Ce, phosphoresc. 8=18600
 Y-B system with 1–1½% Y, structure refinement 8=17429
 $\text{YB}_2(\text{x}=4, 6, 12)$, prep. and props. 8=17384
 $\text{Y}(\text{C}_2\text{H}_5\text{SO}_4)_3$:Nd, dynamic proton polarization 8=2035
 $\text{YCl}(\text{OH})_2$, monoclinic, X-ray diff. exam. 8=17428
 $\text{Y}_3\text{Cl}_2\text{O}(\text{OH})_5$, orthorhombic, X-ray diff. exam. 8=17428
 $\text{Y}_3\text{-Ca-Fe}_5\text{-Sn}_2\text{O}_{12}$, Mössbauer effect of Fe^{57} 8=4677
 YCrO_3 , antiferro- and ferromag. props. 8=18388
 YF_3 , high-temp. stability 8=7617
 $\text{YF}_{0.9}\text{Al}_{0.1}\text{O}_3$ crystal, antiferromag. at 602°K and ferromag. at 600°K 8=14074
 YF, gaseous, electronic states 8=7549
 YF, high-temp. stability 8=7617
 $\text{Y}_3\text{Fe}_5\text{-xCr}_x\text{O}_{12}$, crystal field symmetry by ferromagnetic resonance 8=1636
 YFe garnet, Al and Ga substituted, heat treatment effect on mag. props. 8=14055
 YFe garnet, containing Yb and Ce, magnetostriction 8=2344
 YFe garnet:CuO, preparation and reson. props. 8=21968
 YFe garnet, dielec. loss peaks rel. to check of electron diffusion 8=14050
 YFe garnet domain configs. and rel. to cryst. defects, obs. 8=22863
 YFe garnet, elastic wave optical investigation 8=2070
 YFe garnet, epitaxial film on YAl garnet, chem. vapour deposition 8=13099
 YFe garnet, ferrimag. res. and relax., effects of paramag. impurities 8=2357
 YFe garnet crystal, ferrimag. reson., influence of domain structure 8=5513
 YFe garnet, magnetoelastic wave propag. 8=22861
 YFe garnet, nonlinear photon-magnon interaction under parallel pumping 8=14056
 YFe garnet, refractive index determ. using plane-parallel thin disc 8=18565
 YFe garnet, reflectivity 8=5642
 YFe garnet, Si, doped, photomag. anneal. 8=23022
 YFe garnet single crystal, magnetoacoustic resonance obs. 8=22891
 YFe garnet slab, magnetostatic surface waves 8=22862
 YFe garnet, spheres and powders, determ. of Curie points 8=18367
 YFe garnet, spin and acoustic Bragg diffraction in longitudinal magnetoelastic waves 8=18482
 YFe garnet, spin wave linewidth variations on substitution of rare earths 8=5495
 YFe garnet, spin wave susceptibility saturation above instability threshold, Al and rare earth doping effects, obs. 8=22864
 YFe garnet:Yb $^{3+}$, behaviour on anomalous sites 8=22860
 YFe garnet, Yb doped, bottleneck effects in ferromagnetic resonance 8=9408

Yttrium compounds--contd

- Y₃Fe_{5-x}M_xO₁₂, (M = In, Sc, Al, Ga) Faraday rot. and i.r. modulator appls., 1.15 and 3.39 μ 8=23021
 Y₃Fe₅O₁₂:Ho³⁺, Faraday effect obs. 8=14271
 YGa garnet, Er³⁺ optical obs. intensities and quantum counter action 8=22979
 YGa garnet, reflectivity 8=5642
 YGa garnet:Ru³⁺, e.s.r. 8=18440
 YGaFe garnet, spheres and powders, determ. of Curie points 8=18367
 YH₃, elec. resistivity meas. 1000-1200°K 8=17942
 YH₃, stability of pressed pellets, expansion obs. 8=8871
 YMnO₃, ferroelec., domain struct. made visible by etching 8=2247
 Y₂Ni, alloys, mag. props. 8=18363
 Y₂Ni, cryst. structure 8=13247
 YNi₃ and YNi₅, X-ray diffraction data 8=17426
 Y(OH)₃ polycrystals, light scattering, diffuse, effect of anisotropy 8=23004
 Y₂O₃, addition of ThO₂, inhibition of grain growth during sintering 8=13444
 Y₂O₃ adsorption of ethanol, methanol, ethylene, acetaldehyde and H₂O, i.r. obs. 8=4768
 Y₂O₃, sintering, kinetics, data correlation 8=8258
 Y₂O₃-stabilized ZrO₂, stress relief mechanism 8=17839
 Y₂O₃-Al₂O₃ system, formation of compounds 8=4720
 Y₂O₃-Al₂O₃ system, liquidus curve meas. 8=16921
 Y₂O₃, sintering kinetics, resonant freq. meas. 8=17027
 Y₂O₃-ZrO₂, cubic phase stabilization at low temps. 8=8287
 YS, gaseous, dissociation energies 8=7616
 (Y, Sc)₂Si₂O₇, (thortveitite), e. s. r. 8=9447
 YTaO₄, M²⁺-phase of fergusonite, lattice structure 8=8562
 Y-Tb alloys, susceptibility 8=2299
 YVO₄:Bi, energy transfer and fluoresc. 8=2490
 YVO₄, crystal structure refinement 8=17427
 YVO₄: (Dy or Sm) activated, const. quantum yield 8=5670
 YVO₄:Eu, Bi, energy transfer and fluoresc. 8=2490
 YVO₄:Gd³⁺, e. p. r. spectrum 8=9428
 Y₂W₃, prep., lattice constants and elec. resistivities 8=5709

Yukawa potential. See Field theory, quantum meson field; Nuclear forces; Scattering.

Zeeman effect

- flames, absorption line profiles, Zeeman scanning 8=12044
 fluoroacetylene, molec. g value 8=12246
 ketene, microwave, rotational transitions 8=7581
 rel. to lasers, gaseous, parametric reson., non-linear theory 8=6435
 naphthalenes, substituted, r. m. s. splitting parameter 8=9435
 population transfer and alignment by spontaneous emission 8=20985
 positronium annihilation 8=15739
 rel. to Fe I 6302.5 Å line contours in sunspots, obs. 8=10418
 solid state spectroscopy, crystallographic alignment 8=22936
 in sun spectrum, magnetograph for meas. 8=14865
 Al₂O₃:V³⁺, absorption lines up to 79 kOe at 4.2°K 8=9500
 Br⁷⁹ in p-bromocetanilide, n. q. r. obs. 8=4228
 Ca₂WO₄:Yb³⁺ 8=14205
 Cu₂O n = 1 line in pulsed fields, 4.2°K 8=11157
 D, precise theory for calc. of Lamb shift 8=1158
 Gd I, rel. to g-values of levels 8=4077
 Gd II, rel. to g values for 67 levels 8=4076
 H, precise theory for n=2, calc. of Lamb shift 8=1158
 H₂⁺, sublevels by photodissociation 8=12195
 H₂O vapour laser, 118.65 μ m transition 8=3311
 He atom, aligned, magnetic field saturation, depolarization of scatt. resonance fluorescence 8=20982
 He³, splitting 8=16219
 He-Ne laser, resonances 8=15469
 Hg¹⁹⁸ double reson., Zeeman sublevel transitions shifts, obs. 8=21001
 KBr:Pb, A absorption band 8=9504
 KBr:Ti, A absorption band 8=9504
 KCl:Pb, A absorption band 8=9504
 KI:Ti, A absorption band 8=9504
 Na-D, longitudinal inverse, magneto-optical meas. of profile 8=4057
 α -O, at 4.2°K in 170 kOe mag. field 8=5626
 Tb I spectrum meas. 8=12073

Zener diodes. See Semiconducting devices/diodes.

Zener effect. See Metals; Semiconducting materials; Semiconductors.

Zeta-potential. See Electrokinetic effects.

Zinc

- basal slip, Al impurity effects 8=17836
 concentration gradient near p-n junction in III-IV cpds. 8=8678
 containing Fe, magnetic moment, revision of superconducting props. 8=9344
 crystal interband absorpt., 82° and 295°K 8=18545
 crystal, twinning kinetics in deformation at 8-10°K 8=17211

Zinc--contd

- crystallite nucleation rates rel. to prior adsorpt. on W emitter 8=1746
 crystals, basal dislocation mobility meas. 8=8735
 crystals, effect of mech. vibrs. on growth 8=8430
 crystals in rod form, prep. by recrystn. 8=8431
 damage caused by electric spark discharge machining 8=1959
 deformation at high strain rates in hardening process 8=17837
 de Haas-van Alphen effect, freq. meas. 8=5435
 diffused in GaAs, precipitates formation 8=17617
 diffusion in GaAs, coeff. Fermi level dependence 8=1918
 diffusion in GaAs, under excess As pressure 8=22153
 dislocation density, substructure, effect of Cd addition 8=17295
 dislocations and slip planes in single crystals 8=8725
 dislocations, revealed by etch-pit technique 8=13439
 elasto-plastic behaviour study of pure monocrystalline sheets 8=8848
 estimation in Cu, Pb and Al alloys, atomic absorpt. spectrometry 8=23184
 etch pits at dislocations 8=4985
 in ethylenediamine medium, polarography 8=18761
 Fermi surface and band structure, calc. 8=2111
 Fermi surface study by cyclotron resonance 8=13725
 films, evaporated, oxidation 8=1691
 g factor determ. by de Haas-van Alphen meas. 8=2110
 high-purity, spectrochem. anal., comparison of fine methods 8=23191
 labelled atoms, in crystn. interphase equilib. studies 8=21933
 liquid, cavitation intensity rel. bubble vibration 8=4521
 magnetic properties 8=22755
 molten, ultrasonic velocity 8=12867
 polycrystalline, γ -irrad. and non-irrad. X-ray scattering 8=22253
 pure single crystals, second-order pyramidal slip on {1213} {1212} system 8=22214
 self-diffusion isotope effect 8=4959
 single crystals, stress-wave cleavage 8=21927
 specific heat 8=22121
 spectrum of optically pumped, collision broadening obs. 8=6523
 stacking fault energy calcs. using pseudopotentials 8=17673
 surface corrosion pitting at dislocation sites 8=13440
 texture study by magnetores. and Hall effect 8=8454
 thermal anal. for thermometric fixed point 8=4645
 thermodynamic activity in ϵ -phase Ag-Zn alloys, electronic density of states, dependence 8=22109
 whisker growth from vapour on Zn substrate, and orientation 8=1747
 for Al electroplating, alkaline pretreatment soln. 8=14431
 in CO₂ solns., corrosion rel. to predominance diagrams 8=2523
 in GaAs, photoluminescence, effect of As pressure 8=23053
 K $\beta_{2,5}$ band fine structure 8=23027
 Zn²⁺, pseudopotentials 8=7409
 Zn^{64,66,68} superconducting transitions 8=9062
 Zn⁶⁸ deposition in bone, obs. 8=23766
 Zn-CdS graded band-gap semiconductor, luminescent spectra electric-field dependence 8=9134
 ZnO, impure, with adsorbed O₂, i.r. absorpt. studies 8=4796

Zinc compounds

- alloys atmospheric corrosion prevention, acrylic and polyurethane layers 8=14389
 cellulose, ZnO₂ diffusion and absorpt in cellulose membranes 8=21645
 ferrite form. from Fe(III) oxide at 400°C 8=23117
 gases, electrical resistivity and gas purification 8=4488
 photoconductivity changes, during luminescence excited by alternating field 8=22701
 phthalocyanine, luminesc. singlet-singlet transitions 8=18591
 rare-earth-zinc intermetallic compounds, paramagnetic susceptibilities 8=2298
 sphalerite: Fe²⁺, i.r. absorpt. spectra of Fe²⁺ 8=18570
 wurtzite, symmetrized combinations of plane waves 8=13666
 Cd-Zn solder alloys, high-strength, props. 8=5056
 Zn complexes, tetraphenylporphine and tetraphenylchlorine, as photoconductors 8=9117
 Zn ferrite, intermed. phases in formation 8=17087
 Zn sulphides, standard free energy of formation 8=9712
 Zn tellurite, glass formation, refractive index, optical transmission range 8=5644
 Zn-Ag alloy, Hall effect 8=17941
 Zn-Al alloy, Hall effect 8=17941
 Zn-Al, γ -ray spectrum distrib., compression effects 8=4999
 Zn-Al, superplastic, deformation behaviour 8=5090
 Zn-Bi alloys, solid and liq., thermo-e.m.f. 8=9240
 ZnCl₂, emission spectrum, visible region 8=4171
 ZnCl₂, polymerized with methyl methacrylate, methacrylonitrile and acrylonitrile 8=2527
 Zn-Cu alloy, Hall effect 8=17941
 Zn, Cd, β -Sb, elec. cond., Hall effect and thermoelec. power 8=2131

Zinc compounds—contd

- Zn₂Cd_{1-x}Sb_x, with hole conductivity, thermoelec. efficiency 8=2254
- Zn[Co(CO)₄]₂, cryst. and molec. struct. 8=17431
- ZnCr₂Se₄, magnetic interactions, spiral ground states 8=2296
- ZnF₂:Ni²⁺, i. r. luminesc. emission 8=18626
- ZnFe₂O₄, thermal conductivity rel. to non-stoichiometric vacancies 8=8660
- ZnFe₂O₄, thermal conductivity dependence on anion vacancies (produced by chem. reduction) 8=17543
- Zn₂GeO₄, high pressure transformations 8=13075
- ZnIn₂S₄ monocrystals, photocond. and voltage-controlled negative differential resist. 8=13917
- Zn₃In₂S₆, crystal structure 8=8567
- Zn₃In₂S₆, crystal structure 8=13301
- (Zn, Cu)₂K₂(SO₄)₂·6H₂O, dynamic polarization of protons, non-exponential behaviour 8=18476
- Zn₂Mn₃O₄, cation distrib. determ. 8=17364
- Zn-Mn alloys, low temp. electrical resistivity, influence of magnetic ordering 8=2136
- Zn-Mn alloys, specific heat 8=22121
- Zn(NH₄)₂(SO₄)₂·6H₂O, Co²⁺ e. p. r., forbidden hyperfine spectra 8=9420
- Zn(NO₃)₂·xH₂O, molten, i. r. and Raman spectra 8=16868
- Zn(NO₃)₂·xH₂O (x=4, 2), crystal structures 8=8565
- ZnO, acousto-electric oscillations, 1-5 GHz range 8=22613
- ZnO, attenuation of 3GHz sound waves from 4 to 40°K 8=17490
- ZnO crystal, change in surface conductivity as detector for atomic H beam 8=7475
- ZnO crystal ultrasonic vibrations, diff. of light 8=18514
- ZnO crystals, effect oxygen chemisorption on electrical conductivity 8=5160
- ZnO electrodes, cathodic reduction of aqueous ferri-cyanide ion 8=14423
- ZnO, electroreflectance rel. to gas adsorption 8=9564
- ZnO, formic acid adsorption, i. r. spectra 8=18705
- ZnO, luminescence mechanism 8=5672
- n-ZnO, neutron irradi., resistivity vs time and temp. 8=2109
- Zn-0.03 at. %Cd, Al, Cu or Ag, substructure rel. to impurity distrib. coeff. 8=17296
- ZnO, piezoelectric, microwave rectification 8=9227
- ZnO, polycryst. containing 3% Bi₂O₃, doped, semiconducting and semi-insulating props. 8=18205
- ZnO powder, elec. cond. 8=22612
- ZnO, radiation damage 8=22255
- ZnO, radical-recombination luminescence spectra 8=5673
- ZnO radicaloluminesc. and elec. cond. rel. to excit. mechanism, obs. 8=9635
- ZnO single crystal, transmission spectrum, rel. to exciton absorpt. and exciton-phonon complexes 8=14272
- ZnO single crystal, γ-irradiated, defect structure 8=22168
- ZnO, single crystals, vapour phase growth 8=21970
- ZnO, splitting of exciton lines by uniaxial stress 8=14273
- ZnO:Cu²⁺, absorption spectra 8=14211
- ZnO:(Ni, Co) crystals, Hall effect and conductivity, liquid N₂ to room temp. 8=9132
- ZnO:Ni(Co), lattice-vibration effects 8=9563
- ZnO-NiO ferrite, heating during ferromag. resonance 8=14082
- ZnO:Ni²⁺, i. r. luminesc. emission 8=18626
- ZnO:Zn, H, He, N, Ar and Kr ions energy losses and deterioration depth, obs. 8=18624
- ZnO:Zn phosphor heavy ion irradi. damage deterioration, obs. 8=18623
- ZnO-ZnSe systems, electroluminescence 8=9644
- β-Zn₃(PO₄)₂, cryst. struct. 8=8566
- ZnSO₄ soln. in H₂O-glycol, u. s. relax. 8=8062
- Zn(SO₃F)₂, i. r. spectra and mag. props. 8=9562
- ZnSb and ZnSb-CdSb mixed crystals, growth, elec. and thermal properties, investigation 8=13698
- ZnSe, absorption and reflect spectra in i. r., low temps. 8=23026
- ZnSe crystals, hexagonal, luminesc. 8=9631
- ZnSe crystals, recombination centre parameters 8=18627
- ZnSe, electron mobility rel. to prep. by direct fusion 8=2210
- n-ZnSe, Gunn effect 8=9136
- ZnSe:Ni²⁺, i. r. luminesc. emission 8=18626
- ZnSe, thin films, preparation by flash evaporation 8=13100
- Zn₂Se_{1-x}, LO and TO optical phonons 8=4909
- ZnSe₂Te_{1-x}, thin films, preparation by flash evaporation 8=13100
- ZnSiF₆·6H₂O and analogous cpds., X-ray exam. 8=17432
- Zn₂SiO₄, high pressure transformations 8=13075
- ZnTe, absorption and reflection spectra in i. r., low temps. 8=23026
- ZnTe, electrooptical effect, meas. at 10.6 μ 8=18515
- ZnTe films, electroabsorpt. rel. to determ. of reduced effective mass 8=18566
- ZnTe, i. r. transmission and reflection spectra 8=2460
- ZnTe, melt-grown, edge emission, annealing effects 8=5681
- ZnTe, melt-grown, flash-like thermoluminescence 8=5680

Zinc compounds—contd

- ZnTe, metal vacancies formation energies rel. to Te-Te covalent bonding 8=17608
- ZnTe, phase equilibria 8=16956
- ZnTe, photo-excited paramag. reson. of Cr³⁺ 8=5525
- ZnTe, photoluminescence spectra with anomalous temp. dependence 8=2492
- ZnTe, submillimetre-wave generation by optical difference-frequency mixing of ruby laser lines 8=18569
- ZnTe, thin films, preparation by flash evaporation 8=13100
- ZnTe, vapour press., torsion meas. 8=16963
- ZnTe:Pb, photo-induced paramag. resonance at 77°K 8=9440
- ZnWO₄ crystals, Mn²⁺ impurity, e. p. r. spectra rel. to conc. and temp. 8=5535
- ZnWO₄, e. p. r. spectrum of Cu²⁺ 8=5527
- ZnWO₄:Cr³⁺ (Li⁺), electric broadening of lines 8=18442
- ZnWO₄:Cr³⁺ spin-lattice relax. rel. to maser material 8=10994
- ZnWO₄:Cr³⁺, theory 8=14085
- Zn₂Y single crystals, tuning curve meas. and theoretical agreement 8=5485
- Zn₂Y, (Ba₂Zn₂Fe₁₂O₂₂), single crystals, Bloch wall structure determs. 8=5496
- Zn(II) perchlorates, water solns., u. s. velocity 8=12865
- ZrM₂-H₂ systems, (M = Cr, V, Mo), phase equilibria betw. 0° and 900°C 8=4723
- zinc sulphide
- cathodoluminescence spectra and bands lifetimes obs. 8=9646
- cubic, epitaxial growth by evaporation in ultra-high vac. 8=21893
- electrical conductivity and luminescence changes, alternating voltage effect 8=9259
- electroluminesc., brightness wave 8=9634
- electroluminescence, influence of illumination 8=9630
- electronic band structure rel. to optical props. 8=8928
- electroluminescent lamp, calibrated for use as standard light source 8=20067
- electrolumiphors, radiation-controlled enhancement 8=14344
- films, cathodoluminescence energy losses, rel. to photoluminesc. yield 8=9645
- growth, single crystals, from melt, 1850°C, 50 atm. Ar press. 8=21969
- Hall effect, e and hole mobility obs. 8=8898
- hexagonal → cubic, Cu-induced transformation 8=17107
- hexagonal, electroluminescent intensity distrib. rel. to dislocations 8=18621
- hexagonal, elastic stiffness conductivity dependence, corrections 8=17838
- luminescence reabsorption rel. to equilib. emission kinetics 8=9641
- luminescence, u. v., cryst. prep. conditions for optimum obs. 8=18629
- luminors, effect of Te on emission 8=14336
- minority carriers, photovoltage and photocond. meas. 8=22700
- phase transformations on crushing rel. to luminescent props. 8=17106
- phosphors, carrier redistrib. among traps under i. r. irradi., obs. 8=9135
- phosphors, cryoluminescence 8=14347
- phosphors, glow curves, meas., anal. and origin 8=5675
- phosphors, mech. excited, behaviour of light emissions 8=9633
- phosphors, optical spectra, luminescence and electroluminescence 8=5677
- phosphors, stimulation with i. v. wavelengths 8=5671
- phosphor, vibrational structure in stimulation spectrum 8=2459
- photoconductivity and Hall effect rel. to recomb. mechanisms 8=9258
- photoconductivity, optical quenching spectrum temp. dependence 8=9249
- photoelectret state and Gudden-Pohl effect, correl. 8=5679
- photovoltages, negative differential 8=22702
- polytype families 8=8564
- polytypes of family 24L-72R, unit cell and Zhdanov symbols 8=17194
- polytypes, structure and double refr. 8=8563
- radical-recombination luminescence spectra 8=5673
- self-diffusion of S 8=1931
- semiconductors band structure Green's function method 8=8913
- solution, convective motion due to electrolytic heating, obs. 8=1509
- ultrasonic vibrations, diff. of light 8=18415
- u. v. luminesc. under electron excitation 8=18619
- u. v. two-photon excitation 8=9632
- X-band travelling-wave light-intensity modulator 8=23025
- X-ray microanalysis, atomic number effect. correction, obs. 8=14479
- Cr³⁺ photo-induced e. s. r., decay obs. 77°-325°K 8=18441
- MnS/ZnS mixed crystals, phosphoresc. 8=2484
- S²⁻ photoluminescence, spectra, dark conductivity 8=5000
- β-ZnS film, growth and elect. props. 8=17143

Zinc compounds—contd**zinc sulphide—contd**

- ZnS:Ag, for energy loss of heavy ions obs. in KeV range 8=8758
 ZnS:Ag, red fluorescence, rapidly quenched 8=9648
 ZnS-Ag single crystal, luminescence, influence of i.r. radiation 8=5674
 ZnS:Ag, deterioration depth under prolonged heavy ions bombard. obs. 8=4998
 ZnS:CdS luminors, nonmonotonic var. 8=14337
 ZnS:CdS:Cu phosphor-silicic acid sol. adhesion to glass, obs. 8=8157
 ZnS:Cl colour centres excit. peaks from emission obs. 8=9642
 ZnS:Cu, Al phosphors, electroluminescence rel. to luminescent centre interactions 8=18622
 ZnS-CuAl and ZnS-CuMn freq. depend. of shape of light pulse 8=5675
 ZnS:Cu, brightness wave variations of electro-luminesc. 8=18620
 ZnS/Cu, Cl, luminance and complex dielectric constant, comparison during thermoluminescence 8=13875
 ZnS:Cu colour centres excit. peaks from emission obs. 8=9642
 ZnS-Cu electroluminescent phosphor, filling of traps during electric field excitation 8=14314
 ZnS:Cu electroluminescence brightness non-additivity obs. 8=9636
 ZnS:Cu electroluminesc. cells brightness build-up and ageing, obs. 8=9637
 ZnS:Cu elec. cond. rel. to electroluminesc., obs. 8=9133
 ZnS:Cu²⁺, filled trap distrib. rel. to duration of u.v. irradiation 8=18628
 ZnS:Cu, irradi., electroluminesc. quenching and stimulation rel. to elec. props. 8=9640
 ZnS:Cu phosphor condenser, characts depend on props. of crystal barrier layer 8=9657
 ZnS:Cu photo- and electroluminesc., effects of grinding, obs. 8=9647
 ZnS(Cu), surface temps., exptl determ. by photoluminescent emissions 8=13082
 ZnS:Fe²⁺ i.r. luminescence spectra, 5 and 77°K 8=2491
 ZnS:Ho³⁺ luminesc. and blue centres rel. to lattice-activator energy transfer, obs. 8=9643
 ZnS(Mn, Cu), high-efficiency d.c. electro-luminescence 8=18625
 ZnS:Mn films electroluminesc., pulse excitation characts, obs. 8=9639
 ZnS:Mn films electroluminesc., polarization effects obs. 8=9638
 ZnS:Mn, Cl, electroluminescence i.r. enhancement 8=5678
 ZnS:Mn²⁺, luminescence decay time 8=14326
 ZnS:Ni²⁺, i.r. luminesc. emission 8=18626
 Zn(S, Se)-Ag luminors, interaction of heated luminescence centres 8=14338
 ZnS:Sm³⁺ luminesc. and blue centres rel. to lattice-activator energy transfer, obs. 8=9643
 ZnS/ThO₂ multilayer mirrors, reflectance 8=2461
 ZnS:Tm growth and luminesc. rel. to Zn vacancies, obs. 8=8434

Zirconium

- age hardening and recovery in cold rolled, obs. 8=8872
 band structure, density of states and Fermi surface by cellular method 8=8942
 creep rel. to vacancy diffusion 8=4964
 diffusion of metallic impurities 8=17596
 diffusion in ZrH_{1.7}, ZrH_{0.8}, 800–1000°C 8=17595
 ore deposits in Republic of South Africa 8=9792
 oxidation, low-pressure. 8=14391
 star HR 1105, isotope ratios 8=14759
 H₂ definition, spectral-isotopic method 8=9743
 Ta content, spectrochemical determ. 8=9749
 Zr(IV), polarographic behaviour 8=18735
 α -Zr, deformed, form of polygonized sub-structure 8=22219
 α -Zr, polycrystalline, steady-state creep 8=4986
 α -Zr, H₂ terminal solubility in this, Zircaloy-2 and Zircaloy-4 8=8249
 α -Zr, with and without dissolved O, population anal. of occupied energy bands 8=17878
 β -Zr, diffusion behaviour from thermo and electro-transport meas. 8=17589
 β -Zr, diffusion mechanism 8=17594
 β -Zr, diffusion, summary of ORNL work 8=17593
 Zr⁹⁰, 10–80 MeV He⁴ ions, recoil range 8=13489
 ZrO₂-HfO₂ system, phase equilibria 8=21863

Zirconium compounds

- alloys, creep rel. to vacancy diffusion 8=4964
 carbide, powder, diffusion of Xe¹³³, activation energy, rel. to struct. 8=8686
 electrographic determ. of Zr in alloys 8=18762
 Zircalloy-2, cold rolled, age hardening and recovery, obs. 8=8872
 Zircalloy-2 corrosion in LiOH solns., hydriding rate, 300°C 8=5719
 Zircaloys-2 and -4, H₂ terminal solubility in these and in α -Zr 8=8249
 Zircaloy-2, grain boundary effects in deformation 8=13447

Zirconium compounds—contd

- Zircaloy-2, H₂ terminal solubility, thermal diffusion obs. 8=8250
 Zircaloy-2 tubing, ductility, effect of hydride 8=13615
 zircon, natural, luminescence origin 8=9649
 Zr hydride, effect on Zircaloy-2 tubing ductility 8=13615
 Zr rich alloys, effect of rolling temp. on texture developed 8=22399
 Zr-2.5wt%Nb, H₂ terminal solubility, thermal diffusion obs. 8=8250
 Zr-2.5wt.%Nb, cold rolled, age hardening and recovery rel. to stress relax., obs. 8=8872
 Zr-Al getter cartridge for u.h.v. systems 8=16726
 ZrC powder, in vacuum and Cs vapors, thermal emission props. 8=10843
 ZrC, stoichiometric, enthalpy and specific heat in range 500 to 2400°K 8=13366
 ZrC,H₂, formation in Zr-H-C system, and structure analysis 8=17433
 ZrCr₂Se₃, mag. structure by n-diff. 8=22865
 α -Zr-D solid solns., thermodynamic props. 8=8252
 ZrFe₂, atomic arrangement in homogeneity range of Laves phase 8=1813
 Zr-H alloys, deformation, thermally-activated mechanisms 8=13613
 α -Zr-H equilib. press. of dissolved H 8=8251
 ZrH_{1.69-1.96}, elec. resistivity meas. 1000–1200°K 8=17942
 (Zr,H)_{0.955}N, defect structure by chem. and lattice studies 8=17434
 Zr(HXO₄)₂·H₂O, (X = P, As), synthetic ion exchanger, crystal structure and exchange behaviour 8=13295
 Zr-Nb alloy, oxidation 8=14390
 (Zr_{0.6}Nb_{0.4})Fe₂, Laves cpds., anomaly in magnetization 8=2295
 ZrN₂H₄, formation in Zr-H-N system, and structure analysis 8=17433
 Zr + 4%Nb, transitions during destruction of superconductivity 8=22567
 Zr-Ni-Al system, R(M, X₂ and RMX₂ cpds., crystal structure 8=17435
 Zr-O alloy crystals, deformation rate controlling mechanism at 77–473°K 8=13614
 Zr-O coated W, field-emitted electron distrib. and work function 8=5413
 ZrO, sp. ht. and enthalpy in temp. range 100–2500°K 8=1878
 ZrO₂ between O₂ electrodes, thermoelec. power 8=9241
 ZrO₂, cubic, influence of neutron irradiation on ionic mobility 8=5152
 ZrO₂ films e beam evaporation and dielec. props. 8=22652
 ZrO₂, molec. geometry 8=7550
 ZrO₂, monoclinic, diffuse reflectance characts. as function of purity 8=18568
 ZrO₂, superplasticity during monoclinic \rightleftharpoons tetragonal transform. 8=5091
 ZrO₂-CeO₂ mixtures, high temp. semicond. 8=22614
 ZrO₂-MgO system, phase relations 8=13076
 Zr(OH)₂(MoO₃OH)₂, synthetic ion exchanger, crystal structure and exchange behaviour 8=13295
 ZrO₂-TiO₂ system, change of mineral composition by heat treatment 8=4721
 ZrO₂-TiO, system, phase X-ray obs. 8=17108
 ZrO₂, X-ray and spectrographic investigations of phase transitions and polymorphism 8=4722
 ZrO₂, Y₂O₃- and MgO-stabilized, stress relief mechanism 8=17839
 Zr₃Si₄, prep. and lattice structure 8=17436
 ZrZn₂, magnetic isotherms meas. c.f. band model of ferromagnetism 8=22764
 ZrZn₂ mag. moment rel. to impurity and intrinsic ferromag., \leq 150 kG 8=14041
 ZrZn₂, mag. props., in itinerant electron model of ferromagnetism 8=2336

Zodiacal light

- brightness and polarization distrib., from meteor model of zod. cloud 8=23341
 brightness and polarization, effect of solar activity 8=23690
 large declinations, covariance with 5577 Å OI line 8=14863
 polar, hypothesis of terrestrial origin 8=5961
 and Gegenschein, in tropics, photometric evaluation 8=2630

Zonal heating. See Atmosphere/thermodynamics.**Zone melting and refining**

- alkali halides, removal of OH⁻ and divalent cations 8=21931
 automatic device for multiple passage of a zone 8=4800
 column for crystal purification with cyclic solids movement 8=17223
 electron beam refiner, conversion to r.f. heating 8=23774
 graphite electrodes for spectroscopy, purification by electron beam 8=23187
 naphthalene, effect of ultrasound 8=13139
 Permalloy, possibility of electron-beam vaporization 8=8189
 single-pass, with variable segregation coefficients 8=1732
 zonal melting of thin layers, hydraulic feeding device 8=8394
 Cr-Ni-steels, vacuum melted, effect on electrochem. behaviour 8=9713
 Fe-Ni alloy, refining effect of Ge in vacuum melting, rel. to mag. props. 8=22815

Zone melting and refining—contd

GaP, prep. techniques, effect on luminescence and elec. props. 8=9611

Ge, recryst., by electron beam 8=17235

Ge semiconducting films, prep. 8=8320

InSb, rel. to selective etching in HCl solns. of

FeCl₃ 8=8383

Kr, purification by directional freezing 8=4810

Zone melting and refining—contd

Mo, removal of C and W rel. to residual resistivity 8=17935

Si, temperature field, theory 8=8427

Zone plates. See Diffraction/light.**Zoology**

pig-skin surface contamination by U 8=5987

planarian normal eye, electron microscopy 8=11240

planarian regenerating eye, electron microscopy 8=11241

IEE BOOK

Frequency generation & control for radio systems

IEE CONFERENCE PUBLICATION 31

Atomic clocks and crystal-controlled frequency generators are two of the devices used for the precise frequency control needed for such tasks as the packing of more stations into the radio spectrum and the measurement of time to the required accuracy for navigation and radar aids for aircraft and satellites. At a conference organised by the IEE, the IERE and the IEEE and held in London in May 1967, 32 papers were presented on the following aspects of frequency generation and control:

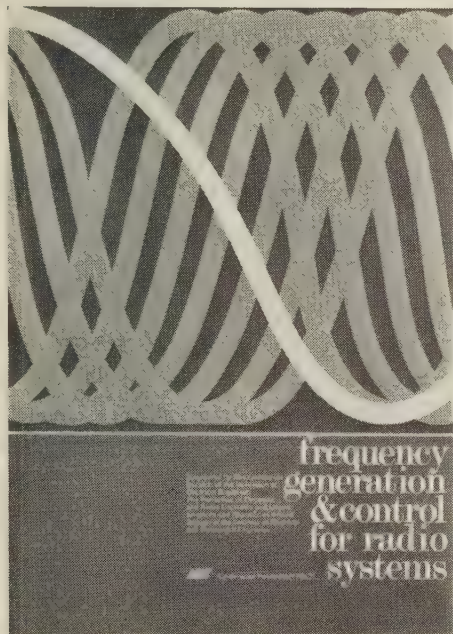
- Oscillators: atomic and transferred-electron sources
- Oscillators: crystal controlled
- Oscillators: measurement and correction
- Control and derivation of frequency: synthesisers
- Control and derivation of frequency: phase and frequency-locking and tracking systems
- Applications.

The papers have been reproduced by photolithography from the authors' manuscripts in IEE Conference Publication 31.

191 pp. A4 size, soft covers. 1967. price £3
(members £2 if ordered through sponsoring society)

Orders, with remittances, should be sent to:

Publications Department, IEE, Savoy Place, London WC2



Great activity in silicon-iron

Intense research activity into silicon-iron is brought to light in this new IEE publication which reviews the whole ambit of magnetic materials and their applications throughout the world.

The book contains 53 papers, presented at a conference held in London in September 1967 and sponsored by the IEE, IPPS and IEEE, which are grouped as follows:

- Orientation and domain structure
- Measurements on silicon-iron
- Permanent magnets
- Magnetostriction in silicon-iron
- Transformer noise
- Losses in silicon-iron
- Nickel-iron and aluminium-iron
- Garnets and ferrites
- Microwave properties of ferrites
- Thin films.

IEE Conference Publication 33: Magnetic materials and their applications.

266 pp. photolitho. A4. soft covers. 1967.

Price £3 15s. (members £2 10s. if ordered through sponsoring society)

Orders, with remittances, should be sent to:

Publications Department, IEE, Savoy Place, London WC2



Magnetic materials and their applications

IEE NEW BOOK



Acoustic noise and its control

IEE CONFERENCE PUBLICATION 26

Excessive noise can cause damage to mechanical structures, but its worst features are its effects on people. These range from annoyance, through interference with speech and communication, to permanent impairment of hearing. An international conference on acoustic noise and its control was organised jointly by the IEE, the IERE, the IEEE, the Institute of Physics & the Physical Society and the British Acoustical Society, and held in London in January 1967. 24 papers were presented by experts from the UK, the USA, Germany and France. The papers were grouped under four headings:

Subjective effects
Measurement analysis
Machines
Noise in buildings.

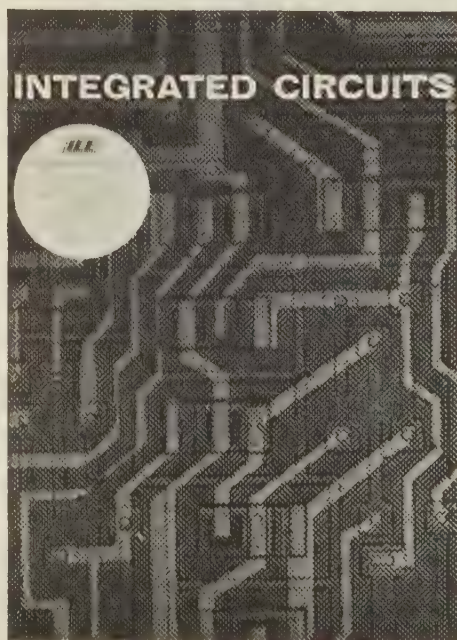
The papers have been reproduced by photolithography from the authors' manuscripts and bound as IEE Conference Publication 26.

101 pp. A4 size. soft covers. 1967. price £2 5s.
(members 30s. if ordered through sponsoring society)

Orders, with remittances, should be sent to:

Publications Department
IEE, Savoy Place, London WC2

IEE BOOK



Integrated circuits

IEE CONFERENCE PUBLICATION 30

'Expensive curiosity' is no longer an accurate description of integrated circuits. Seven years ago, although they had the great advantage of being small and highly reliable, integrated circuits were expensive and limited in capacity. Since then there have been substantial reductions in cost and a great extension of capacity, so that integrated circuits are now an essential part of modern equipments and are causing radical changes in the thinking of design engineers. The latest developments in integrated circuits were reviewed in detail at a conference held in Eastbourne on the 2nd-4th May 1967. The conference, sponsored by the IEE Electronics Division, the IERE and the IEEE, was attended by representatives from 18 countries. The 33 papers presented have been reproduced by photolithography from the authors' manuscripts and bound as IEE Conference Publication 30. The papers are grouped under these headings:

High-speed circuits
Film circuits
Economics: design and characterisation
Large-scale integration
Applications
Design and analysis circuits.

298 pp. A4 size. soft covers. 1967. price £3 15s.
(members £2 10s. if ordered through sponsoring society)

Orders, with remittances, should be sent to:

Publications Department, IEE, Savoy Place, London WC2

IEE Conference Publications

Timely & Authoritative Development & Progress Reviews

The IEE Publications Department, Savoy
Place, London WC2 will be glad to
send you further particulars on any of
our publications.

The papers presented at conferences sponsored by the IEE are regularly reproduced and bound into book form as IEE Conference Publications.

Each conference is organised by one or more of the IEE Divisions, POWER, ELECTRONICS or CONTROL & AUTOMATION, or by the SCIENCE & EDUCATION JOINT BOARD. The conferences thus survey the whole ambit of electrotechnology and control.

IEE Conference Publications are internationally recognised as up-to-date, authoritative reviews of development and progress in the various branches of electrotechnology and control with which they deal.

Conference
Publication
No.

Conference
Publication
No.

12 Components & materials used in electrical engineering

1965, 220 pp., 44 papers, £3

14 Applications of microelectronics

1965, 474 pp., 34 papers, £5

**15 Design criteria & equipment for transmission at 400kV and higher voltages
Part 2**

1965, 163 pp., £3

**16 Automatic control in electricity supply
Part 1**

1966, 349 pp., 29 papers, £3 15s.

Part 2

1966, 87 pp., £2 5s.

**17 Power applications of controllable semiconductor devices.
Part 1**

1965, 256 pp., 42 papers, £3

Part 2

1965, 57 pp., £1 10s.

18 V.H.F. and u.h.f. mobile communication systems & equipment

1966, 136 pp., 20 papers, £2 5s.

19 1966 British Joint Computer Conference

1966, 287 pp., 35 papers, £3 15s.

20 Delay devices for pulse-compression radar

1966, 88 pp., 16 papers, £2 5s.

21 Design & construction of large steerable aerials

1966, 380 pp., 66 papers, £4 10s.

**22 High-voltage d.c. transmission
Part 1**

1966, 454 pp., 92 papers, £7

Part 2

1966, 143 pp., £3

23 Electrical networks

1966, 405 pp., 22 papers, £5

24 Integrated-process-control applications in industry

1966, 140 pp., 15 papers, £3 10s.

25 Automatic operation & control of broadcasting equipment

1966, 163 pp., 30 papers, £3

26 Acoustic noise and its control

1967, 101 pp., 24 papers, £2 5s.

27 Microwave & optical generation & amplification

1966, 531 pp., 112 papers, £7 10s.

28 Air-traffic control

1967, 146 pp., 35 papers, £2 5s.

29 Advances in computer control

1967, 346 pp., 29 papers, £4 10s.

30 Integrated circuits

1967, 298 pp., 33 papers, £3 15s.

31 Frequency generation & control for radio systems

1967, 191 pp., 32 papers, £3

32 Computer technology

1967, 284 pp., 29 papers, £3 15s.

33 Magnetic materials & their applications

1967, 266 pp., 53 papers, £3 15s.

34 The economics of the reliability of supply

1967, 303 pp., 27 papers, £4 5s.

35 Metering & apparatus for modern electricity supply tariffs

1967, 380 pp., 72 papers, £5

36 M.f., l.f., and v.l.f. radio propagation

1967, 354 pp., 43 papers, £5

37 Servocomponents

1967, 264 pp., 27 papers, £4

38 Electrical methods of machining & forming

1967, 261 pp., 22 papers, £3 6s.

39 Interference problems associated with the operation of microwave communication systems

1968, 196 pp., 26 papers, £3 10s.

IEE PERIODICALS

Copies and information can be obtained from the

Publications Department

IEE, Savoy Place, London WC2

Proceedings IEE, published monthly, contains papers of industrial and technological interest from engineers and scientists the world over. Each issue comprises three self-contained groups of papers on Electronics; Power; and Control and Electrical Science, and these can be ordered as separate publications—*Electronics Record*, *Power Record*, and *Control & Science Record*.

Subscriptions to *Proceedings IEE*:

£18 p.a. IEE Associates and Associate Members under 28 and IEE Students: £2 10s. Other IEE members: £5

Separate copies of individual papers are available when they have been published in the *Proceedings*. Price 2s. each.

Electronics Record is published every two months, the papers being taken from the two previous issues of *Proceedings IEE*.

£9 9s. p.a. IEE Associates and Associate Members under 28 and IEE Students: 25s. Other IEE members: £2 10s.

Power Record, quarterly, takes its material from the three preceding issues of *Proceedings IEE*.

£6 p.a. IEE Associates and Associate Members under 28 and IEE Students: 15s. Other IEE members: 30s.

Control & Science Record, quarterly, includes papers on control and automation and electrical science taken from the three previous issues of *Proceedings IEE*.

£6 p.a. IEE Associates and Associate Members under 28 and IEE Students: 15s. Other IEE members: 30s.

Electronics Letters, published fortnightly, is an international journal offering speedy dissemination of research and development results in electronics, control and allied subjects, in the form of communications up to about 1200 words in length. Publication is within two to six weeks of receipt, giving the engineer an immediate picture of the latest developments in the field.

£10 p.a. IEE members: £3

Electronics & Power, published monthly, is a wide-ranging magazine covering the complete field of interest of electrical, electronic, and control technology by means of articles specially written for the busy engineer by experts in every sphere.

Electronics & Power alone: £5 p.a.

Electronics & Power with all issues of *IEE News*: £5 10s. p.a.

IEE members: free

IEE News is a twice-monthly tabloid newspaper for the professional electrical, electronics and control systems engineer. All IEE members receive *IEE News* free. Nonmember subscribers to *Electronics & Power* can also receive *IEE News* for an additional subscription as quoted above. There is no separate subscription to *IEE News*.

Students' Quarterly Journal is received free of further subscription by all IEE Students, Associates and Associate Members under the age of 30. It caters particularly for the younger member, and specialises in concise, topical articles on the latest advances in electrical, electronic and control engineering.

12s. 6d. p.a. Senior members: 8s. 6d. p.a.

SCIENCE ABSTRACTS PUBLICATIONS

Physics Abstracts is the recognised and long-established retrieval service for physicists. Published monthly, it provides 50 000 abstracts annually, drawn from 1000 British, American, Russian and other periodicals. Alphabetical author and subject indexes are given twice yearly.

£50 p.a.

IEE members: £10 p.a.

Electrical & Electronics Abstracts is the comprehensive literature-retrieval service for engineers. It is published monthly and provides 30 000 abstracts annually. Alphabetical author and subject indexes are issued twice yearly.

£40 p.a.

IEE members: £7 10s. p.a.

Control Abstracts is the monthly tool of information retrieval for all aspects of control and automation. It covers cybernetics, the electrical, electronic, mechanical, pneumatic and hydraulic aspects of automatic control, computers and all applications.

£25 p.a.

Cumulative Indexes

Physics Abstracts—subject index for the five years 1955–59 inclusive, bound in one volume, stiff covers and buckram cloth, 800 pp.

£20

Physics Abstracts—author index for the five years 1960–64 inclusive, bound in four parts, stiff covers and buckram cloth, 2300 pp.

£17 set

Members: £10 set

Physics Abstracts—subject index for the five years 1960–64 inclusive, bound in two parts, stiff covers and buckram cloth.

£40 set

Electrical Engineering Abstracts—subject index for the five years 1955–59 inclusive, bound in one volume, stiff covers and buckram cloth, 320 pp.

£15

Members: £9

Electrical Engineering Abstracts—author index for the five years 1960–64 inclusive, bound in two volumes, stiff covers and buckram cloth, 970 pp.

£12 10s. set

Members: £7 10s. set

Electrical Engineering Abstracts—subject index for the five years 1960–64 inclusive, bound in one volume, stiff covers and buckram cloth, 950 pp.

£20

Members: £12

Current Papers in Electrotechnology (CPE) is a monthly 'current-awareness' publication, listing in each issue more than 1300 titles and references of important papers and articles describing new developments in electrical and electronic engineering so that the technologist can see the world's literature at a glance only a few weeks after its appearance.

30s. p.a.

Current Papers in Physics (CPP) is the twice-monthly alerting publication for physicists. More than 1800 titles and references in each issue

£3 p.a.

Current Papers on Control (CPC) displays each month all the important titles and references in the world's literature on control and automation.

20s. p.a.

